Y 3. At 7: 16/19-24

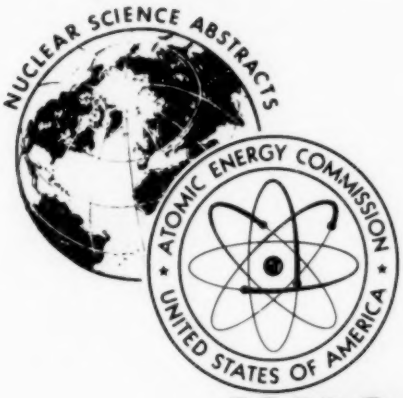

JAN 28 1966

NUCLEAR SCIENCE ABSTRACTS

Volume 19 Number 24

Abstracts 45726-48118

December 31, 1965

UNITED STATES ATOMIC ENERGY COMMISSION
Division of Technical Information

MIAMI UNIVERSITY LIBRARY

USAEC DEPOSITORY LIBRARIES

Collections of USAEC reports are maintained in the libraries of the organizations listed below for reference use by the general public. Facilities for making photocopies are available. The USAEC also makes available through these libraries atomic energy reports of countries other than the U. S. that are abstracted in *Nuclear Science Abstracts*.

ALABAMA
Auburn, Auburn University
ARIZONA
Tucson, University of Arizona
ARKANSAS
Fayetteville, University of Arkansas
CALIFORNIA
Berkeley, University of California
Davis, University of California
Los Angeles, University of California
San Diego, Public Library
Stanford, Stanford University
COLORADO
Boulder, University of Colorado
Denver, Public Library
CONNECTICUT
New Haven, Yale University
DELAWARE
Newark, University of Delaware
DISTRICT OF COLUMBIA
Washington, Library of Congress
FLORIDA
Coral Gables, University of Miami
Gainesville, University of Florida
GEORGIA
Atlanta, Georgia Institute of Technology
HAWAII
Honolulu, University of Hawaii
ILLINOIS
Chicago, John Crerar Library
Chicago, University of Chicago
Evanston, Northwestern University
Urbana, University of Illinois
INDIANA
Bloomington, Indiana University
Lafayette, Purdue University
IOWA
Ames, Iowa State University
KANSAS
Manhattan, Kansas State University
KENTUCKY
Lexington, University of Kentucky
Louisville, University of Louisville
LOUISIANA
Baton Rouge, Louisiana State University
New Orleans, Tulane University
MARYLAND
Baltimore, Johns Hopkins University
College Park, University of Maryland
MASSACHUSETTS
Cambridge, Harvard University
Cambridge, Massachusetts Institute of Technology
MICHIGAN
Ann Arbor, University of Michigan
Detroit, Public Library
East Lansing, Michigan State University
MINNESOTA
Minneapolis, University of Minnesota
MISSISSIPPI
State College, Mississippi State University
MISSOURI
Kansas City, Linda Hall Library
Rolla, University of Missouri School of Mines and Metallurgy
St. Louis, Washington University
MONTANA
Bozeman, Montana State College
NEVADA
Las Vegas, Nevada Southern University
Reno, University of Nevada
NEW JERSEY
Princeton, Princeton University
Teaneck, Fairleigh Dickinson University
NEW MEXICO
Albuquerque, University of New Mexico
NEW YORK
Albany, The University of the State of New York
Buffalo, State University of New York at Buffalo
Ithaca, Cornell University
New York, Atomic Industrial Forum, Inc.
New York, Columbia University
New York, New York University
Rochester, University of Rochester
Schenectady, Union College
Syracuse, Syracuse University
Troy, Rensselaer Polytechnic Institute
NORTH CAROLINA
Charlotte, Public Library of Charlotte and Mecklenburg County
Durham, Duke University
Raleigh, North Carolina State College
NORTH DAKOTA
Grand Forks, University of North Dakota
OHIO
Cincinnati, University of Cincinnati
Cleveland, Public Library
OHIO (CONT.)
Columbus, Ohio State University
Toledo, University of Toledo
Youngstown, Youngstown University
OKLAHOMA
Norman, University of Oklahoma
Stillwater, Oklahoma State University
OREGON
Corvallis, Oregon State University
Portland, Reed College
PENNSYLVANIA
Philadelphia, University of Pennsylvania
Pittsburgh, Carnegie Library
University Park, Pennsylvania State University
PUERTO RICO
Rio Piedras, University of Puerto Rico
RHODE ISLAND
Providence, Brown University
SOUTH CAROLINA
Columbia, University of South Carolina
TENNESSEE
Knoxville, University of Tennessee
Memphis, Public Library
Nashville, Joint University Libraries
Oak Ridge, Oak Ridge Institute of Nuclear Studies
TEXAS
Austin, University of Texas
College Station, Texas A & M University
Dallas, Southern Methodist University
Houston, Rice University
Lubbock, Texas Technological College
San Antonio, Public Library
UTAH
Salt Lake City, University of Utah
VIRGINIA
Blacksburg, Virginia Polytechnic Institute
Charlottesville, University of Virginia
Norfolk, Old Dominion College
WASHINGTON
Pullman, Washington State University
Seattle, University of Washington
WEST VIRGINIA
Morgantown, West Virginia University
WISCONSIN
Madison, University of Wisconsin
Milwaukee, Public Library
WYOMING
Laramie, University of Wyoming

NOTICE

A title page for Volume 19, Numbers 19–24, is included at the back of this issue for use in binding the fourth quarter of this volume.

CORRECTIONS

Vol. 18, No. 13, abst. no. 22516, lines 3 and 4 should read ... sov, and Ya. D. Mikhaylov. Izv. Vysshikh Uchebn. Zavedenii, Tsvetn. Met. 6(5), 116-20(1963).

Vol. 19, No. 6, abst. no. 9640, lines 4 and 5 should read ... shita and Shigeo Aoki (Furukawa Electric Co., Ltd., Japan), FAPIG (Tokyo), No. 31, 39-44(Apr. 1964). (In Japanese).

Vol. 19, No. 7, abst. no. 11536, line 5 should read ... Nara Gakugei Daigaku Kiyo, 12: 51-7(Feb. 1964). (In Japanese).

Vol. 19, No. 7, abst. no. 11820, lines 4 and 5 should read ... 21p. (CONF-640621-1). American Meteorological Society 230th National Meeting, Vancouver, B. C., June 22-4, 1964.

Vol. 19, No. 8, abst. no. 13111, line 4 should read ... and R. Scardino (Ospedale S. Gennaro, Naples). Riforma

Vol. 19, No. 8, abst. no. 13284, line 6 should read ... 9: No. 8, 41-3(1964). 8p. (Includes original, 3p.). Dep.(mn);

Vol. 19, No. 8, abst. no. 13559, line 5 should read ... Tekhn. Nauk, Mekhan. i Mashinostro., No. 4, 124-9

Vol. 19, No. 8, abst. no. 13619, line 1 should read ... (NVO-98-1) TECHNICAL REPORT, TASK 1:

Vol. 19, No. 9, abst. no. 15236, line 2 should read ... P. Wilflingseder (Universitat, Innsbruck). Klin. Med. (Vienna)

Vol. 19, No. 11, abst. no. 19658, lines 3 and 4 should read ... (Univ. of Illinois, Chicago). Am. J. Obstet. Gynecol., 91: 122-31(Jan. 1, 1965).

Vol. 19, No. 14, abst. no. 26305, lines 3 and 4 should read ... E. D. Sinitsyn, and A. P. Popov. Izv. Sibirsk. Otd. Akad. Nauk SSSR, No. 11, Ser. Khim. Nauk, No. 3, 48-54(1964). (In Russian).

Vol. 19, No. 14, abst. nos. 26306, 26307, 26308, lines 5 and 6 should read ... Izv. Sibirsk. Otd. Akad. Nauk SSSR, No. 11, Ser. Khim. Nauk, No. 3, ...

Vol. 19, No. 14, abst. no. 26648, line 2 should read ... NATED CLOTHING MONITOR. A. R. Jones (Atomic Energy of Canada

Vol. 19, No. 16, abst. no. 31536, line 5 should read ... York. Engineering Research Labs.). Mar. 1965. Con-

Vol. 19, No. 18, abst. no. 35045, line 4 should read ... Kniga, 2-Physique, 56(1961/62), 93-117(1963).

Vol. 19, No. 18, abst. no. 35871, line 3 should read ... N. Mex.). (Apr. 1965). Contract AT(29-1)-789. 34p.

Volume 19, Number 24, December 31, 1965

NUCLEAR SCIENCE ABSTRACTS

A semimonthly publication of the USAEC Division of Technical Information, Edward J. Brunenkant, Director.
Published by the USAEC Division of Technical Information Extension, Robert L. Shannon, Extension Manager.

Nuclear Science Abstracts covers the international literature on nuclear science and technology and provides the only comprehensive abstracting and indexing of this body of information. Published twice each month since 1947, *NSA* covers technical reports of the U. S. Atomic Energy Commission and its contractors, technical reports of U. S. Government agencies and other governments, universities, industrial and research organizations, as well as patents, books, and journal literature on a world-wide basis. Nearly 300,000 abstracts have appeared in *NSA* through Volume 18. The subject matter covered in *NSA* is described in issue Number 1 and in TID-4552, *Subject Scope of Nuclear Science Abstracts*, available free from the U. S. Atomic Energy Commission, Division of Technical Information Extension, P. O. Box 62, Oak Ridge, Tennessee 37831.

Abstracts are arranged according to a number of subject categories and subcategories. Definitions of categories appear in issues Number 1 and 13. If the language of the original item is not English, the language will be indicated. Translations are not abstracted where an abstract of the original item has appeared in *NSA*.

INDEXES TO NSA

Corporate author, personal author, subject, and report number indexes appear in each issue and are cumulated quarterly, semiannually, and annually. At the end of Volume 19, report number indexes will be cumulated in two separate publications. Indexes for Vols. 1–15 will be reissued with the latest public availability known at that time. This index will not be reissued. Indexes for Vols. 16–19 will be cumulated as a separate issuance and will be reissued annually to include all volumes beginning with Volume 16.

AVAILABILITY OF PUBLICATIONS ABSTRACTED

The public availability of all U. S. Atomic Energy Commission reports is indicated in the report number indexes. The availability of other reports, when known, is also indicated. The availability of some unnumbered reports is given in the abstract.

Dissertations abstracted in *Dissertation Abstracts* and included in *NSA* are available from University Microfilms, Inc., 315 N. First Street, Ann Arbor, Michigan.

Most of the published literature abstracted in *NSA* is on deposit at the Oak Ridge Institute of Nuclear Studies Library, Oak Ridge, Tennessee, (a USAEC depository library) and is available through interlibrary loan. When requesting papers from this source, it is important that *NSA* volume and abstract number be cited.

HOW TO OBTAIN NUCLEAR SCIENCE ABSTRACTS

NSA is available on an exchange basis to universities, research institutions, industrial firms, and publishers of scientific information. Inquiries should be directed to the U. S. Atomic Energy Commission, Division of Technical Information Extension, P. O. Box 62, Oak Ridge, Tennessee 37831.

Government agencies may obtain *NSA* free of charge.

NSA is available to the general public on a subscription basis from the Superintendent of Documents, U. S. Government Printing Office, Washington, D. C. 20402, as follows:

For the 24 regular issues, $30.00 domestic, $37.00 foreign. A single issue costs $1.75, plus 25 per cent for foreign mailing. Domestic rates apply to the United States, Canada, Mexico, and Central and South American countries except Argentina, Brazil, British and French Guiana, Surinam, and British Honduras. Foreign rates apply to the countries excepted above and to all other countries throughout the world.

For the quarterly, semiannual, and annual indexes, $22.00 domestic, $25.00 foreign.

Multivolume subject and author indexes are available as follows:

Vols. 1–4 (1948–1950) Johnson Reprint Corporation, 111 Fifth Avenue, New York, N. Y. 10003, $30.00.

Vols. 5–10 (1951–1956) Superintendent of Documents, U. S. Government Printing Office, Washington, D. C. 20402, $5.25.

Vols. 11–15, Subjects, Superintendent of Documents, U. S. Government Printing Office, Washington, D. C. 20402, $19.00.

Vols. 11–15, Personal Authors, Superintendent of Documents, U. S. Government Printing Office, Washington, D. C. 20402, $14.25.

Vols. 11–15, Corporate Authors, Superintendent of Documents, U. S. Government Printing Office, Washington, D. C. 20402, $2.50.

Cumulative Report Number Index, Vols. 1–18, is available from the Superintendent of Documents, U. S. Government Printing Office, Washington, D. C. 20402, $5.75.

Annual Indexes are available separately from the U. S. Government Printing Office as follows:

Vol. 16, Subject and Authors, $9.75.
Vol. 17, Subject and Authors, $12.25.
Vol. 18, Subject and Authors, $12.50.

ACKNOWLEDGMENTS

Agreements between the United States Atomic Energy Commission and the following organizations with regard to providing continuing services and specific literature coverage for *Nuclear Science Abstracts* are gratefully acknowledged:

American Institute of Physics; Atomic Energy of Canada Limited; Atomic Energy Research Establishment, United Kingdom; European Atomic Energy Community (EURATOM); Gmelin Institute; International Atomic Energy Agency; Japan Atomic Energy Bureau — Japan Atomic Energy Research Institute; Netherlands Patent Office; Reactor Centrum Nederland.

TABLE OF CONTENTS

Volume 19, Number 24, December 31, 1965

Category	Page
BIOLOGY AND MEDICINE	5715
General	5715
Ecology	5718
Metabolism, Tissue Distribution, and Toxicology	5718
Radiation Effects	5727
Radiation Effects Therapy and Countermeasures	5764
Radiation Hazards and Protection	5768
Radiotherapy and Radiodiagnosis	5769
CHEMISTRY	5791
General	5791
Analytical Procedures	5792
Inorganic and Physical Chemistry	5799
Organic Chemistry	5808
Radiation Chemistry	5811
Radiochemistry	5823
Separation Processes and Procedures	5825
ENGINEERING	5830
General	5830
Applications of Nuclear Explosions	5831
Facilities and Equipment	5832
Heat Transfer and Fluid Flow	5837
Materials Testing	5841
Protective Structures	5842
Space Propulsion	5843
Vacuum Engineering	5844
GEOLOGY AND MINERALOGY	5845
General	5845
Natural Radioactivity and Fallout	5845
Techniques and Equipment	5849
Thorium and Uranium Minerals	5851
HEALTH AND SAFETY	5852
INSTRUMENTATION	5863
General	5863
Radiation Detection	5868
Radiation Effects	5880
ISOTOPE TECHNOLOGY	5882
Industrial Applications	5882
Power Application	5885
Separation and Production	5885
MATHEMATICS AND COMPUTERS	5887
METALS, CERAMICS, AND OTHER MATERIALS	5888
General	5888
Corrosion	5892
Fabrication	5894
Properties and Structure	5897
Radiation Effects	5908
METEOROLOGY	5914
PHYSICS	5915
General	5915
Accelerators	5920
Astrophysics and Cosmology	5923
Atomic Physics	5927
Cosmic Radiation	5934
Criticality Studies	5935
Direct Energy Conversion	5935
Elementary Particles and Radiations	5938
Field Theory and Quantum Mechanics	5950
Geophysics	5954
Low Temperature Physics	5961
Neutron Physics	5966
Nuclear Properties and Reactions	5969
Plasma Physics and Thermonuclear Processes	5986
Shielding	6007
Solid State Physics	6008
REACTOR TECHNOLOGY	6013
General	6013
Auxiliaries and Components	6014
Criticality Studies	6017
Design and Feasibility	6021
Fuels	6021
Power and Power-Breeder Reactors	6023
Propulsion and Space	6030
Research and Test Reactors	6031
WASTE DISPOSAL AND PROCESSING	6035
GENERAL AND MISCELLANEOUS	6037
CORPORATE AUTHOR INDEX	INDEX-1
PERSONAL AUTHOR INDEX	INDEX-12
SUBJECT INDEX	INDEX-62
REPORT NUMBER INDEX	INDEX-163

STAFF OF NUCLEAR SCIENCE ABSTRACTS

MANAGING EDITOR

John W. Norris

ASSISTANT MANAGING EDITOR

Donald D. Davis

ASSOCIATE EDITORS

Lawrence T. Whitehead
David E. Bost
Robert C. Kelly
Lee M. Thompson

SUBJECT INDEX EDITOR

Everett J. Hoffman

EVALUATORS

William D. Matheny
John H. Mitchell
Mary H. Newman

ABSTRACTORS

F. S. Armstrong (AECL)
Jane G. Buchanan
D. Lamar Cason
Helen G. Donald
James R. Dulaney
Wells L. Green
Bernard O. Griggs
Mary Catherine Grissom
Fernando J. Hamilton
Phyllis C. Hansen
Thomas F. Heagerty
Carolyn D. Houston
Rose V. Jermain
Betty L. McDowell
Jean F. Peckham
Mona H. Raridon
Julia Redford
Lila B. Smith
Charles E. Stuber
Martha J. Thomas
Anne G. Ward
David C. West
Milton O. Whitson

SUBJECT HEADING SPECIALIST

Robert E. Upchurch

CORPORATE AUTHOR SPECIALIST

Clara L. Fox

DESCRIPTIVE CATALOGING SPECIALIST

J. Paul Meredith

SCHEDULING AND PUBLISHING COORDINATOR

Brainard L. Patton

Communication concerning the editorial policy and content of *NSA* should be addressed to the Managing Editor, *Nuclear Science Abstracts*, AEC Division of Technical Information Extension, P. O. Box 62, Oak Ridge, Tennessee 37831.

Use of funds for printing this publication approved by the Director of the Bureau of the Budget, May 20, 1963

Volume 19, Number 24 December 31, 1965

NUCLEAR SCIENCE ABSTRACTS

BIOLOGY AND MEDICINE

General

45726 (BNL-9488) PROPERTIES OF GENES. Demerec, M. (Brookhaven National Lab., Upton, N. Y.). [1965]. Contract AT(30-2)-Gen-16. 20p. (CONF-650940-1). Dep. mn; CFSTI $1.00 cy, $0.50 mn.

From Genetics Society of America, Mendel Centennial Conference, Fort Collins, Colo.

Historical aspects of genetic studies by Mendel are discussed. A paper by Mendel supplied evidence, well supported experimentally, that characters carried by two parents segregate in the offspring without undergoing any change. From this evidence Mendel concluded that factors present in the germ cells of the parents are responsible for the transmission of inherited characteristics. From that time forth these factors, the bearers of heredity, later called genes have been pictured as material particles possessing a high degree of stability. Later studies revealed that the genes are located in chromosomes and are, as a rule, present in every living cell of an organism. Until quite recently a good model of physical gene structure was not available. Several geneticists calculated gene size in terms of diameter and radius, reflecting the prevalent visualization of genes as spherical bodies. The same point of view was suggested in Belling's chromomere hypothesis. A new concept was introduced by the Watson-Crick model of DNA and its application to genetic material. But the idea that the gene is the functional unit of a genetic system has remained unchanged and has withstood several attempts at modification. (36 references.) (auth)

45727 (BNL-9506) SPECTRAL CHARACTERISTICS OF A BACTERIOCHLOROPHYLL-PROTEIN COMPLEX FROM GREEN PHOTOSYNTHETIC BACTERIA. Olson, John M. (Brookhaven National Lab., Upton, N. Y.). [1964]. Contract AT(30-2)-Gen-16. 10p. (CONF-650942-1). Dep. mn; CFSTI $1.00 cy, $0.50 mn.

From 2nd Western Europe Conference on Photosynthesis, Zeist, Netherlands.

A water soluble bacteriochlorophyll-protein of molecular weight 1.7×10^5 was isolated from Chloropseudomonas ethylicum. The macromolecular complex contains 21 ± 2 molecules of bchl a, probably buried inside an outer envelope of protein. At 77°K the far red absorption band (809 mμ) of bchl a in the complex splits into 3 peaks at 805, 814, and 824 mμ; and the orange band (603 mμ) splits into 2 peaks at 601 and 607 mμ. Under special conditions at room temperature the bchl-protein complex appears to undergo a conformational change which results in strong interaction between some of the bchl a molecules. This interaction is inferred from the apparent splitting of the 603-mμ band into two bands at 585 and 618 mμ and the splitting of the 809-mμ band into two bands at 785 and 840 mμ. (auth)

45728 (NYO-910-23) BIOLOGICAL EFFECTS OF RADIATION, AND RELATED BIOCHEMICAL AND PHYSICAL STUDIES. Summary Progress Report, July 1, 1950–March 15, 1965. (Sloan-Kettering Inst. for Cancer Research, New York). June 23, 1965. Contract AT(30-1)-910. 196p. Dep. mn; CFSTI $5.00 cy, $1.00 mn.

Summaries of research done in the period July 1, 1950 to March 15, 1965, are presented, and bibliographies of publications resulting from research in the period are included. Separate abstracts were prepared for reports on biophysics, biological chemistry, and clinical investigations. (H.G.D.)

For abstracts of individual sections see: 45729, 45757, and 46158.

45729 (NYO-910-23, pp 1-111) DIVISION OF BIOPHYSICS. (Sloan-Kettering Inst. for Cancer Research, New York).

Progress is reported on: radioisotope metabolism studies; mammalian bone studies; cellular radiation mechanisms, including radioisotope electron spectra determinations, radiation chemistry mechanisms, and theoretical studies of x-ray, γ-ray, and electron penetration; electron spin resonance; intermediary metabolism; element concentrations by special radiation techniques; radioautographic studies of isotope localization; electronics construction; and metabolism of steroid hormones in man. A bibliography of publications resulting from the research is included. (H.G.D.)

45730 (ORNL-3752) THE JOINT NATIONAL INSTITUTES OF HEALTH-ATOMIC ENERGY COMMISSION ZONAL CENTRIFUGE DEVELOPMENT PROGRAM. Semiannual Report, January 1–June 30, 1964. Anderson, N. G. (Oak Ridge National Lab., Tenn.). Mar. 1965. Contract W-7405-eng-26. 66p. Dep. mn; CFSTI $3.00 cy, $0.75 mn.

Work done under the Zonal Centrifuge Development Program on the application to difficult biophysical separation problems of techniques and instruments developed by the AEC is described. Work on zonal centrifuge systems designed to separate particles ranging in size from whole cells to small molecules has progressed with the development of several new rotor systems. The B-IV rotor has been shown to effectively separate quantities of macroglobulin from rat and other animal sera, thereby extending the usefulness of this instrument down to 20S. By application of the two-dimensional S-ρ separation system previously described, a clear spectrum of rat liver glycogen particles has been obtained, and the molecular structure revealed by negative staining is under investigation. Virus-like particles have been recovered from a human breast tumor with the same technique. Further studies on centrifugal fast freezing show that a high percentage of yeast cells survive freezing, but that the lethal damage is done during warming, which must be done rapidly if a high survival rate is to be obtained. Theoretical studies on the particle capacity of gradients in zonal centrifuges are being carried to the point that experimental studies may be designed to examine anomalous sedimentation behavior and band spreading. The low-

speed A-IX rotor has been redesigned and strengthened and is now designated A-XII. Scanning systems that would make this rotor an analytical centrifuge have been completed. Continuous-flow rotors in which the sediment particles are banded in a gradient during the continuous-flow process (rotor B-VIII) have been built and successfully tested. A completely enclosed virus separation facility has been designed for large-scale virus separation. In addition to centrifuges, new countercurrent systems for liquid–liquid extractions and the flame ionization detector for nonvolatile samples are under development. A prototype automated system for carbohydrate analysis has been completed and tested with a variety of sugar-containing samples. With an experimental high-pressure capillary column nucleotide analyzer, it has been demonstrated that rapid analysis of very small samples can be performed with micro ion exchange beads, warm columns, a high flow rate, and columns of very small bore. (auth)

45731 (JPRS-31547) TRANSLATIONS ON BIOPHYSICS AND PHYSIOLOGY. Translated from Dokl. Akad. Nauk SSSR, 162: 688-93; 713-18(1965). 24p. (TT-65-32043). CFSTI $1.00 cy, $0.50 mn.

Separate abstracts were prepared on two articles included. Other articles discuss cortical primary responses and physiological excitation in muscles. (C.H.)

For abstracts of individual papers see: 45821 and 46342.

45732 (JPRS-31602) TRANSLATIONS FROM LIBERATION ARMY MEDICAL JOURNAL, VOL. II, NO. 1, JANUARY 1965. Translation of Chieh-Fang-Chun I-Hsueh Tsa-Chih, 2: No. 1, 1-91(Jan. 1965). 334p. (TT-65-32097). CFSTI $7.00 cy, $1.75 mn.

For an abstract of the individual paper see: 46038.

45733 (JPRS-31933) STUDIES ON THE EFFECTS OF ANTI-RADIATION DRUGS. Translated from Farmakol. i Toksikol., 28: 347-9; 351-5(May-June 1965). 13p. (TT-65-32427). CFSTI $1.00 cy, $0.50 mn.

Separate abstracts were prepared on two papers in this report. (C.H.)

For abstracts of individual papers see: 45823 and 46005.

45734 (TT-64-11407/3) ACTA PHYSIOLOGICA POLONICA. Translated Reprint of Acta Physiologica Polonica, 15: No. 3, 1964. 136p. CFSTI $4.00 cy, $1.00 mn.

45735 THE USE OF ANALOGUE COMPUTERS IN TESTING MODELS IN MEDICINE AND BIOLOGY. Adler, K. H. (Telefunken AG, Konstanz, Ger.). Atompraxis, 11: 424-6(Aug. 1965). (In German).

In studying the dynamic behavior of medical and biological systems, it is possible to establish hypotheses which in turn can lead to mathematical formulations. The validity of such models can be tested with analog computers; this is demonstrated by an example. (auth)

45736 ROLE OF THE ACTION POTENTIAL IN EXCITATION-CONTRACTION COUPLING. Sandow, Alexander; Taylor, Stuart R.; Preiser, Hanna (Inst. for Muscle Disease, New York). Federation Proc., 24: 1116-23 (Sept.-Oct. 1965).

Excitation-contraction (E-C) coupling was studied by considering essentially only the relation between the action potential and its associated twitch under a variety of physiological conditions. Attempts were made to determine the parameters of the action potential's function that are relevant to its role in E-C coupling, and to infer something about the sequence of processes enabling electrical changes to activate mechanical changes. The analysis is based on studies of frog sartorius or toe muscle (fast fiber) responses at room temperature. Caffeine, methylsulfate, Cl^-, NO_3^-, and SCN^- were used to regulate contraction by the mechanical threshold, and Zn^{2+} and UO_2^{2+} were used to regulate contraction by duration of the action potential. The results showed that the role of the action potential in E-C coupling is to swing the membrane potential beyond the prevailing mechanical threshold for the duration of the mechanically effective period and thus initiate the sequence of coupling reactions activating contraction. During the mechanically effective period (MEP) the action potential continuously develops the condition activating contraction in the myofilaments, and this condition is more effective in causing contraction the lower the mechanical threshold and the longer the action potential's duration. (P.C.H.)

45737 THEORETICAL STUDIES ON THE METHODOLOGICAL PROCEDURES OF RADIATION BREEDING. V. PROCEDURES FOR TAKING X_2-SEEDS IN RELATION TO TILLERS FOLLOWING SEED IRRADIATION IN AUTOGAMOUS PLANTS. Yoshida, Yoshio (Kyushu Agricultural Experiment Station, Chikugo, Japan). Idengaku Zasshi, 40: 125-33(Apr. 1965).

To detect at least one desirable mutant with a minimum total number of X_2-plants or of combined X_1- and X_2-plants, two methods were established as suitable in relation to tillers of X_1-plants. They are: a type of the one-plant-two-grain method (method D_2) and of the one-plant-three-grain method (method E_3) in which one grain is taken from each of two or three heads of an X_1-plant respectively. The methods were evaluated by considering the probability that one or more plants with the mutant allele in homozygous recessive form will appear in the total X_2-plants in relation to the number of heads per X_1-plant and to the independent degrees of mutation among the heads of the X_1-plant. The one-plant-one-grain method (method C) proposed by Yoshida (1962) is the best when the number of heads per X_1-plant (t) is equal to or smaller than three and method C or D_2 is the best when $t \geq 4$. No single method is known to cover all of the advantages. However, methods D_2 and E_3 will be better than the one-plant-two-grain method and the one-plant-three-grain method proposed in the first report of this series when $t \geq 2$ and $t \geq 3$ respectively. Generally speaking, it does not seem advantageous to use the one-ear-one-grain method, especially the one-ear-two-grain method and the one-ear-three-grain method. (auth)

45738 EFFECTS OF ACTINOMYCIN D ON THE LENS REGENERATING SYSTEM. Yamada, Tuneo; Roesel, Marion E. (Oak Ridge National Lab., Tenn.). J. Embryol. Exptl. Morphol., 12: 713-25(Dec. 1964).

Autoradiographic studies of transformation of iris into lens during Wolffian lens regeneration of adult Triturus viridescens indicate an enhancement of RNA synthesis in the nucleus of the iris cells in the early phase of regeneration. Activation of protein synthesis and production of lens antigens follow the enhancement of RNA synthesis, suggesting the possibility that lens removal elicits synthesis of specific RNA's which in their turn induce synthesis of proteins essential for transformation of the tissue. Thus it should be possible to suppress lens regeneration by subjecting the system to an inhibitor of RNA synthesis, a possibility which was tested, using actinomycin D as the inhibitor. Actinomycin was injected into the body cavity of adult T. viridescens, in which the tissue transformation had been initiated by lens removal, and the effects of such treatment on the tissue transformation were studied in several sections of the regenerates. One μg/g body weight was injected every day or every other day for a 3- to 12-day period at various phases of lens regeneration. Administration of actinomycin during the early phase of lens regeneration for a period longer than 4 days suppressed the progress of regeneration. Suppression was complete or partial depending upon the experimental conditions. Four daily injections were given at various phases of lens regeneration. When the treatment began after appearance of primary lens fiber cells, differentiation of those cells proceeded normally, while developmental arrest and disintegration were observed in the lens epithelium. The actinomycin treatment given after the regenerate has formed a well-differentiated lens caused a degenerative inhibition of the lens epithelium, but there was no appreciable change in the morphology of lens fibers. The nonregenerating iris and lens did not show any morphological sign of abnormalities after the same treatment. A lens abnormality similar to the one observed here can be produced by x irradiation during the intermediate phase of lens regen-

eration. This finding complements present results in strongly suggesting a capacity of differentiation of the cytoplasm of lens fibers, independent of nuclear activities. (BBB)

45739 THE RADIOISOTOPE PRECIPITATION TEST FOR STUDY OF Q FEVER ANTIBODIES IN HUMAN AND ANIMAL SERA. Tabert, Gayle G.; Lackman, David B. (Rocky Mountain Lab., Hamilton, Mont.). J. Immunol., 94: 959-65(June 1965).

The radioisotope precipitation test (RIPT) was adapted for detecting antibody to Coxiella burnetti. In the RIPT, radiolabeled antigen reacts with specific antibody and anti-γ-globulin (AGG) giving a sedimentable precipitate. The radioactivity of precipitate and/or supernatant fluid is measured and is the criterion of antigen-antibody reaction. Use of a radiolabeled antigen makes this modification of the anti-globulin test highly sensitive for detecting low levels of antibody. The detection of low levels of antibody to C. burnetti is important because the complement fixation test (CFT) is often negative with serum of vaccinated individuals or those who have had subclinical infections with C. burnetti, and the latter may develop severe local reactions when they are subsequently given a dose of vaccine. The purified phase-I Q fever antigen was labeled with ^{131}I by persulfate oxidation; the antigen was washed four times to remove unbound iodine and resuspended in 5 ml of 0.02M phosphate buffered saline, pH 7.1. The labeled antigen was diluted 1:300 to 1:1000 for use, depending on the radioactivity present. After precipitation of the antigen in the test, the remaining ^{131}I-antigen in the supernatant is measured. Results on vaccinated groups and groups occupationally exposed demonstrated that the sensitivity of the RIPT is much greater in man than the CFT or capillary agglutination test. The finding that there are so few cases of Q fever among exposed persons may be partly explained by the high percentage already having antibody detectable by the RIPT. The test was further applied to cattle, guinea pig, and mouse serum but the increased sensitivity observed with human serum was not present with these samples. (BBB)

45740 ERYTHROPOIETIC CAPACITY OF SHORT-TERM MOUSE MARROW CULTURES. Smith, L. H.; McKinley, T. W. Jr. (Oak Ridge National Lab., Tenn.). J. Natl. Cancer Inst., 35: 573-7(Sept. 1965).

Maintenance of erythropoietic activity of mouse bone marrow cells in short-term culture was investigated as part of a study of postradiation environment. Erythropoietic activity was measured by ^{59}Fe uptake by spleens of lethally irradiated mice given injections of normal or cultured marrow cells. Medium composition and physical factors of marrow culture were investigated. Best maintenance at 37°C was obtained with commercial medium TC 199 + 25 percent mammalian serum, and there was a broad pH optimum (6.6 to 8.0). There was an inverse relation between maintenance of erythropoietic activity and culture temperature from 30 to 45°C. Maintenance was improved at temperatures of 2 to 30°C. Decline of activity in culture reflects inability of the stem cell compartment to maintain and replenish itself. (auth)

45741 HIGH RESOLUTION ISOTOPE TRACING IN ELECTRON MICROSCOPY USING INDUCED NUCLEAR REACTIONS. Malmon, A. G. (National Inst. of Health, Bethesda, Md.). J. Theoret. Biol., 9: 77-92(July 1965).

A system for high resolution isotope tracing in the electron microscope is proposed that is based on the detection of tracks of charged particles which are products of induced nuclear reactions of nuclei with desirable properties from a biological standpoint. The tracer atom could be ^{15}N, ^{17}O, or ^{18}O. When ^{17}O is exposed to thermal neutrons, or ^{15}N and ^{18}O to protons of selected energies, there is a relatively high probability that the nucleus will disintegrate into an α particle and a larger residual nucleus. Either of these products may have enough ionizing power to form a track in a thin film which may then be observed in the electron microscope. These tracks would serve as markers indicating the original position of the tracer atom with respect to the biological specimen with a probable resolution in the range of 20 to a few hundred Angstrom units. The experimental and theoretical literature on the electron microscopic observation of tracks found by charged particles is reviewed, and it is shown that it is reasonable to predict that tracks formed by the products of certain induced nuclear reactions may be seen in biological specimens. Experimental details and practical considerations are described. For thermal neutron-induced reactions where the neutron source is a nuclear reactor, large numbers of samples already mounted on electron microscope specimen grids may be conveniently irradiated at one time. In the case of proton-induced reactions, where the source is a positive ion accelerator, only a single beam of protons will be available, and several samples already could be mounted on electron microscope specimen grids side by side. (BBB)

45742 ON THE COUNTING STATISTICS. Potschwadek, B. (Universitaet, Rostock, Ger.). Kernenergie, 8: 478-81(Aug. 1965). (In German).

The relative error for preset counts, preset time, or extremizing is calculated from general points of view as they are valid in medical isotopic laboratories. The results may ever be represented in the form $\epsilon\sqrt{TQ} - 1 = 0$, which shows that the best technique is the method or condition of measuring yielding the highest value of Q. Q is calculated for some conditions occurring in practice and the values are compared. (auth)

45743 CONTRIBUTIONS OF RADIOBIOLOGY TO THE PROGRESS OF CANCEROLOGY. Lacassagne, A. (Foundation Curie, Paris). Minerva Radiol., Fisioterap. Radiobiol., 10: 191-5(June 1965). (In Italian).

The principal progress that radiobiology has contributed to cancerology is reviewed. The mechanism of carcinogenesis indicated by radiobiology and the cure of malignant tumors are considered. (J.S.R.)

45744 BRITISH EMPIRE CANCER CAMPAIGN FOR RESEARCH FORTY-SECOND ANNUAL REPORT COVERING THE YEAR 1964. PART II. THE SCIENTIFIC REPORT. London, British Empire Cancer Campaign for Research, 1965. 727p.

Advances in cancer research in Great Britain during 1964 are summarized. Topics discussed include carcinogenesis, chemotherapy, radiobiology, radiation chemistry, laboratory studies on human cancer, physics, cytogenetic and chromosome studies, tumor virology, hormones, cellular constituents and metabolism, immunology in relation to cancer, general pathology, the concomitants of cancer, cancer diagnosis, and clinico-pathological studies. (C.H.)

45745 NEUE ERGEBNISSE DER BIOPHYSIKALISCHEN FORSCHUNG. (New Results of Biophysical Research). Stuttgart, Georg Thieme Verlag, 1965. 166p.

In addition to the commemorative speeches made on the occasion of the twenty-fifth anniversary of the Max Planck Institute for Biophysics, summary reports were given of the work done by the Institute. These included studies on environmental radiation, whole-body γ-radiation spectrometer, dosimetry of energetic radiation, x irradiation of white mice, biological radiation effects at low temperatures, direct radiation effects, electron spin resonance measurements on biological materials, reaction kinetics investigations on radiochemical systems using pulse-modulated x radiation, synthesis of amino acids and peptides with radiation, radiation effects on the cell, and microradiography — an investigation method used in biophysical research. (J.S.R.)

45746 PROCEEDINGS OF THE FIRST INTERNATIONAL SYMPOSIUM ON BASIC ENVIRONMENTAL PROBLEMS OF MAN IN SPACE, PARIS, 29 OCTOBER–2 NOVEMBER 1962. Bjurstedt, Hilding (ed.). New York, Springer-Verlag, 1965. 513p. (CONF-621006).

Thirty-one articles are included; separate abstracts were prepared for 2. The remaining 29 articles include information on ecophysiology, psychophysiology, and the acquisition, analysis, and control of physiological and psychological data. (P.C.H.)

For abstracts of individual papers see: 46000 and 46001.

Ecology

Refer also to abstracts 46434 and 46587.

45747 (ORNL-TM-1279) CHEMICAL COMPOSITION OF INDIVIDUAL RANGE PLANTS FROM THE U. S. RANGE STATION, MILES CITY, MONTANA, FROM 1955–1960. Van Dyne, G. M.; Payne, G. F.; Thomas, O. O. (Oak Ridge National Lab., Tenn.). Sept. 7, 1965. Contract W-7405-eng-26. 20p. Dep. mn; CFSTI $1.00 cy, $0.50 mn.

Information on chemical composition of some important native plants of the Northern Great Plains is reported. Methods of sample collection, preparation, and chemical analyses are described. Chemical constituents reported include crude protein, ether extract, lignin, crude fiber, carotene, total ash, silica, calcium, phosphorus, and nitrogen-free extract. The data are identified by the Latin name of the plant, phenological stage at which the plant was sampled, and the date of sampling. Data are presented for 459 samples of the entire current year's growth and for 94 samples collected to represent only the portion of the plant which was grazed by cattle. Graphs are presented in which between-year and within-year variations in chemical constituents are reported separately for grasses and grasslike plants and for shrubby plants. Data are tabulated. (P.C.H.)

45748 (TID-22193) ECOLOGY OF ACANTHARIA IN RELATION TO Sr CIRCULATION IN THE SEA. Progress Report, January 23–July 30, 1965. Schreiber, Bruno (Parma Univ. (Italy). Istituto di Zoologia e Anatomia Comparata). Contract AT(30-1)-2607. 14p. Dep. mn; CFSTI $1.00 cy, $0.50 mn.

Progress is reported in an ecological study of plankton in the Mediterranean Sea and Atlantic Ocean. Emphasis was placed on the radioactivity of Acantharia in relation to their capacity to remove ^{90}Sr from sea water. Data are included on the ^{90}Sr content in samples of plankton, sea water, bones of cuttle fish, mussel shell, and marine coastal sediments, and fallout radioactivity in rain water during the first half of 1965. (C.H.)

45749 THE RATIO BETWEEN THE ^{90}Sr CONTENT OF GRASS AND MILK FROM RADIOACTIVE FALLOUT, AS OBSERVED UNDER NATURAL CONDITIONS. Kirchmann, R. (Centre d'Etude de l'Energie Nucleaire, Mol, Belg.). Atompraxis, 11: 382-5(July 1965). (In French).

The OR (observed ratio) values for grass and milk, as obtained under natural conditions from 1959 to 1962, are presented and discussed. Statistical analysis showed that the differences in the mean OR for 1961 on the one hand, and for 1959 and 1962 on the other hand, are significant for the threshold P (0.02). The mean value for the OR in all places during the same period was 0.04. The possible influence of additional fodder during the summer months, and the possible contribution of the bovine skeleton to the Ca and Sr content of the milk are discussed. (auth)

45750 ^{90}Sr ACTIVITY IN GRASS AND ALFALFA DURING 1962 AND 1963 IN WEST SLOVAKIA. Csupka, St.; Petrasova, M.; Carach, J. (Hygienisch-Epidemiologische Institut, Bratislava). Atompraxis, 11: 386-9(July 1965). (In German).

The ^{90}Sr content of grass and alfalfa was studied during the vegetation months in four separate regions of West Slovakia. With the aid of soil analyses, the soil-plant discrimination factors were ascertained, and the influence of the calcium content of the plants and soil on the extent of the Ca–^{90}Sr ratio was determined. (auth)

45751 PINE NEEDLES: AN IDEAL BIOINDICATOR FOR ENVIRONMENTAL RADIOCONTAMINATION. Szepke, R. (Inst. of Nuclear Research, Warsaw). Atompraxis, 11: 391-3(July 1965).

Because of their good proportionality to the radioactivity of fallout, their high concentration of radioactivity, and their easy collection, pine needles are considered a good bioindicator of environmental radiocontamination. The results obtained in the years 1959 to 1964 are presented in comparison with other indicators such as river water, soils, milk, and grass. (auth)

45752 RADIOACTIVITY ON SOUTHEASTERN GRANITE OUTCROPS. McCormick, J. Frank (Univ. of North Carolina, Chapel Hill). Bull. Georgia Acad. Sci., 22: 20-7(Jan. 1964).

Studies of granite outcrop plants and plant communities for radiation ecology research prompted an analysis of background levels of radioactivity on numerous granite outcrops. Levels of radioactivity on the granitic outcrops are largely due to the uranophane content of the rock. Levels of radioactivity were measured with portable scintillation counters. Results reveal that radioactivity levels are greatest in areas which directly receive a large amount of run-off during and following rains. As the amount of run-off decreases, and as soil depth increases, levels of radioactivity decrease. Plants collected in Alabama and Georgia from the top, side, and base of Mount Arabia, and collections from Little Stone Mountain, Mount Rollaway, Almond, and Blake's Ferry were analyzed with a deep well scintillation detector for gross γ activity per g of ash. On the basis of these counts eight of these species were ranked according to greatest activity in descending order as follows: Diamorpha cymosa, Hypericum gentianoides, Caladonia sp., Crotonopsis elliptica, Senecio tomentosus, Viguiera porteri, Polytrichum commune, and Opuntia humifusa. These preliminary data revealed basic differences in the activity of individual species in different locations. A consistent gradient of radioactivity was established from the summit to the base of Mount Arabia. In all species, the lowest readings were found at the top of Mount Arabia and the highest at the base. Likewise, variations in activity were noted within island communities. The highest activities were observed in populations from the outer and upper edges of the communities. Species that ranked highest in bioaccumulation were highest regardless of the location of the community on the outcrop. These data support the conclusions from field observations; that is, gradients in bioaccumulation followed the same gradients observed in the field. (BBB)

Metabolism, Tissue Distribution, and Toxicology

Refer also to abstract 46634.

45753 (AE-191) TRACE ELEMENTS IN THE CONDUCTIVE TISSUE OF BEEF HEART DETERMINED BY NEUTRON ACTIVATION ANALYSIS. Wester, P. O. (Aktiebolaget Atomenergi, Stockholm (Sweden)). 1965. 19p. Dep. mn.

Trace elements were determined by means of neutron activation analysis in samples taken from the bundle of His and adjacent ventricular muscle and from the AV node and adjacent atrial muscle of four beef hearts. The bulk elements K, Na, and P were also determined. Gamma spectrometry subsequent to a recently developed ion-exchange technique were used to determine: Ag, As, Au, Ba, Br, Ca, Cd, Ce, Co, Cr, Cs, Cu, Fe, Hg, La, Mo, Rb, Sb, Sc, Se, Sm, W, and Zn. Calculations on a wet weight basis show a lower concentration of Cs, Cu, Fe, K, P, Rb, and Zn and a higher concentration of Ag, Au, Br, Ca, and Na in conductive tissue than in adjacent muscle tissue. The mean differences (μg/g wet tissue) between the bundle of His and adjacent tissue from the ventricular septum, between the AV node and adjacent atrial muscle, between the ventricular septum and the right atrium, and between the bundle of His and the AV node are given for the elements Cu, Fe, K, Na, P, and Zn. (H.G.D.)

45754 (CEA-R-2787) BILANS THYROIDIENS DE LONGUE DUREE APRES ADMINISTRATION D'IODE RADIOACTIF. (Long-Term Thyroid Values After Intake of Radioactive Iodine). Riviere, Rene (Commissariat a l'Energie Atomique, Saclay (France). Centre d'Etudes Nucleaires). July 1965. 49p. Dep. mn.

A kinetic study of thyroid metabolism in man is described that requires the determination of the specific iodine activity at all accessible levels (plasma, urine, feces), dur-

ing periods of over a month. The basic methods required for such a study are the use of iodine-125 as a tracer, the exact determination of iodine-127 using activation analysis, and the setting-up of a daily diet of constant iodine content. The results are presented for each particular case and the main parameters of thyroid metabolism are calculated. The discussion includes some special considerations concerning the pathological condition of the subject or a break in the thyroid equilibrium. It shows in particular that constant disagreement exists between the experimental curves for the specific iodine activity and the corresponding theoretical curves for a conventional thyroid process based on 3 compartments. These discrepancies concern both the inorganic iodine and the organic iodine eliminated with the feces. (tr-auth)

45755 (CEA-R-2809) EVALUATION EN FONCTION DE L'AGE DES INDIVIDUS DE L'ENERGIE EFFECTIVE DELIVREE A L'UNITE DE MASSE (ϵ/m) DES ORGANES AUTRES QUE LE TRACTUS GASTRO-INTESTINAL PAR LES PRINCIPAUX RADIONUCLIDES SUSCEPTIBLES DE CONTAMINER LA CHAINE ALIMENTAIRE ET LE MILIEU AMBIANT. (Evaluation as a Function of Age of the Effective Energy Absorbed in Any Gram (ϵ/m) of Organs Other Than the Gastrointestinal Tract by the Principal Radionuclides Which Could Eventually Contaminate the Food and the Environment). Garnier, Arlette (Commissariat a l'Energie Atomique, Fortenay-aux-Roses (France). Centre d'Etudes Nucleaires). June 1965. 95p. (EUR-2425.f). Dep. mn.

In order to evaluate internal radiation doses from ingested fission products, it is necessary to know the effective energy dissipated in any gram of the organ of reference, which depends, for any radionuclide, on the physical energy (E) absorbed in the body organ, on the relative biological effectiveness (RBE), on the relative damage factor (n) and on the mass of the organ (m). This effective energy may be evaluated as a function of the size and of the mass of the organs from birth to adult age. This work is done for the principal radionuclides which could eventually contaminate the food and the environment. (auth)

45756 (COO-1170-7) IN VITRO PULMONARY COMPLIANCE AND PHYSIOPATHOLOGY OF GUINEA PIG LUNGS EXPOSED IN VIVO TO GADOLINIUM OXIDE DUST. Abel, B. Michael; Talbot, Richard B. (Iowa State Univ. of Science and Tech., Ames. Inst. for Atomic Research; Iowa State Univ. of Science and Tech., Ames. Coll. of Veterinary Medicine). June 1965. Contract AT(11-1)-1170. 75p. Dep. mn; CFSTI $3.00 cy, $0.75 mn.

Seventy-two guinea pigs were divided into three groups of twenty-four each. Each group consisted of twelve control guinea pigs, and twelve pigs exposed to an aerosol of 20 mg. of gadolinium oxide per M^3 of air for periods of 240, 480, and 720 exposure hours. After the exposure period, the lungs were removed and compliance measurements made. Analysis of the data by a three-way factorial analysis revealed a significant interaction between the treatment and duration of exposure factors. Further analysis for trend disclosed a highly significant linear trend with time in the exposed groups. Histopathological changes in the exposed groups, and the amount of deviation from control lung tissue presuppose a difference in functional ability between the two groups. The histopathological changes included alveolar cell hypertrophy, septal cell thickening, lymphoid hyperplasia, and macrophage formation. (auth)

45757 (NYO-910-23, pp 183-92) [DIVISION OF CLINICAL INVESTIGATIONS]. (Sloan-Kettering Inst. for Cancer Research, New York).

^{47}Ca and ^{85}Sr have been used in patients to study the following aspects of the influence of cancer on bone tissue and calcium metabolism: the effect of tumors involving bone on the kinetic state of calcium in the body; the kinetic state of calcium in cancer patients with hypercalcemia and hyperparathyroidism; the local uptake and kinetic state of ^{47}Ca and ^{85}Sr in bone invaded by tumor and in normal bone; the detection of very early bone lesions; the development of isotope techniques which would increase the accuracy of measurements in vivo and in vitro; and the disappearance rate of tetracycline from blood and its relation to disturbances in calcium homostasis and extensive bone disease associated with cancer, and the comparison of these results with ^{47}Ca kinetic studies. (TCO)

45758 (NYO-2598-24) DECONTAMINATION OF SELECTED VEGETABLE CROPS BY LEACHING WITH REFERENCE TO STRONTIUM [Thesis]. Mechling, William Harrison (Cornell Univ., Ithaca, N. Y.). Feb. 1966. Contract AT(30-1)-2598. 84p. Dep. mn; CFSTI $3.00 cy, $0.75 mn.

Various vegetables were contaminated with ^{89}Sr to see how much could be leached out of the tissue. Bean fruits and leaves accumulated ^{89}Sr only when the bean roots had access to a ^{89}Sr source during the development of the fruit and the leaves; lettuce and tomato plants contained more ^{89}Sr the longer they were growing in an ^{89}Sr-labeled soil; however such was not the case for parsley; translocation of ^{89}Sr applied to one primary bean leaf into the opposite primary leaf did not occur; root-absorbed ^{89}Sr was not leached by an atomized mist of distilled water from bean fruits, lettuce leaves or tomato fruits; however 40 percent of the root-absorbed ^{89}Sr was leached by this method from parsley leaves; when grown in a ^{89}Sr-labeled nutrient solution, leaching of the entire bean plant during the development of the fruit did not prevent contamination of the fruit; bean seeds containing root-absorbed ^{89}Sr were grown in a non-radioactive environment; the resulting fruit from the resulting plants did not contain measurable quantities of ^{89}Sr. Root-absorbed ^{89}Sr was not leached from bean fruits by 1 molar solutions of NaCl, $CaCl_2$, KCl, $MgCl_2$ or HCl, except in the HCl solution at pH 1. Strontium-89 applied in a spray to pea pods was leached off the pod, and did not contaminate the seed within. Both the duration of the leaching period, and the length of time between the foliar contamination and the beginning of the leaching process had an effect on the amount of ^{89}Sr which was leached. Up to 98 percent of the foliar-applied ^{89}Sr was leached from lettuce and parsley leaves and tomato and bean fruits. (132 references.) (auth)

45759 (ORO-631, pp 77-82) ANIMAL NUTRITION. (UT-AEC Agricultural Research Lab., Oak Ridge, Tenn.).

Progress is reported in studies of the metabolism of fission products and chemically related nuclides in domestic animals. Emphasis is placed on the similarity of metabolic pathway within the several species used. Data are reported on the toxic effects of intravenously administered $^{144}Ce-^{144}Pr$ in sheep and swine; the metabolism of ingested ^{90}Sr in sheep; the comparative metabolism of ^{75}Se and ^{127}Te in sheep and swine; the effect of whole-body irradiation on the metabolism of ^{99}Mo and ^{185}W in sheep and swine; the life span of erythrocytes in sheep as determined in ^{75}Se autoradiograms of femur slices; the effects of dietary Ca, Zn, and fat on the metabolism of ^{65}Zn in blood cells of swine; and tracer studies, using $^{35}SO_4$, on the effect of vitamin A on mucopolysaccharides of rat blood platelets. (C.H.)

45760 (ORO-631, pp 83-121) DAIRY NUTRITION. (UT-AEC Agricultural Research Lab., Oak Ridge, Tenn.).

Progress is reported in a study of the pathway of fission product entry into milk and possible metabolic controls. Data are presented on a comparison of ^{131}I metabolism by dairy cows after oral and intramammary administration; the effect of thiocyanate on milk-blood transfer of ^{131}I; placental transfer of ^{131}I; the effects of whole-body γ irradiation at 400 R 2 mo prepartum, 350 R after 18 wk of lactation or lethal doses of neutron-γ radiation on subsequent lactation; the effects of γ irradiation on erythrocyte chimerism and immunologic tolerance of cattle twins; the effects of inorganic composition of the diet on the adsorption of various organic metabolites; and the effects of feeding anion exchange resin on excretion of ^{131}I in rats. A simplified procedure was developed for determining the amounts of 2 mutually interfering radioisotopes in mixed samples. (C.H.)

45761 (ORO-631, pp 122-31) POULTRY NUTRITION. (UT-AEC Agricultural Research Lab., Oak Ridge, Tenn.).

Progress is reported in studies of the metabolism of fission products and chemically related nuclides in poultry and possible metabolic controls of fission product uptake. Data are included on the metabolism of ^{131}I by males and females of various ages and the effects of various doses of ^{131}I on development; the pathological effects of $^{144}Ce-^{144}Pr$ injected into eggs on embryos and chicks; the influence of isolated soy protein and other nutritional factors on calcification and growth of chicks; the metabolism of ^{45}Ca, ^{89}Sr, and ^{32}P in chicks; the influence of dietary Ca and exogenous parathyroid extract on the metabolism of ^{75}Se by parathyroid tissue of chicks; and the toxic effects of Te and Se in chickens, quail, and rats. (C.H.)

45762 (RFP-577) PLUTONIUM BIOASSAY RESULTS FOLLOWING DTPA TREATMENTS ON TWO CASES 7 YEARS AFTER ACCIDENTAL EXPOSURE. Lagerquist, C. R.; Hammond, S. E. (Rocky Flats Div., Dow Chemical Co., Golden, Colo.). Sept. 23, 1965. Contract AT(29-1)-1106. 18p. Dep. mn; CFSTI $2.00 cy, $0.50 mn.

Two employees were given a series of DTPA (diethylenetriaminepentaacetic acid) treatments 7 years after they were exposed to plutonium. Bioassay results show the amount of plutonium excreted during the course of treatment was 1.5% and 1.9% of the estimated body burdens of the two individuals. (auth)

45763 (AD-468388) ON THE RESULTS OF GROWTH-MATERIAL IN HEAVY WATER. Galonska, Helge; Huebner, Gerhard. Translated from Flora, 154: 388-92(1963). 8p. (FTD-TT-65-579). CFSTI.

Growth tests of the Agrostemma hypocotyl cylinders and the Avena coleoptile cylinders were conducted in heavy water. The growth-material induced growth in length was completely inhibited in both test specimens by the heavy water. The results indicate that the inhibition is attributed to the influence of the perception of the growth stimulation by D_2O. (auth)

45764 (JPRS-27544) ANTIRADIATION PROPERTIES OF ARYLAMIDES AND ARYLHYDRAZIDES OF THIOCARBOXYLIC ACIDS. Translated from pp 94-105; 112 of Protivoluchevye Svoystva Arilamidov i Arilgidrazidov Tiokarbonovykh Kislot (a publication of the Publishing House of the Academy of Sciences, Ukrainian SSR, Kiev, 1964). 16p. (TT-64-51793). CFSTI $1.00 cy, $0.50 mn.

For an abstract of the individual paper see: 45765.

45765 (JPRS-27544, pp 1-12) ELIMINATION OF ^{134}Cs FROM THE ORGANISM UNDER THE INFLUENCE OF DERIVATIVES OF 1,5-DIPHENYLTHIOCARBAZONE AND 1,5-DIPHENYLTHIOCARBOHYDRAZIDE. Gorodetskii, A. A.; Pel'kis, P. S.; Ryabova, E. Z.; Dubenko, R. G. Translated from pp 94-105 of Protivoluchevye Svoystva Arilamidov i Arilgidrazidov Tiokarbonovykh Kislot.

Cesium is found in nature only in the stable state in Li minerals and sea water. Cesium has been found in plants and animals and exhibits biological kinship with K. Cesium-137 is among the long-lived fission products of U and presents a possible biological hazard. Data are reviewed from studies on Cs metabolism in animals. Results are reported from studies on the metabolism of ^{134}Cs in guinea pigs and rabbits and the effects of the chelating agents, 1,5-diphenylthiocarbazone and 1,5-diphenylthiocarbohydrazide on the elimination of ^{134}Cs from the animals. Over a 5-day period 26 to 28% of ^{134}Cs was eliminated from control animals and 34 to 36% of ^{134}Cs was eliminated in urine and feces of animals treated with these compounds. (C.H.)

45766 ON THE OCCURRENCE OF METACHROMATIC SUBSTANCE AFTER TREATMENT OF URANYL ACETATE. Selye, Hans; Jamke, Volker (Univ. of Montreal). Acta Histochem., 20: 242-7(1965). (In German).

Experiments are described in which 100-g Sprague-Dawley rats were injected with various metal salts, including $AlCl_3$, $BiCl_3$, $CaCl_2$, $CdCl_2$, $CeCl_3$, $CrCl_3$, $CuCl_2$, $FeCl_3$, $Ga_2(SO_4)_3$, $HgCl_2$, $InCl_3$, $ZnCl_2$, $ZrOCl_2$, $KMnO_4$, $LaCl_3$, $SnCl_2$, $ThCl_4$, Th acetate, Pb acetate, and uranyl acetate. With the exception of the last substance, no significant local changes were seen with staining reactions for connective tissue mucopolysaccharides, such as with toluidine blue and thionine. However, subcutaneously administered uranyl acetate produced intense mast-cell degranulation with diffuse metachromasia of adjacent connective tissue and striated cutaneous musculature at the point of injection. These changes differ from those elicited by the classical mast-cell dischargers, such as compound 48/80, in that the liberated mast-cell granules assume a peculiar yellowish-violet tinge after staining with azure A, and remain demonstrable in the connective tissue for a long-time, without being absorbed or phagocytized. Furthermore, the mast-cell degranulation elicited by uranyl acetate is accompanied by a diffuse metachromasia of the neighboring tissues and an elimination of metachromatic material in the renal tubules. This phenomenon was specific for uranyl ion and could not be elicited with the other metal ions, with the possible exception of Th, which as $ThCl_4$, caused similar mast cell reactions in a few animals but could not be reproduced in later tests. (BBB)

45767 CORONARY COLLATERAL BLOOD FLOW IN RELATION TO THE MASS OF ISCHEMIC MYOCARDIUM, STUDIED WITH KRYPTON. Johansson, Boerje; Linder, Erland; Seeman, Torsten (Univ. of Goteborg). Acta Physiol. Scand., 63: 495-504(Apr. 1965).

An analysis of wash out curves recorded externally during elimination of ^{85}Kr from the myocardium in open chest dogs subjected to acute coronary occlusions was used as a method of measuring coronary collateral blood flow (CCBF). The elimination of ^{85}Kr from the myocardium after close-arterial administration was observed by external recording and wash out curves obtained. As indicated by the results of alternative occlusions at different levels of the left anterior descending artery, the CCBF per unit weight of tissue is dependent upon the size of the ischemic region. During clamping of the trunk of this artery which made 20 to 30 g of myocardium ischemic, collateral blood flows in the range of 6 to 21 ml/min × 100 g were obtained. Distal occlusion of the artery or occulsion of single side branches was associated with relatively higher values of CCBF per unit weight. The results are compared with other isotopic methods using D_2O, ^{86}Rb, and ^{131}I to investigate myocardial blood flow. With ^{85}Kr the values for CCBF after occulsion of the main artery agreed best with those using D_2O. The fact that these two indicators are both inert and rapidly diffusing molecules probably explains this conformity of the results. The comparably high uptake of ^{86}Rb found in ischemic myocardium may be partly explained by the relatively greater extraction of ^{86}Rb at low flow rates. (TCO)

45768 THE TOXICITY OF NIOBIUM SALTS. Downs, William L.; Scott, James K.; Yuile, Charles L.; Caruso, Frank S.; Wong, Lawrence C. K. (Univ. of Rochester, New York). Am. Ind. Hyg. Assoc. J., 26: 337-46(July-Aug. 1965).

The acute and sub-acute toxicity of potassium niobate and niobium pentachloride was investigated. Single intravenous doses of 20 mg Nb/kg or less to rats, rabbits, and dogs were not fatal. The LD_{50} (seven-day) value for mice and rats given a single intraperitoneal injection of potassium niobate was 13 and 92 mg Nb/kg, respectively. The oral LD_{50} (seven-day) value for the rat was 725 mg Nb/kg. Renal injury was observed in all species following parenteral injection at doses ranging from 20 to 50 mg Nb/kg. Repeated intraperitoneal injections of niobium pentachloride or potassium niobate of 30 mg Nb/kg resulted in renal injury and death. Dietary levels as high as 1% of either compound were ingested by rats, for a seven-week period, without effect. The nephrotoxic action of niobium was not observed when the niobium salt was complexed with ascorbic acid prior to injection. (auth)

45769 CHRONIC TOXICITY OF POLYPHENYL MIXTURES. Petkau, A.; Hoogstraaten, J. (Whiteshell Nuclear Research Establishment, Canada). Am. Ind. Hyg. Assoc. J., 26: 380-7(July-Aug. 1965).

In rats the ingestion of Santowax OM, a mixture of ter-

phenyls used as a coolant, and OMRE High Boilers over prolonged periods inhibited weight gain and led to anemia and kidney and liver damage. At a daily dietary intake of 350 mg/kg or more, Santowax OM produced degenerative changes in the nephron; the OMRE High Boilers at a daily dietary intake of 33 mg/kg or more caused histiocytic infiltration and cirrhotic changes in the liver. (auth)

45770 THYROID UPTAKE OF ^{131}I IN RATS CHRONICALLY INTOXICATED WITH CARBON MONOXIDE. Truhaut, R.; Boudene, C.; Claude, J.-R. (Laboratoire de Toxicologie et d'Hygiene Industrielle de la Faculte de Pharmacie, Paris). Ann. Biol. Clin. (Paris), 23: 73-82 (1965). (In French).

Three groups of rats (A', A'', B'') in identical environments were exposed to varying concentrations of carbon monoxide, and their growth rates compared. A fourth group (B') was maintained as a control. Later, two rats from each lot were interperitoneally injected with ^{131}I, and the relative uptakes of ^{131}I in the thyroid were compared. The rats exposed to 250 ppM of CO for 500 hr (A'') showed no retardation of growth rate. Those exposed to 100 ppM of CO for 1000 hr, then maintained in the absence of CO for three months (B'') showed no signs of recovery from the initial retardation. Those exposed to 1000 ppM for 1000 hr, then to 250 ppM for 500 hr (A') showed a significant increase of sensitivity to the effects of CO. All the rats, regardless of age or body weight, exposed to long and recent contact with CO showed a marked diminution in the uptake of ^{131}I in the thyroid. The animals recovering from CO exposure, on the other hand, showed an unexpected augmentation of ^{131}I incorporation that increased as the body weight decreased. The control group (B') showed a ^{131}I uptake by the thyroid of 10.7%, after intraperitoneal injection of 0.5 μC of ^{131}I. The uptake in the A', A'', and B'' groups was 5.2, 6.4, and 13.2%, respectively. The data indicate that CO inhibits the uptake of iodine in the thyroid, and that temporary exposure, although it inhibits the growth rate, stimulates this uptake. It is suggested that CO may depress central nervous system activity, which in turn via hypothalmic mediation may suppress activity of the anterior pituitary. The resulting reduction in thyrotropin secretion would then explain reduced function of the thyroid gland in incorporating inorganic iodine. Reduced body growth would also be accounted for by depressed endocrine activity of the hypophysis and thyroid. (BBB)

45771 SCINTILLATION METHODS FOR METALLIC ION DETERMINATION IN HUMAN SUBJECTS USING COMPUTER TECHNIQUES. Meneely, George R. (Univ. of Texas, Houston); Hayward, Lynn C.; Vinson III, David B.; Rolf, Howard L.; Heyssel, Robert M.; Ball, Con O. T.; Weiland, Raymond L. Ann. N. Y. Acad. Sci., 126: 808-15 (Aug. 6, 1965).

Gamma scintillation spectrometry provided a method to measure total amounts of certain elements within the human body in vivo. Potassium with its naturally occurring radioisotope ^{40}K is one of the most interesting and important metallic ions physiologically and exemplifies the problems encountered in such studies. In order to try to relate the observed amount of this or any other ion so measurable to other anatomical, physiological, or chemical observations simultaneously recorded in the same subject to determine the normal range of its variation and differences to be expected with differences in habitus, etc., it is necessary to accumulate data on large numbers of subjects of different sex and race distributed over as large an age range as possible and representing, hopefully, the whole spectrum of variation characteristic of the population or populations under investigation. The result is a mass of data that are best handled by machine methods. Among 19 variables, there are 171 possible unique pairings. By reason of the primary and necessary separation by race and sex there are therefore four sets of 171 pairings for a total of 684 relations, each with 19 age category data pairs. Since virtually all these relations were complex curvilinear, often also involuted, simple computer techniques for analysis of variance were highly appropriate. To provide a presentation which would be within human capacity to review and comprehend, a program was developed for the IBM-409 computer for detailed graphic presentation. The input to this program was the output from the race-sex category analysis of the means of the 19 variables in each of the 19 age categories. The program generated information and commands for an appropriate x–y plotter. This proved to be a most efficient technique for review of a large body of inter-relations among many variables in a large number of subjects. (auth)

45772 INVESTIGATION ON $^{137}Cs/^{90}Sr$ RATIOS IN MILK. Pfau, A.; Senft, B. (Max-Planck-Institut fuer Tierzucht und Tierernaehrung, Mariensee, Ger.). Atompraxis, 11: 376-82(July 1965). (In German).

The ^{90}Sr radioactivity in milk, which can be determined by radiochemical analysis only, may be estimated by direct physical ^{137}Cs measurements when the $^{137}Cs/^{90}Sr$ ratio in milk is known. However, previously there was no success in deriving a universally approved figure for this ratio. Various foodstuff contaminated by different amounts of ^{137}Cs and ^{90}Sr, and having different contents of calcium or potassium, were investigated for their influence on the $^{137}Cs/^{90}Sr$ ratio in milk. From these inquiries a mathematical function could be derived for the numerical calculation of mean, probable values of this ratio. (auth)

45773 ON THE OCCURRENCE OF ^{55}Fe, ^{60}Co, ^{65}Zn, ^{90}Sr, AND ^{137}Cs IN THE PINE, LARCH, ASPEN, AND BIRCH. Makhonina, G. I. Byul. Mosk. Obshchestva Ispytatelei Prirody, Otd. Biol., 70: 120-3(1965). (In Russian).

Radioisotopes ^{55}Fe, ^{60}Co, ^{65}Zn, ^{90}Sr, and ^{137}Cs were administered to the soil in two fashions: through superficial irrigation, and intrasoil administration. Average data are presented. The highest level of ^{55}Fe was found in the pine needles and birch leaves as well as in the stems + branches and roots of the aspen. ^{60}Co was most abundant in stems + branches of pine and larch needles while being rather uniformly distributed in the organs of the aspen and birch; ^{65}Zn was concentrated in the aspen leaves; ^{90}Sr was concentrated in pine roots and approximately similarly high concentrations were found in the leaves (needles) and stems + branches of the larch and birch; ^{137}Cs was distributed rather uniformly in the major organs of the arboreal plants studied. A comparative study of elimination of radioisotopes by the overground mass of arboreal plants from the soil showed that the greatest amounts of ^{55}Fe were eliminated by the pine and birch, of ^{60}Co — by the larch of ^{65}Zn — by the aspen, and ^{90}Sr — by the birch. ^{137}Cs was eliminated in insignificant amounts by all plants studied. (auth)

45774 INFLUENCE OF RATE OF ^{90}Sr ADDED TO SOIL AT DIFFERENT PHOSPHATE LEVELS ON THE CONCENTRATION OF ^{90}Sr IN PLANTS. Evans, E. J.; Dekker, A. J. (Canada Dept. of Agriculture, Ottawa). Can. J. Plant Sci., 45: 375-81(July 1965).

Studies were made to determine the effects of calcium phosphate both without and with a preliminary wetting and drying treatment, and the effect of different levels of ^{90}Sr added to the soil, on the ^{90}Sr concentrations in oats and alfalfa. Surface soils of Grenville loam and Granby sandy loam were used. Soil (2.5 kg) was treated with three levels of P(0, 0.164, and 0.546 g P/pot as $Ca(H_2PO_4)_2 \cdot H_2O$), four levels of ^{90}Sr(0.05, 0.5, 5, and 50 μC/pot), and two soil pretreatments. These consisted of (1) application of the ^{90}Sr and fertilizer just prior to seeding, and (2) application of the ^{90}Sr and fertilizer, then subjecting the soil to five cycles of wetting to field capacity followed by drying. A reduction in ^{90}Sr concentration in oats of about 50% was effected on Grenville soil by the addition of 0.546 g P per $2\frac{1}{2}$ kg soil. This reduction was caused partly by the effect of Ca in the fertilizer and partly by the dilution caused by a very large increase in yield from the application of the fertilizer. Similar reductions in ^{90}Sr concentration were not found for alfalfa. A wetting and drying pretreatment of the soil caused slight decreases in ^{90}Sr concentration in alfalfa but not in oats compared with samples which received no pretreatment, indicating that the phosphate fixed some ^{90}Sr. In one series of treat-

ments, ^{90}Sr was added to the soils in doses ranging 1000-fold in concentration. The concentration of ^{90}Sr in oats and alfalfa was generally proportional to applied dose, although it was found in some instances to be proportionately higher at the lowest dose added to soil. This conclusion was found to be true whether the results were of ^{90}Sr concentration, ^{90}Sr uptake, or $^{90}Sr/g$ Ca. (BBB)

45775 DETERMINATION OF CONTENTS OF MANGANESE AND COPPER DURING THE LIFE CYCLE OF CHLORELLA CELLS BY NEUTRON ACTIVATION ANALYSIS. Wey, Ming-Tong (Taiwan Provincial Norman Univ., Taipei). Chemistry (Taipei), No. 4, 165-9(1964). (In Chinese).

By the technique of synchronous cell culture of Chlorella ellipsoidea and the nondestructive neutron activation method, changes in content of manganese and copper during the algal life cycle were investigated. About 50 mg of dry chlorella cells was irradiated simultaneously with standards in the Tsing-Hua reactor, at a thermal neutron flux of about 10^{12} N/cm^2 sec, for one half to two hr. After cooling the sample, it was counted with a 2-in. thick, sodium iodide crystal coupled with a 256-channel pulse height analyzer. Manganese and copper were determined by γ-ray spectrometry by comparing the peak heights at 0.85 Mev of the sample with that of a manganese standard and at 0.51 Mev of the sample with a copper standard. Manganese at 40 to 90 ppM and copper at 60 to 160 ppM were present, the levels varying with different cell stages. It was found that the manganese and copper were assimilated more avidly in the ripening stage than the growing stage during the life cycle of chlorella cells. (BBB)

45776 THYROID BURDEN OF RADIOIODINE AFTER RESPIRATOR CONTAMINATION OF MONKEY MACACCUS RHESUS. Thieblemont, P.; Marble, G.; Perrault, G.; Pasquier, Ch. (Centre d'Etudes Nucleaires, Fontenay-aux-Roses, France). Intern. J. Radiation Biol., 9: 233-40 (1965). (In French).

When the Macaccus rhesus monkey inhales Na ^{131}I soluble aerosols, the fraction of the activity retained by the respiratory tract and measured in the thyroid has a value between 24 and 45 per cent. Compared to the inhaled amount, the radioiodine thyroid burden averages 20 per cent, which agrees with the values recommended by the ICRP for the calculation of the permissible doses applying to occupational internal exposure following inhalation of iodine isotopes. In the monkey, the thyroidal iodine decays with a biological half-life close to 8 days. (auth)

45777 OXYGEN CONSUMPTION BY RAT LIVER IN THE PRESENCE OF CYSTAMINE—ROLE OF THE DIAMINO-OXIDASES. Lelievre, P. (Universite, Liege). Intern. J. Radiation Biol., 9: 261-7(1965). (In French).

Rat-liver homogenates incubated with cystamine in a pyruvate-free medium show a slight increase in the oxygen-consumption. This increase varies with the concentration of disulfides. In a medium containing pyruvate, the oxygen-consumption of liver homogenates or mitochondria is increased by small doses of cystamine. On the contrary, higher concentrations of the drug decrease the utilization of oxygen. The increased consumption of oxygen observed in some conditions cannot be ascribed to the activity of diamino- or mono-amino-oxydases, but seems to be related with the activity of –SH containing enzymes. (auth)

45778 THE EFFLUX OF ^{86}Rb FROM THE RABBIT LENS. Becker, Bernard; Cotlier, Edward (Washington Univ., St. Louis). Invest. Ophthalmol., 4: 117-21(Feb. 1965).

Rabbit lenses, freed of vitreous, were incubated in K-free Tyrode's solution containing ^{86}Rb(15 μC/ml) for two hr, to allow for isotopic uptake, then incubated in nonisotopic solution to measure the efflux of ^{86}Rb from the lens. The Tyrode's solution contained either ouabain (0.1 mM) or nonlabeled rubidium (33 mM), concentrations found either to inhibit (ouabain) or saturate (rubidium) the sodium-potassium pump. The runout of ^{86}Rb was estimated by taking 50-μl samples after 30, 60, 120, and 180 min of incubation with gentle shaking in a 37°C. The runout of ^{86}Rb was linear for periods of up to 10 to 12 hr after an initial unstable period of 30 min. The rate of efflux into 0.1 mM ouabain was not influenced by the addition of various concentrations of potassium or nonlabeled rubidium to the medium. Thus, no tendency to saturation of a carrier system could be demonstrated. In the absence of calcium, ^{86}Rb left the lens at a rate four times that found in Tyrode's solution containing the usual concentration of Ca (5 mg%). Levels as high as 10 mg% Ca or more were needed to minimize the rate of runout of ^{86}Rb from the rabbit lens. Various metabolic inhibitors were found to alter the rate of efflux of ^{86}Rb from the lens. Three steroids, deoxycorticosterone acetate, triamcinolone acetonide, and prednisolone hemisuccinate, were capable of increasing runout of ^{86}Rb from the rabbit lens. Lenses incubated in collagenase were found to accumulate ^{86}Rb as well as those not incubated in collagenase. The results show that measurement of the efflux of ^{86}Rb from the rabbit lens permits an evaluation of factors which may influence the concentrations of cations in the lens but without necessarily directly affecting the pump. Metabolic activity is needed in order to minimize the rate of efflux of ^{86}Rb from the lens. Various metabolic inhibitors markedly increased this efflux in concentrations that closely resemble those required to affect the accumulation of ^{86}Rb by the rabbit lens. (BBB)

45779 ^{131}I UPTAKE STUDIES UNDER HOT CLIMATIC CONDITIONS. Lewitus, Zygmunt; Hasenfratz, Julius; Toor, Mordechai; Massry, Shaul; Rabinowitch, Ethel (Beilinson Hospital, Petah Tiqva, Israel). J. Clin. Endocrinol. Metab., 24: 1084-6(Oct. 1964).

To ascertain the state of thyroid function in heat, a study was made of the ^{131}I of uptake under the hot environmental conditions prevailing in summer in Eilat on the Red Sea coast (Negev Area). Part of this study was done in August, on permanent inhabitants of this area, when the average ambient temperature was 38°C. These experiments on the same people were then repeated in February when the average temperature was 24°C. The 24-hr uptake values (as % of dose administered) were 29 and 30% in men and women in August and 40 and 51% in February. The difference of uptake between summer and winter was highly significant. There was no significant difference between the uptakes in winter and those of the controls. The iodine provided by excessive drinking during the heat influences the results of uptake, euthyroid volunteers were given 50, 100, or 150 μg iodine in their drinking water for two to three weeks. No significant difference in their iodine uptake measurements was detected. Although ^{131}I uptake was lower in Eilat during the hot summer months it rose in the same subjects to levels almost identical with those in the Tel Aviv area during the winter months. There was no visible change in their clinical appearance during the lower or the higher uptake. Their protein-bound I (PBI) conversion ratio and PB^{131}I remained in normal ranges. The only change observed was an increase of plasma volume during the summer months. (BBB)

45780 AVAILABILITY OF FALLOUT ^{137}Cs TO DAIRY CATTLE FROM DIFFERENT TYPES OF FEED. Stewart, H. F. (X-Ray Exposure Control Lab., Rockville, Md.); Ward, Gerald M.; Johnson, James E. J. Dairy Sci., 48: 709-13(June 1965).

These studies were designed to evaluate the effect of different diets on the passage of fallout ^{137}Cs from feed to milk as well as the routes of excretion for this nuclide under farm feeding conditions. Cesium-137 balance studies were performed with three cows, two Holsteins and one Guernsey, housed in stalls and fed a ration consisting of hay and grain. The transfer coefficient (^{137}Cs secreted daily per liter of milk as a percentage of total daily ^{137}Cs intake) for individual cows ranged from 0.25 to 0.72 and was found to be closely related to the crude fiber content of the diet. The correlation coefficient between transfer coefficient and crude fiber intake was –0.66. The average percentage of dietary ^{137}Cs found in the milk, urine, and feces was 7.4, 13.5, and 81.5. Previous reports utilizing tracer doses of radio-cesium have found about 1.0% of the

dose secreted in each liter of milk and equal amounts excreted in urine and feces. The results reported here suggest that fallout ^{137}Cs in dairy cattle feeds is considerably less available than suggested by studies with tracers. As a possible explanation for the discrepancy in results between fallout and tracer ^{137}Cs, there may be a fraction of ^{137}Cs in the forage associated with the crude fiber fraction of feeds which is not completely available unless the fiber is completely digested, or that a portion of ^{137}Cs in forage plants exists as insoluble and unavailable particles. Another possibility assumes that all the cesium is available and appears in the feces only because of adsorption on the undigested residue. Since 100% of the ^{137}Cs consumed was accounted for in the three products, milk, urine, and feces, there is no body retention. Potassium balance calculated for these cows indicated an excretion pattern for potassium greatly different than for ^{137}Cs. Urinary excretion of potassium is about three times as high as fecal excretion, whereas fecal excretion of ^{137}Cs is about six times the urinary excretion. Another indication that ^{137}Cs in forage is not as readily absorbed from the intestine as potassium is that a smaller percentage of cesium than potassium is secreted into the milk. If the fallout cesium in the forage was as readily absorbed as potassium, the situation would be reversed. (BBB)

45781 EFFECTS OF FEEDING POTASSIUM IODIDE, 3,5-DIIODOSALICYLIC ACID, OR L-THYROXINE ON IODINE METABOLISM OF LACTATING DAIRY COWS. Miller, J. K.; Swanson, E. W.; Hansen, S. M. (Univ. of Tennessee, Oak Ridge). J. Dairy Sci., 48: 888-94(July 1965).

Three Jersey cows were fed daily 1.3 g iodine as KI, 1.3 g iodine as 3,5-diiodosalicylic acid (DIS), or no supplemental iodine in three periods of a Latin-square design. In each period, $Na^{125}I$ was administered orally twice daily for 21 days. The supplements were added to the capsules containing $Na^{125}I$ from the 8th through the 14th day. A single dose of ^{131}I-labeled L-thyroxine was injected intravenously on the 12th day of $Na^{125}I$ dosing. Iodine-125 excretion was only slightly affected by DIS, but KI caused a 34% reduction in milk ^{125}I and a 38% increase in urine ^{125}I. Both compounds reduced excretion of ^{131}I from thyroxine into milk. Urinary ^{131}I excretion was highest from cows fed KI and lowest from those fed DIS. Neither supplement significantly influenced fecal ^{131}I or ^{125}I excretion. In another experiment, four cows were dosed orally with $Na^{125}I$ twice daily for 31 days. From the 11th through the 26th day, 80 mg of L-thyroxine daily were added to dosing capsules for three cows, and the fourth served as a control. Feeding thyroxine lowered ^{125}I concentration in milk 15%, but this was accompanied by greater milk yields. Total ^{125}I excretion in milk, urine, or feces was not changed by the thyroxine feeding. (auth)

45782 METABOLISM OF DIFFERENT FORMS OF IODINE IN MILK GIVEN TO CALVES BY SUCKLING AND RUMEN INFUSION. Swanson, E. W.; Miller, J. K.; Cragle, R. G. (Univ. of Tennessee, Oak Ridge). J. Dairy Sci., 48: 930-4(July 1965).

Milk labeled with ^{131}I by dosing lactating cows was fed to 25 calves. The percentage of milk ^{131}I in protein-bound form ranged from a normal of 10 up to 90% in anion exchange resin-treated milk. The metabolism of the milk-bound ^{131}I was compared to exchangeable ^{125}I added to the milk just before calves were dosed by nipple pail (suckling), via stomach tube to a nearly empty rumen (infusion), or via stomach tube to a full rumen (drenching). Differences in metabolism of bound and exchangeable iodine were determined from the ratios of percentage of the dose of ^{125}I to ^{131}I which appeared in blood, urine, and feces at successive 24-hr samplings, and in bile, abomasum, and thyroid 24 to 96 hr after dosing. Only slight differences in metabolism of the two forms of iodine resulted after suckling or drenching. After infusion into the rumen, much of the bound iodine was absorbed as such, then it was excreted into the urine about twice as efficiently as was the exchangeable iodine source. This resulted in an increase in the proportion of the exchangeable iodine (^{125}I) in plasma, abomasum, and feces; and about twice as much ^{125}I as ^{131}I was taken up by the thyroid gland. Utilization or excretion of iodine is markedly affected by the form in which it is present in the blood which, in turn, is affected by the manner of consumption, digestion, and absorption. (auth)

45783 AUTORADIOGRAPHY OF DIFFUSIBLE IONS WITH APPLICATION TO THYROIDAL RADIOIODIDE. Andros, George (Massachusetts General Hospital, Boston); Wollman, Seymour H. J. Histochem. Cytochem., 13: 390-5(June 1965).

A new method was developed to determine ^{125}I localization in the mouse thyroid. It is described along with information on tissue preservation and control of artifacts. Thyroid tissue was obtained from hypophysectomized C_3H mice acutely treated with 1 mg of propylthiouracil to prevent formation of organic radioiodine. Carrier-free ^{125}I was administered 10 min before sacrifice (^{125}I in the thyroid was shown to be 99.9% inorganic iodide). The thyroid glands were quickly removed, frozen in isopentane at about −160°C, and transferred to dried degassed paraffin and immersed in liquid nitrogen. After freeze-drying the tissue for at least six days the paraffin was heated in vacuo. Paraffin blocks were assayed in a well-type NaI scintillation counter, and slides were prepared by mounting autoradiographic stripping film on gelatinized slides. This method produced autoradiographs in which the silver grains were in a single focal plane at magnifications as high as 500×. At ten min after radioiodide injection in hypophysectomized mice the autoradiographic image was a ring under the epithelial cells surrounding a less dense lumen. In thyroids removed two or more hours after injection no rings were observed, but only images which were of equal density over lumen and cell. Autoradiographs exhibiting good localization were obtained only by keeping all components such as film, ribbons of tissue, and paper dry. It was also crucial that tissues be kept frozen prior to drying. When tissue was allowed to thaw for one sec prior to freeze-drying, a uniformly diffuse grain pattern under the tissue was obtained. This method yields good autoradiographic localization of ^{125}I in the thyroid gland and should be readily adaptable to autoradiography of other diffusible substances which are insoluble in paraffin. The resolution obtained using the present method is low considering the short range of the electrons from ^{125}I. Limitations on resolution appear to be related to the diffusible nature of ^{125}I. The diffusion of radioiodide in the best autoradiographs was 1 or 2 μ. (BBB)

45784 IODINE IN CHILDREN'S HAIR: ITS RELATION TO URINARY IODINE LEVELS. Ganor, S.; Gedalia, I.; Brand, N. (Hadassah Univ. Hospital, Jerusalem). J. Invest. Dermatol., 43: 5-6(July 1964).

The iodine content of samples of scalp hair and 24-hr urine was determined for 15 children drinking iodine-rich water and for 15 children drinking iodine-poor water. All the children were healthy and between 7 and 17 years of age. Fifteen of the children lived in the Jerusalem area supplied by drinking water containing about 60 μg/1 I; the other 15 children lived in Upper Galilee supplied by drinking water containing less than 7 μg/1 I. In the latter region goiter was endemic. The mean iodine value in the urine of children drinking water with 60 μg/1 I was significantly higher than the mean iodine concentration of the children drinking water with less than 7 μg/1 I. The mean iodine value of the hair samples was not significantly different between these groups, nor between any particular age levels within the groups; nor could any relation to sex be detected. Iodine content of the hair samples in children drinking water of the lower iodine concentration was 150 μg % and in children drinking water of the higher iodine content was 140 μg %. It seems therefore that under normal conditions the hair takes up the amount of iodine it needs, the surplus being mostly excreted in the urine. (BBB)

45785 RADIOHOMOGENEITY OF ^{3}H- AND ^{14}C-LABELED LINOLEIC ACID IN VIVO. Sgoutas, Demetrios; Kim, Moon Ja; Kummerow, Fred A. (Univ. of Illinois, Urbana). J. Lipid Res., 6: 383-9(July 1965).

In the double-label isotope ratio technique, several re-

quirements must be met when it is used to demonstrate the radiotracer stability of ^{3}H-labeled compounds. One of these is that the $^{3}H/^{14}C$ ratio of the administered substrate must be compared to that of the same substrate isolated from the metabolizing system. A mixture of linoleic acid-9,10, 12-13-^{3}H and linoleic acid-1-^{14}C was administered to rats, and the $^{3}H/^{14}C$ ratio in the injected mixture was compared to that found in linoleic acid after isolation from liver and adipose tissue of the rat. In addition, the $^{3}H/^{14}C$ ratio in total lipid and lipid fractions was determined and the differential incorporation of the two labels into different lipids was evaluated. The $^{3}H/^{14}C$ ratio in the linoleic acid recovered from the total lipid material and purified by chromatographic procedures was constant for 10 hr and identical with the $^{3}H/^{14}C$ ratio of the administered mixture. Variations of the $^{3}H/^{14}C$ ratio in the lipid fractions, as separated by silicic acid chromatography, indicated that an increasing incorporation of ^{3}H into cholesterol, diglycerides, and monoglycerides had occurred. A marked change in the $^{3}H/^{14}C$ ratio was seen within the triglyceride peak, indicative of an accumulation of ^{3}H in the tail of the peak. To determine whether there is any discrimination between linoleic-^{3}H and linoleic-^{14}C acid in the conversion of linoleic to arachidonic acid, the latter was isolated as its octabromide. The $^{3}H/^{14}C$ ratio of the octabromide was 9.85. A ratio different from that of the administered linoleic acid (8.0) is to be expected in the isolated arachidonic acid since arachidonic acid is formed in vivo by the addition of acetate to the carboxyl end of linoleic acid. Calculation of the percentage distribution of ^{14}C in the different portions of the arachidonic acid molecule showed that 72% of the ^{14}C activity was contributed by the acetate moiety. On the other hand, the glutaric acid contained all of the ^{14}C radioactivity incorporated into arachidonic acid by both linoleate and acetate portions and all of the tritium radioactivity of acetate. The acetate moiety that was incorporated into arachidonic acid had a $^{3}H/^{14}C$ ratio of 10.6, and the linoleate incorporated had a ratio of 7.75. This last value was indicative of the equivalence of the conversion of the two differently labeled linoleic acids into arachidonic acid. It is concluded that ^{3}H-labeled fatty acids are as stable as ^{14}C-labeled fatty acids in vivo. (BBB)

45786 IODINE METABOLISM IN THE THYROID: A COMPARISON OF WHOLE AND SLICED LOBES. Mack, Robert E.; Bagchi, Nandalal (Wayne State Univ. School of Medicine, Detroit and Woman's Hospital, Detroit). J. Nucl. Med., 6: 142-9(1965).

Thyroids from rats fed a low iodine diet were incubated as whole lobes and sliced lobes in buffer containing iodide ^{131}I. Total uptake of iodide ^{131}I and the fraction of thyroidal ^{131}I bound to protein was determined. The distribution of labeled iodoamino acids was observed following chromatography of pancreatic digest of the thyroid. The values for iodide ^{131}I uptake and protein bound ^{131}I were higher and the ratio of monoiodotyrosine ^{131}I/diiodotyrosine-^{131}I lower in whole lobes as compared to sliced thyroid lobes. When the iodide concentration of the buffer was increased, whole thyroid lobes from rats fed an iodine deficient diet were more sensitive to the inhibitory effect of iodide on protein binding of iodine than was true for sliced lobes. This difference in sensitivity appeared to be related to the greater quantity of stable iodide concentrated by whole thyroid lobes. Neither whole lobes or sliced thyroid lobes from rats maintained on an iodine deficient diet showed any response to TSH. Whole thyroid lobes from rats on a stock laboratory diet demonstrated an increase in iodide ^{131}I uptake and the fraction of ^{131}I bound to protein when incubated in the presence of TSH. It is suggested that in rats on a low iodine diet, endogenous TSH secretion has effected maximal stimulation of some step in the intrathyroidal iodine cycle so that the gland is insensitive to TSH in the buffer. (auth)

45787 ^{65}Zn METABOLISM DURING LOW AND HIGH CALCIUM INTAKE IN MAN. Spencer, Herta; Vankinscott, Vernice; Lewin, Isaac; Samachson, Joseph (Veterans Administration Hospital, Hines, Ill.). J. Nutr., 86: 169-77(June 1965).

The metabolism of orally administered tracer doses of ^{65}Zn was studied in five subjects under strictly controlled dietary conditions. A single tracer dose of 15 to 25 μC ^{65}Zn as the chloride was administered orally with breakfast during low and high calcium intake. The levels of ^{65}Zn in whole blood and plasma were determined at 1, 4, 8, and 25 hr and at less frequent intervals thereafter. Initially, the ^{65}Zn level in plasma was higher than that of whole blood, reached a maximum at 4 hr, and decreased with time thereafter. The plasma concentration of ^{65}Zn continued to decrease with time and less than 0.1% of the dose remained at 10 days. From day 20 to 28 after the oral administration of the dose, the plasma level of ^{65}Zn remained in the same low range. In contrast, the ^{65}Zn level in whole blood continued to increase in the first 5 days after the ingestion of the tracer, and decreased thereafter. The urinary excretion of ^{65}Zn was very low throughout the study. Most of the administered dose, 66%, was passed with the stool in the first 3 days. Thereafter, the fecal excretion of ^{65}Zn was low and less than 1% of the dose was excreted per day. The effect of added calcium on ^{65}Zn absorption was variable and there was no consistent change in the absorption of ^{65}Zn during high calcium intake. Also, there was no consistent relation between the urinary excretion of ^{65}Zn, the intake of calcium, and the increase in urinary calcium excretion in man. (BBB)

45788 THE STABLE MANGANESE CONTENT OF MOLLUSCS FROM LAKE MAGGIORE DETERMINED BY ACTIVATION ANALYSIS. Merlini, Margaret; Girardi, F.; Pietra, R.; Brazzelli, A. (Euratom, C.C.R., Ispra, Italy). Limnol. Oceanog., 10: 371-8(July 1965).

Determinations of stable manganese in four species of freshwater mollusks were made by activation analysis. Significant differences were found between the two species of snails and between the univalves and bivalves. There is a correlation between the accumulation of fallout ^{54}Mn and stable Mn in the different organs of the bivalves. In the clam shell, Mn appears to be nonhomogeneously distributed and to increase in concentration with size. There was a difference in the Mn content of tissues of bivalves collected from different sites. (auth)

45789 UPTAKE AND LOSS OF ^{65}Zn IN THE DRAGONFLY PLATHEMIS LYDIA. Kormondy, Edward J. (Oberlin Coll., Ohio). Limnol. Oceanog., 10: 427-33(July 1965).

Study of uptake and loss of ^{65}Zn in the dragonfly Plathemis lydia employed concentrations of 0.005 to 0.5 μc ^{65}Zn Cl_2/ml water on 200 early, middle, and late instar larvae. Rate and amount of uptake are independent of temperature (10, 20, and 30°C); equilibrium is attained in 24 to 48 hr. Loss rate is significantly greater at 10°C than at 20 and 30°C. Uptake and loss rates are independent of body size (= age), but the amount concentrated is inversely related to body size, the coefficient of accumulation being 68 in small larvae, 28 in larger ones. Total uptake is directly proportional to isotope availability in the medium; owing to experimental error, it could not be determined whether rate of uptake is affected by concentration. Loss rates in the field and the laboratory do not differ. Feeding experiments are inconclusive. Loss rate in dead animals is the same as in live larvae, and 95% of initial activity remains on the cast exuvium at molting and final metamorphosis. Uptake is concluded to be by surface adsorption or cation exchange thereby imposing difficulty in using ^{65}Zn as an indicator of metabolic activity in energy flow studies. Odonata may function significantly in redistributing zinc, the bulk of which localizes in the upper sediments. (auth)

45790 PREPARATION OF MAMMALIAN METAPHASE CHROMOSOMES FOR AUTORADIOGRAPHY. Prescott, D. M.; Bender, M. A. (Oak Ridge National Lab., Tenn.). Methods Cell Physiol., 1: 381-5(1964).

For autoradiographic studies on labeling of DNA, RNA, and proteins of mammalian chromosomes with tritiated precursors, a procedure was developed for preparing cytoplasm-free metaphase chromosomes. The method permits several thousand sets of chromosomes to be

affixed to a single slide. No cytoplasmic layer is present between the chromosomes and the autoradiographic emulsion, thereby increasing the sensitivity and resolution of the autoradiographic detection of incorporated label. Autoradiographic determination of labeled RNA and protein in chromosomes is possible because of the absence of background radioactivity from nonchromosomal RNA and protein. The method was used mainly with the Chinese hamster fibroblast-line CHEF 125 cells, but works equally well with several other mammalian cell types. Colchicine is added to the cell culture (to 10^{-6}M) several hours before isolation of chromosomes. The medium is decanted and the cells washed with balanced salt solution, which is then replaced by hypotonic saline. An important step is complete removal of serum proteins from the culture. After 3 or 4 min in the hypotonic medium, cells arrested in metaphase become dislodged from the glass, and are then concentrated. Isolated chromosomes and well-spread, partial, and complete complements of chromosomes uncontaminated by cytoplasm are obtained by placing the cells on slides in glacial acetic acid. Treatment with the acetic acid takes out much of the protein and RNA from the chromosomes. This loss of material was greatly decreased by substituting a short fixation with neutral formalin for the glacial acetic acid treatment and disrupting the cells with 3:1 fixative. Illustrations show complements of chromosomes in the first metaphase after labeling with ^{3}H-amino acids or uridine-^{3}H. (BBB)

45791 ON THE INCORPORATION OF TRITIATED THYMIDINE AND ON THE KINETICS OF THE PROLIFERATION OF CELLS OF EHRLICH ASCITE TUMOR. Piccotti, F.; Sannazzari, G. L. (Universita, Turin). Minerva Radiol., Fisioterap. Radiobiol., 10: 323-5(July-Aug. 1965). (In Italian).

The use of tritiated thymidine in the study of thymidine incorporation into DNA and in the study of the kinetics of the proliferation of cells of Ehrlich ascite tumor was studied. The results obtained on the numerical increase of tumor cells using tritiated thymidine are given. The numerical increase between the 3rd and the 8th day follows a straight line and the time of doubling is approximately 18 hrs. (J.S.R.)

45792 IODINE METABOLISM AND THE THYROID GLAND. Berson, Solomon A.; Yalow, Rosalyn S. (Veterans Administration Hospital, Bronx, N. Y.). N. Y. State J. Med., 63: 35-42(Jan. 1, 1963).

This review considers the rates of movement of iodine from one physiologic or anatomic compartment of the body to another and with the quantities of iodine held within these compartments, information which has been accumulated largely with the aid of radioiodine during the past two decades. It is emphasized that measurements of radioiodine alone are of relatively limited usefulness, as is true also in other tracer studies; a consideration of the quantities of unlabeled material involved in the processes under study is essential to a meaningful interpretation of isotopic data. The iodide pool includes not only blood and extracellular space but also certain glands, derived from the primitive gastrointestinal tract, that have the capacity to concentrate iodide, in their secretions, 20- to 40-fold above the level of the plasma iodide concentration. Removal from the iodide pool is almost exclusively by way of renal exoretion or thyroid accumulation; therefore, ^{131}I administered as iodide is competed for solely by the thyroid and kidneys, so that the default of one leads to an eventual accumulation by the other of a greater fraction of the administered dose. Thus, in cases of renal failure, thyroidal uptake may account for almost the entire administered dose of ^{131}I. The kinetics of iodide trapping by the gland are discussed, and defects in iodide concentration are considered. Iodide, in large doses, is not effective in overcoming the block of organic binding induced by methimazole (Tapazole) and similar agents and is itself capable of inducing a transient binding block which, in rare cases, persists and leads to hypothyroidism. Radiation that is produced by ^{131}I therapy sometimes induces a transient dissociation of the iodide-trapping and -binding functions of the thyroid. For several months after ^{131}I treatment of Graves disease, the thyroid may continue to trap iodide at an abnormally high rate but fail to bind all into organic form. Presently held concepts of intrathyroidal iodine metabolism are reviewed. (BBB)

45793 HUMAN BONE METABOLISM INFERRED FROM FALL-OUT INVESTIGATIONS. Rivera, J. (Health and Safety Lab., USAEC, New York). Nature, 207: 1330-2 (Sept. 25, 1965).

Measurements of ^{90}Sr accumulation in the skeleton and of ^{90}Sr levels in the diet allowed inferences to be drawn concerning the metabolism of strontium and changes in bone ^{90}Sr concentrations resulting from changes in diet ^{90}Sr concentrations to be predicted. An equation expressing the changes of ^{90}Sr concentrations in bones of adults with changes in ^{90}Sr intake was developed: $B_n = 0.975\ B_{n-1} \rightarrow f0.975\ B_{n-1} + fKZ_{n-1}$, where B_n is the ^{90}Sr/Ca ratio of bone at the beginning of year N, f is the fraction of bone turned over during the year $N-1$, K is the ratio of ^{90}Sr/Ca in newly forming bone to that in the diet, and Z_{n-1} is the ^{90}Sr/Ca ratio of the diet during year $N-1$. The factor 0.975 is introduced to account for the radioactive decay of ^{90}Sr in one year. Equations were also developed for excretion of ^{90}Sr from the skeleton. (M.C.G.)

45794 THE EFFECT OF GROWTH INHIBITORS ON THE INCORPORATION OF ^{32}P INTO THE ALCOHOL SOLUBLE PHOSPHATE FRACTION OF RICE SEEDLINGS. Koeves, E.; Sirokman, F. (Jozsef Attila Univ., Szeged). Naturwissenschaften, 52: 433-4(1965).

The mode of action of two naturally occurring growth inhibitors, salicylic acid and cinnamic acid, was studied to determine whether the decrease of the amount of nucleotide polyphosphates and the accumulation of esters and inorganic phosphate could be correlated with the growth inhibition of these compounds. The studies made on 8 day old rice seedlings showed that the incorporation of ^{32}P increases with respect to the controls with the addition of salicylic or cinnamic acid. The participation of the inorganic phosphorus increases in the total activity. The total nucleotide activity decreases as shown by the percentage of total activity. Salicylic acid increases the incorporation into ^{32}P esters but cinnamic acid decreases it slightly. The percentage activity of glyceric acid phosphate fraction decreases in plants treated with growth inhibitors. Both compounds decrease the phosphorylation of an unknown compound containing indole and sugar. (J.S.R.)

45795 CONTENT OF RADIUM D IN HUMAN BONES AND HAIR. Jaworowski, Zbigniew. Nukleonika, 10: 297-302(1965).

Radium D was determined in human bones and hair samples collected in 1963 in Warsaw. The average concentration of RaD in bones was found to be 0.041 pC/g wet bone and in hair 0.198 pC/g hair. These concentrations are 1.6 and 7 times higher, respectively, than in samples collected in 1960 in the London area and analyzed by the same method. (auth)

45796 IN VITRO ^{131}I UPTAKE BY TISSUES OF RAINBOW TROUT. Maqsood, M.; Reineke, E. P.; Fromm, P. O. (Michigan State Univ., East Lansing). Physiol. Zool., 34: 34-8(1961).

Data on the in vitro ^{131}I uptake by different tissues of rainbow trout (Salmo gairdnerii) under different experimental conditions are presented. Only lower jaw tissue concentrated ^{131}I to a significant degree. The T/M value (cpm/100 mg tissue, divided by 0.1 ml medium) was higher for tissue from the posterior part of the lower jaw than from the anterior part, indicating that the thyroid follicles are comparatively more numerous in the posterior part. The ^{131}I uptake was higher in the lower part of the gill than in the upper part, probably due to the presence of some thyroid follicles in the tissue at the base of the gills at the point of attachment to the lower jaw. Addition of thiouracil to the medium did not affect ^{131}I uptake by any of the tissues studied, whereas KSCN blocked ^{131}I uptake

by lower jaw tissue but had no effect on any other tissues. The T/M values for ^{131}I uptake by different organs of the digestive system, kidney, head kidney, liver, spleen, heart, skeletal muscle, and brain were less than one, indicating that these organs or tissues have a relatively poor ability to concentrate iodide in vitro. In this respect fish differ from mammals, in which thyroidal, mammary gland, salivary gland, and stomach tissues have been shown to concentrate iodide in vitro. The fact that the various fish tissues showed T/M values higher than those for boiled tissues indicates that some uptake of iodide did occur. This small amount of uptake of radioiodine by the various tissues may represent the activity of heterotopic thyroidal tissues, but since KSCN had no effect on the uptake, this process must differ from that occurring in the lower jaw area. (BBB)

45797 EXCRETION OF RADIOACTIVITY BY HUMAN SUBJECTS AFTER INGESTION OF LIVER FROM CATTLE TREATED WITH LABELED POLYDIETHYLSTILBESTROL PHOSPHATE. Perklev, T.; Gassner, F. X.; Martin, R. P.; Huseby, R. A.; Shimoda, W. (AB LEO, Haelsingborg, Sweden; Colorado State Univ., Fort Collins; American Medical Center, Denver). Proc. Soc. Exptl. Biol. Med., 119: 996-8(Aug.-Sept. 1965).

Polydiethylstilbestrol phosphate (PSP), an effective growth promoting agent in beef cattle, tends to accumulate in the animal's liver as indicated by studies in which radioactive PSP was used. Upon ingestion of such liver (cooked) by human beings, 93 to 101% of the radioactivity was found in the feces. No radioactivity could be detected in either blood or urine. It is concluded that neither PSP nor its metabolites ingested under such circumstances are absorbed in detectable amounts during passage through the human intestinal tract. (auth)

45798 THE ^{228}Th DECAY SERIES IN ADULT BEAGLES: ^{224}Ra, ^{212}Pb, AND ^{212}Bi IN SELECTED BONES AND SOFT TISSUES. Stover, Betsy J.; Atherton, David R.; Buster, Dawn S.; Bruenger, Friedrich W. (Univ. of Utah, Salt Lake City). Radiation Res., 26: 132-45(Sept. 1965).

Radium-224 and ^{212}Pb in liver, spleen, kidneys, one humerus, and the third lumbar vertebra, and ^{212}Bi in kidneys, were measured through 3 years after injection of ^{228}Th into young adult beagles. In the liver the activity of ^{212}Pb was slightly higher than that of ^{224}Ra, which was about 30% higher than that of ^{228}Th. All three decrease at about the same rate, and this rate is about the same as observed for the three in blood. In the spleen ^{224}Ra activity was again slightly higher than ^{228}Th activity, but ^{212}Pb activity was only half that of ^{228}Th. The rates of decrease were about the same as for liver and blood. In the kidneys the mean ^{212}Bi activity measured was 17% greater than that of ^{228}Th, which was 3.5 times that of ^{224}Ra and ^{212}Pb, the latter two being equal. There was considerable variation in all four sets of data, and the rates of biological decrease could not be determined. Some of the ^{224}Ra and ^{212}Bi in kidneys and urine must come from extravascular sites. In one humerus and the third lumbar vertebra there was a progressive loss of decay products; the activity of ^{228}Th was greater than that of ^{224}Ra, which exceeded ^{212}Pb. Neither the ^{224}Ra nor the ^{212}Pb data showed a significant rate of biological decrease in either bone. Also the activities of ^{224}Ra and of ^{212}Pb relative to that of ^{228}Th did not show a significant change with time. In general, the biological rates of decrease of ^{224}Ra and ^{212}Pb were found to be about the same as those of ^{228}Th. The biological rate constants for the three nuclides in bone appear to be of the order of 0.1 of the physical decay constant, and for the soft tissues the biological rate constants appear to be of the same order of magnitude. Average radiation dose rates to bone, liver, and kidneys were estimated, and the problem of evaluating the loci of decay of ^{220}Th and ^{216}Po is discussed. (auth)

45799 ^{129}I AS A NONRADIOACTIVE TRACER. Watson, J. Throck; Roe, David K.; Selenkow, Herbert A. (Massachusetts Inst. of Tech., Cambridge; Harvard Medical School and Peter Bent Brigham Hospital, Boston). Radiation Res., 26: 159-63(Sept. 1965).

The nuclide ^{129}I has potential usefulness as an essentially nonradioactive tracer for biological investigations. Neutron activation produces ^{130}I, which can be readily measured by conventional counting equipment. The minimum quantity of ^{129}I detected was 2×10^{-9} g. Further refinements in isolation techniques and in radiation detection should permit accurate measurement of even smaller quantities and will enhance the usefulness of this isotope as a biological tracer. (auth)

45800 A CRITERION ON THE HISTOLOGIC FIXATION FOR RADIOAUTOGRAPHY AND RELEASE OF RADIOACTIVITY FROM THE LIVER TISSUE TREATED WITH ^{35}S-SULFATE. Yamada, Masakazu; Yoshikawa, Kiyoshi; Yamada, Masaoki (Nara Medical Coll., Kashiwara, Japan). Radioisotopes (Tokyo), 14: 319-23(1965).

An attempt was made to study possible relations between histologic fixatives and radioactivity maintained in tissue specimens. The specimens were obtained from the liver of rats treated in vivo with ^{35}S-sodium sulfate. Radioactivities released from or kept in tissues were measured after fixation with various agents. An assumption that fixatives prevent a release of radioactivity from tissue specimens was evaluated. Of the aqueous fluids, trichloroacetic acid and lead acetate showed an inhibition of the release which was denied to formalin. In the case of mixed agents, when aqueous fluids were employed in combination with respective, indicated agents for radioactive substances, the release may be inhibited, as shown by an additional use of barium chloride or calcium chloride for fixing radioactivity of ^{35}S-sulfate in tissue. (auth)

45801 ^{210}Po IN LEAF TOBACCO FROM FOUR COUNTRIES. Gregory, L. P. (National Radiation Lab., Christchurch, N. Z.). Science, 150: 74-6(Oct. 1, 1965).

Tobaccos grown in the United States, Rhodesia, South Africa, and New Zealand were measured for their polonium-210 content. Details of the method of measurement are given and the results are listed. A mean of 0.15 picocurie per gram was found in New Zealand tobacco, compared with 0.49 picocurie per gram in United States tobacco. The concentration in South African tobacco was approximately the same as in United States tobacco, but the level in Rhodesian tobacco appeared to be significantly higher. (auth)

45802 EFFECTS OF BERYLLIUM IN PLANTS AND SOIL. Romney, E. M.; Childress, J. D. (Univ. of California, Los Angeles). Soil Sci., 100: 210-17(Sept. 1965). (UCLA-12-542).

The effects of soluble Be were investigated in plants and soil. Beryllium inhibited the growth of several different crop plants at levels above 2 ppm in nutrient solution and 4 per cent of the cation-exchange capacity in soil. The visible effects of Be in plant tissues are described. Although roots concentrated high levels of Be, this element was not readily translocated to other plant parts. Leaves accumulated more Be than did stems or fruit tissue. The uptake of P was increased and Ca and Mg uptake was decreased in Be-treated plants. Insoluble forms of Be did not inhibit plant growth. Reactions of Be in nutrient solution and soil were influenced by pH. Beryllium was strongly adsorbed by soils and bentonite but not by kaolinite. Previously adsorbed Be was not effectively replaced by Ba, Ca, or Mg; these cations, however, competed with Be for sorption sites under batch-equilibrium conditions. Applications of Be to soil displaced some adsorbed divalent cations, including Ba, Ca, Mg, and Sr. (auth)

45803 HISTOLOGY AND CYTOMORPHOLOGY OF THE EXPERIMENTAL BERYLLIUM GRANULOMA. Gusek, W.; Mestwerdt, W. (Universitaet, Hamburg). Verhandl. Deut. Ges. Pathol., 47: 221-6(1963). (In German).

Electron microscopic and histochemical studies were made of the tissue reactions to Be. The studies were designed to help elucidate the potentially carcinogenic action of Be. The subcutaneous administration to rats and guinea pigs of chemically pure BeO resulted in the development of granulation tissue. These granulation tissues scarred more rapidly in the rat, while in the guinea pig they practically

remained constant, with regard to both quantity and quality, throughout the interval from the first to the sixth month of examination. The essentially proliferative and occasionally tuberculogenic effect of BeO, therefore, was confirmed. The negative statements published in medical literature are due evidently to the animal species used and the dose employed. No histologic relation to silicosis was found to exist. The intranuclear deposits of foreign material in phagocytic cells, in addition to cytoplasmic inclusion bodies, suggests that if Be does have a carcinogenic action, it may arise from direct contact of Be with chromosomes. (BBB)

45804 STUDY OF THE ABSORPTION OF RADIOACTIVE FISSION PRODUCTS BY CULTIVATED CROPS. II. ACCUMULATION OF RADIOACTIVE FISSION PRODUCTS BY CULTIVATED GRAINS AND LEGUMES, AND PERENNIAL GRASSES. Ilyina, G. V.; Rydkii, S. G. Vestn. Mosk. Univ. Ser. VI Biol. Pochoved., 20: 3-9(1965). (In Russian).

Data are presented for the activity found in the pedicles and leaves of 30-day pea plants, those at the beginning of fruit formation, and in the peas for introduction of 1 mC/m^2 of fission product solution (predominantly $^{90}Sr/^{90}Y$) into the ground with and without stable Sr added. Similar data are reported for lupin, including the activity of the flowers. Data are reported for the leaves and stems of 30-day vetch. Activity ranged from 889 cpm/g dried material (peas) to 8845 (lupin leaves at blooming); in every case the value was higher for the solution with stable Sr. Activity for the petioles and leaves of clover, pedicles and leaves of alfalfa, pedicles, and leaves of sweet clover, and orchard grass follows the same pattern and averages 2000 cpm/g dried material. The loss of activity on harvest of clover, alfalfa, sweet clover, and orchard grass is tabulated and averages about 1 mC/ga, considered to be a small amount. Use of lime in the soil decreased the activity in lupin stems and leaves by about 30%. Data are also given for the growth characteristics of orchard grass under these conditions. (BBB)

45805 EFFECTS OF STEROID HORMONES ON STRONTIUM KINETICS IN MAN. Eisenberg, E. (Univ. of California, San Francisco). pp 917-21 of Proc. 2nd Intern. Congr. Endocrinol., Part II, London, August 17-22, 1964. Amsterdam, Excerpta Medica Foundation, 1965.

The kinetics of stable strontium were measured in human subject before and after treatment for four to six weeks with various hormones. Androgens and estrogens were given to 45 women with postmenopausal osteoporosis, 8 men with senile osteoporosis, 11 men with idiopathic osteoporosis, and three elderly men without osteoporosis. Corticoids were given to 59 men and women who were either normal volunteers or patients with diseases requiring large doses of corticoid, such as asthma and generalized exfoliative dermatitis. The androgens and estrogens studied included testosterone enanthate, testosterone caprinoyl acetate, nandrolone phenpropionate, fluoxymesterone, oxandrolone, norethandrolone, oxymetholone, 7,17-dimethyltestosterone, conjugated equine estrogens, ethinyl estradiol, 16α-methylestriol, and 16β,17β,3-methylether. The corticoids included cortisol, prednisone, triamcinolone, 6α-fluoroprednisolone, dexamethasone, and 6α-fluorotriamcinolone. None of the steroids produced a significant change in the miscible pool of strontium during the four to six weeks of therapy. The androgens and estrogens decreased total turnover rate of the pool. With androgens, this was due to a significant decrease in urinary excretion rate. There was a slight decrease in bone deposition rate with androgen therapy but this was not significant. Estrogen therapy caused a significant decrease in both the urinary excretion and the bone deposition rate. All of the corticoids produced a marked increase in urinary excretion rate; most of the corticoids caused an increase in bone deposition rate of Sr. 6α-Fluorotriamcinolone tended to decrease the bone deposition rate. The percentage of administered strontium excreted in the feces before corticoid therapy ranged from 2.3 to 17.0, with a mean of 6.3. Corticoid therapy caused this value to increase in 15, to decrease in 9, and not to change in 5 subjects. Although occasional subjects showed a marked increase in fecal excretion rate of strontium when the corticoid was administered, there was no significant change in fecal excretion rate of strontium in any corticoid-treated group. Thus when fecal clearance rate was not included in bone deposition rate, i.e., when the figure usually calculated for bone deposition rate was corrected by subtracting the fecal clearance rate, the change in bone deposition rate was not affected. (BBB)

Radiation Effects

Refer also to abstracts 46339 and 46695.

45806 (AD-621543) FOCAL ANTIBODY PRODUCTION BY TRANSFERRED SPLEEN CELLS IN IRRADIATED MICE. Playfair, J. H. L.; Papermaster, B. W.; Cole, L. J. (Naval Radiological Defense Lab., San Francisco, Calif.). Aug. 20, 1965. 20p. (USNRDL-TR-887). CFSTI $1.00 cy, $0.50 mn.

Lethally x irradiated mice were injected with various numbers of normal spleen cells, and then immunized with sheep erythrocytes. In their spleens, antibodies appeared in localized areas whose number corresponded to the number of spleen cells injected. When sheep and pig erythrocytes were injected simultaneously, antibody against each was found in separate areas. From these findings it is postulated that single precursor cells are responsible for the areas of antibody, and that the progeny of each is restricted to forming a single antibody. (auth)

45807 (AED-C-04-17) RADIATION EFFECTS ON LIVING TISSUES AND ORGANISMS. Series C. Bibliographies. Stahlhofen, W. (comp.) (Max-Planck-Institut fuer Biophysik, Frankfurt am Main (West Germany)). Jan. 1965. 265p. Dep. mn.

One thousand and forty-seven references are presented to recent literature on the effects of radiation on living organisms and tissues. Author, source, and subject indexes are included. (C. H.)

45808 (NYO-901-36) PROGRESS REPORT NO. 27 [ON RADIOBIOLOGICAL STUDIES], MAY 1, 1964-APRIL 30, 1965. (New England Deaconess Hospital, Boston, Mass. Cancer Research Inst.). Contract AT(30-1)-901. 78p. Dep. mn; CFSTI, $3.00 cy, $0.75 mn

Preliminary investigations of applications of neutron activation analysis in forensic pathology are reported. Progress is reported in studies of the effects of radiation and cancer on adaptive enzyme changes, with emphasis on the control in vivo of the level of liver tryptophan pyrrolase; the induction by tryptophan of tryptophan catabolic enzymes in Pseudomonas; the effects of tryptophan and hydrocortisone on tryptophan pyrrolase content in the liver of young chick embryos; and methods for the purification of tyrosine transaminase for use in the preparation of an antibody for use in studies of tyrosine transaminase. Preliminary analysis of data on the life span and cause of death of American physicians suggests that improved techniques may have increased the life span of radiologists by reduction of the incidence of leukemia and cancer. A survey on the incidence of leukemia after radiotherapy of cancer of the cervix indicates that there may be an increase in leukemia brought about by intensive partial-body radiation. Preliminary results are reported from studies of chromosome patterns of a Marshallese population ten years after exposure to highly-radioactive fallout; aged men, and persons having congenital abnormalities of sex chromosomes; bone pathology in patients with Ra poisoning; the induction of breast tumors in female rats with 7,12-dimethylbenzanthracene; bone pathology and tumor incidence in mice injected with ^{239}Pu; and the protective effects of diethylenetriaminepentaacetic acid (DTPA) against the pathological effects of ^{239}Pu in mice. Sarcomas were induced in mice by treatment with methylcholanthrene and preparations of these tumor cells were tested for their antigen-stimulating properties. The pathological effects of various doses of cortisone in mice of various ages were studied. Preliminary data are re-

ported from a study of the etiology, pathology, and effects of various treatments of cancers of the cervix, urinary bladder, and breast; the effects of tumor transplantation on liver enzyme systems and tumor-host relationships in hamsters; tracer studies of erythrokinetics in hamsters; and a study of radioinduced ovarian tumors in parabiont rats. A study of the possible genetic effects of repeated x irradiation of the testis of male rats over 10 generations is reported. Third and fourth generation rats are being studied. Data are presented from studies on the incidence of tumors of the endocrine system, anastomatic tumors, and on leukemogenesis in parabiotic rats; studies on the carcinogenic effects of chronic γ radiation from a ^{60}Co wire implanted in the lungs of mice, rats, hamsters, guinea pigs, and rabbits; the effects of pre- and post-natal x irradiation of mice on the incidence of leukemia, life-span, and fertility of succeeding generations; the protection afforded by the thymus against the carcinogenic effects of injected ^{131}I in mice; the effects of low-level β doses on the incorporation of tritiated thymidine into the nuclei of thyroid cells in mice; and the effects of ^{131}I or goitrogenic drugs on the pituitary thyrotropic response in mice. Preliminary results are reported from a theoretical investigation of phosphate chemistry based on molecular orbital calculations programmed for the IBM 7090 computer. A list is included of 38 publications during the period covered by this report. (C.H.)

45809 (NYO-1979-12) QUANTITATIVE POPULATION GENETICS OF MICE UNDER IRRADIATION. Progress Report, July 1, 1964–June 30, 1965. Green, Earl L.; Roderick, Thomas H.; Schlager, Gunther (Roscoe B. Jackson Memorial Lab., Bar Harbor, Maine). July 21, 1965. Contract AT(30-1)-1979. 24p. Dep. mn; CFSTI $1.00 cy, $0.50 mn.

Progress is reported in studies of the effects of various doses of x radiation on genetically determined fitness characteristics of mouse populations and the discovery, isolation, and analysis of genetic factors affecting radiation resistance in mouse populations. Data are included on reproductive performance, embryonic mortality, fitness, genetic extinction, genetic differences in radiation resistance of inbred strains, and selection for radiation resistance in experimental populations. Preliminary studies of brain weights of genetically heterogeneous mouse populations indicate a high correlation between brain weight and general fitness. A new mutation, double toes, was determined in populations in which the spermatogonia had received 900 R x radiation for 0, 4, 5, 6, and 7 generations. Life span data on mice in several populations were accumulated. (C.H.)

45810 (NYO-3394-2(Rev.)) FEASIBILITY STUDY OF THE CORRELATION OF LIFETIME HEALTH AND MORTALITY EXPERIENCE OF AEC AND AEC CONTRACTOR EMPLOYEES WITH OCCUPATIONAL RADIATION EXPOSURE. Progress Report No. 1, June 1, 1964–April 2, 1965. Mancuso, Thomas F.; Sanders, Barkev S.; Brodsky, Allen (Pittsburgh Univ., Pa. Graduate School of Public Health. Dept. of Occupational Health). Revised Aug. 10, 1965. Contract AT(30-1)-3394. 164p. Dep. mn; CFSTI $5.00 cy, $1.00 mn.

The objective of this study is to follow cohort employee populations of selected AEC Contractor installations, to test the feasibility of using personnel, employment, medical and radiation records in establishing the relationships, if any, between mortality patterns and levels of radiation exposure. The reason for the study is the absence of empirically tested information pertaining to human populations exposed to recorded low levels of radiation over long periods of time. The procedure devised for the test runs is: to establish a series of cohorts of populations at each facility, those continuously employed as well as those separated, for each year, by tracing these individuals and sibling controls through Social Security records to determine those who have died and their place and date of death; to obtain death certificates to establish age-sex specific death rates; and to analyze causes of death for those with radiation exposure and work-connected health hazards in comparison to appropriate non-exposed controls. The following AEC Contractor facilities have been selected for the test runs: Oak Ridge X10, Oak Ridge Y12, Oak Ridge K25, Hanford Laboratories, and several small feed materials plants. These facilities provide large populations with long intervals of operation. Pilot studies of radiation exposure records of persons exposed in atomic energy facilities will be carried out to determine the average occupational exposure of these populations and appropriate confidence limits in exposure estimates for individuals and various sub-populations. (auth)

45811 (ORO-631) SEMI-ANNUAL PROGRESS REPORT, JULY 1–DECEMBER 31, 1964. (UT-AEC Agricultural Research Lab., Oak Ridge, Tenn.). Aug. 1965. Contract AT(40-1)-Gen-242. 187p. Dep. mn; CFSTI $5.00 cy, $1.00 mn.

Separate abstracts were prepared on 10 sections of this report. A list is included of publications during the period. (C.H.)

For abstracts of individual sections see: 45759–45761, 45812–45817, and 46239.

45812 (ORO-631, pp 1-35) VETERINARIAN MEDICINE. (UT-AEC Agricultural Research Lab., Oak Ridge, Tenn.).

Progress is reported in studies on the survival of domestic animals used for food following a nuclear attack, clinical indications of delayed radiation injury in animals surviving irradiation, and related studies in laboratory animals. Data are presented on the early effects of 700 rads of neutron radiation on the central nervous system of rats and rabbits in which blood pressure response of anesthetized animals to epinephrine was used as the criterion; the effects of 300 or 600 rads of neutrons on blood and cerebrospinal fluid pressure in burros; the effects of head shielding during neutron irradiation of burros on mortality and survival time; and the effects of the body axis relation to the source on the mortality of swine after neutron exposure. The clinical status and mortality data are reviewed for burros surviving neutron-γ irradiation from a nuclear device in 1957; burros surviving lethal doses of γ radiation in 1951; burros exposed in 1953 and 1954 to chronic γ radiation at levels of 25 R/week to a total dose of 375 R; burros exposed to a Godiva reactor in 1959; swine exposed to neutron-γ doses ranging from 15 to 850 rads in 1957; swine surviving exposure to an atomic detonation in 1959; and cattle surviving $LD_{50/30}$ levels of γ radiation in 1959. Mortality in the burros surviving neutron-γ irradiation from an atomic detonation at 7.5 yr post-exposure was comparable in each dose group with an average of 40%. Mortality in burros surviving γ irradiation for periods of 10.5 and 13.5 yr appeared to be dose related. The mortality of swine exposed to neutron-γ radiation was highest of all the animals exposed with 48% mortality at 7.5 yr post exposure. Death of the burros was related to blood dyscrasias, loss of body weight, and enteritis; the mortality of swine was related to enteritis and neoplasias; and mortality in the cattle and sheep was generally associated with infection. Data are included from a comparison of the toxic effects of ^{90}Sr and ^{226}Ra in sheep observed since 1954. The last cow of the herd exposed in 1945 to the radioactive cloud from the first atomic bomb near Alamogordo, New Mexico, was euthanized in Nov. 1964 because of poor health. A malignancy of the bony structure around the left eye was rapidly spreading. The skin, which was marred by lesions caused by β particles, was preserved for a museum specimen. (C.H.)

45813 (ORO-631, pp 36-44) PHYSIOLOGY OF REPRODUCTION. (UT-AEC Agricultural Research Lab., Oak Ridge, Tenn.).

Progress is reported in studies on the effects of radiation on the reproductive cycle in domestic animals and associated studies in laboratory animals. Data are presented on the effects of γ radiation at doses of 200 to 600 R on the reproductive performance of cows and viability of their calves; the effects of prenatal or localized γ

irradiation on ovarian development in heifers; the effects of exposure of pregnant sows to neutrons on development of their offspring; and the effects of various doses of γ radiation on ovarian development in young female swine; and the effects of various doses of γ radiation on spermatogenesis in rabbits. Preliminary results are reported on the effects of 0.5% toxaphene spray and dietary 6% ronnel on the control of horn flies, Siphona irritans, on cattle. Procedures are described for tissue culture studies of peripheral leukocytes of domestic animals. Preliminary results are reported from studies of radioinduced chromosome aberrations in leukocytes in tissue culture. (C.H.)

45814 (ORO-631, pp 45-66) RADIATION PATHOLOGY. (UT-AEC Agricultural Research Lab., Oak Ridge, Tenn.).

The death patterns of irradiated domestic animals were studied through close examination of necropsies of 90 cadavers from 5 species of animals. Eight of the animals were survivors of experimental groups that were subjected to various doses and sources of radiation several years previously. Pathological data are summarized. (C.H.)

45815 (ORO-631, pp 67-76) PHYSIOLOGICAL EFFECTS OF RADIATION. (UT-AEC Agricultural Research Lab., Oak Ridge, Tenn.).

Progress is reported in studies of physiological events that occur in animals as a result of whole-body irradiation. Results are reported from measurements of hippuric acid content in the urine of sheep, swine, and man before and after whole-body γ irradiation at doses of 100 to 300 R. Results indicate a slight decrease in hippuric acid excretion immediately following radiation exposure with an increase between the 7th and 51st post-irradiation day. The effects of ultrafiltrate from normal and irradiated sheep on bone marrow cells in tissue culture and the rate of DNA synthesis in bone marrow cultures as measured by incorporation of ^{14}C-formate were studied. The incidence of tumors in rats injected with irradiated blood plasma or ultrafiltrate was also studied. (C.H.)

45816 (ORO-631, pp 142-4) BIOCHEMISTRY. (UT-AEC Agricultural Research Lab., Oak Ridge, Tenn.).

Data are presented on glucuronide excretion in starved rats after exposure to 1000 R γ radiation. (C.H.)

45817 (ORO-631, pp 145-71) RADIATION GENETICS. (UT-AEC Agricultural Research Lab., Oak Ridge, Tenn.).

Progress is reported in studies of the genetic effects of radiation in plant tissues and environmental factors modifying such effects. Results are reported from a study of the effects of γ radiation on growth and photoperiod requirements of chrysanthemum potted cuttings; the effects of acute γ or neutron exposure on morphogenesis, growth, and somatic mutations in Coleus plants; the relative effectiveness of γ radiation and 2-chloroethyl trimethylammonium chloride (CCC) as plant growth retardants; the effects of exogenous applications of indole acetic acid (IAA) on growth of irradiated Coleus plants; the effects of low temperature and packaging materials on stored irradiated seeds; and species differences in the radiosensitivity of seeds exposed to γ radiation on fission neutrons. A list is included of plant materials irradiated during the period. (C.H.)

45818 (TDCK-33500) PROTECTION AGAINST THE BIOLOGICAL EFFECTS OF THERMAL RADIATION. BIBLIOGRAPHY. Thiessen, J. W.; van Woerden, J. (Technisch Documentatie- en Informatie-Centrum voor de Krijgsmacht, The Hague (Netherlands)). Feb. 1963. 105p. Dep. mn.

Summaries of publications on the physical characteristics of thermal radiation, and the factors of exposure, environment, and skin involved in the production of cutaneous burns, and the protective effect of fabrics, paints, creams, and other interposed materials are presented. Publications on mathematical analyses and prediction techniques and on retinal lesions are also included. (171 references.) (tr-auth)

45819 (TID-22176) DEVELOPMENT OF SELECTION METHODS FOR INDUCED SMALL MUTATIONS IN HIGHER PLANTS (WITH SPECIAL REGARD TO MUTATIONS OF YIELDING CAPACITY). Final Report, February 1, 1961-January 31, 1965. Gaul, Horst (Max-Planck-Institut fuer Zuechtungsforschung, Cologne (West Germany)). Contract AT(30-1)-2619. 51p. Dep. mn; CFSTI $3.00 cy, $0.50 mn.

Barley seeds were x irradiated and 2,024 normal appearing M_2 plants were selected at random along with an equal number of random plants of the untreated barley variety. Individual progenies of these plants were grown from M_3 to M_6 generation. Of main interest were: kernel yield, kernel size, and heading date. The whole material was transferred from the M_3 into the M_4 generation without selection. In M_5 and M_6 generation two selection steps were conducted for yield, both in a positive and in a negative direction. The material was split up in three different experiments in order to obtain information on the relative value of the experimental design used. The analysis of variance in the M_3 and M_4 generation exhibited for the character yield a decrease of the mean values by about 5% and a considerable increase of the genotypic variance of the lines derived from x irradiation compared to the controls. The phenotypic frequency distribution curves indicated that the major part of the induced genetic variability is negative. The shape of the distribution curves suggests that a very large number of micro-mutations is involved and their frequency of occurrence in M_2 generation may be at least 50 times higher than that of macro-mutations. In spite of the low heritability of the character yield a clear response to positive and negative selection was found. There is still a large amount of genotypic variance in M_6 lines whereas no genotypic variance appears to be in the correspondent control lines. Also the phenotypic distribution curves of the M_6 lines indicate clearly that positive yield variance has been selected. From the results it is inferred that it will be possible during following generations to isolate radiation-induced lines with improved yielding potential. (auth)

45820 (TID-22227) STUDIES ON THE EFFECTS OF RADIATION ON MUCOSAL AND FOETAL BRAIN ENZYMES AND RADIATION RECOVERY STUDIES ON SINGLE CELLS. Final Report, November 1, 1964-October 31, 1965. Bernheim, Frederick; Wilbur, Karl M. (Duke Univ., Durham, N. C.). Contract AT(40-1)-2919. 35p. Dep. mn; CFSTI $2.00 cy, $0.50 mn.

Major findings are summarized from a series of studies on the effects of radiation on enzymes in rat tissues and radiation recovery in single cells in which the yeast, Schizosaccharomyces pombe, was used. A method for the estimation of phospholipase activity in tissues is described. Preliminary results with this method indicate that irradiation not only inactivates factors that can activate the enzyme but also changes the distribution of the enzyme in sub-cellular particles. Results of density gradient centrifugation experiments on intestinal mucosa from whole-body x irradiated rats supported the conclusion that the inactive enzyme is not associated with particles and is part of the soluble intracellular protein fraction. The inactive enzyme can be activated to hydrolyze lecithin by addition of fractions from normal mucosa or by treatment with chymotrypsin. Studies on the effects of 2-mercaptoethylamine (MEA) on peroxidation in microsomes showed that the unsaturated lipid of rat liver microsomes is catalyzed by cysteine or thiolacetic acid. The catalysis is increased by the addition of Fe or Cu salts and by exposure to ultraviolet light and MEA inhibits the catalysis under all these conditions. Studies of the growth cycle of S. pombe showed that on transferring cells to a fresh medium there is a period of about 6 hr of cell growth with essentially no division, then a period of rapid, but not synchronized, division followed by a return toward the resting state after about 24 hr. During the pre-division phase the cells showed a marked increase in average length and volume, RNA, and protein. At 12-hr when division was rapid, the RNA and protein values decreased markedly. Exposure to γ radiation at doses of 100,000 to 200,000 R produced cells of increased size. Pre-divisional growth and division were inhibited by O_2, a mixture of O_2 and CO_2, and N. Inhibition of division by O_2 was slightly reduced by 0.01 M glutathione and

0.005 M cysteine, and enhanced by 0.1 M cysteine and 0.001 M thiolacetic acid. The experiments showed that growth rate and division are not closely coupled in S. pombe. A list is included of publications during the period covered by this report. (C.H.)

45821 (JPRS-31547, pp 1-5) ON THE BIOLOGICAL EFFECTS OF HIGH ENERGY PROTONS. Saksonov, P. P.; Antipov, V. V.; Shashkov, V. S.; Razgovorov, B. L.; Murin, G. F.; Morozov, V. S. Translated from Dokl. Akad. Nauk SSSR, 162: 688-90(1965).

Protons are the most widespread form of penetration found in space since they constitute about 85% in the primary cosmic radiation and are generated in great numbers during solar flares. Results are reported from studies of the relative biological effectiveness of protons with energies of 660 and 120 Mev, the specific ionization of which is equal respectively to 6 and 20 pairs of ions/micron, in comparison with γ radiation in mice and rats. The value with respect to LD_{50} was about 0.7, and this value was confirmed by clinical observations and results of previous experiments vs the growth of plants from irradiated seed, mutation rates in Drosophila, and results of chromosome analysis of mouse bone marrow as criteria. (C.H.)

45822 (JPRS-31822) THE BIOLOGICAL ACTION OF NEUTRON RADIATION. Gorodetskii, A. A. (ed.) Translation of Biologicheskoe Deistvie Neitronnogo Izlucheniya from a Publication of Naukova Dumka Publishing House, Kiev, 1965. 133p. (TT-65-32317). CFSTI $4.00 cy, $1.00 mn.

The relative biological effectiveness of fast neutrons is compared with x and γ radiation in a number of biological systems. Data are included from studies of the effects of neutrons on the hematopoietic and cardio-vascular systems of experimental animals; the effects of neutrons on the function of the thyroid and adrenal glands; the morphological effects of neutron irradiation on certain organs of rats; the serological properties of radioinduced mutants of Clostridium perfringens; the effects of fast neutrons on immune properties of toxins produced by Cl. perfringens; the effects of fast neutrons on the physiological and morphological properties of the potato bacillus, B. mesentericus; the development of nitrate gel dosimeters for radiation measurements in mixed neutron-γ fields; and the use of proportional counters in neutron dosimeters. (207 references.) (C.H.)

45823 (JPRS-31933, pp 1-5) PERFORMANCE CAPACITY OF ANIMALS FOLLOWING THEIR IRRADIATION, ADRENALECTOMY AND THE ADMINISTRATION OF ANTI-RADIATION DRUGS. Stashkov, A. M. Translated from Farmakol. i Toksikol., 28: 347-9(May-June 1965).

In adrenalectomized mice and rats, the rate of depression of physical endurance under the action of x radiation, as well as the duration of the barbamyl-induced narcotic sleep, are 20 to 25 percent greater than in intact animals. The duration of the initial phase of cystamine-induced depression of physical endurance is approximately 50 percent greater in adrenalectomized than in intact rats. (auth)

45824 (NASA-TT-F-354) EFFECTS OF IONIZING RADIATION AND OF DYNAMIC FACTORS ON THE FUNCTIONS OF THE CENTRAL NERVOUS SYSTEM. PROBLEMS OF SPACE PHYSIOLOGY. Livshits, N. N. (ed.) Translated for National Aeronautics and Space Administration, Washington, D. C. from Vliyaniye Ioniziruyushchikh Izlucheniy i Dinamicheskikh Faktorov na Funktsii Tsentral'noy Nervnoy Sistemy; Voprosy Kosmicheskoy Fiziologii, Izdatel'stvo Nauka, Moscow, 1964. 195p. CFSTI $5.00 cy, $1.00 mn.

The literature on combined effects of ionizing radiation and nonradiation factors on mammalian organisms is reviewed. The problem of the mechanism of organism response to combined factors is discussed. Published results of experimental investigations of combined effect of vibration and ionizing radiation on some animal organism functions are discussed. These studies are compared with literary data, and the mechanism of higher animal reactions to combined effect of vibration and ionizing radiations is considered. A suggestion is expressed that in responses to vibration and irradiation effects side by side with the mechanisms described in literature, parabiotic processes in the nervous system may be of great importance. (auth)

45825 (NSJ-tr-32) CLINICAL AND EXPERIMENTAL STUDIES ON RADIATION-INJURY TO TASTE. Tanigawa, Kazuo. Translated from Nippon Acta Radiol., 23: 704-12 (Sept. 1963). 18p. Dep. mn; JCL $1.60 fs, $0.80 mf.

The effects of radiation on taste sensitivity was examined in cancer patients before and after ^{60}Co teletherapy treatment. Aqueous solutions of sucrose, acetic acid, sodium chloride, and quinine hydrochloride were used as test solution in this experiment. These solutions were put on a patient's tongue by means of drop method. The patients having normal taste sensitivity were selected out of patients who had cancer of neck or head, especially tongue and maxillary cavity. The taste sensitivity in most of the patients was more or less affected at the doses from 1,000 to 4,000 R, but none of them had a complete loss of taste below a dose of 3,000 R. (auth)

45826 EMBRYONIC ERYTHROPOIESIS AND THE CONTENT OF NUCLEIC ACIDS IN THE EMBRYONIC LIVER IN WHOLE-BODY IRRADIATED RATS. Finck, W.; Theil, S. (Friedrich Schiller Universitaet, Jena, Ger.). Acta Biol. Med. Ger., 12: 354-64(1964). (In German).

These studies were carried out in four- to five-month-old Wistar rats with 200-kv x rays delivered at a dose rate of 40 R/min. After whole-body irradiation of pregnant rats with 400 R on the 17th day of pregnancy, the increase of the liver weight during the following three days was more strongly reduced than weight of the whole fetuses. On the last two days of pregnancy these values were reversed, i.e., liver weight was higher in irradiated than control fetuses. By 24 and 48 hr after irradiation and proportion of proerythroblasts and erythroblasts in embryonic liver was significantly reduced, as compared to the controls, comparable to the depopulation of the bone marrow of adult animals during the same period postirradiation. The increase of the erythrocytes/mm^3 blood was normal up to 24 hr after irradiation; thereafter, the erythrocyte count was significantly lower than in the controls. The number of nucleated red cells in the peripheral blood was significantly higher than in the controls 48 hr after irradiation and later. In the course of pregnancy the absolute and relative RNA and DNA contents in the embryonic liver changed in a characteristic way; the prenatal decrease of the absolute and relative DNA amounts was ascribed to a shifting of the proportion liver cells/precursors of the red blood cells. After irradiation the RNA and DNA content of liver followed the decrease and renewed rise of the proerythroblasts and erythroblasts in the liver. During the period from the 17th to the 22nd day of pregnancy the ratio DNA/RNA changed from 1:1 to 1:2.2; after irradiation the DNA content was more markedly reduced, the ratio being 1:8. (BBB)

45827 THE PRODUCTION OF RESISTANCE AGAINST ISOLOGOUS TRANSPLANTATIONS OF UV-INDUCED SARCOMAS OF THE MOUSE. Graffi, A.; Pasternak, G.; Horn, K.-H. (Deutsche Akademie der Wissenschaften, Berlin). Acta Biol. Med. Ger., 12: 726-8(1964). (In German).

Mice of the XVII/Blu strain were injected in the dorsal area with the UVT 14306 and the UVT 15264 sarcoma cells. After a delay period of about 8 months tumors appeared. Before the tumors appeared the animals were exposed daily for periods of 5 to 30 min to a Hg vapor lamp at a distance of about 40 cm. For immunization the animals studied received subcutaneous injections of the tumor tissue, irradiated in vitro with 14500 R of x ray, at intervals of 14 days. Each injection consisted of 0.2 ml of a 1:4 diluted tissue suspension. The test injections were given 3 days after the final administration of irradiated tissue cells. Control animals did not receive the pretreatment. Pretreatment with x-irradiated tumor tissue produced resistance against the isologous transplants of the

uv sarcomas. In all, 79.6% of the treated animals were made resistant, but only 30% of the control groups were resistant to the tumors. The difference was statistically significant. Although after one of the first test injections resistance to UVT 14306 was not very marked, when the study was repeated at a higher dosage of cells (10^5 cells) in 16 animals, all were resistant. Nine out of 10 unpretreated control animals developed progressively growing tumors. It is known that in isologous systems resistance can be produced against tumors induced by implantation of a foreign body. This study indicates that sarcomas induced by uv irradiation, which is entirely different from any introduction of an external chemical poison, may induce a specific antigenicity. (BBB)

45828 STUDIES OF LIVER FUNCTION IN IRRADIATED RATS AND IN RATS POISONED WITH CARBON TETRACHLORIDE BY MEANS OF ^{131}I-ROSE-BENGAL. Cultrera, G.; Zanolla, W.; Slaviero, G. P. (Universita, Pavia, Italy). Acta Isotopica, 4: 235-45(1964). (In Italian).

Liver function was investigated in groups of normal, irradiated, and carbon tetrachloride-poisoned rats using ^{131}I-rose-bengal. The differences resulting from the analysis of the curves of the three groups are indicative. These differences concerning the disappearance half-time in the blood, the percentage of the injected isotope taken up by the liver, and the liver uptake and excretion half-times suggest that, in rats irradiated with 2000 R and sacrified 12 hours later, there are significant derangements of liver function. (auth)

45829 THE ACUTE RADIATION SYNDROME—THE IMPORTANCE OF THE GASTRO-INTESTINAL INJURY IN THE CATABOLISM AND DISTRIBUTION OF SERUM-ALBUMIN. Wetterfors, J.; Liljedahl, S.-O.; Plantin, L.-O.; Birke, G. (King Gustaf V Research Inst., Stockholm). Acta Med. Scand., 177: 227-42(Feb. 1965).

Rabbits were whole-body irradiated with 275 to 2500 R doses of ^{60}Co γ rays and injected with 70 to 100 μC of ^{131}I-labeled homologous serum albumin to study the effects of irradiation on the distribution and metabolism of albumin, changes in blood volume, and capillary permeability. In irradiated rabbits the plasma volume remained unchanged throughout or increased. The red-cell volume was not determined, but markedly reduced hematocrit values indicated that it is reduced. Pronounced hypoalbuminanemia was induced by radiation, while the decrease of the intravascular albumin pool was less marked because of the increase of the plasma volume. The total protein concentration was unchanged. A gradual rise of albumin catabolism was seen after radiation doses up to and including the LD_{50}. With higher doses an accentuated nonsteady state occurred, which made it impossible to estimate the catabolism by current methods. The ^{131}I-albumin disappears more rapidly from the bloodstream, however. After radiation doses of $>LD_{50}$ this non-steady state was further developed and extravascular retention of ^{131}I-albumin and its degradation products was noted. A considerable retention of activity was noted in the small intestine, which signified an increased loss of ^{131}I-albumin into the intestine as well as a deficient absorption of the degradation products. This points to the central role of intestinal damage in the acute radiation syndrome. The capillary system affected next in order of extent is that of the lungs, where the retention is proportional to the radiation dose. A fundamental disturbance induced by irradiation is not only increased capillary permeability as has been postulated, but possibly also a disturbed inflow into the circulation. (BBB)

45830 SENSITIZATION AND RADIATION RESPONSE IN CASES WITH CARCINOMA OF THE UTERINE CERVIX. INVESTIGATION IN 720 CASES TREATED AT RADIUMHEMMET 1954-1961. Rubio, C. A.; Hertzberg, O.; Kottmeier, H.-L.; Olsson, E.; Zajicek, J. (Karolinska Sjukhuset, Stockholm; National Defense Research Inst., Sundbyberg, Sweden). Acta Radiol. Therapy, Phys., Biol., 3: 241-68(Aug. 1965).

Sensitization response (SR) and radiation response (RR) were studied in 720 patients treated for carcinoma of the uterine cervix. SR was found to have no prognostic significance but was higher in postmenopausal than in premenopausal patients. The maximum and mean values of RR were also proved to bear no relation to the course of the disease. The numerous factors influencing the radiation response are discussed. (auth)

45831 EFFECT OF RADIOSTRONTIUM ON OOCYTES AND FOLLICLES OF ADULT MICE. Henricson, B.; Nilsson, A. (Royal Veterinary Coll., Stockholm; Research Inst. of National Defence, Sundbyberg, Sweden). Acta Radiol. Therapy, Phys., Biol., 3: 296-304(Aug. 1965).

Female CBA mice were injected intravenously with 0.7 μC ^{90}Sr per gram bodyweight at the age of 75 days. The predominating effect seems to be an increased rate of development of oocytes into follicles and of these into later follicular stages. A certain lethal effect on young oocytes cannot be excluded. (auth)

45832 FREQUENCY OF CANCER AND GEOLOGICAL FORMATIONS. Barany, J.; Galacz, L. Acta Unio Intern. Contra Cancrum, 20: 609-11(1964).

The possibility of establishing a relation between occurrence of malignant diseases and the quality of soil was investigated first by local observations made in a town in Hungary where the number of cancer patients and of congenital developmental abnormalities was much higher in certain groups than in other places. On the basis of these preliminary observations, radiation measurements were performed. The number of patients with tumors in the last eight and one-half years were compared to the data of the census taken in 1960. This showed 3401 tumor patients among 393,300 inhabitants living in the 264 localities of the county, which amounts to an 0.865% frequency in this period. When the frequency of cancer was calculated for each locality, it was found that in less than one third the area of the county inhabited by less than one third of the population of the county cancer frequency exceeds the average. On the western plains and in the mountains in the central part of the county, however, cancer frequency is below the average. In the southern district with high cancer frequency the mountains are constituted mostly by quaternary and tertiary rocks partly of volcanic origin, such as basalt, basaltic tufa, limestone, clay, argilaceous marl, and bauxite. Formations originating from Mesozoic age, such as dolomite, flinty limestone, marly-dolomitic sandstone are not so predominant. All these rocks are deposited on a Permian red sandstone, which rises to the surface in several places. This Permian red sandstone is red iron-ochre micaceous quartz sandstone mingled with different minerals, which include radioactive substances. This radioactive material probably accumulated by translocations, sedimentary processes, and by favorable geochemical conditions. Thus, this geologic survey, of the southern part of the county, where the frequency of cancer exceeds the average, shows formations which are fundamentally different from those found in other areas of the county. In this region older formations reach the surface and contain radioactive minerals. However, these preliminary data are not sufficient for establishing causal correlations between these two phenomena. (BBB)

45833 EPIDEMIOLOGY OF LEUKAEMIA. Clemmesen, J. (Finsen Inst., Copenhagen). Acta Unio Intern. Contra Cancrum, 20: 768-73(1964).

Epidemiology statistics of leukemia are considered in terms of its possible etiologic factors, ionizing radiation and viruses. Numerous studies indicate higher leukemia rates with higher urbanization, higher income, and better medical attention, and show higher rates for whites than for nonwhites. Whether such higher rates are due only to the discovery of more cases or whether they can be ascribed to factors such as radiation, myelotoxic drugs, or spread of virus cannot yet be determined. Observations on the leukemogenic effects of irradiation range from mouse experiments to statistics on the mortality among radiologists and casualties from the atomic bomb explosions in Japan in 1945. It is probably significant that the atomic bomb casualties are predominantly myeloid, and this may apply to all leukemias caused by irradiation. The Hiroshima

cases have arisen in a population where lymphatic leukemia is extremely rare. The age distribution of lymphatic leukemia in most countries shows a high incidence for the older age groups, so that there is a long latency period for this form. Possibly, a sufficiently long period of observation has not passed for lymphatic leukemias to appear among the Hiroshima population. A study of 13,352 patients who had received radiotherapy for ankylosing spondylitis revealed 28 cases of leukemia deaths and 12 deaths from aplastic anemia against an expected number of 2.9 and 0.3 cases, respectively. The estimated latency period for leukemia was as low as 2 to 5 yr. This estimate is based on 10 cases, dominated by the myeloid type so that the latency period for lymphatic cases may be longer. The problem of whether x irradiation in clinical doses increases risk of leukemia, mainly myeloid, has been studied by examinations of children, with conflicting results. A preliminary study of the fate of 39,166 children borne by mothers exposed to irradiation during pregnancy revealed 9 cases of leukemia against an expected number of 10.5. Among children exposed to irradiation at pelviometry, 4 deaths were found against an expectation of 5.4. For those exposed to a single abdominal diagnostic irradiation, 5 were found against 4.3 expected. These children had, with one exception, been exposed during the last month of pregnancy. Thus the risk involved in irradiation is rather small measured in numerical values. However, the increase among persons exposed to heavier dose radiation is considerable. Possible etiologic influences of viruses in leukemia are also discussed. (BBB)

45834 THE AFTER-EFFECT OF IRRADIATED HALOGENOPHENOL SOLUTIONS ON THE VIABILITY OF ESCHERICHIA COLI. PART I. EFFECT OF IRRADIATION CONDITIONS ON THE RADIATION INDUCTION OF BACTERICIDAL ACTIVITY. Namiki, Mitsuo; Matsuyama, Akira (Inst. of Physical and Chemical Research, Tokyo). Agr. Biol. Chem. (Tokyo), 29: 525-32(June 1965).

Cobalt-60 γ irradiation induced marked bactericidal activity in an aqueous solution of p-bromophenol even at nontoxic low concentrations. The unirradiated reagent showed some bactericidal effect above the concentration of 3.0mM or 4.0mM by incubation at 30 or 37°C, respectively, whereas the irradiated solution (2.4×10^4 Rad) manifested a marked decrease in viability of bacteria above 0.5mM and 1.5mM at 30 and 37°C, respectively. The effect of temperature during irradiation on the induction of bactericidal activity was determined by exposing 3.0mM and 4.0mM p-bromophenol solutions to 2.4×10^4 Rad at a dose rate of 1.5×10^5 Rad/hr at various temperatures. The maximum induced activity was attained at about 40°C, and the threshold pH value was between pH 9 and 10. The presence of a small amount of L-cysteine or sodium sulfite effectively inhibited the induction of bactericidal activity and similar but less effect was observed with D-glucose and Na glutamate at higher concentrations. In contrast to these inhibitory effects, sodium nitrite apparently enhanced the radiation effect under aerobic condition. Among monosubstituted bromophenols, the para substituted one was most effective while the ortho derivative did not exert any bactericidal activity at the same concentrations. With respect to the substituted halogen the activity increased in the order of Cl < Br < I. It is suggested that the induced activity is attributable to some long-life products, which form as a result of radiolysis of p-bromophenol and radiolysis of water. (BBB)

45835 ELECTROCARDIOGRAPHIC AND PATHOLOGIC CHANGES AFTER CARDIAC X-IRRADIATION IN DOGS. Phillips, Steven J.; Reid, J. Alan; Rugh, Roberts (Coll. of Physicians and Surgeons, New York). Am. Heart J., 68: 524-33(Oct. 1964).

Electrocardiographic (ECG) and pathologic data are presented on dogs precordially x irradiated with 5000 to 8000 R, delivered acutely to the heart. ECG and pathologic evidence of myocardial necrosis was seen in six out of seven irradiated dogs, suggesting that the sensitivity of the heart to radiation is greater than has been reported previously. Hydropericardium was seen in two dogs and gross pericarditis in four, with marked thickening, increase in vascularity, and reactive attachment at the site of the epicardial lesion. The epicardium showed gross indication of damage in six dogs. Histologic changes ranged from moderate extravasation of erythrocytes and hyaline alteration of connective tissue and muscle to marked muscular destruction and fibrosis. Hyaline alteration of the walls of smaller blood vessels, especially veins, was prominent, large areas of eosinophilic exudate often surrounding the veins. In general, the localized changes resembled those seen in myocardial infarction. No immediate ECG changes were seen in any of the dogs, even after larger acute doses as high as 56,000 and 100,000 R, but ECG evidence of myocardial damage appeared 14 days after 7000 to 8000 R. With 5000 R the ECG response in one case was not seen by the 56th day, and in the other, changes were seen on the 70th day. It is concluded that the response of cardiac tissue to irradiation is nonspecific; the final effect is indistinguishable from that produced by conventional infarctions. The damage appears to be related to the high absorption of radiation by extracellular connective tissue, particularly collagen. This is particularly significant in relation to the walls of the blood vessels, so that vascular changes are probably secondary to the alteration and depletion of collagen. (BBB)

45836 EFFECTS OF GAMMA IRRADIATION OF CORN SEED ON THE RESPIRATION AND GROWTH OF THE SEEDLING. Woodstock, Lowell W.; Combs, Michael F. (Agricultural Research Service, Beltsville, Md.). Am. J. Botany, 52: 563-9(July 1965).

As part of an investigation attempting to relate physiological and biochemical changes which occur during the first stages of seed germination to the subsequent growth of the seedling, corn (Zea mays) seed was subjected to various doses of irradiation, after which the growth and respiration of the seedlings were measured during the first 5 days of germination. For irradiation, ^{60}Co γ rays at a dose rate of 5000 rad/min were used. The moisture content of the seeds during irradiation was 24.3%. After irradiation, moisture was reduced to 10.7% by leaving the seeds in shallow containers at room temperature for two days before germination. Exposures of 40 and 80 krad caused marked inhibition in seedling growth and inhibited the rate of respiration, measured as oxygen uptake per seedling. A decrease in respiration rates, at these doses, could be detected within one day after planting, well before emergence of the radicle. Lower doses which were not markedly growth-inhibiting did not appear to inhibit respiration. A highly significant correlation was found between respiration rates at one day and shoot lengths of three-day-old seedlings. The degree of correlation so measured was higher for shoots than for roots and was lowered by growth-inhibiting doses of irradiation. The results indicate that rates of respiration during the first stages of germination may be an important factor in subsequent seedling growth and may provide the basis for predicting the growth of the shoot. The hypothesis that the seed contains oxygen-consuming materials might explain the low correlation between respiration rates and growth in slowly growing seedlings. (BBB)

45837 RETAINED THORIUM DIOXIDE MEDIA IN SEMINAL VESICULOGRAPHY. A FOLLOW-UP STUDY WITH DOSE ESTIMATES. Russell, Walter J.; Hattori, Fumio; Marrow, Lewis B.; Yoshinaga, Haruma; Kogure, Takashi (Atomic Bomb Casualty Commission, Hiroshima and Nagasaki). Am. J. Roentgenol., Radium Therapy Nucl. Med., 95: 479-93(Oct. 1965). (TID-21954).

A brief review of the English and Japanese literature as to the past use of thorium dioxide-containing radiographic contrast media is presented. Physical and laboratory findings, including roentgenography in a follow-up study of 23 cases which received such contrast material for seminal vesiculography 12 to 14 years previously, are also presented. Dose estimates were made for 1 patient typical of the entire group, and for another with a relatively larger residuum. Small amounts of retained contrast material were evident in all cases, but no case of neoplasia attrib-

utable to the presence of the medium was detected. (29 references.) (auth)

45838 THE TIME OF ORIGIN OF THE PARABIOTIC ANASTOMOSIS. Sodiçoff, Marvin; Binhammer, Robert T. (Univ. of Cincinnati). Anat. Record, 148: 625-9(Apr. 1964).

The effect of radiation on the course of development of parabiotic anastomosis was followed in Holtzman (Sprague-Dawley) rats. Rats of similar weight were united surgically, one of the partners being irradiated two hr prior to pairing. Animals received a single 800-R dose directed to their dorsums which represented an $LD_{60/30}$. Radiation was administered with a 250-kvp machine at a dose rate of about 67 R/min. Cross-circulation was studied by following $Na^{51}CrO_4$-tagged red blood cells in some pairs and radioiodinated serum albumin (RISA) in other pairs. The ^{51}Cr-labeled erythrocytes represented a cellular element and RISA a molecule. In nonirradiated controls, erythrocytes were found in the noninjected animal in small numbers at 22 hr after pairing; at 47 hr the rate of transfer became much more rapid. RISA was detected in the noninjected partner as early as five hr after pairing and accumulated steadily thereafter. Irradiation had no effect on the course of development of the parabiotic anastomosis as evidenced by similarity of accumulation rates of ^{51}Cr-labeled erythrocytes and RISA when compared to the nonirradiated pairs. The difference in transfer of erythrocytes and RISA was attributed to the physical characteristics of the labeled particle. The erythrocyte requires a vascular channel of greater size than does the albumin molecule. The abrupt rise in rate of transfer of erythrocytes in nonirradiated rats after 48 hr was interpreted as indicating the time in the development of the capillary anastomosis when lumens of the newly developed capillaries attained sufficient size to permit passage of erythrocytes. RISA showed no similar abrupt increase in rate probably due to its not having a threshold size. (BBB)

45839 INACTIVATION OF PROTEINS BY RADIATION. Dose, K. Angew. Chem., 76: 758(1964). (In German).

In 1% concentrations the primary structure of a protein is damaged by doses greater than 10^7 rad, but inactivation occurs with doses of 10^5 rad; therefore the alterations of secondary and tertiary structure as well as more or less specific alterations in active sites are studied. The following properties of enzymes are examined: sedimentation properties, electrophoretic properties, pH-activity charts, substrate-activity charts, Michaelis constants, reactivity of functional groups, titration curves, D exchange, dispersion of rotation, and absorption spectra. The action of uv light is specific but generally resembles that of ionizing radiation. It is useful to compare the partially quite specific action of monochromatic uv light (e.g., 2537 Å) with the action of x rays. At acid pH values, uv light of this wavelength leads with great selectivity to the rupture of S–S bonds; quite often one observes a close correlation between S–S bond rupture and inactivation. The results are similar to those from chemical reduction studies. The inactivation spectra of proteins stabilized by S–S bonds correspond most nearly to the absorption spectrum of cystine. (BBB)

45840 THE EFFECT OF ULTRAVIOLET RADIATION AND SOME CHEMICALS ON MORPHOGENESIS IN MICRASTERIAS. Kallio, Paavo (Univ. of Turku). Ann. Acad. Sci. Fennicae, Ser. A. IV, 70: 39p.(1963).

Influence of the nucleus on morphogenesis was studied in various species of Micrasterias, and it was shown that the nuclear effect on the cell morphology can be eliminated by uv irradiation. On the other hand, because uv light has only a weak action on an anucleate Micrasterias cell, morphogenetic substances occur only in small amounts, if at all, in this cell type. Some experiments are reported in which uv irradiation was employed to influence the nucleus-controlled morphologic development of the new semicell. Cells of the species Micrasterias thomasiana, M. thomasiana var. notata, and M. torreyi were used. A wavelength of ~2537 Å and an exposure of 6 min at cytokinesis leads to the formation of cells that resemble anucleate cells morphologically. This standard lethal dose given at dividing stage kills the cells within 1 to 3 days. The lethality of the radiation varies with the stage of the life cycle of the cell when the treatment is given. The cell is more sensitive in the first stages of the division, and less sensitive in the last stages of development of the new semicells. Uv radiation produces almost the same effect as denucleation. The exposure of one of the two nuclei in a binucleate cell to the standard lethal dose does not lead to the death of the cell; both nuclei are capable of undergoing division later. If one of the nuclei in a binucleate cell is exposed to the standard lethal dose during cell division and the other nucleus is exposed to the same dose one hr later, the new double cell survives, but the single cells die. The interaction between the two nuclei is discussed. When normal haploid cells are treated with ribonuclease, anucleate-shaped or hypohaploid semicells are formed. These experiments showed that, in contrast to Acetabularia, only small quantities of RNA's are stored in the cytoplasm of Micrasterias cells. (BBB)

45841 ABSORPTION OF D-GLUCOSE BY SEGMENTS OF INTESTINE FROM ACTIVE AND HIBERNATING, IRRADIATED AND NON-IRRADIATED GROUND SQUIRRELS, CITELLUS TRIDECEMLINEATUS. Musacchia, X. J.; Westhoff, D. D. (St. Louis Univ.). Ann. Acad. Sci. Fennicae Ser. A. IV, No. 71, 345-59(1964).

Experiments were designed to compare active absorption of D-glucose in intestine taken from active and hibernating animals, to examine the effects of whole-body x irradiation on these preparations, and to compare the effects of high dose x-irradiation in both hibernating and nonhibernating squirrels to assess the qualities of natural protection offered by hibernal torpor. There were 5 series of experiments: active animals served as controls; animals which had been in hibernation for 7 to 10 days, active animals which were x irradiated, hibernating animals which were x irradiated; and hibernating animals which were x irradiated and then permitted to awaken. The squirrels were subjected to a single, whole-body exposure of 2000 R of x rays (250 kv). Active absorption of D-glucose was observed in the in vitro preparations of duodenum (upper), jejunum (middle), and ileum (lower). Comparison of data from intestinal segments prepared from active and hibernating ground squirrels showed markedly increased levels of active D-glucose absorption in the intestine from the hibernators. All three intestinal areas showed this elevated capacity for uptake and transport of glucose. The data indicate that hibernation has a marked influence on the intestinal cellular mechanisms involved in active absorption of D-glucose, and that enhanced levels of uptake and active transport of sugar occurred in segments taken from ground squirrels in deep hibernal torpor. Upper intestinal segments of irradiated animals clearly showed increased levels of active transport and the lower segments, although not as pronounced, reflected a similar trend. Thus the duodenum and the ileum were found most sensitive to irradiation. (TCO)

45842 EFFECTS OF RADIATIONS ON BLUE-GREEN ALGAE. I. THE PRODUCTION AND CHARACTERIZATION OF STRAIN OF ANACYSTIS NIDULANS RESISTANT TO ULTRAVIOLET RADIATION. Kumar, H. D. (Univ. of Gorakhpur, India). Ann. Botany (London), 27: 723-33(Oct. 1963).

This report describes the morphologic and physiologic characterization of a strain of the unicellular blue-green alga A. nidulans after having been repeatedly exposed to uv radiation during part of successive subcultures. This strain was compared with the untrained parent strain with respect to the following parameters: resistance to uv radiation; cell length and the incidence of long cell formation; pigment production; ability to grow in a medium in which nitrate has been replaced by nitrite; and resistance to streptomycin, penicillin, and isoniazid. From the parental strain, the uv-resistant strain was derived by 24 ten-min exposures to a Hanovia 12-in. quartz-jacketed mercury-vapor lamp which emits most of its energy at a wavelength of 2537 Å. In the untrained strain exposed to uv radiation for 15 min, exponential growth began after a

lag period of 5 days. In the trained strain irradiated for 15, 20, and 25 min on the other hand, the duration of the lag phase was 3 days ±1 day. No increase in cell numbers occurred in the untrained strain exposed for 20, 25, and 30 min, and in the trained strain exposed for 30 min. Whereas in the untrained strain, cells longer than 12 μ were seldom found even in 2-week-old cultures, in the trained strain, cells as long as 20 μ occurred. The uv-trained strain compared with the untrained control was relatively more resistant to penicillin and streptomycin, and more sensitive to isoniazid. It was further characterized by decreased carotenoid/chlorophyll ratio and by not having fully overcome the division-inhibiting effect of uv radiation. It was able to grow better than the untrained strain in a medium containing high concentrations of nitrite as the sole nitrogen source. (BBB)

45843 THE OCULAR EFFECTS OF AN ATOMIC EXPLOSION. Jammet, Henri; Dollfus, Marc Adrien; Haye, Christian (Commissariat a l'Energie Atomique, Paris). Ann. Oculist., 196: 329-61(Apr. 1963). (In French).

Thermal irradiation from an atomic explosion may cause skin burns and retinal burns. This may also produce corneal injuries. The injury of the crystalline lens that is produced among survivors often results in the development of cataracts. The frequency of cataracts is directly related to the distance from the hypocenter that exposure takes place. Out of 159 cases reported, 55% were found in persons exposed in an area extending from the hypocenter to 2-km distance. The percentages of the other cases reported were 20, 15.4, and 9.6% for distances of 2 to 3, 3 to 4, and more than 4 km from the hypocenter. Irradiation cataracts usually appear more frequently in young men as compared to older ones. Out of 113 patients who developed irradiation cataracts after the latent period following exposure to atomic explosion, 37% were an average of 15 yr old, 25% were from 16 to 25 yr old, 25% were from 25 to 40 yr old, and the remainder were more than 40 yr old. The latent period before appearance of irradiation cataract is not less than 10 months and it often is 3 to 5 yrs or more. All patients who developed opacities of the lens had undergone some degree of epilation. The exact dosage of irradiation that produces cataracts is not known. It has been estimated to be of the order of 200 to 500 R, which is sufficient to produce epilation and hematopoietic effects. For neutron exposure the values that induce cataract may be between 20 and 45 rep. The clinical features of irradiation cataracts are similar to those of normally occurring opacities. However, while many irradiation cataracts may regress, some require surgical treatment. (84 references). (BBB)

45844 FURTHER STUDIES ON THE CHANGES IN LACTIC DEHYDROGENASE ACTIVITY IN THE PLASMA OF MICE AFTER WHOLE-BODY X-IRRADIATION. Hori, Yasuharu; Takamori, Yasuhiko; Takeda, Atsuhiko; Nishio, Kazuo. Ann. Rept. Radiation Center Osaka Prefect., 5: 104-6(1964).

Effects of x irradiation on lactic dehydrogenase (LDH) activity in plasma of mice were studied. Assays of LDH activities were done at 2, 4, 6, 8, 10, 12, and 24 hrs after 300 R of whole-body x irradiation of female RF-strain mice, 9–10 weeks of age. A correlation between plasma LDH activity and x radiation dose in the range of 150 to 1200 R was also studied. At the first 2 hrs after irradiation, an increase in the activity of plasma was evident. The plasma LDH activity attained its maximum at 6 hrs, tapered off thereafter, and returned to normal level 24 hrs after irradiation. The activity of plasma LDH 8 hrs after irradiation increased continuously from 150 to 600 R, but the degree of elevation of the activity was not remarkably increased even by irradiation with higher dose than 600 R. A correlation between plasma LDH activity and hemoglobin content in the plasma of irradiated mice was not ascertained. (auth)

45845 DENTAL LESIONS IN RAT INDUCED BY RADIOMIMETIC AGENTS. Hebborn, P.; Mishra, L. C.; Dalton, C.; Williams, J. P. G. (State Univ. of New York, Buffalo). Arch. Pathol., 80: 110-15(Aug. 1965).

The incidence and histology of the lesions which result in tooth loss induced by x rays and alkylating agents were compared. Six N mustard compounds were synthesized and tested, as well as triethylene melamine (TEM), 4-[bis(2-chloroethyl)amino]phenylbutyric acid (Chlorambucil) and 1,4-dimethanesulfonoxybutane busulfan (Myleran). Compounds were administered in cottonseed oil or 10% gum acacia at various dose levels, either as a single injection or daily for three to five days to male rats. The N mustards produced lesions of incisor teeth of adult rats which were similar to those reported to occur after x irradiation. Tooth loss occurred 40 to 70 days after treatment, and in 34% of these cases, atypical regrowth or no regeneration of incisor teeth was observed. Microscopic examination showed degeneration of odontoblasts and dentin niche formation. Body weight loss often preceded overt symptoms of incisor tooth damage and weight loss or death during the second or third month after treatment with radiomimetic agents was probably the result of starvation due to inadequate dentition. No abnormalities were observed after treatment with TEM or busulfan Myleran. X rays produce tooth fractures, generally an incomplete regeneration of fractured teeth and multiple mandibular incisors, and these effects were also observed with the N mustards. Microscopically, degeneration of odontoblasts, formation of osteodentin, and production of typical dentin niches are also produced by x rays. The major effect of moderate doses of x rays on rat incisor teeth probably is damage to cells which would eventually differentiate into mature odontoblasts. The period during which the cells are most sensitive to the effects of irradiation is during the phase of differentiation. Thus the extent of the incisor lesion is determined by the number of differentiating odontoblasts which were damaged. High doses of x rays (3000 rad or more administered locally) are required to produce complete destruction of odontogenic epithelium, resulting in an inability to regenerate tooth bud structures. These doses exceed the whole-body lethal dose by a factor of five or more. In contrast, the N mustards produced complete tooth destruction at a dose less than the LD_{50}. Thus the aromatic N mustards may have a selective action upon developing tooth structures considerably greater than that shown by x rays. In long-term studies of rats treated with radiomimetic agents, the possibility should be considered that death may occur after the initial acute phase as a result of starvation due to inadequate dentition. (BBB)

45846 MORTALITY RATE OF MALIGNANT NEOPLASM IN HIROSHIMA A-BOMB SURVIVORS. Oho, G. (Midorimachi, Hiroshima). Atompraxis, 11: 442-4(Aug. 1965).

During the past ten years (1951 to 1960), a study was made of the mortality rate of malignant neoplasm of the A-bomb survivors in the city of Hiroshima. The results were compared with the ordinary mortality rates in Hiroshima prefecture and the national population provided by the government authorities. The nearer the exposure distance of the A-bomb survivors was, the greater was their mortality rate of leukemia. The mortality rate of malignant neoplasm excluding leukemia was high with those patients who had made an entry into the hypocenter area immediately after the A-bomb explosion, entirely in disregard of the exposure distance. In view of the circumstances, it may reasonably be concluded that the illness of leukemia of those proximally exposed survivors is chiefly due to the irradiation by the primary radiation of the A-bomb, but that the development of the malignant neoplasms excluding leukemia might have been caused by the irradiation to the residual or secondary radiation of the A-bomb. (auth)

45847 STUDIES ON THE USE OF MUTAGENIC AGENTS IN PLANT BREEDING. II. THE EFFECTS OF DOSE AND SEED MOISTURE CONTENT ON MUTATION PRODUCTION IN LUPINUS ANGUSTIFOLIUS BY X-RAYS. Gladstones, J. S.; Francis, C. M. (Univ. of Western Australia, Nedlands). Australian J. Agr. Res., 16: 301-10(May 1965).

Seeds of Lupinus angustifolius were given x-ray doses of 2.5, 5, 10, and 20 kR at each of 12 moisture contents ranging

from 6.1 to 18.1% (wet weight basis). Various measures of injury were recorded in the X_1 generation, and the types and rates of mutations in the X_2. At moisture contents below 16%, total mutation rates were closely correlated with X_1 injury. Injury and mutation rate decreased with increasing moisture up to 11 to 12% moisture, and thereafter remained at a constant minimum up to 16%. Between 16 and 18% moisture there was again an increase in X_1 injury, but not in mutation rate. Between 6 and 12% moisture, a linear relationship was found between moisture content and the logarithm of the dose required to cause a given level of injury or mutation. A possible mechanism for such a pattern of protection is discussed. Lethal mutations increased as a proportion of all mutations as dose and mutation rate increased. There were also proportionately more lethals at high moisture contents than in lower moisture treatments giving the same mutation rates. It is concluded that lethal and seedling chlorophyll-deficient mutations could be misleading when used as indicators of total and viable mutation rates, and that, contrary to the conclusions of some previous authors, no advantage is likely to be gained in practical breeding work from irradiating at high seed moisture contents. (auth)

45848 TEMPORARY INCREASE IN UV-RESISTANCE IN THE COURSE OF SPORE GERMINATION OF BACILLUS SUBTILIS. Irie, Ryozaburo; Yano, Nobuhiro; Morichi, Toshiki; Kembo, Hiroshi (National Inst. of Animal Industry, Chiba, Japan). Biochem. Biophys. Res. Commun., 20: 389-92(Aug. 16, 1965).

A temporary increase in resistance to ultraviolet radiation was noted in the course of germination of spores of Bacillus subtilis. Possible reaction mechanisms involved are discussed. (C.H.)

45849 INTERACTION OF RNA POLYMERASE WITH IRRADIATED DNA. Zimmerman, F. K.; Kroeger, H.; Luecking, T. (Univ., Freiburg i. B.). Biochem. Z., 342: 115-19(1965).

The inhibitory effect of x or ultraviolet irradiated DNA on DNA-directed RNA synthesis was investigated in an RNA polymerase system in vitro. The inhibition of DNA-directed RNA synthesis is not strictly competitive. The degree of inhibition is dependent on the amount of RNA polymerase in the incubation mixture. The inhibitory effect can only be observed if irradiated DNA is added before RNA polymerase has been bound to untreated DNA. The inhibition is due to an irreversible and stronger binding of RNA polymerase to DNA and not to an interference with the copying process. Actinomycin D, in contrast, exerts its inhibitory effect even after RNA polymerase has been bound to its template DNA. (auth)

45850 THE EFFECT OF γ-RADIATION ON SOLUBLE AND INSOLUBLE COLLAGENS. Ramanathan, N.; Mohanaradhakrishnan, V.; Nayudamma, Y. (Central Leather Research Inst., Adyar, Madras). Biochim. Biophys. Acta, 102: 533-41(July 22, 1965).

The effect of γ radiation on soluble and insoluble collagens was studied by the modifications in the electron microscopic appearance, x-ray diffraction pattern, optical birefringence, thermal stability and the tensile properties of collagen fibers obtained from rat and kangaroo tail tendons. The γ ray dosages used were 10 and 30 Mrad. At 10 Mrad collagen fibrils from rat tail tendon did not show any change in the electron microscope while those from kangaroo tail tendon showed partial disorder or disappearance of the cross-striations and exhibited twisting. At 30 Mrad, the latter fibrils appeared gelatinized, while rat tail tendon fibrils retained the fibril form but without the cross-striations. These results are in conformity with the corresponding x-ray diffraction patterns and the data on the optical birefringence and thermal and mechanical stability of these fibrils, and point to the possibility that soluble collagen is more resistant to γ radiation than insoluble collagen. (auth)

45851 ENHANCED NUCLEIC ACID SYNTHESIS IN X-IRRADIATED ESCHERICHIA COLI C DUE TO POST-INFECTION WITH BACTERIOPHAGE PHI X174. Palchoudhury, S. R.; Poddar, R. K. (Saha Inst. of Nuclear Physics, Calcutta). Biochim. Biophys. Acta, 103: 693-5(Aug. 10, 1965).

Phosphorus-32 incorporation studies were used to show that the partial inactivation of E. coli host cells by x irradiation prior to infection with ϕ X174 could be used to alter the pattern of nucleic acid synthesis by infected cells. Initially both the infected and non-infected bacteria took up labeled phosphate at about the same rate. After about 17 min the uptake of labeled phosphate by the infected culture began to slow down rapidly because of the onset of lysis. The x-irradiated non-infected bacteria took up phosphate at a much slower rate than the unirradiated normal controls, but the rate of phosphate uptake by the infected pre-irradiated bacteria was almost equal to that by the unirradiated normal bacteria. Pre-irradiation of phages with 300 Krad of x rays did not qualitatively alter the pattern of phosphate uptake by infected host cells. Chemical fractionation studies revealed an appreciable increase in the amount of incorporated ^{32}P in the nucleic acid fractions of the infected pre-irradiated bacteria compared with the uninfected irradiated controls. The phenol method of RNA fractionation was used to find the distribution of radioactivity into different RNA moieties. Results indicated that the nuclear RNA fraction of the pre-irradiated infected culture incorporated 31.8% more ^{32}P than did that of irradiated non-infected cultures. (H.G.D.)

45852 EFFECTS OF X-IRRADIATION OF MICE EXPOSED IN UTERO DURING DIFFERENT STAGES OF EMBRYOLOGICAL DEVELOPMENT ON DURATION OF MATURE LIFE. Nash, Donald J.; Gowen, John W. (Colorado State Univ., Fort Collins). Biol. Bull., 128: 425-58(June 1965).

Mice exposed to x radiation at different stages of uterine development showed reductions in mean longevity which were dependent on both x-ray dose and embryologic stage. The experiments included five irradiation treatments (0, 20, 80, 160, and 320 R) six embryological stages (untreated, $6\frac{1}{2}$, $10\frac{1}{2}$, $14\frac{1}{2}$, $17\frac{1}{2}$, and newborn ($19\frac{1}{2}$) days of uterine development), two sexes and nine mouse strains. X-ray doses of 160 and 320 R at embryological ages $6\frac{1}{2}$, $10\frac{1}{2}$, and $14\frac{1}{2}$ days were too lethal to obtain the requisite number of progeny in these groups, but 647 completed mouse lives were examined. Mature lifespan ranged downward from 1194 days for the males and 921 days for the females. Both of these two longest lived individuals had been irradiated, the male with 160 R at $14\frac{1}{2}$ days embryologic development and the female with 80 R at $10\frac{1}{2}$ days. The frequency distributions of lifespan were of several types for the different groups, depending on the treatments, strains, or sexes of the individuals. Considering the in utero-treated mice, the average unirradiated female survived for only 69% of the mean male lifespan. This male-to-female difference could not be attributed to irradiation effects but rather to the hazards associated with reproduction. Adjusting for these effects shows that the average female life under irradiation still exhibited greater sensitivities to irradiation in utero. Considering the available data for the doses taken separately, the 20-R females had 85% of the mean lifespan observed for the untreated females, the males 96.7% that of the untreated males. Like comparisons for 80 R were 82% vs 93%; for 160 R, 73% vs 89%; and for 320 R, 30% vs 43%. Intrauterine irradiation, when limited to 20 to 80 R, reduced the female durations of life at all stages of embryological development more than they did those of the males. Genotypic differences, as measured by strain and as separate from sex, had little effect on subsequent mature lifespans when the irradiation was small in amount, 20 including 80 R, or when given at $6\frac{1}{2}$ or $10\frac{1}{2}$ days of embryologic development. The dose became more important to mature life's duration with higher doses. Genotype also interacted with both stages of embryologic development when irradiation occurred and with the dosage of x-rays absorbed. Individually the embryological stages when the irradiations took place had only a small effect on mature lifespan, although they had pronounced effects on survival in the juvenile stage. (BBB)

45853 CHANGES IN THE COLOR OF POTATO TUBERS AFTER IRRADIATION OF ISOLATED SPROUTS. Smalik, M.; Honcariv, R.; Drozd, J.; Kubikova, A. (Selection Station, Velka Lomnice, Czechoslovakia). Biol. Plant. Acad. Sci. Bohemoslov., 4: 207-10(1962).

The reaction of four varieties of potatoes (Solanum tuberosum) after x irradiation of isolated sprouts was examined. A dose causing marked changes was sought. The doses used were: 250, 1000, 1750, 3500, and 5000 R. The irradiated sprouts were wrapped in moistened filter paper and planted in flower pots 16 hr after irradiation. The dose of 250 R generally stimulated the process of sprouting. In the two hybrid varieties this occurred only during the first two days, later there was a marked decrease in the growth of the sprouts. A stimulation of sprouting was seen in the hybrids during the first days even after a dose of 1000 and 1750 R. A dose of 3500 and 5000 R generally seriously slowed sprouting and the percentage of plants which died increased. Irradiation of the sprouts also influenced the all-over growth of the plants; 250 R stimulated the growth of the irradiated plants. After irradiation at higher doses, the plants were smaller. Beginning with a dose of 1000 R, deformation of the leaves and stems and deformation of the tubers was recorded with all four varieties. The normal pairing of the leaves was affected in irradiated plants. Some plants showed a serrated edge on the leaf blade. After higher doses, differentiation in the leaves could no longer be investigated. When the shoots came above ground, the leaves remained near the surface forming a larger or smaller rosette than normal, or the shoot merely became swollen. With all doses including 250 R, changes were observed in the shape of the tubers. In the hybrid strain tubers with pink skin were found. After storing for three weeks on trays, this color changed to the typical color of the red-skinned potatoes with marked intensity especially at the eye end of the tuber. Deformation of the leaves and tubers did not occur in the following generations. The red color of the surface of the tubers was preserved only incompletely in later generations. Because of the limited amount of material, a chemical analysis was not carried out and therefore no conclusion could be reached on the usefulness of this mutation. (BBB)

45854 EFFECT OF ULTRAVIOLET LIGHT ON STOMATAL MOVEMENT. Hercik, Ferdinand (Inst. of Biophysics, Czechoslovak Academy of Sciences, Brno). Biol. Plant. Acad. Sci. Bohemoslov., 6: 70-2(1964).

In experiments with both nonionizing and ionizing radiation on the stomata of Begonia semperflorens it was observed that the open stomata close a few minutes after irradiation. As a source of uv light a Philips tube TUV 15 was used at a distance of 63 cm; this mainly gives a resonance line at 2537 Å. The intensity was 31.6 $\mu w/cm^2$. Very rapid closing of the stomata takes place after a dose of 6900 erg/cm^2. After a dose of 13,800 erg/cm^2, administered in one min, the percentage of closed stomata steeply rises, and after 20 min equilibrium is attained. After higher doses an almost complete closure of the stomata may be observed. The experiments did not show a marked dose-effect relation. After a certain threshold dose (about 10,000 erg/cm^2) changes in the posture of the stomatal apparatus usually occur very rapidly. This points to a mechanism where excitability plays a role. Experiments with the photoreactibility of this phenomenon were not successful. In other experiments, closing of previously opened stomata was found also after irradiation with ^{60}Co source (with a dose of 150 R) and after irradiation with α rays from polonium (with a dose of 3.7×10^6 α particle/cm^2). The closing of the stomata is probably due to the changes of turgor in the guard and/or adjacent cells. It is suggested that the stomata of Begonia semperflorens provide an interesting object for the study of different radiobiological problems. (BBB)

45855 INTERACTIONS OF GAMMA RADIATION AND DROUGHT UPON PINUS ELLIOTTII AND PINUS PALUSTRIS. McCormick, J. Frank (Univ. of North Carolina, Chapel Hill). BioScience, 14: 43-4(1964).

In groups of 100, seeds of the slash pine and longleaf pine were soaked in water and were exposed to each of nine radiation doses (100 to 50,000 R) at the rate of 27 R/min from a ^{60}Co irradiator. Irradiated and control seeds were planted, and 21 days following irradiation, water was withheld from the seedlings for 3 days, reducing the soil moisture content from 10% to 1%. There was an inverse relation between the radiation dose and growth and between the dose and germination, with slash pine appearing to be more sensitive at higher doses than longleaf. Following the drought stress none of the nonirradiated slash seedlings and only 2 of the 78 nonirradiated longleaf seedlings survived 40 days. Of the seedlings which received 100 R, 14 longleaf and no slash seedlings survived; 34 of the 96 slash seedlings and all 69 longleaf seedlings which received 300 R survived the drought for 10 days, but by 40 days, survival was reduced to 20 slash and 60 longleaf seedlings. All plants which were alive at 40 days were still growing after 6 months. All of the slash and longleaf seedlings which had received 500 R survived the drought for 10 days, and most of them survived for 40 days. However, 500 R inhibited formation of true leaves, and all plants died upon completion of the cotyledon stage for lack of a new photosynthetic apparatus. Survival of longleaf following 100 R and drought stress was similar to that of slash following 300 R and drought stress; 100 R inhibited the growth of longleaf, but not slash pine 20 days following irradiation. Forty days after the drought stress, 14 longleaf seedlings which had received 100 R survived but none of the slash seedlings which had received 100 R survived. The greater radiation sensitivity of longleaf rendered it more drought tolerant than slash pine. One stress, irradiation, increased longleaf tolerance to a second stress, drought. (BBB)

45856 THE CELLULAR BASIS OF THE GENETICALLY DETERMINED HEMOPOIETIC DEFECT IN ANEMIC MICE OF GENOTYPE Sl/Sl^d. McCulloch, E. A.; Siminovitch, L.; Till, J. E.; Russell, E. S.; Bernstein, S. E. (Univ. of Toronto; Ontario Cancer Inst., Toronto; Jackson Lab., Bar Harbor, Me.). Blood, 26: 399-410(Oct. 1965).

The proliferation and function of hemopoietic cells derived from genetically anemic Sl/Sl^d mice were studied by the use of cell transplantation technics. It was found that marrow cells derived from anemic Sl/Sl^d or Sl^d/Sl^d mice, when implanted into heavily irradiated mice of genotype $+^{Sl}/+^{Sl}$, are capable of forming macroscopic spleen colonies, with approximately the same frequency as cells derived from normal $+^{Sl}/+^{Sl}$ mice. Marrow cells derived from Sl/Sl^d animals were tested for their capacity to cure the anemia of W/W^v mice and were found to implant as rapidly and to have as long-lasting a beneficial effect as did marrow cells from $+^{Sl}/+^{Sl}$ mice. The radiosensitivity of the colony-forming ability of marrow cells from Sl/Sl^d mice was found to be similar to that found previously for $+^{Sl}/+^{Sl}$ marrow cells, although the anemic animals are known to be more sensitive to whole-body irradiation than are their normal littermates. Marrow cells from $+^{Sl}/+^{Sl}$ mice were found to proliferate more slowly in irradiated mice of genotype Sl/Sl^d than in irradiated $+^{Sl}/+^{Sl}$ littermates, even when the anemic and the normal mice were joined in parabiosis. These observations indicate that the hemopoietic colony-forming cells in mice of genotype Sl/Sl^d are normal, but fail to function adequately because the tissues of mice of this genotype are unable to provide sufficient support for proliferation and differentiation of these progenitor cells. (auth)

45857 PRELIMINARY RESULTS ON THE RELATION BETWEEN HOMOZYGOSIS AND RADIOSENSITIVITY IN THE MOUSE. Stuart, Carlo (Universita, Siena, Italy). Boll. Soc. Ital. Biol. Sper., 41: 369-70(Apr. 15, 1965). (In Italian).

Some radiosensitivity experiments are reported for hybrid mice of the parenteral strains C57BL/6 and NMRI. Although only the F_1 generation is studied here, radiosensitivity studies are contemplated for mice up to the 20th generation (F_{20}) which have been bred over the past five years. In the present experiments, male C57BL/6 mice were mated with NMRI females. The offspring were sepa-

rated from the mother at 30 days of age and subjected to whole-body irradiation at two and one-half months of age. Irradiation was conducted with 200-kv x rays at a dose rate of 46 R/min to total doses of 700 R. For controls, mice of equivalent age to the two parent strains were similarly irradiated. The percentages of animals surviving in the three groups were: male C57BL/6 mice 0%, female NMRI mice 12.5%, and F_1 hybrids 87.8%. The median survival times of the three groups, expressed as the reciprocal of the survival time in hr $\times 10^3$, were: 764.7, 289.7, and 42.8. The differences between the F_1 hybrid and the parental strains are statistically highly significant. (BBB)

45858 THE GROWTH AND INFILTRATION OF EHRLICH'S ASCITES TUMOR IN MICE WITH REDUCED IMMUNOLOGICAL RESPONSES. Wheatley, D. N.; Easty, G. C. (Royal Cancer Hospital, London). Brit. J. Cancer, 18: 743-55(Dec. 1964).

To investigate the role of immune responses in tumor cell invasion from ascites tumors, several different treatments known to reduce the immune responses of host animals were carried out and the effects on tumor growth and infiltration were studied. Cortisone, whole-body irradiation (320 R), and thymectomy and irradiation (700 R) were used for reducing the immunological responsiveness of female BALB/c mice. Animals were inoculated with 10×10^6 Ehrlich's ascites tumor cells intraperitoneally. In all three cases tumor development, as evidenced by daily increase in body weight, ascitic fluid accumulation, and free tumor cell assays, was slower in treated animals than controls. Infiltration of tumor cells into various organs of the abdominal cavity was delayed by these treatments and the delay was greater than could be accounted for by the slower tumor development in treated animals. The most radical treatment (thymectomy and irradiation) suppressed responses in host organs (in particular the body wall) and reduced or prevented the infiltration of tumor cells into these organs. These experiments demonstrated that immunoiogical responses of BALB/c mice to the transplantable Ehrlich's ascites tumor are responsible to a considerable degree for the changes occurring in host tissues which allow the infiltration of tumor cells. Failure of hosts with reduced immune responses to survive untreated hosts after being given the same tumor inoculum was contrary to expectation, especially since the treated hosts developed the tumor more slowly and were less intensively infiltrated. (BBB)

45859 MECHANISMS OF CANCERIZATION BY IRRADIATIONS VISUALIZED AT THE CELLULAR LEVEL. Latarjet, Raymond (Institut du Radium, Paris). Bruxelles-Med., 43: 1281-9(Dec. 1, 1963). (In French).

The author considers several possible mechanisms of induction of tumors by irradiation. Possibilities included are that irradiation itself induces malignant changes or favors induction by another pre-existing agent, such as, for example, a virus, or by a selective clonal mechanism. It would be inappropriate to look for a single cause for the wide variety of cancerogenic actions of irradiation. At the cellular level the most simple explanation is that irradiation produces mutations that are responsible for malignancy. These could be reflected in biochemical alterations of materials normally incorporated into nucleic acid chains. It is also possible that irradiation could affect transfer of cancerogenic substances by altering the permeability of cell membranes. The tissues of irradiated mammals contain large quantities of free nucleic acid and its hydrolysis products. At the same time irradiation may increase cell sensitivity to viruses. These considerations are probably as valid for chemical carcinogens as they are for carcinogenesis by irradiation. (BBB)

45860 EFFECT OF DENATURATING ACTION OF IONIZING RADIATION AND ULTRASOUND ON THE BEHAVIOR OF GAMMA GLOBULINS IN THE REACTION WITH THE RHEUMATOID FACTOR. Zablocki, B.; Skalba, D. (Univ. of Lodz, Poland). Bull. Acad. Polon. Sci. Ser. Sci. Biol., 13: 115-20(1965).

Denaturated human γ-globulin was examined for the presence and level of rheumatoid factor (RF) in the sera of patients with rheumatoid arthritis. Denaturation of γ-globulin was achieved by exposure to ionizing radiation or the action of ultrasound. Solutions of γ-globulin containing 5.6 mg/ml were exposed to 225,000 to 900,000-R doses of ^{60}Co γ radiation or ultrasonication at 800 kHz for one to four hr. The physico-chemical properties of the denaturated γ-globulin were investigated by electrophoresis in agar gel and by immunoelectrophoresis. The serological properties were examined by the hemagglutination of tanned erythrocytes (Boyden's test) and by the BDB-globulin cell test (bisdiazotized benzidine). Exposure to ionizing radiation led to a reduction of the electrophoretic mobility of γ-globulins, whereas treatment with ultrasound had no significant effect on its electrophoretic mobility. The denaturated γ-globulins retained the ability to react with rabbit antiglobulin serum in the gel precipitation test, although they exhibited a reduced ability of diffusion in agar (particularly γ-globulin denaturated by ionizing radiation). Irradiation led to a reduction of the electrophoretic mobility of γ-globulins, whereas treatment with ultrasound had no significant effect on its electrophoretic mobility. The denaturated γ-globulins retained the ability to react with rabbit antiglobulin serum in the gel precipitation test in gel, although they exhibited a reduced ability of diffusion in agar (particularly γ-globulin denaturated by radiation). Denaturation of human γ-globulin by radiation or by ultrasound did not as a rule impair the ability of the γ-globulin to react with the specific antibodies. In the Boyden test, RF did not react with human nondenaturated γ-globulin, but reacted with the denaturated ones. In the BDB method, on the contrary, the action of the RF with denaturated γ-globulins was weaker than with nondenaturated ones. It is concluded that denaturation of γ-globulins leads to an increase of their inhibitory properties. The increased inhibitory ability was found to be dependent on this degree of denaturation. (BBB)

45861 EFFECT OF IONIZING RADIATION ON THE ENDOCRINE SYSTEM IN INSECTS. Piechowska, M. J. (Polish Academy of Sciences, Warsaw). Bull. Acad. Polon. Sci. Ser. Sci. Biol., 13: 139-44(1965).

Celerio euphorbia at different stages of homodynamic development was used to study the effect of ionizing radiation on the functions of the endocrine system in this insect. Caterpillars and pupae were irradiated with γ-rays from ^{60}Co at a dose of 2600 R. All groups studied were affected by this dose but the resulting changes differed widely. The youngest caterpillars were the least resistant; in 95%, growth and increase of weight stopped and death occurred between the 15th and 25th day after irradiation. In older caterpillars the damage by irradiation was less severe. In the surviving caterpillars deficiency in weight was observed, the difference being greater for animals irradiated during instar III than during instar IV. In the groups irradiated at later stages of development the mortality did not differ from that in the control group; after eclosion, however, external malformations of the adult moths appeared. The injuries were the greatest in animals irradiated at the end of the V instar; 40% of the eclosed moths exhibited deformations of head, both pairs of wings and of legs. They could fly only with difficulty, if at all; some could not even walk. In males, only spermatocyte cells in earlier development stages were present. In females, both ovaries and ova were underdeveloped, and only a few ripe eggs, if any, were found. Immaturity of ova was evaluated from the composition and number of protein fractions obtained in paper electrophoresis. In normal ripe ova only four fractions were found, their distribution being similar to that of corresponding hemolymph fractions. In ova from females irradiated during the instar III and IV five fractions were found, their proportions being dependent on the extent of injury caused by irradiation. In the females with no ripe eggs, the amount of fraction I was small and that of fraction IV twice that in the control. When more ova were ripe, the proportion of fraction I was markedly higher. Generally, the less the ovaries were affected and more ripe eggs were present, the greater was the similarity in distribution of the protein fractions with the control, and vice versa. The

underdevelopment of the reproductive organs and ova observed in these experiments in C. euphorbiae may be related to a radiation-induced disturbance in the hormonal system. This suggestion is corroborated by the observation that γ-rays also have an inhibitory effect on the excretion of the juvenile hormone during the molting of caterpillars. (BBB)

45862 EFFECTS OF ULTRAVIOLET RAYS AND CHLORPROMAZINE ON EHRLICH TUMOR CELLS. Carraz, G.; Beriel, H. (Faculté de Medecine, Grenoble, France). Bull. Assoc. Franc. Etude Cancer, 51: 269-76 (Apr.-June 1964). (In French)

The effects of uv rays and chlorpromazine on Ehrlich tumor cells were ascertained from the consumption of O_2 and production of lactic acid. In one test, exposure of the cells for five, ten, 20, or 40 min increased the percentage of lactic acid formed in one hr by 22, 73, 80, or 140% over that formed by the control group. For the same cells, the decrease in O_2 consumption was negligible, whether in the presence or absence of glucose. Exposing Hela cells (another type of tumor cell) to uv rays for 30 min increased lactic acid production 30%. Two suspensions of Brewer's yeast were exposed to uv for 20 min, one with a glucose solution added. In both there was a 20% decrease in CO_2 production. Therefore, uv rays depress the alcoholic fermentation of yeast. To determine if chlorpromazine had an effect analogous to uv on Ehrlich tumor cells, it was added in various concentrations to the cells. At 0.01 and 0.05 mg/ml, lactic acid production increased 70% and 60%. At 0.2 mg there was no difference from the controls, and at 0.4 mg fermentation was blocked. Chlorpromazine had the same effect on O_2 consumption, though not as accentuated. Exposing Ehrlich tumor cells to uv in the presence of chlorpromazine increased lactic acid production, but the effect was not synergistic. In another test series, guinea pig erythrocytes were exposed to uv for five min, but this did not significantly modify their CO_2 production. Erythrocytes do not normally consume O_2, but will do so in the presence of methylene blue. This enables them to utilize glucose through the pentose phosphate cycle. Exposing erythrocytes with methylene blue to uv rays for five min increases O_2 consumption 50%, so it is apparent uv rays stimulate the pentose-phosphate pathway. Uv depresses the consumption of O_2 by muscle tissue. In a guinea pig leg muscle exposed to uv five min, O_2 consumption fell 32%. The liver of male mice exposed to methylene blue, uv rays, or both showed no significant change in O_2 consumption. (BBB)

45863 ROLE OF THE WATER CONTENT IN THE PRODUCTION AND DECAY OF FREE RADICALS IN THE IRRADIATED PEA (PISUM). Houben, J.; Gillet, C.; Depireux, J. (Universite, Liege). Bull. Classe Sci., Acad. Roy. Belg. (5), 50: 1331-30(1964). (In French).

The study of the decay of free radicals in the irradiated flower of peas (Pisum sativum) reveals the existence of at least four types of radicals. The effect of the water content on the yield and the decay period was studied for each of these radicals. (tr-auth)

45864 THE APPLICATION OF BIOLOGICAL INDICATORS TO THE EVALUATION OF RADIOACTIVE INJURY. Altman, Kurt I. (EURATOM-CEN, Mol, Belg.). Bull. Inform. Assoc. Belge Develop. Pacifique Energie At., No. 56, 13-16(June 1965). (In French).

Creatine is used to illustrate in detail the application of a biological indicator to the measurement of radioactive injury. The excretion of creatine by patients receiving radiological treatment is shown. The time behavior of the excretion of creatine in mice and in humans is tabulated and indicated graphically. (J.S.R.)

45865 SOMATICAL RADIOMUTATIONS BY ACER NEGUNDO L. Privalov, G. F. Byul. Mosk. Obshchestva Ispytatelei Prirody, Otd. Biol., 70: 153-60(1965). (In Russian).

The treatment of seeds by Acer negundo L. with ionizing radiation causes an abrupt increase of the frequency of occurrence of mutations in somatic cells of the plants in comparison with spontaneous mutations. Under the influence of ionizing radiation mutations of large systematic features (form of leaves, arrangement of leaf spacing on the shoot, etc.) occur. The spectrum of radiation mutations, developed in Acer negundo in the first generation, was established. It was shown that by means "shooting" unchanged plants, grown from exposed seeds, significant numbers (25%) of latent mutations were also induced, displaced in the process of somatic selection and retained in the wood in parts of the trunks. The study of the basic types of mutations (leaf form, leaf spacing, and leaf chlorophyll) showed that they lead to abrupt changes of the accumulated area of the leaves and rapid growth of the plant. On this basis the creation of forms with delayed or more accelerated growth of the tree was presented as possible. (tr-auth)

45866 CALIFORNIA CHIROPRACTORS: AN EPIDEMIOLOGICAL STUDY OF CAUSES OF DEATH AMONG THEM AND OTHER CHARACTERISTICS. Ravenholt, Reimert T. (Univ. of Washington, Seattle). Calif. Med., 101: 341-7(Nov. 1964).

A study of California chiropractors attempted to ascertain if leukemia and other deleterious effects of ionizing radiation could be observed among this occupational group. During the study period from June 30, 1950 to June 30, 1955, of 599 (14%) of the 4,258 members, death certificates were found for 201 of the 206 members who were deceased. The findings do not indicate that the mortality experience of California chiropractors varies substantially from that of a similar population of non-chiropractors, but the finding of 1.68 times the expected mortality from leukemia is in accord with previous studies which show increased mortality from leukemia among populations which have had unusually great exposure to ionizing radiation. (BBB)

45867 MITOTIC ACTIVITY AND DNA SYNTHESIS IN CLONES DERIVED FROM MAMMALIAN CELL CULTURES IRRADIATED WITH X RAYS. Marin, Guglielmo; Levis, Angelo Gino; Piccinni, Ester (Laboratorio Internazionale di Genetica e Biofisica, Naples). Caryologia, 17: 481-93 (Sept.-Dec. 1965). (In Italian).

Experiments were conducted on RCP cells, originally obtained from guinea pig liver, which have an epitheloid morphology in culture. They are heteroploid, with a modal chromosome no. of 70 to 72. A monocellular suspension was irradiated with 180-kv x rays (at 150 R/min) to doses of 400 and 600 R. Mitotic index and radioautography of ^{3}H-thymidine uptake was examined in clonal cultures. Thus, the mitotic activity and DNA synthetic rate in colonies developed from these irradiated cells were measured at various intervals after irradiation, as an indication of the degree of damage carried by the progeny of irradiated cells. It was found that normal cells belonging to colonies in which giant cells were present displayed a lower mitotic and DNA synthetic activity than those belonging to colonies which did not show such giant cells. This observation is in agreement with previous results indicating that the appearance of giant cells in the progeny of irradiated cells is an indication of lethal damage affecting the whole colony. The possible relations between hereditable, lethal and sublethal lesions induced in cells by x rays are discussed. The reduced capacity for growth of these irradiated cells appears to be a permanent change, presumably in the chromosomes and therefore transmitted to subsequent cell generations. (BBB)

45868 IMMUNOGENICITY OF A GAMMA-IRRADIATED BRUCELLA MELITENSIS VACCINE IN MICE. Nishihara, H.; Ahn, T. H.; Taplin, G. V.; Carpenter, Charles M. (Univ. of California, Los Angeles). Cornell Vet., 54: 573-83(Oct. 1964).

Brucella melitensis and B. abortus were irradiated with ^{60}Co, rendering them nonreproducing and noninfectious, but capable of respiring on suitable substrates. A study was carried out to determine the immunogenicity of such γ-irradiated B. melitensis vaccine (GIV) in mice. Single irradiated vaccine injections of from 0.8 to 0.0001 mg, with and without adjuvant, were highly protective for mice challenged with doses of the homologous B. melitensis

which killed more than half of the unvaccinated controls within 24 hours. Comparative studies with heat and chemically inactivated B. melitensis vaccines demonstrated them to be less effective. Living B. abortus strain 19 and a living R form of B. melitensis showed some immunogenic activity, but at higher doses were themselves lethal for mice. Freund complete adjuvant and a mixture of aluminum potassium sulfate with pectin appeared to enhance the activity of the GIV, but the other adjuvants tested had no effect. A long-term study showed that the immunity developed by 0.4 mg GIV with aluminum hydroxide adjuvant was effective as early as the 4th day after vaccination and persisted as long as one yr. A test was made for possible host reactivation of the nonreproducing irradiated Brucella. Spleen homogenates from mice injected with the vaccine and with the spleen homogenates from vaccinated mice were negative for Brucella on culture and did not produce deaths in the mice. The results of challenging these mice indicated some transfer of immunity with the spleen homogenates from the vaccinated mice. Studies showed that 10^6 r irradiation of lyophilized Brucella rendered the cells incapable of producing visible colonies when cultured on agar, yet these cells continued to respire on suitable substrates at about 50% of the rats of non-irradiated cells capable of normal reproduction. Such irradiated cells are likely to be less damaged than cells subjected to heat or chemical treatment, and genetically and antigenically are more similar to the virulent cells than to attenuated nonvirulent strains. (BBB)

45869 DIFFERENT BEHAVIOR OF THE EPIDERMIS OF THE FLANK AND THE NIPPLE OF THE GUINEA PIG AFTER A 1600-R DOSE OF X RAYS. Maggiora, A.; Bujard, E.; Jadassohn, W. (Hopital Cantonal, Geneva). Dermatologica, 130: 306-11(1965).

Changes in the epidermis of the guinea pig nipple following a single irradiation of 1600 R were compared with those of the epidermis of the guinea pig flank irradiated with the same dose. After an x irradiation dose of 1600 R on the guinea pig flank, severe epidermal alterations could be seen after 7 to 10 days. After 20 and 40 days a marked acanthosis was apparent but apart from this the epidermis is normal. In contrast, the epidermis of the nipple showed little change 4 to 10 days postirradiation. Thickness of the nipple epidermis was normal on the 7th day and slightly augmented on the 10th day. On the 20th day after the irradiation, the flank epidermis was normal, except for the relatively marked acanthosis. On the contrary, on the 20th day after irradiation, severe changes were seen in nipple epidermis that were not noticeable the 10th day after irradiation. The epidermis of the nipple was then more than twice as thick as normal epidermis, but this was not due to a true acanthosis. It was due to a pseudoacanthosis, a thickening not due to an increase of the number of cells, but due to their swelling. By 40 days after irradiation, the epidermis was normal, on the flank as well as on the nipple, exclusive of a thickening of the epidermis. This thickening was due to a true acanthosis of the flank and nipple. No reasons are offered to explain the differences in the evolution of the x-ray effects between the two epidermal areas of the same animals, but it is emphasized they resemble the topographical differences observed in radiation reactions in humans. (BBB)

45870 A POINT OF VIEW ON THE PROBLEM OF THE GENESIS OF RADIOINDUCED LEUKEMIAS IN PULMONARY TUBERCULOSIS. Remmele, W. (Universitaet, Kiel). Deut. Med. Wochschr., 90: 553-7(Mar. 26, 1965). (In German).

Leukemia and tuberculosis can occur together or one may follow the other. Tuberculosis may be a complication of leukemia. However, one question which arises when leukemia is observed in tubercular patients is whether it was produced by repeated exposures to x irradiation during the course of thoracic x ray studies. Recognition of leukemia as the result of diagnostic irradiation in pulmonary tuberculosis would seem to be justified if several prerequisites are fulfilled. The number of times the patient is subjected to fluoroscopy can be important and individual doses to the bone marrow should not exceed 1 R per exposure. This value is often exceeded. Evidence for induced leukemia must be definitely established. Leukemoid reactions that appear with pulmonary tuberculosis can be mistaken for leukemia. The delay between irradiation injury of the bone marrow and appearance of leukemia should accord with an appropriate time interval. An interval less than one yr is improbable, and the shorter the time interval the less probability there is of a causal connection between irradiation and appearance of leukemia. The probability that irradiation may induce acute or chronic myelosis is greater than that it may induce chronic lymphadenosis. The age of the patient may also be considered in evaluating the relation between irradiation and leukemia. If the patient's age is far to one side of the age when the peak of incidence of the leukemia may be expected, then there is more probability of some connection with previous irradiation exposure. In the cases reviewed by the author there appeared to be a positive relation between tuberculosis, irradiation, and leukemia. (BBB)

45871 RADIOSENSITIVITY AND NATURE OF RADIATION INJURY TO MOUSE THYMUS CELLS IN SITU. Rass, I. T. (Inst. of Animal Morphology, Academy of Sciences, USSR). Dokl. Akad. Nauk SSSR, 161: 959-61 (Apr. 1, 1965). (In Russian).

After whole-body x irradiation of mice with doses of 200 to 2000 R, the number of thymus cells with pycnotic nuclei 6 hours after exposure ranged from 50 to 70% of the total. Similarly, irradiation of a suspension of thymocytes with about the same doses killed only 50 to 60% of the cells. It was assumed that the destruction of an equal number of cells by either whole-body irradiation of the animals or irradiation in vitro with a wide range of doses might be caused by the existence of two kinds of cells differing in radiosensitivity. To determine whether the difference was due to the existence of two kinds of cells or to different stages in the life cycle of a homogeneous cell population, the author irradiated mice with a dose lethal to half the cells and then re-irradiated the animals 1 to 2 days later with the same dose. Destruction of new cells after the second exposure would indicate that the given stage of the life cycle was more radioresistant, whereas lack of reaction would suggest that there are two kinds of cells with different radiosensitivity. The results showed that the second exposure did not lead to the destruction of more cells, implying that all the cells were killed by the first exposure. Hence, the thymus gland has at least two kinds of cells that differ sharply from each other in degree of radiosensitivity. (ATD)

45872 THE EFFECT OF DIFFERENT DOSES OF X-RAYS ON THE OSTEOGENESIS IN LONG TUBULAR BONES OF MOUSE EMBRYOS. Neverova, L. G. (Inst. of Experimental Medicine, Academy of Medical Sciences, USSR). Dokl. Akad. Nauk SSSR, 161: 1216-18(Apr. 11, 1965). (In Russian).

Female mice were x-irradiated with 30 to 300 R at times ranging from the eighth to the fourteenth day of pregnancy at a rate of 40.3 to 44.5 R/min. Measurements were made of stained bones of embryos from females autopsied on the seventeenth day and were analyzed statistically. The decrease in the average relative length of the ossification centers was maximum in embryos that were irradiated at 300 R on the eleventh day of development. The effect of 150 R was similar but smaller. A 300 R dose on the fourteenth day also caused some decrease, but 150 R did not. Doses of 150 R on the ninth and thirteenth days increased the length, as did 300 R on the tenth day. Irradiation on the twelfth day had no significant effect. Doses of 100 R on the eleventh day, selected for the lower doses because of the maximum effect already shown on this day, significantly increased the length; 30 R had little effect, and 50 R had no effect on half the animals, and in the other half, increased the length in some and decreased it in others. The results are explained as a stimulating effect of the lower doses, which decreases and then is reversed as the dose increases. (TTT)

45873 SOME OBSERVATIONS ON AN INDUCED ADAPTATION IN A TRANSPLANTABLE TUMOR. Sanford, Barbara H. (Massachusetts General Hospital, Boston; Huntington Memorial Hospital, Boston). Exptl. Cell Res., 39: 97-102(Aug. 1965).

A permanent alteration in tumor transplantability was seen after a single passage of a strain-specific tumor through a first generation hybrid between susceptible and resistant strains. This effect could be observed within the strain of origin either as a change in survival time or in latent period. Since passage through irradiated F_1 hosts was ineffective, an immunological mechanism is suggested. An interpretation in terms of an antigenic adaptation of tumor cells is proposed. (auth)

45874 DISTRIBUTION OF AFFERENT AND EFFERENT FIBERS IN THE CEREBRAL CORTEX OF THE RABBIT REVEALED AT LAMINAR LESIONS PRODUCED BY HEAVY IONIZING PARTICLES. Kruger, Lawrence (Univ. of California, Los Angeles); Malis, Leonard I. Exptl. Neurol., 10: 509-24(Dec. 1964).

Adolescent or mature rabbits were irradiated with deuterons of about 20 Mev. All lesions were situated in the right hemisphere, and in some animals in two different cortical fields. In others, the same cortical field was irradiated twice at different depths by the interposition of aluminum absorbers of appropriate thickness. Most of the lesions were caused by relatively high doses at the peak of energy release ranging from 28,000 to 81,000 rad. Animals were killed at various times after irradiation in order to determine the delay necessary for the occurrence of radionecrosis and changes in myelin constitution. The histological preparations were all stained with the Marchi method. The irradiated zone of the cerebral cortex displayed a dense black region with the Marchi method, interpreted as reflecting degeneration of myelinated nerve fibers. The zone of dense myelin degeneration consisted of a band below the surface in the same lamina in which nerve cells appeared to be destroyed in Nissl-stained sections. This zone corresponds to the peak of ionization or energy release displayed by the Bragg effect. Such laminar lesions were produced with peak doses ranging from 19,000 to 69,000 rad, with the higher doses producing heavy wide bands of necrosis, and displaying small cystic cavities. These patterns of myelin degeneration were observed in all animals with postoperative survival periods ranging from 10 to 32 days. The histological patterns of laminar lesions consisted of two groups on the basis of distribution of rosette-type degeneration, and relation to irradiation dose. The first group displayed fine sprays of pericellular rosette-type degeneration throughout the cellular layers above the laminar lesions, but little in the cortex below, lesions produced with lower doses (average peak dose of 39,000 rad). In the higher-dose group (average peak dose of 53,400) there was consistent coarse granular degeneration in the laminar lesion zone with some rosettes and coarse granules below as well as above the peak dose band. The intensity and extent of degeneration below the lesion increased with higher doses. Irregular cell loss beyond the end of range of deuterons for heavy peak doses were seen in Nissl preparations, interpreted as due to vascular damage. The presence of Marchi granules in the white matter following lesions in any of the cellular layers in several different cortical fields suggests that all cortical laminae contribute efferent fibers to the underlying white matter. The results support the differentiation of the laminar organization of the sensory cortical fields into a predominantly, but not exclusively, afferent role for the granular and supragranular layers, and an efferent role for the infragranular layers. (BBB)

45875 MORPHOLOGICAL AND HISTOENZYMOCHEMICAL STUDIES OF THE AORTA OF RABBITS AFTER LOCALIZED EXPOSURE TO $^{90}Sr-^{90}Y$ BETA RADIATIONS. Kunz, Jochen; Hecht, A.; Hegewald, H. (Humboldt Universitaet, Berlin). Frankfurter Z. Pathol., 74: 293-306 (Jan. 18, 1965). (In German)

The surgically exposed abdominal aortas of 44 rabbits were irradiated locally by means of a $^{90}Sr-^{90}Y$ beta irradiator. After irradiation with 30 kR, extensive injuries of the vessel walls were observed. These included muscle cell destruction, loss of elasticity, and proliferation of the intima. Injury of the irradiated elastic lamellae was indicated additionally by reduced elastic resistance. In irradiated sections of the vessel walls a decrease of acid mucopolysaccharides was demonstrable by histochemical and microfluorescent tests. The acid mucopolysaccharides were increased in the adjacent areas. As the interval between irradiation and final examination was increased, the frequency of appearance of scarification of the vessel walls increased. Macroscopically, this was evidenced by sacculations that resembled aneurysms. After irradiation with 3 kR, only slight morphological changes were observed in the aortic walls. It was not possible to detect early changes in the aorta after exposure to the ionizing irradiations by means of histoenzymochemical methods. The time interval between irradiation and the reduction of activity that was observed in the enzymes studied indicated secondary destruction of enzymatic activity by the irradiation. (BBB)

45876 INDUCTION OF LETHAL MUTATIONS IN DROSOPHILA MELANOGASTER BY DNA. Gershenson, S. (Inst. of Zoology, Ukrainian Academy of Sciences, Kiev). Genet. Res., 6: 157-62(July 1965).

Addition to the food of Drosophila larvae of DNA from calf thymus induced a considerable number of recessive lethal mutations in the 2nd chromosome. An analysis of sixty-six such lethals showed that most of them affect the same segment containing probably some thirty to thirty-five sub-units capable of mutating together or separately. Results were compared with those from x-irradiating 2nd chromosomes (500 R doses). (H.G.D.)

45877 THE NATURE OF LETHALS IN DROSOPHILA WILLISTONI. Magalhaes, L. E.; De Toledo, J. S.; Da Cunha, A. Brito (Universidade de Sao Paulo, Brazil). Genetics, 52: 599-608(Sept. 1965).

The analysis of several natural and radioinduced lethal chromosomes is reported. The same chromosome may behave either as though its lethality were due to a single locus, or as a synthetic lethal, depending upon which chromosome it is tested against. Synthetic lethals are lethal chromosomes produced by recombination between nonlethal chromosomes. Unilocal lethality or synthetic lethality are relative to the rest of the gene constellation, and are not absolute characters. A method is presented for analyzing chromosomes with regard to the locations of lethality factors and their interrelations. (auth)

45878 GENETIC ANALYSIS OF PYRIMIDINE MUTANTS OF SALMONELLA TYPHIMURIUM. Yan, Yanhon; Demerec, M. (Brookhaven National Lab., Upton, N. Y.). Genetics, 52: 643-51(Sept. 1965).

Genetic analyses of 141 pyrimidine (pyr) mutants showed that at least six gene loci control the pathway of biosynthesis leading to production of uridylic acid. Two of these loci, pyrC and D, are close together on the genetic map and are probably members of a cluster of genes controlling related functions. The other four are located in different portions of the chromosome. With respect to function and position on the genetic map, these six pyr loci of S. typhimurium appear to be homologous to six pyr loci described in E. coli (Beckwith et al, J. Mol. Biol., 5: 618-634, 1962; Taylor et al, J. Mol. Biol., 8: 771, 1964). Mutants of the pyrA locus require uracil or orotic acid plus arginine or citrulline, but several of the alleles are able to grow partially on arginine or citrulline. A suppressor has been found that modifies the requirement in certain other pyrA mutants from arginine plus uracil to arginine alone. Genetic mapping within individual loci indicates that multisite mutations are not rare. Pyrimidine mutants are readily induced by 2-aminopurine, diethyl sulfate, ultraviolet radiation, x rays, fast neutrons, and nitrous acid, but they very rarely occur spontaneously. Multisite mutations can occur spontaneously, and are found among the mutants induced by all the mutagens tested except 2-aminopurine. (auth)

45879 THE RELATIVE MUTABILITIES OF DNA IN REGIONS OF THE X CHROMOSOME OF DROSOPHILA MELANOGASTER. Rudkin, George T. (Inst. for Cancer Research, Philadelphia). Genetics, 52: 665-81(Sept. 1965).

The relative DNA contents of ten regions of the X chromosome in four salivary gland nuclei of fully grown larvae and prepupae were determined by cytophotometric measurements of ultraviolet absorbance (λ = 257 nm) of chromosomes treated with ribonuclease. The regions were bounded by the cytogenetic loci of the 11 marker genes, y, z, w, spl, ec, ct, v, g, f, car, and bb. The apparent relative mutability of a chromosome region is defined as the ratio of the percentage of all mutations that were found to occur in the region to the percentage of DNA in the region. Apparent relative mutabilities were determined for seven to ten regions on the basis of eight published sets of sex-linked lethal and visible mutations: five sets produced by x-ray treatment, one set by a mutator gene, one set by incorporated H^3-thymidine, and one set by incorporated ^{32}P. The apparent relative x-ray sensitivities of the regions were not demonstrably different from one another. Lethal mutations induced by Ives' mutator gene hi were not randomly distributed among four chromosome regions; visibles were. Differences between the susceptibilities of the regions to the different mutagenic treatments are suggested but not established by the data. The theory of chromosome evolution by duplication would predict redundance of genetic function in duplicate regions after the duplication event and until the two regions had diverged by mutation to have different functions. No evidence for different degrees of redundance was found, for the distribution of the observed mutations was not related to the number of bands, the ratio of single to double bands, or to the average DNA contents of the bands in the regions analyzed. (auth)

45880 HERITABLE EFFECTS OF RADIATION ON BODY WEIGHT IN RATS. Newcombe, Howard B.; McGregor, John F. (Atomic Energy of Canada Ltd., Chalk River). Genetics, 52: 851-60(Oct. 1965).

Offspring from a group of black-hooded rats, in which male ancestors had received gonadal exposures of 600 Rads of x rays over 13 successive generations, tended to be heavier than their controls, the means of the 90-day weights differing by 0.6 of a standard deviation. The relative incidence of heavy as compared with light animals (defined as those in the upper and lower halves of the weight distribution for irradiated and control groups combined) was higher in the irradiated than in the control group by factors of 3.4 for males and 2.2 for females. This effect of ancestral irradiations on a quantitative physical trait persists when statistical methods are used to remove contributions from differences in sibship size in the two lines. A direct genetic effect is thus indicated, independent of possible differences in the pre- and postnatal environments that might arise as a result of the radioinduced reductions in litter size. The results lend support to the view that a radioinduced reduction in maze-learning ability, may likewise be independent of effects of sibship size, and so be due to hereditary changes that affect directly the character under study. Both the radiation effect on body weight, and that on learning ability, may be regarded as substantial in comparison with the natural variations in these quantitative traits. (auth)

45881 THE SPECTRAL COMPOSITION OF THE ERYTHEMAL PART OF ULTRAVIOLET RADIATION AND ITS DOSE DETERMINATION. Galanin, N. F.; Tyukov, D. M. (Leningrad Research Inst. of Radiation Protection). Gig. Sanit., No. 7, 22-5(July 1965). (In Russian).

Data on the most probable curve for the erythemal action of radiation energy and on the necessity of determining the average erythemal dose for different age groups of the population are presented. Recommendations for design of medical irradiation facilities that were derived for the information on erythemal dose are discussed. (TCO)

45882 INDUCTION OF LEAF SPOTS IN LEGUMINOUS PLANTS BY NUCLEOTOXIC AGENTS. Zacharias, I. M.; Ehrenberg, L. (Universiteit, Stockholm). Hereditas, 48: 284-306(1962).

Further studies were conducted on the earlier observation that after x irradiation of plant seeds, especially of species belonging to the family Leguminosae, a mosaic or variegation of light-green, yellowish, and white color can be found in the seedling leaves. When low or moderate doses are used, the variegation consists of individual light spots, of about equal size; after irradiation at higher doses the spots overlap. Samples of the diploid variety of red clover, Ultuna, were irradiated with fast neutrons. To decrease γ-ray contamination, the seeds were enclosed in a Bi container with 6-cm thick walls. The dose rate amounted to about 2 rad/sec of fast + thermal neutrons contaminated by 0.5 rad/sec of γ radiation. In contradistinction to x rays, neutrons produced, at low doses, leaf spots proportionally to the dose. At higher doses the saturation effect was observed, similar to that found in the earlier x-ray experiments. The rectilinear part of the dose-response curve falls totally within a dose range where no growth inhibition is indicated. Thus, neutrons are many times more effective than x rays in producing leaf spots, the relative biologic effectiveness being about the same as for gene mutations and other disturbances of the genetic material in higher plants. It was shown in red clover that a doubling of the chromosome number afforded protection against the formation of leaf spots after irradiation of seeds. Ethylene oxide and other radiomimetic chemicals induced leaf spots with a high efficiency. For ethylene oxide, as with x rays, the spot frequency is an exponential function of the dose, the exponent being about 1.6. High pressure oxygen exposure produced leaf spots efficiently. This agent is known, in different materials, to produce chromosomal aberrations at high frequencies, and gene mutation. These facts strongly indicate that leaf spots arise through changes of gene material. At the present stage of the experiments, direct effects on plastids or proplastids can not be excluded as responsible for the leaf spots induced by radiations and alkylating substances. However, an action mechanism via the gene material seems at present most plausible, especially considering the high effectiveness and the linear dose-effect relation of neutrons. This leaf-spot method seems to be of value for a rapid estimation of the nucleotoxic activity of various substances. (BBB)

45883 COMPARISON OF FISSION NEUTRONS AND γ-RAYS IN RESPECT TO THEIR EFFICIENCY IN INDUCING MUTATIONS IN SILKWORM GONIA. Murakami, Akio; Kondo, Sohei; Tazima, Yataro (National Inst. of Genetics, Misima, Japan). Idengaku Zasshi, 40: 113-24 (Apr. 1965).

An investigation was made of the effects of fission neutrons on the induction of visible recessive mutations in early and in late gonial cells of the silkworm. The results were compared with those of our pervious reports, in which 14 Mev neutrons and ^{137}Cs γ-rays were used. Dose-mutation frequency curve for fission neutrons was essentially the same as that for other radiations, showing a slow rise in the lower dose range but a rapid rise in the higher dose range. Mutation response to fission neutrons was almost similar for male and female gonial cells, although higher frequencies were observed for fission neutrons than for γ-rays or 14 Mev neutrons. When radiation doses producing a frequency of 10^{-3} of visible recessive egg-color mutations were used as a criterion, the relative biological effectiveness of fission neutrons to γ rays was about 1.7 to 2.4 for early stage gonia and 3.0 to 4.2 for late stage gonia. Similar results have already been reported for 14 Mev neutrons, although the values were smaller. All the dose-frequency curves obtained in the recent series of our work with γ-rays, 14 Mev neutrons and fission neutrons are given in the present paper to make them available for further investigations in this field. (auth)

45884 THEORETICAL STUDIES ON THE METHODOLOGICAL PROCEDURES OF RADIATION BREEDING. IV. DISCUSSION FOR THEORETICAL CONCEPTS OF THE EIN-KORN-RAMSCH METHOD. Yoshida, Yoshio (Kyushu

Agricultural Experiment Station, Chikugo, Japan). Ikushugaku Zasshi, 15: 137-45(1965).

The "Ein-Korn-Ramsch" method proposed by Freisleben and Lein (Z. Pflanz., 25: 255(1943) is discussed in relation to the one-plant-one-grain method, a new method of mutation breeding proposed previously by the author. Proofs are mathematically derived for the basis of their method. In a comparison of their method with the author's, it is seen that the procedure of taking one seed from each of the X_1 plants is identical, but in other respects it is quite different. It is concluded from theoretical arguments and discussions that in this mathematical approach and utility for application to radiation breeding the author's method is superior to the Freisleben and Lein method. It is very common to require two or more different kinds of desirable mutants in practice in radiation breeding. The following three cases are concerned in an X_2 population: (1) detection of at least one mutant belonging to the ith kind of mutants, (2) detection of at least one mutant belonging to any one of all the different kinds of mutants, and (3) obtaining at least one mutant per kind for the different kinds of mutants. In all of these cases, the one-plant-two-grain method, the one-plant-three-grain method, and especially the one-plant-one-grain method will frequently be much better, because of the small total of X_2 plants, and/or X_1 and X_2 plants in the aggregate. These results will be more useful to breeders than those provided by the Ein-Korn-Ramsch method. The latter method aims at the maximum number of mutated X_1 plants by reducing from X_2 lines. In contrast the author's method aims at detecting at least one or two desirable mutants in X_2 with the least number of total X_2 plants and a smaller number of X_1 and X_2 plants in total for any given probability. (BBB)

45885 THE EFFECT OF DIVIDED DOSES OF 15 Mev ELECTRONS ON THE SKIN RESPONSE OF MICE. Fowler, J. F. (Hammersmith Hospital, London); Kragt, Klazien; Ellis, R. E.; Lindop, Patricia J.; Berry, R. J. Intern. J. Radiation Biol., 9: 241-52(1965).

The skin reaction of the irradiated mouse leg was used to determine the sparing effect of dose-fractionation on a normal mammalian tissue. The total dose in two fractions (D_2) required to produce the same effect as a single fraction (D_1) was determined for intervals of 2 to 42 hrs. A rapid increase of D_2-D_1 up to 4 to 5 hrs was observed. Irradiations were carried out in oxygen, air, and nitrogen. The values obtained for (D_2-D_1) at 24 hours in air and oxygen were in the range 300 to 880 rads (15 Mev electrons). These agree well with the findings previously reported on pig and human skin. Hypoxia was demonstrated to affect the response of the mouse skin irradiated when the animal was breathing air or oxygen at normal atmospheric pressure. (auth)

45886 CLONE-SIZE ANALYSIS IN THE STUDY OF CELL GROWTH FOLLOWING SINGLE OR DURING CONTINUOUS IRRADIATION. Nias, A. H. W.; Gilbert, C. W.; Lajtha, L. G.; Lange, C. S. (Christie Hospital and Holt Radium Inst., Manchester, Eng.). Intern. J. Radiation Biol., 9: 275-90(1965).

Analysis of the clone sizes of HeLa cells plated out by the Puck technique showed that the distribution broadened when the cell population included damaged cells with a slower net growth rate. This broadening of the clone-size distribution was found after repeated trypsinization of control cells as well as following single radiation doses and continuous irradiation. The development of these broad clone-size distributions was studied over a number of days. The resultant families of distribution curves reveal additional data about the population kinetics of irradiated cells, that can be related to the growth curves and survival fractions obtained under the same experimental conditions. The more slowly growing clones, which develop after irradiation, were shown to maintain proliferative capacity. The implications of this non-lethal radiation damage are discussed. It is emphasized that the usual parameter of a certain minimum clone size (usually 50 cells) is an arbitrary definition of the reproductive integrity of surviving cells, and that under certain conditions it is more meaningful to study the full clone-size distribution. (auth)

45887 ENZYMATIC AND BIOCHEMICAL STUDIES OF EPIDERMIS FOLLOWING IRRADIATION WITH BETA PARTICLES. Tabachnick, Joseph (Albert Einstein Medical Center, Philadelphia). J. Albert Einstein Med. Center, 11: 17-18(Jan. 1963).

The avascular epidermis is relatively homogeneous, consisting of cells derived from one embryonic type, so that after local irradiation with ^{90}Sr β particles any aberrations observed up to 24 hr or longer reflect changes in the initially irradiated cells or their extracellular matrix, or both. Attempts were made to find some biochemical aberration which would serve as a basis for a sensitivity test for low doses of ionizing radiation. Such a test might be used to replace the less sensitive method of observing the degree of reddening or swelling following irradiation. Studies of the normal epidermis of guinea pigs showed that epidermis contains high concentrations of free amino acids; urocanic acid, a deamination product of the amino acid histidine, accumulates selectively in this tissue; and the enzymes which degrade nucleic acids are present in relatively high concentration on the skin surface and in the hair. These findings were also observed in human epidermis. After a single dose of 3000 rep of β irradiation, guinea pig epidermis showed increases in all three of the items mentioned. Some of these changes were detectable as early as one day after irradiation, well before any visible signs of injury. Irradiation-induced decreases in activity were observed in one of the important nucleases and in several of the alkaline phosphatase enzymes. Some of the epidermal enzymes were purified and characterized. (BBB)

45888 PROBLEMS IN RENAL HOMOTRANSPLANTATION. Starzl, Thomas E.; Marchioro, Thomas L.; Brittain, Robert S.; Holmes, Joseph H.; Waddell, William R. (Univ. of Colorado, Denver). J. Am. Med. Assoc., 187: 734-40(Mar. 7, 1964).

Five successful cases of renal homotransplantation among a total of 12 patients submitted to the procedure are reported. Radiation and/or cytostatic drugs were used to reduce the recipient's immunologic reactivity. Ten patients received homografts from living donors, and in two the renal homografts were obtained from recently deceased cadavers. The patients were all males ranging from 12 to 50 years of age. When convenient, donors were selected of the same major blood type as the recipient. However, in six of the 12 cases, there were major blood group incompatibilities. One patient was treated with 300 R of total-body irradiation preoperatively. Fifty R were given 17, 14, 11, and 5 days before transplantation, culminating in a final dose of 100 R on the day before operation. Four and six days after transplantation, additional doses of 50 R were given, with shielding of the renal transplant. The x-ray doses were given with a 250-kv unit. Despite the resultant suppression of white blood cell count to less than 500/mm^3, vigorous rejection began after two weeks. Therapy was changed to azathioprine (Imuran), actinomycin C, and prednisone with apparent reversal of the rejection. Therapy for the other 11 patients consisted of a combination of azathioprine, actinomycin C, and prednisone. Five of the ten patients who received renal homografts from living donors have good renal function, 7 to 13 months after surgery. All five of the patients have had prednisone discontinued and all receive smaller maintenance doses of azathioprine. Attention was focused on two aspects of the transplantation problem. First, an effort was made to improve the quality of the homograft tissue by reducing its period of ischemia during transfer and by reducing its metabolic requirements during this period by cooling techniques. Second, attempts were made to improve the methods used for prevention and reversal of the rejection crisis which interrupted the recovery of every patient except one. Proper manipulation of drugs is important so that they were maximally effective at the time of greatest need, during the height of the attempted rejection. (BBB)

45889 STUDY OF ADOLESCENTS EXPOSED IN UTERO TO THE ATOMIC BOMB, NAGASAKI, JAPAN. II. GROWTH AND DEVELOPMENT. Burrow, Gerard N.; Hamilton, Howard B.; Hrubec, Zdenek (Yale Univ., New Haven). J. Am. Med. Assoc., 192: 357-64(May 3, 1965). (TID-21765).

Anthropometric measurements and developmental data are given for children who were in utero at the time of the atomic bombing (ATB) in Nagasaki. Three comparison groups were studied: group 1, children whose mothers were within 2000 m of the hypocenter (point on the ground above which the bomb exploded); group 2, whose mothers were located between 3000 to 4999 m; and group 3, whose mothers were not in the city at the time of the bombing. Group-1 males consistently showed smaller measurements than their counterparts in groups 2 and 3, the head circumference generally being significantly smaller. For both sexes within group 1, measurements were generally smaller for those who received higher doses of radiation as judged by estimated radiation dose to the mother, acute radiation syndrome of the mother, or her distance from the hypocenter, and the differences were more often significant in the females than in the males. The most striking differences for both sexes were in the head measurements. The smaller head circumference of those closest to the hypocenter confirmed earlier reports associating exposure to radiation with decreased head size. Along with the apparent smaller size of the high-dose, group 1 females, there was a lag in development as evidenced by delayed menarche and epiphyseal closure of the hand and wrist. The fact that those who received the larger amount of radiation lagged behind suggests that the delay in development may be related either directly or indirectly to radiation of the mothers during gestation. (TCO)

45890 BIOLOGICAL CONSIDERATIONS OF MANNED FLIGHT IN SPACE. Graybiel, Ashton. J. Am. Pharm. Assoc., 368-9, 375(July 1965).

Various factors, including ionizing radiation, which spacecraft personnel must be protected against are reviewed. Radiation is considered as a stress and a hazard to space flight. For example, in orbital flight an inclination of 30° to the geographic equator is chosen to take advantage of the protection afforded by the geomagnetic field and an altitude under 300 mi (nautical) is chosen to avoid the trapped particles, mainly protons, in the Van Allen belts. Within these constraints under ordinary conditions the radiation burden inside a spacecraft is well within acceptable limits. Film emulsion measurements carried out on the MA-9 orbital flight indicate that the total exposure was 40 mrem. Although 40 mrem is far short of the weekly permissible limit of 300 mrad, it is nevertheless tenfold greater than the normal exposure level from cosmic radiation. Even within these orbital constraints and altitude it is necessary to take into account the hazards from solar flares. A solar flare has two important effects. The first is an increase in proton flux which reaches the vicinity of the earth in a characteristic time-intensity pattern. The second effect is in the nature of a geomagnetic storm occurring about 24 hr after the appearance of the solar flare. This storm is characterized by a disturbance in the earth's magnetic field which reduces to a large extent the shielding effect of the geomagnetic field. The prevention or treatment of radiation effects poses a great challenge. Experiments on the protective properties of mercaptopropylamine on the phage-producing activity and genetic apparatus of Escherichia coli show that this agent does not protect the genetic apparatus against lethal effects but does reduce the level of phage-producing activity. (BBB)

45891 ULTRAVIOLET MICROBEAM IRRADIATION IN LIVING CELL MEMBRANES. Montgomery, P. O'B.; Cook, James E.; Karney, David (Univ. of Texas, Dallas). J. Cell Biol., 26: 959-61(Sept. 1965).

Design features are described of a phase-contrast ultraviolet microbeam television microscope. The equipment can be used to generate an ultraviolet microbeam of any desired shape or dimension and to bring it to focus on the specimen. Results are reported from studies of the response of the peripheral cytoplasmic membrane to ultraviolet radiation in which a microbeam of ultraviolet was shaped to fit the entire peripheral membrane of a single Chang liver cell maintained in a tissue culture chamber. The ultraviolet microbeam was continuously applied to the outer edge of the cytoplasmic membrane while the results were recorded by visible light phase-contrast time-lapse motion pictures. The cells were followed until death. Morphological changes are described. (C.H.)

45892 TOLERANCE OF CENTRAL NERVOUS SYSTEM TISSUES TO MEGAVOLTAGE RADIATION. Bradley, J. M. (Peter MacCallum Clinic, Melbourne). J. Coll. Radiologists Australasia, 8: 29-39(Feb. 1964).

The pertinent literature on radioinduced lesions of the central nervous system is reviewed and new data from 38 brain- and spinal cord-irradiated patients are presented. Review of the literature shows that radiation necrosis has been described in the brain stem, spinal cord, hypothalamus, and cerebral hemispheres. Most cases of necrosis, except those arising in the cerebral hemispheres, became clinically apparent within 15 months of irradiation. A table lists the previously reported cases of radiation necrosis of the hypothalamus, brain stem, and spinal cord, together with the intervals, where stated, between the last irradiation and the onset of necrosis. The longest interval was 70 months. A survey of the author's cases submitted to megavoltage (4-Mev) irradiation of the central nervous system showed that the dose of 5000 rad in four weeks, or its biological equivalent, is tolerable to most parts of the nervous system. However, the upper limit of tolerance may be much higher in individual cases. The results were analyzed in three groups of treated patients. (1) Large increments or fractions, the total dose being given in two to three doses; three increments each of 1000 to 1100 rad caused necrosis. Two increments of 1000 rad were tolerated by the lower lumbar cord but should be avoided on the brain stem. Three increments of 875 rad were tolerated by portions of the cervical cord. (2) Treatment given over periods of up to four weeks in 12 to 20 increments; 5000 rad in 20 increments in four weeks appears to be tolerable to the brain stem, hypothalamus, and at least one-third of the volume of one cerebral hemisphere. It also appears to be tolerable to the whole length of the cervical cord and the lower part of the lumbar cord. The same regions would probably tolerate 4000 rad in 12 increments in four weeks, which may be an equivalent effective dose in respect to tumor lethality. That the upper limit of tolerance may be much greater still in some instances is shown by cases which tolerated large doses, and particularly by those which tolerated repeated courses. It is suggested that the dosages mentioned be prescribed as the minimum to those central nervous system tumors whose prognosis is relatively good; e.g., cystic astrocytomas, whereas larger doses may be justifiable for more aggressive tumors of poorer prognosis. (3) Treatment periods of over four weeks. Six thousand rads in six weeks appear to be tolerable to the brain stem, but again the tolerable dose may be much higher. (BBB)

45893 DISCRIMINATION OF BROKEN CIRCLES BY NORMAL AND X-IRRADIATED MONKEYS. Fletcher, Harold J.; Bowman, Robert E.; Boelkins, R. C. (Univ. of Wisconsin, Madison). J. Comp. Physiol. Psychol., 58: 312-14(Oct. 1964).

Three previous studies suggested the possibility of visual defects in monkeys exposed to sublethal doses of ionizing radiation. They required monkeys to discriminate a closed circle from an incomplete circle with a gap ranging from 180° to 0.5°. However in these studies the monkeys' discrimination performance was not consistently related to the size of the gap nor were the conclusions supported by appropriate statistical tests. The present study instituted the procedural change of running subjects to criterion on successively smaller gaps to reveal performance related not only to changes in gap size but also to general learning and transient motivational and situational variables. A random presentation of problems was

employed to elicit performance systematically related only to changes in gap size. The irradiated rhesus monkeys, Macaca mulatta, 5 to 7 yr old, had extensive test experience and had survived an accumulated 3000 R of whole-body x radiation delivered at the rate of 50 R biweekly. After initial training on a single object discrimination problem, they were trained to a 90% criterion successively on 64°-, 32°-, and 16°-gap discrimination problems. Then for five additional 36-trial sessions, these same three problems were presented in a random order. Later, other gap problems were all presented randomly. A 3-factor analysis of variance on the number of correct responses per gap size per week revealed only a statistically significant decrement across gaps and an improvement over weeks of training. There was no significant effect of irradiation. These results are obviously at variance with the three previously mentioned studies which indicated radiation-induced deficits in discrimination performance. Other negative findings are discussed. (BBB)

45894 EFFECTS OF FETAL IRRADIATION ON BEHAVIOR IN THE ALBINO RAT. Fowler, Harry (Univ. of Pittsburgh); Hicks, Samuel P.; D'Amato, Constance J.; Beach, Frank A. J. Comp. Physiol. Psychol., 55: 309-14(1962).

Exposure of pregnant rats to conventional therapeutic x rays in single doses of 150 R results in malformation in the young, and when this treatment is carried out at specific stages of pregnancy, the resulting abnormalities in the young are highly predictable and consistent. Irradiation at days 13.5 to 14.5 of gestation results in, among other things, a very thin cerebral cortex combined with a characteristic subcortical ectopia. The adult behavior of rats with the types of brain abnormalities produced by irradiation at days 13.5 to 14.5 of gestation was studied to determine functional deficiencies which accompany the central nervous system defects. The irradiated rats were inferior to the controls in solving the more difficult problems on the Hebb–Williams maze and in learning a visual discrimination problem. Tests for emotionality revealed that control animals adapted to the open-field situation in the course of several days, whereas the experimental males failed to do so. The controls also showed more of a tendency, over a 5-day series of successive trials, to alternate between the black and white arms of a T maze than did the experimental rats. These findings reflect a general intellectual deficit on the part of the irradiated animals. Postmortem examination of the irradiated animals, including serial sections of the brains and eyes, showed that the chief malformation was a markedly deficient neocortex over the vertex of the brain, an associated subcortical ectopia, and a deficient or absent corpus callosum. (BBB)

45895 RESPONSE OF RADIATED HUMAN GINGIVAL FIBROBLAST-LIKE CELLS TO DILANTIN SODIUM IN TISSUE CULTURE. Shafer, William G. (Indiana Univ., Indianapolis). J. Dental Res., 44: 671-7(July-Aug. 1965).

The mechanism through which diphenylhydantoin (DPH) affects the metabolism of connective-tissue cells to increase their proliferative capacity was investigated in cultures of human gingival fibroblast-like (HGF) cells exposed to x rays. Irradiation of normal HGF cells, in doses between 400 and 1600 R, resulted in a varying degree of diminution of proliferation of the cells. Maintenance of cells irradiated with 400 R in continuous culture resulted in a marked alteration of their metabolic pattern, as evidenced by a gradual alteration of their proliferation rate. Following addition of DPH to actively growing cultures of these previously irradiated cells, complete lack of the usual response to the drug was seen, suggesting severe alteration in the internal metabolism of the cell. Further evidence of this alteration of metabolism was suggested by the somewhat increased resistance to levels of DPH found toxic to the normal HGF cell. Tritiated thymidine uptake studies substantiated the stimulatory effect of DPH on normal HGF cells as reflected by a doubling of labeled nuclei in DPH-treated tubes as compared to control tubes at the 2-day period, probably indicating a marked increase in DNA synthesis. In contrast, while the percentage of labeled cells at the 2-day period was much greater in the irradiated HGF cells than in the normal HGF cells, no increase in nuclear labeling was found in the irradiated HGF cells treated with the drug, thus correlating with mean viable cell counts. In addition, there was a persistent high percentage of labeled nuclei at the 3-day period in the irradiated HGF cell in contrast to the normal HGF cell. These studies provide furthur evidence that DPH is a true cell stimulatory agent for normal fibroblasts and that alteration in the normal metabolic pattern of such cells, as by irradiation or as in neoplasia, can inhibit this effect of the drug. (BBB)

45896 MOISTURE CONTENT OF TISSUES OF NORMAL SURGICALLY TREATED, AND IRRADIATED RATS. Edwards, Cecile H.; Ruffin, Minnie R.; Gadsden, Evelyn L.; Edwards, Gerald A. (Agricultural and Technical Coll. of North Carolina, Greensboro). J. Elisha Mitchell Sci. Soc., 80: 21-2(May 1964).

Rats of the Wistar strain are widely used in radiobiological experiments, and although the moisture content of normal rat tissue is known, it is of interest to know how irradiation affects this parameter. The moisture contents of 25 tissues of normal adult rats were determined under three experimental conditions (postirradiation and after two surgical procedures). Adult rats of Wistar strain, 6 months ±2 weeks of age, were used. In one group of operated rats, an abdominal incision was made one hr prior to sacrifice. In some rats, a polyethylene cannula was inserted, under anesthesia, into the aorta. In others, the organs were manipulated to simulate this procedure. The abdominal incision was closed with silk suture. Two of the sixteen rats were allowed 7-11 days to recover from this operative procedure prior to removal of tissues. Other rats were exposed to a single dose of 700-R whole-body x irradiation six days prior to removal of tissues. At the time of sacrifice, individual tissues were removed quickly; small sections were immediately weighed, then desiccated for four days over calcium oxide, and reweighed. The average water content of thymus and pituitary of surgically treated and recovered rats, and thyroid, pancreas, and pituitary of irradiated rats was slightly greater than that of controls, but differences were not significant. Liver and glandular tissues, such as thymus, thyroid, pancreas, and adrenal, generally contained less water than other tissues, with the exception of bone marrow. The moisture content of small intestine was lower than that of other regions of the gastrointestinal tract. No significant differences were observed between tissues of irradiated rats and normal controls. (BBB)

45897 THE RESPONSE OF X-IRRADIATED LIMBS OF ADULT URODELES TO NORMAL TISSUE GRAFTS. IV. COMPARATIVE EFFECTS OF AUTOGRAFTS AND HOMOGRAFTS OF COMPLETE FOREARM REGENERATES. Stinson, Benjamin D. (Cornell Univ., New York). J. Exptl. Zool., 157: 159-77(Nov. 1964).

As part of a continuing analysis of the mechanism by which normal grafts elicit regenerates on x-irradiated limbs, this investigation was designed to determine the possible differential effects of normal autoplastic and normal homoplastic transplants on irradiated upper arms of adult salamander, Triturus. Both forelimbs of adult newts were amputated through the distal third of the upper arm and allowed to regenerate for two months. Right limbs were then exposed to 2000 R of localized x irradiation on the 61st day. Surgical procedures were performed to test the response of irradiated limbs to (a) simple amputation, (b) amputation and ablation of distal humerus, (c) the same surgery and implantation of irradiated forearm regenerate autografts, (d) normal forearm regenerate autografts, and (e) normal forearm regenerate homografts. Irradiated limbs were reamputated through the grafts 16 to 18 days after transplantation. Most of the grafts had been revascularized and maintained the same orientation with respect to the stump as imposed experimentally. Most unirradiated left limbs, subjected to comparable surgery, underwent normal regeneration. Irradiated

limbs failed to regenerate following procedures (a), (b), and (c). Irradiated limbs formed regenerates with high frequency after procedures (d) and (e), but those formed in response to normal homografts proved abortive and regressed. Those formed in response to normal autografts persisted to yield complete hand regenerates in about half the cases. Such regenerates possessed an asymmetry and a proximodistal pattern of limb components reflecting the structure of the normal autograft, and were disharmonic relative to the irradiated stump. These findings favor the hypothesis that normal grafts mediate the formation of regenerates on irradiated limbs by serving both as a source of normal blastema cells and a source of morphogenetic stimuli. The evidence obtained supports the concept that tissues of the irradiated limb stump recover from radiation damage by virtue of their proximity to the normal transplant, or that diffusible substances emanating from the graft may reactivate or restore the regenerative capacity of the irradiated stump. (BBB)

45898 SEX AS A FACTOR IN AMBIVALENT CUE, DELAYED-RESPONSE PERFORMANCE BY RHESUS MONKEYS. McDowell, A. A.; Brown, W. Lynn (Univ. of Texas, Austin). J. Genet. Psychol., 103: 373-6(Dec. 1963).

Female rhesus monkeys were previously found superior to male rhesus monkeys on identical cue, spatial delayed-response learning and this superiority was attributed to their greater attentiveness, as experimentally demonstrated, rather than to a sex difference in intellectual ability. Of the 64 rhesus monkeys, ranging in age from 36 to 48 months, which were employed, 56 had been exposed to nuclear radiations at the Nevada Test Site 18 months earlier. The radiation doses varied from 119 to 252 R of γ radiation and 77 to 209 rep of neutron exposure, or total doses of 273 to 670 rem. All monkeys had been trained previously on identical cue, spatial delayed-response. Statistical analysis of the error data, using a nonorthogonal analysis of variance procedure, yielded a practice effect which was beyond the 0.001 significance level and a sex-by-practice interaction which was beyond the 0.025 significance level. Performance of the females was immediately almost asymptotic and initially superior to that of the males. The performance of the males gradually improved to the level shown by the females. The effect of previous γ plus neutron irradiation was not statistically evident. (BBB)

45899 RESPONSE PERSEVERATION UNDER CONSTANT STIMULUS-POSITION CONDITIONS BY NORMAL AND PREVIOUSLY IRRADIATED FEMALE RHESUS MONKEYS. McDowell, A. A.; Brown, W. Lynn (Univ. of Texas, Austin). J. Genet. Psychol., 106: 81-4(Mar. 1965).

Previously it was shown that female rhesus monkeys exhibit a greater tendency to position-postremity responses than male monkeys when the requirements of the test situation place no special premium on such responses. Evidence has been presented also for decreased distractibility and for the narrowing of attention in whole-body irradiated monkeys. If decreased distractibility and narrowing of attention are realities in whole-body irradiated subjects, whole-body irradiated females should manifest an accentuation of response perseveration under constant stimulus-position conditions, providing response to any condition is food-rewarded. This hypothesis was tested in monkeys that had been irradiated four years earlier. The training histories of control and irradiated monkeys were identical and included numerous Wisconsin General Test Apparatus (WGTA) tasks. The 13 whole-body irradiated monkeys used were the female survivors of nuclear irradiations. They were sorted into three groups, one of which contained the four controls; a second, the six irradiated subjects that had been exposed to total γ radiation doses of 273, 299, or 355 rem; and the third, the seven irradiated subjects that had been exposed to total doses of 397, 439, or 512 rem. Each monkey was tested in 24 trials per day for 10 days on response under constant stimulus-position conditions. Three test stimuli differing in multiple dimensions were used in constant positions on a three-food well-board with food under each of the three wells on every trial. Each monkey was allowed a single response on any given trial. A significant inverse relation was found between the tendency to shift response direction on successive problems and relative radiation dose. Also, a significant direct relation was found between max number of trials without shifting and relative radiation dose. In support of the hypothesis the results show an accentuation of response perseveration under constant food-rewarded stimulus-position conditions, an accentuation that is dose related. Although such results indicate greater response economy for irradiated than for normal monkeys, they also suggest a radiation-imposed restriction on the exploration of the possibilities inherent in a given situation. (BBB)

45900 RESPONSE-SHIFT LEARNING-SET FORMATION BY NORMAL AND PREVIOUSLY IRRADIATED FEMALE RHESUS MONKEYS. McDowell, A. A.; Brown, W. Lynn (Univ. of Texas, Austin). J. Genet. Psychol., 72: 339-42(Apr. 1965).

Rhesus monkeys will maximize the response-shift tendency after an initial rewarded response if the response shift is rewarded; i.e., they can acquire a response-shift learning set. The prepotent learning mechanism in response-shift learning set is behavioral inhibition of response to previously rewarded cues. This study tested the prediction of facilitated response-shift learning-set formation by previously irradiated monkeys. Four control and 13 whole-body irradiated monkeys were used; the latter were the female survivors of an exposure to nuclear radiations that took place more than four years earlier. Six irradiated monkeys that had been exposed to estimated total radiation doses of 273, 299, or 355 rem were considered together as Group 2, and seven that had been exposed to 397, 439, or 512 rem were considered together as Group 3. The training histories of the subjects were nearly identical and included numerous Wisconsin General Test Apparatus (WGTA) tasks. Each monkey was given 24 object-quality discrimination problems each day for 48 days. Treatment of the error scores over successive eight-day periods of testing, using an analysis-of-variance procedure, yielded a difference between groups beyond the 0.001 significance level and a practice effect also, beyond the 0.001 significance level. Orthogonal comparisons between groups also yielded a difference between control and irradiated subjects beyond the 0.005 significance level and a difference between the two groups exposed to radiations beyond the 0.05 significance level. The results support a hypothesis of facilitated response-shift learning-set formation by previously irradiated female monkeys. Correct responses varied directly with prior relative radiation doses. Thus, whole-body exposure to radiation facilitates behavioral inhibition of response to previously rewarded cues. (BBB)

45901 RADIATION-INDUCED SOMATIC MUTATIONS IN CYATHODIUM. Chatterjee, N. K.; Bhaduri, P. N. (Presidency Coll., Calcutta). J. Heredity, 56: 109-15 (May-June 1965).

Young thalli of Cyathodium tuberosum Kashyap were irradiated with a single acute dose of 4500 or 3000 R of x rays prior to culturing. From these plants, a mutant that remained stable during three vegetative generations was isolated. The following characters of the mutant were markedly different from those of the control plants: erect habit instead of prostrate overlapping habit; yellowish green thalli instead of green thalli; and more-frequent and deep-lobed thalli. Chromosome number ($n = 9$) and morphology were similar in both the mutant and control plants. A tentative explanation of the possible origin of the mutant is discussed in the light of cytoplasmic changes following irradiation. (auth)

45902 INDUCTION OF TOLERANCE TO BOVINE SERUM ALBUMIN BY MEANS OF WHOLE-BODY X-RADIATION. Linscott, William D.; Weigle, William O. (Scripps Clinic and Research Foundation, La Jolla, Calif.). J. Immunol., 94: 430-6(Mar. 1965).

The relation between the amount of antigen given after irradiation and the resulting degree of immunologic unresponsiveness was assessed. Duration of the unresponsive state, and its termination by injections of a cross-reacting antigen, were also investigated. Adult New Zealand rabbits given 500 or 550 R of 210-kv x radiation, followed two and seven days later by intravenous injections totaling 300 mg of bovine serum albumin (BSA), were unable to make antibodies against this antigen when appropriately challenged two months later. The degree of immunologic unresponsiveness observed was related to the amount of BSA injected during the first week after irradiation: 1 mg reduced the subsequent antibody response after challenge by 70%, 12 mg reduced it by 95%, and 300 mg reduced it by more than 99%. The resulting unresponsive state was specific, in that tolerance to BSA did not occur following irradiation and injection of 300 mg of human γ-globulin. The unresponsive state was much less complete four months after irradiation and treatment with BSA than it was at two months. The amount of BSA per kg of body weight required to induce tolerance appeared to be about the same for irradiated adult rabbits and for neonatal rabbits. Neonatal rabbits given 500 mg of BSA during the first week of life became similarly unresponsive, but retained their tolerance longer than irradiated adults. Radioiodinated (^{131}I) BSA was used to determine serum antibody titers by scintillation counting of immune precipitates. (BBB)

45903 RADIOSENSITIVITY OF THE IMMUNE RESPONSE TO SHEEP RED CELLS IN THE MOUSE, AS MEASURED BY THE HEMOLYTIC PLAQUE METHOD. Kennedy, J. C.; Till, J. E.; Siminovitch, L.; McCulloch, E. A. (Univ. of Toronto). J. Immunol., 94: 715-22(May 1965).

The depressant effect of ^{60}Co γ radiation on hemolysin production of spleen cells was studied in C57BL/6J mice given whole-body doses from 0 to 700 rad. The in vitro assay system using the plaque-forming ability of isolated spleen cells on blood-agar plates was employed to measure antibody response. When antigen (sheep red cells) was given within 2 hr after irradiation of the mice, the survival curve was found to be a simple negative exponential, with a D_{37} of 80 rad. No significant change in this curve was found when an interval of 10 days separated irradiation and antigen injection, indicating that radiation-induced damage to the immune system was not repaired during this interval. The capacity of plaque-forming cells to form plaques was found to be much less sensitive to radiation than capacity of the animals to produce plaque-forming cells. No decrease in the capacity of plaque-forming cells to form plaques was found for doses of radiation up to 2 krad. It is suggested that the spleens of normal mice contain a minimum of 10^3 cells which do not themselves produce hemolysin, but respond to the injection of antigen by proliferation and differentiation into hemolysin-producing cells. Further, when these cells (termed antigen-sensitive cells) are rendered incapable of proliferation by radiation they are not replaced to a significant degree for a period of at least 10 days. Failure to demonstrate repair of radiation damage has practical significance, since it indicates that animals that have received 800 rad can serve as inert recipients for the transplantation of isologous cellular grafts whose response to antigen may then be studied. It is possible that the postulated antigen-sensitive cells do not proliferate in the absence of antigen, even in irradiated hosts, and that new antigen-sensitive cells are produced only slowly by the division of more primitive precursor cells which are themselves not sensitive to the presence of antigen. Such a mechanism could account for the long delay in regeneration of the immune response observed. (BBB)

45904 CONTINUOUS IRRADIATION AT LOW DOSE RATE ON EGGS OF BOMBYX MORI AND THE CONCEPT OF EFFECTIVE DOSE RATE. Teulade, P. (Faculte des Sciences, Lyon). J. Insect Physiol., 11: 379-86(Apr. 1965). (In French).

Recovery from low-dose continuous irradiation was investigated in the silkworm. When the eggs are submitted to low-level continuous γ radiation from ^{60}Co at the dose-rates of 15 and 37 R/hr, it was found that for a similar total dose delivered at these dose rates, the effects with 37 R/hr were more pronounced than those with 15 R/hr. The time of development and mortality increased as a linear function of the dose. Recovery took place during irradiation and partly counter-balanced the lethal effect of radiation, thus limiting the efficient dose rate. Therefore, only a fraction of the total dose delivered in a continuous low-level irradiation is effective. This explains the significance of the dose rate. The linear relation between the total dose and the effects seem to be the result of a combination between the efficient dose rate and fluctuations of radiosensitivity in relation to embryonic development. At the higher dose rate (37 R/hr) the mortalities at various total doses were: 18.5% at 900 R, 19.3% at 1820 R, 62.2% at 4460 R, 97.1% at 8230 R, and 98.0% at 12,400 R. At the low dose rate (15 R/hr), mortality was maximum (11.1%) at a total dose of 2160 R. (BBB)

45905 EYE DISEASE FROM NATURAL AND MAN-MADE RADIATION. Dias, John F. J. Intern. Coll. Surgeons, 43: 505-13(May 1965).

The effect of various forms of radiation, encompassing the whole spectrum from radio waves to cosmic rays, on ocular tissues is reviewed. A common mechanism of eye damage operates at all wavelengths: when the photon is absorbed, heat is liberated, and the damage which is done by this heat depends on the transparency of the tissues to the particular wavelength, the density of various tissues (causing some tissues to absorb more photons than others), the energy of the photon, and the degree to which the various tissues are cooled by the blood. The relative transparency and opacity of the optic globe to various wavelengths are illustrated. The globe is essentially pervious to cosmic rays and γ rays as well as to x rays. Cosmic rays, to which the body has adapted since the beginning of life, have no discernible effect on the eye. Beta rays may be absorbed by the eye and produce the greatest effect on the cornea and the lens, two structures that are denser than the rest of the eye and that are not cooled by circulation. The cornea is slightly more resistant than the lens, since it is cooled by evaporation of tears. Again, natural radiation is no hazard. The γ radiation produced by thermonuclear explosions is a small problem as far as the eye is concerned because any quantity of γ rays that will injure the eye usually is fatal to the whole organism. X rays have a similar pattern of absorbability as γ rays. The natural x rays which originate in various interstellar spaces, presumably from neutron stars, present no danger. Usually, the disease produced in the eye by x rays is cataract, which appears as a disc-shaped opacity at the posterior pole, often surrounded by powder-like opacities and sharply demarcated from the rest of the lens. Later, dot-like opacities, vacuoles and opaque striae appear under the anterior capsule, forming a dense white disc, described as asbestos-like. The γ rays released by the atom bombs at Hiroshima and Nagasaki produced 45 cases of radiation cataract in persons who were sufficiently shielded from whole-body irradiation to survive. All of them were epilated by the radiation and several suffered radiation sickness. Other structures of the eye are sensitive to radiation if it is sufficiently intense. It is important to protect the eye whenever tumors of the head are irradiated. The action of uv, ir, and other types of radiation on the eye is also considered. Theoretically, sufficient radiation damage could be sustained by uv light to cause necrosis of the cornea, but this is rare. Large quantities of uv radiation are produced by thermonuclear weapons but the production of the uv as well as ir light is spread over a period of three or four sec, allowing exposed persons time to close their eyes. Consequently, there were no cases of corneal injury reported at Hiroshima or Nagasaki. (BBB)

45906 DIFFERENTIAL CHEMICAL CARCINOGENESIS IN THREE DISTINCT MELANOCYTE SYSTEMS OF SYRIAN (GOLDEN) HAMSTERS. Mishima, Yutaka; Oboler, Allen A.

(Wayne State Univ., Detroit). J. Invest. Dermatol., 44: 157-69(Mar. 1965).

During the course of induction of melanomas in hamster skin by topical application of 7,12-dimethylbenz(a)anthracene (DMBA), melanocyte-activating studies using uv irradiation were carried out with a Mineralight. Untreated hamsters were irradiated over a period of 23 days. The animals' right dorsum was exposed 17 times; each exposure was for 3 min at a distance of ten in. from the uv source. Within the 11th week after the initiation of DMBA painting, minute black flecks were first noted. At about the 18th week the flecks became larger, raised, and more numerous. After 50 weeks every hamster carried between 50 and 150 clinically visible deep blue black melanotic tumors of various sizes. In the epidermis after irradiation, enzymically active melanocytes were found in two previously undescribed sites, the hair sheath and dermal melanocyte foci. The hair sheath melanocyte was observed as a dopa- and premelanin-reaction-positive dendritic melanocyte which is demonstrable in the outer sheath layer of the hair follicle particularly after irradiation. The distinctive dopa- and premelanin-reaction-positive dendritic melanocyte in the hair infundibulum has not been reported before. The previously existing dopa-positive melanocytes of the hair bulb were slightly intensified in melanogenic activity after uv irradiation. Dermal melanocytes were found in irradiated skin as amelanotic oval, bipolar, and/or slightly dendritic dopa- and premelanin-reaction-positive cells. The results suggest that there is an amelanotic (nonpigmented) or minimally active melanocyte system in the hair sheath and diffusely in the dermis in addition to the actively melanin-forming (pigmented) hair bulb melanocytes in normal golden hamster skin. The amelanotic, minimally functional dermal melanocytes, particularly those near hair follicle, in response to DMBA convert to melanotic melanocytes which, simulating the previously proposed melanotic perifollicular melanocyte process, proceed to form blue nevi predominantly around hair follicles. (BBB)

45907 ULTRASTRUCTURAL CHANGES INDUCED BY ULTRAVIOLET LIGHT IN HUMAN EPIDERMIS: BASAL AND SPINOUS LAYERS. Nix, Thomas E. Jr.; Nordquist, Robert E.; Scott, J. Randolph; Everett, Mark Allen (Univ. of Oklahoma, Oklahoma City). J. Invest. Dermatol., 45: 52-64(July 1965).

Four times the minimal erythema dose of medium pressure, mercury vapor irradiation filtered through 2 cm of water was administered to the left lumbar area of a 24-yr-old, healthy Caucasian male. Biopsy specimens were taken from the irradiated site and thin sections were prepared for electron microscopy after uranyl acetate staining. Thick sections were also cut from the same specimens, and crystal violet and periodic acid-Schiff stains were used on these sections examined by light microscopy. Numerous cytoplasmic vacuoles were observed in basal and spinous layer keratinocytes at one, three, and 12 hr postirradiation, but the number of vacuoles had returned to normal by 72 hr except for a few which appeared in the granular layer. Irregular dense bodies, thought to be lipid inclusions, appeared in basal layer keratinocytes 12 hr postirradiation. There, cytoplasmic dense bodies were found in the granular layer at 72 hr, evidently as a result of upward migration of cells containing them. Numerous irregular dense bodies of similar morphology were observed in a few high level branched cells in irradiated epidermis. It is suggested that these postirradiation ultrastructural changes in epidermal cells are not degenerative in nature, but indicate accelerated metabolic activity. Vacuoles and irregular dense bodies are seen in small numbers in normal, unirradiated epidermis. They differ in irradiated cells only by their increased number, and not by any variation in structure. Moreover, no fragmentation or other structural change indicative of degeneration was observed in any of the other organelles of irradiated epidermal cells. No mitoses were seen in the irradiated specimens by either light or electron microscopy. (BBB)

45908 INFLUENCE OF PATHOGENS ON THE LIFE SPAN OF IRRADIATED INSECTS. Jafri, R. H. (Laboratoire de Cytopathologie, St-Christol-Les-Ales, France). J. Invertebrate Pathol., 7: 66-70(Mar. 1963).

Survival of flour beetles after exposure to x radiation and infection with some of their natural pathogenic bacteria was investigated. The beetles infected by A. tribolii were more susceptible to B. thuringiensis infection than were uninfected beetles. T. castaneum adults infected with F. tribolii were more radio-sensitive to 1000, 10,000, 30,000, 50,000, and 90,000 R doses of x rays than noninfected ones. The beetles receiving B. thuringiensis and having F. tribolii infection were much more damaged by sublethal and lethal doses of ionizing radiation. When T. confusum beetles received B. thuringiensis following exposure to sublethal and lethal doses of x rays their life span was shortened to a week or at the most to two weeks. Neither sex showed any significant increased or decreased susceptibility when they received B. thuringiensis immediately and after an interval of 24 and 144 hr following exposure to sublethal and lethal doses of x rays. Ionizing radiation appears to act in the same way as B. thuringiensis, disintegrating the gut tissues and enabling the transgression of midgut bacteria into the body cavity of the host. (TCO)

45909 EVIDENCE FOR REPAIR-REPLICATION OF ULTRAVIOLET DAMAGED DNA IN BACTERIA. Pettijohn, David; Hanawalt, Philip (Stanford Univ., Calif.). J. Mol. Biol., 9: 395-410(Aug. 1964).

Thymine-^{14}C or -^{3}H and 5-bromouracil-^{14}C were used with the density labeling ultracentrifugal technic to follow DNA replication in uv-irradiated bacteria. The partial degradation of the damaged DNA and simultaneous synthesis at random positions in the genome was demonstrated. This nonconservative mode of replication eventually resulted in density heterogeneity (due to differences in the 5-bromouracil-thymine ratio) among the isolated DNA fragments. Normal semiconservative replication was observed if photoreactivating conditions followed the uv irradiation prior to density labeling. Molecular fragments containing these regions of random replication were thermally denatured and/or fragmented by sonication. Density-distribution analysis in the CsCl density-gradient indicated that the density label was incorporated into very short segments along single DNA strands. These findings are consistent with the view that in uv-resistant organisms a mechanism for repair replication exists in which damaged single-strand regions of the chromosome can be excised and replaced, using the undamaged DNA strand as template. Photoreactivation removes blocks to normal DNA replication and presumably eliminates the repair events. Evidently the same lesions repaired by photoreactivation also lead to repair replication. With the uv irradiation dose used, normal replication was not restored during later growth in the dark. This suggests that a portion of the damage, though photoreactivable, is not repaired in the dark. (BBB)

45910 FACTORS AFFECTING MORTALITY FROM SECONDARY DISEASE IN MOUSE RADIATION CHIMERAS. Congdon, C. C.; Kastenbaum, M. A.; Gardiner, D. A. (Oak Ridge National Lab., Tenn.). J. Natl. Cancer Inst., 35: 227-34(July 1965). (ORNL-P-1078).

Cumulative 90-day mortality was determined in (101 × C3H/Anf)F_1 (1C3F_1) male and female mice exposed to 950 R x radiation and treated intravenously with bone marrow transplantation from (C57BL/6 × DBA/2)F_1 (B6D2F_1) male or female donors. In 4 factorial experiments, dose of donor marrow cells, day of injection, age of donor cells, and sex were studied as independent and interacting variables for their relationship to the cumulative mortality. Deaths among cages of mice did not follow a random distribution pattern, which introduced a cage effect problem in the studies. Dose of cells, day of injection, and sex failed to influence 90-day mortality when they were treated as independent or single-factor variables. Age of donor marrow was a significant factor because 7- and 14-day-old donors were associated with fewer 90-day cumulative deaths than 21- or approximately

91-day-old donors. An unusual finding was the low mortality in center point groups that received 30×10^6 cells on day $1\frac{1}{2}$ when the donor marrow was 44 to 61 days old. Presumably these center point groups represent an unexplained and unexpected interaction of variables. Combining the findings in the center point groups with the effect of age of donor cells gave the least 90-day cumulative mortality yet observed in the completed portion of the fourth factorial experiment. All surviving mice tested in these experiments had red blood cells of the donor bone marrow type. (auth)

45911 CHROMOSOMES OF TUMOR CELLS. IV. CELL POPULATION CHANGES IN THYMUS, SPLEEN, AND BONE MARROW DURING X-RAY-INDUCED LEUKEMOGENESIS IN C57BL/6J MICE. Joneja, M. G.; Stich, H. F. (Queen's Univ., Kingston, Ont.). J. Natl. Cancer Inst., 35: 421-34(Sept. 1965).

The incidence of chromosome aberrations and of cells with abnormal chromosome complements was estimated in the thymus, spleen, and bone marrow preleukemic, leukemic, and nonleukemic C57BL/6J mice that received repeated total-body irradiations. In early stages of leukemogenesis the normal cell populations of the thymus, spleen, and bone marrow, consisting predominantly of diploid cells, changed into genetically heterogeneous ones, consisting of cells with abnormal chromosome numbers, marker chromosomes, or both. At 7 weeks after irradiation the incidence of chromosomally abnormal cells in the spleen and bone marrow was greatly reduced, whereas clones of chromosomally abnormal cells became established in the thymus of most irradiated mice. All 10 thymic lymphosarcomas examined consisted of cells with abnormal chromosome complements. The presence of particular marker chromosomes in most leukemic cells of a mouse suggests that they originate from one parent cell. Clones of chromosomally abnormal cells were also observed in the spleen and bone marrow of 2 of 5 irradiated but apparently nonleukemic mice 9 months after irradiation. The particular behavior of the cell population of the thymus, the significance of a genetically heterogeneous cell population in preleukemic mice, and the possible role of environment conditions in tissue are discussed. (auth)

45912 NURSING CARE OF THE PATIENT WITH RADIATION SICKNESS. Korsos, Ruth C. (Brookhaven National Lab., Upton, N. Y.). J. Pract. Nursing, 14: 24-6(Oct, 1964). (BNL-8447).

There is no standard routine to be followed by the nurse treating a patient with radiation sickness. Each patient presents individual problems and requires individual management. The patient whose reactional syndrome results from radiotherapy requires attention also for the disease which necessitated the treatment. The victim of accidental exposure to penetrating rays confronts medical personnel with a different complex picture. Mechanical and thermal injuries may add to his nursing care needs. An early problem confronting the nurse is that of nutrition. The importance of encouraging the patient to eat and drink adequately is emphasized. Visitors should also be restricted. Nausea and vomiting may be lessened if a brief rest period is included before and after each radiation treatment. Meticulous attention must be given to the patient's clinical behavior. The victim of a radiation accident requires a different medical management from that planned for the patient whose radiation sickness is from therapy. The nurse's report on the patient's chart must include pertinent data concerning symptoms of nausea, vomiting, and diarrhea. She must observe the patient carefully and be prompt to report any change in vital signs, such as temperature, pulse, respiration, and blood pressure. (BBB)

45913 ULTRASTRUCTURAL CHANGES INDUCED BY ULTRAVIOLET LIGHT IN HUMAN EPIDERMIS: GRANULAR AND TRANSITIONAL CELL LAYERS. Nix, Thomas E. Jr.; Nordquist, Robert E.; Everett, Mark Allen (Univ. of Oklahoma, Oklahoma City). J. Ultrastruct. Res., 12: 547-73(June 1965).

Electron microscopic findings of epidermal changes studied in biopsies of human skin taken one hr to one week after a single exposure to uv light are presented. The exposure was four times the minimum erythema dose of water-filtered, medium-pressure Hg vapor. The one- and three-hr samples showed no alterations. There were no alterations in either the irradiated or control specimens at one and three hr postirradiation. Changes in the cells of the stratum granulosum at 12 hr postirradiation included increase in numbers and thickness of tonofibrils, and the presence of striations in the infoldings of the granular cell plasma membrane where it adjoins the stratum corneum. The diameter of the striations was 55 Å, and they were separated by electron-light intervals of 42 Å. Changes present at 72 hr postirradiation included: increase in thickness of stratum granulosum and in numbers of dense, round 50- to 200-mμ bodies; vacuolation and presence of occasional granular cells with a diffuse decrease in electron density; presence of irregular dense bodies measuring 0.48μ in longest axis. Peculiar, finger-like extensions of the stratum corneum into the stratum granulosum were observed at 72 hr. Transitional cells were observed at the junction of the stratum granulosum and stratum corneum and were thought to be more numerous than in the control, unirradiated epidermis. Transitional cells varied greatly in structure from one cell to another. Some were comparable in structure to the A_2 and B_1 cells described in hyperkeratotic psoriasis. Several contained large masses of dense material which were dissimilar to keratohyalin. (TCO)

45914 IMMUNE RESPONSE OF EHRLICH ASCITES TUMOR CELLS IRRADIATED IN VITRO. Umehara, Yoji (Kobe Medical Coll., Japan). Kobe J. Med. Sci., 10: 265-76(Dec. 1964).

Since radiation damages cell membranes, the irradiated mammalian cell might show a different response to antibody from that of the nonirradiated cell and the difference might afford a clue for elucidating the mechanism of radiation injury on mammalian cells. It might also have implications on the radiotherapy of malignant tumors from a practical point of view. The immune response of irradiated Ehrlich ascites tumor (EAT) cells exposed to anti-EAT γ-globulin in vitro, was investigated. The viability of cells was examined by staining with crystal violet or nigrosin at various time intervals after ^{60}Co γ irradiation with doses of 50, 100, 300, and 500 R. Percentage survivals after 90-min incubation were 90% at 100 R and 84% at 500 R. Since dead cells would show altered permeability, corrections for these death rates were made in all experiments. Irradiated cells (500 R) take up more anti-whole cell EAT immune γ-globulin (^{131}I labeled) than nonirradiated cells and this effect was exhibited only against immune γ-globulin or radioiodinated human serum albumin (RISA), but not against normal γ-globulin. Among the five subcellular fractions differentiated, only mitochondrial and microsomal fractions showed a significant difference of radioactivity between the irradiated and nonirradiated cells. Since the mitochondrial fraction demonstrated a significant difference of γ-globulin radioactivity between irradiated and nonirradiated cells with anti-whole cell antibody, anti-mitochondrial immune γ-globulin was tested in the same way, but no difference in penetration was observed between them. Thus the antibody to the surface membrane of cells is responsible for the higher penetration of macromolecules by irradiation. With nonirradiated cells the permeability of cells is enhanced by the antigen-antibody reaction in presence of complement, but not in presence of inactivated complement, while, with irradiated cells, permeability is decreased by antigen-antibody reaction in presence of active or inactive complement. Active complement is suppressed by irradiation (inactivation), while heat-inactivated complement is not affected by irradiation. The results demonstrated that membrane permeability of cells is changed by irradiation and more immune γ-globulin penetrated into the interior of the cell across the membrane. (BBB)

45915 CYTOGENETIC STUDIES IN CHRONIC MYELOID LEUKEMIA AND ACUTE LEUKEMIA ASSOCIATED

WITH MONGOLISM. Tough, Ishbel M.; Court Brown, W. M.; Baikie, A. G.; Buckton, Karin E.; Harnden, D. G.; Jacobs, Patricia A.; King, Margaret J.; McBride, J. A. (Western General Hospital Edinburgh). Lancet, 1: 411-17(Feb. 25, 1961).

Results are reported of chromosome cultures in 18 patients with chronic myeloid leukemia, three of which later entered the acute phase. In four cases, chromosome anomalies which were attributed to previous x-ray exposure were seen. These four irradiated cases showed many cells which contained gross structural abnormalities of the chromosomes, including ring chromosomes, dicentric chromosomes, and fragments of chromosome material. In addition, the chromosome count distributions were abnormal in one case. These four patients had all been treated by radiotherapy for their leukemic condition less than eight weeks before their blood was cultured. It was thought that, with the exception of the Ph^1 chromosome, the changes noted in these cases were induced by x-ray exposure. This explanation was supported by the findings in further blood cultures in three cases 14 to 22 weeks after the cessation of radiation exposure. In two cases the abnormalities were appreciably less, and in one case they were no longer present. All of these irradiated patients had been exposed either to localized splenic irradiation or to wide-field irradiation of the abdomen, using medium-kilovoltage x rays. The Ph^1 chromosome was seen in all four untreated cases, in eight of 11 treated cases, and in one of three cases examined after they had passed into a phase of acute leukemia. Thus, the Ph^1 chromosome was found in 12 out of 15 patients diagnosed as having chronic myeloid leukemia, and in one of three patients who had passed from the chronic leukemic state into that of acute leukemia. Five examples of acute leukemia in mongols were also studied, but in none of these was any chromosome abnormality found other than that associated with mongolism. The difference in frequency of the Ph^1 chromosome between those cases showing radiation damage and the other treated cases is significant. One explanation might be that the cells carrying the Ph^1 chromosome were more sensitive to the radiation-induced damage than were cells with a normal chromosome complement. In two cases there was a high probability that the leukemia had been induced by radiation. Both patients had been treated with x rays for ankylosing spondylitis; one with six courses of irradiation 7 to 11 yr before leukemia diagnosis the other having been irradiated one yr before diagnosis of leukemia. (BBB)

45916 QUANTITATIVE STUDIES OF CHROMOSOME ABERRATIONS IN MAN FOLLOWING ACUTE AND CHRONIC EXPOSURE TO X RAYS AND GAMMA RAYS. Court Brown, W. M. (Western General Hospital, Edinburgh); Buckton, Karin E.; McLean, A. S. Lancet, 1: 1239-41(June 12, 1965).

The possibility of using chromosome aberrations in certain types of small lymphocytes to demonstrate human radiation exposure was tested in three populations (normal controls, x-irradiated ankylosing spondylitis patients, and occupationally exposed persons). The latter category consisted of randomly chosen control workers (group A), nonscheduled control workers (B), and three groups (C, D, E) with cumulative doses of 1-9, 23-24, and 76-98 rad of γ rays, respectively. Data were evaluated on the basis of cultured unstable cells (C_u cells), differentiated from other cells (C_s cells) showing stable chromosome rearrangements such as reciprocal translocations. There were no important differences in the frequencies of cells with aberrations for control men aged 15-65 yr. Over 65 yr there was some evidence that the frequency of cells with either type of aberration may increase. The control frequency of C_u cells was taken as about 0.7% and that of C_s cells as about the same. In C_u cells from people in the general population, more than a single acentric fragment is unusual. By definition most C_u cells are visually recognizable, but this is not necessarily true for C_s cells. The frequency of C_u cells would be expected to provide a more reliable indicator of the effect of irradiation. In the irradiated spondylitis cases, the levels were increased in both C_u(23.4%) and C_s(10.3%) cells. The spondylitis data indicated that the level of C_s cells remains unchanged for at least eight years, and earlier data, although less reliable, suggested that a detectable increase in the frequency of C_s cells was present after exposure for up to 20 years. There was no significant difference in the frequency of C_u cells between A, B, and C, and these were combined for comparison with the combined data of groups D and E. The frequency of C_u cells in the latter two groups was found to show a highly significant increase. These changes are reflected also in the frequency of cells containing a dicentric chromosome (2.0% vs 0.7% in controls). The failure to demonstrate a greater difference between the C_u cells of group D and E was not surprising. While there was an ~ threefold difference in cumulative doses, a comparable difference in the yield of unstable aberrations as measured at present is not to be expected. Most of the dose accumulated by the men of group E was received before 1958, after which the mean annual dose was halved. It is concluded that the frequency of certain types of chromosome aberration is increased in small lymphocytes after exposure to ionizing radiations. It may be possible to apply this technique as a quantitative indicator of exposure to low doses of ionizing radiations, but this will depend upon the standardization of the conditions of culture and upon the development of an automated procedure for chromosome analysis. (BBB)

45917 EXPOSURE TO X RAYS AND GAMMA RAYS. Court Brown, W. M. (Western General Hospital, Edinburgh); Buckton, Karin E.; McLean, A. S. Lancet, 1: 1399(June 26, 1965).

Supplementary data are provided to the earlier report of chromosome changes in small lymphocytes caused by ionizing irradiation, by Court Brown, et al. Details of the radiation exposure of the patients treated for ankylosing spondylitis are stated. All the patients whose results are recorded in the earlier article were treated with medium kilovoltage x rays (half-value layer, 2.7 mm Cu), treatment being given through posteriorly placed fields to the whole length of the spine and the sacroiliac joints. The field running the length of the spinal axis was 7.5 cm in width and an average 55 cm long, while that over the sacroiliac region was 15 × 10 cm, the long side at right angles to the spinal axis. The total skin dose was 1500 rad inclusive of back-scatter, and this was mostly given in 10 equal fractions at daily intervals apart from weekends. There was sometimes a gap of a few days between the first fraction and the second, the remaining fractions being given at daily intervals. The dose-rate, which varied slightly depending on the size of the field, was about 67 rad/min. No patient had more than one course of treatment, and all observations were made on cells cultured for 40 to 50 hr. (BBB)

45918 THE RECTAL MUCOSA AS A BIOLOGIC INDICATOR OF RADIATION INJURY. I. PRELIMINARY CYTOPATHOLOGIC OBSERVATIONS. White, David C.; Persing, Ronald L. (Armed Forces Inst. of Pathology, Washington, D. C.). Med. Ann. Distr. Columbia, 34: 68-74(Feb. 1965).

The need and basis for establishment of a sensitive, accurate biologic criterion of radiation injury are discussed, and experiments were conducted in rats to evaluate the usefulness of biopsied rectal mucosa in this regard. A baseline cytopathologic picture was established, and analyses were made of rectal mucosa at two dose levels, 200 and 800 R, with postexposure time intervals of 1, 6, 12, 24, and 48 hr. A duplication of this biopsy study was made with shielding of the thorax, head, and upper extremities to assess any possible variance in response between whole-body and primarily gastrointestinal radiation. The young adult female Sprague-Dawley rats (3 to 4 months of age) were exposed to x rays of 300-kvp at dose rates of 56 to 60 R/min. The sequence of the radiation response at different dose levels, as seen histologically, is described in detail. Certain dose-dependent differential features were evident, and these are discussed. Cellular response to the radiation occurs promptly and is readily detectable with-

in two to three hr down to the 50 to 100 R level. There follows a rapid progression of events; that is, the initial sequence of dynamic histopathology is completed within 48 hours, with subsequent pathologic features developing more slowly and with less distinctive relation to time after exposure. The timing of these early events closely correlates with postexposure interval, and is thus of value. The cytopathologic picture itself is only roughly proportional to the total dose and requires careful interpretation to be meaningful. It is concluded that the characteristic morphologic alterations induced by radiation in the mucosa of the rectum as investigated by biopsy techniques provide a specific post-exposure timetable of histopathologic events and a roughly quantitative relationship to total dose. (BBB)

45919 EFFECT OF ULTRAVIOLET IRRADIATION ON THE PROPERDIN LEVEL OF PIGS' SERA IN VITRO. Szemere, G. (Medical Univ., Szeged, Hungary). Med. Pharmacol. Exptl., 12: 366-72(1965).

The high properdin levels and strong resistance of rats to infections is known. Susceptibility of irradiated rats to severe bacteriemia of intestinal origin suggests that the properdin system may be destroyed by irradiation. The properdin level falls significantly in the early post-irradiation period. While sera of untreated animals have bactericidal and virus-neutralizing effects, sera of irradiated animals have no such properties. As ionizing irradiations reduce the properdin level in vivo, the possibility was examined that in vitro irradiation reduces the properdin level of sera and that treatment of sera either with uv or x rays would provide a method for preparing properdin-deficient (RP) sera required for properdin determinations. In the course of preparing RP serum from pig blood, samples either before or after the zymosan treatment were exposed to uv irradiation for 5, 10, 15, or 20 min. The thickness of the serum layer was 2 mm, a 500-w, S 300 Hanau lamp was used, and irradiation was done from a distance of 30 cm, through a UG-2 filter. A sublytic amount of R'3 serum deficient in the third complement-component, but containing all the others was added to a sensitized sheep erythrocyte suspension for testing serological reactions. The results showed that the properdin titer is not markedly altered even by a prolonged uv irradiation. This, it is suggested, is due to the fact that in course of their evolution living organisms have been exposed to and become adapted to the effect of uv rays, thus their immunological systems are not altered by this kind of radiation. It is considered remarkable that a comparatively labile serum protein like properdin can tolerate the prolonged, direct effect of uv rays without being significantly damaged. (BBB)

45920 BIOLOGICAL FACTORS OF THE RADIOSENSITIVITY OF NEOPLASTIC METASTASES. De Gaetani, G. F. (Universita, Turin, Italy). Minerva Radiol., Fisioterap. Radiobiol., 10: 196-201(June 1965). (In Italian).

Biological factors capable of interferring with metastatic growth and with the radiosensitivity of a metastasis were reviewed to show the complexity of the problem. The factors that can intervene at the level of the tumor itself, at the organ site of the metastases, and the organism were considered. (J.S.R.)

45921 BIOLOGICAL FACTORS OF THE RADIOSENSITIVITY OF METASTASES. Verga, V. (Universita, Naples). Minerva Radiol., Fisioterap. Radiobiol., 10: 201-30(June 1965). (In Italian).

The factors and mechanisms of radiosensitivity are considered in a discussion limited to the metastases of epithelial tumors. The cellular radiosensitivity and the mechanisms that determine it are discussed. The radiosensitivity of tumors in general with emphasis on special factors of the radiosensitivity of the metastases is discussed. The results of an experimental study on the growth of transplanted tumors in white rats after irradiation are reported. The results of histological, histochemical, fluorescence, and electron microscopic investigations are given. Clinical-radiological and clinical-statistical observations on patients suffering with various types of cancers are tabulated and discussed. (J.S.R.)

45922 ANATOMICAL AND FUNCTIONAL MODIFICATIONS OF THE INTESTINE DURING THERAPEUTIC TREATMENTS. De Giuli, G. (Universita, Firenze, Italy). Minerva Radiol., Fisioterap. Radiobiol., 10: 231-4(June 1965). (In Italian).

The studies undertaken at the Instituto di Radiologia of Firenze in the last 5 years on the results of intestinal irradiations in patients are reviewed. The research included the following areas: daily reporting of the clinical symptoms, traditional coprological studies, radiological studies, assimilation studies, investigation of the eventual passage of large molecules from the blood to the intestine, determination of the pancreatic and bile enzymes contained in the daily samples, and histological studies of bioptic samples. (J.S.R.)

45923 EFFECTS OF IONIZING RADIATION ON PROLIFERATING CELLULAR SYSTEMS. Bresciani, F. (Universita, Naples). Minerva Radiol., Fisioterap. Radiobiol., 10: 235-44(June 1965). (In Italian).

The types of proliferating cellular systems are described and the methods used to study cellular proliferation are given. The theoretical model of the radioactive mitotic wave after instantaneous labelling of DNA and the lifetime of various phases of the proliferation cycle are reported. The radioactive mitotic wave after instantaneous labelling of the BNL sarcoma is also reported. The structure of a proliferating cellular system and the effects of radiation on such a system are shown. Experimental studies were made with the BNL sarcoma in vivo and the results are given. These results show that in the BNL sarcoma the irradiation interferes with various stages of the proliferating process. General considerations are made on the mechanism of the inhibition and irradiation aplasia of the proliferating cellular systems. The therapeutic possibilities are indicated. (J.S.R.)

45924 IRRADIATIONS AND SEROPROTEIC PICTURE IN TUMOR CARRIERS. ELECTROFORETIC RESEARCH IN NATURAL AND DENATURED SERA. Dragoni, G. (Universita, Milan). Minerva Radiol., Fisioterap. Radiobiol., 10: 245-55(June 1965). (In Italian).

Electrophoretic studies were made of the natural and denatured sera of 72 patients with malignant tumors. The seroproteic behavior with respect to the radiation treatment was determined. The results were discussed with respect to the type of tumor—neoplasia, mammary neoplasia, connective neoplasia—and not with respect to the type of radiation treatment in the individual cases. The results show that it is possible to know within certain limits the whole of the repercussions of the neoplastic malady on the organism and the course that this can assume following therapeutic treatment. It is shown that thermal denaturation can lead to the distinction between normal sera and pathological sera and to the detection of abnormal conditions of the sera. (J.S.R.)

45925 MORPHOGENESIS OF THE NUCLEAR ANOMALY FROM SMALL DOSES OF X RAYS. Rondanelli, E. G. (Universita, Pavia, Italy); Trenta, A.; Vannini, V.; Parma, A.; Gerna, G. Minerva Radiol., Fisioterap. Radiobiol., 10: 256-61(June 1965). (In Italian).

Morphogenesis of nuclear anomalies from small x-ray doses was studied on various phases of the karyokinesis in erythroblasts of Triton cultivated in vitro and studied in the living state after irradiation of the culture with doses of the order of 12 or 25 R. Observations were made by microphotography, microcinematography, and direct observation. The results showed that the anomalies can be divided into three groups: anomalies of dimension, of form, and of number. The morphogenesis of each of these types of anomalies is briefly described and illustrated. (J.S.R.)

45926 EXPERIMENTAL RESEARCH ON THE POSSIBILITY OF INDUCING CONDITIONS OF RELATIVE RADIORESISTANCE IN INTESTINAL TISSUES. Biagini, C.;

Centi Colella, A.; Trinci, M. (Universita, Rome). Minerva Radiol., Fisioterap. Radiobiol., 10: 273-4(July-Aug. 1965). (In Italian).

Albino rats were exposed to whole-body irradiation of ^{60}Co γ rays administered in single doses of 200, 600, and 700 R after daily irradiations of 50 to 70 rad for 16 to 18 days. Other animals received only the single exposure of 200, 600, or 700 R. The animals were sacrificed after the final exposure and the mitoses in the crypts of intestinal tissues and the number of crypts containing destroyed cells were determined. The results were tabulated and show a reduction of the mitoses per crypt directly proportional to the dose of irradiation for the single exposure. For fractionated exposures the effects on the mitoses are less, with the results proportional to the accumulated dose. The values of the mitotic index expressed in terms of per cent reduction with respect to the control group are also tabulated. The results have not shown the establishment of a condition of radioresistance, understood as an acquired smaller sensitivity to radiation. The increase of the number of destroyed cells in the irradiated animals seems to reach a limiting value at 600 R. The presence of a summation effect was indicated. (J.S.R.)

45927 HISTOCHEMICAL BEHAVIOR OF SOME ENZYMES OF THE INTESTINAL MUCOUS IN IRRADIATED ANIMALS. Calzavara, F.; Pozza, F. (Universita, Padua). Minerva Radiol., Fisioterap. Radiobiol., 10: 274-9(July-Aug. 1965). (In Italian).

The detection of intestinal lesions from the behavior of some enzymes and the possibility of observing a distinction with respect to x and γ radiations were studied on white rats exposed to a single dose of 600 R from an x-ray machine or a Cs γ source. The animals were sacrificed at periods of one hour, 72 hrs, and one week after irradiation. The variations of the alkaline phosphatases, acid phosphatases, and lipase and in the structure of the intestine itself were determined after irradiation. The results showed that the dose of 600 R produces, even an hour after irradiation, significant modifications in the intestine. An early enzymatic modification was observed. A more rapid and complete recovery of the intestine of animals irradiated with x rays was observed in comparison with the slow and partial recovery of the intestine irradiated with γ rays. (J.S.R.)

45928 FIRST RESULTS ON THE BEHAVIOR OF THE TOTAL BILIARY ACIDS AND OF SOME PANCREATIC ENZYMES IN PATIENTS IRRADIATED ON THE ABDOMINAL PELVIC REGION. Dalla Palma, L.; Becciolini, A.; Cappellini, M.; Taddei, L.; Norbi-Bufalini, G. (Universita, Florence). Minerva Radiol., Fisioterap. Radiobiol., 10: 279-87(July-Aug. 1965). (In Italian).

The preliminary results of the study of the biliary and pancreatic secretions in the intestines following irradiation treatment are reported. The samplings were made at the beginning of the irradiation therapy, in the middle of the therapy, and at the end of the irradiation cycle. The methods used for the sampling and the analysis are described. The results reported are limited to the variations of the concentrations/ml either of the bile or of the pancreatic enzymes in the intestine with no consideration of the quantitative variations of the concentrations themselves following processes of dilution and concentration occurring in the intestine. In the middle of the irradiation cycle there is a sharp increase of the biliary concentrations in the first 30 min and a smaller increase toward the end of the first hour. At the end of the irradiation cycle there was observed in almost half the cases a biliary concentration not as high with respect to that observed at the half cycle. In the study of the concentration of some pancreatic enzymes, the increase of the concentration of one enzyme is accompanied by the decrease of the concentration of another enzyme. (J.S.R.)

45929 HISTOLOGICAL STUDY OF THE INTESTINAL MUCOUS MEMBRANE IN PATIENTS IRRADIATED IN EXTRA-ABDOMINAL SITES. De Dominicis, R.; Giannardi, G. F.; Grechi, G. (Universita, Florence). Minerva Radiol., Fisioterap. Radiobiol., 10: 288-9(July-Aug. 1965). (In Italian).

The intestinal mucous membrane of patients irradiated in thoracic or cranial sites was studied. In the majority of the biopsy specimens an absolutely normal aspect was found and only in a few cases were isolated modifications detected. (J.S.R.)

45930 RADIOLOGICAL STUDY OF THE GASTRO-INTESTINAL FUNCTION IN PATIENTS IRRADIATED ON THE ABDOMEN. De Marzi, S. (Universita, Florence). Minerva Radiol., Fisioterap. Radiobiol., 10: 291-3(July-Aug. 1965). (In Italian).

The functional behavior of the gastroenteric system of 68 patients affected with extraintestinal abdominal heteroplasias was studied before, during, and after radiation treatment on the abdomen. The elements taken into consideration for the functional evaluation are the time for gastric emptying, the time for the transition of a dye in the intestine, the duration of the opacity of the dye, the time for the emptying of all the intestine, the progression of the dye in the colon, and modifications of the intestinal functions. The radiation treatments seem to have no effect on the gastric emptying. If the cases are examined according to the irradiation field, there is an acceleration of the emptying in patients treated in the abdominal pelvic site and the abdominal epigastric site. In the same patients there was a significant frequency of acceleration with respect to the transition in the intestine. In the colon generally, a higher velocity of transition was observed. (J.S.R.)

45931 THE ABSORPTION OF GLUCOSE IN PATIENTS IRRADIATED ON THE ABDOMEN FOR EXTRA-INTESTINAL NEOPLASIA. Giannardi, G. F.; De Marzi, S.; Ciampi, G. P. (Universita, Florence; Arcispedale di S. Maria Nouva, Florence). Minerva Radiol., Fisioterap. Radiobiol., 10: 293-4(July-Aug. 1965). (In Italian).

The glucose absorption in patients exposed to abdominal and abdominal pelvic irradiations was determined before and after irradiation after glucose administration by mouth and intravenously. There was a significant decrease of the glucose values for both irradiation sites and for both types of glucose administration. The base curve of the glucose absorption after administration by mouth and by intravenous injection was different. No attempt at interpretation of these preliminary results was made. (J.S.R.)

45932 THE DIGESTION OF PROTEIC AND FATTY SUBSTANCES AND THE TIME OF TRANSITION IN PATIENTS IRRADIATED ON THE ABDOMEN. Pelu, G.; Vichi, G. F.; Pistocchi, F. Minerva Radiol., Fisioterap. Radiobiol., 10: 297-8(July-Aug. 1965). (In Italian).

The digestion of proteins and fatty acids was investigated in 41 patients with respect to the time of the intestinal transition and to the behavior of the stomach. The tests were made before, during, and after radiotherapy of the abdominal region. The degree of digestion of the protein substances can be correlated with the time of intestinal transition. The digestive modifications revealed during radiotherapy upon the abdomen can be correlated to the acceleration of the intestinal transit. A correlation in the time of transition was found with the area of the radiation field. (J.S.R.)

45933 MODIFICATIONS OF THE LYSOZYMIC ACTIVITY IN THE INTESTINE OF IRRADIATED ANIMALS. Rognoni, F.; Poggi Longostrevi, G. (S.P.A., Milan). Minerva Radiol., Fisioterap. Radiobiol., 10: 303-5(July-Aug. 1965). (In Italian).

The lysozymic activity of female rats exposed to a single whole-body dose of 870 R x radiation was determined. The results show that in the period immediately after irradiation a slight increase of the lysozymic activity at the interstitial level is observed and this decreases progressively. The survival curve and the curve of the intestinal lysozymic activity follow the same path. (J.S.R.)

45934 ANALYSIS OF THE BEHAVIOR OF LEUKOCYTES IN THE WHOLE-BODY IRRADIATED RAT. Martinenghi, C.; Castellano, E.; Riccardi, A. (Universita, Milan). Minerva Radiol., Fisioterap. Radiobiol., 10: 320-2(July-Aug. 1965). (In Italian).

Albino rats were exposed to whole-body doses of 250 R from a ^{60}Co γ source. The total leukocyte, lymphocyte,

and granulocyte curves were followed for 65 days after whole-body irradiation. The results are shown graphically. After irradiation, a sharp drop of the number of leukocytes, and in particular of the lymphocyte fraction, was observed with a minimum value reached 72 hrs after irradiation. The number of granulocytes was also reduced but less sharply than the others and its minimum was attained 5 days after the irradiation. Only after the 22nd day did the lymphocyte curve recover. One the 48th day normal values were observed and then a dispersion of the numbers higher than that observed in the animals before the irradiation was detected. The granulocyte curve has an irregular pattern and seems to be affected less by irradiation. (J.S.R.)

45935 CRITICAL CONSIDERATIONS ON THE EVALUATION OF THE RADIOBIOLOGICAL RESPONSE OF IRRADIATED CONNECTIVE TISSUES. Romagnoli, U.; Michaelassi, P. L. (Universita, Pisa, Italy). Minerva Radiol., Fisioterap. Radiobiol., 10: 328-9(July-Aug. 1965). (In Italian).

The problems in the evaluation of the radiobiological response of irradiated connective tissue are discussed. In order for valid comparison to be made between the studies of different workers, a procedure is outlined for the order in which the subdivisions of the tissues would be considered and the dyes that will be used. It is suggested that the work be divided according to histological methods, histochemical methods, and mathematical methods. (J.S.R.)

45936 MODIFICATIONS INDUCED BY IONIZING RADIATIONS ON THE UPTAKE OF TRITIATED THYMIDINE AND ON THE LIFE CYCLE OF CELLS OF EHRLICH ASCITE TUMORS. Sannazzari, G. L.; Piccotti, F. (Universita, Turin). Minerva Radiol., Fisioterap. Radiobiol., 10: 330-1(July-Aug. 1965). (In Italian).

The modifications of the proliferating kinetics and of the synthesis of DNA induced by irradiation in cells of the Ehrlich ascite tumor were studied using tritiated thymidine. The studies were made on mice exposed to radiation doses of 500, 1000, and 2000 rad. The percentage of labeled cells and the number of granules corresponding to the nuclei were determined. The percentage of labeled cells shows a significant drop in animals irradiated with doses from 1000 rad whereas from 1000 and 2000 rad the values are quite similar and the difference is not significant. The evaluation of the granules shows that with doses up to 1000 rad the mean velocity of synthesis per cell does not show any significant variation, but between 1000 and 2000 rad there is a significant inhibition of the labeled thymidine. The uptake of thymidine and the synthesis of DNA in the labeled cells are described briefly. (J.S.R.)

45937 THE BEHAVIOR OF CHOLESTEROL IN IRRADIATED ANIMALS. Villani, G.; Titta, L.; Migliorini, M.; Lertora, M. (Universita, Pisa, Italy; Ospedali Riuniti S. Chiara, Pisa, Italy). Minerva Radiol., Fisioterap. Radiobiol., 10: 342-5(July-Aug. 1965). (In Italian).

Cholesterol content in guinea pigs exposed to doses of 2000, 200, and 50 R on the whole-body, cephalic region, and inferior region was determined. The total cholesterol, the free cholesterol, the esterfied cholesterol, cholesterol bound to the α lipoprotein, and the cholesterol bound to the β lipoprotein, were determined. The results are shown graphically. For doses of 50 R on the whole-body, an increase of all the cholesterol except that bound to the β lipoprotein was detected in the first hours after irradiation. With the administration of 200 R to the whole-body, only the two fractions bound to β and α lipoproteins vary within the first 36 hrs: the first decreases and the second decreases in directly proportional modes. The α and β lipoprotein fractions after exposure to 2000 R behave as the fractions in the irradiation with 200 R for the first 36 hrs. (J.S.R.)

45938 ALTERATIONS OF THE ASCORBIC ACID CONTENT OF LEGUMES CAUSED BY β OR γ IRRADIATION. PART 2. Barakat, M. Z.; Abdel-Wahab, M. F.; Megahed, Y. M. (Cairo Univ.). Monatsh. Chem., 95: 1613-22(1964). (In German)

Samples consisting of 100 g of seeds of Vicia faba Giza I and II, Vigna sinensis, Phaseolus vulgaris, Trigonella foenum graecum, and Lupinus termis were mixed with aqueous solutions containing 100 and 200 μC of $H_3{}^{32}PO_4$, or 1000 and 2000 μC of $Na^{131}I$. The seed samples were removed from the solution after 24 hr. Other samples were irradiated with 5000 and 10000 R from ^{137}Cs and to 1000, 5000, 10,000, 15,000, 20,000, and 50,000 R from ^{60}Co. The vitamin C concentrations of the seedlings that developed from the irradiated seed samples were measured for the initial 30 days following irradiation. In general, the concentrations were slightly less in the irradiated seedlings than in unirradiated controls. The differences increased proportionately to the amounts of irradiation exposure and varied according to the seed types. The maximum differences from control seedling values observed with β irradiation ranged from ~26 to 53%, while the average difference amounted to ~19 to 44%. For seedlings exposed to γ irradiation the ranges of these differences were from ~21 to 53 and ~19 to 50%, respectively. The results indicated that both types of irradiation either inhibited vitamin C formation or accelerated its destruction. (BBB)

45939 IN VITRO EFFECTS ON DIFFERENT TISSUES OF COLLOIDAL CHROMIC RADIOPHOSPHATE. Anghileri, Leopoldo Jose (Comision Nacional de Energia Atomica, Buenos Aires). Naturwissenschaften, 52: 429-30(1965).

Colloidal chromic radiophosphate (^{32}P) was incubated with different rat tissues in order to study the effects of the tissues on the stability of this radiotherapeutic agent. The tissues studied were testis, lung, stomach, intestine, spleen, muscle, liver, bone marrow, and whole blood. Ionic phosphate was observed only in the presence of testis tissue. A diffusely defined peak of activity with a mobility of 0.17 to 0.21 was detected in liver, bone marrow, and whole blood. No change was observed in the other tissues. The results suggest that the testis is the only tissue which releases ionic phosphate in vitro. (J.S.R.)

45940 THE ACTION OF X-RAYS ON NUCLEOLAR STRUCTURES. Herich, Rudolf (Comenius Univ., Bratislava). Naturwissenschaften, 52: 457(1965).

Preliminary results on the effect of x rays on the differentiation and development of nucleolar structures are presented. Seedlings of Cannabis sativa were irradiated at doses of 500, 5000, and 10,000 R. Morphological changes in nucleoli of dividing and resting cells are described. (J.S.R.)

45941 THE BEHAVIOR OF SOME AMINO ACIDS IN GAMMA-IRRADIATED SOILS. Voets, J. P.; Dedeken, M. (State Agricultural Univ., Ghent, Belg.). Naturwissenschaften, 52: 476(1965).

In the study of the behavior of some amino acids in the soil, two techniques were used: the toluene treatment of the soil and the soil sterilization by γ radiation before adding the amino acids to the soil. The activity of urease, saccharase, acid phosphatase, and proteolytic enzymes was not affected by the γ irradiation. The behavior of glycine, dl-α-alanine, l-aspartic acid, and l-glutamic acid were studied after toluene treatment and γ irradiation of the air-dried soil. The results are tabulated and show that the four amino acids tested remain unchanged both in the toluene-treated soil and in the γ-irradiated soil. (J.S.R.)

45942 INDUCTION OF TUMORS BY IONIZING RADIATION. van Bekkum, D. W. (Radiologisch Instituut, Rijswik, Netherlands). Ned. Tijdschr. Geneesk., 108: 1977-82(Oct. 17, 1964). (In Dutch).

The relation between ionizing radiation and tumors is discussed, with some of the early classical examples used as illustrations. Tables of dose rates to various parts of the body from natural sources and doses resulting from the nuclear explosions of 1954 to 1961 are given. The relation between dose and effect in the well-established cases is given, with attention devoted to the latent period. The somatic mutation theory is discussed; pathways for direct and indirect carcinogenesis are discussed. An indirect pathway is better in agreement with the data available;

similarities between radiation and viral causes are noted and several possible pathways for these two methods of induction are outlined. Suggestions for administration of doses to individuals in light of the observed relations are given. (BBB)

45943 THE EFFECT OF THYROID HORMONE ON THE GROWTH OF IRRADIATED AND UNIRRADIATED TUMORS. Siracka, E. (Oncological Research Inst., Bratislava). Neoplasma, 12: 193-7(1965).

In rats with transplanted Jensen's sarcoma the hyperthyroid state was induced by injection of 3,5,3-L-triiodothyronine (T3), and the response of irradiated and unirradiated tumors was followed. X-ray therapy was applied by means of a 60-kv x-ray unit over four consecutive days, fractionated 4 × 1000 R. The T3 was administered subcutaneously in a dose of 1 mg/kg of body weight over three consecutive days. In the group with the combined treatment the first dose of x-ray therapy was given on the last day of T3 application. The volume of tumors was measured on the 1st, 4th, 14th, and 21st day after beginning the irradiation. The tumors irradiated under the influence of T3 exhibited in comparison to the controls (irradiation in a euthyroid state) an increased radiosensitivity. Favorable response to radiation was achieved however only in early, small tumors. On the basis of this observation it is evident that the hyperthyroid state is responsible for increased radiosensitivity through the oxygen effect which is considerably dependent on the blood supply. In animals given T3 the unirradiated tumors exhibited an accelerated growth in comparison to the control groups in which no treatment was given. Possible danger of the enhancement of distant metastases is mentioned in reference to clinical application. (BBB)

45944 THE BIOLOGY OF TISSUE TRANSPLANTATION. [PART] I. Russell, Paul S.; Monaco, Anthony P. (Massachusetts General Hospital, Boston). New Engl. J. Med., 271: 553-62(Sept. 10, 1964).

The graft-vs-host (GVH) reaction and its suppression by various agents, including ionizing radiation, are reviewed. The GVH reaction and concomitant runt disease can be prevented by various immunologic interventions designed to assist the newborn recipient to reject (or possibly inactivate) the graft of adult lymphoid cells. Isogeneic adult splenic cells injected in animals shortly after the foreign splenic cells decrease the mortality from subsequent runt disease, and adult cells from animals preimmunized to the donor strain have an even better protective effect. The possibility of GVH reactions in human renal allografting is considered. Early cellular infiltration of canine allografts is seen by three or four days, the cellular foci being widespread in the renal cortex, and interpreted either as local proliferations of donor cells or as the result of blood-borne invasion from the host. It has been claimed that irradiation before transplantation prevents this cellular proliferation of pyroninophilic cells. However, later investigations failed to confirm this. Doses of 1000 to 1500 R delivered to the kidney do not influence this characteristic interstitial reaction. Furthermore, if the host is irradiated instead of the graft, the interstitial reaction is suppressed as long as the animal lived. A similar result was found after 3000 R, given locally to a kidney 15 min after transplantation, which failed to prevent, or noticeably to reduce, the pyroninophilic reaction. (BBB)

45945 RADIATION-INDUCED CANCER OF THE SKIN (CASE REPORTS AND CONSIDERATIONS). Yamashita, Hisao; Ishida, Osamu. Nippon Igaku Hoshasen Gakkai Zasshi, 21: 656-69(Sept. 25, 1961). (In Japanese).

Data are reported on 23 cases of radiation-induced cancer of the skin and comparison was made with the ordinary cancers of the skin and the radiation-induced cancers of other organs. Radiation was found to be one of the chief causes of cancer of the skin; scarring from wounds was another major cause. Radiation-induced cancer of the skin was found to develop at ages of a little over 50 on the average. Radiation skin cancer developed mainly on the neck, trunk, and upper extremities. Various kinds of skin injury were also seen in the neighboring regions of the cancers. Histological findings included dermatofibrosarcoma, carcinoma simplex, and Bowen's disease in each of three cases, and the other 20 cases were all squamous cell carcinoma in which keratotic and infiltrative reactions and proliferation of fibroblasts were seen. Usually a long time was required for complete healing of the cancers induced by radiation, but the survival rate was good, because most of the patients visited the hospital at relatively early stages, and metastases were seen in only a very few cases. In most cases, skin cancer developed after superficial radiation therapy for benign conditions (various skin diseases or tuberculous disease). In one case treatment with Ra and ^{32}P were additional to x-ray therapy. Cases of radiation-induced cancer of the skin appear to be gradually increasing in number, while cases of ordinary skin cancer are decreasing. The latent period of the radiation-induced cancer of the skin is 23 yr on the average, nearly the same as the 25 yr for radiation cancer of the laryngopharynx, but much longer than the 10 yr for radiation osteosarcoma, radiation cancer of the thyroid, and leukemia. The estimated radiation dose sufficient to induce cancer of the skin is between 5500 to 8500 R in 4 yr, and for radiation cancer of the laryngopharynx between 3000 and 4500 R in 14 months. Thus for skin cancer much more radiation over a longer period is necessary than for radiation cancer of the laryngopharynx. It is concluded that in radiation therapy, especially of benign conditions, care should be taken not to give large doses of radiation even if spread over long periods. Careful observation should also be made of the changes in the irradiated skin and its surroundings. (BBB)

45946 THE EFFECT OF UNSATURATED FATTY ACID EXTRACTED FROM THE LIVER OF IRRADIATED RABBITS ON YOSHIDA SARCOMA CELLS. Shigeo, Nobuki (Okayama Univ., Japan). Nippon Igaku Hoshasen Gakkai Zasshi, 22: 922-8(Nov. 25, 1962). (In Japanese).

A cellular toxin can be extracted from the liver of irradiated rabbits. This fraction (OX) appears to contain unsaturated fatty acid as a major ingredient and may be involved in the in vivo radiation injury to various tissues. It was previously found to cause hypoplasia of rabbit testes, and in the present experiments it was tested in vitro on Yoshida sarcoma cells. Changes in morphology, numbers, nuclear division, growth rate, and metastatic development of transplanted cells were noted. Some experiments are also reported on the effect of OX substance on Brown-Pearce tumor and Ehrlich ascites tumor cells. In the latter, DNA synthesis was inhibited by the OX fraction. Attempts were also made to fractionate OX fraction. A series of four fractions (OX_1, OX_2, OX_3, OX_4) were isolated and found to be more inhibitory on Yoshida sarcoma cells than the crude OX substance. OX_1 and OX_2 were more inhibitory against DNA synthesis than OX_3 and OX_4. All four fractions altered the metabolic apparatus of the cell, as well as causing cellular degeneration and atypical morphology. The intensity of the cytotoxic effect differs with the four fractions. (BBB)

45947 ESR INVESTIGATIONS OF RADIO-INDUCED FREE RADICALS IN MUSCLE TISSUES. Belagyi, J.; Lassmann, G.; Damerau, W. (Medical Univ., Pecs, Hungary; Institut fuer Biophysik, Deutsche Academy der Wissenschaften, Berlin). Monatsber. Deut. Akad. Wiss. Berlin, 7: 131-3(1965). (In German).

Investigations were made on lyophilized rabbit muscles which were irradiated at room temperature by a ^{60}Co source or at the temperature of liquid air with x rays from a 1.5-Mev source. The samples were measured in an X-band spectrometer and the concentration of unpaired spins, the g factor, and the splitting parameters were determined; no ESR signals could be observed before the irradiation. Radical concentrations of about 10^{17} were produced by x or γ irradiation. The samples irradiated at room temperature showed an ESR signal with a hyperfine structure of 4 lines. Irradiation at 80°K gave, however, only one individual line. The occurrence of a hfs with 4 lines was assigned to an interaction of the unpaired electrons with three protons. Irradiation at 80°K and measurement at room tem-

perature showed that at 80°K another radical occurs. This primary radical is irreversibly introduced into a radical structure with a doublet hfs that is stable at room temperature. (J.S.R.)

45948 THE EXCISION OF THYMINE DIMERS FROM DNA, FILAMENT FORMATION AND SENSITIVITY TO ULTRAVIOLET LIGHT IN ESCHERICHIA COLI K-12. Howard-Flanders, P.; Simson, Eva; Theriot, Lee (Yale Univ., New Haven). Mutation Res., 1: 219-26(Oct. 1964).

Strains of Escherichia coli K-12 have been described that lack the ability to excise thymine dimers from DNA after UV irradiation, and are abnormally sensitive to UV light as regards the survival of colony forming ability. These strains carry mutations at the uvrA or uvrB loci which are linked to the loci for methionine requirement and for the λ prophage. Strains with a mutation at the lon locus, which is linked to the marker for T6 resistance, tend to grow in long forms, to form a mucoid capsule and to be abnormally radiosensitive to both UV light and to x rays. The properties of the double mutants uvr lon which are many times more sensitive to UV light than either of the single mutants are described. In genetic crosses with a wild type Hfr and a uvr lon female strain, the radiation resistance of recombinants was found to increase in two steps as the wild-type alleles of the lon and uvr loci entered the zygote. The survival of UV-irradiated T1 phage is affected by uvr, but not lon in the host bacterium used for plating. The results confirm that the uvr and lon genes affect sensitivity to radiation through independent mechanisms. (auth)

45949 EVIDENCE FOR THE TWO-HIT NATURE OF X-RAY INDUCED CROSSING-OVER IN THE CENTROMERIC REGION OF DROSOPHILA MALES. Olivieri, G.; Olivieri, A. (Università, Rome). Mutation Res., 1: 279-95(Oct. 1964).

In order to study the relationship between dosage and frequency of x-ray-induced crossing-over in males of Drosophila melanogaster, four samples of about 130 males each were irradiated with doses of 500, 1000, 2500, and 4000 R respectively. On the 10th to 11th day after irradiation, the two classes of complementary crossovers were found to occur independently of each other in the progeny of the individual males, and the distribution of crossovers per irradiated male followed a Poisson distribution. In consequence, the clusters in this brood were considered as pseudo-clusters, originating from different crossover events in the latest gonial cells. It is this stage that is characterized by the highest sensitivity to the induction of crossing-over. The number of crossovers found on these days has therefore been used as a direct estimate of the number of crossing-overs produced, taking into account the probable induction of crossing-over at the four-strand stage. After logarithmic transformation, a linear relationship was observed between the dose and the percentage of crossovers produced in the late gonial cells in the centromeric region of the second chromosome (regression coefficient = 1.768 ± 0.030). Crossing-over induced in this chromosome region therefore is most probably a two-hit phenomenon, to be explained in terms of two distinct and independent breaks. This conclusion is further supported by the observation that fractionation of the dose significantly reduced the frequency of induced crossing-over. When N_2 was given between the fractions the crossing-over frequency was restored to that of unfractionated radiation. It is thought that N_2 acts by preventing restitution of the breaks required for the pseudo-crossing-over. Post-treatment with N_2 after unfractionated radiation resulted in a significant enhancement of the crossing-over frequency. Irradiation in N_2 reduced the frequency of induced crossing-over to about one-fifth of that observed in air, whereas radiation exposure in oxygen approximately doubled the crossing-over frequency as compared to that induced in air. The radio-sensitivity in O_2 and N_2 differed by a factor of about 10. This is considered to offer further support for the two-hit origin of induced centromeric crossing-over in this stage. (auth)

45950 CYTOGENETIC INVESTIGATIONS ON RADIATION AND CHEMICALLY INDUCED DOMINANT LETHAL MUTATIONS IN OOCYTES AND SPERM OF THE SCREW-WORM FLY. Lachance, Leo E.; Riemann, John G. (Dept. of Agriculture, Mission, Tex.). Mutation Res., 1: 318-33 (Oct. 1964).

Adult females of the screw-worm fly, Cochliomyia hominivorax, containing oocytes in early prophase or early anaphase of the first meiotic division, and day-old males containing mature sperm were exposed to γ radiation or the alkylating agent, 2,4,6-tris(1-aziridinyl)-s.-triazine (= tetramine). The doses used induced nearly 100% dominant lethals in the reproductive cells. Treated insects were crossed with untreated ones. Eggs were collected and fixed after different periods of development at room temperature. Stained whole-mounts of the embryos were studied to determine the kind of chromosome aberrations associated with dominant lethal mutations, the stage of development at which the chromosome aberrations appeared, the stage at which development ceased in embryos containing dominant lethal mutations of either maternal or paternal origin, and whether damage induced by tetramine was cytologically similar to that induced by ionizing radiations. Dominant lethal mutations are characterized by the presence of chromosome bridges and fragments between dividing nuclei in the embryo, but the stage of development at which these first appear differs with the type of mutagen used. The damage produced by irradiation of meiotic oocytes is evident during the first and second meiotic divisions and continues into the early cleavage divisions, at which time development ceases. After treatment of meiotic oocytes with tetramine, the majority of the subsequent meiotic divisions appear normal and the detection of most of the chromosomal damage is first possible in cleavage divisions, or after the treated nucleus undergoes one replication of chromatin material. Treatment of mature sperm with either γ rays or tetramine does not prevent syngamy. Chromosome aberrations become evident at the first cleavage division. It is obvious that chromosome-breakage phenomena formed the basis of dominant lethality in these cells. Each of these treatments stops embryonic development generally after only a few cleavage divisions. Various types of abnormalities were observed in the embryos. The relevance of these observations to the mode of action of the mutagens, the chromosomal basis of dominant lethality, and the differential sensitivity of the three types of germ cells to these mutagens are discussed. (auth)

45951 POST-IRRADIATION RECOVERY OF ESCHERICHIA COLI. Lee, J. S.; Sinnhuber, R. O. (Oregon State Univ., Corvallis). Nature, 207: 1212-14(Sept. 11, 1965).

E. coli strain B was grown in buffered-peptone medium and in Davis's glucose-salts medium. After irradiation, the survivors were further subjected to cold starvation in phosphate buffer at 7°C for 14 days. The effects of such stresses were measured by the loss of colony-forming ability. The cold starvation appeared to exert only a mild stress to healthy cells. The radiation survivors behaved differently. A steady decrease of viable cells was noted during cold starvation when peptone-grown cells were enumerated on the same medium. The cells grown in glucose-salts, after irradiation could be recovered equally well on either peptone or glucose-salts agar. A more rapid viability loss of the non-irradiated population during cold starvation indicated however, that the glucose-salts-grown cells possessed lesser survival potential under this stress. The cells grown in glucose-salts were more radiosensitive than those grown in peptone. (P.C.H.)

45952 INBREEDING AND GENETIC LOADS IN IRRADIATED EXPERIMENTAL POPULATIONS OF DROSOPHILA MELANOGASTER. Sankaranarayanan, K. (Rockefeller Inst., New York, N. Y.). Nature, 207: 1216-17(Sept. 11, 1965).

Results obtained from investigations aimed at comparing the magnitudes of the genetic loads in experimental populations of D. melanogaster. The populations were exposed to a cumulative x-ray dose of 120,000 R for several generations then maintained without further irradiation for varying periods of time. The egg-adult viability in these populations, after the initial rise for 3-4 generations following the cessation of the irradiation, remained at a level

between 70 and 75%, below the level in the control population (80-90%). Experiments investigating the effects of inbreeding on viability were carried out over a period of four consecutive contemporaneous generations. The mean viabilities observed showed the outbred progenies (F = 0) to be the most viable, followed by the progenies of half-sib matings (F = 0.125), and full-sib matings (F = 0.25). The A and B statistics and the B/A ratios and their standard errors are discussed. (P.C.H.)

45953 APPEARANCE OF RAT SLOW ALPHA-TWO GLOBULIN AFTER IRRADIATION. Heim, Werner G. (Wayne State Univ., Detroit). Nature, 207: 1403-4(Sept. 25, 1965).

Studies were made to determine if slow alpha-two globulin (SA_2G) appeared in the sera of rats subjected to irradiation alone or to irradiation followed by the administration of bacterial lipopolysaccharides. The presence or absence of SA_2G was demonstrated by vertical starch-gel electrophoresis. The rats were exposed to approximately 600 R gamma radiation. It was concluded that irradiation at this dose level does not evoke the production of SA_2G to the degree needed to permit its demonstration by vertical starch-gel electrophoresis. All of the irradiated rats tested within 4 days after the administration of lipopolysaccharide showed high levels of SA_2G in their sera. (M.C.G.)

45954 ELECTRON SPIN RESONANCES IN FORMICIDAE. Krebs, A. T.; Benson, B. W. (Walter Reed Army Inst. of Research, Washington, D. C.). Nature, 207: 1412-13(Sept. 25, 1965).

Investigations on the effects of ionizing radiation on survival and behavior of ants were extended into the field of microwave spectroscopy. The electron spin resonance spectra were recorded for 6 species of ants. One species was examined for changes in the signal after exposure to gamma radiation and another for changes after annealing. Irradiation caused an increase in height of the signal, followed by a slow decay with time after irradiation. Annealing, however, completely depressed the 6-peak signal and enhanced the free radical region signal. (M.C.G.)

45955 RELATION OF CELL SIZE TO THE EFFECT OF X-RAYS ON POLIOVIRUS PRODUCTION BY MONKEY-KIDNEY CELLS. Levine, Seymour; Olson, Walter (American Cyanamid Co., Pearl River, N. Y.). Nature, 207: 1413-12(Sept. 25, 1965).

It was found that x-irradiation reduces poliovirus yields from monkey-kidney cells of regular size more than it reduces the yields from grant monkey-kidney cells. (M.C.G.)

45956 THE SPLENIC AND THYMIC WEIGHT RESPONSE TO WHOLE-BODY X IRRADIATION IN THREE STRAINS OF MICE. Hayakawa, Jun-ichiro; Muramatsu, Susumu; Yamada, Junzo; Tsuchiya, Takehiko (National Inst. of Radiological Sciences, Chiba, Japan). Nippon Igaku Hoshasen Gakkai Zasshi, 24: 370-6(July 25, 1964). (In Japanese).

The spleen and thymus weight response to whole-body x irradiation was observed in the three strains (RF, CF1, C57BL/6) of mice of different radiosensitivity (based on LD_{50}) and thyroid function and their F_1 hybrids. RF, CF1, and their F_1 hybrids showed a similar tendency in splenic weight response to x irradiation, while a different response was observed in C57BL and F_1 hybrids from the C57BL strain. The ED_{50} for spleen weight changes (drop followed by rise above normal) of C57BL mice was significantly higher than that of either RF or CF1 mice. The thymic weight response and the ED_{50} for thymus did not significantly differ among the three strains and their F_1 hybrids. The differences of splenic weight response to x irradiation as well as that of LD_{50} for x irradiation in mice presumably result from differences in their genetic constitution. (auth)

45957 EXPERIMENTAL STUDIES ON THE EFFECT OF HIGH-DOSE X IRRADIATION OVER THE SKIN AND SUBCUTANEOUS TISSUE. 1. MACROSCOPIC CHANGES. Toyokawa, Yasuo (Tohoku Univ., Sendai). Nippon Igaku Hoshasen Gakkai Zasshi, 24: 377-86(July 25, 1964). (In Japanese).

Detailed observations were made of gross dermatologic effects of heavy irradiation of rat skin. X rays generated at 150 kvp were given at a dose rate of 100 R/min to total single doses of 4000, 5000, and 6000 R and in fractional doses to a total of 10,000 R. Macroscopic responses in skin appeared in the following order: erythema, ruffled coat, epilation, moist desquamation, ulceration, and, eventually, regrowth of hair. In each group given a single irradiation of 4000 or 5000 R a large individual difference in response was noted, while in each group given a single irradiation of 6000 or fractional irradiation of 10,000 R the individual difference was less. In the groups given a single irradiation, erythema, loss of hair, and desquamation in the early period were not correlated with the radiation dose, but appeared at a definite time. On the other hand, epilation, moist erosion, and ulcers appeared at an interval inversely proportional to the radiation dose. Epilation was observed in all cases. Ulcers appeared in all rats which had received a single irradiation of 6000 R, while in the other irradiated group, it was hardly noted. Recovery in the group with a single irradiation was more delayed in the group with 5000 R than that given 4000 R. In the group given 6000 R a rapid progression to ulcer from moist erosion occurred in all cases, and recovery was not seen. Ulcer in the groups given fractional irradiation was observed in 10 of 12 instances; however, no healing from ulcer occurred in any rats. When the skin reaction of the group given fractional irradiation was compared with that of single irradiation, erythema was less in the former. Desquamation by keratosis in the later period was more marked in the group with fractional irradiation. Indurative changes with scaling were observed in the skin. (BBB)

45958 PATTERNS OF LEUKEMIA IN ISRAEL. Kallner, Gertrude. Pathol. Microbiol., 27: 666-70(1964).

Israel has a high incidence of leukemia, and the groups of various origin among the Jewish population of Israel, distinguished by a different physical background and pattern of life in their past, afford data for epidemiologic studies of leukemia. One situation in particular was studied, i.e., leukemia mortality of children aged 0 to 9 years, born abroad. For this group conditions were extraordinary as they included certain immigration waves principally from North Africa, the children of which were almost all subjected to x-ray treatment for ringworm of the scalp. This, therefore, served as a situation that came very near to being an experimental set up, and attempts were made to determine whether mortality figures of subsequent years would show any specific features concerning this special group. The mortality data for this group, of lymphatic and hematopoietic system cancers in childhood were divided into four groups: children who had been brought to Israel from Oriental and from Occidental countries; children born in Israel to parents of Oriental and of Occidental stock. The data showed that there is a moderate increase by about 25% between the two mortality periods surveyed for children born in Israel independent of their parents' origin. There is further a marked decrease for children who had been brought here from Occidental countries, but there is, on the other hand, an enormous increase by nearly 100% for children who had been born in Asia or North Africa and had been brought to Israel after 1952, i.e., the group including a high proportion of those who received x-ray epilation treatment. (TCO)

45959 SURVEY OF LEUKEMIA IN THE WEST CORNWALL CLINICAL AREA (1948-1961). Wood, Eileen E. (West Cornwall Hospital, Penzance, Eng.). Pathol. Microbiol., 27: 736-8(1964).

The relation between the incidence of leukemia (said to be unduly high) in some parts of Cornwall and the known higher background radioactivity there was investigated. The western two-thirds of the county (population 255,000) was included in the survey. In this area 251 cases of leukemia were studied individually and in relation to their background since 1948. A radiac survey showed considerable activity (0.04–0.06 mR/hr) in association with the

coarse granites found in this county, presumably due to uranium deposits. Within these areas local zones with activity rising to 0.1 mR/hr and over were found; these zones are generally around old mines. Health of individuals living in the vicinity of these mines was studied. At one cottage where the background level reached over 3 mR/hr the present tenant was in good health, as were his parents who lived there. One unusual case of leukemia was seen, that of a radium chemist who worked in the mine at St. Ives 50 years ago and was found to have chronic lymphatic leukemia in 1956. His radium burden during life was 100 times normal, and after death his bones showed activity 100 times greater than normal. A survey of English drinking waters showed that, apart from certain spa waters, the highest levels of radioactivity are found in Cornwall. It is probable that waters containing natural α activity up to 10 μC/l, long-lived ^{226}Ra, and 10 to 20,000 μC/l dissolved ^{222}Rn have been consumed by Cornish populations for a considerable time. Daily intake of ^{226}Ra and its daughters when compared with that of three Welsh counties of comparable surroundings showed the intake to be 1000 times greater in Cornwall. To investigate leukemia distribution in Cornwall, maps were made indicating the exact geographic siting of the cases and the granite outcrops associated with high radioacitivity levels. Two foci of leukemia were noted in association with granite areas and unassociated with population levels, at St. Just and St. Dennis. In two different villages two cases occurred within a few yards of each other, and in one bakery it was found that two cases had been working together. In another town (Newquay) of low radiac background there was a group of three cases. Generally rural areas showed a lower incidence than towns, and in general the towns with the greatest incidence are those where the economic gradient and percentage of retired persons tended to be high. In St. Ives, where only four cases of leukemia have been discovered since 1945, the water supply is from an old uranium mine. (BBB)

45960 NEW WAYS TO CONTROL INSECTS. Lindquist, Arthur W. (Dept. of Agriculture, Beltsville, Md.). Pest Control, 29: 9-19; 36-40(June 1961).

Use of γ radiation and chemical agents in the sterile-male technic of insect eradication is reviewed. The example is cited of the spectacular eradication of the screw-worm in the Southeast by means of the sterile-male technique. The highly successful eradication of this insect from a large area ranks as an outstanding entomological accomplishment. The radio-induced sterility method consists of rearing and sterilizing insects, and releasing males into a natural population. These males mate with native females and destroy their ability to reproduce. For introduction into infested areas, sterile males must be released in numbers greater than exist in nature. The optimum time for sterilizing the screw-worm was found to be 5 to 6 days after pupation at 80°F or 2 to 3 days before adult emergence. A dose of 2500 R caused sterility of males and 5000 R of females without interfering with their normal behavior. Screw-worm females mate only once, which favored use of the method; however, single matings are not a prerequisite to the successful use of the sterile-male method. Theoretically, multiple-mating species may be used, since a population containing up to 10 times as many sterile as normal males gives the advantage to the sterile males even if the females mate more than once. Application of the sterile-male technique to other insects is discussed. Intensive research on the possible uses of the method against the Mediterranean fruit fly (Ceratitis capitata), melon fly (Dacus cucurbitae), and the oriental fruit fly (Dacus dorsalis) has led to field tests. Laboratory tests showed that the common malaria mosquito (Anopheles quadrimaculatus) responds to irradiation and mates in a manner similar to that of the screw-worm. A small field test, initiated on a 5-mile peninsula in Lake Okeechobee, Florida, failed since the natural population of mosquitoes did not decline. Research on the effects of γ radiation and the possible use of the sterile-male method has been conducted on several other insects, such as the boll weevil (Anthonomus grandis), codling moth (Carpocapsa pomenella), European corn borer (Pyrausta nubilalis), and tsetse flies (Glossina spp.). The sterile-male method might be practical with at least some of these insects; however, economical control by this method may not be possible until the natural population is first reduced by other means. Methods of rearing the insects and of producing sterility must be worked out, and the biology and ecology of the insects involved must be understood before the value of this approach can be adequately determined. The possibilities of using radio-induced sterility of male insects for the control of such household pests as cockroaches does not appear practical or very promising at this time. The method of control involves release of more insects than exist in the natural environment, and householders or the owners of business establishments might not tolerate increased numbers of cockroaches, flies, and other pests. Even if the release period involved only a few months with hope of ultimate success, it is doubtful that the method would meet with much favor. Use of chemicals to cause sexual sterility in insects without adversely affecting sexual vigor or behavior is also considered. (BBB)

45961 INACTIVATION OF RHIZOBIUM BACTERIOPHAGE BY ULTRAVIOLET RADIATION OF DIFFERENT WAVE-LENGTHS. Kleczkowski, J.; Kleczkowski, A. (Rothamsted Experimental Station, Harpenden, Eng.). Photochem. Photobiol., 4: 201-7(Mar. 1965).

A strain of clover nodule bacterium (Rhizobium trifolii) and a corresponding bacteriophage were studied. UV irradiations were made with a quartz-prism monochromator, using a 250-w xenon discharge lamp as a source of radiation. The results showed that the action spectrum for inactivation of the bacteriophage by uv radiation follows the shape of the absorption spectrum of DNA between the wavelengths of 240 and 290 mμ (where inactivation probably reflects damage to the nucleic acid only), and deviates sharply upwards at wavelengths shorter than 240 mμ (where inactivation may depend on damage to both the nucleic acid, and protein of the phage). The rate of inactivation follows first-order kinetics at all wavelengths tested. Infectivity of the phage is halved when each mg of the phage nucleic acid has absorbed about 0.08 j of radiation energy at any wavelength between 240 and 290 mμ. The bacteriophage can be photoreactivated after inactivation at any wavelength between 230 and 290 mμ, but less so after inactivation at 230 mμ than at any wavelength above 240 mμ. No evidence was found to suggest that dimerization of thymine residues of the phage DNA plays any part in the mechanism of inactivation of the bacteriophage by uv radiation. (BBB)

45962 INACTIVATION OF A STRAIN OF TOBACCO NECROSIS VIRUS AND OF THE RNA ISOLATED FROM IT, BY ULTRAVIOLET RADIATION OF DIFFERENT WAVE-LENGTHS. Kassanis, B.; Kleczkowski, A. (Rothamsted Experimental Station, Harpenden, Eng.). Photochem. Photobiol., 4: 209-14(Mar. 1965).

Tobacco necrosis virus (TNV) inactivated by uv differs from tobacco mosaic virus in being photoreactivable and, judging from the effect of irradiating inoculated leaves (i.e., of irradiating in vivo), whole virus and infective RNA isolated from it (TNV-RNA) seem equally susceptible to inactivation by uv. A comparison was made of the sensitivities of TNV and of TNV-RNA to inactivation by uv at different wavelengths, and of the extent to which they can be photoreactivated, and to obtain action spectra for their inactivation. The results showed that strain A of TNV and TNV-RNA are equally susceptible to inactivation by uv radiation at all wavelengths tested (230-290 mμ) and can be photoreactivated to the same extent by exposing inoculated host plants to daylight. The shape of the action spectrum for inactivation by uv of TNV and of TNV-RNA follows that of the absorption spectrum of TNV-RNA. Thus, unlike the RNA of tobacco mosaic virus, the RNA of TNV behaves in all these respects in the same way irrespective of whether it is inside or outside the virus particle. To inactivate TNV or TNV-RNA to 50% of their original infectivities, each mg of RNA must absorb about 0.27 j of radiation energy of any wave-length between 230 and 290 mμ, which corresponds to a quantum yield of about 0.65×10^{-3} at 260 mμ. When values of the ratio $r = k_{dark}/k_{light}$ obtained

after irradiation of TNV and of TNV-RNA at different wavelengths were plotted against the wavelengths, the extent of photoreactivation seemed independent of the wavelength used for inactivation, and was about the same with TNV and with TNV-RNA, the average value of r being 1.35. This value is considerably smaller than the value of 2.0 obtained with RNA from tobacco mosaic virus. Thus none of the differences between the behavior of intact tobacco mosaic virus and of the RNA isolated from it were shown by TNV and TNV-RNA. If the bonding between RNA and protein in tobacco mosaic virus protects the RNA from damage by uv and prevents it from undergoing photoreversible changes, there is no such bonding between RNA and protein in TNV. (BBB)

45963 U.V.-DOSAGE MEASUREMENT IN A GEOMETRICALLY COMPLEX SYSTEM WITH LIGHT-SENSITIVE PAPER. QUANTUM YIELD FOR SALMONELLA KILL IN EGG WHITE. Launer, Herbert F.; Hammerle, Olivia O. (Western Regional Research Lab., Albany, Calif.). Photochem. Photobiol., 4: 265-7(Mar. 1965).

A simple method for measurement of germicidal (2537 Å) uv doses in a geometrically complex system is described. It was used to measure the dose in a Centrifilmer, a device used for centrifugally producing thin films, 0.07 mm, of continuously flowing egg white, and for exposing the films to a group of six germicidal lamps, in order to kill Salmonella. The problem was to measure the radiant energy incident on the inside surface of a 95-mm dia stainless steel bowl, rotating at 1750 rpm around the concentric circle of lamps. National Bureau of Standard light-sensitive paper was used which is faded by light and uv to stable endpoints, and which may be evaluated by visual or instrumental comparison with secondary standards produced from the same paper with precisely measured light doses from a standard arc. The number of quanta corresponding to each Salmonella organism killed could be calculated. From the bacteria count it was determined that 2×10^7 organisms per ml were killed at a flowrate of 137 ml/min, corresponding to 1.4×10^5 organisms per cm^2 of 0.070 mm film. Each cm^2 film spent 2.46 sec in the bowl and absorbed $2.46 \times 6.6 \times 10^{15} = 16.2 \times 10^{15}$ quanta. Thus $16.2 \times 10^{15} \div 1.4 \times 10^5 \cong 1.2 \times 10^{11}$ quanta corresponded to each organism killed in egg white. This low apparent quantum efficiency represents a max value and is due to the fact that the egg white absorbed most of the energy, with little transfer of lethal energy to the Salmonella, and with the undesired effect of off-flavor in the egg white. The result shows that films thinner than 0.07 mm of undiluted egg white are required for efficient radiant killing. (BBB)

45964 AN EVALUATION OF THE HEALING PROCESS IN AVIAN DIGITAL FLEXOR TENDONS AND GRAFTS FOLLOWING THE APPLICATION OF AN ARTIFICIAL TENDON SHEATH. Ashley, Franklin L.; McConnell, D. V.; Polak, T.; Stone, R. S.; Marmor, L. (Univ. of California, Los Angeles). Plastic Reconstruct. Surg., 33: 411-21(May 1964).

The use of tendon homografts, exposed to high-energy ionizing radiation to reduce immunogenicity, to repair tendons was investigated by grafting experiments in chickens and turkeys. The use of tendon homografts to perform as growth bridges is prevented by the fact that homologous tendon is significantly antigenic; hence, modification of this antigenicity may be required for such performance. Irradiation and freezing, for example, minimize the stimulus for immune reaction and may permit the transplant to serve its trellis function. Grafting was conducted with frozen, irradiated homogenous tendon in a Silastic sheath. The x-irradiated tendons were prepared by exposure to 1.5 Mrad in 10 sec and then stored at −70°F (for no longer than 3 months prior to use). Postoperatively, the affected limb was immobilized in a light plaster cast until the fourth postoperative week when the tendons were submitted for histologic study. The autografts and irradiated homografts with Silastic sheaths showed no adhesions, but healing seemed delayed in some cases. All of the unirradiated tendon homografts were either necrotic or completely separated from host tendon. (BBB)

45965 FURTHER STUDIES ON THE USE OF IRRADIATED HOMOGRAFTS AND ARTIFICIAL SHEATHS IN AVIAN AND MAMMALIAN TENDON INJURIES. Ashley, Franklin L.; McConnell, D. V.; Polak, T.; Stone, R. S.; Marmor, L. (Univ. of California, Los Angeles). Plastic Reconstruct. Surg., 33: 522-31(June 1964).

Histologic evidence is furnished indicating that frozen, irradiated tendon homografts may serve as a trellis for tendon regeneration. This is in contrast to fresh, unirradiated homografts, which undergo necrosis and fragmentation. Monkeys and Japanese apes were subjected to homograft procedures which consisted of the application of short ($1\frac{1}{2}$ to $2\frac{1}{2}$ cm) or long (4 to 6 cm) frozen, irradiated tendons (with Silastic sheaths at the anastomotic site at either end in the longer grafts). Irradiated tendons were prepared by exposure to 1.5 Mrad in 10 sec. Irradiated tendon homografts were examined at elapsed times of from 2 to 6 months. The sites of anastomosis were almost indistinguishable from the adjacent tendon. The homografts themselves were similar to the host tendon in appearance. No adhesions were noted on the segments of tendon to which Silastic had been applied. Histologically, there were numerous collections of lymphocytes and fibroblasts throughout the substance of the tendons, and on the surface of the tendons there were thin sheaths of flattened fibroblasts. By four months after grafting, irradiated homografts were microscopically almost indistinguishable from adjacent host tendon. The arrangement of the new cells in the graft was strikingly similar to the cellular pattern of the host tendon. Collagen bundles were well aligned and stained normally. Tensiometer measurement of the homografts' tensile strength, with or without Silastic sheathing, showed this to be comparable to the tensile strength of the sutured simple transections and of the autografts. In monkey digits with sheathed, irradiated homografts, function was observed to be satisfactory. Thus, frozen irradiated tendon homografts function in primates as they have previously been shown to function in fowl. That is, they serve as templates for the reconstruction of a tendon-like, fibrous structure between the host tendon ends. In doing this they apparently acquire a new cell population from the host, but whether they also acquire a new population of collagen fibers was not determined. (BBB)

45966 OBSERVATIONS ON RADIOTHYROIDECTOMIZED CHICKENS. Ellen, W. J.; Wentworth, B. C. (Univ. of Massachusetts, Amherst). Poultry Sci., 41: 134-41(Jan. 1962).

Three experiments with radiothyroidectomized (RTx) chickens are reported. In Experiment 1, both sexes of New Hampshire X Delaware chicks were used; in Experiment 2, off-spring of a Rhode Island Red X White Leghorn cross; and in Experiment 3, Hubbard Silver Cross males. When the chicks were about one week of age, they were fed a low-iodine diet containing thiouracil for 2 to 3 days. This pretreatment lowered the iodine content of the thyroids and enhanced the subsequent uptake and retention of ^{131}I. For one day prior to and one day following ^{131}I administration, the low-iodine diet without thiouracil was fed. Radioiodine was injected intraperitoneally as carrier-free Na ^{131}I solution, at a level of 1.5 mC per 100 g of body weight. These RTx chickens showed the following symptoms of extreme hypothyroidism: severely depressed growth, fringed feathers, obesity, shivering and pilomotor response (even in warm environment), subnormal gonadal development and function, lowered resting oxygen consumption, decreased weight of bursae Fabricii, and elevated serum cholesterol. In spite of failure to demonstrate residual thyroid tissue in most RTx chickens, ^{131}I uptake could be detected several months after radiothyroidectomy. It is concluded that the RTx birds were not completely thyroidless, although extremely hypothyroid. There was no evidence of parathyroid damage in RTx birds. (BBB)

45967 GENETIC EFFECTS OF CHRONIC IONIZING RADIATIONS ON MAN. Tanaka, K. (Tokyo Medical and Dental Univ.). Proc. Intern. Congr. Human Genet., 2nd, Rome, 1234-9(1961).

A survey was made by the questionnaire method on

children of radiological technicians in Japan who had worked for 25 yr or more in this field. Items included on the questionnaires were: name, sex, date of birth, address, family registration, locality, details on radiological occupation, spouse, reproductive history, and others. Analysis of the data showed that the sex-ratio among newborn infants conceived after the fathers' exposure was 55.54, which was significantly higher than the sex-ratio among infants conceived before the fathers' exposure, as well as that among a control group and among average Japanese. The average dose of irradiation per yr was estimated at 35 R, or a mean dose rate of 0.1 R/day or 0.7×10^{-4} R/min. The exposures were not continuous, but intermittent. A second, more extensive survey was conducted by sending similar questionnaires to 4793 radiological technicians, i.e., all members of the Japanese Society of Radiation Technology and of the Japanese Association of X-ray Technicians, of which 82% responded. Analysis of these data revealed a higher sex-ratio in children born after fathers' exposure than that in children born before fathers' exposure. The difference is significant at the 5% level. In the first series the rate of increase of the sex-ratio per unit dose of radiation was estimated at 3.8×10^{-5}/R. This value is similar to the estimation of 3.6 to 5.6×10^{-5}/rep for atomic-bomb survivors and also to that of 6 to 12×10^{-5}/rad for patients who had received x-ray therapy. Since the X chromosomes of irradiated fathers would be transmitted to their daughters' children, the sex-linked recessive lethal mutant genes induced in fathers' gonads would increase death of grandsons and, thus, would decrease the sex-ratio in the daughters' children. In previous studies the dominant lethal mutation rate was estimated on the basis of the sex-ratio in children of exposed fathers and the recessive lethal mutation rate on the basis of the sex-ratio in children of exposed mothers. Since sensitivity to radiation and states of exposed germ cells may differ between males and females, some reservation should have been needed to compare the estimated mutation rates. When data on the grandchildren are available, effects of dominant and recessive lethal mutations due to the same irradiations can be estimated on the basis of sex-ratios in children of exposed fathers and that in children of exposed fathers' daughters, respectively. (BBB)

45968 FERTILIZATION IN DROSOPHILA. II. TIME OF INACTIVATION OF A GENE EFFECT. Hildreth, Philip E. (Univ. of California, Berkeley). Proc. Natl. Acad. Sci. U. S., 54: 736-41(Sept. 1965). (UCRL-16198).

Previous experimenters found an inactivation effect of a suppressor gene in Drosophila melanogaster when eggs in early stages after fertilization were irradiated. A repetition of these experiments with presently available stocks did not confirm the original findings. The data do not support the view that the gene action of Su-er is determined very early, or the alternative view that a substance upon which the gene Su-er acts is inactivated by x rays after fertilization of the egg but before cleavage divisions have begun. (auth)

45969 REDUCTION IN LIFE EXPECTANCY AS A MEASURE OF RADIATION-INDUCED GENETIC DAMAGE IN MICE. Spalding, J. F.; Brooks, M. R. (Los Alamos Scientific Lab., N. Mex.). Proc. Soc. Exptl. Biol. Med., 119: 922-5(Aug.-Sept. 1965). (LA-DC-6952).

Life span studies on first generation male and female breeders and on second generation virgin females from 20 generations of x-irradiated mice sires were done. The results of this and other studies strongly suggest that factual statements crediting reduction of life span as being a measure of a radiation-induced genetic decrement in viability are premature and inconsistent with experimental evidence at this date. (auth)

45970 BIOLOGIC RELATIONSHIP OF ENDOTOXIN AND OTHER TOXIC PROTEINS. V. ALTERATIONS OF BLOOD-BRAIN BARRIER AND SUSCEPTIBILITY TO SNAKE VENOM. Staab, Edward V.; Good, Robert A.; Condie, Richard M. (Univ. of Minnesota, Minneapolis). Proc. Soc. Exptl. Biol. Med., 119: 1030-4(Aug.-Sept. 1965).

The blood-brain barrier of normal rabbits was altered by the use of E. coli endotoxin, by x irradiation (whole body or head alone), and by inducing experimental allergic encephalomyelitis. All animals so treated were hypersusceptible to venom. It is concluded that endotoxin induced hypersusceptibility to some snake venoms possibly results from alteration of the so-called blood-brain barrier. (auth)

45971 EFFECT OF GAMMA IRRADIATION ON RESPONSE OF FASTED RATS TO ERYTHROPOIETIN. Eskuche, I.; Hodgson, G. (Universidad de Chile, Santiago). Proc. Soc. Exptl. Biol. Med., 119: 1102-6(Aug.-Sept. 1965).

The effects of γ-irradiation on the response to erythropoietin (EP) of fasted rats depend on the moment irradiation is given in relation to EP injection. Maximum depression of the erythropoietic response is obtained when irradiation is given 3 to 5 hours before and 10 to 24 hours after EP. Minimum effects are obtained when irradiation is given between 1 to 5 hrs after and 24 to 48 hrs before EP. When irradiation is given after EP there is a clear EP dose effect; this is not the case when irradiation is given prior to EP. (auth)

45972 RADIOTHYROIDECTOMY OF LARVAL STEELHEAD TROUT. Norris, David O.; Gorbman, Aubrey (Univ. of Washington, Seattle). Proc. Soc. Exptl. Biol. Med., 119: 1205-7(Aug.-Sept. 1965).

A simplified procedure for radiothyroidectomy of large numbers of juvenile steelhead trout (alevins or fry) is described. Complete destruction of thyroid tissue was achieved 8 to 14 weeks after immersion in a solution of radioiodine in lake water (initial concentration: 12.5 or 25 μC I-131/cc for 8 days). (auth)

45973 THE QUANTITATIVE ASSESSMENT OF HEREDITARY DAMAGE INDUCED BY RADIATION. James, Allen P.; Newcombe, Howard B. (Atomic Energy of Canada Ltd., Chalk River). Progr. Med. Genet., 3: 217-59(1964).

This review, which refers to 161 publications, shows that an abundance of data from lower organisms has failed to provide information that can be applied quantitively to man with assurance, and estimates of the magnitude of the genetic consequences of irradiation of human populations remain uncertain. The animal data are surveyed in terms of locus specificity of gene damage, linearity of dose effects, influence of dose rate and fractionation, cell stage and type, estimates of dose yield, and the general problem of radiation hazards. The three general methods used to obtain quantitative estimates of genetic damage induced by radiation are examined. One utilizes information on the number of loci and their induced mutation rates to estimate the number of genetic deaths expected from a given exposure of radiation. The second utilizes the natural incidence of recognized hereditary defects; the hazard is defined in terms of the expected increase in prevalence of these defects. The third method predicts genetic deaths from information on the natural prevalence of recessive damage as determined in consanguinity studies. Using the first method it is calculated that the exposure of a population having 10^8 births per generation to a dose of 5 R delivered at low intensity would eventually lead to 6000 genetic deaths. By the second method, using a value of 85 R as the doubling dose and 5% as the prevalence of responsive defects, it can be calculated that a dose of 5 R delivered at low intensity to a population which produced 10^8 progeny in a generation would result in the production of about 3000 genetically disabled persons. For the third method, using a value of 0.08 for expressed damage per gamete per generation, a doubling dose of 85 R for exposures of low intensity, and a population giving birth to 10^8 progeny per generation, the estimated number of genetic deaths resulting from 5% is 9000. (BBB)

45974 EFFECTS OF X-IRRADIATION ON THE RESPONSE OF ANIMAL CELLS TO VIRUS. Levine, Seymour

(American Cyanamid Co., Pearl River, N. Y.). Progr. Med. Virol., 5: 127-68(1963).

This review, referring to 101 publications, considers the action of x rays on viruses and their host cells, with particular attention to bacteriophage and certain animal viruses (influenza, polio, vesicular stomatitis, herpes simplex, Newcastle disease, measles, psittacosis, polyoma, and Rous sarcoma). This survey reveals that when cultures of animal cells are irradiated, they lose their ability to multiply by a process that is multi-hit and involves chromosome damage. In most instances the survival curves have an extrapolation number of about two, the D_0 being 50 to 250 R for mammalian cells and 300 to 600 R for chicken embryo cells. A cell that is sterilized by x rays can continue to grow, by a balanced synthesis of the main cellular components (DNA, RNA, and protein), and can form a giant cell. Growth eventually stops, and the cell disintegrates. Giant cells are more sensitive than cells of normal size to the cytopathic action of some viruses, possibly because virus infection accentuates the tendency of such cells to degenerate. Giant cells yield more virus, but the amount of virus synthesized is proportionate to the cell volume, so that the yield of virus per unit volume of protoplasm is the same for giants and normal cells. An increase yield of virus appears to be a general phenomenon of all cells enlarged by growth. Two characteristics of the giant cell (increased sensitivity of the cytopathic effect of virus and increased virus yield) have been advanced to explain the changes in virus susceptibility or adaptability observed in ordinarily resistant or nonsusceptible cells in x-irradiated monolayers. It is suggested that giant cells serve as an enrichment culture for the selection from the virus population of those variants able to grow in the cell line, the greater virus yield per cell from the giants increasing the probability for successful passage of the variants. In every case where radiation has been used to follow the intracellular development of animal viruses (Luria-Latarjet experiment), the curves plotting the surviving infective centers vs the dose of radiation are exponential and remain so throughout most of the growth cycle. Where the curve shifts because of multi-hit inactivation, the extrapolation number is never greater than two even in the case of a virus that accumulates in the cell, like poliovirus. Capacity studies also present a picture that is similar for all the viruses studied. The cells lose their ability to produce virus as a result of either one hit or very few hits, except where secondary effects related to cell survival or the sensitivity of the assay procedure are involved. The curve of the residual capacity vs the radiation dose levels off at high doses. The current explanations advanced for the Luria-Latarjet and capacity studies with bacteriophage are reviewed and discussed in terms of their applicability to similar studies with animal viruses. (BBB)

45975 IMMEDIATE ALTERATION OF UREA PERMEABILITY AFTER ALPHA-IRRADIATION OF ALLIUM EPIDERMIS CELLS. Wattendorff, J. (Freiburg, Switzerland). Protoplasma, 60: 162-8(1965).

The effect of ^{210}Po α particles on permeability of onion (Allium cepa) epidermal cells was studied. The density of radiation was 0.7 to 36×10^{10} α particles/mm^2, corresponding to doses of 3360 to 3700 krad on the basis of 10% absorption in the cuticle. Increasing protoplast length during plasmolysis was measured as a function of time. Urea solution was applied after plasmolysis in glucose solutions of stepwise increased concentrations, the last being equal to the urea concentration. The straight line in the time vs protoplast length diagram seen in the controls was changed in the irradiated samples immediately after irradiation: after high radiation doses deplasmolysis was accelerated suddenly. The diagrams show a break in the straight line at the time of irradiation which leads to another much steeper straight line. This indicates a sudden increase of permeability during irradiation and maintenance of this increased permeability value after irradiation. This was shown by a sudden steepening of the curve after irradiation which returned gradually to a slope similar to that at the beginning. Ultimately there was a straight line nearly parallel to that before irradiation, only at a higher level. After weaker doses, there was a slight increase of the slope of the curve which changed soon to a decrease, falling below the slope of the original straight line. Later on, it increased again, up to nearly the original slope, but at a lower level. After the weakest doses, a persistent decrease of permeability could be seen. The increase of the protoplast length was proportional to the time, both before and after irradiation. Experiments in autumn with onions cultivated in Switzerland showed a higher resistance to α rays than with Italian and Egyptian material in winter and spring. For the straight lines shown in the diagrams, absolute permeability constants could be calculated for the time before and after irradiation. (BBB)

45976 X-RAY INACTIVATION OF PAPAIN COUPLED WITH A SYNTHETIC POLYPEPTIDE. Giovannozzi-Sermanni, G.; Di Marco, G. (Universita, Rome). Radiation Res., 26: 63-8(Sept. 1965).

Free soluble papain was coupled with poly-p-aminophenylalanine obtaining an insoluble product with enzymatic activity. The insoluble enzyme-polymer complex, irradiated with different doses and under different conditions, showed increased radioresistance. This behavior could be explained by a mechanical radioprotection when in aqueous suspension or by an energy transfer when in a dry state. Further evidence is needed to clarify these points. (auth)

45977 SINGLE-DOSE AND SPLIT-DOSE X-RAY STUDIES ON THE RADIOSENSITIVITY OF AUTOCHTHONOUS RADIATION-INDUCED LYMPHOSARCOMAS IN C57BL MICE. Hanks, Gerald E.; Kaplan, Henry S. (Stanford Univ., Palo Alto, Calif.). Radiation Res., 26: 84-94(Sept. 1965).

Single and fractionated doses of x irradiation were used to eradicate permanently early radioinduced thymic lymphosarcomas in C57BL mice. The data indicate that a single dose of 876 R will cure 50% of localized thymic tumors estimated to contain 2×10^7 tumor cells, and that there is no recovery up to 8 days after a conditioning dose of 200 R. Calculations from these results yield a D_{37} of 53 R, with an extrapolation number of 1.0. The pyknotic response of this tumor was studied after single doses of x-irradiation. The dose-response curve constructed from pyknotic cell counts has a D_{37} of 62 R with an extrapolation number of 1.07. (auth)

45978 A STUDY OF THE TIME COURSE OF RECOVERY OF PARAMECIUM AURELIA FROM THE LETHAL EFFECTS OF X-RAYS. Calkins, John (Univ. of Kentucky, Lexington). Radiation Res., 26: 124-31(Sept. 1965).

The time course of recovery of Paramecium aurelia from the lethal effect of x irradiation was investigated. Recovery seems to show the pattern frequently found in other materials; a rapid but transient recovery is followed at about 3 to 4 hours postirradiation by some return to sensitivity, then a recovery to approximately the unirradiated condition ensues. The oscillation in the recovery of Paramecium aurelia does not seem to be the result of the combined effects of synchronization and the normal variation of radiosensitivity during the growth cycle. (auth)

45979 ON THE CHARACTER OF CHANGES OF γ-AMINOBUTYRIC ACID IN BRAIN TISSUES DURING LOCAL IRRADIATION OF CEREBELLUM. Mironova, A. P. (Inst. of Biological Physics, Moscow). Radiobiologiya, 5: 536-9(1965). (In Russian).

Irradiation of the cerebellum of guinea pigs to 8 to 9 kR caused a decrease in the gamma-aminobutyric acid content of the cerebrum and an increase in the cerebellum. The cerebral decrease was immediate, but the cerebellar increase was gradual, reaching a maximum on the second day. Poisoning of the brain of dogs with 1 mg of sodium arsenate decreased the γ-aminobutyric acid content in both the cerebrum and cerebellum. The combined action of arsenic and 8 kR of x radiation decreased this compound somewhat in the cerebrum but had no significant effect on it in the cerebellum. (tr-auth)

45980 LATE EFFECTS AFTER THOROTRAST INJECTION. Schlager, Kurt (Roentgeninstitut des Wil-

helminenspitals, Vienna). Radiol. Austriaca, 14: 285-94 (1963). (In German).

Four cases of late effects of Thorotrast injection are reported by the author. In one male patient who had received Thorotrast 21 yr previously, opaque areas were observed by fluoroscopic examination of the liver, spleen, and in the right inguinal region. In a 63-yr-old patient who had been injected with Thorotrast 33 yr previously the spleen was found to be thickened and small, and the liver exhibited numerous opaque areas with x-ray examination. Liver biopsy indicated fibrosis, and numerous α tracks were detected by autoradiography of the tissue. The patient had a distended left heart, marked esophageal varices, and prostatic carcinoma. The third patient was cachectic and had pain in the right upper abdomen and the right hip. Respiration was labored and was accompanied by a productive cough. X-ray examination showed bilateral cavernous tuberculosis, with multiple foci, osteoclastic foci were observed in the leg and cranial bones. The liver, spleen, and abdominal lymph nodes showed accumulation of Thorotrast from injection 20 yr previously. Upon autopsy of this patient a hypernephroma was found with metastases to lung, pleura, liver, lymph nodes, and bone. The fourth patient had received Thorotrast 17 hr prior to detection of a tumor that contained particulate material in the region of the head of the pancreas, with penetration into adjacent tissues. Large quantities of contrast medium were observed in the spleen, lymth nodes, liver, and gallbladder region. The right lobe of the liver was extensively necrotic and the left lobe was soft and discolored. The surrounding tissues and blood vessels were distorted and thrombosed, with extensive deposits of Thorotrast. In this and the third patient the effects of Thorotrast were definitely shown. 78 references. (BBB)

45981 THE ACUTE EFFECTS OF RADIATION ON INTACT MAMMALS. Evans, Titus C. (Univ. of Iowa, Iowa City). Radiol. Clin. North Am., 3: 219-26(Aug. 1965).

This review considers acute reactions, from moderate to lethal in severity, occurring within 30 days of exposure. The exposure range is from about 100 R to several thousand R. The x-radiation dose to kill 50% of the individuals within 30 days (LD_{50}) varies with species but is usually 400 to 500 rad. The dose-effect curve is S-shaped, and beginning at about 100 rad the increase in mortality is rapid as the dose is increased. The percentage increase with dose becomes lower as the 100% value is approached. Acute effects of radiation in man and experimental animals are described in detail. At exposure rates around 1000 R/min, animals may become highly excitable, lose balance, undergo convulsions, collapse, and die. Pathologically, the effect of several hundred thousand rad of ionizing radiation is complete tissue breakdown. In the exposure range from 10,000 to 100,000 R the animals die within a day or two of damage to the central nervous system (CNS). With 2000 to 10,000 R to the whole body the animals are spared CNS effects and they live for three to six days. The effects on the gastrointestinal tract are marked. In the exposure range from 100 to 1000 R, survival time is reduced as the exposure is increased. Exposures in the 1000 R range result in death in from six to nine days from damage primarily to the hematopoietic system. Use of bone marrow transplantation to prolong survival is described. Other attempts to treat radiation damage are by chemical means; the best protective agents are those that appear to produce hypoxia, which reduces sensitivity to irradiation. Recent research reports in this field are cited. (57 references.) (BBB)

45982 LETHAL EFFECTS OF WHOLE-BODY IRRADIATION IN MICE: THE DOSE-TIME RELATION FOR TERMINATED AND TIME-DEPENDENT EXPOSURE. Sacher, George A. (Argonne National Lab., Ill.). Radiol. Clin. North Am., 3: 227-41(Aug. 1965).

Some experimental and theoretical approaches to the estimation of the lethal effects of whole-body exposure to arbitrary time patterns of irradiation with x or γ rays are considered. Two large bodies of experience about the effects of fractionated radiation exposure are reviewed. Data from radiotherapy trials consistently yield relations of dose to number of fractions that obey about fractional-power rule. Data on death of mice within 30 days after the final fraction just as consistently yield a linear relation of dose for 50% lethality to number of fractions. Increase in fractionation leads to a greater decrease of effectiveness per roentgen for killing of tumors than it does for killing of mice. In view of the computations presented here, it is suggested that consideration must be given to the possibility that the different curves obtained are due not to some unexplained difference in recovery mechanisms in the two situations but rather to the difference between a system in which the risk of death is appreciable for only a short period, as against a system in which mortality can occur over a period of many weeks. The convolution integral for lethality from a rectangular exposure pattern bears out this hypothesis, in that, as originally computed, it embodied the assumption of a sharp endpoint and follows a curve. However, introduction of a correction term based on the known spread of times of death during and following fractionated exposure brings the dose-time relation closer to the form of the experimental curves for $LD_{50/30}$ vs time for irradiated mice. (BBB)

45983 LATE POSTRADIOTHERAPY LESIONS OF THE CENTRAL NERVOUS SYSTEM (CONCERNING ANATOMO-CLINICAL OBSERVATION OF CERVICAL MYELOPATHY). Alajouanine, T.; Lhermitte, Francois; Cambier, J.; Gautier, J. C. Rev. Neurol., 105: 9-21(July 1961). (In French).

A patient suffering from an undifferentiated epithelioma in the right nasal cavity was subjected to telecobalt therapy. He received a total dose of 20,700 R over ~40 days. Several months after tumor recession occurred, the patient showed clinical signs of a central nervous system disorder that later proved to be at the level of the cervical spinal cord, especially on the left side. The patient died nine months later, 21 months after the telecobalt therapy. Lesions in the cervical spinal cord were characterized by a predominance of white matter, by marked and characteristic alterations in the vascular endothelium, the presence of amorphous interstitial substance, and by poor astroglial staining reactions. The level of the spinal cord injury reflected the portals of radiation used in the specific treatment. The cervical cord is the region most heavily exposed in radiation treatment of cancer of the mouth, larynx, and esophagus. These side-effects often occur after conventional doses, and usually do not appear until 9 to 12 months after treatment. Current hypotheses proposed to explain the histogenesis of these nervous system lesions are reviewed. (BBB)

45984 INVESTIGATION OF LATE POSTIRRADIATION CHANGES IN THE REGENERATION POTENTIALITY OF THE BLOOD CELL FORMATION. Simek, Josef (Charles Univ., Hradec Kralove, Czechoslovakia). Sb. Ved. Praci Lekar. Fak. Karlovy Univ. Hradci Kralove, Suppl. 6, 85-118(1963). (In Czech.).

Acute and chronic blood loss (by bleeding or hemolysis induced by phenylhydrazine) was used to investigate the functional capability of the hematopoietic system of rats which had previously undergone heavy irradiation. The tests were conducted at long intervals after irradiation when the peripheral blood picture was almost normal and the bone marrow did not show any morphologic deviations from the normal. The experiments were carried out on 9-week-old white rats irradiated with a 400-R dose of 180-kv x rays. Three main changes were observed in the peripheral blood of rats whose blood formation was stimulated by acute hemorrhage (loss of 2 ml of blood per 100 g of body weight) long after irradiation. These included marked leukocytosis, of both lymphocytes and neutrophils, one month after irradiation before and after acute blood loss. In the experimental rats the red blood cell counts returned to normal more slowly than in the controls after the stress of hemorrhage. Leukocytosis was observed again three months after irradiation before acute hemor-

rhage as well as after it. The most striking finding was the anemia observed before acute blood loss and, as compared with the controls, a slower return of the red cell counts to normal, including the values of hemoglobin concentration after this intervention. No essential differences were found between experimental and control groups six months after irradiation. Similar changes were observed in peripheral blood of rats whose blood formation was stressed with protracted hemolysis (by repeated administration of phenylhydrazine) 1, 3, or 6 months after irradiation. The leukocytosis observed in rats after acute or protracted anemia, 1, or even 3 months after irradiation and induced anemia with a slow return to normal of the red cell counts and the values of hemoglobin concentration which were found in the anemic rats, predominantly three months after irradiation, suggest a late postirradiation abnormality in blood cell formation. This is supported by the findings of changes in the cellularity and content of nucleic acids in spleen and bone marrow of irradiated rats after acute blood loss. The results show that the stress of new blood cell formation gives a better picture of late postirradiation changes in reactivity of the blood-forming tissues than routine hematologic examinations. (TCO)

45985 HOW CELLS REPAIR RADIATION DAMAGE. Moseley, B. E. B. (Cambridge Univ., Eng.). Sci. J., 1: 75-80(Aug. 1965).

A brief historical review is given on studies of the effects of ionizing radiation on bacteria, yeast cells, and isolated mammalian cells in tissue culture. The mechanisms involved in the resistance of bacteria to large doses of ionizing radiation are discussed. The effects of ionizing radiation such as x or gamma radiation on cells is explained, with emphasis on the effects on DNA. Studies of the repair of damaged DNA cells after exposure to ultraviolet radiation are described. The effect of preliminary exposure to gamma radiation before the ultraviolet exposure was discussed. It is believed that the ionizing radiation damage can be repaired enzymatically by a mechanism similar to that shown to operate for the dark repair of ultraviolet damage to DNA. (J.F.P.)

45986 FOCAL ANTIBODY PRODUCTION BY TRANSFERRED SPLEEN CELLS IN IRRADIATED MICE. Playfair, John H. L. (Univ. of California, Berkeley); Papermaster, Ben W.; Cole, Leonard J. Science, 149: 998-1000).

Lethally irradiated mice were injected with small numbers of normal spleen cells and then immunized with sheep erythrocytes. Antibody activity was found in their spleens in localized areas whose number corresponded to the number of spleen cells injected. When sheep and pig erythrocytes were injected together, antibody against each was found in separate areas. Each area may consist of the progeny of a single precursor cell, restricted to forming a single antibody. (auth)

45987 RAPIDLY OCCURRING RECOVERY PROCESSES IN THE SKIN AFTER X-RAY IRRADIATION. Rausch, Ludwig (Universitaet, Giessen, Ger.). Strahlentherapie, 127: 393-404(July 1965). (In German).

Using the ear perforation test of rabbits and mice as models, previously reported results concerning fast recovery events occurring in irradiated skin were confirmed. However, the fast occurring recovery cannot be observed in the rabbit ear after a single irradiation with 3000 R. Quickly developing recovery processes were obtained similarily for the mouse ear. The event in the rabbit ear is considered to be a local process since it is not influenced significantly by a prior whole-body irradiation with sublethal doses. The fast occurring recovery events in the rabbit ear can be decreased considerably by blocking the blood supply during the especially intensive occurring recover (within the first 2 hours after irradiation). Nevertheless, they can still be detected under these conditions. (auth)

45988 EFFECTS OF IONIZING RADIATION ON COMPLEX CELL SYSTEMS AND HIGH ORGANISMS. Rajewsky, Boris (Max-Planck-Institut fuer Biophysik, Frankfurt am Main). Strahlentherapie, 128: 1-10(Sept. 1965). (In German).

The increasing amount of information obtained both in radiobiological research and in clinical investigations urgently requires a systematized classification system. Such a system, applying past experience, is discussed. The experimental results, classified in this way, show the existence of several effect mechanisms in irradiated organisms. These mechanisms can occur simultaneously or successively. They can be independent from or related to each other and they may reinforce each other or act as an antagonist. Experimental results give further proof of this concept. A possible experimental analysis of different mechanisms is shown. Characteristic for each mechanism is its reaction velocity. It may be seen, that each mechanism has its own characteristic velocity. From this it can be concluded, that different irradiation effects, based on the different mechanisms, occur in different dose ranges. The total effect of an irradiation is the sum of the single irradiation effects which may appear at different times. According to this concept, recovery events in the different dose ranges are also different. (tr-auth)

45989 TIME-DEPENDENT RELATION OF DOSE EFFECTS. Schaefer, Peter; Schumacher, Werner; Krokowski, Ernst; Frost, Dietrich (Freie Universitaet, Berlin; Rudolf-Virchow-Krankenhaus, Berlin). Strahlentherapie, 128: 93-7(Sept. 1965). (In German).

The time dependent relationship of dose-effects after a single irradiation, using the tibia of rabbits, with both 200 kv x rays and 35 Mev electrons was not found to be proportional. Under certain conditions, 35 Mev electrons were found to be more effective than 200 kv x rays. In experiments dealing with the Relative Biological Effectiveness (RBE), observation time is highly significant. The variation in dose effects, which was observed, could be the result of qualitative differences in reactions of certain molecular structures with various ionic topographies. (tr-auth)

45990 STUDIES ON THE QUANTITATIVE EFFECTS OF SUBLETHAL AND LETHAL WHOLE-BODY IRRADIATION OF WHITE MICE. Gauwerky, Friedrich (Allg. Krankenhauses St. Georg, Hamburg). Strahlentherapie, 128: 119-35(Sept. 1965). (In German).

The effect of 200 kv x rays and ^{60}Co γ rays on short period lethality of albino mice was investigated. The following conditions were used: sieve irradiation and total-body irradiation without filter, radiation doses between about 400 and 1700 rads, but never exceeding that required for obtaining the 3.5-day-effect. (tr-auth)

45991 STUDIES ON THE DEVELOPMENT OF IMPROVED STRAINS OF STREPTOMYCES CITREUS THROUGH INDUCED MUTATION. Naha, P. M.; Nandi, P. Trans. Bose Res. Inst. (Calcutta), 26: 97-105 (Sept. 1963).

Different doses of ultraviolet and gamma radiations were administered to Streptomyces citreus with a view to obtain better antibiotic-producing mutants. Some of the mutants obtained through γ irradiation only showed higher titre values; the isolates of the UV-irradiated strains were not promising and therefore not selected for further experiments. Four strains, namely M-88, M-1017, M-1038, and M-2042, were preliminarily selected for detailed study as all of them showed higher antibiotic yield. Of these, M-1017 was finally selected for large-scale production of the antibiotic in submerged culture because this strain remained stable through successive generations. (auth)

45992 THE REACTION OF SOMATIC CELL NUCLEI TO IONIZING RADIATION. Fasske, E.; Themann, H. (Universitaet, Munster, Ger.). Verhandl. Deut. Ges. Pathol., 47: 246-53(1963). (In German).

Four studies were conducted in attempts to elucidate the primary site of action of radiation on the cell nucleus. In the first, light and electron microscopic studies were made of mouse tissues after x and ^{60}Co γ irradiation with doses of 250 to 9000 R. Similar examination was made of high-dosage (250-kR) irradiation of isolated cell nuclei in vitro. Uptake of ^{3}H-thymidine by nuclei was investigated

in tissues of the whole-body irradiated mouse. In the fourth experiment quantitative measurements were made of DNA and DNA P content after uptake of ^{32}P at high doses in cell nuclei of rabbit organs. Low doses of both x and γ radiation in mice caused as the first reaction in somatic cell nuclei a swelling, central vacuole formation, and displacement of chromatin to the inner side of the nuclear membrane. The outer nuclear membrane, contiguous with the endoplasmic reticulum, also showed vacuolation. The nucleolus showed little initial change. The in vitro experiments showed that very high dose irradiation degraded the thread-like DNA molecules, not only by rupturing H bonds between the base pairs but by damage to the sugar and phosphate components as well. The studies with ^{3}H-thymidine and ^{32}P showed that irradiation acts on premitotic DNA formation as well as on the performed DNA molecules. The organs with a high rate of DNA replication, such as testis, thymus, and bone marrow, were especially radiosensitive. (BBB)

45993 ON THE BIOLOGICAL EFFECTIVENESS OF ELASTIC NUCLEAR COLLISIONS. I. INACTIVATION OF RIBONUCLEASE BY SLOW PROTONS. Jung, H. (Kernforschungszentrum, Karlsruhe, Ger.). Z. Naturforsch., 20b: 764-72(Aug. 1965). (In German).

Extremely thin layers of ribonuclease were irradiated with slow protons and the differential inactivation cross section determined for various proton energies in the range from 0.8 to 60 kev. At higher proton energies the inactivation cross section is not strongly dependent on energy but with decreasing proton energy it decreases rapidly, reaches a sharp minimum at 1.2 kev and increases again at still smaller energies. By comparing the experimentally determined inactivation cross sections with the cross sections for energy loss in elastic nuclear collisions and in ionizations, respectively, elastic collisions were demonstrated to destroy, in fact, the enzymatic activity of ribonuclease. The energy required for an inactivation by nuclear collision is only one fourth of the energy necessary for an inactivation by ionization. (auth)

45994 STRUCTURAL CHANGES IN THE MEDIA OF THE RABBIT AORTA AFTER LOCAL IRRADIATION ($^{90}Sr-^{90}Y$). David, Heinz; Kunz, Jochen (Humboldt-Universitaet, Berlin). Z. Zellforsch. Mikroskop. Anat., 66: 83-95(1965). (In German).

Localized irradiation of the surgically exposed rabbit aorta was carried out with a $^{90}Sr-^{90}Y$ irradiator. The total dosages administered were 3, 15, and 30 kR, given at a rate of 18 R/sec. The media of the vessels irradiated were studied over several time intervals, ranging from 3 days to 8 months, after the irradiation. The tissues were studied by the light microscope as well as by the electron microscope. In the aortic media the elastic elements became detached from the smooth muscle cells and acquired a moth-eaten appearance. Finally, the elastic lamellas broke down completely, with vacuolization of the muscle cells with subsequent vacuolar disintegration. The changes in the elastic fibers were the result not only of a direct toxic injury, but also of indirect injury from the lack of stimulation substances after the disappearance of muscle cells. After a long interval, hyperplasia of the elastica is observed in the bordering areas. This is accompanied by an increase in function of the smooth muscle cells. Like the increase of collagen fibers observed in the irradiation area, this is an event that could be considered to be a reactive phenomenon. It was detectable only by the electron microscope. It was not possible to assign the exact sequence of events that led up to the increase in elastic substance. Probably the genesis of this is similar to what is seen in embryonic vessel walls. (BBB)

45995 LATE RADIATION NECROSIS OF THE BRAIN. Chandler, Arthur; Tucker, Francis C.; Herzberger, Eugene E. (Monroe Clinic, Monroe, Wis.). Wisconsin Med. J., 63: 297-300(July 1964).

This case report concerns a 59-yr-old woman complaining of frequent headaches in the frontal region of the cranium. Eighteen years previously, 27 radon seeds had been implanted in a subcutaneous neurofibrosarcoma in her right temple. The tumor mass subsequently subsided, leaving atrophic skin and subcutaneous tissues. At subsequent hospitalization severe bilateral frontoparietal headache radiating to the jaw and left arm was present. She also complained of severe pain in the lumbosacral region, and had occasional hallucinations. X-ray films showed the location of the radon seeds, low in the right frontal region superficial to the skull. A right frontotemporal craniotomy was performed and puncture of the brain with a ventricular needle revealed the presence of two large (5-cm dia) intracerebral cysts. One was located in the frontal lobe and extended toward the basal and medial aspects of this lobe. The other was in the temporal pole. The cysts were drained and portions of the abnormal brain overlying the cysts removed for microscopic study. This revealed hemosiderin deposition of the walls of the cysts, perivascular accumulation of lipid phagocytes and protein-rich fluid, hyaline thickening of blood vessel walls, demyelinization of white matter, and proliferation, with swelling and hypertrophy, of astrocytes. These findings were interpreted as late radiation necrosis of the brain. The patient recovered uneventfully. It was estimated that the cumulative dose to the right frontal lobe was about 7000 R (γ rays) at 2-cm depth, 3300 at 3 cm, and 1800 at 4 cm. The tolerance dose of radiation for the brain stem and spinal cord is about 3500 R in 17 days for large fields and 4500 R in 17 days for small fields. Of interest is the long period between the time of implantation and development of symptoms. In most cases, this time interval is under two years. The location of the lesions in the frontal lobe and anterior portion of the temporal lobe probably allowed this patient to pass through the stage of necrosis without symptoms. It is possible that cystic necrosis might be observed more commonly in late radiation necrosis of the brain were it not that significant symptoms usually appear at the time of the demyelinization and encephalomalacia, leading either to death or surgical intervention at that time. (BBB)

45996 SOMATIC HAZARDS FROM ACCIDENTAL EXPOSURE TO RADIATION: RADIOBIOLOGICAL CONSIDERATIONS. Lamerton, L. F. (Inst. of Cancer Research, Sutton, Surrey, Eng.). pp 75-84 of Protection of the Public in the Event of Radiation Accidents. Geneva, World Health Organization, 1965.

The estimates of the carcinogenic risk to man from exposure to radiation are discussed and data are reviewed from the few available studies. It is pointed out that present evidence suggests that acute leukemia and chronic myeloid leukemia are the long-term somatic effects of greatest significance in irradiated human populations. It is assumed that there is a linear relationship between dose and effect and that for some types of somatic effects there may be a threshold dose, but for the induction of leukemia and of many other types of neoplasm it is likely that there is a finite risk even at the lowest doses. In making theoretical deductions, one of the most important problems is the extent of the similarity between the basic carcinogenic mechanisms of radiation and of the chemical, viral, and other factors important in the etiology of spontaneous cancer. Data on the Japanese survivors exposed to radiation from the atomic bombs at Hiroshima and Nagasaki show an increase in cancer of the thyroid in the more heavily exposed persons and it is to be expected that an increased incidence of other forms of neoplasms will become evident in the future. (C.H.)

45997 THE STUDY OF SOMATIC DAMAGE IN MAN FROM EXPOSURE TO HEAVY DOSES OF RADIATION. Court Brown, W. M. (Western General Hospital, Edinburgh). pp 85-96 of Protection of the Public in the Event of Radiation Accidents. Geneva, World Health Organization, 1965.

Clinical data are reviewed on men exposed to high-level doses of radiation. It was found that it is possible to define fairly accurately the interval of time between irradiation and the onset of symptoms, the latter being notably sudden. For a given dose of radiation, the length of this time interval appears directly related to the body size, the larger the

patient the longer the interval. There also appears to be a relation between the length of the interval and the severity of the symptoms, the shorter the interval the more severe the symptoms. These features suggest that the development of symptoms is related to the circulation of some toxic substance or substances that have to reach some critical concentration in the extracellular fluid before symptoms develop. The major types of delayed radiation effects include the development of nephrosclerosis, the development of cataracts, and the development of tumors. Difficulties encountered in handling and interpretation of data on human beings and the establishment of dose-response relationships for delayed radiation effects are discussed. (C.H.)

45998 RELATIVE BIOLOGICAL EFFECTIVENESS. Rossi, H. H. (Columbia Univ., New York). pp 108-13 of Radiation Dosimetry. New York, Academic Press, 1964.

The relative biological effectiveness of some radiation, r, compared to some standard radiation, s, is defined by D_s/D_r, where D_s and D_r respectively are the doses of the standard radiation and the referred radiation required for equal effect. The standard radiation is usually hard γ radiation or sometimes conventional x radiation. The determination of RBE is a difficult procedure requiring great care, and many of the apparent contradictions in the literature concerning RBE values are doubtlessly due to the fact that inadequate attention was paid to dosimetry as well as to radiation characteristics. The most accurate RBE determinations are probably those employing the track segment method. In this technique thin layers of biological material are traversed by charged particles of known energy. The usually linear energy transfer varies very little during traversal, and therefore a very narrow distribution is dealt with. There is not as yet enough physical data to provide an accurate numerical check, but it seems likely that the critical sites for inactivation are a good deal smaller than 1 μm. (J.F.P.)

45999 RADIOBIOLOGY. Gray, L. H. (Mount Vernon Hospital, Northwood, Eng.). pp 304-8 of Radiation Dosimetry. New York, Academic Press, 1964.

Radiobiology is susceptible to generalizations which cut across the usual classifications of biology, that is, plant and animal kingdoms. More usually the important parameters are concerned with questions of uniqueness and redundancy. Part of the similarity in the response of different organisms derives from the fact that genetic damage is often of paramount importance in determining the outcome of an irradiation; and it seems to be a fact that the structure, and the actual chemical composition of genetic material (DNA) is almost universal. Cells are not affected by the amount of radiation which passes through them but only by that part of the energy which is actually absorbed. For this reason the rad which is a measure of the amount of energy absorbed per unit mass of the medium is a very convenient quantity in terms of which the radiobiological response may be considered. Dose and dose rate are discussed. (J.F.P.)

46000 RADIOBIOLOGICAL PROBLEMS OF SPACE FLIGHTS. Frank, G. M.; Saksonov, P. P.; Antipov, V. V.; Dobrov, N. N. (Academy of Sciences, Moscow). pp 254-66 of Proceedings of the First International Symposium on Basic Environmental Problems of Man in Space. New York, Springer-Verlag, 1965.

Radiobiological problems of theoretical and also of great practical importance in solving the problem of protecting a cosmonaut from the harmful effects of cosmic radiation are discussed, along with the genetic effect of cosmic radiation and the biological influence of heavy particles. (P.C.H.)

46001 BIOLOGICAL HAZARDS OF RADIATION APPLICABLE TO MAN IN SPACE. Neary, G. J.; Hulse, E. V. (Medical Research Council Radiobiological Research Unit, Harwell, Eng.). pp 267-84 of Proceedings of the First International Symposium on Basic Environmental Problems of Man in Space. New York, Springer-Verlag, 1965.

The wide range of possible radiation exposure of man in space is noted, and the biological effects of radiation exposure in general are summarized. It appears that among the early effects, the prodromal systoms such as nausea and vomiting may be the limiting factors for an astronaut. The concept of recovery from radiation injury is discussed and it was concluded that there is no simple correlation between degree of recovery from early effects and the risk of delayed effects. Detailed data for recovery from early effects is available only for gross injury. The concept of relative biological effectiveness (RBE) of different types of ionizing particle is discussed. Although RBE varies with dose and dose rate, it probably assumes a constant value for any one effect at low doses or dose rates. The best estimate of the values for man are those given by the International Commission on Radiological Protection (ICRP) for use in the range of permissible exposures. Data relevant to high energy protons are given. The special problem of very heavy particles in space is noted and it was concluded that they are unlikely to be a limiting hazard. The delayed effects of radiation are reviewed. Chemical pre-protection of an astronaut appears to be undesirable. Treatment of radiation injury is summarized. It was concluded that both on general grounds and avoidance of early adverse reactions in flight, the permissible and emergency exposure levels suggested by the ICRP for occupationally exposed persons offer a reasonable guide for planning exposure to man in space. (auth)

46002 REPLICATION OF DNA IN ULTRAVIOLET-IRRADIATED BACTERIA (thesis). Pettijohn, David Everett. (Stanford, Calif., Stanford Univ.). 1964. 117p.

Density labeling with the thymine analog, 5-bromouracil, was used to follow bacterial DNA replication after uv irradiation. Density distribution analysis of the labeled DNA was made by means of density gradient equilibrium sedimentation. In nonirradiated cells the density label is incorporated sequentially into the chromosome at very few (possibly only one) growing points. After irradiation, a partial degradation of the damaged DNA and simultaneous synthesis at random in the genome was demonstrated. The random replication eventually leads to density heterogeneity among the isolated DNA molecules. The heterogeneity is due to differences in the 5-bromouracil/thymine ratio in different DNA molecules. Normal semi-conservative replication was observed if photoreactivating conditions followed the ultraviolet irradiation prior to density labeling. The DNA molecules containing these regions of random replications were thermally denatured and/or fragmented by sonication. The resulting density distribution indicated that the density label was incorporated into very short segments along single DNA strands. The findings are consistent with the view that in uv-resistant organisms a mechanism for repair replication exists in which single-stranded segments of the genome containing photoproducts can be excised and replaced, using the undamaged complementary strand as template. (Dissertation Abstr.)

46003 EFFECT OF BREATHING 5 PERCENT CARBON DIOXIDE AND 95 PERCENT OXYGEN AT ATMOSPHERIC PRESSURE ON TUMOUR RADIOCURABILITY. Inch, W. R.; McCredie, J. A.; Kruuv, J. (Ontario Cancer Treatment and Research Foundation, London, Can.; Univ. of Western Ontario, London, Can.). 19p. (CONF-650219-1). Gmelin, AED-CONF-65-043-1.

From Canadian Association of Radiologists, 28th Annual Meeting, Toronto.

Inhalation of 5% CO_2 and 95% O_2 at atmospheric pressure increased the blood flow and increased the x ray sensitivity of poorly vascularized tumor implants in mice. The radiosensitivity of tumor implants with a better blood supply was increased with air, but not with pure O_2. (C.H.)

46004 METHOD OF TREATING GRASS SEED. Speas, Clarence J. (to Oak Ridge Atom Industries, Inc.). U. S. Patent 3,197,640. July 27, 1965. Filed Oct. 9, 1961.

Grass seed can be treated with radiation to produce improved root systems and more rapid growth in the resulting plants. Total dosages required for maximum stimulation at relative humidities of 30-85% are tabulated for orchard grass, fescues, rye grasses, blue grasses, and red top.

Preferably the rate of irradiation is 100–500 R/min. Gamma sources employed are ^{60}Co and ^{137}Cs. (A.G.W.)

Radiation Effects Therapy and Countermeasures

Refer also to abstracts 45847, 46316, and 46898.

46005 (JPRS-31933, pp 6-12) EFFECT OF ANTI-RADIATION DRUGS ON THE MUSCULAR ACTIVITY OF THE SMALL INTESTINE. Semenov, L. F.; Strelkov, R. B.; Reshetnyak-Moiseeva, V. I. Translated from Farmakol. i Toksikol., 28: 351-5(May-June 1965).

Sulfur-containing preparations, such as cystamine, cysteamine, S-(2-aminoethyl)-isothiuronium, thiourea, and unithiole, introduced in radioprotective doses cause contraction of the isolated segment of the small intestine of the guinea pig. This effect is of a nature close to that of effect of acetylcholine. Serotonin and mexamine cause a specific contraction of the isolated intestinal segment, attenuated by dimedrol and aminazine and, to a lesser degree, by atropine, and hardly attenuated at all by redergam. The possibility of using atropine and dimedrol in the clinic in cases of appearance of side effects of radioprotectors merits attention and requires a special investigation. (auth)

46006 STUDIES ON CHEMICAL PROTECTION AGAINST IONIZING RADIATION. I. STUDIES ON THE TOXICITY OF SODIUM CYSTEINETHIOSULPHONATE FOR C_{57} BLACK MICE. Szczepkowski, Tadeusz; Zebro, Tadeusz; Stachura, Jerzy (Medical Academy, Krakow). Acta Med. Polona, 4: 305-12(1963).

Sodium cysteinethiosulfonate can be obtained synthetically by treating a mixture of cysteine and thiosulfate with iodine. The structure of cysteine thiosulfonate was found to correspond to the formula: $HOOC-CHNH_2CH_2-S-S-SO_3Na$. Experiments showed that sodium cysteine thiosulfonate injected intraperitoneally into C57B1 mice in doses of 0.5 g/kg and 1 g/kg body weight in aqueous solution before irradiating the animals has a protective action, causing longer survival and lower mortality among these animals as compared with control animals injected with 0.9% NaCl solution before irradiation. The protective effect of the compound was observed in mice irradiated with doses of 850, 700, and 520 R. Experimental results were followed by tests of the possible toxicity of sodium cysteine thiosulfonate. The compound was injected intraperitoneally in mice in doses of 2.0 to 20.0 g/kg body weight, and histologic studies were carried out on the kidney, liver, lung, heart, brain, intestine, and bone marrow. Organs of mice which died within 13 hr after receiving injections showed marked capillary hyperemia and extravasation of blood. Focal edema of the lungs and brain was also observed. In the kidney, necrosis and granular degeneration of epithelial cells of the convoluted tubules were seen. Similar, although less extensive, lesions were encountered in the liver cells. It was concluded that doses of 2 g/kg body weight of sodium cysteine thiosulfonate are not toxic in mice. (TCO)

46007 THE AFTER-EFFECT OF IRRADIATED HALOGENOPHENOL SOLUTIONS ON THE VIABILITY OF ESCHERICHIA COLI. PART II. EFFECT OF AFTER-IRRADIATION TREATMENTS ON THE BACTERICIDAL ACTIVITY OF IRRADIATED p-BROMOPHENOL SOLUTION. Namiki, Mitsuo; Matsuyama, Akira (Inst. of Physical and Chemical Research, Tokyo). Agr. Biol. Chem. (Tokyo), 29: 533-9(June 1965).

The bactericidal activity induced by ^{60}Co γ irradiation in p-bromophenol solution was significantly modified by heating after irradiation. A reagent solution, 3.0 mM p-bromophenol in 0.067M phosphate buffer at pH 8.0, was irradiated with a dose of 2.4×10^4 Rad at 10°C. The irradiated solution was then heated on water bath at 80°C, and bactericidal activity estimated by incubation with unirradiated cell suspension at 30°C for 40 min. The survival level was about 1% when cells were incubated with the irradiated solution without heating. The lethal activity of the irradiated reagent solution increased rapidly with increasing periods of heating, that is, with increasing temperatures; it attained a maximum after a few min (0.02% survival). Bactericidal activity then decreased with further heating until it was completely lost by heating for more than 10 min. Some activity remained even after 20-day storage at 4 to 10°C, but at higher temperatures, such as 30°C, the lethal action was almost completely lost by 48-hr storage. Bactericidal activity formed by irradiation was abolished by the presence of a slight amount of L-cysteine or sodium sulfite. The bactericidal factor is unstable at alkaline pH, but is relatively stable at acidic pH. The apparent induced activity depends on the cell concentration and the temperature at the period of contact with the irradiated reagent solution; no lethality was found at concentrations above 10^8 cells per ml. (BBB)

46008 ACTION LEVELS IN MEDICAL TREATMENT OF RADIATION AND RADIOACTIVITY EXPOSURE. Lincoln, T. A. (Oak Ridge National Lab., Tenn.). Am. Ind. Hyg. Assoc. J., 26: 400-3(July-Aug. 1965).

Special medical problems for which action levels might be considered include the handling of the pregnant employee who works in a radiation area, the handling of cases of skin and wound contamination, work restrictions on individuals with internal contamination, and the need for a slit lamp biomicroscopy to detect lens opacities. The medical justifications for action levels are briefly reviewed, and the general practices of medical departments in 17 AEC contractor installations are reported. In general, AEC contractor physicians resisted the idea of using a prescribed exposure level to determine a medical decision. The one area where an action level could be tied to a specific exposure level was the application of restrictions for individuals receiving internal contamination. However, this difficult problem was being handled in many different ways in the installations surveyed. (auth)

46009 TRANSPLANTATION OF HAEMOPOIETIC TISSUES. Loutit, J. F. (Medical Research Council Radiobiological Research Unit, Harwell, Eng.). Brit. Med. Bull., 21: 118-22(May 1965).

Various aspects of bone marrow grafting are discussed, especially with reference to treatment of the radiation syndrome. All the tissues engaged in delivering cells to the circulating blood are highly sensitive to ionizing radiation. Cell death results from disturbances following mitosis. Lymphocytes are readily killed also by radiation during interphase. This may be largely due to interruption of their energy supply which, with a paucity of cytoplasm, depends mainly on phosphorylation in the nucleus. Death from exposure to ionizing radiation is attributable to aplasia of the combined hemopoietic systems, unless the doses are so overwhelming that failure of other systems leads to still earlier death. The circulating blood is the medium by which stem cells are transported, whether a suspension containing the stem cells is injected intravenously or an entire spleen is implanted intraperitoneally or when autogenous spleen or part of the bone marrow is shielded during irradiation. Observations indicate that recovery of the lethally irradiated animals is due to a repopulation by donor's cells, that is, chimeras are produced. Provided that host and donor are syngeneic, i.e., antigenically identical, most animals survive. In allogeneic chimeras where host and donor mice are antigenically different, or in xenogeneic chimeras between mouse and rat, prolonged survival is much less common. After recovery from the primary radiation syndrome during the first week or so after irradiation, the animals develop a secondary wasting disease which frequently leads to death in the second to fourth month. In attempts to avoid these immunological complications, fetal haemopoietic tissue from liver (or spleen) for adult marrow has been used as the seeding suspension. Recent observations at Harwell indicate that even syngeneic fetal liver is not as satisfactory as adult bone marrow for ensuring longevity of the chimeras. In CBA mice a syndrome

apparently identical with secondary disease in clinical, hematological, and histological features results from the use of syngeneic fetal liver or from adult marrow given in suboptimal amounts, as well as after multiple passage in lethally irradiated mice. The common feature at death is aplasia of the lymphatic tissue and in CBA mice this is associated with amyloidosis. Some examples, clinical and experimental, of bone marrow transplantation to treatment of radiation injury are described. (BBB)

46010 THE RADIOPROTECTION OF MAMMALS BY THIOLIC COMPOUNDS. Ciccarone, Pietrangelo. Comit. Nazl. Energia Nucl., Notiziario, 11: 32-7(June 1965). (In Italian).

A bibliographic review is given of the studies made on the radioprotection of mammals using thiolic compounds. The sulfurated compounds with a radioprotective effect—the sulfurated amino acids, mercapto alkyl amines, mercapto alkyl isothiouria, and mercapto alkyl quanidine—are described. 87 references. (J.S.R.)

46011 DISTRIBUTION OF RADIOPROTECTIVE N-/4-NITROPHENYL/-BENZ-^{14}C-AMIDINE IN THE ORGANS OF WHITE RATS. Robev, S.; Baev, I.; Bowev, L. (Scientific-Research Inst. of Radiology and Radiation Protection, Sofia). Compt. Rend. Acad. Bulgare Sci., 18: 51-4(1965). (In Russian).

The HCl salt of NBA tagged with ^{14}C on the amine group was synthesized with a specific activity of 170 μC/g. Aqueous concentrates were injected intravenously into the vein "dorsalis penis" of white rats at a dosage of 1 ml of 0.5% solution, and internally by stomach at a dosage of 2 ml of a 1% solution. Then 8 to 30 minutes after introducing the NBA compound, the white rats were killed by deep ether narcosis, and the content of NBA was determined in the liver, spleen, kidneys, brain, intestine, testicles, and blood by liquid scintillation counting. The tagged NBA was removed from the organ by treating the homogenate with a xylol solution of inactive NBA. The results were quite variable for the organs of different animals due to a difference in individuals. The results did show that local concentration of NBA was not an important factor in explaining the radioprotective effect. (TTT)

46012 INVESTIGATION OF THE EFFECTS OF N-PHENYLBENZAMIDINE ON THE NUMBER OF INVERSE MUTATIONS DURING X IRRADIATION OF E. COLI K_{54} SUSPENSION. Todorov, S.; Robev, S. (Scientific-Research Inst. of Radiology and Radiation Protection, Sofia). Compt. Rend. Acad. Bulgare Sci., 18: 55-8(1965). (In Russian).

A suspension of E. coli K_{54} (10^9 cells/ml) was given an x-ray dose of 20,000 R. Part of the surviving bacteria were grown on a nutrient medium not containing methionine. After 24 to 48 hours of cultivation at 37°C, only the methionine-independent mutants formed colonies. Cysteamine at a dosage of 2.0 μM/ml and N-phenyl-Benzamine Hydrochloride (NBA) at a dosage of 2.0 μM/ml were used to determine if these substances had a radioprotective effect on the independence from methionine induced by the irradiation. In a typical experiment these were 10 mutants independent of methionine out of a total of 450 unirradiated control cells or 2.2%. On irradiating with a dose of 20,000 R there were 30 mutant reversals out of a total of 208 surviving bacteria or 14.5%. With cysteamine added as a radioprotective agent there were 43 mutant reversals out of a total of 300 bacteria or 14.3%. Rather surprisingly cysteamine showed no radioprotective effect. With NBA added as a radioprotector there were 22 mutant reversals out of a total of 280 surviving bacteria or 8%. The NBA had a definite protective effect in preventing the occurrence of the mutation reversal. (TTT)

46013 DNA REPAIR OF RADIATION DAMAGE. I. THE THERAPEUTIC EFFICIENCY OF DNA ADMINISTERED TO RATS AFTER WHOLE-BODY IRRADIATION. Wilczok, Tadeusz; Mendecki, Josef (Inst. of Oncology, Gliwice, Poland). Intern. J. Radiation Biol., 9: 201-11 (1965).

The therapeutic effect of DNA from different sources, such as calf thymus, rat liver, and spleen, herring and salmon sperm and Ehrlich ascites-carcinoma cells was studied on Wistar rats given lethal doses of gamma-irradiation. A single injection of DNA was administered intraperitoneally 24 hours after irradiation. All forms of DNA significantly increased the survival of the irradiated rats. The quantitative differences in the effects of DNA from different sources were directly related to their molecular weight. When native calf-thymus DNA was sheared or denatured, there was a reduction in its therapeutic efficiency proportional to the reduction in molecular size. Therefore heterologous as well as homologous DNA have a marked therapeutic effect which is quantitatively dependent on their molecular weight. (auth)

46014 EFFECT OF PRE- AND POST-IRRADIATION TREATMENT ON THE NUMBER OF BACTERIA SURVIVING X-IRRADIATION AS EVALUATED BY PROBIT ANALYSIS. Van Soestbergen, A. A.; Thompson, Keith H. (Brookhaven National Lab., Upton, N. Y.). Intern. J. Radiation Biol., 9: 213-18(1965). (BNL-8308).

The effect of starvation before irradiation and the effect of plating on a medium containing acriflavine after irradiation was examined for a strain of Pseudomonas aeruginosa. A dose of 3408 rad was given at several different oxygen-concentrations, and the results, measured as the number of surviving bacteria, subjected to probit analysis. A chi-square test gave no evidence of heterogeneity of departure from fitted probit lines obtained after plotting the probits of the fraction of survivors on the logarithm of the oxygen-concentration. It was concluded that starvation increases the sensitivity of Pseudomonas to x-rays under all oxygen-concentrations studied. Plating of irradiated samples on plates containing acriflavine had no effect on the number of survivors at any of the oxygen-concentrations tested. (auth)

46015 RADIOSENSITIVITY OF CULTURES OF ESCHERICHIA FREUNDII GROWN IN THE PRESENCE OF FLUOROACETATE. Liebecq, Claude; Osterrieth, Paul M. (Universite, Liege). Intern. J. Radiation Biol., 9: 253-9 (1965). (In French).

High concentrations of citric acid accumulated in the media of Escherichia freundii (strain EF 5) grown at pH 4.8 in the presence of glucose (5 g/litre) and sodium fluoroacetate (10^{-4} M). Bacteria obtained under these conditions were more radioresistant than controls grown in the absence of fluoroacetate. When only 1 g of glucose was added per litre of medium however, no difference in radiosensitivity was observed although the citric acid level in the media was nearly as high. Moreover, no correlation could be found between the radiosensitivity of the bacteria (or between the dose reduction factor afforded by fluoroacetate) and the concentrations of citrate in the media. At neutral pH and in the presence of 1 g of glucose per litre, fluoroacetate produced a three-fold increase in the intracellular level of citrate. This was accompanied by a moderate reduction in radiosensitivity, of marginal significance. (auth)

46016 TISSUE AND CELLULAR DISTRIBUTION OF TRITIUM-LABELED AET IN MICE. Maisin, J. R.; Leonard, A.; Hugon, J. (Centre d'Etude l'Energie Nucleaire, Mol, Belg.). J. Natl. Cancer Inst., 35: 103-12(July 1965).

It was demonstrated that 2-β-aminoethylisothiourea (AET) penetrates easily and without discrimination into all tissues of mice, regardless of whether they are normal or cancerous. During the first hour after administration, AET appreciably decreased the incorporation of thymidine into DNA but, on the other hand, these substances induced mitochondrial lesions 30 minutes after injection. Also, the diminution of incorporation of ^{3}H-thymidine into the DNA was more pronounced after the simultaneous administration of AET, glutathione, and serotonin than after administration of AET alone. This mixture of compounds also offered a better chemical protection against x-radiation damage than AET alone. (auth)

46017 RECENT ADVANCES IN CHELATION THERAPY. Brugsch, Heinrich G. (Tufts Univ., Boston). J. Occupational Med., 7: 394-401(Aug. 1965).

A review, with 74 references, is given on the use of various metal-binding agents to remove specific metal ions, including those of radionuclides, from the human body. The main chelating agents which have been proven of clinical significance are BAL (dimercaprol), EDTA (ethylenedetate) and its derivatives, DTPA (calcium-trisodiumpentetate), d-penicillamine, and DMFO (desferrioxamine). The study of chelation of radioisotopes has been stimulated by efforts to find means of detoxification and removal of isotopes and fission products from the tissues or body fluids of man. Studies of several rare earths (both as chelates and isotope tracers) showed that Sc forms a stronger linkage with EDTA than La or Y, and removal of rare-earth isotopes by chelation was highest when therapy was instituted early. However, EDTA derivatives are less effective in removing rare-earth isotopes than $CaNa_3$ DTPA. BAETA is suitable for cases of acute exposure to radiostrontium. Side-effects of EDTA therapy are discussed in detail. Studies of $CaNa_3$ DTPA have shown that it effectively chelates Pb, Fe, rare earths, Sr, and Po. (TCO)

46018 THE COMBINED ACTION OF ANTI-TUMOR CHEMICALS AND ^{60}Co GAMMA-RAYS ON MOUSE STRAIN L CELLS CULTURED IN VITRO. II. EFFECT OF ALKYLATING AGENTS AND ANTIBIOTICS. Fujiwara, Yoshisada; Aoyama, Takashi; Kondo, Teruo (Kobe Medical Coll., Japan). Kobe J. Med. Sci., 10: 227-55(Dec. 1964).

Mouse L cells (fibroblasts) were cultured in the presence of various cytostatic drugs and exposed to ^{60}Co γ radiation in doses from 100 to 1000 R. Percentage survival of the cells was determined cytologically seven days postirradiation. Drugs were added in various concentrations before, after, or simultaneously with radiation treatments. Thio-TEPA alone at a concentration of 0.01 μg/ml gave relatively low inhibition of growth, about 30%. After pretreatment with thio-TEPA radiosensitivity was decreased. A significant synergistic action was attained by the simultaneous treatment. With cyclophosphamide a cytocidal effect was observed in vitro with L cells; about 20% inhibition of cell growth was observed in 7 days of culture with 0.01 μg/ml. With the pre- and post-treatments by the drug, radiosensitivity of the cells was diminished; whereas simultaneous treatment caused enhancement of the radiosensitivity. Mitomycin C made the cells radioresistant in both pre- and post-treatments. Enhancement of the radiosensitivity was obtained only by the simultaneous treatment. With chromomycin A_3, an antibiotic obtained from the culture filtrate of Streptomyces griseus, the radiosensitivity of L cells was increased by pretreatment. With actinomycin D only additive effects were attained by post treatment, and this compound and uromycin were most effective when added to the cells simultaneously with irradiation. Thus the highest relative effectiveness was obtained by the simultaneous treatment with all the drugs used. It was concluded that the requisites for an antitumor drug to be used in combination with radiation are: selective affinity to tumor cells; sensitizing action, synchronizing action; and cytocidal action. (TCO)

46019 SKIN PROTECTION AGAINST X RAYS. Bielicky, T.; Zak, M.; Bartak, P.; Malina, L. (Charles Univ., Prague). Lancet, 2: 298(Aug. 7, 1965).

The preventive effects of synthetic antimalarial drugs (chloroquine, hydroxychloroquine, and quinacrine) in some photodermatoses prompted this study of whether a similar effect might also be seen with ionizing radiation. Studies on the effect of antimalarials in vitro and in vivo have shown that chloroquine diphosphate (Resochin) stimulates the activity of the pentose cycle of glucose utilization. Since the pentose cycle is inhibited after irradiation, whether the administration of chloroquine also has a preventive action against x irradiation was also examined. The study was carried out on depilated white male guinea-pigs, x irradiated at 75 kv. The irradiated area, 3 × 5 cm, was delimited with a lead plate. The doses of intraperitoneally administered 5% solution of chloroquine were 0.05, 0.1, 0.3, and 0.4 ml. The lethal dose of chloroquine is 0.025 g, i.e., contained in 0.5 ml of solution. The drug was administered in some animals 2 hr before the irradiation, and in others 30 min after. A radiation dose of 1400 R was sufficient to evoke clinical and histological changes. Examinations carried out on the 7th and 14th days after irradiation showed that chloroquine has a protective effect on the skin against x irradiation. Its effect is proportional to the dose of administered drug, which has pronounced protective activity when given 2 hr before irradiation, and a less pronounced effect when given 30 min later. Among the factors which may be responsible for these effects, the role of the pentose cycle of glucose utilization, on which tissue reparative processes depend, is considered. This enzymatic cycle (which is the only source of ribose-5-phosphate and the main source of reduced nicotinamide-adenine dinucleotide phosphate) is inhibited by ionizing radiation, and chloroquine is one of the factors stimulating its activity. (BBB)

46020 RADIOPROTECTIVE EFFECT OF ATP-DPN IN RATS IRRADIATED WITH DL 85/30 AND DL 100/30. Arghittu, C.; Bragazzi, G. (Centro Nucleare S. Pietro a Grado, Pisa, Italy). Minerva Radiol., Fisioterap. Radiobiol., 10: 309-10(July-Aug. 1965). (In Italian).

The radioprotective effect of a combination of adenosine triphosphate and diphosphopyridine nucleotide (ATP–DPN) was studied in rats exposed to a single dose of 800 R. The rats were inoculated with the ATP–DPN one hr before the irradiation. The results are graphed and show that the mixture used had no radioprotective effect against a whole-body irradiation at lethal doses. This was compared with the 70% protective effect demonstrated in animals irradiated with 700 R. (J.S.R.)

46021 EFFECTS OF NALORPHINE, MORPHINE, AND THEIR ASSOCIATION ON THE MORTALITY IN WHOLE-BODY IRRADIATION IN THE RAT. Caprino, G.; Caprino, L. (Universita, Perugia, Italy). Minerva Radiol., Fisioterap. Radiobiol., 10: 311-15(July-Aug. 1965). (In Italian).

The radioprotective effect of nalorphine, morphine, and nalorphine–morphine combinations was studied in white rats. The drugs were injected before exposure of whole-body doses of 342, 393, 521, and 600 R. The results showed that the increase of the mortality in the animals treated with nalorphine seem to indicate a radiosensitization effect of this drug with respect to the lethal effect. The calculation of the ratio between the DL_{50} of the treated and controlled animals confirms that the pretreatment with nalorphine results in a radiosensitization with respect to mortality. Morphine does not seem to modify appreciably the mortality curve on the 30th day after irradiation. For doses of 10 and 20 mg/kg of morphine the ratio of the DL_{50} of the treated and the controlled animals is respectively greater than and less than 1. For doses of 40 mg/kg of morphine the ratio of treated to controls is greater than 1 on the 30th day. In the case of association of nalorphine and morphine the ratio between dose and effect can be expressed by means of a linear regression line representing the mortality probit-log radiation dose. There was a sharp and significant difference between the frequency of mortality from whole-body irradiation in the animals treated with nalorphine alone and those treated with the same doses of nalorphine combined with morphine. (J.S.R.)

46022 EXPERIMENTAL OBSERVATIONS ON THE RADIOPROTECTIVE ACTION OF RNA. Pini, M.; D'Acunzo, L.; Giudici, G. (Universite, Trieste, Italy; Ospedale Maggiore, Trieste, Italy). Minerva Radiol., Fisioterap. Radiobiol., 10: 326-7(July-Aug. 1965). (In Italian).

The radioprotective effects of RNA for healthy tissues and for tumor tissues were studied in white rats. For the study of healthy tissues the rats were injected with RNA before whole-body exposure to 700 R or electrons. All of the animals not treated with RNA died within the first 6 days. All but three of the treated rats survived more than 30 days after the irradiation. White rats having Ehr-

lich ascite sarcoma were irradiated with fast electrons with doses of 300, 600, and 900 R after injection of RNA. The results showed that there was a marked drop of mitoses of the same order of magnitude as that in irradiated animals not treated with RNA. These results suggest that RNA protects the healthy organism against irradiation but not tumor cells. (J.S.R.)

46023 DELAYED RESULTS OF BIOLOGICAL RADIOPROTECTION IN WHOLE-BODY IRRADIATED RATS. Reggiani, G.; Podesta, A. M.; Pipino, G. (Universita, Genoa). Minerva Radiol., Fisioterap. Radiobiol., 10: 327-8(July-Aug. 1965). (In Italian).

The radioprotective effects of lyophilized tissues of bone marrow, thymus, and spleen were investigated in rats exposed to a whole-body irradiation of 850 R. From 1 to 3 hrs after irradiation the rats were injected with the tissues. The percentages of survival after 2 months and 6 months were determined; the same percentage survived at 6 months as 2 months. The highest protective effect was given by the spleen tissue. (J.S.R.)

46024 EFFECT OF THE TREATMENT WITH HEPATIC DERIVATIVES ON THE SURVIVAL AND ON THE OXIDATIVE PHOSPHORYLATING ACTIVITY OF THE LIVER OF MICE EXPOSED TO WHOLE-BODY IRRADIATION WITH IONIZING IRRADIATION. Rosso, G.; Matli, G. Minerva Radiol., Fisioterap. Radiobiol., 10: 329-30(July-Aug. 1965). (In Italian).

The preliminary experimental results obtained in the exposure of adult mice to massive irradiations followed by intramuscular treatment with hepatic fractions obtained from bovine liver by two different procedures are reported. The white mice were exposed to single doses of 900 R of x rays. The results showed that one hepatic fraction had a much greater radioprotective effect than the other. The components yielding this protective effect are being analyzed. The determination of the oxidative phosphorylating activity made on liver homogenates of the animals sacrificed 5 days after irradiation showed a marked decrease in the oxygen consumption of the control animals and of the animals treated with the first hepatic fraction. (J.S.R.)

46025 EXPERIMENTAL RESULTS AND CONSIDERATIONS ON THE SURVIVAL OF WHITE MICE WHOLE-BODY IRRADIATED AFTER ADMINISTRATION OF NEMBUTAL AT SEDATIVE, HYPNOTIC, AND NARCOTIC DOSES. Stuart, C.; Cittadini, G. (Universita, Siena, Italy). Minerva Radiol., Fisioterap. Radiobiol., 10: 337-41(July-Aug. 1965). (In Italian).

White mice were exposed to whole-body irradiation of 600 and 800 R after administration of 25, 35, and 60 mg/kg of nembutal. For exposures up to 600 R, the results showed no significant differences in the survival of the non-treated rats and the rats treated with the three doses of nembutal. For the exposure to 800 R a highly significant difference was found. Pretreatment with 35 mg/kg was ineffective, pretreatment with 60 mg/kg induces a radioprotective reaction, and pretreatment with 25 mg/kg induces a radiosensitization reaction. (J.S.R.)

46026 MODIFICATION OF RADIATION EFFECTS. Berry, Roger J. (Churchill Hospital, Oxford). Radiol. Clin. North Am., 3: 249-58(Aug. 1965).

The interactions, in mammalian systems, of various categories of radiosensitizing and radioprotective agents with different kinds of radiations are reviewed with emphasis on clinical applications of these interactions. The most drastic modifier of biological response to ionizing radiation remains the presence or absence of oxygen in the irradiated tissue at the time of irradiation. The relation of the oxygen effect to the radiation ionization density (LET) is examined. The effects of high ionization density (high-LET) radiations are relatively independent of the presence or absence of oxygen. A major difference between the biological effects of high- and low-LET radiations is that sparsely ionizing radiations usually require the accumulation of several independent damaging ionization events to be lethal to cells, and much of the accumulated sublethal damage can be repaired rapidly in individual cells within a few hours of the radiation injury. More densely ionizing radiations produce little or no sublethal damage so that much less recovery is achieved. Experimental and clinical data on the action of chemical protective agents and sensitizers are considered. Radioprotective drugs have found only very limited use in conjunction with radiotherapy. Clinical observations that an increased effect of a given radiation dose is seen when that radiation is combined with administration of a drug does not necessarily indicate potentiation of either the radiation or drug effect. Some drugs act additively with radiation, so that the final effect is the sum of that due to the drug and that due to the radiation. Potentiation is shown only when a concentration of drug which does not affect cell reproductive capacity is capable of increasing the effect of single or fractionated radiation doses. Potentiation can also occur when the loss in cell reproductive capacity from combination treatment is greater than the product (not the sum) of the loss of productive capacity produced by each component alone. (BBB)

46027 COMPARATIVE INVESTIGATIONS ON THE PROTECTION MECHANISMS OF CYSTEAMINE AND AET IN INTESTINAL RADIATION DEATH. Zseboek, Zoltan B.; Petranyi, Gyoezoe Jr. (Universitaet, Budapest). Strahlentherapie, 127: 452-62(July 1965). (In German).

The radiation protective mechanisms of AET and cysteamine for intestinal radiation death was investigated in rats. The sodium absorption in the small intestine, the extra-cellular, exchangeable, or the total sodium content as well as the inulin volume and the serum sodium concentration were used as indicators for changes in the sodium- and liquid metabolism. Results obtained with AET and cysteamine were compared. Lethal disturbances in sodium- and liquid metabolism can be inhibited indirectly by cysteamine by means of mobilization of sodium-liquid reserves within the organism. AET did not protect significantly, however, in the small intestine; with the loss in sodium and liquid, only slight protection was observed. The effects on several systems must be studied before the mechanism can be explained completely. (auth)

46028 INVESTIGATIONS ON BIOLOGICAL RADIATION PROTECTION. PART 64. FURTHER INVESTIGATIONS ON THE INFLUENCE OF RADIOPROTECTIVE MATERIALS ON RADIOIRON INCORPORATION AFTER WHOLE-BODY IRRADIATION WITH DOSES UNDER 100 R. Koch, Ruprecht; Seiter, Irma (Universitaet, Freiburg i. B.). Strahlentherapie, 127: 571-7(Aug. 1965). (In German).

The influence of 5′-AMP, pyridoxal-5-phosphate, β-aminoethylisothiuronium-Br, HBr (AET) and homocysteinethiolactone-HCl (HCT), given intraperitoneally, as well as of AET and HCT, given perorally, on the inhibition of radio-iron utilization caused by the total-body irradiation of mice with 75 R was investigated. A protection in bone marrow function was obtained after peritoneal administration of 5′-AMP, pyridoxal-5-phosphate and AET; AET administered orally and HCT administered peritoneally or orally did not protect. No explanation is given for these observations. (tr-auth)

46029 INVESTIGATIONS ON BIOLOGICAL RADIATION PROTECTION. PART 66. THE PROESTROGEN CHLOROTRIANISEN (TACE) AS A RADIOPROTECTIVE SUBSTANCE. Fleming, Kurt; Langendorff, Margarethe (Universitaet, Freiburg i. B.; Heiligenberg-Institut, Ger.). Strahlentherapie, 128: 105-18(Sept. 1965). (In German).

A single subcutaneous injection of chlorotrianisen (Trip-anisylchlorethylene = Tace) increased the survival rate of mice of both sexes 30 days after sublethal total-body x irradiation (640 R). This radioprotective effect was observed when Tace was injected between 5 and 30 days prior to irradiation. A maximum protective effect was obtained when Tace was injected 10 to 15 days prior to irradiation. A protective effect was obtained with 0.02 to 30 mg of Tace per animal; 0.2 to 10.0 mg gave the greatest effect; the effect was the same for this dose interval. Smaller and larger doses were less effective. Tace given orally (2 to 16 mg) was also protective. Tace protected only against middle

to sublethal radiation dosages (590 to 690 R); there was a small protective effect against lethal radiation doses (750 to 810 R). The dose-reduction factor was 1.3 for male animals and 1.2 for females and remained constant for the whole radiation dose area investigated. In future experiments involving the mechanism of Tace, the molecular configuration and the different biological side effects of this substance shall be considered. (tr-auth)

46030 THERAPY OF LETHAL RADIATION WITH RUTIN. PART I. EFFECTS OF RUTIN ON SURVIVAL RATE, BODY WEIGHT, AND OSMOTIC RESISTANCE OF THE ERYTHROCYTES OF FEMALE NMRI MICE UNDER VARIATIONS OF THE WHOLE-BODY IRRADIATION WITH THE USE OF 200-kv RADIATION. Barth, Gunther; Graebner, Herbert; Weise, Hans-Joachim (Universitaet, Giessen, Ger.). Strahlentherapie, 128: 136-47(Sept. 1965). (In German).

It was found that the acute radiation syndrome, obtained after a whole-body irradiation of mice with 650 R, can be treated effectively by an intraperitoneal application of 1 mg of rutin given daily over a period of 9 days. The effect of rutin was less when administered, always after the radiation injury, after an irradiation with a sublethal dose of 550 R. (tr-auth)

46031 SOME WAYS OF CHANGING RADIORESISTANCE IN AN ANIMAL ORGANISM. Yarmomenko, S. P. (Inst. of Labor Health and Occupational Diseases, Moscow). Vestn. Akad. Med. Nauk, No. 7, 66-77(1964).

The literature on the mechanisms of action of chemical radioprotective substances is reviewed. The mechanism of chemical radioprotectors in increasing radioresistance under conditions of large and small (or fractional) radiation doses is discussed. A direct relation between chemical radioprotectors and favorable effect on restorative processes is shown in various studies. With large radiation doses, hemopoiesis is restored to normal in protected animals earlier than in control animals because cell damage is reduced and the restorative processes start at a higher level. However, radioprotector effectiveness is reduced with small radiation doses and fractional doses. Of the two explanations given for reduced effectiveness, the first is that a chemical radioprotector always has a potential capacity for protecting a certain number of bone marrow cells regardless of radiation dose, and with a reduced radiation dose the number of protected cells in relation to the number of remaining cells is decreased. Thus, a small radiation dose produces unfavorable conditions for the radioprotector to realize its full effectiveness which is expressed by a relatively smaller survival rate increase. The second explanation is based on the fact that a radioprotector primarily protects the bone marrow system. With small radiation doses, radiation damage may affect other systems which the radioprotector cannot protect at all or can protect only at certain interkinetic periods. In connection with restorative processes, it is interesting to note that more recent studies indicate that regeneration of chromosome damage in somatic cells is possible with small radiation doses. Thus, reversibility of chromosome damage under certain conditions presents another facet to the problem of increasing radioresistance. The effects of ionizing radiation on different stages of the mitotic cycle and on various organs and systems require further investigation on the cellular level. (CFSTI)

46032 THE DEVELOPMENT OF ULTRAVIOLET-IRRADIATION RESISTANCE BY POLIOVIRUS INFECTIVE CENTERS AND ITS INHIBITION BY GUANIDINE. Eggers, H. J.; Ikegami, N.; Tamm, I. (Rockefeller Inst., New York, N. Y.). Virology, 25: 475-8(Mar. 1965).

The acquisition of uv-irradiation resistance by infective centers was followed in the presence or absence of guanidine, and for comparison, infected cells treated with puromycin were also examined. The results of a typical experiment with guanidine-sensitive poliovirus 1 of the inactivation kinetics of the free virus are reported. Ultraviolet irradiation of infective centers was performed after a total incubation period at 37°C of 50, 110, and 180 min following virus inoculation. By 110 min after infection, the radiation resistance of the untreated infective centers had strikingly increased. In contrast, the radiation resistance of the guanidine- or puromycin-treated infective centers remained unchanged. Inactivation kinetics of the infective centers, like those of free virus, appeared to be first order. The data indicate that a guanidine-sensitive process which is required for acquisition of uv resistance begins between 50 and 110 min after infection. A Luria-Latarjet experiment analogous to that done with guanidine-sensitive poliovirus was also carried out with a guanidine-dependent poliovirus 1 mutant, derived from the Brunenders strain. The development of uv radiation resistance was dependent on the presence of guanidine, but inhibited by puromycin. All available data support the hypothesis that the guanidine-sensitive and guanidine-requiring processes in the multiplication cycle of the respective viruses are biochemically analogous events, involving the synthesis of viral RNA polymerase. (TCO)

46033 RADIOGENIC INJURIES OF THE URINARY TRACT AND THEIR PREVENTION. Langreder, W. (Staedtische Frauenklinik, Rheydt, Ger.). Wiss. Z. Humboldt-Univ. Berlin, Math.-Naturw. Reihe, 12: 173-4 (1963). (In German).

Two approaches to treatment of urological injuries induced by irradiation for gynecological tumors are possible. The prophylactic approach was to inject 50 mg of prednisolone during the periods of Ra implantation. The total Ra dosage was between 7000 and 9000 mg-hr. There was no evidence of hydronephrosis or inflammation of the bladder. A few cases of parametritis were observed. Generally, there was no evidence of irradiation syndrome and the patients had only a slight feeling of sickness. When the prednisolone was given after the irradiation treatment, symptoms of irradiation sickness did not appear. Out of 151 patients treated in this way, 8% developed unilateral hydronephrosis and 3% developed bilateral hydronephrosis. One developed a vesicovaginal fistula. When hydrocortisone treatment was substituted for the prednisolone treatment in bladder tumor, irradiation results were less favorable as compared to the treatment effects in genital tumor irradiation. (BBB)

46034 THE TEMPERATURE DEPENDENCE AND THE EFFECT OF GLYCEROL UPON THE RADIATION SENSITIVITY OF BACTERIOPHAGE-E. COLI COMPLEXES RELATED TO DIRECT AND INDIRECT EFFECT. Shalek, Robert J.; Hunter, Jerry; Smith, Charles E. (Univ. of Texas, Houston). 28p. (CONF-650221-1). ORINS.

From Biophysical Society, 9th Annual Meeting, San Francisco.

A test system of T2r bacteriophage DNA injected into the E. coli host was used in experiments on biologically active DNA in a cellular environment. Irradiation experiments with this system in air at various temperatures using ^{60}Co γ-rays indicated that approximately 33% of the radiation effect upon T2r DNA in a host bacteria is by direct radiation effect. Glycerol conferred radiation protection in the liquid and in the frozen state. The temperature pattern for the radiation inactivation of DNA in this system was qualitatively similar to that for yeast, enzymes and bacterial spores. (auth)

Radiation Hazards and Protection

See also HEALTH AND SAFETY.

46035 (PHS-999-RH-14) ^{131}I IN CHILDREN'S THYROIDS FROM ENVIRONMENTAL EXPOSURE. Wellman, Henry N.; Karches, Gerald J.; Hansen, Warren G.; Laurer, Gerald R.; Eisenbud, Merril; Fooks, Jack H. (Public Health Service, Washington, D. C. Division of Radiological Health). July 1965. 25p. Public Health Service Free.

Balance studies of environmental iodine-131 over a period of 30 days are reported in children ranging from 1 to 6 years of age. Calculations of expected thyroidal accumulations of iodine-131, based on accepted exponential models and thyroid function factors, were compared with

thyroidal iodine-131 measurements performed in a low-background facility. The measured values were lower by a factor of 2 than the calculated accumulation of iodine-131, suggesting a lesser uptake and/or more rapid turnover of iodine in children. The difficulties involved in this type of environmental study and recommendations for improved methodology are discussed. (auth)

46036 IMMEDIATE IMPROVEMENT OF RADIATION PROTECTION. Vogler, Hans (Staedt. Krankenanstalten, Bremen). Strahlentherapie, 127: 629-33(Aug. 1965). (In German).

The use of a movable screen with selective lead values of 1, 2, or more millimeters provided immediate improvement of radiation protection of personnel during radiographic examinations. The screen serves for additional radiation protection and for further reduction of scattered radiation received by personnel. The screen is effective only in certain adjustable directions which have to be considered preferentially. (tr-auth)

46037 TECHNOLOGICAL NEEDS FOR REDUCTION OF PATIENT DOSAGE FROM DIAGNOSTIC RADIOLOGY. A Symposium, Washington, D. C., March 5–6, 1962. Janower, Murray L. (ed.). Springfield, Illinois, Charles C Thomas, 1963. 354p. (CONF-620302).

Seventeen articles are included; separate abstracts have been prepared for each. (P.C.H.)

For abstracts of individual papers see: 46143–46152, 46664, 46744, and 46857–46861.

Radiotherapy and Radiodiagnosis

Refer also to abstracts 45743, 46037, 46678, 46714, 46750, and 46854.

46038 (JPRS–31602, pp 191-7) ^{90}Sr AS A SIMPLE, RAPID, AND INEXPENSIVE TREATMENT FOR AVIATION TYMPANITIS. Yen, Shao; Hsueh, Shan-i. Translated from Chieh-Fang-Chun I-Hsueh Tsa-Chih, No. 1, 43-5 (Jan. 1965).

Pure gamma rays of ^{90}Sr were used to treat aviation tympanitis. Comparisons were made of principal symptoms of the tympani before and after treatment. It was proved that 33 sides out of 41 treated were completely cured, with efficiency rated at 80.5%; 5 sides improved, being 14.5%; and ineffective in 2 sides, comprising 5.0% of the total. The method used and its advantages are described. (P.C.H.)

46039 (JPRS–31667) AN EXAMPLE OF THE USE OF THE RADIOISOTOPE ^{60}Co IN MEDICINE—INTRACAVITARY THERAPY OF CARCINOM PORTIONIS VAGINALIS UTERI WITH RADIOACTIVE ^{60}Co. Merkas, Zlatko; Vujnic, Veselin; Nemoda, Djordje. Translated from Tehnika (Belgrade), No. 7, 1256-60(July 1965). 11p. (TT-65-32162). CFSTI $1.00 cy, $0.50 mn.

The design of a ^{60}Co radioapplicator for use in intercavity therapy of carcinoma of the uterus is described. Advantages over the use of Ra applicators and problems encountered in the activation of metallic Co are discussed. (C.H.)

46040 ACUTE INFLAMMATORY CONDITIONS OF THE UTERINE ADNEXA: CLINICAL, RADIOLOGICAL, AND ISOTOPIC INVESTIGATIONS OF NONGONOCOCCAL ADNEXITIS. Viberg, Lars (Sabbatsberg Hospital, Stockholm). Acta Obstet. Gynecol. Scand., 43: Suppl. 4, 86p. (1964)

Use of x rays and radioisotopes, particularly ^{198}Au, to examine cases of fallopian tubal obstruction as a sequel to inflammatory diseases of the parametrium is considered. Development of a radioisotope method of evaluating tubal patency is described. The ^{198}Au test was developed here to replace older, more difficult, qualitative methods for studies of the transport function of the tube. The test was based on an earlier report of investigators who injected 20 to 50 μC ^{198}Au intra-abdominally and recovered significant amounts in the vagina 2 to 3 days after injection. The injection technique, the radioanalysis procedure, and the dose of radiogold to the patient was dealt with. Ten ml of physiologic saline containing 2μC ^{198}Au in colloidal solution with a negligible amount of ^{197}Au carrier was injected into the abdominal cavity. Intravaginal tampons were changed usually at 24-hr intervals, for at least 3 days, in some cases up to 9 days. The radioactivity of the gauze tampons, which were contained in sealed, thin-walled aluminium tubes, was measured with a well-type scintillation crystal and impulse counter. The radiological dose received by the patient was calculated as follows: The average energy of β rays from ^{198}Au is 0.35 Mev and their average range about 0.1 cm. The total peritoneal area over which the radiogold is distributed is assumed to be 20,000 cm^2. The total dose received is, therefore, on the average, 0.14 rad. This is a well-permissible value for a single exposure. The dose delivered by the γ rays is negligible (about 0.01 rad). The ideal and theoretically expected activity curve is shown, with recovered activity expressed as recovered activity per unit time (ppM/day) plotted against time after injection. There is first a lag time before any activity reaches the vaginal lumen. Then there is an ascending phase until a maximum P_{max}, is reached. The point of time when this occurs is denoted t_{max}. There is then a descending phase due to depletion of the intra-abdominal source of transport material. Some of the resorbed ^{198}Au is retained in the peritoneum or transported by blood and lumph to regional lymph nodes and to liver and spleen. Thus the injected radiogold solution is diluted as a result of such absorption mechanisms. Another factor may contribute to increased dilution, namely irritation of the peritoneum caused by irradition from ^{198}Au available for tubal passage. An important factor determining the radioactivity recovered in the vagina is the transport capacity of the tubes. If none of the tubes is open, exceedingly small recovery of ^{198}Au is expected. If one tube is open, the transported amount is expected to be less than if both tubes are open. Sources of errors in radiometric procedures with ^{198}Au are discussed. Patterns of ^{198}Au recovery in the vagina for various normal and pathologic cases are illustrated and discussed. (BBB)

46041 AUTOMATIC BODY-CONTOURING UNIT FOR DOSE PLANNING IN RADIOTHERAPY. Setaelae, Kai (Univ. of Helsinki). Acta Radiol. Therapy, Phys., Biol., 3: 269-80(Aug. 1965).

A new apparatus is described for dose planning in radiotherapy that provides automatic, rapid and accurate, easily reproducible, life-size, true-to-nature contour equivalents of any desired part of the body from lying patients. The function of the equipment is based on new principles. Examples of the application of the unit are given. (auth)

46042 TWO SPECIAL APPLICATIONS OF HIGH-ENERGY ELECTRON BEAMS. Hultberg, Sven; Walstam, Rune; Asard, Per-Erik (Karolinska Sjukhuset, Stockholm). Acta Radiol. Therapy, Phys., Biol., 3: 287-95 (Aug. 1965).

A method for irradiating areas larger than those covered by the largest standard treatment tube on the Siemens 18 Mev betatron, and a special technique for irradiating intraorbital tumors, are described. Examples of clinical applications are given. (auth)

46043 INTEGRAL ABSORBED DOSES IN ROENTGEN DIAGNOSTIC PROCEDURES. I. THE DOSEMETER. Carlsson, Carl (Univ. of Lund, Sweden). Acta Radiol. Therapy, Phys., Biol., 3: 310-26(Aug. 1965).

Plane-parallel ionization chambers (monitors) and a suitable electrometer circuit for the measurement and recording of integral doses in radiographic examinations are described. The calibration of the monitors is described in detail and the accuracy discussed. The records obtained permit a careful analysis of the contribution to the integral dose from every moment of the examination. (auth)

46044 RADIOACTIVE DRUGS. Kautz, Harold D.; Storey, Robert H.; Zimmermann, Albert J. (Abbott Labs., Chicago). Am. J. Nursing, 64: 124-8(Jan. 1964).

Potential hazards of radiopharmaceuticals in diagnostic as well as in therapeutic uses are discussed and specific

safety precautions for handling them are explained, particularly for nurses. Tables summarize many isotopes currently in common use. Their potential hazard lies in the fact that they emit radiation which cannot be seen or otherwise detected without special equipment; otherwise their use does not differ essentially from the administration of other drugs used daily in hospitals. The diagnostic applications of radiopharmaceuticals rarely pose a serious radiation hazard because of the small doses employed. Since the dose administered is small, precautions are seldom required for nurses or visitors. However, for example, if a patient vomits shortly after oral ingestion of a radiopharmaceutical, precautionary measures will be required. The area must be decontaminated and linens properly disposed. Administration of a radioisotope, such as ^{32}P which emits only β particles creates only a negligible hazard because the β particles are effectively stopped by body tissues and there is thus little chance that β radiation emitted from within a patient will affect other persons. However, an appreciable hazard may exist when a therapeutic dose of a γ-emitting isotope is given. The three methods of protection which can be used alone or in combination to insure personnel safety from exposure to radiation emanating from a patient receiving radioactive therapy involve distance, shielding, and time. The time safety factor refers to the rapid decay of medical radioisotopes and their disposition by the body after administration. Radiation properties of commonly used radioisotopes are tabulated. (BBB)

46045 BETA THERAPY IN FILTERING OPERATIONS FOR THE TREATMENT OF GLAUCOMA. Tribin-Piedrahita, Alfonso. Am. J. Ophthalmol., 60: 140-1(July 1965).

A problem in glaucoma surgery is obstruction of the fistula by cicatricial tissue, most commonly found in races in which pigment formation is marked not only in the eye but throughout the body. As therapy in this situation, β irradiation of the operative field is recommended. The procedure is described. Retrobulbar and local anesthesia is used. The conjunctiva is not infiltrated at the operative site as, occasionally, subconjunctival hemorrhages occur, thus making the surgery difficult and causing some fibrotic reaction during postoperative recovery. A limbal-based flap is formed. A conjunctival and Tenon's capsule incision is made in only one plane 8 mm from the limbus; careful dissection is done downward to the limbus. Bleeding vessels are cauterized. β therapy is applied with a ^{90}Sr applicator (50 mC) over the selera for 30 sec in the area selected for operation. Thirty cases were operated by Scheie's technique and application of ^{90}Sr β therapy, controlling the tension in patients from three months to three years in 96% of the cases. In nine of 10 patients previously operated unsuccessfully without β therapy, the glaucoma was controlled after reoperation with the described technique. (BBB)

46046 CONTOUR BRAIN SCANNING WITH IODINE AND MERCURY COMPOUNDS FOR DETECTION OF INTRACRANIAL TUMORS. Feindel, William; Yamamoto, Lucas; McRae, Donald L.; Zanelli, Joan (McGill Univ., Montreal). Am. J. Roentgenol., Radium Therapy Nucl. Med., 92: 177-86(July 1964).

Scanning technics with ^{131}I and ^{197}Hg or ^{203}Hg for detecting brain tumors are described. Radioiodinated serum albumin (RISA) and radioneohydrin were used. The results showed that radioneohydrin on a quantitative basis is superior to RISA, giving more than double the local uptake in the region of the tumor. In addition, it has the advantage that optimal uptake appears at a shorter interval following injection of the radioisotope into the circulation. The major disadvantage of radioneohydrin tagged with ^{203}Hg (the high level of radiation dosage to the kidney) is eliminated by the use of neohydrin tagged with ^{197}Hg which is considered to be at present the radioisotope of choice for brain scanning. The contour scanning method provides certain advantages over the more familiar rectilinear technique. These are summarized. The injection of 300 to 400 μC of RISA was preceded by Lugol's iodine solution in a dose of 10 drops 3 times a day for 24 hr. Scans were made immediately and at about 24 and 48 hr intervals. With the radioactive mercuric organic compound, the scan was preceded by an intramuscular injection of 2 ml of nonradioactive mercurohydrin on the day before scanning. Neohydrin with ^{203}Hg was used in a dosage of 10 μC/kg of body weight. Neohydrin with ^{197}Hg gave a satisfactory scan with half that dose. Scans were considered positive when a differential increase of 15% or more appeared over a min of 2000 background counts registered from a corresponding region of the opposite side of the head. Since albumin does not permeate normal brain tissue to a significant degree and is less likely to leak out of the circulating blood into extravascular tissues, RISA differentially concentrates in lesions associated either with an increase in vascularity or permeability. Highly vascular lesions such as angiomas or vascular meningiomas show up almost immediately on scanning after RISA is introduced into the blood stream. In other lesions, however, the slow decrease of RISA in the blood stream tends to reduce the differential between the background and target radioactivity. The use of ^{197}Hg which has no β activity and a lower level of γ radiation provides an improvement on the labeling of radioneohydrin. The radiation dosage to the kidneys is almost eliminated and the whole-body dosage is extremely low. Both scanning methods gave a positive scan rate of 88%. (BBB)

46047 NEW METHOD OF TREATING MELANOMA OF THE PECTORAL REGION. Brasfield, Richard D.; Henschke, Ulrich K.; DasGupta, Taposh (Memorial Hospital for Cancer and Allied Diseases, New York). Am. J. Surg., 109: 213-16(Feb. 1965).

In view of the generally poor results of treating melanoma in the pectoral region by conventional methods, a new method has been developed. Four patients are reported who had wide excisional surgery, plus the insertion of a radioactive wire into the internal mammary artery for irradiation of the internal mammary nodes. After radical mastectomy a No. 21 gauge sealed tipped, Nylon catheter was inserted into the left internal mammary artery through the first interspace. On the next day an ^{192}Ir wire was inserted into the catheter which protruded from the skin over the first intercostal space. The total length of the wire was 20 cm, with an active length of 15 cm. The inactive proximal 5 cm was for protecting the skin from excessive irradiation. A calculated dose of 9000 R was delivered to the nodes 0.5 cm from the vessel. In two cases the same technic was used to insert a ^{60}Co wire and to deliver a 9250-R dose, 0.5 cm from the vessel, over seven days. The wound healed well and no residual melanoma was found in the specimen. There is no evidence of irradiation reaction. Melanomas are known to be radioresistant; they will, however, respond to high doses of irradiation. The simple technic of performing a cut-down on the internal mammary artery plus insertion of a Nylon catheter with a fused tip down to the level of the xiphoid, followed by the insertion of a radioactive wire of ^{192}Ir or ^{60}Co, has been used by the authors in the treatment of breast carcinoma since 1957. This technic requires only ten minutes additional operating time and delivers very high doses of radiation to the internal mammary nodes, 97% of which are located within 1.5 cm of the internal mammary vessels. This linear source of irradiation allows very high dosage of these internal mammary nodes. Because the irradiation effect falls off inversely as the square of the distance, a high concentration of irradiation is delivered to the nodes but the surrounding tissue, namely, lung, heart, cartilage, ribs, and skin receive a min amount of irradiation. In 90 patients who have received this method of irradiation, no complications have been seen. (BBB)

46048 COMBINED LUNG-LIVER RADIOISOTOPE SCAN IN THE DIAGNOSIS OF SUBDIAPHRAGMATIC ABCESS. Brown, Donald W. (Univ. of Colorado, Denver). Am. J. Surg., 109: 521-5(Apr. 1965).

A new and comparatively simple radioisotopic method of outlining the space between the lung and liver directly is described and applied to the diagnosis of subdiaphragmatic abscess. Patients are given separate injections of 300 μC of macroaggregated ^{131}I-labeled human serum

albumin (MAA), and 100 μC of either ^{198}Au colloid or colloidal ^{131}I-labeled human serum albumin intravenously. Scanning is begun immediately. The pulse height analyzer is set for ^{131}I with lower and upper windows of 310 and 410 kev respectively, whether or not ^{198}Au is used. Raising the upper window higher to encompass more of the 410-kev photopeak of ^{198}Au was found to introduce too much scatter radiation from higher energy ^{131}I γ rays and to decrease resolution. A scanning speed of 30.5 cm/min and spacing of 0.42 cm were used. An anteroposterior lung-liver scan requires about 90 min to perform. When the patient's condition permits extended scanning time, both anteroposterior and right lateral views should be obtained. A striking difference was seen between the normal pattern and that in patients with right subdiaphragmatic abscesses. Three patients are presented in whom these abscesses were revealed clearly as demarcated areas of decreased radioisotopic concentration. A microscopic autoradiogram is shown from a section of human lung two hr after injection of 300 μC of MAA. The radioactive particles were widely dispersed, most high power fields showing none. There was a complete lack of inflammatory response or ischemic change in the area of microembolization. (BBB)

46049 TREATMENT OF HYPERTHYROIDISM IN THE PREGNANT WOMAN. Ann. Endocrinol. (Paris), 16: 37-43(1964). (In French).

Hazards in the use of ^{131}I to treat thyrotoxicosis in pregnancy are discussed. (BBB)

46050 COMBINED SPLIT-COURSE THERAPY WITH 5-FLUOROURACIL AND MEGAVOLTAGE IRRADIATION. Holsti, Lars R. (Univ. Central Hospital, Helsinki). Ann. Med. Internae Fenniae, 53: 79-87(1964).

Possible synergistic effects of a pyrimidine analog, 5-fluorouracil (5-FU), and radiation were investigated on certain types of cancer. It was previously found that 5-FU potentiates radiation effects in the treatment of lung cancer, and a radiosensitizing effect of 5-FU has been observed in cell culture and animal tumor studies. This report concerns 26 patients treated with combined 5-FU and megavoltage radiotherapy by the split-course technique. There were 19 patients with lung cancer, five with cancer of the colon, one with cancer of the rectum, and one with a retroperitoneal embryonal carcinoma. They were all advanced cases. 5-Fluorouracil was administered by an intravenous 2- to 3-hr infusion of 15 mg/kg of body weight for 4 consecutive days, and thereafter 7.5 mg/kg. Radiation therapy was administered by a 35-Mev Betatron or a ^{60}Co unit, except for one patient who received conventional x-ray therapy. Radiotherapy was given 15 to 60 min after 5-FU infusion. For the Betatron therapy the daily tumor dose was 200 to 270 R, and for the ^{60}Co therapy 170 to 200 R. Radiation therapy was given six times a week. The total tumor dose administered to patients with cancer of the lung was between 5600 and 7100 R, average 6400 R max. Over 7100 R was given in two cases. The total tumor dose administered for cancer of the colon was 3700 to 5990 R, average 5000 R max. The total tumor dose was usually the same as it would have been had radiation been the only treatment. Both 5-FU and radiotherapy were administered by a split-course technique, the treatment being divided into two roughly equal phases separated by a rest interval of 2 to 3 weeks. Treatment was interrupted when the tumor dose was about 3000 R and the 5-FU dose about 6000 mg. After the interval irradiation therapy and 5-FU infusions were repeated in exactly the same way. The effects of radiation and 5-FU on leucocyte and platelet counts, hemoglobin, alkaline phosphatase, serum glutamic-oxalacetic transaminase, serum protein, and uric acid were determined weekly. Side-effects were encountered in 11 out of the 26 patients, but were mild and transient in most cases. However, the leucocyte count of one patient dropped to 700. Regression of the tumor occurred in 18 out of 19 patients with lung cancer, as observed by chest x rays. The disappearance or shrinkage of the tumors was slightly more rapid in combination therapy, often strikingly rapid. On the other hand, metastases sometimes developed in the patients during the treatment or soon after it, indicating that 5-FU therapy does not prevent metastatic spread. These observations show that the combination of 5-FU and megavoltage radiotherapy is useful when administered by a split-course technique and in large doses. Combined therapy gave slightly better primary results than radiotherapy alone. (BBB)

46051 COMBINED RADIATION AND SURGICAL TREATMENT OF CARCINOMA OF THE ESOPHAGUS. Parker, Edward F.; Gregorie, Henry B. Jr. (Medical Coll. of South Carolina, Charleston). Ann. Surg., 161: 710-22(May 1965).

Effectiveness of supervoltage x-ray therapy was evaluated in 134 cases of primary epidermoid carcinoma of the esophagus seen in a 5-yr period ending in 1962 and compared with results in 336 cases previously studied. The total of 471 cases represented three primary methods of treatment: surgical, radiation, and combined radiation and surgical when feasible. When circumstances prevented combining radiation and surgical therapy, results of x ray as the principal mode of therapy were discouraging, with an average survival time of 5.2 months in 77 patients having x-ray treatment solely, 3.5 months in 10 patients having x-ray therapy and gastrostomy, and 6.5 months in 6 patients having x-ray therapy and Gavriliu bypass. Only 4 patients survived for long periods after x-ray therapy alone. The rationale of therapy is now one of primary radiation for all in whom it can be tolerated, followed by resection in all operable cases, regardless of how effective initial x-ray therapy is in view of the high incidence of residual and recurrent carcinoma following x-ray therapy alone. Supervoltage x-ray therapy in a subtumoricidal dose of 4500 R in 3 weeks was delivered to the primary esophageal neoplasm. This dose minimized the risk of spinal cord necrosis which may result from larger doses. There were only 11 (9%) long-term survivors in the present series. However only 30 lesions (22% of 135) were amenable to treatment by radiation and resection. Improvement in results of the treatment of carcinoma of the esophagus by preliminary x-ray therapy followed by resection appeared to be significant. Such preoperative x-ray therapy appears to suppress tumor activity and bulk, possibly reduces transplantability of tumor cells at operation, and enables a nonresectable lesion to be resected. An outstanding benefit of x-ray therapy is restoration of swallowing ability which permits improvement in nutrition by oral alimentation and improved healing potential. The interval between x-ray therapy and resection varied from 10 days to 10 months, with most near two months. No anastomotic leaks or fistulas occurred in any of the patients treated with preoperative irradiation and later resection. (BBB)

46052 TREATMENT OF EYELID CARCINOMA. Domonkos, Anthony N. (Columbia Univ., New York). Arch. Dermatol., 91: 364-71(Apr. 1965).

Use of radiation and other methods of treatment of eyelid cancer is described in 240 patients with attention to doses used, occurrence of radiation injuries, and their prevention. The Philips contact x-ray apparatus was used to treat 105 of the 242 lesions. This apparatus produces x rays having values of energy absorption by the tissue similar to those of radium at 1 cm distance from the skin. The similar sharp drop-off in depth dose with Philips contact x-ray apparatus is achieved mainly by a short focus-skin distance of 18 mm. The tube was operated at 45 kv to give an exposure of either 1000 R daily for eight treatments (total 8000 R) or 1250 R daily for eight treatments (total 10,000 R). During treatment of the eyelid cancers, the lens and cornea were protected from irradiation by insertion of a brass eye shield between the eyelids and the eyeball. The other method of roentgentherapy was the use of conventional, superficial x rays at 60 kv and 100 kv for 37 lesions. This type of roentgentherapy was used mainly for lesions of a greater dia than could be treated with the Philips tube, which has a window only 2 cm in dia. The standard technique was to give 750 R at daily intervals for eight treatments (total 6000 R). This exposure was to lesions 1 cm or less in dia. The dose was reduced

proportionately for wider fields. Another method of treatment was the combination of electrodesiccation and curettage with roentgentherapy. The exposure in these cases was 1000 to 3000 R. Of the 135 carcinomas at the inner canthus, 77% were treated with some form of ionizing radiation. Of the 242 carcinomas, 67% were treated with ionizing radiation. Of these tumors, 64% received contact x-ray therapy. No difference in the results could be detected whether 8000 or 10,000 R total exposure had been given. Irradiation of carcinomas at the inner canthus presents a hazard of stenosis of the lacrimal ducts. Stenosis of the lacrimal duct with resultant persistent lacrimation occurred in five (5%) of 104 cases in which carcinoma of the inner canthus was treated with x rays. Eight % (3 of 37) developed stenosis after conventional x-ray therapy. (BBB)

46053 PHOTOSCANNING IN THE DIAGNOSIS OF INTRACRANIAL LESIONS. Donati, Robert M.; Nelson, Mary L.; Gallagher, Neil I. (St. Louis Veterans Administration Hospital). Arch. Internal Med., 116: 205-11 (Aug. 1965).

Use of ^{203}Hg-labeled chlormerodrin to detect brain lesions in 70 patients is described. Mercury-203 has biologic and physical properties which make it suitable for photoscanning. The physical half-life is 45 days. When incorporated into a mercurial diuretic, excretion is enhanced and one half of the administered dose is excreted in eight hr. Approximately 10% of the labeled diuretic remains bound to the kidneys with a biologic half-life of 28 days. The usual kidney dose of 35 to 40 rad is further reduced to 12 to 13 rad by the prior administration of a mercurial diuretic. Photoscanning of the brain following the administration of ^{203}Hg-chlormerodrin (Neohydrin) has proved to be a more tolerable diagnostic procedure than radiologic contrast studies, and a highly valuable adjunct in the diagnosis and localization of intracranial lesions. Scans were performed utilizing a commercially available photoscanner. To diminish the amount of radioactivity delivered to the kidneys, 2 ml of sodium mercaptomerin (Thiomerin) was administered intramuscularly on the day preceding the scan. On the day of the scan, 700 to 800 μC ^{203}Hg chlormerodrin was injected intravenously two to five hours prior to beginning the scan. Twenty-six scans were positive, 44 were negative. Twenty-one of the positive scans were in patients with intracranial neoplasms, four were in patients with other focal intracranial pathology, and one was in a patient with no apparent organic disease. All patients with the diagnosis of intracranial neoplasm had a positive scan establishing the size and position of the lesion. Complete freedom from complications and discomfort constitute major advantages over cerebral angiography and pneumoencephalography. (BBB)

46054 PREOPERATIVE IRRADIATION IN MANAGEMENT OF LOCALLY ADVANCED BREAST CANCER. Delarue, Norman C.; Ash, C. L.; Peters, Vera; Fielden, Robert (Toronto General Hospital). Arch. Surg., 91: 136-54(July 1965).

The use of irradiation prior to surgery for breast cancer is described with reference to 467 patients. Technical considerations and avoidance of complications are discussed. In the breast the protection of deeper structures, afforded by the pectoral muscles and tissues of the chest wall, is important in minimizing the complications of radiation pneumonitis and destructive skeletal changes that may occur even when careful precautions are taken in radiotherapy. It is stressed that complications following subsequent surgical treatment are not increased if a proper technique is followed in dealing with the irradiated tissue. In the cases presented, an average dose of 4500 R of 400-kv x rays in ~ four weeks, was used, with a waiting period of an additional four to six weeks until the radiation reaction had subsided to avoid technical complications relating to wound healing. During this period the inflammatory reaction enters its fibroblastic phase with fibrotic contracture around the draining vessels and lymphatics. This serves a dual purpose: the vessel becomes considerably less permeable and with the resultant narrowing also less capable of conducting disseminated cells. A five-year survival rate of 35% and a ten-year survival rate of 18.6% were obtained in the entire series of 467 patients. (TCO)

46055 ELECTRONIC COMPUTERS IN NUCLEAR MEDICINE. [PART] I. Habermehl, A.; Graul, E. H. (Philipps-Universitaet, Marburg/Lahn, Ger.). Atompraxis, 11: 419-23(Aug. 1965). (In German).

Electronic computers, both of the analog and the digital type, can be used effectively in nuclear medicine. The present article explains the fundamentals of the analog computing technique, and shows how nuclear-medical studies can be interpreted and put on a quantitative basis by use of model systems. The basic principles involved in the mathematical description of multi-chamber systems by means of systems of differential equations are listed, and examples are given. Here it is found that the analog computer is suitable for a theoretical interpretation of hitherto unknown processes, and also for evaluating clinical examinations on the basis of a model which has been demonstrated to be valid. The digital computer, with its universal applicability, can also be used for such examinations, but its particular advantage lies in the processing of larger amounts of data, as is often necessary in nuclear medicine, e.g., in analyzing complex gamma spectra, in the quantitative evaluation of scintigrams, and in precise calculation of dosages in x ray therapy or after implantation of radioactive seeds. A method is listed by means of which the evaluation of erythrocyte and ferrokinetic examinations can be made more automatic by the use of a digital computer. This latter is equally advantageous in metabolic examinations of radioactivity labeled substances which are rapidly metabolized. (auth)

46056 IMPLANTATION IRRADIATION OF EPITHELIOMATA OF THE EYELIDS AND ADJACENT AREAS. McAuley, F. D. (Dublin Hospital). Brit. J. Ophthalmol., 47: 257-64(May 1963).

Eighteen cases are described to demonstrate the effectiveness with which implanted radiation material eradicates basal cell or squamous epithelioma on the eyelids or in the region surrounding the orbit without causing gross functional impairment or disfigurement. However, a few late complications developed, and are illustrated. Radium needles or Rn seeds were implanted to deliver doses of 5000 to 6000 R over 5 to 6 days. Detailed dose data are given for each case. The complications included lens change in one case in which three radon seeds were implanted to the medial part of the right lower eyelid. A cortical change in the inferonasal quadrant of the lens was detected four yr later. This opacity had not appreciably changed after a further 3½ years, and the visual acuity was then 6/9 in each eye. No other patient developed a lens change. Blockage of the tear ducts, presumably by irradiation, occurred in one case. A late radiation reaction occurred in three cases in the treatment area months afterwards, which presented as areas of induration about 3 mm in dia. These lesions were not painful and cleared in a few weeks with local application of antibiotic ointment. Two cases have an avascular appearance of the skin in the treated areas; the appearance is not very noticeable and not more objectionable cosmetically than the results of plastic surgery might be. One case had a contracture of the conjunctiva in the lower fornix near the punctum, but there was no displacement of the lid margin. Prevention of lens change by the use of a lead shell is not feasible except for short periods since much abrasive damage may be done by the shell unless it has been specially molded; in addition it is questionable if the thickness of the shell rather than the lead is not the main factor in the protection of the crystalline lens from the γ rays. Retraction of the eyelid for a distance of 1 cm from the cornea appeared to have the desired effect. Epiphora is not a usual sequela of implanting radiation material in close proximity to the lacrimal drainage apparatus, provided that the channels are not damaged by surgical trauma. A dose necessary to kill malignant cells does not necessarily lead to the formation of scar tissue. Variation of radiation intensity

with distance from a radium needle is considered. The dose rate is reduced as the distance from the plane of the implant increases. Presuming that at 3 mm the dose rate is 100%, at 5 mm it will be 55%, at 10 mm 17%, and at 20 mm 8%. (BBB)

46057 TREATMENT OF SUPRA-GLOTTIC CARCINOMAS BY TELECOBALT THERAPY. Ennuyer, A.; Bataini, P. (Foundation Curie, Paris). Brit. J. Radiol., 38: 661-6(Sept. 1965).

Results obtained in the treatment of 33 cases of cancer of the laryngeal vestibule by telecobalt therapy are presented. The patients were observed for a minimum of three years. Advantages of telecobalt therapy are listed. A treatment schedule of 1,200 R tumor dose per week was used with 5 or 6 sessions in a week. The usual total tumor dose is of the order of 7,000–8,000 R, protracted over 40 or 50 days. The results were particularly favorable in the states I and II (T1 N0; T1 N1; T2 N0) cases, where there were only two failures among 13 patients. In stages III and IV cases, the results were still worthwhile: 7 survivals out of 20 cases, one of the failures being successfully treated by surgery. (P.C.H.)

46058 THE USE OF ^{131}I-LABELED P.V.P. IN BRAIN SCANNING. Houlder, A. E.; Manning, Gillian; McAlister, Joan M. (St. Bartholomew's Hospital, London). Brit. J. Radiol., 38: 718(Sept. 1965).

Results of the use of ^{131}I-PVP (polyvinylpyrrolidone) for brain-scanning showed that it does not have a half life of 1 day as previously reported, that the liver dose is not insignificant, and that the ratio of tumor-to-brain uptake is not high as previously reported. Its use was discontinued. (P.C.H.)

46059 RECURRENCE OF RODENT ULCERS AFTER RADIOTHERAPY. Cobbett, J. R. (Queen Victoria Hospital, East Grinstead, Eng.). Brit. J. Surg., 52: 347-9 (May 1965).

The effectiveness of radiotherapy in the initial treatment of basal cell carcinoma is analysed in terms of various factors, with reference to 93 cases, and the use of surgery to correct radioinduced skin ulcers or to excise lesions not cured by radiotherapy is described. Basal cell carcinoma is treated by irradiation or excision, with little difference in the recurrence rate which varies between 1 and 10% in five years. Because of preference for nonoperative treatment, most cases are treated initially by irradiation unless this might damage other structures, such as bone, cartilage, and the lacrimal apparatus. Twelve patients had received two, and three patients had received three, courses of radiotherapy to the same lesion. One patient had received a total of 14,500 R x radiation in three courses of irradiation treatment over a period of 8 years. Histological examination in this case showed living neoplastic cells in dense fibrous tissue. Another patient who had received a single dose of 1200 R went 12 years before there was clinical evidence of recurrence. No patient had distant metastases. The 5-yr recurrence rate of 20.5% for patients treated secondarily by surgery is considerably higher than that to be expected by either form of primary treatment. In three cases, late recurrence occurred following secondary surgery in patients with multiple rodent ulcers, and in these patients the recurrence may represent new lesions arising at the margin of the originally treated area, rather than actual recurrence of the lesion. Where possible, surgical repair of the defect by direct suture with undermining of the skin edges usually gave the best cosmetic result. Otherwise the choice was between free skin grafts (either split or full thickness), a local flap, or rarely a distant flap. A flap was necessary in some special sites, such as where there was bare cortical bone to be covered. Where there was no specific indication for either method of repair, it is emphasized that while a local flap will often give a better cosmetic result, it may require later trimming, involving a second operation in an elderly patient. Also, a flap may initially conceal deep recurrence of the basal cell lesion, with consequent delay in the diagnosis of the recurrence. If there is any doubt as to the adequacy of the depth of the excision, a free graft is probably a safer procedure. Recurrence beneath a flap occurred in two patients, both of whom had had scalp flaps to cover bare areas of cortical bone after excision of the pericranium. A survey of published results of similar studies is made. Apparently there is a greater chance of recurrence from irradiation treatment than from primary surgical excision. As many cases are given radiotherapy because they are unsuitable for surgery (including cases where irradiation may be only palliative), recurrence rates for the two methods of treatment cannot easily be compared. A large clinical trial on lesions equally suitable for the two types of treatment would be the only means of assessing comparative results of the two methods in primary treatment. (BBB)

46060 SCANNING THE PANCREAS. Brit. Med. J., 1: 1625-6(June 26, 1965).

Recent developments in use of radioisotopes for scanning the pancreas, one of the few major organs heretofore not amenable to radiologic study, are reviewed. The pancreas takes up selectively methionine tagged with a radioisotope, but none of the elements in amino acids (C, H, N, O, and S) have γ-emitting isotopes with half lives longer than a few minutes. Selenomethionine is readily taken up by the pancreas of dogs one to two hours after administration, and the same applies to man. The technique used is described. The whole-body radiation dose with 250 μC is ~ 0.9 Rad, and the dose to the pancreas 0.2 Rad. A practical difficulty of the scan is that the liver also takes up the isotope, and if the liver is large, its edge tends to overlap part of the head of the pancreas. This can be overcome by scanning the patient supine and rotated slightly to the right side. The two conditions for which scanning has been used particularly are carcinoma and pancreatitis. The normal pancreas takes up the isotope uniformly and thus gives a dark photoscan. Severe pancreatitis largely inhibits the uptake of isotope throughout the organ, and the photoscan shows a spotty distribution of radioactivity of low intensity. If a carcinoma is present, the part of the organ invaded shows almost complete lack of uptake of the isotope, and it is now possible to visualize a lesion as small as 2 cm in dia. (TCO)

46061 THE BLADDER AFTER THE WERTHEIM OPERATION AND IRRADIATION. Kostic, Peter (Gynecological and Obstetrical Hospital, Belgrade). Bull. Federation Soc. Gynecol. Obstet. Langue Franc., 13: 620-3(1961). (In French).

Ninety-one patients, having undergone a Wertheim-Miegs total hysterectomy, were examined, before and after subsequent irradiation, for tumors of the kidney and bladder. Eight to 12 days after the operation and before irradiation, nine cases showed no malfunction of the bladder or kidney, but 62 showed minimal modification of the bladder and kidneys, 20 marked hyperemia of bladder, edema, impaired renal function, pyuria, or hematuria. One month after surgery and before irradiation 65 cases showed normal bladder and renal function; 19 mild hyperemia, edema, pyuria, or moderate hematuria; and seven severe bladder inflammation, abundant pyuria and hematuria, and reduced renal function. After irradiation, 63 cases showed normal bladder and renal function, 23 slight modifications, and five severe vesicular disorders, mainly in the form of acute cystitis. The initial bladder disorders were primarily a consequence of the operation. The most frequent bladder disorders occurred immediately after surgical intervention, and these lesions required little treatment, infectious states being treated with broad-spectrum antibiotics. The immediate postirradiation bladder changes mainly could be attributed to existing acute cystitis exacerbated by irradiation. This cystitis is best treated by warm baths, an appropriate diet, intravesicular instillation of mild disinfectants, and soothing suppositories. This early radiation cystitis is usually responsive to symptomatic treatment, and is to be distinguished from late radiation cystitis and its sequelae which have a less favorable prognosis. (BBB)

46062 RADIATION AND EARLY PREGNANCY. Effer, S. B. Can. Med. Assoc. J., 93: 565(Sept. 4, 1965).

Production of gene mutations as a result of ionizing

radiation has been considered to occur as a nonthreshold phenomenon. Thus even small doses of radiation to the gravid patient in the very earliest stages of pregnancy are not without risk in this respect. Since the gravid patient during the two weeks following conception is seldom aware of the possibility of pregnancy, a simple method is suggested to eliminate one more high-risk group from this radiation hazard. It is suggested that both physicians and diagnostic radiological units incorporate in their requisition forms the date of the last menstrual period and refrain from making requests for radiography during the progestational phase of the menstrual cycle. (auth)

46063 LUNG CHANGES FOLLOWING COBALT TELETHERAPY FOR CARCINOMA OF THE BREAST. Papavasiliou, C.; Garmatis, C.; Elias, C.; Kostouros, D.; Katharios, N. (Alexandra M. Hospital, Athens). Clin. Radiol., 15: 242-5(July 1964).

Incidence of pneumonitis in 68 patients treated for carcinoma of the breast with a telecobalt therapy unit is reported. Radical mastectomy was followed by irradiation three to four weeks postoperatively using two stationary fields. A tumor dose of 4800 rad was given in 32 treatments, 4 cm beneath the surface of the skin, in 150-rad daily increments six days a week. Some patients received less, but not less than 4000 rad; nine patients received more than 4800 rad (up to 6000 rad). Seven patients received preoperative as well as postoperative therapy and the total dose ranged from 6000 to 7500 rad with an interruption of four to five weeks. Forty-seven patients showed no clinical or x-ray signs of lung reaction, but 21 patients (31%) presented x-ray findings of pulmonary fibrosis. Four of these patients (5.9%) developed typical signs of radiation pneumonitis (fever, cough, malaise, dyspnea). The dose was not a crucial factor in the production of lung reactions, but the age of the patients appeared more important, younger people less commonly developing radiation pneumonitis. No patients had pleural effusions attributable to irradiation. Exudative pneumonitis was usually observed in the first film obtained after completion of therapy. The lung changes usually involved the upper lobe, but in three cases the paramediastinal area was also involved. In five patients, the pneumonitis resolved a few months after its appearance and no changes were demonstrable on films obtained later, up to three years after completion of therapy. Five patients developed signs of fibrosis without an initial stage of pneumonitis. Representative x-ray findings of radiation lung changes are illustrated. These changes produced by ^{60}Co teletherapy did not prevent completion of therapy or produce major discomfort with most patients, and in comparison with orthovoltage therapy, sequelae to ^{60}Co irradiation were not more severe. (BBB)

46064 CARCINOMA CORPORIS UTERI: A RADICAL INTRACAVITARY TREATMENT (WITH A NOTE ON THE SENSITIVITY OF ADENOCARCINOMA). Strickland, Paul (Mount Vernon Hospital, Northwood, Eng.). Clin. Radiol., 16: 112-18(Apr. 1965).

A radical radiation treatment was devised for cancer of the uterine body when for various reasons surgery is not used, and the method is compared with earlier methods. The construction of a ^{60}Co intrauterine applicator is described. The applicator is flexible so that it can assume the pyriform shape of the body of the uterus after insertion. From knowledge of the tolerance of various pelvic structures to radiation, it was thought safe to deliver a dose of 6000 R, to a plane of tissue 1.0 cm away from the surface of the applicator. An overall treatment time of 7 days with two separate treatment sessions of not more than 24 hr each was used initially. When the sources were fresh from the atomic pile it was arranged that an insertion of about 15 hr would be sufficient to give a dose of 3000 R to the desired plane in one treatment session. With the passage of time treatment times were lengthened and when they exceeded 24 hr, the sources were discarded. Later, it appeared to be safe to increase the applicator loading so as to deliver 6500 R at 1.5 cm away from the applicator instead of at 1.0 cm, as previously. This involved giving 8500 R. Subsequent experience showed that this increased dose, without any increase in session time or overall time, was justified. The apparatus consists of a spiral of stainless steel wound tightly into a loop. Into the loop are inserted nickel-plated cobalt sources measuring 0.2 cm dia, and an initial activity of 6.5 mC. The usual total loading is 60 mC. A steel pellet is dropped in between each cobalt source, so that radioactive sources are distributed uniformly around the loop. After loading, the applicator is closed with a plug. The improvement in dose distribution is seen by comparing the isodose curves from this applicator and a 100-mg radium tube. Complications of this form of ^{60}Co treatment are described. An experienced operator takes about 5 min to load the applicator during which time his right hand is exposed to about 250 mR and the body to one tenth of this dose. Some degree of vaginal stenosis occurred and sometimes was severe. Telangiectases on the rectal mucosa caused small hemorrhages and similar changes on the bladder mucosa caused hematuria frequently (in 10 to 15% of all cases). In one patient, rectal bleeding was severe enough to require laparotomy. Rectovaginal fistula occurred in two cases. The uterus was removed in 46 of the 105 cases, and the operation performed about 6 weeks after radiation, was not made more difficult as a result. Histologic studies on the radiosensitivity of uterine carcinomas are also reported. (BBB)

46065 RADIATION DAMAGE OF THE SMALL INTESTINE. Halls, J. M. (St. Mark's Hospital, London). Clin. Radiol., 16: 173-6(Apr. 1965).

The literature concerning this condition is reviewed and a new case is presented. The large and small bowel are equally susceptible to damage, but injury to the former is more common, due to the relative fixity of the colon. The segments which are most frequently affected are those which are immobile. The small bowel is mobile and loops may be intermittently withdrawn from the field of irradiation and receive only a fraction of the total dosage. With doses of between 6000 and 6400 rad, the incidence of injury to the transverse colon is 37%. In the case report described, a 41-year-old female with a large anaplastic carcinoma of the rectum was given a course of 6600 rad over ten weeks to the right pelvis. She experienced intermittent attacks of diarrhea and vomiting throughout treatment, but these rapidly subsided with oral prednisolone, 20 mg daily. She was well until about 8 months after the completion of radiotherapy, when she developed mild diarrhea, and later she experienced intermittent attacks of colicky abdominal pain. Several narrowed and fixed loops of ileum were demonstrated, with an unvarying radiological appearance. There was a sharp transition between normal and abnormal bowel, the junction being exaggerated by a failure of the irregular loops to distend during injection. Loss of flexibility was also reflected in the loss of the normal coiled pattern. The diseased segments appeared rigid and straightened. Her condition gradually deteriorated, necessitating surgical intervention, which showed loops of ileum firmly matted together by thick fibrous tissue; the length of the ileum involved being about 4 ft. Its wall was white, edematous, and avascular and there was marked thickening of the mesentery. A segment of jejunum was mobilized and a side-to-side anastomosis with the transverse colon performed. At post-mortem, 52 days later, the pelvis was seen to contain a necrotic mass composed of cecum and small bowel, both studded with perforations. Microscopy revealed extensive loss of mucosa and gross thickening of the submucosa due to fibrous tissue, with extension into the submucosa and mesentery. (BBB)

46066 THE USE OF AN INTRA-ORAL BALLOON IN RADIOTHERAPY. Mowatt, Keith S. (Queensland Radium Inst., Brisbane). Clin. Radiol., 16: 177-9(Apr. 1965).

In oral radiotherapy, after determining the extent of the tumor, it is important to try to confine to the minimum the volume which is irradiated, without prejudicing the tumor coverage, and also to try to spare as much of the normal tissues as possible. An extensive volume of the hard and soft palate, upper alveolus, parotid glands, and their ducts is irradiated when a lesion of the tongue is treated with the

organ lying in its normal situation in the mouth. If the tongue and the structures of the floor of mouth can be widely separated from the roof of the mouth, this will substantially minimize irradiation of the upper structures. This aim may be achieved by the device described here. This cheap, easily constructed device consists of a balloon to separate the upper from the lower parts during irradiation of mouth tumors. This helps to minimize the irradiation of normal tissues, so that the mucosal reaction is diminished, and subsequent mouth dryness is greatly lessened. The lack of palatal radiation reaction also makes swallowing easier and facilitates good nutrition during and immediately following radiotherapy. When the tumor is in the antrum, palate, or upper alveolus, the applicator gives similar advantages in reverse, ensuring that the tongue and much of the lower jaw and submental region are outside the irradiated volume. The rubber balloon used is the fingertip of a surgical glove, which is bound with cotton to a small catheter (No. 7) and inflated by a 20-ml syringe. A Perspex tongue spatula is used to distribute the pressure evenly over the tongue, and a horseshoe-shaped vertical plate may be mounted on this. The balloon is inflated gently and steadily until the patient's maximum tolerance is reached, which occurs at a volume between 60 and 100 cm^3. (BBB)

46067 THE PRESENT PLACE OF RADIOTHERAPY IN THE CURE OF HODGKIN'S DISEASE. Jelliffe, A. M. (Middlesex Hospital, London). Clin. Radiol., 16: 274-7(July 1965).

The effectiveness of x-ray therapy in Hodgkin's disease was assessed in 300 patients, with attention being given to optimal doses, shielding of normal tissue, and prevention of late complications. The series included 187 males and 113 females. The crude survival rate was 31% at 5 years and 20% at 10 years, women having the expected better prognosis. There was a close relation between the extent of the disease and survival. Radiotherapy was at first used in small doses, but later it was applied more intensively. Analysis of the 10-yr survivors reveals two main groups: patients whose disease never reappeared after the initial treatment, and those in whom it recurred for the first time in the originally irradiated site. Comparison of these groups indicated that there is considerable variation in the radiosensitivity of the disease, but that a local recurrence is unlikely after a dose of between 2500 R in 12 days and 4000 R in 28 days (180-to 250-kv x rays). A smaller dose may sterilize the area but is less certain to do so. The concept of prophylactic irradiation is considered. Patients with potentially curable Hodgkin's disease present most commonly with enlarged lymph nodes in the neck and upper mediastinum; sometimes the axillae are involved. When the available evidence indicates that the disease is apparently localized to the upper half of the body, prophylactic irradiation is given to all the main lymph nodes in the upper half of the body, taking the mediastinal field down to the second lumbar vertebra. This is the present practice. With megavoltage equipment, a dose of at least 3000 rad in 3 weeks can be delivered using opposing anterior and posterior fields. Almost all the lung parenchyma is carefully shielded with lead blocks, leaving only an apical cap which must be irradiated down to the fourth rib posteriorly, if all the lymph nodes are to be treated. A small block anteriorly shields the larynx and a long thin posterior block prevents the spinal cord receiving more than 2000 rad. The dose should not be increased to more than 4000 rad in 4 to 5 weeks, because of the risk of late complications in cured patients. At the end of this treatment, residual masses in any area may be given further irradiation with small fields. This prophylactic approach could be extended to include all the main lymphatic nodes of the body, but such a step increases morbidity and greatly prolongs the treatment time. The possibility of inducing leukemia must also receive consideration. At present such intensive treatment appears inadvisable until more limited prophylactic irradiation has been given an adequate trial and its long-term effects assessed. (BBB)

46068 CARCINOMA OF THE LARGE INTESTINE AS A LATE COMPLICATION OF PELVIC RADIOTHERAPY. Black, William C.; Ackerman, Lauren V. (5th U. S. Army Medical Lab., St. Louis). Clin. Radiol., 16: 278-81(July 1965).

Carcinoma of the rectosigmoid is reported in a 77-yr-old woman as a late complication (15 years) after vigorous pelvic radiation therapy. For endometrial adenocarcinoma, the patient had received radiotherapy by both radium and x rays; 75 mg of intracavitary radium (65 mg uterine capsules and 10 mg cervical capsules) were left in place for 60 hr (4500 mg-hr), followed one week later by 40 mg of radium by tandem with 20 mg placed in each lateral position by colpostat and left in place for 50 hr (4000 mg-hr). Soon after, she received 1600 R via x ray bilaterally to the adnexae. Radiation factors were not recorded in sufficient detail to allow estimation of the dose received by the rectosigmoid. A second course of radiation therapy was instituted and 3200 R was delivered to each side including the parametrial areas using inguinal, gluteal, and pelvic ports. During the next year, symptoms of cystitis developed, and there was occasional rectal bleeding, as well as peripheral parasthesiae and mild anema. A segment of bowel, removed surgically because of radiation stricture, showed both radiation changes and carcinoma. Microscopically, there was evidence of severe radiation damage throughout all areas of the bowel and these changes, although general, were accentuated in the immediate vicinity of the carcinoma. The conditions under which this rare complication of radiation therapy can occur have been defined. In this case 8500 mg-hr of radium and 8600 R from external x-ray therapy were delivered to the pelvis in two courses with a 4-yr interval. The amount of radiation delivered to the rectosigmoid was correspondingly significant as evidenced by severe vascular sclerosis of a type characteristic of radiation damage in the bowel. (BBB)

46069 CARCINOMA OF THYROID FOLLOWING IRRADIATION FOR MEDULLOBLASTOMA. Andrew, Douglas S.; Kerr, Ian F. (Western Infirmary, Glasgow). Clin. Radiol., 16: 282-3(July 1965).

Development of a multicentric papillary carcinoma of the thyroid occurring 12 years after irradiation for medulloblastoma is reported. The patient, now 22 years old, was operated on at the age of six for a medulloblastoma, for which postoperative x-ray therapy was given. The 200-kv x rays were given in 19 fractions over 29 days to three spinal fields (2850, 2850, and 3000 R) and to one frontal cerebral field (3000 R). Following treatment she made an excellent recovery and there was no evidence of recurrence. At the age of 18 years, a lump in the right side of her neck was shown by histological examination to be a lymph node replaced by well-differentiated thyroid tissue containing colloid acini. When the thyroid gland was explored surgically, a spherical firm tumor was found at the upper pole of the right lobe. Pathological examination showed a poorly encapsulated well-differentiated carcinoma of the upper pole of the gland with multiple small areas of tumor present throughout the rest of the lobe. Tracer studies with ^{131}I showed activity in the right side of the neck, which was interpreted as evidence of residual tumor. An ablation dose of 100 mC ^{131}I was administered and 3 months later scanning of the neck showed no uptake. She is now in good health. Although this case history is of interest to radiocarcinogenesis, the risk of inducing a thyroid cancer should not weigh too heavily when planning treatment for cerebellar medulloblastoma. (BBB)

46070 INTERPRETATION OF ^{133}Xe LUNG WASH-IN AND WASH-OUT CURVES USING AN ANALOGUE COMPUTER. Matthews, Christine M. E.; Dollery, C. T. (Hammersmith Hospital, London). Clin. Sci., 28: 573-90(June 1965).

A model was developed for use with an analog computer for interpretation of ^{133}Xe regional lung wash-in and wash-out curves in normal subjects and patients with bullous emphysema, taking into account the solubility of this isotope in blood. Results are compared with those obtained with an

insoluble radioactive gas $^{13}N_2$. In normal subjects the later parts of ^{133}Xe wash-out curves are sometimes substantially affected by radioactivity in chest wall. Regional lung volume is underestimated by measuring the count rate over the lung region after rebreathing ^{133}Xe for a few minutes because removal of radioactivity by the blood prevents equilibration with the spirometer. In patients with reduced ventilation the dissolved ^{133}Xe returning to the lungs in systemic venous blood may affect the wash-out curves considerably, but this can be corrected for, using the analog computer. The effect of chest wall ^{133}Xe radioactivity is probably small in patients with reduced ventilation, but it is difficult to distinguish between true low ventilation and apparent low ventilation due to chest wall radioactivity. These errors limit the value of ^{133}Xe wash-out curves for accurate measurement of nonuniform regional ventilation. More accurate measurements of ventilation can be made by matching wash-in curves, but this method also has disadvantages. Although ^{13}N is a much more suitable isotope than ^{133}Xe for measuring regional lung ventilation and volume, it can only be used close to a cyclotron. Also, its more penetrating radiation requires much heavier shielding of the counting equipment than is necessary with ^{133}Xe. (BBB)

46071 THE EVALUATION OF GLOMERULAR FILTRATION RATE IN MAN USING A GAMMA-EMITTING TRACER (HYPAQUE-^{131}I) AND EXTERNAL COUNTING. Bianchi, C.; Toni, P. (Universita, Pisa, Italy). Compt. Rend. Congr. Intern. Nephrol., Prague, 2nd, 1963, 517-23 (1964). (In French).

The evaluation of glomerular filtration rate in man by the use of a γ-emitting tracer, such as the diatrizoate (Hypaque) labeled with ^{131}I, is described. This compound can be used for the determination of glomerular filtration rate since it is excreted by glomerular filtration only and its clearance equals that of inulin and hyposulfate in normal and pathologic conditions. A technique is described for using external counting over the bladder after injection of Hypaque-^{131}I, enabling the determination of glomerular filtration rate without urine collection. Comparison of this method with conventional procedures confirmed its validity. When clearance of Hypaque-^{131}I by external counting was compared with blood assays, the ratio of clearance values for the two methods was found to be 1.07, and the correlation coefficient, 0.94. Comparison with the inulin method gave an average ratio of 1.00 and a correlation coefficient of 0.84. (TCO)

46072 RESULTS OF THYROID FUNCTION DIAGNOSIS WITH RADIOIODINE. Schwartz, K.-D. (Universitaet, Rostock, Ger.). Deut. Gesundheitsw., 19: 1349-53(July 16, 1964). (In German).

In order to establish a firm basis for diagnosis of thyroid function the uptake of ^{131}I is measured at 1, 2, 4, 8, 24, and 48 hr after oral administration of the test dose. In addition, the urinary excretion and the serum concentrations are also measured for this period. At 48 hr normal upper limits for serum ^{131}I and $PB^{131}I$ are 0.35%/l and 0.3%/l. However, 71.8% of the serum ^{131}I values and 78.2% of the $PB^{131}I$ values are less than 0.15%/l. The average values are 0.13%/l and 0.10%/l, respectively. As measured in 335 euthyroid patients the 48-hr excretion was between 15 and 50% of the dose administered. For the first 24 hr the average was 28.4%, and for the second 24 hr the average was 1.2%. For the final 24-hr period the range was between 0 and 4%, with 59.4% of the values amounting to less than 1%. The range for the first 24-hr period was from 12 to 45%. Uptake in the thyroid increased rapidly following administration of ^{131}I. Based on results from 1000 patients, for the first hr the range was from 1 to 19%, with an average of 9.3%. For the second hr the range was from 5 to 31%, with an average of 17%. For the fourth hr the range was 12 to 44%, with an average of 27%. At 8 hr the range was from 18 to 56%, with an average of 37.5%. At 24 hr the uptake ranged from 27 to 68%, and at 48 hr it ranged from 28 to 68%. The average uptakes at these times were 48.5 and 49%, respectively. Values for noneuthyroid patients varied considerably from the norms of uptake and excretion established by these tests. (BBB)

46073 COLOR SCINTIGRAPHY AND COLORED X-RAY IMAGES. Frik, W. (Univ., Erlangen, Ger.). Fortschr. Geb. Roentgenstr. Nuklearmed., 103: 227-8 (1965). (In German).

The successes of the color scintigram based on the color-print process are due to the use of large color contrasts for comparatively coarse impulse-rate steps. In radiography improvements in the rendering of small contrasts are sought. This can not, for physiological reasons, be obtained by converting grey contrasts into fractionally equally small spectral contrasts. (auth)

46074 INTRODUCTORY REMARKS ON THE THEME SURGICAL MEASURES FOR THE EXTENSION OF RADIATION THERAPY AND FOR THE TREATMENT OF RADIATION EFFECTS IN THE FACE-JAW REGION. Schuchardt, Karl (Universitaets-Krankenhaus, Hamburg-Eppendorf, Ger.). Fortschr. Kiefer Gesichtschir., 8: 1-12(1962). (In German).

The author summarizes two main themes of interest to surgeons whose specializations are in the field of facial and jaw surgery, and in plastic surgery. One concerns operations required to remove tumors and to carry out irradiation treatment of tumors. These are relatively standardized procedures. In contrast to these there is another group of procedures that is concerned with repair and reconstruction of defects that result from irradiation treatment. In part, these are the unexpected results of irradiation, but often the patient is irradiated even though there is a definite probability that a radio-induced defect may appear. In particular, injuries to the jaws and teeth may be induced if the irradiation is given during a period of skeletal growth. This applies particularly to infants and children who are often mistakenly treated for hemangiomas and naevi. Although the surgical treatment and repair of radioinduced injuries and defects is an interesting field, it is often difficult. Exceptions that represent simple procedures are radiodermatitis of the face, submandibular, or neck regions. Growth defects induced by radiation are much more difficult to repair surgically. (BBB)

46075 THE CORRECTION OF RADIOINDUCED GROWTH DEFECTS OF THE FACIAL PORTION OF THE SKULL. Schuchardt, Karl (Universitaets-Krankenhaus, Hamburg-Eppendorf, Ger.). Fortschr. Kiefer Gesichtschir., 8: 172-8(1962). (In German).

The most frequent causes of impaired growth of the facial skeleton is irradiation of infants and small children during treatment for hemangiomas and naevi flammeus. Many clinicians feel that the first or second year of life is the optimal time for irradiation treatment of these disorders. However, during this time of life growth centers in cartilage and bones are most sensitive to ionizing irradiation and therefore most susceptible to injury. Impaired growth is evidenced by hypoplasia of the bone structure and by occlusion defects. If the epiphyses of the lower jaw are involved, micrognathy combined with distal bite may result. These types of deformities are usually so marked that it is difficult to normalize the jaw profile or improve occlusion. Correction of radioinduced hypoplasia of the upper jaw with occlusion defect is especially difficult. The author reports case histories, surgical treatment of maxillary and mandibular micrognathia, and discusses methods of prosthesis. For bone defects where there is no functional impairment involved, but where the defect is correctable, near and distant flaps consisting of subcutaneous tissue are frequently very suitable. However, use of distant flaps is justified only when the defect is extensive. For slight defects, such as minor hypoplasias of the os zygomaticum or os frontale, near flaps of subcutaneous tissue are usually adequate. (BBB)

46076 APPLICATION OF THE RADIOISOTOPE PRECIPITATION TEST TO THE STUDY OF Q FEVER IN MAN. Lackman, David B.; Gilda, Gayle; Philip, Robert N. (Public Health Service, Rocky Mountain Lab., Hamilton, Mont.). Health Lab. Sci., 1: 21-8(Jan. 1964).

A radioisotope precipitation test (RIPT) was developed to test for antibodies of Q fever, caused by Coxiella burnetti.

The RIPT is essentially a Coombs' antiglobulin agglutination procedure, but is at least 10 times more sensitive than the Coombs' test as applied to the detection of Q fever antibodies. Iodine-131 is coupled to purified Q fever antigen, the tagged antigen is added to serial dilutions of serum, and the antigen-antibody complex is agglutinated with antiglobulin. The agglutinate is removed by slow-speed centrifugation. Radioactivity is then determined on a measured quantity of supernate. If more than 50% of the radioactivity has been removed in the agglutinate, the test is considered positive. Very small amounts of antigen are used but sufficient antiglobulin to precipitate all of the γ-globulin must be present in the system. As long as all ^{131}I is coupled to the specific antigen, the test procedure seems to be satisfactory and the radioactive antigen is removed from the mixture only by Q fever antibody. Some results from use of the RIPT during a study of Q fever in man are shown. Results of the RIPT in comparison with those obtained by other tests are given. When persons were given antigenic stimulation with a total of 10 to 30 complement-fixing units in one to three doses of vaccine, there was no significant difference in the frequency of positive tests by the RIPT and the capillary-agglutination test (CAT) at 6 and 12 weeks. Overall, 71% were positive by the RIPT and 81% by the CAT. With this amount of antigenic stimulus the CAT measures antibody response fully as well as the RIPT. With the RIPT the results are read by a counter and are printed mechanically on a strip of adding machine paper. The advantages of the RIPT are: sensitivity; the high antibody titers obtained; specificity, especially with sera in poor condition; mechanical reading; and the very small amount of antigen used. The major disadvantages are: the lack of equipment for work with radioisotopes in the usual public health laboratory; and the large quantity of anti-γ-globulin used. The serologist, by use of the RIPT, can provide the epidemiologist and the pathologist with an increasing amount of information regarding the prevalence of C. burnetti infection. (BBB)

46077 TRENDS IN RADIATION THERAPY. **Oeser, H. (Freie Universitaet, Berlin). Internist, 5: 271-7(July 1964). (In German).**

The author traces the history of x irradiation therapy from the time of its discovery by Roentgen in 1895. Many of the early applications of radiotherapy were confined to treatment of various skin diseases or for cosmetic purposes, although it was sometimes used for treatment of tumors. Recognition of its biological effects on internal tissues and organs led to its use for treatment of tumors of the spleen, swollen lymph nodes, and leukoses. Gonadal effects were also studied. Effects of physical factors and radiobiological changes were studied extensively. Modern-day techniques of pendulum irradiation, sieve or raster irradiation, fractionation of doses, use of cascade generators, accelerators, and high-energy nuclides, such as ^{60}Co and ^{137}Cs are itemized. The advantages and disadvantages of high-energy particles are discussed. Methods of direct irradiation of tumor cells are discussed. These include homogeneous tangential irradiation, implantation of radioisotopes, and concentrated tumor irradiation. Basically these are two different approaches to irradiation of tumors. One is distance therapy, where irradiation is used in the form of conventional x irradiation depth therapy, moving irradiation, super or megavolt therapy, or telegamma therapy. The second trend is toward use of contact irradiation by means of Ra, meso-Th, or x irradiation, interstitial implantation of radionuclides, or selective inter- and intracellular irradiation. (BBB)

46078 TUMOR TELE-IRRADIATION WITH ENERGETIC CORPUSCULAR AND WAVE RADIATION. **Becker, J.; Kuttig, H. (Universitaets-Strahlenklinik, Heidelberg). Internist, 5: 276-84(July 1965). (In German).**

The authors review and describe some characteristics of various types and procedures of irradiation with x ray and fast electrons. Early methods of irradiation therapy are described and their relative advantages and disadvantages are compared. Techniques of irradiation, such as cross-fire irradiation and moving irradiation are described. The principles of pendulum convergence irradiation are illustrated, and patterns of dose distribution are compared between pendulum irradiation and cross-fire irradiation procedures when telecobalt therapy is used. The use of tangential pendulum or layer irradiation is described for specialized applications. The advantages of screen or sieve irradiation for skin protection are outlined. Irradiation with x rays with energies greater than 1 Mev, and irradiation from ^{60}Co and ^{137}Cs sources has the advantages that they reach greater depths of tissues and alter the blood picture only relatively infrequently. They are also less affected by absorption in bone and cartilaginous tissues, so that the dose distribution of irradiation can be made more uniform than with less energetic irradiation. The advantage of the higher relative depth dose is that the same focal dose can be administered with a smaller number of fields and less of the healthy tissue is irradiated. As examples of the effects of telecobalt therapy, the percentage survival values with laryngeal carcinoma are 1 yr, 73.5%, 2 yr, 45.5%, 3 yr, 47%, and 4 yr, 32%. These values are somewhat greater than those obtained with epipharyngeal or hypopharyngeal carcinoma. Considerable objective and subjective improvement in treatment of lung tumors, bronchial carcinoma, and abdominal tumors, and many other tumor types have been reported with supervoltage therapy. (BBB)

46079 THE RENAL CLEARANCE OF ^{131}I-LABELLED SODIUM IOTHALAMATE IN MAN. **Sigman, Eugene M.; Elwood, Charles; Reagan, Mark E.; Morris, Arthur M.; Catanzaro, Antonio (Buffalo General Hospital). Invest. Urol., 2: 432-8(Mar. 1965).**

The ^{131}I-labeled sodium iothalamate was prepared from the commercially available product by a method of isotope exchange whereby some of the normal ^{127}I atoms were replaced with ^{131}I atoms. The product was purified by precipitation and then converted to the sodium salt. The sodium ^{131}I iothalamate prepared in this manner had a specific activity of 128 μC/mg and a free ^{131}I content of less than 2% up to 3 weeks after labeling. Simultaneous renal clearances of inulin and ^{131}I-labeled sodium iothalamate were performed on ten patients. Diuresis was induced by oral water loading, as well as by a constant intravenous infusion of lactated Ringer's solution. The total amount of inulin needed for the study was mixed with 150 μC ^{131}I-labeled sodium iothalamate, and then a priming and a sustaining dose was given. In five patients, a carrier substance, meglumine iothalamate, was added to the ^{131}I-labeled sodium iothalamate, in a weight ratio of 50,000 to one. This gave a total amount of contrast medium about three times the usual pyelographic dose. Plasma and urine were analyzed for ^{131}I activity in a well-type scintillation counter. The observed iothalamate-to-inulin clearance ratio varied from 0.74 to 1.23, with an average of 1.06. The data indicate that sodium iothalamate is excreted in man primarily by glomerular filtration. The observation that the clearances of iothalamate, at both low and high plasma concentrations, approximate those of inulin. There are numerous clinical uses for compounds which are excreted only by glomerular filtration and which can be appropriately labeled with a γ-emitting isotope. The quantitation of such radioactive substances in blood and urine can be readily determined by scintillation counting. This technique is far less time-consuming and more accurate than the chemical determination of inulin. Moreover, substances which interfere with the quantitation of inulin, as for example, high concentrations of glucose, pose no problems when radioactivity is measured. (BBB)

46080 GUIDE FOR THE MEDICAL USE OF RADIOACTIVE ISOTOPES: RADIATION PROTECTION. **J. Am. Med. Assoc., 192: 643-5(May 17, 1965).**

This report, prepared by the American Medical Association Committee on Nuclear Medicine, is presented to acquaint the physician with various regulations and recommendations for radiation protection in the medical application of radioactive isotopes. The instrumentation, facilities, procedures, and physician's personal qualifications necessary to comply with existing state and federal regulations are considered. A physician who may wish to use radioactive isotopes should have the services of a radiological safety officer available to him as needed to inspect facili-

ties, ensure against contamination, and ensure the proper and safe handling of radioactive materials. The physician should ensure that he has the necessary equipment and facilities to handle the isotopes safely and also to handle any waste-disposal problems. He should also be sure that his staff is trained in the safe handling of radioactive materials. The physician should familiarize himself with the requirements for record keeping and set up a system whereby records are kept in accordance with applicable state or federal regulations. Before radioisotopes are administered to a patient, determination should be made whether any previously administered radioactive materials are still active in his body. All therapeutic doses of radioisotopes should be administered by a qualified physician. Diagnostic doses of radioisotopes may be administered by a trained technician under the direct supervision of a qualified physician. AEC regulations call for in-hospital administration for doses greater than 30 mC and allow out-patient administration for doses less than 30 mC. When patients are given doses below but near to 30 mC, careful consideration should be given as to adequate maintenance of radiation protection in the home, to determine whether in-hospital administration would be advisable. When doses of radioisotopes above 30 mC are administered, supervision of the radiological health care of the patient by the radiological safety officer is important. Records should be maintained of patient exposure to ionizing radiation, levels of radiation exposure of personnel working in the institution, pre-employment medical examinations, and radioactivity levels measured in the lab and various areas of the institution. Particularly, records should be carefully maintained of pre-employment examinations of all persons occupationally exposed to ionizing radiation. (BBB)

46081 THYROID IODINE DETERMINED BY X-RAY SPECTROPHOTOMETRY. Heedman, Per-Axel; Jacobson, Bertil (St. Goran's Hospital, Stockholm). J. Clin. Endocrinol. Metab., 24: 246-52(Mar. 1963).

With the described method for estimating iodine by x-ray spectrophotometry the total amount of thyroid iodine can be determined both in vivo and in vitro. This x-ray spectrophotometric method was used to determine thyroid iodine in cases of thyrotoxicosis, nontoxic goiter, and normal thyroid function. The radioiodine uptake test was also applied to these subjects, and the protein-bound ^{131}I (PBI) was determined. This made it possible to evaluate correlations between the content of thyroid iodine and radioiodine uptake values, also to compare the specific activity of radioiodine in plasma and thyroid. The x-ray spectrophotometry is based on absorption measurements at selected wavelengths; by determining the absorption difference at two wavelengths, chosen close to and on the opposite sides of the absorption edge of an element, it is possible to determine the amount of this element independently of the presence of other substances. The in vivo determined iodine content of the thyroid gland showed large variations in all three groups of patients investigated: controls, 4.5 to 31.4 mg; nontoxic goiter, 5.8 to 39.2 mg; and thyrotoxicosis, 4.0 to 31.6 mg. The same large variations were found for the in vitro determinations, in which the experimental error was smaller. A comparison between plasma ^{131}I activity and thyroid iodine revealed some correlation. In thyrotoxicosis a high plasma specific activity was obtained when the thyroid iodine content was low, whereas a large thyroid iodine pool was sometimes associated only with a moderately increased plasma activity. In nontoxic goiters, in which the plasma specific activity was generally within the normal range, the same inverse correlation was found. As an explanation for the exceptions, the turnover rate of iodine may differ from one part of the gland to another, and a strict correlation between the total iodine and $PB^{131}I$ therefore cannot be expected. In thyrotoxicosis, iodine taken up from the blood stream and synthesized to thyroid hormone is rapidly secreted again without entering the main thyroid iodine pool. (BBB)

46082 RADIATION, THYROID CELLS AND ^{131}I THERAPY—A HYPOTHESIS. J. Clin. Endrocrinol. Metab., 25: 1141-17(Oct. 1965).

The results of ^{131}I therapy of thyrotoxicosis are unsatisfactory. Many patients require multiple doses and a large minority ultimately develop hypothyroidism. It has been previously emphasized that accurate and optimal ^{131}I dosimetry is impossible and that thyroid cell radiosensitivity may be an important factor in determining the outcome of ^{131}I therapy. These difficulties are re-emphasized and the hypothesis is extended to include the important factors of differential thyroid cell radiosensitivity and cell turnover. Thyroid cell function is reduced by ^{131}I therapy and cell multiplication must be severely impaired, because cell reproductive integrity is much more radiosensitive than cell function. As a result of the latter, thyroid cell renewal is abolished and hypothyroidism is the end result of cell depopulation. The current problems of radiation therapy for thyrotoxicosis are discussed in the light of this hypothesis. (auth)

46083 USE OF AN IMMERSIBLE SCINTILLATION COUNTER IN THE URINARY VITAMIN B_{12} EXCRETION TEST. Gough, J.; Gough, W.; Roath, S. (Royal Infirmary, Manchester, England). J. Clin. Pathol., 18: 250-1(Mar. 1965).

A modified method for conducting this test is described which facilitates counting large volumes of urine containing ^{58}Co-labeled vitamin B_{12}. This urinary excretion test for vitamin B_{12} absorption, devised by Schilling, is the most commonly used method in the assessment of this function of the gut, and particularly in the diagnosis of pernicious anemia. The reproducibility of the results obtained in this manner and the convenience of the procedure compared with others make the urinary excretion method the choice of many laboratories. The urine samples obtained containing labeled B_{12} may be counted in a ring type Geiger-Mueller counter, or by activated crystal scintillation counters in well, annular, or end-on settings. In this study the EKCO type N691 general purpose scintillation detector, fitted with an N609 crystal, was used; it is of a completely immersible design and appeared to be suitable for the counting of large samples of radioactive liquids. Using the technique described, the value of this counter in the Schilling test was assessed, after an initial evaluation of the accuracy of the method. The apparatus was tested in view of its capability of producing adequately high counts in a short time. Schilling tests were carried out on 12 patients in whom pernicious anemia, malabsorption syndromes, or other defects were suspected. The ^{58}Co-labeled vitamin B_{12} of 1.0 μC activity, 1 μg, was given by mouth, followed by 1000 μg of the nonradioactive form by injection, and the urine collected for the following 24 hr. The usual method of counting 10-ml urine samples for 3000 sec in the annular counter, the time found necessary to obtain a significant number of counts, was used, as was the 100-sec count using the immersible detector. The results showed that the immersible detector provided, in 100 sec, figures whose standard errors compare favorably with those obtained by counting 10-ml samples in the annular detector for 3000 sec. When 10-ml samples were counted for only 100 sec, a high standard error was incurred. The ability of the immersible detector to count a large volume of fluid enables significantly high counts to be reached in a conveniently short time. (BBB)

46084 MALIGNANT TUMOURS OF THE EAR. Lederman, M. (Royal Marsden Hospital, London). J. Laryngol. Otol, 79: 85-119(Feb. 1965).

Extensive data are presented on use of radiation in treatment of tumors of the ear with reference to 360 patients. The data include optimal dose data, radiation reactions of normal tissues of the ear and their prevention, and incidence and treatment of postirradiation complications. The structure of the external ear and the special relation of the middle ear to the temporal bone both have a profound influence on the principles of radiation treatment because of the limited tolerance of cartilage and bone to radiation. The loose cancellous bones forming the boundaries of the nasal fossa and upper alveolus or the mucoperiosteum of the ethmoid bone can be irradiated with impunity, since if damaged by radiation their seque-

stration presents little problem to the body. On the other hand, radiation damage to the more dense temporal bone is ill-tolerated and sequestration may cause considerable morbidity. Similarly, the yellow elastic fibrocartilage of the pinna, external nose and suprahyoid epiglottis are far more tolerant of irradiation than are the hyaline thyroid and arytenoid cartilages. While normal cartilage and bone tolerate therapeutic doses of radiation reasonably well, if these tissues be invaded by neoplasm or become infected, their tolerance to radiation is seriously diminished. Wherever surgery and radiotherapy are to be used in combination, radiotherapy should be given first, because its effects are more likely to be beneficial when the blood supply has been least disturbed. Small superficial lesions without cartilage invasion are best treated by low or medium voltage x-ray therapy (45 or 60 kv) with a dose of 6000 R being given in ten applications of 600 R over two weeks. More extensive lesions associated with bone or cartilage involvement can be treated by 140-kv x-rays. Use of megavoltage x rays or ^{60}Co in treatment of a cancer situated in the base of the skull has disadvantages in that it is difficult to localize the max doses of radiation to the diseased tissues without delivering undesirable excessive quantities of radiation to the brain. Some of the problems and disadvantages associated with the use of γ radiation and high energy x rays in the head and neck region can be eliminated by the use of electron beams. The effects of radiation on the ear are described in detail. (BBB)

46085 TEN NEW CASES OF CUTANEOUS RADIONECROSIS. Depaulis, M. J. J. Med. Bordeaux Sud-Ouest, 141: 1703-12(Nov. 1964). (In French).

Results of successful surgical intervention in 10 cases of radionecrosis caused by previous radiotherapy are discussed. Treatment was effected by graft or with a flap of skin introduced over the lesion. Several general conclusions about radiosensitivity and the hazards of radiotherapy, based on these cases, are discussed. In general, irradiation should be avoided when surgical removal of tumors is practical. When irradiation is necessary, all possible attention should be paid to possible consequences. Well-known but often ignored factors that should be taken into consideration prior to irradiation, such as the part of the body irradiated, differences in sensitivity of particular areas of skin, and the possibility of individual radiosensitivity differences, are reviewed. For example, the skin of the axilla, perineum, palms of the hands, and soles of the feet are more radiosensitive; blonds are generally more sensitive than brunettes; and skin affected by previous burns, traumatic scars, hyperkeratosis, and toxic chemicals shows increased sensitivity to radiation. Furthermore the hazards and technical difficulties involved in the surgical treatment of radionecrosis are emphasized. Finally, the relative merits of the graft and the skin flap in the treatment of radionecrosis are discussed. The choice should vary according to the part of the body affected and the extent of the surface to be covered. (BBB)

46086 LOCALIZATION OF INTRACRANIAL VASCULAR LESIONS BY RADIOACTIVE ISOTOPES AND AN AUTOMATIC CONTOUR BRAIN SCANNER. Feindel, William; Rovit, Richard Lee; Stephens-Newsham, Lloyd (McGill Univ., Montreal). J. Neurosurg., 18: 811-21 (Nov. 1961).

This report illustrates, with selected cases, that increased vascularity is a prominent feature of many intracranial lesions that can be detected most readily and localized by a radioisotope method. These studies were made with an automatic contour brain-scanning device that gives reproducible scan records of the total and differential concentration of isotope in the head. By using human serum albumin tagged with ^{131}I (RISA) it was also possible to use the selective permeability of normal brain tissue to albumin, as well as the retention of RISA in the circulation for a biological half-life of 4 days which allows for repeated scans to be carried out. The automatic contour scanner used is described. Using this contour scanner and RISA, it was shown that chronic subdural hematomas give a characteristic pattern of radioactive uptake. The radioactivity of the fluid in the hematoma, as compared to that of peripheral blood, was markedly high. Inert collections of blood within the cranium were associated with lower levels of activity. Highly vascular lesions, such as arteriovenous malformation and vascular tumors, showed the most intense concentration of RISA. This reached a high peak immediately after injection and was maintained over a period of several days until the level of RISA in the circulating blood dropped. These findings are illustrated by selected case reports. The thyroid gland was blocked by Lugol's iodine solution 24 hr before the injection of 300 to 400 μC of RISA. The actual scan takes 30 min, and repeated scans may be carried out up to as long as one week on the basis of the single injection. The total-body radiation dose, using 400 μC of RISA, is 50% less than with the 2000 μC dose used for positron scanning. Registration of activity on the scan chart is by a double row of dots, each row corresponding to one detector. Each dot may represent from 100 to 400 counts. Differences in the accumulated counts from the two detectors with a range of 20 to 100 are indicated by oblique dashes and demonstrate the lateralization of the increased uptake. (BBB)

46087 RECURRENT CYSTIC FORMATION IN CRANIOPHARYNGIOMA TREATED WITH RADIOACTIVE CHROMIC PHOSPHATE. CASE REPORT. Overton III, Marvin C.; Sheffel, Donald D. (Univ. of Texas Medical Branch Hospital, Galveston). J. Neurosurg., 20: 707-10 (Aug. 1963).

The use of ^{32}P, in the form of chromic phosphate, to treat a case of craniopharyngioma is described. Its advantages over ^{198}Au are enumerated. For the intended purpose, chromic phosphate seemed the better of the two because it does not produce γ radiation and has a relatively long half life (14.3 days). Most of the chromic phosphate is plated out homogeneously on the walls of the injected serous cavity, and while the rate and concentration of this process is variable, it is nearly complete in a few days, and its effectiveness is probably because of this plating affinity. The best effects are attained when $Cr^{32}PO_4$ is used to combat malignant effusions which actually have tumor cells present in the fluid, and the percentage of good results is uniformly higher in pleural effusions as compared to peritoneal effusions. Dose estimation has been arbitrary, varying from 4.8 to 20 mC but usually is of the order of 6.9 mC for pleural effusions and 9 to 12 mC for peritoneal effusions. Tendency to localization of the injected substance can be overcome by changing the patient's position frequently during the first few hours after administration. During the time the reaction to radiation is developing, a delay in its effect on fluid secretion occurs, and it is therefore frequently necessary to perform repeated additional aspirations on the patients after the initial instillation of $Cr^{32}PO_4$. Also considered is the use of ^{198}Au and ^{90}Y to produce hypophysectomy and treat pituitary tumors. Radionecrosis hypophysectomy uses 9 to 40 mC by transnasal, transphenoidal, or direct instillation of radioactive chromic phosphate into the pituitary gland. One other case of craniopharyngioma treated with ^{32}P was found in the literature, but no reference could be found to the use of radioactive chromic phosphate for the treatment of recurrent cysts in cases of craniopharyngioma. In the case described here, instillation of 1 mC of ^{32}P was effective. The patient required no further operation and his visual and endocrinological symptomatology improved. This remission was maintained to at least 26 months after the instillation of ^{32}P into the cystic craniopharyngioma. (BBB)

46088 INTRA-ARTERIAL CYTOTOXIC THERAPY AND X-RAY THERAPY FOR CANCER OF THE HEAD AND NECK. Helman, Percy; Sealy, Rossal; Malherbe, Eric; Anderson, John (Univ. of Cape Town, S. Africa). Lancet, 1: 128-30(Jan. 16, 1965).

Results over the past five years in treating 82 patients with advanced cancer of the head and neck by means of intra-arterial cytotoxic therapy, as an adjuvant to radiotherapy, are described. It was found to be of no value to subject patients to intra-arterial infusion whose malignant disease recurred after a course of radiotherapy or failed to respond to irradiation. Best results were obtained in

patients who were treated initially by intra-arterial cytotoxic therapy and who underwent a course of radiotherapy thereafter. Nine patients treated early in the series were infused with nitrogen mustard only. All the rest received methotrexate, usually 50 mg daily. To cut down methotrexate toxicity, folinic acid was also injected. Toward the end of methotrexate treatment many patients were given two or three intra-arterial injections of thioTEPA (15 mg per injection). Radiotherapy was administered by means of conventional deep x-ray therapy (250 kv) as soon as possible after completion of the infusion. A tumor dose of 4000 to 5000 R was delivered in from four to five weeks. Skin reactions were not unduly severe. Serious complications of the treatment are described. They were relatively few compared with the frequency of serious complications in patients whose lesions had been irradiated before infusion. Death due to severe marrow depression occurred in one case. Sloughing of ear happened once, after a nine-day period of infusion in a patient with carcinoma of the maxillary antrum. Six weeks later the whole ear on the ipsilateral side sloughed off. Aneurysm of the carotid artery was observed a month after infusion for squamous carcinoma of lower eyelid and cheek. However, there was a significantly lower frequency of all types of complications when the infusions were the initial form of treatment instead of following x-ray therapy. In 36 patients whose lesions were treated after they had recurred after a course of radiotherapy, not only were there many complications, but also the results of treatment were disappointing, and in many it was quite ineffective. Infusion therapy should not be used in patients previously irradiated. Of the 43 patients treated initially by infusion with subsequent irradiation, 7 failed to respond; in 21 the lesions regressed remarkably, and in 8 of these patients tumor regression was striking; and in 15 there was some objective response. (BBB)

46089 MANAGEMENT OF POLYCYTHAEMIA VERA. Harman, J. B.; Kay, H. E. M.; Ledlie, E. M. (Royal Marsden Hospital, London). Lancet, 1: 1115-16(May 22, 1965).

A previous report on the incidence of leukemia in polycythemia patients treated with ^{32}P is briefly commented on, and it is pointed out that there is not a clear causal relation in this situation. The figures previously quoted show that treated patients live longer than untreated, and that there is no difference between the survival of patients treated with radiophosphorus on the one hand and by venesection and cytotoxic drugs on the other. Yet the conclusion was drawn that drugs should replace radiophosphorus whenever possible. The reason given is the high incidence of so-called leukemia from radiophosphorus, though the non-^{32}P-treated patients had a similarly high incidence of various types of marrow dysplasia. It is suggested that this distinction is based on a confusion of terminology involving the word leukemia. It was concluded that no patient should be treated either with radiophosphorus or cytotoxic drugs merely because the diagnosis of polycythemia vera has been made; but if treatment is required, either because of symptoms or a threat to longevity, then the choice should depend on convenience, and on the quality and duration of remissions. (BBB)

46090 RADIATION AND BREAST CANCER. Gershon-Cohen, J. (Albert Einstein Medical Center, Philadelphia). Lancet, 2: 440-1(Aug. 28, 1965).

Comments are made on a previous report suggesting that any radiation exposure to breast tissues may invoke future mammary cancers. It is pointed out that this alarming implication indicates an unwarranted hazard in a vital diagnostic technique: mammography. It is possible that the conjecture, which is cited, is correct, and certain mammary cancers may have resulted from patient exposure to repeated fluoroscopic examinations during artificial pneumothorax therapy for tuberculosis years previously. Two phthisiologists are cited who died of leukemia, which, it is suspected, resulted from cumulative radiation exposure due to undisciplined fluoroscopy. Mammography, however, which employs low kilovoltages and adequate filtration with sharp collimation of the x-ray beam, cannot be equated with fluoroscopic irradiation (so commonly uncontrolled) by physicians concerned with artificial pneumothorax. In the hands of a skilled radiologist, who exercises all the proper controls, mammography entails insignificant risk. This is true even when repeated x-ray studies are necessary, as in breast screening surveys. Each exposure is of the order of one rad to the skin, limited essentially to the breast, with negligible irradiation of the mediastinum, lungs, or ovaries. It is concluded that mammography is a thoroughly safe and extremely valuable diagnostic procedure. (BBB)

46091 COMBINED 5-FLUOROURACIL AND SUPERVOLTAGE RADIATION THERAPY IN THE PALLIATIVE MANAGEMENT OF ADVANCED GASTROINTESTINAL CANCER: A PILOT STUDY. Moertel, Charles G.; Reitemeier, Richard J.; Childs, Donald S. Jr.; Colby, Malcolm Y.; Holbrook, Margaret A. (Mayo Clinic, Rochester, Minn.). Mayo Clin. Proc., 39: 767-71(Oct. 1964).

Evidence relating to the synergistic effects of 5-fluorouracil and ionizing radiation is discussed, and previous clinical reports are reviewed in which the combination was used for radioresistant carcinomas. A study was made on 44 patients to: determine a safe and tolerable dosage of 5-fluorouracil used in combination with supervoltage radiotherapy; determine whether combined 5-fluorouracil and supervoltage radiation therapy can produce palliation. Radiotherapy was delivered from either ^{60}Co or a 6300-kv linear accelerator. The total tumor dose ranged between 2200 and 5000 R delivered over 10 to 30 days. Field sizes ranged from 10 by 10 cm to 20 by 20 cm. 5-Fluorouracil was administered by a rapid intravenous injection technic in a daily dose of 15 mg/kg. Drug therapy was initiated simultaneously with radiotherapy and was administered on consecutive days until the planned total dosage was completed. In six patients treated with 5-fluorouracil to the point of early stomatitis the late toxicity was most severe. Four patients experienced profound leukopenia and three died as a direct result of drug toxicity. Toxic reactions are listed according to the dosage of 5-fluorouracil administered. At a dose range of 40 to 50 mg/kg the toxicity was usually tolerable and profound leukopenia developed in only 11%. No consistent relation could be established between toxicity and radiation dosage, field size, or field location. A sufficient number of patients (37%) achieved objective and subjective palliation to justify controlled study of the possible additive or synergistic role that 5-fluorouracil may have when combined with radiotherapy. (BBB)

46092 ULCERATED THOROTRASTOMA. Palou, J.; Girbes, J.; Lopez, M. Rodriguez (Servicio de Cirugia Vascular, Barcelona). Med. Clin. (Barcelona), 42: 292-4(Apr. 1964). (In Spanish).

The pertinent literature is reviewed and a new case is presented of an ulcerated tumor diagnosed many years after use of Thorotrast as an intravascular contrast agent. The 60-yr-old patient, whose case history is related in detail, at the age of 42, while suffering from recurrent phlebitis with severe varicosities of the legs, was submitted to phlebography, presumably with Thorotrast. A painful, induration developed in the popliteal region. At subsequent examination of the patient for phlebitis, ulceration of the site was noted, and radiography revealed opaque material at the lower portion of the femur. A hard mass was removed and both radiography and histologic examination revealed the presence of ThO_2 particles in the lesion. Histologically, an area of necrosis was seen, surrounded by macrophages filled with ThO_2. No malignant changes were seen. It is concluded that extravasation of Thorotrast during angiography resulted in formation of this tumorous mass. Its removal was successfully accomplished. (BBB)

46093 DISTRIBUTION OF DOSAGE FIELDS IN PENDULUM GAMMA THERAPY OF THE RECTUM AND URINARY BLADDER TUMORS. Gamaleya, A. N.; Donskoi, M. D.; Stavitskii, R. V.; Shvedov, T. Zh. Med. Radiol., 10: No. 7, 16-19(July 1965). (In Russian).

The distribution of energy in tissues during pendulum γ radiotherapy of tumors of the rectum and urinary bladder was investigated. The dosimetric studies served to plot isodose curves for pendulum irradiation with the swing

angle of the source equalling 90, 120, 180, 240, and 360°. The choice of optimal conditions for irradiation is made with due consideration of the integral absorbed dose in the active bone marrow of the pelvis, femoral neck, urinary bladder, and rectum. (tr-auth)

46094 ON THE CHOICE OF RADIATION ENERGY IN RADIOTELETHERAPY. Sinitsyn, R. V. Med. Radiol., 10: No. 7, 76-83(July 1965). (In Russian).

Recommendations are given for the choice of optimal radiation energies in radioteletherapy of tumors with different localization. Sources of x and gamma-ray emission, as well as those of hard bremsstrahlung and fast electron radiation are considered. The resultant data show that the medical establishment should have at its disposal an assortment of sources within a wide range of radiation energies. (tr-auth)

46095 PHYSICAL AND BIOLOGICAL BASES OF THE EXTERNAL AND INTERNAL IRRADIATION OF SYSTEMIC NEOPLASIA. Bistolfi, F.; Passeri, A. (Universita, Genoa). Minerva Radiol., Fisioterap. Radiobiol., 10: 261-6(June 1965). (In Italian).

The physical and biological base in the external and internal radiotherapy of systemic neoplasia are reviewed. The factors to be considered in whole-body external irradiation and in internal isotope therapy are indicated. The special selectivity of irradiation, the terms radioprotection and radiosensitization, the ratio of equal efficiency, the dose reduction factor, the dose amplification factor, and divergent radiomodification are defined. The association of chemotherapy and radiotherapy is considered. The space and time factors of irradiation are indicated. (J.S.R.)

46096 BIOLOGICAL PROBLEMS IN THE ASSOCIATION OF ANTINEOPLASTIC RADIOTHERAPY-CHEMOTHERAPY. Bergonzini, R.; Torricelli, A. Minerva Radiol., Fisioterap. Radiobiol., 10: 267-71(June 1965). (In Italian).

The basic biological problems—the mechanism of the effect of the associated chemical and radiation treatment and the summation of the separate effects—are discussed under a radiobiological profile. The chronological factors in the combined administration are considered. (J.S.R.)

46097 RADIOSENSITIVITY AND OXYGEN THERAPY IN GYNECOLOGICAL ONCOLOGY. Lagrutta, L.; Reggiani, G.; Grassi, G.; Raimondi, J. (Universita, Florence). Minerva Radiol., Fisioterap. Radiobiol., 10: 294-5(July-Aug. 1965). (In Italian).

Recent results indicating the role of oxygen as an agent increasing the radiosensitivity of tumor cells are briefly reviewed. An apparatus designed for the combined radiotherapy and oxygen therapy of gynecological tumors is shown schematically. The results obtained on 8 patients at oxygen pressures up to 2 atm show no toxic phenomena resulting. (J.S.R.)

46098 CAN THE INDEX OF UPTAKE OF ^{32}P REVEAL THE RADIOSENSITIVITY OF METASTASES. Miceli, R.; Rimondi, C. (Universita, Bologna). Minerva Radiol., Fisioterap. Radiobiol., 10: 296-7(July-Aug. 1965). (In Italian).

The uptake of ^{32}P as a test of the radiosensitivity of metastases was evaluated. For this purpose the uptake of ^{32}P by the metastatic tissues with respect to the healthy tissues was determined. The ratio between the uptake and the radiosensitivity of the metastases was evaluated clinically. The modification of the uptake value of the metastases caused by radiation treatment was determined. The results showed that the test of the uptake of ^{32}P is not an effective test of the index of the radiosensitivity of the metastases. The uptake of ^{32}P can be used in the initial diagnostic evaluation of the metastatic tissues, and is a useful contribution in the evaluation of the evolution of the metastases process. (J.S.R.)

46099 RECTOSIGMOIDOSCOPIC DETECTIONS IN CARCINOMA OF THE CERVIX BEFORE AND AFTER RADIOTHERAPY. Savignoni, R. (Universita, Rome). Minerva Radiol., Fisioterap. Radiobiol., 10: 305-6(July-Aug. 1965). (In Italian).

The effects on the rectosigmoid region of a malignant tumor in adjacent tissues and of radiotherapy of this tissue was studied in 50 patients with cervix carcinoma. The studies made before radiotherapy showed no modification of the rectosigmoid region for tumors of stage one. Beginning with stage two, however, progressive modifications were detected in the rectosigmoid region. After radiotherapy, alterations were observed that are classified according to the Dean and Taylor classification. The results showed that the gravity of the rectal lesion corresponds to the radiation dose. (J.S.R.)

46100 ENDOLYMPHATIC RADIOISOTOPE THERAPY AND PELVIC LYMPHOGRAPHY IN GYNECOLOGICAL CANCEROLOGY. Lagrutta, J.; Grassi, G.; Reggiani, G.; Raimondi, J. (Universita, Genoa). Minerva Radiol., Fisioterap. Radiobiol., 10: 317-20(July-Aug. 1965). (In Italian).

The most significant studies made on the endolymphatic radioisotope therapy in gynecological cancers are reviewed. (J.S.R.)

46101 SOME OBSERVATIONS OF THE RADIOTHERAPY OF METASTASES WITH MASSIVE DOSES. Vallebona, D. (Universita, Genoa). Minerva Radiol., Fisioterap. Radiobiol., 10: 341-2(July-Aug. 1965). (In Italian).

The efficiency of massive x-ray doses in radiotherapy of tumor metastases was evaluated on the basis of palliative results obtained, the rapidity of the appearance of palliative results, and the rates of cure. The massive dose technique has both a clinical and a biological value. There was a rapid appearance of palliative effects. The biological value came from the tissue reactions and of the oncolytic effects following the administration of high doses in a short time. (J.S.R.)

46102 THE USE OF RADIOACTIVE ISOTOPES IN DIAGNOSTIC INTERNAL MEDICINE. Becker, G. (Universitaet, Wuerzburg, Ger.). Muench. Med. Wochschr., 106: 720-6(1964). (In German).

Radioisotopes are diagnostically useful in studies of circulation, hematology, and renal function. The role of radioisotopes in evaluation of kidney function is subject to considerable misinterpretation, under some circumstances the nephrogram can give some indications of the effective renal circulation. Unilateral disturbances are detectable, but false pathological findings occur more frequently than false normals. Disturbance in the region of the efferent ureters and the kidney pelvis, such as pyelonephritis produce alterations of the kidney curve. Estimation of clearance equivalents is rapid and can be carried out without injury to the patient when radioisotopes are used. There are several methods for measurement of blood volumes. These include the use of erythrocytes labelled with ^{32}P or ^{51}Cr, and ^{131}I-labeled serum albumin. Red cell survival is measured by injection of cells labeled with ^{51}Cr. Studies of Fe metabolism are performed with ^{55}Fe or ^{59}Fe. By external counting the greatest activity during the first four days following administration is found over the sacral area. This decreases below the values measured over the spleen and liver, whose activity remains almost constant. In aplastic anemia the liver curve reaches the highest value, while spleen and bone marrow activity is relatively low. Extramedullary blood-forming areas show curves of high activity that are similar to normal bone marrow curves. (BBB)

46103 THE NUCLEOLAR COEFFICIENT OF THE LYMPHOCYTES IN THE PERIPHERAL BLOOD OF PATIENTS WITH HODGKIN'S DISEASE. Potmesil, M.; Smetana, K.; Wienerova, E. (Central Military Hospital, Prague). Neoplasma, 12: 204-14(1965).

The nucleolar coefficient (NC) of the lymphocytes in the peripheral blood, as well as absolute and relative counts of uninucleolar and multinucleolar lymphocytes were studied before and after radiotherapy in 36 patients with Hodgkin's disease and in 100 control subjects. The nucleoli of lymphocytes were stained with toluidine blue, at a constant pH. No sex- or age-specific differences in the values were found in the control group. In patients in an advanced stage of Hodgkin's disease, a rise in the values of NC, a drop in

the absolute uninucleolar lymphocyte count, and a fall in the absolute lymphocyte count were found. Multinucleolar lymphocyte count was not altered. In relapse of the disease, the values of NC were raised as compared to those noted in patients with a remission. In relapse, multinucleolar lymphocytes were in preponderance, as a rule; in remission of the disease, on the contrary, uninucleolar lymphocytes predominated. The value of NC decreased in all patients examined following x-ray treatments and also after chemotherapy during remission by the treatments. The x-ray therapy consisted of 1200- to 8000-R surface doses. For chemotherapy, injections of Trenimon in doses of 3 to 5 mg were used. Therapy was immediately followed in all patients by a drop in NC values. The mean NC value prior to therapy was 1.87, after the end of treatment, 1.72, and at the later control investigation, 1.64. The differences in NC values obtained before and after therapy were statistically significant. Following x-ray therapy and chemotherapy no significant deviations in the absolute numbers of uninucleolar lymphocytes were found in comparison with the results obtained prior to treatment. However, the ratio of uni- and multinucleolar lymphocytes changed in relative as well as absolute values. Before treatment, in 8 patients there was a higher percentage multinucleolar lymphocytes. The value of NC was not related to leukocyte counts, body temperature, red cell sedimentation rate, or anemia. Long-term administration of glucocorticoids did not seem to influence NC. The findings described are in agreement with the concept of lymphocytes participating in the defense mechanisms directed against neoplastic growth. (BBB)

46104 RADIATION TREATMENT OF INOPERABLE THYROID CARCINOMA. Kujawska, Janina (Inst. of Oncology, Krakow). Nowotwory, 14: 265-70(Aug.-Sept. 1964). (In Polish).

To evaluate the adsorbed doses of 250-kv x rays, radiation doses were measured in an anatomical phantom of the neck, simulating three techniques of irradiation of thyroid carcinoma. Measurements were made at points which are considered important in the direction of propagation of thyroid carcinoma metastases in the neck and for post-radiation injury. In the investigated technical conditions, the tumor of the thyroid receives doses from 800 to 3300 R in three to four weeks, and the doses in healthy tissues are close to tolerance dose. Thus x-ray therapy may have only palliative value in the treatment of some forms of inoperable thyroid carcinoma. (BBB)

46105 INTEGRAL DOSE MEASUREMENT USING A PLASTIC SCINTILLATOR. Murai, Takeo (Tokyo Medical and Dental Univ.). Nuclear Eng. (Tokyo), 11: 35-8 (Jan. 1965). (In Japanese).

In the deep x-ray therapy, e.g., for cancers, it is desirable to determine accurately, during the treatment, the radiation absorbed by the patient. A method was developed for estimating the integral dose of a patient, by means of a phantom made of a plastic scintillator and a photomultiplier tube. To measure the integral dose as an electric current of the photomultiplier, an apparatus was constructed, so that the plastic scintillator phantom (28 × 28 × 15 cm) and photomultiplier tube (Du Mont 6292) were located at both ends of a dark box (30 × 15 × 80 cm). The accuracy of this method was shown by the following: the standard integral dose obtained (1.53×10^3 g.r.; at 200 kv, HVL, 2 mm, Cu, F.P.D. 50 cm, field area 78.5 cm^2) was in good agreement with those by Bewley and Meredith, using a celluloid phantom and the theoretical calculations, and single straight lines were obtained by plotting the integral dose (g.r. per r in air at surface of phantom) and the electric current of the photomultiplier and by plotting the field area (0–200 cm^2 at F.P.D. 50 cm) and the electric current of the photomultiplier. The standard integral doses obtained for the various hardness of x rays, i.e., 200 kv, HVL 16 mm Cu, 200 kv, HVL 0.3 mm Cu, and 100 kv, HVL 0.1 mm Cu were 1.49×10^3, 1.06×10^3, and 0.4×10^3 g.r., respectively. The effect of the back-scattered x rays was taken into account. (NSA of Japan)

46106 PELVIC EXENTERATION FOR EXTENSIVE VISCERAL NECROSIS FOLLOWING RADIATION THERAPY FOR GYNECOLOGIC CANCER. Barber, Hugh R. K.; Brunschwig, Alexander (Memorial Hospital for Cancer and Allied Diseases, New York, N. Y.). Obstet. Gynecol., 25: 575-8(Apr. 1965).

Among 794 pelvic exenterations there were 24 instances where the pathologist was unable to identify cancer, and these cases were therefore classified as radiation necrosis. The original diagnoses for which radiation was initially given were: epidermoid carcinoma of the cervix, 20; cervical stump, one; vagina, one; vulva, one; ovary, one. Subjectively, the clinical picture varied considerably from minimum symptoms to severe ones. The operative mortality, death within 30 days of operation regardless of cause, was four among 19. Among the 19 patients operated upon five or more years ago, 13 received total and six had anterior pelvic exenterations. Five among the total exenteration cases survived five or more years (38.4%). Among the six anterior pelvic exenterations, three survived five or more years (50%). The total five-year survivors are 8 among 19 patients (42%). One of the 24 cases treated by pelvic exenteration for radiation necrosis is described in detail to illustrate some of the problems encountered clinically in differentiating radiation necrosis from advanced cancer. It was concluded that pelvic exenterations are indicated in selected patients for radiation necrosis and other damage producing severe symptoms. (TCO)

46107 GONADAL DOSES RESULTING FROM PANORAMIC X-RAY EXAMINATIONS OF THE TEETH. Jung, Till (Universitaets-Klinik, Bonn). Oral Surg., Oral Med., Oral Pathol., 19: 745-56(June 1965).

Gonad doses of scattered radiation were measured in men during various dental radiographic technics with the x-ray tube operated at 55 to 70 kv. Measurements in 600 subjects showed that new x-ray methods bring about important reductions in gonadal dosage when compared with dose values received through the conventional intraoral complete-mouth techniques; the latter doses are already quite low. The dose values in taking roentgenograms with the Orthopantomograph, 0.116 or 0.103 mR at 80 and 76 kv, respectively, amounted to nearly the same values as those obtained from the Panorex with additional lead protection (0.102 to 0.152 mR). Tests of the Panoramix machine were made separately for the upper and lower jaws. Although exposure times in both cases were equally long, the exposure of the upper jaw resulted in a gonadal dose which was less than that of the lower jaw (0.102 vs 0.152 mR); this was true in spite of the fact that the lower jaw was taken at 5 kv less than the upper jaw. Fifteen exposures per examination were used in each instance. From the figures obtained during tests with the Panorex, it was evident that the leakage radiation was of great significance to the gonadal dose. Additional protection of the tube housing by a 0.5-mm sheet of lead reduced the dose to the gonads, when the Panorex machine is used, to about $1/10$ of the value received during an intraoral examination. The gonadal dose produced by an exposure using the Orthopantomograph is approximately the same as that produced by the Panorex with added shielding. (BBB)

46108 REDUCTION OF RADIATION EXPOSURE OF CHILDREN DURING UROLOGIC DIAGNOSIS, INCLUDING A NON-RADIOGRAPHIC METHOD OF DEMONSTRATING VESICOURETERAL REFLUX. Amar, Arjan D.; Chabra, Kamla (Kaiser Foundation Hospital, Walnut Creek, Calif.). Pediatrics, 35: 960-6(June 1965).

Four methods used in the urologic diagnosis of children are presented as examples of methods developed to offset hazards of radiation exposure: limited-area radiographic study; double dose of contrast medium in excretory urography; new, nonradiographic technique for demonstrating vesicoureteral reflux; and cine techniques. The development of similar types of modification to reduce radiation exposure of children is advocated for other specialties relating to the pediatric age group. These include: use of a cone, or a lead rubber, to shield male gonads from direct irradiation; lead rubber shielding of the lower portion of the female abdomen; use of high-speed film and cassettes; beam collimation; filtration, to remove soft irradiation; and

high kilovoltage and low milliamperage. Lead shields should be used, or the x-ray beam collimated, to limit exposure to the site of disease. It is thus possible to reduce radiation received by the abdomen and gonads to one-half or less, for each unilateral or limited area film obtained. Exposure of the fetus in utero can be diminished by shielding as much of the maternal pelvis as is feasible during urographic studies. Radiation exposure can also be decreased by doubling the dose of contrast medium in selected cases. Some new, nonradiographic techniques for demonstrating vesicoureteral reflux are described which avoid irradiation. (TCO)

46109 RADIOISOTOPE RENOGRAPHY IN CHILDREN. I. THE RENOGRAM IN CHILDREN WITHOUT RENAL DISEASE. Wenzl, James E.; Tauxe, Newlon; Burke, Edmund C.; Hunt, James C.; Stickler, Gunnar B. (Mayo Clinic, Rochester, Minn.). Pediatrics, 36: 120-7(July 1965).

Attempts were made to establish a standard technique for performance of radioisotope renograms in children and to establish the normal range of parameters of the renogram curve obtained from children who do not have renal disease. Two scintillation counter probes were positioned at the expected renal positions and after background radioactivity had been recorded, 30 μC of ^{131}I-o-iodohippurate (^{131}I-OIH) was injected rapidly into an antecubital vein and a 30-min renogram was made. Percentage of injected radioactivity excreted in urine was also recorded. Two matched, paired γ-ray-sensitive scintillation counters employing 3 by 2 in. NaI(Tl) crystals with direct-writing recorders were used. The frontal surface of the crystals was placed 20 cm from the body wall by means of stainless steel, flat-field collimators. The injection of OIH-^{131}I was recorded as the difference between injection time and initial rise in radioactivity gave an antecubital-vein-to-kidney circulation time of 10 to 20 sec. The initial increase in radioactivity was rapid, and a peak was reached within a few seconds. Most of the radioactivity measured at this point was assumed to reflect principally the accumulation of ^{131}I-OIH in the vascular system of the kidney and adjacent tissue. After an initial peak, radioactivity normally increased gradually in a slightly convex curve to reach maximal activity in 2.0 to 6.5 min. This gradual rise represents increased accumulation of the radioactive medium within the renal parenchyma and collecting system at a time when radioactivity in the blood is decreasing. Thus, the rise in radioactivity means transfer from blood into renal parenchyma. Values for the point of initial peak (point A), point of maximal radioactivity (point B), and the differences between these points (B-A) were calculated. These values were plotted arithmetically against surface area to obtain regression lines and estimates of the variability of the observations about the line. The time from appearance of radioactivity to peak radioactivity was calculated and found to fall into a relatively narrow range. Similar attempts to correlate mathematically the height of timed segments of the decreasing slope of the renogram with surface area were successful in children with a body surface area of 1.15 m^2 or greater. The state of hydration appeared to influence the excretory slope of the renogram; this effect was most pronounced in children whose total-body surface area was less than 1.15 m^2. (BBB)

46110 REAL AND FICTITIOUS HAZARDS OF PULMONARY RADIOLOGY FOR PATIENTS AND PHYSICIANS. Brun, J.; Beraud, C.; Boijeau, A. (Hopital Sainte-Eugenie, Lyon). Poumon Coeur, 20: 41-70(1964). (In French).

Difficulties of evaluating the hazards of x-ray examinations in pulmonary tuberculosis, carried out periodically or in isolated instances under precise technical and safety conditions, are discussed. The necessity of maintaining proper conditions so that the risks involved in these examinations can be minimized is emphasized. The x-ray doses received by patient and radiologist during fluoroscopy, tomography, and radiography are compared. One min of fluoroscopy is equivalent to 12 exposures in radiocinematography, 20 tomographic scans, and 100 thoracic exposures on radiographic film. About 90% of this dosage is harmful since it is absorbed by the tissues, and only 5 to 10% is useful for radiodiagnosis. The difference between the greater amount of radiation absorbed by the skin and the lesser amount by the gonads is emphasized, and the possibly exaggerated threat to the latter is minimized. The hazards to the patient and physician of mass chest fluoroscopic examinations made at two short intervals are stressed. Finally, the need for extra precautions in the x-ray diagnosis of children and pregnant women is discussed. (TCO)

46111 REMOTE AFTERLOADING FOR INTRACAVITARY RADIATION THERAPY. Henschke, Ulrich K.; Hilaris, Basil S.; Mahan, G. David (Memorial Hospital for Cancer and Allied Diseases, New York). (Progr. Clin. Cancer, 1: 127-36(1965).

Remote afterloading is proposed as a solution to the radiation exposure problem in intracavitary radiotherapy. The many sources of different length and strength required for intracavitary radiotherapy, however, constitute a major obstacle in the design of a satisfactory remote afterloader. By using small sources and moving them during the treatment, any desired active length and isodose pattern can be realized. Small sources also permit the use of sharp curves and angles, such as required in uterus applicators. The design of a device with three identical small moving sources in a remote afterloader is described. It can be operated from the outside of the room like an x-ray machine and thus completely eliminates radiation exposure of personnel. Moving source remote afterloaders can be used with all γ-emitting radioisotopes, but ^{137}Cs appears most suitable except in the case of short treatment times, for which ^{60}Co and ^{192}Ir are preferable because of their higher specific activity, which in turn permits smaller sources and applicators. The choice among these four radioisotopes depends mainly on the shielding of the treatment room and on the desired treatment times. (TCO)

46112 FREQUENCY OF MEDICAL X-RAY EXAMINATIONS IN MONROE COUNTY, NEW YORK. Haddon, William Jr. (New York State Dept. of Health, Albany); Morgan, Russell H. Public Health Rept. (U. S.), 80: 515-25(June 1965).

The doses of ionizing radiation received by the population from medical x ray sources were determined by the numbers and types of examinations performed and by certain dosimetric relationships associated with the techniques employed in each examination type. In Monroe County, N. Y., a survey was undertaken to determine the per capita rates with which the various medical radiological examinations were performed in a large, predominantly urban population with a high level of medical care. Age, sex, and type-specific rates are given for 20 categories of diagnostic examinations. Rates in general increased with age, but the patterns of increase varied considerably by age, sex, and type of examination. Many skeletal and other examinations varied seasonally, in some cases apparently as the result of variations in weather and in athletic activities. In a subsample of those examined, the percentage of women pregnant was similar to that estimated for the general population. Also, the 3-year survival rates of examinees under 35 years of age were essentially the same as those of the general population. (auth)

46113 RADIOTHERAPY OF BLADDER CANCER. IV. RADIOTHERAPY WITH CONVENTIONAL RADIATIONS. Piazza, G.; Bernardi, L. (Universita, Padua). Radiazioni Alta Energia, 4: 99-109(Apr. 1965). (In Italian).

A bibliographic review is presented of the major methods for treating bladder cancer using conventional radiation methods. The percentage of survival after 200-Kv exposure, 500-Kv exposure, and grid therapy are shown in tabular form. (J.S.R.)

46114 RADIOTHERAPY OF BLADDER CANCER. V. ENDOCAVITY AND INTERSTITIAL RADIOTHERAPY. Pozza, F.; Ongaro, M. (Universita, Padua). Radiazioni Alta Energia, 4: 111-28(Apr. 1965). (In Italian).

A bibliographic review is given of the clinical results obtained in the endocavity and interstitial radiotherapy of

bladder cancers using natural and artificial radioisotopes. (J.S.R.)

46115 RADIOTHERAPY OF BLADDER CANCER. VI. EXTERNAL RADIOTHERAPY WITH GAMMA RADIATION. Patrese, P.; Ravasini, R. (Universita, Padua). Radiazioni Alta Energia, 4: 129-55(Apr. 1965). (In Italian).

A bibliographic review is given of the techniques in γ radiotherapy of the bladder and of the clinical results of the treatment. (J.S.R.)

46116 AN INTERNIST COMMENTS ON USE AND ABUSE OF X-RAY EXAMINATIONS OF THE ELDERLY. Alvarez, Walter C. Radiol. Clin. North Am., 3: 261-2 (Aug. 1965).

The necessity of certain diagnostic radiologic tests in older people is pointed out, as well as the excessive use of radiation in diagnostic examinations which may cause needless exposure. It is suggested that all elderly persons should have an x-ray examination once a year of the thorax, stomach, and colon, before symptoms of cancer appear. Differences in needs between men and women are discussed. Abuse of x-ray examinations in the elderly does occur when repeated examinations are made. Another abuse of x-ray examinations is the habit of many physicians who order an almost complete x-ray study of the patient's body when he has just had several such examinations made, one after the other, in perhaps three or four hospitals and in one or two clinics. (TCO)

46117 EXPERIENCE WITH PLACENTOGRAPHY USING HUMAN ALBUMIN LABELLED WITH ^{131}I. Deckart, H.; Pockrandt, H.; Reichel, W. S. (Staedtische Klinikum, Berlin). Radiol. Diagn., 6: 465-72(1965). (In German).

After describing conventional radiological methods for the localization of the placenta (which lead to a relatively high radiation dose of the fetus), experience with the use of ^{131}I-albumin and external counting is reported. The technique of investigation and the results checked by caesarian section or manual palpation post-partum are discussed. Views concerning the problem of radiation dose due to the investigation are expressed. (tr-auth)

46118 ISOTOPE DIAGNOSTICS OF RESPIRATORY INSUFFICIENCY. Murczynski, Cz.; Grec, St.; Brzozkowski, J.; Naroznik, K. Radiol. Diagn., 6: 493-501 (1965). (In German).

Bronchospirography is used for the determination of the percental participation of the right and the left lungs in the respiratory process and for the estimation of the residual volume in both lungs. This circumstantial method may be replaced by the administration of the isotope thulium-170 which due to its weak gamma-radiation (84 kv) indicates the specific air contents of the lung during inspiration and expiration in impulse numbers. A simple device in which 50 mCi thulium-170 and a crystal probe are fixed on a stand allows quick determination of lung transparency at several corresponding points of the thorax and calculation of the difference in ventilation between the right and the left lungs. When the vital capacity of the lung is known and the mass absorption coefficients are calculated, also the residual volume can be determined. By comparing the results of the thulium method with other methods, the suitability of this method for the determination of lung insufficiency was confirmed. The hitherto performed examinations of patients suffering from bronchial carcinoma suggest the application of the thulium method for prophylactic forefield diagnostics of this disease. (tr-auth)

46119 THE DEPENDENCE OF CHARACTERISTIC VALUES OF THE COLLIMATOR ON ENERGY IN SCINTIGRAPHY. Tautz, M. (Staedtische Klinikum, Berlin). Radiol. Diagn., 6: 503-10(1965). (In German).

The dependence of characteristic values of the collimator on quantum energy is proved. The dependence of resolving power on energy is stressed. The limitation of scintigraphy depending on energy and the advantages of scintigraphy in low-energy range should be taken into consideration. The nuclide ^{125}I serves as an example. (tr-auth)

46120 THE RADIOLOGICAL STUDY OF GASTRO-INTESTINAL FUNCTION IN PATIENTS IRRADIATED ON THE ABDOMEN. De Marzi, S. (Universita, Florence). Radiol. Med., 51: 375-401(Apr. 1965). (In Italian).

A photofluorography method was used to examine the functional behavior of the gastroenteric tract in 68 patients suffering from extra-intestinal abdominal neoplasms. The examinations were performed before, during, and at the end of radiological treatment to the abdomen. Gastric emptying appeared to be quickened in subjects irradiated at the abdominal-pelvic and abdominal-epigastric site, and slowed down in those irradiated at the lower part of the abdomen. Passage through the small intestine was most often speeded up, particularly during treatment involving wide abdominal fields. (auth)

46121 EPITHERMAL NEUTRON BEAM ISODOSE CHARTS IN A PHANTOM HEAD. Fairchild, R. G. (Brookhaven National Lab., Upton, N. Y.). Radiology, 85: 555-64(Sept. 1965). (BNL-8957).

Improved depth-dose curves resulting from the deeper penetration of epithermal neutrons in tissue eliminate the problem of rapid neutron attenuation previously encountered when thermal neutron beams were employed in the neutron-capture-therapy procedure. Detailed depth-dose distributions from gamma rays, fast neutrons, and $^{14}N(n,p)^{14}C$ reaction are presented in the form of isodose charts. Isodose charts are shown for each type of radiation so that the data can be multiplied by any RBE desired in order to arrive at an effective dose. In order to facilitate a clinical evaluation of the epithermal neutron beam, the procedure for calculating the additional dose to tumor from a neutron-capturing isotope such as ^{10}B is outlined. The epithermal neutron beam may prove useful in the neutron-capture-therapy procedure, providing an effective localization of neutron-capturing isotope in tumor can be obtained. (auth)

46122 RADIOIODINE THERAPY IN THYROTOXICOSIS: A REVIEW OF 908 CASES. McGirr, E. M.; Thomson, J. A.; Murray, I. P. C. (Royal Infirmary, Glasgow). Scot. Med. J., 9: 505-13(Dec. 1964).

The total amount of ^{131}I required to render patients euthyroid ranged from 5 to 165 mC for males and 5 to 100 for females. In 76.5% of patients the dose did not exceed 15 mC. Three males and 12 females required total doses of more than 50 mC. The average amount of ^{131}I to render patients euthyroid with one dose was 10.6 mC. Of the 543 females, 63.5% had ceased to be thyrotoxic at 3 months, 80.6% at 6 months, 94.0% at 1 year, and 97.8% at 2 years. Of the 118 males, 60.2% had ceased to be thyrotoxic at 3 months, 77.1% at 6 months, 93.2% at 1 year and 98.3% at 2 years. Permanent hypothyroidism developed in 38 males (24.3%) and 204 females (27.1%). Following a single dose of ^{131}I, 28 males (25.0%) and 157 females (26.8%) became hypothyroid. Thirty of the 160 patients (18.8%) became hypothyroid during the subsequent 4 years of follow-up. The average percentage incidence per year of hypothyroidism in patients euthyroid or thyrotoxic at the beginning of the year was 5.2%. Radioiodine therapy failed in 5 (0.6%) patients. One patient died of acute leukemia, but there was no evidence one way or the other whether the leukemia was due to ionizing radiation. In addition to 6 patients who died of malignant disease, 5 more females developed carcinoma. Two of these were of the uterine cervix and three of the breast. In three patients ^{131}I therapy was given inadvertently in early pregnancy, but they had uneventful pregnancies and normal babies. (BBB)

46123 ADDITIVE MEDICAL TREATMENT OF TUMOR BEDS. PART X. HISTOLOGICAL INVESTIGATIONS OF THE CROCKER SARCOMA 180 UNDER COMBINED ACTI-HAEMYL-RADIATION TREATMENT. Barth, Gunther; Graebner, Herbert; Carl, Martin; Ponath, Hans (Universitaet, Giessen, Ger.). Strahlentherapie, 127: 418-29(July 1965). (In German).

A reproducible significant regression in the tumor vol-

ume was observed in comparison to radiation controls up to about half of the administered total irradiation dose in 650 male white mice of a heterozygous commercial strain. Histological studies did not reveal a morphological difference between tumors treated with Actihaemyl and non-treated tumors. Administration of Actihaemyl resulted in a significant increase in survival rates after irradiation when compared with the irradiation controls. With Actihaemyl treatment, histological studies showed an earlier appearance of granulocytes in the tumor bed and an earlier sequestration of necrotic tumor tissue followed by a covering of the skin defect by squamous epithelium. A tumor-specific and in case of a single tumor, always constant environmental reaction, could not be found during progression or regression of the tumor. The favorable effect obtained with Actihaemyl treatment in addition to radiotherapy can be explained by a stimulation of the connective tissue of the tumor beds and by a possibly improved oxygen utilization. (auth)

46124 THE CHANGES IN THE ISOENZYME OF LACTATE DEHYDROGENASE AFTER ACTION OF IONIZING RADIATION. PART III. RESULTS OF INVESTIGATIONS OF THE LDH ISOENZYME DURING RADIOTHERAPY. Kaercher, Karl Heinz; Kato, Helena Toshi (Universitaet, Heidelberg). Strahlentherapie, 127: 439-51(July 1965). (In German).

Changes in distribution pattern of isoenzymes and of total activities of LDH in serum, tumor homogenates, and in melanoma ascites are reported. Clinical results obtained are compared with the experimental results reported previously. Proposals for clinical examinations during irradiation treatment and for future clinical-experimental research are discussed. (auth)

46125 ON THE POSSIBILITY OF THE USE OF RADIOACTIVE DRUGS. Mitchell, Joseph S. (Addenbrooke's Hospital, Cambridge, Eng.; Cambridge Univ., Eng.). Strahlentherapie, 127: 497-509(Aug. 1965). (In German).

Clinical and laboratory studies of the possibility of using tritiated derivatives of Synkayvite, e.g., TRK 219, tetra-sodium-2-methyl-6,7-ditritio-1-4-naphthohydroquinone diphosphate as a therapeutic agent for radiation injuries are reported. The problem is the development of radioactive drugs for selective internal irradiation on the basis of metabolic localization. More than 100 seriously ill patients with very advanced recurrent inoperable malignant tumors and reticuloses were treated. The results proved to be relatively modest. However, in certain cases of some types of malignant tumors, especially melanoma, carcinoma of the colon, and also seminoma, there was substantial inhibition of tumor growth. It may well be that considerably more investigations are needed for assessment of this application of radioactive isotopes. (tr-auth)

46126 A BETATRON FOR ELECTRON DEPTH THERAPY. Schittenhelm, Rudolf; Derndinger, Walter; Groh, Franz; Gscheidlen, Wilhelm; Haubold, Helmut; Petersilka, Franz; Schipper, Philipp; Steinmetz, Otto; Weiss, Robert (Siemens-Reiniger-Werke AG, Erlangen, Ger.). Strahlentherapie, 127: 578-628(Aug. 1965). (In German).

Design features are described of a 42-Mev betatron for use in deep electron therapy. (C.H.)

46127 INVESTIGATIONS WITH IONIZATION CHAMBERS AND FILM DARKENING FOR DETERMINATION OF ISODOSES FOR PENDULUM IRRADIATION WITH ECCENTRICALLY JOINED PENDULUM AXES FOR ULTRAHARD X RADIATION OF A 17-Mev ELECTRON ACCELERATOR (BETATRON). PART I. SHELL IRRADIATION WITH 17-Mev X RADIATION. Heinzler, Franz (Medizinische Akademie, Duesseldorf, Ger.). Strahlentherapie, 128: 148-83(Sept. 1965). (In German)

Using ultrahard x rays from a 17-Mev-betatron, the isodose distribution for shell irradiation was measured in terms of ion doses in the water phantom and as blackening distribution, using film dosimetry, in the Lucite phantom. The dose maximum was found to be displaced to the surface, an effect also observed with concentric pendulum irradiation. The 80%-isodose depended considerably on the field size. A typical shape of isodoses with a critical decrease of the dosage towards the pendulum axis was obtained with increasing pendulum angle and aperture of the central beam. A method usually used for concentric pendulum irradiation has been modified in order to determine the axis depth, the aperture, and the local dose. (tr-auth)

46128 USE OF LABELED VITAMIN B_{12} IN THE CLINIC. Weryha, A. (Faculte de Medecine, Strasbourg). Strasbourg Med., 14: 605-12(July-Aug. 1963). (In French).

The clinical study of vitamin B_1 deficiencies is made possible by the use of vitamin B_{12}, labeled by substituting, by means of microbiological synthesis, a radiocobalt for stable ^{59}Co. The choice of the labeling isotope is based on two factors: the possible hazard to the patient and the efficiency of detection. The ^{57}Co transforms itself into Fe by means of electron capture, as do ^{56}Co and ^{58}Co, but it does not emit β radiation. The Fe emits γ rays rather than β rays in returning to its ground state. Calculation of the absorbed radiation dose to the patient on the basis of the RBE shows that for 1 Rad received by the liver with ^{57}Co, the same dose of ^{58}Co in μC would give 2.1 Rad and ^{60}Co 27 Rad. Also, when the dose to the nonhepatic critical organs, such as gonads and bone marrow, is considered on the basis of the distribution of labeled vitamin B_{12} in the body, ^{57}Co again is the most favorable isotope. Vitamin B_{12} so labeled permits the exploration of intestinal absorption to ascertain the presence or absence of the intrinsic factor, necessary for the optimum absorption of vitamin B_{12}. The Heinle test evaluates absorption by measuring the amount of radiocobalt in the stools two to seven days after absorption. The Glass hepatic test measures the radioactivity of Co fixed in the liver. (TCO)

46129 RADICAL HEAD AND NECK SURGERY IN IRRADIATED PATIENTS: COMPLICATIONS AND SAFEGUARDS. King, G. David (Lahey Clinic, Boston). Surg. Clin. North Am., 45: 567-72(June 1965).

Prevention of complications in extensive surgery after irradiation of the head and neck is discussed. Edema is inevitable following a surgical procedure and in irradiated tissue considerably more edema may be anticipated because of additional interference with previously impaired lymphatic and venous return. This increased tissue pressure will further decrease the vascularity in the operative area, and may cause life-threatening encroachment on the airway. Premature removal of sutures, drains, and nasogastric tubes will lead to wound separation, contamination and breakdown. Thus, before removal of any sutures in patients the lines of incision should be examined carefully. Plastic or plastic-coated sutures should be used which can remain in the tissues indefinitely without causing undue tissue reaction. Necrosis of skin flaps is another complication since extensive dissection of flaps of skin, necessary to obtain good exposure for neck dissection, leads to diminution of the blood supply and interference with lymphatic drainage. When the skin has been exposed to radiation, necrosis in the skin flaps is common. In irradiated patients the trifurcate incision is avoided and a U-shaped flap, which gives excellent exposure but minimizes danger, is utilized. Irradiated tissue is very susceptible to wound infection, and when neck dissection is combined with laryngectomy or excision of an oropharyngeal lesion, mouth secretions inevitably contaminate the operative wound. Therefore, the risk of serious infection is great. Antibiotic therapy at the time of surgery should be withheld but a culture taken. The patient should be observed and if there are indications that an infection is developing, another culture is taken and massive doses of antibiotic therapy are begun immediately. This program has greatly improved the percentage of patients who achieve satisfactory wound healing. Fistula formation, its prevention, and treatment are discussed. In head and neck surgery, rupture of the carotid artery is the most devastating complication seen following surgery upon the irradiated patient. Adequate skin cover protection must be provided for the carotid bulb. The U-shaped type of flap which is described provides healthy,

full-thickness skin which will protect the artery and minimize the possibility of its rupture. (BBB)

46130 RADIOACTIVE SCINTISCANNING IN EVALUATION OF RENAL DISEASE. Motzkin, Donald (Ross-Loos Medical Group, Los Angeles). Texas State J. Med., 61: 401-6(May 1965).

This report describes the use of the renal scan clinically to delineate space-occupying lesions, to demonstrate segmental differences in renal function, to demonstrate obstructive uropathy, and to demonstrate presence or absence of viable renal parenchyma. Chlormerodrin-^{203}Hg or -^{197}Hg were used as the preferred isotopes for space-occupying lesions; radioiodinated o-iodohippuric acid (^{131}I) was preferred for all other uses. These two labeled agents differ sufficiently in their radiologic and biologic properties to allow the use of each for specific clinical problems. The total-body irradiation dose from 250 μC of chlormerodrin-^{203}Hg is 100 mrad. This compares to a total-body irradiation dose of 8 mrad if an equivalent dose of ^{197}Hg, which has a shorter half-life, is used. The residual radioactivity following chlormerodrin-^{203}Hg renal scanning was determined in nine kidneys removed from patients. The percentage uptake of ^{203}Hg was similar (3 to 5% per kidney) in all patients, except for 1.4% in a patient who had chronic pyelonephritis. Thus, after 20 hr, kidney radioactivity remains essentially constant and its slow decrease is mainly a function of radioactive decay of the radioisotope rather than the biological excretion of chlormerodrin ^{203}Hg. From 250 μC of chlormerodrin-^{203}Hg, each kidney absorbs ~12 to 14 rad, which is much higher than the 1.1 rad from a similar dose of chlormerodrin ^{197}Hg. Advantages to using sodium iodohoppurate-^{131}I for all purposes other than tumor localization are enumerated. It is rapidly excreted by the kidneys, with 50% being excreted in the first 30 min. Since ~100% of the dose is excreted in 24 hr, the radiation exposure is extremely low and the study may be repeated as needed. The kidney's radiation dose was calculated as being 31 to 125 mR after a scanning dose of 400 to 800 μC of sodium iodohippurate ^{131}I. As with the lower energy mercury, ^{125}I emits γ rays of low energy which make it difficult to obtain a scan free of the halo effect produced by the close proximity of the primary photo peak and the Compton scattered peak. Because radiation exposure is no problem, the superior scanning characteristics of ^{131}I recommend it over ^{125}I. It is concluded that the renal scan offers a safe and reliable way of determining the presence or absence of viable renal parenchyma since only viable renal parenchyma accumulates and concentrates sodium iodohippurate-^{131}I or chlormerodrin-^{203}Hg. (BBB)

46131 EFFECT OF CHRONIC BRONCHITIS ON CHANGES IN PULMONARY FUNCTION CAUSED BY IRRADIATION OF THE LUNGS. Hoffbrand, B. I. (Whittington Hospital, London); Gillam, P. M. S.; Heaf, P. J. D. Thorax, 20: 303-8(July 1965).

Lung function was followed in patients after radiotherapy of the lungs for carcinoma of the bronchus. The changes found were compared in the three groups of patients, those without bronchitis, those with mild, and those with severe chronic bronchitis. The radiation doses varied from 3000 to 4000 R. There was no evidence that patients with severe chronic bronchitis show any deterioration of the bronchus; nor do they show any greater tendency to develop the functional changes of radioinduced pneumonitis and fibrosis. Gas transference tends to fall one month after the end of treatment in all patients irrespective of the presence of chronic bronchitis. This could represent a subclinical radiation reaction in the lungs. The pulmonary function changes in established radiation pneumonitis and fibrosis are a combination of a restrictive defect and of the alveolar-capillary block syndrome. There are reductions in the static lung volumes, a fall in the diffusing capacity (DL_{CO}), hypoxemia, and alveolar hyperventilation causing a reduced P_{CO_2}. The lung volume changes showed no tendency for patients with severe bronchitis to develop a restrictive abnormality. The DL_{CO} fell in all three groups, but the fall was least in the severely bronchitic patients. The P_{CO_2} changes were small in all three groups, and there is no suggestion that patients with severe chronic bronchitis develop alveolar hyperventilation. It is concluded that radiotherapy should not be withheld from patients with severe chronic bronchitis for fear of exacerbating the bronchitis or inducing radiation pneumonitis and fibrosis. (BBB)

46132 PROTECTION IN RADIODIAGNOSIS. Pons, Henri (Faculte Mixte de Medecine et de Pharmacie, Paris). Toulouse Med., 64: 1107-20(Dec. 1963). (In French).

Three principal effects that result from an overexposure to radiation are discussed: local lesions, systemic injury, and genetic mutation. External or local lesions are usually caused only by error in technique and are, thus, most easily avoided. In dealing with internal injuries, it is important to consider differential cellular radiosensitivity, the gonads and hematopoietic system being the most sensitive. The occurrence of somatic lesions depends directly upon the amount of radiation absorbed, whereas genetic mutation, leukemia, and cancer, on the other hand, presumably can result from even a minimal dose. It is, therefore, impossible to offer complete protection; the concept of the acceptable risk is discussed. The danger of somatic lesions can be avoided in several ways. For example, useless exposure, such as fluoroscopic diagnosis of tuberculosis, should be controlled. Each patient should be provided with an exact up-to-date record of all radiologic exposures to prevent repetitions of needless exposure. Technical error should be eliminated. Methods of protection legislated and supervised by government agencies are discussed with reference to recent French laws regarding radiological protection. Unshielded portable devices should be eliminated. Distinctions of age and condition of health should be carefully considered. Finally, surveillance should be strictly maintained on three levels: in the vicinity of radiation devices by dose-rate meters; of exposed personnel with sensitized film dosimeters; and careful medical and hematologic examinations periodically of all exposed personnel. (BBB)

46133 BONE SCANNING IN THE MANAGEMENT OF CANCER PATIENTS. Wisoff, Carl P. (Norfolk General Hospital, Va.). Virginia Med. Monthly, 92: 166-9(Apr. 1965).

Bone scanning using ^{85}Sr is shown to be a safe and useful procedure in the management of cancer patients. Strontium-85 has a half-life of 64 days; it decays to stable Rb with the emission of a single γ photon with the energy 0.513 Mev. These characteristics of reasonably short half-life and moderately low energy makes ^{85}Sr a convenient and safe isotope to use for scanning. It was administered intravenously in doses of 20 μC to those under 20, and 50 μC to older patients. After injection, scans were made at varying intervals with a commercial photoscanner equipped with a 3 × 2 inch NaI(Tl) crystal, pulse height analyzer, and 19-hole focusing collimator. A 24- to 48-hr interval after injection yielded the most satisfactory scans. Results in several cases are illustrated. Strontium-85 affords a demonstrable increase of isotope activity detectable over a number of different types of bone lesions, including fractures, bone tumors, osteomyelitis, Paget's disease, and eosinophilic granuloma. The bone scan is particularly useful in evaluating patients with localized bone pain who have had carcinoma. In these instances the x-ray examination may be equivocal or negative and the diagnosis can be either confirmed or made by the bone scan. It is useful in planning x-ray therapy to determine the extent of involvement by a lesion, and whether there are other adjacent areas involved to include in the treatments. The radiation dose to bone from a 70-μC dose was calculated to be 3.4 rad in bone, which is the critical organ. This is comparable to doses received by organs during other diagnostic x-ray procedures. The only contraindication to radiostrontium scanning is pregnancy. Thus, the procedure is relatively safe in regard to radiation burden and the tests can be performed over a number of days. (BBB)

46134 COMPUTATION OF RADIATION DOSAGES. Sterling, Theodor D.; Perry, Harold (Univ. of Cincinnati).

pp 439-64 of Computers in Biomedical Research. Vol. 1. New York, Academic Press, 1964.

Methods of determination of radiation dose distribution, especially with computers, are reviewed. Computation methods based on hand-digitized isodose curves are explained in terms of exact summation methods and calculation by interpolation procedures. Estimation of dose values by empirically derived equations is demonstrated, with examples. Two approaches for determining the explicit radiation distribution with interstitial implants are described. In one, the program is designed to accommodate any equally spaced array of radioactive seeds in the shape of a rectangular parallelepiped. The dose at a point with coordinates XYZ is calculated by computing the dose of each individual seed (using the inverse square law and the water-air ratio correction) and summing over the entire array. The other approach is a method for the detailed presentation of radiation distribution around individual radium implants. This computer technique presents calculations which show areas of excessive high or low dosage as well as the distribution throughout and around the implant which would not be apparent with conventional calculation. Until the advent of computers, it was too difficult and laborious to develop adequate treatment plans for each individual patient. This is now possible, and beyond evaluating individual treatments, the radiotherapist can now study the patterns of dose distributions resulting from the configurations of treatment conditions. Depending on these conditions, uniformly high and low dose areas and volumes can be created with relatively sharp breaks between them. The study of these conditions which result in desirable or undesirable dose patterns depends on the way they are manipulated. By studying the dose configurations resulting from changes in conditions of treatment the radiotherapist can begin to optimize treatments factors, i.e. increase of the ratio of dose to tumor divided by dose to tissue which is to be spared an undue amount of radiation. Optimization is possible by planning each case, by making use of the evaluation of the total treatment volume, by replanning treatments in the event change in the tumor should occur during therapy and by optimizing certain conditions through computer calculations. (BBB)

46135 RADIOAKTIVE ISOTOPE IN KLINIK UND FORSCHUNG. BAND VI. VORTRAEGE AM GASTEINER INTERNATIONALEN SYMPOSION 1964. (Radioactive Isotopes in Medicine and Research. Volume VI. Addresses at the Gastein International Symposium, 1964). Fellinger, K.; Hoefer, R. (eds). Munich-Berlin, Urban and Schwarzenberg, 1965. 502p.

Separate abstracts were prepared for nine papers. Two papers were abstracted previously and appeared in NSA Vol. 18 as number 37051 and Vol. 19 as number 36214. Thirty-six additional papers discuss uses of radioisotopes in biological research. (C.H.)

For abstracts of individual papers see: 46136–46142, 46688, and 46862.

46136 USE OF SHORT-LIVED ISOTOPES FOR TRACER DOSE REDUCTION. Brownell, G. L. (Massachusetts General Hospital, Boston). pp 13-21 of Radioaktive Isotope in Klinik und Forschung. Band VI. Munich-Berlin, Urban and Schwarzenberg, 1965.

The use of short-lived isotopes offers marked advantage for dose reduction in medical tracer studies. The use of such isotopes has been limited in the past because of the lack of immediate availability of reactors or cyclotrons for their production. The rapid increase in the number of such devices in recent years has changed this picture, and short-lived isotopes are now available to a larger number of users. Further, improvements in processing and transportation have greatly aided their use. It is obvious that the optimum half life of a radioisotope should be related to the time span of the phenomena being studied. If the half life is too short, the phenomena cannot be adequately observed; whereas, if the half life is too long, the patient receives needless radiation dosage. This and other theoretical considerations are analyzed to relate optimum half life to the biological problem. Production and processing of short-lived isotopes pose many novel problems, particularly if the material is required sterile or in a special chemical form. Examples of specific procedures for processing of short-lived isotopes are discussed. The use of a cow to milk a short-lived daughter from a long-lived parent is particularly promising, and a device for separation of ^{68}Ga from ^{68}Ge by this method is presented. A number of specific applications of short-lived isotopes presented include the use of ^{24}Na, ^{42}K, and ^{38}Cl in electrolyte studies; short-lived positron emitters such as ^{64}Cu, ^{68}Ga, and ^{18}F for scanning problems; and the production and use of ^{15}O, ^{11}C, and ^{13}N in pulmonary and vascular studies. (auth)

46137 COMPARATIVE STUDIES OF THE SENSITIVITY OF LOW BACKGROUND CLINICAL COUNTING SYSTEMS. Trott, N. G.; Parnell, C. J.; Cottrall, M. F. (Royal Cancer Hospital, London; Royal Marsden Hospital, London). pp 22-36 of Radioaktive Isotope in Klinik und Forschung. Band VI. Munich-Berlin, Urban and Schwarzenberg, 1965.

Many problems remain in calculating the radiation dose a patient may receive from particular tracer tests using radionuclides. However, in order to reduce the radiation dose delivered, it is evidently desirable to use measuring equipment of the highest practicable sensitivity. Now it is frequently necessary to combine, in a single test, whole-body, localized body, and sample counting techniques. With this in mind a comparative study was made of the sensitivity of various low background counting systems in use for clinical tracer work. Chalk, which has a low natural radioactive content, was used for bulk shielding of these systems, and some comparative background measurements are reported. It may be noted that, with these systems, detailed clinical tracer tests can be performed with many radionuclides using administered activities of less than 1 μC. The minimum detectable activity and concentration (MDA and MDC) for these counting systems were evaluated; values of approximately 0.05 pC/gm, using ^{47}Ca and ^{131}I, were found for MDC using whole-body and sample counting systems, with somewhat higher values for the localized body counters used. The design and applications of a tissue equivalent rubber phantom, constructed for testing body counting equipment is discussed. Certain special problems that arise in assessing the sensitivity of whole-body counting systems are also considered. These include changes of spectral shape that may arise from redistribution of radionuclides in the body. In addition, a brief analysis is given of the effects of ^{40}K and ^{137}Cs in man on the accuracy obtainable in measurements of low tracer activities, with particular reference to the determination of ^{131}I in the human thyroid at levels of 100 to 1000 pC. (auth)

46138 THE MEASUREMENT OF CALCIUM ABSORPTION BY A DOUBLE ISOTOPE METHOD. Tothill, P.; Dellipiani, A. W. (Royal Infirmary, Edinburgh). pp 86-95 of Radioaktive Isotope in Klinik und Forschung. Band VI. Munich-Berlin, Urban and Schwarzenberg, 1965.

Calcium absorption was measured in a variety of patients following the intravenous injection of ^{47}Ca and the oral administration of ^{45}Ca. The ratio of the activities of the two isotopes in subsequent collections of urine then gives the required information. Calcium was precipitated from urine and the ^{47}Ca measured by well scintillation counting; ^{47}Ca was assayed by liquid scintillation counting after allowing the ^{47}Ca and the ^{47}Sc to decay. Collections were made for 6 days following the administration of the isotopes and the isotope ratios, and therefore the derived figures for absorption, were reasonably constant over this period. Absorption of the oral dose varied from 10 to 50%. Fecal excretion of ^{47}Ca was measured, and by relating this to the specific activity of the urine calcium, an estimate made of endogenous calcium loss. The ^{47}Ca content of some patients was followed with a simple whole-body counter, and the results compared with the figures deduced from accumulated excretion. The loss of ^{47}Ca as indicated by whole-body counting was always greater than that suggested by measurements on excreta, as has been found by other workers. (auth)

46139 ^{99}Mo, A NEW ISOTOPE FOR SCINTILLATION SCANNING OF THE LIVER. Sorensen, Leif B. (Univ. of Chicago). pp 126-35 of Radioaktive Isotope in Klinik und Forschung. Band VI. Munich-Berlin, Urban and Schwarzenberg, 1965.

Recent studies have shown that molybdenum-99 injected in a single tracer dose as ammonium molybdate disappears rapidly from the circulation of man. Six hours after injection of carrier-free material into normal subjects, the blood level of ^{99}Mo falls to less than $1/_{200}$ of the initial concentration. By use of collimated probes, as well as by postmortem radioassay of tissues, this rapid clearance has been shown to be due to a selective concentration of molybdenum in the liver. From excretion data, it is estimated that the uptake of ^{99}Mo by the normal liver is about 80% when carrier free material is injected. The biologic half life of ^{99}Mo determined from whole-body counts is about 20 days. Studies in rats have shown that labeled molybdenum is incorporated as a nondialyzable component of the xanthine oxidase molecule. In man, this enzyme is chiefly located in the liver. The specificity of the liver for molybdate permits scanning of the organ, for which purpose the 0.140 Mev gamma-radiation of the daughter technetium-99m is particularly suitable. Good visualization of the liver is obtained when scans are done 24 hours after injection of 40 μC of ^{99}Mo. At this time, maximal build-up of ^{99m}Tc has taken place in the liver. Space-occupying lesions are readily visualized. In diffuse hepatocellular diseases, the liver accumulates less of the administered dose of ^{99}Mo and leaves more of the isotope available for urinary excretion. Molybdenum-99 has several advantages over colloidal gold and ^{131}I-labeled rose bengal: it accumulates in the hepatic parenchymal cells, and its uptake portrays effectively disease states of parenchymal cells; the concentration of the tracer does not change during the interval of the scan since the isotope has a long biologic half life; and there is superior scanning resolution due of the softer gamma radiation of ^{99m}Tc. (auth)

46140 ^{99m}Tc AS A CLINICAL TRACER MATERIAL. Harper, P. V.; Lathrop, K. A.; Andros, G.; McCardle, R.; Goodman, A.; Beck, R. N.; Covell, J. (Univ. of Chicago). pp 136-45 of Radioaktive Isotope in Klinik und Forschung. Band VI. Munich-Berlin, Urban and Schwarzenberg, 1965.

The physical properties of ^{99m}Tc are ideally suited to many clinical applications. Its short physical half life (6 hours) and virtual absence of particle radiation (only conversion electrons) results in very low radiation dosage. The low energy (140 kev) of its principal (98%) gamma penetrates tissue well and is detectable with a high efficiency by small NaI scintillation crystals. The material is obtained as the daughter of the 67-hour ^{99}Mo fission product. This is absorbed on alumina and the daughter is eluted in pure form with weak acid. As the pertechnetate the localisation is similar to that of perchlorate and iodide, and the thyroid-serum ratio is almost identical with that of iodide under a variety of circumstances. One to 2% of the injected dose is trapped in the thyroid in normals and 10 to 20% in hyperthyroids. This is dischargeable with perchlorate. Thus the trapping phase of iodide metabolism may be studied in vivo by using TcO_4^- without perturbing the gland. Thyroid scans 1 hour following intravenous administration of 1 mC of TcO_4^- in 46 patients were comparable in quality to ^{131}I scans and gave a radiation dose to the gland of only 100 mrads. In the form of thiocyanate dissolved in fat emulsion, ^{99m}Tc localizes largely in the liver. One to 10 mC quantities of isotope may be used without undue radiation dosage, and as a result scans may be made with collimators of much finer resolution producing improved pictures of the liver. This same preparation is suitable for radiocardiography and allows great reduction in the shielding requirements of the detectors. Excellent brain scans are obtained following intravenous administration of 5 to 10 mC of $^{99m}TcO_4$ and the radiocolloid prepared with elemental sulfur gives excellent liver and spleen scans. (auth)

46141 DEVELOPMENT, USING ^{197}Hg, OF A SOURCE OF X RAYS USABLE IN MEDICAL RADIOGRAPHY. THE APPLICATIONS. Kellershohn, C.; Herszberg, B. (Universite, Paris). pp 181-96 of Radioaktive Isotope in Klinik und Forschung. Band VI. Munich-Berlin, Urban and Schwarzenberg, 1965. (In French).

Mercury-197 disintegrates by electron capture emitting essentially a mixture of x ray of 68 kev (the K radiation of gold) and of gamma photons of 77 kev, an energy range which may be used for medical radiography. By irradiating enriched mercury-196 in a flux of 10^{13}n/cm^2/sec of thermal neutrons for some days, a source of ^{197}Hg may be produced. Under such conditions it is, furthermore, possible to produce a source of ^{197}Hg of a size comparable to that of the focus of an x ray tube. The activity obtainable is high enough to make medical radiographs with an exposure time of a few minutes only. However, the source will lose its usefulness in about a week owing to the short physical half life (65 hours) of ^{197}Hg. After irradiation the source might be used again several times. After discussing in some detail the theoretical aspects of the subject, the production of a source of 0.5 mm in diameter is described. A number of radiographs taken with that source are presented. The practical aspects of the procedure are discussed, especially in relation to radiography of the skull. (auth)

46142 PROTEIN RADIOIODINATION BY AN ELECTROLYTIC TECHNIQUE. Rosa, U.; Scassellati, G.; Pennisi, F.; Ambrosino, C.; Liberatori, J.; Federighi, G.; Donato, L.; Bianchi, R. (Universita, Turin; Universita, Pisa, Italy). pp 258-72 of Radioaktive Isotope in Klinik und Forschung. Band VI. Munich-Berlin, Urban and Schwarzenberg, 1965.

An electrolytical method is proposed as a general tool for radioiodine labeling of proteins, in which elemental iodine is set free at the anode by electrolysis of a KI solution in which a protein is dissolved. Preliminary experiments carried out on the amino acids chiefly involved in protein iodination proved that for a proper value of current, i.e. a proper value of elemental iodine in the solution, unwanted oxidative reactions can be minimized. A detailed investigation was carried out on the factors affecting the electrolytic process of human serum albumin iodination. Electrophoresis and microimmuno electrophoresis on agar were adopted to check possible denaturation occurring in the proteins during the iodination process. The results obtained prove that a human serum albumin labeled with ^{131}I at a sufficient specific activity may be produced with a 90% iodination yield and radioiodine content less than 1 atom/protein molecule. Results about gamma globulin, fibrinogen, and insulin iodination are also reported. Iodine-131 labeled albumin and gamma globulin have been used for turnover studies in normal man, using a whole-body counting system. The results obtained are briefly reviewed, and critically analyzed from the point of view of the adequacy of the tracer for protein turnover experiments. (auth)

46143 TECHNIQUES AND INSTRUMENTATION SUITABLE FOR COMMUNITY MONITORING PROGRAMS. Blatz, Hanson (Office of Radiation Control, New York). pp 125-41 of Technological Needs for Reduction of Patient Dosage from Diagnostic Radiology. Springfield, Ill., Charles C Thomas, 1963.

Equipment, standards, and inspection experience for an x-ray control program are discussed. Inspection progress is related to a two year program in New York City. (P.C.H.)

46144 THE EFFECT OF KILOVOLTAGE AND FILTRATION ON DEPTH DOSE. Trout, E. Dale; Kelley, John P.; Lucas, Arthur C. (General Electric Co., Milwaukee). pp 143-57 of Technological Needs for Reduction of Patient Dosage from Diagnostic Radiology. Springfield, Ill., Charles C Thomas, 1963.

Studies were made on the effects of kilovoltage and filtration on depth dose measurements in diagnostic radiology. Isodose data are plotted with these considerations in mind. The results showed that as kilovoltage is increased, contrast decreases and latitude increases, and as filtration is increased, the depth dose, scattered dose, and exit dose stated as percentages of the incident dose all increase. It

was concluded that an extensive physical study could be made to provide information for a wide range of conditions. (P.C.H.)

46145 THE EFFECT OF COLLIMATION: FIELD SIZE, CONE LEAKS, AND SCATTER DOSE OUTSIDE THE USEFUL BEAM. Hale, John (Univ. of Pennsylvania, Philadelphia). pp 159-78 of Technological Needs for Reduction of Patient Dosage from Diagnostic Radiology. Springfield, Ill., Charles C Thomas, 1963.

The hazards of using excessive field size and the benefits of using gonad shields when possible in diagnostic radiology are discussed and emphasized. Recommendations for limitation of field size, beam direction, gonad shields, and immobilizing devices are given. The design of beam defining devices is considered. 63 references are cited. (P.C.H.)

46146 DOSE AND INFORMATION IN DIAGNOSTIC RADIOGRAPHY. Webster, Edward W. (Massachusetts General Hospital, Boston). pp 189-95 of Technological Needs for Reduction of Patient Dosage from Diagnostic Radiology. Springfield, Ill., Charles C Thomas, 1963.

Dose reduction in diagnostic radiography is discussed, and physical problems in dose reduction are considered. (P.C.H.)

46147 THE EVALUATION OF GRIDS. Bates, Lloyd M. (Johns Hopkins Hospital, Baltimore). pp 197-207 of Technological Needs for Reduction of Patient Dosage from Diagnostic Radiology. Springfield, Ill., Charles C Thomas, 1963.

The determination of parameters affecting the ability of the grid to improve contrast is discussed, along with parameter incorporation into the design of the grid to achieve a required increase in contrast with the least increase in patient exposure. The evaluation of grids is based on their ability to adsorb scatter radiation balanced against the absorption of the primary beam that occurs. (P.C.H.)

46148 THE EFFICIENCY OF RADIOGRAPHIC INTENSIFYING SCREENS. Ter-Pogossian, Michel (Washington Univ., St. Louis). pp 215-27 of Technological Needs for Reduction of Patient Dosage from Diagnostic Radiology. Springfield, Ill., Charles C Thomas, 1963.

Studies showed that the efficiency of radiographic intensifying screens can be improved by increasing their absorption of x rays, without altering the thickness of the phosphor layer, and by the use of a more efficient phosphor than conventionally incorporated in screens. The first method can be accomplished by either one or the combination of two factors: use of a lower atomic number phosphor; and better compaction of the phosphor material. Manipulation of these factors may lead at best to a gain in speed of 200 to 300%. The second method may yield a gain in speed of the order of 1000% with only a slight loss in resolution which, in most roentgenological procedures, would probably be of little importance in the diagnostic value of the examination. (P.C.H.)

46149 FACTORS WHICH INFLUENCE IMAGE QUALITY AND SPEED OF FILM-SCREEN COMBINATIONS. Seeman, H. E. (Eastman Kodak Co., Rochester, N. Y.). pp 229-39 of Technological Needs for Reduction of Patient Dosage from Diagnostic Radiology. Springfield, Ill., Charles C Thomas, 1963.

Discussion is presented on the quality of radiographic image and ways to increase the speed of radiographic screen-type film. The principal factors that determine radiographic contrast are the quality of the x rays, as controlled by the kilovoltage and the absorption of the patient, proportion of scattered radiation, and the contrast of the film-developer combination. The speed of a radiographic screen-type film is inversely proportional to the exposure to screen light which will produce a developed net density of 1.0 at a given kilovoltage. (P.C.H.)

46150 THE EVALUATION OF FLUOROSCOPIC SCREENS AND X-RAY IMAGE INTENSIFIERS. Oosterkamp, W. J.; Albrecht, C. (N. V. Philip's Gloeilampenfabrieken, Eindhoven, Netherlands). pp 251-70 of Technological Needs for Reduction of Patient Dosage from Diagnostic Radiology. Springfield, Ill., Charles C Thomas, 1963.

Geometrical resolution expressed as sine wave response functions, the influence of x-ray quanta fluctuations, and their combined effect are discussed. X-ray absorption in powder screens of ZnS, ZnS–CdS, $CaWO_4$, $BaSO_4$–$PbSO_4$, KI, and CaI were calculated and their relative merits are discussed. Advantages and disadvantages of single crystal screens are described. Measurements showed that the dependence of sine wave response upon radiation qualities is, within a wide range, either nil or small for $CaWO_4$ and ZnS–CdS powder screens. (P.C.H.)

46151 CONVERSION EFFICIENCIES OF CONVENTIONAL IMAGE AMPLIFIERS. Niklas, Wilfrid F. (The Rauland Corp., Chicago). pp 271-303 of Technological Needs for Reduction of Patient Dosage from Diagnostic Radiology. Springfield, Ill., Charles C Thomas, 1963.

Possible x-ray image intensifying devices and systems were surveyed, and conclusions were made as to which device may be called a conventional image amplifier. The design of conventional x-ray image intensifiers are described and principles of quantum statistics are discussed. Overall conversion efficiencies of conventional x-ray image intensifiers were compared using manufacturers' quoted values for brightness gain and minification. The importance of the conversion efficiency of individual intensifier components in their effect upon both the overall conversion efficiency and resulting quantum statistics are discussed in detail. Several approaches for the further development of x-ray image intensifiers and intensifying systems are outlined. (P.C.H.)

46152 DOSE ASPECTS OF CINEFLUOROGRAPHY. Henny, George C. (Temple Univ., Philadelphia). pp 319-28 of Technological Needs for Reduction of Patient Dosage from Diagnostic Radiology. Springfield, Ill., Charles C Thomas, 1963.

Methods for the least exposure to the patient in cinefluorography is discussed. The system that is the most satisfactory with the least exposure to the patient is one employing a triggering device to turn the x rays on and off during the open and closed phases of the shutter movement. Methods for this synchronization are described. Other factors affecting patient dose are also discussed. (P.C.H.)

46153 EXTERNAL RADIATION DOSIMETRY IN BONE. Spiers, F. W. (Univ. of Leeds, Eng.). pp 259-68 of Radiation Dosimetry. New York, Academic Press, 1964.

The structure of bone must be considered in relation to dosimetry because it is denser than soft tissues, it is heterogeneous, it includes elements of higher atomic number, and it contains the bone marrow. The presence of bone therefore complicates the problems of dosimetry of external radiation. Absorption of radiation in bone is greater than in soft tissues and hence bone may reduce the dose to soft tissues beyond it and receive a much higher radiation dose itself. Many radioisotopes, the bone seekers, are taken up preferentially, or even exclusively, by bone and can then irradiate bone heavily compared with other tissues. The nature and structure of bone is discussed. The external irradiation of bone is also considered. (J.F.P.)

46154 DOSIMETRY OF RADIOISOTOPES IN SOFT TISSUES AND IN BONE. Spiers, F. W. (Univ. of Leeds, Eng.). pp 269-79 of Radiation Dosimetry. New York, Academic Press, 1964.

The dosimetry of radioisotopes in a complex structure like bone and methods of calculating the dose in soft tissues are briefly presented. The tissue can be considered as a uniform medium with the isotope either distributed throughout it or confined to one part of it. Particle dosimetry under equilibrium conditions, dosimetry of β particles under nonequilibrium conditions, plane surfaces, and cylindrical and spherical sources are discussed. Internal isotopes in bone are considered by a two-component system with the isotope located in one system, bone, and the target tissues being the soft tissues within bone. Dose calcula-

tions are then made on the simplifying assumptions that particle emission is isotropic and uniform over dimensions of the deposit, that particle tracks are regarded as straight, energy loss is uniform along the track, and differences in particle scattering in the two components are neglected. (J.F.P.)

46155 HIGH-ENERGY ELECTRON TREATMENT-PLANNING DOSIMETRY. Laughlin, J. S. (Sloan-Kettering Cancer Center, New York). pp 280-93 of Radiation Dosimetry. New York, Academic Press, 1964.

Some of the dosimetry considerations involved in the therapeutic use of high-energy electrons are treated. In the discussion high-energy electrons are those with a penetration in tissue of at least 2.5 cm, and therefore are those electrons with energies above 6 Mev. Topics covered are characteristics of high-energy electron dose distributions, high-energy electron sources and parameters, calibration of electron energy, relative dose distribution measurement, absorbed dose measurement, treatment planning factors, and inhomogeneity correction for treatment planning. (J.F.P.)

46156 POPULATION DOSE FROM THE MEDICAL USE OF IONIZING RADIATION. Spiers, F. W. (Univ. of Leeds, Eng.). pp 298-303 of Radiation Dosimetry. New York, Academic Press, 1964.

The dose to populations from the medical use of radiations is high, at least in the technically advanced countries; and in these countries it considerably exceeds the dose from other sources, including that from fallout. There is considerable variation in the estimates which are made of the actual magnitude of the medical dose. Determination of population dose in which the significant dose is the average per head of population, the gonad dose weighted to allow for child expectancy, is given. The design of a survey in Great Britain to determine the genetic dose and the mean marrow dose to the population from the sources of general diagnostic radiology, mass miniature radiography (photofluorography), dental radiography, radiotherapy of non-malignant disease, and radiotherapy of malignant disease. The most extensive problem was the determination of dose from diagnostic radiology. The results of the survey are also given. (J.F.P.)

CHEMISTRY

General

46157 (MLM–1254) MOUND LABORATORY PROGRESS REPORT FOR APRIL 1965. Eichelberger, J. F.; Grove, G. R.; Jones, L. V. (Mound Lab., Miamisburg, Ohio). Apr. 30, 1965. Contract AT-33-1-GEN-53. 32p. Dep. mn; CFSTI $2.00 cy, $0.50 mn.

Theoretical intensities computed for the beta phase of $^{208}Po/^{209}Po$ are in good conformity with the corresponding experimental intensities. The rationale of the method of decaying pairs is reviewed. The half-life of ^{227}Th from the power growth curve of ^{227}Ac is 18.718 ± 0.005 days. The fraction of deuterated methane ($^{12}CH_3D$) in CH_4 of high mass 17 enrichment was determined by infrared analysis. C deposited from CO on an Fe catalyst, was purified by contact with wet HCl at 1100°C. In two runs with the CO_2–carbamate chemical exchange system separation factors of 1.58 and 1.62 were obtained. In preparation for experiments on the separation of $^{12}CH_4$ and $^{13}CH_4$ by gas chromatography, two schemes were investigated for control of column temperature at 110°K to room temperature. The charcoal trap used for reducing the tritium content of thermal diffusion product ^3He to less than 2×10^{-10}% was evacuated, heated, and purged with H_2 to lower its contamination. A glass column for enriching low-concentration ^3He–^4He mixtures was built and operated. Considerable difficulty was experienced in maintaining the device leak-free after the Cu seals were replaced with Kovar. An approximate enrichment factor of 40 was obtained in the filtration and 90 in the distillation for an overall enrichment of 3600. Data were obtained on ^3He and ^4He thermomolecular pressures for unsaturated gas with a sensor cold-end temperature of 77°K. A small, fast-response thermopile system was designed and constructed. It is presently being tested as a power integrator. A destructive method of analysis was developed for the simultaneous determination of Si, Cu, and Re in Al alloys. The analysis requires 4 hr and has an error of ±2.5%. A prototype, inverted, Teflon dropping-Hg electrode was made for use in the polarographic investigation of W samples in HF solutions, for which ordinary glass electrodes are unsuitable. An infrared spectrometric method was developed for the determination of $^{12}CH_3D$ in $^{13}CH_4$. The method can be used on samples containing as little as 0.1% deuterated CH_4. A photochemical effect was discovered in which solvated H ions are produced from the interaction of a halogenated hydrocarbon (CCl_4, CH_3Cl, $CHClCCl_2$) and water under the influence of ultraviolet radiation. (auth)

46158 (NYO–910-23, pp 112–82) [DIVISION OF BIOLOGICAL CHEMISTRY]. (Sloan-Kettering Inst. for Cancer Research, New York).

Experience with adenine provided the first demonstration of the incorporation of an organic compound into the nucleic acids. For several years a systematic survey was made of the metabolism of many related purines, pyrimidines, their nucleotides and nucleosides. Demonstrations that the purine ring is incorporated intact, and that pyrimidine ribosyl derivatives are utilized and are reduced to deoxyribosyl derivatives without cleavage of the glycosyl linkage, have furnished the background for many chemotherapeutic trials. A new method for the synthesis of purine nucleosides was developed. This was later extended to pyrimidine nucleosides. The chemotherapeutic possibilities of purine analogs were reviewed. Metabolic studies in microorganisms, resistant mutants, and mammals revealed much information about the mechanisms of action in vivo. Studies of the relation of structure to biological activities and chemical properties included an explanation of the toxicity of adenine and its monohydroxy derivatives; the structural features of adenosine analogs which are necessary for vasodepressor activity; the reasons for the high toxicity of ribosylpurine (deaminoadenosine); and the recognition of the lability to alkali of the imidazole ring of certain purine nucleosides. The metabolism of purine N-oxides, their chemistry, their chemotherapeutic possibilities, and their sensitivity to radiation, are outlined. Differences in the incorporations of adenine and smaller precursors under various conditions suggested that the theoretically necessary inhomogeneity of nucleic acids could be experimentally approached. Physico-chemical techniques have been applied to correlate the physical and biological structure. Cytoplasmic ribonucleoprotein particles from mammalian tissue were studied extensively and the major component has been carefully characterized. (TCO)

46159 (ORNL–3832) CHEMISTRY DIVISION ANNUAL PROGRESS REPORT FOR PERIOD ENDING MAY 20, 1965. (Oak Ridge National Lab., Tenn.). Sept. 1965. Contract W-7405-eng-26. 175p. Dep. mn; CFSTI $5.00 cy, $1.00 mn.

Progress is reported in sections on nuclear chemistry, nuclear and inorganic chemistry of special elements, isotope chemistry, radiation chemistry, organic chemistry, chemistry of aqueous systems, electrochemical kinetics, high-temperature nonaqueous systems, and chemical physics. Separate abstracts were prepared for each of the 9 sections. (J.R.D.)

For abstracts of individual sections see: 46160, 46161, 46237, 46304, 46332, 46899, 46957, 47010, and 47584.

46160 (ORNL–3832, pp 29–32) NUCLEAR AND INORGANIC CHEMISTRY OF SPECIAL ELEMENTS. (Oak Ridge National Lab., Tenn.).

Both $RbPaF_6$ and Rb_2PaF_7 were prepared and characterized by analysis for Rb and Pa as well as by their x-ray powder diffraction patterns. In addition, $(NH_4)_2PaF_7$ was prepared and characterized by its powder pattern, which is almost identical with that of Rb_2PaF_7. The Raman spectra of these crystals have strong, sharp lines at 690 cm^{-1} ($RbPaF_6$), at 645 cm^{-1} (Rb_2PaF_7), and at 650 cm^{-1} [$(NH_4)_2PaF_7$]. The Raman spectra of several solutions of Pa(V) in HF indicate the presence of either the PaF_7^{2-} ion or a complex analogous to an unidentified tantalum fluoro-complex reported earlier. Thermal-neutron activation analysis of ^{99}Tc was examined. For maximum sensitivity the beta decay curve of the reaction product, ^{100}Tc, was measured. Because of impurities in the polystyrene foil sample mounts it was not possible to achieve the full sensitivity inherent in this method, but as little as 10^{-6} g of ^{99}Tc could be determined with good precision. Cross sections for the (n,n′), (n,α), and (n,p) reactions of 14.8-Mev neutrons with ^{99}Tc were found to be 77 ± 4, 7.5, and ~5 mb, respectively. The extraction of Tc(VII) as pertechnetate ion from aqueous acid solutions by cyclohexanone was applied in analytical procedures where the yield of ^{99}Tc was measured to determine the number of ^{235}U fissions and to estimate the burnup of uranium in power reactor fuel elements. (auth)

46161 (ORNL–3832, pp 116–50) CHEMICAL PHYSICS. (Oak Ridge National Lab., Tenn.).

Revised values are presented for the entropy of $K_3Fe(CN)_6$ and for the thermodynamic properties of $Fe(CN)_6^{3-}$(aq) and $Fe(CN)_6^{4-}$(aq). Features of the low-temperature heat capacity of K_2ReBr_6 are briefly presented and discussed. Heats of mixing in the molten LiF–NaF system at 1278°K before and after correction for formation of solid solutions are presented in graphical form. The heat of fusion of $KTcO_4$ was determined to be 6460 ± 20 cal/mole at the melting point, 530.2 ± 0.5°C. A refinement of the structure of dimeric cupric acetate hydrate, $Cu_2(CH_3COO)_4 \cdot 2H_2O$, was nearly finished. Data collection was almost finished for a study of the structure of $(NH_4)_2Cu(SO_4)_2 \cdot 6H_2O$. An analysis of the crystal structure of potassium hydrogen chloromaleate yielded accurate interatomic distances and

angles, a description of the thermal motion of the hydrogen chloromaleate ion, and evidence that the bridging H atom moves in a substantially symmetric potential well. Two new versions of a FORTRAN crystallographic least-squares program based on an existing program, OR FLS, were written. A FORTRAN computer program was written to draw stereoscopic crystal structure illustrations with an X-Y plotter. In studies of photochemically produced free radicals, simple alcohols containing small amounts of H_2O_2 were photolyzed with ultraviolet. Measurements and calculations on single crystals of H_2O_2 and D_2O_2 photolyzed with ultraviolet continued. Crossed molecular beam techniques were used to study a number of alkali-atom–halogen-molecule reactions of the type $M + X_2 \rightarrow M^+X^- + X$. The angular distribution of Cs^+ ions elastically scattered from Ar, Kr, and N_2 was measured in the energy range from 2.3 to 11.6 ev. Measurements of the total scattering cross section of H_2–He and D_2–He were undertaken in an attempt to resolve discrepancies in the interaction potential of H_2 and D_2 as determined from transport properties. The total collision cross section for a 300°K H_2 beam scattered by 77°K He was determined to be 51.5 ± 0.8 A^2, and the corresponding knock-on cross section about 7 A^2. A new energy-calibrated molecular orbital method and theoretical model were developed for calculating ionization potentials and autoionization levels of alkyl free radicals. A charge spectrometer was used to examine the ion fragments and their recoil energies that result from the primary interaction of x rays with CH_3I, HI, and DI. (J.R.D.)

Analytical Procedures

See also Separation Processes and Procedures.

Refer also to abstracts 46324, 46429, and 46941.

46162 (AECL–2262) AN AUTOMATIC POTENTIOMETRIC TITRATOR. Wuschke, E. E.; Stewart, R. B. (Atomic Energy of Canada Ltd.; Pinawa (Manitoba). Whiteshell Nuclear Research Establishment). Apr. 1965. 10p. Dep.; AECL $0.50.

An automatic potentiometric titrator with a sensitivity of 10 microvolts is described. It provides automatic selection of fore or back titration and variable flow rate to ensure rapid titration without overshoot. A timer is included to avoid transient end points. (auth)

46163 (AECL–2263) AN IMPROVED OXY-HYDROGEN BURNER FOR THE DECOMPOSITION OF POLYPHENYL REACTOR COOLANTS. Stewart, R. B.; Smith, G. G. (Atomic Energy of Canada Ltd., Pinawa (Manitoba). Whiteshell Nuclear Research Establishment). June 1965. 8p. Dep.; AECL $0.50.

An oxy-hydrogen burner for the decomposition of polyphenyl reactor coolants and similar organic compounds is described. It consists of a modified large-bore Beckman flame photometer burner surrounded by a water-cooled oxygen annulus designed to fit a Vycor combustion tube whose entrance is a 29/42 standard-taper joint. This burner is used in the destruction of polyphenyls for the determination of chlorine as described in AECL-2137. It permits rapid combustions with minimum dilutions under oxidizing conditions. With it, the sensitivity of the above method is improved by a factor of five. (auth)

46164 (AERE-R-5002) THE DETERMINATION OF NITROGEN IN PLUTONIUM NITRIDE. Milner, G. W. C.; Jones, I. G.; Phillips, G. (Atomic Energy Research Establishment, Harwell (England)). Aug. 1965. 6p. Dep.; BIS $0.20; HMSO 1s. 2d.

Both the Dumas and Kjeldahl methods, developed for the analysis of uranium nitrides, were applied to the analysis of plutonium mononitride for nitrogen content. After slight modifications to the procedures, good agreement was obtained between the two methods on a typical PuN sample. The coefficient of variation for the Kjeldahl method was 0.8%, compared with a value of 1.0% for the Dumas method. (auth)

46165 (CEA-R-2837) DOSAGE DU SODIUM ET DU POTASSIUM DANS LES MILIEUX BIOLOGIQUES PAR ACTIVATION NEUTRONIQUE SANS SEPARATION CHIMIQUE. (Determination of Sodium and Potassium in Biological Media by Neutron Activation Without Chemical Separation). Marble, Georges; Bernier, Michel; Bertet, Michel; Gaude, Gaston (Commissariat a l'Energie Atomique, Fontenay-aux-Roses (France). Centre d'Etudes Nucleaires). July 1965. 28p. Dep. mn.

A relatively simple method for determination of sodium and potassium in biological media was developed. No chemical separation is required. The measurement of the gamma and beta activities induced by activation is carried out using scintillation detectors connected to a multi-channel amplitude selector and a counting unit. The results obtained are excellent for sodium and satisfactory in the case of potassium in biological experiments. (auth)

46166 (DP–980) APPLICATIONS OF ATOMIC ABSORPTION SPECTROSCOPY. Wheat, J. Allen (Du Pont de Nemours (E. I.) and Co., Aiken, S. C. Savannah River Lab.). July 1965. Contract AT(07-2)-1. 20p. Dep. mn; CFSTI $1.00 cy, $0.50 mn.

Procedures were developed for analyzing ten types of samples for numerous elements by atomic absorption spectrometry. Methods of preparing the samples for analysis are described. The procedures can be extended to other types of samples. (auth)

46167 (EUR–1898.e) DATA HANDBOOK FOR SENSITIVITY CALCULATIONS IN NEUTRON ACTIVATION ANALYSIS. Girardi, F.; Guzzi, G.; Pauly, J. (European Atomic Energy Community, Ispra (Italy). Joint Nuclear Research Center). 1965. 316p. Dep. mn.

This handbook enables one to determine whether an analytical problem can be solved by activation analysis or not, and how it can be solved. All the data which are necessary to calculate the sensitivity under different experimental conditions are assembled for most elements. Tables present sensitivity as a function of neutron flux, irradiation time, and decay time. (D.L.C.)

46168 (IA–849) RADIOCHEMICAL PROCEDURES FOR ENVIRONMENTAL MEDIA. Passy, N. (ed.) (Israel Atomic Energy Commission, Yavne. Soreq Research Establishment). Dec. 1964. 65p. Dep. mn.

A compilation is presented of the analytical and radiochemical procedures being used to determine some of the more hazardous radionuclides in the environment. (D.L.C.)

46169 (IDO–14664) SEPARATION OF TELLURIUM AND IODINE FROM OTHER FISSION PRODUCTS: APPLICATION TO LOFT SAMPLES. Anderson, Myra D.; Thomas, T. R. (Phillips Petroleum Co., Idaho Falls, Idaho. Atomic Energy Div.). Sept. 1965. Contract AT(10-1)-205. 24p. Dep. mn; CFSTI $1.00 cy, $0.50 mn.

A simple and rapid procedure for the separation of tellurium and iodine from other fission products and from each other is described. Other biologically significant fission products except ruthenium may be determined in the effluent solution. (auth)

46170 (JEN–148–DQ/I–49) DETERMINACION DE PALADIO POR FOTOMETRIA DE LLAMA. (Determination of Palladium by Flame Photometry). Parellada Bellod, R. (Junta de Energia Nuclear, Madrid (Spain). Division de Quimica). 1964. 13p. Dep. mn.

A study on the determination of palladium by flame photometry, fixing the most convenient experimental conditions and using organic solvents to increase the emission of this element, is carried out. Among the organic solvents, acetone was found the most efficient. The interferences produced by anions and cations were also studied and an analytical method is related, in which lines of calibration for 0 to 100 ppm of palladium are used. (auth)

46171 (KAPL-M–6492) SPECTROPHOTOMETRIC DETERMINATION OF SILICON IN Nb–Si ALLOYS. Kautzman, B. E. (Knolls Atomic Power Lab., Schenec-

tady, N. Y.). Aug. 2, 1965. Contract W-31-109-eng-52. 14p. Dep. mn; CFSTI $1.00 cy, $0.50 mn.

A method is given for the analysis of silicon in niobium–silicon alloys, where the wt % Si is in the range 0.10 to 0.40%. The silicon is determined colorimetrically forming silicomolybdic acid by the addition of ammonium molybdate. Silicomolybdic acid then is reduced with stannous chloride to the molybdenum blue complex which is read at 745 mμ. Niobium, which normally interferes, is precipitated as sodium niobate and filtered off. (auth)

46172 (KR–95) DETERMINATION OF SELENIUM IN ANIMAL TISSUE BY NEUTRON ACTIVATION ANALYSIS. Dahl, J. B.; Steinnes, E. (Institutt for Atomenergi, Kjeller (Norway)). July 1965. 6p. Dep. mn.

A neutron activation method was used to determine trace amounts of selenium in animal tissue. This method is based on radiochemical separation and beta-counting of 18.5 m ^{81}Se. The sensitivity of the method is 2×10^{-8} g at a neutron flux of 2.7×10^{12} n/cm^2 sec. (auth)

46173 (LA–3357) PROCESSING OF PLUTONIUM BY ION EXCHANGE. VII. PLUTONIUM(IV) DESORPTION KINETICS FROM DOWEX 1 x 4 INTO NITRIC ACID SOLUTIONS. James, D. B. (Los Alamos Scientific Lab., Univ. of California, N. Mex.). June 14, 1965. Contract W-7405-eng-36. 20p. Dep. mn; CFSTI $2.00 cy, $0.50 mn.

The experimental desorption of uniformly sorbed plutonium(IV) into nitric acid solutions from Dowex 1 × 4 anion-exchange resin was duplicated by the theory for diffusion in spheres with a constant diffusion coefficient. For the various experiments the diffusion coefficient increased with increasing temperature, decreasing nitric acid in the aqueous phase, and decreasing initial level of plutonium sorption. Desorption into an aqueous phase of less than 0.6M nitric acid, even in the presence of hydroxylamine nitrate, caused the formation of insoluble plutonium polymer in the resin phase, and the desorption rate was controlled by the slow rate of polymer dissolution. One experimental desorption, with the nonuniform initial sorption that resulted from a short sorption time, indicated that such systems are not duplicated by the simple theory. (auth)

46174 (LA-DC–7319) MEASUREMENT OF THE MICROSCOPIC DISTRIBUTION OF OXYGEN AND CARBON IN METALS BY ^{3}He ACTIVATION. Holm, Dale M. (Los Alamos Scientific Lab., Univ. of California, N. Mex.). [1962]. Contract W-7405-eng-26. 4p. (CONF-651101–33). Dep. mn; CFSTI $1.00 cy, $0.50 mn.

From 13th Conference on Remote Systems Technology, Washington, D. C.

Qualitative determination of the microscopic distribution O and C in some metals can be carried out by ^{3}He activation and subsequent autoradiography. Immediately after irradiation, the sample is placed on a microscopic slide with a 10-μ photographic emulsion. The composite decay curve is measured during the emulsion exposure and analyzed to deduce the principal isotope causing the exposure. Using calibrated samples, it is possible to determine C, N, and O. The advantages and disadvantages of the ^{3}He activation method are given. (D.L.C.)

46175 (MLM–1264) A REVIEW OF THE DISSOLUTION OF PLUTONIUM DIOXIDE. Gilman, William S. (Mound Lab., Miamisburg, Ohio). May 7, 1965. Contract AT(33-1)-Gen-53. 12p. Dep. mn; CFSTI $1.00 cy, $0.50 mn.

Methods for the dissolution of plutonium dioxide are reviewed. The methods discussed include the use of mineral acids and complexing agents and by fusion and halogenation. 37 references are cited. (P.C.H.)

46176 (NMI–4997, pp 110-23) METALLOGRAPHY OF FUSED UO_2. Cole, G. R. (Du Pont de Nemours (E. I.) and Co., Aiken, S. C. Savannah River Lab.).

Arc fusion is an excellent method for producing very dense UO_2, but impurities characteristic of the fusion process are often introduced. Metallography has been a valuable supplement to the usual analytical tools for detecting and identifying impurities. Microhardness and tarnishing behavior of microscopic impurities, together with x-ray and chemical techniques, were used to identify excess oxygen, metallic uranium, uranium carbide, and uranium nitride in arc-fused UO_2. The shapes of the second-phase inclusions were of little aid to their identification. Microexamination of randomly selected chunks was employed to estimate the content and distribution of uranium and uranium nitride impurities in as-polished UO_2. Excess oxygen content was estimated by lineal analysis of micrographs of polished-and-etched UO_2; results agreed well with those obtained from weight gain on ignition to U_3O_8. (auth)

46177 (NMI–5025(Pt.I), pp 85–95) QUANTITATIVE METALLOGRAPHY OF HYPOSTOICHIOMETRIC URANIUM MONOCARBIDE. Ritchie, E. E.; Tibbetts, J. L. (Atomics International, Canoga Park, Calif.).

Results from three statistical test methods for determining the amount of excess α-U present in hypostoichiometric UC are summarized. The three test methods were: the grid intercept method, metallographic comparison, and by chemical carbon analysis. (W.L.G.)

46178 (NP–15364) A FEASIBILITY STUDY OF THE METHOD OF NON-DESTRUCTIVE ASSAY OF ^{235}U AND ^{239}Pu IN IRRADIATED FUEL SLUG. Ramanna, R. (Atomic Energy Establishment, Trombay (India). Nuclear Physics Div.). [1964]. 47p. Dep. mn.

A method for the nondestructive analysis of fissile materials is discussed. By using a slowing down time lead spectrometer and making use of the difference in fission cross sections of ^{235}U and ^{239}Pu in the 0.1 to 1 ev region, it is possible to estimate their concentration in case of unirradiated samples. Because of the lack of an intense neutron source, the method could not be applied to the case of an irradiated sample. However, from the data obtained with the plutonium sources, a method of analysis that could be followed in the case of irradiated samples is outlined. (P.C.H.)

46179 (RFP–618) RADIOMETRIC DETERMINATION OF FLUORINE IN BULK PLUTONIUM TETRAFLUORIDE. Long, E. C.; Willoughby, O. H.; Cartwright, D. R. (Rocky Flats Div., Dow Chemical Co., Golden, Colo.). Sept. 17, 1965. Contract AT(29-1)-1106. 10p. Dep. mn; CFSTI $1.00 cy, $0.50 mn.

A radiometric instrument was developed for the determination of the fluoride content in kilogram quantities of impure or nonstoichiometric plutonium tetrafluoride. The radiometric analytical results indicate an accuracy and precision comparable to the fluoride results obtained by the pyrohydrolytic method. The special features of the instrument involve reduced time for the analysis and elimination of sampling error with bulk quantities of the material. (auth)

46180 (UCRL–16254) AMINE HYDROHALIDE EXTRACTION STUDIES. Mueller, Werner (Lawrence Radiation Lab., Univ. of California, Berkeley). July 1965. Contract W-7405-eng-48. 26p. (CONF-650817–1). Dep. mn; CFSTI $2.00 cy, $0.50 mn.

From Gordon Research Conference on Ion Exchange, New London, N. H.

The behavior of amine salt extractants is discussed in the case of a tertiary amine, trilaurylamine (TLA), bound to hydrohalic or pseudohydrohalic acids: HF, HCl, HBr, HI, and HSCN. The organic diluents include cyclohexane, carbon tetrachloride, benzene, toluene, nitrobenzene, and chloroform. Conclusions made concerning metal extraction are stated. Examples given show that the composition and stability of a metal complex after extraction by an amine salt into an organic phase depend on the properties of the system amine salt-diluent and do not only reflect the behavior of the metal ion in the aqueous phase. (P.C.H.)

46181 (WAPD-T–1769) AUTOMATION OF MASS SPECTROMETERS FOR ISOTOPIC ANALYSIS OF REAC-

TOR MATERIALS. Barker, F. B.; Cook, H. D.; Hudgens, J. E. (Bettis Atomic Power Lab., West Mifflin, Pa.). Feb. 12, 1965. Contract AT(11-1)-Gen-14. 15p. (CONF-650401-14). Dep. mn; CFSTI $1.00 cy, $0.50 mn.

From American Chemical Society, Detroit.

A description is given of a versatile on-line computer system which was developed for automatically controlling the mass spectrometer during the data acquisition phase, and simultaneously reducing the data and converting it to the desired form. The functions of the system and the programs for thermal emission and spark-source mass spectrometers are described. (D.L.C.)

46182 (NP-tr-1275) AN EASY METHOD FOR THE ACCURATE DETERMINATION OF THE HEAVY HYDROGEN ISOTOPE BY THERMAL CONDUCTIVITY. Sachsse, H.; Bratzler, K. Translated by H. E. Nowottny (U.K.A.E.A. Atomic Energy Research Establishment, Harwell, Eng.) from Z. Physik. Chem. (Leipzig), A171: 331-40(1934). 18p. Dep. mn; JCL $1.60 fs, $0.80 mf.

A method is described for measuring the thermal conductivity of gases. With this method, the D concentration of hydrogen mixtures containing D can be determined with an accuracy of 0.02%. The method is used at 200 mm total pressure and at 16°C excess temperature. The quantity of gas required for an individual measurement is 0.5 cm^3 at 760 mm. The thermal conductivity values of hydrogen-neon mixtures are measured in the same apparatus, so that it is possible on the basis of these data to calibrate the apparatus for heavy hydrogen without requiring heavy hydrogen of known concentration. (auth)

46183 (NP-tr-1289) ANALYSES OF PARA-ORTHO HYDROGEN AND DEUTERIUM BY GAS CHROMATOGRAPHY. Fujita, Katsuyoshi; Kwan, Takao. Translated by S. G. Brickley (Atomic Energy Research Establishment, Harwell, Eng.), from Bunseki Kagaku, 12: 15-19(1963). 13p. Dep. mn; JCL $1.60 fs, $0.80 mf.

Two methods for the gas chromatographic determination of hydrogen nuclear spin isomers and isotopes were investigated with special reference to their accuracy and practicability. One is based on utilizing two sorts of column packings connected in series as previously proposed (J. Phys. Chem., 65: 190(1961)); the first contains alumina and the second alumina coated with manganese chloride. The chromatogram may yield four peaks corresponding to p-H_2, o-H_2, HD, and D_2. The other needs two acts for the analysis. A portion of hydrogen sample is introduced on alumina column which gives rise to three peaks corresponding to p-H_2, o-H_2 plus HD, and D_2 respectively. The remaining portion is introduced on alumina-manganese chloride column by which three peaks corresponding to H_2, HD, and D_2 may be obtained. By these methods the composition of four hydrogen molecular species may be determined. Both were applied to the quantitative analysis of hydrogen isomers and isotopes of known composition. All peaks appeared within 5-15 min, the composition being agreed with the expected value within ±2% accuracy. (P.C.H.)

46184 (ORNL-tr-841) THE RAPID DETERMINATION OF L-LEUCINE, L-ISOLEUCINE, AND L-VALINE IN A MIXTURE BY INFRARED SPECTROMETRY. Kaga, Shinichiro; Hayashi, Taizo. Translated by H. Kubota (Oak Ridge National Lab., Tenn.) from Nippon Nogeikagaku Kaishi, 37: 116-17(1963). 3p. Dep. mn; JCL $1.10 fs, $0.80 mf.

A rapid method of analysis of mixtures of L-leucine, L-isoleucine, and L-valine was developed. The procedure consists of pressing the material into KBr disks and measuring the infrared absorptivities at selected wavelengths. Good results obtained with the method are reported. (P.C.H.)

46185 ADVANCES IN X-RAY ANALYSIS. VOLUME 8. Proceedings of the Thirteenth Annual Conference on Applications on X-Ray Analysis Held August 12-14, 1964. Mueller, William M.; Mallett, Gavin; Fay, Marie (eds.). New York, Plenum Press, 1965. 481p. $20.65. (CONF-715).

Forty-two papers presented at the Thirteenth Annual Conference on Applications of X-Ray Analysis are given. Separate abstracts were prepared for 4 papers. Six papers were previously abstracted for NSA as 17: 2943, 18: 43384, and 19: 4056, 7973, 12324, and 23111. (M.C.G.)

For abstracts of individual papers see: 46186, 47033, 47034, and 47223.

46186 DETERMINATION OF RUBIDIUM IN CESIUM METAL BY X-RAY FLUORESCENCE SPECTROSCOPY. Laib, Roger D. (U. S. Industrial Chemicals Co., Cincinnati). Advan. X-Ray Anal., 8: 443-7(1965).

A rapid method for the determination of rubidium in cesium metal by x-ray fluorescence is described. Cesium metal is converted to the chloride, and pellets pressed with molybdenum trioxide as an internal standard. The rubidium to molybdenum intensity ratio is used to eliminate the effect of small amounts of the other alkali metals. The analytical curve is linear from 0.05 to 15% rubidium, which covers the range of samples normally encountered. Rubidium can be determined with a coefficient of variation of 1.3% in this range. Good agreement was shown with results obtained by flame photometry. (auth)

46187 A SIMPLE ANALYTICAL METHOD FOR ISOLATING LOW-LEVEL ALPHA ACTIVITY OF ^{241}Am FROM PLUTONIUM IN A ROUTINE URINALYSIS PROCEDURE. Bokowski, D. L. (Dow Chemical Co., Golden, Colorado). Am. Ind. Hyg. Assoc. J., 26: 413-18(July-Aug. 1965).

Plutonium is extracted by thenoyltrifluoroacetone and americium is isolated from the residue. Excess sodium hydroxide redissolves aluminum hydroxide while coprecipitating americium on lanthanum hydroxide. Trivalent americium is oxidized to the hexavalent americyl ion which is stabilized by the addition of ammonium fluoride. After reduction to the trivalent state, the purified americium is recovered by coprecipitation with radiopure cerium. The cerium fluoride is counted in a low-background proportional alpha counter. The method is effective for quantitative separation of americium from the lanthanides, other actinides, iron, and aluminum. Sensitivity is sufficient to detect activities as low as 0.50 disintegration per minute. (auth)

46188 HIGH-SPEED CONTROLLED-POTENTIAL COULOMETRY. APPLICATION TO PRECISE DETERMINATION OF PLUTONIUM. Goode, G. C.; Herrington, J. (Atomic Weapons Research Establishment, Aldermaston, Berkshire, Eng.). Anal. Chim. Acta, 33: 413-17 (Oct. 1965).

An electrolysis cell for high-speed controlled-potential coulometric analysis with conventional magnetic stirring is described. The factors influencing the precision obtainable by this technique with platinum and gold electrodes are discussed with particular reference to the oxidation of Pu(III) to Pu(IV) in 0.5 M sulphuric acid. (auth)

46189 DETERMINATION OF AMERICIUM BY CONTROLLED POTENTIAL COULOMETRY. Koehly, G. (Centre d'Etudes Nucleaires, Fontenay-aux-Roses, France). Anal. Chim. Acta, 33: 418-25(Oct. 1965). (In French).

A coulometric determination of americium by reduction of Am(VI) to Am(V) at a potential of +1.3 v is proposed. The accuracy of the method was evaluated by analyzing ^{241}Am solutions prepared by weighing and dissolving AmO_2 of known purity. The results must be corrected by a factor of 1.017, in order to eliminate the systematic error due to autoreduction. After this correction, the relative standard deviation of the method ranged from 0.44% for americium concentrations of $3.125 \cdot 10^{-3}$ M to 0.96% for those of $1.25 \cdot 10^{-4}$ M. (auth)

46190 METHOD FOR THE ISOLATION OF THORIUM FROM SILICEOUS MATERIALS. Almodovar, Ismael (Univ. of Puerto Rico, Mayaguez). Anal. Chim. Acta, 33: 426-33(Oct. 1965).

A method for the isolation from siliceous materials of carrier-free chemically and radiochemically pure thorium is described. The method was applied and tested on several shale and deep-sea sediment samples used in the application of the thorium isotopes method to the dating

of marine sediments. The chemical procedure consistently produces pure thorium in good yields. Several samples can be prepared simultaneously in a few hours. (auth)

46191 FLAME-PHOTOMETRIC DETERMINATION OF SODIUM IN URANIUM ORES. Kramer, H.; Pinto, J. L. (U. S. Atomic Energy Lab., New Brunswick, N. J.). Anal. Chim. Acta, 33: 438-42(Oct. 1965).

A flame-photometric method of determining sodium in uranium, phosphate, carbonate, and silicate rocks was developed. The mutual enhancement of the alkali metals is overcome by the addition of a radiation buffer added to both the sample and to the standards. The method is rapid and suitable for routine analysis. Results obtained are within ±2% of the sodium content. (auth)

46192 DETERMINATION OF MOLYBDENUM IN HAIR AND WOOL BY NEUTRON ACTIVATION ANALYSIS. Healy, W. B.; Bate, L. C. (Oak Ridge National Lab., Tenn.). Anal. Chim. Acta, 33: 443-8(Oct. 1965). (ORNL-P-158).

Neutron activation analysis was applied to the determination of molybdenum in hair and wool. Ashed samples of hair and wool were irradiated for 15 min at a flux of $5 \cdot 10^{13}$ n/cm^2/sec to produce ^{101}Mo. An acid solution of the ash was first boiled in the presence of sodium bromate to volatilize bromine (^{80}Br and ^{82}Br radioisotopes interfere) and then extracted with 0.1% α-benzoinoxime in chloroform to remove ^{101}Mo from other interfering radionuclides. The ^{101}Tc daughter from ^{101}Mo was measured over the 0.31-Mev γ photopeak after allowing the separated ^{101}Mo to decay for 15 min. The molybdenum concentration in hair varied from 0.02 to 0.13 μg/g while wool was found to contain 0.04–0.58 μg/g. (auth)

46193 NON-DESTRUCTIVE NEUTRON ACTIVATION DETERMINATION OF SILVER AND ANTIMONY IN BISMUTH BY γ,γ-COINCIDENCE SPECTROMETRY. Kim, J. I.; Hoste, J. (Ghent Univ.). Anal. Chim. Acta, 33: 449-58(Oct. 1965).

A non-destructive neutron activation method was developed for the determination of silver and antimony in high-purity bismuth; γ,γ-coincidence counting of ^{110m}Ag or ^{124}Sb was applied. The activity of the matrix or other impurities did not interfere. When I-g samples were irradiated at a neutron flux of $4 \cdot 10^{11}$ n cm^{-2} sec^{-1} 25 days, the sensitivity of the method was in the ppB region. (auth)

46194 GRAVIMETRIC DETERMINATION AND SEPARATION OF THORIUM WITH N-BENZOYL-N-PHENYLHYDROXYLAMINE BY DIRECT WEIGHING. Das, B.; Shome, S. C. (Presidency Coll., Calcutta). Anal. Chim. Acta, 33: 462-4(Oct. 1965).

A detailed study was made on the precipitation of Th with N-benzoyl-N-phenylhydroxylamine (BPHA) under controlled conditions of temperature, and it was found that a granular precipitate of definite composition was formed at 50-55°C. Thorium was determined by direct weighing of the metal-BPHA complex after drying at 105-110°C; the composition of the complex was $Th(C_{13}H_{10}O_2N)_4$. The method was applied for the separation of Th from Ce, Be, U, La, Fe, Al, V, Ti, Zr, Ga, and In by pH adjustment or by using masking agents. (P.C.H.)

46195 THE DETERMINATION OF ACTIVATION PRODUCTS IN IRRADIATED STEELS BY ANION-EXCHANGE SEPARATION AND γ-RAY SPECTROMETRY. Hilton, D. A.; Reed, D. (Berkeley Nuclear Labs., Gloucestershire, Eng.). Analyst, 90: 541-4(Sept. 1965).

A method is described for determining ^{51}Cr, ^{54}Mn, ^{58}Co, ^{60}Co, and ^{59}Fe in irradiated mild and stainless steels. It involves the selective elution of these isotopes with different concentrations of hydrochloric acid from a strongly basic anion-exchange resin column. Each nuclide is determined by γ spectrometry. The precision of the method is better than 2% for each determination. (auth)

46196 A CONTRIBUTION TO THE DETERMINATION OF ^{90}Sr IN EFFLUENTS IN THE PRESENCE OF ^{89}Sr. Zange, E. (Kernforschungsanlage, Juelich, Ger.). Atompraxis, 11: 365-8(July 1965). (In German).

In spite of the presence of sulfate in the effluent radiostrontium was enriched by way of a carbonate precipitation. Prepurification was carried out by a nitrate precipitation. Both the isolation of pure radiostrontium and separation of the ^{90}Y was done by means of an improved ion exchange method. The high chemical total yield (90%) and the high counting efficiency (54%) permitted very small ^{90}Y growth periods. (auth)

46197 DETERMINATION OF RADIOSTRONTIUM (AS SULPHATE) IN THE PRESENCE OF CALCIUM. Narrog, J. (Landesinstitut fuer Arbeitsschutz und Arbeitsmedizin, Karlsruhe, Ger.). Atompraxis, 11: 369-73(July 1965). (In German).

A method for the precipitation of strontium is described, utilizing the isomorphism of strontium and barium sulfates. Under the special conditions of the analysis any interferences in the precipitation of calcium sulfate can be avoided. The methods developed allows yields of 50 to 90% to be obtained in biological samples containing up to 1.5 g Ca. By the determination only of Sr isotopes it is possible to count the radioactivity of the precipitate directly and to determine the chemical yield by weight. In other cases it is possible to isolate other isotopes by known methods. (auth)

46198 A RAPID METHOD FOR DETECTION OF ^{90}Sr/^{90}Y IN URINE. Narrog, J. (Landesinstitut fuer Arbeitsschutz und Arbeitsmedizin, Karlsruhe, Ger.). Atompraxis, 11: 373-6(July 1965). (In German).

Beta particles of >1 Mev in water can be measured by Cherenkov effect in liquid scintillation counting systems. A method was developed, which permits ^{90}Sr determination in urine with a good sensitivity by using the Cherenkov effect of the beta particles of its daughter ^{90}Y. The chemical procedure is quite simple; no α, γ- and β-emitting nuclides interfere. (auth)

46199 A RAPID TECHNIQUE FOR DETERMINATION OF SOFT BETA SOURCES IN SMALL QUANTITIES OF PLANT SUBSTANCE. Knalmann, M. (Technische Hochschule, Hanover). Atompraxis, 11: 393-7(July 1965). (In German).

A fast method for determining soft beta sources in small amounts of plant material is described. Root tips of Vicia fabia (dry weight 0.4 mg) containing tracer quantities of ^{35}S or ^{14}C were pulverized and measured directly. The errors resulting from autoabsorption and backscattering are discussed, and two correction methods are listed. (auth)

46200 QUANTITY OF FOOD REQUIRED FOR THE DETERMINATION OF ^{90}Sr AND ^{137}Cs AND ITS INCINERATION. Ritter, R.; Doerfel, Ch. (Gesellschaft fuer Kernforschung, Karlsruhe, Ger.). Atompraxis, 11: 397-400(July 1965). (In German).

The activity of ^{90}Sr in food can only be determined after enrichment in the radionuclide by incineration and its subsequent radiochemical separation. The same sample serves for the radiochemical determination of ^{137}Cs. Preparations of 6 decays/min are needed for the determination of radioactivity in crude food, i.e., food in its native state, while for prepared products 12 decays/min are required. (The average figures for the corresponding quantities of substance are: potatoes 7.5 kg or 12.5 kg, respectively and salad 1 kg or 1.7 kg, respectively. Figures are also given for milk, flour, apples, and meat.) Routine incineration of the relatively large amounts of samples required an incineration facility, which is operated at a temperature of 450°C (upper limit because of volatility of ^{137}Cs) without producing obnoxious fumes. The off-gas is deodorized by thermocatalytic action. The incineration vessels used are made of porcelain; they are only used once and, therefore, time-consuming cleaning is made unnecessary. (auth)

46201 THE USE OF X-FLUORESCENCE EXCITED BY RADIOACTIVES SOURCES. Martinelli, P. Bull. Inform. Sci. Tech. (Paris), No. 92, 79-90(Apr. 1965). (In French).

Possibilities presented by x-fluorescence analytical methods using radioisotopes as the source of the exciting radiation are discussed. These methods are particularly suitable for continuous control of a given element. They also present special advantages resulting from the variety of sources which may be used and from the simplicity of the equipment required. Particular characteristics of this technique and a few examples of analytical applications, are considered. (auth)

46202 RADIOCRYSTALLOGRAPHIC STUDIES OF RADIOACTIVE MATERIALS. Bloch, J.; Anselin, F.; Solente, P. Bull. Inform. Sci. Tech. (Paris), No. 92, 91-105(Apr. 1965). (In French).

The equipment and techniques of x-ray diffraction were adapted to radiocrystallographic analysis of radioactive materials. Results of typical crystallographic work are presented. Studies were made of irradiated fissile materials and of plutonium. (auth)

46203 USE OF PLASTICS IN THE WITHDRAWING OF SAMPLES OF AIR FOR THE DETECTION OF RADON. Truelle, M. A. (District Hygiene-Epidemiology Station, Ceske Budejovice, Czechoslovakia). Cesk. Hyg., 9: 601-8(Dec. 1964). (In Czech.).

The permeability of several types of collapsible containers used for radon collection was investigated. Six types of bags were tested: three of polyvinyl chloride (PVC) film (0.2 mm thick), one of thicker PVC film (0.5 mm), and two of rubber (0.6 and 0.7 mm). The volumes of these bags varied from 515 to 796 cm^3. Loss of radon from the bags during the transport of air samples was studied. The prepared samples with the content of radon varying from 2.10×10^{-9} to 2.81×10^{-11} C/l (11 different concentrations in all) were stored up to 117 hr in collecting vessels made from the different materials. The radioactivity in 59 cases was followed. It was found from the reduction of the initial activity that higher losses of radon occurred from rubber than from plastic bags. The loss from the rubber bags 24 hr after sampling was 40 to 50% of the initial concentration and the loss from PVC plastic bags (0.5 mm thick) was 5 to 10%. Thus, PVC bags were found to be more suitable for the laboratory detection of radon than rubber ones. Moreover, PVC bags can be used for holding nitrogen, which is used for the bubbling of water samples in the emanometric detection of radon. (BBB)

46204 STABLE ISOTOPE DILUTION ANALYSIS. I. GENERAL DESCRIPTION. Dobkowski, Zbigniew (Katedra Jadrowej Inzynierii Chemicznej Politechniki, Warsaw). Chem. Anal. (Warsaw), 10: 295-300(1965). (In Polish).

Several methods of isotope analysis are compared. In one, the stable isotope is diluted with another stable isotope, which acts as a tracer. The analysis is accomplished by determining either the relative abundance or the total quantity of the tracer isotope taken up by mass spectroscopic methods. In another method, the stable isotope is diluted with a radioactive isotope and radiation counting techniques are used for determining trace quantities of the radioisotope taken up. Activation analysis is also included. Dilution with a stable isotope is quantitatively outlined in terms of its application by means of mass spectrometry. References on mass spectrometry are cited as evidence that all three methods of isotope analysis are comparable. Sensitivities of 10^{-6} g with 1 to 2% accuracy, and even 10^{-12} g is favorable cases are quoted for the method of dilution with a stable isotope. In a method of analyzing the tracks in semiconductor materials, sensitivities of 10^{-11} g are quoted for thorium, 10^{-12} g for rubidium, 10^{-15} g for uranium, and 10^{-15} g for argon. (TTT)

46205 ALKALIMETRIC DETERMINATION OF METALS USING 8-HYDROXYQUINOLINE AS A COMPLEXING AGENT. Koppiker, K. S.; Murthy, T. K. S. (Atomic Energy Establishment, Trombay, Bombay). Indian J. Chem., 3: 393-7(Sept, 1965).

An alkalimetric method is described for the determination of copper, nickel, cobalt, zinc, maganese, aluminum, iron, and uranium, based on the potentiometric titration of acid liberated by complexing the metal with 8-hydroxyquinoline. Free mineral acid, if present, causes error unless corrected for. In the case of copper, nickel, cobalt, manganese, and zinc, the free acid can be potentiometrically titrated before adding 8-hydroxyquinoline. A similar titration and plotting of the data in normal way, i.e. pH versus volume of titrant, or the differential plot did not yield an end point in the case of Al, U, and Fe due to hydrolysis of these ions; a satisfactory end point in the case of Al and U could be obtained by plotting the data according to Gran's method but in the case of Fe sodium oxalate had to be added to complex and suppress the hydrolysis. This procedure enables the determination of free acid and metal by 8-hydroxyquinoline in the same aliquot. (auth)

46206 SPECTROPHOTOMETRIC DETERMINATION OF THORIUM(IV) WITH THE SCHIFF'S BASE DERIVED FROM 1-AMINO-8-NAPHTHOL-3,6-DISULPHONIC ACID AND SALICYLALDEHYDE. Poddar, S. N.; Dey, Kamalendu (Indian Association for the Cultivation of Science, Calcutta). Indian J. Chem., 3: 407-8(Sept. 1965).

A spectrophotometric method for the determination of thorium in weak solutions (0.0003913 g thorium in 1 ml solution) is described. Thorium ions gave a red color with the Schiff's base derived from salicylaldehyde and 1-amino-8-naphthol-3,6-disulfonic acid (monosodium salt) at pH 3.2 to 5.2. The color (λ_{max} 450 mμ; sensitivity 0.032 μg Th/cm^2) of the complex was quite stable and obeyed Beer's law over a wide range of thorium concentration. The red complex was isolated and analyzed to $Th(SB)_2$, where SBH_1 is a molecule of the Schiff's base. (auth)

46207 ACTIVATION ANALYSIS OF TRACE IMPURITIES IN ALUMINUM. Ke, Chiung-Huei; Cheng, Hwa-Sheng (National Tsing Hua Univ., Hsinchu, Taiwan). J. Chinese Chem. Soc. (Taiwan), 12: 39-50(June 1965).

Trace impurities in aluminum were determined. Manganese, nickel, copper, cobalt, and iron were analyzed by the method of activation analysis at the THOR, while sodium was determined by flame photometry. The results were: Mn 0.00066%, Ni 0.00041%, Cu 0.00060%, Co 0.00010%, Fe 0.12%, and Na 0.0048%. (auth)

46208 VERIFICATION OF THE RADIOCHEMICAL PURITY OF A LABELED OPTICAL ISOMER. Verly, Walter G.; Gerday, Charles (Universite, Liege; Univ. of Montreal). J. Labelled Compds., 1: 27-33(Jan.-Mar. 1965). (In French).

A method for evaluating the radiochemical purity of the labeled isomer of an amino acid is described. The method was applied to the case of tritiated L-phenylalanine. The inactive racemic form, added as a carrier, was condensed with L-glutamic acid; the diastereoisomers of the resulting dipeptide were resolved chromatographically on Dowex 50 and the radioactivity of each peak was measured. This process requires only a very little sample and it enables the detection of very minute contaminants. (auth)

46209 SELECTIVE SEPARATION OF ^{65}Zn BY ISOTOPIC EXCHANGE BETWEEN SOLUTION AND GALLIUM-ZINC ALLOY. Toerkoe, J. (Institut fuer Isotope, State Atomic Energy Commission, Budapest). Kernenergie, 8: 494-5(Aug. 1965). (In German).

The isotopic exchange of ^{65}Zn between aqueous solution and Zn–Ga alloy was investigated. The use of the principle for separation of ^{65}Zn present in microquantities from different isotopes is shown. After performing the exchange the re-extraction of ^{65}Zn was carried out with the aid of cupric ions in hydrochloric acid medium; the separation proved to be rapid and rather selective and a yield of 95–96% could be attained. (auth)

46210 METHOD FOR THE CONTROL OF THE RADIOCHEMICAL PURITY OF ^{52}Mn PREPARATES. Svoboda, K.; Mudrova, B. (Inst. for Nuclear Research, Czechoslovak Akademy of Sciences, Rez). Kernenergie, 8: 496-9(Aug. 1965).

A method is described for the chemical separation of Mn, Cr, V, and Zn, allowing the determination of the

radioactivity of ^{51}Cr, ^{48}V, and ^{65}Zn in ^{52}Mn preparates. A simplified procedure for determining the upper limit of the content of interfering radionuclides is presented, based on the measurement of the gamma spectrum of a solution remaining after proceeding removal of ^{52}Mn with a Mn carrier. (auth)

46211 DETERMINATION OF PHOSPHORUS, SULFUR, AND CHLORINE IN ARSENIC BY NEUTRON ACTIVATION ANALYSIS. Niese, S. (Zentralinstitut fuer Kernforschung, Rossendorf, Ger.). Kernenergie, 8: 499-501(Aug. 1965). (In German).

A differential technique for determining phosphorus, sulfur, and chlorine by neutron activation analysis is described. The activities of ^{32}P and ^{35}S obtained by two irradiations using different thermal and fast neutron flux ratios were employed for determining the contents of the elements mentioned. (auth)

46212 ACTIVATION ANALYSIS OF ^{213}Pa FOLLOWED BY γ-RAY SPECTROMETRY OF ^{232}Pa AND ^{233}Pa. Sakanoue, Masanobu; Takagi, Tomoo; Abe, Masao; Oosawa, Masumi (Kanazawa Univ., Japan). Nippon Genshiryoku Gakkaishi, 7: 404-9(Aug. 1965). (In Japanese).

A method for determining ^{231}Pa by neutron irradiation separation of protactinium by solvent extraction with diisobutyl ketone, and γ spectrometry of ^{232}Pa produced by (n,γ) reaction was studied. Preliminary concentration of protactinium before irradiation was carried out by adsorption on quartz powder in a polyethylene column. In the γ spectrum, the total counts in the region from 0.78 to 1.09 Mev decayed with a half life of ^{232}Pa, which can be used as a measure of the relative amount of this nuclide. The total chemical yield was obtained by using the total counts in the region of 0.27 to ~0.36 Mev in that spectrum, which was attributable to the activity of ^{233}Pa added in the sample in the beginning as tracer. The applicability of this activation method for the determination of ^{231}Pa was confirmed by preparing a calibration curve for some samples containing 10^{-8} to 10^{-10} g of ^{231}Pa. The sensitivity of the method is discussed with respect to irradiation time and value of the neutron flux, in comparison with the α counting method for this nuclide. Another method using γ counting with discrimination level was examined and found to also be valid for the determination of ^{232}Pa produced in the irradiated sample. (auth)

46213 ANALYSIS OF LABELED ORGANIC COMPOUNDS BY RADIOGASCHROMATOGRAPHY. Okamoto, Jiro; Dobashi, Genichi (Japan Atomic Energy Res. Inst., Tokyo). Nuclear Eng. (Tokyo), 11: 20-4(Jan. 1965). (In Japanese).

An apparatus with which the gas chromatographic separation and determination of the radioactivity of labeled compounds can be carried out successively was constructed. Each component separated by gas chromatography was mixed with propane and introduced into a gas-flow counter connected to a recording system. Both ends of the counting vessel were sealed, so that the washing-off of the contamination could be done easily. The conditions for operation are reported. A carrier gas consisting of propane and helium had some advantages over a methane-helium system. Examples of the application are given for the analysis of tritium-labeled radiolytic products of isobutyric acid and the separations of tritiated benzene and pyridine, of tritiated toluene and pyridine, and of tritiated chloroform and pyridine. The count was proportional to the amount of sample subjected to the analysis and so it may be possible to use the apparatus for quantitative determinations. (NSA of Japan)

46214 ABSOLUTE COUNTING OF ^{14}C BY EFFICIENCY TRACING TECHNIQUE. Yura, Osamu; Kimura, Miwako (and others) (Electrotech. Lab., Tokyo). Nuclear Eng. (Tokyo), 11: 39-42(Jan. 1965). (In Japanese).

When determining the absolute amount of activity of a sample, either absolute counting of the sample or relative counting in reference to a known standard sample is generally performed. The efficiency tracing technique devised for ^{35}S was applied to the absolute counting of ^{14}C with satisfactory precision. The efficiency tracing technique is a method for the absolute counting of low-energy β emitters with which the 4π β counting is not effective, and was applied to the counting of ^{35}S by using ^{60}Co as the tracer. The tracer must be a nuclide that has an $E_{\beta max}$ similar to that of ^{14}C and that is available for β-γ coincidence counting (e.g., ^{60}Co). A compound or homogeneous mixed system containing both ^{14}C and ^{60}Co is prepared and the counting efficiency of $^{60}Co(\epsilon_{\beta t})$ in the β-channel is obtained by means of the 4π β-γ coincidence counting. The counts of ^{14}C ($N_{\beta m}$) are obtained and $N_{\beta m/m}$ (m: amount of the original ^{14}C solution contained in the sample) is plotted against $\epsilon_{\beta t}$. The disintegration of ^{14}C (absolute activity) per unit mass can be determined from the value of $N_{\beta m/m}$ obtained by extrapolating the line up to $\epsilon_{\beta t} = 100\%$. By the above method, the absolute activity of a solution of glycine-1-^{14}C was estimated to be 3.18×10^6 dps/g-solution. By reference to a standard sample ($Na_2{}^{14}CO_3$ solution) from NBS, using the liquid scintillation technique, the absolute activity of the above sample was found to be 3.08×10^6 dps/g-solution, which was in good agreement with the value obtained by the method. (NSA of Japan)

46215 THE DETERMINATION OF β EMITTERS WITH THE HELP OF CHERENKOV RADIATION. Hoffmann, W. (Farbwerke Hoechst AG., Frankfurt). Radiochim. Acta, 4: 117-19(Aug. 1965). (In German).

The Cherenkov radiation of ^{131}I, ^{24}Na, ^{32}P, and ^{90}Y in aqueous solutions was studied. An analytic method of high sensitivity can be based on the detection of Cherenkov radiation from β emitters with energies > 1 Mev, e.g., ^{32}P, by sensitive photomultipliers. (auth)

46216 GRAVIMETRIC DETERMINATION OF RARE EARTHS WITH DIOXIMALEIC ACID. Spacu, P.; Mavrodin, Maria (Center of Inorganic Chemistry, Bucharest). Rev. Roumaine Chim., 10: 421-4(May 1965).

A gravimetric method for the determination of rare earths by using dihydroxymaleic acid as a reagent was developed. The method is based on the property of certain rare earths to form, in acid medium, precipitates (dihydroxymaleates) that are almost insoluble in water. (J.S.R.)

46217 A REVIEW OF ORGANIC COMPOUNDS CONTAINING P=S AND P(S)SH GROUPS AS SEPARATORY AND ANALYTICAL REAGENTS. Handley, Thomas H. (Oak Ridge National Lab., Tenn.). Talanta, 12: 893-901 (Oct. 1965). (ORNL-P-1115)

A review of separations with, and analytical applications of organic compounds with P=S and P(S)SH groups is presented. (auth)

46218 SIMULTANEOUS DETERMINATION OF $^{65}_{30}Zn$ AND $^{32}_{15}P$ IN SHELLFISH BY RADIOCHEMICAL TECHNIQUES. Setser, J. L.; Rozzell, T. C. (Robert A. Taft Sanitary Engineering Center, Cincinnati). Talanta, 12: 903-11(Oct. 1965).

A radiochemical procedure for the simultaneous determination of ^{65}Zn and ^{32}P in shellfish was devised. Shellfish samples were analyzed for these two nuclides over a period of 8 months. The values obtained by the radiochemical procedure agreed with the ^{65}Zn and ^{65}P values of other investigators. (auth)

46219 PRESENT STATE OF COMPLEXOMETRY. I. DETERMINATION OF QUADRIVALENT AND TERVALENT METALS. Pribil, Rudolf (Czechoslovak Academy of Sciences, Prague). Talanta, 12: 925-39(Oct. 1965).

A review of the visual complexometric determination of quadrivalent and tervalent metals, whether achieved by using indicators, titrants, masking agents, or separatory methods, is presented. Attention is paid to the complexometric behavior of such metals and to the problems of interferences in particular determinations. Older methods, except those which are irreplaceable, are not mentioned. (auth)

46220 A NEW OXIDIMETRIC REAGENT: POTASSIUM DICHROMATE IN A STRONG PHOSPHORIC ACID MEDIUM

V. POTENTIOMETRIC DETERMINATION OF URANIUM (VI). Rao, G. Gopala; Rao, P. Kanta; Rahman, M. A. (Andhra Univ., Waltair, India). Talanta, 12: 953-61(Oct. 1965).

A critical review of the more important methods for the determination of uranium(VI) through reduction to uranium(IV) and subsequent titration with an oxidimetric reagent is given. A method is described involving reduction to uranium(IV) by an excess of iron(II) in a strong phosphoric acid medium followed by potentiometric titration with a standard solution of potassium dichromate. This method has the advantages that the uranium(VI) is reduced quantitatively only to the uranium(IV) stage and that the potentiometric titration could be carried out at room temperature without the need for an inert atmosphere. It is also subject to less interferences than the other methods. (auth)

46221 FACTORS INFLUENCING DETERMINATION OF LITHIUM AND BORON IN ENRICHMENT PRODUCTS IN (n,α) NUCLEAR REACTION. Plaksin, I. N.; Dzhemard'yan, Yu. A.; Malysheva, N. G.; Starchik, L. P. Tsvetn. Metal., No. 6, 18-22(June 1965). (In Russian).

The neutron-absorption technique used for the determination of the Li and B concentrations in products is based on the absorption of thermal neutrons by these elements; however, B can be determined only if other elements possessing a high thermal-neutron capture cross section are not present in the sample. A neutron-induced exothermic reaction forms the basis of the analysis. In the case of ^{6}Li, the energy of the reaction is divided between the 2.05-Mev α particle and the 2.78-Mev T nucleus: $^6Li(n,\alpha)^3H$ + 4.78 Mev. In the case of ^{10}B, the energy of the emitted α particle is 1.49 Mev and that of the Li nucleus 0.85 Mev. The ^{7}Li is formed as an excited nucleus and its transition to the ground state is accompanied by the emission of 0.47-Mev γ quanta: $^{10}B(n,\alpha)^7Li$ + 2.78 Mev. The Li concentration is derived from the count rate of α particles and T; the B content is determined from the α particles and Li. A scintillation counter with a ZnS(Ag) phosphor was used for recording the charged particles, while a 0.25-C Po–Be source placed in paraffin served for the irradiation. The results were very close to those obtained by chemical analysis. It is expected that because of its rapidity, high selectivity, and simplicity, the method will be widely used for mass analyses. (TTT)

46222 ON THE GRAVIMETRIC DETERMINATION OF OXALIC ACID AS THORIUM OXALATE. Sarudi (von Stetina), I. Z. Anal. Chem., 211: 281-2(1965). (In German).

The thorium oxalate precipitated from hot hydrochloric acid solutions is suitable as the weighing form for the oxalic acid determination. The thorium oxalate is precipitated as the hexahydrate, dihydrate, or monohydrate. The conversion of the hydrated thorium oxalate to the oxide was used as proof of the validity of using the hydrates as weighing forms. In all three forms the ThO_2 content found agrees well with the value calculated for the corresponding hydrate. (J.S.R.)

46223 UNIVERSAL METHOD FOR THE ANION EXCHANGE SEPARATION OF URANIUM AND ITS APPLICATION TO THE DETERMINATION OF URANIUM IN SEA WATER, MARINE SEDIMENTS AND OTHER GEOLOGICAL SAMPLES. Hazan, I.; Korkisch, J.; Arrhenius, G. (Univ., Vienna). Z. Anal. Chem., 213: 182-6(1965).

Before the fluorimetric determination of uranium in sea water, marine sediments, and other geological samples an ion exchange procedure was used to separate uranium from interfering elements. This separation was best performed on Dowex 1 in a medium consisting of 90% methyl glycol and 10% 6 N hydrochloric acid. By means of this method easily reproducible and accurate results for determinations of uranium in as little as 250 ml of sea water or in about 0.1 g of solid sample could be obtained. Because of its universal applicability this technique is to be recommended whenever μg and mg quantities of uranium have to be determined. (auth)

46224 THE ANALYTICAL CHEMISTRY OF HAFNIUM AND ZIRCONIUM (thesis). Wardi, Ahmad H. Detroit, Wayne State Univ., 1959. 47p.

The weight of the total oxide (HfO_2 plus ZrO_2) in a mixture was determined by precipitation with mandelic acid. The number of moles of hafnium and zirconium in the mixture were determined also by indirect titration with EDTA. The results obtained from these methods were used to calculate the percentage of hafnium and zirconium in the mixture. Zirconium was separated from all cations except hafnium by the mandelate precipitation. The mandelate was then dissolved in excess EDTA solution. The amount of zirconium was determined by back titration with bismuth nitrate. Hexahydromandelic acid $C_6H_{11}\cdot CH(OH)\cdot COOH$ precipitates zirconium quantitatively by forming a basic salt in weakly acid solution. Atrolactic acid $C_6H_5\cdot C(OH)\cdot CH_3\cdot COOH$ forms two types of compounds with zirconium: (1) chelate compounds, formed at high acidity and high concentration of atrolactic acid and (2) basic salts, formed at low acidity and low concentration of atrolactic acid. Both compounds are soluble in hydrochloric acid and in water. The precipitation of zirconium was not quantitative. (Dissertation Abstr.)

46225 RAF MODEL B TITRATOR (Engineering Materials). (Phillips Petroleum Co. Atomic Energy Div., Idaho Falls, Idaho). (CAPE–1225).

5 drawings.

A remotely operated titrator is described. It is located in a hot cell so that it can be readily removed for decontamination or replacement. It can be easily modified to use either a 50- or 100-ml beaker. The stainless steel stirrer, coated with polyethylene, may be exchanged for a magnetic stirrer. The equipment includes stainless steel acid and caustic probes. Sample sizes are 0.1 ml. (For details, see TID-4100). (M.C.G.)

46226 THE SPECTROCHEMICAL DETERMINATION OF HAFNIUM, TANTALUM AND NIOBIUM IN THORIUM OXIDE. Shuster, E. R. Jr.; Scott, J. E. (Nuclear Materials and Equipment Corp., Apollo, Penna.). 4p. (CONF-650311-3). Gmelin, AED-CONF-65-025-2.

From Conference on Analytical Chemistry and Applied Spectroscopy, Pittsburgh.

The use of parahydroxyphenyl arsonic acid in analysis of thorium oxides for Hf, Ta, and Nb is described. The Hf, Ta, and Nb were precipitated from solutions with thorium oxides and the precipitate was analyzed spectrographically. (M.C.G.)

46227 APPLICATION OF COINCIDENCE METHODS IN ACTIVATION ANALYSIS. Schulze, W. (Freie Universitaet, Berlin). 18p. (CONF-650405–17). Gmelin, AED-CONF-65-040-26.

From International Conference on Modern Trends in Activation Analysis, College Station, Tex.

To what extent the selectivity of nondestructive analysis could be improved by application of coincidence methods was investigated. Distinguishing radiation from one radionuclide without any doubt and without chemical (destructive) means in a mixture of other radionuclides is discussed. Activation of the sample can be done with thermal or with fast (14-Mev) neutrons. The most important types of coincidences resulting from properties of the decay schemes are: ($\gamma_1\gamma_2$), cascade of two γ quanta; β^+, two annihilation quanta with angular correlation; ($\beta\gamma$), β group with γ in cascade; and (eγ), conversion electron with γ in cascade. The selectivity of coincidences is discussed. The decay schemes involved in the activation of the elements Z = 1 to 46 and the ($\gamma\gamma$)-coincidences were investigated; the energy values are given. The simplest equipment for coincidence measurements requires two channels with pulse-height discrimination, which act on a coincidence circuit giving only an output-pulse if events occurring simultaneously enter from the two channels. The measured coincidence-rate consists essentially of two parts, the true coincidence rate C and the random rate R. Values of β^+ activities produced by 14 Mev neutron activation are given for all ele-

ments with Z = 1 to 83 and a selection of the most sensitive cases are given. (F.J.H.)

46228 THE RADIOACTIVATION ANALYSIS OF SILICON AND SILICON COMPOUNDS WITH THE SUCCESSIVE USE OF ION-EXCHANGE CHROMATOGRAPHY. Moiseev, V. V.; Kuznetsov, R. A.; Kalinin, A. I. (Inst. of Silicate Chemistry, Leningrad). 12p. (CONF-650405-10). Gmelin, AED-CONF-65-040-18.

From International Conference on Modern Trends in Activation Analysis, College Station, Tex.

The identification of microimpurities in samples of semiconductor silicon, silicon dioxide, quartz, and some liquid silicon compounds by radioactivation and ion-exchange chromatography is described. Before irradiation liquid products were hydrolyzed in a teflon glass using pure nitric acid at the temperature of liquid nitrogen. The products were then calcinated at 1200°C. The samples were irradiated with a flux of 10^{13} to 10^{14} neutrons per cm^2 sec. The fractions with extracted activities were collected and evaporated by means of an infrared lamp. The activities were recorded either by the γ spectrometer (in the case of the group separation), or by a β counter (in the case of complete scheme of separation). The activity of the extracted fractions was compared with the activity of standards irradiated together with the samples. (F.J.H.)

46229 A NEW APPROACH TO NEUTRON ACTIVATION ANALYSIS THROUGH MICRO AND SUBMICRO ELECTRO-SEPARATION TECHNIQUES. DISCUSSION OF CONDITIONS, PRECAUTIONS, AND PROCEDURES FOR OPTIMUM RESULTS. Mark, Harry B. Jr.; Berlandi, Francis J.; Vassos, Basil H.; Neal, Thomas E. (Univ. of Michigan, Ann Arbor). 34p. (CONF-650405-13). Gmelin, AED-CONF-65-040-10.

From International Conference on Modern Trends in Activation Analysis, College Station, Tex.

The use of electro-separation techniques in activation analysis is described. The combined method has selectivity combined with sensitivity and the advantages of preconcentration, ease of use of short-lived nuclides, and ability to determine several species simultaneously. This method allows for the concentration of trace elements from the bulk of a liquid phase onto an electrode, which is very easy to manipulate. Another advantage is that the gross amount of activity of a sample plus disk electrode is relatively small, which (coupled with no necessity for hot chemical separation) greatly reduces the radiochemical handling facilities required. The difficulty or disadvantages of the method with respect to conventional neutron activation analysis methods is that the sample is dissolved in (or chemically pretreated) and plated out of a solvent-supporting electrolyte system before irradiation. This could give rise to errors resulting from the activation of some trace impurities of the solvent-supporting electrolyte system if they deposit on the electrode. Irradiation of the sample before electrolysis eliminates this problem. Another source of error is the specific adsorption of nonelectroactive species on the electrode surface. (F.J.H.)

Inorganic and Physical Chemistry

Refer also to abstracts 46956, 47025, 47895, and 47921.

46230 (AAEC/E-136) THE ADSORPTION OF BERYLLIUM ON ION-EXCHANGE RESINS FROM INORGANIC SYSTEMS. Fardy, J. J. (Australian Atomic Energy Commission Research Establishment, Lucas Heights). May 1965. 28p. Dep. mn.

Anion-exchange studies revealed that beryllium forms anionic complexes with fluoride, phosphate, carbonate, and thiocyanate. The stabilities of these complexes lie in the order $F^- > H_2PO_4^- \approx CO_3^{=} \gg CNS^-$. Under the conditions of this investigation, BeF_4^{-2} and $Be(H_2PO_4)_4^{-2}$ were identified. Attempts to identify the carbonate complex were prevented by hydrolysis. The anionic thiocyanate complex is very weak and no attempt was made to identify this species. The anion-exchange data obtained in dilute nitric, hydrochloric, and sulphuric acid solutions showed some anionic complex formation but corresponding cation-exchange data showed that in solutions of concentration up to 2.0M the extent of this reaction is negligible. (auth)

46231 (AD-613660) GASEOUS METABORATES. III. THE BERYLLIUM OXIDE-BORON OXIDE SYSTEM. RESEARCH ON THERMODYNAMICS OF THE Al-B-O, Be-B-O AND Al-Be-O SYSTEMS. Interim Technical Report No. 1. Blackburn, Paul E.; Buchler, Alfred (Little (Arthur D.) Inc., Cambridge, Mass.). Mar. 1965. Contracts AF49(638)-1171; DA19 020ORD5584. 26p. CFSTI $2.00 cy, $0.50 mn.

Gaseous beryllium metaborate, $Be(BO_2)_2$, was identified mass spectrometrically in the vapor above the beryllium-boron-oxygen system. A study of this system by differential thermal analysis and Knudsen effusion using a vacuum balance and mass spectrometer, showed solid $Be_3B_2O_6$ to be the only condensed mixed oxide phase present with a melting point of 1495 ± 5°C. The following thermodynamic values were obtained for the formation of gaseous beryllium metaborate from beryllium oxide and gaseous boron oxide: $BeO(c) + B_2O_3(g) = Be(BO_2)_2(g)$; enthalpy at 1500°C = 22 ± 5 kcal/mole; entropy at 1500°C = 6 ± 1 eu/mole. For the formation of solid $Be_3B_2O_6$ from the condensed oxides: $3BeO(c) + B_2O_3(l) = Be_3B_2O_6(c)$; enthalpy = −23 ± 5 kcal/mole; entropy = −13 ± 2 eu/mole. The metal-anion bond strengths in the gaseous lithium and beryllium metaborates show the same relation to each other as the bond strengths in the corresponding chlorides, thus further confirming the pseudohalide character of the gaseous metaborates. (auth)

46232 (BNWL-SA-239) A MULTIPHONON NEUTRON SCATTERING STUDY OF HYDROGEN BONDING IN ZIRCONIUM HYDRIDE. Harling, O. K.; Leonard, B. R. Jr. (Battelle-Northwest, Richland, Wash. Pacific Northwest Lab.). Aug. 2, 1965. Contract AT(45-1)-1830. 22p. (CONF-650932-1). Dep. mn; CFSTI $1.00 cy, $0.50 mn.

From Symposium on the Inelastic Scattering of Neutrons by Condensed Systems, Upton, N. Y.

The Battelle rotating-crystal spectrometer was used to investigate the hydrogen bonding in a sample of ZrH. Scattered neutron spectra were obtained at scattering angles of 15- to 165-degrees for incident energies of 0.504, 0.386, and 0.180 ev. The over-all resolution on energy changes was from 4% to about 20% for neutrons scattered from the first three vibration levels. The observed energies and widths of the first three levels were found to be 141.4 ± 3, 280.9 ± 8, 411 ± 9, and 26.4 ± 0.6, 52.2 ± 3.7, 72 ± 6 mev, respectively. Resolution corrections were applied to these energy widths. The angular distributions of elastic scattering and of the inelastic scattering from the first three vibration levels were compared with theory, assuming that the hydrogen atom is bound in an isotropic harmonic potential well. The experimental elastic scattering distributions agreed with theory to within ±1% to ±6%. For all incident energies, the angular dependence of the total scattering associated with each vibrational level agreed with theory to from ±9% to ±23%. On the basis of these results, it appears that the assumption of harmonic bonding for the first three levels in ZrH is a good first approximation. (auth)

46233 (CEA-R-2752) QUELQUES ASPECTS DE LA TRANSITION SOLIDE-LIQUIDE. (Some Aspects of the Solid-Liquid Transition). Hicter, Pierre; Malmejac, Yves (Commissariat a l'Energie Atomique, Saclay (France). Centre d'Etudes Nucleaires). May 1965. 85p. Dep. mn.

Current theories of fusion were analyzed and grouped by analogies using a unified symbolism to facilitate comparisons. Theories are presented based on solid state vibrational models, nucleation models, order-disorder models, vacancies, and dislocations. For each model, the hypotheses underlying the theoretical analysis were separated and the essential parts of the theoretical development are defined. Principal results are compared with experimental data. (auth)

46234 (COO-1140-123) THERMODYNAMICS OF MATERIALS AT HIGH TEMPERATURE AND LOW PRESSURE. Gilles, Paul W. (Kansas Univ., Lawrence. Dept. of Chemistry). May 24, 1965. Contract AT (11-1)-1140. 23p. (CONF-641124-1). Dep. mn; CFSTI $1.00 cy, $0.50 mn.

From International Conference on Applications of Fundamental Thermodynamics to Metallurgical Processes, Pittsburgh.

A discussion is presented of some of the principles of vaporization phenomena and how they are related to the thermodynamic properties of substances. Some possible purposes of vaporization studies are outlined. Pressure-composition diagrams are discussed with the diagrams of Ti-O, Ti-S, and U-S as examples. Some of the various factors influencing vaporization phenomena are considered, and the stages of a vaporization study are described. (D.L.C.)

46235 (N64-26802) THERMODYNAMIC PROPERTIES OF HIGH TEMPERATURE HELIUM. Report No. 0-71000/3R-11. Hester, J. C.; Sewell, K. G. (Ling-Temco-Vought, Inc., Dallas, Tex.). Aug. 1963. 60p.

The thermodynamic properties of helium were calculated for a range of temperatures from 2,000°K to 100,000°K and for a range of density ratios based on standard atmospheric density from 10^{-10} to 10^{2}. The data are presented in charts which include enthalpy, entropy, pressure, specific heats, speed of sound, compressibility factor, and species concentrations. (auth)

46236 (NIJS-R-430) DIE SYNTHESE VON HYDRAZINIUM-FLUOROZIRKONATEN (IV). (Synthesis of Hydrazine-Fluorozirconates (IV)). Slivnik, J.; Smalc, A.; Sedej, B.; Vilhar, M. (Nuklearni Institut Jozef Stefan, Ljubljana (Yugoslavia)). July 1964. 3p. Dep. mn.

The complex salts $N_2H_6ZrF_6$ and $(N_2H_6)_3Zr_2F_{14}$ were isolated from aqueous solutions of zirconium dioxide solution in hydrofluoric acid and hydrazine fluoride. The thermal stability of the products was studied with a thermal balance. (tr-auth)

46237 (ORNL-3832, pp 76-99) CHEMISTRY OF AQUEOUS SYSTEMS. (Oak Ridge National Lab., Tenn.).

The spectra of light and heavy water are being studied at 0.7 to 2.0 μ. Temperature dependences were measured. The activity coefficient of HCl in HCl-NaCl mixtures was studied to 175°. A computer program was written for calculation of osmotic and activity coefficients from isopiestic data. The program is general (for aqueous solutions) and can be used for any electrolyte type at any temperature. A new set of accurately measured apparent-molal-volume curves of the alkali-metal chlorides was obtained. Equilibrium ultracentrifugation indicates that the degree of polymerization of vanadium(V) species of average formula $VO_2(OH)_{1.5}^{0.5-}$ is about 10, and of average formula $VO_2(OH)_2^{1-}$ in the range of 3 or 4. Anion and cation exchange hyperfiltration membranes were prepared by grafting polyelectrolytes onto cellophane and by amination of polyvinyl chloride. Measurements of selectivity coefficients for the uptake of tetramethylammonium ions at 25° by variously cross-linked sodium polystyrene sulfonates were performed with ^{14}C-labeled tetramethylammonium chloride. Measurements of the weight swelling of a lightly cross-linked, strong-base anion exchanger were employed in thermodynamic calculations of the ionic strength dependence of the selectivity coefficient for the bromide-chloride anion exchange reaction. Measurements of the vapor pressures of aqueous mixtures of the salts of various model compounds for strong-acid cation exchangers and strong-base anion exchangers by the isopiestic vapor-pressure comparison technique were employed in the calculation of thermodynamic activity coefficient ratios, which were compared with the ratios for cross-linked ion exchangers derived from selectivity coefficient measurements or from isopiestic measurements. The selective uptake of Li over Cs ions from dilute aqueous electrolyte solutions by cross-linked polymethacrylic acid-type cation exchangers was shown to be determined by the entropy rather than the enthalpy of the ion exchange reaction. Apparent molal heat contents at 25°C are reported for aqueous solutions of tetramethylammonium chloride, bromide, and iodide; tetraethylammonium chloride, bromide, and iodide; tetrapropylammonium chloride, bromide, and iodide; and tetrabutylammonium chloride and bromide. (auth)

46238 (ORNL-TM-1253) PØLARGRM—A COMPUTER PROGRAM FOR ANALYSIS OF POLAROGRAMS. Savage, Serena; Shults, W. D. (Oak Ridge National Lab., Tenn.). Aug. 31, 1965. Contract W-7405-eng-26. 14p. Dep. mn; CFSTI $1.00 cy, $0.50 mn.

A computer program is given which computes the "least squares" straight line, the slope, the half-wave potential, and the standard deviations for the latter two parameters for the conventional semi-log (Heyrovsky-Ilkovic) plot of current-potential data taken from experimental polarograms. These results, plus the input data and the value of the logarithm term in the Heyrovsky-Ilkovic equation, are printed out to facilitate comparison between theory and experiment. Detailed instructions for the use of the program are given. The program is written in Fortran 63 for the ORNL CDC 1604-A computer. (auth)

46239 (ORO-631, pp 132-41) FISSION PRODUCT CHEMISTRY OF SOILS. (UT-AEC Agricultural Research Lab., Oak Ridge, Tenn.).

Progress is reported in studies of the interactions of fission product elements with mineral clay fractions of the soil. Data are reported from investigations of the rate processes involved in cation movement in clay-water systems using electrical conductance measurements; exchange reactions of Sr and Cs with pure clay minerals and soil clays; exchange diffusion in ion exchanges; and the development of a new technique for measuring self-diffusion in clays. (C.H.)

46240 (TID-22207) HIGH TEMPERATURE SOLID STATE CHEMISTRY AND SUB-SOLIDUS PHASE EQUILIBRIA. Final Technical Progress Report. Vorres, Karl S.; Frushour, Robert; Jaeger, Ralph; Shick, Larry (Purdue Univ., Lafayette, Ind. Dept. of Chemistry). Aug. 1, 1965. Contract AT(11-1)-1246. 61p. Dep. mn; CFSTI $3.00 cy, $0.75 mn.

Six articles are included; separate abstracts were prepared for each. (P.C.H.)

For abstracts of individual papers see: 46241-46246.

46241 (TID-22207, Paper A) PREPARATION AND SOME PROPERTIES OF SODIUM-RARE EARTH MIXED OXIDES. Vorres, Karl S. (Purdue Univ., Lafayette, Ind. Dept. of Chemistry). 5p. (CONF-650804-8).

From 5th Rare Earth Research Conference, Ames, Iowa.

Mixtures of Na_2CO_3 and oxides of Y, La, Nd, Gd, Dy, Ho, Er, or Yb were heated in a dry oxygen or nitrogen stream at 880°C for 15 hours. Reactions took place in all cases yielding products of the type $Na(RE)O_2$. The x-ray data indicated five different structure types. (auth)

46242 (TID-22207, Paper B) STUDIES OF REACTIONS BETWEEN DIVALENT AND TRIVALENT OXIDES. Research Progress Report. Jaeger, Ralph R. (Purdue Univ., Lafayette, Ind. Dept. of Chemistry). 20p.

Barium-rare earth AB_2O_4 type compounds were studied to clarify the applicability of Dietzel's rule and to provide data to help correlate the structures of all compounds of this type. According to Dietzel's rule divalent Ba will not react with trivalent ions larger than 0.89 Å (Ho) and Pb, Sr, and Ca will not react with any rare earth ion. The results showed that Dietzel's rule, as originally written is not applicable to the Ba and Sr-rare earth oxide systems. On the basis of the results with Sr compounds, the critical IFS must be lowered to at least 0.2 to be useful in predicting compound formation between divalent and trivalent metal oxides. $BaCO_3$ reacted with all of the rare earth oxides that were tried (La, Nd, Sm, Gd, Dy, Er, Yb, and Y). The stoichiometry for all of these except for Er and Yb is $BaRe_2O_4$. 78 references are cited. (P.C.H.)

46243 (TID–22207, Paper C) CORRELATION OF THE STRUCTURES OF I-V TYPE ABO_3 COMPOUNDS. Shick, Larry; Vorres, Karl S. (Purdue Univ., Lafayette, Ind. Dept. of Chemistry). 8p.

The structures of ABO_3 compounds where A and B are cations of the valences 1 and 5, respectively, were correlated. A plot of ionic radius of A versus ionic radius of B showed regions of structures similar to those observed for the valence types II–IV and III–III. The Pauling rule relating radius ratio and coordination number was found to be valid most of the time. Similarities and differences between the correlations for the 3 valence types are discussed. (auth)

46244 (TID–22207, Paper D) PREPARATION AND STRUCTURAL STUDY OF ABO_3 COMPOUNDS CONTAINING Cu AND Nb OR Ta. Shick, Larry; Vorres, Karl S. (Purdue Univ., Lafayette, Ind. Dept. of Chemistry). 11p.

Valence isomers of $CuTaO_3$ were prepared. The I-V valence combination was prepared from either CuO_2 or CuO and Ta_2O_5 in vacuum or an inert atmosphere at 970–1100°C. The II-IV compound was obtained by reaction in air. The II-IV compound has a perovskite structure with a = 3.75 Å. A range of composition gave a variable lattice constant. Analogous reactions provide the I-V isomer of $CuNbO_3$. Reactions in air yielded a material with an approximate formula of $CuNbO_{3.12}$. X-ray powder data and qualitative magnetic susceptibility data are given. (auth)

46245 (TID–22207, Paper E) THE PREPARATION AND STRUCTURAL STUDIES OF SOME CUPRIC RARE EARTH AB_2O_4 TYPE COMPOUNDS. Frushour, Robert H.; Vorres, Karl S. (Purdue Univ., Lafayette, Ind. Dept. of Chemistry). 10p.

Ignition of basic cupric carbonate with rare earth oxides in air at 1000°C for 24 hr produced AB_2O_4 compounds with La, Pr, Nd, Sm, Eu, Gd, but not with Ce, Tb, Dy, Ho, Er, Yb, or Y. Except for $CuLa_2O_4$, the AB_2O_4 compounds are apparently isostructural with $NiLa_2O_4$ and have the $K2NiF_4$ structure. The tetragonal space group is number 139, I4/mmm. Lattice constants for the Pr compound are a = 3.96 ± 0.01 and c = 12.23 ± 0.01. The structure of the La compound is more complex and was not determined. The other rare earths gave indications of very slow reactions. (P.C.H.)

46246 (TID–22207, Paper F) IONIC FIELD STRENGTHS AS CRITERIA FOR COMPOUND FORMATION IN OXIDE SYSTEMS. Vorres, Karl S. (Purdue Univ., Lafayette, Ind. Dept. of Chemistry). 4p.

A series of compounds was studied under varying conditions to permit conclusions concerning the validity and region of applicability of the ionic field strength (IFS) rule as proposed by Dietzel. The results indicated that the Dietzel criterion is useful for ionic type compounds such as the Li–rare earth oxide series. Extensions to systems beyond this would depend upon the availability of a lattice with a high degree of covalent bonding which would be more stable than the constituent oxides alone. Such lattices would allow compound formation where the difference in IFS value would indicate no reaction. (P.C.H.)

46247 (UCRL–16349) THE ANALYSIS OF THE NUCLEAR MAGNETIC RESONANCE SPECTRA OF FOUR-MEMBERED RING COMPOUNDS OF THE TYPE A_2B_4 USING BOTH COMPUTER AND DOUBLE-IRRADIATION TECHNIQUES [thesis]. Ferretti, James A. (Lawrence Radiation Lab., Univ. of California, Berkeley). Aug. 1965. Contract W-7405-eng-48. 135p. Dep. mn; CFSTI $4.00 cy, $1.00 mn.

The nuclear magnetic resonance spectra of a series of four-membered ring molecules were analyzed using both computer and double-irradiation techniques. The molecules, trimethylene oxide, trimethylene imine, trimethylene sulfide, and 1,1-dimethylcyclobutanedicarboxylate, were analyzed as A_2B_4 systems. The chemical shifts and vicinal and long range coupling constants were found to be quite normal. Current theories concerning substituent effects on geminal proton coupling constants are presented and the substitutive trends observed in the above series are interpreted in the light of these theories. The effects of bond hybridization on substituent effects were also found to be interpretable in terms of the theory. Nuclear magnetic double resonance spectra were observed both by sweeping the observing r-f field ν_1 and also by sweeping the perturbing field ν_2. When ν_1 is set on a non-degenerate transition frequency and ν_2 subsequently swept to perturb the other lines in the spectrum, intensity changes are observed when any transition which is perturbed by ν_2 has an energy level in common with the line being observed by ν_1. An intensity increase is observed when the energy levels are ordered in a progressive manner and a decrease in intensity is observed when the energy levels are ordered in a regressive manner. This procedure has been used to establish the ordering of the energy levels of the ABC system of protons in 2-chlorothiophene. Pulse experiments were carried out in order to gain a fuller understanding of the phenomena observed in the above double-resonance experiments. These experiments indicate that the observed phenomena are caused by population inversion due to adiabatic rapid passage. A detailed description of the field-frequency spectrometer constructed and used in the above work is presented. (auth)

46248 (FTD-TT–65-591) THERMAL STABILITY OF LITHIUM BOROHYDRIDE. Fedneva, E. M.; Alpatova, V. I.; Mikheeva, V. I. Translated from Zh. Neorgan. Khim., 9: 1519-20(1964). 6p. CFSTI.

A study was made of the behavior of lithium borohydride and its dioxanate up to 600°. The thermogram of lithium borohydride has three endothermic peaks: the peak at 108-112°C apparently is due to a polymorphous conversion, the next peak at 268-286°C is due to melting, and the peak at 480°C is unexplained. Gas liberation begins above 380°C. The dioxanate loses a molecule of dioxane at 85°C with simultaneous H_2 liberation, which becomes more intense above 400°C. It is concluded that the dioxanate is less stable than lithium borohydride. (D.L.C.)

46249 (LA-tr–65-15) THE TERNARY DIAGRAM—URANIUM–URANIUM DIOXIDE–URANIUM OXYCARBIDE. Besson, J.; Blum, P. L.; Morlevat, J.-P. Translated by C. P. Kempter and Gretchen R. Riese (Los Alamos Scientific Lab., N. Mex.) from Compt. Rend., 260: 3390-2 (Mar. 22, 1965). 4p. Dep. mn; JCL $1.00 fs, $0.80 mf.

The U–UO_2–UC area of the ternary U–C–O diagram is described. The different areas constituting the liquidus and the solidus are indicated. The phases obtained after quenching were characterized and determined by chemical and x-ray crystallographic analysis. In this way the paths of crystallization of various ternary liquids were determined. (P.C.H.)

46250 (ORNL-tr–623) ON THE STATE OF SOLUTION OF HYDROGEN IN PALLADIUM AND HYDROGENATION CATALYSIS. Franck, J. Translated for Oak Ridge National Lab., Tenn. from Nachr. Ges. Wiss. Goettingen, Math.-Physik. Kl., 293-6(1933). 6p. Dep. mn; JCL $1.10 fs, $0.80 mf.

Theories on the absorption of hydrogen by palladium are discussed. One theory considers the value of ϕ^+ (desired value for work of extraction of an electron from the metal), which is more than twice the value of ϕ_ϵ (the work of extraction of an electron from the metal). The apparent exceptional position of Pd, which consists of the fact that Pd is capable of absorbing such large quantities of hydrogen, is also considered. It was concluded that a particularly strong cloud formation about each proton should take place due to the high concentration of free electrons, while the cloud formation of protons about electrons, in contrast, is practically negligible. (P.C.H.)

46251 (ORNL-tr–673) ACTION OF CALCIUM CARBIDE ON ALKALINE EARTH CHLORIDES AND FLUORIDES. Bernard, Maurice. Translated by Martha Gerrard and J. J. Pinajian (Oak Ridge National Lab., Tenn.) from Compt. Rend., 221: 296-8(1945). 4p. Dep. mn; JCL $1.10 fs, $0.80 mf.

The reduction reactions of CaC_2 with $BaCl_2$ and $SrCl_2$ are limited by the volatility of the halides. In order to increase the yields, BaF_2 and SrF_2 were substituted for the chlorides; the yield of Ba was increased from 30 to 50% in this way. (D.L.C.)

46252 (ORNL-tr-683) REDUCTION OF ALKALINE EARTH OXIDES WITH ALUMINUM CARBIDE. Bornazyan, A. S.; Darbinyan, M. V. Translated by S. J. Rimshaw and W. D. Box (Oak Ridge National Lab., Tenn.) from Izv. Akad. Nauk Arm. SSSR, Khim. Nauk, 15: No. 1, 25-32(1962). 11p. Dep. mn; CFSTI $1.00 cy, $0.50 mn; JCL $1.60 fs, $0.80 mf.

The reduction of barium and strontium oxides by aluminum carbide was investigated. An aluminate and free carbon are formed in the residue. The free carbon reacts with metal vapor to form the corresponding carbide. Secondary reactions between metal carbide and metal oxide with the evolution of additional amounts of metal and CO begin to occur when the main reaction slows down. Addition of CaF_2 to the mixture significantly accelerated the metal reduction but calcium was found in the condensate as a contaminant. Therefore, it is convenient to use a fluoride of the metal (SrF_2 or BaF_2) being reduced as a catalyzing agent. On using pure SrO or BaO and Al_4C_3 as the reducing agent, the purity of the metal was about the same as the purity of the metal obtained by the aluminothermal reduction. (P.C.H.)

46253 (ORNL-tr-803) PROCESS FOR PREPARING VARIOUS METALS SUCH AS MAGNESIUM BY TREATMENT OF THEIR SALTS WITH ACTIVATED NASCENT HYDROGEN. Delevey, Alfred. Translated by Martha Gerrard (Oak Ridge National Lab., Tenn.) from French Patent 1,199,687, June 16, 1958. 3p. Dep. mn; JCL $1.10 fs, $0.80 mf.

A process is described for preparing various metals, such as Mg, Ca, Ba, or Sr, by treating their salts with a current of catalytic nascent hydrogen, activated in place by a catalyst such as reduced Ni, Co, V, or Cu; molybdenum sulfide; or a mixture of these materials. The sequence of operations by which pure Mg is obtained from anhydrous magnesium sulfate is given as an example of the process. (P.C.H.)

46254 REFRACTOMETRIC STUDY OF THE FORMATION OF COMPLEX NEODYMIUM HALIDES IN AQUEOUS SOLUTION. Spacu, P.; Dragomir, Eugenia; Albescu, Ileana (Centrul de Cercetari Chimice, Academica R.P.R., Bucharest). Acad. Rep. Populare Romine, Studii Cercetari Chim., 11: 277-86(1963). (In Rumanian).

The refractive index vs molarity data for aqueous solutions of $NdCl_3$ were measured and are reported in graphical and tabular form. Similar data are also reported for mixtures of $NdCl_3$ with NaCl, KCl, and CsCl in which the sum of the molarities remained constant at about 1M. Deviations from ideal behavior in the partial refractive indexes indicated the formation of new species. These include $Na_3(NdCl_6)$, $Na_2(NdCl_5)$, $Na(NdCl_4)$, $K(NdCl_4)$, $Cs(NdCl_4)$, and $Cs_3(NdCl_6)$. Experimental data for the refractive index of aqueous $NdBr_3$ are also given in tabular and graphical form. Mixtures of $NdBr_3$ with NaBr and KBr were studied; in solutions where the sum of the molarities equaled 0.5M, no compound formation could be detected. The most stable combination was $M(NdCl_4)$. The data indicated the general tendency for Cl to form more stable complexes than Br. (BBB)

46255 THE CRYSTAL STRUCTURE OF BISNITRATODIAQUODIOXOURANIUM(VI) TETRAHYDRATE (URANYL NITRATE HEXAHYDRATE). Hall, D.; Rae, A. D.; Waters, T. N. (Univ. of Auckland, New Zealand). Acta Cryst., 19: 389-95(Sept. 10, 1965).

The crystal structure of uranyl nitrate hexahydrate was refined in three dimensions. The uranium atom 8-coordinate, with the two nitrate ions (as bidentate ligands) and the two water molecules coordinated in the plane perpendicular to the uranyl group. The molecule is involved with the water of crystallization in an extensive hydrogen-bonding system, which apparently causes some distortion from the ideal molecular shape. (auth)

46256 DETERMINATION OF THE CRYSTAL STRUCTURE OF YTTRIUM ORTHOFERRITE AND REFINEMENT OF GADOLINIUM ORTHOFERRITE. Coppens, P.; Eibschuetz, M. (Weizmann Inst. of Science, Rehovoth, Israel). Acta Cryst., 19: 524-31(Oct. 10, 1965).

The crystal structure of yttrium orthoferrite was determined from full three-dimensional counter data and refined in the space group Pbnm by least squares to an accuracy of about 0.001 and 0.01 Å in the positional parameters of Y^{3+} and O^{2-}, respectively. The parameters were compared with those of $GdFeO_3$, derived by least-squares refinement of Geller's intensity data. It was found that the distortions from the ideal perovskite lattice hardly affect the octahedral environment of the Fe^{3+} ion, which makes it possible to predict $Fe^{3+}-O^{2-}-Fe^{3+}$ angles in other distorted perovskite structures of known cell dimensions. Refinement in the alternative noncentrosymmetric space group $Pbn2_1$, showed small, possible real, deviations from a centric structure. (auth)

46257 A NEUTRON DIFFRACTION STUDY OF URANYL NITRATE HEXAHYDRATE. Taylor, J. C.; Mueller, M. H. (Argonne National Lab., Ill.). Acta Cryst., 19: 536-43(Oct. 10, 1965).

The crystal structure of uranyl nitrate hexahydrate was determined by neutron diffraction. The structure is orthorhombic with $a = 13.197 \pm 0.003$, $b = 8.035 \pm 0.002$, and $c = 11.467 \pm 0.003$ Å, space group $Cmc2_1$. Intensities of 1136 independent reflections with a $2\theta < 105°$ were obtained with $\lambda = 1.065$ Å. The structure was solved from the three-dimensional neutron Patterson and Fourier syntheses, and refined by a full-matrix least squares, using a statistical weighting scheme. The final weighted R index was 3.9%. The uranyl group is surrounded equatorially by a near-planar oxygen hexagon of four oxygen atoms from two nonequivalent bidentate nitrate groups and two equivalent water oxygens. In the nitrate groups, the N–O bonds involving coordinated oxygens are 0.03 to 0.05 Å longer than the N–O bonds involving the noncoordinated oxygen atoms; also the O–N–O angles differ significantly from 120°. All hydrogens are involved in hydrogen bonding and these may be divided into (a) O (water) – O(water) hydrogen bonds of length 2.68 to 2.75 Å and (b) weaker O (water) – O (nitrate) hydrogen bonds of length 2.93 and 2.99 Å. The water molecules associate into sheets perpendicular to the a axis. (auth)

46258 THE CRYSTAL STRUCTURE OF ScB_2C_2. Smith, Gordon S.; Johnson, Quintin; Nordine, Paul C. (Univ. of California, Livermore). Acta Cryst., 19: 668-73(Oct. 10, 1965). (UCRL-12246).

A compound of synthetic composition ScB_2C_2 was prepared, and its crystal structure was established by x-ray diffraction procedures. The presence of graphite lines in powder patterns of this material as well as small variations in lattice constants from preparations on the boron-poor side of ScB_2C_2 indicated some amount of compositional variation. Crystals are orthorhombic with space group Pbam. Lattice constants for the particular crystal used are $a = 5.175 \pm 0.005$, $b = 10.075 \pm 0.007$, and $c = 3.440 \pm 0.005$ Å. A feature of the structure is the incorporation of boron and carbon into nets of aromatic-like five- and seven-membered rings. The scandium atoms lie between the seven-membered rings of adjacent layers. In addition to these 14 light atoms, each Sc is surrounded by 5 other Sc atoms at distances that are nearly the same as in metallic scandium. (auth)

46259 THE CRYSTAL STRUCTURES OF SYNTHETIC ANHYDROUS CARNOTITE, $K_2(UO_2)_2V_2O_8$, AND ITS CESIUM ANALOGUE, $Cs_2(UO_2)_2V_2O_8$. Appleman, Daniel E.; Evans, Howard T. Jr. (Geological Survey, Washington, D. C.). Am. Mineralogist, 50: 825-42(July–Aug. 1965).

The crystal structures of synthetic anhydrous carnotite, $K_2(UO_2)_2V_2O_8$ and its cesium analogue, $Cs_2(UO_2)_2V_2O_8$ were determined, and the latter was refined by Fourier and least-squares techniques to a final R-factor of 0.096 for the 837 observed nonzero reflections. The structures contain tightly bonded sheets made up of uranium and vanadium

coordination polyhedra sharing edges. The sheets, which extend parallel to (001), are held together by bonds from oxygen atoms to the interlayer K^+ or Cs^+ cations. In the cesium compound the linear, symmetrical uranyl ion, with a U-O distance of 1.77 ± 0.06 Å, is coordinated by five oxygen atoms in the form of a plane pentagon, at an average U-O distance of 2.32 Å. The vanadium atom is coordinated by five oxygen atoms in the form of a square pyramid, with V-O distances ranging from 1.71 to 1.97 Å. Two such pyramids share an edge of the base, their apices pointing in opposite directions, to form divanadate groups, V_2O_8. The interlayer bonding consists of eleven Cs-O bonds, with an average length of 3.32 Å, five to one layer and six to the adjacent layer. (auth)

46260 REVERSIBLE AND IRREVERSIBLE PROCESSES IN THE DROPPING-MERCURY ELECTRODE. XIX. URANYL. Sancho, J.; Vidal-Abarca, J. B. Anales Real Soc. Espan. Fis. Quim. (Madrid), Ser. B, 61: 843-8(June 1965). (In Spanish).

The polarographic reduction of uranyl ion was studied in support solutions of $KClO_3$, $KBrO_3$, and KIO_3. (auth)

46261 MEASUREMENT OF DIFFUSION COEFFICIENTS. III. Ce^{3+} AND Pm^{3+} IONS. Sancho, J.; Vidal-Abarca, Juan B.; del Valle, A. Anales Real Soc. Espan. Fis. Quim. (Madrid), Ser. B, 61: 849-51(June 1965). (In Spanish).

By means of capillary techniques the diffusion coefficients of the Ce^{3+} and Pm^{3+} ions in LiCl solutions were measured. The influence of temperature in the 25 to 45°C range was studied. (auth)

46262 DISSOCIATION OF METHYLAMINE MOLECULE IONS FORMED IN CHARGE EXCHANGE COLLISIONS WITH POSITIVE IONS. Sjoegren, H. Arkiv Fysik, 29: 565-72(1965).

Mass spectra of methylamine were obtained after charge exchange with slow positive ions, and the intensities of the peaks were plotted as a function of the energy absorbed by the molecule during the charge exchange. The curves were integrated to give the electron impact mass spectrum, which was compared with experimental values. A region with low probability for ionization seemed to exist between 11 and 12 ev. The structure and dissociation of methylamine are discussed. (auth)

46263 ON THE TRIPLET BANDS OF ND. Kopp, Ingvar; Kronekvist, Mona; Aslund, Nils. Arkiv Fysik, 30: 9-17(1965).

The emission spectrum of ND was generated by pumping heavy ammonia through a water-cooled hollow cathode. Fourth order spectrograms of the region from 2900 to 3600 Å were photographed in a 10.685-meter concave grating spectrograph. The 0–0 and 1–1 bands of the $A^3\Pi - X^3\Sigma^-$ transition were studied. As no satellite branches were observed, the spin splittings of the $^3\Sigma^-$ state could not be obtained directly. A mathematical model of a $^3\Sigma^-$ state was fitted to the term values of the three spin substates. It was not possible to settle a definite numbering of the main Q branches. As a consequence no complete treatment of the $A^3\Pi$ state was carried out. A digital computer was used for the calculations. (auth)

46264 CONCENTRATION AND TEMPERATURE DEPENDENCE OF ISOTOPE EFFECTS IN THE ION MIGRATION OF LITHIUM IN ACETIC ACID SOLUTION. PART V. ON COUNTERCURRENT ELECTROLYSIS. Behne, Von D.; Wagener, K. (Hahn-Meitner-Institut fuer Kernforschung, Berlin). Ber. Bunsenges. Physik. Chem., 69: 378-82 (1965). (In German).

Experimental results are reported for the dependence of the isotope effect on concentration and temperature noted in the migration of lithium ions in n/2 acetic acid. The isotope effects were determined from the stationary degree of separation, attained by a countercurrent electrolysis process. The method was based on relative measurements. For each run the separative tube was calibrated by a Rb–Cs separation. For this purpose the difference of ion mobility for Rb^+ and Cs^+ was determined in the range from 5 to 55°C, for concentrations from 0 to 0.1 molal. The isotope effect in the migration of lithium ions showed only a very small temperature dependence, but an unexpectedly large dependence on the concentration of Li-acetate in the solution was noted. In very dilute solutions the isotope effect was 3.8‰, in 0.056 normal solution 18.6‰. It was supposed that this large increase was caused by an isotope effect in the dissociation equilibrium of the Li acetate. In this case a maximum of the isotope effect is to be expected in about 0.5 normal acetate solution. (auth)

46265 ON THE INTERCALATION OF BASE METALS IN GRAPHITE AS WELL AS IN METAL CHALCOGENIDES OF THE TYPE MeX_2. Ruedorff, Walter (Univ., Tuebingen, Ger.). Chimia (Aarau), 19: 489-99(Sept. 1965). (In German).

Under suitable conditions, strongly electropositive metals, such as the alkali metals, the alkaline earth metals, including beryllium and magnesium, as well as aluminum, europium, and trivalent rare earth metals form intercalation compounds in the carbon planes of the graphite lattice. The preparation, properties, magnetic behavior, structure, and the nature of bonding in these compounds is discussed. Metal sulfides and selenides (MeX_2), which possess a conduction band, react like graphite with metals, if they are dissolved in liquid ammonia, to form non-stoichiometric intercalation compounds. Their magnetic behavior indicates that, while these compounds have metallic character, there is also a transition toward the formation of ionic sulfur and selenide compounds, as shown by the titanium, vanadium, and chromium compounds. (auth)

46266 ISOTOPIC EXCHANGE BETWEEN MOLECULAR OXYGEN AND THE OXIDES OF THE RARE EARTH ELEMENTS. Minachev, Kh. M.; Antoshin, G. V. (Inst. of Organic Chemistry, Academy of Sciences, USSR). Dokl. Akad. Nauk SSSR, 161: 122-4(Mar. 1, 1965). (In Russian).

Because of the interest in the rare earth oxides as oxidation catalysts, the mobility of their oxygen was studied by determining the rate of its exchange with gaseous oxygen enriched in ^{18}O. The kinetic data showed a periodic change in the apparent activation energy in going from La_2O_3 to Lu_2O_3. Data on the effect of aging in oxygen and in a vacuum showed that the mobility of the oxide oxygen increased with removal of part of the oxygen from the oxide surface layer. In the lanthanum oxides the mobility appeared to depend on the presence of a variable valence (the ability to form nonstoichiometric oxides). The oxides whose magnetic susceptibility was closest to maximum had the greatest mobility. The minimum apparent activation energy in the exchange with oxygen was that of Sm_2O_3, and the oxides of the cerium subgroup showed lower values than the ytterbium subgroup. The periodicity of the properties is considered related to the electron structure of the rare earth elements. The data do not agree entirely with magnetic susceptibility data, but the ability of the oxide oxygen to exchange is also related to the conductivity, lattice parameters, particle size, etc. (TTT)

46267 SOLID-PHASE REACTIONS IN THE DECOMPOSITION OF ZIRCONIUM SILICATE BY CALCIUM OXIDE. Chukhlantsev, V. G.; Galkin, Yu. M. (Ural Polytechnical Inst., USSR). Dokl. Akad. Nauk SSSR, 161: 171-4 (Mar. 1, 1965). (In Russian).

Data were tabulated for the reaction of $ZrSiO_4$ with CaO at 1300°C for 50 hr, at 1200°C for 70 hr, and at 1100°C for 120 hr. Both chemical and x-ray analyses of the reaction products formed at the several times and temperatures indicated formation of calcium zirconate and metasilicate. The products identified were $CaZrO_3$, ZrO_2, $Ca_2Si_2O_7$, Ca_3SiO_5, Ca_2SiO_4, $CaSiO_3$, $Ca_3ZrSi_2O_9$, and $CaZrSi_4O_{12}$. The $CaZrSiO_5$ product reported elsewhere was not found. A simplified diagram of the reactions taking place is presented. The experiments were made on powdered materials that were carefully mixed and compressed into tablets at 7 tons/cm². The tablets were heated in a furnace in which the temperature was controlled within 10°C. (TTT)

46268 VOLTAMMETRIC STUDIES OF Eu(III) IN FORMATE BUFFER. THE FORMAL POTENTIAL OF THE Eu(III)–Eu(II) SYSTEM. Macero, Daniel J.; Anderson, Larry B.; Malachesky, Paul (Syracuse Univ., N. Y.). J. Electroanal. Chem., 10: 76-81(July 1965).

Polarographic and chronopotentiometric evidence for the formation of the Eu formate complexes, $Eu(HCOO)^{2+}$ and $Eu(HCOO)_2+$, is given. Values for the corresponding step stability constants were estimated to be 20 and 120, respectively. The effect of such formate complexes on the original determination of the formal potential of the Eu(III) – Eu(II) couple by McCoy (J. Am. Chem. Soc., 58: (1963)) is discussed. The conclusion is that McCoy's result is in error by approximately 70 mv and that the value of −0.35 v vs. N.H.E. is more realistic for the non-complexed system. (auth)

46269 ON THE LUMINESCENT PROPERTIES OF SOME RARE EARTH IONS IN ZINC BORATE AS A HOST. Brixner, L. H. (E. I. du Pont de Nemours and Co., Wilmington, Del.). J. Electrochem Soc., 112: 984-8(Oct. 1965).

Zinc borate, ZnB_2O_4, melting at 1000°C, forms a glass of high optical perfection, which can be cast readily or pulled into almost any shape. Rare earths can be introduced in the cation sites with compensation by Na^{1+} to give glasses of the generic formula $Ln_xNa_xZn_{1-2x}B_2O_4$. The rare earths Sm^{3+}, Eu^{3+}, Tb^{3+}, Dy^{3+}, and Tm^{3+}, all emitting in the visible region, were introduced into zinc borate and emission spectra as well as the optimum x for fluorescent emission were determined. For a rod of the composition $Nd_{0.02}Na_{0.02}Zn_{0.96}B_2O_4$, stimulated emission was observed at room temperature with a threshold of 1500 joules. Rods containing the optimum concentration of Eu^{3+} and Tb^{3+} did not show laser action. (auth)

46270 AN ALL-METAL CELL TECHNIQUE FOR THE MEASUREMENT OF THE EMF OF MOLTEN METAL-METAL HALIDE SOLUTIONS CORROSIVE TO CERAMICS. Bronstein, Harry R. (Oak Ridge National Lab., Tenn.). J. Electrochem. Soc., 112: 1032-40(Oct. 1965). (ORNL-P-1189).

A technique is described, which permits the measurement of emf using an all-metal cell. The applicability of the method to both aqueous systems and molten metal-metal halide systems is demonstrated. This technique will permit measurements of the emf of systems such as the molten alkaline earth-alkaline earth halides and the rare earth-rare earth halides, which are extremely corrosive to ceramics. (auth)

46271 THE THERMAL DECOMPOSITION OF RARE EARTH AND YTTRIUM BROMIDE HYDRATES. Mayer, I.; Zolotov, S. (Hebrew Univ., Jerusalem). J. Inorg. Nucl. Chem., 27: 1905-9(Sept. 1965).

The thermal decomposition of rare earth and yttrium bromide hydrates was studied by the thermogravimetric method. Two groups of reactions were found. The first was $MBr_3 \cdot 6H_2O \rightarrow MBr_3 \cdot H_2O \rightarrow MBr_3 \rightarrow MOBr \rightarrow M_2O_3$. The bromides of Pr to Eu belong to this group. Neither lanthanum nor cerium gave the monohydrate, and cerium did not give the oxybromide. The second was $MBr_3 \cdot 6H_2O \rightarrow (MBr_3 + MOBr) \rightarrow MOBr \rightarrow M_2O_3$. The bromides from Gd to Lu belong to this group. The minimum temperature for oxybromide formation was 350 to 550°C. (auth)

46272 THE PREPARATION AND PROPERTIES OF $TiUO_5$. Marshall, R. H.; Hoekstra, H. R. (Argonne National Lab., Ill.). J. Inorg. Nucl. Chem., 27: 1947-50 (Sept. 1965).

A compound of tetravalent titanium and hexavalent uranium with the formula $TiUO_5$ was synthesized. Two preparative methods are described. The compound is stable to 950°C; loss of oxygen and disproportionation to TiO_2 and U_3O_8 occur above this temperature. X-ray and infrared data for $TiUO_5$ are given. (auth)

46273 PREPARATION OF A NEW TYPE OF NON-STOICHIOMETRIC RARE-EARTH OXIDE. Miller, A. E.; Daane, A. H. (Ames Lab., Ames, Iowa). J. Inorg. Nucl. Chem., 27: 1955-60(Sept. 1965). (IS–1118).

Previously unreported partially reduced rare earth oxides of the type REO_x, $1.450 < x < 1.500$, were prepared by vacuum melting the normal rare earth sesquioxides, RE_2O_3, and by codistilling and comelting the rare earth metals with their respective sesquioxides. The oxygen-to-metal ratio of these materials was determined from the weight gained on reoxidation to the sesquioxide, $REO_{1.500}$. The nature of these materials was explored through x-ray diffraction and density measurements of the cubic (C-type) forms of $GdO_{1.485}$, $YO_{1.491}$, $ErO_{1.489}$, and $LuO_{1.485}$. The x-ray and density data showed that the nonstoichiometry obtained in the partially reduced rare earth sesquioxides could be attributed entirely to the loss of oxygen from the lattice. The loss of oxygen resulted in the formation of vacancies, which greatly affected the properties of these materials. (auth)

46274 THE EFFECT OF LABELLING ON THE SOLUBILITIES OF CRYSTALLINE SUBSTANCES. Bovington, C. H. (Rutherford High Energy Lab., Swindon, Eng.). J. Inorg. Nucl. Chem., 27: 1975-9(Sept. 1965).

The solubilities of $PbSO_4$ and $BaSO_4$ labeled with ^{35}S were measured. In the case of $BaSO_4$ indirect determinations of the solubility were made from kinetic data. $BaSO_4$ showed a 10% increase in solubility over accepted values for inactive material, but $PbSO_4$ showed the same solubility as the inactive material. The measured solubilities were independent of specific activity. Electron microscopic examination of labeled and inactive crystals of $BaSO_4$ and $PbSO_4$ showed what appeared to be radiation damage in the active $BaSO_4$ producing a highly active surface, which may result in increased solubility. (auth)

46275 AN INVERSE DEUTERIUM ISOTOPE EFFECT IN THE DECOMPOSITION OF PERMANGANATE IN ALKALI SOLUTION. Heckner, K. H.; Landsberg, R. (Humboldt-Universitaet, Berlin). J. Inorg. Nucl. Chem., 27: 2037-47 (Sept. 1965). (In German).

Experiment showed that under identical conditions the rate of decomposition of permanganate proceeds more rapidly in KOD than in KOH. The concentration of D_2O was measured by means of the refractive index using the immersion refractometer. The inverse isotope effect [$\alpha = (k_D/k_H) > 1$] was largest in alkaline solutions of low concentration and decreased with rising hydroxide content. This supports the mechanism of reaction proposed in former communications: $MnO_4^- + OH^- \rightleftharpoons MnO_4^{2-} + \cdot OH$ and $OH^- + \cdot OH \rightarrow \cdot O^- + H_2O$. The resultant isotope effect was a product of a kinetic and a thermodynamic isotope effect which counteracted one another. The predominating thermodynamic effect was a result of the stability of the OD radicals, which was higher than that of the OH radicals. The thermodynamic isotope effect of the preceding equilibrium and the kinetic isotope effect relating to the subsequent reaction were theoretically estimated making simplifying assumptions. A comparison with experiment was made. The nonlinear dependence of the isotope effect on the deuterium content of the water was due to the equilibria $H_2O + OD^- = HDO + OH^-$, $HDO + OD^- = D_2O + OH^-$ the constants of which could be calculated from the deviation from linearity. (auth)

46276 THE TERNARY SYSTEM $Li_3(Nb,Sb,Ta)O_4$. Blasse, G. (Philips' Gloeilampenfabrieken, N. V.; Eindhoven, Netherlands). J. Inorg. Nucl. Chem., 27: 2117-19 (Sept. 1965).

Solid solutions between Li_3NbO_4, Li_3SbO_4, and Li_3TaO_4 were studied. X-ray powder diagrams were obtained and the ternary phase diagram is shown. (M.C.G.)

46277 THE EFFECTS OF SEVERAL DICARBOXYLIC ACIDS ON THE RATE OF THE REACTION BETWEEN URANIUM(IV) AND THALLIUM(III) IN AQUEOUS PERCHLORIC ACID SOLUTIONS. Quinn, L. P.; Love, C. M.; Brubaker, C. H. Jr. (Michigan State Univ., East Lansing). J. Inorg. Nucl. Chem., 27: 2119-21(Sept. 1965). (COO–1001-3).

The effects of fumaric, maleic, malic, malonic, oxalic, and succinic acids on the rate of the reaction between uranium (IV) and thallium (III) in perchloric acid were

studied. The addition of oxalic and succinic acids resulted in decreasing rates of reaction. Some acceleration of the rate was observed in the presence of the other acids. (M.C.G.)

46278 MASS TRANSPORT AND GRAIN GROWTH INDUCED BY FISSION FRAGMENTS IN THIN FILMS OF URANIUM DIOXIDE. Rogers, M. D. (Atomic Energy Research Establishment, Harwell, Eng.). J. Nucl. Mater., 16: 298-305(July 1965). (AERE-R-4793).

When fission fragments leave the surface of vacuum-deposited uranium dioxide both the rate of ejection of atoms and the nature of material collected differ considerably from those observed using solid uranium metal. The differences are explained in terms of thermal rods, vaporization, and grain growth as opposed to displacement spikes, ejection of discrete particles, and dynamic equilibrium for uranium metal. (auth)

46279 THE HEATS OF FORMATION OF BERYLLIUM COMPOUNDS. I. BERYLLIUM HYDROXIDES. Bear, I. J.; Turnbull, A. G. (Commonwealth Scientific and Industrial Research Organization, Melbourne). J. Phys. Chem., 69: 2828-33(Sept. 1965).

The heats of solution of ultrapure beryllium metal and of α- and β-beryllium hydroxides in aqueous HF were measured calorimetrically to find $\Delta H^0_{f298}[\alpha\text{-Be(OH)}_2] = -215.75 \pm 0.5$ kcal/mole and $\Delta H^0_{f298}[\beta\text{-Be(OH)}_2] = -216.5 \pm 0.5$ kcal/mole. From the heat of precipitation from beryllium sulfate solution $\Delta H^0_{f298}[\text{Be(OH)}_{2ppt.}]$ was found to equal -213.1 ± 0.6 kcal/mole. Entropies and free energies of the three hydroxides were also estimated and the free energies of several aqueous beryllium ions evaluated. (auth)

46280 EXCHANGE OF DEUTERIUM WITH THE HYDROXYL GROUPS OF ALUMINA. Carter, J. L.; Lucchesi, P. J.; Corneil, P.; Yates, D. J. C.; Sinfelt, J. H. (Esso Research and Engineering Co., Linden, N. J.). J. Phys. Chem., 69: 3070-4(Sept. 1965).

The kinetics of the exchange of deuterium with the surface hydroxyl groups of alumina were studied by infrared spectroscopy. It was observed that the reactivity of the different hydroxyl groups with deuterium varied. Of the three hydroxyl groups present (at 3785, 3740, and 3710 cm^{-1}), the high-frequency one was found to be the most reactive. The kinetics of the exchange obeyed a logarithmic rate law similar to that observed frequently for chemisorption processes. The kinetics may be a consequence of surface heterogeneity. It was observed that the presence of platinum on the surface of the alumina increased the rate of exchange. However, the effect depended on the method of impregnation of the platinum, probably due to the presence or absence of halogen in the platinum salt used for the impregnation. A study of the effect of platinum concentration for samples prepared by impregnation with chloroplatinic acid yielded complex results, which may largely be a consequence of the presence of chlorine in the samples. Some evidence was obtained for a direct reaction (other than exchange) of deuterium with alumina at certain conditions. (auth)

46281 ELECTROKINETIC PHENOMENA AT THE THORIUM OXIDE-AQUEOUS SOLUTION INTERFACE. Holmes, H. F.; Shoup, Charles S. Jr.; Secoy, C. H. (Oak Ridge National Lab., Tenn.). J. Phys. Chem., 69: 3148-55(Sept. 1965). (ORNL-P-1192).

Electrokinetic effects of aqueous solutions in porous plugs of thorium oxide were investigated from the standpoint of irreversible thermodynamics. A kinetic electroosmotic technique was used to determine the electrokinetic potential. This method gave results in agreement with streaming potential data except in the presence of acidic solutions. The cell constant for bulk electrical conductance was observed, in some cases, to be dependent on the nature of the electrolyte within the plugs. Despite variations in cell constants, the measured surface conductances of several plugs and capillaries of thorium oxide could be interpreted in terms of the specific surface conductivity. The specific surface conductivities were much larger than those predicted from the classical theory of surface conductance. The mechanism of surface conductivity in this system was ascribed to the conductivity of ionizable surface hydroxyl groups. (auth)

46282 REVISED THERMODYNAMIC PROPERTIES OF AQUEOUS STRONTIUM ION. Noyes, Richard M. (Univ. of Oregon, Eugene; Max-Planck Institut fuer Physikalische Chemie, Goettingen, Ger.). J. Phys. Chem., 69: 3181-2 (Sept. 1965).

Thermodynamics of hydration of aqueous strontium ions were studied. Examination revealed that an anomaly in the entropy previously observed arose from a mistake in a listed value for the free energy of formation of strontium vapor. The values given were 39.2, 26.3 kcal/mole, and 39.325 cal/mole for ΔH^0_f, ΔF^0_f, and S^0, respectively, for strontium vapor at 1 atm fugacity and 25°C. The entropy of the crystalline standard state at the same temperature is 13.0 cal/mole. Use of 31.2 kcal/mole as the free energy value changed significantly the estimated thermodynamic properties. (F.J.H.)

46283 λ-TYPE THERMAL ANOMALY IN TETRAURANIUM ENNEAOXIDE AT 348°K. Westrum, Edgar F. Jr. (Univ. of Michigan, Ann Arbor); Takahashi, Yoichi; Groenvold, Fredrik. J. Phys. Chem., 69: 3192-6(Sept. 1965).

Heat capacity measurements were made on U_4O_9. The curvature corrected data obtained are presented in terms of the defined thermochemical calorie of 4.1840 joules and in chronological sequence. A λ-type thermal anomaly with a peak near 348°K is shown. The structure of U_4O_9 is related to the fluorite-type structure of UO_2, but with interstitial oxygen atoms. In the zeroth approximation, the extra oxygen atom in U_4O_9 may either be in a fixed position or randomly distributed over four positions, which for $UO_{2.25}$, would lead to an entropy increment of $\frac{1}{4}R \ln 4$ or 0.68 cal/(gfm°K). The thermal effect may be somewhat broadened by radiation damage to the sample accumulated over a 10-yr period at room temperature. (F.J.H.)

46284 A STUDY OF THE VALENCE ELECTRON APPROXIMATION: APPLICATION TO LiH. Stuart, J. D. (Johns Hopkins Univ., Silver Spring, Md.); Hurst, R. P. Mol. Phys., 9: 265-70(1965).

Using the valence bond approach and a six-term wave function, valence electron calculations are made of the energy and dipole moment of lithium hydride. Comparisons are then made with previous two- and with four-electron results. It is found that reasonable agreement with four-electron calculations of the dipole moment is obtained when the valence orbitals are made orthogonal to the orbitals of the neglected lithium inner shell 1s electrons and that an approximate variational theorem for the energy is then valid. On the other hand, when valence orbitals are not required to be orthogonal to the inner shell an energy lower than the "experimental" energy can be obtained and the computed dipole moment is in poor agreement with the computed four-electron moment and with the experimentally determined moment. Finally, as with four-electron calculations, hybridization with the 2p covalent structure is necessary to give a reasonable dipole moment. (auth)

46285 ^{59}Co SPIN-SPIN COUPLING AND ISOTOPE SHIFTS IN $K_3Co(CN)_6$. Loewenstein, A.; Shporer, M. (Israel Inst. of Tech., Haifa). Mol. Phys., 9: 293-4(1965).

The nuclear magnetic resonance spectrum of ^{59}Co was measured in an aqueous solution of $K_3Co(CN)_6$ prepared from KCN enriched to 15 at. % with ^{13}C. The fractions of zero-, mono-, di-, and tri-substituted complexes are 0.377, 0.400, 0.176, and 0.041, respectively. The measurements were performed at two constant frequencies: 4.3 and 14.1 Mc (^{59}Co frequency is 10.1 Mc at 10 kA). The results are shown and the measured data are tabulated. (L.B.S.)

46286 DETERMINATION OF THE ENERGY GAP OF LiD BY SMALL-ANGLE COMPTON SCATTERING. Alex-

andropoulos, N. G.; Alexopoulos, K. D. (Univ. of Athens). Phys. Rev., 140: A597-601(Oct. 18, 1965).

X rays incoherently scattered by electrons at angles of a few degrees transfer energies to them which amount to only a few ev. If the electrons have binding energies of the same order of magnitude, interesting effects are expected which will change the usual form of the Compton spectrum. Theoretical considerations show that in the case of a conductor the spectrum starts from the position of the primary line with the form of a straight line and continues as an inverse parabola. In the case of an insulator the spectrum shows an abrupt limit on the side towards the primary radiation. The energy transfer corresponding to the edge is equal to the energy gap. Experiments are described which allow the determination of the energy gap of LiD by this method. Cu $K\beta$ rays scattered by polycrystalline LiD at 18° were analyzed in a spectrometer employing a Soller slit and a (22$\bar{4}$3) quartz crystal as an analyzer. At this scattering angle the intense diffraction peaks are avoided so that the spectrum of the scattered radiation consists only of thermal diffuse scattering and Compton scattering. By comparing it with the spectrum produced in copper by fluorescence, the two components were separated. The experiment was then repeated with metallic lithium, in which the Compton component starts exactly at the wavelength of the primary radiation. The two Compton profiles show a shift which is put equal to the energy gap. The resulting value is 5.4 ± 0.8 ev. (auth)

46287 PROTON SPIN-LATTICE RELAXATION IN SOLUTIONS OF HYDROGEN CHLORIDE AND DEUTERIUM CHLORIDE. Krynicki, K.; Powles, J. G. (Univ. of Kent, Canterbury, Eng.). Proc. Phys. Soc. (London), 86: 549-60 (Sept. 1965).

Proton spin-lattice relaxation times T_1 for anhydrous solutions of hydrogen chloride and deuterium chloride were measured at 20.8 Mc by a 90°–τ–90° pulse method. The measurements were made, for most solutions, from the supercooled liquid (–116°C) up to the liquid-vapour critical temperature (51.4°C) and a little above. These T_1 results for the HCl–DCl liquid solutions have provided direct evidence of the significant part played by the spin-rotation interaction mechanism of relaxation in liquid HCl and have allowed a detailed analysis. The correlation times for the dipole-dipole intramolecular interaction τ_d and the spin-rotation interaction τ_{sr} were determined independently and shown to vary in the opposite way with temperature. The product $\tau_d\tau_{sr}$ was found to be almost independent of temperature and approximately six times greater than a theoretical value for spherical molecules given by Hubbard. It is suggested that τ_d and τ_{sr} are approximately equal at the critical temperature. The use of viscosity data is remarkably successful in the interpretation of molecular motion in this liquid for which the mean rotational quantum number is quite low. Two new contributions to relaxation, interspin-rotation interactions, are evaluated approximately but they are probably negligible in liquid HCl. (auth)

46288 ON THE COMPOUNDS OF TETRAVALENT NEPTUNIUM AND PLUTONIUM WITH 8-HYDROXYQUINOLINE AND SOME OF ITS DERIVATIVES. Keller, C.; Eberle, S. H. (Technische Hochschule, Karlsruhe, Ger.; Gesellschaft fuer Kernforschung, Karlsruhe, Ger.). Radiochim. Acta, 4: 141-5(Aug. 1965). (In German).

Chelate complexes $Me(ligand)_4$ of Np(IV) and Pu(IV) with 8-hydroxyquinoline and some of its 2-, 5-, and 7-substituted derivatives are formed by precipitation from aqueous solutions. Compounds with more than four ligands per metal atom, known for Th and U(IV), were not found. In extractability, solubility, and absorption spectra, the compounds corresponded to those of the lower actinides. From the distribution of Np in the HOX (2-methyl-8-hydroxyquinoline) or HDCO (5,7-dibromo-8-hydroxyquinoline) chloroform-water system the stability constants of the extracted Np compounds were calculated: $Np(OX)_4$: lg β_4 = 45.28; $Np(DCO)_4$: lg β_4 = 46.05. The distribution curve of Pu showed an anomalous form, which was ascribed to the formation and extraction of basic species. (auth)

46289 NITROGEN ISOTOPE EQUILIBRATION ON TUNGSTEN. Gasser, R. P. H.; Lawrence, C. P.; Newman, D. G. (Oxford Univ.). Trans. Faraday Soc., 61: 1771-4(Aug. 1965).

The isotope equilibration reaction $^{28}N_2 + {}^{30}N_2 = 2{}^{29}N_2$ only occurs at a measurable rate on a tungsten filament when it is heated above 1,000°K. The maximum efficiency of the filament was ca 0.3%. (auth)

46290 NEUTRON-DIFFRACTION STUDY OF $Co_3B_2O_6$. Newnham, R. E.; Redman, M. J.; Santoro, R. P. (Massachusetts Inst. of Tech., Cambridge). Z. Krist., 121: 418-24(July 1965).

Cobalt borate, $Co_3B_2O_6$, is isotypic with the orthorhombic mineral kotoite and is antiferromagnetic below 37°K. Neutron-diffraction patterns were recorded above and below the magnetic transition using a sample enriched in isotope ^{11}B, thereby avoiding the large capture cross section of ^{10}B. A coherent scattering amplitude of $+0.65 \times 10^{-12}$ cm was obtained for ^{11}B from the nuclear intensities. The magnetic reflections in the low-temperature pattern were indexed on an a × 2b × 2c supercell, and calculations based on a four-spin model gave reasonable agreement with the observed intensities. Cobalt moments were arranged in ferromagnetic chains along a having spin directions perpendicular to c. (auth)

46291 PROCEEDINGS OF THE FIRST AUSTRALIAN CONFERENCE ON ELECTROCHEMISTRY HELD IN SYDNEY, 13–15th FEBRUARY AND HOBART, 18–20th FEBRUARY 1963. Friend, J. A.; Gutmann, F.; Hayes, J. W. (eds.). New York, Pergamon Press, 1965. 967p. $30.00. (CONF-387).

Papers presented at the First Australian Conference on Electrochemistry are given. Topics covered include: solid-state chemistry, thermodynamics of electrolytes, corrosion, theory of double layers, electroanalytical methods, applications of electrochemistry, non-aqueous electrolytes, molten salts, fuel cells, electrode processes, electrochemical processes, and electrowinning and electrorefining. A separate abstract was prepared for one paper. Two papers were previously abstracted for NSA as 17: 1817 and 18: 10035. (M.C.G.)

For an abstract of the individual paper see: 46454.

46292 ELECTROCHEMICAL BEHAVIOR OF URANIUM IONS IN VARIOUS ETHANOL–WATER SYSTEMS. I. POLAROGRAPHY OF URANIUM(IV). II. KINETIC STUDY OF THE REACTION BETWEEN URANIUM(VI) AND TIN(II) (thesis). Nolan, George Junior. Fayetteville, Ark., Univ. of Arkansas, 1964. 116p.

The polarography of the uranium (IV)–uranium (III) couple was studied in water at 25°C. The electrode process was found to be reversible in water, 30.0, 60.0, and 80.0 weight per cent ethanol-water above the following acid concentration respectively, 0.05, 0.2, 0.2, and 0.6M. In each of the systems the cathodic wave of the couple was studied as a function of the acid concentration, chloride ion concentration, and uranium (IV) concentration. In water and 30.0 weight per cent ethanol-water the half-wave potential shifts to more negative values as the acid concentration is increased. In 60.0 and 80.0 weight per cent ethanol-water the half-wave potential shifts to more negative values with a decrease in the acidity. In water at chloride ion concentration below 0.2M at 0.2M $HClO_4$ uranium (III) and uranium (IV) form a monochloride complex whereas only uranium (IV) forms a dichloride complex as the chloride ion concentration is increased above 0.2M. In 30.0 weight per cent ethanol-water at chloride ion concentration below 0.2M at 0.2M $HClO_4$ uranium (III) and uranium (IV) form a monochloride complex and above this chloride ion concentration they form a dichloride complex with the uranium (IV) dichloride complex being somewhat more stable than the uranium (III) dichloride complex. The half-wave potential is independent of the uranium (IV) concentration in all the ethanol-water media. The half-wave potential of the uranium (IV)–uranium (III) couple remains fairly constant from 0.0 to 50.0 weight per cent ethanol-water, then it shifts to more negative values and remains

fairly constant to 80.0 weight per cent ethanol-water. The product of the diffusion current constant and square root of the viscosity coefficient behaves in a similar manner. The reaction between uranium (VI) and Sn(II) was studied in water, 86.1, and 99.8 weight per cent ethanol-water media at 25, 30, and 40°C. In 86.1 and 99.8 weight per cent ethanol-water media the reaction was found to be first order with respect to uranium (VI) and Sn(II). In water the order with respect to uranium (VI) and Sn(II) is an unsettled question. At 25°C the observed second order rate constants are 0.67, 6.18, 3.75 liter mole^{-1} min^{-1} for water, 86.1, and 99.8 weight per cent, respectively. The energies of activation are 15.5, 20.3, 15.6 kcal mole^{-1} for water, 86.1, and 99.8 weight per cent, respectively. For these corresponding solvents the entropies of activation are −5.60, −1.11, and −4.77 cal mole^{-1}, respectively. Iron was found to greatly accelerate the reaction. (Dissertation Abstr.)

46293 ISOTOPIC EXCHANGE AND REPLACEMENT REACTIONS OF THE HALOACETIC ACIDS (thesis). Hinton, James Faulk Jr. Athens, Ga., Univ. of Georgia, 1964. 216p.

Isotopic exchange and replacement reactions involving haloacetic acids and halide ions were studied in aqueous solution and in 50% dioxane–50% water solution. Activation enthalpies and entropies were determined. Exchange and replacement reactions in both solvent systems were found to occur through a bimolecular reaction mechanism. For exchange reactions between haloacetic acids and halide ions in aqueous solution, a direct relationship was established between the activation enthalpy for reaction and the bond dissociation enthalpy of the chemical bond broken. Thermochemical parameters were obtained for the replacement reactions in both solvent systems from the experimentally determined activation parameters. The change in enthalpy between forward and reverse replacement reactions was found to be consistent with the difference between the enthalpy of formation for the appropriate chemical species involved. Rate constants for reactions occurring in the 50% dioxane–50% water mixture showed an increase over those obtained for the same reactions in aqueous solution. Exchange and replacement reactions involving chloroacetic, bromoacetic, hydrochloric, and hydrobromic acids were studied in 95% dioxane–5% water solution. Activation enthalpies and entropies were obtained for each reaction. A bimolecular reaction scheme involving molecular species is proposed as one mechanism that is consistent with experimental data. An exchange of chlorine between chloroacetic and chloride ions was induced by 2537 Å light in aqueous solution. This reaction occurs simultaneously with the photo-induced hydrolysis. The quantum yield for exchange depends upon the chloride concentration. The photo-induced exchange may be interpreted in terms of a mechanism involving an activated chloroacetic acid molecule or one that involves a dissociative process. (A.G.W.)

46294 A KINETIC STUDY OF THE ISOTOPE-EXCHANGE BETWEEN ZINC IODIDE AND VARIOUS ALKYL IODIDES IN ACETONITRILE (thesis). Howell, Barbara Fern Fennema. Columbia, Mo., Univ. of Missouri, 1964. 72p.

Rate constants for n-propyl iodide exchange were measured at 40.0°, 47.5°, 50.0°, and 59.1°C. Mean rate constants (in units of 10^{-4} hr^{-1}) found at these temperatures were respectively 1.64 ± 0.16, 3.01 ± 0.50, 5.23 ± 0.25, and 13.29 ± 0.21. The exchange was found to be first order with respect to n-propyl iodide and zero order with respect to zinc iodide. The activation energy for the exchange is 22.9 ± 0.30 kcal/mole and log A is 12.145 ± 0.001. Small amounts of water present in the reacting mixture were found to cause rate acceleration, which was more pronounced at low zinc iodide concentrations. Oxygen present in the reacting solutions caused erratic rate acceleration; the presence of iodine slowed the rate of exchange. When n-propyl iodide exchanged with ZnI_3^-, one-third order kinetics were observed with respect to ZnI_3^-. Rate constants for n-butyl iodide exchange were measured at 40.0°, 47.5°, and 60.0°C. The values of k (in units of 10^{-4} hr^{-1}) were respectively 1.05 ± 0.06, 2.93 ± 0.21, and 7.37 ± 0.50. The activation energy for the exchange was found to be 19.4 ± 0.8 kcal/mole and log A is 9.59 ± 0.23. The reaction order for n-butyl iodide was found to be one and that for zinc iodide was found to be zero. Exchange studies with isopropyl iodide were not successful because the rate of exchange increased with time; therefore no rate constants are reported. In order to explain the order of reactivity of the alkyl iodides investigated, a mechanism is proposed which involves nucleophilic attack by solvent molecules. The rate determining step is the ionization of the alkyl iodide. The kinetics observed for the three alkyl iodides investigated appear to fit the rate expression R = k(RI). (Dissertation Abstr.)

46295 ELECTROCHEMISTRY OF EUROPIUM (thesis). Herman, Harvey Bruce. Syracuse, N. Y., Syracuse Univ., 1964. 144p.

The reduction of Eu(III) to Eu(II) was studied by voltammetry at constant current in sodium acetate and acetic acid buffers. Plots of concentration versus the square root of the transition time, at a current density of .0282 mamp/cm^2, were linear in accordance with the Sand equation. From the slope of this line a diffusion coefficient of 0.45×10^{-5} cm^2/sec was evaluated for Eu(III) in 0.1M acetate buffer at 25°C. The square root of the transition time was found to be linear with i/i_0. The electrode area was evaluated using cadmium(II) ion in 0.1M KNO_3. The electrode reaction for the reduction of Eu(III) to Eu(II) was found to be reversible in this medium. The complex between Eu(III) and acetate ion was studied. Equations were derived that relate complex formation with the quarter wave potential of the reduction. The stability constants of the first and second europium acetate complexes were evaluated; $K_1 = 324$, $K_2 = 20.4$. The formal electrode potential was found to be +0.35 versus NHE. Current reversal studies indicated a possible kinetic or catalytic effect. Reactions with water or residual oxygen are postulated. The potential dependence of a catalytic effect was derived, and the potential dependence of both a catalytic and a kinetic effect are tabulated. An 80-mv difference was found between the polarographic half wave potential and the chronopotentiometric quarter wave potential in the same medium. The difference between the time that the mercury was in contact with the solution was suggested as the reason. A-c polarography experiments indicate a tensammetric wave for acetic acid. Electrocapillary measurements indicate acetic acid is absorbed on mercury. The adsorption appears to have a kinetic step that is not diffusion-controlled at these concentrations. A bridge between acetic acid and europium is proposed, which increases the rate of electron transfer. (Dissertation Abstr.)

46296 GAS-METAL REACTIONS AT HIGH TEMPERATURE WITH PARTICULAR REFERENCE TO NIOBIUM–GAS SYSTEMS. Fromm, E. (Max-Planck-Institut fuer Metallforschung, Stuttgart). Vienna, International Atomic Energy Agency, 1965, Preprint No. SM-66/9, 24p. (CONF-650704-15). ORINS.

From IAEA Symposium on Thermodynamics, Vienna.

One of the most serious disadvantages for the use of niobium as a high-temperature construction material is its relatively high reactivity with gases. When appreciable amounts of gases are dissolved in the metal lattice, a complete embrittlement of the material will occur. The equilibrium states between solid solution and gas phase can be studied by gas-absorption and degassing experiments performed at high temperature and under low pressure. Under these conditions the reaction of nitrogen, oxygen, and water vapor with niobium was evaluated gravimetrically, as well as volumetrically. It was found that in the Nb–N system the condensed phases are in equilibrium with molecular nitrogen, whereas in the Nb–O system the gas phase consists of volatile oxides and the oxygen partial pressure can be neglected. In the Nb–N system equilibrium pressures were measured as a function of nitrogen concentration at tem-

peratures between 1600 and 2200°C. Based on these results, the p–T–c diagram for the metal-rich side of the system was established up to 30 at. % N and some thermodynamic data were calculated. In the Nb–O system evaporation rates of the volatile oxides were measured at temperatures between 1600 and 2300°C under vacuum as well as in an oxygen or water vapor atmosphere at pressures of less than 10^{-2} torr. Under the presence of oxygen or water vapor, a dynamic equilibrium was obtained, in a definite pressure and temperature range, between gas absorption and evaporation of volatile oxides from the niobium–oxygen solid solution. Equations were established showing quantitative relations between oxygen concentration, temperature, and oxygen or water vapor pressure in dynamic equilibrium. In addition, the vapor pressure of the volatile oxides was determined and the respective values of the activation energies of the gas-absorption and degassing reactions were derived. From the oxygen to niobium ratio of the volatile component and from the dependence of this ratio on temperature and concentration it was concluded that the oxides NbO and NbO_2 evaporate. The thermodynamic data obtained for niobium–gas systems were compared with the corresponding values for tantalum, which showed the same behavior with regard to oxygen and nitrogen qualitatively. (auth)

46297 THE APPLICATION OF OXYGEN CONCENTRATION CELLS WITH THE SOLID ELECTROLYTE ZrO_2.CaO TO THERMODYNAMICAL RESEARCH WORK. Matsushita, Y.; Goto, K. (Tokyo Univ.). Vienna, International Atomic Energy Agency, 1965, Preprint No. SM-66/15, 26p. (CONF-650704-16). ORINS.

From IAEA Symposium on Thermodynamics, Vienna.

Oxygen concentration cells with the electrolyte ZrO_2·CaO, which provides a pure anion conduction due to the migration of oxygen defects, were applied to the basic research in process metallurgy. The standard free energies of formation of FeO, Fe_3O_4, SnO, PbO, Cu_2O, CuO, and Ta_2O_5 were measured at 500 to 1300°C and expressed by the functions of temperature with the comparison with the data in the literature. The oxygen pressure in liquid PbO–SiO_2 solution was measured at 800, 900, 1000, and 1100°C in equilibrium with liquid lead. The chemical activities of PbO and SiO_2 and the other thermodynamical properties of PbO–SiO_2 solution were obtained. The chemical activity of tin in liquid Pb–Sn binary solution was measured at 700, 800, and 900°C. The thermodynamical properties of Pb–Sn alloys were also calculated. An oxygen gage was developed to measure the partial pressure of oxygen in high-temperature gases in the range of $Po_2 = 10^{-1}–10^{-30}$ atm at 500 to 1300°C. The self-consistent and reproducible EMF against the gas compositions of CO–CO_2 or Ar–O_2 gas mixtures were obtained with several reference electrodes. The rates of the oxidation or reduction of pure iron and iron oxides by CO–CO_2 gas mixture were measured by the oxygen gage at 900 to 1000°C. The rates were calculated, based on the change of EMF of the cells due to the proceeding of the reactions. The oxygen pressure in liquid iron saturated with with oxygen or with graphite and of intermediate carbon range was measured by the cells with the reference electrodes of graphite or Ni + NiO powder. It seemed that this method could be used to determine the oxygen content in liquid iron at 1500 to 1600°C. The de-oxidation rate of liquid iron by Al and Si was measured by the change of the EMF of the cell constructed in the iron melt. In addition, other possibilities for applying oxygen concentration cells to the basic study of process metallurgy are suggested and industrial applications discussed. (auth)

46298 KNUDSEN EFFUSION STUDIES OF COMPOUNDS OF URANIUM AND THORIUM WITH ELEMENTS OF GROUPS IIIb AND IVb. Alcock, C. B.; Cornish, J. B.; Grieveson, P. (Imperial Coll. of Science and Tech., London). Vienna, International Atomic Energy Agency, 1965, Preprint No. SM-66/35, 34p. (CONF-650704-22). ORINS.

From IAEA Symposium on Thermodynamics, Vienna.

The vaporization of compounds of uranium and thorium with silicon and germanium and of several other compounds of uranium with lead, tin, indium, and gallium under equilibrium conditions was studied. Apart from providing fundamental materials data these studies are of value in a test of the applicability of theories of the stabilities of intermetallic compounds such as that of Kubaschewski and of Mott. It was found that Kubaschewski's theory is semi-quantitatively correct, but a number of difficulties are present in the simple form of this theory and they are given further consideration. The phases for which data are reported are UIn_3, UGa, UGa_2, and UGa_3 together with $ThSi_2$, Th_2Si_3, ThSi, Th_3Si_2, and $ThGe_3$, $ThGe_2$, Th_3Ge_5, ThGe, Th_3Ge_2, and Th_3Ge. The relative stabilities of the uranium and thorium compounds are also explicable in terms of Kubaschewski's theory. Measurements were made of the vapor pressures of gallium and indium metals and the results were different in detail from the literature data. No evidence of volatile oxides could be found, which would vitiate the results. In making these measurements, the values obtained by the Knudsen technique were combined with those from transportation measurements. (auth)

46299 INSOLUBLE CHELATES OF TITANIUM, ZIRCONIUM, HAFNIUM AND THORIUM. Langer, Horst G. (to Dow Chemical Co.). U. S. Patent 3,198,817. Aug. 3, 1965. Filed Nov. 8, 1960.

A method is described for preparing Ti, Zr, Hf, or Th compounds that are tetravalent, water-insoluble chelates of alkylenepolyaminoacetic acid-type chelating agents, such as ethylenediaminetetraacetic acid. The chelates are formed by mixing a concentrated solution of the chelating agent at a temperature near boiling with a solution of the metal compound, and cooling the resulting solution to separate the water-insoluble form of the acid metal chelate. (B.L.M.)

Organic Chemistry

46300 (AECL–2261) THE EFFECT OF p-TERPHENYL ON THE MELTING POINTS OF TERPHENYL–BIPHENYL ORGANIC COOLANTS. Marcinkow, F.; Hollies, R. E. (Atomic Energy of Canada Ltd., Pinawa (Manitoba). Whiteshell Nuclear Research Establishment). June 1965. 10p. Dep.; AECL, $0.50 cy.

The purpose of this study was to widen the known range of melting points in the quaternary system, o-, m-, p-terphenyl, biphenyl, and if possible to further define the composition range where the coolant is liquid at room temperature. These tests were conducted using o-terphenyl, m-terphenyl, and biphenyl near the tertiary eutectic to determine the phase diagram in this area, as well as the effects of p-terphenyl on the phase diagram. The melting points were determined as a function of O:M ratio, biphenyl content, and p-terphenyl content. Both the solidus and liquidus points were recorded. A low-melting quaternary mixture of 30 wt % biphenyl, O:M ratio of 2:1, and p-terphenyl 0.5 to 1.0 wt % was found, but the liquidus point remained above room temperature. Since solids were found in all quaternary mixtures at room temperature, none appear attractive as a start-up coolant for WR-1 reactor. (auth)

46301 (COO–1148–97) POLAROGRAPHIC BEHAVIOR OF PURINES AND PYRIMIDINES. Elving, Philip J. (Michigan Univ., Ann Arbor). June 20, 1965. Contract AT(11-1)-1148. 15p. (CONF-650556-1). Dep. mn; CFSTI $1.00 cy, $0.50 mn.

From Symposium on Electrical Methods and Principles in Molecular Biology, Jena, Ger.

Polarography and the various technics derived from it provide sensitive approaches for investigating the oxidation-reduction behavior of compounds of biological significance, as illustrated by typical examples of electrochemical oxidation and reduction in the purine and pyrimidine series. Reduction of pyrimidine itself at the dropping mercury electrode results in five different waves over the normal pH range. These waves are readily accounted for on the basis of the general mechanistic paths characteristic of the electrochemical reduction of organic compounds. Since the reduction of purines involves reduction of the

pyrimidine moiety, the reduction mechanism of pyrimidine is typical of all pyrimidine and purine derivatives with individual modifications introduced by the presence of substituents. The frequently greater complexity of reaction path for electrochemical oxidation as compared to electrochemical reduction is exemplified by the oxidation of uric acid at the graphite electrode, for which a path can be postulated which is similar to that postulated for its enzymatic oxidation. The latter may be only one instance of a general similarity between enzymatic and electrochemical redox processes, which have many features in common. (auth)

46302 (MLM-1271) PYROLYSIS OF POLYMERS: A BIBLIOGRAPHY. Kohl, Roland W. (Mound Lab., Miamisburg, Ohio). June 8, 1965. Contract AT(33-1)-Gen-53. 39p. Dep. mn; CFSTI $2.00 cy, $0.50 mn.

References (321) are given to journals, reports, and patents published from 1862 through 1963. Separate author and subject indexes are included. (P.C.H.)

46303 (NP-15409) GLYCIDIC ESTERS AND/OR ORGANIC DISULFIDES, AND RELATED SUBSTANCES, AS SOURCES OF ANTI-RADIATION DRUGS. Interim Research Report No. 23, April 1, 1965-June 30, 1965. Barbee, R. B.; Buckman, J. D.; Engelhardt, P. R.; Kim, H. K.; Lacefield, W. B. (Vanderbilt Univ., Nashville, Tenn.). Contract DA-49-193-MD-2030. 29p.

A research program was conducted to prepare organic compounds, particularly sulfur compounds, for testing as radioprotective agents. Studies of the preparation of 1,2-dithiane were continued, including its oxidation to the thiolsulfonate and tetroxide. Reaction of thiolsulfonates with dithiocarbamates gave 2-acetamidoethyl trithiopercarbamate; a sulfinate salt was also synthesized. Thiolsulfonate reactions with thio acids were carried out, and two acyl disulfides were prepared. Disproportionation studies were made on trithiopercarbamates. Work on mercaptodisulfides was concluded. Research was begun on unsymmetrical n-decylaminoethyl disulfides. Studies of the preparation and properties of dithiosulfite esters were concluded. (D.L.C.)

46304 (ORNL-3832, pp 66-75) ORGANIC CHEMISTRY. (Oak Ridge National Lab., Tenn.).

No difference in the rate of oxidative cleavage was found for 1,2-diphenyl ethylene glycol and its α-deuterated form ($C_6H_5CDOHCDOHC_6H_5$). Isotope-effect studies were also made on ^{14}C-labeled ketols and α-diketones. The 2-p-toluenesulfonate ester of 3-phenylnorbornane-2,3-cis-exo-diol was solvolyzed in both acetic acid and water. Photolysis of aroyl cyanides was found to produce the corresponding benzils and, under modified reaction conditions, the benzil dicyanohydrins. Results are reported which do not substantiate earlier findings of large reverse ^{14}C isotope effects for the rearrangement of methylene-labeled benzyl methyl ketoxime and phenyl-1-labeled acetophenone. Two solid photodimers are among the products isolated following photolysis of isophorone. Structures were assigned. Three of the products from treatment of 3-endo-amino-2-exo-phenylnorbornane-2-ol with nitrous acid were definitely characterized, and a mechanism for their formation is proposed. During the pyrolysis of tri-n-butyl phosphate the isomerization of residual groups to sec-butyl groups was observed to occur to a small extent. In a homogeneous system of HNO_2 with nitrobenzene and hydrocarbons, an exothermic reaction was discovered. The temperature of initiation and the intensity of the reaction varied with the structure. (auth)

46305 PREPARATION OF ^{203}Hg LABELED NEOHYDRIN FOR MEDICAL USE. Mani, R. S.; Desai, C. N.; Raghavan, S. V. (Atomic Energy Establishment, Trombay, Bombay). Indian J. Chem., 3: 415-16(Sept. 1965).

A simple and rapid method is described for the preparation of ^{203}Hg-labeled Neohydrin (3-chloromercuri-2-methoxy propylurea) of high specific activity and purity. Mercuric acetate labeled with ^{203}Hg of high specific activity and dissolved in methyl alcohol solution, was refluxed with the requisite amount of allylurea in methyl alcohol. The mixture was treated with sodium chloride and evaporated to near dryness. The residue was dissolved in dilute sodium hydroxide and ^{203}Hg activity was removed by chromatographic adsorption on alumina. The eluant from the alumina column was neutralized, aluminium hydroxide removed by centrifugation, and Neohydrin solution adjusted for isotonicity and sterilized by autoclaving. (auth)

46306 SYNTHESIS OF TRITIUM LABELED ACIDS THROUGH CHAIN ELONGATION AFTER ARNDT-EISTERT. Birkofer, Leonhard; Hempel, Klaus; Nouvertne, Werner (Universitaet, Cologne). J. Labelled Compds., 1: 20-6 (Jan.-Mar. 1965). (In German).

Acids labeled with tritium at the α-C-atom were synthesized through the rearrangement of diazo ketones with TOH-dioxane in the presence of silver oxide. The preparation of p-methoxy-phenylacetic-α-T acid, p-hydroxy-phenylacetic-α-T acid, β-alanine-α-T, γ-aminobutyric-α-T acid, and δ-aminovaleric-α-T acid. (auth)

46307 DEUTERATED ORGANIC COMPOUNDS. XXV. SYNTHESIS OF 1,4,5,8-TETRADEUTERIONAPHTHALENE. Renaud, R. N.; Leitch, L. C. (National Research Council, Ottawa). J. Labelled Compds., 1: 34-41(Jan.-Mar. 1965).

1,4,5,8-Tetradeuterionaphthalene was synthesized from 1,4-dibromonaphthalene by two methods. In the first method naphthalene was repeatedly brominated in chloroform and then debrominated with zinc dust in alkaline deuterium oxide. In the second, 1,4-dibromonaphthalene was nitrated to produce 1,4-dibromo-5-nitronaphthalene which underwent reductive debromination with zinc in alkaline deuterium oxide to 1-amino-5,8-dideuterionaphthalene. The latter was converted into 1-bromo-5,8-dideuterionaphthalene by a modified Sandmeyer reaction in which it was brominated to 1,4-dibromo-5,8-dideuterionaphthalene and then debrominated to 1,4,5,8-tetradeuterionaphthalene. (auth)

46308 DEUTERATED ORGANIC COMPOUNDS. XXV. SYNTHESIS OF CERTAIN DEUTERATED n-UNDECANES AND n-DODECANES. Warner, R. M.; Leitch, L. C. (National Research Council, Ottawa). J. Labelled Compds., 1: 42-53(Jan.-Mar. 1965).

The synthesis of the following n-undecanes and n-dodecanes deuterated in specific positions is described: $CH_3(CH_2)_{10}CD_3$, $CD_3(CH_2)_{10}CD_3$, $CH_3(CD_2)_{10}CH_3$, $[CD_3(CD_2)_4CH_2]_2$, $[CD_3(CD_2)_4]_2CH_2$, $CD_3(CD_2)_3(CH_2)_3(CD_2)_3CD_3$, and $CD_3(CD_2)_3CH_2CD_2CH_2(CD_2)_3CD_3$. The following intermediates were prepared in the course of these syntheses: CCl_3CD_2CD, $CDCD_2CN$, CCl_3CD_2CD, $CDCD_2CO_2H$, CCl_3CD_2CD, $CDCD_2CO_2C_2H_5$, $CCl_3(CD_2)_4CO_2C_2H_5$, $CH_3(CD_2)_4CO_2C_2H_5$, $CD_3(CD_2)_4CO_2C_2H_5$, $CH_3(CD_2)_4CO_2C_2H_5$, $CH_3(CD_2)_4CD_2OH$, $CH_3(CD)_4C_2D_2Br$, $CD_3(CD_2)_4CO_2D$, $[CD_3(CD_2)_4]_2CO$, $[CD_3(CD_2)_4]_2CHOH$, $[CD_3(CD_2)_4]_2CHBr$, $[CD_3(CD_2)_3CH_2]_2CO$, $[CD_3(CD_2)_3CH_2]_2CDOH$, $[CD_3(CD_2)_3CH_2]_2CDBr$, $[CD_3(CD_2)_3CH_2]_2CHOH$, and $[CD_3(CD_2)_3CH_2]_2CHBr$. (auth)

46309 SYNTHESIS OF DOUBLY LABELED CHOLESTERYL LINOLENATE AND ARACHIDONATE. Bardou, L.; Crastes de Paulet, A. (Institut de Biologie, Montpellier, France; Centre Regional de Lutte Contre le Cancer, Montpellier, France). J. Labelled Compds., 1: 54-65(Jan.-Mar. 1965). (In French).

The transesterification method used by Mahadevan and Lundberg for cholesterol ester synthesis, cholesterol acetate + fatty acid methyl ester → cholesterol ester + methyl acetate, was adapted to the microscale (1 to 10 μM) imposed by the use of labeled molecules of high specific activity. This method is particularly suitable for the synthesis of polyethylenic fatty acid cholesterol esters. ^{14}C- + ^{3}H-labeled cholesteryl linolenate and arachidonate were obtained. Mixing these two types of esters of high specific activity gave rise to series of doubly labeled esters. (auth)

46310 USE OF VINYL MAGNESIUM BROMIDE FOR THE SYNTHESIS OF MOLECULES LABELED WITH ^{14}C: NEW METHOD OF PREPARATION OF GLYCEROL 1-^{14}C AND GLYCERIC ACID 1-^{14}C. Pichat, L.; Herbert, M.; Aubert, F. (CEN, Saclay, France). J. Labelled Compds., 1: 66-78(Jan.-Mar. 1965). (In French).

Acrylic acid-1-^{14}C was obtained with an 80% yield by carbonation of vinylmagnesium bromide. In disagreement with the literature it was found that $LiAlH_4$ reduction of acrylic acid does not give rise to allyl alcohol but mainly to n-propanol. By successive additions of bromine and diazomethane acrylic acid-1-^{14}C yields methyl 2-3-dibromopropionate. Reduction by $LiAlH_4$-$AlCl_3$ at –80°C provided 2-3-dibromopropanol, which was converted into 2-3-diacetoxypropanol-1-^{14}C. Saponification followed by partition chromatography gave glycerol-1-^{14}C with an overall yield of 35% calculated on $Ba^{14}CO_3$. Glyceric acid-1-^{14}C was obtained with an overall yield of 43% based on $Ba^{14}CO_3$ from methyl 2-3-dibromopropionate-1-^{14}C. (auth)

46311 TRITIUM LABELLING OF AMINO-ACIDS AND PEPTIDES BY THE WILZBACH METHOD. I. RACEMIZATION OF L-VALINE DURING EXPOSURE TO TRITIUM GAS. Parmentier, J. H. (TNO, Delft, Netherlands). J. Labelled Compds., 1: 93-101(Apr.-June 1965).

Optically pure L-valine was labeled with tritium by the Wilzbach method. Only 4% of the activity of the radiochemically pure valine was found in D-valine. This figure was determined by reverse isotope dilution. The suitability of this method for valine was tested, with good results, with DL-valine also labeled by the Wilzbach method. (auth)

46312 SYNTHESIS OF DL-SHIKIMIC 1-2-^{14}C ACID STARTING FROM METHYL ACRYLATE 2-3-^{14}C. Chabannes, B. (I.N.S.A., Villeurbanne, France); Pichat, L.; Herbert, M.; Pacheco, H. J. Labelled Compds., 1: 102-8 (Apr.-June 1965). (In French).

DL-Shikimic, 1-2-^{14}C acid was prepared by a 5 stage synthesis with a total yield of about 11% from methyl acrylate 2,3-^{14}C. (auth)

46313 SYNTHESIS OF TRITIATED p-TERPHENYLS, LABELLED AT SPECIFIC POSITIONS. Otto, P. Ph. H. L. (TNO, Delft, Netherlands); Juppe, G. J. Labelled Compds., 1: 115-27(Apr.-June 1965).

The tritiated compounds p-terphenyl-4-T, -3-T, -2-T, and -2′-T were synthesized by catalytic reduction of the corresponding bromo-p-terphenyls with tritium gas under mild conditions. For each of the labeled p-terphenyls, the activity distribution over the positions in the molecule was determined by degradation. (auth)

46314 ENZYMATIC IODINATION OF PROTEINS. Numez, J.; Pommier, J.; El Hilali, M.; Roche, J. (College de France, Paris). J. Labelled Compds., 1: 128-40(Apr.-June 1965). (In French).

An iodination enzymatic method was studied, which makes possible the preparation of proteins labeled with ^{125}I or ^{131}I. The optimal enzymatic iodination conditions were studied for various proteins with different biological activities (immunological, hormonal, enzymatic). The enzymatic iodination reaction mechanism was determined. Some molecular characteristics of the iodoproteins prepared were investigated. The iodide oxidation was found to be catalyzed by horseradish peroxydase and not directly caused by H_2O_2 produced by a glucose-glucose oxydase system. When iodide atoms were introduced in a protein under the conditions defined, serumalbumin or thyroglobulin, for instance, no apparent denaturation occurred; but a shift of the sedimentation coefficient established by sucrose gradient ultracentrifugation appeared, which may be due to a change of the proteins' shape. (auth)

46315 SYNTHESIS OF BENZO [RST] PENTAPHENE-5,15-^{14}C AND OF ITS OXIDATION PRODUCTS. Boger, Eliahu; Bernfeld, Peter (Bio-Research Inst., Cambridge, Mass.). J. Labelled Compds., 1: 109-14(Apr.-June 1965).

^{14}C-labeled benzo[rst]pentaphene (V), known as 3,4,9,10-dibenzpyrene, ^{14}C-labeled benzo[rst]pentaphene-5,8-diol, diacetate (VI), and ^{14}C-labeled benzo[rst]pentaphene-5,8-dione (IV) were synthesized for studies of the distribution, the metabolic fate, and the mode of action of the carcinogenic hydrocarbon dibenzpyrene, which appears to differ from other known carcinogens with regard to these factors. (auth)

46316 POTENTIAL ANTIRADIATION AGENTS. PREPARATION AND POLYMERIZATION OF S-VINYL-N-VINYLTHIOCARBAMATES. Overberger, C. G.; Ringsdorf, H.; Avchen, B. (Polytechnic Inst., Brooklyn). J. Org. Chem., 30: 3088-92(Sept. 1965).

Three S-vinyl-N-vinylthiocarbamates (IV) were prepared by dehydrochlorination of the respective S-2-chloroethyl-N-2-chloroethylalkylthiocarbamates (III). The monomers were polymerized under a variety of conditions in an attempt to prepare linear, high-molecular-weight polymers containing a predominant amount of the tetrahydro-1,3-thiazin-2-one moiety along the backbone of the polymer chain. Free-radical-initiated polymerization was found to favor the formation of poly-S-vinyl recurring units, while cationic initiation favored the formation of repeating poly-N-vinyl units. Cyclopolymerization was favored by high dilution and decreasing size of the alkyl substituent. Attempts to isolate polymeric α-amino γ-thiols (VIII) formed on hydrolysis of the resultant "terpolymers" (VII) proved unsuccessful. (auth)

46317 ISOMERIZATION IN RESIDUAL ALKYLS FROM PYROLYTIC AND ESTER INTERCHANGE REACTIONS OF TRIBUTYL PHOSPHATE. Baldwin, W. H.; Higgins, C. E. (Oak Ridge National Lab., Tenn.). J. Org. Chem., 30: 3230-1(Sept. 1965).

Studies were made to determine if ester interchange between TBP and phosphoric acid caused any rearrangement since this method is used for labeling TBP. Virtually pure (99.7%) n-butyl bromide was isolated by distillation when TBP(tributylphosphate) was heated with constant-boiling HBr. The composition of the mixture of butyl bromide isomers recovered from the residue samples was determined by gas chromatography. Results from the ester interchange between TBP and phosphoric acid are given. Very little rearrangement occurred within the alkyl groups. About one-fifth of the butyl groups decomposed to a mixture comprised mainly (62%) of cis- and trans-butene-2. Most isomerization was evident in the gas phase. The distribution of sec-butyl groups in the residue compounds from TBP pyrolysis was uniform. The ratios of butene-2 (cis + trans) and sec-butyl yields are given. There was only ~0.8% yield of sec-butyl groups. (F.J.H.)

46318 THE EFFECT OF D_2O ON THE THERMAL STABILITY OF PROTEINS. THERMODYNAMIC PARAMETERS FOR THE TRANSFER OF MODEL COMPOUNDS FROM H_2O TO D_2O. Kresheck, Gordon C.; Schneider, Henry; Scheraga, Harold A. (Cornell Univ., Ithaca, N. Y.). J. Phys. Chem., 69: 3132-44(Sept. 1965).

Solubility data were obtained for propane, butane, and several amino acids in H_2O and D_2O. The solubility of the hydrocarbons was measured as a function of temperature in order to determine enthalpies and entropies of transfer from H_2O to D_2O, whereas enthalpies of transfer were obtained calorimetrically at 25°C for the amino acids and also for several alcohols. Thermodynamic parameters for the transfer of the nonpolar portions of the amino acids and alcohols were computed on the basis of the assumption that the contributions of the polar and nonpolar portions are additive. The enthalpy of transfer was negative for the hydrocarbons as well as for the hydrocarbon portions of the amino acids and alcohols; the entropy of transfer was negative for the two former classes of compounds. The free energy of transfer was negative (but became less negative with increasing temperature) for hydrocarbons and positive for the nonpolar portions of the amino acids at 25°. Assuming that the behavior of the amino acids most closely reflects the situation, which exists in proteins even though the free amino acids contain charged α-amino and α-carboxyl groups, it was predicted that hydrophobic bonds between protiated amino acid side chains will be stronger in D_2O than in H_2O. This prediction was confirmed by experiments on detergent micelles, in which it was found that the critical micelle concentration is lower in D_2O than in H_2O. (auth)

46319 PREPARATION OF METHANE FOR IONIZING RADIATION DETECTORS. Riedel, Jozef Tadeusz (Inst.

of Nuclear Research, Polish Academy of Sciences, Warsaw). Przeglad Elektrotech., 6: 241-5(May 1965). (In Polish).

A method of producing methane gas of high purity, as required for radiation detectors, is described. The methane is produced by the reaction $CH_3COONa + NaOH \rightarrow CH_4 + NaCO_3$, and is passed over pulverized marble. The gas is dried, after which the methane is condensed. Before cleaning, a typical analysis showed, 89.81 CH_4, 3.24 N_2, 3.54 C_2H_4, 2.051 H_2, 0.7 O_2, and 0.22% CO_2. After passing the methane through two cycles of cleaning, the purity rose to 99.98%. (TTT)

46320 PHYSICS AND CHEMISTRY OF THE ORGANIC SOLID STATE. VOLUME II. Fox, David; Labes, Mortimer M.; Weissberger, Arnold (eds.). New York, Interscience Publishers, 1965. 986p. $27.50.

The properties of organic solids are discussed under the following topics: conductivity, organic polymers that conduct electricity, magnetic properties, luminescence and energy transfer, scintillations in organic solids, solubility and diffusivity, mechanical relaxation phenomena, polymorphism, and radiation effects in polymers. Separate abstracts were prepared for two of the chapters. (F.J.H.)

For abstracts of individual chapters see: 46399 and 46400.

Radiation Chemistry

See also BIOLOGY AND MEDICINE — Radiation Effects.

Refer also to abstracts 46430, 46761, 47092, and 47985.

46321 (AD-611779) AN EPR INVESTIGATION OF RADIATION PROTECTION BY AROMATIC ADDITIVES IN SYNTHETIC POLYMERS [Thesis]. Banaszak, Jerome J. (Pennsylvania State Univ., University Park). Dec. 1964. Contract AF33(608)-954. 75p. CFSTI $3.00 cy, $0.75 mn.

The protective effects against ionizing radiation that aromatic compounds provide when added to a synthetic polymer in various proportions were studied. Since radiation damage in high polymer compounds is usually accompanied by the production of free radicals in the material, electron paramagnetic resonance (EPR) techniques were utilized to measure the extent of the free radical concentration. Comparative measurements were made of the radioprotective effects of different aromatic additives on polymethyl methacrylate. Data obtained from the EPR spectra are correlated with some of the theories currently advanced relating free radical formation, degradation, and crosslinking during polymer irradiation. Degradation or multiple chain scission, is defined as the breaking up of the long molecular chains in a polymer into smaller units, whereas crosslinking is usually associated with increasing the number of lateral linkages between polymer chains. (auth)

46322 (AD-612070) EXCITATION OF ETHYLENE, ACETYLENE, PROPYNE, AND 1-BUTYNE BY LOW-ENERGY ELECTRON IMPACT. Technical Report, October 1, 1963–September 30, 1964. Bowman, C. R.; Miller, W. D. (General Dynamics/Fort Worth, Tex.). Jan. 1965. Contract AF29(601)-6213. 36p. (WL-TR-64-148). CFSTI $2.00 cy, $0.50 mn.

The excitation spectra of ethylene, acetylene, propyne, 1-butyne, 2-butyne, and 3-hexyne were measured by means of a trapped-electron technique which permits the detection of approximately 93% of inelastically scattered electrons independent of scattering angle. Excitation potentials and relative intensities are tabulated for both optically allowed and optically forbidden transitions. Correlation with available ultraviolet absorption data and molecular-orbital theory was used to establish transition assignment. A 1.7-ev excitation in ethylene is attributed to temporary negative-ion formation. In acetylene at 2.0 ev, excitation is postulated as resulting from excitation of the triplet sigma (+) u state. Low-energy maxima occur in propyne, 1-butyne, 2-butyne; however, the complexity of these molecules precludes a meaningful assignment of transitions at this time. (auth)

46323 (AD-613529) LOW TEMPERATURE POLYMERIZATION STUDIES. Progress Report No. 5, January 1–March 31, 1965. Morton, Maurice (Akron Univ., Ohio. Inst. of Rubber Research). Apr. 10, 1965. Contract AF04(611)-9694. 30p. CFSTI $2.00 cy, $0.50 mn.

Results are reported for the polymerization or attempted polymerization of the following monomers by gamma radiation (7.6 rads/hr) at reduced temperatures: acrylonitrile, hexafluoropropylene, fumaronitrile, hexafluoroacetone, trifluoroacetaldehyde, perfluorooctanal, and pentafluoropropionaldehyde. A comprehensive bibliography on the gamma irradiation of potential monomers was almost completed, and a preliminary listing is included. In addition, a differential thermal analysis assembly was constructed for use during polymerization by gamma radiation of acrylonitrile. The results qualitatively indicate that polymerization occurs only in the temperature vicinity of a phase transition. (auth)

46324 (AGN-8132) FISSIOCHEMICAL DEVELOPMENT PROGRAM. Semiannual Progress Report, July 1–December 31, 1964. Hamling, B. H.; Kahn, S.; Meisels, G. G.; Miller, R. I. (Aerojet-General Nucleonics, San Ramon, Calif.). Feb. 1965. Contract AT(04-3)-596, 247p. Dep. mn; CFSTI $6.00 cy, $1.25 mn.

Analytical expressions, based on solid state detector experimental results, are derived relating fragment escape energy to source thickness and geometry. Various micron-sized ceramic and metallic uranium-containing fibers were prepared and tested; Ni-UO_2 fibers underwent 1.8% burnup with no visible damage. A once-through in-reactor fissiochemical gas loop, operable to 400°C, 400 psi, and 25 watts showed the yield of HCN from N_2–CH_4 mixtures to be at least 2 molecules per 100 ev of energy deposited. A variety of investigations examined pressure and track effects, energy transfer mechanism, and free radical production in such systems as ethylene–rare gas, nitrogen, nitrogen–methane, and ammonia. Of a variety of fissiochemical products of interest examined, several (e.g., CO-based compounds, fluorocarbons, aniline) showed initially encouraging results. Equipment and techniques were designed and effectively used to determine the process parameter dependence of hydrazine yield; other systems are under consideration. 85 references are cited. (P.C.H.)

46325 (ANL-7013) LABORATORY INVESTIGATIONS IN SUPPORT OF FLUID-BED FLUORIDE VOLATILITY PROCESSES. PART VII. THE DECOMPOSITION OF GASEOUS PLUTONIUM HEXAFLUORIDE BY ALPHA RADIATION. Wagner, Raymond P.; Shinn, William A.; Fischer, Jack; Steindler, Martin J. (Argonne National Lab., Ill.). May 1965. Contract W-31-109-eng-38. 32p. Dep. mn; CFSTI $2.00 cy, $0.50 mn.

Gaseous plutonium hexafluoride (PuF_6) decomposes at temperatures between 26 and 82°C to plutonium tetrafluoride (PuF_4) and fluorine, at least in part due to irradiation by alpha particles from the plutonium. The rate of decomposition is nonlinear, varying from 1.78 to 0.064% per day in the range from 0.5 to 571 days. Experiments with PuF_6 at initial pressures of 50 and 100 showed that at the lower pressure slightly lower decomposition rates are obtained. Decomposition in large vessels proceeds at slightly lower rates than decomposition in small vessels. The presence of initial PuF_4 decreases the rate of decomposition, but this decrease in rate appears to be independent of the quantity of initial PuF_4. The presence of helium or krypton lowers the rate, but not appreciably. Oxygen or fluorine decreases the PuF_6 decomposition rate. Nitrogen reacts slowly with PuF_6 to form nitrogen trifluoride (NF_3). Higher PuF_6 decomposition rates than those observed in nickel spheres are obtained when quartz or Pyrex spheres are used. Increased nickel surface area gives increased PuF_6 decomposition rates in the absence of initial PuF_4. At 82°C the PuF_6 decomposition rate is higher than at 26°C. No mechanism for the decomposition is postulated because

it is not possible to proportion accurately the contribution of chemical reaction, thermal decomposition, and decomposition due to alpha radiation to the total decomposition observed. (auth)

46326 (CNAEM–28) INVERSION OF THE CYANIDE GROUP INTO ISO-CYANIDE UNDER GAMMA IRRADIATION. Talat-Erben, M.; Uenseren, Envare; Seber, Nurten (Cekmece Nuclear Research Center, Atomic Energy Commission, Istanbul (Turkey)). Sept. 1965. 9p. Dep. mn.

Infrared spectrophotometric evidence indicates that gamma irradiation of the nitriles causes partial inversion of the cyanide group into isocyanide according to the following mechanism: In the gamma flux, some of the cyanide groups are detached from the nitrile as cyan free radicals and, owing to their resonance-hybrid structure, $.C \equiv N - \rightleftharpoons - C \equiv N.$, two distinct recombination processes take place leading partly to the usual cyanide and partly to the isocyanide, respectively. From a comparison of the optical densities at the characteristic frequency of the isocyanide absorption band in irradiated methacrylonitrile and ethyl isocyanide it was concluded that at least 20% of the cyanide groups were transformed into isocyanide in a specific sample of methacrylonitrile irradiated to a total dose of 0.1 megarads. (auth)

46327 (DP–977) RADIOLYSIS OF ION EXCHANGE RESINS USED IN THE PURIFICATION SYSTEMS OF SAVANNAH RIVER REACTORS. Baumann, Elizabeth W. (Du Pont de Nemours (E. I.) and Co., Aiken, S. C. Savannah River Lab.). July 1965. Contract AT(07-2)-1. 17p. Dep. mn; CFSTI $1.00 cy, $0.50 mn.

Loss of ion exchange capacity and the presence of water-soluble materials in depleted deionizer resin from a Savannah River Plant reactor system indicated the resins were degraded during service. Calculations and on-line measurements of radiation dose showed that the threshold dose for resin damage, 10^7 rad, was approached or exceeded in the deionizer beds. Sodium-24, produced by the (n,α) reaction on aluminum fuel cladding, was the major contributor to the radiation dose. (auth)

46328 (EUR–2227.e) MASS SPECTROMETRIC STUDIES ON POLYPHENYLS. PART I. THE MASS SPECTRA OF DIPHENYL, THE TERPHENYLS AND QUATERPHENYLS. Beyrich, W.; Copet, A.; Facchetti, S. (European Atomic Energy Community, Ispra (Italy). Joint Nuclear Research Center). 1965. 24p. Dep. mn.

The 50 and 70 ev mass spectra of diphenyl and the 3 and 6 quaterphenyl isomers, taken with an Atlas CH4 mass spectrometer, are discussed. Comparison of the spectra shows a remarkable difference between the behavior of all compounds containing ortho-bonds with respect to the others and indicates that probably principally different fragmentation processes have to be assumed. Under the given instrumental conditions, para-isomers have the highest, ortho-isomers the lowest stability against electron bombardment. Considerations of the quaterphenyl isomers indicate processes of C_6H_5 loss by simple rupture of the C–C-bond between the rings, for which certain probability values can be obtained in dependence of the isomeric position. The most frequently lost fragments are compiled and compared with literature data on the light products formed in the radiolysis of polyphenyls. (auth)

46329 (EUR–2455.e) STUDIES ON THE EFFECT OF NUCLEAR RADIATIONS ON HETEROGENEOUSLY CATALYZED GAS REACTIONS. (Battelle Institut e. V., Frankfurt am Main (West Germany)). 1965. 60p. Dep. mn.

Studies using various solid catalysts in the presence and absence of beta radiation ($^{90}Sr-^{90}Y$, absorbed dose rate about 8.10^5 rad/hr) were carried out on the decomposition of methanol, ethanol, isopropanol, and formic acid, the hydrogenation of benzene and ethylene, and the oxidation of carbon monoxide. Under the test conditions adopted the radiation was found to have no effect on the reaction rate and the type of reaction products. The results obtained from tests on heterogeneous catalysis in the presence of nuclear or ultraviolet radiation, which are available in the pertinent literature but are in some cases contradictory, indicate that the reason for the occurrence or absence of a radiation effect cannot be ascertained at the moment even in cases of a very similar nature. This is clearly due to the lack of knowledge on the radiation absorption mechanism in solids, especially near the surface. (auth)

46330 (NP–15370) REAKTIONEN VON SPALTRUCKSTOSSATOMEN, INSBESONDERE VON JOD, MIT METHAN UND ANDEREN GASEN. (Reactions of Fission Recoil Atoms, Particularly of Iodine with Methane and Other Gases (thesis)). Denschlag, Johannes-Otto (Mainz Univ. (West Germany). Naturwissenschaftliche Fakultaet). 1965. 199p. Dep. mn.

It was shown that in the interaction of fission recoil nuclei with methane, methyl iodide and methyl bromide are formed. In the reaction on ethane, methyl iodide, methyl bromide, ethyl iodide, and vinyl iodide could be detected. In each case, methyl iodide is the principal reaction product (>60%). The compounds are liquid at room temperature and remain for a long time (at least hours) in the gas space. Elementary iodine and hydrogen iodide also appear to be produced, but they are precipitated within seconds on the vessel walls. Therefore, within minutes after irradiation, only organically bound iodine could be detected. Three reaction processes to the methyl iodide could be identified: (1) a prompt reaction of the fission recoil nuclei of the primary iodine; (2) a prompt reaction of the β-recoil atoms of the secondary iodine; and (3) a delayed reaction of the iodine, that reacted according to neither (1) nor (2) and was fixed on the vessel walls. It can be described as a first-order reaction and was characterized by a half life. The yields on methyl iodide fluctuate greatly. For reaction (1) a yield of 66% of the primary iodine was found for the most favorable case. A yield of only 3 to 4% also was detected. The yield for reaction (2) was only a tenth of the yields of reaction (1) (0 to 2.5%). The half life of reaction (3) was more than 140 days, and this reaction plays no role in short irradiations. The three reactions are not temperature dependent in the range from 20 to 80°C. In a reaction after the end of the irradiation, it was established that the reaction (3) was amplified by γ radiation. Because of the stronger reaction of the primary iodine, the fractional primary yields of the measured iodine isotope were calculated at <3% for ^{131}I, 4.6 ± 2% for ^{133}I, and 25 ± 1% for ^{135}I. They are approximately in agreement with the values expected from the systematics of the independent yield: 0.2, 4, and 37% of the chain yield. Only the ^{135}I value deviates noticeably. The calculation of the primary iodine yield and the reaction yields (or the half life of reaction (3)) was done by an iteration method, that is programmed in "Algol." (tr-auth)

46331 (NYO–1858-1) EFFECT OF RADIATION ON DYNAMIC PROPERTIES OF HIGH POLYMERS. Final Report. Work, Richard N. (Pennsylvania State Univ., University Park. Dept. of Physics). Sept. 1965. Contract AT(30-1)-1858. 13p. Dep. mn; CFSTI $1.00 cy, $0.50 mn.

Significant developments in studies on the solid state behavior of polymeric materials and the effects of radiation on their properties and structure are briefly reviewed. 89 references are cited. (P.C.H.)

46332 (ORNL–3832, pp 50–65) RADIATION CHEMISTRY. (Oak Ridge National Lab., Tenn.).

Because of the interest in gaseous SO_2 as a potential fast-reactor coolant, its radiation stability in the gas phase was investigated. The total yield of reducing radicals in the radiolysis of water was evaluated as 3.13 ± 0.07 molecules/100 ev, with CO and O_2 used as scavengers for the intermediates. In the radiolysis of gaseous CH_4 by gamma rays, N_2O was found to be a satisfactory dosimeter if corrections for stopping power were applied properly. Peroxymonosulfuric acid is capable of oxidizing cerous ion in the presence of radiation and absence of air. Net oxidation does not take place if air is present, indicating that reactivities toward H atoms decrease in the following order: $k(H + O_2) > k(H + H_2SO_5) > k(H + Ce^{4+})$. The ratio of rate constants $k(OH + Ce^{3+})/k(OH + H_2)$ was evaluated to be

7.5 ± 1. Postirradiation reduction of Ce(IV) was observed when concentrated $NaNO_3$ solutions in 0.4 M H_2SO_4 containing Ce(IV) were irradiated with a kilocurie ^{60}Co source. The effects of crystal form, surface area, impurity content, and dose rate on the radiation-induced exchange of deuterium with silanol hydrogen in silica were studied. Doubly isotopically labeled $^7Li^{81}BrO_3$ was prepared and irradiated with thermal neutrons to produce high-specific-activity 35.9-hr ^{82}Br. Detailed measurements on the radiolysis of bromate ion in a typical crystalline alkali-metal bromate, $CsBrO_3$, were completed. Products resulting from the breaking of one, two, and three Br–O bonds were observed. The radiolytic decomposition of bromate ion in crystalline alkaline-earth bromates was shown to give rise to intermediates which are highly unstable thermally; accordingly, their yields are strongly temperature dependent, and their concentrations tend to a steady-state value determined as a balance between their rate of production, their thermal decomposition to Br^- ion and $O_2(g)$, and their recombination to give BrO_3^- ion. Initial 100-ev radiolytic yields for $Ca(BrO_3)_2$ and $Sr(BrO_3)_2$ were estimated to be: $G_0(-BrO_3^-) = 2.4, 2.9$; $G_0(Br^-) = 0.33, 0.51$; $G_0(\text{"Ox"}) = 2.0, 2.4$; $G_0(O_2) = 1.5, 1.9$; $G_0(BrO_2) = 1.2, 1.2$; $G_0(BrO_2^-) = 0.8, 1.1$; and $G_0(BrO^-) = 0, 0$, respectively. (auth)

46333 (SGAE-CH-20/1965) DIE STRAHLENBESTAENDIGKEIT VON ANTHRAZENOELEN. II. RADIOLYSE IM KERNREAKTOR BEI 150 BIS 380 deg C. (The Radiation Stability of Anthracene Oils. Part II. Pile Radiolysis at 150 to 380 deg C). Proksch, E.; Wiesinger, F.; Eschweiler, H.; Szinowatz, W. (Oesterreichische Studiengesellschaft fuer Atomenergie G.m.b.H., Seibersdorf). [1965]. 18p. Dep. mn.

The radiolytic decomposition of anthracene oils in a nuclear reactor was studied using two different fast neutron dose fractions. Assuming additivity of the effects it was found in two series of experiments that the decomposition caused by fast neutrons is higher by a factor of about 2.5 to 5 than by γ radiation. For VÖEST-Anthracene Oil I the G-values for total decomposition and gas production are 0.22 ± 0.04 and 0.016 ± 0.010, respectively, both independent from temperature. The stability of different oils decreases with increasing fraction of non-aromatic protons. The dependence on dose of the decomposition follows a second-order rate law. The main decomposition products are dimers to tetramers of the original hydrocarbons. (auth)

46334 (TID-22231) SOFT X-RAY IRRADIATIONS OF ACETYLENE, METHYLACETYLENE, AND ETHYLACETYLENE IN THE GAS PHASE WITH AND WITHOUT ADMIXTURES OF NOBLE GASES [Thesis]. Cochran, Thomas Brackenridge (Vanderbilt Univ., Nashville, Tenn.). Jan. 1965. Contract AT(40-1)-1327. 172p. Dep. mn; CFSTI $5.00 cy, $1.00 mn.

Acetylene, methylacetylene, and ethylacetylene were irradiated using 50-kvp-50 ma x rays; the products were analyzed using infrared spectra, gas chromatography, and osmometry. Dosimetry measurements were carried out on the x-ray beam, and acetylene ($G(-C_2H_2) = 72$) was used as a standard for the determination of the G's for the other compounds. The effects of Ar, Kr, and Xe on the reaction rates were studied. The G values for the disappearance of methylacetylene and ethylacetylene were found to be 38 and 36 respectively; the G(product gases) = 5 for both, while the G(polymer) = 33 and 31 respectively. Besides the product gases ethylene, propene, acetylene, allene, methane, and hydrogen, methylacetylene also produced ethylacetylene, and ethylacetylene produced methylacetylene. The polymer products exhibited similar properties: yellow-brown color, viscous, soluble in acetone and benzene, and low molecular weights. (D.L.C.)

46335 (TID-22232) RADIATION STUDIES OF 1-BUTENE AND CIS 2-BUTENE USING SOFT X-RAYS AND COBALT-60 GAMMA RAYS [thesis]. Cross, Dan Allan (Vanderbilt Univ., Nashville, Tenn.). Jan. 1965. Contract AT(40-1)-1327. 106p. Dep. mn; CFSTI $4.00 cy, $0.75 mn.

The x-ray irradiation of gaseous 1-butene resulted in an average value G = 21.26; the principal product was a light viscous oil polymer, and the gaseous products were H_2, CH_4, C_2H_4, C_2H_2, and C_3H_6. The effects of added Ar and Xe were to increase greatly the reaction rate; the end product was predominantly C_2H_4. Similar results were obtained in the x irradiation of gaseous cis 2-butene, with the average G being 12.73. Trans 2-butene and an unknown product were also present in addition to the above gaseous products. Gamma-ray irradiations of liquid cis 2-butene gave very low conversions, with a $G \ll 10$. (D.L.C.)

46336 (TID-22236) IRRADIATION OF METHACRYLONITRILE, 1,3-BUTADIENE, AND HEXACHLORO-1,3-BUTADIENE [thesis]. Lintz, John Patrick (Vanderbilt Univ., Nashville, Tenn.). Jan. 1965. Contract AT(40-1)-1327. 72p. Dep. mn; CFSTI $3.00 cy, $0.75 mn.

Liquid methacrylonitrile, liquid 1,3-butadiene, and liquid hexachlorobutadiene were irradiated by cobalt-60 gamma rays (1.17 and 1.33 Mev); 1,3-butadiene gas was irradiated by soft x rays with a peak energy of 50 kev. Gamma irradiation of methacrylonitrile gave an average G-value of 253 ± 12%. No gases were produced by irradiation; the only reaction observed was a polymerization of the monomer. The polymer formed was a light, yellow-brown, crystalline substance which was soluble in methyl ethyl ketone. The molecular weight of the polymer was 1580 ± 5%. Infrared analysis of the polymer indicated a unit structure of $-CH_2-\underset{\displaystyle CH_3}{\overset{\displaystyle |}{C}}(CH_3)-CN$. Cobalt-60 irradiation of liquid 1,3-butadiene yielded an average G-value of 83 ± 12%. No gaseous products were observed. The only reaction noted was that of polymerization of monomer to a highly viscous liquid at ambient conditions. The polymer had a molecular weight of 860 ± 5%, and the infrared spectrum was the same as the spectrum of commercial polybutadiene. The polymer had two unit structures of $-CH_2-CH=CH-CH_2$ and $-CH_2-\underset{\displaystyle CH=CH_2}{\overset{\displaystyle |}{CH}}-$. Gaseous butadiene gave an average G-value of 28.6 ± 12% when irradiated by x rays. Traces of acetylene and 1-butene were produced by irradiation. The structure of the polymer was not determined. Hexachloro-1,3-butadiene yielded an average G-value of 11.1 ± 12% upon cobalt-60 irradiation. No evidence of gaseous products produced by the irradiation was detected. The polymer was a viscous liquid with a molecular weight of 250 ± 5%. The fully chlorinated butadiene had a considerably lower G-value than the unsubstituted butadiene. (D.L.C.)

46337 (TID-22244) THE RADIOLYSIS OF PROPYLENE, HEXAFLUOROPROPYLENE, AND ALLYL ACRYLATE [thesis]. Springer, John Mervin Jr. (Vanderbilt Univ., Nashville, Tenn.). Aug. 1965. Contract AT(40-1)-1327. 79p. Dep. mn; CFSTI $3.00 cy, $0.75 mn.

Allyl acrylate, propylene, and hexafluoropropylene were irradiated by gamma radiation from ^{60}Co; propylene was irradiated in the vapor phase with a 50 kvp x-ray machine. X-ray radiolysis of gaseous propylene yielded a liquid polymer and gaseous products consisting of ethylene, propane, hydrogen, methane, and acetylene. The average G-value was 26.2 molecules/100 ev. IR analysis of the polymer showed it to be atactic polypropylene. Liquid phase gamma radiolysis of propylene resulted in the production of an atactic polymer similar to the x-ray-produced polymer. The only products other than the polymer were small amounts of hydrogen and acetylene. The average G-value was 28.5. The G-value for disappearance of hexafluoropropylene was 12.0. No products other than a liquid polymer were detected. Allyl acrylate polymerized rapidly during irradiation. A polymer and one unidentified liquid were the only products, the polymer being the principal product. Chromatography indicated that the unknown was of lower molecular weight than allyl acrylate. The polymer was a tough, elastic solid, and was insoluble in the monomer. The monomer polymerized rapidly, so only approximate G-values were calculated. Three samples yielded G-values of 48,000, 60,000, and 68,000. The latter two values are believed to be the most accurate. (D.L.C.)

46338 (UCRL-12367) REPRODUCIBILITY STUDIES OF PREPARATION OF A LiF DOSIMETRIC MATERIAL. Jones, D. E.; Burt, A. K. (Lawrence Radiation Lab., Univ. of California, Livermore). July 29, 1965. Contract W-7405-eng-48. 60p. (CONF-650637-3). Dep. mn; CFSTI $3.00 cy, $0.75 mn.

From International Conference on Luminescent Dosimetry, Palo Alto, Calif.

Results of thermoluminescent tests of polycrystalline lithium fluoride with 0.5 mole % (M%) Eu and 0.05 M% Mg added as impurities are presented. Extensive data are given for varying amounts of impurities. (M.O.W.)

46339 (UCRL-16358) FREE RADICAL INDUCED IN ENZYMES BY ELECTRONS AND HEAVY IONS. Henriksen, Thormod (Lawrence Radiation Lab., Univ. of California, Berkeley). Aug. 23, 1965. Contract W-7405-eng-48. 26p. (CONF-650924-2). Dep. mn; CFSTI $2.00 cy, $0.50 mn.

From Workshop Conference on Space Radiation Biology, Berkeley, Calif.

Free radicals produced in three enzymes, ribonuclease, lysozyme, and trypsin, exposed to various types of radiation, were studied by ESR spectroscopy. The enzymes were irradiated in the solid state, in vacuum, at different temperatures in the range 77 to 330°K. For all three enzymes it was found that the resonance spectra at room temperature can be ascribed mainly to sulfur radicals and to a radical in which the unpaired electron is localized on an α-carbon atom in the protein backbone. However, another unidentified resonance was found in all three enzymes. The yield of secondary enzyme radicals increased with increasing irradiation temperature. Good correlation was found between the production of secondary radicals and the inactivation of the three enzymes. (P.C.H.)

46340 (AEC-tr-6570) SOURCES OF GAMMA-RADIATION FOR RADIATION-CHEMICAL INSTALLATIONS. Breger, A. Kh. Translated from Tr. Nauch. Issled. Fiz.-Khim. Inst., [No. 6], 11p.(1963). 11p. Dep. mn; CFSTI $1.00 cy, 1(mn); JCL $1.60 fs, $0.80 mf.

The development of strong gamma sources for radiation-chemical processes in industry is considered. Various gamma sources are compared, and it is found that the fuel elements and the radiation circuits of reactors are the most feasible sources. Calculations are made of the gamma-ray rate of fuel elements. (D.L.C.)

46341 (FTD-TT-65-24) EFFECT OF RADIATION ON CERTAIN CHARACTERISTICS OF ELECTROLUMINESCENT SCREENS. Boyko, L. M. Translated from Ukr. Fiz. Zh., 6: 866-9(1961). 5p. CFSTI.

Electroluminescent screens were investigated with simultaneous electro and photo-excitation. The frequency dependence has a maximum at 12 to 13 kc, on the position of which various forms of radiation—ultraviolet, x and gamma radiation—have no effect. The brightness of the luminescent screen in an alternating electric field decreases during radiation with ultraviolet light and increases during x irradiation, the effect depending on the frequency. The possibility of obtaining "images" on an electroluminescent screen was verified. (auth)

46342 (JPRS-31547, pp 6-12) THE EFFECT OF RADIATION PROTECTIVE SUBSTANCES ON THE PROTRACTED AFTERGLOW OF IRRADIATED SOLUTIONS OF SERUM ALBUMIN. Sapezhinskii, I. I.; Silaev, Yu. V. Translated from Dokl. Akad. Nauk SSSR, 162: 691-3(1965).

Using a continuous-flow apparatus, the authors studied the effect of various kinds of radioprotective agents on the kinetics of the protracted afterglow produced when solutions of serum albumin in phosphate buffer are irradiated with a PRK-4 mercury lamp. Intensity of luminescence decreased sharply when oxygen was removed from the solution. Addition of cysteine after irradiation increased the rate of change in intensity of the afterglow. The magnitude of the effects noted were characterized by the ratio K/K_0 and parameter $\alpha = (K-K_0)\,K_0$, (where K_0 is the constant of the rate of protracted afterglow and K is the rate with the addition of a radioprotective agent). The constant increased linearly with an increase in concentration of cysteine and of the inhibitors of free-radical processes, viz., 2,6-di-tert-butyl-4α-aminoethylphenol and 2-propyl-6-methyl-3-hydroxypyridine. The values of α were determined for 13 substances with a protein concentration of 0.133% in phosphate buffer, pH 7, at 25°. Other protective agents studied included reduced glutathion, β-mercaptoethylamine, thiourea, propylgallate, sodium thiosulfate, aniline, sodium sulfite, ascorbic acid, glucose, and hydroxylamine (all in a concentration of 3.3×10^{-3} M/liter). Those with marked protective action (the sulfur-containing substances, phenol type) had the most potent effect on the kinetics of protracted afterglow. The effect was even more pronounced when they were used prior to irradiation. (ATD)

46343 SOME THERMODYNAMIC CONSIDERATIONS ON THE HYDRATED ELECTRON AND OTHER INTERMEDIATES IN THE RADIOLYSIS OF AQUEOUS SOLUTIONS. Botar, L.; Safarik, I. (Central Research Inst. for Chemistry, Budapest). Acta Chim. Acad. Sci. Hung., 44: 293-9 (1965).

Acid-base dissociation constants for H, H_2, OH, and HO_2 were calculated on the basis of the appropriate oxidation-reduction half reactions by standard thermodynamic methods. The formal half reaction $e^-_{aq} \rightarrow aq + e^-$ was introduced for the calculation of K_H. The importance of these equilibrium processes in the radiolysis of aqueous solutions is discussed. (auth)

46344 RADIATION-INDUCED CHEMILUMINESCENCE. Hoefert, M. Angew. Chem., 76: 826(Oct. 7, 1964). (In German).

Tetralin, cyclohexane, cumene, oleic acid, n-butyl oleate, and linoleic acid in the presence of O_2 exhibit a stationary light emission of ca. 10^3 photons/cm^3 sec which is connected with auto-oxidation. Free radicals are chain carriers in such processes, according to classical descriptions of auto-oxidation; irradiation produces activated molecules and influences the chemical reaction. In all the systems with light and x rays (1 to 10 kR doses) an increase in light emission was observed, with an increase up to 10^4 photons/cm^3 sec noted for the maximum case. At room temperature two decay curves are found; the more rapid has essentially disappeared at 6 min after irradiation. The slower extends over 30 min. Temperature increase represses the rapid process in most cases, and the slower one dominates. The process is explained using an analog computer based on a model of the auto-oxidative chain mechanism combined with recombination emission on collision of two peroxy radicals. Emission maximum for all systems is in the blue-green; ΔH = 55 kcal/mole. The inhibitors ionol, β-naphthol, and thiophenol at 0.05M decrease the intensity of emission after irradiation. (BBB)

47345 FORMATION OF 1-BENZYL-2,3-DIPHENYLINDANES FROM STILBENE IN THE PRESENCE OF TIN TETRACHLORIDE UNDER THE INFLUENCE OF γ-RADIATION. Salzwedel, M.; Werner, V.; Schulte-Frohlinde, D. (Kernforschungszentrum, Karlsruhe, Ger.). Angew. Chem. Intern. Ed. Engl., 3: 803(Dec. 1964).

The irradiation of cis- or trans-stilbene in the presence of tin tetrachloride with γ rays from ^{60}Co led to trimers plus three dimers which were isolated and characterized. The G value for the consumption of the stilbene in an equimolar mixture with tin tetrachloride was 105; the G value for the formation of the mixture of isomers was calculated to be 31.5 on complete reaction. The uv, ir, mass, and proton magnetic resonance spectra of the dimers as well as the products of their oxidative degradation (benzoic acid, o-benzoylbenzoic acid, anthraquinone, 2,3-diphenyl-Δ^2-inden-1-one, and (o-benzoylphenyl) benzoylbenzylmethane) indicate that they are the stereoisomers of 1-benzyl-2,3-diphenylindane. The three isomers, with a molecular weight of 360 had melting point values of 99–100, 114–15, and 147–8°C and uv absorption maxima at 274, 275, and 281 mμ, respectively. (BBB)

46346 PULSE RADIOLYSIS. Sangster, D. F. (Australian Atomic Energy Commission). At. Energy Australia, 8: No. 3, 13-18(July 1965).

The principles, practice, operation, and interpretation of

results in pulse radiolysis are discussed. The scope and value of the technique are illustrated by giving examples of the applications recorded in the chemical literature. One great advantage of the technique is that a qualitative or even a semi-quantitative result is available within 10 sec, the time it takes to develop the photographic record. (P.C.H.)

46347 RADIATION DAMAGE TO CRYSTALLINE RIBONUCLEASE: AN ASSAY METHOD FOR DAMAGE INVOLVED IN THE REFOLDING OF THE REDUCED PROTEIN. Haskill, J. S.; Hunt, J. W. (Univ. of Toronto; Ontario Cancer Inst., Toronto). Biochim. Biophys. Acta, 105: 333-40(Aug. 24, 1965).

The reduction and reoxidation of crystalline ribonuclease (polyribonucleotide 2-oligonucleotidotransferase (cyclizing), EC 2.7.7.16) irradiated in O_2 has indicated the presence of hidden, sublethal damage following irradiation. The ribonuclease preparation arising from reduction and reoxidation of γ irradiated ribonuclease not only had a lower V_{max} than the control preparation from the irradiated enzyme but also possessed a lower K_m, thereby indicating the presence of one or more active, but altered species of ribonuclease. The enzyme irradiated in vacuo showed no evidence of sublethal damage. It is postulated that irradiation in O_2 damages regions of the enzyme which affect the refolding of the enzyme after disulfide-bond cleavage, as well as regions which are involved with the function of the active center. (auth)

46348 IONIZATION AND DISSOCIATION BY ELECTRON IMPACT IN CARBON TETRABROMIDE. Thorburn, R. (Liverpool Coll. of Tech.). Brit. J. Appl. Phys., 16: 1397-1400(Sept. 1965).

The appearance potentials of the positive and negative ions formed by electron impact in CBr_4 were measured. Processes are suggested for their formation and the values of several chemical parameters deduced. The cross section for the production of Br^- in the low-energy resonance capture process was estimated as 6×10^{-16} cm^2. (auth)

46349 THE PRODUCTION OF RADIOELEMENTS AT THE MOL NUCLEAR CENTER. 1963–1964 BALANCE. Constant, R. (Universite Libre, Brussels). Bull. Inform. Assoc. Belge Develop. Pacifique Energie At., 10: No. 55, 21-3(Apr. 1965). (In French).

The development of radioisotope production at Mol since 1961 through 1964 is summarized. A program for the production of radioisotopes can be analyzed on the basis of the number of orders, the activity delivered, or the number of deliveries. Tabulations showing each of these aspects of the Mol Center are given. (J.S.R.)

46350 STUDIES ON THE COPOLYMERIZATION OF VINYL CHLORIDE AND ON THE DECOMPOSITION OF POLYVINYL CHLORIDE. II. γ-RAY INDUCED DECOMPOSITION OF POLYVINYL CHLORIDE. Kimura, Tadashi (Osaka Municipal Techn. Res. Inst.) Bull. Osaka Munic. Techn. Res. Inst., 37: 64-86(Dec. 1964). (In Japanese).

Polyvinyl chloride (PVC) powder was irradiated in air at room temperature with γ rays at total doses up to 2×10^8 r. The dose rate was about 4×10^5 r/hr. The chlorine content of the irradiated PVC decreased steadily down to about 45% at 2×10^8 r. The incipient gel formation was observed at 4×10^7 r and the gel fraction increased rapidly and was about 70% at 2×10^8 r. The predominance of main chain scission over crosslinking may be due to the difficulty of recombination of polymer chain segments in rigid PVC particles, compared with the cases of plasticized PVCs. In addition, main chain scission was accelerated by the polymer peroxide. The PVCs plasticized with dioctyl phthalate (DOP), tricresyl phosphate (TCP), phenyl dicresyl phosphate (PDCP), dioctyl sebacate (DOS), and epoxy safflower oil (ESO) were fabricated into sheets and irradiated in air at room temperature with γ rays. The dose rate was 4×10^5 r/hr with total doses up to 7.7×10^7 r. The tensile strength of the irradiated sheets with DOP decreased markedly. It was confirmed, from the distribution of molecular weight of the soluble fraction of the PVC extracted from the irradiated sheets, that the formation of molecules of lower degree of polymerization by main chain scission occurred parallel with the formation of higher molecules by crosslinking. A higher proportion of DOP in the formulation of the PVC sheets resulted in a higher protective action for the radiation-induced changes of PVC. TCP and PDCP were more effective in the protective action than DOP. DOS and ESO were also very effective in the protective action and ESO was found to add directly to the PVC molecules. (NSA of Japan)

46351 SOME SOLUTION PROPERTIES OF POLYVINYL CHLORIDE POLYMERIZED BY γ-RAY IRRADIATION. Endo, Ryuichi; Goto, Ryuichi (and others) (Tokyo Coll. of Science). Chem. High Polymers (Tokyo), 22: 405-9 (July 1965). (In Japanese).

Vinyl chloride was polymerized by γ irradiation at −78, 0, and 18°C. The solution properties of the polymer were examined. The polymer produced at −78°C was not soluble in tetrahydrofuran at temperatures up to 70°C. The polymer produced at 0°C contained small amounts of tetrahydrofuran insoluble fractions. The polymer produced at 18°C was almost soluble in tetrahydrofuran. The polymers produced at 0 and 18°C were fractionated by the successive fractional precipitation method, using tetrahydrofurane as solvent and water-tetrahydrofuran mixture as nonsolvent. The fractionates were examined osmometrically and viscometrically, and the following equation was obtained: $[\eta] = 5.32 \times 10^{-4} \overline{M}_n^{0.672}$. The value of K obtained by Kawai and Fixman-Stockmayer's method was 2.11×10^{-6}. The γ-induced polymer, as compared with a commercial polymer, kept the linear relation up to the higher molecular weight in the Mark-Houwink equation. (auth)

46352 RADIATION INDUCED CYCLOPOLYMERIZATION OF ACRYLIC ANHYDRIDE. Okada, Mitsuo; Hayashi, Kanae (and others) (Japan Assoc. Radiation on Polymers, Tokyo). Chem. High Polymers (Tokyo), 22: 441-5(July 1965). (In Japanese).

Radioinduced solution and bulk polymerizations of acrylic anhydride were carried out over a wide range of temperatures to study the effects of temperature, phase, conversion, and initial monomer concentration on the degree of cyclization of the polymer obtained. The degree of cyclization increased with increasing conversion and temperature, and decreased with increasing initial monomer concentration. The degree of cyclization of the polymer formed in solid state at −78°C was similar to that of the polymer obtained in toluene solution at the same temperature. But the polymer formed in solid state was crosslinked. Determination of the residual unsaturation of the polymer by bromometry made it possible to evaluate the ratio k_p/k_c of the rate constant of vinyl propagation and that of cyclization; for a solution polymerization in toluene at 30°C, this ratio was equal to 0.09. Similarly, the difference between the activation energies of vinyl propagation and cyclization was evaluated to be 2.3 kcal/mol for solution polymerization in toluene, and 4.7 kcal/mol for bulk polymerization in the liquid state. (auth)

46353 INFLUENCE OF ACETYLENE ON THE RADIO-INDUCED POLYMERIZATION OF ETHYLENE. Munari, S.; Castello, G.; Russo, S. (Universita, Genoa). Chim. Ind. (Milan), 47: 26-9(Jan. 1965). (In Italian).

The influence of acetylene on the polymerization of ethylene by γ rays (^{60}Co source) was studied at ambient temperature in glass ampoules at 45 atm. Using an intensity of 715 r/min, pure ethylene (1.51 g) yielded 0.286 g of polymer in 10 days; with 10 ppm acetylene the yield was 0.271 g, and this steadily decreased to 0.017 g for 50% acetylene. The decrease in rate was much more rapid for initial stages of the addition of acetylene. The melting point of the product decreased with increasing acetylene concentration; 5% acetylene yielded a semi-liquid at 5 days; and 20% yielded a semi-liquid after 10 days. After air oxidation the product contained carbonyl groups and the melting point rose with increasing acetylene concentration. The molecular weight of the polymer increased with absorbed dose and decreased with increasing acetylene concentration. The polymer with acetylene contains unsaturation, and the number of methyl groups per 1000 C atoms increased with increasing acetylene concentration,

reaching 16.78 at 5000 ppm acetylene. Possible reaction steps for the interaction of acetylene with chain radicals were proposed to explain the retarding and chain-transferring properties of acetylene. (BBB)

46354 FILLER MATERIALS IN SYNTHETIC RESIN MASSES AS SHIELDING MATERIAL AGAINST IONIZING RADIATION. Elbel, K. (Feldmuehle AG, Wesseling, Ger.). Chimia, 19: 376-81(June 1965). (In German).

The introduction of filled plastics as a shielding material against ionizing radiation is discussed. The properties of various materials as fillers are discussed and compared. The effect of ionizing radiation on plastics is briefly considered, and the plastics that show the best radiation stability are indicated. (J.S.R.)

46355 STUDIES ON GRAFT-COPOLYMERS OF STYRENE ONTO POLYPROPYLENE PREPARED BY THE USE OF γ RAYS. Kadonaga, Masao; Matsuo, Hiroshi (Elec. Commun. Lab., Tokyo). Elec. Commun. Lab. Tech. J., 13: 1977-2001(Dec. 1964). (In Japanese).

Studies were made on the conditions of graft copolymerization of styrene onto polypropylene (PP) by pre-irradiation in air with γ rays. The degree of crystallization of PP, the preliminary extraction of PP with a solvent, the dose rate, the irradiation atmosphere, the irradiation temperature, the total dose, the concentration of styrene in the methanol in the polymerization reaction, the polymerization, temperature, and the polymerization time are described in connection with the yields of graft-copolymer and styrene homopolymer. The grafting ratio was controlled freely. The mechanism of graft copolymerization is discussed. The ineffective dose below which no graft copolymerization could occur was discovered for graft copolymerization onto PP films. In the curve showing the yield of graft-copolymer against the particle size of PP powder, a minimum appeared, which could be explained by the relative contributions from the polymer peroxide and the frozen free radical. Tensile strengths and elongations at break were measured for the grafted PP films having grafting ratios up to 40%. The stiffness of the films increased as the grafting ratio increased, and elongation at the break decreased rapidly as the grafting ratio increased over 10%, becoming nearly zero at 20% or more. The tensile strength did not depend on the grafting ratio. The main chain scission of PP by irradiation and polymerization was negligible and the polystyrene side chains did not affect the tensile strength but hindered the slipping between the PP main chains. The grafted PP powder was fabricated into sheets, and their mechanical properties were measured and compared with those of sheets fabricated from the blended polymer of PP and polystyrene. The tensile strength, Young's modulus and impact strength of the graft copolymer were higher than those of the blended polymer, whereas the Rockwell hardness was slightly lower. The flow velocity at 200°C, F_x, of the graft copolymer having a PP fraction x is expressed by $F_x = F_0 x^{3.4}$, where F_0 is the flow velocity of PP. The flow velocity of the blended polymer is much higher than that of the graft copolymer of equal PP fraction. The flow temperature of the graft copolymers at constant pressure and constant rate of temperature rise is 10 to 20°C higher than that of PP. (NSA of Japan)

46356 SYNERGISM BETWEEN IONIZING RADIATION AND A CYTOTOXIC METHYLHYDRAZINE DERIVATIVE: EFFECT ON DNA DEGRADATION. Berneis, K.; Bollag, W.; Kofler, M.; Luethy, H. (F. Hoffmann-La Roche and Cie, AG, Basel; Buergerspital, Basel). Experientia, 21: 318-20(1965).

The combined effect of ionizing radiation and N-isopropyl-p-(2-methylhydrazinomethyl)benzamide hydrochloride (Natulan) leads to a significantly increased degradation of DNA from calf thymus than could be expected on the basis of the linear superposition. The synergism is at a maximum when the addition of Natulan is made immediately after the irradiation. This effect can be explained as a result of the formation of instable peroxides during the irradiation. As is known the organic peroxides formed by the irradiation decompose, for the most part, within two or three hours after irradiation with the formation of free radicals. These can act as the initiator in the autoxidation of Natulan and therefore accelerate the decomposition of DNA. (tr-auth)

46357 THE ROLE OF THE TRIPLET EXCITED STATE IN THE PHOTOLYSIS AND RADIOLYSIS OF LIQUID CYCLOPENTANONE. Dunlon, P.; Trumbore, C. N. (Univ. of Delaware, Newark). J. Am. Chem. Soc., 87: 4211-12 (Sept. 20, 1965). (TID-22092).

Studies of the photolysis of cyclopentanone were carried out at both 3130 and 2537 Å and quantum yields for 4-pentanol were 0.37 ± 0.01 and 0.38 ± 0.02, respectively. Minor primary products ($\ll$1%) were found to be 1-butene and CO with 3130 Å radiation and 1/butene, CO, ethylene, and cyclobutane at 2537 Å. Additional experiments showed the 4-pentanol quantum yields to be insensitive to the addition of allyl alcohol, n-hexane, ethylene, carbon monoxide, 1-butene, DPPH, and low concentrations of ferric chloride. The decrease in 4-pentanol resulting from the addition of oxygen was equal to a corresponding increase in the formation of organic peroxide. A mechanism as shown in the equation, $C + h\nu \rightarrow C^1$, $C^1 \rightarrow C^3$, $C^3 \rightarrow$ 4-pentanol, $C^3 + P \rightarrow C + P^3$, and $P^3 \rightarrow$ isomerization of P, could account for the 4-pentanol production. C and P are cyclopentanone and piperylene, respectively, and the superscripts 1 and 3 represent excited singlet and triplet electronic states. Further support for the triplet state precursor of 4-pentanol in the photolysis and radiolysis of cyclopentanone was provided by a comparison of the 4-pentanol yields in deoxygenated vs air-saturated cyclopentanone solutions. (F.J.H.)

46358 THE EFFECTS OF SMALL DOSES OF RADIATION ON THE FLOW AND OTHER PROPERTIES OF ZIEGLER POLYETHYLENES. Ferguson, J.; Wright, B. (Shell Chemical Co. Ltd., Manchester, Eng.). J. Appl. Polymer Sci., 9: 2763-77(Aug. 1965).

The effects of high energy radiation in doses up to 1.0 MRad on the properties of polyethylene were studied. The interactions of some radiation variables and polymer variables were also determined. The results obtained show that the main effects of radiation on polyethylene are to reduce its melt index and concomitantly to increase its flow parameter. The extent of these changes depends on several other factors. It was reduced by many common antioxidants (with the apparent exception of N-stearoyl-p-aminophenol). Under the conditions used it was not affected by the presence of air during irradiation, but was reduced by post-irradiation milling. The data also indicate that it increases with decreasing polymer melt index and with decreasing polymer density, but these apparent effects may be artifacts due to variations of antioxidant content. Radiation in small doses had little effect on any of the other properties of polyethylene, including high shear flow properties, softening point, tensile properties, impact strength, folding endurance, stress cracking resistance, thermal stability, and light stability. (auth)

46359 SELF-RADIOLYSIS OF CLATHRATES CONTAINING TRITIUM-LABELLED MOLECULES. Ciranni, G.; Guarino, A.; Pizzella, R.; Possagno, E. (Universita, Rome). J. Labelled Compds., 1: 1-9(Jan.-Mar. 1965).

Clathrates containing high specific activity methyl stearate-9,10-^{3}H were stored for approximately 70 days. The following "host" molecules were employed: desoxycholic acid, cycloveratryl, tri-o-thymotide, and β-cyclodextrin. The gaseous self-radiolysis products decreased significantly up to $\simeq$90% (HT from choleic clathrate). The total percentage decreases of the decomposition are: 16.95% (choleic clathrate); 27.10 (tri-o-thymotide clathrate); 19.35 (cycloveratryl clathrate); 12.10 (β-cyclodextrin clathrate). (auth)

46360 SELF-RADIOLYSIS OF TRITIUM-LABELLED FATTY ACID ESTERS. Guarino, A.; Pizzella, R.; Possagno, E. (Universita, Rome). J. Labelled Compds., 1: 10-19(Jan.-Mar. 1965).

High-specific-activity methyl butyrate-2,3-^{3}H and methyl stearate-9,10-^{3}H were stored for approximately three months. The products of self-radiolysis were iden-

tified by means of radio-gas chromatographic methods and isotopic dilution techniques. Rather high G-values were found for the parent acids and for the destroyed ester molecules. (auth)

46361 RADIOLYSIS OF ETHYLENE. III. IDENTIFICATION OF IONIC INTERMEDIATES AND FORMATION OF EXCITED SPECIES BY APPLICATION OF ELECTROSTATIC FIELDS. **Meisels, G. G.; Sworski, T. J. (Union Carbide Corp., Tuxedo, N. Y.).** J. Phys. Chem., 69: 2867-74(Sept. 1965).

Formation of both methane and the methyl radical in the radiolysis of ethylene was not significantly affected by application of electrostatic fields too weak to induce secondary ionization. This was attributed to their formation by ionic processes. The marked enhancement in yields of molecular hydrogen, acetylene, and those products requiring hydrogen atoms and/or vinyl radicals as precursors was attributed to formation of excited species of ethylene by secondary electrons accelerated by the field. Dissociation ensues by the processes listed with their normalized probabilities: $C_2H_4^* \rightarrow C_2H_2 + H_2$ 0.38; $C_2H_4^* \rightarrow C_2H_2 + 2H$ 0.46; and $C_2H_4^* \rightarrow C_2H_3 + H$ 0.16. Comparison with mercury-photosensitized decomposition of ethylene indicated the role of excited states above the 4.6 ev triplet state. Comparison with excitation resulting from vacuum ultraviolet and high-energy radiation suggested dissociation of vibrationally excited ground state molecules formed by intersystem crossing and radiationless transitions. (auth)

46362 ENERGY-TRANSFER PROCESSES IN DILUTE SOLUTIONS OF ORGANOMETALLICS IN BENZENE. RADIATION CHEMISTRY AND LUMINESCENCE QUENCHING. **Peterson, D. B.; Arakawa, T.; Walmsley, D. A. G.; Burton, Milton (Univ. of Notre Dame, Ind.).** J. Phys. Chem., 69: 2880-6(Sept. 1965).

The perphenyl compounds of Sn, Pb, As, Sb, and Bi dissolved in benzene experience radio-sensitized decomposition when the solutions are exposed to ^{60}Co γ radiation. The products include biphenyl, the phenylcyclohexadienes, and tetrahydroquaterphenyls. The perphenyl metals have no true effect on $G(H_2)$ or $G(C_2H_2)$ from the benzene itself. It was previously established that these same compounds quench luminescence in benzene solutions containing such scintillators as 1,4-diphenyloxazole or p-terphenyl. The kinetics of the processes were compared, and it is shown that the state of benzene that yields H_2 or C_2H_2 is neither one that yields biphenyl via the metal perphenyls nor one that transfers energy to a scintillator and that the state, which transfers energy to a scintillator (i.e., the $^1B_{2u}$ state of benzene), is a relatively minor contributor to sensitized decomposition of the metal perphenyls. Effects of locally high concentrations of free phenyl radicals were revealed in the relatively large amount of biphenyl produced in the sensitized decomposition. Silicon and germanium tetraphenyls showed none of the reactions exhibited by the other perphenyls; the fact is linked to longer lifetimes of their excited states. (auth)

46363 A STUDY OF THE RADIOLYSIS AND LUMINESCENCE BEHAVIOR OF DIOXANE–BENZENE MIXTURES. **Rojo, Enrique A.; Hentz, Robert R. (Univ. of Notre Dame, Ind.).** J. Phys. Chem., 69: 3024-30(Sept. 1965).

G values for gas products in γ irradiation of pure, liquid dioxane were constant over the range $(0.46-4.6) \times 10^{19}$ ev g^{-1}. These G values for a dose rate of 1.9×10^{18} ev g^{-1} min^{-1} are as follows: H_2, 2.1; C_2H_4, 0.50; C_2H_6, 0.051; CO, 0.23; and CH_4, 0.035. Study of the polymer product indicated that dioxane dimers constitute the initial polymer product. G(monomer → dimer) ≈ 3.9. Hydrogen, biphenyl, polymer, and relative luminescence G values (p-terphenyl as scintillator) were measured for benzene–dioxane mixtures. The parallel behavior of hydrogen and polymer G value curves suggested that a common dioxane precursor of hydrogen and polymer is protected from reaction by some kind of interaction with benzene. Kinetic analysis of the $G(H_2)$ results gave $\alpha = 0.21$ M^{-1} as the ratio of specific rate of excitation transfer to that of decay for the excited dioxane species that yields hydrogen. This analysis also indicated that thermal H atoms make a negligible contribution to the hydrogen yield from dioxane. A similar treatment of relative luminescence G values led to an estimate of 65 M^{-1} as the corresponding ratio for the excited dioxane species that gives rise to luminescence. It was concluded that the latter species makes a negligible contribution to the yield of decomposition products and that the excited species that yields decomposition products is of very short lifetime. For protection to compete with decomposition it may be necessary that a molecule of benzene be a nearest neighbor to the labile excited dioxane species at the time of its formation. (auth)

46364 RADIOLYSIS OF CYCLOHEXANE-d_{12}–CYCLOPENTANE MIXTURES. **Yang, John Y.; Marcus, Inge (North American Aviation Science Center, Thousand Oaks, Calif.).** J. Phys. Chem., 69: 3113-15(Sept. 1965).

The yields of dimers and olefins from irradiation of $C_6D_{12}-C_5H_{10}$ solutions were determined and these values are compared with the corresponding yields from radiolysis of $C_6H_{12}-C_5H_{10}$ solutions. In $C_6D_{12}-C_5H_{10}$ solutions, cyclopentene and bicyclopentyl yields were much higher and, in contrast to $C_6H_{12}-C_5H_{10}$ solutions, the cyclohexene-d_{10} yields were somewhat less than those corrected for energy absorption in the cyclohexane component along. The nature of the solvent-solute interaction between cyclohexane and cyclopentane was accounted for by hydrogen abstraction reactions. The nonideal behavior of the cyclohexene and cyclopentene yields in the radiolysis of $C_6H_{12}-C_5H_{10}$ solutions was attributed to disproportionation processes, $C_6H_{11}\cdot + C_5H_9\cdot \xrightarrow{k_9} C_6H_{10} + C_5H_{10}$ and $C_6H_{11}\cdot + C_5H_9\cdot \xrightarrow{k_{10}} C_6H_{12} + C_5H_8$, in which the rate constant k_9 was greater than k_{10}. (auth)

46365 CHEMICAL SPECIES CONTAINING ^{32}P AND ^{35}S SUBSEQUENT TO THE NEUTRON IRRADIATION OF THIOUREA. **Arrington, Cleon C.; Kiser, Robert W. (Kansas State Univ., Manhattan).** J. Phys. Chem., 69: 3202-4(Sept. 1965).

An investigation was made of the labeled products formed on neutron irradiation of thiourea, the nature of the species resulting from the recoil and radiation damage effects, and the relative quantities for both ^{35}S and ^{32}P in these species. Sample irradiation, counting procedures, and analytical methods are discussed. (F.J.H.)

46366 ACETYLENE PRODUCTION IN THE RADIOLYSIS OF METHANE. **Johnsen, R. H. (Florida State Univ., Tallahassee).** J. Phys. Chem., 69: 3218-19(Sept. 1965). (TID-21774).

Two types of radiation cells were used to study the production of acetylene in radiolysis of methane. Samples were collected and irradiated with 2.0-Mev electrons followed by freezing with liquid nitrogen. The sample was introduced into the gas chromatograph and analysis was by means of a combination silicagel and squalene calibrated with authentic samples. The lowest dose corresponded to about 0.01% decomposition. At lowest doses acetylene was not observed as a product. (F.J.H.)

46367 ON DETERMINING MEGAROENTGEN DOSES FROM RADIATION-INDUCED MOLECULAR WEIGHT DECREASE OF POLYMETHYLMETHACRYLATE. **Boettger, H. G. L. (Institut fuer Angewandte Physik der Reinststoffe der Deutschen Akademie der Wissenschaften, Dresden).** Kernenergie, 8: 349-58(June 1965). (In German).

In the case of polymethylmethacrylate (PMMA) a unique relationship between the average molecular weight $\overline{M}_v$ and the absorbed dose D of high-energy radiation was found to exist. Thus, knowing the energy absorption per main-chain scission E_d, D results from $\overline{M}_{v_0}$ and $\overline{M}_v$ may be determined from the intrinsic viscosity η of a benzene solution of irradiated PMMA. Measurements using a ^{60}Co telecurie unit for medical therapy demonstrated that the degradation of PMMA is independent of dose and dose rate, and that there are no after-effects. The experimental data corresponded to the results of other methods. The method may be employed for reliable dose measurements of a good reproduc-

ibility from 5×10^3 to 10^8 rads using an approximately air- (or water-) equivalent dosimeter system. (auth)

46368 ON THE ABSORBED DOSE RATE DETERMINATION IN VINYLCHLORIDE. PART 2. MEASUREMENTS BY MEANS OF A PARALLEL-PLATE AND A THIMBLE IONIZATION CHAMBER. Hecker, O.; Behrens, H.; Kraak, P. (Institut fuer Physik und Physikalische Chemie der Hochpolymeren, der Deutschen Akademie der Wissenschaften, Berlin). Kernenergie, 8: 358-64 (June 1965). (In German).

The absorbed dose rate in gaseous vinyl chloride was determined using a parallel-plate or a thimble ionization chamber. The design of the chambers is described, and some dose rate curves obtained by using these chambers are given. The W value for vinyl chloride, which must be known for calculating the absorbed dose rate from chamber current by means of a cylindrical chamber, was determined. The energy equivalent of the roentgen for vinyl chloride is given for different radiation qualities. (auth)

46369 CHEMICAL DOSIMETRY OF IONIZING RADIATION WITH THE LEUKO COMPOUNDS OF SOME TRIPHENYLMETHANE DYES IN POLYSTYRENE. Stolz, W.; Prokert, K. (Technische Universitaet, Dresden). Kernenergie, 8: 425-9(July 1965). (In German).

The possibility of chemical dosimetry of gamma and beta radiation with the leuko compounds of benzaurin, fuchsin, Doebner's violet, methyl violet, crystal violet, and malachite green in polystyrene was studied. The dosimeters have the form of a thin polystyrene foil, in which the leuko compound of one of the dyes mentioned together with a heavy volatile halogen hydrogenic carbon is embedded. By the irradiation, amounts of the corresponding triphenylmethane dye proportional to the absorbed dose are formed in the foils. The dose rate and temperature response as well as the reproducibility of the dosimeter reactions were investigated. The reaction mechanism is discussed. (auth)

46370 REACTION OF ETHYLENE WITH METHYLENE CHLORIDE INDUCED BY GAMMA RADIATION. Takehisa, Masaaki; Yasumoto, Masahiko; Urano, Yokichi (Government Chemical Industrial Research Inst., Tokyo) Kogyo Kagaku Zasshi, 68: 968-71(May 1965). (In Japanese).

The G values are given for the 1,1-dichloroalkanes and 1-chloroalkanes obtained by ^{60}Co γ-induced polymerization of ethylene with methylene chloride in the pressure range from 10 to 40 kg/cm^2. The results were interpreted in terms of a free-radical telomerization mechanism, which included the following steps: CH_2Cl_2 (γ rays) $\rightarrow$ $\cdot Cl + \cdot CH_2Cl$; $\cdot Cl + C_2H_4 \rightarrow ClC_2H_4^{\cdot}$; $\cdot CH_2Cl + n(C_2H_4) \rightarrow ClCH_2(C_2H_4)_n^{\cdot}$; $ClC_2H_4^{\cdot} + n(C_2H_4) \rightarrow Cl(C_2H_4)_{n+1}^{\cdot}$; $Cl(CH_2)_{2n+1\text{ or }2n+2} + CH_2Cl_2 \rightarrow Cl(CH_2)_{2n+1\text{ or }2n+2}H + \cdot CHCl_2$; $\cdot CHCl_2 + n(C_2H_4) \rightarrow Cl_2CH(C_2H_4)_n^{\cdot}$; and $Cl_2CH(C_2H_4)_n^{\cdot} + \cdot CH_2Cl \rightarrow Cl_2CH(C_2H_4)_nH + CHCl_2^{\cdot}$. Over the temperature range from 20 to 80°C the chain transfer constant for the reaction $Cl_2CH(C_2H_4)_n^{\cdot} + C_2H_4$, CH_2Cl_2 increased 3- to 5-fold; the degree of polymerization of the radical $Cl_2CH(C_2H_4)_n^{\cdot}$ increased from 1 to 4, and then became constant. (BBB)

46371 X-RAY COLORATION OF KCl CRYSTALS. Ishiguro, Masakazu; Shimada, Toshikazu (and others) (Osaka Univ.). Mem. Inst. Sci. Ind. Res. Osaka Univ., 22: 67-71(Mar. 1965).

Spacial distribution of F centers produced by x-irradiation at room temperature was investigated using a microscopic spectrophotometer. Considerably different results were obtained for pure KCl and KCl : Sr^{2+} crystals. Effects of the surface on coloration were also examined. From the time dependency of coloration at various distances from the surface, it was found that the role of the Sr^{2+} impurity in the second stage process of the coloration depends on the wavelength of the incident x rays. (auth)

46372 E.S.R. STUDY OF IRRADIATED SOLID CYCLOALKANES. Ohmae, Tadayuki (Osaka Univ.); Nitta, Isamu (and others). Mem. Inst. Sci. Ind. Res. Osaka Univ., 22: 97-9(Mar. 1965).

A study of the electron spin resonance spectra of radicals produced by irradiation at −196°C in various polycrystalline cycloalkanes revealed that in all cases the main species observed after irradiation was the cycloalkyl radical corresponding to the parent cycloalkane. Some of these showed appreciable motional narrowing or structural deformation on warming. It was found that the methylenic groups of the cyclopentyl, cyclohexyl, cycloheptyl, and cyclooctyl radicals were twisted in solid state due to the non-planar structure of the parent molecules, while the four β-hydrogens in the cyclobutyl radical were equivalent. (auth)

46373 RADIATION DOSIMETRY WITH SODIUM CACODYLATE AND TRIS. Levinson, Hillel S.; Garber, Esther B. (Army Natick Labs., Mass.). Nature, 207: 751-2 (Aug. 14, 1965).

The values of sodium cacodylate (sodium dimethylarsenate), $(CH_3)_2ASOONa$, and of tris(hydroxymethyl) aminomethane (2-amino-2-hydroxymethyl-1,3-propanediol) as radiation dosimeters were assessed. The results showed that both systems appear to offer promise as simple gamma radiation dosimeters. (P.C.H.)

46374 RELATIONS BETWEEN ACETYLCHOLINE, CHOLINE AND BETAINE CHAINS IN AQUEOUS SOLUTION. Canepa, F. G. (Northern Polytechnic, London). Nature, 207: 1152-4(Sept. 11, 1965).

Evidence from which a mechanism was found for the radiation decomposition of choline chloride (Ch.Cl), attenuated decomposition of choline bromide (Ch.Br), insensitivity of choline iodide (Ch.I) to irradiation, and the temperature effect on the rate of their decomposition is presented. From the results, a similar mechanism for the radiation decomposition of betaine hydrochloride is suggested. (P.C.H.)

46375 PROPERTIES AND STRUCTURE OF RADIATION-POLYMERIZED POLYETHYLENE. Gotoda, Masao; Fujioka, Shuji (and others) (Japan Atomic Energy Res. Inst., Tokyo). Nuclear Eng. (Tokyo), 11: 43-6(Jan. 1965). (In Japanese).

Ethylene was polymerized with ^{60}Co γ rays at dose rates from 5×10^3 to 4.3×10^5 rad/hr at 20 to 30°C under the pressures from 70 to 400 kg/cm^2. In some cases the polymerization was carried out in the presence of methanol. Some of the properties and the infrared spectra of the radiation-polymerized polyethylene were measured and compared with those of the polyethylenes produced by the high- and medium-pressure methods. The relationships between the respective properties and between the molecular structures and the properties are discussed. The infrared spectra of the radiation-polymerized polyethylene showed that numbers of $-CH_3$, $RRC=CH_2$, $RCH=CHR$, and $RCH=CH_2$ groups per 1000 carbon atoms were 4.4, 0.037, 0, and 0, respectively, while the numbers for the high- and medium-pressure polyethylenes were 28.6, 0.377, 0.063, and 0.046, and 0, 0.029, 0, and 1.77, respectively. It was further found that the polyethylene polymerized in the presence of methanol had a strong infrared absorption by −OH of primary alcohol. The relationships between the density, d (g/cm^3), and the degree of crystallinity, X(%), and between X and the molecular weight, $\overline{M}_n$, are shown by the equations $d = 2.0 \times 10^{-3} X + 0.803$ and $X = 96.8 - 5.2 \log \overline{M}_n$. The −OH of the polymers obtained in the presence of methanol had no influence on X. X was influenced by the short branching, and the relationship between X and the number of $-CH_3$ per 100 carbon atoms is expressed by $X = 70.5 - 7.0 \times (-CH_3/100\ C)$ when the $\overline{M}_n$ of the polymer is 1×10^5. The melting points of the radiation-polymerized polyethylenes were approximately the same as those of the high-pressure polyethylenes. The relationship between the melt indices, MI, and $\overline{M}_n$, is expressed by the equation $\log MI = 18.3 - 4.23 \log \overline{M}_n$. (NSA of Japan)

46376 ANTI-ELECTROSTATIC TREATMENT OF TEFLON FILMS BY RADIATION INDUCED GRAFT COPOLYMERIZATION. Nakagawa, Koji; Manaka, Kazuo (Tokyo Shibaura Electric Co., Ltd.). Nuclear Eng. (Tokyo), 11: 47-50(Jan. 1965). (In Japanese).

Teflon films, 0.05-mm thick, were grafted with acrylic acid, acrylamide, or a combination of both by the use of ^{60}Co γ rays. Both the immersion-irradiation technique and the pre-irradiation technique were used for the graft co-

polymerization. The antielectrostatic effect of the surface grafting was evaluated from the decay curves of the surface potential of the films that were charged by a 5000-volt corona discharge. Evaluations were made on four kinds of grafted teflon film. The grafting conditions employed and the half lives for the surface potential were as follows: immersion irradiation, with a dose of 5×10^6 r, of a 40% benzene solution of acrylic acid, a grafting ratio 5.9, and a half-life of 35 sec; immersion irradiation at 1×10^7 r of a benzene solution of mixed acrylic acid (10%) and acrylamide (10%), a grafting ratio of 1.3, and a 6 sec half life; pre-irradiation at 1×10^7 r for an aqueous solution of acrylic acid (20%) and acrylamide (10%), 5.8 ratio, and 200 sec; and pre-irradiation at 1×10^7 r for pure acrylamide and a grafting ratio of 5.6 but with the anti-electrostatic effect apparently inferior to other three. It was obvious that the difference in the anti-electrostatic effect among the different films was not caused by the difference in the grafting ratios; the infrared spectra of the grafted films suggested that better anti-electrostatic effect was obtained when the interaction between $-COOH$ and $-NH_2$ was stronger. (NSA of Japan)

46377 HOMOPOLYMERIZATION OF MALEIC ACID ESTERS AND DIETHYL FUMARATE UNDER THE INFLUENCE OF γ RADIATION. PART I. RADIOCHEMICAL POLYMERIZATION OF MALEATES: DIETHYL, DIBUTYL, AND DIOCTYL, AND COMPARISON OF THE POLYMERIZATION OF DIETHYL MALEATE WITH THAT OF DIETHYL FUMARATE. Orszagh, Andrzej; Czarnodola, Helena (Inst. of Nuclear Research, Polish Academy of Sciences, Warsaw). Nukleonika, 10: 177-85(1965). (In French).

Studies were made on the radioinduced polymerization of diethyl, dibutyl, and dioctyl maleates, and the results were compared with the polymerization of diethyl fumarate under the effects of gamma radiation. The conversion was studied as a function of irradiation time, temperature, and polymerization in the after-effect, as well as the properties of polymers obtained, noting their intrinsic viscosity, mean molecular mass, and degree of polymerization, which for the maleates did not exceed the value of 10, while diethyl fumarate attained the value of 124. Infrared spectra confirmed the formation of polymaleates and polyfumarates with the disappearance of double bonds. (P.C.H.)

46378 ON THE EPR SPECTRA OF SOME IRRADIATED NITRILES. Eliseeva, N. V.; Kotov, B. V.; Sharpatyi, V. A.; Pravednikov, A. N. Opt. Spectry. (USSR) (English Transl.), 18: 470-1(May 1965).

An investigation is made of EPR spectra of radicals formed during radiolysis of aliphatic compounds containing nitrile groups. Acetonitrile and propionitrile were used for the investigation. The samples were outgassed before being irradiated by gamma rays from a cobalt-60 source. The radiation dose varied from 1.5 to 30 Mrad. The anisotropy of the spectra was measured every 10° by rotating the samples about a vertical axis. Certain discrepancies between the experimental and calculated absorption curves are evidently caused by the superposition of several radicals which can be caused by the superposition of the spectra of several radicals which can be formed during the irradiation of propionitrile. Also the existing anisotropic hyperfine structure can possibly change the intensity relations of the components. (J.F.P.)

46379 DE-EXCITATION OF LIGHT SUMS IN X-RAYED ALKALI-HALIDE PHOSPHORS BY STATIONARY F-BAND ILLUMINATION. Shamovskii, L. M.; Maksimova, N. D. Opt. Spectry. (USSR) (English Transl.), 18: 487-90(May 1965).

The optical de-excitation of KCl(Tl) and NaCl(Ni) phosphor crystals x-rayed at room temperature was investigated at different temperatures. It was shown that in NaCl(Ni), optical F-band illumination can de-excite practically the entire stored light sum at liquid-nitrogen temperatures, as well as at room temperature. In KCl(Tl), a considerable light sum is also de-excited at liquid nitrogen temperature, but less than at room temperature. These facts are explained on the basis of the hole scheme of recombination luminescence. A new mechanism of de-excitation of phosphor crystals is proposed. (auth)

46380 ON THE SYMMETRY OF NARROW-BAND LUMINESCENCE AND ABSORPTION CENTERS OF COLORED LiF CRYSTALS. Kaplyanskii, A. A.; Moskvin, N. A. Opt. Spectry. (USSR) (English Transl.), 18: 493-4 (May 1965).

An investigation is made of the effect of deformation on certain lines of LiF colored by gamma rays from cobalt-60. The method is similar to that described previously. The spectra of uniaxially stressed crystals were observed in a direction L which was perpendicular to the compression axis P. Light polarized with E parallel to P and E perpendicular to P was used; the dispersion of the optical instruments was about 5 Å/mm. When the irradiated LiF crystal is heated at 150–200°C and then strongly excited by light from the 436 nm Hg line the intensity of the 5240 Å line increases as compared to the intensities of the lines in the series, the lines of the series being almost invisible in this case. The piezospectroscopic study demonstrates directly that the 5240 Å line is associated with a new kind of rhombohedral center which has a different orientation in the lattice than the principal rhombohedral centers of the luminescence series. The effect of deformation on the main lines of the electron-vibration structure of the R_2-absorption bands of LiF(391 nm) was also examined. (J.F.P.)

46381 NUCLEAR MAGNETIC RESONANCE ABSORPTION OF ^{60}Co γ-RAY IRRADIATED POLYTETRAFLUOROETHYLENE. I. Tutiya, Mituaki; Yamamoto, Kakuji (Tokyo Metropolitan Inst. Radiol. Res.). Oyo Butsuri, 34: 424-8(June 1965). (In Japanese).

Molecular motion in gamma-irradiated polytetrafluoroethylene was investigated by the nuclear magnetic resonance method. With ^{60}Co as radiation source and 10^8 r as the total exposure dose, radiation effects on the line shape of ^{19}F nuclei were investigated. Changes in narrowing of the line width, room temperature transitions in the second moment, and increases in crystallinity were observed. A specimen, heated at 300°C for four hours after irradiation, showed a remarkable increase in crystallinity. The increase in crystallinity is ascribed to the decrease in molecular weight, and the change in molecular motions to the change in molecular arrangement. (auth)

46382 EFFECT OF UV IRRADIATION ON SUSCEPTIBILITY OF SERUM ALBUMINS TO TRYPSIN. Kleczkowski, A. (Rothamsted Experimental Station, Harpenden, Eng.). Photochem. Photobiol., 3: 115-20(June 1964).

To investigate quantitatively the action of uv light on proteins, their solutions were exposed to 2537 Å radiation and various criteria of denaturation were evaluated. Irradiation converts bovine serum albumin (BSA) and rabbit serum albumin (RSA) into forms much more rapidly hydrolyzed by trypsin than the original proteins. The radiation energy required to be absorbed by each mg of a protein to convert half of it into a form susceptible to trypsin ($E_{50\%}$) is about 0.32 j for BSA and 0.62 j for RSA. The average $E_{50\%}$ for inactivation of enzymes and antibodies is 0.7 j so the two processes may depend on similar alterations in irradiated protein molecules. Energy requirements for destruction of the original antigenic structure of proteins, such as serum albumins or the protein of tobacco mosaic virus, seem to be much greater, $E_{50\%}$ being 3–5 j. It is concluded that much more drastic alterations in structure are needed to destroy the original antigenicity of a protein than to inactivate an enzyme, an antibody, or insulin. Inactivation of enzymes or antibodies by uv may result from a stage in the process of denaturation which also increases susceptibility to trypsin. Quantum yields (ϕ) for the conversion of the albumins into forms more susceptible to trypsin were obtained by assuming that $0.5 = e^{-\phi x}$, where x is the number of einsteins absorbed/mole of the albumin when half of it is converted. Taking 70,000 as the molecular weight of the albumins, the quantum yields are about 0.014 for BSA and 0.0073 for RSA. Breakage of some hydro-

gen bonds, and perhaps also of some S-S bonds, resulting in at least a partial unfolding of a protein molecule and in exposure of sites susceptible to the attack by the enzyme, is probably caused by uv. Thus, uv increases susceptibility of a protein to trypsin digestion by affecting its original tertiary structure. (BBB)

46383 THE DIPOLAR BROADENING OF ELECTRON SPIN RESONANCE LINES IN IRRADIATED SOLIDS. Wyard, S. J. (Guy's Hospital Medical School, London). Proc. Phys. Soc. (London), 86: 587-93(Sept. 1965).

The width and the shape of the electron spin resonance absorption line were measured as a function of the spin concentration in irradiated frozen peroxide solutions. Good agreement is found with a modified version of the Kittel and Abrahams formula. It is shown that line-width measurements can be used to obtain the local concentrations of radicals when these are produced by irradiation in clusters. (auth)

46384 CHARGE-TRANSFER COMPLEXES IN THE SCAVENGING BY IODINE OF RADICALS FORMED ON PULSE RADIOLYSIS OF CYCLOHEXANE. Ebert, M.; Keene, J. P.; Land, E. J.; Swallow, A. J. (Christie Hospital and Holt Radium Inst., Manchester, Eng.). Proc. Roy. Soc. (London), Ser. A, 287: 1-14(Aug. 17, 1965).

Pulse radiolysis of solutions of iodine in cyclohexane resulted in the formation of a transient absorption with wavelength maximum at 3300 Å. This transient spectrum was assigned to the $C_6H_{12}\ldots I^-$ charge-transfer complex. The spectrum and extinction coefficients of the complex over the wavelength range 2500 to 6500 Å were obtained. The coefficient at 3300 Å was 2025 l mole^{-1}cm^{-1}. Hydrogen iodide in cyclohexane gave rise to the same transient absorption. Pulse radiolysis of cyclohexane and cyclohexyl iodide alone gave rise to different transient spectra attributed to the cyclohexyl radical, absorbing in the ultraviolet, with an extinction coefficient of 3401 l mole^{-1} cm^{-1} at 2550 Å and of the $C_6H_{11}I\ldots I^-$ charge-transfer complex, with an absorption maximum of 3900 Å and an extinction coefficient of ~10^3 to 10^4 l mole^{-1}cm^{-1}. During the course of the investigations rate constants were obtained for the following reactions: $C_6H_{11}^{\cdot} + I_2 \rightarrow C_6H_{11}I + I^{\cdot}$, $k_{II} = 7 \times 10^9$ l mole^{-1} s^{-1}; $2C_6H_{12}\ldots I^{\cdot} \rightarrow 2C_6H_{12} + I_2$, $k_{II} = 1.06 \times 10^{10}$ l mole^{-1} s^{-1}; or $2I^{\cdot} \rightarrow I_2$; $2C_6H_{11}^{\cdot} \xrightarrow{a} C_6H_{10} + C_6H_{12}$ (or $\xrightarrow{b}$ $C_{12}H_{22}$), $k_{IIa} + k_{IIb} = 2.5 \times 10^9$ l. mole^{-1} s^{-1}. Dilute solutions of iodine (10^{-4} M) in cyclohexane yielded experimental evidence for neutral radical intermediates only. There were, however, indications that ionic radical intermediates occur in more concentrated solutions (>10^{-3} M). (auth)

46385 STUDIES OF RADIATION-INDUCED REACTIONS OF ETHYLENE IN AQUEOUS SOLUTION. I. REACTIONS IN THE ABSENCE OF OXYGEN. Cullis, C. F.; Francis, J. M.; Swallow, A. J. (Imperial Coll., London). Proc. Roy. Soc. (London), Ser. A, 287: 15-26(Aug. 17, 1965).

Studies were made of the effect of ^{60}Co γ radiation on dilute aqueous solutions of ethylene. The influence of the products of dose, ethylene pressure, pH of the solution and additives were systematically investigated. In neutral and acid solutions of pure ethylene, polymerization is the main process, although small amounts of hydrogen peroxide and C_3-C_4 aldehydes are formed simultaneously. Formation of polymer is largely inhibited in the presence of added Fe^{3+} ions of hydrogen peroxide. The velocity constant (k) for the reaction of the solvated electron with ethylene was determined directly by a pulse radiolysis technique and this reaction was shown to proceed slowly if at all ($k < 2.5 \times 10_8$ l. mole^{-1}s^{-1}). It may, therefore, not be involved to any appreciable extent in the radiolysis of ethylene. The results obtained enable deductions to be made as to the principal elementary stages involved in the reaction. It is shown that hydrogen atoms and hydroxyl radicals are the main species which initially attack ethylene and that vinyl, ethyl and β-hydroxyethyl radicals all probably play an important part as intermediates in the reaction mechanism. (auth)

46386 CHEMICAL EFFECTS OF RADIATIVE NEUTRON CAPTURE IN SOME COBALT(III) COMPLEXES WITH 5 OR 6 NITROGEN ATOMS IN THE COORDINATION SPHERE. De Maine, M. M.; Kay, Jack G. (Univ. of Illinois, Urbana). Radiochim. Acta, 4: 149-57(Aug. 1965).

A study of the chemical changes resulting from thermal neutron capture was made for $[Co(NH_3)_6]Cl_3$, $[Co(NH_3)_5Cl]Cl_2$, $[Co(NH_2CH_2CH_2NH_2)_3]Cl_3$, and $[Co(NH_3)_6](NO_3)_3$. Particular note was made of changed yields of certain products that resulted from variation in the irradiation period and from use of neutron pulses in place of a steady-state neutron flux. The effects were greatest by far for $[Co(NH_2CH_2CH_2NH_2)_3]Cl_3$. Comparisons in the extent of thermal annealing were also made. (auth)

46387 ROLE OF WATER OF HYDRATION IN THE ANNEALING BEHAVIOUR OF NEUTRON-IRRADIATED TRIS-DIPYRIDYL COBALT(III) PERCHLORATE, TRIHYDRATE. Shankar, J.; Nath, Amar; Vaish, S. P. (Atomic Energy Establishment, Trombay, India). Radiochim. Acta, 4: 162-4(Aug. 1965).

The annealing behavior of the trihydrate, the anhydrous complex, and the "hydrated" form resulting from the hydration of the anhydrous phase was studied. The rate of thermal annealing for the trihydrate was very much faster than for the anhydrous (dehydrated) complex, while the hydrated form exhibited even a faster rate of annealing than the trihydrate. These observations were interpreted on the basis of the "variable depth electron trapping model" suggested earlier. Exo-electron emission during the phase transformation was invoked for filling up of the shallow electron traps. (auth)

46388 CHEMICAL STATE OF ^{125}Sb FORMED IN NEUTRON IRRADIATED TIN COMPOUNDS. Facetti, J. F. (Puerto Rico Nuclear Center, Mayaguez). Radiochim. Acta, 4: 164-6(Aug. 1965).

The chemical state of ^{125}Sb obtained in the β decay of neutron-irradiated Sn compounds was studied. The compounds irradiated were SnO, SnO_2, and $K_2Sn(OH)_6$. The results obtained suggested that the distribution of Sb^V and Sb^{III} depends on the composition and constitution of the irradiated compounds. (auth)

46389 GAMMA-RAY INITIATED POLYMERIZATION OF VINYL n-BUTYRATE. Kawase, Kaoru; Hayakawa, Kiyoshi (Government Ind. Res. Inst., Nagoya, Japan). Rept. Govt. Ind. Res. Inst., Nagoya, 14: 194-200(May 1965). (In Japanese).

The bulk and solution polymerizations of vinyl-n-butyrate by gamma rays were carried out and the results were compared with the reported values on vinyl acetate. In the bulk polymerization the conversion steadily increased with irradiation time up to about 30%, and neither the gel effect nor the formation of insoluble gel were observed. The initial rate of polymerization showed 0.6-th power dependence on the dose rate, whereas the intensity did not seem to affect the molecular weight of the polymer. The polymerization was inhibited by typical radical scavengers. In the range from −78 to 60°C at 4×10^4 r/hr, the activation energy was 2.6 kcal/mol from the rate, and 1.0 kcal/mol from the rate, and 1.0 kcal-mol from the degree of polymerization of the polyvinyl alcohol obtained from polyvinyl n-butyrate. The effect of carbon tetrachloride and methylene dichloride as solvents on the rate of polymerization was determined. In both solvents the rate of polymerization was rather depressed and did not show any sensitization as is usual in the case of other common monomers. The apparent G-value of the radical formation calculated from the rate of solution polymerization did not coincide with that obtained from DPPH consumption. This discrepancy could not be attributed to the low reactivity of CCl_3 radical with the double bond. (auth)

46390 THE PARAMAGNETIC CENTRES FORMED IN SOME IRRADIATED INORGANIC OXI-COMPOUNDS OF SELENIUM. I. THE e.s.r. SPECTRA OF IRRADIATED SeO_4Na_2. Constantinescu, O.; Pascaru, I.; Constantinescu, M.; Paun, I. (Inst. for Atomic Physics, Academy of the R.P.R., Bucharest). Rev. Roumaine Phys., 10: 251 (1965).

The ESR spectral parameters along with the behavior on heating of irradiated polycrystalline samples of SeO_4Na_2

indicate the possibility of the formation by irradiation of SeO_4^- and SeO_3^- centers. (L.B.S.)

46391 INTERPRETATION OF THE RADIATION AND THERMAL ANNEALING BY PROCESSES GOVERNED BY THE DEFECT CONCENTRATION. Costea, T.; Negoescu, Irina (Inst. for Atomic Physics, Academy of the R.P.R., Bucharest). Rev. Roumaine Phys., 10: 561-72(1965).

The annealing processes, followed by means of the ^{60}Co recoil atom retention, in the hexammino-cobaltic nitrate, concomitantly and after the irradiation in the nuclear reactor, were studied. The kinetics of both radiation and thermal annealing may be explained by the activation energy diminution with the defect concentration. The explanation was made on the assumption that the defect concentration is a function of the radiation dose-rate. (auth)

46392 PLASTIC MATERIAL FOR MEASURING LARGE RADIATION DOSAGE. Matsumoto, Shoichi; Tsukada, Tomomichi (and others) (Tokyo Shibaura Electric Co., Ltd.). Toshiba Rev., 20: 414-18(Apr. 1965). (In Japanese).

Plastic materials for measuring large dosage of radiation (10^4 to 10^7 r) and different dosimeters made of it were developed. The material can be formed into films, sheets, and plates with various thickness and area, into blocks with a wide variety of shape, into fibers, etc., by compression molding, calendering, extrusion molding, and injection molding. The material mainly consists of chlorine-containing polymers, such as, polyvinyl chloride, polyvinyl chloride acetate, polyvinylidene chloride, and chlorinated polyethylene, containing hydrogen chloride-sensitive dye whose color is changed by irradiation of the polymer. The dosimeters made of these plastic materials are characterized by easy radiation dosage evaluation, high performance stability, and low cost. The color of the polymer changes in accordance with radiation dosage; hence, dosage is roughly estimated by observing the coloration with the naked eye, while spectrophotometric measurement may be applied for more precise estimation. The extinction coefficient of the dosimeter at a specific wavelength increases linearly with irradiation on a log-log scale. (auth)

46393 DRIFT VELOCITIES OF SLOW ELECTRONS IN POLYATOMIC GASES. Cottrell, T. L.; Walker, Isobel C. (Univ. of Edinburgh). Trans. Faraday Soc., 61: 1585-93(Aug. 1965).

Drift velocities of low energy electrons were measured in CH_4, CD_4, SiH_4, SiD_4, C_2H_6, C_3H_3, C_2H_4, C_2H_2, C_2D_2, CH_3Cl, AsH_3, CH_3COCH_3, CH_3OCH_3, and C_2H_5OH. The results are interpreted in terms of energy transfer from the electrons to rotational or vibrational modes of the molecules. (auth)

46394 PHOTO- AND RADIATION-CHEMISTRY OF LOW TEMPERATURE AQUEOUS GLASSES. PART I. MINERAL ACID GLASSES CONTAINING N_2O AND Fe^{2+} IONS. Dainton, F. S.; Jones, F. T. (Univ. of Leeds, Eng.). Trans. Faraday Soc., 61: 1681-1700(Aug. 1965).

Measurements were made of $G(N_2)$, $G(O_2)$ and $G(H_2)$ for mineral acid glasses containing N_2O and irradiated at temperatures in the range 77–340°K with cobalt-60 γ rays. Whenever a change of composition or temperature caused a phase change from the crystalline or liquid state to the glassy state, $G(N_2)$ increased sharply but $G(H_2)$ was unaffected. When Fe^{2+} ions were present $G(H_2)$ increased, $G(N_2)$ decreased, and $G(Fe^{3+}) = 2(G(H_2) + G(N_2))$. When glasses containing Fe^{2+} and N_2O were irradiated with uv light similar products were formed. The results combined with measurements of the ESR and uv absorption brought about by irradiation and the effects of increasing temperature on these spectra were consistent with the formation in both the radiation-chemical and the photochemical primary act of a mobile electron e_m^- having energy initially in excess of thermal levels which can migrate linear distances of about 50 Å in the glass and react with a solute which it may encounter. For 5 M H_2SO_4 glass $G_{e_m^-} = 1.7$, $G_{H_3} = 0.63$ based on total energy absorption. e_m^- produced by γ rays had equal rate constants for reaction with N_2O and Fe^{2+} but that generated photochemically reacted twice as rapidly with N_2O as with Fe^{2+}. (auth)

46395 EFFECT OF HYDROGEN ATOM AND ELECTRON SCAVENGERS ON THE RADIOLYSIS OF METHANOL VAPOUR. Meaburn, Malcolm; Mellows, Frank W. (C.E.N., Saclay, France). Trans. Faraday Soc., 61: 1701-8(Aug. 1965).

The ^{60}Co γ radiolysis of methanol vapor was studied at 87 mm pressure and 20°C in the presence of various additives. The yields from pure methanol, $G(H_2) = 11.1 \pm 0.6$, $G(CO) = 1.18 \pm 0.06$ and $G(CH_4) = 0.35 \pm 0.05$ are in reasonable agreement with previously published values. The additives CCl_4, CH_3Br, and O_2 were found to be efficient electron scavengers and the electron yield, $G_{e^-} = 4.1 \pm 0.7$ was determined. The results further indicate that electron scavenging, but not hydrogen atom scavenging, is dose-rate dependent. This finding is consistent with the idea that the electron is reacting with the acid species CH_3OH^+ and not with neutral methanol. (auth)

46396 EFFECT OF ELECTRON SCAVENGERS ON THE FORMATION OF HYDROGEN IN THE RADIOLYSIS OF PROPANE. Johnson, G. R. A.; Warman, J. M. (Univ. of Newcastle upon Tyne, Eng.). Trans. Faraday Soc., 61: 1709-14(Aug. 1965).

The radiolytic yield of H_2 from propane was decreased when N_2O, SF_6, or CCl_4 were present as scavengers, the maximum decrease, $\Delta G(H_2) = 2.6$, being the same for each of these scavengers. Irradiation of propane + N_2O (2–5 mole %) gave $G(N_2) = 8.7$. This fell to zero when CCl_4 (~3 mole %) or SF_6 (10^{-3} to 3 mole %) were present but was not changed by the addition of propene (3 mole %). Propane + propene (3 mole %) gave $G(H_2) = 2.0$. This was not changed by the addition of N_2O. N_2O, SF_6, and CCl_4 can act as electron scavengers, i.e., they can capture electrons to form negative ions. Their effect on $G(H_2)$ is ascribed to a change in the ion-neutralization process, from positive ion + electron recombination in pure propane, to positive ion + negative ion recombination in propane + electron scavenger. It was concluded that ion + ion recombination does not contribute to the formation of H_2 and that ion + electron recombination can give H atoms but not molecular H_2. In propane + N_2O dissociative electron capture by N_2O leads to the formation of N_2. Competition between this process and ion + electron recombination accounts for the dependence of N_2O concentration of $G(N_2)$ and $\Delta G(H_2)$. From a study of this competition it was concluded that $\sqrt{k_r}/k_{e+N_2O} = 3.3 \times 10^{10}$, where k_r is the ion + electron recombination coefficient. SF_6 and CCl_4 can decrease $G(N_2)$ by competing with N_2O for electrons. It was concluded that $k_{e+SF_6}/k_{e+N_2O} \geq 10^4$. (auth)

46397 NITROSOBENZENE-IRON TRICARBONYL DIMERS BY RADIATION CHEMISTRY REDUCTION OF $Fe(CO)_5$ WITH NITROBENZENE. Koerner von Gustorf, E.; Jun, M.-J. (Max-Planck-Institut fuer Kohlenforschung, Muelheim, Ger.). Z. Naturforsch., 20b: 521-3(June 1965). (In German).

The preparation of a complex, dimeric nitrosobenzene-iron tricarbonyl, by irradiation of $Fe(CO)_5$ in nitrobenzene with light or ^{60}Co γ rays is described. According to IR (infrared) spectroscopic data nitrosobenzene molecules are the only bridging ligands in this complex. The mechanism of the reduction of nitrobenzene to nitrosobenzene is discussed. (auth)

46398 BEHAVIOUR OF RECOIL ATOMS IN SEMICONDUCTORS. Costea, T.; Negoescu, Irina (Inst. of Atomic Physics, Bucharest). Z. Physik. Chem. (Frankfurt), 45: 136-9(May 1965).

The behavior of the recoil atoms resulting from n,γ reactions in the nonstoichiometric oxides $CrO_{2.26}$ and $CrO_{2.37}$ was studied. The experimental results concerning the chemical state of the recoil atoms and the thermal annealing process were interpreted by a hypothesis taking into account the contribution of the donor and acceptor levels created by the recoil atoms. (auth)

46399 SCINTILLATIONS IN ORGANIC SOLIDS. Birks, J. B. (Univ. of Manchester, Eng.). pp 433-508

of Physics and Chemistry of the Organic Solid State. Vol. II. New York, Interscience Publishers, 1965.

Scintillations in organic solids are discussed. Topics covered include: scintillation counting, classification of organic scintillators, scintillation phenomena, the scintillation mechanism and absolute scintillation efficiency, practical scintillation efficiency, scintillation response to different ionizing radiations, scintillation decay, the slow scintillation component, radiation damage, and comparison of scintillators. (160 references) (F.J.H.)

46400 RADIATION EFFECTS IN POLYMERS. Alger, Raymond S. (Radiological Defense Lab., San Francisco). pp 769-849 of Physics and Chemistry of the Organic Solid State. Vol. II. New York, Interscience Publishers, 1965.

The radiation effects in polymers are discussed. Energy absorption, thermal equilibrium, chemical equilibrium, radioinduced transients, and permanent radiation effects in polymers are considered. Current models and theories employed in describing the fundamental radioinduced reactions are reviewed. Microscopic and macroscopic radiation effects are described for representative monomeric and polymeric solids. (96 references) (F.J.H.)

46401 CHEMICAL SPECIES IN WATER. Dainton, F. S. (Univ. of Leeds, Eng.). pp 157-66 of Radiation Dosimetry. New York, Academic Press, 1964.

When water is irradiated, molecules close to the track of the radiations are ionized, while some of those further away are electronically excited. Two theories were postulated concerning the fate of these ions so formed. These two theories which are discussed predict different distributions for the H and OH radicals. Evidence for the radical model is presented and the solvated electron is discussed. The present position is given, in which it is shown that if the electron exists long enough for an ionic atmosphere to be built up and then react as such, the rate constants of these reactions may be written as functions of the ionic strength using the limiting form of the Debye-Hückel equation. Types of solute and effects of pH, light absorption of electrons, conversion of H to e_{aq}^-, the electron in aqueous glasses at −196°C, ionization of the OH radical, and the increase of G(H) and G(OH) with $[H^+]$ and $[OH^-]$ are considered. (J.F.P.)

46402 ELECTRON SPIN RESONANCE STUDIES OF RADICALS. Mueller, A. (Kernforschungszentrum, Karlsruhe, Ger.). pp 180-91 of Radiation Dosimetry. New York, Academic Press, 1964.

Although free radicals, that is, molecules containing an odd number of electrons in their valence shell, were shown to play a part in every branch of chemistry, the present survey is essentially restricted to long-lived radicals produced by ionizing radiation in solid organic matter. The restriction to long-lived radicals is imposed by technical difficulties which as yet have prevented electron spin resonance studies of radicals with lifetimes shorter than a minute. This situation also necessitates the limitation to solids. Organic substances attract special interest not only because a detailed knowledge of the mechanisms leading to radiation damage would be very useful for radiation-chemical, radiation-biological, and radiation-medical applications, but also because such studies should lead to a better understanding of the complicated molecular systems of which basic biological structures are composed. Principles of electron spin resonance spectrometry are given. Radicals in organic substances are discussed in detail. Electron spin resonance spectrometry is also discussed. (J.F.P.)

46403 SOLID STATE RADIATION CHEMISTRY OF GLYCINE AND ALANINE CHELATES AND METAL SALTS (thesis). Gottschall, Walter Carl. Boulder, Colo., Univ. of Colorado, 1964. 94p.

Amino acid chelates and salts, carbon-14-labeled in the carboxyl position, were prepared and irradiated in vacuo in the University of Colorado cesium-137 gamma-ray source for periods of 2, 4, 8, and 12 days at a flux of 2.78×10^{19} ev/g hr. After storage in a −15°C freezer for at least two days, carbon-14 dioxide produced was assayed via wet chemical generation and radioactivity determination with ionization chambers on a vibrating reed electrometer. Results obtained, expressed in $G(CO_2)$ were: glycine, 1.02; $Cu(Gly)_2$, 0.45; $Ni(Gly)_2$, 0.34; $Zn(Gly)_2$, 0.28; $Cd(Gly)_2$, 0.21; $Co(Gly)_3$, 0.32; NaGly, 0.43; KGly, 0.54; RbGly, 0.91; alanine, 0.89; $Cu(Ala)_2$, 0.99; $Ni(Ala)_2$, 0.21; $Zn(Ala)_2$, 0.53. The Conway microdiffusion method coupled with the Russell colorimetric procedure indicated comparable $G(NH_3)$ values for the chelates and amino acids. A separate determination of the ratio of amines and NH_3 indicated a constant ratio of 3 or 4 : 1 : : NH_3 : amine, with no other products noticeable. Accordingly $G(NH_3)$ results were: glycine, 4.3; $Cu(Gly)_2$, 1.0; $Cd(Gly)_2$, 0.8; and alanine, 3.3. G(−M) values were determined for glycine and alanine by isotopic dilution and through use of the automatic amino acid analyzer. A value between 5 and 7 was indicated for glycine, and alanine gave results between 4 and 5. Analyses with gas chromatography and mass spectra gave much smaller yields of CO_2 and NH_3 than the "wet" techniques. These differences are felt to reflect extensive trapping of both gases within the crystalline matrix. Hydrolysis of intermediate species is also believed responsible for production of much of the NH_3. Results were correlated with the theory that the greater the electron density on the ionic oxygen atom, the more favored CO_2 production becomes. (Dissertation Abstr.)

46404 GAMMA AND NEUTRON IRRADIATION OF PURE FLUOROCARBONS (thesis). Mailen, James Clifford. Gainesville, Fla., Univ. of Florida, 1964. 201p.

Samples of perfluoromethane, perfluoroethane, perfluoropropane, perfluoro-n-butane, perfluoro-n-pentane, perfluoro-cyclo-pentane, perfluoro-n-hexane, perfluoro-2-methylpentane, and perfluoro-2,3-dimethylbutane were exposed to cobalt-60 gamma rays and the mixed radiation of the Oak Ridge Graphite Reactor and the Oak Ridge LITR reactor. Analysis of the resulting mixtures was by a three-column gas chromatograph allowing essentially complete analysis of all compounds and isomers from C_1 to C_8 and analysis by number of carbon atoms from C_7 to C_{12}. In the irradiation of pure saturated fluorocarbons by gamma rays, the important chemical reactions in the sample are recombination of radicals, disproportionation of small radicals, addition of fluorine and radicals to unsaturated molecules, and the reaction of radicals with molecular fluorine. When fluorocarbons are irradiated to high energy absorption, as in a nuclear reactor, chemical equilibrium considerations are important. The equilibrium depends on the fluorine to carbon ratio of the sample with a ratio of four resulting in nearly pure perfluoromethane. The G values for disappearance of the parent compound are approximately: CF_4, 1.5; C_2F_6, 3.25; C_3F_8, 4.5; $n\text{-}C_4F_{10}$, 5.4; $n\text{-}C_5F_{12}$, 4.9; $cyclo\text{-}C_5F_{10}$, 3.0; $n\text{-}C_6F_{14}$, 6.0; $2\text{-}CF_3C_5F_{11}$, 6.0; and $2,3\text{-}(CF_3)_2C_4F_8$, 9.6. The important products in perfluoromethane are perfluoroethane and perfluoroacetylene produced in about equal amounts. For the other materials for short irradiations the major products are saturated and are those predicted by simple bond rupture and radical recombination reactions. The results for perfluoroethane and larger molecules, excluding cyclo-compounds, can be correlated by statistical recombination calculations using empirically determined radical effectiveness numbers. Since these effectiveness numbers are the same for radicals formed in the same way this method can be used to predict product distributions for other fluorocarbons. (A.G.W.)

46405 RADIOCHEMICAL SEPARATIONS THROUGH RECOIL REACTIONS AND THE PARTIAL CHARACTERIZATION OF ^{133s}Te (thesis). Prussin, Stanley Gerald. Ann Arbor, Univ. of Michigan, 1964. 103p.

The feasibility of performing radiochemical separations based on the organometallic compounds formed when fission fragments and their β-decay products are stopped in an organic liquid was examined. The system chosen for study was comprised of uranium-glass fibers and neohexane (2,2-dimethylbutane). The basic procedure was to irradiate samples of the mixture and then to examine the neohexane for activities of various elements using modifications of standard radiochemical procedures. The data obtained are

discussed and evaluated in terms of the general applicability of the technique to separations of the more electronegative elements formed in fission. As an illustration, a simple and rapid procedure for the isolation of tellurium with the system under investigation is described. A search for the short-lived ^{133}sTe formed in the decay of the 53 min ^{133m}Te resulted in the isolation of an unreported activity of half life 12.45 ± 0.28 min. This activity was shown to be formed in the decay of a parent of half life 54 ± 5 min present in fission product tellurium and was shown to decay to the 21-hr ^{133}I. No activity of half life ≈2 min was isolable in the decay of metastable tellurium isomers produced in fission and none was observed as a result of the decay of the unreported activity. On the basis of these data, the 12.45 ± 0.28 min activity was assigned to the isomer ^{133}sTe. The prominent γ-rays in the decay of this nuclide are 0.154, 0.307, 0.406, 0.73–1.02 (complex), 1.335, 1.709, and 1.85 Mev. A procedure for the rapid isolation of ground-state tellurium isomers based on the change of oxidation state accompanying internal conversion is described. The procedure utilizes the extraction of Te(IV) from hydrochloric acid into TBP–petroleum ether and is applicable to the general separation of Te(IV), Te(VI), and iodine. (Dissertation Abstr.)

46406 METHOD FOR THE INHIBITION OF RADIATION DAMAGE TO THE REPROCESSING SOLVENT TBP. (to Nihon Genshiryoku Kenkyu Sho). British Patent 1,000,798. Aug. 11, 1965. Priority date Dec. 12, 1962, Japan.

The addition of a radical scavenger to TBP minimizes the radiation damage to the TBP used as a reprocessing solvent in the separation of U, Pu, and radioactive fission products. The radical scavenger is added in an amount in the range of 1% w/w to 10% w/w and may be any reagent or mixtures of reagents selected from the following group: hydroquinone, triphenyl methane, tetrachloro-para-benzoquinone, para-phenylene-diamine, tetra-methyl-thiuram disulfide, pyrene, phenanthrene, or terphenyl. (B.L.M.)

Radiochemistry

See also Separation Processes and Procedures.

Refer also to abstracts 46142, 46406, and 47599.

46407 (AAEC/TM-226(Suppl.1)) PURITY OF γ-RAY SOURCES. Watt, J. S. (Australian Atomic Energy Commission Research Establishment, Lucas Heights). Apr. 1965. 9p. Dep. mn.

Purities of γ-ray excited X-ray sources were calculated as a function of energy of the radioisotope γ-ray and atomic number of the target cone. Agreement with experiment is satisfactory. Calculated results of K_α to K_β quanta output, and the ratio of coherent to Compton scattered quanta for the backscattered γ-ray output, are also given. (auth)

46408 (ORNL-tr-770) DEPENDENCE OF THE SEPARATION FACTOR IN ISOTOPE EXCHANGE ON THE PROPERTIES OF THE EXCHANGED MOLECULES. Rozen, A. M.; Mikhailichenko, A. I. Translated for Oak Ridge National Lab., Tenn. from At. Energ. (USSR), 18: 147-56(1965). 23p. Dep. mn; CFSTI $1.00 cy, $0.50 mn; JCL $2.60 fs, $0.89 mf.

An investigation was made of the dependence of the equilibrium constant during isotope exchange in diatomic compounds on the properties of the exchanged molecules: the force constant, dissociation energy, electronegativity, structure of the electron shell, internuclear separation, and masses of the isotopic and supplementary atoms. By means of semiempirical relations, analytical equations were obtained which describe the influence of those factors on the value of the equilibrium constant. Convenient methods of correlation were found which permit predicting the character of the change of the beta-factors in series of analogous compounds. Recommendations are given regarding the selection of systems for the separation of isotopes. An attempt was made to extend some of the conclusions obtained to isotope exchange in multiatomic compounds. (auth)

46409 MICROBIAL PROCESSES FOR PREPARATION OF RADIOACTIVE COMPOUNDS. Perlman, D.; Bayan, Aris P.; Giuffre, Nancy A. (Squibb Inst. New Brunswick, N. J.). Advan. Appl. Microbiol., 6: 27-68(1964).

This review surveys methods used in preparing radioactive compounds by microbial processes, including: (1) methods of addition of precursor to microbial systems, (2) recovery of labeled compounds, (3) determination of the purity of labeled compounds, and (4) stability of labeled compounds. The list of radioactive compounds which have been prepared by microbial processes include: antibiotics, vitamins, amino acids, carbohydrates and related compounds, sterols and related compound, organic acids and alcohols, nucleic acids, and purines. Emphasis is placed on the microbiological aspects of these processes, and technical problems likely to be encountered are mentioned; however, no detailed procedures for preparing the compounds are described. Only radioisotope labeling is considered, and studies with the stable isotopes ^{15}N, ^{13}C, ^{18}O, and deuterium, often used to prepare labeled compounds are only briefly mentioned. Although most labeled compounds produced by microbial processes have been formed as a result of adding ^{14}C-labeled precursors to microbial cells, a few compounds have been made by growing the microorganisms in D_2O. Also considered are techniques adopted to minimize radiation effects. Storage at low temperatures usually reduces the rate of chemical degradation. Dispersion over a large area, such as drying radiochemical solutions on paper, reduces adsorption of radiation energy by the radioactive compound. Dilution of the radioactive compound by either adding the unlabeled form or by introducing other substances, e.g., nonpolar solvents, usually reduces radiolysis. In general, the best practice in working with radioactive compounds is to use them immediately after preparation or receipt from the manufacturer. This will minimize the effects of instability and the complications resulting from impurities caused by radiation. (200 references.) (BBB)

46410 RECENT PROGRESS IN RADIOACTIVE CHEMICAL MANUFACTURE. Chem. Ind. (London), No. 24, 1032-3(June 13, 1964).

Over the last ten years there has been no radical change in the approach to radiochemical manufacture, but much technical progress has been made towards a wider range of products, now available in greater quantity and high quality. More than 150 species of radioisotopes are now available commercially, compared to about 20 ten years ago. For all elements except six there are convenient radioactive tracers, and for some there is a wide choice. With some isotopes the ideal of making them truly carrier-free is now closely approached. The choice of target material is an important factor affecting the isotopic purity of the final product. Although nuclear reactors are still the principal sources of radioisotopes, there has been a reversion to the use of cyclotrons which can provide isotopes in the neutron-deficient group. It was concluded that, in general, the supply of radioactive chemicals is running ahead of the demand. (BBB)

46411 CHEMICAL CHANGES IN THE β-DECAY OF IODINE ISOTOPES AS A METHOD OF SYNTHESIZING XENON COMPOUNDS. Murin, A. N.; Kirin, I. S.; Nefedov, V. D.; Grachev, S. A.; Gusev, Yu. K. (Ioffe Inst. of Physics and Tech., Leningrad). Dokl. Akad. Nauk SSSR, 161: 611-13(Mar. 21, 1965). (In Russian).

The formation of oxygen compounds of xenon on decay of the corresponding ^{131}I compound was demonstrated. In a solution of $K^{131}IO_4$ in dilute sulfuric acid, approximately 40% of the daughter ^{131}Xe that was formed accumulated in chemically combined form. With $K^{131}I$ combined xenon was not found. In these experiments the iodine compounds were dissolved in water or 0.02N H_2SO_4, and the free xenon was removed by a current of helium. Then a reductant was added and helium was again passed through to remove free xenon. The theory is that in the conversion of ^{131}I as iodate or periodate ion, in the first instant of radioactive decay neutral molecules of XeO_3 or XeO_4 are formed. Approximately half these molecules are in the activated state. Cessation of the activation may be accompanied by release

of oxygen and formation of a lower oxidation state, even free xenon. Octavalent xenon is very unstable in acid solution. (TTT)

46412 HOT ATOM CHEMISTRY OF HALOGENS ACTIVATED IN β-DECAY. PART III. REACTIONS OF ^{132}I IN LIQUID MIXTURES OF n-PROPYL HALIDES AND BENZENE OR IODOBENZENE. Halpern, A.; Sokolowska, A. (Inst. of Nuclear Research, Warsaw). J. Inorg. Nucl. Chem., 27: 1893-1903(Sept. 1965).

$^{132}TeCl_4$ was contacted with aliphatic-aromatic mixtures until establishment of the radioactive equilibrium $^{132}Te \rightarrow ^{132}I$. The mole fraction of both organic components was varied from zero to one. The distribution of ^{132}I among the various products was then determined by gas-chromatographic analysis. The specific activity of the aliphatic ^{132}I-labeled products increased with the concentration of the aromatic component (benzene). The results obtained were interpreted in terms of intermolecular energy transfer. (auth)

46413 REVIEWS OF ISOTOPE SEPARATION RESEARCHES IN JAPAN. ACTIVITIES OF THE SPECIAL COMMITTEE ON ISOTOPE SEPARATION. Nippon Genshiryoku Gakkaishi, 7: 429-37(Aug. 1965). (In Japanese).

The Special Committee on Isotope Separation of the Atomic Energy Society of Japan was established in April 1963 and ended in March 1965. Studies were made on the separation of natural isotopes. The isotopes separated included D, ^6Li, ^7Li, ^{10}B, ^{12}C, ^{15}N, ^{18}O, ^{39}K, ^{40}Ar, and ^{235}U. The methods of separation adopted included gaseous diffusion, ultracentrifuge, thermal diffusion, molecular distillation, chemical exchange and electrophoresis. (auth)

46414 SEPARATION AND PURIFICATION OF GASEOUS FISSION PRODUCTS. Ichiha, Sumio (Japan Atomic Energy Res. Inst., Tokyo). Nuclear Eng. (Tokyo), 11: 15-19(Jan. 1964). (In Japanese).

The separation, purification, and uses of gaseous fission products released from ^{235}U bombarded with thermal neutrons are described. These fission products are Xe, Kr, N_2, O_2, H_2, H_2O, CO_2, hydrogen halides, nitrogen oxides, and halogens. Of these, ^{133}Xe and ^{85}Kr are industrially important. Physical or chemical methods are used to separate impurities from Xe and Kr. The separation of ^{133}Xe and ^{85}Kr after the impurities are removed is done either by the distillation or adsorption method. The most widely used is charcoal chromatography. Impurities are first captured in a 900°C charcoal reactor, and then the mixture of Xe and Kr is adsorbed onto an active carbon column (kept at −30 to −125°C) and eluted with He gas. The radioactive inert gases may be used as radiation sources in radiation chemistry, e.g., polymerization of styrene in a liquid phase containing ^{85}Kr; for leak tests, such as radioflow test, and for measurement of gas flow rates. ^{85}Kr can also be fixed in the form of a clathrate compound or used as a kryptonate, i.e., a substance on which Kr is stably fixed by diffusing Kr onto the surface of the solid at high pressure and temperature. (NSA of Japan)

46415 FORMATION OF TRITIUM COMPOUNDS BY IRRADIATION OF BUTANE WITH T^+ IONS AT 2 TO 6 kev. Paulus, J. M.; Adloff, J. P. (Centre de Recherches Nucleaires, Strasbourg). Radiochim. Acta, 4: 146-8(Aug. 1965). (In French).

Tritium ions were generated in a specially designed mass spectrometer in order to study the reactions of these ions with gases at low pressures in a large energy range. Irradiation of butane at pressures from 10^{-2} to 4×10^{-2} mm Hg with 2 to 6 kev T^+ ions led to the following labeled products: CH_3T, C_2H_5T, C_2H_3T, C_3H_7T, C_3H_5T, and C_4H_9T. The yields increased when the tritium ion energy decreased. (auth)

46416 ENRICHMENT OF ^{47}Ca BY THE USE OF SZILARD-CHALMERS PROCESSES OF SOME ORGANOCALCIUM COMPOUNDS. Ebihara, Hiroshi (Japan Atomic Research Inst., Tokyo). Radiochim. Acta, 4: 167-8(Aug. 1965).

It was found to be possible to obtain very useful enrichment of radioactive calcium by heterogeneous extraction (corresponding to a Szilard-Chalmers process) of dehydrated calcium oxinate, oxalate, or citrate. The use of dehydrated oxine and 10% ethanol gave an extraction yield of 44% and an enrichment factor of 40. (auth)

46417 RADIATION-INDUCED CHANGES IN BIOLOGICALLY ACTIVE MACROMOLECULES. Adelstein, S. James (Harvard Medical School, Boston). Radiol. Clin. North Am., 3: 181-95(Aug. 1965).

This is a review of the early biophysical events that occur in the interaction of high energy radiation with isolated and purified macromolecules. Some ultimate chemical changes produced in nucleic acids and proteins are discussed, with reference to 49 previous reports. The relative importance of ionization and excitation in the radiation inactivation of biological macromolecules is considered. Probably, both ionized and excited states are involved in the initial interactions; it seems likely that both intramolecular and intermolecular charge and energy transfer act to funnel the imparted energy to critical loci in macromolecules. The two mechanisms of excitation energy migration which have been proposed, the exciton hypothesis and the proton transfer concept, are outlined. The detection of free radicals and the early radiation events and the ultimate radiochemical damage due to free radicals are examined. These radicals may be produced directly from primary ionizations and excitations or they may derive from the molecular rearrangements and dissociation that follow in the secondary processes. The radiolysis of water and subsequent interactions of the products with biological molecules are discussed. The radicals, and perhaps the molecular products of water, can react with the macromolecular and other organic elements of cells and tissues. Specific modifications of DNA, RNA, and proteins, especially enzymes, are discussed and examples cited. (BBB)

46418 THE RADIO-LABELING OF ORGANIC COMPOUNDS BY $^{12}C(\gamma,n)^{11}C$ REACTIONS BY MEANS OF BREMSSTRAHLUNG OF A 35-Mev BETATRON. Frost, Dietrich; Michel, Lothar; Schwarz, Eberhard (Rudolf-Virchow-Krankenhauses, Berlin; Freie Universitaet, Berlin). Strahlentherapie, 127: 510-15(Aug. 1965). (In German).

The 35-Mev bremsstrahlung from a betatron was utilized in the production of radioactive organic compounds (HLT = 20.5 min) by means of the $^{12}C(\gamma,n)^{11}C$ reaction. Gamma rays can break up chemical bonds as could be shown with urocanic acid in aqueous solution. Free radicals, produced in water, are responsible for the decomposition. Other compounds, such as glycine remain stable and can be used in the investigations. (tr-auth)

46419 CAPACITY DILATOMETER FOR RADIOCHEMICAL INVESTIGATIONS. Ermakov, V. I.; Zakhariev, A. I.; Zagorets, P. A. (Mendeleev Inst. of Chemical Engineering, Moscow). Zh. Fiz. Khim., 39: 1531-5 (June 1965). (In Russian).

The construction of capacity dilatometers designed for radiochemical investigations is proposed. The size of the volume increase of the reaction mixture was obtained by the method of frequency determination of the measuring generator, for a vibrating circuit on which the electrodes of the measuring condenser brass strips, glued to capillaries of the dilatometer, were placed. By virtue of the construction given the possibility of conducting remote determinations and control according to the state of the investigating object was made clear. (tr-auth)

46420 STANDARDS OF ACTIVITY. Newbery, G. R. Amersham, Eng., The Radiochemical Centre, 1965. 27p.

Factors governing the supply of specially measured and certified radioactive material are discussed. Types of standards available, certification, use of standards of activity, absolutely standardized solutions, reference solutions, other standardized solutions, and measurement techniques are considered. (M.C.G.)

46421 THE STANDARDIZATION OF RADIOACTIVE ISOTOPES. Trott, N. G. (Royal Cancer Hospital, London). pp 211-35 of Radiation Dosimetry. New York, Academic Press, 1964.

The term standardization in the field of radioactivity is commonly used to describe the preparation of a sample of a radionuclide having an activity which can be specified, within certain limits of error. Standardization is of considerable importance in the biological and medical applications of radioactivity, especially in calculations of radiation dose. Each radionuclide presents special problems in standardization, and extensive intercomparisons of measurements, nationally and internationally, are necessary to establish the reliability of these methods. The topics discussed include terminology, radium standards, artificial radionuclides, direct methods of determining activity, β-γ coincidence counting, 4π β-γ coincidence counting, internal gas counting, 4π x-ray counting, calorimetry, and ionization methods. Other topics considered are intercomparison of results, maintenance of standards, availability of radioactive standards, and special types of standards. (J.F.P.)

Separation Processes and Procedures

See also Analytical Procedures. ISOTOPE TECHNOLOGY — Separation and Production

Refer also to abstract 47921.

46422 (BNWL-SA-205) STATUS OF THE SALT CYCLE PROCESS FOR PROCESSING OXIDE FUELS. Benedict, G. E.; Bond, W. R.; Jansen, G. Jr.; Morgan, L. G.; Lundquist, J. R. (Battelle-Northwest, Richland, Wash. Pacific Northwest Lab.). Sept. 3, 1965. Contract AT(45-1)-1830. 22p. (CONF-650902-17). Dep. mn; CFSTI $1.00 cy, $0.50 mn.

From American Chemical Society, 150th National Meeting, Atlantic City.

The Salt Cycle process is being developed to reprocess UO_2–PuO_2 based fuels for recycle to thermal heterogeneous reactors. In the recycle scheme short cooled irradiated fuel is reprocessed by remote manipulations. Lately development efforts have been concentrated on remote operations to produce fuel for recycle to the reactor. Decladding, codeposition of mixed oxides, and fuel refabrication have been performed in remote equipment; iodine behavior and plutonium precipitation have been studied in the laboratory; and chlorine recovery has been demonstrated in the cold pilot plant. (P.C.H.)

46423 (DPSPU-64-30-28) PERFORMANCE OF 3% AND 30% TBP PROCESSES. Orth, D. A. (Du Pont de Nemours (E. I.) and Co., Aiken, S. C. Savannah River Plant). Aug. 1965. Contract AT(07-2)-1. 33p. (CONF-650918-4). Dep. mn; CFSTI $2.00 cy, $0.50 mn.

From International Conference on the Chemistry of the Solvent Extraction of Metals, Harwell, Berks, Eng.

The Savannah River Plant (SRP) has two separations plants for the processing of irradiated materials by solvent extraction. One plant utilizes 30% TBP in the typical Purex system that normally is used to recover uranium and plutonium from natural or slightly enriched uranium reactor fuels. The other plant utilizes dilute TBP (nominally 3.5% at present) and is primarily for the recovery of highly enriched uranium; other operations at SRP have included the recovery of plutonium from Pu–Al fuel and of ^{233}U from thorium. An analysis of Purex operating performance at SRP and a review of the experience of some years of operation of the dilute TBP system are presented. The contrast between the systems is quite marked: in the SRP Purex system, decontamination seems to be limited by the level of solvent degradation products in the solvent, and this level changes slowly; in the SRP dilute system, decontamination is a sensitive, inverse function of the feed activity and responds rapidly to changes in feed activity. A laboratory study of the dilute system was made in conjunction with the plant data analysis; the study indicated that plant performance could be explained by the characteristics of zirconium–dibutyl phosphate complexes. The laboratory data on the behavior of this complex as a function of dibutyl and tributyl phosphate and of other variables can explain most of the differences seen between the two plant systems. The difference in decontamination behavior, in which the performance of the dilute TBP system can range from much better to much worse than the Purex system over a fairly small change in feed activity, is credited to radiolytically produced dibutyl phosphate. (auth)

46424 (IS-T-24) REVERSED-PHASE CHROMATOGRAPHIC SEPARATION OF NITROANILINES (thesis). Lehoczky, Marcia Helen (Ames Lab., Iowa State Univ. of Science and Tech.). May 1965. Contract W-7405-eng-82. 59p. Dep. mn; CFSTI $3.00 cy, $0.75 mn.

After a review of liquid-liquid partition and reversed-phase chromatography, results are reported of a study on the following nitroanilines: 2-nitroaniline, 4-nitroaniline, 2,4-dinitroaniline, 2,4-dimethyl-6-nitroaniline, 2,4,6-trinitroaniline, 4-chloro-2,6-dinitroaniline, 2-chloro-4-nitroaniline, and 4-chloro-2-nitroaniline. The problem of determining aniline in aqueous acetic acid–CCl_4 is discussed briefly. Distribution coefficients of the above nitroanilines were determined for aqueous acetic acid–CCl_4 and –$CHCl_3$ on teflon-6 supports. Separations were carried out on one three-component and several two-component mixtures. (D.L.C.)

46425 (K-L-2012) SYSTEMS COMBINING CONTINUOUS-FLOW AND DENSITY GRADIENT CENTRIFUGATION, MODELS B-VIII AND B-IX. Amburgey, John W. Jr. (Oak Ridge Gaseous Diffusion Plant, Tenn.). Aug. 26, 1965. Contract W-7405-eng-26. 13p. Dep. mn; CFSTI $1.00 cy, $0.50 mn.

High inlet flow stream pressures, encountered at steep density gradients and high rotational speeds, are undesirable in the operation of "B" rotor systems since the two-path fluid seal becomes ineffective at these pressures. The operation of centrifuges with combined continuous-flow and density gradient centrifugation is discussed. The B-IX core was designed with smaller core taper and flow channels to reduce the pressure; a detail drawing of the entire assembly is included. Inlet pressure vs rotor speed curves are given for both B-VIII and B-IX rotors. Some typical recovered density gradients from the B-IX rotor system are given together with its dimensions. (D.L.C.)

46426 (NP-15362) THE REMOVAL OF NEUTRON POISONS, IN PARTICULAR ^{135}Xe AND ^{135}I, FROM AN AQUEOUS HOMOGENEOUS SUSPENSION REACTOR. Kreijger, Pieter Job (Technische Hogeschool, Delft (Netherlands)). 1962. 135p. Dep. mn.

Some general considerations on the purification of aqueous homogeneous suspension reactors were studied. An extensive discussion on the possible purification processes for the removal of poisons particularly ^{135}Xe and its precursor ^{135}I is presented. A discussion on the separation of iodine from steam by rectification at high temperature and low concentrations is included. (M.O.W.)

46427 (ORNL-3754) HOT-CELL DISSOLUTION OF HIGHLY IRRADIATED 20% PuO_2–80% UO_2 FAST-REACTOR FUEL SPECIMENS. Goode, J. H. (Oak Ridge National Lab., Tenn.). Oct. 1965. Contract W-7405-eng-26. 23p. Dep. mn; CFSTI $2.00 cy, $0.50 mn.

Hot-cell studies were made at ORNL on prototype fuel specimens to define possible problems in the head-end step in processing fuel from a Fast Breeder reactor. The fuel consisted of stainless-steel-clad PuO_2–UO_2 (20%–80%), swaged or pelletized, made and irradiated by General Electric's Vallecitos Atomic Laboratory. The irradiation levels were as high as 99,000 Mwd/metric ton. It was found that shearing the elements into short pieces and dissolving the core with nitric acid was preferable to chemical decladding with sulfuric acid solutions because of excessive (1.5%) losses of uranium and plutonium. Also, about 60% of the fission-product cesium dissolved in the sulfuric acid; the decay heat from this cesium could cause problems in waste management. More than 99% of the PuO_2–UO_2 dissolved in less than 5 hr in all concentrations of

nitric acid greater than 3M. No fluoride was needed to accelerate the reaction, which is a distinct advantage. Undissolved residues consisted of core oxides and fission-product Mo, Zr, Pd, Ru, and Rh. Feed clarification would be required to remove these solids prior to final recovery of the fissile material by solvent extraction. (auth)

46428 (ORNL–3847) TRANSURANIUM QUARTERLY PROGRESS REPORT FOR PERIOD ENDING NOVEMBER 30, 1964. Burch, W. D. (comp.) (Oak Ridge National Lab., Tenn.). Sept. 1965. Contract W-7405-eng-26. 60p. Dep. mn; CFSTI $3.00 cy, $0.75 mn.

Large-scale production of transuranium elements is centered in the High-Flux Isotope Reactor (HFIR) and the Transuranium Processing Plant (TRU). Target rods irradiated in HFIR are processed in TRU for recovery of transuranium elements and refabrication for further irradiation. The process development included work on the dissolution and metathesis of $NaLa(SO_4)_2$, preparation of dense PuO_2 for HFIR targets, formation of dense rare-earth oxide spheres, and the Talspeak process for separation of actinides from lanthanides. Cold runs and initial hot operations were carried out on the Curium Recovery Facility (Clanex-Tramex cycle). Experimental engineering studies were made on the TRU processing cells. The final design of the HFIR target rod is given, and the equipment for fabricating the rods is described. The irradiation testing program is reported. An account is given of the design and construction of the TRU and chemical process equipment. Corrosion studies were made on Zircaloy-2 in 8M HCl, Hastelloy C and Ta in Hg at 150°C, and plastics in chloride environments. (D.L.C.)

46429 (ORNL-P–1522) ALKYLBENZENE SULFONATE (ABS) CONTROL FOR THE FOAM SEPARATION PROCESS. Laing, W. R.; Lynn, E. C. (Oak Ridge National Lab., Tenn.). [1965]. Contract W-7405-eng-26. 10p. (CONF–650919-3). Dep. mn; CFSTI $1.00 cy, $0.50 mn.

From Technicon Analytical Symposium, New York.

For the decontamination of slightly radioactive process waste water, a foam separation process was developed which involves mixing the water with grundite clay, adding 2–9 ppm Fe^{3+}, adjusting the pH, removing the sludge, adding dodecylbenzene sulfonate (DBS), generating foam, and removing the foam. Decontamination factors are given for Ca, Sr, Cs, Co, Ru, and Ce in the sludge and foam columns. An AutoAnalyzer was used for process control of the DBS concentration in the pilot plant. The method and flow diagram used in the AutoAnalyzer are described, and data on the calibration and accuracy of the method are given. (D.L.C.)

46430 (ORNL-P–1601) STABILITY OF AROMATIC DILUENTS AND SOLVENT EXTRACTION REAGENTS IN RADIOCHEMICAL PROCESSING. Blake, Charles A. Jr.; Schmitt, J. M. (Oak Ridge National Lab., Tenn.). [1965]. Contract W-7405-eng-26. 43p. (CONF-650918–5). Dep. mn; CFSTI $2.00 cy, $0.50 mn.

From International Conference on the Chemistry of the Solvent Extraction of Metals, Harwell, Berks, Eng.

The stabilities of some commercial aromatic diluents, especially the mixed isomers of diethylbenzene, DEB, are determined and examined with respect to their effect on the use of the diluents in solvent extraction processes. Degradation was by mixing the organic phase with an acidic aqueous phase, usually 2M HNO_3, in the presence or absence of ^{60}Co gamma radiation. The degraded solvent was examined by several techniques; measurement of extraction ability, gas liquid and column chromatography, distillation, infrared and nuclear magnetic resonance spectrometry, differential thermal analysis, and elemental analysis. Exposure of 1M TBP/DEB solution while stirring with 2M HNO_3 to 2 watt-hr/l radiation degraded about 0.3% of the DEB. At 70 watt-hr/l about 10% of the DEB degraded. The meta isomer was the most stable. The principal DEB products were ethylacetophenones and 1-nitroethyl-ethylbenzenes and are poor extractants for uranium and fission products. Impurities frequently associated with DEB degraded to compounds which extracted fission products strongly. DEB degraded 2 to 5 times faster when TBP was present in the organic phase, but metals dissolved in both phases retarded degradation slightly. Products in tests where ~10% of the DEB was degraded depressed uranium extraction slightly, decreased the rate of phase disengagement from acidic and alkaline solutions by a factor of 2, did not change the solvent flash point. No satisfactory method of product removal from the organic phase was developed but additional testing is needed to determine rate of buildup during actual processing. Measurement of the heat of degradation of solvents in a new adaptation of the method of differential thermal analysis is described and it is shown how this method should be useful in estimating the requirements of processing apparatus to dissipate heat evolved during degradation. The calculations show little effect of 2 watt hr/l DEB exposure on extraction column temperature, or of degradation of entrained DEB in aqueous phases being concentrated by evaporation. Commercial diisopropylbenzenes and detergent "alkylates" are less stable than DEB. Data are included which summarize the ORNL observations which pertain to the stability of some extraction reagents, e.g., amides, amines, phenols, and a dialkyl phenylphosphonate. (auth)

46431 (ORNL-P–1602) PRIMARY AMINE EXTRACTION OF BERYLLIUM FROM SULFATE LIQUORS. Crouse, D. J.; Brown, K. B.; Seeley, F. G. (Oak Ridge National Lab., Tenn.). [1963]. Contract W-7405-eng-26. 28p. (CONF-650918–6). Dep. mn; CFSTI $2.00 cy, $0.50 mn.

From International Conference on the Chemistry of the Solvent Extraction of Metals, Harwell, Berks, Eng.

Certain amines are potentially useful extractants for recovering beryllium from sulfuric acid digests of low-grade beryllium ores. Of a variety of amines tested, only the primary amines extracted significant amounts of beryllium and, of these, 1-(3-ethylpentyl)-4-ethyloctylamine is the most effective. Beryllium distribution coefficients increase with decreasing acidity and are high enough for practical use in the pH range of 2 to 3. The distribution coefficients increase with increase in sulfate concentration and are proportional to about the 0.7 power of the amine concentration. Aluminum is extracted, but good separation from beryllium can be obtained by saturating the pregnant solvent with beryllium and scrubbing with 0.01M H_2SO_4. Fluoride interferes with beryllium extractions from pure sulfate solutions, but aids extractions from process liquors because it complexes aluminum and reduces the degree of competition by aluminum for the extractant. Beryllium is readily backwashed from the solvent with 0.5–1M H_2SO_4 or with dilute ammonium fluoride solutions. (auth)

46432 (ORNL-P–1603) UNEXPECTED RATE EFFECTS IN THE EXTRACTION OF RARE EARTHS BY DI(2-ETHYLHEXYL)PHOSPHORIC ACID. Crouse, D. J.; Horner, D. E. (Oak Ridge National Lab., Tenn.). [1964]. Contract W-7405-eng-26. 16p. (CONF-650918–7). Dep. mn; CFSTI $1.00 cy, $0.50 mn.

From International Conference on the Chemistry of the Solvent Extraction of Metals, Harwell, Berks, Eng.

In extraction of fission product rare earths with di(2-ethylhexyl) phosphoric acid from tartrate- (or citrate-) complexed waste liquors (pH 5), the rates of extraction are decreased by the presence of certain metal ion contaminants, such as iron, aluminum, and particularly chromium. Apparently, these metal ions react with the rare earths ions and tartrate in the aqueous phase to form non-extractable complexes that are slow to dissociate. The magnitude of the effect is different with each interfering metal ion and also for the different rare earths. Increasing the tartrate concentration increases the rates of extraction. (auth)

46433 (RL-SA–43) ADMINISTERING CRITICALITY CONTROL IN THE HANFORD ATOMIC PRODUCTS OPERATION CHEMICAL PROCESSING DEPARTMENT. (General Electric Co., Richland, Wash. Hanford Atomic Products Operation). Sept. 16, 1965. Contract AT(45-1)-1350. 25p. (CONF-651103–9). Dep. mn; CFSTI $1.00 cy, $0.50 mn.

For Presentation at IAEA Symposium on Criticality Control of Fissile Materials, Stockholm.

A discussion is presented of the administrative procedures used to control safely nuclear criticality during the processing of slightly enriched uranium, uranium-233, and plutonium. Technical criteria, use of water for fire fighting, audits, equipment changes, and personnel training programs are covered. Results of calculations for the reprocessing of 2% enriched uranium are given. (D.L.C.)

46434 ADSORPTION OF ^{90}Sr BY SOIL. Senvar, C. B.; Birguel, O. (Univ. of Ankara). Atompraxis, 11: 389-91 (July 1965).

The adsorption of ^{90}Sr, from aqueous solutions, by three different types of Turkish soils was investigated. These soils were: sand-soil, rich in SiO_2 (92%); calcareous soil, rich in $CaCO_3$ (90%); and clay-soil, rich in aluminum (30% Al_2O_3). The dependence of the adsorption on time, grain size, and initial ^{90}Sr concentration was determined. It was concluded that: efficient adsorption is reached in less than 30 minutes for all three types of soil; the adsorption is independent of the grain size for clay soil but changes with grain size for the other two soils; and clay-soil is the most efficient of all in removing ^{90}Sr from aqueous solutions. (auth)

46435 RADIOACTIVE WASTE PROBLEMS IN THE PROCESSING OF IRRADIATED FUELS. Walrave, W. K. A. Atoomenergie Haar Toepassingen, 7: 135-41(July 1965). (In Dutch).

In the processing of irradiated fuels large quantities of radioactive fission products are released. The matter of storage of the waste presents both economic and safety aspects. In the descriptions given of various types of waste, emphasis is placed on concentrated solutions and on the methods of storing these solutions in solid form. (tr-auth)

46436 CHROMATOGRAPHIC SEPARATION OF RADIOCHEMICALLY PURE ^{90}Y FROM ^{90}Sr. Macasek, F.; Cech, R. (Komensky Univ., Bratislava; Inst. of Conservation of Natural Resources, Bratislava). Chem. Zvesti, 19: 107-14(1965). (In Czech).

The separation factor for the chromatographic separation of ^{90}Y and ^{90}Sr in 10^{-2} M solutions of EDTA in the pH range from 4 to 4.5 attained a value of 10^3 to 10^4. In contrast to the effect that was observed in the case of the separation of macromasses of the ions, the use of the EDTA complex with a mean value of the constants did not improve the stabilities (Zn, Ca) but impaired the condition of separation that was also simultaneously connected with the modification of the sorption of Sr by competing ions. The conditions for the chromatographic separation of ^{90}Y and ^{90}Sr on Dowex 50 × 2 in the NH_4 form (200 and 230 mesh with columns 30 cm × 0.44 cm^2) by elution with 10^2 M EDTA at pH 5.11 were established. With a flow-through velocity of 0.8 ml/min at least a 33-fold elution of the ^{90}Y from equal weights of ^{90}Sr was possible with a radiochemical purity of >99.9998%. This separation is simple and takes only about 2 hr. (tr-auth)

46437 SEPARATION OF LANTHANIDES USING PHTHALATE BUFFER. Krishna Prasad, N. S.; Krishamurthy, M.; Thaiyalanayaki, M. (Atomic Energy Establishment, Trombay, India). Current Sci. (India), 34: 428-9(July 20, 1965).

The behavior of phthalate buffer as an eluent for the separation of lanthanides was investigated, using an equimolar mixture of neodymium and praseodymium oxides. The compositions of the oxides obtained from the effluent fractions through their oxalates were determined spectrophotometrically, and a typical chromatogram of the results is shown. Significant enrichment of the lanthanide fractions was obtained. Similar studies with mixed lanthanide oxides obtained from indium monazite have indicated the feasibility of obtaining the lanthanides individually in pure form. (L.B.S.)

46438 SEPARATION OF SAMARIUM BY THE ION EXCHANGE METHOD. Shiokawa, Jiro; Murakami, Yoichi (Osaka Univ.). Denki Kagaku, 32: 897-900(Dec. 1964). (In Japanese).

The separation of Sm from Y-group elements was carried out by the use of a Dowex 50 (20 – 48 mesh) column. The dimensions of the column were 3.8 × 150 cm and it was filled with 1 to 1.5 liters resin. Elutions were made by 0.1% citric acid at a pH 6.0, 5.5, or 5.0, adjusted with ammonia. The elution efficiency was good at lower pH values, but the pure salt could not be obtained; the procedure was found to be more suitable for the concentrating separation. For 2% EDTA solution (pH = 8.62), in two mixed resin beds, the following results were obtained. When a 2 : 1 $Cu^{2+} - H^+$ form was used, H_4(EDTA) or Cu(EDTA) · $5H_2O$ was precipitated and the separation efficiency $Cu^{2+} - H^+ - NH_4^+$ was not good. For a 2 : 1 : 1 $Cu^{2+} - H^+ - NH_4^+$ form, the elution and separation efficiencies were good. The concentration and purification of Sm from poor ore may be carried out successfully by the following procedure: concentration by 0.1% citric acid, followed by separation and purification with 2% EDTA (pH = 8.62), using a mixed resin bed of Cu^{+2}-form + H^+-form + NH_4^+ = 2 : 1 : 1. (NSA of Japan)

46439 EXTRACTION OF CERIUM WITH TRI-n-OCTYL PHOSPHINE OXIDE. Alian, A.; Moustapha, Z. (Atomic Energy Establishment, Inshas, UAR). Indian J. Chem., 3: 390-2(Sept. 1965).

The extraction of cerium with tri-n-octyl phosphine oxide (TOPO) solution in toluene was investigated as a function of nitric acid and lithium nitrate concentration in aqueous phase and TOPO concentration in the organic phase. It was found that as in the case of tri-n-butyl phosphate (TBP) and di-isoamyl methyl phosphonate (DAMP), cerium is extracted as the trisolvate complex, $Ce(NO_3)_3 \cdot 3TOPO$. The partition data of TOPO extraction of Ce (III) were compared with the data for TBP and DAMP. With increasing lithium nitrate concentration, the cerium partition coefficient (E_a^0Ce) increased initially, attained a maximum value, and then decreased, while in the case of TBP and DAMP E_a^0Ce increased continuously. The values of the stability constants of the extractable cerium complexes increased in the order TBP > DAMP > TOPO. (auth)

46440 THE ISOLATION OF Zr–^{95}Nb FROM MIXED FISSION PRODUCTS BY SOLVENT EXTRACTION WITH OXINE IN BENZENE SOLUTION. Kato, Toyoaki (Tokyo Univ.). J. Chem. Soc. Japan, Pure Chem. Sect., 86: 209-12(Feb. 1965). (In Japanese).

The solvent extraction behavior of ^{95}Zr and ^{95}Nb with oxine in benzene solution was investigated in order to establish the best procedure for the isolation of $^{95}Zr - ^{95}Nb$ from mixed fission products. By an equilibrium extraction with 0.2 mol/l oxine in benzene solution from aqueous acetate media, 92 to 98% of the ^{95}Zr could be transferred to organic phase in the pH region from 4 to 10 and 95% of the ^{95}Nb was extracted between pH 2 and 4.5; hence, the extraction of the both nuclides could be performed from an aqueous solution with a pH of about 4. The presence of citrate, tartrate, and oxalate caused interferences. Among the nuclides tested for their extractabilities with 0.2 mol/l oxine in benzene solution, ^{144}Ce(IV) was quantitatively extracted in the pH range from 7.5 to 11, ^{90}Y was completely extracted between pH 9.5 and 10.5 and about 30% of the ^{90}Sr was also extracted in this pH range, but their extractabilities at a pH of about 4, as well as those of ^{137}Cs, ^{103}Ru, and ^{106}Ru, were negligible. The repeated extraction at pH 4 with 0.2 mol/l oxine in benzene solution from an aqueous acetate solution of the mixed fission products treated with hydrogen potassium sulfate resulted in quantitative transfer of $^{95}Zr - ^{95}Nb$ into organic extract. The decontamination was completed by back washing of the organic extract with an aqueous acetate solution of pH 4. $^{95}Zr - ^{95}Nb$ in the organic extract could be easily removed by agitating it with 0.1 mol/l oxalic acid solution. Thus, the quantitative isolation of $^{95}Zr - ^{95}Nb$ with a high radiochemical purity could be attained by this extraction method. (auth)

46441 SEPARATION OF ^{137}Cs FROM FISSION PRODUCTS BY MEANS OF A KEL-F COLUMN SUPPORTING TETRAPHENYLBORON. Cesarano, C.; Pugnetti, G.; Testa, C. (CNEN, Rome). J. Chromatog., 19: 589-93 (Sept. 1965).

Reversed-phase partition chromatography was applied

to the separation of cesium from fission products, by modification of the tetraphenylboron (TBP) extraction method. Polytrifluorochloroethylene (Kel-F) was used as the inert support for the TPB–amyl acetate solution. By passing the solution of fission products in 0.01M EDTA (pH 6.8) through the column, cesium was strongly retained on the column but could be eluted quantitatively by a 1M HCl–acetone solution. The average cesium recovery was 100.54% ± 0.87%, and was not influenced by the addition of a carrier. The possibility of using this method for either burnup measurements or health physics work is emphasized. (auth)

46442 SEPARATION OF ^{137}Cs FROM FISSION PRODUCTS BY MEANS OF A KEL-F COLUMN SUPPORTING DIPICRYLAMINE. Testa, C.; Cesarano, C. (CNEN, Rome). J. Chromatog., 19: 594-8(Sept. 1965).

The separation of cesium from fission products by a column of Kel-F (polytrifluorochloroethylene) supporting dipicrylamine is described. The average recovery of cesium was 99.95% ± 0.31% and the decontamination factors were greater than 10^3. The column can be regenerated and used for more than 15 consecutive cycles. (auth)

46443 DI n-OCTYL PHOSPHINIC ACID AS A SELECTIVE EXTRACTANT FOR METALLIC CATIONS. SELECTED M(III) AND M(VI) TRACER STUDIES. Peppard, D. F.; Mason, G. W.; Lewey, S. (Argonne National Lab., Ill.). J. Inorg. Nucl. Chem., 27: 2065-73(Sept. 1965).

Hydrogen ion dependencies and extractant dependencies of M(III) elements represented by Ce^{3+}, Eu^{3+}, Tm^{3+}, Yb^{3+}, Y^{3+}, Am^{3+}, and Cm^{3+} and of an M(VI) element, UO_2^{2+}, into a benzene solution of di-n-octyl phosphinic acid, (n-$C_8H_{17})_2PO(OH)$, H[DOP], from an aqueous acidic chloride medium were determined radiometrically. The observed stoichiometries are represented as: $M_A^{+3} + 2.5(HY)_{2O} \rightleftharpoons MY(HY_2)_{2O} + 3H_A^+$ and $UO_{2A}^{+2} + 2(HY)_{2O} \rightleftharpoons UO_2(HY_2)_{2O} + 2H_A^+$, where the subscripts A and O refer, respectively, to the mutually equilibrated aqueous and organic phases and $(HY)_2$ represents the dimeric form of H[DOP]. Values of K_s, defined by the expressions: $K_s = K[H^+]^3/F^{2.5}$, for M(III) and $K_s = K[H^+]^2/F^2$, for U(VI), where $[H^+]$ is the molar hydrogen ion concentration in the aqueous phase, F is the formal concentration of extractant in the organic phase, and K is the observed distribution ratio of the metal, are reported for elements from an aqueous phase 1.0M in (NaCl + HCl). A plot of log K vs Z, in a study involving all of the lanthanides (III) except Gd, showed a slight odd-even effect, the even Z elements lying above a straight line, which acceptably represents the odd-Z elements. (auth)

46444 A RADIOCHEMICAL PROCEDURE FOR OBTAINING RUTHENIUM FREE FROM IRIDIUM. Rengan, K.; Pierson, W. R. (Ford Motor Co., Dearborn, Mich.). J. Inorg. Nucl. Chem., 27: 2113-14(Sept. 1965).

Radiochemical procedures for separation of ruthenium from iridium are described. Irradiated ruthenium metal powder was dissolved in NaOH–NaOCl solution, with gentle heating. Iridium (III) carrier (~5 mg) was added, then $NaBiO_3$ (~100 mg), and the mixture was heated to boiling. Zirconium (IV) carrier (~10 mg in 1 ml solution) was added with stirring, $IrO_2 \cdot xH_2O$ and $ZrO_2 \cdot xH_2O$ were precipitated, separated by centrifuging, and discarded. From the remaining solution, Ru_2O_3 and RuO_2 were precipitated by adding ethanol and heating, and the liquid phase was discarded. The (Ru_2O_3, RuO_2) precipitate was dissolved in HCl, iridium (III) carrier (~5 mg) was added, and RuO_4 was distilled from $HClO_4$ medium. Only about 1 part in 10^9 of the iridium present in the irradiated metal was found in the ruthenium sample obtained by this procedure. (F.J.H.)

46445 SEPARATION OF THE ^{131}I-LABELLED S-SULPHONATED A AND B INSULIN CHAINS BY THIN-LAYER CHROMATOGRAPHY. Massaglia, A.; Rosa, U. (Sorin-Centro Richerche Nucleari, Saluggia, Italy). J. Labelled Compds., 1: 141-4(Apr.-June 1965).

Pure A and B S-sulfochains were prepared from radioiodinated beef insulin. The ^{131}I-labeled insulin was dissolved in 0.03 M $Na_2S_4O_6$, 0.075 M Na_2SO_3, and 8 M urea. Aliquots of the solution were subjected to paper electrophoresis. A and B S-sulfochains were eluted from the paper strips. Mixtures containing different amounts of the two chains were applied 2 cm from the edge of the silicagel plates and developed with various solvents. Autoradiography was employed in order to visualize the true shape of the chromatographic spots. Data are shown in tables and graphs. The A and B chains were completely separated. (M.C.G.)

46446 COUNTER-CURRENT EXTRACTION ON A LABORATORY MIXER-SETTLER. IV. THE CALCULATION OF THE SEPARATION OF URANYL NITRATE AND NITRIC ACID IN THE EXTRACTION WITH TBP. Sraier, Vratislav. Jaderna Energie, 11: 373-8(Oct. 1965). (In Czech).

The separation of uranyl nitrate from nitric acid was calculated for individual stages of the extraction apparatus in countercurrent TBP extractions under Purex Process conditions. The results were compared with those obtained formerly on a laboratory mixer-settler. The composition of random phases and the distribution of uranyl nitrate and nitric acid in individual stages of the mixer-settler may be determined with sufficient accuracy by calculation. Further increases in accuracy may be achieved by more precise determination of the dependence of K'' and K' on the composition of phases in a given system of extractant–diluent. (auth)

46447 THE COMPLEXES FORMED IN THE EXTRACTIONS OF URANIUM(VI) FROM SULFURIC AND NITRIC ACID SOLUTIONS BY TRI-n-OCTYLAMINE. Sato, Taichi (Government Chemical Industrial Research Inst., Tokyo). Naturwissenschaften, 52: 258-9(1965).

The nature of the complexes formed in these extraction systems was studied. The organic phases saturated by uranium were dried in vacuum to evaporate the benzene. Thermogravimetric and differential analyses were made of the compounds, and the complex and its thermal decomposition products were examined by infrared spectroscopy. The results indicated the following compositions for the complexes $(R_3NH)_4UO_2(SO_4)_3(OH_2)_3$ and $(R_3NH)_2UO_2(NO_3)_4$ where R is C_8H_{17}. (J.S.R.)

46448 REPROCESSING OF URANIUM FUELS BY FUSED SALT ELECTROLYSIS. Mukaibo, Takashi; Kanno, Masayoshi; Kokubo, Sanya (Tokyo Univ.). Nippon Genshiryoku Gakkaishi, 7: 410-17(Aug. 1965). (In Japanese).

Purification of U by fused salt electrolysis is one method of pyrometallurgically reprocessing irradiated nuclear fuel. Dummy spent fuel composed of U alloys containing Zr and Mo to simulate fission products were used for the anode. Molten zinc was chosen for cathode, for its adaptability to continuous operation. The electrolytic refining was carried out in a NaCl–KCl–UF_4 fused salt system at 750°C, and a KCl–LiCl–UCl_3 system at 500 to 600°C. In the case of the NaCl–KCl–UF_4 system, at 750°C and with cathodic current densities of 190 to 400 ma/cm^2, the cathodic current efficiencies obtained were 20 to 60% with a bath voltage in the range 1 to 3 v. Continuous operation however was disturbed by dendritic deposits on the cathode container. In the case of the KCl–LiCl–UCl_3 system, the UCl_3 concentration was 10 wt % at 500°C, the cathodic current density was 100 to 250 ma/cm^2, both voltage was 1.2 to 2.5 v, and the cathodic current efficiencies were 40 to 90%. The electrolysis in this case could be maintained for an appreciable period. The U was recovered by vacuum distillation of the U–Zn alloy obtained on the cathode. The decontamination factors were determined to be 10 to 40 for Zr, and 30 for Mo. (auth)

46449 SEPARATION OF THE LANTHANIDES BY HIGH-VOLTAGE ELECTROPHORESIS. Baechmann, K. (Technische Hochschule Darmstadt, Ger.). Radiochim. Acta, 4: 124-7(Aug. 1965). (In German).

Lanthanides were separated by electrophoresis at 90 volt/cm and 5 ma in a short time. The single elements were determined by the impulse rates on the electrophoretic strips. (auth)

46450 EXTRACTION OF URANIUM(VI) BY TRICAPRYLMETHYLAMMONIUM NITRATE. Koch, Guenter (Kernforschungszentrum, Karlsruhe, Ger.). Radiochim. Acta, 4: 128-37(Aug. 1965). (In German).

Uranium(VI) is easily extracted from aqueous nitric acid by solutions of tricaprylmethylammonium nitrate in organic solvents. At about 6 to 7M aqueous HNO_3, the distribution coefficient showed a maximum. From the dependence of the distribution coefficient on the aqueous nitrate activity and on the organic tricaprylmethylammonium nitrate concentration, from the maximum loading of the organic phase, and from the electron spectrum, it was concluded that the organic phase contains tricaprylmethylammonium trinitratodioxouranate(VI), $R_3(CH_3)N[UO_2(NO_3)_3]$. The pure compound was isolated. As shown by the infrared spectrum, the bond between uranium and nitrate in this complex has a rather high degree of covalency. Measurements of molecular weights and of electric conductances in very dilute benzene solution could be tentatively interpreted by the assumption that the compound is associated into ion pairs and higher ion associates. (auth)

46451 INVESTIGATIONS ON THE EXTRACTION OF METALS BY USE OF RADIOACTIVE TRACER ISOTOPES. PART IX. THE EXTRACTION OF TETRAVALENT (Zr, Hf, Th) AND PENTAVALENT (Nb, Ta, Pa) METAL SALTS FROM HCl IN TETRABUTYLPYROPHOSPHATE (TBPP)/HCl AND TETRABUTYLHYPOPHOSPHATE-TETRABUTYL PYROPHOSPHATE (TBHP-TBPP 1:1)/HCl SYSTEMS. Mikulski, Jan (Institut fuer Kernphysik, Krakow). Radiochim. Acta, 4: 137-41(Aug.1965). (In German).

The extraction of zirconium, hafnium, thorium, niobium, tantalum, and protactinium in the systems TBPP–HCl and TBHP–TBPP–HCl was investigated using radioisotopes of ^{95}Zr, ^{181}Hf, ^{234}Th, ^{95}Nb, ^{182}Ta, and ^{233}Pa. The extraction coefficients D for the salts of the tetravalent metals in hydrochloric acid medium may be expressed as $D_{Th} > D_{Hf} > D_{Zr}$ whereas for pentavalent metals the order is: $D_{Ta} > D_{Nb} > D_{Pa}$. The extraction of HCl to the organic phase was also studied and the solvation number was determined for hafnium and thorium. (auth)

46452 A METHOD FOR SEPARATING THE RARE EARTHS FROM URANIUM, IRON, AND MANGANESE. Spacu, P.; Mavrodin, Maria (Center of Inorganic Chemistry, Bucharest). Rev. Roumaine Chim., 10: 425-8(May 1965).

A method for separating rare earths from uranium, iron, and manganese by using dihydroxymaleic acid as precipitating reagent is presented. The rare earths precipitated quantitatively, while uranium, iron, and manganese remained in solution as soluble complexes, under the conditions established. (auth)

46453 EFFECTS OF NUCLEAR RADIATION ON FLOTATION PROCESS. Lebedev, A. T.; Kartushin, V. P.; Uchurkhanov, M. M. Tsvetn. Metal., No. 6, 11-14 (June 1965). (In Russian).

After exposure to the neutron flux of a reactor, the flotation properties of some minerals, such as Zn blend became worse while those of Cu pyrite were improved. However, the radioinduced activity in the materials presented radiation-protection problems. Similar results were obtained with tests using ^{60}Co or a betatron as radiation source. Additional flotation studies were carried out, using a γ source. The experiments involved a study of the surface properties of the ores and flotation agents, the composition and properties of the gas phase within the flotation apparatus, and the kinetics of the flotation process. It was found that Frenkel-type vacancies formed at the surface of the specimens by the radiation follow the law of bimolecular reactions and act as new adsorption centers. The flotation agents underwent radiolysis and formed excited molecules, thereby changing the nature of the dispersive interaction between the mineral and the agent. The toxicity and the order of some of the agents was also affected: exposure of butyl xanthate to 600,000 R caused a marked change in its odor. Industrial flotation agents may be created by exposing otherwise unusable waste materials to radiation. The radiation caused the formation of negative ions in the gas, together with the monomolecular transformation of the primary ions, recombination and neutralization reactions. Excited molecules with an average life of 10^{-9} to 10^{-8} sec were also created, leading to an acceleration of the flotation rate. A weaker temperature dependence of the reaction was noted, as compared with thermally induced reactions. It appears desirable to apply the radiation to pulp at the moment of the flotation in order to make a fuller use of the radiation energy. (TTT)

46454 RECENT DEVELOPMENTS IN THE ELECTROLYTIC EXTRACTION OF LIGHT METALS. Richards, N. E. (Reynolds Metals Co., Sheffield, Ala.). pp 867-81 of Proceedings of the First Australian Conference on Electrochemistry. New York, Pergamon Press, 1965.

Results of research on electrolytic extraction, as it effects Be, B, Mg, Al, and Ti, are discussed. (M.C.G.)

46455 PROCESS FOR THE PURIFICATION OF URANIUM AND PARTICULARLY IRRADIATED URANIUM. Erler, Jean; Peray, Robert; Petit, Jean (to Commissariat a l'Energie Atomique). U. S. Patent 3,205,068. Sept. 7, 1965. Priority date Mar. 18, 1961, France.

A process for the purification of U, particularly irradiated U, consists of melting the U under a thermodynamically stable slag which remains liquid at a temperature lower than the melting point of U, cooling the molten mass to a temperature between the melting temperature of the slag and that of U to solidify the U, and separating the solid purified U from the liquid slag. The slag is constituted by a nearly eutectic composition of BeO and at least one of the oxides that have high thermodynamic stability selected from the group consisting of BaO, CaO, SrO, MgO, Li_2O, and La_2O_3, with the addition of a small quantity of UO_2. During the separation step, the molten slag retains as impurities the fission products to be eliminated. (B.L.M.)

ENGINEERING

General

46456 (AD-425760) MISSILE SHOCK MOUNT SYSTEM WITH SELF-CENTERING PROPERTIES. Grubaugh, R. E. (United Aircraft Corporate Systems Center, Farmington, Conn.). Oct. 10, 1963. 34p. (SCTM-169). CFSTI $3.60.

A linear-elastic, self-centering shock mount system is presented for protecting a missile from the effects of ground motion at 300 psi from a 20-MT weapon burst. The application of the basic mechanical principle is independent of missile configuration or weapon effects, but the design developed is proportioned for a missile and silo geometry representative of the Minuteman. The weapon effects criteria used for design are the ground motion spectra typical of an alluvian deposit over a rock substratum. (CFSTI)

46457 (AD-613674) SIMULATION OF AIR-BLAST-INDUCED GROUND MOTIONS (PHASE II). Period Covered: July 1, 1964–February 1, 1965. Auld, Harry E.; D'Arcy, Gerald P.; Leigh, Gerald G. (Air Force Weapons Lab., Kirtland AFB, N. Mex.). Apr. 1965. 228p. (WL-TR-65-26(Vol.1)). CFSTI $6.00 cy, $1.25 mn.

Results from the Phase II, Long-Duration High-Explosive Simulation Technique (LDHEST) experiment are presented. This experiment simulates the air-blast-induced ground motions from a large-yield nuclear weapon over a plan area 96 by 150 feet. A specially designed matrix of primacord was utilized to produce the desired explosion in a confined volume of air. An overburden, or mass of material, was placed over the explosion to provide a reaction force to shape the resulting wave pulse and to provide the required long durations. The experiment produced an air pressure pulse which had a peak overpressure of 312 psi, a time to one-half peak pressure of 18.2 msec, and a total duration of 170 msec. The shock front traveled at an average velocity of 5,120 ft/sec. On the basis of these results, recommendations are made for future simulation experiments. The measured earth free-field motions and stresses are compared with theoretical calculations, and the validity of the technique for simulating the desired nuclear environment is established. (auth)

46458 (CNLM-6342) SUMMARY OF SNAP-50/SPUR PUMP BEARING DEVELOPMENT PROGRAM. Manfredi, D. V. (Pratt and Whitney Aircraft, Middletown, Conn. Connecticut Advanced Nuclear Engineering Lab.). July 30, 1965. Contract AT(30-1)-2789. 72p. Dep. mn; CFSTI $3.00 cy, $0.75 mn.

A shaft-bearing system design and development program for hermetically sealed liquid metal pumps was conducted as part of the SNAP-50/SPUR space powerplant development program. Three phases of the program were carried out: rotor dynamics tests in water, single bearing tests in water, and single bearing tests in liquid metal. A summary is presented of the work and results of each of the three phases. (D.L.C.)

46459 (CONF-640508, pp 100-57) A STUDY TO INVESTIGATE THE FEASIBILITY OF UTILIZING ELECTRICAL POTENTIALS ON THE SURFACE OF THE SKIN FOR CONTROL FUNCTIONS. Harrison, Lee (Philco Corp., Blue Bell, Pa.).

The advantages of using electromyographic signals to control devices are outlined. Special myographic signal-handling equipment and computer programming were developed to study the feasibility of such uses. A non-deterministic pattern-classification, computer technique was used to study the myographic patterns. The data processing and analysis are still in progress. (D.L.C.)

46460 (CONF-640508, pp 224-32) CONTROL—THE UNIVERSAL PROCESS. Wirta, Roy; Sprince, Richard (General Electric Co., Scranton, Pa. Defense Electronics Div.).

The principles of the control process are outlined. The closed loop of the control process is broken down into five basic units: operator, command data unit, machine, task, and sensory feedback unit. The design hardware for the control process is considered, and the need to match human characteristics with machine characteristics is emphasized. Future trends and the state of art of remote handling are discussed. (D.L.C.)

46461 (RFP-562) AN EVALUATION OF ADJUSTABLE SPEED DRIVE SYSTEMS ON MACHINE TOOLS. Utley, L. W. (Rocky Flats Div., Dow Chemical Co., Golden, Colo.). Aug. 25, 1965. Contract AT(29-1)-1106. 14p. Dep. mn; CFSTI $1.00 cy, $0.50 mn.

The load versus speed characteristics of three machine tools with different drive systems were determined. Included are machines driven by: hydraulic motor, a-c motor, and d-c motor. None of these machine tools had a closed loop feedback system to regulate speed as load was applied. (auth)

46462 (TID-22184) SUMMARY OF INVESTIGATIONS OF ENTRANCE EFFECTS IN CIRCULAR THRUST BEARINGS. Carfagno, S. P.; McCabe, J. T. (Franklin Inst. Research Labs., Philadelphia, Pa.). [nd]. Contracts AT(30-1)-1484; Nonr-2342(00). 157p. (I-A2049-24). Dep. mn; CFSTI $5.00 cy, $1.00 mn.

The pressure depression in the vicinity of the supply hole of an externally pressurized circular thrust bearing having a single, axial supply hole was studied. Most of the experiments were conducted with a 2.750-in. diameter bearing with an 0.020-in. diameter supply hole. The supply hole has had both a square edge and a round edge. The test program was based on a dimensional analysis of the gas flow through the bearing. In accordance with this program, pressure profiles were obtained for clearances between 0.2 and 1.6 mil, and supply pressures between 20 and 215 psia. Flow rates were measured and compared with theoretical values. The load was determined by numerical integration under the pressure profile. Most of the data are presented in nondimensional form as indicated by the dimensional analysis. (auth)

46463 (WAPD-TM-469) INELASTIC BUCKLING OF LONG AXIALLY COMPRESSED CURVED PLATES. Griffin, D. S. (Bettis Atomic Power Lab., Pittsburgh, Pa.). July 1965. Contract AT-11-1-GEN-14. 16p. Dep. mn; CFSTI $1.00 cy, $0.50 mn.

Differential equations are obtained for the inelastic deflections of long curved plates using small deflection theory. The usual assumption of incompressibility of material ($\mu = 1/2$) is avoided by making Poisson's ratio stress dependent beyond the elastic range. Buckling loads are obtained for both clamped and hinged edge conditions assuming a symmetrical mode typical of plates that buckle inelastically. In addition, axial buckling solutions, more rigorous in terms of the variable Poisson's ratio, are obtained for circular cylinders and flat plates with clamped and hinged edge conditions. (auth)

46464 (NSJ-tr-30) RESEARCH ON THE COLLISION-RESISTING CONSTRUCTION OF THE SIDES OF A NUCLEAR POWERED SHIP (REPORT NO. 3). Ooi, Hiroshi; Harima, Tetsuo; Iizuka, Haruhiko; Kataoka, Gunji. Translated from Tech. Rev., Mitsubishi Nippon Heavy-Ind., 4: 145-55(Dec. 1963). 29p. Dep. mn; JCL $2.60 fs, $1.07 mf.

Collision experiments were carried out on model sides of five types of ships, the dimensions of which were of about $1/15$ of the collision-resisting compartment of the Nuclear Powered Oceanographic Research and Tender Ship, subjected to both static and impact loading at the center. The relations between energy absorption and deformation,

mechanism of destruction of bow and side construction, and deformation prediction were made clear. (auth)

Applications of Nuclear Explosions

Refer also to abstracts 46422 and 46580.

46465 (AD-613991) LATERAL-PLATE TESTS WITH PLATE DIAMETER VARIED. Interim Report, August-October 1964. Gill, H. L.; Garcia, T. J. (Naval Civil Engineering Lab., Port Hueneme, Calif.). Apr. 1965. 35p. (R-374). CFSTI $2.00 cy, $0.50 mn.

To further the understanding of the mechanics of soil resistance to horizontal loading, a series of lateral-plate bearing tests was performed in the pit of the NCEL atomic-blast simulator. The tests were a continuation of an earlier test program which considered one plate diameter in one type of soil; during this series of tests, three plate diameters were used, and the results were compared with data from previous tests. In addition, one test was performed with a different type of soil in an attempt to generalize the applicability of the test results. To simulate a variation in the depth of burial of the plate, over-burden pressures were applied to the soil surface by a pneumatic bag. Included in the information gained from this series of tests was the fact that the coefficient of horizontal subgrade reaction, k_h, decreased exponentially with increasing plate deflection and increased exponentially with increasing overburden pressure for all plate diameters. In addition, it was found that plate deflection at a given level of unit load on the plate did not vary directly with plate diameter as has been previously assumed, but was directly proportional to the 1.35 power of plate diameter. In other words, although k_h increases with increasing overburden pressure and decreases with increasing plate deflection for all plate diameters considered, at a given level of pressure on the plate, k_h was found to be inversely proportional to plate diameter raised to the 1.35 power. (auth)

46466 (CEA-Bib-63) APPLICATIONS SCIENTIFIQUES DES EXPLOSIONS NUCLEAIRES. 1ERE PARTIE. EXCAVATIONS (CRATERING). (Scientific Applications of Nuclear Explosions. Part 1. Cratering). Berton, Micheline (Commissariat a l'Energie Atomique, Saclay (France). Centre d'Etudes Nucleaires). Oct. 1965. 90p. Dep. mn.

This bibliography is made up of 283 references to documents, almost all American, on the subject of the formation of craters by nuclear explosives. They are presented in three groups: reports; review articles; and symposia, films, and books. The documents are grouped together according to the important American programs for using the explosions for civil engineering work: extensive excavations, building of ports, canals, dams, drilling of mines. The research concerns the detection of explosions, and the seismological phenomena produced by the explosions have been deliberately omitted. The numerous PLOWSHARE projects have been gathered together up to the last reports cited in May 1965 by the Saclay Central Library. A subject index is included. (D.L.C.)

46467 (NVO-1163-43) A SIMPLIFIED METHOD FOR PREDICTING FREE-FIELD RADIAL DISPLACEMENTS AND STRAINS. Essoglou, M. E.; Rogich, D. G. (Beers (Roland F.), Inc., Alexandria, Va.). May 21, 1965. Contract AT(29-2)-1163. 47p. Dep. mn; CFSTI $2.00 cy, $0.50 mn.

The method for predicting permanent free-field radial displacements and strains caused by contained underground nuclear explosions, is reliable and requires only that the initial chamber and final cavity radii be known. The validity of the method is supported by data from several underground nuclear experiments; the agreement between predicted and actual displacements is discussed. Graphs of displacements and strains as functions of radial distance are included. (D.L.C.)

46468 (POR-1814) THROWOUT STUDY OF AN UNDERGROUND NUCLEAR DETONATION. Project 1.5 [of] PROJECT DANNY BOY. Final Report. Ahlers, Edward B. (Armour Research Foundation, Chicago, Ill.). Sept. 1962. 158p. (WT-1814). Dep. mn; CFSTI $5.00 cy, $1.00 mn.

Project 1.5 of Operation Danny Boy is concerned with measurement of the throwout from an underground nuclear detonation. A series of 1,145 objects were placed at predetermined locations prior to the shot. Objects were placed on the surface, at shallow-burial depths (1 foot deep), and in available drill holes in the crater zone. Surface and shallow-buried objects included a wide range of geometric shapes and sizes, comprising both "ideal" geometric solids and such actual debris objects as bricks and lumber. Placement of surface and shallow-buried objects was made at 10-foot increments from ground zero to the estimated crater radius. Placement of buried objects was selected to cover, as adequately as the availability of drill-holes permitted, the entire estimated crater contour. All ideal objects were serialized and/or color-coded with initial locations recorded. Terminal locations of the emplaced objects were measured after the test area became radsafe. About 18% of surface and shallow-buried objects and 4% of deep-buried objects were recovered. Since only visual inspection was used to locate objects, these percentages are excellent. Various presentations of the measured data are included along with discussions of the results. Trajectory analyses were carried out as a means of presenting these results. Initial velocities were assumed to be radial from the point of burst in the trajectory analyses. The experimental results provide an abundance of data which should be of great use in proving or disproving theories relating to cratering. A particularly significant observation is that the throwout is not symmetrical. This lack of symmetry is secondary with respect to throwout, but may be important in other problem areas. Recommendations are made relating to additional work both in analyzing these results and in obtaining additional information. (auth)

46469 (POR-1815) MASS DISTRIBUTION MEASUREMENTS OF CRATER EJECTA AND DUST. Project 1.6 [of] PROJECT DANNY BOY. Final Report. Rooke, A. D. Jr.; Davis, L. K. (Waterways Experiment Station, Vicksburg, Miss.). July 1963. 108p. (WT-1815). Dep. mn; CFSTI $4.00 cy, $0.75 mn.

An array of tarpaulins was placed in a concentric circular pattern about the ground zero (GZ) of a nuclear device with an intended yield of 470 tons (4.26×10^5 kg). The device was detonated at a depth of 33.5 meters (110 feet) in a basalt medium. After the shot, when the residual radioactivity permitted, samples of ejecta and dust thrown from the crater and deposited on the tarpaulins were recovered, weighed, and analyzed for particle size. The nearest samples to GZ were recovered at a radial distance of 94 meters (≈310 feet) and the most remote at 268 meters (≈ 880 feet). From a total of 158 collector stations, 27 samples were recovered. Mass distribution per unit area and size distribution were tabulated and shown graphically as functions of radial distance from GZ. The amount of deposition was found to decrease sharply with distance; most of the deposition was from within 150 meters (≈ 490 feet) of GZ. Particle size similarly decreased with distance from GZ, the percentage of fines increasing rapidly beyond the 94-meter collector ring. Results of similar experiments are summarized and compared with Danny Boy data by means of dimensionless plots. (auth)

46470 (SC-RR-65-303) A SMALL-SCALE INVESTIGATION OF EXCAVATION WITH PARALLEL ROWS OF EXPLOSIONS. Vortman, L. J. (Sandia Corp., Albuquerque, N. Mex.). Sept. 1965. Contract AT(29-1)-789. 77p. Dep. mn; CFSTI $3.00 cy, $0.75 mn.

Rows of 8-pound spherical charges of TNT buried 3 feet deep and spaced 4 feet apart were fired in parallel configurations. The variations in relative cratering effectiveness of explosives are described as a function of spacing

between rows for both simultaneous and sequential detonation of the rows. The intent was to model at small scale the similar use of nuclear explosives for excavation of overburden from ore bodies to permit open-pit mining. Results indicate that wide craters can be excavated more effectively by parallel row charges fired sequentially than if the rows are fired simultaneously. The data imply that some combinations of closer spacings and deeper burial depths than those tested could increase the efficiency of multiple rows to approach and even exceed that of single rows. (auth)

46471 (UCRL-14123) PROCESS STREAM ANALYSIS SYSTEMS FOR THE SCRUBBER SOLUTIONS USED IN THE PROJECT DRIBBLE VENT GAS TREATMENT PLANT. Rigdon, Lester P.; Harrar, Jackson E. (Lawrence Radiation Lab., Univ. of California, Livermore). May 10, 1965. Contract W-7405-eng-48. 31p. Dep. mn; CFSTI $2.00 cy, $0.50 mn.

Analytical systems are described which provided control information for the Project Dribble vent gas treatment plant. Technicon Instruments Company's AutoAnalyzer equipment was used for continuous monitoring of the components of the plant scrubber solutions. Methods were developed and adapted for the continuous determination of OH^- and $CO_3^{=}$ in the concentration range of 0.05 to 1.5 N; and $SO_3^{=}$, Cl^-, and $SO_4^{=}$ + $SO_3^{=}$ in the range of 0.05 to 3.5 N. The continuous analysis system was incorporated into a glove-box enclosed, trailer-housed facility which also included a capability for manual analyses and pH determination. The performance of this installation with the vent gas treatment plant is characterized. (auth)

46472 (UCRL-14201) MINING BY CAVING WITH NUCLEAR EXPLOSIONS. Hansen, Spenst M.; Lombard, David B. (Lawrence Radiation Lab., Univ. of California, Livermore). June 15, 1965. Contract W-7405-eng-48. 52p. Dep. mn; CFSTI $3.00 cy, $0.50 mn.

A review of the mechanics of underground nuclear explosions demonstrates that they can be used to break large volumes of rock cheaply and safely. A method for mining such broken rock, called nuclear caving, is described. This method utilizes mine workings driven in the solid rock, beneath the broken zone. The workings are connected to the explosion-broken ore by raises, through which the ore is drawn. The method is applicable to large, thick, massive ore bodies, not suitable for open-pit mining. Safety and economic aspects are discussed. It is concluded that nuclear caving has good technical and economic potential. (auth)

46473 (UCRL-14249) NEUTRON ACTIVATION OF THE TERRESTRIAL ENVIRONMENT AS A RESULT OF UNDERGROUND NUCLEAR EXPLOSIONS. Ng, Yook C. (Lawrence Radiation Lab., Univ. of California, Livermore). June 22, 1965. Contract W-7405-eng-48. 41p. Dep. mn; CFSTI $2.00 cy, $0.50 mn.

The neutron activation products induced in the terrestrial environment following underground nuclear explosions are identified, and estimates for their production are presented. These estimates are required for the assessment of the biological implications associated with large-scale nuclear excavations. In the course of this effort all known stable nuclides were considered as parent materials for the more common neutron activation reactions — (n,γ), $(n,2n)$, (n,p), and (n,α) — which result in the production of activities having a half life of one day or greater. The induced radionuclides so identified are numerous and widely distributed in atomic number. Radionuclides of very short half life were thought to lack the potential to contribute significantly to the internal dose and were not considered. Estimates for induced radionuclide production in granite are presented, and the activation products produced in substantial quantity are identified. Adequate estimates can be made for production in rocks differing in composition based on parent element concentrations and yields calculated for granite. When the fission-to-fusion ratio is 0.01, activation products from rock or soil will generally be comparable to fission products in activity if essentially all the fusion neutrons are released to the environment, and will be less prominent if the neutrons released are reduced through the use of nonactivating neutron absorbers. (auth)

46474 NATURAL GAS PRODUCTION FROM UNDERGROUND NUCLEAR EXPLOSIONS. Engineer, 220: 73-4 (July 9, 1965).

Large quantities of gas exist in low-permeability formations in Wyoming, Colorado, New Mexico, Utah, and Arizona. Such reservoirs could conceivably be fractured by nuclear explosives, creating a cylinder or chimney of collapsed rock, and a network of fractures extending beyond the chimney. Gas contained within the fractured radius would flow freely to the chimney and well bore. A preliminary design of an experiment in nuclear stimulation of a gas reservoir was developed as part of the Project Gasbuggy study. Calculations were used for an area in the San Juan Basin of northwestern New Mexico where the natural gas reserves beneath each surface acre are estimated at 33,000,000 ft^3. Estimated recovery from a 160-acre well site is about 10% of these reserves over a 20-year period using conventional industrial practices. Nuclear stimulation is calculated as capable of increasing the recovery to at least 67%. Safety conditions of the project are discussed. It was concluded that a nuclear experiment to test the concept can be executed safely, with no serious inconvenience to residents in the area of the San Juan Basin of New Mexico. (BBB)

Facilities and Equipment

Refer also to abstracts 46928, 47089, 47975, and 47985.

46475 (AD-612113) SUPERCONDUCTORS IN ADVANCED ELECTRONICS. Gaule, Gerhart K.; Breslin, James T.; Ross, Raymond L.; Logan, Roy S. (Army Electronics Labs., Fort Monmouth, N. J.). 1964. 13p. CFSTI $1.00 cy, $0.50 mn.

A novel method for the storage of electrical energy is given by connecting a high current relay switch with a high current, high inductance superconducting solenoid. The basic circuits are derived from analogous capacitor circuits. The inductive energy storage is superior to the capacitive one in the operation of pulsed light sources, for example. A sharp distinction should be made between the cooling methods suitable for the laboratory and those for technical applications. For the latter, greater use should be made of the now available closed cycle refrigerators. Higher operating temperatures for superconducting circuits are sought through improved materials. The development of special low loss dielectric materials for these circuits is also suggested. (TCO)

46476 (AD-613959) DESIGN OF HIGH-ENERGY FAST-PULSE POWER SYSTEM, PHASE II. Period Covered: June 1963–June 1964. Nittrouer, C. A. (Radio Corp. of America, Moorestown, N. J. Missile and Surface Radar Div.). Mar. 1965. Contract AF29(601)-6035. 249p. (WL-TDR-64-94). CFSTI $6.00 cy, $1.50 mn.

A three-part (analytical, experimental, and design) program for development of a high-energy, fast-pulse power system to be used for simulation of certain aspects of high-altitude nuclear detonations is reported. The program was undertaken with objectives of design and cost estimates of the system, and analytical and experimental studies to answer certain remaining questions regarding operation of such a system. It has resulted in a recommended design for a practical system and has provided certain results and conclusions from the experimental and theoretical studies. The findings indicate that such a system can be constructed and have shown what may be expected in regard to output radiation dose rates relative to discharge of the system stored electrical energy. (auth)

46477 (ARL-65-121) STUDIES ON ELECTROMAGNETIC MEANS OF ADDING HEAT AND KINETIC ENERGY TO A GAS. Boedeker, Laurence R.; Coffin, James B. Jr.; Covert, Eugene E.; Haldeman, Charles W.

(Massachusetts Inst. of Tech., Cambridge. Aerophysics Lab.). Mar. 1965. Contract AF33(657)-7975. 350p. CFSTI.

The work completed during the three year contract period on electromagnetic means of adding heat and kinetic energy to a flowing gas stream is presented. Included are discussions of: the nonequilibrium r-f plasma source; the magnetic induction accelerator including the effects of using magnetic core material in the accelerator coils; methods of coil design; numerical results for the one-dimensional flow in the traveling wave pump for various modes of operation; the unsteady axisymmetric flow near the inlet and the resulting velocity profiles; and methods of instrumentation employed to measure plasma properties. A brief discussion of the primary difficulties encountered is also presented. (auth)

46478 (BAW-1280-25) SODIUM-HEATED STEAM GENERATOR DEVELOPMENT. Progress Report No. 23, March 1965. (Babcock and Wilcox Co., Barberton, Ohio. Boiler Div.). Contract AT(11-1)-1280. 57p. Dep. mn; CFSTI $3.00 cy, $0.50 mn.

Background information on various phases of the work and the present status of each phase are summarized. The preliminary design of the Full-Size Steam Generator is complete. The preliminary design of the Prototype Steam Generator is approximately 85% complete. The analysis of sodium-water reaction problems in B&W Full-Size and Prototype Steam Generator, which is being done by APDA under subcontract, is reported. (auth)

46479 (CONF-640508) PROCEEDINGS OF THE 1964 SEMINARS ON REMOTELY OPERATED SPECIAL EQUIPMENT, MAY 26 AND 27, 1964, AEC HEADQUARTERS, GERMANTOWN, MARYLAND. VOLUME I, PARTS I AND II. (Space Nuclear Propulsion Office (AEC/NASA), Washington, D. C.). 382p. Dep. mn; CFSTI $4.00 cy, $1.75 mn. See CONF-641120 for Volume II.

A seminar was held on work on remote manipulation, remote viewing, and man-machine relationships. A total of 14 technical papers was presented, together with a group discussion of future research and development work. Separate abstracts were prepared for the 14 papers. (D.L.C.)

For abstracts of individual papers see: 46459, 46460, 46480–46490, and 48047.

46480 (CONF-640508, pp 4-26) ANALYSIS OF HOSTILE-ENVIRONMENT METHODOLOGIES. Clark, John W. (Battelle Memorial Inst., Columbus, Ohio).

A methodological and functional classification scheme is presented for the tools, methods, and equipment being used in hostile-environment operations. The methodologies are: protective clothing, protective barriers, telechirics (remote control), direct control, and programmed systems. The functions are: manipulation, locomotion, observation, communication, display and control, and power. Definitions and examples of the methodologies and functions are given. (D.L.C.)

46481 (CONF-640508, pp 27-74) SOME WORK ON MANIPULATOR SYSTEMS AT ANL PAST, PRESENT, AND A LOOK AT THE FUTURE. Goertz, Ray (Argonne National Lab., Ill.).

A discussion is presented of development work on general-purpose manipulators and viewing systems. Velocity-controlled unilateral electric manipulators and mechanical or electric master-slave manipulators are covered. Possible future developments, including an increased sense of feel, are considered. A group discussion is included in which the features of a headset television system are described. (D.L.C.)

46482 (CONF-640508, pp 75-99) RATE CONTROLLED MANIPULATORS. Melton, Donald F. (Programmed and Remote Systems Corp., St. Paul, Minn.).

A brief discussion is given of manipulator types, uses, mountings, and operating conditions. A description is given of the design features of rate-controlled manipulators. A group discussion is included in which terminal devices (hands) are considered. (D.L.C.)

46483 (CONF-640508, pp 158-97) DESIGN AND TEST OF A FULL-SCALE WEARABLE EXOSKELETAL STRUCTURE. Mizen, Neil J. (Cornell Aeronautical Lab., Inc., Buffalo, N. Y.).

An exoskeletal device using powered joints is being developed for amplifying a man's muscular strength and increasing his endurance. The joints and their operation are described. Tests were conducted on a nonpowered exoskeleton to determine the number of joints needed, and the velocities at each joint for estimation of power requirements. A group discussion is included, and a description is given of the Case Research Arm-Aid which was developed for studies on man-machine communications multifunction control for orthotic and prosthetic devices. (D.L.C.)

46484 (CONF-640508, pp 198-209) HUMAN FACTORS IN REMOTE HANDLING: A REVIEW OF PAST AND CURRENT RESEARCH AT THE 6570TH AEROSPACE MEDICAL RESEARCH LABORATORIES. Kama, William N. (Aerospace Medical Research Lab. (6570th), Wright-Patterson AFB, Ohio).

The role of remote handling in the problem areas of ground support for nuclear-powered systems and extravehicular space operations is given. A summary is presented of the research carried out on human factor aspects of design and use of remote manipulators. A group discussion is included. (D.L.C.)

46485 (CONF-640508, pp 210-23) A SERVO-RESTRAINT SYSTEM FOR ANTI-G PROTECTION. Loudon, Warren L. (Naval Air Development Center, Johnsville, Pa.).

The problems encountered by operating personnel in aerospace vehicle control are discussed. Two systems for preventing the operator from flailing about prior to ejection are described. The use of General Electric's Handyman control harness to cancel the effects of increased G on a subject is considered. A servo-restraint harness system is being developed, and a hydraulic servo valve which is part of the system is described. The application of servo-restraint to high-speed cross-country travel is considered. (D.L.C.)

46486 (CONF-640508, pp 233-47) AN EVALUATION OF PROPOSED APPLICATIONS OF REMOTE HANDLING IN SPACE. Chubb, Gerald P. (Aerospace Medical Research Lab. (6570th), Wright-Patterson AFB, Ohio).

Encapsulation of astronauts and the use of telechiric systems have been proposed for the maintenance and assembly of orbiting space stations. An evaluation of these methods is made, with emphasis on the human factors design trade-offs. A group discussion is included. (D.L.C.)

46487 (CONF-640508, pp 248-303) ADVANCED DESIGN CONCEPTS FOR A REMOTELY OPERATED MANIPULATOR SYSTEM FOR SPACE-SUPPORT OPERATIONS. Vivian, C. E.; Wilkins, W. H.; Haas, L. L. (Lockheed Missiles and Space Co., Sunnyvale, Calif.).

An advanced design concept of a remotely operated handling system for space operations was developed which is called Space Cargo Handler and Manipulator for Orbital Operations (SCHMOO). The manipulators and control systems of SCHMOO are described, and some of the missions that can be performed by SCHMOO are discussed. (D.L.C.)

46488 (CONF-640508, pp 304-26) PROGRAMMING AND MANUAL CONTROL OF VERSATILE MANIPULATING DEVICES. Holzer, Franz (AMF Atomics, Greenwich, Conn.).

The technical and marketing requirements for design of manipulating devices that could carry out a wide variety of tasks are discussed. Descriptions are given of the two AMF programmed manipulators, VERSATRAN and FLEXIMAN. Manual control of master-slave and servo manipulators is considered, and the types of servodrives considered for the latter are discussed. Computers and bandwidth reduction are discussed in the group discussion. (D.L.C.)

46489 (CONF-640508, pp 327-33) USAF EXPLORATORY DEVELOPMENT OF REMOTE HANDLING EQUIP-

MENT. Tolliver, R. L. (Air Force Weapons Lab., Kirtland AFB, N. Mex.).

A remotely controlled mobile test vehicle was designed for development of capability for recovery of aerospace nuclear power devices under emergency conditions in a high radiation environment. A pair of manipulators and a plasma-arc cutting torch are mounted on the vehicle. The television viewing system is described in some detail. (D.L.C.)

46490 (CONF-640508, pp 340-64) ARCHITECT-ENGINEERING CONSIDERATIONS IN THE DESIGN OF REMOTE HANDLING TOOLS AS TO FUNCTION AND FLEXIBILITY. Colgan, James E. Jr. (Vitro Engineering Co., New York).

The architect-engineering considerations to be made in the design of remote handling devices are discussed for three types of systems: a university gamma cell, a power reactor refueling system, and a wall-mounted handling system for the NERVA program. (D.L.C.)

46491 (CONF-641120) PROCEEDINGS OF THE 1964 SEMINARS ON REMOTELY OPERATED SPECIAL EQUIPMENT HELD AT NUCLEAR ROCKET DEVELOPMENT STATION, JACKASS FLATS, NEVADA, NOVEMBER 4 AND 5, 1964. VOLUME II. (Space Nuclear Propulsion Office (AEC/NASA), Washington, D. C.). 109p. Dep. mn; CFSTI $1.25 cy, $0.75 mn.

See CONF-640508 for Vol. I.

Seventeen articles are included; separate abstracts were prepared for 14. One article on possible remote maintenance and repairs on reactors at NRDS was previously abstracted for NSA as 19: 29740. The other articles include information on methods for spinning-off NASA mission oriented research to life sciences and introduction to work at Case Institute of Technology. (P.C.H.)

For abstracts of individual papers see: 46492–46505.

46492 (CONF-641120, pp 1-3) CURRENT EXPERIMENTS USING PROSTHETIC TERMINAL DEVICES ON MODEL 8 MASTER SLAVES. Stearns, E. H. (Lawrence Radiation Lab., Univ. of California, Livermore).

The adaptation and use of a Dorrance 5XA terminal device on a Model 8 manipulator is discussed. Experience showed that the rubber band closing technique was not readily adapted to a Model 8 and it allowed very little feel of the object that was being picked up. A special adapter was built which offset the hand run out under the ball bearing joint. This made the hand closely coupled to the wrist. Other disadvantages of the model are also mentioned. (P.C.H.)

46493 (CONF-641120, pp 4-5) BRIEF NOTES ON CURRENT TECHNIQUES AND PROBLEMS OF REMOTE HANDLING AT THE REACTOR MAINTENANCE, ASSEMBLY AND DISASSEMBLY FACILITY. York, Don (Los Alamos Scientific Lab., Univ. of California, N. Mex.).

Experience in the use of manipulative equipment in the disassembly of a reactor is reported. Special attention is given to the shielded area and its equipment. (P.C.H.)

46494 (CONF-641120, pp 6-8) REMOTE OPERATIONS AT TEST CELL C. Henshall, J. B. (Los Alamos Scientific Lab., Univ. of California, N. Mex.).

Remote operations at Test Cell "C" at Los Alamos are described. Remote operations are all performed electrically since the distance between the control point and the test cell itself is large. The function of the analog feedback system is also discussed. Camera bunkers are generally located some 600 to 700 ft from the reactor. The cameras are mounted in a protected concrete and earth shield bunker and the pictures are taken through a mirror that is mounted in a support structure above the shield at bunker. Semi-radiation resistant TV cameras are used on the reactor pad. (P.C.H.)

46495 (CONF-641120, pp 9-35) REMOTE HANDLING REQUIREMENTS FOR NERVA (E-MAD AND ETS-1). White, L. E. (Aerojet-General Corp., Jackass Flats, Nev.).

Design criteria related to the Engine Test Stand (ETS-1) and Engine Maintenance, Assembly, and Disassembly (E-MAD) facilities that contribute to the development of significant remote handling systems are presented. The design of the integrated remote handling system for E-MAD is an integration of three basic remote handling systems supplemented by an overhead crane, master slave manipulators at the viewing windows, storage stands, dollies, and fixtures. The ETS-1 provides a test-stand-to-engine interface incorporating remotely operated pneumatic lines and electrical connectors with which the engine counterparts must be accurately mated. Additionally, and since this is a nozzle-down test facility, a method to handle the exhaust gases was developed called the NERVA Exhaust System (NES). This system includes a major sub-system, a deflection duct which deflects the exhaust gases down and away from the facility. The Engine Installation Vehicle (EIV) carries the engine between the engine test stand and the E-MAD Building in a nozzle-down position. Several illustrations of the equipment are given. Remote viewing equipment is also discussed. (P.C.H.)

46496 (CONF-641120, pp 36-8) REPORT ON FMC REMOTE HANDLING VEHICLE. Tolliver, Robert (Air Force Weapons Lab., Kirtland AFB, N. Mex.).

A follow-up report on an experimental fullscale model of a remote controlled salvage system is presented. The equipment has two large manipulators, which are individually capable of picking up in excess of 600 pounds. The arms have 8 different motions and three of these motions may be deleted by actuating switches in the control console. Tests indicate that good remote control can be maintained at a distance of one mile. (P.C.H.)

46497 (CONF-641120, pp 39-40) DISCUSSION OF PROPOSED TELECHIRICS RESEARCH LABORATORY. Clark, John (Battelle Memorial Inst., Columbus, Ohio).

The concept for a Telechirics Research Laboratory (TCRL) in which basic experiments in remote operating techniques and methods will be performed is discussed. The laboratory is proposed in order to avoid reliance upon opinions by generating quantitative measures by which one can tell which system to use in which case. (P.C.H.)

46498 (CONF-641120, pp 41-7) REPORT ON ARGONNE NATIONAL LABORATORY'S ACTIVITIES. Goertz, Ray (Argonne National Lab., Ill.).

Various parameters that are important in general-purpose manipulator systems are discussed with regard to experience at Argonne. The parameters include grasping, friction, speed, and inertia. Progress on the development of an electric master-slave manipulator called the Mark 4 is reported. (P.C.H.)

46499 (CONF-641120, pp 63-6) DISCUSSION OF PNEUMATICALLY ACTUATED MASTER SLAVE MANIPULATOR. Wilson, Kent (Autonetics, Anaheim, Calif.).

Discussion is presented on the development of a manipulator arm and a servo manipulator. The arm is hydraulic, 6 ft long, with a 50 lb capacity, and has a total of nine motions. The manipulator is bilateral and has a force feedback system. In addition to the arm, there are also two pairs of actuators in a shoulder or cylindrical portion that takes the place of the body. In this manipulator each actuator for the seven motions available is a pair of braided tension devices known as McKibben muscles. Range of motions in the manipulator is also discussed. (P.C.H.)

46500 (CONF-641120, pp 67-70) STUDY OF REMOTE HANDLING IN SPACE. Vivian, Charles (Lockheed Missiles and Space Co., Sunnyvale, Calif.).

The Orbital Launch Operation study package is discussed. The primary objective of the study was to develop a conceptual evaluation of an Orbital Launch Operation program to provide the earliest feasible lunar base build-up for reasonable costs and compatible with the early accomplishment of initial manned lunar mission. The recommended support concept involves the use of an Orbital Launch Support Facility (OLF), as an orbital base of operations, providing C/O, countdown, receiving, main-

tenance, and repair services to the Orbital Launch Vehicle. The operational concept of an orbiting launch facility is described. (P.C.H.)

46501 (CONF-641120, pp 73-4) REPORT ON STUDY OF GENERALIZED, PROGRAMMED MANIPULATORS. Mergler, Harry (Case Inst. of Tech., Cleveland, Ohio).

An arm-aid system operating on 500 psi CO_2 in an all pneumatic and electronic system is described. The structure contains five articulated axes, each of which is independently controlled (within the limits of movement of the human arm) and each of which contributes to the generation of a spatial locus. Command data are transmitted to each axis in incremental form over two algebraically-signed lines. The command data are generated by physically moving the splint structure through the desired physical path and recording the algebraically-signed pulses generated by the incremental transducers (pulse generators) associated with each axis. On play-back the transducers act as the feedback signal generators in the individual electromechanical digital servo loops associated with each articulated axis. (P.C.H.)

46502 (CONF-641120, pp 75-7) REPORT ON STUDY OF APPLICATION OF FLUID AMPLIFIERS IN REMOTE CONTROL OPERATIONS. Taft, Charles (Case Inst. of Tech., Cleveland, Ohio).

The use of fluid to transmit power or information is discussed. Work is concerned with a pure digital feedback system. The only mechanical part of the system is the actuator and a disk which serves to interrupt two fluid jets, to provide digital feedback. The system accepts a pulse of fluid. This pulse will command the system to change the output by one increment in the system at an angle of about 15°. A fluid counter sums two pulse trains, one representing the input and one the output, algebraically to produce a difference or error. The difference is converted using fluid elements into an analog fluid signal which is amplified. The fluid signal is then used to drive two turbines, which are just air grinders. These two turbines drive a combination of a worm gear and differential to produce the mechanical output that is used to operate the feedback element. (P.C.H.)

46503 (CONF-641120, pp 78-85) PRELIMINARY CONCEPTS FOR A CENTRAL TEST FACILITY. Whipp, James (Braun (C. F.) and Co., Vienna, Va.).

Considerations relating to the purpose, feasibility, and nature of a central test facility for ROSE systems and elements are discussed. Basic goals of the facility are listed, and a general description of a test facility is given. (P.C.H.)

46504 (CONF-641120, pp 86-97) REMOTE OPERATIONS IN THE SNAP-8 FACILITY AT ATOMICS INTERNATIONAL. Henoch, William; Burton, John (Atomics International, Canoga Park, Calif.).

General background information concerning the SNAP Programs at Atomics International is given, and the complex task of disassembling a SNAP reactor system without visual access after the reactor had been operated in a windowless test vault for a year and a half is described. An example of the type of operations undertaken by the SNAP Remote Handling and Viewing organization is described in the S2DS reactor system disassembly account given. (P.C.H.)

46505 (CONF-641120, pp 98-103) REPORT ON MANIPULATOR CONTROL WORK AT THE MASSACHUSETTS INSTITUTE OF TECHNOLOGY. Sheridan, Thomas; Ferrell, Russ (Massachusetts Inst. of Tech., Cambridge).

A study made on a situation in which there is a long delay between the time a person moved a remote manipulator master control and the time the person could observe the new position of the slave is reported. It was found that even with a delay of $\frac{1}{10}$ of a second, the move and wait strategy is much quicker than trying to predict ahead. The result was somewhat contrary to what linear servo theory predicts. Tactile feedback is also discussed. (P.C.H.)

46506 (CONF-651101-26) EVOLUTION OF THE HIGH LEVEL CAVES AT THE SAVANNAH RIVER LABORATORY. Coogler, A. L.; Deily, G. J.; Hale, R. J. (Du Pont de Nemours (E. I.) and Co., Aiken, S. C. Savannah River Lab.). Aug. 5, 1965. Contract AT(07-2)-1. 39p. Dep. mn; CFSTI $2.00 cy, $0.50 mn.

For Presentation at 13th Conference on Remote Systems Technology, Washington, D. C.

The Hot Cell Facility, which began operations in 1954 with six cell modules, has been expanded in two stages to 16 cell modules with adequate supporting facilities to maintain continuous operation of the cells. Operating experience with the initial facilities established that (a) in-line arrangement of the cells was desirable, (b) transfer of materials and equipment should be through the cell roof, (c) support facilities should be capable of handling peak work loads if efficient use of the cells is expected, (d) simplification of the cell structure would not reduce its usefulness, and (e) all cell equipment should be remotely installed and removed. These criteria were applied to the building expansions to achieve a facility capable of a high output of research and development work. (auth)

46507 (NMI-4997, pp 157-62) A REMOTE METALLOGRAPHIC SPECIMEN GRINDER. Long, E. L. Jr., Richt, A. E.; Holcomb, D. L.; Gray, R. J. (Oak Ridge National Lab., Tenn.).

An investigation to evaluate potential methods of remotely grinding metallographic specimens and to select optimum equipment is described. During this investigation several commercial grinders were considered, none of which could be placed in-cell as purchased. As a result, one grinder was selected and modified for remote grinding. (auth)

46508 (NMI-4998, pp 65-76) MATERIALS RESEARCH WITH THE SCANNING MICROPROBE ANALYZER. Lenke, J. W.; Domagala, R. F. (IIT Research Inst., Chicago, Ill.).

Some of the studies that have been conducted at the IIT Research Institute using a Cambridge Instruments Ltd. electron-beam microprobe analyzer are briefly described. (W.L.G.)

46509 (UCRL-12497-T) LIVERMORE SLUG FABRICATION FACILITY. Hubbell, William H.; Coops, Melvin S. (Lawrence Radiation Lab., Univ. of California, Livermore). July 28, 1965. Contract W-7405-eng-48. 19p. (CONF-651101-22). Dep. mn; CFSTI $1.00 cy, $0.50 mn.

From 13th Conference on Remote Systems Technology, Washington, D. C.

A special water-shielded cave facility was constructed for the fabrication of highly alpha-active capsules which will be irradiated with neutrons in a high flux reactor to form heavier elements. Because neutrons and gamma rays are emitted during spontaneous fission of the target materials, the complete fabrication process is conducted remotely. The primary enclosures are alpha-tight, and the biological shielding consists of steel tanks filled with water. Slugs $\frac{5}{8}$, $1\frac{5}{16}$, and $1\frac{1}{8}$ inches in diameter and up to 6 inches in length may be fabricated. (auth)

46510 (Y-DA-967) A RESEARCH FACILITY FOR THE STUDY AND PREPARATION OF ULTRAPURE MATERIALS. Schreyer, J. M.; Bradford, C. M. (Union Carbide Corp., Oak Ridge, Tenn. Y-12 Plant). Sept. 17, 1965. Contract W-7405-eng-26. 22p. (CONF-651004-4). Dep. mn; CFSTI $1.00 cy, $0.50 mn.

From 9th Conference on Analytical Chemistry in Nuclear Technology, Gatlinburg, Tenn.

A description is given of the High-Purity Laboratory, which was designed for research on the preparation and properties of selected high-purity materials. The Laboratory consists of a clean room surrounded by a laboratory area containing laminar flow devices and equipment for purifying metals and ceramics by different melting techniques. (D.L.C.)

46511 FACILITIES TO SERVICE NUCLEAR INSTRUMENTS. Queer, Paul R. (Westinghouse Electric Corp., Pittsburgh). Atomics, 18: 46-8(July-Aug. 1965).

A survey of laboratory instruments was undertaken and associated maintenance and calibration requirements

established. It was concluded that approximately $50,000 worth of test equipment would be required to properly service the laboratory's instrumentation needs in the development and manufacture of nuclear power reactors and associated equipment. Recruiting instrument technicians, specializations, controlled humidity and temperature, and heat and dust as causes of failure are discussed. (M.C.G.)

46512 X RAYS AND ELECTRONIC MICROSCOPY AT THE GRENOBLE NUCLEAR CENTER. Bertaut, E. F.; Allemand, R.; Pluchery, M. Bull. Inform. Sci. Tech. (Paris), No. 92, 3-78(Apr. 1965). (In French).

Laboratories for electron microscopy and x-ray studies at the Grenoble Nuclear Center gradually extended their services. Characteristic aspects of this development are discussed, especially the role played by this laboratory as a pilot with respect to new instrumental settings and experimental methods. (auth)

46513 PURIFICATION OF HELIUM GAS IN NUCLEAR FACILITIES. Sumitani, Shozo; Ariyoshi, Shigeki. FAPIG (Tokyo), No. 33, 185-9(Aug. 1964). (In Japanese).

Devices used for the purification of helium as coolant, sealing gas, or circulating gas are described. In the O.E.E.C. High-Temperature Reactor (Dragon) it consists of pre-cooler, iodine trap, delay bed, oxygenator, freezer, Kr–Xe delay bed, and Kr–Xe trap. Part of the cooling medium is led to the purifier to remove impurities such as fission products. In the experimental gas-cooled reactor (EGCR) CO_2, H_2, CO, N_2, and H_2O are removed. The device consists of a filter, O_2 supply, catalyst convertor, condenser, and absorber. In the JRR-2 the decomposed gases from heavy water are recombined and contained air is removed. The device consists of a re-combinator, condenser, pre-cooler, main cooler, dessicator, and absorber. In the ANL 350-facility water is absorbed on molecular sieves at high pressure and at room temperature, and oxygen on active carbon at high pressure and at low temperature. A circulating blower, filter, compressor, drying tower, heat exchanger, and active carbon tower make up the purifier. This device is also used for glove-box helium purification. Leakage, selection of an absorbing agent, and pressure loss are discussed. (NSA of Japan)

46514 ELECTROSTATIC ENGINEERING. Felici, N. J. (Universite, Grenoble, France). Sci. J., 1: No. 7, 32-8(Sept. 1965).

A general survey is given of electrostatic engineering. Some electrostatic devices and methods are described such as the four pole electrostatic generator, the electrostatic accelerator, and electrostatic precipitation. Other applications of electrostatics are also mentioned. Although their potential is seldom appreciated, electrostatic devices are already saving western European industry 10 million pounds a year. During the next few years they could lead to a new growth industry. The scope of this field is enormous since it is not restricted to a specific kind of material. (J.F.P.)

46515 CENTRIFUGE TUBES FOR NO. 30 ROTOR (Engineering Materials). (Oak Ridge National Lab., Tenn.). (CAPE–1237).

1 drawing.

Disposable, easily assembled centrifuge tubes were developed to aid in preventing viral and bacterial contamination of the operator and to avoid cross contamination in virus separations using a No. 30 (30,000 rpm) angle-head rotor. Two versions were fabricated from polycarboncite. They differ in the size of the openings at the top; the 30-A has a 0.25-in. dia opening and 30-B has a 0.5-in. opening. Each tube holds 27 ml when spun without liquid pressing the lids. The tubes can be run partially filled or empty without rupturing. Both the tube and the cap can be autoclaved. (For Details, See TID-4100) (M.C.G.)

46516 ELECTRIC MOTOR. (to Brown, Boveri and Co. Ltd.). British Patent 997,197. July 7, 1965. Priority date Sept. 23, 1960, Germany.

An electric motor is provided that is suitable for use in a highly radioactive atmosphere at high temperatures. The motor is suitable for flange mounting to a counter flange and is provided with a closed gas cooling system and a liquid recooling device arranged around the motor casing and intended for cooling the gas. All connecting fixtures and the motor itself are so designed that any part or all of the assembly may be removed by manipulators. (B.L.M.)

46517 AN ARRANGEMENT FOR TRANSFERRING IRRADIATED FUEL ELEMENTS INTO A POOL. (to Commissariat a l'Energie Atomique). British Patent 1,000,777. Aug. 11, 1965. Priority date July 6, 1962, France.

An apparatus is provided for transferring irradiated fuel elements contained in a case resting on a first receptacle at the level of the top of a pool to a suitable storage area, such as racks, fixed at the bottom of the pool, or vice versa. The racks are provided with compartments of the same shape as that of the elements. A rigid bracket is fixed to one of the upper edges of the pool and supports a vertical column that is free to pivot about its axis. An arm may be moved vertically along the column by a system of a chain and pulleys and may pivot with the column. A tubular recess to receive the elements one by one is provided at the free end of the arm. With the fuel elements in the tubular recess, rotation of the column about its axis and raising or lowering the arm along the column serves to transfer the elements from the upper receptacle to the racks or vice versa. (B.L.M.)

46518 A MOVABLE GRIPPING DEVICE. (to EURATOM). British Patent 1,002,171. Aug. 25, 1965. Priority date July 4, 1961, Belgium.

A movable gripping device for handling an object under remote control consists of a movable carrier member, upper and lower gripping jaws, and jaw opening means. The gripping jaws are mounted on the carrier member and movable on it towards and away from one another. Resilient means urge the jaws towards a closed, gripping position, and jaw opening means are operable first to move the upper jaw upwardly from the lower jaw and then to move the lower jaw downwardly. The opening means comprises a separator guided by the carrier member for movement between the jaws and co-operating with inclined cam faces on the jaws. As the separator moves from a jaw-closed position to open the jaws, it engages first the cam face on the upper jaw and then the cam face on the lower jaw. Preferably, the jaws are pivoted to the carrier member for movement, and the pivotal axes of the two jaws are parallel to one another and perpendicular to the direction of movement of the separator. (B.L.M.)

46519 IMPROVEMENTS IN OR RELATING TO CONVEYOR SYSTEMS. Bailey, Peter John; Baines, Bernard Deryck; Lindstaedt, Horst Karl; Webster, Harold (to Nuclear Chemical Plant Limited). British Patent 1,002,601. Aug. 25, 1965. Filed Nov. 10, 1961.

A conveyer system is patented for subjecting objects to penetrating radiation from a source that emits radiation from at least two opposite sides. The system has two substantially parallel upright portions adapted to pass adjacent to the source and on either side of it. Two additional parallel portions are adapted to pass outside and adjacent to the first conveyer portions so that the first conveyer portions are disposed directly between the source and at least one further conveyer portion. A number of supports are spaced apart from each other on the conveyor for carrying objects to be treated. Means are provided for automatically transferring each object laterally on its support means after it has travelled for a pre-determined distance over the upright conveyer portions and for automatically removing the object from the support means after the lateral movement is completed. (B.L.M.)

46520 HANDLING DEVICE HAVING A DETACHABLE GRIPPER. (to Commissariat a l'Energie Atomique). British Patent 1,003,244. Sept. 2, 1965. Priority date Oct. 4, 1962, France.

A manipulator gripper is described that can be easily and rapidly fitted to or detached from a handling device without being withdrawn from the enclosure, such as a

hot cell, where it is being used. The gripper includes a body to which the gripper fingers are pivotally connected and through which extend control means for opening or closing the fingers. A brush is included between the body and the control means, and the brush is free to rotate with respect to the control means, but is lockable against axial and rotational movement of the body. This rotation and locking is accomplished by an element that is displaceable between a position in which it effects the axial and rotational locking and a position in which it locks the brush with respect to rotation only permitting axial movement of the brush and control means relative to the body. Means are also provided rotatable relative to the body and the brush for controlling the displacement of the locking element. Alternatively, the control means are movable in a tube mounted on the gripper axis, and the brush is mounted between the gripper body and the tube and rotates with respect to the tube but is axially rigidly connected to the tube and lockable on the body by an element. (B.L.M.)

46521 MATERIAL EXCHANGE COLUMNS. (to Sulzer Brothers Limited). British Patent 1,004,046. Sept. 8, 1965. Priority date July 31, 1962, Switzerland.

A material exchange column is made up of at least two packing elements one above another. Each element consists of or includes corrugated lamellae that are generally parallel with the column axis. The corrugations of adjacent lamellae extend in different directions, and the corrugations of at least one of each adjacent pair of lamellae are diagonal to the column axis. The elements are so arranged that the planes in which the lamellae of adjacent elements lie are angularly displaced relatively to one another around the column by approximately 90°. Various modifications of the elements are described. (B.L.M.)

46522 FURNACE AND FURNACE WALL. Beattie, John Reginald (to Pilkington Brothers Ltd.). U. S. Patent 3,197,185. July 27, 1965. Priority date May 3, 1962, Great Britain.

A heat treatment furnace is provided that has a low thermal capacity and high speed of response to local applications of heat and exhibits good thermal insulation at temperatures in the range 800 to 1000°C. The furnace includes a cavity wall structure formed by a number of spaced partitions. One or more of the partitions are coated on one surface with a coating of a refractor material to establish a layer on that surface having a surface reflectivity greater than its surface absorptivity at operating temperature. The furnace is particularly applicable to heat treatment of flat glass. (B.L.M.)

46523 CONVEYOR SYSTEMS. Jefferson, Sidney (to United Kingdom Atomic Energy Authority). U. S. Patent 3,200,937. Aug. 17, 1965. Priority date Apr. 27, 1961, Great Britain.

A conveyor system used to move packages past a source of γ radiation is designed to minimize clearance space between adjacent package carriers. Each package carrier is a tubular container pivotally suspended from an overhead railway in such a manner that it can be moved to a horizontal position for loading and rotated to a vertical position during movement along the railway. Preferably packages are loaded through the bottom and removed from the top. The fulcrum around which the container rotates is positioned below and to one side of the center of gravity of the container; the container can thus be brought to rest by gravity against a fixed member on the trolley to reduce swinging during movement. (A.G.W.)

46524 CONSTANT-HEIGHT VERTICAL SUPPORT DEVICE, IN PARTICULAR FOR TANKS. Deleuze, Edouard (to Commissariat a l'Energie Atomique). U. S. Patent 3,201,076. Aug. 17, 1965. Priority date Jan. 25, 1961, France.

A device for supporting tanks such as nuclear reactor vessels consists of equidistant vertical pillars on each of which the bottom of the tank is supported through the intermediary of a universal coupling or Cardan-type coupling. Each pillar is made up of a series of concentric tubular load-transmitting members compensated for expansion to ensure the maintenance of the tank bottom at a constant level. The arrangement has a limited flexibility in the radial direction in order to provide for the radial expansions of the tank. (A.G.W.)

46525 CRYOGENIC TRANSPORT TUBE INCORPORATING LIQUEFACTION APPARATUS. Post, Arthur H. Jr. (to Arthur D. Little, Inc.). U. S. Patent 3,201,947. Aug. 24, 1965. Filed Sept. 6, 1963.

An apparatus is patented for the liquefaction of gases, particularly He, in large quantities within the Dewar storage vessel itself. The apparatus is a modification of the apparatus described in U. S. Pat. 2,458,894, and it eliminates the continuous personal attendance, making it readily adaptable to large-scale production of the liquefied gases. The apparatus is such that it sustains smaller thermodynamic losses than if the liquefied gas were transferred periodically from the liquefaction apparatus to a storage vessel, and it is possible to fill the storage vessel to its maximum capacity. The apparatus is flexible in its application to various sizes of storage vessels and to various locations of the vessel with respect to the cryostat. (B.L.M.)

Heat Transfer and Fluid Flow

See also PHYSICS — General.

Refer also to abstract 48079.

46526 (AECL–2273) TWO-PHASE FLOW MEASUREMENT WITH SHARP-EDGED ORIFICES AND VENTURIS. Bizon, E. (Atomic Energy of Canada Ltd., Chalk River (Ontario)). June 1965. 52p. Dep.; AECL $1.50.

Results are reported of a series of two-phase flow measurements performed at 1200 psig with orifices of diameter ratio 0.45 and 0.70 and a venturi of diameter ratio 0.58 on steam–water mixtures at 1200 psig. Steam weight fractions were between 5 and 50% while mass flow was between 150,000 and 400,000 lb/hr-ft^2. Dimensionless correlations for each device were obtained and a confidence interval for the correlation coefficients was computed. (auth)

46527 (AEEW-R–426) AN EXPERIMENTAL COMPARISON BETWEEN FORCED CONVECTION BURN-OUT IN FREON 12 FLOWING VERTICALLY UPWARDS THROUGH UNIFORMLY AND NON-UNIFORMLY HEATED ROUND TUBES. Stevens, G. F.; Elliott, D. F.; Wood, R. W. (Atomic Energy Establishment, Winfrith (England)). May 1965. 18p. Dep.; BIS $0.50; HMSO 2s. 6d.

Some correlations of forced convection burn-out data are based on the approximate linearity of the relationship between burn-out heat flux and the channel-averaged quality at the burn-out point. These correlations perform satisfactorily on data obtained from uniformly heated configurations. Therefore the further inference is sometimes made that the burn-out heat flux is uniquely related to the quality, and that the burn-out in non-uniformly heated configurations can be calculated from measurements made with uniform heating. This report presents burn-out data for Freon 12 flowing vertically upwards through both uniformly and non-uniformly heated round tubes. These data show that the quality at burn-out does depend on the heat flux profile, and that the inference mentioned above is not justified. (auth)

46528 (ANL–7038) A LIQUID-METAL HEAT-TRANSFER EXPERIMENT. Holtz, R. E. (Argonne National Lab., Ill.). June 1965. Contract W-31-109-eng-38. 34p. Dep. mn; CFSTI $2.00 cy, $0.50 mn.

The utility of thermal-radiation heat transfer as a means of supplying and removing heat from a flowing liquid metal was experimentally investigated and found to be a satisfactory technique for this application. Single-phase heat transfer to liquid NaK during vertical upflow in a tube was also examined. The experimental results are in fair agreement with the semiempirical expressions of others. The effect of the initiation of nucleate boiling in the system was also observed. (auth)

46529 (APDA-175) ANALYSIS OF THE BABCOCK AND WILCOX PROTOTYPE STEAM GENERATOR FOR A SODIUM-WATER REACTION. Ford, J. A.; Chamberlain, H. V.; Chase, W. L. (Atomic Power Development Associates, Inc., Detroit, Mich.). Aug. 23, 1965. Contract AT(11-1)-1280; Subcontract No. 1. 56p. Dep. mn; CFSTI $3.00 cy, $0.50 mn.

An analysis of the effects of a sodium-water reaction in the Babcock & Wilcox Prototype Steam Generator was conducted. A leak in a tube in the Prototype would cause a sodium-water reaction which would result in the rapid generation of quantities of hydrogen and high temperatures. The mathematical model developed to analyze this accident is discussed and data are presented on the effect of (1) leak size, (2) paths for reaction relief, and (3) leak location on hydrogen pressure. A maximum hypothetical accident consisting of the complete and simultaneous severance of all 25 tubes in the boiler section of the unit is discussed and illustrated with curves of the reaction data. Recommendations are presented for (1) improving the method of analysis of a sodium-water reaction in the Prototype and (2) changing the structural design to improve the ability of the unit to withstand such a reaction. (auth)

46530 (BAW-1280-27) SODIUM-HEATED STEAM GENERATOR DEVELOPMENT. Progress Report No. 25, May 1965. (Babcock and Wilcox Co., Barberton, Ohio. Boiler Div.). Contract AT(11-1)-1280. 28p. Dep. mn; CFSTI $2.00 cy, $0.50 mn.

The Preliminary Design of the Prototype Steam Generator is approximately 98% complete. Purchase orders have been placed for almost all of the long-lead materials to be used in fabrication of the Prototype Steam Generator and this material is beginning to be received. Research and development work is being carried out on carbon and mass transfer effects on materials, corrosion of Croloy 2¼ steel in sodium–water, welding of tubes to backside of tube sheet, chemical simulation of sodium environment for leak testing, and analysis of sodium–water reactions. (D.L.C.)

46531 (BAW-1280-28) SODIUM-HEATED STEAM GENERATOR DEVELOPMENT. Progress Report No. 26, June 1965. (Babcock and Wilcox Co., Barberton, Ohio. Boiler Div.). Contract AT(11-1)-1280. 41p. Dep. mn; CFSTI $2.00 cy, $0.50 mn.

The Preliminary Design of the Full-Size Steam Generator is complete. The Preliminary Design of the Prototype Steam Generator is approximately 98% complete. A review meeting was held to review the Steam Generator design prior to beginning fabrication of the Prototype Steam Generator. Some additional work will be required on sodium-water reaction problems in the Full-Size and Prototype Steam Generators. Work is under way on completing the analysis work on these problems. Approval was granted to begin fabrication of the Prototype. Purchase orders have been placed for the materials as required to meet the scheduled beginning of fabrication on July 1. Research and development work on the following subjects are reported: carbon and mass transfer effects on materials, corrosion of Croloy 2¼ by sodium-water reaction products, welding of tubes to back side of tube sheet, chemical simulation of sodium environment for leak testing, and analysis of sodium-water reactions. (D.L.C.)

46532 (BNWL-116) PRESSURIZING VESSEL PERFORMANCE EQUATIONS. Coughren, K. D. (Battelle-Northwest, Richland, Wash. Pacific Northwest Lab.). Aug. 1965. Contract AT(45-1)-1830. 32p. Dep. mn; CFSTI $2.00 cy, $0.50 mn.

Pressurized water systems often use steam-pressurized vessels to control the pressure. In such vessels, a steam-pressurized upper region and a lower region containing saturated water are provided so that a pressure change will cause either the water to flash or the steam to condense. Energy equations relating internal energy to external energy inputs are derived which predict the performance of the pressurizer vessel. The analysis is carried out in two parts: insurge and outsurge. (D.L.C.)

46533 (LA-DC-7373) SOLUTIONS TO NONLINEAR INCOMPRESSIBLE FLOW PROBLEMS THROUGH A FINITE DIFFERENCE METHOD. Fromm, Jacob E. (Los Alamos Scientific Lab., Univ. of California, N. Mex.). [1964]. Contract W-7405-eng-36. 42p. (CONF-650933-1). Dep. mn; CFSTI $2.00 cy, $0.50 mn.

From Symposium on Advanced Problems and Methods in Fluid Dynamics, Jurata, Poland.

A finite difference method of calculating time dependent incompressible fluid flows is described and results from a variety of applications of the technique are illustrated. The objective is to show the diversity of problems that become amenable through the numerical method rather than to develop a complete treatment in any specific area. Included are solutions of Kármán vortex street flows along with examples which involve the transfer of heat in the wake. Stability of shear flows including jets are next considered. Finally results are given from a study of the Bénard problem. In all cases emphasis is placed upon possible directions of research open to numerical treatment by finite difference methods. (auth)

46534 (NP-15437) A STUDY OF SYSTEM-INDUCED INSTABILITIES IN FORCED-CONVECTION FLOWS WITH SUBCOOLED BOILING. Technical Report No. 5382-35. Maulbetsch, John S.; Griffith, Peter (Massachusetts Inst. of Tech., Cambridge. Dept. of Mechanical Engineering). Apr. 15, 1965. Contract AF 49(638)-1468. 166p.

A combined analytical and experimental program was carried out to investigate the problem of hydrodynamic stability of forced-convection flows with boiling. The study was restricted to the flow of water in small channels (< .25" I.D.), high length-to-diameter ratios (25-200), moderate temperature and pressure $T_i \approx 70°F$; $P_{ex} < 60$ psia), and primarily directed toward subcooled, local boiling ($h_{ex} < h_{sat.liq.}$). Two types of instability were recognized: The rist, a non-recurring excursive instability, and the second, an oscillatory instability in which the operating point varies in a sustained, repetitive way around the original condition. The excursive behavior was predicted on the basis of a comparison of the slopes of the pressure drop vs flow rate curve of the heated section and the external system. The criterion for stability was simply that the slope of the external system characteristic be more strongly negative than that of the heated section. This was verified experimentally. This excursion was found to be the limiting condition on the heat flux in a parallel channel system. The oscillatory instability was investigated analytically through the use of a linearized, lumped parameter model in which steady-state measurements of the pressure drop were assumed to be valid in characterizing the transient characteristics of the heated section. For cases in which the energy storage mechanism was a compressible volume either upstream of, or within, the heated section, a critical slope of the pressure drop vs flow rate curve in the heated section could be computed, as well as an associated frequency. The analytical results were verified on a single-tube apparatus with controlled compressibility, and the onset of the instability agreed well with the theoretical predictions. The criterion was applied to the data of a number of other investigations and gave excellent correlation in all cases where the restriction of subcooled or low quality operation was met. In a few isolated cases, the predicted frequencies could be checked against reported values, and the agreement was good. (auth)

46535 (PWAC-386) FINAL REPORT ON DEVELOPMENT OF LCRE LIQUID METAL PUMPS AND SUMPS. Ferguson, C.; Manfredi, D. V.; Milich, J. J.; Welna, H. (Pratt and Whitney Aircraft, Middletown, Conn. Connecticut Advanced Nuclear Engineering Lab.). July 15, 1965. Contract AT(30-1)-2789. 314p. Dep. mn; CFSTI $7.00 cy, $1.50 mn.

The proposed ground test of the Lithium-Cooled Reactor, designated LCRE, required the development of centrifugal pumps mounted in sumps to circulate the lithium primary coolant at 1000°F, the NaK-78 secondary coolant at 700°F and the NaK-78 reflector coolant at 700°F. The

design operating conditions for these pumps were: (a.) 195 gpm at a head rise of 115 feet for the lithium (LP-1) primary coolant pump, (b.) 394 gpm at a head rise of 143 feet for the NaK (NP-1) secondary coolant pump. All three pumps utilized antifriction shaft support bearings lubricated and cooled by Mil-L-7808D oil and were powered by gas-cooled electric motors. Primary sealing of the liquid metal was accomplished with centrifugal dynamic shaft seals, which maintained a liquid metal-to-inert gas interface on the rotating vanes of the dynamic seal impeller. Secondary sealing was provided by inert gas sweep systems and cermet-faced mechanical shaft seals. Extensive testing of pump components, as well as water and liquid metal tests of complete pump assemblies, were accomplished to meet the program objectives of high performance and high reliability for the expected total operating lifetime of 15,000 hours. Over 60,000 hours of component face seal testing and over 74,000 hours of pump testing in liquid metal were conducted. Several successful liquid metal tests of 10,000 hours duration were accomplished with the LP-1 lithium and NP-1 NaK pumps prior to termination of the LCRE program. (auth)

46536 (RT/ING(65)1) ESPERIENZE SUI FLUSSI CRITICI NEL CIRCUITO AD ACQUA PRESSURIZZATA ED A CIRCOLAZIONE NATURALE DEL POLITECNICO DI TORINO. (Experiments on the Critical Flow of a Pressurized Water Loop in Natural Circulation Conditions at the Polytechnic School of Turin). Merelli, A. (Comitato Nazionale per l'Energia Nucleare, Rome (Italy)). June 1965. 49p. Dep. mn.

The results are presented for tests performed on the 100 kw, pressurized water loop of the Polytechnic School of Turin, in natural circulation conditions and at pressures ranging from 50 to 170 kg/cm^2. Experimental data on steady conditions, as well as some on burnout or thermal-hydraulic instability are given; the two latter data were obtained through slight variations in power—or in other quantities—with low fluid subcooling at the test section outlet. The behavior of the loop in the tests described seems to be essentially determined by the quantity of steam present in the terminal part of the test section. (auth)

46537 (SC-RR-65-187) ANALYTICAL METHODS USED IN PREDICTING THE RE-ENTRY ABLATION OF SPHERICAL AND CYLINDRICAL BODIES. Cropp, L. O. (Sandia Corp., Albuquerque, N. Mex.). Sept. 1965. Contract AT(29-1)-789. 98p. Dep. mn; CFSTI $3.00 cy, $0.75 mn.

Heating and ablation of spherical and cylindrical bodies from their initial point of return from earth orbit to that time when all ablation ceases is discussed. A description of the analytical processes currently followed by Sandia Corporation in performing ablation analyses in connection with aerospace nuclear safety studies is presented. Major deficiencies in analytical tools and available data are listed. (P.C.H.)

46538 (TID-22148) A STUDY OF CONVECTION BOILING INSIDE CHANNELS. Progress Report, July 1–September 30, 1964. Ferrell, J. K. (North Carolina State of the Univ. of North Carolina, Raleigh). Sept. 30, 1964. Contract AT(40-1)-2950. 37p. Dep. mn; CFSTI $2.00 cy, $0.50 mn.

Experimental studies were carried out to determine the effects of pertinent variables upon two-phase single component frictional and contraction-expansion pressure losses. The frictional pressure drop relations are studied for both horizontal and vertical, heated and unheated, channel surfaces. Data are presented for a series of runs on a stainless steel tube $\frac{5}{8}$-inch OD and 0.466 ID. The heated length of the test section was eight feet and was preceded by approximately four feet of calming length of the same tubing. (M.O.W.)

46539 (TID-22249) BATTELLE-NORTHWEST STUDIES EXECUTED FOR THE USAEC-AECL COOPERATIVE PROGRAM. Monthly Progress Report, July 1965. Albaugh, F. W. (comp.) (Battelle-Northwest, Richland, Wash. Pacific Northwest Lab.). Aug. 2, 1965. Contract AT(45-1)-1830. 14p. (BNWL-C-27-7). Dep. mn; CFSTI $1.00 cy, $0.50 mn.

Experiments were made to determine boiling burnout conditions for a heated 19-rod bundle test section with subcooled water and fog steam. The data were partially analyzed and are tabulated. Tensile tests were made on specimens from Zr–2.5 Nb pressure tubing at 23, 300, and 400°C and strain rates of 0.002, 0.05, and 0.50 in./in.-min. The effects of hot working Zr–2.5 Nb to 850°C were studied. The status of in-reactor creep measurements in Zr–2.5 Nb is reported. (D.L.C.)

46540 (AD-619382) HIGH TEMPERATURE HEAT-TRANSFER AGENTS. Chechetkin, A. V. Translation of Vysokotemperaturnye Teplonositeli, Gosenergoizdat, 1962, Moscow. 437p. (FTD-MT-63-246). CFSTI.

This book presents information on the properties of both liquid and gaseous heat-transfer agents. Molecular structure, physicochemical properties, thermophysical properties, thermodynamics, hydrodynamics, aerodynamics, and industrial applications are all considered. Diagrams of heating installations and their operation are included. (D.L.C.)

46541 STEAM WATER HEAT TRANSFER—POST-BURNOUT CONDITIONS. Kearsey, H. A. (Atomic Energy Research Establishment, Harwell, Berks). Chem. Process Eng., 455-9(Aug. 1965).

The phenomenon of "burnout" as it occurs in forced-convective boiling of water in a heated tube is described; it is shown to be due to the disappearance of a water film on the heated surface as a result of evaporation, and of net droplet entrainment of water into the steam. At burnout a dry patch occurs, the heat transfer coefficient is reduced, and the surface temperature rises. It is shown that this temperature can rise to such an extent that the entrained water droplets cannot rewet, and hence cool the surface. The heat is thus transferred directly into the steam phase and only a very small fraction of this heat is used to evaporate the entrained droplets. The temperatures of the heated surface and of the bulk steam are therefore higher than would be expected if the cooling were by the steam phase alone in thermodynamic equilibrium with the water phase. An example is given of a suggested method of estimating heater surface temperature in the post-burnout condition. (auth)

46542 FILM THICKNESS, PRESSURE DROP, AND STABILITY IN ANNULAR TWO-PHASE FLOW. Silvestri, M.; Varsi, G. (CESNEF, Milan). Energia Nucl. (Milan), 12: 449-58(Sept. 1965).

The successful test of a correlation between pressure drop and void fraction for annular two-component, two-phase flow in isothermal conditions is described. The correlation was essentially derived from the momentum equation applied to the liquid film in Poiseuille flow. The same correlation, together with a continuity equation, was used to develop a simple analysis of the time behavior of a perturbation of the interface profile. This allowed prediction of the existence of saw-tooth shaped waves and of the boundary between the two types of instabilities shown by experimenters. (auth)

46543 CONTRIBUTION TO COOLING INTENSIFICATION AT HIGH HEAT FLUXES USING A RAGGED HEAT EXCHANGE SURFACE. Zajic, Vladimir. Jaderna Energie, 11: 369-72(Oct. 1965). (In Czech).

Fuel element cooling problems and the analysis of possibilities of power increases in the WWR-S reactor initiated an experimental investigation of heat transfer intensification at a high heat flux using a roughened cooled surface. (auth)

46544 HEAT TRANSFER IN SUBCOOLED STEAM FOR HIGH SYSTEM PRESSURES AND HOT SURFACE CHARGES. Rauber, A. (Siemens-Schuckertwerke A. G., Erlangen, Ger.). Nukleonik, 7: 369-79(Aug. 1965). (In German).

The heat transfer in subcooled steam to the water flowing upward in the ring gap, with the water being heated at the intersurface of the ring gap, was considered. The units used were those that occur in pressurized water reactors.

Heating surface charges between 30 and 400 w/cm², system pressures between 30 and 120 atm, and coolant velocities between 3 and 10 m/sec were used. The problem was formulated completely and the measurement methods were briefly described. The representation and discussion of the results are then given. It was then shown how the coolant throughput and the mean coolant temperature modifies the heat transfer in subcooled steam. The results of the heat transfer measurements were represented and compared with earlier measurement values. The characteristic measurement values are within the range of the results of the literature. In the dimensionless representation the characteristic results show that they can be given sufficient accuracy by none of the reported dimensionless equations. Therefore a new dimensionless equation was derived which approximates satisfactorily the measurement results. (tr-auth)

46545 FORCED CONVECTIVE HEAT TRANSFER IN HORIZONTAL TUBES. I. EXPERIMENTAL STUDY ON THE EFFECT OF BUOYANCY. Mori, Yasuo (Tokyo Inst. of Technol.); Futagami, Kozo (and others). Trans. Japan Soc. Mech. Engrs., 30: 1378-85 (Nov. 1964). (In Japanese).

The effect of buoyancy on forced-convective heat transfer in a horizontal straight pipe was studied with a fully developed flow of air and constant heat flux. Velocity and temperature distributions were measured for large R_eR_a and these are shown to be essentially different from those known so far, for example, the Poiseuille profile for velocity field. Nusselt numbers were calculated from measured velocity and temperature distributions and found to be about twice as large as those calculated by neglecting buoyancy at $R_eR_a = 4 \times 10^5$. In the turbulent region, buoyancy had little effect on velocity and temperature fields, but the critical Reynolds number was affected by buoyancy. (auth)

46546 EFFECTS OF UPSTREAM COMPRESSIBILITY ON SUBCOOLED CRITICAL HEAT FLUX. Daleas, R. S. (Westinghouse Electric Corp., Pittsburgh); Bergles, A. E. New York, American Society of Mechanical Engineers, 1965, Preprint No. 65-HT-67, 7p., $1.00. (CONF-650812-2). ORINS.

From ASME-AIChE Heat Transfer Conference and Exhibit, Los Angeles.

Moderate upstream volumes of subcooled water were found to have sufficient compressibility to promote oscillatory behavior, which produces a large reduction in subcooled critical heat flux for a single channel. When the upstream compressibility is large, the oscillatory instability can be avoided only by operating to the right of the minimum in the overall pressure drop-flow characteristic of the heated section. A flow restriction at the inlet is generally required to alter the overall characteristic so that stable critical heat fluxes can be obtained. (auth)

46547 THE INFLUENCE OF A TRANSVERSE MAGNETIC FIELD ON FORCED CONVECTION LIQUID METAL HEAT TRANSFER. Gardner, R. A.; Uherka, K. L.; Lykoudis, P. S. (Purdue Univ., Lafayette, Ind.). New York, American Inst. of Aeronautics and Astronautics, 1965, Preprint No. 65-539, 12p., $1.00. (CONF-650711-22). ORINS.

From AIAA 2nd Annual Meeting and Technical Demonstration, San Francisco.

Liquid mercury flowing through a stainless steel tube 17.5 in. long and 0.180 in. in dia was subjected to a uniform radial heat flux over the final 9.6 in. of the tube's length for a range of Reynolds numbers from 9,600 to 137,000. It was found that a transverse magnetic field of about 10,000 gauss inhibits the convective mechanism of heat transfer. No appreciable influence of the field was observed at the lower limit of the Reynolds numbers because the convective mechanism was then overshadowed by strong thermal conductivity of mercury. At higher Reynolds numbers where the convective mechanism was significant, the electromagnetic force competed with the inertia force and, in effect, tended to damp out the vigorous fluctuations that enhanced the convective mechanism. The inhibition of the convective mechanism was illustrated by a 20 to 30% decrease in the Nusselt number. The influence of the magnetic field at the upper limit of Reynolds numbers investigated was found to diminish as the inertia force began to overpower the electromagnetic force. (auth)

46548 DRYOUT IN A 19-ROD BUNDLE COOLED BY STEAM/WATER FOG AT 515 PSIA. Moeck, E. O. (Atomic Energy of Canada Ltd., Chalk River, Ont.); Wikhammer, G. A.; Stern, F.; Dempster, R. T. New York, American Society of Mechanical Engineers, 1965, Preprint No. 65-HT-50, 10p., $1.00. (CONF-650812-5). ORINS.

From ASME-AIChE Heat Transfer Conference and Exhibit, Los Angeles.

Measurements were made of the "dryout" heat flux (a term used to describe the "critical" or "burnout" heat flux at high steam qualities) at mass velocities between 0.5 and 1.4×10^6 lb/hr-ft², and outlet qualities in the 38 to 78% range. Two phase inlet conditions were used. Dryout behavior of geometries, simulating power reactor fuels was investigated with angular misalignment between an upstream unheated bundle and the 19.25-in.-long heated bundle; two bundle end geometries (CANDU and flat end); and bundle-mounted stripping rings. Angular misalignment reduced the dryout heat flux on some surfaces (usually inner elements) by up to 20%, but increased it on others (usually outer elements) by up to 70%. Stripping rings raised the dryout heat flux by up to 100%. (auth)

46549 EFFECT OF SURFACE CONDITIONS ON NUCLEATE POOL BOILING OF SODIUM. Marto, Paul J. (Naval Post Graduate School, Monterey, Calif.); Rohsenow, Warren M. New York, American Society of Mechanical Engineers, 1965, Preprint No. 65-HT-51, 11p., $1.00. (CONF-650812-4). ORINS.

From ASME-AIChE Heat Transfer Conference and Exhibit, Los Angeles.

Commercial grade sodium was boiled from a horizontal disk at pressures of 65, 200, and 400 mm Hg absolute with sodium temperatures ranging from 1200 to 1500°F. Heat fluxes as high as 236,000 Btu/hr-ft² were attained. Boiler surface finishes ranged from highly polished mirror finishes to coarse, porous coatings. By following a prescribed cleaning and filling procedure, nucleate boiling results were generally reproducible for a given type surface. The effect of roughness as well as any aging and hysteresis effects were determined experimentally. Incipient nucleate boiling results are discussed as well as the effect of pressure and pool depth on the nucleate boiling curve. (auth)

46550 AN INVESTIGATION OF HEAT TRANSFER TO POOL-BOILING MAGNESIUM. Adams, J. M. (Aerojet-General Corp., Sacramento, Calif.). New York, American Society of Mechanical Engineers, 1965, Preprint No. 65-HT-49, 11p., $1.00. (CONF-650812-6). ORINS.

From ASME-AIChE Heat Transfer Conference and Exhibit, Los Angeles.

The transient-quenching method of determining the critical heat flux and heat-transfer coefficients in film and nucleate-boiling liquid metals is presented, together with a description of the design and fabrication of the apparatus. The apparatus employs a tungsten sphere, instrumented with thermocouples, which is heated to approximately 600°F above the saturation temperature of the liquid metal and quenched in the boiling pool. As the sphere cools, the temperature and heat flux at the surface of the sphere follow the equilibrium boiling curve of the metal being studied. Results on pool-boiling magnesium (subcooled) are presented, which include determination of the critical heat flux and heat-transfer coefficients in the transition and nucleate boiling regimes. (auth)

46551 NUCLEATE BOILING INSTABILITY OF ALKALI METALS. Marto, P. J. (Naval Postgraduate School, Monterey, Calif.); Rohsenow, W. M. New York, American Society of Mechanical Engineers, 1965, Preprint No. 65-HT-22, 11p., $1.00. (CONF-650812-9). ORINS.

From ASME-AIChE Heat Transfer Conference and Exhibit, Los Angeles.

A simplified theoretical model for bubble nucleation stability was proposed, and an approximate stability criterion was developed. This criterion contains both fluid and surface properties, and it predicts that nucleation for sodium should be unstable. Commercial-grade sodium was boiled from a horizontal disk at pressures near 60 mm Hg absolute, with sodium temperatures near 1200°F. Heat fluxes as high as 236,000 Btu/hr ft^2 were attained. Boiler surface finishes ranged from highly polished mirror finishes to coarse, porous coatings. The effects of surface material, chemical treatment, heat flux, and cavity geometry on nucleation stability were measured, and the experimental results agreed with the predictions of the proposed stability model. (auth)

46552 HEAT TRANSFER AND FLOW CHARACTERISTICS OF POROUS MATRICES WITH RADIATION AS A HEAT SOURCE. Chiou, J. P. (AiResearch Mfg. Co., Los Angeles); El-Wakil, M. M. New York, American Society of Mechanical Engineers, 1965, Preprint No. 65-HT-6, 8p., $1.00. (CONF-650812-11). ORINS.

From ASME-AIChE Heat Transfer Conference and Exhibit, Los Angeles.

A theoretical and experimental study of the heat transfer and flow friction characteristics of matrices of high porosity, with incident radiation from one side resulting in an exponential heat source, and with air as a coolant, is reported. In the theory, a transient solution of simultaneous convection and radiation heat transfer equations was worked out. Used with experimental data taken in the unsteady state, it resulted in the calculation of volumetric heat transfer coefficients by convection in the matrices. Correlations with Reynolds numbers, based on a characteristic length obtained by equating pressure drops to the sum of viscous and inertia resistance terms, were obtained. Using the more familiar hydraulic radius did not result in reducing the relationships to a unified form. The matrices used in the experiments were formed from slit-and-expanded aluminum foils, blackened to high radiant absorptivity. The results of the investigation are considered useful in many solar, nuclear, and space applications. (auth)

46553 HEAT TRANSFER TO NaK FLOWING IN-LINE THROUGH A BUNDLE OF CIRCULAR RODS. Kalish, Sheldon; Dwyer, Orrington, E. (Brookhaven National Lab., Upton, N. Y.). New York, American Society of Mechanical Engineers, 1965, Preprint No. 65-HT-11, 9p., $1.00. (CONF-650812-10). ORINS.

From ASME-AIChE Heat Transfer Conference and Exhibit, Los Angeles.

Experimental results are reported for the case of in-line turbulent flow of NaK through an unbaffled bundle of circular rods. The results were compared with theoretical predictions and earlier experimental results obtained under similar conditions with mercury. The bundle consisted of ½-in.-dia rods arranged in an equilateral triangular pattern with a pitch : diameter ratio of 1.75. All rods in the bundle, and the shell, were electrically heated to provide equal and uniform heat fluxes throughout the bundle. Results are reported on nine different test elements, eight of which had copper sheaths and one nickel sheath. Seven of the copper elements had a thin nickel electroplate, and one a chrome plate. The nickel element had a thin copper plating. Results were obtained under conditions of fully-established velocity and temperature profiles and under conditions where they were not established. The results on the first five elements were in fairly good agreement with theory and with the earlier results on mercury; but those on the last four fell low, except at the highest flow rates. The lower the flow rate, the lower they fell. It was concluded that the low coefficients were the result of incomplete wetting of the heating surface, coupled with the release of dissolved or entrained seal gas, from the flowing NaK, at the heating surface. The oxygen concentration in the NaK was below 25 ppm. (auth)

46554 FORCED CONVECTION HEAT TRANSFER AT HIGH PRESSURE AFTER THE CRITICAL HEAT FLUX. Bishop, A. A.; Sandberg, R. O.; Tong, L. S. (Westinghouse Electric Corp., Pittsburgh). New York, American Society of Mechanical Engineers, 1965, Preprint No. 65-HT-31, 12p., $1.00. (CONF-650812-8). ORINS.

From ASME-AIChE Heat Transfer Conference and Exhibit, Los Angeles.

Data were obtained for forced-convection heat transfer to water at high subcritical pressures after the critical heat flux. The coolant entered the cylindrical test sections as a subcooled liquid and during certain test runs left as superheated steam. Emphasis was placed on the region after the critical heat flux where surface temperature oscillations were not large. Pressure ranged from 2420 to 3120 psia, mass-flow rates from 0.5 to 2.5×10^6 lb/hr sq ft, heat flux from 0.1 to 0.65×10^6 Btu/hr sq ft and exit qualities from 7 to 100%. These data were combined with data that extended down to 580 psia and a heat-transfer correlation was obtained for flow rates equal to or greater than 0.8×10^6 lb/hr sq ft over a pressure range of 580 to 3190 psia for steam qualities as high as 100%. (auth)

Materials Testing

46555 (KAPL-M-6493) A TEST APPARATUS AND PROFILE MEASUREMENT SYSTEM FOR RECTANGULAR PLATES SUBJECTED TO IN PLANE THRUSTS. Swota, J. Jr.; Miller, S. H. (Knolls Atomic Power Lab., Schenectady, N. Y.). May 10, 1965. Contract W-31-109-eng-52. 13p. Dep. mn; CFSTI $1.00 cy, $0.50 mn.

Test apparatus designed and constructed to procure information on structural stability of rectangular plates subjected to in-plane thrusts is discussed in some detail. To illustrate the use of the apparatus and the information it can provide, sketches of the equipment components are presented along with typical data obtained for an 1100-0 aluminum plate material. (auth)

46556 (NMI-4997, pp 1-21) METALLOGRAPHY—ALLY OF NONDESTRUCTIVE TESTING IN EVALUATING NUCLEAR FUEL COMPONENTS. Bean, C. H.; McGonnagle, W. J. (Argonne National Lab., Ill.).

Examples of how macro and micro metallography was used to support nondestructive testing methods to determine quantitatively the internal structure of both sound and defective materials are given. (W.L.G.)

46557 (NP-15459) STRESS DISTRIBUTION IN A PERFORATED PLATE OF 10 PERCENT LIGAMENT EFFICIENCY SUBJECTED TO EQUAL BIAXIAL STRESS. Research Report 64-917-520-R1. Leven, M. M. (Westinghouse Research Labs., Pittsburgh, Pa.). Mar. 17, 1964. 16p.

In order to evaluate the method of obtaining the stress distribution in perforated plates subjected to equal biaxial stress by superposition of uniaxial stress results, a hexagonal model was directly loaded by equal forces in six directions. Towards this end, a slice ¼ inch thick was removed from the 10% ligament efficiency portion of the hexagonally-shaped model used for the thermal stress determination. The corners were cut and six equal loads P_a, P_b ... P_f, 60° apart, were applied through plastic bushings. The model in the oven after stress freezing is shown. Two tests were performed at different load levels. In Test 1, the six loads were about four pounds each, while in Test 2, they were about 8¼ pounds. The higher load was used not only to obtain a higher fringe order but also to minimize the unbalance in the applied loads due to the weight of the model (0.21 lbs.). The loads, dimensions and equal biaxial stress applied in the two tests are shown. (auth)

46558 (ORNL-tr-748) RADIOGRAPHY TESTS WITH ACTIVE FUEL ELEMENTS APPLICATION TO TESTING IN HOT LABORATORIES. Brebant, C.; Gautier, M.; Rousel, E. Translation from Symposium International sur les Methodes de Travail Dans les Laboratoires Chauds de Haute Activite, Grenoble, 15-18 Juin 1965. 9p. Dep. mn; JCL $1.10 fs, $0.80 mf.

The G2 reactor, the LECI, and LECA are presently equipped with radiographic instruments. In the first two cases, the x-ray source, the object, and the film are fixed. In the LECA, the object and the film are movable. The

first process permits rapid radiographs to be obtained, but the projections of the ends of large objects are highly distorted. Moreover, special films with a low sensitivity to γ radiation are required. The second process is slow but distortions are avoided and ordinary film can be utilized. (auth)

46559 (ORNL-tr-749) NONDESTRUCTIVE TESTING AT THE HOT LABORATORIES OF THE CEN, GRENOBLE. De Robien, E.; Lachambre, A. Translation from Symposium International sur les Methodes de Travail Dans les Laboratoires Chauds de Haute Activite, Grenoble, 15-18 Juin 1965. 15p. Dep. mn; JCL $1.60 fs, $0.80 mf.

The diversity of irradiation loops studied in the CENG reactors led to the equipping of the hot laboratory with a large number of devices for nondestructive testing. After a definition of the purpose of the hot laboratory, descriptions are given of the different devices utilized under the following categories: macrographic examination, dimensional, radiographic testing, fission gas sampling, and gamma scanning. (auth)

46560 IMPROVED TECHNIQUES IN THE PROJECTION RADIOGRAPHY OF HIGHLY RADIOACTIVE SPECIMENS. Parish, R. W.; Pullen, D. A. W. (Atomic Energy Research Establishment, Harwell, Berks). Brit. J. Non-Destructive Testing, 7: 29-33(June 1965).

Methods of radiographing highly radioactive specimens were improved. A different method of recovering information from a fogged radiograph, by radiography of the film itself, is described. An extension of the use of color film is also discussed. (auth)

46561 PREPARATION OF X-RAY EXPOSURE CHARTS. Gillespie, P. A.; Chrimes, N. W. D. (Australian Atomic Energy Commission, Lucas Heights, New South Wales). Brit. J. Non-Destructive Testing, 7: 34-42(June 1965).

Four procedures for preparation of x-ray exposure charts are described and the results from each method are compared. They are: graphical representation of Lambert's Law, the half value layer method, optimum film density at constant exposure time, and the Gevaert method. The second is preferred, since it allows exposure information to be transposed from one machine to another. For laboratories without precision timing and shuttering devices the Gevaert method is quicker and easier and gives reasonable accuracy. (auth)

46562 APPLICATION OF RADIOGRAPHY TO THE NONDESTRUCTIVE CONTROL OF FUEL ELEMENTS BEFORE AND AFTER IRRADIATION. Allain, C.; Brebant, C.; Gautier, M.; Petit, M.; Prot, A.; Roussel, E. Bull. Inform. Sci. Tech. (Paris), No. 92, 117-35(Apr. 1965). (In French).

The principles of radiography are reviewed. A list is given of various radiographic controls to which the fuel elements are subjected during their fabrication. The role of radiography in the examination of cartridges after passage in the reactor is discussed. Radiography by γ rays of cast uranium bars and tubes is described, along with low-voltage radiography of 1-mm-thick beryllium tubes. Inspection is carried out by passing the irradiated fuel element through the radiographic unit. Equipment being used for the radiography of irradiated elements in the various "hot" laboratories of the CEA both in the research centers (Saclay, Cadarache) and on the production sites (Marcoule) are described. (auth)

46563 NEUTRON RADIOGRAPHY USING A CRYSTAL MONOCHROMATOR. Barton, J. P. (Univ. of Birmingham, Eng.). J. Sci. Instr., 42: 540(Aug. 1965).

By using monochromatic beams of neutrons of selected epithermal energy, the contrast between most parts of elements may be changed. The feasibility of this technique was tested using a special crystal monochromator. The possible advantages of epithermal neutron radiography compared with thermal neutron radiography for particular problems are discussed. (M.C.G.)

46564 THE INFLUENCE OF FLAW SHAPE AND RADIOGRAPHIC TECHNIQUE ON THE DETECTABILITY IN ISOTOPE RADIOGRAPHIC METHODS. Radwan, Maciej; Godlewski, Zbigniew (Inst. of Fundamental Technical Problems, Polish Academy of Sciences, Warsaw). Nukleonika, 10: 145-53(1965).

The influence of the radiographic technique on detectability of different shapes of flaws was studied. The theoretical analysis of the change of density for radiographic images of flaws made it possible to determine decreases in density above the background. Measurement and photometric analysis of density curves for images of flaws were obtained by using an automatic recording photometer. A strong relation was observed between the radiographic technique and the image density curve. By using the density curves it should be possible to determine the kind of flaw. (auth)

46565 ELEVENTH NATIONAL SYMPOSIUM ON RELIABILITY AND QUALITY CONTROL, PROCEEDINGS, MIAMI BEACH, FLORIDA, JANUARY 12, 13, 14, 1965. New York, The Inst. of Electrical and Electronics Engineers, Inc., 1965. 622p. $5.00. (CONF-650115).

Proceedings of the Eleventh National Symposium on Reliability and Quality Control are presented. Reliability in the international market, design techniques, maintainability, training and fundamentals, cost and contracting, mechanical and structural reliability, testing, mathematical techniques, parts reliability, effectiveness of system reliability testing, and commercial applications are discussed. (M.C.G.)

Protective Structures

46566 (AD-425747) RESPONSE SPECTRA FOR HIGH AIR-BLAST LOADS. Grubaugh, R. E.; Orne, D.; Beutjer, W. H. (United Aircraft Corporate Systems Center, Farmington, Conn.). Oct. 1, 1963. Contract AF04(694)-163. 19p. (SCTM-167). CFSTI $2.60.

The computed response of a number of damped single-degree-of-freedom dynamic systems to the side-on air-blast loads from multimegaton explosions is presented. The computations were originally used in the design of protective structures. The computations were carried out on a high-speed digital computer and the results are plotted in the form of response spectra showing maximum displacement versus system frequency for peak overpressures from 300 to 10,000 psi. The basic load used in the computations is a decaying triple exponential pressure time pulse derived by Brode and very recently made available. Moreover, the magnitude and range of loads are much larger than usually considered in such response calculations. (CFSTI)

46567 (NP-15396) DYNAMICALLY LOADED STRIP FOOTING BURIED IN DRY SAND. White, Charles R. (Naval Civil Engineering Lab., Port Hueneme, Calif.). Aug. 1965. 32p. (R-387).

A description is given of the dynamic loading of a 12-inch-wide by 18-inch-deep by 6-foot-long concrete footing, representing the strip footing of a subsurface shelter. Boundary conditions simulated those of a torsionally restrained footing of a flexible arch structure test-loaded at several different depths of burial. Static overburden pressure was applied only on one side to simulate the footing of an exterior wall. Dynamic loads from 5 to 40 kips per square foot were applied to the footing while the adjacent soil was under simulated overburden pressures of zero to 15 psi. A logarithmic relationship between bearing modulus and overburden is demonstrated for downward displacements of the footing ranging from 0.25 to 1.5 inches. The dynamic secant modulus increased exponentially with static overburden pressure. (auth)

46568 (ORNL-TM-1223) ENGINEERING STUDY FOR TUNNEL GRID BLAST-SHELTER CONCEPT FOR A PORTION OF CITY OF DETROIT, MICHIGAN. Robbins, Donald T.; Narver, David L. Jr. (Holmes and Narver, Inc., Los Angeles, Calif.). June 1965. Contract W-7405-eng-26. 125p. Dep. mn; CFSTI $4.00 cy, $1.00 mn.

For Oak Ridge National Lab., Tenn.

The data developed was based on sheltering 10,000 per-

sons per square mile. The total residential population in the area (bounded by 7 Mile, Evergreen, Joy, and Livernois Streets) served by the shelter system is determined to be 259,940, which averages 10,398 per square mile. The additional 398 persons could probably be accommodated in the shelters in the area; however, it may be that surplus space may be available within a reasonable distance outside the study area. Entrances were provided on the basis of the highest day and night populations for each tract. The shelter system can accommodate the extra persons until the surplus people have been able to relocate themselves. Because of the crowded conditions, a final design should consider the ability to expand, after an attack, into the major storm sewer system and basements of major facilities, such as the hospitals and university. As was pointed out earlier, the International Salt Company's mine in the southwest portion of the city has space for over a million people, so it might be used as an expansion or storage area. The estimated cost of $505 per person may be further reduced in a more detailed design study, but even this amount does not seem unreasonable when the benefits of the tunnel-grid system are studied. For example, by making it possible for the population to enter the shelter system at any point and then walk to their assigned shelter space, it is not necessary to provide excess shelter space in order to satisfy the peak population conditions in every area. It also allows for reuniting of the family, redistribution of medical personnel and civil authorities, reducing high density population areas, and egress of the total population at any time into areas that are relatively unaffected by the attack. (auth)

46569 THE STRESS ON THE JOINT OF A BONDED SPHERICAL UNDERGROUND SHELTER BY A COMPRESSIONAL WAVE PROPAGATED THROUGH THE SOIL. Meyer, J. (Fried. Krupp Zentralinstitut fuer Forschung und Entwicklung, Essen). Tech. Mitt. Krupp. Forschungsber., 23: 23-5(June 1965). (In German).

The maximum stress produced by the wave striking the shelter was investigated as a function of the rate of propagation of the compressional wave, as well as its interrelation with the natural frequency of the shelter. (auth)

Space Propulsion

See also REACTOR TECHNOLOGY — Propulsion and Space.

Refer also to abstract 48052.

46570 (AD-614111) PARTICLE GROWTH IN THE IONIC NUCLEATION CONDENSATION COLLOIDAL ION SOURCE. Cox, A. Lucile (Brown Engineering Co., Inc., Huntsville, Ala. Research Labs.). Mar. 1965. 76p. CFSTI $3.00 cy, $0.75 mn.

An analytical treatment of the ionic nucleation condensation colloidal ion source examines the processes involved in the formation and growth of ionic nuclei under controlled conditions. The analysis of the condensation nuclei considers the formation of neutral nuclei, which must be prevented, and the formation of the required ionic nuclei. Several theoretical concepts of nucleation are examined. Since the growth of the nuclei to colloids of a size suitable for use in electrostatic propulsion engines involves a considerable release of heat, the growth process is analyzed on the basis of three different models for the dissipation of the heat of condensation. The conditions and resultant properties are calculated for a mixed propellant flow of cadmium and hydrogen on the basis of these three models. (auth)

46571 (HRL-5249-S) ELECTRODE SURFACE PHYSICS RESEARCH. Wilson, R. G. (Hughes Research Labs., Malibu, Calif.). Jan. 12, 1965. Contract NAS 3-5249. 159p. (NASA-CR-54182).

The metallic elements are analyzed by certain criteria to determine their relative potentials as electrode materials in a device subject to an arrival flux of cesium atoms, high surface electric fields, moderately high temperatures, and energetic cesium ion bombardment. Analytical digital computer calculations are used to determine equilibrium surface coverages as a function of temperature, arrival flux, and adsorbate and substrate species; of composite surface work function and atom and ion desorption energies as functions of surface coverage and adsorbate and substrate species combination; of cesium ion critical temperatures; and of cesium surface ionization efficiencies (neutral fractions). An experimental tube design, a vacuum system, and experimental techniques for studying electron and ion emission from cesiated nonrefractory and refractory metals, semiconductors, and insulators are described. The techniques include fast automated data collection of electron and ion emission currents versus surface temperature. Emitters and collectors are fabricated from the same high-purity materials. Normal electric and magnetic fields are applied. Very low background currents are obtained. A bakeable, all glass, sorption roughed and ion pumped vacuum system was employed, resulting in a clean vacuum environment of 10^{-9} torr, exclusive of cesium and the vapor pressure of the heated emitters. Experimental measurements of effective vacuum work functions, cesium surface ionization current densities and critical temperatures, cesium ion desorption energies (at low coverage), cesiated electron emission S curves and cesiated work functions, the influence of applied surface electric fields, contamination, and temperature, and time hystereses effects were made for molybdenum, molybdenum silicide, copper, iron, chromium, aluminum oxide, and tantalum boride. (auth)

46572 (NASA-TN-D-3041) PERFORMANCE CORRELATION FOR ELECTRON-BOMBARDMENT ION SOURCES. Kaufman, Harold R. (National Aeronautics and Space Administration, Cleveland, Ohio. Lewis Research Center). Oct. 1965. 33p. CFSTI $2.00 cy, $0.50 mn.

A procedure is presented for estimating the gross performance characteristics of a low-density electron-bombardment ion source. Although this ion source was initially investigated for use as a component of an electric-propulsion system, it should also be useful in a variety of other applications. The overall ion source performance was evaluated on the basis of two parameters; the minimum discharge energy (per ion), and the propellant utilization at a discharge energy twice this minimum value. The approach used was to derive generalizing parameters for both of these measures of performance by analysis of the more important ion-source processes. These generalizing parameters involve only overall ion-source measurements and readily available propellant properties. Within certain limits, the use of these generalizing parameters correlates the experimental data within about ±50 percent for minimum discharge energy and within about ±20 percent for the nominal propellant utilization (where the discharge energy is twice the minimum value). Two of these limits are that the discharge potential difference should not be less than about 2.0 times the first ionization potential of the propellant, and that the cyclotron radius of the primary electrons emitted from the cathode should not be more than about 0.45 times the ionization-chamber radius. This correlation, however, is not a substitute for good design. Careful handling of design details is still necessary if the best possible performance is to be obtained. (auth)

46573 (UCRL-12393-T) POROUS METAL ISOLATION TRAPS AND CRYOSORBENTS IN VACUUM TECHNIQUE. Milleron, N. (Lawrence Radiation Lab., Univ. of California, Livermore). Aug. 17, 1965. Contract W-7405-eng-48. 14p. Dep. mn; CFSTI $1.00 cy, $0.50 mn.

Applications of two general forms of porous metals are discussed: applications of forms pierced through by optically dense pores permitting gas to flow through them, and solid core forms with surface porosity only. Among the vacuum uses of appropriate porous metals are: isolation trapping of oil during viscous and Knudsen gas flow; and cryosorbents. For example, tests show that oil contamina-

tion from up-to-air accidents when using diffusion pumps can be reduced by blocking the system flow path completely with a porous metal diaphragm filter. By corrugating a porous diaphragm filter of 150μ pore size and $\frac{1}{16}$ in. thickness and designing optimally, system pumping speeds are increased compared to present common practice. Porous metal isolation traps for fore pumps impede pump down time <10%. Hydrogen cryosorption experiments utilizing porous copper surfaces at ≤6°K are referenced. (auth)

46574 (AD-619323) PRODUCING HIGH-VELOCITY GAS JETS. Voytenko, A. E. Translated from Dokl. Akad. Nauk SSSR, 158: 1278-80(1964). 9p. (FTD-TT-65-564). CFSTI.

The design and performance of a plasma jet for the purposes of creating high velocities and powerful shock waves are discussed. A charge of explosive substance with a plane front of the detonation wave accelerates a metallic plate, which together with a spherical segment forms a compression chamber filled with the actuating gas. In the top of the chamber there is an opening closed by a thin diaphragm, behind which there is the vacuum outlet tube. (M.O.W.)

Vacuum Engineering

46575 (NASA-TN-D-3006) ACCELERATION OF A CONDUCTING FLUID BY A TRAVELING MAGNETIC FIELD. Braun, Willis H. (National Aeronautics and Space Administration, Cleveland, Ohio. Lewis Research Center). Sept. 1965. 32p. CFSTI $2.00.

An analysis is undertaken for the traveling-wave accelerator with the propellant having scalar conductivity. Two configurations of magnetic field are studied. The first employs a field perpendicular to the line of motion and varying sinusoidally. When the conductivity is assumed proportional to the density, the analysis shows that the propellant is ejected in dense pulses, there is an upper limit on efficiency of about one-half, and the acceleration to wave velocity can be performed in one magnetic field wavelength if a defined interaction parameter has a value of order one. Another accelerator using a magnetic wave such as might be produced by coils surrounding the channel has a somewhat lower efficiency, which is due mainly to the loss of propellant to (or through) the boundaries. (auth)

46576 DIFFUSION-CONTROLLED SORPTION IN HIGH-DENSITY DISCHARGES. Maddix, H. S.; Allen, M. A. (Microwave Associates, Inc., Burlington, Mass.). J. Vacuum Sci. Technol., 2: 221-7(Sept.-Oct. 1965).

An experimental technique is described for obtaining reproducible sorption measurements in high-density discharges. Data are given for the sorption of argon, neon, and helium at the quartz walls of an electrodeless discharge for a surface temperature range of 35 to 750°C. The complex dependence of sorption on temperature and discharge power is described in terms of sticking times, depth of ion penetration, diffusion coefficients, and flux rates. A theory is presented which gives good agreement with experiment. Maximum diffusion of gas into the walls occurs when the product of sticking time and ion flux is equal to the number of available trapping sites at the surface. The average depth of ion penetration in quartz was calculated from the theory and data to be in the range of 3 to 7×10^{-8} cm for helium, neon, and argon ions with bombarding energies of 12 to 17 ev. (auth)

46577 VACUUM BREAKDOWN IN THE PRESENCE OF THERMIONIC CATHODES. Brodie, I. (Varian Associates, Palo Alto, Calif.). J. Vacuum Sci. Technol., 2: 249-56(Sept.-Oct. 1965).

Experimental studies of field emission and breakdown with nickel electrodes contaminated by the presence of barium oxide and barium dispenser thermionic cathodes are presented. By comparing field emission and breakdown characteristics in a planar diode system and a cylindrical projection tube, it is demonstrated that minute quantities of material evaporating from the thermionic cathodes activate the tips of already existing whiskers on the nickel thus making them field emit more profusely. Breakdown is apparently caused by whisker disruption which can now occur at lower fields than that to which the surface had previously been conditioned. It is also possible that the new whiskers are formed by preferential condensation of the evaporation products. The areas from which electrons are emitted from the whisker tips usually contain only a few atoms and the regions from which electrons stream from the solid into the vacuum can be resolved in many of the electron images formed on the screen. (auth)

46578 PROBLEM OF MEASURING HYDROGEN PRESSURE IN ULTRAHIGH-VACUUM SYSTEMS. Hickmott, T. W. (General Electric Research Lab., Schenectady, N. Y.). J. Vacuum Sci. Technol., 2: 257-8(Sept.-Oct. 1965).

The problem associated with the accurate measurement of hydrogen pressure in an ultrahigh-vacuum system is discussed in light of techniques using ionization gages and the precautions to be taken to prevent the production of atomic hydrogen. (L.B.S.)

46579 CALIBRATION OF IONIZATION GAGES USING THE DIAMAGNETIC SUSPENSION ABSOLUTE GAGE. Evrard, R.; Beaufils, P. (Laboratoires d'Electronique et de Physique Appliquee, Paris). Vide, 20: 116-20 (Mar.-Apr. 1965). (In French).

The characteristics of the diamagnetic suspension gage are analyzed. It is shown that the apparatus can be used as a molecular manometer of great simplicity, giving rigorously absolute measurements in the presence of a known gas, from 10^{-3} to 5×10^{-7} torr. Use of a thermo-molecular torque makes it possible to extend the limit of pressure measureable to some 10^{-10} torr. The use of the two methods seems suitable for the calibration of other types of gages and for the passive study of the pressure in sealed containers, such as electron tubes. (tr-auth)

GEOLOGY AND MINERALOGY

General

Refer also to abstract 45802.

46580 (AD-613287) STEP LOAD MOVING ON THE SURFACE OF A HALF-SPACE OF A LOCKING MATERIAL: SUBSEISMIC CASE. Period Covered: July 1963-January 1964. Bleich, Hans H. (Air Force Weapons Lab., Kirtland AFB, N. Mex.). Feb. 1965. Contract AF29(601)-6055. 63p. (WL-TDR-64-8). CFSTI $3.00 cy, $0.75 mn.

Considering a locking material prior to compaction as a special case of a nonlinearly hardening elastic material, conditions at a discontinuity—a locking front—are analyzed on the basis of three dimensional theory. It was found that the major compressive principal stress at a locking front must always be normal to the front, even if the front is not plane. Based on this general result, the effect of a uniform step pressure traveling with subseismic velocity on the surface of a half-space was obtained for the case of a locking material which after compaction has elastic-Coulomb behavior. Such a material acts linearly elastic if the state of stress does not overcome internal friction, but slip occurs if the stresses reach a critical state defined by Coulomb friction. As a special case the solution applies also for a material which is linearly elastic after compaction. The stress, velocity and acceleration histories due to the traveling step pressure are discussed and compared to those in the one dimensional case of a suddenly applied uniform surface pressure. (auth)

46581 (UCRL-14292) CHANGES IN THE FRACTURE PERMEABILITY OF A GRANITIC ROCK MASS RESULTING FROM A CONTAINED NUCLEAR EXPLOSION. Boardman, Charles R.; Skrove, James (Lawrence Radiation Lab., Univ. of California, Livermore). Aug. 16, 1965. Contract W-7405-eng-48. 21p. Dep. mn; CFSTI $1.00 cy, $0.50 mn.

In-situ permeability of the rock outside the Hardhat chimney was determined by pressurization of long holes with air. The experimental data indicated a remarkable difference between the fracture permeability of the rock near the chimney and that at a considerable distance. Although permeable fault zones were known to exist in the granite stock, the measurements of background permeability, were quite low on the order of tenths to several millidarcies. The observed increase was about 2 to 3 orders of magnitude above this background in the region 125 to 215 feet radially from the shot point, or 80 to 165 feet radially from the center of the chimney. The presence of a collapsed drift immediately beyond this region precluded measurements which would have defined the maximum extent of the zone of increased permeability. (auth)

46582 LEAD ISOTOPES OF PEGMATITES, GRANITES AND ORES. Brown, John S. Econ. Geol. 60: 1167-84 (Sept.-Oct. 1965).

Assembling of scattered data regarding the lead of pegmatites, granitic rocks, and associated lead ores yielded some significant facts and deductions. Pegmatitic feldspars contain two to twenty times as much lead as granites or their feldspars. The lead in major pegmatites commonly duplicates ore lead isotopically, whereas the lead of granites associated with lead ores is much more variable and often distinctly anomalous. The data do not support the common assumption that ores are derived from igneous rocks by a process of magmatic differentiation. Indeed, they justify the suspicion that pegmatites may not be an end product of differentiation, but instead may result from the external addition of a mineralized fluid to the margins of a cooling intrusive along fracture zones, the reaction producing a low melting eutectic of granitic base with exotic accessories. The few data available for minor pegmatites suggest that their lead is more variable, possibly indicative of diverse origins. The meager data on lead in sedimentary rocks and in igneous rocks outside the granite family are inconclusive. Some appear to contain normal lead and others clearly are anomalous. (auth)

46583 OXYGEN ISOTOPIC COMPOSITION OF ORTHOPHOSPHATE FROM SHELLS OF LIVING MARINE ORGANISMS. Longinelli, A. (Laboratoirio di Geologia Nucleare, Pisa, Italy). Nature, 207: 716-19 (Aug. 14, 1965).

The relation between temperature and oxygen isotopic composition of the phosphate of living shells was investigated. The results showed that the range of the oxygen isotopic composition of the phosphate precipitated by Pelecypoda and other marine animals is rather far from that of the calcium carbonate. A relation between temperature and oxygen isotopic composition of phosphate was found. It is assumed that the precipitation of phosphate takes place under isotopic equilibrium conditions. From the results obtained the fractionation factors were calculated as: $t = 25°C$, $\alpha = 1.1056$, $t = 0°C$, $\alpha = 1.0218$. (P.C.H.)

46584 ISOTOPIC COMPOSITION OF STRONTIUM IN A VARIETY OF ROCKS FROM REUNION ISLAND. Hamilton, E. I. (Univ. of Oxford). Nature, 207: 1188 (Sept. 11, 1965).

The isotopic composition of Sr was determined in a suite of rocks ranging from basalts to quartz-bearing syenites. Studies were made to see whether or not variations in the isotopic composition of Sr were present in a wide range of rock types situated in an oceanic environment. In the samples analyzed no significant differences were observed although the rocks had differing Rb/Sr ratios. This suggests that all the Réunion rocks could be derived from an area in the mantle below Réunion having a constant Rb/Sr ratio. (P.C.H.)

Natural Radioactivity and Fallout

See also HEALTH AND SAFETY.

46585 (AD-410522) FALLOUT AND RADIOLOGICAL COUNTERMEASURES. VOLUME I. Miller, Carl F. (Stanford Research Inst., Menlo Park, Calif.). Jan. 1963. 390p.

Data applicable to civil defense planning for protection against fallout from nuclear explosions are presented. Topics discussed include the nature of fallout, characteristic types of fallout; potential hazards from fallout; the formation of fallout particles; a thermodynamic model of fallout formation; the distribution of fallout particles following a nuclear detonation; the correlation of scaling-model parameters with observed fallout pattern features; and ionization rate contour ratios and the composition of fallout. A subject index is included. (98 references.) (C.H.)

46586 (NP-15361) A SPECTROMETRIC STUDY OF THE ATTENUATION IN AIR OF GAMMA RAYS FROM MINERAL SOURCES. Gregory, A. F.; Horwood, J. L. (Department of Mines and Technical Surveys (Canada). Mines Branch). Sept. 1963. 120p. (R-110). Bureau of Mines and Technical Surveys, Ottawa, $1.25.

The distributions of intensity and energy of the gamma-ray flux about selected sources were measured with a scaler and a 100-channel gamma-ray spectrometer. The sources investigated were: separate mineral concentrates of uranium, thorium and potassium, and pellets of cobalt-60. The observations are compared with established theory. The observed spectrograms showed the following quasi-exponential variations with increasing air distance between source and detector: (1) a decrease in integral count-rate; (2) a decrease in photopeak heights; and (3) an increase in the Compton continuum, especially at low energies. While these changes lead to a gradual loss of photopeak resolution with increasing distance, the major photopeaks are well resolved at distances of at least 700 feet when suitable

counting times are chosen. Some of the conclusions are: Gamma radiations from uranium, thorium, and potassium attenuate at the same rate for air distances from 300 to 1,400 feet. As Berger has shown theoretically, the flux incident on a gamma-ray detector may be significantly altered near a density interface such as the surface of the ground. For simple gamma spectra (e.g. potassium-40), the ratio of photopeak height to integral count may be a useful measure of the distance between source and detector. However, this is not true for the more complex spectra of uranium and thorium. The relative contributions of uranium, thorium, and potassium to the integral response from a mineral source may vary greatly with the counting threshold of the detector and to a lesser extent with the air distance. Airborne surveys with a gamma-ray spectrometer similar to that used in these experiments would be feasible only for regional surveys in which the incident radiation spectra are averaged over a relatively long counting time. However, more detailed surveys may become possible with instruments now under development. (auth)

46587 (NYO-3446-3) THE FIRST ANNUAL PROGRESS REPORT [ON RADIOECOLOGICAL STUDIES]. (Helsinki Univ. (Finland). Dept. of Radiochemistry). July 22, 1965. Contract AT(30-1)-3446. 25p. Dep. mn; CFSTI $1.00 cy, $0.50 mn.

Results are reported from radioecological studies in Finland during the first half of 1965. About 100 Lapps were whole-body counted and an increase of about 15% was found in body radioactivity over that found a year earlier. Data are included on radioactivity in lake waters; ^{137}Cs and ^{90}Sr content in fish from lake waters; inactive elements in lake waters that may serve as carriers of radionuclides; the relation between Ca content of lake waters and ^{90}Sr content of fish; the ^{55}Fe content of fish and meat from elk and reindeer; a comparison of the ^{137}Cs content of meat from elk and reindeer with data on values for caribou and reindeer meat from Alaska in 1964; the analysis of plant samples for 10 micro nutrient elements; and techniques for the determination of ^{55}Fe, ^{210}Po, ^{210}Pb, and ^{40}K in biological samples. (C.H.)

46588 (ORNL-3857) THE ISOTOPIC COMPOSITION OF ATMOSPHERIC NEON. Walton, J. R.; Cameron, A. E. (Oak Ridge National Lab., Tenn.). Sept. 1965. Contract W-7405-eng-26. 16p. Dep. mn; CFSTI $1.00 cy, $0.50 mn.

"Absolute" values for the isotopic abundance ratios of atmospheric neon were determined by mass spectrometry. Calibration standards were prepared by mixing of nearly pure separated nuclides of neon. The percentage abundance of the three nuclides of neon are: ^{20}Ne = 90.5139 ± 0.031, ^{21}Ne = 0.2657 ± 0.005, and ^{22}Ne = 9.2205 ± 0.029. The calculated atomic weight of neon on the unified physical and chemical atomic weight scale (^{12}C = 12) is 20.1794 ± 0.0030. (auth)

46589 (UCRL-14332) GAMMA DOSE CURVES FROM NEUTRON-ACTIVATED SOIL AND SEAWATER COMPARED WITH FISSION-PRODUCT DECAY. Lessler, Richard M.; Guy, Frank W. (Lawrence Radiation Lab., Univ. of California, Livermore). Aug. 1965. Contract W-7405-eng-48. 5p. Dep. mn; CFSTI $1.00 cy, $0.50 mn.

Curves are presented showing total γ-Mev (to 50 years) and γ-Mev/hour resulting from decay of granite, NTS soil, and seawater which have been activated by one mole of 14- or 0.5-Mev neutrons. Curves are graphed as a function of time from 1 hour to 10 years. Fission-product decay curves are shown for purposes of comparison. (auth)

46590 (JPRS-31469) THE MOVEMENT OF RADIOACTIVITY EMANATING FROM ^{40}K IN THE PRECIPITATION AND WATERS ON THE TERRITORY OF VINCA. Radosavljevic, Radoslav; Kovacevic, Miodrag; Djordjevic, Dusan; Vujovic, Veselinka. Translated from Tehnika (Belgrade), No. 6, 1053-6(1965). 9p. (TT-65-31965). CFSTI $1.00 cy, $0.50 mn.

The potassium content in the precipitation and waters on the territory of Vinča was determined during 1964. The origin of the deposited potassium was ascertained. The dynamics of the movement of potassium was analyzed in the water of the Danube, in that of the Mlaka stream which flows across the territory of the "Boris Kidrič" Institute, in that of the small Bolečica River and in the drinking water obtained by treating Danube water. (auth)

46591 (ORNL-tr-642) DEVELOPMENT OF RADIOACTIVE HALOS IN BIOTITE. Hoppe, Gunther. Translated for Oak Ridge National Lab., Tenn. from Mineralog. Sb., L'vovsk. Gos. Univ., No. 16, 328-33(1963). 9p. Dep. mn; CFSTI $1.00 cy, $0.50 mn; JCL $1.10 fs, $0.80 mf.

Several aspects of pleochroic halos in biotites, which are among the best media for studying such halos, are discussed: color changes, age estimation, propagation of α rays, radius of halos, halo formation, secondary changes, and non-uniformity. (D.L.C.)

46592 (ORNL-tr-701) RADIOACTIVE HALOS IN QUARTZ, YTTROFLUORITE AND CASSITERITE AND NEW FINDINGS ON ATOMIC STOPPING POWER OF THE ELEMENTS. Ramdohr, Paul. Translated for Oak Ridge National Lab., Tenn. from Neues Jahr. Mineral., Geol., Beil., 67A: 53-65(1933). 20p. Dep. mn; JCL $1.60 fs, $0.80 mf.

Radioactive halos were investigated in quartz, fluorite, yttrofluorite, and cassiterite. Halos of the uranium decay series were involved in all cases. Quartz showed a very dilute, deep smoky quartz color due to radioactive influences; various uranium minerals made this color disappear again up to the range of the RaC'. Measurements resulted in values that are slightly higher than those determined previously and those of calculations. (P.C.H.)

46593 (ORNL-tr-755) NEW OBSERVATIONS ON RADIOACTIVE HALOS AND RADIOACTIVE FRACTURING. Ramdohr, Paul. Translated for Oak Ridge National Lab., Tenn., from Abhandl. Deut. Akad. Wiss. Berlin, Kl. Chem., Geol. Biol., No. 2, 1-17(1957). 36p. Dep. mn; JCL $3.60 fs, $1.28 mf.

A preliminary review is presented of radioactive halos in various minerals. Halos were found for the first time in the following minerals: triplite, triphylite, astrophyllite and lamprophyllite, hedenbergite, helvite, titanite, chloritoid, orthite, stillwellite, apatite, calcite, cerite, uvarobite, chromium, pyroxene, and ilmenite. Radioactive fractures (circles of cracks in minerals) and the isotropic mechanism are discussed. The possibility of halos produced by the neptunium-bismuth decay series is considered. Halos with uncommon ranges are described. (D.L.C.)

46594 ^{90}Sr IN THE AUSTRALIAN ENVIRONMENT DURING 1963. Bryant, F. J.; Gibbs, W. J.; Moroney, J. R.; Stevens, D. J.; Titterton, E. W. (Australian National Univ., Canberra). Australian J. Sci., 27: 222-6(Feb. 1965).

A survey of ^{90}Sr in the Australian environment has continued since its inception in 1957; this report presents the results for 1963. The survey reports levels of ^{90}Sr in fallout over Australia, and in the diet and bone tissue of the population. Most emphasis is given to major centers of population, Perth, Adelaide, Melbourne, Hobart-Launceston, Sydney, and Brisbane; however, data are also reported for Darwin and Townsville and for agricultural districts in each State. During 1963, 1272 specimens, including rainfall, milk, cabbage, flour, and human and sheep bone tissue, were collected for ^{90}Sr analysis. Strontium-90 levels in precipitation are given from July, 1958, to December, 1963, combined in two-month intervals and plotted as histograms. These figures show that the mean deposition of ^{90}Sr in precipitation over Australia has remained at ~1 mC/km²/annum from 1956 to 1963. There was, however, an overall increase during 1963 at all stations except Hobart. This led to an Australian mean for 1963 of 1.3 mC/km². Of the eight stations, Sydney showed the highest deposition of ^{90}Sr for 1963, namely 2.2 mC/km²; Townsville was lowest at 0.7 mC/km². Measurements, which are tabulated, on foodstuffs collected in the 1963 survey provide a basis for estimating the mean daily per capita intake of ^{90}Sr in diet

in Australia during the year. The small increase in the level of ^{90}Sr in milk in Australia during 1962, previously noted, continued in 1963. In contrast to the small increase in the level of ^{90}Sr in the Australian diet in 1963, those in the U.K. and the U.S. increased sharply during 1963 following nuclear weapon testing by the Soviet Union and by the United States carried out in 1961 and 1962. A slow increase in the levels of ^{90}Sr in Australian human bone tissue of all ages was apparent over the period 1958 to 1963. In many age groups, however, departures from this trend for some six-month sampling periods in the past tended to obscure the small increase. Strontium-90 per g of Ca in sheep bone taken from 21 sites throughout Australia during 1963 showed, at most sites, an increase of about 20% over the 1962 levels. When fallout levels in the Australian environment to the end of 1960 were assessed by the Australian National Radiation Advisory Committee in 1962, it concluded that any biological consequence of those fallout levels would be insignificant in comparison with the normal hazards of everyday life. Fallout levels in Australia during the period 1961 to 1963 were generally similar to those previously assessed. (BBB)

46595 ^{90}Sr IN THE AUSTRALIAN ENVIRONMENT, 1961 TO 1963. Gibbs, W. J.; Moroney, J. R.; Stevens, D. J.; Titterton, E. W.; Wilson, G. U. Australian J. Sci., 28: 44-58(Aug. 1965).

Data are presented on the content of ^{90}Sr in fallout over Australia from 1961 through 1963. The mean annual deposition of ^{90}Sr in precipitation at monitoring stations remained in the region of 1 mCi/km^2 from 1958 to 1962 but rose to about 1.5 mCi/km^2 in 1963. The mean ratio of $^{90}Sr/Ca$ in total diet increased from 3.8 pCi $^{90}Sr/gCa$ in 1957 to 6.4 in 1963 and the ratio of $^{90}Sr/Ca$ in human bone samples also increased during the period 1961 through 1963. Data are included on ^{90}Sr content in samples of soil, milk and other foods such as fruits, vegetables, and grains, and bone samples from sheep and infants and children of various ages. (C.H.)

46596 RECENT DATA ON THE AGE OF ALDANIAN PHLOGOPITES. Firsov, L. V. (Inst. of Geology and Geophysics, Academy of Sciences, Siberian SSR). Dokl. Akad. Nauk SSSR, 161: 679-82(Mar. 21, 1965). (In Russian).

Potassium-argon dating determinations on 21 phlogopite samples are tabulated. The radiological data may be analyzed to show three age groups: 1810 ± 15 million yr for 6 samples, 1750 ± 5 million yr for 4 samples, and 1700 ± 20 million yr for 6 samples. These 16 samples give three points, and this relatively narrow zone may serve as an indication to an actual age variation in the deposits. Only 5 samples were outside these limits, 4 being older (1850, 1875, 1920, and 2220 ± 60 million yr) and 1 younger (1655 million yr). Therefore within 100 million yr the deposits may be considered synchronous, consistent in formation according to time and composition. But in considering the deposits for age grouping, they may be regarded as having formed at different times within intervals of 50 to 60 million yr. The recognition of the approximate synchronism (1790 ± 100 million yr) of the phlogopites of the Aldanian deposits is only the first step in the interpretation. Undoubtedly their distribution into a series of age groups will be more accurate after additional determinations. (TTT)

46597 ATMOSPHERIC ACTIVITY AT THE MONCLOA STATION DURING THE YEAR 1964. Energia Nucl. (Madrid), 9: 139-42(Mar.-Apr. 1965). (In Spanish).

In 1964 the atmospheric activity at the Moncloa Station evolved in a form analogous to that of preceding years but at a considerably lower total level. The activity of the atmospheric dust and of the drinking water is shown graphically for daily and average values. Gamma spectrometry showed the continued presence of ^{144}Ce, ^{125}Sb, $^{106}Ru/^{106}Rh$, ^{137}Cs, $^{95}Zr/^{95}Nb$, and ^{54}Mn. In the period from October 25 to October 30, ^{131}I, ^{140}Ba, and ^{103}Ru were detected in the atmosphere. (J.S.R.)

46598 KRYPTON ISOTOPES IN RADIOACTIVE MINERALS. Shukolyukov, Yu. A.; Tolstikhin, I. N. (Lab. of the Geology of Precambrian, Leningrad). Geokhimiya, No. 9, 1076-84(Sept. 1965). (In Russian).

For use of the uranium–krypton method it is necessary to know the absolute yield of krypton isotopes in the spontaneous fission of ^{238}U. The samarskite investigated had such a high content of rare earth elements that the effect of neutron-induced fission was not great. The absolute age of the samarskite by the uranium–lead method is 330 ± 30 million years. The age by the helium method is 80 million years. The xenon content was determined by the method of isotope dilution: $(22.8 \pm 1.5) \times 10^{-9}$ cm^3/g. The age by the uranium–xenon method is 194 million years. The krypton content was determined by mass spectrometry with a relative sensitivity: $(19.8 \pm 1.0) \times 10^{-10}$ cm^3/g. A method of calculating the true age according to the incompatible uranium–krypton and uranium–xenon age values is proposed. (auth)

46599 AGE OF PLEISTOCENE CARBONATE FORMATION ACCORDING TO THORIUM AND URANIUM ISOTOPES. Cherdyntsev, V. V.; Kazachevskii, I. V.; Kuz'mina, E. A. (Geological Inst., Moscow). Geokhimiya, No. 9, 1085-92(Sept. 1965). (In Russian).

The age of pleistocene formations was determined by the uranium (^{234}U, ^{238}U) and thorium (Io, Rd, Ac, UX_1) ratio. The limited suitableness of fossil bones, soils, peat, and mollusk shells and the good suitableness of calcareous deposits (travertines and stalactite sinter deposits) is shown. Sufficiently reliable data of some events in the pleistocene were obtained. (auth)

46600 ON THE POSSIBLE INTERPRETATION OF THE STRONTIUM ISOTOPIC COMPOSITION AS AN INDICATOR OF MAGMATIC DIFFERENTIATION AND ITS DURATION. Artemov, Yu. M.; Yaroshevskii, A. A. (Vernadskii Inst. of Geochemistry and Analytical Chemistry, Moscow). Geokhimiya, No. 9, 1101-5(Sept. 1965). (In Russian).

Four known examples of the discrepancy between the common strontium isotopic composition in parent rocks and in rock derivates (granites and pegmatites from the Enisei Ridge, Karelia, Adirondack, and gabbro and granophyre from Skaergaard) are incompatible with the idea of rock derivates being a residual product of primary magma differentiation by fractional crystallization. An interpretation of these data based on an assumption of liquid state differentiation of the magma is proposed. It is believed that the process rate is controlled by ion diffusion in the silicate melt. The constructed hypothetic model permits the duration of that differentiation process to be estimated from data of strontium isotopic composition. In the four examples computed durations were from 110 to 500 million years. This estimation might be lowered in assuming some rubidium loss from the system. (auth)

46601 GEOLOGICAL RESULTS AND PROBLEMS OF GAMMA SPECTROGRAPHY OF ROCK SAMPLES (OF HAND SPECIMEN SIZE AND WITHOUT ELEVATED RADIOACTIVITY). Lauterbach, R. Geophys. Geol., No. 6, 51-9 (1964). (In German).

It is possible to obtain reproducible spectra of natural γ radiation from hand specimens of test materials in geological collections and archives without destruction of the sample. Consideration of the results of such investigations indicates the possible study of the stratigraphy, petrogenetics, and tectonics even for weak or nearly inactive samples such as basic or ultrabasic magmatite. The reproducibility is indicated by spectra of various granite samples (including the detectability of high Th content in one sample), samples of quartz and granite porphyry, four samples of gabbrose, and four samples of diabase. Spectra of four samples of melaphyres and five samples of basalt are given. Five samples of sediments are indicated and particular attention is drawn to samples with a relatively high MsTh 2 line. Juvenile basalts may be distinguished from hybrids. A variety of future possible uses of the method are suggested, including the examination of prehistoric ceramics to determine the nature of the raw material. (BBB)

46602 MIGRATION OF ^{90}Sr IN THE GROUND WATERS OF VARIOUS SALT COMPOSITIONS. Orlova, E. I. Gig. Sanit., No. 7, 46-50(July 1965). (In Russian).

The distribution of ^{90}Sr in a water-bearing stratum is determined to a great extent by the salt content of ground waters. The main cations that may influence the migration of ^{90}Sr are natural strontium, calcium, manganese, and sodium. Investigations, carried out under both static and kinetic conditions, showed that the natural cations in natural water may be classified according to their capacity for decreasing the sorption of ^{90}Sr by minerals in the following order: $Sr^{2+} > Ca^{2+} > Mg^{2+} > Na^{+}$. The presence in the water of the most common anions (Cl^{-}, NO_3^{-}, SO_4^{2-}) had practically no effect on the sorption of ^{90}Sr by the sand. On the other hand the anions (PO_4^{3-}, CO_3^{2-}), with which strontium and calcium form weakly soluble compounds increased the sorption of ^{90}Sr by sand and this tended to reduce the migration capacity of the isotope in the water-bearing stratum. (auth)

46603 COSMIC-RAY-PRODUCED AND ARTIFICIAL ^{22}Na IN THE ATMOSPHERE. Roedel, Walter (Univ. of Heidelberg). J. Geophys. Res., 70: 4447-52(Sept. 15, 1965).

The concentration of radioactive ^{22}Na was measured in rain and ground-level air continuously from spring 1962 until fall 1964. Procedures for measuring ^{22}Na are described. The concentration of ^{22}Na in ground-level air varied from 1.4×10^{-4} to 11.9×10^{-4} dpm/m^3, the concentration in rainwater from 0.0065 to 1.02 dpm/l. ^{22}Na is produced by cosmic rays which induce spallation of atmospheric argon. The measurements, however, have shown that ^{22}Na is also produced by nuclear weapons tests. The observed ^{22}Na fallout at Heidelberg was in 1963 about twenty times, and in 1964 about eleven times the estimate of natural production. Some stratospheric air samples collected in spring 1964 showed a ^{22}Na concentration increased by a factor of 10, compared with concentrations observed before the recent nuclear weapons tests. (auth)

46604 HEAVY RADIOACTIVE FALLOUT OVER THE SOUTHERN UNITED STATES, NOVEMBER 1962. Reiter, Elmar R.; Mahlman, J. D. (Colorado State Univ., Ft. Collins). J. Geophys. Res., 70: 4501-20(Sept. 15, 1965).

Radioactive fallout in excess of 320 pc/m^3 of air was observed over the southcentral United States on November 24 to 27, 1962. Atmospheric transport processes leading to these abnormally high values of fallout were studied in detail. In spite of the association of much of this fallout area with rainfall, quasi-adiabatic processes were shown to be responsible for the transport of contaminated air from higher levels to this region. It was estimated that approximately 6×10^{14} kg of air were involved in the sinking process which transported air from the tropopause level to the ground in a matter of approximately two days. The analysis indicated that a low-yield Soviet test on November 17 was responsible for this fallout increase. (auth)

46605 SIMULTANEOUS MEASUREMENTS OF ^{222}Rn, ^{214}Pb, AND ^{214}Bi IN AIR NEAR THE GROUND. Hosler, Charles R. (U. S. Weather Bureau, Washington, D. C.); Lockhart, Luther B. Jr. J. Geophys. Res., 70: 4537-46 (Sept. 15, 1965).

Measurement of the rate of decay of $^{214}Pb + ^{214}Bi$ β-activity collected on a filter provides a means of determining the extent of secular equilibrium between radon and its daughter products in the air; the extent of equilibrium is expressed by the derived atom concentration ratio $\rho = {}^{214}Bi/{}^{214}Pb$ in the air. This parameter is used to obtain a correction factor for relating the β-counting rates on the filter to radon concentration, by comparing the total (corrected) β-count against a known β-count from 100 pc of radon per unit volume. To obtain a calibration of this counting technique simultaneous air sampling, over 20-min durations, for $^{214}Pb + ^{214}Bi$ β-activity by filtration and for radon by α-counting of grab samples, was conducted at elevations of 1 and 91 m above ground. The comparative sampling indicates that for normal weather conditions, by applying a ρ correction for indicated equilibrium departure, the β-counting technique yields radon concentrations equivalent to those obtained by grab samples at an elevation of 91 m; for the 1-m elevation computed concentrations are about 80% of those obtained by grab sample. The depletion of radon daughter product β-activity from the air stream, through impaction or electrostatic effects by polyethylene tubing, is shown to be negligible. Natural atmospheric scavenging processes and dust-loading on filters are discussed as possible mechanisms leading to errors in the comparison of β-counting rates with directly measured radon concentrations. (auth)

46606 ^{230}Th CONTENT OF SOUTH ALLIGATOR RIVER PITCHBLENDE. Awwal, M. A.; Carswell, D. J.; Chorlton, S. (Univ. of New South Wales, Kensington, Australia). J. Inorg. Nucl. Chem., 27: 2125-7(Sept. 1965).

^{230}Th abundance measurements were made on a pitchblende sample from the South Alligator River area of the Northern Territory of Australia. The thorium extraction method is described. A $^{230}Th/^{232}Th$ ratio of 0.0841 ± 0.0014 was found from 16 determinations. (M.C.G.)

46607 THE ISOTOPIC COMPOSITION OF STRONTIUM IN OCEANIC AND CONTINENTAL BASALTS: APPLICATION TO THE ORIGIN OF IGNEOUS ROCKS. Faure, G.; Hurley, P. M. (Massachusetts Inst. of Tech., Cambridge). J. Petrol., 4: 31-50(1963).

For 25 basalts and related volcanic rocks from both oceanic and continental localities, the isotopic abundance of ^{87}Sr, ($^{87}Sr/^{86}Sr$) was found to vary from 0.7047 to 0.7101. The range of variation was outside experimental errors and is considered to be significant. No consistent difference in the value of the $^{87}Sr/^{86}Sr$ ratio was observed for basalts from continental and oceanic localities. The average $^{87}Sr/^{86}Sr$ ratio for 11 oceanic basalts was 0.7072 ± 0.0003, whereas 14 continental basalts and related volcanic rocks averaged 0.7082 ± 0.0003 (standard deviations of the mean). The average $^{87}Sr/^{86}Sr$ ratio for all 25 basalts was 0.7078, with limits of variation of +0.002 and −0.003. The concentrations of Rb and Sr in a representative number of the basalts were determined by isotope dilution. Five olivine basalts averaged 17 ± 6 ppm Rb and 390 ± 55 ppm Sr and Rb/Sr = 0.044 ± 0.018; whereas six tholeiitic basalts were found to contain 30 ± 7 ppm Rb and 504 ± 167 ppm Sr and Rb/Sr = 0.060 ± 0.024. On the basis of the most reliable Rb and Sr analyses of igneous and sedimentary rocks available in the literature the Rb/Sr ratio of the near-surface part of the continental crust was estimated to be 0.25. If its average age is 2 billion years and its initial $^{87}Sr/^{86}Sr$ ratio was 0.704, the present average value would be 0.725. This estimate was compatible with results obtained for two composites of Paleozoic shale, which averaged $^{87}Sr/^{86}Sr = 0.7215 \pm 0.001$. The hypothesis is advanced that there is sufficient enrichment of ^{87}Sr in crustal materials so that the value of the $^{87}Sr/^{86}Sr$ ratio of igneous rocks at the time of crystallization can be used as a criterion for the origin of the material. (BBB)

46608 ON SOME SOURCES OF ERRORS IN LOW ACTIVITY MEASUREMENTS. Klumpar, Josef. Jaderna Energie, 11: 256-9(July 1965). (In Czech).

Standard measurements of total radioactivity of surface or rain water are discussed from the point of view of accuracy needed for purposes of health physics. The sources of error in sample manipulation and in the measurement proper were investigated. The unified evaluation requires the standardization of measurement conditions. (auth)

46609 FREQUENCY MONITORING AND NUCLEAR BURST DETECTION: SOME ASPECTS OF VLF. Haave, C. R.; Shaw, B. W. (Johns Hopkins Univ., Silver Spring, Md.). Johns Hopkins Univ., Appl. Phys. Lab., Tech. Dig., 4: 2-10(Mar.-Apr. 1965).

Very-low-frequency (VLF) monitoring was conducted in 1962, when the U. S. and Soviet high-altitude nuclear tests took place, and a substantial body of nuclear-burst-related VLF perturbation data became available. Analysis of these data has indicated some important connections between VLF perturbations and the trapped radiation from high-altitude nuclear bursts. Delayed perturbations caused by

the two 1962 Soviet high-altitude bursts were monitored by APL facilities on six separate VLF paths; from these data the types and energies of the particles and the extent of the trapped radiation belts were deduced and compared with satellite particle observations. Of the six VLF paths monitored, the path from WWVL (monitoring station in Boulder, Colorado) to APL was the most interesting for analysis. In this path the effects of electrons from radioactive decay of fission fragments and from neutron decay were separately shown in the VLF phase perturbations associated with these two Soviet bursts. The phase anomalies recorded on this path for the Soviet bursts of Oct. 22 and 28 are shown. The first onset on Oct. 22 corresponded to the arrival of electrons having energies typical of the fission-β spectrum; the onsets of 22 and 23 min, related to the arrival of electrons having the endpoint energy of the neutron-decay β spectrum. Electrons with energies characteristic of both the fission-β and neutron-decay β spectra were thus present at geomagnetic latitudes between 49°N (WWVL) and 51°N (APL) for the burst of Oct. 22, but only the neutron-decay betas were observed for the Oct 28 event. This was probably caused by a difference in burst altitude, with the later burst being enough lower than the earlier one that the fission betas were confined to latitudes below 49°N. The onset time of t = 6 min (Oct. 22) on the GBR (Rugby, England) to APL path corresponded with the intersection of particles of 3.5- and 4-Mev energies with the path at a latitude of about 55°N. If these particles had been present in sufficient number at latitudes north of 55°N, an earlier onset than the observed t = 6 min would have been expected. This sets the northern limit of the fission-β belt, insofar as a VLF effect is concerned, at about 55°N for the Oct. 22 burst. No significant perturbation was observed on this path for the Oct. 28 burst, confirming the finding from the WWVL-to-APL path that fission-betas were not present at latitudes north of 49°N for this event and also indicating that the neutron-decay β belt did not extend significantly north of APL. A set of delayed VLF perturbations linked with a high-altitude nuclear burst can thus yield substantial information about the geographical extent and the particle species and energies of trapped radiation associated with the burst. (BBB)

46610 THE ^{90}Sr CONTENTS OF SOILS AND PLANTS ON THE TERRITORY OF THE G.D.R. in 1963. Reissig, H. (Technische Universitaet, Dresden). Kernenergie, 8: 364-78(June 1965). (In German).

The ^{90}Sr contamination of soils and plants in the German Democratic Republic in 1963 is considered. From 1962 to 1963, the ^{90}Sr content of pasture grounds and fields increased significantly. This increase agreed with ^{90}Sr total fallout in this period. Simultaneously, the ^{90}Sr concentration of plants increased in 1963 in comparison with 1962 (except potato bulbs) by a factor of 1.5 to 3. A comparably high increase of ^{90}Sr was observed in rye grain, which was also in good agreement with fallout conditions. The fraction of ^{90}Sr surface contamination in total contamination was higher in 1963 than in 1962 in plants with large specific surface. Its estimation was carried out in 1963 by regression analysis, by determining the ratio of ^{90}Sr contents to residual beta activity, and by determining the ^{137}Cs to ^{90}Sr ratio. The values calculated varied from 40 to 90% in dependence on the plant species. The development of ^{90}Sr contamination of soils and plants is shown for the period from 1960 to 1963. (auth)

46611 CONCENTRATIONS OF GAMMA-EMITTING RADIONUCLIDES PRESENT IN HOLOTHURIAN SAMPLES IN THE COASTAL AREA OF ANTIBES IN CAPE FERRAT IN AUGUST 1962. Chesselet, Roger; Lalou, Claude (Centre d'Etudes Nucleaires, Saclay, France). Radioact. Sea, No. 10, 1-15(June 1964). (In French).

Holothuriae were found to show some characteristics which allow them to be used, in the marine environment, as "witnesses" of accumulation phenomena of some gamma emitters in atmospheric fallout. ^{40}K, ^{95}Zr, ^{95}Nb, ^{141}Ce, ^{144}Ce, and ^{144}Pr contents were measured in the muscles and the viscera of 332 holothuriae gathered during 1962, as well as in the surrounding sand from 6 stations at various depths between Villefranche-sur-Mer and Antibes (western Mediterranean). Concentration factors from 100 to 300 were found in the viscera of those animals in comparison to the contents of the sand on which they live. A comparison between the concentrations of the fission products and those of benzo-3,4 pyrene, points out a dissimilarity, which may be attributed to the different modes of injection of those products in the sea. (auth)

46612 RADIOACTIVE FALLOUT IN GENEVA DURING THE YEAR 1963. Wenger, P.; Soucas, K. (Service Cantonal de Controle des Irradiations, Geneva). Radiol. Clin. Biol., 34: 64-6(1965). (In French).

Tabulated and graphical data are given on ^{137}Cs levels in milk and of body burdens in five subjects followed monthly in 1963. The human subjects were examined in a whole-body counter. In each of the subjects the ^{137}Cs levels rose progressively from the first assay (April 1, 1963) to the last (January 1, 1964). The first and last counts in the five subjects gave increases of ^{137}Cs (expressed as $\mu\mu$C/g K) of 92.9 to 206.5, 76.3 to 172.2, 74.0 to 186.7, 74.3 to 166.7, and 50.9 to 120.7. Concentrations of ^{137}Cs in milk over the same period showed wide fluctuations (from 67.3 to 157.0 $\mu\mu$C/g K). The levels rose from an initial value of 76.9 on May 31, 1963, to a maximum of 157.0 on July 10, 1963, fell irregularly to reach a minimum of 68.5 on October 30, 1963, and then rose again to 125.1 $\mu\mu$C/g K on December 18, 1963. (BBB)

46613 ENRICHMENT OF TRITIUM BY THERMAL DIFFUSION AND MEASUREMENT OF DATED ANTARCTIC SNOW SAMPLES. Buttlar, H. v.; Wiik, B. (Technische Hochschule, Darmstadt, Ger.). Science, 149: 1371-3 (Sept. 17, 1965).

A thermal diffusion column allows a recovery of 99 ± 1 percent of the tritium originally contained in about 50 liters at standard temperature and pressure of hydrogen gas in a final volume of 3.8 liters over a 2-day period. After a tenfold enrichment by electrolysis, a tritium concentration of 10^{-18} with an experimental error of a few percent may be measured with a low-level Geiger counter. The results on some well-dated Antarctic snow samples (between 1941 and 1953) are in general agreement with published data. (auth)

46614 NATURAL GAMMA AERORADIOACTIVITY OF THE DISTRICT OF COLUMBIA AND PARTS OF MARYLAND, VIRGINIA, AND WEST VIRGINIA. Neuschel, Sherman K. Geophysical Investigations Map GP-475. Washington, D. C., Geological Survey, 1965. $0.75.

The survey was made with scintillation detection equipment installed in a twin-engine aircraft. Parallel east-west flights were flown 500 ft above the ground. The scintillation equipment recorded only pulses from gamma radiation with energies greater than 50 kev. The cosmic component was removed from the data by twice daily calibrations. The radioisotopes in the air were considered to be fairly uniform on a given day in a particular area. The ground component came from the upper few inches of the ground. The natural gamma activity in the Washington, D. C. area ranged from 100 to 1500 cps and all changes were due to varying radioisotope contents in rocks and soils. A map is presented. (M.C.G.)

Techniques and Equipment

Refer also to abstract 46777.

46615 (AD-612033) THEORETICAL AND FIELD STUDIES OF SEISMIC WAVES. Final Research Report, April 1, 1962-April 1, 1964. Berg, Joseph W. Jr. (Oregon State Univ., Corvallis). 6p. CFSTI $1.00 cy, $0.50 mn.

Studies were made to determine a method for evaluating the size of a seismic source using amplitudes and/or energy content of the seismic waves generated by the source. Each distance range (local, near-regional, regional, and teleseismic) was considered separately to divide the major problem into several smaller ones. Only the initial seismic

disturbance was considered. Data recorded from Gnome, Hardhat, Haymaker, and Shoal nuclear explosions were chosen to represent the seismic sources. The research that was done for seismic waves recorded in the various distance ranges is discussed. In general, the continuity of energy of the seismic waves recorded from explosions was sought for the entire range of distances over which the seismic waves were recorded. (TAB)

46616 (ORNL-tr-758) NEW OBSERVATIONS ON RADIOACTIVE HALOS IN VARIOUS MINERALS WITH CRITICAL REMARKS FOR THE EVALUATION OF HALOS FOR AGE DETERMINATIONS. Ramdohr, P. Translated for Oak Ridge National Lab., Tenn. from Geol. Rundschau, 49: 253-63(1960). 23p. Dep. mn; JCL $2.60 fs, $0.89 mf.

The physical method of the absolute age determination by radioactive halos is frequently applied to objects which appear to be unsuitable by nature; this applies also to radiating as well as colored minerals. Error sources are found in the corresponding size of the coloring particles, in the difference of their activity which can differ with a zone structure in the mineral itself, in the age of the radiating mineral relative to the rock in which they are found, in the exposure period of the colored material, and in its fate. Age determinations by means of radioactive halos thus must be viewed with great caution essentially due to the insufficient purity of the mineralogical objects. (auth)

46617 THE MEASUREMENT OF RADIOCARBON ACTIVITY AND SOME DETERMINATIONS OF AGES OF ARCHAEOLOGICAL SAMPLES. Agrawal, D. R.; Kusumgar, Sheela; Lal, D. (Tata Inst. of Fundamental Research, Bombay). Current Sci. (India), 34: 394-9(July 5, 1965).

Data from radiocarbon age estimations in India are presented. The method for synthesizing methane gas from carbon atoms of the sample to be dated is described. Proportional counters are filled with the methane prepared by this method. Counting data are given for the radiocarbon activity in the methane. The main advantages in using the present method of methane counting over acetylene are: rapid synthesis, preparation of radon-free gas, and the nonexplosive nature of methane. Six ^{14}C-standard and seven background samples were prepared and counted. The counting rates were found to be the same within the statistical errors of measurements. (F.J.H.)

46618 PRIMARY AND METAMORPHIC Rb–Sr CHRONOLOGY IN CENTRAL COLORADO. Wetherill, G. W.; Bickford, M. E. (Univ. of California, Los Angeles). J. Geophys. Res., 70: 4669-86(Sept. 15, 1965).

Rb–Sr analyses were made on 15 whole rock samples of granitic to granodioritic Precambrian rocks from a region in central Colorado bounded roughly by Independence Pass, Gunnison, Monarch Pass, Leadville, and Red Cliff. Thirteen of these samples define a 1640 ± 35 m.y. isochron with a primary $^{87}Sr/^{86}Sr$ ratio of 0.703 ± 0.002. Analysis of separated minerals from four of these rocks indicates redistribution of strontium and possibly rubidium about 300 m.y. later. In two cases well-defined re-equilibration isochrons are found. Fresh samples of K-feldspar, muscovite, and biotite from pegmatite dikes of the Quartz Creek pegmatite district, near Gunnison, Colorado, give Rb–Sr ages ranging from 1465 to 1380 m.y. These results are interpreted to imply that considerable emplacement of granitic to granodioritic rocks in this area occurred about 1650 m.y. ago. This was followed by intrusion of pegmatites about 200 m.y. later. A subsequent event or series of events about 1350 m.y. ago resulted in extensive redistribution, and in some cases, complete equilibration, of strontium between the mineral phases of these rocks. The results of this study suggest that mineral ages previously measured in central Colorado may largely reflect the 1350-m.y. event and that the primary age of much of the basement is 1650 m.y. or older. (auth)

46619 SOME FUNCTIONS IN THE THEORY OF NEUTRON LOGGING. Allen, L. S. (Socony Mobil Field Research Lab., Dallas); Tittle, C. W. J. Grad. Res. Center (Dallas), 33: 33-54(Apr. 1964).

Solution of the one-energy-group diffusion equation for the case of a point neutron source on the axis of two concentric cylindrical media was programmed for a digital computer. Numerical results for a wide range of values of diffusion length and diffusion coefficient for the outer medium, and for four radii of the inner cylinder, are presented. This program was written for the Remington Rand Univac 1103 computer at Southern Methodist University, and was used to make an extensive study of the numerical behavior. In the course of this work an error was discovered in the normalization procedure described previously. The error can be corrected by setting the quantity U_n, as defined earlier, equal to unity. This correction was incorporated into the work described. A version of the theory, utilizing an expansion into eigenfunctions of z, was also developed and programmed for the Control Data Corporation 1604 computer. Results of a series of calculations in which the diffusion parameters and bore-hole size were variable are presented. Derivation of the mathematical expressions involved is outlined. (BBB)

46620 THE DETECTION OF NUCLEAR EXPLOSIONS IN THE CRUST OF THE EARTH AND THE ATMOSPHERE. Ritsema, A. R. Ned. Tijdschr. Natuurk., 31: 16-21(Jan. 1965). (In Dutch).

The seismic detection of atmospheric and underground nuclear explosions is considered. Typical recordings of seismic waves from nuclear explosions are shown. The propagation velocity of atmospheric waves under various atmospheric conditions is described. It was concluded that atmospheric explosions in the megaton class can be detected by seismic instruments, but underground explosions cannot as yet be determined. (J.S.R.)

46621 ^{14}C DATING OF THE UPPER ANTHROPOGENE IN THE U.S.S.R. Vinogradov, A. P. Radioact. Sea, No. 9, 1-14(Apr. 1964).

Spore pollen analysis was carried out parallel with ^{14}C dating of the upper anthropogenic layer in the USSR. The dating and breakdown of the Holocene in the large peat deposit of Berendeevo, in Franz Josef Land, and in the deposits found in the basin of the lower reaches of the Indigirka River in eastern Siberia, are discussed. Examples are given of the dating of the Taimyr, Chekurovka, and Berezovka mammoths. The way in which a study of sulfur fractionation in the ancient silt deposits on the bed of the Black Sea was used to date the change-over from fresh water to salt water in the sea's basin during the Holocene period is described. ^{14}C dating indicated that organic deposits of this period were approximately 8000 yr old. (auth)

46622 APPARATUS FOR NEUTRON-NEUTRON WELL LOGGING. Youmans, Arthur H. (to Well Surveys, Inc.). U. S. Patent 3,200,251. Aug. 10, 1965. Filed July 7, 1961.

A method and apparatus are provided for making correlative thermal and epithermal neutron logs of subsurface substances during a single trip of the apparatus through a borehole. The apparatus includes a source of fast neutrons suspended in the borehole, detecting means, and recording means. The detecting means responsively produces electrical signals functionally related to incident thermal neutrons and is spaced at a pre-selected distance in the borehole from the source. The detecting means is preferentially exposed to neutrons thermalized in the surrounding substances and preferentially to neutrons thermalized in the borehole, and the recorded signals are compared correlatively with an indication of the depth of the borehole and with an indication of the exposure selected. (B.L.M.)

46623 RADIOACTIVE WELL LOGGING SYSTEM WITH SURFACE CIRCUIT DESIGNED TO ISOLATE A.C. POWER SIGNALS FROM LOGGING SIGNALS. Hoyer, Wilmer A.; Britton, Donald H. (to Esso Production Research Co.). U. S. Patent 3,204,098. Aug. 31, 1965. Filed Dec. 13, 1960.

In a radioactivity well logging system that includes a down-the-hole radiation detector suspended on an electrical conductor cable, a surface circuit is included. The surface circuit includes a ferrite core isolation

choke means for isolating the a-c power source used to power the logging apparatus from the logging signals representative of radiation emanating from subsurface formations and detected by the detector. The surface circuit also includes means for preventing the generation of troublesome power frequency harmonics to preserve the relative amplitude of each pulse logging signal. (B.L.M.)

46624 NEUTRON AND GAMMA RAY WELL LOGGING. Owen, Joe D. (to Phillips Petroleum Co.). U. S. Patent 3,205,356. Sept. 7, 1965. Filed Dec. 12, 1960.

A logging tool is provided that will adjust spacing between the neutron source mounted on the body of the tool and the gamma-ray detector automatically to maintain the gamma-ray detector at a point that has an essentially constant thermal neutron flux. Both the gamma-ray detector and the thermal neutron detector are mounted on the body of the tool. A neutron shield is provided between the source and the detectors. Logging recording means are adapted to record data on a chart from each of the detectors, and the chart is movable relative to the logging recording means in response to the lowering of the body into the well. The apparatus is applicable to surveying a borehole for indications of the presence of oil. (B.L.M.)

Thorium and Uranium Minerals

46625 (ORNL-tr-757) RADIOACTIVITY AND PLEOCHROIC HALOS. Muegge, O. Translated for Oak Ridge National Lab., Tenn. from Centr. Mineral. Geol., 65-71 (1909). 11p. Dep. mn; JCL $1.60 fs, $0.80 mf.

Studies were made on the effects of radium bromide on rock-forming minerals some of which have pleochroic halos. The minerals included: rock salt, cordierite, biotite, chlorite, hornblende, actinolite, and glaucophane. Radiosensitivity of the minerals as related to color intensity is discussed. (P.C.H.)

46626 THE LABORATORY INVESTIGATION OF SOME FACTORS INFLUENCING THE AQUEOUS DISSOLUTION OF THE URANIUM CONTENTS OF ROCKS. [PART] I. Horvath, Eva. At. Kozlemen., 7: 85-93(June 1965). (In Hungarian).

Investigations were made of how the change in the grain size of a certain rock and in the time of contact between rock and water influences the quantity of dissolved uranium. The experiments were made by percolating through andesitic granitic rocks distilled water or water containing 2 g/liter $NaHCO_3$. On the basis of the results of the experiments it was found that the influence of grain size (i.e., the surface of solution) of the examined rocks upon the dissolved uranium quantity is much less than expected. In the case of experiments made under identical circumstances the increase of the surface of solution with two orders of magnitude led only to a triple or fourfold rise in the concentration of the dissolved uranium. In connection with the time-function of the solution it was found that the dissolving concentration which considerably increased in the beginning with the increase of the time of contact, after a certain period of time (in the case of our experiments 150–240 minutes, depending on the rock examined) does not change any more with the increase of time. (auth)

46627 ON THE COMPOSITION OF URANIC–VANADIC MINERALS. Bezrukov, I. Ya.; Zolotavin, V. L.; Askerov, A. B.; Prokopchuk, V. V. (Ural Polytechnical Inst., USSR). Geokhimiya, No. 9, 1120-9(Sept. 1965). (In Russian).

Processes of the interaction of various uranium and vanadium ions in mixing solutions with an identical pH and in titrating mixtures of uranium and vanadium acid solutions with alkali were studied. The existence of the following uranium vanadates: $(UO_2)_3V_{10}O_{28}$, $(U_2O_5)_3V_{10}O_{28}$, $(U_3O_8)_2V_4O_{12}$, $(UO_2)_2V_4O_{12}$, $(UO_2)_2V_2O_7$, $(UO_2)_3(VO_4)_2$, and $K_2(UO_2)_2V_2O_8$ was proved by these experiments, the mechanism of uranyl decavanadate hydrolysis was suggested and considerations concerning the ionic composition of natural uranic–vanadic minerals stated. (auth)

46628 URANIUM AND THORIUM ABUNDANCES IN THE BASALT CORED IN MOHOLE PROJECT (GUADALUPE SITE). Morgan, J. W.; Lovering, J. F. (Australian National Univ., Canberra). J. Geophys. Res., 70: 4724-5 (Sept. 15, 1965).

Two Mohole basalt samples were analyzed for uranium and thorium abundances using a neutron activation technique. It is concluded from the observed Th/v ratio of 1.2 that the Mohole basalt does not have a fundamental relationship to primitive mantle materials. Two possible reasons are given for the low Th/v ratio: that the ratio is a characteristic of its parent magma; and the effects of the contamination of the rock with the abundant secondary calcite which is prominent in the Mohole basalt. (L.B.S.)

46629 EIGHTH ANNUAL URANIUM AND MINERALS SYMPOSIUM, RIVERTON, WYOMING, JUNE 14, 15, 16, 1963. [Riverton, Wyo.,] A.I.M.E., 1963. 91p.

Papers presented at the Eighth Annual Uranium and Minerals Symposium are given. Topics include: education problems in the mineral industry; geology, history, and production of uranium in Wyoming; application of hydrothermal zoning to Wyoming uranium deposits; the 115-yd^3 stripping shovel, the economics of base metal recovery by ion exchange; the comparative economics of self-loading elevating scrapers vs conventional scrapers; industrial applications of acid retardation chelating resins and gel liquid extraction; proposals for modernization of mining law; uranium after 1966; liaison between mining and legal; geologic history and petroleum resources of the Wind River Basin, Wyoming; the time-table for atomic power; and Wyoming bentonite. (M.C.G.)

46630 DIE MIT BUNDESMITTELN UNTERSTUETZTE URANPROSPEKTION DER JAHRE 1956–1962. (The Uranium Prospecting Supported by the State for the Years 1956–1962). Von Braun, Eckart. Munich, Gersbach and Sohn Verlag, 1965. 112p.

From 1956 to the end of 1962 about 12,000,000 DM were made available for uranium prospecting in the German Federal Republic. The purpose of the studies was to establish the occurrences of uranium deposits in the Republic. The work showed that principally the hydrothermal deposits of the variscitic granites in East Bavaria and the Black Forest and the porphyries are of economic interest. Other uranium deposits found had no economic value. (J.S.R.)

HEALTH AND SAFETY

See also BIOLOGY AND MEDICINE — Radiation Hazards and Protection
GEOLOGY AND MINERALOGY — Natural Radioactivity and Fallout

Refer also to abstracts 45747, 45755, 45758, 46080, 46112, 46143, 46473, 46751, 46755, 46839, 46842, and 47569.

46631 (A/AC.82/G/L.986) CONTROLE RADIOLOGIQUE DE L'ENVIRONNEMENT DU C.E.N. A MOL. ORGANISATION ET TECHNIQUES DE MESURES. (Radiological Monitoring of the Surroundings of C.E.N. at Mol. Organization and Techniques of Measurement). Boulenger, R.; Colard, J.; de Maere, X.; Koch, G.; Osipenco, A.; Tytgat, R. (Centre d'Etude de l'Energie Nucleaire, Brussels (Belgium)). Jan. 1964. 88p. (R-2298). Dep. mn.

The radiological monitoring of the C. E. N. environment is done by monitoring chains. The first monitoring chain measures the concentration of mixtures of radioisotopes or of particular isotopes in the effluents of the plant. The second monitoring chain is located at a slight distance from the nuclear installations and makes a continuous measurement of the radioactivity of dust in suspension in the air and the ambient radioactivity. Samplings were also made of milk and of surface water or rain. The third monitoring chain is composed of sampling points of dust in suspension in the air and of precipitations at several tens of km from C. E. N. The techniques and methods used in each of these monitoring chains are described. (J.S.R.)

46632 (A/AC.82/G/L.987) LA RETOMBEE RADIOACTIVE MESUREE A MOL. ANNEE 1963. (Radioactive Fallout Measured at Mol, Annual Report 1963). Boulenger, R. (Centre d'Etude de l'Energie Nucleaire, Brussels (Belgium)). 95p. (R-2302). Dep. mn.

The results of the measurement of the radioactivity of particles in the air at ground level and of the radioactivity of precipitation in Belgium in 1963 are shown graphically. The total α and β activity and the ^{90}Sr and ^{137}Cs activity were determined for both dust and precipitations. The activity of various γ emitters was also determined for the dust suspensions. The results of radioactivity measurements made on milk and data on ^{137}Cs and ^{90}Sr content of milk are also reported graphically and in tabular form. (J.S.R.)

46633 (AD-276187) THE ESTIMATION OF THE INTERNAL RADIATION EXPOSURE RESULTING FROM THE INGESTION OF FALLOUT-CONTAMINATED WATER IN A NUCLEAR WAR. Hawkins, Myron B. (California Univ., Berkeley. Inst. of Engineering Research). June 29, 1961. Contract CD-SR-58-40. 10p. (CONF-610601-1).

From Health Physics Society Meeting, Las Vegas, Nev.

The over-all problem of controlling internal radiation exposure resulting from the ingestion of water contaminated by fallout in wartime is discussed. The limitations of maximum permissible concentration concepts in areas where fallout contamination levels are high are discussed and simplified methods of computing the internal dose are presented. To facilitate the interpretation of such information, the committed dose concept is introduced and its proposed use is described. A brief discussion of the significance of the hazards of fallout-contaminated water supplies relative to other hazards in the nuclear-war situation is presented. (auth)

46634 (AD-423463) THE HAZARD OF ^{90}Sr—A REVIEW. Dacquisto, Michael P.; Jacobus, David P.; McLaughlin, Mary M. (Walter Reed Army Inst. of Research, Washington, D. C. Dept. of Biophysics). June 4, 1958. 20p.

Data are reviewed from experimental studies on the metabolism of strontium-90 in experimental animals and in man. The data indicate that an intravenous or intraperitoneal dose of radiostrontium is 50% excreted in about 10 to 20 days; at the end of the first year only about 10% of a parenteral dose remains, and in 20 years, about 1% remains; an oral dose of strontium is about 10% absorbed. This fraction is then handled as though it had been introduced parenterally. Therefore, from an oral dose 1% remains 1 year later; 0.1%, 20 years later. The concept of a Maximum Permissible Body Burden (MPBB) is valuable but lacks the dimension of time. Failure to consider time as a factor is responsible for an overestimation of body burden. When time is fixed at one year after exposure and the MPBB is assumed to be proportional to body weight, much animal investigation is amenable to an orderly analysis with the following findings: for both radium-226 and strontium-90 there is no evidence of any tumor hazard at 100 MPBB or lower; at 1,000 MPBB the risk is clear (at least 10%) but the area between 100 to 1,000 MPBB appears to be a region of only slightly increased risk. The species used for this type of study seems to be immaterial. The incidence of osteogenic sarcoma due to strontium-90 is dose-dependent. The evidence available concerning the hazard of multiple versus single administration is suggestive of a further safety factor. This may have an important bearing on man's status in the nuclear age. With regard to the MPBB of strontium-90 the total evidence suggests that the current values are too conservative and fail to consider the optimistic experimental data. The Maximum Permissible Body Burden of strontium-90 is therefore probably too low, by at least a factor of 10, possibly more. (35 references.) (auth)

46635 (AD-611764) REQUIREMENTS FOR LOCAL PLANNING TO COVER HAZARDS OF FALLOUT. VOLUME I. Final Report, Vol. 1. (Dunlap and Associates, Inc., Darien, Conn.). Jan. 1965. Contract OCD-OS63-161. 63p. CFSTI $3.00 cy, $0.75 mn.

The development of effective plans for assigning shelters to population, and for bringing the population to the shelter was studied. Two medium-sized towns in Connecticut, Stamford, and Waterbury, were studied in detail. For each town, a study was made on the effectiveness of a number of plans of varying detail and complexity in getting people to shelter. In all plans it was assumed that enough traffic control could be set up to avoid blockages of traffic near shelters, and that the population would know to what shelter areas they had been assigned, and how they were supposed to get there. Two types of shelter assignment were made: the first was by census tract, the second by individual location. In the first, people from shelter-poor census tracts were directed to shelter-rich census tracts, according to a linear programming method aimed at minimizing distance traveled. In the second, a similar method was used to assign people to actual buildings. Studies were made of various speeds of movement to shelter and their effects upon rate at which the population was sheltered. Planning problems associated with primary and secondary fires were given cursory examination. (TAB)

46636 (AD-611765) REQUIREMENTS FOR LOCAL PLANNING TO COVER HAZARDS OF FALLOUT. VOLUME II. APPENDICES. Final Report, Vol. 2. (Dunlap and Associates, Inc., Darien, Conn.). Jan. 1965. Contract OCD-OS63-161. 111p. CFSTI $4.00 cy, $0.75 mn.

Information is included on: civil defense systems, management planning for shelters, mathematical models for traffic, populations, passenger vehicles, and hazards and distribution of radioactive fallout. (TCO)

46637 (AD-612254) LABORATORY INVESTIGATIONS OF SHELTER MANAGEMENT FACTORS. Hale, John F.; Rosenfeld, Michael; Berkowitz, Morris I. (American Institutes for Research, Pittsburgh, Pa. Inst.

for Performance Technology). Jan. 1965. Contract OCD-PS64-57. 246p. CFSTI $6.00 cy, $1.50 mn.

Several shelter exercises were conducted to investigate shelter management factors. The most efficient operation of the shelter occurred when the manager was present from the beginning of the exercise. The effectiveness of operation in the absence of the trained manager depended upon the attitude toward the exercise of the emergent shelter leader, and upon the way in which he employed the in-shelter guidance materials. A management style in which approximately equal attention is given to both technical and non-technical problem areas was much more effective than styles in which more attention is given to one of these areas at the expense of the other. Complete darkness in a shelter was found to be tolerable for 24 hours by a group of volunteers from the research staff of A.I.R. This finding should be viewed, not as a base line, but rather as ceiling. That is, it is very unlikely that a complete shelter naive group would behave nearly as calmly and assuredly as this group. (auth)

46638 (AD-613359) PREDICTION MODELS FOR FIRE SPREAD FOLLOWING NUCLEAR ATTACKS. Final Report. (United Research Services, Inc., Burlingame, Calif.). Jan. 1965. Contract OCD-PS-64-48. 182p. (URS-641-6). CFSTI $5.00 cy, $1.25 mn.

A semiempirical approach is used to predict fire spread beyond the area directly ignited by thermal radiation from nuclear weapons. Mathematical models, both stochastic and deterministic, describe the progress of fires in two-dimensional or one-dimensional space. Application of each model to appropriate cases is discussed. Empirical data needed for evaluation of parameters are specified and methods for acquiring these data suggested. Observed data, accumulated over many years in records of past fires, have proved valuable in determining some of the parameters. The remaining parameters require further observed data. At present approximate prediction can be made by use of a specially designed version. The results of a statistical study on observed rate of spread data are also presented, and a number of specific problems that must be worked out before the method can be used for assessing the fire damage from nuclear attacks are discussed. (auth)

46639 (AECL-2281) PROBLEMS IN BETA DOSE MEASUREMENT AT CRNL. Cross, W. G. (Atomic Energy of Canada Ltd., Chalk River (Ontario)). July 1965. 9p. Dep.; AECL $0.50.

A discussion is given of the beta dose problems at CRNL arising from interpretation of ICRP recommendations and from the energy and angular responses of film dosimeters and dose-rate instruments to beta radiation. (auth)

46640 (BNL-915) 1963 ENVIRONMENTAL RADIATION LEVELS AT BROOKHAVEN NATIONAL LABORATORY. Hull, A. P. (Brookhaven National Lab., Upton, N. Y.). Nov. 1964. Contract AT(30-2)-Gen-16. 19p. Dep. mn; CFSTI $1.00 cy, $0.50 mn.

Measurements were made during 1963 in the environment of Brookhaven National Laboratory and vicinity of natural background radiation levels (including fallout contributions) and of radiation from the ^{41}Ar content of the BGRR cooling-air effluent, from an ecology field gamma source, and from the discharge of low-level liquid wastes. The natural background, as measured 6 in. above roof level, reached 6.22 mR/wk in August. This is attributable to fallout from the large-scale weapons testing conducted during the fall of 1962 and is the highest level on record at this location. The corresponding background at an elevation of 3 ft was ≈65% of that at 6 in. During 1963, radiation levels attributable to Laboratory operations were maintained well below the established MPE, MPC, and RPG levels for whole-body exposures, air particulate concentrations, and liquid effluent concentrations. Radiation levels attributable to fallout were also below these established limits. (TCO)

46641 (CEA-R-2771) ETUDE DES IONS RADIOACTIFS DE L'ATMOSPHERE [Theses]. (Study of Radioactive Ions in the Atmosphere [Thesis]). Renoux, Andre (Commissariat a l'Energie Atomique, Fontenay-aux-Roses (France). Centre d'Etudes Nucleaires). 1965. 86p. Submitted to Paris Univ. (France).

A comparative study was made of active deposits of radon and thoron in suspension in the atmosphere by means of α radiation counting, using ZELENY tubes, scattering equipment, filter papers, or membranes. It was possible to show the existence of small and large ions which are negative and positive, as well as of neutral radioactive nuclei; their properties were studied. A theoretical interpretation of the results is presented. The average content of radon (using the Ra A concentration) and of Th B in the air was determined. The radioactive equilibrium between radon and its daughter products in atmospheric air were examined. The techniques developed for active radon and thoron deposits were applied to the study of artificial radioactivity, the analyses being carried out by means of γ spectrometry. (auth)

46642 (IDO-12043) ENVIRONMENTAL TRITIUM STUDIES AT THE NATIONAL REACTOR TESTING STATION. Hawkins, D. B.; Schmalz, B. L. (Idaho Operations Office (AEC), Idaho Falls, Health and Safety Div.). Aug. 1965. 46p. (CONF-651108-1). Dep. mn; CFSTI $2.00 cy $0.50 mn.

For Presentation at Symposium on Isotope Techniques, Urbana, Ill.

Information on the concentration of tritium in waste, precipitation, and surface and ground water at the National Reactor Testing Station and surrounding areas is presented. These data have been gathered to appraise the effect of NRTS operations on the surrounding region and to elucidate the hydrology of ground water at the NRTS. It is shown that the present concentration of tritium in the environmental water is about 100 times pre-hydrogen-bomb levels. NRTS operations have not noticeably contributed to this contamination except in the case of ground water down gradient from the Chemical Processing Plant. Tritiated water emanating from the Idaho Chemical Processing Plant has been detected down the ground-water gradient over an area of about 75 square miles. A log-log plot of tritium concentration versus time provides a means of estimating first arrival of tritium at an observation well. The tritium concentration in ground water decreases exponentially with distance from the point of injection. An empirical equation has been derived which describes this function. (auth)

46643 (LAL-1136) RAPPORT D'ACTIVITE, OCTOBRE 15, 1964–AVRIL 15, 1965. (Report of Activity, October 15, 1964–April 15, 1965). (Laboratoire de l'Accelerateur Lineaire, Univ. de Paris, Orsay (France)). May 1965. 89p. Dep. mn.

The modification and utilization of the accelerator are summarized, together with research progress on nucleon physics, nuclear spectroscopy, pion physics, and storage rings. Development of storage rings and associated experimental equipment and radiation control are also reported. (J.S.R.)

46644 (ORNL-P-1528) CONTAMINATED FILTER REMOVAL EQUIPMENT. Hahs, Charles A. (Oak Ridge National Lab., Tenn.). [1965]. Contract W-7405-eng-26. 7p. (CONF-651101-10). Dep. mn; CFSTI $1.00 cy, $0.50 mn.

For Presentation at 13th Conference on Remote Systems Technology, Washington, D. C.

A filter removal system was designed for the Thorium-Uranium Fuel Cycle Development Facility. The system provides containment and shielding during removal. Disposable enclosures are designed to contain the filters and are housed in concrete-shielded pits outside the building. The maneuvering of the filter removal carrier is described. (D.L.C.)

46645 (ORNL-TM-1228) ADHESION OF PARTICLES TO SURFACES IN LIQUID AND GASEOUS ENVIRONMENTS. Walker, R. L.; Fish, B. R. (Oak Ridge National Lab., Tenn.). Aug. 30, 1965. Contract W-7405-eng-26. 19p. (CONF-650533-2). Dep. mn; CFSTI $1.00 cy, $0.50 mn.

From American Assn. on Contamination Control, Annual Meeting, Miami.

A review of the adhesive forces that retain particles on surfaces and of forces available to remove them, suggests methods for selecting decontamination techniques. In normal atmospheric environments, the major components of adhesion appear to be capillary, molecular, and electrostatic forces. In liquid systems, electrostatic or molecular forces may predominate; however, it is pointed out that a time dependent force, due to Stefan flow, may affect particle removal from surfaces. Forces available for removing particles from surfaces may be fluid dynamical, inertial, or direct mechanical contact. The efficient choice of a cleaning procedure requires an understanding of the relationships between forces of adhesion and available removal forces. Research on the adhesion of particles in normal atmosphere indicates that the adhesive force depends strongly on the relative humidity. Similar studies in liquids generally show much lower adhesive forces than in air, by approximately two orders of magnitude. (auth)

46646 (PHS-999-RH-13) BEHAVIOR OF CERTAIN RADIONUCLIDES RELEASED INTO FRESH-WATER ENVIRONMENTS. Annual Report, 1959-1960. Friend, Albert G.; Story, Albert H.; Henderson, Croswell R.; Busch, Kenneth A. (Public Health Service, Washington, D. C. Div. of Radiological Health). June 1965. Contract AT(49-5)-1288. 89p. Public Health Service Free.

Radionuclides from various sources, including facilities that produce, process, and handle nuclear material, are entering the fresh-water environment. As part of its assigned responsibilities, the Public Health Service is concerned with the radiological conditions in the various components of the aquatic environment. The Service's Division of Radiological Health, in cooperation with the Atomic Energy Commission, has conducted a number of investigations of streams below atomic energy installations. Two such studies are presented, one on the Mohawk River near Knolls Atomic Power Laboratory and the other on the Clinch and Tennessee Rivers near the Oak Ridge National Laboratory. In general, the results show that all segments of the aquatic environment related to these rivers contain measurable quantities of manmade radionuclides. The results of some uptake studies, carried out in a DRH laboratory, are included to supplement the river studies and to aid in interpreting the results obtained in the field. (auth)

46647 (RISO-104) A MONITORING DESIGN FOR RADIOACTIVE AIR POLLUTION. Flyger, Hans; Rosenbaum, Herbert (Atomenergikomissionen, Risoe (Denmark). Forsoegsinstitut). May 1965. 14p. Dep. mn.

An evaluation is presented of the performance of an installed, continuously measuring air-monitor system for radioactive pollutants in a high-activity handling building at the Danish AEC Research Establishment, Risö. Recent laboratory experiments indicate that the use of long metal tubes in a monitoring system would be disadvantageous owing to the nature and extent of contaminant losses in such conduits. Of special interest are the quite remarkable results obtained concerning the deposition of submicron particles in long, thin tubes. On the basis of these and other recent findings a set of redesign proposals is presented. (auth)

46648 (SC-RR-65-464) FALLOUT REPORT—BETA-GAMMA RADIOACTIVITY IN AIR AT SANDIA LABORATORY JANUARY-JUNE 1965. Womelsduff, R. E. (Sandia Corp., Albuquerque, N. Mex.). Oct. 1965. Contract AT (29-1)-789. 11p. Dep. mn; CFSTI $1.00 cy, $0.50 mn.

Data are reported on the gross beta-gamma radioactivity (expressed as micromicrocuries per cubic meter) of air samples collected at Sandia Laboratory during the first half of 1965. (auth)

46649 (STI/PUB/94) THE PROVISION OF RADIOLOGICAL PROTECTION SERVICES. A Code of Practice Based on the Report of a Panel of Experts. Safety Series No. 13. (International Atomic Energy Agency, Vienna (Austria)). 1965. 90p. IAEA US $2.00; S 42,-; 12/-std; F.Fr. 8,-; DM6.40.

A code of practice is presented for radiation protection in establishments using radiation sources. (C.H.)

46650 (WCAP-1859(Rev.)) SHIPMENT OF IRRADIATED YANKEE FUEL ELEMENTS. (Westinghouse Electric Corp., Pittsburgh, Pa. Atomic Power Dept.). Oct. 1961. Revised Jan. 1962. 123p.

A safeguards evaluation was made of the design and proposed use of a shielded cask for transporting irradiated fuel assemblies from the Yankee reactor site to the Savannah River reprocessing plant. The shipment of irradiated fuel is to be made by special rail car. The cask, which weighs 75 tons when fully loaded, is mounted on the car in a horizontal position, but is lifted to an upright position and removed to a water-filled pit for fuel loading and unloading. The cask is a cylindrical, double-walled stainless steel vessel, in which the space between the inner and outer shells is occupied by lead shielding. Fuel assemblies are positioned within the central cavity by a copper-poison basket with a corrosion resistant cladding, which serves both as a mechanical support and a permanent neutron poison. The bolted closure head contains mechanical components of the cask's internal cooling system, as well as the required thickness of lead for radiation shielding. In the event that the cask cooling systems are disabled by accident, even to the extent that both primary and secondary cooling water are lost, heat dissipation from the finned-outer surface of the cask is sufficient to prevent thermal damage and fission product release from the fuel. It was demonstrated that the cask design and its appurtenances satisfy all applicable regulations by protecting the general public from radiation and the release of radioactive substances. (P.C.H.)

46651 (JPRS-30979) PATHOLOGY, CLINICAL PICTURE AND THERAPY IN AFFECTIONS WITH TOXIC AND RADIOLOGICAL AGENTS. Bogdanov, N. A. (ed.) Translated from pp 1-192 of Patologiya, Klinika i Terapiya Pri Porazheniyakh OV i RV, Leningrad, 1964. 147p. CFSTI $4.00 cy, $1.00 mn.

The characteristics and pathological effects of radiological and chemical warfare agents are reviewed. First-aid treatment methods are outlined for persons exposed to these agents. Topics discussed include acute and chronic radiation sickness; radioinduced skin lesions; internal irradiation; the toxic effects of phosphororganic agents; the toxic effects of hydrocyanic acid; the toxic effects of carbon monoxide; skin irritants, such as Lewisite and yperite; the asphyxiating effects of phosgene, diphosgene, and nitrous oxides; toxic smokes; lacrimators or tear gases; incendiary agents and flame-thrower mixtures; intoxication by smoke-forming agents; poisoning by industrial liquids such as tetraethyl lead, ethylene glycol (antifreeze), methyl alcohol, and dichlorethane; methods for detecting war gases; radiation dosimetry; methods for radiological and gas decontamination; individual and group protective equipment, including gas masks and anti-chemical protection of the skin; and group protective equipment such as shelters for the protection of groups against the effects of nuclear, chemical, and bacteriological warfare agents. (C.H.)

46652 (JPRS-31842) NUCLEAR WEAPONS—PHYSICAL FUNDAMENTALS. Chugasov, A. A. (ed.) Translation of pp 3-112 from Yadernoe Oruzhie—Fizicheskie Osnovy, Moscow, 1965. 102p. (TT-65-32337). CFSTI $4.00 cy, $0.75 mn.

The physical properties of nuclear weapons are discussed. Topics discussed include the atom and its nucleus, the physics of nuclear transformations, the operating principles of nuclear weapons, the shock wave of a nuclear burst, light radiation, penetrating radiations, radioactive contamination by nuclear weapons, and methods of dosimetry of radioactive radiations. (C.H.)

46653 (JPRS-31843) CATALOGUE OF PROTECTIVE EQUIPMENT. Translation of pp 3-189 from Zashchitnaya Tekhnika, Katalog, Atomizdat, Moscow, 1964. 181p. (TT-65-32338). CFSTI $5.00 cy, $1.25 mn.

A list is presented of protective equipment available in the USSR for the protection of individuals working with radioactive materials, chemically active, or toxic materials. Photographs and design details are included for many of the items. (C.H.)

46654 (JPRS-31993) REGULATIONS PERTAINING TO WORK WITH IONIZING RADIATION SOURCES. Translations from Sluzbeni List SFRJ, No. 31, 1198-1205(July 14, 1965). 26p. (TT-65-32487). CFSTI $1.00 cy, $0.50 mn.

Regulations for working with sources of ionizing radiation in Yugoslavia are presented. Standards are discussed for: health examinations and conditions; permissible doses; professional training; and operation and use of sources exceeding designated limits of activity. (H.G.D.)

46655 NATURE OF RADIATION FROM NUCLEAR WEAPONS IN RELATION TO FLASHBLINDNESS. Hill, J. H.; Chisum, Gloria T. (Naval Air Development Center, Johnsville, Penna.). Aerospace Med., 36: 528-32 (June 1965).

A preliminary survey was made, with a view toward developing protective devices, of the transient effects of a nuclear detonation on the retina. Although such a nuclear weapon flash can cause retinal burns, only the nature of the radiation in relation to flashblindness is considered. Required information about a light source to determine whether or not it will produce flashblindness is the luminance, duration, and visual angle subtended by the source. Estimations of these dimensions of a light flash with a nuclear weapon fireball as a source are deduced from available data. The thermal radiation from a nuclear weapon detonated at low altitude amounts to about 35% of the yield of the weapon, the other 65% being in nuclear radiation and mechanical energy. The latter two forms of energy are dissipated to safe levels at much shorter distances than that for the thermal energy. The variation of the ranges with weapon size is shown. Except for their eyes, personnel can be adequately protected up to the point at which they would receive second-degree burns. On this basis, the concept of equal effects of nuclear weapons can be used regardless of weapon size. This concept is illustrated in a hypothetical situation wherein at 0.1 mile from a 1-kt weapon, or 10 miles from a 1-Mt weapon, or anywhere within the second-degree burn level the thermal and mechanical damage may well be so excessive that flashblindness is not a problem. The point at which flashblindness can become a problem is beyond the second-degree burn line. It is shown that for low altitude detonations at the minimum safe distances the eyes can receive more than 5 log mL-sec of visible energy from a 10% reflector before there is time to blink, and the luminance of a fireball viewed directly can be as much as four orders of magnitude greater. It is concluded that from knowledge of the luminance personnel may be expected to encounter in operational situations, adequate flashblindness protection can be devised, and the minimum safe distance for personnel will not have to be extended. (BBB)

46656 WHOLE-BODY GAMMA SPECTROMETRY. Burner, Alvin M.; Thomas, Robert G.; Benson, Richard E. (Radiological Health Lab., Wright-Patterson AFB, Ohio). Arch. Environ. Health, 11: 296-301(Sept. 1965).

The whole-body counting facility has a direct application to the support of the Air Force mission, worldwide, by the Medical Service. Our laboratory has been given the responsibility of providing support in the field of radiological health. This instrument has given us an additional valuable tool with which to fulfill our mission. We feel that any person exposed to a situation under which it is conceivable that radionuclides could either enter the body or be produced within the body is a candidate for examination and evaluation in this facility. We also feel that all personnel that are monitored by neutron film badges should be considered. Persons exposed to conditions requiring the use of such badges will be exposed to levels of neutrons which, in the day-to-day operations, will not be a significant hazard. However, the possibility remains that, because of an unusual combination of circumstances, neutron fluxes may be considerably higher, and these may be a significant biological hazard. The extent of the exposure may be determined most readily by analysis within the whole-body counter for the presence of sodium-24, resulting from neutron activation of the nonradioactive sodium-23 normally present. Personnel in this group will include all Air Force personnel working at Air Force reactors. Personnel routinely exposed to fission products and who use radioisotopes in research should also be examined periodically by whole-body counting. (C.H.)

46657 IRRADIATION AND PROTECTION OF HOSPITAL PERSONNEL EXPOSED TO IONIZING RADIATIONS, ACCORDING TO THEIR OCCUPATIONS. Durgeat, J. (Assistance Publique, Paris). Arch. Maladies Profess., Med. Trav. Securite Sociale, 24: 922-6(Dec. 1963). (In French).

Data furnished by the Laboratoire de Radiologie de l'Assistance Publique reveal that the exposure of hospital personnel to ionizing radiation varies according to their occupation. Film dosimetry was used to estimate these different exposure levels. Two types of sensitized film, Massiot-fluor (for Ra and x-ray therapy) and Chassang-Barroz C-B (for radioisotope diagnosis) were used in a survey of 2000 radiologic personnel. The survey showed that personnel involved in specialized examinations such as arteriography, hysterography, pelvimetry, catheterizations, and spinal and intraventricular radiography received the most significant doses (nine persons, exceeding the maximum permissible dose of 400 mR, averaged 735 mR/month). Next were x-ray technicians working in the operating room and at bedside (seven such persons averaged 707 mR exposure per month). Then follow radiology personnel in children's hospitals (three persons averaged 500 mR/month); next, those involved in Ra therapy (ten persons averaged 592.5 mR per month); personnel in gastrointestinal therapy (three persons averaged 933 mR/month); and finally, x-ray technicians and personnel dealing with isotopes received insignificant doses. The data suggest several protective measures. (TCO)

46658 A COMPUTER PROGRAM FOR AUTOMATIC DETERMINATION OF RADIOACTIVITY IN THE ENTIRE HUMAN BODY. [PART] I. Linden, W. A.; Schneider, C. (Universitaet, Hamburg-Eppendorf, Ger.). Atompraxis, 11: 426-9(Aug. 1965). (In German).

An automatic computing program is presented for determining the radioactivity of the entire human body due to the components of a mixed radiation source using the electronic computer IBM 1620. Computer analysis is made by use of the stripping procedure. In spectra with 4 and 5 components, radiation sources with a characteristic photo peak of energies exceeding 0.4 Mev are determined with a relative error of less than 10%. Scattering bodies (Plexiglas) with a thickness of up to 15 cm have little effect on the accuracy of the analysis if the sources have an energy of more than 0.6 Mev. (auth)

46659 LONG RANGE PROSPECTS OF NUCLEAR ENERGY. Atoomenergie Haar Toepassingen, 7: 144-9 (July 1965). (In Dutch).

Euratom drafted a program for industry in the sphere of nuclear energy in the European community. The program was in the basic form of proposals by Euratom with respect to a common industrial control of nuclear energy. The proposals are summarized. (J.S.R.)

46660 CONCENTRATION OF ^{137}Cs IN AUSTRALIAN MILK DURING 1964. Alsop, R. J. L.; Bonnyman, J.; Keam, D. W.; Molina-Ramos, J. (Commonwealth X-Ray and Radium Lab., Melbourne). Australian J. Sci., 28: 69-71(Aug. 1965).

Weekly samples of milk from 7 major population centers in Australia were analyzed during 1964 for ^{137}Cs content. Data are tabulated. The data show a general increase in the ^{137}Cs content of milk during the period. (C.H.)

46661 THE RADIATION PROTECTION LABORATORY, ONTARIO DEPARTMENT OF HEALTH. Can. J. Public Health, 59: 214-15(May 1965).

The history of radioprotection surveillance in Canada is briefly reviewed, from the time of the establishment of a radium refinery in 1933 to the present, with emphasis on the program of the Ontario Department of Health Radiation Protection Laboratory, which was opened on July 6, 1961. It was designed as a low-level radiation protection to provide maximum flexibility when changes in techniques, equipment, or space might be required. Physical facilities

of this installation are described. Since the 1930's the Division of Industrial Hygiene, Ontario Department of Health, has had varied experience in dealing with health problems in Ra refining, in medical uses, in dial painting, and even in passing judgement on the sale of radioactive water. During the War Years, 1940-1945, many industrial uses were found for radium and new control problems were encountered. Also during this pe.. .d the Division of Industrial Hygiene developed new and more sensitive equipment for the detection of radioactive radiations and in 1944 a small laboratory for testing radioactive materials was established. With the development of the atomic bomb, and the purchase of the Ra refinery at Port Hope by the Government of Canada, the Federal Government entered the field of radiation industrial hygiene. Immediately following the opening in 1961 of the Radiation Laboratory, arrangements were made with the Air Pollution Control section of the Industrial Hygiene Branch to obtain dust-laden air filter samples from each of the 24 stations across Ontario operated by Air Pollution Control. Thus, since July 30, 1961, (prior to the U.S.S.R. series of nuclear weapon tests beginning in September 1961) a continuous record of radioactive fallout has been kept for the 24 representative locations in Ontario. In the three years that have elapsed the facilities of this Radiation Laboratory have been made available to the public, industry, healing professions, and government agencies. (BBB)

46662 RADIONUCLIDES IN WHEAT AND OTHER AGRICULTURAL PRODUCTS—A REVIEW. Pfeifer, V. F. (Northern Regional Research Lab., Peoria, Ill.). Cereal Sci. Today, 9: 354-7(1964).

Iodine-131, ^{140}Ba, and ^{89}Sr have such short half lives that they can be ignored in the consideration of wheat and wheat products. However, ^{90}Sr and ^{137}Cs, with their long half lives, are potentially dangerous. Of these, ^{137}Cs is considered less dangerous, at least to the individual man, because it has a short life in the body (half is eliminated in a few months, owing to rapid replacement of body cells). Strontium-90 thus remains the most important radionuclide. The average ^{90}Sr content of U. S. wheat dropped between 1958 and 1961, then started to increase. The test moratorium of 1959 through the first half of 1961 is clearly reflected in the steady reduction of ^{90}Sr in wheat during this period. In the fall of 1961, Russia resumed testing, and 1962 wheat increased in ^{90}Sr content. The combined effect of 1961 and 1962 testing increased further the levels in 1963 wheat. Most of the fallout radionuclides adhere to foliage and outer seed coverings. Milling is effective in diverting much of the radioactive contamination of the wheat to the feed fractions, so that the flour is quite low in ^{90}Sr. By ordinary milling, ^{90}Sr content of flour can be reduced to 10 to 15% of that present in the starting wheat. The other 85 to 90% is in fractions now fed to animals. If fed to meat-producing animals, most of the ^{90}Sr will be retained in the animal skeleton and will not grossly contaminate the meat. Cereal products account for about 20% of the ^{90}Sr intake in the diet. In case of heavy contamination by radioactive fallout, wheat offers one of the safest sources of raw materials for food, although some mineral supplementation, with stable calcium especially, might be required. With the present ban on nuclear testing, levels of fallout radionuclides in wheat and milled products will drop to lower values. However, soil has been contaminated and will remain so substantially unchanged for years. Wind-borne dust and root absorption will thus continue to be factors for some time. Removal of ^{90}Sr in wheat at its present level of contamination is considered unnecessary and impractical. (BBB)

46663 SAFETY ASPECTS OF TRANSPORT OF RADIOACTIVE MATERIALS. Zahn, L. L. Jr; Junkins, R. L. (General Electric Co.; Richland, Wash.). Chem. Eng. Progr., 61: Symp. Ser., No. 56, 1-6(1965).

The causes and results of potential accidents involving radioactive materials are considered and safeguards, which can be effective against each abnormal condition, are discussed. Safeguards for use in transporting fissile materials, irradiated fuels, and radioisotopes are described. Equivalent risk is discussed. (M.C.G.)

46664 ECONOMICS OF IRRADIATED FUEL SHIPMENT. Salmon, Royes (Oak Ridge National Lab., Tenn.). Chem. Eng. Progr., 61: Symp. Ser., No. 56, 7-15(1965).

A computer code (MYRA) for calculation of costs for shipping spent fuel was constructed. It is written in FORTRAN and can be run on the CDC-1604A or the IBM-7090. The basis for the code is described and some of the results obtained by applying it to typical reactor fuels are shown. Effects of cask weight on costs, cask design, and source strength and heat generation rate are considered. Input data, the calculation sequence, shielding calculations, heat-removal calculations, optimal cooling time, effects of burnup and specific power, effect of allowable fuel temperature, minimum feasible cooling time, avoidance of criticality, and effects of enrichment are discussed. (M.C.G.)

46665 DESIGN OF CONTAINERS FOR SHIPMENT OF RADIOACTIVE MATERIAL INCLUDING IRRADIATED REACTOR FUEL. Peterson, Reuben W. (Knapp Mills, Inc., Wilmington, Del.). Chem. Eng. Progr., 61: Symp. Ser., No. 56, 16-29(1965).

Design requirements and special features required in containers for shipping radioactive material are reviewed. Criticality control, shielding, decay heat removal, structural integrity, fire resistance, accessory equipment, and decontamination are discussed. Characteristics of a number of different types of casks are described. (M.C.G.)

46666 PRACTICES AND PROCEDURES FOR LICENSING. Aikens, A. E. Jr. (Atomic Energy Commission, Washington, D. C.). Chem. Eng. Progr., 61: Symp. Ser. No. 56, 42-9(1965).

Transport regulations for radioactive materials are discussed. Procedures for obtaining approval of an irradiated fuel shipment are outlined. Safety assessments of failure temperature, damage due to impact, and damage due to fire are considered. Acceptable container designs are described. (M.C.G.)

46667 HEAT REMOVAL FROM CASKS. Glynn, James C. (Atomic Energy Commission, Washington, D. C.). Chem. Eng. Progr., 61: Symp. Ser., No. 56, 58-62(1965).

The heat-removal aspects in the design of fuel-element shipping casks are discussed. The amount of fission product decay heat, which will be generated within the irradiated fuel elements, must be established. A method of disposing of this heat must be decided on and a safety analysis made. (M.C.G.)

46668 INTERNATIONAL AND NATIONAL RECOMMENDATIONS, NORMS, GUIDES, ETC. FOR PROTECTION AGAINST IONIZING RADIATION. Rodriguez, Eduardo Ramos (Junta de Energia Nuclear, Madrid). Energia Nucl. (Madrid), 9: 185-99(May-June 1965). (In Spanish).

The evolution of standards in protection against ionizing radiation is briefly indicated. The major recommendations with respect to the lesions of a somatic character, lesions of a genetic character, critical organs, permitted doses, categories of exposure, reduction of the maximum permissible dose, and time interval between permitted doses are summarized. (J.S.R.)

46669 PRACTICAL APPROACH TO SHELTER FROM IONIZING RADIATION, WITH A SPECIAL REFERENCE TO STORAGE ESTABLISHMENT AND MAINTENANCE OF EMERGENCY HOSPITALS. Klinghoffer, Max (Illinois State Medical Society, Chicago). Illinois Med. J., 126: 656-8(Dec. 1964).

A novel approach to civil defense fallout shelter construction is offered. It would take advantage of the nation's highway construction program to provide shielding for the shelters. Most fallout shelters are built below ground, so that the earth serves as a shield, and only an overhead protection is needed to complete the structure. But in many areas, such as metropolitan areas and in low level locations, underground shelters are impractical because of flooding. In many cities, areas below grade become flooded after heavy rains, when storm sewers are overburdened.

in low level areas, such as Florida and Louisiana, ground water may be a problem at all times. Consideration of these problems in construction of both public and private shelters led to the suggestion of a more practical solution which could provide shelter for a moderate proportion of the surviving population and also storage areas and service areas for the emergency hospitals stored throughout the United States. Major highways and superhighways throughout the United States are located such that they are likely to be accessible to most of the surviving population after a nuclear attack. These highways offer the potential of a massive shelter structure which would be below ground, but above earth. By relatively little modification of present construction, each highway built above grade could become a shelter for personnel, material, and hospitals. Further, they could be utilized as dual-purpose structures, such as depots of supply, post offices, and various other governmental offices. A schematic diagram and models of such structures are shown. The construction of shelters for personnel and for medical facilities underneath highways could supplement existing shelter programs, and would also serve to house and to establish the 2000 civil defense emergency hospitals now stored throughout the United States. Since each of these units can be expanded in time of disaster to about 800 beds, such a shelter system, in conjunction with existing hospitals, would provide approximately one and one-half million hospital beds postattack. (BBB)

46670 THE EMANATION OF TRITIUM GAS FROM TWO ELECTRON-CAPTURE DETECTORS. Kahn, Lloyd; Goldberg, Marvin C. (U.S.G.S., Denver Federal Center). J. Gas Chromatogr., 3: 287-8(Aug. 1965).

A study of two gas chromatographic electron-capture detectors indicated that a low-level contamination of the environment by tritium occurs, which exceeds the safety limits set by the Atomic Energy Commission. The extent of the health hazard from these sources is dependent on the amount of activity and the temperature of the tritium foil used in the detector; it is inversely proportional to the size and air-exchange rate of the room. The hazard is eliminated by venting the detectors into a hood or a restricted area commensurate with the Atomic Energy Commission regulations. (auth)

46671 FACTS ON FALLOUT. Dwyer, William A. Jr. J. Med. Soc. New Jersey, 61: 182-5(May 1965).

The three radiation hazards accompanying nuclear explosions are discussed. The first type of hazard occurs only in the area of maximal blast and fire damage. Protection against these factors would prove more than sufficient protection against the associated radiation. In the event of a nuclear war, casualties within 10 to 15 miles of ground zero will closely approximate 100% of persons not sheltered against blast and fire. The second type of hazard, from early fallout, will affect an area downwind from the explosion many times larger than that damaged by blast and fire. Every person inadequately sheltered in this area will be a fatality due to an overdose of radiation. Estimates on the numbers of such casualties runs into the tens of millions, all of them needless deaths. The third type of hazard is delayed fallout. Although it may slightly increase the incidence of leukemia and sarcomas of the bone, the amount of radiation from this source is small and of no immediate consequence. It presents a hazard in the long run because of its incorporation into foodstuffs. The program to locate shelter spaces within existing structures, and to increase the possible number of such spaces in new construction by minor structural modifications, is outlined. The use of locations in different sized buildings for fallout radiation protection is discussed, as well as minor modifications in construction, such as the use of 8-in. concrete inner walls instead of 8-in. outer walls, that could be of substantial aid in reducing the radiation dose. An estimate is made of the potential yield in terms of survivors where an effective fallout shelter system is used. The number of survivors would increase by 50 million in a 5000-Mt attack and in a 10,000-Mt attack by 70,000,000. Thus, staggering numbers of needless deaths are easily preventable by application of knowledge now possessed, and at a cost of $12 per person sheltered, and an estimated $45 per life saved. (BBB)

46672 THE ADSORPTION OF IODINE ON ATMOSPHERIC PARTICLES. Megaw, W. J. (Atomic Energy Research Establishment, Harwell, Berks). J. Nucl. Energy: Pts. A and B, 19: 585-95(Aug. 1965).

Experiments are described in which ^{132}I with ^{127}I was released in the DIDO reactor shell to give an initial concentration of about 0.15 $\mu g\ m^{-3}$. The fraction of the iodine which adsorbed on particles in the shell atmosphere was studied in detail to determine whether there was any preferential adsorption of iodine on particles of a particular size. It was found that only a very small proportion of the particulate iodine was adsorbed on particles greater than 1 μ in diameter, and that in one of the experiments the iodine was adsorbed on particles which were much smaller than the general population of the Aitken nuclei in the shell atmosphere. From this and the low values found for the accommodation coefficient it was concluded that only a small proportion of the particles present was chemically suitable for iodine adsorption. Further work is required to determine whether this is generally true for the atmospheric aerosol. (auth)

46673 THE MAGNETRON—A SOURCE OF X RADIATION. Hlavaty, Vlatislav (Charles Univ., Prague); Trousil, Jaroslav. Jaderna Energie, 11: 223-4(June 1965). (In Czech).

Doses of x radiation were measured around a radar installation designed with magnetrons containing resonant cavities. The doses were measured with the aid of film-badge dosimeters, and the radiation energy to which the radar personnel are exposed was determined. It was found that the ionizing radiation is emitted from various parts of the magnetron. Monitoring of the personnel showed that the tolerance doses specified were not exceeded. With consideration for the x radiation, design modifications are recommended in the production of this type of magnetrons. (CFSTI)

46674 OCCUPATIONAL BODY BURDEN IN THE G.D.R. IN 1963. Kraus, W.; Brasack, G. (Staatliche Zentrale fuer Strahlenschutz, Berlin). Kernenergie, 8: 484-93(Aug. 1965). (In German).

The results of personnel dosimetry of Staatliche Zentrale für Strahlenschutz der DDR controlling 13,619 persons in 1963 are reported. A survey of monthly over-exposures (more than 0.4 rad) as well as of the distribution of annual exposures is given. Owing to a discussion as to the causes of high exposures, information is given on some practical problems of radiation protection. Also attempts were made to answer more detailed questions of radiation hygiene by treating statistically the results of controlling under certain points of view. Finally, the total situation of occupational exposures in the GDR is estimated. (auth)

46675 EVIDENCE FOR RADIO-RUTHENIUM IN MILK. Howard, Alma (Christie Hospital and Holt Radium Inst., Manchester, Eng.). Nature, 207: 776-7(Aug. 14, 1965).

During routine counting for the determination of ^{137}Cs levels, an unexpected gamma peak at about 0.51 Mev was observed in a number of milk samples from different locations throughout Utah. Tests showed the activity was not due to external contamination. A study was made to determine the half life of the unknown nuclide in the milk sample. The results showed the best fit to the data to be a mixture of $^{103}Ru + {}^{106}Ru$. It is expected that if one isotope of Ru were present, the other would also be present. After appropriate corrections, an estimated value of 7 pC $^{106}Ru/l$ was calculated for the sample, using a 365-day half life. The ^{103}Ru in the sample was also computed for the first count based on the calculated contribution from ^{106}Ru. This value was then corrected back to the day of collection, using the 40-day half life and gamma abundances of ^{103}Ru, and this was 34 pC $^{103}Ru/l$. The milk contained 54 pC $^{137}Cs/l$. (P.C.H.)

46676 REVIEW OF THE NEW ICRP RECOMMENDATIONS (1962). Izawa, Masami (National Inst. of Radio-

logical Sciences, Chiba, Japan). Nippon Genshiryoku Gakkaishi, 7: 418-22(Aug. 1965). (In Japanese).

The recommendations of the International Commission on Radiological Protection adopted in 1962 are reviewed. The basic principles are the same as those of the 1958 recommendations, but a number of amendments and clarifications were made. Adoption of the new recommendations to regulations of radiation protection in Japan is discussed. (auth)

46677 METHOD OF USING DETERMINATION OF ^{222}Rn IN THE EXPIRED AIR. Spodenkiewicz, Teresa; Gawronski, Andrzej. Nukleonika, 10: 165-75(1965). (In Polish).

A method of evaluating the ^{226}Ra retention in the body by determination of ^{222}Rn in the expired air is described. Ionization chambers were prepared, connected in a compensating system, with the Zeiss electrometer type EFP. Determinations were carried out in 30 persons not exposed professionally. The results obtained were used for calculating the sensitivity of the method, which amounted to 0.08×10^{-7} C ^{226}Ra in the body. Determinations were made on 154 persons working in contact with the luminous paints containing ^{226}Ra. The contaminations detected did not exceed the figures accepted as safe levels. (auth)

46678 A COUNTY HEALTH DEPARTMENT'S EXPERIENCE WITH A RADIUM MANAGEMENT PROGRAM. Chambers, J. Carroll; Manning, Justice (Jefferson County Dept. of Health, Birmingham, Ala.). Public Health Rept. (U. S.), 80: 545-50(June 1965).

A survey was made of Ra sources in use in Jefferson County, Ala. Data were obtained on the condition of the sources, storage, handling, and record keeping. The structure of the survey method used is discussed. (C.H.)

46679 ROLE OF A RADIOPHYSIOLOGICAL SERVICE IN A UNIVERSITY HOSPITAL. Lerch, P. (Universitaire de Radiophysique Appliquee, Lausanne, Switzerland). Radiol. Clin., 32: 516-24(1963). (In French).

The general duties of a radiophysiological service, including the preparation, control, and detection of radioactive substances, are reviewed. Then, their successful application in the various laboratories of the Institute of Applied Radiophysics is examined. In the radioelements laboratory, the annual no. of doses of radioisotopes rose from 724 in 1960 to 1344 in 1963. Methods for determining the specific activity of various radioelements within 15% accuracy have been improved. The radioprotection laboratory serves both the Lausanne and Vaud cantons, with facilities for developing 100 dosimeter films at one time, and proposed facilities for the automatic processing of 400 films. Clinical dosimetry provided here involves three major activities: regular surveillance of x-ray therapy installations at Lausanne and French Switzerland, and special installations such as the ^{137}Cs source at Fribourg; Ra dosimetry in obstetrics and gynecology, with special attention to the development of the after-loading method, modern means of measuring and calculation in brachytherapy, and the use of solid-state detectors for the dosimetry of x rays and electrons from the University's 35-Mev BBC betatron. The lab for low-level radiation, which runs assays for the whole country in the detection of ^{90}Sr in human bones and infants' teeth, is equipped for measuring very low ^{90}Sr levels. This lab employs devices for automatic measurement by liquid scintillation counting and semiautomatic recording for the simultaneous measurement of twelve specimens, using the Rutschmann and Kalberer method. The nuclear electronics laboratory supports the above-described services through maintenance and repair facilities. Some experimental results are described, and the training of physicists and physicians for service in Swiss hospitals is outlined. (BBB)

46680 RADIOACTIVITY OF THE COLUMBIA RIVER EFFLUENT. Gross, M. Grant; (Univ. of Washington, Seattle); Barnes, Clifford A.; Riel, Gordon K. Science, 149: 1088-90(Sept. 3, 1965).

Chromium-51 and zinc-65 were detected as far as 115 and 15 kilometers, respectively, from the mouth of the Columbia River; zinc-65 also was found at a few isolated stations. Zirconium-95 and niobium-95 from atmospheric fallout occurred in the river effluent but they were most abundant in surface waters further offshore. Distribution of the radionuclides is controlled largely by surface currents and by upwelling of sea water near the coast. (auth)

46681 NATURALLY OCCURRING FIXATION OF ^{137}Cs ON SEDIMENTS OF LACUSTRINE ORIGIN. Lomenick, T. F.; Tamura, T. (Oak Ridge National Lab., Tenn.). Soil Sci. Soc. Am. Proc., 29: 383-7(July-Aug. 1965). (ORNL-P-737).

White Oak Lake formerly served as a final settling basin for contaminated waste water discharged from the Oak Ridge National Laboratory. The site, which now serves as an ecological study preserve, covers an area of 44 acres and contains approximately 1,000,000 ft^3 of contaminated sediment. The most abundant radionuclide present in the sediment of lacustrine origin is ^{137}Cs, 704 ± 35 Curies. Concentrations of ^{137}Cs on the sediment were observed to be as high as 77×10^{-3} $\mu C/g$. More than 80% of the ^{137}Cs is associated with the clay fraction of the material, which was found to be predominantly illite. Significant quantities of ^{137}Cs were removed from the material only by treatment with strong acids. Studies of several selected clays showed illite to have a high affinity for ^{137}Cs at levels of the same order of magnitude as those observed in lake bed sediment and that desorption is only accomplished after disruption of the lattice structure. (auth)

46682 NEW CHALLENGES IN ENVIRONMENTAL HEALTH CONTROL. Gilbertson, W. E. (Public Health Service, Washington, D. C.). Trans. Coll. Physicians Philadelphia, 31: 294-8(Apr. 1964).

Problems in control of atmospheric radionuclides and other air pollutants are considered. (BBB)

46683 PRINCIPLES OF RADIATION PROTECTION ENGINEERING. Translation of Thomas Jaeger's Principles of Radiation Protection Engineering. Dresner, Lawrence. New York, McGraw-Hill Book Co., 1965. 460p. $15.00.

Technical measures designed to limit radiation exposure to a level harmless to both the health of individuals and the genetic constitution of the entire population are considered. Topics covered include: atomic physics fundamentals, radiation detection, radiobiological fundamentals, γ-ray and neutron sources, geometry of radiation sources, reactor radiation shielding measurements, calculation of γ-ray attenuation, calculation of neutron attenuation, heat production by radiation, thermal shielding of nuclear reactors, biological shielding of nuclear reactors, design of radioisotope laboratories, design of chemical separation facilities, design of technical and medical γ-irradiation facilities, shielding of particle accelerators, disposal of radioactive wastes from nuclear research and the nuclear energy industry, reactor accidents and their consequences, and containment of reactor systems. (F.J.H.)

46684 QUANTITIES AND UNITS FOR DOSIMETRY IN DIAGNOSTIC RADIOLOGY. Wyckoff, H. O. (National Bureau of Standards, Washington, D. C.). pp 5-9 of Technological Needs for Reduction of Patient Dosage from Diagnostic Radiology. Springfield, Ill., Charles C Thomas, 1963.

The radiation quantity and unit to be used in diagnostic radiology is summarized. Information is given for the beam before entering the patient, which includes, exposure dose in Roentgens, absorbed dose for soft tissue in rads, the energy in the beam in ergs, joules, or gram-rads (1 gr = 100 ergs); for the radiation at some point in or on the patient-exposure dose in Roentgens, and absorbed dose in rads for soft tissue; for radiation at the detector-exposure dose in Roentgens. (P.C.H.)

46685 RADIATION SAFETY HANDBOOK. Windscale, Eng., United Kingdom Atomic Energy Authority. 26p.

This handbook outlines the nature of radioactivity, the significance of radiation and contamination, and presents guides for radiation safety during the handling of radioactive materials. (C.H.)

46686 CODE OF PRACTICE FOR THE PROTECTION OF PERSONS AGAINST IONISING RADIATIONS ARISING FROM MEDICAL AND DENTAL USE. London, Her Majesty's Stationery Office, 1964. 125p. 12s 6d.

A code is presented for the protection against radiations used in medical and dental practice and allied research in hospitals. (C.H.)

46687 THE RESULTS OF STUDYING RADIOACTIVITY IN THE DISTRICT OF PLZEN IN 1957-1962. Matousek, J.; Mertl, F.; Patocka, S. (Inst. of Medical Physics, Plzen, Czech.). p. 421-9 of Aerosols, Physical Chemistry, and Applications: Proc. 1st Natl. Conf. Aerosols, Liblice, Oct. 8-13, 1962.

Records of atmospheric fallout collections in Plzen from 1957 to 1962 are reported. Also reported is the measurement of natural radioactive products, radon, which was two orders of magnitude higher in Czechoslovakia than that of artificial aerosols (up to the end of 1959 the level of natural radioactivity was 0.4×10^{-10} C/m^3 and the level of artificial radioactivity was 1×10^{-12} C/m^3). There was an apparent dependence of the concentration of Rn on meteorological factors; thus a higher level of Ra emanation was noted with high and decreasing air pressure, inversions of temperature, and on days without precipitation. Neither monthly nor seasonal significant variations were found, and no correlation between air temperature and Rn concentration could be detected. Yearly variation of fallout radioactivity, with a maximum in spring, was observed only in 1962. Dependence of the levels on nuclear weapon tests was observed even in the radioactivity of precipitations, and in weekly and monthly fallout samples. The dependence of long-lived artificial radioactivity of the air on the frequency and amount of precipitation was also studied. A decrease of the fallout level after rain was observed. Rates of decay of various β-emitting nuclides in fallout are also shown. (TCO)

46688 MANS' NATURAL RADIATION ENVIRONMENT. Mayneord, W. V. (Royal Cancer Hospital, London). pp 1-12 of Radioaktive Isotope in Klinik und Forschung. Band VI. Munich-Berlin, Urban and Schwarzenberg, 1965.

A short discussion of radiation dose due to radon in the atmosphere leads to a review of the present situation concerning maximum permissible level of radon in drinking waters. It has been necessary to develop a new approach in mathematical dosimetry, namely that associated with radioactive diffusing materials. The fundamental mathematical theorems concerning dose delivered by alpha, beta, and gamma radiators as they diffuse in a homogeneous medium from a point source are developed and numerical examples discussed. The use of this approach in the solution of more complex problems is discussed. (auth)

46689 THE BASIC REQUIREMENTS FOR PERSONNEL MONITORING. Safety Series No. 14. (International Atomic Energy Agency, Vienna (Austria)). 1965. 46p. (STI/PUB/95). IAEA $1.00; S 21,- (6/-stg; F.Fr. 4,-; DM 3,20).

The objectives and requirements of an adequate system of personnel monitoring in a radiation protection program are presented, and the responsibilities inherent therein are described. In addition to a classification of the monitoring methods, rules that govern their application as well as a choice of techniques and instruments are also included. Reference is also made to the management and use of exposure data, and of personnel monitoring records. (P.C.H.)

46690 PROTECTION OF THE PUBLIC IN THE EVENT OF RADIATION ACCIDENTS. Proceedings of a Seminar, Geneva, 18-22 November 1963. World Health Organization: Monograph Series. Geneva, World Health Organization, 1965. 370p. £1.17.6d, $7.25, Sw. fr. 22.--. (CONF-631105).

Separate abstracts were prepared on 18 papers. An abstract of one paper was prepared previously and appeared in NSA Vol. 19 as No. 20240. (C.H.)

For abstracts of individual papers see: 45996, 45997, 46691–46705, and 46839.

46691 PUBLIC HEALTH ASPECTS OF RADIATION EMERGENCIES: THE NATURE OF THE PROBLEM. Henningsen, E. Juel (National Health Service, Copenhagen). pp 13-23 of Protection of the Public in the Event of Radiation Accidents. Geneva, World Health Organization, 1965.

Problems in handling radiation accidents are compared with the problems in handling natural catastrophes, such as floods and earthquakes, exposure to smallpox, the use of pesticides, etc. It is pointed out that safety precautions taken in connection with the use of ionization radiation are based on criteria formulated by the International Commission on Radiation Protection that demand that all exposure should be kept as low as practicable. It is stressed that the problems involved in a radiation accident are complex and that those called on to handle the situation have probably had no previous experience. However, a knowledge of the risks and hazards will enable those making the decisions to deal with the situation. (C.H.)

46692 SOURCES OF EXPOSURE AND POSSIBLE ACCIDENTS. Adams, C. A. (Central Electricity Generating Board, London). pp 27-41 of Protection of the Public in the Event of Radiation Accidents. Geneva, World Health Organization, 1965.

Possible situations that might result in extensive radiation exposure of the population are reviewed. It is postulated that widespread exposure of the public to dangerously high levels of external radiation is unlikely but the existence of nuclear reactors and high-energy machines, the extensive use of sealed sources, and the transport of irradiated fuels present situations in which an accident might occur that would involve a small number of people. The radiological hazards of contamination, with its potential for producing internal irradiation or highly localized skin doses, and external radiation from a source with which there is no direct contact, are reviewed. (C.H.)

46693 METEOROLOGICAL ASPECTS OF THE SPREAD OF WINDBORNE CONTAMINANTS. Pasquill, F. (Meteorological Office, Bracknell, Berks, Eng.). pp 43-53 of Protection of the Public in the Event of Radiation Accidents. Geneva, World Health Organization, 1965.

The influence of meteorological conditions on the path and dispersion of radioactive materials in the event of an accidental release is considered. The concepts and procedures used in the estimation of the concentration of contamination downwind of the source are discussed. The influence of complex terrain and airflow on atmospheric diffusion and the distribution of windborne contaminants are reviewed. (C.H.)

46694 FOOD AND AGRICULTURAL ASPECTS OF RADIATION EMERGENCIES. Russell, R. Scott (Agricultural Research Council Radiobiological Lab., Letcombe Regis, Berks, Eng.). pp 55-67 of Protection of the Public in the Event of Radiation Accidents. Geneva, World Health Organization, 1965.

The effects of the release of radioactive substances into man's environment are judged in terms of the tissue doses that are imposed on the population and the significance of the contamination of any agricultural product should be assessed in terms of its contribution to the total dose that is received. The control of a radiation accident will be greatly simplified if it can be established that exposure will be primarily due to the presence of a few nuclides in a few foodstuffs. The nuclides likely to deliver the highest radiation doses through their entry into foodstuffs are ^{131}I, ^{89}Sr, ^{90}Sr, and ^{137}Cs. The general nature of food-chain transfer mechanisms is reviewed briefly. Data are presented on the acceptable limits of dietary intake of radioisotopes for peacetime emergencies and the expected contributions of dairy produce, root vegetables, leaf vegetables and fruits, flour, and other sources to the total ^{90}Sr content of a mixed diet. It is pointed out that exclusion of milk from the diet would greatly reduce the amount of radioactivity. The measurement of ^{131}I in milk would give an adequate basis for the emergency assessment of the risk to

the population. It is pointed out that milk judged unsuitable for consumption by children may be diluted by milk from clean supplies or may be used for the manufacture of dried milk, cheese, butter, and other products that are stored for an appreciable period before use. Should the level of ^{90}Sr in milk make it unsuitable for infants, it can be used in the manufacture of butter or cheese, to which little ^{90}Sr is transferred. (C.H.)

46695 ESTIMATION OF THE GENETIC RISK IN THE EVENT OF A RADIATION ACCIDENT AND SOME POSSIBLE COUNTERMEASURES. Schull, William J. (Univ. of Michigan, Ann Arbor). pp 97-105 of Protection of the Public in the Event of Radiation Accidents. Geneva, World Health Organization, 1965.

It is pointed out that most available data on the genetic effects of radiation in man was obtained on groups irradiated for some underlying disease and the data may not be valid for a normal population. Available data are reviewed on the genetic effects of radiation in man, based on studies conducted on samples ranging from a hundred individuals to tens of thousands and doses from one or two R to over 1,000 R chronic low-level or acute exposure. It is concluded that as yet there has been no unequivocal demonstration of genetic effects of radiation in man such as has been demonstrated in other animals, notably the mouse. It is assumed, however, that the principles established in animal studies hold for human beings as well. It is postulated that the genetic damage to a population will be roughly proportional to the total radiation received by members of that population between conception and reproduction. Possible countermeasures against the genetic effects of high-level radiation in the small sample of the total population that may be exposed during a radiation accident are discussed. (C.H.)

46696 SURVEY OF THE MAXIMUM PERMISSIBLE LEVELS THAT HAVE BEEN PROPOSED IN VARIOUS COUNTRIES. Mueller, J. (Charles Univ., Prague). pp 113-19 of Protection of the Public in the Event of Radiation Accidents. Geneva, World Health Organization, 1965.

Problems involved in setting up special maximum permissible emergency levels of radiation are discussed. It is generally accepted that radiation exposure to a group of the population should be kept as low as practicable and therefore permissible dose levels should be kept as low as possible. However, under conditions of radiation accidents this is not possible. The risks to the irradiated individuals and the genetic risks to the population must be considered. Preferential consideration is recommended for children, pregnant women, and adults still capable of procreation, since these are the ones through whom the genetic effects of radiation will have the most influence on the future population. It is pointed out that in most cases of radiation accidents, the genetic risks will be given secondary considerations while primary consideration will be given to the individuals irradiated. It is concluded that priority should be given to countermeasures in those exposed to those nuclides known to accumulate quickly in critical organs. These include ^{131}I, ^{89}Sr, ^{90}Sr, ^{137}Cs, and ^{226}Ra. (C.H.)

46697 ORGANIZATION OF THE EMERGENCY ENVIRONMENTAL SURVEY. Howells, H. (United Kingdom Atomic Energy Authority, Seascale, Cumb., Eng.). pp 141-56 of Protection of the Public in the Event of Radiation Accidents. Geneva, World Health Organization, 1965.

A plan is presented for handling an emergency resulting in a large-scale release of radioactivity into the area surrounding a nuclear installation. The plan is based on experience gained during the accident at the Windscale reactor in Oct. 1957. It is pointed out that future accidents will not necessarily follow the same pattern and before emergency planning can commence the nature and probable effects of the accident for which emergency planning is required must be defined. The important features of any scheme for emergency planning are outlined. Emphasis is placed on the initial emergency environmental survey. (C.H.)

46698 PUBLIC HEALTH AND MEDICAL MEASURES: THEIR PRACTICABILITY AND ASSOCIATED PROBLEMS. Pochin, E. E. (University Coll. Hospital, London). pp 173-82 of Protection of the Public in the Event of Radiation Accidents. Geneva, World Health Organization, 1965.

Public health and medical measures for the protection of the public against radiation hazards in the event of the release of accumulated fission products by a reactor accident are discussed. Emphasis is placed on the protection of persons down-wind from the point of release who may be exposed to radiation from the cloud of fission products, material deposited from the cloud, or radioactive materials taken into the body by inhalation or ingestion after the passage of the radioactive cloud. It is assumed that the radiation exposure of people from food derived from the contaminated area would be of greater importance than their exposure from inhaled material or direct exposure to external radiation. Emphasis on remedial measures is placed on ingestion of ^{131}I, ^{89}Sr, and ^{90}Sr. The justifications for various medical measures are discussed. (C.H.)

46699 SOME POTENTIAL BIOLOGICAL CONSEQUENCES OF A RELEASE OF FISSION PRODUCTS TO THE ATMOSPHERE. Stewart, C. G.; Simpson, S. D. (Atomic Energy of Canada Ltd., Chalk River, Ont.). pp 183-207 of Protection of the Public in the Event of Radiation Accidents. Geneva, World Health Organization, 1965.

products to the atmosphere by the rupture of a reactor fuel core are discussed. There are at least three kinds of hazard to which a population living in the vicinity of a reactor will be exposed in the event of a radiation accident. These include the external radiation dose and the inhalation dose received from the passing cloud, contamination of the ground by fallout from the cloud, and contamination of food produced from land contaminated by radioactive debris. The magnitude of these hazards will be proportional to the kind and amount of radioactivity released. Procedures are described for determining the proportions of fission products released by a reactor accident; the composition of the fission product cloud; the external β or γ dose from the cloud; the external radiation dose from the noble gas fission products in the cloud; the external β or γ dose from the ground due to deposition from the passing cloud; the contamination of food due to deposition of radioactive material from the passing cloud; and the radiation dose from ^{131}I, ^{137}Cs, ^{89}Sr, ^{90}Sr, or tritium oxide released to the environment. (C.H.)

46700 ANIMAL PROTECTION AND CONTROL OF FEEDSTUFFS. Olsen, E. Malling (State Veterinary Service, Copenhagen). pp 257-63 of Protection of the Public in the Event of Radiation Accidents. Geneva, World Health Organization, 1965.

The purpose of protecting domestic animals against external and internal radiation from radioactive substances released in nuclear accidents is to ensure the health and survival of the animals and to secure the human population sufficient amounts of food of a quality safe for consumption. The situations where such protection is important are limited to emergencies in which the intensity of the radiation is sufficiently high to cause radiation sickness in unprotected animals. Doses of lower intensity that are likely to have only long-term effects, such as induction of leukemia or tumors, reduction in life span, changes in fertility, or genetic effects, are of much less importance in domestic animals than in man. The general rules for the protection of domestic animals against ionizing radiation are the same as those for man. Protection against external radiation is provided by shielding, and all domestic animals should be brought into shelter before the arrival of the radioactive cloud, if possible. Protection is most effective during the first 24 to 48 hours from the start of fallout. Decontamination of animals by washing is useful only if done soon after surface contamination of the animal. The radiosensitivity of different species of domestic animals varies from about 650 R for cattle to 1200 R for poultry in a 24-hr period. The protection of animals against

internal radiation must be effected by reducing the intake of contaminated food and measures must be taken to protect the feed against radioactive contamination. Feed harvested but still in the open field, should be covered with dust-tight material. Grain and silage stored in silos are sufficiently protected, as is food in sheds or barns. Once exposed dairy cows are brought into the stall and given uncontaminated feed, they will soon produce milk free of ^{131}I contamination. After the decay of ^{131}I, the major source of contamination is likely to be ^{89}Sr or ^{90}Sr and this can be reduced by adding Ca to the feed. Domestic animals that have been exposed to external radiation may be slaughtered before symptoms of radiation sickness appear and the meat used for human consumption. Normal temperature of the animal should be used as a criterion. (C.H.)

46701 RECLAMATION OF AGRICULTURAL LAND FOLLOWING ACCIDENTAL RADIOACTIVE CONTAMINATION. Reitemeier, R. F. (Atomic Energy Commission, Washington, D. C.); James, P. E.; Menzel, R. G. pp 265-74 of Protection of the Public in the Event of Radiation Accidents. Geneva, World Health Organization, 1965.

Agricultural land may become contaminated with radionuclides owing to the deposition of radioactive debris from the atmosphere, the rupture of vehicles containing radioactive materials, or the contamination of ground water by seepage of radioactive wastes from nuclear installations. The source of contaminants will determine the mechanism of initial contamination of the vegetation. The purpose of land reclamation is to reduce significantly the amounts of radionuclides introduced into the food chains of man by food crops. Treatment of soil or crops for this purpose should be restricted to those situations in which there is a need to lower the concentration of longer-lived nuclides such as ^{137}Cs, ^{89}Sr, and ^{90}Sr. No single decontamination measure is suitable for all situations. Measures may include removal of crops and crop residues, removal of surface soil, deep placement of contaminated soil, the application of fertilizers and soil amendments, and changes in crops and farming systems. The feasibility of the decontamination method used should be based on agricultural, environmental, and economic factors. (C.H.)

46702 PLANNING FOR THE CONTROL OF RADIATION ACCIDENTS. Chadwick, Donald R.; Pecsok, Donald A.; Nelson, Donald J. Jr. (Public Health Service, Washington, D. C.). pp 283-93 of Protection of the Public in the Event of Radiation Accidents. Geneva, World Health Organization, 1965.

The prime objective in planning for radiation accidents is to prevent them. A secondary objective is to provide for an effective orderly action in the event of an accident. Responsibility for the planning and prompt handling of accidents should be clearly delineated. Radiation source users should play a major role in accident planning and health agencies should make certain that adequate plans are made and should assist the radiation users in this objective. (C.H.)

46703 AN EXAMPLE OF PLANNING FOR AN ACCIDENT IN A NUCLEAR POWER STATION. Holbrook, P. H. G. (Trawsfynydd Nuclear Power Station, Merionethshire, Wales). pp 295-310 of Protection of the Public in the Event of Radiation Accidents. Geneva, World Health Organization, 1965.

A plan is presented for handling a radiation accident at a civil nuclear power station using natural U clad in Mg alloy in a graphite-moderated gas-cooled reactor. The actions to be taken by the staff, health physics activities, off-site activities, and collaboration with outside authorities are discussed. (C.H.)

46704 THE ORSEC PLAN FOR RADIATION PROTECTION. Pellerin, P. (Institut National de la Sante et de la Recherce Medicale (INSERM), Le Vesinet, Seine-et-Oise, France). pp 311-18 of Protection of the Public in the Event of Radiation Accidents. Geneva, World Health Organization, 1965.

The National Civil Defense Service of France is responsible for the organization of rescue work at the department level in the case of all possible types of serious accident, including extensive fires, forest fires, train, air, and shipping disasters, floods and other natural disasters, consequences of a state of war to the civilian population, and radiation accidents. In addition to the fire and rescue services of the department, a list of persons with specialized knowledge is maintained and provisions are made for the rapid mobilization of personnel and equipment. Adaptation of the organization to a plan for protection in the event of a radiation accident is discussed. (C.H.)

46705 PLANNING AN ORGANIZATION FOR RADIATION EMERGENCIES, WITH SPECIAL REFERENCE TO SWEDEN. Sievert, R. M. (Inst. of Radiophysics, Stockholm). pp 319-49 of Protection of the Public in the Event of Radiation Accidents. Geneva, World Health Organization, 1965.

The plan for radiation protection in Sweden is reviewed. The emergency plan provides for protection in the case of minor radiation accidents, radiation accidents that may result in exposure of a small number of people, and situations where exposure of a major part of the population may be expected. (C.H.)

46706 RADAR HAZARDS CONTROL ON THE AIR FORCE EASTERN TEST RANGE. Thompson, R. L. (Pan American World Airways, Patrick AFB, Fla.). 22p. (CONF-650540-4). Gmelin, AED-CONF-65-116-3.

From American Industrial Hygiene Association Meeting, Houston, Tex.

Over 50 radar and communications systems are operated on the Air Force Eastern Test Range at frequencies between 400 and 10,000 megacycles per second. Peak power on these systems range from 15 megawatts with the highest effective radiated power being 1330 megawatts. All of these systems are capable of producing biologically hazardous levels of radiation. The harmful effects resulting from excessive exposure to RF radiation are generally attributed to an increase in overall body temperature or to a temperature rise in certain sensitive organs of the body, such as testicles and especially the eyes. The transparent lens of the eye appears to be easily damaged by RF radiated energy, which causes the development of cataracts or opacities of the eye lens. In 1957, the USAF published a directive establishing 10 mw/cm^2 as the maximum safe exposure level (MSEL). The 10 mw/cm^2 MSEL was later adopted by a majority of microwave energy users. Unfortunately research data were not available to consider time in reference to microwave exposure. Therefore, for those groups charged with establishing health criteria the MSEL became the maximum power density for either continuous or intermittent exposure. Recently, new and differing criteria were proposed by USAF/Army, Navy, and ASA. They all agree that time of exposure to various power densities is to be taken into consideration when establishing safety procedures in the vicinity of microwave producing devices. From the information obtained, it appears that this change is based on a reevaluation of prior research results and not on new research data. Differing criteria proposed by these three groups concern time of exposure vs. power densities. All three groups are of the opinion that personnel may be exposed continuously when the power density is 10 mw/cm^2 or less. However, a difference of opinion exists as to the maximum power density above which personnel should not be exposed and the exposure time per unit time for a given power density. (C.H.)

46707 SAFETY ASPECTS OF GROUND TESTING FOR LARGE NUCLEAR ROCKETS. Goldman, Morton I. (Nuclear Utility Services, Inc., Washington, D. C.). 13p. (CONF-650540-3). Gmelin, AED-CONF-65-116-1.

From American Industrial Hygiene Association Meeting, Houston, Tex.

Present nuclear rocket reactors under test in Nevada are operated at nominal power levels of 1000 Mw. It does not seem unreasonable in the future to anticipate reactors with power levels in the range up to 5,000 Mw for space applications. It has been shown that the normal testing of large nuclear rocket engines at NRDS could impose some

restrictions on the fuel performance which would not otherwise be required by space flight operation. The only apparent alternative would require a capability for decontaminating effluent gases prior to release to the atmosphere. In addition to the source restrictions, tests will almost certainly be controlled by wind and atmospheric stability conditions, and the requirements for monitoring and control of off-site exposures will be much more stringent than those presently in force. An analysis of maximum accidents indicates that projections of present credible occurrences cannot be tolerated in larger engine tests. The apparent alternatives to a significant (order of magnitude or better) reduction in credible accident consequences, are the establishment of an underground test facility, a facility in an area equivalent to the Pacific weapons proving ground, or in space. (auth)

INSTRUMENTATION

General

Refer also to abstracts 45891, 46148, 46150, 46151, 46988, 47219, 47717, 47928, and 48059.

46708 (AD-611560) HIGH POWER CYCLOTRON RESONANCE SWITCH. Summary Report, June 15, 1962–February 1, 1963. (Bomac Div., Varian Associates, Beverly, Mass.). May 13, 1963. Contract AF19(604)-7400. 33p. CFSTI $2.00 cy, $0.50 mn.

For Lincoln Lab., Massachusetts Inst. of Tech., Lexington.

Two fundamental prerequisites of a high power cyclotron resonance switch were demonstrated experimentally. Namely, the ability of the switch to hold off the required r-f electric fields and a great reduction of the breakdown voltage upon application of the magnetic field appropriate to cyclotron resonance. The results demonstrated experimentally that the applied magnetic field raises the holdoff power of the tubes, and that the tube holdoff power depends on the tube geometry. The fact that the barrel tube held off the required high power is not considered complete proof that the goal was attained since there is the possibility that current arcing might have detuned the cavity. (TAB)

46709 (AD-614118) PRODUCTION ENGINEERING MEASURE FOR CESIUM BEAM TUBES. Quarterly Progress Report No. 6, August 23–November 23, 1964. George, James (National Co., Inc., Melrose, Mass.). Contract DA36 039AMC01457. 49p. CFSTI $2.00 cy, $0.50 mn.

The life test of the retrofitted PEM-E3 cesium beam tube was continued with satisfactory results. Design and parts fabrication for the original PEM-E5 and PEM-E6 cesium beam tubes were completed. These tubes (PEM-E5 and PEM-E6) were assembled, processed, aligned, tested, and subjected to corrective redesign and retrofitting. The retrofitted PEM-E5 and PEM-E6 tubes were then assembled, processed, aligned, and tested. Only two problem areas remained unresolved in the retrofitted PEM-E5 and PEM-E6 tubes: low signal output and r-f power mismatch. Two completely new beam tubes (incorporating the improved design characteristics of the retrofitted PEM-E5 and PEM-E6 tubes) will be built to resolve these problems. During this reporting period, charts showing the fabrication, assembly, processing, alignment, and testing sequences for the PEM-E5 and PEM-E6 tubes were prepared. (auth)

46710 (BNWL-59) AN INSTRUMENT FOR MEASURING BOWING IN LONG TUBES. Brenden, B. B.; Spanner, J. C. (Battelle-Northwest, Richland, Wash. Pacific Northwest Lab.). Aug. 1965. Contract AT (45-1)-1830. 37p. Dep. mn; CFSTI $2.00 cy, $0.50 mn.

A device, called a Tramek, is described. It is capable of measuring bowing in long tubes that are bent excessively and are otherwise inaccessible for line-of-sight measurement. Tramek has been used to measure the degree of bowing of reactor process tubes. It employs a linear variable differential transformer to measure the radius of curvature of the tube centerline. Measurements at regular intervals along the tube length provide data for calculating bowing distortion. Design parameters affecting the accuracy of computed bowing distortions and the bowing distortions themselves are computed from Tramek data using FORTRAN II computer programs. Data are discussed and examples of typical performance are given. (auth)

46711 (BNWL-SA-161) A ROLL FILM CAMERA FOR REMOTE METALLOGRAPHY. Meyers, D. J.; Gruber, A. J.; Roach, R. J. (Battelle-Northwest, Richland, Wash. Pacific Northwest Lab.). 1965. Contract AT(45-1)-1830. 3p. (CONF-651101-14). Dep. mn; CFSTI $1.00 cy, $0.50 mn.

For Presentation at 13th Conference on Remote Systems Technology, Washington, D. C.

A motor-driven roll film camera was adapted for use with remote metallographs. The camera system includes reflex photographic attachments, roll film magazines, a motorized film advance drive, an electronic interval timer, and an electric shutter. A description is given of the camera and its operation. (D.L.C.)

46712 (BNWL-SA-169) A HIGH TEMPERATURE TENSILE TESTING MACHINE FOR IRRADIATED STRUCTURAL MATERIALS. Teats, R.; Watts, E. C. (Battelle-Northwest, Richland, Wash. Pacific Northwest Lab.). July 1965. Contract AT(45-1)-1830. 9p. (CONF-651101-31). Dep. mn; CFSTI $1.00 cy, $0.50 mn.

From 13th Conference on Remote Systems Technology, Washington, D. C.

A tensile testing system was put into service that is capable of testing irradiated metals at temperatures up to 3000°F. The testing machine, enclosed in a cast iron shielded cell, is equipped with a water-cooled high-vacuum furnace using tantalum strip heating elements. Grips were designed that have successfully held both flat and button head specimens and yet are simple enough to be assembled remotely using a single manipulator. Stress-strain data from a remote extensometer and a load cell are recorded on an XY recorder. (auth)

46713 (CEA-R-2811) DETECTEUR D'ENTRAINEMENT DE LIQUIDE DANS UN GAZ. (Detector for the Liquid Carried Over in a Gas). Delisle, Jean-Paul; Eperonnat, Paul; Lions, Noeel (Commissariat a l'Energie Atomique, Cadarache (France). Centre d'Etudes Nucleaires). July 1965. 23p. Dep. mn.

An optical detector for the detection of a liquid carried over by a gas is described. The device is sensitive to a cumulated quantity of liquid equal to a few cubic millimeters and is capable of operating an alarm from a distance. The prototype was constructed and tested on the oil in the argon compressed by a diaphragm compressor. (auth)

46714 (CONF-640918-1) EFFECT OF COLLIMATOR-SHAPE ON DEPTH DOSE CURVES. Dahler, A. (Norsk Radiumhospital, Oslo; Montefiore Hospital, New York). [nd]. Contract AT(30-1)-2607. 8p. Dep. mn; CFSTI $1.00 cy, $0.50 mn.

From Symposium of High Energy Electrons, Montreux, Switzerland.

A comparison was made of isodose and depth-dose curves for 15-, 25-, and 33-Mev electrons when Cr-plated brass or perspex applicators were used as part of the collimating system. Results indicated that the brass applicators gave a more ideal isodose curve at depths. Design improvements are suggested to increase the performance of collimators used in radiotherapy. (C.H.)

46715 (EUR-2473.f) L'EMPLOI DES JAUGES DE DEFORMATION A HAUTE TEMPERATURE. 1ERE PARTIE. LES CIMENTS. (Application of Strain Gages at High Temperature. Part I. Cements). Legrand, B.; Toux, J.; Bonnet, P.; Grin, M. (European Atomic Energy Community, Ispra (Italy). Joint Nuclear Research Center). Aug. 1965. 30p. Dep. mn.

Some commercial cements were tested under mechanical and thermal stresses. The value of resistance to isolation of the cements in dependence on temperature was plotted. At temperatures higher than 500°C, practically no cement has a resistance to ground sufficient for precise measurements in connection with strain gages. (auth)

46716 (IDO-17081, pp 77-123) INSTRUMENT DEVELOPMENT. (Phillips Petroleum Co. Idaho Falls, Idaho, Atomic Energy Div.).

Descriptions are presented of eddy current proximity detectors and associated circuitry; special purpose nuclear

pulse amplifiers with field-effect transistor (FET) input stages; electrochemical fast data loggers, which interrogate chemical cells and provide digital readouts; automatic ultrasonic flaw detectors which are designed to test curved ATR fuel plates; special input and output stages, designed for operational amplifiers employed in conjunction with electroanalytical potentiostats; and circuit modifications to constant air monitors. The transient behavior of the Power Burst Facility (PBF) was studied on the analog computer in order to estimate the rod motion required for shaping the power burst under various operating conditions. Adiabatic and nonadiabatic thermal models of the reactor core were investigated. Reactor shutdown transients by means of the scram rods were also investigated. Analog studies of the effects of a rupture in the ETR vessel as well as the effects of a power failure in the ETR primary coolant pumps were performed. (auth)

46717 (INSJ–67) A VERY FAST SCALE OF FOUR. Diego, M. (Institute for Nuclear Study, Tokyo Univ. (Japan)). Aug. 8, 1965. 16p. Dep. mn.

The very short switching times of the Esaki (tunnel) diodes make them ideal elements for logic and computer applications. Some scalars were previously developed using as a basic unit the coupled pair circuit, and one of the causes that limit the maximum frequency response of the circuit is the heavy load imposed by the following unit on the preceding one. The problem of isolation between units was solved by the use of a transistor as a coupling element. The analysis is presented. (M.O.W.)

46718 (LA-DC–7015) CAPACITOR BANK CHARGING SYSTEM. Sprague, T. M. (Los Alamos Scientific Lab., Univ. of California, N. Mex.). [nd]. Contract W-7405-eng-36. 16p. (CONF-650512–9). Dep. mn; CFSTI $1.00 cy, $0.50 mn.

From Symposium on Engineering Problems of Controlled Thermonuclear Research, Livermore, Calif.

A brief discussion of problems concerning the charging of capacitor banks is presented. A control system was designed for charging the capacitors. The theory of operation of the control system is discussed. Results from the application of the control system are given. (M.O.W.)

46719 (LA-DC–7030) PROBLEMS ASSOCIATED WITH PULSE CHARGED CAPACITOR BANKS. Schofield, A. E. (Los Alamos Scientific Lab., Univ. of California, N. Mex.). [nd]. Contract W-7405-eng-36. 10p. (CONF-650512–10). Dep. mn; CFSTI $1.00 cy, $0.50 mn.

From Symposium on Engineering Problems of Controlled Thermonuclear Research, Livermore, Calif.

Two areas of pulse charging of capacitors are discussed. The areas include capacitor banks which are designed to be charged in a time which is too short to be convenient using a conventional d-c power supply directly, and capacitors which are charged, due to failures in the circuit, to voltages which may be considerably higher than the system is designed to handle. (M.O.W.)

46720 (NYO-3406-2) DISTRIBUTION OF SINGLE ELECTRON PULSE SIZES FROM MULTIDYNODE ELECTRON MULTIPLIERS. Technical Report No. 2. Reynolds, Geo. T.; Hutchinson, D. P.; Botos, P. Jr. (Princeton Univ., N. J. Elementary Particles Lab.). Aug. 16, 1965. Contract AT(30-1)-3406. 31p. Dep. mn; CFSTI $2.00 cy, $0.50 mn.

The spectrum of light pulse sizes at the anode of a transmission secondary electron multiplier image tube was determined at room temperature and dry ice temperature, for noise, or dark current pulses, as well as for single photoelectrons leaving the cathode. The noise distribution shows two main groups of pulses. The first group obeys a nearly exponential distribution, with a small contribution from the first dynode. The second group consists of a broad distribution of larger pulses, and may be due to ion bombardment of the cathode. The nearly exponential group is reduced by a factor of 4 by cooling, but the second group is not significantly affected. The size distribution of anode pulses from single photoelectrons is monotonically decreasing but deviates significantly from an exponential. The gain of the tube as determined from the pulse height distribution agrees well with that determined by a direct method, and is consistent with a loss of between 10 and 50% of the photoelectrons in the first dynode. (auth)

46721 (ORNL-P–1531) ANALYTICAL LABORATORY HOT-CELL EQUIPMENT. III. A REMOTELY OPERATED FILTER PHOTOMETER. Maddox, W. L. (Oak Ridge National Lab., Tenn.). [1964]. Contract W-7405-eng-26. 7p. (CONF–651101-11). Dep. mn; CFSTI $1.00 cy, $0.50 mn.

For Presentation at 13th Conference on Remote Systems Technology, Washington, D. C.

The photometer consists of a Densichron-1 photometric unit and a remote sensing unit which includes the light source, cuvette compartment, cuvettes and carrier, several interference filters and their holders, and a Densichron phototube probe. Brief descriptions are given of the light source, absorption cell compartment, carrier, and filter holders. (D.L.C.)

46722 (PWAC–462) HIGH TEMPERATURE THERMOMETRY AT PRATT AND WHITNEY AIRCRAFT–CANEL. Bliss, P.; Fanciullo, S. (Pratt and Whitney Aircraft, Middletown, Conn. Connecticut Advanced Nuclear Engineering Lab.). June 2, 1965. Contract AT(30-1)-2789. 45p. Dep. mn; CFSTI $2.00 cy, $0.50 mn.

A description is given of the development of refractory metal-sheathed thermocouples for the in-pile measurement of 2200°F for 10,000 hours at a flux of 10^{13} nvt thermal. Chromel/Alumel thermocouples were developed for this application in liquid metals. The fabrication procedures and equipment are described. Materials compatibility and service experience are discussed, and the problem of transmutation of the thermoelements (W, Re, Mo, and Nb) is considered. Specifications for Nb–1 Zr tubing, W–Re/W–Re wires, various thermocouples, Chromel/Alumel thermocouples, and alumina insulation are included. (D.L.C.)

46723 (RFP-641) STRAIN GAGE APPLICATIONS USING THE ROKIDE PROCESS. Anderson, L. J. (Rocky Flats Div., Dow Chemical Co., Golden, Colo.). Aug. 20, 1965. Contract AT(29-1)-1106. 9p. (CONF-650926–1). Dep. mn; CFSTI $1.00 cy, $0.50 mn.

From 9th Meeting of the IMOG Subgroup on Environmental Testing, Amarillo, Tex.

The Rokide process was developed for attaching strain gages to certain materials under unusual conditions such as high temperature. The advantages and disadvantages of the flame-spraying process are outlined, and the equipment and stages in attaching a strain gage are described. (D.L.C.)

46724 (SC-TM–65-356) HEIGHT-INTERVAL TIMER. Murphy, C. G. (Sandia Corp., Albuquerque, N. Mex.). Aug. 1965. Contract AT(29-1)-789. 10p. Dep. mn; CFSTI $1.00 cy, $0.50 mn.

A circuit which gives a measurement of the time a pulse is above a preset magnitude was developed. Called a height-interval timer, it offers a resolution of ±100 ηseconds, discriminates at levels less than 0.10 volts (with upper limits greater than 10 volts for the circuit tested), and has negligible hysteresis. The output of the circuit is a series of 10 megacycle pulses which, when counted, indicate the desired time. (auth)

46725 (TID–22141, pp 101-10) MASS SPECTROMETER PROGRAM. White, F.; Forman, L. (Rensselaer Polytechnic Inst., Troy, N. Y.).

A multi-stage mass spectrometer was designed and constructed in which two magnets and two electrostatic lenses are used to form two complete double-focusing spectrometers in series. (D.C.W.)

46726 (UCRL–11218(Pt.II)) DESIGN, CONSTRUCTION, AND OPERATION OF A DIFFERENTIAL MICROMANOMETER. PART II. THEORY AND OPERATIONAL CHARACTERISTICS. Rony, Peter R. (Lawrence Radiation Lab., Univ. of California, Berkeley). Apr. 8, 1965. Contract W-7405-eng-48. 119p. Dep. mn; CFSTI $4.00 cy, $0.75 mn.

A differential micromanometer capable of measuring 100 μtorr to an accuracy of ±2% was designed, constructed, and tested. The micromanometer is being used as a Wrede-Harteck gauge, a device that converts an atom concentration into a pressure differential in a low-pressure gaseous system. The pressure difference is sensed by a membrane manometer constructed as a differential capacitor that forms two legs of a resonant-bridge network excited by a radio-frequency source. The bridge output (2.762 Mc/sec) is amplified and fed to a phase-sensitive detector that determines the direction of unbalance and develops a d-c voltage that can be used (a) in a feedback-loop system to restore the diaphragm to its null position, or (b) in an open-loop system and recorded directly. The most favorable system found to date consists of a Decker Corporation Model 306-2A pressure transducer operated open loop with the bridge and electronics. Differential pressures as low as 50 μtorr can be measured with a zero drift of about 30 μtorr or less per hour (approximately 1 μtorr per min) in a room regulated to within ±0.5°C. Differential pressures of 0.5 μtorr are detectable. An attenuator in the amplifier section extends the 306-2A system to differential pressures as large as 35 μtorr. The micromanometer is calibrated electrostatically. The diaphragm constant K in the formula $\Delta P = KV^2$ is determined to ±2% by comparison of the readings produced by a known pressure differential, measured with an accurate McLeod gage, and a voltage of known magnitude applied to one side of the differential capacitor. Once the gage constant is known, the system can be calibrated daily by application of a series of known voltages and a plot of the recorder reading vs the square of the voltages. In the pressure region of 0.1 to 35 μtorr, the system is an excellent secondary pressure standard. The characteristics of the differential micromanometer are compared to those of ten other differential micromanometer systems. (D.L.C.)

46727 (UCRL-16197) ON THE FORMATION OF DONOR-LIKE COMPLEXES IN DIFFUSED SILICON DEVICES. Deshpande, R. Y. (Lawrence Radiation Lab., Univ. of California, Berkeley). June 15, 1965. Contract W-7405-eng-48. 55p. Dep. mn; CFSTI $3.00 cy, $0.50 mn.

An extensive study was made on the electrical characteristics of diffused silicon devices. The effect of the various preparation and treatment conditions on the properties of the devices is discussed at length. A general survey of the work in the field is followed by a description of the effect of various heat and ambient treatments on the properties of silicon–silicon dioxide. The conductivity of the interface was measured as a function of temperature, and from the results the activation energies of the various impurity levels introduced by these treatments were determined. Some of the electrical parameters of the interface were also calculated. A model is proposed, based on the formation of donor-like complexes at the $Si-SiO_2$ interface. A possibility of the bulk properties influencing the electrical characteristics of the interface is also suggested. The point is further investigated by means of the method of double injection in long diffused p^+pn^+ silicon diodes. The formation of donors both in the bulk and at the interface is then tied up. It is also suggested that some of the bulk effects are transferred onto the interface. The characteristics of some diffused silicon devices are finally discussed in the light of these observations. (auth)

46728 (UCRL-16336) HEAT TRANSFER CONSIDERATIONS IN DIFFERENTIAL CALORIMETER DESIGN (thesis). Nicholson, Patrick Stephen (Lawrence Radiation Lab., Univ. of California, Berkeley). Aug. 31, 1965. Contract W-7405-eng-48. 72p. Dep. mn; CFSTI $1.00 cy, $0.50 mn.

Following early work on the development of a differential thermal calorimeter, an attempt was made to eliminate the sources of error inherent in these designs. Previous designs are discussed and criticized in detail, and a set of conditions postulated necessary for accurate work. Following these conditions, a series of modifications of apparatus design are reported. Heat transfer conditions in each system were investigated and are discussed. From these results, an ideal design is proposed which is based primarily on heat flow through packed powders. (auth)

46729 (LA-tr-65-21) THE PRODUCTION OF X-RAY PHOTOGRAPHS WITH VERY SHORT EXPOSURE TIMES. Tsukerman, V. A.; Avdeyenko, A. I. Translated for Los Alamos Scientific Lab., N. Mex. from Zh. Tekhn. Fiz., 12: 185-96(1942). 15p. Dep. mn; CFSTI $1.00 cy, $0.50 mn; JCL $1.60 fs, $0.80 mf.

Existing methods of producing x-ray photographs with exposure times of 10^{-5} to 10^{-6} sec are reviewed, and some of the advantages of employing an electronic x-ray tube for this purpose are set forth. It is shown that microsecond photographs of simple objects can be produced with standard x-ray apparatus, using an ordinary kenotron as the pulse x-ray tube. It is shown that the size of the focus spot is reduced at a high anode current through the kenotron. The results of experiments with a special electronic pulse tube and a 2.89 μF capacitor are given. X-ray photographs of several high-speed objects and simple details, taken with a standard x-ray apparatus at exposures of 2 to 15 microseconds, are reproduced. (auth)

46730 (SC-T-65-760) RADIOACTIVE COLLECTION FOR ATMOSPHERIC ELECTRICITY SOUNDINGS. Roenicke, G. Translated by Marcel I. Weinreich (Sandia Corp., Albuquerque, N. Mex.) from Z. Geophysik, 30: 43-4(1964). 4p. Dep. mn; JCL $1.10 fs, $0.80 mf.

Limitations for field measurement with radioactive collectors are discussed. Special attention is given to the ionic hose issuing from the radioactive collector. Conditions determined for this type collector are: balloon, collector, and the perpendicular ion streamer, produced by the balloon's ascent, move all with the wind, and only shearing forces of the wind are able to tear the ionic hose apart. (P.C.H.)

46731 (SLAC-Trans-21) A NEW METHOD FOR THE DETERMINATION OF MAGNETIC-FIELD DISTRIBUTIONS. Dolega, U.; Pfeifer, H.; Loesche, A. Translated by T. Watt (Stanford Linear Accelerator Center, Stanford Univ., Calif.) from Z. Angew. Phys., 7: 12-13(1955). 5p. Dep. mn; JCL $1.10 fs, $0.80 mf.

A brief discussion reviews the nuclear resonance effect for the measurement of a strong magnetic field. The principle of the new method consists of replacing the single coil previously used by two coils in series, each of which contains an identical sample. One of these coils remains in a fixed position in the magnetic field, while the other is moved around in the field spaces. The use of the double coil permits the direct measurement of the field differences, the results being affected only by the relative time variations of the frequency and magnetic field. (M.O.W.)

46732 ACTA IMEKO, 1964. Proceedings of the 3rd International Measurement Conference [Stockholm, Sept. 1964]. Volumes I, II, and III. Budapest, Hungarian Scientific Society for Measurement and Automation, 1964. 1503p. (CONF-640902).

One hundred and five articles are included; separate abstracts were prepared for 4. 7 articles were previously abstracted in NSA as 19: 4459, 9245, 9246, 9559, 11601, 15850, and 15877. The remaining 94 articles include information on: Vol. I–fundamental problems of metrology; theory and practice of instrument design; technology and organization in instrument manufacture; general electronics as applied to measurements and instruments; border questions of measurement and automation; Vol. II–instruments and methods for measuring geometrical and mechanical quantities, including geodetic measurements; instruments and methods for measuring thermal quantities; Vol. III–instruments and methods for physicochemical measurements; measuring electrical and magnetic quantities; measurements in radio engineering; and radiation measurements. (P.C.H.)

For abstracts of individual papers see: 46733, 46734, 46771, and 46772.

46733 MEASUREMENT AND CALIBRATION TECHNIQUES FOR VERY LOW GAS DENSITIES. Simons, J. C. Jr. Acta IMEKO, 2: 291-303(1964).

Methods for measuring low gas densities were examined to determine their lower limits of detectability and the phenomena responsible for these limits. The hot-cathode suppressor grid gage and the hot-cathode magnetron gage appear at present to be best capable of measuring very low densities. On the other hand, it is likely that outgassing both from the hot-cathode and the complicated gage structure will interfere with measurements at low levels. The cold-cathode gage, while handicapped by non-linear behavior at low levels that is not yet completely understood, is simple and does not appear to enter into the complicated reactions with the gases that a hot filament does. Still in the development phase, it is likely in the long run to be able to measure lower gas densities with greater accuracy and confidence than can the hot-cathode gages. (auth)

46734 THE METHOD AND INSTRUMENT FOR MEASURING TEMPERATURES OF FLAMES, GAS FLOWS AND PLASMAS. Kandyba, V. V. Acta IMEKO, 2: 359-67 (1964).

Principles of the method of flame and gas flow temperature measurements developed in the USSR and applied to the problem of temperature measurements in plasma are reported. Plasma and flame are treated as equilibrium systems the radiation of which is of thermal nature. As an example the low-temperature plasma is considered (flames with the species having low ionization potential) which is of some interest. The device realizing the above mentioned method—a modulation pyrometer MP-59m—is described. The method is based on the temperature measurement of the central part intensity of the spectral line profile. Under certain conditions the intensity attains that of a blackbody and thus presents a measure of the radiator temperature. Decomposition of the radiation into a spectrum and isolation of the central part of the spectral line profile can be performed using the corresponding spectral apparatus with high dispersion and resolving power, for example a diffraction spectrometer. This is realized in MP-59m with the help of a modulation interferometer—a Fabry-Perot etalon. The interferometer has two mirrors: a fixed and a moving one which uses the linear displacement of a piezo-electric ceramic element (barium titanate). In this way the spectral line scanning is obtained. The apparatus may be adjusted at different lines of visual spectrum. The photoelectron system of the device permits the spectral line profile to be recorded on an oscilloscope or a potentiograph direct measurement of the profile ordinate to be performed as a function of temperature using a pointer instrument. The speed of operation of MP-59m is about 0.001 sec., the instrumental error is about 1.5%, and the measured temperature range 2000–6000°C. (auth)

46735 STABILIZED FLASH X-RAY DISCHARGES. Haendel, S. K.; Bergfeldt, J. Arkiv Fysik, 30: 33-44 (1965).

By application of an external axial magnetic field across the electrodes of a flash x-ray tube, it was found that: (i) the hardest x radiation disappears, (ii) the peak current in the discharge tube increases about 20% for $B_{z\max}$, (iii) the discharge time decreases with increasing B_z inside the B_z-interval studied (0–350 gauss), and (iv) the flash x-ray discharge seems to be stabilized. The disappearance of the hardest x radiation is in accordance with the theory for flash x-ray discharges previously reported. (auth)

46736 TIME-AMPLITUDE CONVERTER WORKING WITH TUNNEL DIODES. Scharbert, Tibor. At. Kozlemen., 7: 109-17(June 1965). (In Hungarian).

The resolving time of the time-amplitude converter is 2×10^{-9} sec when used with RCA 6810-A electron multipliers. The apparatus built on the basis of the fast-slow principle works with a tunnel diode fast coincidence circuit. The verification of the time-axis and the examination of linearity was made with the aid of cables of various length, while the calibration of the cables took place on the basis of the velocity of annihilation radiation of the Na-22 isotope. The equipment is linear up to 12 nanoseconds. (auth)

46737 NOTES ON A PHOSPHOROSCOPE. Langouet, Loic (Laboratoire de Luminescence de Rennes, France). Bull. Soc. Sci. Bretagne, 37: 11-15(1962). (In French).

The phosphoroscope directly measures the time sequence of decrease of luminescence produced in a powdered material with a large surface that occurs when the exciting light source is extinguished. It has been used with uranyl salts. It consists of three main components. The first is the excitatory circuit. The light source is a uv lamp. One condenser consisting of two quartz lenses produces an image of the exciting source on a slit. A second quartz condenser forms an image of the slit a little forward of the sample so as to produce uniform excitation of the sample that is positioned horizontally. The second is the observation circuit. A glass condenser forms an image of the sample on a second slit. Then a lens whose focus coincides with this slit produces a beam that is parallel to the beam emitted by the sample. These beams are collected by a photomultiplier that supplies the input resistance of an oscillograph. The third circuit consists of a synchronization system. In order to detect the excitation drop a synchronized shutter system that uses a synchronous motor and a disk with slits which modulates the excitation and the luminescence is observed. It is necessary to produce an angular phase difference between the slits in order to prevent a parasitic effect so that excitation is not terminated at the beginning of the observation. The phase difference corresponds to the dead time. This amounts to 0.5 msec. This equipment has been used to study the decay of luminescence in uranyl sulfate, nitrate, and acetate. For each of these salts the decay takes place exponentially with time. The values obtained for the fluorescence of uranyl sulfate was 1.48 ± 0.07 ($\times 10^{-4}$) sec. For the nitrate and acetate the values obtained were 2.40 ± 0.07 ($\times 10^{-4}$) and 6.5 ± 0.3 ($\times 10^{-4}$) sec, respectively. (BBB)

46738 ON THE COMPONENTS OF THE IMAGE PRODUCED BY AN IONIC OPTICAL SYSTEM. Baril, Marcel; Kerwin, Larkin (Universite Laval, Quebec). Can. J. Phys., 43: 1657-70(Sept. 1965). (In French).

Several theoretical studies were made of the various components of the image formed by a magnetic prism-lens. Experimental measurements of the image formed by a 90° sector magnet are reported. The contributions to the image caused by the finite object width, spherical aberration, chromatic aberration, curvature of fringing field lines, oblique rays, detector slit, and detector response time have been verified quantitatively. When account is taken of image alignment, and focusing locus, and when space charge is absent, the measured resolving power of the system verifies theoretical predictions. (auth)

46739 SUPERCONDUCTING DIODE AS HIGH-FREQUENCY SOUND DETECTOR. Goldstein, Y.; Abeles, B.; Keller, K. R. (Radio Corp. of America, Princeton, N. J.). Electron. Letters, 1: 97(June 1965).

The properties of a broadband sound detector utilizing microwave-phonon-assisted tunnelling in superconductors are described. Using Al–Pb tunnel diodes at 1.3°K, the sensitivity of the detector to 9.3×10^9 c/s sound waves was found to be approximately 2×10^{-4} V/W cm^{-2}. At high frequencies the sensitivity is expected to increase as the square of the sound frequency. (auth)

46740 EXACT SOLUTIONS FOR THE ELECTRON DISTRIBUTION IN PLANE MAGNETRONS. Lindsay, P. A. (Raytheon Co., Burlington, Mass.). Proc. Roy. Soc. (London), Ser. A, 287: 183-200(Aug. 31, 1965).

The old problem of electron distribution in crossed electric and magnetic fields, such as exist in magnetrons, has in the past proved full of pitfalls, owing to the decisive influence which even very small initial electron velocities can have on the character of the solution. A complete analysis of the plane magnetron is presented, with a thermal emitter, i.e. with Maxwellian distribution of the initial velocities. Instead of looking for self-consistent solutions, which vary strongly with the space charge, the solution is given for three simple types of prescribed electric potentials, zero, linear and parabolic. The first two are mainly for orientation, the third is of practical interest as it is approximately self-consistent. For zero or weak electric fields the distribution is triangular, i.e. the function decreases monotonically as we move away from the cathode. For strong electric fields, the distribution has a peak away

from the cathode and strongly resembles that obtained in the so called 'double-stream' flow. Finally, for a parabolic potential distribution (linear field variation) the space charge density exhibits a pronounced plateau which is highly reminiscent of the conditions in a Brillouin or 'single-stream' flow, although the electron motion is anything but rectilinear. (auth)

46741 ON THE HIGH VACUUM DISCHARGE IGNITION MECHANISM IN CROSSED ELECTRIC AND MAGNETIC FIELDS. Reikhrudel', E. M.; Sheretov, E. P. (Moscow State Univ.). Zh. Tekhn. Fiz., 35: 1255-61(July 1965). (In Russian).

Ignition curves were calculated (magnetic field vs. anode potential) for a self-sustained discharge in a plane cold-cathode magnetron, using differential electron elastic scattering and ionization cross sections. It was assumed that an electron executes many cycloidal oscillations between collisions with the residual gas atoms and that these collisions occur at the average distance of the electron from the electrodes. The theoretical elastic scattering cross section was employed in the calculations, and a simple approximate expression was used for the differential ionization cross section, according to which the fraction of the energy transferred to the secondary electron is the square of the sine of the scattering angle. From this form of the ionization cross section it follows that the average energy of the electron is not changed by ionizing collisions as it drifts parallel to the anode, and that the avalanche that develops rotates about the cathode as a whole. This gives rise to space charge oscillations such as have been previously observed. The calculated ignition curves were compared with experimental curves obtained with a cylindrical magnetron. When the theoretical curve is normalized to the experimental data it represents them very well. The effect of outgassing the electrodes at 1600°C was investigated. Outgassing the anode had a much greater influence on the ignition curve than outgassing the cathode. It is suggested that this may be due to the fact that most of the avalanches leading to self-sustained discharge are initiated by ions from the anode rather than by electrons from the cathode. (ATD)

46742 ON SOME PROPERTIES OF AN ELECTRONIC-IONIC OSCILLATORY DISCHARGE. Korsunskii, M. I.; Gorbenko, E. N. (Polytechnic Inst., Khar'kov). Zh. Tekhn. Fiz., 35: 1265-72(July 1965). (In Russian).

In order to investigate discharges analogous to the Penning discharge in which, however, it is ions rather than electrons that oscillate through an opening in one of the electrodes, a four-electrode discharge tube was constructed and operated. The electrodes were four 20 cm diameter, 1 cm thick copper disks mounted parallel to each other on a 6 cm spacing. The edges of the electrodes extended beyond the quartz wall of the chamber and were water cooled. Electrodes 1, 2, and 3 had 2 cm diameter openings in their centers, and electrode 1 carried a hot tungsten filament. Electrodes 2 and 4 were maintained at the same high positive potential (up to 3 kv) with respect to electrode 3 and electrode 1 was kept at a moderate positive potential with respect to electrode 3. A longitudinal magnetic field up to 5×10^4 amp/m was provided. The behavior of the discharge tube for various electrode potentials and gas (air) pressures was observed and is described in considerable detail. The potentials on and the currents to all the electrodes were measured, the heat dissipated at electrode 3 was determined by measuring the temperature rise of the cooling water, and the discharge was observed visually. It was anticipated that electrodes 1, 2, and 3 would give rise to a Penning type discharge and that the ions produced by the oscillating electrons would execute analogous oscillations through the opening in electrode 3. It was found that the discharge was stable when the gas pressure exceeded 6×10^{-4} mm Hg. When electrodes 1 and 3 were maintained at the same or nearly the same potential, the discharge did not differ from that in a two-electrode tube. When the potential difference between electrodes 1 and 2 was considerably less than that between electrodes 2 and 3 and between 3 and 4, however, ion oscillations of the anticipated type occurred, even though the transverse velocities of the ions were considerable. The presence of ionic oscillations was indicated by the presence of cathode sputtering on the side of electrode 3 facing electrode 4. The discharge was stable and the electron and ion oscillations could be independently regulated. In a preliminary discharge chamber with metal walls, currents up to 1 amp were attained at gas pressures from 10^{-4} to 10^{-3} mm Hg with anode potentials up to 3 kv. (ATD)

46743 INVESTIGATION OF HYBRID WAVES IN A CIRCULAR WAVEGUIDE PARTLY FILLED WITH A DIELECTRIC. Bagin, V. A.; Kotov, V. I. Zh. Tekhn. Fiz., 35: 1273-9(July 1965). (In Russian).

A theoretical discussion is presented on the propagation in a waveguide of circular section partly filled with dielectric of "hybrid" waves of the type discussed for a septate waveguide by H. Hahn (Rev. Sci. Instr., 34: 1049, 1963). Such waves are of technical interest in connection with the separation of high energy charged particles and applications to uhf equipment. The circular waveguide of radius b is assumed to be filled from the radius a (less than b) to the wall with a linear dielectric, and those waves are discussed for which the fields are proportional to $\exp i(ft - kz - n\theta)$, where t is the time r, θ, z are cylindrical coordinates, n is an integer, and f, a, k are constants. These waves are found to be a mixture of the hybrid HE and HM modes (H. Hahn, loc. cit.), and the ratio of the two modes is calculated as a function of the waveguide parameters. The dispersion equation is derived and its solution is discussed in some detail for those waves whose phase velocity is the velocity of light. The dependence of the frequency and group velocity of these waves on the waveguide parameters is calculated and presented graphically, and an expression is derived for the energy flux. The focusing action of these waves on ultrarelativistic charged particles is discussed briefly; this action is similar to that of a 2^n-pole lens. (ATD)

46744 TECHNICAL LIMITATIONS OF OPTICAL IMAGE INTENSIFICATION. Coltman, John W. (Westinghouse Research Labs., Pittsburgh). pp 307-18 of Technological Needs for Reduction of Patient Dosage from Diagnostic Radiology. Springfield, Ill., Charles C Thomas, 1963.

A method of expressing in a quantitative fashion the limitations of systems designed to present visual images at high brightness is presented. Consideration is given to a Gaussian white noise, which is characterized by fluctuations that are purely random in nature, and whose spectrum is uniform. (P.C.H.)

46745 PSYCHROMETER PROBE (Engineering Materials). (Sandia Corp., Albuquerque, N. Mex.). (CAPE–1222).

2 drawings.

A probe used with a psychrometer to measure the percentage of relative humidity and temperature by the wet and dry bulb method is described. It contains two precision sensing elements and a blower system. The relative humidity can be measured to an accuracy better than 1% over the range from 5% to 98% in a temperature range from 35 through 140°F. Temperature is measured with an accuracy within 0.05°F over the range from 32 through 212°F. (For Details, See TID-4100). (M.C.G.)

46746 DEW POINTER HYGROMETER (Engineering Materials). (Sandia Corp., Albuquerque, N. Mex.). (CAPE–1223).

1 drawing.

Dew is formed on a polished steel surface in the hygrometer described and then is viewed by a 100-power stereomicroscope. The temperature range is –30 to +30°C. Dew points measured by the hygrometer were compared with calculated values from a two-pressure generator operating at 80°F. The maximum difference was 0.093°C and the arithmetic mean of the difference was 0.028°C. When compared with a 0°C dew-point generator, the maximum difference was 0.105°C and the arithmetic mean of the difference was 0.002°C. (For Details, See TID-4100) (M.C.G.)

46747 STANDARD MODULE SYSTEM (Engineering Materials). (Lawrence Radiation Lab., Univ. of California, Livermore). (CAPE–1226).

21 drawings.

The versatile system of modular plug-in units described conform to the standards adopted by the AEC Committee on Nuclear Instrument Modules. They are easily interchanged or replaced and cost less for updating and expanding. Modules are available in two panel heights, 5.25 and 8.75 in. Panel width are in nominal multiples of 1.35 in., with accommodation for twelve single-width modules in the bin. The 5.25-in. module can plug into an 8.75-in. bin using an adapter plate. The system makes the maximum use of the volume available in a 19 in. relay rack. (F.J.H.)

46748 LOW TEMPERATURE CRYOSTATS FOR MOESSBAUER EXPERIMENTS. Kalvius, Michael (Western Reserve Univ., Cleveland). 31p. (CONF-650101-3). Gmelin, AED-CONF-65-006-5.

From Moessbauer Symposium, New York.

Gas cryostat systems offered the best results for Mössbauer experiments. The temperature varied between 77 and 53°K for nitrogen, between 20 and 10°K for hydrogen, and between 4.2 and 1.2°K for helium as coolants. The gas systems, variation of temperature, feedthrough of mechanical motion, and temperature measurements are discussed. Nitrogen dewars with vacuum insulation, styrofoam insulated dewars, helium glass dewars, helium metal dewars, and helium gas cryostats are described. (F.J.H.)

46749 AIR DENSITY SENSITIVE GAUGES FOR SPACE CRAFT. Wright, Donald E. (to Boeing Airplane Co.). U. S. Patent 3,196,271. July 20, 1965. Filed May 2, 1960.

A combination altimetric system using pressure altimetry at relatively low altitudes and density altimetry at higher altitudes is provided for space craft. In the preferred form of the gage a radioactive source, preferably collimated, is mounted in the free stream of air, and an associated detector is mounted in the free stream in a position to receive subatomic particles, such as beta particles, emitted from the source into the free stream. The beta particles collide with the orbital electrons and the nuclei of the air atoms, and the number of collisions depends on the air density. The source and detector may be placed in relation to each other so that either the absorption or backscattering of the beta particles may be measured. Other forms of electromagnetic and subatomic particle radiation are suitable for use as the energy source. The same gaging apparatus that measures air density may also conveniently be utilized as one element of a Mach number indicator. (B.L.M.)

Radiation Detection

Refer also to abstracts 46105, 46137, 46145, 46338, 46643, 46647, 46670, 47177, 47272, 47336, 47354, and 48033.

46750 (AECL-2270) A GAMMA RAY SCANNER FOR DIAGNOSTIC RADIOGRAPHY. Clarke, R. L. (Atomic Energy of Canada Ltd., Chalk River (Ontario). Chalk River Nuclear Labs.). June 1965. 37p. Dep.; AECL $1.00.

The application of gamma emitting isotopes such as ^{60}Co to diagnostic radiography is considered. It is shown that with high efficiency detectors, such as NaI scintillation counters, it is possible in principle to get equal density resolution over a given volume in the interior of a subject by observation of either the transmitted gamma rays or Compton scattered gammas. The latter system is shown to be less sensitive to interference by objects lying in the path of the incident or emerging beams. Experiments are described which show the resolution of small (2 cc) inclusions whose density differs from the surrounding volume by less than 5%. It is shown that the experimental equipment could be scaled up to give a device which would be practical for medical work. It appears that the major application of the system may be in the resolution of soft tissues. (auth)

46751 (AEEW-M-626) A MULTIWIRE PROPORTIONAL COUNTER FOR THE DETECTION OF ^{239}Pu IN VIVO. Ramsden, D. (Atomic Energy Establishment, Winfrith (England)). May 1965. 20p. Dep.; BIS $0.40; HMSO 2s.

Work is in progress on developing counters to detect plutonium in the human lungs. The need for a low background counter for such work is discussed and the design and construction of a multiwire gas proportional counter described. The performance of the counter with different gas fillings is considered and results obtained on background, resolution, field of view, and efficiency are given. Future work will consist of using the counter in conjunction with a realistic chest phantom. An estimate of the limit of detection is derived. (auth)

46752 (AERE-M-1564) CALIBRATION OF THE NEUTRON SURVEY PROBE 95/0054. Leake, J. W. (Atomic Energy Research Establishment, Harwell (England)). July 1965. 11p. Dep.; BIS $0.50; HMSO 2s. 6d.

The neutron energy response of the survey probe 95/0054-1/6 was measured over a range of energies from thermal to 15 Mev. The response was shown to be substantially constant from thermal to 5 Mev, giving a neutron sensitivity of 0.6 ± 60% cps/n/cm^2 · sec over this region. (auth)

46753 (AERE-R-4895) THE DIDO TRIPLE AXIS CRYSTAL SPECTROMETER. Saunderson, D. H.; Duffill, C.; Sharp, R. I. (Atomic Energy Research Establishment, Harwell (England)). Aug. 1965. 25p. Dep.; BIS $0.80; HMSO 4s.

The theory of triple-axis spectrometry is outlined. The more important mechanical and electronic features and the automatic control system are discussed. The application of triple-axis spectrometry to coherent one-phonon scattering by single crystal samples is described. A summary of the performance of the equipment including count rates and resolution, and examples of the focusing of observed phonon peaks are given. (M.O.W.)

46754 (BNL-9535) GEOMETRIC CONTROL OF SURFACE LEAKAGE CURRENT AND NOISE IN LITHIUM DRIFTED SILICON RADIATION DETECTORS. Llacer, J. (Brookhaven National Lab., Upton, N. Y.). [1964]. Contract AT(30-2)-Gen-16. 23p. (CONF-651001-2). Dep. mn; CFSTI $1.00 cy, $0.50 mn.

From IEEE Nuclear Science Symposium, San Francisco.

Lithium drifted silicon radiation detectors exposed to normal ambient were shown to have a surface n-type layer which extends from the "n" side over to the "p" side of the device. A study of surface problems is presented, and a successful method for the control of leakage current and noise due to surface breakdown is shown. Noise measurements carried out on Li-drifted silicon devices show clearly the existence of two mechanisms for surface noise generation. One has the characteristics of shot noise, while the second one is much noisier than shot noise. Surface potential measurements correlated with light probe scanning give indication as to the origin of the currents which cause the two types of noise. The measurements also suggest the desirability of increasing the resistivity of the surface layer, and show that this can be attained by increasing the magnitude of the internal fields normal to such surface. One possible way of increasing the magnitude of the fields normal to the exposed junction surface consists in shaping the Si crystal so that, after the Li drifting process has been completed, regions of high fields exist within the compensated region. A comparison of cylindrical, planar, and "inverted T" types of p-i-n devices shows the superiority of the third type of device in that it is possible to apply high bias (between 150 and 200 v/mm at room temperature) before the onset of the high noise mechanism. This effect allows good charge collection with short clipping times and a corresponding increase in S/N ratio. A theoretical study of potential and charge distribution in a junction formed by a "p" region–"i" region–"n" surface layer is carried out in order to elucidate the process of increasing the resistivity of a conduction layer on intrinsic material by an increase in the field in the "i" region normal to that surface. (auth)

46755 (BNWL-144) DETECTION OF RADIONUCLIDE CONTAMINATION ON FACE MASKS. Sheen, E. M.; Crouch, G. D. (Battelle-Northwest, Richland, Wash. Pacific Northwest Lab.). Sept. 1965. Contract

AT(45-1)-1830. 10p. Dep. mn; CFSTI $1.00 cy, $0.50 mn.

An experimental monitoring instrument was developed to detect and measure beta-gamma fission product contamination on the inner and outer surfaces of protective face masks. The instrument includes two large scintillation detector assemblies employing light pipes to conform to mask surfaces and one smaller scintillation detector to monitor the nose piece of the mask. All circuitry employed is solid state. The instrument can detect 10 nanocuries (10 nC) of ^{147}Pm, a low energy beta emitter. (auth)

46756 (BNL-9492) USE OF ON-LINE COMPUTERS IN HIGH ENERGY COUNTER EXPERIMENTS. Higinbotham, W. A. (Brookhaven National Lab., Upton, N. Y.). [1965]. Contract AT(30-2)-Gen-16. 15p. (CONF-650923-9). Dep. mn; CFSTI $1.00 cy, $0.50 mn.

From 5th International Conference on High Energy Accelerators, Frascati, Italy.

The experimental use of on-line computers is reviewed briefly, with attention to their use in high energy experiments. The on-line computer facility for high energy physics experiments at Brookhaven is described. Some possible applications and advantages of the on-line technique was discussed. (auth)

46757 (CEA-R-2772) LA TECHNIQUE MULTISPHERE. I. CARACTERISTIQUES GENERALES ET APPLICATIONS. (The Multi-sphere Technique. I. General Characteristics and Applications). Zaborowski, Henryk (Commissariat a l'Energie Atomique, Cadarache (France). Centre d'Etudes Nucleaires). July 1965. 56p. Dep. mn.

A study is made of the general characteristics and the applications of the multisphere technique for flux measurements, dosimetry and the spectrometry of neutron sources ranging from thermal up to 7 Mev neutrons. The equations relating to three fluxmeters (proportional long counters) are given for the measurements of the flux. Other equations were derived for multicollision rad and Rem dosimetry and first collision rad dosimetry; and for the spectrometry and dosimetry of neutrons in five energy bands using a method similar to that used by threshold detectors. (auth)

46758 (CONF-550-99) REMARKS ON THE METHODS OF AUTOMATICAL IONIZATION MEASUREMENT IN A BUBBLE CHAMBER. Davidenko, G. V.; Lomanov, M. F.; Veselovsky, G. S. (Gosudarstvennyi Komitet po Ispol'zovaniyu Atomnoi Energii SSSR, Moscow. Institut Teoreticheskoi Eksperimental'noi Fiziki). 1964. 12p. Dep. mn.

From the International Conference on High-Energy Physics, Dubna, USSR, Aug. 1964.

The possibility of measurements of track density in a bubble chamber is analyzed using automatic scanning devices. By means of addition of diffraction bubble images on film, it is shown how the distribution of small gap lengths (which number is large) is distorted. For calculating the influence of such effects on the observations, the track model was constructed with the aid of a computer. Conformable to the conditions of automatic treatment of bubble chamber photographs the procedure of small gaps cutoff with the least losses in statistics is proposed. The method of the mean gap length, the lacunarity method and the gap counting for stopped particles are discussed. (auth)

46759 (EGG-1183-1017) A STUDY OF THE PANCAKE NEUTRON DETECTOR. Technical Memo L-72. Frisch, A. S. (Edgerton, Germeshausen and Grier, Inc., Las Vegas, Nev.). Jan. 16, 1964. Contract AT(30-1)-1183. 32p. Dep. mn; CFSTI $2.00 cy, $0.50 mn.

Neutron sensitivity calculations, as a function of energy and material thickness, were made on polyethylene with the aid of a computer. Experimental studies were made and the results were compared with the theoretical results. (M.O.W.)

46760 (NP-15462) OTSENKA PREDSTAVITEL'NOSTIVO VREMENI POKAZANII AEROZOL'NYKH RADIOMETROV S NEPRERYVNYM DVIZHENIEM FIL'TRUYUSHCHEI LENTY. (Evaluation of Time-Related Readings of Aerosol Radiometers With a Continuously Moving Filter Strip). Report No. 107. Markov, K. P., Ryabov, N. V.; Stas, K. N. (Institut Atomnoi Energii, Gosudarstvennyi Komitet po Ispol'zovaniyu Atomnoi Energii SSSR, Moscow). [1961]. 5p. Dep. mn.

Analytical expressions were derived for expressing the activity changes in the atmosphere on the basis of the readings on filter strips, onto which radioactive aerosols were deposited. These expressions were examined in order to evaluate the precision of the readings of the detectors, in front of which the strip is passed. The number of atoms derived from the data obtained with instruments with a square-shaped window and a continuously moving filter strip was found to agree within ±10%; thus the results are considered as being comparable with those obtained with a circular window. Calculations were also carried out for determining the activity of the strip when the concentration of a short-lived radioactive species with a decay constant λ changes linearly and for the important case in which the curve describing the concentration changes exhibits maxima and minima; certain simplifying assumptions were used in these calculations. These formulas which take into account the various factors involved in the continuously moving filter technique, were found very useful for establishing that the required precision was indeed achieved in the determination of the concentration of radioactive aerosols. (TTT)

46761 (NYO-2979-34) ORGANOMETALLIC RADIATION DOSIMETRY SYSTEMS. Kivel, Joseph (Atlantic Research Nuclear Corp., Alexandria, Va.). May 31, 1965. Contract AT(30-1)-2979. 52p. Dep. mn; CFSTI $3.00 cy, $0.50 mn.

Certain classes of metal-organic compounds were found to be applicable as gamma radiation dosimetry systems for total doses greater than one megarad. Systems investigated included: metal-acetylacetone chelates, organometallic compounds, and metal cupferrates. The acetylacetonates of chromium(III) and cobalt(III) in toluene were determined to be the most promising dosimetry systems. The yield of aqueous-extractable cobalt(III), by the radiolytic rupture of the metal-to-organic bond of the cobalt(III) acetylacetonate, was determined to be linear with radiation dose over the 0.5–20 megarad range. Irradiations were carried out using 80, 420, and 5000-Curie cobalt-60 sources. Dose rates from 2.5×10^4 to 7.7×10^5 rads per hour were utilized to irradiate samples to total doses of up to 20×10^6 rads. The G (metal ion formation) values for the cobalt(III) and chromium(III) acetylacetonates in toluene were determined to be 0.13 and 0.10, respectively, at 1% chelate concentration, and 0.096 and 0.067 at 0.1% concentration. An 0.8% increase in yield per degree centigrade temperature rise was observed for the Co(III) chelate. Oxygen was shown to slightly decrease the yield of liberated metal and lead to greater scatter in the analytical results. Analysis by dilute nitric acid extraction of the metallic ion from the toluene solution, EDTA complexation, and spectrophotometric determination yielded ±2% reproducibility for the cobalt(III) complex. Direct colorimetric readout of the residual acetylacetonate chelate was applicable for radiation doses above ten megarad. Procedures for the use of these systems as chemical dosimeters are presented. (auth)

46762 (NYO-3474-1) COLOR CENTERS, ENERGY STORAGE, AND THERMOLUMINESCENCE IN LiF CRYSTALS. Progress Report, January 1–September 30, 1965. (Dartmouth Coll., Hanover, N. H.). Sept. 30, 1965. Contract AT(30-1)-3474. 6p. Dep. mn; CFSTI $1.00 cy, $0.50 mn.

Studies were made of thermoluminescence between 25 and 300°C and of optical absorption between 190 and 770 mμ. Measurements were made in the lower gamma-ray dose range, where thermoluminescence is linear with dose. For the impure LiF samples, the F band (250 mμ) and the 310 and 380 mμ bands are produced, while in pure LiF, only the F band is produced. No bands at 340 or 220 mμ were observed at low doses. The 100 and 200° thermoluminescent peaks were identified with the 380 and 310 mμ bands, respectively. Pulse annealing experiments indicate that the F band is involved in the thermolumines-

cent process; it may be the thermoluminescent recombination center. Optical bleaching experiments show that the 250, 310, and 380 mμ bands are each bleached by light absorbed in the band itself, but that the 310 and 380 mμ bands are not bleached by 250 mμ light. The possible existence of trapped-hole centers is considered. (D.L.C.)

46763 (RCN-37) REVIEW OF ACTIVATION METHODS FOR THE DETERMINATION OF FAST NEUTRON SPECTRA. Zijp, W. L. (Reactor Centrum Nederland, Petten). May 1965. 121p. Dep. mn.

A review is given on the possibilities for determining flux densities, fluences, and spectra of fast neutrons from the counting results obtained with threshold detectors. After an introductory chapter on the response of a threshold detector, on the definitions of fast flux density and on effective threshold and effective cross sections, some threshold reactions of interest are considered. The determination of fast flux density and fast fluence is discussed. The various methods mentioned in literature are reviewed for the determination of the spectral distribution from the response integrals. The semi-empirical spectrum representation proposed by Genthon is reviewed. After the mentioning of the activities of the Euratom Working Group on Dosimetry the results of the discussions in the IAEA Panel on In-Pile Dosimetry are mentioned. Tables with nuclear data and an extensive bibliography are included at the end. (auth)

46764 (SZS-6(1965) BESTIMMUNG DER MINDEST-FILTERGROESSE FUER DAS FILTERANALYTISCHE VERFAHREN DER FILMDOSIMETRIE. (Determination of Minimum Filter Size for the Filter Analysis Process of Film Dosimetry). Rothe, W.; Herrmann, D. (Staatliche Zentrale fuer Strahlenschutz, Berlin (East Germany)). July 1965. 18p. Dep. mn.

Investigations are described and results are given of the most favorable number of filters (including window) in film badges. The area of the film covered by metal filters or by the window is not suitable in its whole size for density measurements due to the influence of the filter edges. The width of this edge effect and the linear dimension of the area necessary for density measurement determine the minimum filter size. Minimum filter sizes were investigated for gamma radiation with quantum energies from 84 kev to 1.25 Mev and for beta radiation with average energies from 252 to 940 kev. The material of the filters, the filter thickness, and the angle of incidence of the radiation were varied. Different types of ORWO dosimeter films were used. As a result of the measurements, the minimum filter width is 8 to 10 mm for angles of incidence up to 80° and the minimum window diameter is 15 mm for angles of incidence up to 50°. Therefore, by using a film area of 30×40 mm^2, 5 metal filters and one window can be inserted into a film badge as the optimum. (auth)

46765 (TID-22012, pp 4-21) A TOTAL ABSORPTION GAMMA RAY SPECTROMETER SYSTEM FOR PULSED BEAM n,n γ MEASUREMENTS. Ashe, John B.; Morgan, Ira Lon; Hall, J. D. (Texas Nuclear Corp., Austin).

A gamma ray spectrometer that combines the techniques of particle time-of-flight spectrometers and gamma ray total-absorption spectrometers is described. Gamma ray energy resolution and efficiency are presented along with pulse height spectra obtained from inelastic scattering reactions. (auth)

46766 (TID-22141, pp 67-79) NEW INSTRUMENTATION PROGRAMS. (Rensselaer Polytechnic Inst., Troy, N. Y.).

The spark chamber was studied as a fission detector for use in capture-to-fission ratio measurements; tests were performed on a multiplate wire spark chamber. The use of liquid scintillation detectors in a circle around the scattering sample was proposed for measurement of neutron inelastic scattering cross sections at high energies, and the construction of suitable detectors was begun. The first phase of the Stored Program Data Recorder (on-line computer system) was completed; the delivered system performed according to the specifications. Development also proceeded on a variation of the Moxon-Rae capture-gamma detector. (D.C.W.)

46767 (TID-22256) IDENTIFICATION OF NEUTRON STARS IN NUCLEAR EMULSION [Thesis]. Zych, Allen D. (Case Inst. of Tech., Cleveland, Ohio). 1965. Contract AT(11-1)-818. 104p. Dep. mn; CFSTI $4.00 cy, $0.75 mn.

Direction and ionization measurements on the emitted prongs of 332 proton stars at six different incident energies from 437 Mev to 22.5 Bev were used to develop a method for identifying neutron- and proton-induced stars in cosmic ray emulsion. Neutron-type events were obtained by neglecting the incident proton of the proton stars. The stars are classified according to their prong characteristics and for each class the neutron-to-proton star ratio is introduced as a useful parameter for determining the specific criterion for separating neutron and proton stars. This criterion is obtained by requiring that the number of proton and neutron stars that are identified incorrectly be equal. The proposed self-consistent method for identifying cosmic ray stars will yield a measure of the neutron-to-proton star ratio and also the relative error in identification for both neutron and proton events in each class. For neutron events, the incident neutron direction is predicted to within 20° in most cases. (auth)

46768 (UCRL-14253) ALPHA AIR MONITOR WITH CONSTANT FLOW CONTROL. Beard, E. L.; Petrock, K. F. (Lawrence Radiation Lab., Univ. of California, Livermore). June 30, 1965. Contract W-7405-eng-48. 12p. Dep. mn; CFSTI $1.00 cy, $0.50 mn.

A continuously indicating alpha air monitor featuring a solid-state constant flow control is described. A transistorized detection circuit provides a 30-day record of collected activity. (auth)

46769 (UCRL-16325) NEUTRON SPECTROSCOPY BY THE USE OF NUCLEAR STARS FROM 20 TO 300 Mev [Thesis]. Remy, Rene (Lawrence Radiation Lab., Univ. of California, Berkeley). Aug. 17, 1965. Contract W-7405-eng-48. 68p. Dep. mn; CFSTI $3.00 cy, $0.75 mn.

Stars produced in emulsion by incident neutrons of known average energy (E_n) were used to obtain the average visible energy released per star ($\bar{E}_v$) as a function of E_n. The different neutron average incident energies were 20, 100, 160, 220, and 300 Mev. Although a good discrimination was obtained for $\bar{E}_v$ as a function of E_n, real values of $\bar{E}_v$ depend strongly on the validity of one of the working assumptions (average kinetic energy of grey prongs is independent of neutron incident energy). It was found that a much simpler method could be used to reach the same goal—the average number of grey prongs per star offers, in that range of neutron incident energy, a very good discrimination among the different E_n's. So the use of a simplified method, which consists of counting the number of stars together with the number of grey prongs, should provide a simple way to obtain the average incident neutron energy for an unknown bombarding neutron spectrum in the range 20 to 300 Mev. (auth)

46770 (UCRL-16354) HEAVY-PARTICLE STUDIES WITH SILICON DETECTORS. Raju, Mudundi R. (Lawrence Radiation Lab., Univ. of California, Berkeley). Aug. 20, 1965. Contract W-7405-eng-48. 21p. (CONF-650924-3). Dep. mn; CFSTI $1.00 cy, $0.50 mn.

From Workshop Conference on Space Radiation Biology, Berkeley, Calif.

The response of lithium-drifted silicon semiconductor detectors to alpha and proton beams, and the intermediate energies obtained by placing absorbing materials in the path of the primary beam were studied. The energy distribution at the Bragg peak positions of 910-Mev alpha beam and 49-Mev proton beam is measured in order to evaluate the linear energy transfer distribution at the Bragg peak. (M.O.W.)

46771 A PORTABLE HIGH PRESSURE SPECTROSCOPIC CELL. Malmrud, S.; Claesson, S. Acta IMEKO, 1: 195-201(1964).

A high pressure spectroscopic cell, which is designed to eliminate the inconvenience due to the intensifier, is

described. With this cell there is no need for an intensifier in connection with the cell during the spectroscopic runs and in its absence the cell could be made with only one axial hole through the high pressure vessel and with the optical windows in the pistons. The cell is designed to fit in a Leitz infrared grating spectrometer model III G but may be introduced into various other kinds of spectrometers, provided their sensitivity is high enough. (P.C.H.)

46772 A SEMIAUTOMATICALLY OPERATED RADIOFREQUENCY MASS SPECTROMETER. Harsanyi, Gy. Acta IMEKO, 3: 21-31(1964).

A radiofrequency mass spectrometer was studied under automatic conditions. The energy functions of the selection processes were modelized by electromechanical means, showing the theoretical limits of the resolving power 5–10 times higher — related to the known types of these instruments. The secondary peaks were removed by increasing the phase shifts corresponding to ions of different mass number. It was possible to extend the low and high mass ranges by an especially matched network between the high frequency electrodes and the generator output. With the improved technical data the instrument has lent itself well to automatic operation. The semiautomatically scanned mass spectrum is linear within 0.2%. The mass and time ranges of the scan system are variable. There is a possibility for automatic resetting and starting of the scan. The scanning form of the instrument is constructed for analysing chemical or isotope mixtures. The monitor form allows the continuous monitoring of selected ion masses or recording kinetic changes in gas — phase reactions. The time constant of the sample inlet system has a minimalized value. Mass programing is possible. Control circuits are used to obtain accuracy and reliability. (auth)

46773 ACCELERATION OF ELECTRONS IN THE SEMI-CIRCULAR PHOTOGRAPHIC RECORDING BETA-RAY SPECTROGRAPH. Slaetis, Hilding. Arkiv Fysik, 29: 485-518(1965).

A device for accelerating electrons in a semi-circular photographic recording beta-ray spectrograph is described. The energy of the electrons has been increased by 0.66 kev pre-acceleration and 6.5 to 7.0 kev post-acceleration. Post-accelerated electron trajectories were computed (machine Trask at Datasystem, Stockholm 6) for different arrangements of source, slit, and grid in order to find the most advantageous arrangements. Eighty-five L-Auger lines were found in the beta-ray spectrum of ThB + C + C′. A new arrangement giving the same final energy and almost the same angle of incidence for all electrons is proposed for simple and reliable intensity measurements of Auger and conversion lines. (auth)

46774 MEASUREMENTS AND EXPERIENCES IN CONNECTION WITH A SCINTILLATION FAST NEUTRON DETECTOR. Angeli, Istvan; Hunyadi, Ilona. At. Kozlemen., 7: 95-107(June 1965). (In Hungarian).

An organic scintillator fast neutron detector with reduced γ-background was built devoid of gamma background. The gamma-neutron separation took place with the help of pulse-shape discrimination. The maximum tolerance of the detector for gamma radiation is 10 μR/sec. As an application, the total neutron cross sections of Cs and Rb at 14.08 and 14.69 Mev respectively were measured, and found to be $\sigma_T(Cs) = 4.96\ (\pm 0.21)$ barn $\sigma_T(Rb) = 3.90\ (\pm 0.10)$ barn. (auth)

46775 THE ESSENTIAL SPECIFICATIONS OF THE HAMBURG 4π-LARGE VOLUME RADIOACTIVITY DETECTOR WITH LIQUID ORGANIC SCINTILLATOR. [PART] I. Heinrich, H. C.; Gabbe, E. E.; Whang, D. H. (Universitaet, Hamburg). Atompraxis, 11: 430-8(Aug. 1965). (In German).

The essential specifications for the estimation of the radionuclides ^{57}Co, ^{203}Hg, ^{51}Cr, ^{133}Ba, ^{131}I, ^{85}Sr, ^{137}Cs, ^{58}Co, ^{54}Mn, ^{65}Zn, ^{59}Fe, ^{22}Na, ^{40}K, ^{60}Co, ^{226}Ra, and ^{228}Th in volumes of up to 200 liters, as well as for radionuclides incorporated in the human body, are described for the recently developed module-type of a 4 π-large volume radioactivity detector with liquid scintillator. Depending on radionuclide maximum sensitivities $E\%_\gamma$ of 28% (^{57}Co) to 97% (^{60}Co) are obtained with the 200 cm long 4π counting geometry. Radionuclides incorporated in the human body are measured at optimum E^2/B values with sensitivities $E\%_\gamma$ between 20% (^{203}Hg and ^{51}Cr) and 56% (^{60}Co). Lower border line radioactivities of 0.8 to 2 nC ^{131}I, ^{59}Fe, and ^{60}Co can be measured within the human body within 1000 seconds counting time and a standard error of ±10%. Between 0.13 and 0.38 nC of most radionuclides can be detected if a discrimination from background with 99.9% probability is used as a criterion. (auth)

46776 INSTRUMENTAL AND TECHNICAL NOTES. AN AUTOMATIC ISODOSE CONTOUR RECORDER. Huggett, J. P. (Pembury Hospital, Eng.). Brit. J. Radiol., 38: 701-3(Sept. 1965).

An automatic curve-following isodose recorder utilizing an x, φ co-ordinate system was constructed and is described. Economy and simplicity are two essential features of the device. By direct mechanical linkage between the detecting and recording components, and by the choice of co-ordinate system, the need for duplicating complex and precise scanning equipment was avoided, while possible sources of error arising from mechanical time-constant and slip were eliminated. (P.C.H.)

46777 LOW BACKGROUND COUNTER FOR ^{14}C DATING. Hsu, Yuin-Chi; Huang, Chia-Yi; Lin, Song-Yun; Hsu, Yi-Chuann; Chou, Muh-Chuen; Lu, Shih-Chong; Tai, Yuin-Kwei (National Taiwan Univ., China). Chinese J. Phys. (Taiwan), 3: 1-9(Apr. 1965).

A proportional counting system for radiocarbon dating and procedures for producing carbon dioxide are described. The center counter was filled with carbon dioxide at one atmospheric pressure. The total background is 5.87 ± 0.01 cpm. The value of 95% of the NBS contemporary standard for carbon-14 dating was taken as a standard of dating work. (auth)

46778 PURDUE CONFERENCE ON INSTRUMENTATION FOR HIGH ENERGY PHYSICS, PURDUE UNIVERSITY, LAFAYETTE, INDIANA, MAY 12–14, 1965. IEEE (Inst. Elec. Electron. Engrs.), Trans. Nucl. Sci., NS-12: No. 4, 1-376(Aug. 1965). (CONF-650510).

Fifty-six papers are included; separate abstracts have been prepared for 41. Fifteen of the papers were previously abstracted in NSA, see 18: 35813 and 37949; and 19: 29068, 30532, 30533, 36804, 36812, 36816, 36821, 38970, 38996, 39450, 40869, 41322, and 42721. (T.F.H.)

For abstracts of individual papers see: 46779–46816, 47173, 47962, and 48069.

46779 INNOVATIONS IN VISUAL SPARK CHAMBER TECHNIQUES. Strauch, Karl (Harvard Univ., Cambridge, Mass.). IEEE (Inst. Elec. Electron. Engrs.), Trans. Nucl. Sci., NS-12: No. 4, 1-12(Aug. 1965).

Discharge mechanisms and characteristics of wide-gap track spark chambers operating in the spark mode and streamer mode are reviewed. Characteristics studied include sensitive time, specific ionization, efficiency, accuracy, and reproducibility. (T.F.H.)

46780 PRECISE TRACK MEASUREMENTS IN A WIDE GAP SPARK CHAMBER. Keller, L. P. (Argonne National Lab., Ill.); Schluter, R. A.; Burleson, G. R.; White, T. O. Jr. IEEE (Inst. Elec. Electron. Engrs.), Trans. Nucl. Sci., NS-12: No. 4, 19-21(Aug. 1965).

Cosmic-ray tracks are observed and measured in a wide-gap spark chamber operating in the spark mode. The performance of the apparatus for high-precision reconstruction of vertices occurring outside the detector is discussed. Chamber operation is outlined. (T.F.H.)

46781 DEVELOPMENT OF STREAMER SPARK CHAMBERS. Bulos, F.; Boyarski, A.; Diebold, R.; Richter, B.; Odian, A.; Villa, F. (Stanford Univ., Calif.). IEEE (Inst. Elec. Electron. Engrs.), Trans. Nucl. Sci., NS-12: No. 4, 22-7(Aug. 1965).

Some results obtained with wide-gap streamer-mode track spark chambers are discussed, along with chamber operating characteristics. (T.F.H.)

46782 ELECTRON IDENTIFICATION IN LEAD PLATE SPARK CHAMBERS. McLeod, D. W.; Phelan, J. J.; Roberts, A.; Yurka, G. E. (Argonne National Lab., Ill.). IEEE (Inst. Elec. Electron. Engrs.), Trans. Nucl. Sci., NS-12: No. 4, 28-30(Aug. 1965).

A spark chamber containing Pb, Al, and Cu plates is exposed to momentum-analyzed electron and pion beams at 80 to 340 Mev/c. It is found that the chamber can discriminate electrons from pions with 99 to 99.5% reliability. The chamber geometry and operation for this use are described. (T.F.H.)

46783 MAGNETOSTRICTION WIRE SPARK CHAMBERS. Barbanente, V.; De Blasi, M.; De Marzo, C.; Giannelli, G.; Marangelli, B.; Ricco, M. (Universita, . Bari, Italy). IEEE (Inst. Elec. Electron. Engrs.), Trans. Nucl. Sci., NS-12: No. 4, 31-6(Aug. 1965).

Several concepts of the use of the magnetostrictive effect for localizing tracks in spark chambers are discussed and compared. Pulse propagation is studied. Electronic equipment required is outlined. (T.F.H.)

46784 DIGITIZED PRINTED DISCHARGE PLANES AND THEIR OPERATION AT RAPID RATES. Fischer, Joachim (Brookhaven National Lab., Upton, N. Y.). IEEE (Inst. Elec. Electron. Engrs.), Trans. Nucl. Sci., NS-12: No. 4, 37-48(Aug. 1965). (BNL-9260).

Development of digitized discharge planes, for operation as particle hodoscopes at rapid rates, evolved from small copper wire planes to larger aluminum wire planes and later to printed circuit type thin-wall planes. Construction of the printed circuit planes, design of the vacuum tube pulsers, and factors affecting operation of the planes are described. Recovery time can be on the order of 200 μsec in neon–helium–alcohol mixtures. Factors that affect multi-plane system performance at high rates are discussed. (auth)

46785 AN ON-LINE MEASUREMENT OF MUON DECAY USING WIRE SPARK CHAMBERS. Sherwood, Bruce (Univ. of Chicago). IEEE (Inst. Elec. Electron. Engrs.), Trans. Nucl. Sci., NS-12: No. 4, 49-51(Aug. 1965).

The electron-momentum spectra from muon decay are measured using wire spark chambers with ferrite-core readouts and on-line computation. Systems used and results are printed. (T.F.H.)

46786 THE ANALYSIS OF SPARK CHAMBER PICTURES USING A RASTER SCAN TECHNIQUE. Blackall, P. M.; Macleod, G. R.; Zanella, P. (CERN, Geneva). IEEE (Inst. Elec. Electron. Engrs.), Trans. Nucl. Sci., NS-12: No. 4, 52-68(Aug. 1965).

Raster-scan techniques developed for automatic analysis of spark-chamber film are reviewed. The experiments analyzed, the use of flying-spot digitizers, the use of computers, and the performance of the methods are discussed. (T.F.H.)

46787 ARIANE-AUTOMATIC DEVICE FOR THE ANALYSIS OF SPARK CHAMBER PHOTOGRAPHS. Goldwasser, M.; Michau, J. C.; Mullie, J. (Centre d'Etudes Nucleaires, Saclay, France). IEEE (Inst. Elec. Electron. Engrs.), Trans. Nucl. Sci., NS-12: No. 4, 73-7(Aug. 1965).

Ariane is a flying-spot device that may be controlled in two ways for analyzing spark-chamber photographs. The principle of operation, motion of the spot, measurement method, system components, computer uses, and Ariane performance are discussed. (T.F.H.)

46788 STATUS REPORT ON THE LUND VIDICON SYSTEM. von Dardel, G.; Jarlskog, G.; Henriksson, S. (Univ. of Lund, Sweden). IEEE (Inst. Elec. Electron. Engrs.), Trans. Nucl. Sci., NS-12: No. 4, 78-82(Aug. 1965).

A 60-gap carbon-plate spark chamber is used as a proton polarimeter for measuring the polarization of recoil protons from π^0 photoproduction. The vidicon designed for use in this experiment is described, as regards its general features, logic, data processing, and principles of analysis. (T.F.H.)

46789 FILMLESS AUTOMATIC PROCESSING OF SPARK CHAMBER TRACKS USING STANDARD EQUIPMENT. Hutchinson, G. W.; Seidman, A. (Univ. of Southampton, Eng.). IEEE (Inst. Elec. Electron. Engrs.), Trans. Nucl. Sci., NS-12: No. 4, 83-7(Aug. 1965).

A system is designed that uses a multichannel pulse-height analyzer as a storage and readout and a commercial vidicon television camera for scanning the spark chamber (or spark-chamber photographs). The performance, testing, and circuitry of the system are described. (T.F.H.)

46790 MOVING FILM, FIXED SENSORS, AUTOMATIC SCANNER FOR SPARK PICTURES. Rust, D. R.; Sinclair, C. K.; Talman, R. M. (Cornell Univ., Ithaca, N. Y.). IEEE (Inst. Elec. Electron. Engrs.), Trans. Nucl. Sci., NS-12: No. 4, 88-9(Aug. 1965).

A simple device is described that moves spark-chamber film at a constant rate past a set of sensing devices. The positron of a spark in a gap is located by the time at which it is detected by the appropriate sensor. The output of the scanner can be put on magnetic tape or punched cards. A conceptual diagram of the system is given. (T.F.H.)

46791 SOME CURRENT PERFORMANCE CHARACTERISTICS OF VISUAL SPARK CHAMBER SYSTEMS. Roberts, Arthur (Argonne National Lab., Ill.). IEEE (Inst. Elec. Electron. Engrs.), Trans. Nucl. Sci., NS-12: No. 4, 90-6(Aug. 1965).

The performance of camera and film retrieval techniques for analyzing spark chamber events is reviewed, with particular attention to event identification and selection, particle identification, and measurement accuracy for momentum and direction. The automation of these systems is discussed. (T.F.H.)

46792 ON-LINE DATA ANALYSIS. Miller, R. H. (Univ. of Chicago). IEEE (Inst. Elec. Electron. Engrs.), Trans. Nucl. Sci., NS-12: No. 4, 97-101(Aug. 1965).

A general outline is given of the performance and state-of-the-art of on-line systems for analyzing data from events detected by nuclear detectors. (T.F.H.)

46793 A SYNOPSIS OF THE ARGONNE AUTOMATIC SPARK CHAMBER PROCESSING SYSTEM. Royston, R. J. (Argonne National Lab., Ill.) IEEE (Inst. Elec. Electron. Engrs.), Trans. Nucl. Sci., NS-12: No. 4, 102-4(Aug. 1965).

Chloe is a CRT scanner controlled by a small (ASI 210) computer. It is used with the codes AROMA, AIRWICK, and GRIND to scan and analyze spark-chamber photographs. (T.F.H.)

46794 THE AROMA PROGRAM FOR THE RECOGNITION AND MEASUREMENT OF SPARK IMAGES AND FIDUCIALS. Pennock, Paul (Argonne National Lab., Ill.). IEEE (Inst. Elec. Electron. Engrs.), Trans. Nucl. Sci., NS-12: No. 4, 105-7(Aug. 1965).

AROMA is a FORTRAN program concerned with automatic identification of elements of spark-chamber photographs. The registration marks, fiducial and spark measurements and cell-construction algorithms for AROMA are discussed. (T.F.H.)

46795 MOTION PICTURE ILLUSTRATING THE USE OF GRAPH THEORY IN THE ANALYSIS OF SPARK CHAMBER DATA. Clark, R. (Argonne National Lab., Ill.). IEEE (Inst. Elec. Electron. Engrs.), Trans. Nucl. Sci., NS-12: No. 4, 108-12(Aug. 1965).

Detail photographs are shown from a motion picture illustrating the use of graph theory in the analysis of spark-chamber photographs. (T.F.H.)

46796 A NEW MAGNETIC SPARK CHAMBER SYSTEM. Bernstein, S.; McLeod, D. W., Phelan, J. J.; Rickhoff, W. L.; Roberts, A.; Siljander, W. A.; Yurka, G. E. (Argonne National Lab., Ill.). IEEE (Inst. Elec. Electron. Engrs.), Trans. Nucl. Sci., NS-12: No. 4, 120-9(Aug. 1965).

The design of large spark chambers with surrounding magnets is described, with attention to the magnets, chambers, optics, triggering, pulsers, hydrogen target, and analysis programs. (T.F.H.)

46797 SMP AND FRANCKENSTEIN ON-LINE. McIlwain, R. L. (Purdue Univ., Lafayette, Ind.). IEEE (Inst. Elec. Electron. Engrs.), Trans. Nucl. Sci., NS-12: No. 4, 130-7(Aug. 1965).

Several hardware configurations are described that are in use for on-line computerized analysis of bubble-chamber events. (T.F.H.)

46798 AN APPLICATION OF TELEVISION PICKUP TO BUBBLE-CHAMBER MEASUREMENTS. Condon, P. E.; Herz, A. J. (Naval Research Lab., Washington, D. C.). IEEE (Inst. Elec. Electron. Engrs.), Trans. Nucl. Sci., NS-12: No. 4, 155-9(Aug. 1965).

A semi-automatic, semi-manual prototypical system is described for scanning and analyzing bubble-chamber photographs. (T.F.H.)

46799 A VERY LARGE HEAVY LIQUID BUBBLE CHAMBER. Musset, P. (Ecole Polytechnique, Paris). IEEE (Inst. Elec. Electron. Engrs.), Trans. Nucl. Sci., NS-12: No. 4, 164-9(Aug. 1965).

A 12-m^3 cylindrical bubble chamber is proposed, capable of operation with heavy liquids (e.g., Freon and/or propane), for use in various experiments. (T.F.H.)

46800 A SONIC SPARK CHAMBER SYSTEM WITH ON-LINE COMPUTER. Diddens, A. N. (CERN, Geneva). IEEE (Inst. Elec. Electron. Engrs.), Trans. Nucl. Sci., NS-12: No. 4, 170-9(Aug. 1965).

A system consisting of a scintillation chamber and five sonic spark chambers is used to measure proton scattering distributions in the 2- to 20-mr range at proton energies around 20 Bev. The relevant parameters of each event are written on magnetic tape, after having been checked by a small on-line computer. (T.F.H.)

46801 ON-LINE CONTROL OF BUBBLE CHAMBER MEASURING DEVICES (LIDIAM). Deler, Bernard (Centre d'Etudes Nucleaires, Saclay, France). IEEE (Inst. Elec. Electron. Engrs.), Trans. Nucl. Sci., NS-12: No. 4, 180-1(Aug. 1965).

The Lidiam computerized system is used for control of bubble-chamber photograph-scanning instruments. The means for operator control of measurement accuracy using Lidiam are discussed. (T.F.H.)

46802 INSTRUMENT FOR IONIZATION MEASUREMENTS IN BUBBLE CHAMBER FILMS. Lorenz, Eckart (Max-Planck-Institut fuer Physik, Munich). IEEE (Inst. Elec. Electron. Engrs.), Trans. Nucl. Sci., NS-12: No. 4, 188-95(Aug. 1965).

A device for ionization measurements of elementary particle tracks in bubble chamber films is described. This instrument measures the differential gap length distribution, the total blob number, and the lacunarity. The process is for the most part automatic, using a simple track-following and gap-detecting technique. Maximum speed is about 0.8 mm/sec for a track with an average bubble diameter of 40μ. Except for a power amplifier the device is completely transistorized. The light-sensitive elements are silicon photo elements and a photo resistor. Results from measurements on secondary tracks of the πp interaction in the 81 cm hydrogen bubble chamber show good agreement with the theoretical curves. (auth)

46803 POOR MAN'S SMP. Frisch, O. R. (Cambridge Univ., Eng.). IEEE (Inst. Elec. Electron. Engrs.), Trans. Nucl. Sci., NS-12: No. 4, 196-8(Aug. 1965).

RHODA (Rapid Hand-Operated Digitizing Apparatus) is described. The purpose of RHODA is to digitize, either on- or off-line, accurate positions of particle-track photographs. RHODA is simple and relatively inexpensive. (T.F.H.)

46804 WIRE SPARK CHAMBERS. Higinbotham, W. A. (Brookhaven National Lab., Upton, N. Y.). IEEE (Inst. Elec. Electron. Engrs.), Trans. Nucl. Sci., NS-12: No. 4, 199-205(Aug. 1965).

The status of wire spark chamber devices and techniques is reviewed. Wire-spark-planes have been used as hodoscopes, as spark chambers, and as decision-making devices. Chambers in use have wire spacings of about 1 mm, up to 360 wires, and comparable spatial resolution. Time resolution is less than 1 μsec; efficiencies approach 100%; recovery times are a few hundred microseconds. Large chambers can be built. The most common method of readout is by means of ferrite memory cores. Electrical and acoustic delay lines have also been used, as well as pulse current division and auxiliary discharges. Several techniques are suitable for prompt logical operations. (auth)

46805 ELECTRON AND PHOTON ENERGY MEASUREMENT UP TO 4 Bev. Heusch, Clemens A.; Prescott, Charles Y. (California Inst. of Technology, Pasadena). IEEE (Inst. Elec. Electron. Engrs.), Trans. Nucl. Sci., NS-12: No. 4, 213-21(Aug. 1965).

Developments of Cherenkov detectors and plastic scintillation detectors for measuring the energies of high-energy (up to 10 Bev) cascade-producing electrons and photons are described. (T.F.H.)

46806 CURRENT STATUS OF AN ON-LINE COMPUTER DATA PROCESSING SYSTEM FOR HIGH ENERGY COUNTER AND SPARK CHAMBER EXPERIMENTS. Foley, K. J.; Jones, R. S.; Lindenbaum, S. J.; Love, W. A.; Ozaki, S.; Platner, E. D.; Quarles, C. A.; Willen, E. H.; Yamada, R.; Yuan, L. C. L. (Brookhaven National Lab., Upton, N. Y.). IEEE (Inst. Elec. Electron. Engrs.), Trans. Nucl. Sci., NS-12: No. 4, 222-6(Aug. 1965). (BNL-9184).

Developments in an on-line-computer data-processing system for high-energy events are outlined. The system is designed for use with scintillation hodoscopes, Cherenkov counters, and/or spark chambers. (T.F.H.)

46807 TIME-SHARED MULTI-EXPERIMENT USE OF A SMALL COMPUTER. Brenner, A. E. (Harvard Univ., Cambridge, Mass.). IEEE (Inst. Elec. Electron. Engrs.), Trans. Nucl. Sci., NS-12: No. 4, 241-4(Aug. 1965).

A time-sharing executive system is designed for simultaneous on-line uses of a DEC PDP 1. The time-sharing system permits the shared use of the central processor by several programs, each of which resides simultaneously in magnetic core memory, with a pre-assigned priority hierarchy. The system is designed for on-line use with the Cambridge Electron Accelerator. (T.F.H.)

46808 A PHOTOMULTIPLIER BASE SYSTEM WITH ADJUSTMENTS AND BLEEDER POWER COMPLETELY REMOTE FROM THE PHOTOMULTIPLIER. Davis, Howard F.; Spore, Harold A. (Univ. of Washington, Seattle). IEEE (Inst. Elec. Electron. Engrs.), Trans. Nucl. Sci., NS-12: No. 4, 245-8(Aug. 1965).

The designed base system is comprised by a mechanical-electrical connection at the PM tube, a cable of coaxial cables to the PM for the bias voltages, and a resistance divider module. Only a few electric components, having low power requirements, are located at the PM itself. The advantages of this base design include effective regulation, convenience of replacements, and ease of adjustment. (T.F.H.)

46809 TIME-OF-FLIGHT MEASUREMENTS USING THE RF STRUCTURE OF THE PRINCETON-PENNSYLVANIA ACCELERATOR BEAM. Piroue, P. A.; Smith, A. J. S. (Princeton Univ., N. J.). IEEE (Inst. Elec. Electron. Engrs.), Trans. Nucl. Sci., NS-12: No. 4, 249-50 (Aug. 1965).

The beam from the PPA, as well as secondary beams, is r-f modulated in intensity at about 30 Mc. The use of this modulation as a timing means for time-of-flight measurements on experiments with the secondary beams is discussed. (T.F.H.)

46810 PEPR SYSTEM. Pless, Irwin (Massachusetts Inst. of Tech., Cambridge). IEEE (Inst. Elec. Electron. Engrs.), Trans. Nucl. Sci., NS-12: No. 4, 279-90(Aug. 1965).

The PEPR (Precision Encoding and Pattern Recognition) system is designed for computerized scanning and analyzing of bubble-chamber photographs. The hardware, programming, and operation of PEPR are described. (T.F.H.)

46811 PRELIMINARY PLANS FOR AN AUTOMATIC SCANNING FACILITY FOR BUBBLE AND SPARK CHAMBER PHOTOGRAPHS. von Dardel, G. (CERN, Geneva). IEEE (Inst. Elec. Electron. Engrs.), Trans. Nucl. Sci., NS-12: No. 4, 296-304(Aug. 1965).

The feasibility and possible performance of an instru-

ment for scanning bubble chamber photographs is discussed. A light line from a rotating slit scans the photographs and produces a signal for track segments in near alignment with the line. The picture is reconstructed from these line segments. Fast analog rather than digital methods are used to analyze the output signal. The subsequent reduction of the data before storage on tape can be handled by a small inexpensive computer on-line. Although the instrument can in principle achieve high precision, this will not be needed for the main initial aim, pattern recognition. The design of the instrument allows the scanning parameters to be adapted to the types of photos being scanned and to the event types. (auth)

46812 PRESENT STATUS OF CERN HPD PROGRAMME FOR BUBBLE CHAMBERS. Krischer, W. (CERN, Geneva); Moorhead, W. G.; Seyboth, P. IEEE (Inst. Elec. Electron. Engrs.), Trans. Nucl. Sci., NS-12: No. 4, 305-9 (Aug. 1965).

A description is given of the methods used in the CERN HAZE program for finding average points from HPD digitizings, for use in the geometrical reconstruction program, employing the Milady scan-table rough measurements. Some details of the application of the program to an experiment are given. (auth)

46813 MICROPROGRAMMING FOR DATA ACQUISITION AND CONTROL. McGee, W. C.; Petersen, H. E. (IBM Systems Research and Development Center, Palo Alto, Calif.). IEEE (Inst. Elec. Electron. Engrs.), Trans. Nucl. Sci., NS-12: No. 4, 311-20(Aug. 1965).

An approach to the control of experimental apparatus is presented, in which control is performed by a microprogram controlling a very general register configuration and a single logical element. The basic concepts of microprogram control are described, including how program sequencing is accomplished and used to permit a variety of control capabilities including the generation of non-linear functions within a single system. A short discussion is given of available components, in order to clarify the performance levels that may be achieved and system availability. As an example, a possible microprogram controller for the PEPR film scanning system is described in some detail and its potential performance outlined. (auth)

46814 CONCERNING A SYSTEM OF BUBBLE CHAMBER DATA PROCESSING IN REAL TIME. Ouannes, C. (Institut du Radium, Orsay, France). IEEE (Inst. Elec. Electron. Engrs.), Trans. Nucl. Sci., NS-12: No. 4, 321-2 (Aug. 1965).

A real-time computer system for analyzing bubble-chamber photographs is described that uses both SMP and IEP apparatus. (T.F.H.)

46815 A PHOTOTUBE USING A DIODE AS A MULTIPLIER ELEMENT. Kalibjian, Ralph (Univ. of California, Livermore). IEEE (Inst. Elec. Electron. Engrs.), Trans. Nucl. Sci., NS-12: No. 4, 367-9(Aug. 1965).

The phototube described consists only of a photocathode and a reversed-bias semiconductor diode. All electron multiplication takes place in the space-charge region of the diode. The diode fabrication, electron optics, and phototube operation are discussed. (T.F.H.)

46816 A SIX DECADE LINEAR RESPONSE DIGITIZED ELECTROMETER. Doong, Henry (Goddard Space Flight Center, Greenbelt, Md.). IEEE (Inst. Elec. Electron. Engrs.), Trans. Nucl. Sci., NS-12: No. 4, 370-2(Aug. 1965).

The design of a wide-range digitized electrometer with an operating range from 10^{-12} to 10^{-4} ampere is described. A linear time-base output within ±1% of a decade over a 6-decade operating range has been realized. The design utilizes the input current to charge a small capacitor as the time element. As the capacitor is charged to a predetermined threshold voltage, it causes an astable multivibrator to free-run for one cycle, producing an output pulse. The charging capacitor is then immediately reset and reactivated for the next cycle. (auth)

46817 A MODIFIED PROCEDURE OF SCANNING NUCLEAR EMULSIONS FOR OBTAINING ABSOLUTE NEUTRON YIELDS OF REACTIONS. Sah, J. P. (Univ. of Lucknow, India). Indian J. Phys., 39: 193-4(Apr. 1965).

A modified procedure for scanning nuclear emulsions exposed to neutrons was used, in order to avoid the correction for recoil proton tracks running out of the plate. The absolute yield for the $^{7}Li + {}^{2}H$ reaction was obtained. (auth)

46818 A SYSTEM FOR ACCURATE COUNTING OF SHORT-LIVED ACTIVITIES BY REPETITIVE ACTIVATION. Nicolitsas, A. J.; Chrysochoides, N. G.; Kouvaras, N.; Zikides, C. C. (Democritus Nuclear Research Centre, Athens). J. Sci. Instr., 42: 621-3(Aug. 1965).

A system is described for controlling the irradiation time in a reactor and eliminating the effects of sample transfer time in repetitive activations. (auth)

46819 STUDY OF THE RADIATION DOSIMETRY BY PHOTOGRAPHIC MEASUREMENT. IV. STUDY ON THE SCINTILLATION COLOR SCANNER. Genda, Hidesaburo; Kubo, Souichi (and others) (Chiba Univ., Japan). J. Soc. Sci. Photo. Japan, 27: 14-19(Mar. 1964). (In Japanese).

The scintillation color scanner consists of a motor drive, mechanical scanning system, a spectrometer, a scaler, and an electronical and optical mechanism that translates the count rate to the color. It depicts graphically the actual size and shape of the radioactive distribution as the color map and is used in diagnosing a photological condition. To make a color map a photographic color paper, color filters, and a xenon discharge lamp were used. (auth)

46820 RECENT DEVELOPMENT IN THE FIELD OF NUCLEONICS. Jungclaussen, H. (Zentralinstitut fuer Kernforschung, Rossendorf, Ger.). Kernenergie, 8: 330-6(June 1965). (In German).

The difference between tracking chamber experiments (high information per event, few events per unit time) and counter experiments (low information per event, high counting rate) was reduced. The development of spark chambers and automatic evaluation of chamber records and development of semiconductor counters and multidimensional analysis are discussed. (auth)

46821 A COUNTER TELESCOPE FOR CHARGED PARTICLE MEASUREMENTS BY 14 Mev NEUTRONS. Saeki, Bunzaburo; Fujiwara, Yoshinao (and others) (Konan Univ., Japan). Mem. Konan Univ., Sci. Ser., No. 8, 45-52(1965).

A $dE/dx-E$ counter was constructed for measuring angular distributions of charged particles produced by the reactions with 14-Mev neutrons. This telescope consists of three proportional counters and a silicon solid-state detector. The background of this instrument is particularly low and the energy resolution is fairly good. (auth)

46822 BF_3 PROPORTIONAL COUNTERS. Miyashita, Kyoichi; Ishii, Takemi (Mitsubishi Electric Mfg. Co., Japan). Mitsubishi Denki Giho, 37: 52-60(Dec. 1963). (In Japanese).

The BF_3 proportional counter is a nuclear detector to be used for thermal neutron. Of counters developed by Mitsubishi typical ones are selected to discuss the relations among the following characteristics; gas multiplication, pulse height distribution, plateau characteristics, effect of electron attachment and wall effect. A good counter which is capable of distinguishing neutron pulses subject to the wall effect from gamma pulses shows that there is a region where the plateau slope becomes practically zero. It was confirmed that the counter has a life of 10^{9} counts. It is also found that the background counts free from external neutrons are 0.005 cpm cm^2 and these come from α-radiative material in aluminum cathode. Temperature dependence of the counting rate, in the preliminary experiment, is shown to be fairly large. (auth)

46823 ON THE DESIGN OF A 75 cm-RADIUS IRON-FREE DOUBLE FOCUSING $\sqrt{2}\,\pi$ BETA-SPECTROMETER. Hisatake, Kazuo (Tokyo Inst. of Technol.); Gotoh, Masayuki. Mitsubishi Denki Giho, 39: 805-10(June 1965). (In Japanese).

A 75 cm-radius iron-free double focusing $\sqrt{2}$ π beta-spectrometer is planned to be installed at Institute for Nuclear Study, University of Tokyo. Fundamental design parameters of the beta-spectrometer were examined. The magnetic field shape of the beta-spectrometer can be fitted to the optimum one given by Lee-Whiting and Taylor. In other words, the expansion coefficients of that magnetic field were determined to the fourth order, using three pairs of current loops. Substituting the fitted coefficients of the magnetic field in the equations of motion, the numerical integration of the equations were carried out. Various discrepancies of the trajectories between the numerical and the analytical calculations were examined. These discrepancies are due to the higher order terms which were included in the numerical calculation but not in the analytical one. A trial construction of a medium size coil was made at Kobe Works of Mitsubishi Electric Corp. and the capability of construction within the proposed high precision which is much more severe than ordinary specifications was confirmed. A running test of the coil confirmed that the temperature rise is less than the required value. (auth)

46824 ELECTRON TRANSFER IN SPHERICAL VACUUM CHAMBERS. Randle, K. J. (Edinburgh Univ.). Nature, 207: 743-4(Aug. 14, 1965).

The effects of angular distribution in electron transfer in spherical vacuum chambers were analyzed and the consequences of non-uniform radiation fields was demonstrated. Equations given show that in general the characteristic of the spherical vacuum chamber does not intersect the origin. In the special case of a uniform radiation field and an energy-angular function separable into the form $N(E)\cos\theta$, the current will be zero at zero bias voltage. Thus, the zero-voltage current intercept found by others is a consequence of one or both of the factors: a non-uniform radiation field due to inverse square and exponential attenuation in the chambers walls; or a distribution function $N(E,\theta)$ which cannot be separated into independent energy and angular functions of the type $N(E) \cdot \cos\theta$. The second possibility is considered. (P.C.H.)

46825 REACTOR INSTRUMENTATION IN GERMANY. Schallopp, Bernhard. Nucl. Eng., 10: 338-40(Sept. 1965).

The manufacture of complete reactor instrumentation, neutron detectors, electronics for neutron flux measurements, safety systems, data handling and digital control, radiation monitoring, and process instrumentation is discussed. In Germany there is an absence of any influence from the government or other national bodies on the technical development, except so far as research and development contracts are concerned. This means that the instrument industry receives no developed designs from government authorities and research contracts are not given for items which are adequately available on the world market. (P.C.H.)

46826 APPARATUS FOR MEASURING THE MOESSBAUER EFFECT. Yoshioka, Toru; Goshi, Yoichi (Tokyo Shibaura Elec. Co., Ltd.). Nuclear Eng. (Tokyo), 11: 7-10(Jan. 1965). (In Japanese).

The increasing possibility of the Moessbauer effect in nuclear physics and chemistry has necessitated the development of a more versatile device for the determination of the resonance γ absorption spectra. One based on a velocity-sweep multichannel system was constructed; it consists of a sinusoidal signal generator (63.5 c/s), a γ source (^{57}Co 1 mC deposited on the surface of a copper plate of 3×3 cm^2 and 0.2 mm. thickness) and its vibrator, an absorber (stainless steel of 20 mg./cm.^{2}), a scintillation detector (NaI crystal 0.2 - 0.3 mm thick for detecting the γ rays of 14.4 and 12.4 Mev.), a cathode follower and linear amplifier, a single-channel pulse-height analyzer, a time pulse-height converter, and a multichannel pulse-height analyzer. Although the experimental parameters are quite complicated, an excellent absorption curve is obtainable by regulating the vibrator, single-channel pulse-height analyzer and multichannel pulse-height analyzer. The apparatus constructed may also be used in the measurement of the Debye temperature and the grade of annealing and in many other ways. (NSA of Japan)

46827 HIGH-RESOLUTION, PULSE-HEIGHT ANALYZER. Moriwaki, Yoshio; Ikenuma, Tokuji (and others) (Tokyo Univ.). Nuclear Eng. (Tokyo), 11: 25-8(Jan. 1965). (In Japanese).

The wide use of pulse-height analyzers has required one with a high resolution which reduces the deadtime of radiation counting and operates at high duty. This led to the use of high-speed elements such as a semiconductor and magnetic recording film and to the methods of combining different devices. Two methods in the latter category were attempted, namely, a pulse-distributing system, and a parallel time-delay line system. The block diagrams of the two apparatus constructed are given. The pulse-distributing, multichannel pulse-height analyzer is all transistorized and consists of a pulse amplitude discriminator, linear gates, pulse lengtheners, analog-to-digital converters, counting circuits, out-put gates, a buffer memory, memory circuit, marker generator, and a control circuit. Features of the design are three analog-to-digital converters with 200 channels, a maximum conversion time of 50 μs., a counting-pulse frequency of 40 Mc/s, an inspection-pulse frequency of 1 Mc/s, and a memory-circuit cycle time of 10 μs. The parallel time-delay line, multichannel pulse-height analyzer is also all transistorized and divided in an analog-to-digital converting circuits system, a clock pulse generating system, a time-delay line memory circuits system. Features of the design are three analog-to-digital converters with 120 channels, 15 digital pulses per channel, a digit-pulse frequency of 2 Mc/s, a memory-circuit cycle time of 300 μs., and a channel-pulse frequency of 400 kc/s. (NSA of Japan)

46828 ON THE BACKGROUND STABILITY OF HALOGEN-QUENCHED G-M COUNTERS. Lesinski, Jan (Inst. for Nuclear Research, Polish Academy of Sciences, Warsaw). Nukleonika, 10: 135-44(1965). (In Polish).

The background stability of halogen-quenched G-M counters with cathodes in the form of SnO_2 film on glass was investigated. It was proved that the background instability occurring at the working temperature above 75°C is caused by the exo-electron emission from the cathode. (auth)

46829 A VERSATILE TIME-OF-FLIGHT NEUTRON SPECTROMETER. Hiramoto, Toshiyuki; Inada, Tetsuo (National Inst. Radiol. Scis., Chiba, Japan). Oyo Butsuri, 34: 429-34(June 1965). (In Japanese).

A time-of-flight neutron spectrometer is assembled for radiation researches. It simply consists of a horizontal Van de Graaff accelerator, a deflector, an analyzing magnet, a strong focusing magnet and usual electronic components used widely in time-of-flight system. The post-acceleration pulsing device provides bursts of neutrons. Alternative voltage supplied at deflection plates deflects the accelerated beam with 0.5, 1.0, 2.5 and 5.0 Mc/sec in frequency. The beam slit defines the beam pulse of less than 1.5 nsec in duration and the resultant resolution of the flight time of about 2 Mev neutron in full width at half maximum is 2.2 nsec due to broadenings from plastic scintillator of 3 cm in thickness and electronic circuitry, etc. Supplying about 200 μA of the analyzed beam current of the accelerator, it results in an average beam of about 1 μA on the target at the pulse length of 1.5 nsec in 2.5 Mc pulsing. (auth)

46830 ABSOLUTE MEASUREMENT OF HIGH RATE RADIATION BY IONIZATION METHOD. Moriuchi, Kasuyuki (Electrotech. Lab., Tokyo). Oyo Butsuri, 34: 435-43(June 1965). (In Japanese).

By the use of a parallel-plate ionization chamber with laboratory air and a ^{60}Co γ source that gives an ion density of 0.02 to 1.2 esu/cc, sec, volume recombination characteristics were investigated. With perspex, aluminum, graphite, and copper as the wall material, 0.5 to 5000 volt/cm as the field intensity, and 2 to 15 mm as the plate spacing, the m-value is observed to vary from 39.0 to 27.5 as the collection factor f increased from about 0.2 to nearly

1.0. The m-value seemed dependent not on the wall material, plate spacing or ion density, but on the field intensity alone. Since the m-value remained steady when f > 0.5, intentional use of the intensity range in which the ionization current is not saturated seemed advantageous in obtaining the saturation current with high accuracy. Treating the m-value as a constant was proved to be meaningless. Some stem effects were also investigated. (auth)

46831 AUTOMATIC MOESSBAUER SPECTROMETER. Andreescu, M.; Gelberg, A.; Nistor, C.; Rusu, M. (Bucharest Univ.). Rev. Roumaine Phys., 10: 283-8 (1965).

The working principle of an electrodynamic, constant-speed Mössbauer apparatus is described. The harmonic oscillating source has an approximately constant speed ($\Delta v/v = \pm(1-2)\%$) during $\frac{1}{6}-\frac{1}{6}$ of the oscillation period, the registrations being performed during this time interval. The simplicity of the automation scheme as well as the fact that it does not require the tracing of nonresonant normalization spectra are its main qualities. For testing and calibration of the device the hyperfine splitting of the 14.4 kev level of ^{57}Fe in the Fe_2O_3 compound was measured. (auth)

46832 SENSITOMETRIC STUDIES ON NUCLEAR EMULSION BY MEANS OF BETA-RADIATION. Gizea, F.; Nicolae, Marieta (Institut de Physique Atomique de l'Academie de la R. P. R., Bucharest). Rev. Roumaine Phys., 10: 315-24(1965). (In French).

A study was made of the nuclear emulsion IFA EN_2 sensitivity variation for beta particles. Four beta emitters of different energies were used. These were sulfur-35, calcium-45, cesium-137 with beta energies of 0.169, 0.254, and 0.648 Mev respectively, and ruthenium-rhodium with a range of beta energies 3.51, 3.11, 2.44, and 2.0 Mev. The numbers obtained for the magnitude of 2,000–3,000 ev are comparable to the values given in the literature. The exposure time for the emulsions varied from one minute to several hours. After the exposure, standard development procedure was followed. The mean energy for the development of a grain of emulsion was established, and the emulsion response varied with $1/\beta^2$. The yield of developed grains crossed by a beta particle was, for the emulsion studied, between 0.16 and 0.016. (J.F.P.)

46833 A COUNTER FOR DETECTING RADIOACTIVE SURFACE CONTAMINATION. Otsuka, Iwao (Inst. of Physical and Chemical Research, Tokyo). Rika Gaku Kenkyusho Hokoku, 36: 347-51(1960). (In Japanese).

Problems involved and instruments used in detecting and measuring radioactive surface contamination by α- and β-emitting substances are discussed. The counter-type meter described is based on the concept that by simultaneously changing the applied voltages to the counter tube and the absorbers, it is possible to discriminate α and β rays using only one counter tube. As a counter tube, an end-window alcohol-quenched G-M counter (window thickness 0.4–1.0 mg/cm^2) is used, because it has better counting characteristics in the proportional counter region than those of the halogen quenched type. For example, an alcohol quenched G-M counter with threshold voltage of 1100 v showed an output pulse height of 1 to 10 mv and plateau slope of 1% per 100 v for the proportional counter region with an applied voltage of 700 to 900 v. This contamination detector consists of the following five principal components: a counter tube, an amplifier with a gain of 100, a five-range (0-100 to 0-300, 0-1000, 0-3000, and 0-10000 cpm) linear scale ratemeter with no zero drift, a stabilized high-voltage supply for operation up to 1200 v, and a mechanical device for simultaneous changing of absorbers and applied voltages. The characteristics of this counter-type detector are as follows: (1) counting efficiency for α rays from the RaD + E + F standard source of 12.6%, (2) counting efficiency for β rays from RaD + E + F standard source of 18.2%, (3) little effect of γ rays on α-ray measurement, (4) window thickness 1 mg/cm^2, (5) effective window area 4.8 cm^2, (6) background count <0.17 cpm for α rays and about 30 cpm for β and γ rays, (7) accuracy ±3%, (8) time constant of ratemeter 2, 4, 8, and 16 sec. (BBB)

46834 RESEARCH METHODS IN HIGH-ENERGY PHYSICS. Meriel, Yves. Science Progr.-Nature, No. 3364, 297-304(Aug. 1965). (In French).

The methods used for particle detection at Saclay—the spark chamber and the bubble chamber—are described. The analysis of photographs, with emphasis on automation, determination of geometry, and reaction kinematics, is considered briefly. (J.S.R.)

46835 A TWO-COORDINATE NEUTRON DIFFRACTOMETER. Yamzin, I. I.; Sizov, R. A. (Inst. of Crystallography, Academy of Sciences, USSR). Soviet Phys.-Cryst. (English Transl.), 9: 797-8(May-June 1965).

Translated from Kristallografiya, 9: 946-8(Nov.-Dec. 1964).

A complete description of the diffractometer, and its control system is discussed. The counter can be traversed in vertical and horizontal planes, which makes it possible to examine the complete diffraction pattern with only one setting of the specimen. The stage can rotate at 0.1, 0.5, or 2.5°/min in the vertical plane. The arm and stage can move jointly or independently. An example diffraction pattern is shown. (F.J.H.)

46836 A WHOLE-BODY COUNTER FOR RESEARCH CLINICAL APPLICATIONS, AND RADIATION PROTECTION MEASUREMENTS. Kunkel, Rene; Muth, Hermann; Oberhausen, Erich (Universitaet Saarlandes, Hamburg, Ger.). Strahlentherapie, 128: 98-108(Sept. 1965). (In German).

The design of a whole-body counter and its steel chamber are described. This counter can be used for biophysical research as well as for clinical applications and radiation protection measurements. Two large NaI(Tl) crystals (8 x 4 in.) are used as radiation detectors. A special design, allowing variable speeds of the crystals parallel to the large body axis, improves the counting geometry of these detectors. Normally these detectors are poor compared to liquid scintillators. Several examples concerning the previous use of whole-body counters are briefly discussed. (auth)

46837 NUCLEAR INSTRUMENTS AND RADIATION DOSAGE. Kobayashi, Shigeo; Shimada, Junji (and others) (Tokyo Shibaura Electric Co., Ltd.). Toshiba Rev., 18: 1308-14(Nov. 1963). (In Japanese).

Toshiba, engaged in the research and manufacture of instruments for radiations and radiodosages, has contributed much to the development of nuclear research and techniques of medical treatments and diagnosis. All kinds of radiation and nuclear instruments, covering from tiny instruments like pocket dosimeters to large and deluxe instrumentation like those for reactor control systems or cosmic-ray observation equipment, are now manufactured by Toshiba. An outline is given of the instruments developed, such as, those for detection of radiations, those for radiation counting and dosage, special instruments for radiation, radiation monitors, and personal dosimeters and survey meters. (auth)

46838 ON A RESONANCE COUNTER OF PARTICLES. Suchkin, G. L. Zh. Tekhn. Fiz., 35: 1280-7(July 1965). (In Russian).

A particle counter consisting of a resonator filled with material at a negative temperature is proposed which would amplify by maser action the Cherenkov or other radiation due to the passage of a charged particle; the response of such a system to the passage of a charged particle is analyzed in detail. It is shown that the proposed counter is very sensitive to the velocity of the detected particle. It is found that with a 0.7 cm long cylindrical counter, employing ammonia as the working substance, the energy of a 100 Bev proton can be determined with an accuracy of 10^{-3} Bev. The proposed resonance counters have the advantages over differential gas counters of much higher resolution and very much smaller size and weight. It is concluded that the resonance counters are very promising for energy measurements over a wide range and for cosmic ray investigations, particularly with satellites. (ATD)

46839 MEASUREMENT IN SUCCESSIVE STAGES OF AN EMERGENCY: EQUIPMENT, METHODS AND FACILI-

TIES. Kiefer, H.; Maushart, R. (Kernforschungszentrum, Karlsruhe, Ger.). pp 157-66 of Protection of the Public in the Event of Radiation Accidents. Geneva, World Health Organization, 1965.

The technical requirements of radiation monitoring equipment for use in protecting the public after radiation accidents are reviewed. It is pointed out that monitoring may be divided into the warning stage, the prevention stage, and the recording stage, or assessment of the accumulated dose. It is customary to use measuring equipment that is employed in normal operating conditions in nuclear installations, but special equipment is required for carrying out measurements in particularly adverse conditions. Equipment for use in personnel dosimetry, area dose measurements, direct measurements of activities, the measurement of activities after enrichment, and whole-body counting are discussed, with emphasis on recently-developed equipment. It is pointed out that an adequate staff trained to operate the instruments is a vital factor in emergency radiation monitoring. (C.H.)

46840 RADIATION DOSIMETRY. PROCEEDINGS OF THE INTERNATIONAL SCHOOL OF PHYSICS "ENRICO FERMI," VARENNA ON LAKE COMO, 5th–17th AUGUST 1963. COURSE XXX. Reed, G. W. (ed.). New York, Academic Press, 1964. 315p. $14.00.

The book includes 25 complete papers. Separate abstracts were prepared for each paper. (J.F.P.)

For abstracts of individual papers see: 45998, 45999, 46153–46156, 46401, 46402, 46421, 46841–46855, and 47152.

46841 THE HISTORICAL DEVELOPMENT OF RADIATION DOSIMETRY. Spiers, F. W. (Univ. of Leeds, Eng.). pp 1-6 of Radiation Dosimetry. New York, Academic Press, 1964.

A brief history is given of radiation dosimetry. Early attempts at radiation measurement in which biological methods of dosimetry were commonly employed before their replacement by ionization instruments, and the Roentgen unit are discussed. Ionization chamber techniques, the measurement and expression of radiation doses including gamma-ray dosage are covered. The effects of the advent of the nuclear age on dosimetry problems is also discussed. (J.F.P.)

46842 DOSE CONCEPTS AND UNITS. Rossi, H. H. (Columbia Univ., New York). pp 42-7 of Radiation Dosimetry. New York, Academic Press, 1964.

For purposes of medicine, radiobiology and radiation protection, concepts other than quantities of classical physics are required to characterize ionizing radiation in terms of its potential or actual interaction with matter. With one or two minor exceptions, modern quantities are all based on physical parameters. Averaging procedures and the quantities and units used are given. There is a distinction between directly ionizing particles which are charged particles that ionized the matter which they traverse, and indirectly ionizing particles which are unchanged particles which liberate charged particles. Definition of quantities is discussed; and the quantities used in radiation protection are given. (J.F.P.)

46843 DOSIMETRY AND IONIZATION. Allisy, A. (Bureau International des Poids et Mesures, Sevres, France). pp 48-69 of Radiation Dosimetry. New York, Academic Press, 1964. (In French).

The experimental fact that the average energy lost by a charged particle in producing a pair of ions in a gas is reasonably constant, independent of the energy and, is a certain measure of the nature of the particle, proves that the energy dissipated in excitation is measurably proportional to that dissipated in ionization in the gas. This fundamental property is the basis for all dosimetry by ionization measurement. From knowing the ionization in a gas enclosed in a cavity of a solid, it is possible to infer the energy lost to the solid from the Bragg-Gray relation. Topics included are fundamental definitions, penetration of radiation into matter and equilibrium of the secondary charged particles, relative equilibrium of directly ionizing particles, the slowing-down spectrum of the directly ionizing particles, the case of continuous energy loss, radiation in inhomogeneous media, and Fano's theorem. Other included topics are the Bragg-Gray principle, corrections to the Bragg-Gray relation, remarks on conditions applicable to the Bragg-Gray relation, and some examples of ionization measurement. (J.F.P.)

46844 IONIZATION DOSIMETRY AT HIGH INTENSITY. Boag, J. W. (Mount Vernon Hospital, Northwood, Eng.). pp 70-82 of Radiation Dosimetry. New York, Academic Press, 1964.

There are limits on the dose rate beyond which ionization dosimetry becomes virtually impossible. The limitations imposed by recombination, occurring between positive and negative ions when their concentration in the gas is high, are considered, and also the measures which can be taken to reduce it, and the corrections which can be applied to the measurements to allow for it. Recombination is usually classified as either initial or general. Initial recombination occurs when the positive and negative ions formed in the track of a single ionizing particle meet and recombine. Once the processes of diffusion and drift in the electric field have destroyed the initial track structure, general recombination proceeds. In this positive and negative ions formed by different ionizing particles meet and recombine as they drift toward the opposite electrodes. General recombination, and the dosimetry of pulsed radiation are discussed. (J.F.P.)

46845 HIGH-PRESSURE IONIZATION CHAMBERS. Boag, J. W. (Mount Vernon Hospital, Northwood, Eng.). pp 83-9 of Radiation Dosimetry. New York, Academic Press, 1964.

High-pressure ionization chambers were developed for the measurement of low intensity γ and cosmic radiation. While there are other methods yielding more detailed information, the high pressure ionization chamber is still useful where information on spectral distribution is not required, such as field measurements or inexpensive monitoring. A general description and the performance of such chambers are discussed. The variation of current with pressure and ionic recombination in high-pressure gas are also discussed. Theories of initial recombination and a new theoretical treatment of recombination are given. (J.F.P.)

46846 MICRODOSIMETRY. Rossi, H. H. (Columbia Univ., New York). pp 90-7 of Radiation Dosimetry. New York, Academic Press, 1964.

When ionizing radiations deliver a given absorbed dose to a material, the energy imparted per unit mass of this material is by definition the same. But the microscopic distribution of energy deposition can vary greatly depending on the nature and energy of the directly ionizing particles that deliver the dose. The rate of energy loss along the tracks of these particles known as the linear energy transfer, is a function of charged particle energy, since in most cases of interest the directly ionizing particles are produced by indirectly ionizing radiation with a range of initial energies. Thus the track segments intercepted by a small volume of tissue may show considerable variations in linear energy transfer. Methods of computation of LET distributions of dose are shown. The use of the spherical proportional counter is discussed. Various LET distribution curves are also shown. (J.F.P.)

46847 NEUTRON AND HEAVY-PARTICLE DOSIMETRY. Rossi, H. H. (Columbia Univ., New York). pp 98-107 of Radiation Dosimetry. New York, Academic Press, 1964.

High linear energy transfer (LET) radiations can not only have a far greater biological effectiveness, but also considerable variability of biological effectiveness depending on radiation energy and type. Thus an analysis for purposes of either radiobiology or radiation protection of irradiation by neutrons or heavy particles must include information which is related to the LET of the charged particles that deliver the absorbed dose. This is best done by providing one or several of parameters; most

commonly it would be the distribution of absorbed dose in LET. However when small biological objects are irradiated by neutrons or other heavy particles that are monoenergetic or have known spectral composition, the LET spectrum of dose is unequivocally implied by the particle energy. The principles of dosimetry are discussed; and remarks are made on the interaction between neutrons and heavy particles, and tissue. Various ionization chambers for dosimetry measurements are described. (J.F.P.)

46848 CALORIMETRIC DOSIMETRY. I. INTENSITY. Laughlin, J. S. (Sloan-Kettering Cancer Center, New York). pp 114-23 of Radiation Dosimetry. New York, Academic Press, 1964.

Calorimetric energy measurement systems of two categories were devised, those which measure intensity and those which measure the absorbed dose rate. Such calorimetric systems have a fundamental advantage over other systems in that they measure the locally deposited energy directly. This advantage is realized in those absorbing materials and for those kinds and energy ranges of ionizing radiations for which all of the energy dissipated in ionization and excitation collisions is degraded into thermal energy. It is also desirable that the amount of energy dissipated in the production of bremsstrahlung or of neutrons be small. Energy fluence and intensity units are given. The principles of intensity calorimetry are discussed; and calorimetric determination of energy fluence is shown. Exposure measurements and a summary of measurements of energy fluence exposure are also given. (J.F.P.)

46849 CALORIMETRIC DOSIMETRY. II. ABSORBED DOSE. Laughlin, J. S. (Sloan-Kettering Cancer Center, New York). pp 124-33 of Radiation Dosimetry. New York, Academic Press, 1964.

The design and application of the calorimetric method to the determination of absorbed dose is treated. A brief review of the development and application of calorimeter-absorbed dose measurements is given. Topics covered are calorimetric systems, the local absorbed dose microcalorimeter (design, construction, and circuitry), the results obtained with cobalt-60 gamma rays and high-energy electrons, and the ferrous sulfate dosimeter apparatus and calibration. (J.F.P)

46850 SOLID STATE DOSIMETRY. Laughlin, J. S. (Sloan-Kettering Cancer Center, New York). pp 134-43 of Radiation Dosimetry. New York, Academic Press, 1964.

Solid state dosimetry is taken as applying to all materials in other than the liquid or gaseous state which have a response during or following exposure to ionizing radiation, which can be measured quantitatively. A few of the most useful and promising of the various systems are treated. One of the most promising systems makes use of the luminescence emitted by crystalline powder upon being heated after exposure to radiation. Thermoluminescence may be considered a special case of phosphorescence of long duration intensified by heating. A material which has an ordered or semi-ordered structure and which is either a semi-conductor or insulator is necessary. The action of the radiation produces ions and removes electrons which may move about in the material. The properties of glasses as dosimeters, the dependence of optical absorption on radiation dose in plastic, and p-i-n junction detectors are also discussed. (J.F.P.)

46851 SCINTILLATION DOSIMETRY. Trott, N. G. (Royal Cancer Hospital, London). pp 144-56 of Radiation Dosimetry. New York, Academic Press, 1964.

Scintillation dosimetry represents only one of a number of useful solid state systems. Despite the bulkiness of the photomultiplier, the method has wide practical applications. An advantage of this method over other solid-state systems lies in the considerable variety and reproducibility of the scintillation media; however, sensitivity of the photomultiplier to x and γ radiation remains a limitation. Scintillation spectrometry has made possible detailed experimental measurements of x- and γ-ray spectra, and the data are of considerable importance in the theory and practice of dosimetry. The principle of scintillation dosimetry is given, and scintillator-photomultiplier systems are discussed. Other topics discussed are energy dependence, clinical scintillation dose-rate meters, photomultiplier response to radiation, electron dosimetry, heavy particles, and x-ray and γ-ray spectra. (J.F.P.)

46852 CHEMICAL DOSIMETRY. Dainton, F. S. (Univ. of Leeds, Eng.). pp 167-79 of Radiation Dosimetry. New York, Academic Press, 1964.

There are three ways in which the dose received from a radiation source may be determined, directly, semi-directly, and indirectly. These are described individually. Desirable characteristics of a chemical dosimeter are given, and liquid aqueous systems are discussed in detail. In a dosimeter of this type, a solute is present which can react stoichiometrically with one or more of the primary species while in sufficiently low concentration so as not to influence the rate of energy deposition. Other topics considered are other potential liquid dosimeters, gaseous dosimeters, and dosimeters based on solids. These solids are gels or glasses. (J.F.P.)

46853 PHOTOGRAPHIC DOSIMETRY. Casnati, E. (CSN, Laboratorio Dosimetria e Protezione Sanitaria, Rome). pp 192-210 of Radiation Dosimetry. New York, Academic Press, 1964.

The photographic method of dosimetry proves very useful as it gives a high spatial resolution and makes possible the study of the distribution of the radiation intensity on a surface placed in the ionizing radiation field. The method is examined, including its advantages and disadvantages, and the reduction of the latter. Also some fundamental concepts and definitions are reviewed. A brief outline is given of the photographic process, photographic film processing, and photographic film as a dosimetric device. Characteristics of film dosimeters are given including electron film dosimetry, x and γ radiation film dosimetry, heavy charged particle film dosimetry, and neutron film dosimetry. Applications of photographic dosimetry are also discussed. Film when suitably used is considered a powerful tool. In track analysis the limit to film resolving power is substantially set by the grain dimension and by the resolving power of the optical system employed. The information obtainable on the radiation field produced by heavy particles or fast neutrons can be very accurate. (J.F.P.)

46854 CLINICAL DOSIMETRY. Reed, G. W. (Univ. of Leeds, Eng.). pp 236-58 of Radiation Dosimetry. New York, Academic Press, 1964.

In clinical applications of ionizing radiations the measurements or estimates of dose often have considerably greater uncertainty than those in other applications. This is a consequence of the complexity of the treated region, with respect to nonuniformity of both shape and chemical composition. Another general consideration is that although the cavity ionization principle is of wide application in the clinical field, the primary concern is not with the derivation of absolute values, but with comparisons in which the cavity chamber response is converted into the appropriate values of exposure or absorbed dose from calibrations made under standardized conditions. It is essential then to ensure that the instruments are used only under conditions in which comparison with the calibration is valid. The topics covered are types of measurement in clinical dosimetry, tissue dosage in x- and γ-ray therapy, clinical applications of radiation fields, radium dosimetry, and dosimetry in radioisotope therapy. (J.F.P.)

46855 MEASUREMENT OF RADIATION DOSE FROM ENVIRONMENTAL SOURCES. Spiers, F. W. (Univ. of Leeds, Eng.). pp 294-7 of Radiation Dosimetry. New York, Academic Press, 1964.

A determination of the radiation dose naturally received must be made in order that the additional radiation doses from man-made sources may be compared with it; there is the small chance that it may be possible to study differ-

ences in genetic and somatic effects in populations living at greatly different natural dose levels. There are two problems to be faced in measuring the natural external radiation dose, the provision of a sufficiently sensitive, portable instrument of long-term stability and the final determination of a statistically representative mean dose for any given population. Instrumentation, calibration and testing a background dosimeter, and survey procedures are discussed. (J.F.P.)

46856 SCINTILLATION COUNTERS IN HIGH ENERGY PHYSICS. Akimov, Yu. K. New York, Academic Press, 1965. 205p. $9.50.

Translated from Stsintillyatisonnyye Metody Registratsii Chastits Bol'shikh Energiy.

A systematic discussion of the fundamentals and major problems of the technology of recording high-energy particles is presented. The essential features of counter pulses are examined, and considerable attention is given to the factors responsible for pulse time and amplitude fluctuations. Also the physical characteristics of devices for recording pulse coincidences and anticoincidences are analyzed. Specific examples are used in the discussion of the identification of charged particles produced in accelerator experiments. The identification techniques presented are based on the direction of motion of the particles, their range of flight in the scintillator medium, their momentum, speed, energy, specific ionization, and time of flight. Both layer and filament detectors are described, and some consideration is given to special problems of neutron and gamma radiation recording techniques, and to the use of scintillation counters in hodoscopic systems. (L.B.S.)

46857 IONIZATION CHAMBERS FOR DIAGNOSTIC X-RAY EXPOSURE STUDIES. Laughlin, John S. (Sloan-Kettering Inst., New York). pp 11-40 of Technological Needs for Reduction of Patient Dosage from Diagnostic Radiology. Springfield, Ill., Charles C Thomas, 1963.

The principal parameters involved in the design of ionization chambers and associated apparatus for diagnostic x-ray dose studies are discussed together with limitations and desired future developments. (P.C.H.)

46858 SCINTILLATOR-PHOTOMULTIPLIER COMBINATIONS. Rohrer, Robert H. (Emory Univ., Atlanta). pp 41-59 of Technological Needs for Reduction of Patient Dosage from Diagnostic Radiology. Springfield, Ill., Charles C Thomas, 1963.

Advantages of the scintillation dosimeter as a method of detection of doses over a wide range of intensities in relatively small volumes are given. With liquid and plastic solutions available, scintillating units similating the organs of the body may be developed in order to measure the integral absorbed dose in such organs. Doping, light shield, and light pipe effects are also discussed. The cost of each detector is high compared with the cost of the storage-type detectors, but the rapid readout and adaptability of the instrument to the measurement of doses under patient exposure conditions give the system an advantage for certain applications. (P.C.H.)

46859 GLASS AND THERMOLUMINESCENT DOSIMETERS OF POSSIBLE INTEREST FOR DIAGNOSTIC APPLICATIONS. Attix, Frank H. (Naval Research Lab., Washington, D. C.). pp 61-80 of Technological Needs for Reduction of Patient Dosage from Diagnostic Radiology. Springfield, Ill., Charles C Thomas, 1963.

Discussion is presented on solid state dosimeters that appear most promising over the range of a few milliroentgen to few tens of Roentgens. These systems are: radiophotoluminescence of silver-activated phosphate glass; thermoluminescence of CaF_2: Mn; and thermoluminescence of LiF. The thermoluminescent dosimetry systems seem to have a clear superiority over the radiophotoluminescent glass system because the dose range of the former extends comfortably down to the lower limits required for diagnostic applications. Lithium fluoride has an important advantage over the calcium fluoride from the energy dependence point of view, but at present the calcium fluoride can be more reliably manufactured. (P.C.H.)

46860 CHEMICAL AND FILM MEDIA. Ehrlich, Margarete (National Bureau of Standards, Washington, D. C.). pp 81-100 of Technological Needs for Reduction of Patient Dosage from Diagnostic Radiology. Springfield, Ill., Charles C Thomas, 1963.

A review is presented on sensitive chemical dosimetry systems and photographic dosimetry. Film types, energy dependence, and sensitivity best suited for the measurement of patient exposure during diagnostic radiography are discussed. (P.C.H.)

46861 INSTRUMENTATION FOR MEASUREMENT OF ADMINISTERED RADIATION. Gehret, Edward F. (Johns Hopkins Hospital, Baltimore). pp 109-23 of Technological Needs for Reduction of Patient Dosage from Diagnostic Radiology. Springfield, Ill., Charles C Thomas, 1963.

Instruments that give a measure of the radiant flux projected toward the patient in diagnostic radiology are discussed. Special attention is given to the energy dependent ionization chamber, which measures the radiation projected at the patient in terms of the roentgen-square centimeter and another approach in which the projected radiation is measured in terms of total energy by an energy independent ionization chamber. It was concluded that the combination of a semi-transparent energy independent chamber and a digital type electrometer circuit yields an instrument that satisfies the design criteria. (P.C.H.)

46862 DETECTION OF BETA ACTIVITIES ON A CHROMATOGRAM WITH A THIN LAYER OF ABSORBANT OR OF ION EXCHANGE RESIN, USING A GEL-FORMING SCINTILLATOR. Roucayrol, J. C.; Berger, J. A.; Meyniel, G.; Taillandier, P. (Universite, Paris). pp 474-9 of Radioaktive Isotope in Klinik und Forschung. Band VI. Munich-Berlin, Urban and Schwarzenberg, 1965. (In French).

To detect beta activities on a thin layer chromatogram it is advisable to impregnate the latter with a gel-forming scintillator. Photons are produced and seen by a photomultiplier through a collimator. Means are provided to set the chromatogram lengthwise into motion and thus a continuous record of the activity distribution is obtained. (auth)

46863 MINIATURIZED FISSION CHAMBER AND PREAMPLIFIER/Q-2617/ (Engineering Materials). (Oak Ridge National Lab., Tenn.). (CAPE-1211).

11 drawings.

The assembly described is used as part of a wide-range counting channel, but can also be used as part of a conventional counting system. It consists of a fission chamber, preamplifier, and flexible cables that meet space and environmental requirements of a high-flux reactor. The assembly is waterproof and can operate continuously at 100°C. The inservice life is greater than 1 year and noise-pickup performance is low. (For details, see TID-4100). (M.C.G.)

46864 ORIENTED FISSION EXPERIMENT (Engineering Materials). (Oak Ridge National Lab., Tenn.). (CAPE-1213).

5 drawings.

The circuits described automatically control and record data on a multichannel pulse height analyzer. It is used in a fission fragment experiment to study anisotropy variations with energy that appear to be related to the contributions of the two possible J values. (For details, see TID-4100). (M.C.G.)

46865 GAMMA ION CHAMBER /Q-2204/ (Engineering Materials). (Oak Ridge National Lab., Tenn.). (CAPE-1228).

1 drawing.

The parallel-plate, gamma ion chamber described is used to activate an alarm for personnel protection from high level radiation at the Bulk Shielding Facility. The detector housing is a 1200 cc stainless steel beaker. Nine 1100-H 14 Al plates, are used. The first plate is the HV electrode and the second is the signal electrode. A 5 ×

10 in. Ω resistor is used to aid in maintaining a constant leakage voltage. (For details, see TID-4100). (M.C.G.)

46866 SCANNING MACHINE, MURA A (Engineering Materials). (Argonne National Lab., Ill.). (CAPE-1202).

307 drawings.

The machine described was specifically designed for scanning bubble-chamber film having the MURA "A" format. The MURA "A" format uses a single strip of 70-mm, perforated, Type 2 film; each frame consists of four 60-mm dia views; and there are 67 perforations per frame. The machine consists of a film platen, illumination system, projection lens system, film transport, viewing table, and the necessary electrical controls. The controls allow single frame indexing, forward or reverse. The film transport can be continuously controlled from a slow creep to a speed of ~1000 fpm. Any combination of the four views may be projected simultaneously, and view-pairs 1 to 2 and 3 to 4 can be superimposed. There is also an electronic frame counter with illuminated display. (For details, see TID-4100). (F.J.H.)

46867 G. M. SURVEY METER /Q-2092B/ (Engineering Materials). (Oak Ridge National Lab., Tenn.). (CAPE-1242).

7 drawings.

The G-M survey meter was designed to work in γ intensities ranging to 500 R/hr. There are four ranges that provide full scale calibrations of 500, 5,000, 50,000, and 500,000 counts/min, which correspond roughly to 0.2, 2, 20, and 200 mR/hr. The over-all accuracy is within 7% or better. The calibration sifts only 1%. The detection system functions at high γ levels but has sufficient sensitivity to detect and count small current pulses. It also operates in the Geiger region. The instrument was designed for health physics use. (F.J.H.)

46868 RADIATION MEASURING INSTRUMENT. Thomas, Harold Albert (to General Dynamics Corp.). German Patent 1,196,798. July 15, 1965. Priority date Nov. 21, 1960, United States.

The radiation instrument comprises an integrating-type ionization chamber which is connected to an integrating resistor condenser combination. A series connection of a rectifying element and a second condenser are switched in parallel with the integrating RC-combination so that the second condenser is charged up to a voltage which is proportional to the maximum value of the detector current. An indicating instrument is provided which can be either switched on to the first condenser or to the second condenser. (Gmelin Inst.)

46869 INSTRUMENT FOR THE DETECTION OF RADIOACTIVE RADIATION FROM AEROSOLS IN GASES. Beung, Lorenz; Muennich, K. O. (to Licentia Patent-Verwaltungs-G.m.b.H.). German Patent 1,196,799. July 15, 1965. Filed Aug. 10, 1957.

Two radiation detectors are provided; the outside of one is connected to a negative high voltage and the outside of the other is grounded. The counting rates of each of the detectors are counted separately. (Gmelin Inst.)

Radiation Effects

46870 (AD-612191) STUDY TO REDUCE AND COMPILE USAF NAP RADIATION EFFECTS DATA, SUPPLEMENT 1. Supplemental Report, June 1–December 1, 1964. Emdee, Daniel G. (Air Force Weapons Lab., Kirtland AFB, N. Mex.). Feb. 1965. 24p. (WL-TDR-64-1(Suppl.1)). CFSTI $1.00 cy, $0.50 mn.

The continuing in-house effort to reduce and compile data generated during various irradiation tests of electronic parts is reported. Irradiation tests were performed on approximately 800 electronic piece parts to determine the effects of reactor-produced radiation on their operational characteristics. The devices were subjected to integrated neutron fluxes greater than 10 to the 15th power n/cm^2 (E > 0.1 Mev) and gamma doses in excess of 10^8 rad (C). A few of the devices were tested exclusively in a ^{60}Co gamma source to approximately 8×10^7 rad (C). The data generated in the above tests were reduced to approximately six pertinent data points and recorded on computer library file cards and magnetic tape, along with information such as piece part application, manufacturer, manufacturing process, etc., concerning each part. A limited retrieval and printout program was written for in-house study of the collected data. (auth)

46871 (AD-614268) EVALUATION OF FIELD-EFFECT TRANSISTORS. Final Report. Wong, Harold Y.; Price, William E. (Lockheed Missiles and Space Co., Sunnyvale, Calif.). Oct. 4, 1962. 21p. (LMSD-8-19-62-12). CFSTI $1.00 cy, $0.50 mn.

The electrical parameters of field-effect transistors (FET) due to the effects of nuclear radiation are described. The method of measuring FET electrical parameters is also reported, along with a description of the radiation fields to which the FET's were subjected, and the analysis of the results of subjecting the FET's to a nuclear radiation environment. (TAB)

46872 (AD-621549) ELECTRON TUBES RADIATION RESISTANT PILOT LINE PRODUCTION. Seventh Quarterly Progress Report, December 1, 1964–February 28, 1965. Buchanan, William A. (Tung-Sol Electric Inc., Bloomfield, N. J. Electron Tube Div.). Feb. 28, 1965. Contract DA-36-039-AMC-01476(E). 84p. CFSTI $3.00 cy, $0.75 mn.

Pulse radiation tests were conducted at DORF. The results of this test plus those from the steady state reactor test at Brookhaven are given. Sealing of tube type 6205 using RF or heliarc welding techniques was not successful in improving cathode emission. Although good vacuum tight seals were obtained low emission remains a serious problem. Parts for 6080WB tubes are being fabricated to meet the pre-production quantity and delivery date. The ceramic spacers for tube type 6360 were received and tubes assembled. High temperature bakeout (650°C) on exhaust still affects cathode emission. Modifications to the exhaust equipment, considered at the end of the sixth quarter, were made during December. (auth)

46873 (N64-32322) EFFECTS OF GAMMA-IRRADIATION ON THE CHARACTERISTICS OF A RUBY LASER. Johnson, Vern R.; Grow, Richard W. (Utah Univ., Salt Lake City. Microwave Device and Physical Electronics Lab.). Sept. 1964. 145p. (NSF-7).

An increase in the absorption cross section responsible for optical pumping of a ruby laser was experienced as a result of γ irradiation. As single crystal ruby was irradiated with ^{60}Co γ rays, the usual absorption bands which exist between 200 and 550 mμ changed from four distinct bands to one continuous absorption band inclusive of all wavelengths between 200 and 550 mμ. Similar work on sapphire, the host crystal for ruby, indicated that the majority of this increased absorption is experienced by the Cr^{3+} ion in ruby. Thermoluminescence data are also presented showing that electron traps, metastable states with a high potential barrier, are formed in ruby as a result of γ irradiation. Two of these traps were observed and measurements showed that they have activation energies of about 0.64 and 0.78 ev. These traps remain in the crystal until it is annealed to about 800°C. It was also found that the threshold energy for laser action increases in relation to the amount of γ irradiation. Using the experimental data as a basis, a model was devised to explain mathematically what happens to the Cr^{3+} ions after γ irradiation and how this affects laser action. The theoretical results are supported by experimental data. (P.C.H.)

46874 PREDICTING SEMICONDUCTOR PERFORMANCE IN A NUCLEAR ENVIRONMENT. Rogers, S. C. (Sandia Corp., Albuquerque, N. Mex.). J. Environmental Sci., 7: 19(Apr. 1964).

The most economical way of determining alterations of system performance caused by radiation combines analysis with an experimental technique intended for lab use.

The analytical method requires that the performance of the system be expressed mathematically in terms of component performance. Such equations are then solved using component parameters appropriate to discrete radiation levels. This approach also can be used to determine the probability of system failure as a function of radiation exposure. The experimental technique involves measuring system performance after substituting radiation degraded components. Although this technique only yields the radiation levels for zero and 100% probability of failure, it is a simple and powerful tool. Exposing a system to radiation in order to determine failure levels or failure probabilities is not practical because the large variations normally encountered in semiconductor device parameters may cause failure to occur over a large range of radiation exposure levels. Therefore, a few observations on a specific system are not a reasonable basis for predicting radiation performance of similar systems. (BBB)

46875 RADIATION DAMAGE TO ELECTRICAL MATERIAL AND COMPONENTS. **Epstein, Lewis (Philco Western Development Labs., Palo Alto, Calif.). J. Environmental Sci., 7: 18-22(May 1964).**

Radiation damage likely to occur to space vehicle components is reviewed and an appendix is given, which contains calculations that can be used to estimate the extent of such damage. The radiation source may constitute cosmic rays, the earth's natural proton belt, natural electron belt, and artificial electron belts. The vehicle itself is considered, and a section through the surface of a typical space craft is illustrated. Electron and proton radiation is absorbed principally in the vehicle's skin if not in solar cells outside the skin. On deceleration, the electrons give rise to bremsstrahlung. A sample calculation of bremsstrahlung generation and absorption is presented. Exposed solar cell cover glass and the less-exposed optical elements such as infrared system lenses will brown in the radiation environment, resulting not only in impaired transparency but in perturbed spectral characteristics. Because of the shielding derived from the vehicle's skin, internal packaging, etc., radiation flux inside the vehicle will be reduced several orders of magnitude as compared to the outside flux. Permanent effects of the total dose absorbed, i.e., the time integrated flux, were of the most importance. It was found generally, that a component absorbs radiation up to some threshold without any appreciable effect. Beyond this critical dose, deterioration sets in. The radiation tolerance depends on the material; tolerances for various materials are tabulated. (BBB)

ISOTOPE TECHNOLOGY

Industrial Applications

46876 (AD-613325) RADIATION PRESERVATION OF FOODS PROGRAM. PROCEEDINGS OF CONTRACTORS' MEETING (8TH) U. S. ARMY NATICK LABORATORIES NATICK, MASSACHUSETTS, OCTOBER 7–9, 1963. Fisher, Frank R.; Josephson, Edward S. (eds.) (Army Natick Labs., Mass.). 1964. 196p. (PB-166-166). CFSTI $5.00 cy, $1.25 mn.

Information is included on: army radiation preservation of foods programs: historic highlights, present and future; AEC program; product development; wholesomeness, nutritional adequacy, and microbiology; development of radiation facilities; economic aspects and prospects of commercialization of radiation pasteurized foods; wholesomeness of foods preserved by cold-sterilization and induced radioactivity; present status of the wholesomeness program; biochemical aspects of food radiation; radiation microbiology program philosophy, principles, and objectives; radiation microbiology program progress report; troop acceptance tests of irradiated foods; packaging for radiation sterilized foods; dosimetry and dose distribution; and accelerators for food preservation. (TAB)

46877 (CONF-650552-1) RADIATION TOOLS FOR FOOD PROCESSING. Dietz, George R. (Division of Isotopes Development (AEC), Washington, D. C.). [1965]. 7p. Dep. mn; CFSTI $1.00 cy, $0.50 mn; Gmelin. AED-Conf-65-111-1.

From Institute of Food Technologists, 25th Annual Meeting, Kansas City, Mo.

During 1964 the total sales volume of radiation processed products in the U. S. was only about $70 million, but the volume is growing rapidly. Consumer acceptance of radiation processed foods is critical. The tools for radiation processing are now available for adaptation to food processing and studies have indicated that radiation processing would add only 1 to 3 cents a pound to the cost of fish and about 2 cents per pound to the cost of strawberries and less than one-half cent a pound to the cost of other fruits, such as oranges, tomatoes, and peaches, while resulting in greatly reduced spoilage losses. The cost of radiosterilization of meats of 0.8 to 5 cents a pound is less than 2 to 3.5 cents for frozen and 2 to 8 cents for freeze dehydrated meats. It is pointed out that radiation processing of sutures and medical supplies has become a symbol of assurance of a safe and sterile product and radiation produced polyethylene products, such as shrinkable plastic film used as a food over-wrap, have been accepted by the public without question. It is postulated that radiation processed foods will soon be accepted as a modern processing technology. (C.H.)

46878 (NP-15455) A STUDY OF CHEMICAL CHANGES PRODUCED BY HEAT AND BY IRRADIATION OF MEAT AND MEAT FRACTIONS. Landmann, W. A. (American Meat Inst. Foundation, Chicago, Ill.). Sept. 1965. Contract DA19-129-QM-1972. 9p. (FD-22).

Attempts at identification of the precursor material which gives rise to a specific irradiation odor in beef muscle tissue when subjected to a sterilizing radiation dose (5 megarad) are described. Early work indicated that this irradiation odor was associated with the phospholipid fraction of irradiated meat. Experiments using thin layer chromatography, infrared analysis, and chemical tests, indicate that sphingomyelin or some similar compound could be the precursor material. Efforts to identify the odor by use of infrared analysis, gas chromatography, and chemical tests were unsuccessful. Efforts to reproduce the odor by peroxide oxidation or ozonolysis of sphingomyelin were successful except that other odors were produced in much greater intensities. Irradiation of sphingomyelin and sphingosine sulfate did not produce the irradiation odor, but this could possibly be attributed to differences in conditions. The possibility of a sphingomyelin containing a specific fatty acid linked through the amid nitrogen should not be overlooked as the source of the irradiation odor. (auth)

46879 STERILIZATION WITH COBALT RADIATION OF FASCIA LATA FOR HOMOTRANSPLANT. Gutman, Froncie A. (Univ. Hospital, Ann Arbor, Mich.). Am. J. Ophthalmol., 59: 1095-8(June 1965).

Sterilization of human fascial tissue by ^{60}Co irradiation and its clinical use for homografting procedures are described. The fascia lata is removed at autopsy in a sterile fashion, cut in 10-cm by 0.5-cm strips, and placed in a sterile jar. The separate strips of tissue are then transferred in sterile fashion to polyethylene bags which have been previously soaked in 70% alcohol and rinsed in saline. Ten ml of saline and a sterile glass bead are added to the envelope and it is heat sealed. This package is then placed within a second polyethylene bag which is heat sealed, and the entire package and its contents subsequently receive three Mrad of irradiation. An advantage of this technique over heat sterilization is that it precludes exposing the tissue to an unphysiologic bathing solution, such as exists with the addition of an antibiotic to the stored tissue. The irradiated tissue is stored at room temperature in nonbreakable, heat-sealed bags which are easily kept for prolonged periods. Cobalt-60 sterilized cartilage has been used for successful homotransplant after one year of storage. The glass beads placed in the bags are discolored by the irradiation and thus indicate at surgery that the chosen tissue has actually received irradiation and is sterile. Cobalt-60-sterilized fascia lata was used for homografts in five cases. Three were in children with congenital ptosis, and the tissue was used in the conventional fashion as mechanical struts. After seven months there has been no evidence of host rejection of the grafts and no gross evidence of unsatisfactory character of the grafts insofar as their intended use is concerned. Other possible applications of radiosterilized fascial homotransplants are discussed. (BBB)

46880 THE USE OF IONIZING RADIATION WITH FRUIT PRODUCTS. Dupaigne, P. Ann. Nutr. Aliment, 17: 365-81(1963). (In French).

This is a review of literature concerned with the use of ionizing radiation for prolongation of the market life of fruit, taking into account the physiological and chemical effects as demonstrated by respiration, consistency, and changes in biochemical constituents, mutations induced by irradiation, and changes in products obtained from fruits, such as juice, fruit drinks, pulp, sliced fruit, and concentrates. Studies of the effects of γ irradiation or fast electrons on preservation of fruit showed that irradiations of the order of Mrep produced secondary changes on the surface or within the fruit pulp which were detrimental. Recent studies have resulted in definite stabilization of the fruit without flavor changes if irradiation exposure was from 500 to 700 krep. However, these dosages are insufficient to prevent microbiological changes, or to inactivate the enzymes responsible for over maturation, withering, or decomposition. Almost all recent studies have been devoted to "radiopasteurization," which is irradiation of the entire outer surface of the fruit with a moderate dosage sufficient to destroy most of the microorganisms without producing any marked change in the external or internal condition of the fruit. The purpose of this is to extend the commercially usable life of the fruit as much as possible beyond what it would be if it were not irradiated. The period of conservation that can be reached depends on the nature of the fruit itself, the irradiation dose received, the type of irradiation used (γ irradiation is more penetrating than corpuscular irradiation), the degree of contamination of the fruit, its maturity, and the method of storage used. Ir-

radiation with several hundred Krep may extend the cold storage life of fruit by 3 to 5 times normal. Generally, irradiation with from 300 to 500 Krad will produce marked changes in prolongation of storage life, biochemical changes, and improvement in over-all fruit quality. (103 references.) (BBB)

46881 RADIATION INJURY OF CLOSTRIDIUM BOTULINUM SPORES IN CURED MEAT. Greenberg, Richard A.; Bladel, B. O.; Zingelmann, W. J. (Swift and Co., Chicago). Appl. Microbiol., 13: 743-8(Sept. 1965).

Cans of chopped ham, inoculated with spores of Clostridium botulinum strains 33A and 41B at levels of 2,500 and 250 per gram, were subjected to an enzyme-inactivating heat treatment and irradiation with 0.5, 1.5, 2.5, or 3.5 MRad of ^{60}Co. A portion of the pack was not irradiated, and received a commercial thermal process ($F_0 = 0.2$). Viable spores were enumerated after treatment and after 6 months of incubation at 30 to 37.7 C. Toxic spoilage occurred at 0 and 0.5, but not at 1.5, 2.5, or 3.5 MRad. More spoilage and toxin formation occurred in the product irradiated at 0.5 MRad than in identical product receiving no radiation treatment. Confirmed botulinal spores were isolated from all of the radiation variables of 2,500 per gram-inoculated product and from all but the 3.5 MRad low-inoculum cans. However, neither growth nor toxin was observed in unspoiled product. The injury phenomenon previously described in thermally processed cured meats (survival of botulinal spores without capacity for multiplication or toxigenesis) apparently occurs also in irradiated cured meats. (auth)

46882 APPLICATION OF REPLICA PLATING AND COMPUTER ANALYSIS FOR RAPID IDENTIFICATION OF BACTERIA IN SOME FOODS. II. ANALYSIS OF MICROBIAL FLORA IN IRRADIATED DOVER SOLE (MICROSTOMUS PACIFICUS). Corlett, D. A. Jr.; Lee, J. S.; Sinnhuber, R. O. (Oregon State Univ., Corvallis). Appl. Microbiol., 13: 818-22(Sept. 1965).

An investigation was carried out to determine the nature of the microbial flora shifts in dover sole as a result of irradiation and storage at 6°C. The relationship was determined between the microörganisms which initially survive irradiation and those making up the final spoilage flora. A total of 2,723 isolates were examined by use of the replica-plating and computer analysis method. The spoilage of the unirradiated control samples during storage at 6°C was almost entirely due to the growth of Pseudomonas. This group, which occupied 25% of the fresh flora, grew to nearly 100% in 2 days of storage. In contrast, irradiation doses of 0.1, 0.2, 0.3, and 0.4 MRad favored the growth of Achromobacter and yeasts. The Micrococcus, which survived radiation, did not grow at 6°C. At 0.5 MRad, spoilage of fish samples was due entirely to the growth of yeasts. (auth)

46883 VARIED USES DEVELOPING FOR RADIOISOTOPES. Miller, Barry. Aviation Week Space Technol., 83: 42-3; 45; 49-50(July 19, 1965).

Avionic applications of radioisotope techniques in measurement, detection, and control are discussed. The uses for radioisotopes include: oil gaging systems; V/STOL tactical landing systems; all-weather landing aid; helicopter stationkeeping; air density/altimetry; planetary density sensing; APOLLO/LEM zero-gravity fuel gaging; supercritical liquid level sensor; vent quality gage; metal corrosion detection; ice detection; rendezvous sensor; all-weather missile tracking; missile distance indicators; ablation measurements. (P.C.H.)

46884 ANTIBACTERIAL BACTERIOLOGICAL SWAB. White, W. D. (St. George's Hospital Medical School, London). Brit. Med. J., 2: 229-30(July 24, 1965).

The finding of substances inhibiting bacterial growth in radiosterilized swabs, used for transferring bacterial cultures, is reported. Tests were conducted on the absorbent cotton-tipped sticks before they were either packaged or irradiated. These, when heat-sterilized in glass test-tubes in the usual way, produced swabs as satisfactory as laboratory made swabs. Another brand of commercial swab normally sold unsterilized also proved equally satisfactory when heat sterilized. These findings suggested that either γ radiation or the mode of packaging of the commercial swabs was the cause of the trouble. A variety of swabs packed in paper, plastics, or glass and sterilized by γ radiation was provided by the original commercial firm. These, when tested in the laboratory were all found to be unsatisfactory. Typical findings are shown with experiments done by inoculating various swabs with a saline suspension of Staphylococcus pyogenes so that each swab received about 20 million viable organisms. Some were tested immediately and the others left at room temperature for several hours to simulate normal conditions of use. At set intervals, time batches of swabs were shaken in saline broth in a mechanical shaker for three min. Viable counts were lower with irradiated swabs. These findings suggest that γ radiation, although an effective method of sterilization, is unsuitable for swabs intended for bacteriological use. The irradiation apparently produces a chemical change that renders the swab antibacterial. This matter should be brought to the notice of medical practitioners because of the dangers of false-negative results from swab examinations. Further investigations are in progress to test other makes of commercial swabs treated by γ radiation and other means of sterilization. (BBB)

46885 FOOD STERILIZATION BY IONIZING RADIATIONS. Constant, R. (Centre d'Etudes de l'Energie Nucleaire, Mol, Belg.). Farmaco (Pavia) Ed. Prat., 19: 3-25(Jan. 1964). (In French).

This review, citing 54 references, considers various aspects of the radiation preservation of foodstuffs, such as the doses required, technics and radiation sources used, problems and possible hazards involved, present development of programs in various nations, and likely future trends in research. The maximum doses of γ radiation required for the killing or sterilization of microörganisms with minimum damage to various food products, such as meat, fish, fruits, vegetables, and milk, are stated. The radioisotopes most used in this process are ^{60}Co and ^{137}Cs. Some disadvantages are that large amounts of ^{60}Co are required to obtain suitable dose rates, and ^{137}Cs is quite expensive. Because of their relatively low cost, electron accelerators are of most practical use for industry, but lack sufficient penetrating power. For example, 5-Mev electrons would be required to sterilize a 25-cm thickness of meat. However, at energy levels greater than 5-Mev, there is risk of activation. The optimal average dose would be in the range of 5×10^4 to 10^6 rad, depending on degree of preservation, temperature, and hygrometric conditions. The principal disadvantages of this process are the formation of peroxides through oxidation which cause a rancid odor, a tendency for meats to discolor, and loss of vitamins at doses of 0.5 to 1.5×10^5 rad. These side-effects could be minimized by the elimination of oxygen in the process, use of low temperatures, applications of thermal pretreatments, use of suitable additives and lowering of the dose. Practical problems left to be resolved, such as the risk of formation of toxins and the chemical alteration of the food products as a result of radiation, are discussed. Food sterilization installations using ^{60}Co already in operation in the United States, Canada, U.S.S.R., Great Britain, France, and Germany are briefly described. (BBB)

46886 STORAGE STABILITY OF IRRADIATED MEATS. Heiligman, Fred (U. S. Army Natick Labs., Natick, Mass.). Food Technol., 19: 114-16(July 1965).

Long-term storage studies were made of several types of irradiation-sterilized (4.5 Mrad) enzyme-inactivated meats. Preference tests, in which consumer-type test panels periodically evaluated the various products, showed that the irradiated foods remained stable in storage for long periods. Chicken parts, fresh roast pork, bacon, barbecued pork, and pork chops scored approximately the same after 18-24 months at 70°F as they did initially (shortly after irradiation). At 100°F, some of these items began to decrease in acceptability after 9 to 12 months. Scores indicate that the items were acceptable, since none scored lower than 6.2 (on the 9-point hedonic scale) ini-

tially or after 18 to 24 months at 70°F. Packets of activated charcoal were added to some cans of pork chops at the rate of 0.5, 1.0, and 2.0% based on the cooked weight of the meat. Addition of charcoal was significantly effective in preventing loss in quality during storage. The roast pork loin stored at 100°F began to deteriorate after 10 months of storage. Irradiated chicken had excellent storage stability for at least 21 months at 70°F and for 18 months at 100°F. (BBB)

46887 RADIATION SOURCES FOR IONIZATION DETECTORS IN GAS CHROMATOGRAPHY. Shoemake, G. R.; Fenimore, D. C.; Zlatkis, A. (Univ. of Houston, Tex.). J. Gas Chromatogr., 3: 285-6(Aug. 1965).

The following radiation sources were compared for their utility in gas chromatographic ionization detectors: ^{241}Am, ^{99}Tc, ^{3}H, and ^{226}Ra. The comparisons were made using a typical electron capture detector. (auth)

46888 MEASUREMENT OF THE THICKNESS OF THIN POLYMER FILMS WITH A SEMICONDUCTOR α-PARTICLE DETECTOR. Teranishi, Kazuo (Hitachi Ltd., Japan). Nuclear Eng. (Tokyo), 11: 49-56(Mar. 1965). (In Japanese).

The need for rapid and accurate measurement over a wide range (20 to 0.1μ) of the thicknesses of thin polymer films started an investigation of the α-particle penetration method. The apparatus constructed consists of an α source (^{241}Am, E_α = 5.48 Mev, half life 458 yr, 0.2μC), movable by means of a micrometer mechanism, a silicon n-p junction α counter, a shielding case, and an α counting circuit, which contains a charge sensitive amplifier, proportional amplifier, single-channel pulse-height analyzer, scaler, rate meter, and recorder. The range of thickness measured, the precision and the temperature dependency were measured by determining the energy loss of α particles passing through a polyethylene terephthalate film under various conditions of film thickness (6 to 31 μ), atmospheric pressure (1 atm to 0.1 mm Hg) and room temperature (15 to 40°C). The upper limits of thickness capable of being measured by the apparatus, were 3.0, 1.5, and 1.0 mg/cm^2 for source-detector distances of 6, 20, and 25 mm in the air, respectively. The precision in the measurement in air and in a vaccum (0.1 mm Hg) and theoretical calculations were 0.05, 0.06, and 0.01 mg/cm^2, respectively. The time required for the measurement of one specimen was about five minutes. The pulse heights showed no temperature dependency under the experimental conditions. (NSA of Japan)

46889 INVESTIGATIONS OF THE INFLUENCE OF RADIOACTIVE RAYS ON PHARMACEUTICALS. [PART] II. Buechi, J.; Iconomou, N. (Eidgenoessische Technische Hochschule, Zurich). Pharm. Acta Helv., 40: 374-81 (1965). (In German).

The influence of radiation on the properties of aqueous glucose solutions was examined. Radiolytic changes occur mainly by oxidation of the terminal C atom. The amount of acid as mg of glucuronic acid produced by 2.5×10^6 rad (^{60}Co source) in various glucose solutions is as follows: 5%, 7.76; 10%, 9.14; 20%, 9.74; 40%, 15.73; 50%, 16.45. The pH of the solution after irradiation also changes: 5%, 5.30; 10%, 5.25; 20%, 5.20; 40%, 5.10; 50%, 4.95. The yield of glucuronic acid per g glucose is plotted as a function of radiation dose; this increases from ca. 6 mg/g at 1 rad to ca. 9 mg/g at 2.5 rad. The influence of radiation dose on reducing power of glucose solution was also determined as a function of glucose concentration at 2.5 Mrad and also as a function of radiation dose. The decrease in reducing power is greatest at low concentrations (ca. 3.2% for a 5% solution; ca. 1.6% for a 50% solution) and increases with increasing dose. Only slight changes are reported in the specific rotation of glucose solutions after 2.5 Mrad doses; these values are tabulated and the max change in rotation (for the 5% solution) is less than 1%. Thus only very small radiolytic modifications occur in glucose solutions subjected to doses sufficient for sterilization. (BBB)

46890 A REVIEW OF STERILIZATION AND DISINFECTION AS APPLIED TO MEDICAL, INDUSTRIAL, AND LABORATORY PRACTICE. Rubbo, Sydney D.; Gardner, Jaon F. Chicago, Year Book Medical Publishers, 1965, 250p.

This monograph includes information of recent advances in the use of ionizing and non-ionizing radiations for sterilization. Generally, the term radiation sterilization implies the use of ionizing radiation. Ionizing radiations used for this purpose may be either in the form of particulate high-energy electrons or electromagnetic γ rays. The usual source of γ rays is ^{60}Co; ^{137}Cs is not used in sterilization because of its low energy output, this being only 0.6 Mev compared with 1.3 Mev from ^{60}Co. In contrast to heat, radiation injury does not cause denaturation of protein but induces ionization of vital cell components, particularly the DNA of the nucleus. The extent of ionization of the irradiated molecule depends on the energy level of the radiation used. High-energy radiations (above 5 Mev) may induce radioactivity in the irradiated material and are, therefore, unsuitable for sterilization of medical equipment or foods. Two main theories have been proposed to explain the lethal action of ionizing radiation, and are discussed. A table lists the range of sterilizing doses for different types of microorganisms. For general sterilization a dose of 2.5 Mrad is sufficient and has an inactivation factor of at least 10^6 for highly resistant bacterial spores such as Bacillus pumilus. One important problem that has arisen, particularly in Australia, in regard to dose is the necessity of destruction of the extremely small (10 mμ) virus of foot and mouth disease. In the absence of any precise information, it is assumed that a lethal dose for this virus is between two to four Mrad. The two main types of radiation equipment which are available, ^{60}Co installations and electron accelerators, are described. Both are designed to meet the demands of large-scale industrial production. Their high capital cost precludes any consideration of their installation in hospitals. A comparison of their characteristics is provided. With both installations, irradiation takes place at room temperature. Operation of a typical ^{60}Co installation is shown. Electron accelerators are of two types, the Van de Graaff generator, which gives β rays of one- to three-Mev energy and the microwave linear accelerator, whose output may vary from three to 15 Mev. In contrast to the massive physical dimensions of a ^{60}Co installation, an electron accelerator is small. A beam of electrons is directed on to a conveyor belt carrying small articles of uniform size, such as single packets of sutures or syringes. It is suggested that ionizing radiation will eventually become the main method of sterilizing the bulk of commercially packed medical equipment. Some present applications are listed. At present there are only a few industrial ^{60}Co installations in operation, one of the largest being at Dandenong, Australia. This plant, with a source of 500,000 C, was built with the primary object of sterilizing anthrax spores in intact bales of goat hair. The advantage of radiation sterilization are: the method is highly efficient; the temperature rise is negligible; and articles may be packaged and sealed before sterilization. However, some limitations in its use are: sterilization time is long if ^{60}Co is used (about ca 48 to 72 hr); glassware darkens and textile fibers lose their tensile strength; foods acquire an undesirable flavor at sterilizing doses; color and chemical changes occur in certain pharmaceuticals (e.g., penicillins). Other items of hospital equipment that have been considered for radiation sterilization are textiles such as blankets and mattresses. Blankets deteriorate after 20 treatments at sterilizing doses but withstand 100 radiodisinfecting doses of 0.5 Mrad. Use of nonionizing radiations for sterilization is also reviewed. (BBB)

46891 RADIATION INDUCED CHANGES IN THE KINETICS OF SHRIMP ENZYMES INVOLVED IN SPOILAGE (thesis). Kopfler, Frederick Charles Jr. Baton Rouge, La., Louisiana State Univ., 1964. 84p.

The effects of low-dose gamma irradiation with cobalt-60 on the iced storage life extension of fresh shrimp were investigated. Studies conducted on irradiated solutions of phenolase showed that the enzyme was inactivated. The radiation induced changes were found to be different from those reported to occur upon denaturation of proteins. The

presence of oxygen was shown to enhance inactivation of the enzyme, while the presence of ovalbumin in the phenolase solution protected the activity. The liberation of sulfhydryl groups was not detected after irradiation of 0.5 percent ovalbumin solutions. Irradiation of the substrate, 3,4-dihydroxyphenylalanine, accelerated the reaction. Reports indicated that the phenolase responsible for melanogenesis of shrimp was located in the shell and concentrated primarily at the joints between segments. It was concluded that water and oxygen may diffuse through these joints, and their radiolysis products are responsible for the inactivation of phenolase and subsequent reduction of melanosis. Irradiation of commercial shrimp in which melanogenesis has begun accelerated the reaction. It was postulated that the quinone-like end products of the reaction sequence acted as competitive inhibitors for the reaction, and also functioned as radiation protectors for the enzyme. It was concluded that low-dose gamma irradiation of fresh shrimp reduced melanosis and resulted in a significant extension of their iced-storage life. However, if shrimp were held beyond the onset of melanogenesis, subsequent low-dose irradiation accelerated blackspot formation, which reduced consumer appeal, and therefore was definitely undesirable. (A.G.W.)

46892 METHOD OF DETERMINING DENSITY UTILIZING A GAMMA RAY SOURCE AND A PAIR OF DETECTORS. Kehler, Paul (to Phillips Petroleum Co.). U. S. Patent 3,202,822. Aug. 24, 1965. Filed Nov. 13, 1961.

A method for determining the density of a material consists of passing gamma rays from a source into the material along at least one trajectory at an incident angle ϕ with respect to the reference plane in which the source is positioned; receiving a collimated beam of Compton-scattered photons from within the material, at an angle α with respect to the reference plane, on each of a pair of detectors spaced apart from the source; and measuring the ratio of the responses of the detectors. The detectors are sensitive only to photons that have been scattered at an angle of $\theta = \phi + \alpha$ with respect to the beam of gamma rays. The method is applicable also to well bore logging or to determining the location of the interface between two adjacent materials. (B.L.M.)

Power Application

46893 (DP–974) ^{60}Co HEAT SOURCES FOR 10-60 kw(e) GENERATORS. Dexter, Arthur H. (Du Pont de Nemours (E. I.) and Co., Aiken, S. C. Savannah River Lab.). July 1965. Contract AT(07-2)-1. 10p. Dep. mn; CFSTI $1.00 cy, $0.50 mn.

Cobalt-60 can be produced in large quantities for heat sources that could provide nuclear power in the 10–60 kw(e) range of some SNAP reactors. Potential advantages of ^{60}Co sources over SNAP reactors are: lower costs, longer operating life, more reliable operation, and simpler materials problems. Complete 4π radiation shielding would weigh about the same as the shadow shield for a SNAP reactor of equivalent power, and would provide better protection. (auth)

46894 (GA–5296) DESIGN OF THE SNAP-15A GENERATOR. Campana, R. J. (General Atomic, San Diego, Calif. John Jay Hopkins Lab. for Pure and Applied Science). June 19, 1964. Contract AT(04-3)-167. 36p. Dep. mn; CFSTI $2.00 cy, $0.50 mn.

The considerations and analysis leading to the design of the SNAP-15A generator are summarized. The SNAP-15A generator is a plutonium-238 fueled, metal thermocouple generator providing about 1 milliwatt of output power at greater than 4.5 volts for 5 years with very high reliability even under extreme environmental conditions. An estimation of the performance of the SNAP-15A generators is presented. (M.O.W.)

46895 ISOTOPE-POWERED THERMOELECTRIC GENERATOR FOR RIPPLE I. Thomson, J. M. (Atomic Energy Research Establishment, Harwell, Eng.). Electron. Letters, 1: 93-4(June 1965).

The thermoelectric generator for Ripple I converts the energy from a radioisotope heat source into electrical energy by means of a small module having 36 p- and n-type Bi_2Te_3 thermoelements. This module is mounted to a plug assembly in such a way that any change or maintenance required can be done without elaborately shielded handling facilities. The power from the generator is fed to electronic amplifying equipment to power a xenon flashing light. (auth)

46896 TUNNEL-DIODE INVERTOR FOR RIPPLE I AND II. Third, S. M. (Atomic Energy Research Establishment, Harwell, Eng.). Electron. Letters, 1: 94-5 (June 1965).

The electric output from the thermoelectric generators used in the Ripple I and Ripple II equipments is 75 mw at 400 mv. Because of the low-voltage output, a gallium-arsenide tunnel-diode convertor is used. This unit supplies a trickle charge to a storage battery energizing a pulsed navigation light, which requires a tube voltage of 500 v, a trigger voltage of 8 kv, and has a mean power consumption of 30 mw. (auth)

46897 SELF CHARGING NUCLEAR BATTERY. Goldstein, Melvin M.; Lieb, Harry C. (to U. S. Army). U. S. Patent 3,200,269. Aug. 10, 1965. Filed Jan. 31, 1961.

A nuclear battery consists essentially of a brass housing, a housing insert of Al alloy, a bronze contact pin molded in a thermoplastic resin, a brass insulator cap with an Al alloy insert, an electron emitter consisting of 0.1 cc of ^{90}Sr solution placed in the bottom of the housing and evaporated in place with a minute quantity of binder solution, and a shorting clip. The battery is expected to have a life of approximately 20 yr and a wide range of uses. (A.G.W.)

Separation and Production

See also CHEMISTRY — Separation Processes and Procedures.

Refer also to abstract 46157.

46898 (HMI-B–44) UEBER ISOTOPIE-EFFEKTE BEIM IONENTRANSPORT IN WAESSRIGER LOESUNG—ALS GRUNDLAGE ZUR ISOTOPENTRENNUNG UND ALS HILFSMITTEL PHYSIKALISCH-CHEMISCHER UNTERSUCHUNGEN AN BIOLOGISCHEN MEMBRANEN. (On the Isotope Effect in Ion Transport in Aqueous Solution—as a Basis for Isotope Separation on and as an Instrument in the Physical-Chemical Study on Biological Membranes). Wagener, Klaus (Hahn-Meitner-Institut fuer Kernforschung, Berlin (West Germany)). July 1965. 118p. Dep. mn.

The suitability of ion transport in aqueous solutions for isotope separations is discussed. The electrolytic counter current principle developed by Brewer and Madorsky with respect to methods and apparatus was investigated. The results obtained by the method were, however, unsatisfactory. A modification of the method, however, is described that gives more satisfactory results as the separation results show. The principle of the method is based on the fact that isotopic ions in aqueous solution possess a minute variation in mobility. The explanation for this variation in mobility is discussed with respect to the kinetic mass effect and the effects of dissociation and complex formation equilibrium. The use of this isotope effect in the investigation of active transport through biological membranes is shown on the basis of measurements. (J.S.R.)

46899 (ORNL–3832, pp 33-49) ISOTOPE CHEMISTRY. (Oak Ridge National Lab., Tenn.).

The single-stage separation factor for Li isotopes was 1.00064 for a carboxylic acid resin with 0.2N ammonium acetate as the eluant. The small α can be attributed to similar carboxylic bonding in both phases. Studies of the exchange of B isotopes between BF_3(g) and the $BF_3 \cdot (CH_3)_2Se$(l) complex were completed. Isotopic equilibrium

constants were determined as a function of temperature. The single-stage separation factors for $^{13}C/^{12}C$ and $^{18}O/^{16}O$ were determined for sec-butyl amine carbamate in equilibrium with a slight excess of CO_2. The parameter determining this separation factor in amine carbamates appears to be the temperature of equilibration. The N isotope effect in the decomposition of α,α'-azobisisobutyronitrile varies from 1.046 at 40° to 1.037 at 70°C and is described by the least-squares equation $\log k^{14}/k^{15} = 13.646/T - 0.02385$. The N isotope effect in reduction of NO_3^-, NO_2^-, and NH_2OH to NH_3 by Fe(II) is the same for each species when Cu is present. For boiling aqueous solutions the ratio k^{14}/k^{15} is 1.023. Aqueous boiling suspensions of MgO give various isotope effects for this reduction. For NO_3^-, k^{14}/k^{15} is 1.049; for NH_2OH it is 1.028; and for NO_2^-, 0.990 and 1.017, depending on the amount of Fe reagent used. The single-stage separation factor for Zn isotopes in the reaction $^{67}Zn(Hg) + {}^{66}Zn^{2+}(aq) = {}^{66}Zn(Hg) + {}^{67}Zn^{2+}(aq)$ is 1.0009 ± 0.0005 per mass unit. The heavy isotope concentrates in the aqueous phase. The infrared and Raman spectra of IOF_5 were recorded, and spectral assignments were made on the basis of an octahedral structure with a fourfold symmetry axis. Valence force constants were calculated. Methods used for the vibrational analysis of molecules were compared. Force constants were calculated from spectral data for the molecules XeF_2, XeF_4, $XeOF_4$, NH_3, and BF_3. Rates and activation energies were measured by NMR for the exchange of BF_3 between $(C_2H_5)_2O \cdot BF_3$ and $(C_2H_5)_2S \cdot BF_3$. These data were compared with our previous studies of similar mixtures. Isotopic analyses were performed on BF_3, CO_2, N_2, O_2, and BEt_3 samples. More than 1000 samples were handled during this report period. Conversion of BF_3 to $BeEt_3$ for mass analysis was studied as a means to eliminate the serious memory effects with the former; the results indicate that this would be a useful procedure. Two prototype columns used as the basic unit in a thermal diffusion cascade for the final enrichment of ^{17}O are described. The Oxygen-17 Facility performed well during the past year. The Water Distillation Cascade remained on stream 100% of the time. Maximum concentrations of ^{17}O and ^{18}O reached 13.6 and 99.8%, respectively. (auth)

46900 (RL-SA-46-A and Suppl.) CLEAN ^{233}U PRODUCTION — METHODS AND PARAMETERS. Meichle, R. H. (General Electric Co., Richland, Wash. Hanford Atomic Products Operation). July 26, 1965. Contract AT(45-1)-1350. 12p. CONF-651101-23. Dep. mn; CFSTI $1.00 cy, $0.50 mn.

For Presentation at 13th Conference on Remote Systems Technology, Washington, D. C.

The problem of minimizing the ^{232}U content in ^{233}U produced by irradiation of thoria is considered. Means of minimizing the fast neutrons and prompt gammas are described. The first order buildup equations for ^{232}U and ^{233}U are given. Results are given of test irradiations of 1-g ThO_2 samples in Al and graphite cans with varying ^{230}Th content. (D.L.C.)

46901 ECONOMIC OPTIMUM OF AN ENSEMBLE SATURATOR SEPARATING COLUMN CONDENSER IN AN ISOTOPE SEPARATING PROCESS. Peculea, M. (Institut fuer Atomphysik, Cluj). Rev. Roumaine Phys., 10: 393-401(1965). (In German).

Considerations are given to an isotopic separation apparatus used with phase conversion, and studies were made of an ensemble which consists of a saturator, separation column, and a condenser. The isotopic exchange occurs between a liquid and a gas phase. A thermodynamic study of the ensemble is carried out, and the principle and calculation scheme are established, which allows the degree of reversibility to be expressed in an intuitive form. The economic optimun is obtained in dependence on the saturation temperature, for each of the liquid films, and is dictated by values of the minimal cost price of the isotopes. A numerical example illustrates the use of the obtained equation; a family of curves proportional to the cost price is presented as a function of the saturation temperature. (tr-auth)

MATHEMATICS AND COMPUTERS

Refer also to abstract 48059.

46902 (ANL–7050, pp 207-13) COMMENTS ON COMPUTING. Hammer, Preston C. (Pennsylvania State Univ., University Park).

An outline is given of the relations between mathematics and the science of computers. (T.F.H.)

46903 (BNWL–70) ANALOG COMPUTER METHODS FOR PARAMETER OPTIMIZATION. Harvey, R. A.; Taylor, G. R.; Benham, R. D. (Battelle-Northwest, Richland, Wash. Pacific Northwest Lab.). June 1965. Contract AT(45-1)-1830. 32p. Dep. mn; CFSTI $2.00 cy, $0.50 mn.

Techniques for parameter optimization with analog computers where it is desired to determine the best parameters of a mathematical model are described. Both manual and automatic techniques for analog computer parameter optimization studies are presented. Studies were made on; first order differential equation, extraction column — steady-state model fitting, steady-state — random optimization, and river flow — dynamic model fitting. (M.O.W.)

46904 (EUR–2437.e) APACHE: ANALOG PROGRAMMING AND CHECKING PROGRAMMERS MANUAL. (European Atomic Energy Community, Ispra (Italy). Joint Nuclear Research Center; European Atomic Energy Community, Ispra (Italy). European Scientific Data Processing Center). June 1965. 214p. Dep. mn.

A manual is written to help the analog programmer in writing APACHE programs. It describes in detail the language and its limitations, and gives the procedure for the utilization of the code on the digital computer IBM 7090. The language illustrated is APACHE (Version IV). (auth)

46905 (IDO–17081, pp 125-35) MATHEMATICAL ANALYSIS AND MACHINE COMPUTATIONS. (Phillips Petroleum Co. Idaho Falls, Idaho, Atomic Energy Div.).

Progress continued on Phillips' Monte Carlo program. The input program is now essentially complete. The output includes a complete statistical analysis of the flux in each region. The efficiency of the program for use in reactor physics calculations is being studied. An IBM 7040 program was written to produce a radiation dose report for TRA maintenance. A program was written and checked out to calculate the real and complex roots of a polynomial with real coefficients using a combination of Newton and Bairstow formulas. An IBM 7040 program was developed for calculating the pulse-height response of NaI scintillation detectors. Reactor physics calculations were made on single-, two-, and three-region Westinghouse critical experiments described in WCAP-1433 for support of LOFT and PBF design calculations. (auth)

46906 A HYPERGEOMETRIC FUNCTION OF TWO VARIABLES OF IMPORTANCE IN PERTURBATION THEORY. [PART] II. Olsson, P. O. M. (Royal Inst. of Tech. Stockholm). Arkiv Fysik, 29:. 459-65(1965).

A hypergeometric function of two variables of importance in perturbation theory is continued analytically to a domain of interest in applications. The function has been introduced in a recent paper, where some of its fundamental properties were given. (auth)

METALS, CERAMICS, AND OTHER MATERIALS

General

Refer also to abstracts 47960 and 47993.

46907 (AD-456724) METALLIC BINDERS FOR ZIRCONIUM DIBORIDE: CHROMIUM, MOLYBDENUM, AND TUNGSTEN. Tyrrell, M. E.; Houck, C. W. (Bureau of Mines, Norris, Tenn. Norris Metallurgy Research Lab.). 1964. 14p. (BM-RI-6549). Bureau of Mines Free.

Mixtures of zirconium diboride and refractory metals of group VI were resistance sintered to high-density compacts using modified electric welding equipment. To evaluate the use of chromium, molybdenum, or tungsten as binders for zirconium diboride, the sintered compacts were examined in polished sections and tested for crushing strength, hardness, microhardness, oxidation rate, and resistance to mechanical shock. Chromium yielded the highest compressive strength, the greatest resistance to mechanical shock and oxidation, and a satisfactory Rockwell hardness. Molybdenum did not yield a satisfactory cermet. Tungsten yielded compacts having high microhardness but very low mechanical strength. (auth)

46908 (AD-614464) A SINTER PROCESS, USING MERCURY AS AN AUXILIARY COMPONENT AS APPLIED TO RE-Mn SYSTEMS. (A SUMMARIZING DISCUSSION). DIFFERENTIAL-THERMAL- AND MAGNETO-THERMAL-ANALYSIS OF THE SYSTEM Gd-Mn (0-50 w. percent Mn). Lihl, F. (Technische Hochschule, Vienna (Austria)). July 31, 1964. Contract AF61(052)-609. 62p. CFSTI $3.00 cy, $0.75 mn.

Summarization of the amalgam process is given which turned out to lead to equilibrium states even at higher temperatures than 300-400°C. Applying the amalgam process to higher temperatures (800-1200°C) the mercury, bound by the respective RE-metals, plays the role of an auxiliary component. The amalgam process is the main step of a very particular sinter process. The distillation of mercury out of the amalgam yields intimately mixtures of very fine and reactive powders of RE- and Mn-metal. The different steps of the sinter process are described in detail as well as the results gained applying this alloying method to the RE (Gd, Sm, Dy, Ho, Er)-Mn systems. By means of newly developed methods for differential thermal analysis (DTA) and magnetothermal analysis of small amounts of high reactive materials, the system Gd-Mn was studied and a partial phase diagram (0-50 wt % Gd) is given. (TAB)

46909 (AD-620264) PREPARATION AND EVALUATION OF HIGH PURITY BERYLLIUM. Final Report, October 15, 1963-January 14, 1964. Spangler, G. E.; Herman, M.; Hoover, D. B.; Damiano, V. V. (Franklin Inst. Research Labs., Philadelphia, Pa.). Contract NOw 63-0500-d. 87p. (F-B2098).

An investigation was conducted to produce high-purity Be and to study its deformation and fracture characteristics. Summaries are presented of work on the following topics: zone refining, mechanical property evaluation of single crystals, polycrystalline Be, dislocation structures and slip line markings in deformed single crystals of Be, basal plane fracture of Be single crystals, self-diffusion in Be single crystals, and zone refining heat control system. (D.L.C.)

46910 (AD-620589) FLOW AND FRACTURE STUDIES OF HIGH PURITY AND ALLOYED BERYLLIUM. Quarterly Technical Progress Report, October 7, 1964-January 6, 1965. Herman, M.; London, G.; Damiano, V.; Tint, G. S. (Franklin Inst. Research Labs., Philadelphia, Pa.). Contract NOw 64-0437-d. 11p. CFSTI $1.00 cy, $0.50 mn.

Progress in the zone refining of Be is reported. A theoretical analysis was performed to calculate the Peierls and critical resolved shear stress for various slip planes in Be. The examination of a swaged Be-Cu alloy is described. (D.L.C.)

46911 (AFML-TR-64-392) EXPERIMENTAL STUDY OF FACTORS CONTROLLING THE EFFECTIVENESS OF HIGH-TEMPERATURE PROTECTIVE COATINGS FOR TUNGSTEN. Technical Report, May 15, 1962-August 31, 1964. Brett, J.; Seigle, L. L.; Berkowitz-Mattuck, J.; Lement, B.; Phalen, D. I.; Vaughan, D. A.; Richard, N. A.; Austin, A. E.; Schwartz, C. M. (General Telephone and Electronics Labs. Inc., Palo Alto, Calif.). Nov. 1964. Contract AF 33(657)-8787. 284p.

The restrictions imposed by the processes of diffusion, evaporation, and coating-substrate reactions on the choice of potential protective coating materials for tungsten were studied analytically and experimentally. The diffusive restriction is the most limiting and eliminates many refractory oxides with otherwise satisfactory attributes. The diffusive properties of rare earth sesquioxides and complex refractory oxides were explored by means of oxidation experiments and a layer growth experiment respectively. Mass spectrometric studies of the vaporization of refractory complex oxides were carried out to determine the applicability of the Wagner-Hauffe method of predicting vaporization rates. Provided certain thermodynamic approximations are valid and the vapor species over the complex oxide are the same as those over the pure component oxides, the predictions yield order of magnitude accuracy. A survey and exploration of reactions of possible coating materials with tungsten was performed emphasizing promising materials from the diffusion studies. (auth)

46912 (BMI-1727(Del.)) PROGRESS RELATING TO CIVILIAN APPLICATIONS DURING MAY 1965. Dayton, Russell W.; Paprocki, Stan J. (Battelle Memorial Inst., Columbus, Ohio). June 1, 1965. Contract W-7405-eng-92. 43p. Dep. mn; CFSTI $1.00 cy, $0.50 mn.

Research and development are reported in sections on reactor materials and components, ceramic fuels, radioisotope and radiation applications, coated-particle fuel materials, and gas cooled reactor programs. (J.R.D.)

46913 (BMI-1733(Del.)) PROGRESS RELATING TO CIVILIAN APPLICATIONS DURING JUNE 1965. Dayton, Russell W.; Paprocki, Stan J. (Battelle Memorial Inst., Columbus, Ohio). July 1, 1965. Contract W-7405-eng-92. 46p. Dep. mn; CFSTI $1.00 cy, $0.50 mn.

Progress is reported in sections on reactor materials and components, studies of ceramic fuels, radioisotope and radiation applications, coated-particle fuel materials, and gas cooled reactor programs. (J.R.D.)

46914 (BNWL-141) A STUDY OF TUNGSTEN-TECHNETIUM ALLOYS. Quarterly Progress Report, January 1, 1965-April 1, 1965. (Battelle-Northwest, Richland, Wash. Pacific Northwest Lab.). Sept. 1965. Contract AT(45-1)-1830. 9p. Dep. mn; CFSTI $1.00 cy, $0.50 mn.

Arc-melted W-Tc buttons (0-60 at. % Tc) were radiographed and their density measured. The radiographs showed some porosity, and the density vs composition curve fell below the theoretical curve. The thermal diffusivity and conductivity of an electron-beam-melted Tc wafer were measured at room temperature to 575°C. (D.L.C.)

46915 (BNWL-IR-2) DESCRIPTION OF INVENTION. A METHOD FOR PURIFICATION OF PLUTONIUM METAL. Moore, R. H. (Battelle-Northwest, Richland, Wash. Pacific Northwest Lab.). Aug. 4, 1965. Contract AT(45-1)-1830. 2p. Dep. mn; CFSTI $1.00 cy, $0.50 mn.

A consumable electrode method is described for the purification of plutonium metal containing oxides, carbides, and nitrides. The plutonium consumable electrode is melted through a suitable flux of LiCl-KCl eutectic containing up to 10% KOH to form the ingot. The non-metallic

elements in the consumable electrode material transfer to the flux and are removed from the ingot metal. (P.C.H.)

46916 (BNWL-IR-3) DESCRIPTION OF INVENTION. URANIUM DIOXIDE–LEAD RADIATION SHIELDING. Albrethsen, A. E. (Battelle-Northwest, Richland, Wash. Pacific Northwest Lab.). Aug. 4, 1965. Contract AT (45-1)-1830. 2p. Dep. mn; CFSTI $1.00 cy, $0.50 mn.

The use of a UO_2–Pb composite as a shielding material is shown to have advantages in case of accidents involving fire. Even if the Pb is melted and lost, the UO_2 portion of the shielding would be retained, and excessive pressure due to thermal expansion would not occur. (D.L.C.)

46917 (DP-975) HEAVY WATER MODERATED POWER REACTORS PROGRESS REPORT, MARCH–JUNE 1965. Babcock, D. F.—Hood, R. R. (comp.) (Du Pont de Nemours (E. I.) and Co., Wilmington, Del. Technical Div.). Aug. 1965. Contract AT(07-2)-1. 26p. Dep. mn; CFSTI $2.00 cy, $0.50 mn.

Postirradiation examinations were completed on 14 Zircaloy-clad tubes of mechanically compacted uranium oxide that were irradiated in the Heavy Water Components Test Reactor. The tubes were irradiated at maximum thermal ratings ($\int kd\theta$) of 25 to 40 watts/cm to exposures as high as 17,000 Mwd/mtU. They operated in a satisfactory manner, and nothing was observed in the postirradiation examination to indicate that they would not continue to operate satisfactorily to exposures of 20,000 to 30,000 Mwd/mtU. Collapse tests on Zircaloy-clad UO_2 tubes at temperatures as high as 350°C indicated that the UO_2 core prevents collapse of the inner sheath at stress levels below the proportional limit of the sheath material. The hoop stresses at collapse were 4 to 9 times those at which elastic collapse should occur. Zircaloy-clad tubes of U metal alloyed with small amounts of Fe, Si, and Al increased in volume a maximum of 3% when irradiated to exposures as high as 5600 Mwd/mtU at a maximum U temperature of 425°C. The swelling was much less than that of unalloyed U. The U–Fe–Si–Al alloys showed excellent promise of operating satisfactorily to exposures of the order of 10,000 Mwd/mtU in D_2O-moderated power reactors; however, confirmatory irradiation tests will be necessary. A multigroup, multiregion method was developed for calculating neutron flux spectra and neutron absorptions in a cylindrical lattice cell at epithermal energies. The method is incorporated in a computer code, EPITHET. Another code, HAMMER, was developed that automates some of the calculations for frequently used lattice codes and bases the codes on a common mathematical model. Both EPITHET and HAMMER are available in FORTRAN language. The temperature coefficient of reactivity of a D_2O-moderated lattice of natural U metal (1.00-in.-dia. rods) was measured in an exponential facility. The measured coefficient at 20 to 80°C was -0.75 ± 0.16 $\mu B/°C$. (auth)

46918 (IITRI-B6018-1) A PROTOTYPE MANUAL OF METALLURGICAL PRACTICE. Levinson, David W.; Schwartzbart, Harry; Domagala, Robert F.; Grover, Donald P. (IIT Research Inst., Chicago, Ill.). Mar. 1965. Contract OCD-PS-64-50. 248p. CFSTI.

A manual of metallurgical practice was prepared to serve an educational function for nonprofessionally trained laymen in a post-attack situation. For purposes of this manual it is assumed that normal fabrication facilities and trained metallurgists are unavailable. This document provides information on applications of metals and alloys, identification and recognition, methods of varying the properties, shaping and joining, tool design, and furnace construction. (auth)

46919 (NMI-4996) TECHNICAL PAPERS OF THE FOURTEENTH METALLOGRAPHIC GROUP MEETING, HELD APRIL 5–6, 1960 AT NUCLEAR METALS, INC., WEST CONCORD, MASSACHUSETTS. Roth, H. P. (comp.) (Nuclear Metals, Inc., West Concord, Mass.). Jan. 6, 1964. Contract AT(30-1)-1565. 176p. (CONF-600401). Dep. mn; CFSTI $5.00 cy, $1.00 mn.

Thirteen papers are included; separate abstracts have been prepared for 7. Six papers were previously abstracted in NSA, see 13: 22767, 14: 22013, 15: 618, 28034, 16: 29382, and 30803. (W.L.G.)

For abstracts of individual papers see: 46920, 46951, 46964, 47000–47002, and 47083.

46920 (NMI-4996, pp 27-35c) DECREASING THE ELECTROPOLISHING TIME FOR URANIUM. Robins, L.; Garufi, M. F. (Bridgeport Brass Co., Conn.).

The behavior of mechanically polished uranium was studied during electropolishing to determine the times for preparing satisfactory metallographic samples. Specimens suitable for preferred orientation and microstructural examinations were obtained after 10 minutes in an orthophosphoric acid-ethyl alcohol-ethylene glycol solution, and after about 1.0 minute in a chromic-acetic acid solution. Evaluations were based on x-ray diffractometric and microscopic observations. (auth)

46921 (NMI-4997) TECHNICAL PAPERS OF THE FIFTEENTH METALLOGRAPHIC GROUP MEETING HELD MAY 17–19, 1961, AT SAVANNAH RIVER LABORATORY, AIKEN, SOUTH CAROLINA. Roman, H. Roth (comp.) (Nuclear Metals, West Concord, Mass.). May 1, 1964. Contract AT(30-1)-1565. 241p. (CONF-610501). Dep. mn; CFSTI $6.00 cy, $1.25 mn.

Eighteen papers are included; separate abstracts have been prepared for 16. Two were previously abstracted for NSA, see 15: 7765 and 28031. (W.L.G.)

For abstracts of individual papers see: 46176, 46507, 46556, 46922–46925, 46952, 46953, 47004–47006, and 47084–47087.

46922 (NMI-4997, pp 22-5) METALLOGRAPHIC PREPARATION OF HARD AND BRITTLE MATERIALS. Dvorak, J. R. (Illinois Inst. of Tech., Chicago).

A new and somewhat unconventional method was developed for the metallographic preparation of boron–carbon alloys. These hard and brittle materials are polished in three steps utilizing an automatic mechanical polisher. Two of these operations are performed without the use of conventional cloth-covered wheels. The abrasive is applied directly to a wheel that is fabricated from selected materials. Although the polishing procedure is somewhat time consuming, it would be almost impossible to polish these samples by conventional techniques. The results are excellent; very little relief is produced even in samples of the boron carbide–graphite eutectic. No chipping or pullouts are produced in the extremely brittle phases. This same polishing technique can be successfully applied to other brittle materials. (auth)

46923 (NMI-4997, pp 36-44) PRELIMINARY EVALUATION OF A NEW POLISHING CLOTH. Crouse, R. S. (Oak Ridge National Lab., Tenn.).

The cloth was tested using vibratory and hand polishing methods with several metals and alloys. The polishing action provided is quite rapid and reduces the time for the primary polishing step by about 50%. It was not suitable for polishing aluminum nor for final polishing with Linde B abrasive. The cloth, a mat of fibers apparently held together by a plastic coating, is not as universally applicable as nylon or silk but definitely has a place in metallographic operations. (auth)

46924 (NMI-4997, pp 55-61) MICROSTRUCTURES OF COMPOUNDS OF URANIUM, THORIUM, AND BERYLLIUM. Thompson, C. R.; Farkas, M. S.; Bauer, A. A. (Battelle Memorial Inst., Columbus, Ohio).

The metallography of some of the compounds of uranium, thorium, thorium–uranium, and beryllium is discussed. (auth)

46925 (NMI-4997, pp 85-91) METALLOGRAPHIC PREPARATION OF ALUMINA COATED UO_2 SPHERES IN GRAPHITE. Lott, J. M.; Farkas, M. S.; Bauer, A. A. (Battelle Memorial Inst., Columbus, Ohio).

Three problems arise in the metallographic preparation

of alumina-coated UO_2 in graphite. The maintenance of a flat surface is made difficult by the presence of three materials of different hardness. Secondly, the coated spheres must be retained in the graphite during the cutting and grinding operation. The third problem is that of obtaining the correct, full-density appearance of the alumina and UO_2. Normal preparation methods are discussed and techniques adapted for hot cell preparation are explained. (auth)

46926 (NMI–4998) TECHNICAL PAPERS OF THE SIXTEENTH METALLOGRAPHIC GROUP MEETING, HELD MARCH 28–29, 1962 AT HANFORD ATOMIC PRODUCTS OPERATION, RICHLAND, WASHINGTON. Roman, H. Roth (comp.) (Nuclear Metals, West Concord, Mass.). Aug. 31, 1964. Contract AT(30-1)-1565. 126p. (CONF–620301). Dep. mn; CFSTI $4.00 cy, $0.75 mn.

Eleven papers are included; separate abstracts have been prepared for 5. Six papers were previously abstracted in NSA, see 16: 9165, 20953, 17: 538, 6516, 6680, and 20459. (W.L.G.)

For abstracts of individual papers see: 46508, 46927–46929, and 47088.

46927 (NMI–4998, pp 1-5) MOUNTING OF METALLOGRAPHIC SAMPLES IN EPOXY RESINS USING MULTIPLE CAVITY MOLDS. Hewette II, D. M.; Crouse, R. S. (Oak Ridge National Lab., Tenn.).

Multiple cavity molds were developed for mounting metallographic samples in epoxy resins. For general laboratory use the molds are fabricated from stainless steel. The use of a metal mold requires application of an appropriate mold release for each mounting operation. In glove box facilities where contamination is a problem and where volatile solvents cannot be tolerated, a Teflon mold, which does not require a mold release, was used with moderate success. Flexible molds of silicone rubber vulcanized at room temperature were fabricated and show considerable promise. (auth)

46928 (NMI–4998, pp 14-19) THIRTY-FIVE MILLIMETER COLOR PHOTOMICROGRAPHY. Hopkins, E. N.; Peterson, D. T. (Ames Lab., Iowa State Univ. of Science and Tech.).

A 35 mm camera was simple adapted to a B and L Research Metallograph. This enables the metallographer to take large quantities of color photographs using all the equipment available on the metallograph and at a reasonable cost. (auth)

46929 (NMI–4998, pp 57-64) IDENTIFICATION OF CARBIDES, NITRIDES, AND OXIDES OF COLUMBIUM BY ANODIC STAINING. Crouse, Robert S. (Oak Ridge National Lab., Tenn.).

Carbides, nitrides and oxides in Nb may be identified in metallographic specimens by anodization. Specimens that have been in carefully controlled atmospheres at high temperatures were polished and anodized and identification of the phases correlated with chemical and x-ray diffraction data. It was found that two carbides, two nitrides and three oxides could be differentiated by their characteristic colors. This technique is used to qualitatively identify carbides, nitrides, and oxides in metallographic specimens. More accurate determinations require more conventional chemical analyses. (auth)

46930 (NMI–4999) TECHNICAL PAPERS OF THE SEVENTEENTH METALLOGRAPHIC GROUP MEETING, HELD MAY 21–23, 1963 AT LOS ALAMOS SCIENTIFIC LABORATORY, LOS ALAMOS, NEW MEXICO. Roman, H. Roth (comp.) (Nuclear Metals, West Concord, Mass.). Apr. 1, 1965. Contract AT(30-1)-1565. 166p. (CONF–105). Dep. mn; CFSTI $5.00 cy, $1.00 mn.

Sixteen papers are included; separate abstracts have been prepared for 9. Seven papers were previously abstracted in NSA, see 17: 29251, 29327, 29376, 29389, 34364, 37458, and 19: 18452. (W.L.G.)

For abstracts of individual papers see: 46931–46935, 47003, and 47089–47091.

46931 (NMI–4999, pp 26-9) A PROCEDURE FOR COLOR MICROPHOTOGRAPHY. Gruber, W. J. (General Electric Co., Richland, Wash. Hanford Atomic Products Operation).

The criteria and a procedure for successful color photography with a metallograph is described. Some of the fundamentals of color photography, which are considerations affecting the method selected, are discussed. (auth)

46932 (NMI–4999, pp 60-8) REPLICATION OF MICROSTRUCTURES USING SILICONE RUBBER AND EPOXY RESIN. Crouse, R. S. (Oak Ridge National Lab., Tenn.).

Degassed silicone rubber is poured in a hollow cylinder containing a polished and etched metallographic specimen as the bottom. When the rubber has sufficiently cured to withstand handling, the metallographic specimen is removed and the rubber negative replica becomes the bottom of the cylinder. Epoxy resin is poured on the rubber replica and after setting, is removed and metallized to produce a permanent positive replica. (W.L.G.)

46933 (NMI–4999, pp 78-84) PREPARATION OF THIN FOILS OF URANIUM. Angerman, C. L. (Du Pont de Nemours (E. I.) and Co., Aiken, S. C. Savannah River Lab.).

Foils of uranium suitable for direct observation in the electron microscope were prepared by electropolishing first in a solution containing phosphoric acid, ethylene glycol, and ethyl alcohol and then in a solution containing sulfuric acid, glycerine, and water. Twins, line dislocations, and dislocation loops were observed in typical samples. (auth)

46934 (NMI–4999, pp 104-10) PLUTONIUM METALLOGRAPHIC PRACTICES AT BATTELLE. Snider, R. H.; Storhok, V. W.; Farkas, M. S. (Battelle Memorial Inst., Columbus, Ohio).

A wide variety of plutonium-bearing materials were prepared for metallographic examination at the Battelle Plutonium Laboratory. Operating philosophy, equipment, general metallographic procedures as well as specific techniques for such materials as oxides, nitrides, and several metallic alloys are described. (auth)

46935 (NMI–4999, pp 129-36) A PORTABLE METALLOGRAPHY LABORATORY. Crouse, R. S. (Oak Ridge National Lab., Tenn.).

During the fabrication of large reactor components in the Oak Ridge National Laboratory and other local area shops, need for on-the-spot metallographic examination became apparent. The components were bulky and difficult to move to a central metallography lab. Although they were too valuable to be cut into small sections, it was permissible for specific areas to be ground and polished in situ for examination. These restrictions on standard metallographic procedures required that some means of polishing, etching, and examining be devised to cope with these situations. Two specific instances, the ways in which they were handled, and the portable kit which evolved are described. (auth)

46936 (NMI–5025(Pt.I)) TECHNICAL PAPERS OF THE EIGHTEENTH METALLOGRAPHIC GROUP MEETING HELD JUNE 22–24, 1964, ATOMICS INTERNATIONAL, CANOGA PARK, CALIFORNIA. Roman, H. Roth (comp.) (Nuclear Metals, West Concord, Mass.). Aug. 1965. 212p. (CONF–607(Pt.I)). Dep. mn; CFSTI $2.25 cy, $1.25 mn.

Fourteen papers are included; separate abstracts have been prepared for 6. Eight were previously abstracted in NSA, see 18: 32048, 32049, 32051, 32054, 34047, 44059, 19: 6264, and 7854. (W.L.G.)

For abstracts of individual papers see: 46177, 46937–46939, 46954, and 47007.

46937 (NMI–5025(Pt.I), pp 1-25) METALLOGRAPHIC AND CERAMOGRAPHIC PREPARATION OF NUCLEAR MATERIALS. Filer, E. W.; Asaud, C. A.; Lacefield, K.; Kull, R. B. (General Electric Co., Cincinnati, Ohio. Nuclear Materials and Propulsion Operation).

The polishing and etching procedures for preparing metallic, ceramic and cermet specimens of nuclear materials using the Automet polisher are discussed with some typical examples of the excellent results obtained. The attack-polishing method reported by Ambler and Slattery was successfully adapted to automatic polishing allowing more pressure to be applied to the specimen. This modification has eliminated the difficulties normally encountered in the preparation of specimens containing materials of extreme variations in hardness. The advantages of this technique are discussed. (auth)

46938 (NMI–5025(Pt.I), pp 153–4) A BRIGHT FIELD ETCH FOR ALPHA–PLUTONIUM. Storhok, V. W.; Snider, R. H.; Farkas, M. S. (Battelle Memorial Inst., Columbus, Ohio).

The etchant, which is used electrolytically, consists of 75 cc ethyl alcohol, 20 cc nitric acid, and 5 cc water. The etching technique was not consistently successful. (W.L.G.)

46939 (NMI–5025(Pt.I), pp 185–219) VIBRATORY GRINDING AND POLISHING OF METALLOGRAPHIC SPECIMENS. Matras, S. (Argonne National Lab., Ill.).

The range of metallographic specimen preparation by vibratory polishing was extended to include the grinding operation. A controlled method was developed that reduces the metallographic grinding operation to essentially one step. This was achieved by: (1) controlling the horizontal and vertical components of vibration by changing the springs and the weight of the base of the apparatus to conform to the specific requirements of grinding, (2) providing a special fixture that guides the specimen in a controlled and predetermined manner. The grinding fixture consists of a Lucite bowl that holds an 8 in. dia SiC paper disc and a rotating turret in which the specimens are spaced and loaded with appropriate weights. The grinding produces specimens with surfaces that possess a minimum of disturbed metal with virtually no embedded abrasive. The specimens have flat surfaces and their edges are well preserved. Inclusions and second phases, not normally in evidence at this stage of specimen preparation, are clearly delineated in the matrix. Retention of hard inclusions in a soft matrix is excellent. The commercial vibratory polishers do not always produce a scratch-free final polish, especially with high-purity materials that are soft and ductile. To achieve satisfactory surfaces a final polishing fixture utilizing a center mounted rotating carrier was devised. This fixture replaces the standard stainless steel polishing bowl and retaining ring. The fixture is mounted on a standard vibratory polishing unit. In contrast to standard vibratory polishing units that require specimen loadings of 300 to 600 gm, the new device may be operated without any load on the specimen and will produce a superior polish. Preparing metallographic specimens now involves only three steps: specimen grinding on 400 or 600 grit paper, intermediate polishing, and final polishing. No more hand operations are necessary. The method has broad applicability; for example, it is routinely used for the specimen preparation of cermets; and high-purity Th and Th–Pu alloys have also been successfully prepared. The technique is presently adapted to glovebox work for Pu and its alloys, diffusion couples, and alloys and cermets that are difficult to prepare. (auth)

46940 (NP–15444) DEVELOPMENT AND EVALUATION OF TUNGSTEN-BASE ALLOYS. Final Report, January 10, 1964–March 10, 1965. Semchyshen, M.; Barr, Robert Q.; Kalns, Eric (Climax Molybdenum Co. of Michigan, Ann Arbor). Contract NOw 64-0057-c. 96p.

The investigation is concerned with the development of tungsten-base alloys having high strengths at elevated temperatures. The major portion of the alloys are ternaries containing carbon and up to nominally 0.5% Zr, 1% Hf or 2% Nb as the alloy additions; however, several quaternary alloys are included which contain carbon and the same alloying elements in various combinations. In addition, boron was substituted for carbon in three of the heats. All of the alloys were consolidated by vacuum-arc-melting. Primary working of the as-cast ingots was achieved by extrusion; the tungsten-base alloy blanks were encapsulated in molybdenum prior to extrusion. Additional working of the extruded materials was attempted by swaging. Even though the facilities utilized for swaging had temperatures available for heating of the work up to 3500°F, the working temperatures were too low for successful swaging of the extruded billets, and, as a result, only two alloys yielded reasonable stock after swaging. Strength properties and recrystallization temperatures are reported for the alloys after extrusion and after swaging. It is shown that both strength and recrystallization temperature are dependent on the carbon as well as the metallic alloy content. The highest tensile strength values demonstrated by the alloys investigated were 78,600 psi at 3000°F, 62,300 psi at 3500°F, 34,200 psi at 4000°F, 21,600 psi at 4500°F, and 6,600 psi at 5000°F. (auth)

46941 (NP–15514(Vol.3)) RESEARCH ON PHYSICAL AND CHEMICAL PRINCIPLES AFFECTING HIGH TEMPERATURE MATERIALS FOR ROCKET NOZZLES. Final Report. Volume III. Aspinall, S. R. (Union Carbide Research Inst., Tarrytown, N. Y.). Aug. 1965. Contract DA-30-069-ORD-2787. 203p.

Methods for the preparation of refractory borides, carbides, nitrides, and skeletal refractory-carbide and metal composites, the determination of boron in refractory borides by pyrohydrolysis, and the analysis of hafnium, niobium, tantalum, titanium, and zirconium borides, carbides, and nitrides are presented. A bibliography on the analytical chemistry of the group IV and V borides, carbides, and nitrides is included. (W.L.G.)

46942 (NUMEC–3524-6) DEVELOPMENT AND TESTING OF UO_2–PuO_2 FAST REACTOR FUELS. Quarterly Progress Report, April 1–June 30, 1965. (Nuclear Materials and Equipment Corp., Apollo, Pa.). Contract AT(30-1)-3524. 17p. Dep. mn; CFSTI $1.00 cy, $0.50 mn.

A research program is being conducted on the production, irradiation performance, and physical properties of UO_2–PuO_2 fuels for fast reactors. A list is presented of the specifications for the materials and processes to be used in the production of fuel for the irradiation program. The chemical and physical properties of enriched UO_2 and UNH crystals are tabulated. The particle size distribution of one PuO_2 lot is graphed. The process, equipment, and conditions for the coprecipitation of PuO_2–UO_2 are described. Work on physical property measurements and mixed oxide extrusion is reported. (D.L.C.)

46943 (FTD-TT-65-611) CALCULATION OF RATE OF VAPORIZATION OF METAL FROM CYLINDRICAL VESSELS INTO A VACUUM AND MASS SPECTROMETRIC INVESTIGATION OF VAPOR PRESSURES OF METALS AND ALLOYS. Lyubitov, Yu. N. Translated from Fiz. Khim. Osnovy Proizv. Stali, Akad. Nauk SSSR, Inst. Met., Tr. 6-oi(Shestoi)Konf., Moscow, 358–65(1964). 13p. CFSTI.

Equations are derived for calculating the vaporization coefficients of monomers and dimers from a cylindrical cell. The calculation of necessary and sufficient conditions for the occurrence of saturated vapor above the bottom of the cylinder is also considered. The application of the calculations to the mass spectrometer is described. (D.L.C.)

46944 ELECTROLYTIC NICKEL PLATING BATH. Facquet, Louis; Daboval, Jacques; Chauvin, Guy (to Commissariat a l'Energie Atomique). U. S. Patent 3,203,877. Aug. 31, 1965. Priority date Mar. 22, 1960, France.

A boron and carbon free electrolytic Ni plating bath for pit-free Ni plating of U bars for use in reactors consists of an aqueous solution of approximately 280 g/l of water-soluble Ni salt and an Al alum at a concentration of from 15 to 280 g/l. Preferably, the Ni salt is $NiSO_4 \cdot 7\,H_2O$ and the alum is the K alum, $K_2Al_2(SO_4)_4 \cdot 24\,H_2O$. The bath has a pH of from 3 to 3.5, a temperature between 40 and 60°C, and a current density of from 1 to 10 amp/dm^2. A concentration of chloride ions of not more than 15 g/l can be tolerated in the bath. (B.L.M.)

Corrosion

Refer also to abstracts 46478, 48059, and 48060.

46945 (BNWL-98) NICKEL-PLATED ALUMINUM IN DEIONIZED WATER, pH 10 NH_4OH AND LiOH AT 330°C. Johnson, A. B. Jr. (Battelle-Northwest, Richland, Wash. Pacific Northwest Lab.). Sept. 1965. Contract AT(45-1)-1830. 39p. Dep. mn; CFSTI $2.00 cy, $0.50 mn.

Aluminum alloys, nickel-plated by chemical deposition (electroless process), were diffusion-bonded and exposed to semistatic deionized water and to dynamic (25 ft/sec) pH 10 NH_4OH and pH 10 LiOH at 330°C. The nickel-plated aluminum was compatible with deionized water and pH 10 NH_4OH, but not with dynamic pH 10 LiOH. (auth)

46946 (BNWL-100) HIGH TEMPERATURE CORROSION OF CANDIDATE ATR STRUCTURAL MATERIALS. Charlot, L. A.; Westerman, R. E. (Battelle-Northwest, Richland, Wash. Pacific Northwest Lab.). Sept. 1965. Contract AT(45-1)-1830. 71p. Dep. mn; CFSTI $3.00 cy, $0.75 mn.

The behavior of Hastelloy X-280 and Haynes Alloy 25 in static atmospheres of oxygen, methane, carbon monoxide, carbon dioxide, nitrogen, flowing helium, and water vapor at temperatures of 1120 and 1200°C was studied. Evaporation rates of the alloys and corrosion of weldments in contaminated helium were also studied. At 1200°C, Hastelloy X-280 and Inconel 600 demonstrate an oxidation resistance which would permit their use in oxidizing atmospheres for short periods of time, e.g., a few hours in air, with only moderate attack. Haynes Alloy 25 cannot be exposed to atmospheres containing a higher oxygen partial pressure than about 0.3 torr at 1200°C, even for short times, without risk of catastrophic attack. Haynes Alloy 25, Hastelloy X-280, and Inconel 600 evaporate at similar rates at 1200°C under vacuum conditions (pressures ~10^{-4} torr). It appears that oxidation rates of the superalloys tested would not be too severe at 1200°C if the partial pressure of oxygen did not exceed a pressure of about 0.1 torr. Haynes Alloy 25 exhibited much greater stability in oxygen atmospheres at 1120°C than 1200°C. The relative rate of attack by oxygen is comparable to the attack on Hastelloy X-280. At 1000°C, the oxidation resistance of Hastelloy X-280, Haynes Alloy 25, and Hastelloy C are similar in atmospheres of 3 torr oxygen pressure or greater. In general, however, Hastelloy X-280 seems to be more resistant to internal attack than Haynes Alloy 25 and also shows less dependence on surface preparation than either Haynes Alloy 25 or Hastelloy C. All oxidized alloys tended to spall when cooled from the test temperatures, even in the case of rather thin films. Haynes Alloy 25 was especially susceptible to oxide spallation, particularly when the sample was thermally cycled. Hastelloy X-280 was more stable during thermal cycling, although in both cases more weight was lost from the sample by spalling than gained by oxidation. If Haynes Alloy 25 is to be used as a structural material in the ATR gas loop, cobalt bearing oxide particles can be expected to move within the coolant stream. Other gaseous contaminants such as methane, carbon dioxide, carbon monoxide, and water vapor can be harmful if their concentration reaches a high enough level. At 1200°C, 100 torr nitrogen pressure has no effect on Hastelloy X-280 and Haynes Alloy 25 except to inhibit evaporation. In the case of a system free of oxidizing contaminants, metal vapors from potential evaporating structural materials will be present in the helium gas, especially at temperatures in excess of 2000°F. The metal vapors must then be considered as potentially harmful as the expected gaseous contaminants in their deleterious effects on refractory metal irradiation specimens (solution and subsequent masking of irradiation effects). In the case of Hastelloy X-280–Haynes Alloy 25 weldments at 1200°C, the oxidation resistance of the Haynes Alloy 25 will determine the oxidation resistance of the couple. Hastelloy X-280–Hastelloy X-280 weldments show oxidation resistance equivalent to the parent metal. Grade A helium has a corrosive effect on Haynes Alloy 25 and Hastelloy X-280 at 1038°C. Hastelloy X-280 forms a more tenacious scale and exhibits less internal attack for a given exposure. The superalloys tested exhibit extremely complex corrosion behavior as a function of oxygen pressure. At very low oxidant partial pressures (expected in the ATR loop), it is impossible to predict exactly what degradation phenomenon will be most important especially when the effects of high velocity, high pressure helium are not known. It is of utmost importance that a careful ATR structural material surveillance program be maintained. (D.L.C.)

46947 (CEA-R-2732) CORROSION ATMOSPHERIQUE DES ALLIAGES URANIUM–CARBONE. (Atmospheric Corrosion of Uranium–Carbon Alloys). Rousset, Pierre; Accary, Andre (Commissariat a l'Energie Atomique, Saclay (France). Centre d'Etudes Nucleaires). May 1965. 46p. Dep. mn.

The corrosion of uranium-carbon alloys having compositions close to that of the mono-carbide was studied. It is shown that the extent of the observed corrosion effects increases with the water vapor content of the surrounding gas, and it was concluded that the atmospheric corrosion of these alloys is due essentially to the humidity of the air, the effect of the oxygen being very slight at room temperature. Optimum conditions for preserving U-C alloys are either a vacuum or a perfectly dry argon atmosphere. The type of corrosion involved is one that cracks under stress and is transgranular (it can also be intergranular in the case of substoichiometric alloys). Two hypotheses for explaining this mechanism are proposed, one of which is illustrated by the existence, at the fissure interface, of corrosion products which can play the role of corners in the monocarbide grains. (auth)

46948 (CEA-R-2805) ETUDE COMPARATIVE DE L'OXYDATION DE DIVERSES QUALITES D'URANIUM DANS L'ANHYDRIDE CARBONIQUE AUX TEMPERATURES ELEVEES. (Comparative Study of the Oxidation of Various Qualities of Uranium in Carbon Dioxide at High Temperatures). Desrues, Rene; Paiedassi, Jean (Commissariat a l'Energie Atomique, Saclay (France). Centre d'Etudes Nucleaires). Aug. 1965. 30p. Dep. mn.

Uranium samples of six different qualities were subjected, in the temperature range 400–1000°C, to the action of carbon dioxide carefully purified to eliminate oxygen and water vapor; the resulting oxidation was followed micrographically and also (but only in the range 400–700°C) gravimetrically using an Ugine-Eyraud microbalance. Oxidation of the six uraniums studied obeys a linear law (followed at 700°C by an accelerating law). The rates of reaction differ by a maximum of 100%, the higher purity grades being oxidized more slowly except at 700°C when the reverse is true. Simultaneously with the growth of an approximately uniform film of uranium dioxide on the metal, there occurs a localized attack in the form of blisters in the immediate neighborhood of the monocarbide inclusions in the uranium. The relative importance of this attack is greater for lower oxidation temperatures and for a larger size, number, and inequality of distribution of the inclusions, that is to say for higher carbon concentrations in the uranium (which have values of from 7 to 1000 ppM). For oxidation temperatures above 600°C blistering is much less pronounced, but at 700°C there occurs the beginning of a general deformation of the sample which, above 750°C, becomes much greater; this leads to an acceleration of the reaction rate with respect to the linear law. In view of over-heating, the sample must already be in the γ-phase which is particularly easily deformed; furthermore this expansion phenomenon is more pronounced when the sample is more plastic and therefore purer. (auth)

46949 (CONF-650905-2) THE CORROSIVE POTENTIAL OF WETTED THERMAL INSULATION. Karnes, Herman F. (Knolls Atomic Power Lab., Schenectady, N. Y.). Sept. 1965. Contract W-31-109-eng-52. 44p. Dep. mn; CFSTI $2.00 cy, $0.50 mn.

From American Institute of Chemical Engineers Symposia, Minneapolis.

Practically all thermal insulating materials contain constituents which can be leached from wetted insulation.

Under conditions of moderate heating it has been determined that insulating materials which are wetted continuously can cause stress corrosion cracking of certain materials of construction such as austenitic stainless steel. The corrosion is attributed to the concentration of these leachable constituents at the insulated heated surface. However, not all insulating materials under similar exposure conditions will promote this corrosion. A study was undertaken in an effort to obtain a more quantitative basis for the corrosion potential. Over eighty samples of insulating material were included in the study. The insulating material included block, felt, cements, and lagging items. Each of the samples were analyzed for pertinent leachable constituents such as chloride, silicate, sodium, and hydrogen ion concentration (pH). Approximately 50% of the samples were also corrosion tested through the medium of heated, stressed, U-bend specimens covered with wetted thermal insulation. Some of the samples caused 100% failure within one week whereas others were satisfactory for periods extending to three months. A correlation between the leachable analysis and the corrosion potential was prepared on the basis of the data. (auth)

46950 (LA-DC-7315) HIGH-TEMPERATURE COMPATIBILITY TESTING OF MOLTEN PLUTONIUM FUEL-CONTAINER SYSTEMS. Andelin, R. L. (Los Alamos Scientific Lab., Univ. of California, N. Mex.). [1965]. Contract W-7405-eng-36. 5p. (CONF-651101-28). Dep. mn; CFSTI $1.00 cy, $0.50 mn.

For Presentation at 13th Conference on Remote Systems Technology, Washington, D. C.

The linear relation of Ta capsule lifetime versus temperature obtained for capsules containing Pu and Ga-stabilized Pu–2.5 wt % Fe fuels implies a constant failure mechanism with temperature. The capsules containing Pu had a much shorter lifetime. Carburization of the Ta capsule retarded the Pu intergranular penetration. No difference was observed when using high-purity Na (<1 ppM O_2) or high vacuum (1×10^{-7} torr) as external capsule environments during testing. (W.L.G.)

46951 (NMI-4996, pp 19-26) NOVEL METALLOGRAPHIC UTILIZATION OF REPLICAS AND MICROAUTORADIOGRAPHY. Bierlein, T. K.; Mastel, B. (General Electric Co., Richland, Wash. Hanford Atomic Products Operation).

A method for conducting microautoradiography and metallography on radio and chemically active materials is described and illustrated. In the case of intermetallic compound formation between uranium and AlSi, an etched specimen is coated with Saran which, in turn, is coated with NTB liquid emulsion. After suitable exposure and processing, the Saran and adherent emulsion is stripped with Scotch tape from the specimen. Bright field, reflected light examination of this stripped replica reveals the microstructural detail; polarized light examination of the stripped replica, only the tracks, the reduced silver grains in the emulsion. Correlation of the tracks in the emulsion and microstructural features on the replica is simple and unambiguous. (auth)

46952 (NMI-4997, pp 26-35) MEASUREMENT OF THE THICKNESS OF ALUMINUM OXIDE FILM. Costas, L. P.; Hoxie, E. C. (Du Pont de Nemours (E. I.) and Co., Aiken, S. C. Savannah River Lab.).

A metallographic and a optical technique for measuring the thickness of an alumina film, which was formed as a corrosion product, are described. In the metallographic technique, the sample is dipped into a low-melting Pb–Sn alloy to prevent the rounding of the alumina edges during preparation. The optical method consists of a modification of the Kapernick method, which depends on the differences in the fine focus readings taken between the metal and oxide surfaces. (W.L.G.)

46953 (NMI-4997, pp 62-75) A MICROGRAPHIC STUDY OF THE EFFECT OF MOISTURE IN THE AIR ON ARC-CAST URANIUM MONOCARBIDE AND URANIUM DICARBIDE AT ROOM TEMPERATURE OVER EXTENDED PERIODS. Gray, R. J.; DuBose, C. K. H. (Oak Ridge National Lab., Tenn.).

The development of fissures in uranium carbide metallographic specimens were observed over a four year period. Specimens consisting primarily of uranium monocarbide showed an increase in the severity of fissures after periodic removal from a storage desiccator for examination in ambient laboratory atmosphere. In uranium monocarbide and uranium dicarbide specimens, the amount of fissuring varied inversely with the uranium dicarbide content in the range of 10 to 90%. Uranium monocarbide specimens with minor amounts of α-uranium were observed to develop fissures and minute eruptions in a short time if fully exposed to the ambient atmosphere, but could be sealed in a desiccator and remain inactive for a seemingly indefinite time. (auth)

46954 (NMI-5025(Pt.I), pp 39-58) METALLOGRAPHY OF CERAMIC FUEL AND REFRACTORY METAL COMPATIBILITY COUPLES. McGrath, F. E.; De Mastry, J. A.; Farkas, M. S. (Battelle Memorial Inst., Columbus, Ohio).

The simultaneous compatibility of refractory claddings with UC, UN or UO_2 and liquid Li or Cs vapor was determined by metallographic examination of heated compatibility assemblies. (auth)

46955 (NP-15431) TWO-PHASE MATERIALS ATTRITION PROBLEMS FOR RANKINE CYCLE LIQUID METAL POWER PLANTS. Internal Report 03424-28. Hammitt, Frederick G. (Michigan Univ., Ann Arbor. Lab. for Fluid Flow and Heat Transport Phenomena). July 1965. 27p.

Due to the increasing applications of the liquid metal Rankine cycle powerplants for power in space, compatibility problems between fluid and container materials at operating temperatures were investigated. Those material problems due to the two-phase nature of the fluid flow which will be present in the vapor generator and the condenser are considered. (M.O.W.)

46956 (NP-15514(Vol.1)) RESEARCH ON PHYSICAL AND CHEMICAL PRINCIPLES AFFECTING HIGH TEMPERATURE MATERIALS FOR ROCKET NOZZLES. Final Report. Volume I. Walsh, Patrick N. (Union Carbide Research Inst., Tarrytown, N. Y.). Aug. 1965. Contract DA-30-069-ORD-2787. 342p.

Results are presented for research in the areas of: an induction-heated stagnation-flow reactor for high temperature gas-solid reaction rate measurements; an arc-image stagnation-flow reactor for measuring kinetics of gas-solid reactions from 2000 to 3000°K; stagnation-point velocity distribution for a compressible fluid; numerical solution for stagnation-line flow with heterogeneous chemical reaction; kinetics of the oxidation of W by CO_2; chemical reactivities of refractory carbides and borides; an algorithm for the computation of diffusion-controlled rates of gas-solid reactions; the reaction of microwave-activated N_2 with graphite; the reaction of graphite and refractory carbides with H_2; a mass spectrometric study of the vaporization of Pd; mass spectrometric study of ZrB_2; mass spectrometric measurements of the vaporization of B, Hf, and Ti; a mass spectrometric study of the vaporization of the B–Ti system; a mass spectrometric study of vaporization coefficients of AlN, Si, and Ag; a mass spectrometric study of the oxidation of W; and matrix isolation of high temperature vapors of boric oxide and carbon. (W.L.G.)

46957 (ORNL-3832, pp 100-6) ELECTROCHEMICAL KINETICS AND ITS APPLICATION TO CORROSION. (Oak Ridge National Lab., Tenn.).

A study of electrochemistry of Co metal in the presence of pertechnetate ions was initiated for comparison with corresponding studies on Fe. Effects of anions upon the corrosion behavior of Zr were investigated. The addition of H_2SO_4 to solutions containing HF inhibits the dissolution of Zr by HF. Development of a theory of potentiostatic and galvanostatic transients which occur during charging of the double layer in porous or tubular electrodes of finite length was completed. Boundary-value

problems arising in the theory of induced polarization of porous and tubular electrodes were solved for a number of cases. The relations obtained suggest that induced polarization could be applied to determination of the concentration of oxidizable and reducible substances in flowing streams, to measurement of corrosion rates of pipes, and to the study of certain other situations. The differential capacity of porous C electrodes was measured in 1 M NaCl at 25°C as a function of electrode potential and of concentration of iodide ions. By proper control of electrode potential partial separation of iodide ions from solutions flowing through porous C electrodes was accomplished. Experiments were directed toward establishment of the feasibility of separating organic species from flowing streams by controlled adsorption on porous C electrodes of large surface area. Results showed that a partial separation could be accomplished by proper control of the electrode potential. (auth)

46958 THE OXIDATION OF ZIRCONIUM: AN ELECTRON MICROSCOPY STUDY OF ZIRCONIA FORMED IN THE THIN-FILM REGION. Douglass, D. L. (Studiecentrum voor Kernenergie, Mol, Belg.); Van Landuyt, J. Acta Met., 13: 1069-79(Oct. 1965).

Transmission electron microscopy of stripped oxide films formed by oxidation of zirconium in the interference color region, 250 to 450°C, showed that uniform film growth does not occur. Single crystal monoclinic zirconia films replicated the general grain structure of the metal substrate but also contained a large volume of structural heterogeneities, which were independent of the substrate. Regions of fine-grained about 0.1 μ dia, polycrystalline oxide occupied about 5% of the film area. Preferential oxidation of these areas resulted in massive mounds of oxide at longer times. Pseudo-amorphous patches also existed, at lower temperatures and shorter times, ranging in size from about 0.1 to about 10 μ. Continued oxidation of the amorphous regions gave rise to pustule formation upon breakdown of the patches. The pseudo-amorphous patches contained substructure in the form of grain boundaries and small disk-like crystals, which sometimes changed contrast on tilting in the microscope. Crystallization of the pseudo-amorphous regions by heating in the microscope occurred by the formation of a single layer of crystal plates, having a thickness less than the oxide film. The crystals formed independently of the grain boundaries, and the pre-existing, disk-like crystals did not act as nuclei for crystallization. Prolonged heating eventually removed the boundaries. A tentative explanation for the presence of the boundaries is presented. The non-uniform nature of the thin films can readily account for the numerous rate laws for oxidation reported in the literature and the variations in oxidation behavior for supposedly identical conditions. (auth)

46959 STRESS-CORROSION CRACKING OF AUSTENITIC STAINLESS STEELS IN HIGH TEMPERATURE WATER. Okazaki, Masaomi; Onishi, Shoji (and others) (Mitsubishi Heavy Ind., Ltd., Japan). J. Japan Inst. Metals, (Sendai), 29: 340-5(Apr. 1965). (In Japanese).

Austenitic stainless steels can suffer stress-corrosion cracking under certain conditions of stress and corrosive environment. Some troubles were also caused by the stress-corrosion cracking of austenitic stainless steels under unusual conditions. Marine reactors are in danger of accelerating the occurrence of stress-corrosion cracking that results by repetition of wetting and drying of the reactor wall by cooling water. Various autoclave tests were carried out. Wetting and drying of specimens was found to accelerate the occurrence of stress-corrosion cracking. Additions of Nb and solution treatment reduced the corrosion rate. Disolved oxygen, chloride ion at 5 ppm in water, and surface contamination were found to increase the stress-corrosion cracking. (auth)

Fabrication

Refer also to abstracts 46509, 47976, 47977, 48059, and 48060.

46960 (AD-611837) USE OF REACTIVE ATMOSPHERES FOR THE TREATMENT OF B.C.C. METALS. Quarterly Engineering Progress Reports Nos. 8 and 9, July 1-December 31, 1964. Toth, I. J. (Battersea Coll. of Tech., London (England)). Contract N62558 3591. 4p. CFSTI $1.00 cy, $0.50 mn.

Tungsten test-pieces were sintered, both in hydrogen and hydrogen plus bromine atmospheres, using H.F. heating. The test-pieces were subjected to hot bend tests, hot compression tests, and tests in sealed tubes. The tentative conclusions are reported. (TAB)

46961 (BMI-X-10139) EXPLOSIVE WELDING OF ZIRCALOY TO HAFNIUM. Carlson, Ronald J.; Linse, Vonne D. (Battelle Memorial Inst., Columbus, Ohio). Sept. 7, 1965. Contract W-7405-eng-92. 26p. Dep. mn; CFSTI $2.00 cy, $0.50 mn.

Procedures were developed for cladding 0.250-in.-thick hafnium plates with 0.025-in.-thick Zircaloy. Initial experiments were conducted using Du Pont Detasheet explosive. It was determined that an initial clearance of 0.062 in. between components, a 6 g/in.^{2} charge density, and wedge-shaped buffer of paraffin wax were required to achieve welding. Experiments conducted using Red Cross Extra explosive included charge density, evacuation of joint interface prior to welding, and the use of a metal frame to achieve welding at the edges of the specimens. A charge density of 9 g/in.^{2} and a vacuum of less than 100 μ of mercury were required to achieve the desired welding. The use of a mild steel frame surrounding and in intimate contact with the edges of the hafnium eliminated the edge effects, thus allowing welding to be achieved on the edges of the specimen. These explosively produced welds possess an average tensile strength of 72,200 psi. (auth)

46962 (BNWL-131C) FABRICATION COSTS FOR PLUTONIUM FUEL ELEMENTS. PART C. VARIABLE COSTS OF FABRICATING UO_2-PuO_2 FUEL RODS FOR THE SAXTON REACTOR. Bloomster, C. H. (Battelle-Northwest, Richland, Wash. Pacific Northwest Lab.). Sept. 1965. Contract AT(45-1)-1830. 27p. Dep. mn; CFSTI $2.00 cy, $0.50 mn.

The variable (shop) cost of fabricating plutonium-enriched fuel rods for the Saxton reactor was $255/kg of fuel (as oxide), giving a unit cost of $136 per fuel rod. With a rod length of 1 m, each fuel rod contains 530 g natural UO_2-6.6 wt % PuO_2 fuel. The Zircaloy clad rods were 1 cm OD with a 0.6 mm wall. The costs were based on the fabrication of 150 rods by a well developed, pneumatic impaction-vibrational compaction process. The shop labor requirements for each rod were 4.27 man-hours direct labor and 1.41 man-hours indirect labor. The direct material cost was $43 per fuel rod. The variable costs included direct materials, some processing costs for nuclear materials, shop labor, maintenance, direct overhead, and consumable supplies but did not include the cost of nuclear materials themselves, use charges, administrative overhead, research, development, or engineering costs. (auth)

46963 (CEA-R-2733) ETUDE DE L'USINAGE DE BARREAUX DE CARBURE D'URANIUM OBTENUS PAR COULEE CONTINUE SOUS BOMBARDEMENT ELECTRONIQUE. (Study of the Machining of Uranium Carbide Rods Obtained by Continuous Casting Under Electronic Bombardment). Rousset, Pierre; Accary, Andre (Commissariat a l'Energie Atomique, Saclay (France). Centre d'Etude Nucleaires). July 1965. 39p. Dep. mn.

Various methods of machining uranium monocarbide are considered and critically compared in the case of their application to uranium carbide obtained by fusion under an electronic bombardment and continuous casting. Two mechanical machining methods are proposed: cylindrical rectification and centerless rectification, preceded by a preliminary roughing out of a cylinder, the latter appearing more suitable. A study of the machining yields as a function of the diameter of the rough bars and of the diameter of the finished rods showed that an optimum value of the rough bar diameter exists for each value of the finished rod diameter. It was found that the yield increases as the diameter itself increases, this yield

rising from 45 to around 70% as the diameter of the rough bars increases from 25–26 to 37–38 mm. (auth)

46964 (NMI–4996, pp 149-63) X-RAY FILM DEFECTS AND AUTORADIOGRAPHY OF FUEL ELEMENTS FOR CLADDING THICKNESS MEASUREMENT. Roth, H. P. (Nuclear Metals, Inc., Concord, Mass.).

Radiography of fuel element cladding can be performed by using the natural radioactivity of the core material as the source of exposure. X-ray film is placed in close contact with the surface of the cladding for several hours and the film is exposed by rays from the uranium that penetrate the cladding. The resulting density of the processed film at any specific location is related to the thickness of the cladding at the same location on the fuel element. By measuring photographic film density and comparing it with that of a standard film, which has been exposed and processed at the same time as the subject film, one can determine cladding thickness. The degree of accuracy depends upon carefulness in control of the entire autoradiographic procedure. Plus or minus 10% accuracy is normal for cladding below 20-mils in thickness. This method is not suitable for measuring more than 30-mils of Zircaloy or 50-mils of aluminum. There is a certain defect that is sometimes encountered in photographic supplies "as purchased" and which can be detrimental to fuel element inspection, particularly if these defects are not readily recognized by the testing laboratory. A considerable number of these defects were observed recently during autoradiographic analysis and a few samples of them are shown with this paper. Knowledge of their characteristic appearance and occurrence is sufficient to permit them to be distinguished as separate from metallurgical or fabrication defects in fuel elements in about 80% of all cases. (auth)

46965 (UCRL–16383) X-RAY EXAMINATION OF SQUARE WATER-COOLED COPPER MAGNET-CONDUCTOR BRAZE JOINTS. Nickerson, Richard A. (Lawrence Radiation Lab., Univ. of California, Berkeley). Sept. 1, 1965. Contract W-7405-eng-48. 10p. (CONF-650922–11). Dep. mn; CFSTI $1.00 cy, $0.50 mn.

From the 1st International Symposium on Magnet Technology, Stanford, Calif.

Brazed joint design and fabrication technology was improved by x-ray quality control in early stages of magnet coil production. The x-ray techniques discussed, though simple, require consideration of geometry and of exposure parameters, particularly kilovoltage. A method is described for proper choice of exposure kv, which permits the high-quality radiographs needed for quality control. The joint design which proved to be most reliably manufactured (when a rigidly controlled process is followed) is discussed. (auth)

46966 (WANL-PR(P)–007) DETERMINATION OF THE WELDABILITY AND ELEVATED TEMPERATURE STABILITY OF REFRACTORY METAL ALLOYS. Seventh Quarterly Report, December 21, 1964–March 20, 1965. Lessmann, G. G.; Stoner, D. R. (Westinghouse Electric Corp., Pittsburgh, Pa. Astronuclear Lab.). Contract NAS 3-2540. 57p. (NASA-CR–54434).

The alloys studied included B-66, C-129Y, Cb-752, D-43, FS-85, SCb-291, T-111, T-222, and Ta–10 W. TIG welds were analyzed for C, O, and N pickup; the results indicate that no apparent contamination occurred during welding. The post weld annealing studies were completed, using the bend ductile-to-brittle transition temperature to measure the response of TIG and electron-beam welds to annealing. Welds in T-111, T-222, and FS-85 were screened for thermal stability at 1800°F. An evaluation was initiated of the effect of oxygen contamination on the weldability of T-111, T-222, and FS-85. (D.L.C.)

46967 (Y-KB–62) NUCLEAR SAFETY CONSIDERATIONS IN FABRICATION OF MASSIVE PARTIALLY ENRICHED URANIUM–MOLYBDENUM REACTOR PARTS. Mee, W. T.; Crume, E. C.; McLendon, J. D. (Union Carbide Corp., Oak Ridge, Tenn. Y-12 Plant). Sept. 10, 1965. Contract W-7405-eng-26. 24p. (SM–70/44; CONF-651103–3). Dep. mn; CFSTI $1.00 cy, $.0.50 mn.

For Presentation at IAEA Symposium on Criticality Control of Fissile Materials, Stockholm.

Uranium, enriched to 20% in ^{235}U, has been chemically converted from UF_6 to the metal, alloyed with 10% molybdenum, and cast into massive core components for a prompt burst reactor, Super Kukla. In those areas for which direct criticality data were sparse or lacking, reactor theory-type calculations were made using S_n-type multigroup transport theory machine programs DSN and DTK. Adjustments were made to ensure conservatism in the application of calculations to the resolution of nuclear-safety problems. Using the results of these calculations, the available criticality data, and applying double-contingency analyses to operations, core components weighing up to 400 kg of U–10 Mo alloy were cast and safely manufactured into finished parts. (auth)

46968 (AEC-tr–6615) PHYSICAL AND CHEMICAL PROBLEMS OF THE JOINING OF DISSIMILAR MATERIALS. Rykalin, N. M.; Shorshorov, M. Kh.; Krasulin, Yu. L. Translated from Izv. Akad. Nauk SSSR, Neorgan. Materialy, 1: No. 1, 29-36(1965). 13p. Dep. mn; CFSTI $1.00 cy, $0.50 mn; JCL $1.60 fs, $0.80 mf.

The formation of joints between dissimilar materials with limited mutual solubility is discussed and examples are cited. Methods, equipment, properties of metals, and bonding effects in the formation of joints are considered. (P.C.H.)

46969 PREPARATION OF PURE ZIRCONIUM AND THORIUM BY DIRECT IODINATION OF THEIR CARBIDES. de Tejada, L. S.; Almagro, V.; Lopez Rodriguez, M.; Terraza, J. (Junta de Energia Nuclear, Madrid). Anales Real Soc. Espan. Fis. Quim. (Madrid), Ser. B, 61: 787-94 (June 1965). (In Spanish).

The Kroll process for the production of zirconium is based on this equation: $ZrO_2 \rightarrow ZrC \rightarrow ZrCl_4 \rightarrow Zr$ (sponge). This sponge can be melted or purified by the Van Arkel process to obtain ductile metal. An attempt was made to simplify this global process to obtain ductile zirconium, by iodizing the zirconium carbide in a direct manner. The processes to obtain the zirconium and thorium carbides and further iodination to obtain crystal bar were studied. (auth)

46970 VIBRATORY COMPACTION OF FUSED UO_2. Hirose, Yasuo; Takeda, Seiji (Hitachi, Ltd., Japan). Hitachi Hyoron, (Special Issue), 155-61(Nov. 1964). (In Japanese).

The vibratory compaction method for fabrication of uranium dioxide fuel rods is reviewed. Results obtained with an electrodynamic shaker are given. Combinations of three or four, or multiple particle sizes were found to produce more than 90% bulk density. In the sinusoidal wave vibration, the higher the acceleration the higher is the bulk density, and the frequency for maximum density increased with increasing acceleration. The saw-teeth wave vibration gave a higher density than the sinusoidal vibration. The frequency sweep vibration did not always bring about a high density, but more than 90% density was obtainable by repeated short-period vibration at a resonance frequency after the density was saturated. (NSA of Japan)

46971 EFFECT OF CHROMIUM(III)-OXIDE ON THE SINTERING PROPERTIES OF URANIUM DIOXIDE. Winter, K. (Zentralinstitut fuer Kernforschung, Rossendorf, Ger.). Kernenergie, 8: 413-23(July 1965). (In German).

Sintering experiments on uranium dioxide–chromium oxide mixtures of different uranium dioxide powders and chemical compositions in the temperature range of 1250 to 1700°C showed the possibility of both inhibition and promotion of the sintering as a function of the sintering conditions. The inhibition of sintering is in general due to the isolating effect of the chromium oxide which is inert for the sintering. A comparatively strong decrease of the sintering properties in the case of highly active uranium dioxide powders is caused by the formation of a U_3O_8-chromium oxide compound, the formation conditions and thermal stability of which have been studied. The activation of the sintering process relies on hydrogen atmo-

sphere. The steam generated by reduction of chromium oxide within the sinter-pellet is proved to be due to the promotion of sintering, and a corresponding mechanism is discussed. The role of the results in practical uses is evaluated. (auth)

46972 A 200-kw MULTI-CHAMBER ELECTRON-BEAM FURNACE. Metal Treat. Drop Forging, 30: 407-10(Oct. 1963).

An electron-beam multichamber furnace was designed, which has only one strong diode beam generator. The power can be regulated between 6 and 200 kw, by changing the accelerator potential. The acceleration voltage of 27 kv is so low that no x radiation passes through the walls. The beam generating area is completely decoupled from the melting area by vacuum techniques, so that the pressure level in the melting area can be taken as low as 10^{-2} torr. After each gas emission from the material being remelted the melting vacuum is between 10^{-2} and 10^{-5} torr. Melting takes place in a water-cooled copper crucible and a fixed or movable floor. By a crossed magnetic deflection system the electron beam can be refracted and its braking energy can be distributed between the melting rod and the material in the water-cooled copper crystallizer with a fixed or dropping bottom. The maximum bar charge for steel is about 450 kg. With this furnace it was possible to obtain an almost slag-free high-chrome steel with impact strengths of over 30 kpm/cm^2. It is shown that it is easier to obtain a good outer surface on ingots by using the 200-kw furnace than with the 60-kw furnace. The larger furnace is also justified economically. (BBB)

46973 REACTOR MAINTENANCE BY REMOTE INTERNAL TUBE WELDING. Roberts, J. G.; Newcomb, L. (North American Aviation, Inc., Canoga Park, Calif.). Welding J. (N. Y.), 44: 719-26(Sept. 1965).

Concurrent with the design of a large sodium-graphite nuclear reactor, containing a lattice work of process channels within a calandria core, it became necessary to study and design methods for the installation, maintenance or replacement of the process channels. A development program was initiated to determine joint configuration and replacement processes. Research analysis indicated the gas tungsten-arc process to be the most adaptable to the requirements for remote maintenance within the reactor vessel. Equipment development and the techniques of the operational procedure are outlined. Evaluation of the weld joint necessary for the nuclear application is explained. The need for proper process procedures, precise setup techniques and developed weld parameters is stressed. The development program proved the capabilities of long reach internal tube welds on a slip type lap joint. No edge preparation or filler metal is required. The lap joint is characterized by a free-flow surface without undercutting or concave conditions. (auth)

46974 IMPROVEMENTS IN METHODS OF MAKING BARS OF A URANIUM COMPOUND AND IN PARTICULAR URANIUM CARBIDE. Accary, Andre; Trouve, Jean (to Commissariat a l'Energie Atomique). British Patent 1,002,794. Aug. 25, 1965. Priority date Apr. 4, 1963, France.

A method is described for casting crack-free bars of a U compound, particularly UC, by eliminating excessive thermal stresses during the cooling of the casting. A granular starting material is melted in a mold in such a manner as to leave along the wall of the mold a layer of unmelted grains that form a protective cushion during cooling of the casting. Melting can be obtained by electron bombardment, which is localized so as not to melt the external layer. After removal from the mold, the unmelted grains can be removed from the casting. The method may be used for the continuous casting of bars with the granular material being fed to the molds by a conveyer and the bars extracted from the molds in a continuous fashion. (B.L.M.)

46975 IMPROVEMENTS IN OR RELATING TO METHODS OF EXTRUDING METAL IN THE PLASTIC STATE AND APPARATUS FOR CARRYING OUT THE METHODS. Sauve, Charles (to Commissariat a l'Energie Atomique). British Patent 1,002,900. Sept. 2, 1965. Priority date May 25, 1961, France.

A method of extruding metals in the plastic state, particularly metals that can be deformed only in a relatively small temperature range, comprises the following steps: locating the billet of a metal to be extruded in a lined bore of a billet container having a high heat capacity, heating the container and billet to the temperature of extrusion, and extruding the billet through a die located at one end of the bore. The lining of the bore is of a material that is resistant to chemical attack by the metal. The extrusion die is secured to the billet container, and the metal is extruded by moving a piston along the bore from the end of the bore opposite to the die. A refractory spacer is located between the piston and the billet. (B.L.M.)

46976 HIGH TEMPERATURE COLUMBIUM BASE ALLOYS. Jaffee, Robert I.; Williams, Dean N.; Bartlett, Edwin S.; Bradley, Elihu F. (to United Aircraft Corp.). U. S. Patent 3,193,385. July 6, 1965. Filed May 18, 1962.

Niobium-base alloys are described that have unusually high stress-rupture strength, high tensile strength, and good oxidation resistance at temperatures up to at least 2200°F without any detrimental effect on either fabricability or room-temperature ductility. The alloys consist of 1 to 40 wt.% of one of the elements selected from the group consisting of Ta, W, and Mo; up to 10 wt.% of at least one element selected from the group Hf, Zr, and V; up to 4 wt.% Cr; between 0.05 and 0.15 wt.% Be; and the balance consisting of Nb. (B.L.M.)

46977 GRAPHITIC NEUTRON REFLECTOR CONTAINING BERYLLIUM AND METHOD OF MAKING SAME. Le Baron, Robert (to Great Lakes Carbon Corp.). U. S. Patent 3,202,619. Aug. 24, 1965. Filed Apr. 2, 1962.

A process is reported for the production of carbon or graphite bodies containing Be or Be compounds that are suitable for use as neutron reflectors in atomic reactor cores. At least a few tenths of one percent of a Be compound is uniformly dispersed in the graphitic body by mixmulling raw petroleum coke particles, a hydrocarbon plasticizing agent, and a minor amount of the Be compound. The mixture is cooled, milled, and formed into a compact body. The formed body is then baked and graphitized. (B.L.M.)

46978 PROCESS AND DEVICE FOR THE MANUFACTURE OF A PERMEABLE MEMBRANE. Eyraud, Charles; Counas, Georges; Robinson, Le Plessis; Eudier, Michel; Massignon, Daniel (to Commissariat a l'Energie Atomique). U. S. Patent 3,203,086. Aug. 31, 1965. Priority date Jan. 23, 1960. France.

A process is described for the manufacture of a permeable membrane in which a microporous metallic support of hollow form having a wall thickness between 0.2 and 1 mm and a mean pore radius of from 1μ to several dozen μ is provided with a layer on its internal face of a thickness of 0.05 to 1 mm of a metallic compound admixed with a binder. A rigid core having a polished external surface is fitted against the coated layer, and the assembly is introduced into a casing of such size and shape that there is a clearance of from 0.02 to 1 mm between the support and the casing. The casing is sealed with the exception of at least one opening, and the oxygen is removed from the casing to effect the thermal dissociation of the metallic compound into a subdivided metal having particle dimensions of 0.5 cμ to 0.5μ and a volatile constituent. After the volatile constituents are removed, hydraulic pressure of 1 to 15 T/cm^2 is applied to the external surface of the casing to compress the casing, the support, and the subdivided metal against the core; and the casing is held at a temperature below the sintering temperature of the subdivided metal while the pressure is applied. The membrane is then separated from the core and casing. (B.L.M.)

46979 FORMING OF MATERIALS BY EXTRUSION. Green, Derek (to United Kingdom Atomic Energy Authority). U. S. Patent 3,203,217. Aug. 31, 1965. Priority date June 22, 1962, Great Britain.

An apparatus for the extrusion of materials to form a tube includes a container having a cylindrical bore, and extrusion die located at one end of the bore in the container, and a mandrel rigidly located in the bore of the container in line with the longitudinal axis of the extrusion die. The mandrel has an enlarged head fitting in the bore of the container. Means in the bore of the container position the mandrel longitudinally but also space the head of the mandrel from the extrusion die. A space for a tubular extension billet is defined inside the bore of the container around the mandrel and between the head of the mandrel and the extrusion die. A liquid is pressurized in the bore of the container on the side of the mandrel head remote from the die, and longitudinal passageways are provided through the head of the mandrel to allow pressure in the liquid on the side remote from the die to be transmitted to the liquid on the side of the mandrel head facing the die. (B.L.M.)

Properties and Structure

Refer also to abstracts 46234, 46539, 46573, and 47905.

46980 (AD-611800) CONTROL OF CAST GRAIN SIZE OF STEEL CASTINGS. Interim Report, August 16, 1963–August 15, 1964. Wieser, P.; Church, N.; Wallace, J. F. (Case Inst. of Tech., Cleveland, Ohio). Contract DA33 019AMC273Z. 82p. CFSTI $3.00 cy, $0.75 mn.

Techniques for the quantative evaluation of refinement of a high strength cast steel were evolved and used to test the effectiveness of various inoculants in achieving microstructural and macrostructural refinement. Of the various materials tested only titanium additions produced significant refinement of both the micro and macrostructure. Comparison of the tensile properties of the basic steel with that of a refined steel shows that large additions (0.2-0.6 wt %) of titanium are sufficient to decrease the reduction in area sharply. Further data on castings partially refined with small (0.10 wt %) titanium additions indicate that an improvement in reduction of area is obtained compared to the results with a columnar structure solidified under similar thermal conditions. (auth)

46981 (AD-611821) INTERFACE FRICTION IN HOT METAL DEFORMATION. Bimonthly Progress Report No. 4, November 24, 1964–January 23, 1965. Schey, J. A. (IIT Research Inst., Chicago, Ill.). Feb. 23, 1965. Contract NOw64 0458f. 10p. CFSTI $1.00 cy, $0.50 mn.

An investigation was made on frictional phenomena encountered at the tool-workpiece interface during the hot deformation processing of metals. Progress reported concerns 7075 Al and 6Al-4V-Ti with WC (10% Co) anvils. (TAB)

46982 (AD-611856) SPECTROSCOPIC STUDIES OF THE VAPORIZATION OF REFRACTORY MATERIALS. Quarterly Report No. 3. Linevsky, Milton J. (General Electric Co., Philadelphia, Pa. Missile and Space Div.). Nov. 1, 1963. Contract AF33(615)-1150. 9p. CFSTI $1.00 cy, $0.50 mn.

Matrix isolation spectra in solid argon were obtained on ^{18}O enriched ThO_2. From the resulting spectra it appears that the molecule is highly bent. Frequencies were assigned to the V_1 and V_3 vibrational fundamentals for all the various isotopic species. V_2 was not observed in the frequency region (2 to 55.5 μ) covered and must be presumed to be less than 180/cm. Modifications of the spectroscopic equipment were made and it is now possible to obtain infrared spectra down to 180/cm. Examination of the long wave-length regions of the spectra of MgF_2 and AlF_3 using this modified equipment was made and additional spectra for lithium fluoride obtained. Resonance line studies were initiated on ZrN in a manner completely analogous to that used in the TiN study. However, much difficulty was encountered because of the reaction of the ZrN with carbon. Modifications of the furnace are being made to try to mitigate this reaction. (TAB)

46983 (AD-612159) THE EFFECT OF PRESSURE ON THE STRUCTURE AND PROPERTIES OF METALS. Davidson, T. E.; Uy, J. C.; Lee, A. P. (Watervliet Arsenal, N. Y.). 1964. 15p. CFSTI $1.00 cy, $0.50 mn.

Under certain conditions, sufficiently high hydrostatic pressures can induce localized microscopic deformation in polycrystalline metals. Based on the examination of the effect of hydrostatic pressures to 26 kilobars on several cubic metals, the occurrence of such deformation, which in the early stages is localized along grain boundaries and increases in severity with increasing pressure, results from microscopic shear stresses arising from anisotropy in the linear compressibility. Pressure cycling to 20 kilobars slightly increases the flow stress of polycrystalline zinc. The tensile strength and ductility are not reproducibly affected. As has been observed in other materials, the ductility of magnesium, tungsten, and 1045 steel with an untempered martensitic structure is drastically enhanced when fractured under a superimposed hydrostatic pressure. These materials are also known to undergo abrupt brittle-ductile transitions as a function of temperature, thus indicating that the pressure induced transition may be directly related to the atmospheric pressure phenomenon. (TAB)

46984 (AD-612275) THE STRUCTURE OF METALS AND INTERMETALLIC COMPOUNDS. Final Report, September 1, 1953–August 31, 1964. Samson, Sten (California Inst. of Tech., Pasadena. Div. of Chemistry and Chemical Engineering). Contract Nonr22033. 75p. CFSTI $3.00 cy, $0.75 mn.

Results obtained from the structure investigations resulted in twenty-two publications which are chronologically listed. A brief outline of the research is given. The work on the crystal structure of Beta Mg_2Al_3 is included. (TCO)

46985 (AD-613651) DEVELOPMENT OF TOUGH, HIGH-STRENGTH ALPHA-BETA TITANIUM BASE ALLOYS. Ayvazian, Arthur M.; Colton, Robert M. (Army Materials Research Agency, Watertown Arsenal, Mass.). Mar. 1965. 16p. (AMRA-TR-65-03). CFSTI $1.00 cy, $0.50 mn.

The addition of varying weight percentages of the substitutional elements Cr, Mo, Mn, Ni, U, and Zr and the interstitial elements O, N, C, and B to the basic alloy, Ti–6Al–6V–2Sn–½Fe–¼Cu, resulted in alloys that exhibited mechanical properties superior to those of the basic alloy. The optimum mechanical properties ranged from 198,000 psi yield strength at 0.1% offset, 205,000 psi tensile strength, 5% elongation, 14.0% reduction of area, and 5.4 ft-lb Charpy V-notch impact energy at –40°F for alloy Ti–6Al–6V–2Sn–½Fe–¼Cu, to 221,000 psi yield strength at 0.1% offset, 224,000 psi tensile strength, 11.9% elongation, 32.1% reduction of area, and 5.9 ft-lb Charpy V-notch impact energy at –40°F for alloy Ti–6Al–6V–2Sn–¾Cu–3Zr–0.015N–0.114 02–0.00217H–0.12C. (auth)

46986 (KR-96) CORRELATION BETWEEN CALCULATED AND MEASURED MECHANICAL PROPERTIES OF THIN-WALLED FUEL ELEMENT CANNING TUBES OF STAINLESS STEEL. Brodahl, Erik; Aas, Steinar (Institutt for Atomenergi, Kjeller (Norway)). July 1965. 27p. Dep mn.

Burst and collapse tests were performed on half-hard and annealed tubes of AISI 304 L stainless steel at room temperature and at 300°C. Tensile test specimens were taken from the same tubes and tested at the same temperatures. From stress-strain diagrams, material constants were determined and the yield, burst, and collapse pressures were calculated according to classical formulas and the results correlated with the experimental data. The results showed that the classical formulas predict adequately the critical dimensions or the critical pressures. Internally supported tubes were collapsed at 300°C in order to study the effect of the gap between the support and inner tube wall. (auth)

46987 (AD-614462) INVESTIGATION OF THE SYSTEMS Y–Mn, Gd–Mn AND Sm–Mn. Lihl, F. (Technische Hochschule, Vienna (Austria)). Jan. 31, 1964. Contract AF61(052)-609. 38p. CFSTI $2.00 cy, $0.50 mn.

The mechanism of alloy formation by the amalgam process was studied. It is very likely that at low temperatures manganese metal is formed from the RE–Mn amalgams. This manganese metal is coexistent with the compounds $REHg_2$ and REHg. At higher temperatures (700–800°C) RE-metal is formed from the RE–Hg compounds. The two intimately mixed, fine powdered metals react, yielding the RE–Mn-compounds. The systems Y–Mn, Gd–Mn, and Sm–Mn were studied. The compounds YMn_2, $GdMn_2$, $SmMn_2$, YMn_4, $SmMn_4$, $GdMn_4$, and YMn_{12} were prepared and their lattice spacings were evaluated. The amalgam process is very advantageous for preparing RE–Mn alloys and compounds at temperatures below the melting points of the components. The magnetic transition temperatures (Curie-points) of the ferromagnetic compounds $REMn_4$ were established (YMn_4: 219C; $GdMn_4$: 192C; $SmMn_4$: 170°C). (TAB)

46988 (AD-614465) THEORIES OF THE DIFFERENTIAL-THERMAL-RESP. MAGNETO-THERMAL-ANALYSIS. A DETAILED DESCRIPTION OF THE TWO APPARATUS AND OF FURTHER MEASUREMENTS ON RE–Mn ALLOYS. Lihl, F. (Technische Hochschule, Vienna (Austria)). Oct. 31, 1964. Contract AF61(052)-609. 74p. CFSTI $3.00 cy, $0.75 mn.

An apparatus for measurements on small samples (0.5–1 g) of high reactive RE-alloys (RE-Hg, RE-Mn alloys etc.) was developed. It consists of a platinum-wire furnace, a sample holder with crucibles (made of tantalum), an electronic temperature regulation, and a recorder. The possibilities of this device are discussed. A magnetic balance is described, which allows measurements on RE-alloys from 80°K to 1400°K. Measurements on $GdMn_2$, $GdMn_5$ and $GdMn_{12}$ between 80°K and 1370°K showed that $GdMn_2$ becomes antiferromagnetic at 86°K and that $GdMn_5$ is not ferromagnetic but ferrimagnetic (T_C = 465°K). The results are discussed in terms of the Neel theory. The number of Bohr-magnetons, gained from the measurements at high temperatures (in the paramagnetic region) was compared with theory. (TAB)

46989 (AD-614466) X-RAY-, DTA- AND THERMOMAGNETICAL ANALYSIS OF Y, Sm, Gd, Dy, Ho, Er–Mn-COMPOUNDS. Lihl, F. (Technische Hochschule, Vienna (Austria)). Jan. 31, 1965. Contract AF61(052)-609. 48p. CFSTI $2.00 cy, $0.50 mn.

A summary of the phases that occur in the systems Gd, Sm, Dy, Ho, Er–Mn is presented. In all these systems the phases $REMn_2$, $REMn_4$ (RE_6Mn_{23} or $REMn_5$) and $REMn_{12}$ exist (the compound $SmMn_{12}$ was not detected). The phases $HoMn_2$ and $ErMn_2$ possess (at least at room temperature) the same structure ($MgCu_2$) as the other $REMn_2$ compounds. The lattice spacings of the compounds diminish continuously with atomic number. By DTA the systems Gd–Mn and Dy–Mn were studied and phase diagrams constructed. The x-ray investigations and x-ray fluorescence analysis agree with the diagrams. Magnetic measurements with Y, Sm, Dy, Ho, and Er–Mnx (x = 3, 83 – 5) yielded accurate Curie-points. The saturation magnetization of YMn_5 and $SmMn_5$ was higher than the literature values. By measurements of the paramagnetic properties of $SmMn_5$ and $HoMn_5$ above the Curie temperature the fact that these compounds are ferrimagnetic and not ferromagnetic could be established. The results are discussed in terms of the theory of ferrimagnetic substances. (TAB)

46990 (ARL-65-138) A STUDY OF THE HAFNIUM–OXYGEN SYSTEM. Domagala, R. F.; Ruh, Robert (IIT Research Inst., Chicago, Ill.). May 1965. Contract AF 33(616)-7074. 29p.

A study of annealed and quenched specimens of arc-melted alloys permitted the construction diagram from Hf to HfO_2 and from 700 to 2500°C. The diagram is characterized by the following features: (1) Additions of oxygen to Hf raise the α-β (hcp-bcc) transformation temperature (1775 ± 25°C), resulting in a peritectic reaction L(~1 at. % O) + α(~8 at. % O) → β(~3 at. % O) at ~2250°C. (2) The α phase has a broad solubility for oxygen. The maximum solubility has been positioned at 22 at. % O, decreasing to 20 at. % from 2000°C down to 700°C. The α phase is stabilized to its melting point, 2500°C. A eutectic exists where L(~37 at. % O) → α(~22 at. % O) + HfO_2 at ~2200°C. HfO_2 has a limited homogeneity range extending from ~66 to 66.7 at. % O. No metallographic evidence of the monoclinic–tetragonal inversion in HfO_2 was noted. The lattice parameters of specimens annealed at 1000°C indicate a solubility limit for oxygen in α at 18.6 at. %, in reasonably good agreement with the metallographically determined boundary. (auth)

46991 (AWRE-O-47/65) THE PERMEATION AND DIFFUSION OF HYDROGEN ISOTOPES THROUGH STAINLESS STEELS. PART I. NIOBIUM STABILISED S110 STEEL. Gibson, R.; Jones, P. M. S.; Evans, J. A. (Atomic Weapons Research Establishment, Aldermaston (England)). Sept. 1965. 31p. Dep.; BIS $0.90; HMSO 4s. 6d.

Measurements were made on the passage of hydrogen and deuterium through niobium stablized stainless steel S110 membranes 0.02 in. thick which had been cleaned with hydrogen or contaminated by treatment with nitrogen, oxygen, carbon dioxide, moist oxygen, or argon. Nitrogen and argon had no effect but oxygen reduced the permeation rate significantly. Full experimental results are reported and discussed. Permeation and solubility data agree well with previous results. (auth)

46992 (CEA-R-2792) ETUDES D'ALLIAGES U–Pu–Fe (EXPERIENCE CRITIQUE MASURCA). (Study of U–Pu–Fe Alloys (MASURCA Critical Experiment)). Barthelemy, Pierre; Boucher, Rene (Commissariat a l'Energie Atomique, Fontenay-aux-Roses (France). Centre d'Etudes Nucleaires). July 1965. 48p. (EUR-2449.f). Dep. mn.

Three compositions of U–Pu–Fe alloys were studied. After two weeks in air 74.5 U–25 Pu–0.5 Fe alloys were reduced in powder. As-cast alloys containing 1 and 1.5% Fe were kept undamaged for several months. However, a rapid oxidization of the alloys was observed when the samples underwent phase transformation (at 595 and 590°C, respectively). Ignition tests in the presence of air showed that the oxidization starts at about 250°C and does not spread. Ignition was not observed during heating from 20 to 660°C. The transformation temperature, melting temperature, and thermal expansion coefficients were determined by dilatometry. Below the transformation temperature, the principal phases are U–Pu zêta and $(U, Pu)_6Fe$. Thermal conductibility, Young modulus, density, and heat of fusion were also measured. Compatibility tests showed that between U–Pu–Fe and stainless steel a phase of $(U, Pu)_6Fe$ type is formed. The 74 U–25 Pu–1% Fe alloy seems to behave better than 73.5 U–25 Pu–1.5% Fe alloy because the $(U, Pu)_6Fe$ layer is two or three times smaller. Finally, thermal stability was studied with the 74 U–25 Pu–1% Fe alloy. A dilatometric anomaly (very weak expansion) occurred when the sample was heated above transformation temperature and cooled. (P.C.H.)

46993 (CONF-650810–3) SUBSTRUCTURE MEASUREMENTS BY STATISTICAL FLUCTUATIONS IN X-RAY DIFFRACTION INTENSITY. Sturcken, E. F.; Gettys, W. E.; Bohn, E. M. (Du Pont de Nemours (E. I.) and Co., Aiken, S. C. Savannah River Lab.). Sept. 2, 1965. Contract AT(07-2)-1. 31p. Dep. mn; CFSTI $2.00 cy, $0.50 mn.

From Annual Conference on Applications of X-Ray Analysis, Denver.

B. E. Warren first demonstrated that the statistical fluctuations in x-ray diffraction intensity which occur in coarse-grained samples can be employed to determine grain sizes of greater than 1 micron. Warren also suggested that a modification of this same method might be used to study substructure, i.e., the slight differences in orientation between the subgrains of any one grain. The substructure technique was developed and applied to studies of beta-quenched and recrystallized high purity uranium. The substructure characteristics of both types of uranium were measured and correlated with measurements by optical and transmission electron microscopy, x-ray reflec-

tion microscopy, and conventional and micro Laue diffraction. (auth)

46994 (COO–1149–52) THERMAL ANOMALIES AND THERMODYNAMIC PROPERTIES OF GADOLINIUM HEXABORIDE. Westrum, Edgar F. Jr; Andrews, John T. S.; Clay, Gerald A. (Michigan Univ., Ann Arbor. Dept. of Chemistry). Aug. 1965. Contract AT(11-1)-1149. 10p. (CONF-650804–9). Dep. mn; CFSTI $1.00 cy, $0.50 mn.

From 5th Rare Earth Research Conference, Ames, Iowa.

Previously reported studies on the thermal properties of lanthanum and neodymium hexaborides in the cryogenic region have been extended to gadolinium hexaboride, and are presently in progress on cerium hexaboride. Like its neodymium analog, the gadolinium compound shows a cooperative transition apparently associated with antiferromagnetic ordering, with a peak at 16°K. Moreover, a Schottky effect with a maximum heat capacity at 29°K is apparent. The Schottky effect is attributed to $2\underline{n}$ and $\underline{n}$ degenerate levels, separated by 145 and 230 cal/gfm from the $\underline{n}$ degenerate ground state. The entropy contribution from the Schottky level at 25°C is $\underline{R}$ ln 4, and that associated with the magnetic cooperative transition approximates $\underline{R}$ ln $(2\underline{s} + 1)$ as would be expected for the complete order of the $(2\underline{s} + 1)$ levels associated with the spin, $\underline{s} = 7/2$, of the Gd(III) ion. Partial thermodynamic functions for GdB_6 are derived on the basis of these values. (auth)

46995 (EUR–2424.f) DISPOSITIF DE MESURE DE LA DIFFUSIVITE A HAUTES TEMPERATURES. (Apparatus for the Measurement of Diffusivity at High Temperatures). Van Den Berg, M.; Schmidt, H. E. (European Atomic Energy Community, Karlsruhe (West Germany). Transuranium Inst.). May 1965. 33p. Dep. mn.

An apparatus is described which permits rapid measurement of thermal diffusivity of samples 5 mm in diameter and up to 1 mm thick, at temperatures from 1000°C to 2200°C. The sample is heated by electron bombardment. A periodic small amplitude variation of the beam power produces corresponding temperature variations on the two sample faces. The phase shift is recorded and permits the calculation of the diffusivity. The temperature is measured with a two-color-type pyrometer. Measurements of diffusivity were made on tungsten, graphite, uranium dioxide single crystals, and pure and doped sintered uranium dioxide. The precision of the method was estimated to be of the order of ±10% for all measurements below 2000°C. (auth)

46996 (EUR–2479.e) ELECTRON MICROSCOPY OF SAP FOLLOWING TENSILE DEFORMATION OR QUENCHING. Ruedl, E.; Guyot, P. (European Atomic Energy Community, Ispra (Italy). Joint Nuclear Research Center). Aug. 1965. 36p. (CONF-650631–2). Dep. mn.

From International Powder Metallurgical Conference, New York.

Use is made of transmission electron microscopy to support the mechanisms of plastic deformation of SAP-type alloys previously described. An extruded Al – 4 wt % Al_2O_3 SAP alloy, annealed for 2 hours at +500°C, was studied either before or after tensile deformation at various temperatures. In the extruded and annealed alloy, the grains are elongated along the direction of extrusion with a more or less homogeneous distribution of the alumina particles. The samples deformed in tensile tests at low temperatures (–196°C to +20°C) reveal a high dislocation density, the dislocations tending to arrange in cell boundaries with increasing strain. Evidence for cross-slip of dislocations is given by the direct observation of cross-slip traces in the region between the particles. For low deformations (≤1%) at +20°C, the dislocation density calculated from the activation volume for the dislocation intersection process (forest process) is in agreement with the dislocation density measured by electron microscopy. After deformation at +350°C the dislocation density is also high, while dislocation loops can be recognized both attached to the particles and isolated. After deformation at +500°C the dislocation density is much reduced in most of the grains and the remaining dislocations are pinned principally by the particles. Reactions of attractive dislocations, however, can be recognized in grains where there is still a high dislocation density. A study of the same alloy after cold-rolling, annealing at +640°C, and subsequent cooling either by quenching or more slowly leads to the conclusion that the particle/matrix interface is normally incoherent. This is supported by the fact that a full structural relationship between the larger particles and the matrix which may lead to coherency occurred only rarely and because the strain field surrounding the smaller particles is consistent with differential thermal contraction effects rather than with coherency. (auth)

46997 (JINR–P–2282) ELEKTROFOTOGRAFICHESKII METOD OPREDELENIYA KOEFFITSIENTA DIFFUZII LITIYA V KREMNI p-TIPA. (Electrophotographic Method for Determining the Lithium Diffusion Constant in the p-Type Silicon). Yuskeselieva, L. G.; Antonov, A. S. (Joint Inst. for Nuclear Research, Dubna (USSR). Lab. of Nuclear Problems). 1965. 13p. Dep. mn.

A method is proposed for determining the lithium diffusion constant in the p-type silicon. It is based on applications of electrophotographic developers and is efficient and simple. (auth)

46998 (LA–3331) HEAT CAPACITIES OF $NbC_{0.702}$, $NbC_{0.825}$, $NbC_{0.980}$ AND Nb_2C BELOW 320°K. Sandenaw, T. A.; Storms, E. K. (Los Alamos Scientific Lab., Univ. of California, N. Mex.). July 1965. Contract W-7405-eng-36. 8p. Dep. mn; CFSTI $1.00 cy, $0.50 mn.

The heat capacities of $NbC_{0.702}$, $NbC_{0.825}$, $NbC_{0.980}$, and Nb_2C were measured between 7.5 and 320°K, using an adiabatic calorimeter. Calculated values for entropy and enthalpy are tabulated as functions of composition and temperature. (auth)

46999 (LA-DC–7297) REFRACTORY PLUTONIUM FUEL MATERIALS. Leary, J. A.; Pritchard, W. C.; Nance, R. L.; Shupe, M. W. (Los Alamos Scientific Lab., Univ. of California, N. Mex.). [1965]. Contract W-7405-eng-36. 20p. (CONF-651102–7). Dep. mn; CFSTI $1.00 cy, $0.50 mn.

For Presentation at Royal Commonwealth Society, 3rd International Conference on Plutonium, London.

The plutonium carbides PuC_{1-x}, Pu_2C_3, (U,Pu)C, and $(U,Pu)_2C_3$ were prepared as single phase powders and as dense bodies suitable for fuels. Sintering studies on PuO_2 in inert and in oxidizing atmospheres indicate that dense bodies were produced in either case. However, when an inert atmosphere was used, the less dense bcc form of Pu_2O_3 was produced when the sintering temperature was high. Stoichiometric PuN powders were produced by reaction of $PuH_{0.04}$ with N_2. Densification by sintering in N_2 at 1600°C was trivial. When PuN was co-sintered with PuO_2 in N_2, the PuO_2 was reduced to hexagonal Pu_2O_3 with liberation of N_2. The solid solubility of PuO in PuN is approximately 3 percent. (auth)

47000 (NMI–4996, pp 8-18) METALLOGRAPHIC OBSERVATIONS AT ELEVATED TEMPERATURE. Dvorak, J. R.; Domagala, R. F. (Armour Research Foundation, Chicago, Ill.).

Three factors appear to govern the ability to observe structural changes at elevated temperatures: the effect of thermal etching, the relative emissivity or reflectivity of the phases, and surface contour changes that take place during heating or cooling as a result of volume changes during precipitation or transformation. Attempts to view the allotropic transformation in pure iron, recrystallization and grain growth in pure copper, and isothermal transformation processes in several alloys are described. (auth)

47001 (NMI–4996, pp 36-49) METALLOGRAPHY OF BERYLLIUM OXIDE. Rhodes, Cecil G. (General Electric Co., Cincinnati, Ohio. Aircraft Nuclear Propulsion Dept.).

The metallographic procedures used for preparing Be can be used for BeO samples. Porosity is a major prob-

lem in microstructure interpretation. Mechanical porosity can, however, be distinguished from natural porosity. Impurities are mainly metallic. The ultimate grain size of hot-pressed samples and sintered samples could not be correlated to fabrication times, temperatures, or pressures. Beryllia samples nearly always have equiaxed grains; however, several samples had rod-shaped grains. In an isothermal (1500°C) test conducted in 25 hour increments, the grain sized tripled in 100 hours. (auth)

47002 (NMI-4996, pp 50-76) ELECTRON MICROSCOPE STUDIES OF BERYLLIUM OXIDE POWDERS. Bolinger, M. G. Jr. (General Electric Co., Cincinnati, Ohio. Aircraft Nuclear Propulsion Dept.).

Results are presented to characterize the physical and morphological features of various beryllium oxide powders in relation to parent compounds, calcination conditions, fabricated density and chemical purity. Electron microscope particle size data were tabulated and the results are compared with x-ray diffraction, line-broadening and surface area measurements to facilitate a complete particle size perspective. (auth)

47003 (NMI-4999, pp 111-28) A NEW MICROHARDNESS TECHNIQUE. Kegley, T. M. Jr.; Leslie, B. C. (Oak Ridge National Lab., Tenn.).

Conventional microhardness tests using Kentron and Tukon hardness testers are not adequate for resilient materials such as pyrolytic carbon and pyrolytic graphite, since hardness indentations made on such materials vanish upon removal of the test load. However, if a thin pyroxylin film is placed on the specimen before making the microhardness test, then an image of the indentation is retained on the film. The technique that was developed for coating the pyroxylin film on the specimen so as to record the hardness indentations and some of the test results are described. (auth)

47004 (NMI-4997, pp 45-54) METALLOGRAPHIC STUDIES OF URANIUM-FISSIUM ALLOYS. Zegler, S. T.; Nevitt, M. V.; Wilhelmi, R. P.; Conner, R. A. Jr. (Argonne National Lab., Ill.).

The results of a metallographic study of the effects of Al, Si, Ti, and Y additions on the ductility of a U-5 wt % Fs-2.25 wt % Zr alloy are presented. (W.L.G.)

47005 (NMI-4997, pp 76-84) HIGH-TEMPERATURE METALLOGRAPHY OF URANIUM. Angerman, C. L. (Du Pont de Nemours (E. I.) and Co., Aiken, S. C. Savannah River Lab.).

The changes in the microstructure of uranium that occurred during heating and cooling through the allotropic transformations were recorded by time-lapse photography on 16 mm movie films. Electropolished uranium specimens were heated in a hot stage that was mounted on a metallograph and evacuated to at least 3×10^{-6} mm Hg. During heating, the original grain structure became visible due to relief that resulted from differences in thermal expansion between adjacent grains. At the appropriate temperatures the transformations moved as fronts that emanated from several points in the structure. The α-β transformation occurred at a faster rate than the β-γ transformation. Grain boundaries of the β and γ phases were visible after the respective transformations. (auth)

47006 (NMI-4997, pp 198-207) METALLOGRAPHY OF PYROLYTIC CARBON COATED AND UNCOATED URANIUM CARBIDE SPHERES. DuBose, C. K. H.; Gray, R. J. (Oak Ridge National Lab., Tenn.).

Techniques were developed for the metallographic preparation and examination of carbon-coated and uncoated uranium carbide particles both in the unsupported condition and as-fabricated into graphite matrices. The particle coatings studied were deposited pyrolytically from a hydrocarbon gas, producing two morphological types of pyrolytic carbon coatings. In one type, the coating is smooth on the outer surface and a cross-sectional plane exhibits a laminar onion-ring type structure, while in the outer type, the surface has a pebble-like finish with the cross section exhibiting a columnar or conical grain structure. The microstructures of the carbide particles show variations in the amount of UC and UC_2 with an average ratio of approximately 70% UC_2 and 30% UC. Heat treatments above 1800°C may produce uranium oxides at the particle-coating interface. (auth)

47007 (NMI-5025(Pt.I), pp 127-51) MICROSTRUCTURAL STUDIES OF CAST URANIUM. Bauer, A. A.; Thompson, C. R.; Farkas, M. S. (Battelle Memorial Inst., Columbus, Ohio).

The use of metallographic and electron microscopic techniques for detecting microstructural differences in cast uranium of varied chemistry and casting history is described and some preliminary conclusions drawn. (W.L.G.)

47008 (NP-15429) THE THERMAL-MECHANICAL BEHAVIOR OF STRONTIUM ZIRCONATE. Bimonthly Progress Report No. 4, April 1, 1965-June 1, 1965. Funk, J. E.; Nemeth, J.; Tinklepaugh, J. R. (State Univ. of New York Coll. of Ceramics, Alfred Univ.). Contract NOw 65-0131-d. 8p.

Measurements of high-temperature stress-strain in strontium zirconate were delayed by necessary repairs to the equipment. Experiments are continuing in the study of the stress-strain characteristics of the $CaZrO_3$-$SrZrO_3$ solid solution. Small single crystals of $SrHfO_3$ have been grown. (auth)

47009 (NP-15514(Vol.2)) RESEARCH ON PHYSICAL AND CHEMICAL PRINCIPLES AFFECTING HIGH TEMPERATURE MATERIALS FOR ROCKET NOZZLES. Final Report, Volume II. Aspinall, S. R. (Union Carbide Research Inst., Tarrytown, N. Y.). Aug. 1965. Contract DA-30-069-ORD-2787. 304p.

Results are presented for research in the areas of: a sensitive a-c potentiometer for galvanomagnetic measurements; galvanomagnetic measurements on IVth group carbides; elastic properties of single-crystal and polycrystalline W at 24 to 1800°C; a high temperature furnace for quantitative x-ray intensity measurements; thermal expansion and atomic vibration amplitudes for TiC, TiN, ZrC, ZrN, and pure W; high temperature thermal expansion of certain group IV and V carbides and diborides; static atomic displacements resulting from vacancies in defect structures of TiN_x; high temperature thermal conductivity measurements, theory of Longmire's method and the rectangular bar method; experimental techniques for the rectangular bar method; physical measurements on hot-pressed HfC; measurement of the thermal conductivity and electrical resistivity of ZT-type graphite at high temperatures; high temperature, steady state creep rate in single-crystal MgO; and high temperature creep of polycrystalline TiC and ZrC. (W.L.G.)

47010 (ORNL-3832, pp 107-115) NONAQUEOUS SYSTEMS AT HIGH TEMPERATURES. (Oak Ridge National Lab., Tenn.).

An all-metal apparatus was developed and tested, which allows emf measurements in molten metal-salt systems corrosive to ceramics. The study of metal-metal-halide systems $M\text{-}MX_n$ was extended to the first representative of systems $M\text{-}M_2Y$ (Y is a divalent chalcogenide ion), namely, $K\text{-}K_2S$. At the melting point of the sulfide, the metal and sulfide were found to be miscible in all proportions. K_2O was found to have the low entropy of fusion of only 3.16 eu/mole, similar to those of CaF_2 and $SrCl_2$, with which it is anti-isomorphous. Determination of the melting-point depression of Ca metal produced by dissolving CaF_2 and of the solubility of CaF_2 in solid Ca metal yielded the not unexpected result that in the solution the fluoride ions form separate particles. A similar dissociation is derived for $BaCl_2$ in Ba from vapor-pressure measurements. Experiments were performed in preparation for a study of the K_2O-K and Na_2O-Na systems. Indications were obtained that the melting point of K_2O is in excess of 750°C (literature, 527°) and that of Na_2O in excess of 1015°C (literature, 920°C). (auth)

47011 (ORNL–3862) THE ENERGY OF FORMATION OF A DOUBLE KINK AND AN EXAMINATION OF LOW-TEMPERATURE DEFORMATION. Arsenault, R. J. (Oak Ridge National Lab., Tenn.). Sept. 1965. Contract W-7405-eng-26. 29p. Dep. mn; CFSTI $2.00 cy, $0.50 mn.

The energy of formation of a double kink was calculated as a function of stress for various boundary conditions, values of elastic constants, and different dislocation lengths. The activation energy of the double kink mechanism is considered to be the formation energy of the double kink. Once a double kink has formed, the lateral motion is an athermal process. The interaction energy between the kinks and between the kinks and the remaining portions of the dislocations was found to be small compared to the formation energy of the double kink. There is fair agreement between the calculated activation energies and the experimental values. The potential energy versus displacement curve for the formation of successive double kinks was calculated for a finite dislocation. The potential energy is found to decrease to a minimum and then increase monotonically as the displacement increases. This potential energy profile is examined in terms of low-temperature internal friction and as a possible explanation of the decrease in activation volume with strain for iron deformed at low temperatures. (auth)

47012 (ORNL–TM–1226) STRAIN BEHAVIOR IN ZIRCALOY-2 SHEET-TYPE TENSILE SPECIMENS. Rittenhouse, P. L.; Picklesimer, M. L. (Oak Ridge National Lab., Tenn.). Sept. 1965. Contract W-7405-eng-26. 30p. Dep. mn; CFSTI $2.00 cy, $0.50 mn.

Rolling and transverse direction sheet-type tensile specimens of highly textured Zircaloy-2 were prepared and tested to study strain behavior as a function of specimen geometry. The results of these tests are compared with those obtained from round tensile specimens of the same material. Nonuniform strain is exhibited in the necked region of the sheet specimens. This adds to the difficulty of using this type of specimen as a measure of strain anisotropy through ratios of contractile to axial strain. Some peculiarities in necking behavior are also discussed. (auth)

47013 (PB–171809(Rev.)(Suppl.2)) CRYOGENIC MATERIALS DATA HANDBOOK. Progress Report No. 2. (Martin Co., Denver, Colo.). July 1965. 270p. (ML-TDR–64–280(Suppl.2)). CFSTI.

Data are given for various alloys of aluminum, copper, inconel, inconel X, hastelloy B, hastelloy C, monel, stainless steel, steel, and titanium. The temperature ranges from −400 to 100°F. Some data given include yield strengths, tensile strengths, elongation, notch tensile strengths, notch strength ratios and weld tensile strengths. (M.O.W.)

47014 (RT/MET(64)4) INFLUENCE OF THE HEAT-TREATMENTS ON THE STRUCTURE OF URANIUM-RICH ALLOYS CONTAINING ZIRCONIUM. Fizzotti, C.; Masperoni, A. (Comitato Nazionale per l'Energia Nucleare, Rome (Italy)). Nov. 1964. 17p. Dep. mn.

Uranium alloys containing up to 5 wt % zirconium were heat treated by step-annealing them in the binary phase fields of the system. Aging at 550°C for different periods of time up to 1000 hr was performed on some alloys continuously cooled from the γ phase. Investigations to confirm one of the already published constitutional diagrams for the uranium–zirconium system were also performed. (auth)

47015 (TIM–854) THE ELECTRICAL RESISTIVITY OF LITHIUM AND COLUMBIUM-1 ZIRCONIUM ALLOY TO 1430C. Rigney, D. V.; Kapelner, S. M.; Cleary, R. E. (Pratt and Whitney Aircraft, Middletown, Conn. Connecticut Advanced Nuclear Engineering Lab.). Sept. 1965. Contract AT(30-1)-2789. 19p. Dep. mn; CFSTI $1.00 cy, $0.50 mn.

The electrical resistivities of liquid lithium and niobium-1 zirconium alloy were measured to temperatures of 1430 and 1446°C, respectively. The temperature dependence of the electrical resistivity for each material is given by the equations: lithium (200–1430°C) $\rho = 21.934 + 2.598 \times 10^{-2}\ t + 2.581 \times 10^{-6}t^2 - 1.819 \times 10^{-9}t^3$; and niobium-1 Zr (200–1446°C) $\rho = 16.337 + 4.224 \times 10^{-2}t - 4.922 \times 10^{-6}t^2 - 3.941 \times 10^{-10}t^3$ where ρ is the electrical resistivity in microhm-cm and t is the temperature in degrees Centigrade. The thermal conductivity of lithium, calculated by means of the Wiedemann-Franz-Lorenz relation, has a positive temperature coefficient over the temperature range to 1430°C. (auth)

47016 (TIM–901) REACTION RATE OF COLUMBIUM–1 ZIRCONIUM ALLOY WITH OXYGEN AT LOW PRESSURES. Hogan, J. F.; Limoncelli, E. A.; Cleary, R. E. (Pratt and Whitney Aircraft, Middletown, Conn. Connecticut Advanced Nuclear Engineering Lab.). Aug. 24, 1965. Contract AT(30-1)-2789. 19p. Dep. mn; CFSTI $1.00 cy, $0.50 mn.

The rate of reaction of niobium-1 zirconium alloy with oxygen at 2000°F was determined by thermogravimetric methods in an ultra high vacuum system at oxygen pressures in the range of 7.7×10^{-7} to 5.0×10^{-5} torr. The data indicated that the reaction rate was controlled by pressure and was independent of time up to 6 hours. The reaction rate is given by the equation: $\log R\ (\text{mg cm}^{-2}\ \text{hr}^{-1}) = 22.188 + 11.867 \log P + 2.174\ (\log P)^2 + 0.1414\ (\log P)^3$; (P in torr). The oxygen sticking factors calculated from these data are 0.42 and 0.74 at oxygen pressures of 5.0×10^{-5} torr and 7.7×10^{-7} torr, respectively. (auth)

47017 (UCRL–14316) THE EFFECT OF STRAIN RATE ON THE MECHANICAL PROPERTIES OF GENERAL PURPOSE POLYPROPYLENE. Hoge, K. G. (Lawrence Radiation Lab., Univ. of California, Livermore). July 9, 1965. Contract W-7405-eng-48. 21p. Dep. mn; CFSTI $2.00 cy, $0.50 mn.

The effect of strain rate on the mechanical properties or polypropylene is analyzed. Compressive data were obtained at "static" strain rates from 10^{-4} to 1 per second and at dynamic rates from 650 to 1600 per second on a Dynapak machine utilizing the Hopkinson split-bar technique. The effect of friction on the specimen ends, which produces a triaxial stress state, is analyzed by comparing unlubricated specimens and specimens lubricated with Molykote. Photographs of tests were taken with high speed cameras at 50-μsec intervals to show the mode of deformation. (auth)

47018 (USNRDL–TR–890) DETERMINATION OF THE TOTAL TRITIUM ACTIVITY ADSORBED ON THE SURFACE OF VARIOUS METALS. Balkwell, W. R.; Kubose, D. A. (Naval Radiological Defense Lab., San Francisco, Calif.). Aug. 19, 1965. 22p.

The total tritium activity adsorbed on structural steel, galvanized steel, brass, and aluminum was found to be less than 10 μC of tritium/cm^2 of surface for exposure concentrations of 0.23 mC of tritium/cm^3 in air and an exposure time of one hour. The total tritium activity adsorbed on a carbon steel surface was much greater than for the other surfaces. An increase in the total tritium activity adsorbed with increasing tritium exposure concentration was observed for all the metals studied. The nature of this increase, assuming a clean surface, appears to depend on the surface texture of the material. At a constant exposure concentration (0.11 mC of tritium/cm^3) no significant change in the total tritium activity adsorbed was observed for exposure times from 15 min to 4 hr. (auth)

47019 (AD–619334) THERMOELECTRIC CHARACTERISTICS OF METALLIC SINTERED ALLOYS ON A TUNGSTEN AND MOLYBDENUM BASE. Svede-Shvets, N. I.; Eyduk, Yu. A.; Enina, V. A.; Vodop'yanova, L. S.; Trushin, Yu. V. Translated from Sb. Tr. Tsentr. Nauchn.-Issled. Inst. Chernoi Met., No. 30, 7–16(1963). 15p. (FTD-TT–65–642). CFSTI.

Molybdenum and W alloys were sintered and their thermoelectric properties as electrode materials for creating new thermocouples of special design, for instance the tubular ones, were investigated. Thermocouples with

beryllium, zirconium, magnesium, and aluminum oxides as added materials proved to be insufficient above 1700°C. The best results were found with Mo and W alloys containing Nb, Fe, Ni, and Re. (P.C.H.)

47020 (AEC-tr-6616) RESEARCH IN THE FIELD OF REFRACTORY AND HARD COMPOUNDS. Meyerson, G. A. Translated from Izv. Akad. Nauk SSSR, Neorgan. Materialy, 1: 16-28(1965). 26p. Dep. mn; CFSTI $2.00 cy, $0.50 mn; JCL $2.60 fs, $0.83 mf.

The production, properties, and uses of refractory carbides, nitrides, borides, silicides, and sulfides are discussed. From various examples cited of investigations in the field of refractory and hard compounds, it was concluded that possibilities exist for the production of the compounds in pure form and with exactly set composition and structure. (P.C.H.)

47021 (JPRS-31225) STUDIES IN STRUCTURE OF TUNGSTEN AND MOLTEN IRON, COBALT, AND NICKEL BORIDES. Translated from Dokl. Akad. Nauk SSSR, 162: 64-9(May 1965). 13p. (TT-65-31722). CFSTI $1.00 cy, $0.50 mn.

Two articles are presented on the following topics: study of fine structure of tungsten single crystals by diffraction of ultrafast electrons, and surface tension and structure of molten iron, cobalt, and nickel borides. The article on tungsten single crystals is abstracted separately. (D.L.C.)

For an abstract of the individual paper see: 47022.

47022 (JPRS-31225, pp 1-5) INVESTIGATION OF THE FINE STRUCTURE OF TUNGSTEN SINGLE CRYSTALS BY MICRODIFFRACTION OF ULTRAFAST ELECTRONS. Popov, N. M.; Savitskii, E. M.; Tsarev, G. L. Translated from Dokl. Akad. Nauk SSSR, 162: 64-6(May 1965).

Single crystals of tungsten 99.97% pure were grown by electron beam zone melting and prepared by electrolytic polishing. The specimens were studied with an electron microscope diffraction camera using 557-kev electrons and found to have inclusions varying in size from 0.5 to 2.5μ. Diffraction spectra of these inclusions showed, in addition to tungsten, reflections characteristic of the compound W_2C. Also in specimens cut perpendicular to the growth axis ⟨100⟩, a cellular growth structure with a cell size of 0.2 to 0.4μ was observed. The formation of this structure is caused by reduction of the freezing point by impurities. Diffraction spectra showed that the cell boundaries were rich in impurities, particularly in the W_2C phase. To introduce dislocations, some samples were subjected to slight bending; both screw and edge dislocations were observed. Dislocations whose ends lay along lines in the ⟨110⟩ direction were identified as screw type, and the edge dislocations appeared to form at impurity regions. (D.L.C.)

47023 (LA-tr-65-20) X-RAY DETERMINATION OF THE COEFFICIENT OF THERMAL EXPANSION. Belikov, A. M. Translated by Helen J. Chick and Charles P. Kempter (Los Alamos Scientific Lab., N. Mex.) from Sb. Nauchn.-Tekhn. Tr., Nauchn.-Issled. Inst. Met. Chelyabinsk. Sovnarkhoza, No. 1, 139-44(1960). 9p. Dep. mn; CFSTI $1.00 cy, $0.50 mn; JCL $1.10 fs, $0.80 mf.

Determination of the average thermal expansion coefficients was carried out on microsections and powders of pure metals, as well as on alloys of the system Mo-Nb, and on TiC. The thermal coefficient expansion determined by x-ray was found to be somewhat larger than the coefficient found by dilatometric measurements. The larger the difference, the larger the ratio of the surface to the volume of the material taking part in the reflection of the x-ray beams. (P.C.H.)

47024 (NLCO-tr-6) METALLOGRAPHY—CONCERNING THE EXISTENCE OF AN ALLOTROPIC CHANGE TO CUBIC U_3Si WITHIN THE URANIUM-SILICON SYSTEM. Blum, Pierre L.; Silvestre, Georges; Vangoyeau, Henri. Translated by W. A. Althaus and M. M. Cook (National Lead Co. of Ohio, Cincinnati) from Compt. Rend., 260: 5538-41(May 24, 1965). 5p. Dep. mn; JCL $1.10 fs, $0.80 mf.

Studies at high temperatures by differential thermal analysis, dilatometry, and x-ray diffraction of uranium alloys with a silicon content giving the compound δ U_3Si revealed the existence of a tetragonal ≈ cubic transition at 765°C ± 3°C. The new phase, δ′, is isostructural with Cu_3Au I and its range of stability extends to 930°C, the temperature of the peritectoid decomposition of U_3Si. (auth)

47025 (ORNL-tr-637) THE START OF PRECIPITATION FROM SUPERSATURATED SOLID SOLUTIONS. Hornbogen, Erhard. Translated for Oak Ridge National Lab., Tenn. from Z. Metallk., 56: 133-54(1965). 65p. Dep. mn; JCL $6.60 fs, $2.15 mf.

A survey was made of the phenomena of nucleation in solids. Crystal structure of matrix and nucleus, imperfections present in the matrix after solution treatment, volume change due to phase changes, and nature of the stresses between nucleus and matrix are discussed in relation to nucleation. The nucleation behavior of alloys is discussed considering different types of imperfections and the possibility of formation of metastable phases. To demonstrate the effects, nucleation diagrams are proposed. They show the starting time of nucleation as a function of aging temperature and alloy concentration with lattice imperfections and crystal structures of the nucleated phases as parameters. 79 references are cited. (P.C.H.)

47026 (ORNL-tr-795) CONTRIBUTION TO THE STUDY OF AGEING OF CORROSION-RESISTANT STEELS OF THE TYPE Cr18Ni9Ti. Loebl, Karel; Tuma, Hanus; Rysava, Marie. Translated for Oak Ridge National Lab., Tenn., from Kovove Mater., 2: 433-44(1964). 15p. Dep. mn; JCL $1.60 fs, $0.80 mf.

Studies were made on two 18% Cr-9% Ni steels understabilized (0.21%) and over-stabilized (0.61%) by Ti. The steels were isothermally annealed at 400 to 1000°C for times up to 10,000 hr. The structural changes taking place during annealing, especially carbide precipitation, were followed metallographically, and the individual structural components were isolated electrolytically. A sigma phase is formed in areas of the delta ferrite and high Cr content. At 750-800°C, Cr carbide precipitates in the understabilized steel, while in the over-stabilized steel, it disappears entirely. The isolation of structural components is plotted in the form of space diagrams as functions of temperature and annealing time. The greatest effect of the annealing occurs as a drop in notch toughness. (D.L.C.)

47027 A REFINEMENT OF THE CRYSTAL STRUCTURE OF YTTRIA. Paton, M. G.; Maslen, E. N. (Univ. of Western Australia, Nedlands). Acta Cryst., 19: 307-10 (Sept. 10, 1965).

The crystal structure of yttria, Y_2O_3, was refined using single-crystal x-ray-diffraction data. The results confirmed the general features of earlier analyses using powder diffraction data, but a considerable improvement in accuracy was achieved. (auth)

47028 NEUTRON DIFFRACTION STUDY OF CHEMICAL ORDER-DISORDER IN $PtMn_3$. Sidhu, S. S.; Anderson, K. D.; Zauberis, D. D. (Argonne National Lab., Ill.). Acta Cryst., 19: 413-16(Sept. 10, 1965).

A neutron study of the chemical order-disorder in $PtMn_3$ was made by utilizing the nuclear properties of Mn and Pt nuclei. The $b_{Mn} = -0.36 \times 10^{-12}$ cm and the $b_{Pt} = 0.95 \times 10^{-12}$ cm. In a disordered crystal structure of the stoichiometric $PtMn_3$ alloy, the manganese atoms scatter thermal neutrons 180° out of phase with those of platinum. As a result the structure becomes a nuclear null-matrix, and no diffraction peaks appear in its neutron pattern; however, when even a partial ordering takes place in the structure, diffraction peaks do appear in the pattern, and since their intensities depend on the degree of ordering, they permit a precise determination of the disorder parameter. Numerical values of the disorder parameter of an ordered and a disordered sample of $PtMn_3$ were determined. The

technique of using a nuclear null-matrix to study chemical order-disorder phenomena is described. (auth)

47029 LATTICE CONSTANTS OF Fe–Mo ALLOYS WITH Mo CONTENTS TO 20 wt/percent. Fuchs, Von A.; Ilschner, B. (Universitaet Gottingen, Deutschland). Acta Cryst., 19: 488-9(Sept. 10, 1965). (In German).

Lattice constants are given in tabular and graphical form for Mo–Fe alloys with molybdenum contents from 0 to 19.8 wt %. The lattice constants were determined by a focused back-reflection method. (M.C.G.)

47030 THE CRYSTAL STRUCTURE OF $YbZn_2$. Michel, David J.; Ryba, Earle (Pennsylvania State Univ., University Park). Acta Cryst., 19: 687-9(Oct. 10, 1965). (TID-21746).

The crystal structure of $YbZn_2$ was determined by single-crystal techniques. Stoichiometric amounts of 99.5% ytterbium and 99.999% zinc were sealed under helium in a tantalum crucible, melted, and allowed to furnace-cool. Photographs of a single crystal of the alloy indicated the resulting compound to be orthorhombic, with a = 4.60; b = 7.319, and c = 7.561 Å. A Debye-Scherrer photograph, taken with $FeK_\alpha(\lambda = 1.93728$ Å) radiation, was indexed, and the final lattice parameters were found from least-squares data to be: a = 4.573 ± 0.002, h = 7.325 ± 0.005, and c = 7.569 ± 0.004 Å. All hkl reflections with h + k + l 2n + 1 and hko reflections with h = 2n + 1 were absent on the Weissenberg photographs, indicating that the space group is Im2a (or ma) or Imma. The lattice parameters and possible space group for $YbZn_2$ indicated that it is isostructural with $CeCu_2$. Metallographic examination of the alloy revealed the presence of extensive twinning. A thermal arrest, indicating a possible phase transition in $YbZn_2$, was observed at 683 ± 3°C. (F.J.H.)

47031 INTERACTION OF NIOBIUM WITH ACTIVE GASES AT VERY LOW PRESSURES. I. ADSORPTION OF NITROGEN BY NIOBIUM. Pasternak, R. A.; Gibson, R. (Stanford Research Inst., Menlo Park, Calif.). Acta Met., 13: 1031-8(Oct. 1965).

The interaction of nitrogen with niobium filaments was studied over wide ranges of pressure (6×10^{-9} to 6×10^{-4} torr) and of temperature (25 to 1800°C). At room temperature, the sticking probability on the clean surface was about 0.5 and adsorption led to a saturated surface layer. At high temperatures, the sticking probability was about 0.1, independent of pressure and temperature, and the gas diffused so fast into the bulk that the surface remained virtually clean for an extensive time interval. No significant activation energy was required for adsorption. The dependence of the observed sorption rates on temperature and pressure is discussed in terms of simultaneous adsorption on the surface and diffusion into the bulk. (auth)

47032 DIFFUSION OF ^{63}Ni IN ALPHA-IRRADIATED COPPER. Bonzel, H. P. (Institut fuer Physikalische Chemie, Goettingen, Ger.). Acta Met., 13: 1084-6(Oct. 1965).

The method of decrease in surface activity was used to investigate the diffusion of ^{63}Ni in polycrystalline copper. The copper used for these experiments had a purity of 99.995%. The samples were annealed for 12 hr at 500°C to homogenize the structure. The radioactive nickel was electrolytically deposited on the copper samples. The thickness of the layers was between 30 to 60 au. The diffusion proceeded in a vacuum at ~10^{-6} mm Hg. The radioactively labeled surface of the specimen lay free, so that it could be irradiated during diffusion. ^{210}Po served as the source of α radiation. It had an activity of about 3 C, emitted α-particles with an energy of 5.3 Mev, and produced an α flux of 8×10^9 sec^{-1} cm^{-2}. The temperature dependence for the diffusion of ^{63}Ni in copper was measured and may be expressed as $D = 6.4 \times 10^{-2}$ exp (−45300/RT) cm^2/sec. In the temperature range from 210 to 285°C the diffusion caused by irradiation was found to be independent of temperature and on the order of 10^{-18} cm^2/sec. (J.F.H.)

47033 HIGH-TEMPERATURE MODIFICATIONS OF THORIUM DICARBIDE. Gantzel, P. K.; Langer, S.; Baldwin, N. L.; Kester, F. L. (General Atomic Div., General Dynamics Corp., San Diego, Calif.). Advan. X-Ray Anal., 8: 78-85(1965).

Thermal analyses of samples of thorium dicarbide in equilibrium with graphite showed arrests, which indicated phase transitions at 1427 ± 21 and 1481 ± 28°C. These thermal effects were observed on heating and cooling both in standard thermal analysis and in differential thermal analysis using graphite as a reference material. The microstructure of thorium dicarbide samples showed the characteristic "herringbone" pattern of a material that has undergone a martensitic-type transition. A high-temperature x-ray investigation revealed that the observed thermal arrests correspond to crystallographic transformations. The monoclinic modification found at room temperature was stable to 1427°C, at which temperature a tetragonal modification with $a_0 = 4.235 \pm 0.002$ and $c_0 = 0.002$ Å was formed. At 1481°C, the tetragonal was transformed to cubic with $a_0 = 5.809 \pm 0.002$ Å. The best agreement between observed and calculated intensities was obtained with C–C units of 1.5 Å assumed bond length in space groups $P4_2/mmc$ and Pa3 for the tetragonal and cubic modifications, respectively. (auth)

47034 OXIDATION OF ZIRCONIUM–YTTRIUM ALLOYS. Phalen, D. I.; Vaughan, D. A.; Richard, N. A. (Battelle Memorial Inst., Columbus, Ohio). Advan. X-Ray Anal., 8: 143-50(1965).

The phase and elemental distributions on zirconium alloys loys containing 5, 10, 25, 35, and 50 at. % yttrium, oxidized in dry air at 1200 and 1600°C, were studied by x ray diffraction, fluorescence, and electron-microprobe techniques. Zirconium–yttrium alloys, which were entirely solid at 1200°C, and zirconium 5 and 25 at. % yttrium alloys, which were two-phase solid plus liquid at 1600°C, formed a multiphase scale of ZrO_2, Y_2O_3, and ZrN. The phase distribution varied with yttrium content, while the average metal composition remained constant throughout the oxide scale and base metal. In contrast, zirconium 35 and 50 at. % yttrium alloys, which were entirely liquid at 1600°C, formed a single-phase Y_2O_3 layer. The mechanism of air oxidation of solid zirconium–yttrium alloys, up to 50 at. % yttrium, is one of anion diffusion to the oxide-metal interface with little or no diffusion of the metallic elements. The oxidation of liquid alloys differs in that, as a result of yttrium diffusion to the oxide-liquid interface, Y_2O_3 is the only oxide formed. Ternary Zr–Y–O isotherms are presented to illustrate the phase distribution and mode of formation. (auth)

47035 STRUCTURE OF A THORIUM MONOLAYER ON THE TUNGSTEN (100) SURFACE. Anderson, J.; Estrup, P. J.; Danforth, W. E. (Franklin Inst., Swarthmore, Pa.). Appl. Phys. Letters, 7: 122-3(Sept. 1, 1965).

Previous attempts to explain work-function changes coverage met with a conspicuous lack of data concerning the structure of the absorbed layer. Direct experimental evidence for the structural arrangement of a monolayer of thorium deposited on a tungsten (100) surface is presented. The investigations employed the technique of low-energy electron diffraction. Thorium was deposited on the W(100) substrate and the changes in thermionic emission and in the diffraction pattern were then followed as thorium was desorbed from the surface. Heating of the sample to 700–800°C produced the pattern shown. It consists of 12 spots surrounding the center spot. This is interpreted as arising from two hexagonal patterns rotated 90° from each other. As the sample was heated above about 1100°C the pattern became weak and a simultaneous increase in the thermionic emission was observed. A model of the surface structure is shown. The results may be an illustration of a general tendency of the metal absorbate to form a close-packed monolayer irrespective of the substrate configuration. (J.F.P.)

47036 CRYSTALLOCHEMICAL CHARACTERISTICS OF RHENIUM AND TECHNETIUM AS COMPONENTS OF METALLIC ALLOYS. Niemiec, Jan (Technical Univ., Wroclaw, Poland). Arch. Hutnictwa, 10: 121-41(1965).

A comparison of intermetallic phases occurring in binary systems of technetium and rhenium is shown. The existence

limits of intermetallic phases and boundary solid solutions are given. The electronic concentrations of σ and x phases were calculated in a manner accepted for electronic phases, by consideration of (n − l)d + ns electrons for A and B metals and taking into account the alloy composition. The most common structures in the alloys of rhenium and technetium with other metals are the hexagonal Laves' phases $MgZn_2$(C14), regular x phases (A12-αMn), and tetragonal σ phases (D8b-BU). The participation of Tc and Re in the formation of x and σ phases is very important. There are 9-MRe, 6-MTc, and 2 MOs phases for the entire amount of 18 binary x phases. There are 8-MRe, 5MTc, 5MOs, and MRu phases for 47 binary σ phases. The pairs of metals forming x and σ phases in binary systems are given with respect to the position in the periodic system and their existence range in atomic percentages. Comparison showed that technetium, because of its ability to form intermetallic phases of x and σ type, is more similar to rhenium and osmium than to ruthenium since the latter forms only 3σ phases and does not form x phases. The metals composing x and σ phases came mainly from the VIIth and adjacent Groups. In σ AxBy phases the A atoms belong to the Vth and VIth Groups and the B atoms to the VIIth Group. Manganese, technetium, and rhenium play the role of B or A atoms. In the σ phases A metals are separated from the manganese group by 1 to 2 places to the left and the B metals by 1 to 4 places to the right in the periodic system. (F.J.H.)

47037 HIGH-SPEED THERMAL ANALYSIS OF Zr–Nb ALLOYS. Stewart, D.; Hatt, B. A.; Roberts, J. A. (Fulmer Research Inst. Ltd., Stoke Poges, Eng.). Brit. J. Appl. Phys., 16: 1081-8(Aug. 1965).

The M_s temperature of the ω, "diffuse ω," and α phases in Zr–Nb alloys were studied by recording the thermal arrests obtained on rapid cooling and by electrical resistance measurements. Details of the apparatus which permits heat treatment of specimens in high vacuum, followed by gas quenching, are given together with the temperature of transformation and its dependence on rate of cooling. The transformation temperature is depressed in all alloys with increasing cooling rate, this depression being 100 deg C at 3000 deg C sec^{-1} for pure zirconium. Proof of the dependence of ω formation on cooling rate is given. Hypothetical (M_s, M_f) curves based on the experimental results are shown which account for the sequence of phases observed in as-quenched zirconium alloys. (auth)

47038 WORK FUNCTION MEASUREMENTS ON THE SUBLIMATE FROM URANIUM CARBIDE. Blott, B. H.; Hopkins, B. J. (Univ. of Southampton, Eng.). Brit. J. Appl. Phys., 16: 1215-16(Aug. 1965).

The work function of material sublimed from uranium carbide, measured by the retarding field method, was found in the range 2.9 to 3.6 ev. It is proposed that the higher values were associated with pure uranium, while the lower figures refer to oxidized uranium. (auth)

47039 RADIOLOGICAL SCANNING OF CAST IRON BIOLOGICAL SHIELDINGS. Heath, D. A. Brit. J. Non-Destructive Testing, 7: 44-54(June 1965).

A quality control method of radiography in which counting equipment is utilized as the recording medium is described. Quality control was required for the biological shield castings of the hole preparation, charge and discharge machines of the Hinkley Point reactors. The design required the shield material, cast iron, to have a density of not less than 430 lb/ft^3 at all points. A method of testing was developed in which a preliminary ultrasonic examination of the entire casting was followed by radiological scanning of the suspect areas to determine the density. Principles, equipment, determination of variables, duration of count, method of testing, sensitivity, and radiation hazards are discussed. (M.C.G.)

47040 APPLICATION OF RADIO-CRYSTALLOGRAPHY TO THE TESTING OF NUCLEAR METALS. Baron, J.-L. Bull. Inform. Sci. Tech. (Paris), No. 92, 107-16(Apr. 1965). (In French).

After a review of the physical basis of x-ray diffraction, examples are given of the application of crystallographic methods. The measurement of residual textures in metallic fuels is discussed. These preferential orientations are partly responsible for the dimensional variations, which occur in the fuel element when in-pile. Grain size determinations in uranium alloys are described. Two complementary processes are used: one makes it possible to obtain pictures representing a few grains making up a polycrystalline assembly, the other, using an analytical procedure, leads to an estimation of the average grain size. The problem of textures in structural materials was considered. A description is given of the Schulz method, which gives rapidly a quantitive estimation of the distribution of the normals in the form of a polar figure using beryllium as an example. The identification of phases in the interdiffusion zone was considered. The experimental method is given together with some applications. (auth)

47041 APPLICATION OF RADIOCRYSTALLOGRAPHY TO THE STUDY OF CERAMIC AND REFRACTORY COMPOUNDS. Braun, C.; Conte, M.; Magnier, P. Bull. Inform. Sci. Tech. (Paris), No. 92, 137-43(Apr. 1965). (In French).

Two applications of radiocrystallography are described. X-ray analysis of crystalline phases present on the surface of pellets of sintered uranium oxide yielded precise information about possible re-oxidation of the pellets in the sintering ovens due to the very low oxygen content of the oven atmosphere. This examination, which is very rapid, constitutes a very sensitive control test applicable to production plant conditions. The limits of the domain of existence of UC around the stoichiometric composition $\overline{UC}$ in the uranium–carbon equilibrium diagram were determined. (auth)

47042 THE THERMAL CONDUCTIVITY, THERMOELECTRIC POWER, AND ELECTRICAL RESISTIVITY OF THORIUM BETWEEN 5 AND 100 deg K. Haen, P.; Meaden, G. T. Cryogenics, 5: 194-8(Aug. 1965).

Results of experiments on the thermal conductivity of a high purity thorium specimen between 5 and 100°K are reported and discussed. Electric resistivity measurements carried out on the same sample have enabled Lorenz numbers to be evaluated and have aided the analysis of the thermal conductivity results. It is apparent that an appreciable lattice contribution to the total conductivity is present at all temperatures. An unusual consequence is that this leads to a minimum in the total conductivity at about 50°K. The results were compared with the published works of White and Woods and of Rosenberg on the IVA transition elements and uranium, since these are metals most likely to have similarities with thorium. In addition, the absolute thermoelectric power was studied between 5 and 110°K. (auth)

47043 LOW TEMPERATURE SPECIFIC HEAT OF PLUTONIUM. Lee, J. A. (Atomic Energy Research Establishment, Harwell, Eng.); Mendelssohn, K.; Sutcliffe, P. W. Cryogenics, 5: 227(Aug. 1965).

The specific heat of a sample of high purity plutonium metal in the α-phase was measured from 12.5 to 80°K. The analysis of the results led to a value of 3×10^{-3} cal/mol deg^2, which is compared with other experimental results. (L.B.S.)

47044 HALL EFFECT IN SINGLE CRYSTALS OF GRAPHITE. Bhattacharya, R. (Indian Association for the Cultivation of Science, Jadavpur, Calcutta). Indian J. Phys., 39: 163-9(Apr. 1965).

In view of the apparent differences in the results of Hall effect measurements on natural single crystals of graphite by different workers, it was remeasured with some good crystals before and after the usual chemical purificatory treatments, adopting some special techniques. It was shown that the Hall coefficient which is more or less independent of the magnetic field before the chemical treatments, shows irregular variations with magnetic field after these treatments and that such irregularities are beyond the limits of

experimental errors. Possibility of these anomalies being associated with misalignments produced by chemical treatments was indicated. (auth)

47045 THERMAL EXPANSION OF POLYCRYSTALLINE HfO_2–ZrO_2 SOLID SOLUTIONS. Stansfield, O. M. J. Am. Ceram. Soc., 48: 436-7(Aug. 21, 1965).

Dilatometry was used to determine the thermal expansion of polycrystalline HfO_2–ZrO_2 bodies between 900 and 2500°C. Heating and cooling curves are presented. The thermal expansion below the phase transformation was only slightly composition dependent. At temperatures above the transformation, the expansion coefficients increased significantly as the ZrO_2 content increased. The linear change in specimen length at the monoclinic-tetragonal transformation ranged from about 0.37 to 0.75% but no consistent composition dependence was observed. (M.C.G.)

47046 SURFACE TENSION OF GADOLINIUM AND FLOATING-ZONE SINGLE CRYSTALS. Brissot, J. J.; Martres, R. (Laboratories d'Electronique et de Physique Appliquee, Limeil-Brevannes, France). J. Appl. Phys., 36: 3360-1(Oct. 1965).

Since no published data are available on the surface tension of gadolinium, it was measured by vertically lowering a cylindrical gadolinium rod with a diameter of about 5 mm at a rate of 30 mm/h in a 25-mm-diam and 30-mm long tantalum cylinder which was brought to 1900°C by high-frequency induction heating, keeping the whole system under a pure argon atmosphere. The end of the rod starts to melt slowly, and when the surface-tension forces are exceeded, the drop formed is separated and is collected in a tantalum crucible placed at the foot of the apparatus. Numerical calculation yielded a value of 810[4] dyn/cm. Gadolinium single crystals were prepared by melting gadolinium under a highly purified argon atmosphere, without oxygen, water vapor, or nitrogen, due to the high reactivity of gadolinium. The crystal structure was determined by x-ray diffraction study using the Laue method. (J.F.P.)

47047 INFLUENCE OF URANIUM ADDITION ON IRON AND STEEL. II. URANIUM ADDITION TO MEDIUM CARBON STEELS. Hasegawa, Masayoshi; Onoda, Ichiro J. Iron Steel Inst. (Japan), 50: 48-56(Jan. 1964). (In Japanese).

Laboratory tests on the influence of uranium additions to 0.7% on 0.3 to 0.4% carbon steels are described. In small ingots, no scavenging effect of uranium could be found, but sulfide inclusions decreased, and oxides increased with the addition of uranium. Uranium refined the austenitic grain size insignificantly. Gravitational segregation occurring in a slowly cooled ingot in a melting furnace was revealed by chemical analysis, autoradiography, β-γ counting, and sulfur prints of the longitudinal section. As-normalized hardness showed an increase through the formation of uranium carbides. Transformation temperatures of the steels were not changed by the addition of uranium according to thermal analysis. Microscopic examination showed that uranium scavenged the impurities at the grain boundary, and the pearlite figure was thereby changed with a loss of uniformity. Uranium carbides, UC or UC_2, increased with the content of uranium and precipitated at the austenite grain boundaries. Uranium had no effect on the ability of these steels to harden even at the quenching temperature (1200°C). No secondary hardening effect was caused at the quenching temperature nor on subsequent tempering. It was concluded that uranium carbides were not decomposed and that they were extremely insoluble to the austenite matrix at higher temperature. The effect of uranium on mechanical properties at room temperature was almost negligible, but V-notch Charpy impact strength was reduced with the content of uranium. The effect of uranium on the corrosion resistance to 5% hydrochloric acid was noticeable, but uranium steel suffered a severe pitting in 5% sulfuric acid. Against 3% nitric acid and 3% sodium chloride aqueous solution, it showed no corrosion resistance. (auth)

47048 THE ISOTHERMAL GROWTH OF UAl_2 PRECIPITATES IN URANIUM CONTAINING 250 ppm IRON AND 700 ppm ALUMINUM. Smith, A. F. (Berkeley Nuclear Labs., Eng.). J. Less-Common Metals, 9: 233-43(1965).

The growth of precipitates, identified as essentially UAl_2 in a ternary alloy of uranium containing by weight 250 ppm iron and 700 ppm aluminum, was studied as a function of annealing time and temperature. On heating in the α and β phases the number of precipitates diminished and the average size of those remaining increased. The variation of the average particle radius with time was of the form $r^n = At$. In the α range n varied from about 5 at 590°C to about 4 at 655°C. The exponent n was essentially constant at a value of 3 in the β range and as a consequence the number of particles decreased as the reciprocal of the annealing time. The activation energies for the growth process, interpreted in terms of a diffusion-controlled solubility mechanism, were 3.2 ± 0.2 ev in the α phase and 3.5 ± 0.1 ev in the β phase. (auth)

47049 STRUCTURAL CHANGES DURING CREEP OF A SOLUTION-HARDENED NIOBIUM ALLOY. Harris, Bryan (Pratt and Whitney Aircraft, North Haven, Conn.). J. Less-Common Metals, 9: 244-57(1965).

Vacuum creep-tests were used to study the mechanical behavior of a solution hardened alloy of niobium, containing 20 wt% tantalum, 15 wt% tungsten, and 5 wt% molybdenum, at temperatures between 980 and 1370°C. Standard design data were recorded and the results were analyzed semiquantitatively in an attempt to discover the nature of the deformation mechanism. The mechanical properties were related to structural changes, which were studied by means of optical and x-ray metallography. A picture emerged of a material deforming in a temperature-range where two or more mechanisms compete for control of the creep process. Diffusion-controlled processes such as grain-boundary sliding and substructure formation became increasingly predominant as the test temperature was raised above half the absolute melting point of niobium. Nondiffusion-controlled mechanisms, crystallographic slip for example, which were predominant at 980°C became increasingly unimportant, although still occurring to a slight extent even at 1370°C. (auth)

47050 FIELD ION MICROSCOPE OBSERVATIONS OF STACKING FAULTS IN TUNGSTEN. Ryan, H. F.; Suiter, J. (Univ. of Melbourne). J. Less-Common Metals, 9: 258-62(1965).

Field ion microscope observations made on "as drawn" tungsten wire specimens revealed the presence of defect structures, which exhibit a characteristic behavior. The observed structures are interpreted in terms of stacking faults and impurity segregation; the relevant dislocation reaction is $a/2[\bar{1}11] \rightarrow a/8[\bar{1}0\bar{1}] + a/4[\bar{1}2\bar{1}] + a/8[\bar{1}0\bar{1}]$. The frequency of occurrence of the defects was such that the proposed interpretation requires a dislocation density of the order of 10^{11} cm^{-2}. (auth)

47051 RARE-EARTH INTERMEDIATE PHASES. II. PHASES FORMED WITH PALLADIUM. Harris, I. R.; Raynor, G. V. (Univ. of Birmingham, Eng.). J. Less-Common Metals, 9: 263-9(1965).

Lattice spacings were measured at room temperature for thirteen intermediate phases of the type RE Pd_3. These compounds were found to crystallize in the face-centered cubic type structure. Results indicated that in $CePd_3$ the cerium atoms adopt a valency state similar to that in γ-cerium (effective valency approximately 3.1). Europium and ytterbium appeared to behave as 3-valent elements in the phases $EuPd_3$ and $YbPd_3$. (auth)

47052 RARE EARTH INTERMEDIATE PHASES. III. THE CUBIC LAVES PHASES FORMED WITH ALUMINIUM AND COBALT. Harris, I. R.; Mansey, R. C.; Raynor, G. V. (Univ. of Birmingham, Eng.). J. Less-Common Metals, 9: 270-80(1965).

The lattice spacings of twenty two cubic Laves phases of the $MgCu_2$ type formed by rare earth metals with aluminum and cobalt were measured and are discussed. Hardness and magnetic susceptibility results for the RE Al_2 series are also presented. In $CeAl_2$ cerium adopted an effective atomic diameter consistent with an effective

valency of 3, while in $CeCo_2$ the effective valency was nearer 4. This variable behavior was analogous to that previously observed in solid solutions and intermediate phases containing cerium, and may be interpreted in terms of the opposing tendencies for cerium to change its effective valency towards that of its partner, and to contract by ionization to a higher valency state when subjected to compression. In the Laves phases studied, with the formula AB_2, compressive stresses were exerted on the atoms of the A sublattice by the B sublattice when the ratio r of the atomic diameter of A to that of B exceeded 1.225. Comparison of a number of Laves phases containing cerium suggested that the transition of electrons from the 4*f* levels to the conduction band occurred only for r values exceeding 1.345. The lattice spacing of the $GdCo_2$ phase, which was thought to be ferromagnetic, was abnormally high; this is discussed in terms of magnetic interactions, the elimination of which appeared to lead to a contraction of the atomic diameter of gadolinium. (auth)

47053 THE YTTRIUM–COBALT SYSTEM. Pelleg, J.; Carlson, O. N. (Iowa State Univ., Ames). J. Less-Common Metals, 9: 281-8(1965). (IS-1131).

A constitutional diagram for the yttrium–cobalt system was proposed based on microscopic evidence, thermal analyses, and x-ray diffraction data. Evidence was found for the occurrence of nine intermetallic compounds in this system. The structures of three of these, YCo_5, YCo_3, and YCO_2, were determined and six other intermediate phases were tentatively identified as having the compositions, Y_2Co_{17}, YCo_4, Y_2Co_3, YCo, Y_3Co_2, and Y_3Co. Eutectic reactions occurred at 1340°C and 93 at.% Co and 725°C and 37.5 at.% Co. There appeared to be negligible solid solubility of yttrium in cobalt. (auth)

47054 THE EFFECTS OF SINTERING ON THE MICROSTRUCTURE AND PROPERTIES OF SPRAYED MOLYBDENUM. Sellers, David J.; Levy, Milton (Army Materials Research Agency, Watertown, Mass.). J. Less-Common Metals, 9: 289-98(1965).

Post-sintering treatments in hydrogen were applied to free-standing molybdenum shapes fabricated by the oxy-acetylene and arc-plasma flame-spray processes. Hydrogen sintering at 1350 and 1450°C for periods of 9 to 48 hr yielded substantial improvements in the tensile strength, modulus of elasticity, density, and purity of the sprayed deposits. The low impact energy observed in as-sprayed material was retained in the sintered products. Shrinkage was found to be anisotropic and weight loss equivalent to reduction in MoO_2 content. The sprayed molybdenum was converted from a columnar structure to one typical of recrystallized molybdenum sheet. (auth)

47055 THE CRYSTAL STRUCTURE OF THE SO-CALLED TECHNETIUM DISILICIDE. Wittmann, A.; Nowotny, H. (Universitaet, Vienna). J. Less-Common Metals, 9: 303)1965).

On the basis of x-ray data given for "$TcSi_2$" in technetium–silicon systems, tentative indexing could be done for a = 6.737 and c = 18.099 Å. The unit cell was built of 4 subcells according to a formula of Tc_4Si_7. (M.C.G.)

47056 AN INTERNAL FRICTION PEAK IN BERYLLIUM. Elias, M. J.; Rawlings, R. (Univ. Coll. of South Wales, Cardiff). J. Less-Common Metals, 9: 305-6 (1965).

A survey of the internal friction of Be was made over a wide range of temperature using an inverted torsional pendulum vibrating at about 1 cps in vacuo. The results obtained on extruded Be tested between –20 and +20°C are reported. Three samples of material were tested, two of the samples contained about 0.04% Fe and the other 0.4% Fe. Some of the 0.4% Fe specimens showed a peak in the internal friction/temperature curve at about –3°C whereas the peak was absent during tests on the purer materials. The activation energy for shift of peak temperature with frequency was found to be 15.2 kcal/mol. Using the activation energy and the formula $\omega\tau/(1+\omega\tau)^2$ the internal friction/temperature curve was calculated and found to fit the observed points very well indicating a single time of relaxation. (F.J.H.)

47057 'CAVITIES IN TUNGSTEN. Ryan, H. F.; Suiter, J. (Univ. of Melbourne). J. Less-Common Metals, 9: 307-8(1965).

Cavities in tungsten were observed using a field ion microscope. Wire fabricated from sintered powder was used. The cavities observed were all in the size range from 20 to 400 Å, which was considerably smaller than most of those observed by Wronski and Fourdeux. (F.J.H.)

47058 INTERDIFFUSION IN NIOBIUM–VANADIUM ALLOYS. Geiss, R. C.; Hartley, C. S.; Steedly, J. E. Jr. (Air Force Materials Lab., Wright Patterson Air Force Base, Ohio). J. Less-Common Metals, 9: 309-20(1965).

A determination of the variation of interdiffusion coefficient with composition for Nb–V alloys was made for diffusion temperatures of 1404, 1505, 1630, and 1750°C. Three types of doubly infinite couples were employed: Nb/V, Nb/alloy, and V/alloy, where the alloy was 50 at. % Nb. Compositions in the diffusion zone were determined by electron-beam microanalyzer. Kirkendall shifts were measured in all couples. It was found that the shift in the Nb/alloy couple was greater than the theoretical maximum shift calculated by assuming that the intrinsic diffusion coefficient of Nb is zero. This effect is believed to be due to a current of non-equilibrium vacancies in the diffusion zone, giving rise to a chemical potential gradient to vacancies. (auth)

47059 PHASE RELATIONS IN THE MAGNESIUM-RICH PORTION OF THE CERIUM–MAGNESIUM SYSTEM. Wood, David H.; Cramer, Eugene M. (Univ. of California, Livermore). J. Less-Common Metals, 9: 321-37(1965). (UCRL-12277).

The constitution of alloys up to 50 wt % of cerium in magnesium was studied by conventional methods of differential thermal analysis, metallography, and x ray diffraction. The previously reported compound, $CeMg_4$, is shown not to exist as such, but rather that a series of three compounds formed peritectically ($CeMg_{12}$, Ce_2Mg_{17}, and $CeMg_{8.25}$) exist in this composition region. Approximately 12°C below its formation the compound Ce_2Mg_{17} decomposes into the other two compounds in a eutectoid reaction. The eutectic is between magnesium and $CeMg_{12}$ at about 593°C and 4.2 at. % cerium. The designation $CeMg_{8.25}$ is tentative as the exact stoichiometry is unknown. (auth)

47060 NETWORK STRUCTURES IN URANIUM AND ITS ALLOYS. Angerman, C. L.; Huntoon, R. T. (E. I. du Pont de Nemours and Co., Aiken, S. C.). J. Less-Common Metals, 9: 338-53(1965). (TID-21760).

Network substructures were produced in uranium by the eutectoid decompositions of the gamma and beta phases. One network, corresponding to the beta grain and subgrain boundaries, was composed of either incipient precipitates (zones of segregated impurity or alloying elements) when the cooling rate through the transformation was rapid, or of real particles when the cooling rate was slow or the alloy content high. A second network, corresponding to the gamma grain boundaries, was apparent because the beta phase nucleated at the gamma grain boundaries and, during rapid cooling, either incipient or real precipitates outlined each of the beta regions as they grew into the original gamma grains. The incipient precipitates could be revealed only by certain etchants, such as HNO_3, while the real precipitates could be delineated by either the HNO_3 etch or by electropolishing. The incipient precipitates were readily visible by transmission electron microscopy as tiny zones of high lattice strain. The presence of these network structures increased the work-hardening exponent and embrittled the uranium. (auth)

47061 EVALUATION OF THE PROPERTIES OF PROTECTED MOLYBDENUM AND 0.45% TITANIUM–MOLYBDENUM ALLOY. Glenny, E.; Restall, J. E. (National Gas

Turbine Establishment, Farnborough, Hants, Eng.). J. Less-Common Metals, 9: 367-87(1965).

Preliminary oxidation, stress-to-rupture, thermal fatigue, and vibration fatigue tests in the range 900 to 1200°C, and impact tests at 20°C were carried out on molybdenum and a 0.45% Ti–Mo alloy prepared by both sintering and arc-casting techniques and protectively coated with molybdenum disilicide, a chromium–aluminium–silicon alloy (single and double coats), and a nickel–chromium–boron alloy. The results indicate that the thin silicide coatings are more protective in the absence of external loads than a relatively thick chromium–silicon–aluminium alloy coating, but their behavior is similar in the presence of thermal or alternating mechanical stresses. The presence of coatings considerably reduces the mechanical shock resistance of 0.45% Ti–Mo alloy at 20°C, and this, in combination with the ease of causing damage to these coatings with consequent catastrophic oxidation of the underlying metal, will probably preclude serious consideration of this molybdenum alloy for the turbine blade application. (auth)

47062 RELATION BETWEEN IONIZATION AND COHESIVE ENERGIES OF RARE EARTHS. Wall, L.; Good, R. H. Jr. (Iowa State Univ., Ames). J. Less-Common Metals, 9: 390-1(1965). (IS-978).

A theory previously developed for metallic binding in subgroup A metals was used to predict some of the ionization energies of rare earth atoms. Given the density of the rare earth metal and Z, the number of free electrons per atom, the theory predicts the sum of the cohesive energy of the metal, $-E(r_0)$, and the first Z ionization energies of the atom, I. Z = 2 is assumed for Eu and Yt, Z = 3 for the rest. Given the density and Z, the theory also gives a value for the radius of the ion core inside the metal. (P.C.H.)

47063 THE ELECTRICAL RESISTIVITY AND CHARACTERISTIC TEMPERATURE OF TECHNETIUM. Meaden, G. T. (Univ., Grenoble, France). J. Less-Common Metals, 9: 392(1965).

Using the previously determined value for the thermal conductivity of pure Tc, estimates were made of the electric conductivity and characteristic temperature of the metal. The electric conductivity was found to be about 15 μΩ cm at 295°K. The value of 450 to 500°K was found to be most probable for the characteristic temperature. The result is in keeping with the Debye characteristic temperatures of adjacent and homologous elements. (P.C.H.)

47064 SURFACE TENSION OF LIQUID METALS. Flint, O. (Atomic Energy Research Establishment, Harwell, Eng.). J. Nucl. Mater., 16: 233-48(July 1965). (AERE-M-1479).

Results of surface tension measurements by all reported techniques are collated and examined. The lack of reproducibility and wide scatter is discussed. It is suggested that more fundamental values would be obtained if values for liquid metal density were determined by techniques independent of surface tension corrections. It is also suggested that this reported lack of reproducibility is largely due, as much to variations in choice of liquid metal density and temperature, as to gross impurities and not to traces of unspecified surface-active contaminants. Data are tabulated. 113 references. (auth)

47065 SURFACE TENSION BY PENDANT DROP TECHNIQUE. Flint, O. (Atomic Energy Research Establishment, Harwell, Eng.). J. Nucl. Mater., 16: 260-70 (July 1965). (AERE-R-4782).

The electron bombardment/pendant drop technique for determination of values of surface tension of liquid metals is described and the basic physical disadvantages are enumerated. The method is recommended only for reactive and high melting point metals and then only where other methods have proved inapplicable. Values of surface tension, at the melting point, for 14 materials are quoted; those of 1294 dyn/cm for uranium, 1402 and 1880 dyn/cm for pure and commercial titanium, and 1827 dyn/cm for niobium being of interest, in view of scarcity of published data. (auth)

47066 THE DIFFUSION OF PLUTONIUM IN MAGNESIUM AND MAGNESIUM ALLOYS. Hodkin, D. J.; Mardon, P. G. (Atomic Energy Research Establishment, Harwell, Eng.). J. Nucl. Mater., 16: 271-89(July 1965). (AERE-R-4800).

The diffusion of plutonium in magnesium and magnesium alloys at temperatures of 420–500°C and times of up to 3 months was studied by autoradiographic, metallographic, and x-ray techniques. Diffusion coefficients, calculated by an empirical modification of Hall's technique, were found to vary considerably with plutonium concentration. Differences in behavior between magnesium–aluminum and pure magnesium or magnesium–zirconium alloys are discussed, and in particular the ability of aluminum additions to slow down plutonium penetration by formation of compounds. (auth)

47067 ELECTRICAL RESISTIVITY MEASUREMENTS IN QUENCHED ALUMINIUM–ALUMINA ALLOYS. Nobili, D. (C.C.R. EURATOM, Ispra, Italy); Passari, L. J. Nucl. Mater., 16: 344-6(July 1965).

Electric conductivity measurements were made in order to analyze the recovery spectrum of defects introduced by quenching an Al–Al_2O_3 system. The main concern was with nature of recovery phenomena after cold-work and evaluation of the energy of formation and migration of the defects. After quenching at 515°C for 20 to 30 min. the resistivity decrease was 5 mμ ohm·cm and the half-recovery or centering temperature about 200°C. The hypothesis is advanced that the recovery stage is connected with lattice vacancies. (P.C.H.)

47068 MATERIALS FOR ADVANCED TECHNOLOGIES. Weymueller, Carl R. Metal Progr., 88: No. 3, 57-71(Sept. 1965).

Materials development for aerospace requirements are discussed. Topics covered include: high-strength steels, titanium and aluminum, superalloys, beryllium, refractory metals, oxidation-resistant ceramics, graphites and their coatings, electronic materials, composites, structural plastics and adhesives, fibers and their application, and fluids and lubricants. (M.C.G.)

47069 EFFECTIVE HYPERFINE FIELDS AT THE NUCLEI OF Os AND Pt DISSOLVED IN Fe. Ho, James C.; Phillips, Norman E. (Univ. of California, Berkeley). Phys. Rev., 140: A648-50(Oct. 18, 1965). (UCRL-16119).

The heat capacities of two alloys containing, respectively, 0.75 at. % Os and 3.21 at. % Pt dissolved in Fe were measured from 0.08 to 1.15°K. From the coefficients of the T^{-2} terms, the hyperfine fields at the nuclei were found to be 1400 kOe for Os and 1390 kOe for Pt. (auth)

47070 DIFFUSION OF NON-VOLATILE FISSION PRODUCTS IN UO_2 AND ThO_2 AS DETERMINED BY LEACHING INTO MOLTEN SALTS. Thomas, R.; Lindner, R. (Technical Univ. of Brunswick, Ger.). Radiochim. Acta, 4: 170-1(Aug. 1965).

Reactor-grade UO_2 and ThO_2 with grain sizes of 0.5 and 0.2μ, respectively, was irradiated with an integrated slow neutron flux of 10^{17} and 10^{18}nvt and 3.8×10^{17} fast neutrons sec^{-1} cm^{-2}. After a "cooling time" to decrease the number of fission nuclides observable, samples were immersed in a pure and dry melt of NaCl under a protective argon atmosphere. At various times samples of the melt were taken and measured for radioactivity. The temperature function of the diffusion of various fission products was evaluated. (M.C.G.)

47071 THE DISTRIBUTION OF BERYLLIUM IN SOLID MAGNESIUM ALLOYS CONTAINING BERYLLIUM AT HIGH TEMPERATURES. Ichikawa, Riei; Saito, Reiko (Nagoya Inst. of Tech., Japan). Trans. Japan Inst. Metals, 6: 78-82(Apr. 1965).

The weight increase by heating, the distribution of beryllium in the surface of specimens after heating in the solid state and in the as-cast state, and the effect of the heating atmosphere on the distribution of beryllium were studied on magnesium containing 0.005% beryllium and its alloys containing 1% aluminum, calcium, lantha-

num, thorium, and zinc with beryllium. The weight increase after heating was found to be smaller in magnesium containing beryllium and its alloys containing beryllium than in pure magnesium. The enrichment of beryllium in the surface layer by diffusion was observed in magnesium containing beryllium and in Mg–Be alloys containing aluminum and calcium. The tendency of enrichment in the surface was inconspicuous in the alloys containing zinc and the surface enrichment of beryllium was hardly observable in Mg–Be alloys containing lanthanum and thorium. Such a phenomenon of beryllium enrichment in the surface layer was found in castings of these alloys as well as the solid alloys after heating. The surface enrichment of beryllium was scarcely observed in the alloys heated in vacuum and in argon. (auth)

47072 ADSORPTION OF ARGON IONS BY TITANIUM FILMS. Ivanovskii, G. F.; Radzhabov, T. D. Zh. Tekhn. Fiz., 35: 1312-18(July 1965). (In Russian).

An investigation was made of the adsorption of argon ions on freshly deposited titanium films, regenerated films, and on films that were continuously deposited during the adsorption. The investigation was undertaken because of the technical interest of such adsorption in connection with gettering type ion pumps. The 15 liter measuring chamber was evacuated to better than 5×10^{-9} mm Hg. The titanium films were deposited at from 10 to 50 amp/min on a 3 cm diameter copper base. A beam of up to 10 microamperes of 0.6 to 4.0 kev monoenergetic argon ions was produced by a magnetron type source and directed onto the film. The diameter of the beam at the target was 3 cm. After the adsorption, the titanium film was heated and the desorbed argon was measured. The desorption curves from films that were deposited before they were bombarded showed two maxima, at about 300 and 500°C. The films that were bombarded during deposition showed these two maxima and, in addition, a third rise due to evolution of gas beginning at about 700°C and extending to the melting point of the copper base. Considerably more argon was adsorbed when the film was bombarded during deposition than when it was bombarded only afterward. The quantity of argon adsorbed increased with increasing ion energy at low ion energies, and reached a broad maximum at an ion energy of about 2.5 kev. Adsorption coefficients up to 46% were observed. The experimental results were in good agreement with the theory of A. D. LeClaire and A. H. Rowe (Rev. Metall., 52: 94 (1955)). The high-vacuum deposited titanium films did not adsorb neutral argon that was admitted to the chamber with the ion source inoperative. (ATD)

47073 MECHANISM OF SILICONIZING OF MOLYBDENUM AND TANTALUM BY VAPOR DEPOSITION (thesis). Chu, Gordon Pu Kong. Columbia, Mo., Univ. of Missouri, 1964. 189p.

Molybdenum and tantalum were siliconized in an enclosed system by the hydrogen reduction of silicon tetrachloride with induction heating between 900°C and 1450°C. The siliconizing process was primarily influenced by the gaseous composition, temperature, time, molar flow ratio ($SiCl_4/H_2$), geometrical shape, and ionization charges. The rate of siliconizing, measured as the weight gain by the fused quartz helix balance, generally follows a parabolic law, $y = k t^{\frac{1}{2}}$, where y = weight gain, t = time, and k = rate constant. The activation energy is estimated at 21.6 kcal/mole for siliconizing of molybdenum. Deposition rate is greatly reduced at the later stage of the diffusion-controlled process. Siliconized molybdenum and tantalum were evaluated with metallography, microhardness, x-ray and electron microprobe analysis. Correlation between the coating properties, microstructure, intermetallic phases, and phase diagrams were made. Electron microprobe analysis could determine phases and the sharp concentration variation in one micron range between phases of narrow diffusion zones. However, a variation of 1 to 2 per cent in composition is difficult to resolve. Suggestions for codeposition (such as $TaSi_2$ and TaC), Kirkendall marker determination, diffusion constant, and diffusion barrier studies by electron microprobe analyses as well as the deposition under electrically charged field are proposed. (Dissertation Abstr.)

47074 CREEP AND ATOMIC MOBILITY IN POLYCRYSTALLINE ZIRCONIUM (thesis). Ardell, Alan Jay, Stanford, Calif., Stanford Univ., 1964. 158p.

The elevated temperature creep characteristics of polycrystalline alpha and beta zirconium were studied in vacuum under constant tensile stress. Equipment was designed and constructed so that testing could be conducted in vacuums of less than 10^{-6} mm Hg up to 1500°C. The creep of α–Zr was studied from 660-845°C, with the stresses ranging from 870-5400 psi. The steady-state creep rate, $\dot{\epsilon}_s$, was observed to be related to the applied stress, σ, and temperature, T, by the equation $\dot{\epsilon}_s = C\sigma^4 D \exp(-\eta/\sigma RT)$, where $D = D_0 \exp(-Q/RT)$ is the coefficient of self-diffusion, C is a constant and η ($= 2.54 \times 10^7$ psi-cal) is another constant. The experimental value of Q is about 50,000 cal/mol. The unusual creep behavior of α–Zr is considered in terms of a recent model for steady-state creep. The creep of β–Zr was studied from 975-1425°C, with the stresses ranging from 100-300 psi. The creep characteristics of β–Zr appear normal, and the results of this investigation agree very well with those of another investigation. The activation energy for creep, Q_c, is greater than the activation energy for self-diffusion, Q_d, at all temperatures. However, corrections to Q_c for the variation of Young's modulus with temperature fail to predict realistic values of Q_d. It is concluded, with reservations, that the ring mechanism is not responsible for the anomalous self-diffusion in β–Zr. (A.G.W.)

47075 MECHANISMS OF SOLID FRICTION. A Conference, Kansas City, Missouri, September 16, 17 and 18, 1963. Bryant, P. J.; Lavik, M.; Salomon, G. New York, Elsevier Publishing Co., 1964. 228p. $9.00. (CONF-630912).

Thirteen papers presented at the conference on Mechanisms of Solid Friction are given. The topics covered include: practical uses of the surface energy criterion, probable interface temperatures of solids in sliding contact, the effects of x-ray irradiation on the self-friction of potassium chloride, friction and wear of single crystals, friction and wear of sapphire, mechano-chemical factors in MoS_2-film lubrication, vapor lubrication mechanisms in MoS_2, mechanisms of graphite friction and wear, lubricating properties of lead film on copper, adhesion of metals and factors that influence it, sliding friction of copper, processes of metal transfer and wear, and friction and metal-transfer of heavily deformed sliders. One paper was previously abstracted for NSA as 19: 20011. (F.J.H.)

Radiation Effects

See also CHEMISTRY — Radiation Chemistry.

Refer also to abstracts 46625, 46712, 47576, and 48059.

47076 (AD-612090) RADIATION DAMAGE IN SEMICONDUCTORS. Annual Summary Report No. 3, July 1963-July 1964. Baruch, P. (Paris Univ., Orsay (France). Ecole Normale Superieure). Oct. 10, 1964. Contract AF61(052)-543. 29p. CFSTI $2.00 cy, $0.50 mn.

Three stages of annealing were observed in irradiated silicon between 0 and 120°C, with different defect mobilities. New experimental results on radiation enhanced diffusion in silicon lead to a model of defect diffusion with trapping at impurities. (TCO)

47077 (AD-613471) ANALYSIS OF ASTR RADIATION HEATING IN AEROSPACE STRUCTURAL MATERIALS. Technical Report, October 1, 1963–September 30, 1964. Roberts, I. C.; Goodwin, D. A. (General Dynamics/Fort Worth, Tex.). Feb. 1965. Contract AF29(601)-6213. 105p. (FZK-202; WL-TR-64-152). CFSTI $4.00 cy, $0.75 mn.

To evaluate calculational methods, some typical shielding and structural materials were irradiated by the Aerospace Systems Test Reactor (ASTR) at the Nuclear Aerospace Research Facility (NARF). The materials tested were Inconel-X, aluminum, and 6% borated polyethylene. The difference between the calculated and measured data was

less than 20% of the measured value for Inconel-X and aluminum but was larger for the borated polyethylene. (TCO)

47078 (AD-613643) THE METALLOGRAPHY OF PYROLITIC GRAPHITE. Tarpinian, Aram (Army Materials Research Agency, Watertown Arsenal, Mass.). Dec. 1964. 19p. (AMRA-TR-64-41). CFSTI $1.00 cy, $0.50 mn.

Etching of pyrolytic graphite by both argon ion bombardment and mercury ion bombardment is described. The difference between the microstructures revealed by the two methods is discussed, and an interpretation is suggested. Argon ion bombardment creates a leaf-like pattern reminiscent of stacked shingles. Mercury ion bombardment reveals a laminar structure unlike that produced by argon ion bombardment. Electrochemical polishing and etching reveals microstructures similar to those created by ion bombardment. Using an electrolyte based on phosphoric acid, microstructures similar to those resulting from mercury ion bombardment are revealed. Replacing the phosphoric acid with nitric acid results in microstructures similar to those obtained by argon ion bombardment. Based on the correlation between microstructures developed by ion bombardment and electrochemical etching, it was concluded that the microstructures revealed represent the true structure. (auth)

47079 (AERE-R-5014) STRESS CORROSION OF IRRADIATED STAINLESS STEELS. Davies, M. J.; Landsman, D. A.; Seddon, W. E. (Atomic Energy Research Establishment, Harwell (England)). Aug. 1965. 13p. Dep., BIS $0.50; HMSO 2s. 6d.

Fully annealed specimens of Type-316 stainless steel and of a 20 Cr : 25 Ni : Nb-stabilized stainless steel were subjected to stress corrosion tests in boiling 42% $MgCl_2$ solution; identical specimens were exposed to the same test after receiving doses of fast neutrons up to 2×10^{20} ncm^{-2}. Irradiation of the Type-316 steel greatly increased its susceptibility to stress corrosion cracking at low stress levels, but the 20 : 25 : Nb steel was immune to cracking in both irradiated and unirradiated conditions. It is proposed that the effect on the Type-316 steel is due to fast neutron radiation damage in the oxide film on the metal. (auth)

47080 (EUR-2478.e) DAMAGE AND DIFFUSION IN Al AND Al–Al_2O_3 ALLOY FOLLOWING BOMBARDMENTS WITH OXYGEN OR INERT GAS. Ruedl, E.; Kelly, R. (European Atomic Energy Community, Ispra (Italy). Joint Nuclear Research Center). Aug. 1965. 30p. (CONF-650631-3). Dep. mn.

From International Powder Metallurgical Conference, New York.

Damage and diffusion phenomena in Al and an Al–Al_2O_3 alloy ("SAP") were studied following bombardments with oxygen or inert gas. Use is made of transmission electron microscopy, measurements of gas release, and depth distribution measurements. A dose and dose-rate dependence for the appearance of damage in Al and SAP is found for both O_2 and Ne bombardments at 9 kev. The damage is more aligned, however, when O_2 is used than when Ne is used. The difference in arrangement can be explained by assuming a different mobility of the loops depending on whether O_2 or Ne is present in the Al lattice. The annealing behavior of the damage also depends on which gas is used in the bombardment. In the case of O_2 the damage anneals out roughly in the temperature range for Al self-diffusion (150-200°C). In the case of Ne large loops and tangles are present even at 500°C. Moreover, Ne-bombarded specimens show at high temperatures small bubbles and large undefined features. The latter are assumed to be gas pockets or blisters near the metal/oxide-skin interface. Gas-release experiments following Kr and Xe bombardments at >5 kev show that more than 99% of the gas is retained to the melting point. This is explained by means of depth distributions to be due to trapping near the metal/oxide-skin interface and thus confirms the observation of gas pockets or blisters. After bombardments below ~5 kev, gas is released beginning at the ambient temperature. Such release is analogous to that observed in other systems at low bombardment energies. (auth)

47081 (EURAEC-1432) RESEARCH TO DETERMINE THE LONG-TERM MECHANICAL PROPERTIES OF METALS SUBJECTED TO MECHANICAL STRESS AT ELEVATED TEMPERATURES AND NEUTRON IRRADIATION. Ninth Quarterly Report. Siegfried, W.; Zimering, S. (Battelle Memorial Inst., Geneva (Switzerland)). July 1965. Contracts 100-62-12 RDS and 057-64-7 TEES (RD). 92p. (EUR-2374). Dep. mn; CFSTI $3.00 cy, $0.75 mn.

Work Performed under United States–Euratom Joint Research and Development Program.

The Extrapolation of Time-to-Rupture by Means of the Exponential Function of Real Order. The variation of the parameters of the exponential function with the temperature and the stress is studied. To establish this variation law of the parameters, several experiments of the same alloy and thermical conditions (for example 10 Cr–Mo 910) are studied. A method is being developed for the determination of the stress for a given time-to-rupture and temperature which permits, using the variation law of the parameters, determination of the dispersion before doing the extrapolation. Extension of the Decomposition of the Rupture Process as Described in 2nd Special Report. The influence of the relation between stress and creep rate with respect to the development of a constriction is investigated more in detail. In this way it is possible to draw conclusions on the elementary mechanism taking place during the rupture process on the basis of the shape of time-to-rupture curves. This sort of analysis also permits certain conclusions to be drawn on the embrittlement at high temperatures. (auth)

47082 (NASA-CR-304) EXPERIMENTAL INVESTIGATION OF THERMAL ANNEALING OF NUCLEAR-REACTOR-INDUCED COLORATION IN FUSED SILICA. Douglas, F. C.; Gagosz, R. M. (United Aircraft Corp., East Hartford, Conn.). Sept. 1965. Contract NASw-768. 148p.

An experimental investigation was conducted to determine the spectral transmission characteristics of fused silica over a range of temperatures prior to nuclear irradiation and during thermal annealing of reactor-induced coloration following exposure to a dose of 6×10^{17} nvt fast neutrons per cm^2. The investigation was conducted using commercially supplied specimens of Corning 7940, Amersil Infrasil, and Thermal American Spectrosil brands of fused silica which were selected because of their high purity but which were found to differ slightly in chemical composition. The pre-irradiation studies were carried out at a series of fixed temperatures. The annealing studies were carried out using both ramp variations of temperature with time and stepwise variations of temperature with time for temperatures between 22 and 1000°C. Most of the annealing data were obtained at a wavelength of 0.21 microns, although some annealing data were obtained following step-wise changes in temperature at wavelengths between 0.15 and 4.0 microns. Spectral transmission measurements also were made at wavelengths between 0.15 and 4.0 microns for all samples before nuclear irradiation and after thermal annealing. The results of the tests indicate that nuclear-reactor-induced coloration is greater and more difficult to remove in the ultraviolet portion of the spectrum than in either the visible or the infrared portions of the spectrum. Induced coloration in the ultraviolet is annealed out at temperatures between 700 and 900°C, and the rate of annealing corresponds to activation energies of between 2.2 and 2.8 ev in a first-order kinetic annealing process with a frequency factor of 10^{10} sec^{-1}. The three brands of fused silica in order of their degree of induced coloration and the difficulty of annealing this induced coloration were: Amersil Infrasil, Corning 7940, and Thermal American Spectrosil. (auth)

47083 (NMI-4996, pp 77-85) METALLOGRAPHIC PREPARATION OF IRRADIATED URANIUM CARBIDE. Bauer, A. A.; McGrath, F. E. (Battelle Memorial Inst., Columbus, Ohio).

Uranium carbide is extremely susceptible to corrosive attack by water and moist air. This creates a problem in the hot-cell metallographic preparation of irradiated material, since water alone cannot be used as the abrasive vehicle in vibratory polishing. A solution of 2% chromium trioxide in water was found to provide a satisfactory suspension and polishing medium, although its use for badly cracked specimens is not recommended. Water formed during preparation of plastic replicas also presents a problem in the hot cell. This can be overcome by using methyl acetate as the solvent in preparing cellulose acetate replicas and by desiccating the specimen and replica immediately after application. (auth)

47084 (NMI-4997, pp 124-33) METALLOGRAPHY OF IRRADIATED DISPERSION-TYPE FUEL ELEMENTS. Richt, A. E.; Manthos, E. J.; Sims, E. D. (Oak Ridge National Lab., Tenn.).

Some unusual effects noted in the metallographic examination of irradiated dispersion-type fuel elements are shown and the significance of these observations on the performance of the elements is discussed. (auth)

47085 (NMI-4997, pp 134-56) HOT CELL METALLOGRAPHIC EXPERIENCE AT BATTELLE. McGrath, F. E.; Bauer, A. A. (Battelle Memorial Inst., Columbus, Ohio).

During the operation of the Battelle Hot Cells, a wide variety of irradiated structural, control, and fuel materials were examined. The metallographic procedures are outlined and typical results achieved with various materials are shown. Observed effects of irradiation are noted. (auth)

47086 (NMI-4997, pp 184-8) EXPERIENCE WITH VIBRATORY POLISHERS AND DESIGN FOR HOT-CELL APPLICATION. Long, E. L. Jr.; Gray, R. J.; Meador, J. T. (Oak Ridge National Lab., Tenn.).

Remote equipment was designed, fabricated, and tested for semiproduction type work. Initial results were encouraging. Several necessary design changes were made, which in turn had to be compensated for in the vibratory system to maintain proper polishing action. To complement the remoted polishers, a new specimen holder was designed that allows easy insertion and removal of the specimens using master-slave-type manipulators. (auth)

47087 (NMI-4997, pp 189-97) REMOTE METALLOGRAPHIC PREPARATION OF IRRADIATED ALUMINUM-CLAD LEAD-BONDED CERAMIC FUEL PELLETS. Carlander, R. (Argonne National Lab., Ill.).

Irradiated aluminum-clad lead-bonded thoria–26 wt % urania Borax-IV fuel pellets were prepared for metallographic processing by sectioning on an abrasive cutoff machine and by mounting in cold-setting plastic. Extreme care was exercised in the grinding operations to ensure particle retention by the mounting material. The samples were ground through 600-grit silicon carbide papers and polished, successively, on silk cloths impregnated with 3- and 1-μ diamond abrasive. The samples were final-polished with $\frac{1}{4}$-μ diamond compound on microcloth. This procedure is convenient in that it is also used for uranium and its alloys. Results of this polishing technique are considered quite good, especially taking into account the wide variation in hardness of the materials contained in the fuel plate composite. (auth)

47088 (NMI-4998, pp 95-106) ELECTRON MICROSCOPE STUDIES OF IRRADIATED A-286 ALLOYS. Rau, Robert C. (General Electric Co., Cincinnati, Ohio. Nuclear Materials and Propulsion Operation).

Results of electron microscopy performed on irradiated A-286 alloy specimens are presented. The metallographic polishing and etching techniques used for irradiated and unirradiated control specimens are discussed, together with the replication technique employed for electron microscopy of the specimens. A method of remotely obtaining single-stage direct-stripped replicas from irradiated specimens was developed and is described. (auth)

47089 (NMI-4999, pp 30-50) POST IRRADIATION METALLOGRAPHIC LABORATORY AT GE-NMPO. Leighton, S. A.; Filer, E. W. (General Electric Co., Cincinnati, Ohio. Nuclear Materials and Propulsion Operation).

The construction of the cell and equipment used in preparing irradiated materials for metallographic evaluation are discussed. The mounting, grinding, polishing, etching and photomicrographic procedures used in preparing the various metallic and ceramic materials are given along with representative results. The various pitfalls to be avoided are stressed. The methods used and the results obtained in replicating materials remotely for electron microscopic studies are discussed. (auth)

47090 (NMI-4999, pp 54-9) ONE-STEP REPLICATION IN THE HOT CELL. McGrath, F. E. (Battelle Memorial Inst., Columbus, Ohio).

A technique for obtaining replicas from irradiated material for direct examination is described. The use of this method represents considerable savings of time as compared to the triple replication technique. (auth)

47091 (NMI-4999, pp 69-77) REPLICATION OF IRRADIATED SPECIMENS WITH ROOM-TEMPERATURE VULCANIZING SILICONES. Manthos, E. J. (Oak Ridge National Lab., Tenn.).

Techniques for the replication of irradiated specimens with room-temperature vulcanizing silicones are described. Both unmounted and metallographically mounted specimens were replicated. Silicone rubber molds of the specimen surfaces are cast in the hot cells and, after curing, the molds are removed from the specimens and decontaminated. Positive epoxy replicas are then prepared from the silicone rubber molds in a semi-hot area. The replicas may be used for the verification of hot cell observations and are very useful as models for the location of saw cuts during sectioning of metallographic specimens. Difficulties encountered in the preparation and decontamination of the silicone rubber molds are described, and advantages and disadvantages of the material are discussed. (auth)

47092 (TID-22141) LINEAR ACCELERATOR PROJECT. Annual Technical Report During FY 1965. Gaertner, Erwin R. (Rensselaer Polytechnic Inst., Troy, N. Y.). Contract AT(30-3)-328. 115p. Dep. mn; CFSTI $4.00 cy, $0.75 mn.

Separate abstracts were prepared for seven sections of the report. The remaining papers deal with the radiolysis of carbon monoxide, electron irradiation of germanium and silicon, and transient radiation damage in silicon. (D.C.W.)

For abstracts of individual sections see: 46725, 46766, 47548–47550, 47595, and 47596.

47093 (VDDIT-16(5.2)) RADIATION EFFECTS ON SOLID, URANIUM BASED NUCLEAR FUEL MATERIALS. Vol. 5, No. 2. A Bibliography. Uhlmann, W. (Aktiebolaget Atomenergi, Stockholm (Sweden)). July 1965. 55p. Dep. mn.

A total of 40 abstracts is presented, arranged according to coordinate descriptors. Publication and corporate author indexes are included. (D.L.C.)

47094 (ORNL-tr-668) STUDY OF POINT DEFECTS IN PURE IRON THROUGH ELECTRICAL RESISTIVITY (thesis). Minier-Cassayre, Colette (Grenoble Univ. (France)). Translated by Gregory L. Boisvert. 110p. Dep. mn; JCL $9.10 fs, $3.50 mf.

A study was made of the different recovery phases of point defects produced in pure and doped Fe by neutron or electron irradiation, cold-hardening, and tempering. The point defects were observed by measurements of crystal dimensions and volume changes, magnetic aftereffects, internal friction, stored energy, and electrical resistivity, with emphasis on the latter. The dopants used were Be, Si, Ni, Co, Pt, Sb, and Al. The following identifications of the recovery phases found at low temperatures

were made: I_A, recovery of Frenkel close pairs; I_B, random migrations of interstitial atoms that annihilate themselves in vacancies; II_A, recovery of crowdions; and II_B, recovery of interstitial pairs. The phases at higher temperatures are due to diffusion of vacancies and are characterized more clearly by magnetic aftereffects than by resistivity. (D.L.C.)

47095 EFFECT OF ANNEALING ON MECHANICAL PROPERTIES OF ELECTRON-IRRADIATED ALUMINUM SINGLE CRYSTALS AT 23 deg K. Ono, Kanji; Meshii, M. (Northwestern Univ., Evanston, Ill.). Appl. Phys. Letters, 7: 190-2(Oct. 1, 1965). (COO-1367-4).

Previous investigations of annealing effects are extended to a lower temperature. Aluminum single crystals were irradiated at 23°K with 1-Mev electrons and stress-strain curves of irradiated crystals were determined at 23°K without any intermediate warm up. The effects observed in this study were large increases in both the yield stress and the extent of easy glide. No change in the rate of work hardening in easy glide was observed and there was no sharp yield point immediately after irradiation. As the yield stress increase is proportional to the square root of the defect concentration, the hardening effect is attributed to dispersed interstitials. The effect of intermediate annealing between irradiation and a tensile test on the stress-strain curve is reported. The results clarify the relation between the irradiations at 23 and 80°K in terms of point defect-dislocation interaction and further confirm the operation of a distinct hardening mechanism at each of the irradiation temperatures. (J.F.P.)

47096 EFFECTS OF RADIATION-INDUCED DAMAGE CENTERS IN LEAD ZIRCONATE TITANATE CERAMICS. Glower, Donald D.; Hester, D. L.; Warnke, D. F. (Sandia Corp., Albuquerque, N. Mex.). J. Am. Ceram. Soc., 48: 417-21(Aug. 21, 1965).

A study of reactor irradiation-induced changes in the electrical and lattice properties of ferroelectric Pb $(Zr_{0.65}Ti_{0.35})O_3$ + 1 wt% Nb_2O_5 revealed that these changes in properties are caused by different damage centers. The changes observed were: P_r decreased but P_s remained constant; double (antiferroelectric-type) hysteresis loops were formed; an increase by a factor of 5 in grain size did not affect the radiation damage rate in the ceramics; an increase in irradiation temperature to 100°C above room temperature doubled the damage rate; E_c for unpoled ceramics was insensitive to irradiation until integrated fast neutron fluxes of 10^{18} nvt (and the associated γ-dose) were exceeded and thereafter E_c increased exponentially; aging of the radioinduced damage did not occur at room temperature; the damage centers, which affected the electric properties, were temperature annealed, the annealing temperature depending on the particular material; and the introduction of lattice strain, as observed by changes in the longitudinal wave velocity (phonon mean free path length), did not appear to be related to changes in electrical properties. These changes in electrical and thermal properties were consistent with the published data for irradiated triglycine sulfate, Rochelle salt, barium titanate, and guanidinium aluminum sulfate and it is suggested that a common damage model may be constructed for all these ferroelectric materials. (auth)

47097 LOW-TEMPERATURE RECOVERY SPECTRA OF NEUTRON-IRRADIATED METALS. Burger, G.; Isebeck, K.; Voelkl, J.; Wenzl, H. (Technische Hochschule, Munich). J. Appl. Phys., 36: 3356-8(Oct. 1965).

The low-temperature recovery of the residual resistivity of copper, aluminum, gold, and platinum was investigated after irradiation in the core of a research reactor at 4.6°K in a comparatively hard neutron spectrum. The neutron flux at the same position is given. After irradiation in liquid helium the sample was transferred without warming to a cryostat located outside the reactor. The isochronal anneals were of 10-minute duration, the temperature being held constant to ±0.1°K. The resistivities after each anneal were measured at 4.6°K with a sensitivity of 2×10^{-13} Ω cm. The results for the four metals are shown. It is concluded that irradiation with reactor neutrons produces an annealing spectrum where subpeaks are strongly reduced in magnitude, but more substructure is revealed compared with the more selective population obtained with electron and deuteron irradiation. (J.F.P.)

47098 HYDROGEN EFFECTS IN AN IRRADIATED 1 PERCENT Cr, 1/2 PERCENT Mo PWR PRESSURE VESSEL STEEL. Broomfield, G. H. (Atomic Energy Research Establishment, Harwell, Eng.). J. Nucl. Mater., 16: 249-59(July 1965). (AERE-R-4705).

An investigation was made of the effect of a hydrogen concentration of approximately 1.4 cm^3 (NTP) per 100 g steel on the room and elevated temperature tensile properties, notch strengthening and brittle fracture characteristics, and delayed fracture tendencies, of a 1% Cr, ½% Mo steel in the unirradiated and irradiated ($1.0-1.4 \times 10^{19}$ fission neutrons/cm^2) conditions. The hydrogen embrittles the steel at room temperature and to a diminishing degree with increasing temperature, but the embrittling effect is not completely eliminated even at 250°C. The degree of embrittlement of irradiated steel does not differ significantly from that of unirradiated steel. It was concluded that at all the test temperatures embrittlement is due to a physical effect of the hydrogen in the steel; however, the mechanisms of embrittlement at room temperature and 250°C differ in that the room temperature embrittlement is associated with void formation in the ferrite, while the 250°C embrittlement is apparently due to crack formation in the pearlite. Limited results suggest that the ductile/brittle transition temperatures of the unirradiated and irradiated steel are raised by hydrogen. However, hydrogen has no significant effect on the notch strength and the irradiated steel is not prone to hydrogen-induced delayed fracture. (auth)

47099 THE EFFECT OF GAMMA DOSE ON OXIDE FILMS ON ZIRCONIUM AND ZIRCALOY-2 AND ITS RELEVANCE TO CORROSION. Harrop, P. J.; Wilkins, N. J. M.; Wanklyn, J. N. (Atomic Energy Research Establishment, Harwell, Eng.). J. Nucl. Mater., 16: 290-7(July 1965). (AERE-R-4779).

Oxide films between 2000 and 7000 Å thick, on Van Arkel zirconium and Zircaloy-2, were irradiated to pure gamma doses of up to 2×10^9 Rad; and two films were exposed to 10^{17} nvt of fast neutrons. The electrical conductivity and capacitance (100 c/sec to 20,000 c/sec) and optical absorption (2000 to 20,000 Å) of these films were indistinguishable from those of unirradiated controls. This was taken to indicate that $<10^{19}$ ions/cm^3 were displaced by the radiation. A value of $<10^{17}$ ions/cm^3 was calculated from damage theory. It was reasoned that reactor gamma radiation is unlikely to have an appreciable effect on electron or ion transport in Zircaloy-2 corrosion films a few thousand Ångström thick. Hence, if either electron or ion transport control corrosion in such films, reactor gamma radiation should not affect corrosion. (auth)

47100 THE EFFECTS OF DISLOCATION MOVEMENT IN ENHANCING SWELLING IN α-URANIUM DURING IRRADIATION. Speight, M. V.; Greenwood, G. W. (Central Electricity Generating Board, Berkeley, Eng.). J. Nucl. Mater., 16: 327-32(July 1965).

It is shown that there is a critical temperature range where dislocation movement may contribute to enhanced swelling during the irradiation of α-uranium. This range is one in which the temperature is sufficiently low for deformation to occur on account of internal stresses produced by irradiation growth, but still sufficiently high for fission gas bubble mobility to be adequate for bubbles to remain attached to dislocation lines while they are moving at speeds which enhance the rate of bubble coalescence. An analysis is presented which permits an assessment of the conditions under which swelling may become unacceptably large. (auth)

47101 THE THERMAL CONDUCTIVITY OF IRRADIATED URANIUM. Garlick, A.; Shaw, D. (United King-

dom Atomic Energy Authority, Sellafield, Eng.). J. Nucl. Mater., 16: 333-40(July 1965).

Post-irradiation thermal conductivity measurements were made on uranium specimens cut from fuel rods irradiated in the Calder Hall reactors to levels up to 4500 Mwd/t at temperatures between 250 and 450°C. The measurements were made on specimens 3 in. (7.6 cm) long and 1.15 in. (2.9 cm) diameter in a divided bar apparatus at a mean temperature of 60°C. The thermal conductivity decreased with irradiation dose, the rate of change being much more rapid during the first few hours of irradiation. At fuel temperatures above 320°C, the initial decrease was of the order of 5%, after which the rate of decrease became small at about 0.35% per 1000 Mwd/t. At fuel temperatures of 250°C, the initial decrease was greater, amounting to about 12%. The high initial rate of decrease is ascribed to irradiation growth effects and the smaller subsequent rate of decrease to the combined effect of porosity resulting from inert gas fission product atoms and the accumulation in solid solution of solid fission product atoms. The extent of the decrease is reduced by an enhancement of thermal conductivity due to thermal annealing processes. (auth)

47102 ACCUMULATION OF ELECTRIC CHARGE IN γ-IRRADIATED SHIELDING WINDOW GLASS. Kikuchi, Riichi (Osaka Univ.). Nuclear Eng. (Tokyo), 11: 11-14 (Jan. 1965). (In Japanese).

When irradiated with large doses of γ rays, electric charge is often accumulated in a window shielding glass of a hot cave and this causes breakdown. The cause and state of this accumulation were studied. The electric discharge of the shielding glass irradiated with γ rays is considered to be due to the accumulation of space charge, which is due to the Compton electrons in the direction of the incident γ rays. The temperature dependence of electric resistance was measured for the non-irradiated glass and the activation energy was determined for the charge carriers. The sample glass was exposed to gamma radiation to a total dose of 3×10^7 R and the thermally released current was measured at a heating rate of 100°C/hr. Two current peaks with different signs were obtained, which were attributed to the charge carriers caught in two different kinds of traps (i.e., positive metal ion and electronic current). Thermoluminescence was measured to confirm the fact. Most of the researches carried out so far have concerned the elucidation of the mechanism of accumulation of electric charge, and therefore the methods preventing the breakdown of the shielding glass must be investigated in the future. (NSA of Japan)

47103 DEVELOPMENT OF SWELLING-RESISTANT URANIUM ALLOYS. McDonnell, W. R. (E. I. du Pont de Nemours and Co., Aiken, S. C.). Nucleonics, No. 10, 23: 72(Oct. 1965).

Irradiation tests have defined a series of very dilute uranium alloys with progressively increased resistance to cavitational swelling. These alloys are listed. The approximate exposure thresholds at which cavitational swelling begins during irradiation at 400 to 500°C are given as a measure of their relative stability. At temperatures of 400 to 600°C large cavities form in uranium as a result of changes in the shape of individual grains, anisotropic growth, and related processes. The metal literally tears itself apart as is shown. This is called cavitational swelling as contrasted to fission-gas swelling caused by small fission-gas bubbles. Very few fission bubbles are formed at the low exposures at which cavitation may be severe. (J.F.P.)

47104 DISPLACEMENT PROBABILITIES OF LATTICE ATOMS IN VARIOUS METALS BY REACTOR RADIATION. Koehler, W.; Schilling, W. (Technische Hochschule, Munich). Nukleonik, 7: 389-99(Aug. 1965). (In German).

The recoil spectrum of the primary knock-ons was calculated for reactor irradiations of Al, Fe, Cu, Ag and Au. The neutron flux density and energy distribution is that of the low temperature irradiation facility at the FRM. The contribution of elastic and inelastic scattering processes of fast neutrons was calculated separately. The anisotropy of elastic scattering was taken into account. Using these recoil spectra the expected production rate of Frenkel defects was calculated assuming the displacement model of Kinchin and Pease. These calculated production rates agree with the values deduced from electrical resistivity measurements only, if one uses a mean displacement energy of 50 ev for aluminium, of 160 ev copper, of 190 ev for silver and of 130 ev for gold. A similar comparison of theory and experiment for deuteron irradiation gives quite different displacement energies, using the same displacement model. Therefore it can be deduced that the Kinchin-Pease-model cannot account for the right dependence of the number of stable Frenkel pairs on the energy of the primary knock-ons. Possible explanations of the deviations are discussed. (auth)

47105 AN ELECTRON MICROSCOPE STUDY OF NEUTRON IRRADIATION DAMAGE IN ALPHA-IRON. Eyre, B. L.; Bartlett, A. F. (Atomic Energy Research Establishment, Harwell, Berks, Eng.). Phil. Mag. (8), 12: 261-72(Aug. 1965). (AERE-R-4752).

The technique of transmission electron microscopy was used to study neutron irradiation damage in α-iron. Foils were irradiated to a fission neutron dose of $\sim 2 \times 10^{20}$ cm^{-2} at 60°C and the effects of annealing up to 500°C on the micro-hardness and structure were studied. The irradiated foils contained visible point defect clusters which remained unchanged on annealing up to 300°C. Above 300°C the size of clusters remained fairly constant but the number decreased steadily until they had all disappeared after annealing at 500°C. The micro-hardness also remained unchanged up to 300°C and then recovered steadily until it returned to the unirradiated value at 500°C. The results of a diffraction analysis carried out on loops in annealed foils indicated that their Burgers vector was in a ⟨111⟩ direction and that both interstitial and vacancy loops were present. It is suggested that the visible clusters in the irradiated iron are interstitial in nature, the vacancies being trapped by interstitial impurity atoms. The annealing behavior above 300°C is consistent with the vacancies breaking free from their traps to recombine with the clustered interstitial point defects. (auth)

47106 EFFECT OF NEUTRON RADIATION ON RHENIUM. Brimhall, J. L.; Mastel, B. (Battelle Memorial Inst., Richland, Wash.). Phil. Mag. (8), 12: 419-21(Aug. 1965). (BNWL-SA-115).

Rhenium, a h.c.p. metal, was irradiated to an exposure of 7×10^{18} nvt (E > Mev). Small black spots, visible to transmission electron microscopy, formed during the irradiation. Although the nature of the spots could not be determined, the spots are presumed to be clusters of interstitial atoms. (auth)

47107 MICROSTRAIN IN NEUTRON IRRADIATED COPPER CRYSTALS. Sharp, J. V.; Makin, M. J. (Atomic Energy Research Establishment, Harwell, Eng.). Phil. Mag., (8), 12: 427-30(Aug. 1965). (AERE-M-1581).

It was shown by a sensitive parallel plate condenser technique that no deformation ($>1 \times 10^{-6}$ strain) occurs in neutron irradiated (2.5×10^{18}f.n. cm^{-2}) copper single crystals at stresses lower than the "critical" shear stress at the appropriate strain rate. When the critical stress is reached the deformation occurs entirely by the formation of prominent slip lines, there being no sign of fine slip, viz., the limited movement of dislocations on a large number of slip planes. This result supports the model of slip in neutron irradiated metals proposed by Makin and Sharp and is contrary to the large microstrain observed by Koppenaal in bend tests. (auth)

47108 ANNEALING MECHANISM OF FAST NEUTRON DAMAGED SILICA GLASS. Lungu, S. (Inst. for Atomic Physics, Academy of the R.P.R., Bucharest). Rev. Roumaine Phys., 10: 469-74(1965).

The annealing of fast neutron damaged silica glass is considered as a process with its own activation free energy depending upon the defect concentration and the

annealing temperature. This energy, calculated from the isothermal data of Primak, is identified for zero defect concentrations with the activation free energy of flow. Also the temperature variation of the same calculated energy is identified with the corresponding activation entropy of flow. From the dependence on the concentration it is concluded that there is a nonuniformity in volume distribution of defects. Thus, the local concentration is found to lie between 80% and 125% of the initial average value. These results show that there is a great similarity between damaged state and quenched state of silica glass. (auth)

METEOROLOGY

See also GEOLOGY AND MINERALOGY — Site Survey and Selection.

47109 (RISO–99) A MICROMETEOROLOGICAL DATA-HANDLING SYSTEM AND SOME PRELIMINARY RESULTS. Busch, Niels Eduard (Atomenergikomissionen, Risoe (Denmark). Forsoegsinstitut). May 1965. 93p. Dep. mn.

A description is given of an instrument system that was developed and installed at the meteorological station at Risö. It consists of a recording system for wind and temperature profiles and a turbulence system composed of an electromagnetically damped wind vane in conjunction with an analog computer. To facilitate the statistical treatment of the results the data registration is performed on punched tape in a code directly applicable in the electronic computer GIER available at Risö. A discussion is presented of a sturdy three-cup anemometer well suited for standard measurements of mean wind speed. Digital registration technique was applied to the analog signal from the wind vane. Spectral density estimates, computed for a variety of stability and wind-speed conditions, are presented and discussed. (auth)

47110 (RISO–100) A NOTE ON THE SIMILARITY HYPOTHESIS FOR WIND PROFILES. Busch, Niels Eduard (Atomenergikomissionen, Risoe (Denmark). Forsoegsinstitut). May 1965. 26p. Dep. mn.

From calculations performed on wind and temperature data measured at the Argonne National Laboratories it is concluded that under unstable conditions of stratification the wind and temperature profiles are approximately similar with a tendency for $\alpha_1 = K_M/K_H$ to decrease with increasing height. Here K_M and K_H are the eddy viscosity and eddy heat conductivity respectively. No systematic trends towards variation of the rate of decrease with stability could be noted. A comparison of the results yielded by the Argonne data with results obtained at the Risö site gives evidence of the existence of a free convection regime in very unstably stratified air in which the vertical heat flux is independent of wind shear (Priestley regime). In the case of stable conditions the wind and temperature profiles appear to be approximately similar under stability conditions characterized by Richardson numbers less then 0.1. In a more stable atmosphere the profiles are consistently dissimilar, which indicates a decrease of K_M/K_H with increasing height. In the case of stable stratification the flow changes character at a Richardson number of ca. 0.2, suggesting this to be the critical value for completion of the turbulence decay. (auth)

47111 (UCRL-Trans–1229(L)) STUDIES OF THE DIFFUSION PHENOMENA IN THE ATMOSPHERIC SURFACE LAYER. PART 2. DIFFUSION OF SMOKE PUFFS OF THE FLOATING INSTANTANEOUS-SOURCE TYPE. Inoue, Eiichi. Translated by S. Rundle (Univ. of California Lawrence Radiation Lab., Livermore) from Nogyo Kisho, 16: 20-6(1961). 22p. Dep. mn; JCL $2.60 fs, $0.89 mf.

An attempt was made to establish a connection between floating-source and fixed-source diffusion on the basis of the point of view that the differences that exist could be explained by taking into account the oscillation of the center of gravity of the smoke puff itself in the case of diffusion of the floating-source type. A firm method based on the Similarity Theory is proposed. The results showed that the characteristic figure that differentiates the two types of diffusion is the lifetime of the largest coupling eddy existing within the turbulent area brought about on diffusion. It was also found that the lifetime was characterized by the meandering of the line of smoke and by the change in movement of the degree of density of the smoke at a given point. It is tentatively suggested that the theoretical results and experimental results show a satisfactory degree of agreement. (P.C.H.)

47112 NOTE ON THE AREAL VARIATION OF DEUTERIUM/HYDROGEN RATIOS IN RAINFALL FOR A SINGLE STORM EVENT. Gambell, Arlo W. (Geological Survey, Washington, D. C.); Friedman, Irving. J. Appl. Meteorol., 4: 533-5(Aug. 1965).

Deuterium measurements were made on network rainfall samples from one storm. Rainfall occurred almost exclusively behind a cold front on November 1 and 2, 1963 in eastern North Carolina and southeastern Virginia. The D/H ratios were plotted. There was a decrease in D/H ratios from south to north, which can probably be explained on the basis of the moisture source. Near the coast moisture was picked up directly from the ocean, thereby producing rain with a higher deuterium content. A sharp discontinuity was observed in the northwest corner of the network. Reasons for this discontinuity are postulated. (M.C.G.)

PHYSICS

General

Refer also to abstract 47551.

47113 (AD-612197) FIREBALL PHENOMENOLOGY. Brode, Harold L. (RAND Corp., Santa Monica, Calif.). Oct. 1964. 51p. CFSTI $3.00 cy, $0.50 mn.

The properties of nuclear explosions which influence the predictions and scalings for fireball phenomena, notably fireball sizes, temperatures, densities, and ultimately the thermal radiation output, are discussed. Attention is focused on the initial features of fireball formation, for which scaling with both yield and burst altitude was examined. The scalings were derived from a few theoretical calculations which describe fireball features for several yields and altitudes. (TAB)

47114 (AD-614286) INVESTIGATION OF THE STATISTICS OF BREAKDOWN USING NANOSECOND PULSE TECHNIQUES. Final Report. McDonald, D. F.; Benning, C. J.; Brient, S. J. (Braddock, Dunn, and McDonald, Inc., El Paso, Tex.). Mar. 1965. Contract AF30(602)-2781. 62p. (RADC-TR-64-584). CFSTI $3.00 cy, $0.75 mn.

The experimental equipment, experimental procedures, and test results of a laboratory study on the statistics of discharge initiation in highly over-volted planar spark gaps are presented. The theory of operation of a subnanosecond rise-time multikilovolt pulse generator developed for the study is described. Test data on the electron emission of different electrode materials as a function of gap field strength and electrode conditioning are presented. In addition, a simplified model of the statistics of free-space breakdown in a transmitted microwave beam is described. (auth)

47115 (ANL-6983) PHYSICS DIVISION SUMMARY REPORT, APRIL-DECEMBER 1964. (Argonne National Lab., Ill.). Contract W-31-109-eng-38. 89p. Dep. mn; CFSTI $3.00 cy, $0.75 mn.

A summary of reports on the highlights of the research in physics at the Argonne National Laboratory is presented. A bibliography of physics publications since March 1964 is included. (M.O.W.)

47116 (BNL-9443) ELECTRON DRIFT VELOCITY VARIATIONS IN NEON + 10 percent HELIUM + ALCOHOL, USING SPARK CHAMBER EFFICIENCY AS A SENSITIVE INDICATOR. Fischer, Joachim (Brookhaven National Lab., Upton, N. Y.). [1965]. Contract AT(30-2)-Gen-16. 16p. (CONF-650806-13). Dep. mn; CFSTI $1.00 cy, $0.50 mn.

From 7th International Conference on Phenomena in Ionized Gases, Belgrade.

The disappearance probability of an electron in a gas is very sensitive to variations in transport coefficients. The efficiency of a pulsed nuclear spark chamber is a non-ideal indicator of this probability. Efficiency measurements were used to obtain spark chamber resolving times and measure drift velocity variations in (Ne + 10% He) + C_2H_5OH in a 6.4 mm gap at NTP at E/P of .1 to 2 V/cm/mmHg and vapor pressures of 6 to 48 mmHg. The drift velocities are higher than without alcohol, and show a peak which shifts to higher E/P and velocity with increasing alcohol. The observations are related qualitatively to the reduction of electron energy by alcohol and to changes in collision cross-sections of the gas components. (auth)

47117 (SC-DC-65-1698) AEROSPACE NUCLEAR SAFETY INVESTIGATIONS OF REENTRY ABLATION PHENOMENA. Quarterly Report, [May 1, 1965-July 31, 1965]. Beal, J. L.; Brown, W. R.; Vassallo, F. A.; Adams, D. E. (Cornell Aeronautical Lab., Inc., Buffalo, N. Y.). July 1965. Contract AT(29-1)-789. 47p. Dep. mn; CFSTI $2.00 cy, $0.50 mn.

Initial tests in the development of a target impact method for determining the size distribution of debris particles formed in shock tube tests of disintegration during reentry are described. Bench tests of the heating of zirconium hydride and of preheated and non-preheated zirconium specimens are discussed. (auth)

47118 (UCRL-12018-T) SIMILARITY SOLUTIONS IN 1-D HYDRODYNAMICS. Grover, R. (Lawrence Radiation Lab., Univ. of California, Livermore). Aug. 28, 1964. Contract W-7405-eng-48. 49p. Dep. mn; CFSTI $2.00 cy, $0.50 mn.

A summary of the theory of similarity solutions in one-dimensional hydrodynamics is given in which the limiting role of the equation-of-state is emphasized. A description of a digital computer code (SIMS) for calculating the similarity solutions of a γ-law fluid is given. Two new examples of similarity solutions are described. (auth)

47119 (UCRL-14244) DERIVATION OF A GENERALIZED VON NEUMANN PSEUDO-VISCOSITY WITH DIRECTIONAL PROPERTIES. Richards, Gerald T. (Lawrence Radiation Lab., Univ. of California, Livermore). July 21, 1965. Contract W-7405-eng-48. 21p. Dep. mn; CFSTI $1.00 cy, $0.50 mn.

An absolute scalar pseudo-viscosity ("q") expression for handling shocks automatically in numerical calculations of three-dimensional fluid-dynamics problems is derived. The expression is a generalization of that derived by von Neumann and Richtmyer in the sense that the expressions are identical for a plane shock wave. The basic assumption made is that a shock will be formed in a material when there is compression in the direction of acceleration; this assumption seems reasonable physically, since this condition indicates that a grid established about a point with such compression will collapse, i.e., the "rear" of the grid will overtake the "front." The expression "q" is derived for a generalized curvilinear coordinate space and the expression is given for the three commonly used coordinate systems. The expression is also written for the plane rectangular case and the cylindrical case with no angular motion, to be used in connection with the HEMP code. (auth)

47120 (UCRL-14349) COMPRESSION OF MAGNETIC FIELD INSIDE A HOLLOW EXPLOSIVE-DRIVEN CYLINDRICAL CONDUCTOR. Kidder, Ray E. (Lawrence Radiation Lab., Univ. of California, Livermore). July 27, 1965. Contract W-7405-eng-48. 28p. (CONF-650937-1). Dep.mn; CFSTI $2.00 cy, $0.50 mn.

From Conference on Megagauss Magnetic Field Generation by Explosives and Related Experiments, Frascati, Italy.

Detailed numerical calculations of a flux compression experiment were performed with a one-dimensional magnetohydrodynamics code written for the IBM 7094 computer. Calculated peak magnetic fields of 10-14 megagauss are obtained in approximate agreement with experimental results. The equation of state used to describe the copper liner takes explicit account of the liquid-vapor transition. The temperature coefficient of resistivity of the condensed phase is assumed to be constant and equal to one or three-times the observed value at 1500°C. The effect of the finite resistivity of the vapor phase and of the pressure-dependence of the resistivity of the condensed phase is investigated and found to be small. The distribution of temperature and magnetic field in the liner is described. It is noted that the attainment of large peak magnetic fields requires an implosion with a high degree of cylindrical symmetry to achieve the necessary convergence. (auth)

47121 (UCRL-16080) A METHOD FOR DETERMINING THE GEOMETRY AND CURRENT CONFIGURATION OF A SYSTEM OF CYLINDRICALLY SYMMETRIC SOLENOID COILS FROM A SPECIFIED MAGNETIC FIELD

SHAPE. Halbach, Klaus; Holsinger, Ronald F. (Lawrence Radiation Lab., Univ. of California, Berkeley). July 29, 1965. Contract W-7405-eng-48. 22p. (CONF-650512-11). Dep. mn; CFSTI $1.00 cy, $0.50 mn.

From Symposium on Engineering Problems of Controlled Thermonuclear Research, Livermore, Calif.

Several useful computer programs were developed which, given the geometry and current configuration of a system of coils, calculate with great speed and accuracy the properties of the magnetic field produced by the given coils. Because one experimental program requires a somewhat sophisticated magnetic-field shape, a method and appropriate computer programs were developed which reverse this process. Rather than arrive at a solution for the geometry and current configuration by trial and error, a method was used which systematically solves for the geometry and current configuration required to produce the desired magnetic-field shape. The coil configuration that gives the desired field shape is determined by manipulating with matrix algebra appropriate variables of all individual coils in the coil system. The variables used were currents, relative positions, and lengths of the coils. (auth)

47122 (JPRS-31032) TRANSLATIONS ON COMMUNIST CHINA'S SCIENCE AND TECHNOLOGY. Translation of K'o Hsueh T'ung Pao, No. 4, Apr. 1965. 58p. (TT-65-31530). CFSTI $3.00.

Separate abstracts were prepared for two of the nine included papers. The remaining seven papers were on the separation of niobium and tantalum by chromatography of opposite phases, ion exchange properties of stannic phosphate, cadmium-pyridine complexes, mutually inhibitory rental transient reactions, experimental analysis of the nucleoplasmic relationships in the Stylonychia mytilus, Oncology, and briefs from conference on smelting furnace heat treatment processes. (M.O.W.)

For abstracts of individual papers see: 47123 and 47316.

47123 (JPRS-31032, pp 1-14) STRONG FIELD INTERACTIONS AND NONLINEAR EFFECTS FROM STIMULATED OPTICAL EMISSIONS. T'an, Wei-han. Translated from K'o Hsueh T'ung Pao, No. 4, 339-46(Apr. 1965).

The appearance of high degeneracy coherent light has provided a new tool for the study of microphysics. The interactions between radiation and electrons are no longer due to weak fields, but due to strong ones, hence certain nonlinear effects not noted with weak fields appear. These nonlinear effects are discussed in terms of the following; energy level split and shift problems under strong field actions, two kinds of nonlinear effects, electromagnetic theory of nonlinear media, and problems concerning nonlinear materials. (M.O.W.)

47124 (SLAC-Trans-19) MEAN ENERGIES AND DRIFT VELOCITIES OF ELECTRONS IN NITROGEN, ARGON AND XENON, DETERMINED BY IMAGE INTENSIFIER PHOTOGRAPHS OF ELECTRON AVALANCHES. Wagner, K. H. Translated by J. M. Silberstein (Stanford Linear Accelerator Center, Stanford Univ., Calif.) from Z. Physik, 178: 64-81(1964). 31p. Dep. mn; JCL $3.60 fs, $1.13 mf.

Local and temporal development of electron avalanches in a pulsed discharge gap (d = 3.00 cm) are investigated in N_2, Ar, Xe and in mixtures of N_2 and CH_4 by simultaneously applying high-gain image intensifier- and photomultiplier techniques. Electron-drift velocities are obtained from time-of-flight and path-of-flight measurements in these gases. The mean energy of agitation of the electrons is derived both from electron mobility and avalanche image trace profile (diffusion broadening). (auth)

47125 THE DEPENDENCE OF THE FORMS OF MONOENERGETIC ELECTRON TRANSMISSION CURVES UPON THE MEASURING GEOMETRY. Buday, Iren; Berenyi, Denes; Somogyi, Gyoergy. At. Kozlemen., 7: 119-28(June 1965). (In Hungarian).

In two measuring arrangements of different geometry the transmission curves were taken for 100 and 150 kev monoenergetic electrons, using Al absorbers. A toroid-sector type beta-spectrometer served as electron source. The experimental curves taken at different geometry differ definitely from each other especially at little absorbent thicknesses. At both geometries, however, a deviation can be seen between the experimental and the corresponding theoretical curves. The interpretation of this was attempted. (auth)

47126 NON-EQUILIBRIUM IN THERMALLY IONIZED GASES WITH SMALL SEEDING RATIOS. George, D. W. (Univ. of Sydney). Brit. J. Appl. Phys., 16: 1105-11(Aug. 1965).

Thermally ionized gases which are subjected to electric fields show nonequilibrium effects which can be detected both spectroscopically and electrically through changes in the electron energy distribution and number density. Some experimental results are presented for argon at several atmospheres pressure and low seeding ratios ($<10^{-5}$). At the relatively low electron densities used ($\sim 10^{10}$ cm^{-3}), transitions from diffuse conduction to arc-type discharges occur before any significant increase in conductivity is obtained due to electron temperature enhancement. (auth)

47127 THE INFLUENCE OF A CROSSED MAGNETIC FIELD ON A GASEOUS TOWNSEND DISCHARGE. Heylen, A. E. D. (Univ. of Leeds, Eng.). Brit. J. Appl. Phys., 16: 1151-9(Aug. 1965).

The early treatment by Townsend of the influence of a crossed magnetic field on the movement of an electron swarm in a uniform electric field is extended to high electric fields when ionization occurs and secondary processes can no longer be neglected. It is shown that the discharge moves bodily in the ev × B direction with a velocity, when secondary electron emission by positive ion bombardment of the cathode takes place, given by $\bar{v} = \nu_T^+(\tan\theta^- + \tan\theta^+)\,(\tau_+/\tau_s + \tau_+)$ in which ν_T^+ is the transverse ion drift velocity, θ^- and θ^+ are the electron and ion deflection angles and τ_+ and τ_s are the ion transit and site times. The site time is the delay which occurs between the impact of a positive ion on to a surface and the subsequent emission of an electron; the transit time is the time it takes for the ion to cross the gap. When secondary electron emission by photon bombardment takes place, the propagation velocity of the gaseous discharge is given by $\bar{v} = \nu_\perp^-(\nu^*/\nu_T^- + \nu^*)$ in which ν^* is the photon velocity and $\nu_\perp^-$ and ν_T^- are the electron perpendicular and transverse drift velocity respectively. Because of the importance of θ^-, the dependence of the perpendicular and transverse electron drift velocity on collision cross section, mean energy, E/p and B/p is examined in detail over a wide range and quantitative results obtained for hydrogen. Whereas $\nu_\perp^-$ reaches a maximum with increase in B/p when $\nu_0 \simeq eB/mp$, tan θ^- continues to increase linearly with B/p from low to high magnetic fields. Good agreement is obtained with some but not all of the experimental data reported in the literature. The need for similar data on positive ions is pointed out. (auth)

47128 CURRENT INTERRUPTION IN HYDROGEN AND DEUTERIUM THYRATRONS. Fraser, D. A.; Gowar, J. (M-O Valve Co. Ltd. Research Lab., Wembley, Eng.). Brit. J. Appl. Phys., 16: 1211-12(Aug. 1965).

When a sufficiently high current discharge is struck through a narrow aperture, processes occurring in the discharge lead to a sudden cessation of current after an interval of time. Measurements on thyratrons filled successively with hydrogen and deuterium have shown that in the heavier gas a larger current can pass for a given time without interruption. Heating of the gas, due to elastic collisions between electrons and neutral particles, is suggested as one important mechanism controlling current interruption. (auth)

47129 EXPANSION FORMULAE FOR THE ^{3}He AND ^{4}He VAPOUR PRESSURE SCALES. Montgomery, H. (Atomic Energy Research Establishment, Harwell, Eng.). Cryogenics, 5: 229-30(Aug. 1965).

A formula is presented for converting vapor pressure measurements into temperatures which can be applied to the entire 1958 helium-4 scale and also to the 1962 helium-3 scale. The formula is based on the Clausius-Clapeyron equation, and the fitting procedure used was a standard-least squares method performed on an IBM 9030 computer. The results of some calculations are presented. (L.B.S.)

47130 NEGATIVE ABSORPTION FROM WEAKLY RELATIVISTIC ELECTRONS TRAVERSING A CUCCIA COUPLER. Hsu, T. W.; Robson, P. N. (Univ. of Sheffield, Eng.). Electron. Letters, 1: 84-5(June 1965).

It is shown that a filamentary beam of monoenergetic electrons having a controlled amount of angular momentum and caused to traverse a Cuccia coupler can produce negative energy absorption near the cyclotron frequency, if relativistic effects are taken into account. No threshold angular momentum for the onset of negative absorption is predicted. (auth)

47131 STUDY OF THE PROPERTIES OF AN EXCESS ELECTRON IN LIQUID HELIUM. I. THE NATURE OF THE ELECTRON-HELIUM INTERACTIONS. Jortner, Joshua; Kestner, Neil R.; Rice, Stuart A.; Cohen, Morrel H. (Univ. of Chicago). J. Chem. Phys., 43: 2614-25(Oct. 15, 1965).

A theoretical study of the free and localized states of an excess electron in liquid helium is presented. Electron–helium interactions are treated by the pseudopotential method, while multiple scattering effects on the properties of a quasifree electron in the dense fluid are treated using the Wigner–Seitz model. It is demonstrated that the plane-wave state is not the lowest energy state for an excess electron in liquid helium and that fluid deformation leads to a localized state of lower energy. The large, repulsive helium-atom pseudopotential coupled with the small helium polarization potential lead to electron localization which may be attributed entirely to short-range repulsions. The following experimental observations are adequately interpreted by these results: The energy barrier of liquid helium for electrons, the density-dependent transition from a delocalized state to a localized state of the excess electron, the mobility of an excess electron in normal ^{4}He and in ^{3}He. Pressure and temperature effects on the electron bubble are also discussed. It is concluded that a pressure-induced transition from the localized to the delocalized state of excess electron will not occur in the fluid domain even at high pressures. Finally, some speculations are presented concerning the optical properties of the excess-electron center. (auth)

47132 STUDY OF THE PROPERTIES OF AN EXCESS ELECTRON IN LIQUID HELIUM. II. A REFINED DESCRIPTION OF CONFIGURATION CHANGES IN THE LIQUID. Hiroike, Kazuo; Kestner, Neil R.; Rice, Stuart A.; Jortner, Joshua (Univ. of Chicago). J. Chem. Phys., 43: 2625-32(Oct. 15, 1965).

A study of the structural changes in liquid helium in the vicinity of an excess electron is presented. The formal similarity between the pair distribution function of N-boson system was used, with the wavefunction expressed as the product of pair wavefunctions, and the pair distribution function of a classical fluid. The present model leads to an interfacial surface energy term which is in good agreement with the observed surface tension of liquid helium at 0°K. An important contribution to the bubble energy arises from the volume kinetic energy arising from the excess kinetic energy of the fluid atoms removed from the boundary layer. The bubble radius of 12.4 Å calculated herein is found to be in excellent agreement with the available experimental data. (auth)

47133 SPECTROSCOPIC STUDY OF THE EARLY HELIUM AFTERGLOW. Bickel, William S.; Burnett, C. R. (Pennsylvania State Univ., University Park). J. Opt. Soc. Am., 55: 1504-8(Nov. 1965).

Time-resolved spectroscopic measurements were made of absolute intensities, spectral profiles, and self-absorption for He I lines in the early helium afterglow. Population densities are calculated for the excited states, including metastable states, as a function of time. Electron densities, electron temperatures, and Doppler temperatures are derived from the data. Similar emission and self-absorption measurements of He_2 spectra indicate an increase in molecular populations during the early afterglow. An interpretation identifies the $^3S_1$ atomic metastables as a source of continued ionization and heating of the plasma and a participant in the formation of metastable helium molecules. (auth)

47134 ELECTRODE EROSION AS A PARAMETER OF SPARK DISCHARGE. Kawaguchi, Hiroshi; Nakajima, Tokunosuke (Japan Atomic Energy Res. Inst., Tokyo). J. Spectroscopical Soc. Japan, 13: 125-31(Mar. 1965). (In Japanese).

A neutron-activated zinc electrode is used to measure the electric erosion in a spark discharge. Vapor of the electrode material is collected in a glass capsule and radioactivity of the condensate is measured by a well-type γ spectrometer. The relation between erosion (E) and circuit parameters is found as $E \alpha CBV^{\frac{1}{2}}/R$, where C is the capacitance, B the number of breaks per half cycle, V the break down voltage and R the resistance. Inductance (L) scarcely influences the erosion. These results suggest that erosion is directly proportional to the average current. The latter is measured by the method developed by Schreiber and Fry with a high voltage spark source; with a Raiskii spark source the measurement could not be made. (auth)

47135 PHOTON EMISSION FROM A GIVEN CURRENT. Wergeland, Harald. Kgl. Norske Videnskab. Selskabs, Forh., 37: 69-75(1964).

A very elementary method is given for the solution of the limiting case when field reaction can be neglected in photon emission from a given current. The field reaction can be neglected when either the charged particles are very heavy or the photons are very soft. The simplicity of the exact solution rests upon the premise that the electric current is a prescribed function in space and time. Neglecting thus the reaction upon the sources, the radiation field is an open system whose motion is governed by the hamiltonian. (J.F.P.)

47136 MATTER CREATION BY GRAVITATIONAL WAVES. Brock, M. Clutton (Northampton Coll. of Advanced Tech., London). Nature, 207: 1079-80(Sept. 4, 1965).

It is suggested that matter may be created by the conversion of gravitational energy into mass energy, without violating any conservation laws other than that of baryon number. Although on this model energy is conserved locally, it is not necessarily conserved on a cosmic scale. Since a three-dimensional region does not exist if the gravitational field of the entire universe is considered, there seems to be no reason why the total amount in the universe of mass, and of such energy as may be definable, should remain constant–instead, it may fluctuate from epoch to epoch. Even though the model described may violate the perfect cosmological principle, it still possesses some of the satisfying features of a steady-state model. In particular, it brings the phenomenon of creating within the scope of physical enquiry. (P.C.H.)

47137 IS THERE A CLASSICAL ANALOGUE OF DIRAC'S THEORY? Halbwachs, F. (Faculte des Sciences, Marseille). Nuovo Cimento (10), 36: 832-6(Apr. 1, 1965).

A simple classical picture, deriving from Weyssenhoff's model, is proposed, which generates Dirac's formalism through a generalized hamiltonian procedure. (auth)

47138 REFLECTION AND REFRACTION OF HYDROMAGNETIC PLANE WAVES AT THE BOUNDARY OF TWO COMPRESSIBLE MEDIA. Raju, P. K. (Yale Univ., New Haven). Proc. Natl. Inst. Sci. India, Pt. A, 30: 602-9 (Sept. 26, 1964).

A scalar and a vector potential is defined for the particle velocity of a plane hydromagnetic wave in a homogeneous compressible medium of infinite electrical conductivity. This representation is made use of in the study

of reflection and refraction of plane waves at an interface separating two compressible media. The plane containing the propagation vector and the uniform magnetic field is assumed to be inclined to the interface. The laws of reflection and refraction are given and amplitude relations are worked out for an incident modified plane wave. When incident wave goes from a denser medium to rarer medium, there exists the possibility of total internal reflection. (auth)

47139 ON THE EQUATION OF STATE OF A SYSTEM OF HARD SPHERES. Collins, R. (Royal Coll. of Advanced Tech., Salford, Eng.). Proc. Phys. Soc. (London), 86: 443-9(Sept. 1965).

An approximate equation of state, previously derived on the basis of information theory, is applied to a classical system of non-interacting hard spheres, and the results are compared with those from the cell and tunnel models. By a slight modification of the original statistical argument, it is shown that the cell and tunnel model equations of state are obtained as particular cases. With either approach, at low densities PV/NT is obtained as a power series in $V^{-\frac{1}{3}}$ instead of the correct form in powers of V^{-1}, indicating in this region a break-down in the statistical approximations. (auth)

47140 THE MAGNETOHYDRODYNAMIC BOUNDARY LAYER IN THE PRESENCE OF A PRESSURE GRADIENT. Gribben, R. J. (Univ. of Southampton, Can.). Proc. Roy. Soc. (London), Ser. A, 287: 123-41(Aug. 17, 1965).

A study is made of the two-dimensional, magnetohydrodynamic boundary layer, in steady, incompressible flow, under the influence of an external magnetodynamic pressure gradient (characterized by β) proportional to some power of distance along the boundary. The problem, which has also been considered by Davies (1963), may be regarded as that of extending to conducting fluids the solutions of Falkner and Skan well known in the theory of non-conducting fluids, and here again the "similarity" assumption enables the differential equations to be written with but one independent variable. Solutions of these equations are sought for the cases when ϵ, the ratio of diffusivities (viscous to magnetic), has small or large values. Hence the layers adjacent to the surface in which the diffusion of vorticity and electric current is important have thicknesses which, although both small compared with a typical streamwise length, are of different orders of magnitude. Physically the two cases correspond to fluids whose electric conductivities are sufficiently small or large. Series expansions in ϵ, in each layer, are assumed and the form of the series, as well as boundary conditions satisfied by their coefficients, are determined from "matching" the series in the two layers. The method is equivalent to that used by Glauert (1961, 1962) who, in the former paper, treated the special case to which the present problem reduces when $\beta = 0$. For this case, when $\epsilon \ll 1$, terms of $O(\epsilon \ln \epsilon)$ must be included in the series but the present analysis shows that that is the only case where the "matching" requires this logarithmic term; the presence of a pressure gradient enables the "matching" to be achieved with purely algebraic dependence on ϵ at least up to terms of $O(\epsilon)$. For large ϵ logarithmic terms are present (of $O(\epsilon^{-1} \ln \epsilon)$) and the results include those of Glauert (1961) showing no distinctive features. Throughout, the magnetic field parameter S (ratio of magnetic and dynamic pressures in the main stream) must be restricted so that $1 - S$ is not small. To obtain physically acceptable solutions when the pressure gradient is adverse, further criteria, discussed by Stewartson (1954), may be invoked. Otherwise, the solutions are non-unique and some remarks are made on the effect of this non-uniqueness on the "matching". Results, in the form of series for the skin friction and field intensity at the wall, indicate a reduction of skin friction with increase of magnetic field. (auth)

47141 THE FORMING OF H_3^+ IONS SOURCES BY ELECTRONIC BOMBARDMENT. Ioanoviciu, D.; Ursu, D. Rev. Roumaine Phys., 10: 27-34(1965). (In French).

An approximate theoretical study is made of the formation of H_3^+ in an ion source for electronic bombardment; this was verified by a comparison with experimental results. The graph for $I_3^+/I_2^+ = f(I_2^+)$ with the expressions drawn from theory. By studying the extraction coefficients information can be obtained on the discrimination in the ion source. The length of the ion path in the source can be determined by studying exponent values of derived equations. Increase in the precision of abundance measurements of deuterium is possible by a reduction of the incline of their paths to the right. (J.F.P.)

47142 PRODUCTION OF NEGATIVE H IONS FROM THE ARC ION SOURCE ON A STAND. Indreas, G.; Chein, Kuo Chi; Passyuk, A. S.; Tretyakov, I. P. (Joint Inst. for Nuclear Research, Dubna, USSR). Rev. Roumaine Phys., 10: 101-8(1965).

A study was made on how the parameters and operation conditions of an arc ion source with a hot cathode affect the yield of the negative H ions. The dependencies of H^- ion current upon gas flow rate, arc current and discharge voltage are given. The obtained value of H^- ion current was about 70 μA. (auth)

47143 PARTICLE WITH LOW BINDING ENERGY IN A MAGNETIC FIELD. Demkov, Yu. N.; Drukarev, G. F. (Leningrad State Univ.). Zh. Eksperim. i Teor. Fiz., 49: 257-64(July 1965). (In Russian).

An exact solution is given for the problem of determining the bound state of a charged particle in a zero range force field and in an homogeneous magnetic field. It is shown that if no bound state exists in a potential well in the absence of a magnetic field then turning on the field should result in the appearance of such states. The possibility of detecting the effect in semiconductors is discussed. (auth)

47144 ON THE STRUCTURE OF UNSYMMETRIC TOROIDAL MAGNETIC FIELDS. Graev, M. I.; Mikhailova, M. S.; Morozov, A. I. Zh. Tekhn. Fiz., 35: 1189-92 (July 1965). (In Russian).

Results of calculations on the structure of a three-turn helical magnetic field perturbed by a corrugated field are reported. The fields discussed are those derived from the scalar potential $V = z + 3I_3(3r) \sin 3(\varphi - z) + h_0 I_0(3r) \sin 3z$, where r, φ, z are cylindrical coordinates and h_0 is a parameter. The fields were treated as toroidal by identifying the points r, φ, z and r, φ, $z + 2\pi/3$. The behavior of the magnetic lines of force was characterized by their successive intersection points with the plane z = 0. An S-region is considered for the separatrix of this field. There are two S-regions, of which the inner one has the form of three petals or loops. The results pertain to the region between the inner and outer S-regions outside the loops. The image points of points on the negative x-axis ($\varphi = \pi$) were determined and the displacement function $\delta(x)$ and the function $\varphi_N(x)$ were calculated. A method was developed for calculating the separatrix which is simpler than that of V. K. Mel'nikov (DAN SSSR, 148: No. 6, (1963)). (L.B.S.)

47145 INVESTIGATION OF THE ESCAPE OF ELECTRONS FROM A TRAP WITH A SPATIALLY PERIODIC HELICAL MAGNETIC FIELD. Demirkhanov, R. A.; Kursanov, Yu. V.; Baratov, D. G.; Kharin, G. V. Zh. Tekhn. Fiz., 35: 1250-4(July 1965). (In Russian).

The influence of a pulsed magnetic field on the escape of electrons from a magnetic mirror system with a superimposed helical magnetic field. The magnetic mirror system was established in a 8 cm diameter, 2 m long glass cylinder evacuated to 2×10^{-4} N/m^2. The magnetic field strength in the uniform field region was between 2×10^3 and 2×10^4 A/m and the mirror ratio was between 5 and 7. The mirrors were 1.5 m apart. The helical field was produced by a 12 cm diameter, 16-cm pitch helical winding carrying 600 A. The pulsed field was produced by discharging a capacitor through a one-layer solenoid. This field was in the same direction as the magnetic mirror field; its amplitude was 3×10^3 A/m, its rise time was less than 2 microsec, and its decay time was varied from 10 to 500 microsec. A 1 mm diameter 50 microampere beam of 750 ev elec-

trons was injected for 3.5 microsec parallel to the axis of the system and 1 cm from the axis. The delay between injection of the electrons and pulsing of the field was controlled. The electrons escaping from the magnetic mirror system at the end opposite the injector were collected and analyzed with a two-grid collector probe. Without the pulsed field the electrons escaped from the magnetic mirror system after a few tens of reflections. This rapid escape is ascribed to the reversibility of the resonance interaction of the particles with the helical field. The pulsed magnetic field increased the entrapment time to 25 microsec, corresponding to about 250 reflections. The escape of the electrons when the pulsed field was present appeared to be due to collisions with residual gas molecules. (ATD)

47146 SPARK CHANNEL FORMATION IN AIR. Andreev, S. I.; Sokolov, B. M. Zh. Tekhn. Fiz., 35: 1295-7(July 1965). (In Russian).

Early stages of spark development in an 8-mm gap in air at atmospheric pressure were photographed with a Kerr cell shutter, and the current and voltage in the gap were recorded with an oscilloscope having a resolving time of 10^{-9} sec. The investigation was undertaken mainly to determine the radius of the first spark channel and the current in it at the instant of its formation, when a streamer first bridges the gap. These data are significant because they constitute the initial conditions for the theory of the further development of the channel. The potential on the gap was held at a value slightly below the spontaneous breakdown potential and the discharge was initiated by a trigger electrode in an opening in the cathode. This is believed to produce conditions similar to those obtained when the discharge is initiated by intense ultraviolet illumination of the cathode. Several photographs and drawings of oscilloscope traces are given. The conclusions drawn from the experimental data are discussed. (ATD)

47147 EMISSION PROPERTIES OF A VACUUM SPARK PLASMA. I. ION BEAMS. Suladze, K. V.; Plyutto, A. A. Zh. Tekhn. Fiz., 35: 1298-1307(July 1965). (In Russian).

A vacuum spark was investigated as a source of hydrogen and deuterium ions. The spark source was a slightly modified form of a previously described source (A. A. Plyutto, K. N. Kervalidze, and A. F. Kvartskhava, Atomnaya Energiya, 8: 3(1957)). The spark discharge took place in the 5 mm gap between a copper rod within a porcelain tube and a tungsten or tantalum plate having a 4 mm diameter opening. A channel in the copper electrode contained plexiglas or LiD to provide hydrogen or deuterium ions, respectively. Two sources were investigated, of which one had one such gap and the other had six. The power for the spark was provided by a 50 kv source and a voltage doubler employing two 0.035 microfarad capacitors. Spark potentials up to about 85 kv were employed. The extractor electrode had a 3.5 cm diameter opening covered with a steel grid of 66% transparency. Extraction potentials up to 20 kv were employed. The extracted ions were either caught in a 6 cm diameter Faraday cup, or the central portion of the ion beam was isolated by collimating holes and examined with a Thompson mass spectrometer. The measurements of total ion current and of the ion current to the Faraday cup were supplemented and checked by measurements of the temperature rise of a copper foil collector electrode. Total ion currents up to 100 amp were achieved. The duration of the ion current pulse varied from 0.5 to 5 microsec, depending on the conditions. The pulse was frequently limited by breakdown in the extraction gap. The total ion current at maximum was independent of the extraction potential. This indicates, in agreement with results of investigations reviewed by M. D. Gabovich, that the ion current is not space charge limited. It is suggested that the variation of ion current with extraction potential observed by S. N. Popov may have been due to secondary effects in the source channel. The divergence of the ion beam was determined by observing the current to the Faraday cup at different distances from the source. The divergence of the beam was considerable, but it was much less than was calculated theoretically. It is suggested that this discrepancy may be due to partial neutralization of the space charge by secondary electrons from the extractor grid. The mass spectrometer observations showed that the central portion of the beam contained 80% deuterium ions or 90% hydrogen ions, depending on the material in the copper electrode channel. It is concluded that the chief disadvantage of the vacuum spark ion source is the difficulty of focusing the beam, and that the source is very promising for use with large pulsed resonance accelerators. (ATD)

47148 INHERENT THERMIONIC EMISSION OF LANTHANUM HEXABORIDE AND SURFACE IONIZATION OF CESIUM ATOMS ON IT. Zandberg, E. Ya.; Paleev, V. I. (Ioffe Inst. of Physics and Tech., Leningrad). Zh. Tekhn. Fiz., 35: 1308-11(July 1965). (In Russian).

An investigation was made of the surface ionization of Cs atoms on a cathode made of LaB_6. The use of compressed cathodes made it possible to exclude the influence of backing. Mass-spectrometric methods were used to permit observation of emission of the cathode and to make it possible to measure the temperature dependence of the thermoelectron current for use in determining the thermoelectron work function from the same surface section from which the ion current was taken. LaB_6 rods approximately 14 mm long and 0.8 × 0.8 mm in cross section were used. The electron and ion currents were emitted by a small section of the cathode's surface on which the temperature was assumed to be constant. The cathodes were activated by gradually raising the temperature to 1600 to 1700°K. The following conclusions were drawn: (1) The activated cathode probably has foreign inclusions and nonactivated surface sections on which the work function may exceed 3.9 v. (2) At T > 1400°K, simultaneously with the rise of Cs^+ current, the current of inherent thermoemission of LaO^+ also appears and at T ~ 1600°K the current of La^+ appears. Since the ionization potential of lanthanum $V_{La} = 5.61$ v, it is probable that the main part of the lanthanum atoms evaporating from the surface are desorbed in the atomic state and not in the ionic. The intensity of the La^+ and LaO^+ lines depends on the pressure of the residual gases in the instrument. With increased pressure the intensity of the LaO^+ line increases. The evaporation of La and LaO can lead to a change of the emitter surface, which could be responsible for the rise of the Cs^+ ion current when the temperature is increased. (ATD)

47149 WEAK POSTDISCHARGE EMISSION AS AN INDICATOR OF ELECTRODE SURFACE CONDITION IN VACUUM BREAKDOWN EXPERIMENTS. Chistyakov, P. N.; Tatarinova, N. V. (Moscow Engineering Physics Inst.). Zh. Tekhn. Fiz., 35: 1333-5(July 1965). (In Russian).

It was previously shown that after a gas discharge there occurs a weak emission of electrons from the electrodes (currents from 10^{-13} to 10^{-18}A) which is due to the presence of very thin dielectric films on the electrode surface. The relation between their postdischarge emission and the vacuum breakdown field was investigated. Two identical copper electrodes of approximately the Rogovskiy shape were employed, the gap between which could be varied from 0.2 to 5 mm. The postdischarge emission was measured in a 5 mm gap in argon at 6 mm Hg by the statistical breakdown delay method of H. Paetow (Zs. Physik, 111: 770(1939)) and the vacuum breakdown potential was measured at 10^{-6} mm Hg with the use of a variable voltage (up to 20 kv) rectifier and an 0.6 megohm ballast resistor. The electrodes were subjected to one of the following treatments: (1) high vacuum heating at 250°C; (2) a 1.5 hr 40 mamp pulsed glow discharge in argon at 26 mm Hg; and (3) a 1.5 hr continuous glow discharge in argon at 60 mm Hg during which the current rose from 50 to 120 mamp and the electrodes were heated to 850°C. In passing from treatment (1) to treatment (3), the postdischarge emission decreased by a factor 32 and the vacuum breakdown potential measured in a 0.2 mm gap increased by a factor 3.5; when the electrodes were subjected to treatment (2) the results were intermediate. It is concluded that there is a definite relation between postdischarge emission and vacuum breakdown potential, and that postdischarge emission can serve as a useful indi-

cator of electrode condition in high vacuum breakdown experiments. (ATD)

47150 ASYMPTOTOLOGY. Kruskal, M. (Princeton Univ., N. J.). pp 373-87 of STI/PUB/89.

Asymptotology is defined as the art of dealing with applied mathematical systems in limiting cases. Asymptotology is important because the examination of limiting cases seems to be the only satisfactory effective method of proceeding with the analysis of complicated problems or systems when exact mathematical methods are of no further avail. It is of value both for obtaining qualitative information (insight) about the behavior of a system and its solutions and for obtaining detailed quantitative results. The art of asymptotology lies partly in choosing fruitful limiting cases to examine and in constructing an appropriate generic description for the asymptotic behavior of the solution desired. The scientific element in asymptotology resides in the non-arbitrariness of the asymptotic behavior and of its description, once the limiting case is decided upon. (J.F.P.)

47151 AIR TABLES. Tables of the Compressible Flow Functions for One-Dimensional Flow of a Perfect Gas and of Real Air. Jordan, Duane P.; Mintz, Michael D. New York, McGraw-Hill Book Co., 1965. 843p. $17.50.

The included data tabulations are divided into three sections; one-dimensional compressible flow function of a perfect gas, equation-of-state data of real air, and one-dimensional compressible flow functions of real air. Of these, the first and third sections represent the results of a series of digital computer calculations based on classical thermodynamic derivations of gasdynamic processes for a perfect gas and for real air. (M.O.W.)

47152 FUNDAMENTALS OF RADIATION ABSORPTION PROCESSES. Chiozzotto, M. (Istituto Superiore di Sanita, Rome). pp 7-41 of Radiation Dosimetry. New York, Academic Press, 1964.

Interactions of radiation with matter which are the most important from a dosimetric point of view are discussed. Electromagnetic radiations involved in dosimetric problems are in the photon energy range above a few kev. These radiations originate in several different processes the most important of which are mentioned. Since it may be useful to distinguish electrons according to their origin, electron interactions and other properties are discussed. A pure neutron field is almost never realizable, and neutrons are generally a component of a mixed radiation field on account of the radiations of electromagnetic nature which are almost always emitted by the neutron sources. Some common neutron sources and their interactions with matter are examined. The sources, interactions, and other properties of heavy charged particles are also discussed. (J.F.P.)

47153 SIXTH SYMPOSIUM ON ENGINEERING ASPECTS OF MAGNETOHYDRODYNAMICS, UNIVERSITY OF PITTSBURGH, APRIL 21–22, 1965. Phillipsburg, N. J., American Institute of Aeronautics and Astronautics, 1965. 149p. (CONF-650436).

Thirty-six papers are included: separate abstracts were prepared for 10 papers; two papers were previously abstracted for NSA; see abstracts 19: 23345 and 27591. Papers not abstracted are of two types; complete texts of completed pieces of work and abstracts of work in progress. The papers not abstracted discuss other phases of current research and development in engineering magnetohydrodynamics, such as MHD generation with elevated electrode temperatures, real machine effects in the MHD induction generator, and development of hot shot gas source for pulsed MHD wind tunnel studies. (B.L.M.)

For abstracts of individual papers see: 47289—47296, 47533, and 47801.

47154 HELICAL FIELDS POSSESSING MEAN MAGNETIC WELLS. McNamara, B.; Whiteman, K. J.; Taylor, J. B. (United Kingdom Atomic Energy Authority, Abingdon, Eng.). Vienna, International Atomic Energy Agency, 1965, Preprint No. CN-21/239, 25p. (CONF-650935-33). ORINS.

From 2nd IAEA Conference on Plasma Physics and Controlled Nuclear Fusion Research, Culham, Eng.

A particular magnetic field having helical symmetry could possibly provide a mean magnetic well. Helical fields in general, and the circumstances in which they may exhibit the "well" property, are examined. This investigation is made possible by the use of the stream function formalism, which provides a simple picture of the field geometry. The existence of magnetic wells is related to the topology of the magnetic surfaces, which in turn is connected with the positions of the stationary points of the stream function. (auth)

47155 PARTICLE BEAM MEASUREMENT APPARATUS USING BEAM KINETIC ENERGY TO CHANGE THE HEAT SENSITIVE RESISTANCE OF THE DETECTION PROBE. Baldwin, Lionel V.; Sandborn, Virgil A. (to National Aeronautics and Space Administration). U. S. Patent 3,202,915. Aug. 24, 1965. Filed June 19, 1961.

A particle beam power probe density measuring system includes a probe immersible in the beam. The probe is formed of a pair of spaced rods. The outer ends of the rods are exposed to the particle beam detecting means having its extremities securely fastened to the outer ends for converting the kinetic energy of the particle beam into heat. Tubular means support the probe, and means are provided for dissipating the heat conducted into the outer ends of the rods from the detecting means to maintain the extremities of the detecting means at a substantially constant temperature preventing the destruction of the detecting means. Means are connected to the probe responsive to the electrical variations of the detecting means for developing an electrical signal indicative of the local power density of the beam. (B.L.M.)

47156 BETA RADIATION SOURCE IN A CERAMIC CARRIER. Johnson, James R.; Lahr, Thomas N.; Walz, Richard N. (to Minnesota Mining and Mfg. Co.). U. S. Patent 3,204,103. Aug. 31, 1965. Filed Oct. 4, 1961.

A method is described for fabrication of a beta, gamma, alpha, or bremsstrahlung source that includes a combination of a solid radioisotope forming part of a ceramic carrier and a corrosion-resistant external ceramic shield that is substantially permeable to the radiation of the isotope. The isotope is separated from the shield by an occluding barrier layer substantially permeable to radiation from the isotope but impermeable to radioactive decay products. The barrier layer is substantially nonreactive with the external shield and the isotope at temperatures of the order of those at which the shield is applied. The shield and the barrier are bonded together so as to form an integral construction. (B.L.M.)

Accelerators

Refer also to abstracts 46126, 46514, 46643, and 46809.

47157 (AWRE-NR-1/65) A LOW ENERGY SPREAD NEGATIVE ION RF SOURCE. Garner, G.; Swann, D. (Atomic Weapons Research Establishment, Aldermaston (England)). July 1965. 10p. Dep.; BIS $0.30; HMSO 1s. 9d.

A negative ion r-f source with an ion beam energy spread approaching that of sources of the duoplasmatron type is described. It has a better performance for both pulsed and non-pulsed operation than the negative ion r-f source previously used on the Tandem accelerator. (auth)

47158 (BNL-910) THE FAST BEAM EXTRACTION SYSTEM OF THE ALTERNATING GRADIENT SYNCHROTRON. Forsyth, E. B.; Lasky, C. (Brookhaven National Lab., Upton, N. Y.). Mar. 10, 1965. Contract AT(30-2)-Gen-16. 27p. Dep. mn; CFSTI $2.00 cy, $0.50 mn.

The system provides a fast, single-turn, extracted beam from the AGS at machine energies from 10 to 32 Bev with essentially 100% efficiency. Three pulsed magnets coupled to the beam by coherent betatron oscillations are the major components of the system. Two of the magnets are constructed in the form of a septum, the septum plate dividing

areas of high magnetic field from areas of almost zero field. The field in these magnets is developed relatively slowly, being fully established immediately prior to ejection. Before ejection normal acceleration occurs in the AGS as the beam lies on the zero field side of the septa. The beam is ejected when the third magnet is pulsed; this magnet's field has a rise time shorter than the time between adjacent proton bunches in the AGS. Thus, if the pulsed field is properly synchronized to bunch position, protons are deflected into the high field areas of the septum magnets and out of the AGS. Both septum magnets are withdrawn hydraulically before injection, to avoid restricting the aperture of the machine, and are rammed into place after the transition energy has been attained. The power supply for the fast pulsed magnet consists of low-impedance, high-voltage pulse-forming networks (PFN's) switched by hydrogen thyratrons. One septum magnet is powered by a programmed, constant-current generator using 200 power transistors as the regulating element. The third magnet is pulsed from an 8000-joule capacitor storage bank; its field is regulated to keep the angular jitter of the external beam to <1 part in 1000. (auth)

47159 (BNL-9388) DEVELOPMENT OF SERVO MANIPULATORS FOR HIGH ENERGY ACCELERATOR REQUIREMENTS. Flatau, Carl R. (Brookhaven National Lab., Upton, N. Y.). [nd]. Contract AT(30-2)-Gen-16. 25p. (CONF-651101-25). Dep. mn; CFSTI $1.00 cy, $0.50 mn.

From 13th Conference on Remote Systems Technology, Washington, D. C.

A d-c force reflecting bilateral servo system was developed which will be incorporated into an extremely compact and light servo manipulator for use in high energy accelerators. The compactness is achieved by incorporating the servo actuators within the manipulator arms, thereby giving many additional advantages. By use of force feedback in addition to the customary position and velocity feedback, reflected friction is much reduced so that improved sensitivity and feel will result in the manipulator. (auth)

47160 (BNL-9482) DESIGN OF QUADRUPOLES AND DIPOLES USING PERMANENT MAGNET RINGS. Blewett, J. P. (Brookhaven National Lab., Upton, N. Y.). Aug. 10, 1965. Contract AT(30-2)-Gen-16. 30p. Dep. mn; CFSTI $2.00 cy, $0.50 mn.

A preliminary theoretical analysis of field patterns in permanent magnet quadrupoles was performed in 1954 and 1955. This analysis was refined and is presented. A similar analysis was made of methods for producing uniform fields in permanent magnet rings. The analysis is presented in sections on permanent magnet materials, fields in permanent magnets, quadrupole theory, field patterns in quadrupole magnet rings, dipole theory, and field patterns in dipole magnet rings. (M.O.W.)

47161 (BNL-9483) PLANS FOR A SLOW EXTRACTED BEAM AT AGS. Barton, M. Q. (Brookhaven National Lab., Upton, N. Y.). [1964]. Contract AT(30-2)-Gen-16. 14p. (CONF-650923-5). Dep. mn; CFSTI $1.00 cy, $0.50 mn.

From 5th International Conference on High Energy Accelerators, Frascati, Italy.

The most attractive schemes for obtaining slow extracted beams from circular accelerators consist of variations of the resonant extraction technique originally developed for synchrocyclotrons. The preliminary work towards application of this technique to the Brookhaven AGS is described. (M.O.W.)

47162 (BNL-9503) A COMPARISON OF VARIOUS METHODS FOR DETERMINING PARTICLE BEAM PHASE-SPACE DISTRIBUTION. van Steenbergen, A. (Brookhaven National Lab., Upton, N. Y.). Sept. 3, 1965. Contract AT(30-2)-Gen-16. 16p. (CONF-650923-11). Dep. mn; CFSTI $1.00 cy, $0.50 mn.

From 5th International Conference on High Energy Accelerators, Frascati, Italy.

Various methods to determine the particle density distribution in the two-dimensional space-space intercept are discussed and quantitatively compared. In general the methods yield similar two-dimensional phase-space density contours for typical density distributions encountered experimentally, except in cases where appreciable aberrations are present. (auth)

47163 (BNL-9504) THE PULSED SYNCHROTRON AS AN INSTRUMENT FOR PARTICLE RESEARCH. Green, G. K. (Brookhaven National Lab., Upton, N. Y.). Sept. 3, 1965. 6p. (CONF-650923-7). Dep. mn; CFSTI $1.00 cy, $0.50 mn.

From 5th International Conference on High Energy Accelerators, Frascati, Italy.

Developments in the pulsed synchrotron are reviewed. A listing of some of the more important items and an evaluation of their effects on the overall operation are included. A brief review of the following is given; the magnet system, electric timing markers, injection schemes, radio-frequency acceleration system, and the advent of alternating gradient. (M.O.W.)

47164 (JINR-P-2313) MIKROTRON-INZHEKTOR NA 30 Mev DLYA IBRa. (A 30 Mev Microtron-Injector for the Pulsed Fast Reactor). Anan'ev, V. D.; Antsupov, P. S.; Kapitsa, S. P.; Matora, I. M.; Melekhin, V. N.; Merkulov, L. A.; Khar'yuzov, R. V. (Joint Inst. for Nuclear Research, Dubna (USSR). Lab. of Neutron Physics). 1965. 10p. Dep. mn.

A description is given of the main parts and parameters of the 30-Mev microtron constructed at the Neutron Physics Laboratory of the Joint Institute for Nuclear Research. The microtron produces the pulses of 1–3 μs duration and the current of 40–60 mamp. The pulses are injected into the center of the active zone of the pulsed fast neutron reactor. (auth)

47165 (NIRL/R/99) SERVO THEORY FOR THE CONTROL OF COHERENT BETATRON OSCILLATIONS IN NIMROD. Rees, G. H. (National Inst. for Research in Nuclear Science, Chilton (England). Rutherford High Energy Lab.). Mar. 1965. 16p. Dep. mn; BIS $0.60; HMSO 3s.

A transfer function is derived for the stimulation of coherent vertical betatron oscillations by means of a localized vertical electric field in a synchrotron. There are $(2m + 1)$ resonances in the transfer function (where m is a positive integer or zero). A method of damping all resonant modes, as outlined by F. E. Mills (Mura), is discussed. A modified scheme for Nimrod is presented, providing damping of the $(1 - \nu)$ mode throughout acceleration, where ν is the vertical betatron wave number. There is vertical beam sensing at both points a quarter orbit from the externally applied field to separate the feedback corresponding to m being an odd integer from that where m is even or zero. Some details of the proposed system are given. (auth)

47166 (ORNL-P-1605) EXTRACTION MAGNETS FOR CYCLOTRONS. Hudson, E. D.; Lord, R. S. (Oak Ridge National Lab., Tenn.). [1965]. Contract W-7405-eng-26. 9p. (CONF-650922-8). Dep. mn; CFSTI $1.00 cy, $0.50 mn.

From 1st International Symposium on Magnet Technology, Stanford, Calif.

Three types of magnetic channels meeting the varying requirements for beam extraction from cyclotrons are described. They produce field reductions of up to 9,000 gauss for the deflected beam, but only a few gauss of first harmonic in the region of the circulating beam. The power levels are on the order of 200 kw. (auth)

47167 (ORNL-P-1619) SECTOR MAGNETS FOR A SEPARATED ORBIT CYCLOTRON. Lord, R. S.; Hudson, E. D. (Oak Ridge National Lab., Tenn.). [1965]. Contract W-7405-eng-26. 6p. (CONF-650922-9). Dep. mn; CFSTI $1.00 cy, $0.50 mn.

From 1st International Symposium on Magnet Technology, Stanford, Calif.

The Separated Orbit Cyclotron (SOC) consists of indi-

vidual sector magnets placed alternately with r-f cavities in a circular arrangement. In each magnet sector the beam is bent and focused by alternating gradient fields; ten to twenty pairs of pole tips, depending on design, are mounted on a common yoke and driven by a common coil pair. A variable reluctance device under each pole can be used to adjust the field to the desired value. Model studies were made, and a 50-ton prototype sector magnet for a 50-Mev SOC is being fabricated for further study. (auth)

47168 (TID-22177) A GENERAL ORBIT CODE FOR CYCLOTRON ANALYSIS. Hopp, David I. (California Univ., Los Angeles. Dept. of Physics). May 1965. Contracts AT(11-1)-34; Nonr-233(44). 41p. Dep. mn; CFSTI $2.00 cy, $0.50 mn.

A FORTRAN IV computer program for a 32K system is given which will aid in the analysis of the various types of cyclotrons. The main restriction of this version is that there exists a magnetic median plane above and below which field values may be computed by an expansion involving terms linear in displacement. The field is stored in a point-by-point fashion in polar coordinates. A maximum of 6000 points is allowed in this version. (M.O.W.)

47169 (UCRL-16204) BEVATRON OPERATION AND DEVELOPMENT. 45. JANUARY THROUGH MARCH 1965. Crebbin, Kenneth C. (Lawrence Radiation Lab., Univ. of California, Berkeley). June 23, 1965. Contract W-7405-eng-48. 13p. Dep. mn; CFSTI $1.00 cy, $0.50 mn.

The Bevatron provided beam for physics research for 81% of the scheduled operating time. A more stable operation was achieved than formerly by using a modified inflector-tuning procedure and an inner radius cup with which beam injected into the Bevatron was measured. A major shutdown allowed inspection of bearings and journals on the main motor generator sets. (auth)

47170 (UCRL-16384) MAGNET SYSTEMS—POWER SUPPLIES—COST OPTIMIZATION. Dols, Charles G. (Lawrence Radiation Lab., Univ. of California, Berkeley). Sept. 1, 1965. Contract W-7405-eng-48. 7p. (CONF-650922-3). Dep. mn; CFSTI $1.00 cy, $0.50 mn.

From the 1st International Symposium on Magnet Technology, Stanford, Calif.

As the number of auxiliary magnets for particle accelerators increases, it becomes increasingly important that some of the designs be standardized. More attention will therefore be paid to cost optimization of the standard magnet designs. Significant concepts and elements that enter into such cost optimization are presented. A typical auxiliary-magnet system is first described. Then the factors that enter into cost optimization are discussed, with some examples given. These factors include power duty factors; incremental costs; and present value, including interest rate and useful life. Finally an expression for optimum current density in magnet conductors is derived. (auth)

47171 THE BETATRON RESEARCH PROGRAM AT MELBOURNE UNIVERSITY. Spicer, B. M. (Univ. of Melbourne). At. Energy Australia, 8: No. 3, 2-6(July 1965).

An indication is given of the precision of work possible with the 35-Mev betatron and also of the wide variety of problems it is possible to investigate. Currently the experimental program is majoring on the problems of structure within the giant resonance region, although there are several other interests. (P.C.H.)

47172 HIGH BRILLIANCE ION-SOURCE. Delbarre, J.-P.; Faure, J.; Vienet, R. Bull. Inform. Sci. Tech. (Paris), No. 91, 59-69(Mar. 1965). (In French).

In connection with the 20-Mev injection program for Saturne, a theoretical study was made of the transfer of the proton beam from the source up to the entrance of the 20-Mev linear accelerator. An experimental set-up using these results provided a 30-mamp pulsed beam of 170-kev protons whose brilliance was 30 times greater than that obtained with conventional equipment. (auth)

47173 AN INTERNAL LIQUID HYDROGEN TARGET FOR A PROTON SYNCHROTRON. Hogan, W. J.; Jankowicz, R.; Pigoue, P. A.; Shoemaker, F. C. (Princeton Univ., N. J.). IEEE (Inst. Elec. Electron. Engrs.), Trans. Nucl. Sci., NS-12: No. 4, 251-2(Aug. 1965).

A liquid-hydrogen target, designed for studying p-p interactions at 3 Mev in the Princeton-Pennsylvania Accelerator, is described. The target cooling system, window, and other components are reviewed. (T.F.H.)

47174 ENERGY SPECTRUM OF THE ELECTRON BEAM IN A RACETRACK MICROTRON. Sells, V.; Froelich, H.; Brannen, Eric (Univ. of Western Ontario, London, Can.). J. Appl. Phys., 36: 3264-6(Oct. 1965).

The energy spectrum of the beam of a four-sector racetrack microtron was measured, using a high-resolution double focusing beta-ray spectrometer. For an energy gain per orbit of 750 kev, it was found that 50% of the integrated current in the eighth orbit (6 Mev) was contained in an energy interval of 34 kev and 90% of the beam current in a 73-kev interval. This narrow energy spread (±0.3%) is of particular interest in the generation of submillimeter radiation and in the use of the microtron as an injector for high-energy synchrotrons. (auth)

47175 ON THE DESIGN OF THE VACUUM SYSTEM OF TOKYO ELECTRON SYNCHROTRON. Horikoshi, Gen'ichi (Tokyo Univ.). Japan J. Appl. Phys., 4: 530-7(July 1965).

Design and operation of the vacuum system of the electron synchrotron at the Institute for Nuclear Study, University of Tokyo are described. The number of pumps to be installed around the donut ring of the electron synchrotron was determined by a quantitative estimation based on experimental data. Eight pumping units are installed around the donut ring. These are all linked at the backside, and are backed by one fore-pump system consisting of an oil diffusion pump and a rotary pump. The role of the diffusion pump in the fore-pump system is discussed with results of pressure distribution measurement in the vacuum system under various conditions. Each pump unit used in the vacuum system of the synchrotron is operated without any cold trap. (auth)

47176 A 200 kev ACCELERATOR FOR GENERATING 14 Mev NEUTRONS. Peil, A. (Humboldt-Universitaet, Berlin). Kernenergie, 8: 337-45(June 1965). (In German).

The design and the capacity of a 200-kev accelerator used as a high-output source of monoenergetic fast neutrons are described. A Van de Graaff accelerator or a cascade generator serves as the high-voltage source. Deuterium ions are generated in a high-frequency ion source and meet a zirconium–tritium target after having being accelerated in an ion tube and analyzed in a 90° magnet. The 14-Mev neutrons are generated using the $^3H(d,n)^4He$ reaction. The maximum source output amounts to 10^{10} neutrons/sec. (auth)

47177 FAST ELECTRON DOSIMETRY ON A 2 Mev VAN DE GRAAFF ACCELERATOR. Heinrich, H.-J.; Koch, W. (Institut fuer Angewandte Physik der Reinststoffe der Deutschen Akademie der Wissenschaften, Dresden). Kernenergie, 8: 345-8(June 1965). (In German).

Dose measurements were carried out on a 2-Mev Van de Graaff electron accelerator using a cerium sulfate solution. Using the 0.2M cerium sulfate solution, the upper dose limit was 2×10^7 rad, and using the 0.39M cerium bisulfate solution this limit was about 7×10^7 rad. In comparing the values obtained by means of cerium dosimetry to those of physical measurements (calorimetry, current density) deviations of less than ±5% were found. (auth)

47178 30-Mev FLUX-FORCED FIELD BIASED BETATRON. II. Tanaka, Osamu; Hiro, Sanju (Mitsubishi Electric Mfg. Co., Ltd., Japan). Mitsubishi Denki Giho, 39: 799-804(June 1965). (In Japanese).

From self-expansion phenomena and continuous variation of the nominal orbit radius peculiar to the betatron, information of interest about the electronic orbits of the betatron

has been made available. Characteristics of the x ray output as a function of d-c bias are complicated. The output has been obtained with various bias angles up to 45° (29 Mev). As a typical application of it, the technique of radiography has been developed with the high energy x ray generated by the betatron and its use has been extended to the detection of faults by radiographic operation on heavy metal objects. (auth)

47179 EQUILIBRIUM CHARGE STATES OF ^{16}O IONS. Bernard, D. L.; Bonner, B. E.; Phillips, G. C.; Stelson, P. H. (Rice Univ., Houston, Tex.). Nucl. Phys., 73: 513-21(1965). (TID-21957).

The charge state distributions of an O^{+4} ion beam were measured after passage through thin foils of Au and Ni. The average energy losses in the Au and Ni targets were 4.3 and 3.9 Mev, respectively, and did not change appreciably for the incident bombarding energy range covered. Charge state fractions are calculated as functions of emergent ion velocity. From these fractions, the Z_{rms}/Z is calculated as a function of $V/Z^{\frac{2}{3}}$, where Z_{rms} is the root mean-square of the charge on the ion, Z is the atomic number of the ion, and V is the emergent ion velocity. These results compare favorably with other data taken with ^{16}O ions at higher and lower ion velocities. There appears to be no indication of a decrease of the degree of ionization with atomic number of the stopping material from these comparisons. Preliminary work was done with an incident O^{+5} beam, but inconclusive results were obtained because of small beam intensities. (auth)

47180 A COMPARISON OF THE 30-Mev FIELD-BIASED BETATRON AND 35-Mev CONVENTIONAL BETATRON. Tanaka, Osamu (Mitsubishi Elec. Mfg. Co., Japan). Nuclear Eng. (Tokyo), 11: 29-34(Jan. 1965). (In Japanese).

Compared with the conventional, a flux-forced field-biased betatron has the following advantages: the radius of the stable orbit is variable continuously, it is possible to compare the theoretical estimate of the orbit of accelerated electrons and the experimental results which can be observed easily from the instantaneous diffuse of the orbit due to the phase shift, and it has a high energy output despite the light weight and compactness. However, it has the disadvantage of having very complicated electronic circuits. The comparison of the characteristics of the 30-Mev field-biased betatron and the 35-Mev conventional betatron is presented. (auth)

47181 THE EFFECT OF BACKSCATTERING ON THE TARGET CURRENT OF ELECTRON ACCELERATORS. Okabe, Shigeru; Tabata, Tatsuo (and others) (Radiation Center Osaka Prefecture). Oyo Butsuri, 34: 419-24 (June 1965). (In Japanese).

The ratio of target current to incident electron beam current is studied for thick targets of Al, Fe, Sn, Pb and U in the energy range 4 to 14 Mev. In consideration of practical use, the target is placed in air at about 10 cm from the output window of an electron linear accelerator. The effect of ion current on target current and other errors expected under this experimental condition are verified to be negligible. Therefore, the difference of the observed ratio from unity can be interpreted as the backscattering coefficient of electrons. The backscattering coefficient for a target placed perpendicularly to the beam is found to decrease exponentially with increasing energy in this region. While it increases with the atomic number Z of the target also in the present energy region, the curve of the relation between them does not show such a large change of gradient as observable at $Z \approx 30$ in kev region. (auth)

47182 EXPERIMENTAL OBSERVATIONS OF PULSE SHORTENING IN A LINEAR-ACCELERATOR WAVEGUIDE. Jarvis, T. R. (MEL Equipment Co. Ltd., Crawley, Sussex, Eng.); Saxon, G.; Crowley-Milling, M. C. Proc. Inst. Elec. Engrs. (London), 112: 1795-1802(Sept. 1965).

Experimental observations made of the parasitic oscillations which can occur in electron linear accelerators and which cause the phenomenon known as pulse shortening are described. Measurements were made of the frequency of oscillation, the noise level from which the wave builds up, the rate at which it builds up and the maximum power levels achieved. The presence of resonant conditions was noted during the buildup process. Appendixes give details of an approximate theory of the mechanisms of oscillation. (auth)

47183 THE ITALIAN 35 Mev BETATRON GILBETRON FOR THERAPEUTIC AND SCIENTIFIC-INDUSTRIAL USES. Ascani-Orsini, R.; Gilardoni, A.; Taccani, A. Radiazioni Alta Energia, 4: 87-96(Apr. 1965). (In Italian).

The Gilbetron 35-Mev betatron designed for therapeutic and industrial purposes is described. The practical energy range is examined and it is concluded that the most suitable energy is at 35 Mev. (tr-auth)

47184 PARTICLE ACCELERATORS AND THEIR APPLICATIONS. Kamogawa, Hiroshi (Tokyo Shibaura Electric Co., Ltd.). Toshiba Rev., 18: 1298-1302(Nov. 1963). (In Japanese).

Research and development work on accelerators in Toshiba was begun about 30 years ago. Several accelerators for research purposes such as a 170-Mev strong-focusing cyclotron and a 65-Mev synchrocyclotron have been manufactured and have continued successful service within the country. In addition, betatrons, electrostatic (Van de Graaff type) generators, electron linear accelerators, and a 14-Mev neutron generator have been developed. Among various applications of these accelerators, that for the full-automatic activation analysis apparatus is described. (NSA of Japan)

47185 MAGNETIC FOCUSING OF MEDIUM FAST ELECTRONS IN AIR COILS. Bundke, Werner; Schramm, Herbert (Johann Wolfgang Goethe-Universitaet, Frankfurt am Main). Z. Angew. Physik., 19: 437-42(1965). (In German).

The focusing properties of a double coil system were represented by explicit expression of the potential well by which the particles move. The ratio of axial to radial focusing can be given for various gaps of the coil and for different orbit radii. The axial focusing was significantly improved when the gap of the single coils was made larger than that corresponding to the Helmholtz case. $B_z(\rho)$ and $A(\rho)$ for the median plane of the Helmholtz field was tabulated for $0 \leq \rho \leq 1$ and 0.05. (tr-auth)

47186 THE LIFETIME OF ELECTRON ORBITS IN FOCUSING MAGNETIC FIELDS. [PART] I. Bundke, Werner (Universitaet, Frankfurt am Main). Z. Angew. Physik., 19: 442-5(1965). (In German).

The introduction of particles into focusing fields is a central problem in the planning of tandem accelerators. The present study is concerned with this problem of the storage of accelerated electrons in focusing magnetic fields in the low-energy range. After a description of the measurement principles which use the electron cyclotron as an auxiliary, a simple expression for the depth of the potential well in which the particles moved was derived. The depth of the potential well depends on the field index of the selected air coil configuration. An approximation formula was given for it as a function of the current distribution in the coils. The electron number lifted from the potential well experimentally was represented graphically as a function of the imposed voltage. (J.S.R.)

Astrophysics and Cosmology

Refer also to abstracts 47451 and 47468.

47187 (AD-612182) ABUNDANCES OF ELEMENTS IN STARS AND NEBULAE (DETERMINATION OF RATIO OF GAS PRESSURE TO ELECTRON PRESSURE IN STELLAR ATMOSPHERES). Cowley, C.; Cowley, A.; Aller, L. (Michigan Univ., Ann Arbor. Coll. of Literature, Science and the Arts). July 1962. Contract AF49(638)-807. 13p. (AFOSR-3433). CFSTI $1.00 cy, $0.50 mn.

The ratio of gas pressure (P_g) to electron pressure (P_e) was computed over a range of temperatures by an approximate method and also by a more exact IBM-709 program. The approximate method shows large errors at low temperatures and high gas pressures. Tables give the values of log P_g and log P_e computed by the 709 as well as the relative abundances to which these values refer. (auth)

47188 (AD-613636) ON A SOLAR FLARE MODEL AND ITS LABORATORY EXPERIMENTATION. Technical Information Series. Yen, K. T. (General Electric Co., Philadelphia, Pa. Missile and Space Div.). Apr. 1965. 27p. (R65SD8). CFSTI $2.00 cy, $0.50 mn.

A theoretical model for solar flares is presented to describe the physical processes considered likely to occur in the solar atmosphere above a complex sunspot group leading to the formation and development of a solar flare. Based on the idea that the strong magnetic fields of large sunspots play the dominant role in these processes, a bipolar sunspot group is considered in some detail to show how a very strong magnetic compression can take place to accumulate enough energy to form a solar flare. Estimates of the time scales for solar plasma confinement and the containment of neutral hydrogen atoms are made to show the proposed model to be a feasible one. Physical conditions favorable to the formation of solar flares and the relationship of flares to prominences and filaments are discussed. A laboratory experiment is outlined to verify the validity of the proposed model, and to investigate, within the limitations of laboratory simulation, the physical phenomenon following the flash phase of a flare. (auth)

47189 (N64-31082) THE VELOCITY OF CORPUSCULAR STREAMS IN THE SOLAR CORONA BASED ON OBSERVATIONS OF SOLAR RADIO EMISSION. Moiseev, I. G. Translated from Izv. Krymsk. Astrofiz. Observ., 24: 3-15(1960). 23p. (NASA-TT-F-227). CFSTI $0.75 cy, $0.50 mn.

The velocity of the perturbing agent in the solar corona was estimated from radio bursts of type II, with allowance for coronal condensations. The resulting velocities agree well with the mean velocities of corpuscular streams responsible for the production of magnetic storms of sudden commencement. They indicate that the corpuscular streams are probably ejected from active parts of the solar surface with high initial velocities and are not accelerated in the corona. (auth)

47190 (NASA-TT-F-248) THE NATURE OF A WEAK CHROMOSPHERIC FLARE. Stoyanova, M. N. Translated for National Aeronautics and Space Administration, Washington, D. C. from Byull. Soln. Dannyie, No. 3, 46-55(1963). 14p. CFSTI $1.00 cy, $0.50 mn.

Studies were made on a very weak flare observed on 3 September 1962 at Pulkovo, using a horizontal solar telescope. Spectrograms were obtained for the H_α and HeD_3 segments. Fluctuations in the image did not exceed 2″ in amplitude. The contours of the D_3 line are very shallow, suggesting the possibility that the optical thickness of the flare was slight. The number of atoms along the line of sight (1 cm^2 cross section) for the second and third levels is computed and the ratio was found to be 1.27×10^{-2} (upper level to lower level), which compares favorably with the theoretical value of 1.3×10^{-2}. The contours for emission and absorption of the D_3 line are given. These exhibit a Gaussian form. The contours for H_α are not Gaussian, however. In seeking an explanation for these latter contours, it was found that for any assumed relative optical thickness in the flare, a source function was obtained that was larger throughout the contour than the function obtained from population tables corresponding to the case of photospheric radiation. It was concluded that the observed radiation was not caused by scattering, and for this reason the assumption that the source function changes along the contour does not hold (since the self-radiation does not depend on radiation flux). On the assumption of a constant value of the source function, one-layer models were examined with first a thin, then a thick optical thickness. Neither explained the shape of the contour, and then a two-layer model was investigated. This furnished an explanation, and it was concluded that the emission of hydrogen cannot be explained by scattering of photospheric radiation, but is caused by an increased population at the third level. (auth)

47191 (NASA-TT-F-250) THE NATURE AND LOCALIZATION OF CHROMOSPHERIC FLARES. Slonim, Yu. M. Translated for National Aeronautics and Space Administration, Washington, D. C. from Byull. Soln. Dannyie, No. 4, 67-77(1963). 13p. CFSTI $1.00 cy, $0.50 mn.

The relation of flares to solar prominences was discussed. Three types of flares are considered. Type A is shown to have plasma with sharp, short pulse jets, Type B a strong, contracted radiation burst, and Type C a long-duration pulsating character. The first two appear strictly in the chromosphere, whereas Type C has a coronal origin. In order to compare these various flare types objectively, the flare intensity was replaced by the line width characteristic H_α. It is shown that Type C flares are generated principally in the growth phase of sunspot groups, whereas Types A and B are found in the decaying phase. It is concluded that these facts show the differences between the fast-growing flares of Types A and B, and the pulsating flares of Type C. The analysis is extended to connect Type C flares with loop prominences. Various reasons are given for the hypothesis, emphasizing the similarity between pulsating emission center for Type C flares and the nature of nodal and jet radiation of prominences. (auth)

47192 CURVED SPACE AND GRAVITATION. [PART] II. Brehme, Robert W. (Wake Forest Coll., Winston-Salem, N. C.; Univ. of North Carolina, Chapel Hill). Am. J. Phys., 33: 713-21(Sept. 1965).

The Euclidean and Einstein geodesics are defined for a two-dimensional space–time surface. Both are shown to approach the same classical law of gravitational acceleration, and to preserve the equivalence principle. However, only the Einstein geodesic allows a local time to be defined in such a way that the local velocity of light is constant. The conical surface is discussed and the connection is made between it and the frame of the uniformly accelerated relativistic rocket. Coordinate transformations are discussed to the extent that it is established that the shape of the two-dimensional surface embedded in a Euclidean three-space depends on the choice of coordinate frame. (auth)

47193 THE HELIUM CONTENT OF THE GALAXY. Truran, J. W.; Hansen, C. J.; Cameron, A. G. W. (Yale Univ., New Haven; Goddard Space Flight Center, New York). Can. J. Phys., 43: 1616-35(Sept. 1965).

It is usually assumed in modern theories of nucleosynthesis that the initial composition of the galaxy was pure hydrogen. The large solar and stellar content of helium has appeared to present a difficulty for such an assumption. This problem is examined. Numerical studies are made of the time changes in the compositions of stars and the interstellar medium as a result of stellar evolution. It is concluded that the large helium content of the sun and recently formed stars can be produced only as a result of the evolution of stars of approximately solar mass. Hence the initial hydrogen hypothesis requires a large age for the galaxy ($\geq 2 \times 10^{10}$ years). The content of long-lived radioactivities in the interstellar medium is also followed as a function of time. It is found that the ratios of radioactivities are very insensitive functions of time and are approximately those observed in the solar system when the helium content is satisfactory. However, it is also concluded that these ratios give little useful information about cosmochronology. (auth)

47194 RADIATION AGES OF AUBRITES. Eberhardt, P.; Eugster, O.; Geiss, J. (Univ. of Berne). J. Geophys. Res., 70: 4427-34(Sept. 15, 1965).

The isotopes of helium, neon, and argon were determined in samples of six enstatite achondrites (aubrites). Radiation ages are calculated from these results and from published data for the nine known aubrites. The radiation ages of aubrites are significantly higher than

those of chondrites. Six out of nine fall into a relatively narrow interval around 40 to 50 million years. The significance of these results for the origin of the aubrites is discussed. Four of the aubrites contain large amounts of trapped gases. So far, nothing in the rare gas data of aubrites and enstatite chondrites points toward a common origin of these two meteorite classes. (auth)

47195 COSMIC-RAY-PRODUCED ^{36}S AND ^{33}S IN THE METALLIC PHASE OF IRON METEORITES. Hulston, J. R.; Thode, H. G. (McMaster Univ., Hamilton, Ont.). J. Geophys. Res., 70: 4435-42(Sept. 15, 1965).

Isotopic analysis of sulfur in the iron phase of a number of meteorites has shown the presence of cosmic-ray-produced spallation ^{36}S and ^{33}S. The Clark County meteorite sample yielded about 6×10^{-5} μg/g of $^{36}S_{sp}$ and about 3×10^{-4} μg/g of $^{33}S_{sp}$, samples from the Piñon and Tlacotepec meteorites yielded about 8×10^{-6} μg/g of $^{36}S_{sp}$ and about 2×10^{-5} μg/g of $^{33}S_{sp}$. Spallation sulfur in the Carbo meteorite was diluted considerably by larger quantities of natural sulfur, but it is probable that $^{36}S_{sp}$ is about 2×10^{-5} μg/g. Significant quantities of $^{36}S_{sp}$ or $^{33}S_{sp}$ could not be detected in samples from the Canyon Diablo and Xiquipilco (Toluca) meteorites. These spallation results are in reasonable agreement with predictions based on production rates of the rare gases in these meteorites according to cascade theory for the He isotopes and the Rudstam formula for the Ar isotopes. Detailed comparison of the distribution of the spallation products among the isobars of mass 36 will not be feasible until it is possible to develop methods of increasing the precision of these spallation sulfur measurements. (auth)

47196 LIMITS ON THE DENSITY OF INTERGALACTIC IONIZED HYDROGEN. Kaufman, Michele (Harvard College Observatory, Cambridge, Mass.). Nature, 207: 736-7(Aug. 14, 1965).

Observations of background radiation at radio frequencies were utilized to place limits on the amount of ionized hydrogen that exists in intergalactic space. The intensity to be expected at low frequencies from cosmic sources in an Einstein-de Sitter universe was calculated. With the same value of intergalactic electron temperature and density, general agreement with observation was obtained both near 4,000 Mc/s and in the range 4-100 Mc/s. It was concluded that the density of intergalactic H^+ is probably at least an order of magnitude smaller than the mean density of an Einstein-de Sitter universe, and that the spectrum of background radiation at radio frequencies may be the product of extragalactic sources. (P.C.H.)

47197 CONTRIBUTION OF CHARACTERISTIC X-RAYS TO THE RADIATION OF SOLAR FLARES. Acton, Loren W. (Lockheed Missiles and Space Co., Palo Alto, Calif.). Nature, 207: 737-8(Aug. 14, 1965).

Characteristic x rays emitted as a result of inner-electron transitions is suggested as an important contribution to the x-ray emission of solar flares. The detection of the characteristic radiation of iron atoms in the x radiation from flares would indicate that non-thermal processes are important in the production of x rays in wavelength range 1-3 Å. In order to evaluate the relative contribution of the characteristic radiation excited by non-thermal electrons, this emission was compared to the bremsstrahlung emitted by the same electrons at the same wavelength. From the comparison it was found that if sizeable numbers of energetic electrons are created by a flare then the characteristic radiation from neutral or weakly ionized iron may make a substantial contribution to the x-ray emission of the flare in the wavelength interval around 2 Å. (P.C.H.)

47198 A MODEL OF THE QUASI-STELLAR RADIO VARIABLE CTA 102. Rees, M. J.; Sciama, D. W. (Cambridge Univ., Eng.). Nature, 207: 738-40(Aug. 14, 1965).

A model is proposed that assumes that the observed variations in the quasi-stellar radio source CTA 102 originate in the source itself. This is also consistent with red shift observations. From the model it is predicted that the amplitude of the variations depends on the frequency ν of observation, where ν is in megacycles. For $300 < \nu < 1{,}000$ the intensity reaches a maximum in a time t (ν) days, say, ($t < 50$), and then remains constant for a time (100-2t) days (that is, while the disk is opaque to frequencies between ν and 1,000 Mc/s). The rise-time t (ν) is an increasing function of ν. The times at which the intensity is a minimum should be the same at all frequencies $\nu > 300$ Mc/s, unless there is appreciable dispersion. (P.C.H.)

47199 GAS CLOUDS IN DENSE STAR CLUSTERS: A POSSIBLE QUASAR MODEL. Cameron, A. G. W. (Goddard Space Flight Center, New York). Nature, 207: 1140-2(Sept. 11, 1965).

The properties of gas clouds in dense clusters of stars are discussed, and studies were made to determine if observed properties of quasars are compatible with them. The convention was adopted whereby all the visible quasi-stellar objects are called quasars, and the intense radio-emitting objects are called radio quasars. (P.C.H.)

47200 MAGNETOTURBULENT ENERGY AND STABILITY OF SUPERMASSIVE STARS. Anand, S. P. S. (California Inst. of Tech., Pasadena). Nature, 207: 1345-6(Sept. 25, 1965).

Fowler's binding energy method was used to show that the turbulent kinetic energy associated with internal magnetic disturbances (with conservation of magnetic flux) in quasi-stellar radio objects is also an effective physical mechanism to remove the general relativistic instability. It is shown that magnetoturbulent energy is very useful in removing general relativistic instability. It is shown that stable masses of $10^8 M_\odot$ to $10^{10} M_\odot$ are possible. (M.C.G.)

47201 THE DEVELOPMENT OF STARS. Voigt, H. H. (Universitaets-Sternwarte, Goettingen, Ger.). Naturwissenschaften, 52: 465-70(1965). (In German).

To follow the development of a star it is necessary to investigate what takes place in its interior and how these variations in the interior can be reflected on the surface where they can be observed. After a discussion of the energy sources of stars the internal structure of stars is described together with the hypotheses that make it possible to deduce these processes. The life process of a star from its origin through the various development phases up to its end state is then outlined. (J.S.R.)

47202 HELIUM-BURNING EVOLUTION OF MASSIVE STARS. Giannone, P.; Giannuzzi, M. A. (Osservatorio Astronomico, Rome). Nuovo Cimento (10), 36: 1267-82 (Apr. 16, 1965).

Eight homogeneous equilibrium models were calculated previously for helium-stars with masses ranging between 2.9 and 214 $M_\odot$. Radiation pressure was taken into account in the whole star. The evolution of the models with masses 2.9 and 14.6 $M_\odot$ until helium exhaustion occurs inside the core is studied. Opacity is due entirely to electron scattering and energy generation to the 3α and the subsequent reactions. The relative concentrations of elements produced are studied according to the progressive variation of physical conditions in the core. They change during the evolution, and when helium is exhausted ^{16}O is found to be almost the only product. The production of ^{20}Ne is entirely negligible at 2.9 $M_\odot$; on the contrary at 16.4 $M_\odot$ ^{20}Ne becomes appreciable, and the corresponding luminosity tends to increase very rapidly. Dissipation of energy for neutrino processes is still negligible, being only a small percentage of the total energy (about 1% in the more massive star). Radii are approximately solar, and effective temperatures are about $10^{5.6}$K. The convective core increases in mass, with a tendency to contain the whole mass of the star. Evolution is very fast especially for 14.6 $M_\odot$ and shifts the models to the left of the main sequence of homogeneous equilibrium models in the H-R diagram. (auth)

47203 QUANTUM THEORY AND THE SINGULAR STATE OF COSMOLOGY. Just, K. (Univ. of Arizona, Tucson). Nuovo Cimento (10), 36: 1386-7(Apr. 16, 1965).

It is asserted that the singular state of cosmology cannot

be treated macroscopically but is actually a quantum problem. Relations between the energy density, the world radius, the time measured from the singular moment, the total number of particles, and the gravitational unit are explored, starting from the assumption that the average mass of "elementary" particles under pressure is $m \approx \sqrt[4]{p}$ for $p > p_n \approx 10^{14}$ g/cm^3. (M.J.T.)

47204 INFRARED PHOTONS AND GRAVITONS. Weinberg, Steven (Univ. of California, Berkeley). Phys. Rev., 140: B516-7(Oct. 25, 1965).

It is shown that the infrared divergences arising in the quantum theory of gravitation can be removed by the familiar methods used in quantum electrodynamics. An additional divergence appears when infrared photons or gravitons are emitted from noninfrared external lines of zero mass, but it is proved that for infrared gravitons this divergence cancels in the sum of all such diagrams. (The cancellation does not occur in massless electrodynamics.) The formula derived for graviton bremsstrahlung is then used to estimate the gravitational radiation emitted during thermal collisions in the sun, and this is found to be a stronger source of gravitational radiation (though still very weak) than classical sources such as planetary motion. The conjecture of Dalitz that divergences in the Coulomb-scattering Born series may be summed to an innocuous phase factor is also verified, and it is shown how this result may be extended to processes involving arbitrary numbers of relativistic or nonrelativistic particles with arbitrary spin. (auth)

47205 STRUCTURED COSMOLOGICAL MODELS. Omer, Guy C. Jr.; Starrfield, Sumner G.; Kannenberg, L. C. (Univ. of California, Los Angeles; Univ. of Florida, Gainesville). Proc. Natl. Acad. Sci. U. S., 54: 657-9(Sept. 1965).

It is pointed out that cosmological models which are homogeneous in density are not fair representations for an observed universe in which most of the galaxies appear to be organized into clusters, and a more appropriate model would divide space into cubes of side length L with each cube containing a cluster of galaxies. Two possibilities are considered: a spherical symmetric model, which leads to a homogeneous model; and a cubic model in which the line element can be determined for any specified density. (L.B.S.)

47206 ANTIMATTER AND THE DEVELOPMENT OF THE METAGALAXY. Alfven, H. (Royal Inst. of Tech., Stockholm). Rev. Mod. Phys., 37: 652-65(Oct. 1965).

Elementary particle physics has demonstrated the complete symmetry between particles and antiparticles. From this follows the equivalence between matter and antimatter. It is very unsatisfactory that current cosmological theories are not symmetric with respect to matter and antimatter. It is postulated that a cosmological theory should be matter-antimatter symmetric, and introduce no ad hoc laws of nature. These postulates form part of Klein's theory, but are not satisfied by the "expanding universe" or "continuous creation" theories. Essential properties of an "ambiplasma" consisting of matter and antimatter are studied. It is shown that it emits radio waves but no detectable γ rays. If initially the plasma contains equal amounts of matter and antimatter, the two ingredients can be separated by electromagnetic and gravitational forces. In the present state of the universe there may be coexisting regions of matter and antimatter, separated by thin "Leidenfrost" layers. Klein's theory of the metagalaxy is reviewed and developed. The "initial condition" is supposed to be an extremely thin plasma of matter and antimatter which contracts under the action of gravitation. When the density has reached about 10^{-2} particles cm^{-3}, annihilation produces a radiation pressure which transfers the contraction to the present expansion. The theory leads to a relation between the average density and the Hubble parameter which is in satisfactory agreement with observations. Different ways of detecting antimatter are discussed. It is possible that radio stars consist of ambiplasma. The enormous energy quantities emitted from some celestial objects may be supplied by annihilation. Outside our metagalaxy there may exist other similar systems. The possibility of observing them is discussed. (auth)

47207 X-RAY AND GAMMA-RAY ASTRONOMY. Burbidge, Geoffrey; Sargent, Wallace (Univ. of California, San Diego). Sci. J., 1: 32-7(Aug. 1965).

A brief review is given of x-ray and γ-ray astronomy. Some of the problems in the detection and identification are explained. The method of lunar ocultation for pinpointing radio sources is explained. The observation of the ocultation of the Crab Nebula is described; from these observations theories for the Crab Nebula x-ray source are considered. The future possibilities of x-ray and γ-ray astronomy are also discussed. Thus far it is found that the background x radiation is not high enough for the theory of continuous creation of matter, in the form of neutrons, to be a valid theory. (J.F.P.)

47208 SOLAR MAGNETIC FIELDS. Bumba, V. (Astronomical Inst., Czechoslovak Academy of Sciences, Ondrejov); Howard, Robert. Science, 149: 1331-7(Sept. 17, 1965).

Discussion is presented on the measurement of solar magnetic fields, sunspots, active regions, and decay of active regions. Special attention is given to the development and use of the magnetograph for measurements. (P.C.H.)

47209 GRAVITATION AND SPACE SCIENCE. Dicke, R. H.; Peebles, P. J. (Princeton Univ., N. J.). Space Sci. Rev., 4: 419-60(June 1965).

A review is given of gravitation and space science. Topics discussed are gravitation and relativity, classical tests of general relativity, secular change in G, cosmology, radio galaxies, quasars, and gravitational collapse. It is emphasized that the observational evidence for the presently accepted theory of gravity is meager and of poor quality. The new tools of the space scientist offer more hope for the future than the efforts of laboratory-bound physicists. Space science is needed to improve the understanding of gravitation, and proper understanding of gravitation is essential to the goals of space science. (J.F.P.)

47210 ABSOLUTE INTENSITY MEASUREMENTS IN THE EXTREME ULTRAVIOLET SPECTRUM OF SOLAR RADIATION. Hinteregger, H. E. (Air Force Cambridge Research Labs., Bedford, Mass.). Space Sci. Rev., 4: 461-97(June 1965).

Experimental results and problems of absolute intensity measurements of solar electromagnetic radiation in the extreme ultraviolet (EUV) and soft x-ray region of the spectrum (designated cumulatively as "XUV" for brevity) are reviewed. The numerous practical problems are divided in two major areas, general problems of heterochromatic absolute XUV spectrophotometry in the laboratory and specific problems characteristic of requirements of solar physics, the physics of planetary atmospheres, and existing restrictions of space technology. Within the first area emphasis is placed on recent progress toward justified reliance on ionization detectors without necessary connection to source standards. For the second area, emphasis is placed on the immediate need to have existing exploratory observations followed by a new phase of more systematic experiments of increased accuracy. (auth)

47211 THE POSITION OF THE SOLAR WIND SHOCK BOUNDARY (thesis). Hundhausen, Arthur James. Madison, Wis., Univ. of Wisconsin, 1965. 40p.

A recent discussion by Patterson et al., of the density distribution of neutral hydrogen in interplanetary space includes a method of finding the position of the shock transition that terminates the supersonic solar wind. The requirement that one half of the outward flux of protons through the shock front is returned as an inward flux of fast neutrals permits the matching of the solar wind density to the computed neutral density, and thus the determination of the shock position. In this paper is described a refinement of the method in which a model is developed for the pertinent densities in the shell beyond the shock front, and the resulting flux of neutrals produced in this shell back through the shock front is computed. The shock position is then found by matching the density of these particles at the

shock radius to the density already established there by Patterson et al., with the latter density slightly modified to allow for a non-isotropy in the velocity distribution of the inward moving neutrals. It is noted that the distribution of proton velocities in the entire charge exchange shell could be anisotropic, resulting in a non-isotropic source function for the neutrals produced there. A technique is developed for including such anisotropic source functions in the theory. The position of the shock boundary is computed numerically in the case of a solar wind proton density and velocity of 5 cm^{-3} and 400 km/sec respectively at one astronomical unit. These calculations show that the position of the shock front can be determined only to within a factor of about three. However, it is shown that the shock front must be closer to the sun than the earlier method would indicate. (Dissertation Abstr.)

47212 SPHERICALLY SYMMETRIC COSMOLOGICAL MODELS (thesis). Callan, Curtis Gove Jr. Princeton, N. J., Princeton Univ., 1964. 78p.

Spherically symmetric cosmological models are evolved according to general relativity. The starting point is the derivation of an exact solution in comoving coordinates for the metric tensor of a spherically symmetric pressureless dust cloud. This solution can be applied to a very wide variety of matter distributions and the functions appearing in the metric tensor can be physically interpreted. It is shown that the comoving coordinate system, upon which the solution crucially depends, breaks down after a finite amount of time for inhomogeneous matter distributions. A simple criterion for the validity of the comoving coordinate system is found. The exact solution is applied to several particular model universes in order to show how simply their behavior can be found. The behavior of spherically symmetric dust clouds when comoving coordinates are inapplicable is discussed. The general method is to divide up the matter distribution into concentric thin shells of matter. Each shell falls freely in the central field of the matter interior to it until it collides with another shell. A method of continuing the motion past a collision is worked out. Then this procedure is used to answer two questions of cosmological interest: Can the singularity in the homogeneous universe (Friedmann universe) be avoided by making the matter distribution slightly inhomogeneous? Do slightly inhomogeneous universes become homogeneous in the course of their evolution? In an appendix the exact solution derived in the first part of the thesis is applied to the Schwarzschild problem, and it is shown how a class of comoving metric tensors, equivalent to the Schwarzschild solution can be generated. (Dissertation Abstr.)

47213 ISOTOPIC ANOMALY PATTERNS IN METEORITIC XENON (thesis). Pepin, Robert Osborne. Berkeley, Calif., Univ. of California, 1964. 110p.

Correlated variations in the isotopic composition of xenon from a number of stone meteorites indicate the presence of at least three isotopically distinct xenon components. One component is probably closely related to primordial xenon from the general galactic synthesis of the elements. Data from bronzite, hypersthene, enstatite, carbonaceous and gas-rich chondrites reveal a striking linear correlation of ^{134}Xe and ^{136}Xe abundance anomalies, suggesting the presence of fission xenon as a widely distributed constituent of meteoritic xenon. Neither uranium nor ^{244}Pu fission can readily account for the observed composition and abundance of meteoritic fission xenon within the context of current models of galactic nucleosynthesis. Light isotope abundance anomalies in xenon from chondrules of the Bruderheim meteorite, and all isotopic anomalies in krypton from a bulk sample of this meteorite, are shown to be consistent with the presence of a heavy rare gas component produced by charged-particle irradiation of meteoritic material. Both high energy proton bombardment producing xenon and krypton by spallation reactions, and alpha-particle irradiation leading to $Te(\alpha,xn)Xe$ and $Se(\alpha,xn)Kr$ reactions, are considered. It is noted that the observed light isotope anomaly pattern strongly suggests the operation of a simple mass fractionation process, and that a mixture of fission xenon with a fractionated primordial component adsorbed from the solar wind can quantitatively account for the relative abundances of all isotopes. (Dissertation Abstr.)

Atomic Physics

47214 (AD-612410) RETROFUGAL ELECTRON FLUX FROM MASSIVE TARGETS IRRADIATED WITH A MONOENERGETIC PRIMARY BEAM. Dressel, Ralph W. (White Sands Missile Range, N. Mex. Nuclear Effects Lab.). 1963. 15p. CFSTI $1.00 cy, $0.50 mn.

The term retrofugal flux is introduced to include the backscattering plus the backward secondary emission occurring when a beam of monoenergetic electrons strikes a thick target. A comparison of computations of the angular distribution and the energy spectrum of this flux was made with experimental determinations in order to evaluate the validity of the approximations used in the calculations. (TAB)

47215 (AD-613375) A THEORETICAL STUDY OF THE VIBRATIONAL ENERGY LEVELS OF DIATOMIC MOLECULES. Final Technical Report, January 1960–June 1962. Beckel, Charles L. (Georgetown Univ., Washington, D. C.). 7p. (AFOSR-3031). CFSTI $1.00 cy, $0.50 mn.

A summary of research on vibrational energy levels in diatomic molecules is presented, along with a list of completed theses and papers either presented at scientific meetings or published in scientific journals. (TAB)

47216 (AD-613575) RESEARCH ON SOFT X-RAY ABSORPTION. Status Report. Holcomb, D. F. (Cornell Univ., Ithaca, N. Y.). Feb. 1965. Contract Nonr40137. 8p. CFSTI $1.00 cy, $0.50 mn.

The photoionization cross sections of xenon and krypton are being calculated from the model wave functions of McGuire and Tomboulian (Final States in Photoionization. Technical Report 4. (Cornell Univ., Ithaca, N. Y.). March 1964). By use of the same model, the atomic photoionization cross sections for elements near xenon in the periodic table can be calculated, thereby enabling separation of the atomic and solid state contributions to the cross section. Investigations are planned for extending the model to both higher and lower energies. (TCO)

47217 (AD-613582) ANNIHILATION OF POSITRONS IN METALS [Thesis]. Majumdar, Chanchal Kumar (California Univ., La Jolla, San Diego). Feb. 5, 1965. Contract Nonr221611. 307p. CFSTI $7.00 cy, $1.75 mn.

The theory of positron annihilation in metals, including electron-positron and electron-electron interaction, is discussed. It is well-known that the Coulomb force of the positron causes very major changes in the motion of the electrons. It is established that a sharp break in the angular correlation curve of the two gamma rays resulting from singlet state annihilation occurs at precisely those angles where it should be expected in the absence of electron-positron interaction. This makes positron annihilation in metals a useful tool for the investigation of the true Fermi surface. Taking advantage of such a break in the angular correlation curve, a simple experiment is proposed to measure the effective mass of the positron in metals. The experiment consists in a study of the temperature dependence of the angular correlation curve. It was found that an electron-positron bound state or a positronium-like state does not exist in metals. A more general result was derived: in a non-interacting electron gas in the presence of a localized external potential, there is no sharp distinction between bound and unbound states. (auth)

47218 (AD-613929) DIFFERENTIAL CROSS SECTIONS FOR ELECTRONS ELASTICALLY SCATTERED BY HELIUM ATOMS. Khare, S. P. (Queen's Univ., Belfast (Northern Ireland). Dept. of Applied Mathematics). 1965. Contract N62558 4297. 12p. CFSTI $1.00 cy, $0.50 mn.

The differential cross sections for the elastic scattering of electrons by helium atoms at a few selected electron impact energies, in the 10–50 ev energy range, were calculated by using the adiabatic-exchange phase shifts of Labhan and Callaway (1964) for the l = 0, 1, and 2 partial waves, and the static-dipole phase shifts for the higher partial waves. The calculated values are in satisfactory accord with the experimental data of Bullard and Massey (1931) and of Hughes, McMillen and Webb (1932) and with the theoretical values of Khare and Moiseiwitsch (1965), who included exchange only indirectly. The effect of quadrupole polarizability potential on the differential cross sections was also examined and found to be small. (auth)

47219 (AD-614253) STUDY OF PLASMA AMPLIFIERS. Final Report. Chow, K. K. (Microwave Associates, Inc., Burlington, Mass.). Feb. 15, 1965. Contract AF19(628)-452. 115p. (AFCRL-65-158). CFSTI $4.00 cy, $0.75 mn.

An investigation on the amplification of electromagnetic signals interacting with a plasma was carried out. Specifically, use of recombination radiation at optical frequencies was considered. Theoretical considerations for optical frequencies indicate that a low temperature plasma with high density, high degree of ionization is necessary. Thermal-contact ionization of cesium was chosen as the most suitable means. Fabrication of this plasma generator and the attendant technological problems are discussed in detail. Experimental results show that recombination radiation was obtained in this type of plasma. However, because of the low plasma density attainable, optical oscillation could not be initiated. Schemes are suggested to increase the density and degree of ionization. Studies on gas lasers were also carried out. Optical resonator modes in a Br_2–Ar laser were examined in detail. Excellent agreement between experimental and theoretical results was obtained. (auth)

47220 (NP-15175) MOBILITY OF NEGATIVE IONS IN O_2 AT LOW E/N. Technical Report 29. Voshall, R. E.; Pack, J. L.; Phelps, A. V. (Westinghouse Research Labs., Pittsburgh, Pa.). Apr. 1, 1965. Contract NONR-2584(00). 30p.

Measurement of negative ion mobilities in pure O_2 were made as a function of gas pressure (2-700 Torr), gas temperature (77.4 to 373°K), and electric field. Values of E/N, electric field over gas density, ranged from 6×10^{-18} to 6×10^{-17} v-cm^2 so that the ions were in thermal equilibrium with the gas. The ion mobility times gas density μN is independent of density for 195°K and above. Values of μN for this ion, O_2^-, are 5.7×10^{19}, 6.5×10^{19}, 6.8×10^{19} volt^{-1} sec^{-1}-cm^{-1} for temperatures of 195, 300, and 373°K, respectively. The density dependence of the measured mobilities at 77.4 and 87.6°K is consistent with an equilibrium between the concentrations of O_2^- and O_4^- ions. The low density data yield values of μN for the O_2^- ion of 4.7×10^{19} and 4.9×10^{19} volt^{-1}-sec^{-1}-cm^{-1} at 77.4 and 87.6°K. The μN value of O_4^- ions is $2.6 \pm 0.5 \times 10^{19}$ volt^{-1}-sec^{-1}-cm^{-1} at both temperatures. Correlation with models for the internal motion of O_4^- leads to an estimated dissociation energy of 0.06 ± 0.02 ev. (auth)

47221 (NYO-2403-8) CHEMICAL REACTIONS OF ATOMIC BEAMS AND RELATED PROBLEMS. Final Report. Peterson, N. C.; Marcus, R. A. (Polytechnic Inst. of Brooklyn, N. Y. Dept. of Chemistry). Oct. 3, 1965. Contract AT(30-1)-2403. 5p. Dep. mn; CFSTI $1.00 cy, $0.50 mn.

Modifications were made to the atomic beam apparatus to improve the operating characteristics and to permit operation using argon as well as helium beams. An electron bombardment ionizer was added, together with a beam chopper. This system is designed to permit measurement of inelastic scattering of neutral particles by measurement of the ion current. Experiments to measure the cross sections for scattering helium ions from helium gas were carried out. The results were affected by charging of surfaces in the vacuum system. The measurements will be repeated using a modified vacuum pumping system. (auth)

47222 (ORNL-tr-679) THERMAL IONIZATION OF Cu, Ag AND Ti WITH PURE POLYCRYSTALLINE W AND Re SURFACES AND THOSE COVERED WITH FOREIGN LAYERS. Weiershausen, Walter. Translated for Oak Ridge National Lab., Tenn. from Ann. Physik, 15: 30-48 (1965). 31p. Dep. mn; JCL $3.60 fs, $1.13 mf.

The surface ionization of Cu, Ag, Ti, on W and Re was investigated by means of a mass spectrometer. The degree of ionization α of the Langmuir equation was satisfactory for temperatures above 2000 to 2500°K. From the slope of the curves ln α (1/T) in this temperature range the effective work functions of the polycrystalline W was determined with $\phi_w = (4.55 \pm 0.1)$ ev and of the polycrystalline Re with $\phi_{Re} = (5.2 \pm 0.1)$ ev. In the range of lower temperatures considerable deviations of α result from the course given by the Langmuir equation. These can be attributed to changes in the work function $\Delta\phi$ which is confirmed by direct measurements of $\Delta\phi$ by means of a counter voltage method. This change in the work function is probably caused by the adsorption of residual gas components. However, condensation of the ionizing metals Cu, Ag, and mainly Ti also result in changes in the work function. In the theoretical summary the deviations from the Langmuir equation in the statistical imbalance and the influence of polycrystalline surfaces are discussed. (auth)

47223 A COMPILATION OF BETA-RAY STIMULATED X-RAY SPECTRA. Preuss, L. E.; Collins, H.; Wilson, E. R. (Edsel B. Ford Inst. for Medical Research, Detroit). Advan. X-Ray Anal., 8: 198-203(1965).

Photons resulting from the interaction of beta particles and matter have a certain complexity of origin; but the spectrum is made up, in large part, of two primary components. One of these is the white radiation continuum produced by the external bremsstrahlung mechanism of beta acceleration at the target atom. The second fraction consists of the characteristic K and L x rays of the target atom. Published beta-excited x-ray spectra are centered about a small fraction of the available pure beta emitters and a restricted group of target materials. Furthermore, intercomparisons between references are difficult, due to an infinite variety of source and detector parameters influencing the data. A comprehensive reference compilation of these spectra was begun on a comparative basis and simplified and standardized for cataloging and easy reproduction of the experimental design. The prime purpose is to make available coherent data for many beta-excited x-ray sources in which beta activities, target geometries, and other critical parameters are known, controlled, and constant. Spectral sets for given source–target combinations may, therefore, be intercompared, and application of the beta-excited x ray may be made with the best possible source–target atom combination. The spectra were studied by three proportional counters (operating down to the 1 kev energy range) and two standard scintillation crystals, accumulated in a 256-channel analyzer, and are presented in sets (representing one beta source–target combination) consisting of a minimum of eight spectra, six of which represent the most critical transmission target geometry. Examples of the cataloging of the spectral sets, for the mixture, apposition, and compound isotopic x-ray sources, are presented. (auth)

47224 HARTREE-FOCK WAVE FUNCTIONS FOR EXCITED STATES. THE 2^1S STATE OF HELIUM. Cohen, Maurice (Hebrew Univ., Jerusalem); Kelly, Paul S. Can. J. Phys., 43: 1867-81(Oct. 1965).

Hartree–Fock wave functions for the first-excited singlet states of several members of the helium isoelectronic sequence were calculated. It is shown that unphysically low energies result if the excited-state function is not constrained to be orthogonal to the ground-state eigenfunction, and the excited-state orbitals are chosen orthogonal. If the excited-state orbitals are not chosen orthogonal, the effect of the overall constraint is small, raising the total energy very slightly; however, the effect of imposing both constraints simultaneously is appreciable. It is concluded that the most satisfactory approximation involves nonorthogonal

excited-state orbitals, together with an overall orthogonality constraint towards the ground state. (auth)

47225 A PRECISE MEASUREMENT OF THE RANGE OF 100-Mev PROTONS IN ALUMINIUM. Portner, P. M.; Moore, R. B. (McGill Univ., Montreal). Can. J. Phys., 43: 1904-14(Oct. 1965).

The range of 100-Mev protons in aluminum was determined using the external beam of the McGill synchrocyclotron. The energy and range were determined for a finely collimated pencil beam with an energy spread of 0.12 Mev. Beam energy was measured by the floating-wire technique. Two range determinations yielded values of 9840 ± 9 mg/cm^2 at 99.88 ± 0.08 Mev and 9768 ± 10 mg/cm^2 at 99.58 ± 0.08 Mev. Range straggling was found to be in agreement with theory. The mean excitation potential in aluminum was estimated from these results to be 156 ± 2 ev. (auth)

47226 ON THE STUDY OF ION BEAM MACHINE. Kanaya, Koichi. Denki Shikensho Iho, 29: 109-19(Feb. 1965). (In Japanese).

An ion beam device, which consists of a hot cathode discharge type ion source, a focusing system, and a specimen stage, was designed to be used in such applications as micromachining, surface etching, and color recording. The maximum accelerating voltage and working current are 50 kv and 500 μA, respectively, in experiments using argon gas. It is shown by preliminary experiments that boring a hole in thin metals and metal surface etching without thermal effects are possible by using an ion beam with a high accelerating voltage. A color recording by an ion beam with a low current was tried. The carboneous layer contaminated by ion bombardment on a smooth surface of metal showed a colored pattern by light interference microscopy. By using a metal surface uniformly covered with collodion, color recording of the ion image was found to be more easily performed. It was therefore concluded that an ion color microscope may be realized. (auth)

47227 RESTUDY OF THE MUON CAPTURE IN HYDROGEN. Fujii, Akihiko (Jochi Univ., Japan). Genshikaku Kenkyu, 9: 726-31(Mar. 1965). (In Japanese).

The muon capture rate in hydrogen is reanalyzed with the newly published molecular parameters. The prediction is in good agreement with the experiment. (auth)

47228 COMPUTER STUDIES OF COPPER ATOM RANGES IN COPPER LATTICES. Harrison, D. E. Jr.; Leeds, R. W.; Gay, W. L. (Naval Postgraduate School, Monterey, Calif.). J. Appl. Phys., 36: 3154-61(Oct. 1965).

An n-body collision computer simulation model with a Gibson #2 potential is used to examine various ways in which the lattice nature of the slowing down material influences the motion of a medium-energy copper atom. For normal incidence upon a (110) surface, it is found that the lattice has a significant effect upon the scattering angle when a 10-kev copper atom strikes an atom of a copper lattice. The channel area, which comprises approximately 40% of the representative area in this orientation, is quite insensitive to the copper atom's energy above 1 kev. Total ranges are significantly longer than those reported by Robinson and Oen from calculations based upon a binary collision model. Below 1 kev, total ranges closely approximate the $E^{\frac{1}{2}}$ law reported by Kornelsen et al. Above 1 kev $dE/dx = A - B/E$ appears to describe the motion at all positions in the channel if the values of A and B are specified for the initial point at which the atom enters the channel. This behavior above 1 kev is clearly nonphysical. To be meaningful, even at intermediate energies, computer range studies must include inelastic energy losses. Lattices are known to focus atoms incident near the [110] direction into [110] channels. This mechanism was studied at the center of the channel with 1-kev atoms. The effect is anisotropic in the azimuthal angle, but it was found that atoms inside a 10° cone were always focused, and that 20° focusing occured in one orientation. Angular focusing was less effective at higher energies. Transverse oscillations in the channel were also considered. The "wave lengths" are proportional to $E^{\frac{1}{2}}$, but oscillations are usually not symmetric about the channel axis. Transverse motion is approximately harmonic, but the "vertical" and "horizontal" frequencies are never commensurable. There is evidence for a skimming mechanism in which high energy atoms are confined between (111) planes or to a lesser extent between (100) planes. Trajectories of 5-kev knock-on atoms are shorter than 40 Å unless the moving atom skims. One true channel event was found in 120 trials in which the moving atom started from a lattice site. (auth)

47229 ABSORPTION OF RESONANCE RADIATION AND FORMATION OF MOLECULAR IONS IN CESIUM VAPOR. Pollock, D. H.; Jensen, A. O. (Electro-Optical Systems, Inc., Pasadena, Calif.). J. Appl. Phys., 36: 3184-92(Oct. 1965).

The results of resonance absorption measurements in cesium vapor are reported. It is shown that the half-height width of the absorption (γ) is directly proportional to the neutral cesium density. Over the reduced pressure range of 0.2 to 10 Torr, $\gamma/k = 10^{-22}$ cm^3, where k is the photon-atom absorption cross section. Ionization measurements are reported describing the effect of the absorption of resonance radiation in cesium vapor. On the basis of the results presented, an ionization mechanism was hypothesized for the production of the cesium molecular ion (Cs_2^+) as the dominant ionic species in high-pressure, low-energy cesium vapor thermionic plasmas. The mechanism is based on the collision of two cesium atoms excited to the resonance level (1.45 or 1.38 ev). The excitation mechanism shifts from nearly complete photon-induced excitation at a cathode temperature of 2000°K to equal contributions of photon induced and electron induced excitation at a cathode temperature of 1550°K. At lower cathode temperatures, the excitation is accomplished primarily by electron impact processes. Single impact electron ionization processes are shown to be inadequate for neutralization in the plasma of low-energy discharges such as those found in cesium vapor thermionic converters. It is shown that for a condition of space charge neutralization in the plasma of low-energy cesium vapor discharges the ratio of excited state population density to ion population should be between 2.5 and 5 to 1. (auth)

47230 TRANSPOSITION OF THE THEORIES DESCRIBING SUPERCONDUCTING SYSTEMS TO MOLECULAR SYSTEMS. METHOD OF BIORBITALS. Bratoz, S. (Centre de Mecanique Ondulatoire Appliquee, Paris); Durand, Ph. J. Chem. Phys., 43: 2670-9(Oct. 15, 1965).

A new theory of the electronic structure of molecules is proposed, based on a wavefunction of the following type: $\phi^{SCF-BI} = NA\psi(1,2)\psi(3,4) \ldots \psi(2N \ldots 1,2N)$. This wavefunction is called the self-consistent-field biorbital wavefunction, and the factors $\psi(i,j)$ are called biorbitals. This function is discussed, the corresponding energy expression is derived, and the variational equations leading to the best possible ϕ^{SCF-BI} are presented. This theory is the molecular version of Blatt's theory of superconducting systems. (auth)

47231 ENERGY TRANSFER IN THE REACTION OF He^+ WITH O_2. Moran, T. F.; Friedman, L. (Brookhaven National Lab., Upton, N. Y.). J. Geophys. Res., 70: 4992-4(Oct. 1, 1965). (BNL-9248).

Retarded ion curves are given for oxygen ions resulting from $^3He^+ - O_2$ and $^4He - O_2$ interactions. These curves measure yields of ions at the mass spectrometer detector as a function of retarding repeller voltage in the ion source. The experimental results at low reactant ion velocities indicate that only a very small fraction of the $He^+ - O_2$ reaction can proceed via accidentally resonant dissociative charge transfer. The difference in shapes of the retarded ion curves clearly indicates that He^+ ions when neutralized by reaction with O_2 carry off kinetic energy. (J.F.P.)

47232 INTERFEROMETRIC WAVELENGTHS OF THORIUM LINES BETWEEN 9050 AND 2566 A. Littlefield, T. A.; Wood, Anne (Univ. of Newcastle upon Tyne, Eng.). J. Opt. Soc. Am., 55: 1509-16(Nov. 1965).

486 vacuum wavelengths of the thorium spectrum in the

range 9050–2566 Å were measured by comparison with the isotope Kr 86 line at 6057 Å, by using a reflecting echelon interferometer crossed externally with a Littrow spectrograph. Tests of accuracy by recurring interlevel differences indicate that the average error is about 1 in 10^7. Details are given of the sealed-off Schüler tube used as the thorium source. Difficulties which arose from the use of an Ebert spectrograph to photograph the spectrum are discussed. (auth)

47233 ON THE DISPLACEMENT OF THE ENERGY LEVELS OF ATOMIC SYSTEMS IN STRONG RADIATION FIELDS. Kronig, R.; Ooms, G.; Rijnierse, P. J. Kgl. Norske Videnskab. Selskabs, Forh., 37: 63-8(1964).

The shift produced in the energy levels of an atomic system by a radiation field is extended beyond previous results by considering an atomic system in a degenerate state in which a number of sub-levels coincide. Not only is the energy shift considered, but also the possibility of a partial or complete removal of the degeneracy by the radiation field. The order of magnitude for the shift, calculated from the derived expression, which can be obtained for a polar diatomic molecule with the beam of a strong pulsed laser is of an order of magnitude that falls within the possibility of experimental test. (J.F.P.)

47234 INTERACTION OF INTENSE RADIATION WITH ATOMIC PARTICLES. Gardner, J. W. (English Electric Co. Ltd., Whetsone, Leics, Eng.). Nucl. Energy, 241-8 (Aug. 1965).

For arbitrarily high radiation fluxes there is a significant probability of two or more photons interacting "simultaneously" with a scattering center such as a free electron, atom, ion, molecule or colloidal particle. Numerical orders of magnitude are assessed for the probability of occurrence of such multiphoton processes when scattering centers are exposed to the intense radiation fluxes associated, e.g., with focused laser beams and thermonuclear plasmas. A result of some practical relevance is the prediction of a finite probability for excitation and ionization of atoms or molecules, by multiphoton absorption, in situations where single-photon absorption is energetically forbidden by the quantum rules. (auth)

47235 ON THE SHAPE OF ZEEMAN AND STARK COMPONENTS OF SPECTRAL LINES IN THE MICROWAVE REGION AT LOW PRESSURE AND HIGH TEMPERATURE. Di Giacomo, A. (Scuola Normale Superiore, Pisa, Italy; Universita, Pisa, Italy; Istituto Nazionale di Fisica Nucleare, Pisa, Italy). Nuovo Cimento (10), 36: 916-34(Apr. 1, 1965).

The shape of Zeeman and Stark components of spectral lines in the microwave region for gases at low pressure and high temperature is related to the intermolecular interaction. (auth)

47236 TWO-PHOTON ABSORPTION IN ATOMIC OR MOLECULAR SYSTEMS. Fornaca, G.; Iannuzzi, M.; Polacco, E. (Universita, Pisa, Italy). Nuovo Cimento (10), 36: 1230-6(Apr. 16, 1965).

The possibility of observing two-photon absorption, due to the term $(e^2/2mc^2)A^2$ in the interaction hamiltonian of an atomic or molecular system with an electromagnetic field, is considered. The dependence of these processes on the coherence and polarization of radiation is studied. It is found that two-photon absorption between states with different parity should be readily observable by using a laser. (auth)

47237 CALCULATION OF EFFECTIVE CROSS SECTIONS FOR THE IONIZATION OF HYDROGEN ATOMS BY ELECTRON IMPACT. Veldre, V. Ya.; Vinkalns, I. Zh. Opt. Spectry. (USSR) (English Transl.), 18: 507-8(May 1965).

In order to clarify the question of the capabilities of various approximate methods of calculation, a computer was used to numerically evaluate effective cross sections for ionization of atomic hydrogen by electron impact in the following approximations: the approximation of distorted waves both neglecting polarization effects and considering polarization effects; and the approximation in which both the electrons after ionization are described by Coulomb functions without exchange, with exchange, and considering both exchange and deformation of the incident wave. The results of the calculations of the total ionization cross sections, including the polarization potential are shown. Since the curves differ little from each other, it is concluded that the polarization effects have very little influence upon the total ionization cross section. (J.F.P.)

47238 HIGHER PARTIAL WAVES IN POSITRON-HYDROGEN SCATTERING. Kleinman, Chemia J.; Hahn, Yukap; Spruch, Larry (New York Univ., New York). Phys. Rev., 140: A413-25(Oct. 18, 1965).

The minimum-principle (MP) formulation of scattering theory is applied to the study of the scattering of positrons by atomic hydrogen for a number of incident energies between 0 and 6.8 ev, the threshold for pickup. Rigorous lower bounds, η_1 (MP) and η_2 (MP), are obtained on the p-wave (L = 1) and d-wave (L = 2) phase shifts, η_1 and η_2. The method requires the exact numerical solution of the scattering wave function and of the Green's function of the static (one-body) equation, and the orthogonalization of the trial function $Q\Psi_t$ to the ground-state wave function; at that stage the method proceeds as in a standard variational calculation. $Q\Psi_t$ includes contributions from hydrogenic states with angular momenta l_1 = 0,1,2, and 3 for L = 1, and l_1 = 0,1, and 2 for L = 2; the associated radial functions contain arbitrary, variational parameters, as do the radial functions associated with the positron. Contributions from each l_1 to the total η_L (MP), and the effects of the coupling of different l_1, are studied, and extrapolation estimates of η_1 and η_2 are obtained. The rigorous (variational) bounds and the estimates based on extrapolation are compared with close-coupling and other previous estimates and, at very low energies, with predictions based on long-range polarization effects. (auth)

47239 REARRANGEMENT COLLISIONS—ELECTRON EXCITATION OF He(2^3s). Joachain, Charles J. (Univ. of California, Berkeley); Mittleman, Marvin H. Phys. Rev., 140: A432-6(Oct. 18, 1965). (UCRL-12493).

There are many formal expressions for the T matrix for a rearrangement collision. First-order approximations to the exact wave functions in the different expressions yield different numerical results for the cross section. Eight forms of the T matrix were chosen, and the eight cross sections were evaluated for electron excitation of He(2^3s), which is a pure rearrangement collision when spin-dependent forces are neglected. The projection-operator formalism for T yields good agreement with experiment. (auth)

47240 ELECTRONIC g FACTORS OF LOW-LYING LEVELS OF Fe I, Cr I, AND Mn I. Childs, William J.; Goodman, Leonard S. (Argonne National Lab., Ill.). Phys. Rev., 140: A447-51(Oct. 18, 1965).

The atomic-beam magnetic-resonance technique was used to measure the electronic g factors of 11 low-lying levels in Fe I, Cr I, and Mn I. Both odd-A isotopes (which show hfs) and even-A isotopes were used for the study. The theoretical implications of the results are discussed. (auth)

47241 SINGLET-TRIPLET MIXING CORRECTION TO THE HYPERFINE STRUCTURE OF THE ^{3}He ATOM. Sternheim, Morton M. (Stanford Univ., Calif.). Phys. Rev. Letters, 15: 545-6(Sept. 27, 1965).

The ratio of the hyperfine structure of the He^3 atomic state 2^3S_1 to the hfs of the He^{3+} ionic state $2^2S_{\frac{1}{2}}$ is insensitive to nuclear structure effects. Therefore it provides a clean test of the quantum electrodynamic corrections to hfs and to the two electron system. It is found that including the mixing of the singlet and triplet 2S states by the hyperfine interaction leads to a further 8.9-ppm decrease in the atomic hfs, thereby bringing the calculated and measured atom/ion ratios into agreement. The new value for the difference between the theoretical

and experimental atom/ion hfs ratios is found to be -3 ± 3 ppm. (J.F.P.)

47242 REFLECTION OF VERY SLOW ELECTRONS ON METAL SURFACES. Niedermayer, R.; Hoelzl, J. (Technische Hochschule, Clausthal, Ger.). Phys. Status Solidi, 11: 651-6(Oct. 1965). (In German).

The (110) face of a single crystal of tungsten is bombarded in an ultrahigh vacuum with monochromatic electrons (energy width 0.1 ev). The dependence of the number of elastically reflected electrons on the primary energy in the range 0 to 1.5 ev is studied in the first place as a function of certain gas layers of N_2 and H_2. This measurement is then repeated with the target absolutely free from any gas coverage during measurement. The coefficient of reflected electrons measured using a clean target surface is substantially greater than that calculated by Nordheim on the basis of an image force model. The results are in very good agreement with those of Hutson but disagree with measurements reported by Shelton and Kisliuk. (auth)

47243 EXCITATION AND IONIZATION OF ATOMIC HYDROGEN FROM VARIOUS STATES. Vriens, L. (Universiteit, Utrecht). Physica, 31: 1081-90(July 1965).

For large energies E_1 of the impinging electrons, the cross sections Q for optically allowed excitation and ionization of atoms are given by $Q = A/E_1 \ln cE_1$, where A and c are constants for one transition. For excitation A is proportional to the optical oscillator strength for the transition. For ionization A is proportional to a quantity M_i^2 which can be derived with one of the sum rules for the oscillator strengths. For excitation, values of cU (U is excitation energy) are calculated using known values of Born cross sections for large E_1 or using known values of quantities related to cU. It is indicated how excitation cross sections for small E_1 can be calculated approximately with known values of A and c. It is pointed out that this method probably will be more reliable than classical methods. For ionization, values of M_i^2 and cU_i (U_i is ionization energy) are calculated. Large discrepancies between cU_i values for the same transitions are found, when calculated from (theoretical) cross sections given by different authors. As a possible explanation of these discrepancies, it is indicated that the contribution of the optically disallowed transitions to the total cross sections can be very important, even for large E_1. Further, a comparison with classical collision theories is made. (auth)

47244 BINDING ENERGIES OF POLYATOMIC ^{4}He-MOLECULES. Schmid, E. W. (Max-Planck-Institut fuer Physik und Astrophysik, Munich); Schwager, J.; Tang, Y. C.; Herndon, R. C. Physica, 31: 1143-51(July 1965).

The binding energies, mass distributions and two-particle correlation functions of polyatomic ^{4}He-molecules are investigated with the (12-6) potential LJ1. A variational calculation is performed. Additional information on the energy eigenvalues is obtained from the expectation values of the square of the Hamiltonian. Integrations are carried out by a Monte Carlo method. The results show that three ^{4}He-atoms are bound by about 0.08°K and would be bound even if the well depth parameter of the potential were only 0.95 instead of 0.99. From He_9 to He_{10}, the binding energy per atom increases almost linearly and reaches 10 per cent of the experimental value of that of the liquid. The rms-radius has a minimum of 5.1 Å at He_7 and reaches 5.3 Å at He_{10}. (auth)

47245 ABSOLUTE CROSS SECTIONS FOR SIMULTANEOUS IONIZATION AND EXCITATION OF N_2 BY ELECTRON IMPACT. McConkey, J. W.; Latimer, I. D. (Queen's Univ., Belfast). Proc. Phys. Soc. (London), 86: 463-6(Sept. 1965).

Cross sections for the excitation of the $B\,^2\Sigma$ state of N_2^+ by electron impact on N_2 were measured using a crossed beam technique. Maximum cross sections for the v = 0 and v = 1 levels are 20.5×10^{-18} cm^2 and 1.7×10^{-18} cm^2, respectively. The ratio of effective cross sections of the (0,0), (0,1) and (0,2) bands of the $B\,^2\Sigma - X\,^2\Sigma$ system is 1:0.32:0.075. Comparisons are made with theoretical predictions and the results of other workers. (auth)

47246 THE IONIZATION OF INERT GAS ATOMS BY ELECTRON AND PROTON IMPACT AT HIGH ENERGIES. Kingston, A. E. (Queen's Univ., Belfast). Proc. Phys. Soc. (London), 86: 467-76(Sept. 1965).

At large impact energies E, the cross sections Q, for the electron or proton ionization of the inert gas atoms, are written in the form $QE = A \log E + B$. A is calculated using theoretical and experimental values of the photoionization cross sections. The calculated A's are in good agreement with the proton ionization of Hooper et al. but disagree with the electron ionization data of Schram et al. It is found that the electron ionization data of Golden and Rapp and of Smith are not sufficiently accurate to give reliable values for A. However, when the calculated values of A are normalized to these electron ionization data at impact energies between 20 and 30 atomic units we can obtain estimates for the B's which are in good agreement with the proton ionization data. These B's differ greatly from those of Schram et al. (auth)

47247 THE APPLICATION OF AN ITERATION-VARIATION METHOD TO ATOMIC SCATTERING PROBLEMS. McEachran, R. P. (University Coll., London); Fraser, P. A.; Wallace, J. B. G.; Tull, C. E. Proc. Phys. Soc. (London), 86: 477-89(Sept. 1965).

An iteration-variation method applicable to elastic and inelastic atomic collision problems is described. The method uses trial functions formed from a sequence of Born iterations and, making use of recursion relations, is able to save much computer storage space, particularly in inelastic problems. Convergence is speeded in cases where the iterations themselves converge, and is obtained also from diverging sequences of iterations. Examples are presented from electron-helium collisions (elastic), positron-hydrogen collisions (elastic) and electron-hydrogen collisions (elastic and inelastic). (auth)

47248 A NARROW RESONANCE IN THE ELASTIC SCATTERING OF ELECTRONS BY HELIUM. Kwok, K. L.; Mandl, F. (Univ. of Manchester, Eng.). Proc. Phys. Soc. (London), 86: 501-11(Sept. 1965).

Using a variational principle, a narrow ^2S resonance of the He^- system just below the first excited state of helium was calculated. The position of this resonance is $E_R = 19.5^{+0}_{-0.2}\frac{1}{2}$ ev and the width Γ_R lies in the range 0.8×10^{-2} ev to 3×10^{-2} ev, or possibly a little higher. The dependence of the width on the structure of the resonant state was analyzed for two alternative expressions. (auth)

47249 THE LONG-RANGE INTERACTION OF THREE ATOMS. Bell, R. J. (National Physical Lab., Teddington, Eng.). Proc. Phys. Soc. (London), 86: 519-21(Sept. 1965).

A simple method proposed for evaluating the van der Waals constant is extended to give the non-additive third-order perturbation energy for three interacting atoms separated by large distances. For three hydrogen atoms in their ground states, separated by distances R_1, R_2 and R_3, the leading term is calculated as $\epsilon_0^{(3)} = (43.2854 \pm 0.0020)\Omega R_1^{-3}R_2^{-3}R_3^{-3}\alpha_0^3$ ryd where Ω is an angular factor. This result compares favourably with the previous most accurate estimate $\epsilon_0^{(3)} = 42.8\Omega R_1^{-3}R_2^{-3}R_3^{-3}\alpha_0^3$ ryd obtained by Midzuno and Kihara. (auth)

47250 RELATIVISTIC SELF-CONSISTENT FIELDS. Grant, I. P. (Atlas Computer Lab., Chilton, Eng.; Pembroke Coll., Oxford). Proc. Phys. Soc. (London), 86: 523-7(Sept. 1965).

The work reported by Grant in 1961 on matrix elements of two-electron interactions is extended by providing sum rules for the elements of the magnetic part of the Breit interaction over closed groups. (auth)

47251 ELECTRON INTERACTION COEFFICIENTS IN RELATIVISTIC SELF-CONSISTENT FIELD THEORY. Cooper, J. R. A. (National Physical Lab., Teddington, Eng.). Proc. Phys. Soc. (London), 86: 529-33(Sept. 1965).

Coefficients of direct and exchange integrals occurring in relativistic self-consistent field theory are tabulated for the electrostatic interaction involving electrons of f

or $\bar{g}$ type; reference is made to a recent tabulation of the corresponding coefficients for the magnetic interaction involving electrons up to f type. With these coefficients it is now practicable to calculate relativistic Hartree-Fock self-consistent field wave functions for the ground states of all the naturally occurring elements. (auth)

47252 A METHOD FOR THE DIRECT MEASUREMENT OF SMALL ENERGY LOSSES OF RELATIVISTIC PARTICLES. Aitken, D. K.; Jennings, R. E.; Walker, R. N. F. (University Coll., London). Proc. Phys. Soc. (London), 86: 674-6(Sept. 1965).

A method is described for the measurement of small energy losses of relativistic particles by balancing the signals from two gas Čerenkov detectors. (auth)

47253 THE IONIZATION OF H AND He^+ BY ELECTRON IMPACT. Burke, P. G.; Taylor, A. Joanna (Atomic Energy Research Establishment, Harwell, Berks.). Proc. Roy. Soc. (London), Ser. A, 287: 105-22(Aug. 17, 1965).

The ionization cross-sections of H and He^+ from the ground state and excited 2s state for incident electron energies from threshold to about four times threshold energy are calculated. The strong coupling between the hydrogenic 1s, 2s and 2p states is explicitly allowed for in the initial state, and the final state is taken to be an appropriate combination of Coulomb wave functions of the two outgoing electrons. Comparison with experiment for ground-state ionization shows that the method is an improvement over the Born approximation particularly for He^+. New results are presented for the Born approximation in He^+ ionization and for the Born–Oppenheimer approximation for both H and He^+ ionization. Finally, conclusions are drawn from the results concerning the validity of methods for calculating ionization cross-sections from excited states. (auth)

47254 EFFECTIVE SPIN HAMILTONIAN FOR NONORTHOGONAL ORBITALS. I. LINKED-CLUSTER EXPANSION. Yonezawa, Fumiko (Kyoto Univ.). Progr. Theoret. Phys. (Kyoto), 34: 210-33(Aug. 1965).

The Heitler-London energy is given by a quotient, both the numerator and denominator of which seem to increase without limit when the number of atoms, N, becomes large. The diagram method is used to meet the situation and to show that this difficulty of divergence is spurious; the divergent denominator cancels the corresponding factor from the numerator. As a result, the energy expression as well as the effective expectation value of any operator is represented by certain appropriate linked-clusters, each of which is proportional to N. The linked-cluster expansion not only ensures that the nonorthogonality catastrophe does not really arise but also provides the systematic way to calculate the energy spectra and other physical quantities to a desired order. Now that the present method is free from any restrictions on the magnitude of the overlap integrals, this is a rigorous and general proof on the validity of the Heitler-London scheme for infinite systems. (auth)

47255 TIME DEPENDENT PROBLEMS OF SCATTERING IN LINEAR LATTICE SYSTEM. Sabata, Hideki; Nakazawa, Hiroshi; Teramoto, Ei (Kyoto Univ.). Progr. Theoret. Phys. (Kyoto), 34: 313-14(Aug. 1965).

A harmonically coupled chain is considered with an isotopic impurity atom at the origin. Two special cases are investigated, in order to show the establishment of the stationary case. In both cases the system approaches the stationary state which agrees with the solution of the time independent scattering problem previously mentioned. Damping of the distorted waves which appear at finite t can be also analyzed, especially when $m' > 2m$ there is an additional pole on the negative real axis. This additional pole corresponds to the exponential damping term, discussed previously as a problem of Brownian motion. It is shown that the scattered wave becomes singular for the pure imaginary value of ω and it corresponds to this damping factor. (J.F.P.)

47256 INTEGRATED SPECTRA OF AN ISOTOPICALLY DISORDERED LINEAR CHAIN. Matsuda, Hirotsugu; Teramoto, Ei (Kyoto Univ.). Progr. Theoret. Phys. (Kyoto), 34: 314-15(Aug. 1965).

The exact value of the integrated spectrum per atom was obtained for an elastically coupled isotopically disordered diatomic-linear chain of infinite length. It is pointed out that for any rational number there exists a finite critical value such that if the mass ratio of different isotopes exceeds this critical value then a function of the rational number becomes a special frequency at which frequency the spectrum vanishes independently of the composition ratio and arrangement of the atoms. It is shown that by virtue of the property of special frequencies the integrated spectrum at any frequency can be obtained as long as the ratio of different isotopes is equal to or greater than the function of a ratio of two integers, prime to each other and such that the numerator exceeds the denominator. (J.F.P.)

47257 TWO-ELECTRON SCATTERING DUE TO s-d INTERACTION. Kondo, Jun; Zohta, Yasuhito (Electrotechnical Lab., Tokyo). Progr. Theoret. Phys. (Kyoto), 34: 325-6(Aug. 1965).

It was previously shown that there is an interaction between the conduction electrons when these are interacting with localized spins through the s-d interaction. When the consequent process of two-electron scattering is taken into account by the perturbation theory in calculating the resistivity, the relaxation time of localized spins, etc, the difficulty of the divergence of the results arising from the vanishing denominators is encountered. A solution for the difficulty is shown, and it is noted that the results obtained in a convergent form are of the same magnitude as the first term of the perturbation expansion. The relaxation time of the localized spins are considered. (J.F.P.)

47258 BIBLIOGRAPHY OF ATOMIC AND MOLECULAR COLLISIONS. [PART] I. Takayanagi, Kazuo (Saitama Univ., Urawa, Japan). Sci. Rept. Saitama Univ., Ser. A., 5: 14-48(1965).

A list of published works is given on heavy particle collisions with electronic transitions (theory); rotational and vibrational transitions in collisions (theory); and theory of intermolecular forces. Under heavy particle collisions, atom–atom, atom–molecule, and molecule–molecule (and their ions) collisions are included. Collisions of three heavy particles are also included. A very brief note is given for each reference as an indication of some features of the work. (L.B.S.)

47259 EFFECT OF THE ATOMIC SCREENING FACTOR ON THE INELASTIC SCATTERING OF ELECTRONS. Nakhodkin, N. G.; Ostroukhov, A. A.; Romanovskii, V. A. (Shevchenko State Univ., Kiev). Soviet Phys.-Solid State (English Transl.), 7: 1014-16(Oct. 1965).

Translated from Fiz. Tverd. Tela, 7: 1256-9(Oct. 1965).

The angular dependence of the inelastic reflection coefficient was calculated using the model of continuous losses and allowing for the screening effect. The selected approximation for the scattering cross section made it possible to carry out the calculations by means of a reduction formula. The results are shown for beryllium at initial electron energies $E_0 = 1$ and 100 Mev for aluminum at $E_0 = 2$ and 100 kev, and for gold at $E_0 = 5$, 10, and 100 kev. The data for 100 kev agree with previous calculations carried out without allowance for the screening to within $\leq 1\%$. It is also found that, both for heavy and light substances, the angular dependence of the reflection coefficient varies little with changes in the primary electron energy, when screening is taken into account. (L.B.S.)

47260 STIMULATED RADIATION FROM HYDROGEN AND DEUTERIUM MOLECULES IN THE NEAR INFRARED REGION. Bazhulin, P. A.; Knyazev, I. N.; Petrash, G. G. (Lebedev Inst. of Physics, Moscow). Zh. Eksperim. i Teor. Fiz., 49: 16-23(July 1965). (In Russian).

Results of investigation of stimulated radiation from hydrogen and deuterium molecules or mixtures of them are presented. Stimulated radiation from the latter two gases were obtained for the first time. A mechanism for occupation of the vibrational levels of the operating levels

based on the Franck–Condon principle is discussed in detail for H_2, D_2 and HD molecules. The results are compared with the experiments which confirm the inversion mechanism. (auth)

47261 RADIOOPTICAL RESONANCE OF ATOMS IN STRONG MAGNETIC FIELDS. Pokazan'ev, V. G.; Skrotskii, G. V. (Ural Polytechnical Inst., USSR). Zh. Eksperim. i Teor. Fiz., 49: 163-9(July 1965). (In Russian).

Resonance phenomena are considered in a system processing an electron angular momentum J and nuclear moment I in a strong magnetic field. An expression is derived for the intensity of reradiated light when microwave and radio-frequency fields are applied to the system. It is shown that the light intensity appreciably changes on approach to the nuclear resonance frequency. This phenomenon can be employed for investigating experimentally the hyperfine structure of atoms. (auth)

47262 CONCERNING ANGULAR REGULARITIES IN THE SMALL ANGLE SCATTERING OF INERT GAS IONS. Mashkova, E. S.; Molchanov, V. A. Zh. Tekhn. Fiz., 35: 1321-3(July 1965). (In Russian).

The scattering of 30 kev Ar^+ and Ne^+ ions from a polycrystalline copper surface was investigated at scattering angles from 5 to 28°, employing as a detector an electrostatic analyzer that has been described elsewhere. The investigation was undertaken to obviate possible criticism of earlier work in which ions that were neutralized in the scattering were detected with a secondary electron emission instrument, although it was previously shown that the energy dependence of the secondary emission coefficient and fast sputtered target atoms could not have given rise to significant errors. The scattered ion spectra consisted of narrow peaks corresponding to singly, doubly, and triply charged ions. The angular dependence of the intensity of the singly charged ion peak agreed with that obtained in the previous work for ions that were neutralized in the collision. The energies of the scattered ions were close to the energy expected for an ion that had undergone a single collision with a target atom. The number of ions that increased their charge in the scattering was an order of magnitude less than the number of those that were scattered without change of charge, and the number of sputtered target atoms that became ionized was small compared with the number of ions that were scattered with loss of charge. (ATD)

47263 AN INVESTIGATION OF SECONDARY ELECTRON EMISSION FROM SEVERAL SOLIDS (thesis). Ghalib, Hisham Ali. Cincinnati, Univ. of Cincinnati, 1964. 141p.

Secondary electron emission due to the electron bombardment of copper and aluminum plates, a thin film of copper on an aluminum plate (complex target), and two single crystals of silicon was studied. The secondary emission device used was an electron-gun type tube with a spherical collector. The experimental investigations include the determination of the total secondary yield under both normal and oblique incidence of primary beams and the determination of the energy distribution of the low-energy secondary electrons. The theoretical phase of the work includes a discussion of several theories representing three different approaches to the problem of the production and the escape mechanisms of the secondary electrons. Specifically, the theories discussed are some of the elementary theories, Baroody's free electron theory, and Wooldridge's quantum mechanical theory. (A.G.W.)

47264 A STUDY OF THE SCATTERING OF TWO HYDROGEN ATOMS IN THE BORN-OPPENHEIMER APPROXIMATION (thesis). Lebedeff, Serge). Berkeley, Calif., Univ. of California, 1964. 91p.

Calculations of the scattering amplitude describing collisions of two hydrogen atoms are presented. Only low-energy elastic scattering is considered and all spin interactions are neglected. The problem is discussed within the Born-Oppenheimer approximation, which permits the introduction of a potential for the description of the interaction between the atoms. Most of the calculations were done with the potentials of the Lennard-Jones type, although some calculations were based on the best potential that could be found in the literature. The exact solution is compared in detail with the solutions obtained using several different approximation methods. The J.W.K.B. method is found to be surprisingly accurate at higher than thermal energies. The model of Purcell and Field is shown to be in qualitative but not in quantitative agreement with the exact calculations. Some simple modifications in the model of Purcell and Field are proposed, which improve the accuracy of the model. A detailed analysis of the total scattering cross sections is presented. Certain kinds of maxima that occur in the total scattering cross sections are related to the properties of the phase shifts as functions of energy and angular momentum. The applicability of the semi-classical approximation for the differential cross sections is investigated. The influence of the identity of the atoms on the scattering cross section is discussed. (Dissertation Abstr.)

47265 AN APPROXIMATE METHOD FOR THE EVALUATION OF HOMONUCLEAR DIATOMIC MOLECULAR ORBITALS AT SMALL INTERNUCLEAR SEPARATIONS (thesis). Fenton, David George. Storrs, Conn., Univ. of Connecticut, 1964. 92p.

In Section II there is presented a general review of several important areas of molecular structure including a description of the one-electron molecular orbital approach to the electronic structure of the general diatomic molecule, a description of the molecular states appropriate to the entire molecule, and an accounting of the manifold of molecular terms arising from given initial atomic states of the atoms from which the molecule is derived. In addition, there is presented the accepted theory for the correlation of the electronic states at large separations of the atoms in the molecule with those at vanishingly small separations. Current methods available for the construction of the molecular orbital wave functions, the LCAO and SCF LCAO methods, are reviewed. The well-known exact treatment of the hydrogen molecular ion problem is given in Section III. Correlation of the energy levels in the H_2^+ ion is also discussed. In Section IV is presented an approximate method for the determination of the wave functions and the energy eigenvalues of the molecular orbitals of a homonuclear diatomic molecule at small internuclear separations. Solutions of the wave equation in spheroidal coordinates are derived in simple analytic form under the assumption of a screened two-center Coulomb field, the screening function being given by a certain analytic expression. This can be made to approximate closely the screening function that follows from the Thomas-Fermi statistical model for small internuclear separations. It is shown that with the screening function here set down, the solutions of the Schroedinger equation for an n-electron molecule are readily derived from the known exact solutions for H_2^+ given in Section III. Changes result only in the analogs of the radial parts of the latter solutions, and one obtains approximately self-consistent solutions for the general case at any small internuclear separation. To exemplify the method, computations were carried out for the states of N_2 that are occupied in the ground state of this molecule, and for separations of 0.1, 0.2, 0.4, and 1.1 Bohr radii. The predicted energies are found to lie in the correct region of the energy correlation diagram. (A.G.W.)

47266 AVERAGE IONIC CHARGE OF HELIUM AND HYDROGEN BEAMS IN CADMIUM VAPOR. Torres, P. 10p. (CONF-650410-44). Gmelin, AED-CONF-65-073-80.

From American Physical Society, Washington, D. C.

The experiments reported are part of a study of the relation between the effective electric charge of a beam in the solid and gaseous phases of the same target material. It is hoped ultimately to learn whether the effective charge as obtained by magnetic analysis of the beam and as deduced from the stopping power are the same. The ambient or target material is cadmium because its high

vapor pressure makes the gaseous phase easy to prepare. The beams studied are hydrogen, helium, and deuterium atoms and ions in the velocity range 2.4 to 6.9 × 10^8 centimeters per second. A schematic diagram is shown of the apparatus used. The equilibrium fractions of a hydrogen beam in cadmium vapor are given, and the results for the charge composition of a helium beam in cadmium vapor are shown. (J.F.P.)

47267 COMPOSITION OF NOBLE GAS ION BEAMS PRODUCED WITH A DUOPLASMATRON. Zieske, P. L.; Braams, C. M.; Kofoid, M. J. 6p. (CONF-641108-45). Gmelin, AED-CONF-64-196-78.

From American Physical Society, New York.

The general experimental performance of the duoplasmatron ion source, the analysis of ion species in the beam, the focusing and simultaneous reduction of velocity of the ion beam prior to its entering the plasma, the design of test chamber apparatus, the means for time and power control of the high-frequency power generator, and matching the high-frequency generator to the work load for large power transfer are being studied. Ion beams of the noble gases helium, neon, argon, krypton, and xenon were analyzed using a mass spectrometer. (F.J.H.)

Cosmic Radiation

See also Elementary Particles and Radiations. Nuclear Properties and Reactions.

Refer also to abstract 47451.

47268 (INSJ–86) MEAN SQUARE ANGULAR AND LATERAL SPREADS OF ELECTRONS AND PHOTONS IN A CASCADE SHOWER. Misaki, Akeo (Institute for Nuclear Study, Tokyo Univ. (Japan)). June 6, 1965. 111p. Dep. mn.

Mean square angular and lateral spreads of electrons and photons in a cascade shower initiated by a photon are calculated over wide ranges of energy ratio and observational depth under approximation A with Landau approximation according to Nishimura and Kamata's theory. Corresponding quantities weighted with energy of the shower particle are also obtained. The results are presented in the form of graphs and tables. Results are compared with those of Chartres and Messel, and their results for lateral spreads are indicated to be not reliable. The results are also compared with those of Monte Carlo calculations given by Adachi and others, and the agreement between those results is quite well. (auth)

47269 ASYMPTOTIC DIRECTION OF ARRIVAL OF CHARGED PARTICLES IN THE EARTH'S MAGNETIC FIELD. Lanz, Giovanni (Northwestern Univ., Boston). Am. J. Phys., 33: 740-4(Sept. 1965).

The motion of charged particles in the earth's magnetic field was investigated. Attention was given to the motion in the equatorial plane. It is shown how, from the knowledge of the angle of arrival, particle species and energy, for a value of the impact parameter, the asymptotic direction of arrival can be calculated in closed form. The results of calculations are shown. (auth)

47270 SATELLITE OBSERVATIONS OF LOW-ENERGY PRIMARY COSMIC RAY NUCLEI OF CHARGES Z ≥ 6. Lim, Y. K. (Emmanuel Coll., Boston); Fukui, K. J. Geophys. Res., 70: 4965-7(Oct. 1, 1965).

A study of low-energy heavy nuclei using emulsions exposed in a recoverable satellite are reported. The stack of emulsions was exposed for 4.1 days under 2.1 g/cm^2 of matter in a satellite launched into near-polar orbits, and stopping tracks of primary cosmic ray nuclei of charges Z ≥ 6 were studied. Charge identification was made by means of δ-ray counting, track area, and photometric track width measurements. Differential energy spectra of medium, heavy and very heavy nuclei after extrapolation to outside the vehicle are shown. These data show an apparent lack of evidence of ionization loss to interstellar matter. (J.F.P.)

47271 THE STRONGLY INTERACTING PARTICLES IN AIR SHOWER CORES. Winn, M. M.; Wand, R. H.; Ulrichs, J.; Rathgeber, M. H.; Poole, P. C.; Nelson, D.; McCusker, C. B. A.; Jauncey, D. L.; Crawford, D. F.; Bray, A. D. (Univ. of Sydney). Nuovo Cimento (10), 36: 701-32(Apr. 1, 1965).

The results of an experiment to study the strongly interacting particles in air shower cores are presented. The experiment used 64 large plastic scintillators in three different close configurations, two Wilson cloud chambers, about 600 G-M counters, and 100 tons of lead. It is shown that there is no unique structure function for the strongly interacting particles which fits all showers. Rather, showers can be classed as single-core or multi-core. Single-cored showers appear to be due to proton primaries; multi-cored showers to be due to primaries of A ≥ 2. There is some evidence that deuterons form about 5% of the hydrogen nuclei in the cosmic radiation at total energies of ~4 × 10^{14} ev. Above a shower size of 10^6 particles 47 multi-cored showers and 7 single-cored showers were observed. Between sizes of 10^5 and 10^6 particles 68 multi-cored showers and 85 single-cored showers were seen. It proved possible with this apparatus to study not only individual showers in detail, but also individual nuclear interactions in these showers. In contrast with much emulsion work the surviving baryon can often be easily identified and its momentum determined. It is found that the elasticity in individual nucleon-air nucleus collisions varies from 0.3 to 0.7 with a median value of 0.54. A method of obtaining the average value of the elasticity for energies of 10^{12} to 10^{16} ev is described. In ~400 individual mesons studied none were found with transverse momenta in the region ≥4 Bev/c. Interactions were identified at heights above the array varying from 25 meters to 4 kilometers. This is consistent with an interaction mean free path of protons in air of ~90 g/cm^2. This value is confirmed by an independent measurement of the total number of collisions suffered by 14 proton primaries. The results are compared with previous experiments and their implications discussed. (auth)

47272 THE INTERCALIBRATION OF THE COSMIC-RAY NEUTRON MONITORS AT 9 EUROPEAN SEA-LEVEL STATIONS AND THE DEDUCTION OF A DAILY LATITUDE EFFECT IN 1963. Bachelet, F.; Balata, P.; Dyring, E.; Iucci, N. (Universita, Rome; Istituto Nazionale di Fisica Nucleare, Rome). Nuovo Cimento (10), 36: 762-72(Apr. 1, 1965).

The intercalibration of 9 European monitors of the cosmic-ray nucleonic component from Rome to Bergen (geomagnetic rigidity thresholds from 6.4 to 1 Gv) was carried out in 1963 by means of a standard IGY neutron monitor mounted on a lorry. At each station the ratio of the fixed to the mobile monitor counting rate was measured along with the differences in the simultaneous readings of the official fixed barometer and of the mercury barometer of the expedition. The daily intensity data from each station were normalized and reduced to a single pressure level to draw daily sea-level latitude curves for the period June to October 1963. The curves obtained show the interest the experiment offers for the study of short-term perturbations of the primary spectrum at low rigidities. In fact a displacement of the latitude knee towards high threshold rigidities during Forbush decreases is observed, similar to the one already known to take place in the long-term perturbation. (auth)

47273 EXPECTED VARIATIONS OF COSMIC-RAY INTENSITY ON THE MOON. Biswas, M. M.; Majumdar, D. P. (Univ. of Calcutta). Nuovo Cimento (10), 36: 1039-41(Apr. 1, 1965).

The possible variations of cosmic-ray intensity on the moon are represented from an analysis of these variations on the earth. Discussions are given of variations from solar effects, the solar-flare increase, the Forbush

decrease, the eleven-year variation, the 27-day recurrence tendency, and the 29.5 solar-day variation—and from galactic effects—the sidereal 27-day variation. (M.J.T.)

47274 THE APPARENT SIDEREAL DAILY VARIATION OF COSMIC-RAY INTENSITY AT ~40 M W.E. AT HOBART, TASMANIA. Jacklyn, R. M. (Melbourne Univ. of Tasmania, Hobart, Australia). Nuovo Cimento (10), 36: 1135-48(Apr. 16, 1965).

Changes in the characteristics of the daily variation of vertical cosmic-ray intensity underground at Hobart since 1958 confirm the view that a genuine sidereal component exists. The essential additional evidence since 1958 is a) that a substantial apparent sidereal effect continues to be observed even when seasonal modulation responsible for sideband phenomena is at a low level, and b) that the total daily variation towards the end of 1961 exhibited changes in phase that were consistent with the dominating influence of a sidereal component. It is shown that the phase anomaly was to be expected on the basis of the observed long-term changes in the amplitudes of the solar and apparent sidereal daily variations. The time of maximum of the first harmonic of the observed sidereal effect, averaged over the five years 1958 to 1962, is 0608 ± 0015 local sidereal time. There is also a significant second harmonic which appears to be in phase with the first. With provisional allowance made for the deflection of primaries in the earth's magnetic field, it seems that the right ascension of the direction of maximum intensity of the primaries responsible for the first harmonic observed at Hobart would not be more than about 0700, with a year to year variability of about one hour. (auth)

47275 DETERMINATION OF PRIMARY ENERGY OF JETS BY THE TRANSVERSE MOMENTUM AND ANGULAR DISTRIBUTIONS OF THE SECONDARY. Imaeda, K. (Dublin Inst. for Advanced Studies). Nuovo Cimento (10), 36: 1376-9(Apr. 16, 1965).

In order to avoid difficulties arising in the application of Castagnoli's spectrum-dependent formula to individual events, a formula is derived for determining primary energy by using the p_t distribution, which is independent of the primary energy and the type of interaction. Results of numerical calculations for primary protons, kaons, and pions are presented and show good agreement with experiment. (M.J.T.)

47276 INVESTIGATIONS ON THE MULTIPLY CHARGED NUCLEI OF THE PRIMARY COSMIC RADIATION NEAR THE GEOMAGNETIC EQUATOR USING NUCLEAR EMULSIONS. PART I. FRAGMENTATION PARAMETERS IN GRAPHITE. Badhwar, G. D.; Durgaprasad, N.; Vijayalakshmi, B. (Tata Inst. of Fundamental Research, Bombay). Proc. Indian Acad. Sci., Sect. A, 62: 374-97(June 1965).

The interaction mean-free paths and fragmentation parameters associated with collisions of nuclei of $Z \geq 6$ and $E \geq 7.5$ Bev/n were measured using emulsion-graphite sandwich stacks exposed to the primary cosmic radiation at Hyderabad, India (Geomagnetic latitude $\lambda = 7.6°N$). The results are based on a total of 213 nuclear interactions observed in graphite. Since the atomic number of graphite is very close to the mean atomic number of air, the parameters derived for graphite medium are directly applicable to air. A comparable study was made of the results thus obtained with similar data available for nuclei of $E \geq 1.5$ Bev/n. (auth)

47277 INVESTIGATIONS ON MULTIPLY CHARGED NUCLEI OF THE PRIMARY COSMIC RADIATION NEAR THE GEOMAGNETIC EQUATOR USING NUCLEAR EMULSIONS. PART II. THE CHARGE SPECTRUM OF NUCLEI OF ENERGY $E \geq 7.5$ Gev/NUCLEON. Badhwar, G. D.; Durgaprasad, N.; Vijayalakshmi, B. (Tata Inst. of Fundamental Research, Bombay). Proc. Indian Acad. Sci., Sect. A, 62: 17-33(July 1965).

The charge spectrum obtained from measurements made on tracks of 1329 nuclei of the cosmic radiation of $Z \geq 6$ and $E \geq 7.5$ Bev/n was studied in detail using emulsion stacks exposed over Hyderabad, India (cut off rigidity = 16.8 Gv) at a depth of 6.8 g/cm^2 of air for 7¼ hrs. This spectrum was compared with that available for nuclei of $E \geq 1.5$ Bev/n. Within the limits of experimental errors, no dependence of the flux values or ratios of intensities with energy are noticed. This result has important implications on the origin and history of the cosmic radiation. Integral energy spectra of M and H-nuclei were derived making use of the flux values at the two locations; the spectra thus derived have the least errors associated with these. (auth)

47278 ON THE COSMIC-RAY CUT-OFF RIGIDITIES AND THE EARTH'S MAGNETIC FIELD. Makino, Tadao (Nagoya Univ., Japan). Rept. Ionosphere Space Res. Japan, 17: 173-83(Sept. 1963).

An improved method for deriving geomagnetic cut-off rigidity of cosmic rays is presented by applying some modifications to Quenby-Webber's approximation. Two modifications are considered; one is a correction for the effect of the geomagnetic field at eastern part from the incident point and the other is penumbral correction. The modified cut-off rigidity thus obtained is compared with observed intensity distribution of cosmic rays on the surface of the earth. It shows better agreement than the other theories. The values of the modified cut-off rigidity are tabulated every 5° geographic latitude and every 10° geographic longitude. (auth)

47279 TERRESTRIAL AND SOLAR NEUTRONS. Haymes, R. C. (Rice Univ., Houston, Tex.). Rev. Geophys., 3: 345-64(Aug. 1965).

The study of neutrons in the solar system is reviewed, and the theories and experiments that relate to this study are described. Neutron capture in the atmosphere produces among other isotopes carbon 14 and tritium. The earth's neutron albedo is also a source of Van Allen radiation. The importance of the source is, however, in doubt; therefore, some studies of geomagnetically trapped charged radiation are also reviewed to emphasize the areas of greatest uncertainty in the theory of injection by the neutron albedo. There are conflicting data on the absolute value of the albedo itself, although there is now better agreement on neutron fluxes within the atmosphere. Hence a critical review of the techniques employed in neutron experiments is undertaken, and some possible ways of resolving some of the difficulties are suggested. The search for solar neutrons is also described, and some possible solar-neutron experiments are suggested. In the study of both Van Allen and solar problems, high-energy neutrons are most interesting, and yet this energy region is the least explored. (auth)

Criticality Studies

See also REACTOR TECHNOLOGY — Criticality Studies.

Refer also to abstracts 46967 and 47955.

Direct Energy Conversion

Refer also to abstracts 46571, 47978, and 48053.

47280 (AD-613358) DIRECT ENERGY CONVERSION LITERATURE ABSTRACTS. Bibliography No. 8. (Naval Research Lab., Washington, D. C.). Dec. 1964. 139p. CFSTI $2.75 cy, $1.00 mn.

References from various sources covering the current literature on thermoelectricity, thermionic emission, photoelectric processes, magnetohydrodynamics, electrochemical processes, energy storage, and energy sources are given. (auth)

47281 (ANL-7039) EVALUATION OF A THERMIONIC ENERGY CONVERTER USING FILM-BOILING LIQUID METAL. Ulrich, A. J. (Argonne National Lab., Ill.).

May 1965. Contract W-31-109-eng-38. 25p. Dep. mn; CFSTI $1.00 cy, $0.50 mn.

A thermionic energy-conversion diode was evaluated which uses a liquid metal as the electron collector. Liquids such as cesium, rubidium, or potassium and their alloys, are separated from the hot emitter by the vapor film produced in film boiling. Such a vapor film would maintain electrical separation if the emitter became warped due to radiation damage, thus greatly improving the reliability of the in-core thermionic diode. In an experiment, it was found that stable film boiling occurs for ranges of emitter temperatures and of cesium and potassium vapor pressures which are appropriate for thermionic diodes. The typical thermionic, series-connected, fuel-element geometry can be used in a film-boiling liquid-metal design to produce power in the zero-g field of space. If this is done, the price that must be paid for the improved tolerance to radiation damage and emitter evaporation in this type of space application is primarily more precise control of collector temperatures, a modified startup and shutdown schedule to avoid nucleate boiling, and further development of a new thermal divider to exclude nucleate boiling at the edges of the collector surfaces. (auth)

47282 (NYO-3429-4) THE DEVELOPMENT OF AN IMPROVED THERMIONIC ENERGY CONVERTER. Final Technical Report, June 26, 1964-June 25, 1965. (Radio Corp. of America, Lancaster, Pa. Direct Energy Conversion Dept.). May 1965. Contract AT(30-1)-3429. 84p. Dep. mn; CFSTI $4.00 cy, $0.75 mn.

During this program, fourteen converters similar to the RCA Developmental Converter Type A-1194 were fabricated. This converter design was modified, and new fabrication and processing techniques were developed. The converters were tested and evaluated. The feasibility of operating converters having only two temperature parameters, that of the emitter and the collector, was realized. It was also established that full performance was obtainable from converters without a liquid cesium reservoir. (auth)

47283 (BNL-tr-8) A PROCESS FOR CONVERSION OF IONIZING ENERGY INTO ELECTRICITY. Klein, Siegfried; Preve, Jacques. Translated for Brookhaven National Lab., Upton, N. Y. from J. Phys. Radium, 23: 588-9(Aug.-Sept. 1962). 5p. Dep. mn; JCL $1.00 fs, $0.80 mf.

An apparatus is described permitting direct conversion of energy from an atomic source into electricity by making use of its ionizing properties. A generator of soft x rays was used as an ionizing source with energy varying from zero to 30 kev, irradiating mercury vapor contained in a cell. The vapor is ionized by the x rays from the generator. Results and conclusions are presented. (M.O.W.)

47284 RADIOISOTOPE-PHOTOVOLTAIC ENERGY CONVERSION SYSTEM. Gritton, D. G.; Bourke, R. C. (General Motors Corp., Indianapolis). Advan. Energy Conversion, 5: 119-45(July 1965).

A radiant energy conversion (REC) system based on the electric response of photocells to thermal radiation emanating from a radioisotope-fueled source is described. Some properties and optimization requirements of germanium photovoltaic cells are given. Principal elements of the system and analysis methods of the radiative exchange problem are described along with performance calculations. This system can operate with an efficiency greater than 4 per cent. An upper limit of 12 per cent can be calculated if efficiency values for the photocell are based only on the active cell area and the contacted area is neglected. (auth)

47285 MAGNETOHYDRODYNAMIC ELECTRICAL POWER GENERATION. George, D. W. (Univ. of Sydney). At. Energy Australia, 8: No. 3, 7-12(July 1965).

Large scale commercial power generation from fossil or nuclear fuels by the MHD system is discussed. Convincing demonstrations of the basic feasibility of the technique are described. (P.C.H.)

47286 RECENT RESULTS IN THE DIRECT TRANSFORMATION OF HEAT POWER. Nyerges, Pal. Energia Atomtech., 18: 190-6(Apr. 1965). (In Hungarian).

The direct generation of electricity from heat is considered. Thermoelectric converters based on semiconducting thermocouples and radioactive isotopic sources are widely used, especially for space applications. The Soviet Romashka and the U.S. SNAP-10A generators represent the first reactors based on direct-conversion systems. Even though the conversion efficiency reaches only a few percent, their high specific energy density, relatively long useful life, simple construction, and safety of operation render them very suitable for their intended application. Direct generation of electricity by the magnetohydrodynamic method, using a large reactor as the heat source, is considered to be one of the most promising approaches. Work is being carried out aimed at a better understanding of the properties of equilibrium and nonequilibrium plasma, determination of the atomic and molecular collision cross sections, and at the study of ionization and recombination phenomena. It is hoped that efficiencies up to 60% can be reached, exceeding the current 40 to 45% efficiency of thermal plants. The thermionic generators have a higher efficiency than the thermoelectric converters and when developed are destined primarily to satisfy the higher energy requirements of space ships. (TTT)

47287 PHYSICS OF PLASMA THERMOELEMENTS. Nastoyashchii, A. F. High Temp. (USSR) (English Transl.), 2: 836-50(Nov.-Dec. 1964).

Translated from Teplofiz. Vysokikh Temp., 2: 927-44 (Nov.-Dec. 1964).

A systematic exposition of the main physical phenomena determining the energy conversion process in plasma thermoelements is given. This review represents a compressed account of the physical processes constituting the basis of the thermonuclear method. Technical aspects of the problem are not treated. Experimental material is brought in only to such an extent as is necessary for substantiating theoretical conclusions. The topics discussed are the conversion scheme and leading problems, thermoelectric emission, the physics of surface phenomena, transport processes through the gas space, qualitative theory of plasma thermoelements, and diffusion conditions including fundamental equations and boundary conditions. Also discussed are the conductivity of the isothermal diode, calculating methods in the study of diffusion conditions, the role of gas discharge processes in the gas space plasma, conditions including volume recombination, and the mechanism of arc development. (J.F.P.)

47288 MAGNETOHYDRODYNAMIC GENERATORS. Petschek, H. E. (Avco-Everett Research Lab., Everett, Mass.). pp 253-8 of STI/PUB/89.

A general description is given of MHD generators and of their methods of operation. A discussion of the physics associated with MHD generators is also given. It is apparent from the success of the experiments that the basic physical principles are much more clearly understood in the case of lower temperature than in that of higher temperature plasmas which are of interest for fusion and in space. Some aspects of the basic plasma physics are discussed with particular emphasis on those areas in which problems still remain. These problems arise when the product of electron cyclotron frequency and mean free time exceeds unity by some factor. This might be regarded as the beginning of a collision-free regime in that magnetic effects become comparable to collision effects. (J.F.P.)

47289 ELECTRON BEAM PREIONIZATION IN AN MHD GENERATOR. Shair, F. H.; Sherman, A. (General Electric Co., Valley Forge, Penna.). pp 7-12 of Sixth Symposium on Engineering Aspects of Magnetohydrodynamics. Phillipsburg, N. J., American Institute of Aeronautics and Astronautics, 1965.

Experiments were performed to demonstrate the feasibility of using an electron beam for preionization to achieve a non-equilibrium state of the electrons in a MHD generator operating above atmospheric pressure and at gas temperatures near 1500°K. Argon seeded with cesium was used as a monoatomic working fluid to demonstrate the efficient operation of such a beam. (B.L.M.)

47290 EXPERIMENTAL STUDIES OF STRONG HALL EFFECTS AND U x B INDUCED IONIZATION. II. Klepeis, James; Rosa, Richard J. (Avco-Everett Research Lab.). pp 26-30 of Sixth Symposium on Engineering Aspects of Magnetohydrodynamics. Phillipsburg, N. J., American Institute of Aeronautics and Astronautics, 1965.

Modification of the facility previously described by Klepeis (Proc. Fifth Symp. on Engrg. Asp. MHD (1964)) for experimental studies of strong Hall effects and U × B induced ionization are described. The graphite inert gas heater has been modified to allow experimentation at higher mass flows and at higher stagnation temperatures. The heater can now provide a flow of inert gas at temperatures up to 2000°K and at flow rates up to 500 g of Ar/sec. The principal modifications were the replacement of the rod core with graphite pebbles and increased insulation. (B.L.M.)

47291 EFFICIENCY OF LARGE SCALE OPEN LOOP MHD POWER GENERATION. Rosner, Manfred; Dzung, Lang S. (Brown Boveri Corp., Switzerland). pp 39-48 of Sixth Symposium on Engineering Aspects of Magnetohydrodynamics. Phillipsburg, N. J., American Institute of Aeronautics and Astronautics, 1965.

The range of the efficiency of a MHD-steam power plant is surveyed. In the absence of operating experience, the thermal efficiency represents the only criterion for evaluation of the future prospects of the MHD principle for possible industrial application. A method for optimizing the design parameters to attain high efficiency is indicated, and the results of a number of careful numerical calculations are summarized. The survey shows that at peak temperatures of 2600–2700°K the efficiency does not substantially exceed 0.50, the same efficiency that can be expected with water or steam cooled gas turbines at much lower peak temperature, 1500°K. (B.L.M.)

47292 DC LIQUID-METAL MAGNETOHYDRODYNAMIC POWER GENERATION. Elliott, David G. (Jet Propulsion Lab., Pasadena, Calif.). pp 49-59 of Sixth Symposium on Engineering Aspects of Magnetohydrodynamics. Phillipsburg,N. J., American Institute of Aeronautics and Astronautics, 1965.

A constant-pressure d-c magnetohydrodynamic generator was tested with NaK at inlet velocities up to 300 ft/sec. The maximum output power was 10.8 Kw (18,250 amp at 0.59 v), and the efficiency was 48%. The theoretical efficiency, considering ohmic heating, fluid friction, boundary layer shunting, and end effects, was 58%. The theoretical ultimate efficiency of liquid-metal MHD generators, of the type considered, ranges from 60 to 70%. (auth)

47293 ON THE MODULATED CONDUCTIVITY INDUCTION SYNCHRONOUS MAGNETOGASDYNAMIC GENERATOR. Milewski, J. (Polish Academy of Sciences, Danzig). pp 60-4 of Sixth Symposium on Engineering Aspects of Magnetohydrodynamics. Phillipsburg, N. J., American Institute of Aeronautics and Astronautics, 1965.

In earlier publications (Milewski, "Induction Synchronous Magnetogasdynamic Generators," Trans. Inst. Fluid-Flow Machines, No. 23, 1964, and Milewski, "A Criterion for Applying Low Values of Magnetic Reynolds Number in Induction Magnetogasdynamic Generators," Bull. Acad. Pol. Sci., S.T., No. 11, 1964) the operation of an induction synchronous MGD generator and the criteria that have been formulated for the generator indicating the conditions needed under which certain variants will be independent of the magnitude of the magnetic Reynolds number evaluated for the medium flow in the duct have been described. A more detailed examination concerning the operation of the synchronous generator fed with a jet of varying conductivity working medium is presented. The synchronous generator is compared with an electrode d-c generator and with an asynchronous induction generator. (B.L.M.)

47294 NON-LINEAR EFFECTS OF FLUCTUATIONS ON MHD PERFORMANCE. McCune, James E. (Avco-Everett Research Lab., Everett, Mass.). pp 89-103 of Sixth Symposium on Engineering Aspects of Magnetohydrodynamics. Phillipsburg, N. J., American Institute of Aeronautics and Astronautics, 1965.

An approximate treatment of the effect of correlated a-c fluctuations in reducing MHD performance is given. An elementary method familiar in the theory of gas dynamic turbulence is applied to the generalized Ohm's law for a slightly ionized gas subject to a strong Hall effect. It is shown that the d-c (time-average) current and fields become functions of the space-and-time correlations of the fluctuations in conductivity, Hall parameter, local electric fields, etc. This effect in turn limits the magnitude of the fluctuations. The general formulas are applied to the theory of the MHD oscillator, and it is shown that the a-c power level of that device is extremely limited. The results of this analysis indicate the way in which fluctuations may be controlled. (auth)

47295 TRAVELING WAVE INTERACTION AND WAVE GROWTH. Messerle, Hugo K. (Cornell Univ., Ithaca, New York). pp 104-11 of Sixth Symposium on Engineering Aspects of Magnetohydrodynamics. Phillipsburg, N. J., American Institute of Aeronautics and Astronautics, 1965.

Traveling magnetic wave interaction for one-dimensional flow is investigated using small perturbation theory and assuming that a short circuit path is provided for the induced currents. For a partially ionized gas then the electrical conductivity perturbations are very sensitive to temperature and pressure fluctuations and, as shown, they introduce unstable regions when the relative velocity of magnetic wave and plasma exceeds values well below that of the relative sound velocity. In these regions pressure disturbances traveling against the relative slip velocity are the ones most likely to grow. The Hall effect extends the unstable regions to even lower relative velocities. However, the overall electromechanical interaction is reduced by the Hall effect. Therefore its overall destabilizing influence becomes less pronounced when allowing for the natural damping due to viscosity. (auth)

47296 A GENERALIZED GRAPHICAL PRESENTATION OF MHD GENERATOR AND ACCELERATOR PERFORMANCE CHARACTERISTICS. Powers, W. L.; Dicks, J. B.; Snyder, W. T. pp 115-17 of Sixth Symposium on Engineering Aspects of Magnetohydrodynamics. Phillipsburg,N. J., American Institute of Aeronautics and Astronautics, 1965.

The electric characteristics of MHD generators and accelerators are displayed on a single diagram. The characteristic features of Faraday, Hall, diagonal wall, mixed, and other devices can be represented on the same two-dimensional figure for comparison purposes. For any given power to be generated, each generator represented on the map will have a particular point corresponding to maximum dimensionless power density, and the operating conditions that need be achieved for each generator are easily obtained. From this visual display of Ohm's law, values to about two places can be extracted from the map and the need for exact equations is reduced. If any one of the four: currents, fields, power density, or efficiency is known, then the other three can be obtained. This mapping is useful in evaluating MHD channel performance or for channel design. (B.L.M.)

47297 IMPROVEMENTS IN OR RELATING TO MAGNETOHYDRODYNAMIC GENERATORS. Dyott, Richard Burnaby (to M-O Valve Co., Ltd.; General Electric Co.). British Patent 1,002,842. Sept. 2, 1965. Filed Oct, 8, 1962.

In a MHD generator of the type in which a conducting fluid is forced through a magnetic field in a direction transverse to the direction of the lines of force of the field, means are provided for velocity modulating the flow of the fluid at a position along the path of the flow. The means for velocity modulation is spaced from the position at which the path passes through the magnetic field in such a manner as to cause periodic bunching of the particles in the fluid in the region of the magnetic field. The modulating means comprises an acoustic resonator acoustically coupled with the interior of the tubular enclosure of the generator, and means are provided for maintaining acoustic oscillations within the resonator. This bunching of particles helps to obtain a sufficiently high conductivity in the

conducting fluid to permit the extraction of useful amounts of electric power from the generator. (B.L.M.)

Elementary Particles and Radiations

Refer also to abstracts 46643, 46834, and 47275.

47298 (AD-613934) NATURE OF THE RESONANCE IN THE STATIC PION-NUCLEON SCATTERING IN ONE-MESON APPROXIMATION. Barut, A. O.; Ruei, K. H. (Syracuse Univ., N. Y.). 1961. Contract AF49(638)-801. 12p. (AFOSR-880). CFSTI $1.00 cy, $0.50 mn.

Solution of the Chew-Low integral equation for the static p-wave meson-nucleon scattering was studied as a function of the coupling constant to deduce the nature of the 33-resonance. It is shown that a dynamical resonance must occur in association with either a bound state or with at least one more p-wave resonance. The possibility of a kinematical resonance is also discussed and the effective range formula was derived directly from the dispersion relation. (auth)

47299 (AD-614046) DIFFRACTION AND SCATTERING BY REGULAR BODIES. Final Report, February 1960–January 1965. Kleinman, R. E. (Michigan Univ., Ann Arbor. Radiation Lab.). Feb. 1965. Contract AF19(604)-6655. 22p. (AFCRL-65-199). CFSTI $1.00 cy, $0.50 mn.

Research activities during the period February 1960 to January 1965 are summarized, and work on the preparation of reports presenting the electromagnetic scattering properties of regular bodies as well as original research in basic diffraction theory and nonlinear modeling is included. (TCO)

47300 (BNL-9520) THE $Y_1^*(1660)$ PRODUCED IN K^--p INTERACTIONS AT 2.24 Bev/c. London, G. W.; Rau, R. R.; Samios, N. P.; Goldberg, M.; Primer, M.; Leitner, J. (Brookhaven National Lab., Upton, N. Y.; Syracuse Univ., N. Y.). [1965]. Contract AT(30-2)-Gen-16. 26p. (CONF-650945-1). Dep. mn; CFSTI $2.00 cy, $0.50 mn.

From International Conference on Elementary Particles, Oxford.

The production and decay of the $Y_1^*(1660)^+$ produced in peripheral K^- + p interactions at 2.24 Bev/c is studied. The resonance decays primarily into $Y_0^*(1405) + \pi^+$. A small contribution to the decay through the $\Sigma^+ + \pi^0$ mode is also observed. The Dalitz plot provides no definite information on the spin-parity, but if the K^+ exchange model is assumed, the decay angular distributions provide some evidence against $\frac{3}{2}^+$. (T.F.H.)

47301 (CERN-65-30) WEAK INTERACTIONS. Cabibbo, N.; Veltman, M. (European Organization for Nuclear Research, Geneva (Switzerland)). Aug. 4, 1965. 84p. Dep. mn.

A discussion of the principles involved in the process $\nu + n \rightarrow p + \mu^-$ is presented in the form of theoretical studies on the following; the matrix element (baryonic and leptonic factors), the conserved vector current, the parity, charge conjugation, and time reversal transformations, G-parity (first and second class currents), the Goldberger-Treiman relation, time reversal invariance, and final-state interactions. In addition a review of unitary symmetry and its applications to weak interactions is given. (M.O.W.)

47302 (CU-1932-246) PRECISE HYPERON MASSES. Schmidt, P. (Nevis Labs., Columbia Univ., Irvington-on-Hudson, N. Y.). July 1965. Contract AT(30-1)-1932. 30p. (NEVIS-140; R-512). Dep. mn; CFSTI $2.00 cy, $0.50 mn.

Nine independent measurements were performed on hyperons produced in meson (K^-) capture, and a set of precise hyperon mass measurements was obtained. The mass values are reported. (auth)

47303 (DESY-65/7) ELECTROPRODUCTION OF π-MESONS AND PHOTOPRODUCTION OF DIPIONS. Blechschmidt, H.; Elsner, B.; Heinloth, K.; Ladage, A.; Rathje, J.; Schmidt, D. (Deutsches Elektronen-Synchrotron, Hamburg (West Germany)). Aug. 1965. 27p. Dep. mn.

In a spark chamber experiment, with primary electrons of 5.2 Bev/c, the electroproduction of mesons (π) was measured. At the same time photoproduction of dipions was observed using bremsstrahlung produced by the electrons in the hydrogen target. The experimental setup and the parameters of the experiment are described. Results are presented. (M.O.W.)

47304 (IAE-700) UPRUGOE (p,p)-RASSEYANIE PRI 1.45 Bev. (Elastic (p,p)-Scattering at 1.45 Bev). Kruchinin, S. P.; Mukhin, K. N.; Romantseva, A. S.; Svetlolobov, I. A.; Sulkovskaya, M. M.; Chueva, S. A.; Shlyapnikov, R. S. (Institut Atomnoi Energii, Gosudarstvennyi Komitet po Ispol'zovaniyu Atomnoi Energii SSSR, Moscow). 1964. 16p. Dep. mn.

A propane bubble chamber was used to investigate the angular dependence of elastic scattering of protons by protons at an incident-proton momentum of 2.2 Bev/c, which is higher than the energies used in earlier investigations. A total of 17,000 pairs of stereophotographs was scanned, ~900 cases of elastic π^+p and pp scattering cases were analyzed, and the reduction of these data made it possible to determine the differential cross section of elastic pp scattering at 1.45 Bev over the entire angle interval of 0 to 90° (cms). Calculations based on the optical model with a small region of phase shift gave best agreement with the experimental data with parameter values R_1 = 0.45 F, R_2 = 0.95 F, a = 0.344, and φ = 1.77 rad. (R—interaction radius, φ—phase shift, a—amplitude of transmitted wave for a unit amplitude of incident wave). In the energy region from 0.38 to 30.9 Bev, the differential cross section is proportional to A exp $(-P_{cms}/P_0)$, with A = 115 mb/sr and P_0 = 143 Mev/c. (ATD)

47305 (IC/65/57) THE $\tilde{U}(12)$ SYMMETRY. Delbourgo, R.; Rashid, M. A.; Salam, Abdus; Strathdee, J. (International Centre for Theoretical Physics, Trieste (Italy)). Aug. 1965. 118p. Dep. mn.

The mathematical structure of U(6,6) is covered in great detail. Other detailed discussions include; free particle formalism, supermultiplet field theory and the possible dynamical origin of the $\tilde{U}(12)$, $\tilde{U}(12)$ calculations and experiments, and the inhomogeneous group. (M.O.W.)

47306 (JINR-E-2343) DISPERSION SUM RULES AND SU(6) SYMMETRY. Solov'ev, L. D. (Joint Inst. for Nuclear Research, Dubna (USSR). Lab. of Theoretical Physics). 1965. 5p. Dep. mn.

It is shown that the total magnetic moment of the neutron $\mu_n = -2$ and proton $\mu_p = 3$ (in nuclear magnetons) can be obtained from SU(6) symmetry and the sum rule following from one-dimensional dispersion relations. (auth)

47307 (JINR-P-2278) LEPTONNYE RASPADY BARIONOV V UNIVERSAL'NOI V-A-TEORII. (Leptonic Decays of Baryons in the Universal V-A Theory). Bokov, O. G.; Nguyen Van Hieu; Rerikh, K. V.; Tavkhelidze, A. N.; Khelashvili, A. A. (Joint Inst. for Nuclear Research, Dubna (USSR). Lab. of Theoretical Physics). 1965. 19p. Dep. mn.

In the framework of the universal V-A theory of weak interactions the leptonic decays of baryons are systematically studied. Expressions are obtained for the decay probability, the $l\bar{\nu}$ angular correlation, the energy spectra of leptons and recoil baryons, the asymmetry parameters in the angular distribution of leptons and recoil baryons by the decay of polarized baryons. The contributions from all possible form-factors were considered with account of their linear dependence on the momentum transfer. (auth)

47308 (JINR-P-2284) RASPAD BARIONOV I MEZONOV S OBRAZOVANIEM ELEKTRONNO-POZITRONNOI PARY V SKHEME SIMMETRII U(12). (Decay of Baryons

and Mesons With the Formation of an Electron-Positron Pair in the U(12) Symmetry Scheme). Dao Wong Duc (Joint Inst. for Nuclear Research, Dubna (USSR). Lab. of Theoretical Physics). 1965. 7p. Dep. mn.

The decay of baryons and mesons accompanied by the formation of an electron-positron pair is considered under U(12) symmetry. Expressions for the energy spectrum of finite baryon and meson are found. These can be compared with experiment. (auth)

47309 (JINR-P-2289) RASPADY V SMESHANNOM ANSAMBLE NEITRAL'NYKH K-MEZONOV. (Decays in a Mixed Ensemble of Neutral K-Mesons). Lyuboshits, V. L. (Joint Inst. for Nuclear Research, Dubna (USSR). Lab. of High Energy). 1965. 14p. Dep. mn.

A description of the decay properties of a mixed ensemble of neutral K-mesons is considered with the aid of a two row density matrix. The case when the neutral K meson enters the $K^0\bar{K}^0$ system is investigated in detail. From the new point of view the interference effects occurring by the decay of neutral K mesons into two π mesons are discussed for the case of CP violation. (auth)

47310 (NP-15376) THE BACKWARD ELASTIC SCATTERING OF PIONS ON NEUTRONS WITHIN THE MOMENTUM RANGE 1.2 - 4.5 Bev/C. Alikhanov, A. I.; Bayatyan, G. L.; Brachman, E. V.; Galaktionov, Yu. V.; Joch, F. A.; Landsberg, L. G.; Lyubimov, V. A.; Pavlovskl, F. A.; Sidorov, I. V.; Yeliseev, G. P.; Zeldovich, O. Ya. (Gosudarstvennyi Komiter po Ispol'zovaniyu Atomnoi Energii SSSR, Moscow. Institut Teoreticheskoi i Eksperimental'noi Fiziki). 1964. 10p. Dep. mn.

The cross section of π^- + n elastic backward scattering was measured. The behavior of the cross section over the 1.2-4.5 Bev/c incident momenta is given. (auth)

47311 (NP-15454) POLYUSA REDZHE V POTENTSIALE TIPA KULONOVSKOI YAMY. (Regge Pole in a Coulomb-Well Type Potential). Report No. 302. Kolkunov, V. A.; Lobov, G. A. (Gosudarstvennyi Komitet po Ispol'zovaniyu Atomnoi Energii SSSR, Moscow. Institut Teoreticheskoi i Eksperimental'noi Fiziki). 1964. 28p. Dep. mn.

On the basis of exact solution of Schroedinger equation Regge poles motion depending on the energy for a Coulomb well potential is investigated. This potential coincides with the Coulomb one at small distances and behaves as a square-well potential at large distances. The pole trajectories in a Coulomb well potential at low and mean energies are shown to be of Regge character. The pole trajectories asymptotics at high energies coincide with the Coulomb case. (auth)

47312 (NP-15460) NESOKHRANENIE SR-CHETNOSTI V RASPADE POLYARIZOVANNOGO NEITRONA. (CP-Parity Non-Conservation in Polarized Neutron Decay). Report No. 332. Lobov, G. A. (Gosudarstvennyi Komitet po Ispol'zovaniyu Atomnoi Energii SSSR, Moscow. Institut Teoreticheskoi i Eksperimental'noi Fiziki). 1965. 10p. Dep.mn.

On the basis of the effective hamiltonian containing baryonic currents of the first and second class (six form-factors) the spin correlation $\vec{S}[\vec{P}_p \times \vec{P}_e]$ ($\vec{S}$ – is neutron spin vector, $\vec{P}_p, \vec{P}_e$ – are the proton and electron momenta) in polarized neutron decay was calculated. Models where CP-parity non-conservation is due to the currents of the second class and to the presence of imaginary part in the constant of axial-vector interaction are discussed. The problem of emerging of spin correlation $\vec{S}[\vec{P}_p \times \vec{P}_e]$ due to the Coulomb interaction of proton and electron in final state was investigated. (auth)

47313 (TID-22222) FUTURE THEORETICAL AND EXPERIMENTAL RESEARCH ACTIVITIES IN HIGH ENERGY PHYSICS. Progress Report, September 1964–September 1965. (Pennsylvania Univ., Philadelphia. Dept. of Physics). Contract AT(30-1)-2171. 60p. Dep. mn; CFSTI $3.00 cy, $0.50 mn.

Details of the progress made during the past year, both experimentally and theoretically, are reported. The area of research is elementary particle physics. Separate abstracts were prepared for the experimental and theoretical research discussed. (M.O.W.)

For abstracts of individual sections see: 47314 and 47315.

47314 (TID–22222, pp 3–29) THEORETICAL RESEARCH. (Pennsylvania Univ., Philadelphia. Dept. of Physics).

Theoretical research carried out at the University of Pennsylvania in the area of elementary particle physics is reported. Summaries of work in the following areas are given; weak interactions, broken symmetry structure of field theories, new methods in nuclear structure calculations and theories of collective motion, bootstrap theory of strong interactions and theory of higher symmetries, and higher symmetries, especially SU(6) and its theoretical foundations. (M.O.W.)

47315 (TID–22222 pp 30–45) EXPERIMENTAL RESEARCH. (Pennsylvania Univ., Philadelphia. Dept. of Physics).

Experimental research in elementary particle physics is reported. The work ranges from the discovery of a new particle in strong interaction work to investigation of many aspects of the decays of weakly interacting particles and study of effects of possible CP violations. (M.O.W.)

47316 (JPRS–31032, pp 15–18) ANOMALOUS MAGNETIC MOMENT OF ELEMENTARY PARTICLES DUE TO ELECTROMAGNETIC MASS DIFFERENCE. Hu, Ning. Translated from K'o Hsueh T'ung Pao, No. 4, 347-8(Apr. 1965).

The eightfold theory of the SU(3) group predicts the anomalous magnetic moment μ for the different hyperons. The electromagnetic masses are theoretically found for several baryons and mesons and are tabulated. These calculations can be used to determine the anomalous magnetic moments of the particles. The theoretical electromagnetic masses are compared with experimental ones. (M.O.W.)

47317 (NP-tr-1282) POSSIBLE CP VIOLATION AND THE NATURE OF THE $\Delta T = \frac{1}{2}$ RULE. Zel'dovich, V. Ya.; Okun, L. B. Translated by A. T. Sanders from Phys. Letters, 16: 319-(1965). 6p. Dep. mn; CFSTI $1.00 cy, $0.50 mn; $1.10 fs, $0.80 mf.

The Wolfenstein model is discussed, in which the $K_2^0 \rightarrow 2\pi$ decay is due to the difference in phase of the primary non-leptonic interaction and of the non-leptonic interaction that appears in the second order of perturbation theory due to the virtual lepton exchange. It is shown that in order to get an observable scale of CP violation it is necessary in this model to abandon the non-leptonic interaction Lagrangian in the form of the product of charged currents. This suggests that the primary non-leptonic Lagrangian satisfies the strict $\Delta T = \frac{1}{2}$ rule. (auth)

47318 THE PERIPHERAL ELECTROMAGNETIC INTERACTIONS OF THE FAST CHARGED PARTICLES AND NUCLEONS. Pey, Wang (Szechuan Univ., China). Acta Phys. Sinica, 21: 1533-43(Aug. 1965). (In Chinese).

The influence upon the modification of the theory of equivalent spectrum of photons by Weizsäcker-Williams, given by the electromagnetic structure of the nucleon. To overcome the difficulty caused by the divergence in the calculation with the form factor of the Clementel-Villi's type, a way of modifying the form factor is suggested. The results of the calculation show that within the region in which the method of equivalent spectrum of photons works, our results conform to Weizsäcker-Williams' theory, if the masses for the two particles in collision are considerably different; however, the influence of the structure is very evident, if the masses of the two particles are approximate to each other. (auth)

47319 ANALOGOUS BEHAVIOR OF ELEMENTARY PARTICLES AND SOME SIMPLE WAVEGUIDE AND CAVITY SYSTEMS. Lawson, J. D. (Rutherford High Energy Lab., Chilton, Eng.). Am. J. Phys., 33: 733-9(Sept. 1965).

Instructive parallels may be drawn between the way that electromagnetic cavities and waveguides behave as

the frequency is varied, and the behavior of elementary particle reactions as a function of center-of-mass energy. A series of correspondence between the two types of systems, relating, for example, mode number to quantum number and cutoff wavelength to Compton wavelength are established. A particular cavity and waveguide system are examined in some detail, and their resonant frequencies and decay modes found. Conservation laws are found, and related to the symmetry of the cavity, which is such that "strong," "intermediate," and "weak" decay is possible. Parallels with the interactions, scattering, and decay of elementary particles are discussed. (auth)

47320 REGGE-POLES IN THE NONRELATIVISTIC POTENTIAL SCATTERING. Mueller, Harald J. W. (Universitaet, Munich). Ann. Physik (7), 15: 395-411 (1965). (In German).

Nonrelativistic scattering was investigated using a superposition of Yukawa potentials. For the solution of the radial Schroedinger equation a modified perturbation theory method was used which proved very useful for the preparation of asymptotic developments of higher transcendental functions. After an evaluation of the asymptotic behavior of the Regge poles in the limiting case of infinitely high energies, it was shown that 4 asymptotic solutions of the radial Schroedinger equation, constructed analogously, exist from which the Jost functions and therefore the S matrix can be calculated. For the eigenvalues or poles of the scattering matrix, an asymptotic development for high energies appeared. After a discussion of the analytical properties of the scattering amplitude, its behavior in the limiting case of high energies was derived. (tr-auth)

47321 ONE-PARTICLE SINGULARITIES AND SU(3). Doebner, H. D.; Hegerfeldt, G. C. (Philipps-Universitaet, Marburg, Ger.). Ann. Physik (7), 15: 412-14(1965).

The definition of coupling constants, through residues of one-particle singularities in the amplitude A(s,t) for a process $a + b \rightarrow c + d$ with an SU(3)-invariant S-matrix leads to relations between coupling constants if one uses known SU(3)-properties of a, b, c, d and of the one-particle intermediate states responsible for the singularities. The relations are derived without reference to Lagrangian field theory. It is shown however that they agree with those obtained from an SU(3)-invariant Lagrangian. (auth)

47322 ON THE MATRIX ELEMENTS OF A UNITARY REPRESENTATION OF THE HOMOGENEOUS LORENTZ GROUP. Stroem, Staffan. Arkiv Fysik, 29: 467-83(1965).

The physically interesting unitary irreducible representations of the homogeneous Lorentz group are characterized by two numbers, l_0 and ν. The form of the matrix elements of a finite Lorentz transformation in a unitary representation (l_0,ν) is derived by integration of the infinitesimal relations. It is shown that the matrix elements in a number of cases satisfy a second order differential equation, whose solution can be expressed in terms of hypergeometric polynomials. In particular it is shown, that it is always possible to find a column, whose elements can be written in this way, and thereby simple and explicit expressions are obtained for a set of functions, which forms a basis for a linear representation of the homogeneous Lorentz group. The general matrix element, which satisfies a fourth order differential equation, is determined by an application of the ladder operator technique. (auth)

47323 THE LANDAU THEORY OF FERMI SYSTEMS. I. THE CHARACTERISTIC FEATURES OF THE THEORY. Kisdi, David (MTA Elmeleti Fizikai Kutato Csoport, Budapest). At. Kozlemen., 7: 63-8(Mar. 1965). (In Hungarian).

The Fermi system is defined as a system consisting of particles following the Fermi-Dirac statistics, in which the particles exert a mutual interaction; as an example, the nucleus, the nuclear matter, the electron cloud of atoms and molecules, the electron gas in metals, and liquid ^{3}He may be cited. These systems attracted considerable attention at the time of the development of quantum mechanics. The chief problem requires determination of the eigenvalues of the Hamiltonian operators of the examined systems, on the basis of the multibody problem. Landau's theory outlines the method to be used for determining the system's physical parameters and its reaction to external events on the basis of the excitation levels. The theory provides the link between experimental data and these levels. The theory is especially useful for systems which possess a complicated excitation spectrum. In the study of systems containing limited number of particles, such as a heavy nucleus, the theory was found to be very useful but its role was more restricted in the development of the shell theory. (TTT)

47324 STUDY OF THE L, M, N FUNCTIONS OF THE NON-LINEAR SPINOR THEORY OF ELEMENTARY PARTICLES. David, J. H.; Derem, A. Bull. Classe Sci., Acad. Roy. Belg. (5), 50: 1268-86(1964). (In French).

In the non-linear theory of elementary particles by Heisenberg and coworkers, new functions were introduced, which were called L, M, N. These functions, which depend on two parameters ξ and η, were studied in the general case where ξ is different from η. The method leading to their analytical expressions was reported. (auth)

47325 FINITE TEMPERATURE PROPERTIES OF NORMAL FERMI SYSTEMS. II. A SIMPLE PERTURBATIVE MODEL. Resibois, P. (Universite Libre, Brussels). Bull. Classe Sci., Acad. Roy. Belg. (5), 50: 1287-1301(1964). (In French).

The general transport equation for the normal Fermi systems obtained recently was studied within the framework of a weakly coupled model in which all the parameters in this equation are calculated to the λ^2 order. The ratio between this result and the same approximation of the Landau equation for quasi-particles was analyzed in the limit of a zero temperature. It was shown that the situation is completely analogous to the case of equilibrium: the Wigner distribution function that describes the response of the system to an external field can be decomposed into one part that is singular at the Fermi surface and proportion to the quasi-particle distribution function and into another part that does not contribute to the electric current. (tr-auth)

47326 ACTIVITIES OF THE HIGH ENERGY CORPUSCULAR PHYSICS LABORATORY DURING 1964. Bull. Inform. Sci. Tech. (Paris), No. 91, 3-36(Mar. 1965). (In French).

The principal pieces of equipment (spark and bubble chambers, measurement and data processing methods, and polarized proton target) now being used in the high-energy particle physics laboratory and the most important experiments carried out by this laboratory during 1964 are described. (auth)

47327 A NEW SCATTERING CHAMBER AND ITS INSTALLATION. Delaunay, B.; Delaunay, J.; Meurgues, J.-P.; Passerieux, J.-P.; Perey, F.-J. Bull. Inform. Sci. Tech. (Paris), No. 91, 71-94(Mar. 1965). (In French).

A versatile scattering chamber was built. The system as designed allows remote setting and precise display of the detectors and targets angles. Mechanical standards adhered to in the construction enable rapid modifications of the chamber to suit various experimental needs. Associated equipment includes a particle-identifying system of high resolution. (auth)

47328 THE FIFTEENFOLD WAY OF THE SU(4) SYMMETRY SCHEME OF STRONGLY INTERACTING PARTICLES. Lee, Y. Y.; Chen-Tsai, C. T. (Tsing Hua Univ., Taiwan, China). Chinese J. Phys. (Taiwan), 3: 45-66 (Apr. 1965).

A new model of classification of strongly interacting particles is proposed, in which particles are assigned to those representations of SU(4) that come out from the Kronecker products of the regular $\{15\}$ representations. Mass formulas are derived and new particles are predicted. To account only those particles that have been found experimentally and avoid predicting dubiously too

many new particles, an "N-degeneracy" model is suggested, by which particles of the same "N-spin" multiplet are assumed to be the same particle. Some physical consequences of this model are discussed. (auth)

47329 ABSOLUTE PHOTOELECTRIC CROSS-SECTIONS OF 145, 280 AND 320 kev GAMMA-RAYS. Parthasaradhi, K.; Lakshminarayana, V.; Swami Jnanananda (Andhra Univ., Waltair, India). Current Sci. (India), 34: 427-8(July 20, 1965).

Photoelectric cross sections for Cu, Ag, Sn, Ta, Pt, and Pb at gamma energies of 145, 280, and 320 Kev are computed from expressions developed by Nagel, and a comparative study is made in the light of the values computed from Hertler-Stoble and Sauter-Stobbe expressions as well as with the interpolated values from Grodstein's Tables. The results are tabulated. (L.B.S.)

47330 A NOTE ON THE EFFECT OF NON-ELASTIC PROCESSES ON ELASTIC SCATTERING. Pisut, J.; Noga, M. (Comenius Univ., Bratislava). Czech. J. Phys., 15: 541-8(1965).

The effect of non-elastic processes on elastic scattering is studied by means of Froissart's method. The conditions under which this method leads to a unique solution and those under which inelastic processes lead to the creation of more resonances in the elastic channel are derived. Further the generalization of Levinson's theorem is derived for the case of the existence of nonelastic processes and an illustrative explicitly solvable example is introduced. (auth)

47331 CP VIOLATION AND PT INVARIANCE. Hiida, Kichiro (Tokyo Univ.). Genshikaku Kenkyu, 9: 712-18 (Mar. 1965).

A model of weak interactions is presented such that CP violating weak interactions are invariant universally under PT.* The basis on which the assumption of PT invariance is made and results obtained from the model are discussed. (auth)

47332 PHOTON-PHOTON INTERACTIONS. Gardner, J. W. Nucl. Energy, 254-63(Aug. 1965).

Photon-photon scattering in a vacuum and in material media, plasmas, gases, solids, and liquids is discussed. Applications of these interactions are also discussed. Polarization in a vacuum is described as the polarization of vacuum fluctuations, that is, the appearance and disappearance of an electron-positron pair. The total cross section for photon-photon scattering in a vacuum is always appreciably less than one millionth of the Thompson cross section for electron-photon Compton scattering. Various experiments are proposed for the detection of this scattering. In a plasma the polarization is much greater. Thus the cross section for photon-photon scattering is also greater. Proposed experiments for the scattering detection in plasma are also discussed. The photon interaction in a condensed media is discussed in detail, since this interaction can be readily demonstrated. The case of a crystalline solid is considered. The two main effects which were demonstrated are the generation of optical harmonics and the mixing of light of different frequencies. Experiments, applications, and prospects are also discussed. (J.F.P.)

47333 REPRESENTATION OF THE SYMPLECTIC GROUP OF RANK TWO. Guiasu, I.; Micu, M.; Moisescu, L. (Inst. for Atomic Physics, Bucharest). Nucl. Phys., 73: 522-8(1965).

The matrix elements of the generators of the four dimensional symplectic group are obtained by using the generators of two subgroups with the view of labeling uniquely the states of an irreducible representation. The two independent invariants of the group are also given in order to determine the highest weight of an irreducible representation. (auth)

47334 STUDIES OF THE PAIRING HAMILTONIAN WITH VARIABLE INTERACTION MATRIX ELEMENTS. Chasman, R. R. (Argonne National Lab., Ill.). Nucl. Phys., 73: 588-92(1965).

Approximate solutions are obtained for the pairing hamiltonian having variable interaction matrix elements. The adequacy of these solutions is considered in detail. (auth)

47335 ON THE REGGE SYMMETRIES OF THE 3j-SYMBOLS. Kleima, D.; Van Wageningen, R. (Rijksuniversiteit, Groningen, Netherlands). Nucl. Phys., 73: 625-30(1965).

A simple derivation of the Regge symmetries for 3j-symbols is given. It is also shown that there is essentially only one Regge symmetry. It is discussed whether these symmetries can be used for extending the range of validity of well-known approximate expressions for 3j-symbols. (auth)

47336 MATCHING THE COMPUTER TO THE MAN. Mollenauer, James F. (Bell Telephone Labs., Inc., Murray Hill, N. J.). Nucleonics, No. 10, 23: 66-71(Oct. 1965).

To get the most out of an on-line system, information transfer between experimenter and machine must be efficient and flexible. A cathode-ray-tube display coupled to a light-pen feedback looks best thus far. In general, any effort devoted to further improvements should be guided by the principle that the ultimate criterion of success for an on-line system is not an efficient mechanical process from input to output within the hardware, but the most suitable match between the man and the computer for information transfer between them. The emphasis must be on convenience to the user not to the machine, if the computer's potential as a tool is to be fully utilized. Topics discussed are input to output matching, cathode-ray-tube and light pen applications, and the experimenter's use of the computer. Specific applications including particle identification, time-of-flight neutron spectral analysis event sorting, and track analysis are discussed. (J.F.P.)

47337 S-WAVE Λ-Λ INTERACTION AND A SCALAR DIPION RESONANCE. Bose, Subir (Univ. of Allahabad, India); Khare, H. C. Nuovo Cimento(10), 36: 805-12 (Apr. 1, 1965).

The N/D method of dispersion theory is used to calculate the S-wave zero-energy Λ-Λ scattering length. The calculated value of the scattering length comes in close agreement with the value obtained by Dalitz and Rajasekaran from an analysis of the $^{10}Be_{\Lambda\Lambda}$ event. The inclusion of the contribution of a scalar meson σ is, however, necessary in order to reproduce the correct sign and magnitude of the scattering length. (auth)

47338 MARGINALLY SINGULAR FORCES AND THEIR ROLE IN PRODUCING PSEUDOVECTOR RESONANCES. Morgan, D. (CERN, Geneva). Nuovo Cimento (10), 36: 813-31(Apr. 1, 1965).

The problem of two equal-mass scalar bosons scattering in a P-state under the influence of marginally singular forces is studied. Such forces arise from the exchange of a vector boson. It is shown that the solutions of the N/D equations have a one-parameter ambiguity, which is related to the existence in the theory of quasi-elementary particles. It is speculated that the observed vector bosons might belong to this category. The possibility of a special form of left-hand cut with the property that all solutions of the N/D equations would contain a resonance is also discussed. It is pointed out that if this were to occur in the bootstrap context, it could provide a new mechanism for the determination of the coupling constant by crossing symmetry. (auth)

47339 HYPERFRAGMENT FORMATION IN $K^- + d \rightarrow \pi^+ + \Sigma^- + n$ REACTIONS AT REST. Chand, Ramesh (Syracuse Univ., N. Y.; Wayne State Univ., Detroit). Nuovo Cimento (10), 36: 837-47(Apr. 1, 1965).

In the multiple scattering formalism of $\bar{K},\mathcal{N}$ system, the ratio of bound to free Σ^--n systems in $K^- + d \rightarrow \pi^+ + \Sigma^- +$ n capture reactions at rest is calculated, using the sum rule method in terms of Σ-nucleon isospin states. The s-wave $\bar{K}\mathcal{N}$ scattering parameters of the solution X1 are used as input to find that, in order to explain the experimentally

known ratio of less than one percent, the binding energy of this hyperfragment must be less than one kev. (auth)

47340 SPECTRAL REPRESENTATION AND MASS FORMULA FOR SPIN-3/2 PARTICLES. Galindo, A.; Hadjioannou, F.; Pascual, P. (CERN, Geneva). Nuovo Cimento (10), 36: 848-56(Apr. 1, 1965).

A canonical quantization of a spin-$\frac{3}{2}$ field is considered. Lehmann's representation is used to derive sum rules connecting the spectral functions with the mass and renormalized constant, assuming that the interaction lagrangian does not violate the Rarita-Schwinger subsidiary conditions and the current commutes with the field. By considering the inverse Green's function a 1/m mass formula is obtained. The result is applied to the decuplet of spin-$\frac{3}{2}$ resonances. (auth)

47341 HIGH-ENERGY BEHAVIOUR OF PRODUCTION AMPLITUDES IN PERTURBATION THEORY. Polkinghorne, J. C. (Cambridge Univ., Eng.). Nuovo Cimento (10), 36: 857-65(Apr. 1, 1965).

A unified method for extracting the high energy behavior of production amplitudes in perturbation theory is developed with the aid of Mellin transforms. A wide range of limits is evaluated including that possible in the physical region. (auth)

47342 AN SU_3 ESTIMATE OF THE EFFECTIVE NON-LEPTONIC PARITY-VIOLATING COUPLING IN STRANGENESS-CONSERVING WEAK PROCESSES. Kummer, W. (CERN, Geneva). Nuovo Cimento (10), 36: 884-95(Apr. 1, 1965).

It is assumed that nonleptonic weak interactions contain a product of SU_3 octets which are the natural generalization of the octet currents in semileptonic interactions. If the representation 27 is suppressed, this leads to a prediction of the effective coupling in the weak nucleon-pion vertex, which contributes to nonleptonic strangeness-conserving (NLSC) weak processes. Both nonderivative and derivative effective coupling are discussed. In the latter case, which seems the more important one, an argument can be given that the effective parity-violating vertex coupling for the NLSC reactions, which follows from the experimental parameters of hyperon decays, is likely to be not very different for any other effective coupling. (auth)

47343 INELASTIC BOUND-STATE SCATTERING IN SEPARABLE APPROXIMATION. Cushing, J. T. (Imperial Coll. of Science and Tech., London). Nuovo Cimento (10), 36: 905-15(Apr. 1, 1965).

The inelastic contributions to the scattering amplitude describing the scattering of an elementary particle from a bound state are calculated explicitly from the Fadeev equations for separable interactions. The inelastic terms are then combined with the previously calculated elastic amplitude, and the analytic properties of the complete amplitude are investigated in the static limit. The trajectories of the singularities of the partial-wave amplitude are shown to be bounded in the right-half plane of the total angular momentum. The model is applied to the scattering of a spinless elementary particle from a spinless compound one. The resulting amplitude is bounded by a finite power of $\cos\theta_1$ and independent of $\cos\theta_2$, where θ_1 and θ_2 are the scattering angles of the scattered elementary particle and ejected bound particle, respectively. The possible applicability of the separable approximation used is discussed. (auth)

47344 BREAKING OF SU_3 SYMMETRY IN THE ELECTROMAGNETIC DECAY OF THE DECUPLET. Barrett, B. (Columbia Univ., New York); Tanaka, K. Nuovo Cimento (10), 36: 965-7(Apr. 1, 1965). (COO-1261-10).

The interaction responsible for the electromagnetic decays of the decuplet of $\frac{3}{2}^+$ baryon resonances is assumed to contain a symmetry-breaking part transforming as the I = 0, Y = 0 member of an octet, and relations between the amplitudes for these decays are presented. The effect of an interaction transforming as a member of the 27 representation is also discussed. (auth)

47345 QUANTUM FIELD THEORY OF THE BOOTSTRAP MECHANISM. Guettinger, W. (Universitaet, Munich). Nuovo Cimento (10), 36: 968-1001(Apr. 1, 1965).

It is shown that a self-supporting mechanism operates in a conventional quantum field theory which fixes the coupling constants and mass ratios and reproduces the bootstrap mechanism of dispersion theory in some approximation. This self-supporting mechanism is closely related to the Z = 0 physics of composite elementary particles. A restatement of the concept of mass renormalization in other terms is shown to produce finite values for the masses of physical elementary particles in the limit where they become composite. Finiteness of the particle masses is the consequence of a resonance effect. The bootstrap mechanism of field theory and that of dispersion theory turn out to be equivalent to a field theory with direct Fermi interaction, the bare Fermi constant of which vanishes if the theory is to describe interacting particles of finite mass. (auth)

47346 ELECTROMAGNETIC INTERACTION OF MESONS RESULTING FROM A BROKEN SYMMETRY. Guralnik, G. S. (Imperial Coll. of Science and Tech., London). Nuovo Cimento (10), 36: 1002-15(Apr. 1, 1965).

The Nambu, Jona-Lasinio broken symmetry theory is restated in terms of Green's functions in the presence of an external current source. By using these Green's functions, it is possible to calculate the lowest-order effects of electromagnetic interactions on the initially massless pseudoscalar mesons induced by the broken symmetry. It is found that the uncharged meson acquires no mass, and hence the results are consistent with the Goldstone theorem applied to the fully interacting system. (auth)

47347 S-WAVE PION-PION SCATTERING IN THE STATE T = 0. Nath, Ravinder; Pande, L. K. (Univ. of Delhi). Nuovo Cimento (10), 36: 1035-8(Apr. 1, 1965).

An attempt is made to reproduce the correct scattering length for the possible S-wave, T = 0 $\pi\pi$ resonance, the σ meson, in a simple N/D method, using a knowledge of the forces due to the low-mass intermediate states in the crossing channel. One- and two-channel calculations are made for the $\pi\pi \to \pi\pi$ and $\pi\pi \to K\bar{K}$ scattering; it is not found possible to obtain the σ meson in this way. (M.J.T.)

47348 LOW-ENERGY Σ^-n INTERACTIONS. Dass, Guru Vachan (Univ. of Delhi). Nuovo Cimento (10), 36: 1045-6(Apr. 1, 1965).

The possibility of a sigma-nucleon bound state in the T = $\frac{3}{2}$ state is discussed on the basis of an N/D calculation within the framework of the one-boson-exchange model. The $^1S_0$, the $^3S_1$, and the $^3P_0$ phase shifts are evaluated, using the Zemach approximation. It is concluded that there is no bound state in either S state; since inelastic unitarity is not considered, no conclusion can be made about a possible P resonance. (M.J.T.)

47349 VERTEX PARTS AND COMPOSITENESS. Dowker, J. S. (Univ. of Manchester, Eng.). Nuovo Cimento (10), 36: 1050-1(Apr. 1, 1965).

Comments are made on a previous suggestion that a dynamical pole in the two-particle scattering amplitude may not induce a pole in the vertex and self-energy functions of the bound state corresponding to the pole or of the particle with the same quantum numbers as the bound state. The pole locations of the scattering amplitudes with off-mass-shell external lines and with on-shell lines are discussed. Problems connected with the inclusion of composite particles in the lagrangian are also considered. (M.J.T.)

47350 A POSSIBLE MODEL FOR A STRONG INTERACTION IN THE P_{11} PION-NUCLEON STATE. Clegg, A. B. (Oxford Univ.). Nuovo Cimento (10), 36: 1052-4 (Apr. 1, 1965).

An explanation for the observed rapid rise in the P_{11} phase in pion-nucleon scattering near 500-Mev pion energy is offered. A conceivable model for a strong interaction of two pions with the nucleon at the same

time is discussed. It is proposed that both pions may each spend an appreciable part of the time in the (I, J) = (3/2, 1/2) state with respect to the nucleon. It is shown that it is possible to find a wave function for an (I, J) = (1/2, 1/2) state of the Nππ system in which both pions have a large probability of being in an (I, J) = (3/2, 3/2) state with respect to the nucleon at the same time. (M.J.T.)

47351 POSSIBLE TEST OF CP VIOLATION AND THE $|\Delta T| = 1/2$ RULE FOR RADIATIVE K-MESON DECAYS. Cline, D. (Univ. of Wisconsin, Madison). Nuovo Cimento (10), 36: 1055-8(Apr. 1, 1965). (COO-881-44).

It is pointed out that if the lowest-order multipole radiation dominates the decay $K_2^0 \rightarrow \pi^+ + \pi^- + \gamma$ as well as the direct emission amplitude for the decay $K^+ \rightarrow \pi^+ + \pi^0 + \gamma$ and if the $|\Delta T| = 1/2$ rule is valid, then the decay mode $K_2^0 \rightarrow \pi^+ + \pi^- \rightarrow \pi^+ + \pi^- + \gamma$ should be observable. Photon spectra for the various decay modes are shown, assuming different branching ratios, and the effect of CPT invariance or CP violation on the decay rates of the various modes is considered. (M.J.T.)

47352 MASS FORMULA IN THE COVARIANT SPIN-UNITARY SPIN SCHEME. Roman, P.; Aghassi, J. J. (Boston Univ.). Nuovo Cimento (10), 36: 1062-5(Apr. 1, 1965).

A rigorous justification of a modified powerful mass formula is given. The full symmetry group, SV(12) ⊗ U_1^B, where U_1^B is the baryon gauge group, is considered and broken into combinations of the SU(3), L(5), and U_1 groups to obtain a quadratic mass formula for both bosons and fermions. This formula is applied to the baryon supermultiplet 364 and the meson supermultiplet 143; results of computed baryon and meson masses are tabulated. (M.J.T.)

47353 HIGH-ENERGY BEHAVIOUR OF TOTAL CROSS-SECTIONS. Jameel, M. (Univ. of Sydney). Nuovo Cimento (10), 36: 1066-8(Apr. 1, 1965).

A property of the total cross section for any elementary process dominated by the exchange of a Regge pole is reported. The photoproduction of pions on nucleons is considered as an example. It is found that the total cross section decreases at least as fast as the forward differential cross section at high energy. (M.J.T.)

47354 THE DETECTION AND THE MEASUREMENT OF ENERGY OF ELECTRON CASCADES IN A SMALL LEAD-PLATE SPARK CHAMBER. Agrinier, B. (CEA, Saclay, France); Koechlin, Y.; Parlier, B.; Boella, G.; Delgi Antoni, G.; Dilworth, C.; Scarsi, L.; Sironi, G. Nuovo Cimento (10), 36: 1077-88(Apr. 16, 1965).

The development of electron showers in a small lead-plate spark chamber was observed in the energy ranges 0.5 to 1.45 Bev and 3 to 8 Bev during exposures at the Saclay and C.E.R.N. protosynchrotrons. The possibility of discrimination between electron showers and nuclear interactions is discussed, and an empirical relation between electron shower size and energy is established. (auth)

47355 COHERENT PRODUCTION OF PION TRIDENTS BY A PRIMARY BEAM OF 16.2 Gev/c NEGATIVE PIONS IN NUCLEAR EMULSION. Rinaldo, J. D.; Jain, P. L.; Bharadwaj, P. D. (State Univ. of New York, Buffalo). Nuovo Cimento (10), 36: 1089-1100(Apr. 16, 1965).

Predictions were made recently of a special type of inelastic interaction between a high energy particle and a nucleus which acts coherently. By using a primary beam of 16.2-Bev/c negative pions, events with only three outgoing relativistic tracks (tridents) were selected by along-the-track scanning. A total of 13 tridents were found out of 503 interactions. From these 13 tridents only two pion tridents were positively identified; one for Coulomb dissociation and the other for diffraction dissociation by two independent methods i.e. 1) by the longitudinal momentum transfer to the target nucleus computed from measurements and 2) by the measurement of the space angles of the shower tracks. The cross section for pion-pion interactions was estimated for one event and was found to be in good agreement with previous results. (auth)

47356 THE REACTION $K^+p \rightarrow K^0p\pi^+$ AT 3 Gev/c. Ferro-Luzzi, M.; George, R.; Goldschmidt-Clermont, Y.; Henri, V. P.; Jongejans, B.; Leith, D. W. G.; Lynch, G. R.; Muller, F.; Perreau, J.-M. (CERN, Geneva). Nuovo Cimento (10), 36: 1101-20(Apr. 16, 1965).

The reaction $K^+p \rightarrow K^0p\pi^+$ was studied at 3.0 Bev/c. The two dominant reactions in this final state are $K^+p \rightarrow K^*p$, $K^* \rightarrow K^0\pi^+$ and $K^+p \rightarrow \Delta^{++}K^0$, $\Delta^{++} \rightarrow p\pi^+$ accounting each for (38 ± 3)% of the events and corresponding to a cross section of (0.8 ± 0.1) mb. The production angular distributions for both K^* and Δ^{++} are suggestive of a peripheral mechanism of production. Within the framework of a simple one-meson-exchange model, the decay angular distributions for K^* are consistent with the assumption that these events are predominantly produced by the exchange of a vector meson with only (7 ± 6)% of the events being produced by the exchange of a pion. The Δ^{++} decay distributions agree with the prediction of the model of Stodolsky and Sakurai. For both K^* and Δ^{++}, a form factor of the type $\exp[-\Delta^2/t^2]$, with t equal to about 0.6 Bev/c, is needed to fit the very sharply peaked production distributions. A modified one-meson-exchange model, taking into account absorption effects due to competing processes, derived by Gottfried, Jackson, and Svensson, gives a reasonable account of the production angular distribution and of the decay correlations for both K^* and Δ^{++}. (auth)

47357 ANALYSIS OF EXPERIMENTAL DATA CONCERNED WITH PION-PION SCATTERING. Baton, J. P.; Regnier, J. (CEN, Saclay, France). Nuovo Cimento (10), 36: 1149-63(Apr. 16, 1965). (In French).

Experimental information concerning the $\pi^-\pi^0$ and $\pi^-\pi^+$ elastic scatterings are analyzed with the goal of making precise the phase shifts of the first partial waves and in particular that of the I = 1, l = 1 state. It is shown that the results depend critically on the hypothesis made as to the connections between the actual ππ scattering and the observed phenomenon. As an example, two series of phase shifts are given, one corresponding to the approximation said to be of the physical region, the other corresponding to the assumption that the ρ is a resonance in the I = 1, l = 1 state. (tr-auth)

47358 Σ-Λ CONVERSION IN K⁻-DEUTERIUM ABSORPTIVE PROCESSES AT REST. Chand, Ramesh (Wayne State Univ., Detroit). Nuovo Cimento (10), 36: 1237-56(Apr. 16, 1965).

In the multiple scattering formalism for $\bar{K}\Lambda\Lambda$ system, the pion momentum spectra and the total rates for the at-rest absorption processes $K^- + d \rightarrow \pi^- + \Sigma^+ + n$, $\pi^- + \Sigma^0 + p$, and π^- + indirect Λ + p are calculated using the s-wave $\bar{K}$-nucleon scattering parameters of the solution XI as input. The calculations are performed using the zero-range boundary conditions method of Dalitz for coupled $\bar{K}\Lambda$, πY and $\Sigma\Lambda$, $\Lambda\Lambda$ systems. By imposing a constraint of $\Sigma\Lambda$ bound state description of $\Lambda\Lambda$ resonance in I = 1/2, $^3s_1$-state for determining the $\Sigma\Lambda \rightarrow \Sigma\Lambda$ and $\Sigma\Lambda \rightarrow \Lambda\Lambda$ amplitudes, no evidence of a $\Lambda\Lambda$ resonance in the at-rest K^--deuterium absorptive reactions is found on comparing the calculated and the experimental values of the π^--momentum spectra associated with the production of indirect Λ-hyperons. (auth)

47359 SPIN-ONE WAVE EQUATION. Sankaranarayanan, A.; Good, R. H. Jr. (Ames Lab., Ames, Iowa). Nuovo Cimento (10), 36: 1303-15(Apr. 16, 1965). (IS-1000).

A manifestly covariant wave equation for a spin-one particle is given in which the wave function has six components. The thirty-six bilinear covariants are exhibited. Formulas for the three-vector, four-vector, and antisymmetric tensor polarization operators are given which are valid for any spin. The connections with other spin-one formalisms are shown. (auth)

47360 SINGULAR POTENTIALS IN CO-ORDINATE SPACE. Cornille, H. (CERN, Geneva). Nuovo Cimento (10), 36: 1316-36(Apr. 16, 1965).

With the help of the Laplace transform, the possibility of useful approximate methods for the Jost functions was

shown previously in the case of Yukawa generalized potentials, where the most singular term near the origin is like G^2r^{-2n} ($n \geq 1$, $G^2 > 0$ for $n > 1$). The same problem of the construction of the Jost function is studied directly in coordinate space for families of singular potentials where the most singular term near the origin is repulsive. The same family of short-range potentials, as previously made with the use of Laplace transform, and also a family of arbitrary power potentials more singular than r^{-2} are considered. The key is to define new Jost solutions asymptotically ingoing (or outgoing) and going to constant (Jost function) near the origin. If the perturbation expansion of these new Jost functions is considered, it is found that, if the order of the perturbation p and the radial coordinate are connected in a certain manner, then the Jost function is the limit of convergent sequences. More explicitly, it is found that there exists a limiting dependence $r_L(p) = \text{const}/p^{(1/(n-1))-\epsilon'}$ ($\epsilon' > 0$ arbitrary small), such that if r(p) goes to zero less rapidly than $r_L(p)$ these sequences are convergent. Arbitrary cut-off or hard-core procedures are not used, and only when p is infinite is it obtained that these r(p) dependences are 0. (auth)

47361 ON THE INVERSION PROBLEM IN THE λ-PLANE. Burdet, G. (Faculte des Sciences, Lyon); Giffon, M.; Predazzi, E. Nuovo Cimento (10), 36: 1337-47(Apr. 16, 1965).

The inversion problem in the complex angular momentum plane is treated for a class of potentials behaving near the origin less singularly than the centrifugal term. The method follows the one of Jost and Kohn in the complex linear momentum plane. Equations of the Gel'fand and Levitan type are established which allow the potential to be constructed from the knowledge of both the discrete and continuum spectra in the complex angular momentum plane for a given physical angular momentum. (auth)

47362 ON CORBEN'S QUANTUM THEORY OF ELEMENTARY PARTICLES. Castell, L. (Univ. of London). Nuovo Cimento (10), 36: 1348-50(Apr. 16, 1965).

It is pointed out that the linear field equations proposed by Corben can be interpreted consistently only in the framework of an indefinite metric in Hilbert space. In addition the lowest energy level trajectories are calculated for arbitrary high spin. (auth)

47363 LEPTONIC NEUTRON DECAY OF Ω^-. Gupta, K. C.; Mathur, V. S. (Univ. of Delhi). Nuovo Cimento (10), 36: 1359-64(Apr. 16, 1965).

In an attempt to clarify the roles of the $\Delta I = \frac{1}{2}$ rule and the $\Delta S = \Delta Q$ rule in semileptonic weak interactions, the decay $\Omega^- \rightarrow n + e^- + \bar{\nu}$ is considered. The characteristics of this decay mode are calculated and compared with those of the leptonic decay of Ω^- to Ξ^0. (auth)

47364 HIGH-ENERGY ELECTRON-POSITRON SCATTERING. Vigier, J. P. (Institut Henri Poincare, Paris); Wataghin, V. Nuovo Cimento (10), 36: 1380-3(Apr. 16, 1965).

Theoretical predictions of a model of electrodynamics are stated for the case of high-energy electron-positron elastic scattering. The model preserves both macroscopic causality and Lorentz invariance and introduces in momentum space form factors which modify the local matrix elements and depend both on the square of the momentum transfer and on the square of the total cms energy involved. The model is formulated in terms of Feynman diagrams. Results of calculations of the angular distributions of Bhabha scattering at various energies and angular momenta are plotted. (M.J.T.)

47365 Y_0^* RESONANCE AND $\bar{K}$-N $^1S_0$, T = 0 SCATTERING LENGTH. Pal, B. K. (National Physical Lab., New Delhi, India). Nuovo Cimento (10), 36: 1392-4(Apr. 16, 1965).

The scattering length for the $\bar{K}$-N interaction is calculated using a modified Khuri representation and introducing Born terms where possible. Equations for the modified scattering amplitudes are presented. Results of the calculation are compared with those of previous works. (M.J.T.)

47366 THE ELECTROMAGNETIC Σ^0-Λ^0 MIXING AND THE Y_0^* DECAYS. Chan, C. H.; Sarker, A. Q. (Univ. of California, San Diego, La Jolla). Nuovo Cimento (10), 36: 1402-4(Apr. 16, 1965).

The SU(3) prediction that the physical eigenstates, Λ_p^0 and Σ_p^0, are definite combinations of the isospin-pure Λ^0 and Σ^0 states, with the mixing due to electromagnetic interactions, is discussed. Consequences of this mixing in the decay of Y_0^* resonances are considered. Equations for the mixing parameters are found in terms of the electromagnetic transition masses $(\Sigma^0|\Lambda^0)$ and $(\pi^0|\eta^0)$ and used to calculate the decay branching ratio for the processes $Y_0^* \rightarrow \Sigma_p^0 + \pi_p^0$ and $Y_0^* \rightarrow \Lambda_p^0 + \pi_p^0$, for the various observed Y_0^* resonances. It is found that the branching ratio for $Y_0^*(1520)$ is measurable, assuming that the $Y_0^*(1520)$ is a member of an SU(3) octet and that the mass transitions $(\Sigma^0|\Lambda^0)$ and $(\pi^0|\eta^0)$ are as large as predicted by SU(3). (M.J.T.)

47367 A NOTE ON THE SU_6 SYMMETRY FOR STRONG INTERACTION. Ohnuki, Y.; Toyoda, A. (Nagoya Univ., Japan). Nuovo Cimento (10), 36: 1405-7(Apr. 16, 1965).

The SU(6) supermultiplet theory is examined, assuming, for simplicity, a four-fermion interaction among quarks. The strong-coupling approach, in which only the interaction hamiltonian H' is invariant and where the quark kinetic energy in the compound state is small compared with the interaction energy, leads to results contradicting the experimental situation. The weak-coupling or nonrelativistic approach, leaving H_0 invariant and dividing H' into two parts H_1' and H_2' and $H_0 + H_1'$ SU(6)-invariant, is found more suitable. (M.J.T.)

47368 PHOTOPRODUCTION OF π^0 FROM HYDROGEN NEAR THE SECOND PION-NUCLEON RESONANCE. De Staebler, H. Jr.; Erickson, E. F.; Hearn, A. C.; Schaerf, C. (Standford Univ., Calif.). Phys. Rev., 140: B336-48 (Oct. 25, 1965).

Angular distributions for π^0 photoproduction from hydrogen at energies between 660 and 800 Mev and proton center-of-mass angles from 0 to 140° were measured and analyzed. Some variation from a pure $d_{\frac{5}{2}}$ state is seen in the resonance region. A possible high-momentum-transfer enhancement of the cross section is discussed. (auth)

47369 ELECTROMAGNETIC MASS DIFFERENCES OF VECTOR BOSONS. Bose, Sudesh (Univ. of Delhi). Phys. Rev., 140: B349-51(Oct. 25, 1965).

The recent method of Dashen and Frautschi is applied to calculate the ρ^+-ρ^0 and K^{*+}-K^{*0} mass differences. In the SU(3) relation, the calculated values of the above-mentioned mass differences are substituted to estimate the ρ^0-ω_8^0 transition mass. The decay rates of $\omega \rightarrow 2\pi$ and $\phi \rightarrow 2\pi$ are briefly discussed. (auth)

47370 RARE $\Delta Q = 0$, $\Delta S = 1$ DECAY MODES OF HYPERONS AND K MESONS. Tanaka, K. (Ohio State Univ., Columbus). Phys. Rev., 140: B463-5(Oct. 25, 1965). (COO-1261-8).

The $\Delta Q = 0$, $\Delta S = 1$ component of the unitary spin current is used in interactions that are both weak and electromagnetic. The effective coupling constant is determined from the experimental decay rate $\Sigma^+ \rightarrow p + \gamma$. With the aid of symmetry arguments, the rare decay rates of the modes $B \rightarrow B' + \gamma$, $B \rightarrow B' + e^+ + e^-$, and $K \rightarrow \pi + e^+ + e^-$ are computed. (auth)

47371 $\pi\rho$ AND $K\bar{K}$ CONTRIBUTION TO THE ISOSCALAR FORM FACTOR OF THE NUCLEON. Uchiyama-Campbell, Fumiyo (Univ. of California, San Diego, La Jolla). Phys. Rev., 140: B473-9(Oct. 25, 1965).

The isoscalar form factors of the nucleon are calculated assuming that the low-energy part of the spectral functions is determined by the three-pion ($\pi\rho$ in this approximation) and $K\bar{K}$ intermediate states. The effect of the ω and φ mesons is evaluated using the relativistic effective-range approximation. The $\langle\pi\rho|N\bar{N}\rangle$ and $\langle K\bar{K}|N\bar{N}\rangle$ amplitudes are considered in the approximation of a one-baryon exchange interaction. The results are compared with experiments, and a qualitative discussion of the relative weight of the ω and φ contributions is given. (auth)

47372 SEARCH FOR C-INVARIANCE VIOLATION IN η(958 Mev) AND η(549 Mev) DECAYS. Rittenberg, Alan (Univ. of California, Berkeley); Kalbfleisch, George R. Phys. Rev. Letters, 15: 556-60(Sept. 27, 1965). (UCRL-16297)

A search for C-nonconserving decay modes and asymmetries in η(549) and η(958) decays was made. No C-invariance violating effects are observed, although the sensitivity of the measurement is such that even a maximal violation in electromagnetism cannot be ruled out. But it is noted that the $\pi^0 \to e^+e^-$ decays may be suppressed relative to current crude estimates. The η(958) mesons were produced in the reaction $K^- + p \to \Lambda + \eta(958)$. About 700,000 pictures of 2.1-, 2.45-, 2.55-, 2.63-, and 2.70-Bev/c mesons (K^-) incident upon the 72-in bubble chamber were used. The η(958) mesons subsequently decay, $\eta(958) \to \eta(549) + \pi^+ + \pi^-$, producing η(549) mesons. (J.F.P.)

47373 POLARIZATION IN $\pi^- + p$ ELASTIC SCATTERING AT 2.08 Gev/c. Suwa, Shigeki (Argonne National Lab., Ill.); Yokosawa, Akihiko; Booth, Norman E.; Esterling, Robert J.; Hill, Roger E. Phys. Rev. Letters, 15: 560-3(Sept. 27, 1965).

The differential cross section and polarization $\pi^- + p$ elastic scattering is measured at an incident meson (π) laboratory momentum of 2.08 Bev/c. This momentum is interesting because it is near the center of a 2-mb peak observed in the $\pi^- + p$ total cross section measured previously as a function of energy. At this energy considerable scattering at larger angles is also found including a prominent peak. The polarization measurements show that the usual assumption of a single scalar amplitude to describe elastic scattering in this energy region is not valid. The experiment was carried out with a zero gradient synchrotron with polarized proton target. Negative mesons (π) were directed into the apparatus by a standard beam transport system. The results for the differential cross section and polarization were plotted against cos θ_π in the center of mass system. (J.F.P.)

47374 $p\bar{p}$ ANNIHILATION INTO TWO MESONS IN THE SPURION SCHEME OF BROKEN U(6,6) SYMMETRY. Lai, Chai S. (Univ. of Chicago). Phys. Rev. Letters, 15: 563-7(Sept. 27, 1965).

It is pointed out that the inclusion of the U(6) symmetry-breaking spurions previously reported $(\gamma_5 \otimes \gamma_5) \otimes \epsilon_1$ and $(\gamma_\mu \otimes \gamma_\mu) \otimes \epsilon_1$ which are still SU(3) singlets as indicated by the factor ϵ_1, gives rise to quite different and more reasonable predictions. Since $p\bar{p}$ annihilation at rest into two mesons is forbidden in the $U(6)_q$-invariant pole dominance model, the following two models are considered: In the first case it is assumed that the $U(6)_q$-invariant amplitude is supplemented by terms obtained with a U(6)-breaking spurion $(\gamma_5 \otimes \gamma_5) \otimes \epsilon_1$ in arbitrary order. There remains invariance under a group U(3) $\otimes$ U(3) with generators $(1 \pm \vec{\sigma} \cdot \vec{\xi}) \otimes \lambda_a$. For the other model, the $U(6)_q$-breaking (with spurions $(\gamma_5 \otimes \gamma_5 \otimes \epsilon_1$ and $\gamma_\mu \otimes \gamma_\mu) \otimes \epsilon_1$) pole terms are dominant compared to other symmetry-breaking non-pole terms. In this model, it is important to assume the meson-pole dominance, because otherwise the symmetry is broken down to SU(3). The $U(6)_q$-symmetric term is included, since it is assumed to be comparable with the $U(6)_q$-breaking pole terms. It is concluded that the first model is not empirically favorable, but the sum rules for the second model are compatible to the present experimental data. (J.F.P.)

47375 EXTRA RESTRICTION ON THE FORWARD SCATTERING AMPLITUDES. Sawada, Tetsuo (International Centre for Theoretical Physics, Trieste). Phys. Rev. Letters, 15: 567-71(Sept. 27, 1965).

In the case of the first sheet function the value of the function itself cannot be computed in a small neighborhood of certain points from the unitary condition alone without introducing any approximation, since although the pole term dominates, there still remains finite background contribution and there is no way to compute it exactly. The discussion is restricted to the case of meson (π)-nucleon scattering, and the spin of the nucleon is neglected for reasons of simplicity. A new method is developed which may be used not only to obtain the relation between the total cross section and the coupling constant, but also to compute the subtraction constant from the total cross section without introducing any approximation. (J.F.P.)

47376 THEORY OF BOUND STATES. II. FOUR-DIMENSIONAL DEUTERON WAVE FUNCTION. Kawaguchi, Masaaki (Osaka Univ.). Progr. Theoret. Phys. (Kyoto), 34: 243-51(Aug. 1965).

The four-dimensional deuteron wave function is obtained based on the method of solving the Bethe-Salpeter equation. It is shown that the three-dimensional deuteron wave function obtained from our four-dimensional function exactly coincides with the ordinary wave function of the S state. Our approximation turns out to be very good for the wave function of bound states. (auth)

47377 CHARGE RATIO OF PRODUCED PIONS IN NEUTRINO INELASTIC SCATTERING. Fukawa, Mineo (Sophia Univ., Tokyo). Progr. Theoret. Phys. (Kyoto), 34: 252-5(Aug. 1965).

In the neutrino inelastic scattering the predominance of the production of π^+, compared with that of π^0 is likely due to the associate appearance of N**, not to the only effect of 3-3 resonance state that gives rise to the ratio 5 to 1. The charge ratio is calculated to be 3.1 on the basis of the SU(3) $\otimes$ SU(3) symmetry scheme. (auth)

47378 ON THE NATURE OF MUON. Nakamura, Seitaro (Tokyo Univ.; Nihon Univ., Tokyo); Itami, Kunio; Ugai, Hiroyuki. Progr. Theoret. Phys. (Kyoto), 34: 256-62(Aug. 1965).

By assuming that a neutral intermediate boson $W^{0\prime}$ with the particle number ± 2 interacts between muon and electron in the following channels: $(\mu^+)^c \to e^- + (W^{0\prime})^c$, $\mu^+ \to (e^-)^c + W^{0\prime}$, their effects on the anomalous magnetic moments of muon and electron are calculated. With regard to the μ-e decay and the anomalous magnetic moments, a consistent solution of the coupling constants is found for the theory in which the intermediate boson interacts with neutrino in the super-weak coupling and with the fermions (other than neutrino) in the meso-strong coupling. (auth)

47379 INTRINSICALLY BROKEN $\tilde{U}(18)$ SYMMETRY. Miyazawa, Hironari; Sugawara, Hirotaka (Tokyo Univ.). Progr. Theoret. Phys. (Kyoto), 34: 263-73(Aug. 1965).

The SU(9) symmetry is extended to SL(9) so that the Lorentz invariance is preserved. Discrete operations P, C, and T are also extended. An adjoint representation of $\tilde{U}(18)$ contains $(1/2)^+$, 0^- and 1^- particles of the SU(3) singlet and of the octet. Totally symmetric representation is also examined. Ordinary SU(6) results concerning the baryon currents are reproduced if the latter representation is chosen. In our theory the baryon number is included in the SL(3) algebra which is extended from the SL(2) (covering group of the Lorentz group) algebra. The second quantization is done so that it violates the SL(9) symmetry. The quantization of this system consistent with the symmetry seems difficult and is not attempted. (auth)

47380 SHRINKAGE OF EFFECTIVE CORE AND LARGE ANGLE SCATTERING AT HIGH ENERGY. Yamamoto, Kunio (Osaka Univ.). Progr. Theoret. Phys. (Kyoto), 34: 274-83(Aug. 1965).

It is shown that, by improving a previous theorem, the first $l_0(s)$ partial wave amplitudes determine the scattering amplitude for the scattering angle θ within an error smaller than exp [–const $l_0(s)\sin\theta/\ln l_0(s)$] provided that $l_0(s) >$ const $\ln s/\sin\theta$, s being the square of the center-of-mass energy. The improvement of the error is important for the investigation of the large angle scattering at high energy. In connection with this improvement, a field theoretical model of the high-energy large-angle scattering is presented. The improvement of the lower limit of $l_0(s)$ immediately gives us the high energy bound of Kinoshita, Loeffel and Martin. The scattering of particles with spin is also discussed. (auth)

47381 K-MATRIX FORMALISM FOR THREE-BODY SCATTERING AND BOUND-STATE SCATTERING. Mishima, Nobuhiko; Yamazaki, Miwae (Tokyo Metropolitan Univ.). Progr. Theoret. Phys. (Kyoto), 34: 284-8(Aug. 1965).

The K-matrix formalism corresponding to the T-matrix formalism given by Faddeev is described for the three-body and bound-state scatterings. (auth)

47382 SYMMETRY CHARACTER OF BOUND STATES WITH MULTICHANNELS. Okabayashi, Takao (Tokyo Univ.). Progr. Theoret. Phys. (Kyoto), 34: 289-98(Aug. 1965).

It is pointed out from the standpoint of the Green function formalism that the existence of bound states in multichannel problems always introduces a group which is restricted by the degeneracies of bound states and their constituent particles. The vertex function of the secondary interaction between a bound state and its constituent particles is proportional to the Clebsch-Gordan coefficients of the group. Further, it is shown that the bootstrap philosophy can be seen as a formalism in which the elementary (or, more strictly speaking, fundamental) particles and their interactions are eliminated from the usual formalism of the field theory. (auth)

47383 ON THE MASS SPLITTING UNDER SU(3). Kawamura, Ryuji (Tokyo Metropolitan Univ.). Progr. Theoret. Phys. (Kyoto), 34: 312-13(Aug. 1965).

It is shown that the output mass splitting for the vector meson originates from the input mass splitting for the PS meson and a symmetric property. The symmetric interaction is assumed and only the lowest self-energy diagram is considered. It is concluded that, if the SU(3) type interaction and the mass splitting for the PS meson due to the Gell-Mann Okubo mass formula are assumed, the derived mass splitting for the vector meson has the same relation as the one given by the Gell-Mann Okubo mass formula. Also, if $\delta m_8^2 = \delta m_3^2 = \delta m_0^2$ is assumed for the PS meson $\delta m_3^1 = \delta m_0^2 = \delta m_x^2$ is obtained. It is expected that the output mass splitting calculated by the bootstrap method also originates from the input mass splitting as was previously discussed. (J.F.P.)

47384 MASS FORMULA FOR RESONANCE STATES. Ihara, Chiaki; Nakazawa, Kazo (Kyoto Univ.). Progr. Theoret. Phys. (Kyoto), 34: 316-17(Aug. 1965).

The mass formula for the resonance states was investigated based on the group-theoretical considerations and from an empirical point of view. An empirical mass formula is proposed for the presently discovered resonance states from the latter standpoint. The boson resonance states and the baryon resonance states are considered. (J.F.P.)

47385 SU(6) AND RP INVARIANCE IN NONLEPTONIC BARYON DECAYS. Itoh, Chiaki (Tokyo Univ.). Progr. Theoret. Phys. (Kyoto), 34: 318-19(Aug. 1965).

RP invariance is applied to nonleptonic baryon decays in SU(6). It assumed that parity-violating and parity-conserving interactions transform as (8,1) and (8,3) members of the 35-dimensional representations, respectively, and also that weak interactions are CP invariant. Baryons which are 56-dimensional may be described by a mixture of tensors which are symmetric with respect to the indices α, β and γ. These tensors are reducible under SU(3) $\otimes$ SU(2) and are expressed, in the rest frame, in terms of spin wave functions and SU(3) tensors. It is emphasized that SU(6) and RP invariance now give the same relations without assuming the pole approximation, as was done in the previously obtained relations. The results are given. The theory predicts the nonleptonic weak vertices between baryons and vector mesons, which are important in the nonmesonic decays of hyperfragments, as was previously found. (J.F.P.)

47386 ON A 3*-PLET MODEL OF ELEMENTARY PARTICLES. Nakagawa, Masami (Nagoya Univ., Japan). Progr. Theoret. Phys. (Kyoto), 34: 323-5(Aug. 1965).

Another possible scheme for elementary particles is considered in which ξ^0, ξ^-, and λ^0 are assumed as urbaryons. In the strong interaction a full symmetry, mentioned previously, is assumed for the urbaryons in the strong interactions. In order to examine mass values, a mass operator is assumed, which includes a symmetry breaking in interaction up to the second order. (J.F.P.)

47387 CHARGE FORM FACTOR AND THE COULOMB ENERGY OF ^{3}He. Okamoto, Kazuto (North Japan Coll., Tagajo) Progr. Theoret. Phys. (Kyoto), 34: 326-8(Aug. 1965).

It was previously pointed out that the Coulomb energy of Helium-3 is smaller than the binding energy difference between ^{3}He and ^{3}H. However there is a question about the validity of the SS′ interference, on which the discussion was based. Also the accuracy of variational calculation, which was used to deduce the final result, is not good. Therefore, the Coulomb energy is estimated directly from the observed charge form factor of ^{3}He to see if the conclusion is reliable. The resulting energy value is in good agreement with that of the previous discussion, unless charge symmetry is considered in which case there is disagreement with the experiment. The conclusion is independent of the existence of the S′ state and of the accuracy of the variational calculations. That is, it is almost certain that the Coulomb energy of ^{3}He is smaller than the binding energy difference between ^{3}He and ^{3}H, as far as the wave function which reproduces the observed charge form factor of ^{3}He is assumed. (J.F.P.)

47388 FIXED VARIABLE DISPERSION RELATIONS FOR THE PION–NUCLEON SYSTEM. Lyth, D. H. (NORDITA, Copenhagen). Rev. Mod. Phys., 37: 709-23 (Oct. 1965).

It is shown that an earlier study by Hamilton and Woolcock of fixed momentum-transfer dispersion relations may be complemented by a study of fixed energy dispersion relations. Two main results are obtained. First, by demanding that the two types of relation give the same value for the amplitude, nontrivial restrictions are obtained on the amplitude (the f_0-N-N coupling constants and the values of certain integrals over the high-energy πN amplitude are obtained). Secondly, the fixed energy relation enables one to discuss quantitatively the validity of the "CGLN" approximate method which Hamilton and Woolcock had used to calculate the partial-wave amplitudes at low energies from the fixed momentum-transfer dispersion relation alone. The terms neglected by this approximation are evaluated, and found to be large except at low energies. Even when these terms are included, undesirable cancellations occur, and the conclusion in fact is that fixed variable relations are not suitable for calculating the partial-wave amplitudes (except at low energies), but only for providing sum rules. (auth)

47389 PHOTO-PRODUCTION OF TWO MESONS ON NUCLEON AT HIGH ENERGY. Mihul, Eleonora; Ion, D. B. (Institute for Atomic Physics, Academy of the R. P. R., Bucharest). Rev. Roumaine Phys., 10: 267-74(1965).

The interactions of high-energy photons and nucleons in which two π (K)-mesons are produced are dealt with using the Regge pole hypothesis. The isoscalar and isovector contribution was estimated, as well as their ratio at high energies. The momentum – transfer distributions of the final nucleons were calculated for 4 Bev energy in the cms. At the same energy the invariant-mass distribution of the produced pions was calculated for the case when the ρ-resonance appears. The results offer a check of the Regge pole hypothesis for photoproduction processes and can also be used for obtaining certain information on the Regge trajectories. (auth)

47390 ON THE SIGN OF THE EFFECTIVE RANGE PARAMETER. Radescu, E.; Visinescu, M. (Inst. for Atomic Physics, Academy of the R.P.R., Bucharest). Rev. Roumaine Phys., 10: 573-9(1965).

The effective range parameter r_0 is written in terms of cut-contributions corresponding to Yukawian-potential and poles corresponding to bound, anti-bound and resonant states of the scattering amplitude in complex k-plane. It

is shown that r_0 has different signs in different physical situations. (auth)

47391 TIME REVERSAL. Christenson, J. H. (Columbia Univ. Irvington-on-Hudson, N. Y.). Sci. J., 1: 52-7(Aug. 1965).

Serious doubt was recently cast upon the basic physical principle of time reversal invariance, that physical laws are unchanged when the direction of flow of time is reversed. The results of an experiment indicate that there is at least one exception to this rule. Numerous theories were advanced to explain the experimental results by other means. Even a new fundamental force of nature was suggested. But this proposal was refuted by more recent experiments, leaving the problem unsolved. An explanation of time reversal invariance and the CPT theorem is given. A detailed description of the experiment in which mesons (K_2^0) were found to decay into two mesons (π) showing the time reversal violation, is given. The various theories proposed to explain this phenomena are mentioned; and the theory proposing the new force in nature is discussed together with the experiments disproving it. (J.F.P.)

47392 ANALYTICITY AND THRESHOLD BEHAVIOURS OF FERMION REGGE TRAJECTORIES. Lee, Hwa-chung (Chung-Shan Univ., China). Wu Li Hsueh Pao, 21: 1387-1405(July 1965). (In Chinese).

Starting from π-N scattering amplitude and based on the Mandelstam's representation and unitary condition, analyticity and threshold properties of fermion Regge trajectories of baryon quantum number 1 and strangeness 0 are investigated. The following preliminary results are obtained: (1) The position parameter of the Regge trajectories $\alpha(s)$ has a right-hand physical cut and no left-hand dynamical cut, but has a kinematical left-hand cut at $s = 0$; (2) $\alpha(s)$ in the region $s < 0$ are complex; $\alpha_+(s)$ and $\alpha_-(s)$, being of opposite space parity, are complex conjugate to each other. In the region $0 < s < (M + \mu)^2$, $\alpha_+(s)$ are real but the dependence on s may be different; (3) The energy dependence of $\alpha(s)$ at the threshold is obtained; (4) Two kinds of Regge poles are distinguished. Those with $\alpha(W_0) \neq 0$ (W_0 – threshold energy) are responsible for dynamical resonances and bounded states. There are other kinds of the Regge trajectories for which $\alpha(W_0) = 0$ and whose threshold behaviors are also investigated. As energy approaches the threshold from energy below the threshold, there are infinite pairs of poles approaching Re $J = 0$ from the left half J-plane, each pair containing a couple of conjugate complex poles. While as energy approaches from above the threshold, there are also infinite pairs of poles approaching Re $J = 0$, each pair containing poles in the first and third quadrant of the J-plane. For all these poles, Re $\alpha(s) \to 0$ faster than Im $\alpha(s) \to 0$ by one or two orders. The poles condense at the origin of the J-plane. The Gribov-Pomeranchuk condensation of the Regge poles is obtained in the case of Fermion trajectories. This kind of poles has a purely kinematical origin. They reflect the general properties of the S-matrix at the threshold. (auth)

47393 PHOTOPRODUCTION OF π^+-MESONS ON PROTONS AT E_γ = 230 Mev AND DETERMINATION OF THE $\gamma\pi\rho$-INTERACTION CONSTANT. Aleksandrov, Yu. M.; Grushin, V. F.; Zapevalov, V. A.; Leikin, E. M. (Lebedev Inst. of Physics, Moscow). Zh. Eksperim. i Teor. Fiz., 49: 54-65(July 1965). (In Russian).

The differential cross sections for photoproduction π^+-mesons on protons at an energy E_γ = 230 Mev are measured for angles of 0, 38, 82, 90, 116, 138, 146 and 180° in the c.m.s. A magnetic spectrometer and stop detector for identification of the mesons according to their momentum and range are employed. Stopped π^+-mesons are recorded on basis of the $\pi \to \mu$-decay. On the average the statistical accuracy of the results is ±(3–4)%. The magnitude of the constant $\Lambda_{\gamma\pi\rho}$ is estimated by comparing the experimental data and theoretical calculations based on the dispersion relations; the valuo $\Lambda_{\gamma\pi\rho}$ = (0.63 ± 0.11) ef is obtained. (auth)

47394 RAREFIED FERMI GAS AND THE TWO BODY SCATTERING PROBLEM. Efimov, V. N. (Ioffe Inst. of Physics and Tech., Leningrad). Zh. Eksperim. i Teor. Fiz., 49: 188-92(July 1965). (In Russian).

The difficulties in solving the three-body problem restrict the possibilities of investigation of the properties of a rarefied Fermi gas. With a gas of hard spheres taken as an example, it is shown that expansion of the energy of the ground state in a small parameter $\gamma = p_F a$ (p_F is the Fermi momentum, and a the sphere diameter) can be carried out only to terms of the order of γ^4. Calculation of the latter is equivalent to solving the three-body scattering problem at zero energy. An expansion term preceding γ^4 and proportional to $\gamma^4 \ln \gamma$ is detected and evaluated. Preceding expansion terms have been evaluated earlier. The results are extended to a gas with an arbitrary repulsive interaction. (auth)

47395 THE NUCLEON AS A REGGE POLE (thesis). Dilley, James Paul. Syracuse, N. Y., Syracuse Univ., 1964. 60p.

A calculation is made of the pion-nucleon, $T = 1/2$, p-wave scattering amplitude on the assumption that the nucleon lies on a Regge trajectory and dominates the process at low energies. The parameters of the trajectory are calculated from the threshold behavior of the amplitude and these results are then used to determine the amplitude higher energies and to calculate the pion-nucleon coupling constant. It is found under these conditions, that although the coupling constant is predicted rather well, the computed amplitude differs somewhat from the analyzed experimental values. It is shown that a possible explanation for this discrepancy is that the physical p-wave amplitude is not an analytic continuation from the higher partial waves, and that if the difference of these quantities is approximated by the pole contribution from a fixed energy dispersion relation, the agreement with accepted values is considerably improved. The final determination of whether this explanation is actually correct necessarily depends upon a more detailed knowledge of the other singularities in the complex angular momentum plane and their contribution in this energy region. (Dissertation Abstr.)

47396 UNITARITY AND DISPERSION RELATIONS IN QUANTUM ELECTRODYNAMICS (thesis). Blade, Richard Allen. Boulder, Colo., Univ. of Colorado, 1964. 101p.

The quantum electrodynamic processes $e\gamma \to e\gamma$, $ee \to ee$, and $\gamma\gamma \to \gamma\gamma$ are studied using Lorentz invariance and various conservation laws, and it is shown that $e\gamma \to e\gamma$ has six independent invariant amplitudes, while $ee \to ee$ has five. Possible spinor bases are demonstrated, and invariant variables for analytic continuation are set up. The physical regions for the crossed reactions are shown in terms of these variables. A pole approximation to unitarity is applied to the $e\gamma \to e\gamma$ and $ee \to ee$ processes, and the results are seen to be identical with first order perturbation theory. Unitarity in second order is then studied for the $e\gamma \to e\gamma$, $ee \to ee$, $\gamma\gamma \to \gamma\gamma$ processes using a successive pole approximation. Furthermore, the anomalous magnetic moment of the electron is calculated, and it is shown that $\sigma(\gamma\gamma \to \gamma\gamma)$ is proportional to $e^8\omega^6$ at low energies in the center-of-mass frame. Finally, perturbation methods are reviewed and compared to the successive pole approximation in unitarity. The single pole approximation and first order perturbation results are shown to be always identical, while in second order the dispersion relations are shown to eliminate the need for renormalization. Other methods of approximating unitarity are discussed in connection with the convergence of the perturbation series. (Dissertation Abstr.)

47397 INTERNAL SYMMETRIES IN S-MATRIX THEORY (thesis). Branscomb, Elbert Warren. Syracuse, N. Y., Syracuse Univ., 1964. 126p.

An essential element of S-matrix theory is the postulate that all channels of a given process are described by a single (analytic) amplitude function. The feasibility of this postulate rests on the fact that the amplitudes for the various channels transform equivalently under all invariance

transformations. In view of this fact a channel independent formulation of invariance requirements is given, which is the basis for a discussion of the analytically extended Pauli-principle, crossing symmetries, the expansion of the amplitude tensor into scalar amplitudes and basis tensors, the general crossing matrix, and the extension of the "one amplitude" postulate to quantum numbers other than the four-momenta. These results are applied to the proposed higher symmetry of strong interactions, SU_3, which is first given a short exposition. Numerical values for the components of the basis tensors and the elements of the associated crossing matrices are given for the SU_3 symmetric processes of physical interest. The contrasting roles of Lorentz invariance and the so-called internal symmetries, and the general restrictions that must be satisfied by the representations of the invariance group, are discussed in the appendices. (Dissertation Abstr.)

47398 POSSIBLE EXISTENCE OF VERY MASSIVE, ALMOST BARE, UNSTABLE PARTICLES (thesis). Leiter, Darryl Jay. Waltham, Mass., Brandeis Univ., 1964. 133p.

The possible existence of a hierarchy of very massive, almost bare, unstable particles in scalar, vector, and spinor fields is investigated. Particular attention is paid to the possible existence of a "heavy photon" (Γ_0) and its experimental implications. "Heavy pions" and "heavy nucleons" are also discussed as well as "heavy vectons" in a strong coupling vector gauge theory. (Dissertation Abstr.)

47399 AN APPROXIMATE SOLUTION OF A FINITE MANY PARTICLE SYSTEM WITH TRANSLATIONAL INVARIANCE (thesis). Vassell, Milton Oliver. New York, New York Univ., 1964. 69p.

A formal technique is developed to study internal properties of finite many-particle systems possessing translational invariance. The formalism is based on the method of redundant variables, in which the shell model wave function describes the internal degrees of freedom of the system while a superfluous variable is introduced to satisfy the conservation law and to handle the collective motion. The spurious degeneracy that results from the introduction of the extra variable is removed by suitable subsidiary conditions. With the aid of these restricted solutions it is shown that the density with respect to the center-of-mass can be calculated in terms of a one-body operator. The dynamics of the system is then formulated in terms of density matrices suitably defined from these restricted solutions. Within the context of the modified shell model the density matrices consist of the Dirac density matrices of the shell model plus correction terms that depend nonlinearly on these Dirac matrices and matrix elements of the coordinate, X. The single particle states of the shell model are finally chosen to minimize the expectation of the Hamiltonian. The resulting variational equation contains a homogeneous part that has the structure of the conventional Hartree-Fock equation together with an inhomogeneous term depending nonlinearly on the single-particle states. The solution of this equation is finally expanded about the non-translationally invariant Hartree-Fock solution to first order in perturbation theory. As illustrations of the formalism and the possible utility of the method the problem of N particles interacting via harmonic pair forces is studied, and the possibility of obtaining non-translationally invariant solutions of the Thomas Fermi equation for systems with Coulomb and Yukawa pair interactions is investigated. (Dissertation Abstr.)

47400 A MODIFIED STATISTICAL MODEL FOR ULTRA-HIGH ENERGY INTERACTIONS (thesis). Settles, Ronald Dean. Baton Rouge, La., Louisiana State Univ., 1964. 122p.

A modified statistical model has been used to generate meson showers about which physical information is rather complete. This statistical model is "modified" by constraints consisting of input information based largely on experimentally determined average properties of showers produced by nuclear interactions at about 10^{12} ev. The Monte Carlo method is used to determine properties of the produced particles in the center-of-mass system from the following input information: the angular distribution in the center-of-mass system, the transverse momentum distribution and energy-momentum conservation. The average properties of the resulting meson showers have symmetry between forward and backward directions in the center-of-mass system, and the produced particles possess only those correlations introduced by energy-momentum conservation. The showers are transformed to the laboratory system using the Lorentz transformation corresponding to a nucleon-nucleon collision of 3×10^{12} ev (laboratory energy). Some conventional analysis procedures are carried out with the resulting Monte Carlo jets using parameters calculated from the angular distributions of the charged particles. The results give insight into the sensitivity of the parameters to approximations used in interpreting the parameters and indicate how well, on the average as well as for individual jets, a parameter $Y(\theta)$ is a measure of the physical quantity y which the parameter is expected to represent. The Castagnoli energy is found, rather independently of details of the input information, to overestimate the energy of a jet by an average factor of about 1.8, with statistical fluctuations causing approximately 68% of the measurements to be within a factor of 2.3 of this average factor. Other parameters are examined and are found to be generally more sensitive to the details of the input information. Also studied are methods used for observing the angular distribution in the center-of-mass system; these methods are found to provide average information expected of them. A rather complete investigation using the Monte Carlo jets is made of the four-momentum transfer between two groups of the particles produced in ultrahigh energy interactions. (Dissertation Abstr.)

47401 THE PRODUCTION OF η-MESONS IN PION-NUCLEON COLLISIONS (thesis). Moss, Thomas Alan. Baton Rouge, La., Louisiana State Univ., 1964. 48p.

The $\pi + N \rightarrow \eta + N$ reaction in the neighborhood of threshold is studied from a field-theoretical viewpoint. The effects of the second resonant state of the pion-nucleon system are taken into account, and a parameter study of the reaction is performed in which the variable parameters are the coupling constants involved in the reaction and the resonance width of the second resonant state. The angular distributions and excitation function for the reaction are calculated for various relative magnitudes of the coupling constants and two values of the width. A comparison between these calculated data and experimental angular distributions and excitation functions in the neighborhood threshold is suggested when experimental data in this energy range become available. This comparison may give an indication of the importance of the effect of the second resonant state on the $\eta-N$ interaction thus suggesting the possibility of strong d-wave $\eta-N$ interaction at low energy. (Dissertation Abstr.)

47402 AN INVESTIGATION OF THE L.S.Z. FORMALISM IN THE LEE MODEL (thesis). Maxon, Marshall Stephen. Bloomington, Ind., Indiana Univ., 1964. 47p.

The Lehmann, Szymanzik, and Zimmerman (LSZ) axiomatic approach to field theory is investigated for the Lee model, a theory describing two fermions, the V and N particles, interacting with a relativistic, spin 0 boson, the θ particle. Spin and recoil are neglected for the fermions and the interaction gives rise to scattering independent of direction. First it is shown that the LSZ asymptotic condition, relating matrix elements of the "in" and "out" fields to matrix elements of the Heisenberg fields, is equivalent to a formal solution of the eigenvalue equation for the scattering states. The asymptotic condition is then used to derive a formula relating a given S-matrix element to a τ-function, the vacuum expectation of a time ordered product of Heisenberg fields. From the field equations and commutation relations, a set of coupled, first-order differential equations can be derived for the τ-functions of the Lee model. These equations break up into an infinite number of closed systems of equations. The first set describes the first non-trivial sector where the V particle state and the N-θ scattering states form a complete set. The equa-

tions are transformed into momentum space and solved algebraically. The two renormalization constants are obtained by studying the analytic structure of the V propagator. The structure of the τ-functions is discussed. Then the S-matrix element for N-θ scattering is written down. The results agree with those in the literature, where the problem was treated by directly solving the eigenvalue equation for the V particle and N-θ scattering states. Proceeding to the next higher sector, there is an additional θ particle in initial, final, and intermediate states giving rise to V-θ and N-2θ scattering as well as V$\theta \rightarrow$ N2θ production. The equations for the appropriate τ-functions in momentum space yield a singular integral equation, which is reduced to the inhomogeneous Hilbert problem. The solution is obtained in terms of quadratures. (Dissertation Abstr.)

47403 A STUDY OF SINGLE PARTICLE EXCHANGE MODELS IN PION-PROTON INTERACTIONS AT 2.16 Bev/c (thesis). Bussian, Alfred Erich. Boulder, Colo., Univ. of Colorado, 1964. 72p.

An experimental study of 2.16-Bev/c negative pions on protons was made. The reactions considered were single pion production and elastic scattering processes. The emphasis was on determining which Feynman diagrams are important in the production of excited meson and baryon states. At this energy the inelastic processes studied are dominated by the production of the rho meson. Previous experiments show this to be a one-pion exchange process. Significant production of the Δ (1920) isobar in this experiment, however, makes it difficult to test the mechanism. In order to explain the production of the Δ (1920) isobar, a baryon exchange mechanism is proposed. It correctly predicts the isotopic spin states found, as well as the preferred forward direction of the isobar in the barycentric system. Further impetus is given to the model by examining the results of a number of previously reported experiments. Some indication is also found for the production of the Δ (1238) isobar via the rho exchange mechanism. Finally a study of the elastic differential cross section shows a second maximum at $\cos\theta \sim 0.2$ in the barycentric system. Possible explanations for this maximum are discussed. (Dissertation Abstr.)

47404 TESTS OF EXCHANGE MODELS, INCLUDING SPIN (thesis). Goldhaber, Alfred Scharff. Princeton, N. J., Princeton Univ., 1964. 210p.

Several new tests of one-particle exchange models are presented. For spin-zero-exchange (SZE), the cross section at fixed bombardment energy for the reaction $1 + 2 \rightarrow 3 + 4$ must factor into two parts, one depending only on invariants constructed from the spins and momenta of 1 and 3, the other depending only on 2 and 4. As a result there may be no correlations between scalars in the 1–3 system and scalars in the 2–4 system. If the collision amplitude is a superposition of several SZE amplitudes, there may be correlations of 1–3 scalars with 2–4 scalars. If the exchanged particles have both parities, there may be correlations between 1–3 pseudoscalars and 2–4 pseudoscalars. For spin-J-exchange, the cross section may contain up to 2J factors that are scalar products of 1–3 four-vectors with 2–4 four-vectors. Therefore it may be a polynomial of degree 2J in the bombardment energy. For an appropriate choice of the other independent variables of the collision, the only additional dependence on bombardment energy is a kinematic factor $(p_{2L}^2)^{-1}$, where p_{2L} is the momentum of the bombarding particle. The maximum number of factors of a cosine or sine of a Treiman-Yang angle in the 1–3 (or 2–4) system is 2J. Results of an analysis of data for the reaction $\pi + N \rightarrow 2\pi + N$ with the final dipion mass in the neighborhood of the resonance are presented. These data taken mainly at bombarding momenta of 1.38, 1.71, and 3.0 Bev/c, are almost completely consistent with the Treiman-Yang criterion for one-pion-exchange. A detailed exposition of the tensor-spinor formalism for coupling of angular momenta is included. The ordinary three-dimensional form is developed, and then extended to provide a systematic method of finding the independent couplings of Lorentz covariants. (Dissertation Abstr.)

47405 LECTURES ON PARTICLES AND FIELD THEORY. VOLUME TWO. Johnson, K.; Lichtenberg, D. B.; Schwinger, J.; Weinberg, S.; Yock, P.; Mubayi, V.; Nieh, H.; Davis, F.; Mitter, H.; Weaver, D. Englewood Cliffs, N. J., Prentice-Hall, Inc., 1965. 488p. $5.00.

Five lectures are included; separate abstracts have been prepared for each. (L.B.S.)

For abstracts of individual chapters see: 47406–47409 and 47442.

47406 SPECTROSCOPY OF THE STRONGLY INTERACTING PARTICLES. Lichtenberg, D. B. (Indiana Univ., Bloomington). pp 77-143 of Lectures on Particles and Field Theory. Vol. II. Englewood Cliffs, N. J., Prentice-Hall, Inc., 1965.

The strongly interacting particles are discussed, with primary consideration given to experimental information and its interpretation. The theory that is needed to correlate experimental measurements with physically important quantities is presented, which includes conservation laws, spin and statistics, CPT invariance, quantum numbers C and G, parity, superselection rules and intrinsic parity, Dalitz plot, and some theorems about spin and parity. Emphasis is then given to the quantum numbers of the strongly interacting particles and how they are determined. (L.B.S.)

47407 FIELD THEORY OF PARTICLES. Schwinger, Julian (Harvard Univ., Cambridge, Mass.). pp 145-288 of Lectures on Particles and Field Theory. Vol. II. Englewood Cliffs, N. J., Prentice-Hall, Inc., 1965.

Some general aspects of quantum field theory are reviewed, including the quantum action principle, fields, and Lorentz invariance. Various analogies and arguments are exploited to construct a dynamical field theory. An attempt is made to establish, in a qualitative phenomenological way, the connection between the fundamental theory and the observed strong, electromagnetic, and weak phenomena. (L.B.S.)

47408 QUASIPARTICLES AND PERTURBATION THEORY. Weinberg, Steven (Univ. of California, Berkeley). pp 289-403 of Lectures on Particles and Field Theory. Vol. II. Englewood Cliffs, Prentice-Hall, Inc., 1965.

The questions on what distinguishes composite and elementary particles, and how to diagnose and correct the failures of perturbation theory in scattering problems are explored in detail. A brief review of some essentials of scattering theory is given, and the question of elementarity versus compositeness is treated. The field renormalization constant Z is introduced in a nonrelativistic context to provide a quantitative basis for answering the question on elementarity. The measurement of Z for the case of the deuteron is discussed. Investigations are made of perturbation theory in two-particle nonrelativistic scattering problems, and examples are given to elucidate application of the quasi-particle method. Certain difficulties that arise in the analysis of multiparticle scattering which are intrinsic to many-body problems are discussed and dealt with systematically. A partial answer to the question of elementarity in the relativistic case is given and several other questions are raised. (L.B.S.)

47409 THE QUANTUM THEORY OF MASSLESS PARTICLES. Weinberg, Steven (Univ. of California, Berkeley). pp 405-85 of Lectures on Particles and Field Theory. Vol. II. Englewood Cliffs, N. J., Prentice-Hall, Inc., 1965.

The quantum theory of massless particles is presented in a manner as to minimize the gap between this theory and the rest of particle physics. It is shown how to define particles as irreducible representations of the inhomogeneous Lorentz group, and the neutrino, photon, graviton states are defined as those particular representations characterized by mass zero and spins $\frac{1}{2}$, 1, or 2. The type of interaction which will yield a Lorentz invariant S-matrix can be deduced from information on how the particle states transform. The simplest possibility is explored, in which the particle operators enter the interaction on the form of free fields which transform according to various representa-

tions of the homogeneous Lorentz group, and commute with each other at spacelike separations. It is shown how these two requirements uniquely dictate the form of the fields, also lead to the spin-statistics connection, the existence and properties of antiparticles, and the Feynman rules. It is shown that for massless particles of spins j = 1 and j = 2 the only Lorentz invariant theories are those of Maxwell and Einstein. Finally, S-matrix theory for photons and gravitons is treated. (L.B.S.)

47410 RELATIVISTIC CORRECTIONS IN ELECTRON-DEUTERON SCATTERING. Adler, R. J. (Univ. of Washington, Seattle); Erickson, E. F. 9p. (CONF-650410-41). Gmelin, AED-CONF-65-073-77.

From American Physical Society, Washington, D. C.

The simplest example of the estimate of relativistic corrections is considered; this is a direct extension of previous work. It is expected intuitively that for very low momentum transfer and small angle electron scattering the cross section for elastic electron-deuteron scattering should not depend on the detailed inner structure of the deuteron. It is therefore natural to use the simplest possible model of the deuteron, the tail approximation, as used previously. (J.F.P.)

Field Theory and Quantum Mechanics

47411 (NP-15486) THEORIES OF GRAVITATION. Narlikar, J. V. (Institute of Mathematical Science, Madras (India)). [1965]. 54p. Dep. mn.

Separate discussions are presented on the following; the electromagnetic field, principle of equivalence, the curvature tensor, Einstein's equations, experimental verification, Mach's principle, steady state cosmology, action at a distance, Maxwell's field from direct particle interactions, radiation damping, retarded and advanced potentials in curved space-time, "C" field theory, and Hoyle-Narlikar theory of gravitation. (M.O.W.)

47412 ON SINGULARITIES OF AMPLITUDES IN A PERTURBATION THEORY. Chang, T. S.; Wu, T. F.; Jiu, T. C. (Academia Sinica, China). Acta Phys. Sinica, 21: 1544-51(Aug. 1965). (In Chinese).

Two remarks on the singularities of the scattering amplitudes in a perturbation theory are given. First, it is pointed out that if the condition of stability is violated at several corners of a Feynmann diagram so that analytic extensions with respect to several external masses must be made, different sequences of carrying out the analytic extensions may lead to different positions of the singularities with respect to the final position of the integration contour (in a dispersion integral) and hence to different expressions for the amplitudes. Next, it is pointed out that the non-Landau singularities fall into two classes, of which one, say the first, is given by Cutkosky. For singularities in the first class, it is shown that they may be independent of the internal masses if and only if all the internal masses are equal or if the diagram is a loop. Their positions for the latter case are given. For singularities in the second class, it is shown that they are always independent of the internal masses and that they occur only for a very restricted set of diagrams. (auth)

47413 CANONICAL TRANSFORMATIONS IN QUANTUM MECHANICS. Levine, Arnold D. (West Virginia Univ., Morgantown). Am. J. Phys., 33: 728-32(Sept. 1965).

A review of canonical transformations in quantum mechanics is outlined with a view toward their use in the solution of specific problems. Several typical problems are worked out by the method of canonical transformations to emphasize the utility of this approach. In this way an insight may be obtained into the nature and limitation of the connection that exists between the canonical transformations of classical mechanics and the unitary transformations of quantum mechanics. Certain expository and pedagogical objectives are achieved, and no original contribution to the theory is intended. (auth)

47414 ELASTIC COLLISION WAVES IN THE FRAMEWORK OF THE GENERAL RELATIVITY THEORY. Schoepf, Hahs-Georg (Universitaet, Greifswald, Ger.). Ann. Physik (7), 15: 348-56(1965). (In German).

Elastic collision waves were defined through the requirement that the third derivative of the metric tensor on a 2-type hypersurface in the direction of the normal undergo a non-strong transformable discontinuity. This requirement was fulfilled through the assumption of discontinuities which the second derivatives of the Lagrange coordinates undergo. For a suitably defined isotropic body formulas were derived on this basis for the wave velocity. These assume approximately the classical form. In the case of an ideal liquid the classical formula is exactly valid for the wave velocity. (tr-auth)

47415 ON THE QUANTUM-MECHANICAL FOKKER-PLANCK EQUATION. Davis, H. Ted (Univ. of Minnesota, Minneapolis); Hiroike, Kazuo; Rice, Stuart A. J. Chem. Phys., 43: 2633-42(Oct. 15, 1965).

Taking the Wigner function as the basic N-body distribution function, quantum-mechanical modifications to the Fokker–Planck equation are studied using the two different approaches introduced, respectively, by Kirkwood and Prigogine. The weak coupling limit is studied using the time-smoothing technique first introduced by Kirkwood; the results of this section can perhaps form the basis of an approximate treatment of the transport phenomena of pure liquids. The problem of the Brownian motion of a heavy particle is treated employing the perturbation techniques developed by Prigogine and co-workers; in this section it is found that the form of the quantum-mechanical Fokker–Planck equation is identical to the classical equation, but that the friction coefficient contains quantum-mechanical corrections. Finally, it is noted that the weak coupling result obtained by the time-smoothing technique is identical to the approximation of small momentum transfer, if in the latter case the scattering cross section is represented in the Born approximation. (auth)

47416 QUANTUM-MECHANICAL BOLTZMANN EQUATION. Hoffman, David K.; Mueller, John J.; Curtiss, C. F. (Univ. of Wisconsin, Madison). J. Chem. Phys., 43: 2878-84(Oct. 15, 1965).

A Boltzmann equation is derived from the N-particle Schrödinger equation. The development is based on the solution of the two-particle quantum-mechanical Liouville equation due to Green. The various approximations involved in the derivation are discussed and the collision integral and corrections are compared to their classical analogs. Further development of the collision integral yields the standard result, the usual Boltzmann collision integral in which the classical differential cross section is replaced by its quantum-mechanical counterpart. (auth)

47417 PERTURBATION THEORY USING CANONICAL TRANSFORMATIONS IN CLASSICAL EIGENVALUE PROBLEMS. Pegel, B. (Institut fuer Angewandte Physik der Reinststoffe, Dresden). Monatsber. Deut. Akad. Wiss. Berlin, 7: 99-103(1965). (In German).

A systematic perturbation theory for linear classical eigenvalue problems was given on the basis of canonical transformations. Some necessary principles of the canonical transformations are tabulated. The general scheme for the perturbation calculation is derived. The perturbation formalism for the present problem is then carried out. (J.S.R.)

47418 THE KINEMATICS OF THE ANGULAR MOMENTUM OF A PARTICLE. I. TRANSLATION BROADENING OF ANGULAR MOMENTUM. Moses, H. E.; Wang, S. C. (Massachusetts Inst. of Tech., Lexington). Nuovo Cimento (10), 36: 788-804(Apr. 1, 1965).

The way a particle changes its angular momentum under inhomogeneous Lorentz transformations is well known classically. The problem is considered quantum-mechanically for particles of any mass and any spin. The case where a particle has a definite angular momentum in one frame of reference is studied, and the probability distri-

bution of angular momentum in a frame translated with respect to the original frame is calculated. The basic mathematical tool is the form for the infinitesimal generators of the inhomogeneous Lorentz group devised by Lomont and Moses in which the hamiltonian, square of the angular momentum, z-component of angular momentum, and helicity are diagonal. The results can be used to take into account, to a certain degree at least, the effect of the selection rules. For example, it is shown that when the density of a gas is sufficiently low, radiative cooling goes on at a much faster rate when selection rules are taken into account than when they are ignored. (auth)

47419 NONPOSITIVITY OF THE ENERGY DENSITY IN QUANTIZED FIELD THEORIES. Epstein, H.; Glaser, V.; Jaffe, A. (Institut des Hautes Etudes Scientifiques, Bures-sur-Yvette, France). Nuovo Cimento (10), 36: 1016-22(Apr. 1, 1965).

It is shown that a positive definite local energy density is incompatible with the usual postulates of local field theory. The question whether it can be bounded below is briefly discussed but not solved. (auth)

47420 INEQUIVALENT REPRESENTATIONS IN THE MANY-BOSON PROBLEM. Orzalesi, C. A. (Universita, Pavia, Italy; Istituto Nazionale di Fisica Nucleare, Pavia, Italy). Nuovo Cimento (10), 36: 1047-9(Apr. 1, 1965).

Some of the properties of the canonical Bogoliubov transformation as it is applied in the study of a finite-volume system of many bosons with weak or hard-core interaction are demonstrated. It is shown that in the cases considered the use of the Bogoliubov transformations may lead to inequivalent representations if a cut-off assumption for the momentum spectrum is not made. Applications of the creation and destruction boson operators to the problem of many bosons at low temperatures are considered in diagonalization of the hamiltonian and in dealing with nonhermitian hamiltonians. (M.J.T.)

47421 ON THE INVARIANCE PROPERTIES OF THE DIRAC EQUATION. Sen Gupta, N. D. (Tata Inst. of Fundamental Research, Bombay). Nuovo Cimento (10), 36: 1181-1216(Apr. 16, 1965).

The mappings of the Dirac matrices $\gamma_\mu \rightarrow \gamma'_\mu = \Lambda\gamma_\mu\Lambda^{-1}$, where Λ is an element of the group D of 4×4 unimodular matrices, studied. It is shown that the unitary subgroup of D consists of elements of the type i) $\exp[i\gamma_5\psi]$, ii) $u_\mu\gamma_\mu$ $(1+\gamma_5)/2 + v_\mu\gamma_\mu(1-\gamma_5)/2$, and iii) $\cos\theta\gamma_5 + n_\mu\gamma_\mu \sin\theta$ and their products. The nonunitary factors of any element of D are reducible to the hermitian matrices i) $\exp[\gamma_5\psi]$ and ii) $\exp[i\gamma_4(n\cdot\gamma)]$ and their products. The mappings induced by them and the corresponding transformations of the Dirac equation together with their physical significances are discussed. Further D is shown to be isomorphic to the (group) extension of an abelian group of 5 parameters, by a 5-dimensional rotation group. Finally the expression for the matrix for the transposition operation is derived, and different representations of γ's with respect to transposition are discussed. (auth)

47422 REPRESENTATIONS OF THE POINCARE GROUP ASSOCIATED WITH COMPLEX ENERGY-MOMENTUM. Beltrametti, E. G.; Luzzatto, G. (Universita, Genoa; Istituto Nazionale di Fisica Nucleare, Genoa). Nuovo Cimento (10), 36: 1217-29(Apr. 16, 1965).

A possible extension to unstable systems of the usual connection between the irreducible representations of the Poincaré group and the mass and spin numbers of stable particles is analyzed. This is done by a study of nonunitary representations of the real Poincaré group associated to complex values of the energy-momentum four-vector π. The representations turn out to be one-dimensional and exhibit some similarities with the unitary representations corresponding to zero mass. (auth)

47423 ON PRIMITIVE ANALYTICITY DOMAINS FOR HIGH-ORDER WIGHTMAN FUNCTIONS. Manoharan, A. C. (Princeton Univ., N. J.). Nuovo Cimento (10), 36: 1283-1302(Apr. 16, 1965).

Boundary surfaces are investigated for analyticity domains in scalar product space, without using local commutativity, for those Wightman functions where the number of difference vector variables exceeds the spacetime dimension. Contrary to what might be naively expected, it is shown that in (1 + 3) spacetime the leading-order hypersurface pieces of the boundaries for the 8-point and every higher-order function have 8-point structure with respect to natural stability properties under complex Lorentz transformations. These results are related to the question as to whether the extended tubes and primitive domains are natural domains of holomorphy. (auth)

47424 NOTE ON THE MAJORIZATION OF FEYNMAN DIAGRAMS. Aganovic, I. (Faculty of Science, Zagreb; Inst. Rudjer Boskovic, Zagreb). Nuovo Cimento (10), 36: 1384-5(Apr. 16, 1965).

The majorization of Feynman diagrams with only meson external lines is considered. It is found that a set of strongly connected diagrams of a meson process is majorized in the euclidean region of external momenta by a one-loop diagram and by a set of loops with chords, with at least two external vertices lying on each chord. (M.J.T.)

47425 A SIMPLE DERIVATION OF THE REPRESENTATION OF THE INHOMOGENEOUS LORENTZ GROUP IN THE ANGULAR-MOMENTUM SYSTEM. Raszillier, I. (Physikalisches Institut der Akademie, Bucharest). Nuovo Cimento (10), 39: 967-74(Oct. 1, 1965). (In German).

A simple derivation of the irreducible representation of the inhomogeneous Lorentz group in the angular-momentum system with an arbitrary normalization is given, starting from the momentum system. The properties of the functions $D^j_{M\lambda}(\varphi,\theta,-\varphi)$ of the rotation group are essential in this presentation. The results of Lomont and Moses are rederived as a special case. (tr-auth)

47426 THE COVARIANT DEFINITION OF SPIN IN RELATIVISTIC QUANTUM FIELD THEORY. Hilgevoord, J.; De Kerf, E. A. (Universiteit, Amsterdam). Physica, 31: 1002-16(July 1965).

Spin and orbital angular momentum densities are defined in the relativistic quantum theories of free fields with nonvanishing rest mass and arbitrary spin, in such a way that the corresponding space integrals are conserved tensors which satisfy the Frenkel condition. (auth)

47427 PROBABILITY OF VIOLATION OF THE EHRENFEST PRINCIPLE IN FAST PASSAGE. Wannier, Gregory H. (Bell Telephone Labs., Inc., Murray Hill, N. J.). Physics, 1: 251-3(May–June 1965).

Adiabatic passage through an almost degenerate intermediate state is a common experimental technique. It is based on the Ehrenfest principle which states that if the external conditions for a system are changed slowly enough, the change of the system can be predicted by computing quasistatically the modification of its initial quantum state. It was shown recently that if the external change is measured by a slowness parameter inversely proportional to the time taken to effect the change then the Ehrenfest principle is valid to all orders in this parameter. A rigorous formula is derived for the probability that the adiabatic path is followed in the simple case of the near crossing of two quantum levels. The general problem of two levels crossing in time contains several parameters. After the irrelevant parameters are disposed of, the two essential parameters of the problem are left, namely, the sweeping rate at which energy difference of the two levels changes at a distance from the crossing, and the minimum value which this difference takes at the time of closest approach. These parameters are shown in an energy plot. (J.F.P.)

47428 THE RIGID ROTATOR ACCORDING TO RELATIVISTIC QUANTUM MECHANICS. Rao, K. N. Srinivasa; Saroja, D. (Central Coll., Bangalore, India). Proc. Indian Acad. Sci., Sect. A, 62: 398-406(June 1965).

The eigenvalues of a rigid rotator are determined according to both the Klein-Gordon and Dirac equations. The trivial case of a single Klein-Gordon at a fixed distance from a center of rotation and with a given rest mass and moment of inertia is considered. Then the more

realistic case of a dumb-bell shaped rotator is considered. The problem can be solved if it is assumed that the two particles of the rotator are of equal mass. The eigenvalues are then found according to the Dirac equation and then according to that of Klein-Gordon. (J.F.P.)

47429 NUMERICAL INTEGRATION OF SCHROEDINGER'S EQUATION FOR A SQUARE WELL POTENTIAL USING AN IBM 1620 COMPUTER. Adams, Richard D.; Ganfield, Edgar; Sprouse, Gerald (Upper Iowa Univ., Fayette). Proc. Iowa Acad. Sci., 71: 392-8(1964).

For pedagogical purposes, numerical integration methods are applied to a simple eigenvalue problem in quantum mechanics. Computer programming of the problem is discussed, the effect of different choices of initial conditions is mentioned, and the sensitivity of the method to the difference interval width is discussed. (auth)

47430 SHADOW SCATTERING AT LARGE ANGLES. Serber, R. (Brookhaven National Lab., Upton, N. Y.). Proc. Nati. Acad. Sci. U. S., 54: 692-6(Sept. 1965). (TID-22116).

Two expressions are given for the scattering amplitude, which contain Legendre and Bessel functions, and it is pointed out that while the approximations are valid for small angles, at large angles the equality between the Legendre and Bessel functions is in error by terms of order $\sin^2 \theta/2$. The relations between the results given by each expression is investigated for a class of problems for which an asymptotic expansion exists for large momentum transfer. (L.B.S.)

47431 CLASSICAL RADIATION THEORY AND POINT CHARGES. Cornish, F. H. J. (Univ. of Leeds, Eng.). Proc. Phys. Soc. (London), 86: 427-42(Sept. 1965).

The usual theory for a continuous system may not be applied without some alteration to a system of point charges because the orthodox electromagnetic energy-momentum tensor for the field leads to infinite self energies. The method adopted is to assume that Maxwell's equations hold for point charge sources but to regard the equations of motion of the charges as dependent on the energy-momentum tensor chosen. A class of modified energy-momentum tensors are constructed in such a way that the field singularities do not lead to difficulty and the corresponding equations of motion are derived. Thus a class of equations is obtained each of which is capable of describing the history of a point-charge system in terms of energy and momentum flow. In this theory named the interaction theory, the equations of motion do not contain radiation reaction terms and whereas a group of charges may radiate on account of their mutual interactions, an isolated point charge cannot. When certain conditions are satisfied it is shown that the interaction theory leads to the same results as the orthodox theory for the dipole radiation involved in a wide range of processes. (J.F.P.)

47432 ON A PARALLELISM BETWEEN CLASSICAL MECHANICS AND QUANTUM MECHANICS. Nishiyama, Yoshio (Osaka Univ.). Progr. Theoret. Phys. (Kyoto), 34: 299-311(Aug. 1965).

Striking parallelism between classical mechanics and quantum mechanics is evidenced for several bound systems in a rather general form by introducing resonably "quantum-mechanical momentum" from the Schrödinger equation. The following are proved: The "quantum-mechanical momentum" which is nearly equal to the corresponding classical momentum in "classical region" can be defined in the whole range of validity of the coordinate for the bound systems. In the same way as in classical mechanics, in quantum mechanics one can construct an associated wave accompanying a motion of a quantum particle and obeying the Schrödinger equation. The uniqueness condition on the associated wave throughout an orbit leads to the boundary condition on the wave function which is composed of the associated wave and to "quantum-mechanical quantization condition", equivalently. In addition, all these quantum-mechanical quantities are approximately equal to the corresponding classical ones in the "classical region" of the coordinate. In particular it is demonstrated that even for a bound system of a singular (central) potential exists the ground state with the lowest energy eigenvalue. It is proved in one dimension that to any physical system obeying the Schrödinger equation always exists the corresponding classical system. (auth)

47433 THE CONCEPTUAL BASIS AND USE OF THE GEOMETRIC INVARIANCE PRINCIPLES. Houtappel, R. M. F. (Instituut Lorentz, Leiden); Van Dam, H.; Wigner, E. P. Rev. Mod. Phys., 37: 595-632(Oct. 1965).

Invariance principles are used, in physics, in two distinct manners. First, they are used as superlaws of nature in that, once their validity is suggested by their consistency with the known laws of nature, they serve as guides in our search for as yet unknown laws of nature. Second, they can serve as tools for obtaining properties of the solutions of the equations provided by the laws of nature. It is desirable for the first use to give a formulation of invariances directly in terms of the primitive concepts of physical theory, i.e., in terms of observations, or measurements, and their results. Invariances which can be so formulated are called geometric invariances. An attempt at such a formulation of geometric invariances is presented. This formulation is then applied, in detail, to the classical mechanics of point particles, to a relativistic mechanics of interacting point particles, and to quantum theory. With the exception of the relativistic mechanics of point particles, these applications form a review, from a single point of view, of earlier work on this subject. A review of the second use of invariances is also given. (auth)

47434 THE REGGE CUTS IN A PERTURBATION THEORY. Chang, T. S. Wu Li Hsueh Pao, 21: 1381-6(July 1965). (In Chinese).

With the help of perturbation theories the asymptotic properties of a ladder in the s channel are studied as the momentum transfer $t \to \infty$ and some external masses $M^2 \to t^{\frac{1}{2}}$. The knowledge of such a property is essential to the calculation of the asymptotic property (as the momentum transfer $t \to \infty$) of a diagram which connects a ladder (in the s channel) and an ordinary pole in parallel. The absorptive part in the t channel of the diagram which connects a ladder in the s channel and an ordinary pole in parallel is also studied. It proves that if the partial waves in the s channel possesses a Regge cut, the starting point of such a cut must lie to the left of the position given by current theories. (auth)

47435 EXACT INTEGRATION OF THE EQUATIONS OF MOTION FOR RELATIVISTIC CHARGED PARTICLES FOR A CERTAIN CLASS OF VARIABLE ELECTROMAGNETIC FIELDS. Glikman, L. G.; Kel'man, V. M.; Yakushev, E. M. (Inst. of Nuclear Physics, Academy of Sciences, Kazakh SSR). Zh. Eksperim. i Teor. Fiz., 49: 210-13(July 1965). (In Russian).

An exact solution is found for the equations of motion of relativistic charged particles in the middle plane of a cylindrically symmetric electromagnetic field. The magnetic potential of the field in a cylindrical coordinate system ρ, φ, z possesses only one nonvanishing component in this plane, $A_\varphi = \rho^{-1}\omega(t/\rho)$ where ω is an arbitrary function and t is time. The electrostatic potential is zero. (auth)

47436 FINITE QUANTUM ELECTRODYNAMICS: A FIELD-THEORETIC MODEL USING AN INDEFINITE METRIC (thesis). Arons, Michael Eugene. Rochester, N. Y., Univ. of Rochester, 1964. 168p.

A model for quantum electrodynamics free from ultraviolet divergencies is constructed. The basic technique utilized involves the use of two auxiliary fermion fields with anti-commutation relations of opposite sign from the normal fermion (electron). This results in a Hilbert space with an indefinite metric. Together with the electron, the two auxiliary fermions are coupled to the electromagnetic field so as to make the contribution to the matrix element from any diagram finite. Although the Lagrangian of the

theory is not gauge invariant, the electromagnetic field is quantized in a manner to yield a propagator in the Landau gauge, and it is proved that this is sufficient to insure that the physical vector particles are zero-mass perpendicular quanta. Mass and charge renormalizations are discussed, and the former is carried out by a technique that uses a Taylor expansion in the mass. The physical fermion mass and the electric charge are put into the theory, leaving only the masses of the two auxiliary fermions as parameters (called ghost masses). The anomalous magnetic moment of the electron and the differential and total cross sections for Compton scattering are calculated to lowest order. It is required that the predictions of this model agree with the conventional predictions to the extent that the latter correspond to experiment and that the charge and mass renormalization effects be truly small so that there is no explicit contradiction to the validity of the perturbation expansion. A range of the ghost mass parameters is found for which the above conditions are satisfied. Thus a finite quantum electrodynamics, using an indefinite metric, is accomplished. The question of a test between this model and conventional QED is discussed as is the possibility of unusual mass solutions. (Dissertation Abstr.)

47437 ASYMPTOTIC BEHAVIOR OF COUPLED GRAVITATIONAL FIELDS (thesis). Winicour, Jeffrey Harold. Syracuse, N. Y., Syracuse Univ., 1964. 51p.

The Bondi-Sachs approach to asymptotic investigations of the gravitational field is generalized to include coupled fields. The coupled Einstein equations separate, as in the vacuum case, into 4 hypersurface equations, 2 standard equations, 1 trivial equation, and 3 supplementary conditions. The coupled energy momentum tensor serves to identify the supplementary conditions as conservation laws of total energy and angular momentum. The outgoing radiation condition that the fluxes of energy and angular momentum be asymptotically radial and equal in magnitude to their corresponding densities implies the outgoing radiation condition of Sachs in terms of the asymptotic algebraic structure of the Weyl tensor. For asymptotically traceless coupled fields the converse is also true. The coupled Einstein-Maxwell fields are investigated in detail. With the proper gauge condition, Maxwell's equations in terms of the vector potential separate into 1 hypersurface equation, 2 standard equations, and 1 supplementary condition. By virtue of the charge constant of the motion, the gauge group can be reduced to a one-parameter group in analogy with the reduction to a one-parameter group in analogy with the reduction of the generalized Bondi-Metzner group to the ten-parameter Lorentz group when the mass is constant. The electromagnetic news function plays a role similar to that of the gravitational news function. (Dissertation Abstr.)

47438 P STATES OF THREE-PARTICLE SYSTEMS WITH COULOMB INTERACTION (thesis). Machacek, Milos. Austin, Tex., Univ. of Texas, 1964. 55p.

Center-of-mass coordinates are employed to determine the dependence of energy and other physical properties of systems with three Coulombic particles (two identical) on the masses of the particles. No adiabatic approximation is needed, since the non-relativistic and spin-free Hamiltonian with the exact mass dependence is used in the eigenvalue problem. The total angular momentum of the particles is quantized to unity. Both symmetry states with the space-z-component of angular momentum $M_z = 0$ are considered. The computations cover the entire range of the mass ratio as well as several different charges of the particles. In most cases the energies obtained are either the lowest yet found or the first to be reported. (Dissertation Abstr.)

47439 QUANTUM STATISTICS OF FULLY IONIZED GASES (thesis). Grandy, Walter Thomas Jr. Boulder, Colo., Univ. of Colorado, 1964. 200p.

A recently developed theory of the quantum statistical mechanics of multicomponent systems is applied to a fully ionized gas in thermal equilibrium. Essential features of this theory are the removal of inherent singularities due to the Coulomb interaction, and the nonrelativistic renormalization of charged particle energy contributions so as to remove all electromagnetic self-energy terms. The grand potential and equation of state of a fully ionized gas are calculated through fifth order in e, the electronic charge. This result is valid in regions of moderately high temperature and moderately low density and has the form of a virial expansion. It is observed that the master-graph formulation of quantum statistics developed by Mohling is quite necessary for studying the general ionized gas. Although this formalism was developed in order to treat the many-body self-energy difficulties that arise in low temperature systems due to momentum space ordering, it is apparent that the long range nature of the Coulomb force requires a similar analysis. The correct treatment of this aspect of the problem leads to the conclusion that the lowest-order (e^2) contributions to the equation of state due to Coulomb interactions come from exchange integrals. This term, among others, introduces a new parameter into the theory, which indicates that a quantum mechanical screening of the Coulomb interaction occurs in the ionized gas, over and above the classical Debye screening. The present results are used to examine the so-called electron gas, and the limiting case of a classical system. Application to ionized hydrogen is considered briefly in connection with the Saha ionization equilibrium equation. (Dissertation Abstr.)

47440 CONTRIBUTIONS TO THE EINSTEIN-KURSUNOGLU FIELD EQUATIONS (thesis). Pizzo, Joseph Francis Jr. Gainesville, Fla., Univ. of Florida, 1964. 61p.

Certain aspects of Einstein's unified field theory are investigated. This theory aims to derive all fields from one single tensor. However, here the problem is restricted to deriving the electromagnetic together with the gravitational field. It is found that the general problem, on which Einstein spent the last twenty or more years of his life, is not at the present time soluble. Certain linearized cases were investigated by Einstein, Strauss, and others. Here a new approach is utilized which may be termed a first order perturbation of the "gravitational tensor" by means of an antisymmetric part added to it. This case is found to be completely soluble, and the covariant electromagnetic field equations for the general space and a complete solution for these in the space of constant positive curvature with uncurved time are obtained. It is shown that this solution, in the limit of an infinite radius of the universe, goes into the ordinary Maxwell's equations, known to exist in Minkowski space and invariant under the Lorentz group. (Dissertation Abstr.)

47441 COVARIANT FORMULATION OF THE LAGRANGIAN THEORY OF FIELDS (thesis). Ray, John Robert. Athens, Ohio, Ohio Univ., 1964. 98p.

The variational principle of classical field theory is introduced and discussed. The variation of the action is carried out in the same way each time, namely, by introducing a one-parameter family of variations. Noether's theorem and two useful lemmas from differential calculus are used throughout to find the invariants associated with the variational principle under consideration. In special relativity these invariants are the ten integrals of the motion, and in a generally covariant field theory, such as general relativity, these are differential identities. Two different formulations are considered: a formulation in which all quantities are kept in obviously covariant notation, and a formulation in which non-tensorial quantities are used. This latter formulation is conventional. In the obviously covariant formulation, the Lagrangian density is taken to be a function of the covariant derivatives of the fields instead of their ordinary derivatives. From this Lagrangian density an obviously covariant form of Lagrange's equations is obtained. The obviously covariant form of Lagrange's equations and the usual form of Lagrange's equations can be shown to be equivalent. A covariant form of the identities of a generally convariant field theory is also obtained. These covariant identities can be shown to be

equivalent to the usual expressions. A completely covariant formulation of the general theory of relativity is given as an example of the methods introduced. It is suggested that progress in formulating global, covariant, conserved quantities must await progress in the theory of the observables of covariant field theories, primarily general relativity. (Dissertation Abstr.)

47442 QUANTUM ELECTRODYNAMICS. Johnson, K. (Massachusetts Inst. of Tech., Cambridge). pp 1-75 of Lectures on Particles and Field Theory. Vol. II. Englewood Cliffs, N. J., Prentice-Hall, Inc., 1965.

The general formulation of the theory is presented with emphasis on the possible choices of gauge to be used. The electromagnetic field interacting with a given external current is discussed, and the complementary situation, where the electron field interacts with an external electromagnetic field, is then considered. The care that is needed to ensure that the formulation is gauge invariant at each stage is emphasized. The Schwinger-Dyson equations are derived in order to examine the relations between the various Green's functions that are introduced in the theory. The high-energy behavior of the Schwinger-Dyson equations is then investigated. (L.B.S.)

47443 MICROSCOPIC THEORY OF A FERMI LIQUID (thesis). Tuttle, Elizabeth Rose. Boulder, Colo., Univ. of Colorado, 1964. 167p.

The quasi-particle model of a low-temperature, single-component, Fermi liquid was examined. This study was centered about two different, low temperature theories, and the relationship existing between these two theories was investigated. The first of these is Landau's phenomenological theory of a Fermi liquid; its relation to the quasi-particle description of a Fermi liquid was studied in detail. A generalization of the theory was made in order to include higher order energy distribution functions. The second theory is the microscopic theory formulated by Mohling and based upon the work of Lee and Yang. The Λ-transformation introduced by Mohling to eliminate some of the low temperature difficulties is discussed. Explicit expressions for the ground state energy, the particle momentum distribution, and Δ (k), the transformation function defined by the Λ-transformation, were derived through third order in the two-quasi-particle reaction matrix, $g_1(k_1k_2|k_3k_4)$. It was shown that the resulting expressions satisfy Landau's equations. The interaction energy of two quasi-particles was derived, and it was shown that this interaction energy cannot be interpreted as a simple two-body potential energy. There is a two-body contribution to the interaction energy of two quasi-particles, but there is also a contribution from other, many-body potential energies. These potential energies are related to each other in a very complicated manner. The limits of applicability of the particular reaction matrix expansion were considered and the expansion function $g_1(k_1k_2|k_3k_4)$ was analyzed for a potential composed of a repulsive core surrounded by an attractive square well. (Dissertation Abstr.)

Geophysics

47444 (AD-611629) A RESEARCH PROGRAM TO INVESTIGATE ARTIFICIALLY INJECTED TRAPPED RADIATION. Final Report. Giacconi, R.; Paolini, F. R.; Hadley, W. C.; Talbot, R. Jr. (American Science and Engineering, Inc., Cambridge, Mass.). Oct. 30, 1964. Contract AF19(628)-2799. 148p. (ASE-759; AFCRL-64-917). CFSTI $4.00 cy, $1.00 mn.

An experimental research program to measure the intensity, angular distribution, and energy spectra of particles trapped in the Earth's magnetic field is described. Particular attention was focused on the measurement of particles artificially injected by high altitude nuclear detonations during the series of nuclear tests conducted by the USSR and the USA during the summer and fall of 1962. A detailed description of the instrumentation and calibration procedures are given. Measurements obtained by instrumentation identical to the one described, flown on an Air Force satellite, are given. The method of data handling is discussed and machine programs for data reduction are described. Results from these measurements have appeared in several documents, a listing of which is included in the test. A summary of the results and conclusions is given. (auth)

47445 (AD-611828) ION CYCLOTRON WHISTLERS [Thesis]. Report No. 65-2. Gurnett, D. A. (State Univ. of Iowa, Iowa City). June 1965. Contracts Nonr93803; Nonr150906. 96p. CFSTI $3.00 cy, $0.75 mn.

An experimental study of the proton-whistler, a new vlf phenomenon observed in satellite data, is presented and an explanation of this new effect is given. It is proposed that the proton-whistler is simply a dispersed form of the original lightning impulse and that the dispersion can be explained by considering the effect of ions on the propagation of an electromagnetic wave in the ionosphere. The propagation of a wave in a multicomponent plasma for frequencies on the order of the ion gyrofrequencies is discussed. It is shown that the proton-whistler is an ion cyclotron wave which occurs via a polarization reversal process. Near the altitude and frequencies for which polarization reversal occurs it is shown that the right-hand polarized wave and the ion cyclotron wave may be strongly coupled. For frequencies on the order of the ion gyrofrequencies this coupling process plays an important part in determining what regions of the ionosphere are accessible to waves from a given source location. (TAB)

47446 (AD-612013) ANALYSIS AND EVALUATION OF MEASUREMENTS OF GEOMAGNETICALLY TRAPPED ELECTRONS FROM HIGH-ALTITUDE NUCLEAR EXPLOSIONS. Final Report. Report No. 3-25-64-1. Imhof, William L.; Gaines, Edward E.; King, David R.; Nakano, George H.; Smith, Ray V. (Lockheed Missiles and Space Co., Palo Alto, Calif.). July 1964. Contract DA49 146XZ-205. 136p. (DASA-1540). CFSTI $4.00 cy, $1.00 mn.

The Starfish detonation on 9 July 1962 dramatically demonstrated, by producing significant damage to several space missions, the important military implications of geomagnetically trapped electrons. Results on the spatial distribution, spectrum, angular distribution, and time history of electrons artificially injected and trapped in the earth's field as a result of not only the Starfish detonation but also some Soviet high-altitude detonations are presented. (TAB)

47447 (AD-612083) GEOPHYSICS AND SPACE DATA BULLETIN NO. 3. Carrigan, Anne L.; Oliver, Norman J. (eds.) (Air Force Cambridge Research Labs., L. G. Hanscom Field, Mass.). Jan. 1965. 199p. CFSTI $5.00 cy, $1.25 mn.

Information is included on: component magnetometer; cosmic neutron intensity monitor; oblique backscatter radar; oblique H-F propagation; riometer; and solar radio emission-spectral observations. (TAB)

47448 (AD-612119) DETERMINATION OF THE IONOSPHERIC ELECTRON CONTENT UTILIZING SATELLITE SIGNALS. Arendt, Paul R.; Papayoanou, Aristole; Soicher, Haim (Army Electronics Labs., Fort Monmouth, N. J.). 1964. 15p. CFSTI $1.00 cy, $0.50 mn.

Ionospheric electron content may be determined from satellite signals by both active and passive methods: the former involve measurements by the satellite itself, the latter involve measurements by ground stations. Both methods are discussed, although limited to topside ionospheric sounding, for the active case, and to c-w transmission from the satellite and ground reception, for the passive case. Active methods, which yield complete information about the altitude profile of the electron density, depend on specific information regarding the satellite's position and the geomagnetic field strength along the radio path. Under restricted circumstances, passive methods are independent of such specific information. (TAB)

47449 (AD-613199) APPROXIMATE SERIES SOLUTIONS OF THE THREE-SPECIES ATMOSPHERIC DEIONIZATION DIFFERENTIAL EQUATIONS. Bogusch,

R, L. (Technical Military Planning Operation, General Electric Co., Santa Barbara, Calif.). Feb. 1, 1965. Contract DA49 146XZ281. 37p. (DASA-1597). CFSTI $2.00 cy, $0.50 mn.

In the course of investigating the effects of a nuclear explosion on electromagnetic wave propagation, it is often convenient to consider the ionized constituents of the atmosphere to be represented by a single species of positive ions, a single negative ion species, and electrons. The number densities of these charged particles at a specific time after detonation are then obtained from the solution of a system of three differential equations which describe the time rate of change of each particle density. An exact analytic solution was not found for these equations, and hence either approximate analytic forms or numerical integration methods are employed. The latter offers high accuracy but is often too time-consuming for general application. A new set of approximate analytic solutions are derived which provide accuracies approaching that of numerical integration for many cases, but which retain the advantage of rapid computation. (auth)

47450 (LA-DC-7365) VELA SATELLITE MEASUREMENTS. Coon, James H. (Los Alamos Scientific Lab., Univ. of California, N. Mex.). [1965]. Contract W-7405-eng-36. 47p. (CONF-650816-2). Dep. mn; CFSTI $2.00 cy, $0.50 mn.

From Conference on Radiation Trapped in the Earth's Magnetic Field, Bergen, Norway.

The Vela satellite program is briefly reviewed. A description of orbital coverage and coordinate systems is presented. A brief description of the characteristics of the instruments employed on the Vela satellites for making observations of low or moderate energy charged particles is given. A summary of some of the more significant results is presented in five sections entitled, interplanetary medium, low shock, transition region, magnetospheric boundary, and magnetospheric cavity. (M.O.W.)

47451 (SC-M-65-419) SANDIA CORPORATION EXPEDITION FOR AIRBORNE SCIENTIFIC OBSERVATION OF THE ECLIPSE OF THE QUIET SUN OF MAY 30, 1965. Anderholm, N. C. (Sandia Corp., Albuquerque, N. Mex.). Sept. 1965. Contract AT(29-1)-789. 48p. Dep. mn; CFSTI $2.00 cy, $0.50 mn.

The preparations for and operations of expedition to observe the total solar eclipse of May 30, 1965 are described. Of the other observations made on the expedition, brief summaries are given on the measurements of the cosmic ray induced neutron flux and the twinkle experiment. Brief statements of expected results are included. (auth)

47452 (NASA-TT-F-204) AURORAE AND AIRGLOW. Krasovskii, V. I. (ed.) Translation of Polyarnyye Siyaniya i Svecheniye Nochnogo Neba from IGY Program, Section IV, No. 10, Izdatel'stvo Akademii Nauk SSSR, Moscow, 1963. 283p. CFSTI $4.00.

The following topics are discussed; spectral distribution of extra-atmospheric and atmospheric components of the night-airglow continuum, background measurements during photoelectric observations of [01] emission at λ 5777 Å, an anomalous increase in the intensity of natural atmospheric airglow in the region λ 5577 Å, night airglow emission in the ultraviolet region of the spectrum, hydroxyl emission with different vibrational excitation, hydroxyl emission in the upper atmosphere, the spatial distribution and variations of H_α emission in night airglow, observation of certain weak emissions of the night sky by the electron telescopy method, an attempt to detect atmospheric emission during the solar eclipse of February 15, 1961, photoelectric recording of infrared spectra, patrol observations on the contours of the H_α line, proton intrusion in aurorae, determining the relative populations of vibrational levels and rotational temperature of the system of bands $A^2\pi - X^2\Sigma$ of N_2^+, results of visual observations of aurorae in 1957-1958, morphology of aurorae and geomagnetism, auroral isochasms, making allowance for errors in measurements of auroral positions based on ascafilms, a study of the S-180 camera, and behavior of λ 10830 Å helium emission at twilight. (M.O.W.)

47453 FURTHER STUDY ON POSSIBLE EFFECTS OF THE DYNAMO-ELECTRIC FIELD ON ELECTRONS TRAPPED IN THE MAGNETOSPHERE. Maeda, Ken-ichi (Kyoto Univ.). J. Geomagnet. Geoelec., 17: 1-21(1965).

The electrostatic field communicated from the dynamo region (the E region) into the magnetosphere will affect the motion of the trapped electrons. The case of electrons with energy ranging from 300 ev to 30 kev is treated. The electron orbit between two conjugate mirror points shifts earthward (inward) during night and outward during daytime. At the same time the mirror points shifts downwards and equatorwards (or upwards and polewards) during night (or daytime). The integrated effect on the apex height of an orbit and its diurnal variation are given. The number of inelastic collisions of an electron is calculated and the effective lifetime of a trapped electron is estimated. By the use of this result a possibility is studied whether the trapped electrons, coming down to the mirror point as low as 300-500 km, can be the principal cause of ionization of the F region during night. (auth)

47454 A NEW INDEX OF GEOMAGNETIC PULSATION AND ITS RELATION TO SOLAR M-REGIONS, II, ANALYSIS OF THE DATA FROM 1959 TO 1964. Saito, Takao (Tohoku Univ., Sendai). J. Geomagnet. Geoelec., 17: 23-44(1965).

Data are given from Dec. 1959 to Dec. 1964. The superposed epoch method which was used for the solar M-region study may draw many diverse conclusions. Controversy among four hypotheses, Allen's, Mustel's, Dessler-Fejer's, and Piddington's, on the mechanism of 27-day recurrent geomagnetic disturbance is partly due to obscurity in the superposed epoch method. In order to obtain exact locations of M-regions in relation to solar active regions, a geomagnetic pulsation pc 3 and calcium plage are applied as the representatives among various solar and terrestrial phenomena. An M-region temporally obtained by putting ΣKc 3, the daily sum of pc 3 index, back by three days is called an apparent M- (or AM-) region. All diverse relations between AM-region and active region obtained by the superimposed method cannot be uniquely interpreted by any of the above four hypotheses. It is shown that such the different relations cannot be interpreted by a radial solar wind emission from the sun, which is the fundamental assumption especially in both Allen's and Mustel's hypotheses. Thus, the deflection hypothesis based on the following assumptions is introduced. The solar winds with high velocity responsible for M-disturbances are emitted generally in the nonradial direction with respect to the solar surface. Most of the wind particles are supplied from a region of Ca plage or of its remnant (abbreviated to PR-region). This hypothesis is applied for a practical explanation of the different relations between AM- and PR-regions which have appeared during the present solar cycle. (auth)

47455 STUDIES ON PRE-SC POLAR IONOSPHERE AND HF RADIO PROPAGATION OVER POLAR PATHS. II. PRE-SC INCREASE OF WWV 20 AND 25 Mc/s FIELD INTENSITY AND OF f_0F_2 IN HIGH LATITUDES. Ondoh, Tadanori; Obu, Koji (Radio Research Labs., Nakaminato-shi, Japan). J. Geomagnet. Geoelec., 17: 45-57(1965).

Storm-time variations of WWV 25, 20, 15, 10, 5, and 2.5 Mc, and of the average deviations of f_0F_2 from the monthly median are examined for fifty geomagnetic storms during August 1957-February 1959. Abnormal increases of field intensity of WWV 20 and 25 Mc/s, and Δf_0F_2 occur from about 18 hours before a geomagnetic storm sudden commencement. Such field intensity increases were not statistically found previously below 15 Mc. The abnormal increases of field intensity at 20 and 25 Mc may be interpreted as being due to a decrease in deviative absorption associated with an increase in f_0F_2 for the penetration frequency near 20-25 Mc. The low latitude boundary of the pre-sc increase of f_0F_2 lies around 57°.0 N in geomagnetic latitude. A pre-sc increase of Δf_0F_2 in high latitudes is also found for geo-

magnetic storms associated with PCA during August 1957–February 1959. (auth)

47456 SUDDEN COMMENCEMENTS OF GEOMAGNETIC STORMS AND THEIR LOCAL IRREGULARITIES. Maeda, Rikio; Rikitake, Tsuneji; Nagata, Takesi (Tokyo Univ.). J. Geomagnet. Geoelec., 17: 69-93(1965).

The vertical components of geomagnetic variations at times of sudden commencements of magnetic storms apparently show an irregular distribution over the world, in contrast to the simultaneous horizontal field-change. The geomagnetic vertical field-change depends on the topographic condition at magnetic observatories, and this seems to be explained from the viewpoint of electromagnetic induction within the earth's outermost layer. An earth model with uniform electric conductivities is the zero-order approximation, with which the behavior of sudden commencements of geomagnetic storms at continental stations can be explained. The earth seems to act as a perfect conductor to screen the geomagnetic-field-change under the earth surface ($|\dot{H}|/|\dot{E}| \to 1/2$) for sudden commencements of extremely short risetime, so far as the data of continental stations are concerned. In a higher-order approximation for the electrical conductivity-distribution of the earth's outermost layer, the conductivity is non-uniform owing to the sea-land contrast over the world. When the non-uniformity of electric conductivity in the earth's outermost layer is simply taken into account, the observed tendency of the vertical geomagnetic variation at most non-continental stations can also be reasonably explained by the electromagnetic induction, except in special areas such as the Japan Islands and the Antarctic coast. (auth)

47457 SOME CHARACTERISTICS OF GEOMAGNETIC VARIATION ANOMALY IN JAPAN. Rikitake, T. (Tokyo Univ.). J. Geomagnet. Geoelec., 17: 95-7(1965).

Close comparisons were undertaken of the deviation from a straight line connecting the beginning of an event to the end, denoted as ΔH, found at an observatory to that at Kakioka. It is thought that the distribution of ΔH might provide a clue for investigating the cause of geomagnetic variation anomaly in Japan. Some 100 bay-like events during 1959 were chosen for most of the observatories shown, although events during different periods were used for observatories from which no observations were obtained during 1959. It noted that the ratio is large in the southern part of Japan and small in north eastern Japan. The outline of the anomaly is given, but nothing definite can be said about the cause of this geomagnetic variation anomaly in Japan. (J.F.P.)

47458 ABSENCE OF 40-kev ELECTRONS IN THE EARTH'S MAGNETOSPHERIC TAIL AT 3300 EARTH RADII. Van Allen, J. A. (Univ. of Iowa, Iowa City). J. Geophys. Res., 70: 4731-9(Oct. 1, 1965).

The Mars-bound spacecraft Mariner 4 drifted westward through the presumed region of an extended magnetospheric tail of the earth during late January and early February 1965 at a geocentric radial distance of ~3300 R_E (earth radii). A pair of thin-window Geiger tubes with wide-angle collimators, which had shown the presence of electrons $E_e > 40$ kev out to 23 R_E in the morning fringe of the magnetosphere during the early phase of the flight, failed to detect any effects of a magnetospheric tail during 7 days of flight within a geocentric angle between 1 and 5° from its presumed center line. (auth)

47459 ENERGETIC ELECTRON FLUXES IN THE TAIL OF THE GEOMAGNETIC FIELD. Anderson, K. A. (Univ. of California, Berkeley). J. Geophys. Res., 70: 4741-63 (Oct. 1, 1965).

Fluxes of energetic electrons up to 10^7 cm^{-2} sec^{-1} above 45 kev frequently appear in the tail of the geomagnetic field out to distances of 31.5 earth radii. They characteristically occur as isolated patches, not directly attached to other particle distributions around the earth. It is shown that these particles are usually injected into regions of space at least a few earth radii in size in an impulsive manner. The buildup time for these fluxes at a fixed point in space is typically a few minutes or less. The fluxes then decay away in times of several minutes up to a few hours, during which they may exhibit highly unstable behavior. The frequency of appearance of these fluxes has a radial dependence that rapidly falls off with increasing distance from the earth's center. The island fluxes are sensitive to geomagnetic activity but are present with low frequency even in quiet times. Their relation to other features of the distant radiation zone is discussed. (auth)

47460 EFFECTS OF SOLAR-WIND COMPOSITION ON THE THRESHOLD FOR PLASMA INSTABILITY IN THE TRANSITION REGION. Fredricks, R. W.; Scarf, F. L. (TRW Space Technology Labs., Redondo Beach, Calif.). J. Geophys. Res., 70: 4765-76(Oct. 1, 1965).

The effect of a small concentration of solar-wind α particles on the conditions for drift instability in the transition region is investigated. It is shown that, for α-particle concentrations less than about 20%, the proton-electron threshold curve is sufficiently accurate, for the range of relative electron-proton-α-particle drift speeds of interest. Recent transition region plasma measurements are interpreted in terms of the conditions for marginal stability with respect to electrostatic plasma oscillations. (auth)

47461 DIFFUSION OF PROTONS IN THE OUTER RADIATION BELT. Nakada, M. P.; Mead, G. D. (Goddard Space Flight Center, Greenbelt, Md.). J. Geophys. Res., 70: 4777-91(Oct. 1, 1965).

The diffusion of protons in the outer radiation belt due to violation of the third adiabatic invariant was examined. The particular mechanism studied is one in which variations in the intensity of the solar wind produce magnetic disturbances causing motion of particles between L shells. A Fokker-Planck diffusion equation is used with terms describing Coulomb energy degradation and charge-exchange losses with the ambient atmosphere. A source near the magnetopause is assumed. The diffusion constant is numerically evaluated by an analysis of observed frequencies of sudden impulses and commencements. The equation is solved to obtain radial and energy distributions. A comparison of the results with the measured proton fluxes of Davis, Hoffman, and Williamson indicates that a diffusion process of this general nature seems to be responsible for the observed outer-belt protons. For the parameters selected, the magnetic disturbances studied may not be sufficient to produce the required diffusion rate. The effects of possible changes in parameters are discussed. (auth)

47462 THE RADIATION BELT BOUNDARY NEAR SOLAR CYCLE MAXIMUM AS DETERMINED FROM THE TRAPPING OF ENERGETIC ELECTRONS. Rosen, Alan (TRW Space Technology Labs., Redondo Beach, Calif.). J. Geophys. Res., 70: 4793-4816(Oct. 1, 1965).

The termination of the radiation belt, as defined by the trapping boundary for electrons greater than 500 kev, is studied during the solar cycle maximum period of August 8, to September 10, 1959, using Explorer 6 scintillation counter data. The region investigated is on the evening side with respect to the earth-sun direction. The daily fluctuation in the position of the radiation belt boundary is presented for magnetically stormy and nonstormy periods. The boundary is compressed to low L values during magnetic storms and expands to high L values during periods of low magnetic activity. Evidence is presented to show that the expansion of the boundary is due to the addition of new particles at high L values. It is concluded that the mechanism active in injecting electrons of E > 500 kev into the radiation belt is effective during periods of low magnetic activity. Thus the local acceleration, diffusion or injection of particles into the radiation belt is a more or less continuous process. The fluctuation in the position of the boundary and the appearance of large fluxes of energetic electrons for short periods of time imply gross changes in the characteristics of the region. (J.F.P.)

47463 PARTIAL ELECTRON VELOCITY SPECTRUMS FROM CYCLOTRON ABSORPTION OF WHISTLER POWER. Liemohn, H. B. (Southwest Center for Advanced Studies, Dallas). J. Geophys. Res., 70: 4817-22(Oct. 1, 1965).

A method is proposed for the determination of partial electron velocity spectrums from the power spectrums of whistler signals at their upper cutoff. It is assumed that the only frequency-dependent attenuation of the signal is cyclotron resonance absorption by the non-thermal electron component (around 1 kev) in the magnetosphere. According to the theory, the differential density $F = [dN/dv_{||}]_{v_{||}=-u(\omega)}$ is related by an integral equation to the power loss $L(\omega)$ of each whistler, where $v_{||}$ is the velocity component parallel to the local geomagnetic field, u is the resonance speed, and ω is the propagation frequency. The equation is too difficult to solve analytically for F, but over a narrow frequency band $\omega_1 \leq \omega \leq \omega_2$ at the cutoff, where L is measurable, an approximate solution is obtained in the form $F = Au^{-n}$ in the range $u_1 \leq u \leq u_2$. The power spectrum of whistlers is not measured accurately yet, but the sharp cutoffs observed on sonograph traces suggest that $n \geq 9$. The results are compared with previous applications of the theory. (auth)

47464 WHISTLER-HYDROMAGNETIC EXTENSION OF MAGNETOIONIC THEORY. Kantor, Gideon (Air Force Cambridge Research Labs., Lawrence G. Hanscom Field, Bedford, Mass.). J. Geophys. Res., 70: 4823-46(Oct. 1, 1965).

This detailed study of the whistler-hydromagnetic extension of magnetoionic theory is based on exact derivations. The conductivity tensor formulation is reviewed. A resistivity tensor formulation that is derived is used to obtain a relatively simple wave polarization expression and an exact quadratic equation for the phase refractive index at ion gyrofrequency. A frequency slightly above the ion gyrofrequency is proposed as a condition for the transition between the whistler and hydromagnetic extensions. The four modes are defined from the two equal solutions of the transverse case. Standard curves and the corresponding phase refractive index surfaces are presented for protons. Although without apparent immediate practical application, being primarily of theoretical interest, the curves should encourage heuristic studies aimed at extending magnetoionic theory to whistler and hydromagnetic frequencies. (auth)

47465 IONOSPHERIC ELECTRON DENSITY AND BODY POTENTIAL MEASUREMENTS BY A CYLINDRICAL LANGMUIR PROBE. Nagy, A. F.; Faruqui, A. Z. (Univ. of Michigan, Ann Arbor). J. Geophys. Res., 70: 4847-58(Oct. 1, 1965).

The results of a detailed analysis of the experimental electron current characteristics of a cylindrical Langmuir probe carried by NASA rocket 6.05 (2325 LT, December 21, 1961, Wallops Island, Va.) are presented. Three different data reduction techniques are used to derive the ambient electron density and the equilibrium potential of the reference body. The results obtained by the different methods are critically discussed. The considerable difference between the upleg and downleg parameters (e.g., density and temperature) as measured by the probe, as well as supplementary information from the ionosonde, indicates that the measurements were made at a time when traveling ionospheric disturbances were present. It is concluded that the electron current characteristics of such a cylindrical probe do give reliable information and thus provide a useful technique for direct measurements of electron density in the ionosphere. (auth)

47466 TRANSMISSION OF GEOMAGNETIC MICROPULSATIONS THROUGH THE IONOSPHERE AND LOWER EXOSPHERE. Field, E. C.; Greifinger, C. (Rand Corp., Santa Monica, Calif.). J. Geophys. Res., 70: 4885-99 (Oct. 1, 1965).

The propagation of hydromagnetic waves at altitudes below about 2000 km is considered. This work is an extension of a previous paper in which heights below about 500 km were considered. The case of plane wave propagation in the vertical direction is treated, and the geomagnetic field is assumed to be vertical (polar propagation). Currently used models indicate that the ionosphere (the height region between about 80 and 500 km) may be reasonably represented by a constant Alfvén speed and locally exponential ion-neutral collision frequency, while the lower exosphere (the region between about 500 and 2000 km) can be adequately described by an Alfvén speed which increases exponentially with height. By using these approximate forms, the solutions of the relevant forms of the electromagnetic wave equation can be expressed in terms of known functions. Analytic expressions for the magnetic transmission and reflection coefficients are derived and analyzed, and numerical results are obtained. These results, although strictly applicable only to high magnetic latitudes, compare favorably with many geographically widespread experimental data. Of particular interest is the prediction of a prominent double transmission resonance in the daytime and a single strong resonance at night. This agrees with the measurements of various workers. Many lesser resonances are also found. The advantage of the analytic representation is the ease of interpretation of the physical results. For example, simple expressions describing the transmission resonances found by Jacobs and Watanabe for a grounded exosphere are found to be a limiting case of the equations derived here. (auth)

47467 IMPULSE RESPONSE OF THE MAGNETOSPHERIC COLUMN. Prince, C. E. Jr.; Bostick, F. X. Jr.; Smith, H. W. (Univ. of Texas, Austin). J. Geophys. Res., 70: 4901-8(Oct. 1, 1965).

The transmission characteristics of a plane stratified model of the earth's magnetospheric to plane hydromagnetic waves incident at the uppermost layer interface were computed. The computations, performed as a function of the angular frequency of the wave, are used to obtain the ratio of the amplitudes of the tangential magnetic fields in the specified incident waves to the magnetic field amplitudes computed at the layer interface representing the earth's surface. This steady-state transfer function is then Fourier-transformed to obtain simulated time records of the magnetic field at the earth's surface excited by impulsive inputs at the top of the magnetospheric column. Models representing both daytime and nighttime atmospheres during conditions of sunspot minimum are considered. The simulated time records are compared with experimental recording of the geomagnetic field obtained by other investigators. (auth)

47468 GEOMAGNETIC AND SOLAR DATA. Lincoln, J. Virginia (ed.) (National Bureau of Standards, Boulder, Colo.). J. Geophys. Res., 70: 4963-4(Oct. 1, 1965).

Data are presented for geomagnetic and solar activity in May 1965. Range indices and sunspot numbers are given. Sudden commencements and solar-flare effects are given for the fourth quarter, 1964. (J.F.P.)

47469 GEOMETRY OF THE MAGNETOSPHERIC TAIL AND AURORAL CURRENT SYSTEMS. Fejer, J. A. (Southwest Center for Advanced Studies, Dallas). J. Geophys. Res., 70: 4972-5(Oct. 1, 1965).

Certain consequences of the measured magnetic field configuration are considered, and it is suggested that, if the energetic charged particles in the neutral sheet were predominantly of one sign with charge neutrality maintained by low energy particles of the opposite sign, ionospheric current systems would result as well as important modifications of the co-rotation of low-energy plasma in the magnetosphere. The manner in which the energetic particles in the neutral sheet originate is not essential in the present discussion, but the presence of a neutral sheet containing neutral particles, and the possibility of the energy density of particles of one sign predominating over the energy density of particles of the other sign are vital. The suggested association between the geometry of the magnetospheric tail and the auroral electrojet current system, and the accompanying magnetospheric motions of the low-energy plasma could be an important feature of high-latitude geophysical processes. (J.F.P.)

47470 SPATIAL ASYMMETRY AND PERIODIC TIME VARIATIONS OF X-RAY MICROBURSTS IN THE AURORAL ZONE. Parks, G. K.; Hudson, H. S.; Milton, D. W.; Anderson, K. A. (Univ. of California, Berkeley). J. Geophys. Res., 70: 4976-8(Oct. 1, 1965).

Two microburst episodes were observed on September 8, 1964. The first, which is discussed, occurred for 15 minutes centered about 1300 UT. These microbursts showed high peak intensities at these times and were well resolved from all backgrounds. It is shown that the microburst sources moved about in the production layer. At 1329 UT the northeast detector counting rate exceeded the northwest detector counting rate. Some 18 seconds later, the reverse was true. Such fluctuations in the counting rates of detectors viewing separate parts of the production layer persisted throughout the entire episode; they can be attributed to motions associated with the precipitating region of the microburst. To reveal periodicities associated with this microburst episode, power spectrum analysis was employed. There are no conclusive ideas of why electrons of 25–100 kev travel in bunches along the L = 0 shell, but results obtained show evidence that they do. (J.F.P.)

47471 DETERMINATIONS OF THE AURORAL-ZONE X-RAY SPECTRUM. Hudson, H. S.; Parks, G. K.; Milton, D. W.; Anderson, K. A. (Univ. of California, Berkeley). J. Geophys. Res., 70: 4979-82(Oct. 1, 1965).

A portion of the bremsstrahlung spectrum of electrons precipitating into the auroral-zone atmosphere is accessible to precise spectrum measurements from balloon borne scintillation detectors. Such measurements were made during local daytime on a magnetically disturbed day. The design of the detector embodied several features that made possible to reliable extrapolation from the spectrum observed at balloon altitude to the true spectrum at the stopping level of the electrons. The counting-rate profile of the x rays observed with this detector is shown. The mean spectrum of several microburst events, and for comparison the spectrum of adjacent unstructured activity are shown. The main conclusion drawn is that the microbursts, although strikingly different in time structure, do not deviate appreciably in energy spectrum from the associated precipitation. (J.F.P.)

47472 THE DEPENDENCE OF OCCURRENCE OF MID-LATITUDE AURORA ON THE SUNSPOT CYCLE. Bellew, W. (Northeastern Univ., Boston); Silverman, S. M. J. Geophys. Res., 70: 4985-6(Oct. 1, 1965).

Data are presented from 1955 to 1963 in geographic latitude 32°43'N, geomagnetic latitude 41.6°N, bearing on the relation between northern enhancements of the 6300 Å line observed photometrically and magnetic activity for different phases of the sunspot cycle. The midlatitude aurora is most evident as an enhancement of the red line of atomic oxygen, normally to the north-northeast. The number of auroras, the number of observing nights, and the fraction of observing nights on which auroras were observed, are all presented as a function of the planetary magnetic index. Since the table given refers to enhancements to the red line observed photometrically, the data include a number of fainter auroras which might be expected to occur at lower magnetic activity and which would not be included in a count of visual auroras. Also the number of nights from March 1955 to March 1963 by year for which observations were made and for which auroral activity was observed according to the highest K_p on that night. It is evident from the table that a strong dependency of the occurrence on sunspot cycle exists. (J.F.P.)

47473 CONTINUOUS OBSERVATION OF THE AURORAL BELT BY MEANS OF RADIO. Bates, H. F.; Belon, A. E.; Romick, G. J.; Stringer, W. J. (Univ. of Alaska, College). Nature, 207: 1081-2(Sept. 4, 1965).

It is shown that the southern edge of the auroral belt (the latitudinal range over which aurorae occur at a given time and longitude) can be reliably tracked by radio means. Results from the all-sky-camera network north of College, Alaska, the College and Fort Yukon meridian scanning photometers (5577 Å) and the 4–64 Mc/s College step sounder were used. The results showed that the observed radio-wave scattering region is closely associated with the nighttime auroral belt. No appreciable diurnal difference was found between backscatter records obtained when the ionosphere was dark or sunlit for a given level of magnetic activity. Thus, the determination of the spatial and temporal variations of the auroral belt is possible from multi-frequency high-frequency backscatter records during daylight hours, and in particular during the Arctic summer, when ground-based optical observations cannot be made. (P.C.H.)

47474 EQUATORIAL ANGLE DISTRIBUTION BETWEEN THE ELECTRONS CAPTURED IN THE OUTER VAN ALLEN RADIATION BELT. Calamai, G. (Osservatorio Astrofisico di Arcetri, Firenze, Italy). Nature, 207: 1179-80(Sept. 11, 1965).

Properties of the trajectories corresponding to $\chi_e = 35°$ (χ_e = equatorial pitch) are discussed. Considering the geomagnetic field as produced by a dipole, and using perturbation theory, an equation was written for the angle χ between the velocity v and the magnetic field H, as a function of the magnetic latitude φ. As a result, the existence of a repulsing force from the equator is suggested. (P.C.H.)

47475 POWER SPECTRUM OF SPORADIC-E AT WILKES AND BYRD STATIONS, ANTARCTICA. Noel, T. M.; Bennett, S. M. (Avco Corp., Wilmington, Mass.). Nature, 207: 1182-3(Sept. 11, 1965).

Periodic variations of the ionospheric sporadic-E layer in Antarctica with similar frequency and latitude characteristics are reported. It is suggested that periodicities observed are real and that they may be similar to the absorption variations noted by others. The results may have considerable importance in suggesting a theory of high-latitude sporadic-E. (P.C.H.)

47476 SURVEY OF SOME ASPECTS OF EXPERIMENTAL AND THEORETICAL GEOMAGNETICS. Prince, Clarence E. Jr. (Taejon Coll., Korea). New Phys. (Korea), 5: No. 1, 29-36(May 1965).

Work on geomagnetic micropulsations is discussed. Some theoretical considerations, which may contribute to the formation of an acceptable model of the mechanism behind geomagnetic variations, are presented. Geomagnetic micropulsations can be regarded as minute fluctuations in the earth's main field or simply as ultra-low-frequency electromagnetic waves impinging on the surface of the earth. The roles of the solar wind and the Chapman-Ferraro cavity in the formation of micropulsations are discussed. A mathematical analysis of the geomagnetic micropulsations is presented. (M.C.G.)

47477 DIRECT DETECTION OF AMBIENT ELECTRON PLASMA OSCILLATION FIELDS IN THE MAGNETOSPHERE. Scarf, F. L.; Fredricks, R. W. (Thompson Ramo Wooldridge Inc., Redondo Beach, Calif.). Planetary Space Sci., 13: 921-2(Sept. 1965).

A possible interpretation is given for event D, previously observed, in which the most intense noise burst appeared only in the lower channel and at an altitude for which the local electron plasma frequency approached 700 kc/s. It is suggested that the antennas were simply responding to the electrostatic fields associated with the thermal or equilibrium level of electron plasma oscillations rather than to any local resonance. (J.F.P.)

47478 ON THE PROPAGATION OF WEAK HYDROMAGNETIC SHOCK WAVES IN THE EXOSPHERE AND THE SUDDEN COMMENCEMENT OF GEOMAGNETIC STORM. PART I. FAST SHOCK. Namikawa, Tomikazu (Osaka City Univ.); Okuzawa, Takashi (and others). Rept. Ionosphere Space Res. Japan, 17: 21-34(Mar. 1963).

The propagation of weak hydromagnetic shock discontinuities, of fast mode, in the dipole magnetic field is investigated, and the results obtained are applied to the weak shock propagation in a model exosphere. It is

shown that: (1) If the initial discontinuity surface is chosen as a concentric spherical surface with the earth, the characteristic rays propagate along radial direction under a first order approximation. (2) If the initial discontinuity surface is taken in the form of semi-infinite plane intersecting perpendicularly the geomagnetic equatorial plane, the characteristic rays toward the earth are most passable in the equatorial region under the approximation that the Alfvén wave velocity is regarded only as a function of radial distance from the center of the earth. From these results the equatorial enhancement of SSC in the day time is discussed. (auth)

47479 GEOMAGNETIC PULSATIONS AND THE EXOSPHERE. PART I. STATISTICAL RESULTS. Kitamura, Tai-ichi (Doshisha Univ., Japan). Rept. Ionosphere Space Res. Japan, 17: 67-76(June 1963).

Frequency-time analysis of geomagnetic giant pulsations (Pg's) is made on the basis of IGY data and the following four types are found: a type having an increasing frequency with time (ascending tone); a type having a constant frequency with time (descending tone); a type having a constant frequency with time; and a type having an irregular frequency with time. By examining in more detail the frequency character of Pg's from this point of view, a phenomenon is found like a beat having regularly varying amplitudes with time. The first half of it shows the ascending tone character and the latter half shows the descending tone, or vice versa. On the other hand, if the occurrence frequency of Pg's is plotted against local time, two maxima are found; one is in the morning (9h LT) and the other, in the evening (19h LT). The ascending type Pg's have a tendency to occur more often in the morning, whereas the descending ones, more frequently in the evening. In order to interpret these phenomena, the dispersion mechanism, Doppler mechanism, variable frequency mechanism, and the cavity mechanism are considered; and it is found that the cavity mechanism may be most reliable. (auth)

47480 SOLAR FLARE EFFECT ON GEOMAGNETIC VARIATION. Ohshio, Mitsuo; Fukushima, Naashi (and others) (Tokyo Univ.). Rept. Ionosphere Space Res. Japan, 17: 77-114(June 1963).

From the analysis of world-wide data at the time of 15 selected events during the IGY, the important characteristics of the geomagnetic solar flare effect are found. Progressive change in the ionospheric current-system during the geomagnetic solar flare effect is illustrated for some typical examples. The geomagnetic solar flare effect is shown not to be a mere augmentation of Sq. On considering also the simultaneous ionospheric effect, the effective current-flowing layer of geomagnetic s.f.e. is concluded to be situated at the bottom of the ionospheric E-region, a little lower than the layer for Sq current-system. By combining the effects of the electron production by intensified solar x ray and of the electromagnetic induction within the ionosphere, the world-wide aspect of individual geomagnetic solar flare effect seems to be reasonably explained. It is also shown that the introduction of spectrum and intensity of the x ray to interpret the observed geomagnetic effect is also reasonable to explain the simultaneous ionospheric effect. The origin of the geomagnetic solar flare effect is therefore interpreted to be the solar x ray with wavelength of 1 to 20 Å, the flux intensity of which increases suddenly within about one minute and then decreases gradually. (L.B.S.)

47481 DYNAMIC MORPHOLOGY OF AURORAS. Akasofu, Syun-Ichi (Univ. of Alaska, College). Space Sci. Rev., 4: 498-540(June 1965).

Simultaneous changes of auroral forms, brightness, and motions over the whole polar region are studied, using IGY all-sky camera records from widely distributed stations in eastern Siberia, Alaska, Canada and the northern United States. It is found that the auroral system centered in the midnight sector in the auroral zone repeatedly undergoes an expansion and subsequent contraction; during the maximum stage of the activity, the whole auroral system extends over a substantial portion of the darkened polar region. Such extensive auroral activity as a whole may be regarded as a single event, and is described in terms of the auroral substorm. The substorm has two characteristic phases, an expansive phase and a recovery phase. Characteristic auroral displays over the entire polar region during the substorm are described in detail. The basic physical processes involved for the auroral substorm are also discussed. Geomagnetic disturbances associated with the auroral substorm are also described in detail in terms of the polar magnetic substorm, and it is shown that both the auroral substorm and the polar magnetic substorm are different aspects of the manifestation of a large-scale plasma motion in the magnetosphere. The distribution of the aurora for different degrees of the geomagnetic activity is also discussed in terms of the auroral belt. It is shown that the center line of the auroral belt moves greatly with respect to its average location (namely the auroral zone), depending on the degree of the magnetic activity. (auth)

47482 APPEARANCE OF pc PULSATIONS IN EARTH'S MAGNETIC FIELD IN RELATION TO THE GEOMAGNETIC ACTIVITY. Muench, J. (Universitaet, Goettingen, Ger.). Z. Geophys., 31: 192-9(1965). (In German).

In the pulsation-records of the geomagnetic observatories Wingst, Göttingen, and Fürstenfeldbruck the appearance of pc-type pulsations was studied with regard to intervals of different geomagnetic activity measured in Kp. The following results were obtained as far as the H-component of pc's is concerned: at a given station the behavior of pc's systematically varies with different Kp's, and it also varies with geomagnetic latitude for a distinct Kp-value. The probability of appearance of sinusoidal pc's increases with increasing Kp, at the southern stations more than at the northern ones. The analysis of pc-periods yields a rather broad spectrum at all stations under consideration. The position of the maxima in the three spectra is dependent on geomagnetic latitude and Kp. The periods decrease with increasing Kp, however, this shift does not seem to happen continuously and above all not simultaneously at the three stations. The amplitudes of pc's strongly depend on the periods belonging to them. Comparing the amplitudes of the three stations, they rather vary with period and Kp than with latitude. (auth)

47483 INCREASE OF EARTH'S RADIUS. Eder, G. (Universitaet, Giessen, Ger.). Z. Geophys., 31: 206-11 (1965). (In German).

The increase of the length of the day and the frequency of radioactive elements within the earth can be used to estimate an increase of about 0.07 cm per year for the radius of the earth. A simple model yields an increase of the surface of the earth from 213 to 510 million km^2 since the stiffening of the earth-crust. This has far-reaching consequences for the continental drift and for the distribution of the oceans during the history of the earth. (auth)

47484 PLASMA THEORY AND OBSERVATIONS IN SPACE. Dungey, J. W. (Imperial Coll. of Science and Tech., London). pp 341-7 of STI/PUB/89.

The magnetosphere is described. The measurements made by probes in the magnetosphere are explained. These measurements are different from those made in the laboratory. The magnetic field is easy to measure, the electric field difficult, and the measurements of particles of the collisionless plasma very interesting. All plasma theory flows from either the Vlasov equation, the Boltzmann equation, or the Fokker-Plank equation, each of which has for its dependent variable the velocity distribution function. The instruments used in space essentially measure this function. Some detectors accept particles from only a small cone of directions and only in a small range of energy. (J.F.P.)

47485 EFFECTS OF ELECTROMAGNETIC PERTURBATIONS ON PARTICLES TRAPPED IN THE RADIATION BELTS. Dungey, J. W. (Imperial Coll. of Science and Tech., London). pp 349-72 of STI/PUB/89.

Magnetic field disturbances in the radiation belts are

weak compared with the undisturbed field except near the outer boundary of the magnetosphere. Thus the disturbance can be treated as a perturbation. The adiabatic theory of trajectories is given with relativistic corrections omitted. Numerical values are also given. Change of the magnetic moment invariant by disturbances and applications of the change in magnetic moment invariant are treated. The change of the longitudinal invariant by disturbances, and disturbances which change only the third invariant are considered. The form of the diffusion terms is discussed. (J.F.P.)

47486 AN ASTRONOMICAL AND GEOPHYSICAL SEARCH FOR SCALAR GRAVITATIONAL WAVES (thesis). Morgan, William Jason. Princeton, N. J., Princeton Univ., 1964. 159p.

Several gravity-sensitive mechanisms—the rotation of the earth, the motion of the moon, the motions of the outer planets, earthquakes, and data from a gravimeter—are examined to see if fluctuations occur in more than one of these mechanisms simultaneously. The simultaneous occurrence of such events could be due to fluctuations in G, the gravitational constant. From the amplitude of the fluctuations in the length of day, for which good data exists since 1820, an upper limit on gravity fluctuations with periods of a few years to a few decades was found to be $\delta G/G = 4 \times 10^{-8}$. The outer planets and earthquake rates both correlate with the changes in the length of day in a manner consistent with the varying gravity hypothesis, but the significance of these correlations is not very large. From modern comparisons of the rotation of the earth with the motion of the moon, it was found that most of the changes in the rotation rate must be due to a non-gravitational effect and that gravity fluctuations with periods of from two to five years were less than $\delta G/G = 5 \times 10^{-9}$ in the interval 1955 to 1962. From the gravimeter data, an upper limit on gravity fluctuations with periods of from one to six months in 1960 and 1961 of $\delta G/G = 1 \times 10^{-8}$ is found. (Dissertation Abstr.)

47487 MODIFIED FERMI HEATING IN THE OUTER VAN ALLEN BELT (thesis). Hord, Charles William. Boulder, Colo., Univ. of Colorado, 1964. 50p.

An energy distribution for the electrons in the outer portion of the Van Allen radiation zone is calculated. A previously proposed heating process involving the interaction of electrons with the electric field accompanying whistlers is examined and is found to be incapable of giving the observed electron energy distribution. A modified Type "A" Fermi acceleration process is examined as a possible means of heating low energy electrons. The distribution function so obtained agrees with the Explorer 12 experimental intensities. The existence of a modified Fermi heating mechanism is shown to qualitatively predict the existence of a radiation belt. (Dissertation Abstr.)

47488 PHYSICS OF THE EARTH'S UPPER ATMOSPHERE. Hines, C. O.; Paghis, I.; Hartz, T. R.; Fejer, J. A. (eds.). Englewood Cliffs, N. J., Prentice-Hall, Inc., 1965. 445p. $17.35.

Sixteen chapters and two appendices are included; separate abstracts have been prepared for 14. Chapters not abstracted for NSA deal with general aspects of atmospheric structure, geomagnetic field, ionospheric research and the sun; solar optical radiation; and motions of the neutral atmosphere. (L.B.S.)

For abstracts of individual chapters see: 47489–47502.

47489 THE LOWER IONOSPHERIC REGIONS. Belrose, J. S. (Defence Research Telecommunications Establishment, Ottawa). pp 46-72 of Physics of the Earth's Upper Atmosphere. Englewood Cliffs, N. J., Prentice-Hall, Inc., 1965.

An introductory discussion on the formation of ionization layers is presented, followed by a treatment of the ionospheric D region and E region. The treatment includes electron distributions and seasonal variations in the D and E regions, diurnal variations, variations with solar activity, and the nocturnal E layer. Recombinations and collisional frequencies are also discussed. (L.B.S.)

47490 THE IONOSPHERIC F REGION. Belrose, J. S. (Defence Research Telecommunications Establishment, Ottawa). pp 73-95 of Physics of the Earth's Upper Atmosphere. Englewood Cliffs, N. J., Prentice-Hall, Inc., 1965.

The global morphology of the F region during magnetically quiet times is outlined, and its structure is discussed in terms of the composition of the atmosphere. Physical conditions, such as temperature, effective electron loss rates, and collision frequencies are briefly reviewed. Some F-region irregularities, not obviously associated with magnetic storms, are considered. The F region below the F2 peak is mainly dealt with, but on occasion, the discussion is concerned with physical processes that are continuous across the F2 peak. (L.B.S.)

47491 THE OUTER IONOSPHERIC REGIONS. Heikkila, W. J. (Southwest Center for Advanced Studies, Dallas); Axford, W. I. pp 96-133 of Physics of the Earth's Upper Atmosphere. Englewood Cliffs, N. J., Prentice-Hall, Inc., 1965.

The present picture of the outer ionospheric regions is summarized, including new information resulting from rocket and satellite experiments. The neutral and the charged components are considered separately, and the charged components are discussed according to their energies, whether low (thermal) or high (trapped). Several distinct classes of trajectories of the neutral particle in the exosphere are distinguished. A short review of some relevant elements of plasma physics is included for the understanding of the trapped particle phenomenon. The inner and outer radiation belts, and the geomagnetic effects of trapped particles are discussed. (L.B.S.)

47492 MOTIONS OF IONIZATION. Fejer, J. A. (Southwest Center for Advanced Studies, Dallas). pp 155-75 of Physics of the Earth's Upper Atmosphere. Englewood Cliffs, N. J., Prentice-Hall, Inc., 1965.

A study is made of the ionization movements at E-region levels and above. General expressions for the mean drift velocities of the charged particles are derived theoretically. The results are then used to determine the conductivity and to derive the equations governing ambipolar diffusion in the ionosphere. Different atmospheric current systems whose existence is inferred from magnetic observations are discussed. Emphasis is placed on the dynamo current system which is thought to be the main cause of the daily variations (both solar and lunar) of the earth's magnetic field during magnetically quiet days. It is shown that, although the dynamo current system is generally restricted to heights below about 150 km, electric fields and electron drifts associated with it extend upward throughout the magnetosphere. The redistribution of electrons is studied, with emphasis of F2 layer effects. A discussion of motions on ionization due to horizontal winds in the neutral gas is presented. (L.B.S.)

47493 IONOSPHERIC NOISE AND GEOMAGNETIC MICROPULSATIONS. Barrington, R. E. (Defence Research Telecommunications Establishment, Ottawa); Fejer, J. A. pp 176-97 of Physics of the Earth's Upper Atmosphere. Englewood Cliffs, N. J., Prentice-Hall, Inc., 1965.

The characteristics of ionospheric noise are discussed, and a comprehensive system of classifying discrete emissions, according to the specific form of the frequency-time variation, is illustrated. Investigations of the occurrence in relations to other geophysical phenomena are considered. Some of the theories which have been advanced to explain the origin of ionospheric noise are discussed. The various types and characteristic of micropulsations are outlined, and some theories are briefly discussed. (L.B.S.)

47494 SOLAR ACTIVITY AND SHORT-LIVED TERRESTRIAL EFFECTS (SID). Collins, W. C. (National Research Council, Ottawa); Herzberg, L. pp 198-215 of Physics of the Earth's Upper Atmosphere. Englewood Cliffs, N. J., Prentice-Hall, Inc., 1965.

A broad-survey is given of the various aspects of abnormal solar activity revealed by optical phenomena. The type of solar radiation producing sudden ionospheric disturbances (SID's) is discussed, and a description of SID's is

given in terms of vlf and l–f, h–f, vhf, and geomagnetic effects. Ionization during SID's is treated. (L.B.S.)

47495 PARTICLE EMISSIONS FROM THE DISTURBED SUN, AND THE SUN-EARTH ENVIRONMENT. Hartz, T. R. (Defence Research Telecommunications Establishment, Ottawa). pp 216-44 of Physics of the Earth's Upper Atmosphere. Englewood Cliffs, N. J., Prentice-Hall, Inc., 1965.

The common environment of the sun and the earth, the interplanetary gas and magnetic field, is briefly discussed along with the influence on the solar particles in their flight. Observations which have provided information on the ejected solar material at various distances from the sun are summarized, and causal relationship between unusual events of the sun and terrestrial disturbances is discussed. (L.B.S.)

47496 SOLAR COSMIC RAYS AND THE IONOSPHERE. Reid, G. C. (National Bureau of Standards, Boulder, Colo.). pp 245-70 of Physics of the Earth's Upper Atmosphere. Englewood Cliffs, N. J., Prentice-Hall, Inc., 1965.

The nature of the link between solar cosmic rays and ionospheric absorption and its implications for both cosmic-ray and ionospheric physics are discussed. Observational techniques for measuring ionospheric absorption are briefly described. Ionospheric effects and the nature of solar cosmic rays are briefly discussed. Some typical features of polar cap absorption (PCA) as observed on riometer recordings are discussed and an account of current ideas concerning the interpretation of these features is given. The use of ionospheric sounding to investigate PCA and the effects of ionization produced in the lower ionosphere by solar protons on the propagation characteristics of low-frequency radio waves are discussed. (L.B.S.)

47497 MAGNETIC AND IONOSPHERIC STORMS. Paghis, I. (Defence Research Telecommunications Establishment, Ottawa). pp 271-98 of Physics of the Earth's Upper Atmosphere. Englewood Cliffs, N. J., Prentice-Hall, Inc., 1965.

The relation between solar activity and storms, and the information which it provides about the classification of storms are discussed. The magnetic and ionospheric storms are then described, both as individual events and as averaged world-wide disturbances. (L.B.S.)

47498 OPTICAL AURORA. Montalbetti, R. (Defence Research Telecommunications Establishment, Ottawa). pp 299-318 of Physics of the Earth's Upper Atmosphere. Englewood Cliffs, N. J., Prentice-Hall, Inc., 1965.

The geographical distribution of auroras in both the northern and southern hemispheres is briefly considered, and the classification which distinguishes forms on the basis of the general shape and structure of the luminosity and on certain characteristic time and spatial variations is discussed. Measurements are briefly described of the height of auroral forms, their particular orientation in space, the distribution of luminosity, and motion of displays as a whole or of the individual forms, which give information about the disturbed atmosphere and are necessary in formulating auroral theories. The influence of solar activity, associated geophysical phenomena, the auroral spectrum, temperature measurements, hydrogen emissions, and auroral particles are treated. (L.B.S.)

47499 RADIO AURORA. Blevis, B. C. (Defence Research Telecommunications Establishment, Ottawa); Collins, W. C. pp 319-33 of Physics of the Earth's Upper Atmosphere. Englewood Cliffs, N. J., Prentice-Hall, Inc., 1965.

The information that can be obtained from a study of the reflection and scattering of radio waves for h–f ionosondes and for vhf and uhf radar systems is discussed. The general eral characteristics and structure of radio aurora, their relation to other geophysical phenomena, and their likely generation mechanisms, are described. Radio emissions from aurora are briefly considered. (L.B.S.)

47500 THEORY OF GEOMAGNETIC AND AURORAL STORMS. Hines, C. O. (Univ. of Chicago); Reid, G. C. pp 334-62 of Physics of the Earth's Upper Atmosphere. Englewood Cliffs, N. J., Prentice-Hall, Inc., 1965.

Hydromagnetic processes and charged-particle drifts in inhomogeneous magnetic fields are considered in discussions on geomagnetic storms, which include sudden commencements, initial phase, main-phase DS behavior, main phase Dst behavior, and elementary polar storms. Some of the major theories of the aurora are examined, and an attempt is made to indicate their principal successes and shortcomings. (L.B.S.)

47501 WAVE PROPAGATION IN A HOMOGENEOUS IONIZED GAS. Barrington, R. E. (Defence Research Telecommunications Establishment, Ottawa). pp 371-95 of Physics of the Earth's Upper Atmosphere. Englewood Cliffs, N. J., Prentice-Hall, Inc., 1965.

Several idealizations which are applicable in ionospheric problems are introduced in the mathematical treatment of wave propagation in an ionized gas. The assumptions reduce the discussion to a consideration of waves in an infinite, partially ionized low-temperature gas pervaded by a steady magnetic field. The treatment is mainly devoted to radio waves; the dispersion equation, reflection conditions, the effects of collisions on the refractive indices, and whistler dispersion are considered. The dispersion equation for hydromagnetic waves is also developed. (L.B.S.)

47502 WAVE PROPAGATION IN AN INHOMOGENEOUS MEDIUM. Fejer, J. A. (Southwest Center for Advanced Studies, Dallas). pp 396-423 of Physics of the Earth's Upper Atmosphere. Englewood Cliffs, N. J., Prentice-Hall, Inc., 1965.

The propagation of radio waves in a horizontally stratified medium is treated, and certain approximate solution of the differential equations, the ray solutions, are described. It is shown how double refraction by the earth's magnetic field complicates the ray-tracing procedure by splitting up an incident wave packet into two separate packets, corresponding to two characteristic waves. The conditions for which the ray solutions are no longer valid are discussed. Irregular variations, such as fluctuations caused by turbulence, superimposed on the regular variation of ionospheric properties with height and the slower variation with geographical position are considered; a detailed introduction to the methods used for dealing with irregular variations is given. (L.B.S.)

Low Temperature Physics

47503 (BNL-9478) THE SUPERCONDUCTING TRANSITION TEMPERATURE OF THIN Al FILMS. Strongin, Myron; Kammerer, O. F.; Paskin, A. (Brookhaven National Lab., Upton, N. Y.). [1965]. Contract AT(30-2)-Gen-16. 19p. (CONF-650936-2). Dep. mn; CFSTI, $1.00 cy, $0.50 mn.

From 1st International Symposium on Basic Problems in Thin Film Physics, Clausthal-Gottingen, Ger.

The superconducting transition temperature T_c of thin aluminum films was measured. The variation of T_c with thickness is presented, and a model is discussed that explains these results in terms of the surface superconductivity ideas introduced by Ginzburg. Large rises in T_c of room temperature evaporated films of aluminum are reported and discussed. (M.O.W.)

47504 (JPL-TR-32-650(Pt.2)) THE ROTATING SUPERCONDUCTOR. PART II. THE FREE ENERGY. Saffren, M. M. (Jet Propulsion Lab., Calif. Inst. of Tech., Pasadena). May 14, 1965. Contract NAS 7-100. 11p.

The free energies appropriate for stationary and rotating superconductors with and without an external applied field are derived. A general theorem is deduced that determines the fluxoids of a multiply connected superconductor in its equilibrium state. Also shown is that an isolated stationary superconductor rotates when made superconducting in an external field. This is an effect that was not noticed pre-

viously. In the derivation of free energies from the point of view of London theory, which is to treat the superelectrons as having a uniform density, it is shown that even from the point of view of the Ginzburg-Landau theory, in which this restriction is not imposed, the obtained conclusions are essentially unaltered. In the derivation of the free energies, an expression for the magnetic enthalpy is required. This expression is obtained in a novel way through use of the concept of a "magnetic reservoir." (auth)

47505 THERMAL EXPANSION OF COMPRESSED He II. Mills, R. L.; Sydoriak, S. G. (Univ. of California, Los Alamos, N. Mex.). Ann. Phys. (N.Y.), 34: 276-90 (Sept. 1965). (LA-DC-7034).

Measurements of the isobaric thermal expansion coefficient, α_p, of compressed He II are considered. The experimental details are described and the results of measurements of α_p from 0.5 to 1.5°K at pressures of 3, 6, 12, and 24 atm. are presented. A p-T locus of $\alpha_p = 0$ is found to intersect the melting curve at 0.59°K. The entropy of compression is calculated over the region investigated. Finally the implication of a volume maximum on the melting curve is discussed. (auth)

47506 MICROSCOPIC THEORY OF SUPERFLUID HELIUM. Hohenberg, P. C.; Martin, P. C. (Harvard Univ., Cambridge, Mass.; Ecole Normale Superieure, Paris). Ann. Phys. (N.Y.), 34: 291-359(Sept. 1965).

The properties of an interacting condensed Bose system are discussed emphasizing those aspects which do not depend on the weakness of the potential, and which therefore apply to superfluid helium. A physical and mathematical characterization of Bose condensation is presented in terms of an additional macroscopic quantity, the wave function of the condensed mode, which is defined in terms of microscopic quantities. It is shown that in equilibrium the assumption of Bose condensation leads to a two-fluid model. The hydrodynamic generalization applicable to slowly varying disturbances from equilibrium is then discussed and rigorous microscopic expressions are derived for the parameters of this theory (including dissipative coefficients). The elementary excitation spectrum in this collision dominated regime is exhibited. The Landau quasi-particle theory is examined, as well as the relation of condensation and the excitation spectrum, to the property of superfluidity. Under certain regularity assumptions the form of the long-wave length excitation spectrum at vanishing temperature is deduced. The corresponding derivation at finite temperature is presented and criticized. Finally, techniques are discussed for evaluating properties of the Bose system starting from the interaction potential. Approximation schemes consistent with the conservation laws and with the absence of a gap in the elementary excitation spectrum are discussed. Previous approximations for the weakly interacting Bose gas are classified and summarized and additional approximations are examined. (auth)

47507 THE PROPAGATION OF PERSISTENT CURRENT DECAY IN Nb-Zr WIRES. Walker, M. S.; Hulm, J. K. (Westinghouse Research Labs., Pittsburgh). Appl. Phys. Letters, 7: 114-16(Sept. 1, 1965).

The persistent currents which are induced in the interior of a strongly pinned type-II superconductor by a magnetic field form a local store of energy. The controlled release of persistent current energy by local heat injection was studied. The experiments indicate that once current decay is initiated in a small region, the resulting disturbance may propagate indefinitely through the material, feeding upon the stored energy. From the observed pattern of flux changes the arrangement of persistent current domains for a wire in a transverse field can be deduced. Potential leads were attached to a short length Nb-Zr wire. A heater was mounted near one end. With the sample at 4.2°K and a magnetic field perpendicular to the axis of the wire, it was found that less than an erg of electric energy injected rapidly into the heater would produce the time sequence of signal shown. (J.F.P.)

47508 THE SUPERCONDUCTIVITY OF SINTERED Nb_3Sn AT TEMPERATURES ABOVE 4.2 deg K. Hancox, R. (Culham Lab., Abingdon, Eng.). Appl. Phys. Letters, 7: 138-9(Sept. 1, 1965).

It was previously demonstrated that a cylinder of sintered Nb_3Sn of average density 5.5 g/cm^3 was stable for a field change greater than 55 kG, but was unstable for a field change greater than 17 kG when impregnated with wax to prevent absorption of liquid helium. A further consequence of this dependence on the thermal capacity is that the rapid change in specific heat with temperature of a specimen from which liquid helium is excluded should be reflected in a temperature dependence of its stability in an increasing magnetic field. To check this, measurements of the field which could be screened by a cylinder of sintered Nb_3Sn before the flux motion became unstable, were made in a vacuum calorimeter. The specific heat and critical current were also measured. The resulting specific heat, critical current density, and screening field are each plotted as a function of temperature. (J.F.P.)

47509 ON THE BOGOLIUBOV-ZUBAREV-TSERKOVNIKOV METHOD IN THE THEORY OF SUPERCONDUCTIVITY. Chen-Tsai, C. T. (Tsing Hua Univ., Taiwan, China). Chinese J. Phys. (Taiwan), 3: 22-34(Apr. 1965).

An alternative proof of the asymptotic exactness of the BCS theory of superconductivity within the framework of perturbation theory is made by employing the Bloch Statistical mechanical pertubation theory in the Bogoliubov-Zubarev-Tserkovnikov method. (auth)

47510 SURVEY OF TYPE II SUPERCONDUCTORS. Lowell, J. Cryogenics, 5: 185-93(Aug. 1965).

A survey is presented of recent work on superconductors of the second kind. Evidence for the GLAG theory and its ramifications is considered, followed by an account of the models which attempt to account for magnetic hysteresis and related effects. The motion of fluxoids under the influence of the Lorentz force and the phenomenon of flux-jumping are discussed briefly. (auth)

47511 EFFECT OF THE OMEGA TRANSFORMATION ON CRITICAL CURRENTS IN A ZIRCONIUM-RICH NIOBIUM ALLOY. King, A. H. (A. D. Little, Inc., Cambridge, Mass.); O'Brien, J. L.; Roberts, J. A.; Roberts, P. R. Cryogenics, 5: 230-1(Aug. 1965).

Measurements were made of the change of critical current versus field up to 28 kG for various heat treatments of zirconium-rich alloys containing niobium, in order to determine the effect of the highly faulted quenched structure as well as the aged structure. It was found for a sample containing 15 at. % niobium that the lowest critical current at high field values occurs in the quenched alloy, and that aging increased the critical current values. It is concluded that a highly faulted structure does not necessarily lead to a high critical current. (L.B.S.)

47512 SUPERCONDUCTING COIL DEGRADATION. Taquet, B. (United Kingdom Atomic Energy Authority, Abingdon, Eng.). J. Appl. Phys., 36: 3250-5(Oct. 1965).

Experiments carried out to try to explain the degradation phenomenon of superconducting coils are described. It is established that flux jumps occurring in a low-field zone cause a sudden decrease in the series current, which in turn causes a disturbance of field throughout the coil and thus probably results in a quench in a high-field zone. Degradation of short samples is obtained by following a peculiar cycle of magnetization similar to that observed in a coil. An explanation is given to explain the difference of degradation observed between a short sample and a coil. A measurement of the apparent resistance of a superconducting wire under changing field conditions gives an equivalent resistivity of 10^{-14} Ω · cm for dB/dt = 200 G/sec. (auth)

47513 EFFECT OF PROCESSING HISTORY ON THE SUPERCONDUCTING PROPERTIES AND LONG-RANGE ORDER OF Ta_3Sn. Courtney, T. H.; Pearsall, G. W.; Wolff, J. (Massachusetts Inst. of Tech., Cambridge). J. Appl. Phys., 36: 3256-60(Oct. 1965).

Variations of the transition temperature and long-range order parameter of Ta_3Sn compacts were studied as func-

tions of sintering time and temperature. Reacting the compacts for 4 days at 900°C produced a maximum in the order parameter (0.68) and the maximum transition temperature observed (8.35°K). Transition temperatures could be lowered to less than 4.2°K by vacuum heat treating presintered compacts at elevated temperatures. Ta_3Sn was the only intermediate phase observed to form in the Ta–Sn system between 700° and 1450°C. (auth)

47514 ADSORBED ^{3}He: HEAT CAPACITY AT LOW TEMPERATURES. Lambert, Marcel H. (Univ. of California, Berkeley). J. Chem. Phys., 43: 2913-14(Oct. 15, 1965).

Heat-capacity data are presented on adsorbed ^{3}He for different coverages, since they provide general information on the properties of adsorbed helium. These properties are expected to result from a competition between the high zero-point energy of the atoms and their interaction with the adsorbant. The heat capacity of different amounts of ^{3}He adsorbed on 0.183 grams of zeolite plotted as hc/T versus T, where T is temperature, is shown, with the heat capacity of the empty cell subtracted. Curves are shown for 1.9×10^{-4}, 4.7×10^{-4}, and 8.3×10^{-4} mole helium-3. Data for higher coverages are also shown. These data differ in two respects. The heat capacity increases very fast above 0.3°K, and it presents a sharp peak at 0.12°K which is probably related to isotopic ordering. These data indicate that adsorbed He at low temperatures has solidlike properties. No nuclear (^{3}He) contribution to the heat capacity is apparent down to 0.1°K. (J.F.P.)

47515 ANOMALOUS BEHAVIORS IN JOSEPHSON CURRENT. Shigi, Toyoichiro (Osaka City Univ.); Saji, Yoshiro; Nakaya, Shigehisa; Uchiho, Kousuke; Aso, Takeshi. J. Phys. Soc. Japan, 20: 1276(July 1965).

Tunneling d-c currents were observed at zero voltage (Josephson currents) while measuring the magnetic field dependence of the energy gap by electron tunneling through a very thin oxide barrier in Sn–SnO–Pb junctions with various thicknesses. The lead and tin films are 1500 and 2900 Å respectively, evaporated onto a glass substrate at room temperature. The pressure during evaporation was $2(10)^{-5}$ mm Hg or less. The direction of the field is parallel to the plane of the films. The ordinate at H = 0 does not coincide with the symmetrical axis of the curve; and the periodicity of the Josephson current with the magnetic field cannot be seen. This may be due to no shielding of the magnetic field of the earth and the latter due to too large a width of the films compared with the Josephson penetration distance. The anomalous behavior of the Josephson current is shown. The reason for this behavior must be examined; but it is supposed that it may be due to the large area of the junctions or inhomogeneity of film thickness. (J.F.P.)

47516 VORTICES IN AN IMPERFECT BOSE GAS. III. SCATTERING OF SINGLE-PARTICLE EXCITATIONS. Fetter, Alexander L. (Univ. of California, Berkeley). Phys. Rev., 140: A452-60(Oct. 18, 1965).

The scattering of single-particle excitations by a vortex in the condensate of an imperfect Bose gas is studied using the Bogoliubov approximation. The S matrix is calculated as in conventional scattering theory, and the phase shifts are determined with the Schwinger variational principle. The differential cross section in the long-wavelength limit is found to be $d\sigma/d\chi = \frac{1}{2}\pi(\hbar/mc)^2 k \cot^2(\frac{1}{2}\chi)$, where m is the mass of one atom and c is the speed of sound. This cross section agrees precisely with that found previously for scattering of sound by a classical vortex with circulation h/m. (auth)

47517 SUPERCONDUCTING PROPERTIES OF TIN, INDIUM, AND MERCURY BELOW 1 deg K. Finnemore, D. K.; Mapother, D. E. (Univ. of Illinois, Urbana). Phys. Rev., 140: A507-18(Oct. 18, 1965).

The superconducting critical field curves for pure Sn, In, and Hg were measured down to about 0.3°K. In the low-temperature region where the superconducting electronic entropy is negligible, the entropy difference (and hence the normal electronic entropy) is linear in temperature, as expected for a free electron gas. The measurements provide a sensitive test for details of the BCS theory in that the accuracy obtainable is much higher than in other experiments. A simple scaling of the energy-gap-to-temperature ratio brings the theoretical predictions into good agreement with experiment. The results are critically analyzed in the light of a possible lattice contribution to the entropy change at the superconducting transition of In, but no evidence for such a lattice contribution is found. (auth)

47518 COLLECTIVE EXCITATIONS IN STRONG-COUPLING SUPERCONDUCTING ALLOYS. Fulde, Peter; Strassler, Sigfrid (Univ. of California, Berkeley). Phys. Rev., 140: A519-22(Oct. 18, 1965).

The mean-free-path dependence of collective excitations in strong-coupling superconducting alloys is investigated by extension of the Fermi-liquid theory, which was developed by Larkin and Migdal for pure strong-coupling superconductors. Numerical results, which are presented, show that the dependence of the energy of transverse collective excitations on mean free path is large enough to suggest that the precursor in the infrared absorption spectrum of lead alloys is not due to collective excitations. (auth)

47519 SERIES SOLUTION OF THE GINZBURG-LANDAU EQUATIONS FOR THE ABRIKOSOV MIXED STATE. Lasher, Gordon (International Business Machines Corp., Yorktown Heights, N. Y.). Phys. Rev., 140: A523-8(Oct. 18, 1965).

Periodic solutions of the Ginzburg-Landau (GL) equations in the form of a power series in the quantity $(H_{c2} - B)/B$ are found. The lowest order term of the series satisfies the linearized GL equation. The order parameter, the free energy, and the magnetic moment are explicitly evaluated to the next higher order for the regular triangular lattice and the square lattice. These results evaluate the error in using the solutions of the linearized equation and extend the range of magnetic field for which the mixed-state configuration is known. An orthonormal set of functions in which the order parameter may be expanded is generated. The mixed-state solutions of the linearized equation with fluxoid quantum numbers greater than unity are determined and shown to have higher free energy than the unit-fluxoid solutions of the same symmetry. (auth)

47520 SUPERCONDUCTIVITY IN THE TIN–GALLIUM SYSTEM. Knapp, Gordon; Merriam, M. F. (Univ. of California, San Diego, La Jolla). Phys. Rev., 140: A528-30(Oct. 18, 1965).

Superconducting transition temperatures were measured for a number of Sn-Ga compositions in both the quenched (quick cast) and annealed states. The increases in T_c in the quenched samples are not large (usually about 0.1 to 0.2°K) and can be accounted for on the basis of internal stresses in the sample. The equilibrium transition temperatures are consistent with the known phase diagram of Predel. Within the Sn solid solution T_c first drops (mean-free-path effect), then rises to 3.9°K. Compositions in the neighborhood of the eutectic show depressed and broadened transitions; these are attributed to proximity effects. (auth)

47521 OBSERVATION OF PERSISTENT CURRENTS IN A SUPERCONDUCTING CIRCUIT CONTAINING A JOSEPHSON JUNCTION. Smith, T. I. (Rice Univ., Houston, Tex.). Phys. Rev. Letters, 15: 460-2(Sept. 6, 1965).

The I-V characteristics of Josephson tunnel junctions were always obtained by potentiometric techniques. The observation of the superconductivity of a junction by the much more sensitive method of incorporating it in a persistent current loop is described. That the junction should support a persistent current equal in magnitude to the maximum indicated by the I-V characteristic is not immediately evident. In the latter case, the boundary conditions for the wave function are determined by the external

current source, while in the former case the wave function must be single valued around the loop. The measurements described show that superconducting loops containing $Pb-Pb_xO_y-Pb$ junctions will support persistent currents equal to the maximum supercurrent obtained from the I-V characteristic. Single-particle tunneling is indicated by a sharp rise in current when the voltage is near 2.5 mv. In zero applied field it was found possible to trap a Josephson current in the persistent current loop. (J.F.P.)

47522 DIRECT MEASUREMENTS OF MULTIPLE QUANTIZATION IN He II. Steyert, W. A.; Taylor, R. D.; Kitchens, T. A. (Los Alamos Scientific Lab., N. Mex.). Phys. Rev. Letters, 15: 546-9(Sept. 27, 1965).

The experiments reported use a probe small enough to examine properties of individual vortex lines in He II. Particles of the frozen H-D gas are used to investigate the pressure and velocity fields near the vortex core. Adjustments are made such that the motion of the particles of gas is considered entirely due to the motion of the helium. While most of the particles move very slowly and smoothly through the liquid, one in 10^3 is perturbed and executes a single loop similar to that shown schematically. It then continues on along a smooth path. Rarely will a particle execute two loops around the same center. For purposes of analysis the motion is thought of as a one-turn helix viewed microscopically. The results show that this highly sensitive method of examination clearly establishes the existence of quantized circulation of $n > 1$ and further, direct observations of vortices created in helium counter flow show that vortex generation does contribute to Gorter-Mellink mutual friction supporting previous conclusions. (J.F.P.)

47523 THERMAL EXPANSION COEFFICIENT AND COMPRESSIBILITY OF SOLID ^{3}He. Adams, E. D.; Straty, G. C.; Wall, E. L. (Univ. of Florida, Gainesville). Phys. Rev. Letters, 15: 549-51(Sept. 27, 1965).

Direct observations of the thermal expansion coefficient and compressibility of solid helium-3 are reported. The measurements are all in the bcc phase for molar volumes from 22.39 to 24.61 cm^3/mode and over the temperature range from 0.3°K to the melting point. A capacitance-type strain gage which permitted observations of changes in pressure on the solid sample of less than 10^{-3} atmospheres was used. A plot is shown of the compressibility versus the molar volume of helium-3. The thermal expansion coefficient was then found from the slopes of the isochores. A plot of this coefficient versus temperature for various molar volumes is also given. It is noted that no negative expansion coefficients were observed in contrast to theoretical predictions. (J.F.P.)

47524 MAGNETIC PROPERTIES OF SUPERCONDUCTING TANTALUM. Bots, G. J. C.; Pals, J. A.; Blaisse, B. S.; De Jong, L. N. J.; Van Engelen, P. P. J. (Technische Hogeschool, Delft, Netherlands). Physica, 31: 1113-23(July 1965).

Magnetization curves of a single wire of tantalum were measured at various temperatures between 1.3°K and 4.2°K. The unannealed tantalum showed a very strong hysteresis. The magnetization curve in increasing field of the annealed material was very similar to an Abrikosov curve; some hysteresis was still present, but much less pronounced than in the unannealed tantalum. During the annealing process some nitrogen has been absorbed leading to an increase of the electrical resistance at low temperatures, to a decrease of T_c and to an increase of the H_{c2} values. (auth)

47525 THE TEMPERATURE DEPENDENCE OF THE NUCLEATION FIELDS IN DIRTY ANISOTROPIC SUPERCONDUCTORS. Tilley, D. R. (Mullard Research Labs., Redhill, Eng.). Proc. Phys. Soc. (London), 86: 678-9(Sept. 1965).

It is shown that the calculations previously made for H_{c2} and H_{c3} in the Ginzburg–Landau temperature region can be extended to all temperatures using the methods given by de Gennes and by Maki. (auth)

47526 SUPERCONDUCTING ELECTROMAGNET OF Nb_3Sn. Kuan, Wei-yen; Liu, Ti-hang; Cheng, Guo-kuang, Wu Li Hsueh Pao, 21: 1345-54(July 1965). (In Chinese).

Results of study on tubular Nb_3Sn magnets are presented. Magnetic flux jumping was observed as usual. The "frozen" field distribution is closely related to the external field distribution and previous history. The distribution need not be symmetrical with respect to the mid-plane perpendicular to the cylindrical axis, as in the case of soft superconductors. This confirms the suggestion that the sintered Nb_3Sn material is not a homogeneous medium. A new magnet structure with which magnetic flux jumping can be avoided is described. With these magnets, besides the use of the iron core for trapping magnetic flux, there are also special features in both the excitation and the measurement of magnetic fields. Utilizing the tubular Nb_3Sn as a piston, a highest magnetic field of 28.5kG at 1.5°K was obtained. (auth)

47527 A NONLOCAL EXTENSION OF THE GINZBURG-LANDAU EQUATIONS IN THE THEORY OF SUPERCONDUCTIVITY. Wu, Hang-sheng; Lei, Hsiao-lin. Wu Li Hsueh Pao, 21: 1355-69(July 1965). (In Chinese).

The necessary conditions in the microscopic derivation of the Ginzburg-Landau (GL) equations are discussed, by showing that for a Pippard- or an intermediate-type superconductor the GL equations are valid only in a rather narrow region. Basing on the Gorkov equations for the thermodynamic Green functions of superconductor and using a nonlocal series of the "Green function of normal metal" in the magnetic field, a pair of coupled integro-differential equations was derived for the energy-gap function and vector potential. The equations are valid for the Pippard- and intermediate-type superconductors in the same region near T_c as that for the London-type. The equations are applied to a semi-infinite superconductor in a static magnetic field. The integral expressions for energy-gap function and penetration depth are given. In the London and Pippard limit the integrals are performed analytically. For a superconductor of the Pippard-type, the corrections of energy-gap function and penetration depth due to magnetic field are calculated in the whole region near T_c. It is shown that the behavior of a a Pippard-type superconductor differs much from that predicted by the GL theory. (auth)

47528 THERMAL CONDUCTIVITY OF Gd AND Tb AT LOW TEMPERATURES. Aliev, N. G.; Volkenshtein, N. V. (Inst. of Physics, Academy of Sciences, Azerbaidzhan SSR). Zh. Eksperim. i Teor. Fiz., 49: 24-6(July 1965). (In Russian).

The temperature dependence of the thermal conductivity of Gd and Tb samples is measured at 2 to 100°K. Maxima in the thermal conductivity are observed at temperatures of 16 to 20°K. The Lorentz number calculated for 4.2°K is found to greatly exceed the theoretical value. It is suggested that at these temperatures besides electron thermal conductivity there exist other transfer mechanisms which contribute to the total thermal conductivity of these rare earth metals. Anomalies in the thermal conductivity and electric conductivity of Tb are observed at temperatures below 5°K. (auth)

47529 EFFECT OF IMPURITIES ON THE PRESSURE EFFECT IN THALLIUM. [PART] II. Brandt, N. B.; Ginzburg, N. I.; Ignat'eva, T. A.; Lazarev, B. G.; Lazareva, L. S.; Makarov, V. I. (Moscow State Univ.; Inst. of Physics and Tech., Kiev). Zh. Eksperim. i Teor. Fiz., 49: 55-9(July 1965). (In Russian).

The effect of pressure P, up to 28,000 atm on the superconductivity transition temperature T_k for pure thallium and thallium with mercury impurities is investigated. It is found that at high pressures (20,000–28,000 atm) the dependence of T_k on P in thallium with mercury impurities is similar to that for pure thallium ($dT_k/dP = -1.4 \cdot 10^{-6}$ degree/atm). At low pressures (up to ~7000 atm) the dependence of T_k on P in pure thallium and thallium with impurities is different (the sign of the effect changes at a certain concentration of the impurity). It is suggested

that such a behavior of thallium and its alloys is connected with peculiarities in the dependence of the state density on the Fermi surface on pressure. It is possible that these features correspond to a change in topology of the Fermi surface of thallium. (auth)

47530 CHANGES IN THE RESISTANCE OF TIN FILMS ON DESTRUCTION OF SUPERCONDUCTIVITY BY A CURRENT. Smirnov, A. P.; Totubalin, V. N.; Parshina, I. S. (Ioffe Inst. of Physics and Tech., Leningrad). Zh. Eksperim. i Teor. Fiz., 49: 117-23(July 1965). (In Russian).

It is shown that destruction of the superconductivity of tin films $(3-8) \times 10^{-5}$ cm thick occurs in a broad range of current values. The critical current criteria are discussed. When the critical current is determined on basis of the appearance of a certain fraction of the resistance, the temperature dependence of the critical current can be described by a formula down to temperatures of 2.9°K. (auth)

47531 SUPERCONDUCTIVITY IN Ag–Ga SYSTEM. Alekseevskii, N. E. (Inst. of Problems in Physics, Academy of Sciences, USSR). Zh. Eksperim. i Teor. Fiz., 49: 159-62(July 1965). (In Russian).

It is shown that Ag–Ga alloys containing ≈30 atm % of Ga become superconductive. The specificity of the superconducting properties and phase composition of the alloys is discussed. (auth)

47532 He II FILM TRANSFER RATES UNDER VARIOUS CONDITIONS (thesis). Selden, Robert Wentworth. Madison, Wis., Univ. of Wisconsin, 1965. 103p.

The volume rates of transfer of liquid helium II through the film were studied under isothermal and quiescent conditions, and with temperature differences between and mechanical agitation in the two bodies of bulk liquid that served as the source and sink for the film. Measurements were made for film transfer into and out of glass capillary breakers over barrier heights up to 34 cm, at temperatures ranging from 1.3 to 2.0°K. Experiments performed under isothermal and quiescent conditions show that the transfer rate, R, depends on the barrier height above the source liquid, H, and the gravitational pressure head, ΔH. Unusual effects such as the persistence of rates, jumps to other rates, and unstable behavior seem to be characteristic of film flow. Comparison of emptying and filling rates indicates that normalization of the flow to the smallest periphery above the source liquid is not sufficient. The dependence of R on ΔH is found to vary with temperature, the method of filling the beaker, and the geometry of the reservoir supplying the film. Temperature differences created by electric heaters in the bulk liquids produce only distillation and thermomechanical effects for values of heat flux up to 10^{-4} watts/cm^2. Mechanical agitation increases the unstable behavior of the flow, but does not affect the general dependence of R on ΔH. A change in the transfer rate, ΔR, existed only as long as the agitation continued, but the "normal" rate to which the flow returns when agitation is discontinued depends on the method of filling the beaker. These results support the idea that microscopic turbulence or vorticity in the superfluid plays an important role in film flow phenomena. (Dissertation Abstr.)

47533 SUPERCONDUCTING MAGNET FACILITY FOR PLASMA PHYSICS RESEARCH. Roth, J. Reece (National Aeronautics and Space Administration, Cleveland); Freeman, Donald C. Jr.; Haid, David A. pp 146-8 of Sixth Symposium on Engineering Aspects of Magnetohydrodynamics. Phillipsburg, N. J., American Institute of Aeronautics and Astronautics, 1965.

A split pair of superconducting coils with a maximum field of 25 kG on the axis and an accessible diameter of 7 in. is described for plasma physics research. The coils are operated in a magnetic bottle configuration that may be either symmetric or asymmetric about the midplane. The mirror ratio of the symmetric configuration may be altered by varying the spacing of the coils. At an operating current of 14.7 amp, 150 min are required to bring the coils up to the rated field when operated in series with 6-in. spacers. Both coils withstood six normal transitions while installed in multilayer dewars. Each Dewar consists of an inner stainless steel cannister enclosing the superconducting coils and a liquid He reservoir and an outer Al canister containing a reservoir for liquid N_2. The superconducting magnet system fits into a vacuum tank that forms the outer canister of the Dewar. This vacuum tank is fabricated of nonmagnetic stainless steel. An air lock system attached to the vacuum system reduces the number of times that the system must be brought to atmospheric pressure and accommodates the insertion of a Langmuir probe, a Faraday cup, a hot-wire probe, and an emissive probe. A double Faraday cup and the ion source are mounted on sliding seals that permit the two-degree-of-freedom manipulation of both. Comparison of the superconducting magnet system with four conventional magnet systems with respect to installation and operation costs is included. (B.L.M.)

47534 ELECTRON TRANSPORT PHENOMENA IN TIN AT LIQUID HELIUM TEMPERATURES (thesis). Bordoloi, Kiron Chandra. Baton Rouge, Louisiana State Univ., 1964. 99p.

The magnetic field dependences of the electrical and thermal resistances, the thermoelectric power, the Hall, the Righi-Leduc and the Ettinghausen-Nernst effects at liquid helium temperatures in magnetic fields up to 17.5 kG, were studied in a pure single crystal of tin. The measurements were taken with either a constant heat current or a constant electric current flowing perpendicular to the tetragonal axis and with the magnetic field parallel to the tetragonal axis. All the above mentioned effects showed Shubnikov-de Haas type oscillations. The electrical, the Hall, the thermal, and the Righi-Leduc conductivities showed saturation effects around 11 kG. Both the Hall and the Righi-Leduc conductivities were negative in the entire field of measurement. The thermoelectric power and the Ettinghausen-Nernst effects were purely oscillatory. The longitudinal and transverse Lorenz numbers showed complex behaviors suggesting that the lattice conductivity is not necessarily field independent. Several possible explanations of the behavior of the lattice conductivity were considered. (A.G.W.)

47535 INVESTIGATION OF THE DENSITY OF STATES IN SUPERCONDUCTORS CONTAINING MAGNETIC IMPURITIES (thesis). Woolf, Michael Andrew. Berkeley, Calif., Univ. of California, 1964. 48p.

The technique of electron tunneling was applied to a systematic study of the density of states in superconductors containing magnetic impurities. The experiments measured directly the tunneling conductance, and hence the density of states, down to 0.4°K. The present data can therefore be compared with the predictions of the Abrikosov-Gorkov theory worked out in detail by Skalski, Betbeder-Matibet, and Weiss. Qualitatively, the addition of magnetic impurities causes a reduction of the energy gap and a broadening of the peak in the density of states. The detailed shape of the density of states curves agrees reasonably well with the theory, at least for a rare earth impurity system like Gd in lead. The transition element impurities Fe (in indium) and Mn (in lead) have a more pronounced effect than predicted, the energy gap being substantially more filled in and less well-defined than in the Pb-Gd system. Experiments on pure superconducting films with superimposed layers of magnetic metal atoms yield similar marked effects on the density of states. The experiments indicate that it is the presence of strong correlations between electrons rather than the existence of a well-defined energy gap that is the essential feature of the superconducting state. (Dissertation Abstr.)

47536 THERMODYNAMIC PROPERTIES OF STRONG-COUPLING SUPERCONDUCTORS. Wada, Yasushi (Univ. of Maryland, College Park). 11p. (CONF-650317-8). Gmelin, AED-CONF-65-039-7.

From American Physical Society Meeting, Kansas City, Mo.

Energy gap equations had to be solved numerically in

order to determine the thermodynamic properties of strong-coupling superconductors. It appeared that the various thermodynamic quantities except the tunneling characteristics did not depend so sensitively on the detailed form of the phonon spectrum. At nonzero temperature a negative bump was observed at the energy that corresponded to the difference between phonon energy and the energy gap at the gap edge. This was due to the recombination process with a thermally excited quasiparticle emitting a phonon. The reduced energy gap as a function of temperature is very close to BCS weak coupling expression. The ratios between effective electron-phonon coupling strengths and typical transverse phonon energies were found to be the quantities that distinguish strong-coupling superconductors from weak-coupling ones. The free energy difference between normal and superconducting phases was calculated. Expressions were also derived for the specific heat jump and the isotope effect. (M.C.G.)

Neutron Physics

See also REACTOR TECHNOLOGY — Criticality Studies.

Refer also to abstracts 47868, 47945, and 47949.

47537 (AD-613468) DYNAMIC PROGRAMMING AND AN INVERSE PROBLEM IN NEUTRON TRANSPORT THEORY. Bellman, R. E.; Kagiwada, H. H.; Kalaba, R. E. (RAND Corp., Santa Monica, Calif.). Mar. 1965. Contract AF49(638)-700. 23p. (RM-4495-PR). CFSTI $1.00 cy, $0.50 mn.

Since it has long been recognized that inverse problems, in which some aspects of the radiation field are measured and properties of the sources and the media deduced, are of great significance in the areas of neutron transport, radiative transfer in planetary atmospheres, and astrophysics, among others. An approach along the line of dynamic programming to the neutron theory of transport processes is presented. (TAB)

47538 (ANL-7050, pp 33-49) THE CALCULATION OF THERMAL-NEUTRON SPECTRA—GENERALIZED FREE-GAS THEORY. Schaefer, G. W.; Allsopp, K. (English Electric Co., Ltd., Whetstone (England). Atomic Power Div.).

The direct solution of the complete Boltzmann equation for thermal neutron spectra in reactor lattice cells, by the multigroup collision probability method, for example, is undesirable for two reasons. Firstly, since the spectrum is insensitive to nearly all of the detail of the scattering law, the essential physics is hidden, making physical insight nearly impossible. Secondly, as a corollary, the calculations are excessively wasteful of machine time and storage capacity. A second-order differential thermalization operator is derived from the Boltzmann equation and designated the Generalized Free Gas operator. It contains all the important physics to sufficient accuracy, avoids massive compilations, and gives rise to band matrix equations that are easy to solve. When applied along with a judicious combination of collision probability and diffusion theory, spectra can be calculated about one hundred times faster. Examples of the application of the neuroses code are given, including the spatial variation within a cell of the temperature coefficient of reactivity. (auth)

47539 (ANL-7050, pp 51-76) THE CALCULATION OF NEUTRON SPECTRA IN THE DOPPLER REGION. Brissenden, R. J.; Durston, C. (Atomic Energy Establishment, Winfrith (England)).

A completely numerical method is presented for calculating Doppler coefficients in reactors, based on the use of large computers. The capabilities and drawbacks of this method are discussed. (T.F.H.)

47540 (ANL-7050, pp 93-112) THE SOLUTION OF THE TRANSPORT EQUATION BY COLLISION PROBABILITY METHODS. Beardwood, J. E.; Clayton, A. J.; Pull, I. C. (Atomic Energy Establishment, Winfrith (England))

Methods are developed for calculating the neutron flux within a lattice cell as a function of space and energy, based on a representation of neutron transport in terms of first-collision probabilities. The method provides a description of neutronics phenomena directly, without recourse to the Boltzmann integrodifferential equation. The transport and collision mechanics parts of the problem are completely dissociated. Thus the form of the final equations that are solved numerically is independent of geometry. The computer codes used in these calculations are described. (T.F.H.)

47541 (ANL-7050, pp 179-89) THE APPLICATION OF THE EQUIPOISE ITERATIVE METHOD TO DIFFUSION AND TRANSPORT THEORY. Tobias, Melvin L.; Fowler, T. B. (Oak Ridge National Lab., Tenn.).

The iterative procedure known as Equipoise is probably the simplest technique for the solution of the finite-difference analogs of the neutron-diffusion equations. The original method (and variants upon it) are successful in transport calculations of the discrete-ordinate type. The Equipoise method is based on the idea that error modes in an iterative calculation will be significantly reduced if known facts concerning the final solution to the problem are made a part of the problem-solving process. A condition that can be used as an accelerative device is the requirement that final answers should contain the idea of balance, that is, that all residues should be as close to zero as permitted by round-off error in the machine computation. The central concept of the Equipoise method is that iterative procedures can often be significantly accelerated if blocks of equations are forced to satisfy this overall balance condition. (auth)

47542 (ANL-7050, pp 457-70) A FAMILY OF FORTRAN ROUTINES FOR THE ANALYSIS OF NEUTRON RESONANCE EFFECTS. Adler, D. B.; Adler, F. T.; Lewis, E. E. (Illinois Univ., Urbana).

In problems connected with the evaluation of neutron resonance effects, such as resonance escape probability in homogeneous and heterogeneous media, and correlated quantities, such as reaction rates, group cross sections, fluxes, and slowing-down densities, two concurrent aspects have to be considered. These aspects, however, are based on independent physical approaches. One is the mathematical form chosen for the actual evaluation of such quantities, and the other is the choice of a physically plausible model to describe the resonance cross sections. This diversity, in turn, has consequences on the mathematical mechanism chosen to evaluate integral properties. A family of self-consistent FORTRAN routines for the analysis of neutron resonance effects is presented. (auth)

47543 (ANL-7050, pp 471-85) COMPUTATION OF SCATTERING CROSS SECTIONS FOR USE IN THERMAL-NEUTRON TRANSPORT CALCULATIONS. Hutchinson, P.; Schofield, P. (Atomic Energy Research Establishment, Harwell (England)).

In the past, the inelastic scattering cross sections for use in thermal-neutron transport calculations have, basically, been calculated in two stages. First, the "scattering law" $S(\alpha,\beta)$ is computed from data that give details of the chemical binding of the moderator atoms which affect the thermalizing properties, and then the required Legendre coefficients $\sigma_l(E' \rightarrow E)$ of the cross sections $\sigma(E' \rightarrow E,\mu)$ are obtained by numerical integration over the variable α. This procedure has several drawbacks. Unless great care is taken, serious numerical errors occur in the results, especially for high incident neutron energy. To overcome these difficulties, the FORTRAN code SCAT is written, which uses a specially designed integration routine to evaluate the cross sections $\sigma_l(E' \rightarrow E)$ directly from the data used in the calculation of $S(\alpha,\beta)$, without the intermediate step of evaluating $S(\alpha,\beta)$ itself. The method of computation for a complex distribution $\rho(\beta)$, compares favorably in computer time with other methods for the evaluation

of scattering matrices, and is generally of much greater numerical reliability. Details of calculations with SCAT are given, together with a general discussion of the numerical problems associated with the evaluation of thermal scattering cross sections. (auth)

47544 (KAPL-M-6467) DISC. A PROGRAM TO COMPUTE INELASTIC SCATTERING MATRICES FOR MULTIGROUP REACTOR CODES. Lubitz, C. R. (Knolls Atomic Power Lab., Schenectady, N. Y.). Aug. 1965. Contract W-31-109-eng-52. 24p. Dep. mn; CFSTI $1.00 cy, $0.50 mn.

DISC is a Fortran program which constructs a multigroup transfer matrix from inelastic scattering data. It accepts data on the excitation of individual levels, if available, and augments this with an evaporation model to yield a desired total inelastic cross section. The level-inelastic or evaporation model calculations can also be run separately. The program will not handle anisotropic angular distributions and also neglects recoil of the target nucleus. (auth)

47545 (KFK-297) LOESUNG DER TRANSPORTGLEICHUNG MIT HILFE DER MONTE-CARLO-METHODE. (Solution of the Transport Equation with the Help of the Monte-Carlo Method). Moeller, Ulrich (Kernforschungszentrum, Karlsruhe (West Germany). Institut fuer Neutronenphysik und Reaktortechnik). Feb. 1965. 28p. Dep. mn.

The theoretical and practical principles of a Monte Carlo code for the treatment of neutron physics problems are given. Monte Carlo methods for Fredholm integral equations of the second type are first considered. A general representation of the Monte Carlo method for Fredholm integral equations of the second type is given. The problem was to produce random samples of given distribution coherent with the solution functions of the integral equations. The usual statistical methods can then be used on these random samples. This makes possible, under some conditions, a very effective utilization of the random transport processes. Monte Carlo methods for the solution of the homogeneous transport equation were also considered. The theoretical principles for a program for the solution of the time-dependent transport equation was given. The use of expected values in place of the straightforward estimated functions which leads to simplification of the program or shortening of the calculation time was treated. It was shown how, with the help of so-called influence factors, the statistics in the individual reactor regions and energy and angular groups can be modified in various ways. The time dependence and the corresponding eigenvalue calculation were discussed extensively. The types of calculations (reaction rates, leakage rates, neutron fluxes, neutron densities, and energy transfer rates) were described. The effective cross section was calculated. (tr-auth)

47546 (KFK-298) UNTERPROGRAMME ZUR LOESUNG NEUTRONENPHYSIKALISCHER PROBLEME MIT HILFE DER MONTE-CARLO-METHODE. (On Programs for Solution of Neutron Physics Problems with the Help of Monte-Carlo Method). Moeller, Ulrich (Kernforschungszentrum, Karlsruhe (West Germany). Institut fuer Neutronenphysik und Reaktortechnik). Feb. 1965. 19p. Dep. mn.

Within the framework of a study for the development of a general Monte Carlo code for reactor physics investigations, a description is given of two auxiliary programs used. The first is a realization of distributions of neutron transport for Monte Carlo problems. For the treatment of neutron transport using the Monte Carlo method, random samples of a series of distributions defined by the integral core are necessary. Methods for the realization of all distributions necessary for neutron transport were given. The methods used were all selected with respect to a decimal computer. Effective cross sections for the Monte Carlo problems were also considered. For the solution of the neutron transport equation used in the Monte Carlo method, the cross section as a stable function of the neutron energy is necessary; a scheme is given for the solution of this problem. An IBM-7070 program is described with which, from the neutron energy, the temperature of the material, and a list of isotopes and their densities (atoms/cm^3), the microscopic cross sections in cm^{-1} (capture, elastic scattering, inelastic scattering, fission, and (n,2n) reactions) can be calculated for each isotope given. Constituents of the program are the nuclear data such as resonance parameters, atomic weights, etc. In energy ranges in which the thermal motion of the nucleus plays a role, the cross sections averaged over a Maxwell spectrum of the nuclear velocities are given. The cross sections calculated in the area of statistical resonances are, in the statistical sense, random numbers. In the energy range in which only measurement values of the cross section are present, polynomials were used. (tr-auth)

47547 (LA-DC-7320) MOMENTS EQUATIONS AND EQUIVALENT DISCRETE ORDINATES EQUATIONS. PART I. GENERALIZED MOMENTS EQUATIONS. PART II. EQUIVALENT DISCRETE ORDINATES EQUATIONS. Carlson, B. G.; Lathrop, K. D. (Los Alamos Scientific Lab., Univ. of California, N. Mex.). [1964]. Contract W-7405-eng-36. 11p. (CONF-651101-29). Dep. mn; CFSTI $1.00 cy, $0.50 mn.

For Presentation at 13th Conference on Remote Systems Technology, Washington, D. C.

There are two common means of approximating the analytic Boltzmann transport equation: by a finite set of coupled equations among angular moments of the distribution function, and by a discrete ordinates representation of the angular dependence. The derivation of moments equations is illustrated in which the assumed form of the angular representation may be freely chosen. Such moments equations have the advantage that the angular dependence assumed may be tailored to suit the requirements of a specific problem without altering the form of the moments equations themselves. Discrete ordinates equations are established that are equivalent to the moments equations that were firstly derived. The equivalent discrete ordinates system may usefully be solved instead of the moments system; in addition, the requirements of equivalence provide guidelines for the selection of quadrature coefficients in discrete ordinates systems. (auth)

47548 (TID-22141, pp 3-33) NEUTRON THERMALIZATION. (Rensselaer Polytechnic Inst., Troy, N. Y.).

Some research on neutron thermalization is summarized dealing with the effects of coherent scattering on thermalization in Be, analysis of time-dependent spectra in D_2O, asymptotic and steady-state spectra in multiplying media, spatially dependent asymptotic spectra in H_2O, the upscattering fraction, temperature dependence of scattering kernels, analysis of pulsed-neutron experiments in moderating assemblies, interpretation of time-dependent spectra in Be, non-1/v thermalization parameters, pulsed-neutron calculations in the P_N approximation, and the relation between the diffusion cooling coefficient and the asymptotic neutron spectrum temperature. (D.C.W.)

47549 (TID-22141, pp 34-49) LOW ENERGY NEUTRON INELASTIC SCATTERING (LENIS). (Rensselaer Polytechnic Inst., Troy, N. Y.).

The cross section and scattering law for neutron inelastic scattering from high-density polyethylene at room temperature were measured at neutron energies from 0.15 to 1.81 ev, and the differential inelastic scattering cross section of water was measured relative to vanadium over the same energy range. The results were compared with predictions of both bound-atom and free-gas models. The inelastic scattering of slow neutrons by thorium hydrides, titanium hydrides, and zirconium hydrides was also studied. (D.C.W.)

47550 (TID-22141, pp 81-93) HIGH ENERGY NEUTRON CROSS SECTIONS. Andrews, J.; Augustson, R. H.; Hockenbury, R. (and others).

Preliminary studies of experimental arrangements for the measurement of neutron total cross sections from about 0.50 to 50 Mev were made. Data for carbon were compared with data from other laboratories. (D.C.W.)

47551 (UJV–1354/65) MINIMUM ENTROPY PRODUCTION PRINCIPLE AND LINEAR TRANSPORT EQUATION. Grmela, M. (Ustav Jaderneho Vyzkumu, Ceskoslovenska Akademie VED, Rez). July 1965. 17p. Dep. mn.

The non-equilibrium thermodynamics especially minimum entropy production rate principle for stationary processes is founded on the basis of the linear transport equation. Transport theory approximation being equivalent to non-equilibrium thermodynamics is discovered. The mentioned method enables one to generalize simply non-equilibrium thermodynamics to states which are deviated from the local equilibrium. In conclusion the discovered variational principle is used for solving the stationary, space and energy dependent neutron transport. (auth)

47552 DETERMINATION OF MANGANESE SULPHATE CONTENT FOR NEUTRON SOURCE MEASUREMENTS. De Volpi, A.; Armani, R. J.; Porges, K. G. (Argonne National Lab., Ill.). J. Nucl. Energy: Pts. A and B, 597-9 Aug. 1965).

Present technology for neutron source calibration leans heavily on manganese bath measurements. Since the manganese concentration enters directly into the calculations, a simple and accurate method of obtaining the $MnSO_4$ content is required. Obtaining solution density at a standard temperature would fulfill such objectives. A polynomial representation of the concentration as a function of the solution density at 30°C is provided. In addition, the results are displayed graphically and compared with experimental data. (auth)

47553 A CALCULATION OF UPPER BOUNDS ON TIME-DECAY CONSTANTS IN PULSED NEUTRON EXPERIMENTS. Williams, M. M. R.; Wood, J. (Univ. of Birmingham, Eng.). J. Nucl. Energy: Pts. A and B, 19: 601-5(Aug. 1965).

Numerical values of $(v\Sigma)$ min were obtained for a liquid and a crystal in the incoherent approximation. The liquid calculations are based on the effective width model and results for water are given. The crystal results are obtained from the Gaussian approximation, with multi-phonon terms approximated by the central limit theorem of statistics. Beryllium and graphite were studied using the Debye and Egelstaff phonon frequency spectra, respectively. The limitations of the heavy crystal model are stressed. (auth)

47554 ON THE MEASUREMENT OF THE NEUTRON ASYMPTOTIC DECAY CONSTANT IN SMALL CRYSTALLINE ASSEMBLIES. Ghatak, A. K.; Goyal, I. C.; Kothari, L. S. (Univ. of Delhi). J. Nucl. Energy, Pts. A and B, 19: 679-85(Sept. 1965).

The consequences of trapping of neutrons in the Bragg peak on the measured values of λ_0, the fundamental mode decay constant, for large B^2 are investigated. The reason why the measured values of λ_0 in small crystalline assemblies exceed the theoretical upper bound [viz.$(v\Sigma_a)_{min}$] is discussed. A theoretical upper bound for λ_0, which will be observed in experiments, is obtained. An explanation is given of the reason the calculated transient spectra in graphite even after about 5 msec do not approach the theoretical asymptotic distribution. The consequence of this on the interpretation of the diffusion cooling coefficient is briefly discussed. (auth)

47555 ENERGY DISTRIBUTION OF THERMAL NEUTRONS IN SEMI-INFINITE AND FINITE BLOCKS OF BERYLLIUM OXIDE ASSEMBLY. Trikha, S. K. (Univ. of Delhi). J. Nucl. Energy, Pts. A and B, 19: 687-92(Sept. 1965).

Energy distributions of thermal neutrons in semi-infinite and finite blocks of beryllium oxide assembly were studied by solving the Boltzmann equation in the diffusion approximation by numerical iteration. In the steady-state problem a constant source of thermal neutrons in contact with the free face of the semi-infinite block was assumed. Different absorptions of the medium were considered. For pure beryllium oxide moderator, the value of diffusion length obtained is in good agreement with the experimental results. The decay rates of neutrons in assemblies of different sizes are calculated by using two different scattering kernels. Placzek kernel is found to give higher values of decay constant λ. The value of the diffusion constant D agrees well with the experimental results but the diffusion cooling constant C comes out to be about twice the experimentally observed value. (auth)

47556 THE TRANSPORT MEAN-FREE PATH AND THE DIFFUSION LENGTH OF THERMAL NEUTRONS IN GRAPHITE IN THE TEMPERATURE RANGE 100–300 deg K. Ahmed, F. (Univ. of Delhi). J. Nucl. Energy, Pts. A and B, 19: 703-5(Sept. 1965).

Previous calculations of the transport mean-free path and diffusion length in graphite are extended to temperatures of 300, 200, 150, and 100°K. The one-phonon coherent scattering cross section is plotted as a function of neutron energy up to the Bragg cutoff. The transport cross sections are plotted as a function of energy for energies higher than the Bragg cutoff at a graphite temperature of 300°K. From this, the values of the transport mean-free path and the diffusion length are found. It is noted that in going from 300 to 100°K, the transport mean free path increases by a factor of four. This effect is explained. (J.F.P.)

47557 ON A SYNTHETIC SCATTERING KERNEL FOR CALCULATING THE ENERGY DISTRIBUTION OF THERMAL NEUTRONS. Meyer, K. (VEB Atomkraftwerk, Berlin). Kernenergie, 8: 404-10(July 1965). (In German).

The synthetic scattering kernel is of the Wigner-Wilkins type. Matching the scattering kernel to real models was done in such a manner that the equality of the zero and first moments of the differential scattering cross section for the real and the synthetic kernel was postulated. The consequences resulting from this statement are discussed, especially with regard to H_2O. It is advantageous to define the scattering kernels of this kind separately for each component of a molecular compound in order to produce a correct matching to the asymptotic spectrum. Possibilities for a more general application of the method are discussed. (auth)

47558 ON THE CALCULATION OF THE THERMAL UTILIZATION FACTOR IN THE ENERGY-DEPENDENT DIFFUSION APPROXIMATION. Meyer, K. (VEB Atomkraftwerk, Berlin). Kernenergie, 8: 467-70(Aug. 1965). (In German).

Starting from some difficulties occurring in connection with the formulation of the energy-dependent diffusion approach for calculating the thermal utilization factor, an approximation method is described allowing the calculation of utilization factors by means of a multi-group theory. The method is based on a generalization of the statement for the space-coordinate independent collision equation, in which the neutron flux density is expanded into a series of powers of absorption cross section. In the two-group approximation a solution is obtained containing (in addition to a Maxwell constituent) a transient and another function which, for high neutron energies, describes the transition of the neutron spectrum into the slowing-down spectrum. (auth)

47559 THE ROLE OF INTERFERENCE SCATTERING IN NEUTRON THERMALIZATION BY HEAVY WATER. Koppel, J. U.; Young, James A. (General Atomic Div., General Dynamics Corp., San Diego, Calif.). Nukleonik, 7: 408-15(Aug. 1965). (GA–6103).

The influence of interference scattering on the thermalization and transport of thermal neutrons in D_2O was numerically investigated. The scattering kernel used in these calculations was given previously in analogy to Nelkin's model for water. Suitable approximations were introduced in order to reduce the computing time to reasonable limits. From the results obtained it can be concluded that because of the accidental cancellation of inner and outer interference terms, coherent effects can be neglected altogether in nearly all cases encountered in practice. The angular cross section $d\sigma/d\vartheta$, however, shows strong interference peaks at

small angles, in quite good agreement with experiment. (auth)

47560 MEASUREMENT OF THE DIFFUSION LENGTH IN TIME-DECAYING NEUTRON FIELDS. Arai, Eiichi; Kuchle, Marko (Kernforschungszentrum, Karlsruhe, Ger.). Nukleonik, 7: 416-21(Aug. 1965). (In German).

The diffusion length in water was measured in neutron fields that decay exponentially with time. The decay constant expressed by the source was $\alpha < (\Sigma_\alpha \nu)H_2O$ according to Joest and Memmert. The diffusion length should then be $L = D_0/\Sigma_\alpha \nu - \alpha > D_0/\Sigma_\alpha \cdot \nu$ which was verified in the measurements. The time-decaying neutron source was constructed of a graphite block introduced before a large square water container in which a neutron pulse from an accelerator was injected. After the transients from this pulse are decayed, the neutron density in water and graphite decays with the same time constant α. The measurement of the diffusion length is made with a small counter in this asymptotic time interval. By the combination of these results with other pulsed measurements and poisoned measurements, the accuracy in the determination of the diffusion parameter of water could be significantly improved. (tr-auth)

47561 MEASURED AND PREDICTED VARIATIONS IN FAST NEUTRON SPECTRUM WHEN PENETRATING LAMINATED Fe–D_2O. Aalto, E.; Sandlin, R.; Fraeki, R. (AB Atomenergi, Stockholm). Nukleonik, 7: 421-6(Aug. 1965).

Variations of the fast neutron spectrum in thin regions of alternating Fe and D_2O were studied using threshold detectors (In(n,n'), S(n,p), Al(n,α)). The results were compared to those calculated by two shielding codes (NRN and Rash D) of multigroup removal-diffusion type. The absolute fast spectrum calculated in our rather complicated configurations was found to agree with measurements within the same accuracy (a factor of two) as did the thermal flux. The calculated spectrum is slightly harder than the measured one, but the detailed variations (covering the range 1 : 5) in the form of the spectrum when penetrating Fe agree with observations to within 15–20%. In and Al activities were found to be proportional to the integrated flux over 1 Mev throughout the whole configuration, while S showed the least proportionality. (auth)

47562 PROPAGATION OF BRAGG-REFLECTED NEUTRONS IN LARGE MOSAIC CRYSTALS AND THE EFFICIENCY OF MONOCHROMATORS. Werner, S. A. (Univ. of Michigan, Ann Arbor); Arrott, Anthony. Phys. Rev., 140: A675-86(Oct. 18, 1965).

The general integral equations for describing the multiple Bragg reflections in a mosaic crystal are given. The solutions of the general problem are in the form of infinite series. For the particular problem of a delta-function beam striking a semi-infinite crystal, these series are summed to give modified Bessel function as the appropriate solutions. The modified Bessel-function solution serves as a Green's function for the generation of solutions of a general beam striking a semi-infinite crystal. Discussed in some detail are the effects of absorption and of crystal-cutting angle on the efficiency of monochromating crystals. The concept of the asymptotic value of neutron current density is stressed to show the importance of not collimating the beam between the neutron source and the monochromating crystal. (auth)

47563 A NOTE ON NEUTRON SLOWING DOWN AND DIFFUSION PROBLEM IN A MEDIUM CONTAINING HOLES. Murase, Hirokazu (Kawasaki Dockyard Co., Ltd., Japan); Sekiya, Tamatsu (and others). Technol. Rept. Osaka Univ., 15: 161-5(Mar. 1965).

The calculation method of the second spatial moment of the neutron distribution in homogeneous moderators was generalized to include the case of heterogeneous moderators containing holes. The method is also a generalization of one group theory developed by several authors. A method of measuring τ and M^2 in an anisotropic medium is proposed. (auth)

Nuclear Properties and Reactions

Refer also to abstracts 46157, 46407, 46643, 46774, and 46817.

47564 (AD-612038) NUCLEAR STRUCTURE. Final Progress Report, April 1–December 31, 1964. (Stanford Univ., Calif.). Feb. 26, 1965. Contract Nonr22575. 6p. CFSTI $1.00 cy, $0.50 mn.

Nuclear energy levels and nuclear reaction mechanisms were studied, including proton, deuteron, ^{3}He, and α reactions on ^{6}Li, ^{7}Li, and ^{9}Be. A gamma detector was used which features cosmic-ray anticoincidence shielding and anti-pile-up circuitry. Cluster effects are described. It was found that the levels in ^{8}Be between 16 and 18 Mev can apparently be described by simple shell model wave functions. Lifetimes of the first excited states of the mirror nuclei ^{7}Li and ^{7}Be were determined by Doppler shift measurements using Li-drifted germanium detectors. (TAB)

47565 (AD-614270) ELECTRON SCATTERING ON NUCLEONS, THREE-BODY NUCLEI, AND ^{40}Ca. Hofstadter, R. (Stanford Univ., Calif. High-Energy Physics Lab.). Nov. 24, 1964. 35p. (HEPL-355). CFSTI $2.00 cy, $0.50 mn.

Results from electron elastic scattering measurements are given. The nucleon structure was studied using the form factor given by relativity theory and the electron scattering amplitude. Two mirror nuclei, ^{3}He and ^{3}H, were studied as examples of the three-body problem. The shape of the charge distribution in ^{40}Ca is discussed. (TAB)

47566 (AERE-R-5009) THE FORMATION OF ^{89m}Y BY 14 Mev NEUTRON IRRADIATION OF ZIRCONIUM. Fern, C.; Gibbons, D.; Olive, G. (Atomic Energy Research Establishment, Harwell (England)). July 1965. 11p. Dep.; BIS $0.50; HMSO 2s. 6d.

A gamma ray of 0.92 Mev energy and 16 sec half-life was observed in the spectrum of zirconium irradiated with 14 Mev neutrons. This was attributed to yttrium-89m produced by the ^{90}Zr(n,pn)^{89m}Y reaction. The cross section for this reaction was measured relative to the ^{90}Zr(n,2n)^{89m}Zr and ^{90}Zr(n,2n)^{89}Zr reactions and an average value of 27.5 ± 0.8 mb obtained. This value may, however, include a contribution from the ^{91}Zr(n,t)^{89m}Y reaction. (auth)

47567 (CEA-R-2775) MESURES DES SECTIONS DE FISSION DE ^{235}U ET DE ^{239}Pu EN NEUTRONS THERMIQUES. (Measurement of the Fission Cross Section of ^{235}U and ^{239}Pu for Thermal Neutrons). Fraysse, Georges; Prosdocimi, Armando, Netter, Francis; Samour, Claude (Commissariat a l'Energie Atomique, Saclay (France). Centre d'Etudes Nucleaires). Apr. 1965. 90p. Dep. mn.

Improved techniques of fast detection were applied for determining the fission cross sections of ^{235}U and ^{239}Pu with reference to the absorption cross section of boron. Monochromatic neutron beams of 0.0322 ev, 0.0626 ev, and 0.275 ev were employed. Use was made of a Xe-filled gaseous scintillator and of a low-geometry solid state ion chamber. Both measured alpha and fission rates. (auth)

47568 (CEA-R-2779) CALCUL DE L'ENERGIE DES PARTICULES EMISES PAR LES REACTIONS ^{3}T(d,n)^{4}He, D(d,n)^{3}He ET D(d,p)T. (Calculation of the Energy of Particles Emitted by the Reactions ^{3}T(d,n)^{4}He, D(d,n)^{3}He and D(d,p)T). Oria, Michel; Sorriaux, Andre (Commissariat a l'Energie Atomique, Saclay (France). Centre d'Etudes Nucleaires). Mar. 1965. 103p. Dep. mn.

With a view to ease the work of research workers using 150 kv electrostatic accelerators, the energy and the emission angle of particles emitted during the reactions ^{3}T(d,n)^{4}He, ^{2}D(d,n)^{3}He and ^{2}D(d,p)^{3}T were calculated. The results are tabulated and arranged according to the acceleration energy of the deuterons. Since the energies considered are relatively low the study was limited to the nonrelativistic domain; this simplification results in a maximum energy variation with respect to the real energy values of 1 percent. Two curves representing the varia-

tions in the total cross sections for the reactions T(d,n)^{4}He and D(d,n)^{3}He are given. (auth)

47569 (CEX.62-50) NEUTRON-FIELDS AND INDUCED-ACTIVITY MEASUREMENTS. Tomnovec, F. M.; Ferguson, J. M. (Naval Radiological Defense Lab., San Francisco, Calif.). Sept. 1965. 40p. Dep. mn; CFSTI $1.00 cy, $0.50 mn.

Operation BREN (Bare Reactor Experiment, Nevada) was an experiment that used a 1500-ft tower and a bare (no shielding) fast nuclear reactor patterned on Godiva to simulate a nuclear weapon detonated at various heights above the ground. Certain characteristics of the neutron field from this unshielded reactor were measured. The activation of gold, manganese, sulfur, cadmium-covered gold, and cadmium-covered manganese was determined as a function of distance from the reactor and of depth in the ground. The data show how those parameters, important for calculating neutron-induced activity in the soil, vary as a function of the height of the source and the slant range from the source. (auth)

47570 (COO-7-0361) POLARIZATION OF 4.4 Mev NEUTRONS SCATTERED ELASTICALLY FROM ^{6}Li AND ^{7}Li. Steuer, M. F.; Kelsey, C. A. (Wisconsin Univ., Madison). [1964]. Contract AT(11-1)-Gen-7. 6p. (CONF-650928-1). Dep. mn; CFSTI $1.00 cy, $0.50 mn.

From International Conference on Polarization Phenomena of Nucleons, Karlsruhe, Ger.

The angular dependence of the polarization of 4.4 Mev neutrons scattered by ^{6}Li and ^{7}Li were investigated. The experimental procedure is discussed. Results are included. (M.O.W.)

47571 (EUR-2456.e) (n,2n) EXCITATION FUNCTIONS FOR NUCLEI AROUND Z = 28. Liskien, H.; Paulsen, A. (European Atomic Energy Community, Ispra (Italy). Joint Nuclear Research Center; European Atomic Energy Community, Geel (Belgium). Central Nuclear Measurements Bureau). 1965. 8p. (CONF-650706-23). Dep. mn.

From International Conference on the Study of Nuclear Structure with Neutrons, Antwerp.

Excitation functions for (n,2n) reactions of six nuclei around Z = 28 (^{55}Mn, ^{59}Co, ^{58}Ni, ^{63}Cu, ^{65}Cu, and ^{64}Zn) were determined experimentally with an accuracy of about ±6%. These experimental results are compared with theoretical calculations based on the complete statistical concept of the compound nucleus model. The discrepancy between theoretical and experimental results is shown to be consistent with the inaccuracy of the knowledge of level density parameters. (auth)

47572 (GA-6547) EXPERIMENTAL DETERMINATION OF NEUTRON INELASTIC SCATTERING IN POLYETHYLENE. Whittemore, W. L. (General Atomic, San Diego, Calif. John Jay Hopkins Lab. for Pure and Applied Science). July 22, 1965. Contract AT(04-3)-167. 22p. (CONF-650932-3). Dep. mn; CFSTI $1.00 cy, $0.50 mn.

From Symposium on the Inelastic Scattering of Neutrons by Condensed Systems, Upton, N. Y.

The cross sections for inelastic scattering of neutrons by polyethylene at 0.167, 0.233, 0.408, and 0.499 ev were measured at angles of 30, 60, 90, and 150°. The results were compared with theoretical calculations. (D.C.W.)

47573 (IAE-717) IZOTOPICHESKOE SMESHCHENIE I KVADRUPOL'NYE MOMENTY OKOLOSFERICHESKIKH YADER. (Isotope-Shift and Quadrupole Moments of Near-Spherical Nuclei). Bunatyan, G. G.; Mikulinskii, M. A. (Institut Atomnoi Energii, Gosudarstvennyi Komitet po Ispol'zovaniyu Atomnoi Energii SSSR, Moscow). 1964. 15p. Dep. mn.

The isotopic shift and the quadrupole moments of nuclei that are close to spherical were calculated on the basis of the theory developed by A. B. Migdal for the Fermi liquid of finite systems. Use was made in the calculations of eigenfunctions and eigenvalues of an effective hamiltonian with a Woods-Saxon potential and with spin-orbit coupling. The matrix elements were calculated and the linear equations solved by means of an electronic computer. An analysis of the results leads to the conclusion that in order to reconcile the data with experiment it is necessary to introduce an interaction amplitude which changes sign and magnitude on the boundary of the nucleus. The values of the internal and external constants involved in the theory are determined. (ATD)

47574 (IAE-836) REAKTSII ^{7}Li(p,t)^{5}Li I ^{6}Li(α,t)^{7}Be. (The Reaction ^{7}Li(p,t)^{5}Li and ^{6}Li(α,t)^{7}Be). Ogloblin, A. A.; Chuev, V. I. (Institut Atomnoi Energii, Gosudarstvennyi Komitet po Ispol'zovaniyu Atomnoi Energii SSSR, Moscow). 1965. 16p. Dep. mn.

The differential cross sections of the reaction ^{7}Li(p,t)^{5}Li at E_p = 16.6 Mev and ^{6}Li(α,t)^{7}Be at E_α = 40 Mev were measured. Comparison of the (p,t) reaction on ^{7}Li with the (n,t) reactions on ^{6}Li and ^{7}Li testifies in favor of the triton knock-out mechanism in the interaction of protons and neutrons with ^{7}Li. A ^{7}Be level with energy 5.0 ± 0.3 Mev was observed in the reaction ^{6}Li(α,t)^{7}Be. The excitation of this state and also of the 4.53-Mev level proceeds roughly with the same probability as of the first two states of ^{7}Be. In this respect the reaction (α,t) on ^{6}Li strongly differs from the (d,p) reaction. An evaluation of the results obtained from the point of view of the dispersion theory of direct processes is presented. Established triangle diagrams can apparently be correlated with the reactions studied. However, a qualitative explanation of the experimental data encounters some difficulties. (tr-auth)

47575 (IDO-16986) RESONANCE ABSORPTION OF NEUTRONS IN MIXTURES OF ^{232}Th AND ^{238}U: AN INVESTIGATION OF INTERFERENCE BETWEEN ABSORBERS BY MEANS OF REACTIVITY MEASUREMENTS IN THE ADVANCED REACTIVITY MEASUREMENT FACILITIES [Thesis]. Foell, Wesley K. (Phillips Petroleum Co. Idaho Falls, Idaho. Atomic Energy Div.). Aug. 1965. Contract AT(10-1)-205. 152p. Dep. mn; CFSTI $5.00 cy, $1.00 mn.

Resonance integrals of single absorber samples of uranium-238 dioxide and thorium-232 dioxide, each in admixture with a lead dioxide diluent, were measured by means of static reactivity techniques in the ARMF-II. The experimental results for the uranium dioxide/lead dioxide samples were in good agreement over a wide range of absorber concentrations with the results predicted with the aid of Nordheim's treatment. There was quantitative disagreement between the experimental results for the thorium dioxide/lead dioxide samples and the corresponding predicted values. The infinite dilution resonance integral of thorium-232, adjusted to a cutoff energy of 0.5 ev, and including the 1/v contribution, was measured as 81.2 ± 4 barns. The concept of interference between resonances of two absorbers was formulated and defined as the effect on the resonance integral caused by the lack of complete flux recovery between the resonances. Interference was measured in a series of uranium-238/thorium-32 mixtures. The experimental results indicated slightly more than three percent interference in the samples of highest absorber concentration. Interference was also predicted for this series of mixtures by means of multiresonance solutions of the first-flight coupled equations. These calculations predicted an interference of approximately 1.3 percent in the samples of highest absorber concentration. It is believed that the underestimate of interference in the calculations may result from the use of the narrow resonance approximation in the moderator terms of the first-flight coupled equations. On the basis of the experimental and theoretical results, interference was predicted for uranium-238/thorium/232 metal rods of theoretical density. Also described are numerous experimental techniques and methods of analyses generally applicable to reactivity and activation measurements in low power reactors. (auth)

47576 (IDO-17081, pp 49-76) NUCLEAR TECHNOLOGY. (Phillips Petroleum Co. Idaho Falls, Idaho, Atomic Energy Div.).

The beta decay of ^{139}Pt to ^{139}Au was studied using Li-drifted Ge, NaI(Tl), permanent-field spectrographs, and γ-γ and β-γ coincidence techniques. The half-life of ^{139}Pt was measured to be 31.4 ± 0.5 min. The energies of the

prominent transitions (and their photon intensities relative to the 543-kev gamma ray) are 54.9, 74.6, 185.6 (401), 219 (22), 226 (30), 246.5 (163), 316.9 (358), 417 (14), 425 (23), 467 (133), 474.2 (99), 493.6 (379), 542.8 (1000), 644 (6), 665 (12), 715 (122), 791 (76), 836 (1), 889 (2), 967 (63) kev. Conversion electrons were observed for the 55-, 75-, 186-, 246-, 317-, and 543-kev transitions. No photons were observed corresponding to the 55-kev transition. On the basis of the experimental results, tentative levels were placed in ^{190}Au at 74.6, 316.9, 321.1, 540.2, 542.8, 728.4, 733.8, 788.1, 790.6, 930, and 967 kev. Evidence was found for an isomeric state in ^{190}Au with a half-life greater than 200 msec and less than 1 sec. The total neutron cross section of ^{232}U was measured for neutrons of energies between 0.01 and 10,000 ev. Preliminary values of resonance parameters were obtained for five resonances below 28 ev. A small, 1 mg, sample of the ^{228}Th daughter of ^{232}U was chemically separated from the latter and used for positive identification of the 2 ev resonance which grows into ^{232}U after initial purification. Measurements were made of the relative yield of high total kinetic energy fragments of the fission of ^{235}U induced by neutrons of energy between 0.1 and 10 ev. Alpha spectra of ^{229}Th and its daughters were obtained. A new chemistry isolation box was built and installed in the MTR hot alpha cave. The box is capable of processing several different radioactive nuclides prepared for fast chopper cross section measurements and replaces the original box designed only for ^{233}Pa chemistry. A sample of irradiated Tl was discharged from the ETR, processed through the alpha cave, and the material prepared for fast chopper measurement of the cross section of ^{204}Tl. Slow neutron scattering calculations were made for ethane and n-butane. As a result, better agreement between experimentally measured and theoretically calculated data was obtained. Further theoretical computations were completed on a model formulated to describe the scattering of slow neutrons by methane. Using the ARMF-II, infinitely dilute resonance absorption integrals were measured for Tb, Ho, Er, Tm, and Yb in their natural isotopic ratios. (auth)

47577 (IDO–17107) EFFECTIVE CROSS-SECTION FACTORS. Nisle, R. G. (Phillips Petroleum Co. Idaho Falls, Idaho. Atomic Energy Div.). Aug. 1965. Contract AT(10-1)-205. 90p. Dep. mn; CFSTI $3.00 cy, $0.75 mn.

An alternative to the cadmium ratio concept is reviewed and the advantages are discussed. The basis for this alternative concept is Westcott's conventional flux, Campbell and Freemantle's description of the joining function between Maxwellian and 1/E flux components, and a proposal of Gavin's for the measurement of neutron temperature. The derived formalism leads to an effective cross-section factor, $P_x(F_1,T)$ that amounts to a flux weighted average. $P_x(F_1,T)$ may be calculated for any isotope, x, from differential cross-section data by direct integration, or in special cases by a simplified formula. Tables of the factor $P_x(F_1,T)$ for ten values of F_1 and fourteen values of T were calculated and are presented for most of the elements and isotopes of interest to reactor engineers. (auth)

47578 (IS-T-28) PHOTODISINTEGRATION OF ^{40}Ca (thesis). Anderson, David Walter (Ames Lab., Iowa State Univ. of Science and Tech.). July 1965. Contract W-7405-eng-82. 147p. Dep. mn; CFSTI $4.00 cy, $1.00 mn.

The bremsstrahlung beam from the Iowa State University electron synchrotron was used to study the photodisintegration of ^{40}Ca to 65 Mev. A sample of calcium metal was bombarded and the positron activities produced were counted using NaI scintillation detectors and a multichannel analyser. The yield from the one second activities, mainly due to the reactions ^{40}Ca (γ,n) ^{39}Ca, ^{40}Ca (γ,pn) ^{38m}K and ^{40}Ca (γ,2n) ^{38}Ca was separated from the yield due to longer lived activities. Analysis for the cross section using the least structure technique shows seven resonances in the region above the giant resonance. The resonance energies are 28.4 ± 0.5, 34.7 ± 0.6, 39.7 ± 1.3, 43.1 ± 0.4, 48.3 ± 0.3, 54.5 ± 0.3, and 60.0 ± 1.0 Mev. (auth)

47579 (JINR-P-2275) OB IZOTOPAKH ^{156}Er I ^{157}Ho. OBRAZOVANIE ^{162}Ho V REAKTSII Ta + p (660 Mev). (On ^{156}Er and ^{157}Ho Isotopes. The Formation of ^{162}Ho in the Ta + p (660 Mev) Reaction). Gromov, K. Ya.; Muzhtasimov, F. N. (Joint Inst. for Nuclear Research, Dubna (USSR). Lab. of Nuclear Problems). 1965. 6p. Dep. mn.

The spectrum of conversion electrons arising by the decay of neutron-deficient isotopes of Er and Ho was investigated with a β-spectrograph. The resolving power of the device was about 0.06%, the accuracy in the energy determination was about 0.05%. The data confirming the existence of the ^{156}Er and ^{157}Ho were obtained. It is established for the first time that in the bombardment of Ta with 660 Mev protons an isotope ^{162}Ho is created. (auth)

47580 (LA–3352) FISSION FRAGMENT REMOVAL OF URANIUM FROM A FISSIONING SURFACE. Peterson, P. J.; Thorpe, M. M. (Los Alamos Scientific Lab., Univ. of California, N. Mex.). July 5, 1965. Contract W-7405-eng-36. 21p. Dep. mn; CFSTI $2.00 cy, $0.50 mn.

A model is proposed whereby U is removed from a fissioning U metal source by deposition of fission fragment energy in UO_2 crystallites of a critical size range on the source surface. It is also suggested that a second method of U removal is also operative. This concept is represented by the equation $M' = M_0(1 - e^{-\lambda'(\Phi t)}) + c'(\Phi t)$, where M' is micrograms of U removed, M_0 is micrograms of U originally present in UO_2 crystallites of a certain size, λ' is a calculated removal constant for UO_2 crystallites of a given size, and Φt is the integrated thermal neutron flux seen by the source. The term $c'(\Phi t)$ represents the second method of removal where the amount removed per unit of Φt is the constant, c'. This curve is fitted to data gathered in a series of irradiation capsule experiments. (auth)

47581 (LA-DC-6730) EXPERIMENTS WITH POLARIZED PROTONS AND THE NEUTRON-NUCLEUS POTENTIAL DERIVED THEREFROM. Rosen, L. (Los Alamos Scientific Lab., Univ. of California, N. Mex.). [nd]. Contract W-7405-eng-36. 55p. (CONF-650706-24). Dep. mn; CFSTI $3.00 cy, $0.50 mn.

From International Conference on the Study of Nuclear Structure With Neutrons, Antwerp.

The spin dependence of elastic scattering of protons was measured for a large number of nuclei and the results used to determine the average parameters for a proton-nucleus optical model potential. The potential so deduced is capable of describing many of the observables in proton-nucleus interactions, over a large range of energy and nuclear species. Holding fixed all the geometrical parameters and the spin-orbit depth, 14-Mev neutron elastic-scattering data were fit to determine the real and imaginary well-depths of the central potential for neutrons. The resulting neutron-nucleus potential, with fixed parameters, is evaluated by comparison of its predictions with a large amount of neutron data over the energy region 0.3 to 24 Mev and for nuclei ranging from Li to U. With the exception of inelastic scattering at low energies, the general features of representative experimental data are reproduced and quantitative agreement is obtained over a major portion of the periodic table. (auth)

47582 (NEVIS–129) ISOTOPIC DIFFERENCES IN THE MU-MESIC K X-RAY ENERGIES OF ^{16}O–^{18}O, ^{40}Ca–^{44}Ca, ^{116}Sn–^{124}Sn, ^{155}Gd–^{160}Gd (thesis). Nissim-Sabat, Charles (Nevis Labs., Columbia Univ., Irvington-on-Hudson, N. Y.). Mar. 1965. Contract Nonr-266(72). 85p. (R-483; CU-235).

The isotopic differences in the μ-mesic K x-ray energies of ^{16}O–^{18}O, ^{40}Ca–^{44}Ca, ^{116}Sn–^{124}Sn, and ^{155}Gd–^{160}Gd were measured in order to obtain information about the change in the radius of the nuclear proton distribution as the neutron number is increased. The essential feature of the experimental method is the simultaneous measurement of the spectra of the two isotopes by means of a conventional NaI(Tl) crystal γ-ray spectrometer. Great care was taken to aviod any bias or nonstatistical errors in measurements and analysis by treating the two isotope targets in an exactly similar fashion.

Probable contributions to the isotopic shifts from nuclear polarization effects are examined and are found to be negligible. The relevance of isotope shift measurements to the understanding of general nuclear properties, such as compressibility, is also considered. A review is made of the theory of optical isotopic shift measurements in order to determine how they can best be complemented by future high accuracy μ-mesic x-ray measurements. (auth)

47583 (NP-15467) ODNOCHASTICHNYE EFFEKTY V NEITRONNOI FIZIKI I TONKAYA STRUKTURA YADERNYKH MASS. III. KORRELYATSII V POLOZHENIYAKH NEITRONNYKH UROVNEI. (Single-Particle Effects in Neutron Physics and the Fine Structure of Nuclear Masses. III. Correlations in Positions of Neutron Levels). Report No. 347. Sukhoruchkin, S. I. (Gosudarstvennyi Komitet po Ispol'zovaniyu Atomnoi Energii SSSR, Moscow. Institut Teoreticheskoi i Eksperimental'noi Fiziki). 1965. 28p. Dep. mn.

Comparison of neutron levels position for all nuclei shows a certain grouping effect, more pronounced for levels with relatively large reduced neutron widths. If one analyzes all nuclei; the coincidences of resonances lying close to binding energy are frequently obtained. (auth)

47584 (ORNL-3832, pp 1-28) NUCLEAR CHEMISTRY. (Oak Ridge National Lab., Tenn.).

A measurement was made of the cross section of ^{248}Cm in the pneumatic tube facility of the LITR. Isotopically enriched samples of Ru were irradiated to flux-times of $\sim 3 \times 10^{20}$ neutrons/ cm^2. The thermal-neutron capture cross sections and resonance integrals for three isotopes are: ^{99}Ru, 4.4 and 195 barns; ^{100}Ru, 6.1 and 11.2 barns; ^{101}Ru, 5.5 and 79.1 barns. The activation cross sections of stable ^{102}Ru, σ_{th} = 1.23 barns and I_0 = 4.14 barns, were obtained with an error of ±10%. Measurements showed that thermal-neutron cross sections and resonance integrals of ^{154}Gd and ^{156}Gd are $\sigma_{th} \approx 23$ and 9, and $I_0 \approx 530$ and 23 barns, respectively. The 70-min Pr assigned in the current literature to ^{136}Pr was shown to be ^{137}Pr. It decays by electron capture and positron emission to a complex energy-level structure in ^{137}Ce. In the decay of ^{101}Tc, 25 gamma rays were assigned to transitions involving excited levels in ^{101}Ru. Ten gamma rays in the decay of ^{101m}Rh were assigned to transitions associated with levels at 127.0 ± 0.3, 306.8 ± 0.3, 311.0 ± 0.5, 545.2 ± 0.5, and 639 ± 1 kev. A 59.7 ± 2.0 nsec level with decay energy of 344 kev in ^{117}In was measured using time-to-pulse-height techniques. An analysis of the energy levels in ^{132}Xe populated by the decay of ^{132}I was made. The proposed level scheme involves 33 gamma transitions and 12 excited states in ^{132}Xe. Independent fission yields of ^{95}Zr from thermal-neutron fission of ^{233}U and ^{235}U were determined. Half lives of 6 ± 2 sec and 16.87 ± 0.05 hr were determined for ^{97}Y and ^{97}Zr, respectively. (J.R.D.)

47585 (ORNL-3851) ELASTIC AND INELASTIC SCATTERING OF 12.0-Mev PROTONS FROM ^{62}Ni, ^{63}Cu, AND ^{64}Zn: TABULATED DIFFERENTIAL CROSS SECTIONS. Dickens, J. K.; Silva, R. J. (Oak Ridge National Lab., Tenn.). Sept. 1965. Contract W-7405-eng-26. 38p. Dep. mn; CFSTI $2.00 cy, $0.50 mn.

Numerical values of differential cross sections for elastic and inelastic scattering of 12.0-Mev protons from ^{62}Ni, ^{63}Cu, and ^{64}Zn are reported in tabular form. Cross sections were determined at 5° intervals between laboratory angles of 20 and 165° for ^{62}Ni and ^{64}Zn, and between laboratory angles of 20 and 110° for ^{63}Cu. Inelastic-scattering data are reported for 2 excited states of ^{62}Ni (Q = -1.17 and -2.74 Mev); for 17 excited states of ^{63}Cu (Q = -0.668, -0.961, -1.327, -1.412, -1.547, -1.862, -2.012, -2.080, -2.210, -2.337, -2.405, -2.50, -2.69, -3.28, -3.45, -3.69, and -4.11 Mev); and for 21 excited states of ^{64}Zn (Q = -0.993, -1.804, -1.904, -2.31, -2.61, -2.74, -2.79, -3.00, -3.08, -3.20, -3.30, -3.37, -3.45, -3.55, -3.60, -3.71, -3.86, -3.93, -4.03, -4.16, and -4.31 Mev). (auth)

47586 (ORNL-TM-1218) SINGLE AND MULTINUCLEON TRANSFER REACTIONS INDUCED BY ^{14}N [thesis]. Gaedke, Rudolph M. (Oak Ridge National Lab., Tenn.). Sept. 1965. Contract W-7405-eng-26. 77p. Dep. mn; CFSTI $3.00 cy, $0.75 mn.

Submitted to Univ. of South Carolina, Columbia.

A survey is presented of excitation functions of ^{14}N-induced reactions. Studied are (^{14}N,^{13}N) reactions with ^{12}C, ^{16}O, ^{31}P, ^{51}V, and ^{55}Mn; (^{14}N,^{15}N) reactions with ^{16}O, ^{19}F, ^{45}Sc, and ^{55}Mn; and the reaction ^{16}O(^{14}N,^{12}F)^{12}C. (T.F.H.)

47587 (TID-22012) NUCLEAR PHYSICS DIVISION ANNUAL PROGRESS REPORT FOR PERIOD ENDING AUGUST 1, 1964. (Texas Nuclear Corp., Austin). Aug. 15, 1964. Contract AT(40-1)-2791. 332p. Dep. mn; CFSTI, $7.00 cy, $1.75 mn.

Separate abstracts were prepared for the eight included papers. (M.O.W.)

For abstracts of individual sections see: 46765, 47588, and 47589–47594.

47588 (TID-22012, pp 22-52) GAMMA RAYS PRODUCED IN THE INELASTIC SCATTERING. III. THE ^{27}Al(n,n'γ)^{27}Al REACTION. Mathur, S. C.; Tucker, W. E.; Morgan, I. L. (Texas Nuclear Corp., Austin). (TID-21477).

The angular distributions of gamma rays produced by inelastic scattering of neutrons with ^{27}Al were measured in the neutron energy range of 3.5 to 4.5 Mev. The angular distributions and differential cross sections were also calculated on the basis of the Satchler formalism and comparisons made with the experimental results. (auth)

47589 (TID-22012, pp 53-66) GAMMA RAYS PRODUCED IN THE INELASTIC SCATTERING OF NEUTRONS WITH MAGNESIUM AND SILICON. Mathur, S. C.; Morgan, I. L.; Benjamin, R. W. (Texas Nuclear Corp., Austin).

The angular distributions of gamma rays produced by inelastic scattering of neutrons with magnesium and silicon were measured in the incident neutron energy range of 3.0 to 4.35 Mev. The angular distributions and differential cross sections were also calculated on the basis of Satchler formalism and comparisons made with the experimental results. (auth)

47590 (TID-22012, pp 67-98) ANGULAR DISTRIBUTION OF GAMMA RAYS PRODUCED IN THE INELASTIC SCATTERING OF NEUTRONS FROM ^{40}Ar. Mathur, Suresh C.; Morgan, Ira Lon (Texas Nuclear Corp., Austin).

The excitation function for the production of gamma rays in the inelastic scattering of neutrons from Argon-40 was measured in the neutron energy range of 3.0 to 4.5 Mev. The angular distributions were measured for neutron energies 3.0 and 3.5 Mev. From a comparison of the experimental angular distributions and the distributions calculated on the basis of Satchler's theory, a spin of 2^+ was assigned to the 3rd excited level in ^{40}Ar at 2.53 Mev and a spin of 4^+ to the 5th excited level at 3.22 Mev. The branching ratio of the gamma rays produced in the de-excitation of the 2.53-Mev level was also determined. (auth)

47591 (TID-22012, pp 99-128) CROSS SECTIONS AND ANGULAR DISTRIBUTIONS OF NEUTRON PRODUCED GAMMA RAYS IN Fe FROM E_n = .96 TO 4.75 Mev. Benjamin, R. W.; Morgan, I. L. (Texas Nuclear Corp., Austin).

The production cross sections and angular distributions of several gamma rays produced in ^{56}Fe by inelastic neutron scattering at various energies ranging from 0.96 to 4.0 Mev were measured. These data were compared with the theoretical predictions of Satchler using three different sets of neutron penetrabilities. The general shape of the angular distributions is reproduced with any of the three sets of penetrabilities, but the Beyster values agree most closely with the experimental results. In addition, cross sections at 90° for all the prominent gamma rays are given for the energies included above, and 90° cross sections for the 0.845 Mev gamma ray are given to 4.750 Mev. (auth)

47592 (TID-22012, pp 129-55) INELASTIC NEUTRON SCATTERING IN ^{208}Pb, ^{207}Pb, AND ^{206}Pb. Nellis, Donald O.; Morgan, Ira L. (Texas Nuclear Corp., Austin).

Gamma rays from (n,n'γ) reactions in separated isotopes of lead were observed at several neutron energies. Previously unreported gamma rays having energies of 1.65 and 2.62 Mev in ^{208}Pb, 2.12 and 2.64 Mev in ^{207}Pb and 1.36 and 1.60 Mev in ^{206}Pb were observed. Angular distributions of some of the more prominent gamma rays were measured. (auth)

47593 (TID-22012, pp 156-75) ANGULAR DISTRIBUTION OF GAMMA RAYS FROM C, O AND N AT E_n = 14.8 Mev. Morgan, I. L.; Ashe, J. B.; Nellis, D. O. (Texas Nuclear Corp., Austin).

The cross sections and angular distributions of the gamma rays produced by the reactions ^{12}C(n,n'γ)^{12}C, ^{14}N(n,n'γ)^{14}N, ^{14}N(n,αγ)^{11}B, ^{14}N(n,dγ)^{13}C, ^{14}N(n,pγ)^{14}C, ^{16}O(n,n'γ)^{16}O, ^{16}O(n,αγ)^{13}C, and ^{16}O(n,n'αγ)^{12}C were measured for an incident neutron energy of 14.8 Mev at angles from 30 to 140°. A pulsed beam time-of-flight technique was used in conjunction with a total absorption gamma ray spectrometer. Probable assignments were made for most of the observed gamma rays from nitrogen and oxygen. Angular distributions of the more intense gamma rays indicate that they are in general anisotropic. (auth)

47594 (TID-22012, pp 176-205) NEUTRON PRODUCED GAMMA RAYS FROM ^{10}B, ^{11}B, Ca, Co, Ce AND U. (Texas Nuclear Corp., Austin).

Results from various neutron reactions (n,Gγ) with boron-10 and -11, calcium, cobalt, cerium, and uranium are presented. The gamma angular distributions and cross sections for incident neutron energies from 3.0 to 14.8 Mev are presented. (M.O.W.)

47595 (TID-22141, pp 50-66) NEUTRON CROSS SECTIONS. (Rensselaer Polytechnic Inst., Troy, N. Y.).

The capture-to-fission cross section ratio of ^{235}U was measured, and preliminary values of the neutron resonance parameters for Hf isotopes were obtained by analysis of total cross section measurements on Hf. Neutron scattering and total cross sections of ^{239}Pu, ^{233}U, and ^{235}U were measured from 10 to 100 ev. The analysis of the cross section data for enriched samples of ^{182}W, ^{183}W, ^{184}W, and ^{186}W was almost completed; resonances were identified and assigned by isotopes from 100 ev to 4 kev using a computer program. (D.C.W.)

47596 (TID-22141, pp 94-7) PHOTONUCLEAR REACTION STUDIES BY ACTIVATION METHODS. Medicus, H. A.; Tatarczuk, J. R.; Mosel, D. K.; Bernatowicz, H.; Raymond, D. J.; Weglarz, L. (Rensselaer Polytechnic Inst., Troy, N. Y.).

The spin cutoff parameter which characterizes the spin dependence of the nuclear level density was determined for ^{46}Sc through the reactions ^{45}Sc(γ,n)^{44}Sc, ^{46}Ti(γ,pn)^{44}Sc, and ^{45}Sc(n,2n)^{44}Sc. The yield ratio for the (γ,n), (γ,2n), and (γ,2p) reactions on ^{45}Sc at 45 Mev was determined. The relative yields for bremsstrahlung reactions with ^{51}V at 25, 29, and 37 Mev were also measured, and integrated cross sections were obtained from the yields. Statistical model calculations using a level density formula similar to that of Erickson and transmission coefficients from optical model calculations agree with the values for the (γ,2n) and (γ,2p) reactions. For the (γ,α) reaction, however, the experimental yield is approximately five times as large as the theoretical value. The yields of (γ,t) reactions at 37 Mev on Ag, Cd, In, Sn, and Sb were also measured, and a (γ,3p) reaction on ^{31}P was observed at 50 Mev. (D.C.W.)

47597 (UCRL-16187) THEORETICAL ALPHA DECAY RATES OF DEFORMED NUCLEI (thesis). Poggenburg, John Kenneth Jr. (Lawrence Radiation Lab., Univ. of California, Berkeley). Aug. 1965. Contract W-7405-eng-48. 206p. Dep. mn; CFSTI $6.00 cy, $1.25 mn.

The shell-model theory of alpha decay developed by Mang is summarized. The calculation of the alpha formation entails the use of the pairing-force wave functions of superconductivity theory, and their calculation with a delta-force approximation. The penetration of the alpha particle through the anisotropic potential barrier is considered in detail. The approximate treatment of Fröman is studied, and the results clearly justify the method. The particular features of the potential barrier are examined in terms of the WKB expression for barrier transmission. The Woods-Saxon potential $V = -74/(1 + \exp\{(r - 1.17A^{\frac{1}{3}} - 1.6)/(a)\})$ is chosen after a survey of recent optical model analyses of alpha scattering experiments. The Woods-Saxon potential results in penetrability factors that are ≈45% lower than those calculated with the Igo potential. Modification of the Coulomb potential has little effect on the penetrability. Extensive numerical calculations are given. The theory gives reasonable agreement with experiment, and has provided a clear example of its value in the analysis of the alpha decay of ^{241}Am. The calculations predict relative amplitudes and phases of importance in interpretation of angular correlation experiments. They also predict the l-wave mixing in the transition to final states of odd-mass nuclei. Comparisons of theoretical and experimental transition rates indicate the nature of the errors in the calculations. Suggestions are given for future improvement. (auth)

47598 (USNRDL-TR-876) GAMMA-EMISSION DATA FOR THE CALCULATION OF EXPOSURE RATES FROM NUCLEAR DEBRIS. VOLUME I. FISSION PRODUCTS. Crocker, G. R.; Connors, M. A. (Naval Radiological Defense Lab., San Francisco, Calif.). June 10, 1965. Contract AT(49-7)-1963. 82p. Dep. mn; CFSTI $3.00 cy, $0.75 mn.

Photon energies and abundances were compiled and summarized for some fission-product and other radionuclides, using data reported in the literature up to June 1963. The data are presented in tabular form, listing photon energies and abundances for gamma rays, beta rays, and x rays emitted. A list of multipliers is also presented for converting activities of the radionuclides to infinite-plane exposure rates. (auth)

47599 (ORNL-tr-707) A NEW INTERPRETATION OF THE MATHEMATICAL INTERRELATIONSHIPS OF RADIOACTIVE DECAY. Wolfke, M. Translated for Oak Ridge National Lab., Tenn. from Physik, Z., 30: 899-901(1929). 5p. Dep. mn; JCL $1.10 fs, $0.80 mf.

From the decay law of atoms of a uniform radioactive substance ($-dn/dt = \lambda n$), it is generally concluded from this equation that the decay probability for the individual atom at a given moment is independent of its age and is constant at any time during its life. It is shown that the conclusion mentioned above is not binding because this equation can also be obtained when the role of coincidence is limited only to the moment of formation of the atom and when its further fate is considered to be a consequence of a singularly proceeding mechanism. (M.O.W.)

47600 A SHELL MODEL INTERPRETATION OF THE SPECTRA OF $2s_{\frac{1}{2}}$-$1d_{\frac{3}{2}}$ NUCLEI. Yang, Shan-teh (Chilin Univ., Japan). Acta Phys. Sinica, 21: 1522-32(Aug. 1965). (In Japanese).

Taking account of the mixing of states within the subshells $2s_{\frac{1}{2}}$ and $1d_{\frac{3}{2}}$, we have systematically calculated the spectra of nuclei with A = 30, 31, 32 and A = 37, 38, according to Talmi's method. The calculated results are in good agreement with the experimental data. (auth)

47601 CRITERIA FOR THE DESIGN OF EXPERIMENTS TO MEASURE DIFFERENTIAL CROSS SECTIONS AND OTHER POLYNOMIAL DISTRIBUTIONS. Monahan, J. E.; Langsdorf, A. Jr. (Argonne National Lab., Ill.). Ann. Phys. (N.Y.), 34: 238-75(Sept. 1965).

The criteria presented enable an experimenter to select a set of positions at which a distribution should be measured in order that the resulting set of measurements should determine the distribution most efficiently, i.e., with minimum uncertainty for a given expenditure of time, effort, or money. The results are applicable to the measurement of any distribution that can be represented by a finite-degree polynomial in the independent variable or in some function of the independent variable. Thus, for example, the criteria can be used to select a set of angles at which measurements of the particle flux would most efficiently determine the corresponding differential cross

section or polarization distribution. In particular, we determine the positions at which a polynomial distribution should be sampled in order to minimize a given linear combination of the sample variances in the resultant estimated values of the polynomial coefficients. It is shown that an approximate minimum of this quantity can be obtained even when the only a priori information about the distribution to be measured is that it is a polynomial of finite degree. Criteria are given also for the selection of measurements that provide "most sensitive" tests of hypotheses about the degree of the distribution. The analysis makes possible the use of a computer to program (and control) suitable experiments in order to attain a desired objective most efficiently. (auth)

47602 STUDY OF THE ISOTOPIC DISPLACEMENT OF URANIUM (235 TO 238). CONTRIBUTION TO THE CLASSIFICATION OF THE ARC AND SPARK SPECTRA OF URANIUM. Diringer, Michele (Centre National de la Recherche Scientifique, Bellevue, France). Ann. Phys. (Paris)(13), 10: 89-120(Mar.-Apr. 1965). (In French).

After a review of the results of the theory of isotopic shift it is shown in a general fashion how they are applied to classification problems. Previous works on isotopic shift in U I and II spectra are summarized. The experimental method used and the results obtained are described. The arc and spark spectra are then classified. An attempt is made, from the results obtained, to evaluate the order of magnitude of the characteristic experimental isotopic shift constant of the $^{235}U-^{238}U$ couple. (tr-auth)

47603 THE β^+ RADIOACTIVITY OF THE ISOTOPES ^{14}O, ^{19}Ne, ^{26}Si, AND ^{30}S. Frick, Georges (Institut de Recherches Nucleaires, Strasbourg). Ann. Phys. (Paris) (13), 10: 155-90(Mar.-Apr. 1965). (In French).

The β^+ radioactivity of ^{14}O, ^{19}Ne, ^{26}Si, and ^{30}S were studied using a high-precision magnetic spectrometer with intermediate focusing and scintillation detectors. The maximum energies, the half lives, and the branching ratios were determined. The theory of radioactivity established by theoretical and experimental studies is presented, and the calculation methods used to explore the experimental measurements and their interpretations are reported. The methods and apparatus used are described in detail. The maximum energy of the two branches of β^+ decay are 4.085 and 1.821 Mev. The branching ratios are 0.65% and 99.35%. The half life is 71.3 sec. The maximum energy of the branch going to ^{19}F from ^{19}Ne is 3.416 Mev and the half life is 1.47 sec. The existence of a second branch at 1.04 Mev was shown with scintillation detectors. The branching ratios calculated were 99% and 9%. ^{26}Si decays in two branches to ^{26}Al. The more energetic has the maximum energy of 3.828 Mev, but the second branch is masked by other activities. Its half life is 2.1 sec. ^{30}S decays in two branches with the energies 5.085 and 4.422 Mev. It has a half life of 1.4 sec and branching ratios of 20% and 80%. (J.S.R.)

47604 (d,p) REACTIONS AND EXPERIMENTAL STUDIES OF THE EXCITED LEVELS OF SOME LIGHT NUCLEI. Fintz, Pierre (Centre de Recherches Nucleaires, Strasbourg). Ann. Phys. (Paris)(13), 10: 435-74(July-Aug. 1965). (In French).

The (d,p) reactions of ^{11}B, ^{12}C, and ^{14}N were studied. The predictions of the shell model with respect to the nuclei studied were indicated. The formulations of the resonance reactions are given and the concept of the penetrability factor is described. The theory of stripping angular distributions with plane waves and its generalization taking into consideration exchange effects and Coulomb and nuclear effects are reported. The theory of p-γ angular correlations in a direct d-p reaction is considered. The experimental techniques are described. The experimental results are given and the reactions are analyzed by the theories cited. The results are compared with the predictions of the shell model and with results of others. The angular distribution of protons going to the ground level and to the 0.95 and 1.67-Mev levels of ^{12}B and the p-γ angular correlations for 0.95-Mev level of ^{12}B were measured in the reaction $^{11}B(d,p)^{12}B$. The photon spectra from the reaction $^{13}C(d,p)^{13}C$ were analyzed. Angular distributions of protons and the intensity of the γ radiations were measured. The excitation curves were deduced. The excitation curves and the angular distributions of the protons going to the ground level of ^{15}N were studied in the $^{14}N(d,p)^{15}N$ reaction. The angular distribution of the protons going to the 5.28-5.31 and 6.33-Mev levels and the p-γ angular correlations for the 6.33-Mev level of ^{15}N were also measured. (J.S.R.)

47605 β-γ CIRCULAR POLARIZATION CORRELATION IN PERMITTED β TRANSITIONS: ^{58}Co, ^{95}Zr, AND ^{95}Nb. Collin, W.; Daniel, H.; Schmitt, H. (Max-Planck-Institut fuer Kernphysik, Heidelberg). Ann. Physik (7), 15: 383-8 (1965). (In German)

The β-(circularly polarized γ) correlations of ^{58}Co, ^{95}Zr, and ^{95}Nb were measured by Compton forward scattering. The effects arising from positron annihilation in the case of ^{58}Co were investigated and corrected. The two cascades of ^{95}Zr, hitherto unresolved, were resolved by suitable β energy discrimination. The asymmetry parameters A were found to be -0.103 ± 0.032 (^{58}Co), -0.57 ± 0.08 (^{95}Zr β 362 - γ760), -0.41 ± 0.04 (^{95}Zr β 396 $-$ γ726), and 0.52 ± 0.10 (^{95}Nb). The ^{58}Co result implies a ratio X between Fermi and Gamow-Teller contributions to the decay of $X = -0.077 \pm 0.038$ while all other β transitions are pure Gamow-Teller ($\Delta I = 1$). The mixing ratios δ(E2/M1) were found to be 0.08 ± 0.09 or $1.85^{+0.09}_{-0.11}$ (^{95}Zr γ 760), -0.09 ± 0.04 or $3.0^{+0.3}_{-0.4}$ (^{95}Zr γ 726), and $-0.02^{+0.11}_{-0.13}$ or $-2.1^{+0.3}_{-0.4}$ (^{95}Nb). (auth)

47606 ANALYSIS OF NUCLEAR DIPOLE MOMENTS DETERMINED WITH NUCLEAR MAGNETIC RESONANCE. Lindgren, Ingvar (Univ. of Uppsala). Arkiv Fysik, 29: 553-63(1965).

A new analysis of measurements of nuclear magnetic dipole moments with nuclear magnetic resonance was performed. Due to the presence of mainly unknown chemical shifts a modified least-square method was used. The results are compared with the previously accepted values of the nuclear moments, based on calculations of Walchli. The new values are found to fall outside the limits of error of the previous values in 26 cases. Particularly large discrepancies are observed for the moments of ^{41}K, ^{95}Mo, ^{97}Mo and ^{187}Re due to errors in earlier compilations. The values obtained in the present work are also compared with moments measured independently with other techniques in a few cases, where such information is available. The difficulty in estimating the uncertainty of the moments is discussed, and different estimations are made, which can only be regarded as lower limits of the uncertainty. (auth)

47607 MEASUREMENTS OF COMBINED MAGNETIC AND ELECTRIC PERTURBATIONS OF ANGULAR CORRELATIONS OF γ-RAYS FROM POLYCRYSTALLINE SOURCES. Matthias, E.; Karlsson, E.; Svensson, A. G.; Johansson, K.; Gustafsson, S. Arkiv Fysik, 30: 19-31 (1965).

The integral angular correlation of the 133-482 kev-cascade in ^{181}Ta was studied with polycrystalline sources of $(NH_4)_3HfF_7$ and metallic Hf in longitudinally and transversally applied magnetic fields. The purpose of these investigations was to check experimentally some of the theoretical predictions for combined magnetic and electric interactions. While the electric quadrupole interaction in a Hf-metal source was found to be static with a frequency $\omega_L \approx 350 \times 10^6$ rad/sec the observed perturbation in $(NH_4)_3$ Hf F_7 indicates the presence of both a static and a time-dependent interaction. (auth)

47608 CONTRIBUTION OF STUDIES OF INELASTIC SCATTERING OF α PARTICLES TO THE STRUCTURE OF THE NUCLEUS. Faraggi, H. (Centre d'Etudes Nucleaires, Saclay, France). Bull. Inform. Sci. Tech. (Paris), No. 91, 37-47(Mar. 1965). (In French).

Experimental data were collected on collective states of spherical nuclei by inelastic scattering of 44-Mev alpha particles. Experiments using the Saclay fixed-frequency cyclotron showed that the vibrational picture of these states is far from satisfactory. (auth)

47609 SCIENTIFIC RESEARCH IN THE NUCLEAR PHYSICS LABORATORY. Bouchez, R. Bull. Inform. Sci. Tech. (Paris), No. 91, 49-58(Mar. 1965). (In French).

Recent results obtained in the Nuclear Physics Laboratory at Grenoble concern: a Coulomb stripping (d,p) process observed at very low energy on ^{16}O and ^{11}B; $\Delta 1 = 2$ inelastic scattering of 14-Mev neutrons on ^{12}C, ^{6}Li, and ^{7}Li; the two-step process $^{9}Be(n,n')\ ^{9}Be^{*}(n'')\ ^{8}Be^{*}$ observed with 14-Mev neutrons; measurements of polarized β-γ angular correlation and of the shape of the forbidden β spectra of ^{42}K and ^{86}Rb; and experiments carried out at C.E.R.N. (visitor group). (auth)

47610 APPLICATION OF THE HELICITY REPRESENTATION TO ANGULAR CORRELATIONS WITH RECOIL EFFECT. Baghdikian, M. Bull. Classe Sci., Acad. Roy. Belg. (5), 50: 1302-14(1964). (In French).

The helicity representation has many advantages, compared to conventional representations, when applied to angular correlations. It was used by Micu for the decay $A \rightarrow B + d_1$, $B \rightarrow C + d_2$. This problem is generalized to the case where the recoil of nucleus B cannot be neglected. The helicity representation is also applied to neutron capture and Coulomb excitation (with and without recoil). (auth)

47611 INDEPENDENT YIELDS OF ^{124}Sb AND ^{126}Sb IN THERMAL NEUTRON INDUCED FISSION AND THEIR IMPLICATION ON THE EMPIRICAL Z_p FUNCTION. Strom, P. O.; Grant, G. R.; Pappas, A. C. (Univ. of Oslo). Can. J. Chem., 43: 2493-2507(Sept. 1965).

The independent fission yields in thermal neutron induced fission of ^{235}U were measured to be $(9.5 \pm 1.4) \times 10^{-4}\%$ and $(1.04 \pm 0.17) \times 10^{-3}\%$ for ^{124g}Sb and ^{126g}Sb, respectively. The total independent yields for all isomers of these nuclides were estimated to be $(1.2 \pm 0.2) \times 10^{-5}\%$ for ^{124}Sb and $(3.7 \pm 0.6) \times 10^{-3}\%$ for ^{126}Sb using a Huizenga–Vandenbosch approach for estimating population of isomeric states. These data do not seem to support a 50 proton shell effect on the Z_p function, using the unique charge distribution curve of Wahl. A revised Wahl plot based on recent information on neutron emission from individual fission fragments is given and discussed in view of shell effects in fission. It is shown that the effect of the Z_p function of the 50 proton shell is very small. (auth)

47612 LIFETIMES OF THE ^{16}O 6.13-Mev LEVEL AND THE ^{17}O 0.871-Mev LEVEL. Alexander, T. K.; Allen, K. W. (Chalk River Nuclear Labs., Ontario). Can. J. Phys., 43: 1563-73(Sept. 1965).

The mean lifetimes of the 0.871-Mev state of ^{17}O(E2) and the 6.13-Mev state of ^{16}O(E3) were measured by a new recoil method using a Ge(Li) gamma-ray detector. The data yield mean lifetimes of $(2.33 \pm 0.27) \times 10^{-10}$ and $(2.5 \pm 0.2) \times 10^{-11}$ sec for the states in ^{17}O and ^{16}O respectively. The recoil method is generally applicable to the measurement of lifetimes greater than about 5×10^{-12} sec and provides a technique for a region of time where neither direct electronic timing nor Doppler-shift attenuation methods are accurate. (auth)

47613 NEW INFORMATION ON THE EMISSION OF DELAYED PROTONS FOLLOWING THE DECAY OF ^{17}Ne, ^{21}Mg, AND ^{25}Si. Hardy, J. C.; Bell, R. E. (McGill Univ., Montreal). Can. J. Phys., 43: 1671-7(Sept. 1965).

The spectrum of delayed protons from the decay of ^{17}Ne was extended up to 8 Mev; an additional peak corresponding to the decay of a level at (7.99 ± 0.05) Mev in ^{17}F was found. The delayed-proton spectrum observed following 80-Mev proton bombardment of magnesium and sodium targets, previously attributed solely to the decay of ^{21}Mg, was shown to contain components due to the decay of ^{17}Ne. The lifetime of ^{21}Mg was remeasured to be (121 ± 5) msec. The contribution of other decays was shown to be small compared with that of ^{25}Si in the delayed-proton spectrum observed following bombardment of aluminum and silicon targets at 80 Mev. (auth)

47614 SYSTEMATICS OF FISSION BASED ON THE EXPONENTIAL MASS FORMULA. Cameron, A. G. W. (Goddard Space Flight Center, New York). Can. J. Phys., 43: 1723-31(Oct. 1965).

A simple function of the fissionability parameter Z^2/A is found, which enables fission thresholds to be calculated relative to the exponential mass formula reference surface (with shell and pairing corrections omitted). From these thresholds, systematics of spontaneous fission rates and of the ratios of neutron to fission widths are developed. A discussion is given of multiple neutron capture experiments in the light of these fission characteristics. (auth)

47615 THE POSSIBILITY OF USING THE MOESSBAUER EFFECT TO MEASURE CROSS RELAXATION OF ^{57}Co COUPLED TO AN UNPAIRED ELECTRON SPIN. Misra, Sushil K.; Daniels, J. M. (Univ. of Toronto). Can. J. Phys., 43: 1843-52(Oct. 1965).

A parameter R(v), relevant to velocity-sensitive Mössbauer spectroscopy, was computed for the case where the orientation of ^{57}Co nuclei is produced dynamically by the Overhauser effect. This particular pumping scheme for producing nuclear orientation brings out two features. It allows the determination of η, the ratio of flip-flop to flip-flip thermal relaxations, by an experimental measurement of R(v), since the theoretical expressions for R(v) are found to be quite sensitive to the value of η. A numerical evaluation for three cases of overlap between absorber and emitter lines indicates wide variation in R(v) for increasing values of η from 10^{-7} to 10^{7}: R(v) increases monotonically from 8.5×10^{-7} to 1.07×10^{6} when emission line $3/2 \rightarrow 1/2$ overlaps absorption line $-1/2 \rightarrow -3/2$; R(v) decreases monotonically from 1.34×10^{14} to 8.91×10^{-6} when emission line $-1/2 \rightarrow 1/2$ overlaps absorption line $-1/2 \rightarrow 1/2$; R(v) decreases monotonically from 1.62×10^{2} to 6.14×10^{-3} when source lines $-1/2 \rightarrow -1/2$, $1/2 \rightarrow -1/2$, $1/2 \rightarrow 1/2$, and $3/2 \rightarrow 1/2$ overlap absorber lines $-1/2 \rightarrow -3/2$, $-1/2 \rightarrow 1/2$, $1/2 \rightarrow -1/2$, and $1/2 \rightarrow 1/2$ respectively. Since these R(v)'s are found to be much different from those that would be achieved through a pumping scheme using the Jeffries–Abragam effect, the possibility of using the Mössbauer effect to distinguish between the various ways of producing the nuclear orientation is suggested. (auth)

47616 INFLUENCE OF THE PAIRING INTERACTION ON THE NUCLEAR ENERGY LEVEL DENSITY. Hwang, Jenn-Lin (National Taiwan Univ., China). Chinese J. Phys. (Taiwan), 3: 35-44(Apr. 1965).

The modern theory of superconductivity developed by BCS and BZT is employed to examine the pairing interaction on the nuclear energy level density. A statistical model of nucleus is assumed to obtain the over-all character of the excited states. The empirical formula for the pairing energy proposed by Nemirovsky and Adamchuck and the semi-empirical formula for the single particle level density proposed by Abdelmaleck and Stavinsky are used to calculate the transition temperature, excitation energy, entropy, specific heat and the total level density. Except for the extremely light and heavy nuclei, a phase transition is predicted all at an energy of 2.73 Mev or so for a wide range of the mass number. This is remarkably different from the one calculated by Sano and Yamasaki. The level density below the transition energy is far smaller than that expected on extrapolating it from the higher energy side. (auth)

47617 ON THE ENERGY LEVELS OF ^{92}Mo WITH DIFFERENT POTENTIALS. Kumar, Vijay; Kumar, Naresh (Panjab Univ., Chandigarh, India). Current Sci. (India), 34: 427(July 20, 1965).

Calculations were made of the energy levels of ^{92}Mo arising due to the configuration $(g_{9/2})^2$, using the Gaussian, Yukawa, and Coulomb potential. The results show good agreement with each other. (L.B.S.)

47618 INFLUENCE OF THE NUCLEAR SHELLS ON THE THERMAL NEUTRON CROSS-SECTIONS. Raju, B. B. Venkatapathi; Swami Jnanananda (Andhra Univ., Waltair, India). Current Sci. (India), 34: 503-4(Sept. 5, 1965).

A number of elements were studied and the experimentally obtained values of the neutron cross sections are

given. The following conclusions can be drawn about the influence of nuclear shells on thermal neutron cross sections: The cross section is a maximum near the closing-up of the proton shell. Besides the stable neutron number, a stable proton number must also be passed before high values are reached. As soon as the proton shell is closed the cross section falls off sharply. The cross section is found to increase rapidly near the beginning of a shell as can be seen from the data on rare-earth elements. Besides the shell effects, the high cross sections may be attributed to the presence of energy levels in the compound nucleus corresponding to the neutron energy which causes the occurrence of large absorption. (J.F.P.)

47619 DECAY OF ^{51}Cr. Dhingra, K. C.; Gupta, U. C.; Sidhu, N. P. (Atomic Energy Establishment, Trombay, India). Current Sci. (India), 34: 504(Sept. 5, 1965).

The branching ratio of the decay of chromium-51 to the 0.323-Mev state is of great importance in the standardization of the radioisotope by the gamma spectrometer. Appreciable variation in the values of this branching ratio were reported previously. Thus the branching ratio was redetermined. A NaI scintillation crystal was used for the detection of x rays in view of its higher efficiency and shorter dead time compared to the proportional counter. Very thin NaI crystals were used in order to reduce to a considerable extent the contribution from 0.323-Mev gamma rays to the x-ray channel. The total disintegration rate was measured. A gamma spectrometer was used to determine the disintegration rate to the 0.323-Mev state of vanadium-51. A branching ratio value of 10.20 ± 0.63 was obtained. (J.F.P.)

47620 NUCLEAR STRUCTURE EFFECTS ON INTERNAL CONVERSION COEFFICIENTS. Sharma, R. P.; Thosar, B. V. (Tata Inst. of Fundamental Research, Bombay). Current Sci. (India), 34: 524-7(Sept. 20, 1965).

Measurements were carried out on the K-shell internal conversion coefficients for pure E2 transitions for rare earth nuclei from emission spectra. There are certain uncertainties which are very important in the low-energy region. These are due to photoelectron angular distribution and its effect on the photoelectric absorption cross section, scattering in the beta-absorber, the ratio of the internal and external source strengths, and the difference in geometries in internal and external measurements. A logarithmic plot of the incident particle energy versus the charge is also given. (J.F.P.)

47621 A MODERN WAY TO TEACH NUCLEAR PHYSICS. Siering, R. (Phywe AG, Goettingen, Ger.). Euro-Nucl., 2: 384-7(Aug. 1965).

Some basic experiments that can be performed with standard equipment to teach nuclear physics are described. Detection of alpha and beta particles, measurement of beta energy, registration of high pulse rates, and use of radiation sources are discussed. (M.C.G.)

47622 A NEW METHOD FOR CALCULATING NUCLEAR MATRIX ELEMENTS. Ikeda, Kiyomi; Fujita, Junichi (Tokyo Univ.). Genshikaku Kenkyu, 9: 731-45(Mar. 1965). (In Japanese).

A new method for calculating nuclear matrix elements is proposed, which turns out to be especially useful for the allowed unfavored transitions. (auth)

47623 SCATTERING OF ALPHA PARTICLES BY MEDIUM-WEIGHT NUCLEI. Kumabe, Isao; Ogata, Hiroshi (and others) (Kyoto Univ.). Genshikaku Kenkyu, 9: 785-802(Mar. 1965). (In Japanese).

The angular distributions of the elastic and inelastic scattering of 34.4 Mev alpha particles by ^{58}Ni, ^{60}Ni, ^{90}Zr, ^{91}Zr, ^{92}Zr, ^{96}Sn, ^{117}Sn, ^{118}Sn, ^{119}Sn, and ^{120}Sn were measured using a broad range magnetic analyzer having array detectors and/or a semiconductor detector. For ^{58}Ni and ^{60}Ni, it was found that the angular distribution of inelastic scattering leading to the two-phonon 4^+ state has intermediate phase between the elastic distribution and the first 2^+ inelastic distribution, and the angular distribution of inelastic scattering leading to the two-phonon 0^+ state in ^{60}Ni is out of phase with the two-phonon 4^+ inelastic distribution. On the other hand, the inelastic distribution to the two-phonon 2^+ state is in phase with the corresponding elastic distribution, and the inelastic distribution to the three-phonon 2^+ state is out of phase with the elastic distribution. The angular distribution of inelastic scattering leading to the 5^- state in ^{90}Zr was obtained. The differential cross sections are considerably large and the oscillation period is somewhat longer than the period for the elastic scattering. For Sn isotopes, the angular distributions for the quadrupole and octupole excitations were obtained for both even–even nuclei and odd–mass nuclei. Optical–model analyses and distorted–wave calculations are in process. (auth)

47624 INCOHERENT SCATTERING OF 280-kev GAMMA RAYS. Rao, P. V. Ramana; Rao, J. Rama; Lakshminarayana, V. (Andhra Univ., Waltair, India). Indian J. Phys., 39: 195-8(Apr. 1965).

Incoherent scattering cross sections σ_b in elements carbon, aluminum, copper, and cadmium are determined at the photon energy 280 kev and compared with the corresponding Klein-Nishina cross section σ_f. Progressively increasing deviation is observed between the two cross sections with increasing atomic number. This deviation is attributed to the influence of electron binding. The ratio (σ_b/σ_f) is computed theoretically on the basis of Thomas-Fermi atomic charge distribution and compared with the experimentally observed ratio. A fair agreement is noticed. (auth)

47625 CROSS-SECTIONS FOR PRODUCTION OF ^{7}Be FROM LIGHT TARGETS BY 2.2 Gev PROTONS. Reeder, P. L. (Brookhaven National Lab., Upton, N. Y.). J. Inorg. Nucl. Chem., 27: 1879-80(Sept. 1965). (BNL-8940).

The cross sections for the production of ^{7}Be from ^{14}N, ^{15}N, ^{16}O, and ^{18}O by bombardment with 2.2-Bev protons were measured to be 8.6 ± 0.8 ± 5.4 ± 0.5, 8.8 ± 0.4, and 5.5 ± 0.4 mb, respectively. (auth)

47626 HALF-LIFE OF ^{223}Ra. Kirby, H. W.; Jordan, K. C.; Braun, J. Z.; Curtis, M. L.; Salutsky, M. L. (Monsanto Research Corp., Miamisburg, Ohio). J. Inorg. Nucl. Chem., 27: 1881-7(Sept. 1965). (TID-20867; MLM-1229J).

The half life of ^{223}Ra was determined simultaneously by microcalorimetry and proportional alpha counting, with 5 mC of ^{223}Ra separated from ^{227}Ac and ^{227}Th by cation exchange. A 4-mC fraction of the purified ^{223}Ra was transferred to a tantalum capsule, dried, ignited at red heat, and hermetically sealed. The remainder was distributed among ten stainless steel disks in fractions ranging from 0.15 to 0.001 mC. The heat output of the tantalum capsule was measured in an isothermal resistance bridge microcalorimeter for 35 days, and in an isothermal thermoelectric microcalorimeter for 96 days. The stainless steel disks were alpha-counted in a windowless gas-flow proportional counter for 172 days. The half life of ^{223}Ra was found to be 11.4347 ± 0.0011 days by microcalorimetry and 11.4267 ± 0.0062 days by proportional counting. The weighted average was 11.4346 ± 0.0011 days. (auth)

47627 HALF-LIFE OF ^{53}Mn FROM METEORITE OBSERVATIONS. Kaye, J. H.; Cressy, P. J. (Carnegie Inst. of Tech., Pittsburgh). J. Inorg. Nucl. Chem., 27: 1889-92(Sept. 1965).

The half life of ^{53}Mn was estimated from measurements of the deficiency of this nuclide in a terrestrially old iron meteorite and in a stone meteorite of short cosmic-ray-exposure age. The respective estimates are (1.4 ± 0.2) and (2.4 ± 0.6) million years. These may be considered more properly as a lower and an upper limit, respectively, with the best estimate of the half life of ^{53}Mn being (1.9 ± 0.5) × 10^6 years. (auth)

47628 DISCOVERY OF PROTON RADIOACTIVITY. Petrzilka, Vaclav. Jaderna Energie, 11: 361-88(Oct. 1965). (In Czech).

The discovery of a proton decay of atomic nuclei having an excess of protons is reported. These nuclei were pro-

duced by bombarding atoms of some elements either in a beam of heavy ions or in a beam of fast protons. Radioactive nuclei emitted protons either in a process analogous to the radioactive α decay, or after the β^+ transition, by a mechanism similar to the delayed neutron emission during fission of nuclei. It is shown that there exists the possibility of producing nuclei decaying with the proton emission from practically all elements. (auth)

47629 PROBLEMS OF LOW-ENERGY NUCLEAR PHYSICS. Alexander, K. F. (Zentralinstitut fuer Kernforschung, Rossendorf, Ger.). Kernenergie, 8: 393-403 (July 1965). (In German).

Information is included on: experimental techniques (accelerators, spectrometers, and detectors); conceptions of nuclear structure (weak interaction and beta-decay, nucleon-nucleon interaction and the problem of nuclear matter, nuclear spectra, nuclear reactions). (auth)

47630 A NEW METHOD FOR DEUTERON STRIPPING CALCULATIONS. [PART] I. Butler, S. T. (Univ. of Sydney). Nature, 207: 1346-7(Sept. 25, 1965).

An approach to deuteron stripping calculations different from that of the distorted wave Born approximation theories is discussed. An equation was derived for the basic matrix for a (d,p) reaction, which involves a bound-state-neutron wave function characterized by a given orbital angular momentum and the neutron optical model wave function. The angle integrations in this equation may be trivially performed leaving a one-dimensional integral over the neutron radial coordinate. (M.C.G.)

47631 A NEW METHOD FOR DEUTERON STRIPPING CALCULATIONS. [PART] II. May, Robert M. (Univ. of Sydney). Nature, 207: 1348-9(Sept. 25, 1965).

The impulse approximation method for use in deuteron stripping and pickup calculations presented by Butler is discussed. A square well was used for the neutron-nucleus interaction to effect an exploration of the consequences of the approximation. The results were compared with the B-B (Butler-Born) theory with respect to: absolute magnitudes of cross sections, angular variation in differential cross section, and zeros in the differential cross section. (M.C.G.)

47632 GAMMA-RAY CASCADES IN ^{21}Ne. Pelte, D.; Povh, B.; Schuerlein, B. (Universitaet, Freiburg i. B.). Nucl. Phys., 73: 481-91(1965).

The gamma cascades from the excited states up to 4.73-Mev excitation energy in ^{21}Ne were studied using the ^{19}F(^{3}He,p)^{21}Ne reaction at ^{3}He energies of 4.4 and 4.7 Mev and the ^{20}Ne(d,p)^{21}Ne reaction at deuteron energies of 1.8 and 2.2 Mev. The 2.80-Mev state was found to decay dependent on the way the state was populated. This suggests that there are two states at 2.80 Mev. One with $J^\pi = 1/2^+$ decays predominantly to the $J^\pi = 3/2^+$ ground state. The other state of unknown spin and parity decays with the branching ratio $\leq 40 : \geq 60$ to the ground state and 0.35-Mev state, respectively. The 3.67-Mev state decays to the ground state, the first excited state, and the 2.80-Mev states with branching ratios $\leq 12 : 49 : 39$. The 3.89-Mev excited state decays to the ground state with 75% probability and to the first excited state with 25% probability. The 4.44-Mev state was found to decay partially through the 2.87-Mev state. The two closely spaced states at 4.7 Mev decay to the ground state, the first excited state, and the $J^\pi = 1/2^+$ state at 2.80 Mev with branching ratios $\leq 6 : 75 : 19$. The angular-correlation measurement for the 3.89-Mev state limits the spin for this state to $J \leq 5/2$. (auth)

47633 EXCITED STATES IN ^{21}Ne BY THE ^{23}Na(d,α)^{21}Ne REACTION. Pelte, D.; Povh, B. (Universitaet, Freiburg i.B.). Nucl. Phys., 73: 492-8(1965).

The probable spin assignments to the states in ^{21}Ne below 4.53 Mev excitation energy were deducted, applying the $2J + 1$ rule to the averaged cross sections of the ^{23}Na(d,α)^{21}Ne reaction. The spin assignments so obtained are $J = 1/2$ for both states at 2.80 Mev, $J = 3/2$ for the 3.67-Mev state, $J = 5/2$ for the 3.74- and 4.53-Mev states. The spin of the 3.89-Mev state can be $J = 3/2, 5/2$ with preference to the assignment $J = 5/2$. The states of ^{21}Ne are discussed in the framework of the unified model. (auth)

47634 SEARCH FOR DIRECT NEUTRON CAPTURE IN MANGANESE. Wasson, O. A.; Draper, J. E. (Yale Univ., New Haven). Nucl. Phys., 73: 499-512(1965).

A search for the existence of the direct neutron capture reaction mechanism in the radiative capture of low-energy neutrons in manganese is reported. An electron Linac was used to produce pulsed neutrons, the neutron energies were selected by the time-of-flight technique, and the γ rays were detected in a NaI(Tl) anticoincidence spectrometer. The shape of the partial capture cross section for emission of the 7.16-Mev ground state γ ray was measured as a function of neutron energy. The amount of direct capture was to be identified by the expected interference between direct and resonance capture near the 337-ev resonance. At 1-ev neutron energy an upper limit of 160 mb was established for the direct capture cross section. If it is assumed that the partial radiation widths and phase factors for the bound level at −2830 ev and for the 337-ev resonance are the same, then the upper limit of ≈30 mb is obtained. The accuracy of these results was limited by the multiple scattering in the sample and by the uncertainty in the bound level parameters. However, the experimental results can not be accounted for without interference effects in the capture mechanism. (auth)

47635 INELASTIC SCATTERING OF DEUTERONS FROM ^{60}Ni AND ^{114}Cd. Dickens, J. K.; Perey, F. G.; Satchler, G. R. (Oak Ridge National Lab., Tenn.). Nucl. Phys., 73: 529-38(1965). (ORNL-P-1402).

Differential cross sections for inelastic scattering of deuterons from the first excited states of ^{114}Cd and ^{60}Ni were measured for deuteron bombarding energies between 8 and 15 Mev for ^{114}Cd, and 9.9 and 13.6 Mev for ^{60}Ni. The data were analyzed by the distorted-wave method using the collective model of excitation. Good agreement with experiment for all cases is obtained, but only by deforming both real and imaginary parts of the optical potential and including Coulomb excitation. Real coupling alone considerably underestimates the magnitude of the cross sections even though for Ni it reproduces slightly better the experimental angular distributions. At the lower energies there are large contributions from Coulomb excitation and its interference with the nuclear excitation. (auth)

47636 GAMMA-GAMMA ANGULAR CORRELATIONS IN ^{124}Te. Dorikens-Vanpraet, L.; Demuynck, J.; Dorikens, M. (Rijksuniversiteit, Ghent). Nucl. Phys., 73: 539-47(1965).

The spin and parity of five levels and the nature of ten transitions in ^{124}Te were determined by means of gamma-gamma angular correlations and by making use of the experimental conversion coefficients mentioned in Nuclear Data Sheets. The results for the spin and parity of the levels are 2865-kev level, 3^-; 2691-kev level, 3^-; 2295-kev level, 3^-; 1962-kev level, 4^+; 1248-kev level, 3^+. The following characteristics of the transitions were obtained: 645-kev gamma, 95% M1 + 5% E2; 714-kev gamma, E2; 722-kev gamma, 15% M1 + 85% E2; 1361-kev gamma, E2; 1370-kev gamma, E1; 1540-kev gamma, E1; 1690-kev gamma, E1; 2090-kev gamma, E1; 2260-kev gamma, E1. (auth)

47637 DIRECT PROCESSES IN (n,α) REACTIONS. Kulisic, P. (Inst. Ruder Boskovic, Zagreb); Cindro, N.; Strohal, P.; Lalovic, B. Nucl. Phys., 73: 548-60(1965).

The energy and angular distributions of alpha particles produced by 14.6-Mev neutron bombardment of ^{103}Rh, ^{139}La, ^{141}Pr, ^{159}Tb, and ^{209}Bi were measured. While data on ^{103}Rh are inconclusive, both the energy spectra and the angular distributions of all other reactions show a surface direct process, possibly of a knock-out nature. A simple model is used to calculate the probability of formation of alpha particle clusters on the surface of heavy nuclei, and the lifetime of these clusters is estimated. (auth)

47638 ANGULAR DISTRIBUTIONS OF GAMMA RAYS PRODUCED BY NEUTRON BOMBARDMENT OF Al, Mg AND Si. Mathur, S. C.; Tucker, W. E.; Benjamin, R. W.;

Morgan, I. L. (Texas Nuclear Corp., Austin). Nucl. Phys., 73: 561-78(1965). (TID-21906).

The angular distributions of gamma rays produced by inelastic scattering of neutrons with magnesium, aluminum, and silicon were measured in the neutron energy range of 3.0 to 4.5 Mev. An attempt is made to determine the validity of the statistical assumption in the compound nucleus formation with ^{27}Al, ^{24}Mg, ^{26}Mg, and ^{28}Si nuclei. In order to do so, the angular distributions and differential cross sections are calculated on the basis of the Satchler formalism and comparisons made with the experimental results. (auth)

47639 ANGULAR DISTRIBUTION OF GAMMA RAYS PRODUCED IN THE ^{40}Ar(n,n'γ)^{40}Ar REACTION. Mathur, S. C.; Morgan, I. L. (Texas Nuclear Corp., Austin). Nucl. Phys., 73: 579-87(1965). (TID-21602; TID-21905).

The excitation functions for the production of gamma rays in the inelastic scattering of neutrons from ^{40}Ar were measured in the neutron energy range of 3.0 to 4.5 Mev. The angular distributions were measured for neutron energies of 3.0 and 3.5 Mev. From a comparison of the experimental angular distributions and the distributions calculated on the basis of the Satchler formalism, a spin of 2^+ was assigned to the third excited level in ^{40}Ar at 2.53 Mev and a spin of 4^+ to the fifth excited level at 3.22 Mev. The branching ratio of the gamma rays produced in the de-excitation of the 2.53-Mev level was also determined. (auth)

47640 ISOMERS IN ODD-MASS Lu ISOTOPES, ASCRIBED TO THE [541]$1/2^-$ NILSSON CONFIGURATION. Bjoernholm, S.; Borggreen, J.; Frahm, H. J.; Hansen, N. J. Sigurd (Universiteit, Copenhagen). Nucl. Phys., 73: 593-603(1965).

Irradiation of Yb isotopes with pulsed beams of 8 to 13-Mev protons and deuterons led to the discovery of the following new isomeric transitions in the Lu isotopes: a 29-kev, 160-sec, E3 transition in ^{169}Lu; a 70-kev, 76-sec, E3 transition in ^{171}Lu; a 345-kev, 1.3-μsec, E1 transition in ^{175}Lu; a 0.67-sec level in ^{170}Lu decaying by a 48-kev, M2 transition and a 44-kev, E2 transition; and a 64-kev, 430-μsec, E1 transition in ^{172}Lu. The isomerism in the odd-mass isotopes is ascribed to the [541]$1/2^-$ Nilsson state, in analogy to the well-studied case in ^{173}Lu. The results are discussed in relation to the parameters of the Nilsson model. (auth)

47641 SHELL MODEL CALCULATIONS OF NUCLEAR MAGNETIC MOMENTS AND M1 TRANSITION PROBABILITIES IN THE $2s_{1/2}1d_{3/2}$ SHELL. Wiechers, G. (Univ. of Cape Town); Brussaard, P. J. Nucl. Phys., 73: 604-12 (1965).

Recently, shell model wave functions for low-lying nuclear states in the range ^{29}Si to ^{40}Ca, with intermediate coupling and configurational mixing, were calculated. These wave functions are used to obtain numerical values for magnetic dipole moments and magnetic dipole transition rates. Expressions are given for the matrix elements of the magnetic dipole operator in terms of single-particle matrix elements. The ground state magnetic moments and the widths for M1 transitions to the ground state are calculated with single-particle g values and with effective g values for the nuclei in the range ^{29}Si to ^{40}Ca. The results are tabulated. (auth)

47642 INELASTIC SCATTERING OF DEUTERONS FROM Zn AND Se ISOTOPES. Lin, E. K. (Univ. of Pittsburgh). Nucl. Phys., 73: 613-24(1965).

The level structures of ^{64}Zn, ^{66}Zn, ^{67}Zn, ^{68}Zn, ^{76}Se, ^{78}Se, ^{80}Se, and ^{82}Se below 4 Mev were studied with 40 to 120-kev resolution by inelastic scattering of 15-Mev deuterons. The collective behavior of even nuclei of these isotopes were investigated, and most of the one-phonon and two-phonon groups were observed. Parity assignments were tentatively made for several new levels by the Blair phase rule. The previously unknown 4^+ state of the two-phonon triplet and the collective 3^- state in ^{82}Se were found at 1.75 and 3.08 Mev, respectively. (auth)

47643 THE K-CONVERSION COEFFICIENT OF THE 328 kev E2 TRANSITION IN ^{194}Pt. Lewin, W. H. G.; Lettinga, J.; Wapstra, A. H. (Laboratorium voor Technische Fysika, Delft, Netherlands). Nucl. Phys., 73: 627-47 (1965).

The K-conversion coefficient of the 328-kev E2 transition in ^{194}Pt was determined by means of K-conversion electron-gamma coincidence measurements. The result $\alpha_K = (505 \pm 20) \times 10^{-4}$ is in good agreement with the theoretical values of 495×10^{-4} computed by Rose, Sliv, and Band. (auth)

47644 THE (n,d) REACTIONS INDUCED BY 14 Mev NEUTRONS ON ^{19}F, ^{31}P AND ^{23}Na. Saeki, Bunzabro (Konan Univ., Kobe, Japan). Nucl. Phys., 73: 631-6 (1965).

A counter telescope consisting of three proportional counters and a solid state detector was employed to study the angular distribution of deuterons from the reactions ^{19}F(n,d)^{18}O, ^{31}P(n,d)^{30}Si, and ^{23}Na(n,d)^{22}Ne. The angular distributions for transition to the ground state of ^{18}O and ^{30}Si were measured for laboratory angles between 0 and 160°, and they are compared with the theoretical cross sections based on the theory of Butler. The differential cross sections were measured on a ^{23}Na target for angles between 0 and 60° and for transitions to the three lowest states of ^{22}Ne. (auth)

47645 A STUDY OF THE J = 2 EXCITED LEVEL OF ^{6}Li. Lovitch, L. (Istituto Nazionale di Fisica Nucleare, Pisa, Italy); Rosati, S. Nucl. Phys., 73: 648-56(1965).

The $J = 2^+$ level of ^{6}Li is studied using a three-body (proton, neutron, and alpha particle) model, where the alpha-nucleon pairs are described by trial normalizable wave functions. The experimental energy implies that the level, when regarded as a three-body state, is unbound. A search is made for the resonance by solving the effective Schrödinger equation associated with the neutron-proton pair. With the Pease and Feshbach neutron-proton potential an improved value of the total energy is obtained, as compared with the previous variational calculation of Wackman and Austern. The use of a neutron-proton potential containing a hard core does not introduce any additional complexity in the calculation, and it is found that the results are not independent of the particular potential chosen. (auth)

47646 THE (d,α) REACTIONS ON ^{19}F AT DEUTERON ENERGIES OF ABOUT 1 Mev. Stanojevic, D. M.; Cirilov, S. D.; Ninkovic, M. M. (Inst. of Nuclear Sciences Boris Kidrich, Belgrade). Nucl. Phys., 73: 657-63(1965).

The angular distributions of four alpha groups from the ^{19}F(d,α)^{17}O reaction were measured at five deuteron energies, ranging from 950 to 1250 kev. All angular distributions showed marked asymmetry about 90° and changed their shape rapidly with bombarding energy. The experimental data were analyzed in terms of Legendre polynomials. The α_1, α_2, and α_3 groups have total cross-sections consistent with the 2J + 1 law, as is expected from a statistical compound nucleus mechanism. (auth)

47647 THE MASS-SEVEN HYPERNUCLEI AND THE MASS-SIX NUCLEI. Bodmer, A. R. (Argonne National Lab., Ill.); Murphy, J. W. Nucl. Phys., 73: 664-80(1965).

The mass-seven hypernuclei are studied with a two-body model consisting of the Λ and the core nucleus. The Λ-core potentials are obtained with the use of two-body Λ-N Yukawa forces and of density distributions for the A = 6 core nuclei obtained from s-shell oscillator distributions and both oscillator and square-well wave functions for the p nucleons. The resulting Λ-core eigenvalue problems are solved numerically. The results are interpreted as strong evidence that the structure of the A = 6 nuclei can be described as an α particle plus two nucleons. To obtain significant information about the Λ-N interaction, a model would have to be used which takes into account the structure and dynamics of the cores in a reasonable way. It is shown that it is quite unlikely that the low experimental value of the separation energy $B_\Lambda(_\Lambda^7\text{He})$ in $_\Lambda^7$He compared with $B_\Lambda(_\Lambda^7\text{Be})$ is due to differences in the rearrangement energies of the ^{6}He and ^{6}Be cores. (auth)

47648 MECHANISM OF HYPERFRAGMENT FORMATION IN K^- CAPTURE. Patrick, J. W.; Jain, P. L. (Univ. of California, Berkeley). Nucl. Phys., 73: 681-94 (1965). (UCRL-11328).

In an attempt to understand the mechanism of hyperfragment production, a sample of 63 parent stars of hyperfragment production was studied. These were selected to have a fast pion accompanying the HF emission. The pion charges and energy distributions as well as the proton spectrum are used to establish the HF production process. Hyperfragments are emitted preferentially opposite to the direction of emission of associated pions or fast protons. The energy spectrum of the negative pions emitted from the K^--capture stars in association with hyperfragments can be separated into two groups, the one of lower energy being larger. On the other hand, the fact that all the π^+ mesons have energies typical of the lower-energy group confirms the assumption that the π^+ must originate in association with Σ^- hyperons. It is thus deduced that majority (71%) of the Λ's originate in Σ-conversion processes. The frequency of π^0 emission in association with hyperfragment production is evaluated. The reactions for the production of Λ's by K^- absorption on one or two nucleons are discussed. Attempts to separate K^- captures in C, N, or O from those in Ag or Br are almost completely successful. It is estimated that less than 20% of the multinucleon absorption occurred in heavy elements. (auth)

47649 MEASUREMENTS OF GAMMA-GAMMA ANGULAR CORRELATION IN ^{140}La. Zuk, Wlodzimierz; Goworek, Tomasz; Skorzynski, Zbigniew (Madam-Curie-Sklodowska Univ., Lublin). Nukleonika, 10: 261-8(1965).

Measurements of gamma-gamma angular correlation for ^{140}La were carried out by means of a gamma-gamma directional correlation apparatus consisting of a coincidence spectrometer with two detectors, one fixed and the other movable. The movable detector was adjusted at angles 90, 135, 180, and 225° with respect to the fixed detector. For the 304-162 kev cascade about 25,000 coincidences were collected for each position of the movable counter. This allowed determination of the angular correlation coefficients: $A_2 = 0.060 \pm 0.007$, $A_4 = 0.020 \pm 0.014$. Assuming the spin sequence 1-2-3 for the 304-162 kev cascade, the radiation should have a mixed multipolarity (D,Q) for both transitions of this cascade. The measurements of a low energy line 30 kev + x-ray correlation with the 537 kev gamma line also showed a distinct anisotropy, and allowed for determination of $A_2 = 0.030 \pm 0.013$ without correction for the x-ray component. (auth)

47650 STUDY OF HYPERFRAGMENTS. II. SHORT-RANGE HYPERFRAGMENTS AND SHORT TRACKS. Burte, D. P.; Ganguli, S. N.; Rao, N. K.; Ray, A. K.; Rengarajan, T. N.; Swami, M. S. (Tata Inst. of Fundamental Research, Bombay). Nuovo Cimento (10), 36: 733-50 (Apr. 1, 1965).

From a sample of 553 hyperfragments produced in 23-Bev/c proton interactions with emulsion nuclei, the hyperfragments of range ≤ 10 μm were studied. In order to understand the nature of these short-range hyperfragments, the emission of short tracks ($R \leq 10$ μm) and ^{8}Li fragments from interactions of 23-Bev/c protons and 3.5-Bev/c pions with emulsion nuclei were also studied; for this 596 ^{8}Li fragments were used. From these studies it was concluded that the effective Coulomb barrier for the emission of ^{8}Li fragments is smaller by a factor of ~3 than the classical one; a broad mass spectrum of nuclei is required to understand the range distribution of short tracks; this conclusion also follows from the N_h distribution of the parent stars; and among the hyperfragments of range (0 to 5) μm and (5 to 10) μm, at least 34% and 74% respectively have mass numbers $\lesssim 50$. (auth)

47651 THE EMISSION OF LIGHT CHARGED PARTICLES FROM HIGHLY EXCITED COMPLEX NUCLEI IN NUCLEAR EMULSION. Fliedner, A.; Harmsen, D. M.; Schink, L. (Institut fuer Experimentalphysik, Hamburg). Nuovo Cimento (10), 36: 751-61(Apr. 1, 1965).

The emission frequencies of the light nuclei p, d, t, ^{3}He, and ^{4}He from Ag and Br nuclei in emulsion were measured using the elastic scattering on protons in the emulsion for the identification of the particles. Results are: $(d + t)/(p + d + t) = 0.445 \pm 0.086$ and $(^3He + ^4He)/(p + d + t) = 0.457 \pm 0.138$. (auth)

47652 A STUDY OF EXCITED LEVELS IN ^{28}Si BY RANDOM PHASE APPROXIMATION. Di Porto, P.; Di Toro, M. (Universita, Rome; Scuola di Perfezionamento in Fisica Nucleare, Rome). Nuovo Cimento (10), 36: 873-83(Apr. 1, 1965).

The isotopic spin formalism is introduced in the first and second RPA. A simple calculation of the levels 2^+ $T = 0$ and 4^+ $T = 0$ of ^{28}Si is performed. The application of the first RPA gives results in agreement with the values obtained by a shell-model calculation. The introduction of double excitations of the particle-hole type does not affect appreciably the results. (auth)

47653 FURTHER ANALYSIS OF α-^{12}C SCATTERING PROCESS BY REGGE REPRESENTATION. Bertero, M. (Universita, Genoa; Istituto Nazionale di Fisica Nucleare, Genoa); Carrassi, M.; Passatore, G.; Viano, G. A. Nuovo Cimento (10), 36: 954-64(Apr. 1, 1965).

An analysis of two resonances in low-energy α-^{12}C scattering is made by Regge's representation. It is shown that by one- and two-pole approximations all the relevant features of the process are satisfactorily described. The background integral appears to be negligible except near the forward direction. Some discrepancies met in previous analyses of this type are overcome. The results indicate that a Regge description for this process can be made successfully when there is no interference of too many resonances belonging to different trajectories. (auth)

47654 ON SOME FEATURES OF MOESSBAUER ABSORPTION IN TIN METAL. Lamborizio, C.; Ortalli, I. (Universita, Parma, Italy). Nuovo Cimento (10), 36: 1059-61(Apr. 1, 1965).

Results of measurements of Moessbauer absorption spectra in tin, using a ^{119m}Sn source and a 6-mg/cm^2 absorber enriched in ^{119m}Sn, are discussed. Effects of impurities, especially tin oxides, of temperature conditions, and of etching in an attempt to remove impurities are considered. (M.J.T.)

47655 SINGLE-PARTICLE ELECTROMAGNETIC DECAY OF NUCLEI WITH HIGH ANGULAR MOMENTUM. Sperber, D. (Illinois Inst. of Tech., Chicago). Nuovo Cimento (10), 36: 1164-72(Apr. 16, 1965). (IITRI-A6034-2(App.I)).

The spectra and angular distribution of γ rays from nuclei with high angular momentum are calculated. The calculation is based on one single-particle transition. It is indicated how these results can be generalized for a cascade of γ rays. (auth)

47656 NUCLEAR CORRELATION FUNCTIONS AND MUON CAPTURE. Foldy, L. L.; Walecka, J. D. (CERN, Geneva). Nuovo Cimento (10), 36: 1257-66(Apr. 16, 1965).

Properties of certain nuclear correlation functions which enter into the theory of muon capture in complex nuclei in the closure approximation are examined. The reliability of certain suggested methods for evaluating these correlation functions involving the Fermi gas approximation, and refinements of it, are assessed both from the point of view of internal theoretical self-consistency and by comparison with pertinent empirical information available from photodisintegration data on nuclei. (auth)

47657 ON THE EFFECT OF n-p TENSOR FORCES IN $^3H_\Lambda$ [PART] II. Rosati, S. (Universita, Pisa, Italy; Istituto Nazionale di Fisica Nucleare, Pisa, Italy). Nuovo Cimento (10), 36: 1351-8(Apr. 16, 1965).

A study is made of the effect of the tensor part of the neutron-proton interaction in hypertritium. It is found that the corrections obtained for the volume integral of the Λ-nucleon interaction result in appreciable variation of the parameters of the Λ-nucleon potential as derived from studies of light hypernuclei. (auth)

47658 ON THE LOW-LYING LEVELS OF ODD-ODD SPHERICAL NUCLEI. Prosperi, D. (Centro di Studi Nucleari della Casaccia, Rome); Salusti, E. Nuovo Cimento (10), 36: 1372-5(Apr. 16, 1965).

A model to reproduce the general features of the low-energy spectra of intermediate and heavy odd-odd spherical nuclei is presented. A hamiltonian including the main effects of the short-range forces is introduced; the n-n and p-p interactions are the usual pairing forces, and the n-p interaction reproduces the contact interaction. A matrix equation for the eigenvalue problem is obtained; applications to nuclei are discussed. Results are similar to those of the quasi-particle method. (M.J.T.)

47659 PROBABILITY DISTRIBUTIONS OF FLUCTUATIONS IN THE REACTION $^{25}Mg(d,\alpha)^{23}Na$. Omar, H. M.; Gontchar, V. Y.; Bakr, M. H. S. (Atomic Energy Establishment, Cairo). Nuovo Cimento (10), 36: 1388-91 (Apr. 16, 1965).

The fluctuations in the differential cross section of the $^{25}Mg(d,\alpha)^{23}Na$ reaction are used to obtain the probability distribution. This is compared with the theoretical histogram obtained from integration of the equation for the Thomas-Porter distribution. The autocorrelations and cross correlations of the fluctuations in the differential cross sections for five separate alpha groups and their summation, measured at 1.5 to 2.5 Mev and 150°, are shown. The derived experimental histograms of the probability distribution of the cross-section fluctuations are compared with the calculated ones. The coherent widths and derived and calculated effective channel numbers are given. It is concluded that the reaction takes place through compound-nucleus formation and that the cross-section fluctuations are in good agreement with the theory of Ericson. (M.J.T.)

47660 A MODEL FOR DOUBLE CHARGE-EXCHANGE NUCLEAR REACTIONS WITH PIONS. Becker, F.; Maric, Z. (Universite de Paris, Orsay, France). Nuovo Cimento (10), 36: 1395-7(Apr. 16, 1965).

An attempt is made to describe the mechanism of the double charge-exchange nuclear reaction with pions by imagining that the process is a double-scattering process. The impulse approximation is assumed for both steps of the reaction, each being the simple scattering of pion on nucleon with unit exchange of charge. An expression for the matrix element of the reaction is obtained by treating the graphs of the reaction by the perturbation-theory method and approaching phenomenologically the energy-dependence of the scattering amplitude inside the nuclear matter. The differential cross section of the $^{7}Li(\pi^{+},\pi^{-})^{7}B$ reaction was calculated using this expression. (M.J.T.)

47661 COLLECTIVE AND PARTICLE-STATE IN ^{174}Yb FROM THE DECAY OF ^{174}Lu. Ricci, R. A.; Pautrat, M.; Drosi, M.; Chilosi, G.; Cuzzocrea, P. (Istituto Nazionale di Fisica Nucleare, Naples; Universita, Naples). Nuovo Cimento (10), 36: 1398-1401(Apr. 16, 1965).

The gamma spectrum of radioactive Lu sources produced by 25-Mev deuteron bombardment of ^{175}Lu was studied. Results are presented of gamma peaks and coincidences, assignments of gamma rays to the various isotopes ^{173}Lu, ^{174}Lu, ^{172}Yb, and ^{174}Yb, and energies and spin-parity of the collective and two-particle states of ^{174}Yb from the ^{174}Lu decay. (M.J.T.)

47662 HALF-LIFE AND g FACTOR OF THE 75-kev LEVEL IN ^{100}Rh. Mathias, E. (Univ. of California, Berkeley); Shirley, D. A.; Evans, J. S.; Naumann, R. A. Phys. Rev., 140: B264-7(Oct. 25, 1965). (UCRL-16069).

The half life of the 74.8-kev level in ^{100}Rh was measured by delayed-coincidence techniques. The result is $T_{\frac{1}{2}}$ = 235 ± 3 nsec. The time dependence of the 84 – 74.8-kev angular correlation in an external magnetic field was used to obtain the g factor of the 74.8-kev level as g = +2.13 ± 0.03. (auth)

47663 DECAY SCHEME OF 25-MINUTE ^{131g}Te. Walters, W. B.; Bemis, C. E. Jr.; Gordon, G. E. (Massachusetts Inst. of Tech., Cambridge). Phys. Rev., 140: B268-76(Oct. 25, 1965). (MIT-905-33).

The decay of 25-min ^{131g}Te produced by ^{130}Te (n,γ) was investigated with the use of Ge(Li) and NaI(Tl) γ-ray detectors. Coincidence relations among the γ rays were determined in γ-γ and sum-peak coincidence experiments. Because of the good resolution of the Ge(Li) detector complex γ-ray peaks observed in the ~350- and 950- to 1000-kev regions could be resolved, and additional γ rays were observed. The energies (in kev) of observed γ rays and their percentage intensities relative to 150-kev (in parentheses) are: 279 (1), 343 (1.1), 384 (1.1), 453 (24.0), 493 (7.0), 544 (0.4), 603 (5.9), 654 (1.8), 695 (0.5), 727 (0.4), 842 (0.2), 898 (0.3), 933 (1.2), 948 (3.0), 952 (0.6), 997 (5.1), 1007 (1.5), 1098 (0.8), 1147 (9.4), 1295 (1.4). The main changes from previous level schemes for ^{131}I are the lowering of the ~350-kev transitions to near the ground state and the addition of levels at 877, 1188, and 1445 kev. Preliminary measurements on the γ rays of 1.2-day ^{131m}Te are reported. Trends of the low-lying levels of odd-A iodine isotopes from mass 127 to mass 131 are discussed. The half life of ^{131g}Te was determined to be 25.0 ± 0.1 min. (auth)

47664 DECAY PROPERTIES OF THE NUCLIDES ^{256}Fm AND ^{257}Fm AND ^{255}Md, ^{256}Md, AND ^{257}Md. Sikkeland, T.; Ghiorso, A.; Latimer, R.; Larsh, A. E. (Univ. of California, Berkeley). Phys. Rev., 140: B277-82(Oct. 25, 1965). (UCRL-16086).

The decay properties of fermium and mendelevium nuclides produced by ^{11}B, ^{12}C, and ^{13}C ion bombardments of californium were studied. Those observed for ^{256}Fm, ^{257}Fm, ^{255}Md, and ^{256}Md agree well with previously reported results. For the first time alpha particles were recorded in the decay of ^{256}Fm (6.85 Mev) and ^{256}Md (7.17 Mev). In the course of the experiments the nuclide ^{257}Md was discovered. It decays with a half life of about 3 hr with the emission of 7.07-Mev alpha particles. Evidence is presented that its main mode of decay is electron capture. Attempts to produce and identify the isotope ^{258}Fm failed. A brief discussion of the results is given. (auth)

47665 SHORT-RANGE CORRELATIONS IN NUCLEAR MATTER. Moszkowski, S. A. (Univ. of California, Los Angeles). Phys. Rev., 140: B283-6(Oct. 25, 1965).

It is shown that a wave function which is a simple product of two-particle correlation functions gives a smaller short-range three-body correlation energy (calculated as the ground-state expectation value of the kinetic energy and short-range part of the interactions) than the approximate Faddeev wave function used in the recent work of Bethe. Thus for a plausible nucleon-nucleon interaction, the short-range three-body correlations contribute less than 1 Mev per particle to the energy of nuclear matter. (auth)

47666 OFF-ENERGY-SHELL EFFECTS IN THE BRUECKNER THEORY OF NUCLEAR MATTER. Coon, Sidney A. (Univ. of California, San Diego, La Jolla); Dabrowski, Janusz. Phys. Rev., 140: B287-96(Oct. 25, 1965).

The binding energy of nuclear matter at the equilibrium density determined by Brueckner and Gammel is calculated with the Brueckner-Gammel-Thaler nuclear forces. The Brueckner theory is applied. It is found that a solution exists for the coupled equations which determine the off-energy-shell elements of the K matrix of the Brueckner theory. This exact treatment of the off-energy-shell effects increases drastically the single-particle potential at high momenta. The calculated binding energy per nucleon, 7.5 Mev, is much smaller than the value of 15.2 Mev obtained by Brueckner and Gammel. This result is discussed. Two methods of treating the repulsive core—hard core and hollow hard core—are compared. (auth)

47667 EXCITATION FUNCTIONS FOR NUCLEON AND ALPHA-PARTICLE TRANSFER REACTIONS INDUCED BY ^{14}N IONS. Gaedke, R. M.; Toth, K. S.; Williams, I. R. (Oak Ridge National Lab., Tenn.). Phys. Rev., 140: B296-304(Oct. 25, 1965). (ORNL-P-1315).

Nitrogen ions, accelerated in the ORNL 63-in. cyclotron and tandem Van de Graaff, were utilized in a study of nucleon and alpha-particle transfer reactions. The reaction products were identified by means of their characteristic gamma rays and half lives and quantitatively studied by radioactive assay. In all, 21 reactions were investigated. The following nucleon transfer reactions were studied: $^{12}C(^{14}N,^{13}N)^{13}C$; $^{16}O(^{14}N,^{13}N)^{17}O$; $^{16}O(^{14}N,^{15}N)^{15}O$; $^{19}F(^{14}N,^{15}N)^{18}F$; $^{31}P(^{14}N,^{13}N)^{32}P$; $^{45}Sc(^{14}N,^{15}N)^{44m}Sc$; $^{45}Sc(^{14}N,^{15}N)^{44g}Sc$; $^{51}V(^{14}N,^{13}N)^{52}V$; $^{55}Mn(^{14}N,^{13}N)^{56}Mn$; and $^{55}Mn(^{14}N,^{15}N)^{54}Mn$. For the ^{45}Sc target it was found that the isomer yield ratio, $^{44m}Sc/^{44g}Sc$, remained constant at a value of ~0.8 over the bombarding range 20–42 Mev. The ^{31}P reaction was investigated by the detection of both products. The yields obtained in these two ways were found to be equal, within experimental error, thus indicating that the ^{13}N (whose excited states are unstable with respect to particle emission) is left in its ground state. Three new values were determined for the ratio of the neutron reduced width in ^{14}N and ^{19}F by comparing $(^{14}N,^{13}N)$ reactions on ^{19}F, ^{51}V, and ^{55}Mn with $(^{19}F,^{18}F)$ data obtained by Perkin et al. on the same three target nuclei. Excitation functions were determined for $(^{14}N,^{18}F)$ reactions on the following targets: ^{6}Li, ^{7}Li, ^{12}C, ^{16}O, ^{19}F, and ^{27}Al. These data were examined together with previously available results for the same reaction on ^{9}Be and ^{10}B. It was noted that the cross sections at the Coulomb barrier energies show a strong dependence on the alpha-particle binding energy of the target nucleus; this suggests that at low incident energies the ^{18}F may be at least partially produced by the pickup of an alpha particle by the incident ^{14}N ion. Cross-section measurements were also made for the production of: ^{15}O from ^{6}Li and ^{7}Li; ^{21}Na and ^{24}Na from ^{12}C; ^{22}Na from ^{16}O; and ^{38}K from ^{27}Al. (auth)

47668 $^{54}Fe(n,p)$, (n,α), AND (n,2n) CROSS SECTIONS. Salisbury, S. R.; Chalmers, R. A. (Lockheed Missiles and Space Co., Palo Alto, Calif.). Phys. Rev., 140: B305-10(Oct. 25, 1965).

Absolute cross sections for the $^{54}Fe(n,p)$ ^{54}Mn and ^{54}Fe (n,α) ^{51}Cr reactions were measured for the neutron energy intervals 2.2 to 6.2 Mev and 13.1 to 16.8 Mev. The cross section for the $^{54}Fe(n,2n)^{53}Fe$ reaction was measured at 14.0 and 16.8 Mev. Ten samples 1 by 2 by 0.45 cm enriched to 97% in ^{54}Fe were irradiated. Neutrons were produced with the D(d,n) and T(d,n) reactions, using gas targets and a Van de Graaff accelerator. Samples were placed 9 cm from the gas cell at angles from 0 to 122°. The absolute neutron flux at 11° was measured with a proton-recoil telescope. Relative neutron angular distributions were obtained from published D(d,n) and T(d,n) cross sections by integrating over source and target dimensions; the effect of scattering in the gas-cell window foil was also included. These angular distributions were normalized to the telescope values. The induced gamma activity following the decay of ^{54}Mn, ^{51}Cr, and ^{53}Fe was counted with a large calibrated NaI scintillation spectrometer. The (n,p), (n,α), and (n,2n) results at 14 Mev agree with previous experimental work. Previous measurements of the (n,p) cross section from 2 to 6 Mev give values somewhat lower than the present work. All experimental results are somewhat higher than cross sections obtained by a statistical-model calculation based on optical-model potentials, while a more empirical calculation gives good agreement with the (n,2n) data. (auth)

47669 COHERENT KNOCKOUT AMPLITUDES IN DEUTERON STRIPPING REACTIONS. Strobel, George L.; Scott, Bruce L. (Univ. of Southern California, Los Angeles). Phys. Rev., 140: B311-23(Oct. 25, 1965).

The knockout amplitude, which is present with the stripping amplitude in a properly antisymmetrized formulation of the (d,p) stripping reaction, is computed for the $^{12}C(d,p)$ ^{13}C and $^{32}S(d,p)^{33}S$ reactions. It is found to be much smaller than previous rough estimates had indicated, and it is argued that this is a general occurrence. The calculation uses the distorted-wave Born approximation with a zero-range perturbation interaction, although the deuteron is approximated by a Hulthén wave function for the computation of the knockout amplitude. The stripping-forbidden $^{10}B(d,p)^{11*}B$ (2.14 Mev) reaction is computed assuming it to be a pure knockout process. Poor agreement with the experimental data is obtained in forward directions. It is concluded that knockout can not be the sole reaction mechanism. (auth)

47670 DIRECT-INTERACTION (p,α) REACTIONS IN ^{89}Y AND ^{90}Zr. Fulmer, C. B.; Ball, J. B. (Oak Ridge National Lab., Tenn.). Phys. Rev., 140: B330-6(Oct. 25, 1965). (ORNL-P-1296).

Alpha-particle energy spectra from (p,α) reactions in ^{89}Y and ^{90}Zr were obtained at 5° intervals between 15 and 90°. Bombarding energies of 20.2 and 22.5 Mev were used. Differential cross sections for reactions leading to the ground and first excited states were determined. Distorted-wave calculations were done for the angular distributions for the reactions leading to each of the ground states and the 0.38-Mev first excited state in ^{87}Y. The calculated angular distributions reproduce the general features of the experimental angular distributions. Spectroscopic factors, obtained from normalization of the calculated angular distributions to the experimental data, are consistent with triton pickup as the dominant mechanism for direct-interaction (p,α) reactions. The normalization factors also indicate the ^{90}Zr ground-state proton configuration to be 70% $(2p_{\frac{1}{2}})$ and 30% $(1g_{\frac{9}{2}})$. (auth)

47671 NEW ISOTOPE OF FLUORINE: ^{22}F. Vaughn, F. J.; Chalmers, R. A.; Chase, L. F. Jr.; Salisbury, S. R. (Lockheed Aircraft Corp., Palo Alto, Calif.). Phys. Rev. Letters, 15: 555-6(Sept. 27, 1965).

Evidence for the production of fluorine-22 by the reaction $^{22}Ne(n,p)^{22}F$ was obtained, using 14.8-Mev neutrons. The half-life of fluorine was measured, and information about its decay scheme was obtained. The gamma-ray spectrum from fluorine-22 decay is shown. β-ray spectra were also observed. The end-point energy for ^{22}F β rays was found to be 11.2 ± 0.6 Mev. Observations were consistent with the two spectra having the same end point, implying that no β-ray transitions directly to the ground state of neon-22 occur. Measurements of the half life of fluorine-22 were made by observing the number of β rays emitted from the isotope as a function of time. The observed half life is 4.0 ± 0.4 seconds. A proposed decay scheme is shown. From the observed data the mass difference of neon-22 and fluorine-22 is 12.5 ± 0.6 Mev. (J.F.P.)

47672 PROTONS FROM THE ALPHA-PARTICLE BOMBARDMENT OF ^{27}Al. Kuperus, J. (Rijksuniversiteit, Utrecht). Physica, 31: 1069-80(July 1965).

Energies and strengths are reported of ninety-one ^{27}Al $(\alpha,p)^{30}Si$ resonances, observed in the energy range E_α = 1.0–3.3 Mev. The natural width of thirteen resonances and the partial widths of one resonance are reported. The observed level density of ^{31}P is in agreement with theory. Angular distributions of ground-state protons, measured at twenty-six resonances, yield unique spin values for ten levels and the parity of five of these. At twelve resonances the angular distributions exhibit level-interference effects. (auth)

47673 SOME ACTIVATION CROSS SECTIONS FOR 14 Mev NEUTRONS. Nagel, W.; Aten, A. H. W. Jr. (Instituut voor Kernphysisch Onderzoek, Amsterdam). Physica, 31: 1091-5(July 1965).

A number of reaction cross sections for 14 Mev neutrons were measured relative to the standard reactions $^{56}Fe(n,p)$ ^{56}Mn and $^{65}Cu(n,2n)^{64}Cu$. (auth)

47674 SEARCH FOR ANOMALOUS ELECTRIC DIPOLE TRANSITIONS IN ^{187}Re. Bashandy, E.; Mousa, M. G.; Migahed, M. (Atomic Energy Establishment, Cairo). Physica, 31: 1125-32(July 1965).

The internal conversion lines of the 72, 552 and 686 kev transitions in ^{187}Re were measured by means of a high resolution iron free double focusing spectrometer. It was found from the L-subshell ratios that the 72 kev transition is a pure E1 transition without any anomalous conversion observed. The K-conversion coefficient of the

552 kev transition was determined to be $\alpha_K^{552} = 0.0050 \pm 0.0004$ in good agreement with the theoretical value for pure E1 transition calculated by Sliv and Band. No penetration effects were found in the conversion process of the retarded 686 kev E1 transition. (auth)

47675 ON THE QUADRUPOLE MOMENTS OF NUCLEAR PARTICLE-HOLE STATES. Boeker, E. (Vrije Universiteit, Amsterdam). Physica, 31: 1133-42(July 1965).

A method is proposed to calculate in a simple way quadrupole moments and deformations of nuclear particle-hole states. The method can be applied to states described by any linear combination of isotropic harmonic oscillator wave functions belonging to the same energy. The method is illustrated by calculating the quadrupole moments of the $1^-(T = 1)$ and $1^-(T = 0)$ states in ^{16}O, which are described by the wave functions that Gillet obtained by diagonalizing an adjusted residual interaction. The largest deformations with $\beta \approx 0.18$ and $\beta \approx -0.16$ are found for the 18 Mev and 19 Mev $1^-(T = 1)$ states respectively. The largest deformations of the $T = 0$ states are somewhat smaller. (auth)

47676 A SEPARATION-TYPE CALCULATION IN A FINITE NUCLEUS. Bhaduri, R. K.; Tomusiak, E. L. (Oxford Univ.). Proc. Phys. Soc. (London), 86: 451-61(Sept. 1965).

The first-order terms in a separation-type calculation applied to a nuclear spectrum are investigated in detail. The assumption that the separation distance is independent of state is not satisfied well in the particular case considered (^{16}O, using the Kallio–Kolltveit singlet S potential); allowance for its variation makes an appreciable change in the predicted spectrum. (auth)

47677 SHELL MODEL PARAMETERS AND ENERGY LEVELS IN THE 2s-1d SHELL FROM HIGH ENERGY ELECTRON SCATTERING. Shaw, Rosemary R.; Swift, R.; Elton, L. R. B. (Battersea Coll. of Technology, London). Proc. Phys. Soc. (London), 86: 513-18(Sept. 1965).

Elastic electron scattering data were analyzed by means of charge distributions derived from single-particle proton wave functions in a central potential of the Saxon–Woods type, and it was found that it is possible to fit both the electron scattering and the proton binding energies as far as these are known from (p,2p) scattering experiments. Results for ^{40}Ca and ^{32}S, are reported, and, in the case of ^{40}Ca, the electron scattering results are compared with those obtained using phenomenological charge distributions. (auth)

47678 A FOUR-BODY OPERATOR IN NUCLEAR SPECTROSCOPY. Flowers, B. H.; Szpikowski, S. (Univ. of Manchester, Eng.). Proc. Phys. Soc. (London), 86: 672-4 (Sept. 1965).

A four-body operator is constructed which allows a physically significant and complete classification of states of all irreducible representations of the rotation group R(5) appropriate to jj coupling in the nuclear shell model with charge-independent pairing interactions. The corresponding operator for R(8) allows complete classification of some important irreducible representations required in LS coupling. (auth)

47679 NUCLEON PAIRS EMITTED BY NEGATIVE PION CAPTURE AND CHARGE-DEPENDENT NUCLEAR WAVE FUNCTIONS IN LIGHT NUCLEI. Kohmura, Toshitake (Tokyo Univ.). Progr. Theoret. Phys. (Kyoto), 34: 234-42(Aug. 1965).

The ratio of nn pair to pn pair emitted by π^- capture in light nuclei, $R = P(\pi^- + pn \rightarrow nn)/P(\pi^- + pp \rightarrow pn)$, is investigated, and it is shown that the ratio is seriously influenced by charge dependence of nuclear wave functions. From the experimental value of the ratio, it is concluded that the range of the wave function for a ^3S pair is shorter than that for a ^1S pair by about five percent. (auth)

47680 A REMARK ON THE HIGHER ORDER CORRECTIONS IN THE CRANKING MODEL. Shono, Yoshiyuki (Hokkaido Univ., Sapporo). Progr. Theoret. Phys. (Kyoto), 34: 321-3(Aug. 1965).

If the higher corrections are taken into account, in the cranking model, deviations from pure rotational energy appear. But such discussions are based on a model which has not a clear physical ground. Attempts were previously made to clarify the theoretical ground of the cranking model within the framework of the Q–Q interaction model. There, wave functions in the cranking model and an exact wave function in the Q–Q interaction model are linked together in a definite way. An example is shown in which the inclusion of the higher correction terms leads to an erroneous answer for the value of the moment of inertia. The origins of this error are mentioned briefly with the aid of previous results. The final conclusion as to the physical meaning of the higher correction terms must be drawn after the investigations of more general systems. But since models have their own limits of applicability, it is pointed out that physical reality cannot be given to the higher correction terms in the cranking model without qualification. (J.F.P.)

47681 ON THE DECAY OF ^{158}Eu AND ^{159}Eu. Muenzel, H.; Gantner, E. (Kernforschungszentrum, Karlsruhe, Ger.). Radiochim. Acta, 4: 119-24(Aug. 1965). (In German).

^{158}Eu and ^{159}Eu decay was studied with a β counter and NaI scintillation spectrometer. Analysis of the γ spectra gave the energies and relative intensities of the γ peaks of ^{158}Eu and ^{159}Eu. With a fast coincidence circuit the γ-γ-coincidences of the ^{158}Eu peaks > 0.9 Mev were measured. From the decay curves the following half lives were calculated: ^{158}Eu, 45.9 ± 0.2 min; and ^{159}Eu, 18.07 ± 0.09 min. Rapid europium extraction from the ^{160}Gd target by sodium amalgam is described. (auth)

47682 SEARCH FOR THE 5-MIN ISOMER OF ^{78}As. Fritze, K.; Kiefer, W. (Universitaet, Mainz). Radiochim. Acta, 4: 166-7(Aug. 1965). (In German).

A search was made for a 5-min isomer of ^{78}As but it was not observed. Nemilor et al. reported the existence of a γ line of 500 kev and a half life of 5 to 6 min in the irradiation of ^{78}Se with 14-Mev neutrons, which was ascribed to an isomer of ^{78}As. In a similar study no line at 500 kev was observed. (M.C.G.)

47683 NOTE ON DECAY OF ^{162}Tb. Schneider, Th.; Muenzel, H. (Kernforschungszentrum, Karlsruhe, Ger.). Radiochim. Acta, 4: 171-2(Aug. 1965). (In German).

The gamma lines appearing in the decay of ^{162}Tb were studied. The ^{162}Tb was prepared by the reaction $^{162}Dy(n,p)$ ^{162}Tb and the gamma spectra observed with a NaI(Tl) crystal and a 512-channel pulse-height analyzer. The energies of the gamma lines and their relative intensities are given. (M.C.G.)

47684 DISPERSION RELATIONS AND DIRECT NUCLEAR REACTIONS. Schnitzer, Howard J. (Univ. of California, Berkeley; Brandeis Univ., Waltham, Mass.). Rev. Mod. Phys., 37: 666-78(Oct. 1965).

This review is concerned with the application of dispersion relation methods to direct nuclear reactions. A discussion of the assumptions required to relate analyticity properties to the conventional descriptions of direct-reaction amplitudes is given. This leads naturally to a description of phenomenological methods such as extrapolation to poles and similar topics. The use of the unitarity condition provides a framework for the discussion of the distorted wave Born approximation from the S-matrix point of view. Finally attention is called to some dynamical calculations of relevance to the discussion. (auth)

47685 ANALYSES OF THE SCATTERING OF NUCLEAR PARTICLES BY COLLECTIVE NUCLEI IN TERMS OF THE COUPLED-CHANNEL CALCULATION. Tamura, Taro (Oak Ridge National Lab., Tenn.). Rev. Mod. Phys., 37: 679-708(Oct. 1965). (ORNL-P-416).

The formalism of the coupled-channel analysis of the scattering of nuclear projectiles by nuclei is presented in detail. Since the necessity for coupled-channel calculations increases with the degree of collectivity exhibited by the target nucleus, the presentation is particularly suited to collective nuclei, with the target states described by phe-

nomenological collective coordinates. Within this restriction the formalism given here is quite general so that the following cases can be considered: The target can be any (collective) nucleus, even-A or odd-A, vibrational or rotational; the projectile can be either charged or uncharged, and can have any spin; either or both the projectile and the target can be polarized; finally, the energy of the projectile can be very low since the contribution of the compound-state formation to the cross section can be included. Using a computer program which was written following the above formalism (which can be used to do any of the calculations enumerated above) scattering cross sections for several typical cases were obtained and are presented to show their contrasting behavior when different targets (and different coupling schemes) and different projectiles are chosen. Realistic calculations were also made in order to fit a large number of existing experimental data. Good fits were obtained in most cases which indicate that the coupled-channel calculation is a very powerful tool in explaining various complicated scattering data, and further in extracting useful spectroscopic information about the target nucleus. Possible future developments of the present analyses are discussed. (auth)

47686 ON THE DECAY OF ^{101}Tc (14 MIN). Cretu, T.; Funke, L. (Zentralinstitut fuer Kernforschung, Dresden). Rev. Roumaine Phys., 10: 67-76(1965). (In German).

The decay of technetium-101 was studied from scintillations of a gamma spectrometer. The gamma-gamma coincidences were detected. A two-dimensional coincidence selector, having a 2048-channel ferrite memory is described. The principle of this selector is explained. In general the results are compatible with the decay scheme indicated. The 635 kev-transition is ambiguous at present, but can be located in the decay scheme with certainty. The relative intensities of the gamma transitions are indicated. (J.F.P.)

47687 SOME INFORMATION CONCERNING THE STRUCTURE OF THE 16.7 Mev-LEVEL OF ^{5}He OR ^{5}Li OBTAINED FROM THE REDUCED WIDTHS OF THE REACTIONS ^{3}H(d,n)^{4}He AND ^{3}He(d,p)^{4}He. Dumitrescu, Ovidiu (Bucharest Univ.); Sandulescu, Aurel. Rev. Roumaine Phys., 10: 77-94(1965).

The reduced widths for the decay of ^{5}He or ^{5}Li into a deuteron and a triton are calculated, from the 16.7 Mev energy level in the assumption that the configuration of this level is given by an alpha particle and a neutron in a d-shell model state. The result shows that the value of the reduced width is one eighth as large as the corresponding value obtained on the basis of the shell model configuration s^3p^2. Taking into account the experimental value it is concluded that in a rough approximation the structure of the 16.7 Mev energy level is given by the configuration s^3p^2. (auth)

47688 THE EXCITATION FUNCTION AND THE ISOMERIC YIELD RATIO FOR THE 14 msec FISSIONING ISOMER FROM DEUTERON IRRADIATION OF PLUTONIUM. Flerov, G. N. (Joint Inst. for Nuclear Research, Dubna, USSR); Pleve, A. A.; Polikanov, S. M.; Ivanov, E.; Martalogu, N.; Poenaru, D.; Vilcov, N. Rev. Roumaine Phys., 10: 217-22(1965).

Further studies on the excitation of the 14 msec spontaneously fissioning isomeric state by the deuteron bombardment of a plutonium target are presented. The cross-section exciting the isomeric state, as well as the isomeric yield ratio, were measured at deuteron energies from about 7 to 12 Mev. The excitation function shapes verify the assumption that the isomer is produced via the (d,2n) process. The small values of the isomeric yield ratio ($<5.10^{-4}$) lead to the conclusion that the total angular momentum of the excited state, responsible for fission, is high. (auth)

47689 INTERACTION MEAN FREE PATH OF 9 Gev/c NEGATIVE PIONS IN XENON. Friedlaender, E. M.; Nitu, R. (Inst. for Atomic Physics, Academy of the R.P.R., Bucharest). Rev. Roumaine Phys., 10: 381-6 (1965).

The interaction mean free path of 9 Bev/c negative pions was measured in a xenon bubble chamber by two independent methods, under conditions excluding observational bias. The resulting cross-section (1578 ± 61) mb is in disagreement with previous measurements and slightly larger than the best interpolated proton value. (auth)

47690 ^{9}Be, ^{11}B AND ^{31}P(p,p') ANGULAR DISTRIBUTIONS. Hulubei, H.; Ivascu, M.; Berinde, A.; Neamu, I.; Scintei, N.; Francz, I.; Martalogu, N.; Marincu, E. (Inst. for Atomic Physics, Academy of the R.P.R., Bucharest). Rev. Roumaine Phys., 10: 403-13(1965).

The energy dependence of the angular distributions of inelastically scattered protons from ^{9}Be, ^{11}B and ^{31}P in the 5.80 to 6.15 Mev energy range was studied, in order to obtain information on the reaction mechanism. In the ^{9}Be(p,p')^{9*}Be, Q = 2.43 Mev reaction, the smooth variation of the excitation function at $\theta_{CM} = 94°$ at 5.60 to 6.15 Mev and the shape of the angular distributions suggest a direct interaction mechanism. Butler's theoretical curves computed for an interaction radius R = 2fm fit the shape of the measured angular distributions. The angular distributions of the ^{11}B(p,p')^{11*}B, Q = −2.13 Mev reaction are asymmetric about $\theta_{CM} = 90°$, the differential cross-sections showing an increase at large angles. This behavior may be explained by the excitation of a small number of resonances in the ^{12}C compound nucleus. The angular distributions of the ^{31}P(p,p')^{31*}P, Q = −2.23 Mev reaction are practically isotropic, suggesting a compound nucleus mechanism which can be described with good approximation by the statistical model. However, the anomaly of the angular distribution of inelastically scattered protons on the first energy level of ^{31}P, Q = −1.27 Mev at 5.8 Mev incident energy shows that the statistical theory must be used carefully in this domain of energy and mass number. (auth)

47691 THE POLARIZATION OF ELASTICALLY SCATTERED PROTONS ON ^{16}O AT 4.5 Mev ENERGY. Boca, I.; Cenja, M; Iliescu, E.; Martalogu, N. (Inst. for Atomic Physics, Academy of the R.P.R., Bucharest). Rev. Roumaine Phys., 10: 415-18(1965).

The angular distribution of the elastically scattered proton polarization on ^{16}O was measured from 50 to 128° laboratory angles at an energy of 4.5 Mev. The results are compared with the polarizations predicted on the basis of phase shift analysis of the elastic scattering data. (auth)

47692 THE POLARIZATION OF ELASTICALLY SCATTERED PROTONS ON Al AND Mg AT 4.5 Mev ENERGY. Boca, I.; Cenja, M.; Iliescu, E.; Martalogu, N. (Inst. for Atomic Physics, Academy of the R.P.R., Bucharest). Rev. Roumaine Phys., 10: 419-24(1965).

The angular distributions of the elastically scattered proton polarization on Mg and Al were measured from 50 to 128° laboratory angles at an energy of 4.5 Mev. The results on Al are compared with the optical model calculations. (auth)

47693 FINITE SOLID ANGLE CORRECTIONS IN γ-γ ANGULAR CORRELATION MEASUREMENTS. Deciu, N.; Kemeny, P.; Mihai, R. (Inst. for Atomic Physics, Academy of the R.P.R., Bucharest). Rev. Roumaine Phys., 10: 456-67(1965).

The solid angle correction coefficients in γ-γ angular correlation measurements were determined for the whole spectrum, and for the photopeak with and without a lead shielding around the crystal. These measurements were performed for different crystal sizes, for various γ-ray energies and source-crystal distances. Using an approximation proposed by Berényi et al., the correction coefficients were tabulated for large limits of the parameters (δ, $\delta - A$). The results are given in graphs and tables. (auth)

47694 POSITIVE PARITY STATES OF T = 3/2 IN A = 15 NUCLEI. Guiasu, Ileana; Micu, M. (Inst. for Atomic Physics, Academy of the R.P.R., Bucharest). Rev. Roumaine Phys., 10: 555-60(1965).

The T = 3/2 states of A = 15 nuclei are constructed by

adding a nucleon to the lowest T = 1 state of A = 14 nuclei. This approximation together with the pure j−j coupling approximation permits the semiempirical relations between the levels of A = 16 nuclei and those of A = 15 to be given. (auth)

47695 THE POLARIZATION OF ELASTICALLY SCATTERED PROTONS ON ^{12}C AT 6 Mev ENERGY. Boca, I.; Borsaru, M.; Cenja, M.; Iliescu, E. (Inst. for Atomic Physics, Academy of the R.P.R., Bucharest). Rev. Roumaine Phys., 10: 581-4(1965).

The angular distribution of the polarization of elastically scattered protons on ^{12}C was measured from 55 to 85° laboratory angles at the energy of 6 Mev. (auth)

47696 ON SOME LEVELS OF LOW EXCITATION ENERGY IN ^{55}Fe. Alevra, A.; Dumitrescu, R.; Lukas, Ingrid R.; Magda, Tatiana M.; Martalogu, N.; Plostinaru, D.; Trutia, Elena; Vilcov, Isabela; Vilcov, N. (Inst. for Atomic Physics, Academy of the R.P.R., Bucharest). Rev. Roumaine Phys., 10: 593-6(1965).

Some low energy levels in ^{55}Fe were excited by the ^{55}Mn (p,n) reaction and the energies of the neutron groups were measured using a time-of-flight method. Besides the known levels in ^{55}Fe (0.41; 0.94; 1.34 and 1.41 Mev) a level at 0.51 Mev was determined, which was not observed in the ^{54}Fe (d,p)^{55}Fe reaction. (auth))

47697 THE POLARIZATION OF THE ELASTICALLY AND INELASTICALLY SCATTERED PROTONS ON ^{24}Mg AT 5.8 Mev ENERGY. Boca, I.; Borsaru, M.; Cenja, M.; Hateganu, C.; Iliescu, E.; Martalogu, N. (Inst. for Atomic Physics, Academy of the R.P.R., Bucharest). Rev. Roumaine Phys., 10: 597-9(1965).

The polarization of the elastically and inelastically scattered protons on ^{24}Mg at 5.88 Mev was measured in a double scattering experiment at eight angles between 48 and 125°, in order to obtain information about the reaction mechanism on the ^{24}Mg nucleus. The angular distributions of the proton polarization are tabulated. An argument for a direct interaction with channel coupling is offered on the basis of the analysis of the data, which shows a strong correlation between the polarization of the elastically and inelastically scattered protons. It is also observed that the value of the spin-orbit potential in the elastic channel is greater than the value in the inelastic channel. (L.B.S.)

47698 EVIDENCE FOR HIGH FOUR-MOMENTUM TRANSFER FROM π^--Xe INTERACTIONS AT 9 Gev. Anghelescu, D. (Polytechnic Inst., Bucharest); Datcu, V.; Friedlaender, E. M.; Nitu, R.; Preda, A. Rev. Roumaine Phys., 10: 599-600(1956).

A search was made on frames of a xenon bubble chamber exposed to a 9 Bev/c π^- beam for inelastic π^--nucleon interactions with high four-momentum transfers Δ^2 to the recoil nucleon, for events in which the recoil nucleon appears as a neutron and interacts in the vicinity of the parent star. Evidence was obtained for a significant number of correlated high-energy neutron stars with $\Delta^2 \gtrsim 1$ (Bev/c)^2, and a lower limit of 0.76 ± 0.27 mb/nucleon was assigned for the partial cross section. (L.B.S.)

47699 ENERGY SPECTRA OF PHOTOPROTONS FROM ^{12}C, ^{24}Mg, ^{28}Si, ^{32}S AND ^{40}Ca. Ishizuka, Takeo (Saitama Univ., Urawa, Japan); Kageyama, Kosuke; Kawamura, Nobuaki; Abe, Ken; Mutsuro, Naoshi. Sci. Rept. Saitama Univ., Ser. A., 5: 8-11(1965).

Measurements were made of the photoproton energy spectra from ^{12}C, ^{24}Mg, ^{28}Si, ^{32}S, and ^{40}Ca at 25.5 Mev, using a lithium-drift type semiconductor detector. The cross sections obtained from the (γ,p) spectra, on the assumption that the residual nucleus is left in its ground state, show fine structure, which is in good agreement with both the (γ,p_0) cross sections obtained from detailed balances relations for (p,γ_0) reactions and the (γ,n) cross section derived from previous works on the same assumption. It is observed that as Z increases in even Z nuclei from 8 to 20, the branching ratio to the ground state seems to decrease. (L.B.S.)

47700 THE LOW ENERGY OPPOSITE PARITY COHERENT STRUCTURE OF ^{17}O AND ^{17}F. Lee, Ching-run, Wu Li Hsueh Pao, 21: 1370-80(July 1965). (In Chinese).

The low energy opposite parity states of ^{17}O and ^{17}F are calculated using the shell model. The residual interaction between nucleons is considered as the δ-type force. First, the equations are solved under the L−S coupling approximation, and the result reveals that the low energy states possess the pairing coherent structure. Next, the spin-orbit coupling force is introduced by a certain approximate method, and an energy spectrum comparable with experiment is obtained. The transition probabilities corresponding to the existing experimental data are also calculated. (auth)

47701 INVESTIGATION OF THE INTENSITIES OF HARD γ TRANSITIONS IN THE CAPTURE OF RESONANCE NEUTRONS BY ^{135}Ba. Urbanec, Jan; Vrzal, Jan; Liptak, Jan (Joint Inst. for Nuclear Research, Dubna, USSR). Zh. Eksperim. i Teor. Fiz., 49: 80-4(July 1965). (In Russian).

The spectra of hard γ quanta with energies lying between 4 and 10 Mev and emitted as a result of capture of 18 to 1500 ev resonance neutrons by ^{135}Ba are measured with a single-crystal scintillation spectrometer and a three-dimensional analyzer. An appreciable anomaly is observed in the intensity of the transitions to the ground and first excited levels. The intensities of these two transitions for 11 resonances in ^{135}Ba are determined and possible explanations of the observed anomaly of the 24.5 ev resonance are presented. (auth)

47702 INELASTIC PROTON SCATTERING FROM ^{40}Ca, ^{50}Ti, AND ^{54}Fe (thesis). Gray, Walter Steven. Boulder, Colo., Univ. of Colorado, 1964. 158p.

Inelastic proton scattering from ^{40}Ca, ^{50}Ti, and ^{54}Fe was studied at bombarding energies ranging from 14.6 to 18.2 Mev, using protons accelerated in the University of Colorado variable-energy cyclotron. The inelastic angular distributions obtained were compared with distorted-wave predictions from the Oak Ridge computer code TSALLY. An interaction form factor corresponding to first-order collective excitations was employed. The distorted waves used in the analysis were the solutions for a free particle in the optical potential well that gave the best fit to the elastic scattering. The optical potential employed was of the Woods-Saxon form with pure surface-derivative absorption and no spin-orbit term. On the basis of the distorted-wave treatment spin and parity assignments were made to the following levels: ^{40}Ca−3.73 Mev(3−), 3.90 Mev(2+), 6.29 Mev(3−), 6.55 Mev(3−), 6.94 Mev(2+), and 7.10 Mev(3−); ^{50}Ti−1.55 Mev(2+), 2.67 Mev(4+), 4.42 Mev(3−), and 5.20 Mev(3−); ^{54}Fe−1.41 Mev(2+), 2.56 Mev (4+?), 2.96 Mev(2+), 3.16 Mev(2+), 3.84 Mev(4+), and 4.08 Mev(5−?). These results are compared with some of the theoretical level calculations for the three nuclei studied. The results of the distorted-wave analysis for states with well-established spins indicate that the first-order, collective interaction model is most successful in describing the scattering to 2+ and 3− states. The agreement for 4+ states was less satisfactory, and in the only cases in which states with spins known to be different from 2, 3, or 4 were encountered, the theory was in marked disagreement with the experimental angular distributions. It is suggested that a calculation in which the form factor would be constructed from the individual interactions between the incident particle and a limited number of nucleons in the target might be more successful in describing the excitation of these states. (A.G.W.)

47703 MEASUREMENTS AND ANALYSIS OF ANGULAR DISTRIBUTION INTERFERENCE EFFECTS IN THE $^7Li(p,\gamma)^8Be$ REACTION (thesis). Schlueter, Donald Jerome. Manhattan, Kan., Univ. of Kansas, 1964. 64p.

Measurements were made that extend angular distribution information to E_p = 1700 kev in the $^7Li(p,\gamma)^8Be$ reaction. An excitation curve at 0° does not confirm the presence of new resonances recently proposed at E_p = 720 kev and 870 kev. Yield curves for the γ rays corresponding to transitions to the ground state and first excited state are

resonant at both the 441- and 1030-kev resonances. The analysis of the angular distributions shows that a satisfactory fit can be made for the $a_1(E)$ coefficient in the expression $W(\theta,E) = 1 + a_1(E)P_1 + \ldots$ by assuming that the interference results from overlapping compound states of opposite parity. The best fits are obtained for four cases for which the spins and parities of the 441-, 1030-, 2100-, and 5800-kev resonances are given respectively by the values (1+, 1+, 1−, 1−), (1+, 1+, 1−, 2−), (1+, 1+, 2−, 1−), and (1+, 1+, 2−, 2−). (Dissertation Abstr.)

47704 TENSOR POLARIZATION OF DEUTERONS SCATTERED FROM ^{4}He (thesis). McIntyre, Laurence Cook Jr. Madison, Wis., Univ. of Wisconsin, 1965. 193p.

The spin tensor moments $\langle T_{20}\rangle$, $\langle T_{21}\rangle$, and $\langle T_{22}\rangle$ of deuterons elastically scattered from ^{4}He were measured in the energy range 2-9 Mev. Measurements were made at laboratory scattering angles of 45°, 60°, 75°, and 90°. The ^{3}He(d,p)^{4}He reaction was used as the polarization analyzer. At 45°, 60°, and 75°, $\langle T_{20}\rangle$ and $\langle T_{22}\rangle$ exhibit single broad peaks of fairly large magnitude. This is a maximum in all cases except for $\langle T_{20}\rangle$ at 45° where a minimum is observed. The largest observed polarization occurs at 5.35 Mev, 60°, where $\langle T_{20}\rangle$ is 64% of its maximum possible value. At 90°, smaller polarization with little structure was observed. The moment $\langle T_{21}\rangle$ was essentially zero at all energies and angles except below 5 Mev at 75° and 90°. A phase-shift analysis of d-α elastic scattering was done using the measured tensor polarization parameters as well as available differential cross-section data. A FORTRAN language computer program was used in a search for phase shifts that best fit the experimental data. Complex s, p, and d waves plus a real parameter ϵ, coupling the s- and d-wave J = 1 phase shifts were used. The s-wave phase shift exhibits hard-sphere behavior requiring an interaction radius of 4.3 fm. The three p waves remain less than 10° in magnitude. The d waves J = 1 and J = 2 both resonate, while the d-wave J = 3 phase shift, which corresponds to a known resonance near 1 Mev, has hard-sphere behavior in the energy range investigated. An analysis of the two d-wave resonances using the single-level approximation of R-matrix theory reveals that they correspond to the known 2^+ and 1^+ levels in ^{6}Li at excitation energies of 4.6 and 5.7 Mev respectively. Resonance parameters that best fit the complex phase shifts were obtained. No evidence for the previously reported T = 0 level at 7.4 Mev excitation was found. (Dissertation Abstr.)

47705 ELASTIC SCATTERING CROSS-SECTIONS OF 14.5 Mev PROTONS FOR MEDIUM WEIGHT NUCLEI (thesis). Kelly, John Gordon. Boulder, Colo., Univ. of Colorado, 1964. 105p.

The differential cross-sections for elastic scattering of 14.5-Mev protons by twenty-two separated isotopes of medium weight nuclei were measured. The targets were rolled foils of ^{49}Ti, ^{54,56,57,58}Fe, ^{58,60,62}Ni, ^{63,65}Cu, ^{64,66,68}Zn, ^{90,91,92,94}Zr, and ^{116,117,118,119,120}Sn. The proton beam from the University of Colorado variable-energy sector-focused cyclotron was directed into a 36-inch scattering chamber where the scattered protons were identified and counted with silicon surface-barrier solid state detectors. The cross sections were measured at five-degree intervals from 20 to 160 degrees. Corrections were applied for multiple scattering in the targets, for finite angular resolution of the detector, for isotopic impurities, and for oxygen contamination. The polarization was measured by Rosen of Los Alamos National Laboratory on these targets at the same energy, but the optical model parameters that he obtained would not yield differential cross-sections in satisfactory agreement with those of this experiment. As a consequence of this disagreement a preliminary investigation was made using a computer program that searches for optical model parameters which will fit the polarization and differential cross-sections simultaneously. The parameters obtained by this procedure appear to be more sensitive to the form factors of the potential, and possibly to shell effects in the spin orbit potential with less ambiguity than previously possible. A preliminary determination of the symmetry energy term in the real potential was found. (Dissertation Abstr.)

47706 A STUDY OF (p,d) AND (p,t) REACTIONS ON NICKEL AND IRON AT 28 Mev (thesis). Hoot, Charles Glen. Boulder, Colo., Univ. of Colorado, 1964. 132p.

An experiment was performed to investigate single and double neutron pickup reactions induced by 28-Mev protons in thin self-supporting metallic targets of nickel and iron. The proton beam was generated with the University of Colorado 52-inch sector-focussed cyclotron and the pickup reactions were observed in a 36-inch scattering chamber using an E times ΔE charged particle identification system. The energy resolution of this system was about 100 kev. The results obtained included the Q-value of −13.987 ± 0.018 Mev for the ^{58}Ni(p,t)^{56}Ni ground state reaction, which yields a better value for the mass of ^{56}Ni than that previously estimated from beta-decay systematics. Levels at 2.71, 3.94, 6.62, and possibly 5.35 Mev (all ±0.05 Mev) in ^{56}Ni were also observed. Angular distributions were measured for these triton groups and for the (p,t) reaction on targets of ^{56}Fe, ^{58}Fe, and ^{60}Ni leading to prominent levels in ^{54}Fe at 0, 1.41, 2.57, and 2.97 Mev, in ^{56}Fe at 0, 0.85, 2.06, and 2.65 Mev (all ±0.05 Mev), and to the ground and first excited states of ^{58}Ni. The (p,d) reaction on the same targets showed deuteron groups from levels in ^{55}Fe at excitations of 0, 0.41, 0.94, 1.41, 2.97, 4.55, 4.88, and 7.74 Mev, in ^{57}Fe at 0.02, 0.13, 0.37, 1.33, 1.41, 2.18, 3.16, 4.98, 5.27, and 10.56 Mev, in ^{57}Ni at 0, 0.77, 1.11, 2.57, 5.25, and 6.01 Mev, and in ^{59}Ni at 0, 0.39, 0.90, 1.08, 1.30, 2.62, 3.02, and 4.50 Mev (all ±0.05 Mev). The previously unreported states in ^{55}Fe, ^{57}Fe, and ^{57}Ni at 7.74, 10.56, and 5.25 Mev are identified as isobaric spin analogue states by their excitation energy, l = 3 angular distributions, and relative strengths. (Dissertation Abstr.)

47707 MUON CAPTURE IN OXYGEN (thesis). Jenkins, David Albert. Berkeley, Calif., Univ. of California, 1964. 72p.

The muon-capture rate in oxygen, $\mu^- + {}^{16}O - {}^{16*}N + \nu$, is used as a means for measuring the induced-pseudoscalar-coupling constant (C_P) of weak interactions. The capture rates between the $J^P = 0^+$ state of ^{16}O and the 0^- and 1^- states of ^{16}N are measured by the stopping of muons in water where some of these muons are captured by ^{16}O and form excited states of ^{16}N. Capture into the excited states of ^{16}N is identified by counting the gamma rays that are emitted in the nuclear transition to the ground state. A rate of $(1.6 \pm 0.2) \times 10^3$ sec^{-1} for the capture rate into the 0^- state was obtained and used to calculate C_P with different nuclear models for the ^{16}O wave functions. The transition rate, and therefore C_P, depends strongly on the nuclear model. It is concluded that $5 < C_P/C_A < 20$. (Dissertation Abstr.)

47708 A BUBBLE CHAMBER STUDY OF K^--NUCLEUS INTERACTIONS AT REST (thesis). Davis, Herbert Sidney. Boulder, Colo., Univ. of Colorado, 1964. 73p.

A study of K^--nucleus interactions at rest was carried out in the Berkeley 30-inch propane-freon bubble chamber. The event configurations, restricted to those having a positive pion as a final state particle at the K^- interaction vertex, fall naturally into two categories: positive pions accompanied by a Σ^- and positive pions not accompanied by a Σ^-. The pion momentum distributions of these two categories indicated the production and decay of the 1405-Mev Y_1^* hyperon resonance. An estimate of the relative number of Y_1^* decays outside the production nuclei leads, by a time-of-flight technique, to a Y_1^* mean lifetime of $(6.2 \pm 2.6) \times 10^{-23}$ sec. The data were corrected for scanning losses, and it is proposed that the high rate of cryptofragment formation is due to the trapping of Λ-hyperons produced by the reaction $\Sigma^- + p \rightarrow \Lambda + n + \gamma$. Information on nucleon correlations within the nucleus is obtained by means of strange particle interactions. (Dissertation Abstr.)

47709 POLARIZATION OF PROTONS SCATTERED BY HELIUM (thesis). Weitkamp, William George. Madison, Wis., Univ. of Wisconsin, 1965. 131p.

The proton polarization in p-He^4 scattering was measured at six laboratory scattering angles ψ_s from 45° to 115° at proton energies from 17.5 to 27 Mev. The ^{3}He(d,p)^{4}He reac-

tion, with incident deuterons from 5.55 to 10.68 Mev, provided, at a reaction angle of 30°, the source of polarized protons from 22 to 27 Mev. Polyethylene energy absorbers were used to obtain proton energies less than 22 Mev. Scattered protons were detected in two counter telescopes. Corrections were applied to the data for the effects of finite gas target volumes and finite detector areas. The same apparatus was used to measure the polarization of the protons produced in the $^3He(d,p)^4He$ reaction. The measured extremes of p-^{4}He polarization at 17.5 Mev are -0.682 ± 0.030 at $\psi_3 = 75°$ and 0.922 ± 0.044 at $\psi_3 = 115°$. Polarization magnitudes decrease slowly with increasing energy, except that a substantial anomaly in the polarization is observed at proton energies near 23 Mev. The polarization measurements at 22 Mev are consistent with previous measurements. A phase shift search was carried out at proton energies of 17.5 and 20.0 Mev. The polarization anomaly near 23 Mev was attributed to the $^3/_2{}^+$ excited state in ^{5}Li. The energy dependence of the polarization in the vicinity of the anomaly was calculated from a set of resonance parameters for this level. (Dissertation Abstr.)

47710 THE POLARIZATION OF NEUTRONS FROM THE $^{13}C(p,n_0)^{13}N$ AND $^{15}N(p,n_0)^{15}O$ REACTIONS (thesis). Walker, Bryan Dale. Berkeley, Calif., Univ. of California, 1964. 59p.

The polarizations of neutrons from the $^{13}C(p,n_0)^{13}N$ and $^{15}N(p,n_0)^{15}O$ reactions were measured for several proton energies in the region between 6.9 and 12.3 Mev and neutron emission angles between 0 and 90°. The neutrons were detected using the Livermore time-of-flight facility incorporating pulse-shape discrimination to reduce the time-independent background. The "left" and "right" measurements were obtained by employing a solenoid for spin precession. Liquid helium was utilized as an analyzer. Large polarizations (50 to 70%) were noted for both reactions at several energies and angles. Corrections for multiple scattering in the analyzer were made. The energy dependence of the polarizations tends to confirm the "twin" reaction hypothesis of Bloom et al. Comparisons with polarization predictions of the quasi-elastic model of the (p,n) process are also shown. (Dissertation Abstr.)

47711 ZERO-FIELD LEVEL CROSSINGS IN EXCITED OPTICAL STATES OF ^{87}Rb (thesis). Feichtner, John David. Boulder, Colo., Univ. of Colorado, 1964. 97p.

Zero-field crossings (Hanle Effect) of magnetic sublevels of the excited optical states $5^2P_{\frac{1}{2}}$ and $5^2P_{\frac{3}{2}}$ of rubidium-87 in the vapor phase were studied at temperatures from 0°C to 40°C. The magnetic field of the earth was cancelled to within 30 milligauss by three mutually perpendicular sets of Helmholtz coils surrounding the apparatus. The crossing signals exhibited the behavior to be expected of a quantum-mechanical interference phenomenon involving $^2P_{\frac{1}{2},\frac{3}{2}}$ states populated by optical excitation from the $^2S_{\frac{1}{2}}$ ground state. The experiment yields, for the lifetimes of the $5^2P_{\frac{1}{2}}$ and $5^2P_{\frac{3}{2}}$ states of rubidium-87 atoms, $(2.8 \pm .2) \times 10^{-8}$ sec and $(3.0 \pm .3) \times 10^{-8}$ sec, respectively. The corresponding oscillator strengths are $f(5^2P_{\frac{1}{2}} - 5^2S_{\frac{1}{2}}) = (.32 \pm .03)$ and $f(5^2P_{\frac{3}{2}} - 5^2S_{\frac{1}{2}}) = (.65 \pm .05)$. Studies of the temperature dependence of the width of the $5^2P_{\frac{1}{2}}$ and $5^2P_{\frac{3}{2}}$ sublevels indicate a sudden increase in level width beginning at 27°C. Although this temperature dependence of the level width exhibits the general characteristics of collisional broadening, the relatively low temperature rules out this possibility on theoretical grounds. The temperatures are those at which one would expect trapping of resonance radiation to be important, but theory predicts in that case a decrease of the level width. The data also indicate a higher field level crossing in the $5^2P_{\frac{1}{2}}$ state in the region of 57 gauss, which is far enough removed from the zero-field crossing to cause little effect on the determination of the $5^2P_{\frac{1}{2}}$ lifetime. (Dissertation Abstr.)

47712 A RADIOCHEMICAL STUDY OF BISMUTH FISSION INDUCED WITH 36- AND 58-Mev PROTONS (thesis). Roesmer, Josef. Worcester, Mass., Clark Univ., 1964. 133p.

Radiochemical determinations of fission yields of bismuth with 36-Mev protons were performed for 13 mass chains in the mass region 66 to 113 and for 16 mass chains in the mass region 67 to 140 with 58-Mev protons. The total fission cross sections at these two energies were measured to be 1.8 and 11 mb, respectively. The mass-yield distributions are peaked at about mass 103 at 36 Mev and at about mass 102 at 58 Mev. Both mass distributions are narrow. The width at half height of the 36-Mev mass-yield curve is 18 mass units, while that of the 58-Mev distribution is 22 mass units. A resolvable asymmetric mode of mass division was observed in the region of masses 66 to 73 in 36-Mev bismuth fission. The asymmetric fission cross section was found to be about 6 μb. The narrowness of the asymmetric peak of about 7 mass units suggests that the asymmetric mode of bismuth fission is due to fission of a single species. Arguments are presented in support of the assumption that the asymmetric fission mode at 36 Mev occurs from a fairly high level of excitation. (Dissertation Abstr.)

47713 PARALLEL PLATE FISSION CHAMBER /Q-2207/ (Engineering Materials). (Oak Ridge National Lab., Tenn.). (CAPE-1229).

4 drawings.

The parallel plate fission chamber described is used in determining the ratio of the capture cross section to the fission cross section for ^{233}U, ^{235}U, and ^{239}Pu in the energy region from 1 ev to 30 kev. There are 29 plates that are 2.75 in. in dia and are fabricated of 0.005-in.-thick magnesium. The plates are coated on both sides, excluding the end plates, to a thickness of 1 mg/cm^2 with fissile material (^{235}U). The plates are in a spherical container with a magnesium shell. (For details, see TID-4100). (M.C.G.)

Plasma Physics and Thermonuclear Processes

Refer also to abstracts 47154 and 47533.

47714 (AD-613307) RESEARCH ON PLASMA ACCELERATION BY ELECTRIC FIELD GRADIENT. Semi-annual Technical Report, December 15, 1959-June 15, 1960. (RCA Labs., Radio Corp. of America, Princeton, N. J.). Contract AF49(638)-658. 72p. (AFOSR-TR-60-120). CFSTI $3.00 cy, $0.75 mn.

Theoretical studies of plasma acceleration by an r-f field gradient indicated that a plasma will be accelerated toward the low-field region if the applied frequency is greater than the critical frequency of the plasma, and toward the high-field region if the frequency is less than the critical frequency. Calculations for the acceleration of plasma spheres and ellipsoids of arbitrary orientation with respect to the r-f field were completed. Experiments with plasmas of various densities have demonstrated both the acceleration and deceleration of the plasmas as predicted by theory. Mercury plasma was accelerated with a 140-mC r-f field gradient to a velocity of 25 × 100,000 cm/sec, equivalent to a specific impulse of 2500 seconds. (auth)

47715 (AD-613622) THE JUELICH PLASMA SYMPOSIUM. Cap, Ferdinand; Lackner, Karl (Innsbruck Univ. (Austria)). July 14, 1964. Contract AF61(052)-675. 23p. CFSTI $1.00 cy, $0.50 mn.

Papers presented at the meeting of the European Study Group on Fusion are summarized under four topics: pinch discharges and related investigations; plasma acceleration; plasma confinement; and plasma diagnostics. (TAB)

47716 (AD-614283) THE ADIABATIC LINEAR STARK EFFECT IN A PLASMA. Wilke, K. H.; Hunger, K.; Larenz, R. W. (Technische Hochschule, Hanover (West Germany)). Dec. 1, 1964. Contract AF61(052)-161. 17p. (AFCRL-65-192). CFSTI $1.00 cy, $0.50 mn.

The electrical microfield in a plasma changes rapidly in space and time. For this reason the linear Stark effect of hydrogen spectral lines emitted from a plasma cannot be treated by a pure static theory as this is usually done assuming that the shift of atomic energy levels corresponds

to the instantaneous electric field. A more rigorous treatment has to consider the simultaneous action of the long range Coulomb fields of many particles. Only the low frequency part of this composed field leads to adiabatic energy shifts. On obtaining an expression for the mean square low frequency field some Belmer line profiles are computed as far as the adiabatic Stark effect is concerned. On account of some new results on the probability distribution of the microfield a Gaussian distribution has to be used for the adiabatic shift of a single energy term. The resulting profiles are compared with those of the static 'Holtsmark-Theory' and some experimental material. It turns out that the formula obtained here for adiabatic line broadening coincides nearly with the 'Lindholm Formula' for the Coulomb case but derived originally to account for collision broadening. (auth)

47717 (AD-614285) PLASMA KINETIC ENERGY—RF CONVERSION. Final Report. (Advanced Kinetics, Inc., Costa Mesa, Calif.). Feb. 1965. Contract AF30 (602)-2981. 128p. (RADC-TDR-64-550). CFSTI $4.00 cy, $1.00 mn.

An experimental and theoretical investigation was made on microwave energy produced by cyclotron radiation from a plasma medium. Power densities several orders of magnitude higher than had been obtained previously were experimentally measured. Power densities of hundreds of watts per cubic centimeter of X-band power were produced in the form of 100-500 nanosecond pulses. These high power densities indicate some ordering or coherency mechanism in this interaction. If this coherency can be enhanced and if this proves to be a true volume instead of surface interaction, this effort could result in microwave generators which are capable of producing power outputs far beyond any of those available from present generators. (auth)

47718 (AD-614442) ELECTROMAGNETIC WAVE PROPAGATION IN ANISOTROPIC PLASMAS ALONG THE DIRECTION OF A STATIC MAGNETIC FIELD. Bachynski, M. P.; Gibbs, B. W. (RCA Victor Co., Ltd., Montreal (Quebec). Research Labs.). Dec. 1964. Contract AF19(628)-4071. 164p. (AFCRL-65-84). CFSTI $5.00 cy, $1.25 mn.

An experimental and theoretical investigation of the propagation of electromagnetic waves in an anisotropic plasma along the direction of the applied static magnetic field was conducted. Experimental measurements of electron density and attenuation using circularly polarized waves (left-hand or right-hand) show good agreement with theory and with each other over all ranges of parameters. For the right-hand mode at radio frequencies above the electron cyclotron frequency, cut-off occurs at much lower electron densities than in the absence of a magnetic field. For the left-hand wave, both the phase change and attenuation decrease with magnetic field and the wave is affected much less by the plasma than the right-hand wave over the range of parameters encountered in the experiments. The theory of propagation of a linearly polarized wave in a lossy anisotropic plasma was derived. Investigations of the collisional effects on electromotive propagation in the region of the electron cyclotron frequency show a reversal in phase of the wave passing through the plasma as the electron density is increased. This phenomenon occurs only for the right-hand circularly polarized wave at frequencies very near but just above the electron cyclotron frequency. Collisional effects based on cold plasma theory can account for this behavior. (TAB)

47719 (ARL-65-131) RESEARCH ON PLASMA BOUNDARY STUDIES. Final Report, March 1, 1961–February 28, 1965. Kino, G.; Self, S.; Pavkovich, J. (Stanford Univ., Calif.). July 1965. Contract AF 33(616)-8121. 64p.

A review of the theoretical and experimental work on the properties of the plasma sheath is presented. This work led to further investigations of other effects within plasmas. A theory of the d-c properties of the plasma sheath is presented, and was used as a basis for setting up a small signal r-f theory to determine r-f field variations in the sheath. The direct orbital integration of Boltzmann's equation was obtained, and results for frequencies below the plasma frequency presented for both the field variations of the sheath and the effective impedance of the sheath. Experimental measurements were carried out, using the deflection of an electron beam as a diagnostic tool, to measure both the r-f and d-c field variations in the sheath when r-f is applied to a metal plate immersed in a plasma, the sheath being formed on the metal plate. The results are in good agreement with the experiment. An experiment on a theory of a new mode of beam plasma interaction which involves the growing deflection waves of a beam passing through a plasma is described. New methods of forming laboratory plasmas suitable for r-f measurements are described. Two new types of plasmas were used: a diffusion type of plasma produced from sources at each end of the system, and an electron neutralized ion beam. Both methods produced stable plasmas with a low collision frequency. Various diagnostic techniques for measurements of a plasma are given. A new analog device for reducing Langmuir probe data quickly was constructed and is in use throughout this lab. Another analog device for differentiating Langmuir probe characteristics, and for determination of the velocity distribution of the electrons was also constructed. Experiments to measure direct propagation of Bohm and Gross waves through the plasma volume are also described; the results indicate the presence of such waves. (auth)

47720 (LA-3347) COMPUTER PROGRAM FOR SOLUTION OF THE ENERGY BALANCE AND HEAT TRANSFER OF A PULSED THERMONUCLEAR REACTOR. Powers, J. E.; Ribe, F. L. (Los Alamos Scientific Lab., Univ. of California, N. Mex.). June 1, 1965. Contract W-7405-eng-36. 17p. Dep. mn; CFSTI $1.00 cy, $0.50 mn.

A summary is given of the function and use of a Fortran program for use on the IBM-7094. The program is used to solve the energy balance and heat transfer of the pulsed reactor discussed in LA-3294-MS, "Feasibility Study of a Pulsed Thermonuclear Reactor." (auth)

47721 (LA-3385) NEUTRON BLANKET CALCULATIONS FOR THERMONUCLEAR REACTORS. Bell, George I. (Los Alamos Scientific Lab., Univ. of California, N. Mex.). Aug. 30, 1965. Contract W-7405-eng-36. 13p. Dep. mn; CFSTI $1.00 cy, $0.50 mn.

Calculations are made of the production of tritium by 14-Mev neutrons incident on various neutron blankets. Neutron migration and reactions are computed with a 25-group DSN calculation. Blankets are considered containing normal Li, Be, C, and F, sometimes with Cu or Mo between the neutron source and blanket. Blankets of mostly Be, containing enough Li to absorb all slow neutrons, appear attractive for tritium regeneration. For example, a 60 cm thick blanket of 50 vol.% Be and 50% Li, having 3.3 cm of Mo between source and blanket, gives a production of 1.79 tritons per incident neutron. It is concluded that by use of Be, tritium regeneration can be achieved with considerable flexibility of blanket design. (auth)

47722 (LA-DC-7039) STABILITY, HEATING AND END LOSS OF A 3.5-MEGAJOULE THETA PINCH (SCYLLA IV). Quinn, W. E.; Little, E. M.; Ribe, F. L.; Sawyer, G. A. (Los Alamos Scientific Lab., Univ. of California, N. Mex.). [1965]. Contract W-7405-eng-36. 16p. (CONF-650935-2). Dep. mn; CFSTI $1.00 cy, $0.50 mn.

From 2nd IAEA Conference on Plasma Physics and Controlled Nuclear Fusion Research, Culham, Eng.

Experiments on stable, high-density, high-temperature, drift-free plasmas produced at initial deuterium filling pressures of 10 to 50 mtorr without bias magnetic fields (low-density regime), as well as at initial filling pressures of 50 to 125 mtorr with negative bias magnetic fields (high-density regime) were reported. These measurements on the plasma generated by a "primary" capacity bank of the Scylla-IV theta pinch (570-kJ at 50 kv with a 7.4-μsec half period) included the following: Mach-Zehnder interferometer measurements of the plasma electron density, shape, stability, and end losses; x-ray absorption measurements

of the electron temperature and impurity levels; neutron yields and collimation measurements of plasma length; shadowgraphs showing sharp plasma boundaries; and streak photographs showing gross plasma stability. In the low pressure regime without magnetic bias fields, characteristic plasma parameters are: density, 2 to 4 × 10^{16} cm^{-3}; electron temperature, 300 ev; mean ion energies, 3 to 9 kev; plasma length, 80 cm; plasma volume, 60 cm^3; and plasma impurities <0.1%. Plasma end losses were found to be the predominant loss mechanism. The extension of these measurements to the higher magnetic field and longer half-period provided by a 3-MJ, 20-kv "secondary" capacitor bank of Scylla IV is reported. In this case the plasma containment is no longer limited by the duration of the applied field. The end loss proceeds as indicated by the loss rates measured in the earlier experiments, and all plasma disappears by ~17 μsec. During this time no flute instability or appreciable drift of the plasma core are observed. Some effects, attributed to cold plasma diffusing in from the ends, are seen during the longer compression times. Closed, theta-pinches without end loss are discussed as a means of reaching the long containment times in which the eventual stability limitation can be tested. (auth)

47723 (LA-DC-7112) QUANTITATIVE SPECTROSCOPY OF CESIUM PLASMAS. Agnew, Lewis; Summers, C. (Los Alamos Scientific Lab., Univ. of California, N. Mex.). [1964]. Contract W-7405-eng-36. 28p. (CONF-650806-11). Dep. mn; CFSTI $2.00 cy, $0.50 mn.

From 7th International Conference on Phenomena in Ionized Gases, Belgrade.

Quantitative spectroscopic measurements were made of the line and continuum intensities and line profiles observed in an isothermal cesium plasma oven at plasma conditions up to 2300°K, 6.5 torr and 10^{14} ions/cm^3. Absolute oscillator strengths for 50 lines are given. Results are larger than Stone's calculated values by approximately 35% for the sharp series and 12% for the diffuse and fundamental series. Radiative recombination cross sections measured for the first two excited states (6P and 5D) are $\sigma_{6P}(v) = 3.74 \times 10^{-6}/v^2$ cm^2 and $\sigma_{5D}(v) = 8.3 \times 10^{-6}/v^2$ cm^2 (v in cm/sec). Widths of Stark-broadened fundamental series lines are in good agreement with theory. (auth)

47724 (MATT-267) TRANSITION FROM LANDAU DAMPING TO VISCOUS DAMPING OF ION ACOUSTIC WAVES. Motley, R. W.; Wong, A. Y. (Princeton Univ., N. J. Plasma Physics Lab.). July 1965. Contract AT(30-1)-1238. 5p. (CONF-630701-1). Dep. mn; CFSTI $1.00 cy, $0.50 mn.

From 6th International Conference on Ionization Phenomenon in Gases, Paris.

Previous experimental work on the propagation of ion acoustic waves in highly-ionized cesium plasma was extended to denser plasma ($n \gtrsim 4 \times 10^{12}$ cm^{-3}). In these plasmas the ion-ion collision frequency should exceed the wave frequency (<60 kc/sec), so that the fluid equations, rather than the collisionless equations, should better describe the wave propagation. The waves are excited by a tungsten grid immersed in the plasma column and are detected by a similar grid. There is a slow drift of plasma between the grids which gives rise to an asymmetry in the two directions of propagation. The "downstream" phase velocity was found to decrease from 1.3 × 10^5 cm/sec to 1.0 × 10^5 cm/sec and the "upstream" velocity from 6.9 × 10^5 cm/sec to 0.3 × 10^5 cm/sec as $\omega\tau$ decreases from 40 to 0.15, where τ is (related to) the ion-ion collision time. For the forward wave the damping distance δ increases from 0.55 λ to ~2.5 λ with decreasing $\omega\tau$. The damping distance for the backward wave is much shorter, and does not change significantly with $\omega\tau$. The results are compared with the predictions of the fluid equations. (auth)

47725 (NP-15355) WILLS PLASMA PHYSICS DEPARTMENT NINTH SIX-MONTHLY PROGRESS REPORT, JANUARY 1–JUNE 30, 1965. (Sydney Univ. (Australia). School of Physics). 6p. (PR-9). Dep. mn.

Progress is reported on preionization and shock wave ionization processes in SUPPER I, Alfven wave studies, current induced instability, a 2 mm interferometer, and lasers. (M.O.W.)

47726 (NP-15394) NELINEINAYA STABILIZA PUCHKOVYKH NEUSTOICHIVOSTEI PLAZMY. (Nonlinear Stabilization of Plasma Bunch Instabilities). Tsytovich; V. N. Shapiro, V. D. (Akademiya Nauk Ukrainskoi SSR, Kharkov. Fiziko-Tekhnicheskii Institut). 1964. 14p. Dep.mn.

In some cases of the passage of low-density beams through a plasma, the effects of nonlinear wave interaction may be small, the interaction being followed by longer intervals of the quasilinear relaxation of the beam. In such a case the energy of the beam-generated oscillations is identical with the original beam energy and the nonlinear wave interaction results in the transformation of the spectrum formed during the quasilinear stage. Excitation of plasma oscillations leads turbulent heating, generation of microwave and other effects. The calculations carried out indicate that within a certain range of the plasma parameters it is possible to stabilize the beam instabilities at the expense of the nonlinear effects. Thus, the beam may pass through the plasma without substantial energy losses and may be accelerated by internal fields. The stabilization is based on the fact that when the nonlinear effects become strong, the generated oscillations are transferred to the nonresonance region of the spectrum where they do not interact directly with the beam. If the process takes place within a time interval that is shorter than the characteristic time of generation of the waves by the beam, the wave energy acting on the beam will remain small and the beam will not be affected markedly. The mathematical criteria of the instability are derived. (TTT)

47727 (NP-15434) DETERMINATION OF DEUTERIUM DENSITY PROFILE IN A DEUTERIUM PLASMA USING AN ENERGETIC D^+ BEAM. Hickok, R. L.; Jobes, F. C.; Marshall, J. F. (Socony Mobil Oil Co., Princeton, N. J. Central Research Div. Lab.). [1965]. 19p.

A method is described for obtaining deuterium density profiles in a cylindrically symmetric deuterium plasma by probing the plasma with an energetic deuteron beam and observing the proton production rate from the $D(d,p)^3H$ reaction. It was used to investigate the density of a high current arc as a function of current and gas feed. For a given gas feed the maximum density decreases and the radial half-width increases as the current is reduced. A comparison of density and optical intensity profiles shows that the optical intensity decreases more rapidly with radius than the deuterium density. (auth)

47728 OPERATION AND DIAGNOSTICS OF A CLOSED LOOP MPD POWER GENERATOR. Schneider, Richard T.; Wilhelm, Horst E. Allison Res. Eng., 4: 10-22(1964).

A report is made of a fundamental research program, instituted to obtain basic information regarding plasmas in closed loop MPD power generators. The working fluid is helium, seeded with cesium. Measurements with argon are planned during a later stage of the program. The design of the device, which is described, becomes more complicated because of the specific task. These complications arise because the device must serve as an MPD power generator as well as a diagnostic device. In addition to performing the design, it was necessary to adopt existing diagnostic methods and to develop a new spectroscopic method for measuring temperatures in the range between 1000 and 3000°K. (auth)

47729 AN IMAGE INTENSIFYING SHUTTER FOR OBSERVING TRANSIENT PLASMAS. Roberts, James R. (Univ. of Michigan, Ann Arbor). Appl. Optics, 4: 1179-83(Sept, 1965).

A pulsed image intensifying tube is described for use as a shutter in a snapshot spectroscopic investigation of a shock-heated hydrogen plasma. The shutter was placed at the image plane of a spectrograph to obtain snapshot photographs of the H_δ line profile and the underlying hydrogen continuum. Electron density measurements of 0.8–2 × 10^{17} cm^{-3} were obtained from the width of the Stark

broadened H_β line. Plasma temperatures in the range 2 ev to 6 ev were obtained from the H_β line to hydrogen continuum ratio. An independent and simultaneous electron density measurement was obtained photo-electrically from the absolute specific intensity of the hydrogen continuum as a check on the image intensifying shutter measurements. This agreement was within the 10% experimental error. Time-resolved photographs of the plasma structure were also taken with this shutter. (auth)

47730 A LASER INTERFEROMETER FOR REPETITIVELY PULSED PLASMAS. Hooper, E. B. Jr.; Bekefi, G. (Massachusetts Inst. of Tech., Cambridge). Appl. Phys. Letters, 7: 133-5(Sept. 1, 1965).

A laser interferometer operating in the optical and near infrared was developed to measure phase changes as small as $2\pi \times 10^{-3}$ rad. The device was used in measurements of time and spatial variations of a repetitively pulsed plasma. The use of synchronous detection and of a null method for phase measurement makes this instrument more than an order of magnitude more sensitive than earlier laser interferometers. The interferometer consists of a three-mirror optical resonator, which is shown. The intensity of the laser depends upon the optical distance between two mirrors. A small modulation of the dielectric between the mirrors causes a corresponding intensity change which can be used to determine this modulation. Small drifts in the apparatus are compensated by using a calibrated dielectric as well as the plasma to be measured. Measurements made with a helium-neon laser are shown. (J.F.P.)

47731 THERMODYNAMIC PROPERTIES OF AIR AT HIGH TEMPERATURES (WITH CONSIDERATION OF RADIATION CONTRIBUTIONS). Kuthe, R.; Neumann, Kl.-K. (Technische Hochschule, Brunswick). Ber. Bunsenges. Physik. Chem., 69: 414-25(1965). (In German).

Results for an air plasma (21 mole % O_2; 79 mole % N_2) with inclusion of contributions from radiation are reported. Starting from the previously determined data, as the internal energy, the enthalpy per unit volume, the compressibility factor, the ratio of "effective specific heats" were determined and the number of electrons per unit volume were calculated. The temperature ranges were determined in which, at a given pressure, certain kinds of particles (atoms and ions) occurred at concentrations greater than 1 mole %. The translational enthalpy, the enthalpy of electronic excitation, the radiation enthalpy, and the contributions of the zero point enthalpies of neutral atoms and of the various ionization stages were calculated. The calculations were based on the assumption of complete thermodynamic equilibrium (i.e., also equilibrium between particles of matter and radiation), as well as the validity of the ideal gas law. The results are given in diagrammatic form for a temperature range from 20,000 to 150,000°K at pressures of 10^3, 10^2, 10^1 bar, and at pressures of 1, 10^{-1}, and 10^{-2} bar for a temperature range from 10,000°K to just below the temperature at which the radiation pressure became equal to the total pressure. (auth)

47732 ON THE APPLICATION OF PLASMA KINETIC THEORY TO IONIC SOUND-WAVE EXPERIMENTS IN MAGNETIC FIELDS. Haggerty, M. J. (Polytechnic Inst. of Brooklyn, Farmingdale, N. Y.). Can. J. Phys., 43: 1750-65(Oct. 1965).

The kinetic theoretical results for a homogeneous plasma in a uniform magnetic field are discussed qualitatively. The role of the mean cyclotron radius as a natural long-range cutoff is clarified. A relation between a critical frequency for ionic sound waves and the magnetic-field intensity is predicted. (auth)

47733 HELMHOLTZ INSTABILITY OF A VISCOUS COMPRESSIBLE PLASMA. Bhutani, O. P.; Sundaram, A. K. Can. J. Phys., 43: 1891-1903(Oct. 1965).

An attempt was made to discuss the Helmholtz instability of a viscous compressible plasma considered to be a perfect electrical conductor. Initially, the plasma is assumed to be in contact with a uniform magnetic field along a plane boundary that is parallel to the field and is assumed to flow with uniform velocity V_0 perpendicular to the field. By using the normal mode technique, the amplitudes of the perturbed quantities are obtained. The conditions for the validity of the principle of exchange of stability and overstability are obtained also. Finally, the growth-rate curves for different values of the viscosity parameter λ' have been drawn and it has been found that the effect of viscosity adds to the stability of the system. (auth)

47734 USE OF SCREEN CATHODES TO OBTAIN PLASMA/ELECTROMAGNETIC-WAVE INTERACTION STRUCTURES WITH FREE PLASMA BOUNDARIES. Lian, K. T. (Polytechnic Inst. of Brooklyn, Farmingdale, N. Y.). Electron. Letters, 1: 47(Apr. 1965).

A gas-discharge structure which uses a screen cathode is described. The plasma, which is formed between two equipotential metallic surfaces, has geometrically well defined planar plasma–gas boundaries (free boundary). Electron densities greater than 10^{12} cm^{-3} were obtained. (auth)

47735 HIGH-SPEED DIAGNOSTICS OF A PLASMA JET. Kurtmullaev, R. Kh.; Nesterikhin, Yu. E.; Pil'skii, V. I.; Ponomarenko, A. G. (Inst. of Nuclear Physics, Academy of Sciences, USSR). High Temp. (USSR) (English Transl.), 2: 753-7(Nov.-Dec. 1964).

Translated from Teplofiz. Vysokikh Temp., 2: 837-41 (Nov.-Dec. 1964).

There are a number of microwave diagnostic schemes, but the majority of these are subject to limitations when studying dense plasma and rapid processes. The latter problem, the setting up of a high-speed recording system is considered. A description of a rapid-acting microwave interferometer is presented. A description of the interferometer system, and some results of studying plasma jets with the microwave interferometer are given. It is concluded that fairly prolonged use of the interferometer described under working conditions shows that the apparatus corresponds fully to the parameters given. This offers the possibility of recording a process with a minimum duration of 150 to 300 nsec, rates of change of charged particle concentration up to 10^{13} cm^{-3} μsec^{-1} minimum concentration 5×10^{10} cm^{-3} (for effective plasmoid diameter of order of 50 mm), and velocity of boundaries 1.4×10^6 cm sec^{-1}. The accuracy of the measurements does not depend on the absorption of the probing signal, up to 15 to 20 db, and external noise. The recording system of the apparatus may be used in various wave bands. (J.F.P.)

47736 INSTABILITY OF THE PONDEROMOTIVE FORCE IN A WEAKLY IONIZED PLASMA. Eliseev, B. V. High Temp. (USSR) (English Transl.), 2: 767-73(Nov.-Dec. 1964).

Translated from Teplofiz. Vysokikh Temp., 2: 852-9 (Nov.-Dec. 1964).

Instabilities arising in a plasma bearing a current flowing perpendicular to a magnetic field are investigated. These arise in particular when the electron flow rate exceeds the velocity of sound in the neutral gas, or when the ion slip rate relative to the neutral particles exceeds the velocity of sound. Besides the "beam instabilities" mentioned, instability associated with the heating of electrons and the rise in their concentration in a nonisothermal plasma is studied. This is called ionization instability. The development of this instability is determined by the relation between the relaxation time for the electron density to reach equilibrium, the inflow of energy for ionization into unit volume, and the time in which inhomogeneities in the plasma average out during their macroscopic motion. The increments of all the instabilities and their dependence on the plasma parameters are determined. (auth)

47737 EFFECT OF A NITROGEN IMPURITY ON THE ELECTRON ENERGY LOSSES IN A NONEQUILIBRIUM ARGON–CESIUM PLASMA. Zhibritskii, V. K. High Temp. (USSR) (English Transl.), 2: 851-6(Nov.-Dec. 1964).

Translated from Teplofiz. Vysokikh Temp., 2: 945-6 (Nov.-Dec. 1964).

A study was made of a steady-state discharge in argon

containing different concentrations of nitrogen and an admixture of cesium. The pressure of the cesium was determined from the temperature of the coldest part of the discharge tube. The total gas pressure in the discharge tube was constant for all values of nitrogen concentration, and equaled 100 mm Hg. The discharge current was also held constant and equal to 0.5 A. As a result of the measurements made, a relation was obtained between the values of the conductivity and the nitrogen concentration. Calculations were also made of the inelastic loss coefficient of the electrons. It was found that as the concentration of impurity increases, the inelastic loss coefficient increases. These experiments show that molecular impurities have a substantial effect on the nonequilibrium conductivity of an argon-cesium plasma. Characteristics were also found for technically and spectrally pure argon. (J.F.P.)

47738 THE ELECTRON TEMPERATURE OF THE POSITIVE COLUMN IN HYDROGEN AT LOW PRESSURE. Ben-Yosef, N.; Shartiel, Y.; Kaufman, A. S. (Hebrew Univ., Jerusalem). Intern. J. Electron. (1), 18: 595-7(June 1965).

Measurements are extended to lower pressures for the device MAYA, previously reported, in which the ionized gas originates in the positive column of the arc discharge. A brief account of the results obtained is reported. The measurements of electron temperature were performed using axial plane electrostatic probes in two hot-cathode arcs of different diameter, the gas being hydrogen. The arc current was kept constant at 0.43 amp; and no stationary striations were observed visually for the range of pressures investigated. The results are shown. These results are compared with a previous theory of the positive column for the case where the mean free path of the ions is greater than the tube radius. While the experimental and theoretical curves are of the same form, they differ in magnitude to an extent which is greater than the experimental error. Some measure of diffusion to the walls could qualitatively account for this difference. (J.F.P.)

47739 BRUSH CATHODE PLASMA—A WELL-BEHAVED PLASMA. Persson, Karl-Birger (National Bureau of Standards, Boulder, Colo.). J. Appl. Phys., 36: 3086-94(Oct. 1965).

Results of probe, spectroscopic, and microwave studies are used to describe properties of a novel cold-cathode discharge. The use of a brush cathode allows stable operation in the abnormal glow region where some of the usual cold-cathode mechanisms are greatly exaggerated and determine the features of the produced plasma. The cathode fall is about an order of magnitude larger than for the corresponding normal cold cathode. The brush cathode generates a uniform electron beam in the energy range 1 to 10 kv and a corresponding negative glow with a longitudinal dimension (reaching distance of the beam) one to two orders of magnitude larger than for the normal cathode glow. The large dimensions of the negative glow and the fact that it is well-behaved (no instabilities and no striations) make it ideal for a whole series of investigations in plasma physics and spectroscopy. The electron density in the helium plasma is in the range 10^{10} to 10^{11} cm^{-3}, the electron temperature in the range 0.05 to 0.10 ev. The negative glow is beam generated (essentially field free) and recombination dominated making it a practically uniform plasma ideal for the study of rate and transport coefficients. Preliminary measurements of the particle balance give a recombination rate of 5×10^{-10} cm^3 sec^{-1} at 1100°K and an electron density of 3×10^{12} cm^{-3} in agreement with the collisional-radiative recombination theory developed by Bates, Kingston, and McWhirter. The recombination light emitted by the plasma is sufficiently strong to make spectroscopic methods useful for measurements of the electron density and the electron temperature. Lines in the helium series $2s^3S - np^3P^0$ are observed up to the quantum level n = 30. (auth)

47740 BEAM PROBING OF RF BEAM/PLASMA INTERACTIONS. Cannara, A. B.; Crawford, F. W. (Stanford Univ., Calif.). J. Appl. Phys., 36: 3132-5(Oct. 1965).

Experimental measurement of r-f electric fields in electron-beam/plasma interactions requires a nonperturbing probing technique. Such a technique is described and is applied to study cathodic electron beam break-up and meniscus formation phenomena observed in a low-pressure mercury-vapor discharge. Experiments are described in which the deflection of a fine electron-beam probe directed parallel to the cathode surface is measured to determine the spatial variations of the low- and high-frequency electric fields. A number of supporting experiments are reported which help to clarify the various phenomena occurring in the beam/plasma interaction region. (auth)

47741 OSCILLATIONS AND NOISE GENERATION IN A BEAM-GENERATED PLASMA. Dunn, D. A.; Nichparenko, W.; Simpson, J. E.; Thomassen, K. I. (Stanford Univ., Calif.). J. Appl. Phys., 36: 3273-5(Oct. 1965).

An electron beam at a few kilovolts is used to generate a plasma in helium or argon at 10^{-4} to 10^{-2} torr in a glass tube aligned with an axial uniform magnetic field of 0.3 to 2 kG. At and above a critical beam current and gas pressure, the discharge changes from a glow region the size of the beam to a glow discharge filling or nearly filling the glass tube (total glow). Measurements of the plasma density, the velocity distribution of the beam, and the spectrum of the rf noise generated in the plasma as functions of beam current, voltage, and gas pressure were made. These data are consistent with an explanation of the effect involving a convective forward-wave beam-plasma oscillation which has a starting current equal to the measured critical current for the transition to total glow and which is determined by the net gain of the system including reflections at the ends. The oscillation, once started, is not a coherent oscillation, but can have a very wide noise bandwidth extending essentially from zero frequency to near the electron plasma frequency. (auth)

47742 HYDROMAGNETIC WAVE IN A TOROIDAL DISCHARGE WITH LONGITUDINAL MAGNETIC FIELD. Itoh, Satoshi; Fujisawa, Noboru; Miyajima, Shigeki; Yamamoto, Kenzo (Nagoya Univ., Japan). J. Appl. Phys., 36: 3295-9(Oct. 1965).

A regular hydromagnetic oscillation in a simple toroidal discharge is found for the first time. The externally applied longitudinal magnetic field and high degree of ionization are essential to generation of the oscillation. The observation by magnetic probes and streak camera shows that a plasma column of the m = 1 helix rotates in the direction of right-handed screw to the applied magnetic field. The wavelength of helix and rotational frequency depend on the pressure, ion mass, and applied magnetic field. The phase velocity of the plasma helix coincides with the Alfvén velocity. (auth)

47743 ISOTROPIC PLASMA GUIDE—TE_{11} MODE. Johnston, T. W.; Gore, J. V.; Osborne, F. J. F. (RCA Victor Research Labs., Montreal). J. Appl. Phys., 36: 3354-5(Oct. 1965).

The fast-wave quasi-TE_{11} mode behavior of two circular guides of different size with the same discharge plasma within them was studied experimentally. When the plasma container dielectric effects were properly accounted for, the results for the two guides for various discharge conditions gave a good check on the consistency of the theory for the partially filled plasma guide. The calculated results for the two guides are given, with the guide diameters indicated and the assumed uniform plasma column diameter of 1.6 cm for a field frequency of 9.2 Bc. It is concluded that the theory is adequate and noted that the proper calculation of dielectric effects is apparently worthwhile. Unmagnetized plasma perturbation theory gives a reasonable result for bulk modes provided the guide is fairly well filled. Obtaining actual values of wavenumber and of the square of the refractive index n^2, rather than only the phase shifts, is good practice since the n^2 vs electron density curve is nearly straight and the dielectric effect on n^2 is nearly constant. (J.F.P.)

47744 COLLISIONLESS NON-LINEAR COUPLING OF ELECTROMAGNETIC WAVES NEAR THE ELECTRON GYROFREQUENCY BY PLASMA ELECTRONS. Hamberger,

S. M. (Culham Lab., Abingdon, Eng.). J. Nucl. Energy, Pt. C, 7: 445-54(Sept.–Oct. 1965).

A collisionless mechanism is suggested which can lead to the mixing of two electromagnetic waves in a magnetoplasma at frequencies near the electron gyrofrequency. Some preliminary experiments are described which support the predictions of the theory, namely that the difference frequency wave amplitude $\propto$ (difference frequency)$^{-2}$ when collisions are rare, but is independent of difference frequency when collisions occur frequently during a beat period. (auth)

47745 UTILIZATION OF TRANSVERSE MODES IN THE SPHERICAL LASER INTERFEROMETER. Gerardo, J. B.; Verdeyen, J. T. (Univ. of Illinois, Urbana). J. Nucl. Energy Pt. C, 7: 475(Sept.–Oct. 1965).

It is noted that no conflict exists between the results obtained by using the transverse modes in laser interferometer measurements of plasma density with those of Quinn (1965). It is also noted that the transverse modes were recently utilized to increase the sensitivity of the interferometer by a factor of 27 greater than the sensitivity obtained using only the longitudinal modes. (L.B.S.)

47746 QUASI-STATIC OSCILLATIONS IN A HOT ASYMMETRICAL PLASMA SLAB. Nihoul, J. C.; Vandenplas, P. E. (Ecole Royale Militaire, Brussels). J. Nuclear Energy, Pt. C, 7: 341-52(July–Aug. 1965).

A simple model is introduced to investigate the influence of a transverse magnetic field on the resonance peaks of a hot plasma drifting along its axis. The model adopted is such that the results are valid in any asymmetrical plasma whatever the origin of the asymmetry. The second set of temperature resonances which one observes experimentally is qualitatively explained by the theory. This analysis is also an opportunity to apply carefully the method of using successive moments of the Boltzmann equation and interrupting the series to a given order in the dimensionless temperature when a steady magnetic field is present. (auth)

47747 STABILITY OF A PLASMA WITH A PLANE BOUNDARY. Krishan, S. (Univ. of Delhi). J. Nuclear Energy, Pt. C, 7: 353-8(July–Aug. 1965).

An attempt is made to study the stability of a semi-infinite plasma in the longitudinal approximation, i.e., k parallel to E, where k is the wave vector and E the perturbed electric field. A suitable equilibrium distribution is chosen which preserves charge neutrality, becomes Maxwellian away from the boundary and corresponds to current over the interface. If $\Omega > \omega_p$ the system is stable in the low-frequency magnetohydrodynamic limit: $\omega/\Omega \ll 1$, $(kR)^2 \ll 1$; and unstable in the high-frequency limit $\omega \gg \Omega$. Here ω is the characteristic frequency of the wave, R the Larmor radius, ω_p the plasma frequency and Ω the cyclotron frequency. (auth)

47748 A NUMERICAL STUDY OF PARTICLE BEHAVIOUR IN NON-ADIABATIC MAGNETIC TRAPS. Dunnett, D. A. (Glasgow Univ.); Laing, E. W.; Roberts, S. J.; Robson, A. E. J. Nuclear Energy, Pt. C, 7: 359-80(July–Aug. 1965).

The behavior of charged particles in a mirror machine with a spatially-modulated central field is examined by adopting a model in which the modulation has the form of a square wave. This enables the equations of motion to be solved algebraically and particle orbits may be computed for long periods in the machine. The non-conservation of magnetic moment allows particles injected through the mirror to be temporarily trapped, and by considering that mirror reflections randomize the Larmor phase of a particle, a statistical distribution of lifetimes is obtained corresponding to the injection of a beam having a finite spread in initial parameters. Containment properties are derived for a variety of resonant and non-resonant modulation systems. (auth)

47749 HIGH REFRACTIVE INDEX AT ELECTRON CYCLOTRON HARMONICS IN A PLASMA. Furutani, Y.; Kalman, G. (Universite, Paris). J. Nuclear Energy, Pt. C, 7: 381-97(July–Aug. 1965).

A theoretical explanation for the enhanced emissions of electron cyclotron harmonics from a nonrelativistic plasma immersed in an external magnetic field, is considered. An asymptotic resolution of the general dispersion equation for the cyclotron harmonics and for quasi-perpendicular propagation is systematically studied. A quasi-longitudinal and a quasi-extraordinary mode are obtained, the refractive index of both modes being very large. The limiting condition of applicability of the solutions obtained is investigated for a small angular deviation from $\theta = \pi/2$, θ being the angle of the wave vector k with the magnetic field H_0. (auth)

47750 EXCITATION OF DRIFT INSTABILITIES IN THERMIONIC PLASMAS. Chen, F. F. (Princeton Univ., N. J.). J. Nuclear Energy, Pt. C, 7: 399-417(July-Aug. 1965). (MATT-313).

Low-frequency oscillations travelling near the electron pressure gradient drift velocity in Cs or K plasmas were observed to exist only in the presence of an ion sheath at the cathodes. It is suggested that these waves are self-exciting 'universal' instabilities in the presence of finite resistivity and that their excitation is connected with the insulating properties of an ion sheath, which allow the perturbation amplitude to be finite at the sheath edge. This leads to overstable oscillations with $\lambda_{||}$ longer than the length of the machine, a strange concept which is explained physically. Although the solution of the problem involves sheath-type boundary conditions, for an isothermal plasma the criterion for onset of instability can be stated rather simply. The predicted critical sheath voltage agrees well with observations. It appears that alkali-metal plasmas with electron sheaths are quiescent only by virtue of stabilization by conducting end-plates; however, this feature makes such plasmas particularly valuable for the study of the onset of long-wavelength drift instabilities. (auth)

47751 ELECTROLYTIC RESISTORS IN PLASMA PHYSICS RESEARCH. Bishop, A. E.; Edmonds, G. D. (Culham Lab., Abingdon, Eng.). J. Nuclear Energy, Pt. C, 7: 423-6 (July–Aug. 1965).

The electrolytic resistor offers the principal advantage of high-energy absorption with flexibility in the choice of resistor value over a very wide range. With a series of standard electrodes and tubes this range can be extended still further. The principal disadvantage is that there is a liquid to be contained. On direct current for one filling of electrolyte, the resistors have a limited though long life depending on duty. Eventually the solution gets deprived of copper ions. On pulsed or alternating current no limits were found. Three types of electrolytic resistors are shown and their resistivities given. Energy, current ratings, electrodes, and the effect of air bubbles in the solutions are also discussed. (J.F.P.)

47752 A NOTE ON HIGH-ENERGY NEUTRAL INJECTION. Luce, J. S.; Lafferty, D. L. (Aerojet-General Nucleonics, San Ramon, Calif.). J. Nuclear Energy, Pt. C, 7: 427-30(July-Aug. 1965).

Theory and experiments in controlled fusion research show that density-limiting velocity space instabilities arise from monoenergetic ions trapped in magnetic bottles. All of such instabilities appear to be caused by injection conditions which place the trapped ions in the same energy shell with the same magnetic moment and with $W_\perp/W \sim 1$. The injection of particles with many velocities and magnetic moments which could be provided by a multi-momentum neutral beam should alleviate these instabilities. Preliminary experiments are described which have produced multi-momentum neutrals simultaneously from monoenergetic generator. In the initial experiments only hydrogen and deuterium were used. When these ions are accelerated to an energy E and converted to neutrals by dissociation and charge exchange, the range of final energies is from E/5 to E, resulting in nine momentum levels. The various ions in the beam and the neutrals produced are listed; and also the final energy, velocity, and momentum of H^+ and D^+ ions resulting from injection and ionization trapping of the various neutral particles is shown. (J.F.P.)

47753 THE VLASOV EQUATION IN HIGH MAGNETIC FIELDS. Rowlands, G. (Culham Lab., Abingdon, Eng.). J. Nuclear Energy, Pt. C, 7: 430-3(July–Aug. 1965).

A well-known method for the solution of the Vlasov equation is one essentially based on expansions in inverse powers of the magnetic field. Usually this expansion was carried only to the lowest order, although higher order terms were considered in special cases. A further restriction previously made was that all terms in the Vlasov equation, except those explicitly dependent on the magnetic and perpendicular electric fields, are treated as small and also of the same order. It is shown that the results obtained with this ordering scheme include those appropriate to other schemes. The expansion procedure is carried to the next significant order in the most general case. (J.F.P.)

47754 A SPECTROSCOPIC METHOD FOR THE DETERMINATION OF ELECTRON DENSITY. Vanhauwermeiren, R. (Universite, Brussels). J. Nuclear Energy, Pt. C, 7: 433-6(July–Aug. 1965).

A method for the experimental determination of the density and the electron temperature of a hydrogen plasma from the intensity of a spectral line and of the continuous spectrum region near the line is given. This only requires relative measurements. The region of the method's application is fixed in the lower limit by the local thermal equilibrium criteria previously found and in the upper limit by the validity of a previous theory of line broadening. The method is based on the systematic use of calculated contours. An additional approximation permits the simple determination of density and temperature at the same time, using only a number obtained from the channel width. (J.F.P.)

47755 MEASUREMENT OF LOW ELECTRON DENSITY PLASMA BY THE MICROWAVE FREE SPACE METHOD. Shiobara, Shinji (Inst. of Physical and Chemical Research, Tokyo). Japan. J. Appl. Phys., 4: 513-22 (July 1965).

Electron density measurements of steady state helium plasmas in glass cylinders 17 to 96 mm in diameter are made at 34 GC and at pressures of 0.08 to 1.0 mmHg and densities of about 5×10^{10} to $10^{12} cm^{-3}$. Standard pyramidal horns of 20 db gain and teflon lenses about 75 mm in diameter are used. Errors arising from the multiple reflection between antennas and the spreading of microwave beams incident on plasmas are investigated. It is shown that over 90% reliability by Langmuir probe method criterion is attainable for low density plasmas when an appropriate use is made of the free space method. (auth)

47756 ANOMALOUS DIFFUSION AND OSCILLATIONS OF THE POSITIVE COLUMN IN A MAGNETIC FIELD. Yatsui, Kiyoshi; Inuishi, Yoshio (Osaka Univ.). Kakuyugo Kenkyu, 14: 490-509(May 1965). (In Japanese).

Relation between anomalous diffusion and oscillations of the positive column located in the longitudinal magnetic field in the range 0 to 2,200 gauss was studied to examine the theory of Kadomtsev and Nedospasov. By investigation of intensity and spectrum of oscillations in the region of anomalous diffusion, higher harmonics of high frequency oscillation of the order 1 mC/s were detected. It is concluded that the excitation of high-frequency oscillation is the essential cause of anomalous diffusion phenomenon in opposition to the theory of Kadomtsev and Nedospasov. In addition, the set-in-magnetic-field of helical instability was investigated by changing the intensity of low-frequency oscillation and it was found that the set-in-magnetic-field decreases with increasing intensity of pre-helical oscillations. It may relate to the hysteresis characteristics of E_z–B first proposed by Nakano et al. (auth)

47757 SPECTROSCOPIC MEASUREMENTS OF IMPURITIES IN THE PLASMA STREAM. I. Inoue, Kenji; Mori, Sigeru (and others) (Japan Atomic Energy Res. Inst., Tokyo). Kakuyugo Kenkyu, 14: 510-20(May 1965). (In Japanese).

The plasma stream produced by a coaxial plasma gun includes various impurity components of which copper and carbon are very serious. Emission lines from these impurities are measured by a 3.4M Fastie-Ebert type polychromator. In order to reduce copper ions, a longitudinal magnetic field is applied along the passage of the plasma stream. For example, relative intensity of Cu(II) 2247A to He(II) 4686A is reduced to 1/30 after passing through a magnetic field of 1000 gauss. Also, this relative intensity varies with operation conditions of the gun. (auth)

47758 PROBE MEASUREMENT OF ELECTRON DENSITY IN MAGNETIZED PLASMA. Miyoshi, Syoichi; Shiobara, Shinji (and others) (Inst. Phys. Chem. Res., Tokyo). Kakuyugo Kenkyu, 14: 521-35(May 1965). (In Japanese).

Electrostatic probe measurement of electron density in magnetized plasma is discussed. Experiments are made in helium at pressures ranging from 0.3 to 1.6 mm Hg with plasma electron density of 10^{11} to 10^{12}/cc and magnetic field strength of 0 to 5000 gauss. The influence of magnetic field, pressure and discharge current on the saturation electron current to cylindrical probe is investigated, for which the plasma electron density determined by the following two methods is taken as the true density: one is based on probe characteristic of ion current almost free from the effect of magnetic field, the other is with a microwave cavity devised to become free from the effect of magnetic field. Results of experiment show that the thickness of sink region around the probe perpendicular to the magnetic field is given by $V_e/(\omega_p^2 + \omega_B^2)^{1/2}$ where V_e is the thermal velocity of electron, and ω_p and ω_B are respectively the angular frequencies of electron plasma and cyclotron. Use of this region and the theory developed by Dote enables the numerical determination of electron density of magnetized plasma. The electron density calculated by using electron current characteristics of the probe with its axis parallel to the magnetic flux agrees well with the true electron density of magnetized plasma. The electron density measurement with the probe perpendicular to the magnetic line of force is also investigated. (auth)

47759 DENSITY MEASUREMENT OF PINCH PLASMA USING INFRARED He–Ne LASER INTERFEROMETER (B.S.G.-1). Miyamoto, Kenro; Fujita, Junji (and others) (Nagoya Univ., Japan). Kakuyugo Kenkyu, 14: 559-66 (May 1965). (In Japanese).

Two wavelength He–Ne gas laser interferometer is used to measure the plasma density produced by θ pinch. The laser beam passes through the plasma in the direction perpendicular to the magnetic field. The product of the plasma density and the thickness is estimated to be 3×10^{16} cm^{-2}. (auth)

47760 AN APPROACH TO CONTROLLED FUSION. Kawai, Tadashi; Kondo, Hiromichi (and others) (Mitsubishi Electric Co., Japan). Mitsubishi Denki Lab. Rept., 6: 251-60(Apr. 1965).

A brief summary is presented of the experience on the magnetic compression (θ-pinch) of the toroidal plasma column and a theoretical investigation to search for the inherently restoring force field for a charged particle. The importance of the investigations on the interactions of plasmas and the high frequency multipole field when the frequency of the field is high enough for the ions to lose their adiabaticy of the motion is discussed. (auth)

47761 SPATIALLY PERIODIC PLASMA STRUCTURES APPEARING IN FAST HEAVY-CURRENT DISCHARGES. Kvartskhava, I. F.; Kervalidze, K. N.; Gvaladze, Yu. S.; Zukakishvili, G. G. (Inst. of Physics and Tech., Sukhumi, USSR). Nucl. Fusion, 5: 181-91(Sept. 1965). (In Russian).

Recent theta- and z-pinch experiments performed to investigate the spatially periodic structure of a heavy-current plasma are discussed. A heavy-current plasma seeks to form a periodic structure whose basic elements are the E filaments (oriented along the electric field) and the H filaments (oriented perpendicular to the electric field). By means of Rogowski belts and magnetic probes the distributions of plasma currents and magnetic fields were measured. Almost all the plasma current was concentrated in the E filaments that are the elementary z

pinches, whereas relatively very small currents flowed along the H filaments. The initial magnetic field stimulated plasma breakup into filaments that were parallel to the field lines. The E- and H-filament systems had a certain stability and they affected the discharge dynamics in a definite manner. Related to them in particular was the excitation of a "tongue" plasma instability in theta pinches. A qualitative study was made of several mechanisms that are possible in forming E- and H-filament systems and are based on plasma drift motion in sheared electric and magnetic fields. (auth)

47762 TOPOLOGY OF STEADY-STATE PLASMA CONFIGURATIONS IN TRANSVERSE SELF-CONSISTENT FIELDS: SPATIAL-PERIODIC STRUCTURES. [PART] II. Komarov, N. N.; Kvartskhava, I. F.; Fadeev, V. M. (Inst. of Physics and Tech., Sukhumi, USSR). Nucl. Fusion, 5: 192-201(Sept. 1965). (In Russian).

A theoretical study is made of steady-state plasma configurations with a spatially periodic structure. The conditions for the existence of those configurations are analyzed, their concrete forms are described and compared with experimental findings. It is shown that, for given parameter values, plasmoids with a smooth and with a periodic (filament) structure can exist, that is, a diversity of configuration occurs. States with a spatially periodic structure of order n + 1 represent a system of n + 1 periodically spaced and mutually balanced self-constricted current filaments for which the equilibrium conditions of a linear pinch [3-5, 7, 10, 15-19] are individually satisfied. The energy advantage of plasma states with a spatially periodic structure over those having a smooth configuration is discussed. In strong-current discharges conditions are created that are necessary for the appearance of spatially periodic structures, that is for the formation of a system of local pinches possessing a certain symmetry of distribution. Experiments performed with linear pinches [1a, 2, 20] show that for appropriate current values a fairly stable system of E-filaments (oriented along the electric field) does indeed occur in both z pinches and theta pinches. This system is the simplest and corresponds to the theoretical results obtained. A comparison of experiment with calculation shows that they are in satisfactory qualitative agreement. For higher current values, a still more complex system of stable mutually perpendicular filaments appears; this requires a further development of theory for its elucidation. (auth)

47763 SELF-FOCUSING OF LOCAL PLASMA CURRENTS. Fadeev, V. M.; Kvartskhava, I. F.; Komarov, N. N. (Inst. of Physics and Tech., Sukhumi, USSR). Nucl. Fusion, 5: 202-9(Sept. 1965). (In Russian).

For a Boltzmann distribution function, neglecting collisions and in the presence of a longitudinal external magnetic field, the self-consistent equilibrium configuration is found for a plasma with components s; this configuration represents an infinitely extended plane layer consisting of periodically recurring quasi-filaments of current for each of which the Bennett self-focusing condition $I = 2\theta_s/q_s\beta_s$ is fulfilled. The filaments may be considered the result of the continuous topological transformation of a homogeneous plane layer having the characteristic dimension $k_{s0}^2 = 2\pi_0\Sigma(q_s^2\beta_s^2/\theta_s^2)$ since the condition indicated is fulfilled for an element of the homogeneous layer in the range $-\infty \leq x \leq \infty, -\pi/k_{s0} \leq y \leq \pi/k_{s0}$. During this transformation the characteristic dimensions, the total current and the energy of the y component of the magnetic field of the filaments remain constant. With increasing depth of the modulation, characterized by the parameter $\gamma = (\sqrt{n_{max}} - \sqrt{n_{min}})/(\sqrt{n_{max}} + \sqrt{n_{min}})$ only the energy of the x component of the magnetic field grows (proportionally to γ in the linear case). The stability of a homogeneous plane layer is examined with respect to perturbations of the type $j_s = j_s(x) \exp(\omega t + 1 ky)$, as well as the factors giving rise to filaments in high current discharge processes. (auth) (auth)

47764 LAGRANGIAN FORMULATION OF WAVE KINETICS IN A WEAKLY TURBULENT PLASMA. Suramlishvili, G. I. (Inst. of Cybernetics, Academy of Sciences, Tbilise, Georgian SSR). Nucl. Fusion, 5: 210-14(Sept. 1965). (In Russian).

Kinetic equations for plasma oscillations are derived. The method is the following: the complete Lagrangian function for a system of charged particles in an electromagnetic field is written down; the amplitude of the oscillations is defined explicitly and an expansion in powers of it is performed. As a result, a power series for the Lagrangian is obtained. The zeroth order Lagrangian gives only the equilibrium state: the first order Lagrangian vanishes identically; the second order Lagrangian contains the natural oscillations of the plasma; the higher order Lagrangians give the interactions of the natural oscillations. The distribution for oscillators in phase space is introduced and the oscillation interaction Lagrangian is written in the second quantization representation. The kinetic equation for the oscillation distribution function is then obtained by the usual method. (auth)

47765 THE EFFECT OF SHEAR ON FLUTE INSTABILITY IN A DILUTE PLASMA. Mikhailovskaya, L. V.; Mikhailovskii, A. B. (Kurchatov Inst. of Atomic Energy, Moscow). Nucl. Fusion, 5: 234-9(Sept. 1965). (In Russian).

The flute oscillation of a plasma is considered in a helical, cylindrically symmetrical magnetic field, with shear not equal to zero, at an arbitrary value of the parameter $\beta = 8\pi p/B^2$, particularly where $\beta \to 0$. Suydam's familiar stabilization criterion loses its validity if $\beta < (M_e/M_i)(k_\perp\rho)^2$ (in a low-density plasma), and that it is replaced by the criterion $\theta > 4(M_e/M_i)^{1/2}(a/R)[1 + (c/c_A)^2]^{1/2}$. The combined stabilizing action of shear and a finite ion Larmor radius makes it possible to eliminate flute instability over the whole range of densities. (A plasma without shear, on the other hand, and with a density in the range $a/R < (c/c_A)^2 \lesssim 1$ would be unstable no matter how large the Larmor radius of the ions.) (auth)

47766 FLUTE INSTABILITY OF A PLASMA WITH NONZERO ION LARMOR RADIUS AND NONZERO PRESSURE. Mikhailovskii, A. B.; Tsypin, V. S. (Kurchatov Inst. of Atomic Energy, Moscow). Nucl. Fusion, 5: 240-1 (Sept. 1965). (In Russian).

From a system of equations for description of the flute instability, it is shown that the stabilizing effect of the nonzero Larmor radius occurs not only in a zero, but also in a nonzero (finite) pressure plasma. (auth)

47767 HEATING A PLASMA BY MEANS OF MAGNETIC PUMPING. Dawson, John M.; Uman, Myron F. (Princeton Univ., N. J.). Nucl. Fusion, 5: 242-8(Sept. 1965). (MATT-294).

Two models for the heating of a cylindrical plasma by an oscillating magnetic field are presented. The model for collisional heating, applicable at low temperatures and high densities, is extended to include dissipative effects. Both linear and nonlinear numerical calculations yield heating times which agree for moderate values of the modulation index. A model for collisionless transit-time heating, applicable at high temperatures, is extended to include the self-consistent electric fields: the ions are treated by means of a Vlasov equation and the electrons are treated as a fluid in equilibrium. Inclusion of the electric fields enhances the heating rate by as much as a factor of four. Heating rates calculated from the two theories are in essential agreement when the mean free path of the ions is comparable to the length of the pumping section. (auth)

47768 CORRECTIONS TO FLUTE INSTABILITY OF AN AXIALLY-SYMMETRIC PLASMA WITH A FINITE ION LARMOR RADIUS. Mikhailovskaya, L. V.; Mikhailovskii, A. B. (Kurchatov Inst. of Atomic Energy, Moscow). Nucl. Fusion, 5: 249-50(Sept. 1965). (In Russian).

It is shown in the case of a large ion Larmor radius that the first mode of flute perturbations is unstable (for arbitrary distributions of the pressure and density of the plasma). (auth)

47769 DOPPLER-BROADENED SPECTRAL LINES FROM A THETA PINCH. Bogen, P.; Schlueter, J. (Kernforschungsanlage, Juelich, Ger.). Nucl. Fusion, 5: 251-2 (Sept. 1965).

The profile of a Doppler-broadened spectral line emitted from impurity ions in a high-temperature hydrogen plasma was measured. By observation in the axial and radial directions the distribution of the respective velocity components are obtained. The profile of the Cu 2270.6 Å spectral line is shown, and the results are summarized. (L.B.S.)

47770 INTERACTION BETWEEN A RADIO WAVE AND A PLASMA. Krishan, S. (Univ. of Delhi). Nuovo Cimento (10), 36: 896-904(Apr. 1, 1965).

The interaction between a wave and a warm plasma is studied by making use of Langevin's equation. Collisions between electrons and heavy ions and the electric field caused by the group displacement are taken into account. The propagation of a radio wave in the plasma is investigated. The relation between the current density and the oscillating electric field is obtained. In the limit of the electric field caused by displacement of charges approaching zero, the results become as those obtained by Margenau. The effect of variable collision frequency is also included in the theory. (auth)

47771 ELECTROMAGNETIC PROPERTIES OF A QUANTIZED RELATIVISTIC ELECTRON-POSITRON GAS. Steinert, L. A. (Univ. of Lund, Sweden). Nuovo Cimento (10), 36: 935-53(Apr. 1, 1965).

A description of linearized electromagnetic wave propagation and oscillations in a relativistic electron-positron gas is given. Special emphasis is placed on the long wavelength region. The behavior of the relativistic gas is shown to contrast sharply with its nonrelativistic counterpart with respect to the existence of collisionless damping effects. (auth)

47772 SPECTROSCOPIC INVESTIGATIONS OF A HIGH-FREQUENCY DISCHARGE IN HELIUM. Bochkova, O. P.; Razumovskaya, L. P. Opt. Spectry. (USSR) (English Transl.), 18: 438-41(May 1965).

Cylindrical discharge tubes made from molybdenum glass were used to measure a high-frequency discharge in helium. The luminescence was excited with a VG-2 generator operating at a constant frequency of 6 Mc. The power of the generator was 150 W, and the range of pressures investigated was 0.1 to 7 mm Hg. The excited atom concentration was determined by reabsorption and emission methods. The two-probe method was used to measure electron concentrations and temperatures. Data concerning the population of the first excited levels of helium were obtained by the reabsorption method applied to the strongest lines with the highest transition probabilities. Concentrations of excited helium atoms are given as a function of pressure and as a function of the diameter of the discharge tube. Concentrations of atoms in various excited states are also given as a function of the quantum number n. The concentrations of excited atoms for each level were calculated separately, assuming a Maxwellian distribution of electron velocities and using the measured electron temperatures and electron concentrations for the 12 mm diameter tube. (J.F.P.)

47773 SPECTRAL DETERMINATION OF THE ELECTRON TEMPERATURE OF CESIUM PLASMA IN A THERMOELECTRIC DIODE. Morgulis, N. D.; Babich, I. L.; Ayadyun, Yu. A.; Kovalenko, V. P. Opt. Spectry. (USSR) (English Transl.), 18: 527-8(May 1965).

The problem of determining the plasma electron temperature is explored with two spectroscopic methods: the distribution of intensity in the continuous recombination spectrum and in the line emission spectrum. The object of the investigation was a short thermoelectric diode containing cesium vapor without the positive anode voltage applied. Between the tube containing the plasma and the spectroscopic device there was located a synchronous rotating vane whose speed was so adjusted that the radiation could pass only during the no-current half-period of the rectified alternating current heating the cathode. For negative anode voltages the voltage-current characteristic of the diode is shown. In the second part of the investigation, a spectrometer with a DFS-4 grating and photographic and photoelectric recording was used. The observed emission spectra of the cesium plasma under short-circuited conditions in the range 4200-6300 Å is similar to the usual arc discharge in cesium vapor. It is found that both the probe method, reported previously, and these two spectroscopic methods yield the same values of the electron temperature. (J.F.P.)

47774 RADIATION FROM A CURRENT FILAMENT IN AN ANISOTROPIC PLASMA. Ohba, Yujiro; Ikezaki, Kazuo (Keio Univ., Japan). Oyo Butsuri, 34: 486-92 (July 1965). (In Japanese).

The radiation field from a current filament is calculated. The filament is located in a homogeneous, unbounded plasma medium under an impressed magnetic field and carries travelling electric or magnetic current. The usual formula of the dielectric tensor of the plasma is used, where the temperature effect is neglected and the constancy of the collision frequency is assumed. There exist two sets of wave modes to be excited. The field from the current filament is made up by superposition of these two sets of wave modes in both cases of electric and magnetic current filaments. The approximate formulae for the attenuation length are obtained in several cases. (auth)

47775 CLASSICAL THEORY OF THE PAIR DISTRIBUTION FUNCTION OF PLASMAS. DeWitt, Hugh E. (Univ. of California, Livermore). Phys. Rev., 140: A466-70 (Oct. 18, 1965). (UCRL-14175).

The diagrammatic method used by Abe to obtain the Helmholtz free energy of the classical electron gas is used to derive the pair distribution function beyond the Debye-Hückel result. The calculation can be done systematically either in configuration space or wave-number space and is carried out exactly to $O(\Lambda^2)$ where $\Lambda = \frac{1}{4}\pi\rho\lambda_D^3$ is the classical plasma parameter. It is shown that $g(r)$ has the form $g(r) = e^{-\beta u_s}[1 + g_0^0(r) + g_0^2(r)]$, where $u_s = (e^2/r)\exp(-r/\lambda_D)$ is the Debye screened potential, and g_0^0 and g_0^2 are functions of r/λ_D which are evaluated analytically to $O(\Lambda^2)$. For the region $\beta e^2 < r < \lambda_D$ the correction in brackets multiplying the Boltzmann factor $\exp(-\beta u_s)$ is less than 1. A surprising result is that for $r >> \lambda_D$ the linear Debye-Hückel theory does not correctly describe the disappearance of particle correlations, and instead the correction function g_0^0 dominates. As $r \to \infty$ it is found that $g(r) - 1 \sim \frac{1}{8}(\ln 3)\,\Lambda^2 \exp(-r/\lambda_D)$. (auth)

47776 MICROWAVE SCATTERING DUE TO ACOUSTIC-ION-PLASMA-WAVE INSTABILITY. Arunasalam, V.; Brown, Sanborn C. (Massachusetts Inst. of Tech., Cambridge). Phys. Rev., 140: A471-9(Oct. 18, 1965).

An analysis is presented of an experimental study of microwave scattering from nonequilibrium plasmas in which the electrons had a large steady drift velocity v_d with respect to the ions. According to theory, such plasmas must support relatively undamped acoustic-ion-plasma waves due to a two-stream instability type of mechanism. Measurements of the frequency-power spectrum of the scattered signal show agreement with theory. In particular, as predicted, the measured scattering cross sections were large in comparison with the Thomson cross section. The effects of collisions predicted by theory did not show up in the experimental results. As expected from theoretical considerations of nonlinear effects (such as the nonlinear coupling between the plasma modes of different wave numbers), the relative drift velocity and the electron-ion temperature ratio tend toward a saturation value as the plasma current is increased. The experimental results indicate that the nonlinear effects are relatively weak. (auth)

47777 LASER-INDUCED PERTURBATION IN A PLASMA. Paik, S. F.; Ben-Dov, O. (Northwestern Univ., Ev-

anston, Ill.). Proc. IEEE (Inst. Elec. Electron. Engrs.), 53: 1145-6(Aug. 1965).

Experimental observations of Thomson scattering of optical radiation from a laser by free electrons in a plasma found a gross variation of the probe potential indicating a large perturbation of the plasma by the laser beam. The experimental arrangement is shown. A d-c discharge plasma containing helium at approximately 100 micron pressure is irradiated by a laser beam from a ruby in an elliptical cavity. The effect of the incident beam is observed by measuring the change in the floating potential of the probe. The variation of this potential is shown. It is observed to increase slowly for the duration of the laser pulse, which seems to indicate an integrating effect. Two unusual discontinuities are noted in the decaying portion of the wave form which are independent of the external circuit effect. The potential at two probes were measured with identical results. Whatever the cause of the disturbance, the perturbation caused by the ruby laser is large enough to affect the result of Thomson scattering experiments appreciably. (J.F.P.)

47778 OSCILLATION OF THE RF-EXCITED POSITIVE COLUMN IN A LONGITUDINAL MAGNETIC FIELD. Nagao, Shigeo; Sugita, Keiichiro (and others) (Nagoya Univ., Japan). Technol. Rept. Tohoku Univ., 29: 87-93 (Dec. 1964).

The experimental results that are obtained using r-f electric field (1 Mc/s) parallel to the discharge tube axis in a longitudinal magnetic field are in agreement with the helical instability model proposed by Kadomtsev et al. In the plasma which is r-f excited but with a small amount of d-c current (4 mA), the oscillation, whose rotating direction and frequency (several 10 kc/s) are the same as those of d-c discharges, is observed at the magnetic field corresponding to the critical one in d-c charges, and is found not to be magnetohydrodynamic wave. On the other hand, there is no onset of oscillation with r-f field only. Such phenomena are ascribed to the existence of d-c current. (auth)

47779 PRELIMINARY OPERATION OF THE THERMONUCLEAR FUSION ASSEMBLY OF SCALLOPED TORUS TYPE. Matsuda, Nisaku (Tokyo Shibaura Electric Co., Ltd.). Toshiba Rev., 18: 1315-19(Nov. 1963). (In Japanese).

The configuration of the assembly is unique scalloped U-bent sections with an internal axial magnetic field successively connected to form a weaved torus. The equilibrium conditions of tenuous plasmas in the configuration were investigated. The dipole charge separation can be eliminated by the scalloping in the radial direction and the remnant quadrupole by the scalloping in the axial direction of the torus. Moreover, the higher-order poles can be neutralized by making the torus figure 8-shaped by changing the orders of connection of each arc section. The vessel of torus is fabricated with glass tubes of 7.5 cm in diameter and 1,524.8 cm in axial length. Solenoids wound around the vessel can be energized by the 35,000-kv amp short-circuit generator. Upon application of the electric field, the plasma current reaches about 800 amp at the confining field which is 6,000 gauss at its maximum. Spectroscopic data of helium spectrum lines were obtained by means of photomultiplier systems. The light generation, up to 80 μsec after the disappearance of accelerating field, indicated effective plasma confinement by the magnetic field. Electron temperatures of 12 to 16 ev, from the relative intensities of corresponding singlet and triplet lines in the spectrum, and the ion temperature of 2 ev, from Doppler line widths, were measured. (auth)

47780 STABILIZATION OF A POWERFUL PENNING DISCHARGE BY A MAGNETIC FIELD INCREASING ALONG THE RADIUS. Dubovoi, L. V.; Popov, P. G. Zh. Eksperim. i Teor. Fiz., 49: 27-30(July 1965). (In Russian).

A study is made of the effect of a magnetic field increasing along the radius and produced by a system of six rods with currents moving in opposite directions in each neighboring pair on development of instabilities in a powerful penning discharge with cold cathodes. It is shown that when the stabilizing system is turned off, the discharge is completely ionized and is strongly unstable. The discharge oscillations range from 10^4 to 3.10^7 c/s. The level of the oscillations connected with instability of the discharge is lowered by at least two orders of magnitude when the stabilization system is turned on. The electron temperature in the discharge strongly drops in this case, the plasma density remaining constant. It is concluded that the high values of T_e in penning discharges are related to the turbulent character of the processes in the discharge. (auth)

47781 INVESTIGATION OF A SPARK DISCHARGE IN AIR PRODUCED BY FOCUSSING THE RADIATION FROM A LASER. [PART] II. Mandel'shtam, S. L.; Pashinin, P. P.; Prokhorov, A. M.; Raizer, Yu. P.; Sukhodrev, N. K. (Lebedev Inst. of Physics, Moscow). Zh. Eksperim. i Teor. Fiz., 49: 127-34(July 1965). (In Russian).

Results are presented of an experimental investigation of the initial stage of a discharge in air induced by focusing the radiation from a laser. The plasma temperature produced in the region of the focus is determined on basis of the spectrum of recombination radiation in the soft-x ray range, $\lambda \approx 10$Å and is found to be $T_e = 50 \div 60$ ev. A study of the laser radiation scattered on the plasma indicated that the ionization front moves towards the focusing lens. The velocity of the front, $v \approx 10^7$ cm/sec is measured on basis of the Doppler shift of the scattered light. A hydrodynamic mechanism of broadening of the ionization region is considered. Values for the velocity of the detonation wave front and the plasma temperature behind the plasma estimated on basis of this mechanism are in satisfactory agreement with those found experimentally. (auth)

47782 THEORY OF TRANSVERSE DIFFUSION AND STATIC AND HIGH FREQUENCY CONDUCTIVITY OF A PLASMA IN A STRONG MAGNETIC FIELD. Silin, V. P.; Shister, A. R. (Lebedev Inst. of Physics, Moscow). Zh. Eksperim. i Teor. Fiz., 49: 193-209(July 1965). (In Russian).

It is shown that in a completely ionized plasma with an electron temperature T_e which considerably exceeds the ion temperature T_i, the effective collision frequency of the particles is proportional to $T_e^{-3/2}T_i^{-1}$. The effect of Coulomb interaction between the particles on the time they spend in the region of action of the forces is taken into account. Weak nonlinear effects of removal of the particles from the interaction region as a result of electric drift are detected. (auth)

47783 RUN-AWAY ELECTRONS IN A NONEQUILIBRIUM PLASMA. Gurevich, A. V.; Zhivlyuk, Yu. N. (Commission of Spectroscopy, Academy of Sciences, USSR). Zh. Eksperim. i Teor. Fiz., 49: 214-24(July 1965). (In Russian).

A solution is found for the kinetic equation for electrons in a plasma in a stationary electric field. Interaction between the electrons and nonequilibrium oscillations of the plasma are taken into account. The flux of run-away electrons and the magnitude of the critical field are determined. (auth)

47784 ON EFFECTS DUE TO INTERACTION OF PLASMONS. Kovrizhnykh, L. (Lebedev Inst. of Physics, Moscow). Zh. Eksperim. i Teor. Fiz., 49: 237-47(July 1965). (In Russian).

Explicit expressions are derived for the probabilities of four-plasmon decays of longitudinal waves with a random phase in the plasma. Some particular cases are considered. Qualitative analysis of the effects of four-plasmon decays is carried out for longitudinal waves and it is shown that they result in a broadening of the noise spectrum. (auth)

47785 ON THE FLUCTUATIONS IN A MAGNETIZED PLASMA THAT IS NOT IN EQUILIBRIUM. Sitenko, A. G.; Radzievskii, V. N. (Inst. of Physics, Kiev). Zh. Tekhn. Fiz., 35: 1165-76(July 1965). (In Russian).

The electric field and current fluctuations in a uniform rarefied plasma in a uniform magnetic field are discussed.

The plasma is assumed to be in a quasi-equilibrium state in which the ion and electron velocity distributions are different and non-Maxwellian, so that the fluctuation-dissipation theorem is not applicable. The electron and ion fluctuations are first treated as independent and their coupling through the action of the self-consistent field is subsequently taken into account. Collisions between the ions and electrons are neglected throughout. The general equations derived for the current and field fluctuations are rewritten for the specific case of a plasma that is traversed by a neutral beam of charged particles moving parallel to the applied magnetic field. Simple approximate expressions are derived for those fluctuations of this system that are associated with Langmuir waves and with magnetic sound. The interaction of different kinds of waves with the fluctuations is discussed. There is possible not only incoherent scattering but also a quasicoherent scattering with frequency change, associated with Langmuir and Alfven waves and with magnetic sound. It is also possible for waves of one kind to give rise to waves of another kind by interaction with the fluctuations. Equations describing these processes are derived. The interaction of a moving charged particle with the fluctuations of a (not necessarily magnetized) plasma is discussed. When the velocity of the particle is less than the thermal velocities in the plasma the fluctuations accelerate the particle. A more rapidly moving particle loses energy to the fluctuations, and these energy losses can become anomalously large under certain circumstances, which are discussed in some detail. (ATD)

47786 ON THE INTERACTION OF CIRCULAR WAVES IN A COLD PLASMA. Giorgadze, N. P. (Inst. of Physics, Academy of Sciences, Georgian SSR). Zh. Tekhn. Fiz., 35: 1177-81(July 1965). (In Russian).

The interactions of circular waves in a cylindrical waveguide with a perfectly conducting wall filled with a cold plasma are discussed. By a circular wave is understood a disturbance that propagates only in the azimuthal direction. The calculations were undertaken to complete the picture of wave process development in plasma waveguides which was previously developed. The plasma is treated in the hydrodynamic self-consistent field approximation. The equations for circular waves are solved first in the linear approximation and then in the succeeding approximation, so that nonlinear effects are treated in the first order in which they appear. Waves in which the plasma density is constant and those in which the density participates in the oscillation are treated separately. It is found that in the latter case a disturbance, which in the linear approximation would have a single definite frequency, can give rise not only to higher frequency components (overtones), but also, under certain circumstances, to lower frequency components. (ATD)

47787 DIFFUSION THEORY OF A BEAM PLASMA. Levitskii, S. M.; Shashurin, I. P. (Kiev State Univ.). Zh. Tekhn. Fiz., 35: 1182-8(July 1965). (In Russian).

The stable behavior of a beam plasma produced by an electron beam traversing a gas parallel to an applied magnetic field is treated. The theory of J. E. Hopson (J. Appl. Phys. 34:(8) 2425(1963)) is regarded as unsatisfactory because Hopson assumed that the plasma ions could diffuse freely in the axial direction (whereas the plasma diffusion is ambipolar in all directions), and because he employed the diffusion equation at pressures below which its use is justified. Hopson's conclusion that there is a limiting pressure below which a beam plasma cannot be formed is regarded as erroneous and the agreement between his experimental results and his theory as fortuitous. A theory of the stable beam plasma is developed on the assumptions that the electron beam is uniform, that the secondary electrons do not ionize, and that charged particles leave a volume element only by ambipolar diffusion (i.e., that recombination is negligible). The diffusion equations are solved for the two limiting cases that the diffusion is overwhelmingly radial (high pressure and weak magnetic field) or axial (low pressure and strong magnetic field), and the solution for the intermediate case is discussed briefly. The theoretical results are compared with experimentally measured densities of the plasmas produced by a 3-3 mm diameter 4 mamp beam of 900 ev electrons traversing a 33 to 35 cm long 1 cm diameter glass tube containing hydrogen at pressures up to 0.08 mm Hg. The electron density in the plasma was determined by observing the resonant frequency shift of a cavity resonator through which passed a portion of the tube. (ATD)

47788 HIGH-PRESSURE ELECTRODELESS DISCHARGE. Mitin, R. V.; Pryadkin, K. K. Zh. Tekhn. Fiz., 35: 1205-9(July 1965). (In Russian).

High-frequency electrodeless discharge was investigated in argon and krypton at pressures from 10^4 to 10^6 n/m^2. The discharge took place in a 3-cm-diameter, 25-cm-long quartz tube surrounded in its upper third by a coaxial winding for introducing radio frequency power and in its lower third by the field winding of an electric motor by means of which the gas could be caused to rotate at 400 rad/sec. The r-f power was provided by a nominal 1.5-kw, 10-Mc/sec push-pull oscillator. The discharge was initiated as a glow discharge at low pressure, and the pressure was gradually increased. As the pressure increased the discharge pulled away from the walls, brightened, and changed color. At about atmospheric pressure the discharge took the form of a bright, nearly spherical plasmoid perhaps 2 cm in diameter. Further increase of pressure led to an increase in the size and brightness of the plasmoid. Stable discharges were obtained at pressures up to 10^6 n/m^2 in argon and to 6×10^5 n/m^2 in krypton. The r-f power absorbed by the 10^6 n/m^2 argon discharge was only about 600 w. Provision was made to set the gas into rotation in order to increase the stability of the discharge, but the discharge was found to be less stable when the gas was rotating than when it was not. The stability of the discharge was found to depend strongly on the axial symmetry of the exciting winding and the discharge chamber, and the position of the winding with respect to the flat top of the chamber. The total radiation from the plasma was measured with a thermopile and its spectrum was examined from 0.2 to 2.5 μ. The plasma appeared to be very similar to that of a high pressure arc. The radiation loss from the 10^6 n/m^2 argon plasma was 30% of the absorbed r-f power and the luminous efficiency of this radiation was 40 lumen/w. From these data the temperature of the plasma was calculated to be 9000°K and its ionization to be between 0.1 and 1%. (ATD)

47789 PULSE HEATING OF A HIGH-PRESSURE ARGON ARC. [PART] I. Mitin, R. V.; Knyazev, Yu. R.; Petrenko, V. I.; Borovik, E. S. Zh. Tekhn. Fiz., 35: 1210-17(July 1965). (In Russian).

Previous investigations of high pressure argon arcs are continued and experiments are reported in which a 4500 μ microfarad capacitor charged to 3 kv or less was discharged through the low voltage arc. The low voltage arcs up to 16 cm long burned between tungsten electrodes in argon at pressures from 5×10^5 to 8×10^6 N/cm^2. The arcs were stabilized by rotation of the gas; the rotation was effected either by rotating vanes within the chamber or by tangential injection of the gas. The arc chamber was provided with two 2 cm diameter observation ports, through which the arc was photographed, the luminous intensity was measured, the spectrum (from 250 to 650 mμ) was recorded, and streak photographs showing the time variation of the arc diameter were made. The current through the arc, the voltage across it, and the luminous flux were displayed on an oscilloscope. It is concluded that by pulsing a long stable high pressure arc with millisecond current pulses having amplitudes of tens of kiloamperes, rather large volumes of highly ionized dense plasma in a quasistationary state can be produced. (L.B.S.)

47790 PULSE HEATING OF A HIGH-PRESSURE ARGON ARC. [PART] II. Mitin, R. V.; Knyazev, Yu. R.; Petrenko, V. I.; Borovik, E. S. Zh. Tekhn. Fiz., 35: 1218-24(July 1965). (In Russian).

Experimental data are reported on high pressure pulsed argon arcs. The properties of the arcs at different pressures and of different lengths when pulsed with pulses of different amplitudes were compared at their respective points of maximum current where they were in equilibrium. At fixed pressure and current the voltage across the arc

was a linear function of its length. The constant electric field in the arc column derived from this relation was found to be approximately proportional to $I^{\frac{1}{2}}P^{\frac{1}{4}}$, where I is the current and P is the pressure. When P was 4×10^4 N/cm^{-2} and I was 40 kamp, the electric field was 60 v/cm. The luminance of the pulsed arc was found to be proportional to the power dissipated per unit length, and the proportionality constant (1.3×10^4 nit cm/w) was the same as for low voltage arcs. The luminance of the brightest arcs (carrying 40 kamp) was about 4×10^{10} nit; this corresponds to a black body surface temperature of 12000°K. The conductivity of the arc column was derived from the electric field strength and the current by assuming the column diameter to be approximately 1 cm. The conductivity of the 40 kA 4×10^6 N/cm^2 arc was approximately 275 mho/cm. From this was derived a charged particle density of 10^{19} cm^{-3} and a temperature of 30,000°K. The temperature of the arc plasma was also derived from the energy balance equation with the two limiting assumptions of transparency and radiative heat transport; the limiting temperatures derived in this way were 25,000 and 70,000°K. (ATD)

47791 THE TRANSITION MECHANISM OF A CORONA DISCHARGE INTO A SPARK DISCHARGE IN LONG AIR GAPS. Aleksandrov, G. N. (Leningrad Polytechnic Inst.). Zh. Tekhn. Fiz., 35: 1225-9(July 1965). (In Russian).

The formation of a spark channel in long air gaps with a sharply inhomogeneous field was investigated. Such formations are preceded by "avalanche" and "streamer" corona discharges. In both cases the ionization is accomplished by the electron avalanches. Both forms of corona discharge require the presence of a region of high-intensity field (of the order of 30 kv/cm and stronger). Corona discharge is a cold discharge, while the channel of the spark discharge is highly heated. Thus, a thermal ionization occurs which determines the high conductivity of the channel. The transition from corona to spark discharge is therefore conditioned by the air heating up to a temperature sufficient for thermal ionization of the gas. A phenomenological picture of a discharge in a long gap is given. (L.B.S.)

47792 ON THE ENERGY DISSIPATED IN A HIGH-CURRENT VACUUM DISCHARGE. Osadin, B. A. Zh. Tekhn. Fiz., 35: 1230-5(July 1965). (In Russian).

An investigation was made of the vacuum (10^{-5} mm Hg) discharge of a 180 microfarad capacitor charged to 3 kv or less between a 25 mm inner diameter cylindrical copper electrode and 8 mm diameter rods of lead, tin, zinc, aluminum, copper, steel, and tungsten. The investigation was undertaken because of interest in the behavior of cylindrical plasma guns. The two electrodes were coaxial and their ends were coplanar with the end of a 16 and 19 mm inner and outer diameter insulating quartz tube. The inductance of the external circuit was 4×10^{-8} henry and the maximum current reached 160 kamp. The inner electrode was always the anode during the first half period. The current in the discharge (measured with a Rogovskiy band and an integrating circuit), the voltage across it, and the luminous intensity were observed with an oscilloscope. The plasma emitted in the discharge was observed and the speed of the plasma bursts were measured by means of high-speed streak photography. The energy evolved in the discharge was measured with a specially constructed calorimeter. It was found that 54% of the energy stored in the capacitor was transferred to the electrode erosion products (plasma, unionized vapor, and metal droplets). The most rapid plasma bursts (6×10^6 cm/sec for the aluminum electrode) were emitted in the very early stage of the discharge long before the current had reached its maximum. This is ascribed to the presence in the later stages of the discharge of a much greater mass of eroded electrode material to be accelerated. A very brief discussion of the efficiencies of plasma guns is given. (ATD)

47793 INVESTIGATION OF A TITANIUM PLASMA SOURCE. Andryukhina, E. D.; Shpigel', I. S. (Lebedev Inst. of Physics, Moscow). Zh. Tekhn. Fiz., 35: 1242-9 (July 1965). (In Russian).

The operation under different conditions of a titanium plasma source of the type described by F. H. Coensgen, W. F. Cummings, and A. E. Sherman (Phys. Fluids, 2(4): 350(1959)) was investigated in order to determine how to improve the purity of the hydrogen plasma obtainable from it. The source contained a 50 mm stack of 20 titanium disks 19 mm in diameter which were outgassed and saturated with hydrogen. A 1.6 microfarad capacitor charged to 10 kv or less was discharged through the stack. The period of the discharge circuit was 3.9 microsec. The plasma was analyzed with a time of flight mass spectrometer provided with an electrostatic gate so that the plasma could be sampled at different parts of the cycle, and with a large (10 cm diameter) three-electrode probe. It was found that the hydrogen content of the plasma jet increased with decreasing duration of the current pulse. The energy of the hydrogen ions was considerably greater than that of the impurity ions, and the transverse velocity of the hydrogen ions was an order of magnitude less than that of the impurity ions. There results, accordingly, a self-purification of the plasma as it travels from the source. There were two peaks in the energy distribution of the hydrogen ions; at 25 cm from the source the high energy group contained 30% of the total number of protons produced by the source. (ATD)

47794 CONCERNING THE RADIAL DISTRIBUTION OF ELECTRIC CONDUCTIVITY IN AN IONIZED GAS JET. Pavlov, S. M.; Shevchenko, S. A. (State Inst. of Applied Chemistry, USSR). Zh. Tekhn. Fiz., 35: 1262-4(July 1965). (In Russian).

The effect of the radial distribution of the electric conductivity of a cylinder of ionized gas on the effective conductivity is discussed as measured by the loading effect of the ionized gas on a resonant circuit. The effective conductivity measured in this way is a weighted average of the true conductivity, the weight being proportional to the square of the local electric field strength. It is assumed that the measurements are made in such a way that the electric field strength is proportional to the radius (the distance from the axis of the ionized gas cylinder). The radial distribution of the conductivity is related to that of the temperature by a known equation for a weakly ionized gas, and the effective conductivities of ionized gas cylinders with different assumed temperature distributions were calculated. Some of these rather simple computations were (successfully) checked by electrolytic tank measurements. It is concluded that the effective conductivity as measured in the assumed manner is more characteristic of the cooler outer portions of the jet than of the hot inner (axial) region. (ATD)

47795 ON THE INVESTIGATION BY UHF METHODS OF THE MOTION OF A PLASMA IN A RADIATION ACCELERATOR. Gekker, I. R.; Luk'yanchikov, G. S. Zh. Tekhn. Fiz., 35: 1323-7(July 1965). (In Russian).

The motion of the plasma in a radiation accelerator was investigated by observing the reflection from the plasma of the accelerating microwaves. The plasmas, containing 10^{15} to 10^{16} ions of which approximately half were H^+ ions, were produced by a spark source on the axis of a stainless steel waveguide of circular section and 1 mm wall thickness and were accelerated by H_{01} waves in the 10 cm region. The uhf oscillator was operated on 9 microsec pulses. The output was taken as H_{10} waves in a rectangular waveguide; these waves passed through a ferrite gate and a King type $H_{10} - H_{01}$ converter, and entered the accelerator waveguide through a vacuum window. A longitudinal magnetic field was provided in the accelerating waveguide, but it was not always employed. Probe measurements at the end of the accelerating waveguide showed that approximately 10^{12} ions were accelerated to energies of several kev. The microwaves reflected by the plasma were recorded with two probes located in the rectangular waveguide preceding the wave converter, at different known distances from it. The use of two probes made it possible to derive both the reflection coefficient and the phase difference (at a fixed location) between the incident and reflected waves. The phase difference was found to remain nearly constant during the full 9 microsec duration of the microwave pulse.

From this it is concluded that the main mass of the plasma remained practically stationary; this is in agreement with the probe measurements, which indicated the acceleration of only a small fraction of the plasma ions. The reflection coefficient increased rapidly, reached a maximum of some 80 or 90% at from 1 to 6 microsec from the beginning of the pulse, then fell to a deep minimum, and finally increased again. It is suggested that this behavior may be due to a temporary matching of the waveguide section as a result of the changing size of the plasma. (ATD)

47796 CONCERNING THE FORMATION OF CLUMPS IN PULSED PLASMA ACCELERATORS. Osadin, B. A. Zh. Tekhn. Fiz., 35: 1327-9(July 1965). (In Russian).

Longitudinal time resolution streak photographs of the plasma issuing from a coaxial plasma gun show a banded structure which has had different interpretations. I. F. Kvartskhava, R. D. Meladze, and K. V. Suladze ascribe the bands to the successive ejection of separate plasma clumps or plasmoids, whereas Yu. V. Skvortsov, V. S. Komel'kov and S. S. Tserevitinov regard the bands as due to the helical structure of a continuously emitted plasma. The transverse streak photographs and high-speed motion picture records were made of vacuum (10^{-5} mm Hg) sparks between coaxial cylindrical electrodes of different metals and between plane electrodes. The outer diameter of the inner electrode and the inner diameter of the outer electrode were either 8 and 25 mm, respectively, or 4 and 14 mm, respectively. The outer electrode was of copper and the inner of lead, tin, zinc, aluminum, copper, steel, or tungsten. The plane electrodes were of brass; they were 2 cm in diameter and were separated by an undisclosed distance. The sparks were produced by discharge of a 180 microfarad capacitor charged to 3 kv, or a 1.4 microfarad capacitor charged to 30 kv. The inner electrode was always the anode during the first half-cycle. All the longitudinal streak photographs (including those made with plane electrodes) showed the familiar banded structure, the details of which varied with the electrode material. Since it seems unlikely that plane electrodes could give rise to a helical plasma, it is concluded that the bands are due to successively ejected plasmoids. This conclusion is confirmed by the transverse streak photographs. The formation of separate plasmoids is ascribed to the discontinuous vaporization of the electrode material. Electrode vapor is important also when the spark occurs in the presence of gas, for the gas would be expelled from the discharge region during the initial stages of the spark. (ATD)

47797 ON THE POLARIZATION OF A PLASMA MOVING IN A CURVED MAGNETIC FIELD. Voitsenya, V. S.; Gorbanyuk, A. G.; Onishchenko, I. N.; Shkoda, V. V.; Safronov, B. G. Zh. Tekhn. Fiz., 35: 1330-2(July 1965). (In Russian).

Probe measurements were previously made of the electric fields in plasma (from a conical plasma gun) which were moving in a uniform magnetic field (ZhTF, 34: 847 (1964)) and it was shown that there is present a "radial" electric field directed toward the axis of the plasma. Similar measurements are reported on plasmas moving in a toroidal magnetic field. In both groups of experiments the plasmas were produced by a conical plasma gun, passed through 2-cm diameter openings in two grounded plane electrodes, and drifted in a 6-cm diameter glass tube. The drift tube was bent into a 50 cm radius circle, thus forming a torus. Electric potentials were measured along the two principal diameters of the drift tube, i.e., parallel to the axis and to the large radius of the torus, respectively. When the radial field that was previously found to arise in a plasma moving in a uniform magnetic field was subtracted, the residual electric field was found to be in qualitative agreement with the polarization field expected theoretically in a plasma moving in a curved magnetic field. In a 600 Oe magnetic field the residual polarization field was 8 v/cm in the direction of the torus axis and 6 v/cm in the direction of the large radius. This latter value is several times larger than that calculated by N. A. Khizhnyak. This discrepancy can be due either to a less efficient short circuiting of the polarization field than was assumed in the theoretical derivation, or to the presence in the experimental plasmas of significant quantities of heavy ions. (ATD)

47798 THE CYLINDRICAL MAGNETOHYDRODYNAMIC WAVES IN PLASMA (thesis). Seto, Yeb Jo, Austin, Tex., Univ. of Texas, 1964. 155p.

The presence of static magnetic fields in plasma volumes results in a dyadic electrical conductivity. Propagation of electromagnetic waves in such magnetoactive plasma is described by a dyadic-vector helmholtz equation. Separability of the dyadic-vector Helmholtz equation was studied to facilitate fitting of boundary conditions. It was found that four coordinate systems, namely, rectangular, circular cylindrical, elliptical cylindrical, and parabolic cylindrical, permit separation of the dyadic-vector Helmholtz equation into terms of longitudinal and transverse vector components. A dispersion relation appropriate for the boundary condition is obtained through separation. The longitudinal and the transverse vectors are generated by differential vector operation on scalar functions, each of which satisfies a scalar Helmholtz equation and its boundary conditions. Solutions so obtained are expressed in terms of complete sets of eigenfunctions. When current sources are presented in the bounded magneto-plasma volume, the waves excited by these sources are obtainable through a Green's dyadic. The conditions that the Green's dyadic must satisfy were determined. The Green's dyadic is generated from three orthogonal vector components derivable from the longitudinal and the transverse vector operations on a scalar Green's function. The formulation developed is applied to analyze the radially propagating waves in a bounded magnetoactive plasma slab. A macroscopical analysis of the plasma medium is effected. The results enable numerical computation of the dispersion relation for some arbitrarily chosen values of plasma medium parameters. Waves excited by each of three different sources of various configurations and spatial current distribution in the bounded magnetoplasma are qualitatively analyzed. The three types of sources considered are the line source with constant spatial current distribution, the line source with spatial sinusoidal current distribution, and the loop source with constant spatial current distribution. (A.G.W.)

47799 TRANSPORT PROPERTIES OF AN ELECTRON GAS IN A MAGNETIC FIELD (thesis). Dworin, Lowell. New York, Columbia Univ., 1964. 334p.

The Luttinger-Ward propagator formalism is used to obtain the transport coefficients from the Kubo expression for a system of independent electrons interacting with a set of fixed, but randomly located, impurity centers in the usual thermodynamic limit $Ne \to \infty$, $Ni \to \infty$, $\Omega \to \infty$ in such a way that both the electron density $n_e = (Ne/\Omega)$ and the impurity density $n_i = (Ni/\Omega)$ remain finite. Both the weak field case, in which the magnetic field is assumed to be weak enough that the magnetic energy is small compared to the chemical potential, and the strong field case, in which the magnetic field is assumed to be large compared to the density of impurities, are considered. (A.G.W.)

47800 TWO PROBLEMS IN THE KINETIC THEORY OF PLASMAS: PROPAGATION OF A TEST PARTICLE IN A PLASMA AND THE SPECTRUM OF ELECTRON-DENSITY FLUCTUATIONS FOR A NON-MAXWELLIAN ELECTRON GAS (thesis). Perkins, Francis William Jr. Ithaca, N. Y., Cornell Univ., 1964. 175p.

Let a test particle of arbitrary mass, charge, and velocity be introduced at a specific point in a uniform plasma otherwise in thermal equilibrium. The possible trajectories of this test particle are described by a distribution function that spreads out in velocity and coordinate space as time increases. A convergent kinetic equation for the distribution function was obtained by dividing the correlations that result from the interaction between the test particle and the plasma particles into a long-range part and a short-range part. For short ranges the correlations are given by binary collision theory, whereas for long ranges an expansion in powers of the interaction energy similar to the Debye-Huckel theory is appropriate. The

errors introduced by the division of the correlations and by assuming a kinetic form for the distribution function equation were estimated. Explicit expressions for the energy loss and dynamical friction were obtained. In the second problem the spectrum of electron density fluctuations for a non-Maxwellian electron gas was studied for frequencies near the electron plasma frequency. The effect of electron-ion collisions was included by using a model of the plasma that describes the electrons by the Vlasov equation and assumes the ions are discrete, infinitely massive, and stationary particles. All terms except the logarithmically dominant ones were neglected. The resulting spectrum shows that electron plasma waves are excited not only by fast particles but also by random collisions and that the damping of plasma waves is caused both by Landau damping and by collisional damping. In an important special case where the Landau damping is greater than the collisional damping and the electron velocity distribution is flatter than a Maxwellian near the phase velocity of the plasma wave, the magnitude of the electron density fluctuations near the plasma frequency can be much greater than in the thermal equilibrium case. (Dissertation Abstr.)

47801 RECOMBINATION RATES AND NON-EQUILIBRIUM ELECTRICAL CONDUCTIVITY IN A SEEDED PLASMA. Cool, T. A.; Zukoski, E. E. (California Inst. of Tech., Pasadena). pp 122-34 of Sixth Symposium on Engineering Aspects of Magnetohydrodynamics. Phillipsburg, N. J., American Institute of Aeronautics and Astronautics, 1965.

Experimentally determined values of electric conductivity and electron temperature have been measured in a non-equilibrium seeded plasma. These results are in good agreement over a wide range of parameters with values calculated from a two-temperature model of the plasma. There is no doubt that the two-temperature model is valid over a wide range of gas temperatures, seed concentrations, and current densities for the argon-potassium and helium-potassium plasmas. However, the model does not give an accurate description of the plasma when the current density is below about 0.4 amp/cm^2; in this range the omission of the influence of atom-atom excitation and the influence of non-equilibrium excited state populations may explain the discripancy between experiment and theory. The electron-electron-ion collisional recombination rate for potassium has been measured in the argon-potassium system. The range of electron temperatures investigated was between 1900° and 3000°K with electron densities between 3×10^{13} and 4×10^{14}/cm^3. The measured values show a scatter of 60 per cent about theoretical values calculated from present recombination-rate theory employing the Gryzinski classical collision cross sections. (auth)

47802 PLASMA PHYSICS. Lectures Presented at the Seminar on Plasma Physics Organized by and Held at the International Centre for Theoretical Physics, Trieste, from 5–13 October 1964. (International Atomic Energy Agency, Vienna). June 1965. 654p. (STI/PUB/89; CONF-641008). IAEA $13.00; S 273,-; £ 3.18.0; F.Fr. 52,-; DM 45,50 cy.

The conference included 34 complete papers and one paper, "Magnetohydrodynamics and Shock Waves," which was mentioned only by title. Separate abstracts were prepared for 32 papers. Two of the papers previously appeared in NSA as 19: 17145 and 45383. (J.F.P.)

For abstracts of individual papers see: 47150, 47288, 47484, 47485, and 47805–47830.

47803 INTRODUCTION TO PLASMA PHYSICS. Thompson, W. B. (Oxford Univ.). pp 7-20 of STI/PUB/89.

The general properties of plasma are reviewed. A definition of plasma is given, and its range of application is summarized both in the ionosphere and universe, and in its technological applications. The basic properties and methods of investigation are given including its electric properties, conductivity, the Langmuir probe, and high frequency response. The production of plasma and magnetized plasma are also mathematically described. (J.F.P.)

47804 MACROSCOPIC THEORY OF PLASMA WAVES. Trehan, S. K. (Univ. of Delhi). pp 21-46 of STI/PUB/89.

The simplest case of electron oscillations in a uniform plasma is first considered neglecting in the first instance the thermal motions of the particles. The ions are assumed to form a uniform fluid providing the neutralizing background for the electron fluid in equilibrium. Experimental evidence is then given for plasma oscillations; and the effect of thermal motions is considered. Finite temperature effects of the plasma on electron oscillations is described assuming that the electrons form a charged fluid obeying the basic hydrodynamic equations. The discussion of ion oscillations is restricted to the case of longitudinal oscillations. The complex behavior of a plasma in an external magnetic field is also considered. Hydromagnetic waves are studied by considering the plasma to be a hydromagnetic fluid characterized by a finite pressure, viscosity, and conductivity. The effect of thermal conductivity, and hydromagnetic waves from the Chew, Goldberger, and Low theory are also discussed. (J.F.P.)

47805 MAGNETOHYDRODYNAMICS. Jukes, J. D. (United Kingdom Atomic Energy Authority, Abingdon, Eng.). pp 47-63 of STI/PUB/89.

Some basic electromagnetic concepts are revised; dimensional analysis is derived in a simple physical way; and finally, basic MHD equations are given, in various approximations, with the boundary conditions. Certain solutions of the equations which are relevant to laboratory plasma physics are considered, such as the equilibrium and dynamics of highly conducting plasma in magnetic fields from an elementary point of view. MHD wave propagation and high speed flows are also considered. These include phenomena in which small perturbations are propagated according to linearized approximate theories and also phenomena in which finite amplitude, quasi discontinuities, occur. (J.F.P.)

47806 ELEMENTARY ORBIT AND DRIFT THEORY. Kruskal, M. (Princeton Univ., N. J.). pp 67-90 of STI/PUB/89.

The general equations of classical plasma are given from which the Vlasov equations are obtained. Single particle motion is discussed with constant uniform fields and with slightly varying fields. Motion of lines of magnetic force is considered with the proof of line preservation and proof of flux preservation presented. The motion of particles with lines of force is also discussed. (J.F.P.)

47807 ADVANCED THEORY OF GYRATING PARTICLES. Kruskal, M. (Princeton Univ., N. J.). pp 91-102 of STI/PUB/89.

The nonrelativistic motion of a charged test particle is considered in the guiding center approximation. This applies when the motion of the particle may be treated approximately as a gyration (having uniform circular motion) orthogonal to the magnetic field, of small radius but finite velocity, hence large frequency, superimposed on the finite velocity motion of a guiding center. The electromagnetic fields at the position of the particle change only a little during one gyration period. (J.F.P.)

47808 DERIVATION OF MACROSCOPIC EQUATIONS. Oberman, C. (International Centre for Theoretical Physics, Trieste, Italy). pp 103-13 of STI/PUB/89.

Since it is a problem of prohibitive difficulty to follow the detailed motion of all the particles interacting with their self-created and/or externally imposed electromagnetic fields, the behavior of the plasma system must be described in some average or statistical sense. It is often desirable to use a hydrodynamic description in terms of mean number density, mean-velocity, pressure, etc., modified to include electromagnetic effects. Thus insight into the plasma behavior and a large body of qualitative results may be obtained. A totally ionized plasma is assumed to consist of electrons and positive ions, of one species. The generalization to more complex systems

with ions in various stages of ionization is made in a straightforward manner as long as the internal dynamics of an ion is negligible. (J.F.P.)

47809 EQUILIBRIUM OF A MAGNETICALLY CONFINED PLASMA IN A TOROID. Kruskal, M. (Princeton Univ., N. J.). pp 115-36 of STI/PUB/89.

A variety of properties possessed by solutions of the magnetostatic equations, describing a static equilibrium of plasma, are derived; and additional conditions are established which together with the magnetostatic equations, and the boundary conditions, determine a unique solution for these equations. An experiment is imagined in which an ideal viscous hydromagnetic fluid exhibits a damped motion until coming to rest in an equilibrium configuration. A number of invariants with respect to any such motion is described. These lead to constraints on the admissible trial states in a variational principle suggested by the experiment. The quantity varied is the potential energy, the sum of the magnetic and the internal fluid energies. The variational principle provides a potentially powerful tool for providing the existence of solutions of the magnetostatic equations and for obtaining them numerically; it also characterizes the solutions by their invariant values. Equations governing a steady state of magnetic field and slowly diffusing plasma are introduced. The system of equations obtained is expected to have a solution which is unique, and this is verified. (J.F.P.)

47810 HYDROMAGNETIC STABILITY THEORY. Oberman, C. (International Centre for Theoretical Physics, Trieste, Italy). pp 137-62 of STI/PUB/89.

Ideal hydromagnetics is studied. The stability of those hydrodynamic equilibria in which the mass flow vanishes is considered; then a small motion about an equilibrium state is followed. The double adiabatic theory and the adiabatic particle theory are also discussed. (J.F.P.)

47811 LINEAR OSCILLATIONS OF A COLLISIONLESS PLASMA. Simon, A. (General Atomic Div., General Dynamics Corp., San Diego, Calif.). pp 163-95 of STI/PUB/89.

The approximate derivation of the Vlasov equation is given. It is noted that because of the long range nature of the Coulomb force, the assumption of binary collisions is inadequate. Also the collision terms are considerably smaller than the streaming terms. Linear oscillations are discussed, and some examples of Vlasov instabilities are given. (J.F.P.)

47812 BINARY PROCESSES IN PLASMA. Thompson, W. B. (Oxford Univ.). pp 197-206 of STI/PUB/89.

Certain fundamental processes in plasma require a knowledge of the effects of particle collisions. To establish a plasma, electron bombardment of a neutral gas is usually used to ionize it. Once a plasma is formed collisions between electrons and ions lead to an equipartition of energy, while collisions with ions, especially with partially stripped ions, lead to energy radiation. Finally, when a plasma decays it usually does so by the recombination of ions and electrons. Topics discussed are inelastic collisions between electrons and atoms, inelastic collisions between ions and atoms, and elastic collisions between charged particles. (J.F.P.)

47813 THE TRANSPORT EQUATION FOR A PLASMA. Thompson, W. B. (Oxford Univ.). pp 207-29 of STI/PUB/89.

The discussion of the transport equation for a plasma covers the following topics, transport equations, test particles and particle correlation in plasma, Landau's form for the collision integral, the Fokker-Planck equation, and calculation of the spectrum. The dominant approximation, and correlation functions and scattering of radiation from a plasma are also considered. (J.F.P.)

47814 HIGH-FREQUENCY CONDUCTIVITY AND THE EMISSION AND ABSORPTION COEFFICIENTS OF A FULLY IONIZED PLASMA. Oberman, C. (International Centre for Theoretical Physics, Trieste, Italy). pp 231-9 of STI/PUB/89.

The frequency dependence of the resistivity, and the associated processes of absorption and emission of radiation is investigated by means of a simple model. The validity of this simple treatment in a large part rests upon the fact that the electron motion is inertia dominated, or in other words, to the lowest approximation the current response to the driving electric field is mainly reactive. Collective effects are properly included. Most previous results have not treated the collective aspects consistently and so are incorrect particularly near the plasma frequency. The validity of this model is borne out by an exact treatment. (J.F.P.)

47815 CYCLOTRON RADIATION. Drummond, W. E. (General Atomic Div., General Dynamics Corp., San Diego, Calif.). pp 241-50 of STI/PUB/89.

It is found that the only way a thermonuclear reactor can produce more energy than is lost by cyclotron radiation is for the reactor to be big enough so that most of the cyclotron radiation is absorbed within the plasma; that is, the plasma must be at least as thick as the mean free path for the absorption of the cyclotron radiation. Thus the essential result that is to be obtained is the critical size of a reactor which is the size at which the cyclotron radiation loss is just balanced by the thermonuclear energy production. It is found that for frequencies large compared to the plasma frequency the electrons radiate as though they were in a vacuum, as was previously assumed. Although the total radiation loss is found to be very strongly dependent on the magnetic field, there is often a critical field which must not be exceeded if stability is to be maintained. (J.F.P.)

47816 INTRODUCTION TO CONTROLLED THERMONUCLEAR RESEARCH. Thompson, W. B. (Oxford Univ.). pp 259-71 of STI/PUB/89.

The advantages of thermonuclear reactions are presented, and some of the requirements for a thermonuclear reactor are discussed in a simple, approximate, semiquantitative way. The discussion includes energetic considerations, and the geometry of magnetic confinement. In the latter the magnetostatic approximation, low β systems, and stability are considered. (J.F.P.)

47817 EXPERIMENTS ON PLASMA. Francis, G. (United Kingdom Atomic Energy Authority, Abingdon, Eng.). pp 273-85 of STI/PUB/89.

Methods of measurement are given for total currents, local current density, electric field, and electron density and temperature in plasma. Probes in a magnetic field are discussed with their range, use, and construction. Measurements on moving plasma and experiments on magnetic wells are described. (J.F.P.)

47818 PLASMA DIAGNOSTICS BASED ON REFRACTIVITY. Ascoli-Bartoli, U. (EURATOM-CNEN, Rome). pp 287-321 of STI/PUB/89.

The discussion of the use of a light beam to diagnose a discharge in a plasma is limited to the refractivity, and this implies that the spatial density distribution of plasma, and hence the refractive index, does not undergo abrupt variations within distances of many light wavelengths. The refractivity of plasma is discussed, and a review of methods and techniques in refractivity diagnosis is given, with some limits to these methods. Interferometric measurements, the Schlieren method, and the shadowgraph methods of diagnosis are considered. (J.F.P.)

47819 TOROIDAL MAGNETIC FIELD CONFIGURATIONS AND FINITE RESISTIVITY. Furth, H. P. (Univ. of California, Livermore). pp 391-409 of STI/PUB/89.

The confinement of low-β plasma in closed vacuum-magnetic-field configurations, is discussed with particular reference to the finite-resistivity hydromagnetic stability problem. Shear stabilization and maximum $\int dl/B$ stabilization is described. Some $\int dl/B$-stable configurations are given including periodic multiple stagnation-point and floating-ring solutions. The $\int dl/B$ stability in the presence of shear and finite resistivity is also discussed. (J.F.P.)

47820 EXPERIMENTS IN TOROIDAL PLASMA CONFINEMENT. Furth, H. P. (Univ. of California, Livermore). pp 411-20 of STI/PUB/89.

The nature of the stability problem is stated and illustrated, and a probable direction of experimental progress indicated. The principal problem in the experimental study of stable toroidal confinement is the difficulty of reliable diagnosis, in the sense of the inability to interpret cooperative phenomena reliably and to prove points about the basic feasibility of the theoretical configurational stabilization techniques. Much progress is made in understanding and eliminating the gross hydromagnetic instabilities that occur when confinement is based to a considerable extent on the self-field of plasma currents. But if toroidal confinement experiments are to attain a level of clarity and significance similar to that which the open-ended experiments have achieved, it seems probable that similar advantages must be built into future toroidal apparatus. The stability problem and hard-core configurations are discussed. (J.F.P.)

47821 MIRROR TRAPS. Ioffe, M. S. (Kurchatov Atomic Energy Inst., Moscow). pp 421-48 of STI/PUB/89.

Magnetic mirror configurations are considered. The basic physical principle is that charged particles placed in a longitudinal axially-symmetric magnetic field bounded at both ends by sections with a stronger field, can be reflected from these sections of stronger field when moving along the lines of force. Stronger field regions are therefore called magnetic mirrors. The reflection from mirrors is connected with the adiabatic invariance of the charged particles' magnetic moment. General information is given on mirror traps. Other topics discussed include plasma instabilities in mirror traps, methods of injecting high-temperature plasma into traps, the hybrid magnetic field experiments, hybrid trap with minimum H, the study of plasma stability in the PR5 device, and plasma lifetime measurements. (J.F.P.)

47822 PLASMA CONFINEMENT IN MAGNETIC WELLS. Taylor, J. B. (United Kingdom Atomic Energy Authority, Abingdon, Eng.). pp 449-81 of STI/PUB/89.

The problem of confinement and stability of plasma in a special type of magnetic field is considered. Fields of this type are variously known as magnetic wells, hybrid traps, or minimum-B fields. They are of special interest because they combine the adiabatic containment properties of the simple mirror field with the stability of the cusp field. The stability of the cusp is related to the fact that its field strength decreases as the center is approached, so that the class of fields considered are those which have the basic feature that there is a region in which the field is nowhere zero, so that adiabatic containment is possible, and the magnetic field strength increases outward. Topics discussed are special equilibria, general equilibria, and stability at finite pressure. (J.F.P.)

47823 MICROINSTABILITIES. Rosenbluth, M. N. (General Atomic Div., General Dynamics Corp., San Diego, Calif.; Univ. of California, San Diego). pp 485-513 of STI/PUB/89.

Linear stability of a confined equilibrium is discussed. It is not known for certain whether any confined plasma can be made linearly stable against all possible microinstabilities. General considerations are given. Other included topics are loss-cone instability, dispersion relation for microinstabilities of inhomogeneous plasma, and special cases of microinstabilities of homogeneous plasmas. Microinstability calculations, even in their linear phase, are based on very highly idealized models and simplifications so that considerably more work is required to apply the results with confidence to inhomogeneous laboratory plasmas. (J.F.P.)

47824 PLASMA STABILITY. Vuillemin, M. (EURATOM-CEA, Fontenay-aux-Roses, France). pp 515-25 of STI/PUB/89.

Conservative systems are considered for which the linearized equations of the perturbed motion can be written in the compact form $H(\omega)\xi = 0$, in which ξ is a set of perturbed variables and H is an operator depending on the equilibrium quantitites and function of ω as a parameter. Two main topics are considered. They are problems in plasma stability and instabilities of a plane current sheet. (J.F.P.)

47825 QUASI-LINEAR THEORY OF PLASMA TURBULENCE. Drummond, W. E. (General Atomic Div., General Dynamics Corp., San Diego). pp 527-41 of STI/PUB/89.

The dynamics of a low-β, collisionless, unstable plasma are examined from the time of onset of the instability to the final quiescent equilibrium state. The time development of this process is roughly broken into four phases. During the first phase the linearized theory applies and the unstable waves grow exponentially. In the second phase the quasi-linear theory applies and the background particle distribution diffuses in such a way as to bring the growth rate of the unstable waves to zero, leaving a quasi-stationary spectrum of waves. In the third phase the waves in the quasi-stationary spectrum interact in such a way, called resonant mode coupling, as to distort the spectrum but to keep the energy in the spectrum roughly constant. In the fourth phase the waves interact to produce virtual waves which in turn lose energy to the bulk of the particles by Landau damping. The nonlinear Landau damping produces a slow decay of the wave energy and a slow heating of the plasma, together with diffusion of the plasma across the magnetic field until all of the wave energy is given up to the particles and the plasma is in a quiescent, stable state. (J.F.P.)

47826 PLASMA TURBULENCE. Kadomtsev, B. B. (Inst. of Nuclear Energy, Moscow). pp 543-54 of STI/PUB/89.

It is known that under experimental conditions plasma often shows a chaotic motion. Such motion, when many degrees of freedom are excited to levels considerably above the thermal level, is called turbulent. The appearance of various anomalies in plasma behavior indicates the presence of turbulence. In order to verify directly the presence of turbulent motion in plasma, the fluctuation of some microscopic parameters must be measured. A precise theory exists at present only for the weak turbulence of plasma, when perturbation methods can be used. A short survey of this theory is given and the strong turbulence is discussed. (J.F.P.)

47827 LANDAU DAMPING AND FINITE RESISTIVITY INSTABILITY IN PLASMAS. Sagdeev, R. Z. (Inst. of Nuclear Physics, Novosibirsk, USSR). pp 555-66 of STI/PUB/89.

Anomalous damping in collision-free plasmas of finite amplitude disturbances and, in particular, of shock waves are discussed. Topics included are Landau damping and finite amplitude waves, and the connection between finite resistivity instability (precise theory) and Bohm diffusion (speculations). (J.F.P.)

47828 SHOCK WAVES IN COLLISION FREE PLASMAS. Petschek, H. E. (Avco-Everett Research Lab., Everett, Mass.). pp 567-76 of STI/PUB/89.

In a plasma with a mean free path large compared to the gyroradius, shock waves have thicknesses less than a mean free path. In this case, the mechanisms by which the directed flow energy ahead of the shock is converted to random energy behind the shock are more complex. Some of the mechanisms by which this dissipation can occur are discussed. This treatment includes hydraulic analogy, plasma wave trains, turbulent plasma shocks, and experiments. (J F.P.)

47829 ADVANCED KINETIC THEORY. Balescu, R. (Universite Libre, Brussels). pp 577-94 of STI/PUB/89.

A simple model of a plasma consisting of N particles of charge e, mass m, enclosed in a cubic box of volume Ω, the average density being $C = N/\Omega$. The total charge is neutralized by a continuous background of opposite charge, which otherwise plays no role in the dynamics. An outline of the general theory is given. Non-Markoffian kinetic

equation for plasmas and the dielectric constant and the theory of Brownian motion are discussed. (J.F.P.)

47830 ASYMPTOTIC METHODS IN THE HYDRODYNAMIC THEORY OF STABILITY. Sagdeev, R. Z. (Inst. of Nuclear Physics, Novosibirsk, USSR). pp 625-43 of STI/PUB/89.

It is shown that there is a simple asymptotic approach to the analysis of the equation: $\alpha\beta^2\phi^{IV} - \beta U_2(x,k,\omega)\phi'' + U_1(x,k,\omega)\phi = 0$. This equation models the problems of U becoming infinite at some point in the region considered. A statement of the problem is given, and the weak and strong cases are considered. Some characteristic features of a plasma instability in the field of gravity are also discussed. (J.F.P.)

47831 PRODUCTION OF A HOT PLASMA BY DISCHARGE IN A STRONGLY INHOMOGENEOUS MAGNETIC FIELD. Angerth, B.; Ehrensvaerd, J.; Persson, H. (Royal Inst. of Tech., Stockholm). Vienna, International Atomic Energy Agency, 1965, Preprint No. CN-21/5, 17p. (CONF-650935-4). ORINS.

From 2nd IAEA Conference on Plasma Physics and Controlled Nuclear Fusion Research, Culham, Eng.

If, in an inhomogeneous magnetic field, ions and electrons have different angular distributions, they will have different ability to penetrate deeply into the strong parts of the magnetic field. Hence quasi-neutrality cannot be maintained without a parallel electric field. The theory of a plasma in an inhomogeneous magnetic field shows that a considerable electric field parallel to the magnetic field may be produced if the velocity distributions are anisotropic. The electric field necessary to maintain quasi-neutrality is given in a few typical cases. The loss region in velocity space is described. It should be possible to produce a plasma with a very high ion energy by a discharge in an inhomogeneous magnetic field. Therefore, a Penning discharge in a magnetic mirror field has been studied. Two cathodes are placed at the points of maximum B. Between them there is a ring-shaped anode. The mirror ratio (γ) is high, between 30 and 60. Measurements with $\gamma \approx 1$ are made for comparison. The pressure is 10^{-4} to 10^{-3} torr. Hydrogen and deuterium are used. With γ high, the burning voltage is high during 1 to 2 msec after ignition. Up to 14 kv burning voltage has been measured with an applied voltage of 17 kv. The current is a few amperes. After 1 to 2 msec the voltage suddenly breaks down to a low value (0.3 to 3 kv). With γ low, the burning voltage always drops down to a low value immediately after ignition. Measurements of the heating of a cathode show that at the high-voltage mode the ions impinging upon it have an energy corresponding to a substantial fraction of the burning voltage. A lower estimate of the density is obtained from the measured electric current. There is some indication that near the cathode a plasma is produced with a density of 10^{10} to 10^{11}/cm^3 and an ion energy of the order of 10 kev. (auth)

47832 ION HEATING IN THE MODEL C STELLARATOR. Yoshikawa S.; Sinclair, R. M.; Rothman, M. A. (Princeton Univ., N. J.). Vienna, International Atomic Energy Agency, 1965, Preprint No. CN-21/121, 22p. (CONF-650935-42). ORINS.

From 2nd IAEA Conference on Plasma Physics and Controlled Nuclear Fusion Research, Culham, Eng.

Ion cyclotron resonance heating (ICRH) is applied to the C stellarator plasma previously formed by ohmic heating. Slow Alfvén waves are generated by a Stix coil with r-f power up to several hundred kilowatts. The waves are damped in regions of reduced field (magnetic beaches) where the local ion cyclotron frequency equals the fixed 25-Mc generator frequency. Nonresonant plasma loading, presumably caused by electrostatic coupling between the plasma and the Stix coil, and the associated impurity influx were enormously reduced by employing a Faraday shield. Wave generation was confirmed by r-f magnetic probes and by the variation of Stix coil loading and of plasma heating with magnetic field. The temperature of ions confined by the magnetic mirrors of the "local beaches" reached 2 to 3 kev at 5×10^{12} cm^{-3} density. The electron conductivity temperature rose, due to ICRH, above the ohmic heating value of 15 ev typically to about 50 ev. Electrons are apparently heated directly by the waves as well as by the hot ions. With small ohmic heating currents, diamagnetic pressure decay times after ICRH exceeds 1 msec and can be attributed to ion-electron cooling and ion-ion scattering from the mirrors. Neutron production typically shows 500-μsec decay times. Heating is also observed at higher harmonics and subharmonics, the latter being attributable to H_2^+. In this same fashion deuterons ($\sim 10^{12}$ cm^{-3}) mixed with protons can be preferentially heated to 10 kev. With the "long beach" configuration, ion temperatures up to 200 ev were attained almost uniformly around the stellarator with 1 to 2 msec confinement times, indicating evidently that pumpout may not be sensitive to ion temperature. (auth)

47833 ENERGY DISTRIBUTION OF PARTICLES LEAVING A θ-PINCH. Bingham, R. L.; Goldman, L. M.; Kilb, R. W. (General Electric Research Lab., Schenectady, N. Y.). Vienna, International Atomic Energy Agency, 1965, Preprint No. CN-21/87, 15p. (CONF-650935-10). ORINS.

From 2nd IAEA Conference on Plasma Physics and Controlled Nuclear Fusion Research, Culham, Eng.

Ion energies in θ-pinches are determined by measuring the energy distribution of the ions escaping through the mirror. An electrostatic analyzer, a 127° focusing type, is used. The contribution of fast ions other than deuterium was checked by using a magnetic momentum analyzer following the energy analyzer. No measurable quantity of contaminant was found. Measurements are made both with and without reversed trapped field. The most significant result of the experiment is the broadness of energy distribution suggesting a plasma in which the bulk of the particles are heated, rather than a select few in a far tail. In the zero trapped field cases, both the mean energy and the dispersion of the distribution increased with time up to peak field time. For reversed field cases the heating occurred at a much earlier part of the cycle with the peak of the mean energy occurring well before peak field. The peak energy was 25 per cent greater than for the zero trapped field case. To determine the velocity distribution inside the plasma, an assumption must be made about the energy dependence of the loss. If it is assumed the losses are dominated by coulomb collisions, then the mean energy of the ions in the plasma is about 5 kev for a peak field of 44 kG. (auth)

47834 PLASMA FLOW IN A THETA-PINCH. Wesson, J. A. (United Kingdom Atomic Energy Authority, Abingdon, Eng.). Vienna, International Atomic Energy Agency, 1965, Preprint No. CN-21/43, 21p. (CONF-650935-41). ORINS.

From 2nd IAEA Conference on Plasma Physics and Controlled Nuclear Fusion Research, Culham, Eng.

In the absence of instabilities the loss of plasma in a theta-pinch is almost wholly due to flow along the magnetic field to the ends of the coil. Thus in order to understand the containment of the plasma it is necessary to study the transient axial flow of the plasma. This is done by setting up a simple model of the plasma in which the problem is reduced to that of studying a one-dimensional flow. (auth)

47835 PLASMA STABILITY IN A MAGNETIC MIRROR MACHINE WITH STABILIZING RODS. Trubnikov, B. A. (Kurchatov Inst. of Atomic Energy, Moscow). Vienna, International Atomic Energy Agency, 1965, Preprint No. CN-21/125, 21p. (In Russian). (CONF-650935-40). ORINS.

From 2nd IAEA Conference on Plasma Physics and Controlled Nuclear Fusion Research, Culham, Eng.

A stability criterion is generalized for the general case of axially asymmetric fields. This criterion is applied to plasma stability in a magnetic mirror machine with stabilizing rods. Systems with 4 and 6 stabilizing rods are discussed in detail. The calculated results for the 6-rod system agree with experiments. In addition to infinite

rods, stabilizing rods are considered of finite length, which can be realized with multipole magnets of finite length. Stabilization can be achieved even in the extreme case of very short rods, where they can be regarded as a system of magnetic point dipoles located in the central plane of the magnetic mirror machine, and directed along the radius. (auth)

47836 CHARACTERISTICS OF THE BEAM-PLASMA DISCHARGE. Smullin, L. D.; Getty, W. D. (Massachusetts Inst. of Tech., Cambridge). Vienna, International Atomic Energy Agency, 1965, Preprint No. CN-21/122, 20p. (CONF-650935-38). ORINS.

From 2nd IAEA Conference on Plasma Physics and Controlled Nuclear Fusion Research, Culham, Eng.

The electron-beam/plasma interaction is studied. When an electron beam passes through a plasma, it excites oscillations at the plasma frequency. These microwave oscillations sustain a microwave discharge, and we have named the entire process the "beam-plasma discharge." Ionization of the ambient gas is carried on by energetic plasma electrons that have been accelerated by the oscillatory fields. The result is the production of a hot-electron plasma inside the magnetic mirror. Results are discussed on plasma stability; density, average energy, and peak energy of the plasma electrons; and ion heating. (auth)

47837 ENERGETIC NEUTRAL INJECTION INTO AN ELECTRON-CYCLOTRON PLASMA. Dandl, R. A.; Ard, W. B.; Becker, M. C.; Eason, H. O.; England, A. C.; Haas, G. M.; Lazar, N. H. (Oak Ridge National Lab., Tenn.). Vienna, International Atomic Energy Agency, 1965, Preprint No. CN-21/101, 11p. (CONF-650935-5). ORINS.

From 2nd IAEA Conference on Plasma Physics and Controlled Nuclear Fusion Research, Culham, Eng.

A beam of twenty-kev hydrogen atoms has been directed through an electron-cyclotron plasma (ECP) contained in a magnetic mirror. The observed density is more than a factor of ten greater than that obtainable from neutral gas trapping under comparable conditions. The measured currents of charge-exchanged 20-kev protons and the decay of these currents are in experimental agreement with the calculated neutral density inside the ECP. The experiments were performed with a large volume (50 liter) ECP in order to ascertain the effectiveness of plasma shielding against thermal neutral gas. The extension of this work to higher densities of hot ions by the employment of much denser ECP and the effect of such critical parameters as thermal neutral reflux and energetic beam current are discussed. The density, power, and stability bounds on mm wavelength ECP's currently under investigation are also described. (auth)

47838 COLLISIONAL AND ANOMALOUS DIFFUSION. Eldridge, O. C.; Harris, E. G. (Univ. of Tennessee, Knoxville). Vienna, International Atomic Energy Agency, 1965, Preprint No. CN-21/108, 22p. (CONF-650935-16). ORINS.

From 2nd IAEA Conference on Plasma Physics and Controlled Nuclear Fusion Research, Culham, Eng.

The diffusion coefficients for the transport of a plasma across a magnetic field are calculated directly from the motion of test particles. The method is sufficiently general to describe anomalous diffusion as well as collisional diffusion. A consistent perturbation theory is developed for calculating particle orbits, in which secular terms are eliminated. These secular terms (quantities that increase linearly with time) appear when conventional perturbation theory is applied to the orbits, and invalidate the basis of the theory. (auth)

47839 INTERACTION BETWEEN AND CAPTURE OF PLASMOIDS IN A MAGNETIC MIRROR MACHINE DUE TO COLLECTIVE PROCESSES IN A PLASMA. Galeev, A. A.; Iskoldskii, A. M.; Lukyanov, V. I.; Nesterikhin, Yu. E.; Ponomarenko, A. G. (Inst. of Nuclear Physics, Novosibirsk, USSR). Vienna, International Atomic Energy Agency, 1965, Preprint No. CN-21/215, 39p. (In Russian). (CONF-650935-21). ORINS.

From 2nd IAEA Conference on Plasma Physics and Controlled Nuclear Fusion Research, Culham, Eng.

The injection into a magnetic mirror machine of hot plasmoids, the collective interactions between which may be used to provide a capture mechanism, is studied. A theoretical evaluation of the relative importance of different types of instability in the given conditions shows that capture occurs as a result of the development of a "hose-type" magnetohydrodynamic instability of the two colliding plasmoids. By varying the experimental conditions the qualitative picture of the theoretically predicted capture mechanism is confirmed. One of the principal problems is that of measuring the magnetic field pulsations. Possible particle acceleration mechanisms in a turbulent plasma are discussed on the basis of the experimental data. The experiment is carried out using deuterium or hydrogen plasma. (auth)

47840 STABILITY OF NON-UNIFORM PLASMA IN A MAGNETIC FIELD GRADIENT. Jukes, J. D. (United Kingdom Atomic Energy Authority, Abingdon, Eng.). Vienna, International Atomic Energy Agency, 1965, Preprint No. CN-21/39, 20p. (CONF-650935-25). ORINS.

From 2nd IAEA Conference on Plasma Physics and Controlled Nuclear Fusion Research, Culham, Eng.

Both shear Alfven waves and electro-acoustic waves become strongly distorted at very low frequencies in a low pressure plasma having a density gradient and confined by a strong magnetic field. These waves can become unstable (either hydrodynamically, or because of resonance with electrons moving along field lines) when finite ion orbit size is taken into account. The effect of a gradient in the magnetic field, which may form a magnetic well, is studied. Distributions of ion velocities in velocity space are considered that approximate the situation in an ion injection mirror machine where the mean ion energy much exceeds T_e. In this case the magnetic well has a pronounced stabilizing effect on the above waves. For the inhomogeneous plasma, weakly unstable to electron resonance, a nonlinear limiting effect is considered and the resultant diffusion coefficient estimated. (auth)

47841 CONTAINMENT OF A HIGH-TEMPERATURE PLASMA OBTAINED BY TURBULENT HEATING IN A TRAP OF COMPOSITE TYPE. Simonov, V. A.; Abozovik, V. V.; Ignat'ev, V. V. (Kurchatov Inst. of Atomic Energy, Moscow). Vienna, International Atomic Energy Agency, 1965, Preprint No. CN-21/167, 27p. (In Russian). (CONF-650935-37). ORINS.

From 2nd IAEA Conference on Plasma Physics and Controlled Nuclear Fusion Research, Culham, Eng.

A method is investigated of obtaining a plasma with ion and electron temperatures of several kev by fast internal injection from a turbulent plasma jet, and of containing the plasma in mirror and composite type traps with absorbing walls of the vacuum vessel. The method of producing the plasma and the containment vacuum conditions are chosen with a view to using the plasma so obtained for the capture, with small losses, of externally-injected fast particles and for the production of a hot plasma under steady-state conditions. (auth)

47842 DYNAMIC STABILIZATION OF A PLASMA COLUMN. Orlinskii, D. V.; Osovets, S. M.; Sinitsyn, V. I. (Kurchatov Inst. of Atomic Energy, Moscow). Vienna, International Atomic Energy Agency, 1965, Preprint No. CN-21/136, 19p. (In Russian). (CONF-650935-34). ORINS.

From 2nd IAEA Conference on Plasma Physics and Controlled Nuclear Fusion Research, Culham, Eng.

An investigation is performed with a view to checking experimentally the principle of dynamic stabilization. The investigation bore on a plasma column with a current stabilized by high-frequency magnetic fields of various configurations. The experiments were carried out in two directions. In the first experiment the stabilizing circuit was fed from a high-frequency tube generator, and in the second from a damped capacitor-bank discharge. Comparison of the discharge photographs with the curves showing the

density distribution of the quasi-constant current and the high-frequency magnetic field, and also comparison of the discharge in the high-frequency field with a discharge in the stationary field of the same configuration, and with a discharge without an external field, point to the stabilizing effect of the high-frequency field. It was ascertained that the hydrodynamic instabilities appearing in the pinch, revealed as deformations in the bending and the twisting, do not appear if the stabilizing field is supplied at a certain moment of the development of the main discharge, just before instability begins to develop. Satisfactory agreement with the theory of the method is observed in both cycles of the investigations performed, though only on the assumption that the instabilities which appear are those with the maximum possible wavelength, and that shorter-wave perturbations do not appear. (auth)

47843 HIGH DENSITY DEUTERIUM PLASMA. Mather, J. W. (Los Alamos Scientific Lab., N. Mex.). Vienna, International Atomic Energy Agency, 1965, Preprint No. CN-21/80, 23p. (CONF-650935-32). ORINS.

From 2nd IAEA Conference on Plasma Physics and Controlled Nuclear Fusion Research, Culham, Eng.

Dense plasma foci are formed beyond the end of the inner electrode of a coaxial electrode discharge as a result of a strong pinch effect (z pinch). The plasma has the following properties: an electron temperature of ~2 to 5 kev; plasma volume of 1 to 5 mm^3; duration of ~0.2 to 0.3 μsec; and neutron yields $\sim 5 \times 10^{10}$/burst. Neutron production scales almost linearly with energy up to ~36 kJ (neutron yields $\sim 10^{11}$); the larger energies require initial gas pressures up to ~6 torr. (auth)

47844 ELECTROMAGNETIC INSTABILITY OF COLLISIONLESS PLASMA. Laval, G.; Pellat, R.; Vuillemin, M. (Centre d'Etudes Nucleaires, Fontenay-aux-Roses, France). Vienna, International Atomic Energy Agency, 1965, Preprint No. CN-21/71, 33p. (In French). (CONF-650935-30). ORINS.

From 2nd IAEA Conference on Plasma Physics and Controlled Nuclear Fusion Research, Culham, Eng.

The stability of inhomogeneous collisionless plasmas in plane or cylindrical geometries is studied. The method employed limits the choice of perturbations, but makes it possible to write an energy integral and to show that theta pinches with a reversed field are unstable and have a growth rate comparable to those observed. The macroscopic equilibrium parameters depend only on one coordinate of an orthogonal system, the current carried by the plasma being directed along another co-ordinate axis. The perturbations considered are constant along the current lines. The equilibrium is inhomogeneous in the x direction and the deformations are constant along the z axis, the direction of the currents. (auth)

47845 PLASMA HEATING MECHANISM BY COLLISIONLESS SHOCK WAVES. Kurtmullaev, R. Kh.; Nesterikhin, Yu. E.; Pil'skii, V. I.; Sagdeev, R. Z. (Inst. of Nuclear Physics, Novosibirsk, USSR). Vienna, International Atomic Energy Agency, 1965, Preprint No. CN-21/218, 26p. (In Russian). (CONF-650935-28). ORINS.

From 2nd IAEA Conference on Plasma Physics and Controlled Nuclear Fusion Research, Culham, Eng.

A "magnetic piston" formed by a rapidly increasing magnetic field at the boundary of a preionized cylindrical plasma column with density varying from 10^{12} to 10^{14} cm^{-3} was used to produce convergent cylindrical shock waves. The convergence and structure of the cylindrical shock wave and the heating of the plasma in conditions under which normal binary collisions are unimportant are investigated. The experiments show agreement with the theoretical concepts of the structure of collisionless shock waves in a tenuous plasma in a strong magnetic field, and emphasize the decisive part played by collective interactions in the dynamics of rapid processes in similar plasmas. (auth)

47846 PLASMAS FOR THERMONUCLEAR RESEARCH PRODUCED BY LASER BEAM IRRADIATION OF SINGLE SOLID PARTICLES. Haught, A. F.; Polk, D. H. (United Aircraft Corp., East Hartford, Conn.). Vienna, International Atomic Energy Agency, 1965, Preprint No. CN-21/110, 20p. (CONF-650935-24). ORINS.

From 2nd IAEA Conference on Plasma Physics and Controlled Nuclear Fusion Research, Culham, Eng.

A ruby laser was used to form a high-temperature, high density plasma from a single, solid particle of lithium hydride suspended in a vacuum. The 10 to 50 micron diameter particle was charged by an electron beam and suspended in a vacuum in the electric field produced by a cubical array of electrodes of which opposite pairs were connected to the terminals of a Y-connected, three-phase alternating current supply. The focused 20 nanosecond, 30 megawatt giant pulse beam from a Q-spoiled ruby laser irradiated the suspended particle and produced the plasma. Charge collection measurements showed that complete single ionization of the 10^{15} atoms in the lithium hydride was achieved in the plasmas produced. Time-of-flight studies of the expanding plasma yield initial plasma temperatures of 10 to 100 electron volts. Since the ionization was produced in a vacuum, there was no collisional cooling of this high-energy plasma. (auth)

47847 RECENT DEVELOPMENTS IN THE TRANSVERSE INJECTION EXPERIMENT. Hammel, J. E.; Baker, D. A. (Los Alamos Scientific Lab., N. Mex.). Vienna, International Atomic Energy Agency, 1965, Preprint No. CN-21/85, 19p. (CONF-650935-23). ORINS.

From 2nd IAEA Conference on Plasma Physics and Controlled Nuclear Fusion Research, Culham, Eng.

The motion of a plasma stream injected transverse to a magnetic field, as it crosses a region where magnetic field lines reverse direction about a field null line, is studied. As the stream proceeds across the separatrix between the two field line directions, the electric field must change direction if the stream drift is to continue. The stream halts in the region of the separatrix while large currents are measured along magnetic field lines connecting the front of the stream with the following portions. Insulators placed to interrupt the current allow the stream to proceed into the reversed-field region. By making use of the inductance associated with the depolarization current when magnetic field lines are tied at some distance to the side of the stream, a separation of fast and slow stream components can be made. The cutoff of the slow stream component is observed with He–Ne laser interferometry techniques. Preliminary data from a matrix of electric field probes and readout circuits are given. (auth)

47848 THE CONTAINMENT OF PLASMA TRAPPED IN A MAGNETIC WELL. Francis, G.; Hill, J. W.; Mason, D. W. (United Kingdom Atomic Energy Authority, Abingdon, Eng.). Vienna, International Atomic Energy Agency, 1965, Preprint No. CN-21/30, 15p. (CONF-650935-18). ORINS.

From 2nd IAEA Conference on Plasma Physics and Controlled Nuclear Fusion Research, Culham, Eng.

Plasma from a coaxial gun is guided along an injection line by a converging magnetic field into a central glass vacuum chamber. Here part of the plasma is reflected from a magnetic mirror, and then trapped by the application of another rapidly-pulsed mirror field. Stabilizing fields can also be applied by currents in six Ioffe bars parallel to the axis. The fields, of short rise time, are maintained roughly constant for 1 msec. A rotating flute instability is present. With stabilizing fields applied, the lifetime of energetic ions (measured by the emission of charge exchanged neutral atoms) is increased. This decay rate is faster than that owing to charge exchange at the background gas pressure, indicating a large transient influx of gas from the walls of the chamber. The fast atom flux lasts 140 to 200 microseconds in both simple mirror and complex fields. The signal due to charge exchange emission peaks about 30 μsec after the instant of trapping. This signal measures the product of the fast ion and neutral gas densities. (auth)

47849 ROTATION OF A PLASMA JET IN A MAGNETIC FIELD. Demichev, V. F.; Matyukhin, V. D.; Nikologorskii, A. V.; Strunnikov, V. M. (Kurchatov Inst. of Atomic Energy, Moscow). Vienna, International Atomic

Energy Agency, 1965, Preprint No. CN-21/138, 21p. (In Russian). (CONF-650935-14). ORINS.

From 2nd IAEA Conference on Plasma Physics and Controlled Nuclear Fusion Research, Culham, Eng.

The motion was investigated of a plasma jet in a magnetic field set up by a current flowing through four bars such that the directions of flow were opposite in adjacent bars. In their central region the conductors were bent through 90°. The field strength along the axial line of a similar system of conductors equals zero, while the maximum field strength in the slit between two adjacent rods is 6 kOe. The plasma jet produced by a coaxial gun was injected along the axis of the magnetic system at a time near the maximum of the field. The jet was not fully ionized and contained, in addition to hydrogen ions, also considerable quantities of impurities. (auth)

47850 ROTATING PLASMA EXPERIMENTS. Bergstroem, J.; Holmberg, S.; Lehnert, B. (Royal Inst. of Tech., Stockholm). Vienna, International Atomic Energy Agency, 1965, Preprint No. CN-21/3, 35p. (CONF-650935-8). ORINS.

From 2nd IAEA Conference on Plasma Physics and Controlled Nuclear Fusion Research, Culham, Eng.

Experiments are performed in a rotating plasma device with a curved magnetic field, having large mirror ratios and radial ratios. The plasma is created by a discharge applied across the magnetic field. When the power input is below a certain level, there is only a partially ionized plasma with a small kinetic energy stored in its rotation. However, as soon as the power input exceeds a certain critical level, a burnout takes place of the neutral gas in the confinement region, and a fully ionized plasma is created. The momentum balance of the fully ionized plasma is explained by classical theory. It is determined by transverse losses due to viscous drag between the plasma and the electrodes, and by longitudinal losses due to particles escaping to the end insulators. When the plasma is released from its energy source, the velocity of rotation decays exponentially. The corresponding time constant increases with the magnetic field. Further, the time constant of the azimuthal current is half as large as that of the velocity. Thus, there is a radial balance of forces at a ratio of about 0.1 between the centrifugal and magnetic "pressures". The voltage across the plasma cannot exceed a certain critical value. This limitation can be explained by a plasma-insulator interaction. (auth)

47851 THE INSTABILITY OF A ROTATING PLASMA FROM THE TWO FLUID EQUATIONS INCLUDING FINITE RADIUS OF GYRATION EFFECTS. Berge, G. (Universitet, Bergen, Norway). Vienna, International Atomic Energy Agency, 1965, Preprint No. CN-21/230, 10p. (CONF-650935-7). ORINS.

From 2nd IAEA Conference on Plasma Physics and Controlled Nuclear Fusion Research, Culham, Eng.

A macroscopic treatment is given of instabilities of rotating plasmas, based on the two-fluid equations for a plasma. The finite radius of gyration effects for ions are included in the pressure tensor for this particle species. The equations governing the perturbed state are analyzed by the methods of normal modes in time and in the azimuthal co-ordinate. The resulting set of ordinary differential equations is solved consistently as an eigenvalue problem when terms are neglected of order higher than one in the parameter $\omega/\omega_i \ll 1$, where ω is the characteristic frequency of the system and ω_i the frequency of gyration for ions. The eigenvalue problem is solved. Moreover the "universal mode" appears as a special case of the more general solution, and is shown to be the most unstable mode of motion. (auth)

47852 PLASMA HEATING AND BURNOUT IN BEAM-PLASMA INTERACTION. Alexeff, I.; Jones, W. D.; Neidigh, R. V.; Peed, W. F.; Stirling, W. L. (Oak Ridge National Lab., Tenn.). Vienna, International Atomic Energy Agency, 1965, Preprint No. CN-21/102, 30p. (CONF-650935-3). ORINS.

From 2nd IAEA Conference on Plasma Physics and Controlled Nuclear Fusion Research, Culham, Eng.

Experiments using beam-plasma interaction to generate fully ionized plasma and enhance the temperature of the components are described. The electron beam is directed through high-pressure gas. Such a dense cloud of electrons is produced that neutral gas streaming inward from the walls is almost completely ionized or burned out before reaching the center of the apparatus. The most spectacular feature of the burnout transition is the sudden decrease of spectral light by a factor about one thousand. Neutral-beam transmission experiments give electron densities greater than 10^{12} cm^{-3}. Microwave cut-off measurements agree with this lower limit. Direct measurements of the electron plasma frequency and the ion plasma frequency give a density of 5×10^{12} cm^{-3}. (auth)

47853 THE INTER-DIFFUSION OF PLASMA AND MAGNETIC FIELDS IN PINCH AND HARDCORE DISCHARGES. Reynolds, P.; Lees, D. J.; Bickerton, R. J.; Hardcastle, R. A.; Wetherell, A. T.; White, B. M. (United Kingdom Atomic Energy Authority, Abingdon, Eng.). Vienna, International Atomic Energy Agency, 1965, Preprint No. CN-21/29, 20p. (CONF-650935-9). ORINS.

From 2nd IAEA Conference on Plasma Physics and Controlled Nuclear Fusion Research, Culham, Eng.

Experiments made using two discharge tubes are described. The first, Tiber, is a large linear tube, used with pinch and hard-core discharges. The original aim of obtaining a thin-skinned stabilized pinch is not achieved because of the rapid diffusion of the initially separated magnetic fields. The rate of diffusion increases with increase of energy input per particle in the discharge. The theoretical conditions for stability are not satisfied, and it is found that the current channel suffers from gross instabilities. Experiments to determine the cause of the rapid field diffusion are continuing in the same tube fitted with a hard-core, since some of the instabilities present in the pinch, possibly responsible for the diffusion, should not appear in the hard-core geometry. The second tube, Faust, is a linear hard-core tube. The discharge is set up by a rapidly rising axial field which causes the inward collapse of a cylindrical plasma shell onto an initially established azimuthal field. Experiments show that the plasma stability decreases as the current is increased. At all currents, however, the plasma is well confined radially. Diffusion of the magnetic fields is slow. Self-consistent measurements of plasma density, temperature, pressure, and resistivity are described. (auth)

47854 MEASUREMENTS OF POWER BALANCE AND PARTICLE LOSS RATE IN OHMICALLY-HEATED DISCHARGES IN THE C STELLARATOR. Bishop, A. S.; Hinnov, E. (Princeton Univ., N. J.). Vienna, International Atomic Energy Agency, 1965, Preprint No. CN-21/119, 19p. (CONF-650935-11). ORINS.

From 2nd IAEA Conference on Plasma Physics and Controlled Nuclear Fusion Research, Culham, Eng.

Measurements are made in the C stellarator to compare the ohmic power supplied to helium and hydrogen plasmas with that expended in the various loss processes, namely radiation, ionization, heating, charge-exchange, and particle loss across the sheath potential. Power into radiation is determined by means of absolutely calibrated monochromators for visible and ultraviolet light, appropriate corrections being made for axial and radial inhomogeneities. Power expended in ionization is, in turn, computed from the radiation measurements through a knowledge of the relative rate coefficients for excitation and ionization. The rates of change of temperature and particle densities are likewise determined from time measurements of plasma conductivity, electron densities, and radiation intensities. From these quantities the power expended in heating and charge-exchange processes can be determined. For helium discharges these measurements show that the power input can be satisfactorily accounted for in terms of power dissipated in radiation, ionization, and heating of the plasma. Similar power-balance measurements carried out in hydrogen discharges yield conclusions are essentially the same as those for helium. A high-speed computer is used to simulate the time development of discharges in the stel-

larator. Agreement is found between experimental and computer results. (auth)

47855 INVESTIGATION OF THE PLASMA IN THE AC DEVICE. Bortnikov, A. V.; Brevnov, N. N.; Zhukovskii, V. G.; Romanovskii, M. K. (Kurchatov Inst. of Atomic Energy, Moscow). Vienna, International Atomic Energy Agency, 1965, Preprint No. CN-21/139, 20p. (In Russian). (CONF-650935-12). ORINS.

From 2nd IAEA Conference on Plasma Physics and Controlled Nuclear Fusion Research, Culham, Eng.

The Adiabatic Compression trap is intended for the study of a plasma produced by the injection of fast ions. The ions are injected into a magnetic field which is constant in time and increases towards the end away from the injector. The plasma so obtained is then detached from the injector by a pulsed magnetic mirror, driven towards the steady magnetic mirror and compressed by a magnetic field of mirror geometry increasing in time. Depending on the method of injection, the plasma can be obtained in the form of a cylinder about the system axis (as in DCX-1), or in the shape of a "rosette" of Larmor orbits passing close to the system axis (as in "Ogrenok" or "Ogra 1"). The results are described of measurements of the plasma density and potential, the lifetime of the fast ions, the origin and development of oscillations at ion-cyclotron frequency, etc. Measurements were made: during the filling of the system with ions; after the separation of the plasma and its capture in the uniform magnetic field region between the stationary and the pulsed magnetic mirrors; and after the driving and compression of the plasma by the magnetic field increasing in time. (auth)

47856 THE CONDITIONS FOR IMPROVED STABILITY IN ZETA. Butt, E. P.; Cole, H. C.; Gibson, A.; Rusbridge, M. G.; Wort, D. J. H. (United Kingdom Atomic Energy Agency, Abingdon, Eng.). Vienna, International Atomic Energy Agency, 1965, Preprint No. CN-21/32, 16p. (CONF-650935-13). ORINS.

From 2nd IAEA Conference on Plasma Physics and Controlled Nuclear Fusion Research, Culham, Eng.

The influence of initial conditions on the onset of a relatively quiescent period in the Zeta discharge are investigated and the plasma parameters during this time are determined. The "quiescent" period is characterized by a marked reduction in the amplitude of fluctuations in the rate of change of current; in visible light output; and in the velocity of turbulent elements. The effect occurs soon after peak current. The magnetic field profile is obtained from multi-channel probe measurements; densities are obtained from infrared emission and by means of an infrared laser interferometer. Electron temperatures are estimated from spectroscopic and resistivity measurements. These measurements lead to estimates of β, where $\beta = 4NkT/I^2$. Comparison is made between hydrogen and deuterium discharges, and containment measurements are made in a helium discharge. The magnetic center is close to the geometric center under quiescent conditions. Observations on the residual fluctuations are made using correcting fields to move the magnetic center of the discharge. Experiments using an active clamp circuit, which can maintain the current constant for times >1 Msec, show the effect of rate of fall of current and the absence of a reversed electric field in the outer regions of the discharge on quiescence. Comparison is made with a theoretical model of the diffuse pinch. (auth)

47857 EXPERIMENTS ON THE ACCUMULATION OF A HOT ION PLASMA IN PR-5. Gott, Yu. V.; Ioffe M. S.; Yushmanov, E. E. (Kurchatov Inst. of Atomic Energy, Moscow). Vienna, International Atomic Energy Agency, 1965, Preprint No. CN-21/143, 21p. (In Russian). (CONF-650935-22). ORINS.

From 2nd IAEA Conference on Plasma Physics and Controlled Nuclear Fusion Research, Culham, Eng.

Experiments on PR-5 show that in a trap with magnetic mirrors the flute instability is completely suppressed when a radially increasing hybrid magnetic field (minimum-H trap) is set up. A hydrogen plasma with hot ions (5 kev) and density up to 10^{10} cm^{-3} has been produced by the magnetron injection method; the confinement time τ was limited only by charge-exchange losses. The possibility is explored of achieving prolonged containment of the plasma at densities $\gtrsim 10^{11}$ cm^{-3} and $T \simeq 5$ kev. (auth)

47858 INJECTION EXPERIMENTS IN JUTPHAAS. de Kluiver, H.; Brandt, H. B.; Strijland, W.; Huizenga, W. (FOM-Instituut voor Plasma-Fysica, Rijnhuizen, Jutphaas, Netherlands). Vienna, International Atomic Energy Agency, 1965, Preprint No. CN-21/124, 14p. (CONF-650935-27). ORINS.

From 2nd IAEA Conference on Plasma Physics and Controlled Nuclear Fusion Research, Culham, Eng.

Experiments are performed on injection parallel to the axis of a cusped magnetic field in a nonadiabatic regime. In a model experiment using an electron beam, half of the injected current gets temporarily trapped. Containment time versus magnetic field is found to agree with orbit analysis. With external electrostatic fields, complete containment is obtained except for losses associated with collisions with the background gas. Proton beams of 75 mA at 15 kv were extracted from a protruding plasma ion-source in pulses with falloff times of 2 μsec. Decay time is found to be 50 μsec. The measurements suggest that during injection a positive space charge is built up in the center. This fills continuously the outer, more adiabatic, region of the cusp. After beam turnoff, the particles in the nonadiabatic region are depleted quickly, while particles in the adiabatic region leave much more slowly (50 μsec). (auth)

47859 INVESTIGATION OF THE UNIVERSAL INSTABILITY IN A THERMAL PLASMA DEVICE (Q-MACHINE). Lashinsky, H. (Univ. of Maryland, College Park). Vienna, International Atomic Energy Agency, 1965, Preprint No. CN-21/107, 23p. (CONF-650935-29). ORINS.

From 2nd IAEA Conference on Plasma Physics and Controlled Nuclear Fusion Research, Culham, Eng.

The fully ionized column in a thermal plasma device (Q-machine) provides a convenient medium for studying the universal (drift-wave) instability arising from the joint effect of the finite ion Larmor radius and the density gradient perpendicular to the magnetic confining field. The pertinent dimensionless parameters can be varied over a range such that the results can be scaled to make comparisons with plasmas of thermonuclear interest, and the instability can be excited in controlled fashion by appropriate adjustment of the sheath conditions at the metal end plates. (auth)

47860 HIGH ENERGY PLASMA SOURCE. (to Vitro Corp.). British Patent 1,003,964. Sept. 8, 1965. Priority date Apr. 19, 1962, United States.

A high-energy plasma source includes a concentric anode and cathode positioned radially with respect to each other by means of an intervening hollow with insulating material. The cathode surface projects forwardly of the anode surface and tapers to a tip from which the electrical discharge formed during operation extends to the anode surface over paths largely parallel to the tapering cathode surface. The tip of the cathode is recessed to form a sharp circumferential line. The anode surface is the forward, narrow-diameter end surface of a hollow truncated cone of a porous conducting material to permit the introduction of a fluid flow. (B.L.M.)

47861 ARC INITIATOR FOR PLASMA GENERATOR. Martinson, Paul E. (to Standard Oil Co.). U. S. Patent 3,202,852. Aug. 24, 1965. Filed Apr. 3, 1961.

An improved arc initiator or starting head for plasma stream apparatus is described. The apparatus is simple, durable, reliable, relatively inexpensive, and relieves the personnel of the hazard of manual manipulation and exposure to high-current electrodes or the resultant high heat and hazardous radiation from the electrodes. More efficient cooling means are provided for the plasma stream apparatus, and provision is made for readily replacing worn parts without the destruction of the remainder of the apparatus. (B.L.M.)

47862 EQUIPMENT FOR FORMING HIGH TEMPERATURE PLASMAS. Sunnen, Jean Albert Francois (to La Soudure Electrique Autogene). U. S. Patent 3,205,338. Sept. 7, 1965. Priority date Oct. 6, 1961, France.

Equipment is described for the production of a high-temperature plasma by means of an arc powered by an alternating current rather than the usual practice of sustaining the arc by a direct current. The equipment includes a source of direct current, one pole of which is connected to a first electrode while the other pole is connected to a hollow second electrode. Means to direct the plasma formed by the arc adjoining the two electrodes through the hollow electrode to come in contact with a third electrode is connected at one side to a source of alternating current passed through the plasma and capable of sustaining an arc fed by the alternating current. The apparatus permits instantaneous restriking of the a-c arc after each zero value of the main current. The alternating current is not superimposed on the direct current between the two electrodes connected to the source of direct current, and the ionized plasma formed by the permanent arc created between the two electrodes connected to the direct current source and discharged at the gap where the alternating arc must strike will be sustained permanently in the gap. (B.L.M.)

Shielding

Refer also to abstract 47102.

47863 (AD-613480) ANALYSIS OF RADIATION STREAMING THROUGH SINGLE-BEND DUCTS. Period Covered: October 1, 1963–September 30, 1964. Marshall, J. D. (General Dynamics/Fort Worth, Tex.). Jan. 1965. Contract AF29(601)-6213. 106p. (WL-TR-64-136). CFSTI $4.00 cy, $0.75 mn.

An experimental study was performed to obtain data for verification of the Monte Carlo Multibend-Duct Procedure and to obtain data for a parametric study of radiation transported through a ducted shield. To accomplish these objectives, a 14-Mev neutron source and ^{60}Co gamma sources were used in conjunction with single-bend aluminum ducts in water shields. The duct bends were varied from 30 to 60° and the top-leg-to-bottom-leg ratio from 0.3 to 3.0. The calculation procedure was verified within certain limitations, which were mainly a function of shield thickness. Experimental results were integrated over the exit plane of the ducted shields. The scattered component of the dose rate was obtained by subtraction of the calculated direct-beam component from the integrated experimental dose rates. The scattered component was 70 to 90% of the total radiation dose and increased with increasing shield thickness. No other general tendencies were noted over the range of the parameters considered. (auth)

47864 (ANL-7050, pp 113-22) A NUMERICAL SOLUTION OF THE GAMMA TRANSPORT EQUATION APPLIED TO CONCRETE SLABS. Penkuhn, H. (European Atomic Energy Community, Ispra (Italy). Joint Nuclear Research Center).

The gamma transport equation is solved numerically in plane multislab geometry. A monoenergetic source is assumed on one surface, with isotropic or collimated angular distribution. After computing the unscattered flux, the fluxes at lower energies are calculated from those at higher energies without iteration. Integration of the differential fluxes gives the energy spectra and buildup factors. Source energies ≤10 Mev and thicknesses of some dozen mfp can be handled with the program, BIGGI 3. As an application, buildup factors for normal and heavy concretes are calculated and compared with those of Al, Ar, and Fe. The so-called Z_{eff} values for heavy concretes are found to be a function of the source energy. (auth)

47865 (ANL-7061) A GENERAL THEORY OF FIRST-PASSAGE DISTRIBUTIONS IN TRANSPORT AND MULTIPLICATIVE PROCESSES. Moyal, J. E. (Argonne National Lab., Ill.). June 1965. Contract W-31-109-eng-38. 24p. Dep. mn; CFSTI $1.00 cy, $0.50 mn.

The "Milne problem," expressed in probabilistic terms, is solved for general transport and multiplicative processes. If a particle initially in a given state at a given position inside a surface τ is multiply scattered while traveling through a fixed medium, then, given the scattering cross sections and, if required, the probability distribution for a change of state between collisions (e.g., by diffusion or ionization), the problem is to obtain the probability that the particle eventually effects a first passage through a specified position on the surface τ and in a specified state. In the case of a multiplicative process, given, in addition, the rates of creation and annihilation of particles (considering the nature of the particle as a state variable), the problem is to obtain the probability that eventually n particles will emerge for the first time through specified positions on τ and in specified states (with n = 0, 1, 2, . . .). A general solution is given in the form of a convergent series whose terms are obtained by iteration; this solution is unique if and only if the probability θ_∞ of an infinity of atomic events before a first passage (which is the limit of a certain nonincreasing sequence) is identically zero; in the multiplicative case, $\theta_\infty \neq 0$ may be taken to mean that the process is "supercritical." The mathematical theory that leads to this solution is a generalization of the corresponding theory for time-dependent Markov processes in which the time variable is replaced by a set of surfaces ordered by inclusion of their "insides," and is valid for Euclidean space of any number of dimensions. Applying it to the four-dimensional space of special relativity with ordered sets of space-like surfaces, one obtains a Lorentz-invariant formulation of the theory of physical Markov processes. A few examples are given. (auth)

47866 (KAPL-M-6460) SOSH-5. A COMPUTER PROGRAM FOR SHIELDING CALCULATIONS. Pendergast, M. S.; Mueller, G. O. (Knolls Atomic Power Lab., Schenectady, N. Y.). June 30, 1965. Contract W-31-109-eng-52. 50p. Dep. mn; CFSTI $2.00 cy, $0.50 mn.

SOSH-5 is a computer program that can be used to calculate the neutron flux at a point P (e.g., an ion chamber) due to many neutron sources distributed so as to approximate a reactor core. The use of the program is mainly in relative matters rather than absolute quantities; i.e., determining the ion chamber sensitivity to water temperature, location of the ion chamber, location of the discrete neutron sources within the reactor, and the contribution to the ion chamber flux from various regions of the reactor core. SOSH-5 allows for fuel cells which are not parallel to the reactor centerline and for variable water density in the axial direction in the outer reflector. The program is capable of calculating the flux distribution along the centerline of the instrument tube for optimizing the location of the ion chamber. SOSH-5 is also capable of integrating the flux distribution over specified lengths of the instrument tube to yield a number proportional to the ion chamber response. (auth)

47867 (NP-15384) PROGRAM DESCRIPTION AND USER'S MANUAL FOR PROTOS, A COMPUTER PROGRAM FOR TREATING PROTON SLOWING-DOWN DUE TO ATOMIC COLLISIONS. Johansson, C. (Forsvarets Forskiningsanstalt, Stockholm (Sweden)). July 1965. 28p. Dep. mn.

The PROTOS program is given. Instructions on the use of the program are given. It is recommended that the manual be used in conjunction with the report FOA 4A 4411-411 which describes the computational method. (M.O.W.)

47868 (RRA-T52) NEUTRON TRANSPORT DATA FOR SINGLE AND MULTILAYER SLABS OF ALUMINUM, POLYETHYLENE, AND CARBON. Wells, M. B.; Newell, J. M. (Radiation Research Associates, Inc., Fort Worth, Tex.). May 28, 1965. Contract NAS 8-11047. 96p.

Dose rate transmission data for 18-Mev plane isotropic neutron sources embedded in slabs of aluminum, polyethylene, and carbon are presented for slab thicknesses to 30 cm. These data as well as the neutron transmission data previously reported for monoenergetic sources be-

tween 0.5 and 18 Mev were integrated over the evaporation neutron spectrum to provide transmission data for use in evaporation neutron transport calculations. To illustrate the application of the transmission data, neutron doses behind slabs of aluminum, polyethylene, and carbon were computed for evaporation neutrons produced by normal incident protons with an energy spectrum defined by the equation $\phi(E) = 3.49 \times 10^8\ E^{-3.12}$ (protons cm^{-2} Mev^{-1} $flare^{-1}$). Simplified calculational methods are outlined for use in predicting the transmission of neutrons from plane isotropic sources embedded in multilayer slabs. The simplified methods, which make use of the results of the single-layer slab calculations, were found to produce results which are in good agreement with dose rate transmission data from Monte Carlo calculations for two and three layer slabs. (auth)

47869 (ORNL-tr-710) MEASUREMENT OF GAMMA BACKSCATTERING ON CONCRETE WALLS. Ito, Kazuo. Translated for Oak Ridge National Lab., Tenn. from Genshiryoku Kogyo, 10: 22-5(1964). 12p. Dep. mn; JCL $1.60 fs, $0.80 mf.

When the useful flux of gamma rays which possess a relatively high energy is highly directional, care must be exercised in insulating the walls opposite to the side of incidence, and at the same time, one must also consider the inevitable phenomenon of gamma-ray backscattering. Several experimental observations of gamma-ray backscattering on those concrete walls frequently used as radiation shields are discussed. (auth)

47870 INVESTIGATION OF HYDROGENLESS SHIELDING FOR NUCLEAR REACTORS. Tsypin, S. G.; Sinitsyn, B. I.; Daruga, V. K. (Inst. of Power Engineering, Obninsk, USSR). Jaderna Energie, 11: 201-6(June 1965). (In Czech).

Experimental investigations and computations of neutron transmission through hydrogenless shields are reviewed. The possibilities of using simple empirical formulas to estimate the shielding properties of some materials, particularly of mixtures were examined. The values obtained showed good agreement with the experimental results, within an accuracy of 10 to 20 percent. (CFSTI)

47871 STOPPING CROSS SECTIONS OF CARBON AND HYDROCARBON SOLIDS FOR LOW-ENERGY PROTONS AND HELIUM IONS. Sautter, C. A.; Zimmerman, E. J. (Univ. of Nebraska, Lincoln). Phys. Rev., 140: A490-8 (Oct. 18, 1965). (COO-35-78).

Experimental determinations of stopping cross sections of carbon, polyvinyltoluene, and polypropylene were made for protons and helium ions in the energy range 30 to 350 kev. Previous measurements on polyethylene, polystyrene, and a styrene-butadiene copolymer (Pliolite S-5A) were refined for protons above 160 kev. The data are in reasonable agreement with earlier experimental work, and have standard deviations between 1.7 and 4.3%. Application of the Bragg rule to the hydrocarbon data yields atomic-carbon cross sections about 13% too large at the highest beam energies, demonstrating the failure of additivity. Extrapolation of the proton data to higher energies gives results in excellent agreement with Brandt's theoretical values. A mean excitation energy $I = 96 \pm 4$ ev independent of proton energy down to 150 kev was found for carbon. Analysis of available hydrocarbon data indicates that gases have on the average approximately 8% larger proton stopping than solids of similar chemical binding. Furthermore, differences up to 23% in ratios of He to H stopping power (at the same velocities) show that the assumption that this ratio should be independent of the stopping material is untenable. These ϵ_{He}/ϵ_H ratios, extending from beam velocities of 1.2 to 1.7 (in units of $e^2/\hbar$), are greater for hydrocarbon solids than for gases, in agreement with the finding of Mechbach and Allison for Cd. (auth)

47872 GAMMA-RAY PENETRATION OF IRON-LEAD SHIELDS (thesis). Chitnis, Vishvanath Dattatraya. Ames Iowa, Iowa State Univ., 1964. 76p.

A laminated shield with alternate layers of two different materials designed to absorb radiation from a point source of gamma radiation is analyzed. The shield consists of alternate layers of iron and lead of constant thickness. An estimate of the total thickness of the shield is made from an approximate calculation in the case of a shield consisting of iron only. The energy of gamma rays emitted by the source is 10 m_0c^2. The total thickness of the shield is kept constant and the ratio of the thickness of the iron to that of the lead is varied. For four such different ratios the penetration of gamma rays through the composite shield is studied using the techniques of the Monte Carlo approach. The shield is infinite in two dimensions and finite in one dimension. Along the finite dimension of the shield the transport of gamma rays is studied and the energy deposited at various points along the finite dimension of the shield is determined. The interactions responsible for the penetration of gamma rays through the shield are Compton scattering and elastic scattering. The total number of layers used in this investigation is six. A large number of histories are generated for gamma rays and the results are presented. (Dissertation Abstr.)

Solid State Physics

See also CHEMISTRY — Inorganic and Physical Chemistry
METALS, CERAMICS, AND OTHER MATERIALS — Properties and Structure

Refer also to abstract 46753.

47873 (AD-612384) NUCLEAR MAGNETIC RESONANCE IN BORON TRIOXIDE AT ELEVATED TEMPERATURES. McDade, James C. (Harry Diamond Labs., Washington, D. C.). Jan. 15, 1965. 57p. CFSTI $3.00 cy, $0.75 mn.

The magnetic resonance of the ^{11}B nucleus in vitreous boron trioxide was observed at 10 Mcps and at temperatures ranging from room temperature to 800°C. The resonance line narrows with increasing temperature to about 600°C, above which it broadens again. The narrowing below the glass-transition temperature T_g is attributed to lattice vibrations; that above T_g, to molecular rotation. The broadening above 600°C is ascribed to the decrease in the lifetime of the energy states. Theory is given relating the line width to the molecular motion of the liquid. There is no evidence for a proposed change in molecular structure. (auth)

47874 (AD-613606) SPIN WAVE-SPIN WAVE SCATTERING IN A HEISENBERG FERROMAGNET [Thesis]. Boyd, Robert Gerald (California Univ., Riverside. Dept. of Physics). Jan. 1965. 54p. CFSTI $3.00 cy, $0.75 mn.

Consideration is given to scattering on one spin wave from another in a perfect simple cubic Heisenberg ferromagnet with nearest neighbor exchange only. An orthonormal set of two-spin-wave states is displayed, and the exchange hamiltonian is divided into a diagonal part and an off-diagonal part. The Lippmann-Schwinger scattering equation was solved for two spin derivations, and an exact exchange scattering cross section was obtained. The "Golden Rule" was used to derive, in Born approximation, the dipole scattering cross section. It was concluded that if the Born approximation is valid for dipole scattering and if the ratio of cross sections is similar for face centered cubic lattices, then in EuS dipole scattering swamps out exchange scattering at low temperatures. (TAB)

47875 (AD-614136) FUNDAMENTAL PROBLEMS OF SOLIDS. Final Report, September 1, 1961-August 31, 1964. Ferrell, Richard A.; Myers, Ralph D. (Maryland Univ., College Park). 11p. (AFOSR-65-0656). CFSTI $1.00 cy, $0.50 mn.

The problem of electronic correlations and the correlations of lattice vibrations with electrons and other lattice vibrations is discussed. Special attention is given to the

description of such correlations in terms of the collective motions of the system. (TCO)

47876 (AD-614435) GROWTH AND CHARACTERIZATION OF SINGLE CRYSTALS OF RARE EARTH COMPOUNDS. Quarterly Technical Report No. 7. (Westinghouse Research Labs., Pittsburgh, Pa.). 1965. Contract AF49(638)-1245. 9p. CFSTI $1.00 cy, $0.50 mn.

The spin disorder effect on scattering of the conduction electrons was examined together with increases in the residual resistivity of Gd observed in various intrarare earth alloys. It was found that the extrapolated values of the spin-disorder resistivity previously reported were much too small to account for the inelastic scattering with spin flip. This large discrepancy between the calculated and extrapolated value of spin-disorder resistivity has heretofore been overlooked. It may imply the existence of short-range order of spins in the paramagnetic state at temperatures considerably higher than the Curie point. Resistance measurements were conducted on a polycrystalline sample of Si-doped $CrBr_3$. The electrical data revealed that the compound became a semiconductor only in the paramagnetic state. Below the Curie temperature it remained an insulator. The excess electrons detonated by the Si atoms in $CrBr_3$ thus behave markedly differently from those detonated by La in EuS. Experimental work was continued on the growth of crystals of La-doped EuS. An investigation was begun on Ba-doped NdS. Further progress was made in the study of the magnetic structures of the solid solutions of CrTe and CrSb. (auth)

47877 (LA-3335) AN INTEGRATED SERIES OF CRYSTALLOGRAPHIC COMPUTER PROGRAMS. X. ANISOTROPIC STRUCTURE FACTOR CALCULATION AND POWDER PATTERN GENERATION. Larson, Allen C.; Roof, R. B. Jr.; Cromer, Don T. (Los Alamos Scientific Lab., Univ. of California, N. Mex.). Jan. 1965. Contract W-7405-eng-36. 50p. Dep. mn; CFSTI $3.00 cy, $0.50 mn.

A program for calculation of structure factors for any space group is described. The program is used to compute phases for Fourier electron density maps, to compute exact data to test our least-squares program subroutines, and to calculate powder patterns. (auth)

47878 (LA-3379) A SIMPLE EXPRESSION FOR THE QUARTIC ANHARMONIC CONTRIBUTION TO THE HELMHOLTZ FREE ENERGY OF A SPECIAL MODEL OF AN F.C.C. CRYSTAL. Maradudin, A. A. (Los Alamos Scientific Lab., Univ. of California, N. Mex.). Aug. 1965. Contract W-7405-eng-36. 9p. Dep. mn; CFSTI $1.00 cy, $0.50 mn.

In general, the calculation of the quartic anharmonic contribution F_4 (T) to the free energy of a crystal involves double summation over the Brillouin zone. Thus, its usefulness is often limited because of the enormous amount of numerical work required for its evaluation. However, for many crystals one obtains a satisfactory approximation by considering only nearest-neighbor interactions. For this case, it is shown that F_4 (T) simplifies to an expression involving the square of a single summation over the zone. The proof is for a face-centered cubic crystal. The expression is valid at all temperatures and can be written as an integral over the frequency spectrum; furthermore, it is unnecessary to calculate the eigenvectors. This result enables simple calculations of the thermodynamic properties corresponding to F_4 (T) to be carried out. (auth)

47879 (LA-DC-7277) CHARGED BOND CORRECTION TO THE DISPERSION CURVES OF DIAMOND. Warren, John L. (Los Alamos Scientific Lab., Univ. of California, N. Mex.). [1964]. Contract W-7405-eng-36. 14p. (CONF-650932-2). Dep. mn; CFSTI $1.00 cy, $0.50 mn.

From Symposium on the Inelastic Scattering of Neutrons by Condensed Systems, Upton, N. Y.

In an attempt to find a model for the phonon dispersion curves for diamond, it was noted that the charge-density about any atom in a diamond-type lattice is not spherically symmetric. An electrostatic model for the lowest order of approximation was derived. The formulas for the second neighbor Born-von Karman model which forms the basis of the included short range interaction are summarized. The calculation of the electrostatic contribution to the dynamical model is described. Conclusions from the calculation are given. (M.O.W.)

47880 (LA-DC-7353) ELECTRONIC BAND STRUCTURES OF PLUTONIUM AND ITS MONOCARBIDE. Kmetko, E. A.; Waber, J. T. (Los Alamos Scientific Lab., Univ. of California, N. Mex.). [1965]. Contract W-7405-eng-36. 31p. (CONF-651102-9). Dep. mn; CFSTI $2.00 cy, $0.50 mn.

For Presentation at Royal Commonwealth Society, 3rd International Conference on Plutonium, London.

The band structure of delta-phase plutonium was calculated by the tight binding and Augmented Plane Wave methods. The band width, density of states curve, and the Fermi surface were obtained from these calculations. The width of the 5f bands from the tight binding results is in better agreement with the width Kmetko deduced from a heuristic study than with that deduced from the Augmented Plane Wave results. The width of the 5f band in PuC was found by the tight binding method to be about two-thirds as large as that in delta-phase plutonium. (auth)

47881 (ORNL-P-585) LATTICE VIBRATION FREQUENCY SPECTRUM OF GRAPHITE. Wilson, John V. (Oak Ridge National Lab., Tenn.). [1964]. Contract W-7405-eng-26. 3p. Dep. mn; CFSTI $1.00 cy, $0.50 mn.

The frequency spectrum of the lattice vibrations of graphite was calculated by computer using the root-sampling method. Results are plotted in the form of histograms for modes of vibration in the plane of the hexagon of the lattice and for modes normal to that plane. The differences between the results and previous work with respect to their effects on neutron spectra are shown to be less than 2% at all energies. (D.L.C.)

47882 (RISO-103) ON THE DETERMINATION OF INTERATOMIC POTENTIALS IN METALS BY ELECTRON IRRADIATION EXPERIMENTS. Andersen, H. H.; Sigmund, P. (Atomenergikomissionen, Risoe (Denmark). Forsoegsinstitut). May 1965. 23p. Dep. mn.

The repulsive interaction between two atoms in a crystal is described by a Born-Mayer potential $V(r) = A \exp(-r/a)$. The parameters A and a are determined by an interpretation of measured threshold energies for displacement due to irradiation with electrons. The method is similar to that of Lucasson and makes use of the theory of collision sequences and of computer calculations on slowing-down. Measurements by Sosin and Garr on Cu single crystals suggest that $.18\text{Å} \lesssim a \lesssim .23\text{Å}$ for Cu. Several schemes of scaling potential parameters as a function of the atomic number are examined. The best one appears to be a = const., $A \propto Z^{\frac{1}{2}}$. The potential parameters finally adopted are a = .219Å, $A = 52\ Z^{\frac{1}{2}}$ ev. The agreement of estimated and experimental E_d values for several FCC and BCC metals is satisfactory. The resulting parameters are compared with Born-Mayer constants determined by other methods, and the origin of some discrepancies is discussed. The present potentials prove to be similar to those of Lucasson, but a final decision on their validity requires some more experimental work on single crystals. (auth)

47883 (UCRL-16279) QUADRUPOLE COUPLING IN RARE EARTH CRYSTALS (thesis). Blok, Johan (Lawrence Radiation Lab., Univ. of California, Berkeley). Sept. 1965. Contract W-7405-eng-48. 120p. Dep. mn; CFSTI $4.00 cy, $0.75 mn.

The electric field gradient at the nucleus was obtained for the rare earth ethylsulfates and double nitrates of La^{+3}, Eu^{+3}, Gd^{+3}, and Lu^{+3} by measuring the quadrupole coupling constants via nuclear orientation. From a comparison with the calculated antishielding factor and the measured crystal field gradients, ionic shielding factors were obtained for the rare earths. These shielding factors are observed to vary considerably through the rare earths. These experiments also yielded the nuclear quadrupole moment of

^{140}La, Q = +0.121(12) barns. These measurements required a precise knowledge of the temperature susceptibility relationship for cerium magnesium nitrate and for neodymium ethylsulfate. The temperature scale for cerium magnesium nitrate has recently been determined quite accurately; thus it was used without reservations. For neodymium ethylsulfate, however, the temperature scale was determined at low temperatures using gamma-ray heating and nuclear orientation. Considerable discrepancy with the previously published work was found. An exhaustive study was made of the decay of 155-day ^{177}Lu. The relative intensities and precise energies of many of the gamma rays in this complex decay were determined. From nuclear orientation of the 7-day and the 155-day ^{177}Lu isomers, the ratio of the nuclear quadrupole moments of the 155-day metastable state and the 7-day ground state was determined to be $Q_m/Q_g = +2.33(25)$. For gamma rays following the 1-second intermediate state in ^{177}Hf, the unattenuated value of the anisotropy was found. It is concluded that no reorientation takes place in this 1-second state. (auth)

47884 (IS-Trans-18) ATOMIC ABSORPTION CENTERS AND LUMINESCENCE PHENOMENA IN HEAVY-ELEMENT ACTIVATED ALKALI-HALIDE PHOSPHORS, AND THEIR PREPARATION UNDER THE INFLUENCE OF BAND RADIATION. Kats, M. L. Translated for Ames Lab., Ames, Iowa from Opt. i Spektroskopiya, 3: 602-9(1957). 10p. Dep. mn; CFSTI $1.00 cy, $0.50 mn; JCL $1.10 fs, $0.80 mf.

Crystalline alkali phosphors activated by silver, nickel, and tin ions were investigated. The absorption spectra of these phosphors consist of characteristic bands caused by activating admixtures. Excepting the case of nickel-activated phosphors, the light corresponding to the absorption bands of the activator induces fluorescence having a specific spectral composition. After exposure of the above-mentioned phosphors to band radiation, a sharp change was noted in their absorption spectra which exhibited a new band. New luminescence bands were also formed in the phosphors. The nature of these absorption and luminescence centers formed under the influence of band radiation is discussed on the basis of the results. (auth)

47885 (N64-21857) TRANSLATIONS ON COMMUNIST CHINA'S SCIENCE AND TECHNOLOGY NO. 81. Translated from K'o Hsueh T'ung Pao, No. 1, 52-6; 71-3; 76-7 (1964). 27p. (JPRS-24372; OTS-64-31167). CFSTI $0.75 cy, $0.50 mn.

For abstracts of individual papers see: 47886 and 47887.

47886 (N64-21857, pp 1-6) LIGHT AND SPECTROSCOPIC PROPERTIES OF INORGANIC VITREOUS RARE EARTH OXIDES. Kan, Fu-hsi; Chiang, Chung-hung; T'sai, Ying-shih; Hsiao, Kao-yen. Translated from K'o Hsueh T'ung Pao, No. 1, 52-4(1964).

The fluorescent spectra of rare earth ions in silicate glass were measured. The fluorescent emissions of the vitreous rare earth ions were separated according to fluorescence in the visible-light zone: Ce, Sm, Eu, Dy, Tm, Tb, and Er; fluorescence near the infrared zone: Nd, Yb, Ho, and Pr; and fluorescence near the uv zone: Gd. From the results it was concluded that the fluorescent spectra of rare earth ions in different base materials (crystals and glass) are not similar. The function of the base material was also indicated in its effect on the leaping process between different energy levels. (P.C.H.)

47887 (N64-21857, pp 7-12) PHYSICAL RESEARCH OF IRRADIATIVE RADIATION EMANATION OF Nd^{3+} ACTIVATED INORGANIC VITREOUS STATES. Kan, Fu-hsi; Chiang, Chung-hung; T'sai, Ying-shih. Translated from K'o Hsueh T'ung Pao, No. 1, 54-6(1964).

Studies were made on neodymium oxide concentration effects on the intensity and duration of fluorescence; temperature eruptive deactivation of fluorescence, and the radiation emanation of Nd^{3+} activated glass. Because of the effectiveness of shielding in the 4f layer, Nd^{3+} activated glass produced linear fluorescence and also radiation emanation at 1.06 μ under the condition that the energy input was not too large. Different vitreous base materials affected the absorption spectra of vitreous Nd^{3+} ions. The vitreous base material with a higher polarization ability can increase the vitreous absorption of irradiative radiation energy. Highly concentrated Nd_2O_3 (7 wt %) did not affect the fluorescence efficiency and the homogeneity of the vitreous base material. (P.C.H.)

47888 THE SCATTERING LENGTH OF YTTRIUM FOR THERMAL NEUTRONS. Paton, M. G.; Maslen, E. N. (Univ. of Western Australia, Nedlands). Acta Cryst., 19: 679-80(Oct. 10, 1965).

The thermal neutron scattering length of yttrium was determined using more accurate data on the structure of yttria. The neutron beam produced by reflection from the face of a copper crystal, had a mean wavelength of 1.067 Å. The powder sample which was cylindrical was held in an aluminum container, and the intensities of the diffracted beams were measured with a two-inch BF_3 proportional counter coupled to a ratemeter and chart recorder. A relatively large sample was necessary to produce scattered beams strong enough to be measurable. The intensities of the scattered neutron lines depended on the neutron scattering length, and the atomic coordinates and thermal vibration parameters of the atoms. The structural parameters are known from the x-ray analysis, and the neutron scattering length of oxygen was accurately determined to be 0.577×10^{-12}cm. The scale factor and b_y were refined through several cycles of least squares until the values were stationary. The final value was $0.781 \pm 0.008 \times 10^{-12}$cm. The intensities calculated for the value of b_y are given. (F.J.H.)

47889 NUCLEAR TECHNIQUES APPLIED TO THE SOLID-STATE PROBLEMS. [PART] II. Agullo Lopez, F. (Junta de Energia Nuclear, Madrid). Energia Nucl. (Madrid), 9: 119-36(Mar.-Apr. 1965). (In Spanish).

The application of nuclear techniques to solid-state problems was analyzed with a consideration of the techniques of elastic and inelastic scattering of slow neutrons and the deterioration of solids by radiation. (tr-auth)

47890 PIEZOSPECTROSCOPIC DETERMINATION OF THE SYMMETRY OF THE CRYSTAL FIELD ACTING ON TRIVALENT IONS OF RARE EARTHS IN THE FLUORITE LATTICE. Kaplyanskii, A. A.; Medvedev, V. N. Opt. Spectry. (USSR) (English Transl.), 18: 451-6(May 1965).

The effect of the deformation by a uniaxial compression upon the absorption spectra of monocrystals of CaF_2-Ho^{3+} and CaF_2-Ce^{3+}, grown under different physico-chemical conditions, was experimentally investigated at 4.2°K. The existence of three types of local crystal field in which the TR^{3+} ions are situated in the CaF_2 lattice was established by the deformation splitting of the lines. In two cases the crystal field has trigonal symmetry, and in the remaining case it is tetragonal. Rare-earth centers of a different type in CaF_2 are also discussed. (auth)

47891 INFLUENCE OF LEAD IMPURITY ON THE LOW-TEMPERATURE COLOR-CENTER PRODUCTION IN KCl. Sonder, E.; Sibley, W. A. (Oak Ridge National Lab., Tenn.). Phys. Rev., 140: A539-46(Oct. 18, 1965). (ORNL-P-1300).

The growth of optical absorption bands in the visible and ultraviolet as a function of 1.5-Mev electron irradiation at liquid-nitrogen temperature was measured for high-purity and lead-doped KCl. Dissolved lead causes the coloration near 360 nm to be enhanced; the rate of growth increases monotonically with Pb concentration, in agreement with previous studies of trapped holes. The F coloration is also enhanced by small amounts of impurity; however, the F-growth enhancement saturates at impurity levels of 20 to 100 ppm lead. An actual lowering of the F-center production rate is observed when samples doped with more than 100 ppm lead are used. This lowering is shown to be due to an increase in the α-center-to-F-center ratio in highly doped KCl. An explanation is proposed for the increased F-center coloration in terms of intersti-

tial–F-center recombination and interstitial stabilization by the impurities. (auth)

47892 INVESTIGATIONS OF OXYGEN-DEFECT INTERACTIONS BETWEEN 25 AND 700°K IN IRRADIATED GERMANIUM. Whan, R. E. (Sandia Lab., Albuquerque, N. Mex.). Phys. Rev., 140: A690-?(Oct. 18, 1965).

Oxygen impurity atoms interact with radiation-induced defects in germanium over a wide temperature range, producing a variety of optically active oxygen-defect complexes. Two complexes with bands at 719 and 736 cm^{-1}, not present after irradiation at 25°K, develop on annealing between 58 and 73°K in oxygen-doped Ge. One of these complexes is shown by isotopic substitution to contain oxygen and demonstrates conclusively that impurity-defect interactions occur in germanium at low temperatures. A third band at 620 cm^{-1}, which develops near 120°K with the disappearance of the first two bands, is also associated with a complex containing oxygen. By analogy to oxygen-defect interactions in silicon, these complexes are postulated to be oxygen-vacancy complexes, formed as the vacancy moves at ~65°K. Many other species develop at temperatures above 273°K. Their annealing behavior indicates that existing complexes react with additional defects or impurity atoms to form new species. Some of the annealing stages occur at temperatures corresponding to annealing stages reported for germanium containing other dopants, suggesting that analogous interactions occur between defects and a variety of impurities. (auth)

47893 REFLECTION STUDIES OF EXCITONS IN LIQUID AND SOLID XENON. Beaglehole, David (Univ. of Chicago). Phys. Rev. Letters, 15: 551-3(Sept. 27, 1965).

A comparison between the liquid and solid xenon spectra is reported. The liquid exciton spectrum is found to be very similar to that of the solid just below the melting point. The lower lying exciton states are broadened by increased disorder, and the extra exciton at 10.3 ev is still present in the liquid. The light reflected from a lithium fluoride window was measured when the cell is first empty then filled, the back surface of the window forming an interface between the xenon and the lithium fluoride. Measurements were made in the region 7.8 to 11 ev. This region covers the hydrogenic exciton lines and just includes the lower of the extra excitons. Curves showing the reflectivity of an Xe-LiF interface are shown. It appears that the deep extra excitons must have more of an atomic than kinematic band origin. (J.F.P.)

47894 THE TIME-OF-FLIGHT METHOD FOR INVESTIGATIONS OF SINGLE-CRYSTAL STRUCTURES. Buras, B. (Inst. of Nuclear Research, Swierk, Poland); Mikke, K.; Lebech, B.; Leciejewicz, J. Phys. Status Solidi, 11: 567-73(Oct, 1965). (RISO-106).

A new method is described for neutron diffraction structure investigations of single crystals using the time-of-flight technique. A pulsed incident neutron beam is used, and the neutrons scattered from a single-crystal sample within an angular range of $\Delta\theta$ are counted by means of a multi-time-channel analyzing system. In this way the integrated intensities are measured for several reciprocal lattice points simultaneously. Two cases are discussed, one involving a large and the other a small range of scattering angles. The feasibility of the method has been demonstrated for single crystals of aluminum and chromium at the DR 3 reactor at Risö and at the EWA reactor at Swierk. (auth)

47895 COVALENCY EFFECTS IN NEUTRON DIFFRACTION FROM FERROMAGNETIC AND ANTIFERROMAGNETIC SALTS. Hubbard, J.; Marshall, W. (Atomic Energy Research Establishment, Harwell, Eng.). Proc. Phys. Soc. (London), 86: 561-72(Sept. 1965).

It is shown that covalent bonding affects the absolute intensities and form factors for neutron diffraction from antiferromagnetic and ferromagnetic salts. The general effect is to reduce the absolute intensity below the theoretical values for a purely ionic salt and to make the form-factor curve somewhat flatter (except in directions very close to the forward direction). In the case of Ni^{2+} and Cr^{3+} salts the reductions in absolute intensities observed by Nathans, Alperin and others are roughly consistent with the degree of covalency indicated by the nuclear magnetic resonance measurements of Shulman and Knox. Furthermore, Alperin's observed form-factor curve for NiO can be largely explained by allowing for the same degree of covalency. On the other hand, we have not been able to explain the observed absolute intensities or the form factors for Mn^{2+} salts in these terms. It is also shown that Bragg scattering experiments on crystals with large unit cells or measurements of diffuse elastic scattering should reveal a sharp forward peak in the form factor. (auth)

47896 THE FERMI SURFACE OF CAESIUM. Okumura, K.; Templeton, I. M. (National Research Council, Ottawa). Proc. Roy. Soc. (London), Ser. A, 287: 89-104 (Aug. 17, 1965).

A study of the de Haas-Van Alphen effect in cesium by the pulsed field method, under carefully controlled experimental conditions, has yielded information about the orientation dependence of the Fermi surface cross-section. A computer analysis of the results in terms of cubic harmonic series has indicated a probable radial distortion of some +3.3% in the [110] direction, −0.9% in the [100] direction, and −1.4% in the [111] direction; this is compared with the predictions of band structure calculations which, though indicating approximately the correct shape of Fermi surface, are appreciably in error as to the magnitude of the deviations from a sphere. The observed Fermi surface distortion is also discussed in terms of its effect on the low temperature thermoelectric power of cesium. The volume of the Fermi surface is found to be within a few tenths of 1% of that calculated from published lattice constant data. Strong variations of signal strength with orientation were observed; these have been attributed in part to the effect of spin-splitting of the Landau levels. (auth)

47897 s-d SCATTERING AT LOW TEMPERATURES. Kondo, Jun (Electro-Technical Lab., Tokyo). Progr. Theoret. Phys. (Kyoto), 34: 204-9(Aug. 1965).

Based on a simple model which can be solved exactly, the electrical resistivity due to the s-d interaction in dilute alloys has been found to be expressed by $[\pi^3 S(S+1)c\hbar/ze^2k_F][\{\log(T/T_c)\}^2 + (\pi/2)^2]^{-1}$, where $kT_c \sim \epsilon_F e^{1/J\rho}$, for both signs of J. From this four conclusions are drawn as follows; the resistivity shows a maximum at T_c, which is independent of the concentration of impurity; when $J < 0$, T_c is usually so low that increasing resistivity is observed with decreasing temperature, while, when $J > 0$, T_c is so high that decreasing resistivity is observed with decreasing temperature; the resistivity at T_c is independent of J, the s-d exchange integral; and the resistivity due to the s-d interaction tends to zero as the temperature tends to zero. An available experiment is analyzed using the above formula, and T_c is estimated to be 0.0006°K in this case. The possibility of observing the maximum is discussed. (auth)

47898 EPR SPECTRA OF THE Gd^{3+} ION IN SINGLE CRYSTALS OF CeO_2. Vinokurov, I. V.; Zonn, Z. N.; Ioffe, V. A. (Inst. of Silicate Chemistry, Leningrad). Soviet Phys.-Solid State (English Transl.), 7: 814-17(Oct. 1965).

Translated from Fiz. Tverd. Tela, 7: 1012-16(April 1965).

Studies were made of the EPR spectra of Gd^{3+} in single crystals of CeO_2 having a fluorite-type structure. It was found from the angular dependence of the fine structure lines that regardless of the conditions of crystal growth or the concentration of Gd^{3+} ions in CeO_2, one kind of centers is formed in which the local field has cubic symmetry. Hyperfine structure spectra from the odd isotopes Gd_{155} and Gd_{157} were obtained and studied. Values were obtained for the g-factor, the hyperfine interaction constants of Gd_{155} and Gd_{157}, and the crystal-field constants. (auth)

47899 SLOW NEUTRON SCATTERING IN ANTIFERROMAGNETS HAVING WEAK FERROMAGNETISM. Bar'yakhtar, V. G.; Kvirikadze, A. G. (Inst. of Physics, Tiflis, Academy of Sciences, Georgian SSR). Soviet Phys.-Solid State (English Transl.), 7: 891-3(Oct. 1965).

Translated from Fiz. Tverd. Tela, 7: 1110-13(April 1965).

A calculation is made of the line broadening for an inelastic neutron scattering in antiferromagnets having weak ferromagnetism, accompanied by emission or absorption of nonactivated spin waves. (auth)

47900 THE BEHAVIOR OF ADSORBED Cs FILMS ON SINGLE-CRYSTAL SPIKES OF Ta AND Ta_2C. Gorbatyi, N. A.; Ryabchenko, E. M. (Lenin State Univ., Tashkent). Soviet Phys.-Solid State (English Transl.), 7: 921-6(Oct. 1965).

Translated from Fiz. Tverd. Tela, 7: 1150-6(April 1965).

A single-crystal spike of tantalum carbide was produced in the field emission microscope and the mean value of its work function was determined. The work functions for optimum coverage were also determined for the Ta–Cs and Ta_2Cs systems as 1.6 and 1.4 ev, respectively. The mean heat of evaporation of Cs from Ta_2C was found to be 2.8 ev. The heat of evaporation of Cs from Ta was estimated as 2.5 ev. (auth)

47901 PERMITTIVITIES AND ATOMIC CHARGES OF RARE-EARTH METAL OXIDES. Batsanov, S. S.; Dulepov, E. V. (Inst. of Inorganic Chemistry, Novosibirsk, Siberia). Soviet Phys.-Solid State (English Transl.), 7: 995-6(Oct. 1965).

Translated from Fiz. Tverd. Tela, 7: 1239-41(April 1965).

Measurements were made of the permittivity ϵ of rare earth metal oxides by the immersion method, using samples in the form of crystalline powders, in order to obtain additional information on the nature of the chemical binding in these oxides. The Syigeti formula was used to calculate the effective atomic charge from the values of ϵ, and the results are found to be in good agreement with the electronegativity concept. (L.B.S.)

47902 MEASUREMENT OF THE THERMAL CONDUCTIVITY OF CRYSTAL ^4He. Mezhov-Deglin, L. P. (Inst. of Problems in Physics, Academy of Sciences, USSR; Inst. of Solid State Physics, Academy of Sciences, USSR). Zh. Eksperim. i Teor. Fiz., 49: 66-79(July 1965). (In Russian).

The thermal conductivity of crystal ^4He is measured between 0.5 and 2.5°K and at pressures up to 185 atm. The samples were grown in a glass ampule under constant pressure and continuous visual and temperature control. In this way single crystals with a small concentration of lattice defects could be obtained. The temperature dependence and also the maximal values of the thermal conductivity of such single crystals significantly differs from those usually observed and are in good agreement with the results of Gurzhi who made a theoretical study of transfer processes in ideal crystals. (auth)

47903 ON BOUND ELECTRON AND NUCLEAR SPIN OSCILLATIONS IN ANTIFERROMAGNETICS. Turov, E. A.; Kuleev, V. G. (Inst. of Physics of Metals, Academy of Sciences, USSR). Zh. Eksperim. i Teor. Fiz., 49: 248-56(July 1965). (In Russian).

The spectrum of bound (due to hyperfine interaction) oscillations of the electron and nuclear spins of an antiferromagnetic are calculated and investigated for the case when the axis of the antiferromagnetic lies in the plane of small magnetic anisotropy. The relaxation mechanism is considered for oscillations of the nuclear-like branch which appears as a result of the hyperfine binding if damping in the electron spin system is taken into account. The ultra high frequency magnetic susceptibility of the whole spin system is calculated, and the nuclear magnetic resonance amplification coefficient is determined. Space dispersion of nuclear-like spin waves is investigated and the possibility of excitation of such waves by a homogeneous ultra high frequency field (nuclear spin wave resonance) is indicated. (auth)

47904 CRITICAL NEUTRON SCATTERING FROM β-BRASS. Dietrich, O. W.; Als-Nielsen, J. (Danish AEC Research Establishment, Risoe, Denmark). 12p. (CONF-650428-2). Gmelin, AED-CONF-65-078-5.

From Conference on Phenomena in the Neighborhood of the Critical Point, Washington, D. C.

In a study of the critical neutron scattering from β-brass, monochromatic neutrons were extracted from the polyenergetic reactor beam by Bragg reflection in a Be single crystal. The monochromatic beam intensity was 2.5×10^5 neutrons/sec. The spherical crystal, one inch in diameter, was tightly encapsuled in a thin stainless steel container to avoid Zn evaporation. A 5% variation of the Zn content changes T_c 14°C but in the six-months duration of the experiment T_c remained constant within a few tenths of a degree. Two different scan types through a superlattice reflection in reciprocal space are sketched. The following results can be deduced from the experiment: the temperature dependence of LRO in the close vicinity of T_c, the absolute value and the temperature dependence of the SRO correlation range, and some conclusions concerning the shape of the pair correlation function. (J.F.P.)

47905 THE INTERACTION OF LOCAL MODES WITH STRESS FIELDS. Girifalco, L. A. (Univ. of Pennsylvania, Philadelphia). 19p. (CONF-650423-5). Gmelin, AED-CONF-65-058-12.

From International Conference on Physics of Solids and High Pressures, Tucson, Ariz.

A discussion is given of the application of the lattice dynamics of defect crystals to the theory of entropy of defect formation and migration in the presence of stresses. A brief presentation of the lattice dynamics of defect crystals is given, with emphasis on the defect-induced changes in mass and force constants necessary for local mode formation. The problem of determining numerical criteria for the formation of local modes in copper is examined. Consideration is restricted to the vacancy, the vacancy saddle point configuration, the split-interstitial and the split interstitial saddle-point configuration. A generalized Gruneisen method for describing the strain dependence of the vibration frequency is developed. The results are incorporated into the theory of defect formation and migration, and numerical results are presented for copper. (J.F.P.)

REACTOR TECHNOLOGY

General

Refer also to abstract 46493.

47906 (AECL–2282) ACCOUNTING SYSTEMS FOR HEAVY WATER AND FISSIONABLE MATERIALS. Fletcher, G. W.; Reid, H. B.; Jenkinson, W. G. (Atomic Energy of Canada Ltd., Chalk River (Ontario)). July 1965. 30p. (CONF-650803–8). Dep. AECL $1.00.

From IAEA Symposium on Nuclear Materials Management, Vienna.

Detailed accounting and reporting procedures used by Atomic Energy of Canada Limited (A.E.C.L.) for maintaining adequate records and control of heavy water supplies and stocks of fissionable materials are described, along with the duties and responsibilities of those administering the system. An appraisal is made of these procedures with respect to their adaptability for use in rapidly expanding research and power programs. In particular the use of electronic data processing equipment is evaluated. (auth)

47907 (ANL–7050) PROCEEDINGS OF THE CONFERENCE ON THE APPLICATION OF COMPUTING METHODS TO REACTOR PROBLEMS, MAY 17–19, 1965. (Argonne National Lab., Ill.). Aug. 1965. Contract W-31-109-eng-38. 572p. (CONF-650501). Dep. mn; CFSTI $6.00 cy, $2.50 mn.

Thirty-eight papers are included; separate abstracts have been prepared for 25. Thirteen of the papers were previously abstracted in NSA, see 19: 21638, 29166, 29180, 29696, 31423, 31467, 31505, 31513, 33566, 33569, 38130, 40149, and 45469. (T.F.H.)

For abstracts of individual papers see: 46902, 47538–47543, 47864, 47908–47919, and 47945–47949.

47908 (ANL–7050, pp 125-39) ACTIVITIES OF THE ANL-ENEA COMPUTER PROGRAM LIBRARIES AND THE ORNL RADIATION SHIELDING INFORMATION CENTER. Butler, Margaret (Argonne National Lab., Ill.); Maskewitz, Betty (Oak Ridge National Lab., Tenn.); Rosen, Johnny (European Atomic Energy Community, Ispra (Italy). Joint Nuclear Research Center).

The histories and operations of the information centers are outlined. The ANL-ENEA libraries contain computer programs relating to reactor problems, while the NSIC compiles information on radiation shielding. 27 references. (T.F.H.)

47909 (ANL–7050, pp 217-30) USE OF DIGITAL PROGRAMS IN REACTOR PLANT DESIGNS. Halsey, G. H.; Jordan, W. B.; Mueller, G. O.; Stevens, H. E. Jr. (Knolls Atomic Power Lab., Schenectady, N. Y.).

Techniques are presented for coordinating digital-computer programs for analyzing overall design of nuclear power plants. The advantages and disadvantages of several techniques are compared. (T.F.H.)

47910 (ANL–7050, pp 299-307) MAFIA II—A ONE-DIMENSIONAL BURNUP CODE. Massimo, L. (European Atomic Energy Community, Ispra (Italy). Joint Nuclear Research Center).

MAFIA-II is a one-dimensional burnup code written in Fortran II language for a 32-k-word computer. The limitations may be expressed as: 150 meshpoints for the diffusion calculation, 20 burnup regions, and 25 isotopes per region. Calculations may be made in slab or cylinder geometry. The basic multigroup library is used in a zero-dimensional neutron-spectrum calculation in which the actual reactor size appears only through energy-dependent bucklings and the cell structure through energy- and concentration-dependent self-shielding factors. The resonance absorption is treated as in the GAM-I code by the methods developed by L. W. Nordheim. The neutron spectrum calculated in this way is used for producing averaged few-group (from 2 to 4) cross sections, which allow a fast diffusion calculation giving the power distribution across the core. The few-group energy boundaries are given as input. The burnup calculation is performed by treating separately a maximum of 20 core regions, whose relative power is determined at each time step by the diffusion calculation. Control poisons in various regions of the reactor can be automatically adjusted according to some specified sequence. Reshuffling and recharging of fuel regions can be performed. A simplified flow diagram is shown. (auth)

47911 (ANL–7050, pp 309-13) MECHANISED HANDLING OF NUCLEAR DATA. Pull, I. C. (Atomic Energy Establishment, Winfrith (England)).

Techniques devised for computer handling of nuclear data are outlined briefly. The GALAXY code is described as an example. (T.F.H.)

47912 (ANL–7050, pp 347-68) A NEW APPROACH TO WATER REACTOR LIFETIME WITH SPATIAL VARIATION STUDIES. Console, M. (FIAT, Turin (Italy). Sezione Energia Nucleare); Salina, E.

The solution of the burnup problem coupled with the few-group diffusion in one and two dimensions is studied, for pressurized water reactors. A family of monodimensional digital computer programs, MELE-1, MELE-2, and MELE-3 (Modal Expansion Lifetime Evaluation) is running on the IBM 7090. A bidimensional program, CONDOR, is being tested. The chosen approach assumes, as a starting point, the series expansion of the spatial flux and the variational technique for the solution of the diffusion equations. The potential rapidity implicit in the modal expansion is able to be used to generate fast computer programs for lifetime evaluation. (auth)

47913 (ANL–7050, pp 369-78) BISTRO, AN INTEGRATED COMPUTATIONAL SYSTEM FOR PREDICTION OF THE HISTORY OF BOILING WATER REACTORS. Moen, H. (Institutt for Atomenergi, Kjeller (Norway)).

The BISTRO system is designed in order to facilitate reactor history calculations for light-water boiling reactors. BISTRO is a system of computer programs and routines. The BISTRO program itself performs the necessary data transmission and various auxiliary calculations associated with the various codes used in the BISTRO system. BISTRO is developed for the one-bank version of the CDC 3600 and is written as an overlay program in FORTRAN 63. The various aspects of the system are described. Scope, configuration of parameters used, and physical models used in connection with particular problems are described. The data-transmission system is discussed. (auth)

47914 (ANL–7050, pp 379-94) A REACTOR SYSTEM DYNAMICS CODE: AIROS. Blaine, R. A.; Berland, R. F. (Atomics International, Canoga Park, Calif.).

The AIROS system is designed for reactor-dynamics investigations, and is comprised of: a fast numerical integration system; flexible means for representing a multitude of physical phenomena; and special programming features. (T.F.H.)

47915 (ANL–7050, pp 413-27) A TIME-DEPENDENT MULTIGROUP DIFFUSION CODE WITH AUTOMATIC RESONANCE SELF-SHIELDING OF CROSS SECTIONS. Brickstock, A.; Davies, A. R.; Smith, I. C. (Atomic Weapons Research Establishment, Aldermaston (England)).

The one-dimensional diffusion code SWANTIME is described. SWANTIME uses the input routines and data libraries of the multigroup, steady-state diffusion code SWAN. Any number of compositions and regions are allowed, each composition being separately "self-shielded." A full downscatter matrix is included that can usually be truncated after relatively few groups in many cases. The

outer boundary condition is usually logarithmic, although zero flux is also allowed. (T.F.H.)

47916 (ANL–7050, pp 429–41) PINETO—A FORTRAN CODE DESIGNED FOR THE SOLUTION OF NONLINEAR DIFFERENTIAL EQUATIONS IN NEUTRON DYNAMICS. Tamagnini, C. Mongini (European Atomic Energy Community, Ispra (Italy). Joint Nuclear Research Center); Bona, C.; Mathis, A.; Modonesi, O. (Comitato Nazionale per l'Energia Nucleare, Casaccia (Italy). Centro di Studi Nucleari).

PINETO integrates concurrently the one-group one-region kinetic equation, as many as 11 delayed-neutron equations, and as many as 98 nonlinear inhomogeneous first-order differential equations. PINETO describes the time variations of mean spatial values of the variables involved in reactor dynamics. (T.F.H.)

47917 (ANL–7050, pp 487–502) EXTENSIONS OF THE POWER-CONTROL METHOD FOR SOLUTION OF LARGE INHOMOGENEOUS REACTOR PROBLEMS. Crowther, R. L. (General Electric Co., San Jose, Calif. Atomic Power Equipment Dept.).

A power-control method is described for computerized calculation of critical control-element distributions in large boiling-water reactors. The input to the computer program is the desired power distribution. (T.F.H.)

47918 (ANL–7050, pp 503–14) A COMPUTER CALCULATION OF THE ENERGY YIELD PRODUCED BY A HYPOTHETICAL FAST REACTOR ACCIDENT. Russell, L. M.; Morris, E. (Atomic Weapons Research Establishment, Aldermaston (England)).

The zero-energy fast reactor VERA is used in various integral experiments and can accommodate a variety of cores. In the consideration of the safety aspects of this reactor, computer code COOT is written in the S2 language (the AWRE dialect of Fortran II for the IBM-7030). In general principles the code is similar to the AX-1 code and is at the moment still a little unsophisticated in its overall control, owing to the manner in which it was put together. The effect of changing the equation of state used for the core material is studied. This study is important, because it can affect greatly the amount of kinetic energy produced, and change the total energy yield. (auth)

47919 (ANL–7050, pp 581–92) A MONTE CARLO APPROACH TO THE CALCULATION OF CHARACTERISTIC REACTOR PARAMETERS IN THREE-DIMENSIONAL ASSEMBLIES. Rief, H.; Kschwendt, H. (European Atomic Energy Community, Ispra (Italy). Joint Nuclear Research Center).

The TIMOC code calculates stationary and time-dependent reactor parameters by the Monte Carlo method. Non-equilibrium processes can be taken into account by the code. (T.F.H.)

47920 (ANL–7090) REACTOR DEVELOPMENT PROGRAM PROGRESS REPORT, AUGUST 1965. (Argonne National Lab., Ill.). Sept. 21, 1965. Contract W-31-109-eng-38. 86p. Dep. mn; CFSTI $3.00 cy, $0.75 mn.

Separate abstracts were prepared for the four included sections on: liquid metal cooled reactors, general reactor technology, advanced systems research and development, and nuclear safety. (M.O.W.)

For abstracts of individual sections see: 47921, 47950, 47989, and 48053.

47921 (ANL–7090, pp 30–54) GENERAL REACTOR TECHNOLOGY. (Argonne National Lab., Ill.).

Several areas of the reactor development program are discussed. Among them are theoretical reactor physics, high-temperature materials, nondestructive testing of reactor fuels, engineering development, chemical separations, sodium coolant chemistry, and plutonium recycle reactors. (M.O.W.)

47922 THERMAL STRESS TECHNIQUES IN THE NUCLEAR INDUSTRY. Zudans, Zenons; Yen, Tsi Chu; Steingelmann, William H. (Franklin Inst. Research Labs., Philadelphia, Pa.). [1965]. Contract AT(30-1)-1484. 583p. American Elsevier Publishing Co., Inc., New York.

The basic facts and theories necessary for handling thermal stress problems encountered in the nuclear industry are presented. Topics discussed include the nuclear power plant, temperature distributions in reactor systems components, thermoelasticity, analysis of creep and thermal fatigue, analysis of axisymmetric structures, and applications to plant components. (M.O.W.)

47923 THE ATOMIC ENERGY MARKET IN EUROPE. PART VIII. THE NETHERLANDS. Hoekstra, E. K.; Verbiest, A. J. (Reactor Centrum Nederland, The Hague). Atomwirtschaft, 10: 471-2(Sept. 1965). (In German).

The growing energy requirements accompanying population and industrial expansion in Holland play a special role with respect to the nuclear market. As yet no reactor type can supply electricity that is competitive with conventionally produced power. The discovery of mineral gas in the northern part of the country postponed a need for the development of a nuclear power supply system. However the advanced conversion reactor, which uses a homogeneous suspension of uranium oxide and thorium oxide in heavy water, was studied. A pressurized-water reactor for ship propulsion with 20,000 shp is being developed and a boiling-water nuclear power station with a capacity of 50 Mw(e) is being constructed. The Dutch industry is closely following the developments in the field on nuclear energy. (J.S.R.)

47924 REACTOR WITH TUBES DISPLACED FROM CORE AXES. Dickinson, John R. (to Atomic Energy of Canada Ltd.). U. S. Patent 3,201,318. Aug. 17, 1965. Filed July 8, 1963.

In a fuel channel lattice for a right circular cylindrical nuclear reactor core, the fuel channels are skewed at an angle with respect to the central axis of the core and the lattice is tighter in the central regions of the core than in the outer regions. Such a lattice may be constructed with a uniform skew angle throughout the lattice, or a number of discrete regions of uniform skew angles may be provided. Two fueling machines are used to insert and remove fuel elements, and the refueling is so timed as to assist in achieving a radial flattening of the neutron flux. (A.G.W.)

Auxiliaries and Components

47925 (GA–6505) PRESTRESSED CONCRETE STRUCTURES FOR LARGE POWER REACTORS. Marsh, R. O.; Rockenhauser, W. (General Atomic, San Diego, Calif. John Jay Hopkins Lab. for Pure and Applied Science). June 30, 1965. Contract AT(04-3)-167. 31p. (CONF-651110–1). Dep. mn; CFSTI $2.00 cy, $0.50 mn.

For Presentation at American Society of Mechanical Engineers, Annual Winter Meeting, Chicago.

Prestressed concrete reactor structures are rapidly coming of age in the nuclear field, especially for gas-cooled reactors. The analysis, design, and construction aspects of such a structure are discussed on the basis of a design study recently performed for a 1000 Mw(e) gas-cooled reactor. Basic design philosophy is presented, particular emphasis being given to those points where the design philosophy departs from that for conventional steel primary systems. Methods in use for the stress analysis of concrete reactor structures are described, in particular a numerical method for the thick-walled, heterogeneous case. The use of subscale-model tests to predict the behavior of a full-size structure is discussed. Proposed construction methods are described. In conclusion, a brief resume is given of the design, analysis, and construction planning currently under way for the concrete structure of a 330 Mw(e) reactor plant. (auth)

47926 NEW SHOP TO MEET FUTURE NEED FOR LARGER REACTOR VESSELS. Reimer, R.; Gaines, A. L. (Combustion Engineering, Inc., New York). Elec. Light Power, 41: No. 11, 42-3(Nov. 1963).

Weights to be handled and sizes to be inspected far ex-

ceed the present day capabilities. Since it was recognized that pressure-vessel manufacturing facilities could be a limiting factor in the growth of nuclear power, a manufacturing bay was constructed specifically designed for the purpose of handling the required weights and sizes. The 530- by 86-foot manufacturing bay specializes in the fabrication of ferrous-metal products and components that are extremely large, heavy or thick, made of stainless steel and other alloys, intricate or require a high degree of finish and strict adherence to extremely close tolerances, and required to be clean to nuclear standards or optically flat. Machine tools at this plant are the largest of their type available. However, even larger facilities must now be planned. There is no reason why nuclear-power unit sizes should not continue to grow at the accelerated pace of the past few years. Since the major limiting factor to unit-size growth is turbine-generator capability and reactor vessel size, 1500-Mw units are considered for the future. (J.F.P.)

47927 THE EXPERIMENTAL STUDY ON THE PERFORMANCE OF PRESSURE SUPPRESSION CONTAINMENT SYSTEM. Ishikawajima-Harima Eng. Rev., No. 24, 369-76(July 1965). (In Japanese).

To obtain information on transient behavior and to observe the condensation of steam in pool water, a non-nuclear small-scale facility was constructed. Forty test runs were made on this model simulating rupture accidents in the primary system under various conditions. Under all conditions there was almost complete condensation of the steam injected into the pool water. The transient pressure in the containment system was dependent mainly on primary system pressure before rupture and on the rupture area, except in case where there was very little water in the pool. The maximum pressure occurring inside the containment system was below the design pressure of the prototype, even when the rupture area was three times that assumed for the maximum credible accident. Reliability of this containment system was thus established for the whole range of conditions tested. (auth)

47928 A THREE-DECADE EXPONENTIAL CURRENT GENERATOR FOR TESTING REACTOR PERIOD METERS. Talboy, James H. (Argonne National Lab., Ill.). Nucl. Appl., 1: 356-8(Aug. 1965).

A single generator for producing currents that are exponential functions of time is described. The signals have a range of three decades, starting at 2.5×10^{-9} amp. Six periods, between 3.8 and 168 sec, are available. The generator is useful for calibrating and testing instruments, e.g. reactor period meters that measure currents, which are exponential functions of time. (auth)

47929 RELIABILITY OF SAFETY SYSTEMS. Bierman, George; Karish, Peter (Metropolitan Edison Co., Reading, Penna.). Nucleonics, No. 10, 23: 60-3(Oct. 1965).

Reliability, which is the probability that performance will at least equal the design criteria, is steadily improving. Features such as automatic testing are being included to further improve systems performance. Reliability obtained in the operation of nuclear equipment is found substantially better than that obtained with similar conventional equipment. Improvements in reliability could be made from increased feedback of performance information from plant to designer, digital control of nuclear plants, and research programs. Topics discussed are calculating reliability, designing for reliability, testing safeguards, and consequence-limiting safeguards. (J.F.P.)

47930 IMPROVEMENTS IN OR RELATING TO PRESSURE VESSELS AND TO PRESSURISERS USING SUCH VESSELS. (to Babcock and Wilcox Co.). British Patent 1,003,714. Sept. 8, 1965. Priority date May 31, 1961, United States.

A pressure vessel is described that is applicable to use with a pressurizer used in pressurized water nuclear steam generators. The pressure vessel is provided with a number of heating units each of which comprises at least one elongated tubular member mounted on a closure member and arranged to be heated internally along its length. The tubular member is inserted through an opening in the pressure vessel wall that is closed by the closure member. The tubular members may have various forms and may be heated by several different methods. The vessel may be formed of structural metal lined internally with corrosion-resistant material with the opening in the vessel being closed by a diaphragm of the corrosion-resistant material provided at its outer side with the closure member of structural material attached to the wall of the vessel to maintain the diaphragm in position to seal the opening. (B.L.M.)

47931 DEVICE FOR CHARGING AND DISCHARGING THE CHANNELS OF A PRESSURIZED, GAS-COOLED NUCLEAR REACTOR. Alliot, Paul; Charon, Michel; Tiberghien, Rene (to INDATOM S.A.R.L.). German Patent 1,192,333. May 6, 1965. Priority date Mar. 27, 1959.

Two gas-tight auxiliary vessels constructed in the shape of locks are provided which can be connected to the reactor pressure vessel. One of these auxiliary vessels serves for charging and the other for discharging the fuel elements. The two vessels are connected to each other by means of a piping system equipped with a compressor and valves so that the pressure in the auxiliary vessels can be alternatively adjusted to the operation pressure in the reactor vessel and to the atmospheric pressure. (Gmelin Inst.)

47932 CHARGING AND DISCHARGING INSTALLATION FOR A GAS-COOLED NUCLEAR REACTOR. Ayre, James Lewis; Gledhill, Peter Raymond (Simon-Carves Ltd. and General Electric Co. Ltd.). German Patent 1,192,334. May 6, 1965. Priority date Nov. 23, 1959, Great Britain.

An auxiliary vessel containing a magazine of fuel elements is connected to the reactor vessel by means of a charging tube. In order to facilitate a circulation of the gaseous reactor coolant through the auxiliary vessel during the charging and discharging operation an additional tube is attached to the auxiliary vessel which is also connected to the reactor vessel. (Gmelin Inst.)

47933 FUEL AND CONTROL ROD CHANNEL ARRANGEMENT IN A GRAPHITE-MODERATED NUCLEAR REACTOR. Kirkpatrick, Alan Robert (to C. A. Parsons and Co. Ltd.). German Patent 1,194,993. June 16, 1965. Priority date Dec. 4, 1956, Great Britain.

The nuclear reactor given comprises a shell formed by a radiation shield surrounding a vessel, a core of graphite, channels disposed within the core, a proportion of which are used for housing nuclear fuel in the form of uranium while others house control means for varying the neutron flux. Ducts penetrating the shell and in axial alignment with the channels housing the control means through which the control means may be inserted in or removed from the reactor are provided. There are also charging tubes for inserting the fuel into or removing it from the reactor, the tubes comprising a fixed portion for alignment with a fuel channel and a movable portion capable of being moved in any or substantially any direction away from the axis of the fixed portion to permit loading and unloading of adjacent fuel channels. The channels are disposed in a series of parallel equidistant rows in two mutually perpendicular directions, the pitch (p) of the channels being the same in each direction. Further ducts are provided penetrating the shell, each of which is aligned with a fuel channel and through which a charge tube may be introduced, the arrangement being that the further ducts are located with their axes forming the apices of isosceles triangles of base 6p and side $\sqrt{45}p$, the movable portion of the charge tube being capable of movement in a plane at right angles to the axes of the channels so as to be able to load and unload channels within a radius equal to $\sqrt{10}p$. The channels outside the sweep of a movable tube are used to house the means for controlling the neutron flux. (Gmelin Inst.)

47934 CONTROL ROD DRIVE FOR NUCLEAR REACTORS. Hawke, Basil Cromey; Liederbach, Fred Joseph; Lones, Walter (to General Dynamics Corp.). German Patent 1,198,945. Aug. 19, 1965. Priority date Aug. 23, 1961, United States.

The control rod drive comprises a guide spindle to which the control rod is attached, an electric motor activating the guide spindle during normal operation of the reactor, and a second, hydraulic motor which rotates the guide spindle with a much higher rotating speed than the electric motor and which serves for the emergency shutdown of the reactor. There is a coupling between the electric motor and the guide spindle which releases automatically the guide spindle as soon as a predetermined rotating speed is surpassed. (Gmelin Inst.)

47935 ARRANGEMENT FOR THE GENERATION OF AN INITIATING ELECTRICAL SIGNAL FOR FAST SHUTDOWN IN A NUCLEAR REACTOR. Uhrig, Hans (to Gesellschaft fuer Kernforschung m.b.H.). German Patent 1,198,946. Aug. 18, 1965. Filed July 23, 1964.

The circuit arrangement comprises a neutron detector, a logarithmic amplifier, and a comparator comparing the measured value after logarithmation and differentiation with a demand signal and generating the electrical signal which initiates the shutdown. The invention is characterized in that two differentiating circuits switched in series are switched between the logarithmic amplifier and the comparator. (Gmelin Inst.)

47936 PROCESS FOR PRODUCING POWER. Stern, David R.; Stewart, Robert D. (to American Potash and Chemical Corp.). U. S. Patent 3,195,304. July 20, 1965. Filed July 16, 1962.

The preparation of a ternary alkali metal alloy containing from 2 to 7 wt% Na, 16 to 36 wt% K, and 60 to 80 wt% Cs is discussed. The alloy is a liquid from about −73 to 740°C under atmospheric pressure. The alloy is prepared by mechanically mixing the metals at a temperature above their melting point in an inert atmosphere. The alloy may be used to produce power by heating the ternary mixture to provide a stream of Cs rich vapor and a liquid residue, extracting the energy from the vapor, and condensing the cooled vapor to liquid Cs for remixing with the liquid residue. The resulting mixture of the condensed Cs with the liquid residue has the composition of the ternary mixture. (B.L.M.)

47937 METHOD AND APPARATUS FOR REACTOR LEAK DETECTION. Ralfe, Leonard George; Paget, Francis Thomas William (to United Kingdom Atomic Energy Authority). U. S. Patent 3,200,041. Aug. 10, 1965. Priority date Jan. 20, 1959, Great Britain.

A method of testing for the presence of a damaged fuel cartridge in a fluid-cooled nuclear reactor consists of sampling coolant that has passed over fuel cartridges, passing the sample over a surface under the influence of an electric field so that solid daughter products of long-lived fission products are precipitated on the surface, and monitoring the surface to detect β particles and γ rays of >3 Mev. Sampling pipes for continuously taking two samples of coolant from each fuel channel in the reactor are coupled with a cross matrix of sampling ducts so that coolant issuing from any channel is identified by its coordinates in the matrix. Flow between the sampling ducts and the monitors is retarded to permit decay of induced activity and short-lived fission products so that the principal active solid constituent monitored is ^{88}Rb. An arrangement is included that permits continuous monitoring of a single channel only. (A.G.W.)

47938 PLANT FOR REMOTE HANDLING OF NUCLEAR FUEL ELEMENTS. Franco, Gianfranco; Lockett, George Edward; Kinkead, Norman; Sorensen, Viggo Henning (to United Kingdom Atomic Energy Authority). U. S. Patent 3,200,043. Aug. 10, 1965. Priority date June 24, 1960, Great Britain.

A system for remote handling of nuclear fuel elements is integrated with a reactor enclosed within a pressure vessel. An inner containment structure containing the pressure vessel includes also a loading bay and a transfer chamber for fuel elements and a storage magazine located below ground level. A loading route for fuel elements and an unloading route for irradiated fuel elements are made up of a series of locations aligned with one another. A transfer flask supported on a carriage is arranged to run on rails over the locations on the routes. Motors for operating the system are located in a control room in an outer containment building. (A.G.W.)

47939 CHARGING SYSTEM FOR NUCLEAR REACTOR. Long, Everett (to English Electric Co. Ltd.). U. S. Patent 3,200,044. Aug. 10, 1965. Priority date Feb. 1, 1961, Great Britain.

An apparatus for providing access to a group of fuel element channels in a nuclear reactor through an access duct in the biological shield includes a rotatable charge chute mounted in the duct and an assembly of fixed fuel-element guide tubes positioned adjacent the servicing ends of the fuel channels. Each guide tube is aligned at one end with one of the reactor fuel channels, and the other end is so positioned that access may be obtained to any desired fuel channel through the opening in the charge chute and the appropriate guide tube by simple rotation of the charge chute. The charge chute may also have a guide member capable of angular movement with respect to the axis of the charge chute. (A.G.W.)

47940 NUCLEAR REACTOR WITH PRESSURIZER. Hackney, Stanley; Williams, Ronald Peter (to United Kingdom Atomic Energy Authority). U. S. Patent 3,201,319. Aug. 17, 1965. Priority date July 5, 1962, Great Britain.

The reactor patented has a liquid primary coolant as an intermediary between the fuel elements and a secondary coolant passing through the core. The primary coolant is contained separately from the secondary coolant and is in communication with a pressure chamber arranged to enable the primary coolant to be pressurized against bulk boiling. Preferably the chamber encompasses the core outline. It may take the form of a coil of ducting with its turns close together, or it may take the form of several superposed endless ducts intercommunicating through pipes of smaller cross section. The circuit further includes a pump to induce forced circulation in the primary coolant. (A.G.W.)

47941 REEL-TYPE CONTROL ROD DRIVE AND BRAKE AND BRAKING MECHANISM. Fortescue, Peter; Bell, Francis R. (to General Dynamics Corp.). U. S. Patent 3,202,580. Aug. 24, 1965. Filed Feb. 11, 1963.

An apparatus is provided for controlling the quick fall of a vertical-type control rod during an emergency shutdown of the reactor. The control mechanism prevents the control rod from arriving at a desired final position at excessive speed while not unduly slowing down the fall of the rod to a safe position. The apparatus is designed for use with a cable-suspended rod, a clutch for connecting the motor to the cable for adjusting the operating height of the rod, and means for promptly disengaging the clutch in case of an emergency. The apparatus controls the fall of the rod by disengaging the clutch to permit the rod to fall quickly to a safe position and using a percentage of the energy developed in the emergency fall to effect uni-directional rotary movement of a flywheel geared to and driven by the cable. After the rod reaches a safe position, the apparatus progressively increases the percentage automatically during the later period of emergency fall of the rod to progressively decelerate the fall of the rod during the final period to a safe speed before the rod reaches its bottom position. The cable is then disconnected from the flywheel permitting it to continue its uni-directional movement. (B.L.M.)

47942 CHARGING APPARATUS FOR NUCLEAR REACTORS. Greaves, Thomas Cyril; Orszak, Peter (to English Electric Co., Ltd.). U. S. Patent 3,205,142. Sept. 7, 1965. Priority date Sept. 6, 1961, Great Britain.

An apparatus is described that provides access to a group of fuel element channels through an access duct in the biological shield of the reactor. A rotatable charge chute is adapted to be mounted in the duct, and an assembly of fixed element guide tubes are positioned adjacent to the servicing ends of the fuel channels. Each guide tube is aligned at one end with one of the fuel channels within the group, and the other ends are arranged on two pitch circles

concentric with the axis of the charge chute. A movable flap is mounted on the charge chute for angular movement across the chute between two positions, in one position to provide access to guide tubes on one of the pitch circles and in the other position to provide access to guide tubes on the other pitch circle. Actuating means are included for automatically causing appropriate angular movement of the movable flap in response to rotational movement of the charge chute. (B.L.M.)

47943 ROD CLUSTER FUEL ASSEMBLY SUPPORT STRUCTURE FOR NUCLEAR REACTOR. Waine, Peter; Waters, James Duncan (to United Kingdom Atomic Energy Authority). U. S. Patent 3,205,148. Sept. 7, 1965. Priority date Oct. 27, 1960, Great Britain.

A rod cluster fuel assembly is fabricated from strip material troughed transversely at intervals. The strip material is assembled juxtaposed in parts to form webs of double thickness with the troughs coming together to define a number of spaced openings bounded with single thickness of strip material to receive the fuel rods of the cluster. The lengths of strip material forming the webs are secured together at some point(s) remote from the openings. The components of strip material are fashioned to the outline of a closed, generally polygonal figure with the troughs at its corners. (B.L.M.)

Criticality Studies

See also PHYSICS — Criticality Studies.

47944 (ANL–7034) THE RATIO OF ^{238}U CAPTURE AND ^{235}U FISSION CROSS SECTIONS IN FAST REACTORS. Davey, William G. (Argonne National Lab., Idaho Falls, Idaho). May 1965. Contract W-31-109-eng-38. 31p. Dep. mn; CFSTI $2.00 cy, $0.50 mn.

An activation technique was developed for the measurement of the ratio of the capture cross section of ^{238}U and the fission cross section of ^{235}U in zero-energy fast reactors. This work was initiated because of the long-standing discrepancy between calculated values of this ratio and radiochemically measured values. The new technique is a direct counting method which does not involve chemical separation in any way. Measurements were made in four ZPR-3 fast reactor assemblies, two with hard spectra and two with soft spectra. In all four cases the measured ratio was slightly (4%) higher, on the average, than the calculated value. This is in strong contrast with the past radiochemical measurements in ZPR-3 assemblies, which gave values 16% less than calculation. The present measurements, therefore, support the general correctness of the calculated ratio, and hence indicate that there are no gross errors in the assumed average microscopic values of the ^{238}U capture cross section and the ^{235}U fission cross section. (auth)

47945 (ANL–7050, pp 159-77) VARIATIONAL METHODS FOR THE SOLUTION OF PROBLEMS OF REACTOR KINETICS. Galligani, Ilio (European Atomic Energy Community, Ispra (Italy). Joint Nuclear Research Center).

The solution of the time-dependent multigroup, multiregion diffusion equations may be obtained by searching for the functions that render stationary a particular functional. These functions are determined numerically by Kantorovich's method and by Euler's method. With the Kantorovich method the flux and the adjoint flux are expanded in a set of space-dependent trial functions with time-dependent coefficients. These coefficients are determined by solving with a "one-step method" a system of ordinary differential equations. The Euler method consists in searching for the functions that render stationary the above functional in the class of piecewise linear functions. These functions satisfy a large system of ordinary differential equations and are determined numerically by three different methods, the "implicit" method, the "implicitly explicit" method, and the Saul'yev "alternating" method. A comparison between the Kantorovich method and the Euler method is made by means of some numerical examples. (auth)

47946 (ANL–7050, pp 231-49) METHODS FOR THE INTERPRETATION AND PREDICTION OF REACTOR POWER DISTRIBUTIONS WITH AN APPLICATION TO FUEL CYCLE CALCULATIONS. Blackburn, D.; Griggs, C. F. (Reactor Group, United Kingdom Atomic Energy Authority, Sellafield (England)).

Methods for the solution of the two-dimensional diffusion equations are discussed. The most elaborate method is an extension of the source-sink method to finite fuel channels, but this is reformulated in terms of the conventional finite-difference equations plus some extra terms. Results of sufficient accuracy for many purposes are, however, obtained in AGR situations from a method that solves the conventional finite-difference equations using one in-channel mesh point per lattice. As an application of this last method a program for studying fuel cycles in AGR is described. (auth)

47947 (ANL–7050, pp 395-412) FREAK—A FAST REACTOR MULTIGROUP KINETICS PROGRAM. Perks, M. A. (Reactor Group, United Kingdom Atomic Energy Authority, Risley (England)).

A program is written to deal with multienergetic neutrons with two-dimensional spatial distribution, in order to check the normal treatment of kinetics of fast neutron reactors for integral disturbances (e.g., step and ramp changes in reactivity), and to investigate those types of local disturbances (e.g., movement of some of the fuel elements and partial flow blockage) for which the point model is clearly unacceptable. Since the program is intended to deal specifically with fast power reactors, it was considered necessary to treat multienergetic neutrons and also to be able to follow in some detail the movements of fuel elements, since this can be a major source of reactivity feedback in such systems. The general basis of the program is described, along with the steady-state calculations. Treatment of time-dependent behavior is given. The Doppler effect, reactor control and scram, and editing routines associated with the main program are studied. Comparisons are made between results obtained from the program and those from a point reactor treatment. (auth)

47948 (ANL–7050, pp 517-39) THE PROCESSING OF NUCLEAR DATA FOR REACTOR CALCULATIONS. Parker, K. (Atomic Weapons Research Establishment, Aldermaston (England)); Honeck, H. C. (Brookhaven National Lab., Upton, N. Y.).

The nuclear data used in reactor calculations are outlined, particular emphasis being given to neutron cross sections. Problems involved in converting nuclear physics measurements and calculations into a form suitable for use in reactor calculations are discussed. The need for computer processing of the data is demonstrated. Examples of existing punched card/magnetic tape libraries of microscopic neutron cross sections and associated computer processing codes are described. The desirability of international cooperation in the exchange of libraries and processing codes is discussed as a logical consequence of the scale of effort involved. The concept and development of the Evaluated Nuclear Data File at Brookhaven National Laboratory as an effort in this direction is described. (auth)

47949 (ANL–7050, pp 557-79) TECHNIQUES USED IN THE GEM CODE FOR MONTE CARLO NEUTRONICS CALCULATIONS IN REACTORS AND OTHER SYSTEMS OF COMPLEX GEOMETRY. Woodcock, E. R.; Murphy, T. (Reactor Group, United Kingdom Atomic Energy Authority, Risley (England)).

A number of codes is under development to exploit the advantages of the Monte Carlo technique. The GEM code was designed initially to study criticality-safety problems in chemical plants, and a primary objective was to use nuclear data in as fine a detail as possible. Its geometrical capabilities were extended to carry out a survey of the factors affecting the nuclear safety of arrays of transport

containers carrying fissile materials. Developments since that time have enabled virtually all geometrical restrictions to be removed. The resulting program has proved versatile enough to make neutronic calculations for a complete reactor, incorporating all the significant structural features. (auth)

47950 (ANL–7090, pp 69-78) NUCLEAR SAFETY. (Argonne National Lab., Ill.).

Discussions on reactor kinetics, TREAT, and chemical and associated energy-transfer problems in reactor safety are given. The discussion on reactor kinetics concerns; the fast-neutron hodoscope, meltdown experiments with sodium, and fast reactor control and safety. (M.O.W.)

47951 (APDA–173) FAST REACTOR FUEL MELTDOWN TEST FACILITY REQUIREMENTS. Branyan, C. E.; Ball, G. L. (Atomic Power Development Associates, Inc., Detroit, Mich.). Aug. 31, 1965. Contract AT(11-1)-865. 35p. Dep. mn; CFSTI $2.00 cy, $0.50 mn.

To provide a basis for the evaluation of existing or proposed reactor facilities for fast reactor meltdown testing, a study was conducted to establish the nuclear characteristics and supporting auxiliaries required of a test reactor facility to enable it to make a significant contribution to existing data on meltdown phenomena for fast reactor safety studies. The range of meltdown accident types of interest to fast reactor safety analysts is discussed in detail. It is concluded that, in addition to burst-type operation, a test facility must be capable of brief periods of high-power operation. It is necessary to approximate steady-state temperature conditions in a fuel test sample prior to initiation of meltdown such as by reduction of coolant flow or an increase in power. A minimum-sized oxide fuel test bundle containing 19 pins 0.25 inch in outside diameter is specified, to be tested in a sodium or NaK loop capable of removing up to 1/2 Mw of heat from the test bundle. The data required from typical meltdown tests are indicated, with primary emphasis placed on obtaining information on the distribution of the molten and particulate test fuel as a function of time. These data are of major importance in assessing the probability and extent of an energy release resulting from the meltdown of a fast reactor core. (auth)

47952 (APDA–177) APPLICATION OF THE POWER BURST FACILITY TO FAST REACTOR FUEL MELTDOWN TESTS. Branyan, C. E.; Ball, G. L.; MacLeod, R. A.; Nicholson, R. B.; Ross, T. P. (Atomic Power Development Associates, Inc., Detroit, Mich.). Aug. 31, 1965. Contract AT(11-1)-865. 94p. Dep. mn; CFSTI $3.00 cy, $0.75 mn.

The initial core planned for the Power Burst Facility (PBF) is evaluated with respect to the extent of its application as a test facility for stimulating various types of fast reactor fuel meltdown accidents of interest in fast reactor safety analysis. It is concluded that the application of PBF is limited to the simulation of rapid reactivity insertions from low power and to the simulation of a meltdown accident resulting from decay heat in the absence of sodium. Various second-core concepts are evaluated, based upon increasing the heat capacity of the PBF core to facilitate simulation of at-power temperature conditions in the fuel test sample before meltdown. A driver-core fuel mixture of uranium oxide and beryllium oxide is potentially capable of providing the necessary heat capacity to simulate a number of important meltdown accidents. It is determined that a UO_2–BeO heat-capacity-type core using a nonhydrogenous coolant such as perchlorethylene, or a related chemical compound, is feasible for application to PBF. The conceptual design of a large sodium loop necessary for fast reactor fuel meltdown tests is presented, and methods of directly or indirectly determining the progress of the test fuel sample meltdown are discussed. Cost estimates are presented for utilizing the initial PBF core for fast reactor fuel meltdown tests. Likewise, cost estimates are given for an expanded program utilizing a UO_2–BeO core and a large sodium loop. (auth)

47953 (BNL–9393) INTERMEDIATE RESONANCE ABSORPTION IN HETEROGENEOUS MEDIA INCLUDING MODERATOR SCATTERING. Sehgal, Bal Raj; Goldstein, Rubin (Brookhaven National Lab., Upton, N. Y.). July 1965. Contract AT(30-2)-Gen-16. 5p. (CONF-651101-32). Dep. mn; CFSTI $1.00 cy, $0.50 mn.

From 13th Conference on Remote Systems Technology, Washington, D. C.

In the resonance absorption theory the restriction of treating the moderator in a narrow resonance approximation was recently removed. The intermediate resonance previously developed is extended to include moderator scattering in heterogeneous media. The brief procedure for the extension is given. Calculations were done with this method for a series of ^{238}U metal lattices for the 6.7-ev resonance, and some of the results are presented. (M.O.W.)

47954 (BNWL–127) MONTE CARLO CALCULATED MATERIAL BUCKLINGS OF 3 wt PERCENT ENRICHED URANIUM-WATER LATTICES WITH URANIUM IN THE WATER MODERATOR. Carter, L. L. (Battelle-Northwest, Richland, Wash. Pacific Northwest Lab.). Sept. 1965. Contract AT(45-1)-1830. 33p. Dep. mn; CFSTI $2.00 cy, $0.50 mn.

A difficult technical problem of importance in processing reactor fuels involves criticality of uranium rods in uranium solution (problem of uranium dissolution). The material buckling for such a mixture is difficult to evaluate by standard methods. Monte Carlo techniques were used to evaluate the material bucklings for 3 wt % enriched uranium–water lattices with various uranium concentrations in the moderator. The maximum material buckling that may be obtained under optimum geometry conditions was calculated to occur with uranium absent from the moderator. These results apply to solid rods only since tubular fuel elements were not considered. (auth)

47955 (CONF-651103-6) MAXIMUM SAFE LIMITS FOR SLIGHTLY ENRICHED URANIUM AND URANIUM OXIDE. Clark, H. K. (Du Pont de Nemours (E. I.) and Co., Aiken, S. C. Savannah River Lab.). Sept. 9, 1965. Contract AT(07-2)-1. 21p. (SM-70/31). Dep. mn; CFSTI $1.00 cy, $0.50 mn.

For Presentation at IAEA Symposium on Criticality Control of Fissile Materials, Stockholm.

A simple, approximate method is used for the calculation of safe limits for lattices of slightly enriched uranium and uranium oxide in water. The material buckling is calculated by an asymptotic multigroup transport code and the extrapolation distances by a two-group diffusion theory code. Data from exponential and critical experiments on these lattices in water are reviewed briefly. The calculations and experimental data were used to calculate critical and safe dimensions for spheres, infinite cylinders, and infinite slabs. (D.L.C.)

47956 (IAE-723) VLIYANIE TEMPERATURY ZAMEDLYAYUSHCHEI SREDY NA PROSTRANSTVENNO-ENERGETICHESKOE RASPREDELENIE POTOKOV NEITRONOV. (Effect of the Moderating-Medium Temperature on the Space-Energy Distribution of Neutron Flux). Isaev, A. N.; Chernilin, Yu. F. (Institut Atomnoi Energii, Gosudarstvennyi Komitet po Ispol'zovaniyu Atomnoi Energii SSSR, Moscow). 1964. 12p. Dep.mn.

The possibility of increasing the neutron flux in the energy interval 0.1 to 0.5 ev by modifying the neutron energy spectrum and by changing the temperature of the reactor reflector is estimated. The analysis begins with an estimate of the influence of the variation of the temperature and the energy distribution of neutron fluxes in an infinite moderating medium without absorption of neutrons during the course of moderation. Such a neutron spectrum can be produced in the reactor with sufficiently thick reflector and small absorption cross section. In the next step it is assumed that the neutron spectrum of the reaction is such that the slowing-down neutrons have a Fermi distribution and the thermal neutrons have a Maxwellian distribution. The transition between the Fermi and the Maxwell spectra

occurs in some energy region in which the neutron spectrum differs somewhat from Maxwellian. The results show that when the reflector temperature is increased from 350 to 1700°K the flux of the 0.2 to 0.6 ev neutrons increases 100 times. Corrections are introduced to allow for the neutron distribution in actual reactors (type IRT and type SM). The results confirm the appreciable increase in the integral flux of thermal neutrons resulting from the increase in the reflector temperature. (ATD)

47957 (IAE-724) OPTIMAL'NYE METODY OBRABOTKI PEREKHOTSNYKH PROTSESSOV. (Optimum Methods for Handling Transient Processes in Nuclear Reactors). Isaev, A. N.; Ostapenko, V. V.; Chernilin, Yu. F. (Institut Atomnoi Energii, Gosudarstvennyi Komitet po Ispol'zovaniyu Atomnoi Energii SSSR, Moscow). 1964. 15p. Dep. mn.

The transients occurring in a nuclear reactor were used to determine its kinetic and physical constants. It is pointed out that earlier methods are based on a solution of elementary kinetic equations for some specified law of reactivity variation. Some of the difficulties involved in earlier methods are pointed out. The method described consists of deriving the coefficients of the system of elementary kinetic equations by applying optimal methods for the reduction of the transient curves. The theory of the method is based on the application of variational analysis and probability theory to automatic control, as developed by various authors. It is shown that by constructing a reactor model in analog form it is possible to obtain information on the reactivity state of the reactor, provided the model is part of a feedback control loop based on the difference between the output of the nuclear reactor and its model. The optimization is obtained if extremal parametric control of the model is employed. The coefficients of the system of elementary kinetic equations are thus determined without the need for experimental equipment. The use of high-speed computers, which can search rapidly for a solution of the differential equations satisfying the specified optimality criterion, can provide the solutions of concrete problems in reactor control. Some of the premises discussed are illustrated by concrete examples of calculations performed with an electronic computer. (ATD)

47958 (PWAC-475) OPERATING LIMITS AND SAFETY ANALYSIS FOR SPLIT-TABLE, DRY, FLEXIBLE CRITICAL EXPERIMENTS AT THE CANEL NUCLEAR PHYSICS LABORATORY. Paradis, E. L.; Welsh, W. F.; Kapinos, L. E. (and others) (Pratt and Whitney Aircraft, Middletown, Conn. Connecticut Advanced Nuclear Engineering Lab.). Aug. 16, 1965. Contract AT(30-1)-2789. 53p. Dep. mn; CFSTI $3.00 cy, $0.50 mn.

Operating limits are presented for split-table, dry, and flexible critical experiments. The operating limits cover those operating variables which are measurable and under the control of the operating group, and those operating and administrative procedures which can significantly influence safe operation. The potential operational hazards and countermeasures of these operating limits are discussed. (M.O.W.)

47959 (WCAP-3269-52) EVALUATION OF A COMPUTATIONAL SYSTEM APPLICABLE TO THE NUCLEAR ANALYSIS OF CRITICAL EXPERIMENTS AND POWER REACTORS. Eich, W. J.; Williams, H. T. Jr.; Radcliffe, R. E. (Westinghouse Electric Corp., Pittsburgh, Pa. Atomic Power Div.). June 1965. Contract AT(30-1)-3269. 57p. Dep. mn; CFSTI $3.00 cy, $0.50 mn.

A computational system which has proven to be extremely consistent in the nuclear analysis of practical configurations involving light water moderated lattices is described. The assemblies which have been analyzed consist of either UO_2 or U-metal clad in aluminum, steel or zirconium; single enrichment, multi-region and borated room-temperature experiments as well as actual reactor (Yankee Core I) zero-power configurations have been studied. The computational scheme applied to the analysis of these experiments makes use not only of a refined specification of lattice cell reaction rates but also of auxiliary multigroup calculations to account for the various spectral and transport effects always present near lattice discontinuities such as the core-reflector interface in critical assemblies or the control rods in a large reactor. Neutron multiplication factors for most of the room temperature critical assemblies subjected to analysis average to the value of 0.9979 with a standard deviation of 0.0019. Neutron multiplication factors which are outside this band correspond to two sets of experiments. One set is a group of high buckling experiments with 0.300" diameter fuel rods. The second set involves the Yankee reactor at a temperature of 514°F. (auth)

47960 (ORNL-tr-694) NUCLEAR REACTOR SAFETY: THE MELTDOWN OF METALS AT HIGH TEMPERATURES AND METAL-WATER REACTIONS. Liimatainen, Robert C. Translated for Oak Ridge National Lab., Tenn. from Arkhimedes, No. 1, 27-36(1964). 15p. Dep. mn; JCL $1.60 fs, $0.80 mf.

The significance of chemical energy is evaluated in relation to a water-cooled reactor wherein the nuclear energy release during a power excursion or loss of coolant incident is sufficient to melt the fuel elements which may then react exothermically with the water. Experimental results are summarized from both laboratory and TREAT in-pile studies on reaction of molten aluminum, magnesium, stainless steel, uranium, and zirconium with water. The data show that there are three interrelated parameters pertinent to the metal-water hazards analysis problems for a given core material; they are: the energy input as determined by the integrated power of the reactor pulse, the reactor period, and the particle size into which the fragmented core materials are dispersed. Finally, rate limiting mechanisms and approaches to correlating and predicting metal-water reactions are presented. (auth)

47961 CRITICAL AND EXPONENTIAL EXPERIMENTS. Caro, R. (Junta de Energia Nuclear, Madrid). Energia Nucl. (Madrid), 9: 113-17(Mar.-Apr. 1965). (In Spanish).

The necessity of experimentation with critical and exponential assemblies as a preliminary step to the construction of a nuclear reactor is analyzed. Such a step, apart from the experience which bears on the technology of the system, is used to adjust the calculation model used and in some cases to gain information on physical magnitudes. An inadequate calculation model can lead to inadmissible cost imprecisions. (tr-auth)

47962 AN ANALYSIS OF A NONLINEAR REACTOR CONTROL SYSTEM. Beltracchi, L. (Pratt and Whitney Aircraft, Middletown, Conn.). IEEE (Inst. Elec. Electron. Engrs.), Trans. Nucl. Sci., NS-12: No. 4, 323-42(Aug. 1965). (TID-21638).

The stability criteria and stability margin for a nonlinear reactor control system are developed. The nonlinear reactor control system contains a position feedback of the reactivity control element. The position feedback is around the motor and results in an enhancement of stability. A qualitative analysis of the effects of control characteristics upon stability is conducted. A similar analysis is conducted to evaluate the performance of the control. (auth)

47963 KINETIC EQUATIONS FOR NEUTRON DISTRIBUTIONS. Osborn, R. K.; Natelson, M. (Univ. of Michigan, Ann Arbor). J. Nucl. Energy: Pts. A and B, 19: 619-39(Aug. 1965).

Kinetic equations for neutrons and some of the other kinds of particles important to neutron balance in reactors and reactor-like systems are derived from a quantum Liouville equation. In particular, equations for some of the relevant singlet and doublet densities in phase space are deduced for the purpose of studying neutron density fluctuations. The equations describing neutron densities, ignoring delayed neutron precursors, are then singled out for special attention. These equations are reduced to "one-speed" or mono-energetic analogues, and are then approximated by equations for the zeroth and first angular moments of these densities. During the process, points of connection with the descriptions of neutron density fluc-

tuations from previous work are made. Formal solutions of the equations in phase space are displayed, along with an explicit solution of the reduced equations. Properties of these solutions are discussed, with particular interest paid to the implications for the "critical limit." (auth)

47964 APPROXIMATE TREATMENT OF THE FAST NEUTRON SPECTRUM IN A TWO-COMPONENT HOMOGENEOUS MEDIUM. Yousef, M. Y. A.; Amin, E. A.; Lukyanov, A. A. (Atomic Energy Establishment, Cairo). J. Nucl. Energy, Pts. A and B, 19: 693-701(Sept. 1965).

On the basis of the Goertzel-Greuling method, a simple formula for the fast neutron spectrum in a bare homogeneous reactor with a two-component moderator is obtained. Application of this formula to spectrum calculations in H_2O and D_2O gives results in good agreement with exact numerical calculations. (auth)

47965 ACTIVITIES OF SPECIAL COMMITTEE ON EXPERIMENTAL REACTOR PHYSICS. Nippon Genshiryoku Gakkaishi, 7: 306-16(May 1965). (In Japanese).

A summary is given of the activities performed by the Special Committee on Experimental Reactor Physics over the two years from its formation in May 1963 to its termination in March 1965. The areas covered included reactivity measurements, pulsed-neutron experiments, neutron spectra analysis, and criticality analyses. The status of experimental reactor physics in Japan, including both critical and subcritical systems moderated by light water, heavy water, and graphite, was reviewed. (auth)

47966 SOME TOPICS FROM ACTIVITIES OF SPECIAL COMMITTEE ON REACTOR NOISE ANALYSIS. Nippon Genshiryoku Gakkaishi, 7: 359-66(July 1965). (In Japanese).

The Special Committee on Reactor Noise Analysis of the Atomic Energy Society of Japan was established in May 1963. Surveys were made on reactor noise studies in Japan and abroad. Work related to the theoretical aspects of reactor noise and the relation between reactor noise and control was carried out. (auth)

47967 PLUTONIUM CRITICALITY EXPERIMENTS. Clayton, E. D. (Battelle-Northwest, Hanford, Wash.). Phys. Today, 18: 46-8; 50-2(Sept. 1965).

For both reactor design and safety in nuclear-fuel processing, the masses, concentrations, and dimensions of critical plutonium systems must be known. Behavior is similar to that of uranium, but different enough that extrapolation is difficult and experiments are necessary. These experiments have examined criticality in water solutions and plutonium assemblies. The reasons for plutonium study, critical mass, volume, and size, criticality in ^{239}Pu and ^{235}U, plutonium isotopes, critical experiments, and safety are discussed. (J.F.P.)

47968 A SIMPLIFIED CELL THEORY APPLIED TO THE CALCULATION OF THERMAL NEUTRON SPECTRA IN LIGHT WATER LATTICES (thesis). Mac Vean, Charles Robert. Ithaca, N. Y., Cornell Univ., 1964. 214p.

A simplified polyenergetic cell theory is formulated to determine spatially averaged energy-dependent thermal fluxes in the moderator, cladding, and fuel regions within the unit cell of a reactor lattice. The derived spectra are then utilized in the calculations of the thermal integral parameters and average cross sections required for reactor computations. The cell theory, as formulated, postulates an infinite moderator region with the absorption cross section of this region appropriately modified to account for the neutron leakage into and absorption by the fuel element. The modifications to the moderator absorption cross section are formulated both in terms of the net current at the fuel element-moderator interface and in terms of energy-dependent moderator and fuel element escape probabilities. Analytic expressions for the escape probabilities are presented, integral transport theory being applied to the fuel element region, while diffusion theory is utilized in the moderator region. The theory is applied to actual lattices in the form of the light-water-moderated and uranium-dioxide-fueled cores of the Cornell University Zero Power Reactor. Room temperature parameters and their temperature coefficients are determined using both the monatomic gas model and the Nelkin water kernel to describe the energy transfer process in the moderator. Calculations are made with PROGRAM COUTH, a Fortran-63 program written for use with the Control Data Corporation 1604 digital computer. A study of the sensitivity of the calculated integral parameters to variations in the input data leads to the assignment of rather small uncertainties in the results calculated with the simplified cell theory. (Dissertation Abstr.)

47969 A MEASUREMENT OF THE RESONANCE ESCAPE PROBABILITY OF NEUTRONS IN A HOMOGENEOUS THORIUM REACTOR (thesis). Anthony, Lee Saunders. Blacksburg, Va., Virginia Polytechnic Inst., 1962. 64p.

A determination of the resonance escape probability of thorium as thorium nitrate in aqueous solution was made as a function of thorium concentration. The physical system used was an aluminum box surrounded by successive layers of cadmium, paraffin, and borated paraffin. Neutrons were obtained from a Cockcroft-Walton type accelerator by the $D(d,n)^3He$ reaction. Neutron density was measured at nine spatial positions in the direction of the neutron beam with a bare boron trifluoride detector. The area under a curve of neutron density versus spatial position was obtained for various concentrations of absorber. This process was carried out for the thorium solution and for a mock solution, whose cross section was similar to that of thorium except that it had no resonances in the thorium resonance region. By taking ratios of the neutron densities in the thorium solution to the neutron density in the mock solution, it was possible to determine the resonance escape probability of neutrons in a homogeneous, aqueous solution of thorium nitrate. It is shown that, for the absorber concentrations used, the resonance escape probability for an infinite geometry may be obtained by the above ratio method. Before taking the above ratios of neutron densities, it was necessary to compensate for the spectral shift of the thermal flux in the two solutions. Over the range covered by the experiment ($0 - 1 \times 10^{21}$ atoms of thorium per cubic centimeter), experimental results agree with Monte Carlo predictions to within one percent. Calculations of effective resonance integrals from the experimentally determined values of the resonance escape probability show good agreement with published measurements on other systems. (Dissertation Abstr.)

47970 A MONTE CARLO CALCULATION OF THE RESONANCE ESCAPE PROBABILITY OF THORIUM IN A HOMOGENEOUS REACTOR (thesis). Bushnell, David Lewis. Blacksburg, Va., Virginia Polytechnic Inst., 1961. 146p.

A method is developed for determining the resonance escape probability of homogeneous reactors containing aqueous solutions of a resonance absorber. $Th(NO_3)_4$ was selected as a salt since it is readily dissolvable in water. The atomic densities of thorium and nitrogen are small compared to hydrogen and oxygen; therefore, a water Monte Carlo serves adequately as the neutron supply to the resonance region of thorium. In order to find an escape probability the ratio of the number of neutrons that attain energies below the resonance region to the number that appear in the resonance region for the first time is determined. The water Monte Carlo provides a set of data cards that can be used as the input data to a second Monte Carlo designed to calculate the resonance escape probability. The resonance escape Monte Carlo is a direct analog type using known physical distributions and laws. The detailed effect of the thorium resonances on the number of neutrons absorbed is described by the cross section as a function of energy. A Breit-Wigner Doppler broadened single level formulation gives the scattering and absorption parts of the cross section as a function of energy. The heart of the Monte Carlo method lies in the determination of a random variable, distributed according to some known probability function. This requires a source of random numbers which in our case is provided by the IBM-650

computer. The resonance escape probability as a function of thorium number density fits very closely to a straight line with small negative slope throughout the whole range of stable concentrations. The Monte Carlo statistics provide probable errors of less than 0.3% for all five points calculated. A theoretical determination of the resonance escape probability based on resonance integral theory for the eight peaks used in the Monte Carlo calculation gives good enough agreement to make both methods plausible. (A.G.W.)

Design and Feasibility

47971 STABILITY OF THE REACTOR WHICH HAS THE EXTERNAL CONTROL SYSTEM. Ogawa, Yuichi (Hokkaido Univ., Japan). Nippon Genshiryoku Gakkaishi, 7: 290-7(May 1965). (In Japanese).

When a reactor is externally controlled, parameters governing the control must be chosen in close connection with the nuclear and thermal properties and output of the reactor, in order to attain stability in the vicinity of operating power. To get this relation, nonlinear integral equations containing the effects of fast- and slow-responding internal feedbacks and delayed neutrons were adopted and related to the external control system. The method of introducing the special Liapunov function developed by Lur'ye, et al. was applied to the whole system and the required relation was obtained. Results of numerical calculations are presented in the form of diagrams. Some modifications to the dynamic reactor equations to obtain a more concrete representation of the dynamic behavior of heterogeneous reactors are discussed. It is desirable that the equations contain directly the effect of the moderator temperature, which consists of three thermal time constants and is the solution of heat equations between the heterogeneous elements of the reactor. These equations were solved by expansion, and the region of stability was determined. (auth)

47972 NUCLEAR REACTOR. Lemesle, Georges; Patarin, Louis; Rouge, Pierre (to Commissariat a l'Energie Atomique). British Patent 1,003,395. Sept. 2, 1965. Priority date Aug. 1, 1963, France.

A heterogeneous reactor includes a core and a heat exchanger that are separated from one another by a radiation shield and that are disposed in a reactor pressure vessel adapted to withstand the pressure of the reactor cooling fluid. The core and the heat exchanger are received in a secondary cell that coöperates with the pressure vessel to bound an annular zone and comprises a double side wall bounding the annular space. Means are provided to provide a flow of secondary cooling fluid in the annular zone between the pressure vessel and the secondary cell at a temperature below the temperature of the fluid leaving the heat exchanger. Preferably from a structural standpoint, the secondary cell is borne by the base end of the pressure vessel and transfers the weight of the reactor core to this base end. (B.L.M.)

47973 GAS COOLED NUCLEAR REACTOR WITH IMPROVED FUEL ELEMENT ARRANGEMENT. Fortescue, Peter; Rickard, Corwin L. (to General Dynamics Corp.). U. S. Patent 3,201,320. Aug. 17, 1965. Filed Dec. 7, 1960.

A fuel element arrangement particularly adapted for large-capacity power reactors having a large number of fuel elements is patented. Individual elongated vertically disposed fuel elements are arranged in side-by-side relation to form a cluster, which is supported in a manner preventing displacement of the elements during operation of the reactor and affording removal of the cluster as a unit for refueling. A passage is provided for the purge flow of fission products. (A.G.W.)

47974 PRESSURIZED WATER REACTOR PLANT WITH IMPROVED JET PUMP ARRANGEMENT. Bogaardt, Maarten; Bonsel, Wouter G.; Muysken, Matthijs; Nijs, Wilhelmus W.; Bahbout, Abraham (to Reactor Centrum Nederland). U. S. Patent 3,202,584. Aug. 24, 1965. Priority date Jan. 26, 1961, Netherlands.

A pressurized-water reactor comprises a vertical casing, a number of elongated fuel elements in the casing means supporting the elements in spaced relation to define a number of vertical passages, a heat exchanger, and conduits interconnecting the casing and heat exchanger to form a closed circuit. The circuit is filled with water acting both as moderator and coolant. A jet pump is provided in the space surrounding the core and includes a jet tube connected to the pressure outlet of a main pump located in one of the conduit means for circulating the water. The jet pump has a suction inlet directed towards the upper space in the casing into which the outlet end of the core opens and a pressure outlet directed towards the lower space in the casing to which the inlet end of the core communicates. The reactor is compact with a relatively high thermal efficiency and is adapted to propel vessels. (B.L.M.)

Fuels

47975 (BNL-9450) ALPHA GAMMA FACILITY FOR FUEL STUDIES. Banslaben, A. J.; Chow, J. G. Y. (Brookhaven National Lab., Upton, N. Y.). [1964]. Contract AT(30-2)-Gen-16. 11p. (CONF-651101-21). Dep. mn; CFSTI $1.00 cy, $0.50 mn.

From 13th Conference on Remote Systems Technology, Washington, D. C.

An alpha gamma facility was constructed at Brookhaven National Laboratory to study fast reactor fuel materials. The facility consists of three Argonne type DDD boxes, a welding dry box, and five shielded containment boxes. All the boxes will operate with a nitrogen gas atmosphere to avoid oxidation of fuel and to prevent NaK fire. In the design of the facility care was not used to duplicate functions for hot and cold testing of the fuel pellets. (auth)

47976 (BNWL-131A) FABRICATION COSTS FOR PLUTONIUM FUEL ELEMENTS. PART A: VARIABLE COSTS OF FABRICATION UO_2–PuO_2 FUEL RODS FOR THE PLUTONIUM RECYCLE CRITICAL FACILITY. Bloomster, C. H. (Battelle-Northwest, Richland, Wash. Pacific Northwest Lab.). Sept. 1965. Contract AT (45-1)-1830. 24p. Dep. mn; CFSTI $2.00 cy, $0.50 mn.

Based on the fabrication of 500 rods by a well developed, pneumatic-impaction, vibrational-impaction process, the variable cost of fabricating plutonium-enriched fuel rods for PRCF was determined to be $88/kg of fuel (as oxide). This represents a unit cost of $99 per fuel rod. Each rod contains 1.1 kg of UO_2–2 wt % PuO_2 fuel, is 3 ft long and ½ in. ID with Zircaloy cladding. For each rod the shop labor requirements were 3.79 man-hours direct labor and 1.37 man-hours indirect labor. The variable costs included direct materials, some processing costs for nuclear materials, shop labor, direct overhead, analytical services, and consumable supplies, but did not include the cost of nuclear materials themselves, use charges, administrative overhead, research, development, or engineering costs. (auth)

47977 (BNWL-131B) FABRICATION COSTS FOR PLUTONIUM FUEL ELEMENTS. PART B. VARIABLE COSTS OF FABRICATING UO_2–PuO_2 FUEL RODS FOR THE EXPERIMENTAL BOILING WATER REACTOR. Bloomster, C. H. (Battelle-Northwest, Richland, Wash. Pacific Northwest Lab.). Sept. 1965. Contract AT(45-1)-1830. 28p. Dep. mn; CFSTI $2.00 cy, $0.50 mn.

The variable cost of fabricating plutonium-enriched fuel rods for the EBWR came to $198 per kg of fuel (as oxide). This represents a unit cost of $164 per fuel rod. The costs were based on the fabrication of 200 fuel rods by a well developed, pneumatic impaction, vibrational compaction process. With a core length of 1.23 m, each fuel rod contained 829 grams of depleted UO_2–1.5 wt % PuO_2 fuel. The shop labor requirements for each rod were 5.53 man-hours direct labor and 1.61 man-hours indirect labor. Although the costs included the cost of replacing one end cap in each fuel rod, techniques were later developed to eliminate this need. The direct material cost was $48 per fuel rod. The variable costs included direct materials,

some processing costs for nuclear materials, shop labor, maintenance, direct overhead, and consumable supplies. (P.C.H.)

47978 (CEA-R-2782) REPARTITION DES FLUX ET DES TEMPERATURES DANS LES CONVERTISSEURS THERMOIONIQUES NUCLEAIRES SIRENE 50 ET SIRENE 100. (Flux and Temperature Distribution in the Nuclear Thermionic Converters Sirene 50 and Sirene 100). Bliaux, Jean; Jamet, Jean-Michel (Commissariat a l'Energie Atomique, Saclay (France). Centre d'Etudes Nucleaires). May 1965. 55p. Dep. mn.

A preliminary calculation concerning the perturbed neutron flux in a nuclear thermionic converter is given; the true flux value makes it possible to check the real conversion efficiency. Then, another calculation to determine the temperatures distribution in the fuel pin is presented (assuming several conditions about the neutron flux repartition). A comparative neutronical and thermal study makes it possible to judge the interest of an annular fuel pin converter. (auth)

47979 NUCLEAR ENERGY DEVELOPMENT AND ITS DEPENDENCE ON NUCLEAR FUEL RESERVES. van Staveren, J. C.; Went, J. J. At. Strom, 11: 45-8(May 1965). (In German).

The relations between the amount of reserves, consumption, and the future uranium and thorium costs are discussed. The price of nuclear energy is also considered. The effect of tube-material cost on the development of a nuclear energy program and on current nuclear energy production is also considered. (J.S.R.)

47980 IMPROVEMENTS IN OR RELATING TO SHEATHS FOR NUCLEAR FUEL ELEMENTS. Gauthron, Maurice; Ringot, Claude; Stohr, Jacques Andre (to Commissariat a l'Energie Atomique). British Patent 997,190. July 7, 1965. Priority data July 12, 1961, France.

A sheath for a cylindrical fuel element in the form of pellets is shaped in such a way to have sufficient flexibility to compensate for the effects of differential expansion between the sheath and the fuel. The shaping of the sheath material may take any of the following forms: circumferential folds, longitudinal folds material, spiral folds, or a combination of circumferential and longitudinal folds. The circumferential folds are arranged opposite the end pellets of the fuel or opposite the contact planes of the pellets in the fuel element. The sheath is closed at its ends by flexible stoppers. (B.L.M.)

47981 IMPROVEMENTS IN NUCLEAR REACTORS. (to Babcock and Wilcox Ltd.). British Patent 1,000,931. Aug. 11, 1965. Priority date Nov. 9, 1960, Germany.

A nuclear reactor includes a core of moderator material surrounded by a layer of reflector material and provided with fuel elements. Each fuel element is made up of a can containing the nuclear fuel and an absorber material, active carbon, adapted to absorb gaseous fission products emanating from the fuel under irradiation. The fuel element is positioned in the core with the absorber material located in or beyond the layer of reflector material. The can includes walls of impermeable graphite, and the portion of the can immediately adjacent to the absorber material and arranged to be positioned beyond the reflector material is stainless steel. The fuel may be contained in short, cylindrical containers made of permeable graphite and having longitudinally grooved enlarged ends arranged to position the containers within the can. The fuel element can is positioned in a channel extending through the core provided with longitudinally extending grooves for the flow of coolant. (B.L.M.)

47982 NUCLEAR FUEL ASSEMBLY. Rigg, Shepherd; Dodd, John Allan (to Societe Anglo-Belge Vulcain S.A.). British Patent 1,000,933. Aug. 11, 1965. Filed Feb. 25, 1963.

A nuclear fuel assembly has a cluster of fuel rods spaced laterally by a cellular spacing grid through which the rods extend. At least one key fuel rod is in mechanical engagement with its surrounding cell so that the grid is axially supported by the key rod while other cells carry projections to locate fuel rods passing through them without restraining axial movement of the rods. The term "mechanical engagement" excludes thermal methods of attachment such as welding that could damage the rod. The preferred method of engagement between the grid and key rod is crimping a cell wall into a recess in the key rod. (B.L.M.)

47983 PROCESS FOR COATING NUCLEAR FUEL PARTICLES WITH PYROLYTIC GRAPHITE. Finicle, Robert Lee (to Union Carbide Corp.). British Patent 1,002,078. Aug. 25, 1965. Priority date Dec. 18, 1962, United States.

A process for coating nuclear fuel particles with pyrolytic graphite by the pyrolysis of a gaseous hydrocarbon consists of heating the particles to a temperature slightly below the surface sintering temperature of the particles in an atmosphere of an inert gas diluent mixed with a hydrocarbon gas. The volume ratio of the inert gas to the hydrocarbon is 3 to 1 to 20 to 1. The particles are maintained in the atmosphere for a period of time sufficient to deposit a first layer of graphite of a thickness of 5 to 50μ on the particles. The coated particles are heated further to a temperature of 1800°C in an atmosphere consisting of the mixed gases in a volume ratio of inert gas to hydrocarbon of from 7 to 1 to 20 to 1 for a period of time sufficient to deposit a second layer of graphite of the desired thickness. (B.L.M.)

47984 METHOD FOR OPERATING FUEL ELEMENTS OF AN ATOMIC REACTOR AND FOR MANUFACTURING SUCH ELEMENTS. Schludi, Harry N. U. S. Patent 3,200,042. Aug. 10, 1965. Priority date Apr. 14, 1960, Germany.

A method of manufacturing and operating reactor fuel elements is intended to avoid large changes in temperature and the resultant stresses. Uranium metal is fed into fuel cans at a temperature of above 772°C and the canned fuel elements are maintained at a temperature sufficient to prevent a phase change until they are in the reactor and at operating temperature. If the power of the reactor is not sufficient to maintain the desired temperature of the fuel material or if the reactor is switched off, heat is supplied from an external source to the fuel elements. (A.G.W.)

47985 NUCLEAR REACTOR FUEL ELEMENT FOR NITROGEN FIXATION. Morrison, Willard L. (to Union Stock Yard and Transit Co. of Chicago). U. S. Patent 3,201,322. Aug. 17, 1965. Filed Feb. 13, 1958.

A reaction chamber provides a passage for the flow of a fluid, in which both the cross sectional area of the passage and the clearance between the fuel or other reactive bodies may be conveniently changed. The ends of fibers are attached to two parallel relatively rigid walls so that the fibers are held in tension and generally parallel to each other. The walls are so supported that they move longitudinally with respect to one another and also approach to and from one another. When one wall is moved longitudinally, the distance between the walls and the inclination of the fibers with respect to the walls are changed. The fibers may contain fissionable material; they may contain a catalyst; or the arrangement may be used as a filter. One example of the use of the chamber is the fixation of nitrogen from air by reactor radiation. (A.G.W.)

47986 NUCLEAR FUEL MATERIALS INCLUDING VITREOUS PHASE. Hope, Christopher Cameron; George, Dennis; Lloyd, Henry; Williams, Jack (to United Kingdom Atomic Energy Authority). U. S. Patent 3,205,174. Sept. 7, 1965. Priority date May 30, 1958, Great Britain.

A method for the preparation of a ceramic nuclear fuel material consisting of particles of at least one oxide of a fissile or fertile metal and particles of at least one refractory oxide of an element of low neutron absorption cross section selected from the group consisting of alumina, magnesia, beryllia, and hafnium-free zirconia uniformly

dispersed in a vitreous material of high melting point is described. The dispersion in the vitreous material renders the fuel material less permeable to gaseous fission products. A suitable vitreous material is a glass formed from alumina, silica, and one or more oxides such as lime or magnesia. (B.L.M.)

Power and Power-Breeder Reactors

Refer also to abstracts 46917 and 46962.

47987 (AD-612409) CLOSED CYCLE GAS TURBINE. Crim, W. M. Jr. (Nuclear Power Field Office, Fort Belvoir, Va.). 1963. 16p. CFSTI $1.00 cy, $0.50 mn.

The closed cycle gas turbine power plant has been under development since 1940. During this time some dozen or more central station type plants have been put into operation, in the 1200 kw class. The concept, theories explored, design, fabrication, construction, and initial testing in the first experimental compact closed cycle (AK process) thermodynamic system are reported. (TAB)

47988 (ANL-6776) PHYSICS PERFORMANCE OF THE EBWR IN ITS OPERATION FROM ZERO TO 100 MWt. Iskenderian, H. P. (Argonne National Lab., Ill.). May 1965. Contract W-31-109-eng-38. 27p. Dep. mn; CFSTI $2.00 cy, $0.50 mn.

Experimental results taken from the EBWR during its power operation from zero to 100 Mw(t) are presented. Brief discussions on the completion of loading core 1A, initial operation of stripping spike fuel elements, and calibration of the control rod system are discussed. A discussion of the power runs from zero to 60 and from 60 to 100 Mw(t) is included. Measurements presented include reactivity control rod worths and void coefficients. (M.O.W.)

47989 (ANL-7090, pp 1-29) LIQUID-METAL-COOLED REACTORS. (Argonne National Lab., Ill.).

Progress on the reactor development program is reported. Various aspects of the following reactor programs are discussed; EBR-II, FARET, ZPR-6, ZPR-9, and ZPPR. Doppler measurements and the fat-man effect are given for the ZPR-6. Critical masses of the ZPR-9 assembly according to reflector thickness are given. Further developments in fast reactor fuels are discussed. (M.O.W.)

47990 (BNWL-105) MINIMIZED FUEL CYCLE COST FOR A SIMULATED BOILING WATER REACTOR. PART I. Deonigi, D. E.; Horton, P. A.; McConiga, A. F. (Battelle-Northwest, Richland, Wash. Pacific Northwest Lab.). Apr. 1965. Contract AT(45-1)-1830. 90p. Dep. mn; CFSTI $3.00 cy, $0.75 mn.

For specified power reactor types, sizes, lattice configurations, and fuel-to-moderator ratios, minimum fuel costs are determined as functions of economic conditions. The economic conditions considered include costs of fuel fabrication, reprocessing, uranium cascading, separative duty, and working capital interest rates. Results are presented graphically for a 1000-Mw(e) single-cycle boiling-water reactor. (T.F.H.)

47991 (GA-6126) CHEMICAL ENGINEERING IN THE HTGR. Simon, R. H.; Gitterman, M.; Webb, G. B. (General Atomic, San Diego, Calif. John Jay Hopkins Lab. for Pure and Applied Science). Apr. 1, 1965. Contract AT(04-3)-187. 19p. (CONF-650559). Dep. mn; CFSTI $1.00 cy, $0.50 mn; Gmelin, AED-Conf-65-086-16.

From American Institute of Chemical Engineers, 56th National Meeting, San Francisco.

A review is presented of some of the chemical engineering aspects of the High Temperature Gas Cooled Reactor concept with special reference to the Peach Bottom power plant. The fuel elements, steam generator, and helium purification system are discussed together with possible ways of increasing the efficiency and economics. (D.L.C.)

47992 (KEA-311) DIE LOKALE NEUTRONENFLUSSVERTEILUNG IN EINEM BUENDEL AUS SEGMENTIERTEM BRENNSTOFF. (The Local Neutron Flux Distribution in a Bundle from Segmented Fuel Elements). Kilian, P.; Andres, R.; Sauer, A. (Kernenergieanlagen, Allgemeine Elektricitaets-Gesellschaft, Frankfurt am Main (West Germany)). Oct. 1964. 32p. Dep. mn.

In the measurement channel of the AEG test reactor with quadratic constructed core, three-dimensional flux distributions at the connector zone of a bundle from segmented fuel elements were investigated. The neutron flux was measured with Dy-Al foils between the fuel elements. Two different connector heights with and without Dy poisoning in the end elements were investigated. The flux distribution was calculated with a three-dimensional diffusion program and by flux sensitization. A good agreement was obtained between the two methods with 5% accuracy. Deviations between experiment and calculation occur in the flux structure directly at the boundary surface on the connector zone, since, in the calculation, the continuous variation of the cell fine structure in the actual direction was not sufficiently accurately considered. (tr-auth)

47993 (NAA-SR-10751) CARBIDE FUELS IN FAST REACTORS. Wheelock, C. W. (Atomics International, Canoga Park, Calif.). Sept. 15, 1965. Contract AT(11-1)-Gen-8. 78p. Dep. mn; CFSTI $3.00 cy, $0.75 mn.

Plutonium-uranium carbide shows promise of becoming an outstanding fuel for Fast Breeder Reactors (FBR). The requirements for FBR fuels, including specific power, fuel rod size, temperature, burnup levels, and processing costs are discussed; insofar as they are interrelated and affect fuel cycle costs. Applicable laboratory and irradiation data and observations for uranium carbide fuels are integrated with the more limited data available on mixed carbides, (U,Pu)C. Cladding and fuel material processing prospects are reviewed, and fuel system possibilities for near-term (~1 mill/kwh) and long-range (<0.5 mill/kwh) fuel cycles are described. (auth)

47994 (NP-15393) EKSPERIMENTAL'NOE ISSLEDOVANIE NA MODELYAKH POLEI TEMPERATURY TEPLOVYDELYAYUSHCHIKH ELEMENTOV AKTIVNOI ZONY I EKRANA REAKTORA BN-350. (Experimental Investigation of Models of the Temperature Fields of Heat Exchange Elements in the Active Zone and Shielding of the BN-350 Reactor). Subbotin, V. I.; Ushakov, P. A.; Zhukov, A. V.; Talanov, V. D.; Kudryavtseva, L. K.; Sviridenko, E. Ya., Vasil'eva, L. V. (Gosudarstvennyi Komitet po Ispol'zovaniyu Atomnoi Energii SSSR, Obninsk. Fiziko-Energeticheskii Institut). 1965. 23p. Dep.

The core of the Na-cooled Bn-350 reactor contains 211 hexagonal holders, each of which holds 169 cylindrical fuel elements in a straight triangular lattice. In order to prevent buckling, the elements are spaced by means of spiral-shaped fins. A similar design was used for the elements of the blanket grid at the side of the core; in that location the holders contain 37 rods. The safe operation of the reactor depends on the reliability of the heat removal from the fuel elements. The presence of the fins affects the heat transfer process; they facilitate mixing of the coolant but also may cause local overheating. The problem was experimentally examined on core models, determining the temperature fields formed at the central and peripheral elements. The 2 circuits of the test assembly operated with Na and with NaK (22% Na + 78% K), circulating the coolant by means of electromagnetic and centrifugal pumps, at a rate of up to 150 m^3/hr and a pressure of 6 kg/cm^2. Tests were carried out under various flow conditions. The results indicated a more marked temperature inhomogeneity in the peripheral elements as compared to the central ones. At the same Reynolds number, the temperature differences in the peripheral elements in the blanket were higher than in the elements of the core. This was attributed to the larger distance between the peripheral elements and the wall, resulting in a higher flow rate and a higher heat transfer from individual units; the increased wall thickness in the elements of the blanket was also a factor. (TTT)

47995 (NP-15473) DUNGENESS B—AGR NUCLEAR POWER STATION. (Central Electricity Generating Board, London (England)). [nd]. 12p. Dep. mn.

The design of Dungeness B which employs the Advanced Gas Cooled Reactor (AGR) as used at Windscale is described. Discussions on the AGR include the following; improved fuel, on-load fueling, operating characteristics, and safety aspects. (M.O.W.)

47996 (NP-15474) AN APPRAISAL OF THE TECHNICAL AND ECONOMIC ASPECTS OF DUNGENESS B NUCLEAR POWER STATION. (Central Electricity Generating Board, London (England)). [1965]. 26p. Dep. mn.

It is reported that an advanced gas-cooled reactor (AGR) will be used at the nuclear power station Dungeness B. A study of the economical and technical aspects of the AGR is presented. In addition the cost of power produced from the accepted design for Dungeness B is compared with that available from Wylfa, the latest magnox station now being built, and from a coal fired station of the latest available design situated in an area where fuel costs are low. Results are presented. (M.O.W.)

47997 (NP-15478) ACTIVITY REPORT OF THE FIRST QUARTER OF 1965. FAST NEUTRONS PROJECT. (Commissariat a l'Energie Atomique, Cadarache (France). Centre d'Etudes Nucleaires). [nd]. 125p. Dep. mn.

Fast-reactor studies in Rapsodie, Masurca, and Harmonie are described, with emphasis on construction, operation, and experimentation (particularly neutronic, dynamic, mechanical, sodium- and fuel-technological, metallurgical, and loop experimentation and analyses). Theoretical studies on neutron cross sections and Doppler shifts are reported, as applicable to fast reactors. Design studies are reported on 1000-Mw(e) reactor concepts. (T.F.H.)

47998 (SRO-118) HEAVY WATER POWER REACTOR PROGRAM MONTHLY STATUS AND PROGRESS REPORT, JULY 1965. (Savannah River Operations Office (AEC), Aiken, S. C.). 13p. Dep. mn; CFSTI $1.00 cy, $0.50 mn.

Research and development in the heavy water organic cooled reactor program (HWOCR) are reported on fuel channel assemblies, fuel elements, reactor materials, coolants, reactor physics, reactor control and on-power fueling, and plant engineering. Development work on Th fuel cycles is reported on fuel element parameterization, and design of Th-optimized 1000 Mw(e) HWOCR. In the AEC/AECL cooperative program, experiments were performed to determine burnout conditions in 19-rod fog-cooled bundles. Critical heat flux data were obtained on annular test sections at 1000 psia. Results of investigations of hydride platelets, Zr–Nb pressure tubes, and in-reactor creep of Zr–Nb and Zircaloy-2–Nb are reported. Operation of the CVTR is summarized. (J.R.D.)

47999 (TRG-Report-227) METHODS OF CONTROL ROD CALCULATION FOR GRAPHITE MODERATED REACTORS. Buckler, A. (Atomic Energy Establishment, Winfrith (England)); Nichols, P.; O'Dell, F. P. (Reactor Group, United Kingdom Atomic Energy Authority, Risley (England)). Feb. 6, 1962. 28p. (NPCC-RKWP/P.435; CONF-620404-1). Dep. mn.

From Symposium on the Physics of Graphite Moderated Reactors, Bournemouth, Eng.

The appropriate boundary conditions for the solution of control rod problems using diffusion theory are discussed, and a comparison with transport theory is given. The problems associated with epithermal absorption are considered, particularly the calculation of extrapolation length boundary conditions at the control rod channel wall. Two approaches to the solution of this problem are described: first a multigroup treatment using fundamental data, and second an empirical approach based on a correlation of experiments in the Calder and NERO reactors. Comparison with experiment is made for both methods of calculation. (auth)

48000 (WCAP-3738) LARGE CLOSED-CYCLE WATER REACTOR RESEARCH AND DEVELOPMENT PROGRAM. Progress Report, January 1, 1963–March 31, 1963. (Westinghouse Electric Corp., Pittsburgh, Pa. Atomic Power Div.). Contract AT(30-1)-3269. 131p. Dep. mn; CFSTI $4.00 cy, $1.00 mn.

Program development during the period January 1, 1963–March 31, 1963 is reported on various topics under the following subject headings: reactor physics development, reactor core-design and fabrication development, chemical shim development, plant development, reactor hazards analysis, and critical experiments. (M.O.W.)

48001 (WCAP-3743) LARGE CLOSED-CYCLE WATER REACTOR RESEARCH AND DEVELOPMENT PROGRAM. Progress Report, July 1–September 30, 1963. (Westinghouse Electric Corp., Pittsburgh, Pa. Atomic Power Div.). Contract AT(30-1)-3269. 290p. Dep. mn; CFSTI $6.00 cy, $1.50 mn.

Activities during the quarter are summarized including reactor physics calculations, core design and fabrication efforts, chemical shim studies, coolant and control system development, reactor hazards analysis, and critical experiments. (D.C.W.)

48002 (ORNL-tr-747) NON-DESTRUCTIVE UNDERWATER TESTING IN THE BR2 REACTOR. Pele, J.-P.; Hoyaux, G.; Baugnet, J.-M. Translation of Report No. 17 from Symposium International sur les Methodes de Travail Dans les Laboratoires Chauds de Haute Activite, Grenoble, 15–18 Juin 1965. 16p. Dep. mn; JCL $1.60 fs, $0.80 mf.

The BR2 reactor in Mol (Belgium) is jointly operated by the Center of Nuclear Energy Research (C.E.N.) and EURATOM. In connection with this, non-destructive tests were developed for examining the reactor core and testing highly radioactive materials, such as fuel elements. As these tests have many problems in common (e.g., high dose rate, remote control, underwater working), they were studied in parallel. The problems involved, the solutions adopted, and the knowledge acquired in the operation of the equipment are described. (auth)

48003 THE NEW TARGET PROGRAM OF EURATOM. Michaelis, H. (EURATOM, Brussels). Atomwirtschaft, 10: 420-4(Sept. 1965). (In German).

The studies carried out within the European Economic Community on the type and extent of the energy demand and the structure of the electrical economy to meet these demands are reviewed. The present situation with respect to power reactors in the Community is given. The target program for development of nuclear power production proposed by the Euratom Commission in 1960 provided for a nuclear capacity of 40,000 Mw(e). It is estimated that the nuclear capacity at the turn of the century will be at least half of the total electrical capacity expected at that time. The target reactor models that could be developed for the achievement of the target goals are reviewed. The Commission favored the development of proven types of reactors, supplemented by advance convertors and then by breeders so that by the end of century breeder reactors would represent about one half of the nuclear energy capacity. The advantages of the program are discussed. (J.S.R.)

48004 THE ATOMIC ENERGY MARKET IN EUROPE. PART III. DENMARK. Lundgren, C.-E. (DANATOM, Copenhagen). Atomwirtschaft, 10: 451-2(Sept. 1965). (In German).

There is no nuclear market in Denmark as yet but there are plans for its development. The power companies decided to build nuclear power stations of the largest possible capacity as soon as sufficient operating experience was available and their economic competitiveness was established with certainty. A comprehensive investigation to determine the size of such a station showed that at the beginning of the next decade a 500 Mw(e) nuclear power station with an annual utilization of over 7000 hr at full load could be introduced into the two Danish grids. The study indicated that the introduction of nuclear power stations after 1970 would be economically sound and justifiable. Danish industry is contributing to about half of the conventional power construction for the heavy water reactors

being constructed in collaboration with the Swedish government in Sweden. (J.S.R.)

48005 THE ATOMIC ENERGY MARKET IN EUROPE. PART IV. FINLAND. Rehbinder, B. Atomwirtschaft, 10: 454-5(Sept. 1965). (In German).

Because of rapid industrialization since the war, the rate of increase in power demand in Finland was higher than in most European countries. The power demand was chiefly satisfied by hydroelectrical power. However, it was concluded that steam electric power generation must be developed. As there are no coal or oil deposits in Finland, all fossil fuels have to be imported. Economic studies showed that a 300 Mw nuclear power plant could compete with a conventional steam electric station at the prevailing fossil fuel cost in Finland. Preplanning and site evaluations for the construction of such a reactor are underway. The possibilities for the use of process heat reactors was also investigated, but the results were nor promising. Finnish manufacturers have the capacity to fabricate a considerable proportion of the components for nuclear power station but the first nuclear power plant will call for foreign responsibility for the reactor portion of the plant, including fuel fabrication. (J.S.R.)

48006 THE ATOMIC ENERGY MARKET IN EUROPE. PART V. FRANCE. Huet, P. Atomwirtschaft, 10: 456-60(Sept. 1965). (In German).

The French nuclear market was defined for the next few years by a five-year plan in which account was taken of political and economic considerations such as security of the energy supply, easing of the balance of payments situation, and the rate of expansion of the nuclear industry. The French program is based on graphite-moderated and gas-cooled natural uranium reactors. However there was long-term research and development work on fast neutron reactors and on the design and construction of a heavy-water-moderated gas-cooled natural uranium reactor. The economic outlook for these natural uranium reactors justifies the view that in France these reactors are competitive today with traditional power stations. The expansions proposed for auxiliary industries, such as civil engineering and the metal, electrical, and electronic industries, are indicated. (J.S.R.)

48007 THE ATOMIC ENERGY MARKET IN EUROPE. PART VI. GREAT BRITAIN. Raby, G. W. Atomwirtschaft, 10: 462-5(Sept. 1965). (In German).

The first 5000 Mw nuclear power program of Great Britain is reviewed and the second 5000 Mw nuclear power program from 1970 to 1975 is outlined. The long-term plans for the future development of advanced gas-cooled reactors, the steam-generating heavy-water reactor, and fast breeder reactors are described. The need for nuclear power in Great Britain is indicated. The capacity of British industry is considered ample to meet the nuclear needs of the country. (J.S.R.)

48008 THE ATOMIC ENERGY MARKET IN EUROPE. PART VII. ITALY. - Bullio, P. Atomwirtschaft, 10: 467-70(Sept. 1965). (In German).

The lack of coal and oil and the limitations on commercially usable sites for hydroelectric stations provided good prerequisites for the introduction of nuclear power plants into Italy. The first-generation nuclear power plants were installed in 1957 and 1958. The nuclear market appears to be in an expanding stage. The Italian industry acquired experience in the construction of three different reactor types: pressurized-water reactors, boiling-water reactors, and gas-graphite reactors. The competence of the Italian industry in development work and in the supply reactor components is indicated. (J.S.R.)

48009 THE ATOMIC ENERGY MARKET IN EUROPE. PART X. SWITZERLAND. Choisy, E. Atomwirtschaft, 10: 475-7(Sept. 1965). (In German).

The energy needs of Switzerland and the manner in which these needs are met are reviewed. The characteristics of nuclear power that are of interest for Switzerland are indicated. The three commercial power stations being constructed are described. As Swiss industry is primarily concerned with export, its industry must be in a position to export nuclear power equipment. The founding of the nuclear research center in Wurenlingen with the construction of the DIORIT research reactor was used as a base for obtaining competence in the field of D_2O technology. The future reactor construction program of Switzerland is indicated. The competence of the Swiss nuclear industry is discussed and the opportunities for foreign firms in the Swiss market are described. (J.S.R.)

48010 THE ATOMIC ENERGY MARKET IN EUROPE. PART XI. AUSTRIA. Kloiber, H. Atomwirtschaft, 10: 479(Sept. 1965). (In German).

In the immediate future Austria's base load requirements will be met chiefly by hydroelectrical power with thermal power stations playing a merely complementary role. Therefore there is no firm program for the construction of power reactors. A preliminary design study was completed on a small scale experimental power plant incorporating a 15 Mw(e) pressurized-water reactor. Several industries in Austria engage in the supply of components for nuclear facilities with their efforts concentrated in the fabrication of fuel elements. (J.S.R.)

48011 THE ATOMIC ENERGY MARKET IN EUROPE. PART XII. SPAIN. de Oriol y Urquijo, J. M. Atomwirtschaft, 10: 481-2(Sept. 1965). (In German).

The growth of the Spanish power needs above that predicted is indicated. In 1962 the Spanish government announced a program for further construction of three 300 Mw nuclear power plants within 10 years. The power utilities companies submitted plans for approval within the framework of this program; these plans are outlined. The competence of the Spanish industry in the nuclear field is indicated. (J.S.R.)

48012 PROBLEMS IN THE NUCLEAR SUPERHEATING OF STEAM. Kleijn, H. R. Atoomenergie Haar Toepassingen, 7: 100-11(May 1965). (In Dutch).

A review is given of the investigations in many countries on the problems of nuclear superheating in steam and illustrated with many examples. The problems on the fission elements used, the reactor physics aspects, corrosion problems, and fuel element covering are described. A short review is given of the reactors now in use utilizing nuclear superheating of steam. (tr-auth)

48013 THE POSSIBLE INFLUENCE OF MHD GENERATORS ON THE DEVELOPMENT IN POWER STATION DESIGN. Denzel, P.; Buecken, R. (Technische Hochschule, Aachen). Brennstoff-Waerme-Kraft, 17: 399-401 (Aug. 1965). (In German).

To the competition which can be expected between orthodox power stations and nuclear power plants to meet the increased demands for electrical energy, aspects are added by the MHD (magnetohydrodynamic) generator. These aspects are, however, very different for coal and for nuclear stations. For coal-fired stations there are strong incentives for combination with the MHD generator, while for nuclear stations the direct transformation methods are considered less attractive because of the completely different cost structure of the former. (auth)

48014 THE ECONOMY. SOVIET ATOMIC POWER STATIONS. Vvedenskii, G. A. Bull. Inst. Study USSR, 12: No. 2, 33-8(Feb. 1965).

Nuclear power stations in the Soviet Union are described briefly. Economic aspects of using nuclear energy as a source of electric power are discussed. The program for use of heat from nuclear reactors for desalination of seawater is reviewed. (M.C.G.)

48015 NUCLEAR TESTS AT FERMI CONFIRM BASIC PREDICTIONS. McCarthy, Walter J. Jr. (Power Reactor Development Co., Detroit). Elec. Light Power, 41: No. 11, 36-9(Nov. 1963).

The objectives of the nuclear test procedures at the Enrico Fermi Atomic Power Plant are to provide calibration information and information to verify mechanical

and nuclear design uncertainties. The complete program is expected to take from 6 to 9 months depending on the outcome of individual tests. At the present time, after approximately 1 month of operation, the results of test procedures are very satisfactory. The reactor, which is a sodium-cooled fast breeder, utilized U–10 wt% Mo alloy as its fuel. The principal testing procedures, together with their purposes and the method of conducting the test are given. Each test is described briefly. (J.F.P.)

48016 REACTOR AUXILIARY SYSTEMS FILL SPECIAL NEEDS. Chittenden, W. A. (Sargent and Lundy Engineers, Chicago). Elec. Light Power, 41: No. 11, 44-7(Nov, 1963).

Since the pressurized-water-reactor concept represents the largest installed or ordered nuclear-plant capacity in the United States, this concept is utilized to illustrate some reactor-plant auxiliary-system functional requirements and their manifestation. The energy-conversion cycle and some of the auxiliary systems are indicated diagrammatically. Many of these auxiliary-system requirements are similar for the boiling-water, liquid-metal-cooled and the gas-cooled reactor systems. But in many cases the manifestation or fulfillment of these requirements would be accomplished by different types of equipment. The problem of heat decay, the maintenance of coolant volume and pressure, the design of the purification system, and the backup-shutdown system are discussed. Other topics considered are heat removal from spent fuel, cooling for radiation shield, and radioactive waste disposal. (J.F.P.)

48017 ADVANCES IN TECHNIQUES AND AUXILIARY EQUIPMENT FOR ATOMIC POWER STATIONS. Elec. Light Power, 41: No. 11, 48-55(Nov. 1963).

The success of nuclear power revolves arcund technological improvements in present systems, new hardware, and better ways of following existing procedures. These improvements result in better performance, lower cost or increased efficiency in operating a nuclear power plant. Developments reported by the manufacturers named represent many of the most significant recent technological improvements in this field. These developments are discussed in detail and many of them are shown pictorially. (J.F.P.)

48018 RESEARCH NEEDED ON NUCLEAR STATION GAS BLOWERS. (METAL FATIGUE FAILURES AT HINKLEY POINT). Elec. Rev., 176: 623(Apr. 23, 1965).

Investigations into the failures of gas blowers at the Hinkley Point (U.K.) nuclear power station showed that the knowledge available for predicting the acoustic behavior of designs is inadequate. The failures at Hinkley Point were caused primarily by metal fatigue arising from acoustic excitations due to aerodynamic interactions between the fixed and moving blades of the blower. The failures occurred in August, 1963, during the hot run testing on No. 1 reactor. The first indication of trouble occurred on No. 5 blower when a drop in the mass flow as well as in driving motor current occurred. Later, a severe drop took place in the mass flow with an accompanying rise in gas temperature, and the tests were terminated on this machine. The speed was reduced to 300 rpm with the pony motor driving the blower during the six days' cooling period. One day later, No. 3 blower began to show similar symptoms. The damage to the blower diffuser and the blading in Nos. 3 and 5 circuits was severe. A large section of the No. 5 diffuser had broken away and extensive fatigue cracking was found. The other four blowers also showed some cracks but no pattern of failure could be determined. Examinations of inlet guide vanes showed that the blades were subjected to severe vibration and suffered extensive damage to their shanks on the inner dia. Tests on scale models indicated the presence of two contrarotating vortices in the upper half of the blade annulus caused mainly by the severe change in angle from the vertical inlet duct to the horizontal main casing with consequent lack of flow in the upper third of the inlet to the blower. To correct this the inlet guide vanes were removed and egg-box flow-straighteners were added to all blowers at Hinkley Point. In addition, the major components involved in the failures, such as the diffuser, were replaced by new units of modified design. (BBB)

48019 SATISFACTORY PERFORMANCE OF BRITISH NUCLEAR POWER STATIONS. Berry, D. J. Elec. Rev., 177: 47-8(July 9, 1965).

Operating difficulties encountered and overcome at Berkeley (4 × 83 Mw sets), Bradwell (6 × 50 Mw sets), and Hunterston (6 × 56 Mw sets) led to improved design and performance at later stations. Among the developments were: concrete pressure vessels, increased gas coolant pressures, changes in the steam cycle, and improvements in fuel design. A brief survey of experience with reactor cores and materials at Berkeley and Bradwell is presented. Core instabilities, which occur as a result of plutonium build-up in the fuel as irradiation proceeds, were controlled satisfactorily by manual adjustment of sector control rods. Experience with the fuel was satisfactory and the fuel element can failure rate was low. The more serious form of fuel element failure, the fast burst, occurred in five instances at Bradwell and once at Berkeley. In all cases the failures were caused by handling damage to the end welds. The load factors achieved in the first year of operation (Berkeley 49%, Bradwell 67%, and Hunterston 74%) compared favorably with those of conventional power stations (31 to 49%). Faults occurring on the conventional items of the plants, especially the boilers and turbines, were the principal cause of loss of output. On-load refueling experience was not very satisfactory because of difficulties encountered with the refueling machine grabs. (BBB)

48020 FIRST DETAILED COMPARATIVE ASSESSMENT OF COMMERCIAL NUCLEAR POWER. Elec. Rev., 177: 198-201(Aug. 6, 1965).

Economic and technical information is provided on the planned advanced gas-cooled reactor (AGR) design, which was approved for the projected U.K. Dungeness B nuclear power generator. The station will incorporate two AGR reactors with a combined output of 1200 Mw(e), and is planned to be in operation by 1971. Although the station will cost nearly twice as much as a coal-fired station of comparable output, generating costs will be 10% lower than those of the most efficient coal station. Reasons for selection of the AGR over the boiling-water reactor (BWR) and other designs are cited, and a table is given showing detailed economic comparison of the two designs. Capital costs per kilowatt are over £7 higher than those for the BWR. The BWR cannot be fuelled while on load and therefore has an inherently lower load factor than the AGR. The AGR design was the only one to include provision for on-load fuelling. In assessing capital charges and operating costs an operating life of 20 yr and load factor of 75% were assumed. The two reactors at Dungeness B were designed for channel gas inlet and outlet temperatures of 320 and 675°C, respectively, with a peak can temperature of 800°C and a circulator outlet pressure of 450 psia. The steam conditions are 2315 psia and 565°C with reheat to 565°C at 556 psia. The complete reactor, including core, gas circulators, and boilers, is housed within a prestressed vessel. An inner pressure cylinder separates the core from the boilers. The circulators deliver into the region within this cylinder, some of the flow passing downwards through the core to keep the graphite and its restraint structure close to inlet temperature. The total flow then passes upwards through the 465 fuel channels and charge tubes, and is discharged through ports into the plenum above the pressure cylinder, whence it passes down through the boilers back to the circulator inlets. The UO_2 fuel is contained in stainless steel cans arranged in three-ring clusters of 36 pins 0.57-in. dia within graphite sleeves, to form 40-in. long fuel elements. The initial enrichment is 1.47 to 1.76% and the feed enrichment 1.99 to 2.42%. The lattice pitch is 15.5 in. The mean fuel rating (9.5 Mw/ton) is three times greater than for the Magnox system and the axial shuffling of fuel elements part way through their

irradiation period leads to uniform irradiation of all fuel. A single fuelling machine serves both reactors and is designed to operate with the reactor at full load. The plant was arranged to control contamination and to dispose of all solid active waste within the building. (BBB)

48021 FRENCH PREFABRICATE A-POWER PLANT. Eng. News-Record, 175: 42(Aug. 5, 1965).

Ways in which prefabrication methods have cut a year from the construction time of the new French nuclear power plant (EDF-4, being built by Electricité de France on the Loire River) are described and illustrated. The success of prefabrication is attributed to relocation of the reactor above the heat exchangers. Since the connecting channels do not extend outside the vessel, there is no need to reinforce them strongly. To produce the prefabricated sections, EDF engineers built assembly plants on three sides of the reactor, leaving the fourth side open for the turbine building. The prefabricated sections roll on railroad tracks to within reach of six bridge cranes mounted on the previously erected reactor superstructure. A grill structure incorporates vertical pipes for the CO_2 coolant and the steam that drives the turbogenerator. Later the 640-ton steel cap plate for the exchanger-reactor, and 500-ton concrete and graphite shield that will insulate the exchanger from the reactor, will be positioned. Steel plates will form the reactor's 118-ft-high inner shell. As the inner shell rises, it is lined with vertically post-tensioned concrete sections prefabricated in the assembly plants. After the cables are threaded through the conduit and stressed, the tendons are pressure-grouted and tested for bond. While the inner shell is rising, the 28 heat-exchanger sections will be prefabricated on the ground; then, one of the 60-ton sections will be dropped in place each day. Cost of the temporary assembly sites was considered offset by improved efficiency. (BBB)

48022 FUELLING AT SIZEWELL NUCLEAR POWER-STATION. Engineer, 220: 99(July 16, 1965).

Fuel loading in No. 1 reactor of Sizewell started on June 21, 1965. This station illustrates the advantages of the innovation of enclosing the two natural-uranium, graphite-moderated gas-cooled reactors in one building where they can share the services of a central control block, fuel-handling machinery, and a fuel-element cooling pond. There are two fueling machines, each designed to carry out the fueling program of the two reactors. By having a common pile cap floor one machine is in service; the other acts as standby. Apart from this economy there is a saving in structural materials. The single reactor building, aluminium clad, is 350 ft long, 280 ft wide, and 200 ft high. In the fueling arrangements, the charge chutes form a channel between the pile cap floor and the reactor core and each is used for fueling, gas sampling, and control rod movement. The charge chutes are designed to be normally retained within the 64-ft dia pressure vessels. Accordingly, the fueling machine itself is simpler, smaller, and lighter than in previous stations. There is also a servicing machine designed for the handling of reactor components which need to be removed for maintenance. Illustrations show the fuel handling machines, servicing machines, and the handling of charge chutes. The vertical storage racks which hold the charge chutes, each 30 ft long by 15 in., are also illustrated. (BBB)

48023 APPRAISAL OF REACTORS FOR DUNGENESS-B. Engineer, 220: 217-18(Aug. 6, 1965).

The detailed appraisal of the technical and economic aspects of the projected Dungeness-B nuclear power-station, issued by the Central Electricity Generating Board (CEGB), is reviewed. It shows how the tenders for this station were compared and assessed, and explains why the AGR (advanced gas-cooled reactor) was chosen in preference to the light-water reactors that were offered. The CEGB assessment gives a generating cost of 0.457d/unit for the AGR compared with 0.505d/unit for the nearest rival, the BWR (boiling water reactor), and 0.53d/unit for an efficient contemporary coal-fired power station. Assessment of technical problems for the AGR is also made. Under AGR conditions the irradiation-induced chemical reaction between graphite and the carbon dioxide coolant causes rapid corrosion. Even with the special low porosity graphite developed for Dungeness-B, it is necessary to inhibit the reaction to keep corrosion to acceptably low levels. It was necessary to know the magnitude of the dimensional changes which occur with irradiation and to show that the consequential internal stresses in the graphite bricks will not result in serious cracking. Of the reactors considered, the AGR is the only one that can be refueled on load and the effect of this on the operating characteristics can be expressed partly in financial terms in the assessment. (BBB)

48024 BRITAIN'S SEVENTH NUCLEAR POWER STATION. Engineering, 200: 70(July 16, 1965).

The Sizewell power station will reach full power early in 1966, giving the Central Electricity Generating board an added 2000 Mw of nuclear generating capacity. The station, situated near Aldeburgh on the Suffolk Coast, follows Trawsfynydd, Hinckley Point, and Dungeness A stations into service. It is a twin Magnox reactor station with a net electrical output of 580 Mw. The two reactors are located in one building, sharing a single control block, and each drives a single 325 Mw set. The pressure vessels are steel spheres 63 ft 6 in. ID and 4.125-in. thick, enabling the coolant gas pressure to be raised to 279 psi. The length of fuel rod was increased to 42 in., and the number of channels reduced to 3800. The temperature at the surface of the fuel can will be 454°C. These design improvements increased the efficiency from 25.5 to 30.5%. The most notable design change, apart from that of the reactors, was in the boilers. At Sizewell there are four boilers per reactor, each 22 ft 6 in. in dia by 91 ft long and their combined output is 5.5 million lb of steam per hr. Two 325-Mw turbo-alternators were installed. They are designed to operate from steam conditions of 646 psi and 700°F. A common shield floor enables economies to be made with the fuel handling and maintenance plant. Fuel replacement on load is to be performed by a machine of relatively simple construction. The generating cost estimate is 0.73d per unit, but the ultimate cost, based on revised estimates of life and load factor, may be as low as 0.59d per unit. (BBB)

48025 SWEDEN'S LARGEST NUCLEAR POWER STATION. Engineering, 200: 141(July 30, 1965).

Plans for a 400-Mw(e) nuclear power station at Oskarshamn, Sweden, the largest station in Europe with a boiling water reactor, are described. The station, planned for commissioning in the autumn of 1970, is to be situated on the Baltic coast, about 130 miles south of Stockholm. The estimated total cost of £24 million is equivalent to £63/kw; the generating cost is calculated to be as low as that for a coal- or oil-fired station at the site. The proposed reactor is a water-cooled and -moderated boiling-water type in which the fuel consists of uranium oxide, enriched by 2.5% ^{235}U, canned in zirconium alloy tubes. The water moderator is of ordinary light water contained in a cylindrical pressure vessel. The reactor is fundamentally an American design, but the fuel rods will be manufactured and assembled in Sweden. A diagram of how the station will be constructed is shown. The reactor will be located in a separate building from the rest of the plant, so that, in an emergency, it can be isolated from the remainder of the station. Treatment and storage of radioactive waste will be carried out in a separate building. After treatment the waste will be discharged. Work on the station is expected to start in the spring of 1966 and it is expected that during 1970 generation will start, initially at 350 Mw(e) with progressive uprating to the full design power level during the following year. (BBB)

48026 PROGRESS IN THE DEVELOPMENT OF NUCLEAR POWER. Moore, R. V. (U. K. Atomic Energy Authority, Windscale, Eng.). Engrs. Digest, 26: 289-92 (June 1965).

The U.K. program for nuclear power development is traced from its inception in 1946, through its present

status, to future projects. Construction began with two reactors at Calder Hall, Cumberland, with the dual purpose of producing plutonium for defense purposes and for generating electricity. Subsequently, the number of reactors was increased to eight. The eight graphite-moderated, CO_2-cooled reactors use natural uranium in magnox cans for fuel, and all proved to be reliable and well suited to base-load operation. Advances in the design of nuclear power stations are illustrated by a table that shows how the (electric) power outputs of the twin-reactor plants built under this program have increased and how their capital costs and generating costs were progressively reduced. Advanced gas-cooled reactor (AGR) development in the U.K. is outlined. Construction of the prototype AGR began late in 1958, and it achieved its design thermal output of 100 Mw(t) in January 1963. The British government established in April, 1964, the second nuclear-power program of stations (AGR) to be commissioned from 1970 to 1975. A gas-cooled reactor operating at even higher temperatures (750°C, Dragon project) was developed that necessitated a change from carbon dioxide to helium gas as the coolant and the elimination of metal cans by using a fuel element in which the fuel particles of ^{235}U and ^{233}Th are coated with pyrolytic carbon and compacted in a graphite matrix. The building of a prototype D_2O-moderated reactor, with an output of 100 Mw(e), was initiated in February 1963. (BBB)

48027 AGR SUCCESS IN THE UK. EuroNucl., 2: 371a-d(Aug. 1965).

The general design of the reactor selected for the Dungeness B station is described. The complete reactor, including core, gas circulators, and steam-raising units, is housed within the concrete pressure vessel. An inner pressure cylinder in the shape of a bell separates the core from the boilers and circulators. The internal walls of the concrete pressure vessel are clad with a stainless steel thermal insulation. The coolant circulators are of the centrifugal type. The fuel is UO_2 pellets clad with stainless steel. Each fuel element assembly consists of 36 fuel pins arranged in 3 concentric rings and contained within a graphite sleeve. The site plan of the twin-reactor complex is described and operational control discussed. (M.C.G.)

48028 OSKARSHAMN NUCLEAR POWER STATION. EuroNucl., 2: 382-3(Aug. 1965).

The design of the third Swedish nuclear power station, at Oskarshamn on the Simpevarp peninsula on the Baltic coast, is described. It will be a light boiling water type with a capacity of 400 Mw(e) and is expected to begin commercial operation in 1970. The fuel is 2.0 to 2.5% enriched UO_2 with zirconium alloy tubing as the canning. The direct heating requirements are discussed. (M.C.G.)

48029 BIOLOGICAL SHIELD COOLING. Ide, Akira. Fuji Elec. J., 37: 178-83(Jan. 1964). (In Japanese).

A method of calculation and design criteria of shield cooling system are outlined. Solving heat-balance equations in the system, the heat distribution in concrete is obtained, and then stress distribution assuming concrete as a perfect elastic body. Changing each variable independently, the most preferable combination of variables is found to retain maximum stress and temperature in the concrete below permissible levels. As an example, the configuration of shield cooling system and some results of calculation for Tokai Reactor are given. (auth)

48030 NEUTRON DOSE MEASUREMENT IN GRAPHITE IRRADIATIONS IN BR-2. Martin, W. H.; Brocklehurst, J. E.; Clare, D. M. (United Kingdom Atomic Energy Authority, Culcheth, Eng.). J. Nucl. Energy, Pts. A and B, 19: 673-7(Sept. 1965).

Fast and thermal neutron doses were measured in graphite irradiation experiments in the Belgian Reactor BR-2 using iron (enriched in ^{54}Fe) and cobalt activation monitors respectively. These data are analyzed to derive peak neutron fluxes at full power for inner and outer ring positions in the BR-2 core in 5-plate fuel elements with central support tubes. (auth)

48031 A CALORIMETER FOR GRAPHITE DOSE RATE IN ADVANCED GAS-COOLED REACTORS. Todd, M. J.; Bishop, J.; Cartwright, D. K. (United Kingdom Atomic Energy Authority, Risley, Lancs). J. Sci. Instr., 42: 576-83(Aug. 1965).

A steady-state calorimeter of simple design, for determining absolutely the total energy deposition rate in a graphite sample inside the core of an advanced gas-cooled reactor, was developed, and three were tested in continuous operation in the Windscale reactor. The operating conditions are: temperature of 300 to 400°C, pressure of 270 lb $in.^{-2}$, and energy deposition (or dose) rate between 100 and 200 Mw g^{-1} at full reactor power. The performance was good and, despite subsequent heater failure, no significant change in the original calibration by electrical heating was found. The average total dose to each of the instruments now exceeds 5×10^{11} rad (1 rad = 100 erg g^{-1}). The major correction (about 10%), necessary to the measured graphite dose rate, arises from the effect of neutron captures by the stainless steel can. The overall experimental accuracy (standard error) in the dose rate at full reactor power was estimated as ±3%. There could be an additional uncertainty in the deduced quantity, which is the CO_2 (pore gas) dose rate, of up to about 4%, mainly because the fast neutron stopping powers of CO_2 and graphite differ slightly. Reasonable agreement was obtained between semi-empirical calculations of moderator dose rate, based on relative channel power outputs, and the actual measurements in the core. (auth)

48032 ON THE PROBLEM OF THE PRICE OF PLUTONIUM. Fuchs, K. (Zentralinstitut fuer Kernforschung, Rossendorf, Ger.). Kernenergie, 8: 325-30(June 1965). (In German).

A method for treating the problem of the price of plutonium is presented and applied to the special case of an exponentially increasing production. The method is based on the economically optimum problem under the conditions of expanded production. The production cost of plutonium in a nuclear power station equipped with a breeding reactor can be uniquely defined. It depends on the rate of expansion of the production and on the characteristic economic and technical characteristics of the power station as functions of the breeding rate. (auth)

48033 THE FAST COUNTING CHANNEL AT PEOPLE-OWNED ENTERPRISE (VEB) VAKUTRONIK WIB IN DRESDEN. Lange, W. Kernenergie, 8: 379-82(June 1965). (In German).

The construction, operation, performance, and applications of a fast counting channel are described and illustrated with circuit diagrams, block diagrams, photographs, and diagrams. The channel is used for measuring the neutron flux in the inlet of a power reactor. The principal components include a nuclear fission chamber, a preamplifier, a counting amplifier, a high-voltage source, and a logarithmic density meter. Some findings obtained with the aid of the counting channel described are presented and discussed. (CFSTI)

48034 SAFETY ASPECTS OF THE EXPERIMENTAL POWER STATION KNK. Nucl. Eng., 10: 335-7(Sept. 1965).

The layout of the experimental power station with a sodium-cooled zirconium hydride-moderated reactor (Type KNK) is described with special attention to the safety aspects. The essential control-safety measures are combined within the reactor safety system which serves to protect the reactor and the heat transfer systems from dangerous operating conditions, wherein normal operation might be disrupted either through human errors in manual operation, or on automatic control by a fault in a part of the plant. According to the extent and seriousness of the fault either an alarm or an appropriate automatic action is put in effect. (P.C.H.)

48035 THE CEGB'S APPRAISAL OF DUNGENESS B TENDERS. Nucl. Eng., 10: 344-6(Sept. 1965).

Three AGR tenders were received. The chosen design submitted by Atomic Power Constructions Ltd. (APC) re-

tained very largely those features of the Windscale AGR and the earlier magnox stations which had been embodied in the CEGB's inquiry specification. Operating characteristics, safety and siting, economic assessment, method of costing, construction cost, amortization period and load factor, availability adjustment, fuel costs, replacement fuel, and insurance are discussed. (P.C.H.)

48036 EVALUATION AND REFLECTION ON THE DESIGN STUDIES MADE ON THE DOMESTIC POWER REACTOR. Takeda, Eichi (Tokyo Inst. Technol.); Furuhashi, Akira (and others). Nucl. Power (Tokyo), 8: 15-27(Sept. 1964). (In Japanese).

Various designs and their studies made for the development of a domestic power reactor are described, reflecting on the works performed. The study and design concerned most the selection of a suitable cooling system for the reactor. The types of cooling system considered in the design study were pressurized heavy water, low-pressure boiling light water, high-pressure boiling light water, organic substance, and CO_2 gas. In connection with the above are also described the nuclear calculations, the lattice structure, burn-up calculations, etc. (NSA of Japan)

48037 POWER REACTOR CONTAINMENT. Schmitz, Paul; Griffin, Roger (Bechtel Corp., San Francisco). Nucleonics, No. 10, 23: 50-5(Oct. 1965).

Containment and design are becoming increasingly important in the design and siting of nuclear power plants. Judgment and experience are the basis of good containment design. Containment types are basically pressure containment and pressure suppression. Since there are no absolute standards for comparison there is no precise method of calculating the containment required for a reactor at a given site. Criteria guides are concerned with calculated radiation doses at the edge of a site and at nearby communities subsequent to serious contained accidents of very low probability of occurrence. Containment design concepts are discussed including pressure, multiple-barrier, and pressure-suppression containment. Design considerations including design pressure for a containment structure, the rate and time of energy release, pressure transients, leakage rate, and periodic integrated tests are discussed. (J.F.P.)

48038 REACTOR SAFEGUARD SYSTEMS. Gitterman, Henry (Burns and Roe, Inc., New York). Nucleonics, No. 10, 23: 56-9; 63-4(Oct. 1965).

In order to site reactors near populated areas, a whole spectrum of devices and procedures are evolved to protect the plant and population in a variety of normal and abnormal situations. The development of these safeguards along different lines, as exemplified by particle filters and after-heat-removal systems, reflects a broadening of philosophy to include steps to limit an incident and its consequences as well as more sophisticated systems to indicate the existence of a condition which might lead to an accident. Since current U. S. interest in power reactors for near-term use is almost exclusively directed toward boiling and pressurized water reactors, the safeguards for these plants are discussed primarily. Accident-prevention systems are considered including reactor instrumentation, control-rod, sampling and monitoring, failed fuel detection, fuel handling systems, emergency power, mechanical protective devices, and administrative procedures. Accident-limiting systems are also discussed including afterheat removal, and injection or core spray. (J.F.P.)

48039 DUAL-PURPOSE OPERATION OF HANFORD REACTOR. Flehn, A. J.; Dupont, F. M.; Zizza, M.; Bucalo (Burns and Roe, Inc., New York). Power, 109: 68-9(Sept. 1965).

Plans are being made for dual-purpose operation of the Hanford NPR reactor. While plutonium production continues to take precedence, electric power will be generated as a by-product in two 430-Mw turbine generators. Operating procedures, process conditions, and control settings will favor plutonium production by holding the primary coolant entering the reactor at a constant optimum temperature, and by keeping steam pressure as low as possible. Starting in 1972, the entire facility will be devoted to electric power generation. Heat dissipation systems, reactor safety, coolant flow regulation, and water level control are discussed. (M.C.G.)

48040 THE CONTRIBUTION OF A 5-CURIE Pu–Be SOURCE TO THE SUBCRITICAL SM-1 STRUCTURE. Meloni, Sandro (Universita, Pavia, Italy). Ric. Sci. Rend., Sez. B, 8: 213-24(Mar.-Apr. 1965). (In Italian).

Neutron flux measurements in the SM-1 subcritical assembly were carried out. The neutron sources used were: a 1-curie Ra–Be source, a 5-curie Pu–Be source, and a source the sum of the two preceding ones. The method employed was irradiation and absolute beta counting of indium foils. Thermal flux distribution was studied as a function of the distance from the sources. The measurements were carried out on the equatorial plane and orthogonally. The results are shown in tables and graphs and are discussed. (auth)

48041 NUCLEAR POWER IN DEVELOPING AREAS. Balligand, P. L.; Khan, M. A.; Krymm, R.; Kuhn, D.; Pedersen, O. E.; Webb, J. C. (International Atomic Energy Agency, Vienna). Sci. World, 8: 18-22,30(1964).

In June 1962, 19 power stations utilizing five reactor types with a total capacity of 1600 Mw(e) were in operation in six countries. By the end of 1963, 55 stations in ten countries with a total capacity of 4500 Mw(e) were expected. To aid in determining the most advantageous time for starting power reactor programs, data were summarized from a consideration of the technical status of different power reactors, their cost aspects, materials required for nuclear power production, and steps to be taken by a country interested in a nuclear power program. The power reactors considered are in three broad categories: (a) those already in commercial use, (b) those considered promising for the near future, and (c) those based on advanced concepts under technological and experimental development. Development of water-cooled and gas-cooled reactors is described. Also discussed are several reactor concepts that have advanced beyond the experimental stage and are being demonstrated in the form of full-scale prototype power plants. These types include heavy water, organic-moderated, and sodium graphite reactors. Other advanced design systems include aqueous homogeneous reactors, molten salt reactors, and breeder reactors of both fast and thermal types. Certain steps that a developing country interested in a nuclear power program should take towards the actual construction of a power station are enumerated. (BBB)

48042 WATER TREATMENT ON THE DRAGON REACTOR. Gray, P. S. Steam Heating Engr., 34: No. 403, 10-16(June 1965).

The thermal shield of the Dragon Reactor is a 13-in. sandwich construction of alternate 1-in. layers of mild steel and water. Auxiliary cooling circuits also use water. Water for process use is treated in an automatic ion exchange plant. The resin is too weakly acidic to remove calcium or magnesium from their sulfates and so only the temporary hardness is removed. The water is stripped of excess CO_2 in a tower by air blowing and the pH adjusted to 8 to 8.5 to minimize iron corrosion, then passed to a reservoir for distribution through the site process system. Demineralized water is prepared from the treated water by complete demineralization in a 1,000 gal/hr mixed-bed unit. Chemical deoxygenation is accomplished by reacting the oxygen in the water with sulfite ions adsorbed on a strongly basic ion exchange resin. Any sulfate picked up and any other dissolved contaminants are removed by passing the water through a mixed bed of strong acidic and basic resins. Operation of the secondary coolant circuits was planned to minimize water capacity of the circuits to limit the release of water into the reactor in the event of a primary heat exchanger tube failure. Operation of the tertiary and emergency circuits and water treatment for use in them are discussed. (M.C.G.)

48043 DEVELOPMENTAL INVESTIGATION OF POWER REACTOR PLANT. Satoyama, Shozo (Tokyo

Shibaura Electric Co., Ltd.). Toshiba Rev., 20: 617-21 (June 1965). (In Japanese).

Japan has come to the stage of materializing commercial nuclear power plants, several being under way. Their general tendency is toward utilization of the light-water type on account of its economic superiority. In view of the same account, Toshiba, with the co-operation of the affiliated companies, such as NAIG, advanced research on nuclear power reactors, especially of the boiling water type. Furthermore, Toshiba, as a manufacturer, has established the technique on a profound and extensive basis for the construction of nuclear power reactors and related instruments. With an aim at the domestic production of reactors of this type, programs are steadily on foot at the Company. Some of the major subjects included in the programs are discussed. (auth)

48044 BOILING WATER REACTOR, 1,000 MWe, FEASIBILITY STUDY (Engineering Drawings). (General Electric Co., Atomic Power Equipment Dept., San Jose, Calif.). (CAPE-1203).

24 drawings.

The feasibility of a 1,000-Mw(e) boiling water reactor plant utilizing one or two reactors, and the reheat or non-reheat steam cycle, was established. Designs were based, with minor extrapolations, on components in operating nuclear power plants. The reactor building houses the reactor, associated nuclear steam supply system equipment, reactor pressure-suppression containment vessel, fuel storage and refueling areas, and other reactor auxiliary and emergency systems. The reactor is contained in a dry-well pressure vessel, which is connected by means of vent piping to a chamber partly filled with water. The radwaste building houses the collection, monitoring, processing, and disposal facilities for the radioactive liquid waste products from the plant. The outside height of the stainless steel-clad, carbon steel reactor pressure vessel is 67 ft 2 in. and it is 23 ft 4 in. in dia. It was designed for a pressure of 1,250 psi and operates at 1,000 psi. Fuel material is UO_2 contained in Zircaloy tubing. The four plant arrangements are: single reactor non-reheat cycle–reference plant; single reactor reheat cycle; twin reactor non-reheat cycle; and twin reactor reheat cycle. Reactors are of the single-cycle type with internal steam separation. Saturated steam is sent directly to twin turbine generators. (M.C.G.)

48045 NUCLEAR REACTOR. Fortescue, Peter; Rickard, Corwin L. (to General Dynamics Corp.). U. S. Patent 3,201,321. Aug. 17, 1965. Filed Dec. 7, 1960.

In the reactor patented, the fuel and moderator are mixed to eliminate metal cladding of the fuel elements. The reactor core is so arranged that the coolant circulates upwardly along the walls of the reactor vessel and downwardly through the fuel-element-containing portion of the core. As the gas leaves the core, it is directed to means for converting the heated gas into usable energy. A fission product trapping system prevents contamination of the primary coolant circuit. A storage area for spent fuel elements is provided in the upper half of the reactor pressure vessel (coolant circulation is confined to the lower half). (A.G.W.)

Propulsion and Space

See also ENGINEERING — Space Propulsion.

Refer also to abstracts 46458, 46494, 46495, 46500, and 46504.

48046 (AD-613998) CAVITY NUCLEAR REACTORS. Paper No. 1738. Holl, R. J.; Plunkett, T. F. (Douglas Aircraft Co., Inc., Santa Monica, Calif.). July 11, 1963. 17p. CFSTI $1.00 cy, $0.50 mn.

A nuclear analysis was performed for cavity nuclear reactors suitable for space propulsion. Calculational methods were evaluated and multigroup diffusion theory was selected. A survey in spherical geometry evaluated reflector materials, nuclear fuels, reactor dimensions, and temperature effects. Two-dimensional results for a finite cylindrical reactor are included. The study showed that extremely high fuel loadings were required for a propulsion reactor. (auth)

48047 (CONF-640508, pp 334-9) EVOLUTION OF REMOTE HANDLING CAPABILITIES AT NRDS. Neder, M. J.; Montgomery, C. D. (Aerojet-General Corp., Azusa, Calif.).

A description is given of the equipment that was developed for the transportation, assembly and disassembly, post mortem, and recovery from major malfunctions for the KIWI/NRX reactors and the NERVA engines. Future developments are considered briefly. (D.L.C.)

48048 (GE-65SD4251) STUDY OF NUCLEAR BRAYTON CYCLE POWER SYSTEM. Freedman, S. I. (General Electric Co., Philadelphia, Pa. Missile and Space Div.). Aug. 5, 1965. Contract NASw-980. 210p. (NASA-CR-54397).

A parametric analysis and system optimization was made of reactor-heated Brayton-cycle space powerplants in the 50 to 200 kwe range. Models of gas and liquid-metal cooled reactors, shields, turbomachinery, heat exchangers, piping, and gas and liquid-metal filled radiators were synthesized. Application to manned and unmanned missions enabled evaluations to be made of reactors and shield configurations and system integration influences over a wide range of requirements. Turbomachinery performance was based on the efficiencies of the NASA/Lewis two-shaft solar Brayton system. Dependence of optimized system specific weight on shield requirements, turbine inlet temperature, and power rating were determined. (auth)

48049 (LA-3301) NRDS ANALYSIS OF THE KIWI B-4D-202 NUCLEAR REACTOR CONTROL SYSTEM. Hearn, Thomas O. (Los Alamos Scientific Lab., Univ. of California, N. Mex.). Aug. 1964. Contract W-7405-eng-36. 103p. Dep. mn; CFSTI $4.00 cy, $0.75 mn.

The technique used in controlling nuclear rocket engines at NRDS is summarized. The control systems used with the KIWI B-4D-202 reactor series are evaluated through the use of an analog computer simulation. The three modes of control discussed are: automatic reactor startup, power control, and power-temperature control. A brief analysis of the B-4E-301 temperature control system is also included. (auth)

48050 (NAA-SR-9908) THE DEVELOPMENT AND QUALIFICATION OF THERMAL CONTROL COATINGS FOR SNAP SYSTEMS. Crosby, J. R. (Atomics International, Canoga Park, Calif.). Sept. 30, 1965. Contract AT(11-1)-Gen-8. 69p. Dep. mn; CFSTI $1.75 cy, $0.75 mn.

Components of the (SNAP 2) Mercury-Rankine and SNAP 10A systems require various radiation control coatings which exhibit particular thermal emittance and solar reflectance properties. A specialty coating system, designated AI93, was developed for the SNAP 2 radiator-condenser and the SNAP 10A thermoelectric module and pump radiator fins. This coating exhibits a thermal emittance of 0.91 (400 to 700°F) and a solar absorptance of 0.30. Stability of this coating system in a nuclear and simulated space environment was demonstrated. Other coating systems which were developed and qualified are: gold foil and gold on molybdenum foil for use as radiative insulation, high-thermal-emittance coatings for use on heat-sensitive components, and a mosaic coating pattern for use on the SNAP 10A ejectable heat shield. Data generated during the development of these coating systems along with the associated equipment descriptions are included. (auth)

48051 GERMANY'S NUCLEAR SHIP. Salander, C.; Ulken, D. (GKSS Inst. for Nuclear Ship Propulsion, Geesthacht, Ger.). Nucl. Eng., 10: 324-9(Sept. 1965).

The planning, design, construction, and dimensions, and

machinery of the German nuclear ship, Otto Hahn, is reported. Location of the reactor within the ship, FDR nuclear power plant, and research program are described. (P.C.H.)

48052 NUCLEAR SPACE PROPULSION. Crouch, Holmes F. Granada Hills, Calif., Astronuclear Press, 1965. 445p.

The concepts presented are founded on solid-fueled nuclear rockets. This is a class of nuclear space propulsion distinct from such forms as gas-core, pulse-charge, and electric-ion types. Topics discussed are technology, fuel properties, reactor basics, neutron criticality, fission control, propellant flow, engine control, thrust maneuvering, reactor potentials, vehicle aspects, space missions, and reactor recovery. (J.F.P.)

Research and Test Reactors

48053 (ANL-7090, pp 55-68) ADVANCED SYSTEMS RESEARCH AND DEVELOPMENT. (Argonne National Lab., Ill.).

The Argonne Advanced Research Reactor is discussed in terms of the following; critical experiments, analyses of transients, heat transfer, fuel and materials development, and the primary system and components. The feasibility of using a liquid-metal MHD generator as a topping unit for a fast reactor central power station is discussed. (M.O.W.)

48054 (BNL-9308) REPORT ON HFBR MODIFICATIONS AND TESTS PREPARATORY TO OPERATING AUTHORIZATION. Hendrie, J. M.; Sheehan, T. V. (eds.) (Brookhaven National Lab., Upton, N. Y.). Aug. 1965. Contract AT(30-2)-Gen-16. 75p. Dep. mn; CFSTI $3.00 cy, $0.75 mn.

A safety review is made of the High Flux Beam Reactor (HFBR). It is concluded that the HFBR can be operated without undue risk to the health and safety of the public, subject to the completion of several modifications to the plant, to demonstrations of the required containment leak rate and the successful operation of various plant equipment, and to the development of procedures for the safety of visitors and experimenters. The required modifications, tests, and procedure formulations are described. (auth)

48055 (BNL-9402) CHEMONUCLEAR LOOP REMOVAL FROM THE BGRR USING A SEMI-REMOTE CUTTING TECHNIQUE. Waide, C. H.; Klein, J. H. (Brookhaven National Lab., Upton, N. Y.). July 1965. Contract AT(30-2)-Gen-16. 13p. (CONF-651101-27). Dep. mn; CFSTI $1.00 cy, $0.50 mn.

From 13th Conference on Remote Systems Technology, Washington, D. C.

A cutting technique was developed for use in removing the 40-ft long Chemonuclear Loop in-pile section from the BGRR. The in-pile section will be a complex assembly of stainless steel pipe, tubing, cable, foil, wire, and insulation and will have a 4-in. square cross section. At the time of removal, it will be contaminated along its length with fission products and could contain an irradiated uranium fuel package. The procedure developed is based on the use of a guillotine shear which will cut the in-pile section into 4-ft lengths. The equipment and procedures developed for this task provide for positioning the guillotine, manipulating the in-pile section, controlling the cutting, shielding personnel and transporting the cut sections. (auth)

48056 (BNL-9510) NEUTRON DYNAMICS OF BROOKHAVEN'S HIGH FLUX BEAM REACTOR. Chernick, Jack (Brookhaven National Lab., Upton, N. Y.). Sept. 1965. Contract AT(30-2)-Gen-16. 27p. (CONF-651105-2). Dep. mn; CFSTI $2.00 cy, $0.50 mn.

From Conference on Nuclear Electronics, Bombay.

A brief review of the High Flux Beam Reactor design features is presented. Results from studies on reactor control and safety are presented. The results and conclusions from various accident studies are discussed. Several tests which were made in preparation for reactor startup are discussed. (M.O.W.)

48057 (BNWL-109) PRTR CONTAINMENT VESSEL PRESSURE TEST EXPERIENCE. Clark, R. G.; Koberg, D. R. (Battelle-Northwest, Richland, Wash. Pacific Northwest Lab.). Aug. 1965. Contract AT (45-1)-1830. 76p. Dep. mn; CFSTI $3.00 cy, $0.75 mn.

A leakage rate of slightly less than 0.9% per 24 hr at the design pressure (15 psig) was determined for the containment completed in May 1964, using the Reference Volume Method in which 475 ft of 3/4 in. thin-walled copper tubing constituted the reference volume. Results from tests conducted at 3, 6, and 15 psig showed that the leakage rates on this vessel at different pressures varied approximately as the square roots of the ratios of the gage pressures. The test installation and the method of testing were verified by superimposing a 0.9% leakage rate on the vessel having an existing leakage rate of 1.3%. The superimposed leakage rate was measured by a rotameter. The measured leakage rate increased from 1.3 to 2.1%, giving an 0.8% increase. Comparisons of leakage rates determined by the Absolute Method and the Reference Volume Method showed agreement within the limits of the errors inherent in the testing on all tests completed at different pressures. The resolution of the differential pressure manometer and the stable temperatures and vapor pressures in the vessel during the testing permitted reliable estimates of leakage rates (based on a 24 hr interval), to be determined in tests as short as 3 to 15 min at the magnitude of the leakage rates measured in these tests. Leakage rate tests, it was shown, need not extend through 24 hr periods and longer to provide reliable results. (auth)

48058 (BNWL-130) SAFETY ROD INTERACTION IN THE PRCF. Sakata, H.; Schmid, L. C. (Battelle-Northwest, Richland, Wash. Pacific Northwest Lab.). Aug. 1965. Contract AT(45-1)-1830. 18p. Dep. mn; CFSTI $1.00 cy, $0.50 mn.

The Plutonium Recycle Critical Facility has 3 vertical safety rods. The reactivity worths of the rods are measured singly and in combinations by correlations of flux transients with reactivity changes. The safety rods are distributed symmetrically with respect to the core. The interactions of the rods are calculated theoretically and compared with the measured values. (T.F.H.)

48059 (IDO-17081) NUCLEAR TECHNOLOGY BRANCHES QUARTERLY REPORT, OCTOBER 1-DECEMBER 31, 1964. (Phillips Petroleum Co. Idaho Falls, Idaho, Atomic Energy Div.). Contract AT(10-1)-205. 147p. Dep. mn; CFSTI $4.00 cy, $1.00 mn.

Progress is reported in sections on reactor engineering, nuclear technology, instrument development, and mathematical analysis and machine computations. Separate abstracts were prepared for each section. (J.R.D.)

For abstracts of individual sections see: 46716, 46905, 47576, and 48060.

48060 (IDO-17081, pp 1-47) REACTOR ENGINEERING. (Phillips Petroleum Co. Idaho Falls, Idaho, Atomic Energy Div.).

The reactivity effects of the experiment mock-ups in the ATRC were measured. Experimental and calculated distributions of excess reactivity for the ATR are compared. The reactivity effect of a possible radial shift of fuel elements in the ATR due to hydraulic stresses was less than 0.1$. A diagram shows the measured power distribution in the ATRC core. The hot-spot power density normalized to full-power (250 Mw) in the ATR is 27,000 w/g ^{235}U. The effects on the core hot spot due to venting or slotting the fuel element side plates are depicted graphically in radial, axial, and azimuthal profiles. The shutdown reactivity in the ATRC safety rods is greater than 7$ in all cases measured. Interaction effects between the shims and safety rods were investigated. An experimental program was conducted to determine the reactivity effect of displacing different volumes of water at various locations in the ARMF-I central experimental hole. Initial operation of a

once-through loop in the ETR core was executed in support of ATR fuel materials development. A computer code was written to calculate axial wall and bulk coolant temperatures for fuel elements of the ATR design. Analyses of the pressure and thermally induced stresses and deflections of the ATR fuel element generating the maximum power density are reported. It is shown that axial thermal stresses may exceed the yield strength of the fuel plates in some areas under maximum peak power (hot spot) conditions. The microprobe was applied successfully to the identification of fission products in two highly irradiated MTR fuel materials. One of these materials consisted of UO_2 particles in an aluminum matrix and had undergone a burnup of 83%. Fission-product Ce and Ba were found in the UO_2 fuel particles and in the Al matrix immediately adjacent to them. No indication of chemical reaction between the UO_2 and Al matrix was found. A U–Al alloy, consisting of uranium aluminide particles suspended in an Al matrix was irradiated to 24% burnup. In this material, Ce was found within the fuel particles and in the immediately adjacent Al matrix. Ba was not detected. Examination of two ATR-type fuel elements which were previously tested in the Hydraulic Facility and one MTR-type fuel element in which U-bearing Fiberglas was used as the fuel material are reported. (auth)

48061 (ORNL–3848) EFFECTS OF REACTOR OPERATION ON HFIR COOLANT. Jenks, G. H. (Oak Ridge National Lab., Tenn.). Oct. 1965. Contract W-7405-eng-26. 86p. Dep. mn; CFSTI $3.00 cy, $0.75 mn.

A dilute solution of nitric acid (ph 5) in water will be employed as the coolant-moderator in the High Flux Isotope Reactor (HFIR). The solution will be pressurized, and O_2 or H_2O_2 can be added if required to stabilize the HNO_3 during irradiation. The average rate of absorption of radiation energy in core water will be about 100 w/cm^3, and the temperature of water leaving the core will be about 80°C or less. A study employing available experimental and theoretical information was made to obtain estimates of: the pressures of dissolved gases which will develop in the coolant as a result of the radiolytic decomposition of water, and the possibility that the hydrogen ion concentration will be affected in solutions containing excess oxygen at concentrations up to a few thousandths molar. Interaction of radical and molecular species formed in the decomposition of water leads to formation of steady states in pressurized systems in which rates of formation and disappearance of a species are equal. Steady-state concentrations in the HFIR were calculated using: published information on reactions, published values for rate constant at about 25°C and estimated activation energies for reactions, and G-values for radiolytic species obtained from published values and from analyses of reported experimental data for steady-state concentrations of H_2, O_2, and H_2O_2 formed under irradiation. Available information on steady-state concentrations in the coolant solutions of the Oak Ridge Research Reactor and the Engineering Test Reactor was among the information used to evaluate G-values, activation energies, and the all around agreement between calculated and experimental values. Nitrate ion and its reduction products react with the radicals formed in radiolysis of water, and it is expected that steady-state concentrations of the several possible ionic and neutral species will be formed, and that these concentrations will depend upon the concentrations of the oxidizing and reducing radicals formed in water radiolysis. However, the radiation and thermal chemistry of the various nitrogen compounds is not completely understood. Estimates of concentrations of excess oxidant necessary to assure substantial stability of the HNO_3 near fuel elements were based on comparisons between calculated steady-state concentrations of oxidizing and reducing radicals formed in the HFIR and in another reactor where a solution of 10^{-3}M HNO_3 was used as the coolant and the HNO_3 found to be substantially stable in the solution outside the core. It was concluded that excess oxidant concentrations of about 10^{-3}M O_2 or the equivalent H_2O_2 will be required to provide reasonable assurance that the $[H^+]$ near the fuel element surfaces does not differ appreciably from 10^{-4}M. The expected steady-state concentrations of H_2, O_2, and H_2O_2 with this excess oxidant are near 10^{-3}M. (auth)

48062 (SC–4522(RR)) FINAL HAZARDS SUMMARY FOR THE SANDIA ENGINEERING REACTOR FACILITY (SERF). Hasenkamp, A. (Sandia Corp., Albuquerque, N. Mex.). Sept. 1961. Contract AT(29-1)-789. 195p. Dep. mn; CFSTI $5.00 cy, $1.00 mn.

An analysis of the hazards associated with the proposed operation of the Sandia Engineering Reactor Facility (SERF) is presented. The analysis includes descriptions of the reactor and facility, considerations of the reactor site in relation to hazards to the public, evaluations of safety factors, and a description of supervisory practices and operating procedures. (auth)

48063 (SC-RR-65-344) SANDIA PULSED REACTOR SPR-II-1 CORE CALCULATIONS. Schmidt, W. H. (Sandia Corp., Albuquerque, N. Mex.). Oct. 1965. Contract AT (29-1)-789. 30p. Dep. mn; CFSTI $2.00 cy, $0.50 mn.

The SPR-II-1 Sandia Pulsed Reactor design is described and evaluated in light of the results of problems solved on the Sandia Laboratory IBM 7090 computer. The calculations, which also provided insight into previously unexplored areas of fast-burst reactor technology, clearly indicated the inadequacy of the design presently proposed. (auth)

48064 (TID–22204) FINAL HAZARDS SUMMARY REPORT FOR AMES LABORATORY RESEARCH REACTOR. (AMF Atomics, Greenwich, Conn.). Mar. 1964. Contract AT(11-1)-855. 348p. Dep. mn; CFSTI $7.00 cy, $1.75 mn.

The design and safeguards of the Ames Laboratory Research Reactor and its associated facilities are reviewed. The causes and consequences of serious accidents are considered. It is found that the maximum credible accident for the ALRR is a quiet melt-down of the aluminum core, which results from loss of D_2O coolant. The accident is assumed to release 60% of the noble gases, 25% of the halogens, and 1% of the particulate fission products stored in the core. Downwind doses to persons outside the exclusion area are calculated on the basis of the above fission product release and the attenuation of activity provided by the containment system. Extreme inversion, fumigation and rainfall conditions are assumed. The restrictive effect of strontium fallout on surrounding agriculture is considered. It is found that the maximum credible accident, in combination with the specified containment and exclusion criteria, does not endanger the health and safety of persons outside the exclusion area, and does not impose restrictions upon agriculture. (auth)

48065 ON THE EFFICIENT UTILIZATION OF THE NUCLEAR REACTOR FOR RESEARCH OF THE VENEZUELAN INSTITUTE OF SCIENTIFIC RESEARCH. Rada, G. (Instituto Venezolano de Investigaciones Cientificas, Caracas). Acta Cient. Venezolana, 16: 14-17(1965). (In Spanish).

Certain problems related to the programming and utilization of nuclear research reactors are discussed. In particular, an analysis is made of the situation for the RV-1, the research reactor of the IVIC. The previous history of the acquisition and installation of the reactor under the Atoms for Peace program is related. Some possible uses of the instrument in the natural sciences and technology are mentioned as examples of scientific research. Propositions of the International Atomic Energy Organization are considered, and it is recommended that studies be directed to the effects of radiation on matter. It is particularly important that the staff be well integrated into the IVIC. Thus the cost of construction and personnel development, in excess of 20,000,000 bolivars, must be justified by rational use of the instrument; the IVIC is capable of efficient exploitation of the instrument because of its staff and capability in general; and the absence of energy problems in Venezuela directs use of the instrument to interdisciplinary areas, certain areas of physics,

and disciplinary equilibrium within the institute. Contributions to health, industry, economics, and technical education should be directed to the problems of Venezuela. (BBB)

48066 MODIFICATIONS OF SORIN'S POOL TYPE REACTOR AVOGADRO RS1 FOR HIGHER POWER OPERATION. Orsoni, L.; Custodero, S.; Walther, H. (SORIN, Saluggia, Italy). Energia Nucl. (Milan), 12: 459-70(Sept. 1965).

The principal modifications recently performed with reasonable costs on the Avogadro RS1 reactor of SORIN, which allow operation at considerably higher power (up to 10 Mw instead of 2 Mw), are briefly described. The criteria adopted for technical solutions are outlined. The following topics are discussed: reactor core (MTR fuel element with addition of graphite reflector elements, modification of the control rod system, reactor physics data, etc.); radiation shielding (warm water surface layer, modifications of Pb thermal shields, etc.); heat exchange (modifications to the primary and secondary circuits); control system (addition of a power channel based on ^{16}N activity, improvement of the alarm systems, etc.); increase of the irradiation facilities; and safety aspects. (auth)

48067 NUCLEAR REACTOR FOR IMPERIAL COLLEGE. Engineering, 200: 12(July 2, 1965).

The 100-kw Consort reactor Mark 2, which was installed at the Silwood Park field station of the Imperial College of Science and Technology is described and illustrated. It is being used to provide a source of neutrons for a wide range of experimental purposes. A cylindrical aluminum tank houses the core, fuel storage facilities, and the water for the pool-type reactor. Shielding is provided radially by concrete blocks and vertically by a combination of the water above the core and two concrete filled shield trolleys which run on rails over the top of the reactor. Four stainless-steel clad cadmium rods which run in aluminum guide tubes in spaces between the fuel boxes are used for control; natural convection cooling is employed. Fuel elements consist of an enriched U–Al alloy (80% ^{235}U) clad in aluminum. Control and safety instrumentation ensures that at least three safety circuits are always in use. After the reactor went critical on April 9, 1965, the power output was progressively raised, and full power was reached in mid-May, when the first experiments were begun. Some difficulties with radiation levels were overcome. (BBB)

48068 NEUTRON BEAM UTILIZATION AT THE PETTEN HFR. Goedkoop, J. A.; Loopstra, B. O. (Reactor Centrum Nederland, Petten). EuroNucl., 2: 376-8(Aug. 1965).

Work carried out at the Petten High Flux Research Reactor is described and the manner in which relations with the universities are organized is reviewed. At two of the five beam holes in use there are neutron diffractometers, which are used for solid-state investigations. One beamhole is being used to study gamma-rays emitted on capture of a thermal neutron. Another beam hole is being used for investigating solids and liquids by inelastic scattering of neutrons. The fifth beam hole is used for (n,γ) measurements by angular correlation. (M.C.G.)

48069 DIGITAL START-UP CONTROL OF A RESEARCH REACTOR. Takahashi, Yoshizo; Takamatsu, Shigeyuki (Tokyo Shibaura Electric Co., Ltd.). IEEE (Inst. Elec. Electron. Engrs.), Trans. Nucl. Sci., NS-12: No. 4, 355-66(Aug. 1965).

The automatic start-up of the Toshiba Training Reactor, a 100-kw swimming-pool reactor, from source level to the power level is facilitated by a digital computer. The digital computer designed for this purpose is used to count pulse signals of the neutron detector at fixed time intervals and, at the same time, to calculate reactor period for the indication and inverse period for the control using an approximate formula. The calculated inverse period together with the number of counts is compared with the program of start-up which is preset on push-buttons on the control signals to the control-rod servomechanisms. The control signal is so determined that the speed of the control rod is in proportion to the deviation of the inverse period from the preset value. (auth)

48070 CALIBRATION OF THE GRAPHITE DAMAGE FLUX IN A REPLACED FUEL ELEMENT POSITION IN DR-3 AT RISO. Gray, B. S. (UKAEA Reactor Materials Lab., Culcheth, Lancs, Eng.); Sorensen, H. J. Nucl. Energy: Pts. A and B, 19: 641-2(Aug. 1965).

An experimental comparison of a Mk. I Wigner rig loaded in a Zircaloy thimble in a replaced fuel element (RFE) or empty lattice position in DR-3 with a standard facility in BEPO is reported. Six graphite specimens were irradiated for 72 hours in each of the three specimen magazines of a Wigner rig with DR-3 operating at 600 kw. The specimen temperature was controlled to ±1°C in a helium atmosphere while their electric resistivity was measured before and after irradiation. The discrepancy between the two results obtained is expected from previous work. (J.F.P.)

48071 RADIATION MONITORS FOR INPILE GAS LOOP EXPERIMENTAL APPARATUS. Goto, Masayuki; (Mitsubishi Electric Corp. Res. Lab., Japan); Ogura, Shigeyoshi (and others). Mitsubishi Denki Giho, 37: 39-46 (Dec. 1963). (In Japanese).

Radiation monitors were developed for use with the so called Inpile Gas Loop for the testing of the semi-homogeneous uranium fuel in the reactor JRR-2 of the Japan Atomic Energy Research Institute. They consist of a failed fuel detector, a gamma-radiation detector, a gamma-ray in a water detector and radiation monitors in gas and dust. The failed fuel detector, built in a new concept, is for detecting the fission fragments of uranium fuel and expected to detect beta-radiation of 10$\mu\mu$C/cc in helium gas. The gamma-radiation detector with a logarithmic amplifier covers the range from 1 mR/h to 1 R/h for a 5 l chamber and from 10 mR/h to 10 R/h for a 0.5 l chamber. The gamma ray in water has a sensitivity at least as much as 5×10^{-5} μC/cc radioactive detectability calibrated by ^{137}Cs aqua. (auth)

48072 THE CALCULATION OF FLUX DISTRIBUTION IN THE VVR-S REACTOR BY S_n APPROXIMATION. Pavelescu, M.; Rosescu, T. (Inst. for Atomic Physics, Academy of the R.P.R., Bucharest). Rev. Roumaine Phys., 10: 193-200(1965).

The neutron flux distribution at WWR-S reactor was calculated in initial configuration, by the S_n method. The calculations were made for two neutron groups, fast and slow, with n = 5, I = K = 20, in cylindrical geometry with a reflector using a CIFA–101 computer. (auth)

48073 CRITICAL SIZE CALCULATION BY A FIRST COLLISION PROBABILITY METHOD. Rosescu, T.; Pavelescu, M. (Inst. for Atomic Physics, Academy of the R.P.R., Bucharest). Rev. Roumaine Phys., 10: 387-92 (1965).

A critical size calculation was made by a first collision probability method, at the VVR-S reactor, with three and five concentric annuli fuel elements. It was found that only the five concentric annuli fuel elements variant permits, for 36% enrichment, the allowed critical size and an acceptable $\Delta\rho$ to be obtained. It was also found that for a power increase of 2 to 10 Mw the thermal flux increased only 2.5 times. (auth)

48074 AN EXPERIMENTAL HETEROGENEOUS NUCLEAR REACTOR. (to Licentia Patent-Verwaltungs-GmbH). British Patent 1,000,982. Aug. 11, 1965. Priority date Sept. 24, 1960, Germany.

An experimental nuclear reactor is provided in which the moderator and reflector are built up of individual graphite blocks, some of which have recesses in the form of grooves so that channels for the reception of the fuel elements or of control rods can be formed by rows of recessed graphite blocks. The blocks are arranged in the form of a polygon around the longitudinal axis of the reactor core. The blocks are so shaped that they remain

in their place after the removal of some of the blocks to form stable cavities in the graphite core without any additional structural means. The fuel element unit may be made up of a can containing the fuel and water as a moderator; or the fuel may be embedded in a hydrogen containing synthetic plastics moderator material, such as polyethylene. The reactor shield that surrounds the graphite core is built up of individual concrete blocks, and the operating mechanism for the control rods is arranged outside this shield. (B.L.M.)

WASTE DISPOSAL AND PROCESSING

See also BIOLOGY AND MEDICINE — Ecology.
CHEMISTRY — Radiochemistry.
CHEMISTRY — Separation Processes and Procedures.
HEALTH AND SAFETY.

48075 (BNWL-68) SOLVENT EXTRACTION OF CESIUM FROM HANFORD ALKALINE SUPERNATE BY 4-SEC-BUTYL-2(α-METHYLBENZYL)PHENOL. LABORATORY STUDIES. Bray, L. A. (Battelle-Northwest, Richland, Wash. Pacific Northwest Lab.). Aug. 1965. Contract AT(45-1)-1830. 18p. Dep. mn; CFSTI $1.00 cy, $0.50 mn.

A cesium solvent extractant, 4-sec-butyl-2(α-methylbenzyl)phenol, was investigated for possible use at Hanford. The substituted phenol, diluted with a kerosene, was found to be a very selective extractant for cesium, both in the laboratory and, subsequently, by G. L. Richardson in pilot-plant-scale pulse column demonstrations. The extractant provides an efficient method for cesium recovery from the very large volumes of Alkaline Supernate now being stored at the separations facilities. The extraction of cesium depends upon the concentration of phenol, the pH of the aqueous waste solution, the temperature of the equilibration, and the aqueous Na^+ concentration. Approximately 0.3 of a mole of additional OH^- was required per liter of synthetic Alkaline Supernate (9M Na^+, pH 10.3) for maximum cesium extraction. Cesium distribution values are enhanced by an equilibration temperature decrease. The heat of extraction, $-\Delta H$, was found to be approximately 19 kcal. The cesium distribution ratio was also inversely dependent on the sodium concentration with a slope of slightly less than –2 over the range of 1 to 8M sodium. (auth)

48076 (DPSPU-62-30-3A) BENTONITE AS A PROTECTIVE COVER FOR BURIED RADIOACTIVE WASTE. Hawkins, R. H. (Du Pont de Nemours (E.I.) and Co., Aiken, S. C. Savannah River Plant). May 1962. Contract AT(07-2)-1. 9p. (CONF-32-3). Dep. mn; CFSTI $1.00 cy, $0.50 mn.

From Health Physics Society 7th Annual Meeting, Chicago, June 1962.

Laboratory tests, lysimeter tests, and field tests indicate that bentonite is an effective barrier to the movement of soil moisture. As such it appears to offer improved protection of buried solid radioactive waste from this primary cause of radionuclide migration. Bentonite studies are being continued. (auth)

48077 (IDO-12024) AN APPRAISAL OF GASEOUS WASTE DISPOSAL INTO THE LITHOSPHERE AT THE NATIONAL REACTOR TESTING STATION, IDAHO. Mudra, Paul J.; Schmalz, Bruce L. (Idaho Operations Office (AEC), Idaho Falls. Health and Safety Div.). Sept. 1965. 141p. Dep. mn; CFSTI $4.00 cy, $1.00 mn.

A series of gas-injection field tests were performed at the National Reactor Testing Station, Idaho, during the summer of 1964, to determine the feasibility of discharging radioactive gaseous waste to the lithosphere. Specific objectives included the determination of the: (a) storage capacity of the lithosphere, (b) direction and velocity of migration of the injected gas, (c) dilution and dispersion effects on the initial concentration of the injected gas, and (d) pressures required for injection. A cost estimate using this concept under hypothetical circumstances was also developed. Helium was used as a tracer gas to identify approximately 33 million standard cubic feet of air injected into porous zones both above and below the regional water table within the subsurface basalts underlying the station and into the unconsolidated sandy regolith materials. The maximum depth of injection was 400 feet below land surface. A mean pressure of 15 psig was required to maintain an injection rate of 1000 cubic feet per minute into the unsaturated basalt zones. Observations indicated that no finite geological reservoir existed in the subsurface and that the regolith materials offered the most restrictive barrier to vertical movement. Although injected gas could eventually arrive at land surface, the amount of dispersion and dilution observed indicates that lithospheric gas disposal is feasible at the NRTS for single injection volumes of up to 6 million standard cubic feet. The cost for a lithospheric disposal system is estimated at a maximum of $250,000. (auth)

48078 (JUL-261-DE) WASSERWIRTSCHAFT UND ABWASSERBEHANDLUNG DER KERNFORSCHUNGSANLAGE JUELICH IN DEN JAHREN 1960–1962. (Water Economy and Waste Water Treatment of the Juelich Nuclear Research Installation in the Years 1960–1962). Schulze-Rettmer, R.; Rattay, K. H. (Kernforschungsanlage, Juelich (West Germany)). Apr. 1965. 30p. Dep. mn.

The water economic relations at the research institution were reviewed. The methods used for the monitoring and treatment of domestic sewage, waste waters from laboratories and workshops, and waste waters from hot laboratories are reported. The methods used for the monitoring of drinking water, ground water, rain water, and rivers and lakes are described. The analytical monitoring of boiler water is also reported. (J.S.R.)

48079 (NP-15371) CHEMICAL ENGINEERING STUDIES ON THE PROCESSING OF RADIOACTIVE LIQUID WASTES BY EVAPORATION. Final Report, January 1, 1964–March 31, 1965. Yamamoto, Yutaka; Miyauchi, T.; Kunii, D.; Kiyose, R. (Tokyo Univ. (Japan). Faculty of Engineering). Contract 250/RB. 27p. Dep. mn.

In studies on the use of the fluidized-bed spray-type evaporator for economical processing of radioactive liquid wastes, cold experiments were conducted to obtain fundamental data on evaporation and solidification processes of solutions sprayed and heated in superheated steam. Heat transfer rate in the preheating stage is quite rapid as the process is considered to be condensation heat transfer. In the vaporization process, sensible heat transfer through the film around the liquid drops is considered dominant and the process is somewhat slower than the preheating stage. Engineering data for the fluidized-bed are correlated. It was concluded that the selection of the position of injection point of the feed liquid is not a critical problem in this type of evaporator. Liquid drop size has, however, an important effect on the operation characteristics of the bed. From a bench scale experiment it was concluded that the minimum recycling steam is necessary to maintain the good fluidizing condition. (P.C.H.)

48080 (ORNL-2873) THE COSTS OF PERMANENT DISPOSAL OF POWER-REACTOR FUEL-PROCESSING WASTES IN TANKS. Blomeke, J. O.; Frederick, E. J.; Salmon, R.; Arnold, E. D. (Oak Ridge National Lab., Tenn.). Sept. 1965. Contract W-7405-eng-26. 118p. Dep. mn; CFSTI $4.00 cy, $0.75 mn.

The costs of permanent storage of reactor fuel processing wastes are estimated for a 22,400-Mw(e) nuclear power economy. The wastes arise from chemical dissolution of the fuel cladding and solvent extraction purification of a combination of uranium and thorium converter fuels. The economics are examined for three representative types of financing: government ownership, private ownership, and a combination of government and private owner-

ship. Total costs for storing raffinate waste, in terms of the cost of electricity generated, were least for storage of acid wastes in tanks of 75-yr life with government ownership, and greatest for storage of alkaline wastes in tanks of 25-yr life with private ownership. For acid wastes, the optimum tank capacity is about a million gallons, and minimum total costs range from 0.0165 to 0.0272 mill/kwh. For alkaline wastes, the optimum tank capacity is 2.5 million gallons, and minimum total costs range from 0.0177 to 0.0294 mill/kwh. Doubling the concentration of fission products in the wastes, as stored, reduced the total costs between 15 and 30%. Total costs for storing cladding wastes ranged from 0.0215 to 0.0398 mill/kwh. These costs were greater than those for raffinate storage because of the greater volumes of cladding wastes. (P.C.H.)

48081 (RT/PROT(65)19) A STUDY ON THE SORPTION PROPERTIES OF NATURAL TUFFS OCCURRING IN THE LAKE BRACCIANO REGION (ROME). Boenzi, D.; Diouhy, Z., Lenzi, G. (Comitato Nazionale per l'Energia Nucleare, Rome (Italy)). June 1965. 18p. Dep. mn.

This study includes a preliminary classification of natural tuffs from the Lake Bracciano Region, according to their ability to take in microamounts of cesium and strontium. The materials studied were classified by means of criteria of distribution coefficients for both radionuclides. The most promising among these sorbents were studied in more detail. The influence of granulometry, of pH, and of the concentration of competing Na^+ and Ca^{++} ions, as well as the sorption kinetics, were the main criteria for comparing the selected materials. (auth)

48082 (UJV–1296/65) THE SORPTION OF FISSION PRODUCTS ON THE SUSPENSION OF THE NATURAL SORBENTS COAGULATED IN AN ELECTRIC FIELD. Napravnik, J.; Kepak, F. (Ustav Jaderneho Vyzkumu, Ceskoslovenska Akademie Ved, Rez). Feb. 1965. 35p. Dep. mn.

Results are reported of the laboratory and pilot plant experiments of the sorption of fission products on the suspension of natural aluminosilicates coagulated in an electric field. This method proved to be very suitable for natural sorbents, because no losses of their sorption capacity occurred in contradiction with the chemical coagulation. The influence of the nature of electrodes, current density, temperature, and of pH on the electrocoagulation was determined. The influence of the mode of the coagulation on the sorption properties of used sorbents was investigated. Attention was also paid to the sedimentation time and to the volume of the resulting sludge. (auth)

48083 RADIOACTIVE WASTE RESEARCH AND DEVELOPMENT ACTIVITIES—A REPORT OF PROGRESS. Belter, Walter G.; Regan, William H. (Atomic Energy Commission, Washington, D. C.). J. Water Pollution Control Federation, 37: 316-35(Mar. 1965).

Basic objectives of the radioactive waste management research and development program are discussed. The nature of radioactive wastes is reviewed. Objectives of the waste management operations are outlined. The use of a scavenging-precipitation ion-exchange process for waste processing is discussed. Foam separation methods of waste processing are described. Hydraulic fracturing of shale for waste disposed is considered. High-level waste solidification by the various methods of calcination and the phosphate glass process is described. Economic aspects of high-level waste treatment and disposal are discussed. Disposal of gaseous effluents is also considered. Environmental studies in support of the waste-disposal program are described. (M.C.G.)

48084 EFFECT OF A SYNTHETIC DETERGENT ON THE WATER TREATMENT OF RADIOACTIVE WASTES BY THE COAGULATION PRECIPITATION PROCESS. Ito, Fumio (National Inst. Radiol. Scis., Chiba, Japan). J. Water Waste (Tokyo), 6: 921-6(Dec. 1964). (In Japanese).

The effect of ABS-Na (sodium alkylbenzenesulfonate) on the water treatment of radioactive wastes was studied. Water (1000 cmp/ml) containing ^{89}Sr and 1% ABS-Na was used as the test solution. Two coagulants, $FeCl_3$ (300 ppm) and Na_3PO_4 (300 ppm + auxiliary coagulant $Ca(OH)_2$ 150 ppm), were used. The pH of the solution was varied between 10, 11, and 12. The synthetic detergent in the radioactive waste affected the water treatment by coagulation precipitation. When the ABS-Na concentration exceeded 240 ppm and pH was higher than 10, the decontamination efficiency increased considerably. The effect of ABS-Na on the coagulation precipitation became larger as the pH was lowered. In the case of Na_3PO_4, the decontamination efficiency was not varied considerably if the pH exceeded 9. (NSA of Japan)

48085 STUDY OF THE SORPTION PROPERTIES OF PYROCLASTIC ROCKS, FOR THE DECONTAMINATION OF RADIOACTIVE WASTE WATER. PART 2. STUDY UNDER STATIC CONDITIONS. Diouhy, Zdenek (Inst. of Nuclear Research, Czechoslovak Academy of Sciences, Rez). Jaderna Energie, 11: 207-12(June 1965). (In Czech.).

It was previously found that rhyodacite tuff from Nizny Hrabovec is the most suitable pyroclastic rock for the decontamination of radioactive waste water. Therefore, this mineral was investigated in greater detail, and the dependence of the adsorption of the radionuclide ion on the Ca^{2+} and Na^+ ions present was determined. The results obtained were in good agreement with the published data, except for the value of the distribution coefficient for Cs. It was concluded that for Cs the proportionality condition, as reported in the literature, of ion activities and molar fractions of these ions in solid phase is probably invalid. (CFSTI)

48086 A PLANT FOR THE DISPOSAL OF RADIOACTIVE WASTE WATER. Vesely, Vladimir (Inst. of Nuclear Research, Czechoslovak Academy of Sciences, Rez); Napravnik, Jiri; Jansa, Jindrich. Jaderna Energie, 11: 213-18(June 1965). (In Czech.).

When work with radioisotopes was begun at the Nuclear Research Institute in Rez, the storage tanks designed originally only for reactor waste water proved inadequate. A waste water disposal plant was built, with a boiler and a film evaporator. The disposal plant is described, and experience with its operation over a period of several years is reviewed. (CFSTI)

GENERAL AND MISCELLANEOUS

48087 (AD-613537) AIR FORCE RESEARCH OBJECTIVES. (Office of Aerospace Research, Washington, D. C.). 1964. 70p. CFSTI $3.00 cy, $0.75 mn.

Information is given on programs for physical sciences, environmental sciences, mathematical sciences, psychological and social sciences, and biological and medical sciences. (TCO)

48088 (BNWL-113-6) PLUTONIUM ABSTRACTS. Volume 5, Number 6. (Battelle-Northwest, Richland, Wash. Pacific Northwest Lab.). July 30, 1965. Contract AT(45-1)-1830. 41p. Dep. mn; CFSTI $2.00 cy, $0.50 mn.

A total of 92 abstracts is presented on new developments in plutonium technology. The abstracts are arranged under the following headings: biology and medicine, chemistry, health and safety, metallurgy, miscellaneous, physics, and reactor technology. (D.L.C.)

48089 (CALT-473-4) BASAL DISLOCATION MOBILITY IN HIGH PURITY ZINC SINGLE CRYSTALS. Report No. 3. Adams, K. H.; Vreeland, T. Jr.; Wood, D. S. (California Inst. of Tech., Pasadena. W. M. Keck Lab. of Engineering Materials). June 1965. Contract AT(04-3)-473. 77p. Dep. mn; CFSTI $3.00 cy, $0.75 mn.

Experimental measurements of dislocation mobility and density, and the strain-rate sensitivity of the flow stress were made on 99.999 per cent pure zinc crystals. Dislocation mobility in the $\langle 11\bar{2}0 \rangle \{0001\}$ basal slip system was measured by observing slip band growth produced by load pulses of controlled amplitude and duration. The results of the experimental measurements of dislocation mobility are discussed in relation to current theories. A comparison of the strain-rate sensitivity and mobility measurements shows that a significant change in the density of moving dislocations is associated with a change in strain-rate. A dislocation model is proposed to explain the observed strain-rate sensitivity. (auth)

48090 (COO-1149-53) THERMODYNAMICS OF TRIMETHYLACETONITRILE AND DIMETHYLMALONONITRILE [Thesis]. Ribner, Aaron (Michigan Univ., Ann Arbor. Dept. of Chemistry). Sept. 1965. Contract AT (11-1)-1149. 101p. Dep. mn; CFSTI $4.00 cy, $0.75 mn.

The thermodynamic properties of trimethylacetonitrile ["TMAN," $(CH_3)_3CCN$] and dimethylmalononitrile ["DMMN," $(CH_3)_2C(CN)_2$] were measured and compared with those calculated from spectroscopic frequencies. Vapor pressure measurements from 40 to 100°C were made on both compounds. The data were fit by the following equations: TMAN: $\log_{10} P(atm) = 21.6423 - 2703.45/T - 5.624 \log_{10} T$. DMMN: $\log_{10} P(atm) = 26.5509 - 3506.24/T - 7.0462 \log_{10} T$. The heat capacities of TMAN and DMMN were determined by the adiabatic technique from 5 to 350°K. The smoothed heat capacity at saturated vapor pressure (C_s), entropy (S^0), and Gibbs free energy ($-[G^0 - H]/T$) at 300°K are 42.96, 55.45, and 24.50 cal/(mole °K), respectively, for the liquid phase of TMAN. The corresponding values for the solid phase of DMMN at 298.15°K are 42.87, 44.92, and 22.97 cal/(mole °K). The experimental standard (third law) entropy of gaseous TMAN, $S^0_{298.15} = 79.63$, was compared with that, $S^0_{298.15} = 79.86$, calculated from molecular spectroscopic frequencies. It was found that TMAN undergoes two transitions, one at about 213°K with $\Delta S_t = 0.26$ cal/(mole °K), and the second at 232.74°K with $\Delta S_t = 1.86$ cal/(mole °K); melting occurs at 292.13°K with $\Delta S_m = 7.60$ cal/(mole °K). The transitions are interpreted in terms of rotation about the C-CN axis. The mechanism adopted gives a calculated $\Delta S_t = 2.12$ cal/(mole °K). The experimental entropy for gaseous DMMN, $S^0_{298.15} = 83.43$ cal/(mole °K), is in good agreement with that, 83.55 cal/(mole °K), calculated from molecular spectroscopic data. In DMMN, one transition occurs at 302.60°K with $\Delta S_t = 7.79$ cal/(mole °K) and melting at 307.47°K with $\Delta S_m = 3.15$ cal/(mole °K). Thus, by Timmerman's definition, DMMN is a plastic crystal. The transition in this compound was interpreted in terms of the alignment of symmetry features of the DMMN molecule at the site which it occupies in the crystalline lattice. On this basis, the calculated ΔS_t is 7.69 cal/(mole °K). Density measurements were made on both TMAN and DMMN at various temperatures. The experimental values for TMAN agree with those found in the literature [$P = 0.7618 - 9.75 \times 10^{-4}$ (t-20)], and those for DMMN fit the equation $P = 0.8900 - 11.0 \times 10^{-4}$ (t-35). (D.L.C.)

48091 (NP-15418) ATOMIC ENERGY BOARD EIGHTH ANNUAL REPORT, 1964. (Atomic Energy Board, Pretoria (South Africa)). 54p. Dep. mn.

An account is given of the atomic energy activities in 1964, which saw the ending of the first 5-year program and the beginning of another program. The areas in which research was carried out included geology, extraction metallurgy, reactor engineering, physical metallurgy, chemistry, physics, isotopes and radiation, and life sciences. Administrative and technical activities are also reported along with the construction program. Production and control of radioactive materials are discussed briefly. (D.L.C.)

48092 (NP-15477) AUSTRALIAN ATOMIC ENERGY COMMISSION THIRTEENTH ANNUAL REPORT, JUNE 30, 1965. (Australian Atomic Energy Commission). 100p. Dep. mn.

Activities in the following fields are discussed: nuclear power, raw materials, feasibility of high-temperature gas-cooled reactors, research establishment operations and services, and radioisotopes. Administrative and financial reports are included together with a bibliography of technical papers. (D.L.C.)

48093 (RFP-654) SPINDLE DESIGN. Green, H. S. (Rocky Flats Div., Dow Chemical Co., Golden, Colo.). Oct. 11, 1965. Contract AT(29-1)-1106. 8p. (CONF-651011-1). Dep. mn; CFSTI $1.00 cy, $0.50 mn.

From IMOG and Metrology Subgroup Meeting, Las Vegas, Nev.

Spindle specifications, types of spindles, tests, and available equipment are discussed. (P.C.H.)

48094 (SC-DC-65-1646) [AN ATMOSPHERIC STATIC ELECTRICITY WARNING SYSTEM]. Gentzler, R. F. (Sandia Corp., Albuquerque, N. Mex.). Aug. 19, 1965. Contract AT(29-1)-789. 11p. (CONF-650442-2). Dep. mn; CFSTI $1.00 cy, $0.50 mn.

From 2nd Space Congress, Cocoa Beach, Fla.

An atmospheric static electricity warning system is described which provides basic data on potential gradient at selected stations in Sandia Corporation's Albuquerque testing area. The measurements are transmitted over telephone wires to a master control station for recording and monitoring. Repeater stations located in certain test areas sequentially present the basic data from the master control station and give a warning signal both visual and aural when certain preset limits are exceeded. Data samples are presented. (auth)

48095 (SC-DR-64-539) DEVELOPMENT REPORT FOR TP82. Platt, L. W. (Sandia Corp., Albuquerque, N. Mex.). Apr. 1964. Contract AT(29-1)-789. 13p. Dep. mn; CFSTI $1.00 cy, $0.50 mn.

The TP82 is a battery charger designed to operate on 115-volt, 60-cps power, to fast charge from one to four 16-cell, wet nickel-cadmium, 2 ampere-hour batteries and to hold them on float charge for an indefinite time. (auth)

48096 (SC-DR-65-271) AN INTRODUCTION TO THE TTA GENERALIZED RIGID BODY TRAJECTORY PROGRAM FOR DIGITAL COMPUTER. Allensworth, J. A. F. (Sandia Corp., Albuquerque, N. Mex.). May 1965. Contract AT(29-1)-789. 40p. Dep. mn; CFSTI $1.00 cy, $0.50 mn.

Much valuable information concerning the movement of bodies in space can be obtained by the computation of theoretical trajectories. The TTA program was designed to meet the developing requirements for trajectories. TTA permits requesting the trajectory by means of a flexible language which is similar to English. The language and data structure of TTA places a useful tool into the hands of the user. (auth)

48097 (SC-DR-65-338) THE VOLTAGE-SWITCHING CLASS-D AMPLIFIER. Caffey, T. W. H. (Sandia Corp., Albuquerque, N. Mex.). July 1965. Contract AT(29-1)-789. 7p. Dep. mn; CFSTI $1.00 cy, $0.50 mn.

Circuit operation of the voltage-switching type of the Class-D amplifier and details of comparison with Class-C service are discussed. Some practical work with the Class-D amplifier is described and a problem pointed out. (auth)

48098 (SC-R-65-902) NAMDA—A NEW METHOD OF COMPUTERIZED MANAGEMENT CONTROL. Morrisroe, G. L. (Sandia Corp., Albuquerque, N. Mex.). June 1965. Contract AT(29-1)-789. 12p. (CONF-650327-2). Dep. mn; CFSTI $1.00 cy, $0.50 mn.

From American Society of Tool and Mfg. Engineers, Annual Conference, Cleveland.

Programming and scheduling the development of hundreds of different types of product testers pose problems which do not lend themselves to conventional PERT methods. A new technique developed by Sandia Corporation to resolve these problems is known as NAMDA (Network Analysis in Multiple, Dissimilar Applications). This system employs the same IBM/PERT computer program used for weapon programming modified to standardize and separate all activities related to product tester development. Each tester is treated as a separate network, and the resulting reports compile data to show slack times and work loads at each stage of development. NAMDA has improved "on-time" deliveries of product testers, and refinements to the technique promise still further improvement. (auth)

48099 (SC-TM-64-653) INVESTIGATIONS OF HIGH-INTENSITY HEAT FLUX GRAPHITE RESISTORS, 1960–1962. Dresser, John C. (Sandia Corp., Albuquerque, N. Mex.). July 1964. Contract AT(29-1)-789. 86p. Dep. mn; CFSTI $3.00 cy, $0.75 mn.

Machined graphite resistors of flat single-phase and cylindrical three-phase configurations were tested as possible high-intensity radiant heat sources. Results indicate that these resistors may be electrically heated to surface temperatures around 5000°F and above, where they act as effective heat emitters. Undesirable effects include nonuniform surface temperatures, structural deformation, short life, and sluggish response to changes in power levels. Photos and all test data are presented. (auth)

48100 (SC-TM-65-294) A GUIDE FOR THE APPLICATION OF HERMETICALLY SEALED, DIRECT CURRENT, ELECTROMAGNETIC RELAYS. Bates, C. C. (Sandia Corp., Albuquerque, N. Mex.). Aug. 1965. Contract AT(29-1)-789. 61p. Dep.mn; CFSTI $3.00 cy, $0.75 mn.

A guide for circuit design engineers for the proper application of hermetically sealed, direct current, electromagnetic relays is presented. It covers relay input, relay output, operating characteristics, and contact protection. (auth)

48101 (SC-TM-65-332) SUPPLEMENT REPORT ON COMARS (COORDINATE MEASURING AND RECORDING SYSTEM). Rosborough, J. R.; Stoner, C. L. (Sandia Corp., Albuquerque, N. Mex.). July 1965. Contract AT(29-1)-789. 15p. Dep. mn; CFSTI $1.00 cy, $0.50 mn.

This Report Supersedes SC-TM-352-63(24).

A system is described for digitally measuring and recording linear dimensions accurately to ±0.0001 inch. The system is rugged enough to be used in a normal factory environment. The results of an error-of-measurement study made on this system are also reported. (auth)

48102 (TID-22175) THE BIOCHEMISTRY OF SENESCENCE IN PLANT CELLS. Final Report, June 15, 1963–June 14, 1965. Varner, J. E.; Chandra, G. Ram; Chrispeels, M. J. (Martin Co., Baltimore, Md. Research Inst. for Advanced Studies). Contract AT(30-1)-3232. 12p. Dep. mn; CFSTI $1.00 cy, $0.50 mn.

The effects of gibberellic acid on the in vivo incorporation of ^{14}C-uridine, ^{14}C-adenosine, ^{14}C-adenine, and $^{32}PO_4$ into the RNA of aleurone cells of pea seeds were investigated. A time course study revealed that gibberellic acid enhances the in vivo incorporation of RNA precursors into the RNA of aleurone layers during the first 24 hr of treatment of dry seeds. Actinomycin D and 5-bromouracil inhibited the incorporation of the precursors into RNA. Results are included from a study of the synthesis and secretion of α-amylase by aleurone cells of barley seeds, in which ^{14}C-amino acids were used as tracers and a number of protein-synthesis-inhibitors were applied at various times after treatment with gibberellic acid. Results showed that gibberellic acid not only leads to the production of α-amylase but of protease as well, and this hydrolyzes the cellular proteins of the aleurone layers and of the starchy endosperm. This releases a flood of amino acids and for this reason the incorporation of ^{14}C-amino acids cannot conveniently be used as a measure of protein synthesis. (C.H.)

48103 (UCRL-16260) A PRECISION TECHNIQUE FOR MEASURING AZIMUTHAL DISTORTION IN OPTICAL LENSES. Hohenstein, Jack; Norgren, Duane (Lawrence Radiation Lab., Univ. of California, Berkeley). July 14, 1965. Contract W-7405-eng-48. 11p. Dep. mn; CFSTI $1.00 cy, $0.50 mn.

Apparatus and techniques were developed for accurately measuring azimuthal distortion in camera lenses. Great care was taken in fabricating the camera, which was made cylindrical so that the lens could be rotated. The experimental setup included a collimating telescope, the cylindrical camera containing the lens to be tested, and the test pattern. By rotation of the cylindrical camera, the same portion of the test pattern could be used for checking azimuthal distortion in different sectors of the lens. The distortion was recorded on film plates, which were then measured with a linear micrometer. Results were obtained to an accuracy of 1 part in 100,000. (auth)

48104 (UCRL-16278) DISPERSION OF OPTICAL ROTATION AND BIREFRINGENCE OF BIOPOLYMERS. I. THEORY OF FARADAY ROTATION IN POLYMERS. II. ELECTRICAL BIREFRINGENCE OF TOBACCO MOSAIC VIRUS. III. OPTICAL ROTATION OF DINUCLEOSIDE PHOSPHATES (thesis). Bush, C. Allen (Lawrence Radiation Lab., Univ. of California, Berkeley). July 1965. Contract W-7405-eng-48. 210p. Dep. mn; CFSTI $6.00 cy, $1.25 mn.

The optical properties of biological polymers in the ultraviolet and the interpretation of results to give information on the structure of biopolymers in solution are discussed. The theory of Faraday effect in organic molecules is developed and Faraday rotational strengths are defined. An exciton theory of the interaction of groups in a polymer is applied to Faraday rotation. This theory is used to predict how the Faraday effect changes with polymer conformation. Experiments on the optical properties of tobacco mosaic virus (TMV) and TMV protein are described. The optical rotatory dispersion (ORD) of TMV, of TMV protein subunits, and of TMV protein in aggregated rods is reported and discussed in terms of absorbing groups. The electrical birefringence of TMV and TMV protein rods is determined as a function of wavelength of light in an attempt to determine the orientation of the absorbing groups. A calculation is included of the ORD of

dinucleoside phosphates from an exciton model. The method assumes that the circular dichroism has the same dependence on wavelength as does the absorption. The ORD is obtained from a Kronig-Kramers transformation of the circular dichroism. The results of the Faraday rotation theory are applied to the effect observed in ketones. The interpretation leads to the conclusion that the 280 mμ absorption is composed of two distinct electronic transitions. In polymers, the theory predicts a structure-dependent Faraday effect. The ORD of TMV and its protein is interpreted as implying that the rods of aggregated protein resemble the native virus. The interpretation of the birefringence of TMV and the aggregated protein as a function of wavelength proved to be ambiguous. This ambiguity results partly from the small amount of RNA in the virus and partly from difficulties in separating the intrinsic birefringence from the form birefringence. The calculation of the ORD of dinucleoside phosphates gives reasonably good agreement with experiment, indicating that the exciton interaction is the origin of the large Cotton effects observed in some dinucleosides. It was also concluded that ApA and UpU are right handed helices and that, by implication, poly A at pH 7 also forms a right handed helix. The calculations suggest very strongly that all dinucleoside phosphates of the four RNA bases (A, U, G, and C) are right handed in conformation, and that they have helical increment angles of 28 to 40°. The calculation also predicts that certain dinucleoside phosphates may have very large rotations at low temperature. (auth)

48105 (UCRL–16290) STABLE-FLOW FREE-BOUNDARY ELECTROPHORESIS THEORY AND PRACTICE AS APPLIED TO THE STUDY OF HUMAN SERUM LIPOPROTEINS [Thesis]. Tippetts, Roger D. (Lawrence Radiation Lab., Univ. of California, Berkeley). Aug. 28, 1965. Contract W-7405-eng-48. 122p. Dep. mn; CFSTI $4.00 cy, $1.00 mn.

A review of electrophoretic methods is presented, pointing out their general inadequacy for the study of serum lipoproteins because of small sample size, instabilities for free-boundary (zone) methods, and sorption effects of those requiring solid supporting material. The Stable-Flow Free-Boundary (Staflo) Electrophoretic method is described and the Staflo theory of Howard C. Mel is reviewed. This includes aspects of density-gradient stability, self-balancing hydrostatic-hydrodynamic feedback, and the laminar flow pattern. New phenomena involving the dynamics of fluid flow are described, and their effect upon the design of Staflo apparatus and experiments are discussed. These include: the characteristic vertical and horizontal velocity profiles, solute migration profiles and the phenomena called "diffusion-convection," "laminar defocusing," and "central sharpening." Novel methods of Staflo sample handling and observation are described. These include the "thin sample" technique, the programmed electric field, and the thin-slit illumination method for observation of the Staflo sample migration profiles. The experimental conditions necessary for Staflo electrophoresis of the low-density lipoproteins (S_f 0–10^5) are described. This study has coupled Staflo electrophoresis of serum lipoproteins with ultraviolet spectrophotometry, lipid analysis, preparative and analytical ultracentrifugation, and electron microscopy. The principal results of this study demonstrated that low-density lipoprotein fractions may be preparatively or analytically (or both) Staflo electrophoresed. This study also indicates methods by which dense lipoproteins and proteins might be Staflo electrophoresed. These methods should be of more general application than only to lipoproteins. The observations and theory concerning the Staflo method should be valid for almost any soluble or suspendable solute, whether in an aqueous or other environment, and for a variety of forces causing the migration, e.g., electrical, gravitational, magnetic, and diffusional. (auth)

48106 (Y–1488) AN ACCELERATION SWITCHING VALVE CONTROL SYSTEM WITH MACHINE TOOL APPLICATION [Thesis]. Mankin, J. B. (Union Carbide Corp., Oak Ridge, Tenn. Y-12 Plant). Aug. 11, 1965. Contract W-7405-eng-26. 119p. Dep. mn; CFSTI $4.00 cy, $0.75 mn.

Submitted to Univ. of Tennessee, Knoxville.

With equal emphasis on practice and theory, the application of the acceleration switching valve to machine tool control systems is examined. Utilizing basic hydraulic concepts and electrical analogy techniques, the differential equation describing the acceleration switching valve and its associated load is developed. Root locus techniques are then utilized to synthesize a feedback control system with desirable transient responses and steady-state errors. Physical tests are performed to verify all results. (auth)

48107 (AEC-tr–6487) NUKLEONIKA. Translation of Nukleonika, 10: No. 1, 1–68, 1965. 63p. Dep. mn; CFSTI $3.00 cy, $0.75 mn.

48108 (ORNL-tr–754) STATISTICAL PROPERTIES OF NONLINEAR STRING. Izrailev, F. M.; Chirikov, B. V. (Akademiya Nauk SSSR, Novosibirsk. Institut Yadernoi Fiziki). Translated for Oak Ridge National Lab., Tenn. from preprint, 1965. 21p. Dep. mn; CFSTI $1.00 cy, $0.50 mn; JCL $2.60 fs, $0.83 mf.

The qualitative behavior of the longitudinal oscillations of a nonlinear string with fixed ends and satisfying the equation $\partial^2X/\partial t^2 = (\partial^2X/\partial Z^2)\,[1 + 3\beta\,(\partial X/\partial Z)^2]$ is investigated. This problem was previously examined by the method of numerical integration for a chain of nonlinear oscillators approximately representing a string and satisfying the following system of ordinary differential equations: $\ddot{X}_e = (X_{e+1} + X_{e-1} - 2X_e)\,\{1 + \beta\,[(X_{e+1} - X_e)^2 + (X_e - X_{e-1})^2 + (X_{e+1} - X_e)(X_e - X_{e-1})]\}$ where $l = 1, 2, \ldots, N-1$; $Q = L$ and $L = N$. The boundary of stochastic instability for this system of oscillators is estimated. (M.O.W.)

48109 (SC-T–65-749) THE TRIPLE IMPULSE ASYMPTOTIC PATHS. Siegel, Carl Ludwig. Translated by Marcel I. Weinreich (Sandia Corp., Albuquerque, N. Mex.) from Ann. Math., 42: 156-62(1941). 10p. Dep. mn; JCL $1.10 fs, $0.80 mf.

The solutions for a system of differential equations of the form $d\delta_K/dS = \Sigma_{l=1}^{n} a_{Kl}\,\delta_l + \Psi_K$ (K = 1, ..., n), were obtained. Two assumptions are made: a_{Kl} is a real constant, and Ψ_K is a power series of the variables $\delta_1, \ldots, \delta_n$ with real coefficients which converge in a certain neighborhood of the zero point and which contain neither constant non linear members. (M.O.W.)

48110 (SC-T–65-750) MODULATION OF LIGHT BY MEANS OF ELECTRICALLY BIREFRINGENT CRYSTALS. EXCERPT. Grau, Gerhard; Guers, Karl; Mueller, Rudolph. Translated by Marcel I. Weinreich (Sandia Corp., Albuquerque, N. Mex.) from Z. Angew. Phys., 17: 16-20(1964). 8p. JCL $1.10 fs, $0.80 mf.

A systematic investigation of the electro-optical effect suitable for modulation of light shows that certain crystal types are particularly appropriate. Various modulation methods and crystal types were examined. A procedure is described which makes it possible to establish a wide-band modulation with a low modulation power. Experiments are described with gas and ruby lasers based on continuous dash or wave signals. The utilized modulation frequencies attain a level of up to 2 Bc. (M.O.W.)

48111 ATOMIC ENERGY FOR AFRICA—A STUDY FOR EURATOM. To the Berlin Meeting on the Savary Report. Atomwirtschaft, 10: 425-6(Sept. 1965). (In German).

The economic possibilities for utilization of nuclear energy in the African countries associated with the European Common Market were investigated. The use of power reactors for electricity production, desalination of sea water, and for industrial heating and cooling, and the use of radioisotopes for agriculture and hydrology were studied. (J.S.R.)

48112 THE ATOMIC ENERGY MARKET IN EUROPE. PART I. FEDERAL REPUBLIC OF GERMANY. Winnacker, K. Atomwirtschaft, 10: 442-6(Sept. 1965). (In German).

The development of nuclear energy in the Federal Republic of Germany is reviewed. The market for the reactor

industry, based on the projected electrical needs up to 1980, is considered. The development of industry dealing with the fuel cycle and the utilization of radiation did not develop as rapidly as the construction of power reactors. Installations, however, for the reprocessing of reactor fuels are under construction. The disposal of radioactive waste is in the study stage in the Federal Republic. The long range view of radioisotopes in medicine, biology, agriculture, and technology indicates that they will have a considerable economic significance. (J.S.R.)

48113 THE ATOMIC ENERGY MARKET IN EUROPE. PART II. BELGIUM. Smits, P. Atomwirtschaft, 10: 448-50(Sept. 1965). (In German).

The status of the energy needs of Belgium and the available fuel supply to meet these needs are reviewed. Proposed future developments include two 600 Mw(e) nuclear power plants to be constructed for start-up in 1970 and 1973. The development of the nuclear industry in Belgium began with the construction of the Mol Nuclear Research Center. The component supply industry has reached a high standard and facilities were constructed for the fabrication of special nuclear products, especially nuclear fuels and fuel elements, uranium processing, and plutonium processing. The development specialized in components for pressurized water reactors. (J.S.R.)

48114 THE ATOMIC ENERGY MARKET IN EUROPE. PART IX. NORWAY. Moeller, F. Atomwirtschaft, 10: 474(Sept. 1965). (In German).

The nuclear market in Norway is composed of the requirements of equipment laboratories, etc. by the Institutt for Atomenergi, that is operating three research reactors – JEEP-I, the Halden Heavy Water Boiling Reactor, and the NORA Research Reactor. A plutonium extraction plant and a waste treatment plant are also in operation. The design and proposal for a 65,000 ton tanker was developed in cooperation with Sweden. The study indicated that a balance in economy could be achieved with a reactor. The main occupation of the Norwegian industry in the field of radioisotope application is laboratories and instruments for use in handling the radioisotopes. (J.S.R.)

48115 RESEARCH CENTRES IN EUROPE. NO. 8. HARWELL. EuroNucl., 2: 395-406(Aug. 1965).

The Harwell Atomic Energy Research Establishment is described. Its organization, reactors, accelerators, research program, and general services are discussed. (M.C.G.)

48116 PRESENT STATUS AND FUTURE PLAN OF ATOMIC ENERGY RESEARCH IN UNIVERSITIES. Oyama, Akira (Tokyo Univ.). Nippon Genshiryoku Gakkaishi, 7: 423-8(Aug. 1965). (In Japanese).

The present status of the organization, research facilities, and educational system on nuclear engineering and related arts in major universities is discussed. Activities of the Research Reactor Institute of Kyoto University and at the facilities of JAERI in Tokai-mura are described. Five-year plans for universities and research centers for universities were proposed. (auth)

48117 USES OF HIGH ENERGY RADIATION IN GERMANY. Rosinger, S. (Farbwerke Hoechst AG, Frankfurt am Main). Nucl. Eng., 10: 341-2(Sept. 1965).

The use of high energy radiation in Germany for synthesis, polymerizations, irradiation of polymers, and food preservation and biology, is discussed. The development of radiation sources is briefly discussed. Reactions and procedures that have been successful as preparative methods and may prove to be of practical value are included. (P.C.H.)

48118 GROUPING OF THE INDUSTRIES NECESSARY FOR THE REALIZATION FOR NUCLEAR PROGRAM. Rivoluzione Ind., No. 146, 19-21; 36(May-June 1965). (In Italian).

Two documents published by the Euratom Commission are reviewed. One is an indicative program for the electronuclear industry of the community and the second is on the elements of an industrial policy for the community in the nuclear energy sector. The indicative program includes estimates for the energy needs for the community, the reactors to be constructed, and the prospects for the various types of reactors. The elements of an industrial policy reviews the structural and organizational problems in the transition of nuclear energy to an industrial character with proposals on the actions to be undertaken in the industrial field. (J.S.R.)

CORPORATE AUTHOR INDEX

This index contains entries for this period for all report literature and, in addition, for certain published literature items for which it is felt that a corporate approach is especially desirable, e.g., symposia, conference proceedings, and meetings.

Each entry under a corporate author is a shortened version of the title of the publication, followed by the *NSA* volume and abstract number. Report numbers are given in parentheses.

The phrase "Progress report" is abbreviated as "Prog. rpt.," permitting a more rapid and complete alphabetical arrangement of the titles without changing the location of the progress report titles in relation to the other titles.

A

ADVANCED KINETICS INC., COSTA MESA, CALIF.
Final rpt. on plasma r-f energy conversion, 2/65, 19: 47717 (AD-614285)

AEROJET-GENERAL CORP., AZUSA, CALIF.
Evolution of remote handling capabilities at NRDS, 19: 48047 (CONF-640508, pp 334-9)

AEROJET-GENERAL CORP., JACKASS FLATS, NEV.
Remote handling requirements for NERVA (E-MAD and ETS-1), 19: 46495 (CONF-641120, pp 9-35)

AEROJET-GENERAL NUCLEONICS, SAN RAMON, CALIF.
Prog. rpt. on fissiochemical development, semiannual, 7–12/64, 19: 46324 (AGN-8132)

AEROSPACE MEDICAL RESEARCH LAB. (6570TH), WRIGHT-PATTERSON AFB, OHIO.
Evaluation of proposed applications of remote handling in space, 19: 46486 (CONF-640508, pp 233-47)
Human factors in remote handling, 19: 46484 (CONF-640508, pp 198-209)

AIR FORCE CAMBRIDGE RESEARCH LABS., L. G. HANSCOM FIELD, MASS.
Geophysics and Space Data Bull. No. 3, 19: 47447 (AD-612083)

AIR FORCE WEAPONS LAB., KIRTLAND AFB, N. MEX.
FMC remote handling vehicle, 19: 46496 (CONF-641120, pp 36-8)
Prog. rpt. on simulation of air-blast-induced ground motions, 7/64–1/65, 19: 46457 (AD-613674)
Step load moving on surface of half-space of a locking material: subseismic case, 19: 46580 (AD-613287)
Study to reduce and compile USAF NAP radiation effects data, 19: 46870 (AD-612191)
USAF exploratory development of remote handling equipment, 19: 46489 (CONF-640508, pp 327-33)

AKADEMIYA NAUK SSSR, NOVOSIBIRSK. INSTITUT YADERNOI FIZIKI.
Statistical properties of nonlinear string, 19: 48108 (ORNL-tr-754)

AKADEMIYA NAUK UKRAINSKOI SSR, KHARKOV. FIZIKO-TEKHNICHESKII INSTITUT.
Nonlinear stabilization of plasma bunch instabilities, 19: 47726 (NP-15394)

AKRON UNIV., OHIO. INST. OF RUBBER RESEARCH.
Prog. rpt. on low-temperature polymerization, 1–3/65, 19: 46323 (AD-613529)

AKTIEBOLAGET ATOMENERGI, STOCKHOLM (SWEDEN).
Bibliography on radiation effects on solid, U based nuclear fuel materials, Vol. 5, No. 2, 19: 47093 (VDDIT-16(5.2))
Trace elements in the conductive tissue of beef heart determined by neutron activation analysis, 19: 45753 (AE-191)

AMERICAN INSTITUTES FOR RESEARCH, PITTSBURGH, PA. INST. FOR PERFORMANCE TECHNOLOGY.
Laboratory investigations of shelter management factors, 19: 46637 (AD-612254)

AMERICAN MEAT INST. FOUNDATION, CHICAGO, ILL.
Chemical changes produced by heat and by irradiation of meat and meat fractions, 19: 46878 (NP-15455)

AMERICAN SCIENCE AND ENGINEERING, INC., CAMBRIDGE, MASS.
Research program to investigate artificially injected trapped radiation, 19: 47444 (AD-611629)

AMES LAB., IOWA STATE UNIV. OF SCIENCE AND TECH.
Photodisintegration of ^{40}Ca, 19: 47578 (IS-T-28)
Reversed-phase chromatographic separation of nitroanilines, 19: 46424 (IS-T-24)
Thirty-five millimeter color photomicrography, 19: 46928 (NMI-4998, pp 14-19)

AMF ATOMICS, GREENWICH, CONN.
Final hazards summary report for Ames Lab. Research Reactor, 19: 48064 (TID-22204)
Programming and manual control of versatile manipulating devices, 19: 46488 (CONF-640508, pp 304-26)

ARGONNE NATIONAL LAB., IDAHO FALLS, IDAHO.
Ratio of ^{239}U capture and ^{238}U fission cross sections in fast reactors, 19: 47944 (ANL-7034)

ARGONNE NATIONAL LAB., ILL.
A reactor system dynamics code: AIROS, 19: 47914 (ANL-7050, pp 379-94)
Activities of ANL-ENEA computer program libraries and the ORNL Radiation Shielding Information Center, 19: 47908 (ANL-7050, pp 125-39)
Advanced systems research and development, 19: 48053 (ANL-7090, pp 55-68)
ANL activities in [remote-control equipment], 19: 46498 (CONF-641120, pp 41-7)
Application of the Equipoise iterative method to diffusion and transport theory, 19: 47541 (ANL-7050, pp 179-89)
BISTRO, an integrated computational system for prediction of history of boiling water reactors, 19: 47913 (ANL-7050, pp 369-78)
Calculation of neutron spectra in the Doppler region, 19: 47539 (ANL-7050, pp 51-76)
Comments on computing, 19: 46902 (ANL-7050, pp 207-13)
Computation of scattering cross sections for use in thermal-neutron transport calculations, 19: 47543 (ANL-7050, pp 471-85)
Computer calculation of energy yield produced by hypothetical fast reactor accident, 19: 47918 (ANL-7050, pp 503-14)
Conference on applications of computing methods to reactor problems, Argonne National Lab., 5/65, 19: 47907 (ANL-7050)
Decomposition of gaseous PuF_6 by α radiation. VII., 19: 46325 (ANL-7013)
Evaluation of thermionic energy converter using film-boiling liquid metal, 19: 47281 (ANL-7039)
Extensions of power-control method for solution of large inhomogeneous reactor problems, 19: 47917 (ANL-7050, pp 487-502)
Family of FORTRAN routines for analysis of neutron resonance effects, 19: 47542 (ANL-7050, pp 457-70)
FREAK—fast reactor multigroup kinetics program, 19: 47947 (ANL-7050, pp 395-412)
General reactor technology, 19: 47921 (ANL-7090, pp 30-54)
General theory of first-passage distributions in transport and multiplicative processes, 19: 47865 (ANL-7061)
Interpretation and prediction of reactor power distributions with application to fuel cycle calculations, 19: 47946 (ANL-7050, pp 231-49)
Liquid-metal-cooled reactors, 19: 47989 (ANL-7090, pp 1-29)
Liquid-metal heat-transfer experiment, 19: 46528 (ANL-7038)

MAFIA II—a one-dimensional burnup code, 19: 47910 (ANL-7050, pp 299-307)
Manipulator systems at ANL, 19: 46481 (CONF-640508, pp 27-74)
Mechanized handling of nuclear data, 19: 47911 (ANL-7050, pp 309-13)
Metallographic studies of uranium-fissium alloys, 19: 47004 (NMI-4997, pp 45-54)
Metallography—ally of nondestructive testing in evaluating nuclear fuel components, 19: 46556 (NMI-4997, pp 1-21)
Monte Carlo approach to calculation of characteristic reactor parameters in three-dimensional assemblies, 19: 47919 (ANL-7050, pp 581-92)
New approach to water reactor lifetime with spatial variation studies, 19: 47912 (ANL-7050, pp 347-68)
Nuclear safety, 19: 47950 (ANL-7090, pp 69-78)
Numerical solution of γ transport equation applied to concrete slabs, 19: 47864 (ANL-7050, pp 113-22)
Physics performance of the EBWR in its operation from 0 to 100 Mwt, 19: 47988 (ANL-6776)
PINETO—FORTRAN code designed for the solution of nonlinear differential equations in neutron dynamics, 19: 47916 (ANL-7050, pp 429-41)
Processing of nuclear data for reactor calculations, 19: 47948 (ANL-7050, pp 517-39)
Prog. rpt. on physics, 4–12/64, 19: 47115 (ANL-6983)
Prog. rpt. on reactor development, 8/65, 19: 47920 (ANL-7090)
Remote metallographic preparation of irradiated aluminum-clad lead-bonded ceramic fuel pellets, 19: 47087 (NMI-4997, pp 189-97)
Solution of the transport equation by collision probability methods, 19: 47540 (ANL-7050, pp 93-112)
Techniques used in GEM code for Monte Carlo neutronics calculations in reactors and other systems of complex geometry, 19: 47949 (ANL-7050, pp 557-79)
The calculation of thermal-neutron spectra—generalized free-gas theory, 19: 47538 (ANL-7050, pp 33-49)
Time-dependent multigroup diffusion code with automatic resonance self-shielding of cross sections, 19: 47915 (ANL-7050, pp 413-27)
Use of digital programs in reactor plant designs, 19: 47909 (ANL-7050, pp 217-30)
Variational methods for solution of problems of reactor kinetics, 19: 47945 (ANL-7050, pp 159-77)
Vibratory grinding and polishing of metallographic specimens, 19: 46939 (NMI-5025(Pt.I), pp 185-219)

ARMOUR RESEARCH FOUNDATION, CHICAGO, ILL.
Metallographic observations at elevated temperature, 19: 47000 (NMI-4996, pp 8-18)
Throwout study of underground nuclear detonation, 19: 46468 (POR-1814)

ARMY ELECTRONICS LABS., FORT MONMOUTH, N. J.
Determination of the ionospheric electron content utilizing satellite signals, 19: 47448 (AD-612119)
Superconductors in advanced electronics, 19: 46475 (AD-612113)

ARMY ENGINEER WATERWAYS EXPERIMENT STATION, VICKSBURG, MISS.
Mass distribution measurements of crater ejecta and dust, 19: 46469 (POR-1815)

ARMY MATERIALS RESEARCH AGENCY, WATERTOWN ARSENAL, MASS.
Development of tough, high-strength α-β titanium base alloys, 19: 46985 (AD-613651)
Metallography of pyrolitic graphite, 19: 47078 (AD-613643)

ARMY NATICK LABS., MASS.
Meeting on radiation preservation of foods, Natick Mass., 10/63, 19: 46876 (AD-613325)

ATLANTIC RESEARCH CORP., ALEXANDRIA, VA.
Organometallic radiation dosimetry systems, 19: 46761 (NYO-2979-34)

ATOMENERGIKOMMISSIONEN, RISOE (DENMARK). FORSOEGSINSTITUT.
Determination of interatomic potentials in metals by electron irradiation experiments, 19: 47882 (RISÖ-103)
Micrometeorological data-handling system and some preliminary results, 19: 47109 (RISO-99)
Monitoring design for radioactive air pollution, 19: 46647 (RISO-104)
Similarity hypothesis for wind profiles, 19: 47110 (RISO-100)

ATOMIC ENERGY BOARD, PRETORIA (SOUTH AFRICA).
Prog. rpt., annual, 1964, 19: 48091 (NP-15418)

ATOMIC ENERGY ESTABLISHMENT, TROMBAY (INDIA). NUCLEAR PHYSICS DIV.
Feasibility of method of nondestructive assay of ^{235}U and ^{239}Pu in irradiated fuel slug, 19: 46178 (NP-15364)

ATOMIC ENERGY ESTABLISHMENT, WINFRITH (ENGLAND).
Calculation of neutron spectra in the Doppler region, 19: 47539 (ANL-7050, pp 51-76)
Forced convection burnout in Freon-12 flow, 19: 46527 (AEEW-R-426)
Mechanized handling of nuclear data, 19: 47911 (ANL-7050, pp 309-13)
Methods of control rod calculation for graphite moderated reactors, 19: 47999 (TRG-Report-227)

Multiwire proportional counter for the detection of ^{239}Pu, 19: 46751 (AEEW-M-526)
Solution of the transport equation by collision probability methods, 19: 47540 (ANL-7050, pp 93-112)

ATOMIC ENERGY OF CANADA LTD., CHALK RIVER (ONTARIO).
Accounting systems for heavy water and fissionable materials, 19: 47906 (AECL-2282)
Problems in β dose measurement at CRNL, 19: 46639 (AECL-2281)
Two-phase flow measurement with sharp-edged orifices and venturis, 19: 46526 (AECL-2273)

ATOMIC ENERGY OF CANADA LTD., CHALK RIVER (ONTARIO). CHALK RIVER NUCLEAR LABS.
Gamma-ray scanner for diagnostic radiography, 19: 46750 (AECL-2270)

ATOMIC ENERGY OF CANADA LTD., PINAWA (MANITOBA). WHITESHELL NUCLEAR RESEARCH ESTABLISHMENT.
Automatic potentiometric titrator, 19: 46162 (AECL-2262)
Effect of p-terphenyl on melting points of terphenyl-biphenyl organic coolants, 19: 46300 (AECL-2261)
Improved oxy-hydrogen burner for decomposition of polyphenyl reactor coolants, 19: 46163 (AECL-2263)

ATOMIC ENERGY RESEARCH ESTABLISHMENT, HARWELL (ENGLAND).
Calibration of the neutron survey probe, 19: 46752 (AERE-M-1564)
Computation of scattering cross sections for use in thermal-neutron transport calculations, 19: 47543 (ANL-7050, pp 471-85)
Determination of nitrogen in plutonium nitride, 19: 46164 (AERE-R-5002)
DIDO triple axis crystal spectrometer, 19: 46753 (AERE-R-4895)
Formation of ^{88m}Y by 14-Mev neutron irradiation of Zr, 19: 47566 (AERE-R-5009)
Stress corrosion of irradiated stainless steels, 19: 47079 (AERE-R-5014)

ATOMIC POWER DEVELOPMENT ASSOCIATES, INC., DETROIT, MICH.
Analysis of Babcock and Wilcox prototype steam generator for sodium-water reaction, 19: 46529 (APDA-175)
Application of Power Burst Facility to fast reactor fuel meltdown tests, 19: 47952 (APDA-177)
Fast reactor fuel meltdown test facility requirements, 19: 47951 (APDA-173)

ATOMIC WEAPONS RESEARCH ESTABLISHMENT, ALDERMASTON (ENGLAND).
Computer calculation of energy yield produced by hypothetical fast reactor accident, 19: 47918 (ANL-7050, pp 503-14)
Low-energy spread negative ion r-f source, 19: 47157 (AWRE-NR-1/65)
Permeation and diffusion of hydrogen isotopes through stainless steels. I, 19: 46991 (AWRE-O-47/65)
Processing of nuclear data for reactor calculations, 19: 47948 (ANL-7050, pp 517-39)
Time-dependent multigroup diffusion code with automatic resonance self-shielding of cross sections, 19: 47915 (ANL-7050, pp 413-27)

ATOMICS INTERNATIONAL, CANOGA PARK, CALIF.
A reactor system dynamics code: AIROS, 19: 47914 (ANL-7050, pp 379-94)
Carbide fuels in fast reactors, 19: 47993 (NAA-SR-10751)
Development and qualification of thermal control coatings for SNAP systems, 19: 48050 (NAA-SR-9908)
Quantative metallography of hypostoichiometric UN, 19: 46177 (NMI-5025(Pt.I), pp 85-95)
Remote operations in SNAP-8 facility at AI, 19: 46504 (CONF-641120, pp 86-97)

AUSTRALIAN ATOMIC ENERGY COMMISSION.
Prog. rpt. on AEC activities, annual, 1964–1965, 19: 48092 (NP-15477)

AUSTRALIAN ATOMIC ENERGY COMMISSION RESEARCH ESTABLISHMENT, LUCAS HEIGHTS.
Adsorption of beryllium on ion-exchange resins from inorganic systems, 19: 46230 (AAEC/E-136)
Purity of γ-ray sources, 19: 46407 (AAEC/TM-226(Suppl.1))

AUTONETICS, ANAHEIM, CALIF.
Pneumatically actuated master slave manipulator, 19: 46499 (CONF-641120, pp 63-6)

B

BABCOCK AND WILCOX CO., BARBERTON, OHIO. BOILER DIV.
Prog. rpt. on Na-heated steam generator development, 3/65, 19: 46478 (BAW-1280-25)
Prog. rpt. on Na-heated steam generator, 5/65, 19: 46530 (BAW-1280-27)
Prog. rpt. on Na-heated steam generator, 6/65, 19: 46531 (BAW-1280-28)

BATTELLE INSTITUT E. V., FRANKFURT AM MAIN (WEST GERMANY).
Effect of nuclear radiations on heterogeneously catalyzed gas reactions, 19: 46329 (EUR-2455.e)

BATTELLE MEMORIAL INST., COLUMBUS, OHIO.
Analysis of hostile-environment methodologies, 19: 46480 (CONF-

640508, pp 4-26)
Bright field etch for α plutonium, 19: 46938 (NMI-5025(Pt.I), pp 153-4)
Explosive welding of Zircaloy to Hf, 19: 46961 (BMI-X-10139)
Hot cell metallographic experience at Battelle, 19: 47085 (NMI-4997, pp 134-56)
Metallographic preparation of alumina-coated UO_2 spheres in graphite, 19: 46925 (NMI-4997, pp 85-91)
Metallographic preparation of irradiated uranium carbide, 19: 47083 (NMI-4996, pp 77-85)
Metallography of ceramic fuel and refractory metal compatibility couples, 19: 46954 (NMI-5025(Pt.I) pp 39-58)
Microstructural studies of cast uranium, 19: 47007 (NMI-5025(Pt.I), pp 127-51)
Microstructures of compounds of uranium, thorium, and beryllium, 19: 46924 (NMI-4997, pp 55-61)
One-step replication in the hot cell, 19: 47090 (NMI-4999, pp 54-9)
Plutonium metallographic practices at Battelle, 19: 46934 (NMI-4999, pp 104-10)
Prog. rpt. on civilian applications, 5/65, 19: 46912 (BMI-1727(Del.))
Prog. rpt. on civilian applications, 6/65, 19: 46913 (BMI-1833(Del.))
Proposed telechirics research laboratory, 19: 46497 (CONF-641120, pp 39-40)

BATTELLE MEMORIAL INST., GENEVA (SWITZERLAND).
Prog. rpt. on mechanical properties of metals subjected to mechanical stress and neutron irradiation, 7/65, 19: 47081 (EURAEC-1432)

BATTELLE-NORTHWEST, RICHLAND, WASH. PACIFIC NORTHWEST LAB.
Analog computer methods for parameter optimization, 19: 46903 (BNWL-70)
Detection of radionuclide contamination on face masks, 19: 46755 (BNWL-144)
High-temperature tensile testing machine for irradiated structural materials, 19: 46712 (BNWL-SA-169)
High-temperature corrosion of ATR structural materials, 19: 46946 (BNWL-100)
Instrument for measuring bowing in long tubes, 19: 46710 (BNWL-59)
Minimized fuel cycle cost for simulated boiling water reactor, 19: 47990 (BNWL-105)
Monte Carlo calculated material bucklings of enriched uranium–water lattices with uranium in the water moderator, 19: 47954 (BNWL-127)
Multiphonon neutron scattering study of hydrogen bonding in zirconium hydride, 19: 46232 (BNWL-SA-239)
Nickel-plated aluminum in deionized water, NH_4OH, and LiOH at 330°C, 19: 46945 (BNWL-98)
Plutonium Abstracts, Vol. 5, No. 6, 19: 48088 (BNWL-113-6)
Pressurizing vessel performance equations, 19: 46532 (BNWL-116)
Prog. rpt. on Battelle-Northwest studies executed for USAEC-AECL cooperative program, 7/65, 19: 46539 (TID-22249)
Prog. rpt. on W–Tc alloys, 1–4/65, 19: 46914 (BNWL-141)
PRTR containment vessel pressure test experience, 19: 48057 (BNWL-109)
Purification of Pu metal, 19: 46915 (BNWL-IR-2)
Roll film camera for remote metallography, 19: 46711 (BNWL-SA-161)
Safety rod interaction in the PRCF, 19: 48058 (BNWL-130)
Solvent extraction of Cs from Hanford alkaline supernate, 19: 48075 (BNWL-68)
Status of salt cycle process for processing oxide fuels, 19: 46422 (BNWL-SA-205)
Uranium dioxide–Pb radiation shielding, 19: 46916 (BNWL-IR-3)
Variable costs of fabricating UO_2–PuO_2 fuel rods for PRCF, 19: 47976 (BNWL-131A)
Variable costs of fabricating UO_2–PuO_2 fuel rods for EBWR, 19: 47977 (BNWL-131B)
Variable costs of fabricating UO_2–Pu_2 fuel rods for Saxton reactor, 19: 46962 (BNWL-131C)

BATTERSEA COLL. OF TECH., LONDON (ENGLAND).
Prog. rpt. on treatment of bcc metals, 7–12/64, 19: 46960 (AD-611837)

BEERS (ROLAND F.), INC., ALEXANDRIA, VA.
Predicting free-field radial displacements and strains, 19: 46467 (NVO-1163-43)

BETTIS ATOMIC POWER LAB., PITTSBURGH, PA.
Inelastic buckling of long axially compressed curved plates, 19: 46463 (WAPD-TM-469)

BETTIS ATOMIC POWER LAB., WEST MIFFLIN, PA.
Automation of mass spectrometers for isotopic analysis of reactor materials, 19: 46181 (WAPD-T-1769)

BOMAC DIV., VARIAN ASSOCIATES, BEVERLY, MASS.
Prog. rpt. on high-power cyclotron resonance switch, 6/15/62–1/63, 19: 46708 (AD-611560)

BRADDOCK, DUNN, AND MCDONALD, INC., EL PASO, TEX.
Statistics of breakdown using nanosecond pulse techniques, 19: 47114 (AD-614286)

BRAUN (C. F.) AND CO., VIENNA, VA.
Preliminary concepts for a central test facility, 19: 46503 (CONF-641120, pp 78-85)

BRIDGEPORT BRASS CO., CONN.
Decreasing electropolishing time for uranium, 19: 46920 (NMI-4996, pp 27-35c)

BROOKHAVEN NATIONAL LAB., UPTON, N. Y.
Alpha-gamma facility for fuel studies, 19: 47975 (BNL-9450)
Chemonuclear loop removal from BGRR using a semi-remote cutting technique, 19: 48055 (BNL-9402)
Comparison of various methods for determining particle beam phase-space distribution, 19: 47162 (BNL-9503)
Design of quadrupoles and dipoles using permanent magnet rings, 19: 47160 (BNL-9482)
Development of servo manipulators for high-energy accelerator requirements, 19: 47159 (BNL-9388)
Electron drift velocity variations in neon + 10% helium + alcohol, 19: 47116 (BNL-9443)
Fast beam extraction system of the alternating-gradient synchrotron, 19: 47158 (BNL-910)
Geometric control of surface leakage current and noise in Li-drifted Si radiation detectors, 19: 46754 (BNL-9535)
HFBR modifications and tests preparatory to operating authorization, 19: 48054 (BNL-9308)
Intermediate resonance absorption in heterogeneous media including moderator scattering, 19: 47953 (BNL-9393)
Neutron dynamics of Brookhaven's High Flux Beam Reactor, 19: 48056 (BNL-9510)
Plans for slow extracted beam at AGS, 19: 47161 (BNL-9483)
Processing of nuclear data for reactor calculations, 19: 47948 (ANL-7050, pp 517-39)
Properties of genes, 19: 45726 (BNL-9488)
Pulsed synchrotron as instrument for particle research, 19: 47163 (BNL-9504)
Spectral characteristics of a bacteriochlorophyll-protein complex from green photosynthetic bacteria, 19: 45727 (BNL-9506)
Superconducting transition temperature of thin Al films, 19: 47503 (BNL-9478)
The $Y_1^*(1660)$ produced in K^--p interactions at 2.24 Bev/c, 19: 47300 (BNL-9520)
Use of on-line computers in high-energy counter experiments, 19: 46756 (BNL-9492)
1963 environmental radiation levels at BNL, 19: 46640 (BNL-915)

BROWN ENGINEERING CO., INC., HUNTSVILLE, ALA. RESEARCH LABS.
Particle growth in the ionic nucleation condensation colloidal ion source, 19: 46570 (AD-614111)

BUREAU OF MINES, NORRIS, TENN. NORRIS METALLURGY RESEARCH LAB.
Metallic binders for zirconium diboride: chromium, molybdenum, and tungsten, 19: 46907 (AD-456724)

C

CALIFORNIA INST. OF TECH., PASADENA. DIV. OF CHEMISTRY AND CHEMICAL ENGINEERING.
Prog. rpt. on structure of metals and intermetallic compounds, final, 9/53–8/64, 19: 46984 (AD-612275)

CALIFORNIA INST. OF TECH., PASADENA. W. M. KECK LAB. OF ENGINEERING MATERIALS.
Basal dislocation mobility in high-purity zinc single crystals, 19: 48089 (CALT-473-4)

CALIFORNIA UNIV., BERKELEY. INST. OF ENGINEERING RESEARCH.
Estimation of internal radiation exposure resulting from ingestion of fallout-contaminated water in a nuclear war, 19: 46633 (AD-276187)

CALIFORNIA UNIV., LA JOLLA, SAN DIEGO.
Annihilation of positrons in metals, 19: 47217 (AD-613582)

CALIFORNIA UNIV., LOS ANGELES. DEPT. OF PHYSICS.
General orbit code for cyclotron analysis, 19: 47168 (TID-22177)

CALIFORNIA UNIV., RIVERSIDE. DEPT. OF PHYSICS.
Spin wave-spin wave scattering in a Heisenberg ferromagnet, 19: 47874 (AD-613606)

CASE INST. OF TECH., CLEVELAND, OHIO.
Application of fluid amplifiers in remote control operations, 19: 46502 (CONF-641120, pp 75-7)
Control of cast grain size of steel castings, 19: 46980 (AD-611800)
Generalized, programmed manipulators, 19: 46501 (CONF-641120, pp 73-4)
Identification of neutron stars in nuclear emulsion, 19: 46767 (TID-22256)

CEKMECE NUCLEAR RESEARCH CENTER, ATOMIC ENERGY

COMMISSION, ISTANBUL (TURKEY).
Inversion of cyanide group into iso-cyanide under γ irradiation, 19: 46326 (CNAEN-28)
CENTRAL ELECTRICITY GENERATING BOARD, LONDON (ENGLAND).
Appraisal of technical and economic aspects of Dungeness B nuclear power station, 19: 47996 (NP-15474)
Dungeness B—AGR nuclear power station, 19: 47995 (NP-15473)
CENTRE D'ETUDE DE L'ENERGIE NUCLEAIRE, BRUSSELS (BELGIUM).
Radioactive fallout measured at Mol. Annual report, 1963, 19: 46632 (A/AC.82/G/L.987)
Radiological monitoring of the surroundings of CEN at Mol, 19: 46631 (A/AC.82/G/L.986)
CLIMAX MOLYBDENUM CO. OF MICHIGAN, ANN ARBOR.
Prog. rpt. on tungsten-base alloys, final, 1/10/64–3/10/65, 19: 46940 (NP-15444)
COMITATO NAZIONALE PER L'ENERGIA NUCLEARE, CASACCIA (ITALY). CENTRO DI STUDI NUCLEARI.
PINETO—FORTRAN code designed for the solution of nonlinear differential equations in neutron dynamics, 19: 47916 (ANL-7050, pp 429-41)
COMITATO NAZIONALE PER L'ENERGIA NUCLEARE, ROME (ITALY).
Experiments on critical flow of a pressurized water loop in natural circulation conditions, 19: 46536 (RT/ING(65)1)
Influence of heat-treatments on structure of uranium-rich alloys containing zirconium, 19: 47014 (RT/MET(64)4)
Sorption properties of natural tuffs occurring in the Lake Bracciano region (Rome), 19: 48081 (RT/PROT(65)19)
COMMISSARIAT A L'ENERGIE ATOMIQUE, CADARACHE (FRANCE). CENTRE D'ETUDES NUCLEAIRES.
Detector for liquid carried over in a gas, 19: 46713 (CEA-R-2811)
Multi-sphere technique. I., 19: 46757 (CEA-R-2772)
Prog. rpt. on fast neutron project, 1–3/65, 19: 47997 (NP-15478)
COMMISSARIAT A L'ENERGIE ATOMIQUE, FONTENAY-AUX-ROSES (FRANCE). CENTRE D'ETUDES NUCLEAIRES.
Determination of sodium and potassium in biological media by neutron activation without chemical separation, 19: 46165 (CEA-R-2837)
Effective energy of radionuclides absorbed in organs other than G-I tract, 19: 45755 (CEA-R-2809)
Radioactive ions in the atmosphere, 19: 46641 (CEA-R-2771)
Study of U–Pu–Fe alloys (MASURCA critical experiment), 19: 46992 (CEA-R-2792)
COMMISSARIAT A L'ENERGIE ATOMIQUE, SACLAY (FRANCE). CENTRE D'ETUDES NUCLEAIRES.
Atmospheric corrosion of uranium–carbon alloys, 19: 46947 (CEA-R-2732)
Calculation of energy of particles emitted by reactions $^{3}T(d,n)^{4}He$, $D(d,n)^{3}He$ and $D(d,p)T$, 19: 47568 (CEA-R-2779)
Comparative study of the oxidation of various qualities of uranium in carbon dioxide at high temperatures, 19: 46948 (CEA-R-2805)
Flux and temperature distribution in nuclear thermionic converters Sirene 50 and Sirene 100, 19: 47978 (CEA-R-2782)
Long-term thyroid values after intake of radioactive iodine, 19: 45754 (CEA-R-2787)
Machining of uranium carbide rods obtained by continuous casting under electronic bombardment, 19: 46963 (CEA-R-2733)
Measurement of fission cross section of ^{235}U and ^{239}Pu for thermal neutrons, 19: 47567 (CEA-R-2775)
Scientific applications of nuclear explosions. I., 19: 46466 (CEA-Bib-63)
Some aspects of the solid-liquid transition, 19: 46233 (CEA-R-2752)
CORNELL AERONAUTICAL LAB., INC., BUFFALO, N. Y.
Design and test of full-scale wearable exoskeletal structure, 19: 46483 (CONF-640508, pp 158-97)
Prog. rpt. on aerospace nuclear safety investigations of reentry ablation phenomena, 5–7/65, 19: 47117 (SC-DC-65-1698)
CORNELL UNIV., ITHACA, N. Y.
Decontamination of selected vegetable crops by leaching with reference to Sr, 19: 45758 (NYO-2598-24)
Research on soft x-ray absorption, 19: 47216 (AD-613575)

D

DARTMOUTH COLL., HANOVER, N. H.
Prog. rpt. on color centers, energy storage, and thermoluminescence in LiF crystals, 1/1–9/30/65, 19: 46762 (NYO-3474-1)
DEPARTMENT OF MINES AND TECHNICAL SURVEYS (CANADA). MINES BRANCH.
Spectrometric study of attenuation in air of γ-rays from mineral sources, 19: 46586 (NP-15361)
DEUTSCHES ELEKTRONEN-SYNCHROTRON, HAMBURG (WEST GERMANY).

Electroproduction of π mesons and photoproduction of dipions, 19: 47303 (DESY-65/7)
DIVISION OF ISOTOPES DEVELOPMENT (AEC), WASHINGTON, D. C.
Radiation tools for food processing, 19: 45877 (CONF-650552-1)
DOUGLAS AIRCRAFT CO., INC., SANTA MONICA, CALIF.
Cavity nuclear reactors, 19: 48046 (AD-613998)
DU PONT DE NEMOURS (E. I.) & CO., AIKEN, S. C. SAVANNAH RIVER LAB.
Applications of atomic absorption spectroscopy, 19: 46166 (DP-980)
Cobalt-60 heat sources for 10- to 60-kw(E) generators, 19: 46893 (DP-974)
Evolution of high level caves at Savannah River Laboratory, 19: 46506 (CONF-651101-26)
High-temperature metallography of uranium, 19: 47005 (NMI-4997, pp 76-84)
Maximum safe limits for slightly enriched uranium and uranium oxide, 19: 47955 (CONF-651103-6)
Measurement of the thickness of aluminum oxide film, 19: 46952 (NMI-4997, pp 26-35)
Metallography of fused UO_2, 19: 46176 (NMI-4997, pp 110-23)
Preparation of thin foils of uranium, 19: 46933 (NMI-4999, pp 78-84)
Radiolysis of ion exchange resins used in the purification systems of Savannah River reactors, 19: 46327 (DP-977)
Substructure measurements by statistical fluctuations in x-ray diffraction intensity, 19: 46993 (CONF-650810-3)
DU PONT DE NEMOURS (E. I.) & CO., AIKEN, S. C. SAVANNAH RIVER PLANT.
Bentonite as protective cover for buried radioactive waste, 19: 48076 (DPSPU-62-30-3A)
Performance of 3% and 30% TBP processes, 19: 46423 (DPSPU-64-30-28)
DU PONT DE NEMOURS (E. I.) AND CO., WILMINGTON, DEL. TECHNICAL DIV.
Prog. rpt. on D_2O-moderated power reactors, 3–6/65, 19: 46917 (DP-975)
DUKE UNIV., DURHAM, N. C.
Prog. rpt. on effects of radiation on mucosal and fetal brain enzymes and radiation recovery, final, 11/1/64–10/31/65, 19: 45820 (TID-22227)
DUNLAP AND ASSOCIATES, INC., DARIEN, CONN.
Requirements for local planning to cover hazards of fallout. I., 19: 46635 (AD-611764)
Requirements for local planning to cover hazards of fallout. II. Appendices, 19: 46636 (AD-611765)

E

EDGERTON, GERMESHAUSEN AND GRIER, INC., LAS VEGAS, NEV.
Pancake neutron detector, 19: 46759 (EGG-1183-1017)
ENGLISH ELECTRIC CO., LTD., WHETSTONE (ENGLAND). ATOMIC POWER DIV.
The calculation of thermal-neutron spectra—generalized free-gas theory, 19: 47538 (ANL-7050, pp 33-49)
EUROPEAN ATOMIC ENERGY COMMUNITY.
APACHE: Analog programming and checking programmers manual, 19: 46904 (EUR-2437.e)
Apparatus for measurement of diffusivity at high temperatures, 19: 46895 (EUR-2424.f)
Application of strain gages at high temperature. I., 19: 46715 (EUR-2473.f)
Damage and diffusion in Al and Al–Al_2O_3 alloy following bombardment with oxygen or inert gas, 19: 47080 (EUR-2478.e)
Data handbook for sensitivity calculations in neutron activation analysis, 19: 46167 (EUR-1898.e)
Effect of nuclear radiations on heterogeneously catalyzed gas reactions, 19: 46329 (EUR-2455.e)
Electron microscopy of SAP following tensile deformation or quenching, 19: 46996 (EUR-2479.e)
Mass spectrometric studies on polyphenyls. I., 19: 46328 (EUR-2227.e)
EUROPEAN ATOMIC ENERGY COMMUNITY, GEEL (BELGIUM). CENTRAL NUCLEAR MEASUREMENTS BUREAU.
Excitation functions for nuclei around Z = 28, 19: 47571 (EUR-2456.e)
EUROPEAN ATOMIC ENERGY COMMUNITY, ISPRA (ITALY). EUROPEAN SCIENTIFIC DATA PROCESSING CENTER.
APACHE: Analog programming and checking programmers manual, 19: 46904 (EUR-2437.e)
EUROPEAN ATOMIC ENERGY COMMUNITY, ISPRA (ITALY). JOINT NUCLEAR RESEARCH CENTER.
Activities of ANL-ENEA computer program libraries and the ORNL Radiation Shielding Information Center, 19: 47908 (ANL-7050, pp 125-39)
APACHE: Analog programming and checking programmers manual, 19: 46904 (EUR-2437.e)
Application of strain gages at high temperature. I., 19: 46715 (EUR-

2473.f)
Damage and diffusion in Al and Al–Al_2O_3 alloy following bombardments with oxygen or inert gas, 19: 47080 (EUR-2478.e)
Data handbook for sensitivity calculations in neutron activation analysis, 19: 46167 (EUR-1898.e)
Electron microscopy of SAP following tensile deformation or quenching, 19: 46996 (EUR-2479.e)
Excitation functions for nuclei around Z = 28, 19: 47571 (EUR-2456.e)
MAFIA II—a one-dimensional burnup code, 19: 47910 (ANL-7050, pp 299-307)
Mass spectrometric studies on polyphenyls. I., 19: 46328 (EUR-2227.e)
Monte Carlo approach to calculation of characteristic reactor parameters in three-dimensional assemblies, 19: 47919 (ANL-7050, pp 581-92)
Numerical solution of γ transport equation applied to concrete slabs, 19: 47864 (ANL-7050, pp 113-22)
PIKETO—FORTRAN code designed for the solution of nonlinear differential equations in neutron dynamics, 19: 47916 (ANL-7050, pp 429-41)
Variational methods for solution of problems of reactor kinetics, 19: 47945 (ANL-7050, pp 159-77)

EUROPEAN ATOMIC ENERGY COMMUNITY, KARLSRUHE (WEST GERMANY). TRANSURANIUM INST.
Apparatus for measurement of diffusivity at high temperatures, 19: 46995 (EUR-2424.f)

EUROPEAN ORGANIZATION FOR NUCLEAR RESEARCH, GENEVA (SWITZERLAND).
Weak interactions, 19: 47301 (CERN-65-30)

F

FIAT, TURIN (ITALY). SEZIONE ENERGIA NUCLEARE.
New approach to water reactor lifetime with spatial variation studies, 19: 47912 (ANL-7050, pp 347-68)

FORSVARETS FORSKNINGSANSTALT, STOCKHOLM (SWEDEN).
PROTOS—computer program for treating proton slowing-down due to atomic collisions, 19: 47867 (NP-15384)

FRANKLIN INST. RESEARCH LABS., PHILADELPHIA, PA.
Entrance effects in circular thrust bearings, 19: 46462 (TID-22184)
Prog. rpt. on flow and fracture of alloyed Be, 10/7/64–1/6/65, 19: 46910 (AD-620589)
Prog. rpt. on preparation and evaluation of Be, 10/15/63–1/14/64, 19: 46909 (AD-620264)

G

GENERAL ATOMIC, SAN DIEGO, CALIF. JOHN JAY HOPKINS LAB. FOR PURE AND APPLIED SCIENCE.
Chemical engineering in the HTGR, 19: 47991 (GA-6126)
Design of SNAP-15A generator, 19: 46894 (GA-5296)
Experimental determination of neutron inelastic scattering in polyethylene, 19: 47572 (GA-6547)
Prestressed concrete structures for large power reactors, 19: 47925 (GA-6505)

GENERAL DYNAMICS/FORT WORTH, TEX.
Analysis of ASTR radiation heating in aerospace structural materials, 19: 47077 (AD-613471)
Analysis of radiation streaming through single-bend ducts, 19: 47863 (AD-613480)
Excitation of ethylene, acetylene, propyne, and 1-butyne by low-energy electron impact, 19: 46322 (AD-612070)

GENERAL ELECTRIC CO., CINCINNATI, OHIO. AIRCRAFT NUCLEAR PROPULSION DEPT.
Electron microscope studies of beryllium oxide powders, 19: 47002 (NMI-4996, pp 50-76)
Metallography of beryllium oxide, 19: 47001 (NMI-4996, pp 36-49)

GENERAL ELECTRIC CO., CINCINNATI, OHIO. NUCLEAR MATERIALS AND PROPULSION OPERATION.
Electron microscope studies of irradiated A-286 alloys, 19: 47088 (NMI-4998, pp 95-106)
Metallographic and ceramographic preparation of nuclear materials, 19: 46937 (NMI-5025(Pt.I), pp 1-25)
Post-irradiation metallographic laboratory at GE-NMPO, 19: 47089 (NMI-4999, pp 30-50)

GENERAL ELECTRIC CO., PHILADELPHIA, PA. MISSILE AND SPACE DIV.
Nuclear Brayton cycle power system, 19: 48048 (GE-65SD4251)
Prog. rpt. on vaporization of refractory materials, 7–9/63, 19: 46982 (AD-611856)
Solar flare model and its laboratory experimentation, 19: 47188 (AD-613636)

GENERAL ELECTRIC CO., RICHLAND, WASH. HANFORD ATOMIC PRODUCTS OPERATION.
Administering criticality control in HAPO chemical processing department, 19: 46433 (RL-SA-43)
Clean ^{233}U production—methods and parameters, 19: 46900 (RL-SA-46-A)
Novel metallographic utilization of replicas and microautoradiography, 19: 46951 (NMI-4996, pp 19-26)
Procedure for color microphotography, 19: 46931 (NMI-4999, pp 26-9)

GENERAL ELECTRIC CO., SAN JOSE, CALIF. ATOMIC POWER EQUIPMENT DEPT.
Extensions of power-control method for solution of large inhomogeneous reactor problems, 19: 47917 (ANL-7050, pp 487-502)

GENERAL ELECTRIC CO., SCRANTON, PA. DEFENSE ELECTRONICS DIV.
Control—the universal process, 19: 46460 (CONF-640508, pp 224-32)

GENERAL TELEPHONE AND ELECTRONICS LABS. INC., PALO ALTO, CALIF.
Factors controlling effectiveness of high-temperature protective coatings for tungsten, 19: 46911 (AFML-TR-64-392)

GEORGETOWN UNIV., WASHINGTON, D. C.
Theoretical study of vibrational energy levels of distonic molecules, 19: 47215 (AD-613375)

GOSUDARSTVENNYI KOMITET PO ISPOL'ZOVANIYU ATOMNOI ENERGII SSSR, MOSCOW. INSTITUT TEORETICHESKOI I EKSPERIMENTAL'NOI FIZIKI.
Backward elastic scattering of pions on neutrons at 1.2 to 4.5 Bev, 19: 47310 (NP-15376)
CP parity non-conservation in polarized neutron decay, 19: 47312 (NP-15460)
Regge pole in a Coulomb-well type potential, 19: 47311 (NP-15454)
Single-particle effects in neutron physics and fine structure of nuclear masses. III., 19: 47583 (NP-15467)

GOSUDARSTVENNYI KOMITET PO ISPOL'ZOVANIYU ATOMNOI ENERGII SSSR, OBNINSK. FIZIKO-ENERGETICHESKII INSTITUT.
Models of temperature fields of heat exchange elements in active zone and shielding of the BN-350 reactor, 19: 47994 (NP-15393)

GRENOBLE UNIV. (FRANCE).
Point defects in pure iron through electrical resistivity, 19: 47094 (ORNL-tr-668)

H

HAHN-MEITNER-INSTITUT FUER KERNFORSCHUNG, BERLIN (WEST GERMANY).
Isotope effect in ion transport in aqueous solution—an basis for isotope separation and an instrument, 19: 46898 (HMI-B-44)

HARRY DIAMOND LABS., WASHINGTON, D. C.
Nuclear magnetic resonance in boron trioxide at elevated temperatures, 19: 47873 (AD-612384)

HELSINKI UNIV. (FINLAND). DEPT. OF RADIOCHEMISTRY.
Prog. rpt. on [radioecological studies], annual, 7/65, 19: 46587 (NYO-3446-3)

HOLMES AND NARVER, INC., LAS VEGAS, NEV.
Engineering study for tunnel grid blast-shelter concept for Detroit, 19: 46568 (ORNL-TM-1223)

HUGHES RESEARCH LABS., MALIBU, CALIF.
Electrode surface physics research, 19: 46571 (HRL-5249-S)

I

IDAHO OPERATIONS OFFICE (AEC), IDAHO FALLS. HEALTH AND SAFETY DIV.
Appraisal of gaseous waste disposal into the lithosphere at NRTS, 19: 48077
Environmental tritium studies at the National Reactor Testing Station, 19: 46642 (IDO-12043)

IIT RESEARCH INST., CHICAGO, ILL.
Hafnium–oxygen system, 19: 46990 (ARL-65-138)
Materials research with scanning microprobe analyzer, 19: 46508 (NMI-4998, pp 65-76)
Prog. rpt. on interface friction in hot metal deformation, 11/24/64–1/23/65, 19: 46981 (AD-611821)
Prototype manual of metallurgical practice, 19: 46918 (IITRI-B6018-1)

ILLINOIS INST. OF TECH., CHICAGO.
Metallographic preparation of hard and brittle materials, 19: 46922 (NMI-4997, pp 22-5)

ILLINOIS UNIV., URBANA.
Family of FORTRAN routines for analysis of neutron resonance effects, 19: 47542 (ANL-7050, pp 457-70)

INNSBRUCK UNIV. (AUSTRIA).
Juelich plasma symposium, 19: 47715 (AD-613622)

INSTITUT ATOMNOI ENERGII, GOSUDARSTVENNYI KOMITET PO

ISPOL'ZOVANIYU ATOMNOI ENERGII SSSR, MOSCOW.
Effect of temperature on space-energy distribution of neutron flux, 19: 47956 (IAE-723)
Elastic (p,p) scattering at 1.45 Bev, 19: 47304 (IAE-700)
Evaluation of time-related readings of aerosol radiometers with a continuously moving filter strip, 19: 46760 (NP-15462)
Isotope shift and quadrupole moments of near spherical nuclei, 19: 47573 (IAE-717)
Optimum methods for handling transient processes in reactors, 19: 47957 (IAE-724)
Reaction $^{7}Li(p,t)^{5}Li$ and $^{6}Li(\alpha,t)^{7}Be$, 19: 47574 (IAE-836)
INSTITUTE FOR NUCLEAR STUDY, TOKYO UNIV. (JAPAN).
Mean square angular and lateral spreads of electrons and photons in a cascade shower, 19: 47268 (INSJ-86)
Very fast scale of four, 19: 46717 (INSJ-87)
INSTITUTE OF MATHEMATICAL SCIENCE, MADRAS (INDIA).
Theories of gravitation, 19: 47411 (NP-15486)
INSTITUTT FOR ATOMENERGI, KJELLER (NORWAY).
BISTRO, an integrated computational system for prediction of history of boiling water reactors, 19: 47913 (ANL-7050, pp 369-78)
Correlation between calculated and measured mechanical properties of thin-walled fuel element canning tubes of stainless steel, 19: 46986 (KR-96)
Determination of selenium in animal tissue by neutron activation analysis, 19: 46172 (KR-95)
INTERNATIONAL ATOMIC ENERGY AGENCY, VIENNA (AUSTRIA).
Basic requirements for personnel monitoring, 19: 46689
Provision of radiological protection services, 19: 46649 (STI/PUB/94)
Seminar on plasma physics, Trieste, 10/64, 19: 47802
INTERNATIONAL CENTRE FOR THEORETICAL PHYSICS, TRIESTE (ITALY).
$\bar{U}(12)$ symmetry, 19: 47305 (IC/65/57)
IOWA STATE UNIV. OF SCIENCE AND TECH., AMES. COLL. OF VETERINARY MEDICINE.
Pulmonary compliance and physiopathology of guinea pig lungs exposed to gadolinium oxide dust, 19: 45756 (COO-1170-7)
IOWA STATE UNIV. OF SCIENCE AND TECH., AMES. INST. FOR ATOMIC RESEARCH.
Pulmonary compliance and physiopathology of guinea pig lungs exposed to gadolinium oxide dust, 19: 45756 (COO-1170-7)
ISRAEL ATOMIC ENERGY COMMISSION, YAVNE. SOREQ RESEARCH ESTABLISHMENT.
Radiochemical procedures for environmental media, 19: 46168 (IA-849)

J

JET PROPULSION LAB., CALIF. INST. OF TECH., PASADENA.
Rotating superconductor, 19: 47504 (JPL-TR-32-650(Pt.2))
JOINT INST. FOR NUCLEAR RESEARCH, DUBNA (USSR). LAB OF HIGH ENERGY.
Decays in a mixed ensemble of neutral K mesons, 19: 47309 (JINR-P-2289)
JOINT INST. FOR NUCLEAR RESEARCH, DUBNA (USSR). LAB. OF NEUTRON PHYSICS.
30-Mev microtron-injector for pulsed fast reactor, 19: 47164 (JINR-P-2313)
JOINT INST. FOR NUCLEAR RESEARCH, DUBNA (USSR). LAB OF NUCLEAR PROBLEMS.
Electrophotographic method for determining the lithium diffusion constant in p-type silicon, 19: 46997 (JINR-P-2282)
Formation in Ho-162 in Ta + p at 660 Mev, 19: 47579 (JINR-P-2275)
JOINT INST. FOR NUCLEAR RESEARCH, DUBNA (USSR). LAB OF THEORETICAL PHYSICS.
Decay of baryons and mesons with formation of an electron-positron pair in the U(12) symmetry scheme, 19: 47308 (JINR-P-2284)
Dispersion sum rules and SU(6) symmetry, 19: 47306 (JINR-E-2343)
Leptonic decays of baryons in the universal V-A theory, 19: 47307 (JINR-P-2278)
JUNTA DE ENERGIA NUCLEAR, MADRID (SPAIN). DIVISION DE QUIMICA.
Determination of palladium by flame photometry, 19: 46170 (JEN-148-DQ/I-49)

K

KANSAS UNIV., LAWRENCE. DEPT. OF CHEMISTRY.
Thermodynamics of materials at high temperature and low pressure, 19: 46234 (COO-1140-123)
KERNENERGIEANLAGEN, ALLGEMEINE ELEKTRICITAETS-GESELLSCHAFT, FRANKFURT AM MAIN (WEST GERMANY).
Local neutron flux distribution in a bundle from segmented fuel elements, 19: 47992 (KEA-311)
KERNFORSCHUNGSANLAGE, JUELICH (WEST GERMANY).
Water economy and waste water treatment of the Juelich Research Installation, 1960–1962, 19: 48078 (JÜL-261-DE)
KERNFORSCHUNGSZENTRUM, KARLSRUHE (WEST GERMANY). INSTITUT FUER NEUTRONENPHYSIK UND REAKTORTECHNIK.
Programs for solution of neutron physics problems with help of Monte Carlo Method, 19: 47546 (KFK-298)
Solution of the transport equation with help of the Monte Carlo Method, 19: 47545 (KFK-297)
KNOLLS ATOMIC POWER LAB., SCHENECTADY, N. Y.
Corrosive potential of wetted thermal insulation, 19: 46949 (CONF-650905-2)
Program to compute inelastic scattering matrices for multigroup reactor codes, 19: 47544 (KAPL-M-6467)
SOSH-5. Computer program for shielding calculations, 19: 47866 (KAPL-M-6460)
Spectrophotometric determination of silicon in Nb–Si alloys, 19: 46171 (KAPL-M-6492)
Test apparatus and profile measurement system for rectangular plates subjected to in-plane thrusts, 19: 46555 (KAPL-M-6493)
Use of digital programs in reactor plant designs, 19: 47909 (ANL-7050, pp 217-30)

L

LABORATOIRE DE L'ACCELERATEUR LINEAIRE, UNIV. DE PARIS, ORSAY (FRANCE).
Report of activity, October 15, 1964–April 15, 1965, 19: 46643 (LAL-1136)
LAWRENCE RADIATION LAB., UNIV. OF CALIFORNIA, BERKELEY.
A precision technique for measuring azimuthal distortion in optical lenses 19: 48103 (UCRL-16260)
Amine hydrohalide extraction studies, 19: 46180 (UCRL-16254)
Analysis of NMR spectra of four-membered ring compounds of type A_2B_4, 19: 46247 (UCRL-16349)
Design, construction, and operation of differential micromanometer. II., 19: 46726 (UCRL-11218(Pt.II))
Determining geometry and current configuration of cylindrically symmetric solenoid coils from a specified magnetic field shape, 19: 47121 (UCRL-16080)
Dispersion of optical rotation and birefringence of biopolymers. I and II., 19: 48104 (UCRL-16278)
Formation of donor-like complexes in diffused Si devices, 19: 46727 (UCRL-16197)
Free radical induced in enzymes by electrons and heavy ions, 19: 46339 (UCRL-16358)
Heat transfer considerations in differential calorimeter design, 19: 46728 (UCRL-16336)
Heavy-particle studies with silicon detectors, 19: 46770 (UCRL-16354)
Magnet systems—power supplies—cost optimization, 19: 47170 (UCRL-16384)
Neutron spectroscopy by use of nuclear stars from 20 to 300 Mev, 19: 46769 (UCRL-16325)
Prog. rpt. on Bevatron operations and development, 1–3/65, 19: 47169 (UCRL-16204)
Quadrupole coupling in rare earth crystals, 19: 47883 (UCRL-16279)
Stable-flow free-boundary electrophoresis theory and practice as applied to study of human serum lipoproteins, 19: 48105 (UCRL-16290)
Theoretical α decay rates of deformed nuclei, 19: 47597 (UCRL-16187)
X-ray examination of square water-cooled copper magnet-conductor brass joints, 19: 46965 (UCRL-16383)
LAWRENCE RADIATION LAB., UNIV. OF CALIFORNIA, LIVERMORE.
Alpha air monitor with constant flow control, 19: 46768 (UCRL-14253)
Changes in fracture permeability of granitic rock mass resulting from a contained nuclear explosion, 19: 46581 (UCRL-14292)
Compression of magnetic field inside hollow explosive-driven cylindrical conductor, 19: 47120 (UCRL-14349)
Current experiments using prosthetic terminal devices on Model 8 master slaves, 19: 46492 (CONF-641120, pp 1-3)
Derivation of generalized Von Neumann pseudo-viscosity with directional properties, 19: 47119 (UCRL-14244)
Effect of strain rate on the mechanical properties of general purpose polypropylene, 19: 47017 (UCRL-14316)
Gamma dose curves from neutron-activated soil and seawater compared with fission-product decay, 19: 46589 (UCRL-14332)
Livermore slag fabrication facility, 19: 46509 (UCRL-12497-T)
Mining by caving with nuclear explosions, 19: 46472 (UCRL-14201)
Neutron activation of terrestrial environment as result of underground nuclear explosions, 19: 46473 (UCRL-14249)
Porous metal isolation traps and cryosorbents in vacuum technique,

19: 46573 (UCRL-12393-T)
Process stream analysis systems for scrubber solutions used in Project Dribble vent gas treatment plant, 19: 46471 (UCRL-14123)
Reproducibility studies of preparation of a LiF dosimetric material, 19: 46338 (UCRL-12367)
Similarity solutions in hydrodynamics, 19: 47118 (UCRL-12018-T)
LINCOLN LAB., MASSACHUSETTS INST. OF TECH., LEXINGTON.
Prog. rpt. on high-power cyclotron resonance switch, 6/15/62–1/63, 19: 46708 (AD-611560)
LING-TEMCO-VOUGHT, INC., DALLAS, TEX.
Thermodynamic properties of high-temperature helium, 19: 46235 (N64-26802)
LITTLE (ARTHUR D.) INC., CAMBRIDGE, MASS.
Gaseous metaborates. III., 19: 46231 (AD-613660)
LOCKHEED MISSILES AND SPACE CO., PALO ALTO, CALIF.
Analysis and evaluation of measurements of geomagnetically trapped electrons from high-altitude nuclear explosions, 19: 47446 (AD-612013)
LOCKHEED MISSILES AND SPACE CO., SUNNYVALE, CALIF.
Advanced design concepts for a remotely operated manipulator system for space-support operations, 19: 46487 (CONF-640508, pp 248-303)
Evaluation of field-effect transistors, 19: 46871 (AD-614268)
Remote handling in space, 19: 46500 (CONF-641120, pp 67-70)
LOS ALAMOS SCIENTIFIC LAB., UNIV. OF CALIFORNIA, N. MEX.
Capacitor bank charging system, 19: 46718 (LA-DC-7015)
Charged bond correction to dispersion curves of diamond, 19: 47879 (LA-DC-7277)
Computer program for solution of energy balance and heat transfer of pulsed thermonuclear reactor, 19: 47720 (LA-3347)
Current techniques and problems of remote handling at reactor maintenance, assembly and disassembly facility, 19: 46493 (CONF-641120, pp 4-5)
Electronic band structures of plutonium and its monocarbide, 19: 47880 (LA-DC-7353)
Experiments with polarized protons and the neutron-nucleus potential derived therefrom, 19: 47581 (LA-DC-6730)
Expression for quartic anharmonic contribution to Helmholtz free energy of a special model of an fcc crystal, 19: 47878 (LA-3379)
Fission fragment removal of uranium from a fissioning surface, 19: 47580 (LA-3352)
Heat capacities of Nb carbides below 320°K, 19: 46998 (LA-3331)
High-temperature compatibility testing of molten plutonium fuel-container systems, 19: 46950 (LA-DC-7315)
Integrated series of crystallographic computer programs. X., 19: 47877 (LA-3335)
Measurement of microscopic distribution of oxygen and carbon in metals by ^{3}He activation, 19: 46174 (LA-DC-7319)
Moments equations and equivalent discrete ordinates equations. I and II., 19: 47547 (LA-DC-7320)
Neutron blanket calculations for thermonuclear reactors, 19: 47721 (LA-3385)
NRDS analysis of the Kiwi B-4D-202 nuclear reactor control system, 19: 48049 (LA-3301)
Problems associated with pulse charged capacitor banks, 19: 46719 (LA-DC-7030)
Processing of plutonium by ion exchange. VII., 19: 46173 (LA-3357)
Quantitative spectroscopy of cesium plasmas, 19: 47723 (LA-DC-7112)
Refractory plutonium fuel materials, 19: 46999 (LA-DC-7297)
Remote operations at Los Alamos Test Cell C, 19: 46494 (CONF-641120, pp 6-8)
Solutions to nonlinear incompressible flow problems through a finite difference method, 19: 46533 (LA-DC-7373)
Stability, heating, and end loss of a 3.5-megajoule θ pinch (Scylla IV), 19: 47722 (LA-DC-7039)
Vela satellite measurements, 19: 47450 (LA-DC-7365)

M

MAINZ UNIV. (WEST GERMANY). NATURWISSENSCHAFTLICHE FAKULTAET.
Reactions of fission recoil atoms, particularly of iodine with methane and other gases, 19: 46330 (NP-15370)
MARTIN CO., BALTIMORE, MD. RESEARCH INST. FOR ADVANCED STUDIES.
Prog. rpt. on biochemistry of senescence in plant cells, final, 6/15/63–6/14/65, 19: 48102 (TID-22175)
MARTIN CO., DENVER, COLO.
Cryogenic materials data handbook, 19: 47013 (PB-171809(Rev.) (Suppl.2))
MARYLAND UNIV., COLLEGE PARK.
Final rpt. on fundamental problems of solids, 9/61–8/64, 19: 47875 (AD-614136)
MASSACHUSETTS INST. OF TECH., CAMBRIDGE.
Manipulator control work at MIT, 19: 46505 (CONF-641120, pp 98-103)
MASSACHUSETTS INST. OF TECH., CAMBRIDGE. AEROPHYSICS LAB.
Electromagnetic means of adding heat and kinetic energy to a gas, 19: 46477 (ARL-65-121)
MASSACHUSETTS INST. OF TECH., CAMBRIDGE. DEPT. OF MECHANICAL ENGINEERING.
Study of system-induced instabilities in forced-convection flows with subcooled boiling, 19: 46534 (NP-15437)
MAX-PLANCK-INSTITUT FUER BIOPHYSIK, FRANKFURT AM MAIN (WEST GERMANY).
Bibliography on radiation effects on living tissues and organisms, 19: 45807 (AED-C-04-17)
MAX-PLANCK-INSTITUT FUER ZUECHTUNGSFORSCHUNG, COLOGNE (WEST GERMANY).
Prog. rpt. on selection methods for induced small mutations in higher plants, final, 2/61–1/65, 19: 45819 (TID-22176)
MICHIGAN UNIV., ANN ARBOR.
Polarographic behavior of purines and pyrimidines, 19: 46301 (COO-1148-97)
MICHIGAN UNIV., ANN ARBOR. COLL. OF LITERATURE, SCIENCE AND THE ARTS.
Abundances of elements in stars and nebulae (determination of ratio of gas pressure to electron pressure in stellar atmospheres), 19: 47187 (AD-612182)
MICHIGAN UNIV., ANN ARBOR. DEPT. OF CHEMISTRY.
Thermal anomalies and thermodynamic properties of gadolinium hexaboride, 19: 46994 (COO-1149-52)
Thermodynamics of trimethylacetonitrile and dimethylmalononitrile, 19: 48090 (COO-1149-53)
MICHIGAN UNIV., ANN ARBOR. LAB. FOR FLUID FLOW AND HEAT TRANSPORT PHENOMENA.
Two-phase materials attrition problems for Rankine cycle liquid metal power plants, 19: 46955 (NP-15431)
MICHIGAN UNIV., ANN ARBOR. RADIATION LAB.
Prog. rpt. on diffraction and scattering by regular bodies, final 2/60–1/65, 19: 47299 (AD-614046)
MICROWAVE ASSOCIATES, INC., BURLINGTON, MASS.
Final rpt. on plasma amplifiers, 2/65, 19: 47219 (AD-614253)
MONTEFIORE HOSPITAL, NEW YORK.
Effect of collimator-shape on depth dose curves, 19: 46714 (CONF-640918-1)
MOUND LAB., MIAMISBURG, OHIO.
Bibliography on pyrolysis of polymers, 19: 46302 (MLM-1271)
Prog. rpt., 4/65, 19: 46157 (MLM-1254)
Review of dissolution of plutonium dioxide, 19: 46175 (MLM-1264)

N

NATIONAL AERONAUTICS AND SPACE ADMINISTRATION, CLEVELAND, OHIO. LEWIS RESEARCH CENTER.
Acceleration of conducting fluid by traveling magnetic field, 19: 46575 (NASA-TN-D-3006)
Performance correlation for electron-bombardment ion sources, 19: 46572 (NASA-TN-D-3041)
NATIONAL CO., INC., MELROSE, MASS.
Prog. rpt. on production engineering measure for Cs beam tube, 8/23–11/23/64, 19: 46709 (AD-614118)
NATIONAL INST. FOR RESEARCH IN NUCLEAR SCIENCE, CHILTON (ENGLAND). RUTHERFORD HIGH ENERGY LAB.
Servo theory for the control of coherent betatron oscillations in Nimrod, 19: 47165 (NIRL/R/99)
NAVAL AIR DEVELOPMENT CENTER, JOHNSVILLE, PA.
Servo-restraint system for anti-G protection, 19: 46485 (CONF-640508, pp 210-23)
NAVAL CIVIL ENGINEERING LAB., PORT HUENEME, CALIF.
Dynamically loaded strip footing buried in dry sand, 19: 46567 (NP-15396)
Lateral-plate tests with plate diameter varied, 19: 46465 (AD-613991)
NAVAL RADIOLOGICAL DEFENSE LAB., SAN FRANCISCO, CALIF.
Determination of total tritium activity adsorbed on surface of various metals, 19: 47018 (USNRDL-TR-890)
Focal antibody production by transferred spleen cells in irradiated mice, 19: 45806 (AD-621543)
Gamma-emission data for calculation of exposure rates from nuclear debris. I., 19: 47598 (USNRDL-TR-876)
Neutron fields and induced-activity measurements, 19: 47569 (CEX-62-50)
NAVAL RESEARCH LAB., WASHINGTON, D. C.
Direct energy conversion literature abstracts, 19: 47280 (AD-613358)
NEVIS LABS., COLUMBIA UNIV., IRVINGTON-ON-HUDSON, N. Y.
Isotopic differences in the μ-mesic K x-ray energies of ^{16}O–^{18}O, ^{40}Ca–

^{44}Ca, ^{116}Sn–^{124}Sn, ^{155}Gd–^{160}Gd, 19: 47582 (NEVIS-129)
Precise hyperon masses, 19: 47302 (CU-1932-246)
NEW ENGLAND DEACONESS HOSPITAL, BOSTON, MASS. CANCER RESEARCH INST.
Prog. rpt. on [radiobiological studies], 5/64–4/65, 19: 45808 (NYO-901-36)
NORSK RADIUMHOSPITAL, OSLO.
Effect of collimator-shape on depth dose curves, 19: 46714 (CONF-640918-1)
NORTH CAROLINA STATE OF THE UNIV. OF NORTH CAROLINA, RALEIGH.
Prog. rpt. on convection boiling inside channels, 7–9/64, 19: 46538 (TID-22148)
NUCLEAR MATERIALS AND EQUIPMENT CORP., APOLLO, PA.
Prog. rpt. on development and testing of UO_2–PuO_2 fast reactor fuels, 4/1–6/30/65, 19: 46942 (NUMEC-3524-6)
NUCLEAR METALS, WEST CONCORD, MASS.
A new microhardness technique, 19: 47003 (NMI-4999, pp 111-28)
Bright field etch for α plutonium, 19: 46938 (NMI-5025(Pt.I), pp 153-4)
Conference on metallurgy, Savannah River, 5/61, 19: 46921 (NMI-4997)
Conference on metallurgy, Richland, 3/62, 19: 46926 (NMI-4998)
Conference on metallurgy, Los Alamos, 5/63, 19: 46930 (NMI-4999)
Effect of moisture in the air on arc-cast UC and UC_2 at room temperature over extended periods, 19: 46953 (NMI-4997, pp 62-75)
Electron microscope studies of irradiated A-286 alloys, 19: 47088 (NMI-4998, pp 95-106)
Experience with vibratory polishers and design for hot-cell application, 19: 47086 (NMI-4997, pp 184-8)
High-temperature metallography of uranium, 19: 47005 (NMI-4997, pp 76-84)
Hot cell metallographic experience at Battelle, 19: 47085 (NMI-4997, pp 134-56)
Identification of carbides, nitrides, and oxides of Nb by anodic staining, 19: 46929 (NMI-4998, pp 57-64)
Materials research with scanning microprobe analyzer, 19: 46508 (NMI-4998, pp 65-76)
Measurement of the thickness of aluminum oxide film, 19: 46952 (NMI-4997, pp 26-35)
Metallographic and ceramographic preparation of nuclear materials, 19: 46937 (NMI-5025(Pt.I), pp 1-25)
Metallographic preparation of hard and brittle materials, 19: 46922 (NMI-4997, pp 22-5)
Metallographic preparation of alumina-coated UO_2 spheres in graphite, 19: 46925 (NMI-4997, pp 85-91)
Metallographic studies of uranium-fissium alloys, 19: 47004 (NMI-4997, pp 45-54)
Metallography—ally of nondestructive testing in evaluating nuclear fuel components, 19: 46556 (NMI-4997, pp 1-21)
Metallography of fused UO_2, 19: 46176 (NMI-4997, pp 110-23)
Metallography of ceramic fuel and refractory metal compatibility couples, 19: 46954 (NMI-5025(Pt.I) pp 39-58)
Metallography of pyrolytic carbon-coated and uncoated uranium carbide spheres, 19: 47006 (NMI-4997, pp 198-207)
Metallography of irradiated dispersion-type fuel elements, 19: 47084 (NMI-4997, pp 124-33)
Microstructural studies of cast uranium, 19: 47007 (NMI-5025(Pt.I), pp 127-51)
Microstructures of compounds of uranium, thorium, and beryllium, 19: 46924 (NMI-4997, pp 55-61)
Mounting of metallographic samples in epoxy resins using multiple cavity molds, 19: 46927 (NMI-4998, pp 1-5)
One-step replication in the hot cell, 19: 47090 (NMI-4999, pp 54-9)
Plutonium metallographic practices at Battelle, 19: 46934 (NMI-4999, pp 104-10)
Portable metallography laboratory, 19: 46935 (NMI-4999, pp 129-36)
Post-irradiation metallographic laboratory at GE-NMPO, 19: 47089 (NMI-4999, pp 30-50)
Preliminary evaluation of a new polishing cloth, 19: 46923 (NMI-4997, pp 36-44)
Preparation of thin foils of uranium, 19: 46933 (NMI-4999, pp 78-84)
Procedure for color microphotography, 19: 46931 (NMI-4999, pp 26-9)
Proceedings of the 18th metallographic meeting, Canoga Park, Calif, 6/64, 19: 46936 (NMI-5025(Pt.I))
Quantative metallography of hypostoichiometric UN, 19: 46177 (NMI-5025(Pt.I), pp 85-95)
Remote metallographic specimen grinder, 19: 46507 (NMI-4997, pp 157-62)
Remote metallographic preparation of irradiated aluminum-clad lead-bonded ceramic fuel pellets, 19: 47087 (NMI-4997, pp 189-97)
Replication of irradiated specimens with room-temperature vulcanizing silicones, 19: 47091 (NMI-4999, pp 69-77)
Replication of microstructures using silicone rubber and epoxy resin, 19: 46932 (NMI-4999, pp 60-8)
Thirty-five millimeter color photomicrography, 19: 46928 (NMI-4998, pp 14-19)
Vibratory grinding and polishing of metallographic specimens, 19: 46939 (NMI-5025(Pt.I), pp 185-219)
NUCLEAR METALS, INC., WEST CONCORD, MASS.
Conference on metallurgy, Nuclear Metals, Inc., 4/60, 19: 46919 (NMI-4996)
Decreasing electropolishing time for uranium, 19: 46920 (NMI-4996, pp 27-35c)
Electron microscope studies of beryllium oxide powders, 19: 47002 (NMI-4996, pp 50-76)
Metallographic observations at elevated temperature, 19: 47000 (NMI-4996, pp 8-18)
Metallographic preparation of irradiated uranium carbide, 19: 47083 (NMI-4996, pp 77-85)
Metallography of beryllium oxide, 19: 47001 (NMI-4996, pp 36-49)
Novel metallographic utilization of replicas and microautoradiography, 19: 46951 (NMI-4996, pp 19-26)
X-ray film defects and autoradiography of fuel elements for cladding thickness measurement, 19: 46964 (NMI-4996, pp 149-63)
NUCLEAR POWER FIELD OFFICE, FORT BELVOIR, VA.
Closed cycle gas turbine, 19: 47987 (AD-612409)
NUKLEARNI INSTITUT "JOZEF STEFAN," LJUBLJANA (YUGOSLAVIA).
Synthesis of hydrazine-fluorozirconates, 19: 46236 (NIJS-R-430)

O

OAK RIDGE GASEOUS DIFFUSION PLANT, TENN.
Systems combining continuous-flow and density gradient centrifugation, 19: 46425 (K-L-2012)
OAK RIDGE NATIONAL LAB., TENN.
A new microhardness technique, 19: 47003 (NMI-4999, pp 111-28)
Activities of ANL-ENEA computer program libraries and the ORNL Radiation Shielding Information Center, 19: 47908 (ANL-7050, pp 125-39)
Adhesion of particles to surfaces in liquid and gaseous environments, 19: 46645 (ORNL-TM-1228)
Alkylbenzene sulfonate control for foam separation process, 19: 46429 (ORNL-P-1522)
Analytical laboratory hot-cell equipment. III., 19: 46721 (ORNL-P-1531)
Application of the equipoise iterative method to diffusion and transport theory, 19: 47541 (ANL-7050, pp 179-89)
Chemical composition of individual range plants from the U. S. Range Station, Miles City, Montana, from 1955–1960, 19: 45747 (ORNL-TM-1279)
Chemical physics, 19: 46161 (ORNL-3832, pp 116-50)
Chemistry of aqueous systems, 19: 46237 (ORNL-3832, pp 76-99)
Contaminated filter removal equipment, 19: 46644 (ORNL-P-1528)
Costs of permanent disposal of power-reactor fuel-processing wastes in tanks, 19: 48080 (ORNL-2873)
Effect of moisture in the air on arc-cast UC and UC_2 at room temperature over extended periods, 19: 46953 (NMI-4997, pp 62-75)
Effects of reactor operation on HFIR coolant, 19: 48061 (ORNL-3848)
Elastic and inelastic scattering of 12.0-Mev protons from ^{62}Ni, ^{63}Cu, and ^{64}Zn: Tabulated differential cross sections, 19: 47585 (ORNL-3851)
Electrochemical kinetics and its application to corrosion, 19: 46957 (ORNL-3832, pp 100-6)
Energy of formation of a double kink and an examination of low-temperature deformation, 19: 47011 (ORNL-3862)
Engineering study for tunnel grid blast-shelter concept for Detroit, 19: 46568 (ORNL-TM-1223)
Experience with vibratory polishers and design for hot-cell application, 19: 47086 (NMI-4997, pp 184-8)
Extraction magnets for cyclotrons, 19: 47166 (ORNL-P-1605)
Hot-cell dissolution of highly irradiated PuO_2 and UO_2 fast-reactor fuel specimens, 19: 46427 (ORNL-3754)
Identification of carbides, nitrides, and oxides of Nb by anodic staining, 19: 46929 (NMI-4998, pp 57-64)
Isotope chemistry, 19: 46899 (ORNL-3832, pp 33-49)
Isotopic composition of atmospheric neon, 19: 46588 (ORNL-3857)
Lattice vibration frequency spectrum of graphite, 19: 47881 (ORNL-P-585)
Metallography of pyrolytic carbon-coated and uncoated uranium carbide spheres, 19: 47006 (NMI-4997, pp 198-207)
Metallography of irradiated dispersion-type fuel elements, 19: 47084 (NMI-4997, pp 124-33)
Mounting of metallographic samples in epoxy resins using multiple cavity molds, 19: 46927 (NMI-4998, pp 1-5)

Homogeneous systems at high temperatures, 19: 47010 (ORNL-3832, pp 127-50)
Nuclear and inorganic chemistry of special elements, 19: 46160 (ORNL-3832, pp 29-32)
Nuclear chemistry, 19: 47584 (ORNL-3832, pp 1-28)
Organic chemistry, 19: 46304 (ORNL-3832, pp 66-75)
POELARGRM—A computer program for analysis of polarograms, 19: 46238 (ORNL-TM-1253)
Portable metallography laboratory, 19: 46935 (NMI-4999, pp 129-36)
Preliminary evaluation of a new polishing cloth, 19: 46923 (NMI-4997, pp 36-44)
Primary amine extraction of beryllium from sulfate liquors, 19: 46431 (ORNL-P-1602)
Prog. rpt. on chemistry, annual, 5/21/64–5/20/65, 19: 46159 (ORNL-3832)
Prog. rpt. on transuranium research, 11/64, 19: 46428 (ORNL-3847)
Prog. rpt. on zonal centrifuge development, 1–6/64, 19: 45730 (ORNL-3752)
Radiation chemistry, 19: 46332 (ORNL-3832, pp 50-65)
Remote metallographic specimen grinder, 19: 46507 (NMI-4997, pp 157-62)
Replication of irradiated specimens with room-temperature vulcanizing silicones, 19: 47091 (NMI-4999, pp 69-77)
Replication of microstructures using silicone rubber and epoxy resin, 19: 46932 (NMI-4999, pp 60-8)
Sector magnets for a separated orbit cyclotron, 19: 47167 (ORNL-P-1619)
Single and multi-nucleon transfer reactions induced by ^{14}N, 19: 47586 (ORNL-TM-1218)
Stability of aromatic diluents and solvent extraction reagents in radiochemical processing, 19: 46430 (ORNL-P-1601)
Strain behavior in Zircaloy-2 sheet-type tensile specimens, 19: 47012 (ORNL-TM-1226)
Unexpected rate effects in extraction of rare earths by di(2-ethylhexyl)-phosphoric acid, 19: 46432 (ORNL-P-1603)

OESTERREICHISCHE STUDIENGESELLSCHAFT FUER ATOMENERGIE G.M.B.H., SEIBERSDORF.
The radiation stability of anthracene oils. II., 19: 46333 (SGAE-CH-20/1965)

OFFICE OF AEROSPACE RESEARCH, WASHINGTON, D. C.
Air Force research objectives, 19: 48087 (AD-613537)

ONTARIO CANCER INST., TORONTO.
Methods of automatic ionization measurement in a bubble chamber, 19: 46758 (CONF-550-99)

OREGON STATE UNIV., CORVALLIS.
Final rpt. on seismic waves, 4/62–3/64, 19: 46615 (AD-612033)

P

PARIS UNIV. (FRANCE).
Radioactive ions in the atmosphere, 19: 46641 (CEA-R-2771)

PARIS UNIV., ORSAY (FRANCE). ECOLE NORMALE SUPERIEURE.
Prog. rpt. on radiation damage in semiconductors, annual, 7/63–6/64, 19: 47076 (AD-612090)

PARMA UNIV. (ITALY). ISTITUTO DI ZOOLOGIA E ANATOMIA COMPARATA.
Prog. rpt. on ecology of Acantharia in relation to Sr circulation in sea, 1/23–7/30/65, 19: 45748 (TID-22193)

PENNSYLVANIA STATE UNIV., UNIVERSITY PARK.
Comments on computing, 19: 46902 (ANL-7050, pp 207-13)
EPR investigation of radiation protection by aromatic additives in synthetic polymers, 19: 46321 (AD-611779)

PENNSYLVANIA STATE UNIV., UNIVERSITY PARK. DEPT. OF PHYSICS.
Prog. rpt. on radiation effects on high polymers, final, 1955-65, 19: 46331 (NYO-1858-1)

PENNSYLVANIA UNIV., PHILADELPHIA. DEPT. OF PHYSICS.
Experimental research, 19: 47315 (TID-22222 pp 30-45)
Prog. rpt. on high-energy physics, 9/64–9/65, 19: 47313 (TID-22222)
Theoretical research, 19: 47314 (TID-22222, pp 3-29)

PHILCO CORP., BLUE BELL, PA.
Possibility of utilizing electrical potentials on surface of skin for control functions, 19: 46459 (CONF-640508, pp 100-57)

PHILLIPS PETROLEUM CO. IDAHO FALLS, IDAHO., ATOMIC ENERGY DIV.
Effective cross-section factors, 19: 47577 (IDO-17107)
Instrument development, 19: 46716 (IDO-17081, pp 77-123)
Mathematical analysis and machine computations, 19: 46905 (IDO-17081, pp 125-35)
Nuclear technology, 19: 47576 (IDO-17081, pp 49-76)
Prog. rpt. on nuclear technology, 10–12/64, 19: 48059 (IDO-17081)
Reactor engineering, 19: 48060 (IDO-17081, pp 1-47)
Resonance absorption of neutrons in mixtures of ^{232}Th and ^{238}U, 19: 47575 (IDO-16986)
Separation of tellurium and iodine from other fission products, 19: 46169 (IDO-14664)

PITTSBURGH UNIV., PA. DEPT. OF OCCUPATIONAL HEALTH.
Prog. rpt. on occupational radiation exposure, 6/64–4/2/65, 19: 45810 (NYO-3394-2(Rev.))

POLYTECHNIC INST. OF BROOKLYN, N. Y. DEPT. OF CHEMISTRY.
Chemical reactions of atomic beams and related problems, 19: 47221 (NYO-2403-8)

PRATT AND WHITNEY AIRCRAFT, MIDDLETOWN, CONN. CONNECTICUT ADVANCED NUCLEAR ENGINEERING LAB.
Electrical resistivity of lithium and columbium-1 zirconium alloy to 1430°C, 19: 47015 (TIM-854)
High-temperature thermometry at Pratt and Whitney canel, 19: 46722 (PWAC-462)
Operating limits and safety analysis for split-table, dry, flexible critical experiments at CANEL Nuclear Physics Lab., 19: 47958 (PWAC-475)
Prog. rpt. on LCRE pumps and sumps, final, 7/65, 19: 46535 (PWAC-386)
Reaction rate of Nb–1Zr alloy with oxygen at low pressures, 19: 47016 (TIM-901)
Summary of SNAP-50/SPUR pump bearing development program, 19: 46458 (CNLM-6342)

PRINCETON UNIV., N. J. ELEMENTARY PARTICLES LAB.
Distribution of single electron pulse sizes from multidynode electron multipliers, 19: 46720 (NYO-3406-2)

PRINCETON UNIV., N. J. PLASMA PHYSICS LAB.
Transition from Landau damping to viscous damping of ion acoustic waves, 19: 47724 (MATT-267)

PROGRAMMED AND REMOTE SYSTEMS CORP., ST. PAUL, MINN.
Rate controlled manipulators, 19: 46482 (CONF-640508, pp 75-99)

PUBLIC HEALTH SERVICE, WASHINGTON, D. C. DIV. OF RADIOLOGICAL HEALTH.
Iodine-131 in children's thyroids from environmental exposure, 19: 46035 (PHS-999-RH-14)
Prog. rpt. on behavior of radionuclides released into fresh-water environments, annual, 1959–60, 19: 46646 (PHS-999-RH-13)

PURDUE UNIV., LAFAYETTE, IND. DEPT. OF CHEMISTRY.
Correlation of structures of I-V type ABO_3 compounds, 19: 46243 (TID-22207, Paper C)
Ionic field strengths as criteria for compound formation in oxide systems, 19: 46246 (TID-22207, Paper F)
Preparation and some properties of sodium-rare earth mixed oxides, 19: 46241 (TID-22207, Paper A)
Preparation and structural study of ABO_3 compounds containing Cu and Nb or Ta, 19: 46244 (TID-22207, Paper D)
Preparation and structural studies of some cupric rare earth AB_2O_4 type compounds, 19: 46245 (TID-22207, Paper E)
Prog. rpt. on high-temperature solid-state chemistry and sub-solidus phase equilibria, final, 8/65, 19: 46240 (TID-22207)
Studies of reactions between divalent and trivalent oxides, 19: 46242 (TID-22207, Paper B)

Q

QUEEN'S UNIV., BELFAST (NORTHERN IRELAND). DEPT. OF APPLIED MATHEMATICS.
Differential cross sections for electrons elastically scattered by helium atoms, 19: 47218 (AD-613929)

R

RADIATION RESEARCH ASSOCIATES, INC., FORT WORTH, TEX.
Neutron transport data for single and multilayer slabs of aluminum, polyethylene, and carbon, 19: 47868 (RRA-T52)

RADIO CORP. OF AMERICA, LANCASTER, PA. DIRECT ENERGY CONVERSION DEPT.
Prog. rpt. on improved thermionic energy converter, final, 6/64–6/65, 19: 47282 (NYO-3429-4)

RADIO CORP. OF AMERICA, MOORESTOWN, N. J. MISSILE AND SURFACE RADAR DIV.
Design of high-energy fast-pulse power system, 19: 46476 (AD-613959)

RAND CORP., SANTA MONICA, CALIF.
Dynamic programming and an inverse problem in neutron transport theory, 19: 47537 (AD-613468)
Fireball phenomenology, 19: 47113 (AD-612197)

RCA LABS., RADIO CORP. OF AMERICA, PRINCETON, N. J.
Prog. rpt. on plasma acceleration, 12/15/59–6/15/60, 19: 47714 (AD-613307)

RCA VICTOR CO., LTD., MONTREAL (QUEBEC). RESEARCH LABS.

Electromagnetic wave propagation in anisotropic plasmas along direction of static magnetic field, 19: 47718 (AD-614442)

REACTOR CENTRUM NEDERLAND, PETTEN.
Review of activation methods for determination of fast neutron spectra, 19: 46763 (RCN-37)

REACTOR GROUP, UNITED KINGDOM ATOMIC ENERGY AUTHORITY, RISLEY (ENGLAND).
FREAK—fast reactor multigroup kinetics program, 19: 47947 (ANL-7050, pp 395-412)
Methods of control rod calculation for graphite moderated reactors, 19: 47999 (TRG-Report-227)
Techniques used in GEM code for Monte Carlo neutronics calculations in reactors and other systems of complex geometry, 19: 47949 (ANL-7050, pp 557-79)

REACTOR GROUP, UNITED KINGDOM ATOMIC ENERGY AUTHORITY, SELLAFIELD (ENGLAND).
Interpretation and prediction of reactor power distributions with application to fuel cycle calculations, 19: 47946 (ANL-7050, pp 231-49)

RENSSELAER POLYTECHNIC INST., TROY, N. Y.
High-energy neutron cross sections, 19: 47550 (TID-22141, pp 81-93)
Low-energy neutron inelastic scattering (Lenis), 19: 47549 (TID-22141, pp 34-49)
Mass spectrometer program, 19: 46725 (TID-22141, pp 101-10)
Neutron cross sections, 19: 47595 (TID-22141, pp 50-66)
Neutron thermalization, 19: 47548 (TID-22141, pp 3-33)
New instrumentation programs, 19: 46766 (TID-22141, pp 67-79)
Photonuclear reaction studies by activation methods, 19: 47596 (TID-22141, pp 94-7)
Prog. rpt. on linear accelerator project, annual, 1965, 19: 47092 (TID-22141)

ROCKY FLATS DIV., DOW CHEMICAL CO., GOLDEN, COLO.
Evaluation of adjustable speed drive systems on machine tools, 19: 46461 (RFP-562)
Plutonium bioassay results following DTPA treatments, 19: 45762 (RFP-577)
Radiometric determination of fluorine in bulk PuF_4, 19: 46179 (RFP-618)
Spindle design, 19: 48093 (RFP-654)
Strain gage applications using the Rokide process, 19: 46723 (RFP-641)

ROSCOE B. JACKSON MEMORIAL LAB., BAR HARBOR, MAINE.
Prog. rpt. on quantitative population genetics of mice under irradiation, 7/64–6/65, 19: 45809 (NYO-1979-12)

S

SANDIA CORP., ALBUQUERQUE, N. MEX.
Analytical methods used in predicting re-entry ablation of spherical and cylindrical bodies, 19: 46537 (SC-RR-65-187)
Atmospheric static electricity warning system, 19: 48094 (SC-DC-65-1646)
Development report for TP82, 19: 48095 (SC-DR-64-539)
Excavation with parallel rows of explosions, 19: 46470 (SC-RR-65-303)
Fallout report—β-γ radioactivity in air at Sandia, 1–6/65, 19: 46648 (SC-RR-65-464)
Final hazards summary for Sandia Engineering Reactor Facility (SERF), 19: 48062 (SC-4522(RR))
Guide for application of hermetically sealed, direct current, electromagnetic relays, 19: 48100 (SC-TM-65-294)
Height-interval timer, 19: 46724 (SC-TM-65-356)
Introduction to TTA generalized rigid-body trajectory program for digital computer, 19: 48096 (SC-DR-65-271)
Investigations of high-intensity heat flux graphite resistors, 1960–1962, 19: 48099 (SC-TM-64-653)
NAMDA—new method of computerized management control, 19: 48098 (SC-R-65-902)
Sandia Corporation expedition for airborne scientific observation of the eclipse of the quiet sun of May 30, 1965, 19: 47451 (SC-M-65-419)
Sandia Pulsed Reactor SPR-II-1 core calculations, 19: 48063 (SC-RR-65-344)
Supplement report on COMARS (coordinate measuring and recording system), 19: 48101 (SC-TM-65-332)
Voltage-switching class-D amplifier, 19: 48097 (SC-DR-65-338)

SAVANNAH RIVER OPERATIONS OFFICE (AEC), AIKEN, S. C.
Prog. rpt. on heavy water power reactor program, 7/65, 19: 47998 (SRO-118)

SLOAN-KETTERING INST. FOR CANCER RESEARCH, NEW YORK.
Biophysics Div. [radiobiology research], 19: 45729 (NYO-910-23, pp 1-111)
Division of biological chemistry, 19: 46158 (NYO-910-23, pp 112-82)
Division of clinical investigations, 19: 45757 (NYO-910-23, pp 183-92)
Prog. rpt. on biological effects of radiation, 7/50–3/65, 19: 45728 (NYO-910-23)

SOCONY MOBIL OIL CO., INC., PRINCETON, N. J. CENTRAL RESEARCH DIV. LAB.
Determination of deuterium density profile in a deuterium plasma using an energetic D^+ beam, 19: 47727 (NP-15434)

SOUTH CAROLINA UNIV., COLUMBIA.
Single and multi-nucleon transfer reactions induced by ^{14}N, 19: 47586 (ORNL-TM-1218)

SPACE NUCLEAR PROPULSION OFFICE (AEC/NASA), WASHINGTON, D. C.
Advanced design concepts for a remotely operated manipulator system for space-supported operations, 19: 46487 (CONF-640508, pp 248-303)
Analysis of hostile-environment methodologies, 19: 46480 (CONF-640508, pp 4-26)
ANL activities in [remote-control equipment], 19: 46498 (CONF-641121, pp 41-7)
Application of fluid amplifiers in remote control operations, 19: 46502 (CONF-641120, pp 75-7)
Conference on remotely operated special equipment, AEC Headquarters, Germantown, Md., 5/64. Vol. I, Pts. I and II., 19: 46479 (CONF-640508)
Conference on remotely operated special equipment, Jackass Flats, Nevada, 11/64. II., 19: 46491 (CONF-641120)
Control—the universal process, 19: 46460 (CONF-640508, pp 224-32)
Current experiments using prosthetic terminal devices on Model 8 master slaves, 19: 46492 (CONF-641120, pp 1-3)
Current techniques and problems of remote handling at reactor maintenance, assembly and disassembly facility, 19: 46493 (CONF-641120, pp 4-5)
Design and test of full-scale wearable exoskeletal structure, 19: 46483 (CONF-640508, pp 158-97)
Design of remote handling tools as to function and flexibility, 19: 46490 (CONF-640508, pp 340-64)
Evaluation of proposed applications of remote handling in space, 19: 46486 (CONF-640508, pp 233-47)
Evolution of remote handling capabilities at NRDS, 19: 48047 (CONF-640508, pp 334-9)
Feasibility of utilizing electrical potentials on surface of skin for control functions, 19: 46459 (CONF-640508, pp 100-57)
FMC remote handling vehicle, 19: 46496 (CONF-641120, pp 36-8)
Generalized, programmed manipulators, 19: 46501 (CONF-641120, pp 73-4)
Human factors in remote handling, 19: 46484 (CONF-640508, pp 198-209)
Manipulator control work at MIT, 19: 46505 (CONF-641120, pp 98-103)
Manipulator systems at ANL, 19: 46481 (CONF-640508, pp 27-74)
Pneumatically actuated master slave manipulator, 19: 46499 (CONF-641120, pp 63-6)
Preliminary concepts for a central test facility, 19: 46503 (CONF-641120, pp 78-85)
Programming and manual control of versatile manipulating devices, 19: 46488 (CONF-640508, pp 304-26)
Proposed telechirics research laboratory, 19: 46497 (CONF-641120, pp 39-40)
Rate controlled manipulators, 19: 46482 (CONF-640508, pp 75-99)
Remote handling in space, 19: 46500 (CONF-641120, pp 67-70)
Remote handling requirements for NERVA (E-MAD and ETS-1), 19: 46495 (CONF-641120, pp 9-35)
Remote operations at Los Alamos Test Cell C, 19: 46494 (CONF-641120, pp 6-8)
Remote operations in SNAP-8 facility at AI, 19: 46504 (CONF-641120, pp 86-97)
Servo-restraint system for anti-G protection, 19: 46485 (CONF-640508, pp 210-23)
USAF exploratory development of remote handling equipment, 19: 46489 (CONF-640508, pp 327-33)

STAATLICHE ZENTRALE FUER STRAHLENSCHUTZ, BERLIN (EAST GERMANY).
Determination of minimum filter size for the filter analysis process of film dosimetry, 19: 46764 (SZS-6(1965))

STANFORD RESEARCH INST., MENLO PARK, CALIF.
Fallout and radiological countermeasures. I., 19: 46585 (AD-410522)

STANFORD UNIV., CALIF.
Final rpt. on plasma boundaries, 3/61–2/65, 19: 47719 (ARL-65-131)
Prog. rpt. on nuclear structure, 4–12/64, 19: 47564 (AD-612038)

STANFORD UNIV., CALIF. HIGH-ENERGY PHYSICS LAB.
Electron scattering on nucleons, three-body nuclei, and ^{40}Ca, 19: 47565 (AD-614270)

STATE UNIV. OF IOWA, IOWA CITY.
Ion cyclotron whistlers, 19: 47445 (AD-611828)

STATE UNIV. OF NEW YORK COLL. OF CERAMICS, ALFRED UNIV.
Prog. rpt. on behavior of $SrZrO_3$, 4–6/65, 19: 47008 (NP-15429)

SYDNEY UNIV. (AUSTRALIA). SCHOOL OF PHYSICS.

Prog. rpt. on plasma physics, 1–6/65, 19: 47725 (NP-15355)
SYRACUSE UNIV., N. Y.
Nature of resonance in static pion-nucleon scattering in one-meson approximation, 19: 47298 (AD-613934)
The $Y_1^*(1660)$ produced in K^--p interactions at 2.24 Bev/c, 19: 47300 (BNL-9520)

T

TECHNICAL MILITARY PLANNING OPERATION, GENERAL ELECTRIC CO., SANTA BARBARA, CALIF.
Approximate series solutions of the three-species atmospheric deionization differential equations, 19: 47449 (AD-613199)
TECHNISCH DOCUMENTATIE- EN INFORMATIE-CENTRUM VOOR DE KRIJGSMACHT, THE HAGUE (NETHERLANDS).
Bibliography on protection against biological effects of thermal radiation, 19: 45818 (TDCK-33500)
TECHNISCHE HOCHSCHULE, HANOVER (WEST GERMANY).
Adiabatic linear Stark effect in a plasma, 19: 47716 (AD-614283)
TECHNISCHE HOCHSCHULE, VIENNA (AUSTRIA).
Analysis of Y, Sm, Gd, Dy, Ho, Er–Mn-compounds, 19: 46989 (AD-614466)
Measurements on rare earth–Mn alloys, 19: 46988 (AD-614465)
Sintering process for rare earth–Mn systems, 19: 46908 (AD-614464)
Systems Y–Mn, Gd–Mn and Sm–Mn, 19: 46987 (AD-614462)
TECHNISCHE HOGESCHOOL, DELFT (NETHERLANDS).
Removal of neutron poisons from aqueous homogeneous suspension reactor, 19: 46426 (NP-15362)
TENNESSEE UNIV., KNOXVILLE.
Acceleration switching valve control system with machine tool application, 19: 48106 (Y-1488)
TEXAS NUCLEAR CORP., AUSTIN.
Angular distribution of γ rays produced in inelastic scattering of neutrons from ^{40}Ar, 19: 47590 (TID-22012, pp 67-98)
Angular distribution of gamma rays from C, O and N at 14.8 Mev, 19: 47593 (TID-22012, pp 156-75)
Cross sections and angular distributions of neutron-produced γ rays in Fe from .96 to 4.75 Mev, 19: 47591 (TID-22012, pp 99-128)
Gamma rays produced in inelastic scattering. III., 19: 47588 (TID-22012, pp 22-52)
Gamma rays produced in the inelastic scattering of neutrons with magnesium and silicon, 19: 47589 (TID-22012, pp 53-66)
Inelastic neutron scattering in ^{206}Pb, ^{207}Pb, and ^{208}Pb, 19: 47592 (TID-22012, pp 129-55)
Neutron produced gamma rays from ^{10}B, ^{11}B, Ca, Co, Ce and U, 19: 47594 (TID-22012, pp 176-205)
Prog. rpt. on nuclear physics, annual, 8/63–7/64, 19: 47587 (TID-22012)
Total absorption γ spectrometer system for pulsed beam n,n γ measurements, 19: 46765 (TID-22012, pp 4-21)
TOKYO UNIV. (JAPAN). FACULTY OF ENGINEERING.
Prog. rpt. on chemical engineering studies on processing radioactive wastes, final, 1/64–3/65, 19: 48079 (NP-15371)
TUNG-SOL ELECTRIC INC., BLOOMFIELD, N. J. ELECTRON TUBE DIV.
Prog. rpt. on radiation-resistant electron tube production, 12/1/64–2/28/65, 19: 46872 (AD-621549)

U

UNION CARBIDE CORP., OAK RIDGE, TENN. Y-12 PLANT.
Acceleration switching valve control system with machine tool application, 19: 48106 (Y-1488)
Nuclear safety considerations in fabrication of massive partially enriched U–Mo reactor parts, 19: 46967 (Y-KB-62)
Research facility for study and preparation of ultrapure materials, 19: 46510 (Y-DA-967)
UNION CARBIDE RESEARCH INST., TARRYTOWN, N. Y.
Physical and chemical principles affecting high-temperature materials for rocket nozzles, 19: 46941 (NP-15514(Vol.3))
Physical and chemical principles affecting high-temperature materials for rocket nozzles, 19: 46956 (NP-155614(Vol.1))
Physical and chemical principles affecting high-temperature materials for rocket nozzles, 19: 47009 (NP-15514(Vol.2))
UNITED AIRCRAFT CORPORATE SYSTEMS CENTER, FARMINGTON, CONN.
Missile shock mount system, 19: 46456 (AD-425760)
Response spectra for high air-blast loads, 19: 46566 (AD-425747)
UNITED AIRCRAFT CORP., EAST HARTFORD, CONN.
Experimental investigation of thermal annealing of nuclear-reactor-induced coloration in fused silica, 19: 47082 (NASA-CR-304)
UNITED RESEARCH SERVICES, INC., BURLINGAME, CALIF.
Prediction models for fire spread following nuclear attacks, 19: 46638 (AD-613359)
UNITED STATES–EURATOM JOINT RESEARCH AND DEVELOPMENT PROGRAM.
Prog. rpt. on mechanical properties of metals subjected to mechanical stress and neutron irradiation, 7/65, 19: 47081 (EURAEC-1432)
USTAV JADERNEHO VYZKUMU, CESKOSLOVENSKA AKADEMIE VED, REZ.
Minimum entropy production principle and linear transport equation, 19: 47551 (UJV-1354/65)
The sorption of fission products on the suspension of the natural sorbents coagulated in an electric field, 19: 48082 (UJV-1296/65)
UT-AEC AGRICULTURAL RESEARCH LAB., OAK RIDGE, TENN.
Animal nutrition, 19: 45759 (ORO-631, pp 77-82)
Biochemistry, 19: 45816 (ORO-631, pp 142-4)
Dairy nutrition, 19: 45760 (ORO-631, pp 83-121)
Fission product chemistry of soils, 19: 46239 (ORO-631, pp 132-41)
Physiological effects of radiation, 19: 45815 (ORO-631, pp 67-76)
Physiology of reproduction, 19: 45813 (ORO-631, pp 36-44)
Poultry nutrition, 19: 45761 (ORO-631, pp 122-31)
Prog. rpt., 7–12/64, 19: 45811 (ORO-631)
Radiation genetics, 19: 45817 (ORO-631, pp 145-71)
Radiation pathology, 19: 45814 (ORO-631, pp 45-66)
Veterinarian medicine, 19: 45812 (ORO-631, pp 1-35)
UTAH UNIV., SALT LAKE CITY. MICROWAVE DEVICE AND PHYSICAL ELECTRONICS LAB.
Effects of γ-irradiation on characteristics of a ruby laser, 19: 46873 (N64-32322)

V

VANDERBILT UNIV., NASHVILLE, TENN.
Irradiation of methacrylonitrile, 1,3-butadiene, and hexachloro-1,3-butadiene, 19: 46336 (TID-22236)
Prog. rpt. on anti-radiation drugs, 4–6/65, 19: 46303 (NP-15409)
Radiation studies of 1-butene and cis-2-butene using soft x-rays and cobalt-60 gamma rays, 19: 46335 (TID-22232)
Radiolysis of propylene, hexafluoropropylene, and allyl acrylate, 19: 46337 (TID-22244)
Soft x-ray irradiations of acetylene, methylacetylene, and ethylacetylene in the gas phase with and without admixtures of noble gases, 19: 46334 (TID-22231)
VITRO ENGINEERING CO., NEW YORK.
Design of remote handling tools as to function and flexibility, 19: 46490 (CONF-640508, pp 340-64)

W

WALTER REED ARMY INST. OF RESEARCH, WASHINGTON, D. C. DEPT. OF BIOPHYSICS.
Hazard of ^{90}Sr—a review, 19: 46634 (AD-423463)
WATERVLIET ARSENAL, N. Y.
Effect of pressure on structure and properties of metals, 19: 46983 (AD-612159)
WESTINGHOUSE ELECTRIC CORP., PITTSBURGH, PA. ASTRO-NUCLEAR LAB.
Prog. rpt. on weldability and temperature stability of refractory metal alloys, 12/21/64–3/20/65, 19: 46966 (WANL-PR(P)-007)
WESTINGHOUSE ELECTRIC CORP., PITTSBURGH, PA. ATOMIC POWER DEPT.
Shipment of irradiated Yankee fuel elements, 19: 46650 (WCAP-1859 (Rev.))
WESTINGHOUSE ELECTRIC CORP., PITTSBURGH, PA. ATOMIC POWER DIV.
Evaluation of computational system applicable to the nuclear analysis of critical experiments and power reactors, 19: 47959 (WCAP-3269-52)
Prog. rpt. on large closed-cycle water reactor research, 1–3/63, 19: 48000 (WCAP-3738)
Prog. rpt. on large closed-cycle H_2O reactor, 7–9/63, 19: 48001 (WCAP-3743)
WESTINGHOUSE RESEARCH LABS., PITTSBURGH, PA.
Growth and characterization of single crystals of rare earth compounds, 19: 47876 (AD-614435)
Mobility of negative ions in O_2 at low E/N, 19: 47220 (NP-15175)
Stress distribution in a perforated plate of 10% ligament efficiency subjected to equal biaxial stress, 19: 46557 (NP-15459)
WHITE SANDS MISSILE RANGE, N. MEX. NUCLEAR EFFECTS LAB.
Retrofugal electron flux from massive targets irradiated with monoenergetic primary beam, 19: 47214 (AD-612410)
WISCONSIN UNIV., MADISON.
Polarization of 4.4-Mev neutrons scattered elastically from ^6Li and ^7Li, 19: 47570 (COO-7-0361)

PERSONAL AUTHOR INDEX

Each entry after an author's name is a shortened version of the title of the report or article, followed by the *NSA* volume and abstract number. Report numbers are given in parentheses.

The phrase "Progress report" is abbreviated as "Prog. rpt.," permitting a more rapid and complete alphabetical arrangement of the titles without changing the location of the progress report titles in relation to the other titles.

Because of problems involving the mechanical preparation of this index, all accent marks are omitted. The following changes in spelling have been introduced to reduce some of the confusion which might result from omitting the accents:

Ä	becomes	ae
Ö		oe
ø		oe
Ü		ue (except in transliterated Chinese names)

A

AALTO, E., Measured and predicted variations in fast neutron spectrum when penetrating laminated Fe–D_2O, 19: 47561

AAS, Steinar, Correlation between calculated and measured mechanical properties of thin-walled fuel element canning tubes of stainless steel, 19: 46986 (KR-96)

ABDEL-WAHAB, M. F., Alterations of ascorbic acid content of legumes caused by β or γ irradiation. II., 19: 45938

ABE, Kea, Energy spectra of photoprotons from ^{12}C, ^{24}Mg, ^{28}Si, ^{32}S and ^{40}Ca, 19: 47699

ABE, Masao, Activation analysis of ^{231}Pa followed by γ spectrometry of ^{232}Pa and ^{233}Pa, 19: 46212

ABEL, B. Michael, Pulmonary compliance and physiopathology of guinea pig lungs exposed to gadolinium oxide dust, 19: 45756 (COO-1170-7)

ABELES, B., Superconducting diode as high-frequency sound detector, 19: 46739

ABOZOVIK, V. V., Containment of a high-temperature plasma, 19: 47841

ACCARY, Andre, Atmospheric corrosion of uranium–carbon alloys, 19: 46947 (CEA-R-2732)

ACCARY, Andre, Machining of uranium carbide rods obtained by continuous casting under electronic bombardment, 19: 46963 (CEA-R-2733)

ACCARY, Andre, Making bars of uranium compound, in particular uranium carbide, 19: 46974

ACKERMAN, Lauren V., Carcinoma of large intestine as late complication of pelvic radiotherapy, 19: 46068

ACTON, Loren W., Contribution of characteristic x rays to radiation of solar flares, 19: 47197

ADAMS, C. A., Sources of exposure and possible accidents, 19: 46692

ADAMS, D. E., Prog. rpt. on aerospace nuclear safety investigations of reentry ablation phenomena, 5–7/65, 19: 47117 (SC-DC-65-1698)

ADAMS, E. D., Thermal expansion coefficient and compressibility of solid ^3He, 19: 47523

ADAMS, J. M., Heat transfer to pool-boiling magnesium, 19: 46550

ADAMS, K. H., Basal dislocation mobility in high-purity zinc single crystals, 19: 48089 (CALT-473-4)

ADAMS, Richard D., Numerical integration of Schroedinger's equation for square-well potential using an IBM 1620 computer, 19: 47429

ADELSTEIN, S. James, Radiation-induced changes in biologically active macromolecules, 19: 46417

ADLER, D. B., Family of FORTRAN routines for analysis of neutron resonance effects, 19: 47542 (ANL-7050, pp 457-70)

ADLER, F. T., Family of FORTRAN routines for analysis of neutron resonance effects, 19: 47542 (ANL-7050, pp 457-70)

ADLER, K. H., Use of analog computers in testing models in medicine and biology, 19: 45735

ADLER, R. J., Relativistic corrections in electron-deuteron scattering, 19: 47410

ADLOFF, J. P., Formation of tritium compounds by irradiation of butane with T^+ ions at 2 to 6 kev, 19: 46415

AGANOVIC, I., Majorization of Feynman diagrams, 19: 47424

AGHASSI, J. J., Mass formula in the covariant spin-unitary spin scheme, 19: 47352

AGNEW, Lewis, Quantitative spectroscopy of cesium plasmas, 19: 47723 (LA-DC-7112)

AGRAWAL, D. R., Measurement of radiocarbon activity and some determinations of ages of archaeological samples, 19: 46617

AGRINIER, B., Energy of electron cascades in a small lead-plate spark chamber, 19: 47354

AGULLO LOPEZ, F., Nuclear techniques applied to solid-state problems. II., 19: 47889

AHLERS, Edward B., Throwout study of underground nuclear detonation, 19: 46468 (POR-1814)

AHMED, F., Diffusion length of thermal neutrons in graphite, 19: 47556

AHN, T. H., Immunogenicity of a γ-irradiated Brucella melitensis, 19: 45868

AIKENS, A. E. Jr., Practices and procedures for licensing, 19: 46666

AITKEN, D. K., Direct measurement of small energy losses of relativistic particles, 19: 47252

AKASOFU, Syun-Ichi, Dynamic morphology of auroras, 19: 47481

AKIMOV, Yu. K., Scintillation counters in high-energy physics, 19: 46866

ALAJOUANINE, T., Late postradiotherapy lesions of the central nervous system, 19: 45983

ALBAUGH, F. W., Prog. rpt. on Battelle-Northwest studies executed in USAEC-AECL cooperative program, 7/65, 19: 46539 (TID-22249)

ALBESCU, Ileana, Refractometric study of formation of complex neodymium halides in aqueous solution, 19: 46254

ALBRECHT, C., Evaluation of fluoroscopic screens and x-ray image intensifiers, 19: 46150

ALBRETHSEN, A. E., Uranium dioxide–Pb radiation shielding, 19: 46916 (BNWL-IR-3)

ALCOCK, C. B., Knudsen effusion studies of compounds of uranium and thorium with elements of groups IIIb and IVb, 19: 46298

ALEKSANDROV, G. N., Transition mechanism of corona discharge into spark discharge in long air gaps, 19: 47791

ALEKSANDROV, Yu. M., Photoproduction of π^+ mesons on protons at 230 Mev, 19: 47393

ALEKSEEVSKII, N. E., Superconductivity in Ag–Ga system, 19: 47531

ALEVRA, A., Levels of low excitation energy in ^{56}Fe, 19: 47696

ALEXANDER, K. F., Problems of low-energy nuclear physics, 19: 47629

ALEXANDER, T. K., Lifetimes of the ^{16}O 6.13-Mev level and the ^{17}O 0.871-Mev level, 19: 47612

ALEXANDROPOULOS, N. G., Determination of energy gap of LiD by small-angle Compton scattering, 19: 46286

ALEXEFF, I., Plasma heating and burnout in beam-plasma interaction, 19: 47852

ALEXOPOULOS, K. D., Determination of energy gap of LiD by small-angle Compton scattering, 19: 46286

ALFVEN, H., Antimatter and the development of the metagalaxy, 19: 47256

ALGER, Raymond S., Radiation effects in polymers, 19: 46400

ALIAN, A., Extraction of cerium with tri-n-octyl phosphine oxide, 19: 46491

ALIEV, N. G., Thermal conductivity of Gd and Tb at low temperatures,

19: 47528
ALIKHANOV, A. I., Backward elastic scattering of pions on neutrons at 1.2 to 4.5 Bev, 19: 47310 (NP-15376)
ALLAIN, C., Application of radiography to nondestructive control of fuel elements before and after irradiation, 19: 46562
ALLEMAND, R., X rays and electronic microscopy at the Grenoble Nuclear Center, 19: 46512
ALLEN, K. W., Lifetimes of the ^{16}O 6.13-Mev level and the ^{17}O 0.871-Mev level, 19: 47612
ALLEN, L. S., Some functions in theory of neutron logging, 19: 46619
ALLEN, M. A., Diffusion-controlled sorption in high-density discharges, 19: 46576
ALLENSWORTH, J. A. F., Introduction to TTA generalized rigid-body trajectory program for digital computer, 19: 48096 (SC-DR-65-271)
ALLER, L., Abundances of elements in stars and nebulae (determination of ratio of gas pressure to electron pressure in stellar atmospheres), 19: 47187 (AD-612182)
ALLIOT, Paul, Device for charging and discharging channels of a pressurized, gas-cooled nuclear reactor, 19: 47931
ALLISY, A., Dosimetry and ionization, 19: 46843
ALLSOPP, K., The calculation of thermal-neutron spectra—generalized free-gas theory, 19: 47538 (ANL-7050, pp 33-49)
ALMAGRO, V., Preparation of pure Zr and Th by direct iodination of their carbides, 19: 46969
ALMODOVAR, Ismael, Method for isolation of Th from siliceous materials, 19: 46190
ALPATOVA, V. I., Thermal stability of lithium borohydride, 19: 46248 (FTD-TT-65-591)
ALS-NIELSON, J., Critical neutron scattering from β brass, 19: 47904
ALSOP, R. J. L., Concentration of ^{137}Cs in Australian milk during 1964, 19: 46660
ALTHAUS, W. A., Metallography—concerning existence of an allotropic change to cubic U_3Si within U–Si, 19: 47024 (NLCO-tr-6)
ALTMAN, Kurt I., Application of biological indicators to the evaluation of radioactive injury, 19: 45864
ALVAREZ, Walter C., Use and abuse of x-ray examinations of the elderly, 19: 46116
AMAR, Arjan D., Reduction of radiation exposure of children during urologic diagnosis, 19: 46108
AMBROSINO, C., Protein radioiodination by an electrolytic technique, 19: 46142
AMBURGEY, John W. Jr., Systems combining continuous-flow and density centrifugation, 19: 46425 (K-L-2012)
AMIN, E. A., Approximate treatment of fast neutron spectrum in two-component homogenous medium, 19: 47964
AMND, S. P. S., Magnetoturbulent energy and stability of supermassive stars, 19: 47200
AMAN'EV, V. D., 30-Mev microtron-injector for pulsed fast reactor, 19: 47164 (JINR-P-2313)
ANDELIN, R. L., High-temperature compatibility testing of molten plutonium fuel-container systems, 19: 46950 (LA-DC-7315)
ANDERHOLM, N. C., Sandia Corporation expedition for airborne scientific observation of the eclipse of the quiet sun of May 30, 1965, 19: 47451 (SC-M-65-419)
ANDERSEN, H. H., Determination of interatomic potentials in metals by electron irradiation experiments, 19: 47882 (RISO-103)
ANDERSON, David Walter, Photodisintegration of ^{40}Ca, 19: 47578 (IS-T-28)
ANDERSON, J., Structure of thorium monolayer on the tungsten (100) surface, 19: 47035
ANDERSON, John, Intra-arterial cytotoxic therapy and x-ray therapy for cancer of head and neck, 19: 46088
ANDERSON, K. A., Determinations of auroral-zone x-ray spectrum, 19: 47471
ANDERSON, K. A., Energetic electron fluxes in tail of geomagnetic field, 19: 47459
ANDERSON, K. A., Spatial asymmetry and periodic time variations of x-ray microbursts in auroral zone, 19: 47470
ANDERSON, K. D., Neutron-diffraction study of chemical order-disorder in $PtBi_2$, 19: 47028
ANDERSON, L. J., Strain gage applications using the Rokide process, 19: 46723 (RFP-641)
ANDERSON, Larry B., Voltammetric studies of Eu(III) in formate buffer, 19: 46268
ANDERSON, Myra D., Separation of tellurium and iodine from other fission products, 19: 46169 (IDO-14664)
ANDERSON, N. G., Prog. rpt. on zonal centrifuge development, 1–6/64, 19: 45730 (ORNL-3752)
ANDREESCU, M., Automatic Moessbauer spectrometer, 19: 46831
ANDREEV, S. I., Spark channel formation in air, 19: 47146
ANDRES, R., Local neutron flux distribution in a bundle from segmented fuel elements, 19: 47992 (KEA-311)
ANDREW, Douglas S., Carcinoma of thyroid following irradiation for medulloblastoma, 19: 46069
ANDREWS, J., High-energy neutron cross sections, 19: 47550 (TID-22141, pp 81-93)
ANDREWS, John T. S., Thermal anomalies and thermodynamic properties of gadolinium hexaboride, 19: 46994 (COO-1149-52)
ANDROS, G., Technetium-99m as clinical tracer material, 19: 46140
ANDROS, George, Autoradiography of diffusible ions with application to thyroidal radioiodide, 19: 45783
ANDRYUKHINA, E. D., Investigation of titanium plasma source, 19: 47793
ANGELI, Istvan, Measurements and experiences in connection with scintillation fast neutron detector, 19: 46774
ANGERMAN, C. L., High-temperature metallography of uranium, 19: 47005 (NMI-4997, pp 76-84)
ANGERMAN, C. L., Network structures in uranium and its alloys, 19: 47060
ANGERMAN, C. L., Preparation of thin foils of uranium, 19: 46933 (NMI-4999, pp 78-84)
ANGERTH, B., Production of hot plasma by discharge in strongly inhomogeneous magnetic field, 19: 47831
ANGHELESCU, D., Evidence for high four-momentum transfer from π^--Xe interactions at 9 Bev, 19: 47698
ANGHILERI, Leopoldo Jose, In vitro effects on different tissues of colloidal chromic radiophosphate, 19: 45939
ANSELIN, F., Radiocrystallographic studies of radioactive materials, 19: 46202
ANTHONY, Lee Saunders, Resonance escape probability of neutrons in a homogeneous Th reactor, 19: 47969
ANTIPOV, V. V., Biological effects of high energy protons, 19: 45821 (JPRS-31547, pp 1-5)
ANTIPOV, V. V., Radiobiological problems of space flights, 19: 46000
ANTONOV, A. S., Electrophotographic method for determining the lithium diffusion constant in p-type silicon, 19: 46997 (JINR-P-2282)
ANTOSHIN, G. V., Isotopic exchange between molecular oxygen and oxides of rare earth elements, 19: 46266
ANTSUPOV, P. S., 30-Mev microtron-injector for pulsed fast reactor, 19: 47164 (JINR-P-2313)
AOYAMA, Takashi, Combined action of anti-tumor chemicals and ^{60}Co γ rays on mouse strain L cells cultured in vitro. II., 19: 46018
APPLEMAN, Daniel E., Structures of $K_2(UO_2)_2V_2O_8$ and $Ca_2(UO_2)_2V_2O_8$, 19: 46259
ARAI, Eiichi, Measurement of diffusion length in time-decaying neutron fields, 19: 47560
ARAKAWA, T., Energy-transfer processes in dilute solutions of organometallics in benzene, 19: 46362
ARD, W. B., Energetic neutral injection into an electron-cyclotron plasma, 19: 47837
ARDELL, Alan Jay, Creep and atomic mobility in polycrystalline Zr, 19: 47074
ARENDT, Paul R., Determination of the ionospheric electron content utilizing satellite signals, 19: 47448 (AD-612119)
ARGHITTU, C., Radioprotective effect of ATP-DPN in rats irradiated with DL 85/30 and DL 100/30, 19: 46020
ARIYOSHI, Shigeki, Purification of helium gas in nuclear facilities, 19: 46513
ARMANI, R. J., Determination of manganese sulfate content for neutron source measurements, 19: 47552
ARNOLD, E. D., Costs of permanent disposal of power-reaction fuel-processing wastes in tanks, 19: 48080 (ORNL-2873)
ARONS, Michael Eugene, Finite quantum electrodynamics, 19: 47436
ARRHENIUS, G., Anion exchange separation of uranium and its application to determination of uranium in sea water, marine sediments, and other geological samples, 19: 46223
ARRINGTON, CLEON C., Chemical species containing ^{32}P and ^{35}S subsequent to neutron irradiation of thiourea, 19: 46365
ARROTT, Anthony, Propagation of Bragg-reflected neutrons in large mosaic crystals and efficiency of monochromators, 19: 47562
ARSENAULT, R. J., Energy of formation of a double kink and an examination of low-temperature deformation, 19: 47011 (ORNL-3862)
ARTEMOV, Yu. M., Interpretation of strontium isotopic composition as indicator of magmatic differentiation and its duration, 19: 46600
ARUNASALAM, V., Microwave scattering due to acoustic-ion-plasma-wave instability, 19: 47776
ASARD, Per-Erik, Two special applications of high-energy electron beams, 19: 46042
ASAUD, C. A., Metallographic and ceramographic preparation of nuclear materials, 19: 46937 (NMI-5025(Pt.I), pp 1-25)
ASCANI-ORSINI, R., Italian 35-Mev betatron Gilbetron for therapeutic and scientific-industrial uses, 19: 47183
ASCOLI-BARTOLI, U., Plasma diagnostics based on refractivity, 19: 47818

ASH, C. L., Preoperative irradiation in management of locally advanced breast cancer, 19: 46054

ASHE, J. B., Angular distribution of gamma rays from C,O and N at 14.8 Mev, 19: 47593 (TID-22012, pp 156-75)

ASHE, John B., Total absorption γ spectrometer system for pulsed beam $n,n\gamma$ measurements, 19: 46765 (TID-22012, pp 4-21)

ASHLEY, Franklin L., Evaluation of healing process in avian digital flexor tendons and grafts following application of artificial tendon sheath, 19: 45964

ASHLEY, Franklin L., Use of irradiated homografts and artificial sheaths in avian and mammalian tendon injuries, 19: 45965

ASKEROV, A. B., Composition of uranic–vanadic minerals, 19: 46627

ASLUND, Nils, Triplet bands of ND, 19: 46263

ASO, Takeshi, Anomalous behaviors in Josephson current, 19: 47515

ASPINALL, S. R., Physical and chemical principles affecting high-temperature materials for rocket nozzles, 19: 46941 (NP-15514(Vol.3))

ASPINALL, S. R., Physical and chemical principles affecting high-temperature materials for rocket nozzles, 19: 47009 (NP-15514(Vol.2))

ATEH, A. H. W. Jr., Activation cross sections for 14-Mev neutrons, 19: 47673

ATHERTON, David R., Thorium-228 decay series in adult beagles, 19: 45798

ATTIX, Frank H., Glass and thermoluminescent dosimeters, 19: 46859

AUBERT, F., Use of vinyl magnesium bromide for synthesis of molecules labeled with ^{14}C, 19: 46310

AUGUSTSON, R. H., High-energy neutron cross sections, 19: 47550 (TID-22141, pp 81-93)

AULD, Harry E., Prog. rpt. on simulation of air-blast-induced ground motions, 7/64–1/65, 19: 46457 (AD-613674)

AUSTIN, A. E., Factors controlling effectiveness of high-temperature protective coatings for tungsten, 19: 46911 (AFML-TR-64-392)

AVCHEN, B., Potential antiradiation agents, 19: 46316

AVDEYENKO, A. I., Production of x-ray photographs with very short exposure times, 19: 46729 (LA-tr-65-21)

AWWAL, M. A., Thorium-230 content of South Alligator River pitchblende, 19: 46606

AXFORD, W. I., Outer ionospheric regions, 19: 47491

AYADYUN, Yu. A., Spectral determination of electron temperature of Cs plasma in a thermoelectric diode, 19: 47773

AYRE, James Lewis, Charging and discharging installation for a gas-cooled nuclear reactor, 19: 47932

AYVAZIAN, Arthur M., Development of tough, high-strength α-β titanium base alloys, 19: 46985 (AD-613651)

B

BABCOCK, D. F., Prog. rpt. on D_2O-moderated power reactors, 3–6/65, 19: 46917 (DP-975)

BABICH, I. L., Spectral determination of electron temperature of Cs plasma in a thermoelectric diode, 19: 47773

BACHELET, F., Intercalibration of cosmic-ray neutron monitors, 19: 47272

BACHYNSKI, M. P., Electromagnetic wave propagation in anisotropic plasmas along direction of static magnetic field, 19: 47718 (AD-614442)

BADHWAR, G. D., Multiply charged nuclei of the primary cosmic radiation. I., 19: 47276

BADHWAR, G. D., Multiply charged nuclei of primary cosmic radiation. II., 19: 47277

BAECHMANN, K., Separation of lanthanides by high-voltage electrophoresis, 19: 46449

BAEV, I., Distribution of radioprotective N-4-nitrophenyl/-beta-^{14}C-amidine in organs of white rats, 19: 46011

BAGCHI, Nemdelal, Iodine metabolism in the thyroid, 19: 45786

BAGHDIKIAN, M., Application of helicity representation to angular correlations with recoil effect, 19: 47610

BAGIN, V. A., Investigation of hybrid waves in circular waveguide partly filled with a dielectric, 19: 46743

BAHBOUT, Abraham, Pressurized water reactor plant with improved jet pump arrangement, 19: 47974

BAIKIE, A. G., Cytogenetic studies in chronic myeloid leukemia and acute leukemia associated with mongolism, 19: 45915

BAILEY, Peter John, Improvements in or relating to conveyor systems, 19: 46519

BAINES, Bernard Deryck, Improvements in or relating to conveyor systems, 19: 46519

BAKER, D. A., Recent developments in transverse injection experiment, 19: 47847

BAKR, M. H. S., Probability distributions of fluctuations in reaction $^{25}Mg(d,\alpha)^{23}Na$, 19: 47659

BALATA, P., Intercalibration of cosmic-ray neutron monitors, 19: 47272

BALDWIN, Lionel V., Particle beam measurement apparatus using beam kinetic energy to change heat sensitive resistance of the detection probe, 19: 47155

BALDWIN, N. L., High-temperature modifications of ThC_2, 19: 47033

BALDWIN, W. H., Isomerization in residual alkyls from pyrolytic and ester interchange reactions of tributyl phosphate, 19: 46317

BALESCU, R., Advanced kinetic theory, 19: 47829

BALKWELL, W. R., Determination of total tritium activity adsorbed on surface of various metals, 19: 47018 (USNRDL-TR-890)

BALL, Con O. T., Scintillation methods for metallic ion determination in human subjects using computer techniques, 19: 45771

BALL, G. L., Application of Power Burst Facility to fast reactor fuel meltdown tests, 19: 47952 (APDA-177)

BALL, G. L., Fast reactor fuel meltdown test facility requirements, 19: 47951 (APDA-173)

BALL, J. B., Direct-interaction (p,α) reactions in ^{89}Y and ^{90}Zr, 19: 47670

BALLIGAND, P. L., Nuclear power in developing areas, 19: 48041

BANASZAK, Jerome J., EPR investigation of radiation protection by aromatic additives in synthetic polymers, 19: 46321 (AD-611779)

BANSLABEN, A. J., Alpha-gamma facility for fuel studies, 19: 47975 (BNL-9450)

BARAKAT, M. Z., Alterations of ascorbic acid content of legumes caused by β or γ irradiation. II., 19: 45938

BARANY, J., Frequency of cancer and geological formations, 19: 45832

BARATOV, D. G., Investigation of escape of electrons from trap with a spatially periodic helical magnetic field, 19: 47145

BARBANENTE, V., Magnetostriction wire spark chambers, 19: 46783

BARBEE, R. B., Prog. rpt. on anti-radiation drugs, 4–6/65, 19: 46303 (NP-15409)

BARBER, Hugh R. K., Pelvic exenteration for extensive visceral necrosis following radiation therapy for gynecologic cancer, 19: 46106

BARDOU, L., Synthesis of doubly labeled cholesteryl linolenate and arachidonate, 19: 46309

BARIL, Marcel, Components of the image produced by an ionic optical system, 19: 46738

BARKER, F. B., Automation of mass spectrometers for isotopic analysis of reactor materials, 19: 46181 (WAPD-T-1769)

BARNES, Clifford A., Radioactivity of Columbia River effluent, 19: 46680

BARON, J.-L., Application of radiocrystallography to testing of nuclear metals, 19: 47040

BARR, Robert Q., Prog. rpt. on tungsten-base alloys, final, 1/10/64–3/10/65, 19: 46940 (NP-15444)

BARRETT, B., Breaking of SU_3 symmetry in electromagnetic decay of the decuplet, 19: 47344

BARRINGTON, R. E., Ionospheric noise and geomagnetic micropulsations, 19: 47493

BARRINGTON, R. E., Wave propagation in a homogeneous ionized gas, 19: 47501

BARTAK, P., Skin protection against x rays, 19: 46019

BARTH, Gunther, Additive medical treatment of tumor beds. X., 19: 46121

BARTH, Gunther, Therapy of lethal radiation with rutin. I., 19: 46030

BARTHELEMY, Pierre, Study of U–Pu–Fe alloys (MASURCA critical experiment), 19: 46992 (CEA-R-2792)

BARTLETT, A. F., Electron microscope study of neutron irradiation damage in α-iron, 19: 47105

BARTLETT, Edwin S., High-temperature Nb-base alloys, 19: 46976

BARTON, J. P., Neutron radiography using crystal monochromator, 19: 46563

BARTON, M. Q., Plans for slow extracted beam at AGS, 19: 47161 (BNL-9483)

BARUCH, P., Prog. rpt. on radiation damage in semiconductors, annual, 19: 47076 (AD-612090)

BARUT, A. O., Nature of resonance in static pion-nucleon scattering in one-meson approximation, 19: 47298 (AD-613934)

BAR'YAKHTAR, V. G., Slow neutron scattering in antiferromagnets having weak ferromagnetism, 19: 47899

BASHANDY, E., Search for anomalous electric dipole transitions in ^{197}Hg, 19: 47674

BATAINI, P., Treatment of supraglottic carcinomas by telecobalt therapy, 19: 46057

BATE, L. C., Determination of Mo in hair and wool by neutron activation analysis, 19: 46192

BATES, C. C., Guide for application of hermetically sealed, direct current, electromagnetic relays, 19: 48100 (SC-TM-65-294)

BATES, H. F., Continuous observation of auroral belt by means of radio, 19: 47473

BATES, Lloyd M., Evaluation of grids, 19: 46147

BATON, J. P., Analysis of experimental data concerned with pion-pion scattering, 19: 47357

BATSANOV, S. S., Permittivities and atomic charges of rare-earth metal oxides, 19: 47901

BAUER, A. A., Hot cell metallographic experience at Battelle, 19: 47085

(NMI-4997, pp 134-56)
BAUER, A. A., Metallographic preparation of irradiated uranium carbide, 19: 47083 (NMI-4996, pp 77-85)
BAUER, A. A., Metallographic preparation of alumina-coated UO_2 spheres in graphite, 19: 46925 (NMI-4997, pp 85-91)
BAUER, A. A., Microstructures of compounds of uranium, thorium, and beryllium, 19: 46924 (NMI-4997, pp 55-61)
BAUER, A. A., Microstructural studies of cast uranium, 19: 47007 (NMI-5025(Pt.I), pp 127-51)
BAUGNET, J.-M., Nondestructive underwater testing in the BR2 reactor, 19: 48002 (ORNL-tr-747)
BAUMANN, Elizabeth W., Radiolysis of ion exchange resins used in the purification system of Savannah River reactors, 19: 46327 (DP-977)
BAYAN, Aris P., Microbial processes for preparation of radioactive compounds, 19: 46409
BAYATYAN, G. L., Backward elastic scattering of pions on neutrons at 1.2 to 4.5 Bev, 19: 47310 (NP-15376)
BAZHULIN, P. A., Stimulated radiation from hydrogen and deuterium molecules in near-infrared region, 19: 47260
BEACH, Frank A., Effects of fetal irradiation on behavior in the albino rat, 19: 45894
BEAGLEHOLE, David, Reflection studies of excitons in liquid and solid xenon, 19: 47893
BEAL, J. L., Prog. rpt. on aerospace nuclear safety investigations of reentry ablation phenomena, 5–7/65, 19: 47117 (SC-DC-65-1698)
BEAN, C. H., Metallography—ally of nondestructive testing in evaluating nuclear fuel components, 19: 46556 (NMI-4997, pp 1-21)
BEAR, I. J., Heats of formation of Be compounds. I., 19: 46279
BEARD, E. L., Alpha air monitor with constant flow control, 19: 46768 (UCRL-14253)
BEARDWOOD, J. E., Solution of the transport equation by collision probability methods, 19: 47540 (ANL-7050, pp 93-112)
BEATTIE, John Reginald, Furnace and furnace wall, 19: 46522
BEAUFILS, P., Calibration of ionization gages using diamagnetic suspension absolute gage, 19: 46579
BECCIOLINI, A., Behavior of total biliary acids and of some pancreatic enzymes in patients irradiated on the abdominal pelvic region, 19: 45928
BECK, R. N., Technetium-99m as clinical tracer material, 19: 46140
BECKEL, Charles L., Theoretical study of vibrational energy levels of diatomic molecules, 19: 47215 (AD-613375)
BECKER, Bernard, Efflux of ^{86}Rb from rabbit lens, 19: 45778
BECKER, F., Model for double charge-exchange nuclear reactions with pions, 19: 47660
BECKER, G., Use of radioactive isotopes in diagnostic internal medicine, 19: 46102
BECKER, J., Tumor tele-irradiation with energetic corpuscular and wave radiation, 19: 46078
BECKER, M. C., Energetic neutral injection into an electron-cyclotron plasma, 19: 47837
BEHNE, Von D., Concentration and temperature dependence of isotope effects in ion migration of Li in acetic acid solutions. V., 19: 46264
BEHRENS, H., Absorbed dose rate determination in vinylchloride. II., 19: 46368
BEKEFI, G., Laser interferometer for repetitively pulsed plasmas, 19: 47730
BELAGYI, J., ESR investigations of radioinduced free radicals in nucle tissues, 19: 45947
BELIKOV, A. M., X-ray determination of coefficient of thermal expansion, 19: 47023 (LA-tr-65-20)
BELL, Francis R., Reel-type control rod drive and brake and braking mechanism, 19: 47941
BELL, George I., Neutron blanket calculations for thermonuclear reactors, 19: 47721 (LA-3385)
BELL, R. E., New information on the emission of delayed protons following decay of ^{17}Ne, ^{21}Mg, and ^{25}Si, 19: 47613
BELL, R. J., Long-range interaction of three atoms, 19: 47249
BELLEW, W., Dependence of occurrence of mid-latitude aurora on sunspot cycle, 19: 47472
BELLMAN, R. E., Dynamic programming and an inverse problem in neutron transport theory, 19: 47537 (AD-613468)
BELON, A. E., Continuous observation of auroral belt by means of radio, 19: 47473
BELROSE, J. S., Ionospheric F region, 19: 47490
BELROSE, J. S., Lower ionospheric regions, 19: 47489
BELTER, Walter G., Radioactive waste research and development activities, 19: 48083
BELTRACCHI, L., Analysis of a nonlinear reactor control system, 19: 47962
BELTRAMETTI, E. G., Representations of Poincaré group associated with complex energy-momentum, 19: 47422
BEMIS, C. E. Jr., Decay scheme of 25-minute ^{131g}Te, 19: 47663
BENDER, M. A., Preparation of mammalian metaphase chromosomes for autoradiography, 19: 45790
BEN-DOV, O., Laser-induced perturbation in plasma, 19: 47777
BENEDICT, G. E., Status of salt cycle process for processing oxide fuels, 19: 46422 (BNWL-SA-205)
BENHAM, R. D., Analog computer methods for parameter optimization, 19: 46903 (BNWL-70)
BENJAMIN, R. W., Angular distributions of γ rays produced by neutron bombardment of Al, Mg and Si, 19: 47638
BENJAMIN, R. W., Cross sections and angular distributions of neutron-produced γ rays in Fe from .96 to 4.75 Mev, 19: 47591 (TID-22012, pp 99-128)
BENJAMIN, R. W., Gamma rays produced in the inelastic scattering of neutrons with magnesium and silicon, 19: 47589 (TID-22012, pp 53-66)
BENNETT, S. M., Power spectrum of sporadic E at Wilkes and Byrd Stations, Antarctica, 19: 47475
BENNING, C. J., Statistics of breakdown using nanosecond pulse techniques, 19: 47114 (AD-614286)
BENSON, B. W., Electron spin resonances in formicidae, 19: 45954
BENSON, Richard E., Whole-body gamma spectrometry, 19: 46656
BEN-YOSEF, N., Electron temperature of positive column in hydrogen at low pressure, 19: 47738
BERAUD, C., Real and fictitious hazards of pulmonary radiology for patients and physicians, 19: 46110
BERENYI, Denes, Dependence of forms of monoenergetic electron transmission curves on measuring geometry, 19: 47125
BERG, Joseph W. Jr., Final rpt. on seismic waves, 4/62–3/64, 19: 46615 (AD-612033)
BERGE, G., Instability of a rotating plasma, 19: 47851
BERGER, J. A., Detection of β activities on chromatogram with thin layer of absorbent or of ion exchange resin, using gel-forming scintillator, 19: 46862
BERGFELDT, J., Stabilized flash x-ray discharges, 19: 46735
BERGLES, A. E., Effects of upstream compressibility on subcooled critical heat flux, 19: 46546
BERGONZINI, R., Biological problems in association of antineoplastic radiotherapy-chemotherapy, 19: 46096
BERGSTROEM, J., Rotating plasma experiments, 19: 47850
BERIEL, H., Effects of uv rays on Ehrlich tumor cells, 19: 45862
BERINDE, A., ^9Be, ^{11}B and $^{31}P(p,p')$ angular distributions, 19: 47690
BERKOWITZ, Morris I., Laboratory investigations of shelter management factors, 19: 46637 (AD-612254)
BERKOWITZ-MATTUCK, J., Factors controlling effectiveness of high-temperature protective coatings for tungsten, 19: 46911 (AFML-TR-64-392)
BERLAND, R. F., A reactor system dynamics code: AIROS, 19: 47914 (ANL-7050, pp 379-94)
BERLANDI, Francis J., New approach to neutron activation analysis through micro and submicro electroseparation techniques, 19: 46229
BERNARD, D. L., Equilibrium charge states of ^{16}O ions, 19: 47179
BERNARD, Maurice, Action of calcium carbide on alkaline earth chlorides and fluorides, 19: 46251 (ORNL-tr-673)
BERNARDI, L., Radiotherapy of bladder cancer. IV., 19: 46113
BERNATOWICZ, H., Photonuclear reaction studies by activation methods, 19: 47596 (TID-22141, pp 94-7)
BERNEIS, K., Synergism between ionizing radiation and a cytotoxic methylhydrazine derivative: effect on DNA degradation, 19: 46356
BERNFELD, Peter, Synthesis of benzo[rst]pentaphene-5,15-^{14}C and of its oxidation products, 19: 46315
BERNHEIM, Frederick, Prog. rpt. on effects of radiation on mucosal and fetal brain enzymes and radiation recovery, final, 11/1/64–10/31/65, 19: 45820 (TID-22227)
BERNIER, Michel, Determination of sodium and potassium in biological media by neutron activation without chemical separation, 19: 46165 (CEA-R-2837)
BERNSTEIN, S., Magnetic spark chamber system, 19: 46796
BERNSTEIN, S. E., Hemopoietic defect in anemic mice of genotype Sl/Sl^4, 19: 45856
BERRY, D. J., Satisfactory performance of British nuclear power stations, 19: 48019
BERRY, R. J., Effect of divided doses of 15-Mev electrons on skin response of mice, 19: 45885
BERRY, Roger J., Modification of radiation effects, 19: 46026
BERSON, Solomon A., Iodine metabolism and thyroid gland, 19: 45792
BERTAUT, E. F., X rays and electronic microscopy at the Grenoble Nuclear Center, 19: 46512
BERTERO, M., Analysis of α-^{12}C scattering process by Regge representation, 19: 47653
BERTET, Michel, Determination of sodium and potassium in biological media by neutron activation without chemical separation, 19: 46165 (CEA-R-2837)

BERTON, Michelino, Scientific applications of nuclear explosions. I., 19: 46466 (CEA-Bib-63)
BESSON, J., Ternary diagram—uranium–uranium dioxide–uranium oxycarbide, 19: 46249 (LA-tr-65-15)
BEUNG, Lorentz, Instrument for detection of radioactive radiation from aerosols in gases, 19: 46869
BEUTJER, W. H., Response spectra for high air-blast loads, 19: 46566 (AD-425747)
BEYRICH, W., Mass spectrometric studies on polyphenyls. I., 19: 46328 (EUR-2227.e)
BEZRUKOV, I. Ya., Composition of uranic–vanadic minerals, 19: 46627
BHADURI, P. N., Radiation-induced somatic mutations in Cyathodium, 19: 45901
BHADURI, R. K., Separation-type calculation in finite nucleus, 19: 47676
BHARADWAJ, P. D., Coherent production of pion tridents by a primary beam of 16.2 Bev/c π^- in nuclear emulsion, 19: 47355
BHATTACHARYA, R., Hall effect in single crystals of graphite, 19: 47044
BHUTANI, O. P., Helmholtz instability of viscous compressible plasma, 19: 47733
BIAGINI, C., Inducing conditions of relative radioresistance in intestinal tissues, 19: 45926
BIANCHI, C., Evaluation of glomerular filtration rate in man using γ-emitting tracer (Hypaque-^{131}I) and external counting, 19: 46071
BIANCHI, R., Protein radioiodination by an electrolytic technique, 19: 46142
BICKEL, William S., Spectroscopic study of the early helium afterflow, 19: 47133
BICKERTON, R. J., Inter-diffusion of plasma and magnetic fields in pinch and hardcore discharges, 19: 47853
BICKFORD, M. E., Primary and metamorphic Rb–Sr chronology in central Colorado, 19: 46618
BIELICKY, T., Skin protection against x rays, 19: 46019
BIERLEIN, T. K., Novel metallographic utilization of replicas and micro-autoradiography, 19: 46951 (NMI-4996, pp 19-26)
BIERMAN, George, Reliability of safety systems, 19: 47929
BINGHAM, R. L., Energy distribution of particles leaving a θ pinch, 19: 47833
BINHAMMER, Robert T., Time of origin of the parabiotic anastomosis, 19: 45838
BIRGUEL, O., Adsorption of ^{90}Sr by soil, 19: 46434
BIRKE, G., Acute radiation syndrome, 19: 45829
BIRKOFER, Leonhard, Synthesis of tritium-labeled acids through chain elongation after Arndt-Eistert, 19: 46306
BIRKS, J. B., Scintillations in organic solids, 19: 46399
BISHOP, A. A., Forced convection heat transfer at high pressure after critical heat flux, 19: 46554
BISHOP, A. E., Electrolytic resistors in plasma physics research, 19: 47751
BISHOP, A. S., Power balance and particle loss rate in C Stellarator, 19: 47854
BISHOP, J., Calorimeter for graphite dose rate in advanced gas-cooled reactors, 19: 48031
BISTOLFI, F., Physical and biological bases of external and internal irradiation of systemic neoplasia, 19: 46095
BISWAS, M. M., Expected variations of cosmic-ray intensity on the moon, 19: 47273
BIZON, E., Two-phase flow measurement with sharp-edged orifices and venturis, 19: 46526 (AECL-2273)
BJOERNHOLM, S., Isomers in odd-mass Lu isotopes ascribed to $\frac{1}{2}^-$ Nilsson configuration, 19: 47640
BJURSTEDT, Hilding, Symposium on man in space, Paris, 10/62, 19: 45746
BLACK, William C., Carcinoma of large intestine an late complication of pelvic radiotherapy, 19: 46068
BLACKALL, P. M., Analysis of spark chamber pictures using raster-scan technique, 19: 46786
BLACKBURN, D., Interpretation and prediction of reactor power distributions with application to fuel cycle calculations, 19: 47946 (ANL-7050, pp 231-49)
BLACKBURN, Paul E., Gaseous metaborates. III., 19: 46231 (AD-613660)
BLADE, Richard Allen, Unitarity and dispersion relations in quantum electrodynamics, 19: 47396
BLADEL, B. O., Radiation injury of Clostridium botulinum spores in cured meat, 19: 46881
BLAINE, R. A., A reactor system dynamics code, AIROS, 19: 47914 (ANL-7050, pp 379-94)
BLAISSE, B. S., Magnetic properties of superconducting Ta, 19: 47524
BLAKE, Charles A. Jr., Stability of aromatic diluents and solvent extraction reagents in radiochemical processing, 19: 46430 (ORNL-P-1601)
BLASSE, G., Ternary system $Li_3(Nb,Sb,Ta)O_4$, 19: 46276

BLATZ, Hannes, Techniques and instrumentation suitable for community monitoring programs, 19: 46143
BLECHSCHMIDT, H., Electroproduction of π-mesons and photoproduction of dipions, 19: 47303 (DESY-65/7)
BLEICH, Hans H., Step load moving on surface of half-space of a locking material: subseismic case, 19: 46580 (AD-613287)
BLEVIS, B. C., Radio aurora, 19: 47499
BLEWETT, J. P., Design of quadrupoles and dipoles using permanent magnet rings, 19: 47160 (BNL-9482)
BLIAUX, Jean, Flux and temperature distribution in nuclear thermionic converters Sirene 50 and Sirene 100, 19: 47978 (CEA-R-2782)
BLISS, P., High-temperature thermometry at Pratt and Whitney canel, 19: 46722 (PWAC-462)
BLOCH, J., Radiocrystallographic studies of radioactive materials, 19: 46202
BLOK, Johan, Quadrupole coupling in rare earth crystals, 19: 47883 (UCRL-16279)
BLOMEKE, J. O., Costs of permanent disposal of power-reactor fuel-processing wastes in tanks, 19: 48080 (ORNL-2873)
BLOOMSTER, C. H., Variable costs of fabricating UO_2–PuO_2 fuel rods for Saxton reactor, 19: 46962 (BNWL-131C)
BLOOMSTER, C. H., Variable costs of fabricating UO_2–PuO_2 fuel rods for PRCF, 19: 47976 (BNWL-131A)
BLOOMSTER, C. H., Variable costs of fabricating UO_2–PuO_2 fuel rods for EBWR, 19: 47977 (BNWL-131B)
BLOTT, B. H., Work function measurements on the sublimate from uranium carbide, 19: 47038
BLUM, P. L., Ternary diagram—uranium–uranium dioxide–uranium oxycarbide, 19: 46249 (LA-tr-65-15)
BLUM, Pierre L., Metallography—concerning existence of an allotropic change to cubic U_3Si within U–Si, 19: 47024 (NLCO-tr-6)
BOAG, J. W., High-pressure ionization chambers, 19: 46845
BOAG, J. W., Ionization dosimetry at high intensity, 19: 46844
BOARDMAN, Charles R., Changes in fracture permeability of granitic rock mass resulting from a contained nuclear explosion, 19: 46581 (UCRL-14292)
BOCA, I., Polarization of elastically scattered protons on ^{16}O at 4.5-Mev energy, 19: 47691
BOCA, I., Polarization of elastically scattered protons on Al and Mg at 4.5 Mev, 19: 47692
BOCA, I., Polarization of elastically scattered protons on ^{12}C at 6 Mev, 19: 47695
BOCA, I., Polarization of elastically and inelastically scattered protons on ^{26}Mg at 5.8 Mev, 19: 47697
BOCHKOVA, O. P., Spectroscopic investigations of high-frequency discharge in helium, 19: 47772
BODMER, A. R., Mass-seven hypernuclei and the mass-six nuclei, 19: 47647
BOEDEKER, Lawrence R., Electromagnetic means of adding heat and kinetic energy to a gas, 19: 46477 (ARL-65-121)
BOEKER, E., Quadrupole moments of nuclear particle-hole states, 19: 47675
BOELKINS, R. C., Discrimination of broken circles by x-irradiated monkeys, 19: 45893
BOELLA, G., Energy of electron cascades in a small lead-plate spark chamber, 19: 47354
BOENZI, D., Sorption properties of natural tuffs occurring in the Lake Bracciano region (Rome), 19: 48081 (RT/PROT(65)19)
BOETTGER, H. G. L., On determining megaroentgen doses from radiation-induced molecular weight decrease of polymethylmethacrylate, 19: 46367
BOGAARDT, Maarten, Pressurized water reactor plant with improved jet pump arrangement, 19: 47974
BOGDANOV, N. A., Pathology, clinical picture and therapy in affection with toxic and radiological agents, 19: 46651 (JPRS-30979)
BOGEN, P., Doppler-broadened spectral lines from theta pinch, 19: 4780
BOGER, Elisha, Synthesis of benzo[rst]pentapheno-5,15-^{14}C and of its oxidation products, 19: 46315
BOGUSCH, R. L., Approximate series solutions of the three-species atmospheric deionization differential equations, 19: 47449 (AD-613189)
BOHN, E. M., Substructure measurements by statistical fluctuations in x-ray diffraction intensity, 19: 46993 (CONF-650810-3)
BOIJEAU, A., Real and fictitious hazards of pulmonary radiology for patients and physicians, 19: 46110
BOISVERT, Gregory L., Point defects in pure iron through electrical resistivity, 19: 47094 (ORNL-tr-668)
BOKOV, O. G., Leptonic decays of baryons in the universal V-A theory, 19: 47307 (JINR-P-2278)
BOKOWSKI, D. L., Method for isolating low-level alpha activity of americium-241 from plutonium in routine urinalysis procedure, 19: 4615
BOLINGER, M. G. Jr., Electron microscope studies of beryllium oxide

powders, 19: 47002 (NMI-4996, pp 50-76)
BOLLAG, W., Synergism between ionizing radiation and a cytotoxic methylhydrazine derivative: effect on DNA degradation, 19: 46356
BONA, C., PINETO—FORTRAN code designed for the solution of nonlinear differential equations in neutron dynamics, 19: 47916 (ANL-7050, pp 429-41)
BOND, W. R., Status of salt cycle process for processing oxide fuels, 19: 46422 (BNWL-SA-205)
BONEV, L., Distribution of radioprotective N-/4-nitrophenyl/-benz-^{14}C-amidine in organs of white rats, 19: 46011
BONNER, B. E., Equilibrium charge states of ^{16}O ions, 19: 47179
BONNET, P., Application of strain gages at high temperature. I. Cements, 19: 46715 (EUR-2473.f)
BONNYMAN, J., Concentration of ^{137}Cs in Australian milk during 1964, 19: 46660
BONSEL, Wouter G., Pressurized water reactor plant with improved jet pump arrangement, 19: 47974
BONZEL, H. P., Diffusion of ^{63}Ni in α-irradiated copper, 19: 47032
BOOTH, Norman E., Polarization in $\pi^- + p$ elastic scattering at 2.08 Bev/c, 19: 47373
BORDOLOI, Kiren Chandra, Electron transport phenomena in tin at liquid helium temperatures, 19: 47534
BORGGREEN, J., Isomers in odd-mass Lu isotopes ascribed to ½⁻ Nilsson configuration, 19: 47640
BORNAZYAN, A. S., Reduction of alkaline earth oxides with aluminum carbide, 19: 46252 (ORNL-tr-683)
BOROVIK, E. S., Pulse heating of high-pressure argon arc. I., 19: 47789
BOROVIK, E. S., Pulse heating of high-pressure argon arc. II., 19: 47790
BORSARU, M., Polarization of elastically scattered protons on ^{12}C at 6 Mev, 19: 47695
BORSARU, M., Polarization of elastically and inelastically scattered protons on ^{24}Mg at 5.8 Mev, 19: 47697
BORTNIKOV, A. V., Investigation of plasma in the AC device, 19: 47855
BOSE, Subir, S-wave Λ–Λ interaction and a scalar dipion resonance, 19: 47337
BOSE, Sudesh, Electromagnetic mass differences of vector bosons, 19: 47369
BOSTICK, F. X. Jr., Impulse response of the magnetospheric column, 19: 47467
BOTAR, L., Thermodynamic considerations on hydrated electron and other intermediates in radiolysis of aqueous solutions, 19: 46343
BOTOS, P. Jr., Distribution of single electron pulse sizes from multidynode electron multipliers, 19: 46720 (NYO-3406-2)
BOTS, G. J. C., Magnetic properties of superconducting Ta, 19: 47524
BOUCHER, Rose, Study of U–Pu–Fe alloys (MASURCA critical experiment), 19: 46992 (CEA-R-2792)
BOUCHEZ, R., Scientific research in the nuclear physics laboratory, 19: 47609
BOUDENE, C., Thyroid uptake of ^{131}I in rats chronically intoxicated with CO, 19: 45770
BOULENGER, R., Radiological monitoring of the surroundings of CEN at Mol, 19: 46631 (A/AC.82/G/L.986)
BOULENGER, R., Radioactive fallout measured at Mol, Annual report, 1963, 19: 46632 (A/AC.82/G/L.987)
BOURKE, R. C., Radioisotope-photovoltaic energy conversion system, 19: 47284
BOVINGTON, C. H., Effect of labeling on solubilities of crystalline substances, 19: 46274
BOWMAN, C. R., Excitation of ethylene, acetylene, propyne, and 1-butyne by low-energy electron impact, 19: 46322 (AD-612070)
BOWMAN, Robert E., Discrimination of broken circles by x-irradiated monkeys, 19: 45893
BOX, W. D., Reduction of alkaline earth oxides with aluminum carbide, 19: 46252 (ORNL-tr-683)
BOYARSKI, A., Development of streamer spark chambers, 19: 46781
BOYD, Robert Gerald, Spin wave-spin wave scattering in a Heisenberg ferromagnet, 19: 47874 (AD-613606)
BOYKO, L. M., Effect of radiation on certain characteristics of electroluminescent screens, 19: 46341 (FTD-TT-65-24)
BRAAMS, C. M., Composition of noble gas ion beams produced with a duoplasmatron, 19: 47267
BRACHMAN, E. V., Backward elastic scattering of pions on neutrons at 1.2 to 4.5 Bev, 19: 47310 (NP-15376)
BRADFORD, C. M., Research facility for study and preparation of ultrapure materials, 19: 46510 (Y-DA-967)
BRADLEY, Elihu F., High-temperature Nb-base alloys, 19: 46976
BRADLEY, J. M., Tolerance of central nervous system tissues to radiation, 19: 45892
BRAGAZZI, G., Radioprotective effect of ATP-DPN in rats irradiated with DL 85/30 and DL 100/30, 19: 46020
BRAND, N., Iodine in children's hair: its relation to urinary iodine levels, 19: 45784
BRANDT, H. B., Injection experiments in Jutphaas, 19: 47858
BRANDT, H. B., Effect of impurities on pressure effect in thallium. II., 19: 47529
BRANNEN, Eric, Energy spectrum of the electron beam in a racetrack microtron, 19: 47174
BRANSCOMB, Elbert Warren, Internal symmetries in S-matrix theory, 19: 47397
BRANYAN, C. E., Application of Power Burst Facility to fast reactor fuel meltdown tests, 19: 47952 (APDA-177)
BRANYAN, C. E., Fast reactor fuel meltdown test facility requirements, 19: 47951 (APDA-173)
BRASACK, G., Occupational body burden in the G.D.R. in 1963, 19: 46674
BRASFIELD, Richard D., Treating melanoma of pectoral region, 19: 46047
BRATOZ, S., Transposition of theories describing superconducting systems to molecular systems, 19: 47230
BRATZLER, K., Accurate determination of the heavy hydrogen isotope by thermal conductivity, 19: 46182 (NP-tr-1275)
BRAUN, C., Application of radiocrystallography to study of ceramic and refractory compounds, 19: 47041
BRAUN, J. Z., Half life of ^{223}Ra, 19: 47626
BRAUN, Willis H., Acceleration of conducting fluid by traveling magnetic field, 19: 46575 (NASA-TN-D-3006)
BRAY, A. D., Strongly interacting particles in air shower cores, 19: 47271
BRAY, L. A., Solvent extraction of Cs from Hanford alkaline supernate, 19: 48075 (BNWL-68)
BRAZZELLI, A., Stable manganese content of mollusks from Lake Maggiore, 19: 45788
BREBANT, C., Application of radiography to nondestructive control of fuel elements before and after irradiation, 19: 46562
BREBANT, C., Radiography tests with active fuel elements application to testing in hot laboratories, 19: 46558 (ORNL-tr-748)
BREGER, A. H., Sources of γ radiation for radiation-chemical installations, 19: 46340 (AEC-tr-6570)
BREHME, Robert W., Curved space and gravitation. II., 19: 47192
BRENDEH, B. B., Instrument for measuring bowing in long tubes, 19: 46710 (BNWL-59)
BRENNER, A. E., Time-shared multi-experiment use of a small computer, 19: 46807
BRESCIANI, F., Effects of ionizing radiation on proliferating cellular systems, 19: 45923
BRESLIN, James T., Superconductors in advanced electronics, 19: 46475 (AD-612113)
BRETT, J., Factors controlling effectiveness of high-temperature protective coatings for tungsten, 19: 46911 (AFML-TR-64-392)
BREVNOV, N. N., Investigation of plasma in the AC device, 19: 47855
BRICKLEY, S. G., Analyses of para-ortho hydrogen and deuterium by gas chromatography, 19: 46183 (NP-tr-1289)
BRICKSTOCK, A., Time-dependent multigroup diffusion code with automatic resonance self-shielding of cross sections, 19: 47915 (ANL-7050, pp 413-27)
BRIENT, S. J., Statistics of breakdown using nanosecond pulse techniques, 19: 47114 (AD-614286)
BRIMHALL, J. L., Effect of neutron radiation on Re, 19: 47106
BRISSENDEN, R. J., Calculation of neutron spectra in the Doppler region, 19: 47539 (ANL-7050, pp 51-76)
BRISSOT, J. J., Surface tension of gadolinium and floating-zone single crystals, 19: 47046
BRITTAIN, Robert S., Problems in renal homotransplantation, 19: 45888
BRITTON, Donald H., Radioactive well logging system with surface circuit designed to isolate a-c power signals from logging signals, 19: 46623
BRIXNER, L. H., Luminescent properties of rare earth ions in zinc borate as host, 19: 46269
BROCK, M. Clutton, Matter creation by gravitational waves, 19: 47136
BROCKLEHURST, J. E., Neutron dose measurement in graphite irradiations in BR-2, 19: 48030
BRODAHL, Erik, Correlation between calculated and measured mechanical properties of thin-walled fuel element canning tubes of stainless steel, 19: 46986 (KR-96)
BRODE, Harold L., Fireball phenomenology, 19: 47113 (AD-612197)
BRODIE, I., Vacuum breakdown in presence of thermionic cathodes, 19: 46577
BRODSKY, Allen, Prog. rpt. on occupational radiation exposure, 6/64–4/2/65, 19: 45810 (NYO-3394-2(Rev.))
BRONSTEIN, Harry R., All-metal cell technique for measurement of the emf of molten metal–metal halide solutions corrosive to ceramics, 19: 46270
BROOKS, M. R., Reduction in life expectancy as a measure of radiation-induced genetic damage in mice, 19: 45969
BROOMFIELD, G. H., Hydrogen effects in an irradiated PWR pressure vessel steel, 19: 47098

BROWN, Donald W., Combined lung-liver radioisotope scan in the diagnosis of subdiaphragmatic abcess, 19: 46048
BROWN, John S., Lead isotopes of pegmatites, granites, and ores, 19: 46582
BROWN, K. B., Primary amine extraction of beryllium from sulfate liquors, 19: 46431 (ORNL-P-1602)
BROWN, Sanborn C., Microwave scattering due to acoustic-ion-plasma-wave instability, 19: 47776
BROWN, W. Lyan, Response perseveration under constant stimulus-position conditions by normal and previously irradiated female rhesus monkeys, 19: 45899
BROWN, W. Lyan, Response-shift learning-set formation by normal and previously irradiated female rhesus monkeys, 19: 45900
BROWN, W. Lyan, Sex as factor in ambivalent cue, delayed-response performance by rhesus monkeys, 19: 45898
BROWN, W. R., Prog. rpt. on aerospace nuclear safety investigations of re-entry ablation phenomena, 5–7/65, 19: 47117 (SC-DC-65-1698)
BROWNELL, G. L., Use of short-lived isotopes for tracer dose reduction, 19: 46136
BRUBAKER, C. H. Jr., Rate of the reaction between U(IV) and Ti(III), 19: 46277
BRUENGER, Friedrich W., Thorium-228 decay series in adult beagles, 19: 45798
BRUGSCH, Heinrich G., Recent advances in chelation therapy, 19: 46017
BRUN, J., Real and fictitious hazards of pulmonary radiology for patients and physicians, 19: 46110
BRUNSCHWIG, Alexander, Pelvic exenteration for extensive visceral necrosis following radiation therapy for gynecologic cancer, 19: 46106
BRUSSAARD, P. J., Shell model calculations of nuclear magnetic moments and M1 transition probabilities $2s_{1/2}$ $1d_{3/2}$, 19: 47641
BRYANT, F. J., Strontium-90 in Australian environment during 1963, 19: 46394
BRYANT, P. J., Conference on mechanisms of solid friction, Kansas City, 9/63, 19: 47075
BRZOZKOWSKI, J., Isotope diagnostics of respiratory insufficiency, 19: 46118
BUCALO, Dual-purpose operation of Hanford reactor, 19: 48039
BUCHANAN, William A., Prog. rpt. on radiation-resistant electron tube production, 12/1/64–2/28/65, 19: 46872 (AD-621549)
BUCHLER, Alfred, Gaseous metaborates. III., 19: 46231 (AD-613660)
BUCKLER, A., Methods of control rod calculation for graphite moderated reactors, 19: 47999 (TRG-Report-227)
BUCKMAN, J. D., Prog. rpt. on anti-radiation drugs, 4–6/65, 19: 46303 (NP-15409)
BUCKTON, Karin E., Chromosome aberrations in man following acute and chronic exposure to x and gamma rays, 19: 45916
BUCKTON, Karin E., Cytogenetic studies in chronic myeloid leukemia and acute leukemia associated with mongolism, 19: 45915
BUCKTON, Karin E., Exposure to x and gamma rays, 19: 45917
BUDAY, Ivan, Dependence of forms of monoenergetic electron transmission curves on measuring geometry, 19: 47125
BUECHI, J., Influence of radioactive rays on pharmaceuticals. II., 19: 46889
BUECKEN, R., Influence of MHD generators on development in power station design, 19: 48013
BUJARD, E., Different behavior of epidermis of flank and nipple of the guinea pig after a 1600-R dose of x rays, 19: 45869
BULLIO, P., Atomic energy market in Europe. VII. Italy, 19: 48008
BULOS, F., Development of streamer spark chambers, 19: 46781
BUMBA, V., Solar magnetic fields, 19: 47208
BUNATYAN, G. G., Isotope shift and quadrupole moments of near-spherical nuclei, 19: 47573 (IAE-717)
BUNDKE, Werner, Lifetime of electron orbits in focusing magnetic fields. I., 19: 47186
BUNDKE, Werner, Magnetic focusing of medium fast electrons in air coils, 19: 47185
BURAS, B., Time-of-flight method for investigations of single-crystal structures, 19: 47894
BURBIDGE, Geoffrey, X-ray and gamma-ray astronomy, 19: 47207
BURCH, W. D., Prog. rpt. on transuranium research, 11/64, 19: 46428 (ORNL-3847)
BURDET, G., Inversion problem in the λ plane, 19: 47361
BURGER, G., Low-temperature recovery spectra of neutron-irradiated metals, 19: 47097
BURKE, Edmund C., Radioisotope renography in children. I., 19: 46109
BURKE, P. G., Ionization of H and He^+ by electron impact, 19: 47253
BURLESON, G. R., Precise track measurements in a wide gap spark chamber, 19: 46780
BURNER, Alvin M., Whole-body gamma spectrometry, 19: 46656
BURNETT, C. R., Spectroscopic study of the early helium afterflow, 19: 47133
BURROW, Gerard N., Study of adolescents exposed in utero to the atomic bomb, Nagasaki, Japan. II., 19: 45889
BURT, A. K., Reproducibility studies of preparation of a LiF dosimetric material, 19: 46338 (UCRL-12367)
BURTE, D. P., Study of hyperfragments. II., 19: 47650
BURTON, John, Remote operations in SNAP-8 facility at AI, 19: 46504 (CONF-641120, pp 86-97)
BURTON, Milton, Energy-transfer processes in dilute solutions of organometallics in benzene, 19: 46362
BUSCH, Kenneth A., Prog. rpt. on behavior of radionuclides released into fresh-water environments, annual, 1959–60, 19: 46646 (PHS-999-RH-13)
BUSCH, Niels Eduard, Micrometeorological data-handling system and some preliminary results, 19: 47109 (RISO-99)
BUSCH, Niels Eduard, Similarity hypothesis for wind profiles, 19: 47110 (RISO-100)
BUSH, C. Allen, Dispersion of optical rotation and birefringence of biopolymers. I and II., 19: 48104 (UCRL-16278)
BUSHNELL, David Lewis, Resonance escape probability of Th in a homogeneous reactor, 19: 47970
BUSSIAN, Alfred Erich, Single particle exchange models in n–p interaction, 19: 47403
BUSTER, Dawn S., Thorium-228 decay series in adult beagles, 19: 45798
BUTLER, Margaret, Activities of ANL-ENEA computer program libraries and the ORNL Radiation Shielding Information Center, 19: 47908 (ANL-7050, pp 125-39)
BUTLER, S. T., Method for deuteron stripping calculations. I., 19: 47630
BUTT, E. P., Conditions for improved stability in Zeta, 19: 47856
BUTTLAR, H. V., Enrichment of tritium by thermal diffusion and measurement of dated Antarctic snow samples, 19: 46613

C

CABIBBO, N., Weak interactions, 19: 47301 (CERN-65-30)
CAFFEY, T. W. H., Voltage-switching class-D amplifier, 19: 48097 (SC-DR-65-338)
CALAMAI, G., Equatorial angle distribution between electrons captured in outer Van Allen radiation belt, 19: 47474
CALKINS, John, Time course of recovery of Paramecium aurelia from lethal effects of x rays, 19: 45978
CALLAN, Curtis Gove Jr., Spherically symmetric cosmological models, 19: 47212
CALZAVARA, F., Histochemical behavior of some enzymes of intestinal mucous in irradiated animals, 19: 45927
CAMBIER, J., Late postradiotherapy lesions of the central nervous system, 19: 45983
CAMERON, A. E., Isotopic composition of atmospheric neon, 19: 46588 (ORNL-3857)
CAMERON, A. G. W., Gas clouds in dense star clusters: a possible quasar model, 19: 47199
CAMERON, A. G. W., Helium content of the galaxy, 19: 47193
CAMERON, A. G. W., Systematics of fission based on exponential mass formula, 19: 47614
CAMPANA, R. J., Design of SNAP-15A generator, 19: 46894 (GA-5296)
CANARA, A. B., Beam probing of r-f beam-plasma interactions, 19: 47740
CANEPA, F. G., Relations between acetylcholine, choline, and betaine chains in aqueous solution, 19: 46374
CAP, Ferdinand, Juelich plasma symposium, 19: 47715 (AD-613622)
CAPPELLINI, M., Behavior of total biliary acids and of some pancreatic enzymes in patients irradiated on the abdominal pelvic region, 19: 45928
CAPRINO, G., Effects of nalorphine, morphine, and their association on the mortality in whole-body irradiation in the rat, 19: 46021
CAPRINO, L., Effects of nalorphine, morphine, and their association on the mortality in whole-body irradiation in the rat, 19: 46021
CARACH, J., Strontium-90 activity in grass and alfalfa during 1962 and 1963 in West Slovakia, 19: 45750
CARFAGNO, S. P., Entrance effects in circular thrust bearings, 19: 46462 (TID-22184)
CARL, Martin, Additive medical treatment of tumor beds. X., 19: 46123
CARLANDER, R., Remote metallographic preparation of irradiated aluminum-clad lead-bonded ceramic fuel pellets, 19: 47087 (NMI-4997, pp 189-97)
CARLSON, B. G., Moments equations and equivalent discrete ordinates equations. I and II., 19: 47547 (LA-DC-7320)
CARLSON, O. H., Yttrium–cobalt system, 19: 47053
CARLSON, Ronald J., Explosive welding of Zircaloy to Hf, 19: 46961 (BMI-X-10139)
CARLSSON, Carl, Integral absorbed doses in roentgen diagnostic procedures. I., 19: 46043
CARO, R., Critical and exponential experiments, 19: 47961
CARPENTER, Charles M., Immunogenicity of a γ-irradiated Brucella melitensis, 19: 45868

CARRASSI, M., Analysis of α-^{12}C scattering process by Regge representation, 19: 47653
CARRAZ, G., Effects of uv rays on Ehrlich tumor cells, 19: 45862
CARRIGAN, Anne L., Geophysics and Space Data Bull. No. 3, 19: 47447 (AD-612083)
CARSWELL, D. J., Thorium-230 content of South Alligator River pitchblende, 19: 46606
CARTER, J. L., Exchange of deuterium with hydroxyl groups of alumina, 19: 46280
CARTER, L. L., Monte Carlo calculated material bucklings of enriched uranium–water lattices with uranium in the water moderator, 19: 47954 (BNWL-127)
CARTWRIGHT, D. K., Calorimeter for graphite dose rate in advanced gas-cooled reactors, 19: 48031
CARTWRIGHT, D. R., Radiometric determination of fluorine in bulk PuF_4, 19: 46179 (RFP-618)
CARUSO, Frank S., Toxicity of niobium salts, 19: 45768
CASNATI, E., Photographic dosimetry, 19: 46853
CASTELL, L., Corben's quantum theory of elementary particles, 19: 47362
CASTELLANO, E., Analysis of behavior of leukocytes in the whole-body irradiated rat, 19: 45934
CASTELLO, G., Influence of acetylene on radioinduced polymerization of ethylene, 19: 46353
CATANZARO, Antonio, Renal clearance of ^{131}I-labeled sodium iothalamate in man, 19: 46079
CECH, R., Chromatographic separation of radiochemically pure ^{90}Y from ^{90}Sr, 19: 46436
CENJA, M., Polarization of elastically scattered protons on ^{16}O at 4.5-Mev energy, 19: 47691
CENJA, M., Polarization of elastically scattered protons on Al and Mg at 4.5 Mev, 19: 47692
CENJA, M., Polarization of elastically scattered protons on ^{12}C at 6 Mev, 19: 47695
CENJA, M., Polarization of elastically and inelastically scattered protons on ^{24}Mg at 5.8 Mev, 19: 47697
CENTI COLELLA, A., Inducing conditions of relative radioresistance in intestinal tissues, 19: 45926
CESARANO, C., Separation of ^{137}Cs from fission products, 19: 46441
CESARANO, C., Separation of ^{137}Cs from fission products, 19: 46442
CHABANNES, B., Synthesis of DL-shikimic 1-2-^{14}C acid starting from methyl acrylate 2-3-^{14}C, 19: 46312
CHABRA, Kamla, Reduction of radiation exposure of children during urologic diagnosis, 19: 46108
CHADWICK, Donald R., Planning for the control of radiation accidents, 19: 46702
CHALMERS, R. A., Cross sections for $^{54}Fe(n,p)$, (n,α), and (n,2n), 19: 47668
CHALMERS, R. A., New isotope of fluorine: ^{22}F, 19: 47671
CHAMBERLAIN, H. V., Analysis of Babcock and Wilcox prototype steam generator for sodium–water reaction, 19: 46529 (APDA-175)
CHAMBERS, J. Carroll, Radium management program in county Health Dept., 19: 46678
CHAN, C. H., Electromagnetic Σ^0–Λ^0 mixing and the Y_0^0 decays, 19: 47366
CHAND, Ramesh, Hyperfragment formation in $K^- + d \rightarrow \pi^+ + \Sigma^- + n$ reactions at rest, 19: 47339
CHAND, Ramesh, Σ^-–Λ conversion in K^--deuteron absorptive processes at rest, 19: 47358
CHANDLER, Arthur, Late radiation necrosis of the brain, 19: 45995
CHANDRA, G. Ram, Prog. rpt. on biochemistry of senescence in plant cells, final, 6/15/63–6/14/65, 19: 48102 (TID-22175)
CHANG, T. S., Regge cuts in perturbation theory, 19: 47434
CHANG, T. S., Singularities of amplitudes in perturbation theory, 19: 47412
CHARLOT, L. A., High-temperature corrosion of ATR structural materials, 19: 46946 (BNWL-100)
CHARON, Michel, Device for charging and discharging channels of a pressurized, gas-cooled nuclear reactor, 19: 47931
CHASE, L. F. Jr., New isotope of fluorine: ^{22}F, 19: 47671
CHASE, W. L., Analysis of Babcock and Wilcox prototype steam generator for sodium–water reaction, 19: 46529 (APDA-175)
CHASMAN, R. R., Pairing Hamiltonian with variable interaction matrix elements, 19: 47334
CHATTERJEE, H. K., Radiation-induced somatic mutations in Cyathodium, 19: 45901
CHAUVIN, Guy, Electrolytic nickel-plating bath, 19: 46944
CHECHETKIN, A. V., High temperature heat-transfer agents, 19: 46540 (AD-619382)
CHEN, Kuo Chi, Production of H^- ions from arc ion source on a stand, 19: 47142
CHEN, F. F., Excitation of drift instabilities in thermionic plasmas, 19: 47750
CHENG, Guo-kuang, Superconducting electromagnet of Nb_3Sn, 19: 47526
CHENG, Hwo-Sheng, Activation analysis of trace impurities in Al, 19: 46207
CHEN-TSAI, C. T., Bogoliubov-Zubarev-Tserkov-Nikov method in theory of superconductivity, 19: 47509
CHEN-TSAI, C. T., Fifteenfold way of the SU(4) symmetry scheme of strongly interacting particles, 19: 47328
CHERDYNTSEV, V. V., Age of pleistocene carbonate formation according to thorium and uranium isotopes, 19: 46599
CHERNICK, Jack, Neutron dynamics of Brookhaven's High Flux Beam Reactor, 19: 48056 (BNL-9510)
CHERNILIN, Yu. F., Effect of temperature on space-energy distribution of neutron flux, 19: 47956 (IAE-723)
CHERNILIN, Yu. F., Optimum methods for handling transient processes in reactors, 19: 47957 (IAE-724)
CHESSELET, Roger, Concentrations of γ-emitting radionuclides present in holothurian samples in coastal area of Antibes in Cape Ferrat in August 1962, 19: 46611
CHIANG, Chung-hung, Light and spectroscopic properties of inorganic vitreous rare earth oxides, 19: 47886 (N64-21857, pp 1-6)
CHIANG, Chung-hung, Physical research of irradiative radiation emanation of Nd^{3+} activated inorganic vitreous states, 19: 47887 (N64-21857, pp 7-12)
CHICK, Helen J., X-ray determination of coefficient of thermal expansion, 19: 47023 (LA-tr-65-20)
CHILDRESS, J. D., Effects of Be in plants and soil, 19: 45802
CHILDS, Donald S. Jr., Combined 5-fluorouracil and supervoltage radiation therapy in the palliative management of advanced G-I cancer, 19: 46091
CHILDS, William J., Electronic g factors of low-lying levels of Fe I, Cr I, and Mn I, 19: 47240
CHILOSI, G., Collective and particle-state in ^{174}Yb from decay of ^{174}Lu, 19: 47661
CHIOU, J. P., Heat transfer and flow characteristics of porous matrices with radiation as a heat source, 19: 46552
CHIOZZOTTO, M., Fundamentals of radiation absorption processes, 19: 47152
CHIRIKOV, B. V., Statistical properties of nonlinear string, 19: 48108 (ORNL-tr-754)
CHISTYAKOV, P. N., Weak postdischarge emission as indicator of electrode surface condition in vacuum breakdown experiments, 19: 47149
CHISUM, Gloria T., Nature of radiation from nuclear weapons in relation to flashblindness, 19: 46655
CHITNIS, Vishvanath Dattatraya, Gamma penetration of iron–lead shields, 19: 47872
CHITTENDEN, W. A., Reactor auxiliary systems fill special needs, 19: 48016
CHOISY, E., Atomic energy market in Europe. X. Switzerland, 19: 48009
CHORLTON, S., Thorium-230 content of South Alligator River pitchblende, 19: 46606
CHOU, Meh-Chwen, Low-background counter for ^{14}C dating, 19: 46777
CHOW, J. G. Y., Alpha-gamma facility for fuel studies, 19: 47975 (BNL-9450)
CHOW, K. K., Final rpt. on plasma amplifiers, 2/65, 19: 47219 (AD-614253)
CHRIMES, N. W. D., Preparation of x-ray exposure charts, 19: 46561
CHRISPEELS, M. J., Prog. rpt. on biochemistry of senescence in plant cells, final, 6/15/63–6/14/65, 19: 48102 (TID-22175)
CHRISTENSON, J. H., Time reversal, 19: 47391
CHRYSOCHOIDES, N. G., System for accurate counting of short-lived activities by repetitive activation, 19: 46818
CHU, Gordon Pu Kong, Mechanism of siliconizing of molybdenum and tantalum by vapor deposition, 19: 47073
CHUBB, Gerald P., Evaluation of proposed applications of remote handling in space, 19: 46486 (CONF-640508, pp 233-47)
CHUEV, V. I., Reaction $^7Li(p,t)^5Li$ and $^6Li(\alpha,t)^7Be$, 19: 47574 (IAE-836)
CHUEVA, S. A., Elastic (p,p) scattering at 1.45 Bev, 19: 47304 (IAE-700)
CHUGASOV, A. A., Nuclear weapons—physical fundamentals, 19: 46652 (JPRS-31842)
CHUKHLANTSEV, V. G., Solid-phase reactions in the decomposition of zircon by calcium oxide, 19: 46267
CHURCH, N., Control of cast grain size of steel castings, 19: 46980 (AD-611800)
CIAMPI, G. P., Absorption of glucose in patients irradiated on the abdomen for extra-intestinal neoplasia, 19: 45931
CICCARONE, Pietrangelo, Radioprotection of mammals by thiolic compounds, 19: 46010
CINDRO, N., Direct processes in (n,α) reactions, 19: 47637
CIRANNI, G., Self-radiolysis of clathrates containing tritium-labeled molecules, 19: 46359
CIRILOV, S. D., Reactions (d,α) on ^{19}F at 1 Mev, 19: 47646
CITTADINI, G., Survival of white mice whole-body irradiated after administration of nembutal at sedative, hypnotic, and narcotic doses,

19: 46025
CLAESSON, S., Portable high-pressure spectroscopic cell, 19: 46771
CLARE, D. M., Neutron dose measurement in graphite irradiations in BR-2, 19: 48030
CLARK, H. K., Maximum safe limits for slightly enriched uranium and uranium oxide, 19: 47955 (CONF-651103-6)
CLARK, John, Proposed telechirics research laboratory, 19: 46497 (CONF-641120, pp 39-40)
CLARK, John W., Analysis of hostile-environment methodologies, 19: 46480 (CONF-640508, pp 4-26)
CLARK, R., Motion picture illustrating use of graph theory in analysis of spark chamber data, 19: 46795
CLARK, R. G., PRTR containment vessel pressure test experience, 19: 48057 (BNWL-109)
CLARKE, R. L., Gamma-ray scanner for diagnostic radiography, 19: 46750 (AECL-2270)
CLAUDE, J.-R., Thyroid uptake of ^{131}I in rats chronically intoxicated with CO, 19: 45770
CLAY, Gerald A., Thermal anomalies and thermodynamic properties of gadolinium hexaboride, 19: 46994 (COO-1149-52)
CLAYTON, A. J., Solution of the transport equation by collision probability methods, 19: 47540 (ANL-7050, pp 93-112)
CLAYTON, E. D., Plutonium criticality experiments, 19: 47967
CLEARY, R. E., Electrical resistivity of lithium and columbium-1 zirconium alloy to 1430°C, 19: 47015 (TIM-854)
CLEARY, R. E., Reaction rate of Nb–1Zr alloy with oxygen at low pressures, 19: 47016 (TIM-901)
CLEGG, A. B., Possible model for strong interaction in the P_{11} pion-nucleon state, 19: 47350
CLEMMENSEN, J., Epidemiology of leukemia, 19: 45833
CLINE, D., Possible test of CP violation, 19: 47351
COBBETT, J. R., Recurrence of rodent ulcers after radiotherapy, 19: 46059
COCHRAN, Thomas Brackenridge, Soft x-ray irradiations of acetylene, methylacetylene, and ethylacetylene in the gas phase with and without admixtures of noble gases, 19: 46334 (TID-22231)
COFFIN, James B. Jr., Electromagnetic means of adding heat and kinetic energy to a gas, 19: 46477 (ARL-65-121)
COHEN, Maurice, Hartree-Fock wave functions for excited states, 19: 47224
COHEN, Morrel H., Properties of an excess electron in liquid He. I., 19: 47131
COLARD, J., Radiological monitoring of the surroundings of CEN at Mol, 19: 46631 (A/AC.82/G/L.986)
COLBY, Malcolm Y., Combined 5-fluorouracil and supervoltage radiation therapy in the palliative management of advanced G-I cancer, 19: 46091
COLE, G. H., Metallography of fused UO_2, 19: 46176
COLE, H. C., Conditions for improved stability in Zeta, 19: 47856
COLE, L. J., Focal antibody production by transferred spleen cells in irradiated mice, 19: 45806 (AD-621543)
COLE, Leonard J., Focal antibody production by transferred spleen cells in irradiated mice, 19: 45986
COLGAN, James E. Jr., Design of remote handling tools as a function and flexibility, 19: 46490 (CONF-640508, pp 340-64)
COLLIN, W., Circular polarization (β-γ) correlation in permitted β transitions: ^{58}Co, ^{95}Zr, and ^{95}Nb, 19: 47605
COLLINS, H., Compilation of β-stimulated x-ray spectra, 19: 47223
COLLINS, R., Equation of state of system of hard spheres, 19: 47139
COLLINS, W. C., Radio aurora, 19: 47499
COLLINS, W. C., Solar activity and short-lived terrestrial effects, 19: 47494
COLTMAN, John W., Technical limitations of optical image intensification, 19: 46744
COLTON, Robert M., Development of tough, high-strength α-β titanium base alloys, 19: 46985 (AD-613651)
COMBS, Michael F., Effects of γ irradiation of corn seed on respiration and growth of seedling, 19: 45836
CONDIE, Richard M., Biologic relationship of endotoxin and other toxic proteins. V., 19: 45970
CONDON, P. E., Application of television pickup to bubble-chamber measurements, 19: 46798
CONGDON, C. C., Factors affecting mortality from secondary disease in mouse radiation chimeras, 19: 45910
CONNER, R. A. Jr., Metallographic studies of uranium-fissium alloys, 19: 47004 (NMI-4997, pp 45-54)
CONNORS, M. A., Gamma-emission data for calculation of exposure rates from nuclear debris. I. Fission products, 19: 47598 (USNRDL-TR-876)
CONSOLE, M., New approach to water reactor lifetime with spatial variation studies, 19: 47912 (ANL-7050, pp 347-68)
CONSTANT, R., Food sterilization by ionizing radiations, 19: 46885
CONSTANT, R., Production of radioelements at Mol nuclear center. 1963–1964 balance, 19: 46349
CONSTANTINESCU, M., Paramagnetic centers formed in irradiated inorganic oxycompounds of selenium. I., 19: 46390
CONSTANTINESCU, O., Paramagnetic centers formed in irradiated inorganic oxycompounds of selenium. I., 19: 46390
CONTE, M., Application of radiocrystallography to study of ceramic and refractory compounds, 19: 47041
COOGLER, A. L., Evolution of high level caves at Savannah River Laboratory, 19: 46506 (CONF-651101-26)
COOK, H. D., Automation of mass spectrometers for isotopic analysis of reactor materials, 19: 46181 (WAPD-T-1769)
COOK, James E., Ultraviolet microbeam irradiation in living cell membranes, 19: 45891
COOK, M. M., Metallography—concerning existence of an allotropic change to cubic U_3Si within U–Si, 19: 47024 (NLCO-tr-6)
COOL, T. A., Recombination rates and non-equilibrium electrical conductivity in a seeded plasma, 19: 47801
COON, James H., Vela satellite measurements, 19: 47450 (LA-DC-7365)
COON, Sidney A., Off-energy-shell effects in Brueckner theory of nuclear matter, 19: 47666
COOPER, J. R. A., Electron interaction coefficients in relativistic self-consistent field theory, 19: 47251
COOPS, Melvin S., Livermore slug fabrication facility, 19: 46509 (UCRL-12497-T)
COPET, A., Mass spectrometric studies on polyphenyls. I., 19: 46328 (EUR-2227.e)
COPPENS, P., Crystal structure of yttrium orthoferrite and refinement of gadolinium orthoferrite, 19: 46256
CORLETT, D. A. Jr., Replica plating and computer analysis for rapid identification of bacteria in foods. II., 19: 46882
CORNEIL, P., Exchange of deuterium with hydroxyl groups of alumina, 19: 46280
CORNILLE, H., Singular potentials in coordinate space, 19: 47360
CORNISH, F. H. J., Classical radiation theory and point charges, 19: 47011
CORNISH, J. B., Knudsen effusion studies of compounds of uranium and thorium with elements of groups IIIb and IVb, 19: 46298
COSTAS, L. P., Measurement of the thickness of aluminum oxide film, 19: 46952 (NMI-4997, pp 26-35)
COSTEA, T., Behavior of recoil atoms in semiconductors, 19: 46398
COSTEA, T., Interpretation of radiation and thermal annealing by processes governed by defect concentration, 19: 46391
COTLIER, Edward, Efflux of ^{86}Rb from rabbit lens, 19: 45778
COTTRALL, M. F., Comparative studies of sensitivity of low-background clinical counting systems, 19: 46137
COTTRELL, T. L., Drift velocities of slow electrons in polyatomic gases, 19: 46393
COUGHREN, K. D., Pressurizing vessel performance equations, 19: 46532 (BNWL-116)
COUNAS, Georges, Process and device for manufacture of a permeable membrane, 19: 46978
COURT BROWN, W. M., Chromosome aberrations in man following acute and chronic exposure to x and gamma rays, 19: 45916
COURT BROWN, W. M., Cytogenetic studies in chronic myeloid leukemia and acute leukemia associated with mongolism, 19: 45915
COURT BROWN, W. M., Exposure to x and gamma rays, 19: 45917
COURT BROWN, W. M., Somatic damage in man from exposure to heavy doses of radiation, 19: 45997
COURTNEY, T. H., Effect of processing history on the superconducting properties and long-range order of Ta_3Sn, 19: 47513
COVELL, J., Technetium-99m as clinical tracer material, 19: 46140
COVERT, Eugene E., Electromagnetic means of adding heat and kinetic energy to a gas, 19: 46477 (ARL-65-121)
COWLEY, A., Abundances of elements in stars and nebulae (determination of ratio of gas pressure to electron pressure in stellar atmospheres), 19: 47187 (AD-612182)
COWLEY, C., Abundances of elements in stars and nebulae (determination of ratio of gas pressure to electron pressure in stellar atmospheres), 19: 47187 (AD-612182)
COX, A. Lucile, Particle growth in the ionic nucleation condensation colloidal ion source, 19: 46570 (AD-614111)
CRAGLE, R. G., Metabolism of different forms of I in milk, 19: 45782
CRAMER, Eugene M., Phase relations in magnesium-rich portion of cesium-magnesium system, 19: 47059
CRASTES DE PAULET, A., Synthesis of doubly labeled cholesteryl linolenate and arachidonate, 19: 46309
CRAWFORD, D. F., Strongly interacting particles in air shower cores, 19: 47271
CRAWFORD, F. W., Beam probing of r-f beam-plasma interactions, 19: 47740
CREBBIN, Kenneth C., Prog. rpt. on Bevatron operations and development, 1–3/65, 19: 47169 (UCRL-16204)
CRESSY, P. J., Half life of ^{53}Mn from meteorite observations, 19: 47627

CRETU, T., Decay of ^{101}Tc, 19: 47686
CRIM, W. M. Jr., Closed cycle gas turbine, 19: 47987 (AD-612409)
CROCKER, G. R., Gamma-emission data for calculation of exposure rates from nuclear debris. I. Fission products, 19: 47598 (USNRDL-TR-876)
CROMER, Don T., Integrated series of crystallographic computer programs. I., 19: 47877 (LA-3335)
CROPP, L. O., Analytical methods used in predicting re-entry ablation of spherical and cylindrical bodies, 19: 46537 (SC-RR-65-187)
CROSBY, J. R., Development and qualification of thermal control coatings for SNAP systems, 19: 48050 (NAA-SR-9908)
CROSS, Don Allen, Radiation studies of 1-butene and cis 2-butene using soft x-rays and cobalt-60 gamma rays, 19: 46335 (TID-22232)
CROSS, W. G., Problems in β dose measurement at CRNL, 19: 46639 (AECL-2281)
CROUCH, G. D., Detection of radionuclide contamination on face masks, 19: 46755 (BNWL-144)
CROUCH, Holmes F., Nuclear space propulsion, 19: 48052
CROUSE, D. J., Primary amine extraction of beryllium from sulfate liquors, 19: 46431 (ORNL-P-1602)
CROUSE, D. J., Unexpected rate effects in extraction of rare earths by di(2-ethylhexyl)phosphoric acid, 19: 46432 (ORNL-P-1603)
CROUSE, R. S., Mounting of metallographic samples in epoxy resins using multiple cavity molds, 19: 46927 (NMI-4998, pp 1-5)
CROUSE, R. S., Portable metallography laboratory, 19: 46935 (NMI-4999, pp 129-36)
CROUSE, R. S., Preliminary evaluation of a new polishing cloth, 19: 46923 (NMI-4997, pp 36-44)
CROUSE, R. S., Replication of microstructures using silicone rubber and epoxy resin, 19: 46932 (NMI-4999, pp 60-8)
CROUSE, Robert S., Identification of carbides, nitrides, and oxides of Nb by anodic staining, 19: 46929 (NMI-4998, pp 57-64)
CROWLEY-MILLING, M. C., Experimental observations of pulse shortening in a linear-accelerator waveguide, 19: 47182
CROWTHER, R. L., Extensions of power-control method for solution of large inhomogeneous reactor problems, 19: 47917 (ANL-7050, pp 487-502)
CRUME, E. C., Nuclear safety considerations in fabrication of massive partially enriched U–Mo reactor parts, 19: 46967 (Y-KB-62)
CSUPKA, Št., Strontium-90 activity in grass and alfalfa during 1962 and 1963 in West Slovakia, 19: 45750
CULLIS, C. F., Studies of radiation-induced reactions of ethylene in aqueous solution. I., 19: 46385
CULTRERA, G., Studies of liver function in irradiated rats, 19: 45828
CURTIS, M. L., Half life of ^{223}Ra, 19: 47626
CURTISS, C. F., Quantum-mechanical Boltzmann equation, 19: 47416
CUSHING, J. T., Inelastic bound-state scattering in separable approximation, 19: 47343
CUSTODERO, S., Modifications of SORIN's pool-type reactor Avogadro RS1 for higher power operation, 19: 48066
CUZZOCREA, P., Collective and particle-state in ^{174}Yb from decay of ^{174}Lu, 19: 47661
CZARNODOLA, Helena, Homopolymerization of maleic acid esters and diethyl fumarate. I., 19: 46377

D

DAANE, A. H., Preparation of new type of nonstoichiometric rare-earth oxide, 19: 46273
DABOVAL, Jacques, Electrolytic nickel-plating bath, 19: 46944
DABROWSKI, Janusz, Off-energy-shell effects in Brueckner theory of nuclear matter, 19: 47666
DACQUISTO, Michael P., Hazard of ^{90}Sr—a review, 19: 46634 (AD-423463)
DA CUNHA, A. Brito, Nature of lethals in Drosophila willistoni, 19: 45877
D'ACUNZO, L., Experimental observations on radioprotective action of RNA, 19: 46022
DAHL, J. B., Determination of selenium in animal tissue by neutron activation analysis, 19: 46172 (KR-95)
DAHLER, A., Effect of collimator-shape on depth dose curves, 19: 46714 (CONF-640918-1)
DAINTON, F. S., Chemical dosimetry, 19: 46852
DAINTON, F. S., Chemical species in water, 19: 46401
DAINTON, F. S., Photo- and radiation-chemistry of low-temperature aqueous glasses. I., 19: 46394
DALEAS, R. S., Effects of upstream compressibility on subcooled critical heat flux, 19: 46546
DALLA PALMA, L., Behavior of total biliary acids and of some pancreatic enzymes in patients irradiated on the abdominal pelvic region, 19: 45928
DALTON, C., Dental lesions in rat induced by radiomimetic agents, 19: 45845
D'AMATO, Constance J., Effects of fetal irradiation on behavior in the albino rat, 19: 45894
DAMERAU, W., ESR investigations of radioinduced free radicals in muscle tissues, 19: 45947
DAMIANO, V., Prog. rpt. on flow and fracture of alloyed Be, 10/7/64–1/6/65, 19: 46910 (AD-620589)
DAMIANO, V. V., Prog. rpt. on preparation and evaluation of Be, 10/15/63–1/14/64, 19: 46909 (AD-620264)
DANDL, R. A., Energetic neutral injection into an electron-cyclotron plasma, 19: 47837
DANFORTH, W. E., Structure of thorium monolayer on the tungsten (100) surface, 19: 47035
DANIEL, H., Circular polarization (β-γ) correlation in permitted β transitions: ^{58}Co, ^{95}Zr, and ^{95}Nb, 19: 47605
DANIELS, J. M., Cross relaxation of ^{57}Co coupled to an unpaired electron spin, 19: 47615
DAO WONG DUC, Decay of baryons and mesons with formation of an electron-positron pair in the U(12) symmetry scheme, 19: 47308 (JINR-P-2284)
DARBINYAN, M. V., Reduction of alkaline earth oxides with aluminum carbide, 19: 46252 (ORNL-tr-683)
D'ARCY, Gerald P., Prog. rpt. on simulation of air-blast-induced ground motions, 7/64–1/65, 19: 46457 (AD-613674)
DARUGA, V. K., Investigation of hydrogenless shielding for nuclear reactors, 19: 47870
DAS, B., Gravimetric determination and separation of Th with N-benzoyl-N-phenylhydroxylamine by direct weighing, 19: 46194
DAS GUPTA, Taposh, Treating melanoma of pectoral region, 19: 46047
DASS, Guru Vachan, Low-energy Σ^-n interactions, 19: 47348
DATCU, V., Evidence for high four-momentum transfer from π^--Xe interactions at 9 Bev, 19: 47698
DAVEY, William G., Ratio of ^{238}U capture and ^{235}U fission cross sections in fast reactors, 19: 47944 (ANL-7034)
DAVID, Heinz, Structural changes in media of rabbit aorta after local irradiation (^{90}Sr–^{90}Y), 19: 45994
DAVID, J. H., L, M, N functions of non-linear spinor theory of elementary particles, 19: 47324
DAVIDENKO, G. V., Methods of automatic ionization measurement in a bubble chamber, 19: 46758 (CONF-550-99)
DAVIDSON, T. E., Effect of pressure on structure and properties of metals, 19: 46983 (AD-612159)
DAVIES, A. R., Time-dependent multigroup diffusion code with automatic resonance self-shielding of cross sections, 19: 47915 (ANL-7050, pp 413-27)
DAVIES, M. J., Stress corrosion of irradiated stainless steels, 19: 47079 (AERE-R-5014)
DAVIS, F., Lectures on particles and field theory. II., 19: 47405
DAVIS, H. Ted, Quantum-mechanical Fokker-Planck equation, 19: 47415
DAVIS, Herbert Sidney, Bubble chamber study of K^--nucleus interactions at rest, 19: 47708
DAVIS, Howard F., Photomultiplier base system remote from photomultiplier, 19: 46808
DAVIS, L. K., Mass distribution measurements of crater ejecta and dust, 19: 46469 (POR-1815)
DAWSON, John M., Heating plasma by magnetic pumping, 19: 47767
DAYTON, Russel W., Prog. rpt. on civilian applications, 5/65, 19: 46912 (BMI-1727(Del.))
DAYTON, Russell W., Prog. rpt. on civilian applications, 6/65, 19: 46913 (BMI-1733(Del.))
DE BLASI, M., Magnetostriction wire spark chambers, 19: 46783
DECIU, N., Finite solid-angle corrections in γ-γ angular correlation measurements, 19: 47693
DECKART, H., Experience with placentography using human albumin labeled with ^{131}I, 19: 46117
DEDEKEN, M., Behavior of some amino acids in γ-irradiated soils, 19: 45941
DE DOMINICIS, R., Histological study of intestinal mucous membrane in patients irradiated in extra-abdominal sites, 19: 45929
DE GAETANI, G. F., Biological factors of the radiosensitivity of neoplastic metastases, 19: 45920
DE GIULI, G., Anatomical and functional modifications of the intestine during therapeutic treatments, 19: 45922
DEILY, G. J., Evolution of high level caves at Savannah River Laboratory, 19: 46506 (CONF-651101-26)
DE JONG, L. N. J., Magnetic properties of superconducting Ta, 19: 47524
DE KERF, E. A., Covariant definition of spin in relativistic quantum field, 19: 47426
DEKKER, A. J., Influence of rate of ^{90}Sr added to soil at different phosphate levels on the concentration of ^{90}Sr in plants, 19: 45774
DE KLUIVER, H., Injection experiments in Jutphaas, 19: 47858
DELARUE, Norman C., Preoperative irradiation in management of locally advanced breast cancer, 19: 46054
DELAUNAY, B., New scattering chamber and its installation, 19: 47327
DELAUNAY, J., New scattering chamber and its installation, 19: 47327

DELBARRE, J.-P., High-brilliance ion source, 19: 47172
DELBOURGO, R., U(12) symmetry, 19: 47305 (IC/65/57)
DELER, Bernard, On-line control of bubble chamber measuring devices (Lidian), 19: 46801
DELEUZE, Edouard, Constant-height vertical support device, in particular for tanks, 19: 46524
DELEVEY, Alfred, Process for preparing metals by treatment of their salts with activated nascent hydrogen, 19: 46253 (ORNL-tr-803)
DELGI ANTONI, G., Energy of electron cascades in a small lead-plate spark chamber, 19: 47354
DELISLE, Jean-Paul, Detector for liquid carried over in a gas, 19: 46713 (CEA-R-2811)
DELLIPIANI, A. W., Measurement of Ca asborption by double isotope method, 19: 46138
DEL VALLE, A., Measurement of diffusion coefficients. III., 19: 46261
DE MAERE, X., Radiological monitoring of the surroundings of CEN at Mol, 19: 46631 (A/AC.82/G/L.986)
DE MAGALHAES, L. E., Nature of lethals in Drosophila willistoni, 19: 45877
DE MAINE, M. M., Chemical effects of radiative neutron capture in some cobalt(III) complexes with 5 or 6 nitrogen atoms in coordination sphere, 19: 46336
DE MARZI, S., Absorption of glucose in patients irradiated on the abdomen for extra-intestinal neoplasia, 19: 45931
DE MARZI, S., Radiological study of gastrointestinal function in patients irradiated on the abdomen, 19: 46120
DE MARZI, S., Radiological study of the gastrointestinal function in patients irradiated on the abdomen, 19: 45930
DE MARZO, C., Magnetostriction wire spark chambers, 19: 46783
DE MASTRY, J. A., Metallography of ceramic fuel and refractory metal compatibility couples, 19: 46954 (NMI-5025(Pt.I) pp 39-58)
DEMEREC, M., Properties of genes, 19: 45726 (BNL-9488)
DEMERIC, M., Genetic analysis of pyrimidine mutants of Salmonella typhimurium, 19: 45878
DEMICHEV, V. F., Rotation of plasma jet in magnetic field, 19: 47849
DEMIRKHANOV, R. A., Investigation of escape of electrons from trap with a spatially periodic helical magnetic field, 19: 47145
DEMKOV, Yu. N., Particle with low binding energy in a magnetic field, 19: 47143
DEMPSTER, R. T., Dryout in a 19-rod bundle cooled by steam/water fog at 515 psia, 19: 46548
DEMUYNCK, J., Gamma-gamma angular correlations in ^{124}Te, 19: 47636
DENSCHLAG, Johannes-Otto, Reactions of fission recoil atoms, particularly of iodine with methane and other gases, 19: 46330 (NP-15370)
DENZEL, P., Influence of MHD generators on development in power station design, 19: 48013
DEOMIGI, D. E., Minimized fuel cycle cost for simulated boiling water reactor. I., 19: 47990 (BNWL-105)
DE ORIOL Y URQUIJO, J. M., Atomic energy market in Europe. XII. Spain, 19: 48011
DEPAULIS, M. J., Ten new cases of cutaneous radionecrosis, 19: 46085
DEPIREUX, J., Role of water content on production and decay of free radicals in irradiated peas, 19: 45863
DEREM, A., L, M, N functions of non-linear spinor theory of elementary particles, 19: 47324
DERNDINGER, Walter, Betatron for electron depth therapy, 19: 46126
DE ROBIEN, E., Nondestructive testing at hot laboratories of the CEN, Grenoble, 19: 46559 (ORNL-tr-749)
DESAI, C. N., Preparation of ^{203}Hg-labeled neohydrin for medical use, 19: 46305
DESHPANDE, R. Y., Formation of donor-like complexes in diffused Si devices, 19: 46727 (UCRL-16197)
DESRUES, Rene, Comparative study of the oxidation of various qualities of uranium in carbon dioxide at high temperatures, 19: 46948 (CEA-R-2805)
DE STAEBLER, H. Jr., Photoproduction of π^0 from H near the second π–N resonance, 19: 47368
DE TEJADA, L. S., Preparation of pure Zr and Th by direct iodination of their carbides, 19: 46969
DE TOLEDO, J. S., Nature of lethals in Drosophila willistoni, 19: 45877
DE VOLPI, A., Determination of manganese sulfate content for neutron source measurements, 19: 47552
DE WITT, Hugh E., Classical theory of pair distribution function of plasmas, 19: 47775
DEXTER, Arthur H., Cobalt-60 heat sources for 10- to 60-kw(e) generators, 19: 46893 (DP-974)
DEY, Kameleada, Spectrophotometric determination of Th(IV), 19: 46206
DHINGRA, K. C., Decay of ^{51}Cr, 19: 47619
DIAS, John F., Eye disease from natural and man-made radiation, 19: 45905
DICKE, R. H., Gravitation and space science, 19: 47209
DICKENS, J. K., Elastic and inelastic scattering of 12.0-Mev protons from ^{62}Ni, ^{63}Cu, and ^{64}Zn: tabulated differential cross sections, 19: 47585 (ORNL-3851)
DICKENS, J. K., Inelastic scattering of deuterons from ^{60}Ni and ^{114}Cd, 19: 47635
DICKINSON, John R., Reactor with tubes displaced from core axes, 19: 47924
DICKS, J. B., Generalized graphical presentation of MHD generator and accelerator performance characteristics, 19: 47296
DIDDENS, A. N., Sonic spark chamber system with on-line computer, 19: 46800
DIEBOLD, R., Development of streamer spark chambers, 19: 46781
DIEGO, M., Very fast scale of four, 19: 46717 (INSJ-87)
DIETRICH, O. W., Critical neutron scattering from β brass, 19: 47904
DIETZ, George R., Radiation tools for food processing, 19: 46877 (CONF-650552-1)
DI GIACOMO, A., Shape of Zeeman and Stark components of spectral lines in the microwave region, 19: 47235
DILLEY, James Paul, Nucleon as a Regge pole, 19: 47395
DILWORTH, C., Energy of electron cascades in a small lead-plate spark chamber, 19: 47354
DI MARCO, G., X-ray inactivation of papain coupled with a synthetic polypeptide, 19: 45976
DI PORTO, P., Excited levels in ^{28}Si by random phase approximation, 19: 47652
DIRINGER, Michele, Isotopic displacement of uranium (235 to 238), 19: 47602
DI TORO, M., Excited levels in ^{28}Si by random phase approximation, 19: 47652
DJORDJEVIC, Dusan, Movement of radioactivity emanating from ^{40}K in precipitation and waters on territory of Vinca, 19: 46590 (JPRS-31469)
DLOUHY, Zdenek, Sorption properties of pyroclastic rocks. II., 19: 48085
DLOUHY, Z., Sorption properties of natural tuffs occurring in the Lake Bracciano region (Rome), 19: 48081 (RT/PROT(65)19)
DOBASHI, Genichi, Analysis of labeled organic compounds by radio gas chromatography, 19: 46213
DOBKOWSKI, Zbigniew, Stable isotope dilution analysis. I., 19: 46204
DOBROV, N. N., Radiobiological problems of space flights, 19: 46000
DODD, John Allan, Nuclear fuel assembly, 19: 47982
DOEBNER, H. D., One-particle singularities and SU(3), 19: 47321
DOERFEL, Ch., Quantity of food required for determination of ^{90}Sr and ^{137}Cs and its incineration, 19: 46200
DOLEGA, U., Determination of magnetic-field distributions, 19: 46731 (SLAC-Trans-21)
DOLLERY, C. T., Interpretation of ^{133}Xe lung washin and washout curves using an analog computer, 19: 46070
DOLLFUS, Marc Adrien, Ocular effects of an atomic explosion, 19: 45841
DOLS, Charles G., Magnet systems—power supplies—cost optimization, 19: 47170 (UCRL-16384)
DOMAGALA, R. F., Hafnium–oxygen system, 19: 46990 (ARL-65-138)
DOMAGALA, R. F., Materials research with scanning microprobe analyzer, 19: 46508 (NMI-4998, pp 65-76)
DOMAGALA, R. F., Metallographic observations at elevated temperature, 19: 47000 (NMI-4996, pp 8-18)
DOMAGALA, Robert F., Prototype manual of metallurgical practice, 19: 46918 (IITRI-B6018-1)
DOMONKOS, Anthony N., Treatment of eyelid carcinoma, 19: 46052
DONATI, Robert M., Photoscanning in the diagnosis of intracranial lesions, 19: 46053
DONATO, L., Protein radioiodination by an electrolytic technique, 19: 46142
DONSKOI, M. D., Distribution of dosage fields in pendulum γ therapy of rectum and urinary bladder tumors, 19: 46093
DOONG, Henry, Six-decade linear response digitized electrometer, 19: 46816
DORIKENS, M., Gamma-gamma angular correlations in ^{124}Te, 19: 47636
DORIKENS-VANPRAET, L., Gamma-gamma angular correlations in ^{124}Te, 19: 47636
DOSE, K., Inactivation of proteins by radiation, 19: 45839
DOUGLAS, F. C., Experimental investigation of thermal annealing of nuclear reactor-induced coloration in fused silica, 19: 47082 (NASA-CR-304)
DOUGLASS, D. L., Oxidation of zirconium, 19: 46958
DOWKER, J. S., Vertex parts and compositeness, 19: 47349
DOWNS, William L., Toxicity of niobium salts, 19: 45768
DRAGOMIR, Eugenia, Refractometric study of formation of complex neodymium halides in aqueous solution, 19: 46254
DRAGONI, G., Irradiations and seroproteic picture in tumor carriers. Electroforetic research in natural and denatured sera, 19: 45924
DRAPER, J. E., Search for direct neutron capture in manganese, 19: 47634
DRESNER, Lawrence, Principles of radiation protection engineering, 19: 46683
DRESSEL, Ralph W., Retrofugal electron flux from massive targets insid-

ated with monoenergetic primary beam, 19: 47214 (AD-612410)
DRESSER, John C., Investigations of high-intensity heat flux graphite resistors, 1960–1962, 19: 48099 (SC-TM-64-653)
DROSI, M., Collective and particle-state in ^{174}Yb from decay of ^{174}Lu, 19: 47661
DROZD, J., Changes in color of potato tubers after irradiation, 19: 45853
DRUKAREV, G. F., Particle with low binding energy in a magnetic field, 19: 47143
DRUMMOND, W. E., Cyclotron radiation, 19: 47815
DRUMMOND, W. E., Quasi-linear theory of plasma turbulence, 19: 47825
DUBENKO, R. G., Elimination of ^{134}Cs from organism under influence of derivatives of 1,5-diphenylthiocarbazone and 1,5-diphenylthiocarbohydraziде, 19: 45765 (JPRS-27544, pp 1-12)
DU BOSE, C. K. H., Effect of moisture in the air on arc-cast UC and UC_2 at room temperature over extended periods, 19: 46953 (NMI-4997, pp 62-75)
DU BOSE, C. K. H., Metallography of pyrolytic carbon-coated and uncoated uranium carbide spheres, 19: 47006 (NMI-4997, pp 198-207)
DUBOVOI, L. V., Stabilization of powerful Penning discharge by a magnetic field increasing along the radius, 19: 47780
DUFFILL, C., DIDO triple axis crystal spectrometer, 19: 46753 (AERE-R-4895)
DULEPOV, E. V., Permittivities and atomic charges of rare-earth metal oxides, 19: 47901
DUMITRESCU, Ovidiu, Structure of 16.7 Mev-level of ^{5}He or ^{5}Li, 19: 47687
DUMITRESCU, R., Levels of low excitation energy in ^{56}Fe, 19: 47696
DUNGEY, J. W., Effects of electromagnetic perturbations on particles trapped in radiation belts, 19: 47485
DUNGEY, J. W., Plasma theory and observations in space, 19: 47484
DUPUIS, P., Photolysis and radiolysis of liquid cyclopentanone, 19: 46357
DU'A, D. A., Oscillations and noise generation in beam-generated plasma, 19: 47741
DUNNET, D. A., Numerical study of particle behavior in non-adiabatic magnetic traps, 19: 47748
DUPAIGNE, P., Use of ionizing radiation with fruit products, 19: 46880
DUPONT, F. M., Dual-purpose operation of Hanford reactor, 19: 48039
DURAND, Ph., Transpositon of theories describing superconducting systems to molecular systems, 19: 47230
DURGAPRASAD, N., Multiply charged nuclei of the primary cosmic radiation. I., 19: 47276
DURGAPRASAD, N., Multiply charged nuclei of primary cosmic radiation. II., 19: 47277
DURGEAT, J., Irradiation and protection of hospital personnel exposed to ionizing radiations, 19: 46657
DURSTON, C., Calculation of neutron spectra in the Doppler region, 19: 47539 (ANL-7050, pp 51-76)
DVORAK, J. R., Metallographic preparation of hard and brittle materials, 19: 46922 (NMI-4997, pp 22-5)
DVORAK, J. R., Metallographic observations at elevated temperature, 19: 47000 (NMI-4996, pp 8-18)
DWORIN, Lowell, Transport properties of an electron gas in a magnetic field, 19: 47799
DWYER, Orrington E., Heat transfer to NaK flowing in-line through a bundle of circular rods, 19: 46553
DWYER, William A. Jr., Facts on fallout, 19: 46671
DYOTT, Richard Bunnaby, Improvements in or relating to magnetohydrodynamic generators, 19: 46297
DYRING, E., Intercalibration of cosmic-ray neutron monitors, 19: 47272
DZHEMARD'YAN, Yu. A., Factors influencing determination of lithium and boron in enrichment products in (n,α) nuclear reaction, 19: 46221
DZUNG, Long S., Efficiency of large-scale open-loop MHD power generation, 19: 47291

E

EASON, H. O., Energetic neutral injection into an electron-cyclotron plasma, 19: 47837
EASTY, G. C., Growth and infiltration of Ehrlich's ascites tumor in mice with reduced immunological responses, 19: 45858
EBERHARDT, P., Radiation ages of subrites, 19: 47194
EBERLE, S. H., Compounds of Np(IV) and Pu(IV) 8-hydroxyquinoline, 19: 46288
EBERT, M., Charge-transfer complexes in scavenging by iodine of radicals formed on pulse radiolysis of cyclohexane, 19: 46384
EBIHARA, Hiroshi, Enrichment of ^{47}Ca by use of Szilard-Chalmers processes of some organocalcium compounds, 19: 46416
EDER, G., Increase of earth's radius, 19: 47483
EDMONDS, G. D., Electrolytic resistors in plasma physics research, 19: 47751
EDWARDS, Cecile H., Moisture content of tissues of normal surgically treated, and irradiated rats, 19: 45896
EDWARDS, Gerald A., Moisture content of tissues of normal surgically treated, and irradiated rats, 19: 45896
EFFER, S. B., Radiation and early pregnancy, 19: 46062
EFIMOV, V. N., Rarefied Fermi gas and the two-body scattering problem, 19: 47394
EGGERS, H. J., Development of uv radiation resistance by poliovirus infective centers, 19: 46032
EHRENBERG, L., Induction of leaf spots in leguminous plants by nucleotoxic agents, 19: 45882
EHRENSVAERD, J., Production of hot plasma by discharge in strongly inhomogeneous magnetic field, 19: 47831
EHRLICH, Margarete, Chemical and film media, 19: 46860
EIBSCHUETZ, M., Crystal structure of yttrium orthoferrite and refinement of gadolinium orthoferrite, 19: 46256
EICH, W. J., Evaluation of computational system applicable to the nuclear analysis of critical experiments and power reactors, 19: 47959 (WCAP-3269-52)
EICHELBERGER, J. F., Prog. rpt., 4/65, 19: 46157 (MLM-1254)
EISENBERG, E., Effects of steroid hormones on strontium kinetics in man, 19: 45805
EISENBUD, Merril, Iodine-131 in children's thyroids from environmental exposure, 19: 46035 (PHS-999-RH-14)
ELBEL, K., Filler materials in synthetic resin masses as shielding material against ionizing radiation, 19: 46354
ELDRIDGE, O. C., Collisional and anomalous diffusion, 19: 47838
EL HILALI, M., Enzymatic iodination of proteins, 19: 46314
ELIAS, C., Lung changes following cobalt teletherapy for carcinoma of the breast, 19: 46063
ELIAS, M. J., Internal friction peak in beryllium, 19: 47056
ELISEEV, B. V., Instability of ponderomotive force in weakly ionized plasma, 19: 47736
ELISEEV, G. P., Backward elastic scattering of pions on neutrons at 1.2 to 4.5 Bev, 19: 47310 (NP-15376)
ELISEEVA, N. V., EPR spectra of some irradiated nitriles, 19: 46378
ELLEN, W. J., Observations on radiothyroidectomized chickens, 19: 45966
ELLIOTT, D. F., Forced convection burnout in Freon-12 flow, 19: 46527 (AEEW-R-426)
ELLIOTT, David G., D-c liquid-metal magnetohydrodynamic power generation, 19: 47292
ELLIS, R. E., Effect of divided doses of 15-Mev electrons on skin response of mice, 19: 45885
ELSNER, B., Electroproduction of π-mesons and photoproduction of dipions, 19: 47303 (DESY-65/7)
ELTON, L. R. B., Energy levels in the 2s-1d shell from high energy electron scattering, 19: 47677
ELVING, Philip J., Polarographic behavior of purines and pyrimidines, 19: 46301 (COO-1148-97)
EL WAKIL, M. M., Heat transfer and flow characteristics of porous matrices with radiation as a heat source, 19: 46552
ELWOOD, Charles, Renal clearance of ^{131}I-labeled sodium iothalamate in man, 19: 46079
EMDEE, Daniel G., Study to reduce and compile USAF NAP radiation effects data, 19: 46870
ENDO, Ryuichi, Solution properties of polyvinyl chloride polymerized by γ irradiation, 19: 46351
ENGELHARDT, P. R., Prog. rpt. on anti-radiation drugs, 4–6/65, 19: 46303 (NP-15409)
ENGLAND, A. C., Energetic neutral injection into an electron-cyclotron plasma, 19: 47837
ENINA, V. A., Thermoelectric characteristics of metallic sintered alloys on tungsten and molybdenum base, 19: 47019 (AD-619334)
ENNUYER, A., Treatment of supraglottic carcinomas by telecobalt therapy, 19: 46057
EPERONNAT, Paul, Detector for liquid carried over in a gas, 19: 46713 (CEA-R-2811)
EPSTEIN, H., Nonpositivity of the energy density in quantized field theories, 19: 47419
EPSTEIN, Lewis, Radiation damage to electrical material and components, 19: 46875
ERICKSON, E. F., Photoproduction of π^0 from H near the second π–N resonance, 19: 47368
ERICKSON, E. F., Relativistic corrections in electron-deuteron scattering, 19: 47410
ERLER, Jean, Purification of uranium and particularly irradiated uranium, 19: 46455
ERMAKOV, V. I., Capacity dilatometer for radiochemical investigations, 19: 46419
ESCHWEILER, H., The radiation stability of anthracene oils. II., 19: 46333 (SGAE-CH-20/1965)
ESKUCHE, I., Effect of γ irradiation on response of fasted rats to erythropoietin, 19: 45971

ESSOGLOU, M. E., Predicting free-field radial displacements and strains, 19: 46467 (NVO-1163-43)
ESTERLING, Robert J., Polarization in $\pi^- + p$ elastic scattering at 2.08 Bev/c, 19: 47373
ESTRUP, P. J., Structure of thorium monolayer on the tungsten (100) surface, 19: 47035
EUDIER, Michel, Process and device for manufacture of a permeable membrane, 19: 46978
EUGSTER, O., Radiation ages of aubrites, 19: 47194
EVANS, E. J., Influence of rate of ^{90}Sr added to soil at different phosphate levels on the concentration of ^{90}Sr in plants, 19: 45774
EVANS, Howard T. Jr., Structure of $K_2(UO_2)_2V_2O_8$ and $Cs_2(UO_2)_2V_2O_8$, 19: 46259
EVANS, J. A., Permeation and diffusion of hydrogen isotopes through stainless steels. I., 19: 46991 (AWRE-O-47/65)
EVANS, J. S., Half life and g factor of 75-kev level in ^{100}Rh, 19: 47662
EVANS, Titus C., Acute effects of radiation on intact mammals, 19: 45981
EVERETT, Mark Allen, Ultrastructural changes induced by ultraviolet light in human epidermis: basal and spinous layers, 19: 45907
EVERETT, Mark Allen, Ultrastructural changes induced by uv light in human epidermis: granular and transitional cell layers, 19: 45913
EVRARD, R., Calibration of ionization gages using diamagnetic suspension absolute gage, 19: 46579
EYDUK, Yu. A., Thermoelectric characteristics of metallic sintered alloys on tungsten and molybdenum base, 19: 47019 (AD-619334)
EYRAUD, Charles, Process and device for manufacture of a permeable membrane, 19: 46978
EYRE, B. L., Electron microscope study of neutron irradiation damage in α-iron, 19: 47105

F

FACCHETTI, S., Mass spectrometric studies on polyphenyls. I., 19: 46328 (EUR-2227.e)
FACETTI, J. F., Chemical state of ^{125}Sb formed in neutron irradiated tin compounds, 19: 46388
FACQUET, Louis, Electrolytic nickel-plating bath, 19: 46944
FADEEV, V. M., Self-focusing of local plasma currents, 19: 47763
FADEEV, V. M., Topology of steady-state plasma configurations in transverse self-consistent fields. II., 19: 47762
FAIRCHILD, R. G., Epithermal neutron beam isodose charts in phantom head, 19: 46121
FANCIULLO, S., High-temperature thermometry at Pratt and Whitney canel, 19: 46722 (PWAC-462)
FARAGGI, H., Contribution of studies of inelastic scattering of α particles to structure of the nucleus, 19: 47608
FARDY, J. J., Adsorption of beryllium on ion-exchange resins from inorganic systems, 19: 46230 (AAEC/E-136)
FARKAS, M. S., Bright field etch for α plutonium, 19: 46938 (NMI-5025 (Pt.I), pp 153-4)
FARKAS, M. S., Metallographic preparation of alumina-coated UO_2 spheres in graphite, 19: 46925 (NMI-4997, pp 85-91)
FARKAS, M. S., Metallography of ceramic fuel and refractory metal compatibility couples, 19: 46954 (NMI-5025(Pt.I) pp 39-58)
FARKAS, M. S., Microstructures of compounds of uranium, thorium, and beryllium, 19: 46924 (NMI-4997, pp 55-61)
FARKAS, M. S., Microstructural studies of cast uranium, 19: 47007 (NMI-5025(Pt.I), pp 127-51)
FARKAS, M. S., Plutonium metallographic practices at Battelle, 19: 46934 (NMI-4999, pp 104-10)
FARUQUI, A. Z., Ionospheric electron density and body potential measurements by a cylindrical Langmuir probe, 19: 47465
FASSKE, E., Reaction of somatic cell nuclei to radiation, 19: 45992
FAURE, G., Isotopic composition of strontium in oceanic and continental basalts: application to origin of igneous rocks, 19: 46607
FAURE, J., High-brilliance ion source, 19: 47172
FAY, Marie, Conference on advances in x-ray analysis, Denver, 8/64. VIII., 19: 46185
FEDERIGHI, G., Protein radioiodination by an electrolytic technique, 19: 46142
FEDNEVA, E. M., Thermal stability of lithium borohydride, 19: 46248 (FTD-TT-65-591)
FEICHTNER, John, Zero-field level crossings in excited optical states of ^{87}Rb, 19: 47711
FEINDEL, William, Automatic contour brain scanner, 19: 46086
FEINDEL, William, Contour brain scanning with I and Hg compounds for detection of intracranial tumors, 19: 46046
FEJER, J. A., Geometry of magnetospheric tail and auroral current systems, 19: 47469
FEJER, J. A., Ionospheric noise and geomagnetic micropulsations, 19: 47493

FEJER, J. A., Motions of ionization, 19: 47492
FEJER, J. A., Physics of earth's upper atmosphere, 19: 47488
FEJER, J. A., Wave propagation in an inhomogeneous medium, 19: 47502
FELICI, N. J., Electrostatic engineering, 19: 46514
FELLINGER, K., Radioactive isotopes in medicine and research. VI., 19: 46135
FENIMORE, D. C., Radiation sources for ionization detectors in gas chromatography, 19: 46887
FENTON, David George, Homonuclear diatomic molecular orbitals at small internuclear separations, 19: 47265
FERGUSON, C., Prog. rpt. on LCRE pumps and sumps, final, 7/65, 19: 46535 (PWAC-386)
FERGUSON, J., Effects of small doses of radiation on flow and other properties of Ziegler polyethylenes, 19: 46358
FERGUSON, J. M., Neutron fields and induced-activity measurements, 19: 47569 (CEX-62-50)
FERN, C., Formation of ^{89m}Y by 14-Mev neutron irradiation of Zr, 19: 47566 (AERE-R-5009)
FERRELL, J. K., Prog. rpt. on convection boiling inside channels, 7–9/64, 19: 46538 (TID-22148)
FERRELL, Richard A., Final rpt. on fundamental problems of solids, 9/61–8/64, 19: 47875 (AD-614136)
FERRELL, Russ, Manipulator control work at MIT, 19: 46505 (CONF-641120, pp 98-103)
FERRETTI, James A., Analysis of NMR spectra of four-membered ring compounds of the type A_2B_4, 19: 46247 (UCRL-16349)
FERRO-LUZZI, M., Reaction $K^+p \rightarrow K^0p\pi^+$ at 3 Bev, 19: 47356
FETTER, Alexander L., Vortices in an imperfect Bose gas. III., 19: 47516
FIEHN, A. J., Dual-purpose operation of Hanford reactor, 19: 48039
FIELD, E. C., Transmission of geomagnetic micropulsations through the ionosphere and lower exosphere, 19: 47466
FIELDEN, Robert, Preoperative irradiation in management of locally advanced breast cancer, 19: 46054
FILER, E. W., Metallographic and ceramographic preparation of nuclear materials, 19: 46937 (NMI-5025(Pt.I), pp 1-25)
FILER, E. W., Post-irradiation metallographic laboratory at GE-NMPO, 19: 47089 (NMI-4999, pp 30-50)
FINCK, W., Embryonic erythropoesis and content of nucleic acids in embryonic liver in whole-body irradiated rats, 19: 45826
FINICLE, Robert Lee, Process for coating nuclear fuel particles with pyrolytic graphite, 19: 47983
FINNEMORE, D. K., Superconducting properties of tin, indium, and mercury below 1°K, 19: 47517
FINTZ, Pierre, Reactions (d,p) and experimental studies of excited levels of some light nuclei, 19: 47604
FIRSOV, L. V., Recent data on age of Aldanian phlogopites, 19: 46596
FISCHER, Jack, Decomposition of gaseous PuF_6 by α radiation. VII., 19: 46325 (ANL-7013)
FISCHER, Joachim, Digitized printed discharge planes and their operation at rapid rates, 19: 46784
FISCHER, Joachim, Electron drift velocity variations in neon + 10% helium + alcohol, 19: 47116 (BNL-9443)
FISH, B. R., Adhesion of particles to surfaces in liquid and gaseous environments, 19: 46645 (ORNL-TM-1228)
FISHER, Frank R., Meeting on radiation preservation of foods, Natick, Mass., 10/63, 19: 46876 (AD-613325)
FIZZOTTI, C., Influence of heat-treatments on structure of uranium-rich alloys containing zirconium, 19: 47014 (RT/MET(64)4)
FLATAU, Carl R., Development of servo manipulators for high-energy accelerator requirements, 19: 47159 (BNL-9388)
FLEMMING, Kurt, Investigations on biological radiation. LXVI., 19: 46029
FLEROV, G. N., Yield ratio for fissioning isomer from deuteron irradiation of Pu, 19: 47688
FLETCHER, G. W., Accounting systems for heavy water and fissionable materials, 19: 47906 (AECL-2282)
FLETCHER, Harold J., Discrimination of broken circles by x-irradiated monkeys, 19: 45893
FLIEDNER, A., Emission of light charged particles from highly excited complex nuclei in nuclear emulsion, 19: 47651
FLINT, O., Surface tension of liquid metals, 19: 47064
FLINT, O., Surface tension by pendant drop technique, 19: 47065
FLOWERS, B. H., Four-body operator in nuclear spectroscopy, 19: 47678
FLYGER, Hans, Monitoring design for radioactive air pollution, 19: 46847 (RISO-104)
FOELL, Wesley K., Resonance absorption of neutrons in mixtures of ^{232}Th and ^{238}U, 19: 47575 (IDO-16986)
FOLDY, L. L., Nuclear correlation functions and muon capture, 19: 47688
FOLEY, K. J., On-line computer data processing system for counter and spark chamber experiments, 19: 46806
FOOKS, Jack H., Iodine-131 in children's thyroids from environmental exposure, 19: 46035 (PHS-999-RH-14)

FORD, J. A., Analysis of Babcock and Wilcox prototype steam generator for sodium–water reaction, 19: 46529 (APDA-175)
FORMAN, L., Mass spectrometer program, 19: 46725 (TID-22141, pp 101-10)
FORNACA, G., Two-photon absorption in atomic or molecular systems, 19: 47236
FORSYTH, E. B., Fast beam extraction system of the alternating-gradient synchrotron, 19: 47158 (BNL-910)
FORTESCUE, Peter, Gas-cooled reactor with improved fuel element arrangement, 19: 47973
FORTESCUE, Peter, Nuclear reactor, 19: 48045
FORTESCUE, Peter, Reel-type control rod drive and brake and braking mechanism, 19: 47941
FOWLER, Harry, Effects of fetal irradiation on behavior in the albino rat, 19: 45894
FOWLER, J. F., Effect of divided doses of 15-Mev electrons on skin response of mice, 19: 45885
FOWLER, T. B., Application of the equipoise iterative method to diffusion and transport theory, 19: 47541 (ANL-7050, pp 179-89)
FOX, David, Physics and chemistry of the organic solid state. II., 19: 46320
FRAAK, P., Absorbed dose rate determination in vinylchloride. II., 19: 46368
FRAEKI, R., Measured and predicted variations in fast neutron spectrum when penetrating laminated Fe–D_2O, 19: 47561
FRAHN, H. J., Isomers in odd-mass La isotopes ascribed to ½⁻ Nilsson configuration, 19: 47640
FRANCIS, C. M., Studies on the use of mutagenic agents in plant breeding. II., 19: 45847
FRANCIS, G., Containment of plasma trapped in a magnetic well, 19: 47848
FRANCIS, G., Experiments on plasma, 19: 47817
FRANCIS, J. M., Studies of radiation-induced reactions of ethylene in aqueous solution. I., 19: 46385
FRANCK, J., Solution of hydrogen in palladium and hydrogenation catalysis, 19: 46250 (ORNL-tr-623)
FRANCO, Gianfranco, Plant for remote handling of nuclear fuel elements, 19: 47938
FRANCZ, I., ^{7}Be, ^{12}B and ^{31}P(p,p′) angular distributions, 19: 47690
FRANK, G. M., Radiobiological problems of space flights, 19: 46000
FRASER, D. A., Current interruption in hydrogen and deuterium thyratrons, 19: 47128
FRASER, P. A., Application of iteration-variation method to atomic scattering problems, 19: 47247
FRAYSSE, Georges, Measurement of fission cross section of ^{235}U and ^{239}Pu for thermal neutrons, 19: 47567 (CEA-R-2775)
FREDERICK, E. J., Costs of permanent disposal of power-reactor fuel-processing wastes in tanks, 19: 48080 (ORNL-2873)
FREDRICKS, R. W., Direct detection of ambient electron plasma oscillation fields in the magnetosphere, 19: 47477
FREDRICKS, R. W., Effects of solar-wind composition on threshold for plasma instability in transition region, 19: 47460
FREEDMAN, S. I., Nuclear Brayton cycle power system, 19: 48048 (GE-65SD4251)
FREEMAN, Donald C. Jr., Superconducting magnet facility for plasma physics research, 19: 47533
FRICK, Georges, Radioactivity (β^+) of ^{14}O, ^{18}Ne, ^{26}Si, and ^{30}S, 19: 47603
FRIEDLAENDER, E. M., Evidence for high four-momentum transfer from π^--Xe interactions at 9 Bev, 19: 47698
FRIEDLAENDER, E. M., Interaction mean free path of 9-Bev π^- in Xe, 19: 47689
FRIEDMAN, Irving, Areal variation of deuterium/hydrogen ratios in rainfall for a single storm event, 19: 47112
FRIEDMAN, L., Energy transfer in reaction of He^+ with O_2, 19: 47231
FRIEND, Albert G., Prog. rpt. on behavior of radionuclides released into fresh-water environments, annual, 1959–60, 19: 46646 (PHS-999-RH-13)
FRIEND, J. A., First Australian conference on electrochemistry, Sydney, 2/63, 19: 46291
FRIX, W., Color scintigraphy and colored x-ray images, 19: 46073
FRISCH, A. S., Pancake neutron detector, 19: 46759 (EGG-1183-1017)
FRISCH, O. R., Poor man's SMP, 19: 46803
FRITZE, K., Search for 5-min isomer of ^{78}As, 19: 47682
FROELICH, H., Energy spectrum of the electron beam in a nuclear track microtome, 19: 47174
FROMM, E., Gas-metal reactions at high temperature with particular reference to niobium–gas systems, 19: 46296
FROMM, Jacob E., Solutions to nonlinear incompressible flow problems through a finite difference method, 19: 46533 (LA-DC-7373)
FROMM, P. O., Iodine-131 uptake by tissues of rainbow trout, 19: 45796
FROST, Dietrich, Radio-labeling of organic compounds by $^{12}C(\gamma,n)^{11}C$ reactions by means of bremsstrahlung of 35-Mev betatron, 19: 46418
FROST, Dietrich, Time-dependent relation of dose effects, 19: 45989
FRUSHOUR, Robert, Prog. rpt. on high-temperature solid-state chemistry and sub-solidus phase equilibria, final, 8/65, 19: 46240 (TID-22207)
FRUSHOUR, Robert H., Preparation and structural studies of some cupric rare earth AB_2O_4 type compounds, 19: 46245 (TID-22207, Paper E)
FUCHS, K., Problem of the price of plutonium, 19: 48032
FUCHS, Von A., Lattice constants of Fe–Mo alloys, 19: 47029
FUJII, Akihiko, Muon capture in hydrogen, 19: 47227
FUJIOKA, Shuji, Properties and structure of radiation-polymerized polyethylene, 19: 46375
FUJISAWA, Hobaro, Hydromagnetic wave in toroidal discharge with longitudinal magnetic field, 19: 47742
FUJITA, Junichi, Calculating nuclear matrix elements, 19: 47622
FUJITA, Junji, Density measurement of pinch plasma using infrared He–Ne laser interferometer, 19: 47759
FUJITA, Katsuyoshi, Analyses of para-ortho hydrogen and deuterium by gas chromatography, 19: 46183 (NP-tr-1289)
FUJIWARA, Yoshisco, Counter telescope for charged particle measurements by 14-Mev neutrons, 19: 46821
FUJIWARA, Yoshisada, Combined action of anti-tumor chemicals and ^{60}Co γ rays on mouse strain L cells cultured in vitro. II., 19: 46018
FUKAWA, Minoo, Charge ratio of produced pions in neutrino inelastic scattering, 19: 47377
FUKUI, K., Satellite observations of low-energy primary cosmic-ray nuclei of charges $Z \geq 6$, 19: 47270
FUKUSHIMA, Noshi, Solar flare effect on geomagnetic variation, 19: 47480
FULDE, Peter, Collective excitations in strong-coupling superconducting alloys, 19: 47518
FULMER, C. B., Direct-interaction (p,α) reactions in ^{89}Y and ^{90}Zr, 19: 47670
FUNK, J. E., Prog. rpt. on behavior of $SrZrO_3$, 4–6/65, 19: 47008 (NP-15429)
FUNKE, L., Decay of ^{101}Tc, 19: 47686
FURTH, H. P., Experiments in toroidal plasma confinement, 19: 47820
FURTH, H. P., Toroidal magnetic field configurations and finite resistivity, 19: 47819
FURUHASHI, Akira, Evaluation and reflection on design studies made on the domestic power reactor, 19: 48036
FURUTANI, Y., High refractive index at electron cyclotron harmonics in plasma, 19: 47749

G

GABBE, E. E., Essential specifications of Hamburg 4π large-volume radioactivity detector with liquid organic scintillator. I., 19: 46775
GADSDEN, Evelyn L., Moisture content of tissues of normal surgically treated, and irradiated rats, 19: 45896
GAEDKE, R. M., Excitation functions for nucleon and α-particle transfer reactions induced by ^{14}N ions, 19: 47667
GAEDKE, Rudolph M., Single and multinucleon transfer reactions induced by ^{14}N, 19: 47586 (ORNL-TM-1218)
GAERTTNER, Erwin R., Prog. rpt. on linear accelerator project, annual, 1965, 19: 47092 (TID-22141)
GAGOSZ, R. M., Experimental investigation of thermal annealing of nuclear-reactor-induced coloration in fused silica, 19: 47082 (NASA-CR-304)
GAINES, A. L., New shop to meet future need for larger reactor vessels, 19: 47926
GAINES, Edward E., Analysis and evaluation of measurements of geomagnetically trapped electrons from high-altitude nuclear explosions, 19: 47446 (AD-612013)
GALACZ, L., Frequency of cancer and geological formations, 19: 45832
GALAKTIONOV, Yu. V., Backward elastic scattering of pions on neutrons at 1.2 to 4.5 Bev, 19: 47310 (NP-15376)
GALANIN, N. F., Spectral composition of erythemal part of uv radiation, 19: 45881
GALEEV, A. A., Capture of plasmoids in a magnetic mirror machine, 19: 47839
GALINDO, A., Spectral representation and mass formula for spin-½ particles, 19: 47340
GALKIN, Yu. M., Solid-phase reactions in the decomposition of zircon by calcium oxide, 19: 46267
GALLAGHER, Neil I., Photoscanning in the diagnosis of intracranial lesions, 19: 46053
GALLIGANI, Ilio, Variational methods for solution of problems of reactor kinetics, 19: 47945 (ANL-7050, pp 159-77)
GALONSKA, Helge, On the results of growth-material in heavy water, 19: 45763 (AD-468388)
GAMALEYA, A. N., Distribution of dosage fields in pendulum γ therapy of rectum and urinary bladder tumors, 19: 46093
GAMBELL, Arlo W., Areal variation of deuterium/hydrogen ratios in rainfall

for a single storm event, 19: 47112
GANFIELD, Edgar, Numerical integration of Schroedinger's equation for square-well potential using an IBM 1620 computer, 19: 47429
GANGULI, S. N., Study of hyperfragments. II., 19: 47650
GANOR, S., Iodine in children's hair: its relation to urinary iodine levels, 19: 45784
GANTNER, E., Decay of ^{156}Eu and ^{159}Eu, 19: 47681
GANTZEL, P. K., High-temperature modifications of ThC_2, 19: 47033
GARBER, Esther B., Radiation dosimetry with sodium cacodylate and TRIS, 19: 46373
GARCIA, T. J., Lateral-plate tests with plate diameter varied, 19: 46465 (AD-613991)
GARDINER, D. A., Factors affecting mortality from secondary disease in mouse radiation chimeras, 19: 45910
GARDNER, J. W., Interaction of intense radiation with atomic particles, 19: 47234
GARDNER, J. W., Photon-photon interactions, 19: 47332
GARDNER, Jane F., Review of sterilization and disinfection as applied to medical, industrial, and laboratory practice, 19: 46890
GARDNER, R. A., Influence of transverse magnetic field on forced convection liquid metal heat transfer, 19: 46547
GARLICK, A., Thermal conductivity of irradiated uranium, 19: 47101
GARMATIS, C., Lung changes following cobalt teletherapy for carcinoma of the breast, 19: 46063
GARNER, G., Low-energy spread negative ion r-f source, 19: 47157 (AWRE-NR-1/65)
GARNIER, Arlette, Effective energy of radionuclides absorbed in organs other than G-I tract, 19: 45755 (CEA-R-2809)
GARUFI, M. F., Decreasing electropolishing time for uranium, 19: 46920 (NMI-4996, pp 27-35c)
GASSER, R. P. H., Nitrogen isotope equilibration on tungsten, 19: 46289
GASSNER, F. X., Excretion of radioactivity by human subjects after ingestion of liver from cattle treated with labeled polydiethylstilbestrol phosphate, 19: 45797
GATO, Ryuichi, Solution properties of polyvinyl chloride polymerized by γ irradiation, 19: 46351
GAUDE, Gaston, Determination of sodium and potassium in biological media by neutron activation without chemical separation, 19: 46165 (CEA-R-2837)
GAUL, Horst, Prog. rpt. on selection methods for induced small mutations in higher plants, final, 2/61–1/65, 19: 45819 (TID-22176)
GAULE, Gerhart K., Superconductors in advanced electronics, 19: 46475 (AD-612113)
GAUTHRON, Maurice, Improvements in or relating to sheaths for nuclear fuel elements, 19: 47980
GAUTIER, J. C., Late postradiotherapy lesions of the central nervous system, 19: 45983
GAUTIER, M., Application of radiography to nondestructive control of fuel elements before and after irradiation, 19: 46562
GAUTIER, M., Radiography tests with active fuel elements application to testing in hot laboratories, 19: 46558 (ORNL-tr-748)
GAUWERKY, Friedrich, Quantitative effects of sublethal and lethal whole-body irradiation of white mice, 19: 45990
GAWRONSKI, Andrzej, Method of using determination of ^{222}Rn in expired air, 19: 46677
GAY, W. L., Computer studies of copper atom ranges in copper lattices, 19: 47228
GEDALIA, I., Iodine in children's hair: its relation to urinary iodine levels, 19: 45784
GEHRET, Edward F., Instrumentation for measurement of administered radiation, 19: 46861
GEISS, J., Radiation ages of subrites, 19: 47194
GEISS, R. C., Interdiffusion in niobium–vanadium alloys, 19: 47058
GEKKER, I. R., Investigation by uhf methods of motion of plasma in a radiation accelerator, 19: 47795
GELBERG, A., Automatic Moessbauer spectrometer, 19: 46831
GELLESPIE, P. A., Preparation of x-ray exposure charts, 19: 46561
GENDA, Hidesaburo, Radiation dosimetry by photographic measurement. IV., 19: 46819
GENTZLER, R. F., Atmospheric static electricity warning system, 19: 48094 (SC-DC-65-1646)
GEORGE, D. W., Magnetohydrodynamic electrical power generation, 19: 47285
GEORGE, D. W., Non-equilibrium in thermally ionized gases with small seeding ratios, 19: 47126
GEORGE, Dennis, Nuclear fuel materials including vitreous phase, 19: 47986
GEORGE, James, Prog. rpt. on production engineering measure for Cs beam tube, 8/23–11/23/64, 19: 46709 (AD-614118)
GEORGE, R., Reaction $K^+p \rightarrow K^0p\pi^+$ at 3 Bev, 19: 47356
GERARDO, J. B., Utilization of transverse modes in spherical laser interferometer, 19: 47745
GERDAY, Charles, Verification of radiochemical purity of labeled optical isomer, 19: 46208
GERNA, G., Morphogenesis of nuclear anomaly from small doses of x rays, 19: 45925
GERRARD, Martha, Action of calcium carbide on alkaline earth chlorides and fluorides, 19: 46251 (ORNL-tr-673)
GERRARD, Martha, Process for preparing metals by treatment of their salts with activated nascent hydrogen, 19: 46253 (ORNL-tr-803)
GERSHENSON, S., Induction of lethal mutations in Drosophila melanogaster by DNA, 19: 45876
GERSHON-COHEN, J., Radiation and breast cancer, 19: 46090
GETTY, W. D., Characteristics of the beam-plasma discharge, 19: 47836
GETTYS, W. E., Substructure measurements by statistical fluctuations in x-ray diffraction intensity, 19: 46993 (CONF-650810-3)
GHALIB, Hishem Ali, Secondary electron emission from several solids, 19: 47263
GHATAK, A. K., Measurement of the neutron asymptotic decay constant in small crystalline assemblies, 19: 47554
GHIORSO, A., Decay properties of ^{256}Fm and ^{257}Fm and ^{255}Md, ^{256}Md, and ^{257}Md, 19: 47664
GIACCONI, R., Research program to investigate artificially injected trapped radiation, 19: 47444 (AD-611629)
GIANNARDI, G. F., Absorption of glucose in patients irradiated on the abdomen for extra-intestinal neoplasia, 19: 45931
GIANNARDI, G. F., Histological study of intestinal mucous membrane in patients irradiated in extra-abdominal sites, 19: 45929
GIANNELLI, G., Magnetostriction wire spark chambers, 19: 46783
GIANNONE, P., Helium-burning evolution of massive stars, 19: 47202
GIANNUZZI, M. A., Helium-burning evolution of massive stars, 19: 47202
GIBBONS, D., Formation of ^{88m}Y by 14-Mev neutron irradiation of Zr, 19: 47566 (AERE-R-5009)
GIBBS, B. W., Electromagnetic wave propagation in anisotropic plasmas along direction of static magnetic field, 19: 47718 (AD-614442)
GIBBS, W. J., Strontium-90 in Australian environment during 1963, 19: 46594
GIBBS, W. J., Strontium-90 in Australian environment, 1961 to 1963, 19: 46595
GIBSON, A., Conditions for improved stability in Zeta, 19: 47856
GIBSON, R., Interaction of niobium with active gases at very low pressures. I., 19: 47031
GIBSON, R., Permeation and diffusion of hydrogen isotopes through stainless steels. I., 19: 46991 (AWRE-0-47/65)
GIFFON, M., Inversion problem in the λ plane, 19: 47361
GILARDONI, A., Italian 35-Mev betatron Gilbetron for therapeutic and scientific-industrial uses, 19: 47183
GILBERT, C. W., Clone-size analysis in the study of cell growth following single or during continuous irradiation, 19: 45886
GILBERTSON, W. E., New challenges in environmental health control, 19: 46682
GILDA, Gayle, Application of radioisotope precipitation test to study Q fever in man, 19: 46076
GILL, H. L., Lateral-plate tests with plate diameter varied, 19: 46465 (AD-613991)
GILLAM, P. M. S., Effect of chronic bronchitis on changes in pulmonary function caused by irradiation of the lungs, 19: 46131
GILLES, Paul W., Thermodynamics of materials at high temperature and low pressure, 19: 46234 (COO-1140-123)
GILLET, C., Role of water content on production and decay of free radicals in irradiated peas, 19: 45863
GILMAN, William S., Review of dissolution of plutonium dioxide, 19: 46175 (MLM-1264)
GINZBURG, N. I., Effect of impurities on pressure effect in thallium. II., 19: 47529
GIORGADZE, N. P., Interaction of circular waves in cold plasma, 19: 47786
GIOVANNOZZI-SERMANNI, G., X-ray inactivation of papain coupled with a synthetic polypeptide, 19: 45976
GIRARDI, F., Data handbook for sensitivity calculations in neutron activation analysis, 19: 46167 (EUR-1898.e)
GIRARDI, F., Stable manganese content of mollusks from Lake Maggiore, 19: 45788
GIRBES, J., Ulcerated thorotrastoma, 19: 46092
GIRIFALCO, L. A., Interaction of local modes with stress fields, 19: 47905
GITTERMAN, Henry, Reactor safeguard systems, 19: 48038
GITTERMAN, M., Chemical engineering in the HTGR, 19: 47991 (GA-6120)
GIUDICI, G., Experimental observations on radioprotective action of RNA, 19: 46022
GIUFFRE, Nancy A., Microbial processes for preparation of radioactive compounds, 19: 46409

GIZEA, F., Sensitometric studies on nuclear emulsion by means of β radiation, 19: 46832
GLADSTONES, J. S., Studies on the use of mutagenic agents in plant breeding. II., 19: 45847
GLASER, V., Nonpositivity of the energy density in quantized field theories, 19: 47419
GLEDHILL, Peter Raymond, Charging and discharging installation for a gas-cooled nuclear reactor, 19: 47932
GLENNY, E., Evaluation of the properties of protected Mo and 0.45% Ti–Mo alloy, 19: 47061
GLIKMAN, L. G., Exact integration of equations of motion for relativistic charged particles for a certain class of variable electromagnetic fields, 19: 47435
GLOVER, Donald D., Effects of radiation-induced damage centers in lead zirconate titanate ceramics, 19: 47096
GLYNN, James C., Heat removal from casks, 19: 46667
GODLEWSKI, Zbigniew, Detectability in isotope radiographic methods, 19: 46564
GOEDKOOP, J. A., Neutron beam utilization at the Petten HFR, 19: 48068
GOERTZ, Ray, ANL activities in (remote-control equipment), 19: 46498 (CONF-641120, pp 41-7)
GOERTZ, Ray, Manipulator systems at ANL, 19: 46481 (CONF-640508, pp 27-74)
GOLDBERG, M., The Y_1^0(1660) produced in K⁻-p interactions at 2.24 Bev/c, 19: 47300 (BNL-9520)
GOLDBERG, Marvin C., Emanation of tritium from two electron-capture detectors, 19: 46670
GOLDHABER, Alfred Scharff, Tests of exchange models, including spin, 19: 47404
GOLDMAN, L. M., Energy distribution of particles leaving a θ pinch, 19: 47833
GOLDMAN, Morton I., Safety aspects of ground testing for large nuclear rockets, 19: 46707
GOLDSCHMIDT-CLERMONT, Y., Reaction $K^+p \rightarrow K^0p\pi^+$ at 3 Bev, 19: 47356
GOLDSTEIN, Melvin M., Self-charging nuclear battery, 19: 46897
GOLDSTEIN, Robin, Intermediate resonance absorption in heterogeneous media including moderator scattering, 19: 47953 (BNL-9393)
GOLDSTEIN, Y., Superconducting diode as high-frequency sound detector, 19: 46739
GOLDWASSER, M., Ariane-automatic device for analysis of spark chamber photographs, 19: 46787
GONTCHAR, V. Y., Probability distributions of fluctuations in reaction $^{25}Mg(d,\alpha)^{23}Na$, 19: 47659
GOOD, R. H. Jr., Relation between ionization and cohesive energies of rare earths, 19: 47062
GOOD, R. H. Jr., Spin-one wave equation, 19: 47359
GOOD, Robert A., Biologic relationship of endotoxin and other toxic proteins. V., 19: 45970
GOODE, G. C., High-speed controlled-potential coulometry. Application to precise determination of Pu, 19: 46188
GOODE, J. H., Hot-cell dissolution of highly irradiated PuO_2–UO_2 fast-reactor fuel specimens, 19: 46427 (ORNL-3754)
GOODMAN, A., Technetium-99m as clinical tracer material, 19: 46140
GOODMAN, Leonard S., Electronic g factors of low-lying levels of Fe I, Cr I, and Mn I, 19: 47240
GOODWIN, D. A., Analysis of ASTR radiation heating in aerospace structural materials, 19: 47077 (AD-613471)
GORBANYUK, A. G., Polarization of plasma moving in curved magnetic field, 19: 47797
GORBATYI, N. A., Behavior of adsorbed Cs films on single-crystal spikes of Ta and Ta_2C, 19: 47900
GORBENKO, E. N., Properties of an electronic-ionic oscillatory discharge, 19: 46742
GORMAN, Aubrey, Radiothyroidectomy of larval steel-head trout, 19: 45972
GORDON, G. E., Decay scheme of 25-minute ^{131g}Te, 19: 47663
GORE, J. V., Isotropic plasma guide—TE_{11} mode, 19: 47743
GORODETSKII, A. A., Biological action of neutron radiation, 19: 45822 (JPRS-31822)
GORODETSKII, A. A., Elimination of ^{134}Cs from organism under influence of derivatives of 1,5-diphenylthiocarbazone and 1,5-diphenylthiocarbohydrazide, 19: 45765 (JPRS-27544, pp 1-12)
GOSHI, Yoichi, Apparatus for measuring the Mossbauer effect, 19: 46826
GOTO, K., Application of oxygen concentration cells with solid electrolyte ZrO_2 · CaO to thermodynamical research work, 19: 46297
GOTO, Masayuki, Radiation monitors for in-pile gas loop experimental apparatus, 19: 48071
GOTODA, Masao, Properties and structure of radiation-polymerized polyethylene, 19: 46375
GOTOH, Masayuki, Design of 75-cm-radius iron-free double-focusing β spectrometer, 19: 46823
GOTT, Yu. V., Experiments on accumulation of hot ion plasma in PR-5, 19: 47857
GOTTSCHALL, Walter Carl, Solid-state radiation chemistry of glycine and alanine chelates and metal salts, 19: 46403
GOUGH, J., Use of immersible scintillation counter in urinary vitamin B_{12} excretion test, 19: 46083
GOUGH, W., Use of immersible scintillation counter in urinary vitamin B_{12} excretion test, 19: 46083
GOWAR, J., Current interruption in hydrogen and deuterium thyratrons, 19: 47128
GOWEN, John W., Effects of x irradiation of mice exposed in utero during different stages of embryological development on duration of mature life, 19: 45852
GOWOREK, Tomasz, Measurements of γ-γ angular correlation in ^{140}La, 19: 47649
GOYAL, I. C., Measurement of the neutron asymptotic decay constant in small crystalline assemblies, 19: 47554
GRACHEV, S. A., Chemical changes in β decay of I isotopes, 19: 46411
GRAEBNER, Herbert, Additive medical treatment of tumor beds. X., 19: 46123
GRAEBNER, Herbert, Therapy of lethal radiation with rutin. I., 19: 46030
GRAEV, M. I., Structure of unsymmetric toroidal magnetic fields, 19: 47144
GRAFFI, A., Production of resistance against isologous transplantations of uv-induced sarcomas of the mouse, 19: 45827
GRANDY, Walter Thomas Jr., Quantum statistics of fully ionized gases, 19: 47439
GRANT, G. R., Independent yields of ^{124}Sb and ^{126}Sb in thermal-neutron-induced fission and their implication on the empirical Z_p function, 19: 47611
GRANT, I. P., Relativistic self-consistent fields, 19: 47250
GRASSI, G., Endolymphatic radioisotope therapy and pelvic lymphography in gynecological cancerology, 19: 46100
GRASSI, G., Radiosensitivity and oxygen therapy in gynecological oncology, 19: 46097
GRAU, Gerhard, Modulation of light by means of electrically birefringent crystals, 19: 48110 (SC-T-65-750)
GRAUL, E. H., Electronic computers in nuclear medicine. I., 19: 46055
GRAY, B. S., Calibration of graphite damage flux in a replaced fuel element position in DR-3 at Risoe, 19: 48070
GRAY, L. H., Radiobiology, 19: 45999
GRAY, P. S., Water treatment on the Dragon reactor, 19: 48042
GRAY, R. J., Effect of moisture in the air on arc-cast UC and UC_2 at room temperature over extended periods, 19: 46953 (NMI-4997, pp 62-75)
GRAY, R. J., Experience with vibratory polishers and design for hot-cell application, 19: 47086 (NMI-4997, pp 184-8)
GRAY, R. J., Metallography of pyrolytic carbon-coated and uncoated uranium carbide spheres, 19: 47006 (NMI-4997, pp 198-207)
GRAY, R. J., Remote metallographic specimen grinder, 19: 46507 (NMI-4997, pp 157-62)
GRAY, Walter Steven, Inelastic proton scattering from ^{46}Ca, ^{50}Ti, and ^{54}Fe, 19: 47702
GRAYBIEL, Ashton, Biological considerations of manned flight in space, 19: 45890
GREAVES, Thomas Cyril, Charging apparatus for nuclear reactors, 19: 47942
GREC, St., Isotope diagnostics of respiratory insufficiency, 19: 46118
GRECHI, G., Histological study of intestinal mucous membrane in patients irradiated in extra-abdominal sites, 19: 45929
GREEN, Derek, Forming of materials by extrusion, 19: 46979
GREEN, Earl L., Prog. rpt. on quantitative population genetics of mice under irradiation, 7/64–6/65, 19: 45809 (NYO-1979-12)
GREEN, G. K., Pulsed synchrotron as instrument for particle research, 19: 47163 (BNL-9504)
GREEN, H. S., Spindle design, 19: 48093 (RFP-654)
GREENBERG, Richard A., Radiation injury of Clostridium botulinum spores in cured meat, 19: 46881
GREENWOOD, G. W., Effects of dislocation movement in enhancing swelling in γ-uranium during irradiation, 19: 47100
GREGORIE, Henry B. Jr., Combined radiation and surgical treatment of carcinoma of the esophagus, 19: 46051
GREGORY, A. F., Spectrometric study of attenuation in air of γ rays from mineral sources, 19: 46586 (NP-15361)
GREGORY, L. P., Polonium-210 in leaf tobacco from four countries, 19: 45801
GREIFINGER, C., Transmission of geomagnetic micropulsations through the ionosphere and lower exosphere, 19: 47466
GRIBBEN, R. J., Magnetohydrodynamic boundary layer in presence of a pressure gradient, 19: 47140
GRIEVESON, P., Knudsen effusion studies of compounds of uranium and

thorium with elements of groups IIIb and IVb, 19: 46298
GRIFFIN, D. S., Inelastic buckling of long axially compressed curved plates, 19: 46463 (WAPD-TM-469)
GRIFFIN, Roger, Power reactor containment, 19: 48037
GRIFFITH, Peter, Study of system-induced instabilities in forced-convection flows with subcooled boiling, 19: 46534 (NP-15437)
GRIGGS, C. F., Interpretation and prediction of reactor power distributions with application to fuel cycle calculations, 19: 47946 (ANL-7050, pp 231-49)
GRIN, M., Application of strain gages at high temperature. I. Cements, 19: 46715 (EUR-2473.f)
GRITTON, D. G., Radioisotope-photovoltaic energy conversion system, 19: 47284
GRMELA, M., Minimum entropy production principle and linear transport equation, 19: 47551 (UJV-1354/65)
GROH, Franz, Betatron for electron depth therapy, 19: 46126
GROMOV, K. Ya., Formation in Ho-162 in Ta + p at 660 Mev, 19: 47579 (JINR-P-2275)
GROSS, M. Grant, Radioactivity of Columbia River effluent, 19: 46680
GROVE, G. R., Prog. rpt. 4/65, 19: 46157 (MLM-1254)
GROVER, Donald P., Prototype manual of metallurgical practice, 19: 46918 (IITRI-B6018-1)
GROVER, R., Similarity solutions in hydrodynamics, 19: 47118 (UCRL-12018-T)
GROW, Richard W., Effects of γ-irradiation on characteristics of a ruby laser, 19: 46873 (N64-32322)
GRUBAUGH, R. E., Missile shock mount system, 19: 46456 (AD-425760)
GRUBAUGH, R. E., Response spectra for high air-blast loads, 19: 46566 (AD-425747)
GRUBER, A. J., Roll film camera for remote metallography, 19: 46711 (BNWL-SA-161)
GRUBER, W. J., Procedure for color microphotography, 19: 46931 (NMI-4999, pp 26-9)
GRUSHIN, V. F., Photoproduction of π^+ mesons on protons at 230 Mev, 19: 47393
GSCHEIDLEN, Wilhelm, Betatron for electron depth therapy, 19: 46126
GUARINO, A., Self-radiolysis of clathrates containing tritium-labeled molecules, 19: 46359
GUARINO, A., Self-radiolysis of tritium-labeled fatty acid esters, 19: 46360
GUERS, Karl, Modulation of light by means of electrically birefringent crystals, 19: 48110 (SC-T-65-750)
GUETTINGER, W., Quantum field theory of the bootstrap mechanism, 19: 47345
GUIASU, I., Representation of the symplectic group of rank two, 19: 47333
GUIASU, Ileana, Positive parity states of T = 3/2 in A = 15 nuclei, 19: 47694
GUPTA, K. C., Leptonic neutron decay of Ω^-, 19: 47363
GUPTA, U. C., Decay of ^{51}Cr, 19: 47619
GURALNIK, G. S., Electromagnetic interaction of mesons resulting from a broken symmetry, 19: 47346
GUREVICH, A. V., Run-away electrons in a nonequilibrium plasma, 19: 47783
GURNETT, D. A., Ion cyclotron whistlers, 19: 47445 (AD-611828)
GUSEK, W., Histology and cytomorphology of experimental beryllium granuloma, 19: 45803
GUSEV, Yu. K., Chemical changes in β decay of I isotopes, 19: 46411
GUSTAFSSON, S., Angular correlations of γ rays from polycrystalline sources, 19: 47607
GUTMAN, Francis A., Sterilization with cobalt radiation of face tissue for homotransplant, 19: 46879
GUTMANN, F., First Australian conference on electrochemistry, Sydney, 2/63, 19: 46291
GUY, Frank W., Gamma dose curves from neutron-activated soil and seawater compared with fission-product decay, 19: 46589 (UCRL-14332)
GUYOT, P., Electron microscopy of SAP following tensile deformation or quenching, 19: 46996 (EUR-2479.e)
GUZZI, G., Data handbook for sensitivity calculations in neutron activation analysis, 19: 46167 (EUR-1898.e)
GVALADZE, Yu. S., Spatially periodic plasma structures appearing in fast heavy-current discharges, 19: 47761

H

HAAS, G. M., Energetic neutral injection into an electron-cyclotron plasma, 19: 47837
HAAS, L. L., Advanced design concepts for a remotely operated manipulator system for space-support operations, 19: 46487 (CONF-640508, pp 248-303)
HAAVE, C. R., Frequency monitoring and nuclear burst detection: some aspects of vlf, 19: 46609

HABERMEHL, A., Electronic computers in nuclear medicine. I., 19: 46055
HACKNEY, Stanley, Nuclear reactor with pressurizer, 19: 47940
HADDON, William Jr., Frequency of medical x-ray examinations, 19: 46112
HADJIOANNOU, F., Spectral representation and mass formula for spin-½ particles, 19: 47340
HADLEY, W. C., Research program to investigate artificially injected trapped radiation, 19: 47444 (AD-611629)
HAEN, P., Electrical resistivity of Th, 19: 47042
HAENDEL, S. K., Stabilized flash x-ray discharges, 19: 46735
HAGGERTY, M. J., Application of plasma kinetic theory to ionic sound-wave experiments in magnetic fields, 19: 47732
HAHAN, Yukap, Higher partial waves in positron-hydrogen scattering, 19: 47238
HAHS, Charles A., Contaminated filter removal equipment, 19: 46644 (ORNL-P-1528)
HAID, David A., Superconducting magnet facility for plasma physics research, 19: 47533
HALBACH, Klaus, Determining geometry and current configuration of cylindrically symmetric solenoid coils from a specified magnetic field shape, 19: 47121 (UCRL-16080)
HALBWACHS, F., Is there a classical analog of Dirac's theory?, 19: 47137
HALDEMAN, Charles W., Electromagnetic means of adding heat and kinetic energy to a gas, 19: 46477 (ARL-65-121)
HALE, John, Effect of collimation: field size, cone leaks, and scatter dose outside the useful beam, 19: 46145
HALE, John F., Laboratory investigations of shelter management factors, 19: 46637 (AD-612254)
HALE, R. J., Evolution of high level caves at Savannah River Laboratory, 19: 46506 (CONF-651101-26)
HALL, D., Crystal structure of bisnitratodisquodioxouranium(VI) tetrahydrate (uranyl nitrate hexahydrate), 19: 46255
HALL, J. D., Total absorption γ spectrometer system for pulsed beam n,nγ measurements, 19: 46765 (TID-22012, pp 4-21)
HALLS, J. M., Radiation damage of the small intestine, 19: 46065
HALPERN, A., Hot atom chemistry of halogens activated in β decay. III., 19: 46412
HALSEY, G. H., Use of digital programs in reactor plant designs, 19: 47909 (ANL-7050, pp 217-30)
HAMBERGER, S. M., Collisionless non-linear coupling of electromagnetic waves near electron gyrofrequency by plasma electrons, 19: 47744
HAMILTON, E. I., Isotopic composition of Sr in variety of rocks from Reunion Island, 19: 46584
HAMILTON, Howard B., Study of adolescents exposed in utero to the atomic bomb, Nagasaki, Japan. II., 19: 45889
HAMING, B. H., Prog. rpt. on fissiochemical development, semiannual, 7–12/64, 19: 46324 (AGN-8132)
HAMMEL, J. E., Recent developments in transverse injection experiment, 19: 47847
HAMMER, Preston C., Comments on computing, 19: 46902 (ANL-7050, pp 207-13)
HAMMERLE, Olivia O., Uv-dosage measurement in geometrically complex system with light-sensitive paper, 19: 45963
HAMMITT, Frederick G., Two-phase materials attrition problems for Rankine cycle liquid metal power plants, 19: 46955 (NP-15431)
HAMMOND, S. E., Plutonium bioassay results following DTPA treatments, 19: 45762 (RFP-577)
HANAWALT, Philip, Evidence for repair-replication of uv-damaged DNA in bacteria, 19: 45909
HANCOX, R., Superconductivity of sintered Nb_3Se at temperatures above 4.2°K, 19: 47508
HANDLEY, Thomas H. Organic compounds containing P = S and P(S)SH groups as separatory and analytical reagents, 19: 46217
HANKS, Gerald E., Radiosensitivity of autochthonous radiation-induced lymphosarcomas in C57BL mice, 19: 45977
HANSEN, C. J., Helium content of the galaxy, 19: 47193
HANSEN, H. J. Sigurd, Isomers in odd-mass La isotopes ascribed to ½⁻ Nilsson configuration, 19: 47640
HANSEN, S. M., Iodine metabolism of lactating dairy cows, 19: 45781
HANSEN, Spencer M., Mining by caving with nuclear explosions, 19: 46472 (UCRL-14201)
HANSEN, Warren G., Iodine-131 in children's thyroids from environmental exposure, 19: 46035 (PHS-999-RH-14)
HARDCASTLE, R. A., Inter-diffusion of plasma and magnetic fields in pinch and hardcore discharges, 19: 47853
HARDY, J. C., New information on the emission of delayed protons following decay of ^{17}Ne, ^{21}Mg, and ^{25}Si, 19: 47613
HARIMA, Tetsuo, Collision-resisting construction of sides of a nuclear powered ship, 19: 46464 (NSJ-tr-30)
HARLING, O. K., Multiphonon neutron scattering study of hydrogen bonding in zirconium hydride, 19: 46232 (BNWL-SA-239)
HARMAN, J. B., Management of polycythaemia vera, 19: 46089

HARMSEN, D. M., Emission of light charged particles from highly excited complex nuclei in nuclear emulsion, 19: 47651

HARNDEN, D. G., Cytogenetic studies in chronic myeloid leukemia and acute leukemia associated with mongolism, 19: 45915

HARPER, P. V., Technetium-99m as clinical tracer material, 19: 46140

HARRAR, Jackson E., Process stream analysis systems for scrubber solutions used in Project Dribble vent gas treatment plant, 19: 46471 (UCRL-14123)

HARRIS, Bryan, Structural changes during creep of solution-hardened Nb alloy, 19: 47049

HARRIS, E. G., Collisional and anomalous diffusion, 19: 47838

HARRIS, I. R., Rare-earth intermediate phases. II., 19: 47051

HARRIS, I. R., Rare earth intermediate phases. III., 19: 47052

HARRISON, D. E. Jr., Computer studies of copper atom ranges in copper lattices, 19: 47228

HARRISON, Lee, Feasibility of utilizing electrical potentials on the surface of skin for control functions, 19: 46459 (CONF-640508, pp 100-57)

HARROP, P. J., Effect of γ dose on oxide films on Zr and Zircaloy-2, 19: 47099

HARSANYI, Gy., Semiautomatically operated radiofrequency mass spectrometer, 19: 46772

HARTLEY, C. S., Interdiffusion in niobium–vanadium alloys, 19: 47058

HARTZ, T. R., Particle emissions from disturbed sun, and the sun-earth environment, 19: 47495

HARTZ, T. R., Physics of earth's upper atmosphere, 19: 47488

HARVEY, R. A., Analog computer methods for parameter optimization, 19: 46903 (BNWL-70)

HASEGAWA, Masayoshi, Influence of uranium addition on iron and steel. II., 19: 47047

HASENFRATZ, Julius, Iodine-131 uptake studies under hot climatic conditions, 19: 45779

HASENKAMP, A., Final hazards summary for Sandia Engineering Reactor Facility (SERF), 19: 48062 (SC-4522(RR))

HASKILL, J. S., Radiation damage to crystalline ribonuclease, 19: 46347

HATEGANU, C., Polarization of elastically and inelastically scattered protons on ^{26}Mg at 5.8 Mev, 19: 47697

HATT, B. A., High-speed thermal analysis of Zr–Nb alloys, 19: 47037

HATTORI, Fumio, Retained ThO_2 media in seminal vesiculography. Follow-up study with dose estimates, 19: 45837

HAUBOLD, Helmut, Betatron for electron depth therapy, 19: 46126

HAUGHT, A. F., Plasmas for thermonuclear research produced by laser beam irradiation of single solid particles, 19: 47846

HAWKE, Basil Cromey, Control rod drive for nuclear reactors, 19: 47934

HAWKINS, D. B., Environmental tritium studies at the National Reactor Testing Station, 19: 46642 (IDO-12043)

HAWKINS, Myron B., Estimation of internal radiation exposure resulting from ingestion of fallout-contaminated water in a nuclear war, 19: 46633 (AD-276187)

HAWKINS, R. H., Bentonite as protective cover for buried radioactive waste, 19: 48076 (DPSPU-62-30-3A)

HAYAKAWA, Jun-ichiro, Splenic and thymic weight response to whole-body x irradiation in three strains of mice, 19: 45956

HAYAKAWA, Kiyoshi, Gamma-ray initiated polymerization of vinyl n-butyrate, 19: 46389

HAYASHI, Kenso, Radiation-induced cyclopolymerization of acrylic anhydride, 19: 46352

HAYASHI, Teizo, Rapid determination of L-leucine, L-isoleucine, and L-valine in a mixture by infrared spectrometry, 19: 46184 (ORNL-tr-841)

HAYE, Christian, Ocular effects of an atomic explosion, 19: 45843

HAYES, J. W., First Australian conference on electrochemistry, Sydney, 2/63, 19: 46291

HAYNES, R. C., Terrestrial and solar neutrons, 19: 47279

HAYWARD, Lynn C., Scintillation methods for metallic ion determination in human subjects using computer techniques, 19: 45771

HAZAN, I., Anion exchange separation of uranium and its application to determination of uranium in sea water, marine sediments, and other geological samples, 19: 46223

HEAF, P. J. D., Effect of chronic bronchitis on changes in pulmonary function caused by irradiation of the lungs, 19: 46131

HEALY, W. B., Determination of Mo in hair and wool by neutron activation analysis, 19: 46192

HEARN, A. C., Photoproduction of π^0 from H near the second π–N, 19: 47368

HEARN, Thomas O., NRDS analysis of the Kiwi B-4D-202 nuclear reactor control system, 19: 48049 (LA-3301)

HEATH, D. A., Radiological scanning of cast iron biological shieldings, 19: 47039

HEBBORN, P., Dental lesions in rat induced by radiomimetic agents, 19: 45845

HECHT, A., Morphological and histoenzymochemical studies of aorta of rabbits after localized exposure to ^{90}Sr–^{90}Y β radiations, 19: 45875

HECKER, O., Absorbed dose rate determination in vinylchloride. II., 19: 46368

HECKNER, K. H., Inverse deuterium isotope effect in decomposition of permanganate in alkali solution, 19: 46275

HEEDMAN, Per-Axel, Thyroid iodine determined by x-ray spectrophotometry, 19: 46081

HEGERFELDT, G. C., One-particle singularities and SU(3), 19: 47321

HEGEWALD, H., Morphological and histoenzymochemical studies of aorta of rabbits after localized exposure to ^{90}Sr–^{90}Y β radiations, 19: 45875

HEIKKILA, W. J., Outer ionospheric regions, 19: 47491

HEILIGMAN, Fred, Storage stability of irradiated meats, 19: 46886

HEIM, Werner G., Appearance of rat slow alpha-two globulin after irradiation, 19: 45953

HEINLOTH, K., Electroproduction of π-mesons and photoproduction of dipions, 19: 47303 (DESY-65/7)

HEINRICH, H. C., Essential specifications of Hamburg 4π large-volume radioactivity detector with liquid organic scintillator. I., 19: 46775

HEINRICH, H.-J., Fast electron dosimetry on a 2-Mev Van de Graaff accelerator, 19: 47177

HEINZLER, Franz, Isodoses for pendulum irradiation for ultrahard x radiation. I., 19: 46127

HELMAN, Percy, Intra-arterial cytotoxic therapy and x-ray therapy for cancer of head and neck, 19: 46088

HEMPEL, Klaus, Synthesis of tritium-labeled acids through chain elongation after Arndt-Eistert, 19: 46306

HENDERSON, Croswell R., Prog. rpt. on behavior of radionuclides released into fresh-water environments, annual, 1959–60, 19: 46646 (PHS-999-RH-13)

HENDRIE, J. M., HFBR modifications and tests preparatory to operating authorization, 19: 48054 (BNL-9308)

HENNINGSEN, E. Juel, Public health aspects of radiation emergencies: nature of the problem, 19: 46691

HENNY, George C., Dose aspects of cinefluorography, 19: 46152

HENOCH, William, Remote operations in SNAP-8 facility at AI, 19: 46504 (CONF-641120, pp 86-97)

HENRI, V. P., Reaction $K^+p \rightarrow K^0p\pi^+$ at 3 Bev, 19: 47356

HENRICSON, B., Effect of radiostrontium on oocytes and follicles of adult mice, 19: 45831

HENRIKSEN, Thormod, Free radical induced in enzymes by electrons and heavy ions, 19: 46339 (UCRL-16358)

HENRIKSSON, S., Status report on Lund vidicon system, 19: 46788

HENSCHKE, Ullrich K., Remote afterloading for intracavitary radiation therapy, 19: 46111

HENSCHKE, Ulrich K., Treating melanoma of pectoral region, 19: 46047

HENSHALL, J. B., Remote operations at Los Alamos Test Cell C, 19: 46494 (CONF-641120, pp 6-8)

HENTZ, Robert R., Radiolysis and luminescence behavior of dioxane–benzene mixtures, 19: 46363

HERBERT, M., Synthesis of DL-shikimic 1-2-^{14}C acid starting from methyl acrylate 2-3-^{14}C, 19: 46312

HERBERT, M., Use of vinyl magnesium bromide for synthesis of molecules labeled with ^{14}C, 19: 46310

HERCIK, Ferdinand, Effect of uv light on stomatal movement, 19: 45854

HERDON, R. C., Binding energies of polyatomic ^{4}He-molecules, 19: 47244

HERICH, Rudolf, Action of x rays on nucleolar structures, 19: 45940

HERMAN, Harvey Bruce, Electrochemistry of europium, 19: 46295

HERMAN, M., Prog. rpt. on preparation and evaluation of Be, 10/15/63–1/14/64, 19: 46909 (AD-620264)

HERMAN, M., Prog. rpt. on flow and fracture of alloyed Be, 10/7/64–1/6/65, 19: 46910 (AD-620589)

HERRINGTON, J., High-speed controlled-potential coulometry. Application to precise determination of Pu, 19: 46188

HERRMANN, D., Determination of minimum filter size for the filter analysis process of film dosimetry, 19: 46764 (SZS-6(1965))

HERSZBERG, B., Development of source of x rays usable in medical radiography, 19: 46141

HERTZBERG, O., Sensitization and radiation response in cases with carcinoma of the uterine cervix, 19: 45830

HERZ, A. J., Application of television pickup to bubble-chamber measurements, 19: 46798

HERZBERG, L., Solar activity and short-lived terrestrial effects, 19: 47494

HERZBERGER, Eugene E., Late radiation necrosis of the brain, 19: 45995

HESTER, D. L., Effects of radiation-induced damage centers in lead zirconate titanate ceramics, 19: 47096

HESTER, J. C., Thermodynamic properties of high-temperature helium, 19: 46235 (N64-26802)

HEUSCH, Clemens A., Electron and photon energy measurement up to 4 Bev, 19: 46805

HEWETTE II, D. M., Mounting of metallographic samples in epoxy resins

using multiple cavity molds, 19: 46927 (NMI-4998, pp 1-5)
HEYLEN, A. E. D., Influence of crossed magnetic field on gaseous Townsend discharge, 19: 47127
HEYSSEL, Robert M., Scintillation methods for metallic ion determination in human subjects using computer techniques, 19: 45771
HICKMOTT, T. W., Problem of measuring hydrogen pressure in ultrahigh-vacuum systems, 19: 46578
HICKOK, R. L., Determination of deuterium density profile in a deuterium plasma using an energetic D^+ beam, 19: 47727 (NP-15434)
HICKS, Samuel P., Effects of fetal irradiation on behavior in the albino rat, 19: 45894
HICTER, Pierre, Some aspects of the solid-liquid transition, 19: 46233 (CEA-R-2752)
HIGGINS, C. E., Isomerization in residual alkyls from pyrolytic and ester interchange reactions of tributyl phosphate, 19: 46317
HIGINBOTHAM, W. A., Use of on-line computers in high-energy counter experiments, 19: 46756 (BNL-9492)
HIGINBOTHAM, W. A., Wire spark chambers, 19: 46804
HIIDA, Kichiro, CP violation and PT invariance, 19: 47331
HILARIS, Basil S., Remote afterloading for intracavitary radiation therapy, 19: 46111
HILDRETH, Philip E., Fertilization in Drosophila. II., 19: 45968
HILGEVOORD, J., Covariant definition of spin in relativistic quantum field theory, 19: 47426
HILL, J. H., Nature of radiation from nuclear weapons in relation to flash-blindness, 19: 46655
HILL, J. W., Containment of plasma trapped in a magnetic well, 19: 47848
HILL, Roger E., Polarization in $\pi^- + p$ elastic scattering at 2.08 Bev/c, 19: 47373
HILTON, D. A., The determination of activation products in irradiated steels by anion-exchange separation and γ spectrometry, 19: 46195
HINES, C. O., Physics of earth's upper atmosphere, 19: 47488
HINES, C. O., Theory of geomagnetic and auroral storms, 19: 47500
HINNOV, E., Power balance and particle loss rate in C Stellarator, 19: 47854
HINTEREGGER, H. E., Absolute intensity measurements in extreme ultraviolet spectrum of solar radiation, 19: 47210
HINTON, James Faulk Jr., Isotopic exchange and replacement reactions of the haloacetic acids, 19: 46293
HIRAMOTO, Toshiyuki, Versatile time-of-flight neutron spectrometer, 19: 46829
HIRO, Sunjo, 30-Mev flux-forced field biased betatron. II., 19: 47178
HIROIKE, Kazuo, Properties of an excess electron in liquid He. II., 19: 47132
HIROIKE, Kazuo, Quantum-mechanical Fokker-Planck equation, 19: 47415
HIROSE, Yasuo, Vibratory compaction of fused UO_2, 19: 46970
HISATAKE, Kazuo, Design of 75-cm-radius iron-free double-focusing β spectrometer, 19: 46823
HLAVATY, Vlatislav, Magnetron—a source of x radiation, 19: 46673
HO, James C., Effective hyperfine fields at the nuclei of Os and Pt dissolved in Fe, 19: 47069
HOCKENBURY, R., High-energy neutron cross sections, 19: 47550 (TID-22141, pp 81-93)
HODGSON, G., Effect of γ irradiation on response of fasted rats to erythropoietin, 19: 45971
HODKIN, D. J., Diffusion of plutonium in magnesium and magnesium alloys, 19: 47066
HOEFER, R., Radioactive isotopes in medicine and research. VI., 19: 46135
HOEFERT, M., Radiation-induced chemiluminescence, 19: 46344
HOEKSTRA, E. K., Atomic energy market in Europe. VIII. The Netherlands, 19: 47923
HOEKSTRA, H. R., Preparation and properties of $TiUO_3$, 19: 46272
HOELZL, J., Reflection of very slow electrons on metal surfaces, 19: 47242
HOFFBRAND, B. I., Effect of chronic bronchitis on changes in pulmonary function caused by irradiation of the lungs, 19: 46131
HOFFMAN, David K., Quantum-mechanical Boltzmann equation, 19: 47416
HOFFMANN, W., Determination of β emitters with help of Cherenkov radiation, 19: 46215
HOFSTADTER, R., Electron scattering on nucleons, three-body nuclei, and ^{40}Ca, 19: 47565 (AD-614270)
HOGAN, J. F., Reaction rate of Nb–1Zr alloy with oxygen at low pressures, 19: 47016 (TIM-901)
HOGAN, W. J., Internal liquid hydrogen target for a proton synchrotron, 19: 47173
HOGE, K. G., Effect of strain rate on the mechanical properties of general purpose polypropylene, 19: 47017 (UCRL-14316)
HOHENBERG, P. C., Microscopic theory of superfluid helium, 19: 47506
HOHENSTEIN, Jack, A precision technique for measuring azimuthal distortion in optical lenses, 19: 48103 (UCRL-16260)

HOLBROOK, Margaret A., Combined 5-fluorouracil and supervoltage radiation therapy in the palliative management of advanced G-I cancer, 19: 46091
HOLBROOK, P. H. G., Planning for an accident in a nuclear power station, 19: 46703
HOLCOMB, D. F., Research on soft x-ray absorption, 19: 47216 (AD-613575)
HOLCOMB, D. L., Remote metallographic specimen grinder, 19: 46507 (NMI-4997, pp 157-62)
HOLL, R. J., Cavity nuclear reactors, 19: 48046 (AD-613998)
HOLLIES, R. E., Effect of p-terphenyl on melting points of terphenyl–biphenyl organic coolants, 19: 46300
HOLM, Dale M., Measurement of microscopic distribution of oxygen and carbon in metals by ^3He activation, 19: 46174 (LA-DC-7319)
HOLMBERG, S., Rotating plasma experiments, 19: 47850
HOLMES, H. F., Electrokinetic phenomena at thorium oxide–aqueous solution interface, 19: 46281
HOLMES, Joseph H., Problems in renal homotransplantation, 19: 45888
HOLSINGER, Ronald F., Determining geometry and current configuration of cylindrically symmetric solenoid coils from a specified magnetic field shape, 19: 47121 (UCRL-16080)
HOLSTI, Lars R., Combined split-course therapy with 5-fluorouracil and megavoltage irradiation, 19: 46050
HOLTZ, R. E., Liquid-metal heat-transfer experiment, 19: 46528 (ANL-7038)
HOLZER, Franz, Programming and manual control of versatile manipulating devices, 19: 46488 (CONF-640508, pp 304-26)
HONCARIV, R., Changes in color of potato tubers after irradiation, 19: 45853
HONECK, H. C., Processing of nuclear data for reactor calculations, 19: 47948 (ANL-7050, pp 517-39)
HOOD, R. R., Prog. rpt. on D_2O-moderated power reactors, 3–6/65, 19: 46917 (DP-975)
HOOGSTRAATEN, J., Chronic toxicity of polyphenyl mixtures, 19: 45769
HOOPER, E. B. Jr., Laser interferometer for repetitively pulsed plasmas, 19: 47730
HOOT, Charles Glen, Reactions (p,d) and (p,t) on nickel and iron at 28 Mev, 19: 47706
HOOVER, D. B., Prog. rpt. on preparation and evaluation of Be, 10/15/63–1/14/64, 19: 46909 (AD-620264)
HOPE, Christopher Cameron, Nuclear fuel materials including vitreous phase, 19: 47986
HOPKINS, B. J., Work function measurements on the sublimate from uranium carbide, 19: 47038
HOPKINS, E. N., Thirty-five millimeter color photomicrography, 19: 46930 (NMI-4998, pp 14-19)
HOPP, David I., General orbit code for cyclotron analysis, 19: 47168 (TID-22177)
HOPPE, Gunther, Development of radioactive halos in biotite, 19: 46591 (ORNL-tr-642)
HORD, Charles William, Modified Fermi heating in outer Van Allen belt, 19: 47487
HORI, Yasuharu, Changes in lactic dehydrogenase activity in plasma of mice after whole-body x irradiation, 19: 45844
HORIKOSHI, Gen'ichi, Design of vacuum system of Tokyo electron synchrotron, 19: 47175
HORN, K.-H., Production of resistance against isologous transplantations of uv-induced sarcomas of the mouse, 19: 45827
HORNBOGEN, Erhard, Start of precipitation from supersaturated solid solutions, 19: 47025 (ORNL-tr-637)
HORNER, D. E., Unexpected rate effects in extraction of rare earths by di(2-ethylhexyl)phosphoric acid, 19: 46432 (ORNL-P-1603)
HORTON, P. A., Minimized fuel cycle cost for simulated boiling water reactor. I., 19: 47990 (BNWL-105)
HORVATH, Eva, Aqueous dissolution of U contents of rocks. I., 19: 46626
HORWOOD, J. L., Spectrometric study of attenuation in air of γ rays from mineral sources, 19: 46586 (NP-15361)
HOSLER, Charles R., Simultaneous measurements of ^{222}Rn, ^{214}Pb, and ^{214}Bi in air near the ground, 19: 46605
HOSTE, J., Nondestructive neutron activation determination of Ag and Sb in bismuth by $\gamma\gamma$ coincidence spectrometry, 19: 46193
HOUBEN, J., Role of water content on production and decay of free radicals in irradiated peas, 19: 45863
HOUCK, C. W., Metallic binders for zirconium diboride: chromium, molybdenum, and tungsten, 19: 46907 (AD-456724)
HOULDER, A. E., Use of ^{131}I-labeled PVP in brain scanning, 19: 46051
HOUTAPPEL, R. M. F., Electron-kinetics in irradiated dipolar systems. (T), 19: 47433
HOWARD, Alma, Evidence for radio-ruthenium in milk, 19: 46675
HOWARD, Robert, Solar magnetic fields, 19: 47208

HOWARD-FLANDERS, P., Excision of thymine dimers from DNA, filament formation, and sensitivity to ultraviolet light in E. coli, 19: 45948
HOWELL, Barbara Fern Fonnema, Isotope exchange between zinc iodide and various alkyl iodides in acetonitrile, 19: 46294
HOWELLS, H., Organization of the emergency environmental survey, 19: 46697
HOXIE, E. C., Measurement of the thickness of aluminum oxide film, 19: 46952 (NMI-4997, pp 26-35)
HOYAUX, G., Nondestructive underwater testing in the BR2 reactor, 19: 48002 (ORNL-tr-747)
HOYER, Wilmer A., Radioactive well logging system with surface circuit designed to isolate a-c power signals from logging signals, 19: 46623
HRUBEC, Zdenek, Study of adolescents exposed in utero to the atomic bomb, Nagasaki, Japan. II., 19: 45889
HSIAO, Kuo-yen, Light and spectroscopic properties of inorganic vitreous rare earth oxides, 19: 47886 (N64-21857, pp 1-6)
HSU, T. W., Negative absorption from weakly relativistic electrons traversing Cuccia coupler, 19: 47130
HSU, Yi-Chuana, Low-background counter for ^{14}C dating, 19: 46777
HSU, Yuh-Chi, Low-background counter for ^{14}C dating, 19: 46777
HSUEH, Shan-i, Strontium-90 as simple, rapid, and inexpensive treatment for aviation tympanitis, 19: 46038 (JPRS-31602, pp 191-7)
HU, Ning, Anomalous magnetic moment of elementary particles due to electromagnetic mass difference, 19: 47316 (JPRS-31032, pp 15-18)
HUANG, Chio-Yi, Low-background counter for ^{14}C dating, 19: 46777
HUBBARD, J., Covalency effects in neutron diffraction from ferromagnetic and antiferromagnetic salts, 19: 47895
HUBBELL, William H., Livermore slug fabrication facility, 19: 46509 (UCRL-12497-T)
HUDGENS, J. E., Automation of mass spectrometers for isotopic analysis of reactor materials, 19: 46181 (WAPD-T-1769)
HUDSON, E. D., Extraction magnets for cyclotrons, 19: 47166 (ORNL-P-1605)
HUDSON, E. D., Sector magnets for a separated orbit cyclotron, 19: 47167 (ORNL-P-1619)
HUDSON, H. S., Determinations of auroral-zone x-ray spectrum, 19: 47471
HUDSON, H. S., Spatial asymmetry and periodic time variations of x-ray microbursts in auroral zone, 19: 47470
HUEBNER, Gerhard, On the results of growth-material in heavy water, 19: 45763 (AD-468388)
HUET, P., Atomic energy market in Europe. V. France, 19: 48006
HUGGETT, J. P., Automatic isodose contour recorder, 19: 46776
HUGON, J., Tissue and cellular distribution of tritium-labeled AET in mice, 19: 46016
HUIZENGA, W., Injection experiments in Jutphaas, 19: 47858
HULL, A. P., 1963 environmental radiation levels at BNL, 19: 46640 (BNL-915)
HULM, J. K., Propagation of persistent current decay in Nb–Zr wires, 19: 47507
HULSE, E. V., Biological hazards of radiation applicable to man in space, 19: 46001
HULSTON, J. R., Cosmic-ray-produced ^{36}S and ^{33}S in metallic phase of iron meteorites, 19: 47195
HULTBERG, Sven, Two special applications of high-energy electron beams, 19: 46042
HULUBEI, H., ^{9}Be, ^{11}B and $^{31}P(p,p')$ angular distributions, 19: 47690
HUNDHAUSEN, Arthur Jones, Position of solar wind shock boundary, 19: 47211
HUNGER, K., Adiabatic linear Stark effect in a plasma, 19: 47716 (AD-614283)
HUNT, J. W., Radiation damage to crystalline ribonuclease, 19: 46347
HUNT, James C., Radioisotope renography in children. I., 19: 46109
HUNTER, Jerry, Radiation sensitivity of bacteriophage-E. coli complexes, 19: 46034
HUNTOON, R. T., Network structures in uranium and its alloys, 19: 47060
HUNYADI, Ilona, Measurements and experiences in connection with scintillation fast neutron detector, 19: 46774
HURLEY, P. M., Isotopic composition of strontium in oceanic and continental basalts: application to origin of igneous rocks, 19: 46607
HURST, R. P., Valence electron approximation: application to LiH, 19: 46284
HUSEBY, R. A., Excretion of radioactivity by human subjects after ingestion of liver from cattle treated with labeled polydiethylstilbestrol phosphate, 19: 45797
HUTCHINSON, D. P., Distribution of single electron pulse sizes from multidynode electron multipliers, 19: 46720 (NYO-3406-2)
HUTCHINSON, G. W., Filmless automatic processing of spark chamber tracks using standard equipment, 19: 46789
HUTCHINSON, P., Computation of scattering cross sections for use in thermal-neutron transport calculations, 19: 47543 (ANL-7050, pp 471-85)
HWANG, Jeun-Lin, Influence of pairing interaction on nuclear energy level density, 19: 47616

I

IANNUZZI, M., Two-photon absorption in atomic or molecular systems, 19: 47236
ICHIHA, Sumio, Separation and purification of gaseous fission products, 19: 46414
ICHIKAWA, Riei, Distribution of Be in solid Mg alloys containing Be at high temperatures, 19: 47071
ICONOMOU, N., Influence of radioactive rays on pharmaceuticals. II., 19: 46889
IDE, Akira, Biological shield cooling, 19: 48029
IGNAT'EV, V. V., Containment of a high-temperature plasma, 19: 47841
IGNAT'EVA, T. A., Effect of impurities on pressure effect in thallium. II., 19: 47529
IHARA, Chiaki, Mass formula for resonance states, 19: 47384
IIZUKA, Harohiko, Collision-resisting construction of sides of a nuclear powered ship, 19: 46464 (NSJ-tr-30)
IKEDA, Kiyomi, Calculating nuclear matrix elements, 19: 47622
IKEGAMI, H., Development of uv radiation resistance by poliovirus infective centers, 19: 46032
IKENUMA, Tokuji, High-resolution, pulse-height analyzer, 19: 46827
IKEZAKI, Kazuo, Radiation from current filament in anisotropic plasma, 19: 47774
ILIESCU, E., Polarization of elastically scattered protons on ^{16}O at 4.5-Mev energy, 19: 47691
ILIESCU, E., Polarization of elastically scattered protons on Al and Mg at 4.5 Mev, 19: 47692
ILIESCU, E., Polarization of elastically scattered protons on ^{12}C at 6 Mev, 19: 47695
ILIESCU, E., Polarization of elastically and inelastically scattered protons on ^{24}Mg at 5. 8 Mev, 19: 47697
ILSCHNER, B., Lattice constants of Fe–Mo alloys, 19: 47029
ILYINA, G. V., Absorption of radioactive fission products by cultivated crops. II., 19: 45804
IMAEDA, K., Determination of primary energy of jets, 19: 47275
IMHOF, William L., Analysis and evaluation of measurements of geomagnetically trapped electrons from high-altitude nuclear explosions, 19: 47446 (AD-612013)
INADA, Tetsuo, Versatile time-of-flight neutron spectrometer, 19: 46829
INCH, W. R., Effect of breathing 5% CO_2 and 95% O on tumor radiocurability, 19: 46003
INDREAS, G., Production of H^- ions from arc ion source on a stand, 19: 47142
INOUE, Eiichi, Diffusion phenomena in atmospheric surface layer. II., 19: 47111 (UCRL-Trans-1229(L))
INOUE, Kenji, Spectroscopic measurements of impurities in plasma stream. I. 19: 47757
INUISHI, Yoshio, Anomalous diffusion and oscillations of positive column in magnetic field, 19: 47756
IOANOVICIU, D., Forming of H_2^+ ions sources by electronic bombardment, 19: 47141
IOFFE, M. S., Experiments on accumulation of hot ion plasma in PR-5, 19: 47857
IOFFE, M. S., Mirror traps, 19: 47821
IOFFE, V. A., EPR spectra of Gd^{3+} ion in single crystals of CeO_2, 19: 47898
ION, D. B., Photoproduction of two mesons on nucleons at high energy, 19: 47389
IRIE, Ryozaburo, Temporary increase in uv resistance in course of spore germination of Bacillus subtilis, 19: 45848
ISAEV, A. N., Effect of temperature on space-energy distribution of neutron flux, 19: 47956 (IAE-723)
ISAEV, A. N., Optimum methods for handling transient processes in reactors, 19: 47957 (IAE-724)
ISEBECK, K., Low-temperature recovery spectra of neutron-irradiated metals, 19: 47097
ISHIDA, Osamu, Radiation-induced cancer of the skin, 19: 45945
ISHIGURO, Masakazu, X-ray coloration of KCl crystals, 19: 46371
ISHII, Takemi, BF_3 proportional counters, 19: 46822
ISHIZUKA, Takeo, Energy spectra of photoprotons from ^{12}C, ^{24}Mg, ^{28}Si, ^{32}S and ^{40}Ca, 19: 47699
ISKENDERIAN, H. P., Physics performance of the EBWR in its operation from 0 to 100 mwt, 19: 47988 (ANL-6776)
ISKOLDSKII, A. M., Capture of plasmoids in a magnetic mirror machine, 19: 47839
ITO, Fumio, Effect of synthetic detergent on water treatment of radioactive wastes by coagulation precipitation process, 19: 48084
ITO, Kazuo, Measurement of γ backscattering on concrete walls, 19: 47869

(ORNL-tr-710)
ITOH, Chiaki, SU(6) and RP invariance in nonleptonic baryon decays, 19: 47385
ITOH, Satoshi, Hydromagnetic wave in toroidal discharge with longitudinal magnetic field, 19: 47742
ITOMI, Kunio, Nature of the muon, 19: 47378
IUCCI, H., Intercalibration of cosmic-ray neutron monitors, 19: 47272
IVANOV, E., Yield ratio for fissioning isomer from deuteron irradiation of Pu, 19: 47688
IVANOVSKII, G. F., Adsorption of argon ions by titanium films, 19: 47072
IVASCU, M., ^{7}Be, ^{12}B and ^{32}P(p,p') angular distributions, 19: 47690
IZAWA, Masami, Review of ICRP recommendations (1962), 19: 46676
IZRAILEV, F. M., Statistical properties of nonlinear string, 19: 48108 (ORNL-tr-754)

J

JACKLYN, R. M., Apparent sidereal daily variation of cosmic-ray intensity at ~40 Mwe at Hobart, Tasmania, 19: 47274
JACOBS, Patricia A., Cytogenetic studies in chronic myeloid leukemia and acute leukemia associated with mongolism, 19: 45915
JACOBSON, Bertil, Thyroid iodine determined by x-ray spectrophotometry, 19: 46681
JACOBUS, David P., Hazard of ^{90}Sr—a review, 19: 46634 (AD-423463)
JADASSOHN, W., Different behavior of epidermis of flank and nipple of the guinea pig after a 1600-R dose of x rays, 19: 45869
JAEGER, Ralph, Prog. rpt. on high-temperature solid-state chemistry and sub-solidus phase equilibria, final, 8/65, 19: 46240 (TID-22207)
JAEGER, Ralph R., Studies of reactions between divalent and trivalent oxides, 19: 46242 (TID-22207, Paper B)
JAFFE, A., Nonpositivity of the energy density in quantized field theories, 19: 47419
JAFFEE, Robert I., High-temperature Nb-base alloys, 19: 46976
JAFRI, R. H., Influence of pathogens on life span of irradiated insects, 19: 45908
JAHNKE, Volker, Occurrence of metachromatic substance after treatment of uranyl acetate, 19: 45766
JAIN, P. L., Coherent production of pion tridents by a primary beam of 16.2 Bev/c π^- in nuclear emulsion, 19: 47355
JAIN, P. L., Mechanism of hyperfragment formation in K$^-$ capture, 19: 47648
JAMEEL, M., High-energy behavior of total cross sections, 19: 47353
JAMES, Allen P., The quantitative assessment of hereditary damage induced by radiation, 19: 45973
JAMES, D. B., Processing of plutonium by ion exchange. VII., 19: 46173 (LA-3357)
JAMES, P. E., Reclamation of agricultural land following accidental radioactive contamination, 19: 46701
JAMET, Jean-Michel, Flux and temperature distribution in nuclear thermionic converters Sirene 50 and Sirene 100, 19: 47978 (CEA-R-2782)
JAMMET, Henri, Ocular effects of an atomic explosion, 19: 45843
JANKOWICZ, R., Internal liquid hydrogen target for a proton synchrotron, 19: 47173
JANOWER, Murray L., Symposium on reduction of patient dosage from radiology, Washington, D. C., 3/62, 19: 46037
JANSA, Jindrich, Plant for disposal of radioactive waste water, 19: 48086
JANSEN, G. Jr., Status of salt cycle process for processing oxide fuels, 19: 46422 (BNWL-SA-205)
JARLSKOG, G., Status report on Lund vidicon system, 19: 46788
JARVIS, T. R., Experimental observations of pulse shortening in a linear-accelerator waveguide, 19: 47182
JAUNCEY, D. L., Strongly interacting particles in air shower cores, 19: 47271
JAWOROWSKI, Zbigniew, Content of radium D in human bones and hair, 19: 45795
JEFFERSON, Sidney, Conveyor systems, 19: 46523
JELLIFFE, A. M., Present place of radiotherapy in cure of Hodgkin's disease, 19: 46067
JENKINS, David Albert, Muon capture in oxygen, 19: 47707
JENKINSON, W. G., Accounting systems for heavy water and fissionable materials, 19: 47906 (AECL-2282)
JENKS, G. H., Effects of reactor operation on HFIR coolant, 19: 48061 (ORNL-3848)
JENNINGS, R. E., Direct measurement of small energy losses of relativistic particles, 19: 47252
JENSEN, A. O., Absorption of resonance radiation and formation of molecular ions in cesium vapor, 19: 47229
JIU, T. C., Singularities of amplitudes in perturbation theory, 19: 47412
JOACHAIN, Charles J., Rearrangement collisions—electron excitation of He(2^{3}s), 19: 47239
JOBES, F. C., Determination of deuterium density profile in a deuterium plasma using an energetic D$^+$ beam, 19: 47727 (NP-15434)
JOCH, F. A., Backward elastic scattering of pions on neutrons at 1.2 to 4.5 Bev, 19: 47310 (NP-15376)
JOHANSSON, Bosrje, Coronary collateral blood flow in relation to mass of ischemic myocardium, 19: 45767
JOHANSSON, C., PROTOS—computer program for treating proton slowing-down due to atomic collisions, 19: 47867 (NP-15384)
JOHANSSON, K., Angular correlations of γ rays from polycrystalline sources, 19: 47607
JOHNSEN, R. H., Acetylene production in the radiolysis of methane, 19: 46366
JOHNSON, A. B. Jr., Nickel-plated aluminum in deionized water, NH_4OH, and LiOH at 330°C, 19: 46945 (BNWL-98)
JOHNSON, G. R. A., Effect of electron scavengers on formation of hydrogen in radiolysis of propane, 19: 46396
JOHNSON, James E., Availability of fallout ^{137}Cs to dairy cattle from different types of feed, 19: 45780
JOHNSON, James R., Beta radiation source in a ceramic carrier, 19: 47156
JOHNSON, K., Lectures on particles and field theory. II., 19: 47405
JOHNSON, K., Quantum electrodynamics, 19: 47442
JOHNSON, Quintin, Crystal structure of ScB_2C_2, 19: 46258
JOHNSON, Vern R., Effects of γ-irradiation on characteristics of a ruby laser, 19: 46873 (N64-32322)
JOHNSTON, T. W., Isotropic plasma guide—TE_{11} mode, 19: 47743
JONEJA, M. G., X-ray-induced leukemogenesis in C57BL/6J mice, 19: 45911
JONES, D. E., Reproducibility studies of preparation of a LiF dosimetric material, 19: 46338 (UCRL-12367)
JONES, F. T., Photo- and radiation-chemistry of low-temperature aqueous glasses. I., 19: 46394
JONES, I. G., Determination of nitrogen in plutonium nitride, 19: 46164 (AERE-R-5002)
JONES, L. V., Prog. rpt., 4/65, 19: 46157 (MLM-1254)
JONES, P. M. S., Permeation and diffusion of hydrogen isotopes through stainless steels. I., 19: 46991 (AWRE-O-47/65)
JONES, R. S., On-line computer data processing system for counter and spark chamber experiments, 19: 46806
JONES, W. D., Plasma heating and burnout in beam-plasma interaction, 19: 47852
JONGEJANS, B., Reaction $K^+p \to K^0p\pi^+$ at 3 Bev, 19: 47356
JORDAN, Duane P., Air tables. Tables of compressible flow functions, 19: 47151
JORDAN, K. C., Half life of ^{223}Ra, 19: 47626
JORDAN, W. B., Use of digital programs in reactor plant designs, 19: 47909 (ANL-7050, pp 217-30)
JORTNER, Joshua, Properties of an excess electron in liquid He. I., 19: 47131
JORTNER, Joshua, Properties of an excess electron in liquid He. II., 19: 47132
JOSEPHSON, Edward S., Meeting on radiation preservation of foods, Natick, Mass., 10/63, 19: 46876 (AD-613325)
JUKES, J. D., Magnetohydrodynamics, 19: 47805
JUKES, J. D., Stability of non-uniform plasma in magnetic field gradient, 19: 47840
JUN, M.-J., Nitrosobenzene–iron tricarbonyl dimers by radiation chemistry reduction of $Fe(CO)_5$ with nitrobenzene, 19: 46397
JUNG, H., Biological effectiveness of elastic nuclear collisions. I., 19: 45993
JUNG, Till, Gonadal doses resulting from panoramic x-ray examinations of teeth, 19: 46107
JUNGCLAUSSEN, H., Recent development in field of nucleonics, 19: 46820
JUNKINS, R. L., Safety aspects of transport of radioactive materials, 19: 46663
JUPPE, G., Synthesis of tritiated p-terphenyls, labeled at specific positions, 19: 46313
JUST, K., Quantum theory and the singular state of cosmology, 19: 47283

K

KADOMTSEV, B. B., Plasma turbulence, 19: 47826
KADONAGA, Masao, Studies on graft copolymers of styrene onto polypropylene prepared by use of γ rays, 19: 46355
KAERCHER, Karl Heinz, Changes in isoenzyme of lactate dehydrogenase after action of ionizing radiation. III., 19: 46124
KAGA, Shinichiro, Rapid determination of L-leucine, L-isoleucine, and L-valine in a mixture by infrared spectrometry, 19: 46184 (ORNL-tr-941)
KAGEYAMA, Kosuke, Energy spectra of photoprotons from ^{12}C, ^{24}Mg, ^{28}Si, ^{32}S and ^{40}Ca, 19: 47699
KAGIWADA, H. H., Dynamic programming and an inverse problem in neutron transport theory, 19: 47537 (AD-613468)

KAHN, Lloyd, Emanation of tritium from two electron-capture detectors, 19: 46670
KAHN, S., Prog. rpt. on fissiochemical development, semiannual, 7-12/64, 19: 46324 (AGN-8132)
KALABA, R. E., Dynamic programming and an inverse problem in neutron transport theory, 19: 47537 (AD-613468)
KALBFLEISCH, George R., Search for C-invariance violation in η(958 Mev) and η(549 Mev) decays, 19: 47372
KALIBJIAN, Ralph, Phototube using diode as a multiplier element, 19: 46815
KALININ, A. I., The radioactivation analysis of silicon and silicon compounds with the successive use of ion-exchange chromatography, 19: 46228
KALISH, Sheldon, Heat transfer to NaK flowing in-line through a bundle of circular rods, 19: 46553
KALLIO, Paavo, Effect of uv radiation and some chemicals on morphogenesis in micrasterias, 19: 45840
KALLNER, Gertrude, Patterns of leukemia in Israel, 19: 45958
KALMAN, G., High refractive index at electron cyclotron harmonics in plasma, 19: 47749
KALNS, Eric, Prog. rpt. on tungsten-base alloys, final, 1/10/64–3/10/65, 19: 46940 (NP-15444)
KALVIUS, Michael, Low-temperature cryostats for Moessbauer experiments, 19: 46748
KAMA, William N., Human factors in remote handling, 19: 46484 (CONF-640508, pp 198-209)
KAMMERER, O. F., Superconducting transition temperature of thin Al films, 19: 47503 (BNL-9478)
KAMOGAWA, Hiroshi, Particle accelerators and their applications, 19: 47184
KAN, Fu-hsi, Light and spectroscopic properties of inorganic vitreous rare earth oxides, 19: 47886 (N64-21857, pp 1-6)
KAN, Fu-hsi, Physical research of irradiative radiation emanation of Nd^{3+} activated inorganic vitreous states, 19: 47887 (N64-21857, pp 7-12)
KANAYA, Koichi, Study of ion beam machine, 19: 47226
KANDYBA, V. V., Measuring temperatures of flames, gas flows and plasmas, 19: 46734
KANNENBERG, L. C., Structured cosmological models, 19: 47205
KANNO, Masayoshi, Reprocessing of uranium fuels by fused salt electrolysis, 19: 46448
KANTOR, Gideon, Whistler-hydromagnetic extension of magnetoionic theory, 19: 47464
KAPELNER, S. M., Electrical resistivity of lithium and columbium-1 zirconium alloy to 1430°C, 19: 47015 (TIM-854)
KAPINOS, L. E., Operating limits and safety analysis for split-table, dry, flexible critical experiments at CANEL Nuclear Physics Lab., 19: 47958 (PWAC-475)
KAPITSA, S. P., 30-Mev microtron-injector for pulsed fast reactor, 19: 47164 (JINR-P-2313)
KAPLAN, Henry S., Radiosensitivity of autochthonous radiation-induced lymphosarcomas in C57BL mice, 19: 45977
KAPLYANSKII, A. A., Piezospectroscopic determination of symmetry of crystal field acting on trivalent ions of rare earths in fluorite lattice, 19: 47890
KAPLYANSKII, A. A., Symmetry of narrow-band luminescence and absorption centers of colored LiF crystals, 19: 46380
KARCHES, Gerald J., Iodine-131 in children's thyroids from environmental exposure, 19: 46035 (PHS-999-RH-14)
KARISH, Peter, Reliability of safety systems, 19: 47929
KARLSSON, E., Angular correlations of γ rays from polycrystalline sources, 19: 47607
KARNES, Herman F., Corrosive potential of wetted thermal insulation, 19: 46949 (CONF-650905-2)
KARNEY, David, Ultraviolet microbeam irradiation in living cell membranes, 19: 45891
KARTUSHIN, V. P., Effects of radiation on flotation process, 19: 46453
KASSANIS, B., Inactivation of a strain of tobacco and of RNA isolated from it, by uv radiation, 19: 45962
KASTENBAUM, M. A., Factors affecting mortality from secondary disease in mouse radiation chimeras, 19: 45910
KATAOKA, Gunji, Collision-resisting construction of sides of a nuclear powered ship, 19: 46464 (NSJ-tr-30)
KATHARIOS, H., Lung changes following cobalt teletherapy for carcinoma of the breast, 19: 46063
KATO, Helena Toshi, Changes in isoenzyme of lactate dehydrogenase after action of ionizing radiation. III., 19: 46124
KATO, Toyoaki, Isolation of ^{95}Zr–^{95}Nb from mixed fission products by solvent extraction with oxine in benzene solution, 19: 46440
KATS, M. L., Atomic absorption centers and luminescence phenomena in alkali halide phosphors, 19: 47884 (IS-Trans-18)
KAUFMAN, A. S., Electron temperature of positive column in hydrogen at low pressure, 19: 47738
KAUFMAN, Harold R., Performance of correlation for electron-bombardment ion sources, 19: 46572 (NASA-TN-D-3041)
KAUFMAN, Michele, Limits on density of intergalactic ionized hydrogen, 19: 47196
KAUTZ, Herold D., Radioactive drugs, 19: 46044
KAUTZMAN, B. E., Spectrophotometric determination of silicon in Nb–Si alloys, 19: 46171 (KAPL-M-6492)
KAWAGUCHI, Hiroshi, Electrode erosion as parameter of spark discharge, 19: 47134
KAWAGUCHI, Masaaki, Theory of bound states. II., 19: 47376
KAWAI, Tadashi, Approach to controlled fusion, 19: 47760
KAWAMURA, Nobuaki, Energy spectra of photoprotons from ^{12}C, ^{24}Mg, ^{28}Si, ^{32}S and ^{40}Ca, 19: 47699
KAWAMURA, Ryuji, Mass splitting under SU(3), 19: 47383
KAWASE, Kaoru, Gamma-ray initiated polymerization of vinyl n-butyrate, 19: 46389
KAY, H. E. M., Management of polycythaemia vera, 19: 46089
KAY, Jack G., Chemical effects of radiative neutron capture in some cobalt(III) complexes with 5 or 6 nitrogen atoms in coordination sphere, 19: 46386
KAYE, J. H., Half life of ^{53}Mn from meteorite observations, 19: 47627
KAZACHEVSKII, I. V., Age of pleistocene carbonate formation according to thorium and uranium isotopes, 19: 46599
KE, Chiung-Huei, Activation analysis of trace impurities in Al, 19: 46207
KEAM, D. W., Concentration of ^{137}Cs in Australian milk during 1964, 19: 46660
KEARSEY, H. A., Steam–water heat transfer—post-burnout conditions, 19: 46541
KEENE, J. P., Charge-transfer complexes in scavenging by iodine of radicals formed on pulse radiolysis of cyclohexane, 19: 46384
KEGLEY, T. M. Jr., A new microhardness technique, 19: 47003 (NMI-4999, pp 111-28)
KEHLER, Paul, Method of determining density utilizing a γ source and pair of detectors, 19: 46892
KELLER, C., Compounds of Np(IV) and Pu(IV) 8-hydroxyquinoline, 19: 46288
KELLER, K. R., Superconducting diode as high-frequency sound detector, 19: 46739
KELLER, L. P., Precise track measurements in a wide gap spark chamber, 19: 46780
KELLERSHOHN, C., Development of source of x rays usable in medical radiography, 19: 46141
KELLEY, John P., Effect of kilovoltage and filtration on depth dose, 19: 46144
KELLY, John Gordon, Elastic scattering cross sections of 14.5-Mev protons for medium-weight nuclei, 19: 47705
KELLY, Paul S., Hartree-Fock wave functions for excited states, 19: 47224
KELLY, R., Damage and diffusion in Al and Al–Al_2O_3 alloy following bombardments with oxygen or inert gas, 19: 47080 (EUR-2478.e)
KEL'MAN, V. M., Exact integration of equations of motion for relativistic charged particles for a certain class of variable electromagnetic fields, 19: 47435
KELSEY, C. A., Polarization of 4.4-Mev neutrons scattered elastically from ^6Li and ^7Li, 19: 47570 (COO-7-0361)
KEMBO, Hiroshi, Temporary increase in uv resistance in course of spore germination of Bacillus subtilis, 19: 45848
KEMENY, P., Finite solid-angle corrections in γ-γ angular correlation measurements, 19: 47693
KEMPTER, C. P., Ternary diagram—uranium–uranium dioxide–uranium oxycarbide, 19: 46249 (LA-tr-65-15)
KEMPTER, Charles P., X-ray determination of coefficient of thermal expansion, 19: 47023 (LA-tr-65-20)
KENNEDY, J. C., Radiosensitivity of the immune response to sheep red cells in the mouse, 19: 45903
KEPAK, F., The sorption of fission products on the suspension of the natural sorbents coagulated in an electric field, 19: 48082 (UJV-1296/65)
KERR, Ian F., Carcinoma of thyroid following irradiation for medulloblastoma, 19: 46069
KERVALIDZE, K. N., Spatially periodic plasma structures appearing in fast heavy-current discharges, 19: 47761
KERWIN, Larkin, Components of the image produced by an ionic optical system, 19: 46738
KESTER, F. L., High-temperature modifications of ThC_2, 19: 47033
KESTNER, Neil R., Properties of an excess electron in liquid He. I., 19: 47131
KESTNER, Neil R., Properties of an excess electron in liquid He. II., 19: 47132
KHAN, M. A., Nuclear power in developing areas, 19: 48041
KHARE, H. C., S-wave Λ–Λ interaction and a scalar dipion resonance, 19: 47337

KHARE, S. P., Differential cross sections for electrons elastically scattered by helium atoms, 19: 47218 (AD-613929)
KHARIN, G. V., Investigation of escape of electrons from trap with a spatially periodic helical magnetic field, 19: 47145
KHAR'YUZOV, R. V., 30-Mev microtron-injector for pulsed fast reactor, 19: 47164 (JINR-P-2313)
KHELASHVILI, A. A., Leptonic decays of baryons in the universal V-A theory, 19: 47307 (JINR-P-2278)
KIDDER, Ray E., Compression of magnetic field inside hollow explosive-driven cylindrical conductor, 19: 47120 (UCRL-14349)
KIEFER, H., Measurement in successive stages of an emergency: equipment, methods and facilities, 19: 46839
KIEFER, W., Search for 5-min isomer of ^{78}As, 19: 47682
KIKUCHI, Riichi, Accumulation of electric charge in γ-irradiated shielding window glass, 19: 47102
KILB, R. W., Energy distribution of particles leaving a θ pinch, 19: 47833
KILIAN, P., Local neutron flux distribution in a bundle from segmented fuel elements, 19: 47992 (KEA-311)
KIM, H. K., Prog. rpt. on anti-radiation drugs, 4–6/65, 19: 46303 (NP-15409)
KIM, J. I., Nondestructive neutron activation determination of Ag and Sb in bismuth by $\gamma\gamma$ coincidence spectrometry, 19: 46193
KIM, Moon Ja, Radiohomogeneity of ^{3}H- and ^{14}C-labeled linoleic acid, 19: 45785
KIMURA, Miwako, Absolute counting of ^{14}C by efficiency tracing technique, 19: 46214
KIMURA, Tadashi, γ-Ray induced decomposition of polyvinyl chloride. II., 19: 46350
KING, A. H., Effect of omega transformation on critical currents in a Zr-rich Nb alloy, 19: 47511
KING, David R., Analysis and evaluation of measurements of geomagnetically trapped electrons from high-altitude nuclear explosions, 19: 47446 (AD-612013)
KING, G. David, Radical head and neck surgery in irradiated patients: complications and safeguards, 19: 46129
KING, Margaret J., Cytogenetic studies in chronic myeloid leukemia and acute leukemia associated with mongolism, 19: 45915
KINGSTON, A. E., Ionization of inert gas atoms by electron and proton impact at high energies, 19: 47246
KINKEAD, Norman, Plant for remote handling of nuclear fuel elements, 19: 47938
KINO, G., Final rpt. on plasma boundaries, 3/61–2/65, 19: 47719 (ARL-65-131)
KIRBY, H. W., Half life of ^{223}Ra, 19: 47626
KIRCHMANN, R., Ratio between the ^{90}Sr content of grass and milk from radioactive fallout, 19: 45749
KIRIN, I. S., Chemical changes in β decay of I isotopes, 19: 46411
KIRKPATRICK, Alan Robert, Fuel and control rod channel arrangement in a graphite-moderated nuclear reactor, 19: 47933
KISDI, David, Landau theory of Fermi systems. I., 19: 47323
KISER, Robert W., Chemical species containing ^{32}P and ^{35}S subsequent to neutron irradiation of thiourea, 19: 46365
KITAMURA, Tei-ichi, Geomagnetic pulsations and the exosphere. I., 19: 47479
KITCHENS, T. A., Direct measurements of multiple quantization in He II, 19: 47522
KIVEL, Joseph, Organometallic radiation dosimetry systems, 19: 46761 (NYO-2979-34)
KIYOSE, R., Prog. rpt. on chemical engineering studies on processing radioactive wastes, final, 1/64–3/65, 19: 48079 (NP-15371)
KLECZKOWSKI, A., Effect of uv irradiation on susceptibility of serum albumins to trypsin, 19: 46382
KLECZKOWSKI, A., Inactivation of Rhizobium bacteriophage by uv radiation of different wave lengths, 19: 45961
KLECZKOWSKI, A., Inactivation of a strain of tobacco and of RNA isolated from it, by uv radiation, 19: 45962
KLECZKOWSKI, J., Inactivation of Rhizobium bacteriophage by uv radiation of different wave lengths, 19: 45961
KLEIJN, H. R., Problems in nuclear superheating of steam, 19: 48012
KLEIMA, D., Regge symmetries of the 3j-symbols, 19: 47335
KLEIN, J. H., Chemonuclear loop removal from BGRR using a semi-remote cutting technique, 19: 48055 (BNL-9402)
KLEIN, Siegfried, Process for conversion of ionizing energy into electricity, 19: 47283(T) (BNL-tr-8)
KLEINMAN, Chemia J., Higher partial waves in positron-hydrogen scattering, 19: 47238
KLEINMAN, R. E., Prog. rpt. on diffraction and scattering by regular bodies, final, 2/60–1/65, 19: 47299 (AD-614046)
KLEPEIS, James, Experimental studies of strong Hall effects and U × B induced ionization. II., 19: 47290
KLINGHOFFER, Max, Practical approach to shelter from radiation, with special reference to storage establishment and maintenance of emergency hospitals, 19: 46669
KLOIBER, H., Atomic energy market in Europe. XI. Austria, 19: 48010
KLUMPAR, Josef, Sources of errors in low activity measurements, 19: 46608
KMETKO, E. A., Electronic band structures of plutonium and its monocarbide, 19: 47880 (LA-DC-7353)
KNALMANN, M., Determination of soft β sources in small quantities of plant substance, 19: 46199
KNAPP, Gordon, Superconductivity in the tin–gallium system, 19: 47520
KNYAZEV, I. N., Stimulated radiation from hydrogen and deuterium molecules in near-infrared region, 19: 47260
KNYAZEV, Yu. R., Pulse heating of high-pressure argon arc. I., 19: 47789
KNYAZEV, Yu. R., Pulse heating of high-pressure argon arc. II., 19: 47790
KOBAYASHI, Shigeo, Nuclear instruments and radiation dosage, 19: 46837
KOBERG, D. R., PRTR containment vessel pressure test experience, 19: 48057 (BNWL-109)
KOCH, G., Radiological monitoring of the surroundings of CEN at Mol, 19: 46631 (A/AC.82/G/L. 986)
KOCH, Guenter, Extraction of uranium(VI) by tricaprylmethylammonium nitrate, 19: 46450
KOCH, Ruprecht, Investigations on biological radiation protection. LXIV., 19: 46028
KOCH, W., Fast electron dosimetry on a 2-Mev Van de Graaff accelerator, 19: 47177
KOECHLIN, Y., Energy of electron cascades in a small lead-plate spark chamber, 19: 47354
KOEHLER, W., Displacement probabilities of lattice atoms in various metals by reactor radiation, 19: 47104
KOEHLY, G., Determination of Am by controlled potential coulometry, 19: 46189
KOERNER VON GUSTORF, E., Nitrosobenzene–iron tricarbonyl dimers by radiation chemistry reduction of $Fe(CO)_5$ with nitrobenzene, 19: 46397
KOEVES, E., Effect of growth inhibitors on incorporation of ^{32}P into alcohol-soluble phosphate fraction of rice seedlings, 19: 45794
KOFLER, M., Synergism between ionizing radiation and a cytotoxic methylhydrazine derivative: effect on DNA degradation, 19: 46356
KOFOID, M. J., Composition of noble gas ion beams produced with a duoplasmatron, 19: 47267
KOGURE, Takashi, Retained ThO_2 media in seminal vesiculography. Follow-up study with dose estimates, 19: 45837
KOHL, Roland W., Bibliography on pyrolysis of polymers, 19: 46302 (MLM-1271)
KOHMURA, Toshitake, Nucleon pairs emitted by negative pion capture in light nuclei, 19: 47679
KOKUBO, Sonyo, Reprocessing of uranium fuels by fused salt electrolysis, 19: 46448
KOLKUNOV, V. G., Regge pole in a Coulomb-well type potential, 19: 47311 (NP-15454)
KOMAROV, N. N., Self-focusing of local plasma currents, 19: 47763
KOMAROV, N. N., Topology of steady-state plasma configurations in transverse self-consistent fields. II., 19: 47762
KONDO, Hiromichi, Approach to controlled fusion, 19: 47760
KONDO, Jun, s-d Scattering at low temperatures, 19: 47897
KONDO, Jun, Two-electron scattering due to s-d interaction, 19: 47257
KONDO, Sohei, Comparison of fission neutrons and γ rays in respect to their efficiency in inducing mutations in silkworm gonia, 19: 45883
KONDO, Teruo, Combined action of anti-tumor chemicals and ^{60}Co γ rays on mouse strain L cells cultured in vitro. II., 19: 46018
KOPFLER, Frederick Charles Jr., Radiation-induced changes in the kinetics of shrimp enzymes involved in spoilage, 19: 46891
KOPP, Ingvar, Triplet bands of ND, 19: 46263
KOPPEL, J. U., Role of interference scattering in neutron thermalization by heavy water, 19: 47559
KOPPIKER, K. S., Alkalimetric determination of metals using 8-hydroxyquinoline as complexing agent, 19: 46205
KORKISCH, J., Anion exchange separation of uranium and its application to determination of uranium in sea water, marine sediments, and other geological samples, 19: 46223
KORMONDY, Edward J., Uptake and loss of ^{65}Zn in dragonfly Plathemis lydia, 19: 45789
KORSOS, Ruth C., Nursing care of the patient with radiation sickness, 19: 45912
KORSUNSKII, M. I., Properties of an electronic-ionic oscillatory discharge, 19: 46742
KOSTIC, Peter, Bladder after the Wertheim operation and irradiation, 19: 46061
KOSTOUROS, D., Lung changes following cobalt teletherapy for carcinoma of the breast, 19: 46063

KOTHARI, L. S., Measurement of the neutron asymptotic decay constant in small crystalline assemblies, 19: 47554
KOTOV, B. V., EPR spectra of some irradiated nitriles, 19: 46378
KOTOV, V. I., Investigation of hybrid waves in circular waveguide partly filled with a dielectric, 19: 46743
KOTTMEIER, H.-L., Sensitization and radiation response in cases with carcinoma of the uterine cervix, 19: 45830
KOUVARAS, N., System for accurate counting of short-lived activities by repetitive activation, 19: 46818
KOVACEVIC, Miodrag, Movement of radioactivity emanating from ^{40}K in precipitation and waters on territory of Vinca, 19: 46590 (JPRS-31469)
KOVALENKO, V. P., Spectral determination of electron temperature of Cs plasma in a thermoelectric diode, 19: 47773
KOVRIZHNYKH, L., Effects due to interaction of plasmons, 19: 47784
KOZO, Fotogami, Forced convective heat transfer in horizontal tubes. I., 19: 46545
KRAGT, Klaxies, Effect of divided doses of 15-Mev electrons on skin response of mice, 19: 45885
KRAMER, H., Flame-photometric determination of Na in U ores, 19: 46191
KRASOVSKII, V. I., Aurorae and airflow, 19: 47452 (NASA-TT-F-204)
KRASULIN, Yu. L., Physical and chemical problems of joining of dissimilar materials, 19: 46968 (AEC-tr-6615)
KRAUS, W., Occupational body burden in the G.D.R. in 1963, 19: 46674
KREBS, A. T., Electron spin resonances in formicidae, 19: 45954
KREIJGER, Pieter Job, Removal of neutron poisons from aqueous homogeneous suspension reactor, 19: 46426 (NP-15362)
KRESHECK, Gordon C., Effect of D_2O on thermal stability of proteins, 19: 46318
KRISCHER, W., Status of CERN HPD program for bubble chambers, 19: 46812
KRISHAMURTHY, M., Separation of lanthanides using phthalate buffer, 19: 46437
KRISHAN, S., Interaction between a radio wave and a plasma, 19: 47770
KRISHAN, S., Stability of plasma with plane boundary, 19: 47747
KRISHNA PRASAD, N. S., Separation of lanthanides using phthalate buffer, 19: 46437
KROEGER, H., Interaction of RNA polymerase with irradiated DNA, 19: 45849
KROKOWSKI, Ernst, Time-dependent relation of dose effects, 19: 45989
KRONEKVIST, Mona, Triplet bands of ND, 19: 46263
KRONIG, R., Displacement of energy levels of atomic systems in strong radiation fields, 19: 47233
KRUCHININ, S. P., Elastic (p,p) scattering at 1.45 Bev, 19: 47304 (IAE-700)
KRUGER, Lawrence, Afferent and efferent fibers in cerebral cortex of rabbit, 19: 45874
KRUSKAL, M., Advanced theory of gyrating particles, 19: 47807
KRUSKAL, M., Asymptotology, 19: 47150
KRUSKAL, M., Elementary orbit and drift theory, 19: 47806
KRUSKAL, M., Equilibrium of magnetically confined plasma in a toroid, 19: 47809
KRUUV, J., Effect of breathing 5% CO_2 and 95% O on tumor radiosusbility, 19: 46003
KRYNN, R., Nuclear power in developing areas, 19: 48041
KRYNICKI, K., Proton spin-lattice relaxation in solutions of hydrogen chloride and deuterium chloride, 19: 46287
KSCHWENDT, H., Monte Carlo approach to calculation of characteristic reactor parameters in three-dimensional assemblies, 19: 47919 (ANL-7850, pp 581-92)
KUAN, Wei-yen, Superconducting electromagnet of Nb_3Sn, 19: 47526
KUBIKOVA, A., Changes in color of potato tubers after irradiation, 19: 45853
KUBO, Soichi, Radiation dosimetry by photographic measurement. IV., 19: 46819
KUBOSE, D. A., Determination of total tritium activity adsorbed on surface of various metals, 19: 47018 (USNRDL-TR-890)
KUBOTA, H., Rapid determination of L-leucine, L-isoleucine, and L-valine in a mixture by infrared spectrometry, 19: 46184 (ORNL-tr-841)
KUCKLE, Marko, Measurement of diffusion length in time-decaying neutron fields, 19: 47560
KUDRYAVTSEVA, L. K., Models of temperature fields of heat exchange elements in active zone and shielding of the BN-350 reactor, 19: 47994 (NP-15393)
KUHN, D., Nuclear power in developing areas, 19: 48041
KUJAWSKA, Janina, Radiation treatment of inoperable thyroid carcinoma, 19: 46104
KULEEV, V. G., Bound electron and nuclear spin oscillations in antiferromagnetics, 19: 47903
KULISIC, P., Direct processes in (n,α) reactions, 19: 47637
KULL, R. B., Metallographic and ceramographic preparation of nuclear materials, 19: 46937 (NMI-5025(Pt.I), pp 1-25)
KUMABE, Isao, Scattering of α particles by medium-weight nuclei, 19: 47623
KUMAR, H. D., Effects of radiations on blue-green Algae. I., 19: 45842
KUMAR, Naresh, Energy levels of ^{92}Mo with different potentials, 19: 47617
KUMAR, Vijay, Energy levels of ^{92}Mo with different potentials, 19: 47617
KUMMER, W., SU_3 estimate of effective nonleptonic parity-violating coupling in strangeness-conserving weak processes, 19: 47342
KUMMEROW, Fred A., Radiohomogeneity of ^{3}H- and ^{14}C-labeled linoleic acid, 19: 45785
KUNII, D., Prog. rpt. on chemical engineering studies on processing radioactive wastes, final, 1/64–3/65, 19: 48079 (NP-15371)
KUNKEL, Rene, Whole-body counter for research, clinical applications, and radiation protection measurements, 19: 46836
KUNZ, Jochen, Morphological and histoenzymochemical studies of aorta of rabbits after localized exposure to ^{90}Sr–^{90}Y β radiations, 19: 45875
KUNZ, Jochen, Structural changes in media of rabbit aorta after local irradiation (^{90}Sr–^{90}Y), 19: 45994
KUPERUS, J., Protons from α bombardment of ^{27}Al, 19: 47672
KURSANOV, Yu. V., Investigation of escape of electrons from trap with a spatially periodic helical magnetic field, 19: 47145
KURTMULLAEV, R. Kh., High-speed diagnostics of a plasma jet, 19: 47735
KURTMULLAEV, R. Kh., Plasma heating mechanism by collisionless shock waves, 19: 47845
KUSUMGAR, Shoolo, Measurement of radiocarbon activity and some determinations of ages of archaeological samples, 19: 46617
KUTHE, R., Thermodynamic properties of air at high temperatures (with consideration of radiation contributions), 19: 47731
KUTTIG, H., Tumor tele-irradiation with energetic corpuscular and wave radiation, 19: 46078
KUZ'MINA, E. A., Age of pleistocene carbonate formation according to thorium and uranium isotopes, 19: 46599
KUZNETSOV, R. A., The radioactivation analysis of silicon and silicon compounds with the successive use of ion-exchange chromatography, 19: 46228
KVARTSKHAVA, I. F., Self-focusing of local plasma currents, 19: 47763
KVARTSKHAVA, I. F., Spatially periodic plasma structures appearing in fast heavy-current discharges, 19: 47761
KVARTSKHAVA, I. F., Topology of steady-state plasma configurations in transverse self-consistent fields. II., 19: 47762
KVIRIKADZE, A. G., Slow neutron scattering in antiferromagnets having weak ferromagnetism, 19: 47899
KWAN, Takao, Analyses of para-ortho hydrogen and deuterium by gas chromatography, 19: 46183 (NP-tr-1289)
KWOK, K. L., Narrow resonance in elastic scattering of electrons by helium, 19: 47248

L

LABES, Mortimer M., Physics and chemistry of the organic solid state. II., 19: 46320
LACASSAGNE, A., Contributions of radiobiology to the progress of cancerology, 19: 45743
LACEFIELD, K., Metallographic and ceramographic preparation of nuclear materials, 19: 46937 (NMI-5025(Pt.I), pp 1-25)
LACEFIELD, W. B., Prog. rpt. on anti-radiation drugs, 4–6/65, 19: 46303 (NP-15409)
LACHAMBRE, A., Nondestructive testing at hot laboratories of the CEN, Grenoble, 19: 46559 (ORNL-tr-749)
LACHANCE, Leo E., Induced dominant lethal mutations in oocytes and sperm of screw-worm fly, 19: 45950
LACKMAN, David B., Application of radioisotope precipitation test to study of Q fever in man, 19: 46076
LACKMAN, David B., Radioisotope precipitation test for study of Q fever antibodies in human and animal sera, 19: 45739
LACKNER, Karl, Juelich plasma symposium, 19: 47715 (AD-613622)
LADAGE, A., Electroproduction of π-mesons and photoproduction of dipions, 19: 47303 (DESY-65/7)
LAFFERTY, D. L., High-energy neutral injection, 19: 47752
LAGERQUIST, C. R., Plutonium bioassay results following DTPA treatments, 19: 45762 (RFP-577)
LAGRUTTA, J., Endolymphatic radioisotope therapy and pelvic lymphography in gynecological cancerology, 19: 46100
LAGRUTTA, L., Radiosensitivity and oxygen therapy in gynecological oncology, 19: 46097
LAHR, Thomas N., Beta radiation source in a ceramic carrier, 19: 47156
LAI, Chai S., $p\bar{p}$ annihilation into two mesons in the spurion scheme of broken U(6,6) symmetry, 19: 47374
LAIB, Roger D., Determination of Rb in Cs by x-ray fluorescence spectroscopy, 19: 46186
LAING, E. W., Numerical study of particle behavior in non-adiabatic

magnetic traps, 19: 47748

LAING, W. R., Alkylbenzene sulfonate control for foam separation process, 19: 46429 (ORNL-P-1522)

LAJTHA, L. G., Close-size analysis in the study of cell growth following single or during continuous irradiation, 19: 45886

LAKSHMINARAYANA, V., Absolute photoelectric cross sections of 145-, 280-, and 320-kev γ rays, 19: 47329

LAKSHMINARAYANA, V., Incoherent scattering of 280-kev γ rays, 19: 47624

LAL, D., Measurement of radiocarbon activity and some determinations of ages of archaeological samples, 19: 46617

LALOU, Claude, Concentrations of γ-emitting radionuclides present in holothurian samples in coastal area of Antibes in Cape Ferrat in August 1962, 19: 46611

LALOVIC, B., Direct processes in (n,α) reactions, 19: 47637

LAMBERT, Marcel H., Adsorbed ^{3}He: heat capacity at low temperatures, 19: 47514

LAMBORIZIO, C., Features of Moessbauer absorption in tin metal, 19: 47654

LAMERTON, L. F., Somatic hazards from accidental exposure to radiation: radiobiological considerations, 19: 45996

LAND, E. J., Charge-transfer complexes in scavenging by iodine of radicals formed on pulse radiolysis of cyclohexane, 19: 46384

LANDMANN, W. A., Chemical changes produced by heat and by irradiation of meat and meat fractions, 19: 46878 (NP-15455)

LANDSBERG, L. G., Backward elastic scattering of pions on neutrons at 1.2 to 4.5 Bev, 19: 47310 (NP-15376)

LANDSBERG, R., Inverse deuterium isotope effect in decomposition of permanganate in alkali solution, 19: 46275

LANDSMAN, D. A., Stress corrosion of irradiated stainless steels, 19: 47079 (AERE-R-5014)

LANGE, C. S., Close-size analysis in the study of cell growth following single or during continuous irradiation, 19: 45886

LANGE, W., Fast counting channel at Vakutronik in Dresden, 19: 48033

LANGENDORFF, Margarethe, Investigations on biological radiation protection. LXVI., 19: 46029

LANGER, Horst G., Insoluble chelates of titanium, zirconium, hafnium, and thorium, 19: 46299

LANGER, S., High-temperature modifications of ThC_2, 19: 47033

LANGOUET, Loic, Notes on a phosphoroscope, 19: 46737

LANGREDER, W., Radiogenic injuries of urinary tract and their prevention, 19: 46033

LANGSDORF, A. Jr., Experiments to measure differential cross sections, 19: 47601

LANZ, Giovanni, Asymptotic direction of arrival of charged particles in earth's magnetic field, 19: 47269

LARENZ, R. W., Adiabatic linear Stark effect in a plasma, 19: 47716 (AD-614283)

LARSH, A. E., Decay properties of ^{256}Fm and ^{257}Fm and ^{255}Md, ^{256}Md, and ^{257}Md, 19: 47664

LARSON, Allen C., Integrated series of crystallographic computer programs. X., 19: 47877 (LA-3335)

LASHER, Gordon, Series solution of Ginzburg-Landau equations for the Abrikosov mixed state, 19: 47519

LASHINSKY, H., Universal instability in thermal plasma device (Q machine), 19: 47859

LASKY, C., Fast beam extraction system of the alternating-gradient synchrotron, 19: 47158 (BNL-910)

LASSMANN, G., ESR investigations of radioinduced free radicals in muscle tissues, 19: 45947

LATARJET, Raymond, Mechanisms of cancerization by irradiations visualized at cellular level, 19: 45859

LATHROP, K. A., Technetium-99m as clinical tracer material, 19: 46140

LATHROP, K. D., Moments equations and equivalent discrete ordinates equations. I and II., 19: 47547 (LA-DC-7320)

LATIMER, I. D., Absolute cross sections for simultaneous ionization and excitation of N_2 by electron impact, 19: 47245

LATIMER, R., Decay properties of ^{256}Fm and ^{257}Fm and ^{255}Md, ^{256}Md, and ^{257}Md, 19: 47664

LAUGHLIN, J. S., Calorimetric dosimetry. I., 19: 46848

LAUGHLIN, J. S., Calorimetric dosimetry. II., 19: 46849

LAUGHLIN, J. S., High-energy electron treatment-planning dosimetry. 19: 46155

LAUGHLIN, J. S., Solid-state dosimetry, 19: 46850

LAUGHLIN, John S., Ionization chambers for diagnostic x-ray exposure studies, 19: 46857

LAUNER, Herbert F., Uv-dosage measurement in geometrically complex system with light-sensitive paper, 19: 45963

LAURER, Gerald R., Iodine-131 in children's thyroids from environmental exposure, 19: 46035 (PHS-999-RH-14)

LAUTERBACH, R., Geological results and problems of gamma spectrography or rock samples, 19: 46601

LAVAL, G., Electromagnetic instability of collisionless plasma, 19: 47844

LAVIK, M., Conference on mechanisms of solid friction, Kansas City, 9/63, 19: 47075

LAWRENCE, C. P., Nitrogen isotope equilibration on tungsten, 19: 46209

LAWSON, J. D., Analogous behavior of elementary particles and some simple waveguide and cavity systems, 19: 47319

LAZAR, N. H., Energetic neutral injection into an electron-cyclotron plasma, 19: 47837

LAZAREV, B. G., Effect of impurities on pressure effect in thallium. II., 19: 47529

LAZAREVA, L. S., Effect of impurities on pressure effect in thallium. II., 19: 47529

LEAKE, J. W., Calibration of the neutron survey probe, 19: 46752 (AERE-M-1564)

LEARY, J. A., Refractory plutonium fuel materials, 19: 46999 (LA-DC-7297)

LE BARON, Robert, Graphitic neutron reflector containing Be and method of making same, 19: 46977

LEBECH, B., Time-of-flight method for investigations of single-crystal structures, 19: 47894

LEBEDEFF, Sergej, Scattering of two H atoms in the Born-Oppenheimer approximation, 19: 47264

LEBEDEV, A. T., Effects of radiation on flotation process, 19: 46453

LECIEJEWICZ, J., Time-of-flight method for investigations of single-crystal structures, 19: 47894

LEDERMAN, M., Malignant tumors of the ear, 19: 46084

LEDLIE, E. M., Management of polycythaemia vera, 19: 46089

LEE, A. P., Effect of pressure on structure and properties of metals, 19: 46983 (AD-612159)

LEE, Ching-run, Low-energy opposite-parity coherent structure of ^{17}O and ^{17}F, 19: 47700

LEE, Hwa-chung, Analyticity and threshold behaviors of fermion Regge trajectories, 19: 47392

LEE, J. A., Low-temperature specific heat of plutonium, 19: 47043

LEE, J. S., Post-irradiation recovery of E. coli, 19: 45951

LEE, J. S., Replica plating and computer analysis for rapid identification of bacteria in foods. II., 19: 46882

LEE, Y. Y., Fifteenfold way of the SU(4) symmetry scheme of strongly interacting particles, 19: 47328

LEEDS, R. W., Computer studies of copper atom ranges in copper lattices, 19: 47228

LEES, D. J., Inter-diffusion of plasma and magnetic fields in pinch and hardcore discharges, 19: 47853

LEGRAND, B., Application of strain gages at high temperature. I. Cements, 19: 46715 (EUR-2473.f)

LEHNERT, B., Rotating plasma experiments, 19: 47850

LEHOCZKY, Marcia Helen, Reversed-phase chromatographic separation of nitroanilines, 19: 46424 (IS-T-24)

LEI, Hsiao-lin, Nonlocal extension of the Ginzburg-Landau equations in theory of superconductivity, 19: 47527

LEIGH, Gerald G., Prog. rpt. on simulation of air-blast-induced ground motions, 7/64–1/65, 19: 46457 (AD-613674)

LEIGHTON, S. A., Post-irradiation metallographic laboratory at GE-NMPO, 19: 47089 (NMI-4999," pp 30-50)

LEIKIN, E. M., Photoproduction of π^+ mesons on protons at 230 Mev, 19: 47393

LEITCH, L. C., Deuterated organic compounds. XXV., 19: 46307

LEITCH, L. C., Deuterated organic compounds. XXV., 19: 46308

LEITER, Darryl Jay, Possible existence of very massive, almost bare, unstable particles, 19: 47398

LEITH, D. W. G., Reaction $K^+p \rightarrow K^0p\pi^+$ at 3 Bev, 19: 47356

LEITNER, J., The $Y_1^*(1660)$ produced in K^-p interactions at 2.24 Bev/c, 19: 47300 (BNL-9520)

LELIEVRE, P., Oxygen consumption by rat liver in presence of cystamine-role of diaminooxidases, 19: 45777

LEMENT, B., Factors controlling effectiveness of high-temperature protective coatings for tungsten, 19: 46911 (AFML-TR-64-392)

LEMESLE, Georges, Nuclear reactor, 19: 47972

LENKE, J. W., Materials research with scanning microprobe analyzer, 19: 46508 (NMI-4998, pp 65-76)

LENZI, G., Sorption properties of natural tuffs occurring in the Lake Bracciano region (Rome), 19: 48081 (TR/PROT(65)19)

LEONARD, A., Tissue and cellular distribution of tritium-labeled AET in mice, 19: 46016

LEONARD, B. R. Jr., Multiphonon neutron scattering study of hydrogen bonding in zirconium hydride, 19: 46232 (BNWL-SA-239)

LERCH, P., Role of radiophysiological service in a university hospital, 19: 46679

LERTORA, M., Behavior of cholesterol in irradiated animals, 19: 45937

LESINSKI, Jan, Background stability of halogen-quenched G-M counters, 19: 46828

LESLIE, B. C., A new microhardness technique, 19: 47003 (NMI-4999, pp 111-28)

LESSLER, Richard M., Gamma dose curves from neutron-activated soil and seawater compared with fission-product decay, 19: 46589 (UCRL-14332)

LESSMANN, G. G., Prog. rpt. on weldability and temperature stability of refractory metal alloys, 12/21/64–3/20/65, 19: 46966 (WANL-PR(P)-007)

LETTINGA, J., K-conversion coefficient of 328-kev E2 transition in ^{194}Pt, 19: 47643

LEVEN, M. M., Stress distribution in a perforated plate of 10% ligament efficiency subjected to equal biaxial stress, 19: 46557 (NP-15459)

LEVINE, Arnold D., Canonical transformations in quantum mechanics, 19: 47413

LEVINE, Seymour, Effects of x irradiation on the response of animal cells to virus, 19: 45974

LEVINE, Seymour, Relation of cell size to effect of x rays on poliovirus production by monkey kidney cells, 19: 45955

LEVINSON, David W., Prototype manual of metallurgical practice, 19: 46918 (IITRI-B6018-1)

LEVINSON, Hillel S., Radiation dosimetry with sodium cacodylate and TRIS, 19: 46373

LEVIS, Angelo Gino, Mitotic activity and DNA synthesis in clones derived from mammalian cell cultures irradiated with x rays, 19: 45867

LEVITSKII, S. M., Diffusion theory of a beam plasma, 19: 47787

LEVY, Milton, Effects of sintering on microstructure and properties of sprayed molybdenum, 19: 47054

LEVEY, S., Di n-octyl phosphinic acid as a selective extractant for metallic cations, 19: 46443

LEVIN, Isaac, Zinc-65 metabolism during low and high Ca intake in man, 19: 45787

LEVIN, W. H. G., K-conversion coefficient of 328-kev E2 transition in ^{194}Pt, 19: 47643

LEWIS, E. E., Family of FORTRAN routines for analysis of neutron resonance effects, 19: 47542 (ANL-7050, pp 457-70)

LEWITUS, ZYGMUNT, Iodine-131 uptake studies under hot climatic conditions, 19: 45779

LHERMITTE, Francois, Late postradiotherapy lesions of the central nervous system, 19: 45983

LIAN, K. T., Plasma/electromagnetic-wave interaction structures with free plasma boundaries, 19: 47734

LIBERATORI, J., Protein radioiodination by an electrolytic technique, 19: 46142

LICHTENBERG, D. B., Lectures on particles and field theory. II., 19: 47405

LICHTENBERG, D. B., Spectroscopy of the strongly interacting particles, 19: 47406

LIEB, Harry C., Self-charging nuclear battery, 19: 46897

LIEBECQ, Claude, Radiosensitivity of cultures of E. freundii grown in presence of fluoroacetate, 19: 46015

LIEDERBACH, Fred Joseph, Control rod drive for nuclear reactors, 19: 47934

LIEHOHN, H. B., Partial electron velocity spectrums from cyclotron absorption of Whistler power, 19: 47463

LIHL, F., Analysis of Y, Sm, Gd, Dy, Ho, Er–Mn-compounds, 19: 46989 (AD-614466)

LIHL, F., Measurements on rare earth–Mn alloys, 19: 46988 (AD-614465)

LIHL, F., Sinter process for rare earth–Mn systems, 19: 46908 (AD-614464)

LIHL, F., Systems Y–Mn, Gd–Mn and Sm–Mn, 19: 46987 (AD-614462)

LIIMATAINEN, Robert C., Nuclear reactor safety: the meltdown of metals at high temperatures and metal-water reactions, 19: 47960 (ORNL-tr-694)

LILJEDAHL, S.-O., Acute radiation syndrome, 19: 45829

LIN, Y. K., Satellite observations of low-energy primary cosmic-ray nuclei of charges $Z \geq 6$, 19: 47270

LINONCELLI, E. A., Reaction rate of Nb–1Zr alloy with oxygen at low pressures, 19: 47016 (TIM-901)

LIN, E. K., Inelastic scattering of deuterons from Zn and Se isotopes, 19: 47642

LIN, Song-Yun, Low-background counter for ^{14}C dating, 19: 46777

LINCOLN, J. Virginia, Geomagnetic and solar data, 19: 47468

LINCOLN, T. A., Action levels in medical treatment of radiation and radioactivity exposure, 19: 46008

LINDEN, W. A., Computer program for automatic determination of radioactivity in entire human body, 19: 46658

LINDENBAUM, S. J., On-line computer data processing system for counter and spark chamber experiments, 19: 46806

LINDER, Erland, Coronary collateral blood flow in relation to mass of ischemic myocardium, 19: 45767

LINDGREN, Ingvar, Analysis of nuclear dipole moments determined with nuclear magnetic resonance, 19: 47606

LINDNER, R., Diffusion of non-volatile fission products in UO_2 and ThO_2 as determined by leaching into molten salts, 19: 47070

LINDOP, Patricia J., Effect of divided doses of 15-Mev electrons on skin response of mice, 19: 45885

LINDQUIST, Arthur W., New ways to control insects, 19: 45960

LINDSAY, P. A., Exact solutions for the electron distribution in plane magnetrons, 19: 46740 6–0

LINDSTAEDT, Horst Karl, Improvements in or relating to conveyor systems, 19: 46519

LINEVSKY, Milton J., Prog. rpt. on vaporization of refractory materials, 7–9/63, 19: 46982 (AD-611856)

LINSCOTT, William D., Induction of tolerance to bovine serum albumin by means of whole-body x radiation, 19: 45902

LINSE, Vonne D., Explosive welding of Zircaloy to Hf, 19: 46961 (BMI-X-10139)

LINTZ, John Patrick, Irradiation of methacrylonitrile, 1,3-butadiene, and hexachloro-1,3-butadiene, 19: 46336 (TID-22236)

LIONS, Nosel, Detector for liquid carried over in a gas, 19: 46713 (CEA-R-2811)

LIPTAK, Jan, Investigation of the intensities of hard γ transitions in capture of resonance neutrons by ^{135}Ba, 19: 47701

LISKIEN, H., (n,2n) Excitation functions for nuclei around Z = 28, 19: 47571 (EUR-2456.e)

LITTLE, E. M., Stability, heating, and end loss of a 3.5-megajoule theta pinch (Scylla IV), 19: 47722 (LA-DC-7039)

LITTLEFIELD, T. A., Interferometric wavelengths of thorium lines between 9050 and 2566 Å, 19: 47232

LIU, Ti-hong, Superconducting electromagnet of Nb_3Sn, 19: 47526

LIVSHITS, N. N., Effects of ionizing radiation and of dynamic factors on the functions of the central nervous system, 19: 45824 (NASA-TT-F-354)

LLACER, J., Geometric control of surface leakage current and noise in Li-drifted Si radiation detectors, 19: 46754 (BNL-9535)

LLOYD, Henry, Nuclear fuel materials including vitreous phase, 19: 47986

LOBOV, G. A., CP parity non-conservation in polarized neutron decay, 19: 47312 (NP-15460)

LOBOV, G. A., Regge pole in a Coulomb-well type potential, 19: 47311 (NP-15454)

LOCKETT, George Edward, Plant for remote handling of nuclear fuel elements, 19: 47938

LOCKHART, Luther B. Jr., Simultaneous measurements of ^{222}Rn, ^{214}Pb, and ^{214}Bi in air near the ground, 19: 46605

LOEBL, Karel, Ageing of corrosion-resistant steels of the type $Cr^{18}Ni^{9}Ti$, 19: 47026 (ORNL-tr-795)

LOESCHE, A., Determination of magnetic-field distributions, 19: 46731 (SLAC-Trans-21)

LOEWENSTEIN, A., Cobalt-59 spin-spin coupling and isotope shifts in $K_3Co(CN)_6$, 19: 46285

LOGAN, Roy S., Superconductors in advanced electronics, 19: 46475 (AD-612113)

LOMANOV, M. F., Methods of automatic ionization measurement in a bubble chamber. 19: 46758 (CONF-550-99)

LOMBARD, David B., Mining by caving with nuclear explosions, 19: 46472 (UCRL-14201)

LOMENICK, T. F., Naturally occurring fixation of ^{137}Cs on sediments of lacustrine origin, 19: 46681

LONDON, G., Prog. rpt. on flow and fracture of alloyed Be, 10/7/64–1/6/65, 19: 46910 (AD-620589)

LONDON, G. W., The Y*(1660) produced in K⁻-p interactions at 2.24 Bev/c, 19: 47300 (BNL-9520)

LONES, Walter, Control rod drive for nuclear reactors, 19: 47934

LONG, E. C., Radiometric determination of fluorine in bulk PuF_4, 19: 46179 (RFP-618)

LONG, E. L. Jr., Experience with vibratory polishers and design for hot-cell application, 19: 47086 (NMI-4997, pp 184-8)

LONG, E. L. Jr., Remote metallographic specimen grinder, 19: 46507 (NMI-4997, pp 157-62)

LONG, Everett, Charging system for nuclear reactor, 19: 47939

LONGINELLI, A., Oxygen isotopic composition of orthophosphate from shells of living marine organisms, 19: 46583

LOOPSTRA, B. O., Neutron beam utilization at the Petten HFR, 19: 48068

LOPEZ, M. Roderiguez, Ulcerated thorotrastoma, 19: 46092

LOPEZ RODRIGUEZ, M., Preparation of pure Zr and Th by direct iodination of their carbides, 19: 46969

LORD, R. S., Extraction magnets for cyclotrons, 19: 47166 (ORNL-P-1605)

LORD, R. S., Sector magnets for a separated orbit cyclotron, 19: 47167 (ORNL-P-1619)

LORENZ, Eckart, Instrument for ionization measurements in bubble chamber films, 19: 46802

LOTT, J. M., Metallographic preparation of alumina-coated UO_2 spheres in graphite, 19: 46925 (NMI-4997, pp 85-91)

LOUDON, Warren L., Servo-restraint system for anti-G protection, 19: 46485 (CONF-640508, pp 210-23)

LOUTIT, J. F., Transplantation of hemopoietic tissues, 19: 46009
LOVE, C. M., Rate of the reaction between U(IV) and Ti(III), 19: 46277
LOVE, W. A., On-line computer data processing system for counter and spark chamber experiments, 19: 46806
LOVERING, J. F., Uranium and thorium abundances in basalt cored in Mohole Project (Guadalupe Site), 19: 46628
LOVITCH, L., Study of the J = 2 excited level of ^{6}Li, 19: 47645
LOWELL, J., Survey of type II superconductors, 19: 47510
LU, Shih-Cheng, Low-background counter for ^{14}C dating, 19: 46777
LUBITZ, C. R., Disc. Program to compute inelastic scattering matrices for multigroup reactor codes, 19: 47544 (KAPL-M-6467)
LUCAS, Arthur C., Effect of kilovoltage and filtration on depth dose, 19: 46144
LUCCHESI, P. J., Exchange of deuterium with hydroxyl groups of alumina, 19: 46280
LUCE, J. S., High-energy neutral injection, 19: 47752
LUECKING, T., Interaction of RNA polymerase with irradiated DNA, 19: 45849
LUETHY, H., Synergism between ionizing radiation and a cytotoxic methylhydrazine derivative: effect on DNA degradation, 19: 46356
LUKAS, Ingrid R., Levels of low excitation energy in ^{57}Fe, 19: 47696
LUK'YANCHIKOV, G. S., Investigation by uhf methods of motion of plasma in a radiation accelerator, 19: 47795
LUKYANOV, A. A., Approximate treatment of fast neutron spectrum in two-component homogenous medium, 19: 47964
LUKYANOV, V. I., Capture of plasmoids in a magnetic mirror machine, 19: 47839
LUNDGREN, C.-E., Atomic energy market in Europe. III. Denmark, 19: 48004
LUNDQUIST, J. R., Status of salt cycle process for processing oxide fuels, 19: 46422 (BNWL-SA-205)
LUNGU, S., Annealing mechanism of fast-neutron-damaged silica glass, 19: 47108
LUZZATTO, G., Representations of Poincaré group associated with complex energy-momentum, 19: 47422
LYKOUDIS, P. S., Influence of transverse magnetic field on forced convection liquid metal heat transfer, 19: 46547
LYNCH, G. R., Reaction $K^{+}p \rightarrow K^{0}p\pi^{+}$ at 3 Bev, 19: 47356
LYNN, E. C., Alkylbenzene sulfonate control for foam separation process, 19: 46429 (ORNL-P-1522)
LYTH, D. H., Fixed variable dispersion relations for the π–N system, 19: 47388
LYUBIMOV, V. A., Backward elastic scattering of pions on neutrons at 1.2 to 4.5 Bev, 19: 47310 (NP-15376)
LYUBITOV, Yu. N., Calculation of rate of vaporization of metal from cylindrical vessels into a vacuum and mass spectrometric investigation of vapor pressures of metals and alloys, 19: 46943 (FTD-TT-65-611)
LYUBOSHITS, V. T., Decays in a mixed ensemble of neutral K mesons, 19: 47309 (JINR-P-2289)

M

MACASEK, F., Chromatographic separation of radiochemically pure ^{90}Y from ^{90}Sr, 19: 46436
MACERO, Daniel J., Voltammetric studies of Eu(III) in formate buffer, 19: 46268
MACHACEK, Miles, P states of three-particle systems with Coulomb interaction, 19: 47438
MACK, Robert E., Iodine metabolism in the thyroid, 19: 45786
MACLEOD, G. R., Analysis of spark chamber pictures using raster-scan technique, 19: 46786
MAC LEOD, R. A., Application of Power Burst Facility to fast reactor fuel melt-down tests, 19: 47952 (APDA-177)
MAC VEAN, Charles Robert, Calculation of thermal neutron spectra in light water lattices, 19: 47968
MADDIX, H. S., Diffusion-controlled sorption in high-density discharges, 19: 46576
MADDOX, W. L., Analytical laboratory hot-cell equipment. III., 19: 46721 (ORNL-P-1531)
MAEDA, Ken-ichi, Effects of dynamo-electric field on electrons trapped in magnetosphere, 19: 47453
MAEDA, Rikio, Sudden commencements of geomagnetic storms and their local irregularities, 19: 47456
MAGDA, Tatiana M., Levels of low excitation energy in ^{56}Fe, 19: 47696
MAGGIORA, A., Different behavior of epidermis of flank and nipple of the guinea pig after a 1600-R dose of x rays, 19: 45869
MAGNIER, P., Application of radiocrystallography to study of ceramic and refractory compounds, 19: 47041
MAHAN, G. David, Remote afterloading for intracavitary radiation therapy, 19: 46111
MAHLMAN, J. D., Heavy radioactive fallout over southern United States, November, 1962, 19: 46604
MAILEN, James Clifford, Gamma and neutron irradiation of pure fluorocarbons, 19: 46404
MAISIN, J. R., Tissue and cellular distribution of tritium-labeled AET in mice, 19: 46016
MAJUMDAR, Chanchal Kumar, Annihilation of positrons in metals, 19: 47217 (AD-613582)
MAJUNDAR, D. P., Expected variations of cosmic-ray intensity on the moon, 19: 47273
MAKAROV, V. I., Effect of impurities on pressure effect in thallium. II., 19: 47529
MAKHONINA, G. I., Occurrence of ^{59}Fe, ^{60}Co, ^{65}Zn, ^{90}Sr, and ^{137}Cs in pine, larch, aspen, and birch, 19: 45773
MAKIN, M. J., Microstrain in neutron-irradiated copper crystals, 19: 47107
MAKINO, Tadao, Cosmic-ray cut-off rigidities and earth's magnetic field, 19: 47278
MAKSIMOVA, N. D., De-excitation of light sums in x-rayed alkali-halide phosphors by stationary F-band illumination, 19: 46379
MALACHESKY, Paul, Voltammetric studies of Eu(III) in formate buffer, 19: 46268
MALHERBE, Eric, Intra-arterial cytotoxic therapy and x-ray therapy for cancer of head and neck, 19: 46088
MALINA, L., Skin protection against x rays, 19: 46019
MALIS, Leonard I., Afferent and efferent fibers in cerebral cortex of rabbit, 19: 45874
MALLETT, Gavin, Conference on advances in x-ray analysis, Denver, 8/64. VIII., 19: 46185
MALMEJAC, Yves, Some aspects of the solid-liquid transition, 19: 46233 (CEA-R-2752)
MALMON, A. G., High resolution isotope tracing in electron microscopy using induced nuclear reactions, 19: 45741
MALMRUD, S., Portable high-pressure spectroscopic cell, 19: 46771
MALYSHEVA, N. G., Factors influencing determination of lithium and boron in enrichment products in (n,α) nuclear reaction, 19: 46221
MANAKA, Kazuo, Anti-electrostatic treatment of teflon films by radiation-induced graft copolymerization, 19: 46376
MANCUSO, Thomas F., Prog. rpt. on occupational radiation exposure, 6/64–4/2/65, 19: 45810 (NYO-3394-2(Rev.))
MANDEL'SHTAM, S. L., Investigation of spark discharge in air produced by focusing radiation from a laser, 19: 47781
MANDELSSOHN, K., Low-temperature specific heat of plutonium, 19: 47041
MANDL, F., Narrow resonance in elastic scattering of electrons by helium, 19: 47248
MANFREDI, D. V., Prog. rpt. on LCRE pumps and sumps, final, 7/65, 19: 46535 (PWAC-386)
MANFREDI, D. V., Summary of SNAP-50/SPUR pump bearing development program, 19: 46458 (CNLM-6342)
MANI, R. S., Preparation of ^{203}Hg-labeled neohydrin for medical use, 19: 46305
MANKIN, J. B., Acceleration switching valve control system with machine tool application, 19: 48106 (Y-1488)
MANNING, Gillian, Use of ^{131}I-labeled PVP in brain scanning, 19: 46058
MANNING, Justice, Radium management program in county Health Dept., 19: 46678
MANOHARAN, A. C., Primitive analyticity domains for high-order Wightman functions, 19: 47423
MANSEY, R. C., Rare earth intermediate phases. III., 19: 47052
MANTHOS, E. J., Metallography of irradiated dispersion-type fuel elements, 19: 47084 (NMI-4997, pp 124-33)
MANTHOS, E. J., Replication of irradiated specimens with room-temperature vulcanizing silicones, 19: 47091 (NMI-4999, pp 69-77)
MAPOTHER, D. E., Superconducting properties of tin, indium, and mercury below 1°K, 19: 47517
MAQSOOD, M., Iodine-131 uptake by tissues of rainbow trout, 19: 45796
MARADUDIN, A. A., Expression for quartic anharmonic contribution to Helmholtz free energy of a special model of an fcc crystal, 19: 47878 (LA-3379)
MARANGELLI, B., Magnetostriction wire spark chambers, 19: 46783
MARBLE, G., Thyroid burden of radioiodine after respirator contamination of monkey Macaccus rhesus, 19: 45776
MARBLE, Georges, Determination of sodium and potassium in biological media by neutron activation without chemical separation, 19: 46165 (CEA-R-2837)
MARCHIORO, Thomas L., Problems in renal homotransplantation, 19: 45880
MARCINKOW, F., Effect of p-terphenyl on melting points of terphenyl–biphenyl organic coolants, 19: 46300 (AECL-2261)
MARCUS, Inge, Radiolysis of cyclohexane-d_{12}–cyclopentane mixtures, 19: 46364
MARCUS, R. A., Chemical reactions of atomic beams and related problems, 19: 47221 (NYO-2403-8)
MARDON, P. G., Diffusion of plutonium in magnesium and magnesium alloys,

19: 47066
MARIC, Z., Model for double charge-exchange nuclear reactions with pions, 19: 47660
MARIN, Guglielmo, Mitotic activity and DNA synthesis in clones derived from mammalian cell cultures irradiated with x rays, 19: 45867
MARINCU, E., ^{9}Be, ^{11}B and $^{31}P(p,p')$ angular distributions, 19: 47690
MARK, Henry B. Jr., New approach to neutron activation analysis through micro and submicro electroseparation techniques, 19: 46229
MARKOV, K. P., Evaluation of time-related readings of aerosol radiometers with a continuously moving filter strip, 19: 46760 (NP-15462)
MARMOR, L., Evaluation of healing process in avian digital flexor tendons and grafts following application of artificial tendon sheath, 19: 45964
MARMOR, L., Use of irradiated homografts and artificial sheaths in avian and mammalian tendon injuries, 19: 45965
MARROW, Lewis B., Retained ThO_2 media in seminal vesiculography. Follow-up study with dose estimates, 19: 45837
MARSH, R. O., Prestressed concrete structures for large power reactors, 19: 47925 (GA-6505)
MARSHALL, J. D., Analysis of radiation streaming through single-bend ducts, 19: 47863
MARSHALL, J. F., Determination of deuterium density profile in a deuterian plasma using an energetic D^+ beam, 19: 47727 (NP-15434)
MARSHALL, R. H., Preparation and properties of $TiUO_5$, 19: 46272
MARSHALL, W., Covalency effects in neutron diffraction from ferromagnetic and antiferromagnetic salts, 19: 47895
MARTALOGU, N., Levels of low excitation energy in ^{58}Fe, 19: 47696
MARTALOGU, N., Polarization of elastically scattered protons on ^{16}O at 4.5-Mev energy, 19: 47691
MARTALOGU, N., Polarization of elastically scattered protons on Al and Mg at 4.5 Mev, 19: 47692
MARTALOGU, N., Polarization of elastically and inelastically scattered protons on ^{24}Mg at 5.8 Mev, 19: 47697
MARTALOGU, N., Yield ratio for fissioning isomer from deuteron irradiation of Pu, 19: 47688
MARTALOGU, N., ^{9}Be, ^{11}B and $^{31}P(p,p')$ angular distributions, 19: 47690
MARTIN, P. C., Microscopic theory of superfluid helium, 19: 47506
MARTIN, R. P., Excretion of radioactivity by human subjects after ingestion of liver from cattle treated with labeled polydiethylstilbestrol phosphate, 19: 45797
MARTIN, W. H., Neutron dose measurement in graphite irradiations in BR-2, 19: 48030
MARTINELLI, P., Use of x fluorescence excited by radioactive sources, 19: 46201
MARTINENGHI, C., Analysis of behavior of leukocytes in the whole-body irradiated rat, 19: 45934
MARTINSON, Paul E., Arc initiator for plasma generator, 19: 47861
MARTO, P. J., Nucleate boiling instability of alkali metals, 19: 46551
MARTO, Paul J., Effect of surface conditions on nucleate pool boiling of sodium, 19: 46549
MARTRES, R., Surface tension of gadolinium and floating-zone single crystals, 19: 47046
MASHKOVA, E. S., Concerning angular regularities in small-angle scattering of inert gas ions, 19: 47262
MASKEWITZ, Betty, Activities of ANL-ENEA computer program libraries and the ORNL Radiation Shielding Information Center, 19: 47908 (ANL-7050, pp 125-39)
MASLEN, E. N., Refinement of crystal structure of yttria, 19: 47027
MASLEN, E. N., Scattering length of yttrium for thermal neutrons, 19: 47888
MASON, D. W., Containment of plasma trapped in a magnetic well, 19: 47848
MASON, G. W., Di n-octyl phosphinic acid as a selective extractant for metallic cations, 19: 46443
MASPERONI, A., Influence of heat-treatments on structure of uranium-rich alloys containing zirconium, 19: 47014 (RT/MET(64)4)
MASSAGLIA, A., Separation of ^{131}I-labeled S-sulfonated A and B insulin chains by thin-layer chromatography, 19: 46445
MASSIGNON, Daniel, Process and device for manufacture of a permeable membrane, 19: 46978
MASSIMO, L., MAFIA II—a one-dimensional burnup code, 19: 47910 (ANL-7050, pp 299-307)
MASSRY, Shawl, Iodine-131 uptake studies under hot climatic conditions, 19: 45779
MASTEL, B., Effect of neutron radiation on Re, 19: 47106
MASTEL, B., Novel metallographic utilization of replicas and microautoradiography, 19: 46951 (NMI-4996, pp 19-26)
MATHER, J. W., High-density deuterium plasma, 19: 47843
MATHIAS, E., Half life and g factor of 75-kev level in ^{100}Rh, 19: 47662
MATHIS, A., PINETO—FORTRAN code designed for the solution of nonlinear differential equations in neutron dynamics, 19: 47916 (ANL-7050, pp 429-41)
MATHUR, S. C., Angular distributions of γ rays produced by neutron bombardment of Al, Mg and Si, 19: 47638
MATHUR, S. C., Angular distribution of γ rays produced in the $^{40}Ar(n,n'\gamma)^{40}Ar$ reaction, 19: 47639
MATHUR, S. C., Gamma rays produced in inelastic scattering. III., 19: 47588 (TID-22012, pp 22-52)
MATHUR, S. C., Gamma rays produced in the inelastic scattering of neutrons with magnesium and silicon, 19: 47589 (TID-22012, pp 53-66)
MATHUR, Suresh C., Angular distribution of γ rays produced in inelastic scattering of neutrons from ^{40}Ar, 19: 47590 (TID-22012, pp 67-98)
MATHUR, V. S., Leptonic neutron decay of Ω^-, 19: 47363
MATLI, G., Effect of treatment with hepatic derivatives on survival and on oxidative phosphorylating activity of liver of mice exposed to whole-body irradiation, 19: 46024
MATORA, I. M., 30-Mev microtron-injector for pulsed fast reactor, 19: 47164 (JINR-P-2313)
MATOUSEK, J., Radioactivity studies in Plzen, 1957–1962, 19: 46687
MATRAS, S., Vibratory grinding and polishing of metallographic specimens, 19: 46939 (NMI-5025(Pt.I), pp 185-219)
MATSUDA, Hirotsugu, Integrated spectra of an isotopically disordered linear chain, 19: 47256
MATSUDA, Nisaku, Preliminary operation of thermonuclear fusion assembly of scalloped torus type, 19: 47779
MATSUMOTO, Shoichi, Plastic material for measuring large radiation dosage, 19: 46392
MATSUO, Hiroshi, Studies on graft copolymers of styrene onto polypropylene prepared by use of γ rays, 19: 46355
MATSURO, Naoshi, Energy spectra of photoprotons from ^{13}C, ^{24}Mg, ^{28}Si, ^{32}S and ^{40}Ca, 19: 47699
MATSUSHITA, Y., Application of oxygen concentration cells with solid electrolyte $ZrO_2 \cdot CaO$ to thermodynamical research work, 19: 46297
MATSUYAMA, Akira, Aftereffect of irradiated halogenophenol solutions on the viability of Escherchia coli. II., 19: 46007
MATSUYAMA, Akira, After-effect of irradiated halogenophenol solutions on viability of E. coli, 19: 45834
MATTHEWS, Christine M. E., Interpretation of ^{133}Xe lung washin and washout curves using an analog computer, 19: 46070
MATTHIAS, E., Angular correlations of γ rays from polycrystalline sources, 19: 47607
MATYUKHIN, V. D., Rotation of plasma jet in magnetic field, 19: 47849
MAULBETSCH, John S., Study of system-induced instabilities in forced-convection flows with subcooled boiling, 19: 46534 (NP-15437)
MAUSHART, R., Measurement in successive stages of an emergency: equipment, methods and facilities, 19: 46839
MAVRODIN, Maria, Gravimetric determination of rare earths with dioximaleic acid, 19: 46216
MAVRODIN, Maria, Separating rare earths from uranium, iron, and manganese, 19: 46452
MAXON, Marshall Stephen, Investigation of the L.S.Z. formalism in Lee model, 19: 47402
MAY, Robert M., Method for deuteron stripping calculations. II., 19: 47631
MAYER, I., Thermal decomposition of rare earth and yttrium bromide hydrates, 19: 46271
MAYNEORD, W. V., Mans' natural radiation environment, 19: 46688
MC ALISTER, Joan M., Use of ^{131}I-labeled PVP in brain scanning, 19: 46058
MC AULEY, F. D., Implantation irradiation of epitheliomata of eyelids and adjacent areas, 19: 46056
MC BRIDE, J. A., Cytogenetic studies in chronic myeloid leukemia and acute leukemia associated with mongolism, 19: 45915
MC CABE, J. T., Entrance effects in circular thrust bearings, 19: 46462 (TID-22184)
MC CARDLE, R., Technetium-99m as clinical tracer material, 19: 46140
MC CARTHY, Walter J. Jr., Nuclear tests at Fermi confirm basic predictions, 19: 48015
MC CONIGA, A. F., Minimized fuel cycle cost for simulated boiling water reactor. I., 19: 47990 (BNWL-105)
MC CONKEY, J. W., Absolute cross sections for simultaneous ionization and excitation of N_2 by electron impact, 19: 47245
MC CONNELL, D. V., Evaluation of healing process in avian digital flexor tendons and grafts following application of artificial tendon sheath, 19: 45964
MC CONNELL, D. V., Use of irradiated homografts and artificial sheaths in avian and mammalian tendon injuries, 19: 45965
MC CORMICK, J. Fronk, Interactions of γ radiation and drought upon Pinus elliottii and Pinus palustris, 19: 45855
MC CORMICK, J. Fronk, Radioactivity on southeastern granite outcrops, 19: 45752
MC CREDIE, J. A., Effect of breathing 5% CO_2 and 95% O on tumor radiocurability, 19: 46003

MC CULLOCH, E. A., Hemopoietic defect in anemic mice of genotype Sl/Sl^{d}, 19: 45856
MC CULLOCH, E. A., Radiosensitivity of the immune response to sheep red cells in the mouse, 19: 45903
MC CUNE, James E., Non-linear effects of fluctuations on MHD performance, 19: 47294
MC CUSKER, C. B. A., Strongly interacting particles in air shower cores, 19: 47271
MC DADE, James C., Nuclear magnetic resonance in boron trioxide at elevated temperatures, 19: 47873 (AD-612384)
MC DONALD, D. F., Statistics of breakdown using nanosecond pulse techniques, 19: 47114 (AD-614286)
MC DONNELL, W. R., Development of swelling-resistant uranium alloys, 19: 47103
MC DOWELL, A. A., Response perseveration under constant stimulus-position conditions by normal and previously irradiated female rhesus monkeys, 19: 45899
MC DOWELL, A. A., Response-shift learning-set formation by normal and previously irradiated female rhesus monkeys, 19: 45900
MC DOWELL, A. A., Sex as factor in ambivalent cue, delayed-response performance by rhesus monkeys, 19: 45898
MC EACHRAN, R. P., Application of iteration-variation method to atomic scattering problems, 19: 47247
MC GEE, W. C., Microprogramming for data acquisition and control, 19: 46813
MC GIRR, E. M., Radioiodine therapy in thyrotoxicosis: review of 908 cases, 19: 46122
MC GONNAGLE, W. J., Metallography—ally of nondestructive testing in evaluating nuclear fuel components, 19: 46556 (NMI-4997, pp 1-21)
MC GRATH, F. E., Hot cell metallographic experience at Battelle, 19: 47085 (NMI-4997, pp 134-56)
MC GRATH, F. E., Metallographic preparation of irradiated uranium carbide, 19: 47083 (NMI-4996, pp 77-85)
MC GRATH, F. E., Metallography of ceramic fuel and refractory metal compatibility couples, 19: 46954 (NMI-5025(Pt.I) pp 39-58)
MC GRATH, F. E., One-step replication in the hot cell, 19: 47090 (NMI-4999, pp 54-9)
MC GREGOR, John F., Heritable effects of radiation on body weight in rats, 19: 45880
MC ILWAIN, R. L., SMP and Frankenstein on-line, 19: 46797
MC INTYRE, Lawrence Cook Jr., Tensor polarization of deuterons scattered from ^{4}He, 19: 47704
MC KINLEY, T. W. Jr., Erythropoietic capacity of short-term mouse marrow cultures, 19: 45740
MC LAUGHLIN, Mary M., Hazard of ^{90}Sr—a review, 19: 46634 (AD-423463)
MC LEAN, A. S., Chromosome aberrations in man following acute and chronic exposure to x and gamma rays, 19: 45916
MC LEAN, A. S., Exposure to x and gamma rays, 19: 45917
MC LENDON, J. D., Nuclear safety considerations in fabrication of massive partially enriched U–Mo reactor parts, 19: 46967 (Y-KB-62)
MC LEOD, D. W., Electron identification in lead plate spark chambers, 19: 46782
MC LEOD, D. W., Magnetic spark chamber system, 19: 46796
MC NAMARA, B., Helical fields possessing mean magnetic wells, 19: 47154
MC RAE, Donald L., Contour brain scanning with I and Hg compounds for detection of intracranial tumors, 19: 46046
MEABURN, Malcolm, Effect of hydrogen atom and electron scavengers on radiolysis of methanol vapor, 19: 46395
MEAD, G. D., Diffusion of protons in outer radiation belt, 19: 47461
MEADEN, G. T., Electrical resistivity of Th, 19: 47042
MEADEN, G. T., Electrical resistivity and characteristic temperature of technetium, 19: 47063
MEADOR, J. T., Experience with vibratory polishers and design for hot-cell application, 19: 47086 (NMI-4997, pp 184-8)
MECHLING, William Harrison, Decontamination of selected vegetable crops by leaching with reference to Sr, 19: 45758 (NYO-2598-24)
MEDICUS, H. A., Photonuclear reaction studies by activation methods, 19: 47596 (TID-22141, pp 94-7)
MEDVEDEV, V. N., Piezospectroscopic determination of symmetry of crystal field acting on trivalent ions of rare earths in fluorite lattice, 19: 47890
MEE, W. T., Nuclear safety considerations in fabrication of massive partially enriched U–Mo reactor parts, 19: 46967 (Y-KB-62)
MEGAHED, Y. M., Alterations of ascorbic acid content of legumes caused by β or γ irradiation. II., 19: 45938
MEGAW, W. J., The adsorption of iodine on atmospheric particles, 19: 46672
MEICHLE, R. H., Clean ^{233}U production—methods and parameters, 19: 46900 (RL-SA-46-A)
MEISELS, G. G., Prog. rpt. on fissiochemical development, semiannual, 7–12/64, 19: 46324 (AGN-8132)

MEISELS, G. G., Radiolysis of ethylene. III., 19: 46361
MELEKHIN, V. N., 30-Mev microtron-injector for pulsed fast reactor, 19: 47164 (JINR-P-2313)
MELLOWS, Frank W., Effect of hydrogen atom and electron scavengers on radiolysis of methanol vapor, 19: 46395
MELONI, Sandro, Contribution of a 5-curie Pu–Be source to the subcritical SM-1 structure, 19: 48040
MELTON, Donald F., Rate controlled manipulators, 19: 46482 (CONF-640508, pp 75-99)
MENDECKI, Josef, DNA repair of radiation damage. I., 19: 46013
MENEELY, George R., Scintillation methods for metallic ion determination in human subjects using computer techniques, 19: 45771
MENZEL, R. G., Reclamation of agricultural land following accidental radioactive contamination, 19: 46701
MERELLI, A., Experiments on critical flow of a pressurized water loop in natural circulation conditions, 19: 46536 (RT/ING(65)1)
MERGLER, Harry, Generalized, programmed manipulators, 19: 46501 (CONF-641120, pp 73-4)
MERIEL, Yves, Research methods in high-energy physics, 19: 46834
MERKAS, Zlatko, Intracavitary therapy of uterine carcinoma with Co-60, 19: 46039 (JPRS-31667)
MERKULOV, L. A., 30-Mev microtron-injector for pulsed fast reactor, 19: 47164 (JINR-P-2313)
MERLINI, Margaret, Stable manganese content of mollusks from Lake Maggiore, 19: 45788
MERRIAM, M. F., Superconductivity in the tin–gallium system, 19: 47521
MERTL, F., Radioactivity studies in Plzen, 1957-1962, 19: 46687
MESHII, M., Effect of annealing on mechanical properties of electron-irradiated Al single crystals at 23°K, 19: 47095
MESSERLE, Hugo K., Traveling-wave interaction and wave growth, 19: 47295
MESTWERDT, W., Histology and cytomorphology of experimental beryllium granuloma, 19: 45803
MEURGUES, J.-P., New scattering chamber and its installation, 19: 47127
MEYER, J., Stress on joint of bonded spherical underground shelter by compressional wave propagated through soil, 19: 46569
MEYER, K., Calculation of thermal utilization factor in energy-dependent diffusion approximation, 19: 47558
MEYER, K., Synthetic scattering kernel for calculating the energy distribution of thermal neutrons, 19: 47557
MEYERS, D. J., Roll film camera for remote metallography, 19: 46711 (BNWL-SA-161)
MEYERSON, G. A., Research on refractory and hard compounds, 19: 47010 (AEC-tr-6616)
MEYNIEL, G., Detection of β activities on chromatogram with thin layer of absorbent or of ion exchange resin, using gel-forming scintillator, 19: 46862
MEZHOV-DEGLIN, L. P., Measurement of the thermal conductivity of crystal ^{4}He, 19: 47902
MICELI, R., Can the index of uptake of ^{32}P reveal radiosensitivity of metastases, 19: 46098
MICHAELASSI, P. L., Critical considerations on the evaluation of the radiobiological response of irradiated connective tissues, 19: 45935
MICHAELIS, H., New targe program of euratom, 19: 48003
MICHAU, J. C., Ariane-automatic device for analysis of spark chamber photographs, 19: 46787
MICHEL, David J., Crystal structure of $YbZn_2$, 19: 47030
MICHEL, Lothar, Radio-labeling of organic compounds by $^{12}C(\gamma,n)^{11}C$ reactions by means of bremsstrahlung of 35-Mev betatron, 19: 46413
MICU, M., Positive parity states of T = ½ in A = 15 nuclei, 19: 47694
MICU, M., Representation of the symplectic group of rank two, 19: 47333
MIGAHED, M., Search for anomalous electric dipole transitions in ^{197}Hg, 19: 47674
MIGLIORINI, M., Behavior of cholesterol in irradiated animals, 19: 45917
MIHAI, R., Finite solid-angle corrections in γ-γ angular correlation measurements, 19: 47693
MIHUL, Eleonora, Photoproduction of two mesons on nucleons at high energy, 19: 47389
MIKHAILICHENKO, A. I., Dependence of the separation factor in isotope exchange on the properties of the exchanged molecules, 19: 46408 (ORNL-tr-770)
MIKHAILOVA, M. S., Structure of unsymmetric toroidal magnetic fields, 19: 47144
MIKHAILOVSKAYA, L. V., Corrections to flute instability of axially symmetric plasma with finite ion Larmor radius, 19: 47768
MIKHAILOVSKAYA, L. V., Effect of shear on flute instability in dilute plasma, 19: 47765
MIKHAILOVSKII, A. B., Corrections to flute instability of axially symmetric plasma with finite ion Larmor radius, 19: 47768
MIKHAILOVSKII, A. B., Effect of shear on flute instability in dilute plasma, 19: 47765

MIKHAILOVSKII, A. B., Flute instability of plasma with nonzero ion Larmor radius and nonzero pressure, 19: 47766
MIKHEEVA, V. I., Thermal stability of lithium borohydride, 19: 46248 (FTD-TT-65-591)
MIKKE, K., Time-of-flight method for investigations of single-crystal structures, 19: 47894
MIKULINSKII, M. A., Isotope shift and quadrupole moments of near-spherical nuclei, 19: 47573 (IAE-717)
MIKULSKI, Jan, Extraction of metals by use of tracer isotopes. IX., 19: 46451
MILEWSKI, J., Modulated conductivity induction synchronous magnetogasdynamic generator, 19: 47293
MILICH, J. J., Prog. rpt. on LCRE pumps and sumps, final, 7/65, 19: 46535 (PWAC-386)
MILLER, A. E., Preparation of new type of nonstoichiometric rare-earth oxide, 19: 46273
MILLER, Barry, Varied uses developing for radioisotopes, 19: 46883
MILLER, Carl F., Fallout and radiological countermeasures. I., 19: 46585 (AD-410522)
MILLER, J. K., Iodine metabolism of lactating dairy cows, 19: 45781
MILLER, J. K., Metabolism of different forms of I in milk, 19: 45782
MILLER, R. H., On-line data analysis, 19: 46792
MILLER, R. I., Prog. rpt. on fissiochemical development, semiannual, 7-12/64, 19: 46324 (AGN-8132)
MILLER, S. H., Test apparatus and profile measurement system for rectangular plates subjected to in-plane thrusts, 19: 46555 (KAPL-M-6493)
MILLER, W. D., Excitation of ethylene, acetylene, propyne, and 1-butyne by low-energy electron impact, 19: 46322 (AD-612070)
MILLERON, N., Porous metal isolation traps and cryosorbents in vacuum technique, 19: 46573 (UCRL-12393-T)
MILLS, R. L., Thermal expansion of compressed He, II., 19: 47505
MILNER, G. W. C., Determination of nitrogen in plutonium nitride, 19: 46164 (AERE-R-5002)
MILTON, D. W., Determinations of auroral-zone x-ray spectrum, 19: 47471
MILTON, D. W., Spatial asymmetry and periodic time variations of x-ray microbursts in auroral zone, 19: 47470
MINACHEV, Kh. M., Isotopic exchange between molecular oxygen and oxides of rare earth elements, 19: 46266
MINIER-CASSAYRE, Colette, Point defects in pure iron through electrical resistivity, 19: 47094 (ORNL-tr-668)
MINTZ, Michael D., Air tables. Tables of compressible flow functions, 19: 47151
MIRONOVA, A. P., Character of changes of γ-aminobutyric acid in brain tissues during local irradiation of cerebellum, 19: 45979
MITAKI, Akio, Mean square angular and lateral spreads of electrons and photons in a cascade shower, 19: 47268 (INSJ-86)
MIYAJIMA, Nobuhiko, K-matrix formalism for three-body and bound-state scattering, 19: 47381
MIYAJIMA, Yutaka, Differential chemical carcinogenesis in three distinct melanocyte systems of Syrian (golden) hamsters, 19: 45906
MISHRA, L. C., Dental lesions in rat induced by radiomimetic agents, 19: 45845
MISRA, Sushil K., Cross relaxation of ^{57}Co coupled to an unpaired electron spin, 19: 47615
MITCHELL, Joseph S., Possibility of use of radioactive drugs, 19: 46125
MITIN, R. V., High-pressure electrodeless discharge, 19: 47788
MITIN, R. V., Pulse heating of high-pressure argon arc. I., 19: 47789
MITIN, R. V., Pulse heating of high-pressure argon arc. II., 19: 47790
MITTER, H., Lectures on particles and field theory. II., 19: 47405
MITTLEMAN, Marvin H., Rearrangement collisions—electron excitation of He(2^3s), 19: 47239
MIYAJIMA, Shigeki, Hydromagnetic wave in toroidal discharge with longitudinal magnetic field, 19: 47742
MIYAMOTO, Kenro, Density measurement of pinch plasma using infrared He-Ne laser interferometer, 19: 47759
MIYASHITA, Kyoichi, BF_3 proportional counters, 19: 46822
MIYAUCHI, T., Prog. rpt. on chemical engineering studies on processing radioactive wastes, final, 1/64-3/65, 19: 48079 (NP-15371)
MIYAZAWA, Hironari, Intrinsically broken U(18) symmetry, 19: 47379
MIYOSHI, Syoichi, Probe measurement of electron density in magnetized plasma, 19: 47758
MIZEN, Neil J., Design and test of full-scale wearable exoskeletal structure, 19: 46483 (CONF-640508, pp 158-97)
MODONESI, O., PINETO—FORTRAN code designed for the solution of nonlinear differential equations in neutron dynamics, 19: 47916 (ANL-7050, pp 429-41)
MOECK, E. O., Dryout in a 19-rod bundle cooled by steam/water fog at 515 psia, 19: 46548
MOELLER, F., Atomic energy market in Europe. IX. Norway, 19: 48114
MOELLER, Ulrich, Programs for solution of neutron physics problems with help of Monte Carlo method, 19: 47546 (KFK-298)
MOELLER, Ulrich, Solution of the transport equation with help of the Monte Carlo method, 19: 47545 (KFK-297)
MOEN, H., BISTRO, an integrated computational system for prediction of history of boiling water reactors, 19: 47913 (ANL-7050, pp 369-78)
MOERTEL, Charles G., Combined 5-fluorouracil and supervoltage radiation therapy in the palliative management of advanced G-I cancer, 19: 46091
MOHANARADHAKRISHNAN, V., Effect of γ radiation on soluble and insoluble collagens, 19: 45850
MOISEEV, I. G., The velocity of corpuscular streams in the solar corona based on observations of solar radio emission, 19: 47189 (N64-31082)
MOISEEV, V. V., The radioactivation analysis of silicon and silicon compounds with the successive use of ion-exchange chromatography, 19: 46228
MOISESCU, L., Representation of the symplectic group of rank two, 19: 47333
MOLCHANOV, V. A., Concerning angular regularities in small-angle scattering of inert gas ions, 19: 47262
MOLINA-RAMOS, J., Concentration of ^{137}Cs in Australian milk during 1964, 19: 46660
MOLLENAUER, James F., Matching the computer to the man, 19: 47336
MONACO, Anthony P., Biology of tissue transplantation. I., 19: 45944
MONAHAN, J. E., Experiments to measure differential cross sections, 19: 47601
MONTALBETTI, R., Optical aurora, 19: 47498
MONTGOMERY, C. D., Evolution of remote handling capabilities at NRDS, 19: 48047 (CONF-640508, pp 334-9)
MONTGOMERY, H., Expansion formulae for the ^{3}He and ^{4}He vapor pressure scales, 19: 47129
MONTGOMERY, P. O'B., Ultraviolet microbeam irradiation in living cell membranes, 19: 45891
MOORE, R. B., Measurement of range of 100-Mev protons in Al, 19: 47225
MOORE, R. H., Purification of Pu metal, 19: 46915 (BNWL-IR-2)
MOORE, R. V., Progress in development of nuclear power, 19: 48026
MOORHEAD, W. G., Status of CERN HPD program for bubble chambers, 19: 46812
MORAN, T. F., Energy transfer in reaction of He^+ with O_2, 19: 47231
MORGAN, D., Marginally singular forces and their role in producing pseudovector resonances, 19: 47338
MORGAN, I. L., Angular distribution of gamma rays from C, O and N at 14.8 Mev, 19: 47593 (TID-22012, pp 156-75)
MORGAN, I. L., Angular distributions of γ rays produced by neutron bombardment of Al, Mg and Si, 19: 47638
MORGAN, I. L., Angular distribution of γ rays produced in the ^{40}Ar(n,n'γ)^{40}Ar reaction, 19: 47639
MORGAN, I. L., Cross sections and angular distributions of neutron-produced γ rays in Fe from .96 to 4.75 Mev, 19: 47591 (TID-22012, pp 99-128)
MORGAN, I. L., Gamma rays produced in inelastic scattering. III., 19: 47588 (TID-22012, pp 22-52)
MORGAN, I. L., Gamma rays produced in the inelastic scattering of neutrons with magnesium and silicon, 19: 47589 (TID-22012, pp 53-66)
MORGAN, Ira L., Inelastic neutron scattering in ^{206}Pb, ^{207}Pb, and ^{209}Pb, 19: 47592 (TID-22012, pp 129-55)
MORGAN, Ira Lee, Angular distribution of γ rays produced in inelastic scattering of neutrons from ^{40}Ar, 19: 47590 (TID-22012, pp 67-98)
MORGAN, Ira Lee, Total absorption γ spectrometer system for pulsed beam n,nγ measurements, 19: 46765 (TID-22012, pp 4-21)
MORGAN, J. W., Uranium and thorium abundances in basalt cored in Mohole Project (Guadalupe Site), 19: 46628
MORGAN, L. G., Status of salt cycle process for processing oxide fuels, 19: 46422 (BNWL-SA-205)
MORGAN, Russell H., Frequency of medical x-ray examinations, 19: 46112
MORGAN, William Jason, Search for scalar gravitational waves, 19: 47486
MORGULIS, N. D., Spectral determination of electron temperature of Cs plasma in a thermoelectric diode, 19: 47773
MORI, Sigeru, Spectroscopic measurements of impurities in plasma stream. I. 19: 47757
MORI, Yasuo, Forced convective heat transfer in horizontal tubes. I., 19: 46545
MORICHI, Toshiki, Temporary increase in uv resistance in course of spore germination of Bacillus subtilis, 19: 45848
MORIUCHI, Kazuyoshi, Absolute measurement of high rate radiation by ionization method, 19: 46830
MORIWAKI, Yoshio, High-resolution, pulse-height analyzer, 19: 46827
MORLEVAT, J.-P., Ternary diagram—uranium-uranium dioxide-uranium oxycarbide, 19: 46249 (LA-tr-65-15)
MORONEY, J. R., Strontium-90 in Australian environment during 1963, 19: 46594
MORONEY, J. R., Strontium-90 in Australian environment, 1961 to 1963, 19: 46595

MOROZOV, A. I., Structure of unsymmetric toroidal magnetic fields, 19: 47144
MOROZOV, V. S., Biological effects of high energy protons, 19: 45821 (JPRS-31547, pp 1-5)
MORRIS, Arthur M., Renal clearance of ^{131}I-labeled sodium iothalamate in man, 19: 46079
MORRIS, E., Computer calculation of energy yield produced by hypothetical fast reactor accident, 19: 47918 (ANL-7050, pp 503-14)
MORRISON, Willard L., Nuclear reactor fuel element for nitrogen fixation, 19: 47985
MORRISROE, G. L., NAMDA—new method of computerized management control, 19: 48098 (SC-R-65-902)
MORTON, Maurice, Prog. rpt. on low-temperature polymerization, 1–3/65, 19: 46323 (AD-613529)
MOSEL, D. K., Photonuclear reaction studies by activation methods, 19: 47596 (TID-22141, pp 94-7)
MOSELEY, B. E. B., How cells repair radiation damage, 19: 45985
MOSES, H. E., Kinematics of angular momentum of a particle. I., 19: 47418
MOSKVIN, N. A., Symmetry of narrow-band luminescence and absorption centers of colored LiF crystals, 19: 46380
MOSS, Thomas Alan, Production of η mesons in π–N collisions, 19: 47401
MOSZKOWSKI, S. A., Short-range correlations in nuclear matter, 19: 47665
MOTLEY, R. W., Transition from Landau damping to viscous damping of ion acoustic waves, 19: 47724 (MATT-267)
MOTZKIN, Donald, Radioactive scintiscanning in evaluation of renal disease, 19: 46130
MOUSA, M. G., Search for anomalous electric dipole transitions in ^{187}Re, 19: 47674
MOUSTAPHA, Z., Extraction of cerium with tri-n-octyl phosphine oxide, 19: 46439
MOWATT, Keith S., Use of an intra-oral balloon in radiotherapy, 19: 46066
MOYAL, J. E., General theory of first-passage distributions in transport and multiplicative processes, 19: 47865 (ANL-7061)
MUBAYI, V., Lectures on particles and field theory. II., 19: 47405
MUDRA, Paul J., Appraisal of gaseous waste disposal into the lithosphere at NRTS, 19: 48077 (IDO-12024)
MUDROVA, B., Control of radiochemical purity of ^{52}Mn preparates, 19: 46210
MUEGGE, O., Radioactivity and pleochroic halos, 19: 46625 (ORNL-tr-757)
MUELLER, A., Electron spin resonance studies of radicals, 19: 46402
MUELLER, G. O., SOSH-5. Computer program for shielding calculations, 19: 47866 (KAPL-M-6460)
MUELLER, G. O., Use of digital programs in reactor plant designs, 19: 47909 (ANL-7050, pp 217-30)
MUELLER, Harold J. W., Regge poles in nonrelativistic potential scattering, 19: 47320
MUELLER, J., Survey of maximum permissible levels that have been proposed in various countries, 19: 46696
MUELLER, John J., Quantum-mechanical Boltzmann equation, 19: 47416
MUELLER, M. H., Neutron-diffraction study of uranyl nitrate hexahydrate, 19: 46257
MUELLER, Rudolph, Modulation of light by means of electrically birefringent crystals, 19: 48110 (SC-T-65-750)
MUELLER, Werner, Amine hydrohalide extraction studies, 19: 46180 (UCRL-16254)
MUELLER, William M., Conference on advances in x-ray analysis, Denver, 8/64. VIII., 19: 46185
MUENCH, J., Appearance of pc pulsations in earth's magnetic field in relation to geomagnetic activity, 19: 47482
MUENNICH, K. O., Instrument for detection of radioactive radiation from aerosols in gases, 19: 46869
MUENZEL, H., Decay of ^{150}Eu and ^{150}Eu, 19: 47681
MUENZEL, H., Decay of ^{160}Tb, 19: 47683
MUKAIBO, Takeshi, Reprocessing of uranium fuels by fused salt electrolysis, 19: 46448
MUKHIN, K. N., Elastic (p,p) scattering at 1.45 Bev, 19: 47304 (IAE-700)
MULLER, F., Reaction $K^+p \rightarrow K^0p\pi^+$ at 3 Bev, 19: 47356
MULLIE, J., Ariane-automatic device for analysis of spark chamber photographs, 19: 46787
MUNARI, S., Influence of acetylene on radioinduced polymerization of ethylene, 19: 46353
MURAI, Takeo, Integral dose measurement using a plastic scintillator, 19: 46105
MURAKAMI, Akio, Comparison of fission neutrons and γ rays in respect to their efficiency in inducing mutations in silkworm gonia, 19: 45883
MURAKAMI, Yoichi, Separation of samarium by the ion exchange method, 19: 46438
MURAMATSU, Susumu, Splenic and thymic weight response to whole-body x irradiation in three strains of mice, 19: 45956
MURASE, Hirokazu, Neutron slowing down and diffusion problem in medium containing holes, 19: 47563

MURCZYNSKI, Cz., Isotope diagnostics of respiratory insufficiency, 19: 46118
MURIN, A. N., Chemical changes in β decay of I isotopes, 19: 46411
MURIN, G. F., Biological effects of high energy protons, 19: 45821 (JPRS-31547, pp 1-5)
MURPHY, C. G., Height-interval timer, 19: 46724 (SC-TM-65-356)
MURPHY, J. W., Mass-seven hypernuclei and the mass-six nuclei, 19: 47647
MURPHY, T., Techniques used in GEM code for Monte Carlo neutronics calculations in reactors and other systems of complex geometry, 19: 47949 (ANL-7050, pp 557-79)
MURRAY, I. P. C., Radioiodine therapy in thyrotoxicosis: review of 908 cases, 19: 46122
MURTHY, T. K. S., Alkalimetric determination of metals using 8-hydroxyquinoline as complexing agent, 19: 46205
MUSACCHIA, X. J., Absorption of D-glucose by segments of intestine from irradiated ground squirrels, 19: 45841
MUSSET, P., Large heavy liquid bubble chamber, 19: 46799
MUTH, Hermann, Whole-body counter for research, clinical applications, and radiation protection measurements, 19: 46836
MUYSKEN, Matthijs, Pressurized water reactor plant with improved jet pump arrangement, 19: 47974
MUZHTASIMOV, F. N., Formation in Ho-162 in Ta + p at 660 Mev, 19: 47579 (JINR-P-2275)
MYERS, Ralph D., Final rpt. on fundamental problems of solids, 9/61–8/64, 19: 47875 (AD-614136)

N

NAGAO, Shigeo, Oscillation of the rf-excited positive column in longitudinal magnetic field, 19: 47778
NAGATA, Takesi, Sudden commencements of geomagnetic storms and their local irregularities, 19: 47456
NAGEL, W., Activation cross sections for 14-Mev neutrons, 19: 47673
NAGY, A. F., Ionospheric electron density and body potential measurements by a cylindrical Langmuir probe, 19: 47465
NAHA, P. M., Development of improved strains of Streptomyces citreus through induced mutation, 19: 45991
NAKADA, M. P., Diffusion of protons in outer radiation belt, 19: 47461
NAKAGAWA, Koji, Anti-electrostatic treatment of teflon films by radiation-induced graft copolymerization, 19: 46376
NAKAGAWA, Masami, 3^a-Plet model of elementary particles, 19: 47386
NAKAJIMA, Tokuosuke, Electrode erosion as parameter of spark discharge, 19: 47134
NAKAMURA, Seitaro, Nature of the muon, 19: 47378
NAKANO, George H., Analysis and evaluation of measurements of geomagnetically trapped electrons from high-altitude nuclear explosions, 19: 47446 (AD-612013)
NAKAYA, Shigehisa, Anomalous behaviors in Josephson current, 19: 47515
NAKAZAWA, Hiroshi, Time-dependent problems of scattering in linear lattice system, 19: 47255
NAKAZAWA, Kozo, Mass formula for resonance states, 19: 47384
NAKHODKIN, N. G., Effect of atomic screening factor on inelastic scattering of electrons, 19: 47259
NAMIKAWA, Tomikazu, Propagation of weak hydromagnetic shock waves in the exosphere. I., 19: 47478
NAMIKI, Mitsuo, Aftereffect of irradiated halogenophenol solutions on the viability of Escherichia coli. II., 19: 46007
NAMIKI, Mitsuo, After-effect of irradiated halogenophenol solutions on viability of E. coli, 19: 45834
NANCE, R. L., Refractory plutonium fuel materials, 19: 46999 (LA-DC-7297)
NANDI, P., Development of improved strains of Streptomyces citreus through induced mutation, 19: 45991
NAPRAVNIK, J., The sorption of fission products on the suspension of the natural sorbents coagulated in an electric field, 19: 48082 (UJV-1236/65)
NAPRAVNIK, Jiri, Plant for disposal of radioactive waste water, 19: 48086
NARLIKAR, J. V., Theories of gravitation, 19: 47411 (NP-15486)
NAROZNIK, K., Isotope diagnostics of respiratory insufficiency, 19: 46118
NARROG, J., Determination of radiostrontium in presence of Ca, 19: 46197
NARROG, J., Rapid method for detection of ^{90}Sr/^{90}Y in urine, 19: 46198
NARVER, David L. Jr., Engineering study for tunnel grid blast-shelter concept for Detroit, 19: 46568 (ORNL-TM-1223)
NASH, Donald J., Effects of x irradiation of mice exposed in utero during different stages of embryological development on duration of mature life, 19: 45852
NASTOYASHCHII, A. F., Physics of plasma thermoelements, 19: 47207
NATELSON, M., Kinetic equations for neutron distributions, 19: 47963
NATH, Amar, Role of water of hydration in annealing behavior of neutron-irradiated trisdipyridyl cobalt(III) perchlorate, trihydrate, 19: 46387

NATH, Ravinder, S-wave pion-pion scattering in state T = 0, 19: 47347
NAUMANN, R. A., Half life and g factor of 75-kev level in ^{100}Rh, 19: 47662
NAYUDAMMA, Y., Effect of γ radiation on soluble and insoluble collagens, 19: 45850
NEAL, Thomas E., New approach to neutron activation analysis through micro and submicro electroseparation techniques, 19: 46229
NEAMU, I., ^{9}Be, ^{11}B and $^{31}P(p,p')$ angular distributions, 19: 47690
NEARY, G. J., Biological hazards of radiation applicable to man in space, 19: 46001
NEDER, M. J., Evolution of remote capabilities at NRDS, 19: 48047 (CONF-640508, pp 334-9)
NEFEDOV, V. D., Chemical changes in β decay of I isotopes, 19: 46411
NEGOESCU, Irina, Behavior of recoil atoms in semiconductors, 19: 46398
NEGOESCU, Irina, Interpretation of radiation and thermal annealing by processes governed by defect concentration, 19: 46391
NEIDIGH, R. V., Plasma heating and burnout in beam-plasma interaction, 19: 47852
NELLIS, D. O., Angular distribution of gamma rays from C, O and N at 14.8 Mev, 19: 47593 (TID-22012, pp 156-75)
NELLIS, Donald O., Inelastic neutron scattering in ^{206}Pb, ^{207}Pb, and ^{208}Pb, 19: 47592 (TID-22012, pp 129-55)
NELSON, D., Strongly interacting particles in air shower cores, 19: 47271
NELSON, Donald J. Jr., Planning for the control of radiation accidents, 19: 46702
NELSON, Mary L., Photoscanning in the diagnosis of intracranial lesions, 19: 46053
NEMETH, J., Prog. rpt. on behavior of $SrZrO_3$, 4–6/65, 19: 47008 (NP-15429)
NEMODA, Djordje, Intracavitary therapy of uterine carcinoma with Co-60, 19: 46039 (JPRS-31667)
NESTERIKHIN, Yu. E., Capture of plasmoids in a magnetic mirror machine, 19: 47839
NESTERIKHIN, Yu. E., High-speed diagnostics of a plasma jet, 19: 47735
NESTERIKHIN, Yu. E., Plasma heating mechanism by collisionless shock waves, 19: 47345
NETTER, Francis, Measurement of fission cross section of ^{235}U and ^{239}Pu for thermal neutrons, 19: 47567 (CEA-R-2775)
NEUMANN, Kl.-K., Thermodynamic properties of air at high temperatures (with consideration of radiation contributions), 19: 47731
NEUSCHEL, Sherman K., Natural γ aeroradioactivity of D. C. and parts of Md., Va., and W. Va., 19: 46614
NEVEROVA, L. G., Effect of different doses of x rays on osteogenesis in long tubular bones of mouse embryos, 19: 45872
NEVITT, M. V., Metallographic studies of uranium-fissium alloys, 19: 47004 (NMI-4997, pp 45-54)
NEWBERY, G. R., Standards of activity, 19: 46420
NEWCOMB, L., Reactor maintenance by remote internal tube welding, 19: 46973
NEWCOMBE, Howard B., Heritable effects of radiation on body weight in rats, 19: 45880
NEWCOMBE, Howard B., The quantitative assessment of hereditary damage induced by radiation, 19: 45973
NEWELL, J. M., Neutron transport data for single and multilayer slabs of aluminum, polyethylene, and carbon, 19: 47868 (RRA-T52)
NEWMAN, D. G., Nitrogen isotope equilibration on tungsten, 19: 46289
NEWNHAM, R. E., Neutron-diffraction study of $Co_3B_2O_6$, 19: 46290
NG, Yook C., Neutron activation of terrestrial environment as result of underground nuclear explosions, 19: 46473 (UCRL-14249)
NGUYEN, Van Hieu, Leptonic decays of baryons in the universal V-A theory, 19: 47307 (JINR-P-2278)
NIAS, A. H. W., Clone-size analysis in the study of cell growth following single or during continuous irradiation, 19: 45886
NICHOLS, P., Methods of control rod calculation for graphite moderated reactors, 19: 47999 (TRG-Report-227)
NICHOLSON, Patrick Stephen, Heat transfer considerations in differential calorimeter design, 19: 46728 (UCRL-16336)
NICHOLSON, R. B., Application of Power Burst Facility to fast reactor fuel meltdown tests, 19: 47952 (APDA-177)
NICHPARENKO, W., Oscillations and noise generation in beam-generated plasma, 19: 47741
NICKERSON, Richard A., X-ray examination of square water-cooled copper magnetconductor braze joints, 19: 46965 (UCRL-16383)
NICOLAE, Mariete, Sensitometric studies on nuclear emulsion by means of β radiation, 19: 46832
NICOLITSAS, A. J., System for accurate counting of short-lived activities by repetitive activation, 19: 46818
NIEDERMAYER, R., Reflections of very slow electrons on metal surfaces, 19: 47242
NIEH, N., Lectures on particles and field theory. II., 19: 47405
NIEMIEC, Jan, Crystallochemical characteristics of Re and Te as components of metallic alloys, 19: 47036
NIESE, S., Determination of phosphorus, sulfur, and chlorine in arsenic by neutron activation analysis, 19: 46211
NIHOUL, J. C., Quasi-static oscillations in hot asymmetrical plasma slab, 19: 47746
NIJS, Wilhelmus W., Pressurized water reactor plant with improved jet pump arrangement, 19: 47974
NIKLAS, Wilfrid F., Conversion efficiencies of conventional image amplifiers, 19: 46151
NIKOLOGORSKII, A. V., Rotation of plasma jet in magnetic field, 19: 47849
NILSSON, A., Effect of radiostrontium on oocytes and follicles of adult mice, 19: 45831
NINKOVIC, M. M., Reactions (d,α) on ^{19}F at 1 Mev, 19: 47646
NISHIHARA, H., Immunogenicity of a γ-irradiated Brucella melitensis, 19: 45868
NISHIO, Kozoo, Changes in lactic dehydrogenase activity in plasma of mice after whole-body x irradiation, 19: 45844
NISHIYAMA, Yoshio, On a parallelism between classical mechanics and quantum mechanics, 19: 47432
NISLE, R. G., Effective cross-section factors, 19: 47577 (IDO-17107)
NISSIM-SABAT, Charles, Isotopic differences in the μ-mesic K x-ray energies of ^{16}O–^{18}O, ^{40}Ca–^{44}Ca, ^{116}Sn–^{124}Sn, ^{155}Gd–^{160}Gd, 19: 47582 (NEVIS-129)
NISTOR, C., Automatic Moessbauer spectrometer, 19: 46831
NITTA, Isamu, ESR study of irradiated solid cycloalkanes, 19: 46372
NITTROUER, C. A., Design of high-energy fast-pulse power system, 19: 46476 (AD-613959)
NITU, R., Evidence for high four-momentum transfer from π^--Xe interactions at 9 Bev, 19: 47698
NITU, R., Interaction mean free path of 9-Bev π^- in Xe, 19: 47689
NIX, Thomas E. Jr., Ultrastructural changes induced by ultraviolet light in human epidermis: basal and spinous layers, 19: 45907
NIX, Thomas E. Jr., Ultrastructural changes induced by uv light in human epidermis: granular and transitional cell layers, 19: 45913
NOBILI, D., Electrical resistivity measurements in quenched aluminum–alumina alloys, 19: 47067
NOEL, T. M., Power spectrum of sporadic E at Wilkes and Byrd Stations, Antarctica, 19: 47475
NOGA, M., Effect of nonelastic processes on elastic scattering, 19: 47330
NOLAN, George Junior, Electrochemical behavior of U ions in various ethanol–water systems. I and II., 19: 46292
NORBI-BUFALINI, G., Behavior of total biliary acids and of some pancreatic enzymes in patients irradiated on the abdominal pelvic region, 19: 45928
NORDINE, Paul C., Crystal structure of ScB_2C_2, 19: 46258
NORDQUIST, Robert E., Ultrastructural changes induced by ultraviolet light in human epidermis: basal and spinous layers, 19: 45907
NORDQUIST, Robert E., Ultrastructural changes induced by uv light in human epidermis: granular and transitional cell layers, 19: 45913
NORGREN, Duane, A precision technique for measuring azimuthal distortion in optical lenses, 19: 48103 (UCRL-16260)
NORRIS, David O., Radiothyroidectomy of larval steel-head trout, 19: 45972
NOUVERTNE, Werner, Synthesis of tritium-labeled acids through chain elongation after Arndt-Eistert, 19: 46306
NOWOTNY, H., Crystal structure of so-called technetium ditilicide, 19: 47055
NOWOTTNY, H. E., Accurate determination of the heavy hydrogen isotope by thermal conductivity, 19: 46182 (NP-tr-1275)
NOYES, Richard M., Revised thermodynamic properties of aqueous strontium ion, 19: 46282
NUMEZ, J., Enzymatic iodination of proteins, 19: 46314
NYERGES, Pal, Direct transformation of heat power, 19: 47286

O

OBERHAUSEN, Erich, Whole-body counter for research, clinical applications, and radiation protection measurements, 19: 46836
OBERMAN, C., Derivation of macroscopic equations, 19: 47808
OBERMAN, C., High-frequency conductivity and the emission and absorption coefficients of a fully ionized plasma, 19: 47814
OBERMAN, C., Hydromagnetic stability theory, 19: 47810
OBOLER, Allen A., Differential chemical carcinogenesis in three distinct melanocyte systems of Syrian (golden) hamsters, 19: 45906
O'BRIEN, J. L., Effect of omega transformation on critical currents in a Zr-rich Nb alloy, 19: 47511
OBU, Koji, Pre-SC polar ionosphere and h-f radio propagation over polar paths. II., 19: 47455
O'DELL, F. P., Methods of control rod calculation for graphite moderated reactors, 19: 47999 (TRG-Report-227)
ODIAN, A., Development of streamer spark chambers, 19: 46781

OESER, H., Trends in radiation therapy, 19: 46077
OGATA, Hiroshi, Scattering of α particles by medium-weight nuclei, 19: 47623
OGAWA, Yuichi, Stability of reactor which has external control system, 19: 47971
OGLOBLIN, A. A., Reaction $^{7}Li(p,t)^{5}Li$ and $^{6}Li(\alpha,t)^{7}Be$, 19: 47574 (IAE-836)
OGURA, Shigeyoshi, Radiation monitors for in-pile gas loop experimental apparatus, 19: 48071
ONBA, Yujiro, Radiation from current filament in anisotropic plasma, 19: 47774
OHMAE, Tadayuki, ESR study of irradiated solid cycloalkanes, 19: 46372
OHNUKI, Y., Note on the SU_6 symmetry for strong interaction, 19: 47367
OHO, G., Mortality rate of malignant neoplasm in Hiroshima A-bomb survivors, 19: 45846
OHSHIO, Mitsuo, Solar flare effect on geomagnetic variation, 19: 47480
OKABAYASHI, Tokuo, Symmetry character of bound states with multichannels, 19: 47382
OKABE, Shigeru, Effect of backscattering on target current of electron accelerators, 19: 47181
OKADA, Mitsuo, Radiation-induced cyclopolymerization of acrylic anhydride, 19: 46352
OKAMOTO, Jiro, Analysis of labeled organic compounds by radio gas chromatography, 19: 46213
OKAMOTO, Kazuto, Charge form factor and Coulomb energy of ^{3}He, 19: 47387
OKAZAKI, Masaomi, Stress-corrosion cracking of austenitic stainless steels in high-temperature water, 19: 46959
OKUMURA, K., Fermi surface of cesium, 19: 47896
OKUN, L. B., CP violation and nature of $\Delta T = \frac{1}{2}$ rule, 19: 47317 (NP-tr-1282)
OKUZAWA, Takeshi, Propagation of weak hydromagnetic shock waves in the exosphere. I., 19: 47478
OLIVE, G., Formation of ^{89m}Y by 14-Mev neutron irradiation of Zr, 19: 47566 (AERE-R-5009)
OLIVER, Norman J., Geophysics and Space Data Bull. 3, 19: 47447 (AD-612063)
OLIVIERI, A., X-ray induced crossing-over in centromeric region of Drosophila males, 19: 45949
OLIVIERI, G., X-ray induced crossing-over in centromeric region of Drosophila males, 19: 45949
OLSEN, E. Melling, Animal protection and control of feedstuffs, 19: 46700
OLSON, John M., Spectral characteristics of a bacteriochlorophyll-protein complex from green photosynthetic bacteria, 19: 45727 (BNL-9506)
OLSON, Walter, Relation of cell size to effect of x rays on poliovirus production by monkey kidney cells, 19: 45955
OLSSON, E., Sensitization and radiation response in cases with carcinoma of the uterine cervix, 19: 45830
OLSSON, P. O. M., Hypergeometric function of two variables of importance in perturbation theory. II., 19: 46906
OMAR, H. M., Probability distributions of fluctuations in reaction $^{25}Mg(d,\alpha)^{23}Na$, 19: 47659
OMER, Guy C. Jr., Structured cosmological models, 19: 47205
ONDOH, Tadamori, Pre-SC polar ionosphere and b-f radio propagation over polar paths. II., 19: 47455
ONGARO, M., Radiotherapy of bladder cancer. V., 19: 46114
ONISHCHENKO, I. N., Polarization of plasma moving in curved magnetic field, 19: 47797
ONISHI, Shoji, Stress-corrosion cracking of austenitic stainless steels in high-temperature water, 19: 46959
ONO, Kanji, Effect of annealing on mechanical properties of electron-irradiated Al single crystals at 23°K, 19: 47095
ONODA, Ichiro, Influence of uranium addition on iron and steel. II., 19: 47047
OOI, Hiroshi, Collision-resisting construction of sides of a nuclear powered ship, 19: 46464 (NSJ-tr-30)
OOMS, G., Displacement of energy levels of atomic systems in strong radiation fields, 19: 47233
OOSAWA, Masumi, Activation analysis of ^{231}Pa followed by γ spectrometry of ^{232}Pa and ^{233}Pa, 19: 46212
OOSTERKAMP, W. J., Evaluation of fluoroscopic screens and x-ray image intensifiers, 19: 46150
ORIA, Michel, Calculation of energy of particles emitted by reactions $^{3}T(d,n)^{4}He$, $D(d,n)^{3}He$ and $D(d,p)T$, 19: 47568 (CEA-R-2779)
ORLINSKII, D. V., Dynamic stabilization of plasma column, 19: 47842
ORLOVA, E. I., Migration of ^{90}Sr in ground waters of various salt composition, 19: 46602
ORNE, D., Response spectra for high air-blast loads, 19: 46566 (AD-425747)
ORSONI, L., Modifications of SORIN's pool-type reactor Avogadro RS1 for higher power operation, 19: 48066

ORSZAGH, Andrzej, Homopolymerization of maleic acid esters and diethyl fumarate. I., 19: 46377
ORSZAK, Peter, Charging apparatus for nuclear reactors, 19: 47942
ORTALLI, I., Features of Moessbauer absorption in tin metal, 19: 47654
ORTH, D. A., Performance of 3% and 30% TBP processes, 19: 46423 (DPSPU-64-30-28)
ORZALESI, C. A., Inequivalent representations in the many-boson problem, 19: 47420
OSADIN, B. A., Energy dissipated in high current vacuum discharge, 19: 47792
OSADIN, B. A., Formation of clumps in pulsed plasma accelerators, 19: 47796
OSBORN, R. K., Kinetic equations for neutron distributions, 19: 47963
OSBORNE, F. J. F., Isotropic plasma guide—TE_{11} mode, 19: 47743
OSIPENCO, A., Radiological monitoring of the surroundings of CEN at Mol, 19: 46631 (A/AC.82/G/L.986)
OSOVETS, S. M., Dynamic stabilization of plasma column, 19: 47842
OSTAPENKO, V. V., Optimum methods for handling transient processes in reactors, 19: 47957 (IAE-724)
OSTERRIETH, Paul M., Radiosensitivity of cultures of E. freundii grown in presence of fluoroacetate, 19: 46015
OSTROUKHOV, A. A., Effect of atomic screening factor on inelastic scattering of electrons, 19: 47259
OTSUKA, Iwao, Counter for detecting radioactive surface contamination, 19: 46833
OTTO, P. Ph. H. L., Synthesis of tritiated p-terphenyls, labeled at specific positions, 19: 46313
OUANNES, C., Concerning system of bubble chamber data processing in real time, 19: 46814
OVERBERGER, C. G., Potential antiradiation agents, 19: 46316
OVERTON III, Marvin C., Recurrent cystic formation in craniopharyngioma treated with radioactive chromic phosphate, 19: 46087
OWEN, Joe D., Neutron and gamma ray well logging, 19: 46624
OYAMA, Akira, Present status and future plan of atomic energy research in universities, 19: 48116
OZAKI, S., On-line computer data processing system for counter and spark chamber experiments, 19: 46806

P

PACHECO, H., Synthesis of DL-shikimic 1-2-^{14}C acid starting from methyl acrylate 2-3-^{14}C, 19: 46312
PACK, J. L., Mobility of negative ions in O_2 at low E/N, 19: 47220 (NP-15175)
PAGET, Francis Thomas William, Method and apparatus for reactor leak detection, 19: 47937
PAGHIS, I., Magnetic and ionospheric storms, 19: 47497
PAGHIS, I., Physics of earth's upper atmosphere, 19: 47488
PAIEDASSI, Jean, Comparative study of the oxidation of various qualities of uranium in carbon dioxide at high temperatures, 19: 46948 (CEA-R-2805)
PAIK, S. F., Laser-induced perturbation in plasma, 19: 47777
PAL, B. K., Y_8^8 resonance and $K-N_{S_{1/2}}$, T = 0, 19: 47365
PALCHOUDHURY, S. R., Enhanced nuclei acid synthesis in x-irradiated E. coli, 19: 45851
PALEEV, V. I., Inherent thermionic emission of lanthanum hexaboride and surface ionization of cesium atoms on it, 19: 47148
PALOU, J., Ulcerated thorotrastoma, 19: 46092
PALS, J. A., Magnetic properties of superconducting Ta, 19: 47524
PANDE, L. K., S-wave pion-pion scattering in state T = 0, 19: 47347
PAOLINI, F. R., Research program to investigate artificially injected trapped radiation, 19: 47444 (AD-611629)
PAPAVASILIOU, C., Lung changes following cobalt teletherapy for carcinoma of the breast, 19: 46063
PAPAYOANOU, Aristole, Determination of the ionospheric electron content utilizing satellite signals, 19: 47448 (AD-612119)
PAPERMASTER, B. W., Focal antibody production by transferred spleen cells in irradiated mice, 19: 45805 (AD-621543)
PAPERMASTER, Bea W., Focal antibody production by transferred spleen cells in irradiated mice, 19: 45986
PAPPAS, A. C., Independent yields of ^{124}Sb and ^{126}Sb in thermal-neutron-induced fission and their implication on the empirical Z_p function, 19: 47611
PAPROCKI, Stan J., Prog. rpt. on civilian applications, 5/65, 19: 46912 (BMI-1727(Del.))
PAPROCKI, Stan J., Prog. rpt. on civilian applications, 6/65, 19: 46913 (BMI-1733(Del.))
PARADIS, E. L., Operating limits and safety analysis for split-table, dry, flexible critical experiments at CANEL Nuclear Physics Lab., 19: 47959 (PWAC-475)
PARELLADA BELLOD, R., Determination of palladium by flame photometry, 19: 46170 (JEN-148-DQ/I-49)

PARISH, R. W., Improved techniques in the projection radiography of highly radioactive specimens, 19: 46560
PARKER, Edward F., Combined radiation and surgical treatment of carcinoma of the esophagus, 19: 46051
PARKER, K., Processing of nuclear data for reactor calculations, 19: 47948 (ANL-7050, pp 517-39)
PARKS, G. K., Determinations of auroral-zone x-ray spectrum, 19: 47471
PARKS, G. K., Spatial asymmetry and periodic time variations of x-ray microbursts in auroral zone, 19: 47470
PARLIER, B., Energy of electron cascades in a small lead-plate spark chamber, 19: 47354
PARMA, A., Morphogenesis of nuclear anomaly from small doses of x rays, 19: 45925
PARMENTIER, J. H., Tritium labeling of amino acids and peptides by Wilzbach method. I., 19: 46311
PARNELL, C. J., Comparative studies of sensitivity of low-background clinical counting systems, 19: 46137
PARSHINA, I. S., Changes in resistance of tin films on destruction of superconductivity by current, 19: 47530
PARTHASARADHI, K., Absolute photoelectric cross sections of 145-, 280-, and 320-kev γ rays, 19: 47329
PASCARU, I., Paramagnetic centers formed in irradiated inorganic oxy-compounds of selenium. I., 19: 46390
PASCUAL, P., Spectral representation and mass formula for spin-$\frac{3}{2}$ particles, 19: 47340
PASHININ, P. P., Investigation of spark discharge in air produced by focusing radiation from a laser. II., 19: 47781
PASKIN, A., Superconducting transition temperature of thin Al films, 19: 47503 (BNL-9478)
PASQUIER, Ch., Thyroid burden of radioiodine after respirator contamination of monkey Mecaccus rhesus, 19: 45776
PASQUILL, F., Meteorological aspects of the spread of windborne contaminants, 19: 46693
PASSARI, L., Electrical resistivity measurements in quenched aluminum–alumina alloys, 19: 47067
PASSATORE, G., Analysis of α-^{12}C scattering process by Regge representation, 19: 47653
PASSERI, A., Physical and biological bases of external and internal irradiation of systemic neoplasia, 19: 46095
PASSERIEUX, J.-P., New scattering chamber and its installation, 19: 47327
PASSY, N., Radiochemical procedures for environmental media, 19: 46168 (IA-1347)
PASSYUK, A. S., Production of H^- ions from arc ion source on c stand, 19: 47142
PASTERNAK, G., Production of resistance against isologous transplantations of uv-induced sarcomas of the mouse, 19: 45827
PASTERNAK, R. A., Interaction of niobium with active gases at very low pressures. I., 19: 47031
PATARIN, Louis, Nuclear reactor, 19: 47972
PATOCKA, S., Radioactivity studies in Plzen, 1957-1962, 19: 46687
PATON, M. G., Refinement of crystal structure of yttria, 19: 47027
PATON, M. G., Scattering length of yttrium for thermal neutrons, 19: 47888
PATRESE, P., Radiotherapy of bladder cancer. VI., 19: 46115
PATRICK, J. W., Mechanism of hyperfragment formation in K^- capture, 19: 47648
PAULSEN, A., (n,2n) Excitation functions for nuclei around Z = 28, 19: 47571 (EUR-2456.e)
PAULUS, J. M., Formation of tritium compounds by irradiation of butane with T^+ ions at 2 to 6 kev, 19: 46415
PAULY, J., Data handbook for sensitivity calculations in neutron activation analysis, 19: 46167 (EUR-1898.e)
PAUN, I., Paramagnetic centers formed in irradiated inorganic oxycompounds of selenium. I., 19: 46390
PAUTRAT, M., Collective and particle-state in ^{174}Yb from decay of ^{174}Lu, 19: 47661
PAVELESCU, M., Calculation of flux distribution in VVR-S reactor by S_n approximation, 19: 48072
PAVELESCU, M., Critical size calculation by a first collision probability method, 19: 48073
PAVKOVICH, J., Final rpt. on plasma boundaries, 3/61–2/65, 19: 47719 (ARL-65-131)
PAVLOV, S. M., Concerning the radial distribution of electric conductivity in ionized gas jet, 19: 47794
PAVLOVSKI, F. A., Backward elastic scattering of pions on neutrons at 1.2 to 4.5 Bev, 19: 47310 (NP-15376)
PAYNE, G. F., Chemical composition of individual range plants from the U. S. Range Station, Miles City, Montana, from 1955–1960, 19: 45747 (ORNL-TM-1279)
PEARSALL, G. W., Effect of processing history on the superconducting properties and long-range order of Ta_3Sn, 19: 47513
PECSOK, Donald A., Planning for the control of radiation accidents, 19: 46702
PECULEA, M., Economic optimum of an ensemble saturator separating column condenser in isotope separating process, 19: 46901
PEDERSEN, O. E., Nuclear power in developing areas, 19: 48041
PEEBLES, P. J., Gravitation and space science, 19: 47209
PEED, W. F., Plasma heating and burnout in beam-plasma interaction, 19: 47852
PEGEL, B., Perturbation theory using canonical transformations in classical eigenvalue problems, 19: 47417
PEIL, A., 200-Kev accelerator for generating 14-Mev neutrons, 19: 47176
PELE, J.-P., Nondestructive underwater testing in the BR2 reactor, 19: 48002 (ORNL-tr-747)
PEL'KIS, P. S., Elimination of ^{134}Cs from organism under influence of derivatives of 1,5-diphenylthiocarbazone and 1,5-diphenylthiocarbohydrazide, 19: 45765 (JPRS-27544, pp 1-12)
PELLAT, R., Electromagnetic instability of collisionless plasma, 19: 47844
PELLEG, J., Yttrium–cobalt system, 19: 47053
PELLERIN, P., ORSEC plan for radiation protection, 19: 46704
PELTE, D., Excited states in ^{21}Ne by the ^{23}Na(d,α)^{21}Ne reaction, 19: 47633
PELTE, D., Gamma-ray cascades in ^{21}Ne, 19: 47632
PELU, G., Digestion of proteic and fatty substances and time of transition in patients irradiated on the abdomen, 19: 45932
PENDERGAST, M. S., SOSH-5. Computer program for shielding calculations, 19: 47866 (KAPL-M-6460)
PENKUHN, H., Numerical solution of γ transport equation applied to concrete slabs, 19: 47864 (ANL-7050, pp 113-22)
PENNISI, F., Protein radioiodination by an electrolytic technique, 19: 46142
PENNOCK, Paul, AROMA program for recognition and measurement of spark images and fiducials, 19: 46794
PEPIN, Robert Osborne, Isotopic anomaly patterns in meteoritic xenon, 19: 47213
PEPPARD, D. F., Di n-octyl phosphinic acid as a selective extractant for metallic cations, 19: 46443
PERAY, Robert, Purification of uranium and particularly irradiated uranium, 19: 46455
PEREY, F. G., Inelastic scattering of deuterons from ^{60}Ni and ^{114}Cd, 19: 47635
PEREY, F.-J., New scattering chamber and its installation, 19: 47327
PERKINS, Francis William Jr., Two problems in kinetic theory of plasmas, 19: 47800
PERKLEV, T., Excretion of radioactivity by human subjects after ingestion of liver from cattle treated with labeled polydiethylstilbestrol phosphate, 19: 45797
PERKS, M. A., FREAK—fast reactor multigroup kinetics program, 19: 47947 (ANL-7050, pp 395-412)
PERLMAN, D., Microbial processes for preparation of radioactive compounds, 19: 46409
PERRAULT, G., Thyroid burden of radioiodine after respirator contamination of monkey Mecaccus rhesus, 19: 45776
PERREAU, J.-M., Reaction $K^+p \rightarrow K^0p\pi^+$ at 3 Bev, 19: 47356
PERRY, Harold, Computation of radiation dosages, 19: 46134
PERSING, Ronald L., Rectal mucosa as biologic indicator of radiation injury. I., 19: 45918
PERSSON, H., Production of hot plasma by discharge in strongly inhomogeneous magnetic field, 19: 47831
PERSSON, Karl-Birger, Brush cathode plasma—a well-behaved plasma, 19: 47739
PETERS, Vera, Preoperative irradiation in management of locally advanced breast cancer, 19: 46054
PETERSEN, H. E., Microprogramming for data acquisition and control, 19: 46813
PETERSILKA, Franz, Betatron for electron depth therapy, 19: 46126
PETERSON, D. B., Energy-transfer processes in dilute solutions of organometallics in benzene, 19: 46362
PETERSON, D. T., Thirty-five millimeter color photomicrography, 19: 46928 (NMI-4998, pp 14-19)
PETERSON, H. C., Chemical reactions of atomic beams and related problems, 19: 47221 (NYO-2403-8)
PETERSON, P. J., Fission fragment removal of uranium from a fissioning surface, 19: 47580 (LA-3352)
PETERSON, Reuben W., Design of containers for shipment of radioactive material including irradiated reactor fuel, 19: 46665
PETIT, Jean, Purification of uranium and particularly irradiated uranium, 19: 46455
PETIT, M., Application of radiography to nondestructive control of fuel elements before and after irradiation, 19: 46562
PETKAU, A., Chronic toxicity of polyphenyl mixtures, 19: 45769

PETRANYI, Gyorgy Jr., Comparative investigations on protection mechanisms of cysteamine and AET in intestinal radiation death, 19: 46027
PETRASH, G. G., Stimulated radiation from hydrogen and deuterium molecules in near-infrared region, 19: 47260
PETRASOVA, M., Strontium-90 activity in grass and alfalfa during 1962 and 1963 in West Slovakia, 19: 45750
PETRENKO, V. I., Pulse heating of high-pressure argon arc. I., 19: 47789
PETRENKO, V. I., Pulse heating of high-pressure argon arc. II., 19: 47790
PETROCK, K. F., Alpha air monitor with constant flow control, 19: 46768 (UCRL-14253)
PETRZILKA, Vaclav, Discovery of proton radioactivity, 19: 47628
PETSCHEK, H. E., Magnetohydrodynamic generators, 19: 47288
PETSCHEK, H. E., Shock waves in collision-free plasmas, 19: 47828
PETTIJOHN, David, Evidence for repair-replication of uv-damaged DNA in bacteria, 19: 45909
PETTIJOHN, David Everett, Replication of DNA in uv-irradiated bacteria, 19: 46002
PEY, Wang, Peripheral electromagnetic interactions of fast charged particles and nucleons, 19: 47318
PFAU, A., Investigation on $^{137}Cs/^{90}Sr$ ratios in milk, 19: 45772
PFEIFER, H., Determination of magnetic-field distributions, 19: 46731 (SLAC-Trans-21)
PFEIFER, V. F., Radionuclides in wheat and other agricultural products—a review, 19: 46662
PHALEN, D. I., Factors controlling effectiveness of high-temperature protective coatings for tungsten, 19: 46911 (AFML-TR-64-392)
PHALEN, D. I., Oxidation of zirconium–yttrium alloys, 19: 47034
PHELAN, J. J., Electron identification in lead plate spark chambers, 19: 46782
PHELAN, J. J., Magnetic spark chamber system, 19: 46796
PHELPS, A. V., Mobility of negative ions in O_2 at low E/N, 19: 47220 (NP-15175)
PHILIP, Robert H., Application of radioisotope precipitation test to study of Q fever in man, 19: 46076
PHILLIPS, G., Determination of nitrogen in plutonium nitride, 19: 46164 (AERE-R-5002)
PHILLIPS, G. C., Equilibrium charge states of ^{16}O ions, 19: 47179
PHILLIPS, Herman E., Effective hyperfine fields at the nuclei of Os and Pt dissolved in Fe, 19: 47069
PHILLIPS, Steven J., Changes after cardiac x irradiation in dogs, 19: 45835
PIAZZA, G., Radiotherapy of bladder cancer. IV., 19: 46113
PICCINNI, Ester, Mitotic activity and DNA synthesis in clones derived from mammalian cell cultures irradiated with x rays, 19: 45867
PICCOTTI, F., Incorporation of tritiated thymidine and kinetics of proliferation of cells of Ehrlich ascite tumor, 19: 45791
PICCOTTI, F., Modifications induced by ionizing radiations on uptake of tritiated thymidine and on life cycle of cells of Ehrlich ascite tumors, 19: 45936
PICHAT, L., Synthesis of DL-shikimic 1-2-^{14}C acid starting from methyl acrylate 2-3-^{14}C, 19: 46312
PICHAT, L., Use of vinyl magnesium bromide for synthesis of molecules labeled with ^{14}C, 19: 46310
PICKLESIMER, M. L., Strain behavior in Zircaloy-2 sheet-type tensile specimens, 19: 47012 (ORNL-TM-1226)
PIECHOWSKA, M. J., Effect of ionizing radiation on endocrine system in insects, 19: 45861
PIERSON, W. R., Radiochemical procedure for obtaining ruthenium free from iridium, 19: 46444
PIETRA, R., Stable manganese content of mollusks from Lake Maggiore, 19: 45788
PIL'SKII, V. I., High-speed diagnostics of a plasma jet, 19: 47735
PIL'SKII, V. I., Plasma heating mechanism by collisionless shock waves, 19: 47845
PINAJIAN, J. J., Action of calcium carbide on alkaline earth chlorides and fluorides, 19: 46251 (ORNL-tr-673)
PINI, M., Experimental observations on radioprotective action of RNA, 19: 46072
PINTO, J. L., Flame-photometric determination of Na in U ores, 19: 46191
PIPINO, G., Delayed results of biological radioprotection in whole-body irradiated rats, 19: 46023
PIROUE, P. A., Internal liquid hydrogen target for a proton synchrotron, 19: 47173
PIROUE, P. A., Time-of-flight measurements using r-f structure of Princeton-Pennsylvania accelerator beam, 19: 46809
PISTOCCHI, F., Digestion of proteic and fatty substances and time of transition in patients irradiated on the adbomen, 19: 45932
PISUT, J., Effect of nonelastic processes on elastic scattering, 19: 47330
PIZZELLA, R., Self-radiolysis of clathrates containing tritium-labeled molecules, 19: 46359
PIZZELLA, R., Self-radiolysis of tritium-labeled fatty acid esters, 19: 46360
PIZZO, Joseph Francis Jr., Contributions to the Einstein-Kursunoglu field equations, 19: 47440
PLAKSIN, I. N., Factors influencing determination of lithium and boron in enrichment products in (n,α) nuclear reaction, 19: 46221
PLANTIN, L.-O., Acute radiation syndrome, 19: 45829
PLATNER, E. D., On-line computer data processing system for counter and spark chamber experiments, 19: 46806
PLATT, L. W., Development report for TP82, 19: 48095 (SC-DR-64-539)
PLAYFAIR, J. H. L., Focal antibody production by transferred spleen cells in irradiated mice, 19: 45806 (AD-621543)
PLAYFAIR, John H. L., Focal antibody production by transferred spleen cells in irradiated mice, 19: 45986
PLESS, Irwin, PEPR system, 19: 46810
PLEVE, A. A., Yield ratio for fissioning isomer from deuteron irradiation of Pu, 19: 47688
PLOSTINARU, D., Levels of low excitation energy in ^{56}Fe, 19: 47696
PLUCHERY, M., X rays and electronic microscopy at the Grenoble Nuclear Center, 19: 46512
PLUNKETT, T. F., Cavity nuclear reactors, 19: 48046 (AD-613998)
PLYUTTO, A. A., Emission properties of a vacuum spark plasma. I., 19: 47147
POCHIN, E. E., Public health and medical measures: their practicability and associated problems, 19: 46698
POCKRANDT, H., Experience with placentography using human albumin labeled with ^{131}I, 19: 46117
PODDAR, R. K., Enhanced nuclei acid synthesis in x-irradiated E. coli, 19: 45851
PODDAR, S. N., Spectrophotometric determination of Th(IV), 19: 46206
PODESTA, A. M., Delayed results of biological radioprotection in whole-body irradiated rats, 19: 46023
POENARU, D., Yield ratio for fissioning isomer from deuteron irradiation of Pu, 19: 47688
POGGENBURG, John Kenneth Jr., Theoretical α decay rates of deformed nuclei, 19: 47597 (UCRL-16187)
POGGI LONGOSTREVI, G., Modifications of lysozymic activity in intestine of irradiated animals, 19: 45933
POKAZAN'EV, V. G., Radiooptical resonance of atoms in strong magnetic fields, 19: 47261
POLACCO, E., Two-photon absorption in atomic or molecular systems, 19: 47236
POLAK, T., Evaluation of healing process in avian digital flexor tendons and grafts following application of artificial tendon sheath, 19: 45964
POLAK, T., Use of irradiated homografts and artificial sheaths in avian and mammalian tendon injuries, 19: 45965
POLIKANOV, S. M., Yield ratio for fissioning isomer from deuteron irradiation of Pu, 19: 47688
POLK, D. H., Plasmas for thermonuclear research produced by laser beam irradiation of single solid particles, 19: 47846
POLKINGHORNE, J. C., High-energy behavior of production amplitudes in perturbation theory, 19: 47341
POLLOCK, D. H., Absorption of resonance radiation and formation of molecular ions in cesium vapor, 19: 47229
POMMIER, J., Enzymatic iodination of proteins, 19: 46314
PONATH, Hans, Additive medical treatment of tumor beds. X., 19: 46121
PONOMARENKO, A. G., Capture of plasmoids in a magnetic mirror machine, 19: 47839
PONOMARENKO, A. G., High-speed diagnostics of a plasma jet, 19: 47735
PONS, Henri, Protection in radiodiagnosis, 19: 46132
POOLE, P. C., Strongly interacting particles in air shower cores, 19: 47271
POPOV, N. M., Fine structure of tungsten single crystals by microdiffraction of ultrafast electrons, 19: 47022 (JPRS-31225, pp 1-5)
POPOV, P. G., Stabilization of powerful Penning discharge by a magnetic field increasing along the radius, 19: 47780
PORGES, K. G., Determination of manganese sulfate content for neutron source measurements, 19: 47552
PORTNER, P. M., Measurement of range of 100-Mev protons in Al, 19: 47225
POSSAGNO, E., Self-radiolysis of clathrates containing tritium-labeled molecules, 19: 46359
POSSAGNO, E., Self-radiolysis of tritium-labeled fatty acid esters, 19: 46360
POST, Arthur H. Jr., Cryogenic transport tube incorporating liquefaction apparatus, 19: 46525
POTMESIL, M., Nucleolar coefficient of lymphocytes in peripheral blood of patients with Hodgkin's disease, 19: 46103
POTSCHWADEK, B., Counting statistics, 19: 45742

POYN, B., Excited states in ^{21}Ne by the $^{23}Na(d,\alpha)^{21}Ne$ reaction, 19: 47633
POYN, B., Gamma-ray cascades in ^{21}Ne, 19: 47632
POWERS, J. E., Computer program for solution of energy balance and heat transfer of pulsed thermonuclear reactor, 19: 47720 (LA-3347)
POWERS, W. L., Generalized graphical presentation of MHD generator and accelerator performance characteristics, 19: 47296
POWLES, J. G., Proton spin-lattice relaxation in solutions of hydrogen chloride and deuterium chloride, 19: 46287
POZZA, F., Histochemical behavior of some enzymes of intestinal mucous in irradiated animals, 19: 45927
POZZA, F., Radiotherapy of bladder cancer. V., 19: 46114
PRAVEDNIKOV, A. N., EPR spectra of some irradiated nitriles, 19: 46378
PREDA, A., Evidence for high four-momentum transfer from π^--Xe interactions at 9 Bev, 19: 47698
PREDAZZI, E., Inversion problem in the λ plane, 19: 47361
PREISER, Hanno, Role of the action potential in excitation-contraction coupling, 19: 45736
PRESCOTT, Charles Y., Electron and photon energy measurement up to 4 Bev, 19: 46805
PRESCOTT, D. M., Preparation of mammalian metaphase chromosomes for autoradiography, 19: 45790
PREUSS, L. E., Compilation of β-stimulated x-ray spectra, 19: 47223
PREVE, Jacques, Process for conversion of ionizing energy into electricity, 19: 47283 (BNL-tr-8)
PRIBIL, Rudolf, Present state of complexometry. I., 19: 46219
PRICE, William E., Evaluation of field-effect transistors, 19: 46871 (AD-614268)
PRIMER, M., The $Y\mathring{1}(1660)$ produced in K⁻-p interactions at 2.24 Bev/c, 19: 47300 (BNL-9520)
PRINCE, C. E. Jr., Impulse response of the magnetospheric column, 19: 47467
PRINCE, Clarence E. Jr., Aspects of experimental and theoretical geomagnetics, 19: 47476
PRITCHARD, W. C., Refractory plutonium fuel materials, 19: 46999 (LA-DC-7297)
PRIVALOV, G. F., Somatical radiomutations by Acer negundo, 19: 45865
PROKERT, K., Chemical dosimetry of ionizing radiation, 19: 46369
PROKHOROV, A. M., Investigation of spark discharge in air produced by focusing radiation from a laser. II., 19: 47781
PROKOPCHUK, V. V., Composition of uranic–vanadic minerals, 19: 46627
PROKSCH, E., The radiation stability of anthracene oils. II., 19: 46333 (SGAE-CH-20/1965)
PROSDOCIMI, Armando, Measurement of fission cross section of ^{235}U and ^{239}Pu for thermal neutrons, 19: 47567 (CEA-R-2775)
PROSPERI, D., Low-lying levels of odd-odd spherical nuclei, 19: 47658
PROT, A., Application of radiography to nondestructive control of fuel elements before and after irradiation, 19: 46562
PRUSSIN, Stanley Gerald, Radiochemical separations through recoil reactions, 19: 46405
PRYADKIN, K. K., High-pressure electrodeless discharge, 19: 47788
PUGHETTI, G., Separation of ^{137}Cs from fission products, 19: 46441
PULL, I. C., Mechanized handling of nuclear data, 19: 47911 (ANL-7050, pp 309-13)
PULL, I. C., Solution of the transport equation by collision probability methods, 19: 47540 (ANL-7050, pp 93-112)
PULLEN, D. A. W., Improved techniques in the projection radiography of highly radioactive specimens, 19: 46560

Q

QUARLES, C. A., On-line computer data processing system for counter and spark chamber experiments, 19: 46806
QUEER, Paul R., Facilities to service nuclear instruments, 19: 46511
QUINN, L. P., Rate of the reaction between U(IV) and Tl(III), 19: 46277
QUINN, W. E., Stability, heating, and end loss of a 3.5-megajoule theta pinch (Scylla IV), 19: 47722 (LA-DC-7039)

R

RABINOWITCH, Ethel, Iodine-131 uptake studies under hot climatic conditions, 19: 45779
RABY, G. W., Atomic energy market in Europe. VI. Great Britain, 19: 48007
RABA, G., Efficient utilization of reactor of Venezuelan Institute of Scientific Research, 19: 48065
RADCLIFFE, R. E., Evaluation of computational system applicable to the nuclear analysis of critical experiments and power reactors, 19: 47959 (WCAP-3269-52)
RADESCU, E., Sign of the effective range parameter, 19: 47390
RADOSAVLJEVIC, Radoslav, Movement of radioactivity emanating from ^{40}K in precipitation and waters on territory of Vinca, 19: 46590 (JPRS-31469)
RADWAN, Maciej, Detectability in isotope radiographic methods, 19: 46564
RADZHABOV, T. D., Adsorption of argon ions by titanium films, 19: 47072
RADZIEVSKII, V. N., Fluctuations in magnetized plasma not in equilibrium, 19: 47785
RAE, A. D., Crystal structure of bisnitratodiaquodioxouranium(VI) tetrahydrate (uranyl nitrate hexahydrate), 19: 46255
RAGHAVAN, S. V., Preparation of ^{203}Hg-labeled neohydrin for medical use, 19: 46305
RAHMAN, M. A., New oxidimetric reagent: potassium dichromate in a strong phosphoric acid medium. V., 19: 46220
RAIMONDI, J., Endolymphatic radioisotope therapy and pelvic lymphography in gynecological cancerology, 19: 46100
RAIMONDI, J., Radiosensitivity and oxygen therapy in gynecological oncology, 19: 46097
RAIZER, Yu. P., Investigation of spark discharge in air produced by focusing radiation from a laser. II., 19: 47781
RAJEWSKY, Boris, Effects of ionizing radiation on complex cell systems and high organisms, 19: 45988
RAJU, B. B. Venkatapathi, Influence of nuclear shells on thermal neutron cross sections, 19: 47618
RAJU, Mudundi R., Heavy-particle studies with silicon detectors, 19: 46770 (UCRL-16354)
RAJU, P. K., Reflection and refraction of hydromagnetic plane waves at boundary of two compressible media, 19: 47138
RALFE, Leonard George, Method and apparatus for reactor leak detection, 19: 47937
RAMANATHAN, N., Effect of γ radiation on soluble and insoluble collagens, 19: 45850
RAMANNA, R., Feasibility of method of nondestructive assay of ^{235}U and ^{239}Pu in irradiated fuel slug, 19: 46178 (NP-15364)
RAMDOHR, P., Radioactive halos in various minerals with critical remarks for the evaluation of halos for age determinations, 19: 46616 (ORNL-tr-758)
RAMDOHR, Paul, Observations on radioactive halos and radioactive fracturing, 19: 46593 (ORNL-tr-755)
RAMDOHR, Paul, Radioactive halos in quartz, yttrofluorite, and cassiterite and new findings on atomic stopping power of the elements, 19: 46592 (ORNL-tr-701)
RAMSDEN, D., Multiwire proportional counter for detection of ^{239}Pu, 19: 46751 (AEEW-M-526)
RANDLE, K. J., Electron transfer in spherical vacuum chambers, 19: 46824
RAO, G. Gopala, New oxidimetric reagent: potassium dichromate in a strong phosphoric acid medium. V., 19: 46220
RAO, J. Rama, Incoherent scattering of 280-kev γ rays, 19: 47624
RAO, K. N. Srinivasa, Rigid rotator according to relativistic quantum mechanics, 19: 47428
RAO, N. K., Study of hyperfragments. II., 19: 47650
RAO, P. Kesta, New oxidimetric reagent: potassium dichromate in a strong phosphoric acid medium. V., 19: 46220
RAO, P. V. Ramana, Incoherent scattering of 280-kev γ rays, 19: 47624
RASHID, M. A., $\bar{U}(12)$ symmetry, 19: 47305 (IC/65/57)
RASS, I. T., Radiosensitivity and nature of radiation injury to mouse thymus cells, 19: 45871
RASZILLIER, I., Simple derivation of representation of the inhomogeneous Lorentz group in the angular momentum system, 19: 47425
RATHGEBER, M. H., Strongly interacting particles in air shower cores, 19: 47271
RATHJE, J., Electroproduction of π-mesons and photoproduction of diplons, 19: 47303 (DESY-65/7)
RATTAY, K. H., Water economy and waste water treatment of the Juelich research installation, 1960–1962, 19: 48078 (JUL-261-DE)
RAU, R. R., The $Y\mathring{1}(1660)$ produced in K⁻-p interactions at 2.24 Bev/c, 19: 47300 (BNL-9520)
RAU, Robert C., Electron microscope studies of irradiated A-286 alloys, 19: 47088 (NMI-4998, pp 95-106)
RAUBER, A., Heat transfer in subcooled steam for high system pressures and hot surface charges, 19: 46544
RAUSCH, Ludwig, Rapidly occurring recovery processes in skin after x irradiation, 19: 45987
RAVASINI, R., Radiotherapy of bladder cancer. VI., 19: 46115
RAVENHOLT, Reimert T., California chiropractors: epidemiological study of causes of death among them and other characteristics, 19: 45866
RAWLINGS, R., Internal friction peak in beryllium, 19: 47056
RAY, A. K., Study of hyperfragments. II., 19: 47650
RAY, John Robert, Covariant formulation of the Lagrangian theory of fields, 19: 47441
RAYMOND, D. J., Photonuclear reaction studies by activation methods, 19: 47596 (TID-22141, pp 94-7)

RAYNOR, G. V., Rare-earth intermediate phases. II., 19: 47051
RAYNOR, G. V., Rare earth intermediate phases. III., 19: 47052
RAZGOVOROV, B. L., Biological effects of high energy protons, 19: 45821 (JPRS-31547, pp 1-5)
RAZUMOVSKAYA, L. P., Spectroscopic investigations of high-frequency discharge in helium, 19: 47772
REAGAN, Mark E., Renal clearance of ^{131}I-labeled sodium iothalamate in man, 19: 46079
REDMAN, M. J., Neutron-diffraction study of $Co_3B_2O_6$, 19: 46290
REED, D., The determination of activation products in irradiated steels by anion-exchange separation and γ spectrometry, 19: 46195
REED, G. W., Clinical dosimetry, 19: 46854
REED, G. W., Radiation dosimetry. Fermi International School of Physics, Varenna, 8/63, 19: 46840
REEDER, P. L., Cross sections for production of ^{7}Be from light targets by 2.2-Bev protons, 19: 47625
REES, G. H., Servo theory for the control of coherent betatron oscillations in Nimrod, 19: 47165 (NIRL/R/99)
REES, M. J., Model of the quasi-stellar radio variable CTA 102, 19: 47198
REGAN, William H., Radioactive waste research and development activities, 19: 48083
REGGIANI, G., Delayed results of biological radioprotection in whole-body irradiated rats, 19: 46023
REGGIANI, G., Endolymphatic radioisotope therapy and pelvic lymphography in gynecological cancerology, 19: 46100
REGGIANI, G., Radiosensitivity and oxygen therapy in gynecological oncology, 19: 46097
REGNIER, J., Analysis of experimental data concerned with pion-pion scattering, 19: 47357
REHBINDER, B., Atomic energy market in Europe. IV. Finland, 19: 48005
REICHEL, W. S., Experience with placentography using human albumin labeled with ^{131}I, 19: 46117
REID, G. C., Solar cosmic rays and the ionosphere, 19: 47496
REID, G. C., Theory of geomagnetic and auroral storms, 19: 47500
REID, H. B., Accounting systems for heavy water and fissionable materials, 19: 47906 (AECL-2282)
REID, J. Alan, Changes after cardiac x irradiation in dogs, 19: 45835
REIKHRUDEL', E. M., High-vacuum discharge ignition mechanism in crossed electric and magnetic fields, 19: 46741
REIMER, R., New shop to meet future need for larger reactor vessels, 19: 47926
REINEKE, E. P., Iodine-131 uptake by tissues of rainbow trout, 19: 45796
REISSIG, H., Strontium-90 contents of soils and plants on the territory of the G.D.R. in 1963, 19: 46610
REITEMEIER, R. F., Reclamation of agricultural land following accidental radioactive contamination, 19: 46701
REITEMEIER, Richard J., Combined 5-fluorouracil and supervoltage radiation therapy in the palliative management of advanced G-I cancer, 19: 46091
REITER, Elmer R., Heavy radioactive fallout over southern United States, November, 1962, 19: 46604
REMMELE, W., Genesis of radioinduced leukemias in pulmonary tuberculosis, 19: 45870
REMY, Rene, Neutron spectroscopy by use of nuclear stars from 20 to 300 Mev, 19: 46769 (UCRL-16325)
RENAUD, R. N., Deuterated organic compounds. XXV., 19: 46307
RENGAN, K., Radiochemical procedure for obtaining ruthenium free from iridium, 19: 46444
RENGARAJAN, T. N., Study of hyperfragments. II., 19: 47650
RENOUX, Andre, Radioactive ions in the atmosphere, 19: 46641 (CEA-R-2771)
RERIKH, K. V., Leptonic decays of baryons in the universal V-A theory, 19: 47307 (JINR-P-2278)
RESHETNYAK-MOISEEVA, V. I., Effect of antiradiation drugs on muscular activity of small intestine, 19: 46005 (JPRS-31933, pp 6-12)
RESIBOIS, P., Finite temperature properties of normal Fermi systems. II., 19: 47325
RESTALL, J. E., Evaluation of the properties of protected Mo and 0.45% Ti–Mo alloy, 19: 47061
REYNOLDS, Geo. T., Distribution of single electron pulse sizes from multidynode electron multipliers, 19: 46720 (NYO-3406-2)
REYNOLDS, P., Inter-diffusion of plasma and magnetic fields in pinch and hardcore discharges, 19: 47853
RHODES, Cecil G., Metallography of beryllium oxide, 19: 47001 (NMI-4996, pp 36-49)
RIBE, F. L., Computer program for solution of energy balance and heat transfer of pulsed thermonuclear reactor, 19: 47720 (LA-3347)
RIBE, F. L., Stability, heating, and end loss of a 3.5-megajoule theta pinch (Scylla IV), 19: 47722 (LA-DC-7039)
RIBNER, Aaron, Thermodynamics of trimethylacetonitrile and dimethylmalononitrile, 19: 48090 (COO-1149-53)

RICCAFORDI, A., Analysis of behavior of leukocytes in the whole-body irradiated rat, 19: 45934
RICCI, R. A., Collective and particle-state in ^{174}Yb from decay of ^{174}Lu, 19: 47661
RICCO, M., Magnetostriction wire spark chambers, 19: 46783
RICE, Stuart A., Properties of an excess electron in liquid He. I., 19: 47131
RICE, Stuart A., Properties of an excess electron in liquid He. II., 19: 47132
RICE, Stuart A., Quantum-mechanical Fokker-Planck equation, 19: 47415
RICHARD, H. A., Factors controlling effectiveness of high-temperature protective coatings for tungsten, 19: 46911 (AFML-TR-64-392)
RICHARD, N. A., Oxidation of zirconium–yttrium alloys, 19: 47034
RICHARDS, Gerald T., Derivation of generalized Von Neumann pseudo-viscosity with directional properties, 19: 47119 (UCRL-14244)
RICHARDS, N. E., Electrolytic extraction of light metals, 19: 46454
RICHT, A. E., Metallography of irradiated dispersion-type fuel elements, 19: 47084 (NMI-4997, pp 124-33)
RICHT, A. E., Remote metallographic specimen grinder, 19: 46507 (NMI-4997, pp 157-62)
RICHTER, B., Development of streamer spark chambers, 19: 46781
RICKARD, Corwin L., Gas-cooled reactor with improved fuel element arrangement, 19: 47973
RICKARD, Corwin L., Nuclear reactor, 19: 48045
RICKHOFF, W. L., Magnetic spark chamber system, 19: 46796
RIEDEL, Jozef Tadeusz, Preparation of methane for radiation detectors, 19: 46319
RIEF, H., Monte Carlo approach to calculation of characteristic reactor parameters in three-dimensional assemblies, 19: 47919 (ANL-7050, pp 581-92)
RIEL, Gordon K., Radioactivity of Columbia River effluent, 19: 46680
RIEMANN, John G., Induced dominant lethal mutations in oocytes and sperm of screw-worm fly, 19: 45950
RIESE, Gretchen R., Ternary diagram—uranium–uranium dioxide–uranium oxycarbide, 19: 46249 (LA-tr-65-15)
RIGDON, Lester P., Process stream analysis systems for scrubber solutions used in Project Dribble vent gas treatment plant, 19: 46471 (UCRL-14123)
RIGG, Shepherd, Nuclear fuel assembly, 19: 47982
RIGNEY, D. V., Electrical resistivity of lithium and columbium-1 zirconium alloy to 1430°C, 19: 47015 (TIM-854)
RIJNIERSE, P. J., Displacement of energy levels of atomic systems in strong radiation fields, 19: 47233
RIKITAKE, T., Characteristics of geomagnetic variation anomaly in Japan, 19: 47457
RIKITAKE, Tsuneji, Sudden commencements of geomagnetic storms and their local irregularities, 19: 47456
RIMONDI, C., Can the index of uptake of ^{32}P reveal radiosensitivity of metastases, 19: 46098
RINSHAW, S. J., Reduction of alkaline earth oxides with aluminum carbide, 19: 46252 (ORNL-tr-683)
RINALDO, J. D., Coherent production of pion tridents by a primary beam of 16.2 Bev/c π^- in nuclear emulsion, 19: 47355
RINGOT, Claude, Improvements in or relating to sheaths for nuclear fuel elements, 19: 47980
RINGSDORF, H., Potential antiradiation agents, 19: 46316
RITCHIE, E. E., Quantitative metallography of hypostoichiometric UN, 19: 46177 (NMI-5025(Pt.I), pp 85-95)
RITSEMA, A. R., Detection of nuclear explosions in crust of earth and in the atmosphere, 19: 46620
RITTENBERG, Alan, Search for C-invariance violation in η(958 Mev) and η(549 Mev) decays, 19: 47372
RITTENHOUSE, P. L., Strain behavior in Zircaloy-2 sheet-type tensile specimens, 19: 47012 (ORNL-TM-1226)
RITTER, R., Quantity of food required for determination of ^{90}Sr and ^{137}Cs and its incineration, 19: 46200
RIVERA, J., Human bone metabolism inferred from fallout investigations, 19: 45793
RIVIERE, Rene, Long-term thyroid values after intake of radioactive iodine, 19: 45754 (CEA-R-2787)
ROACH, R. J., Roll film camera for remote metallography, 19: 46711 (BNWL-SA-161)
ROATH, S., Use of immersible scintillation counter in urinary vitamin B_{12} excretion test, 19: 46083
ROBBINS, Donald T., Engineering study for tunnel grid blast-shelter concept for Detroit, 19: 46568 (ORNL-TM-1223)
ROBERTS, A., Electron identification in lead plate spark chambers, 19: 46782
ROBERTS, A., Magnetic spark chamber system, 19: 46796
ROBERTS, Arthur, Current performance characteristics of visual spark chamber systems, 19: 46791

ROBERTS, I. C., Analysis of ASTR radiation heating in aerospace structural materials, 19: 47077 (AD-613471)

ROBERTS, J. A., Effect of omega transformation on critical currents in a Zr-rich Nb alloy, 19: 47511

ROBERTS, J. A., High-speed thermal analysis of Zr–Nb alloys, 19: 47037

ROBERTS, J. G., Reactor maintenance by remote internal tube welding, 19: 46973

ROBERTS, James R., Image-intensifying shutter for observing transient plasmas, 19: 47729

ROBERTS, P. R., Effect of omega transformation on critical currents in a Zr-rich Nb alloy, 19: 47511

ROBERTS, S. J., Numerical study of particle behavior in non-adiabatic magnetic traps, 19: 47748

ROBEY, S., Distribution of radioprotective N-/4-nitrophenyl/-benz-^{14}C-amidine in organs of white rats, 19: 46011

ROBEY, S., Investigation of the effects of N-phenylbenzamidine on the number of inverse mutations during x irradiation of E. coli K suspension, 19: 46012

ROBINS, L., Decreasing electropolishing time for uranium, 19: 46920 (NMI-4996, pp 27-35c)

ROBINSON, Le Plessis, Process and device for manufacture of a permeable membrane, 19: 46978

ROBSON, A. E., Numerical study of particle behavior in non-adiabatic magnetic traps, 19: 47748

ROBSON, P. N., Negative absorption from weakly relativistic electrons traversing Cuccia coupler, 19: 47130

ROCHE, J., Enzymatic iodination of proteins, 19: 46314

ROCKENHAUSER, W., Prestressed concrete structures for large power reactors, 19: 47925 (GA-6505)

RODERICK, Thomas H., Prog. rpt. on quantitative population genetics of mice under irradiation, 7/64–6/65, 19: 45809 (NYO-1979-12)

RODRIGUEZ, Eduardo Ramos, International and national recommendations, norms, guides, etc., for protection against ionizing radiation, 19: 46668

ROE, David K., ^{129}I as a nonradioactive tracer, 19: 45799

ROEDEL, Walter, Cosmic-ray-produced and artificial ^{22}Na in the atmosphere, 19: 46603

ROENICKE, G., Radioactive collection for atmospheric electricity soundings, 19: 46730 (SC-T-65-760)

ROESEL, Marion E., Effects of actinomycin D on lens regenerating system, 19: 45738

ROESMER, Josef, Bismuth fission induced with 36- and 58-Mev protons, 19: 47712

ROGERS, M. D., Mass transport and grain growth induced by fission fragments in thin films of uranium dioxide, 19: 46278

ROGERS, S. C., Predicting semiconductor performance in a nuclear environment, 19: 46874

ROGICH, D. G., Predicting free-field radial displacements and strains, 19: 46467 (NVO-1163-43)

ROGNONI, F., Modifications of lysozymic activity in intestine of irradiated animals, 19: 45933

ROHRER, Robert H., Scintillator-photomultiplier combinations, 19: 46858

ROHSENOW, Warren M., Effect of surface conditions on nucleate pool boiling of sodium, 19: 46549

ROJO, Enrique A., Radiolysis and luminescence behavior of dioxane–benzene mixtures, 19: 46363

ROLF, Howard L., Scintillation methods for metallic ion determination in human subjects using computer techniques, 19: 45771

ROMAGNOLI, U., Critical considerations on the evaluation of the radiobiological response of irradiated connective tissues, 19: 45935

ROMAN, H. Roth, Conference on metallurgy, Savannah River, 5/61, 19: 46921 (NMI-4997)

ROMAN, H. Roth, Conference on metallurgy, Richland, 3/62, 19: 46926 (NMI-4998)

ROMAN, H. Roth, Conference on metallurgy, Los Alamos, 5/63, 19: 46930 (NMI-4999)

ROMAN, H. Roth, Proceedings of the 18th metallographic meeting, Canoga Park, Calif., 6/64, 19: 46936 (NMI-5025(Pt.I))

ROMAN, P., Mass formula in the covariant spin-unitary spin scheme, 19: 47352

ROMANOVSKII, M. K., Investigation of plasma in the AC device, 19: 47855

ROMANOVSKII, V. A., Effect of atomic screening factor on inelastic scattering of electrons, 19: 47259

ROMANTSEVA, A. S., Elastic (p,p) scattering at 1.45 Bev, 19: 47304 (IAE-700)

ROMICK, G. J., Continuous observation of auroral belt by means of radio, 19: 47473

ROMNEY, E. M., Effects of Be in plants and soil, 19: 45802

RONDANELLI, E. G., Morphogenesis of nuclear anomaly from small doses of x rays, 19: 45925

RONY, Peter R., Design, construction, and operation of differential micromanometer. II., 19: 46726 (UCRL-11218(Pt.II))

ROOF, R. B. Jr., Integrated series of crystallographic computer programs. X., 19: 47877 (LA-3335)

ROOKE, A. D. Jr., Mass distribution measurements of crater ejecta and dust, 19: 46469 (POR-1815)

ROSA, Richard J., Experimental studies of strong Hall effects and U × B induced ionization. II., 19: 47290

ROSA, U., Protein radioiodination by an electrolytic technique, 19: 46142

ROSA, U., Separation of ^{131}I-labeled S-sulfonated A and B insulin chains by thin-layer chromatography, 19: 46445

ROSATI, S., Effect of n-p tensor forces in $^{4}_{\Lambda}$H Λ hyperfragment. II., 19: 47657

ROSATI, S., Study of the J = 2 excited level of ^{6}Li, 19: 47645

ROSBOROUGH, J. R., Supplement report on COMARS (coordinate measuring and recording system), 19: 48101 (SC-TM-65-332)

ROSEN, Alex, Radiation belt boundary near solar cycle maximum as determined from trapping of energetic electrons, 19: 47462

ROSEN, Johnny, Activities of ANL-ENEA computer program libraries and the ORNL Radiation Shielding Information Center, 19: 47908 (ANL-7050, pp 125-39)

ROSEN, L., Experiments with polarized protons and the neutron-nucleus potential derived therefrom, 19: 47581 (LA-DC-6730)

ROSENBAUM, Herbert, Monitoring design for radioactive air pollution, 19: 46647 (RISO-104)

ROSENBLUTH, M. N., Microinstabilities, 19: 47823

ROSENFELD, Michael, Laboratory investigations of shelter management factors, 19: 46637 (AD-612254)

ROSESCU, T., Calculation of flux distribution in VVR-S reactor by S_n approximation, 19: 48072

ROSESCU, T., Critical size calculation by a first collision probability method, 19: 48073

ROSINGER, S., Uses of high energy radiation in Germany, 19: 48117

ROSNER, Manfred, Efficiency of large-scale open-loop MHD power generation, 19: 47291

ROSS, Raymond L., Superconductors in advanced electronics, 19: 46475 (AD-612113)

ROSS, T. P., Application of Power Burst Facility to fast reactor fuel meltdown tests, 19: 47952 (APDA-177)

ROSSI, H. H., Dose concepts and units, 19: 46842

ROSSI, H. H., Microdosimetry, 19: 46846

ROSSI, H. H., Neutron and heavy-particle dosimetry, 19: 46847

ROSSI, H. H., Relative biological effectiveness, 19: 45998

ROSSO, G., Effect of treatment with hepatic derivatives on survival and on oxidative phosphorylating activity of liver of mice exposed to whole-body irradiation, 19: 46024

ROTH, H. P., Conference on metallurgy, Nuclear Metals, Inc., 4/60, 19: 46919 (NMI-4996)

ROTH, H. P., X-ray film defects and autoradiography of fuel elements for cladding thickness measurement, 19: 46964 (NMI-4996, pp 149-63)

ROTH, J. Reece, Superconducting magnet facility for plasma physics research, 19: 47533

ROTHE, W., Determination of minimum filter size for the filter analysis process of film dosimetry, 19: 46764 (SZS-6(1965))

ROTHMAN, M. A., Ion heating in the model C Stellarator, 19: 47832

ROUCAYROL, J. C., Detection of β activities on chromatogram with thin layer of absorbent or of ion exchange resin, using gel-forming scintillator, 19: 46862

ROUGE, Pierre, Nuclear reactor, 19: 47972

ROUSSEL, E., Application of radiography to nondestructive control of fuel elements before and after irradiation, 19: 46562

ROUSSEL, E., Radiography tests with active fuel elements application to testing in hot laboratories, 19: 46558 (ORNL-tr-748)

ROUSSET, Pierre, Atmospheric corrosion of uranium–carbon alloys, 19: 46947 (CEA-R-2732)

ROUSSET, Pierre, Machining of uranium carbide rods obtained by continuous casting under electronic bombardment, 19: 46963 (CEA-R-2733)

ROVIT, Richard Lee, Automatic contour brain scanner, 19: 46086

ROWLANDS, G., Vlasov equation in high magnetic fields, 19: 47753

ROYSTON, R. J., Synopsis of Argonne automatic spark chamber processing system, 19: 46793

ROZEN, A. M., Dependence of the separation factor in isotope exchange on the properties of the exchanged molecules, 19: 46408 (ORNL-tr-770)

ROZZELL, T. C., Simultaneous determination of Zn-65 and P-32 in shellfish by radiochemical techniques, 19: 46218

RUBBO, Sydney D., Review of sterilization and disinfection as applied to medical, industrial, and laboratory practice, 19: 46890

RUBIO, C. A., Sensitization and radiation response in cases with carcinoma of the uterine cervix, 19: 45830

RUDKIN, George T., The relative mutabilities of DNA in regions of X chromosome of Drosophila melanogaster, 19: 45879

RUEDL, E., Damage and diffusion in Al and Al–Al_2O_3 alloy following bombardments with oxygen or inert gas, 19: 47080 (EUR-2478.e)

RUEDL, E., Electron microscopy of SAP following tensile deformation or quenching, 19: 46996 (EUR-2479.e)
RUEDORFF, Walter, Intercalation of base metals in graphite as well as in metal chalcogenides of type MeX_2, 19: 46265
RUEI, K. H., Nature of resonance in static pion-nucleon scattering in one-meson approximation, 19: 47298
RUFFIN, Minnie R., Moisture content of tissues of normal surgically treated, and irradiated rats, 19: 45896
RUGH, Roberts, Changes after cardiac x irradiation in dogs, 19: 45835
RUH, Robert, Hafnium–oxygen system, 19: 46990 (ARL-65-138)
RUNDLE, S., Diffusion phenomena in atmospheric surface layer. II., 19: 47111 (UCRL-Trans-1229(L))
RUSBRIDGE, M. G., Conditions for improved stability in Zeta, 19: 47856
RUSSELL, E. S., Hemopoietic defect in anemic mice of genotype Sl/Sl^d, 19: 45856
RUSSELL, L. M., Computer calculation of energy yield produced by hypothetical fast reactor accident, 19: 47918 (ANL-7050, pp 503-14)
RUSSELL, Paul S., Biology of tissue transplantation. I., 19: 45944
RUSSELL, R. Scott, Food agricultural aspects of radiation emergencies, 19: 46694
RUSSELL, Walter J., Retained ThO_2 media in seminal vesiculography. Follow-up study with dose estimates, 19: 45837
RUSSO, S., Influence of acetylene on radioinduced polymerization of ethylene, 19: 46353
RUST, D. R., Moving film, fixed sensors, automatic scanner for spark pictures, 19: 46790
RUSU, M., Automatic Moessbauer spectrometer, 19: 46831
RYABCHENKO, E. M., Behavior of adsorbed Cs films on single-crystal spikes of Ta and Ta_2C, 19: 47900
RYABOV, N. V., Evaluation of time-related readings of aerosol radiometers with a continuously moving filter strip, 19: 46760 (NP-15462)
RYABOVA, E. Z., Elimination of ^{134}Cs from organism under influence of derivatives of 1,5-diphenylthiocarbazone and 1,5-diphenylthio-carbohydrazide, 19: 45765 (JPRS-27544, pp 1-12)
RYAN, H. F., Cavities in tungsten, 19: 47057
RYAN, H. F., Field ion microscope observations of stacking faults in tungsten, 19: 47050
RYBA, Earle, Crystal structure of $YbZn_2$, 19: 47030
RYDKII, S. G., Absorption of radioactive fission products by cultivated crops. II., 19: 45804
RYKALIN, N. M., Physical and chemical problems of joining of dissimilar materials, 19: 46968 (AEC-tr-6615)
RYSAVA, Marie, Ageing of corrosion-resistant steels of the type $Cr^{18}Ni^9Ti$, 19: 47026 (ORNL-tr-795)

S

SABATA, Hideki, Time-dependent problems of scattering in linear lattice system, 19: 47255
SACHER, George A., Lethal effects of whole-body irradiation in mice, 19: 45982
SACHSSE, H., Accurate determination of the heavy hydrogen isotope by thermal conductivity, 19: 46182 (NP-tr-1275)
SAEKI, Bunzobro, Reactions (n,d) induced by 14-Mev neutrons on ^{19}F, ^{31}P and ^{23}Na, 19: 47644
SAEKI, Bunzobro, Counter telescope for charged particle measurements by 14-Mev neutrons, 19: 46821
SAFARIK, I., Thermodynamic considerations on hydrated electron and other intermediates in radiolysis of aqueous solutions, 19: 46343
SAFFREN, M. M., Rotating superconductor, 19: 47504 (JPL-TR-32-650 (Pt.2))
SAFRONOV, B. G., Polarization of plasma moving in curved magnetic field, 19: 47797
SAGDEEV, R. Z., Asymptotic methods in hydrodynamic theory of stability, 19: 47830
SAGDEEV, R. Z., Landau damping and finite resistivity instability in plasmas, 19: 47827
SAGDEEV, R. Z., Plasma heating mechanism by collisionless shock waves, 19: 47845
SAH, J. P., Modified procedure of scanning nuclear emulsions for obtaining absolute neutron yields of reactions, 19: 46817
SAITO, Raiko, Distribution of Be in solid Mg alloys containing Be at high temperatures, 19: 47071
SAITO, Takao, Index of geomagnetic pulsation and its relation to solar M regions. II., 19: 47464
SAJI, Yoshiro, Anomalous behaviors in Josephson current, 19: 47515
SAKANOUE, Masanobu, Activation analysis of ^{231}Pa followed by γ spectrometry of ^{232}Pa and ^{233}Pa, 19: 46212
SAKATA, H., Safety rod interaction in the PRCF, 19: 48058 (BNWL-130)
SAKSONOV, P. P., Biological effects of high energy protons, 19: 45821 (JPRS-31547, pp 1-5)

SAKSONOV, P. P., Radiobiological problems of space flights, 19: 46000
SALAM, Abdus, Ū(12) symmetry, 19: 47305 (IC/65/57)
SALANDER, C., Germany's nuclear ship, 19: 48051
SALINA, E., New approach to water reactor lifetime with spatial variation studies, 19: 47912 (ANL-7050, pp 347-68)
SALISBURY, S. R., Cross sections for $^{54}Fe(n,p)$, (n,α), and (n,2n), 19: 47668
SALISBURY, S. R., New isotope of fluorine: ^{23}F, 19: 47671
SALMON, R., Costs of permanent disposal of power-reactor fuel-processing wastes in tanks, 19: 48080 (ORNL-2873)
SALMON, Royce, Economics of irradiated fuel shipment, 19: 46664
SALOMON, G., Conference on mechanisms of solid friction, Kansas City, 9/63, 19: 47075
SALUSTI, E., Low-lying levels of odd-odd spherical nuclei, 19: 47658
SALUTSKY, M. L., Half life of ^{223}Ra, 19: 47626
SALZWEDEL, M., Formation of 1-benzyl-2,3-diphenylindanes from stilbene in presence of tin tetrachloride under influence of γ radiation, 19: 46345
SAMACHSON, Joseph, Zinc-65 metabolism during low and high Ca intake in man, 19: 45787
SAMIOS, N. P., The $Y_1^0(1660)$ produced in K⁻-p interactions at 2.24 Bev/c, 19: 47300 (BNL-9520)
SAMOUR, Claude, Measurement of fission cross section of ^{235}U and ^{239}Pu for thermal neutrons, 19: 47567 (CEA-R-2775)
SAMSON, Stan, Prog. rpt. on structure of metals and intermetallic compounds, final, 9/53–8/64, 19: 46984 (AD-612275)
SANCHO, J., Measurement of diffusion coefficients. III., 19: 46261
SANCHO, J., Reversible and irreversible processes in the dropping-Hg electrode. XIX., 19: 46260
SANDBERG, R. O., Forced convection heat transfer at high pressure after critical heat flux, 19: 46554
SANDBORN, Virgil A., Particle beam measurement apparatus using beam kinetic energy to change heat sensitive resistance of the detection probe, 19: 47155
SANDENAW, T. A., Heat capacities of Nb carbides below 320°K, 19: 46998 (LA-3331)
SANDERS, A. T., CP violation and nature of $\Delta T = \frac{1}{2}$ rule, 19: 47317 (NP-tr-1282)
SANDERS, Barkev S., Prog. rpt. on occupational radiation exposure, 6/64–4/2/65, 19: 45810 (NYO-3394-2(Rev.))
SANDLIN, R., Measured and predicted variations in fast neutron spectra when penetrating laminated Fe–D_2O, 19: 47561
SANDOW, Alexander, Role of the action potential in excitation-contraction coupling, 19: 45736
SANFORD, Barbara H., Induced adaptation in a transplantable tumor, 19: 45873
SANGSTER, D. F., Pulse radiolysis, 19: 46346
SANKARANARAYANAN, A., Spin-one wave equation, 19: 47359
SANKARANARAYANAN, K., Inbreeding and genetic loads in irradiated experimental populations of Drosophila melanogaster, 19: 45952
SANNAZZARI, G. L., Incorporation of tritiated thymidine and kinetics of proliferation of cells of Ehrlich ascite tumor, 19: 45791
SANNAZZARI, G. L., Modifications induced by ionizing radiations on uptake of tritiated thymidine and on life cycle of cells of Ehrlich ascite tumors, 19: 45936
SANTORO, R. P., Neutron-diffraction study of $Co_3B_2O_6$, 19: 46290
SAPEZHINSKII, I. I., Effect of radiation protective substances on pro-tracted afterglow of irradiated solutions of serum albumin, 19: 46342 (JPRS-31547, pp 6-12)
SARGENT, Wallace, X-ray and gamma-ray astronomy, 19: 47207
SARKER, A. Q., Electromagnetic Σ^0–Λ^0 mixing and the Y_1^0 decays, 19: 47366
SAROJA, D., Rigid rotator according to relativistic quantum mechanics, 19: 47428
SARUDI (VON STETINA), I., Gravimetric determination of oxalic acid as Th oxalate, 19: 46222
SATCHLER, G. R., Inelastic scattering of deuterons from ^{60}Ni and ^{114}Cd, 19: 47635
SATO, Taichi, Complexes formed in the extractions of uranium(VI) from sulfuric and nitric acid solutions by tri-n-octylamine, 19: 46447
SATOYAMA, Shozo, Developmental investigation of power reactor plant, 19: 48043
SAUER, A., Local neutron flux distribution in a bundle from segmented fuel elements, 19: 47992 (KEA-311)
SAUNDERSON, D. H., DIDO triple axis crystal spectrometer, 19: 46753 (AERE-R-4895)
SAUTTER, C. A., Stopping cross sections of carbon and hydrocarbon solids for low-energy protons and helium ions, 19: 47871
SAUVE, Charles, Improvements in extruding metal in the plastic state and apparatus for carrying out the methods, 19: 46975
SAVAGE, Serene, POELARGRM—a computer program for analysis of polarograms, 19: 46238 (ORNL-TM-1253)

SAVIGNONI, R., Rectosigmoidoscopic detections in carcinoma of cervix before and after radiotherapy, 19: 46099
SAVITSKII, E. M., Fine structure of tungsten single crystals by microdiffraction of ultrafast electrons, 19: 47022 (JPRS-31225, pp 1-5)
SAWADA, Tetsuo, Extra restriction on forward scattering amplitudes, 19: 47375
SAWYER, G. A., Stability, heating, and end loss of a 3.5-megajoule theta pinch (Scylla IV), 19: 47722 (LA-DC-7039)
SAXON, G., Experimental observations of pulse shortening in a linear-accelerator waveguide, 19: 47182
SCARF, F. L., Direct detection of ambient electron plasma oscillation fields in the magnetosphere, 19: 47477
SCARF, F. L., Effects of solar-wind composition on threshold for plasma instability in transition region, 19: 47460
SCARSI, L., Energy of electron cascades in a small lead-plate spark chamber, 19: 47354
SCASSELLATI, G., Protein radioiodination by an electrolytic technique, 19: 46142
SCHAEFER, G. W., The calculation of thermal-neutron spectra—generalized free-gas theory, 19: 47538 (ANL-7050, pp 33-49)
SCHAEFER, Peter, Time-dependent relation of dose effects, 19: 45989
SCHAERF, C., Photoproduction of π^0 from H near the second π–N, 19: 47368
SCHALLOPP, Bernhard, Reactor instrumentation in Germany, 19: 46825
SCHARBERT, Tibor, Time-amplitude converter working with tunnel diodes, 19: 46736
SCHERAGA, Harold A., Effect of D_2O on thermal stability of proteins, 19: 46318
SCHEY, J. A., Prog. rpt. on interface friction in hot metal deformation, 11/24/64–1/23/65, 19: 46981 (AD-611821)
SCHILLING, W., Displacement probabilities of lattice atoms in various metals by reactor radiation, 19: 47104
SCHINK, L., Emission of light charged particles from highly excited complex nuclei in nuclear emulsion, 19: 47651
SCHIPPER, Philipp, Betatron for electron depth therapy, 19: 46126
SCHITTENHELM, Rudolf, Betatron for electron depth therapy, 19: 46126
SCHLAGER, Gunther, Prog. rpt. on quantitative population genetics of mice under irradiation, 7/64–6/65, 19: 45809 (NYO-1979-12)
SCHLAGER, Kurt, Late effects after Thorotrast injection, 19: 45980
SCHLUDI, Harry N., Method for operating fuel elements of an atomic reactor and for manufacturing such elements, 19: 47984
SCHLUETER, Donald Jerome, Interference effects in the $^7Li(p,\gamma)^8Be$ reaction, 19: 47703
SCHLUETER, J., Doppler-broadened spectral lines from theta pinch, 19: 47769
SCHLUTER, R. A., Precise track measurements in a wide gap spark chamber, 19: 46780
SCHMALZ, B. L., Environmental tritium studies at the National Reactor Testing Station, 19: 46642 (IDO-12043)
SCHMALZ, Bruce L., Appraisal of gaseous waste disposal into the lithosphere at NRTS, 19: 48077 (IDO-12024)
SCHMID, E. W., Binding energies of polyatomic ^{4}He-molecules, 19: 47244
SCHMID, L. C., Safety rod interaction in the PRCF, 19: 48058 (BNWL-130)
SCHMIDT, D., Electroproduction of π-mesons and photoproduction of dipions, 19: 47303 (DESY-65/7)
SCHMIDT, H. E., Apparatus for measurement of diffusivity at high temperatures, 19: 46995 (EUR-2424.f)
SCHMIDT, P., Precise hyperon masses, 19: 47302 (CU-1932-246)
SCHMIDT, W. H., Sandia Pulsed Reactor SPR-II-1 core calculations, 19: 48063 (SC-RR-65-344)
SCHMITT, H., Circular polarization (β-γ) correlation in permitted β transitions: ^{58}Co, ^{95}Zr, and ^{95}Nb, 19: 47605
SCHMITT, J. M., Stability of aromatic diluents and solvent extraction reagents in radiochemical processing, 19: 46430 (ORNL-P-1601)
SCHMITZ, Paul, Power reactor containment, 19: 48037
SCHNEIDER, C., Computer program for automatic determination of radioactivity in entire human body, 19: 46658
SCHNEIDER, Henry, Effect of D_2O on thermal stability of proteins, 19: 46318
SCHNEIDER, Richard T., Operation and diagnostics of closed-loop MPD power generator, 19: 47728
SCHNEIDER, Th., Decay of ^{152}Tb, 19: 47683
SCHNITZER, Howard J., Dispersion relations and direct nuclear reactions, 19: 47684
SCHOEPF, Hans-Georg, Elastic collision waves in framework of the general relativity theory, 19: 47414
SCHOFIELD, A. E., Problems associated with pulse charged capacitor banks, 19: 46719 (LA-DC-7030)
SCHOFIELD, P., Computation of scattering cross sections for use in thermal-neutron transport calculations, 19: 47543 (ANL-7050, pp 471-85)
SCHRAMM, Herbert, Magnetic focusing of medium fast electrons in air coils, 19: 47185
SCHREIBER, Bruno, Prog. rpt. on ecology of Acantharia in relation to Sr circulation in sea, 1/23–7/30/65, 19: 45748 (TID-22193)
SCHREYER, J. M., Research facility for study and preparation of ultrapure materials, 19: 46510 (Y-DA-967)
SCHUCHARDT, Karl, Correction of radioinduced growth defects of facial portion of the skull, 19: 46075
SCHUCHARDT, Karl, Surgical measures for extension of radiation therapy and for treatment of radiation effects in face-jaw region, 19: 46074
SCHUERLEIN, B., Gamma-ray cascades in ^{21}Ne, 19: 47632
SCHULL, William J., Estimation of genetic risk in event of radiation accident and some possible countermeasures, 19: 46695
SCHULTE-FROHLINDE, D., Formation of 1-benzyl-2,3-diphenylindanes from stilbene in presence of tin tetrachloride under influence of γ radiation, 19: 46345
SCHULZE, W., Application of coincidence methods in activation analysis, 19: 46227
SCHULZE-RETTMER, R., Water economy and waste water treatment of the Juelich research installation, 1960–1962, 19: 48078 (JUL-261-DE)
SCHUMACHER, Werner, Time-dependent relation of dose effects, 19: 45989
SCHWAGER, J., Binding energies of polyatomic ^{4}He-molecules, 19: 47244
SCHWARTZ, C. M., Factors controlling effectiveness of high-temperature protective coatings for tungsten, 19: 46911 (AFML-TR-64-392)
SCHWARTZ, K.-D., Results of thyroid function diagnosis with radioiodine, 19: 46072
SCHWARTZBART, Harry, Prototype manual of metallurgical practice, 19: 46918 (IITRI-B6018-1)
SCHWARZ, Eberhard, Radio-labeling of organic compounds by $^{12}C(\gamma,n)^{11}C$ reactions by means of bremsstrahlung of 35-Mev betatron, 19: 46418
SCHWINGER, J., Lectures on particles and field theory. II., 19: 47405
SCHWINGER, Julian, Field theories of particles, 19: 47407
SCIAMA, D. W., Model of the quasi-stellar radio variable CTA 102, 19: 47198
SCINTEI, N., ^{9}Be, ^{11}B and $^{31}P(p,p')$ angular distributions, 19: 47690
SCOTT, Bruce L., Coherent knockout amplitudes in deuteron stripping reactions, 19: 47669
SCOTT, J. E., Spectrochemical determination of hafnium, tantalum, and niobium in thorium oxide, 19: 46226
SCOTT, J. Randolph, Ultrastructural changes induced by ultraviolet light in human epidermis: basal and spinous layers, 19: 45907
SCOTT, James K., Toxicity of niobium salts, 19: 45768
SEALY, Russel, Intra-arterial cytotoxic therapy and x-ray therapy for cancer of head and neck, 19: 46088
SEBER, Norton, Inversion of cyanide group into iso-cyanide under γ irradiation, 19: 46326
SECOY, C. H., Electrokinetic phenomena at thorium oxide–aqueous solution interface, 19: 46281
SEDDON, W. E., Stress corrosion of irradiated stainless steels, 19: 47079 (AERE-R-5014)
SEDEJ, B., Synthesis of hydrazine–fluorozirconates, 19: 46236 (NIJS-R-430)
SEELEY, F. G., Primary amine extraction of beryllium from sulfate liquors, 19: 46431 (ORNL-P-1602)
SEEMAN, H. E., Factors which influence image quality and speed of film-screen combinations, 19: 46149
SEEMAN, Torsten, Coronary collateral blood flow in relation to mass of ischemic myocardium, 19: 45767
SEHGAL, Bal Raj, Intermediate resonance absorption in heterogeneous media including moderator scattering, 19: 47953 (BNL-9393)
SEIDMAN, A., Filmless automatic processing of spark chamber tracks using standard equipment, 19: 46789
SEIGLE, L. L., Factors controlling effectiveness of high-temperature protective coatings for tungsten, 19: 46911 (AFML-TR-64-392)
SEITER, Irma, Investigations on biological radiation protection. LXIV., 19: 46028
SEKIYA, Tomatsu, Neutron slowing down and diffusion problem in medium containing holes, 19: 47563
SELDEN, Robert Wentworth, Helium II film transfer rates under various conditions, 19: 47532
SELENKOW, Herbert A., ^{129}I as a nonradioactive tracer, 19: 45799
SELF, S., Final rpt. on plasma boundaries, 3/61–2/65, 19: 47719 (ARL-65-131)
SELLERS, David J., Effects of sintering on microstructure and properties of sprayed molybdenum, 19: 47054
SELLS, V., Energy spectrum of the electron beam in a racetrack microtron, 19: 47174
SELYE, Hans, Occurrence of metachromatic substance after treatment of uranyl acetate, 19: 45766
SEMCHYSHEN, M., Prog. rpt. on tungsten-base alloys, final, 1/10/64–3/10/65, 19: 46940 (NP-15444)
SEMENOV, L. F., Effect of antiradiation drugs on muscular activity of

small intestine, 19: 46005 (JPRS-31933, pp 6-12)
SENFT, B., Investigation on $^{137}Cs/^{90}Sr$ ratios in milk, 19: 45772
SEN GUPTA, N. D., Invariance properties of the Dirac equation, 19: 47421
SENVAR, C. B., Adsorption of ^{90}Sr by soil, 19: 46434
SERBER, R., Shadow scattering at large angles, 19: 47430
SETAELAE, Kai, Automatic body-contouring unit for dose planning in radiotherapy, 19: 46041
SETO, Yeh Jo, Cylindrical MHD waves in plasma, 19: 47798
SETSER, J. L., Simultaneous determination of Zn-65 and P-32 in shellfish by radiochemical techniques, 19: 46218
SETTLES, Ronald Dean, Modified statistical model for ultra-high energy interactions, 19: 47400
SEWELL, K. G., Thermodynamic properties of high-temperature helium, 19: 46235 (N64-26802)
SEYBOTH, P., Status of CERN HPD program for bubble chambers, 19: 46812
SGOUTAS, Demetrios, Radiohomogeneity of ^{3}H- and ^{14}C-labeled linoleic acid, 19: 45785
SHAFER, William G., Response of radiated human gingival fibroblast-like cells to dilantin sodium in tissue culture, 19: 45895
SHAIR, F. H., Electron beam preionization in an MHD generator, 19: 47289
SHALEK, Robert J., Radiation sensitivity of bacteriophage-E. coli complexes, 19: 46034
SHANOVSKII, L. M., De-excitation of light sums in x-rayed alkali-halide phosphors by stationary F-band illumination, 19: 46379
SHANKAR, J., Role of water of hydration in annealing behavior of neutron-irradiated trisdipyridyl cobalt(III) perchlorate, trihydrate, 19: 46387
SHAPIRO, V. D., Nonlinear stabilization of plasma bunch instabilities, 19: 47726 (NP-15394)
SHARMA, R. P., Nuclear structure effects on internal conversion coefficients, 19: 47620
SHARP, J. V., Microstrain in neutron-irradiated copper crystals, 19: 47107
SHARP, R. I., DIDO triple axis crystal spectrometer, 19: 46753 (AERE-R-4395)
SHARPATYI, V. A., EPR spectra of some irradiated nitriles, 19: 46378
SHARTIEL, Y., Electron temperature of positive column in hydrogen at low pressure, 19: 47738
SHASHKOV, V. S., Biological effects of high energy protons, 19: 45821 (JPRS-31547, pp 1-5)
SHASHURIN, I. P., Diffusion theory of a beam plasma, 19: 47787
SHAW, B. W., Frequency monitoring and nuclear burst detection: some aspects of vlf, 19: 46609
SHAW, D., Thermal conductivity of irradiated uranium, 19: 47101
SHAW, Rosemary R., Energy levels in the 2s-1d shell from high energy electron scattering, 19: 47677
SHEEHAN, T. V., HFBR modifications and tests preparatory to operating authorization, 19: 48054 (BNL-9308)
SHEEN, E. M., Detection of radionuclide contamination on face masks, 19: 46755 (BNWL-144)
SHEFFEL, Donald D., Recurrent cystic formation in craniopharyngioma treated with radioactive chromic phosphate, 19: 46087
SHERETOV, E. P., High-vacuum discharge ignition mechanism in crossed electric and magnetic fields, 19: 46741
SHERIDAN, Thomas, Manipulator control work at MIT, 19: 46505 (CONF-641120, pp 98-103)
SHERMAN, A., Electron beam preionization in an MHD generator, 19: 47289
SHERWOOD, Bruce, On-line measurement of muon decay using wire spark chambers, 19: 46785
SHEVCHENKO, S. A., Concerning the radial distribution of electric conductivity in ionized gas jet, 19: 47794
SHICK, Larry, Correlation of structures of I-V type ABO_3 compounds, 19: 46243 (TID-22207, Paper C)
SHICK, Larry, Preparation and structural study of ABO_3 compounds containing Cu and Nb or Ta, 19: 46244 (TID-22207, Paper D)
SHICK, Larry, Prog. rpt. on high-temperature solid-state chemistry and sub-solidus phase equilibria, final, 8/65, 19: 46240 (TID-22207)
SHIGEO, Nobuki, Unsaturated fatty acid extracted from the liver of irradiated rabbits, 19: 45946
SHIGI, Toyoichiro, Anomalous behaviors in Josephson current, 19: 47515
SHIMADA, Junji, Nuclear instruments and radiation dosage, 19: 46837
SHIMADA, Toshikazu, X-ray coloration of KCl crystals, 19: 46371
SHIMODA, W., Excretion of radioactivity by human subjects after ingestion of liver from cattle treated with labeled polydiethylstilbestrol phosphate, 19: 45797
SHINN, William A., Decomposition of gaseous PuF_6 by α radiation. VII., 19: 46325 (ANL-7013)
SHIOBARA, Shinji, Measurement of low electron density plasma by microwave free space method, 19: 47755
SHIOBARA, Shinji, Probe measurement of electron density in magnetized plasma, 19: 47758
SHIOKAWA, Jiro, Separation of samarium by the ion exchange method, 19: 46438
SHIRLEY, D. A., Half life and g factor of 75-kev level in ^{100}Rh, 19: 47662
SHISTER, A. R., Theory of transverse diffusion and static and high frequency conductivity of plasma in strong magnetic field, 19: 47782
SHKODA', V. V., Polarization of plasma moving in curved magnetic field, 19: 47797
SHLYAPNIKOV, R. S., Elastic (p,p) scattering at 1.45 Bev, 19: 47304 (IAE-700)
SHOEMAKE, G. R., Radiation sources for ionization detectors in gas chromatography, 19: 46887
SHOEMAKER, F. C., Internal liquid hydrogen target for a proton synchrotron, 19: 47173
SHOME, S. C., Gravimetric determination and separation of Th with N-benzoyl-N-phenylhydroxylamine by direct weighing, 19: 46194
SHONO, Yoshiyuki, Remark on higher-order corrections in cranking model, 19: 47680
SHORSHOROV, M. Kh., Physical and chemical problems of joining of dissimilar materials, 19: 46968 (AEC-tr-6615)
SHOUP, Charles S. Jr., Electrokinetic phenomena at thorium oxide–aqueous solution interface, 19: 46281
SHPIGEL', I. S., Investigation of titanium plasma source, 19: 47793
SHPORER, M., Cobalt-59 spin-spin coupling and isotope shifts in $K_3Co(CN)_6$, 19: 46285
SHUKOLYUKOV, Yu. A., Krypton isotopes in radioactive minerals, 19: 46598
SHULTS, W. D., POELARGRM—a computer program for analysis of polarograms, 19: 46238 (ORNL-TM-1253)
SHUPE, M. W., Refractory plutonium fuel materials, 19: 46999 (LA-DC-7297)
SHUSTER, E. R. Jr., Spectrochemical determination of hafnium, tantalum, and niobium in thorium oxide, 19: 46226
SHVEDOV, T. Zh., Distribution of dosage fields in pendulum γ therapy of rectum and urinary bladder tumors, 19: 46093
SIBLEY, W. A., Influence of lead impurity on low-temperature color-center production in KCl, 19: 47891
SIDHU, N. P. S., Decay of ^{51}Cr, 19: 47619
SIDHU, S. S., Neutron-diffraction study of chemical order-disorder in $PtMn_3$, 19: 47028
SIDOROV, I. V., Backward elastic scattering of pions on neutrons at 1.2 to 4.5 Bev, 19: 47310 (NP-15376)
SIEGEL, Carl Ludwig, Triple impulse asymptotic paths, 19: 48109 (SC-T-65-749)
SIEGFRIED, W., Prog. rpt. on mechanical properties of metals subjected to mechanical stress and neutron irradiation, 7/65, 19: 47081 (EURAEC-1432)
SIERING, R., Modern way to teach nuclear physics, 19: 47621
SIEVERT, R. M., Planning an organization for radiation emergencies, with special reference to Swedes, 19: 46705
SIGMAN, Eugene M., Renal clearance of ^{131}I-labeled sodium iothalamate in man, 19: 46079
SIGMUND, P., Determination of interatomic potentials in metals by electron irradiation experiments, 19: 47882 (RISO-103)
SIKKELAND, T., Decay properties of ^{256}Fm and ^{257}Fm and ^{255}Md, ^{256}Md, and ^{257}Md, 19: 47664
SILAEV, Yu. V., Effect of radiation protective substances on protracted afterglow of irradiated solutions of serum albumin, 19: 46342 (JPRS-31547, pp 6-12)
SILBERSTEIN, J. M., Mean energies and drift velocities of electrons in nitrogen, argon and xenon, determined by image intensifier photographs of electron avalanches, 19: 47124 (SLAC-Trans-19)
SILIN, V. P., Theory of transverse diffusion and static and high frequency conductivity of plasma in strong magnetic field, 19: 47782
SILJANDER, W. A., Magnetic spark chamber system, 19: 46796
SILVA, R. J., Elastic and inelastic scattering of 12.0-Mev protons from ^{62}Ni, ^{63}Cu, and ^{64}Zn: tabulated differential cross sections, 19: 47585 (ORNL-3851)
SILVERMAN, S. M., Dependence of occurrence of mid-latitude aurora on sunspot cycle, 19: 47472
SILVESTRE, Georges, Metallography—concerning existence of an allotropic change to cubic U_3Si within U–Si, 19: 47024 (NLCO-tr-6)
SILVESTRI, M., Film thickness, pressure drop, and stability in annular two-phase flow, 19: 46542
SIMEK, Josef, Late postirradiation changes in regeneration potentiality of blood cell formation, 19: 45984
SIMINOVITCH, L., Hemopoietic defect in anemic mice of genotype Sl/Sl^{d}, 19: 45856
SIMINOVITCH, L., Radiosensitivity of the immune response to sheep red cells in the mouse, 19: 45903
SIMON, A., Linear oscillations of collisionless plasma, 19: 47811
SIMON, R. H., Chemical engineering in the HTGR, 19: 47991 (GA-6128)
SIMONOV, V. A., Containment of a high-temperature plasma, 19: 47841

SIMONS, J. C. Jr., Measurement and calibration techniques for very low gas densities, 19: 46733

SIMPSON, J. E., Oscillations and noise generation in beam-generated plasma, 19: 47741

SIMPSON, S. D., Potential biological consequences of release of fission products to the atmosphere, 19: 46699

SIMS, E. D., Metallography of irradiated dispersion-type fuel elements, 19: 47084 (NMI-4997, pp 124-33)

SIMSON, Eva, Excision of thymine dimers from DNA, filament formation, and sensitivity to ultraviolet light in E. coli, 19: 45948

SINCLAIR, C. K., Moving film, fixed sensors, automatic scanner for spark pictures, 19: 46790

SINCLAIR, R. M., Ion heating in the model C Stellarator, 19: 47832

SINFELT, J. H., Exchange of deuterium with hydroxyl groups of alumina, 19: 46280

SINITSYN, B. I., Investigation of hydrogenless shielding for nuclear reactors, 19: 47870

SINITSYN, R. V., Choice of radiation energy in radioteletherapy, 19: 46094

SINITSYN, V. I., Dynamic stabilization of plasma column, 19: 47842

SINNHUBER, R. O., Post-irradiation recovery of E. coli, 19: 45951

SINNHUBER, R. O., Replica plating and computer analysis for rapid identification of bacteria in foods. II., 19: 46882

SIRACKA, E., Effect of thyroid hormone on the growth of irradiated and unirradiated tumors, 19: 45943

SIROKMAN, F., Effect of growth inhibitors on incorporation of ^{32}P into alcohol-soluble phosphate fraction of rice seedlings, 19: 45794

SIRONI, G., Energy of electron cascades in a small lead-plate spark chamber, 19: 47354

SITENKO, A. G., Fluctuations in magnetized plasma not in equilibrium, 19: 47785

SIZOV, R. A., Two-coordinate neutron diffractometer, 19: 46835

SJOEGREN, H., Dissociation of methylamine molecule ions formed in charge exchange collisions with positive ions, 19: 46262

SKALBA, D., Effect of radiation on behavior of gamma globulins in reaction with the rheumatoid factor, 19: 45860

SKORZYNSKI, Zbigniew, Measurements of γ-γ angular correlation in ^{140}La, 19: 47649

SKROTSKII, G. V., Radiooptical resonance of atoms in strong magnetic fields, 19: 47261

SKROVE, James, Changes in fracture permeability of granitic rock mass resulting from a contained nuclear explosion, 19: 46581 (UCRL-14292)

SLAETIS, Hilding, Acceleration of electrons in semi-circular photographic recording β spectrograph, 19: 46773

SLAVIERO, G. P., Studies of liver function in irradiated rats, 19: 45828

SLIVNIK, J., Synthesis of hydrazine--fluorozirconates, 19: 46236 (NIJS-R-430)

SLOMIN, Yu. M., Nature and localization of chromospheric flares, 19: 47191 (NASA-TT-F-250)

SMALC, A., Synthesis of hydrazine--fluorozirconates, 19: 46236 (NIJS-R-430)

SMALIK, M., Changes in color of potato tubers after irradiation, 19: 45853

SMETANA, K., Nucleolar coefficient of lymphocytes in peripheral blood of patients with Hodgkin's disease, 19: 46103

SMIRNOV, A. P., Changes in resistance of tin films on destruction of superconductivity by current, 19: 47530

SMITH, A. F., The isothermal growth of UAl_2 precipitates in uranium containing 250 ppm iron and 700 ppm aluminum, 19: 47048

SMITH, A. J. S., Time-of-flight measurements using r-f structure of Princeton-Pennsylvania accelerator beam, 19: 46809

SMITH, Charles E., Radiation sensitivity of bacteriophage-E. coli complexes, 19: 46034

SMITH, G. G., Improved oxy-hydrogen burner for decomposition of polyphenyl reactor coolants, 19: 46163 (AECL-2263)

SMITH, Gordon S., Crystal structure of ScB_2C_2, 19: 46258

SMITH, H. W., Impulse response of the magnetospheric column, 19: 47467

SMITH, I. C., Time-dependent multigroup diffusion code with automatic resonance self-shielding of cross sections, 19: 47915 (ANL-7050, pp 413-27)

SMITH, L. H., Erythropoietic capacity of short-term mouse marrow cultures, 19: 45740

SMITH, Roy V., Analysis and evaluation of measurements of geomagnetically trapped electrons from high-altitude nuclear explosions, 19: 47446 (AD-612013)

SMITH, T. I., Observation of persistent currents in superconducting circuit containing Josephson junction, 19: 47521

SMITS, P., Atomic energy market in Europe. II. Belgium, 19: 48113

SMULLIN, L. D., Characteristics of the beam-plasma discharge, 19: 47836

SNIDER, R. H., Bright field etch for α plutonium, 19: 46938 (NMI-5025 (Pt.I), pp 153-4)

SNIDER, R. H., Plutonium metallographic practices at Battelle, 19: 46934 (NMI-4999, pp 104-10)

SNYDER, W. T., Generalized graphical presentation of MHD generator and accelerator performance characteristics, 19: 47296

SODICOFF, Marvin, Time of origin of the parabiotic anastomosis, 19: 45838

SOICHER, Haim, Determination of the ionospheric electron content utilizing satellite signals, 19: 47448 (AD-612119)

SOKOLOV, B. M., Spark channel formation in air, 19: 47146

SOKOLOWSKA, A., Hot atom chemistry of halogens activated in β decay. III., 19: 46412

SOLENTE, P., Radiocrystallographic studies of radioactive materials, 19: 46202

SOLOVSEV, L. D., Dispersion sum rules and SU(6) symmetry, 19: 47306 (JINR-E-2343)

SOMOGYI, Gyoergy, Dependence of forms of monoenergetic electron transmission curves on measuring geometry, 19: 47125

SONDER, E., Influence of lead impurity on low-temperature color-center production in KCl, 19: 47891

SORENSEN, H., Calibration of graphite damage flux in a replaced fuel element position in DR-3 at Risoe, 19: 48070

SORENSEN, Leif B., Molybdenum-99, a new isotope for scintillation scanning of the liver, 19: 46139

SORENSEN, Viggo Henning, Plant for remote handling of nuclear fuel elements, 19: 47938

SORRIAUX, André, Calculation of energy of particles emitted by reactions $^3T(d,n)^4He$, $D(d,n)^3He$ and $D(d,p)T$, 19: 47568 (CEA-R-2779)

SOUCAS, K., Radioactive fallout in Geneva during 1963, 19: 46612

SPACU, P., Gravimetric determination of rare earths with dioximaleic acid, 19: 46216

SPACU, P., Refractometric study of formation of complex neodymium halides in aqueous solution, 19: 46254

SPACU, P., Separating rare earths from uranium, iron, and manganese, 19: 46452

SPALDING, J. F., Reduction in life expectancy as a measure of radiation-induced genetic damage in mice, 19: 45969

SPANGLER, G. E., Prog. rpt. on preparation and evaluation of Be, 10/15/63--1/14/64, 19: 46909 (AD-620264)

SPANNER, J. C., Instrument for measuring bowing in long tubes, 19: 46710 (BNWL-59)

SPEAS, Clarence J., Method of treating grass seed, 19: 46004

SPEIGHT, M. V., Effects of dislocation movement in enhancing swelling in γ-uranium during irradiation, 19: 47100

SPENCER, Herta, Zinc-65 metabolism during low and high Ca intake in man, 19: 45787

SPERBER, D., Single-particle electromagnetic decay of nuclei with high angular momentum, 19: 47655

SPICER, B. M., Betatron research program at Melbourne Univ., 19: 47171

SPIERS, F. W., Dosimetry of radioisotopes in soft tissues and in bone, 19: 46154

SPIERS, F. W., External radiation dosimetry in bone, 19: 46153

SPIERS, F. W., Historical development of radiation dosimetry, 19: 46841

SPIERS, F. W., Measurement of radiation dose from environmental sources, 19: 46155

SPIERS, F. W., Population dose from medical use of ionizing radiation, 19: 46156

SPODENKIEWICZ, Teresa, Method of using determination of ^{222}Rn in expired air, 19: 46677

SPORE, Harold A., Photomultiplier base system remote from photomultiplier, 19: 46808

SPRAGUE, T. M., Capacitor bank charging system, 19: 46718 (LA-DC-7015)

SPRINCE, Richard, Control---the universal process, 19: 46460 (CONF-640508, pp 224-32)

SPRINGER, John Mervin Jr., Radiolysis of propylene, hexafluoropropylene, and allyl acrylate, 19: 46337 (TID-22244)

SPROUSE, Gerald, Numerical integration of Schroedinger's equation for square-well potential using an IBM 1620 computer, 19: 47429

SPRUCH, Larry, Higher partial waves in positron-hydrogen scattering, 19: 47238

SRAIER, Vratislav, Counter-current extraction on a laboratory mixer-settler. IV., 19: 46446

STAAB, Edward V., Biologic relationship of endotoxin and other toxic proteins. V., 19: 45970

STACHURA, Jerzy, Chemical protection against ionizing radiation. I., 19: 46006

STAHLHOFEN, W., Bibliography on radiation effects on living tissues and organisms, 19: 45807 (AED-C-04-17)

STANOJEVIC, D. M., Reactions (d,α) on ^{19}F at 1 Mev, 19: 47646

STANSFIELD, O. M., Thermal expansion of polycrystalline HfO_2--ZrO_2 solid solutions, 19: 47045

STARCHIK, L. P., Factors influencing determination of lithium and boron in enrichment products in (n,α) nuclear reaction, 19: 46221

STARRFIELD, Sumner G., Structured cosmological models, 19: 47205

STARZL, Thomas E., Problems in renal homotransplantation, 19: 45888

STAS, K. H., Evaluation of time-related readings of aerosol radiometers with a continuously moving filter strip, 19: 46760 (NP-15462)

STASHKOV, A. M., Performance capacity of animals following irradiation, adrenalectomy and administration of antiradiation drugs, 19: 45823 (JPRS-31933, pp 1-5)

STAVITSKII, R. V., Distribution of dosage fields in pendulum γ therapy of rectum and urinary bladder tumors, 19: 46093

STEARNS, E. H., Current experiments using prosthetic terminal devices on Model 8 master slaves, 19: 46492 (CONF-641120, pp 1-3)

STEEDLY, J. E. Jr., Interdiffusion in niobium–vanadium alloys, 19: 47058

STEINDLER, Martin J., Decomposition of gaseous PuF_6 by α radiation. VII., 19: 46325 (ANL-7013)

STEINERT, L. A., Electromagnetic properties of quantized relativistic electron-positron gas, 19: 47771

STEINGELMANN, William H., Thermal stress techniques in the nuclear industry, 19: 47922 (TID-22119)

STEINMETZ, Otto, Betatron for electron depth therapy, 19: 46126

STEINNES, E., Determination of selenium in animal tissue by neutron activation analysis, 19: 46172 (KR-95)

STELSON, P. H., Equilibrium charge states of ^{16}O ions, 19: 47179

STEPHENS-NEWSHAM, Lloyd, Automatic contour brain scanner, 19: 46086

STERLING, Theodor D., Computation of radiation dosages, 19: 46134

STERN, David R., Process for producing power, 19: 47936

STERN, F., Dryout in a 19-rod bundle cooled by steam/water fog at 515 psia, 19: 46548

STERNHEIM, Morton M., Singlet-triplet mixing correction to hyperfine structure of the ^3He atom, 19: 47241

STEUER, M. F., Polarization of 4.4-Mev neutrons scattered elastically from ^6Li and ^7Li, 19: 47570 (COO-7-0361)

STEVENS, D. J., Strontium-90 in Australian environment during 1963, 19: 46594

STEVENS, D. J., Strontium-90 in Australian environment, 1961 to 1963, 19: 46595

STEVENS, G. F., Forced convection burnout in Freon-12 flow, 19: 46527 (AEEW-R-426)

STEVENS, H. E. Jr., Use of digital programs in reactor plant designs, 19: 47909 (ANL-7050, pp 217-30)

STEWART, C. G., Potential biological consequences of release of fission products to the atmosphere, 19: 46699

STEWART, D., High-speed thermal analysis of Zr–Nb alloys, 19: 47037

STEWART, H. F., Availability of fallout ^{137}Cs to dairy cattle from different types of feed, 19: 45780

STEWART, R. B., Automatic potentiometric titrator, 19: 46162 (AECL-2262)

STEWART, R. B., Improved oxy-hydrogen burner for decomposition of polyphenyl reactor coolants, 19: 46163 (AECL-2263)

STEWART, Robert D., Process for producing power, 19: 47936

STEYERT, W. A., Direct measurements of multiple quantization in He II, 19: 47522

STICH, H. F., X-ray-induced leukemogenesis in C57BL/6J mice, 19: 45911

STICKLER, Gunnar B., Radioisotope renography in children. I., 19: 46109

STINSON, Benjamin D., Response of x-irradiated limbs of adult urodeles to normal tissue grafts. IV., 19: 45897

STIRLING, W. L., Plasma heating and burnout in beam-plasma interaction, 19: 47852

STOHR, Jacques Andre, Improvements in or relating to sheaths for nuclear fuel elements, 19: 47980

STOLZ, W., Chemical dosimetry of ionizing radiation, 19: 46369

STONE, R. S., Evaluation of healing process in avian digital flexor tendons and grafts following application of artificial tendon sheath, 19: 45964

STONE, R. S., Use of irradiated homografts and artificial sheaths in avian and mammalian tendon injuries, 19: 45965

STONER, C. L., Supplement report on COMARS (coordinate measuring and recording system), 19: 48101 (SC-TM-65-332)

STONER, D. R., Prog. rpt. on weldability and temperature stability of refractory metal alloys, 12/21/64–3/20/65, 19: 46966 (WANL-PR(P)-007)

STOREY, Robert H., Radioactive drugs, 19: 46044

STORHOK, V. W., Bright field etch for α plutonium, 19: 46938 (NMI-5025 (Pt.I), pp 153-4)

STORHOK, V. W., Plutonium metallographic practices at Battelle, 19: 46934 (NMI-4999, pp 104-10)

STORMS, E. K., Heat capacities of Nb carbides below 320°K, 19: 46998 (LA-3331)

STORY, Albert H., Prog. rpt. on behavior of radionuclides released into fresh-water environments, annual, 1959-60, 19: 46646 (PHS-999-RH-13)

STOVER, Betsy J., Thorium-228 decay series in adult beagles, 19: 45798

STOYANOVA, M. N., Nature of a weak chromospheric flare, 19: 47190

STRASSLER, Sigfrid, Collective excitations in strong-coupling superconducting alloys, 19: 47518

STRATHDEE, J., Ū(12) symmetry, 19: 47305 (IC/65/57)

STRATY, G. C., Thermal expansion coefficient and compressibility of solid ^3He, 19: 47523

STRAUCH, Karl, Innovations in visual spark chamber techniques, 19: 46779

STRELKOV, R. B., Effect of antiradiation drugs on muscular activity of small intestine, 19: 46005 (JPRS-31933, pp 6-12)

STRICKLAND, Paul, Carcinoma corporis uteri: a radical intracavitary treatment, 19: 46064

STRIJLAND, W., Injection experiments in Jutphaas, 19: 47858

STRINGER, W. J., Continuous observation of auroral belt by means of radio, 19: 47473

STROBEL, George L., Coherent knockout amplitudes in deuteron stripping reactions, 19: 47669

STROEM, Steffen, Matrix elements of a unitary representation of the homogeneous Lorentz group, 19: 47322

STROHAL, P., Direct processes in (n,α) reactions, 19: 47637

STROM, P. O., Independent yields of ^{124}Sb and ^{126}Sb in thermal-neutron-induced fission and their implication on the empirical Z_p function, 19: 47611

STRONGIN, Myron, Superconducting transition temperature of thin Al films, 19: 47503 (BNL-9478)

STRUNNIKOV, V. M., Rotation of plasma jet in magnetic field, 19: 47849

STUART, C., Survival of white mice whole-body irradiated after administration of nembutal at sedative, hypnotic, and narcotic doses, 19: 46025

STUART, Carlo, Relation between homozygosis and radiosensitivity in the mouse, 19: 45857

STUART, J. D., Valence electron approximation: application to LiH, 19: 46284

STURCKEN, E. F., Substructure measurements by statistical fluctuations in x-ray diffraction intensity, 19: 46993 (CONF-650810-3)

SUBBOTIN, V. I., Models of temperature fields of heat exchange elements in active zone and shielding of the BN-350 reactor, 19: 47994 (NP-15393)

SUCHKIN, G. L., Resonance counter of particles, 19: 46838

SUGAWARA, Hirotaka, Intrinsically broken U(18) symmetry, 19: 47379

SUGITA, Keiichiro, Oscillation of the rf-excited positive column in longitudinal magnetic field, 19: 47778

SUITER, J., Cavities in tungsten, 19: 47057

SUITER, J., Field ion microscope observations of stacking faults in tungsten, 19: 47050

SUKHODREV, N. K., Investigation of spark discharge in air produced by focusing radiation from a laser. II., 19: 47781

SUKHORUCHKIN, S. I., Single-particle effects in neutron physics and fine structure of nuclear masses. III., 19: 47583 (NP-15467)

SULADZE, K. V., Emission properties of a vacuum spark plasma. I., 19: 47147

SULKOVSKAYA, M. M., Elastic (p,p) scattering at 1.45 Bev, 19: 47304 (IAE-700)

SUMITANI, Shozo, Purification of helium gas in nuclear facilities, 19: 46513

SUMMERS, C., Quantitative spectroscopy of cesium plasmas, 19: 47723 (LA-DC-7112)

SUNDARAM, A. K., Helmholtz instability of viscous compressible plasma, 19: 47733

SUNNEN, Jean Albert Francois, Equipment for forming high-temperature plasmas, 19: 47862

SURAMLISHVILI, G. I., Lagrangian formulation of wave kinetics in weakly turbulent plasma, 19: 47764

SUTCLIFFE, P. W., Low-temperature specific heat of plutonium, 19: 47043

SUWA, Shigeki, Polarization in $\pi^- + p$ elastic scattering at 2.08 Bev/c, 19: 47373

SVEDE-SHVETS, N. I., Thermoelectric characteristics of metallic sintered alloys on tungsten and molybdenum base, 19: 47019 (AD-619334)

SVENSSON, A. G., Angular correlations of γ rays from polycrystalline sources, 19: 47607

SVETLOLOBOV, I. A., Elastic (p,p) scattering at 1.45 Bev, 19: 47304 (IAE-700)

SVIRIDENKO, E. Ya., Models of temperature fields of heat exchange elements in active zone and shielding of the BN-350 reactor, 19: 47994 (NP-15393)

SVOBODA, K., Control of radiochemical purity of ^{52}Mn preparates, 19: 46210

SWALLOW, A. J., Charge-transfer complexes in scavenging by iodine of radicals formed on pulse radiolysis of cyclohexane, 19: 46384

SWALLOW, A. J., Studies of radiation-induced reactions of ethylene in aqueous solution. I., 19: 46385

SWAMI, M. S., Study of hyperfragments. II., 19: 47650

SWAMI JNANANANDA, Absolute photoelectric cross sections of 145-, 285-,

120-kev γ rays, 19: 47329
SWAMI JNANANANDA, Influence of nuclear shells on thermal neutron cross sections, 19: 47618
SWANN, D., Low-energy spread negative ion r-f source, 19: 47157 (AWRE-NR-1/65)
SWANSON, E. W., Iodine metabolism of lactating dairy cows, 19: 45781
SWANSON, E. W., Metabolism of different forms of I in milk, 19: 45782
SWIFT, R., Energy levels in the 2s-1d shell from high energy electron scattering, 19: 47677
SWORSKI, T. J., Radiolysis of ethylene. III., 19: 46361
SWOTA, J. Jr., Test apparatus and profile measurement system for rectangular plates subjected to in-plane thrusts, 19: 46555 (KAPL-M-6493)
SYDORIAK, S. G., Thermal expansion of compressed He, II., 19: 47505
SZCZEPKOWSKI, Tadeusz, Chemical protection against ionizing radiation. I., 19: 46006
SZEMERE, G., Effect of uv irradiation on properdin level of pigs' sera in vitro, 19: 45919
SZEPKE, R., Pine needles as bioindicator for environmental radiocontamination, 19: 45751
SZINOWATZ, W., The radiation stability of anthracene oils. II., 19: 46333 (SGAE-CH-20/1965)
SZPIKOWSKI, S., Four-body operator in nuclear spectroscopy, 19: 47678

T

TABACHNICK, Joseph, Studies of epidermis following β irradiation, 19: 45887
TABATA, Tatsuo, Effect of backscattering on target current of electron accelerators, 19: 47181
TABERT, Gayle G., Radioisotope precipitation test for study of Q fever antibodies in human and animal sera, 19: 45739
TACCANI, A., Italian 35-Mev betatron Gilbetron for therapeutic and scientific-industrial uses, 19: 47183
TADDEI, L., Behavior of total biliary acids and of some pancreatic enzymes in patients irradiated on the abdominal pelvic region, 19: 45928
TAFT, Charles, Application of fluid amplifiers in remote control operations, 19: 46502 (CONF-641120, pp 75-7)
TAI, Yuin-Kwei, Low-background counter for ^{14}C dating, 19: 46777
TAILLANDIER, P., Detection of β activities on chromatogram with thin layer of absorbent or of ion exchange resin, using gel-forming scintillator, 19: 46862
TAKAGI, Tomoo, Activation analysis of ^{231}Pa followed by γ spectrometry of ^{232}Pa and ^{233}Pa, 19: 46212
TAKAHASHI, Yoshizo, Digital startup control of research reactor, 19: 48069
TAKAMATSU, Shigeyuki, Digital startup control of research reactor, 19: 48069
TAKAMORI, Yasuhiko, Changes in lactic dehydrogenase activity in plasma of mice after whole-body x irradiation, 19: 45844
TAKAYANAGI, Kozuo, Bibliography of atomic and molecular collisions. I., 19: 47258
TAKEDA, Atsuhiko, Changes in lactic dehydrogenase activity in plasma of mice after whole-body x irradiation, 19: 45844
TAKEDA, Eichi, Evaluation and reflection on design studies made on the domestic power reactor, 19: 48036
TAKEDA, Seiji, Vibratory compaction of fused UO_2, 19: 46970
TAKEHISA, Masaaki, Reaction of ethylene with methylene chloride induced by γ radiation, 19: 46370
TALANOV, V. D., Models of temperature fields of heat exchange elements in active zone and shielding of the BN-350 reactor, 19: 47994 (NP-15393)
TALAT-ERBEN, M., Inversion of cyanide group into iso-cyanide under γ irradiation, 19: 46326 (CNAEM-28)
TALBOT, R. Jr., Research program to investigate artificially injected trapped radiation, 19: 47444 (AD-611629)
TALBOT, Richard B., Pulmonary compliance and physiopathology of guinea pig lungs exposed to gadolinium oxide dust, 19: 45756 (COO-1170-7)
TALBOY, James H., Three-decade exponential current generator for testing reactor period meters, 19: 47928
TALMAN, R. M., Moving film, fixed sensors, automatic scanner for spark pictures, 19: 46790
TAMAGNINI, C. Mongini, PINETO—FORTRAN code designed for the solution of nonlinear differential equations in neutron dynamics, 19: 47916 (ANL-7050, pp 429-41)
TAMM, I., Development of uv radiation resistance by poliovirus infective centers, 19: 46032
TAMURA, T., Naturally occurring fixation of ^{137}Cs on sediments of lacustrine origin, 19: 46681
TAMURA, Toro, Analyses of scattering of nuclear particles by collective nuclei in terms of coupled-channel calculation, 19: 47685
T'AN, Wei-han, Strong field interactions and nonlinear effects from stimulated optical emissions, 19: 47123 (JPRS-31032, pp 1-14)
TANAKA, K., Breaking of SU_3 symmetry in electromagnetic decay of the decuplet, 19: 47344
TANAKA, K., Genetic effects of chronic ionizing radiations on man, 19: 45967
TANAKA, K., Rare $\Delta Q = 0, \Delta S = 1$ decay modes of hyperons and K mesons, 19: 47370
TANAKA, Osamu, A comparison of the 30-Mev field biased betatron and 35-Mev conventional betatron, 19: 47180
TANAKA, Osamu, 30-Mev flux-forced field biased betatron. II., 19: 47178
TANG, Y. C., Binding energies of polyatomic ^4He-molecules, 19: 47244
TANIGAWA, Kozuo, Clinical and experimental studies on radiation injury to taste, 19: 45825 (NSJ-kr-32)
TAPLIN, G. V., Immunogenicity of a γ-irradiated Brucella melitensis, 19: 45868
TAQUET, B., Superconducting coil degradation, 19: 47512
TARPINIAN, Aram, Metallography of pyrolitic graphite, 19: 47078 (AD-613643)
TATARCZUK, J. R., Photonuclear reaction studies by activation methods, 19: 47596 (TID-22141, pp 94-7)
TATARINOVA, N. V., Weak postdischarge emission as indicator of electrode surface condition in vacuum breakdown experiments, 19: 47149
TAUTZ, M., Dependence of characteristic values of the collimator on energy in scintigraphy, 19: 46119
TAUXE, Newlon, Radioisotope renography in children. I., 19: 46109
TAVHELIDZE, A. N., Leptonic decays of baryons in the universal V-A theory, 19: 47307 (JINR-P-2278)
TAYLOR, A. Joanna, Ionization of H and He^+ by electron impact, 19: 47253
TAYLOR, G. R., Analog computer methods for parameter optimization, 19: 46903 (BNWL-70)
TAYLOR, J. B., Helical fields possessing mean magnetic wells, 19: 47154
TAYLOR, J. B., Plasma confinement in magnetic wells, 19: 47822
TAYLOR, J. C., Neutron-diffraction study of uranyl nitrate hexahydrate, 19: 46257
TAYLOR, R. D., Direct measurements of multiple quantization in He II, 19: 47522
TAYLOR, Stuart R., Role of the action potential in excitation-contraction coupling, 19: 45736
TAZIMA, Yotoro, Comparison of fission neutrons and γ rays in respect to their efficiency in inducing mutations in silkworm gonia, 19: 45883
TEATS, R., High-temperature tensile testing machine for irradiated structural materials, 19: 46712 (BNWL-SA-169)
TEMPLETON, I. M., Fermi surface of cesium, 19: 47896
TERAMOTO, Ei, Integrated spectra of an isotopically disordered linear chain, 19: 47256
TERAMOTO, Ei, Time-dependent problems of scattering in linear lattice system, 19: 47255
TERANISHI, Kozuo, Measurement of thickness of thin polymer films with semiconductor α-particle detector, 19: 46888
TER-POGOSSIAN, Michel, Efficiency of radiographic intensifying screens, 19: 46148
TERRAZA, J., Preparation of pure Zr and Th by direct iodination of their carbides, 19: 46969
TESTA, C., Separation of ^{137}Cs from fission products, 19: 46441
TESTA, C., Separation of ^{137}Cs from fission products, 19: 46442
TEULADE, P., Continuous irradiation at low dose rate on eggs of Bombyx mori and concept of effective dose rate, 19: 45904
THAIYALANAYAKI, M., Separation of lanthanides using phthalate buffer, 19: 46437
THEMANN, H., Reaction of somatic cell nuclei to radiation, 19: 45992
THERIOT, Lee, Excision of thymine dimers from DNA, filament formation, and sensitivity to ultraviolet light in E. coli, 19: 45948
THIEBLEMONT, P., Thyroid burden of radioiodine after respirator contamination of monkey Macaccus rhesus, 19: 45776
THIEL, S., Embryonic erythropoesis and content of nucleic acids in embryonic liver in whole-body irradiated rats, 19: 45826
THIESSEN, J. W., Bibliography on protection against biological effects of thermal radiation, 19: 45818 (TDCK-33500)
THIRD, S. M., Tunnel-diode invertor for Ripple I and II, 19: 46896
THODE, H. G., Cosmic-ray-produced ^{36}S and ^{33}S in metallic phase of iron meteorites, 19: 47195
THOMAS, Harold Albert, Radiation measuring instrument, 19: 46868
THOMAS, O. O., Chemical composition of individual range plants from the U. S. Range Station, Miles City, Montana, from 1955–1960, 19: 45747 (ORNL-TM-1279)
THOMAS, R., Diffusion of non-volatile fission products in UO_2 and ThO_2 as determined by leaching into molten salts, 19: 47070
THOMAS, Robert G., Whole-body gamma spectrometry, 19: 46656
THOMAS, T. R., Separation of tellurium and iodine from other fission products, 19: 46169 (IDO-14664)
THOMASSEN, K. I., Oscillations and noise generation in beam-generated plasma, 19: 47741

THOMPSON, C. R., Microstructures of compounds of uranium, thorium, and beryllium, 19: 46924 (NMI-4997, pp 55-61)
THOMPSON, C. R., Microstructural studies of cast uranium, 19: 47007 (NMI-5025(Pt.I), pp 127-51)
THOMPSON, J. M., Isotope-powered thermoelectric generator for Ripple I, 19: 46895
THOMPSON, Keith H., Effect of pre- and post-irradiation treatment on bacteria surviving x irradiation as evaluated by probit analysis, 19: 46014
THOMPSON, R. L., Radar hazards control on the Air Force Eastern Test Range, 19: 46706
THOMPSON, W. B., Binary processes in plasma, 19: 47812
THOMPSON, W. B., Introduction to plasma physics, 19: 47803
THOMPSON, W. B., Introduction to controlled thermonuclear research, 19: 47816
THOMPSON, W. B., Transport equation for a plasma, 19: 47813
THOMSON, J. A., Radioiodine therapy in thyrotoxicosis: review of 908 cases, 19: 46122
THORBURN, R., Ionization and dissociation by electron impact in CBr_4, 19: 46348
THORPE, M. M., Fission fragment removal of uranium from a fissioning surface, 19: 47580 (LA-3352)
THOSAR, B. V., Nuclear structure effects on internal conversion coefficients, 19: 47620
TIBBETTS, J. L., Quantitative metallography of hypostoichiometric UN, 19: 46177 (NMI-5025(Pt.I), pp 85-95)
TIBERGHIEN, Rene, Device for charging and discharging channels of a pressurized, gas-cooled nuclear reactor, 19: 47931
TILL, J. E., Hemopoietic defect in mosaic mice of genotype Sl/Sl^d, 19: 45856
TILL, J. E., Radiosensitivity of the immune response to sheep red cells in the mouse, 19: 45903
TILLEY, D. R., Temperature dependence of the nucleation fields in dirty anisotropic superconductors, 19: 47525
TINKLEPAUGH, J. R., Prog. rpt. on behavior of $SrZrO_3$, 4–6/65, 19: 47008 (NP-15429)
TINT, G. S., Prog. rpt. on flow and fracture of alloyed Be, 10/7/64–1/6/65, 19: 46910 (AD-620589)
TIPPETTS, Roger D., Stable-flow free-boundary electrophoresis theory and practice as applied to study of human serum lipoproteins, 19: 48105 (UCRL-16290)
TITTA, L., Behavior of cholesterol in irradiated animals, 19: 45937
TITTERTON, E. W., Strontium-90 in Australian environment during 1963, 19: 46594
TITTERTON, E. W., Strontium-90 in Australian environment, 1961 to 1963, 19: 46595
TITTLE, C. W., Some functions in theory of neutron logging, 19: 46619
TOBIAS, Melvin L., Application of the equipoise iterative method to diffusion and transport theory, 19: 47541 (ANL-7050, pp 179-89)
TODD, M. J., Calorimeter for graphite dose rate in advanced gas-cooled reactors, 19: 48031
TODOROV, S., Investigation of the effects of N-phenylbenzamidine on the number of inverse mutations during x irradiation of E. coli K suspension, 19: 46012
TOERKOE, J., Selective separation of ^{65}Zn by isotopic exchange between solution and gallium–zinc alloy, 19: 46209
TOLLIVER, R. L., USAF exploratory development of remote handling equipment, 19: 46489 (CONF-640508, pp 327-33)
TOLLIVER, Robert, FMC remote handling vehicle, 19: 46496 (CONF-641120, pp 36-8)
TOLSTIKHIN, I. N., Krypton isotopes in radioactive minerals, 19: 46598
TOMNOVEC, F. M., Neutron fields and induced-activity measurements, 19: 47569 (CEX-62-50)
TOMUSIAK, E. L., Separation-type calculation in finite nucleus, 19: 47676
TONG, L. S., Forced convection heat transfer at high pressure after critical heat flux, 19: 46554
TONI, P., Evaluation of glomerular filtration rate in man using γ-emitting tracer (Hypaque-^{131}I) and external counting, 19: 46071
TOOR, Mordechai, Iodine-131 uptake studies under hot climatic conditions, 19: 45779
TORRES, P., Average ionic charge of helium and hydrogen beams in cadmium vapor, 19: 47266
TORRICELLI, A., Biological problems in association of antineoplastic radiotherapy-chemotherapy, 19: 46096
TOTH, I. J., Prot. rpt. on treatment of bcc metals, 7–12/64, 19: 46960 (AD-611837)
TOTH, K. S., Excitation functions for nucleon and α-particle transfer reactions induced by ^{14}N ions, 19: 47667
TOTHILL, P., Measurement of Ca absorption by double isotope method, 19: 46138
TOTUBALIN, V. N., Changes in resistance of tin films on destruction of superconductivity by current, 19: 47530
TOUGH, Ishbel M., Cytogenetic studies in chronic myeloid leukemia and acute leukemia associated with mongolism, 19: 45915
TOUX, J., Application of strain gages at high temperature. I. Cements, 19: 46715 (EUR-2473.f)
TOYODA, A., Note on the SU_6 symmetry for strong interaction, 19: 47367
TOYOKAWA, Yasuo, Experimental studies on effect of high-dose x irradiation over skin and subcutaneous tissue. I., 19: 45957
TREHAN, S. K., Macroscopic theory of plasma waves, 19: 47804
TRENTA, A., Morphogenesis of nuclear anomaly from small doses of x rays, 19: 45925
TRETYAKOV, I. P., Production of H^- ions from arc ion source on a stand, 19: 47142
TRIBIN-PIEDRAHITA, Alfonso, Beta therapy in filtering operations for treatment of glaucoma, 19: 46045
TRIKHA, S. K., Energy distribution of thermal neutrons in semi-infinite and finite blocks of beryllium oxide assembly, 19: 47555
TRINCI, Inducing conditions of relative radioresistance in intestinal tissues, 19: 45926
TROTT, N. G., Comparative studies of sensitivity of low-background clinical counting systems, 19: 46137
TROTT, N. G., Scintillation dosimetry, 19: 46851
TROTT, N. G., Standardization of radioactive isotopes, 19: 46421
TROUSIL, Jaroslav, Magnetron—a source of x radiation, 19: 46673
TROUT, E. Dale, Effect of kilovoltage and filtration on depth dose, 19: 46144
TROUVE, Jean, Making bars of uranium compound, in particular uranium carbide, 19: 46974
TRUBNIKOV, B. A., Plasma stability in magnetic mirror machine with stabilizing rods, 19: 47835
TRUELLE, M. A., Use of plastics in withdrawing of samples of air for the detection of radon, 19: 46203
TRUHAUT, R., Thyroid uptake of ^{131}I in rats chronically intoxicated with CO, 19: 45770
TRUMBORE, C. N., Photolysis and radiolysis of liquid cyclopentanone, 19: 46357
TRURAN, J. W., Helium content of the galaxy, 19: 47193
TRUSHIN, Yu. V., Thermoelectric characteristics of metallic sintered alloys on tungsten and molybdenum base, 19: 47019 (AD-619334)
TRUTIA, Elena, Levels of low excitation energy in ^{58}Fe, 19: 47696
T'SAI, Ying-shih, Light and spectroscopic properties of inorganic vitreous rare earth oxides, 19: 47886 (N64-21857, pp 1-6)
T'SAI, Ying-shih, Physical research of irradiative radiation emanation of Nd^{3+} activated inorganic vitreous states, 19: 47887 (N64-21857, pp 7-12)
TSAREV, G. L., Fine structure of tungsten single crystals by micro-diffraction of ultrafast electrons, 19: 47022 (JPRS-31225, pp 1-5)
TSUCHIYA, Takehiko, Splenic and thymic weight response to whole-body x irradiation in three strains of mice, 19: 45956
TSUKADA, Tomomichi, Plastic material for measuring large radiation dosage, 19: 46392
TSUKERMAN, V. A., Production of x-ray photographs with very short exposure times, 19: 46729 (LA-tr-65-21)
TSYPIN, S. G., Investigation of hydrogenless shielding for nuclear reactors, 19: 47870
TSYPIN, V. S., Flute instability of plasma with nonzero ion Larmor radius and nonzero pressure, 19: 47766
TSYTOVICH, V. N., Nonlinear stabilization of plasma bunch instabilities, 19: 47726 (NP-15394)
TUCKER, Francis C., Late radiation necrosis of the brain, 19: 45995
TUCKER, W. E., Angular distributions of γ rays produced by neutron bombardment of Al, Mg and Si, 19: 47638
TUCKER, W. E., Gamma rays produced in inelastic scattering. III., 19: 47588 (TID-22012, pp 22-52)
TULL, C. E., Application of iteration-variation method to atomic scattering problems, 19: 47247
TUMA, Hanus, Ageing of corrosion-resistant steels of the type $Cr^{18}Ni^9Ti$, 19: 47026 (ORNL-tr-795)
TURNBULL, A. G., Heats of formation of Be compounds. I., 19: 46279
TUROV, E. A., Bound electron and nuclear spin oscillations in antiferromagnetics, 19: 47903
TUTIYA, Mitsuki, NMR absorption of ^{60}Co γ-irradiated polytetrafluoroethylene. I., 19: 46381
TUTTLE, Elizabeth Rose, Microscopic theory of a Fermi liquid, 19: 47403
TYRRELL, M. E., Metallic binders for zirconium diboride: chromium, molybdenum, and tungsten, 19: 46907 (AD-456724)
TYTGAT, R., Radiological monitoring of the surroundings of CEN at Mol, 19: 46631 (A/AC.82/G/L.986)
TYUKOV, D. M., Spectral composition of erythemal part of uv radiation, 19: 45881

U

UCHINO, Kousuke, Anomalous behaviors in Josephson current, 19: 47515

UCHIYAMA-CAMPBELL, Fumiye, sp and KK contribution to isoscalar form factor of the nucleon, 19: 47371

UCHURKHANOV, M. M., Effects of radiation on flotation process, 19: 46453

UENSEREN, Enver, Inversion of cyanide group into iso-cyanide under γ irradiation, 19: 46326 (CNAEM-28)

UGAI, Hiroyuki, Nature of the muon, 19: 47378

UHERKA, K. L., Influence of transverse magnetic field on forced convection liquid metal heat transfer, 19: 46547

UHLMANN, W., Bibliography on radiation effects on solid, U based nuclear fuel materials, Vol. 5, No. 2, 19: 47093 (VDDIT-16(5.2))

UHRIG, Hess, Signal for fast shutdown in a nuclear reactor, 19: 47935

ULKEN, D., Germany's nuclear ship, 19: 48051

ULRICH, A. J., Evaluation of thermionic energy converter using film-boiling liquid metal, 19: 47281 (ANL-7039)

ULRICHS, J., Strongly interacting particles in air shower cores, 19: 47271

UMAN, Myron F., Heating plasma by magnetic pumping, 19: 47767

UMEHARA, Yoji, Immune response of Ehrlich ascites tumor cells irradiated in vitro, 19: 45914

URANO, Yukichi, Reaction of ethylene with methylene chloride induced by γ radiation, 19: 46370

URBANEC, Jan, Investigation of the intensities of hard γ transitions in capture of resonance neutrons by ^{138}Ba, 19: 47701

URSU, D., Forming of H_2^+ ions sources by electronic bombardment, 19: 47141

USHAKOV, P. A., Models of temperature fields of heat exchange elements in active zone and shielding of the BN-350 reactor, 19: 47994 (NP-15393)

UTLEY, L. W., Evaluation of adjustable speed drive systems on machine tools, 19: 46461 (RFP-562)

UY, J. C., Effect of pressure on structure and properties of metals, 19: 46983 (AD-612159)

V

VAISH, S. P., Role of water of hydration in annealing behavior of neutron-irradiated trisdipyridyl cobalt(III) perchlorate, trihydrate, 19: 46387

VALLEBONA, D., Radiotherapy of metastases with massive doses, 19: 46101

VAN ALLEN, J. A., Absence of 40-kev electrons in earth's magnetospheric tail at 3300 earth radii, 19: 47458

VAN BEKKUM, D. W., Induction of tumors by ionizing radiation, 19: 45942

VAN DAM, H., Electrons-kinetics in irradiated dipolar systems, (T), 19: 47433

VAN DEN BERG, M., Apparatus for measurement of diffusivity at high temperatures, 19: 46995 (EUR-2424.f)

VANDENPLAS, P. E., Quasi-static oscillations in hot asymmetrical plasma slab, 19: 47746

VAN DYNE, G. M., Chemical composition of individual range plants from the U. S. Range Station, Miles City, Montana, from 1955–1960, 19: 45747 (ORNL-TM-1279)

VAN ENGELEN, P. P. J., Magnetic properties of superconducting Ta, 19: 47524

VANGOYEAU, Henri, Metallography—concerning existence of an allotropic change to cubic U_3Si within U–Si, 19: 47024 (NLCO-tr-6)

VANHAUWERMEIREN, R., Spectroscopic method for determination of electron density, 19: 47754

VANKINSCOTT, Vernice, Zinc-65 metabolism during low and high Ca intake in man, 19: 45787

VAN LANDUYT, J., Oxidation of zirconium, 19: 46958

VANNINI, V., Morphogenesis of nuclear anomaly from small doses of x rays, 19: 45925

VAN SOESTBERGEN, A. A., Effect of pre- and post-irradiation treatment on bacteria surviving x irradiation as evaluated by probit analysis, 19: 46014

VAN STAVEREN, J. C., Nuclear energy development and dependence on nuclear fuel reserves, 19: 47979

VAN STEENBERGEN, A., Comparison of various methods for determining particle beam phase-space distribution, 19: 47162 (BNL-9503)

VAN WAGENINGEN, R., Regge symmetries of the 3j-symbols, 19: 47335

VAN WOERDEN, J., Bibliography on protection against biological effects of thermal radiation, 19: 45818 (TDCK-33500)

VARNER, J. E., Prog. rpt. on biochemistry of senescence in plant cells, final, 6/15/63–6/14/65, 19: 48102 (TID-22175)

VARSI, G., Film thickness, pressure drop, and stability in annular two-phase flow, 19: 46542

VASIL'EVA, L. V., Models of temperature fields of heat exchange elements in active zone and shielding of the BN-350 reactor, 19: 47994 (NP-15393)

VASSALLO, F. A., Prog. rpt. on aerospace nuclear safety investigations of reentry ablation phenomena, 5–7/65, 19: 47117 (SC-DC-65-1698)

VASSELL, Milton Oliver, Solution of finite many-particle system with translational invariance, 19: 47399

VASSOS, Basil H., New approach to neutron activation analysis through micro and submicro electroseparation techniques, 19: 46229

VAUGHAN, D. A., Factors controlling effectiveness of high-temperature protective coatings for tungsten, 19: 46911 (AFML-TR-64-392)

VAUGHAN, D. A., Oxidation of zirconium–yttrium alloys, 19: 47034

VAUGHN, F. J., New isotope of fluorine: ^{23}F, 19: 47671

VELDRE, V. Ya., Calculation of effective cross sections for the ionization of hydrogen atoms by electron impact, 19: 47237

VELTMAN, M., Weak interactions, 19: 47301 (CERN-65-30)

VERBIEST, A. J., Atomic energy market in Europe. VIII. The Netherlands, 19: 47923

VERDEYEN, J. T., Utilization of transverse modes in spherical laser interferometer, 19: 47745

VERGA, V., Biological factors of the radiosensitivity of metastases, 19: 45921

VERLY, Walter G., Verification of radiochemical purity of labeled optical isomer, 19: 46208

VESELOVSKY, G. S., Methods of automatic ionization measurement in a bubble chamber, 19: 46758 (CONF-550-99)

VESELY, Vladimir, Plant for disposal of radioactive waste water, 19: 48086

VIANO, G. A., Analysis of α-^{12}C scattering process by Regge representation, 19: 47653

VIBERG, Lars, Acute inflammatory conditions of the uterine adnexa, 19: 46040

VICHI, G. F., Digestion of proteic and fatty substances and time of transition in patients irradiated on the abdomen, 19: 45932

VIDAL-ABARCA, J. B., Reversible and irreversible processes in the dropping-Hg electrode. XIX., 19: 46260

VIDAL-ABARCA, Juan B., Measurement of diffusion coefficients. III., 19: 46261

VIENET, R., High-brilliance ion source, 19: 47172

VIGIER, J. P., High-energy electron-positron scattering, 19: 47364

VIJAYALAKSHMI, B., Multiply charged nuclei of the primary cosmic radiation. I., 19: 47276

VIJAYALAKSHMI, B., Multiply charged nuclei of primary cosmic radiation. II., 19: 47277

VILCOV, Isabela, Levels of low excitation energy in ^{56}Fe, 19: 47696

VILCOV, N., Levels of low excitation energy in ^{56}Fe, 19: 47696

VILCOV, N., Yield ratio for fissioning isomer from deuteron irradiation of Pu, 19: 47688

VILHAR, M., Synthesis of hydrazine–fluorozirconates, 19: 46236 (NIJS-R-430)

VILLA, F., Development of streamer spark chambers, 19: 46781

VILLANI, G., Behavior of cholesterol in irradiated animals, 19: 45937

VINKALNS, I. Zh., Calculation of effective cross sections for the ionization of hydrogen atoms by electron impact, 19: 47237

VINOGRADOV, A. P., Carbon-14 dating of Upper Anthropogene in the USSR, 19: 46621

VINOKUROV, I. V., EPR spectra of Gd^{3+} ion in single crystals of CeO_2, 19: 47898

VINSON III, David B., Scintillation methods for metallic ion determination in human subjects using computer techniques, 19: 45771

VISINESCU, M., Sign of the effective range parameter, 19: 47390

VIVIAN, C. E., Advanced design concepts for a remotely operated manipulator system for space-support operations, 19: 46487 (CONF-640508, pp 248-303)

VIVIAN, Charles, Remote handling in space, 19: 46500 (CONF-641120, pp 67-70)

VODOP'YANOVA, L. S., Thermoelectric characteristics of metallic sintered alloys on tungsten and molybdenum base, 19: 47019 (AD-619334)

VOELKL, J., Low-temperature recovery spectra of neutron-irradiated metals, 19: 47097

VOETS, J. P., Behavior of some amino acids in γ-irradiated soils, 19: 45941

VOGLER, Hans, Immediate improvement of radiation protection, 19: 46036

VOIGT, H. H., Development of stars, 19: 47201

VOITSENYA, V. S., Polarization of plasma moving in curved magnetic field, 19: 47797

VOLKENSHTEIN, N. V., Thermal conductivity of Gd and Tb at low temperatures, 19: 47528

VON BRAUN, Eckart, Uranium prospecting supported by German Federal Republic, 1956–1962, 19: 46630

VON DARDEL, G., Automatic scanning facility for bubble and spark chamber photographs, 19: 46811

VON DARDEL, G., Status report on Lund vidicon system, 19: 46788

VORRES, Karl S., Correlation of structures of I-V type ABO_3 compounds, 19: 46243 (TID-22207, Paper C)

VORRES, Karl S., Ionic field strengths as criteria for compound formation

in oxide systems, 19: 46246 (TID-22207, Paper F)
VORRES, Karl S., Preparation and some properties of sodium–rare earth mixed oxides, 19: 46241 (TID-22207, Paper A)
VORRES, Karl S., Preparation and structural study of ABO_3 compounds containing Cu and Nb or Ta, 19: 46244 (TID-22207, Paper D)
VORRES, Karl S., Preparation and structural studies of some cupric rare earth AB_2O_5 type compounds, 19: 46245 (TID-22207, Paper E)
VORRES, Karl S., Prog. rpt. on high-temperature solid-state chemistry and sub-solidus phase equilibria, final, 8/65, 19: 46240 (TID-22207)
VORTMAN, L. J., Excavation with parallel rows of explosions, 19: 46470 (SC-RR-65-303)
VOSHALL, R. E., Mobility of negative ions in O_2 at low E/N, 19: 47220 (NP-15175)
VOYTENKO, A. E., Producing high-velocity gas jets, 19: 46574 (AD-619323)
VREELAND, T. Jr., Basal dislocation mobility in high-purity zinc single crystals, 19: 48089 (CALT-473-4)
VRIENS, L., Excitation and ionization of atomic hydrogen from various states, 19: 47243
VRZAL, Jan, Investigation of the intensities of hard γ transitions in capture of resonance neutrons by ^{138}Ba, 19: 47701
VUILLEMIN, M., Electromagnetic instability of collisionless plasma, 19: 47844
VUILLEMIN, M., Plasma instability, 19: 47824
VUJNIC, Veselin, Intracavitary therapy of uterine carcinoma with Co-60, 19: 46039 (JPRS-31667)
VUJOVIC, Veselinka, Movement of radioactivity emanating from ^{40}K in precipitation and waters on territory of Vinca, 19: 46590 (JPRS-31469)
VVEDENSKII, G. A., The economy. Soviet atomic power stations, 19: 48014

W

WABER, J. T., Electronic band structures of plutonium and its monocarbide, 19: 47880 (LA-DC-7353)
WADA, Yasushi, Thermodynamic properties of strong-coupling superconductors, 19: 47536
WADDELL, William R., Problems in renal homotransplantation, 19: 45888
WAGENER, K., Concentration and temperature dependence of isotope effects in ion migration of Li in acetic acid solutions. V., 19: 46264
WAGENER, Klaus, Isotope effect in ion transport in aqueous solution—as basis for isotope separation and as instrument, 19: 46898 (HMI-B-44)
WAGNER, K. H., Mean energies and drift velocities of electrons in nitrogen, argon and xenon, determined by image intensifier photographs of electron avalanches, 19: 47124 (SLAC-Trans-19)
WAGNER, Raymond P., Decomposition of gaseous PuF_6 by α radiation. VII., 19: 46325 (ANL-7013)
WAIDE, C. H., Chemonuclear loop removal from BGRR using a semi-remote cutting technique, 19: 48055 (BNL-9402)
WAINE, Peter, Rod cluster fuel assembly support structure for nuclear reactor, 19: 47943
WALECKA, J. D., Nuclear correlation functions and muon capture, 19: 47656
WALKER, Bryce Dale, Polarization of neutrons from $^{12}C(p,n_0)^{12}N$ and $^{15}N(p,n_0)^{15}O$ reactions, 19: 47710
WALKER, Isobel C., Drift velocities of slow electrons in polyatomic gases, 19: 46393
WALKER, M. S., Propagation of persistent current decay in Nb–Zr wires, 19: 47507
WALKER, R. L., Adhesion of particles to surfaces in liquid and gaseous environments, 19: 46645 (ORNL-TM-1228)
WALKER, R. M. F., Direct measurement of small energy losses of relativistic particles, 19: 47252
WALL, E. L., Thermal expansion coefficient and compressibility of solid ^3He, 19: 47523
WALL, L., Relation between ionization and cohesive energies of rare earths, 19: 47062
WALLACE, J. B. G., Application of iteration-variation method to atomic scattering problems, 19: 47247
WALLACE, J. F., Control of cast grain size of steel castings, 19: 46980 (AD-611800)
WALMSLEY, D. A. G., Energy-transfer processes in dilute solutions of organometallics in benzene, 19: 46362
WALRAVE, W. K. A., Radioactive waste problems in processing of irradiated fuels, 19: 46435
WALSH, Patrick N., Physical and chemical principles affecting high-temperature materials for rocket nozzles, 19: 46956 (NP-15514(Vol.I))
WALSTAM, Rune, Two special applications of high-energy electron beams, 19: 46042
WALTERS, W. B., Decay scheme of 25-minute ^{131g}Te, 19: 47663
WALTHER, H., Modifications of SORIN's pool-type reactor Avogadro RS1 for higher power operation, 19: 48066

WALTON, J. R., Isotopic composition of atmospheric neon, 19: 46588 (ORNL-3857)
WALZ, Richard H., Beta radiation source in a ceramic carrier, 19: 47156
WAND, R. H., Strongly interacting particles in air shower cores, 19: 47271
WANG, S. C., Kinematics of angular momentum of a particle. I., 19: 47418
WANKLYN, J. H., Effect of γ dose on oxide films on Zr and Zircaloy-2, 19: 47099
WANNIER, Gregory H., Probability of violation of the Ehrenfest principle in fast passage, 19: 47427
WAPSTRA, A. H., K-conversion coefficient of 328-kev E2 transition in ^{194}Pt, 19: 47643
WARD, Gerald M., Availability of fallout ^{137}Cs to dairy cattle from different types of feed, 19: 45780
WARDI, Ahmad H., Analytical chemistry of hafnium and zirconium, 19: 46224
WARMAN, J. M., Effect of electron scavengers on formation of hydrogen in radiolysis of propane, 19: 46396
WARNER, R. M., Deuterated organic compounds. XXV., 19: 46308
WARNKE, D. F., Effects of radiation-induced damage centers in lead zirconate titanate ceramics, 19: 47096
WARREN, John L., Charged bond correction to dispersion curves of diamond, 19: 47879 (LA-DC-7277)
WASSON, O. A., Search for direct neutron capture in manganese, 19: 47634
WATAGHIN, V., High-energy electron-positron scattering, 19: 47364
WATERS, James Duncan, Rod cluster fuel assembly support structure for nuclear reactor, 19: 47943
WATERS, T. N., Crystal structure of bisnitratodiaquodioxouranium(VI) tetrahydrate (uranyl nitrate hexahydrate), 19: 46255
WATSON, J. Throck, ^{129}I as a nonradioactive tracer, 19: 45799
WATT, J. S., Purity of γ-ray sources, 19: 46407 (AAEC/TM-226(Suppl.1))
WATT, T., Determination of magnetic-field distributions, 19: 46731 (SLAC-Trans-21)
WATTENDORFF, J., Immediate alteration of urea permeability after α irradiation of Allium epidermis cells, 19: 45975
WATTS, E. C., High-temperature tensile testing machine for irradiated structural materials, 19: 46712 (BNWL-SA-169)
WEAVER, D., Lectures on particles and field theory. II., 19: 47405
WEBB, G. B., Chemical engineering in the HTGR, 19: 47991 (GA-6126)
WEBB, J. C., Nuclear power in developing areas, 19: 48041
WEBSTER, Edward W., Dose and information in diagnostic radiography, 19: 46146
WEBSTER, Harold, Improvements in or relating to conveyor systems, 19: 46519
WEGLARZ, L., Photonuclear reaction studies by activation methods, 19: 47596 (TID-22141, pp 94-7)
WEIERSHAUSEN, Walter, Thermal ionization of Cu, Ag, and Ti with pure polycrystalline W and Re surfaces and those covered with foreign layers, 19: 47222 (ORNL-tr-679)
WEIGLE, William O., Induction of tolerance to bovine serum albumin by means of whole-body x radiation, 19: 45902
WEILAND, Raymond L., Scintillation methods for metallic ion determination in human subjects using computer techniques, 19: 45771
WEINBERG, S., Lectures on particles and field theory. II., 19: 47405
WEINBERG, Steven, Infrared photons and gravitons, 19: 47204
WEINBERG, Steven, Quantum theory of massless particles, 19: 47409
WEINBERG, Steven, Quasiparticles and perturbation theory, 19: 47408
WEINREICH, Marcel I., Modulation of light by means of electrically birefringent crystals, 19: 48110 (SC-T-65-750)
WEINREICH, Marcel I., Radioactive collection for atmospheric electricity soundings, 19: 46730 (SC-T-65-760)
WEINREICH, Marcel I., Triple impulse asymptotic paths, 19: 48109 (SC-T-65-749)
WEISE, Hans-Joachim, Therapy of lethal radiation with rutin. I., 19: 46030
WEISS, Robert, Betatron for electron depth therapy, 19: 46126
WEISSBERGER, Arnold, Physics and chemistry of the organic solid state. II., 19: 46320
WEITKAMP, William George, Polarization of protons scattered by helium, 19: 47709
WELLMAN, Henry N., Iodine-131 in children's thyroids from environmental exposure, 19: 46035 (PHS-999-RH-14)
WELLS, M. B., Neutron transport data for single and multilayer slabs of aluminum, polyethylene, and carbon, 19: 47869 (RRA-T52)
WELNA, H., Prog. rpt. on LCRE pumps and sumps, final, 7/65, 19: 46535 (PWAC-386)
WELSH, W. F., Operating limits and safety analysis for split-table, dry, flexible critical experiments at CANEL Nuclear Physics Lab., 19: 47958 (PWAC-475)
WENGER, P., Radioactive fallout in Geneva during 1963, 19: 46612
WENT, J. J., Nuclear energy development and dependence on nuclear fuel reserves, 19: 47979
WENTWORTH, B. C., Observations on radiothyroidectomized chickens,

19: 45966
VENZL, H., Low-temperature recovery spectra of neutron-irradiated metals, 19: 47097
VENZL, James E., Radioisotope renography in children. I., 19: 46109
VERGELAND, Harold, Photon emission from a given current, 19: 47135
VERNER, S. A., Propagation of Bragg-reflected neutrons in large mosaic crystals and efficiency of monochromators, 19: 47562
VERNER, V., Formation of 1-benzyl-2,3-diphenylindanes from stilbene in presence of tin tetrachloride under influence of γ radiation, 19: 46345
VERYHA, A., Use of labeled vitamin B_{12} in the clinic, 19: 46128
VESSOT, J. A., Plasma flow in a θ pinch, 19: 47834
VESTER, P. O., Trace elements in the conductive tissue of beef heart determined by neutron activation analysis, 19: 45753 (AE-191)
VESTERMAN, R. E., High-temperature corrosion of ATR structural materials, 19: 46946 (BNWL-100)
VESTHOFF, D. D., Absorption of D-glucose by segments of intestine from irradiated ground squirrels, 19: 45841
VESTRUM, Edgar F. Jr., Thermal anomalies and thermodynamic properties of gadolinium hexaboride, 19: 46994 (COO-1149-52)
VESTRUM, Edgar F. Jr., Thermal anomaly in U_4O_9 at 348°K, 19: 46283
VETHERELL, A. T., Inter-diffusion of plasma and magnetic fields in pinch and hardcore discharges, 19: 47853
VETHERILL, G. W., Primary and metamorphic Rb–Sr chronology in central Colorado, 19: 46618
VETTERFORS, J., Acute radiation syndrome, 19: 45829
VEY, Ming-Tong, Determination of contents on Mn and Cu during life cycle of Chlorella cells by neutron activation analysis, 19: 45775
VEYMUELLER, Carl R., Materials for advanced technologies, 19: 47068
VHAN, R. E., Investigations of oxygen-defect interactions between 25 and 700°K in irradiated Ge, 19: 47892
VHANG, D. H., Essential specifications of Hamburg 4π large-volume radioactivity detector with liquid organic scintillator. I., 19: 46775
VHEAT, J. Allen, Applications of atomic absorption spectroscopy, 19: 46166 (DP-980)
VHEATLEY, D. H., Growth and infiltration of Ehrlich's ascites tumor in mice with reduced immunological responses, 19: 45858
VHEELOCK, C. W., Carbide fuels in fast reactors, 19: 47993 (NAA-SR-10751)
VHIPP, James, Preliminary concepts for a central test facility, 19: 46503 (CONF-641120, pp 78-85)
VHITE, B. M., Inter-diffusion of plasma and magnetic fields in pinch and hardcore discharges, 19: 47853
VHITE, CHARLES R., Dynamically loaded strip footing buried in dry sand, 19: 46567 (NP-15396)
VHITE, David C., Rectal mucosa as biologic indicator of radiation injury. I., 19: 45918
VHITE, F., Mass spectrometer program, 19: 46725 (TID-22141, pp 101-10)
VHITE, L. E., Remote handling requirements for NERVA (E-MAD and ETS-1), 19: 46495 (CONF-641120, pp 9-35)
VHITE, T. O. Jr., Precise track measurements in a wide gap spark chamber, 19: 46780
VHITE, W. D., Antibacterial bacteriological swab, 19: 46884
VHITEMAN, K. J., Helical fields possessing mean magnetic wells, 19: 47154
VHITTEMORE, W. L., Experimental determination of neutron inelastic scattering in polyethylene, 19: 47572 (GA-6547)
VIECHERS, G., Shell model calculations of nuclear magnetic moments and M1 transition of probabilities $2s_{1/2}$ $1d_{3/2}$, 19: 47641
VIENEROVA, E., Nucleolar coefficient of lymphocytes in peripheral blood of patients with Hodgkin's disease, 19: 46103
VIESER, P., Control of cast grain size of steel castings, 19: 46980 (AD-611800)
VIESINGER, F., The radiation stability of anthracene oils. II., 19: 46333 (SGAE-CH-20/1965)
VIGNER, E. P., Electron-kinetics in irradiated dipolar systems, (T), 19: 47433
VIK, B., Enrichment of tritium by thermal diffusion and measurement of dated Antarctic snow samples, 19: 46613
VIKHAMMER, G. A., Dryout in a 19-rod bundle cooled by steam/water fog at 515 psia, 19: 46548
VILBUR, Karl M., Prog. rpt. on effects of radiation on mucosal and fetal brain enzymes and radiation recovery, final, 11/1/64–10/31/65, 19: 45820 (TID-22227)
VILCZOK, Tadeusz, DNA repair of radiation damage. I., 19: 46013
VILHELM, Horst E., Operation and diagnostics of closed-loop MPD power generator, 19: 47728
VILHELMI, R. P., Metallographic studies of uranium-fission alloys, 19: 47004 (NMI-4997, pp 45-54)
VILKE, K. H., Adiabatic linear Stark effect in a plasma, 19: 47716 (AD-614283)
VILKINS, M. J. M., Effect of γ dose on oxide films on Zr and Zircaloy-2, 19: 47099
WILKINS, W. H., Advanced design concepts for a remotely operated manipulator system for space-support operations, 19: 46487 (CONF-640508, pp 248-303)
WILLEN, E. H., On-line computer data processing system for counter and spark chamber experiments, 19: 46806
WILLIAMS, Dean N., High-temperature Nb-base alloys, 19: 46976
WILLIAMS, H. T. Jr., Evaluation of computational system applicable to the nuclear analysis of critical experiments and power reactors, 19: 47959 (WCAP-3269-52)
WILLIAMS, I. R., Excitation functions for nucleon and α-particle transfer reactions induced by ^{14}N ions, 19: 47667
WILLIAMS, J. P. G., Dental lesions in rat induced by radiomimetic agents, 19: 45845
WILLIAMS, Jack, Nuclear fuel materials including vitreous phase, 19: 47986
WILLIAMS, M. M. R., Calculation of upper bounds on time-decay constants in pulsed neutron experiments, 19: 47553
WILLIAMS, Ronald Peter, Nuclear reactor with pressurizer, 19: 47940
WILLOUGHBY, O. H., Radiometric determination of fluorine in bulk PuF_4, 19: 46179 (RFP-618)
WILSON, E. R., Compilation of β-stimulated x-ray spectra, 19: 47223
WILSON, G. U., Strontium-90 in Australian environment, 1961 to 1963, 19: 46595
WILSON, John V., Lattice vibration frequency spectrum of graphite, 19: 47881 (ORNL-tr-585)
WILSON, Kent, Pneumatically actuated master slave manipulator, 19: 46499 (CONF-641120, pp 63-6)
WILSON, R. G., Electrode surface physics research, 19: 46571 (HRL-5249-S)
WINICOUR, Jeffrey Harold, Asymptotic behavior of coupled gravitational fields, 19: 47437
WINN, M. M., Strongly interacting particles in air shower cores, 19: 47271
WINNACKER, K., Atomic energy market in Europe. I. Federal Republic of Germany, 19: 48112
WINTER, K., Effect of chromium(III)-oxide on sintering properties of UO_2, 19: 46971
WIRTA, Roy, Control—the universal process, 19: 46460 (CONF-640508, pp 224-32)
WISOFF, Carl P., Bone scanning in management of cancer patients, 19: 46133
WITTMANN, A., Crystal structure of so-called technetium disilicide, 19: 47055
WOLFF, J., Effect of processing history on the superconducting properties and long-range order of Ta_3Se, 19: 47513
WOLFKE, M., Interpretation of mathematical interrelationships of radioactive decay, 19: 47599 (ORNL-tr-707)
WOLLMAN, Seymour H., Autoradiography of diffusible ions with application to thyroidal radioiodide, 19: 45783
WOMELSDUFF, R. E., Fallout report—β-γ radioactivity in air at Sandia, 1–6/65, 19: 46648 (SC-RR-65-464)
WONG, A. Y., Transition from Landau damping to viscous damping of ion acoustic waves, 19: 47724 (MATT-267)
WONG, Harold Y., Evaluation of field-effect transistors, 19: 46871 (AD-614268)
WONG, Lawrence C. K., Toxicity of niobium salts, 19: 45768
WOOD, Anne, Interferometric wavelengths of thorium lines between 9050 and 2566 Å, 19: 47232
WOOD, D. S., Basal dislocation mobility in high-purity zinc single crystals, 19: 48089 (CALT-473-4)
WOOD, David H., Phase relations in magnesium-rich portion of cerium–magnesium system, 19: 47059
WOOD, Eileen E., Survey of leukemia in West Cornwall clinical area (1948–1961), 19: 45959
WOOD, J., Calculation of upper bounds on time-decay constants in pulsed neutron experiments, 19: 47553
WOOD, R. W., Forced convection burnout in Freon-12 flow, 19: 46527 (AEEW-R-426)
WOODCOCK, E. R., Techniques used in GEN code for Monte Carlo neutronics calculations in reactors and other systems of complex geometry, 19: 47949 (ANL-7050, pp 557-79)
WOODSTOCK, Lowell W., Effects of γ irradiation of corn seed on respiration and growth of seedling, 19: 45836
WOOLF, Michael Andrew, Investigation of the density of states in superconductors, 19: 47535
WORK, Richard N., Prog. rpt. on radiation effects on high polymers, final, 1955–1965, 19: 46331 (NYO-1858-1)
WORT, D. J. H., Conditions for improved stability in Zeta, 19: 47856
WRIGHT, B., Effects of small doses of radiation on flow and other properties of Ziegler polyethylenes, 19: 46358
WRIGHT, Donald E., Air density sensitive gages for space craft,

19: 46749
WU, Hung-sheng, Nonlocal extension of the Ginzburg-Landau equations in theory of superconductivity, 19: 47527
WU, T. F., Singularities of amplitudes in perturbation theory, 19: 47412
WUSCHKE, E. E., Automatic potentiometric titrator, 19: 46162 (AECL-2262)
WYARD, S. J., Dipolar broadening of electron spin resonance lines in irradiated solids, 19: 46383
WYCKOFF, H. O., Quantities and units for dosimetry in diagnostic radiology, 19: 46684

Y

YAKUSHEV, E. M., Exact integration of equations of motion for relativistic charged particles for a certain class of variable electromagnetic fields, 19: 47435
YALOW, Rosalyn S., Iodine metabolism and thyroid gland, 19: 45792
YAMADA, Junzo, Splenic and thymic weight response to whole-body x irradiation in three strains of mice, 19: 45956
YAMADA, Masakazu, Histologic fixation for radioautography and release of radioactivity from liver tissue treated with ^{35}S-sulfate, 19: 45800
YAMADA, Masaaki, Histologic fixation for radioautography and release of radioactivity from liver tissue treated with ^{35}S-sulfate, 19: 45800
YAMADA, R., On-line computer data processing system for counter and spark chamber experiments, 19: 46806
YAMADA, Tunao, Effects of actinomycin D on lens regenerating system, 19: 45738
YAMAMOTO, Kakuji, NMR absorption of ^{60}Co γ-irradiated polytetrafluoroethylene. I., 19: 46381
YAMAMOTO, Kenzo, Hydromagnetic wave in toroidal discharge with longitudinal magnetic field, 19: 47742
YAMAMOTO, Kunio, Shrinkage of effective core and large-angle scattering at high energy, 19: 47380
YAMAMOTO, Lucas, Contour brain scanning with I and Hg compounds for detection of intracranial tumors, 19: 46046
YAMAMOTO, Yutaka, Prog. rpt. on chemical engineering studies on processing radioactive wastes, final, 1/64–3/65, 19: 48079 (NP-15371)
YAMASHITA, Hisao, Radiation-induced cancer of the skin, 19: 45945
YAMAZAKI, Miwao, K-matrix formalism for three-body and bound-state scattering, 19: 47381
YAMZIN, I. I., Two-coordinate neutron diffractometer, 19: 46835
YAN, Youhou, Genetic analysis of pyrimidine mutants of Salmonella typhimurium, 19: 45878
YANG, John Y., Radiolysis of cyclohexane-d_{12}–cyclopentane mixtures, 19: 46364
YANG, Shan-tah, Shell-model interpretation of spectra of $2s_{1/2}$-$1d_{3/2}$ nuclei, 19: 47600
YANO, Nobuhiro, Temporary increase in uv resistance in course of spore germination of Bacillus subtilis, 19: 45848
YARMOMENKO, S. P., Radioresistance in an animal organism, 19: 46031
YAROSHEVSKII, A. A., Interpretation of strontium isotopic composition as indicator of magmatic differentiation and its duration, 19: 46600
YASUMOTO, Masahiko, Reaction of ethylene with methylene chloride induced by γ radiation, 19: 46370
YATES, D. J. C., Exchange of deuterium with hydroxyl groups of alumina, 19: 46280
YATSUI, Kiyoshi, Anomalous diffusion and oscillations of positive column in magnetic field, 19: 47756
YEN, K. T., Solar flare model and its laboratory experimentation, 19: 47188 (AD-613636)
YEN, Shao, Strontium-90 as simple, rapid, and inexpensive treatment for aviation tympanitis, 19: 46038 (JPRS-31602, pp 191-7)
YEH, Tsi Chu, Thermal stress techniques in the nuclear industry, 19: 47922 (TID-22119)
YOCK, P., Lectures on particles and field theory. II., 19: 47405
YOKOSAWA, Akihiko, Polarization in $\pi^- + p$ elastic scattering at 2.08 Bev/c, 19: 47373
YONEZAWA, Fumiko, Effective spin Hamiltonian for nonorthogonal orbitals. I., 19: 47254
YORK, Don, Current techniques and problems of remote handling at reactor maintenance, assembly and disassembly facility, 19: 46493 (CONF-641120, pp 4-5)
YOSHIDA, Yoshio, Theoretical studies on methodological procedures of radiation breeding. V., 19: 45737
YOSHIDA, Yoshio, Theoretical studies on the methodological procedures of radiation breeding. IV., 19: 45884
YOSHIKAWA, Kiyoshi, Histologic fixation for radioautography and release of radioactivity from liver tissue treated with ^{35}S-sulfate, 19: 45800
YOSHIKAWA, S., Ion heating in the model C Stellarator, 19: 47832
YOSHINAGA, Haruso, Retained ThO_2 media in seminal vesiculography. Follow-up study with dose estimates, 19: 45837

YOSHIOKA, Toru, Apparatus for measuring the Moessbauer effect, 19: 46826
YOUMANS, Arthur H., Apparatus for neutron-neutron well logging, 19: 46622
YOUNG, James A., Role of interference scattering in neutron thermalization by heavy water, 19: 47559
YOUSEF, M. Y. A., Approximate treatment of fast neutron spectrum in two-component homogenous medium, 19: 47964
YUAN, L. C. L., On-line computer data processing system for counter and spark chamber experiments, 19: 46806
YUILE, Charles L., Toxicity of niobium salts, 19: 45768
YURA, Osamu, Absolute counting of ^{14}C by efficiency tracing technique, 19: 46214
YURKA, G. E., Electron identification in lead plate spark chambers, 19: 46782
YURKA, G. E., Magnetic spark chamber system, 19: 46796
YUSHMANOV, E. E., Experiments on accumulation of hot ion plasma in PR-5, 19: 47857
YUSKESELIEVA, L. G., Electrophotographic method for determining the lithium diffusion constant in p-type silicon, 19: 46997 (JINR-P-2282)

Z

ZABLOCKI, B., Effect of radiation on behavior of gamma globulins in reaction with the rheumatoid factor, 19: 45860
ZABOROWSKI, Henryk, Multi-sphere technique. I., 19: 46757 (CEA-R-2772)
ZACHARIAS, I. M., Induction of leaf spots in leguminous plants by nucleotoxic agents, 19: 45882
ZAGORETS, P. A., Capacity dilatometer for radiochemical investigations, 19: 46419
ZAHN, L. L. Jr., Safety aspects of transport of radioactive materials, 19: 46663
ZAJIC, Vladimir, Contribution to cooling intensification at high heat fluxes using a ragged heat exchange surface, 19: 46543
ZAJICEK, J., Sensitization and radiation response in cases with carcinoma of the uterine cervix, 19: 45830
ZAK, M., Skin protection against x rays, 19: 46019
ZAKHARIEV, A. I., Capacity dilatometer for radiochemical investigations, 19: 46419
ZANDBERG, E. Ya., Inherent thermionic emission of lanthanum hexaboride and surface ionization of cesium atoms on it, 19: 47148
ZANELLA, P., Analysis of spark chamber pictures using raster-scan technique, 19: 46786
ZANELLI, John, Contour brain scanning with I and Hg compounds for detection of intracranial tumors, 19: 46046
ZANGE, E., Determination of ^{90}Sr in effluents in presence of ^{89}Sr, 19: 46196
ZANOLLA, W., Studies of liver function in irradiated rats, 19: 45828
ZAPEVALOV, V. A., Photoproduction of π^+ mesons on protons at 230 Mev, 19: 47393
ZAUBERIS, D. D., Neutron-diffraction study of chemical order-disorder in $PtMn_3$, 19: 47028
ZEBRO, Tadeusz, Chemical protection against ionizing radiation. I., 19: 46006
ZEGLER, S. T., Metallographic studies of uranium-fissium alloys, 19: 47004 (NMI-4997, pp 45-54)
ZELDOVICH, O. Ya., Backward elastic scattering of pions on neutrons at 1.2 to 4.5 Bev, 19: 47310 (NP-15376)
ZEL'DOVICH, V. Ya., CP violation and nature of $\Delta T = \frac{1}{2}$ rule, 19: 47317 (NP-tr-1282)
ZHIBRITSKII, V. K., Effect of nitrogen impurity on electron energy losses in nonequilibrium argon–cesium plasma, 19: 47737
ZHIVLYUK, Yu. N., Run-away electrons in a nonequilibrium plasma, 19: 47783
ZHUKOV, A. V., Models of temperature fields of heat exchange elements in active zone and shielding of the BN-350 reactor, 19: 47994 (NP-15393)
ZHUKOVSKII, V. G., Investigation of plasma in the AC device, 19: 47855
ZIESKE, P. L., Composition of noble gas ion beams produced with a duoplasmatron, 19: 47267
ZIJP, W. L., Review of activation methods for determination of fast neutron spectra, 19: 46763 (RCN-37)
ZIKIDES, C. C., System for accurate counting of short-lived activities by repetitive activation, 19: 46818
ZIMERING, S., Prog. rpt. on mechanical properties of metals subjected to mechanical stress and neutron irradiation, 7/65, 19: 47081 (EURAEC-1432)
ZIMMERMAN, E. J., Stopping cross sections of carbon and hydrocarbon solids for low-energy protons and helium ions, 19: 47871
ZIMMERMAN, F. K., Interaction of RNA polymerase with irradiated DNA, 19: 45849

ZIMMERMANN, Albert J., Radioactive drugs, 19: 46044
ZINGELMANN, W. J., Radiation injury of Clostridium botulinum spores in cured meat, 19: 46881
ZIZZA, M., Dual-purpose operation of Hanford reactor, 19: 48039
ZLATKIS, A., Radiation sources for ionization detectors in gas chromatography, 19: 46887
ZONTA, Yasuhito, Two-electron scattering due to s-d interaction, 19: 47257
ZOLOTAVIN, V. L., Composition of uranic–vanadic minerals, 19: 46627
ZOLOTOV, S., Thermal decomposition of rare earth and yttrium bromide hydrates, 19: 46271
ZONN, Z. N., EPR spectra of Gd^{3+} ion in single crystals of CeO_2, 19: 47898
ZSEBOEK, Zoltan B., Comparative investigations on protection mechanisms of cysteamine and AET in intestinal radiation death, 19: 46027
ZUDANS, Zenons, Thermal stress techniques in the nuclear industry, 19: 47922 (TID-22119)
ZUK, Wlodzimierz, Measurements of γ-γ angular correlation in ^{140}La, 19: 47649
ZUKAKISHVILI, G. G., Spatially periodic plasma structures appearing in fast heavy-current discharges, 19: 47761
ZUKOSKI, E. E., Recombination rates and non-equilibrium electrical conductivity in a seeded plasma, 19: 47801
ZYCH, Allen D., Identification of neutron stars in nuclear emulsion, 19: 46767 (TID-22256)

SUBJECT INDEX

Main entries in this index are generally specific materials, things, and processes. These are followed by modifiers that describe the properties of, and processes applied to, the main entries.

The number preceding the colon is the *NSA* volume number, and the number following is the abstract number. The designation (R) following the abstract number indicates that the abstract is of a progress report; (P) indicates a patent; and (T) indicates a translation. Abstracts for reports other than progress reports carry no letter designation. References to report numbers, where appropriate, are included after the abstract number of the citation. Published literature (journal article or book) is identifiable by the absence of a report number.

The user should bear in mind that the ideas presented in the original literature, rather than key words, have been indexed. The indexers have tried to select what seemed the most probable and logical place to look for typical information. Since it is not possible to anticipate where a user would look for information, numerous cross references are included to assist him in his search.

Experience in using an index of this type will be the best guide in obtaining the desired information, and a consideration of synonymous or closely related terms will prove valuable.

Information must be so indexed as to be of the greatest use to the greatest number of users. This requires that a topic be indexed to headings that most specifically describe it and not ordinarily to the headings that describe its ultimate use, nor to the general class headings that include the specific headings. For example, information on the treatment of thyroid disease with I-131 would be indexed under Thyroid Diseases and under Iodine Isotopes I-131, but not necessarily under Radiotherapy. A study of the effects of x radiation on hair would be indexed under both X Radiation and Hair.

The broad, general class headings are used only for general information or for comprehensive reports or articles.

Subject Heading Styles

Generally, the direct form of subject entry is used rather than inverted headings or, in some cases, subheadings; e.g., Amino Acids rather than Acids, amino; Helium Isotopes He-4 rather than Helium — isotopes He-4 or Helium — He-4 isotopes. Note, however, that in some cases modifying terms are used parenthetically in preference to a more direct type of entry which would result in the scattering of information. Organic compounds, however, are usually entered in the index in the inverted form so that substituted compounds can be listed near the parent compound; e.g., Benzene, Bromo- rather than Bromobenzene. In general, the style of nomenclature used is that of *Chemical Abstracts*, except that some items listed in that publication as subheadings are elevated to form part of the main heading; e.g., Butyric Acid, Methyl Ester rather than Butyric Acid — methyl ester.

Alphabetization

Main headings are arranged according to the widely accepted word-by-word alphabetic system. A parenthetic qualifier following a main heading is disregarded in alphabetizing unless there are two or more headings identical except for the parenthetic qualifier, in which case the qualifier determines the order. Headings involving Greek letters are arranged as if the names of the letters were spelled out, e.g., Mesons (π), Mesons (ζ).

Nomenclature of Inorganic Compounds

Inorganic compounds are indexed in the direct form, listing cations in the order of increasing valence in the case of polycationic salts of varying valence and in alphabetic order for polycationic salts in which all cations have the same valence; e.g., Sodium Aluminum Silicates and Potassium Sodium Sulfates.

Multicomponent Systems

Multicomponent alloys, except well-known trade names, are indexed under each element in the alloy.

Example: Aluminum–Chromium Alloys are indexed

ALUMINUM ALLOYS
Al–Cr ...
CHROMIUM ALLOYS
Al–Cr ...

Well-known alloys such as Hastelloy are indexed directly. Cross references appear in the index cumulations. Multicomponent systems of elements are indexed similarly.

Example: Silicon–Tungsten Systems are indexed

SILICON SYSTEMS
Si–W ...
TUNGSTEN SYSTEMS
Si–W ...

Multicomponent systems of compounds are similarly indexed under the compound.

Physical States of Materials

Specification of the physical state of the material, if other than normal, is included in the modifying phrase.

Modifying Phrases (Subheadings)

Whenever it appears that such information would be useful, descriptive phrases (modifiers), rather than ordinary subheadings, are used under the main headings to give a better indication of the material covered in an abstract. Such phrases are written so that the idea considered most important is presented first. However, when using this index, the reader is advised to scan all modifiers under a main heading to determine whether any abstracts in addition to the most obvious should be consulted for the desired information. Many of the modifiers are designed to be read in inverted order or to be read with the main heading inserted at the position of the comma in order to obtain a meaningful phrase; e.g., Uranium–allotropic transformation temperatures of, effect of cooling rate on is read "effect of cooling rate on allotropic transformation temperatures of uranium." In many cases, the prepositions have been

omitted from such phrases provided no ambiguity results from the omission.

For entries concerned with physics, if the modifier does not indicate whether the reference is experimental or theoretical, a symbol E or T or E/T is given.

Conferences

Proceedings of conferences and conference papers are included in the Report Number Index.

A

A-286 ALLOY
radiation effects on structure of, electron microscope studies of fast and thermal neutron, 19: 47088 (NMI-4998, pp 95-106)
sample preparation for electron microscope studies, irradiated, 19: 47088 (NMI-4998, pp 95-106)
ABDOMEN
radiotherapy of tumors of, effects on gastrointestinal function, 19: 45930
radiotherapy of tumors of, effects on glucose absorption after intravenous oral administration, 19: 45931
radiotherapy of tumors of, effects on gastrointestinal function, 19: 45932
radiotherapy of, effects on function of gastrointestinal tract, 19: 46120
ABSTRACTS
on direct energy conversion, 19: 47280 (AD-613358)
on plutonium technology, 19: 48088 (BNWL-113-6)
on radiation effects on solid uranium-based fuel materials, 19: 47093 (VDDIT-16(5.2))
ACCELERATORS
beam storage for tandem, orbit lifetime in, 19: 47186
design of 200-kev, for producing 14-Mev neutrons, 19: 47176
development and uses of Japanese, 19: 47184
equipment development for, servomechanism, 19: 47159 (BNL-9388)
magnet systems and power supplies for, cost optimization of, 19: 47170 (UCRL-16384)
storage rings for, development of, 19: 46643(R) (LAL-1136)
ACCIDENTS
conference on nuclear, 19: 46690
decontamination of agricultural lands after radiation, 19: 46701
energy release from fast-reactor, computer analysis of, 19: 47918 (ANL-7050, pp 503-14)
environmental survey after radiation, 19: 46697
food contamination by radiation, 19: 46694
genetic effects of radiation, 19: 46695
meteorological aspects, radiation, 19: 46693
monitoring equipment for radiation, 19: 46839
pathological effects of criticality, 19: 45997
planning for nuclear power station, 19: 46703
planning for radiation, 19: 46702
protection in radiation, French plans for, 19: 46704
protection in radiation, Swedish plans for, 19: 46705
protection of domestic animals in radiation, 19: 46700
public health aspects of radiation, 19: 46691
public health aspects of radiation, 19: 46698
public health aspects of radiation, 19: 46699
radiation, analysis of maximum possible during testing of rocket reactors, 19: 46707
sources of radiation, 19: 46692
ACETATE COMPLEXES
with europium, formation and stability, 19: 46295
ACETATES, FLUORO-
radiosensitivity effects on *Escherichia freundii*, x, 19: 46015
ACETIC ACID
diffusion of lithium ions in, in electrolysis, isotope effects on, 19: 46264
ACETIC ACID, BROMO-
reactions with halide ions, isotopic exchange and replacement, 19: 46293
ACETIC ACID, [(CARBOXYMETHYLIMINO) BIS(ETHYLENENITRILO)] TETRA-
effects on excretion of plutonium, delayed administration, 19: 45762 (RFP-577)
protective effects of, against pathological effects of plutonium-239 in mice, 19: 45808(R) (NYO-901-36)
ACETIC ACID, CHLORO-
reactions with halide ions, isotopic exchange and replacement, 19: 46293
ACETIC ACID, (ETHYLENEDIAMINE) TETRA-
uses in determination of quadrivalent and tervalent metal by complexometric methods, 19: 46219
ACETIC ACID, (ETHYLENEDIAMINE) TETRA- COMPLEXES
with hafnium in aqueous solutions, preparation, 19: 46299(P)
with thorium in aqueous solutions, preparation, 19: 46299(P)
with titanium in aqueous solutions, preparation, 19: 46299(P)
with zirconium in aqueous solutions, preparation, 19: 46299(P)
ACETIC ACID, IODO-
reactions with halide ions, isotopic exchange and replacement, 19: 46293
ACETIC ACID, METHOXYPHENYL-
labeling with tritium at α-carbon atom, 19: 46306
ACETIC ACID, TRICHLORO-
effects on sulfur-35 fixation in rat liver, 19: 45800
ACETONE
effects on sulfur-35 fixation in rat liver, 19: 45800
electron drift velocities in, at low energy, 19: 46393
ACETONITRILE
iodine exchange in, alkyl iodide–zinc iodide, 19: 46294
radiation effects on cyanide group inversion in, infrared spectra of, 19: 46326 (CNAEM-28)
radiolysis of, EPR spectra from radicals formed in gamma, (E), 19: 46379
ACETOPHENONE
oxime, Beckmann rearrangement of, isotope effects on, 19: 46304(R) (ORNL-3832, pp 66-75)
ACETYLENE
effects on radioinduced polymerization of ethylene, 19: 46353
electron drift velocities in deuterated and normal, at low energy, 19: 46393
electron reactions with, spectra of energy level transitions in, 19: 46322 (AD-612070)
radiolysis of, x, 19: 46334 (TID-22231)
yields from radiolysis of ethylene, 19: 46361
yields from radiolysis of methane, 19: 46366
yields in electron radiolysis of ethylene, nitric oxide effects on, 19: 46324(R) (AGN-8132)
yields in electron radiolysis of ethylene–oxygen systems, 19: 46324(R) (AGN-8132)
yields in radiolysis of ethylene–methane–nitric oxide, 19: 46324(R) (AGN-8132)
ACOUSTIC WAVES
interactions with magnetic fields, plasma kinetic correlations with, (T), 19: 47732
propagation in dense plasma, damping transitions in, (E/T), 19: 47724 (MATT-267)
ACRIFLAVINE
radiosensitivity effects in *Pseudomonas aeruginosa*, effects of oxygen concentration on, 19: 46014
ACRYLAMIDE
radioinduced grafting to teflon, antielectrostatic effect of, 19: 46376
ACRYLIC ACID
labeling with carbon-14, use of vinylmagnesium bromide in, 19: 46310
radioinduced grafting to teflon, antielectrostatic effect of, 19: 46376
ACRYLIC ACID, ALLYL ESTERS
radioinduced polymerization of, gamma, 19: 46337 (TID-22244)
ACRYLIC ANHYDRIDE
radioinduced cyclopolymerization, 19: 46352
ACRYLONITRILES
radioinduced polymerization of, at low temperatures, 19: 46323(R) (AD-613529)
ACTINIUM
separation from radium by ion exchange, 19: 47626
ACTINIUM ISOTOPES Ac-225
alpha spectra, (E), 19: 47576(R) (IDO-17081, pp 49-76)
ACTINIUM ISOTOPES Ac-227
growth curve of, use in determining half lives of radium-233 and thorium-227, 19: 46157(R) (MLM-1254)
ACTINOMYCIN
effects on lens regeneration in salamanders, 19: 45738
effects on radiation damage in cultured mouse fibroblasts, 19: 46018
ACTIVATION ANALYSIS
forensic applications of, 19: 45808(R) (NYO-901-36)
methods for trace-element, in beef heart, 19: 45753 (AE-191)
sensitivity calculations in, data handbook for, 19: 46167 (EUR-1898.e)
sensitivity of, effects of coincidence methods on, 19: 46227
sensitivity of, effects of electrolytic separation techniques on, 19: 46229
use of helium-3 in determination of carbon, nitrogen, and oxygen in metals, 19: 46174 (LA-DC-7319)
ACTIVATION DETECTORS
performance for fast neutron spectra determination, 19: 46763 (RCN-37)
ADDITION COMPOUNDS
isotopic exchange and vapor pressures of boron trifluoride, 19: 46899(R) (ORNL-3832, pp 33-49)
radiolysis of, containing tritium-labeled methyl stearate, self-, 19: 46389
ADENINE
effects on pyrimidine mutation induction in *Salmonella typhimurium*, genetic analysis of, 19: 45878
ADENOSINEPHOSPHORIC ACIDS
protective effects of injected, against radiation injuries in rats, 19: 46020
radiation effects on aqueous solution of, x, 19: 45729(R) (NYO-910-23, pp 1-111)

ADRENAL GLANDS
properties for aerospace uses, 19: 47068
radiosensitivity effects in mice and rats, x, 19: 45823(T) (JPRS-31933, pp 1-5)
ADVANCED REACTIVITY MEASUREMENT FACILITY
neutron resonance absorption measurements in, (E/T), 19: 47575 (IDO-16986)
reactivity of, water displacement coefficient for, 19: 48060(R) (IDO-17081, pp 1-47)
ADVANCED TEST REACTOR
gas loop materials, corrosion studies of, 19: 46946 (BNWL-100)
physics experiments in critical facilities for, 19: 48060(R) (IDO-17081, pp 1-47)
AEROSOLS
monitoring radioactivity in, detector for, 19: 46869(P)
radioactivity of, performance of radiometers for measuring, (T), 19: 46760 (NP-15462)
sorptive properties of atmospheric, for iodine, 19: 46672
AFRICA
nuclear energy uses in, 19: 48111
AGE ESTIMATION
evaluation of radioactive halo, 19: 46616(T) (ORNL-tr-768)
method of carbon-14 for Upper Anthropogene in Soviet Union, 19: 46621
radiation detector for use in carbon-14, low-background, 19: 46777
radiocarbon methods of, using methane-filled proportional counter, 19: 46617
uranium–krypton and uranium–xenon methods of, for samarskite, 19: 46598
uranium–thorium method of, for pleistocene formations, 19: 46599
AGRICULTURE
land reclamation after radioactive contamination, 19: 46701
radioisotopes in African, 19: 48111
AIR
corrosive effects on superalloys at high temperatures, 19: 46946 (BNWL-100)
electric breakdown in, spark channel formation by, 19: 47146
electric breakdown by laser beams, (E), 19: 47781
electric breakdown of long gap of, transition from corona to spark discharge in, 19: 47791
flow function tables for one-dimensional, compressible, 19: 47151
gamma attenuation by, spectrometric study, 19: 46586 (NP-15361)
monitoring for alpha emitters, instrument design for, (E), 19: 46768 (UCRL-14253)
radiation effects on thermodynamic properties of, at 20000 to 50000°K, 19: 47731
reactions with plutonium nitride at 540 to 1000°C, 19: 46912(R) (BMI-1727(Del.))
AIRCRAFT
materials development for, 19: 47068
AIRCRAFT EQUIPMENT
radioisotopes in, review on, 19: 46883
ALANINE
complexes of, solid state radiation chemistry of, 19: 46403
labeling with tritium at α-carbon atom, 19: 46306
poly-p-aminophenyl-, radiation effects on inactivation of complex with papain, 19: 45976
radiation effects on, in soil, 19: 45941
thermodynamic properties of, in water and heavy water, 19: 46318
ALANINE, PHENYL-
analysis of tritium-labeled, for radiochemical impurities, 19: 46208
thermodynamic properties of, in water and heavy water, 19: 46318
ALARM SYSTEMS
description of atmospheric static electricity, 19: 48094 (SC-DC-65-1646)
design of gamma, engineering drawings of, 19: 46865
ALBUMINS
radiation effects on metabolism of, in rabbits, 19: 45829
radiation effects on rabbit tolerance to bovine serum, 19: 45902
radioinduced luminescence in solutions of blood serum, uv, 19: 46342(T) (JPRS-31547, pp 6-12)
use of iodine-131 labeled, in clinical studies, 19: 46142
ALCOHOLS
effects on photolysis of cyclopentanone, 19: 46357
preparation of labeled, by microbial processes, 19: 46409
ALFALFA
strontium-90 content in, effects of plant calcium content and soil in, 19: 45750
ALGAE
analysis of *Chlorella ellipsoidea* for copper content during life cycle, neutron activation, 19: 45775
analysis of *Chlorella ellipsoidea* for manganese content during life cycle, neutron activation, 19: 45775
radioinduced mutations of, 19: 45842
ALKALI METAL COMPOUNDS
isotope exchange in, effects of separation factor on properties of exchanged molecules in, 19: 46408(T) (ORNL-tr-770)
ALKALI METALS
reactions with graphite to form intercalation compounds, 19: 46265
ALKALINE EARTH METALS
reactions with graphite to form intercalation compounds, 19: 46265
ALKANES
radiolysis of sodium compounds of, yields in, 19: 46324(R) (AGN-8132)
ALKENE ADDITION COMPOUNDS
radiolysis of, yields in, 19: 46324(R) (AGN-8132)
ALKYL IODIDES
iodine exchange with zinc iodide, 19: 46294
ALLENES
yields in radiolysis of ethylene–methane–nitric oxide, 19: 46324(R) (AGN-8132)
ALLOYS
electric conductivity of dilute, from s-d scattering, (T), 19: 47897
excitations in strong-coupling superconducting, Fermi-liquid theory for collective, 19: 47518
nucleation of precipitates from supersaturated solutions of, review on, 19: 47025(T) (ORNL-tr-637)
time-to-rupture tests of, analysis, 19: 47081 (EURAEC-1432)
ALPHA PARTICLES
angular and energy distributions from (n,α) reactions at 14.6 Mev, (E/T), 19: 47637
angular distributions from fluorine-19 (d,α) reactions at 0.95 to 1.25 Mev, (E/T), 19: 47646
angular distributions from magnesium-25 (d,α) reactions at 1.5 to 2.5 Mev, fluctuations in, (T), 19: 47659
angular distributions and energy spectra from yttrium-89 and zirconium-90 (p,α) reactions, (E/T), 19: 47670
attenuation by aluminum, titanium, and zirconium absorbers, energy-range relations in, 19: 46324(R) (AGN-8132)
detection and measurement in air, monitor design for, (E), 19: 46768 (UCRL-14253)
detection and measurement of, performance of silicon for, 19: 46770 (UCRL-16354)
effects on decomposition of plutonium hexafluoride at 26 to 82°C, extent and rate of, 19: 46325 (ANL-7013)
effects on diffusion of nickel-63 in copper, 19: 47032
effects on membrane permeability of plant cells by urea, 19: 45975
effects on stomatal movement of Begonia leaves, 19: 45854
effects on sulfur dioxide, 19: 46332(R) (ORNL-3832, pp 50-65)
rates of deformed nucleus, (T), 19: 47597 (UCRL-16187)
reactions (α,p) with aluminum-27 at 1.0 to 3.3 Mev, resonances in, (E), 19: 47672
reactions (α,t) with lithium-6 at 40 Mev, differential cross sections for, (E/T), 19: 47574 (IAE-836)
reactions with beryllium-9 and lithium-6 and -7, energy levels and mechanisms of, 19: 47564(R) (AD-612038)
reactions with meteoritic materials, krypton and xenon production by, 19: 47213
scattering by carbon-12 at 2.5 to 7.5 Mev, Regge representation analysis of, 19: 47653
scattering by nickel, tin, and zirconium isotopes at 34.4 Mev, angular distributions for, (E), 19: 47623
scattering by nuclei at 44 Mev, data on collective states from inelastic, (E), 19: 47608
ALPHA SOURCES
fabrication of, in a ceramic carrier, 19: 47156(P)
uses in measuring thickness of thin polymer films, 19: 46888
uses of americium-241 and radium-226 for gas chromatographic ionization detectors, 19: 46887
ALPHA SPECTRA
catalog development, 19: 47576(R) (IDO-17081, pp 49-76)
measurement of thorium-229 and daughters, (E), 19: 47576(R) (IDO-17081, pp 49-76)
ALTIMETERS
design of radiometric pressure- and density-sensitive, for space vehicles, 19: 46749(P)
ALUMINUM
alpha attenuation by, energy-range relations in, 19: 46324(R) (AGN-8132)
analysis for thorium using *N*-benzoyl-*N*-phenylhydroxylamine, gravimetric, 19: 46194
analysis for trace impurities, activation and flame photometric, 19: 46207
bonding analysis of rectangular plates of, apparatus for, 19: 46555 (KAPL-M-6493)
bonding at 900 to 1000°F, self, 19: 46912(R) (BMI-1727(Del.))

corrosion by mercury, 19: 48060(R) (IDO-17081, pp 1-47)
corrosion of nickel-plated, by water and hydroxide solutions at 330°C, 19: 46945 (BNWL-98)
deformation of, interface friction in hot, 19: 46981(R) (AD-611821)
determination by complexometric methods using EDTA, 19: 46219
determination by potentiometric titration of acid liberated by complex formation, 19: 46205
determination in aluminum oxide, method for, 19: 46324(R) (AGN-8132)
effects on crystal structure of uranium, 19: 47048
effects on ductility of fissium–uranium–zirconium alloys, 19: 47004 (NMI-4997, pp 45-54)
effects on network structure in uranium, 19: 47060
effects on point defects in iron, 19: 47094(T) (ORNL-tr-668)
electron beam backscattering at 4 to 14 Mev, effects on target current of, (E), 19: 47181
electron inelastic scattering at 2 and 100 kev, effect of atomic screening on, (T), 19: 47259(T)
electron secondary emission from, after electron bombardment, 19: 47263
electron transmission at 100 and 150 kev, geometric dependence of, (E), 19: 47125
excitation potential from proton range measurements, (E), 19: 47225
gamma incoherent scattering at 280 kev, cross sections for, (E), 19: 47624
gamma transport in slabs of, dose buildup factors for, (T), 19: 47864 (ANL-7050, pp 113-22)
mechanical properties at cryogenic temperatures, 19: 47013 (PB-171809(Rev.)(Suppl.2))
neutron transport in single and multilayer slabs of, (T), 19: 47868 (RRA-T52)
preparation of irradiated composite of lead-bonded ceramic fuel clad with, for metallography, 19: 47087 (NMI-4997, pp 189-97)
properties for aerospace uses, 19: 47068
proton elastic scattering at 4.5 Mev, polarization in, (E), 19: 47692
proton ranges in, at 100 Mev, (E), 19: 47225
radiation damage induced by oxygen and inert gas bombardment, 19: 47080 (EUR-2478.e)
radiation effects on, for use as aerospace structural materials, (E/T), 19: 47077 (AD-613471)
radiation effects on mechanical properties of single crystals of, annealing effects on electron, 19: 47095
radiation effects on electric conductivity of, low-temperature recovery of neutron, (E), 19: 47097
radiation effects on, lattice atom displacement probabilities in deuteron and neutron, (T), 19: 47104
radiation transport through single-bend ducts of, in water shields, (E), 19: 47863 (AD-613480)
reactions with graphite to form intercalation compounds, 19: 46265
reactions with water at high temperatures during core meltdown, (E/T), 19: 47960(T) (ORNL-tr-694)
reactor criticality effects, 19: 48053(R) (ANL-7090, pp 55-68)
separation from other materials by electrolytic extraction, 19: 46454
sorptive properties for tritium, effects of texture on, 19: 47018 (USNRDL-TR-890)
superconducting properties of, 19: 47536
thermal expansion coefficient of, x-ray determination of, 19: 47023(T) (LA-tr-65-20)
thickness measurement, autoradiographic technique for, 19: 46964 (NMI-4996, pp 149-63)

ALUMINUM ALLOYS
analysis for copper, iron, and silicon, activation, 19: 46157(R) (ML-M-1254)
properties for aerospace uses, 19: 47068
Al–Ce, crystal structure of Laves phases in, 19: 47052
Al–Cu–Fe–Sn–Ti–V, additive and alloying effects on mechanical properties of, 19: 46985 (AD-613651)
Al–Dy, crystal structure of Laves phases in, 19: 47052
Al–Er, crystal structure of Laves phases in, 19: 47052
Al–Eu, crystal structure of Laves phases in, 19: 47052
Al–Fe–U, radioinduced swelling in, resistance to, 19: 47103
Al–Gd, crystal structure of Laves phases in, 19: 47052
Al–Ho, crystal structure of Laves phases in, 19: 47052
Al–La, crystal structure of Laves phases in, 19: 47052
Al–Mg, crystal structure of Mg_2Al_3 in, 19: 46984(R) (AD-612275)
Al–Mg, diffusion of plutonium at 420 to 500°C, 19: 47066
Al–Mg, diffusion of beryllium to surface of, on heating at 300 to 500°C, 19: 47071
Al–Nd, crystal structure of Laves phases in, 19: 47052
Al–Pr, crystal structure of Laves phases in, 19: 47052
Al–Sm, crystal structure of Laves phases in, 19: 47052
Al–Tb, crystal structure of Laves phases in, 19: 47052
Al–Ti–V, interface friction in hot deformation of, 19: 46981(R) (AD-611821)
Al–Tm, crystal structure of Laves phases in, 19: 47052
Al–U, radiation effects on, 19: 48060(R) (IDO-17081, pp 1-47)

ALUMINUM CARBIDES
reduction of barium and strontium oxides by, catalytic effects of calcium fluoride on, 19: 46252(T) (ORNL-tr-683)

ALUMINUM COUPLES
Al/Pb, performance of superconducting diodes of, as h-f sound detector, 19: 46739

ALUMINUM FLUORIDES
spectra of vaporized, 19: 46982(R) (AD-611856)

ALUMINUM ISOTOPES Al-26
energy levels of, 19: 47603

ALUMINUM ISOTOPES Al-27
alpha reactions (α,p) at 1.0 to 3.3 Mev, resonances in, (E), 19: 47672
neutron inelastic scattering at 3 to 4.5 Mev, angular distributions and energy levels from, (E/T), 19: 47638
neutron reactions (n,n′γ) at 3.5 to 4.5 Mev, gamma angular distributions from, (E/T), 19: 47588(R) (TID-22012, pp 22-52)
nitrogen-14 reactions at 20 to 42 Mev, excitation functions for, (E), 19: 47667
proton reactions (p,γ) with, giant dipole resonance of gamma yield from, 19: 47115(R) (ANL-6983)

ALUMINUM NITRIDES
vaporization coefficients, 19: 46956 (NP-15514(Vol.1))

ALUMINUM OXIDES
analysis for aluminum, method for, 19: 46324(R) (AGN-8132)
corrosion product films from, metallographic and optical technique for measuring thickness of, 19: 46952 (NMI-4997, pp 26-35)
deuterium exchange with hydroxyl groups on surface of, 19: 46280
effects on sorptive properties of soils for strontium, 19: 46434
materials testing for cesium ion engine, 19: 46571 (HRL-5249-S)
preparation of, coated spheres of uranium in graphite for metallography, 19: 46925 (NMI-4997, pp 85-91)
preparation procedures, ceramographic, 19: 46937 (NMI-5025(Pt.I), pp 1-25)
radiation effects on catalytic effects of, on gaseous reactions, 19: 4629 (EUR-2455.e)
Al–Al_2O_3, electric conductivity measurements on quenched, 19: 47067
Al_2O_3–H, radiolysis yields in, 19: 46324(R) (AGN-8132)
Al_2O_3–UO_2, radiation effects on fibrous fissiochemical fuels of, 19: 46324(R) (AGN-8132)
Al_2O_3–UO_3, radiation effects on fibrous fissiochemical fuels of, 19: 46324(R) (AGN-8132)

ALUMINUM SILICATES
joining to glasses, techniques for, 19: 46872(R) (AD-621549)
radiation testing of glass of, 19: 46872(R) (AD-621549)
sorptive properties of electrocoagulated tuff particles for fission products, 19: 48082 (UJV-1296/65)

ALUMINUM SYSTEMS
Al–Al_2O_3, electric conductivity measurements on quenched, 19: 47067
Al–Be–O, thermodynamics of, 19: 46231 (AD-613660)
Al–B–O, thermodynamics of, 19: 46231 (AD-613660)
Al–C–Cu–H–N–Sn–Ti–V–Zr, mechanical properties of, 19: 46985 (AD-613651)
Al–Cr–Fe–Si–U, radioinduced swelling in, resistance to, 19: 47103
Al–Cr–Si, protective effects as coating on molybdenum and molybdenum-titanium alloy, 19: 47061
Al–Fe–Mo–Si–U, radioinduced swelling in, resistance to, 19: 47103
Al–Fe–Si–U, radioinduced swelling in, resistance to, 19: 47103
Al–Si, reactions with uranium, metallographic and microautoradiographic study of, 19: 46951 (NMI-4996, pp 19-20)
Al–Si–U, radiation effects on structure of dispersion-type fuel elements of, 19: 47084 (NMI-4997, pp 124-33)
Al–Si–U, radioinduced swelling in, resistance to, 19: 47103
Al–UO_2, radiation effects on, 19: 48060(R) (IDO-17081, pp 1-47)

AMERICIUM
determination by controlled potential coulometry, 19: 46189
separation from aqueous chloride solutions by solvent extraction using di-n-octyl phosphinic acid, tracer studies of, 19: 46443
separation from lanthanides, development of Talspeak process for, 19: 46428(R) (ORNL-3847)

AMERICIUM ISOTOPES Am-241
radioinduced production of americium-242 from, (E), 19: 47576(R) (IDO-17081, pp 49-76)
separation from plutonium in urinalysis, method for, 19: 46187
uses as radiation source for ionization detectors in gas chromatography, 19: 46887

AMERICIUM ISOTOPES Am-242
production in plutonium-242 (d,2n) reactions at 7 to 12 Mev, excitation function and isomeric yield ratio in, (E), 19: 47688

radioinduced production from americium-241, (E), 19: 47576(R) (IDO-17081, pp 49-76)
AMES LAB., AMES, IOWA
description, 19: 48064 (TID-32204)
AMES RESEARCH REACTOR
design, 19: 48064 (TID-32204)
experimental facilities for, description of, 19: 48064 (TID-32204)
hazards analysis for, 19: 48064 (TID-32204)
operation procedures for, 19: 48064 (TID-32204)
reactivity effects in, 19: 48064 (TID-32204)
site description, 19: 48064 (TID-32204)
AMINES
methyl-, charge transfer collisions with positive ions, mass spectra of products from, 19: 46262
solvent properties for beryllium from sulfate liquors, 19: 46431 (ORNL-P-1602)
tert-, mutagenic effects in screw-worm fly, 19: 45950
yields from solid state irradiation of alanine and glycine chelates and metal salts, 19: 46403
AMINO ACIDS
analysis of labeled, for radiochemical impurities, 19: 46208
preparation of labeled, by microbial processes, 19: 46409
radiation effects on skin, 19: 45887
AMINO ALCOHOLS
3-*endo*-amino-2-*exo*-phenylnorbomane-2-ol, deamination mechanisms, 19: 46304(R) (ORNL-3832, pp 66-75)
AMMONIA
force constants of, calculation of molecular, 19: 46899(R) (ORNL-3832, pp 33-49)
radiolysis of, hydrazine yield in electron, 19: 46324(R) (AGN-8132)
yields from solid state irradiation of alanine and glycine chelates and metal salts, 19: 46403
NH_3–ammonium acetate, radiolysis yields in, 19: 46324(R) (AGN-8132)
NH_3–benzene, radiolysis yields in, 19: 46324(R) (AGN-8132)
NH_3–benzene, radiolysis yields in, 19: 46324(R) (AGN-8132)
NH_3–CO, radiolysis yields in, 19: 46324(R) (AGN-8132)
NH_3–D, radiolysis yields in, 19: 46324(R) (AGN-8132)
NH_3–dimethylamine, radiolysis yields in, 19: 46324(R) (AGN-8132)
NH_3–methane, radiolysis yields in, 19: 46324(R) (AGN-8132)
AMMONIUM ACETATES
NH_3–ammonium acetate, radiolysis yields in, 19: 46324(R) (AGN-8132)
AMMONIUM COMPOUNDS, QUATERNARY
heats of dilution of alkyl halide, 19: 46237(R) (ORNL-3832, pp 76-99)
ion exchange with polystyrene sulfonates, thermodynamics of sodium, 19: 46237(R) (ORNL-3832, pp 76-99)
solvent properties of tricaprylmethylammonium nitrate for uranium, 19: 46450
AMMONIUM COPPER SULFATES
molecular structure of hydrated, neutron diffraction studies of, 19: 46161(R) (ORNL-3832, pp 116-50)
AMMONIUM HEPTAFLUOROHAFNATE(IV)
tantalum-181 gamma angular correlations from, (E), 19: 47607
AMMONIUM HYDROXIDES
corrosive effects of solutions of, on nickel-plated aluminum at 330°C, 19: 46945 (BNWL-98)
AMMONIUM PROTACTINIUM FLUORIDES
preparation and properties, 19: 46160(R) (ORNL-3832, pp 29-32)
spectra in hydrofluoric acid, Raman, 19: 46160(R) (ORNL-3832, pp 29-32)
AMPLIFIERS
design of field-effect transistor, 19: 46716(R) (IDO-17081, pp 77-123)
design of miniaturized pre-, engineering drawings for, 19: 46863
development for semiconductor detectors, 19: 46643(R) (LAL-1136)
operation of voltage-switching class-D, 19: 48097 (SC-DR-65-338)
AMYL ALCOHOL
thermodynamic properties of, in water and heavy water, 19: 46318
AMYLASES
metabolism in alleurone cells of seeds, tracer study, 19: 48102(R) (TID-22175)
ANALYSIS
isotopic dilution methods of, review of, 19: 46204
ANESTHETICS
radiation effects on response to, in mice and rats, 19: 45823(T) (JPRS-31933, pp 1-5)
response of mice and rats to, effects of adrenalectomy on, 19: 45823(T) (JPRS-31933, pp 1-5)
ANILINE, 4-CHLORO-2,6-DINITRO-
separation from other nitroanilines, chromatographic, 19: 46424 (IS-T-24)
ANILINE, 2-CHLORO-4-NITRO-
separation from other nitroanilines, chromatographic, 19: 46424 (IS-T-24)
ANILINE, 4-CHLORO-2-NITRO-
separation from other nitroanilines, chromatographic, 19: 46424 (IS-T-24)
ANILINE, 2,4-DIMETHYL-6-NITRO-
separation from other nitroanilines, chromatographic, 19: 46424 (IS-T-24)
ANILINE, 2,4-DINITRO-
separation from other nitroanilines, chromatographic, 19: 46424 (IS-T-24)
ANILINE, 2-NITRO-
separation from other nitroanilines, chromatographic, 19: 46424 (IS-T-24)
ANILINE, 4-NITRO-
separation from other nitroanilines, chromatographic, 19: 46424 (IS-T-24)
ANILINE, 2,4,6-TRINITRO-
separation from other nitroanilines, chromatographic, 19: 46424 (IS-T-24)
ANIMAL CELLS
genetic structure of, 19: 45726 (BNL-9488)
radiation effects on proliferating, 19: 45923
radiation effects on cultured mouse fibroblasts, effects of alkylating agents and antibiotics on, 19: 46018
radiation effects on nuclei of, 19: 45992
radiation effects on poliovirus production by monkey-kidney, 19: 45955
radiation effects on growth of virus in, 19: 45974
radiation effects on desoxyribonucleic acid synthesis of, in tissue culture, 19: 45867
radiation effects on reproduction of HeLa, clone-size analysis of, 19: 45886
radiation effects on membrane of, uv, 19: 45891
radiation effects in connective tissue, metabolic, 19: 45895
radiation effects on granular and transitional layers of, in human skin, 19: 45913
radiation effects on tissue cultures of mammalian, 19: 45729(R) (NYO-910-23, pp 1-111)
radiation effects on mitotic activity of, in tissue cultures, 19: 45867
radioinduced toxin effects on morphology and growth of, in tissue culture, 19: 45946
radiosensitivity of intestinal, in rats, 19: 45926
radiosensitivity of, in thymus gland of mice, 19: 45871
ANIMAL REPRODUCTION
radiation effects on, of mice, 19: 45808(R) (NYO-901-36)
radiation effects on, in mice, 19: 45809(R) (NYO-1979-12)
radiation effects on, in domestic animals, 19: 45813(R) (ORO-631, pp 36-44)
ANIMAL RESPIRATION
measurements in single lung, using thulium-170 and crystal detector probe, 19: 46118
ANIMALS
analysis for selenium in tissues of, by activation, 19: 46172 (KR-95)
radiation effects on immune reactions to transplanted hematopoietic tissue in, 19: 46009
radiation effects on immune reactions to tissue transplants, 19: 45944
radiation effects in, genetic, 19: 45973
radiation effects on response of, to virus infections, 19: 45974
radiation effects on, bibliography, 19: 45807 (AED-C-04-17)
radiosensitivity of, effects of radioprotective compounds, 19: 46031
strontium-90 metabolism by, 19: 46634 (AD-423463)
ANION EXCHANGE MATERIALS
ingestion by rats, effects on iodine-131 excretion, 19: 45760(R) (ORO-631, pp 83-121)
ANIONS
effects on Amberlite selectivity for lithium and sodium ions, 19: 46899(R) (ORNL-3832, pp 33-49)
effects on corrosion of zirconium by hydrofluoric acid, 19: 46957(R) (ORNL-3832, pp 100-6)
ANISOLE
anisole–BF_3, boron isotopic exchange thermodynamics of, 19: 46899(R) (ORNL-3832, pp 33-49)
ANOXIA
radiosensitivity effects on mouse skin, electron, 19: 45885
ANTHRACENE
use for determining beta energy spectra, 19: 45729(R) (NYO-910-23, pp 1-111)
ANTIBIOTICS
effects on radiation damage in cultured mouse fibroblasts, 19: 46018
preparation of labeled, by microbial processes, 19: 46409
production from radioinduced mutations of *Streptomyces citreus*, 19: 45991
radiosensitivity effects of puromycin on poliovirus infective centers, 19: 46032
ANTIBODIES
determination in animal and human sera, radioisotope precipitation test for, 19: 45739
determination of, by radioisotope precipitation test, 19: 46076
radiation effects on production of, by transferred spleen cells in mice, 19: 45986
radiation effects on production of, in mice, 19: 45806 (AD-621543)

radiation effects on formation of, in mice, 19: 45903
radioinduced inactivation of, ultraviolet, 19: 46382
ANTIFERROMAGNETIC MATERIALS
electron and nuclear spin oscillations in, bound, 19: 47903
neutron diffraction from, covalency effects on, (T), 19: 47895
neutron inelastic scattering in, with weak ferromagnetism, (T), 19: 47899(T)
ANTIGENS
radiation effects on immune response to, in mice, 19: 45903
reactions with antibodies in Q fever, radioisotope precipitation test for detecting, 19: 45739
ANTIMONY
content and distribution in beef heart, 19: 45753 (AE-191)
determination in bismuth by γ, γ-coincidence counting, activation, 19: 46193
effects on point defects in iron, 19: 47094(T) (ORNL-tr-668)
ANTIMONY ALLOYS
Sb–Cr, magnetic structure of, 19: 47876 (AD-614435)
ANTIMONY ISOTOPES Sb-124
yields in thermal neutron fission of uranium-235, implication on empirical Z_p function, (E), 19: 47611
ANTIMONY ISOTOPES Sb-125
content in atmosphere and drinking water, Moncloa Station, Spain, 1964, 19: 46597
production by beta decay of neutron-irradiated tin compounds, 19: 46388
ANTIMONY ISOTOPES Sb-126
yields in thermal neutron fission of uranium-235, implication on empirical Z_p function, (E), 19: 47611
ANTINEUTRINOS
energy spectra, (E), 19: 46643(R) (LAL-1136)
ANTINUCLEONS
form factors of, ($K\bar{K}$) and (np) contributions to isoscalar, (T), 19: 47371
ANTIPROTONS
interactions with protons in spurion scheme of broken U(6,6), two-meson annihilation, (T), 19: 47374
ARACHIDONIC ACID
labeling cholesterol ester of, with carbon-14 and tritium, 19: 46309
ARCHAEOLOGICAL SPECIMENS
age estimation by carbon-14 counting technique, 19: 46617
ARGON
determination by isotopic dilution techniques, 19: 46204
effects on x radiolysis of acetylene, methylacetylene, and ethylacetylene, 19: 46334 (TID-22231)
electric arcs in, pulse heating of high pressure, (E), 19: 47789
electric arcs in, pulse heating of high-pressure, 19: 47790
electric discharges in, electrode surface characteristics from vacuum breakdown by, (E), 19: 47149
electric discharges in, plasmoid production by h-f electrodeless, (E), 19: 47788
electron drift velocity and mean energy in, determination of, 19: 47124(T) (SLAC-Trans-19)
equilibrium in thermally ionized gases of, with small seeding ratios, (E), 19: 47126
gamma transport in slabs of, dose buildup factors for, (T), 19: 47864 (ANL-7050, pp 113-22)
ionization by, electron and proton impact at high energies, cross sections for, (T), 19: 47246
noise and oscillations in beam-generated plasma of, (E), 19: 47741
scattering by copper at 30 kev, (E), 19: 47262
scattering of cesium ions by, angular distribution of elastic, 19: 46161(R) (ORNL-3832, pp 116-50)
sorption by quartz walls in high-density discharges, (E/T), 19: 46576
ARGON IONS
beams of, analysis of duoplasmatron, 19: 47267
effects on etching of pyrolytic graphite, 19: 47078 (AD-613643)
effects on free radical formation in lysozyme, ribonuclease, and trypsin, spectra of, 19: 46339 (UCRL-16358)
sorption by titanium films, (E), 19: 47072
ARGON ISOTOPES Ar-35
magnetic moments and M1 transition probabilities in $2s_{1/2}$ $1d_{1/2}$ shell, (T), 19: 47641
ARGON ISOTOPES Ar-37
magnetic moments and M1 transition probabilities in $2s_{1/2}$ $1d_{1/2}$ shell, (T), 19: 47641
ARGON ISOTOPES Ar-40
neutron inelastic scattering at 3 to 4.5 Mev, angular distributions and excitation functions from, (E/T), 19: 47639
neutron reactions (n,n'γ) at 3.0 to 4.5 Mev, gamma angular distributions from, (E/T), 19: 47590(R) (TID-22012, pp 67-98)
production of, methods for, 19: 46413
ARGON SYSTEMS
Ar–Br, resonator modes in laser of, (E/T), 19: 47219 (AD-614253)
Ar–Cs, electron energy losses in nonequilibrium plasma of, nitrogen impurity effects on, (E), 19: 47737(T)
Ar–K, electron recombination rates and nonequilibrium conductivity in, (E), 19: 47801
ARGONNE ADVANCED RESEARCH REACTOR
criticality studies in, 19: 48053(R) (ANL-7090, pp 55-68)
ARGONNE FAST REACTOR EXPERIMENT TEST
development, 19: 47989(R) (ANL-7090, pp 1-29)
ARMY REACTORS (SM-1)
neutron flux in, with plutonium–beryllium source, 19: 48040
ARSENIC
analysis for chlorine, phosphorus, and sulfur, activation, 19: 46211
content and distribution in beef heart, 19: 45753 (AE-191)
ARSENIC ISOTOPES As-78
gamma spectra of 5-min isomer of, search for, 19: 47682
ARSINE
electron drift velocities in, at low energy, 19: 46393
ARSINE, TRIPHENYL-
effects on scintillation quenching in benzene, 19: 46362
radiolysis of, in benzene, 19: 46362
ASCORBIC ACID
radiation effects on content of, in legumes, 19: 45938
ASPARTIC ACID
radiation effects on, in soil, 19: 45941
ASTRONAUTS
radiation protection of, 19: 45890
ASTRONOMY
methods for gamma- and x-ray, review of, 19: 47207
ASTROPHYSICS
gravitational fluctuations in, search for, 19: 47486
hydrogen density in intergalactic space, limits on ionized, (T), 19: 47196
model of quasi-stellar radio source CTA 102, (T), 19: 47198
ATLANTIC OCEAN
plankton ecology in, 19: 45748(R) (TID-22193)
ATMOSPHERE
airglow and brightness during solar eclipse, (E), 19: 47451 (SC-M-65-419)
airglow in, research on, 19: 47452(T) (NASA-TT-F-204)
auroral phenomena in, optical, 19: 47498
auroral phenomena in, radio, 19: 47499
book: *Physics of the Earth's Upper Atmosphere*, 19: 47488
chemical contaminants in, control of, 19: 46682
diffusion of smoke puffs in, floats instantaneous-source type, (T), 19: 47111(T) (UCRL-Trans-1229(L))
disturbances of upper, from solar particle emissions, 19: 47495
electric fields in, use of radioactive collector for measuring, 19: 46730(T) (SC-T-65-760)
electricity in, warning system for detecting static, 19: 48094 (SC-DC-65-1646)
fallout monitoring in Moncloa Station, Spain, 1964, 19: 46597
fallout monitoring in Pizen, 1957–1962, 19: 46687
iodine-131 uptake by thyroid in children from, 19: 46035 (PHS-999-RH-14)
ionization by nuclear explosions in, series solutions of three-species differential equations for, (T), 19: 47449 (AD-613199)
monitoring at Sandia Lab., Jan.–June 1965, 19: 46648(R) (SC-RR-65-464)
neon isotopic composition in, 19: 46588 (ORNL-3857)
particle adhesion to surfaces in, decontamination methods for removal of, 19: 46645 (ORNL-TM-1228)
radioactive contamination of, in reactor accidents, 19: 46699
radioactivity distribution in, meteorological factors in radiation accident, 19: 46693
radioactivity from radon and radon-220 in suspension in, 19: 46641 (CEA-R-2771)
radioactivity in, control of, 19: 46682
radioactivity of Belgian, 1963, 19: 46632(R) (A/AC.82/G/L.987)
sodium-22 content and production in, 19: 46603
temperature and wind measurements in, similarity of, 19: 47110 (RISO-100)
x-ray microbursts in auroral zone, spatial asymmetry and time variations of, (E), 19: 47470
x-ray spectra in auroral zone, (E), 19: 47471
ATMOSPHERES
monitoring in high-activity handling cell, system for, 19: 46647 (RISO-104)
ATOMIC BEAMS
reactions of, research program on chemical, 19: 47221 (NYO-2403-8)
ATOMIC CLOUDS
from nuclear explosions, hazards of, 19: 46671
radiation dose measurements for reactor accident, 19: 46699
radiation hazards of, from reactor accidents, 19: 46698

ATOMIC ENERGY
activities in Australia, 1964-65 report on, 19: 48092 (NP-15477)
activities in South Africa, 1964 report on, 19: 48091(R) (NP-15418)
control of industrial, in European Atomic Energy Community, 19: 46659
personnel, effects of radiation exposure on lifetime health and mortality patterns, 19: 45810(R) (NYO-3394-2(Rev.))
research programs on, in Japanese universities, 19: 48116
use in Belgium, 19: 48113
use in industry, Euratom studies of industry grouping for, 19: 48118
ATOMIC EXPLOSIONS
bibliography on cratering by underground, 19: 46466 (CEA-Bib-63)
blast effects on single-degree-of-freedom dynamic systems, response spectra, 19: 46566 (AD-425747)
blast loading of soils by simulated, lateral-plate bearing tests on mechanics of, 19: 46465 (AD-613991)
detection of atmospheric and underground, seismic methods for, 19: 46620
effects of contained, on fracture permeability of granite rock mass, 19: 46581 (UCRL-14292)
effects of radiation from, on Hiroshima population, 19: 45846
ground motions from atmospheric, simulation of, 19: 46457 (AD-613674)
radial displacements and strains produced by contained underground, method for predicting, 19: 46467 (NVO-1163-43)
radiation effects of, delayed pathological, 19: 45812(R) (ORO-631, pp 1-35)
radiation hazards to eyes from, 19: 45843
throwout from Danny Boy, measurements of, 19: 46468 (POR-1814)
use in mining ore bodies by caving, 19: 46472 (UCRL-14201)
use of underground, in natural gas production, Project Gasbuggy studies of, 19: 46474
vent gas treatment plant for Dribble, analytical systems for, 19: 46471 (UCRL-14123)
ATOMIC STRUCTURE
energy levels of diatomic molecules, vibrational, (T), 19: 47215 (AD-613375)
ATOMIC WEAPONS
book: *Nuclear Weapons—Physical Fundamentals*, 19: 46652(T) (JPRS-31842)
ATOMS
absorption spectra in systems of, two photon, (T), 19: 47236
collisions of, bibliography on, 19: 47258
electron and ion reactions in plasma, inelastic, (T), 19: 47812
electron interactions in, sum rules for two-body, (T), 19: 47250
electron interaction coefficients in relativistic self-consistent field theory for, (T), 19: 47251
electron interactions in, s-d, (T), 19: 47257
electron orbitals in, spin hamiltonian for nonorthogonal, (T), 19: 47254
photon reactions with, excitation and ionization by multi-, 19: 47234
radiation effects on energy level shifts in, laser, (T), 19: 47233
reactions in three-body systems of, long-range, (T), 19: 47249
resonance in strong magnetic fields, radio-optical, 19: 47261
scattering in linear lattice systems, time-dependent, (T), 19: 47255
shell vacancies in, charge spectrometry of inner, 19: 46161(R) (ORNL-3832, pp 116-50)
spectra of isotopically disordered linear chain, integrated, (T), 19: 47256
AUDITORY ORGANS
radiation effects on, 19: 46084
radiotherapy of tumors of the ear, injuries in, 19: 46084
therapy of aviation tympanitis, use of strontium-90 in, 19: 46038(T) (JPRS-31602, pp 191-7)
AURORAL STORMS
kinetics and structure of, 19: 47481
observation of auroral belt using radio, (E), 19: 47473
occurrence of, sunspot cycle effects on, 19: 47472
properties of optical, 19: 47498
properties of radio, 19: 47499
research on, 19: 47452(T) (NASA-TT-F-204)
theory, 19: 47500
AUSTRALIA
atomic energy activities in, 1964-65 report on, 19: 48092 (NP-15477)
fallout monitoring, 1963, 19: 46594
fallout monitoring, 1961 to 1963, 19: 46595
thorium-230 content of pitchblendes in South Alligator River area, 19: 46606
AUSTRALIA. COMMONWEALTH X-RAY AND RADIUM LAB., MELBOURNE
tritium in, uses of, 19: 45729(R) (NYO-910-23, pp 1-111)
AUSTRIA
nuclear power development in, 19: 48010
AUTORADIOGRAPHY
methods of tissue, 19: 45729(R) (NYO-910-23, pp 1-111)
of chromosomes, using tritium-labeled metabolites, 19: 45790
of iodine-125 distribution in thyroid gland of mice, 19: 45783
technique for measuring thickness of fuel element cladding, 19: 46964 (NMI-4996, pp 149-63)
techniques for micro-, of chemical reactions in radioactive materials, 19: 46951 (NMI-4996, pp 19-26)
AVIATION PERSONNEL
protection against G forces, servo-restraint system for, 19: 46485 (CONF-640508, pp 210-23)
AZETIDINE
nuclear magnetic resonance spectra of, analysis, 19: 46247 (UCRL-16349)

B

BACTERIA
chlorophyll-protein complex from, spectral characteristics of, 19: 45727 (BNL-9506)
radiation damage in, repair mechanisms for, 19: 45985
radiation effects on *Pseudomonas aeruginosa*, protective effects of acriflavin and diet against x, 19: 46014
radiation effects on *Escherichia freundii*, protective effects of fluoroacetate against x, 19: 46015
radiation effects on immunogenicity of *Brucella abortus* and *Brucella melitensis*, 19: 45868
radiation effects on desoxyribonucleic acid replication in, ultraviolet, 19: 45909
radiation effects on DNA replication in, uv, 19: 46002
radiation effects on growth of *Staphylococcus pyogens*, 19: 46884
radioinduced inactivation of *Rhizobium trifolii*, ultraviolet, 19: 45961
radiosensitivity effects of pathogenic, on flour beetles, 19: 45908
radiosensitivity of spores of *Bacillus subtilis*, uv, 19: 45848
radiosensitivity of pathological, 19: 46890
radiosterilization effects on *Clostridium botulinum* spores in cured meat, 19: 46881
radiosterilization of cotton bacteriological swabs, 19: 46884
tryptophan metabolism in, enzyme systems for, 19: 45808(R) (NYO-901-36)
BACTERIOPHAGES
radiation effects on nucleic acid synthesis in *E. coli* infected with ϕX174, x, 19: 45851
radioinduced inactivation of *Rhizobium trifolii*, ultraviolet, 19: 45961
radiosensitivity of, in *Escherichia coli*, effects of glycerol on, 19: 46034
radiosensitivity of, in *Escherichia coli*, effects of temperature, 19: 46034
BARIUM
content and distribution in beef heart, 19: 45753 (AE-191)
preparation by reduction of barium salt using catalytic nascent hydrogen, 19: 46253(T) (ORNL-tr-803)
BARIUM BROMATES
radiolysis products from, gamma, 19: 46332(R) (ORNL-3832, pp 50-65)
BARIUM CARBONATES
reactions with rare earth oxides, ternary oxide formation in, 19: 46242(R) (TID-22207, Paper B)
reactions with rare earth oxides, ionic field strengths as criteria for compound formation in, 19: 46246(R) (TID-22207, Paper F)
BARIUM CHLORIDES
reduction by calcium carbide, 19: 46251(T) (ORNL-tr-673)
$BaCl_2$–NaCl–H_2O, activity coefficient determination by ultracentrifugation, 19: 46237(R) (ORNL-3832, pp 76-99)
BARIUM FLUORIDES
reduction by calcium carbide, 19: 46251(T) (ORNL-tr-673)
BARIUM IONS
displacement in soils by beryllium, 19: 45802
BARIUM ISOTOPES Ba-132
energy level schemes for cesium-132 decay-produced, (E), 19: 47584(R) (ORNL-3832, pp 1-28)
BARIUM ISOTOPES Ba-135
neutron capture at 18 to 1500 ev, gamma transitions from resonance, (E), 19: 47701
BARIUM ISOTOPES Ba-140
content in atmosphere and drinking water, Monclos Station, Spain, 1964, 19: 46597
BARIUM OXIDES
reduction by aluminum carbide, catalytic effects of calcium fluoride on, 19: 46252(T) (ORNL-tr-683)
BARIUM SULFATES
solubility of, effects of labeling with sulfur-35 on, 19: 46274
$BaSO_4$–$PbSO_4$, sorptive properties for x rays as function of photon energy, 19: 46150
BARLEY
radioinduced mutations of, 19: 45819(R) (TID-22176)

BARYONS
decay in SU(6) symmetry, RP invariance in nonleptonic, (T), 19: 47385
decay of, U(12) symmetry for electron-positron production in, (T), 19: 47308 (JINR-P-2284)
decay of, V-A theory for leptonic, (T), 19: 47307 (JINR-P-2278)
decays of, unitary symmetry for $\Delta Q = 0$ $\Delta S = 1$ ($B'\gamma$) and ($B'e^+e^-$), (T), 19: 47370
mass formula for, in covariant spin-unitary-spin scheme, 19: 47352
models of, 3^*-plet, (T), 19: 47386
properties of, 19: 47406
symmetry for strongly interacting, fifteenfold way of SU(4), (T), 19: 47328
BARYONS, RESONANCE
decay and production of $Y_1^*(1660)$, (E), 19: 47300 (BNL-9520)
decay branching ratios of Y_0^*, electromagnetic Σ^0-Λ^0 mixing in, (T), 19: 47366
decay of $\frac{3}{2}^+$ decuplet, SU(3)-symmetry breaking in electromagnetic, 19: 47344
mass formula for, in covariant spin-unitary-spin scheme, 19: 47352
mass formula for, empirical, (T), 19: 47384
mass formulas and spectral representation of spin-$\frac{3}{2}$ decuplet, 19: 47340
production of Λ (1238) and (1820) in meson (π^-)-proton interactions at 2.16 Bev/c, 19: 47403
production of N^*, in meson (K^+)-proton interactions at 3 Bev/c, (E/T), 19: 47356
production of Y_0^* in $S_{1/2}$ T = 0 meson (K^0)-nucleon interactions, (T), 19: 47365
production of Y_1^* (1405), in meson (K^-) reactions with nuclei, 19: 47708
properties of, 19: 47406
symmetry for strongly interacting, fifteenfold way of SU(4), (T), 19: 47328
BATTERIES
charger for nickel–cadmium, development of fast, 19: 48095 (SC-DR-64-539)
BEANS
radiation effects on ascorbic acid content of, beta and gamma seed, 19: 45938
BEARINGS
development for SNAP-50/SPUR liquid-metal pumps, 19: 46458 (CNLM-6342)
pressure profiles and flow characteristics of externally pressurized circular thrust, 19: 46462(R) (TID-22184)
BEHAVIOR
radiation effects on, of monkeys, 19: 45893
radiation effects on, of rats, fetal exposure, 19: 45894
radiation effects on, of monkeys, 19: 45898
radiation effects on response to stimulus of female monkeys, 19: 45899
radiation effects on learning, of monkeys, 19: 45900
BELGIAN REACTOR-2
components testing in, non-destructive underwater, 19: 48002(T) (ORNL-tr-747)
neutron dose measurement in graphite irradiations in, 19: 48030
BELGIUM
fallout monitoring, 1963, 19: 46632(R) (A/AC.82/G/L.987)
nuclear energy development and uses in, review of, 19: 48113
radiation monitoring at Center for Nuclear Energy, Mol, 19: 46631 (A/AC.82/G/L.986)
BENTONITES
beryllium sorption in, effects of acidity on, 19: 45802
evaluation of, as moisture barrier in buried wastes, 19: 48076 (DPSPU-62-30-3A)
sorptive properties of electrocoagulated, for fission products, 19: 48082 (UJV-1296/65)
BENZAMIDINE, *N*-(*o*-NITROPHENYL)-
distribution in rat tissues, tracer study of, 19: 46012
radiosensitivity effects in rats, 19: 46011
BENZAMIDINE, *N*-PHENYL-
radiosensitivity effects in *E. coli* mutants, x, 19: 46012
BENZANTHRACENES
carcinogenic effects in female mice, 19: 45808(R) (NYO-901-36)
BENZENE
benzene-8-quinolinol, solvent properties for fission products, 19: 46440
effects on metal extraction by tridodecylamine in presence of hydrohalic or thiocyanic acid, 19: 46180 (UCRL-16254)
radiation effects on hydrogenation of, by copper catalyst, 19: 46329 (EUR-2455.e)
radiolysis of, yields in, 19: 46324(R) (AGN-8132)
separation of tritiated, from tritiated pyridine, by gas chromatography, 19: 46213
benzene–2-propanol, NMR spectra, 19: 46157(R) (MLM-1254)
benzene–N, radiolysis yields in, 19: 46324(R) (AGN-8132)
benzene–dioxane, radiolysis and luminescence behavior, 19: 46363
benzene–iodopropane–$TeCl_4$, technetium-132 decay in, chemical reactions of iodine-132 from, 19: 46412
NH_3–benzene, radiolysis yields in, 19: 46324(R) (AGN-8132)
NH_3–benzene, radiolysis yields in, 19: 46324(R) (AGN-8132)
BENZENE, DIETHYL-
radiation effects on solvent properties of, gamma, 19: 46430 (ORNL-P-1601)
BENZENE, IODO-
iodobenzene–iodopropane–$TeCl_4$, technetium-132 decay in, chemical reactions of iodine-132 from, 19: 46412
BENZENE, NITRO-
effects on metal extraction by tridodecylamine in presence of hydrohalic or thiocyanic acid, 19: 46180 (UCRL-16254)
BENZENE, NITROSO-
complexes with iron carbonyls, radioinduced formation of, 19: 46397
BENZENEARSONIC ACID
hydroxy-, analytical use for determination of hafnium, niobium, and tantalum in thorium oxides, 19: 46226
BENZENESULFONIC ACID, DODECYL ESTER
determination in foam separation process, 19: 46429 (ORNL-P-1522)
BENZENETHIOL
effects of radioinduced chemiluminescence in organic compounds in presence of oxygen, 19: 46344
BENZOHYDROXAMIC ACID, *N*-PHENYL-
analytical use in gravimetric determination of thorium, 19: 46194
BENZOIC ACID, SODIUM SALTS
sorption on carbon electrodes, effects of potential on, 19: 46957(R) (ORNL-3832, pp 100-6)
BENZOPENTAPHENE
labeling with carbon-14, 19: 46315
BENZOQUINONE
tetrachloro-*p*-, use as radical scavenger reagent to minimize radiation effects on TBP, 19: 46406(P)
BENZYL ALCOHOL
thermodynamic properties of, in water and heavy water, 19: 46318
BEPO
design and operation, 19: 48115
BERYLLIUM
analysis for thorium using *N*-benzoyl-*N*-phenylhydroxylamine, gravimetric, 19: 46194
crystal structure and texture of, x-ray diffraction studies of, 19: 47040
deformation of single crystals of, dislocation structures and slip lines in, 19: 46909(R) (AD-620264)
diffusion in, tracer study of self-, 19: 46909(R) (AD-620264)
diffusion to surface in magnesium and its alloys on heating at 300 to 500°C, 19: 47071
effects of plant and soil, 19: 45802
effects on guinea pig and rat tissues, cytomorphology and histology of, 19: 45803
effects on point defects in iron, 19: 47094(T) (ORNL-tr-668)
electron inelastic scattering at 1 and 100 kev, effect of atomic screening on, (T), 19: 47259(T)
fracture of single crystals of, effects of impurities on basal-plane, 19: 46909(R) (AD-620264)
internal friction peak in, at −20 to +20°C, 19: 47056
mechanical properties of single crystals of, 19: 46909(R) (AD-620264)
neutron reactions at 14 Mev, tritium yields from, 19: 47721 (LA-3385)
neutron spectra in, time-dependent, (T), 19: 47548(R) (TID-22141, pp 3-33)
neutron thermalization in, coherent scattering effects on, (E), 19: 47548(R) (TID-22141, pp 3-33)
neutron time-decay constants in, upper bounds for pulsed, (T), 19: 47553
plastic flow on slip planes in, Peierls stress calculations for, 19: 46910(R) (AD-620589)
preparation and mechanical properties of polycrystalline, 19: 46909(R) (AD-620264)
preparation of high-purity, by zone refining, 19: 46909(R) (AD-620264)
properties for aerospace uses, 19: 47068
radiography of tubes, 19: 46562
radioinduced swelling of, effects of high temperatures on, 19: 47576(R) (IDO-17081, pp 49-76)
separation from other materials by electrolytic extraction, 19: 46454
separation from sulfate liquors by solvent extraction using primary amines, 19: 46431 (ORNL-P-1602)
zone refining of, 19: 46910(R) (AD-620589)
BERYLLIUM ALLOYS
Be–Cu, examination of swaged, 19: 46910(R) (AD-620589)
Be–Cu, mechanical properties of single crystals of, 19: 46909(R) (AD-620264)
Be–Th–U, preparation for metallography, 19: 46924 (NMI-4997, pp 5561)
BERYLLIUM CARBIDES
neutron reactions at 14 Mev, tritium yields from, 19: 47721 (LA-3385)

BERYLLIUM CARBONATES
reactions with rare earth oxides, ionic field strengths as criteria for compound formation in, 19: 46246(R) (TID-22207, Paper F)
BERYLLIUM COMPLEXES
with anions, ion exchange studies of, 19: 46230 (AAEC/E-136)
BERYLLIUM HYDROXIDES
crystal structure of, x-ray diffraction studies of, 19: 46279
heats of formation of, 19: 46279
BERYLLIUM ISOTOPES Be-7
energy level lifetime, first, 19: 47564(R) (AD-612038)
energy levels from lithium-6 (α,t) reactions at 40 Mev, (E/T), 19: 47574 (IAE-836)
model of hyperon(Λ) hypernucleus, two-body, 19: 47647
production by proton reactions with nitrogen-14, nitrogen-15, oxygen-16, and oxygen-18 at 2.2 Bev, cross sections for, 19: 47625
BERYLLIUM ISOTOPES Be-8
energy levels from lithium-7 (p,γ), 19: 47703
energy levels of, shell model analysis, 19: 47564(R) (AD-612038)
BERYLLIUM ISOTOPES Be-9
charged particle reactions with, energy levels and mechanisms of, 19: 47564(R) (AD-612038)
neutron scattering at 14 Mev, (E), 19: 47609
proton inelastic scattering at 5.8 to 6.15 Mev, angular distributions from, (E), 19: 47690
BERYLLIUM OXIDES
density of sintered, effects of grade on, 19: 46912(R) (BMI-1727(Del.))
neutron energy distribution in finite and semi-infinite blocks of, (T), 19: 47555
particle size measurement, methods for, 19: 47002 (NMI-4996, pp 50-76)
particle size, effects of calcining temperature on, 19: 47002 (NMI-4996, pp 50-76)
preparation procedures, ceramographic, 19: 46937 (NMI-5025(Pt.I), pp 1-25)
properties of powders of, effects of processing on, 19: 47002 (NMI-4996, pp 50-76)
sample preparation, metallographic, 19: 47001 (NMI-4996, pp 36-49)
use as base for slag for purification of uranium, 19: 46455(P)
BeO–PuO_2, melting point of, eutectic, 19: 46913(R) (BMI-1733(Del.))
BeO–PuO_2, phase studies, 19: 46912(R) (BMI-1727(Del.))
BeO–PuO_2–ThO_2, melting point of, eutectic, 19: 46913(R) (BMI-1733 (Del.))
BeO–UO_2, diffusion of fission products from, 19: 46913(R) (BMI-1733 (Del.))
BeO–UO_2, meltdown studies in PBF, feasibility of, 19: 47952 (APDA-177)
BeO–UO_2, radiation effects on stability of, 19: 46912(R) (BMI-1727 (Del.))
BeO–UO_2–Y_2O_3, preparation procedures, ceramographic, 19: 46937 (NMI-5025(Pt.I), pp 1-25)
BERYLLIUM SYSTEMS
Al–Be–O, thermodynamics of, 19: 46231 (AD-613660)
Be–B–O, thermodynamics of beryllium metaborate formation in, 19: 46231 (AD-613660)
Be–C, fabrication of reactor reflectors from, 19: 46977(P)
Be–graphite, fabrication of reactor reflectors from, 19: 46977(P)
BETA PARTICLES
angular correlations in potassium-42 and rubidium-86 decay, (E), 19: 47609
detection of, nuclear emulsion sensitivity for, 19: 46832
dosimetry of, problems at ORNL in, 19: 46639 (AECL-2281)
effects on amino acids and enzymes in guinea pig skin, 19: 45887
effects on aorta of rabbits, pathological, 19: 45875
effects on ascorbic acid content of legumes, seed, 19: 45938
effects on clathrates from tritium decay in incorporated labeled methyl stearate, 19: 46359
effects on fish thyroid, surgical, 19: 45972
effects on heterogeneously catalyzed gas reactions, 19: 46329 (EUR-2455.e)
effects on leuko compounds of triphenylmethane dyes in polystyrene, 19: 46369
effects on methyl butyrate and methyl stearate from tritium decay in labeled, 19: 46360
effect on ovarian follicles in mice, 19: 45831
effects on rabbit aorta, morphological, 19: 45994
effects on skin, pathological, 19: 45887
effects on thymidine metabolism in cell nuclei, 19: 45808(R) (NYO-901-36)
reactions with matter, compilation of x-ray spectra stimulated in, 19: 47223
spectra from lead-212–bismuth-212 and thallium-208 source, Auger, 19: 46773
BETA SOURCES
detection on thin-layer chromatograms using gel-forming scintillators, 19: 46862
fabrication of, in a ceramic carrier, 19: 47156(P)
uses of technetium-99 and tritium for gas chromatographic ionization detectors, 19: 46887
BETA SPECTRA
determination using tissue-equivalent anthracene crystals, 19: 45729(R) (NYO-910-23, pp 1-111)
BETA SPECTROMETERS
design of iron-free double-focusing, 19: 46823
electron acceleration and intensity measurement in semi-circular photographic recording, (E), 19: 46773
BETAINE HYDROCHLORIDE
radioinduced decomposition of aqueous solutions of, mechanism of, 19: 46374
BETATRONS
characteristics of 30-Mev field-biased and 35 Mev conventional, 19: 47180
design for deep electron therapy, 19: 46126
research program for 35-Mev, at Melbourne Univ., 19: 47171
use in radiochemistry, 19: 46418
use of 35 Mev Gilbetron, for industry and therapy, 19: 47183
x-ray production and uses from 30-Mev flux-forced field-biased, 19: 47178
BEVATRON
development and operation, January to March 1965, 19: 47169(R) (UCRL-16204)
BIBLIOGRAPHIES
on analytical chemistry relating to borides, carbides, and nitrides of certain group IV and V elements, 19: 46941 (NP-15514(Vol.3))
on atomic and molecular collisions, 19: 47258
on chelation therapy for radioisotopes in man, 19: 46017
on crater formation by nuclear explosions, 19: 46466 (CEA-Bib-63)
on direct energy conversion, 19: 47280 (AD-613358)
on dissolution of plutonium dioxide, 19: 46175 (MLM-1264)
on fallout hazards and properties, 19: 46585 (AD-410522)
on fissiochemistry, 19: 46324(R) (AGN-8132)
on nucleation of precipitates from supersaturated solid solutions, 19: 47025(T) (ORNL-tr-637)
on plutonium technology, 19: 48088 (BNWL-113-6)
on preparation and structure of ternary oxides, 19: 46242(R) (TID-22207, Paper B)
on pyrolysis of polymers, 19: 46302 (MLM-1271)
on radiation effects on living organisms and tissues, 19: 45807 (AED-C-04-17)
on radiation effects on dynamic properties of polymers, 19: 46331(R) (NYO-1858-1)
on radiation effects on solid uranium-based fuel materials, 19: 47093 (VDDIT-16(5.2))
on radioactive halos in minerals, 19: 46593(T) (ORNL-tr-755)
on radioinduced polymerization at low temperatures, 19: 46323(R) (AD-613529)
on radioprotection of mammals by thiolic compounds, 19: 46010
on radiotherapy of bladder cancer by conventional methods, 19: 46113
on radiotherapy of bladder cancer, 19: 46114
on radiotherapy of bladder cancer, 19: 46115
on reactor and shielding information compilations, 19: 47908 (ANL-7050, pp 125-39)
on surface tension of liquid metals, 19: 47064
on thermal radiation protection, 19: 45818 (TDCK-33500)
on x radiation effects on viruses and host cells, 19: 45974
BICYCLOPENTYL
yields from radiolysis of cyclohexane-d_{12}–cyclopentane, 19: 46364
BILE ACIDS
radiation effects on excretion of, 19: 45928
BIOCHEMISTRY
research programs at Sloan-Kettering, review of, 19: 46158(R) (NYO-910-23, pp 112-82)
BIOLOGICAL MATERIALS
analysis for mineral elements, fluorescence, 19: 45729(R) (NYO-910-23, pp 1-111)
analysis for potassium and sodium, neutron activation, 19: 46165 (CEA-R-2837)
analysis for strontium, 19: 46197
autoradiographic methods for, 19: 45729(R) (NYO-910-23, pp 1-111)
book: *The Biological Action of Neutron Radiation*, 19: 45822(T) (JPRS-31822)
electron energy distribution in, 19: 45729(R) (NYO-910-23, pp 1-111)
optical properties of polymers, ultraviolet spectroscopic study, 19: 48104 (UCRL-16278)

ultraviolet dosimetry in, 19: 45963
BIOLOGICAL MODELS
data from, computer analysis of, 19: 45735
for radioactive mitotic wave following instantaneous DNA labeling, 19: 45923
BIOLOGICAL SYSTEMS
dynamics of, computer analysis of data on, 19: 45735
radiosensitivity of, effects of oxygen, 19: 46026
use of iodine-129 as nonradioactive tracer in, 19: 45799
BIOLOGICAL WARFARE AGENTS
effects of, pathology, clinical picture, and therapy in, 19: 46651(T) (JPRS-30979)
BIOLOGY
research on, Air Force, 19: 48087 (AD-613537)
BIOMETRY
counting statistics in, 19: 45742
BIOPHYSICS
research programs of Max Planck Institute, 19: 45745
BIOSYNTHESIS
hydrogen fractionation in, 19: 45729(R) (NYO-910-23, pp 1-111)
radiation effects on nucleic acid, in phage-injected *E. coli*, 19: 45851
BIOTITES
radioactive halos in, 19: 46591(T) (ORNL-tr-642)
BIPHENYL
mass spectra of, after electron bombardment, 19: 46328 (EUR-2227.e)
yields from radiolysis of benzene–dioxane mixtures, 19: 46363
biphenyl–terphenyl, melting points of, effects of *p*-terphenyl on, 19: 46300 (AECL-2261)
BIRDS
immune reactions to irradiated tendon grafts in, 19: 45964
immune reactions to irradiated tendon grafts in, 19: 45965
BIREFRINGENCE
of biological polymers, 19: 48104 (UCRL-16278)
BISMUTH
analysis for antimony and silver by γ, γ-coincidence counting, activation, 19: 46193
determination by complexometric methods using EDTA, 19: 46219
electron scattering by, (E), 19: 46643(R) (LAL-1136)
positron scattering by, (E), 19: 46643(R) (LAL-1136)
proton fission at 36 and 58 Mev, 19: 47712
BISMUTH ISOTOPES Bi-209
neutron reactions (n,α) at 14.6 Mev, angular and energy distributions from, (E/T), 19: 47637
BISMUTH ISOTOPES Bi-212
alpha spectra, (E), 19: 47576(R) (IDO-17081, pp 49-76)
uptake and distribution in beagle bones, kidneys, liver, and spleen from thorium-228 decay, 19: 45798
BISMUTH ISOTOPES Bi-213
alpha spectra, (E), 19: 47576(R) (IDO-17081, pp 49-76)
BISMUTH ISOTOPES Bi-214
content in atmosphere, 19: 46605
BISMUTHINE, TRIPHENYL-
effects on scintillation quenching in benzene, 19: 46362
radiolysis of, in benzene, 19: 46362
BLADDER
radiotherapy of cancer of, 19: 46114
radiotherapy of cancer in, gamma, 19: 46115
radiotherapy of tumors in, x, 19: 46113
radiotherapy of tumors of, gamma dosimetry for, 19: 46093
BLAST EFFECTS
from nuclear explosions, hazards of, 19: 46671
ground motions from atmospheric nuclear explosion, simulation of, 19: 46457 (AD-613674)
loading resistance of soils, lateral-plate bearing tests on mechanics of, 19: 46465 (AD-613991)
on geologic discontinuity, acceleration, stresses, and velocity in, 19: 46580 (AD-613287)
protection of missile against, shock mount system for, 19: 46456 (AD-425760)
response spectra of single-degree-of-freedom dynamic systems to multi-megaton nuclear explosions, 19: 46566 (AD-425747)
BLOOD
diethylstilbenediol uptake by human, 19: 45797
nitrophenylbenzamine content in rat, 19: 46011
toxic effects of OMRE High Boilers and Santowax OM on rat, 19: 45769
zinc-65 metabolism in human, effects of dietary calcium on, 19: 45787
BLOOD CELLS
function and proliferation of transplanted, from anemic mice, 19: 45856
radiosensitivity of, 19: 46009
zinc-65 metabolism in swine, 19: 45759(R) (ORO-631, pp 77-82)
BLOOD CIRCULATION
in lungs, tracer study using nitrogen-13 or xenon-133 in normal subjects and patients with emphysema, 19: 46070
measurement of coronary, in dogs using deuterium, iodine-131, krypton-85, and rubidium-86, 19: 45767
radiation effects on, in parabiotic rats, 19: 45838
tracer studies of, 19: 46102
BLOOD DISEASES
radiation effects on morphology of lymphocytes in patients with Hodgkin's disease, 19: 46103
radiodiagnosis of, 19: 46102
BLOOD PICTURE
radiation effects on leukocyte, in rats, 19: 45934
BLOOD PLASMA
iodine-125 and -131 content in, following uptake from milk, 19: 45782
iodine-131 content of proteins of, 19: 46081
radiation effects on lactic dehydrogenase activity in mouse, 19: 45844
zinc-65 metabolism in human, effects of dietary calcium on, 19: 45787
BLOOD PLATELETS
polysaccharide metabolism in rat, effects of vitamin A, 19: 45759(R) (ORO-631, pp 77-82)
BLOOD PRESSURE
radiation effects on rabbit and rat, 19: 45812(R) (ORO-631, pp 1-35)
radiation effects on burro, 19: 45812(R) (ORO-631, pp 1-35)
BLOOD SERUM
analysis for antibodies in animal and human, radioisotope precipitation test for, 19: 45739
radiation effects on isoenzymes and lactate dehydrogenase in human, 19: 46124
radiation effects on denaturation of, following malignant tumor therapy, 19: 45924
radiation effects on appearance of slow alpha-two globulin in, in rats, 19: 45953
radiation effects on properdin content of, ultraviolet, 19: 45919
radiation effects on immune properties of, ultraviolet, 19: 45919
rheumatoid factor in gamma globulin of, from patients with rheumatoid arthritis, 19: 45860
BLOOD VESSELS
localization of lesions in, radioisotope tracer methods for, 19: 46086
radiation effects on rabbit aorta, morphological, 19: 45994
radiation effects on aorta, of rabbits, 19: 45875
BLOOD VOLUME
radiation effects on, in rabbits, 19: 45829
BLOWERS
failures at Hinkley Point Reactor, effects of acoustic excitations on, 19: 48018
BOILERS
corrosion of PWR 1B, causes and extent of, 19: 46912(R) (BMI-1727 (Del.))
corrosion of PWR 1-B, causes and extent of, 19: 46913(R) (BMI-1733 (Del.))
development of sodium-heated, 19: 46478(R) (BAW-1280-25)
development of sodium-heated, 19: 46530(R) (BAW-1280-27)
development of sodium-heated, 19: 46531(R) (BAW-1280-28)
sodium–water reactions in prototype sodium-cooled, analysis, 19: 46529 (APDA-175)
BOILING
analysis of convection, inside channels, (E), 19: 46538(R) (TID-22148)
burnout in forced-convective, in heated tubes, 19: 46541
burnout in upward flow of Freon 12 through uniformly and non-uniformly heated tubes, forced-convection, 19: 46527 (AEEW-R-426)
burnout in 19-rod bundle with subcooled water and fog, 19: 46539(R) (TID-22249)
effects of surface conditions on sodium nucleate, 19: 46549
instability of subcooled, in forced-convection flows through small tubes, 19: 46534 (NP-15437)
nucleate, effects on heat transfer to liquid metals during vertical upflow, 19: 46528 (ANL-7038)
stability of liquid sodium nucleate, 19: 46551
BOILING REACTORS
criticality of large, computer calculations of, 19: 47917 (ANL-7050, pp 487-502)
design of 1000-Mw(e), engineering drawings for, 19: 48044
development in Italy, 19: 48008
development of 50 Mw(e), 19: 47923
fuel cycle costs for 1000-Mwe single-cycle, minimization of, 19: 47990 (BNWL-105)
reactivity lifetime calculations for, BISTRO code for, 19: 47913 (ANL-7050, pp 369-78)
safety systems for power, 19: 48038
BONDING
problems in dissimilar-metal, chemical and physical, 19: 46968(T) (AEC-

tr-6615)
BONE MARROW
deoxyribonucleic acid metabolism in tissue culture cells of, tracer study using carbon-14-formate, 19: 45815(R) (ORO-631, pp 67-76)
erythropoiesis maintenance in cultures of mouse, method for, 19: 45740
growth of tissue culture cells of, effects of ultrafiltrate from irradiated animals on, 19: 45815(R) (ORO-631, pp 67-76)
protective effects of injected tissues of, against radiation injuries in rats, 19: 46023
radiation effects on mouse, protective effects of pyridoxal-5-phosphate, aminoethylisothiouronium, and homocysteinethiolaction against, 19: 46028
radiation effects on mouse, protective effects of sodium cysteisethiosulfonate against, 19: 46006
radioinduced chromosomal aberrations in mouse, x, 19: 45911
radiosensitivity of, 19: 46031
radiosensitivity of, 19: 46009
radiosensitivity of genotype S1/S1 anemic mouse, cellular basis of hemopoietic defect in, 19: 45856
radiosensitivity of, in tuberculosis patients, 19: 45870
BONE TUMORS
effects on calcium kinetics in cancer patients, 19: 45757(R) (NYO-910-23, pp 183-92)
effects on calcium-47 uptake, 19: 45757(R) (NYO-910-23, pp 183-92)
effects on strontium-85 uptake, 19: 45757(R) (NYO-910-23, pp 183-92)
induced by plutonium-239 in mice, 19: 45808(R) (NYO-901-36)
localization of, with strontium-85 and external scanning, 19: 46133
pathology of, induced by radium poisoning, 19: 45808(R) (NYO-901-36)
BONES
calcium-47 uptake by tumorous, measurement of, 19: 45757(R) (NYO-910-23, pp 183-92)
lead-210 content in human, Warsaw, 1963, 19: 45795
radiation dosimetry for, external, 19: 46153
radiation dosimetry for, from internal isotopes, 19: 46154
radiation effects on rabbit, time factors in, 19: 45989
radiation effects on osteogenesis of, in mouse embryos, 19: 45872
radiation effects on mineral metabolism in mouse, x, 19: 45729(R) (NYO-910-23, pp 1-111)
radiation effects on alkaline phosphatase production in mouse, x, 19: 45729(R) (NYO-910-23, pp 1-111)
radiodiagnosis of lesions of, using strontium-85 and external counting, 19: 46133
radiodiagnosis of metastases in, using calcium-45 and strontium-85, 19: 45729(R) (NYO-910-23, pp 1-111)
radiodiagnosis of lesions in, using calcium-47 and strontium-85, 19: 45757(R) (NYO-910-23, pp 183-92)
radiosensitivity of face and jaw, in children, 19: 46074
radiosensitivity of face and jaw, in children, 19: 46075
strontium metabolism in, effects of steroid hormones, age, and sex on, 19: 45805
strontium-85 uptake by tumorous, measurement of, 19: 45757(R) (NYO-910-23, pp 183-92)
strontium-90 content of, in adults, effects of diet on, 19: 45793
strontium-90 content of Australian, 1963, 19: 46594
strontium-90 content of, in Australia, 19: 46595
thorium-228 decay in beagle, metabolism of bismuth-212, lead-212, and radium-224 from, 19: 45798
BORANE, TRIETHYL-
analysis for boron-10 and boron-11, mass spectrometric, 19: 46899(R) (ORNL-3832, pp 33-49)
BORIDES
analysis for carbon, graphite, nitrogen, and oxygen in refractory, method for, 19: 46941 (NP-15514(Vol.3))
bibliography on analytical chemistry of certain group IV and V, 19: 46941 (NP-15514(Vol.3))
production, properties, and uses of refractory, 19: 47020(T) (AEC-tr-6616)
BORON
determination by thermal neutron capture, 19: 46221
determination in hafnium, niobium, tantalum, titanium, and zirconium borides, method for, 19: 46941 (NP-15514(Vol.3))
heat of vaporization, 19: 46956 (NP-15514(Vol.1))
neutron cross sections of, shell effects on thermal, (E), 19: 47618
separation from other materials by electrolytic extraction, 19: 46454
BORON CARBIDES
preparation for metallography, 19: 46922 (NMI-4997, pp 22-5)
BORON FLUORIDES
analysis for boron-10 and boron-11, mass spectrometric, 19: 46899(R) (ORNL-3832, pp 33-49)
reactions with tungsten, 19: 46956 (NP-15514(Vol.1))
seisole–BF_3, boron isotopic exchange thermodynamics of, 19: 46899(R) (ORNL-3832, pp 33-49)
BF_3–butyl sulfide, boron isotopic exchange thermodynamics of, 19: 36899(R) (ORNL-3832, pp 33-49)
BF_3–dimethyl selenide, boron isotopic exchange reactions of, 19: 46899(R) (ORNL-3832, pp 33-49)
BF_3–ethyl ether, boron isotopic exchange thermodynamics of, 19: 46899(R) (ORNL-3832, pp 33-49)
BF_3–ethyl sulfide, boron isotopic exchange thermodynamics of, 19: 46899(R) (ORNL-3832, pp 33-49)
BF_3–ethyl ether–ethyl sulfide, boron trifluoride exchange in, 19: 46899(R) (ORNL-3832, pp 33-49)
BF_3–methyl ether, boron isotopic exchange thermodynamics of, 19: 46899(R) (ORNL-3832, pp 33-49)
BF_3–methyl sulfide, boron isotopic exchange thermodynamics of, 19: 46899(R) (ORNL-3832, pp 33-49)
BF_3–phenol, boron isotopic exchange thermodynamics of, 19: 46899(R) (ORNL-3832, pp 33-49)
BF_3–tetrahydrofuran, boron isotopic exchange thermodynamics of, 19: 46899(R) (ORNL-3832, pp 33-49)
BF_3–triethylamine, boron isotopic exchange thermodynamics of, 19: 46899(R) (ORNL-3832, pp 33-49)
BORON ISOTOPES B-10
determination in boron trifluoride and triethyl boron, mass spectrometric, 19: 46899(R) (ORNL-3832, pp 33-49)
deuteron reactions (d,p) with, coherent knockout amplitudes in, (T), 19: 47669
electron scattering by, 19: 46643(R) (LAL-1136)
form factors, (T), 19: 46643(R) (LAL-1136)
neutron reactions (n,n′γ) at 3.0 to 4.5 Mev, gamma angular distributions and cross sections from, (E/T), 19: 47594(R) (TID-22012, pp 176-205)
production of, methods for, 19: 46413
BORON ISOTOPES B-11
determination in boron trifluoride and triethyl boron, mass spectrometric, 19: 46899(R) (ORNL-3832, pp 33-49)
deuteron reactions (d,p) at 1.3 to 5.5 Mev, boron-12 excited levels from, (E), 19: 47604
deuteron reactions (d,p) with, (E), 19: 47609
electron scattering by, 19: 46643(R) (LAL-1136)
form factors, (T), 19: 46643(R) (LAL-1136)
neutron reactions (n,n′γ) at 3.0 to 4.75 Mev, differential cross sections for, (E/T), 19: 47594(R) (TID-22012, pp 176-205)
nuclear magnetic resonance in boron trioxide to 800°C, 19: 47873 (AD-612384)
proton inelastic scattering at 5.8 to 6.15 Mev, angular distributions from, (E), 19: 47690
proton reactions (p,γ) with, giant dipole resonance of gamma yield from, 19: 47115(R) (ANL-6983)
BORON ISOTOPES B-12
energy levels of parity and spin of excited, (E), 19: 47604
BORON OXIDES
boron-11 NMR in, to 800°C, 19: 47873 (AD-612384)
infrared spectra of high temperature vapors of, 19: 46956 (NP-15514 (Vol.1))
BORON SYSTEMS
Al–B–O, thermodynamics of, 19: 46231 (AD-613660)
B–Cr–Ni, protective effects as coating on molybdenum and molybdenum–titanium alloy, 19: 47061
B–C–Sc, crystal structure of ScB_2C_2, 19: 46258
Be–B–O, thermodynamics of beryllium metaborate formation in, 19: 46231 (AD-613660)
B–W–Zr, fabrication and mechanical properties of, 19: 46940(R) (NP-15444)
BOSONS
interactions at high energy, perturbation theory for production amplitudes in, 19: 47341
interactions of many, Bogoliubov transformation and inequivalent representations in, 19: 47420
interactions with bosons under marginally singular forces, pseudovector-resonance production in, 19: 47338
interactions with fermions, axiomatic approach to Lee model for, 19: 47402
mass formula and spectral representation of vector, 19: 47340
scattering of single-particle excitations by vortices in condensate of imperfect gas of, (T), 19: 47516
wave equations for spin-one, manifestly covariant, 19: 47359
BRAIN
deuteron effects in rabbit, 19: 45874
localization of vascular lesions in, radioisotope tracer methods for, 19: 46086
nitrophenylbenzamine content in rat, 19: 46011
radiation effects on mouse, protective effects of sodium cysteinethiosulfonate against, 19: 46006

radiation effects on 4-aminobutyric acid content in guinea pig, 19: 45979
radioinduced lesion of, in man, 19: 45995
radiosensitivity of human, 19: 45892
weight, correlation with fitness in mice, 19: 45809(R) (NYO-1979-12)
BRAIN TUMORS
radiodiagnosis of, by scanning with iodine-131, mercury-197, or mercury-203, 19: 46046
radiodiagnosis using technetium-99, 19: 46140
radiodiagnosis using iodine-131-polyvinylpyrrolidone for scanning, hazards of, 19: 46058
radiodiagnosis, using mercury-203 scanning, 19: 46053
radiotherapy of intraorbital, method for, 19: 46042
radiotherapy, using phosphorus-32–chromic phosphate, 19: 46087
BRASS
neutron scattering from beta, critical, (E), 19: 47904
sorptive properties for tritium, effects of texture on, 19: 47018 (USNRDL-TR-890)
BRAZED JOINTS
radiography of copper magnet-conductor, 19: 46965 (UCRL-16383)
BREASTS
radiotherapy of cancer of, combined with surgery, 19: 46054
BREATH
analysis for radon-222, determination of radium-226 body burden by, 19: 46677
BREEDER REACTORS
development in Great Britain, 19: 48007
fuels for fast, performance of carbide, 19: 47993 (NAA-SR-10751)
BREMSSTRAHLUNG
emission from beta reactions with matter, 19: 47223
energy spectra in auroral zone atmosphere, (E), 19: 47471
fabrication of, in a ceramic carrier, 19: 47156(P)
interactions with protons, dipion production in, (E), 19: 47303 (DESY-65/7)
interactions with protons at 660 to 800 Mev, meson (π^0) angular distributions from, (E), 19: 47368
reactions (γ,n), (γ,2n), and (γ,pn) with calcium-40 at 15 to 65 Mev, yields from, 19: 47578 (IS-T-23)
reactions (γ,n) with scandium-45 at 48 Mev, (E), 19: 47596(R) (TID-22141, pp 94-7)
reactions (γ,pn) with titanium-46 at 48 Mev, (E), 19: 47596(R) (TID-22141, pp 94-7)
reactions (γ,t) with elements at 37 Mev, (E), 19: 47596(R) (TID-22141, pp 94-7)
reactions (γ,3p) with phosphorus-31 at 50 Mev, (E), 19: 47596(R) (TID-22141, pp 94-7)
reactions with scandium-45 and vanadium-51, (E), 19: 47596(R) (TID-22141, pp 94-7)
BREN OPERATION
soil radioactivity produced in, 19: 47569 (CEX-62-50)
BROMIDE IONS
reactions with haloacetic acids, isotopic exchange and replacement, 19: 46293
BROMINE
content and distribution in beef heart, 19: 45753 (AE-191)
meson (K^-) reactions at 1.5 to 3 Bev/c, light charged particle emission in, (E), 19: 47651
BROMINE FLUORIDES
reactions with uranium(IV-VI) oxides, partial pressure effects on rate constant for, 19: 47921(R) (ANL-7090, pp 30-54)
BROMINE IONS
reactions with cesium and potassium in crossed-beam experiments, 19: 46161(R) (ORNL-3832, pp 116-50)
BROMINE SYSTEMS
Ar–Br, resonator modes in laser of, (E/T), 19: 47219 (AD-614253)
BROOKHAVEN ALTERNATING-GRADIENT SYNCHROTRON
beam extraction system for, slow, 19: 47161 (BNL-9483)
beam injection systems for, design of permanent magnets for, (T), 19: 47160 (BNL-9482)
magnets for, design of beam-extracting septum, (E), 19: 47158 (BNL-910)
BROOKHAVEN BEAM RESEARCH REACTOR
neutron kinetics in, 19: 48056 (BNL-9510)
safety hazards analysis for, 19: 45054 (BNL-9308)
BROOKHAVEN REACTOR
contamination from 1963 argon-41, 19: 46640 (BNL-915)
loop removal from, cutting technique for, 19: 48055 (BNL-9402)
BUBBLE CHAMBERS
design of large, heavy-liquid, (E), 19: 46799
development, 19: 46643(R) (LAL-1136)
ionization measurements in, methods for automatic, 19: 46758 (CONF-550-99)
particle track analysis in, using computers, 19: 47336
particle track analysis in, using on-line computers, (E), 19: 46797
particle track analysis in, using semi-automatic scanning systems, (E), 19: 46798
particle track analysis systems for, design of Lidiam, (E), 19: 46801
particle track analysis in, using PEPR system, (E), 19: 46810
particle track analysis in photographs from, on-line computer system for, (E), 19: 46811
particle track analysis in, using CERN HAZE program, (E), 19: 46812
particle track analysis in photographs from, computer systems for, (E), 19: 46814
particle track ionization in photographs from, devices for measuring, (E), 19: 46802
photographs from, engineering drawings of scanner for, 19: 46866
use in high-energy physics, 19: 46834
BULK SHIELDING FACILITY
radiation monitoring of, engineering drawings of gamma ion chamber for, 19: 46865
BURNS
pathology of, 19: 45818 (TDCK-33500)
BURROS
protection against fallout, 19: 46700
radiation effects on, delayed pathological, 19: 45812(R) (ORO-631, pp 1-35)
radiation effects on, pathological, 19: 45814(R) (ORO-631, pp 45-66)
BUTADIENE
radioinduced polymerization of gaseous and liquid, gamma and x, 19: 46336 (TID-22236)
1,3-BUTADIENE, HEXACHLORO-
radioinduced polymerization of liquid, gamma, 19: 46336 (TID-22236)
BUTANE
neutron scattering by, calculation methods for, (E/T), 19: 47576(R) (IDO-17081, pp 49-76)
reactions with tritium ions at 2 to 6 kev, preparation of labeled hydrocarbons by, 19: 46415
thermodynamic properties of, in water and heavy water, 19: 46318
yields in electron radiolysis of ethylene, nitric oxide effects on, 19: 46324(R) (AGN-8132)
yields in radiolysis of ethylene–methane–nitrogen, 19: 46324(R) (AGN-8132)
BUTANE, 1-BROMO-
radioinduced reactions with tin, effects of dose and other metals on, 19: 46912(R) (BMI-1727(Del.))
radioinduced reactions with tin, effects of heat on, 19: 46913(R) (BMI-1733(Del.))
yields from pyrolysis and ester interchange reactions of tributyl phosphate, 19: 46317
BUTANE, 2,2-DIMETHYL-
use in radiochemical separation of fission products, 19: 46405
1-BUTANOL
thermodynamic properties of, in water and heavy water, 19: 46318
2-BUTANOL
thermodynamic properties of, in water and heavy water, 19: 46318
1-BUTENE
effects on photolysis of cyclopentanone, 19: 46357
radiolysis of gaseous, x, 19: 46335 (TID-22232)
yields from photolysis and radiolysis of cyclopentanone, 19: 46357
yields in electron radiolysis of ethylene, nitric oxide effects on, 19: 46324(R) (AGN-8132)
yields in radiolysis of ethylene–methane–nitric oxide, 19: 46324(R) (AGN-8132)
2-BUTENE
radiolysis of gaseous and liquid *cis*-, x and gamma, 19: 46335 (TID-22232)
yields in electron radiolysis of ethylene, nitric oxide effects on, 19: 46324(R) (AGN-8132)
yields in radiolysis of ethylene–methane–nitric oxide, 19: 46324(R) (AGN-8132)
BUTENES
yields from pyrolysis and ester interchange reactions of tributyl phosphate, 19: 46317
BUTYL GROUP
isomerization of, in pyrolysis and reactions of TBP, 19: 46317
BUTYL PHOSPHATES
pyrolysis of, and reactions with phosphoric acid, yields of alkyl isomers from, 19: 46317
pyrolysis of, isomerization of residual butyl groups in, 19: 46304(R) (ORNL-3832, pp 66-75)
radiation effects on, radical scavenger reagent for minimization of, 19: 46406(P)
solvent properties for cerium, 19: 46439

solvent properties for uranium, 19: 46446
D2EHPA–kerosene–TBP, solvent properties for rare earths from complexed waste solutions, 19: 46432 (ORNL-P-1603)

BUTYL SULFIDES
BF_3–butyl sulfide, boron isotopic exchange thermodynamics of, 19: 46899(R) (ORNL-3832, pp 33-49)

1-BUTYNE
electron reactions with, spectra of energy level transitions in, 19: 46322 (AD-612070)
radiolysis of, x, 19: 46334 (TID-22231)

2-BUTYNE
electron reactions with, spectra of energy level transitions in, 19: 46322 (AD-612070)

BUTYRIC ACID, 2-AMINO-
thermodynamic properties of, in water and heavy water, 19: 46318

BUTYRIC ACID, 4-AMINO-
labeling with tritium at α-carbon atom, 19: 46306
radiation effects on content in brain of guinea pigs, 19: 45979

BUTYRIC ACID, METHYL ESTER
radiolysis of tritium-labeled, self-, 19: 46360

BUTYRIC ACID, VINYL ESTER
radioinduced polymerization of, in bulk and solution, 19: 46389

C

CACODYLIC ACID, SODIUM SALT
properties for use as gamma dosimeter, 19: 46373

CADARACHE REACTORS (RAPSODIE)
uses for fast-reactor studies, 19: 47997(R) (NP-15478)

CADMIUM
bremsstrahlung reactions (γ,t) at 37 Mev, yields in, (E), 19: 47596(R) (TID-22141, pp 94-7)
content and distribution in beef heart, 19: 45753 (AE-191)
ion beam average charge in vapors of, (E), 19: 47266
neutron cross sections of, shell effects on thermal, (E), 19: 47618
radiation effects on shielding properties of, 19: 47576(R) (IDO-17081, pp 49-76)

CADMIUM CHLORIDES
Cd–$CdCl_2$, emf in molten lithium chloride-potassium chloride, measurement method for, 19: 47010(R) (ORNL-3832, pp 107-50)
Cd–$CdCl_2$, EMF of molten, equipment for measuring, 19: 46270

CADMIUM ISOTOPES Cd-109
gamma reactions with, K x-ray purity from, 19: 46407 (AAEC/TM-226 (Suppl. 1))

CADMIUM ISOTOPES Cd-114
deuteron inelastic scattering at 8 to 15 Mev, differential cross sections for, (E/T), 19: 47635

CADMIUM SYSTEMS
Cd–$CdCl_2$, emf in molten lithium chloride-potassium chloride, measurement method for, 19: 47010(R) (ORNL-3832, pp 107-50)
Cd–$CdCl_2$, EMF of molten, equipment for measuring, 19: 46270
Cd–H, particle growth in flow of propellant of, 19: 46570 (AD-614111)

CADMIUM ZINC SULFIDES
absorptive properties for x rays as function of photon energy, 19: 46150

CAFFEINE
effects on contraction regulation by mechanical threshold in frog muscles, 19: 45736

CALCIUM
content and distribution in beef heart, 19: 45753 (AE-191)
content in range plants, Miles City, Montana, 1955 to 1960, 19: 45747 (ORNL-TM-1279)
effects of bone tumors on, kinetic, 19: 45757(R) (NYO-910-23, pp 183-92)
effects of dietary, on zinc-65 metabolism in man, 19: 45787
effects of metabolic diseases in cancer patients on, kinetic, 19: 45757(R) (NYO-910-23, pp 183-92)
effects on cesium-137 ratio to strontium-90 in milk, 19: 45772
effects on determination of strontium, 19: 46197
effects on distribution of strontium-90 in water-bearing strata by ground waters, 19: 46602
effects on selenium-75 metabolism in chickens, 19: 45761(R) (ORO-631, pp 122-31)
effects on strontium-90 content in grass and alfalfa in West Slovakia, USSR, 19: 45750
melting point of, effects of calcium fluoride on, 19: 47010(R) (ORNL-3832, pp 107-50)
metabolism, 19: 45729(R) (NYO-910-23, pp 1-111)
metabolism in man, double tracer method for analyzing, 19: 46138
preparation by reduction of barium salt using catalytic nascent hydrogen, 19: 46253(T) (ORNL-tr-803)
uptake by plants, effects of beryllium on, 19: 45802

CALCIUM ALLOYS
Ca–Mg, diffusion of beryllium to surface of, on heating at 300 to 500°C, 19: 47071

CALCIUM BROMATES
radiolysis products from, gamma, 19: 46332(R) (ORNL-3832, pp 50-65)

CALCIUM CARBIDES
reactions with barium and strontium halides, 19: 46251(T) (ORNL-tr-673)

CALCIUM CARBONATES
effects on sorptive properties of soils for strontium, 19: 46434
reactions with rare earth oxides, ionic field strengths as criteria for compound formation in, 19: 46246(R) (TID-22207, Paper F)

CALCIUM COMPOUNDS
calcium-47 enrichment in organic, by Szilard-Chalmers reaction, 19: 46416

CALCIUM FLUORIDES
catalytic effects on reduction of barium and strontium oxides by aluminum carbide, 19: 46252(T) (ORNL-tr-683)
crystal field effects on rare earth ions in lattices of, (E), 19: 47890(T)
effects on melting point of calcium, 19: 47010(R) (ORNL-3832, pp 107-50)
properties as thermoluminescent dosimeter, 19: 46859
Ca–CaF_2, phase studies, 19: 47010(R) (ORNL-3832, pp 107-50)
CaF_2–propane, radiolysis yields in, 19: 46324(R) (AGN-8132)

CALCIUM IONS
displacement in soils by beryllium, 19: 45802
effects on sorptive properties of rhyodacite tuff for radioisotopes, 19: 48085

CALCIUM ISOTOPES Ca-40
bremsstrahlung reactions (γ,n), (γ,2n), and (γ,pn) at 15 to 65 Mev, yields from, 19: 47578 (IS-T-23)
bremsstrahlung reactions (γ,p) at 25.5 Mev, energy spectra from, (E), 19: 47699
electron scattering by, energy levels and shell-model parameters from, (T), 19: 47677
meson (μ^-) capture by, K x ray energies from, 19: 47582 (NEVIS-129)
neutron reactions (n,n′γ) and (n,p′γ) at 4.2 and 4.43 Mev, gamma angular distributions and cross sections from, (E/T), 19: 47594(R) (TID-22012, pp 176-205)
nuclear charge distribution in, (E), 19: 47565 (AD-614270)
nuclear charge distribution radius, 19: 47582 (NEVIS-129)
proton inelastic scattering at 14.6 to 18.2 Mev, (E/T), 19: 47702

CALCIUM ISOTOPES Ca-44
meson (μ^-) capture by, K x ray energies from, 19: 47582 (NEVIS-129)
nuclear charge distribution radius, 19: 47582 (NEVIS-129)

CALCIUM ISOTOPES Ca-45
metabolism in chickens, 19: 45761(R) (ORO-631, pp 122-31)
use in metabolic studies in man, 19: 46138

CALCIUM ISOTOPES Ca-47
concentration in organocalcium compounds by Szilard-Chalmers reaction, 19: 46416
diagnostic use for bone metastases, 19: 45729(R) (NYO-910-23, pp 1-111)
diagnostic use for bone lesions, 19: 45757(R) (NYO-910-23, pp 183-92)
uptake by tumorous bone, measurement of, 19: 45757(R) (NYO-910-23, pp 183-92)
use in metabolic studies in man, 19: 46138

CALCIUM ISOTOPES Ca-48
deuteron reactions (d,α) at 12 Mev, potassium-46 production in, 19: 47115(R) (ANL-6983)

CALCIUM OXIDES
reactions with zirconium silicate at 1300°C for 50 hr, 1200°C for 70 hr, or 1100°C for 120 hr, 19: 46267
CaO–UO_2–ZrO_2, enthalpy and thermal conductivity at 100 to 2000°C, 19: 46912(R) (BMI-1727(Del.))
CaO–ZrO_2, uses as electrolyte in oxygen reaction cells, 19: 46297

CALCIUM SYSTEMS
Ca–CaF_2, phase studies, 19: 47010(R) (ORNL-3832, pp 107-50)

CALCIUM TUNGSTATES
absorptive properties for x rays as function of photon energy, 19: 46150

CALCIUM ZIRCONATES
$CaZrO_3$–$SrZrO_3$, stress-strain characteristics of, 19: 47008(R) (NP-15429)

CALDER HALL REACTORS
blower failures at Hinkley Point, effects of acoustic excitations on, 19: 48018
control rod worths of, methods for calculating, 19: 47999 (TRG-Report-227)
design of advanced gas-cooled Dungeness B, 19: 48020
design of AGR for Dungeness B, 19: 47995 (NP-15473)
design of Dungeness B, 19: 48027
design of Sizewell, 19: 48024
economic and technical aspects of Dungeness-B, 19: 48023
economics of AGR, for Dungeness B, 19: 47996 (NP-15474)

loading at Sizewell, 19: 48022
performance at Berkeley, Bradwell, and Hunterston, 19: 48019
proposals and specifications for Dungeness B, 19: 48035

CALIFORNIUM ISOTOPES Cf-248
neutron capture cross sections and resonances of, measurement of thermal, (E), 19: 47584(R) (ORNL-3832, pp 1-28)
production from plutonium-242, scheme for, (E/T), 19: 47584(R) (ORNL-3832, pp 1-28)

CALORIMETERS
design for determining graphite radiation dose absorption rate in gas-cooled reactors, 19: 48031
design of differential thermal, heat transfer considerations in, 19: 46728 (UCRL-16336)
design of fast-response micro, 19: 46157(R) (MLM-1254)
performance of local absorbed dose, 19: 46849
performance for radiation dosimetry, 19: 46848

CALORIMETRY
use for standardization of isotopic radiation sources, 19: 46421

CAMBRIDGE SYNCHROTRON
data analysis from, using PDP 1 computer with time sharing, (E), 19: 46807

CAMERAS
description of motor-driven roll-film, for remote metallography, 19: 46711 (BNWL-SA-161)

CANADA
radiation protection program of, 19: 46661

CAPTURE-TO-FISSION RATIOS
measurement of engineering drawings of instrument for, 19: 47713

CARBAMIC ACID ESTERS
separation of carbon and oxygen isotopes in carbon dioxide mixtures of, by fractionation, 19: 46900 (ORNL-3832, pp 33-49)

CARBAMIC ACID, THIO-, *S*-VINYL-*N*-VINYL ESTER
preparation and polymerization of, for use as protective agent against radiation, 19: 46316

CARBIDES
analysis for carbon, graphite, nitrogen, and oxygen in refractory, method for, 19: 46941 (NP-15514(Vol.3))
bibliography on analytical chemistry of certain group IV and V, 19: 46941 (NP-15514(Vol.3))
production, properties, and uses of refractory, 19: 47020(T) (AEC-tr-6616)
separation from plutonium by consumable electrode method, 19: 46915 (BNWL-IR-2)

CARBOHYDRATES
analysis of, automated system for, 19: 45730(R) (ORNL-3752)
preparation of labeled, by microbial processes, 19: 46409

CARBON
determination in liquids or solids, flame ionization detector for, 19: 45730(R) (ORNL-3752)
determination in metals by helium-3 activation, 19: 46174 (LA-DC-7319)
determination in refractory borides, carbides, and nitrides, method for, 19: 46941 (NP-15514(Vol.3))
effects on mechanical properties of aluminum–copper–iron–tin–titanium–vanadium alloys, 19: 46985 (AD-613651)
effects on network structure in uranium, 19: 47060
hardness of pyrolytic, technique for measuring micro-, 19: 47003 (NMI-4999, pp 111-28)
helium-ion absorption cross sections at 30 to 350 kev, (E), 19: 47871
infrared spectra of high temperature vapors of, 19: 46956 (NP-15514 (Vol.1))
neutron reactions at 14 Mev, tritium yields from, 19: 47721 (LA-3385)
neutron total cross section at 0.75 to 50 Mev, (E), 19: 47550(R) (TID-22141, pp 81-93)
neutron transport in single and multilayer slabs of, (T), 19: 47868 (RRA-T52)
preparation of uranium carbide spheres coated with pyrolytic, for metallography, 19: 47006 (NMI-4997, pp 198-207)
proton absorption cross sections at 30 to 350 kev, (E), 19: 47871
reactions with zirconium diboride, thermodynamic data for, 19: 46956 (NP-15514(Vol.1))
sorption of benzoate ions on porous electrodes of, effects of potential on, 19: 46957(R) (ORNL-3832, pp 100-6)
sorption of iodides on porous electrodes of, double-layer capacity for, 19: 46957(R) (ORNL-3832, pp 100-6)
spectra of impurity ions of, in plasma streams, 19: 47757
structure of uranium carbide spheres coated with pyrolytic, metallography, 19: 47006 (NMI-4997, pp 198-207)

CARBON (ACTIVATED)
decontamination for helium purification traps, 19: 46157(R) (MLM-1254)
use in reactor fuel elements for fission gas absorption, 19: 47981(P)

CARBON DIOXIDES
corrosive effects on silver–tungsten composite at 2250°C, 19: 46956 (NP-15514(Vol.1))
corrosive effects on superalloys at high temperatures, 19: 46946 (BNWL-100)
oxidation of graphite, 19: 46956 (NP-15514(Vol.1))
oxidation of hafnium, tantalum, and titanium carbides at 2250°C, 19: 46956 (NP-15514(Vol.1))
oxidation of hafnium, niobium, tantalum, titanium, and zirconium diborides at 2250°C, 19: 46956 (NP-15514(Vol.1))
oxidation of niobium and zirconium carbides at 2250°C, 19: 46956 (NP-15514(Vol.1))
oxidation of niobium carbide–zirconium carbide at 2250°C, 19: 46956 (NP-15514(Vol.1))
oxidation of tungsten at 2330 to 2850°K, reaction kinetics for, 19: 46956 (NP-15514(Vol.1))
oxidative effects on uranium at 400 to 1000°C, 19: 46948 (CEA-R-2805)
performance in proportional counters, 19: 46777
separation from carbamate chemical exchange systems, effects of heater voltage on, 19: 46157(R) (MLM-1254)
separation of carbon and oxygen isotopes in carbamate mixtures of, by fractionation, 19: 46899(R) (ORNL-3832, pp 33-49)
yields from solid state irradiation of alanine and glycine chelates and metal salts, 19: 46403
$CO–CO_2$, reactions with iron and iron oxides, 19: 46297

CARBON IONS
effects on free radical formation in lysozyme, ribonuclease, and trypsin, spectra of, 19: 46339 (UCRL-16358)

CARBON ISOTOPES
separation by fractionation in butylamine carbamate–carbon dioxide systems, temperature effects on, 19: 46899(R) (ORNL-3832, pp 33-49)

CARBON ISOTOPES C-11
incorporation into organic compounds using carbon-12 (γ,n) reactions, 19: 46418
use in medical diagnostics, 19: 46136

CARBON ISOTOPES C-12
alpha scattering at 2.5 to 7.5 Mev, Regge representation analysis of, 19: 47653
bremsstrahlung reactions (γ,n) with, radiochemical use of, 19: 46418
bremsstrahlung reactions (γ,p) at 25.5 Mev, energy spectra from, (E), 19: 47699
deuteron reactions (d,p) with, coherent knockout amplitudes in, (T), 19: 47669
deuteron reactions (d,p) at 1.3 to 5.5 Mev, carbon-13 excited levels from, (E), 19: 47604
electron scattering by, 19: 46643(R) (LAL-1136)
neutron inelastic scattering at 14 Mev, (E), 19: 47609
neutron reactions (n,n′γ) at 14.8 Mev, gamma angular distributions from, (E/T), 19: 47593(R) (TID-22012, pp 156-75)
nitrogen-14 reactions with, excitation functions for one-neutron-transfer, (E/T), 19: 47586 (ORNL-TM-1218)
nitrogen-14 reactions at 20 to 42 Mev, excitation functions for, (E), 19: 47667
production in thermonuclear helium-4 reactions during massive-star evolution, 19: 47202
proton elastic scattering at 6 Mev, angular distribution of polarization of, (E), 19: 47695
separation from carbon-13 in deuterated methane, by thermal diffusion, 19: 46157(R) (MLM-1254)

CARBON ISOTOPES C-13
concentration in natural carbon by conversion of enriched methane, 19: 46157(R) (MLM-1254)
energy levels of parity and spin of excited, (E), 19: 47604
production of, methods for, 19: 46413
proton reactions (p,n) with, neutron polarization in, 19: 47710
separation from carbon-12 in deuterated methane, by thermal diffusion, 19: 46157(R) (MLM-1254)

CARBON ISOTOPES C-14
determination by absolute beta counting, use of efficiency tracing technique in, 19: 46214
determination in plant material by beta counting, 19: 46199
incorporation in acrylic and glyceric acids and glycerol, use of vinylmagnesium bromide in, 19: 46310
incorporation in benzo[rst]pentaphene and its oxidation products, 19: 46315
incorporation in cholesterol esters of arachidonic and linoleic acids, 19: 46309
incorporation in DL-shikimic acid, 19: 46312
incorporation into linoleic acid of, 19: 45785
incorporation into organic compounds of, by microbial processes, 19: 46409
isotope effects on oxidation of benzoin, 19: 46304(R) (ORNL-3832,

pp 66-75)
use in age estimation, low-background counter for, 19: 46777
CARBON MONOXIDES
corrosive effects on superalloys at high temperatures, 19: 46946 (BNWL-100)
effects on iodine-131 uptake by rat thyroid, 19: 45770
effects on photolysis of cyclopentanone, 19: 46357
radiation effects on oxidation of, by zinc oxide catalyst, 19: 46329 (EUR-2455.e)
radiolysis, (E), 19: 47092(R) (TID-22141)
yields from photolysis and radiolysis of cyclopentanone, 19: 46357
yields from radiolysis of benzene–dioxane mixtures, 19: 46363
CO–CO_2, reactions with iron and iron oxides, 19: 46297
CO–H–N, radiolysis yields in, 19: 46324(R) (AGN-8132)
NH_3–CO, radiolysis yields in, 19: 46324(R) (AGN-8132)
CARBON STEEL
corrosion resistance of, effects of uranium on, 19: 47047
mechanical properties of, effects of uranium on, 19: 47047
stress corrosion cracking by wetted thermal insulation, 19: 46949 (CONF-650905-2)
Cr–Mo, corrosion of Croloy 2¼ by sodium–water reaction products, 19: 46478(R) (BAW-1280-25)
CARBON SYSTEMS
Al–C–Cu–H–N–Sn–Ti–V–Zr, mechanical properties of, 19: 46985 (AD-613651)
B–C–Sc, crystal structure of ScB_2C_2, 19: 46258
Be–C, fabrication of reactor reflectors from, 19: 46977(P)
C–Hf–Nb–W, fabrication and mechanical properties of, 19: 46940(R) (NP-15444)
C–Hf–Ta–W, weldability studies of T-222, 19: 46966(R) (WANL-PR(P)-007)
C–Hf–W, fabrication and mechanical properties of, 19: 46940(R) (NP-15444)
C–Nb–W, fabrication and mechanical properties of, 19: 46940(R) (NP-15444)
C–Nb–W–Zr, fabrication and mechanical properties of, 19: 46940(R) (NP-15444)
C–Nb–W–Zr, weldability studies of D-43, 19: 46966(R) (WANL-PR(P)-007)
C–N–Ti, Hall coefficients, 19: 47009 (NP-15514(Vol.2))
C–U, atmospheric corrosion of, 19: 46947 (CEA-R-2732)
C–W–Zr, fabrication and mechanical properties of, 19: 46940(R) (NP-15444)
CARBON TETRACHLORIDE
effects on hydrogen yields in propane radiolysis, 19: 46396
effects on liver function in rats, use of iodine-131-labeled rose bengal for analysis of, 19: 45828
effects on metal extraction by tridodecylamine in presence of hydrohalic or thiocyanic acid, 19: 46180 (UCRL-16254)
effects on radioinduced polymerization of vinyl butyrate, 19: 46389
effects on radiolysis of methanol vapor, 19: 46395
electron drift velocities in deuterated and normal, at low energy, 19: 46393
radioinduced dissociation and ionization in, electron, 19: 46348
solvent properties for nitroanilines in aqueous acetic acid solutions, 19: 46424 (IS-T-24)
CCl_4–2-propanol, NMR spectra of, 19: 46157(R) (MLM-1254)
CARBON TETRAFLUORIDE
ionization potentials, calculated, 19: 46161(R) (ORNL-3832, pp 116-50)
CARBONACEOUS ROCKS
age estimation of pleistocene, from uranium–thorium ratio, 19: 46599
analysis for sodium, flame photometric, 19: 46191
CARBONATE COMPLEXES
with beryllium, ion exchange studies of, 19: 46230 (AAEC/E-136)
CARBONATES
determination in scrubber solutions used in Dribble vent gas treatment plant, 19: 46471 (UCRL-14123)
effects on distribution of strontium-90 in water-bearing strata by ground waters, 19: 46602
CARBONIUM COMPOUNDS
solvolytic effects on exo-norbornyl derivatives, mechanisms of, 19: 46304(R) (ORNL-3832, pp 66-75)
CARCINOGENESIS
chemical, in hamster skin, synergistic effects of ultraviolet radiation, 19: 45906
role of radiation and viruses in, 19: 45942
role of radiation in, 19: 45859
CARCINOGENS
mechanism in, radiobiological, 19: 45743
CARCINOMAS
pathology of, induced by Thorotrast, 19: 45980
radiation response in patients with cervical, 19: 45830
radiodiagnosis of pancreatic, method for, 19: 46060
radioinduced in intestine, by therapy, 19: 46068
radioinduced thyroid, after radiotherapy of medulloblastoma, 19: 46069
radiotherapy effects combined with 5-fluorouracil on palliative management of gastrointestinal, 19: 46091
radiotherapy of basal cell, 19: 46059
radiotherapy of breast, using cobalt-60 or iridium-192 wire applicators, 19: 46047
radiotherapy of breast, combined with surgery, 19: 46054
radiotherapy of breast, pathological effects on lungs, 19: 46063
radiotherapy of esophagus, 19: 46051
radiotherapy of eyelid, 19: 46052
radiotherapy of gynecologic, pelvic exenteration for extensive visceral necrosis after, 19: 46106
radiotherapy of head and neck, synergistic effects of cytotoxic chemicals, 19: 46088
radiotherapy of inoperable thyroid, evaluation of, 19: 46104
radiotherapy of lung, late effects of, 19: 46131
radiotherapy of supraglottic, using telecobalt, 19: 46057
radiotherapy of uterine, using cobalt-60 intercavitary applicator, 19: 46039(T) (JPRS-31667)
radiotherapy of uterine, late effects on urinary tract, 19: 46061
radiotherapy of uterine, 19: 46064
radiotherapy of uterine, effects on rectum, 19: 46099
research programs on, Great Britain, 1964, 19: 45744
sensitization response in patients with cervical, 19: 45830
surgery of uterine, late effects on urinary tract, 19: 46061
CARNOTITES
crystal structure of synthetic anhydrous, 19: 46259
CAROLINAS-VIRGINIA TUBE REACTOR
operation, 19: 47998(R) (SRO-118)
CAROTENE
content in range plants, Miles City, Montana, 1955 to 1960, 19: 45747 (ORNL-TM-1279)
CASCADE SHOWERS
electron and photon angular and lateral distributions in photon-initiated, (T), 19: 47268 (INSJ-86)
CAST IRON
density for use as radiation shielding, radiological scanning methods for determination of, 19: 47039
CASTINGS
inspection of, radiographic methods of, 19: 46564
CATARACTS
radioinduced, etiology of, 19: 45905
radioinduced, pathology of, 19: 45843
CATHODES
field emission by nickel thermionic, vacuum breakdown by, 19: 46577
performance of brush, for uniform plasma production, (E), 19: 47739
use of screen, for plasma structures with free boundary, 19: 47734
CATIONS
motion in clay-water systems, rate processes for, 19: 46239(R) (ORO-631, pp 132-41)
reactions with methylamine, charge exchange in, 19: 46262
CATTLE
cesium-137 metabolism by, effects of diet on, 19: 45780
control of horn flies on, effects of dietary roxnel, 19: 45813(R) (ORO-631, pp 36-44)
diethylstilbenediol uptake by liver in, 19: 45797
iodine metabolism in lactating, effects of diiodosalicylic acid, potassium iodide, or L-thyroxine feeding on, 19: 45781
iodine-131 metabolism by dairy, 19: 45760(R) (ORO-631, pp 83-121)
protection against fallout, 19: 46700
protective effects of liver homogenates from, against radiation injuries in mice, 19: 46024
radiation effects on lactation by dairy, whole-body, 19: 45760(R) (ORO-631, pp 83-121)
radiation effects on, delayed pathological, 19: 45812(R) (ORO-631, pp 1-35)
radiation effects on reproduction of, 19: 45813(R) (ORO-631, pp 36-44)
radiation effects on, pathological, 19: 45814(R) (ORO-631, pp 45-66)
CAVES
atmosphere monitoring system for, 19: 46647 (RISO-104)
description of expanded high-level facilities at Savannah River Laboratory, 19: 46506 (CONF-651101-26)
design and construction of, for slug fabrication, 19: 46509 (UCRL-12497-T)
design of chemistry isolation box for MTR alpha, 19: 47576(R) (IDO-17081, pp 49-76)
metallographic cell for irradiated materials, 19: 47089 (NMI-4999, pp 30-50)

radiation effects on glass windows of, gamma, 19: 47102
CAVITY RESONATORS
use with MHD generator to bunch particles in the conducting fluid, 19: 47297(P)
wave behavior in, correlation to elementary particle behavior, 19: 47319
CELLOPHANE
properties for hyperfiltration, effects of metal salts on, 19: 46237(R) (ORNL-3832, pp 76-99)
CEMENTS
testing of, for high-temperature strain gages, 19: 46715 (EUR-2473.f)
CENTRIFUGAL PUMPS
development for Lithium Cooled Reactor Experiment, 19: 46535(R) (PWAC-386)
CENTRIFUGATION
density inversion during, (T), 19: 45730(R) (ORNL-3752)
use of ultra, in activity coefficients determination, 19: 46237(R) (ORNL-3832, pp 76-99)
CENTRIFUGES
design and performance of rotor systems for combined continuous-flow and density-gradient centrifugation, 19: 46425 (K-L-2012)
development of zonal, for biomedical applications, 19: 45730(R) (ORNL-3752)
tubes for, engineering drawings for, 19: 46515
CERAMIC MATERIALS
properties for aerospace uses, 19: 47068
CERIUM
analysis for thorium using *N*-benzoyl-*N*-phenylhydroxylamine, gravimetric, 19: 46194
cohesive energy and ionization of, relation between, (T), 19: 47062
content and distribution in beef heart, 19: 45753 (AE-191)
diffusion in thorium and uranium dioxides, 19: 47070
neutron reactions $(n,n'\gamma)$ at 3.0 to 4.5 Mev, gamma angular distributions and cross sections for, (E/T), 19: 47594(R) (TID-22012, pp 176-205)
separation from aqueous chloride solutions by solvent extraction using di-n-octyl phosphinic acid, tracer studies of, 19: 46443
separation from nitric acid solutions by solvent extraction using tri-n-octyl phosphine oxide, 19: 46439
separation from other fission products by solvent extraction using benzene–oxine solutions, 19: 46440
CERIUM ALLOYS
Al–Ce, crystal structure of Laves phases in, 19: 47052
Ce–Co, crystal structure of Laves phases in, 19: 47052
Ce–Mg, phase studies, 19: 47059
Ce–Pd, phase studies, 19: 47051
CERIUM BROMIDES
thermal decomposition of hydrates of, mechanisms of, 19: 46271
CERIUM IONS
diffusion in lithium chloride solutions at 25 to 45°C, 19: 46261
spectra in calcium fluoride crystals, deformation effects on absorption, (E), 19: 47890(T)
spectra in silicate glass, fluorescence, 19: 47886(T) (N64-21857, pp 1-6)
CERIUM ISOTOPES Ce-137
distribution and fixation in sediments of lacustrine origin, 19: 46681
CERIUM ISOTOPES Ce-141
content in holothuriae, western Mediterranean, 1962, 19: 46611
CERIUM ISOTOPES Ce-144
content in atmosphere and drinking water, Monclon Station, Spain, 1964, 19: 46597
content in holothuriae, western Mediterranean, 1962, 19: 46611
effects on chicken embryos, pathological, 19: 45761(R) (ORO-631, pp 122-31)
CERIUM OXIDES
atomic charge and permittivity of, (E/T), 19: 47901(T)
gadolinium ion EPR spectra in single crystals of trivalent, 19: 47898(T)
CeO_2–UO_2, radiation effects at high burnup, 19: 46912(R) (BMI-1727 (Del.))
CeO_2–UO_2, radiation effects on, at high burnups, 19: 46913(R) (BMI-1733(Del.))
CERIUM SULFATES
radiation effects on, electron dosimetry by, 19: 47177
CERMETS
preparation procedures, ceramographic, 19: 46937 (NMI-5025(Pt.I), pp 1-25)
radiation effects on aluminum–urania, 19: 48060(R) (IDO-17061, pp 1-47)
CESIUM
analysis for rubidium by x-ray fluorescence spectroscopy, 19: 46186
content and distribution in beef heart, 19: 45753 (AE-191)
electron temperature in plasma of, spectral determination of, (E), 19: 47773(T)
Fermi surface of, 19: 47896
ionization on lanthanum hexaboride surfaces, 19: 47148
neutron total cross section at 14.08 Mev, 19: 46774
photon absorption in vapors of, molecular ions production in resonance, (E), 19: 47229
properties in electron tubes, 19: 46709(R) (AD-614118)
reactions with clays, exchange, 19: 46239(R) (ORO-631, pp 132-41)
reactions with materials in thermionic cells, tracer studies of, 19: 47282(R) (NYO-3429-4)
reactions with refractory metal alloys at 3400°C, metallographic specimen preparation of, 19: 46954 (NMI-5025(Pt.I), pp 39-58)
separation from other fission products by solvent extraction using benzene–oxine solutions, 19: 46440
separation from other fission products by reversed-phase chromatography using tetraphenylboron, 19: 46441
separation from other fission products by chromatography using dipicrylamine, 19: 46442
separation from Purex Alkaline Supernate waste by solvent extraction using 4-*sec*-butyl-2(α-methylbenzyl)phenol, 19: 48075 (BNWL-68)
sorption from solutions by tuffs, 19: 48081 (RT/PROT(65)19)
sorption on tantalum and tantalum carbides, 19: 47900(T)
spectra of plasma of, absolute oscillator strengths for, 19: 47723 (LA-DC-7112)
stability of thermionic plasma of, drift, (T), 19: 47750
CESIUM ALLOYS
Cs–K–Na, preparation and use for power production, 19: 47936(P)
CESIUM BROMATES
radiolysis products from, properties of, 19: 46332(R) (ORNL-3832, pp 50-65)
CESIUM CHLORIDES
molal volume and salt-induced structure transitions of aqueous, 19: 46237(R) (ORNL-3832, pp 76-99)
CsCl–$NdCl_3$, complex formation in, refractometric studies of, 19: 46254
CESIUM IODIDES
absorptive properties for x rays as function of photon energy, 19: 46150
CESIUM IONS
desorption from electrode materials for cesium ion engines, 19: 46571 (HRL-5249-S)
reactions with bromine in crossed-beam experiments, 19: 46161(R) (ORNL-3832, pp 116-50)
scattering by argon, krypton, and nitrogen, angular distributions of elastic, 19: 46161(R) (ORNL-3832, pp 116-50)
CESIUM ISOTOPES Cs-132
decay schemes and gamma spectra of, (E), 19: 47584(R) (ORNL-3832, pp 1-28)
CESIUM ISOTOPES Cs-134
excretion by rats, effects of dithizone derivatives on, 19: 45765(T) (JPRS-27544, pp 1-12)
CESIUM ISOTOPES Cs-137
contamination of food by, after radiation accident, 19: 46694
content in atmosphere and drinking water, Monclon Station, Spain, 1964, 19: 46597
content in dust and precipitation, 19: 46632(R) (A/AC.82/G/L.987)
content in fish from lake waters in Finland, 1965, 19: 46587(R) (NYO-3446-3)
content in man, whole-body, 19: 46612
content in meat from caribou, elk, and reindeer, 19: 46587(R) (NYO-3446-3)
content in milk, 19: 46612
content in milk, 19: 46632(R) (A/AC.82/G/L.987)
content in milk in Australia, 1964, 19: 46660
content in milk in Utah, 19: 46675
content in milk, effects of various foodstuffs on, 19: 45772
determination in food after incineration, 19: 46200
metabolism by dairy cattle, effects of diet on, 19: 45780
radiation hazards of, released by accident, 19: 46696
uptake by tree branches, leaves, needles, roots, and stems from soil, 19: 45773
CESIUM ISOTOPES Cs-144
toxic effects on sheep and swine, 19: 45759(R) (ORO-631, pp 77-82)
CESIUM SYSTEMS
Ar–Cs, electron energy losses in nonequilibrium plasma of, nitrogen impurity effects on, (E), 19: 47737(T)
CESIUM URANYL VANADATES
crystal structure, 19: 46259
CHALKS
shielding properties, 19: 46137
CHARGED PARTICLE BEAMS
focusing of ultrarelativistic, by circular waveguides, 19: 46743
reactions of modulated, time-of-flight analyses of, (E), 19: 45809
CHARGED PARTICLES
absorption in matter, mechanisms of, 19: 47152

beam interactions with plasma waves, 19: 47785
binding energy of, in magnetic field, 19: 47143
density and energy distributions in geomagnetic fields, measurements from Vela Project, 19: 47450 (LA-DC-7365)
detection and measurement of, design of high-resolution resonance counter for, 19: 46838
dosimetry of heavy, equipment for, 19: 46847
dosimetry of heavy, photographic, 19: 46853
electromagnetic perturbation effects on, in Van Allen belts, (T), 19: 47485
interactions with nucleons, peripheral electromagnetic, (T), 19: 47318
kinetics in plasma, statistical, (T), 19: 47808
motion in electromagnetic fields, nonrelativistic gyration, (T), 19: 47807
motion in geomagnetic fields, 19: 47491
motion in nonadiabatic magnetic traps, (T), 19: 47748
motion in plasma, drift and orbit theory for, 19: 47806
motion of relativistic, in electromagnetic fields, (T), 19: 47435
photon interactions with, 19: 47234
production in neutron reactions at 14 Mev, counter telescope for measurement of, 19: 46821
properties of systems of three Coulombic, dependence on particle mass, (T), 19: 47438
reactions in plasma, elastic, (T), 19: 47812
reactions with magnetic mirror fields, (T), 19: 47821
scattering in plasma, equations for, 19: 47800
spectra of trapped, in magnetosphere, 19: 47444 (AD-611629)

CHELATES
alanine, solid state radiation chemistry of, 19: 46403
glycine, solid state radiation chemistry of, 19: 46403
therapeutic use for radioisotope removal from human body, 19: 46017

CHEMICAL ANALYSIS
method for analyzing odors in irradiated beef, 19: 46878 (NP-15455)
methods for radioisotopes in environmental samples, 19: 46168 (IA-849)

CHEMICAL RADIATION DETECTORS
development of chromium and cobalt acetylacetonate systems as gamma, 19: 46761 (NYO-2979-34)
performance for dosimetry, 19: 46852
performance of leuko compounds of triphenylmethane dyes in polystyrene, 19: 46369
performance of sodium cacodylate and *tris*-(hydroxymethyl)aminomethane as gamma, 19: 46373
performance of, for diagnostic exposures, 19: 46860
properties of cerium sulfate, for 2-Mev electrons, 19: 47177

CHEMICAL WARFARE AGENTS
effects of, pathology, clinical picture, and therapy in, 19: 46651(T) (JPRS-30979)

CHEMICALS AND REAGENTS
contamination of atmosphere by, control of, 19: 46682
protection against toxic, catalog of equipment for, 19: 46653(T) (JPRS-31843)

CHEMISTRY
preparation, properties, and structure of ternary oxides, 19: 46240(R) (TID-22207)
research on, Air Force, 19: 48087 (AD-613537)
research programs at ORNL June 1964 to May 1965, 19: 46159(R) (ORNL-3832)

CHEMOTHERAPY
effects of combined radiotherapy and, on tumors, 19: 46095
effects of combined radiotherapy and, on neoplasia, 19: 46096
effects on neoplasia, mechanism for synergistic radiotherapy in, 19: 46096
of cancers of head and neck, synergistic effects with radiotherapy, 19: 46088

CHERENKOV DETECTORS
design for electron and photon spectroscopy up to 10 Bev, (E), 19: 46805
performance with on-line computers for analyzing nuclear events, (E), 19: 46806
use for measuring electron beam energy losses in gases, 19: 47252

CHERENKOV RADIATION
detection of, for determination of strontium-90 in urine, 19: 46198
detection of, for determination of beta emitters in aqueous solutions, 19: 46215

CHICKENS
growth of, effects of soy proteins on, 19: 45761(R) (ORO-631, pp 122-31)
iodine-131 ablation of thyroid gland in, 19: 45966
iodine-131 metabolism in, 19: 45761(R) (ORO-631, pp 122-31)
metabolism of, calcium-45, strontium-89, and phosphorus-32, 19: 45761(R) (ORO-631, pp 122-31)
selenium toxicity in, 19: 45761(R) (ORO-631, pp 122-31)
selenium-75 metabolism in parathyroid glands of, 19: 45761(R) (ORO-631, pp 122-31)
technetium toxicity in, 19: 45761(R) (ORO-631, pp 122-31)

CHIMERAS
immune reactions in, 19: 46009
radiation effects on erythrocyte twine cattle, 19: 45760(R) (ORO-631, pp 83-121)
radiation mouse, mortality from secondary disease in, 19: 45910

CHLORELLA
analysis for copper during life cycle, neutron activation, 19: 45775
analysis for manganese during life cycle, neutron activation, 19: 45775

CHLORIDE COMPLEXES
with beryllium, ion exchange studies of, 19: 46230 (AAEC/E-136)

CHLORIDE IONS
effects on contraction regulation by mechanical threshold in frog muscles, 19: 45736
effects on electrochemical behavior of uranium (IV) in ethanol–water, 19: 46292
reactions with haloacetic acids, isotopic exchange and replacement, 19: 46293

CHLORIDES
determination in scrubber solutions used in Dribble vent gas treatment plant, 19: 46471 (UCRL-14123)
effects on distribution of strontium-90 in water-bearing strata by ground waters, 19: 46602

CHLORINE
determination in arsenic, activation, 19: 46211
determination in polyphenyl reactor coolants, oxy-hydrogen burner for decomposition in, 19: 46163 (AECL-2263)
reactions with potassium, chemiluminescence from, 19: 46161(R) (ORNL-3832, pp 116-50)

CHLORINE ISOTOPES Cl-32
magnetic moments and M1 transition probabilities in $2s_{1/2}$ $1d_{1/2}$ shell, (T), 19: 47641

CHLORINE ISOTOPES Cl-33
magnetic moments and M1 transition probabilities in $2s_{1/2}$ $1d_{1/2}$ shell, (T), 19: 47641

CHLORINE ISOTOPES Cl-35
magnetic moments and M1 transition probabilities in $2s_{1/2}$ $1d_{1/2}$ shell, (T), 19: 47641

CHLORINE ISOTOPES Cl-36
magnetic moments and M1 transition probabilities in $2s_{1/2}$ $1d_{1/2}$ shell, (T), 19: 47641

CHLORINE ISOTOPES Cl-37
magnetic moments and M1 transition probabilities in $2s_{1/2}$ $1d_{1/2}$ shell, (T), 19: 47641

CHLORINE ISOTOPES Cl-38
use in medical diagnostics, 19: 46136

CHLOROFORM
effects on metal extraction by tridodecylamine in presence of hydrohalic or thiocyanic acid, 19: 46180 (UCRL-16254)
separation of tritiated, from tritiated pyridine, by gas chromatography, 19: 46213
solvent properties for nitroanilines in aqueous acetic acid solutions, 19: 46424 (IS-T-24)

CHLOROPHYLLS
spectral characteristics of, from green photosynthetic bacteria, 19: 45727 (BNL-9506)

CHLOROTRIANISENE
radiosensitivity effects in mice, 19: 46029

CHOLANTHRENE, 3-METHYL-
carcinogenic effects in mice, 19: 45808(R) (NYO-901-36)

CHOLESTEROL
radiation effects on content of, in guinea pigs, 19: 45937

CHOLESTEROL ESTERS
labeling of arachidonate and linolenate with carbon-14 and tritium, 19: 46309
radiation effects on content of, in guinea pigs, 19: 45937

CHOLINE, ACETYL-
radioinduced decomposition of aqueous solutions of, mechanism of, 19: 46374

CHOLINE BROMIDE
radioinduced decomposition of aqueous solutions of, 19: 46374

CHOLINE CHLORIDE
radioinduced decomposition of aqueous solutions of, mechanism of, 19: 46374

CHOLINE IODIDE
radiation effects on, 19: 46374

CHROMATOGRAPHIC SEPARATIONS
capillary columns for nucleotides, 19: 45730(R) (ORNL-3752)
reversed-phase nitroaniline, 19: 46424 (IS-T-24)
temperature control in columns for carbon isotope, methods of, 19: 46157(R) (MLM-1254)

CHROMATOGRAPHY
ionization detectors for gas, comparison of radiation sources for, 19: 46887
method for analyzing odors in irradiated beef, 19: 46878 (NP-15455)
method for beta activity using gel-forming scintillators, 19: 46862
CHROMIUM
content and distribution in beef heart, 19: 45753 (AE-191)
determination by complexometric methods using EDTA, 19: 46219
effects on mechanical properties of sintered zirconium diboride, 19: 46907 (AD-456724)
effects on mechanical properties of aluminum–copper–iron–tin–titanium–vanadium alloys, 19: 46985 (AD-613651)
electron emission from surface of, thermionic, 19: 46571 (HRL-5249-S)
mechanical properties of, effects of nitrogen on, 19: 46912(R) (BMI-1727 (Del.))
neutron diffraction by, time-of-flight method for, (E), 19: 47894
CHROMIUM ALLOYS
properties for aerospace uses, 19: 47068
Cr–Fe–Ni, stress corrosion cracking of Alloy 600 by wetted thermal insulation, 19: 46949 (CONF-650905-2)
Cr–Re, fabrication for internal friction studies, 19: 46913(R) (BMI-1733 (Del.))
Cr–Y, fabrication for internal friction studies, 19: 46913(R) (BMI-1733 (Del.))
Sb–Cr, magnetic structure of, 19: 47876 (AD-614435)
CHROMIUM BORIDES
preparation and purification, 19: 46941 (NP-15514(Vol.3))
CHROMIUM BROMIDES
electric conductivity of silicon-activated, 19: 47876 (AD-614435)
CHROMIUM COMPLEXES
with 2,4-pentanedione, use in gamma dosimetry, 19: 46761 (NYO-2979-34)
CHROMIUM IONS
electronic g factors of low-lying levels of singly ionized, (E), 19: 47240
CHROMIUM ISOTOPES Cr-51
decay of, branching ratio to 0.323-Mev state in, (E), 19: 47619
determination in irradiated steel by ion-exchange separation and gamma spectrometry, 19: 46195
distribution in Columbia River effluent, 19: 46680
separation from manganese-52, method for, 19: 46210
use in radiodiagnosis, 19: 46102
CHROMIUM OXIDES
effects on sintering properties of uranium dioxide, 19: 46971
reactions of recoils from neutron (n,γ) reactions in, 19: 46398
CHROMIUM PHOSPHATES
metabolism by rat tissues *in vitro*, 19: 45939
CHROMIUM STEEL
Cr–Mo, corrosion of Croloy-2¼ by sodium hydroxide solutions at high temperatures, 19: 46530(R) (BAW-1280-27)
Cr–Mo, effects of hydrogen on embrittlement of irradiated pressure vessels of, 19: 47098
Cr–Ni–Nb, radiation effects on stress corrosion by magnesium chloride, 19: 47079 (AERE-R-5014)
Cr–Ni–Ti, ageing of corrosion-resistant, structural changes in, 19: 47026(T) (ORNL-tr-795)
CHROMIUM SYSTEMS
Al–Cr–Fe–Si–U, radioinduced swelling in, resistance to, 19: 47103
Al–Cr–Si, protective effects as coating on molybdenum and molybdenum–titanium alloy, 19: 47061
B–Cr–Ni, protective effects as coating on molybdenum and molybdenum–titanium alloy, 19: 47061
CHROMIUM TELLURIDES
magnetic structure of solid, 19: 47876 (AD-614435)
CHROMOSOMES
mutations in Drosophila 2nd, effects of DNA-feeding on, 19: 45876
nucleic acid and protein metabolism in, tracer studies, 19: 45790
pattern of human, 19: 45808(R) (NYO-901-36)
patterns in leukemic leukocytes, 19: 45915
preparation of cytoplasm-free, 19: 45790
properties of, 19: 45726 (BNL-9488)
radiation effect on mouse, aberrant x, 19: 45911
radiation effects on complements of mouse, during leukemia induction, x, 19: 45911
radioinduced aberrations in Drosophila, 19: 45949
radioinduced aberrations in screw-worm, 19: 45950
radioinduced aberrations of, 19: 45915
radioinduced aberrations of lymphocyte, in man, 19: 45916
radioinduced aberrations of lymphocyte, in man, 19: 45917
radioinduced aberrations in leukocyte, 19: 45813(R) (ORO-631, pp 36-44)
radioinduced lethal *D. willistoni*, nature of lethal, 19: 45877
radioinduced mutations in Drosophila 2nd, x, 19: 45876
radiosensitivity of, 19: 46031

CIRCUITS
performance of transistorized coupled pair, 19: 46717 (INSJ-87)
CIRCULATORY DISEASES
radiodiagnosis of intracranial vascular lesions, 19: 46086
radiodiagnosis of, 19: 46102
CITRIC ACID
effects on radioprotective properties of fluoroacetates in *Escherichia freundii*, 19: 46015
CIVILIAN DEFENSE
fallout protection planning, 19: 46585 (AD-410522)
metallurgical practice manual for laymen after nuclear attack, 19: 46918 (IITRI-B6018-1)
population assignment and traffic to shelters, plans for, 19: 46635 (AD-611764)
population direction to and management in shelters, 19: 46636 (AD-611765)
protection against radiological and toxic agents, 19: 46651(T) (JPRS-30979)
shelter development under highways, 19: 46669
shelter evaluation, 19: 46671
shelter operation, management factors for efficient, 19: 46637 (AD-612254)
CLAYS
cation diffusion in, measurement of, 19: 46239(R) (ORO-631, pp 132-41)
reactions with cesium and strontium, exchange, 19: 46239(R) (ORO-631, pp 132-41)
clay–H_2O, cation movement in, 19: 46239(R) (ORO-631, pp 132-41)
CLEAN ROOMS
description of high-purity, at Y-12, 19: 46510 (Y-DA-967)
CLINCH RIVER
radioactive contamination in, 19: 46646(R) (PHS-999-RH-13)
CLOUD CHAMBERS
development, 19: 46820
CLOUD-ION CHAMBERS
design of gamma, engineering drawings for, 19: 46865
COATINGS
corrosion and fretting of Zircaloy, effects of fuel spacer clips on water, 19: 46913(R) (BMI-1733(Del.))
deposition and radiation effects on fuel particle, 19: 46912(R) (BMI-1727(Del.))
deposition of pyrolytic graphite, on nuclear fuel particles, process for, 19: 47983(P)
for high-temperature protection of tungsten, restrictions on materials for, 19: 46911 (AFML-TR-64-392)
COBALT
content and distribution in beef heart, 19: 45753 (AE-191)
determination by complexometric methods using EDTA, 19: 46219
determination by potentiometric titration of acid liberated by complex formation, 19: 46205
determination in aluminum, activation, 19: 46207
dissolution in noninhibiting solutions, mechanisms of, 19: 46957(R) (ORNL-3832, pp 100-6)
effects on point defects in iron, 19: 47094(T) (ORNL-tr-668)
neutron cross sections of, shell effects on thermal, (E), 19: 47618
neutron reactions (n,n′γ) at 3.0 to 4.5 Mev, gamma angular distributions and cross sections for, (E/T), 19: 47594(R) (TID-22012, pp 176-205)
properties of, effects of pertechnetate ions on electrochemical, 19: 46957(R) (ORNL-3832, pp 100-6)
COBALT ALLOYS
properties for aerospace uses, 19: 47068
CONDOR, for reactor burnup and diffusion analyses, (T), 19: 47912
CHLOE, for analyzing spark-chamber photographs, (E), 19: 46793 (ANL-7050, pp 347-68)
description of PEPR system for particle track analysis in bubble-chamber
Ce–Co, crystal structure of Laves phases in, 19: 47052
Co–Dy, crystal structure of Laves phases in, 19: 47052
Co–Er, crystal structure of Laves phases in, 19: 47052
Co–Eu, crystal structure of Laves phases in, 19: 47052
Co–Gd, crystal structure of Laves phases in, 19: 47052
Co–Ho, crystal structure of Laves phases in, 19: 47052
Co–La, crystal structure of Laves phases in, 19: 47052
Co–Lu, crystal structure of Laves phases in, 19: 47052
Co–Nd, crystal structure of Laves phases in, 19: 47052
Co–Pr, crystal structure of Laves phases in, 19: 47052
Co–Sm, crystal structure of Laves phases in, 19: 47052
Co–Tb, crystal structure of Laves phases in, 19: 47052
Co–Tm, crystal structure of Laves phases in, 19: 47052
Co–Y, phase diagram, 19: 47053
Co–Yb, crystal structure of Laves phases in, 19: 47052
COBALT BORATES
crystal structure and magnetic properties, neutron diffraction studies of,

19: 46290
COBALT BORIDES
surface tension of molten, 19: 47021(T) (JPRS-31225)
COBALT COMPLEXES
radiation effects on, role of water of hydration in annealing, 19: 46387
radiation effects of neutron capture in nitrogen-containing, 19: 46386
COBALT(III) COMPLEXES
with 2,4-pentanedione, use in gamma dosimetry, 19: 46761 (NYO-2979-34)
COBALT ISOTOPES Co-57
orientation by Overhauser effect, Mössbauer spectroscopy for determining, (T), 19: 47615
use in vitamin B_{12} for radiodiagnosis, 19: 46128
COBALT ISOTOPES Co-58
beta decay of, β-γ circular polarization correlation in permitted transitions in, (E), 19: 47605
determination in irradiated steel by ion-exchange separation and gamma spectrometry, 19: 46195
tracer use of, for vitamin B_{12} metabolism, 19: 46083
COBALT ISOTOPES Co-59
neutron reactions (n,2n) at 12.6 to 19.6 Mev, excitation function for, (E/T), 19: 47571 (EUR-2456.e)
nuclear magnetic resonance in potassium cyanocobaltates (III), 19: 46285
COBALT ISOTOPES Co-60
determination in irradiated steel by ion-exchange separation and gamma spectrometry, 19: 46195
gamma rays from, attenuation by air, 19: 46586 (NP-15361)
performance as heat source for producing nuclear power, 19: 46893 (DP-974)
therapeutic use as applicator, for uterine carcinomas, 19: 46064
therapeutic use of wires of, for pectoral tumors, 19: 46047
uptake by tree branches, leaves, needles, roots, and stems from soil, 19: 45773
use for intercavitary therapy of uterine carcinomas, 19: 46039(T) (JPRS-31667)
use in transmission diagnostic radiography, 19: 46750 (AECL-2270)
COBALT NITRATES
ammine complexes of, radiation effects on, neutron, 19: 46391
COCKCROFT-WALTON ACCELERATORS
use as high-voltage source in 200-kev accelerator for generating 14-Mev neutrons, 19: 47176
COILS
magnetic flux degradation phenomena in superconducting, (E), 19: 47512
COINCIDENCE COUNTERS
design and performance for charged particles produced by 14-Mev neutrons, 19: 46821
design of two-dimensional selector, (E), 19: 47686
performance in reactor core meltdown analysis, 19: 47950(R) (ANL-7090, pp 69-78)
performance with on-line computers for analyzing nuclear events, (E), 19: 46806
use in standardization of isotopic radiation sources, 19: 46421
COINCIDENCE MEASUREMENTS
of platinum-199 decay, (E), 19: 47576(R) (IDO-17081, pp 49-76)
uses of, in activation analysis, 19: 46227
COLLAGEN
radiation effects on soluble and insoluble, gamma, 19: 45850
COLLIMATORS
design of, effects on measurements of low-energy gamma radiation using scintillation detector, 19: 46119
effectiveness in diagnostic radiology, 19: 46145
shape of, effects on depth-dose curves, 19: 46714 (CONF-640918-1)
COLUMBIA RIVER
radioactivity from chromium-51, niobium-95, zinc-65, and zirconium-95, 19: 46680
COMPUTER PROGRAMS
AIROS, for reactor dynamics analyses, (T), 19: 47914 (ANL-7050, pp 379-94)
AIRWICK, for analyzing spark-chamber photographs, (E), 19: 46793
AROMA, for analysis of spark-chamber photographs, FORTRAN, (E), 19: 46794
AROMA, for analyzing spark-chamber photographs, (E), 19: 46793
BISTRO, lifetime calculations on boiling-water reactors, FORTRAN 63 for CDC 3600, 19: 47913 (ANL-7050, pp 369-78)
BM FLS and XFLS, for crystallography, 19: 46461(R) (ORNL-3832, pp 116-50)
COOT, for energy released by fast-reactor accidents, 19: 47918 (ANL-7050, pp 503-14)
COREMAP, for ETR critical facility flux data, 19: 48060(R) (IDO-17081, pp 1-47)
photographs, (E), 19: 46810
DISC, for neutron inelastic scattering matrices, in FORTRAN, 19: 47544 (KAPL-M-6467)
EPITHET, for neutron absorption and spectra in cylindrical lattices, 19: 46917 (DP-975)
EQUIPOISE, for neutron diffusion and transport, 19: 47541 (ANL-7050, pp 179-89)
for analysis of bubble chamber photographs, 19: 46643(R) (LAL-1136)
for analysis of electron scattering, 19: 46643(R) (LAL-1136)
for analysis of human whole-body radioactivity data, IBM 1620, 19: 46658
for analysis of physiological data on man, IBM-409, 19: 45771
for anisotropic structure factor calculation and powder pattern generation, in FORTRAN II for IBM-IBSYS, 19: 47877 (LA-3335)
for buildup in sequential nuclear reactions, 19: 47584(R) (ORNL-3832, pp 1-28)
for calculation of multicomponent chemical equilibria, FORTRAN II for IBM 7090, 19: 46956 (NP-15514(Vol.1))
for collision-probability calculations of neutron transport in reactors, (T), 19: 47540 (ANL-7050, pp 93-112)
for critical control-element distributions in large boiling reactors, 19: 47917 (ANL-7050, pp 487-502)
for electrolyte activity and osmotic coefficients from isopiestic data, 19: 46237(R) (ORNL-3832, pp 76-99)
for neutron detector sensitivity calculations, in FORTRAN for CDC 1604, 19: 46759 (EGG-1183-1017)
for neutron resonance effects in matter, 19: 47542 (ANL-7050, pp 457-70)
for neutron transport calculations using Monte Carlo method, 19: 47545 (KFK-297)
for neutron transport calculations using Monte Carlo method, 19: 47546 (KFK-298)
for numerical integration of Schroedinger equation for square well potential, in FORTRAN for IBM 1620, 19: 47429
for personnel exposure in reactor maintenance, 19: 46905(R) (IDO-17081, pp 125-35)
for pulsed thermonuclear reactor energy balance and heat transfer, in FORTRAN II for IBM 7094, 19: 47720 (LA-3347)
for radiation effects on electronic equipment, 19: 46870(R) (AD-612191)
for roots of polynomial equations, 19: 46905(R) (IDO-17081, pp 125-35)
for shapes of single-energy gamma spectra, 19: 46905(R) (IDO-17081, pp 125-35)
for stereoscopic crystal-structure illustrations, 19: 46161(R) (ORNL-3832, pp 116-50)
FREAK, two-dimensional reactor kinetics analysis, (T), 19: 47947 (ANL-7050, pp 395-412)
GALAXY, for nuclear-data handling, (T), 19: 47911 (ANL-7050, pp 309-13)
GEM, Monte Carlo analysis of criticality, (T), 19: 47949 (ANL-7050, pp 657-79)
GOC, for cyclotron orbit analysis, in FORTRAN IV, 19: 47168 (TID-22177)
GRIND, for analyzing spark-chamber photographs, (E), 19: 46793
HAMMER, for automation of lattice codes, 19: 46917(R) (DP-975)
HAZE, for analysis of HPD data from bubble-chamber photographs, (E), 19: 46812
HEMP, anisotropic pseudo-viscosity expression for use in, (T), 19: 47119 (UCRL-14244)
MAFIA-II, one-dimensional burnup in reactors, (T), 19: 47910 (ANL-7050, pp 299-307)
MELE-1, for reactor burnup and diffusion analyses, (T), 19: 47912 (ANL-7050, pp 347-68)
MELE-2, for reactor burnup and diffusion analyses, (T), 19: 47912 (ANL-7050, pp 347-68)
MELE-3, for reactor burnup and diffusion analyses, (T), 19: 47912 (ANL-7050, pp 347-68)
MYRA, for calculating shipping costs of irradiated fuels, in FORTRAN on CDC-1604A or IBM-7090, 19: 46664
NAMDA, management control for product tester development, 19: 48098 (SC-R-65-902)
NEUROSES, for free-gas-theory calculations of thermal neutron spectra in lattices, (T), 19: 47538 (ANL-7050, pp 33-49)
PINETO, reactor dynamics analysis by solution of nonlinear differential equations, 19: 47916 (ANL-7050, pp 429-41)
POLARGRM, for analysis of polarograms, Fortran 63 for CDC 1604-A, 19: 46238 (ORNL-TM-1253)
PROTOS, for proton slowing down due to atomic collisions, in FORTRAN II for IBM 7090, 19: 47867 (NP-15384)
SCAT, for inelastic scattering cross sections for thermal neutrons by matter, 19: 47543 (ANL-7050, pp 471-85)
SIMS, for γ-law similarity solutions in one-dimensional hydrodynamics, for IBM 7094, 19: 47118 (UCRL-12018-T)
SOSH-5, for shielding calculations, for Philco 2000-2121, 19: 47866

(KAPL-M-6460)
SWANTIME, one-dimensional time-dependent neutron diffusion in reactors, (T), 19: 47915 (ANL-7050, 413-27)
TIMOC, for Monte Carlo calculations of reactor parameters, 19: 47919 (ANL-7050, pp 581-92)
TTA, for generalized rigid body trajectory calculations, for CDC 3600, 19: 48096 (SC-DR-65-271)
TURBO, for fuel depletion, 19: 48060(R) (IDO-17081, pp 1-47)
uses in reactor design analysis, 19: 47909 (ANL-7050, pp 217-30)
COMPUTERS
design for on-line analysis of radiation-detector data, (E), 19: 46792
design for use in startup of Toshiba Training Reactor, (E), 19: 48069
design of Lidian system for particle track analysis in bubble chamber photographs, (E), 19: 46801
design of PHYLIS, for on-line nuclear data processing, 19: 47115(R) (ANL-6983)
language for analog-digital conjunction, description of APACHE, 19: 46904 (EUR-2437.e)
performance for control of experimental devices, using microprogramming techniques, (E), 19: 46813
performance for micrometeorological data processing, 19: 47109 (RISO-99)
performance in semi-automatic bubble-chamber particle-track scanning systems, (E), 19: 46798
performance of analog, for parameter optimization, 19: 46903 (BNWL-70)
performance of IEP and SMP systems for particle-track analysis in bubble-chamber photographs, (E), 19: 46814
programming PEPR system for track analysis, (E), 19: 46813
radiation dose calculations using, 19: 46134
time-sharing systems for PDP 1, (E), 19: 46807
use for neutron logging theory calculations, 19: 46619
use in analysis of data from metabolic tracer studies, 19: 46055
use in analysis of data from tracer studies of blood circulation in lungs, 19: 46070
use in analysis of data on biological systems, 19: 45735
use in automation of mass spectrometers for isotopic analysis of reactor materials, 19: 46181 (WAPD-T-1769)
use in neutron spectra calculations for light-water lattices, 19: 47968
use in therapeutic radiation dose calculations, 19: 46055
use of IBM 7090 for molecular orbital calculations on phosphates, 19: 45808(R) (NYO-901-36)
use of, information transfer in, 19: 47336
use on-line in high energy counter experiments, 19: 46756 (BNL-9492)
uses for neutron-spectrum calculations in Doppler region, (T), 19: 47539 (ANL-7050, pp 51-76)
uses for nuclear-data handling, (T), 19: 47911 (ANL-7050, pp 309-13)
uses for processing reactor data, 19: 47948 (ANL-7050, pp 517-39)
uses for reactor calculations, conference, 19: 47907 (ANL-7050)
uses in pure mathematics, outline, 19: 46902 (ANL-7050, pp 207-13)
uses of Frankenstein and SMP on-line with bubble chambers, (E), 19: 46797
uses on-line for processing data from high-energy nuclear reactions, (E), 19: 46806
CONCRETES
gamma backscattering by, measurement of, (E), 19: 47869(T) (ORNL-tr-710)
gamma transport in slabs of, dose buildup factors for, (T), 19: 47864 (ANL-7050, pp 113-22)
use of prestressed, in pressure vessels for large power reactors, 19: 47925 (GA-6505)
CONES
electromagnetic wave scattering by, (T), 19: 47299(R) (AD-614046)
CONFERENCES
see also introduction to Report Number Index
Electrochemistry, First Australian Conference on Sydney and Hobart Feb. 1963, 19: 46291
Jülich Plasma Symposium, Innsbruck Univ., Austria, July 14, 1964, 19: 47715 (AD-613622)
Mechanisms of Solid Friction, Conference on, Kansas City, Mo., Sept. 16 to 18, 1963, 19: 47075
Metallography, Canoga Park, California, June 22 to 24, 1964, 19: 46936 (NMI-5025(Pt.I))
Radiation Preservation of Foods Program, Natick, Mass., Oct. 7–9, 1963, 19: 46876 (AD-613325)
Radioactive Isotopes in Medicine and Research, Munich-Berlin, 1965, 19: 46135
Seventeenth Metallographic Group Meeting, May 21-23, 1963, Los Alamos, New Mexico, 19: 46930 (NMI-4999)
Uranium and Minerals Symposium, Eighth Annual, Riverton, Wyoming, June 14 to 16, 1963, 19: 46629
X-Ray Analysis, Thirteenth Annual Conference on Applications of, Denver, Colorado, Aug. 12 to 14, 1965, 19: 46185
CONNECTIVE TISSUE
metabolic effects of diphenylhydantoin in, 19: 45895
radiation effects on, pathological, 19: 45935
CONVECTION
analysis of, for boiling inside channels, (E), 19: 46538(R) (TID-22148)
CONVECTION (FORCED)
boiling burnout in upward flow of Freon 12 through uniformly and non-uniformly heated tubes, 19: 46527 (AEEW-R-426)
boiling instability in flows through small tubes, subcooled, 19: 46534 (NP-15437)
CONVERSION ELECTRONS
energy spectra of platinum-199, (E), 19: 47576(R) (IDO-17081, pp 49-76)
CONVEYERS
design of, for subjecting objects to irradiation, 19: 46519(P)
COPPER
argon ion scattering at 30 kev, (E), 19: 47262
content and distribution in beef heart, 19: 45753 (AE-191)
copper atom ranges in crystal lattices of, at 10 kev, (T), 19: 47228
crystal defect formation and migration in, (T), 19: 47905
determination by potentiometric titration of acid liberated by complex formation, 19: 46205
determination in aluminum, activation, 19: 46207
determination in algae, neutron activation, 19: 45775
determination in aluminum alloys by activation, 19: 46157(R) (MLM-1254)
effects on ductility of beryllium, 19: 46909(R) (AD-620264)
electron emission from surfaces of, thermionic, 19: 46571 (HRL-5249-5)
electron reactions with crystals of, determination of interatomic potentials in, (T), 19: 47882 (RISO-103)
electron secondary emission from, after electron bombardment, 19: 47263
gamma incoherent scattering at 280 kev, cross sections for, (E), 19: 47624
ionization on rhenium and tungsten, effects of condensed layers and residual gases on, (T), 19: 47222(T) (ORNL-tr-679)
mechanical properties at cryogenic temperatures, 19: 47013 (PB-171809(Rev.)(Suppl.2))
neon ion scattering at 30 kev, (E), 19: 47262
neutron reactions (n,2n) at 14 Mev, use in fusion-reactor blankets, 19: 47721 (LA-3385)
photoelectron production by 145, 280 and 320 kev gamma rays, cross sections for, (T), 19: 47329
properties of porous, for use as isolation traps in vacuum systems, 19: 46573 (UCRL-12393-T)
radiation effects on catalytic effects of, on gaseous reactions, 19: 46329 (EUR-2455.e)
radiation effects on diffusion of nickel-63 in, alpha, 19: 47032
radiation effects on electric conductivity of, low-temperature recovery of neutron, (E), 19: 47097
radiation effects on, lattice atom displacement probabilities in deuteron and neutron, (T), 19: 47104
radiation effects on crystalline, microstrain from neutron, (E), 19: 47107
spectra of impurity ions of, in plasma streams, 19: 47757
surface tension of, measurement by pendant drop method, 19: 47065
COPPER ACETATES
molecular structure of hydrated, neutron diffraction studies of, 19: 46161(R) (ORNL-3832, pp 116-50)
COPPER ALLOYS
Al–Cu–Fe–Sn–Ti–V, additive and alloying effects on mechanical properties of, 19: 46985 (AD-613651)
Be–Cu, examination of swaged, 19: 46910(R) (AD-620589)
Be–Cu, mechanical properties of single crystals of, 19: 46909(R) (AD-620264)
Cu–Ni, stress corrosion cracking of Alloy 400 by wetted thermal insulation, 19: 46949 (CONF-650905-2)
COPPER CARBONATES
reactions with rare earth oxides, structure of AB_2O_4 type compounds in, 19: 46245(R) (TID-22207, Paper E)
COPPER ISOTOPES
proton elastic scattering at 14.5 Mev, cross sections for, 19: 47705
COPPER ISOTOPES Cu-63
alpha inelastic scattering at 44 Mev, collective states in, 19: 47608
alpha inelastic scattering by, excited states from, 19: 47608
neutron reactions (n,2n) at 12.6 to 19.6 Mev, excitation function for, (E/T), 19: 475.1 (EUR-2456.e)
proton scattering at 12 Mev, cross sections for, 19: 47585 (ORNL-3851)
COPPER ISOTOPES Cu-64
use in medical diagnostics, 19: 46136
COPPER ISOTOPES Cu-65
alpha inelastic scattering by, excited states from, 19: 47608
energy levels of, isobaric analog, 19: 47115(R) (ANL-6983)
neutron reactions (n,2n) at 14 Mev, cross sections for, (E), 19: 47673

neutron reactions (n,2n) at 12.6 to 19.6 Mev, excitation function for, (E/T), 19: 47571 (EUR-2456.e)

COPPER OXIDES
reactions with niobium and tantalum oxides, structure of ABO_3 type compounds formed in, 19: 46244(R) (TID-22207, Paper D)
thermodynamic properties of, at 500 to 1300°C, 19: 46297

COPPER SYSTEMS
Al–C–Cu–H–N–Sn–Ti–V–Zr, mechanical properties of, 19: 46985 (AD-613651)

CORTISONE
pathological effects in mice of, effects of age, 19: 45808(R) (NYO-901-36)

COSMIC MESONS (π)
interactions in jet showers, secondary angular distribution and momenta for primary energy of, (T), 19: 47275

COSMIC NEUTRONS
book: *Geophysics and Space Data Bulletin No. 3*, 19: 47447 (AD-612083)
detection by emulsions, identification of stars in, (E), 19: 46767 (TID-22256)
intensity variations in 1963, latitude effect in, 19: 47272
spectra in atmosphere, 19: 47279

COSMIC NUCLEONS
intensity variations in 1963, latitude effect in, 19: 47272

COSMIC PARTICLES
charge spectra of nuclei in primary, (E), 19: 47277
effects on man in space flight, 19: 46000
energy spectra and identities of strongly interacting, in air shower cores, (E), 19: 47271
flux intensity ratios of multiply charged primary nuclei in, (E), 19: 47277
motion in geomagnetic fields, determination of arrival direction from, (T), 19: 47269
reactions with graphite, fragmentation parameters and mean free path for, 19: 47276

COSMIC PROTONS
detection by emulsions, identification of stars in, (E), 19: 46767 (TID-22256)
interactions in jet showers, secondary angular distribution and momenta for primary energy of, (T), 19: 47275

COSMIC RADIATION
detection and measurement of, design of high-resolution resonance counter for, 19: 46838
effects on electric materials and components in space vehicles, 19: 46875
effects on man in space flight, 19: 46000
energy spectra of nuclei ($Z \geq 6$), (E), 19: 47270
geomagnetic cut-off rigidity of, 19: 47278
intensity during solar eclipse, (E), 19: 47451 (SC-M-65-419)
intensity variations on moon, 19: 47273
intensity variations of, sidereal daily, 19: 47274

COSMIC SHOWERS
electron and photon angular and lateral distributions in photon-initiated, (T), 19: 47268 (INSJ-86)
energy of jet, from secondary angular distributions and momenta, (T), 19: 47275
particle energies and identities in cores of air, strongly interacting, (E), 19: 47271

COSMOLOGY
models in, spherically symmetric, 19: 47212
models of universe, structured, 19: 47205
quantum effects in singular state of, 19: 47203
review, 19: 47209
theory of antimatter and development of metagalaxy in, (T), 19: 47206

COTTON
radiosterilization of bacteriological swabs, 19: 46884

CRATERS
ejecta and dust from Danny Boy, mass distribution measurements of, 19: 46469 (POR-1815)
formation by nuclear explosions, bibliography on, 19: 46466 (CEA-Bib-63)
formation by parallel rows of TNT charges, 19: 46470 (SC-RR-303)
throwout from Danny Boy, measurements of, 19: 46468 (POR-1814)

CREATINE
radiation effects on human and mouse excretion of, use as damage indication, 19: 45864

o-CRESOL
effects on radioinduced chemiluminescence in organic compounds in presence of oxygen, 19: 46344

CRISTOBALITES
radiolysis of surface silanols on, effects of dose, impurities, and surface area on, 19: 46332(R) (ORNL-3832, pp 50-65)

CRITICAL ASSEMBLIES
criticality studies of ZPR-6 and -9, 19: 47989(R) (ANL-7090, pp 1-29)
criticality studies in PWR core, 19: 48000(R) (WCAP-3738)
criticality studies on plutonium, 19: 47967
design and operation at Harwell, 19: 48115
development of ZPPR, 19: 47989(R) (ANL-7090, pp 1-29)
fuel core fabrication for Super Kukla, safety in, 19: 46967 (Y-KB-62)
neutron resonance effects in, 19: 47542 (ANL-7050, pp 457-70)
operation and safety analysis of split-table, dry, (E), 19: 47958 (PWAC-475)
physics calculations on, for LOFT and PBF design, 19: 46905(R) (IDO-17081, pp 125-35)
physics of light-water-, heavy-water-, and graphite-moderated, in Japan, 19: 47965
power calibration of ATR, 19: 48060(R) (IDO-17081, pp 1-47)
reactivity at ATR quarter-core mock-up, 19: 48060(R) (IDO-17081, pp 1-47)
reactivity of heavy-water-moderated natural uranium, temperature coefficients of, 19: 46917(R) (DP-975)
safety of VERA, computer analysis of, 19: 47918 (ANL-7050, pp 503-14)
use in reactor design, 19: 47961
uses of Harmonie and Masurca, for fast-reactor studies, 19: 47997(R) (NP-15478)

CRITICALITY STUDIES
maximum safe limits of slightly enriched uranium and uranium oxide in water, 19: 47955 (CONF-651103-6)
methods of, review of Japanese, 19: 47965
Monte Carlo methods in, 19: 47949 (ANL-7050, pp 657-79)
of uranium–water and uranium dioxide–water lattices, method for analyzing, 19: 47959 (WCAP-3269-52)
reactivity worths of cadmium–indium–silver rods in tungsten–uranium lattices, 19: 48001(R) (WCAP-3743)

CROSS SECTIONS
measurement of differential, criteria for polynomial distributions with minimum uncertainty for, (T), 19: 47601

CRUSTACEA
oxygen-18 content of orthophosphate from shells of living, 19: 46583

CRYOSTATS
design of low-temperature, for Mössbauer experiments, 19: 46748

CRYSTAL STRUCTURE
analysis by neutron scattering, 19: 47889
electron and lattice vibration correlations in, problems in, 19: 47875 (AD-614136)
research programs on, at Harwell, 19: 48115

CRYSTALLOGRAPHY
methods of, for studies of irradiated fissile materials and plutonium, 19: 46202
neutron diffraction determination of α-monodeuteroglycolate configuration, 19: 46161(R) (ORNL-3832, pp 116-50)

CRYSTALS
free energy of, nearest-neighbor approximation of quartic contributions to, (T), 19: 47878 (LA-3379)
lattice dynamic interactions with defect stress fields in, local mode, (T), 19: 47905
light frequency modulation by electrically birefringent, 19: 48110(T) (SC-T-65-750)
neutron multiple Bragg reflection in large mosaic, (T), 19: 47562
neutron time-decay constants in, upper bounds for pulsed, (T), 19: 47553

CUMENE
radioinduced chemiluminescence of, in presence of oxygen, 19: 46344

CUPFERRON COMPLEXES
with zirconyl, radiation effects on, 19: 46761 (NYO-2979-34)

CURIUM
separation from aqueous chloride solutions by solvent extraction using di-n-octyl phosphinic acid, tracer studies of, 19: 46443

CURIUM ISOTOPES Cm-244
separation in Curium Recovery Facility, 19: 46428(R) (ORNL-3847)

CURRENT REGULATORS
design of constant-current, 19: 46157(R) (MLM-1254)

CUTTING TOOLS
design for removing chemonuclear loop from BGRR, 19: 48055 (BNL-9402)

CYANIDES
aroyl, photolytic products of, 19: 46304(R) (ORNL-3832, pp 66-75)

CYANOGEN
yields in radiolysis of methane–nitrogen systems in fissiochemical loop, 19: 46324(R) (AGN-8132)

CYBERNETICS
principles of control processes, 19: 46460 (CONF-640508, pp 224-32)

CYCLOALKANES
radiolysis of, at −196°C, ESR of free radicals produced in, 19: 46372

CYCLOBUTANE
yields from photolysis and radiolysis of cyclopentanone, 19: 46357

1,1-CYCLOBUTANEDICARBOXYLIC ACID, DIMETHYL ESTER

nuclear magnetic resonance spectra of, analysis, 19: 46247 (UCRL-16349)
CYCLOHEPTANE
radiolysis of, at −196°C, ESR of free radicals produced in, 19: 46372
CYCLOHEXANE
cyclohexane-d_{12}–cyclopentane, radiolysis of, yields dimers and olefins from, 19: 46364
effects on metal extraction by tridodecylamine in presence of hydrohalic or thiocyanic acid, 19: 46180 (UCRL-16254)
radioinduced chemiluminescence of, in presence of oxygen, 19: 46344
radiolysis of, at −196°C, ESR of free radicals produced in, 19: 46372
solvent properties for technetium, 19: 46160(R) (ORNL-3832, pp 29-32)
yields of deuterated (d_{10}), in irradiation of cyclohexane-d_{12}–cyclopentane mixtures, 19: 46364
cyclohexane–I, charge-transfer complexes in pulse radiolysis of, 19: 46384
cyclohexane–HI, charge-transfer complexes in pulse radiolysis of, 19: 46384
2-CYCLOHEXEN-1-ONE, 3,5,5-TRIMETHYL-
photodimerization mechanisms of, 19: 46304(R) (ORNL-3832, pp 66-75)
CYCLOOCTANE
radiolysis of, at −196°C, ESR of free radicals produced in, 19: 46372
CYCLOPENTANE
cyclohexane-d_{12}–cyclopentane, radiolysis of, yields dimers and olefins from, 19: 46364
radiolysis of, at −196°C, ESR of free radicals produced in, 19: 46372
CYCLOPENTANONE
photolysis and radiolysis of liquid, yields of 4-pentenal from, 19: 46357
photolysis of liquid, role of triplet excited state in, 19: 46357
CYCLOPENTENE
yields from radiolysis of cyclohexane-d_{12}–cyclopentane, 19: 46364
CYCLOPROPANE
yields in radiolysis of ethylene–methane–nitric oxide, 19: 46324(R) (AGN-8132)
CYCLOTRON RADIATION
emission from plasma in thermonuclear reactor, (T), 19: 47815
CYCLOTRONS
beam energy spectra from four-sector racetrack microtron, (E), 19: 47174
beam extraction from, properties of magnets for, 19: 47166 (ORNL-P-1605)
beam orbit analysis of, computer program for, 19: 47168 (TID-22177)
design and operation of variable, at Harwell, 19: 48115
design of 30-Mev microtron-injector, for pulsed fast reactors, 19: 47164 (JINR-P-2313)
magnets for 50-Mev separated-orbit, development of, 19: 47167 (ORNL-P-1619)
CYLINDERS
electromagnetic wave scattering by, (T), 19: 47299(R) (AD-614046)
magnetic flux compression in hollow explosive-driven conducting, (T), 19: 47120 (UCRL-14349)
CYSTEINE
complexes with sodium thiosulfate, protective effects against radiation injuries in mice, 19: 46006
effects of bactericidal activity of irradiated *p*-bromophenol, 19: 45834
effects on bactericidal activity in irradiated *p*-bromophenol, 19: 46007
radiosensitivity effects on mouse bone marrow, 19: 46028
CYTOLOGY
radiation effects on, dosimetry for, 19: 45999
CZECHOSLOVAKIA
fallout monitoring in atmosphere in Pizen, 1957–1962, 19: 46687

D

DATA RECORDING SYSTEMS
design for chemical cell interrogation, 19: 46716(R) (IDO-17081, pp 77-123)
design of automatic isodose contour, for radiation dosimetry, 19: 46776
development of on-line, 19: 46766(R) (TID-22141, pp 67-79)
use in nuclear materials management at AECL, 19: 47906 (AECL-2282)
DATA TABULATIONS
alpha, neutron, proton, and triton energy distributions from deuterium (d,n) and (d,p) and tritium (d,n) reactions, 19: 47568 (CEA-R-2779)
book: *Air Tables*, 19: 47151
gamma energies and intensities from fission products, 19: 47598 (USNRDL-TR-876)
geomagnetic pulsation and solar H region parameters for 1959 to 1964, 19: 47454
lithium fluoride properties as dosimetric materials, 19: 46338 (UCRL-12367)
mechanical properties of materials at cryogenic temperatures, 19: 47013 (PB-171809(Rev.)(Suppl.2))
neutron effective cross section factors, 19: 47577 (IDO-17107)
neutron levels in nuclei, 19: 47583 (NP-15467)
neutron transport in aluminum, carbon, and polyethylene slabs, 19: 47868 (RRA-T52)
nuclear magnetic dipole moments, (T), 19: 47606
nuclear quadrupole moments and isotopic shifts of near-spherical nuclei, 19: 47573 (IAE-717)
on management of civilian defense systems, 19: 46636 (AD-611765)
proton scattering cross sections for copper-63, nickel-62, and zinc-64 at 12 Mev, 19: 47585 (ORNL-3851)
sensitivities in activation analysis, 19: 46167 (EUR-1898.e)
thermodynamic properties of helium at 2,000 to 100,000°K, 19: 46235 (N64-26802)
DECAY SCHEMES
equations for radioisotopes, analysis of, (T), 19: 47599(T) (ORNL-tr-707)
DECONTAMINATION
method for vegetable, leaching, 19: 45758 (NYO-2598-24)
methods for agricultural land, 19: 46701
methods for, of surfaces in gaseous and liquid environments, 19: 46645 (ORNL-TM-1228)
process for radioactive water, foam, 19: 46429 (ORNL-P-1522)
DEER
cesium-137 content in, Finland, 1964, 19: 46587(R) (NYO-3446-3)
DEHYDROGENASES
radiation effects on, in human melanoma ascites, serum, and tumor homogenates, 19: 46124
radiation effects on activity of lactic, in mouse blood plasma, 19: 45844
DENMARK
nuclear power development in, 19: 48004
DENSITY
measurement of, using gamma sources, 19: 46892(P)
DETERGENTS
effects on waste processing by coagulation precipitation method, 19: 48084
DEUTERIUM
content in rainfall, North Carolina and Virginia, Nov. 1 and 2, 1963, 19: 47112
density profile of plasma of, method for determining, (E), 19: 47727 (NP-15434)
determination by gas chromatography, methods for, 19: 46183(T) (NP-tr-1289)
determination in hydrogen, thermal conductivity method for, 19: 46182 (NP-tr-1375)
deuteron reactions (d,n) and (d,p) at 10 to 150 kev, alpha, neutron, and proton energies from, 19: 47568 (CEA-R-2779)
diffusion and permeation in niobium stainless steel S110, oxygen effects on, 19: 46991 (AWRE-O-47/65)
effects on decomposition of permanganates in alkaline solutions, 19: 46275
effects on radiolysis of cyclohexane–cyclopentane mixtures, 19: 46364
electric current interruptions in thyratron gases of, (E), 19: 47128
exchange with hydroxyl groups on surface of alumina, 19: 46280
incorporation in dodecanes and undecanes, 19: 46308
incorporation in naphthalene, 19: 46307
incorporation into organic compounds of, by microbial processes, 19: 46409
isotope effects on oxidation of 1,2-diphenylethylene glycol, 19: 46304(R) (ORNL-3832, pp 66-75)
plasma production in, in coaxial-electrode discharge, (E), 19: 47843
production of, methods for, 19: 46413
radiation from molecular, stimulated near-infrared, (E/T), 19: 47260
scattering by helium, cross sections for elastic, 19: 46161(R) (ORNL-3832, pp 116-50)
used in coronary blood circulation measurement in relation to ischemic myocardium in dogs, 19: 45767
DEUTERIUM HYDRIDES
determination by gas chromatography, methods for, 19: 46183(T) (NP-tr-1289)
production of ions of, in electron-bombardment sources, (T), 19: 47141
yields in radiolysis of ammonia–deuterium, 19: 46324(R) (AGN-8132)
DEUTERIUM IONS
charge in cadmium vapor, average, (E), 19: 47266
production by vacuum spark source, 19: 47147
production of negative, source for, 19: 47157 (AWRE-NR-1/65)
DEUTERIUM SYSTEMS
D–H, radiation for molecular, stimulated near-infrared, (E/T), 19: 47260
NH_3–D, radiolysis yields in, 19: 46324(R) (AGN-8132)
DEUTERON BEAMS
reactions with deuterium plasma, density profile determination by, (E), 19: 47727 (NP-15434)
DEUTERONS
angular distributions from (n,d) reactions at 14 Mev, (E/T), 19: 47644

biological effects in rabbit brain, 19: 45874
effects on lattice atom displacement probabilities in copper, gold, iron, and silver, (T), 19: 47104
emission from excited emulsion nuclei, (E), 19: 47651
interactions with mesons (K⁻) at rest, Σ-Λ conversion in, (T), 19: 47358
interactions with electrons, relativistic corrections for, (T), 19: 47410
interactions with mesons (K⁻) at rest, hyperfragment (Σ⁻n) production in, (T), 19: 47339
reactions (d,α) with calcium-48 at 12 Mev, potassium-46 production in, 19: 47115(R) (ANL-6983)
reactions (d,α) on fluorine-19 at 0.95 to 1.25 Mev, angular distributions from, (E/T), 19: 47646
reactions (d,α) with magnesium-25 at 1.5 to 2.5 Mev, differential cross section fluctuations in, (T), 19: 47659
reactions (d,α) with sodium-23 at 4.9 to 5.5 Mev, neon-21 excited states from, (E), 19: 47633
reactions (d,He-3) with nuclei, residual nucleon interactions in, 19: 47115(R) (ANL-6983)
reactions (d,n) with iron-54, neutron spectra from, 19: 47115(R) (ANL-6983)
reactions (d,n) with lithium-7, neutron yields from, (E), 19: 46817
reactions (d,n) with tritium, level structure from, (T), 19: 47687
reactions (d,n) with deuterium and tritium at 10 to 15 kev, alpha and neutron energies from, 19: 47568 (CEA-R-2779)
reactions (d,p) with nuclei, coherent knockout amplitudes in, (T), 19: 47669
reactions (d,p) with helium-3 level structure from, (T), 19: 47687
reactions (d,p) with helium-3, proton polarization in, 19: 47709
reactions (d,p) with deuterium at 10 to 150 kev, proton and triton energies from, 19: 47568 (CEA-R-2779)
reactions (d,p) with boron-11, carbon-12, and nitrogen-14, at 1.3 to 5.5 Mev excited states from, (E), 19: 47604
reactions (d,p) with boron-11 and oxygen-16, (E), 19: 47609
reactions (d,p) with nuclei, equation for matrix element of, 19: 47630
reactions (d,p) with nuclei, impulse approximation for calculating, 19: 47631
reactions (d,p) with neon-20 at 1.8 and 2.2 Mev, neon-21 energy levels from, (E), 19: 47632
reactions (d,2n) with plutonium-242 at 7 to 12 Mev, excitation function and yield ratio for fissioning isomer from, (E), 19: 47688
reactions with beryllium-9 and lithium-6 and -7, energy levels and mechanisms of, 19: 47564(R) (AD-612038)
scattering by cadmium-114 and nickel-60 at 10 to 15 Mev, differential cross sections for inelastic, (E/T), 19: 47635
scattering by helium-4 at 2 to 9 Mev, tensor polarization in elastic, 19: 47704
scattering by selenium and zinc at 15 Mev, energy levels from inelastic, (E), 19: 47642
wave functions for, four-dimensional, (T), 19: 47376

DIAMONDS
phonon dispersion curves of, charged bond correction for, 19: 47879 (LA-DC-7277)

DIDO REACTORS
design and operation, 19: 48115

DIELECTRIC BREAKDOWN
statistics of, using nanosecond pulse techniques, 19: 47114 (AD-614286)
vacuum breakdown in presence of thermionic cathodes, 19: 46577

DIELECTRICS
properties for aerospace uses, 19: 47068

DIES
design for extruding tubes, 19: 46979(P)

DIET
effects of inorganic composition of cattle, on adsorption of organic nutrients, 19: 45760(R) (ORO-631, pp 83-121)
effects on cesium-137 metabolism by cattle, 19: 45780
radiosensitivity effects in *Pseudomonas aeruginosa*, effects of oxygen concentration on, 19: 46014
strontium-90 content of Australian, 1963, 19: 46594

DIFFERENTIAL EQUATIONS
solution of sets of nonlinear first-order, code for, 19: 47916 (ANL-7050, pp 429-41)
solutions for triple impulse asymptotic paths, (T), 19: 48109(T) (SC-T-65-749)
solutions of three-species, for atmospheric ionization in high-altitude explosions, (T), 19: 47449 (AD-613199)

DILATOMETERS
design for radiochemistry, 19: 46419

DIMETHYLAMINE
NH_2–dimethylamine, radiolysis yields in, 19: 46324(R) (AGN-8132)

DIODES
development of in-pile thermionic, using liquid-metal electron collectors, 19: 47281 (ANL-7039)
performance of semiconductor, as photomultiplier-tube anode, (E), 19: 46815
performance of tunnel, with time-amplitude converter, 19: 46736
use of tunnel, in fast switching circuits, 19: 46717 (INSJ-87)
vacuum breakdown in, with nickel electrodes, 19: 46577

DIOXANE
benzene–dioxane, radiolysis and luminescence behavior, 19: 46363

DIPHENYLAMINE, 2,2',4,4',6,6'-HEXANITRO-
solvent properties for cesium, 19: 46442

DIRECT ENERGY CONVERSION DEVICES
development for ionizing energy conversion, (E), 19: 47283(T) (BNL-tr-8)
development of, review of, 19: 47286

DISEASES
radiodiagnosis of kidney, using labeled compounds and external scanning, 19: 46130
therapy of aviation tympanitis, use of strontium-90 in, 19: 46038(T) (JPRS-31602, pp 101-7)

DISTRICT OF COLUMBIA
gamma aeroradioactivity at 500 ft over, mapping of, 19: 46614

DISULFIDES
bis(dimethylthiocarbamoyl)-, use as radical scavenger reagent to minimize radiation effects on TBP, 19: 46406(P)
synthesis of, for use as radioprotective agents, 19: 46303(R) (NP-15409)

DITHIZONE
chelation of cesium-134 by, 19: 45765(T) (JPRS-27544, pp 1-12)
derivatives of, effects on elimination of cesium-134 from rabbits and rats, 19: 45765(T) (JPRS-27544, pp 1-12)

DODECANE
labeling with deuterium, 19: 46308

DOGS
blood circulation in relation to ischemic myocardium in heart of, tracer studies, 19: 45767
metabolism of bismuth-212, lead-212, and radium-224 in, from thorium-228 decay, 19: 45798
radiation effects on 4-aminobutyric acid content of brain, 19: 45979
radiation effects on heart of, pathological, 19: 45835
radiation effects on calcium metabolism in, electron, 19: 45729(R) (NYO-910-23, pp 1-111)
thorium-228 decay and metabolism in bones, kidneys, liver, and spleen in, 19: 45798
toxic effects of niobium pentachloride and potassium niobate on, 19: 45768

DOSIMETERS
book: *Radiation Dosimetry*, 19: 46840
design and performance for neutrons and heavy particles, 19: 46847
design and performance of calorimetric, 19: 46848
design and performance of local absorbed dose calorimeter, 19: 46849
design and performance of Fricke ferrous sulfate system, 19: 46849
design and performance for clinical use, 19: 46854
design for contour equivalents in radiotherapy, 19: 46041
design of scintillation color scanner, 19: 46819
development of chromium and cobalt acetylacetonate systems as gamma, 19: 46761 (NYO-2979-34)
development of, review of, 19: 46841
filter size for film badges, 19: 46764 (SZS-6(1965))
performance in environmental dose measurements, 19: 46855
performance of calcium and lithium fluorides thermoluminescent and phosphate glass, 19: 46859
performance of chemical, 19: 46852
performance of ionization chamber, 19: 46844
performance of nitrous oxide, at low dose rates, 19: 46332(R) (ORNL-3832, pp 50-65)
performance of photographic, 19: 46853
performance of scintillator-photomultiplier systems, 19: 46851
performance of solid state, 19: 46850
performance of spherical tissue-equivalent proportional counter, 19: 46846
response of beta, angular, 19: 46639 (AECL-2281)
use for radioisotopes in bones, 19: 46154
use in radiobiology, 19: 45999

DROSOPHILA
mutagenesis in 2nd chromosomes of, effects of DNA-feeding on, 19: 45876
radiation effects on genetic loads and inbreeding in populations of, 19: 45952
radiation effects on suppressor genes in, x, 19: 45968
radioinduced lethal chromosomes in *D. willistoni*, nature of, 19: 45877
radioinduced mutations of, 19: 45949
radioinduced mutations in, x, 19: 45876
radioinduced mutations in region of X chromosome in *D. melanogaster*

DNA, 19: 45879
DRUGS
effects of Actinomycin D combined with radiotherapy on sarcomas in mice, histology of, 19: 46123
effects of cytostatic, on immune response to transplanted kidneys in man, 19: 45888
effects of goitrogenic, on pituitary hormones in mice, 19: 45808(R) (NYO-901-36)
use in treatment of polycythemia vera, comparison of phosphorus-32 therapy with, 19: 46089
DUSTS
pathological effects of inhaled gadolinium oxide, in guinea pig lungs, 19: 45756 (COO-1170-7)
DYSPROSIUM
cohesive energy and ionization of, relation between, (T), 19: 47062
luminescence in zinc borate glass, 19: 46269
neutron cross sections of, shell effects on thermal, (E), 19: 47618
DYSPROSIUM ALLOYS
Al–Dy, crystal structure of Laves phases in, 19: 47052
Co–Dy, crystal structure of Laves phases in, 19: 47052
Dy–Mn, phase studies by differential thermal, thermo-magnetical, and x-ray analysis of, 19: 46989 (AD-614466)
Dy–Mn, preparation by sinter process using mercury, 19: 46908 (AD-614464)
Dy–Pd, phase studies, 19: 47051
DYSPROSIUM BROMIDES
thermal decomposition of hydrates of, mechanisms of, 19: 46271
DYSPROSIUM FERRATES(III)
crystal structure, 19: 46256
DYSPROSIUM IONS
spectra in silicate glass, fluorescence, 19: 47886(T) (N64-21857, pp 1-6)
DYSPROSIUM ISOTOPES Dy^{160}
internal conversion coefficients for E2 transitions in, nuclear structure effects on, (T), 19: 47620
DYSPROSIUM OXIDES
atomic charge and permittivity of, (E/T), 19: 47901(T)
oxygen-18 exchange between molecular oxygen and, 19: 46266
reactions with barium carbonates, ternary oxide formation in, 19: 46242(R) (TID-22207, Paper B)

E

EARTH
radius increase of, model for, (T), 19: 47483
ECHINODERMS
radioisotope content of western Mediterranean, 1962, 19: 46611
ECOLOGY
of plants of Southeastern granite outcrops, 19: 45752
EGGS
radiosensitivity of silkworm, *Bombyx mori*, 19: 45904
ELECTRIC ARC FURNACES
design of stagnation-flow, for high temperature gas-solid reaction rate measurement, 19: 46956 (NP-15514(Vol.1))
ELECTRIC ARCS
electrode erosion in, neutron-activated zinc, 19: 47134
plasma production in argon and krypton, 19: 47788
plasma production in high-pressure argon, by pulse heating, (E), 19: 47789
plasma production in high-pressure argon, by pulse heating, (E), 19: 47790
ELECTRIC CELLS
design for emf measurements in molten metal-salt solutions, 19: 47010(R) (ORNL-3832, pp 107-50)
ELECTRIC CHARGES
radiation theory for point, (T), 19: 47431
ELECTRIC CONDENSERS
charging of problems associated with pulsed, 19: 46719 (LA-DC-7030)
charging of, control system for, 19: 46718 (LA-DC-7015)
electric discharges in, high-current, plasma production by, 19: 47792
ELECTRIC CONDUCTIVITY
electron interaction effects in dilute alloys, s-d, (T), 19: 47897
ELECTRIC CURRENTS
photon emission from, (T), 19: 47135
ELECTRIC DISCHARGE
diffusion and oscillations of positive-column, in magnetic fields, 19: 47756
diffusion-controlled sorption in high-density, 19: 46576
hydromagnetic wave propagation in toroidal, with longitudinal magnetic field, (E), 19: 47742
ignition mechanism in crossed electric and magnetic fields, 19: 46741
in air, spark channel formation by, 19: 47146
in air, transition from corona to spark, 19: 47791
in argon and krypton, plasmoid production by h-f, (E), 19: 47788
in argon, electrode surface characteristics from vacuum breakdown by, (E), 19: 47149
in electric condensers, plasma production by, 19: 47792
magnet field effects on gaseous Townsend, (T), 19: 47127
plasma excitation in r-f, in longitudinal magnetic field, 19: 47778
plasma production by, 19: 47831
production by electron-beam–plasma interactions, (E), 19: 47836
properties of electronic-ionic oscillatory, 19: 46742
stability of penning, effect of magnetic field on, (E), 19: 47780
vacuum breakdown in presence of thermionic cathodes, 19: 46577
ELECTRIC FIELDS
effects of dynamo-, on geomagnetically trapped electrons, (T), 19: 47453
effects on electron and ion emission by electrodes in cesium ion engines, 19: 46571 (HRL-5249-S)
measurement in atmosphere, use of radioactive collectors for, 19: 46730(T) (SC-T-65-760)
plasma acceleration by, (E/T), 19: 47714(R) (AD-613307)
ELECTRIC GENERATORS
analysis of nuclear Brayton-cycle, for space vehicles, 19: 48048 (GE-65SD4251)
design of three-decade exponential, for testing reactor period meters, 19: 47928
development of MHD, for power generation, 19: 47285
ELECTRIC POTENTIAL
measurement of, design of all-metal cell for, 19: 46270
ELECTRIC POWER
generation by magnetohydrodynamics, developments in, 19: 47285
generation of, effects of magnetohydrodynamic generators on plant design for, 19: 48013
storage using relay switch connection to superconducting solenoid, 19: 46475 (AD-612113)
ELECTRIC PROBES
performance for plasma diagnostics, 19: 47817
performance of Langmuir, for ionospheric electron density measurements, (E), 19: 47465
use of scanning microprobe analyzer for materials research, description of, 19: 46508 (NMI-4998, pp 65-76)
ELECTRICITY
detection of atmospheric static, warning system for, 19: 48094 (SC-DC-65-1646)
production by ionizing energy conversion, (E), 19: 47283(T) (BNL-tr-9)
ELECTROCHEMISTRY
conference on, Sydney and Hobart, Australia, Feb. 1963, 19: 46291
ELECTRODES
charging of double layer, theory of galvanostatic and potentiostatic, 19: 46957(R) (ORNL-3832(p.100-6)
electron emission by, factors influencing, 19: 47114 (AD-614286)
electron emission from vacuum breakdown, post-, (E), 19: 47149
erosion of neutron-activated zinc, in spark discharge, 19: 47134
polarization of porous and tubular, 19: 46957(R) (ORNL-3832, pp 100-6)
response of cation-sensitive glass, 19: 46237(R) (ORNL-3832, pp 76-99)
sorption of iodides on porous carbon, double-layer capacity for, 19: 46957(R) (ORNL-3832, pp 100-6)
ELECTROLUMINESCENCE
radiation effects on, gamma, uv, and x, 19: 46341(T) (FTD-TT-65-24)
ELECTROLYTIC CELLS
design of all-metal for measuring EMF of molten metal-metal halide solutions, 19: 46270
development of, for high-speed controlled potential coulometry, 19: 46188
performance as resistors in plasma research, 19: 47751
ELECTROLYTIC SEPARATION PROCESSES
uses in activation analysis, 19: 46229
ELECTROMAGNETIC FIELDS
charged-particle gyrations in, nonrelativistic, (T), 19: 47807
charged-particle motion in, relativistic, (T), 19: 47435
ion motion in, (T), 19: 47464
plasma acceleration and heating by, (E/T), 19: 46477 (ARL-65-121)
ELECTROMAGNETIC LENSES
electron focusing in coil, 19: 47185
ion optics in, image components in, 19: 46738
ELECTROMAGNETIC WAVES
emission by current filaments in plasma, (T), 19: 47774
interactions in plasma near electron gyrofrequency, coupling, 19: 47744
interactions with plasma, amplification in, (E/T), 19: 47219 (AD-614253)
interactions with free plasma boundary, use of screen cathode for obtaining, 19: 47734
oscillations and propagation in relativistic quantized electron-positron

gas, (T), 19: 47771
propagation from high-altitude explosions, series solutions for atmospheric ionization in, (T), 19: 47449 (AD-613199)
propagation in anisotropic plasma along static magnetic field, (E/T), 19: 47718 (AD-614442)
propagation in dielectric-layer circular waveguides, (T), 19: 46743
propagation in ionosphere, ion effects on, 19: 47445 (AD-611828)
scattering by regular bodies, (T), 19: 47299(R) (AD-614046)

ELECTROMETERS
design for radiographic dosimetry, 19: 46043
design of digitized, for pico- to microampere range, (E), 19: 46816
use in energy independent ionization chamber for diagnostic radiology dosimetry, 19: 46861

ELECTRON BEAMS
attenuation of high energy, 19: 45729(R) (NYO-910-23, pp 1-111)
effects of 1.5-Mev, on low-temperature color centers in lead-doped and pure potassium chlorides, (E), 19: 47891
effects on calcium metabolism in dogs, 19: 45729(R) (NYO-910-23, pp 1-111)
effects on cyclohexane–iodine systems, 19: 46384
effects on ethylene, 19: 46361
effects on germanium and silicon, (E), 19: 47092(R) (TID-22141)
effects on methane, yields of acetylene from, 19: 46366
effects on mouse skin, effects of dose-fractionation on, 19: 45885
effects on pure and doped iron, point defects produced by, 19: 47094(T) (ORNL-tr-668)
effects on rabbit tibia, time factors for, 19: 45989
energy absorption traversing a Cuccia coupler, negative, (T), 19: 47130
energy losses in gases, method for measuring small, 19: 47252
energy spectra of, in four-sector racetrack microtron, (E), 19: 47174
interactions with plasma, electric discharge from, (E), 19: 47836
interactions with plasma, ionization from, (E), 19: 47852
radiation dose from therapeutic, effects of collimator shape on depth-, 19: 46714 (CONF-640916-1)
reactions with hydrogen at 900 ev, plasma production by, (E/T), 19: 47787
reactions with mercury plasma, diagnostics by nonperturbing probe, (E), 19: 47740
scattering from aluminum, iron, lead, tin and uranium targets at 4 to 14 Mev, effects of back-, (E), 19: 47181
therapeutic use, 19: 46078
use for preionization in high temperature MHD generators, 19: 47289
use of betatron, therapeutic, 19: 46126

ELECTRON MICROSCOPY
development at Grenoble Nuclear Center, 19: 46512
isotope tracing in, using nuclear reactions, 19: 45741
sample preparation for transmission, uranium, 19: 46933 (NMI-4999, pp 78-84)
sample preparation of irradiated A-286 alloy, 19: 47088 (NMI-4998, pp 95-106)
sample preparation in hot cell, one-step replication, 19: 47090 (NMI-4999, pp 54-9)
sample preparation for irradiated materials, 19: 47089 (NMI-4999, pp 30-50)
uses for microstructural studies of cast uranium, 19: 47007 (NMI-5025 (Pt.I), pp 127-51)

ELECTRON PAIRS
production in baryon and meson decay, U(12) symmetry for, (T), 19: 47308 (JINR-P-2284)

ELECTRON SHOWERS
detection and measurement at 0.5 to 8 Bev, spark-chamber efficiency for, 19: 47354

ELECTRON TUBES
current interruption in hydrogen and deuterium, (E), 19: 47128
development of radiation resistant, 19: 46872(R) (AD-621549)
electric-discharge ignition mechanism in magnetron, 19: 46741
electron and ion oscillations in four-electrode discharge, 19: 46742
electron distribution in magnetron, analysis of, 19: 46740
production and testing of cesium-beam, 19: 46709(R) (AD-614118)
radiation testing of alumino-silicate enclosed, 19: 46872(R) (AD-621549)
vacuum breakdown in, with nickel electrodes, 19: 46577

ELECTRONIC EQUIPMENT
design and operation of digitized discharge planes for spark chambers, 19: 46784
design of analyzer-scanner for spark-chamber photographs, (E), 19: 46790
design of particle track analyzers for spark-chamber photographs, (E), 19: 46791
design of visual scanner for analyzing spark-chamber events, 19: 46789
development, 19: 46643(R) (LAL-1136)
radiation effects on, computer program for data retrieval in, 19: 46870(R) (AD-612191)
radiation effects on, methods of predicting, 19: 46874
radiation effects on, in space vehicles, 19: 46875

ELECTRONS
absorption in matter, mechanisms of, 19: 47152
acceleration and intensity measurement in semi-circular photographic recording beta spectrograph, 19: 46773
capture in outer Van Allen belt, equatorial angle distribution between, (T), 19: 47474
content in ionosphere, determination using satellite signals, 19: 47448 (AD-612119)
correlation with lattice vibration in solids, problems in, 19: 47875 (AD-614136)
cyclotron radiation from plasma, (T), 19: 47815
density and temperature in helium early afterglow, (E), 19: 47133
density and temperature in uniform helium plasma, (E), 19: 47739
density and temperature in hydrogen plasma, spectroscopic method for, (T), 19: 47754
density and temperature in helium plasma, (E), 19: 47772(T)
density and temperature measurements in plasma, (T), 19: 47817
density fluctuations in non-Maxwellian plasma, spectrum of, 19: 47800
density in helium plasma, probe measurement of, (E), 19: 47758
density in ionosphere, Langmuir probe measurements of, (T), 19: 47465
density of 40-kev, in magnetospheric tail, (E), 19: 47458
detection and discrimination from pions at 80 to 340 Mev/c, (E), 19: 46782
detection and measurement of, produced by meson (μ) decay, (E), 19: 46785
detection and measurement of geomagnetically trapped, from high-altitude nuclear explosions, 19: 47446 (AD-612013)
dissociation during hydrogen diffusion in palladium, (T), 19: 46250(T) (ORNL-tr-623)
distribution in plane magnetrons, exact solution for, 19: 46740
dosimetry above 6 Mev, for therapeutic use, 19: 46155
dosimetry of 2-Mev, using cerium sulfate solution, 19: 47177
dosimetry of, photographic, 19: 46853
drift velocities in polyatomic gases, at low energy, 19: 46393
drift velocity and mean energy determination in argon, nitrogen, and xenon, 19: 47124(T) (SLAC-Trans-19)
drift velocity variations in ethanol–helium–neon mixtures, 19: 47116 (BNL-9443)
effects of excess, on structure of liquid helium, (T), 19: 47132
effects on aluminum crystal mechanical properties, annealing effects on, 19: 47095
effects on carbon tetrabromide, dissociation and ionization in, 19: 46348
effects on deuterated and natural hydrogen peroxides, dipolar broadening of ESR lines in, 19: 46383
effects on ethylene, effects of nitric oxide on yields in, 19: 46324(R) (AGN-8132)
effects on free radical formation in lysozyme, ribonuclease, and trypsin, spectra of, 19: 46339 (UCRL-16358)
effects on gaseous ammonia, hydrazine yields in, 19: 46324(R) (AGN-8132)
effects on polyphenyls, mass spectra of fragments produced in, 19: 46328 (EUR-2227.e)
electric field effects on geomagnetically trapped, dynamo-, (T), 19: 47453
electromagnetic-wave propagation in relativistic quantized electron-positron gas, (T), 19: 47771
emission by electrodes materials in cesium ion engines, thermionic, 19: 46571 (HRL-5249-S)
emission of secondary, by electron-bombarded aluminum, copper, and silicon, 19: 47263
energy distribution in outer Van Allen belt, calculation of, 19: 47487
energy losses in nonequilibrium argon–cesium plasma, nitrogen impurity effects on, (E), 19: 47737(T)
flux of energetic, in geomagnetic tail, (E), 19: 47459
focusing of medium fast, in magnetic coils, (E), 19: 47185
geomagnetic trapping of energetic, Van Allen belt boundary from, (E), 19: 47462
interaction coefficients in relativistic self-consistent field theory, (T), 19: 47251
interaction frequency and lifetime of geomagnetically trapped, (T), 19: 47453
interactions of, sum rules for two-body, (T), 19: 47250
interactions with protons, (E), 19: 46643(R) (LAL-1136)
interactions with positrons in metals, (E/T), 19: 47217 (AD-513582)
interactions with positrons at high energy, nonlocal model for elastic, 19: 47364
interactions with electrons and gamma radiation, dispersion relations and unitarity in, (T), 19: 47396

interactions with deuterons, relativistic corrections for, (T), 19: 47410
interactions with electrons in metals, (E/T), 19: 47217 (AD-613582)
interactions with protons at 5.2 Bev/c, meson (π) production in, (E), 19: 47303 (DESY-65/7)
kinetics in plasma, equation for, 19: 47783
magnetic moments of, (T), 19: 47378
magnetic moments of, calculation of anomalous, 19: 47396
magnetic moments of, calculation of anomalous, 19: 47436
motion and loss mechanism in magnetic mirrors with helical magnetic field, 19: 47145
motion in auroral zone atmosphere, x-ray microburst for, (E), 19: 47470
motion in two-component plasma, (T), 19: 47747
neutron diffraction by, time-of-flight method for, (E), 19: 47894
orbits in focusing magnetic fields, lifetime of, 19: 47186
oscillation fields in ambient plasma of, in magnetosphere, (T), 19: 47477
oscillations of bound, in antiferromagnetics, 19: 47903
pressures in stellar atmospheres, 19: 47187 (AD-612182)
reactions of excess, in liquid helium, (T), 19: 47131
reactions with alkynes and ethylene, spectra of energy level transitions in, 19: 46322 (AD-612070)
reactions with atomic hydrogen, excitation and ionization in, (T), 19: 47243
reactions with atoms in plasma, inelastic, (T), 19: 47812
reactions with helium-ions and hydrogen, ionization cross sections for, (T), 19: 47253
reactions with hydrogen atoms, ionization cross sections for, (T), 19: 47237(T)
reactions with inert gases at high energies, ionization cross sections for, (T), 19: 47246
reactions with methylamine, charge exchange in, 19: 46262
reactions with metals, determination of interatomic potentials in, (T), 19: 47882 (RISO-103)
reactions with nitrogen at 20 to 500 ev, excitation and ionization cross sections for, (E), 19: 47245
scattering by bismuth, (E), 19: 46643(R) (LAL-1136)
scattering by calcium-40 and sulfur-32, energy levels and shell model parameters from, (T), 19: 47677
scattering by calcium-40, helium-3, and tritium, elastic, (E), 19: 47565 (AD-614270)
scattering by helium at 10 to 50 ev, differential cross sections for elastic, (T), 19: 47218 (AD-615929)
scattering by helium, T matrix for (2^3s) excitation in, (T), 19: 47239
scattering by helium and hydrogen, iteration-variation method for, (T), 19: 47247
scattering by helium, resonance in elastic, (T), 19: 47248
scattering by nuclei, (E/T), 19: 46643(R) (LAL-1136)
scattering by thick targets, angular distribution and energy spectrum of, 19: 47214 (AD-612410)
scattering of conduction, from s-d interaction, (T), 19: 47257
scattering on aluminum at 2 and 100 kev, effect of atomic screening on inelastic, (T), 19: 47259(T)
scattering on beryllium at 1 and 100 kev, effect of atomic screening on inelastic, (T), 19: 47259(T)
scattering on gold at 5, 10, and 100 kev, effect of atomic screening on, (T), 19: 47259(T)
scattering on tungsten single crystals at 0 to 1.5 ev, 19: 47242
spectroscopy up to 10 Bev, (E), 19: 46805
temperature in cesium plasma, spectral determination of, (E), 19: 47773(T)
temperature in positive column of hydrogen discharge plasma, (E), 19: 47738
transfer in spherical vacuum chambers, angular distribution in, (T), 19: 46824
transmission in aluminum at 100 and 150 kev, geometric dependence of, (E), 19: 47125
transport in magnetic fields, equations for, 19: 47799
transport in tin, effects of magnetic fields on, 19: 47534
velocity spectra of magnetospheric, from cyclotron absorption of whistler power, (E), 19: 47463

ELECTROPHORESIS
isotope separation by, 19: 46413
review of stable-flow free-boundary, for study of human serum lipoproteins, 19: 48105 (UCRL-16290)
use in analyzing denaturation in irradiated serum, 19: 45924

ELECTROPLATING
process for pit-free nickel on uranium bars, 19: 46944(P)

ELECTROSTATIC FIELDS
effect on product yields in radiolysis of ethylene, 19: 46361
production from ambient electron plasma oscillations in magnetosphere, 19: 47477

ELECTROSTATIC GENERATORS
performance of, 19: 46514

ELECTROSTATICS
use in engineering, review of, 19: 46514

ELEMENTARY PARTICLES
book: *Lectures on Particles and Field Theory*, 19: 47405
decay of, research on CP-violation in, (E), 19: 47315(R) (TID-22222, pp 30-45)
existence of heavy unstable, possibility of, 19: 47398
field theory of, 19: 47407
interaction potentials in coordinate space, Jost functions for singular, 19: 47360
interaction potentials in complex angular momentum plane, inversion in, 19: 47361
interactions and properties of, research on, (E/T), 19: 47313(R) (TID-22222)
interactions at high energy, perturbation theory for production amplitudes in, 19: 47341
interactions at high energy, behavior of total cross sections in Regge-pole-exchange, (T), 19: 47353
interactions at ultra-high energies, modified statistical model for, 19: 47400
interactions kinematics of, determination in bubble and spark chambers, 19: 46834
interactions of two, compositeness and vertex parts of dynamical poles in, (T), 19: 47349
interactions of, CP violation and PT invariance in weak, (T), 19: 47331
interactions of, computer analysis of kinematics of, 19: 47336
interactions of, internal symmetries in S-matrix theory of, 19: 47397
interactions of, K matrix for three-body and bound-state, 19: 47381
interactions of, majorization of Feynman diagrams for, 19: 47424
interactions of, nonelastic processes in, (T), 19: 47330
interactions of, one-particle singularities in SU(3) for coupling constants of, 19: 47321
interactions of, pairing hamiltonian with variable matrix elements for, 19: 47334
interactions of, quantum field theory of bootstrap mechanism for, 19: 47345
interactions of, quark model for SU(6) symmetry in strong, 19: 47367
interactions of, research on, (T), 19: 47314(R) (TID-22222, pp 3-29)
interactions of, research on, (E), 19: 47315(R) (TID-22222, pp 30-45)
interactions of, Regge poles in Coulomb-well potential for, (T), 19: 47311 (NP-15454)
interactions of, SU(3) estimate of nonleptonic parity-violating coupling in weak, 19: 47342
interactions of, shrinkage of effective core in large-angle, (T), 19: 47380
interactions of, tests of one-particle exchange models for, 19: 47404
interactions of, weak, (T), 19: 47301 (CERN-65-30)
interactions with bound state, separable approximation for inelastic, (T), 19: 47343
kinematics of angular momentum of, translation broadening in relativistic quantum-mechanical, 19: 47418
magnetic moments of, due to electromagnetic mass difference, (T), 19: 47316(T) (JPRS-31032, pp 15-18)
models of, 3°-plet, (T), 19: 47386
perturbation theory for interactions of, quasi-particle method in, 19: 47408
properties of many-body systems of, with translational invariance, 19: 47399
properties of strongly interacting, 19: 47406
properties of, cavity and waveguide analog to, (T), 19: 47319
quantum theory of massless, 19: 47409
quantum theory of, field equations in Corben, 19: 47362
Regge symmetries of 3j-symbols, 19: 47335
symmetries for, research on, (T), 19: 47314(R) (TID-22222, pp 3-29)
symmetry for strongly interacting, fifteenfold way of SU(4), (T), 19: 47328
symmetry for, complex energy-momentum in Poincaré group for, 19: 47422
symmetry for, extension of SU(9) to SL(9), 19: 47379
symmetry for, intrinsically broken $\bar{U}(18)$, 19: 47379
symmetry for, U(12), (T), 19: 47305 (IC/65/57)
symmetry for, unitary, (T), 19: 47301 (CERN-65-30)
symmetry of bound states with multichannels, (T), 19: 47382
symmetry of, matrix elements of homogeneous Lorentz group, (T), 19: 47322
symmetry of, representation of rank-two symplectic group for, 19: 47333
theory of, L, M, N functions of non-linear spinor, 19: 47324
transport in matter, solution to Milne problem for, (T), 19: 47865 (ANL-7061)
wave equations for spin-one, manifestly covariant, 19: 47359

ELEMENTS
abundance in nebulae and stars, 19: 47187 (AD-612182)

EMBRYOS

cerium-144 effects in developing chicken, 19: 45761(R) (ORO-631, pp 122-31)
protactinium-144 effects in developing chicken, 19: 45761(R) (ORO-631, pp 122-31)
radiation effects on nucleic acid content in liver of rat, 19: 45826
radiation effects on erythropoiesis in rat, 19: 45826
radiation effects on mouse, pathological, 19: 45852
radiation effects on osteogenesis in long bones of mouse, 19: 45872
ENDOCRINE GLANDS
radiation effects on, in insects, 19: 45861
ENDOXAN
effects on radiation damage in cultured mouse fibroblasts, 19: 46018
ENERGY
conversion of, bibliography on direct, 19: 47280 (AD-613358)
ENGINEERING
electrostatic, review of, 19: 46514
ENGINEERING TEST REACTOR
operation of, effects of coolant pump failure and reactor vessel rupture on, 19: 46716(R) (IDO-17081, pp 77-123)
ENTROPY
production principle for non-equilibrium thermodynamics, (T), 19: 47551 (UJV-1354/65)
ENZYMES
determination of phospholipase activity in tissues, 19: 45820(R) (TID-22227)
effects of cancer on liver, 19: 45808(R) (NYO-901-36)
properties of, 19: 45839
purification of tyrosine transaminase, 19: 45808(R) (NYO-901-36)
radiation effects on iso-, in human melanoma ascites, serum, and tumor homogenates, 19: 46124
radiation effects on content of, in rat intestine, 19: 45927
radiation effects on excretion of pancreatic, 19: 45928
radiation effects on, in soil, 19: 45941
radiation effects on DNA interactions with RNAse, 19: 45849
radiation effects on skin, 19: 45887
radiation effects on bile and pancreatic, following intestinal irradiation, 19: 45922
radiation effects on, 19: 46417
radiation effects on liver, 19: 45808(R) (NYO-901-36)
radiation effects on shrimp, involved in spoilage, 19: 46891
radioinduced inactivation of, ultraviolet, 19: 46382
reactions with tryptophan of, 19: 45808(R) (NYO-901-36)
EPIDEMIOLOGY
of leukemia in Israel, 19: 45958
of radiation effects as cause of death in California chiropractors, 19: 45866
EQUATION OF STATE
for system of hard spheres, 19: 47139
EQUIPMENT AND PROCEDURES
description and tests of wearable exoskeletal device for amplification of human capacity, 19: 46483 (CONF-640508, pp 158-97)
ERBIUM
cohesive energy and ionization of, relation between, (T), 19: 47062
resonance absorption integrals, (E), 19: 47576(R) (IDO-17081, pp 49-76)
ERBIUM ALLOYS
Al–Er, crystal structure of Laves phases in, 19: 47052
Co–Er, crystal structure of Laves phases in, 19: 47052
Er–Mn, phase studies by differential thermal, thermo-magnetical, and x-ray analysis of, 19: 46989 (AD-614466)
Er–Mn, preparation by sinter process using mercury, 19: 46908 (AD-614464)
Er–Pd, phase studies, 19: 47051
ERBIUM BROMIDES
thermal decomposition of hydrates of, mechanisms of, 19: 46271
ERBIUM FERRITES
crystal structure, 19: 46256
ERBIUM IONS
spectra in silicate glass, fluorescence, 19: 47886(T) (N64-21857, pp 1-6)
ERBIUM ISOTOPES Er-156
decay of, conversion electron and gamma spectra and half life for, (E), 19: 47579 (JINR-P-2275)
ERBIUM ISOTOPES Er-166
internal conversion coefficients for E2 transitions in, nuclear structure effects on, (T), 19: 47620
ERBIUM OXIDES
atomic charge and permittivity of, (E/T), 19: 47901(T)
oxygen-18 exchange between molecular oxygen and, 19: 46266
preparation and crystal structure of nonstoichiometric, 19: 46273
reactions with barium carbonates, ternary oxide formation in, 19: 46242(R) (TID-22207, Paper B)
ERYTHROCYTES
life span of sheep, tracer study, 19: 45759(R) (ORO-631, pp 77-82)
ERYTHROPOIESIS
kinetics of, in hamsters, tracer study, 19: 45808(R) (NYO-901-36)
maintenance in short-term cultures of mouse marrow cells, method for, 19: 45740
radiation effects on nuclei during, x, 19: 45925
radiation effects on, in rat embryos, 19: 45826
ERYTHROPOIETIN
radiation effects on response to, in fasted rats, 19: 45971
ESCHERICHIA COLI
effects of irradiated *p*-bromophenol on viability of, 19: 45834
radiation effects on mutants of, protective effects of phenylbenzamidine against x, 19: 46012
radiation effects on nucleic acid synthesis in ϕX174-infected, tracer study of x, 19: 45851
radiosensitivity of bacteriophage in, effects of glycerol, 19: 46034
radiosensitivity of bacteriophage in, effects of temperature, 19: 46034
radiosensitivity of, genetic factors affecting, 19: 45948
radiosensitivity of, effects of glucose-salt and peptone media on, 19: 45951
ESOPHAGUS
radiotherapy of carcinoma of, 19: 46051
ESTERS
3-phenylnorbornane-2,3-*cis-exo*-diol-2-p-toluenesulfonate, solvolysis mechanisms of, 19: 46304(R) (ORNL-3832, pp 66-75)
ETHANE
electron drift velocities in, at low energy, 19: 46393
neutron scattering by, calculation methods for, (E/T), 19: 47576(R) (IDO-17081, pp 49-76)
reactions with fission recoils, 19: 46330 (NP-15370)
yields in electron radiolysis of ethylene, nitric oxide effects on, 19: 46324(R) (AGN-8132)
ethane–N, radiolysis yields in, 19: 46324(R) (AGN-8132)
ETHANETHIOL, 2-AMINO-
protective effects against intestinal radiation death in rats, 19: 46027
radiosensitivity effects in *E. coli* mutants, x, 19: 46012
ETHANOL
effects on sulfur-35 fixation in rat liver, 19: 45800
electron drift velocities in, at low energy, 19: 46393
radiation effects on decomposition of, in presence of catalysts, 19: 46329 (EUR-2455.e)
thermodynamic properties of, in water and heavy water, 19: 46318
ethanol-H_2O, electrochemical properties of uranium (IV) in, 19: 46292
ethanol–He–Ne, electron drift velocity variations in, 19: 47116 (BNL-9443)
ETHYL ETHER
BF_3–ethyl ether, boron isotopic exchange thermodynamics of, 19: 46899(R) (ORNL-3832, pp 33-49)
BF_3–ethyl ether–ethyl sulfide, boron trifluoride exchange in, 19: 46899(R) (ORNL-3832, pp 33-49)
ETHYL ISOCYANIDE
radiation effects on cyanide group inversion in, infrared spectra of, 19: 46326 (CNAEM-28)
ETHYL SULFATES
effects on pyrimidine mutation induction in *Salmonella typhimurium*, genetic analysis of, 19: 45878
ETHYL SULFIDES
BF_3–ethyl sulfide, boron isotopic exchange thermodynamics of, 19: 46899(R) (ORNL-3832, pp 33-49)
BF_3–ethyl ether–ethyl sulfide, boron trifluoride exchange in, 19: 46899(R) (ORNL-3832, pp 33-49)
ETHYLAMINE, 2,2'-DITHIOBIS-
effects on oxygen metabolism in rat mitochondria, 19: 45777
ETHYLENE
effects on photolysis of cyclopentanone, 19: 46357
electron drift velocities in, at low energy, 19: 46393
electron reactions with, spectra of energy level transitions in, 19: 46322 (AD-612070)
ion-molecule reactions in, 19: 46324(R) (AGN-8132)
radiation effects on hydrogenation of, by copper catalyst, 19: 46329 (EUR-2455.e)
radioinduced polymerization of, effects of acetylene on, 19: 46353
radioinduced polymerization of, with methylene chloride, yields of 1-chloroalkanes and 1,1-dichloroalkanes from, 19: 46370
radioinduced polymerization, 19: 46375
radioinduced reactions in aqueous solutions of, gamma, 19: 46385
radiolysis of effects of electrostatic fields on yields from, 19: 46361
radiolysis of, nitric oxide effects on butene production in, 19: 46324(R) (AGN-8132)
reactions of ions and molecules in, 19: 46161(R) (ORNL-3832, pp 116-50)

yields from photolysis and radiolysis of cyclopentanone, 19: 46357
ethylene–N, radiolysis yields in, 19: 46324(R) (AGN-8132)
ethylene–methane–N, radiolysis of, 19: 46324(R) (AGN-8132)
ethylene–O, radiolysis of, 19: 46324(R) (AGN-8132)
ethylene–methane–NO, radiolysis of, 19: 46324(R) (AGN-8132)
ethylene–N, radiolysis of, 19: 46324(R) (AGN-8132)
ETHYLENE, CHLORO-
radiation dose absorption by, design of parallel-plate and thimble ionization chambers for measuring, 19: 46368
radioinduced polymerization of, at –78, 0, and 18°C, 19: 46351
ETHYLENE, CHLORO- POLYMERS
radiolysis of, effects of plasticizers on gamma, 19: 46350
solubility in tetrahydrofuran, 19: 46351
uses of, as bags for, air samples for radon determination, 19: 46203
ETHYLENE POLYMERS
neutron inelastic scattering by, epithermal, (E/T), 19: 47549(R) (TID-22141, pp 34-49)
neutron inelastic scattering at 0.167 to 0.499 ev, 19: 47572 (GA-6547)
neutron transport in single and multilayer slabs of, (T), 19: 47868 (RRA-T52)
performance for neutron detection, 19: 46759 (EGG-1183-1017)
properties and structure of radiation-polymerized, 19: 46375
radiation effects on flow and other properties of, 19: 46358
radiation effects on borated, for use as aerospace structural materials, (E/T), 19: 47077 (AD-613471)
use as moderator in reactor fuel elements, 19: 48074(P)
polyethylene–polypropene, radiation effects on flow and other properties of, 19: 46358
ETHYLENE, TETRAFLUORO- POLYMERS
performance as electrode for polarography, 19: 46157(R) (MLM-1254)
radiation effects on, NMR studies of, 19: 46381
radioinduced grafting of acrylic acid and acrylamide to, antielectrostatic effect of, 19: 46376
reactor criticality effects, 19: 48053(R) (ANL-7090, pp 55-68)
EUROPEAN ATOMIC ENERGY COMMUNITY
nuclear industry program in, 19: 46659
nuclear power development by, target program for, 19: 48003
EUROPIUM
cohesive energy and ionization of, relation between, (T), 19: 47062
electrochemistry, 19: 46295
luminescence in zinc borate glass, 19: 46269
separation from aqueous chloride solutions by solvent extraction using di-n-octyl phosphinic acid, tracer studies of, 19: 46443
EUROPIUM ALLOYS
Al–Eu, crystal structure of Laves phases in, 19: 47052
Co–Eu, crystal structure of Laves phases in, 19: 47052
Eu–Pd, phase studies, 19: 47051
EUROPIUM BROMIDES
thermal decomposition of hydrates of, mechanisms of, 19: 46271
EUROPIUM COMPLEXES
with acetate ion, formation and stability, 19: 46295
with formic acid, chronopotentiometry and polarography of formation of, 19: 46268
EUROPIUM FERRATES(III)
crystal structure, 19: 46256
EUROPIUM IONS
quadrupole coupling in cerium magnesium nitrate and neodymium ethylsulfate lattices, 19: 47883 (UCRL-16279)
spectra in silicate glass, fluorescence, 19: 47886(T) (N64-21857, pp 1-6)
EUROPIUM ISOTOPES Eu-156
internal conversion coefficients for E2 transitions in, nuclear structure effects on, (T), 19: 47620
EUROPIUM ISOTOPES Eu-158
decay of, gamma-gamma coincidences in, 19: 47681
half life, 19: 47681
EUROPIUM ISOTOPES Eu-159
decay of, gamma spectra and half life of, 19: 47681
EUROPIUM OXIDES
atomic charge and permittivity of, (E/T), 19: 47901(T)
oxygen-18 exchange between molecular oxygen and, 19: 46266
preparation procedures, ceramographic, 19: 46937 (NMI-5025(Pt.I) pp 1-25)
EUROPIUM SULFIDES
crystal growth in lanthanum-activated, 19: 47876 (AD-614435)
spin wave–spin wave scattering in Heisenberg ferromagnetic, cross sections in, (T), 19: 47874 (AD-613606)
EVAPORATORS
heat transfer properties of fluidized-bed spray-type, for waste processing, 19: 48079(R) (NP-15371)
EXOSPHERE
geomagnetic micropulsation transmission in lower, (T), 19: 47466
geomagnetic pulsations in, analysis of, 19: 47479
hydromagnetic shock wave propagation in, 19: 47478
properties of, 19: 47491
EXPERIMENTAL BOILING WATER REACTOR
fuel rod fabrication for, variable costs of plutonium dioxide–uranium dioxide, 19: 47977 (BNWL-131B)
reactivity excursion to 100 Mw(t), (E), 19: 47988 (ANL-6776)
EXPERIMENTAL BREEDER REACTOR-II
development, 19: 47989(R) (ANL-7090, pp 1-29)
EXPERIMENTAL GAS COOLED REACTOR
coolant purification system for, helium, 19: 46513
EXPLOSIONS
use for magnetic flux compression, (T), 19: 47120 (UCRL-14349)
EXTRACTION APPARATUS
development of countercurrent distribution cells, 19: 45730(R) (ORNL-3752)
EXTRUSION
method and apparatus for, of metals in the plastic state, 19: 46975(P)
of tubes, equipment design for, 19: 46979(P)
EYE LESIONS
radioinduced, pathology of, 19: 45843
radioinduced, pathology of, 19: 45905
radiotherapy and surgical treatment of glaucoma, beta, 19: 46045
radiotherapy, using radium needles or radon seeds, 19: 46056
EYES
effects of actinomycin on regenerating lens in salamanders, 19: 45738
radiosensitivity of, thermal, 19: 45818 (TDCK-33500)
radiosensitivity of, 19: 45843
radiosensitivity of monkey, 19: 45893
radiosensitivity of, 19: 45905
radiosensitivity of, 19: 46655
radiotherapy of cancers of eyelid, 19: 46052
rubidium-85 metabolism in lens of rabbit, during incubation, 19: 45778

F

FALLOUT
content of gamma-emitting, in holothuriae, western Mediterranean, 1962, 19: 46611
distribution and hazards of radioactive, 19: 46636 (AD-611765)
from nuclear explosions, hazards of, 19: 46671
hazards and properties of, 19: 46585 (AD-410522)
measurement in southern U. S., Nov. 1962, 19: 46604
monitoring at Brookhaven, 1963, 19: 46640 (BNL-915)
monitoring in Australia, 1963, 19: 46594
monitoring in Australia, 1961 to 1963, 19: 46595
monitoring in Belgium, 1963, 19: 46632(R) (A/AC.82/G/L.987)
monitoring in Finland, 1965, 19: 46587(R) (NYO-3446-3)
monitoring in pine needles, 1959 to 1964, 19: 45751
monitoring in Spain, 1964, 19: 46597
monitoring in Switzerland, 1963, 19: 46612
monitoring of atmospheric, in Pizen, 1957–1962, 19: 46687
monitoring of, from high-altitude thermonuclear explosions in 1962, 19: 46609
monitoring strontium-90, in grass and milk, 1959 to 1962, 19: 45749
protection of domestic animals against, 19: 46700
radiation hazards from ingestion in water, 19: 46633 (AD-276187)
shelters, development under highways, 19: 46669
FAST REACTORS
accidents in, computer analysis of energy release from, 19: 47918 (ANL-7050, pp 503-14)
design and development of, in 1000-Mwe range, 19: 47997(R) (NP-15478)
development in Great Britain, 19: 48007
fuel development for, 19: 47989(R) (ANL-7090, pp 1-29)
fuel meltdown in, performance of PBF for studies on, 19: 47952 (APDA-177)
fuel meltdown tests in, analysis of facilities for, 19: 47951 (APDA-173)
fuels for breeder-type, performance of carbide, 19: 47993 (NAA-SR-10751)
fuels for, development of plutonium dioxide–uranium dioxide, 19: 46942(R) (NUMEC-3524-6)
neutron cross sections in, method for measuring, 19: 47944 (ANL-7034)
FATTY ACIDS
radiation effects on digestion of, 19: 45932
radiation effects on properties of, in rabbit liver, 19: 45946
FECES
iodine-125 and -131 content in, following uptake from milk, 19: 45782
zinc-65 excretion in human, effects of dietary calcium on, 19: 45787
FERMI FAST BREEDER REACTOR
criticality studies, 19: 48015
FERMIONS

interactions in finite quantum electrodynamics, (T), 19: 47436
interactions in system of rarefied gas of, two-body, 19: 47394
interactions with bosons, axiomatic approach to Lee model for, 19: 47402
mass formulas and spectral representation of spin-½, 19: 47340
model for system of, finite temperature properties from perturbative, 19: 47325
Regge trajectories for, analyticity and threshold properties of, 19: 47392
systems of, Landau theory for, 19: 47323

FERMIUM ISOTOPES Fm-256
decay properties and production, (E), 19: 47664

FERMIUM ISOTOPES Fm-257
decay properties and production, (E), 19: 47664

FERMIUM ISOTOPES Fm-258
decay properties and production, (E), 19: 47664

FERRICYANIDES
thermodynamic properties of aqueous, at 298°K, 19: 46161(R) (ORNL-3832, pp 116-50)

FERROCYANIDES
thermodynamic properties of aqueous, at 298°K, 19: 46161(R) (ORNL-3832, pp 116-50)

FERROMAGNETIC MATERIALS
neutron diffraction from, covalency effects on, (T), 19: 47895
spin wave–spin wave scattering in Heisenberg, cross section ratios in, (T), 19: 47874 (AD-613606)

FETUSES
radiosensitivity of, 19: 46117
radiosensitivity of, 19: 46062
radiosensitivity of nervous system in rat, 19: 45894

FIELD THEORY
analyticity domains for high-order Wightman functions in relativistic quantum, 19: 47423
book: *Lectures on Particles and Field Theory*, 19: 47405
bootstrap mechanism in quantum, 19: 47345
covariant formulation of Lagrangian, 19: 47441
energy density in quantized local, nonpositivity of, 19: 47419
equations in Corben quantum, for elementary particles, 19: 47362
equations in Einstein-Kursunoglu, 19: 47440
Feynman diagrams in, majorization of, 19: 47424
for elementary particles, 19: 47407
Jost functions for singular potentials in coordinate space, 19: 47360
Lee model in, axiomatic approach to, 19: 47402
quantum, spin and orbital angular momentum in relativistic, 19: 47426

FILTERS
design with adjustably spaced fibers, 19: 47985(P)
performance of cellophane, effects of metal salts on, 19: 46237(R) (ORNL-3832, pp 76-99)
removal of contaminated, equipment for, 19: 46644 (ORNL-P-1528)

FINLAND
fallout monitoring, 1965, 19: 46587(R) (NYO-3446-3)
nuclear power plant development in, 19: 48005

FIRES
spread following nuclear attacks, models for, (T), 19: 46638 (AD-613359)

FISH
iodine-131 metabolism by *Salmo gairdnerii*, 19: 45796
radioactivity in Finland, 1965, 19: 46587(R) (NYO-3446-3)
radiothyroidectomy of larval steelhead trout, beta, 19: 45972
strontium-90 content in, 1965, 19: 45748(R) (TID-22193)

FISSION
properties of, neutron ratios, rates, and thresholds in, (T), 19: 47614

FISSION CHAMBERS
design of miniaturized, engineering drawings for, 19: 46863
design of parallel plate, engineering drawings for, 19: 47713

FISSION FRAGMENTS
detection of, engineering drawings of circuits for, 19: 46864
diffusion in uranium dioxide, effects on grain growth and mass transport, 19: 46278
energy deposition and range from uranium dioxide in cylindrical, slab, and spherical geometries, 19: 46324(R) (AGN-8132)
energy of uranium-235, from fission by neutrons at 0.1 to 10 ev, 19: 47576(R) (IDO-17081, pp 49-76)
reactions of iodine with gases, 19: 46330 (NP-15370)

FISSION PRODUCTS
diffusion from carbon-coated urania particles, effects of irradiation temperature on, 19: 46912(R) (BMI-1727(Del.))
diffusion from carbon-coated thorium-uranium carbide particles, 19: 46913(R) (BMI-1733(Del.))
diffusion from coated urania particles, 19: 46913(R) (BMI-1733(Del.))
diffusion of non-volatile in thorium and uranium dioxides, 19: 47070
gamma emission from, energies and intensities of, 19: 47598 (USNRDL-TR-876)
plant metabolism of, 19: 45804
radiation dose from ingested, effects of age and organ weight on, 19: 45755 (CEA-R-2809)
radiation hazards of ingested and inhaled, 19: 46698
radiation hazards of reactor-accident, 19: 46699
separation and uses of gaseous, 19: 46414
separation from irradiated fuel elements, waste problems in, 19: 46435
separation from irradiated uranium by melting and solidification under a slag, 19: 46455(P)
separation from technetium by solvent extraction using cyclohexane, 19: 46160(R) (ORNL-3832, pp 29-31)
separation of cesium-137 from, by reversed-phase chromatography, 19: 46441
separation of cesium from, by chromatography using dipicrylamine, 19: 46442
separation of iodine and tellurium from, method for, 19: 46169 (IDO-14664)
separation of, using recoil reactions with organic liquids, 19: 46405
sorption by electrocoagulated aluminosilicates, 19: 48082 (UJV-1296/65)
sorption of gaseous, use of activated carbon in fuel elements for, 19: 47981(P)
yield from plutonium and uranium, 19: 46585 (AD-410522)

FISSIONABLE MATERIAL
management of, accounting systems at AECL for, 19: 47906 (AECL-2282)
shipping of, safety aspects in, 19: 46663

FISSIUM
decay of, gamma dose curves from, (T), 19: 46589 (UCRL-14332)
fissium–U–Zr, ductility of, effects of aluminum, silicon, titanium, and yttrium additions on, 19: 47004 (NMI-4997, pp 45-54)

FLAMES
temperature measurements on, design of modulation pyrometer for, 19: 46734

FLOTATION REAGENTS
radiolysis of, in mineral flotation process, 19: 46453

FLUID FLOW
effects of two-phase, on materials in Rankine cycle power plants, 19: 46955 (NP-15431)
film thickness, pressure drop, and stability in two-phase, 19: 46542
heat transfer by, effects of upstream compressibility on, 19: 46546
heat transfer by, in porous materials with radiation heat source, 19: 46552
heat transfer from bundle of circular rods to liquid potassium–sodium alloy in, 19: 46553
instability in forced-convection flows through small tubes with subcooled boiling, 19: 46534 (NP-15437)
magnetohydrodynamic, effect of pressure gradient on boundary layer in conducting viscous, 19: 47140
two-phase, orifice and venturi measurements in steam–water at 1200 psig, 19: 46526 (AECL-2273)

FLUID FUEL REACTORS
neutron poisons in homogeneous, removal of, 19: 46426 (NP-15362)

FLUID PROPELLANTS
particle growth in, models for, 19: 46570 (AD-614111)

FLUORAL
radioinduced polymerization of, at low temperatures, 19: 46323(R) (AD-613529)

FLUORESCENCE
use in determining mineral elements in biological materials, 19: 45729(R) (NYO-910-23, pp 1-111)
use in radiation dosimetry, 19: 45729(R) (NYO-910-23, pp 1-111)

FLUORIDE COMPLEXES
with beryllium, ion exchange studies of, 19: 46230 (AAEC/E-136)

FLUORIMETERS
screens and image intensifiers for, evaluation of, 19: 46150

FLUORINE
determination in bulk plutonium tetrafluoride, 19: 46179 (RFP-618)
effects on radioinduced decomposition of plutonium hexafluoride, 19: 46325 (ANL-7013)
neutron reactions at 14 Mev, tritium yields from, 19: 47721 (LA-3385)

FLUORINE ISOTOPES F-17
energy levels from neon-17 decay, spins and parities of, (E), 19: 47613
energy levels of oxygen-17 and, opposite parity low, (T), 19: 47700

FLUORINE ISOTOPES F-18
energy levels of, 19: 47603
use in medical diagnostics, 19: 46136

FLUORINE ISOTOPES F-19
chemical shifts in boron trifluoride addition compounds, 19: 46899(R) (ORNL-3832, pp 33-49)
deuteron reactions (d,α) at 0.95 to 1.25 Mev, angular distributions from, (E/T), 19: 47646
helium-3 reactions (He-3, pγ) at 4.4 and 4.7 Mev, neon-21 energy levels

from, (E), 19: 47632
neutron reactions (n,d) at 14 Mev, angular distributions from, (E/T), 19: 47644
nitrogen-14 reactions with, excitation functions for one-neutron-transfer, (E/T), 19: 47586 (ORNL-TM-1218)
nitrogen-14 reactions at 20 to 42 Mev, excitation functions for, (E), 19: 47667
proton reactions (p,γ) with, giant dipole resonance of gamma yield from, 19: 47115(R) (ANL-6983)

FLUORINE ISOTOPES F-22
beta decay of, gamma spectra and half life for, (E), 19: 47671
production in neutron reactions (n,p) with neon-22 at 14.8 Mev, (E), 19: 47671

FLUOROCARBONS
radiation effects on saturated, gamma and neutron, 19: 46404

FLUOROMETRY
dose reduction in cino-, 19: 46152

FOOD
analysis for cesium-137 and strontium-90 by radiochemical separation after incineration, 19: 46200
radiation dose from fallout-contaminated, 19: 45755 (CEA-R-2809)
radiation effects on shrimp spoilage, 19: 46891
radiation processing of, economic aspects, 19: 46877 (CONF-650552-1)
radiation processing of, review, 19: 46885
radiation processing of meats, effects of storage at room temperature on wholesomeness, 19: 46886
radiation processing, 19: 46890
radiation processing of fruits, effects on storage life and quality, 19: 46880
radioactive contamination of U. S., 19: 46662
radioactive contamination of, by radiation accident, 19: 46694
radioactive contamination in reactor accidents, 19: 46698
radioactive contamination of, in reactor accidents, 19: 46699
radiosterilization of, conference on, 19: 46876 (AD-613325)
radiosterilization effects on *Clostridium botulinum* spores in cured meat, 19: 46881
radiosterilization effects with storage on microbial flora in dover sole fillets, 19: 46882
strontium-90 content of, in Australia, 19: 46595

FOOD IRRADIATION FACILITIES
design of, 19: 46885
design of, 19: 46890

FORMALDEHYDE
determination of, colorimetric, 19: 46324(R) (AGN-8132)
effects of aqueous solution of, on sulfur-35 fixation in rat liver, 19: 45800

FORMAMIDE
determination of, colorimetric, 19: 46324(R) (AGN-8132)

FORMIC ACID
complexes with europium, chronopotentiometry and polarography of formation of, 19: 46268
radiation effects on decomposition of, in presence of catalysts, 19: 46329 (EUR-2455.e)

FOWLS
protection against fallout, 19: 46700

FRANCE
nuclear power development in, 19: 48006
radiation protection plan for, 19: 46704

FRANCIUM ISOTOPES Fr-221
alpha spectra, (E), 19: 47576(R) (IDO-17081, pp 49-76)

FREE RADICALS
electron spin resonance of radioinduced, in rabbit muscle tissue, 19: 45947
electron spin resonance of, in irradiated solid cycloalkanes, 19: 46372
ionization potentials of butyl, ethyl, methyl, and propyl, 19: 46161(R) (ORNL-3832, pp 116-50)
photoinduced in alcohols, paramagnetic resonances of, 19: 46161(R) (ORNL-3832, pp 116-50)
radioinduced in lysozyme, ribonuclease, and trypsin, ESR spectra of, 19: 46339 (UCRL-16358)
radioinduced in nuclei acids, radiosensitivity effects of, 19: 45729(R) (NYO-910-23, pp 1-111)
radioinduced in peas, effects of water content on, 19: 45863
radioinduced, in nucleic acids and proteins, 19: 46417

FRICTION
conference on mechanisms of solid, Kansas City, Mo., Sept. 16 to 18, 1963, 19: 47075
phenomena of, in hot metal deformation, 19: 46981(R) (AD-611821)

FROGS
excitation-contraction coupling in muscles in, chemical effects and role of action potential in, 19: 45736

FRUITS
radiation processing of, effects on storage life and quality, 19: 46880

FUMARIC ACID
effects on rate of reaction between uranium(IV) and thallium(III), 19: 46297

FUMARIC ACID, DIETHYL ESTER
radioinduced polymerization of, properties of polymer obtained in, 19: 46377

FUMARONITRILE
radioinduced polymerization of, at low temperatures, 19: 46323(R) (AD-613529)

FUNGI
radioinduced mutations of *Streptomyces citreus*, antibiotic properties of, 19: 45991

FURAN, TETRAHYDRO-
solvent properties for polyvinyl chloride, 19: 46351
BF_3–tetrahydrofuran, boron isotopic exchange thermodynamics of, 19: 46899(R) (ORNL-3832, pp 33-49)

FURNACES
design and performance of electron-beam, 19: 46972
design for heat treatment, 19: 46522(P)
design of, for x-ray diffraction intensity measurements on, 19: 47009 (NP-15514(Vol.2))

G

GADOLINIUM
cohesive energy and ionization of, relation between, (T), 19: 47062
crystal structure, (E), 19: 47046
effects on density of states in superconductors, 19: 47535
neutron cross sections of, shell effects on thermal, (E), 19: 47618
surface tension, (E), 19: 47046
thermal conductivity at low temperature, (E), 19: 47528

GADOLINIUM ALLOYS
electric conductivity and conduction scattering in, spin disorder effects on, 19: 47876 (AD-614435)
Al–Gd, crystal structure of Laves phases in, 19: 47052
Co–Gd, crystal structure of Laves phases in, 19: 47052
Gd–Mn, magnetic properties of, 19: 46988 (AD-614465)
Gd–Mn, phase studies by differential thermal, thermo-magnetical, and x-ray analysis of, 19: 46989 (AD-614466)
Gd–Mn, phase studies, 19: 46908 (AD-614464)
Gd–Mn, preparation, phase studies, and properties of, 19: 46987 (AD-614462)
Gd–Mn, preparation by sinter process using mercury, 19: 46908 (AD-614464)
Gd–Pd, phase studies, 19: 47051

GADOLINIUM BORIDES
thermodynamic properties of hexa-, 19: 46994 (COO-1149-52)

GADOLINIUM BROMIDES
thermal decomposition of hydrates of, mechanisms of, 19: 46271

GADOLINIUM FERRATES(III)
crystal structure, 19: 46256

GADOLINIUM IONS
electron paramagnetic resonance spectra in cerium dioxide crystals, 19: 47898(T)
quadrupole coupling in cerium magnesium nitrate and neodymium ethylsulfate lattices, 19: 47883 (UCRL-16279)
spectra in silicate glass, fluorescence, 19: 47886(T) (N64-21857, pp 1-5)

GADOLINIUM ISOTOPES Gd-153
gamma reactions with, K x-ray purity from, 19: 46407 (AAEC/TM-226 (Suppl.1))

GADOLINIUM ISOTOPES Gd-154
neutron activation cross sections and integrals of, thermal, (E), 19: 47584(R) (ORNL-3832, pp 1-28)

GADOLINIUM ISOTOPES Gd-155
meson (μ^-) capture by, K x ray energies from, 19: 47582 (NEVIS-129)
nuclear charge distribution radius, 19: 47582 (NEVIS-129)

GADOLINIUM ISOTOPES Gd-156
neutron activation cross sections and integrals of, thermal, (E), 19: 47584(R) (ORNL-3832, pp 1-28)

GADOLINIUM ISOTOPES Gd-160
meson (μ^-) capture by, K x ray energies from, 19: 47582 (NEVIS-129)
nuclear charge distribution radius, 19: 47582 (NEVIS-129)

GADOLINIUM OXIDES
atomic charge and permittivity of, (E/T), 19: 47901(T)
oxygen-18 exchange between molecular oxygen and, 19: 46266
pathological effects of inhaled dust of, in guinea pig lungs, 19: 45756 (COO-1170-7)
preparation and crystal structure of nonstoichiometric, 19: 46273

reactions with barium carbonates, ternary oxide formation in, 19: 46242(R) (TID-22207, Paper B)
GALAXIES
evolution of radio-, gravitation theory for, 19: 47209
helium content of, 19: 47193
theory of meta-, containing antimatter, 19: 47206
GALLIUM
analysis for thorium using *N*-benzoyl-*N*-phenylhydroxylamine, gravimetric, 19: 46194
determination by complexometric methods using EDTA, 19: 46219
vapor pressure, 19: 46298
GALLIUM ALLOYS
Ag–Ga, superconductivity of, (E), 19: 47531
Ga–Fe–Pu, reactions with tantalum at 900 to 1150°C, 19: 46950 (LA-DC-7315)
Ga–Sn, superconducting transition temperatures in, (E), 19: 47520
Ga–U, vaporization of, stability of intermetallic compounds in, 19: 46298
Ga–Zn, isotopic exchange of zinc-65 between aqueous solution and, 19: 46209
GALLIUM ISOTOPES Ga-68
separation from germanium-68, 19: 46136
use in medical diagnostics, 19: 46136
GAMMA RADIATION
absorption of, apparatus for measuring resonance, 19: 46826
angular correlations of cascade, finite solid angular corrections to, (E), 19: 47693
angular correlations from tantalum-181 in ammonium hafnium fluorides, (E), 19: 47607
angular correlations in potassium-42 and rubidium-86 decay, (E), 19: 47609
angular distributions from aluminum-27 (n,n′γ) reactions at 3.5 to 4.5 Mev, (E/T), 19: 47588(R) (TID-22012, pp 22-52)
angular distributions from magnesium and silicon (n,n′γ) reactions at 3.0 to 4.5 Mev, (E/T), 19: 47589(R) (TID-22012, pp 53-66)
angular distributions from argon-40 (n,n′γ) reactions at 3.0 to 4.5 Mev, (E/T), 19: 47590 (TID-22012, pp 67-98)
angular distributions from iron-56 (n,n′γ) reactions at .97 to 4.76 Mev, (E/T), 19: 47591(R) (TID-22012, 99-128)
angular distributions from lead-206, -207, and -208 (n,n′γ) reactions at 1.0 to 4.6 Mev, (E/T), 19: 47592(R) (TID-22012, pp 129-55)
angular distributions from carbon-12, nitrogen-14, and oxygen-16 (n,n′γ) reactions at 14.8 Mev, (E/T), 19: 47593(R) (TID-22012, pp 156-75)
angular distributions from (n,n′γ) reactions with nuclei, (E/T), 19: 47594(R) (TID-22012, pp 176-205)
angular distribution and energy spectra from single-particle decay of nuclei, (T), 19: 47655
attenuation by air, spectrometric study, 19: 46586 (NP-15361)
carcinogenic effects in lungs of mammals, 19: 45808(R) (NYO-901-36)
design for pulsed beam (n,nγ) measurements, 19: 46765(R) (TID-22012, pp 4-21)
detection and measurement in urine of, use of immersible scintillation counter for, 19: 46083
detection and measurement of, using scintillation counters at 500 ft over District of Columbia, Maryland, Virginia, and West Virginia, 19: 46614
detection and measurement after transmission through man, scanner for, 19: 46750 (AECL-2270)
detection and measurement of low-level, 19: 46775
detection and measurement of, effects of volume recombination on ionization chamber, 19: 46830
detection and measurement of, engineering drawings of G-M survey meter for, 19: 46867
detection of low-energy, performance of scintillation detector and collimator in, 19: 46119
dose for mice, determination of lethal, 19: 45990
doses of, from neutron-activated granite, seawater, and soils, (T), 19: 46589 (UCRL-14332)
dosimetry in pendulum therapy of urinary bladder and rectum, 19: 46093
dosimetry of neutron-capture, in tissue, 19: 46121
dosimetry of, for therapy of eye lesions, 19: 46056
dosimetry of, photographic, 19: 46853
dosimetry using metal-organic compounds, 19: 46761 (NYO-2979-34)
dosimetry using nitrous oxide, 19: 46332(R) (ORNL-3832, pp 50-65)
effects in corn seed, physiological, 19: 45836
effects in insects, genetic, 19: 45960
effects in mice and rats, biological, 19: 45821(T) (JPRS-31547, pp 1-5)
effects in mice, lethal, 19: 45982
effects in rats, hematological, 19: 45934
effects in screw-worm fly, genetic, 19: 45950
effects on absorption and luminescence spectra of activated alkali halide phosphors, 19: 47884(T) (IS-Trans-18)
effects on acetonitrile, ethyl isocyanide, and methacrylonitrile, infrared spectra of, 19: 46326 (CNAEM-28)
effects on albumin metabolism in rabbits, tracer study, 19: 45829
effects on allyl acrylate, propene, and hexafluoropropene, 19: 46337 (TID-22244)
effects on amino acids and enzymes in soil, 19: 45941
effects on antibody production by transferred spleen cells in mice, 19: 45986
effects on appearance of slow alpha-two globulin in rat sera, 19: 45953
effects on aqueous sulfuric acid, products from, 19: 46332(R) (ORNL-3832, pp 50-65)
effects on aqueous glucose solutions, chemical, 19: 46889
effects on aromatic diluents and extractants for radiochemical processing, 19: 46430 (ORNL-P-1601)
effects on ascorbic acid content of legumes, seed, 19: 45938
effects on bacteriophage desoxyribonucleic acid in a host bacteria, 19: 46034
effects on bactericidal activity of *p*-bromophenol, effects of cysteine, heat, and sodium sulfite on, 19: 46007
effects on bacteria cells, damage repair in, 19: 45985
effects on bactericidal activity of *p*-bromophenol, factors affecting, 19: 45834
effects on behavior of monkeys, 19: 45898
effects on benzene addition compound, yields in, 19: 46324(R) (AGN-8132)
effects on bladder cancer, therapeutic, 19: 46115
effects on blood volume in rabbits, 19: 45829
effects on cell nuclei, biological, 19: 45992
effects on chromosomes of lymphocytes in man, morphological, 19: 45916
effects on chromosomes of lymphocytes in man, morphological, 19: 45917
effects on *cis*- and *trans*-stilbene in tin tetrachloride, spectra of yields in, 19: 46345
effects on *Clostridium botulinum* spores in cured meat, 19: 46881
effects on collagens, 19: 45850
effects on cotton bacteriological swabs, 19: 46884
effects on cultured mouse fibroblasts, effects of alkylating agents and antibiotics on, 19: 46018
effects on cyclohexane-d_{12}–cyclopentane mixtures, 19: 46364
effects on dioxane–benzene mixtures, 19: 46363
effects on DNA, synergistic effects of methylhydrazine derivatives in, 19: 46356
effects on domestic animals, delayed pathological, 19: 45812(R) (ORO-631, pp 1-35)
effects on *E. coli* B, effects of glucose-salt and peptone media on, 19: 45951
effects on eggs of silkworm, *Bombyx mori*, biological, 19: 45904
effects on electron spin resonance spectra of ants, 19: 45954
effects on electroluminescent screens, (E), 19: 46341(T) (FTD-TT-65-24)
effects on electronic equipment, computer program for data retrieval on, 19: 46870(R) (AD-612191)
effects on endocrine system in insects, 19: 45861
effects on enzyme content in rat intestine, 19: 45927
effects on erythropoietin response in fasted rats, effects of injection time on, 19: 45971
effects on erythrocyte chimerism of twin cattle, 19: 45760(R) (ORO-631, pp 83-121)
effects on ethylene reactions in aqueous solutions, 19: 46385
effects on ethylene, 19: 46375
effects on field-effect transistors, 19: 46871 (AD-614268)
effects on flotation properties of ores, 19: 46453
effects on formation of dimeric nitrosobenzene–irontricarbonyl, 19: 46397
effects on glass shielding windows of caves, 19: 47102
effects on glucuronide excretion by rats, whole-body, 19: 45816(R) (ORO-631, pp 142-4)
effects on grass seed, 19: 46004(P)
effects on growth of *Schizosaccharomyces pombe*, 19: 45820(R) (TID-22227)
effects on heats of transition and surface properties of ice, 19: 46332(R) (ORNL-3832, pp 50-65)
effects on immunogenicity of *Brucella abortus* and *Brucella melitensis*, 19: 45868
effects on immune properties of gamma globulins, 19: 45860
effects on immune reactions in mice, 19: 45903
effects on immune response and membrane permeability in Ehrlich ascites tumor cells, 19: 45914
effects on intestinal cells of rats, whole-body single or multiple exposures, 19: 45926
effects on ion exchange resins used in purification systems, 19: 46327 (DP-977)
effects on lactation by dairy cows, whole-body, 19: 45760(R) (ORO-631, pp 83-121)

effects on lethal chromosome induction in *D. willistoni*, nature of, 19: 45877
effects on leuko compounds of triphenylmethane dyes in polystyrene, 19: 46369
effects on leukocyte chromosomes, 19: 45813(R) (ORO-631, pp 36-44)
effects on liquid *cis* 2-butene, 19: 46335 (TID-22232)
effects on liquid butadiene, hexachlorobutadiene, and methacrylonitrile, 19: 46336 (TID-22236)
effects on lithium fluoride crystals, absorption and luminescence centers from, 19: 46380(T)
effects on lithium fluoride crystals, thermoluminescence and color center, 19: 46762(R) (NYO-3474-1)
effects on lungs, pathological, 19: 46063
effects on metal-organic compounds, 19: 46761 (NYO-2979-34)
effects on methanol vapor, scavenging effects of carbon tetrachloride, bromomethane, and oxygen on, 19: 46395
effects on mice, 19: 45990
effects on mineral acid glasses, effects of iron ions and nitrous oxide on yields in, 19: 46394
effects on nitriles, EPR spectra from radicals formed in, 19: 46378
effects on NMR of polytetrafluoroethylene, 19: 46381
effects on organometallics in benzene, 19: 46362
effects on oxide film corrosion on Zircaloy-2 and zirconium, 19: 47099
effects on plant growth, 19: 45817(R) (ORO-631, pp 145-71)
effects on polymerization of organic compounds at low temperature, 19: 46323(R) (AD-613529)
effects on polymerization of ethylene in presence of acetylene, 19: 46353
effects on polymerization of dialkyl malestes and diethyl fumarate, properties of polymers obtained in, 19: 46377
effects on polymerization of vinyl butyrate, 19: 46389
effects on polymethylmethacrylate, 19: 46367
effects on polyvinyl chloride, 19: 46350
effects on propane, effects of carbon tetrachloride, nitrous oxide, and sulfur hexafluoride on hydrogen yields in, 19: 46396
effects on rabbit muscle tissues, ESR of free radicals produced in, 19: 45947
effects on rats, protective effects of DNA against, 19: 46013
effects on reproduction in domestic animals, 19: 45813(R) (ORO-631, pp 36-44)
effects on response of monkeys to stimulus-position conditions, whole-body, 19: 45899
effects on ribonuclease, in oxygen and *in vacuo*, 19: 46347
effects on ruby lasers, (E/T), 19: 46873 (N64-32322)
effects on saturated fluorocarbons, chemical, 19: 46404
effects on seeds of Pinus, physiological, 19: 45855
effects on seeds, species differences in, 19: 45817(R) (ORO-631, pp 145-71)
effects on shrimp spoilage, 19: 46891
effects on stomatal movement of Begonia leaves, 19: 45854
effects on *Streptomyces citreus*, genetic, 19: 45991
effects on taste sensitivity of man, 19: 45825(T) (NSJ-tr-32)
effects on vinyl chloride at −78, 0, and 18°C, 19: 46351
effects on water, production of reducing radicals from, 19: 46332(R) (ORNL-3832, pp 50-65)
effects with storage on microbial flora in dover sole fillets, 19: 46882
emission from fission products, energies and intensities of, 19: 47598 (USNRDL-TR-876)
emission in proton reactions (p,γ) giant dipole resonance of, 19: 47115(R) (ANL-6983)
interactions with nucleons at high energies, meson production and momentum-transfer distributions in, (T), 19: 47389
interactions with protons at 230 Mev, meson (π^+) production in, (E), 19: 47393
interactions with electrons and gamma radiation, dispersion relations and unitarity in, (T), 19: 47396
monitoring in man, use of whole-body spectrometry for, 19: 46656
photoelectric effect on copper, silver, tin, tantalum, platinum, and lead at 145, 280, and 320 kev, cross sections for, (T), 19: 47329
radiolytic effects on alkaline-earth bromates, 19: 46332(R) (ORNL-3832, pp 50-65)
reactions with cadmium-109 and gadolinium-153, K x-ray from, 19: 46407 (AAEC/TM-226(Suppl.1))
scattering by aluminum, cadmium, copper, and gold at 280 kev, cross sections for incoherent, (E), 19: 47624
scattering by concretes, measurement of reflected, (E), 19: 47869(T) (ORNL-tr-710)
spectroscopy up to 10 Bev, (E), 19: 46805
therapeutic use of, for cancers, 19: 46050
transitions in barium-135 from resonance neutron capture at 18 to 1500 ev, (E), 19: 47701
transmission by iron-lead laminates, 19: 47872

transport in concretes, (T), 19: 47864 (ANL-7050, pp 113-22)
transport through single-bend aluminum ducts in water shields, (E), 19: 47863 (AD-613480)
use in astronomy, 19: 47207

GAMMA SHIELDING
analysis of laminated iron-lead, 19: 47872
gamma transport in slabs of, dose buildup factors for, (T), 19: 47864 (ANL-7050, pp 113-22)

GAMMA SOURCES
design of cobalt-60 applicators, for uterine carcinomas, 19: 46064
development of strong, for industrial radiation-chemical processes, 19: 46340(T) (AEC-tr-6570)
effects on silkworm gonial cells, mutagenic, 19: 45883
energy spectra from, theoretical calculation of, 19: 45729(R) (NYO-910-23, pp 1-111)
fabrication of, in a ceramic carrier, 19: 47156(P)
for therapeutic use, 19: 46078
monitoring, environmental at Brookhaven, 1963, 19: 46640 (BNL-915)
radiation hazards from handling and storage of radium, 19: 46678
use in density determinations, 19: 46892(P)
use in therapy, 19: 46077

GAMMA SPECTRA
analysis of human whole-body, computer program for, 19: 46658
analysis of, computer, 19: 46055
from decay of metastable technetium-95, 19: 47584(R) (ORNL-3832, pp 1-28)
measurement of natural, without sample destruction, 19: 46601
measurement of platinum-199, coincidence, (E), 19: 47576(R) (IDO-17081, pp 49-76)

GAMMA SPECTROMETERS
design and performance of automatic, for Mössbauer effect, 19: 46831
use for whole-body counting of man, 19: 46656

GAMMA SPECTROSCOPY
use in human physiology, 19: 45771

GAS COOLED REACTORS
accident planning for, 19: 46703
design of high-temperature, 19: 48045(P)
design with moderated core reflector, 19: 47981(P)
development in Italy, 19: 48008
development of advanced, in Great Britain, 19: 48007
fuel element arrangement for large-capacity power, 19: 47973(P)
kinetics of, fuel-cycle and power-distribution calculations, (T), 19: 4798 (ANL-7050, pp 231-49)
loading device for pressurized, design of, 19: 47931(P)
loading installation for, design of, 19: 47932(P)
materials for, properties of stainless steel as, 19: 46913(R) (BMI-1733 (Del.))

GAS FLOW
flow function tables for one-dimensional, compressible, 19: 47151
heat transfer by, in horizontal tubes, effects of buoyancy on, 19: 46545
models for stagnation-line, with heterogeneous chemical reaction, 19: 46956 (NP-15514(Vol.1))
temperature measurements on, design of modulation pyrometer for, 19: 46734

GAS MASKS
monitoring for radioactive contamination, design of detector for, 19: 46755 (BNWL-144)

GASEOUS DIFFUSION PLANTS
isotope separation by, 19: 46413

GASES
acceleration and heating ionized, using electromagnetic devices, (E/T), 19: 46477 (ARL-65-121)
analysis for transported liquids, detector for, 19: 46713 (CEA-R-2811)
book: *High Temperature Heat-Transfer Agents*, 19: 46540(T) (AD-619382)
clouds in dense star clusters, quasar model for, (T), 19: 47199
densities of, calibration and measurement methods for low, 19: 46733
electromagnetic properties of relativistic quantized electron-positron, (T), 19: 47771
equation of state of hard-sphere, 19: 47139
liquefaction of, apparatus for, 19: 46525(P)
photon interactions in, properties of, (T), 19: 47332
pressures in stellar atmospheres, 19: 47187 (AD-612182)
quantum statistics of fully ionized, 19: 47439
scattering of rarefied Fermi, two-body, 19: 47394
scattering of single-particle excitations by vortices in condensate of imperfect Bose, (T), 19: 47516
spectra at low pressure and high temperature, Stark and Zeeman components of microwave, (T), 19: 47235

GASTROINTESTINAL TRACT
diethylstilboestrol uptake by human, 19: 45797
radiation effects on function of, 19: 45930

radiation effects on digestion of proteins in, 19: 45932
radiosensitivity of, in mammals, 19: 45981
radiotherapy effects on function of, photofluorography of, 19: 46120
radiotherapy effects combined with 5-fluorouracil on palliative management of cancer of, 19: 46091
radiotherapy of rectal tumors of, gamma dosimetry for, 19: 46093
GEIGER-MUELLER TUBES
background stability of halogen-quenched, 19: 46828
performance of, for monitoring surface alpha and beta contamination, 19: 46833
GENES
properties of, 19: 45726 (BNL-9488)
radiation effects on Drosophila suppressor, x, 19: 54968
GENETICS
cellular basis of hemopoietic defect in anemic mice of genotype S1/S1, 19: 45856
contribution by Mendel to, 19: 45726 (BNL-9488)
effects of genetic constitution on radiation effects on weight of spleen and thymus in mice, 19: 45956
radiation effects in manned space flight, cosmic, 19: 46000
radiation effects on genetic loads and inbreeding in *D. melanogaster* populations, 19: 45952
radiation effects on mouse, effects on life spans of, 19: 45969
radiation effects on litter sizes in rats, 19: 45880
radiation effects on human, factors in, 19: 46695
radiosensitivity and, 19: 45857
selection methods for mutations in higher plants, 19: 45819(R) (TID-22176)
GEOLOGY
crater ejecta and dust in project Danny Boy, mass distribution measurements of, 19: 46469 (POR-1815)
effects on cancer incidence of, 19: 45832
gamma spectra measurement without sample destruction, 19: 46601
seismic wave attenuation in discontinuities, acceleration, stresses, and velocity in, 19: 46580 (AD-613287)
GEOMAGNETIC FIELDS
charged particle measurements in, from Vela Project, 19: 47450 (LA-DC-7365)
charged particle motion in, 19: 47491
charged particles in, angular distribution, energy, and intensity of trapped, 19: 47444 (AD-611629)
cosmic particle motion in, determination of arrival direction from, (T), 19: 47269
cosmic ray cut-off rigidity in, 19: 47278
electron flux in tail of, energetic, (E), 19: 47459
electrons trapped in, effects of nuclear high-altitude explosions on, 19: 47446 (AD-612013)
micropulsation transmission in lower exosphere and ionosphere, (T), 19: 47466
micropulsations in, mechanisms of, 19: 47476
pulsations in exosphere, analysis of, 19: 47479
pulsations of, correlation with solar M regions, 19: 47454
pulsations of, correlation of storm activity with pc, 19: 47482
GEOMAGNETIC STORMS
commencement of, local irregularities in sudden, (T), 19: 47456
data for fourth quarter, 1964 and May 1965, 19: 47468
intensity of, correlation with geomagnetic field pc pulsations, 19: 47482
intensity variation anomaly in Japan, 19: 47457
occurrence of, sunspot cycle effects on, 19: 47472
properties of and solar activity effects on, 19: 47497
sudden commencement of, hydromagnetic studies of, 19: 47478
theory, 19: 47500
GEOPHYSICS
book: *Geophysics and Space Data Bulletin No. 3*, 19: 47447 (AD-612083)
gravitational fluctuations in, search for, 19: 47486
research on, Air Force, 19: 48087 (AD-613537)
GERMAN REACTORS
instrumentation of, review, 19: 46825
GERMANE, TETRAPHENYL-
effects on scintillation quenching in benzene, 19: 46362
radiolysis of, in benzene, 19: 46362
GERMANIUM
performance radioisotope-photovoltaic energy conversion system, 19: 47284
radiation effects on, electron, (E), 19: 47092(R) (TID-22141)
radiation effects on defect-oxygen interactions at 25 to 700°K, (E), 19: 47892
GERMANIUM ALLOYS
Ge–Th, vaporization of, stability of intermetallic compounds in, 19: 46298
Ge–U, vaporization of, stability of intermetallic compounds in, 19: 46298
GERMANY
nuclear energy development and uses in Federal Republic, 19: 48112
radiation body burden to personnel in Democratic Republic of, occupational, 19: 46674
strontium-90 content of plants and soils of Democratic Republic, 1963, 19: 46610
uranium deposits in Federal Republic, 19: 46630
GIBBERELLIC ACID
effects on RNA synthesis in aleurone cells of seeds, tracer study, 19: 48102(R) (TID-22175)
GLASS
heat treatment of flat, design of furnace for, 19: 46522(P)
joining to alumino-silicate glass, techniques for, 19: 46872(R) (AD-621549)
neodymium spectra in, concentration dependence of fluorescence, 19: 47887(T) (N64-21857, pp 7-12)
performance for radiation dosimetry, 19: 46850
photo- and radiation chemistry of mineral acid, effects of iron ions and nitrous oxide on yields in, 19: 46394
radiation effects on shielding window, gamma, 19: 47102
radiation effects on silica, annealing of fast neutron, (E), 19: 47108
radiation testing of ordinary and alumino-silicate enclosed, 19: 46872(R) (AD-621549)
rare earth spectra in silicate, 19: 47886(T) (N64-21857, pp 1-6)
GLEEP
design and operation, 19: 48115
GLOBULIN
effects of denaturation of, on immune properties of, 19: 45860
radiation effects on appearance of alpha-two, in rat sera, 19: 45953
radiation effects on electrophoretic mobility of, 19: 45860
radiation effects on immune properties of, 19: 45860
separation and properties of rat macro-, 19: 45730(R) (ORNL-3752)
use of iodine-131 labeled, in clinical studies, 19: 46142
GLOVE BOXES
helium purification system for, 19: 46513
GLUCOSE
radiation effects on absorption of, after oral or intravenous administration, 19: 45931
radiation effects on absorption of, by intestines in active and hibernating ground squirrels, 19: 45841
radiolysis of aqueous solutions of, 19: 46889
GLUCURONIDES
determination in urine of rats, 19: 45816(R) (ORO-631, pp 142-4)
radiation effects on excretion of, in rats, 19: 45816(R) (ORO-631, pp 142-4)
GLUTAMIC ACID
radiation effects on, in soil, 19: 45941
GLUTATHIONE
effects on thymidine uptake by mouse DNA, 19: 46016
protective effects against radiation damage in mammals, review on, 19: 46010
protective effects against radiation damage in mice, 19: 46016
GLYCERIC ACID
labeling with carbon-14, use of vinylmagnesium bromide in, 19: 46310
GLYCEROL
labeling with carbon-14, use of vinylmagnesium bromide in, 19: 46310
protective effects of, against radioinduced inactivation of desoxyribonucleic acid, 19: 46034
GLYCINE
complexes of, solid state radiation chemistry of, 19: 46403
determination, colorimetric, 19: 46324(R) (AGN-8132)
preparation of carbon-11 labeled, using carbon-12 (γ,n) reactions, 19: 46418
radiation effects on, in soil, 19: 45941
radioactivity of carbon-14-labeled, absolute measurement of, 19: 46214
thermodynamic properties of, in water and heavy water, 19: 46318
GLYCOGEN
separation of rat liver, by zonal centrifuge, 19: 45730(R) (ORNL-3752)
GLYCOLIC ACID, LITHIUM SALT
molecular configuration of, neutron diffraction studies of, 19: 46161(R) (ORNL-3832, pp 116-50)
GLYCOLS
1,2-diphenylethylene, deuterium isotope effects in oxidation of, 19: 46304(R) (ORNL-3832, pp 66-75)
GOLD
content and distribution in beef heart, 19: 45753 (AE-191)
electron inelastic scattering at 5, 10, and 100 kev, effect of atomic screening on, 19: 47259(T)
electron reactions with crystals of, determination of interatomic potentials in, (T), 19: 47882 (RISO-103)
gamma incoherent scattering at 280 kev, cross sections for, (E),

19: 47624
neutron cross sections of, shell effects on thermal, (E), 19: 47618
oxygen-ion transmission through thin foils of, charge-state distribution after, (E), 19: 47179
performance of foils of, for thermal insulation, 19: 48050 (NAA-SR-9903)
radiation effects on electric conductivity of low-temperature recovery of neutron, (E), 19: 47097
radiation effects on, lattice atom displacement probabilities in deuteron and neutron, (T), 19: 47104
surface tension of, measurement by pendant drop method, 19: 47065
GOLD ALLOYS
Au–Pt, radiation effects on catalytic effects of, on gaseous reactions, 19: 46329 (EUR-2455.e)
GOLD ISOTOPES Au-194
beta decay of, conversion-electron and gamma spectra in, (E), 19: 47643
GOLD ISOTOPES Au-197
neutron reactions (n,γ) in soil, activity induced by, 19: 47569 (CEX-62-50)
GOLD ISOTOPES Au-198
diagnostic use of, for localization of subdiaphragmatic abscess, 19: 46048
production in soil by neutron reactions (n,γ) on gold-197, activity from, 19: 47569 (CEX-62-50)
use of injected, for diagnosis of fallopian tube obstruction, 19: 46040
GOLD ISOTOPES Au-199
energy level scheme, (E/T), 19: 47576(R) (IDO-17081, pp 49-76)
gamma spectra from transitions in, (E), 19: 47576(R) (IDO-17081, pp 49-76)
GONADS
nitrophenylbenzamine content in rat, 19: 46011
radiation dose to, during dental radiography, 19: 46107
radiation dose to, shielding effects on diagnostic radiology, 19: 46145
radiation hazards to, during radiodiagnosis of lung diseases, 19: 46110
radiodiagnosis of fallopian tube obstruction, 19: 46040
radiosensitivity of screw-worm fly, 19: 45950
radiosensitivity of, in male rats, 19: 45808(R) (NYO-901-36)
radiosensitivity of, in domestic animals, 19: 45813(R) (ORO-631, pp 36-44)
GRANITE DEPOSITS
fracture permeability of, effects of contained nuclear explosion on, 19: 46581 (UCRL-14292)
GRANITES
lead isotope composition in, review on, 19: 46582
neutron activation of, gamma dose curves from, (T), 19: 46589 (UCRL-14332)
radioactivity of, effects on plant growth on, 19: 45752
GRAPHITE
corrosion by hydrogen chloride at 2250°C, 19: 46956 (NP-15514 (Vol.1))
corrosion by hydrogen and hydrogen fluoride, calculation of, 19: 46956 (NP-15514(Vol.1))
cosmic nuclei fragmentation parameters in, (E), 19: 47276
crystal lattice vibration frequency spectrum, (T), 19: 47881 (ORNL-P-585)
deposition of pyrolytic, on nuclear fuel particles, process for, 19: 47983(P)
determination in refractory borides, carbides, and nitrides, method for, 19: 46941 (NP-15514(Vol.3))
electric conductivity of highly anisotropic, at 1200 to 2800°K, 19: 47009 (NP-15514(Vol.2))
emissivity of highly anisotropic, at 1200 to 2800°K, 19: 47009 (NP-15514(Vol.2))
etching of pyrolytic, effects of argon and mercury ion bombardment on, 19: 47078 (AD-613643)
Hall effect in single crystals of, (E), 19: 47044
hardness of pyrolytic, technique for measuring micro-, 19: 47003 (NMI-4999, pp 111-28)
intercalation of strongly electropositive metals in, 19: 46265
neutron absorption by gas-cooled reactor, calorimeter for determining, 19: 48031
neutron asymptotic decay constant in crystalline, (E), 19: 47554
neutron diffusion length and transport mean free path at 100 to 300°K, thermal, (T), 19: 47556
neutron time-decay constants in, upper bounds for pulsed, (T), 19: 47553
oxidation by carbon dioxide and oxygen, 19: 46956 (NP-15514(Vol.1))
performance of resistors of, as heat sources, 19: 48099 (SC-TM-64-653)
properties for aerospace uses, 19: 47068
radiation damage flux calibrations for, neutron, 19: 48070
reactions with hydrogen at 1900 to 2500°C, 19: 46956 (NP-15514(Vol.1))
reactions with microwave-activated nitrogen at 1694 to 2365°K, 19: 46956 (NP-15514(Vol.1))
research programs on, at Harwell, 19: 48115
thermal conductivity of highly anisotropic, at 1200 to 2800°K, 19: 47009 (NP-15514(Vol.2))
thermal diffusivity at 1200 to 1950°C, 19: 46995 (EUR-2424.f)
GRAPHITE (IMPREGNATED)
preparation of, with alumina-coated uranía spheres for metallography, 19: 46925 (NMI-4997, pp 85-91)
GRAPHITE MODERATED REACTORS
control rod worths of, methods for calculating, 19: 47999 (TRG-Report-227)
core structure for, 19: 47933(P)
development in Italy, 19: 48008
GRAPHITE SYSTEMS
Be–graphite, fabrication of reactor reflectors from, 19: 46977(P)
GRASS
radiation effects on seeds of, gamma, 19: 46004(P)
strontium-90 content in, 1959 to 1962, 19: 45749
strontium-90 content in, effects of plant calcium content and soil in, 19: 45750
GRAVITATION
coupled fields of, asymptotic behavior of, (T), 19: 47437
effects on geodesics of space-time surface, (T), 19: 47192
fluctuations in, astronomical and geophysical study of, 19: 47486
gravitons in, quantum theory for, 19: 47409
radiation of gravitons, quantum electrodynamics for infrared divergences in, 19: 47204
theory of, lectures on, 19: 47411 (NP-15436)
theory of, review of, 19: 47209
waves of, creation of matter by, (T), 19: 47136
GREAT BRITAIN
cancer research activities in, 1964, 19: 45744
leukemia incidence in Cornwell, 19: 45959
nuclear power development in, 19: 48007
nuclear power development in, review of, 19: 48026
radioactivity of Cornwell area, natural, 19: 45959
GRENOBLE REACTORS
irradiated specimens from, nondestructive testing of, 19: 46559(T) (ORNL-tr-749)
GRINDING
equipment for metallographic sample, 19: 46507 (NMI-4997, pp 157-62)
equipment for metallographic sample preparation, description of vibratory, 19: 46939 (NMI-5025(Pt.I), pp 185-219)
GROSSWELZHEIM SUPERHEAT REACTOR
neutron flux distributions in fuel bundles of, local, (E/T), 19: 47992 (KEA-311)
GROUND
motions of, simulation of air-blast-induced, 19: 46457 (AD-613674)
radiation contamination of, in reactor accident, 19: 46699
GROUND WATERS
fallout monitoring in, Moncloa Station, Spain, 1964, 19: 46597
strontium-90 migration in, effects of various ions on, 19: 46602
GROWTH
radiation effects on reproduction of HeLa, clone-size analysis of, 19: 45886
GUANIDINE
mercapto alkyl-, protective effects against radiation damage in mammals, 19: 46010
radiosensitivity effects on poliovirus infective centers, 19: 46032
GUIDED MISSILES
shock mount system for protection against ground motion, design of self-centering, 19: 46456 (AD-425760)
GUINEA PIGS
effects of beryllium on tissues of, cytomorphology and histology of, 19: 45803
effects of radioprotective compounds on muscular activity of intestine of, 19: 46005(T) (JPRS-31933, pp 6-12)
pathological effects of inhaled gadolinium oxide dust in lungs of, 19: 45756 (COO-1170-7)
radiation effects on cholesterol content of, 19: 45937
radiation effects on 4-aminobutyric acid content of brain, 19: 45979
radiation injuries of skin of, protective effects of chloroquinine, 19: 46019
radioinduced skin lesions of, pathology, 19: 45869
radioinduced skin lesions in, 19: 45887

H

HAFNIUM
determination in hafnium carbide–niobium carbide, method for, 19: 46941 (NP-15514(Vol.3))
determination in thorium oxide, spectrochemical, 19: 46226

determination using mandelic acid, 19: 46224
heat of vaporization, 19: 46956 (NP-15514(Vol.1))
separation from hydrochloric acid solutions by solvent extraction using tetrabutylpyrophosphate and tetrabutylhypophosphate, tracer studies of, 19: 46451
solvent extraction from nitric acid solutions, effects of solvent degradation on, 19: 46430 (ORNL-P-1601)
welding of Zircaloy sheet to plates of, explosive, 19: 46961 (BMI-X-10139)
HAFNIUM ALLOYS
Hf–Nb–W–Y, weldability studies of C-129Y, 19: 46966(R) (WANL-PR(P)-007)
Hf–Ta–W, reactions with cesium at 3400°C, metallographic specimen preparation of T-111, 19: 46954 (NMI-5025(Pt.I), pp 39-58)
Hf–Ta–W, reactions with uranium carbide, nitride, and dioxide, metallographic specimen preparation of T-111, 19: 46954 (NMI-5025 (Pt.I), pp 39-58)
Hf–Ta–W, weldability studies of T-111, 19: 46966(R) (WANL-PR(P)-007)
HAFNIUM BORIDES
analysis for boron, method for, 19: 46941 (NP-15514(Vol.3))
corrosion by hydrogen chloride at 2250°C, 19: 46956 (NP-15514 (Vol.1))
lattice parameters and thermal expansion at 25 to 2041°C, 19: 47009 (NP-15514(Vol.2))
oxidation by carbon dioxide at 2250°C, 19: 46956 (NP-15514(Vol.1))
preparation and purification, 19: 46941 (NP-15514(Vol.3))
HAFNIUM CARBIDES
corrosion by hydrogen chloride at 2250°C, 19: 46956 (NP-15514 (Vol.1))
electric conductivity at 1000 to 2800°K, 19: 47009 (NP-15514(Vol.2))
emissivity at 1100 to 2800°K, total, 19: 47009 (NP-15514(Vol.2))
oxidation by carbon dioxide at 2250°C, 19: 46956 (NP-15514(Vol.1))
preparation and purification, 19: 46941 (NP-15514(Vol.3))
thermal capacity at 1200 to 1800°K, 19: 47009 (NP-15514(Vol.2))
thermal conductivity at 1100 to 2800°K, 19: 47009 (NP-15514(Vol.2))
thermal expansion at 25 to 2030°C, 19: 47009 (NP-15514(Vol.2))
HfC–NbC, analysis for hafnium and niobium, method for, 19: 46941 (NP-15514(Vol.3))
HAFNIUM COMPLEXES
with alkylenepolyaminoacetic acid type chelating agents, preparation, 19: 46299(P)
HAFNIUM ISOTOPES
neutron resonance parameters, (E), 19: 47595(R) (TID-22141, pp 50-66)
HAFNIUM ISOTOPES Hf-176
internal conversion coefficients for E2 transitions in, nuclear structure effects on, (T), 19: 47620
neutron resonance parameters, (E), 19: 47595(R) (TID-22141, 50-66)
HAFNIUM ISOTOPES Hf-177
neutron resonance parameters, (E), 19: 47595(R) (TID-22141, pp 50-66)
HAFNIUM ISOTOPES Hf-178
neutron resonance parameters, (E), 19: 47595(R) (TID-22141, pp 50-66)
HAFNIUM ISOTOPES Hf-179
neutron resonance parameters, (E), 19: 47595(R) (TID-22141, pp 50-66)
HAFNIUM ISOTOPES Hf-180
neutron resonance parameters, (E), 19: 47595(R) (TID-22141, pp 50-66)
HAFNIUM NITRIDES
preparation and purification, 19: 46941 (NP-15514(Vol.3))
HAFNIUM OXIDES
HfO_2–ZrO_2, thermal expansion of solid solutions of, at 900 to 2500°C, 19: 47045
HAFNIUM SYSTEMS
C–Hf–Nb–W, fabrication and mechanical properties of, 19: 46940(R) (NP-15444)
C–Hf–Ta–W, weldability studies of T-222, 19: 46966(R) (WANL-PR(P)-007)
C–Hf–W, fabrication and mechanical properties of, 19: 46940(R) (NP-15444)
Hf–O, phase studies, 19: 46990 (ARL-65-138)
HAIR
analysis for molybdenum, activation, 19: 46192
iodine content of, from children, 19: 45784
lead-210 content in human, Warsaw, 1963, 19: 45795
HALDEN BOILING REACTOR
development and operation of, industrial requirements for, 19: 48114
HALL EFFECT
in MHD generators at high mass flows and high stagnation temperatures, 19: 47290
measurement in transition-metal carbides, borides, and nitrides, design and operation of potentiometer for, 19: 47009 (NP-15514(Vol.2))
HAMSTERS
effects of transplanted tumors on liver enzyme systems in, 19: 45808(R) (NYO-901-36)
erythropoiesis in, tracer study, 19: 45808(R) (NYO-901-36)
pathology of melanomas in skin of, 19: 45906
HANDBOOKS AND MANUALS
catalog of protective equipment, USSR, 19: 46653(T) (JPRS-31843)
Code of Practice for the Protection of Persons Against Ionizing Radiations Arising from Medical and Dental Use, 19: 46686
cryogenic materials data handbook, 19: 47013 (PB-171809(Rev.) (Suppl.2))
for applications of hermetically sealed, d-c, electromagnetic relays, 19: 48100 (SC-TM-65-294)
for sensitivity calculations in activation analysis, 19: 46167 (EUR-1898.e)
for using computer code PROTOS, 19: 47867 (NP-15384)
on basic requirements for personnel monitoring, 19: 46689
on metallurgical practice, for laymen after nuclear attack, 19: 46918 (IITRI-B6018-1)
Radiation Safety Handbook, 19: 46685
HANDLING AND STORAGE
equipment for irradiated fuel element, 19: 46517(P)
of radium sources, 19: 46678
HANFORD PRODUCTION REACTORS (N)
operation of, procedures for dual-purpose, 19: 48039
HANFORD WORKS, RICHLAND, WASH.
chemical processing department, administration of criticality control in, 19: 46433 (RL-SA-43)
HARWELL SYNCHROTRON
betatron oscillations in, servo theory for control of, (T), 19: 47165 (NIRL/R/99)
HASTELLOY B
mechanical properties at cryogenic temperatures, 19: 47013 (PB-171809(Rev.)(Suppl.2))
HASTELLOY C
corrosion by gaseous contaminants in helium at high temperatures, 19: 46946 (BNWL-100)
corrosion by mercury at 150°C, 19: 46428(R) (ORNL-3847)
mechanical properties at cryogenic temperatures, 19: 47013 (PB-171809(Rev.)(Suppl.2))
HASTELLOY X
corrosion by gaseous contaminants in helium at high temperatures, 19: 46946 (BNWL-100)
HAYNES 25 ALLOY
corrosion by gaseous contaminants in helium at high temperatures, 19: 46946 (BNWL-100)
HEAD
radiography of, use of mercury-197 as x-ray source for, 19: 46141
radiosterilization of face tissue for homografting procedures, 19: 46879
radiotherapy of tumors, 19: 46129
radiotherapy of tumors of face and jaw, 19: 46074
shielding of burro, radiosensitivity effects of, 19: 45812(R) (ORO-631, pp 1-35)
HEALTH PHYSICS
conference on public protection, 19: 46690
personnel training, 19: 46839
program for hospitals, 19: 46679
radiation exposure levels, survey of maximum permissible, 19: 46696
HEART
analysis for trace elements, neutron activation, 19: 45753 (AE-191)
blood circulation in relation to ischemic myocardium in dogs, tracer studies, 19: 45767
radiation effects on mouse, protective effects of sodium cysteinethiosulfonate against, 19: 46006
radiation effects on dog, pathological, 19: 45835
HEAT
effects on bactericidal activity in irradiated *p*-bromophenol, 19: 46007
HEAT TRANSFER
ablation testing device for re-entering bodies, (E), 19: 47117(R) (SC-DC-65-1698)
burnout heat flux and pressure drop in reactor test sections, 19: 47998(R) (SRO-118)
by fluid flow through porous material with radiation heat source, 19: 46552
by rough surfaces at high heat fluxes, 19: 46543
calculation for pulsed thermonuclear reactor, computer program for, 19: 47720 (LA-3347)
determination in film and nucleate-boiling liquid metals, transient-quenching method of, 19: 46550
dryout in 19-rod bundle in steam–water flow at 515 psia, 19: 46548
effects of magnetic field on liquid mercury, 19: 46547
in fluidized-bed spray-type evaporator for liquid waste processing,

19: 48079(R) (NP-15371)
in horizontal tubes, effects of buoyancy on forced-convective, 19: 46545
of cylindrical and spherical re-entry bodies, analytical methods for predicting, 19: 46537 (SC-RR-65-187)
to liquid metals during vertical upflow, nucleate boiling effects on single phase, 19: 46528 (ANL-7038)
to liquid potassium–sodium alloy flowing through bundle of circular rods, 19: 46553
to water at high pressures after critical heat flux, 19: 46554
to water in boiling channels, effects of upstream compressibility on, 19: 46546
HEAT TRANSFER SYSTEMS
boiling burnout in pressurized water, in natural circulation conditions, 19: 46536 (RT/ING(65)1)
book: *High Temperature Heat-Transfer Agents*, 19: 46540(T) (AD-619382)
HEATERS
performance of graphite resistors as, 19: 48099 (SC-TM-64-653)
HEAVY WATER REACTORS
development in Great Britain, 19: 48007
development of organic-cooled, 19: 47998(R) (SRO-118)
development of, using fuel suspensions, 19: 47923
HELIUM
corrosive effects on superalloys at high temperatures, 19: 46946 (BNWL-100)
effects on radioinduced decomposition of plutonium hexafluoride, 19: 46325 (ANL-7013)
electric discharge in, spectroscopy of early afterglow from, (E), 19: 47133
electric discharge in, spectroscopic investigations of high-frequency, (E), 19: 47772(T)
electron density in plasma of, probe measurement of, (E), 19: 47758
electron density in plasma of, microwave free space method for measuring, (E), 19: 47755
electron elastic scattering at 10 to 50 ev, differential cross sections for, (T), 19: 47218 (AD-615929)
electron elastic scattering by, iteration-variation method for, (T), 19: 47247
electron elastic scattering by, resonances in, (T), 19: 47248
electron reactions in liquid, properties of excess, (T), 19: 47131
electron scattering by, T matrix for (2^3s) excitation in, (T), 19: 47239
energy levels of, Hartree-Fock wave functions for excited, (T), 19: 47224
film transfer rates of liquid II, 19: 47532
helium ion scattering, 19: 47221 (NYO-2403-8)
ionization by, electron and proton impact at high energies, cross sections for, (T), 19: 47246
liquefaction of, apparatus for, 19: 46525(P)
magnetohydrodynamic cells for diagnostics of plasma of, 19: 47728
motion of liquid II, multiple quantization of, (E), 19: 47522
noise and oscillations in beam-generated plasma of, (E), 19: 47741
properties of brush cathode plasma of, (E), 19: 47739
properties of plasma of, in C Stellarator, (E), 19: 47854
purification of, design of equipment for, 19: 46513
scattering of deuterium and hydrogen by, cross sections for elastic, 19: 46161(R) (ORNL-3832, pp 116-50)
scattering of single-particle excitations by vortices in liquid II, (T), 19: 47516
sorption by quartz walls in high-density discharges, (E/T), 19: 46576
structure of liquid, near excess electron, (T), 19: 47132
theory of superfluid, microscopic, 19: 47506
thermal expansion of liquid II, (E), 19: 47505
thermodynamic properties at 2,000 to 100,000°K, 19: 46235 (N64-26802)
HELIUM IONS
absorption cross sections in carbon and hydrocarbon solids at 30 to 350 kev, (E), 19: 47871
beams of, analysis of duoplasmatron, 19: 47267
charge in cadmium vapor, average, (E), 19: 47266
effects on free radical formation in lysozyme, ribonuclease, and trypsin, spectra of, 19: 46339 (UCRL-16358)
electron reactions with, ionization cross sections for, (T), 19: 47253
reactions with oxygen, energy transfer in, (E), 19: 47231
scattering by atomic helium, 19: 47221 (NYO-2403-8)
HELIUM ISOTOPES He-3
compressibility and thermal expansion of solid, (E), 19: 47523
deuteron reactions (d,p) with, level structure from, (T), 19: 47687
deuteron reactions (d,p), proton polarization in, 19: 47709
electron elastic scattering by, nucleon structure from, (E), 19: 47565 (AD-614270)
emission from excited emulsion nuclei, (E), 19: 47651
form factor for, Coulomb energy from charge, (T), 19: 47387
hyperfine structure of, singlet-triplet mixing correction to, (T), 19: 47241
pressure at 77°K, thermomolecular, 19: 46157(R) (MLM-1254)
reactions (He-3,$p\gamma$) with fluorine-19 at 4.4 and 4.7 Mev, neon-21 energy levels from, (E), 19: 47632
reactions with beryllium-9 and lithium-6 and -7, energy levels and mechanisms of, 19: 47564(R) (AD-612038)
separation from superfluid helium-4 by filtration, apparatus for, 19: 46157(R) (MLM-1254)
thermal capacity at low temperatures, (E), 19: 47514
use in determination of carbon, nitrogen, and oxygen in metals by activation, 19: 46174 (LA-DC-7319)
vapor pressure scales for, expansion formula for, (T), 19: 47129
HELIUM ISOTOPES He-4
binding energies of polyatomic molecules of, (T), 19: 47244
deuteron elastic scattering at 2 to 9 Mev, tensor polarization in, 19: 47704
emission from excited emulsion nuclei, (E), 19: 47651
meson (π^0) photoproduction on, (E), 19: 46643(R) (LAL-1136)
pressure at 77°K, thermomolecular, 19: 46157(R) (MLM-1254)
proton scattering at 17.5 to 27 Mev by, polarization in, 19: 47709
reactions in massive-star evolution, thermonuclear, (T), 19: 47202
separation of superfluid, from helium-3 by filtration, 19: 46157(R) (MLM-1254)
thermal conductivity of single crystals of, (E), 19: 47902
vapor pressure scales for, expansion formula for, (T), 19: 47129
HELIUM ISOTOPES He-5
energy levels of, structure of 16.7 Mev, (T), 19: 47687
HELIUM ISOTOPES He-7
model of hyperon(Λ) hypernucleus, two-body, 19: 47647
HELIUM SYSTEMS
ethanol–He–Ne, electron drift velocity variations in, 19: 47116 (BNL-9443)
He–K, electron recombination rates and nonequilibrium conductivity in, (E), 19: 47801
HEMATOLOGY
tracer studies of, 19: 46102
HEMATOPOIETIC SYSTEM
radiation effects on function of rat, 19: 45984
radiosensitivity of, 19: 46031
radiosensitivity of, in mammals, 19: 45981
radiosensitivity of, in domestic animals, 19: 45812(R) (ORO-631, pp 1-35)
transplantation of tissues of, 19: 46009
HENDECANE
labeling with deuterium, 19: 46308
HETEROGENEOUS REACTORS
design, 19: 47972(P)
design of experimental, with graphite block moderator and reflector, 19: 48074(P)
design using skewed fuel lattice, 19: 47924(P)
HEXANE
effects on photolysis of cyclopentanone, 19: 46357
radiolysis in presence of sodium, yields in, 19: 46324(R) (AGN-8132)
3-HEXYNE
electron reactions with, spectra of energy level transitions in, 19: 46322 (AD-612070)
HIBERNATION
effects on radiation effects on glucose absorption in ground squirrel intestines, 19: 45841
HIGH-ALTITUDE EXPLOSIONS
atmospheric ionization by nuclear, series solutions of three-species differential equations for, (T), 19: 47449 (AD-613199)
charged particle injection into magnetosphere by nuclear, 19: 47444 (AD-611629)
electrons from, evaluation of measurements on geomagnetically trapped, 19: 47446 (AD-612013)
fallout monitoring of 1962, 19: 46609
fireball evolution from nuclear, 19: 47113 (AD-612197)
simulation of nuclear, design of high-energy fast-pulse power system for, (E/T), 19: 46476 (AD-613959)
HIGH TEMPERATURE GAS COOLED REACTOR EXPERIMENT
coolant purification system for, helium, 19: 46513
cooling systems of, water treatment for secondary and tertiary, 19: 48042
HIGH-TEMPERATURE REACTIONS
studies of, using vaporization at high temperatures, 19: 46234 (COO-1140-123)
HIGH TEMPERATURE SEPARATION PROCESSES
zone refining equipment for purifying beryllium, 19: 46909(R) (AD-620264)
HIPPURIC ACID
radiation effects on content in urine, whole-body, 19: 45815(R) (ORO-631, pp 67-76)
HIROSHIMA

mortality rate of malignant neoplasms of residents of, effects of atomic explosion on exposure, 19: 45846
HISTOLOGY
of connective tissues, 19: 45935
HOLMIUM
cohesive energy and ionization of, relation between, (T), 19: 47062
resonance absorption integrals, (E), 19: 47576(R) (IDO-17081, pp 49-76)
HOLMIUM ALLOYS
Al–Ho, crystal structure of laves phases in, 19: 47052
Co–Ho, crystal structure of Laves phases in, 19: 47052
Ho–Mn, phase studies by differential thermal, thermo-magnetical, and x-ray analysis of, 19: 46989 (AD-614466)
Ho–Mn, preparation by sinter process using mercury, 19: 46908 (AD-614464)
Ho–Pd, phase studies, 19: 47051
HOLMIUM BROMIDES
thermal decomposition of hydrates of, mechanisms of, 19: 46271
HOLMIUM FERRATES(III)
crystal structure, 19: 46256
HOLMIUM IONS
spectra in calcium fluoride crystals, deformation effects on absorption, (E), 19: 47890(T)
spectra in silicate glass, fluorescence, 19: 47886(T) (N64-21857, pp 1-6)
HOLMIUM ISOTOPES Ho-157
decay of, conversion electron and gamma spectra and half life for, (E), 19: 47579 (JINR-P-2275)
HOLMIUM ISOTOPES Ho-162
decay of, conversion electron and gamma spectra and half life for, (E), 19: 47579 (JINR-P-2275)
production by proton reactions with tantalum at 660 Mev, (E), 19: 47579 (JINR-P-2275)
HOLMIUM OXIDES
atomic charge and permittivity of, (E/T), 19: 47901(T)
oxygen-18 exchange between molecular oxygen and, 19: 46266
HOMOGENEOUS REACTORS
neutron resonance escape probability in thorium, 19: 47969
neutron resonance escape probability in thorium, Monte Carlo calculation of, 19: 47970
HORMONES
metabolism of steroid, effects of disease on, 19: 45729(R) (NYO-910-23, pp 1-111)
radiation effects on, in insects, 19: 45861
therapeutic use of, 19: 45729(R) (NYO-910-23, pp 1-111)
HOSPITALS
radiation exposure of personnel in, according to occupation, 19: 46657
radiation protection programs for, 19: 46679
radiation protection of personnel, 19: 46686
shielding of emergency, for use in event of radiological warfare, 19: 46669
HUMIDITY
measurement of, engineering drawings of psychrometer probe for, 19: 46745
radiosensitivity effects on Lupinus mutations, x, 19: 45847
radiosensitivity effects on grass seed, 19: 46004(P)
HUNGARY
cancer incidence in, 19: 45832
geology, 19: 45832
HYDANTOINS
metabolic effects in connective tissue cells, 19: 45895
HYDRAULICS
fluid amplifiers for remote-control operations, 19: 46502 (CONF-641120, pp 75-7)
HYDRAZINE
complexes with zirconium fluoride, preparation and stability of, 19: 46236 (NIJS-R-430)
yields in electron radiolysis of gaseous ammonia, 19: 46324(R) (AGN-8132)
HYDRAZINE, METHYL–
radiosensitivity effects on DNA, synergistic, 19: 46356
HYDRAZYL, DIPHENYLPICRYL-
effects on photolysis of cyclopentanone, 19: 46357
HYDRIODIC ACID
effects on metal extraction by tridodecylamine in organic diluent, 19: 46180 (UCRL-16254)
radioinduced decomposition of, distribution and energies of fragments from, 19: 46161(R) (ORNL-3832, pp 116-50)
radioinduced decomposition of deuterated, distribution and recoil energies of fragments from, 19: 46161(R) (ORNL-3832, pp 116-50)
cyclohexane–HI, charge-transfer complexes in pulse radiolysis of, 19: 46384
HYDROAROMATIC COMPOUNDS
effects on radiation effects on polymethyl methacrylate, 19: 46321 (AD-611779)
HYDROBROMIC ACID
effects on metal extraction by tridodecylamine in organic diluent, 19: 46180 (UCRL-16254)
reactions with halide ions, isotopic exchange and replacement, 19: 46293
HYDROCARBONS
determination by gas chromatography, 19: 46324(R) (AGN-8132)
preparation of tritium-labeled, by reactions of tritium ions with butane at 2 to 6 kev, 19: 46415
HYDROCHLORIC ACID
corrosive effects of 8 *M* solution of, on Zircaloy-2 at 35 to 105°C, 19: 46428(R) (ORNL-3847)
corrosive effects on tungsten and graphite at 2250°C, 19: 46956 (NP-15514(Vol.1))
corrosive effects on hafnium, niobium, tantalum, titanium, and zirconium carbides and diborides at 1250°C, 19: 46956 (NP-15514(Vol.1))
effects on metal extraction by tridodecylamine in organic diluent, 19: 46180 (UCRL-16254)
proton spin-lattice relaxation in deuterated and natural, (E), 19: 46287
reactions with halide ions, isotopic exchange and replacement, 19: 46293
HCl–NaCl, thermodynamic properties of, 19: 46237(R) (ORNL-3832, pp 76-99)
HYDROCYANIC ACID
yields in radiolysis of methane–nitrogen systems in fissiochemical loop, 19: 46324(R) (AGN-8132)
HYDRODYNAMICS
equations similarity solutions for one-dimensional, computer program for calculating, 19: 47118 (UCRL-12918-T)
shock waves in, calculations of pseudo-viscosity for, (T), 19: 47119 (UCRL-14244)
HYDROFLUORIC ACID
corrosive effects on zirconium, effects of nitric and sulfuric acid on, 19: 46957(R) (ORNL-3832, pp 100-6)
corrosive effects on graphite, calculation of, 19: 46956 (NP-15514 (Vol.1))
effects on metal extraction by tridodecylamine in organic diluent, 19: 46180 (UCRL-16254)
reactions with tungsten, 19: 46956 (NP-15514(Vol.1))
HF–methane, radiolysis yields in, 19: 46324(R) (AGN-8132)
HF–propane, radiolysis yields in, 19: 46324(R) (AGN-8132)
HF–S, radiolysis yields in, 19: 46324(R) (AGN-8132)
HYDROGEN
analysis for deuterium, thermal conductivity method for, 19: 46182 (NP-tr-1375)
catalytic effects of nascent, on metal preparation by reduction of salt, 19: 46253(T) (ORNL-tr-803)
containment of neutral solar plasma of, model for, (T), 19: 47188 (AD-613636)
containment of plasma of, in magnetic mirrors, 19: 47857
corrosive effects on graphite, calculation of, 19: 46956 (NP-15514 (Vol.1))
density of intergalactic ionized, limits on, (T), 19: 47196
density of neutral, near solar wind shock boundary, 19: 47211
determination by gas chromatography, methods for, 19: 46183(T) (NP-tr-1289)
diagnostics of transient plasma of, image-intensifying shutter for spectroscopic, 19: 47729
diffusion and permeation in niobium stainless steel S110, oxygen effects on, 19: 46991 (AWRE-O-47/65)
diffusion in palladium, electron and proton dissociation in, (T), 19: 46250(T) (ORNL-tr-623)
effects on embrittlement of irradiated chromium–molybdenum steel pressure vessel, 19: 47098
effects on sprayed molybdenum at 1350 and 1450°C, 19: 47054
electric current interruptions in thyratron gases of, (E), 19: 47128
electron beam reactions at 900 ev, plasma production by, (E/T), 19: 47787
electron density and temperature in plasma of, spectroscopic method for, (T), 19: 47754
electron elastic scattering by, interation-variation method for, (T), 19: 47247
electron reactions with atomic, ionization cross sections for, (T), 19: 47237(T)
electron reactions with atomic excitation and ionization in, (T), 19: 47243
electron reactions with, ionization cross sections for, (T), 19: 47253
electron temperature in positive column of discharge plasma of, (E),

19: 47738
injection of 20-kev neutral atoms of, into electron-cyclotron plasma, 19: 47837
ionization by, electron and proton impact at high energies, cross sections for, (T), 19: 47246
meson (K^-) capture by, hyperon mass determinations in, 19: 47302 (CU-1932-246)
meson (μ) capture rate in, 19: 47227
microwave reflection from plasma of, (E), 19: 47795
plasma production using titanium source, 19: 47793
positron scattering at 0 to 6.8 ev, higher partial waves in, (T), 19: 47238
pressure in ultrahigh-vacuum systems, measurement of, 19: 46578
properties of plasma of, in C Stellarator, (E), 19: 47854
radiation from molecular, stimulated near-infrared, (E/T), 19: 47260
reactions in three-body systems of atomic, long-range, (T), 19: 47249
reactions with graphite at 1900 to 2500°C, 19: 46956 (NP-15514(Vol.1))
scattering by helium, cross sections for elastic, 19: 46161(R) (ORNL-3832, pp 116-50)
scattering by hydrogen atoms, calculations of low-energy elastic, 19: 47264
spectral line broadening in theta-pinch plasma of, impurity, (E), 19: 47769
spectral of plasma of, adiabatic linear Stark effect, 19: 47716 (AD-614283)
yields from radiolysis of water, thermodynamics of, 19: 46343
yields from radiolysis of ethylene, 19: 46361
yields from radiolysis of benzene–dioxane mixtures, 19: 46363
yields in photo- and radiation chemistry of mineral acid glasses, effects of iron ions and nitrous oxide on, 19: 46394
yields in radiolysis of propane, scavenging effects of carbon tetrachloride, nitrous oxide, and sulfur hexafluoride on, 19: 46396
yields in radiolysis of ethylene–methane–nitrogen, 19: 46324(R) (AGN-8132)
yields in radiolysis of ammonia–deuterium, 19: 46324(R) (AGN-8132)

HYDROGEN ION CONCENTRATION
effects on electrochemical behavior of uranium (IV) in ethanol–water, 19: 46292

HYDROGEN IONS
charge in cadmium vapor, average, (E), 19: 47266
production by vacuum spark source, 19: 47147
production of di- and triatomic, in electron-bombardment sources, (T), 19: 47141
production of negative, from arc source, 19: 47142
production of negative, source for, 19: 47157 (AWRE-NR-1/65)
yields from radiolysis of water, thermodynamics of, 19: 46343

HYDROGEN ISOTOPES
fractionation in biosynthesis and chemical reactions, 19: 45729(R) (NYO-910-23, pp 1-111)

HYDROGEN PEROXIDES
magnetic resonance of photolyzed single-crystal, 19: 46161(R) (ORNL-3832, pp 116-50)
production in radiolysis of water containing carbon monoxide and oxygen, 19: 46332(R) (ORNL-3832, pp 50-65)
radiation effects on deuterated and natural, dipolar broadening of ESR lines in, 19: 46383

HYDROGEN SYSTEMS
Al–C–Cu–H–N–Sn–Ti–V–Zr, mechanical properties of, 19: 46985 (AD-613651)
Al_2O_3–H, radiolysis yields in, 19: 46324(R) (AGN-8132)
Cd–H, particle growth in flow of propellant of, 19: 46570 (AD-614111)
CO–H–N, radiolysis yields in, 19: 46324(R) (AGN-8132)
D–H, radiation for molecular, stimulated near-infrared, (E/T), 19: 47260

HYDROLOGY
radioisotopes in African, 19: 48111

HYDROMAGNETIC WAVES
analysis of cylindrical, in plasma, 19: 47798
propagation in ionosphere, (T), 19: 47501
propagation in toroidal discharge with longitudinal magnetic field, (E), 19: 47742
reflection and refraction at boundary of two compressible media, 19: 47138
theory for, magnetoionic, (T), 19: 47464
transmission in magnetosphere, impulse response to, (T), 19: 47467

HYDROPEROXIDES
yields from radiolysis of water, thermodynamics of, 19: 46343

HYDROQUINONE
use as a radical scavenger reagent to minimize radiation effects on TBP, 19: 46406(P)

HYDROXIDES
determination in scrubber solutions used in Dribble vent gas treatment plant, 19: 46471 (UCRL-14123)

HYDROXYL IONS
production in water radiolysis, (T), 19: 46401
yields from radiolysis of water, thermodynamics of, 19: 46343

HYDROXYL RADICAL
production in water radiolysis, (T), 19: 46401

HYDROXYLAMINE
reduction by iron in alkaline solutions, mechanisms of, 19: 46899(R) (ORNL-3832, pp 33-49)

HYGROMETERS
design of dew-pointer, engineering drawings for, 19: 46746
design of, engineering drawings for, 19: 46745

HYPERFRAGMENTS
model for mass-7 hyperon(Λ), two-body, 19: 47647
potentials in tritium-Λ, neutron-proton tensor, (T), 19: 47657
production of (Σ^-n), in deuteron-meson (K^-) interactions at rest, (T), 19: 47339
production of short-range, in meson (π^-) and proton reactions with emulsion nuclei, (E), 19: 47650
production on meson (K^-) capture by nuclei, (E/T), 19: 47648

HYPERONS
production and properties of Y_1^* in meson (K^-)-nucleus reactions, 19: 47708

HYPERONS (Λ^0)
binding in tritium hypernucleus, neutron-proton tensor forces in, (T), 19: 47657
interactions in mass-7 hypernuclei, two-body model for, 19: 47647
interactions with hyperons (Λ^0), scalar dipion resonance in S-wave zero-energy, (T), 19: 47337
interactions with hyperons (Σ^0), Y_0^*, decay from mixing in electromagnetic, (T), 19: 47366
mass determination of, by meson (K^-) capture in hydrogen, 19: 47302 (CU-1932-246)
production in deuteron-meson (K^-) interactions at rest, (T), 19: 47358

HYPERONS (Ω^-)
decay of, leptonic neutron, (T), 19: 47363

HYPERONS (Σ)
interactions with nucleons at low energy, T = ⅔ bound state in, (T), 19: 47348

HYPERONS (Σ^-)
binding in hyperfragments with neutrons, deuteron-meson (K^-) interactions for, (T), 19: 47339
mass determination of, by meson (K^-) capture in hydrogen, 19: 47302 (CU-1932-246)
production in meson (K^-)-nucleus reactions, 19: 47708

HYPERONS (Σ^0)
interactions with hyperons (Λ^0), Y_0^* decay from mixing in electromagnetic, (T), 19: 47366
mass determination of, by meson (K^-) capture in hydrogen, 19: 47302 (CU-1932-246)
production in deuteron-meson (K^-) interactions at rest, (T), 19: 47358

HYPERONS (Σ^+)
mass determination of, by meson (K^-) capture in hydrogen, 19: 47302 (CU-1932-246)
production in deuteron-meson (K^-) interactions at rest, (T), 19: 47358

HYPOPHOSPHORIC ACID, ALKYL ESTERS
tetrabutylhypophosphate–tetrabutylpyrophosphate, solvent properties for tetra- and pentavalent metals, 19: 46451

I

ICE
radiation effects on heats of transition and surface properties of low-temperature, gamma, 19: 46332(R) (ORNL-3832, pp 50-65)

IGNEOUS ROCKS
lead isotope composition in, review on, 19: 46582

IMAGE BRIGHTNESS INTENSIFIERS
conversion efficiencies of conventional x-ray, 19: 46151
efficiency of radiographic, 19: 46148
evaluation of x-ray, 19: 46150
limitations of optical, technical, 19: 46744

IMIDOGEN
spectra of deuterated, triplet bands in, 19: 46263

IMMUNE REACTIONS
antibody determination in Q fever, radioisotope precipitation test for, 19: 45739
antigenic adaptation in transplantable radioinduced tumors in mice, 19: 45873
radiation effects on, to transferred spleen cells in mice, 19: 45986
radiation effects on, to tissue transplants, 19: 45944
radiation effects on snake venom, x, 19: 45970
radiation effects on, in mice, 19: 45806 (AD-621543)

radiation effects on, to transplanted ultraviolet-induced sarcomas in mice, 19: 45827
radiation effects on, to transplanted tumors in mice, 19: 45858
radiation effects on, to kidney transplants in man, 19: 45888
radiation effects on, to bovine serum albumin in rabbits, 19: 45902
radiation effects on, in Ehrlich ascites tumor cells, 19: 45914
radiation effects on, in blood serum of swine, ultraviolet, 19: 45919
radiation effects on, in cattle twins, 19: 45760(R) (ORO-631, pp 83-121)
radiosensitivity of, in mice, 19: 45903
to Brucella vaccines prepared from irradiated bacteria, in mice, 19: 45868
to *Coxiella burnetii*, radioisotope precipitation test for, 19: 46076
to tendon grafts, effects of radiation exposure of grafts on, 19: 45964
to tendon grafts, effects of radiation exposure grafts on, 19: 45965
to transplanted hematopoietic tissues in animals, 19: 46009

IN-PILE LOOPS
construction and operation of ETR, 19: 48060(R) (IDO-17081, pp 1-47)
design and construction of, for fissiochemical fuels, 19: 46324(R) (AGN-8132)
materials for ATR gas, corrosion studies of, 19: 46946 (BNWL-100)
radiation monitors for, 19: 48071
removal from BGRR by remote cutting, 19: 48055 (BNL-9402)

INCONEL
corrosion of 600, by gaseous contaminants in helium at high temperatures, 19: 46946 (BNWL-100)
mechanical properties at cryogenic temperatures, 19: 47013 (PB-171809(Rev.)(Suppl.2))

INCONEL X
corrosion and fretting of fuel spacer-clips of, by water at 550° F, 19: 46913(R) (BMI-1733(Del.))
corrosion by water at high temperatures, 19: 46912(R) (BMI-1727(Del.))
mechanical properties at cryogenic temperatures, 19: 47013 (PB-171809(Rev.)(Suppl.2))
radiation effects on, for use as aerospace structural materials, (E/T), 19: 47077 (AD-613471)

INDIAN POINT POWER REACTOR
fuel handling equipment and operations, 19: 46490 (CONF-640508, pp 340-64)

INDIUM
analysis for thorium using *N*-benzoyl-*N*-phenylhydroxylamine, gravimetric, 19: 46194
bremsstrahlung reactions (γ,t) at 37 Mev, yields in, (E), 19: 47596(R) (TID-22141, pp 94-7)
determination by complexometric methods using EDTA, 19: 46219
neutron cross sections of, shell effects on thermal, (E), 19: 47618
superconducting properties to 0.3°K, (E), 19: 47517
superconducting properties of, 19: 47536
vapor pressure, 19: 46298

INDIUM ALLOYS
In–U, vaporization of, stability of intermetallic compounds in, 19: 46298

INDIUM ISOTOPES In-117
decay schemes, half-life of 89 kev transition in, 19: 47584(R) (ORNL-3832, pp 1-28)

3-INDOLEACETIC ACID
effects on plant growth, 19: 45817(R) (ORO-631, pp 145-71)

5-INDOLOL, 3-(2-AMINOETHYL)-
effects on thymidine uptake by mouse DNA, 19: 46016
protective effects against radiation damage in mice, 19: 46016

INDUCTION FURNACES
design of stagnation-flow, for high temperature gas-solid reaction rate measurement, 19: 46956 (NP-15514(Vol.1))

INFECTIONS
radiation effects on response of animals to virus, 19: 45974
radioinduced in domestic animals, 19: 45812(R) (ORO-631, pp 1-35)

INFLAMMATION
effects of bronchitis on pulmonary function after radiotherapy of lung carcinomas, 19: 46131
of uterus, late pathology of, 19: 46040

INFORMATION RETRIEVAL SYSTEMS
description of ANL-ENEA and NSIC systems, 19: 47908 (ANL-7050, pp 125-39)

INFRARED SPECTROMETERS
cell design for high pressure, portable, 19: 46771

INFRARED SPECTROSCOPY
method for analyzing odors in irradiated beef, 19: 46878 (NP-15455)

INSECTICIDES
effectiveness of toxaphene and ronnel for control of horn flies on cattle, 19: 45813(R) (ORO-631, pp 36-44)

INSECTS
chemically induced mutations of screw-worm fly, 19: 45950
control of *Siphona irritans* on cattle, 19: 45813(R) (ORO-631, pp 36-44)
radiation control of populations of, by sterile male technique, 19: 45960
radiation control of screw-worm populations, 19: 45960
radiation control of Mediterranean fruit fly (*Ceratitis capitata*) populations, 19: 45960
radiation control of melon fly (*Dacus cucurbitae*) populations, 19: 45960
radiation control of oriental furit fly (*Dacus dorsalis*) populations, 19: 45960
radiation control of malaria mosquito (*Anopheles quadrimaculatus*) populations, 19: 45960
radiation control of boll weevil (*Anthonomus grandis*) populations, 19: 45960
radiation control of codling moth (*Carpocapsa pomonella*) populations, 19: 45960
radiation control of European corn borer (*Pyrausta nubilalis*) populations, 19: 45960
radiation control of tsetse fly (*Glossina* spp.) populations, 19: 45960
radiation effects and annealing effects on electron spin resonances in ants, 19: 45954
radiation effects on endocrine system in *Celerio euphorbia*, 19: 45861
radioinduced mutations of screw-worm fly, 19: 45950
radiosensitivity of flour beetles, effects of pathogenic bacteria on, 19: 45908
zinc-65 metabolism in dragonfly, effects of body size and temperature on, 19: 45789

INSPECTION AND CONTROL
computer program for, of product tester development, 19: 48098 (SC-R-65-902)

INSTRUMENTATION
calibration and maintenance of, facilities for, 19: 46511
conference on Stockholm, Sept. 1964, 19: 46732
design for accurate counting of short-lived radioactivities, 19: 46818
development of reactor, in Germany, 19: 46825
module system for, engineering drawings of standard, 19: 46747

INSTRUMENTS
control by microprogrammed computers, (E), 19: 46813
design and operation for research on high-energy particle physics, 19: 47326
design and performance for digitally measuring and recording linear dimensions, 19: 48101 (SC-TM-65-332)
design for measuring azimuthal distortion in optical lenses, 19: 48103 (UCRL-16260)
design for measuring bowing in long tubes, 19: 46710 (BNWL-59)
design for obtaining integral of ω^2 dt, 19: 45730(R) (ORNL-3752)

INSULIN
separation of iodine-131-labeled A and B chains of, by thin-layer chromatography, 19: 46445

INTERFEROMETERS
design and performance of laser, for repetitively pulsed plasma, 19: 47730
design and performance of microwave, for high-speed plasma jet diagnostics, (E), 19: 47735(T)
use of laser, for plasma diagnostics in transverse modes, 19: 47745

INTERMETALLIC COMPOUNDS
crystal structure, 19: 46984(R) (AD-612275)

INTESTINE
muscular activity of guinea pigs, effects of radioprotective compounds on, 19: 46005(T) (JPRS-31933, pp 6-12)
nitrophenylbenzamine content in rat, 19: 46011
radiation effects on enzyme content in rat, 19: 45927
radiation effects on lysozyme activity of rat, 19: 45933
radiation effects on liquid and sodium metabolism in rat, protective effects of AET and cysteamine against, 19: 46027
radiation effects on glucose absorption by, in active and hibernating ground squirrels, 19: 45841
radiation effects on human, review, 19: 45922
radiation effects on mouse, protective effects of sodium cysteinethiosulfonate against, 19: 46006
radiation effects on phospholipase activity of mucosa of rats, 19: 45820(R) (TID-22227)
radiation injuries of, after radiotherapy of pelvic tumors, 19: 46065
radioinduced carcinoma of, after pelvic radiotherapy, 19: 46068
radiosensitivity of cells of rat, 19: 45926
radiosensitivity of mucosa of, 19: 45929
radiosensitivity of, in domestic animals, 19: 45812(R) (ORO-631, pp 1-35)

IODIDE IONS
reactions with haloacetic acids, isotopic exchange and replacement, 19: 46293

IODINE
content of, in hair of children, 19: 45784
content of, in urine of children, 19: 45784
determination in thyroid gland, x-ray spectrophotometric, 19: 46081

metabolism in lactating cows, effects of diiodosalicylic acid, potassium iodide, or L-thyroxine feeding on, 19: 45781
metabolism in man, tracer study, 19: 45754 (CEA-R-2787)
metabolism in thyroid gland, tracer study, 19: 45792
metabolism of, bound and exchangeable, in milk, 19: 45782
metabolism of, in children, 19: 45784
reactions of fission-recoil, with gases, 19: 46330 (NP-15370)
separation from fission products, method for, 19: 46169 (IDO-14664)

IODINE BROMIDES
reactions with rubidium ions in crossed-beam experiments, 19: 46161(R) (ORNL-3832, pp 116-50)

IODINE FLUORIDE OXIDES
spectra of, calculation of bonding and structure from Raman, 19: 46899(R) (ORNL-3832, pp 33-49)

IODINE IONS
reactions with potassium in crossed-beam experiments, 19: 46161(R) (ORNL-3832, pp 116-50)

IODINE ISOTOPES
exchange between alkyl iodides and zinc iodide, 19: 46294

IODINE ISOTOPES I-125
detection and measurement of, performance of scintillation detector and collimator for, 19: 46119
determination in thyroid tissue, autoradiographic, 19: 45783
incorporation in proteins by enzymatic iodination, 19: 46314
metabolism in thyroid gland of mice, 19: 45783
metabolism of sodium iodide-incorporated, in lactating cows, 19: 45781
uptake by abomasum, feces, plasma, thyroid, and urine from milk, 19: 45782

IODINE ISOTOPES I-127
sorption on atmospheric particles, 19: 46672

IODINE ISOTOPES I-129
energy levels of, magnetic moment of 26.8-kev, 19: 47115(R) (ANL-6983)
properties for use as nonradioactive tracer in biological systems, 19: 45799

IODINE ISOTOPES I-131
beta decay in potassium iodate, formation of xenon compounds from, 19: 46411
carcinogenic effects in mice, 19: 45808(R) (NYO-901-36)
contamination of food by, after radiation accident, 19: 46694
content in atmosphere and drinking water, Moncloa Station, Spain, 1964, 19: 46597
content in blood plasma proteins, 19: 46081
determination in aqueous solutions by detection of Cherenkov radiation, 19: 46215
diagnostic use for localization of brain tumors, 19: 46046
diagnostic use of, for localization of subdiaphragmatic abscess, 19: 46048
diagnostic use of, for thyroid diseases, 19: 46072
effects of therapeutic doses of, on thyroid function, 19: 46082
effects on chickens, age dependence of, 19: 45761(R) (ORO-631, pp 122-31)
effects on pituitary hormones in mice, 19: 45808(R) (NYO-901-36)
energy levels and gamma transitions from tellurium-131g decay, (E), 19: 47663
excretion by rats, effects of ingestion of anion exchange materials on, 19: 45760(R) (ORO-631, pp 83-121)
incorporation in proteins by enzymatic iodination, 19: 46314
incorporation into proteins, electrolytical method for, 19: 46142
metabolism by chickens, 19: 45761(R) (ORO-631, pp 122-31)
metabolism by dairy cows, 19: 45760(R) (ORO-631, pp 83-121)
metabolism by man, effects of climatic temperature on, 19: 45779
metabolism by rainbow trout, 19: 45796
metabolism of L-thyroxine-incorporated, in lactating cows, 19: 45781
metabolism of sodium iodide-incorporated, in monkey respiratory tract and thyroid, 19: 45776
placental transfer in dairy cows, 19: 45760(R) (ORO-631, pp 83-121)
radiation hazards of, released by accident, 19: 46696
therapeutic use of, for thyrotoxicosis, 19: 46122
thyroid ablation induced by, in chickens, 19: 45966
thyroid metabolism of, in whole and sliced lobes of rats, 19: 45786
tracer use for kidney function tests, 19: 46130
uptake by abomasum, feces, plasma, thyroid, and urine from milk, 19: 45782
uptake by rat thyroid, effects of carbon monoxide exposure on, 19: 45770
uptake by thyroid in children, environmental, 19: 46035 (PHS-999-RM-14)
use as label for iothalamate for kidney function tests, 19: 46079
use for kidney function tests in children, 19: 46109
use in determining glomerular filtration rate in man, 19: 46071
use in radiodiagnosis, 19: 46102
use in therapy of thyroid diseases, 19: 45792
use in treatment of thyroid diseases during pregnancy, 19: 46049
use with polyvinylpyrrolidone in brain scanning, hazards and ineffectiveness of, 19: 46058
used in coronary blood circulation measurement in relation to ischemic myocardium in dogs, 19: 45767

IODINE ISOTOPES I-132
chemical reactions of, from beta decay of technetium-132 in technetium chlorides in aliphatic-aromatic mixture, 19: 46412
sorption on atmospheric particles, 19: 46672

IODINE ISOTOPES I-133
decay schemes, (E), 19: 47584(R) (ORNL-3832, pp 1-28)
gamma spectra from 21-hour, (E), 19: 47584(R) (ORNL-3832, pp 1-28)

IODINE ISOTOPES I-135
separation from homogeneous suspension reactor fuels, method for, 19: 46426 (NP-15362)

IODINE SYSTEMS
cyclohexane–I, charge-transfer complexes in pulse radiolysis of, 19: 46384

ION BEAMS
production and uses, 19: 47226
production using duoplasmatron, 19: 47267

ION EXCHANGE
analytical use for trace elements in beef heart, 19: 45753 (AE-191)
isotope separation by, 19: 46413

ION EXCHANGE MATERIALS
ionic selectivity of organic, mechanisms of, 19: 46237(R) (ORNL-3832, pp 76-99)
sorptive properties for anionic complexes of beryllium, 19: 46230 (AAEC/E-136)
sorptive properties of Amberlite for lithium and sodium ions, effects of anions on, 19: 46899(R) (ORNL-3832, pp 33-49)

ION EXCHANGERS
diffusion in, exchange, 19: 46239(R) (ORO-631, pp 132-41)
physical chemistry of, 19: 46237(R) (ORNL-3832, pp 76-99)

ION SOURCES
design, 19: 47226
design and operation at Harwell, 19: 48115
design and performance of arc, for negative hydrogen ion production, 19: 47142
design and performance of r-f negative, 19: 47157 (AWRE-NR-1/65)
design of high-brilliance, for use with Saturne Accelerator, 19: 47172
operation of duoplasmatron, 19: 47267
particle growth in ionic nucleation condensation colloidal, 19: 46570 (AD-614111)
performance of electron-bombardment, for propulsion, 19: 46572 (NASA-TN-D-3041)
properties of vacuum spark, for hydrogen and deuterium ions, 19: 47147

IONIZATION CHAMBERS
design and performance for neutron and heavy particle dosimetry, 19: 46847
design and performance for clinical dosimetry, 19: 46854
design for radiographic dosimetry, 19: 46043
design of energy independent, with digital type electrometer circuit for use in diagnostic radiology, 19: 46861
design of parallel-plate and thimble, for measuring absorbed dose rate in vinyl chloride, 19: 46368
development and performance for diagnostic x-ray dosimetry, 19: 46857
development for radiation dosimetry, 19: 46841
dosimetry with, radiographic, 19: 46043
performance for dosimetry, 19: 46844
performance in environmental dose measurements, 19: 46855
performance of high-pressure, 19: 46845
performance of transistorized, for measuring α and neutron fission rates, 19: 47567 (CEA-R-2775)
use in standardization of isotopic radiation sources, 19: 46421
volume recombination characteristics of parallel-plate, 19: 46830

IONOSPHERE
current systems in, magnetospheric effects on, (T), 19: 47469
disturbances in, properties of and solar activity effects on, 19: 47497
disturbances in, solar activity effects on sudden, 19: 47494
electron content in, determination using satellite signals, 19: 47448 (AD-612119)
electron density in, Langmuir probe measurements of, (E), 19: 47465
emission by, geomagnetic micropulsations and noise, 19: 47493
geomagnetic micropulsation transmission in, (T), 19: 47466
ionization increases in, pre-SC, 19: 47455
ionization motions in, in E region and above, 19: 47492
properties and structure of F region of, 19: 47490
properties of D and E regions of, 19: 47489
properties of outer region of, 19: 47491
solar flare effects on, geomagnetic, 19: 47480
solar radiation effects on, 19: 47496

variations in sporadic-E layer in, spectrum of, (E), 19: 47475
wave propagation in, (T), 19: 47501
wave propagation in, (T), 19: 47502
whistler production in, ion-cyclotron, (E/T), 19: 47445 (AD-611828)
IONS
collisions of, bibliography on, 19: 47258
effects on electromagnetic wave propagation in ionosphere, 19: 47445 (AD-611828)
motion of singly-charged, in two-component plasma, (T), 19: 47747
motions in electromagnetic fields, (T), 19: 47464
reactions with atoms in plasma, inelastic, (T), 19: 47812
reactions with molecules in ethylene, mass spectrometry of, 19: 46161(R) (ORNL-3832, pp 116-50)
transport in aqueous solutions, isotope effects in, 19: 46898 (HMI-B-44)
IRIDIUM
separation from ruthenium by radiochemical methods, 19: 46444
IRIDIUM ISOTOPES Ir-192
therapeutic use of wires of, for pectoral tumors, 19: 46047
IRON
analysis for thorium using *N*-benzoyl-*N*-phenylhydroxylamine, gravimetric, 19: 46194
analysis of liquid, for oxygen, 19: 46297
content and distribution in beef heart, 19: 45753 (AE-191)
crystal deformations in, analysis of double kink, (T), 19: 47011 (ORNL-3862)
defects in pure and doped, recovery phases of point, 19: 47094(T) (ORNL-ti-668)
determination by complexometric methods using EDTA, 19: 46219
determination by potentiometric titration of acid liberated by complex formation, 19: 46205
determination in aluminum, activation, 19: 46207
determination in aluminum alloys by activation, 19: 46157(R) (MLM-1254)
dissolution in noninhibiting solutions, mechanisms of, 19: 46957(R) (ORNL-3832, pp 100-6)
effects on crystal structure of uranium, 19: 47048
effects on density of states in superconductors, 19: 47535
effects on internal friction peak in beryllium, 19: 47056
effects on network structure in uranium, 19: 47060
effects on reaction between tin (II) and uranium (IV), 19: 46292
electron beam backscattering at 4 to 14 Mev, effects on target current of, (E), 19: 47181
electron emission from surfaces of, thermionic, 19: 46571 (HRL-5249-S)
gamma transport in slabs of, dose buildup factors for, (T), 19: 47864 (ANL-7050, pp 113-22)
metabolism of, tracer studies, 19: 46102
oxidation by carbon monoxide–carbon dioxide systems, 19: 46297
phase transformations in, metallographic observations of, 19: 47000 (NMI-4996, pp 8-18)
radiation damage in α, neutron, 19: 47105
radiation effects on, lattice atom displacement probabilities in deuteron and neutron, (T), 19: 47104
separation from rare earths by precipitation using dehydroxymaleic acid, 19: 46452
surface tension of, measurement by pendant drop method, 19: 47065
IRON ALLOYS
properties for aerospace uses, 19: 47068
Al–Cu–Fe–Sn–Ti–V, additive and alloying effects on mechanical properties of, 19: 46985 (AD-613651)
Al–Fe–U, radioinduced swelling in, resistance to, 19: 47103
Cr–Fe–Ni, stress corrosion cracking of Alloy 600 by wetted thermal insulation, 19: 46949 (CONF-650905-2)
Fe–Mo, crystal structure of, effects of molybdenum content on, 19: 47029
Fe–Os, hyperfine fields at osmium nuclei in, 19: 47069
Fe–Pt, hyperfine fields at platinum nuclei in, 19: 47069
Fe–Pu–U, properties and structure of, 19: 46992 (CEA-R-2792)
Ge–Fe–Pu, reactions with tantalum at 900 to 1150°C, 19: 46950 (LA-DC-7315)
IRON BORIDES
surface tension of molten, 19: 47021(T) (JPRS-31225)
IRON CARBONYLS
complexes with nitrosobenzene, radioinduced formation of, 19: 46397
IRON(III) CHLORIDES
effects on photolysis of cyclopentanone, 19: 46357
IRON IONS
effects of divalent, on hydroxylamine, nitrates, and nitrites, 19: 46899(R) (ORNL-3832, pp 33-49)
effects of yields in photo- and radiation chemistry of mineral acid glasses, 19: 46394
electronic g factors of low-lying levels of singly ionized, (E), 19: 47240
IRON ISOTOPES
proton elastic scattering at 14.5 Mev, cross sections for, 19: 47705
IRON ISOTOPES Fe-54
alpha inelastic scattering at 44 Mev, collective states in, 19: 47608
deuteron reactions (d,n) with, spectra from, 19: 47115(R) (ANL-6983)
energy levels from iron-56 (p,t) at 28 Mev, 19: 47706
neutron reactions (n,α), (n,2n), and (n,p) at 2.2 to 16.8 Mev, cross sections for, (E/T), 19: 47668
proton inelastic scattering at 14.6 to 18.2 Mev, (E/T), 19: 47702
IRON ISOTOPES Fe-55
content in fish from lake waters in Finland, 1965, 19: 46587(R) (NYO-3446-3)
energy levels from proton reactions (p,n) with manganese-55 at 3.315 and 3.525 Mev, (E), 19: 47696
energy levels from iron-56 (p,d) at 28 Mev, 19: 47706
use in radiodiagnosis, 19: 46102
IRON ISOTOPES Fe-56
energy levels from iron-58 (p,t) at 28 Mev, 19: 47706
neutron reactions (n,n'γ) at .97 to 4.76 Mev, gamma angular distributions and cross sections from, (E/T), 19: 47591(R) (TID-22012, pp 99-128)
neutron reactions (n,p) at 14 Mev, cross sections for, (E), 19: 47673
proton reactions (p,d) and (p,t) at 28 Mev, (E), 19: 47706
uptake by tree branches, leaves, needles, roots, and stems from soil, 19: 45773
IRON ISOTOPES Fe-57
energy levels from iron-58 (p,d) at 28 Mev, 19: 47706
IRON ISOTOPES Fe-58
energy levels of, parity and spin of, 19: 47605
proton reactions (p,d) and (p,t) at 28 Mev, (E), 19: 47706
IRON ISOTOPES Fe-59
determination in irradiated steel by ion-exchange separation and gamma spectrometry, 19: 46195
use in radiodiagnosis, 19: 46102
IRON OXIDES
oxidation and reduction by carbon monoxide–carbon dioxide systems, 19: 46297
IRON(II) OXIDES
thermodynamic properties of, at 500 to 1300°C, 19: 46297
IRON(III) OXIDES
thermodynamic properties of, at 500 to 1300°C, 19: 46297
IRON(II) SULFATES
performance in calorimetric dosimeters, 19: 46849
IRON SYSTEMS
Al–Cr–Fe–Si–U, radioinduced swelling in, resistance to, 19: 47103
Al–Fe–Mo–Si–U, radioinduced swelling in, resistance to, 19: 47103
Al–Fe–Si–U, radioinduced swelling in, resistance to, 19: 47103
Fe–D_2O, neutron energy spectra in laminated, variations in, (E/T), 19: 47561
Fe–Pb, gamma transmission by laminated, 19: 47872
Fe–Si–U, radioinduced swelling in, resistance to, 19: 47103
IRRADIATION FACILITIES
conveyor system design for package, 19: 46523(P)
design and construction of alpha-gamma, for fuel studies, 19: 47975 (BNL-9450)
design for medical use, effects of erythemal dose data on, 19: 45881
design of betatron, 19: 46042
design of conveyor system for, 19: 46519(P)
remote handling in gamma cell, 19: 46490 (CONF-640508, pp 340-64)
IRRADIATION TECHNIQUES
for grass seed using gamma radiation, 19: 46004(P)
ISOBUTYRIC ACID
radiolysis of tritium-labeled, separation of products from self-, 19: 46213
ISOLEUCINE
determination in mixture with leucine and valine by infrared spectrometry, 19: 46184(T) (ORNL-*tr*-341)
ISOTOPE EFFECTS
carbon-14, on oxidation of benzoin, 19: 46304(R) (ORNL-3832, pp 66-75)
deuterium, on oxidation of 1,2-diphenylethylene glycol, 19: 46304(R) (ORNL-3832, pp 66-75)
in Beckmann rearrangement of acetophenone oxime and benzyl methyl ketoxime, 19: 46304(R) (ORNL-3832, pp 66-75)
of deuterium on decomposition of permanganates in alkaline solutions, 19: 46275
of deuterium on radiolysis of cyclohexane-d_{12}–cyclopentane mixtures, 19: 46364
on migration of lithium ions in acetic acid, at 5 to 55°C, 19: 46264
ISOTOPE SEPARATION METHODS
economic optimum of saturator separation column condenser in, 19: 46901
ion transport in aqueous solutions, 19: 46898 (HMI-B-44)
research programs on, in Japan, 19: 46413

ISOTOPIC EQUILIBRATION
uses in chemical analysis, 19: 46204
ISOTOPIC EXCHANGE
between molecular oxygen and rare earth oxides, 19: 46266
effects of separation factor in, on properties of exchanged molecules, 19: 46408(T) (ORNL-tr-770)
mechanisms of, in haloacetic acids, 19: 46293
of deuterium with hydroxyl groups on surface of alumina, 19: 46280
thermodynamics of boron isotope, in boron trifluoride addition compounds, 19: 46899(R) (ORNL-3832, pp 33-49)
ISOVALERONE
solvent properties for protactinium, 19: 46212
ISRAEL
leukemia incidence in, epidemiology of, 19: 45958
ITALY
manganese-54 in mollusks from Lake Maggiore, 19: 45788
nuclear power developments in, 19: 48008
sorptive properties of tuffs from Lake Bracciano region for cesium and strontium, 19: 48081 (RT/PROT(65)19)

J

JAPAN
atomic energy research programs at universities in, 19: 48116
isotope separation research in, review of, 19: 46413
reactor physics studies in, report of special committee on, 19: 47965
JAWS
radiosensitivity of bones of, in children, 19: 46074
radiosensitivity of bones of, in children, 19: 46075
JEEP REACTOR
development and operation of, industrial requirements for, 19: 48114
JET PUMPS
design of, for pressurized-water reactors, 19: 47974(P)

K

KAOLINITES
beryllium sorption in, effects of acidity on, 19: 45802
KEROSENE
D2EHPA–kerosene–TBP, solvent properties for rare earths from complexed waste solutions, 19: 46432 (ORNL-P-1603)
kerosene–4-*sec*-butyl-2(α-methylbenzyl)phenol, solvent properties for cesium from alkaline waste solutions, 19: 48075 (BNWL-68)
KIDNEYS
function tests in children, using radioisotopes as tracers, 19: 46109
function tests of, using radioisotopes, 19: 46102
function tests using iodine-131–sodium iothalamate, 19: 46079
glomerular filtration in human, use of iodine-131-labeled Hypaque for determining, 19: 46071
nitrophenylbenzamine content in rat, 19: 46011
radiation effects on mouse, protective effects of sodium cysteinethiosulfonate against, 19: 46006
radiation effects on poliovirus production by monkey, 19: 45955
radiation effects on immune reactions to transplanted, in man, 19: 45888
radiodiagnosis of diseases of, using labeled compounds and external scanning, 19: 46130
thorium-228 decay in beagle, metabolism of bismuth-212, lead-212, and radium-224 from, 19: 45798
toxic effects of OMRE High Boilers and Santowax OM on rat, 19: 45769
KRYPTON
content in samarskites, 19: 46598
effects on radioinduced decomposition of plutonium hexafluoride, 19: 46325 (ANL-7013)
effects on x radiolysis of acetylene, methylacetylene, and ethylacetylene, 19: 46334 (TID-22231)
electric discharges in, plasmoid production by h-f electrodeless, (E), 19: 47788
ionization by, electron and proton impact at high energies, cross sections for, (T), 19: 47246
photoionization cross sections for, calculation from model wave functions, (T), 19: 47216 (AD-613675)
scattering of cesium ions by, angular distribution of elastic, 19: 46161(R) (ORNL-3832, pp 116-50)
KRYPTON IONS
beams of, analysis of duoplasmatron, 19: 47267
diffusion in aluminum at high bombardment energies, 19: 47080 (EUR-2478.e)
KRYPTON ISOTOPES
abundance in meteorites, anomalies in, 19: 47213
KRYPTON ISOTOPES Kr-84
concentration in krypton isotopic mixtures by thermal diffusion, 19: 46157(R) (MLM-1254)
KRYPTON ISOTOPES Kr-85
separation from other fission products, 19: 46414
used in coronary blood circulation measurement in relation to ischemic myocardium in dogs, 19: 45767
uses of, survey of, 19: 46414
KRYPTON ISOTOPES Kr-86
concentration in krypton isotopic mixtures by thermal diffusion, 19: 46157(R) (MLM-1254)

L

LABORATORIES
description of ultrapure materials, at Y-12, 19: 46510 (Y-DA-967)
design and operation for research on high-energy particle physics, 19: 47326
development for electron microscopic and x-ray studies at Grenoble Nuclear Center, 19: 46512
helium purification system for ANL 350, 19: 46513
proposal of, for telechirics research, 19: 46497 (CONF-641120, pp 39-40)
LABORATORY EQUIPMENT
design of reaction chamber with catalyst-containing fibers, 19: 47985(P)
economics of, for servicing nuclear instruments, 19: 46511
LAMINATES
gamma transmission by iron–lead, 19: 47872
LANTHANUM
analysis for thorium using *N*-benzoyl-*N*-phenylhydroxylamine, gravimetric, 19: 46194
cohesive energy and ionization of, relation between, (T), 19: 47062
content and distribution in beef heart, 19: 45753 (AE-191)
LANTHANUM ALLOYS
Al–La, crystal structure of Laves phases in, 19: 47052
Co–La, crystal structure of Laves phases in, 19: 47052
La–Mg, diffusion of beryllium to surface of, on heating at 300 to 500°C, 19: 47071
La–Pd, phase studies, 19: 47051
LANTHANUM BORIDES
preparation and purification, 19: 46941 (NP-15514(Vol.3))
thermionic emission and cesium atom surface ionization of, 19: 47148
LANTHANUM BROMIDES
thermal decomposition of hydrates of, mechanisms of, 19: 46271
LANTHANUM FERRITES
crystal structure, 19: 46256
LANTHANUM IONS
quadrupole coupling in cerium magnesium nitrate and neodymium ethylsulfate lattices, 19: 47883 (UCRL-16279)
LANTHANUM ISOTOPES La-139
neutron reactions (n,α) at 14.6 Mev, angular and energy distributions from, (E/T), 19: 47637
LANTHANUM ISOTOPES La-140
gamma-gamma angular correlation in, (E), 19: 47649
nuclear quadrupole moment, 19: 47883 (UCRL-16279)
LANTHANUM OXIDES
atomic charge and permittivity of, (E/T), 19: 47901(T)
oxygen-18 exchange between molecular oxygen and, 19: 46266
reactions with barium carbonates, ternary oxide formation in, 19: 46242(R) (TID-22207, Paper B)
LARVAE
radiation effects on endocrine system in insect, 19: 45861
LEAD
electron beam backscattering at 4 to 14 Mev, effects on target current of, (E), 19: 47181
photoelectron production by 145, 280 and 320 kev gamma rays, cross sections for, (T), 19: 47329
preparation of irradiated composite of aluminum-clad ceramic fuel bonded with, for metallography, 19: 47087 (NMI-4997, pp 189-97)
radiation effects on color centers in potassium chlorides doped with, electron, (E), 19: 47891
shielding properties of, 19: 46036
superconducting currents in junctions of, Josephson, 19: 47515
superconducting persistent currents in Josephson junction of, (E), 19: 47521
superconducting properties of, 19: 47536
LEAD ACETATES
effects on sulfur-35 fixation in rat liver, 19: 45800
LEAD ALLOYS
excitations in strong-coupling superconducting, Fermi-liquid theory for collective, 19: 47518
Pb–Sn, thermodynamic properties, 19: 46297
Pb–U, vaporization of, stability of intermetallic compounds in,

19: 46298
LEAD CARBONATES
reactions with rare earth oxides, ionic field strengths as criteria for compound formation in, 19: 46246(R) (TID-22207, Paper F)
LEAD COUPLES
Al/Pb, performance of superconducting diodes of, as sound detector, 19: 46739
LEAD ISOTOPES
composition in granites, lead ores, and pegmatites, 19: 46582
LEAD ISOTOPES Pb-206
neutron reactions (n,n'γ) at 1.0 to 4.6 Mev, gamma angular distributions from, (E/T), 19: 47592(R) (TID-22012, pp 129-55)
LEAD ISOTOPES Pb-207
neutron reactions (n,n'γ) at 1.0 to 4.6 Mev, gamma angular distributions from, (E/T), 19: 47592(R) (TID-22012, pp 129-55)
LEAD ISOTOPES Pb-208
alpha inelastic scattering at 44 Mev, cross section angular dependence in, 19: 47608
neutron reactions (n,n'γ) at 3.0 to 4.5 Mev, gamma angular distributions from, (E/T), 19: 47592(R) (TID-22012, pp 129-55)
LEAD ISOTOPES Pb-210
content in human bones and hair in Warsaw, 1963, 19: 45795
LEAD ISOTOPES Pb-212
uptake and distribution in beagle bones, kidneys, liver, and spleen from thorium-228 decay, 19: 45798
LEAD ISOTOPES Pb-214
content in atmosphere, 19: 46605
LEAD ORES
lead isotope composition in, review on, 19: 46582
LEAD OXIDES
thermodynamic properties of, at 500 to 1300°C, 19: 46297
$PbO–SiO_2$, thermodynamic properties and oxygen pressure in, at 800, 900, 1000, and 1100°C, 19: 46297
$PbO_2–ThO_2$, neutron resonance absorption in, (E/T), 19: 47575 (IDO-16986)
$PbO_2–UO_2$, neutron resonance absorption in, (E/T), 19: 47575 (IDO-16986)
LEAD SULFATES
solubility of, effects of labeling with sulfur-35 on, 19: 46274
$BaSO_4–PbSO_4$, sorptive properties for x rays as function of photon energy, 19: 46150
LEAD SYSTEMS
Fe–Pb, gamma transmission by laminated, 19: 47872
$Pb–UO_2$, use as radiation shielding, 19: 46916 (BNWL-IR-3)
LEAD, TETRAPHENYL-
effects on scintillation quenching in benzene, 19: 46362
radiolysis of, in benzene, 19: 46362
LEAD ZIRCONIUM TITANATES
$Pb(Zr_{0.65}Ti_{0.35})O_3–Nb_2O_5$, radiation effects on crystal structure and electric properties, 19: 47096
LEAK DETECTORS
design of, for liquid in gas, 19: 46713 (CEA-R-2811)
LEAKS
rates in PRTR containment vessel, 19: 48057 (BNWL-109)
LEAVES
fallout monitoring in pine needles, 1959 to 1964, 19: 45751
polonium-210 content in tobacco, from four countries, 19: 45801
radiation effects on stomatal movement of Begonia, 19: 45854
LECTURES
book: *Lectures on Particles and Field Theory*, 19: 47405
on gravitational field theory, 19: 47411 (NP-15436)
LEPTONS
production in baryon decays, V-A theory for, (T), 19: 47307 (JINR-P-2278)
LEUCINE
determination in mixture with isoleucine and valine by infrared spectrometry, 19: 46184(T) (ORNL-tr-341)
LEUKEMIA
development in polycythemia vera, terminology in, 19: 46089
epidemiology of, in Israel, 19: 45958
epidemiology of, in chiropractors, 19: 45866
etiology of, role of radiation in, 19: 45833
etiology of, role of viruses in, 19: 45833
incidence in Great Britain of, 19: 45959
induced by radiotherapy, 19: 45808(R) (NYO-901-36)
radioinduced in man, 19: 45996
radioinduced in mice, effects on chromosomal aberrations of x, 19: 45911
radioinduced in mice, 19: 45808(R) (NYO-901-36)
radioinduced in tuberculosis patients, 19: 45870
radioinduced, chromosome studies of, 19: 45915
radioinduced, in residents of Hiroshima exposed to atomic explosion, 19: 45846
LEUKOCYTES
chromosome patterns in leukemic, 19: 45915
chromosome studies of, in tissue culture, 19: 45915
radiation effects on, in rats, 19: 45934
radioinduced chromosome aberrations of lymphocytes, in man, 19: 45916
radioinduced chromosome aberrations of lymphocytes, in man, 19: 45917
radioinduced chromosome aberrations in, 19: 45813(R) (ORP-631, pp 36-44)
tissue cultures of, from domestic animals, 19: 45813(R) (ORO-631, pp 36-44)
LIDO
design and operation, 19: 48115
LIFE SPANS
of mice, 19: 45809(R) (NYO-1979-12)
radiation effects on mouse, embryonic exposure, 19: 45852
radiation effects on, of mice, 19: 45808(R) (NYO-901-36)
radiation effects on, of personnel exposed to radiation during employment at nuclear energy installations, 19: 45810(R) (NYO-3394-2(Rev.))
radiation effects on domestic animal, 19: 45814(R) (ORO-631, pp 45-66)
radioinduced reduction in mouse effects of genetic damage on, 19: 45969
LIGHT
distortion in lenses, instrument for measuring azimuthal, 19: 48103 (UCRL-16260)
effects on chemiluminescence induction in organic compounds in presence of oxygen, 19: 46344
effects on formation of dimeric nitrosobenzene–irontricarbonyl, 19: 46397
frequency modulation of, by electrically birefringent crystals, 19: 48110(T) (SC-T-65-750)
hazards of flashblindness from viewing, from nuclear detonation, 19: 46655
refraction by plasma, diagnostics from, (T), 19: 47818
scattering by plasma, (E), 19: 47781
LIGNIN
content in range plants, Miles City, Montana, 1955 to 1960, 19: 45747 (ORNL-TM-1279)
LIMBS
description of artificial arm-aid for paralyzed patients, 19: 46483 (CONF-640508, pp 158-97)
LINEAR ACCELERATORS
beam pulse shortening in wave guide of electron, (E), 19: 47182
design and operation at Harwell, 19: 48115
development at University of Paris, 19: 46643(R) (LAL-1136)
target current of electron, effect of backscattering at 4 to 14 Mev on, (E), 19: 47181
LINOLEIC ACID
carbon-14 labeled, stability in rats of, 19: 45785
labeling cholesterol ester of, with carbon-14 and tritium, 19: 46309
stability of labeled, in rats, 19: 45785
tritium labeled, stability in rats of, 19: 45785
LINOLENIC ACID
radioinduced chemiluminescence of, in presence of oxygen, 19: 46344
LIPIDS
metabolism in rats, tracer study, 19: 45785
LIPOPROTEINS
electrophoresis of human serum, review of Staflow, 19: 48105 (UCRL-16290)
LIQUID FLOW
calculation of nonlinear, difference method for, (T), 19: 46533 (LA-DC-7373)
LIQUID METAL COOLED REACTORS
fuel elements of BN-350, temperature distributions in, (E), 19: 47994 (NP-15393)
safety of sodium cooled, zirconium hydride moderated, 19: 48034
LIQUIDS
book: *High Temperature Heat-Transfer Agents*, 19: 46540(T) (AD-619382)
determination in gases, detector for, 19: 46713 (CEA-R-2811)
neutron time-decay constants in, upper bounds for pulsed, (T), 19: 47553
particle adhesion to surfaces in, decontamination methods for removal of, 19: 46645 (ORNL-TM-1228)
photon interactions in, properties of, (T), 19: 47332
theory of Fermi, quasi-particle, 19: 47443
wave velocity in, general relativity theory for elastic collision, (T), 19: 47414
LITHIUM
determination by thermal neutron capture, 19: 46221
diffusion in p-type silicon, electrophotographic determination of, 19: 46997 (JINR-P-2282)
electric conductivity at 200 to 1430°C, 19: 47015 (TID-854)
neutron reactions at 14 Mev, tritium yields from, 19: 47721 (LA-3385)

LITHIUM ANTIMONATES
Li_3SbO_4–Li_3NbO_4–Li_3TaO_4, phase diagram, 19: 46276
LITHIUM BOROHYDRIDES
thermal stability of, and its dioxanate, 19: 46248(T) (FTD-TT-65-591)
LITHIUM CHLORIDES
diffusion of cerium and promethium ions in solutions of, at 25 to 45°C, 19: 46261
molal volume and salt-induced structure transitions of aqueous, 19: 46237(R) (ORNL-3832, pp 76-99)
LiCl–KCl–UCl_3, uses in electrolytic processing of irradiated uranium fuels, 19: 46448
LITHIUM COOLED REACTOR EXPERIMENT
liquid-metal pumps and sumps for, development of, 19: 46535(R) (PWAC-386)
LITHIUM DEUTERIDES
x-ray small-angle Compton scattering by, energy-gap determination from, (E), 19: 46286
LITHIUM FLUORIDES
properties as thermoluminescent dosimeter, 19: 46859
radioinduced color centers in, symmetry of narrow-band absorption centers and luminescence from gamma, 19: 46380(T)
radioinduced thermoluminescence in, use for dosimetry, 19: 46338 (UCRL-12367)
radioinduced thermoluminescence and color centers in crystals of, gamma, 19: 46762(R) (NYO-3474-1)
spectra of vaporized, 19: 46982(R) (AD-611856)
thermoluminescent properties of, 19: 46338 (UCRL-12367)
LiF–NaF, mixing enthalpies of molten, molar, 19: 46161(R) (ORNL-3832, pp 116-50)
LITHIUM HYDRIDES
electric moments of molecular, valence electron approximation for, (T), 19: 46284
production of plasma of, by laser irradiation, (E), 19: 47846
LITHIUM HYDROXIDES
corrosive effects of solutions of, on nickel-plated aluminum at 330°C, 19: 46945 (BNWL-98)
LITHIUM IONS
electrolysis of acetic acid solutions of, isotope effects on migration in, 19: 46264
sorption by Amberlite, effects of anions on, 19: 46899(R) (ORNL-3832 pp 33-49)
LITHIUM ISOTOPES
separation by ion exchange chromatography, single-stage separation factors for, 19: 46899(R) (ORNL-3832, pp 33-49)
LITHIUM ISOTOPES Li-5
energy levels of, structure of 16.7-Mev, (T), 19: 47687
LITHIUM ISOTOPES Li-6
alpha reactions (α,t) at 40 Mev, differential cross sections for, (E/T), 19: 47574 (IAE-836)
charged particle reactions with, energy levels and mechanisms of, 19: 47564(R) (AD-612038)
effects on migration of lithium ions in acetic acid solutions in electrolysis, 19: 46264
energy levels of, three-body model for 2^+, (T), 19: 47645
neutron inelastic scattering at 14 Mev, (E), 19: 47609
neutron scattering at 4.4 Mev, polarization from, (E/T), 19: 47570 (COO-7-0361)
nitrogen-14 reactions at 20 to 42 Mev, excitation functions for, (E), 19: 47667
production of, methods for, 19: 46413
LITHIUM ISOTOPES Li-7
charged particle reactions with, energy levels and mechanisms of, 19: 47564(R) (AD-612038)
deuteron reactions (d,n) with neutron yields from, (E), 19: 46817
energy level lifetime, first, 19: 47564(R) (AD-612038)
meson (π^+) reactions (π^+,π^-), differential cross section for, (T), 19: 47660
model of hyperon(Λ) hypernucleus, two-body, 19: 47647
neutron inelastic scattering at 14 Mev, (E), 19: 47609
neutron scattering at 4.4 Mev, polarization from, (E/T), 19: 47570 (COO-7-0361)
nitrogen-14 reactions at 20 to 42 Mev, excitation functions for, (E), 19: 47667
production of, methods for, 19: 46413
proton (p,γ) reactions, angular distribution interference effects in, 19: 47703
proton reactions (p,t) at 16.6 Mev, differential cross sections for, (E/T), 19: 47574 (IAE-836)
LITHIUM ISOTOPES Li-8
production of hyperfragments of, in meson (π^-) and proton reactions with emulsion nuclei, (E), 19: 47650
LITHIUM NIOBATES
Li_3SbO_4–Li_3NbO_4–Li_3TaO_4, phase diagram, 19: 46276
LITHIUM RARE EARTH OXIDES
formation of, ionic field strengths as criteria for, 19: 46246(R) (TID-22207, Paper F)
LITHIUM TANTALATES
Li_3SbO_4–Li_3NbO_4–Li_3TaO_4, phase diagram, 19: 46276
LIVER
diethylstilbenediol uptake by cattle, 19: 45797
effects of carbon tetrachloride on function of rat, use of iodine-131-labeled rose bengal for analysis of, 19: 45828
oxygen metabolism in rat, effects of cystamine on, 19: 45777
protective effects of injected homogenates of bovine, against radiation injuries in mice, 19: 46024
radiation effects on mouse, protective effects of sodium cysteinethiosulfonate against, 19: 46006
radiation effects on function of rat, use of iodine-131-labeled rose bengal for analysis of, 19: 45828
radiation effects on content of nucleic acids in, of rat embryos, 19: 45826
sulfur-35 uptake by rat, histologic fixation and release of, 19: 45800
thorium-228 decay in beagle, metabolism of bismuth-212, lead-212, and radium-224 from, 19: 45798
toxic effects of OMRE High Boilers and Santowax OM on rat, 19: 45769
LIVER DISEASES
radiodiagnosis of, using molybdenum-99, 19: 46139
radiodiagnosis using technetium-99, 19: 46140
LIVERWORTS
radioinduced mutations in *Cyathodium tuberosum*, x, 19: 45901
LUBRICANTS
properties for aerospace uses, 19: 47068
LUMINESCENCE
measurement of chemi-, from chlorine-potassium reactions, 19: 46161(R) (ORNL-3832, pp 116-50)
radioinduced in albumin solutions, uv, 19: 46342(T) (JPRS-31547, pp 6-12)
LUMINESCENT MATERIALS
radiation effects on electro-, gamma, uv, and x, 19: 46341(T) (FTD-TT-65-24)
LUNG DISEASES
radiodiagnosis of, radiation hazards from, 19: 46110
LUNG INJURIES
radioinduced by therapy of carcinoma of breast, 19: 46063
LUNGS
analysis for plutonium-239, development of multiwire proportional counter for external, 19: 46751 (AEEW-M-526)
blood circulation in, tracer study using nitrogen-13 or xenon-133, effects of emphysema on, 19: 46070
pathological effects of inhaled gadolinium oxide dust in, of guinea pigs, 19: 45756 (COO-1170-7)
radiation effects on mouse, protective effects of sodium cysteinethiosulfonate against, 19: 46006
radiodiagnosis of respiratory insufficiency using thulium-170, 19: 46118
radioinduced tumors of, after chronic gamma exposure, 19: 45808(R) (NYO-901-36)
radiotherapy of carcinomas of, late effects of, 19: 46131
LUTETIUM
cohesive energy and ionization of, relation between, (T), 19: 47062
LUTETIUM ALLOYS
Co–Lu, crystal structure of Laves phases in, 19: 47052
Lu–Pd, phase studies, 19: 47051
LUTETIUM BROMIDES
thermal decomposition of hydrates of, mechanisms of, 19: 46271
LUTETIUM FERRATES(III)
crystal structure, 19: 46256
LUTETIUM IONS
quadrupole coupling in cerium magnesium nitrate and neodymium ethylsulfate lattices, 19: 47883 (UCRL-16279)
LUTETIUM ISOTOPES Lu-169
energy levels and isomeric transitions in, Nilsson configuration for, (E/T), 19: 47640
LUTETIUM ISOTOPES Lu-171
energy levels and isomeric transitions in, Nilsson configuration for, (E/T), 19: 47640
LUTETIUM ISOTOPES Lu-173
beta decay of, gamma spectra from, (E), 19: 47661
energy levels and isomeric transitions in, Nilsson configuration for, (E/T), 19: 47640
LUTETIUM ISOTOPES Lu-174
beta decay of, gamma spectra and ytterbium-174 levels from, (E), 19: 47661

LUTETIUM ISOTOPES Lu-175
energy levels and isomeric transitions in, Nilsson configuration for, (E/T), 19: 47640
LUTETIUM ISOTOPES Lu-177
decay of, 19: 47883 (UCRL-16279)
LUTETIUM OXIDES
atomic charge and permittivity of, (E/T), 19: 47901(T)
oxygen-18 exchange between molecular oxygen and, 19: 46266
preparation and crystal structure of nonstoichiometric, 19: 46273
LYMPH CELLS
radiation effects on morphology of, in patients with Hodgkin's disease, 19: 46103
LYMPH DISEASES
radiation effects on morphology of lymphocytes in patients with Hodgkin's disease, 19: 46103
radiotherapy of Hodgkin's disease, 19: 46067
LYMPH SYSTEM
radioinduced tumors in mouse, radiosensitivity of, 19: 45977
LYSOZYME
radiation effects on activity of, in rat intestine, 19: 45933
radioinduced free radicals in, spectra of, 19: 46339 (UCRL-16358)

M

MACHINE TOOLS
control system acceleration switching valve for, 19: 48106 (Y-1488)
drive system evaluation for machining round parts, 19: 46461 (RFP-562)
spindle design, 19: 48093 (RFP-654)
MAGNESIUM
diffusion of beryllium to surface of, on heating at 300 to 500°C, 19: 47071
diffusion of plutonium in, at 420 to 500°C, 19: 47066
ductility of, pressure effects on, 19: 46983 (AD-612159)
heat transfer to pool-boiling, 19: 46550
from, (E/T), 19: 47589(R) (TID-22012, pp 53-66)
neutron reactions (n,n'γ) at 3.0 to 4.5 Mev, gamma angular distributions
preparation by reduction of magnesium sulfate using catalytic nascent hydrogen, 19: 46253(T) (ORNL-tr-803)
proton elastic scattering at 4.5 Mev, polarization in, (E), 19: 47692
reactions with water at high temperatures during core meltdown, (E/T), 19: 47960(T) (ORNL-tr-694)
separation from other materials by electrolytic extraction, 19: 46454
uptake by plants, effects of beryllium on, 19: 45802
MAGNESIUM ALLOYS
diffusion of plutonium in, at 420 to 500°C, 19: 47066
Al–Mg, crystal structure of Mg_2Al_3in, 19: 46984(R) (AD-612275)
Al–Mg, diffusion of plutonium at 420 to 500°C in, 19: 47066
Al–Mg, diffusion of beryllium to surface of, on heating at 300 to 500°C, 19: 47071
Ca–Mg, diffusion of beryllium to surface of, on heating at 300 to 500°C, 19: 47071
Ce–Mg, phase studies, 19: 47059
La–Mg, diffusion of beryllium to surface of, on heating at 300 to 500°C, 19: 47071
Mg–Pu, diffusion of plutonium at 420 to 500°C, 19: 47066
Mg–Th, diffusion of beryllium to surface of, on treating at 300 to 500°C, 19: 47071
Mg–Zn, diffusion of beryllium to surface of, on heating at 300 to 500°C, 19: 47071
Mg–Zr, diffusion of plutonium at 420 to 500°C in, 19: 47066
MAGNESIUM BROMATES
radiolysis products from, gamma, 19: 46332(R) (ORNL-3832, pp 50-65)
MAGNESIUM BROMIDES
vinyl-, uses in preparation of carbon-14-labeled acrylic and glyceric acids and glycerol, 19: 46310
MAGNESIUM CARBONATES
reactions with rare earth oxides, ionic field strengths as criteria for compound formation in, 19: 46246(R) (TID-22207, Paper F)
MAGNESIUM CERIUM NITRATES
rare earth ion quadrupole coupling in lattices of, 19: 47883 (UCRL-16279)
MAGNESIUM CHLORIDES
radiation effects on corrosive effects of, on stainless steels, 19: 47079 (AERE-R-5014)
MAGNESIUM FLUORIDES
spectra of vaporized, 19: 46982(R) (AD-611856)
MAGNESIUM IONS
displacement in soils by beryllium, 19: 45802
MAGNESIUM ISOTOPES Mg-21
decay of, delayed proton emission in, (E), 19: 47613
MAGNESIUM ISOTOPES Mg-24
bremsstrahlung reactions (γ,p) at 25.5 Mev, energy spectra from, (E), 19: 47699
energy levels of, parity and spin of, (E/T), 19: 47589(R) (TID-22012, pp 53-66)
neutron inelastic scattering at 3 to 4.5 Mev, angular distributions and energy levels from, (E/T), 19: 47638
proton elastic and inelastic scattering at 5.8 Mev, polarization in, (E), 19: 47697
MAGNESIUM ISOTOPES Mg-25
deuteron reactions (d,α) at 1.5 to 2.5 Mev, differential cross section fluctuations in, (T), 19: 47659
MAGNESIUM ISOTOPES Mg-26
neutron inelastic scattering at 3 to 4.5 Mev, angular distributions and energy levels from, (E/T), 19: 47638
MAGNESIUM OXIDES
creep in single-crystal, at 1450 to 1700°C, steady-state, 19: 47009 (NP-15514(Vol.2))
MAGNET COILS
design of superconducting, for plasma research, 19: 47533
design of, determination from specified magnetic fields, (T), 19: 47121 (UCRL-16080)
fabrication of large copper, x radiography of brazed joints in, 19: 46965 (UCRL-16383)
MAGNETIC FIELDS
acoustic wave interactions with, plasma kinetic correlations with, (T), 19: 47732
configuration of, determination of geometry and current of coils for producing specified, (T), 19: 47121 (UCRL-16080)
description of helical-symmetry, having potential wells, 19: 47154
effect on binding energy of charged particles, 19: 47143
effect on stability of penning discharge, (E), 19: 47780
effects of crossed, on gaseous Townsend discharge, (T), 19: 47127
effects of transverse, on resonance peaks of hot asymmetric plasma, (T), 19: 47746
effects on electron and ion emission from electrode materials for cesium ion engines, 19: 46571 (HRL-5249-S)
effects on electron transport phenomena in tin at liquid helium temperatures, 19: 47534
effects on heat transfer by liquid mercury, 19: 46547
effects on hydromagnetic waves in toroidal plasma, (E), 19: 47742
electron cyclotron harmonics in nonrelativistic plasma in, (T), 19: 47749
electron orbits in focusing, 19: 47186
electron transport in, equations for, 19: 47799
in hollow explosive-driven cylindrical conductor, (T), 19: 47120 (UCRL-14349)
measurement of, double-coil method for, (E), 19: 46731(T) (SLAC-Trans-21)
measurements of solar, review on, 19: 47208
plasma acceleration from pulsing, analysis of, 19: 46575 (NASA-TN-D-3006)
plasma containment in toroidal, low-β, (T), 19: 47819
plasma containment in toroidal, (T), 19: 47820
plasma containment in magnetic wells, (T), 19: 47822
plasma diffusion across, (T), 19: 47838
plasma equilibrium in toroidal, (T), 19: 47809
plasma heating by oscillating, (T), 19: 47767
plasma injection into cusped, (E), 19: 47858
plasma kinetics in high, Vlasov equation for, (T), 19: 47753
plasma motion near zeros of, 19: 47847
plasma polarization in curved, (E), 19: 47797
plasma rotation in, from coaxial guns, (E), 19: 47849
plasma stability in spatially varying, (T), 19: 47840
structure of unsymmetric toroidal, (T), 19: 47144
uses for dynamic stabilization of plasma, (E), 19: 47842
MAGNETIC MIRROR MACHINES
injection of 20-kev neutral hydrogen atoms into electron-cyclotron plasma in, (E), 19: 47837
plasma capture by, (E/T), 19: 47839
plasma containment in PR-5, 19: 47857
plasma properties in Scylla IV theta pinch, (E), 19: 47722 (LA-DC-7039)
plasma stability in, effects of stabilizing rods on, (T), 19: 47835
MAGNETIC MIRRORS
charged-particle motion in nonadiabatic, (T), 19: 47748
charged-particle reactions with, (T), 19: 47821
electron loss from, with superimposed helical magnetic field, 19: 47145
plasma containment in, (E), 19: 47848
MAGNETIC PROBES
performance for plasma diagnostics, 19: 47817
MAGNETIC PROPERTIES
measurement in transition-metal carbides, borides, and nitrides, design

and operation of potentiometer for, 19: 47009 (NP-15514(Vol.2))

MAGNETO-OPTICAL ROTATION
of biological polymers, 19: 48104 (UCRL-16278)

MAGNETOHYDRODYNAMIC CELLS
design with acoustic resonator for bunching particles in conducting fluid, 19: 47297(P)
development for direct conversion of heat to electricity, 19: 47286
developments in, 19: 47285
diagnostics and operation of closed-loop, 19: 47728
feasibility studies of liquid–metal, 19: 48053(R) (ANL-7090, pp 55-68)
Hall effect and induced ionization in, 19: 47290
ionization in, use of electron beam, 19: 47289
operation, (T), 19: 47288
performance as generator and accelerator, graphical presentation of, 19: 47296
performance of modulated conductivity induction synchronous, 19: 47293
performance of, nonlinear effects of fluctuations on, (T), 19: 47294
plasma wave growth and interactions in, 19: 47295
power generation by large-scale open loop, efficiency of, 19: 47291
testing of d-c, liquid metal, 19: 47292
use in electric power stations, 19: 48013

MAGNETOHYDRODYNAMICS
bibliography, 19: 47280 (AD-613358)
conference on, 19: 47153
flow of conducting viscous fluid in boundary layers, effect of pressure gradient on, 19: 47140
stability of supermassive stars, effects of magnetoturbulent energy on, 19: 47200

MAGNETOMETERS
book: *Geophysics and Space Data Bulletin No. 3*, 19: 47447 (AD-612083)
development of double-coil proton magnetic resonance, 19: 46731(T) (SLAC-Trans-21)

MAGNETOSPHERE
charged particle measurements in, from Vela Project, 19: 47450 (LA-DC-7365)
charged particles in, angular distribution, energy, and intensity of trapped, 19: 47444 (AD-611629)
effects on auroral and geomagnetic storms, 19: 47481
electric field effects on electrons trapped in, dynamo-, (T), 19: 47453
electron content in tail of, 40-kev, (E), 19: 47458
electron interaction frequency and lifetime in, (T), 19: 47453
electron plasma oscillation fields in, ambient, (T), 19: 47477
electron velocity spectra in, from cyclotron absorption of whistler power, (E), 19: 47463
hydromagnetic wave, transmission in impulse response in, (T), 19: 47467
magnetic field configuration in tail of, effects on auroral current systems, (T), 19: 47469
properties of, measurements of, (T), 19: 47484
solar wind effects on threshold for plasma instability in transition region of, (T), 19: 47460

MAGNETS
cost analysis for accelerator systems of, 19: 47170 (UCRL-16384)
design and performance of niobium–tin superconducting, 19: 47526
design of septum, for beam extraction from Brookhaven AGS, (E), 19: 47158 (BNL-910)
development, 19: 46643(R) (LAL-1136)
properties of permanent, for AGS injection beam focusing, (T), 19: 47160 (BNL-9482)
properties of sector, for 50-Mev separated-orbit cyclotron, 19: 47167 (ORNL-P-1619)
properties of, for cyclotron beam extraction, 19: 47166 (ORNL-P-1605)

MAIZE
radiation effects in seeds of, physiological, 19: 45836

MALEIC ACID
effects on rate of reaction between uranium(IV) and thallium(III), 19: 46277

MALEIC ACID, DERIVATIVES
dibutyl- and dioctyl-, radioinduced polymerization of, 19: 46377
potassium hydrogen chloromaleate, molecular structure by neutron diffraction, 19: 46161(R) (ORNL-3832, pp 116-50)

MALEIC ACID, DIETHYL ESTER
radioinduced polymerization of, properties of polymer obtained in, 19: 46377

MALEIC ACID, DIHYDROXY-
analytical uses for determination of rare earths, 19: 46216
uses in separation of rare earths from iron, manganese, and uranium, 19: 46452

MALIC ACID
effects on rate of reaction between uranium(IV) and thallium(III), 19: 46277

MALONIC ACID
effects on rate of reaction between uranium(IV) and thallium(III), 19: 46277

MALONONITRILE
dimethyl-, thermodynamic properties of, 19: 48090 (COO-1149-53)

MAMMALS
radiation effects on, protective effects of thiolic compounds against, 19: 46010
radiation effects in, acute pathological, 19: 45981
radiation effects combined with nonradiation factors on, mechanism of response for, 19: 45824(T) (NASA-TT-F-354)
radioinduced lung tumors in, 19: 45808(R) (NYO-901-36)
radioinduced tumors in, etiology of, 19: 45859

MAMMARY GLAND
radiosensitivity of, 19: 46090
radiosensitivity of skin of, of guinea pigs, 19: 45869
radiotherapy of carcinomas of, using cobalt-60 or iridium-192 wire applicator, 19: 46047
radiotherapy of carcinoma of, pathological effects on lungs, 19: 46063
radiotherapy of melanoma of, using iridium-192 wire applicator, 19: 46047

MAN
calcium metabolism in, double tracer method for analyzing, 19: 46138
cancer in, radiological and clinical statistics for, 19: 45921
cesium-137 content of, whole-body, 19: 46612
chromosome patterns in mongols, 19: 45915
chromosome patterns in leukemia, 19: 45915
effects of space flight on, problems of environmental, 19: 45746
glomerular filtration rate in, use of iodine-131-labeled Hypaque for determining, 19: 46071
iodine metabolism in, tracer study, 19: 45754 (CEA-R-2787)
iodine metabolism in children, 19: 45784
iodine metabolism in thyroid gland of, tracer study, 19: 45792
iodine-131 metabolism in, effects of climatic temperature, 19: 45779
metabolism of carbon-14-labeled diethylstilbenediol in, 19: 45797
microwave exposure criteria for, 19: 46706
organ weight in, effects of age on, 19: 45755 (CEA-R-2809)
pathological effects of Thorotrast in, 19: 45980
physiology of, computer analysis of gamma spectroscopic data on, 19: 45771
radiation dosage in diagnostic radiology, reduction of, 19: 46037
radiation dosage to, problems in reduction of diagnostic, 19: 46146
radiation dose from diagnostic radiography, 19: 46112
radiation dose to, from ingested fission products, 19: 45755 (CEA-R-2809)
radiation dose to, from ingestion of water contaminated by fallout, 19: 46633 (AD-276187)
radiation dose to, from natural radioactivity, 19: 46688
radiation effects on, in space flight, 19: 46001
radiation effects in, genetic, 19: 45967
radiation effects in, genetic, 19: 45973
radiation effects on immune response to transplanted kidneys in, 19: 45888
radiation effects in skin of, ultraviolet, 19: 45907
radiation effects on granular and transitional cell layers in skin of, 19: 45913
radiation effects on intestine in, review, 19: 45922
radiation effects in, genetic, 19: 46695
radiation effects on chromosome pattern, 19: 45808(R) (NYO-901-36)
radiation effects on lifetime health and mortality patterns of, employed in nuclear energy installations, 19: 45810(R) (NYO-3394-2(Rev.))
radiation effects on, physiological, 19: 45815(R) (ORO-631, pp 67-76)
radiation effects on creatine excretion by, use as damage indicator, 19: 45864
radiation hazards of diagnostic radiography of pregnant women, 19: 46062
radiation injuries of, after high-level exposure, 19: 45997
radiation injuries in, diagnosis by lymphocyte chromosome studies, 19: 45916
radiation injuries in, diagnosis by lymphocyte chromosome studies, 19: 45917
radiation response and sensitization in, with cervical carcinoma, 19: 45830
radiation sickness from accidental and therapeutic exposure, nursing care of, 19: 45912
radioactivity in, whole-body counting of, 19: 46656
radioactivity in, computer program for analyzing whole-body data on, 19: 46658
radioactivity in, performance of large liquid scintillation detector for whole-body measurement of, 19: 46775
radioactivity of Lapps, whole-body, 19: 46587(R) (NYO-3446-3)
radioactivity of, whole-body counting of tracer, 19: 46137

radiodiagnosis of elderly, use and abuse of, 19: 46116
radiography of, using gamma transmission, 19: 46750 (AECL-2270)
radioinduced brain lesion of, 19: 45995
radioinduced erythema in, dose determinations for uv, 19: 45881
radioinduced skin cancers in, 19: 45945
radioinduced tumor after injection of Thorotrast, 19: 46092
radioinduced tumors in, 19: 45942
radioisotope renography in children, 19: 46109
radiosensitivity of brain and central nervous system of, 19: 45892
radiosensitivity of eyes of, 19: 46655
radiotherapy effects on central nervous system in, late nasal cavity, 19: 45983
radiotherapy of, effects on isoenzymes and lactate dehydrogenase in melanoma ascites, serum, and tumor homogenates, 19: 46124
radium-226 content in, determination from radon-222 in expired air, 19: 46677
removal of radioisotopes from, developments in chelation therapy for, 19: 46017
strontium metabolism in, effects of steroid hormones, age, and sex on, 19: 45805
strontium-90 maximum permissible body burden for, 19: 46634 (AD-423463)
strontium-90 metabolism by, 19: 45793
strontium-90 metabolism by, 19: 46634 (AD-423463)
taste radiosensitivity in, 19: 45825(T) (NSJ-tr-32)
zinc-65 metabolism in, effects of dietary calcium on, 19: 45787

MANDELIC ACID
hexahydro-, reaction with zirconium, 19: 46224
labeling with tritium at α-carbon atom, 19: 46306
use in hafnium and zirconium determination, 19: 46224

MANGANESE
determination by potentiometric titration of acid liberated by complex formation, 19: 46205
determination in aluminum, activation, 19: 46207
determination in algae, neutron activation, 19: 45775
determination in mollusks from Lake Maggiore, activation, 19: 45788
distribution in mollusk tissues, 19: 45788
effects on density of states in superconductors, 19: 47535
effects on distribution of strontium-90 in water-bearing strata by ground waters, 19: 46602
effects on mechanical properties of aluminum–copper–iron–tin–titanium–vanadium alloys, 19: 46985 (AD-613651)
separation from rare earths by precipitation using dehydroxymaleic acid, 19: 46452

MANGANESE ALLOYS
Dy–Mn, phase studies by differential thermal, thermo-magnetical, and x-ray analysis of, 19: 46989 (AD-614466)
Dy–Mn, preparation by sinter process using mercury, 19: 46908 (AD-614464)
Er–Mn, phase studies by differential thermal, thermo-magnetical, and x-ray analysis of, 19: 46989 (AD-614466)
Er–Mn, preparation by sinter process using mercury, 19: 46908 (AD-614464)
Gd–Mn, magnetic properties of, 19: 46988 (AD-614465)
Gd–Mn, phase studies by differential thermal, thermo-magnetical, and x-ray analysis of, 19: 46989 (AD-614466)
Gd–Mn, phase studies, 19: 46908 (AD-614464)
Gd–Mn, preparation, phase studies, and properties of, 19: 46987 (AD-614462)
Gd–Mn, preparation by sinter process using mercury, 19: 46908 (AD-614464)
Ho–Mn, phase studies by differential thermal, thermo-magnetical, and x-ray analysis of, 19: 46989 (AD-614466)
Ho–Mn, preparation by sinter process using mercury, 19: 46908 (AD-614464)
Mn–Pt, crystal structure of intermetallic compound $PtMn_3$ in, neutron diffraction studies of disorder in, 19: 47028
Mn–rare earths, properties of, equipment for measuring, 19: 46988 (AD-614465)
Mn–Sm, phase studies by differential thermal, thermo-magnetical, and x-ray analysis of, 19: 46989 (AD-614466)
Mn–Sm, preparation, phase studies, and properties of, 19: 46987 (AD-614462)
Mn–Sm, preparation by sinter process using mercury, 19: 46908 (AD-614464)
Mn–Y, phase studies by differential thermal, thermo-magnetical, and x-ray analysis of, 19: 46989 (AD-614466)
Mn–Y, preparation, phase studies, and properties of, 19: 46987 (AD-614462)

MANGANESE CARBONATES
reactions with rare earth oxides, ionic field strengths as criteria for compound formation in, 19: 46246(R) (TID-22207, Paper F)

MANGANESE IONS
electronic g factors of low-lying levels of singly ionized, (E), 19: 47240

MANGANESE ISOTOPES Mn-52
separation from chromium-51, vanadium-48, and zinc-65, method for, 19: 46210

MANGANESE ISOTOPES Mn-53
half life of, from meteorite observations, 19: 47627

MANGANESE ISOTOPES Mn-54
content in atmosphere and drinking water, Moncloa Station, Spain, 1964, 19: 46597
determination in irradiated steel by ion-exchange separation and gamma spectrometry, 19: 46195
distribution in mollusk tissues, 19: 45788

MANGANESE ISOTOPES Mn-55
neutron reactions (n,γ) in soil, activity induced by, 19: 47569 (CEX-62-50)
neutron reactions (n,2n) at 12.6 to 19.6 Mev, excitation function for, (E/T), 19: 47571 (EUR-2456.e)
neutron reactions (n,γ) to 10 kev, cross sections for, (E/T), 19: 47634
nitrogen-14 reactions with, excitation functions for one-neutron-transfer, (E/T), 19: 47586 (ORNL-TM-1218)
nitrogen-14 reactions at 20 to 42 Mev, excitation functions for, (E), 19: 47667
proton reactions (p,n) at 3.315 and 3.525 Mev, iron-55 energy levels from, (E), 19: 47696

MANGANESE ISOTOPES Mn-56
production in soil by neutron reactions (n,γ) on manganese-55, activity from, 19: 47569 (CEX-62-50)

MANGANESE SULFATES
content in baths for neutron source calibration, determination of, (E/T), 19: 47552

MANOMETERS
development of differential micro-, 19: 46726 (UCRL-11218(Pt.II))

MARCOULE REACTORS (G-2)
fuel elements from, radiography of, 19: 46558(T) (ORNL-tr-748)

MARITIME REACTORS
design for German ships, 19: 48051
design of pressurized-water, 19: 47923

MARYLAND
gamma aeroradioactivity at 500 ft over, mapping of, 19: 46614

MASERS (OPTICAL)
beam effects on atomic energy level shifts, (T), 19: 47233
beam interactions with plasma, 19: 47234
beam interactions in air, spark discharge from, (E), 19: 47781
beam reactions with, plasma, perturbation induced in, (E), 19: 47777
design and performance of interferometers of, for repetitively pulsed plasma, 19: 47730
plasma density measurement using helium–neon, 19: 47759
radiation effects on properties of ruby, (E/T), 19: 46873 (N64-32322)
radiation field from, nonlinear effects of, 19: 47123(T) (JPRS-31032, pp 1-14)
resonator modes in argon–bromine, (E/T), 19: 47219 (AD-614253)
use for interferometer measurement of plasma density in transverse mode, 19: 47745
uses of ruby, for vaporization of lithium hydride plasma, (E), 19: 47846

MASS SPECTROGRAPHY
vaporization of metals in, calculations, 19: 46943(T) (FTD-TT-65-611)

MASS SPECTROMETERS
automation of, for isotopic analysis of reactor materials, 19: 46181 (WAPD-T-1769)
design of multi-stage, 19: 46725(R) (TID-22141, pp 101-10)
performance of semiautomatic radiofrequency, 19: 46772

MATERIALS TESTING
ablation testing device for re-entering bodies, (E), 19: 47117(R) (SC-DC-65-1698)
metallography in nondescructive, 19: 46556 (NMI-4997, pp 1-21)
methods for radiographic flaw detection, 19: 46564
nondestructive equipment for irradiated specimens from Grenoble reactors, 19: 46559(T) (ORNL-tr-749)
nondestructive method for density determination using gamma sources, 19: 46892(P)

MATHEMATICS
computer uses in, outline, 19: 46902 (ANL-7050, pp 207-13)
research on, Air Force, 19: 48087 (AD-613537)
solutions for limiting cases in applied systems in, asymptotology for, (T), 19: 47150

MATTER
creation by gravitational waves, (T), 19: 47136
neutron resonance effects in, 19: 47542 (ANL-7050, pp 457-70)
neutron scattering by, cross sections for inelastic thermal, 19: 47543

(ANL-7050, pp 471-85)
theory of antimatter, 19: 47206
MEATS
cesium-137 content in, Finland, 1964, 19: 46587(R) (NYO-3446-3)
radiation processing of, effects of storage at room temperature on wholesomeness, 19: 46886
radioinduced odor in beef, chemical analysis of, 19: 46878 (NP-15455)
MECHANICS
Dirac formalism in classical, Weyssenhoff model for, 19: 47137
dynamic properties of nonlinear string, (T), 19: 48108(T) (ORNL-tr-754)
invariance principles for classical and relativistic point particles in, (T), 19: 47433
quantum mechanics, correlations with classical, (T), 19: 47432
MEDICAL SUPPLIES
radiosterilization of cotton bacteriological swabs, 19: 46884
radiosterilization, 19: 46890
MEDICINE
action levels in treatment of radiation and radioactivity exposure, 19: 46008
facilities for radiation, effects of erythemal dose data on, design of, 19: 45881
life span and cause of death of American physicians, 19: 45808(R) (NYO-901-36)
nursing care of patients with accidental and therapy induced radiation sickness, 19: 45912
radiation protection during intracavitary radiotherapy, design of remote afterloader for, 19: 46111
radiation protection of personnel using radioisotopes, 19: 46080
radiation protection of personnel, 19: 46686
MEDITERRANEAN SEA
plankton ecology in, 19: 45748(R) (TID-22193)
MEMBRANES
fabrication of permeable, of subdivided metallic particles, 19: 46978(P)
ion transport through biological, isotope effects in, 19: 46898 (HMI-B-44)
radiation effects on permeability of plant cell, by urea, 19: 45975
radiation effects on animal cell, uv, 19: 45891
MENDELEVIUM ISOTOPES Md-255
decay properties and production, (E), 19: 47664
MENDELEVIUM ISOTOPES Md-256
decay properties and production, (E), 19: 47664
MENDELEVIUM ISOTOPES Md-257
decay properties and production, (E), 19: 47664
MERCHANT VESSELS
description of German nuclear-powered, 19: 48051
development of nuclear-powered, 19: 48114
MERCURY
acceleration of plasma of, by electric field gradient, (E), 19: 47714(R) (AD-613307)
content and distribution in beef heart, 19: 45753 (AE-191)
corrosive effects on aluminum, 19: 48060(R) (IDO-17081, pp 1-47)
corrosive effects on Hastelloy C and tantalum at 150°C, 19: 46428(R) (ORNL-3847)
electron beam reactions with plasma of, diagnostics by nonperturbing probe, (E), 19: 47740
heat transfer by flowing, effects of magnetic fields on, 19: 46547
superconducting properties to 0.3°K, (E), 19: 47517
superconducting properties of, 19: 47536
x-ray reactions with vapors of, electricity production in, (E), 19: 47283(T) (BNL-tr-8)
MERCURY ALLOYS
Hg–Tl, superconducting transition temperature of, pressure effect on, (E), 19: 47529
MERCURY IONS
effects on etching of pyrolytic graphite, 19: 47078 (AD-613643)
MERCURY ISOTOPES Hg^{-197}
diagnostic use for localization of brain tumors, 19: 46046
nuclear properties, 19: 46141
properties as x-ray source for diagnostic radiography, 19: 46141
tracer use for kidney function tests, 19: 46130
MERCURY ISOTOPES Hg^{-199}
gamma spectra from transitions in, (E), 19: 47576(R) (IDO-17081, pp 49-76)
MERCURY ISOTOPES Hg^{-203}
diagnostic use for localization of brain tumors, 19: 46046
diagnostic use of, for brain tumor scanning, 19: 46053
incorporation in 3-(chloromercuri)-2-methoxypropylurea for medical uses, 19: 46305
tracer use for kidney function tests, 19: 46130
MESIC ATOMS
meson (μ) capture rate in hydrogen, 19: 47227
x ray emission from, isotope effects on energy spectra of, 19: 47582 (NEVIS-129)
MESON SHOWERS
properties of, produced by ultra-high energy interactions, (T), 19: 47400
MESONS
decay of, 8(12) symmetry for electron-positron production in, (T), 19: 47308 (JINR-P-2284)
decay of, unitary symmetry for $\Delta Q = 0$ $\Delta S = 1$ ($\pi e^+ e^-$), (T), 19: 47370
interactions of massless pseudoscalar, broken symmetry for electromagnetic, 19: 47346
mass formula for, in covariant spin-unitary-spin scheme, 19: 47352
mass splitting of vector, under SU(3), 19: 47383
properties of, 19: 47406
symmetry for strongly interacting, fifteenfold way of SU(4), (T), 19: 47328
MESONS, RESONANCE
mass differences of vector, K^{*+}-K^{*0} and ρ^+-ρ^0 electromagnetic, (T), 19: 47369
mass formula for, in covariant spin-unitary-spin scheme, 19: 47352
mass formula for, empirical, (T), 19: 47384
production of K^*, in meson (K^+)-proton interactions at 3 Bev/c, (E/T), 19: 47356
properties of, 19: 47406
MESONS (η)
decay of (958) and (549), C-invariance violation in, (E), 19: 47372
production in meson (π)-nucleon interactions, (T), 19: 47401
MESONS (K)
interactions in jet showers, secondary angular distribution and momenta for primary energy of, (T), 19: 47275
interactions with mesons ($\bar{K}$), nucleon isoscalar form factor from elastic, (T), 19: 47371
photoproduction on nucleons at high energies, momentum-transfer distributions in, (T), 19: 47389
MESONS (K^-)
capture in hydrogen, hyperon mass determinations in, 19: 47302 (CU-1932-246)
interactions with protons at 2.24 Bev/c, $Y_1^*(1660)$ resonance from, (E), 19: 47300 (BNL-9520)
interactions with deuterons at rest, hyperfragment (Σ^-n) production in, (T), 19: 47339
interactions with deuterons at rest, Σ-Λ conversion in, (T), 19: 47358
interactions with mesons (K), nucleon isoscalar form factor from elastic, (T), 19: 47371
interactions with protons at 2.1 to 2.7 Bev/c, mesons (η) (958) production in, (E), 19: 47372
reactions with emulsion nuclei, hyperfragment production in capture, (E/T), 19: 47648
reactions with emulsion nuclei at 1.5 to 3 Bev/c, light charged particle emission in, (E), 19: 47651
reactions with nuclei at rest, 19: 47708
MESONS (K^0)
decay in mixed ensembly, (T), 19: 47309 (JINR-P-2289)
decay of K_2^0, CP violation and $\Delta T = \frac{1}{2}$ rule in, (T), 19: 47317(T) (NP-tr-1282)
decay of K_2^0, time reversal invariance violation in 2π, (E/T), 19: 47391
decay of, CP violation in 2π, (T), 19: 47309 (JINR-P-2289)
MESONS ($\bar{K}^0$)
decay in mixed ensemble, (T), 19: 47309 (JINR-P-2289)
interactions with nucleons, scattering length for $S_{1/2}$ T = 0, (T), 19: 47365
MESONS (K^+)
interactions with protons at 3 Bev/c, resonance production in ($K^0\pi^+$), (E/T), 19: 47356
photoproduction, (E), 19: 46643(R) (LAL-1136)
MESONS ($K^0_{1,2}$)
decay of, test of CP violation and $|\Delta T| = \frac{1}{2}$ rule for radiative, 19: 47351
MESONS ($K^0_{\pi\pi}$)
decay of, test of CP violation and $|\Delta T| = \frac{1}{2}$ rule for radiative, 19: 47351
MESONS (μ)
capture by complex nuclei, correlation functions in, (T), 19: 47656
capture rate in, 19: 47227
decay of, coupling constants for, (T), 19: 47378
decay of, electron spectra from, 19: 46785
magnetic moments of, (T), 19: 47378
MESONS (μ^-)
capture by nuclei, isotope effects on K x rays from, 19: 47582 (NEVIS-129)
capture by oxygen-16, pseudoscalar coupling constant from, 19: 47707
MESONS (ω^0)
decay rate of, (2π), (T), 19: 47369
MESONS (ϕ)
decay rate of, (2π), (T), 19: 47369
MESONS (π)

detection and discrimination from electrons at 80 to 340 Mev/c, (E), 19: 46782
existence of heavy unstable, possibility of, 19: 47398
interactions in jet showers, secondary angular distribution and momenta for primary energy of, (T), 19: 47275
interactions with nucleons, resonance in static, (T), 19: 47298 (AD-613934)
interactions with mesons (σ), Λ-Λ scattering length from meson (σ) resonance in, (T), 19: 47337
interactions with mesons (π), meson (σ) production in S-wave, (T), 19: 47347
interactions with nucleons, model for P_{11}-state strong, 19: 47350
interactions with mesons (ρ), nucleon isoscalar form factor from elastic, (T), 19: 47371
interactions with nucleons, restriction on forward amplitudes of, (T), 19: 47375
interactions with nucleons, fixed-variable dispersion relations for, (T), 19: 47388
interactions with nucleons, calculation using Regge trajectory, 19: 47395
interactions with nucleons, meson (η) production in, (T), 19: 47401
interactions with nucleons, analysis of data for, 19: 47404
photoproduction of di-, in spark chambers, 19: 47303 (DESY-65/7)
photoproduction on nucleons at high energy, total cross section for, (T), 19: 47353
photoproduction on nucleons at high energies, momentum-transfer distributions in, (T), 19: 47389
production in electron-proton interactions at 5.2 Bev/c, (E), 19: 47303 (DESY-65/7)
production in meson (π^-)-nuclear field interactions at 16.2 Bev/c, coherent trident, (E), 19: 47355
production in neutrino-nucleon inelastic interactions, charge radio of, (T), 19: 47377

MESONS (π^-)
capture by nuclei, nucleon pair emission from, (T), 19: 47679
interactions with protons at 8 Bev/c, (E), 19: 46643(R) (LAL-1136)
interactions with neutrons at 1.2 to 4.5 Bev/c, cross sections for backward elastic, (E), 19: 47310 (NP-15376)
interactions with nuclear field at 16.2 Bev/c, coherent production of meson (π) tridents in, (E), 19: 47355
interactions with mesons (π^0) and (π^0), phase shifts in elastic, (T), 19: 47357
interactions with protons at 2.08 Bev/c, differential cross section and polization for, (E), 19: 47373
interactions with protons at 2.16 Bev/c, single-particle exchange models in, (E), 19: 47403
production in deuteron-meson (K$^-$) interactions at rest, (T), 19: 47358
reactions with emulsion nuclei at 3.5 Bev/c, hypefragment production in, (E), 19: 47650
reactions with xenon at 9 Bev/c, cross section for, (E), 19: 47689
reactions with xenon at 9 Bev/c, neutron emission in high four-momentum transfer, (E), 19: 47698

MESONS (π^0)
interactions with mesons (π^-), phase shifts in elastic, (T), 19: 47357
photoproduction on protons, (E), 19: 46643(R) (LAL-1136)
photoproduction on helium-4, (E), 19: 46643(R) (LAL-1136)
photoproduction on nuclei, (E), 19: 46788
photoproduction on protons at 660 to 800 Mev, angular distributions for, (E), 19: 47368
production in neutrino-nucleon inelastic interactions, (T), 19: 47377

MESONS (π^+)
interactions with protons at 1.45 Bev/c, differential cross section for, (E/T), 19: 47304 (IAE-700)
interactions with mesons (π^-), phase shifts in elastic, (T), 19: 47357
photoproduction on protons, (E), 19: 46643(R) (LAL-1136)
production in gamma interactions with protons at 230 Mev, cross sections for, 19: 47393
production in meson (K$^-$)-nucleus reactions, 19: 47708
production in neutrino-nucleon inelastic interactions, (T), 19: 47377
production of separated beams of 2 Bev/c, 19: 46643(R) (LAL-1136)
reactions (π^+,π^-) with nuclei, model for, 19: 47660

MESONS (ρ)
interactions with mesons (π), nucleon isoscalar form factor from elastic, (T), 19: 47371
production in meson (π^-)-proton interactions, (E), 19: 47403
production of, electromagnetic, (E), 19: 46643(R) (LAL-1136)

MESONS (ρ^0)
mass difference, ρ^+-ρ^0, (T), 19: 47369

MESONS (ρ^+)
mass difference, ρ^+-ρ^0, (T), 19: 47369

MESONS (σ)
production in meson (π)-meson (π) interactions, Λ-Λ scattering length from, (T), 19: 47337
production in S-wave meson (π)-meson (π) scattering, (T), 19: 47347

METABOLIC DISEASES
effects on calcium kinetics in cancer patients, hypercalcemia and hyperparathyroid, 19: 45757(R) (NYO-910-23, pp 183-92)
radiodiagnosis of, involving calcium, 19: 46138
radiodiagnosis of, involving proteins, 19: 46142

METABOLISM
analysis of, computer analysis of data from tracer, 19: 46055
radiation effects on, in connective tissue cells, 19: 45895
radiotherapy of thyrotoxicosis, iodine-131, 19: 46082

METALLOGRAPHY
camera for remote, motor-driven roll-film, 19: 46711 (BNWL-SA-161)
camera for, use of 35 mm, 19: 46928 (NMI-4998, pp 14-19)
conference, 19: 46936 (NMI-5025(Pt.I))
facilities for, description of portable, 19: 46935 (NMI-4999, pp 129-36)
methods at high temperatures, 19: 47000 (NMI-4996, pp 8-18)
methods for color microphotography, 19: 46931 (NMI-4999, pp 26-9)
polishing cloth for, evaluation of commercial, 19: 46923 (NMI-4997, pp 36-44)
preparation procedures for ceramic, cermet, and metallic specimens, 19: 46937 (NMI-5025(Pt.I), pp 1-25)
replication of irradiated samples using silicone rubbers, 19: 47091 (NMI-4999, pp 69-77)
replication of using silicone rubber and epoxy resin, 19: 46932 (NMI-4999, pp 60-8)
sample mounting in epoxy resins using multiple cavity molds, 19: 46927 (NMI-4998, pp 1-5)
sample preparation, description of remote grinder for, 19: 46507 (NMI-4997, pp 157-62)
sample preparation procedures, vibratory grinding and polishing, 19: 46939 (NMI-5025(Pt.I), pp 135-219)
sample preparation of irradiated A-286 alloy, 19: 47088 (NMI-4998, pp 95-106)
sample preparation for irradiated materials, 19: 47089 (NMI-4999, pp 30-50)
sample preparation for irradiated material, 19: 47085 (NMI-4997, pp 134-56)
sample preparation by vibratory polishing, techniques for hot-cell, 19: 47086 (NMI-4997, pp 184-8)
techniques for chemically and radioactive materials, replication, 19: 46951 (NMI-4996, pp 19-20)
techniques for irradiated uranium carbide, 19: 47083 (NMI-4996, pp 77-85)
uses for microstructural studies of cast uranium, 19: 47007 (NMI-5025 (Pt.I), pp 127-51)
uses in nondestructive testing methods, 19: 46556 (NMI-4997, pp 1-21)

METALLURGICAL EQUIPMENT
design for rectangular plate bending analysis, 19: 46555 (KAPL-M-6493)

METALLURGY
manual on practice of, for laymen after nuclear attack, 19: 46918 (IITRI-B6018-1)

METALS
analysis for carbon, nitrogen, and oxygen by helium-3 activation, 19: 46174 (LA-DC-7319)
corrosive effects of liquid, on materials in Rankine cycle power plants, 19: 46955 (NP-15431)
crystal deformations in, analysis of double kink, (T), 19: 47011 (ORNL-3862)
crystal structure, 19: 46984(R) (AD-612275)
deformation of, interface friction in hot, 19: 46981(R) (AD-611821)
determination in uranium, heavy water, and water using atomic absorption spectroscopy, 19: 46166 (DP-980)
extrusion of, method and apparatus for, 19: 46975(P)
heat transfer during vertical upflow of liquid, nucleate boiling effects in single-phase, 19: 46528 (ANL-7038)
joining dissimilar, chemical and physical problems in, 19: 46968(T) (AEC-tr-6615)
phase studies on, liquid-solid transitions in, (T), 19: 46233 (CEA-R-2752)
positron annihilation in, (E/T), 19: 47217 (AD-613582)
properties and structure of, pressure effects on, 19: 46983 (AD-612159)
properties of porous, for use as isolation traps in vacuum systems, 19: 46573 (UCRL-12393-T)
radiation effects on tensile properties of, design of equipment for measuring, 19: 46712 (BNWL-SA-169)
radiation effects on microstructure, use of silicon rubber for replication of, 19: 47091 (NMI-4999, pp 69-77)
solvent partition in hydrohalic acid–organic diluent–tridodecylamine

system, 19: 46180 (UCRL-16254)
surface tension of liquid, review on measurement of, 19: 47064
time-to-rupture tests of, analysis, 19: 47081 (EURAEC-1432)
use of liquid, in d-c MHD generators, 19: 47292
vaporization from cylindrical cells, calculation of rates of, 19: 46943(T) (FTD-TT-65-611)

METASTASES
radiodiagnosis in bones using calcium-45 and strontium-85, 19: 45729(R) (NYO-910-23, pp 1-111)
radiosensitivity in neoplastic, biological factors affecting, 19: 45920
radiosensitivity of epithelial tumor, biological factors affecting, 19: 45921

METEORITES
manganese-53 content of, half-life calculations from, 19: 47627
radiation exposure ages of, from rare gas isotopic content, 19: 47194
sulfur-33 and -36 in iron, cosmic-ray-produced, 19: 47195
xenon isotope abundances in, anomaly patterns in, 19: 47213

METEOROLOGY
effects on radioactive particles after radiation accident, 19: 46693
measurements in, data processing system for, 19: 47109 (RISO-99)

METHACRYLIC ACID, METHYL ESTER POLYMERS
radiation effects on, spectra of protective effects of aromatic additives against, 19: 46321 (AD-611779)
radiation effects on, dose determination from, 19: 46367

METHACRYLONITRILE
radiation effects on cyanide group inversion in, infrared spectra of, 19: 46326 (CNAEM-28)
radioinduced polymerization of liquid, gamma, 19: 46336 (TID-22236)

METHANE
corrosive effects on superalloys at high temperatures, 19: 46946 (BNWL-100)
determination of deuterated in normal, by infrared spectrometry, 19: 46157(R) (MLM-1254)
neutron scattering by, calculation methods for, (E/T), 19: 47576(R) (IDO-17081, pp 49-76)
preparation of high-purity, for use in radiation detectors, 19: 46329
radiolysis of, yields acetylene from, 19: 46366
reactions with fission recoils, 19: 46330 (NP-15370)
yields from radiolysis of ethylene, 19: 46361
yields from radiolysis of benzene–dioxane mixtures, 19: 46363
ethylene–methane–N, radiolysis of, 19: 46324(R) (AGN-8132)
ethylene–methane–NO, radiolysis of, 19: 46324(R) (AGN-8132)
HF–methane, radiolysis yields in, 19: 46324(R) (AGN-8132)
methane–N, electron drift velocity and mean energy in, determination of, 19: 47124(T) (SLAC-Trans-19)
methane–Na_2SiF_6, radiolysis yields in, 19: 46324(R) (AGN-8132)
methane–SiF_4, radiolysis yields in, 19: 46324(R) (AGN-8132)
methane–N, radiolysis of, 19: 46324(R) (AGN-8132)
methane–N, radiolysis in fissiochemical loop, 19: 46324(R) (AGN-8132)
NH_3–methane, radiolysis yields in, 19: 46324(R) (AGN-8132)

METHANE, BROMO-
effects on radiolysis of methanol vapor, 19: 46395

METHANE, CHLORO-
electron drift velocities in, at low energy, 19: 46393

METHANE, DICHLORO-
effects on radioinduced polymerization of vinyl butyrate, 19: 46389
radioinduced polymerization of, with ethylene, yields of 1-chloroalkanes and 1,1-dichloroalkanes from, 19: 46370

METHANE, DICHLORODIFLUORO-
boiling burnout in upward flow through uniformly and non-uniformly heated tubes, forced-convection, 19: 46527 (AEEW-R-426)

METHANE, IODO-
radioinduced decomposition of, distribution and energies of fragments from, 19: 46161(R) (ORNL-3832, pp 116-50)
yields in reactions of fission-recoil iodine with gases, 19: 46330 (NP-15370)

METHANE, TRIPHENYL-
use as a radical scavenger reagent to minimize radiation effects on TBP, 19: 46406(P)

METHANE, TRIPHENYL-, DERIVATIVES
properties of, in polystyrene as chemical dosimeters, 19: 46369

METHANES, HALO-
ionization potentials, calculated, 19: 46161(R) (ORNL-3832, pp 116-50)

METHANOL
determination of, method for, 19: 46324(R) (AGN-8132)
radiation effects on decomposition of, in presence of catalysts, 19: 46329 (EUR-2455.e)
radiolysis of vaporous, scavenging effects of carbon tetrachloride, bromomethane, and oxygen on, 19: 46395
thermodynamic properties of, in water and heavy water, 19: 46318
methanol–naphthalene, radiolysis yields in, 19: 46324(R) (AGN-8132)

METHYL ETHER
electron drift velocities in, at low energy, 19: 46393
BF_3–methyl ether, boron isotopic exchange thermodynamics of, 19: 46899(R) (ORNL-3832, pp 33-49)

METHYL RADICALS *(Free Radicals)*
yields from radiolysis of ethylene, 19: 46361
yields in radiolysis of ethylene–methane–nitrogen, 19: 46324(R) (AGN-8132)

METHYL SELENIDES
BF_3–dimethyl selenide, boron isotopic exchange reactions of, 19: 46899(R) (ORNL-3832, pp 33-49)

METHYL SULFIDES
BF_3–methyl sulfide, boron isotopic exchange thermodynamics of, 19: 46899(R) (ORNL-3832, pp 33-49)

METHYLAMINE
radiolysis of, analysis of yields in, 19: 46324(R) (AGN-8132)

METROLOGY
equipment and methods for, conference on, 19: 46732

MICA
age estimation of phlogopites, in Aldanian deposits, Russia, 19: 46596

MICE
autoradiography of iodine-125 distribution in thyroid gland of, 19: 45783
bone tumors induced by plutonium-239 in, 19: 45808(R) (NYO-901-36)
erythropoiesis maintenance in marrow cultures from, 19: 45740
immune reactions to Brucella vaccine prepared from irradiated bacteria, 19: 45868
life span of, 19: 45809(R) (NYO-1979-12)
pathological effects of cortisone in, effects of age, 19: 45808(R) (NYO-901-36)
performance capacity of, effects of adrenalectomy on, 19: 45823(T) (JPRS-31933, pp 1-5)
pituitary hormones in, effects of iodine-131 and goitrogens on, 19: 45808(R) (NYO-901-36)
radiation chimeras in, mortality from secondary disease in, 19: 45910
radiation effects on metabolism of desoxyribonucleic acid in tumor cells of, tracer study, 19: 45936
radiation effects on bone marrow of, protective effects of pyridoxal-5-phosphate, aminoethylisothiouronium, and homocysteinethiolaction against, 19: 46028
radiation effects on ear of, skin recovery processes in, 19: 45987
radiation effects on, 19: 45990
radiation effects on cell nuclei in, 19: 45992
radiation effects on, protective effects of sodium cysteinethiosulfonate against, 19: 46006
radiation effects on, protective effects of AET, glutathione, and serotonin against, 19: 46016
radiation effects on spleen weight in, genetic factors, 19: 54956
radiation effects on thymus weight in, genetic factors, 19: 45956
radiation effects on life spans in, effects of genetic damage on, 19: 45969
radiation effects in, lethal, 19: 45982
radiation effects on antibody production by transferred spleen cells in, 19: 45986
radiation effects on immune reactions in, 19: 45806 (AD-621543)
radiation effects on, gamma and proton, 19: 45821(T) (JPRS-31547, pp 1-5)
radiation effects on performance capacity of, 19: 45823(T) (JPRS-31933, pp 1-5)
radiation effects on immune reactions to transplanted ultraviolet-induced sarcomas, 19: 45827
radiation effects on oocytes in, beta, 19: 45831
radiation effects on lactic dehydrogenase activity in blood plasma in, 19: 45844
radiation effects on embryos of, pathological, 19: 45852
radiation effects on growth of tumor transplants in, 19: 45858
radiation effects on immune reactions in, 19: 45858
radiation effects on osteogenesis in long bones of embryos of, 19: 45872
radiation effects on skin of, effects of dose-fractionation on electron, 19: 45885
radiation effects on immune reactions in, 19: 45903
radiation effects on mineral metabolism in, x, 19: 45729(R) (NYO-910-23, pp 1-111)
radiation effects on alkaline phosphatase production in bones of, 19: 45729(R) (NYO-910-23, pp 1-111)
radiation effects on, genetic, 19: 45809(R) (NYO-1979-12)
radiation effects on creatine excretion by, use as damage indicator, 19: 45864
radiation injuries, protective effects of injected bovine liver homogenates, 19: 46024
radiation injuries of, protective effects of chlorotrianisene against, 19: 46029

radiation sickness using rutin, 19: 46030
radioinduced leukemia in, effects on chromosomal aberrations of x, 19: 45911
radioinduced leukemia in, 19: 45808(R) (NYO-901-36)
radioinduced tumors in, antigenic adaptation in transplantable, 19: 45873
radioinduced tumors in, 19: 45808(R) (NYO-901-36)
radiosensitivity of tumor implants in, effects of oxygen on, 19: 46003
radiosensitivity of autochthonous radioinduced lymphosarcomas in, single- and split-dose, 19: 54977
radiosensitivity of genotype S1/S1 anemic, cellular basis of hemopoietic defect in, 19: 45856
radiosensitivity of, genetic factors in, 19: 45857
radiosensitivity of cells of thymus gland of, 19: 45871
radiotherapy effects combined with Actihaemyl in sarcomas in, histology, 19: 46123
thymidine uptake by DNA in, effects of AET, glutathione, and serotonin on, 19: 46016
toxic effects of niobium pentachloride and potassium niobate on, 19: 45768
tumors induced by chemicals in, 19: 45808(R) (NYO-901-36)
MICROORGANISMS
incorporation of radioisotopes by, 19: 46409
radiosterilization effects with storage on microbial flora in dover sole fillets, 19: 46882
MICROSCOPES
design of phase-contrast uv microbeam, with television equipment, 19: 45891
hot stage design for metallographic, 19: 47000 (NMI-4996, pp 8-16)
MICROSCOPY
methods for membrane radiation injuries, 19: 45891
MICROWAVE EQUIPMENT
development of high-power cyclotron resonance switch, 19: 46708(R) (AD-611560)
electromagnetic wave-plasma interactions in, amplification in, (E/T), 19: 47219 (AD-614253)
electromagnetic-wave propagation in dielectric-layer circular wave-guides, (T), 19: 46743
plasma oscillation modes in circular waveguides, (E), 19: 47743
waveguide behavior in, correlation with elementary particle behavior, 19: 47319
MICROWAVE OSCILLATORS
x radiation production by, in radar installations, 19: 46673
MICROWAVES
maximum safe exposure criteria for man, 19: 46706
production by energy conversion in plasma, (E/T), 19: 47717 (AD-614285)
propagation in dielectric-layer circular waveguides, 19: 46743
reflection from hydrogen plasma, (E), 19: 47795
scattering by plasma, from acoustic-ion-plasma-wave instability, (E/T), 19: 47776
use for plasma diagnostics, free space method for, (E), 19: 47755
MILK
cesium-137 content of, effects of diet of cows on, 19: 45780
cesium-137 content of, 19: 46612
cesium-137 content of Australian, 1964, 19: 46660
cesium-137 ratio to strontium-90 in, effects of various foodstuffs on, 19: 45772
iodine content of, bound and exchangeable, 19: 45782
iodine-125 and -131 in, uptake by abomasum, feces, plasma, thyroid, and urine of, 19: 45782
radioactive contamination of, by radiation accident, 19: 46694
radioactivity of Belgian, 1963, 19: 46632(R) (A/AC.82/G/L.987)
radioactivity of Utah, cesium-137 and ruthenium-103 and -106, 19: 46675
strontium-90 content in, 1959 to 1962, 19: 45749
MINERAL METABOLISM
radiation effects on mouse, x, 19: 45729(R) (NYO-910-23, pp 1-111)
MINERALS
age determination by radioactive halos in, evaluation of, 19: 46616(T) (ORNL-tr-768)
determination in biological materials, fluorescence, 19: 45729(R) (NYO-910-23, pp 1-111)
radiation processing by flotation method, 19: 46453
radioactive halos in cassiterite and yttrofluorite, measurements of, 19: 46592(T) (ORNL-tr-701)
radioactive halos in, review, 19: 46593(T) (ORNL-tr-755)
radioinduced coloration in, with and without pleochroic halos, 19: 46625(T) (ORNL-tr-757)
sorptive properties for strontium-90 in ground waters, 19: 46602
MINING
caving method using nuclear explosions, 19: 46472 (UCRL-14201)
methods of, uranium, 19: 46629
MITOCHONDRIA
oxygen metabolism in rat, effects of cystamine on, 19: 45777
MITOMYCINS
effects on radiation damage in cultured mouse fibroblasts, 19: 46018
MITOSIS
radiation effects on, in proliferating cellular systems, 19: 45923
radiation effects on, in intestinal cells of rats, 19: 45926
radiation effects on, in animal cells in tissue culture, 19: 45867
MOHAWK RIVER
radioactive contamination in, 19: 46646(R) (PHS-999-RH-13)
MOLECULAR BEAMS
reactions in crossed alkali-halogen, 19: 46161(R) (ORNL-3832, pp 116-50)
MOLECULAR STRUCTURE
review of diatomic, 19: 47265
valence electron approximations in, 19: 46284
MOLECULAR WEIGHTS
effects on radioprotective properties of heterologous and homologous DNA in mice, 19: 46013
MOLECULES
absorption spectra in systems of, two photon, (T), 19: 47236
collisions of, bibliography on, 19: 47258
electron orbitals in, spin hamiltonian for nonorthogonal, (T), 19: 47254
electron orbitals of homonuclear diatomic, at small internuclear separations, 19: 47265
electron structure of, superconducting theory for, (T), 19: 47230
energy levels of diatomic, vibrational, (T), 19: 47215 (AD-613375)
isotope exchange of, effects of separation factor on properties of, 19: 46408(T) (ORNL-tr-770)
photon reactions with, excitation and ionization by multi-, 19: 47234
radiation effects on diffusion of, 19: 45922
reactions with ions in ethylene, mass spectrometry of, 19: 46161(R) (ORNL-3832, pp 116-50)
scattering in linear lattice systems, time-dependent, (T), 19: 47255
spectra at low pressure and high temperature, Stark and Zeeman components of microwave, (T), 19: 37235
spectra of isotopically disordered linear chain, integrated, (T), 19: 47256
MOLLUSKS
analysis for zinc-65 and phosphorus-32 by radiochemical techniques, 19: 46218
manganese and manganese-54 distributions in tissues of Lake Maggiore, 19: 45788
manganese content in Lake Maggiore, activation determination of, 19: 45788
strontium-90 content in, 1965, 19: 45748(R) (TID-22193)
MOLYBDENUM
content and distribution in beef heart, 19: 45753 (AE-191)
determination in hair and wool, activation, 19: 46192
effects on mechanical properties of sintered zirconium diboride, 19: 46907 (AD-456724)
effects on mechanical properties of aluminum–copper–iron–tin–titanium–vanadium alloys, 19: 46985 (AD-613651)
electron emission from surfaces of, thermionic, 19: 46571 (HRL-5249-S)
microstructure of, effects of sintering on, 19: 47054
neutron reactions (n,2n) at 14 Mev, use in fusion-reactor blankets, 19: 47721 (LA-3385)
oxidation and properties of, effects of protective coatings on, 19: 47061
properties for aerospace uses, 19: 47068
siliconizing by vapor deposition, mechanism of, 19: 47073
surface tension of, measurement by pendant drop method, 19: 47065
tensile properties of, effects of sintering on, 19: 47054
thermal expansion coefficient of, x-ray determination of, 19: 47023(T) (LA-tr-65-20)
Mo–W, reactions with cesium at 3400°F, metallographic specimen preparation of, 19: 46954 (NMI-5025(Pt.I), pp 39-58)
MOLYBDENUM ALLOYS
properties for aerospace uses, 19: 47068
thermoelectric properties of sintered, for use as thermocouples at high temperatures, 19: 47019(T) (AD-619334)
Fe–Mo, crystal structure of, effects of molybdenum content on, 19: 47029
Mo–Nb, thermal expansion coefficient determination by x-ray method, 19: 47023(T) (LA-tr-65-20)
Mo–Nb–Ta–W, creep slip of solution-hardened, at 980 to 1370°C, 19: 47049
Mo–Nb–V–Zr, reactions with cesium at 3400°F, metallographic specimen preparation of B-66, 19: 46954 (NMI-5025(Pt.I), pp 39-58)
Mo–Nb–V–Zr, reactions with uranium carbide, nitride, and dioxide, metallographic specimen preparation of B-66, 19: 46954 (NMI-5025 (Pt.I), pp 39-58)

Mo–Nb–V–Zr, weldability studies of B-66, 19: 46966(R) (WANL-PR(P)-007)
Mo–Ti, effects of protective coatings on oxidation and properties of, 19: 47061
Mo–Ti–Zr, reactions with cesium at 3400°F, metallographic specimen preparation of TZM, 19: 46954 (NMI-5025(Pt.I), pp 39-58)
Mo–Ti–Zr, reactions with uranium carbide, nitride, and dioxide, metallographic specimen preparation of TZM, 19: 46954 (NMI-5025 (Pt.I), pp 39-58)
Mo–U, fabrication into massive enriched core components for Super Kukla, safety in, 19: 46967 (Y-KB-62)
Mo–U, radioinduced swelling in clad tubular, 19: 46917(R) (DP-975)
Mo–U, separation of uranium from, by fused salt electrolysis, 19: 46448
Mo–W, reactions with uranium carbide, nitride, and dioxide, metallographic specimen preparation of, 19: 46954 (NMI-5025(Pt.I), pp 39-58)

MOLYBDENUM BORIDES
preparation and purification, 19: 46941 (NP-15514(Vol.3))

MOLYBDENUM ISOTOPES Mo-92
energy levels from $(g_{9/2})^2$ configuration, (T), 19: 47617

MOLYBDENUM ISOTOPES Mo-95
energy levels of, parity and spin of, 19: 47605

MOLYBDENUM ISOTOPES Mo-99
metabolism in sheep and swine, 19: 45759(R) (ORO-631, pp 77-87)
physical properties of, 19: 46139
use in liver scanning, 19: 46139

MOLYBDENUM OXIDES
analytical uses as standard in rubidium determination in cesium by x-ray fluorescence spectroscopy, 19: 46186

MOLYBDENUM SELENIDES
intercalation of strongly electropositive metals in, 19: 46265

MOLYBDENUM SILICIDES
electron emission from surfaces of, thermionic, 19: 46571 (HRL-5249-S)
protective effects as coating on molybdenum and molybdenum–titanium alloy, 19: 47061

MOLYBDENUM STEEL
Cr–Mo, corrosion of Croloy 2¼ by sodium hydroxide solutions at high temperatures, 19: 46530(R) (BAW-1280-27)
Cr–Mo, corrosion of Croloy 2¼ by sodium–water reaction products, 19: 46478(R) (BAW-1280-25)
Cr–Mo, effects of hydrogen on embrittlement of irradiated pressure vessels of, 19: 47098

MOLYBDENUM SULFIDES
intercalation of strongly electropositive metals in, 19: 46265

MOLYBDENUM SYSTEMS
Al–Fe–Mo–Si–U, radioinduced swelling in, resistance to, 19: 47103

MONAZITES
analysis for uranium by ion exchange separation and fluorimetry, 19: 46223

MONEL
mechanical properties at cryogenic temperatures, 19: 47013 (PB-171809(Rev.)(Suppl.2))

MONKEYS
immune reactions to irradiated tendon grafts in, 19: 45965
iodine-131 uptake in respiratory tract and thyroid of, 19: 45776
radiation effects on performance tests requiring visual discrimination, by *Macaca mulatta*, 19: 45803
radiation effects on behavior of, sex factors, 19: 45898
radiation effects on response to stimulus-position conditions, of female rhesus, 19: 45899
radiation effects on learning by Rhesus, 19: 45900

MONTE CARLO METHOD
computer program for, general purpose, 19: 46905(R) (IDO-17081, pp 125-35)
use for buckling calculations in uranium-water lattices, 19: 47954 (BNWL-127)
use in meson-shower analysis, 19: 47400
use in neutron resonance escape probability calculations, 19: 47970
use in neutron transport calculations, 19: 47545 (KFK-297)
use in neutron transport calculations, computer program for, 19: 47546 (KFK-298)
uses in GEM code for criticality studies, 19: 47949 (ANL-7050, pp 657-79)
uses in TIMOC code for calculating reactor parameters, 19: 47919 (ANL-7050, pp 581-92)

MOON
cosmic-ray intensity variations on, 19: 47273

MORPHINES
protective effects of, against radiation injuries in rats, 19: 46021

MORPHOLOGY
radiation effects on sea urchin, ultraviolet, 19: 45840

MOSQUITOES
radiation control of malaria mosquito (*Anopheles quadrimaculatus*) populations, 19: 45960

MÖSSBAUER EFFECT
detection of, design and performance of automatic spectrometer for, 19: 46831
measurement of, design of low-temperature cryostat for, 19: 46748
measurement of, equipment for, 19: 46826
use for nuclear orientation production diagnostics, (T), 19: 47615

MOTORS
design of electric, for use at high temperatures in radioactive atmosphere, 19: 46516(P)
evaluation of drive systems for machining of round parts, 19: 46461 (RFP-562)

MOUTH
radiotherapy of tumors of, 19: 46066

MUCOSA
radiation effects on phospholipase activity in intestinal, of rats, 19: 45820(R) (TID-22227)
radiosensitivity of intestinal, 19: 45929
radiosensitivity of rectal, in rats, 19: 45918

MULTIPLICATION FACTOR
measurement of, instrumentation for, 19: 46716(R) (IDO-17081, pp 77-123)

MUSCLES
activity of guinea pig intestine, effects of radioprotective compounds on, 19: 46005(T) (JPRS-31933, pp 6-12)
excitation-contraction coupling in frog, chemical effects and role of action potential in, 19: 45736
radioinduced free radicals in tissues of rabbit, ESR of gamma and x, 19: 45947
use of myographic signals for control functions, study of feasibility of, 19: 46459 (CONF-640508, pp 100-57)

MUTAGENS
effects of 2-chloroethyl trimethylammonium chloride on plant growth, 19: 45817(R) (ORO-631, pp 145-71)

MUTATIONS
chemically induced, for screw-worm fly, 19: 45950
chemically induced in *Salmonella typhimurium*, genetic analysis of pyrimidine, 19: 45878
detection in plants, methods for, 19: 45737
induced in Drosophila 2nd chromosomes by DNA feeding, 19: 45876
radioinduced in *Acer negundo*, 19: 45865
radioinduced in algae, 19: 45842
radioinduced in animals, review, 19: 45973
radioinduced in *Cyathodium tuberosum*, x, 19: 45901
radioinduced in Drosophila, 19: 45949
radioinduced in Drosophila 2nd chromosomes, x, 19: 45876
radioinduced in Lupinus, protective effects of moisture against x, 19: 45847
radioinduced in man, 19: 45967
radioinduced in region of X chromosome in *D. melanogaster* DNA, 19: 45879
radioinduced in red clover, Ultuna, 19: 45882
radioinduced in *Salmonella typhimurium*, genetic analysis of pyrimidine, 19: 45878
radioinduced in silkworm gonial cells, fission neutron and gamma, 19: 45883
radioinduced in *Streptomyces citreus*, antibiotic properties of, 19: 45991
radioinduced mutations of, 19: 45853
radioinduced somatic, in plants, 19: 45817(R) (ORO-631, pp 145-71)
radioinduced, in barley, 19: 45819(R) (TID-22176)
radioinduced, in mice, 19: 45809(R) (NYO-1979-12)
radioinduced, in plants, 19: 45884
radioinduced, of screw-worm fly, 19: 45950
radiosensitivity of *Escherichia coli*, uv, 19: 45948

N

NAGASAKI
radiation effects from bomb on development and growth of adolescents exposed *in utero*, 19: 45889

NAPHTHALENE
labeling with deuterium, 19: 46307
methanol–naphthalene, radiolysis yields in, 19: 46324(R) (AGN-8132)

1,4-NAPHTHALENEDIOL, 2-METHYL- DIPHOSPHATE, SODIUM SALTS
use of tritiated, in radiotherapy of tumors, 19: 46125

NAPHTHOL
determination of, method for, 19: 46324(R) (AGN-8132)
effects on radioinduced chemiluminescence in organic compounds in presence of oxygen, 19: 46344

NATIONAL REACTOR TESTING STATION
environs monitoring, 1965, 19: 46642 (IDO-12043)
hydrology, 19: 46642 (IDO-12043)
waste gas injection into lithosphere at, appraisal, 19: 48077 (IDO-12024)
NATURAL GAS
production of, Project Gasbuggy studies of underground nuclear explosions in, 19: 46474
NATURAL WATERS
monitoring of, at Juelich research center, 19: 48078 (JUL-261-DE)
potassium-40 content in, in Vinca, Yugoslavia, 19: 46590(T) (JPRS-31469)
NEBULAE
element abundances in, 19: 47187 (AD-612182)
NECK
radiotherapy of supraglottic carcinomas using telecobalt, 19: 46057
radiotherapy of tumors, 19: 46129
NEODYMIUM
cohesive energy and ionization of, relation between, (T), 19: 47062
separation from praseodymium using phthalate buffer, 19: 46437
NEODYMIUM ALLOYS
Al–Nd, crystal structure of Laves phases in, 19: 47052
Co–Nd, crystal structure of Laves phases in, 19: 47052
Nd–Pd, phase studies, 19: 47051
NEODYMIUM BROMIDES
refractive index of, in aqueous solutions, 19: 46254
thermal decomposition of hydrates of, mechanism of, 19: 46271
NdBr–KBr, complex formation in, refractometric studies of, 19: 46254
$NdBr_3$–NaBr, complex formation in, refractometric studies of, 19: 46254
NEODYMIUM CHLORIDES
refractive index of, in aqueous solutions, 19: 46254
CsCl–$NdCl_3$, complex formation in, refractometric studies of, 19: 46254
$NdCl_3$–KCl, complex formation in, refractometric studies of, 19: 46254
$NdCl_3$–NaCl, complex formation in, refractometric studies of, 19: 46254
NEODYMIUM ETHYL SULFATES
magnetic temperature scale, 19: 47883 (UCRL-16279)
rare earth ion quadrupole coupling in lattices of, 19: 47883 (UCRL-16279)
NEODYMIUM FERRATES(III)
crystal structure, 19: 46256
NEODYMIUM IONS
spectra in glass, concentration dependence of fluoresence, 19: 47887(T) (N64-21857, pp 7-12)
spectra in silicate glass, fluorescence, 19: 47886(T) (N64-21857, pp 1-6)
NEODYMIUM OXIDES
atomic charge and permittivity of, (E/T), 19: 47901(T)
oxygen-18 exchange between molecular oxygen and, 19: 46266
reactions with barium carbonates, ternary oxide formation in, 19: 46242(R) (TID-22207, Paper B)
spectra of, absorption and fluorescence, 19: 47887(T) (N64-21857, pp 7-12)
NEODYMIUM SULFIDES
crystal growth in barium-activated, 19: 47876 (AD-614435)
NEON
atomic weight, 19: 46588 (ORNL-3857)
ionization by, electron and proton impact at high energies, cross sections for, (T), 19: 47246
isotopic composition of atmospheric, 19: 46588 (ORNL-3857)
scattering by copper at 30 kev, (E), 19: 47262
sorption by quartz walls in high-density discharges, (E/T), 19: 46576
NEON IONS
beams of, analysis of duoplasmatron, 19: 47267
effects on aluminum and SAP at 9 kev, 19: 47080 (EUR-2478.e)
NEON ISOTOPES Ne-17
decay of, delayed proton emission in, (E), 19: 47613
NEON ISOTOPES Ne-18
beta decay of, branching ratios, energies, and half lives, 19: 47603
NEON ISOTOPES Ne-20
content in atmospheric neon, 19: 46588 (ORNL-3857)
deuteron reactions (d,p) at 1.8 and 2.2 Mev, neon-21 energy levels from, (E), 19: 47632
production in thermonuclear helium-4 reactions during massive-star evolution, 19: 47202
NEON ISOTOPES Ne-21
content in atmospheric neon, 19: 46588 (ORNL-3857)
energy levels and gamma cascades, (E), 19: 47632
energy levels from sodium-23 (d,α) reactions at 4.9 to 5.5 Mev, (E), 19: 47633
separation from thermal diffusion cascades, system for, 19: 46157(R) (MLM-1254)
NEON ISOTOPES Ne-22
content in atmospheric neon, 19: 46588 (ORNL-3857)
neutron reactions (n,p) at 14.8 Mev, fluorine-22 production in, (E), 19: 47671
NEON SYSTEMS
ethanol–He–Ne, electron drift velocity variations in, 19: 47116 (BNL-9443)
NEPTUNIUM COMPLEXES
with 8-quinolinol, preparation and properties, 19: 46288
NERVES
radiation effects on, deuterons, 19: 45874
NERVOUS SYSTEM
radiation effects on rabbit and rat, pathological, 19: 45812(R) (ORO-631, pp 1-35)
radiosensitivity of, in mammals, 19: 45981
radiosensitivity of human, 19: 45892
radiosensitivity of, in rat fetuses, 19: 45894
radiotherapy effects on human, late nasal cavity, 19: 45983
NETHERLANDS
nuclear power development in, 19: 47923
NEUTRINOS
energy spectra, (E), 19: 46643(R) (LAL-1136)
interactions with neutrons, analysis of, (T), 19: 47301 (CERN-65-30)
interactions with nucleons, charge ratio of mesons (π) produced in, (T), 19: 47377
quantum theory for, 19: 47409
NEUTRON ACTIVATION CROSS SECTIONS
measurement for gadolinium-154, gadolinium-156, and ruthenium-102, (E), 19: 47584(R) (ORNL-3832, pp 1-28)
NEUTRON BEAMS
dosimetry in tissue, isodose charts for, 19: 46121
NEUTRON CAPTURE CROSS SECTIONS
measurement for californium-248, (E), 19: 47584(R) (ORNL-3832, pp 1-28)
measurement for ruthenium-96, 99, 100, and 101, (E), 19: 47584(R) (ORNL-3832, pp 1-28)
measurement for tungsten isotopes, (E), 19: 47595(R) (TID-22141, pp 50-66)
measurement in fast reactors, method for, 19: 47944 (ANL-7034)
measurement of, detector systems for, 19: 46566(R) (TID-22141, pp 67-79)
NEUTRON CROSS SECTIONS
measurements of, effective factors for, (T), 19: 47577 (IDO-17107)
tabulation of 16 groups, for Sandia Pulsed Reactor II, 19: 48063 (SC-RR-65-344)
NEUTRON DIFFRACTOMETERS
design and operation of two-coordinate, 19: 46835(T)
NEUTRON FISSION CROSS SECTIONS
measurement in fast reactors, method for, 19: 47944 (ANL-7034)
of uranium-235 at 0.1 to 10 ev, 19: 47576(R) (IDO-17081, pp 49-76)
NEUTRON MONOCHROMATORS
efficiency of, from multiple Bragg reflection in large mosaic crystals, (T), 19: 47562
use of crystal, in epithermal-neutron radiography, 19: 46563
NEUTRON PHOTOGRAPHY
methods of, using crystal monochromator, 19: 46563
NEUTRON SCATTERING CROSS SECTIONS
measurement for plutonium-239, uranium-233, and uranium-235, (E), 19: 47595(R) (TID-22141, pp 50-66)
measurement of inelastic, liquid scintillation detectors for, 19: 46766(R) (TID-22141, pp 67-79)
NEUTRON SOURCES
calibration of, determination of manganese sulfate content in baths for, (E/T), 19: 47552
dosimetry, flux measurements, and spectrometry of, multisphere technique for, 19: 46757 (CEA-R-2772)
neutron flux in SM-1 reactor with plutonium–beryllium, 19: 48040
use for well logging, 19: 46624(P)
NEUTRON SPECTRA
determination of fast, review of activation methods for, 19: 46763 (RCN-37)
NEUTRON SPECTROMETERS
design and performance of DIDO triple-axis, 19: 46753 (AERE-R-4895)
design and performance of time-of-flight, 19: 46829
development of multisphere, 19: 46757 (CEA-R-2772)
development of time-of-flight with large memory capacity, 19: 47115(R) (ANL-6983)
development of time-of-flight, using computers, 19: 47336
NEUTRON SPECTROSCOPY
use of nuclear emulsion stars for, from 20 to 300 Mev, (E/T), 19: 46769 (UCRL-16325)
NEUTRON TOTAL CROSS SECTIONS
measurement at high energies, 19: 47550(R) (TID-22141, pp 81-93)
measurement for plutonium-239, uranium-233, and uranium-235, (E),

19: 47595(R) (TID-22141, pp 50-66)
measurement of thorium-228 and uranium-232, (E), 19: 47576(R) (IDO-17081, pp 49-76)
NEUTRONS
absorption by graphite in gas-cooled reactors, calorimeter for determining, 19: 48031
absorption in heterogeneous media including moderator scattering, intermediate resonance, (T), 19: 47953 (BNL-9393)
absorption in matter, mechanisms of, 19: 47152
book: *The Biological Action of Neutron Radiation*, 19: 45822(T) (JPRS-31822)
capture by nuclei, helicity representation for, 19: 47610
decay of polarized, CP-parity non-conservation in, (T), 19: 47312 (NP-15460)
density distributions in reactors, kinetic equations for, (T), 19: 47963
detection and measurement of, calibration of survey probe for, 19: 46752 (AERE-M-1564)
detection and measurement of, multisphere technique for, 19: 46757 (CEA-R-2772)
detection and measurement of, performance of polyethylene for, 19: 46759 (EGG-1183-1017)
diffraction from antiferromagnetic and ferromagnetic salts, covalency effects on, 19: 47895
diffusion and slow down in heterogeneous moderators containing holes, (T), 19: 47563
diffusion in reactors, computer calculations of, (T), 19: 47912 (ANL-7050, pp 347-68)
diffusion in reactors, variational calculations of, (T), 19: 47945 (ANL-7050, pp 159-77)
diffusion in reactors, use for fuel-cycle and power-distribution calculations, (T), 19: 47946 (ANL-7050, pp 231-49)
diffusion length in water, from time-decaying fields, (E), 19: 47560
diffusion of, calculation of thermal utilization factor in energy-dependent, (T), 19: 47558
dosimetry of, equipment for, 19: 46847
dosimetry of, photographic, 19: 46853
effects on aluminum, copper, gold, and platinum, low-temperature recovery of residual resistivity from, (E), 19: 47097
effects on behavior of monkeys, 19: 45898
effects on copper crystals, microstrain from, (E), 19: 47107
effects on crystal structure and electric properties of lead zirconium titanate–niobium oxide systems, 19: 47096
effects on domestic animals, delayed pathological, 19: 45812(R) (ORO-631, pp 1-35)
effects on eyes, pathological, 19: 45843
effects on hexamminocobalt nitrate, annealing of, 19: 46391
effects on lactation by dairy cows, whole-body, 19: 45760(R) (ORO-631, pp 83-121)
effects on leukocyte chromosomes, 19: 45813(R) (ORO-631, pp 36-44)
effects on nervous system in rabbits and rats, pathological, 19: 45812(R) (ORO-631, pp 1-35)
effects on pure and doped iron, point defects produced by, 19: 47094(T) (ORNL-tr-668)
effects on reproduction in domestic animals, 19: 45813(R) (ORO-631, pp 36-44)
effects on rhenium, 19: 47106
effects on saturated fluorocarbons, chemical, 19: 46404
effects on thermal conductivity of uranium, 19: 47101
effects on thiourea yields of compounds labeled with phosphorus-32 and sulfur-35 from, 19: 46365
effects on time-to-rupture of metals and alloys, 19: 47081(R) (EURAEC-1432)
effects on tin compounds, yields of antimony-125 from, 19: 46388
emission in meson (π^-) reactions with xenon at 9 Bev/c, high four-momentum transfer in, (E), 19: 47698
energy states in nuclei, correlation of positions of, 19: 47583 (NP-15467)
escape probability in homogeneous thorium reactors, resonance, 19: 47969
escape probability in homogeneous thorium reactor, resonance, 19: 47970
flux calculations in Sandia Pulsed Reactor II, tabulations of, 19: 48063 (SC-RR-65-344)
flux decay constant in graphite crystalline assemblies, asymptotic, 19: 47554
flux distribution in WWR-S, (T), 19: 48072
flux distributions in thermionic fuel elements, 19: 47978 (CEA-R-2782)
flux distributions in Grosswelzheim Superheat Reactor, (E/T), 19: 47992 (KEA-311)
flux in power reactors, design of fast counting channel for, 19: 48033
flux in reactors, calibration of graphite damage, (E), 19: 48070
flux measurement in reactors, computer program for, 19: 47866 (KAPL-M-6460)
interactions with neutrinos, analysis of, (T), 19: 47301 (CERN-65-30)
interactions with mesons (π^-) at 1.2 to 4.5 Bev/c, cross sections for backward elastic, (E), 19: 47310 (NP-15376)
interactions with neutrinos, charge ratio of mesons (π) produced in, (T), 19: 47377
interactions with protons in tritium-Λ hypernucleus, tensor, (T), 19: 47657
kinetics in BBRR, 19: 48056 (BNL-9510)
lifetime in crystals and liquids, upper bounds for time-decay constants of, (T), 19: 47553
magnetic moment from sum rules and SU(6) symmetry, (T), 19: 47306 (JINR-E-2343)
polarization in proton reactions (p,n) with carbon-13 and nitrogen-15 at 6.9 to 12.3 Mev, 19: 47710
production of 14-Mev, design of accelerator for, 19: 47176
reactions ($n,\alpha\gamma$), ($n,d\gamma$), ($n,n'\gamma$), ($n,p\gamma$), and ($n,n'\alpha\gamma$) with carbon-12, nitrogen-14, and oxygen-16 at 14.8 Mev, gamma angular distributions from, (E/T), 19: 47593(R) (TID-22012, pp 156-75)
reactions (n,α), (n,2n), and (n,p) with iron-54 at 2.2 to 16.8 Mev, cross sections for, (E/T), 19: 47668
reactions (n,α) with nuclei at 14.6 Mev, angular and energy distributions from, (E/T), 19: 47637
reactions (n,d) with fluorine-19, phosphorus-31, and sodium-23 at 14 Mev, (E/T), 19: 47644
reactions (n,γ) in chromium oxides, reactions of recoils from, 19: 46398
reactions (n,γ) with manganese-55 to 10 kev, cross sections for, (E/T), 19: 47634
reactions (n,n'γ) with aluminum-27 at 3.5 to 4.5 Mev, gamma angular distributions from, (E/T), 19: 47588(R) (TID-22012, pp 22-52)
reactions (n,n'γ) with magnesium and silicon at 3.0 to 4.35 Mev, gamma angular distributions from, (E/T), 19: 47589(R) (TID-22012, pp 53-66)
reactions (n,n'γ) with argon-40 at 3.0 to 4.5 Mev, gamma angular distributions from, (E/T), 19: 47590(R) (TID-22012, pp 67-98)
reactions (n,n'γ) with iron-56 at .97 to 4.76 Mev, gamma angular distributions and cross sections from, (E/T), 19: 47591(R) (TID-22012, pp 99-128)
reactions (n,n'γ) with lead-206, -207, and -208 at 1.0 to 4.6 Mev, gamma angular distributions from, (E/T), 19: 47592(R) (TID-22012, pp 129-55)
reactions (n,n'γ) with boron-10 and -11, calcium-40, cerium, cobalt, and uranium at 3.0 to 14.8 Mev, gamma angular distributions and cross sections from, (E/T), 19: 47594(R) (TID-22012, pp 176-205)
reactions (n,pn) with zirconium-90 at 14 Mev, production of yttrium-89 isomers in, (E), 19: 47566 (AERE-R-5009)
reactions (n,p) with neon-22 at 14.8 Mev, fluorine-22 production in, (E), 19: 47671
reactions (n,p) with iron-56 at 14 Mev, cross sections for, (E), 19: 47673
reactions (n,p) with copper-65 at 14 Mev, cross sections for, 19: 47673
reactions (n,2n) with scandium-45 at 14 Mev, (E), 19: 47596(R) (TID-22141, pp 94-7)
reactions (n,2n) with nuclei (Zr – 28) at 12.6 to 19.6 Mev, excitation functions for, (E/T), 19: 47571 (EUR-2456.e)
reactions at 14 Mev, counter telescope for charged-particle production in, 19: 46821
reactions with α-iron, damage from, 19: 47105
reactions with matter, resonance effects in, 19: 47542 (ANL-7050, pp 457-70)
reactions with nuclei, fission systematics for, (T), 19: 47614
reactions with technetium-99 at 14 Mev, 19: 46160(R) (ORNL-3832, pp 29-32)
reactions with uranium dioxide surfaces, uranium atom ejection during fission, (T), 19: 47580 (LA-3352)
reflection in large mosaic crystals, monochromator efficiency and multiple Bragg, (T), 19: 47562
resonance absorption in thorium-232 and uranium-238 mixtures, (E/T), 19: 47575 (IDO-16986)
scattering by aluminum and chromium single crystals, time-of-flight method for, (E), 19: 47894
scattering by aluminum, magnesium, and silicon at 3 to 4.5 Mev, gamma angular distributions from inelastic, (E/T), 19: 47638
scattering by argon-40 at 3 to 4.5 Mev, gamma angular distributions from inelastic, (E/T), 19: 47639
scattering by beryllium-9 at 14 Mev, (E), 19: 47609
scattering by beta brass, critical, (E), 19: 47904
scattering by carbon-12, lithium-6, and lithium-7 at 14 Mev, inelastic, (E), 19: 47609
scattering by ethylene polymers at 0.167 to 0.499 ev, inelastic, (E), 19: 47572 (GA-6547)
scattering by lithium-6 and -7 at 4.4 Mev, polarization from, (E/T), 19: 47570 (COO-7-0361)
scattering by nuclei, computer program for matrices of inelastic, (T), 19: 47544 (KAPL-M-6467)

scattering by nuclei, Coulomb field and magnetic moment interactions in, 19: 47115(R) (ANL-6983)
scattering in antiferromagnets with weak ferromagnetism, (T), 19: 47899(T)
scattering in single crystals, measurement of one-phonon, 19: 46753 (AERE-R-4895)
scattering on nuclei, potential model for elastic, (E/T), 19: 47581 (LA-DC-6730)
spectra in Doppler region, calculation of, (T), 19: 47539 (ANL-7050, pp 51-76)
spectra in light-water lattices, cell theory calculation of, 19: 47968
strength function for nuclei $220 \leq A \leq 248$, peak in s-wave, 19: 47115(R) (ANL-6983)
structure of, from form factors and scattering amplitudes, (E/T), 19: 47565 (AD-614270)
thermalization, (E/T), 19: 47548(R) (TID-22141, pp 3-33)
thermalization in heavy water, interference scattering effects on, (T), 19: 47559
transmission by hydrogenless shielding materials, 19: 47870
transport equation for, relation to non-equilibrium thermodynamics, 19: 47551 (UJV-1354/65)
transport in aluminum, carbon, and polyethylene slabs, data tabulations for, (T), 19: 47868 (RRA-T52)
transport in lattices, EQUIPOISE method for calculating, 19: 47541 (ANL-7050, pp 179-89)
transport in reactors, (T), 19: 47921(R) (ANL-7090, pp 30-54)
transport in reactors, collision-probability calculations of, (T), 19: 47540 (ANL-7050, pp 93-112)
transport of, for computer program, Monte Carlo calculations, 19: 47546 (KFK-298)
transport of, moments and discrete ordinates equations for, (T), 19: 47547 (LA-DC-7320)
transport of, Monte Carlo calculations of, 19: 47545 (KFK-297)
transport theory for, dynamic programming and inverse problem in, (T), 19: 47537 (AD-612468)
transport through single-bend aluminum ducts in water shields, (E), 19: 47863 (AD-613480)

NEUTRONS, EPITHERMAL
absorption and flux spectra in cylindrical lattice cells, computer program for, 19: 46917(R) (DP-975)
scattering by polyethylene and water, inelastic, (E/T), 19: 47549(R) (TID-22141, pp 34-49)

NEUTRONS, FAST
detection of, performance of organic scintillation detector for, 19: 46774
dose measurements of, in graphite irradiation in Belgian Reactor-2, 19: 48030
effects on color of fused silica, 19: 47082 (NASA-CR-304)
effects on electronic equipment, computer program for data retrieval on, 19: 46870(R) (AD-612191)
effects on lattice atom displacement probabilities in copper, gold, iron, and silver, (T), 19: 47104
effects on oxide film corrosion on Zircaloy-2 and zirconium, 19: 47099
effects on pyrimidine mutation induction in *Salmonella typhimurium*, genetic analysis of, 19: 45878
effects on seeds of red clover, Ultuna, genetic, 19: 45882
effects on silica glass, annealing of, (E), 19: 47108
effects on stability of anthracene oils, 19: 46333 (SGAE-CH-20/1965)
effects on stress corrosion of stainless steels by magnesium chloride, 19: 47079 (AERE-R-5014)
effects on structure of A-286 alloy, electron microscope studies of, 19: 47088 (NMI-4998, pp 95-106)
effects on zirconium by hydrofluoric acid, 19: 46957(R) (ORNL-3832, pp 100-6)
effects on 347 stainless steel, 19: 46912(R) (BMI-1727(Del.))
effects on 347 stainless steel, 19: 46913(R) (BMI-1733(Del.))
energy spectra in bare homogeneous reactor with two-component moderator, equations for, (T), 19: 47964
energy spectra of, penetrating layers of iron and heavy water, (E/T), 19: 47561
reactions with granite, seawater, and soils, gamma dose curves from, (T), 19: 46589 (UCRL-14332)
reactions with light nuclei, tritium yields from, 19: 47721 (LA-3385)
spectra of, activation methods for determining, 19: 46763 (RCN-37)

NEUTRONS, FISSION
effects on seeds, species differences in, 19: 45817(R) (ORO-631, pp 145-71)
effects on silkworm gonial cells, mutagenic, 19: 45883

NEUTRONS, RESONANCE
capture by barium-135 at 18 to 1500 ev, gamma transitions from, (E), 19: 47701

NEUTRONS, THERMAL
capture by strontium-88, radiation widths of gamma emission from, 19: 47115(R) (ANL-6983)
capture of nitrogen-containing cobalt complexes, chemical effects of, 19: 46386
diffusion length and transport mean-free path in graphite at 100 to 300°K, (T), 19: 47556
detection using boron trifluoride proportional counters, 19: 46822
dose measurements of, in graphite irradiation in Belgian Reactor-2, 19: 48030
effects on fibrous fissiochemical fuels, 19: 46324(R) (AGN-8132)
effects on seeds of red clover, Ultuna, genetic, 19: 45882
effects on structure of A-286 alloy, electron microscope studies of, 19: 47088 (NMI-4998, pp 95-106)
energy distribution in beryllium oxide finite and semi-infinite blocks, (T), 19: 47555
energy distribution of, synthetic scattering model for calculating, 19: 47557
flux distribution in soil in Operation Bren, 19: 47569 (CEX-62-50)
flux distributions in reactor moderators and reflectors, temperature effects on, (T), 19: 47956 (IAE-723)
reactions with nuclei, shell effects on cross sections for, (E), 19: 47618
reactions with plutonium-239 and uranium-235, fission cross sections for, 19: 47567 (CEA-R-2775)
reactions with uranium-235, yields of antimony-124 and -126 and implication on empirical Z_p function in fission, (E), 19: 47611
scattering by butane, ethane, and methane, calculation methods for, (E), 19: 47576(R) (IDO-17081, pp 49-76)
scattering by matter, cross sections for inelastic, 19: 47543 (ANL-7050, pp 471-85)
scattering by thorium, titanium, and zirconium hydrides, inelastic, (E/T), 19: 47549(R) (TID-22141, pp 34-49)
scattering by yttrium, 19: 47888
scattering of, solid-state studies by, 19: 47889
spectra in lattices, free-gas-theory calculations of, (T), 19: 47538 (ANL-7050, pp 33-40)

NEVADA TEST SITE
neutron activation of soils of, gamma dose curves from, (T), 19: 46589 (UCRL-14332)
nuclear rocket reactor tests at, safety aspects, 19: 46707

NICKEL
corrosion of plated coatings of, on aluminum by water and hydroxide solutions at 330°C, 19: 46945 (BNWL-98)
determination by potentiometric titration of acid liberated by complex formation, 19: 46205
determination in aluminum, activation, 19: 46207
effects on mechanical properties of aluminum–copper–iron–tin–titanium–vanadium alloys, 19: 46985 (AD-613651)
effects on point defects in iron, 19: 47094(T) (ORNL-tr-668)
electrodeposition on uranium bars, bath for, 19: 46944(P)
oxygen-ion transmission through thin foils of, charge-state distribution after, (E), 19: 47179
surface tension of, measurement by pendant drop method, 19: 47065
thermal expansion coefficient of, x-ray determination of, 19: 47023(T) (LA-tr-65-20)

NICKEL ALLOY COUPLES
Alumel/Chromel, development for in-pile measurements, 19: 46722 (PWAC-462)

NICKEL ALLOYS
properties for aerospace uses, 19: 47068
Cr–Fe–Ni, stress corrosion cracking of Alloy 600 by wetted thermal insulation, 19: 46949 (CONF-650905-2)
Cu–Ni, stress corrosion cracking of Alloy 400 by wetted thermal insulation, 19: 46949 (CONF-650905-2)

NICKEL BORIDES
surface tension of molten, 19: 47021(T) (JPRS-31225)

NICKEL ISOTOPES
proton elastic scattering at 14.5 Mev, cross sections for, 19: 47705

NICKEL ISOTOPES Ni-56
energy levels from nickel-58 (p,t) at 28 Mev, 19: 47706
mass, 19: 47706
proton reactions (p,d) and (p,t) at 28 Mev, (E), 19: 47706

NICKEL ISOTOPES Ni-57
energy levels from nickel-58 (p,d) at 28 Mev, 19: 47706

NICKEL ISOTOPES Ni-58
alpha scattering at 34.4 Mev, angular distributions for, (E), 19: 47623
energy levels from nickel-60 (p,t) at 28 Mev, 19: 47706
neutron reactions (n,2n) at 12.6 to 19.6 Mev, excitation function for, (E/T), 19: 47571 (EUR-2456.e)
proton reactions (p,d) and (p,t) at 28 Mev, (E), 19: 47706

NICKEL ISOTOPES Ni-59
energy levels from nickel-60 (p,d) at 28 Mev, 19: 47706

NICKEL ISOTOPES Ni-60
alpha inelastic scattering at 44 Mev, cross section angular dependence in, 19: 47608
alpha scattering at 34.4 Mev, angular distributions for, (E), 19: 47623
deuteron inelastic scattering at 9.9 to 13.6 Mev, differential cross sections for, (E/T), 19: 47635

NICKEL ISOTOPES Ni-62
alpha inelastic scattering at 44 Mev, collective states in, 19: 47608
proton scattering at 12 Mev, cross sections for, 19: 47585 (ORNL-3851)

NICKEL ISOTOPES Ni-63
diffusion in alpha-irradiated copper, 19: 47032

NICKEL STEEL
Cr–Ni–Nb, radiation effects on stress corrosion by magnesium chloride, 19: 47079 (AERE-R-5014)
Cr–Ni–Ti, ageing of corrosion-resistant, structural changes in, 19: 47026(T) (ORNL-tr-795)

NICKEL SYSTEMS
B–Cr–Ni, protective effects as coating on molybdenum and molybdenum–titanium alloy, 19: 47061
Ni–UO_2, radiation effects on fibrous fissiochemical fuels of, 19: 46324(R) (AGN-8132)

NIOBIUM
analysis for carbides, nitrides, and oxides by anodic staining, 19: 46929 (NMI-4998, pp 57-64)
determination in hafnium carbide–niobium carbide, method for, 19: 46941 (NP-15514(Vol.3))
determination in niobium carbide–zirconium carbide, method for, 19: 46941 (NP-15514(Vol.3))
determination in thorium oxide, spectrochemical, 19: 46226
diffusion in thorium and uranium dioxides, 19: 47070
properties for aerospace uses, 19: 47068
reaction with nitrogen, oxygen, and water vapor, embrittling effects of, 19: 46296
separation from hydrochloric acid solutions by solvent extraction using tetrabutylpyrophosphate and tetrabutylhypophosphate, tracer studies of, 19: 46451
separation from other fission products by solvent extraction using benzene–oxine solutions, 19: 46440
solvent extraction from nitric acid solutions, effects of solvent degradation on, 19: 46430 (ORNL-P-1601)
sorptive properties for nitrogen at 25 to 1800°C and 6×10^{-9} to 6×10^{-8} torr, 19: 47031
surface tension of, measurement by pendant drop method, 19: 47065
thermal expansion coefficient of, x-ray determination of, 19: 47023(T) (LA-tr-65-20)

NIOBIUM ALLOYS
fabrication of, with high stress-rupture strength up to 2200°F, 19: 46976(P)
properties for aerospace uses, 19: 47068
Hf–Nb–W–Y, weldability studies of C-129Y, 19: 46966(R) (WANL-PR(P)-007)
Mo–Nb, thermal expansion coefficient determination by x-ray method, 19: 47023(T) (LA-tr-65-20)
Mo–Nb–Ta–W, creep slip of solution-hardened, at 980 to 1370°C, 19: 47049
Mo–Nb–V–Zr, reactions with cesium at 3400°F, metallographic specimen preparation of B-66, 19: 46954 (NMI-5025(Pt.I), pp 39-58)
Mo–Nb–V–Zr, reactions with uranium carbide, nitride, and dioxide, metallographic specimen preparation of B-66, 19: 46954 (NMI-5025 (Pt.I), pp 39-58)
Mo–Nb–V–Zr, weldability studies of B-66, 19: 46966(R) (WANL-PR(P)-007)
Nb–Sn, superconductivity of intermetallic compounds of, above 4.2°K, (E), 19: 47508
Nb–Sn, superconducting electromagnetic of, 19: 47526
Nb–Ta–W, weldability studies of SCb-291, 19: 46966(R) (WANL-PR(P)-007)
Nb–Ta–W–Zr, weldability studies of FS-85, 19: 46966(R) (WANL-PR(P)-007)
Nb–V, interdiffusion in, 19: 47058
Nb–W, reactions with cesium at 3400°F, metallographic specimen preparation of, 19: 46954 (NMI-5025(Pt.I), pp 39-58)
Nb–W, reactions with uranium carbide, nitride, and dioxide, metallographic specimen preparation of, 19: 46954 (NMI-5025(Pt.I), pp 39-58)
Nb–W–Zr, weldability studies of Cb-752, 19: 46966(R) (WANL-PR(P)-007)
Nb–Zircaloy-4–Zr, fabrication of tubular, methods for, 19: 47998(R) (SRO-118)
Nb–Zr, critical currents in, effect of omega transformation on, (E), 19: 47511
Nb–Zr, current decay propagation in superconducting, persistent, (E), 19: 47507
Nb–Zr, electric conductivity at 200 to 1446°C, 19: 47015 (TIM-854)
Nb–Zr, magnetic flux degradation in superconducting coils of, (E), 19: 47512
Nb–Zr, pressure testing of tubular, 19: 47998(R) (SRO-118)
Nb–Zr, reactions with oxygen at 2000°F, 19: 47016 (TIM-901)
Nb–Zr, tensile properties of pressure tubing of, effects of hot working on, 19: 46539(R) (TID-22249)
Nb–Zr, thermal analysis of ω phase of, 19: 47037

NIOBIUM BORIDES
analysis for boron, method for, 19: 46941 (NP-15514(Vol.3))
corrosion by hydrogen chloride at 2250°C, 19: 46956 (NP-15514 (Vol.1))
lattice parameters and thermal expansion at 25 to 1700°C, 19: 47009 (NP-15514(Vol.2))
oxidation by carbon dioxide at 2250°C, 19: 46956 (NP-15514(Vol.1))
preparation and purification, 19: 46941 (NP-15514(Vol.3))

NIOBIUM CARBIDES
corrosion by hydrogen chloride at 2250°C, 19: 46956 (NP-15514 (Vol.1))
determination in niobium by anodic staining, 19: 46929 (NMI-4998, pp 57-64)
Fermi level, 19: 47009 (NP-15514(Vol.2))
oxidation by carbon dioxide at 2250°C, 19: 46956 (NP-15514(Vol.1))
preparation and purification, 19: 46941 (NP-15514(Vol.3))
thermal capacity of, at 7.5 to 320°K, 19: 46998 (LA-3331)
thermal expansion at 25 to 2030°C, 19: 47009 (NP-15514(Vol.2))
HfC–NbC, analysis for hafnium and niobium, method for, 19: 46941 (NP-15514(Vol.3))
NbC–NbN–ZrC, Hall coefficient for solid solutions of, 19: 47009 (NP-15514(Vol.2))
NbC–ZrC, analysis for niobium and zirconium, method for, 19: 46941 (NP-15514(Vol.3))
NbC–ZrC, oxidation by carbon dioxide at 2250°C, 19: 46956 (NP-15514(Vol.1))

NIOBIUM CHLORIDES
toxic effects on dogs, mice, rabbits, and rats, 19: 45768

NIOBIUM ISOTOPES Nb-95
beta decay of, β-γ circular polarization correlation in permitted transitions in, (E), 19: 47605
content in atmosphere and drinking water, Moncloa Station, Spain, 1964, 19: 46597
content in holothuriae, western Mediterranean, 1962, 19: 46611
distribution in Columbia River effluent, 19: 46680
energy levels of, parity and spin of, 19: 47605

NIOBIUM NITRIDES
determination in niobium by anodic staining, 19: 46929 (NMI-4998, pp 57-64)
Fermi level, 19: 47009 (NP-15514(Vol.2))
NbC–NbN–ZrC, Hall coefficient for solid solutions of, 19: 47009 (NP-15514(Vol.2))

NIOBIUM OXIDES
determination in niobium by anodic staining, 19: 46929 (NMI-4998, pp 57-64)
effects on thermal conductivity of sintered uranium dioxide at 1000 to 2000°C, 19: 46995 (EUR-2424.f)
reactions with copper oxides, structure of ABO_3 type compound formed in, 19: 46244(R) (TID-22207, Paper D)
$Pb(Zr_{0.65}Ti_{0.35})O_3$–$Nb_2O_5$, radiation effects on crystal structure and electric properties, 19: 47096

NIOBIUM STEEL
diffusion and permeation of deuterium and hydrogen in S110, oxygen effects on, 19: 46991 (AWRE-O-47/65)
Cr–Ni–Nb, radiation effects on stress corrosion by magnesium chloride, 19: 47079 (AERE-R-5014)

NIOBIUM SYSTEMS
C–Hf–Nb–W, fabrication and mechanical properties of, 19: 46940(R) (NP-15444)
C–Nb–W, fabrication and mechanical properties of, 19: 46940(R) (NP-15444)
C–Nb–W–Zr, fabrication and mechanical properties of, 19: 46940(R) (NP-15444)
C–Nb–W–Zr, weldability studies of D-43, 19: 46966(R) (WANL-PR(P)-007)
Nb–N, phase studies at 1600 to 2200°C, 19: 46296
Nb–O, phase studies at 1600 to 2200°C, effect on crystal structure, 19: 46296
Nb–Si, analysis for silicon, spectrophotometric, 19: 46171 (KAPL-M-6492)

NITRATE COMPLEXES
with beryllium, ion exchange studies of, 19: 46230 (AAEC/E-136)

NITRATE IONS
effects on contraction regulation by mechanical threshold in frog muscles, 19: 45736
reduction by iron in alkaline solutions, mechanisms of, 19: 46899(R) (ORNL-3832, pp 33-49)
NITRATES
effects on distribution of strontium-90 in water-bearing strata by ground waters, 19: 46602
NITRIC ACID
effects on etching of pyrolytic graphite, 19: 47078 (AD-613643)
performance of dilute, as HFIR coolant-moderator, 19: 48061 (ORNL-3848)
reactions with hydrocarbon diluents for phosphates, scouting experiments on, 19: 46304(R) (ORNL-3832, pp 66-75)
solubility for sodium lanthanum sulfate, 19: 46428(R) (ORNL-3847)
solvent properties for irradiated stainless steel clad plutonium dioxide–uranium dioxide fuels, 19: 46427 (ORNL-3754)
sorptive properties for plutonium in ion exchange resin, 19: 46173 (LA-3357)
NITRIDES
analysis for carbon, graphite, nitrogen, and oxygen in refractory, method for, 19: 46941 (NP-15514(Vol.3))
bibliography on analytical chemistry of certain group IV and V, 19: 46941 (NP-15514(Vol.3))
production, properties, and uses of refractory, 19: 47020(T) (AEC-tr-6616)
separation from plutonium by consumable electrode method, 19: 46915 (BNWL-IR-2)
NITRILES
α–α′ azobisisobutyro-thermal decomposition of, nitrogen isotope effects on, 19: 46899 (ORNL-3832, pp 33-49)
NITRITE IONS
radioinduced production in nitrate solutions, mechanisms of, 19: 46332(R) (ORNL-3832, pp 50-65)
reduction by iron in alkaline solutions, mechanisms of, 19: 46899(R) (ORNL-3832, pp 33-49)
NITROGEN
content in range plants, Miles City, Montana, 1955 to 1960, 19: 45747 (ORNL-TM-1279)
corrosive effects on superalloys at high temperatures, 19: 46946 (BNWL-100)
determination in metals by helium-3 activation, 19: 46174 (LA-DC-7319)
determination in plutonium mononitride, methods for, 19: 46164 (AERE-R-5002)
determination in refractory borides, carbides, and nitrides, method for, 19: 46941 (NP-15514(Vol.3))
effects on electron energy losses in argon–cesium nonequilibrium plasma, (E), 19: 47737(T)
effects on mechanical properties of chromium, 19: 46912(R) (BMI-1727 (Del.))
effects on mechanical properties of aluminum–copper–iron–tin–titanium–vanadium alloys, 19: 46985 (AD-613651)
effects on radioinduced decomposition of plutonium hexafluoride, 19: 46325 (ANL-7013)
electron drift velocity and mean energy in, determination of, 19: 47124(T) (SLAC-Trans-19)
electron orbitals of molecular, calculation of, 19: 47265
electron reactions at 20 to 500 ev, excitation and ionization cross sections for, (E), 19: 47245
radioinduced fixation of, equipment for, 19: 47985(P)
reactions with graphite at 1694 to 2365°K, microwave-activated, 19: 46956 (NP-15514(Vol.1))
reactions with niobium, embrittling effects of, 19: 46296
scattering of cesium ions by, angular distribution of elastic, 19: 46161(R) (ORNL-3832, pp 116-50)
sorption by niobium at 25 to 1800°C and 6×10^{-9} to 6×10^{-5} torr, 19: 47031
yields in photo- and radiation chemistry of mineral acid glasses, effects of iron ions and nitrous oxide on, 19: 46394
yields in radiolysis of ammonia–deuterium, 19: 46324(R) (AGN-8132)
NITROGEN ISOTOPES
effects on thermal decomposition of α–α′-azobisisobutyro nitride, 19: 46899(R) (ORNL-3832, pp 33-49)
equilibration reactions on tungsten, 19: 46289
NITROGEN ISOTOPES N-13
tracer use for measurement of blood circulation in lungs, 19: 46070
use in medical diagnostics, 19: 46136
NITROGEN ISOTOPES N-14
deuteron reactions (d,p) at 1.3 to 5.5 Mev nitrogen-15 excited levels from, (E), 19: 47604
energy levels of, 19: 47603
equilibration reactions with nitrogen-15 on tungsten, 19: 46289
neutron reactions (n,αγ), (n,dγ), and (n,pγ) at 14.8 Mev, gamma angular distributions from, (E/T), 19: 47593(R) (TID-22012, pp 156-75)
proton reactions at 2.2 Bev with, cross sections for beryllium-7 production in, 19: 47625
reactions with nuclei, excitation functions for nucleon-transfer, (E/T), 19: 47586 (ORNL-TM-1218)
reactions with nuclei at 20 to 42 Mev, excitation functions for alpha- and nucleon-transfer, (E), 19: 47667
NITROGEN ISOTOPES N-15
energy levels of parity and spin of excited, (E), 19: 47604
equilibration reactions with nitrogen-14 on tungsten, 19: 46289
production of, methods for, 19: 46413
proton reactions (p,n) with, neutron polarization in, 19: 47710
proton reactions at 2.2 Bev with, cross sections for beryllium-7 production in, 19: 47625
tracer use in electron microscopy using nuclear reactions, 19: 45741
NITROGEN MUSTARDS
tooth lesions induced by, in rats, 19: 45845
NITROGEN OXIDES
effects on hydrogen yields in propane radiolysis, 19: 46396
effects on radiolysis yields in ethylene, 19: 46324(R) (AGN-8132)
effects on yields in photo- and radiation chemistry of mineral acid glasses, 19: 46394
use of nitrous, for low gamma dosimetry, 19: 46332(R) (ORNL-3832, pp 50-65)
ethylene–methane–NO, radiolysis of, 19: 46324(R) (AGN-8132)
NO–N, radiolysis of, 19: 46324(R) (AGN-8132)
NITROGEN SYSTEMS
Al–C–Cu–H–N–Sn–Ti–V–Zr, mechanical properties of, 19: 46985 (AD-613651)
benzene–N, radiolysis yields in, 19: 46324(R) (AGN-8132)
C–N–Ti, Hall coefficients, 19: 47009 (NP-15514(Vol.2))
CO–H–N, radiolysis yields in, 19: 46324(R) (AGN-8132)
ethane–N, radiolysis yields in, 19: 46324(R) (AGN-8132)
ethylene–N, radiolysis yields in, 19: 46324(R) (AGN-8132)
ethylene–methane–N, radiolysis of, 19: 46324(R) (AGN-8132)
ethylene–N, radiolysis of, 19: 46324(R) (AGN-8132)
methane–N, electron drift velocity and mean energy in, determination of, 19: 47124(T) (SLAC-Trans-19)
methane–N, radiolysis of, 19: 46324(R) (AGN-8132)
methane–N, radiolysis in fissiochemical loop, 19: 46324(R) (AGN-8132)
Nb–N, phase studies at 1600 to 2200°C, 19: 46296
NO–N, radiolysis of, 19: 46324(R) (AGN-8132)
N–propene, radiolysis yields in, 19: 46324(R) (AGN-8132)
NITROUS ACID
effects on pyrimidine mutation induction in *Salmonella typhimurium*, genetic analysis of, 19: 45878
NORTH CAROLINA
deuterium content in rainfall in, Nov. 1 and 2, 1963, 19: 47112
NORVALINE
thermodynamic properties of, in water and heavy water, 19: 46318
NORWAY
nuclear power development and uses in, 19: 48114
NOSE
radiotherapy of, late effects on central nervous system from, 19: 45983
NUCLEAR BATTERIES
design using strontium-90, 19: 46897(P)
NUCLEAR ELECTRIC MOMENTS
calculations of quadrupole, for near-spherical nuclei, (T), 19: 47573 (IAE-717)
NUCLEAR EMULSIONS
neutron star identification in, method for, (E), 19: 46767 (TID-22256)
performance for neutron spectroscopy from 20 to 30 Mev, (E/T), 19: 46769 (UCRL-16325)
proton star identification in, method for, (E), 19: 46767 (TID-22256)
scanning procedure for absolute neutron yields, (E), 19: 46817
sensitivity for beta particles, 19: 46832
NUCLEAR ENGINEERING
book: *Principles of Radiation Protection Engineering*, 19: 46683(T)
research programs on, 19: 48059(R) (IDO-17081)
NUCLEAR MAGNETIC MOMENTS
analysis of dipole, determined with NMR, (T), 19: 47606
NUCLEAR MAGNETIC RESONANCE
spectra of four-membered ring compounds, analysis, 19: 46247 (UCRL-16349)
spectrometer for, resolving power and sensitivity of, 19: 46157(R) (MLM-1254)
use in nuclear dipole moment studies, (T), 19: 47606
NUCLEAR MATERIALS MANAGEMENT
accounting systems for, at AECL, 19: 47906 (AECL-2282)
criticality control in chemical processing department at Hanford, adminis-

tration of, 19: 46433 (RL-SA-43)
isotopic analysis, automation of mass spectrometers for, 19: 46181 (WAPD-T-1769)
NUCLEAR MODELS
energy levels in cranking, higher order corrections to rotational, (T), 19: 47680
NUCLEAR MODELS (SHELL)
alpha decay of deformed nuclei, (T), 19: 47597 (UCRL-16187)
energy levels in, four-body operator for classification ν, (T), 19: 47678
use in studying many-particle systems with translational invariance, 19: 47399
NUCLEAR PARTICLES
scattering by collective nuclei, coupled-channel calculations for, (T), 19: 47685
NUCLEAR PHYSICS
equipment for low-energy, 19: 47629
research, (E/T), 19: 47587(R) (TID-22012)
research programs on high-energy, equipment and methods for, 19: 47326
teaching of, experiments for use in, 19: 47621
NUCLEAR POWER
performance of Berkeley, Bradwell, and Hunterston, 19: 48019
NUCLEAR POWER PLANTS
design of Brayton-cycle, for space vehicles, 19: 48048 (GE-65SD4251)
design of Dungeness B, 19: 47995 (NP-15473)
development in Austria, 19: 48010
development in Belgium, 19: 48113
development in Denmark, 19: 48004
development in European Atomic Energy Community, target program for, 19: 48003
development in France, 19: 48006
development in Great Britain, 19: 48007
development in Italy, 19: 48008
development in Netherlands, 19: 47923
development in Spain, 19: 48011
development in Switzerland, 19: 48009
development of Dungeness-B 1200-Mw(e), 19: 48020
development of Japanese, 19: 48043
development of 300 Mw(e), in Finland, 19: 48005
development of, effects of magnetohydrodynamic generators on, 19: 48013
development of, Euratom studies of industry grouping for, 19: 48118
economic and technical aspects of Dungeness-B, 19: 48023
economic aspects of, effects of fuel reserves and costs of tubing on, 19: 47979
economic aspects of, in Soviet Union, 19: 48014
economics of Dungeness B, 19: 47996 (NP-15474)
planning for accidents, 19: 46703
turbines for, closed-cycle gas, 19: 47987 (AD-612409)
NUCLEAR REACTIONS
analysis of high-energy, using detectors with on-line computers, (E), 19: 46806
analysis of, using PDP 1 computer with time sharing, (E), 19: 46807
dispersion relations for direct, (T), 19: 47684
NUCLEAR SPIN
oscillations in antiferromagnetics, 19: 47903
NUCLEAR STRUCTURE
analysis by alpha inelastic scattering, (E), 19: 47608
binding energy at equilibrium density, off-energy-shell effects in Brueckner theory for, 19: 47666
correlation energy in, wave function for short-range three-body, 19: 47665
problems in, 19: 47629
NUCLEAR THEORY
matrix elements for allowed unfavored transitions in, (T), 19: 47622
quasar model for gas clouds in dense star clusters, 19: 47199
NUCLEI
alpha decay of deformed, (T), 19: 47597 (UCRL-16187)
alpha inelastic scattering at 44 Mev, data on collective states from, (E), 19: 47608
binding energy at equilibrium density, off-energy-shell effects in Brueckner theory for, 19: 47666
charge spectra of, in primary cosmic radiation, (E), 19: 47277
correlation energy of, wave function for short-range three-body, 19: 47665
decay of high-angular-momentum, gamma spectra from single-particle electromagnetic, (T), 19: 47655
decay of, helicity representation for angular correlations with recoil effect in, 19: 47610
deuteron (d,p) reactions with, impulse approximation for calculating, 19: 47631
deuteron reactions (d,p) with, equation for matrix element of, 19: 47630
electric quadrupole moment and spectral isotopic shift calculations of near-spherical, (T), 19: 47573 (IAE-717)
energy level density of, pairing effects on, (T), 19: 47616
energy levels in A = 15, positive parity T = ½, 19: 47694
energy levels in, four-body operator for classification of, (T), 19: 47678
energy-level spectra of odd-odd spherical, low-lying, (T), 19: 47658
flux intensity ratios of multiply charged, in primary cosmic radiation, (E), 19: 47277
interactions with mesons (π^-) at 16.2 Bev/c, coherent meson (π) trident production in, (E), 19: 47355
meson (K^-) reactions with, at rest, 19: 47708
meson (μ) capture by complex, correlation functions in, (T), 19: 47656
meson (π^-) capture by, nucleon pair emission in, (T), 19: 47679
meson (π^+) reactions (π^+,π^-), model for, 19: 47660
mesons (K^-) reactions with emulsion, hyperfragment production in, (E/T), 19: 47648
neutron elastic scattering on, model for, (E/T), 19: 47581 (LA-DC-6730)
neutron inelastic scattering by, computer program for matrices of, (T), 19: 47544 (KAPL-M-6467)
neutron levels in, correlation of positions of, 19: 47583 (NP-15467)
neutron reactions with, effective cross section factors for, (T), 19: 47577 (IDO-17107)
neutron scattering by, Coulomb field and magnetic moment interactions in, 19: 47115(R) (ANL-6983)
nuclear particle scattering by collective, coupled-channel calculations for, (T), 19: 47685
photon reactions with, meson (π^0) production in, (E), 19: 46788
proton decay of, following bombardment by heavy ions or fast protons, 19: 47628
proton elastic scattering at 10.5 and 14.5 Mev, neutron-nucleus potential from polarized, (E/T), 19: 47581 (LA-DC-6730)
spectra of $2s_{1/2} - 1d_{1/2}$, shell model for, (T), 19: 47600
transitions in, matrix elements for, (T), 19: 47622
wave functions in light, charge-dependent nuclear, (T), 19: 47679
NUCLEI (CELLS)
radiation effects on Triton erythroblast, x, 19: 45925
radiation effects on morphology of, in *Cannabis sativa* seedlings, 19: 45940
radiation effects on, biological, 19: 45992
radiation effects on thymidine metabolism in, 19: 45808(R) (NYO-901-36)
NUCLEIC ACIDS
physiological chemistry of, 19: 46158(R) (NYO-910-23, pp 112-82)
radiation chemistry of, 19: 46417
radiation effects on synthesis in ϕX174-infected *E. coli*, tracer study of x, 19: 45851
radiosensitivity effects of irradiated, 19: 45729(R) (NYO-910-23, pp 1-111)
NUCLEONS
emission of pairs of, in meson (π^-) capture by nuclei, (T), 19: 47679
existence of heavy unstable, possibility of, 19: 47398
form factor for, electromagnetic, 19: 47318
form factors of, ($K\bar{K}$) and ($n\rho$) contributions to isoscalar, (T), 19: 47371
interactions with mesons (π), resonance in static, (T), 19: 47298 (AD-613934)
interactions with charged particles, peripheral electromagnetic, (T), 19: 47318
interactions with hyperons (Σ) at low energy, T = ½ bound state in, (T), 19: 47348
interactions with mesons (π), model for P_{11}-state strong, 19: 47350
interactions with photons at high energy, total cross section for (πN), (T), 19: 47353
interactions with mesons (K^0), scattering length for $S_{1/2}$ T = 0, (T), 19: 47365
interactions with mesons (π), restriction on forward amplitudes of, (T), 19: 47375
interactions with mesons (π), fixed-variable dispersion relations for, (T), 19: 47388
interactions with gamma rays at high energies, meson production and momentum-transfer distributions in, (T), 19: 47389
interactions with mesons (π) calculation using Regge trajectory, 19: 47395
interactions with mesons (π), meson (η) production in, (T), 19: 47401
interactions with mesons (π), analysis of data for, 19: 47404
pairing interactions in nuclei, effects on level densities, (T), 19: 47616
NUCLEOSIDES
optical rotation of dinucleoside phosphates, 19: 48104 (UCRL-16278)
synthesis of purine method for, 19: 46158(R) (NYO-910-23, pp 112-82)
NUCLEOTIDES
separation by capillary column chromatography, 19: 45730(R) (ORNL-3752)
NUCLEOTIDES, PYRIDINE DIPHOSPHATE

protective effects of injected, against radiation injuries in rats, 19: 46020

O

OAK RIDGE NATIONAL LAB., TENN.
transuranic element production program, 19: 46428(R) (ORNL-3847)
OCTANAL, PENTADECAFLUORO-
radioinduced polymerization of, at low temperatures, 19: 46323(R) (AD-613529)
ODOR
radioinduced in beef, chemical analysis of, 19: 46878 (NP-15455)
OIL DEPOSITS
prospecting for, by radiometric well logging, 19: 46624(P)
OILS
radiation effects on stability of anthracene, fast neutron, 19: 46333 (SGAE-CH-20/1965)
OLEIC ACID
butyl ester, radioinduced chemiluminescence of, 19: 46344
radioinduced chemiluminescence of, in presence of oxygen, 19: 46344
OOCYTES
radiation effects on mouse, beta, 19: 45831
OPTICAL SYSTEMS
design of analyzer-scanner for spark-chamber photographs, (E), 19: 46790
design of particle track analyzers for spark-chamber photographs, (E), 19: 46791
design of visual scanner for analyzing spark-chamber events, 19: 46789
distortion in, instrument for measuring azimuthal, 19: 48103 (UCRL-16260)
image components from ionic, 19: 46738
ORES
radiation effects on flotation properties, 19: 46453
ORGANIC ACIDS
preparation of labeled, by microbial processes, 19: 46409
ORGANIC COMPOUNDS
analysis of labeled, by gas chromatography and radiation counting, 19: 46213
book: *Physics and Chemistry of the Organic Solid State*, Vol. II, 19: 46320
preparation of carbon-11 labeled, using carbon-12 (γ,n) reactions, 19: 46418
properties and uses of, containing thiophosphoryl groups, 19: 46217
radiolysis of, ESR studies of radicals produced in, 19: 46402
scintillation properties of solid, review of, 19: 46399
ORGANIC COMPOUNDS, METALLO-
radioinduced formation of butyl tin bromate, effects of atmosphere, metals, and temperature on, 19: 46913(R) (BMI-1733(Del.))
ORGANIC COOLED REACTORS
development of heavy water, 19: 47998(R) (SRO-118)
ORGANS
weight of human, effects of age on, 19: 45755 (CEA-R-2809)
ORIFICES
use in measurements of two-phase flow, 19: 46526 (AECL-2273)
ORNL HIGH FLUX ISOTOPE REACTOR
coolant-moderator for, effects of reactor operation on, 19: 48061 (ORNL-3848)
target rod development for, 19: 46428(R) (ORNL-3847)
OSKARSHAMN POWER REACTOR
design, 19: 48028
design of 400-Mwe boiling-water, 19: 48025
OSMIUM ALLOYS
Fe–Os, hyperfine fields at osmium nuclei in, 19: 47069
OSMIUM ISOTOPES Os-186
internal conversion coefficients for E2 transitions in, nuclear structure effects on, (T), 19: 47620
OSMIUM ISOTOPES Os-188
internal conversion coefficients for E2 transitions in, nuclear structure effects on, (T), 19: 47620
OXALIC ACID
determination as thorium oxalate, gravimetric, 19: 46222
effects on rate of reaction between uranium(IV) and thallium(III), 19: 46277
OXAZOLE, DIPHENYL-
radioinduced luminescence in benzene, quenching effects of organometallics on, 19: 46362
OXIDES
deposition of refractory, on tungsten, 19: 46911 (AFML-TR-64-392)
formation of ternary, ionic field strengths as criteria for, 19: 46245(R) (TID-22207, Paper F)
preparation, properties, and structure of ternary, 19: 46240(R) (TID-22207)
separation from plutonium by consumable electrode method, 19: 46915 (BNWL-IR-2)
structure of ternary, bibliography on, 19: 46242(R) (TID-22207, Paper B)
structures of I-V type ABO_3, correlation of, 19: 46243(R) (TID-22207, Paper C)
OXIMES
keto, Beckmann rearrangement of, isotope effects on, 19: 46304(R) (ORNL-3832, pp 66-75)
OXYGEN
corrosive effects on superalloys at high temperatures, 19: 46946 (BNWL-100)
determination in liquid iron at 1500 to 1600°C, 19: 46297
determination in metals by helium-3 activation, 19: 46174 (LA-DC-7319)
determination in refractory borides, carbides, and nitrides, method for, 19: 46941 (NP-15514(Vol.3))
determination of excess, in arc-fused urania, metallographic, 19: 46176 (NMI-4997, pp 110-23)
effects on deuterium and hydrogen diffusion and permeation in niobium stainless steel S110, 19: 46991 (AWRE-O-47/65)
effects on mechanical properties of aluminum–copper–iron–tin–titanium–vanadium alloys, 19: 46985 (AD-613651)
effects on photolysis of cyclopentanone, 19: 46357
effects on radiation chemistry of ribonuclease, 19: 46347
effects on radioinduced chemiluminescence in organic compounds, 19: 46344
effects on radioinduced decomposition of plutonium hexafluoride, 19: 46325 (ANL-7013)
effects on radioinduced defects in germanium at 25 to 700°K, (E), 19: 47892
effects on radiolysis of methanol vapor, 19: 46395
effects on radiolysis of chromium and cobalt acetylacetonate, 19: 46761 (NYO-2979-34)
effects on radiosensitivity of biological systems, 19: 46026
metabolism in rat, effects of cystamine on, 19: 45777
oxidation of graphite, 19: 46956 (NP-15514(Vol.1))
oxidation of tungsten at 1400 to 3150°K, reaction kinetics of, 19: 46956 (NP-15514(Vol.1))
oxygen ion mobilities in, at low electric field/density ratios, 19: 47220 (NP-15175)
radiosensitivity effects on tumor implants in mice, 19: 46003
radiosensitivity effects of, on tumors, 19: 46097
reactions with helium ions, energy transfer in, (E), 19: 47231
reactions with niobium, embrittling effects of, 19: 46296
reactions with niobium–zirconium alloy at 2000°F, rate of, 19: 47016 (TIM-901)
yields in photo- and radiation chemistry of mineral acid glasses, effects of iron ions and nitrous oxide on, 19: 46394
OXYGEN IONS
charge state distribution of beam of, equilibrium, (E), 19: 47179
effects on aluminum and SAP at 9 kev, 19: 47080 (EUR-2478.e)
mobilities in oxygen at low electric field/density ratios, 19: 47220 (NP-15175)
production of, source for, 19: 47157 (AWRE-NR-1/65)
OXYGEN ISOTOPES
separation by fractionation in butylamine carbamate–carbon dioxide systems, temperature effects on, 19: 46899(R) (ORNL-3832, pp 33-49)
OXYGEN ISOTOPES O-14
beta decay of, branching ratios, energies, and half lives, 19: 47603
OXYGEN ISOTOPES O-15
production in nitrogen-14 reactions on lithium-6 and -7, cross sections for, (E), 19: 47667
use in medical diagnostics, 19: 46136
OXYGEN ISOTOPES O-16
charge-state distribution of ion beam of, equilibrium, (E), 19: 47179
deuteron reactions (d,p) with, (E), 19: 47609
electron scattering by, 19: 46643(R) (LAL-1136)
energy levels in, quadrupole moments and deformation of particle-hole, 19: 47675
energy levels of lifetime of 6.13-Mev, (E), 19: 47612
meson (μ^-) capture rate in, pseudoscalar coupling constant from, 19: 47707
meson (μ^-) capture by, K x ray energies from, 19: 47582 (NEVIS-129)
neutron reactions (n,n′γ), (n,αγ), and (n,n′αγ) at 14.8 Mev, gamma angular distributions from, (E/T), 19: 47593(R) (TID-22012, pp 156-75)
nitrogen-14 reactions with, excitation functions for one-neutron-transfer, (E/T), 19: 47586 (ORNL-TM-1218)
nitrogen-14 reactions (N-14, F-18) with, excitation functions, (E/T), 19: 47586 (ORNL-TM-1218)
nitrogen-14 reactions at 20 to 42 Mev, excitation functions for, (E), 19: 47667

nuclear charge distribution radius, 19: 47582 (NEVIS-129)
production in thermonuclear helium-4 reactions during massive-star evolution, 19: 47202
proton elastic scattering at 4.5 Mev, polarization in, (E), 19: 47691
proton reactions at 2.2 Bev with, cross sections for beryllium-7 production in, 19: 47625

OXYGEN ISOTOPES O-17
energy levels of fluorine-17 and opposite parity low, (T), 19: 47700
energy levels of, lifetime of 0.871-Mev, (E), 19: 47612
separation from natural oxygen by thermal diffusion, 19: 46899(R) (ORNL-3832, pp 33-49)
tracer use in electron microscopy using nuclear reactions, 19: 45741

OXYGEN ISOTOPES O-18
content in orthophosphate from living marine organism shells, 19: 46583
energy levels of separation-type calculations for, (T), 19: 47676
exchange between rare earth oxides and molecular oxygen, 19: 46266
meson (μ^-) capture by, K x ray energies from, 19: 47582 (NEVIS-129)
nuclear charge distribution radius, 19: 47582 (NEVIS-129)
production of, methods for, 19: 46413
proton reactions at 2.2 Bev with, cross sections for beryllium-7 production in, 19: 47625
tracer use in electron microscopy using nuclear reactions, 19: 45741

OXYGEN SYSTEMS
Al–Be–O, thermodynamics of, 19: 46231 (AD-613660)
Al–B–O, thermodynamics of, 19: 46231 (AD-613660)
Be–B–O, thermodynamics of beryllium metaborate formation in, 19: 46231 (AD-613660)
ethylene–O, radiolysis of, 19: 46324(R) (AGN-8132)
Hf–O, phase studies, 19: 46990 (ARL-65-138)
Nb–O, phase studies at 1600 to 2200°C, effect on crystal structure, 19: 46296

P

PACKED COLUMNS
design of elements for, 19: 46521(P)

PALLADIUM
determination of, flame photometric, 19: 46170 (JEN-148-DQ/I-49)
diffusion of hydrogen in, electron and proton dissociation in, (T), 19: 46250(T) (ORNL-tr-623)
heat of sublimation, 19: 46956 (NP-15514(Vol.1))
neutron cross sections of, shell effects on thermal, (E), 19: 47618

PALLADIUM ALLOYS
Ce–Pd, phase studies, 19: 47051
Dy–Pd, phase studies, 19: 47051
Er–Pd, phase studies, 19: 47051
Eu–Pd, phase studies, 19: 47051
Gd–Pd, phase studies, 19: 47051
Ho–Pd, phase studies, 19: 47051
La–Pd, phase studies, 19: 47051
Lu–Pd, phase studies, 19: 47051
Nd–Pd, phase studies, 19: 47051
Pd–Pr, phase studies, 19: 47051
Pd–Sm, phase studies, 19: 47051
Pd–Tb, phase studies, 19: 47051
Pd–Y, phase studies, 19: 47051

PANCREAS
radiation effects on enzyme excretion by, 19: 45928
radiation effects on enzymes from, 19: 45922
radiodiagnosis of carcinoma and inflammation of, method for, 19: 46060

PAPAIN
radiation effects on inactivation of, coupled with poly-p-aminophenyl-alanine, 19: 45976

PARABIOSIS
effects on radioinduced tumors in rats, 19: 45808(R) (NYO-901-36)
radiation effects on blood circulation between rats joined by, 19: 45838

PARAMECIUM
radiation effects on, time course of recovery from lethal x-ray, 19: 45978

PARATHYROID EXTRACTS
effects on selenium-75 metabolism in chickens, 19: 45761(R) (ORO-631, pp 122-31)

PARATHYROID GLANDS
selenium-75 metabolism in chicken, 19: 45761(R) (ORO-631, pp 122-31)

PARTICLE BEAMS
density distribution in, methods for determining phase-space, (T), 19: 47162 (BNL-9503)
injection of high-energy neutral, in fusion experiments, (E), 19: 47752
power density of, apparatus for measurement of, 19: 47155(P)

PARTICLE COLLECTORS
use of radioactive, for atmospheric electricity soundings, 19: 46730(T) (SC-T-66-760)

PARTICLE TRACKS
analysis in bubble chambers, use of computers for, 19: 47336
analysis in bubble chambers using on-line computers, (E), 19: 46797
analysis in bubble chambers, using semi-automatic scanning systems, (E), 19: 46798
analysis in bubble-chamber photographs, using PEPR system, (E), 19: 46810
analysis in bubble-chamber photographs, computer systems for, (E), 19: 46814
analysis in photographs, using flying-spot devices, (E), 19: 46787
analysis in spark chambers, systems for, 19: 46789
analysis in spark chambers, use of AROMA code for, (E), 19: 46794
analysis in spark-chamber photographs, using raster-scan methods, (E), 19: 46786
analysis in spark-chamber photographs, using CHLOE scanner, (E), 19: 46793
analysis in spark-chamber photographs, use of graph theory for, (T), 19: 46795
analysis of bubble-chamber, design of Lidian system for, (E), 19: 46801
analysis of bubble-chamber, using CERN HAZE program, (E), 19: 46812
analysis of high-energy, using track spark chambers, (E), 19: 46780
analysis of photographic, semi-automatic device for, (E), 19: 46803
analysis of photographic, using on-line computer system, (E), 19: 46811
analysis of photographs of, computer programming for PEPR system, (E), 19: 46813
detection and measurement in spark chambers, (E), 19: 46779
detection in electron microscope using tracers, method for, 19: 45741
ionization analysis of, in bubble-chamber photographs, (E), 19: 46802

PARTICLES
adhesion to surfaces in gaseous and liquid environments, decontamination methods for, 19: 46645 (ORNL-TM-1228)
deposition in long thin tubes, 19: 46647 (RISO-104)
distribution of radioactive, atmospheric, 19: 46693
kinematics of angular momentum of, translation broadening in relativistic quantum-mechanical, 19: 47418
separation of virus-like, from tumors, 19: 45730(R) (ORNL-3752)
sorptive properties of atmospheric, for iodine, 19: 46672

PEACH BOTTOM POWER REACTOR
chemical engineering aspects of, 19: 47991 (GA-6126)

PEAS
radiation effects on ascorbic acid content of, beta and gamma seed, 19: 45938
radioinduced free radicals in, effects of water content on, 19: 45863

PEAT
age of USSR, estimation of, 19: 46621

PEGMATITES
lead isotope composition in, review on, 19: 46582

2,4-PENTANEDIONE COMPLEXES
with chromium(III) and cobalt(III), use in gamma dosimetry, 19: 46761 (NYO-2979-34)

4-PENTENAL
yields from photolysis and radiolysis of cyclopentanone, 19: 46357

PENTOBARBITAL SODIUM
protective effects against radiation injuries in rats, effects of dose, 19: 46025

PERMANGANATES
decomposition in alkaline solutions, deuterium isotope effects on, 19: 46275

PERSONNEL
protection against toxic chemicals, catalog of USSR equipment for, 19: 46653(T) (JPRS-31843)
protection of Bulk Shielding Facility, engineering drawings of gamma ion chamber alarm for, 19: 46865
radiation dosimetry of occupational, in East Germany, 19: 46674
radiation exposure to, action levels in medical treatment of, 19: 46008
radiation exposure of hospital, according to occupation, 19: 46657
radiation monitoring, use of whole-body gamma spectrometry for, 19: 46656
radiation monitoring of, basic requirements for, 19: 46689
radiation protection of diagnostic radiography, 19: 46036
radiation protection of medical, during use of radioisotopes, 19: 46080
radiation protection of, using radiation sources, 19: 46649 (STI/PUB/94)
radiation protection of, catalog of USSR equipment for, 19: 46653(T) (JPRS-31843)
radiation protection standards for, in Yugoslavia, 19: 46654(T) (JPRS-31993)
radiation protection of, in radar installations using magnetrons, 19: 46673
radiation protection of medical, 19: 46686
radium-226 uptake by, in work with luminous paints, 19: 46677
training radiation monitoring, 19: 46839

PERTECHNETATE IONS
effects on electrochemical properties of cobalt, 19: 46957(R) (ORNL-3832, pp 100-6)
PERTURBATION THEORY
eigenvalue problems in, canonical transformations for linear classical, (T), 19: 47417
hypergeometric function of two variables in, 19: 46906
Regge cuts in, 19: 47434
scattering amplitudes in, singularities of, 19: 47412
PHANTOMS
design of tissue-equivalent rubber, 19: 46137
neutron isodose charts for head, 19: 46121
radiation dosimetry in, design of automatic isodose contour recorder for, 19: 46776
use of lucite and water, for x radiation isodose distribution measurements, 19: 46127
PHARMACEUTICALS
radiation hazards from use of labeled, in diagnosis and therapy, 19: 46044
radiosterilization of glucose solutions, effects on stability, 19: 46889
radiosterilization, 19: 46890
PHASE STUDIES
liquid-solid transitions in, (T), 19: 46233 (CEA-R-2752)
nucleation of precipitates from supersaturated solid solutions, review on, 19: 47025(T) (ORNL-tr-637)
PHENANTHRENE
use as a radical scavenger reagent to minimize radiation effects on TBP, 19: 46406(P)
PHENOL
BF_3–phenol, boron isotopic exchange thermodynamics of, 19: 46899(R) (ORNL-3832, pp 33-49)
PHENOL, p-BROMO-
radiation effects on bactericidal activity of, effects of cysteine, heat, and sodium sulfite on, 19: 46007
radiation effects on bactericidal activity of, factors affecting, 19: 45834
PHENOL, 4-*sec*-BUTYL-2-α-METHYLBENZYL-
kerosene–4-*sec*-butyl-2(α-methylbenzyl)phenol, solvent properties for cesium from alkaline waste solutions, 19: 48075 (BNWL-68)
PHENOTHIAZINE, 3-CHLORO-10-(3'-DIMETHYLAMINOPROPYL)-
effects on respiration in tumor cells and other biological systems, 19: 45862
PHENYLENEDIAMINE
use as radical scavenger reagent to minimize radiation effects on TBP, 19: 46406(P)
PHONONS
dispersion curves for diamond, charged bond correction for, 19: 47879 (LA-DC-7277)
PHOSPHATASES
radiation effects on production in mouse bone of alkaline, x, 19: 45729(R) (NYO-910-23, pp 1-111)
PHOSPHATE COMPLEXES
with beryllium, ion exchange studies of, 19: 46230 (AAEC/E-136)
PHOSPHATE GLASS
properties of silver-activated, in diagnostic dosimetry, 19: 46859
PHOSPHATE ROCKS
analysis for sodium, flame photometric, 19: 46191
PHOSPHATES
chemical properties, computer calculations of, 19: 45808(R) (NYO-901-36)
effects on distribution of strontium-90 in water-bearing strata by ground waters, 19: 46602
effects on strontium-90 uptake from soil, 19: 45774
optical rotation of dinucleoside phosphates, 19: 48104 (UCRL-16278)
oxygen-18 content of, from living marine organism shells, 19: 46583
PHOSPHATIDES
radiation effects on enzyme activity of, in rat intestinal mucosa, 19: 45820(R) (TID-22227)
PHOSPHINE OXIDE, TRIOCTYL-
solvent properties for cerium, 19: 46439
PHOSPHINE SULFIDE, TRIS(1-AZIRIDINYL)-
effects on radiation damage in cultured mouse fibroblasts, 19: 46018
PHOSPHINIC ACID, DIOCTYL-
solvent properties for actinides and rare earths, 19: 46443
PHOSPHONIC ACID, METHYL, DIISOAMYL ESTER
solvent properties for cerium, 19: 46439
PHOSPHORESCENCE
measurement of, design of phosphoroscope for, 19: 46737
PHOSPHORIC ACID
effects on etching of pyrolytic graphite, 19: 47078 (AD-613643)
PHOSPHORIC ACID, BIS(2-ETHYLHEXYL) ESTERS
D2EHPA–kerosene–TBP, solvent properties for rare earths from complexed waste solutions, 19: 46432 (ORNL-P-1603)
PHOSPHORS
efficiency of radiographic intensifying, methods for improving, 19: 46148
performance of gel-forming in thin-layer beta chromatography, 19: 46862
properties of organic, review of, 19: 46399
use of plastic, for x-ray integral dose measurement, 19: 46105
PHOSPHORUS
content in range plants, Miles City, Montana, 1955 to 1960, 19: 45747 (ORNL-TM-1279)
determination in arsenic, activation, 19: 46211
determination in beef heart, neutron activation, 19: 45753 (AE-191)
uptake by plants, effects of beryllium on, 19: 45802
PHOSPHORUS COMPOUNDS
analytical uses of organic sulfur-containing, 19: 46217
PHOSPHORUS ISOTOPES P-29
magnetic moments and M1 transition probabilities in $2s_{1/2}$ $1d_{1/2}$ shell, (T), 19: 47641
PHOSPHORUS ISOTOPES P-30
magnetic moments and M1 transition probabilities in $2s_{1/2}$ $1d_{1/2}$ shell, (T), 19: 47641
PHOSPHORUS ISOTOPES P-31
bremsstrahlung reactions (γ,3p) at 50 Mev, (E), 19: 47596(R) (TID-22141, pp 94-7)
magnetic moments and M1 transition probabilities in $2s_{1/2}$ $1d_{1/2}$ shell, (T), 19: 47641
neutron reactions (n,d) at 14 Mev, angular distributions from, (E/T), 19: 47644
nitrogen-14 reactions with, excitation functions for one-neutron-transfer, (E/T), 19: 47586 (ORNL-TM-1218)
nitrogen-14 reactions at 20 to 42 Mev, excitation functions for, (E), 19: 47667
proton inelastic scattering at 5.8 to 6.15 Mev, angular distributions from, (E), 19: 47690
PHOSPHORUS ISOTOPES P-32
determination in aqueous solutions by detection of Cherenkov radiation, 19: 46215
determination in shellfish by radiochemical techniques, 19: 46218
effects on mutation induction in region of X chromosome in *D. melanogaster* DNA, 19: 45879
magnetic moments and M1 transition probabilities in $2s_{1/2}$ $1d_{1/2}$ shell, (T), 19: 47641
metabolism by rat tissues *in vitro*, 19: 45939
metabolism by rice seedlings, effects of chemical growth inhibitors on, 19: 45794
metabolism in chickens, 19: 45761(R) (ORO-631, pp 122-31)
metabolism of, in tumor metastases, 19: 46098
production in soil by neutron reactions (n,p) on sulfur-32, activity from, 19: 47569 (CEX-62-50)
radiation effects on distribution in RNA moieties, x, 19: 45851
therapeutic use of, for brain tumor, 19: 46087
use in radiodiagnosis, 19: 46102
use in treatment of polycythemia vera, comparison of drugs with, 19: 46089
yields from radiolysis of thiourea by neutrons, 19: 46365
PHOTOELECTRIC CELLS
performance of radioisotope-fueled, 19: 47284
PHOTOGRAPHIC FILM
analysis for spark-chamber tracks, using raster-scan methods, (E), 19: 46786
defects in x-ray, identification of, 19: 46964 (NMI-4996, pp 149-63)
exposure time in x-ray cameras, 19: 46729(T) (LA-tr-65-21)
particle track analysis in, using flying-spot devices, (E), 19: 46787
particle track analysis in, from spark chambers, (E), 19: 46790
particle track analysis in, from spark chambers, (E), 19: 46791
particle track analysis in spark-chamber, using CHLOE scanner, (E), 19: 46793
particle track analysis in spark-chamber, use of graph theory for, (T), 19: 46795
particle track analysis in bubble-chamber, Lidiam system for, (E), 19: 46801
particle track analysis ionization in bubble-chamber, devices for, (E), 19: 46802
particle track analysis in, semi-automatic device for, (E), 19: 46803
particle track analysis in bubble-chamber, using PEPR system, (E), 19: 46810
particle track analysis in, using on-line computer, (E), 19: 46811
particle track analysis in, using CERN HAZE program, (E), 19: 46812
particle track analysis in, computer programming for PEPR system, (E), 19: 46813
particle track analysis in bubble-chamber, computer systems for, (E),

19: 46814
scanning of, engineering drawings of equipment for, 19: 46866
use in projection radiography of highly radioactive specimens, 19: 46560
PHOTOGRAPHIC FILM DETECTORS
filter size for badge dosimeters, 19: 46764 (SZS-6(1965))
performance for dosimetry, 19: 46853
performance of, for diagnostic exposures, 19: 46860
response to beta particles, angular dependence of, 19: 46639 (AECL-2281)
PHOTOGRAPHY
camera for metallographic, 35-mm color, 19: 46928 (NMI-4998, pp 14-19)
PHOTOMETERS
description of remotely operated filter, 19: 46721 (ORNL-P-1531)
PHOTOMULTIPLIER TUBES
base design for, with remote power connections, (E), 19: 46808
design of, using semiconductor diode as anode, (E), 19: 46815
electron pulse sizes from multidynode, distributions of, 19: 46720 (NYO-3406-2)
PHOTONS
absorption in cesium vapors, molecular ion production in resonance, (E), 19: 47229
absorption in matter, mechanisms of, 19: 47152
absorption of two, in atomic or molecular systems, (T), 19: 47236
emission from electric current, (T), 19: 47135
existence of heavy unstable, possibility of, 19: 47398
interactions with protons, meson (π) production in, (E), 19: 46643(R) (LAL-1136)
interactions with charged particles, 19: 47234
interactions with photons in condensed media, plasma, and vacuum, (T), 19: 47332
interactions with plasma, 19: 47234
interactions with nucleons at high energy, total cross section for (πN), (T), 19: 47353
interactions with protons at 660 to 800 Mev, meson (π^0) angular distributions from, (E), 19: 47368
quantum theory for, 19: 47409
reactions with nuclei, meson (π^0) production in, (E), 19: 46788
PHOTOSYNTHETIC PRODUCTS
spectra of chlorophyll-protein complex in bacterial, 19: 45727 (BNL-9506)
PHTHALATES
solvent properties for lanthanides separation, 19: 46437
PHYSICS
dynamic properties of nonlinear string, (T), 19: 48108(T) (ORNL-tr-754)
invariance principles in, conceptual use and basis of geometric, (T), 19: 47433
mathematical systems in limiting cases in, asymptotology for, (T), 19: 47150
research in Communist China, 19: 47122(T) (JPRS-31032)
research on, Air Force, 19: 48087 (AD-613537)
PHYSIOLOGY
computer methods in human, 19: 45771
radiation effects combined with vibrations on animal, 19: 45824(T) (NASA-TT-F-354)
PINCH DEVICES
plasma properties in theta, (E), 19: 47722 (LA-DC-7039)
plasma properties in hard-core and no-core, (E), 19: 47853
plasma transient flow in theta-, (T), 19: 47834
PINCH EFFECT
particle losses from theta, spectral distributions in, (E), 19: 47833
plasma in, dynamic stabilization methods for, (E), 19: 47842
production in coaxial-electrode discharge, in deuterium, (E), 19: 47843
PIPES
radiation streaming through single-bend aluminum, in water shields, (E), 19: 47863 (AD-613480)
PITCHBLENDES
separation of thorium from, by solvent extraction and ion exchange, 19: 46606
thorium-230 content of, in South Alligator River area, Australia, 19: 46606
PITUITARY HORMONES
effects of iodine-131 and goitrogenic drugs on, in mice, 19: 45808(R) (NYO-901-36)
PIVALONITRILE
thermodynamic properties of, 19: 48090 (COO-1149-53)
PLACENTA
iodine-131 transfer by, of dairy cows, 19: 45760(R) (ORO-631, pp 83-121)
localization of, using iodine-131 albumin and external counting, 19: 46117
PLANKTON
ecology of Atlantic and Mediterranean, 19: 45748(R) (TID-22193)

strontium-90 metabolism by, 19: 45748(R) (TID-22193)
PLANT CELLS
genetic structure of, 19: 45726 (BNL-9488)
radiation effects on nucleolar structures in *Cannabis sativa* seedlings, 19: 45940
radiation effects on membrane permeability of *Allium cepa*, by urea, 19: 45975
PLANT METABOLISM
effects of chemical growth inhibitors on, in rice seedlings, 19: 45794
effects of gibberellic acid on protein, in aleurone cells of seeds, 19: 48102(R) (TID-22175)
PLANT RESPIRATION
radiation effects on, in corn seedlings, 19: 45836
PLANTS
analysis for beta-emitting radioisotopes, 19: 46199
analysis for tracer elements, 19: 46587(R) (NYO-3446-3)
chemical composition of range, from Miles City, Montana, 1955 to 1960, 19: 45747 (ORNL-TM-1279)
ecology of, of Southeastern granite outcrops, 19: 45752
effects of chemical growth inhibitors on rice, 19: 45794
growth of Agrostemma hypocotyl and Avena coleoptile cylinders, effects of heavy water on, 19: 45763(T) (AD-468388)
growth of crop, effects of beryllium on, 19: 45802
mutation detection in, 19: 45737
radiation effects on, bibliography, 19: 45807 (AED-C-04-17)
radiation effects on, genetic, 19: 45817(R) (ORO-631, pp 145-71)
radiation effects on growth of coleus and chrysanthemum, 19: 45817(R) (ORO-631, pp 145-71)
radioactivity of agricultural, due to fission product absorption, 19: 45804
radioactivity of, effects of species on, 19: 45752
radioinduced mutations in Lupinus, protective effects of moisture against x, 19: 45847
strontium-89 leaching and metabolism in vegetable, 19: 45758 (NYO-2598-24)
strontium-90 content of, in German Democratic Republic, 1963, 19: 46610
strontium-90 metabolism in alfalfa and oat, 19: 45774
strontium-90 metabolism by agricultural, 19: 45804
yttrium-90 metabolism by agricultural, 19: 45804
PLASMA
acceleration by electric field gradient, (E/T), 19: 47714(R) (AD-613307)
capture in magnetic mirror machines, (E/T), 19: 47839
charged particle motion in theta pinch, restoring force field for, 19: 47760
charged-particle beam interactions with waves in magnetoactive, 19: 47785
charged-particle collision processes in, binary, (T), 19: 47812
charged-particle kinetics in, statistical, (T), 19: 47808
charged-particle scattering in, equations for, 19: 47800
conference, 19: 47802
conference on, summary of Innsbruck Univ., Austria, July 14, 1964, 19: 47715 (AD-613622)
containment by traps, (E), 19: 47841
containment in magnetic wells, (T), 19: 47822
containment in pulsed magnetic mirrors, (E), 19: 47848
containment in toroids, equilibrium in, (T), 19: 47809
containment of hydrogen, in magnetic mirrors, 19: 47857
containment of low-β, in closed vacuum-magnetic field configurations, (T), 19: 47819
containment of, superconducting magnetic battle apparatus for, 19: 47533
containment of, toroidal, (T), 19: 47820
current filaments in anisotropic, radiation field from, (T), 19: 47774
current stability in, (T), 19: 47763
cyclotron radiation from, (T), 19: 47815
density measurement of θ-pinch, using infrared helium–neon laser interferometer, 19: 47759
density profile of deuterium, method for determining, (E), 19: 47727 (NP-15434)
diagnostics of magnetospheric, (T), 19: 47484
diagnostics of repetitively pulsed, laser interferometer for, 19: 47730
diagnostics of transient, image-intensifying shutter for spectroscopic, 19: 47729
diagnostics of, light beam refraction for, (T), 19: 47818
diagnostics of, probes for, (T), 19: 47817
diffusion across magnetic fields, (T), 19: 47838
diffusion and high-frequency conductivity of, in strong magnetic field, (T), 19: 47782
electric conductivity of seeded, measurement of, 19: 47801
electric conductivity of fully ionized, h-f, (T), 19: 47814
electric current and field fluctuations in magnetoactive, 19: 47785
electric discharges in, effect of magnetic field on stability of pessing,

(E), 19: 47780
electromagnetic properties of relativistic quantized electron-positron, (T), 19: 47771
electromagnetic signal amplification by, (E/T), 19: 47219 (AD-614253)
electromagnetic wave interactions with free boundary of, use of screen cathodes for obtaining, 19: 47734
electromagnetic wave coupling near electron gyrofrequency in, 19: 47744
electromagnetic wave propagation in anisotropic, along static magnetic field, (E/T), 19: 47718 (AD-614442)
electron and ion motion in, equations for, 19: 47747
electron beam reactions with mercury, diagnostics by nonperturbing probe, (E), 19: 47740
electron cyclotron harmonics in nonrelativistic, high refractive index at, (T), 19: 47749
electron density and temperature in hydrogen, spectroscopic method for, (T), 19: 47754
electron density and temperature in helium, (E), 19: 47772(T)
electron density fluctuations in non-Maxwellian, spectrum of, 19: 47800
electron density in, use of transverse modes in laser interferometers for, 19: 47745
electron density in helium, microwave free space method for measuring, (E), 19: 47755
electron density in helium, probe measurement of, (E), 19: 47758
electron energy losses in nonequilibrium argon–cesium, nitrogen-impurity effects on, (E), 19: 47737(T)
electron kinetics in, equation for, 19: 47783
electron temperature in, cesium spectral determination of, (E), 19: 47773(T)
electron temperatures in seeded, measurement of, 19: 47801
flow in theta-pinch devices, models for transient, (T), 19: 47834
heating by magnetic pumping, models for, (T), 19: 47767
heating cylindrical, by axially imploding shock waves, (E), 19: 47845
heating, losses, and stability in Scylla IV theta pinch, (E), 19: 47722 (LA-DC-7039)
hydromagnetic wave propagation in toroidal discharge with longitudinal magnetic field, (E), 19: 47742
hydromagnetic waves in, theoretical analysis of cylindrical, 19: 47798
injection into cusped fields, (E), 19: 47858
injection of 20-kev neutral hydrogen atoms into electron-cyclotron, (E), 19: 47837
interactions with electron beams, electric discharge from, (E), 19: 47836
interactions with electron beams, ionization by, (E), 19: 47852
ion acoustic wave propagation in dense, damping transitions in, (E/T), 19: 47724 (MATT-267)
ion heating by ion-cyclotron-resonance methods in, in C Stellarator, (E), 19: 47832
kinetics, (T), 19: 47829
kinetics in high magnetic fields, Vlasov equation for, (T), 19: 47753
kinetics in thermoelectric cells, (T), 19: 47287(T)
kinetics of homogeneous, correlation with sound wave phenomena in magnetic field, (T), 19: 47732
laser beam reactions with, induced perturbations in, (E), 19: 47777
losses from theta-pinch, spectral distributions in, (E), 19: 47833
magnetohydrodynamic cells for diagnostics of helium, 19: 47728
magnetohydrodynamics of, (T), 19: 47805
microwave scattering by nonequilibrium, acoustic-ion-plasma waves in, (E/T), 19: 47776
motion in magnetic fields, near field zeros, 19: 47847
motion of hydrogen, in radiation accelerator, (E), 19: 47795
noise and oscillations in beam-generated, (E), 19: 47741
oscillation modes in circular waveguides, (E), 19: 47743
oscillations in hot asymmetric slab of, quasi-static, (T), 19: 47746
oscillations in weakly turbulent, kinetic equations for, (T), 19: 47764
oscillations in, energy conversion by, (E/T), 19: 47717 (AD-614285)
oscillations of collisionless, linear, (T), 19: 47811
oscillations of *n*-fold-excited, in longitudinal magnetic field, 19: 47778
pair distribution function of, classic theory of, 19: 47775
particle bunching in, use of acoustic resonator to obtain, 19: 47297(P)
particle motion in, drift and orbit theory for, (T), 19: 47806
photon interactions with, multi-, 19: 47234
pinch effect in, compression in theta, 19: 47760
polarization in curved magnetic field, (E), 19: 47797
production by electronic discharge, 19: 47831
production by laser beam interactions in air, (E), 19: 47781
production by laser induced vaporization of lithium hydride, (E), 19: 47846
production in high-pressure argon arc by pulse heating, 19: 47789
production in high-pressure argon arc by pulse heating, (E), 19: 47790
production of argon and krypton, by electrodeless, (E), 19: 47788
production of deuterium, in coaxial-electrode discharge, (E), 19: 47843
production of high-temperature, equipment for, 19: 47862(P)
production of hydrogen, using titanium source, 19: 47793
production of rotating, (E), 19: 47850
properties in Adiabatic Compression (AC) device, (E), 19: 47855
properties in C Stellarator, (E), 19: 47854
properties in magnetic traps, (T), 19: 47821
properties of sheath of, research on, (E/T), 19: 47719 (ARL-65-131)
properties of uniform helium brush cathode, (E), 19: 47739
properties of, summary of, (T), 19: 47803
radiation absorption and emission by fully ionized, (T), 19: 47814
radiation effects on thermodynamic properties of air, 19: 47731
radio-wave interactions with warm, Langevin's equation for, (T), 19: 47770
research, (E), 19: 47725(R) (NP-15355)
resistors for study of, electrolytic, 19: 47751
shock waves in collisionless, dissipation mechanisms for, (T), 19: 47828
source design for, 19: 47860(P)
source of, arc initiator for, 19: 47861(P)
spectra of cesium, absolute oscillator strengths for, 19: 47723 (LA-DC-7112)
spectral line broadening in theta-pinch hydrogen, impurity, (E), 19: 47769
stability, (T), 19: 47824
stability in hard-core and no-core pinch devices, (E), 19: 47853
stability in low-density, effect of shear on flute, (T), 19: 47765
stability in magnetic mirror machines with stabilizing rods, (T), 19: 47835
stability in Q machines, (T), 19: 47859
stability in thermionic, excitation of drift, (T), 19: 47750
stability in weakly ionized, ponderomotive, (T), 19: 47736(T)
stability in Zeta, 19: 47856
stability of axially-symmetric, effect of large ion Larmor radius on, (T), 19: 47768
stability of beam-produced hydrogen, diffusion theory for, 19: 47787
stability of collisionless, (T), 19: 47844
stability of compressible viscous, Helmholtz, (T), 19: 47733
stability of confined, linear, (T), 19: 47823
stability of nonuniform, in magnetic field gradients, (T), 19: 47840
stability of rotating, two-fluid analysis of, (T), 19: 47851
stability of spatially periodic structure in heavy-current, (E), 19: 47761
stability of spatial-periodic structures in, (T), 19: 47762
stability of, asymptotic methods in hydrodynamic theory of, (T), 19: 47830
stability of, dynamic methods for increasing, (E), 19: 47842
stability of, effect of nonzero ion Larmor radius and nonzero pressure on flute, (T), 19: 47766
stability of, finite resistivity, (T), 19: 47827
stability of, hydromagnetic theory for, (T), 19: 47810
stability of, with plane boundary, (T), 19: 47747
Stark effect in, adiabatic linear, 19: 47716 (AD-614283)
structure in pulsed plasma accelerators, (E), 19: 47796
temperature measurements on, design of modulation pyrometer for, 19: 46734
transport equation for, 19: 47813
transport in magnetic fields, equations for, 19: 47799
turbulence in, (T), 19: 47826
turbulence in, quasi-linear theory of, (T), 19: 47825
wave damping in, Landau, (T), 19: 47827
wave interaction in cold, in cylindrical waveguide, 19: 47786
wave interactions in, nonlinear stabilization of, (T), 19: 47726 (NP-15394)
wave interactions in, four-plasmon decays in longitudinal, 19: 47784
waves in, macroscopic, (T), 19: 47804

PLASMA JETS

carbon and copper impurities in streams from coaxial, spectra of, 19: 47757
design and performance of high-velocity, 19: 46574(T) (AD-619323)
development for re-entry simulation, (E/T), 19: 46477 (ARL-65-121)
diagnostics of, microwave interferometer for high-speed, (E), 19: 47735(T)
electric conductivity of, radial distribution of, (E/T), 19: 47794
electric discharges in coaxial, 19: 47792
performance of magnetic traveling-wave, 19: 46575 (NASA-TN-D-3006)
plasma from, rotation in magnetic fields, (E), 19: 47849
plasma injection into traps from, (E), 19: 47841
plasma structure in coaxial, (E), 19: 47796

PLASTIC FILMS

thickness of, alpha source-semiconductor detector arrangement for measuring, 19: 46888

PLASTICIZERS

effects on radiolysis of polyvinyl chloride, 19: 46350

PLASTICS
corrosion by chloride environments, 19: 46428(R) (ORNL-3847)
performance for radiation dosimetry, 19: 46850
properties for aerospace uses, 19: 47068
properties of chlorine-containing, for radiation dosimetry, 19: 46392
properties of filled, for use as shielding material, 19: 46354
radiation effects on, 19: 46354
use of scintillating, in x-ray dosimetry, 19: 46105

PLATES
bending analysis of rectangular, apparatus for, 19: 46555 (KAPL-M-6493)
buckling of long axially compressed curved, analysis of inelastic, (T), 19: 46463 (WAPD-TM-469)
stress distribution in perforated, subjected to equal biaxial stress, 19: 46557 (NP-15459)

PLATINUM
effects on exchange of deuterium with hydroxyl groups on surface of alumina, 19: 46280
effects on point defects in iron, 19: 47094(T) (ORNL-tr-668)
neutron cross sections of, shell effects on thermal, (E), 19: 47618
photoelectron production by 145, 280 and 320 kev gamma rays, cross sections for, (T), 19: 47329
radiation effects on electric conductivity of, low-temperature recovery of neutron, (E), 19: 47097

PLATINUM ALLOYS
Au–Pt, radiation effects on catalytic effects of, on gaseous reactions, 19: 46329 (EUR-2455.e)
Mn–Pt, crystal structure of intermetallic compound $PtMn_3$ in, neutron diffraction studies of disorder in, 19: 47028

PLATINUM CATALYSTS
radiation effects on, in gaseous reactions, 19: 46329 (EUR-2455.e)

PLATINUM ISOTOPES Pt-194
gamma transitions in, K-conversion coefficient of 328-kev E2, (E), 19: 47643

PLATINUM ISOTOPES Pt-197
gamma spectra from transitions in, (E), 19: 47576(R) (IDO-17081, pp 49-76)

PLATINUM ISOTOPES Pt-199
decay of, beta and gamma spectra from, (E), 19: 47576(R) (IDO-17081, pp 49-76)
decay spectra computer analysis, (E), 19: 47576(R) (IDO-17081, pp 49-76)
half life, (E), 19: 47576(R) (IDO-17081, pp 49-76)

PLOWSHARE PROJECT
bibliography on cratering by nuclear explosions, 19: 46466 (CEA-Bib-63)
crater ejecta and dust in Danny Boy, mass distribution measurements of, 19: 46469 (POR-1815)
mining of ore bodies by nuclear caving, 19: 46472 (UCRL-14201)
natural gas production from underground nuclear explosions in Project Gasbuggy, 19: 46474
radioactivity induced in rocks and soil in, 19: 46473 (UCRL-14249)

PLUTONIUM
analysis of, radiocrystallographic, 19: 46202
bibliography on technology of, 19: 48088 (BNWL-113-6)
desorption by nitric acid solution from ion exchange resin, rate of, 19: 46173 (LA-3357)
determination by high-speed controlled potential coulometry, 19: 46188
diffusion in magnesium and its alloys at 420 to 500°C, 19: 47066
electron band structure of delta, calculations of, 19: 47880 (LA-DC-7353)
etchant for bright field studies of alpha-, 19: 46938 (NMI-5025(Pt.I), pp 153-4)
excretion of deposited, effects of diethylenetriaminepentaacetic acid on, 19: 45762 (RFP-577)
metallography of, for sample preparation, 19: 46934 (NMI-4999, pp 104-10)
production in power reactors, economic aspects of, 19: 48032
purification of, consumable electrode method for, 19: 46915 (BNWL-IR-2)
reactions with tantalum at 900 to 1150°C, 19: 46950 (LA-DC-7315)
separation from americium-241 alpha activity in urinalysis, method for, 19: 46187
separation from fuels; operation of Norwegian plant for, 19: 48114
thermal capacity at low temperature, (E), 19: 47043

PLUTONIUM ALLOYS
metallography of, for sample preparation, 19: 46934 (NMI-4999, pp 104-10)
Fe–Pu–U, properties and structure of, 19: 46992 (CEA-R-2792)
Ga–Fe–Pu, reactions with tantalum at 900 to 1150°C, 19: 46950 (LA-DC-7315)
Mg–Pu, diffusion of plutonium at 420 to 500°C in, 19: 47066

PLUTONIUM CARBIDES
electron band structure of, calculation of, 19: 47880 (LA-DC-7353)
fabrication and properties of dense bodies and powders of, for use as fuels, 19: 46999 (LA-DC-7297)
PuC–UC, fabrication and properties for use as fuels, 19: 46999 (LA-DC-7297)
Pu_2C_3–U_2C_3, fabrication and properties for use as fuels, 19: 46999 (LA-DC-7297)
PuC–UC, performance as fast breeder reactor fuel, 19: 47993 (NAA-SR-10751)

PLUTONIUM COMPLEXES
with 8-quinolinol, preparation and properties, 19: 46288

PLUTONIUM(IV) FLUORIDES
analysis for fluorine, radiometric instrument for, 19: 46179 (RFP-618)
effects of solid, on radioinduced decomposition of gaseous plutonium hexafluoride, 19: 46325 (ANL-7013)

PLUTONIUM(VI) FLUORIDES
radioinduced decomposition at 26 to 82°C, extent and rate of alpha, 19: 46325 (ANL-7013)

PLUTONIUM ISOTOPES
criticality studies, 19: 47967

PLUTONIUM ISOTOPES Pu-239
carcinogenic effects in mice, 19: 45808(R) (NYO-901-36)
criticality studies, 19: 47967
detection in lungs, development of multiwire proportional counter for external, 19: 46751 (AEEW-M-526)
determination in irradiated fuel slugs, nondestructive spectrometric, 19: 46178 (NP-15364)
fission product yield from, 19: 46585 (AD-410522)
neutron capture-to-fission ratio in, engineering drawings of fission chamber for measuring, 19: 47713
neutron fission cross sections of, technique for measuring thermal, 19: 47567 (CEA-R-2775)
neutron scattering and total cross sections of, (E), 19: 47595(R) (TID-22141, pp 50-66)

PLUTONIUM ISOTOPES Pu-242
deuteron reactions (d,2n) at 7 to 12 Mev, excitation function and yield rates for fissioning isomeric from, (E), 19: 47688

PLUTONIUM NITRIDES
analysis for nitrogen, methods for, 19: 46164 (AERE-R-5002)
fabrication and properties for use as fuels, 19: 46999 (LA-DC-7297)
oxidation by air at 540 to 1000°C, 19: 46912(R) (BMI-1727(Del.))
oxidation by flowing carbon dioxide at 340 to 400°C, 19: 46913(R) (BMI-1733(Del.))

PLUTONIUM OXIDES
fabrication and properties for use as fuels, 19: 46999 (LA-DC-7297)

PLUTONIUM(IV) OXIDES
dissolution of, methods for, 19: 46175 (MLM-1264)
preparation of dense plutonium-242-enriched, for HFIR targets, 19: 46428(R) (ORNL-3847)
BeO–PuO_2, melting point of, eutectic, 19: 46913(R) (BMI-1733(Del.))
BeO–PuO_2, phase studies, 19: 46912(R) (BMI-1727(Del.))
PuO_2–PuO_2–ThO_2, melting point of, eutectic, 19: 46913(R) (BMI-1733 (Del.))
PuO_2–ThO_2, melting point of, eutectic, 19: 46913(R) (BMI-1733(Del.))
PuO_2–UO_2, cost analysis for fuel rod fabrication of, 19: 47976 (BNWL-131A)
PuO_2–UO_2, developments in salt-cycle process for reprocessing, 19: 46422 (BNWL-SA-205)
PuO_2–UO_2, development as fast reactor fuel, 19: 46942(R) (NUMEC-3524-6)
PuO_2–UO_2, dissolution by nitric acid on irradiated stainless steel clad, 19: 46427 (ORNL-3754)
PuO_2–$UL_{.4}$, fabrication into fuel rods for Saxton reactor, costs of, 19: 46962 (BNWL-131C)
PuO_2–UO_2, variable costs for fabricating fuel rods of, 19: 47977 (BNWL-131B)

PLUTONIUM POISONING
effectiveness of delayed treatment with diethylenetriaminepentaacetic acid, 19: 45762 (RFP-577)

PLUTONIUM RECYCLE CRITICAL FACILITY
fuel rod fabrication for, cost analysis for plutonium dioxide–uranium dioxide, 19: 47976 (BNWL-131A)
safety rod worths in, in combinations and singly, (E), 19: 48058 (BNWL-130)

PLUTONIUM RECYCLE TEST REACTOR
containment vessel leak rate tests, 19: 48057 (BNWL-109)

PLUTONIUM SULFIDES
thermal diffusivity, 19: 47921(R) (ANL-7090, pp 30-54)

PNEUMATIC SYSTEMS
development for master-slave, 19: 46499 (CONF-641120, pp 63-6)

POLAND
monitoring lead-210 content in human bones and hair in Warsaw, 1963, 19: 45795

POLAROGRAPHY
analysis of polarograms, computer program for, 19: 46238 (ORNL-TM-1253)
POLISHING
equipment for metallographic sample preparation, description of vibratory, 19: 46939 (NMI-5025(Pt.I), pp 185-219)
method of vibratory, for metallographic samples, 19: 47086 (NMI-4997, pp 184-8)
POLONIUM ISOTOPES Po-210
content in tobacco leaves, 19: 45801
half life determination by decaying pairs, 19: 46157(R) (MLM-1254)
POLYCYTHEMIA
treatment of, use of drugs versus phosphorus-32 for, 19: 46089
POLYMERS
biological, optical properties of, ultraviolet spectroscopic study, 19: 48104 (UCRL-16278)
book: *Physics and Chemistry of the Organic Solid State*, Vol. II, 19: 46320
properties of chlorine-containing, for radiation dosimetry, 19: 46392
pyrolysis of, bibliography on, 19: 46302 (MLM-1271)
radiation effects on chlorine-containing, 19: 46392
radiation effects on, review of, 19: 46400
radiation effects on dynamic properties of, review on developments in, 19: 46331(R) (NYO-1858-1)
yields from radiolysis of benzene–dioxane mixtures, 19: 46363
POLYPHENYLS
analysis for chlorine, oxy-hydrogen burner for decomposition in, 19: 46163 (AECL-2263)
toxic effects of OMRE High Boilers on rat blood, kidneys, and liver, 19: 45769
POLYSACCHARIDES
metabolism in blood platelets of rats, effects of vitamin A, 19: 45759(R) (ORO-631, pp 77-82)
POPULATIONS
assignment and management in fallout shelters, plans for, 19: 46635 (AD-611764)
data on human, computer analysis of, 19: 45771
direction to and management in shelters, 19: 46636 (AD-611765)
radiation control of insect, by sterile male technique, 19: 45960
radiation dose from diagnostic radiography, 19: 46112
radiation dose to, diagnostic and therapeutic, 19: 46156
radiation effects on human, somatic, 19: 45996
radiation effects on genetic loads and inbreeding in *D. melanogaster*, 19: 45952
radiation effects in animal, genetic, 19: 45973
radiation effects in human, genetic, 19: 46695
radiation effects in mouse, genetic, 19: 45809(R) (NYO-1979-12)
radiation effects on lifetime health and mortality patterns of, employed in nuclear energy installations, 19: 45810(R) (NYO-3394-2(Rev.))
radiation exposure standards for, 19: 46696
radiation hazards to, reactor-accident, 19: 46699
radiation monitoring in diagnostic radiology, instrumentation and methods for, 19: 46143
radiation protection of, after radiation accident, 19: 46691
radiation protection of, after radiation accident, 19: 46692
radiation protection planning for, 19: 46697
radiation protection after reactor accidents, 19: 46698
radioinduced leukemia and tumors in Hiroshima, 19: 45846
POROUS MATERIALS
fabrication into permeable membranes, 19: 46978(P)
properties of metallic, for vacuum system traps, 19: 46573 (UCRL-12393-T)
POSITRONS
annihilation in metals, (E/T), 19: 47217 (AD-613582)
electromagnetic-wave propagation in relativistic quantized electron-positron gas, (T), 19: 47771
interactions with protons, (E), 19: 46643(R) (LAL-1136)
interactions with electrons at high energy, nonlocal model for elastic, 19: 47364
interactions with electrons in metals, (E/T), 19: 47217 (AD-513582)
scattering by atomic hydrogen at 0 to 6.8 ev, higher partial waves in, (T), 19: 47238
scattering by bismuth, (E), 19: 46643(R) (LAL-1136)
scattering by helium and hydrogen, iteration-variation method for, (T), 19: 47247
spectroscopy up to 10 Bev, (E), 19: 46805
POTASSIUM
content in precipitation and waters in Vinca, Yugoslavia, 19: 46590(T) (JPRS-31469)
determination in biological materials, neutron activation, 19: 46165 (CEA-R-2837)
determination in beef heart, neutron activation, 19: 45753 (AE-191)
effects on cesium-137 ratio to strontium-90 in milk, 19: 45772
electron recombination rate in plasma of, (E), 19: 47801
gamma rays from, attenuation by air, 19: 46586 (NP-15361)
reactions with chlorine, chemiluminescence from, 19: 46161(R) (ORNL-3832, pp 116-50)
stability of thermionic plasma of, drift, (T), 19: 47750
POTASSIUM ALLOYS
Cs–K–Na, preparation and use for power production, 19: 47936(P)
K–Na, heat transfer during vertical upflow of, 19: 46528 (ANL-7038)
K–Na, heat transfer to, flowing through bundle of circular rods, 19: 46553
K–Na, performance in MHD cells, 19: 48053(R) (ANL-7090, pp 55-68)
POTASSIUM BROMATES
uranyl ion polarographic reduction in, 19: 46260
POTASSIUM BROMIDES
radiation effects on absorption and luminescence spectra of nickel-, silver-, or tin-activated, 19: 47884(T) (IS-Trans-18)
NdBr–KBr, complex formation in, refractometric studies of, 19: 46254
POTASSIUM BROMORHENATES
heat capacity and thermal behavior at 7 to 300°K, 19: 46161(R) (ORNL-3832, pp 116-60)
POTASSIUM CHLORATES
uranyl ion polarographic reduction in, 19: 46260
POTASSIUM CHLORIDES
molal volume and salt-induced structure transitions of aqueous, 19: 46237(R) (ORNL-3832, pp 76-99)
radiation effects on absorption and luminescence spectra of nickel-, silver-, or tin-activated, 19: 47884(T) (IS-Trans-18)
radiation effects on low-temperature color centers in lead-doped and pure, 1.5-Mev electron, (E), 19: 47891
radioinduced color center formation in, effects of strontium ions on, 19: 46371
radioinduced luminescence in, de-excitation of light sums from x, 19: 46379(T)
KCl–NaCl–UF_4, uses in electrolytic processing of irradiated uranium fuels, 19: 46448
LiCl–KCl–UCl_3, uses in electrolytic processing of irradiated uranium fuels, 19: 46448
$NdCl_3$–KCl, complex formation in, refractometric studies of, 19: 46254
POTASSIUM CHROMATES
analytical uses in determination of uranium, 19: 46220
POTASSIUM CYANOCOBALTATES(III)
cobalt-59 NMR in, 19: 46285
POTASSIUM FERRICYANIDES
thermodynamic properties at 298°K, 19: 46161(R) (ORNL-3832, pp 116-60)
POTASSIUM HYDROXIDES
permanganate decomposition in, deuterium isotope effects on, 19: 46275
POTASSIUM IODATES
iodine-131 beta decay in formation of xenon compounds from, 19: 46411
uranyl ion polarographic reduction in, 19: 46260
POTASSIUM IODIDES
absorptive properties for x rays as function of photon energy, 19: 46150
effects on iodine metabolism in lactating cows, 19: 45781
POTASSIUM IONS
reactions with bromine and iodine in crossed-beam experiments, 19: 46161(R) (ORNL-3832, pp 116-50)
POTASSIUM ISOTOPES K-37
magnetic moments and M1 transition probabilities in $2s_{1/2}$ $1d_{1/2}$ shell, (T), 19: 47641
POTASSIUM ISOTOPES K-38
magnetic moments and M1 transition probabilities in $2s_{1/2}$ $1d_{1/2}$ shell, (T), 19: 47641
production in nitrogen-14 reactions on aluminum-27, cross sections for, (E), 19: 47667
POTASSIUM ISOTOPES K-39
magnetic moments and M1 transition probabilities in $2s_{1/2}$ $1d_{1/2}$ shell, (T), 19: 47641
production of, methods for, 19: 46413
POTASSIUM ISOTOPES K-40
activity in precipitation and waters in Vinca, Yugoslavia, 19: 46590(T) (JPRS-31469)
content in holothuriae, western Mediterranean, 1962, 19: 46611
determination in man by whole-body gamma counting, computer analysis of data on, 19: 45771
POTASSIUM ISOTOPES K-42
decay of, polarized beta-gamma angular correlations in, (E), 19: 47609
use in medical diagnostics, 19: 46136
POTASSIUM ISOTOPES K-46
production in calcium-48 (d,α) reactions at 12 Mev, 19: 47115(R) (ANL-6983)

POTASSIUM NIOBATES
toxic effects on dogs, mice, rabbits, and rats, 19: 45768
POTASSIUM OXIDES
thermal properties, 19: 47010(R) (ORNL-3832, pp 107-50)
POTASSIUM SULFIDES
entropy and heat content at 298 to 1260°K, 19: 47010(R) (ORNL-3832, pp 107-50)
K–K_2S, phase studies, 19: 47010(R) (ORNL-3832, pp 107-50)
POTASSIUM SYSTEMS
Ar–K, electron recombination rates and nonequilibrium conductivity in, (E), 19: 47801
He–K, electron recombination rates and nonequilibrium conductivity in, (E), 19: 47801
K–K_2S, phase studies, 19: 47010(R) (ORNL-3832, pp 107-50)
POTASSIUM TECHNETATES
heat of fusion and melting point, 19: 46161(R) (ORNL-3832, pp 116-50)
POTASSIUM URANYL VANADATES
crystal structure, 19: 46259
preparation and hydrolysis, 19: 46627
POTATOES
radioinduced mutations of, 19: 45853
POTENTIOMETERS
design and operation for measuring Hall effect in transition-metal carbides, borides, and nitrides, 19: 47009 (NP-15514(Vol.2))
POWDERS
x-ray diffraction analysis of, computer program for intensity calculations of, 19: 47877 (LA-3335)
POWER BREEDER REACTORS
plutonium production in, economic aspects of, 19: 48032
POWER BURST FACILITY
coolant loop for, design of sodium, 19: 47952 (APDA-177)
performance for fast reactor fuel meltdown studies, 19: 47952 (APDA-177)
transient behavior of, computer analysis of, 19: 46716(R) (IDO-17081, pp 77-123)
POWER CYCLES
materials attrition testing for Rankine systems, 19: 46955 (NP-15431)
POWER PLANTS
efficiency of large-scale open loop magnetohydrodynamic, 19: 47291
materials attrition testing in Rankine cycle, 19: 46955 (NP-15431)
POWER REACTORS
accident planning for gas-cooled, 19: 46703
components and auxiliary equipment for, development of, 19: 48017
containment design for, 19: 48037
criticality of large boiling-water, computer calculations of, 19: 47917 (ANL-7050, pp 487-502)
design and development of fast, in 1000-Mwe range, 19: 47997(R) (NP-15478)
design of gas-cooled, 19: 48045(P)
design of Japanese, 19: 48036
design of 1000-Mw(e) boiling-water, engineering drawings for, 19: 48044
design using skewed fuel lattice, 19: 47924(P)
development in Great Britain, 19: 48026
development of gas-cooled graphite-moderated, 19: 48006
development of large closed-cycle pressurized-water, 19: 48001(R) (WCAP-3743)
development programs for, survey of, 19: 48041
fuel cycle costs for 1000-Mwe boiling-water, minimization of, 19: 47990 (BNWL-105)
fuel element arrangement for large gas-cooled, 19: 47973(P)
neutron flux measurements in, design of fast counting channel for, 19: 48033
pressure vessels for large, review of prestressed concrete, 19: 47925 (GA-6505)
safety of sodium cooled, zirconium hydride moderated, 19: 48034
safety systems for boiling and pressurized-water, 19: 48038
use in Africa, 19: 48111
POWER SUPPLIES
analysis of nuclear Brayton-cycle, for space vehicles, 19: 48048 (GE-65SD4251)
cost analysis for accelerator systems of, 19: 47170 (UCRL-16384)
design of high-energy fast-pulse, (E/T), 19: 46476 (AD-613959)
PRASEODYMIUM
cohesive energy and ionization of, relation between, (T), 19: 47062
separation from neodymium using phthalate buffer, 19: 46437
PRASEODYMIUM ALLOYS
Al–Pr, crystal structure of Laves phases in, 19: 47052
Co–Pr, crystal structure of Laves phases in, 19: 47052
Pd–Pr, phase studies, 19: 47051
PRASEODYMIUM BROMIDES
thermal decomposition of hydrates of, mechanisms of, 19: 46271
PRASEODYMIUM FERRITES
crystal structure, 19: 46256
PRASEODYMIUM IONS
spectra in silicate glass, fluorescence, 19: 47886(T) (N64-21857, pp 1-6)
PRASEODYMIUM ISOTOPES Pr-137
energy levels and estimated half life of, 19: 47584(R) (ORNL-3832, pp 1-28)
PRASEODYMIUM ISOTOPES Pr-141
neutron reactions (n,α) at 14.6 Mev, angular and energy distributions from, (E/T), 19: 47637
PRASEODYMIUM ISOTOPES Pr-144
content in holothuriae, western Mediterranean, 1962, 19: 46611
effects on chicken embryos, pathological, 19: 45761(R) (ORO-631, pp 122-31)
toxic effects on sheep and swine, 19: 45759(R) (ORO-631, pp 77-82)
PRASEODYMIUM OXIDES
oxygen-18 exchange between molecular oxygen and, 19: 46266
PRECIPITATION, ATMOSPHERIC
potassium-40 content in, in Vinca, Yugoslavia, 19: 46590(T) (JPRS-31469)
radioactivity of Belgian, 1963, 19: 46632(R) (A/AC.82/G/L.987)
strontium-90 content of Australian, 1963, 19: 46594
PREDNISOLONE
effects on radiation injuries in urinary tract, 19: 46033
PREGNANCY
placenta localization during, use of iodine-131 albumin and external counting, 19: 46117
radiation effects on osteogenesis of bones of embryos during, of mice, 19: 45872
radiation hazards from use of iodine-131 for treatment of thyrotoxicosis during, 19: 46049
radiation hazards of diagnostic radiography during, 19: 46062
PRESSURE
effects on properties and structure of metals, 19: 46983 (AD-612159)
PRESSURE DROP
void fraction relation to, in annular two-phase flow, 19: 46542
PRESSURE REGULATORS
design of absolute, for thermal diffusion columns, 19: 46157(R) (MLM-1254)
PRESSURE VESSELS
design criteria, 19: 48037
design for pressurized water reactors, 19: 47930(P)
fabrication facility for, 19: 47926
leak rate tests of PRTR containment, 19: 48057 (BNWL-109)
radiation effects on embrittlement of chromium–molybdenum steel, hydrogen effects on, 19: 47098
review of prestressed concrete, for large power reactors, 19: 47925 (GA-6505)
rupture of ETR, computer analysis of effects of, 19: 46716(R) (IDO-17081, pp 77-123)
testing of, in pressure suppression containment system, 19: 47927
PRESSURIZED WATER REACTORS
components and auxiliary equipment for, description of, 19: 48016
control rod power distributions and worth calculations for, (E/T), 19: 48000(R) (WCAP-3738)
cooling system design for, primary, 19: 47940(P)
criticality studies in assemblies of, 19: 48000(R) (WCAP-3738)
design for German ships, 19: 48051
design of compact, with jet pump arrangement, 19: 47974(P)
development and research on large closed-cycle, 19: 48000(R) (WCAP-3738)
development for ship propulsion, 19: 47923
development in Belgium, 19: 48113
development in Italy, 19: 48008
development of large closed-cycle power, 19: 48001(R) (WCAP-3743)
development of 15-Mw(e), 19: 48010
fuel assemblies for, strain testing of, 19: 48000(R) (WCAP-3738)
fuel element cladding of, determination of strain limits of, 19: 48000(R) (WCAP-3738)
kinetics of, computer calculations of, (T), 19: 47912 (ANL-7050, pp 347-68)
pressure vessel for, 19: 47930(P)
pressurizing vessel performance equations, 19: 46532 (BNWL-116)
safety systems for power, 19: 48038
PRESSURIZERS
design for primary reactor cooling systems, 19: 47940(P)
performance equations for steam-pressurized vessel, 19: 46532 (BNWL-116)
PRINCETON SYNCHROTRON
beam modulation from, uses for time-of-flight measurements, (E),

19: 46809
targets for, design of liquid-hydrogen, (E), 19: 47173
PROCESS HEAT REACTORS
use in Africa, 19: 48111
use in Finland, 19: 48005
PROMETHIUM IONS
diffusion in lithium chloride solutions at 25 to 45°C, 19: 46261
PROMETHIUM OXIDES
oxygen-18 exchange between molecular oxygen and, 19: 46266
PROPANE
electron drift velocities in, at low energy, 19: 46393
radiolysis of, scavenging effects of carbon tetrachloride, nitrous oxide, and sulfur hexafluoride on hydrogen yield in, 19: 46396
thermodynamic properties of, in water and heavy water, 19: 46318
yields in radiolysis of ethylene–methane–nitrogen, 19: 46324(R) (AGN-8132)
CaF_2–propane, radiolysis yields in, 19: 46324(R) (AGN-8132)
HF–propane, radiolysis yields in, 19: 46324(R) (AGN-8132)
PROPANE, 1-IODO-
benzene–iodopropane–$TeCl_4$, technetium-132 decay in, chemical reactions of iodine-132 from, 19: 46412
iodobenzene–iodopropane–$TeCl_4$, technetium-132 decay in, chemical reactions of iodine-132 from, 19: 46412
1,3-PROPANEDIOL, 2-AMINO-2-HYDROXYMETHYL-
properties for use as gamma dosimeter, 19: 46373
2-PROPANETHIOL, 1-AMINO-
protective effects of, against radiation injuries to bacteria and bacteriophage, 19: 45890
radiosensitivity effects on mouse bone marrow, 19: 46028
1-PROPANOL
thermodynamic properties of, in water and heavy water, 19: 46318
2-PROPANOL
nuclear magnetic resonance spectra of, 19: 46157(R) (MLM-1254)
radiation effects on decomposition of, in presence of catalysts, 19: 46329 (EUR-2455. e)
thermodynamic properties of, in water and heavy water, 19: 46318
benzene–2-propanol, NMR spectra, 19: 46157(R) (MLM-1254)
CCl_4–2-propanol, NMR spectra of, 19: 46157(R) (MLM-1254)
2-PROPANOL, 2-METHYL-
thermodynamic properties of, in water and heavy water, 19: 46318
2-PROPANONE, HEXAFLUORO-
radioinduced polymerization of, at low temperatures, 19: 46323(R) (AD-613529)
PROPENE
radioinduced polymerization of, gamma and x, 19: 46337 (TID-22244)
radiolysis of, yields in, 19: 46324(R) (AGN-8132)
N–propene, radiolysis yields in, 19: 46324(R) (AGN-8132)
PROPENE, HEXAFLUORO-
radioinduced polymerization of, at low temperatures, 19: 46323(R) (AD-613529)
radioinduced polymerization of, gamma, 19: 46337 (TID-22244)
PROPENE POLYMERS
helium-ion absorption cross sections at 30 to 350 kev, (E), 19: 47871
mechanical properties of, effects of strain rate on, 19: 47017 (UCRL-14316)
proton absorption cross sections at 30 to 350 kev, (E), 19: 47871
radioinduced grafting of styrene, 19: 46355
polyethylene–polypropene, radiation effects on flow and other properties of, 19: 46358
PROPIOLONITRILE
radiolysis of, EPR spectra from radicals formed in gamma, (E), 19: 46378
PROPIONALDEHYDE, PENTAFLUORO-
radioinduced polymerization of, at low temperatures, 19: 46323(R) (AD-613529)
PROPORTIONAL DETECTORS
design and performance of low-background, for carbon-14 dating, 19: 46777
design and performance for neutron and heavy particle dosimetry, 19: 46847
development of multiwire, for plutonium-239 in lungs, 19: 46751 (AEEW-M-526)
performance of boron trifluoride, for thermal neutrons, 19: 46822
performance of spherical tissue-equivalent, for dosimetry, 19: 46846
tritium release from, safety hazards from, 19: 46670
uses in gas chromatography, radiation sources for, 19: 46887
PROPULSION
book: *Nuclear Space Propulsion*, 19: 48052
ion engines for space, electrode materials testing for, 19: 46571 (HRL-5249-S)
performance of electron-bombardment sources for, 19: 46572 (NASA-TN-D-3041)
reactors for space, cavity nuclear, 19: 48046 (AD-613998)
PROPYNE
electron reactions with, spectra of energy level transitions in, 19: 46322 (AD-612070)
radiolysis of, x, 19: 46334 (TID-22231)
PROTACTINIUM
separation from hydrochloric acid solutions by solvent extraction using tetrabutylpyrophosphate and tetrabutylhypophosphate, tracer studies of, 19: 46451
separation from radiation targets by solvent extraction using diisobutyl ketone, 19: 46212
PROTACTINIUM ISOTOPES Pa-231
determination by activation methods and gamma spectroscopy, 19: 46212
PROTACTINIUM ISOTOPES Pa-232
determination by gamma spectroscopy, 19: 46212
PROTACTINIUM ISOTOPES Pa-233
determination by gamma spectroscopy, 19: 46212
PROTECTIVE CLOTHING
shielding properties of, thermal, 19: 45818 (TDCK-33500)
PROTECTIVE OINTMENTS
shielding properties of, thermal, 19: 45818 (TDCK-33500)
PROTEINS
content of crude, in range plants, Miles City, Montana, 1955 to 1960, 19: 45747 (ORNL-TM-1279)
effects of soy, on growth of chickens, 19: 45761(R) (ORO-631, pp 122-31)
iodine-131 content of blood plasma, 19: 46081
labeling with iodine-131, electrolytical method for, 19: 46142
labeling with iodine-125 or iodine-131 by enzymatic iodination, 19: 46314
metabolism in chromosomes, tracer study, 19: 45790
metabolism in seeds, tracer study, 19: 48102(R) (TID-22175)
radiation chemistry of, ultraviolet, 19: 46382
radiation chemistry of, 19: 46417
radiation effects on digestion of, 19: 45932
radiation effects on properdin content of blood serum of swine, ultraviolet, 19: 45919
radioinduced inactivation of, 19: 45839
spectra of chlorophyll complex of, from green photosynthetic bacteria, 19: 45727 (BNL-9506)
thermal stability of, effects of heavy water on, 19: 46318
PROTON BEAMS
effects on ribonuclease, inactivation, 19: 45993
PROTONS
absorption cross sections in carbon and hydrocarbon solids at 30 to 350 kev, (E), 19: 47871
angular distributions from alpha reactions (α,p) with aluminum-27 at 1.0 to 3.3 Mev, (E), 19: 47672
density near solar wind shock boundary, 19: 47211
detection and measurement of, performance of silicon for, 19: 46770 (UCRL-16354)
detection and measurement around 20 Bev, using sonic spark chambers, (E), 19: 46800
detection and measurement of, design of high-resolution resonance counter for, 19: 46838
diffusion in outer Van Allen belt, (T), 19: 47461
dissociation during hydrogen diffusion in palladium, (T), 19: 46250(T) (ORNL-tr-623)
effects on mice and rats, biological, 19: 45821(T) (JPRS-31547, pp 1-5)
emission from excited emulsion nuclei, (E), 19: 47651
interactions at 3 Mev, target design for measurement of, (E), 19: 47173
interactions in jet showers, secondary angular distribution and moments for primary energy of, (T), 19: 47275
interactions with photons, meson (π) production in, (E), 19: 46643(R) (LAL-1136)
interactions with electrons and positrons, (E), 19: 46643(R) (LAL-1136)
interactions with mesons (π^-) at 8 Bev/c, (E), 19: 46643(R) (LAL-1136)
interactions with mesons (K-) at 2.24 Bev/c, Y*(1660) resonance from, 19: 47300 (BNL-9520)
interactions with electrons at 5.2 Bev/c, meson (π) production in, (E), 19: 47303 (DESY-65/7)
interactions with mesons (π^+) and protons at 1.45 Bev/c, differential cross sections for, (E/T), 19: 47304 (IAE-700)
interactions with mesons (K^+) at 3 Bev/c, resonance production in ($K^0p\pi^+$), (E/T), 19: 47356
interactions with photons at 660 to 800 Mev, meson (π^0) angular distributions from, (E), 19: 47368
interactions with mesons (K^-) at 2.1 to 2.7 Bev/c, mesons (η) (958) production in, (E), 19: 47372
interactions with mesons (π^-) at 2.08 Bev/c, differential cross section and polarization for, (E), 19: 47373
interactions with antiprotons in spurion scheme of broken U(6,6), two-meson annihilation, (T), 19: 47374

interactions with neutrinos, charge ratio of mesons (π) produced in, (T), 19: 47377
interactions with gamma radiation at 230 Mev, meson (π^+) production in, (E), 19: 47393
interactions with mesons (π^-) at 2.16 Bev/c, single-particle exchange models in, (E), 19: 47403
interactions with neutrons in tritium-Λ hypernucleus, tensor, (T), 19: 47657
interactions with bremsstrahlung, dipion production in, (E), 19: 47303 (DESY-65/7)
magnetic moment from sum rules and SU(6) symmetry, (T), 19: 47306 (JINR-E-2343)
motion in electromagnetic fields, (T), 19: 47464
polarization in elastic and inelastic scattering on magnesium-24 at 5.8 Mev, (E), 19: 47697
polarization in elastic scattering on aluminum and magnesium at 4.5 Mev, (E), 19: 47692
polarization in helium-3 (d,p) reactions, 19: 47709
ranges in aluminum at 100 Mev, (T), 19: 47225
reactions (p,α) with yttrium-89 and zirconium-90 at 20.2 to 22.5 Mev, angular distributions from, (E/T), 19: 47670
reactions (p,d) and (p,t) with iron and nickel at 28 Mev, (E), 19: 47706
reactions (p,γ) with aluminum-27, boron-11, and giant dipole resonance of gamma yield from, 19: 47115(K) (ANL-6983)
reactions (p,γ) with lithium-7, angular distribution interference effects in, 19: 47703
reactions (p,n) with manganese-55 at 3.315 and 3.525 Mev, iron-55 energy levels from, (E), 19: 47696
reactions (p,n) with carbon-13 and nitrogen-15, neutron polarization in, 19: 47710
reactions (p,t) with lithium-7 at 16.6 Mev, differential cross sections for, (E/T), 19: 47574 (IAE-836)
reactions with beryllium-9 and lithium-6 and -7, energy levels and mechanisms of, 19: 47564(R) (AD-612038)
reactions with bismuth at 36 and 58 Mev, fission yields in, 19: 47712
reactions with emulsion nuclei at 23 Bev/c, hyperfragment production in, (E), 19: 47650
reactions with inert gases at high energies, ionization cross sections for, (T), 19: 47246
reactions with meteoritic materials, krypton and xenon production by, 19: 47213
reactions with nitrogen-14, nitrogen-15, oxygen-16, and oxygen-18 at 2.2 Bev, cross sections for beryllium-7 production in, 19: 47625
reactions with tantalum at 660 Mev, holmium-162 production by, (E), 19: 47579 (JINR-P-2275)
scattering by beryllium-9, boron-11, and phosphorus-31, angular distributions from, (E), 19: 47690
scattering by calcium-40, iron-54, and titanium-50 at 14.6 to 18.2 Mev, inelastic, (E/T), 19: 47702
scattering by copper-63, nickel-62, and zinc-64 at 12 Mev, cross sections for elastic and inelastic, (E), 19: 47585 (ORNL-3851)
scattering by helium-4 at 17.5 to 27 Mev, polarization in, 19: 47709
scattering by medium-weight nuclei at 14.5 Mev, cross sections for elastic, 19: 47705
scattering on aluminum and magnesium at 4.5 Mev, polarization in elastic, (E), 19: 47692
scattering on carbon-12 at 6 Mev, angular distribution of polarization of elastic, (E), 19: 47695
scattering on magnesium-24 at 5.8 Mev, polarization in elastic and inelastic, (E), 19: 47697
scattering on nuclei ($12 \leq A \leq 120$) at 10.5 and 14.5 Mev, neutron-nucleus potential from elastic polarized, (E/T), 19: 47581 (LA-DC-6730)
slowing down due to atomic collisions, computer program for calculating, 19: 47867 (NP-15384)
spectra from bremsstrahlung reactions (y,p) with carbon-12, magnesium-24, silicon-28, sulfur-32, and calcium-40, (E), 19: 47699
spectra of delayed, in magnesium-21, neon-17, and silicon-25 decay, (E), 19: 47613
spin-lattice relaxation in deuterium chloride and hydrogen chloride, (E), 19: 46287
structure of, from form factors and scattering amplitudes, (E/T), 19: 47565 (AD-614270)

PSEUDOUREA, 2-(2-AMINOETHYL)-2-THIO-
effects on thymidine uptake by mouse DNA, 19: 46016
protective effects against intestinal radiation death in rats, 19: 46027
protective effects against radiation damage in mice, 19: 46016
radiosensitivity effects on mouse bone marrow, 19: 46028

PSYCHOLOGY
radiation effects on performance of tests by monkeys, 19: 45893
radiation effects on response performance of monkeys, 19: 45898
radiation effects on response to stimulus of female monkeys, 19: 45899
radiation effects on learning by monkeys, 19: 45900

PULSE ANALYZERS
design for fission-fragment studies, engineering drawings for, 19: 46854
design for measurement of lifetimes in nuclear transitions, 19: 47584(R) (ORNL-3832, pp 1-28)
design of high resolution transistorized multichannel, 19: 46827
performance time-amplitude converter with tunnel diodes, 19: 46736
use in measuring Mössbauer effect, 19: 46826

PULSE GENERATORS (ELECTRONICS)
breakdown initiation using pulse techniques, statistics of, 19: 47114 (AD-614286)
design of three-decade exponential, for testing reactor period meters, 19: 47928

PUMPS (LIQUID METAL)
bearing development for SNAP-50/SPUR, 19: 46458 (CNLM-6342)
development for Lithium Cooled Reactor Experiment, 19: 46535 (PWAC-386)

PUPAE
radiation effects on endocrine system in insect, 19: 45861

PUREX PROCESS
cesium recovery from alkaline supernate waste by solvent extraction using 4-sec-butyl-2(α-methylbenzyl)phenol, 19: 48075 (BNWL-68)
performance of 3 and 30% TBP process in, at Savannah River Plant, 19: 46423 (DPSPU-64-30-28)

PURINES
N-oxides, chemistry and metabolism of, 19: 46158(R) (NYO-910-23, pp 112-82)
polarographic behavior of, 19: 46301 (COO-1148-97)
synthesis of nucleosides of, method for, 19: 46158(R) (NYO-910-23, pp 112-82)
therapeutic uses of analogs, 19: 46158(R) (NYO-910-23, pp 112-82)
uptake by DNA, tracer study, 19: 46158(R) (NYO-910-23, pp 112-82)

PYRENE
use as a radical scavenger reagent to minimize radiation effects on TBP, 19: 46406(P)

PYRIDINE
separation of tritiated, from tritiated benzene, chloroform, and toluene, by gas chromatography, 19: 46213

PYRIMIDINE
electrochemical reduction, 19: 46301 (COO-1148-97)

PYRIMIDINES
polarographic behavior of, 19: 46301 (COO-1148-97)
uptake by DNA, tracer study, 19: 46158(R) (NYO-910-23, pp 112-82)

PYROMETERS
design of modulation, for temperature measurements on flames, gas flows, and plasmas, 19: 46734

PYROPHOSPHORIC ACID, ALKYL ESTERS
solvent properties for tetra- and pentavalent metals, 19: 46451
tetrabutylhypophosphate--tetrabutylpyrophosphate, solvent properties for tetra- and pentavalent metals, 19: 46451

PYRROLIDONE, VINYL- POLYMERS
use of iodine-131-labeled, in brain scanning, 19: 46058

Q

QUALITY CONTROL
conference on, Miami Beach, Jan. 1965, 19: 46565

QUANTUM ELECTRODYNAMICS
dispersion relations and unitarity in, 19: 47396
gravitational theory of, for infrared gravitons, 19: 47204
model for finite, using indefinite metric, 19: 47436
theory of, 19: 47442

QUANTUM MECHANICS
Boltzmann equation in, derivation from N-particle Schrödinger equation, (T), 19: 47416
canonical transformations in, (T), 19: 47413
classical mechanics correlations with, (T), 19: 47432
Dirac equation in, invariance properties of, 19: 47421
Ehrenfest principle in, probability of violation of, 19: 47427
field theory in, spin and orbital angular momentum in relativistic, 19: 47426
Fokker-Planck equation in, modifications to, (T), 19: 47415
invariance principles for point particles in, (T), 19: 47433
kinematics of particle angular momentum in relativistic, 19: 47418
Poincaré group associated with complex energy-momentum in, representations of, 19: 47422
rotators in relativistic, eigenvalues for rigid, (T), 19: 47428
scattering of single-particle excitations by vortices in imperfect Bose gas, 19: 47516
statistical, of fully ionized gases, 19: 47439
wave equations for square well potentials in, numerical integration of

Schroedinger, 19: 47429
QUARTZ
analysis for impurities by radioactivation and ion-exchange chromatography, 19: 46228
radioactive halos in, measurements of, 19: 46592(T) (ORNL-tr-701)
radiolysis of surface silanols on, effects of dose, impurities, and surface area on, 19: 46332(R) (ORNL-3832, pp 50-65)
sorptive properties for argon, helium, and neon in high-density discharges, (E/T), 19: 46576
QUATERPHENYL
mass spectra of, after electron bombardment, 19: 46328 (EUR-2227.e)
QUININE
protective effects of synthetic, against radiation injuries of skin of guinea pigs, 19: 46019
8-QUINOLINOL
analytical use in determination of aluminum, cobalt, copper, iron, manganese, nickel, uranium, and zinc, 19: 46205
benzene-8-quinolinol, solvent properties for fission products, 19: 46440
8-QUINOLINOL COMPLEXES
with neptunium and plutonium, preparation and properties, 19: 46288

R

RABBITS
cesium-134 excretion by, effects of dithizone derivatives on, 19: 45765(T) (JPRS-27544, pp 1-12)
deuteron effects in brain of, 19: 45874
radiation effects on ear of, skin recovery processes in, 19: 45987
radiation effects on tibia of, time factors in, 19: 45989
radiation effects on cell nuclei in, 19: 45992
radiation effects on blood-brain barrier in, x, 19: 45970
radiation effects on albumin metabolism in, 19: 45829
radiation effects on blood volume in, 19: 45829
radiation effects on aorta of, 19: 45875
radiation effects on tolerance to bovine serum albumin in, 19: 45902
radiation effects on nervous system of, neutron, 19: 45812(R) (ORO-631, pp 1-35)
radiation effects on reproduction of, 19: 45813(R) (ORO-631, pp 36-44)
radiation effects on, pathological, 19: 45814(R) (ORO-631, pp 45-66)
radioinduced free radicals in muscle tissues of, ESR of gamma and x, 19: 45947
rubidium-85 metabolism in incubated lens of, 19: 45778
toxic effects of niobium pentachloride and potassium niobate on, 19: 45768
RADAR
biological hazards in man, 19: 46706
maximum safe exposure levels for man, 19: 46706
RADIATION
absorption and emission by fully ionized plasma, (T), 19: 47814
adsorption by vinyl chloride, design of parallel-plate and thimble ionization chambers for measuring, 19: 46368
book: *Radiation Dosimetry*, 19: 46840
cancer of skin induced by, 19: 45945
carcinogenic effects of, 19: 45859
dose concepts and units for, 19: 46842
dose distributions to populations in diagnostic and therapeutic use, 19: 46156
dose rates from Saxton components, 19: 48000 (WCAP-3738)
dosimetry in diagnostic radiology, quantities and units for, 19: 46684
dosimetry in radiography using ionization chambers and electrometer circuits, 19: 46043
dosimetry of personnel in Democratic Republic of Germany, 19: 46674
dosimetry of, by computer calculations, 19: 46134
dosimetry of, by radioinduced molecular weight decreases of polymethylmethacrylate, 19: 46367
dosimetry of, calorimetric, 19: 46848
dosimetry of, calorimetric methods for, 19: 46849
dosimetry of, chemical, 19: 46852
dosimetry of, clinical, 19: 46854
dosimetry of, design of automatic isodose contour recorder for, 19: 46776
dosimetry of, equipment development for, 19: 46841
dosimetry of, from ingestion of water contaminated by fallout, 19: 46633 (AD-276187)
dosimetry of, from ionization measurements, 19: 46843
dosimetry of, from ionization measurements, 19: 46844
dosimetry of, from environmental sources, 19: 46855
dosimetry of, in bones, 19: 46153
dosimetry of, linear energy transfer distributions for microscopic, 19: 46846
dosimetry of, properties of plastics for, 19: 46392
dosimetry of, scintillation, 19: 46851
dosimetry of, solid state, 19: 46850
effectiveness of, relative biological, 19: 45998
effects combined with nonradiation factors on mammals, 19: 45824(T) (NASA-TT-F-354)
effects in animals, genetic, 19: 45973
effects in mammals, acute pathological, 19: 45981
effects in man, carcinogenic, 19: 45942
effects in man, genetic, 19: 46695
effects in plants, genetic, 19: 45884
effects in seeds, genetic, 19: 45884
effects in solid organic matter, ESR of radicals in, 19: 46402
effects of high-level, on man, somatic, 19: 45997
effects of laser beam, on atomic energy level shifts, (T), 19: 47233
effects of occupational exposure to, on lifetime health and mortality patterns, 19: 45810(R) (NYO-3394-2(Rev.))
effects of therapeutic iodine-131, on thyroid gland function, 19: 46082
effects on *Acer negundo*, genetic, 19: 45865
effects on acetylcholine, betaine hydrochloride, and choline halides, mechanism of, 19: 46374
effects on aerospace structural materials, (E/T), 19: 47077
effects on animals, physiological, 19: 45815(R) (ORO-631, pp 67-76)
effects on bacteria cells, damage repair in, 19: 45985
effects on beef odor, 19: 46878 (NP-15455)
effects on bile and pancreatic enzymes following intestinal irradiation, 19: 45922
effects on cervical carcinoma patients, response and sensitization, 19: 45830
effects on cholesterol content of guinea pigs, 19: 45937
effects on chromosome pattern of man, 19: 45808(R) (NYO-901-36)
effects on creatine excretion in humans and mice, use as damage indicator, 19: 45864
effects on cyclopolymerization of acrylic anhydride, 19: 46352
effects on defect-oxygen interactions at 25 to 700°K, (E), 19: 47892
effects on desoxyribonucleic acid metabolism in tumor cells in mice, tracer study, 19: 45936
effects on development and growth of adolescents exposed *in utero* in Nagasaki bombing, 19: 45889
effects on domestic animals, pathological, 19: 45814(R) (ORO-631, pp 45-66)
effects on dynamic properties of polymers, review on developments in, 19: 46331(R) (NYO-1858-1)
effects on excretion of pancreatic enzymes, 19: 45928
effects on eyes of atomic bomb, pathological, 19: 45843
effects on fatty acids in rabbit liver, 19: 45946
effects on flow and other properties of polyethylene and polypropene, 19: 46358
effects on gastrointestinal function, 19: 45930
effects on gastrointestinal function, 19: 45932
effects on glucose absorption, after intravenous or oral administration, abdominal exposure, 19: 45931
effects on growth of tumor transplants in mice, 19: 45858
effects on growth in HeLa cells, clone-size analysis of, 19: 45886
effects on growth of transplanted tumors in rats, 19: 45921
effects on humans, carcinogenic, 19: 45996
effects on immune reactions to tissue transplants, 19: 45944
effects on immune reactions in mice, 19: 45858
effects on intestinal mucosa, 19: 45929
effects on learning by monkeys, 19: 45900
effects on liquid and sodium metabolism in rat intestines, protective effects of AET and cysteamine against, 19: 46027
effects on liver function in rats, use of iodine-131-labeled rose bengal for analysis of, 19: 45828
effects on mammals, protective effects of thiolic compounds against, 19: 46010
effects on man in space flight, 19: 46001
effects on mice, protective effects of sodium cysteinethiosulfonate against, 19: 46006
effects on molecular diffusion, 19: 45922
effects on peas, effects of water content on, 19: 45863
effects on plants, genetic, 19: 45817(R) (ORO-631, pp 145-71)
effects on polymers, review of, 19: 46400
effects on polymethyl methacrylate, EPR spectra of protective effects of aromatic additives against, 19: 46321 (AD-611779)
effects on proliferating cellular systems, 19: 45923
effects on secretion of biliary acids, 19: 45928
effects on semiconductor performance, methods of predicting, 19: 46874
effects on serum denaturation following cancer therapy, electrophoretic study of, 19: 45924
effects on silicon semiconductors, 19: 47076(R) (AD-612090)
effects on solid uranium-based fuel materials, bibliography on, 19: 47093 (VDDIT-16(5.2))

effects on swelling in alpha-uranium, dislocation movement effects in, 19: 47100
effects on tensile properties of metals to 3000°F, equipment for measuring, 19: 46712 (BNWL-SA-169)
effects on thermodynamic properties of air plasma at 20000 to 50000°K, 19: 47731
effects on urania-base fuels, 19: 46912(R) (BMI-1727(Del.))
effects on water, decomposition and ionization in, (T), 19: 46401
emission by point charges, (T), 19: 47431
epidemiology of, as cause of death in California chiropractors, 19: 45866
exposure to, survey of national maximum permissible, 19: 46696
hazards of space, 19: 45890
hazards to hospital personnel according to occupation, 19: 46657
monitoring at Brookhaven, 1963 background, 19: 46640 (BNL-915)
production of, mechanisms of, 19: 47152
role in leukemia etiology, 19: 45833
use in nitrogen fixation, equipment for, 19: 47985(P)
use of high-energy, in Germany, 19: 48117

RADIATION CHEMISTRY

alanine and glycine chelate, solid-state, 19: 46403
developments in aqueous solution, 19: 45729(R) (NYO-910-23, pp 1-111)
developments in Germany, review on, 19: 48117
gamma sources for industrial processes, 19: 46340(T) (AEC-tr-6570)
of nucleic acids, 19: 46417
of proteins, 19: 46417
radiolysis in, advantages and method of pulse, 19: 46346
radiolysis of hydriodic acid and methyl iodide, distribution and energies of fragments from, 19: 46161(R) (ORNL-3832, pp 116-50)
radiolysis of saturated fluorocarbons, gamma and neutron, 19: 46404

RADIATION DETECTION INSTRUMENTS

data analysis from, on-line systems for, (E), 19: 46792
data from, improved methods of analyzing, 19: 46820
design and operation of digitized discharge planes for spark chambers, 19: 46784
design for monitoring airborne alpha activity, (E), 19: 46768 (UCRL-14253)
development for multiplication experiments, 19: 46716(R) (IDO-17081, pp 77-123)
development for neutron capture cross section measurements, 19: 46766(R) (TID-22141, pp 67-79)
development for use with storage rings, 19: 46643(R) (LAL-1136)
evaluation of, for monitors in radiation accidents, 19: 46839
particle track analysis in photographs from, semi-automatic device for, (E), 19: 46803
performance of whole-body, 19: 46137
review of Toshiba, 19: 46837
uses of time-of-flight, with modulated accelerator beams, (E), 19: 46809

RADIATION DETECTION INSTRUMENTS (ION CURRENT TYPE)

design for gamma monitoring at 0.2 to 500 R/hr, engineering drawings of, 19: 46867
design with integrating resistor condenser and integrating-type ionization chamber, 19: 46868(P)
performance in high-activity handling cell monitoring system, 19: 46647 (RISO-104)
performance of, for monitoring surface alpha and beta contamination, 19: 46833
tritium release from, safety hazards from, 19: 46670

RADIATION DETECTION INSTRUMENTS (PULSE TYPE)

book: *Scintillation Counters in High Energy Physics*, 19: 46856(T)
calibration of cosmic-neutron monitors, 19: 47272
calibration of neutron survey probe, 19: 46752 (AERE-M-1564)
design and performance of, with large liquid scintillator, 19: 46775
design and performance of whole-body, 19: 46836
design for gamma transmission radiography, 19: 46750 (AECL-2270)
design for monitoring radioactive contamination on protective face masks, 19: 46755 (BNWL-144)
design of fast counting channel, for neutron flux measurements, 19: 48033
use with computers in high energy experiments, 19: 46756 (BNL-9492)

RADIATION DETECTORS

design for monitoring aerosols in gases, 19: 46869(P)
design of high-resolution resonance, for charged particles, 19: 46838
development for alpha spectra measurement, 19: 47576(R) (IDO-17081, pp 49-76)
development for monitoring of JRR-2 in-pile gas loop, 19: 48071
development of, conference, 19: 46778
evaluation of, for monitors in radiation accidents, 19: 46839

RADIATION INJURIES

book: *The Biological Action of Neutron Radiation*, 19: 45822(T) (JPRS-31822)
diagnosis in man, by lymphocyte chromosome studies, 19: 45916
diagnosis in man, by lymphocyte chromosome studies, 19: 45917
diagnosis of, by examination of rectal mucosa, 19: 45918
effects of moisture on Lupinus, 19: 45847
effects of prednisolone on, in urinary tract, 19: 46033
indicator for estimation of, use of creatine as, 19: 45864
mechanisms of, in animals, 19: 46031
of brain, induced by implanted radon seeds in man, 19: 45995
of eyes, pathology of, 19: 45905
of intestine, induced by radiotherapy of pelvic tumors, 19: 46065
of skin, effects on amino acids and enzymes, 19: 45887
pathology of deuteron, in rabbit brain, 19: 45874
pathology of high-level exposure, in man, 19: 45997
pathology of rectal, induced by radiotherapy, 19: 46099
pathology of thermal, 19: 45818 (TDCK-33500)
pathology of thyroid gland, induced by iodine-131 therapy, 19: 46082
pathology of ultraviolet-induced, in human skin, 19: 45907
pathology of, in domestic animals, 19: 45814(R) (ORO-631, pp 45-66)
pathology of, in heart, 19: 45835
pathology of, in rabbit aorta, 19: 45994
pathology of, in rat skin, 19: 45957
pathology of, in rabbit aorta, 19: 45875
pathology of, induced by Thorotrast, 19: 45980
pathology of, induced by deposited thorium oxides, 19: 45837
protection against skin, effects of chloroquinine in guinea pigs, 19: 46019
protection against, effects of mixture of adenosine triphosphate and diphosphopyridine nucleotide in rats, 19: 46020
protection against, effects of morphines in rats, 19: 46021
protection against, effects of injected ribonucleic acid in rats, 19: 46022
protection against, effects of injected bone marrow, spleen, or thymus tissues in rats, 19: 46023
protection against, effects of injected bovine liver homogenates in mice, 19: 46024
protection against, protective effects of nembutal in rats, 19: 46025
protection against, effectiveness of chlorotrianisene in, 19: 46029
protection against, effects of transplanted hematopoietic tissues, 19: 46009
protection against, in mammals, 19: 45981
protection against thermal, 19: 45818 (TDCK-33500)
protection against, effects of chemical radioprotective compounds, 19: 46026
protection against, recommended methods for, 19: 46668
reaction mechanisms of, classification system for, 19: 45988
time factors in rabbit tibia, 19: 45989

RADIATION MONITORING

equipment for air, design of, 19: 46716(R) (IDO-17081, pp 77-123)
equipment for, engineering drawings of alarm, 19: 46865
equipment for, in radiation accidents, 19: 46839
equipment for, of high-activity handling cells, 19: 46647 (RISO-104)
instrumentation and methods for community-wide diagnostic, 19: 46143
instruments for in-pile gas loop of JRR-2, 19: 48071
methods for accident, 19: 46697
of radium sources, 19: 46678
procedures at CEN, Mol, 19: 46631 (A/AC.82/G/L.986)
program at BNL, 1963, 19: 46640 (BNL-915)
requirements for personnel, 19: 46689
spectrometry for, whole-body gamma, 19: 46656

RADIATION PROTECTION

bibliography on thermal, 19: 45818 (TDCK-33500)
book: *Principles of Radiation Protection Engineering*, 19: 46683(T)
code for users of radiation sources, 19: 46649 (STI/PUB/94)
during intracavitary radiotherapy, design of remote afterloader for, 19: 46111
during radiodiagnosis, 19: 46132
equipment for, catalog of USSR, 19: 46653(T) (JPRS-31843)
from microwaves, 19: 46706
handbook for medical personnel, 19: 46686
manual on, 19: 46685
methods for fallout, 19: 46700
methods for personnel during diagnostic radiography, 19: 46036
methods for population, in reactor accidents, 19: 46698
methods for, after radiation accident, 19: 46692
methods for, during radiodiagnosis of urinary tract in children, 19: 46108
methods for, in radiation accidents, 19: 46691
methods for, of hospital personnel exposed according to occupation, 19: 46657
of medical personnel using radioisotopes, 19: 46080
of personnel at accelerators, 19: 46643(R) (LAL-1136)
of personnel using radioactive pharmaceuticals, 19: 46044

planning for in Sweden, 19: 46705
planning for, in radiation accidents, 19: 46697
planning for, in radiation accidents, 19: 46702
plans for, French, 19: 46704
program for hospitals, 19: 46679
program in Canada, 19: 46661
regulations for, review of ICRP, 19: 46676
standards and recommendations for, 19: 46668
standards for, in Yugoslavia, 19: 46654(T) (JPRS-31993)
use of thiolic compounds for, of mammals, 19: 46010

RADIATION SICKNESS
nursing care of patients with accidental and therapy induced, 19: 45912
therapy using rutin in mice, 19: 46030

RADIATION SOURCES
design, for radiosterilization facilities, 19: 46890
fabrication of, in a ceramic carrier, 19: 47156(P)
protection code for, 19: 46649 (STI/PUB/94)
standardization of isotopic, methods for, 19: 46421
use in Yugoslavia, standards for, 19: 46654(T) (JPRS-31993)

RADIATION TARGET CANS
design for fissiochemical fuel studies, 19: 46324(R) (AGN-8132)

RADIATION TARGETS
design for analysis of 3-Mev proton-proton interactions, (E), 19: 47173
development for HFIR, 19: 46428(R) (ORNL-3847)
development of liquid deuterium and liquid hydrogen, 19: 46643(R) (LAL-1136)

RADICALS
production in radiolysis of solid organic matter, ESR studies of, 19: 46402

RADIO WAVES
book: *Geophysics and Space Data Bulletin No. 3*, 19: 47447 (AD-612083)
interactions with warm plasma, Langevin's equation for, (T), 19: 47770
propagation in ionosphere, (T), 19: 47501
propagation in ionosphere, (T), 19: 47502
propagation over polar paths, pre-SC field intensity increases in, (E), 19: 47455
scattering of, association with nighttime auroral belt, (E), 19: 47473

RADIOACTIVE CONTAMINATION
countermeasures for agricultural land, 19: 46701
detection on face masks, design of detector for, 19: 46755 (BNWL-144)
dose estimations for ingested, 19: 45755 (CEA-R-2809)
medical treatment of, action levels in, 19: 46008
monitoring in Clinch and Mohawk Rivers, 19: 46646(R) (PHS-999-RH-13)
monitoring in high-activity handling cell, system for, 19: 46647 (RISO-104)
monitoring, on surfaces, 19: 46833
of atmosphere, control of, 19: 46682
of foods in U. S., 19: 46662
radiation dose to man from, of water supplies, 19: 46633 (AD-Z76187)

RADIOACTIVE MATERIALS
analysis of, radiocrystallographic, 19: 46202
distribution after radiation accident, meteorological factors in, 19: 46693
organic, preparation by microbial processes, 19: 46409
shipping of, design of containers for, 19: 46665
shipping of, regulations and licensing procedures for, 19: 46666
use in USSR, catalog of protective equipment, 19: 46653(T) (JPRS-31843)
use in Yugoslavia, standards for, 19: 46654(T) (JPRS-31993)

RADIOACTIVE MINERALS
effects on cancer incidence of, 19: 45832

RADIOACTIVE WATERS
decontamination of, foam separation process for, 19: 46429 (ORNL-P-1522)
in Great Britain, 19: 45959

RADIOACTIVITY
data on human whole-body, computer program for analysis of, 19: 46658
halos in biotites, 19: 46591(T) (ORNL-tr-642)
halos in minerals, review, 19: 46593(T) (ORNL-tr-755)
measurement of halos of, in cassiterite, quartz, and yttrofluorite, 19: 46592(T) (ORNL-tr-701)
measurement of, in rain and surface waters, errors in, 19: 46608
of eyes, 19: 45905
of Great Britain, natural, 19: 45959
radiation dose to man from natural, 19: 46688

RADIOAPPLICATORS
design of cobalt-60, for intercavitary therapy of carcinoma of uterus, 19: 46039(T) (JPRS-31667)
design of cobalt-60, 19: 46064
radiation dose from, computer calculations of, 19: 46055
radiation hazards from handling and storage of radium, 19: 46678
use of cobalt-60 as, 19: 46047
use of iridium-192 wire as, 19: 46047
use of radium needle for treatment of eye lesions, 19: 46056
use of radon seeds for treatment of eye lesions, 19: 46056

RADIOBIOLOGY
contributions to cancer study, 19: 45743
developments in Germany, review on, 19: 48117
dosimetry for, 19: 45999
problems in manned space flight, 19: 46000
radiation injury and recovery mechanisms, classification system for, 19: 45988

RADIOCHEMICAL PROCESSING PLANTS
development of Curium Recovery Facility, 19: 46428(R) (ORNL-3847)
development of TRU facility for transuranium elements, 19: 46428(R) (ORNL-3847)

RADIOCHEMISTRY
development in, review on, 19: 46410
dilatometers design for, 19: 46419
standards of activity in, 19: 46420

RADIODIAGNOSIS
color scintigraphy and x-radiography in, 19: 46073
counters for, evaluation of whole-body, 19: 46137
data from, computer analysis of, 19: 46055
data from, computer analysis of, 19: 45735
dose reduction during, short-lived radioisotopes for, 19: 46136
method for respiratory insufficiency, thulium-170, 19: 46118
method for, of carcinoma and inflammation of pancreas, 19: 46960
methods using iodine-131-labeled proteins and whole-body counting, 19: 46142
of bone lesions using strontium-85 and external counting, 19: 46133
of brain tumors by scanning with iodine-131, mercury-197, or mercury-203, 19: 46046
of brain tumors, using mercury-203 scanning, 19: 46053
of fallopian tube obstruction using injected gold-198, 19: 46040
of kidney diseases, using iodine-131–sodium iothalamate as tracer, 19: 46079
of Q fever induced by *Coxiella burnetii*, radioisotope precipitation test, 19: 46076
of subdiaphragmatic abscess, by liver-lung scanning with iodine-131 and gold-198, 19: 46048
of thyroid diseases using iodine-131, 19: 46072
of thyroid diseases, 19: 46081
of tumor metastases, by phosphorus-32 uptake, 19: 46098
of vascular lesions of brain, 19: 46086
radiation hazards in, of lung diseases, 19: 46110
radiation hazards from use of labeled pharmaceuticals for, 19: 46044
radiation protection during, 19: 46132
tracer for, properties of technetium-99, 19: 46140
urinary cobalt-58-labeled vitamin B_{12} excretion test, 19: 46083
urologic, methods for reduction of exposure time in children during, 19: 46108
use and abuse of, in elderly persons, 19: 46116
use of cobalt-57-labeled vitamin B_{12} for, 19: 46128
use of radioisotopes for, radiation protection of medical personnel, 19: 46080
uses of radioisotopes for, 19: 46102

RADIOFREQUENCY SPECTROMETERS
description of field-frequency, for nuclear magnetic resonance spectra, 19: 46247 (UCRL-16349)
performance of semiautomatic, 19: 46772

RADIOGRAPHY
color contrasts in, 19: 46073
dental, radiation dose of gonads from, 19: 46107
diagnostic use of gamma-transmission, 19: 46750 (AECL-2270)
dosimetry in, ionization chambers and electrometer circuits in, 19: 46043
equipment and methods for active fuel elements, 19: 46558(T) (ORNL-tr-748)
methods of projection, for highly radioactive specimens, 19: 46560
methods using counting equipment as recording medium in, 19: 47039
radiation dose from repeated diagnostic, in tuberculosis patients, 19: 45870
radiation dose to population from diagnostic, 19: 46112
radiation hazards of diagnostic, in pregnant women, 19: 46062
radiation hazards of diagnostic, of breast, 19: 46090
radiation protection of personnel during diagnostic, 19: 46036
use for flaw detection, methods for, 19: 46564
use in inspection of brazed joints in copper magnet coils, 19: 46965 (UCRL-16383)
x-ray exposure conditions for, preparation of charts for determining, 19: 46561
x-ray source for diagnostic, use of mercury-197, 19: 46141

RADIOISOTOPES
activity of short-lived, instrumentation for measuring, 19: 46818

activity of, methods for standardization of, 19: 46421
decay law for, analysis of, (T), 19: 47599(T) (ORNL-tr-707)
determination in environmental samples, radiochemical procedures for, 19: 46168 (IA-849)
determination of beta-emitting, in plant materials, 19: 46199
dosimetry of, in soft tissues and bones, 19: 46154
effects on bladder cancer, therapeutic, 19: 46114
energy transfer by internally administered, LET for, 19: 45729(R) (NYO-910-23, pp 1-111)
gamma emission from, energies and intensities of, 19: 47598 (USNRDL-TR-876)
measurement in Cinch and Mohawk Rivers, 19: 46646(R) (PHS-999-RH-13)
occurrence of gamma-emitting, in District of Columbia, Maryland, Virginia, and West Virginia, 19: 46614
performance in photovoltaic energy conversion system, 19: 47284
production at Mol nuclear center, review on, 19: 46349
production by Szilard-Chalmers reactions, problems of, 19: 46332(R) (ORNL-3832, pp 50-65)
production in rocks and soil from underground explosions, 19: 46473 (UCRL-14249)
production of, developments in, 19: 46410
proton decay, 19: 47628
removal from human body, developments in chelation therapy for, 19: 46017
shipping of, safety aspects in, 19: 46663
sorption from waste water by rhyodacite tuff, 19: 48085
therapeutic use in neoplasias, mechanisms for, 19: 46095
uptake by biological materials, energy distributions of electrons from, 19: 45729(R) (NYO-910-23, pp 1-111)
use in agriculture and hydrology in Africa, 19: 48111
use in agriculture, biology, industry, and medicine in Federal Republic of Germany, 19: 48112
use in avionics, review on, 19: 46883
use in Norway, 19: 48114
use in therapy of gynecological cancers, 19: 46100
uses in x-ray fluorescence analysis, 19: 46201
uses of, standards of activity for, 19: 46420

RADIOLOGICAL DEFENSE
shelter development, 19: 46669

RADIOLOGICAL WARFARE
book: *Nuclear Weapons—Physical Fundamentals*, 19: 46652(T) (JPRS-31842)

RADIOLOGICAL WARFARE AGENTS
effects of, pathology, clinical picture, and therapy in, 19: 46651(T) (JPRS-30979)

RADIOLOGY
diagnostic, efficiency of intensifying screens in, 19: 46148
dose reduction in diagnostic, problems in, 19: 46146
dosimetry in diagnostic, instrumentation and methods for, 19: 46143
dosimetry in diagnostic, filtration and kilovoltage effects on depth, 19: 46144
dosimetry in diagnostic, collimation effects on, 19: 46145
dosimetry in diagnostic x-ray, ionization chambers for, 19: 46857
dosimetry in diagnostic, performance of chemicals and films for, 19: 46860
dosimetry in diagnostic, instrumentation for, 19: 46861
dosimetry in, properties of calcium and lithium fluoride and phosphate glass for, 19: 46859
dosimetry in, scintillator-photomultiplier combination for, 19: 46858
grid evaluation for diagnostic, 19: 46147
image quality and speed of film-screen combinations in diagnostic, 19: 46149
life span and cause of death of radiologists, 19: 45808(R) (NYO-901-36)
radiation dose to patients in, reduction of, 19: 46037
radiation dosimetry units for, 19: 46684
screens and intensifiers for evaluation of fluoroscopic, 19: 46150

RADIOMETERS
performance for monitoring aerosols, determination of, (T), 19: 46760 (NP-15462)

RADIOMETRIC ANALYSIS
equipment for fluorine in plutonium tetrafluoride, 19: 46179 (RFP-618)
methods for radioisotope, solutions, 19: 45760(R) (ORO-631, pp 83-121)

RADIOMIMETIC SUBSTANCES
genetic effects in red clover seeds, 19: 45882
tooth lesions induced by, in rats, 19: 45845

RADIOPROTECTIVE COMPOUNDS
effects of chlorotrianisene in mice, 19: 46029
effects of mixture of adenosine triphosphate and diphosphopyridine nucleotide in rats, 19: 46020
effects of sulfur-containing, on muscular activity of intestine of guinea pigs, 19: 46005(T) (JPRS-31933, pp 6-12)
effects on radiosensitivity of animals, 19: 46031
effects on uv-induced luminescence in albumin solutions, 19: 46342(T) (JPRS-31547, pp 6-12)
preparation and polymerization of S-vinyl-N-vinylthiocarbamates, 19: 46316
radiosensitivity effects on mouse bone marrow, 19: 46028
reaction mechanisms of, 19: 46026
reaction mechanisms in animals, 19: 46031
synthesis of sulfur compounds, 19: 46303(R) (NP-15409)

RADIOSENSITIVITY
biological factors in neoplastic metastasis, 19: 45920
biological factors in metastatic epithelial tumor, 19: 45921
genetic factors in, 19: 45857
of animals, effects of radioprotective compounds, 19: 46031
of autochthonous radioinduced lymphosarcomas in mice, single- and split-dose, 19: 45977
of bone marrow and mice with genotype S1/S1 anemia, cellular basis of hemopoietic defect in, 19: 45856
of cells of rat intestine, 19: 45926
of cells of thymus gland of mice, 19: 45871
of connective tissues, 19: 45935
of *Escherichia coli*, effects of genetic factors, 19: 45948
of immune reactions in mice, 19: 45903
of rectal mucosa in rats, 19: 45918
of Salmonella, ultraviolet, 19: 45963
of skin of nipple and flank, in guinea pigs, 19: 45869
of tissues, effects of desoxyribonucleic acid metabolism on, 19: 45992
of tumors, effects of oxygen, 19: 46097
of tumors, evaluation of metastatic, 19: 46098

RADIOSTERILIZATION
book: *A Review of Sterilization and Disinfection as Applied to Medical, Industrial, and Laboratory Practice*, 19: 46890
conference on food, Natick, Mass., Oct. 7–9, 1963, 19: 46876 (AD-613325)
developments in Germany, review on, 19: 48117
economics of food, 19: 46877 (CONF-650552-1)
effects on *Clostridium botulinum* spores in cured meat, 19: 46881
effects with storage on microbial flora in dover sole fillets, 19: 46882
of foods, review, 19: 46885
of fruits, effects on storage life and quality, 19: 46880
of glucose solutions, effects on stability, 19: 46889
of meats, wholesomeness after storage at room temperature, 19: 46886
of tissues, for use in homografting procedures, 19: 46879

RADIOTHERAPY
betatron design for, 19: 46126
carcinoma of thyroid induced by, 19: 46069
conventional x, of bladder cancer, 19: 46113
dose distribution for shell irradiation using ultrahard x rays, phantom studies, 19: 46127
dose in electron-beam, effects of collimator shape on depth-, 19: 46714 (CONF-640918-1)
dose measurements in, equipment and methods for, 19: 46854
dosimetry for x, using plastic scintillator, 19: 46105
dosimetry in neutron capture, 19: 46121
dosimetry in pendulum gamma, of urinary bladder and rectum, 19: 46093
dosimetry in, equipment designed for, 19: 46041
dosimetry of high-energy electrons for, 19: 46155
effects combined with 5-fluorouracil on palliative management of gastrointestinal cancer, 19: 46091
effects of combined chemotherapy and, on tumors, 19: 46095
effects of combined chemotherapy and, on neoplasia, 19: 46096
effects of malignant tumors, on serum denaturation, 19: 45924
effects on central nervous system in man, late nasal cavity, 19: 45983
effects on function of gastrointestinal tract, photofluorography of, 19: 46120
effects on isoenzymes and lactate dehydrogenase in human melanoma ascites, serum, and tumor homogenates, 19: 46124
effects on lung function, late, 19: 46131
effects on morphology of lymphocytes in patients with Hodgkin's disease, 19: 46103
effects on neoplasia, mechanism for synergistic chemotherapy in, 19: 46096
effects on rat sarcoma, effects of 3,5,3-L-triiodothyronine on, 19: 45943
effects on visceral necrosis development, pelvic exenteration for, 19: 46106
electron beam, techniques, 19: 46078
evaluation of, in treatment of inoperable thyroid carcinoma, 19: 46104
factors affecting external and internal, of systemic neoplasia, 19: 46095
gamma sources for, 19: 46078

injuries from intestinal, 19: 45922
leukemia induced by, 19: 45808(R) (NYO-901-36)
method for large-area, 19: 46042
methods for bladder cancer, 19: 46114
methods for, of bladder cancer, 19: 46115
computer calculations of radiation doses for, 19: 46134
of abdominal lesions, effects on gastrointestinal function, 19: 45930
of abdominal lesions, effects on gastrointestinal function, 19: 45932
of abdominal region, physiological effects, 19: 45928
of abdominal tumors, effects on absorption of glucose after oral or intravenous administration, 19: 45931
of brain tumor, using phosphorus-32–chromic phosphate, 19: 46087
of cancers of eyelid, 19: 46052
of cancers of head and neck region, synergistic effects with cytotoxic chemicals, 19: 46088
of cancers, synergistic effects of 5-fluorouracil, 19: 46050
of cancers, use of radioisotopes for gynecological, 19: 46100
of carcinoma of breast, pneumonitis induced by, 19: 46063
of carcinoma of uterus, design of cobalt-60 intercavitary applicator for, 19: 46039(T) (JPRS-31667)
of carcinoma of uterus, late radiation injury to urinary tract after, 19: 46061
of carcinomas of esophagus, 19: 46051
of carcinomas of the uterus, effects on rectum, 19: 46099
of carcinomas of uterus, 19: 46064
of carcinomas, recurrence of basal cell, 19: 46059
of eye lesions, using radium needles, 19: 46056
of eye lesions, using radon seeds, 19: 46056
of head and thorax lesions, effects on intestinal mucosa, 19: 45929
of Hodgkin's disease, 19: 46067
of lesions resulting in exposure of brain and central nervous system, pathological effects in man, 19: 45892
of pelvic tumors, radiation injuries of intestine induced by, 19: 46065
of thyroid diseases during pregnancy, 19: 46049
of thyrotoxicosis using iodine-131, 19: 46122
of tumor metastases, 19: 46101
of tumors, 19: 46077
of tumors of face and jaw, 19: 46074
of tumors of face, in children, 19: 46075
of tumors of head and neck, 19: 46129
of tumors of oral cavity, use of balloon for, 19: 46066
of tumors of pectoral region, using wire radioapplicators, 19: 46047
of tumors of the ear, 19: 46084
of tumors, design of apparatus for simultaneous oxygenation of gynecological, 19: 46097
pelvic, carcinoma of intestine induced by, 19: 46068
radiation dose for, computer calculations of, 19: 46055
radiation energy selection for, 19: 46094
radiation hazards from use of labeled pharmaceuticals for, 19: 46044
radiation protection in intracavitary, design of remote afterloader for, 19: 46111
skin lesions induced by, surgical repair, 19: 46085
tritiated Synkayvite for tumor, 19: 46125
use of beta, with surgery in treatment of glaucoma, 19: 46045
use of radioisotopes for, radiation protection of medical personnel, 19: 46080
use of telecobalt, in treatment of supraglottic carcinomas, 19: 46057
used in combination with surgery for breast cancer, 19: 46054
x radiation, techniques, 19: 46078

RADIUM
radiation hazards from handling and storage of sources of, 19: 46678
separation from actinium and thorium by ion exchange, 19: 47626

RADIUM BROMIDES
effects on coloration in minerals with and without pleochroic halos, 19: 46625(T) (ORNL-tr-757)

RADIUM ISOTOPES Ra-223
half life determination from actinium-227 power growth curve, 19: 46157(R) (MLM-1254)
half life of, determination by microcalorimetry and proportional alpha counting, 19: 47626

RADIUM ISOTOPES Ra-224
uptake and distribution in beagle bones, kidneys, liver, and spleen from thorium-228 decay, 19: 45798

RADIUM ISOTOPES Ra-226
content in body, determination from radon-222 in expired air, 19: 46677
radiation hazards of, released by accident, 19: 46696
toxic effects in sheep, 19: 45812(R) (ORO-631, pp 1-35)
uses as radiation source for ionization detectors in gas chromatography, 19: 46887

RADIUM POISONING
pathology of bone lesions induced by, 19: 45808(R) (NYO-901-36)

RADON
content in suspension in atmosphere, equilibrium with daughter products, 19: 46641 (CEA-R-2771)
determination of, use of polyvinylchloride and rubber bags for holding air samples, 19: 46203
pathological effects of implanted seeds of, 19: 45995
radiation doses to man from environmental, 19: 46688

RADON ISOTOPES Rn-220
alpha spectra, (E), 19: 47576(R) (IDO-17081, pp 49-76)
content in suspension in atmosphere, 19: 46641 (CEA-R-2771)

RADON ISOTOPES Rn-222
content in atmosphere in equilibrium with lead-214 and bismuth-214, 19: 46605
determination in expired air, estimation of radium-226 content in body from, 19: 46677

RAIN WATER
deuterium content in, North Carolina and Virginia, Nov. 1 and 2, 1963, 19: 47112
radioactivity of, sources of errors in measurement of, 19: 46608
strontium-90 content in, 1965, 19: 45748(R) (TID-22193)

RARE EARTH ALLOYS
Mn–rare earths, properties of, equipment for measuring, 19: 46988 (AD-614465)

RARE EARTH BROMIDES
thermal decomposition of hydrates of, mechanisms of, 19: 46271

RARE EARTH FERRATES(III)
crystal structure, 19: 46256

RARE EARTH OXIDES
atomic charge and permittivity of, (E/T), 19: 47901(T)
formation of dense spheres of, 19: 46428(R) (ORNL-3847)
oxygen-18 exchange between molecular oxygen and, 19: 46266
preparation and crystal structure of nonstoichiometric, 19: 46273
reactions with cupric carbonate, structure of AB_2O_4 type compounds formed in, 19: 46245(R) (TID-22207, Paper E)
reactions with metal carbonates, ionic field strengths as criteria for compound formation in, 19: 46246(R) (TID-22207, Paper F)
reactions with sodium carbonates, properties and structure of compounds formed in, 19: 46241(R) (TID-22207, Paper A)

RARE EARTHS
determination using dihydroxymaleic acid, gravimetric, 19: 46216
luminescence in zinc borate glass, 19: 46269
reactions with graphite to form intercalation compounds, 19: 46265
separation by electrophoresis at 90 volt/cm and 5 ma, 19: 46449
separation from complexed waste solutions by solvent extraction using di(2-ethylhexyl)phosphoric acid, effects of contaminants on, 19: 46432 (ORNL-P-1603)
separation from iron, manganese, and uranium by precipitation using dehydroxymaleic acid, 19: 46452
separation of americium from, development of Talspeak process for, 19: 46428(R) (ORNL-3847)
separation of samarium from, by ion exchange using citric acid and EDTA elutants, 19: 46438

RATE METERS
angular response of beta, angular, 19: 46639 (AECL-2281)
use in clinical dosimetry, 19: 46854

RATS
cesium-134 excretion by, effects of dithizone derivatives on, 19: 45765(T) (JPRS-27544, pp 1-12)
effects of beryllium on tissues of, cytomorphology and histology of, 19: 45803
effects of carbon tetrachloride on liver function in, use of iodine-131-labeled rose bengal for analysis of, 19: 45828
effects of parabiosis on radioinduced tumors in, 19: 45808(R) (NYO-901-36)
effects of phosphorus-32–chromium phosphate on *in vitro* tissues of, 19: 45939
effects of thorium chloride on mast cell reactions in tissues in, 19: 45766
effects of uranyl acetate on induction of metachromasia in tissues in, 19: 45766
effects of 3,5,3-L-triiodothyronine on growth of irradiated sarcoma in, 19: 45943
iodine-131 excretion by, effects of anion exchange material ingestion on, 19: 45760(R) (ORO-631, pp 83-121)
iodine-131 metabolism in whole and sliced thyroid lobes from, 19: 45786
iodine-131 uptake by thyroid in, effects of carbon monoxide exposure on, 19: 45770
lipid metabolism in, tracer study, 19: 45785
nitrophenylbenzamine distribution in, 19: 46011
oxygen metabolism in mitochondria of, effects of cystamine on,

19: 45777
performance capacity of, effects of adrenalectomy on, 19: 45823(T) (JPRS-31933, pp 1-5)
polysaccharide metabolism in blood platelets of, effects of vitamin A, 19: 45759(R) (ORO-631, pp 77-82)
radiation effects on enzyme content of intestine of, 19: 45927
radiation effects on lysozyme activity of intestine in, 19: 45933
radiation effects on leukocytes in, 19: 45934
radiation effects on liquid and sodium metabolism in intestines in, protective effects of AET and cysteamine against, 19: 46027
radiation effects on, protective effects of DNA against γ, 19: 46013
radiation effects on appearance of slow alpha-two globulin in sera of, 19: 45953
radiation effects on erythropoietin response in fasted, of injection time on gamma, 19: 45971
radiation effects on function of hematopoietic system, 19: 45984
radiation effects on, gamma and proton, 19: 45821(T) (JPRS-31547, pp 1-5)
radiation effects on performance capacity of, 19: 45823(T) (JPRS-31933, pp 1-5)
radiation effects on embryos of, 19: 45826
radiation effects on liver function in, use of iodine-131-labeled rose bengal for analysis of, 19: 45828
radiation effects on blood circulation in parabiotic, 19: 45838
radiation effects on body weight of, heritable, 19: 45880
radiation effects on behavior of, fetal exposure, 19: 45894
radiation effects on moisture content of tissues of, 19: 45896
radiation effects on growth of transplanted tumors in, 19: 45921
radiation effects in, genetic, 19: 45808(R) (NYO-901-36)
radiation effects on nervous system of, neutron, 19: 45812(R) (ORO-631, pp 1-35)
radiation effects on glucuronide excretion by, 19: 45816(R) (ORO-631, pp 142-4)
radiation effects on phospholipase activity of intestinal mucosa of, 19: 45820(R) (TID-22227)
radiation injuries in, protective effects of injected nucleic acids in, 19: 46020
radiation injuries, protective effects of morphines in, 19: 46021
radiation injuries, protective effects of injected ribonucleic acid, 19: 46022
radiation injuries, protective effects of injected bone marrow, spleen, or thymus tissues, 19: 46023
radiation injuries, protective effects of nembutal, 19: 46025
radiation injuries of skin, pathology of, 19: 45957
radiosensitivity of intestinal cells in, 19: 45926
radiosensitivity of, 19: 46022
radiosensitivity of, effects of nitrophenylbenzamine on, 19: 46011
radiosensitivity of rectal mucosa in, 19: 45918
sulfur-35 uptake by liver tissue in, histologic fixation and release of, 19: 45800
toxic effects of niobium pentachloride and potassium niobate on, 19: 45768
toxic effects of OMRE High Boilers and Santowax OM on blood, kidneys, and liver in, 19: 45769
tumor production in, by injected materials from irradiated donors, 19: 45815(R) (ORO-631, pp 67-76)

REACTION MECHANISMS
classification of radiation injury and recovery, 19: 45988
measurement of gas-solid, design of stagnation-flow furnaces for, 19: 46956 (NP-15514(Vol.1))
models for calculating rates of diffusion-controll, film, 19: 46956 (NP-15514(Vol.1))

REACTOR BREEDING BLANKETS
materials evaluation for tritium-regenerating, for fusion reactors, 19: 47721 (LA-3385)

REACTOR CONTROL RODS
calibration of ATR critical facility, 19: 48060(R) (IDO-17081, pp 1-47)
design for graphite moderated reactor, 19: 47933(P)
development for large closed-cycle pressurized-water reactors, 19: 48001(R) (WCAP-3743)
drive mechanism for, design of, 19: 47934(P)
drive mechanism for, with brake and braking mechanism, 19: 47941(P)
motion in PBF for power-burst shaping, computer analysis of, 19: 46716(R) (IDO-17081, pp 77-123)
reactivity of, in PWR, (E/T), 19: 48000(R) (WCAP-3738)
reactivity worths in graphite moderated reactors, methods for calculating, 19: 47999 (TRG-Report-227)

REACTOR CONTROL SYSTEMS
design of rod-drive and braking mechanism for, 19: 47941(P)
development for BWR and PWR, 19: 48038
development for large closed-cycle pressurized-water reactors, 19: 48001(R) (WCAP-3743)
electric signal for shutdown, generator for, 19: 47935(P)
performance reliability of, 19: 47929
period meters in, three-decade exponential current generator for testing, 19: 47928
stability of nonlinear, using position feedback, 19: 47962

REACTOR COOLANTS
analysis of polyphenyl, for chlorine, oxy-hydrogen burner for decomposition in, 19: 46163 (AECL-2263)
development for organic-cooled heavy water reactor program, 19: 47998(R) (SRO-118)
heat transfer in subcooled steam, for high system pressures and hot surface charges, (T), 19: 46544
monitoring for fuel rupture detection, system for, 19: 47937(P)
preparation of cesium–potassium–sodium alloy, 19: 47936(P)

REACTOR COOLING SYSTEMS
design using pressurized primary coolant, 19: 47940(P)
development for large closed-cycle pressurized-water reactors, 19: 48001(R) (WCAP-3743)
development of closed-cycle water, 19: 48000(R) (WCAP-3738)
pump failure in ETR, computer analysis of effects of, 19: 46716(R) (IDO-17081, pp 77-123)

REACTOR ENGINEERING
design methods for heavy water organic-cooled reactor program, 19: 47998(R) (SRO-118)

REACTOR FUEL ALLOYS
radiation effects on aluminum–uranium, 19: 48060(R) (IDO-17081, pp 1-47)

REACTOR FUEL ELEMENTS
analysis for plutonium-239 and uranium-235 in irradiated, nondestructive spectrometric, 19: 46178 (NP-15364)
cladding strain limits of, determination of, 19: 48000(R) (WCAP-3738)
cladding thickness measurement, autoradiographic technique for, 19: 46964 (NMI-4996, pp 149-63)
corrosion and fretting by water at 550°F, effects of spacer clips on, 19: 46913(R) (BMI-1733(Del.))
corrosion by water at high temperatures, effects of metallic spacer clips on, 19: 46912(R) (BMI-1727(Del.))
deflection and vibration of, transducer for measurement of, 19: 46716(R) (IDO-17081, pp 77-123)
design and development for 1000-Mwe organic cooled heavy water reactor, 19: 47998(R) (SRO-118)
design of assembly of, for gas-cooled power reactors, 19: 47973(P)
design of canned, with fission gas absorber, 19: 47981(P)
design of rod-cluster, with cellular spacing grid, 19: 47982(P)
design of, with can containing fuel and water moderator for heterogeneous reactors, 19: 48074(P)
design of, with fuel embedded in plastic moderator material for heterogeneous reactors, 19: 48074(P)
design with fuel-containing fibers, 19: 47985(P)
development for large closed-cycle pressurized-water reactors, 19: 48001 (WCAP-3743)
fabrication in Austria, 19: 48010
fabrication of, Belgian facilities for, 19: 48113
fabrication of, maintenance of constant temperature during, 19: 47984(P)
failure in reactors, detection system for, 19: 47937(P)
handling system for, design of remote, 19: 47938(P)
heat transfer by, effects of rough surface on, 19: 46543
inspection of hydraulically tested ATR, destructive, 19: 48060(R) (IDO-17081, pp 1-47)
meltdown in fast reactors, testing facilities for, 19: 47951 (APDA-173)
performance of ATR, analysis of, 19: 48060(R) (IDO-17081, pp 1-47)
processing of high- and low-enrichment, 19: 47921(R) (ANL-7090, pp 30-54)
processing of irradiated, economic and safety aspects of waste from, 19: 46435
processing of irradiated, construction of installations for, in Federal Republic of Germany, 19: 48112
radiation effects on, alpha-gamma facility for studying, 19: 47975 (BNL-9450)
radiation effects on MTR-type Fiberglas, sonic and radiographic inspection of, 19: 48060(R) (IDO-17081, pp 1-47)
radiography for nondestructive control of, before and after irradiation, 19: 46562
radiography of active, equipment and methods for, 19: 46558(T) (ORNL-tr-748)
reactivity of HWCTR driver, 19: 46917(R) (DP-975)
shipping cask design for irradiated Yankee, evaluation of, 19: 46650 (WCAP-1859(Rev.))
shipping of irradiated, safety aspects in, 19: 46663
shipping of irradiated, economic aspects of, 19: 46664

shipping of irradiated, regulations and licensing procedures for, 19: 46666
shipping of irradiated, heat removal from casks for, 19: 46667
transfer to storage pools equipment for, 19: 46517(P)
use of irradiated, as gamma sources in industrial radiation-chemical processes, 19: 46340(T) (AEC-tr-6570)
venting at ATR, effects on fission rates in, 19: 48060(R) (IDO-17081, pp 1-47)

REACTOR FUEL ELEMENTS (CERAMIC)
development, 19: 46913(R) (BMI-1733(Del.))
fabrication of oxide-type, with vitreous material as dispersing agent, 19: 47986(P)
fission fragment energy deposition and range in differential geometries of uranium dioxide, 19: 46324(R) (AGN-8132)
performance of plutonium–uranium carbides, for fast breeder reactors, 19: 47993 (NAA-SR-10751)
processing plutonium dioxide–uranium dioxide, problems in head-end step in, 19: 46427 (ORNL-3754)
radiation effects on Zircaloy-clad urania, at high exposures, 19: 46917(R (DP-975)

REACTOR FUEL ELEMENTS (DISPERSION)
radiation effects on, metallography of, 19: 47084 (NMI-4997, pp 124-33)

REACTOR FUEL ELEMENTS (THERMOELECTRIC)
design of Sirene 50 and 100, 19: 47978 (CEA-R-2782)
neutron flux and temperature distributions in Sirene 50 and 100, 19: 47978 (CEA-R-2782)

REACTOR FUEL PLATES
flow detection in, ultrasonic equipment for, 19: 46716(R) (IDO-17081, pp 77-123)
reactivity of ATR, effects of bowing on, 19: 48060(R) (IDO-17081, pp 1-47)
vibration of ATR, measuring device for, 19: 46716(R) (IDO-17081, pp 77-123)

REACTOR FUEL RODS
arrangement for graphite moderated reactor, design of, 19: 47933(P)
buckling calculations for uranium and water moderated, 19: 47954 (BNWL-127)
design of web support for assembly of, 19: 47943(P)
fabrication costs of Zircaloy-clad plutonium dioxide–uranium dioxide, for Saxton reactor, 19: 46962 (BNWL-131C)
fabrication of plutonium dioxide–uranium dioxide, cost analysis for, 19: 47976 (BNWL-131A)
fabrication of plutonium dioxide–uranium dioxide, variable costs for, 19: 47977 (BNWL-131B)
fabrication of uranium dioxide, by vibratory compaction, 19: 46970
heat transfer dryout in bundles of, in steam–water flow at 515 psia, 19: 46548
heat transfer from bundle of, to flowing potassium–sodium alloy, 19: 46553

REACTOR FUEL SPHERES
preparation for metallography, 19: 46925 (NMI-4997, pp 85-91)

REACTOR FUEL TUBES
deformation of Zircaloy-clad, effects of urania filler density on, 19: 46917(R) (DP-975)
radiation effects on compacted urania, effects on fabrication on, 19: 46917(R) (DP-975)

REACTOR FUELS
burnup code for, MAFIA II, (T), 19: 47910 (ANL-7050, pp 299-307)
burnup of, computer calculations of, (T), 19: 47912 (ANL-7050, pp 347-68)
cans for pellet, design of, 19: 47980(P)
coating of particulate, with pyrolytic graphite, process for, 19: 47983(P)
crystal structure and residual textures of metallic, x-ray diffraction studies of, 19: 47040
cycle costs for 1000-Mwe boiling-water, minimization of, 19: 47990 (BNWL-105)
cycles in reactors, diffusion calculations of, (T), 19: 47946 (ANL-7050, pp 231-49)
development for fast reactors, 19: 47989(R) (ANL-7090, pp 1-29)
development in Federal Republic of Germany, 19: 48112
economic aspects of, in development of nuclear energy, 19: 47979
fabrication of massive enriched uranium–molybdenum core components for Super Kukla, safety in, 19: 46967 (Y-KB-62)
processing in Belgium, development of facilities for, 19: 48113
radiation effects on solid uranium-based, bibliography on, 19: 47093 (VDDIT-16(5.2))
reprocessing at Hanford, administration of criticality control in, 19: 46433 (RL-SA-43)
reprocessing of irradiated, performance of 3 and 30% TBP processes for, 19: 46423 (DPSPU-64-30-28)
research programs on, at Harwell, 19: 48115

REACTOR MATERIALS
analysis of, automation of mass spectrometers for isotopic, 19: 46181 (WAPD-T-1769)
development for organic-cooled heavy water reactor program, 19: 47998(R) (SRO-118)
properties of stainless steel as, 19: 46913(R) (BMI-1733(Del.))
properties of, for cavity reactors, 19: 48046 (AD-613998)

REACTOR MATRICES
criticality calculations on uranium–water and uranium dioxide–water, method for, 19: 47959 (WCAP-3269-52)
design for graphite reactor, 19: 47933(P)
design with nonaxial elements, 19: 47924(P)
neutron absorption and spectra in cylindrical computer program for epithermal, 19: 46917(R) (DP-975)
neutron spectra in light-water, cell theory calculation of, 19: 47968

REACTOR MODERATORS
neutron energy spectra in two-component, (T), 19: 47964
neutron flux distributions in, temperature effects on, (T), 19: 47956 (IAE-723)
neutron scattering from, resonance effects of, (T), 19: 47953 (BNL-9393)

REACTOR REFLECTORS
fabrication of beryllium-containing carbon or graphite, process for, 19: 46977(P)
neutron flux distributions in, temperature effects on, (T), 19: 47956 (IAE-723)

REACTOR SAFETY
hazards analysis for large closed-cycle pressurized-water reactor, 19: 48001(R) (WCAP-3743)
planning for accidents, 19: 46703
public health aspects of, 19: 46698
public health aspects, 19: 46699
system for, at experimental power station KNK, 19: 48034

REACTOR SAFETY EXPERIMENTS
core meltdown in TREAT, 19: 47950(R) (ANL-7090, pp 69-78)
core meltdown in TREAT, metal–water reactions in, 19: 47960(T) (ORNL-tr-694)

REACTOR SHIELDING
calculations for, computer program for, 19: 47866 (KAPL-M-6460)

REACTOR SIMULATORS
use in study of ETR coolant pump failure and reactor vessel rupture effects, 19: 46716(R) (IDO-17081, pp 77-123)
use in study of PBF transient behavior, 19: 46716(R) (IDO-17081, pp 77-123)

REACTOR SLURRIES
separation of iodine- and xenon-135 from, method for, 19: 46426 (NP-15362)

REACTOR THERMAL COLUMNS
use of Petten HFR, 19: 48068

REACTOR TUBES
fabrication and testing, 19: 47998(R) (SRO-118)
welding of, gas tungsten-arc process for remote internal, 19: 46973

REACTORS
analysis using computerized calculations, (T), 19: 47911 (ANL-7050, pp 309-13)
analysis using computers, data-processing techniques for, 19: 47948 (ANL-7050, pp 517-39)
book: *Thermal Stress Techniques in the Nuclear Industry*, 19: 47922 (TID-22119)
charging machine for, 19: 47942(P)
computer uses with, conference, 19: 47907 (ANL-7050)
containment system for, testing of pressure suppression, 19: 47927
criticality of, GEM code for, 19: 47949 (ANL-7050, pp 657-79)
criticality studies of, review of Japanese, 19: 47965
design of, analysis of use of computer programs in, 19: 47909 (ANL-7050, pp 217-30)
design of, use of critical assemblies in, 19: 47961
development program, 19: 47920(R) (ANL-7090)
disassembly of, use of remote-control equipment for, 19: 46493 (CONF-641120, pp 4-5)
fuel burnup in, MAFIA II code for, (T), 19: 47910 (ANL-7050, pp 299-307)
information centers for problems of, 19: 47908 (ANL-7050, pp 125-39)
kinetics of, AIROS computer code for analyzing, (T), 19: 47914 (ANL-7050, pp 379-94)
kinetics of, two-dimensional code for analysis of, (T), 19: 47947 (ANL-7050, pp 395-412)
loading system design for, 19: 47938(P)
loading system design for, 19: 47939(P)
neutron density distributions in, kinetic equations for, (T), 19: 47963
neutron diffusion in, SWANTIME code for, (T), 19: 47915 (ANL-7050, pp 413-27)
neutron diffusion in, variational calculations of, (T), 19: 47945 (ANL-

7050, pp 159-77)
neutron flux measurements in, computer program for, 19: 47866 (KAPL-M-6460)
neutron spectra in, free-gas-theory calculations of thermal, (T), 19: 47538 (ANL-7050, pp 33-49)
neutron spectra in, in Doppler region, 19: 47539 (ANL-7050, pp 51-76)
neutron thermal utilization factor in, (T), 19: 47558
neutron transport analysis in, using PINETO code, 19: 47916 (ANL-7050, pp 429-41)
neutron transport in, (T), 19: 47921(R) (ANL-7090, pp 30-54)
neutron transport in, collision-probability calculations of, (T), 19: 47540 (ANL-7050, pp 93-112)
neutron transport in, EQUIPOISE method for calculating, 19: 47541 (ANL-7050, pp 179-89)
operation of, preventing thermal stress in fuel elements during, 19: 47984(P)
parameters of, Monte Carlo code for calculating, 19: 47919 (ANL-7050, pp 581-92)
reactivity noise analysis for, survey of, 19: 47966
reactivity transients in, optimal methods for processing, (T), 19: 47957 (IAE-724)
safety systems reliability, 19: 47929
shutdown of, device for generation of electric signal for, 19: 47935(P)
stability of externally controlled, (T), 19: 47971

REFRACTORY MATERIALS
deposition of oxides on tungsten, 19: 46911 (AFML-TR-64-392)
production, properties, and uses of hard compounds of, 19: 47020(T) (AEC-tr-6616)
vaporization at high temperatures, use in thermodynamic studies, 19: 46234 (COO-1140-123)

RELATIVITY THEORY
Dirac equation in, invariance properties of, 19: 47421
formalism for elastic collision waves, 19: 47414
kinematics of particle angular momentum in quantum, 19: 47418
Lorentz group in angular-momentum basis, irreducible representation of, 19: 47425
Poincaré group associated with complex energy-momentum in, representations of, 19: 47422
quantum effects in singular state of cosmology, 19: 47203
review, 19: 47209

RELAYS
use of hermetically sealed, d-c, electromagnetic, guide for, 19: 48100 (SC-TM-65-294)
use with superconducting solenoids for electric energy storage, 19: 46475 (AD-612113)

REMOTE-CONTROL EQUIPMENT
amplifiers for, use of fluid, 19: 46502 (CONF-641120, pp 75-7)
classification of techniques for operating in hostile environments, 19: 46480 (CONF-640508, pp 4-26)
conference on, 19: 46479 (CONF-640508)
conference on, 19: 46491 (CONF-641120)
description of filter photometer, 19: 46721 (ORNL-P-1531)
description of programmed manipulators, 19: 46488 (CONF-640508, pp 304-26)
description of, for handling Kiwi rocket reactors, 19: 48047 (CONF-640508, pp 334-9)
description of, for space operations, 19: 46487 (CONF-640508, pp 248-303)
design features of rate-controlled manipulators, 19: 46482 (CONF-640508, pp 75-99)
design for NERVA project, 19: 46495 (CONF-641120, pp 9-35)
design for remote handling vehicle, 19: 46496 (CONF-641120, pp 36-8)
design of detachable manipulator gripper for handling device, 19: 46520(P)
design of electric motor for use at high temperatures in radioactive atmosphere, 19: 46516(P)
design of handling devices, architect-engineer considerations in, 19: 46490 (CONF-640508, pp 340-64)
design of mobile vehicle for recovery of aerospace nuclear power devices, 19: 46489 (CONF-640508, pp 327-33)
design of movable gripper for, 19: 46518(P)
design of, for afterloading in intracavitary radiotherapy, 19: 46111
development and operation in SNAP program, 19: 46504 (CONF-641120, pp 86-97)
development for salt-cycle process for oxide fuels, 19: 46422 (BNWL-SA-205)
development for use in space, 19: 46500 (CONF-641120, pp 67-70)
development of generalized, programmed manipulators, 19: 46501 (CONF-641120, pp 73-4)
development of manipulators at Argonne, 19: 46481 (CONF-640508, pp 27-74)
development of pneumatically actuated master-slave, 19: 46499 (CONF-641120, pp 63-6)
development of, Telechirics Research Laboratory for, 19: 46497 (CONF-641120, pp 39-40)
human factors in design of manipulators, 19: 46484 (CONF-640508, pp 198-209)
manipulator control using, psychology of, 19: 46505 (CONF-641120, pp 98-103)
principles of control processes, 19: 46460 (CONF-640508, pp 224-32)
prosthetic terminal devices on Model 8 master slaves, 19: 46492 (CONF-641120, pp 1-3)
systems of, parameters of general, 19: 46498 (CONF-641120, pp 41-7)
test facility for, concept of central, 19: 46503 (CONF-641120, pp 78-85)
use in operation of test cell for rocket reactors, 19: 46494 (CONF-641120, pp 5-8)
use in reactor disassembly, experience in, 19: 46493 (CONF-641120, pp 4-5)
use in space, evaluation of proposed methods for, 19: 46486 (CONF-640508, pp 233-47)
use of myographic signals for control functions, study of feasibility of, 19: 46459 (CONF-640508, pp 100-57)
viewing system for master-slave, TV, 19: 47921 (ANL-7090, pp 30-54)

REMOTE-VIEWING EQUIPMENT
description of, for NERVA project, 19: 46495 (CONF-641120, pp 9-35)
development, 19: 46481 (CONF-640508, pp 27-74)
development and operation in SNAP program, 19: 46504 (CONF-641120, pp 86-97)
development of slave television for master-slave manipulators, 19: 47921(R) (ANL-7090, pp 30-54)

RESEARCH REACTORS
coolant purification system for JRS-2, helium, 19: 46513
criticality studies for WWR-S, 19: 48073
design of heterogeneous water-moderated, 19: 48074(P)
development and operation of NORA, industrial requirements for, 19: 48114
experimental facilities of Petten HFR, review of research programs for, 19: 48068
experimental facilities for, radiation monitors for inpile, 19: 48071
heat transfer in WWR-S, effects of rough heat-exchanger surface on, 19: 46543
neutron flux distribution in WWR-S, (T), 19: 48072
neutron graphite damage flux in DR-3, calibration of, (E), 19: 48070
startup of Toshiba Training Reactor, computer uses in, (E), 19: 48069
uses of Venezuelan, efficient, 19: 48065

RESINS
desorption of plutonium from ion exchange, by nitric acid, 19: 46173 (LA-3357)
radiolysis of ion exchange, use in purification systems, 19: 46327 (DP-977)
sample mounting in epoxy, molds for metallographic, 19: 46927 (NMI-4998, pp 1-5)
use of epoxy, in metallographic replication, 19: 46932 (NMI-4999, pp 60-8)

RESISTORS
performance of electrolytic, in plasma research, 19: 47751
performance of graphite, for use as heat sources, 19: 48099 (SC-TM-64-653)

RESPIRATION
effects of chlorpromazine on, in tumor cells and other biological systems, 19: 45862
radiation effects on, in tumor cells and other biological systems, 19: 45862

RESPIRATORY TRACTS
iodine-131 uptake in monkey, following inhalation of labeled sodium iodide, 19: 45776

RHENIUM
ionization of copper, silver, and titanium on, effects of condensed layers and residual gases on, 19: 47222(T) (ORNL-tr-679)
radiation effects on, 19: 47106
Re–W, reactions with cesium at 3400°F, metallographic specimen preparation of, 19: 46954 (NMI-5025(Pt.I), pp 39-58)

RHENIUM ALLOYS
phase studies of, crystallochemical, 19: 47036
Cr–Re, fabrication for internal friction studies, 19: 46913(R) (BMI-1733 (Del.))
Re–W, reactions with uranium carbide, nitride, and dioxide, metallographic specimen preparation of, 19: 46954 (NMI-5025(Pt.I), pp 39-58)

RHENIUM ISOTOPES Re-187
internal conversion coefficients for electric dipole transitions in, (E), 19: 47674

RHODIUM
neutron cross sections of, shell effects on thermal, (E), 19: 47618
RHODIUM ISOTOPES Rh-100
energy levels of, g factor and half life of 75-kev, (E), 19: 47662
RHODIUM ISOTOPES Rh-101
gamma spectra from metastable, 19: 47584(R) (ORNL-3832, pp 1-28)
RHODIUM ISOTOPES Rh-103
neutron reactions (n,α) at 14.6 Mev, angular and energy distributions from, (E/T), 19: 47637
RHODIUM ISOTOPES Rh-106
content in atmosphere and drinking water, Moncloa Station, Spain, 1964, 19: 46597
RIBONUCLEASE
radiation chemistry of, effects of oxygen on, 19: 46347
radiation effects on DNA interactions with RNAse, 19: 45849
radiation inactivation of, energy levels for proton, 19: 45993
radioinduced free radicals in, spectra of, 19: 46339 (UCRL-16358)
RIBONUCLEIC ACID
metabolism in aleurone cells of seeds, effects of gibberellic acid on, 19: 48102(R) (TID-22175)
metabolism in chromosomes, tracer study, 19: 45790
protective effects of, against radiation injuries in rats, 19: 46022
radiation chemistry of, 19: 46417
radiation effects on content of, in liver of rat embryos, 19: 45826
radiation effects on phosphorus-32 distribution in moieties of, tracer study of x, 19: 45851
radiation effects on synthesis of, in animal cells, 19: 45867
radioinduced inactivation of infective, from tobacco necrosis virus, ultraviolet, 19: 45962
RIBONUCLEIC ACID, DESOXY-
content in genes, 19: 45726 (BNL-9488)
effects on 2nd chromosomes in Drosophila, mutagenic, 19: 45876
labeling of proliferating cell, theoretical model for instantaneous, 19: 45923
metabolism in bone marrow cells in tissue culture, tracer study using carbon-14-formate, 19: 45815(R) (ORO-631, pp 67-76)
metabolism in chromosomes, tracer study, 19: 45790
metabolism in tumor cells, tracer study, 19: 45791
radiation chemistry of, 19: 46417
radiation effects on metabolism of, in tumor cells in mice, tracer study, 19: 45936
radiation effects on metabolism of, in mice and rabbits, 19: 45992
radiation effects on metabolism in *Escherichia coli*, uv, 19: 45948
radiation effects on content of, in liver of rat embryos, 19: 45826
radiation effects on replication in bacterial, uv, 19: 46002
radiation effects on aqueous solutions of, x, 19: 45729(R) (NYO-910-23, pp 1-111)
radioinduced degradation of, synergistic effects of methylhydrazine derivatives in, 19: 46356
radioinduced mutations in region of X chromosome in *D. melanogaster*, 19: 45879
radiosensitivity effects in rats of heterologous and homologous, x, 19: 46013
replication of, in ultraviolet-irradiated bacteria, 19: 45909
thymidine uptake by, effects of AET, glutathione, and serotonin on, 19: 46016
uptake of purines and pyrimidines by, tracer study, 19: 46158(R) (NYO-910-23, pp 112-82)
RICE
effects of chemical growth inhibitors on, 19: 45794
RICKETTSIA
radioisotope precipitation test for antibodies of *Coxiella burnetii*, 19: 46076
ROCKET REACTORS
analysis of cavity, 19: 48046 (AD-613998)
book: *Nuclear Space Propulsion*, 19: 48052
operation of, remote, 19: 46494 (CONF-641120, pp 5-8)
ROCKET REACTORS (KIWI)
control system for, analog simulation of, 19: 48049 (LA-3301)
handling equipment for, design of remote, 19: 46495 (CONF-641120, pp 9-35)
remote handling equipment for, 19: 48047 (CONF-640508, pp 334-9)
remote handling system for NERVA, wall-mounted, 19: 46490 (CONF-640508, pp 340-64)
testing at Nevada Test Site, safety aspects, 19: 46707
ROCKETS
materials development for, 19: 47068
ROCKS
age determination by rubidium–strontium method, 19: 46618
analysis for thorium and uranium, in basalt from Mohole Project, 19: 46628
gamma spectra measurement on, without destruction, 19: 46601
radioactivity induced in, by underground explosions, 19: 46473 (UCRL-14249)
rubidium and strontium abundances in, estimation of origin of material by, 19: 46607
sorptive properties of tuff for cesium and strontium, 19: 48081 (RT/PROT(65)19)
sorptive properties of rhyodacite tuff for radioisotopes in waste water, 19: 48085
strontium isotopic composition in Réunion Island, 19: 46584
strontium isotopic composition of, effects of magmatic differentiation on, 19: 46600
strontium-86/87 abundance ratio in basalts, 19: 46607
uranium aqueous dissolution in, 19: 46626
RODS
boiling burnout in 19-rod bundle with subcooled water and fog, 19: 46539(R) (TID-22249)
ROOTS
analysis for beta-emitting radioisotopes, 19: 46199
radioactivity in tree, from cesium-137, cobalt-60, iron-56, strontium-90, and zinc-65 uptake from soil, 19: 45773
ROSE BENGAL
use of iodine-131-labeled, in analysis of rat liver function, 19: 45828
ROTORS
centrifuge tubes for, engineering drawings for, 19: 46515
design and performance of, for combined continuous-flow and density-gradient centrifugation, 19: 46425 (K-L-2012)
development for zonal centrifuges, 19: 45730(R) (ORNL-3752)
RUBBER
uses of, as bags for, air samples for radon determination, 19: 46203
RUBIDIUM
abundance in rocks, determination of rock origin from, 19: 46607
content and distribution in beef heart, 19: 45753 (AE-191)
determination by isotopic dilution techniques, 19: 46204
determination in cesium by x-ray fluorescence spectroscopy, 19: 46186
neutron total cross section at 14.69 Mev, 19: 46774
RUBIDIUM CHLORIDES
molal volume and salt-induced structure transitions of aqueous, 19: 46237(R) (ORNL-3832, pp 76-99)
RUBIDIUM IONS
reactions with iodine bromide in crossed-beam experiments, 19: 46161(R) (ORNL-3832, pp 116-50)
RUBIDIUM ISOTOPES Rb-85
metabolism in lens of incubated rabbit eye, 19: 45778
RUBIDIUM ISOTOPES Rb-86
decay of, polarized beta-gamma angular correlations in, (E), 19: 47609
used in coronary blood circulation measurement in relation to ischemic myocardium in dogs, 19: 45767
RUBIDIUM ISOTOPES Rb-87
excited optical states of, zero-field level crossings in, 19: 47711
RUBIDIUM PROTACTINIUM FLUORIDES
preparation and properties, 19: 46160(R) (ORNL-3832, pp 29-32)
RUBIES
radiation effects on properties of laser, (E/T), 19: 46873 (N64-32322)
RUPTURE
time-to-rupture tests on metals and alloys, analysis of, 19: 47081(R) (EURAEC-1432)
RUTHENIUM
diffusion in thorium and uranium dioxides, 19: 47070
separation from iridium by radiochemical methods, 19: 46444
separation from other fission products by solvent extraction using benzene–oxine solutions, 19: 46440
RUTHENIUM-94
decay schemes, (E), 19: 47584(R) (ORNL-3832, pp 1-28)
RUTHENIUM ISOTOPES Ru-96
neutron capture cross sections and resonances of, measurement of thermal, (E), 19: 47584(R) (ORNL-3832, pp 1-28)
RUTHENIUM ISOTOPES Ru-99
neutron capture cross sections and resonances of, measurement of thermal, (E), 19: 47584(R) (ORNL-3832, pp 1-28)
RUTHENIUM ISOTOPES Ru-100
neutron capture cross sections and resonances of, measurement of thermal, (E), 19: 47584(R) (ORNL-3832, pp 1-28)
RUTHENIUM ISOTOPES Ru-101
energy levels, 19: 47584(R) (ORNL-3832, pp 1-28)
energy levels of, parity and spin of, (E), 19: 47686
neutron capture cross sections and resonances of, measurement of thermal, (E), 19: 47584(R) (ORNL-3832, pp 1-28)
RUTHENIUM ISOTOPES Ru-102
neutron activation cross sections and integrals of, thermal, (E), 19: 47584(R) (ORNL-3832, pp 1-28)

RUTHENIUM ISOTOPES Ru-103
content in atmosphere and drinking water, Monclos Station, Spain, 1964, 19: 46597
content in milk in Utah, 19: 46675
RUTHENIUM ISOTOPES Ru-106
content in atmosphere and drinking water, Monclos Station, Spain, 1964, 19: 46597
content in milk in Utah, 19: 46675
RUTIN
effects on radiation sickness in mice, 19: 46030

S

SACLAY PROTON SYNCHROTRON
beam injection in, high-brilliance ion source for, 19: 47172
SAFETY
criticality control in chemical processing department at Hanford, administration of, 19: 46433 (RL-SA-43)
in fabrication of massive enriched uranium–molybdenum core components for Super Kukla, 19: 46967 (Y-KB-62)
manual for radiation, 19: 46685
SAFETY HAZARDS
evaluation of, in transport of radioactive materials, 19: 46663
from tritium release by electron-capture detectors, 19: 46670
SAINT LAURENT-DES-EAUX REACTOR (EDF-4)
construction of, use of prefabricated sections in, 19: 48021
SALAMANDERS
lens regeneration in, effects of actinomycin, 19: 45738
radiation effects on response to tissue grafts, 19: 45897
SALICYLIC ACID
3,5-diiodo-, effects on iodine metabolism in lactating cows, 19: 45781
SALMONELLA
chemically induced pyrimidine mutations in, *S. typhimurium*, genetic analysis of, 19: 45878
radioinduced pyrimidine mutations in *S. typhimurium*, genetic analysis of, 19: 45878
radiosensitivity of, ultraviolet, 19: 45963
SALTS
effects on cellophane filter performance, 19: 46237(R) (ORNL-3832, pp 76-99)
SAMARIUM
cohesive energy and ionization of, relation between, (T), 19: 47062
content and distribution in beef heart, 19: 45753 (AE-191)
luminescence in zinc borate glass, 19: 46269
neutron cross sections of, shell effects on thermal, (E), 19: 47618
separation from other rare earths and ores by ion exchange using citric acid and EDTA eluants, 19: 46438
SAMARIUM ALLOYS
Al–Sm, crystal structure of Laves phases in, 19: 47052
Co–Sm, crystal structure of Laves phases in, 19: 47052
Mn–Sm, phase studies by differential thermal, thermo-magnetical, and x-ray analysis of, 19: 46989 (AD-614466)
Mn–Sm, preparation, phase studies, and properties of, 19: 46987 (AD-614462)
Mn–Sm, preparation by sinter process using mercury, 19: 46908 (AD-614464)
Pd–Sm, phase studies, 19: 47051
SAMARIUM BORIDES
preparation and purification, 19: 46941 (NP-15514(Vol.3))
SAMARIUM BROMIDES
thermal decomposition of hydrates of, mechanisms of, 19: 46271
SAMARIUM FERRATES(III)
crystal structure, 19: 46256
SAMARIUM IONS
spectra in silicate glass, fluorescence, 19: 47886(T) (N64-21857, pp 1-6)
SAMARIUM OXIDES
atomic charge and permittivity of, (E/T), 19: 47901(T)
oxygen-18 exchange between molecular oxygen and, 19: 46266
reactions with barium carbonates, ternary oxide formation, 19: 46242(R) (TID-22207, Paper B)
SAMARSKITES
age estimation of, by uranium–krypton and uranium–xenon methods, 19: 46598
krypton and xenon contents of, 19: 46598
SANDIA CORP., ALBUQUERQUE, N. MEX
atmospheric radioactivity, Jan. to June 1965, 19: 46648(R) (SC-RR-65-464)
SANDIA ENGINEERING REACTOR
design, 19: 48062 (SC-4522(RD))
experimental facilities for, description of, 19: 48062 (SC-4522(RD))
hazards analysis for, 19: 48062 (SC-4522(RD))
operation procedures for, 19: 48062 (SC-4522(RD))
site description, 19: 48062 (SC-4522(RD))
SANDIA PULSED REACTOR II
criticality calculations for, 19: 48063 (SC-RR-65-344)
SANDS
sorptive properties for strontium-90 in ground water, 19: 46602
SAP (SINTERED ALUMINUM PRODUCTS)
deformation of, electron microscopic study of dislocation structures in tensile, 19: 46996 (EUR-2479.e)
radiation damage induced by oxygen and inert gas bombardment, 19: 47080 (EUR-2478.e)
SARCOMAS
effects of 3,5,4-L-triiodothyronine on growth of rat, 19: 45943
radiation effects on proliferation of, mechanisms for, 19: 45923
radiation effects on immune reactions to transplanted ultraviolet-induced in mice, 19: 45827
radioinduced in mouse lymph system, radiosensitivity of, 19: 45977
radioinduced lympho-, chromosome complements in x, 19: 45911
radiotherapy effects combined with Actihaemyl in mouse, histology of, 19: 46123
research programs on, Great Britain, 1964, 19: 45744
SAVANNAH RIVER COMPONENTS TEST REACTOR
shutdown status of, 19: 46917(R) (DP-975)
SAVANNAH RIVER PLANT
fuels reprocessing, performance of 3 and 30% TBP processes for, 19: 46423 (DPSPU-64-30-28)
SAXTON POWER REACTOR
fuel assemblies for, design of, 19: 48000(R) (WCAP-3738)
fuel rods for, fabrication costs of plutonium, 19: 46962 (BNWL-131C)
radiation dose rates from components of, 19: 48000 (WCAP-3738)
SCANDIUM
content and distribution in beef heart, 19: 45753 (AE-191)
SCANDIUM ISOTOPES Sc-43
energy levels of, lifetime of low-lying hole, 19: 47115(R) (ANL-6983)
SCANDIUM ISOTOPES Sc-44
energy level density in, spin dependence of, (E), 19: 47596(R) (TID-22141, pp 94-7)
SCANDIUM ISOTOPES Sc-45
bremsstrahlung reactions (γ,n) at 48 Mev, (E), 19: 47596(R) (TID-22141, pp 94-7)
bremsstrahlung reactions at 45 Mev, (E), 19: 47596(R) (TID-22141, pp 94-7)
energy levels of, lifetime of low-lying hole, 19: 47115(R) (ANL-6983)
neutron reactions (n,2n) at 14 Mev, (E), 19: 47596(R) (TID-22141, pp 94-7)
nitrogen-14 reactions with, excitation functions for one-neutron-transfer, (E/T), 19: 47586 (ORNL-TM-1218)
nitrogen-14 reactions at 20 to 42 Mev, excitation functions for, (E), 19: 47667
SCANDIUM ISOTOPES Sc-47
energy levels of, lifetime of low-lying hole, 19: 47115(R) (ANL-6983)
SCANDIUM SYSTEMS
B–C–Sc, crystal structure of ScB_2C_2, 19: 46258
SCATTERING
amplitudes for large-angle, 19: 47430
amplitudes in complex K-plane, effective range parameter in S-matrix theory for, 19: 47390
amplitudes in perturbation theory, singularities of, 19: 47412
model for calculating energy distribution in thermal neutron, 19: 47557
potential, Regge poles in nonrelativistic, (T), 19: 47320
potentials for, in complex angular momentum plane, inversion in, 19: 47361
potential in coordinate space, Jost functions for singular, 19: 47360
Regge pole trajectories in Coulomb-well type potential, (T), 19: 47311 (NP-15454)
research facilities for, 19: 47327
theory for elastic, nonelastic processes in, 19: 47330
theory of spin wave–spin wave, in Heisenberg ferromagnet, (T), 19: 47874 (AD-613606)
SCHIFF BASES
analytical use for determination of thorium by spectrophotometric method, 19: 46206
SCINTILLATION
mechanisms of, in organic solids, 19: 46399
SCINTILLATION DETECTORS
book: *Scintillation Counters in High Energy Physics*, 19: 46856(T)
design and performance of large liquid, 19: 46775
design for electron and photon spectroscopy up to 10 Bev, (E), 19: 46805
development of liquid, for measurement of neutron inelastic scattering cross sections, 19: 46766(R) (TID-22141, pp 67-79)

performance for low-energy gamma radiation, effects of collimator design on, 19: 46119
performance for radiation dosimetry, 19: 46851
performance in molybdenum-99 liver scanning in man, 19: 46139
performance in Mössbauer effect spectrometer, 19: 46831
performance of gaseous, for measuring α and neutron fission rates, 19: 47567 (CEA-R-2775)
performance of immersible, for radiometric analysis of urine, 19: 46083
performance of organic, for fast neutrons, 19: 46774
performance of whole-body, 19: 46836
performance with on-line computers for analyzing nuclear events, (E), 19: 46806
performance with sonic spark chambers for proton detection at 20 Bev, (E), 19: 46800
use in diagnostic x-ray dosimetry, 19: 46858
uses in color scanner for radiation dosimetry, 19: 46819
SEA URCHINS
radiation effects on morphogenesis in, ultraviolet, 19: 45840
SEA WATER
analysis for uranium by ion exchange separation and fluorimetry, 19: 46223
desalination of, using reactor heat, in Soviet Union, 19: 48014
desalination using nuclear energy, 19: 48111
neutron activation of, gamma dose curves from, (T), 19: 46589 (UCRL-14332)
radioactivity from Columbia River effluent, 19: 46680
strontium-90 content in, 1965, 19: 45748(R) (TID-22193)
SEED
effects of temperature and packaging on stored irradiated, 19: 45817(R) (ORO-631, pp 145-71)
metabolism of RNA in aleurone cells of, effects of gibberellic acid on, 19: 48102(R) (TID-22175)
mutation analysis of, methods for, 19: 45737
radiation effects in corn, on seedling growth, 19: 45836
radiation effects on Pinus, physiological, 19: 45855
radiation effects on *Acer negundo*, genetic, 19: 45865
radiation effects on red clover, genetic, 19: 45882
radiation effects on barley, genetic, 19: 45819(R) (TID-22176)
radiosensitivity of, 19: 45884
radiosensitivity of, species differences in, 19: 45817(R) (ORO-631, pp 145-71)
SEEDLINGS
effects of chemical growth inhibitors on rice, 19: 45794
radiation effects on growth of corn, 19: 45836
radiation effects on respiration in corn, 19: 45836
radiation effects in seed on growth of Pinus, 19: 45855
SEIGHETTOELECTRIC MATERIALS
radiation effects on ascorbic acid content in legume, beta and gamma seed, 19: 45938
SEISMIC WAVES
amplitudes and energy content of, use for evaluating seismic source size, 19: 46615 (AD-612033)
attenuation in geologic discontinuity, acceleration, stresses, and velocity in, 19: 46580 (AD-613287)
SEISMOLOGY
use for detection of atmospheric and underground nuclear explosions, 19: 46620
SELENIUM
content and distribution in beef heart, 19: 45753 (AE-191)
determination in animal tissue by activation, 19: 46172 (KR-95)
toxic effects on chickens, 19: 45761(R) (ORO-631, pp 122-31)
SELENIUM ISOTOPES Se-75
metabolism in parathyroid gland of chickens, 19: 45761(R) (ORO-631, pp 122-31)
metabolism in sheep and swine, 19: 45759(R) (ORO-631, pp 77-82)
SELENIUM ISOTOPES Se-76
deuteron inelastic scattering at 15 Mev, energy levels from, (E), 19: 47642
SELENIUM ISOTOPES Se-77
deuteron inelastic scattering at 15 Mev, energy levels from, (E), 19: 47642
SELENIUM ISOTOPES Se-78
deuteron inelastic scattering at 15 Mev, energy levels from, (E), 19: 47642
SELENIUM ISOTOPES Se-80
deuteron inelastic scattering at 15 Mev, energy levels from, (E), 19: 47642
SELENIUM ISOTOPES Se-82
deuteron inelastic scattering at 15 Mev, energy levels from, (E), 19: 47642
SEMICONDUCTOR DETECTORS
amplifiers for, development of, 19: 46643(R) (LAL-1136)
current leakage and noise in lithium-drifted silicon, geometric control of, 19: 46754 (BNL-9535)
development, 19: 46820
development, 19: 46643(R) (LAL-1136)
performance for radiation dosimetry, 19: 46850
performance of lithium-drifted silicon, for alpha particles and protons, 19: 46770 (UCRL-16354)
uses in measuring thickness of thin polymer films, 19: 46888
SEMICONDUCTORS
charged-particle binding energy in, effect of magnetic field on, 19: 47143
electric properties of diffused silicon, effects of processes and treatments on, 19: 46727 (UCRL-16197)
magnetic properties of tantalum, (E), 19: 47524
radiation effects on, 19: 47076 (AD-612090)
radiation effects on, system performance predictions from, 19: 46874
radiation effects on, in space vehicles, 19: 46875
reactions of recoils from neutron (n,γ) reactions in, 19: 46398
use of niobium–tin, for high field magnets, 19: 47526
SEPARATION PROCESSES
design and control of dodecylbenzene sulfonate foam, 19: 46429 (ORNL-P-1522)
developments in salt-cycle, for plutonium dioxide–uranium dioxide fuels, 19: 46422 (BNWL-SA-205)
SERVOMECHANISMS
development for high energy accelerator requirements, 19: 47159 (BNL-9388)
development of restraint system for anti-G protection, 19: 46485 (CONF-640508, pp 210-23)
SHALES
separation of thorium from, method for chemical, 19: 46190
SHEEP
cerium-144 toxicology in, 19: 45759(R) (ORO-631, pp 77-82)
erythrocyte life span in, tracer study, 19: 45759(R) (ORO-631, pp 77-82)
protection against fallout, 19: 46700
radiation effects on molybdenum-99 metabolism in, 19: 45759(R) (ORO-631, pp 77-82)
radiation effects on tungsten-185 metabolism in, 19: 45759(R) (ORO-631, pp 77-82)
radiation effects on, delayed pathological, 19: 45812(R) (ORO-631, pp 1-35)
radiation effects on, pathological, 19: 45814(R) (ORO-631, pp 45-66)
radiation effects on, physiological, 19: 45815(R) (ORO-631, pp 67-76)
selenium-75 metabolism in, 19: 45759(R) (ORO-631, pp 77-82)
strontium-90 metabolism in, 19: 45759(R) (ORO-631, pp 77-82)
tellurium-127 metabolism in, 19: 45759(R) (ORO-631, pp 77-82)
SHELTERS
cost factors for, 19: 46671
design for protection against biological, chemical, and radiological warfare agents, 19: 46651(T) (JPRS-30979)
design of, under highways, 19: 46669
design study of tunnel-grid blast, for portion of Detroit, 19: 46568 (ORNL-TM-1223)
dynamic loading of strip footing of flexible arch structure in sand, simulation tests, 19: 46567 (NP-15396)
effectiveness of, for protection against radiation hazards from thermonuclear explosions, 19: 46671
management factors for efficient operation of, 19: 46637 (AD-612254)
population assignment and traffic to, plans for, 19: 46635 (AD-611764)
population direction to and management in, 19: 46636 (AD-611765)
properties of fallout, for domestic animals, 19: 46700
SHIELDED CONTAINERS
design for shipment of radioactive material, 19: 46665
design for shipping irradiated Yankee fuel elements, evaluation of, 19: 46650 (WCAP-1859(Rev.))
heat removal from, for shipping irradiated fuel elements, 19: 46667
SHIELDING
book: *Principles of Radiation Protection Engineering*, 19: 46683(T)
design of portable, for personnel during diagnostic radiography, 19: 46036
effectiveness of gonad, during diagnostic radiology, 19: 46145
information centers for problems of, 19: 47908 (ANL-7050, pp 125-39)
of fallout shelters, use of highways for, 19: 46669
radiation streaming through single-bend aluminum ducts in, 19: 47863 (AD-613480)
SHIELDING MATERIALS
density of cast iron, radiographical methods for determination of, 19: 47039
neutron transmission by hydrogenless, 19: 47870
particle multiplication and transport in, solution to Milne problem for, (T),

19: 47865 (ANL-7061)
properties of filled plastics as, 19: 46354
radiation effects on cadmium, 19: 47576(R) (IDO-17081, pp 49-76)
use of lead–uranium dioxide as, 19: 46916 (BNWL-IR-3)
SHIKIMIC ACID
labeling with carbon-14, 19: 46312
SHIPPING
cask design for radioactive material, 19: 46665
economic irradiated fuel, 19: 46664
heat removal in irradiated fuel element, 19: 46667
licensing procedure for radioactive material, 19: 46666
safety hazards in radioactive material, 19: 46663
SHIPPINGPORT PRESSURIZED WATER REACTOR
boiler corrosion in, causes and extent of, 19: 46913(R) (BMI-1733(Del.))
corrosion in 1B boiler of, causes and extent of, 19: 46912(R) (BMI-1727 (Del.))
SHIPS
nuclear-powered, research on collision-resisting sides of, 19: 46464(T) (NSJ-tr-30)
SHOCK WAVES
dissipation in collisionless plasma, mechanisms for, (T), 19: 47828
effects on underground structures, 19: 46569
fluid-dynamics calculations of pseudo-viscosity for, (T), 19: 47119 (UCRL-14244)
uses of axially imploding, for heating cylindrical plasma, (E), 19: 47845
SILANE, TETRAPHENYL-
effects on scintillator quenching in benzene, 19: 46362
radiolysis of, in benzene, 19: 46362
SILICATE ROCKS
analysis for sodium, flame photometric, 19: 46191
SILICIDES
production, properties, and uses of refractory, 19: 47020(T) (AEC-tr-6616)
production, properties, and uses of refractory, 19: 47020(T) (AEC-tr-6616)
SILICON
analysis for impurities by radioactivation and ion-exchange chromatography, 19: 46228
current leakage and noise in lithium-drifted detectors of, geometric control of, 19: 46754 (BNL-9535)
deposition on molybdenum and tantalum, process for, 19: 47073
determination in aluminum alloys by activation, 19: 46157(R) (MLM-1254)
determination in niobium–silicon systems, spectrophotometric, 19: 46171 (KAPL-M-6492)
effects on ductility of fissium–uranium–zirconium alloys, 19: 47004 (NMI-4997, pp 45-54)
effects on network structure in uranium, 19: 47060
effects on point defects in iron, 19: 47094(T) (ORNL-tr-668)
electron emission by single crystals of, after electron bombardment, 19: 47263
neutron reactions (n,n′γ) at 3.0 to 4.5 Mev, gamma angular distributions from, (E/T), 19: 47589(R) (TID-22012, 53-66)
performance of lithium-drifted, for alpha particles and protons, 19: 46770 (UCRL-16554)
radiation effects on semiconductors of, 19: 47076 (AD-612090)
radiation effects on, electron, (E), 19: 47092(R) (TID-22141)
vaporization coefficients of single crystal, 19: 46956 (NP-15514(Vol.1))
SILICON COMPOUNDS
analysis for impurities by radioactivation and ion-exchange chromatography, 19: 46228
SILICON FLUORIDES
methane–SiF_4, radiolysis yields in, 19: 46324(R) (AGN-8132)
SILICON HYDRIDES
electron drift velocities in deuterated and normal, at low energy, 19: 46393
SILICON ISOTOPES Si-25
decay of, delayed proton emission in, (E), 19: 47613
SILICON ISOTOPES Si-26
beta decay of, branching ratios, energies, and half lives, 19: 47603
SILICON ISOTOPES Si-28
bremsstrahlung reactions (γ,p) at 25.5 Mev, energy spectra from, (E), 19: 47699
electron scattering by, 19: 46643(R) (LAL-1136)
energy levels of, parity and spin of, (E/T), 19: 37589(R) (TID-22012, pp 53-66)
energy levels of, random phase approximation for excited, 19: 47652
neutron inelastic scattering at 3 to 4.5 Mev, angular distributions and energy levels from, (E/T), 19: 47638
SILICON ISOTOPES Si-29
magnetic moments and M1 transition probabilities in $2s_{1/2}$ $1d_{1/2}$ shell, (T), 19: 47641
SILICON ISOTOPES Si-30
energy levels from alpha reactions (α,p) with aluminum-27 at 1.0 to 3.3 Mev, resonance, (E), 19: 47672
SILICON ISOTOPES Si-31
magnetic moments and M1 transition probabilities in $2s_{1/2}$ $1d_{1/2}$ shell, (T), 19: 47641
SILICON JUNCTIONS
diffusion of lithium in p-type, electrophotographic determination of, 19: 46997 (JINR-P-2282)
electric properties of diffused, effects of processes and treatments on, 19: 46727 (UCRL-16197)
SILICON OXIDES
analysis for impurities by radioactivation and ion-exchange chromatography, 19: 46228
content in range plants, Miles City, Montana, 1955 to 1960, 19: 45747 (ORNL-TM-1279)
effects on sorptive properties of soils for strontium, 19: 46434
radiation effects of glass of, annealing of fast neutron, (E), 19: 47108
radioinduced coloration of fused, thermal annealing of reactor, 19: 47082 (NASA-CR-304)
radiolysis of surface silanols on, effects of dose, impurities, and surface area on, 19: 46332(R) (ORNL-3832, pp 50-65)
PbO–SiO_2, thermodynamic properties and oxygen pressure in, at 800, 900, 1000, and 1100°C, 19: 46297
Si–SiO_2, electric properties of interfaces in, 19: 46727 (UCRL-16197)
SILICON SYSTEMS
Al–Cr–Fe–Si–U, radioinduced swelling in, resistance to, 19: 47103
Al–Cr–Si, protective effects as coating on molybdenum and molybdenum–titanium alloy, 19: 47061
Al–Fe–Mo–Si–U, radioinduced swelling in, resistance to, 19: 47103
Al–Fe–Si–U, radioinduced swelling in, resistance to, 19: 47103
Al–Si, reactions with uranium, metallographic and microautoradiographic study of, 19: 46951 (NMI-4996, pp 19-26)
Al–Si–U, radiation effects on structure of dispersion-type fuel elements of, 19: 47084 (NMI-4997, pp 124-33)
Al–Si–U, radioinduced swelling in, resistance to, 19: 47103
Fe–Si–U, radioinduced swelling in, resistance to, 19: 47103
Nb–Si, analysis for silicon, spectrophotometric, 19: 46171 (KAPL-M-6492)
Si–SiO_2, electric properties of interfaces in, 19: 46727 (UCRL-16197)
Si–Tc, crystal structure of $TcSi_2$ in, 19: 47055
Si–U, radioinduced swelling in, resistance to, 19: 47103
SILICONE RUBBERS
use in metallographic replication, 19: 46932 (NMI-4999, pp 60-8)
use in replication of irradiated samples, 19: 47091 (NMI-4999, pp 69-77)
SILKWORMS
radiation effects on gonial cells in, mutagenic fission neutron and gamma, 19: 45883
radiosensitivity of eggs of *Bombyx mori*, 19: 45904
SILTS
age of, Black Sea and Indigirka River, USSR, 19: 46621
analysis for uranium by ion exchange separation and fluorimetry, 19: 46223
cesium-137 distribution and fixation in, of lacustrine origin, 19: 46681
separation of thorium from, method for chemical, 19: 46190
strontium-90 content in, 1965, 19: 45748(R) (TID-22193)
SILVER
bremsstrahlung reactions (γ,t) at 37 Mev, yields in, (E), 19: 47596(R) (TID-22141, pp 94-7)
content and distribution in beef heart, 19: 45753 (AE-191)
determination in bismuth by γ, γ-coincidence counting, activation, 19: 46193
electron reactions with crystals of, determination of interatomic potentials in, (T), 19: 47882 (RISO-103)
ionization on rhenium and tungsten, effects of condensed layers and residual gases on, 19: 47222(T) (ORNL-tr-679)
meson (K^-) reactions at 1.5 to 3 Bev/c, light charged particle emission in, (E), 19: 47651
neutron cross sections of, shell effects on thermal, (E), 19: 47618
photoelectron production by 145, 280 and 320 kev gamma rays, cross sections for, (T), 19: 47329
radiation effects on, lattice atom displacement probabilities in deuteron and neutron, (T), 19: 47104
surface tension of, measurement by pendant drop method, 19: 47065
vaporization coefficients of single crystal, 19: 46956 (NP-15514(Vol.1))
SILVER ALLOYS
Ag–Ga, superconductivity of, (E), 19: 47531
Ag–W, corrosion by carbon dioxide at 2250°C, 19: 46956 (NP-15514 (Vol.1))
SILVER SYSTEMS
Ag–TaC, production and properties of skeletal carbide composites of, 19: 46941 (NP-15514(Vol.3))

SINGLE CRYSTALS
neutron scattering in, measurement of one-phonon, 19: 46753 (AERE-R-4895)
SKIN
pathology of melanomas in hamster, 19: 45906
radiation effects on mouse and rabbit, recovery processes in, 19: 45987
radiation effects on mouse, effects of dose-fractionation on electron, 19: 45885
radiation effects on granular and transitional cell layers in human, 19: 45913
radiation hazards to, during radiodiagnosis of lung diseases, 19: 46110
radiation injuries of, protective effects of chloroquinine in guinea pigs, 19: 46019
radiation injuries of rat, pathology of, 19: 45957
radiation injuries of, thermal, 19: 45818 (TDCK-33500)
radioactive contamination of, action levels in medical treatment of, 19: 46008
radioinduced cancer of, 19: 45945
radiosensitivity of human, 19: 46085
radiosensitivity of, of nipple and flank of guinea pigs, 19: 45869
radiosensitivity of human, ultraviolet, 19: 45907
use of myographic signals for control functions, study of feasibility of, 19: 46459 (CONF-640508, pp 100-57)
SKIN LESIONS
radioinduced during therapy, surgical repair, 19: 46085
radioinduced in guinea pigs, pathology of, 19: 45869
radioinduced in guinea pigs, effects on amino acids and enzymes, 19: 45887
radioinduced in man, dose determinations for erythemal uv, 19: 45881
radiotherapy of carcinomas of eyelid, 19: 46052
SLUG ELEMENTS
fabrication of, design of cave for, 19: 46509 (UCRL-12497-T)
SMOKES
diffusion of, floating instantaneous-source type, (T), 19: 47111(T) (UCRL-Trans-1229(L))
SNOW
tritium measurement in, after enrichment by thermal diffusion, 19: 46613
SODIUM
boiling instabilities in liquid, nucleate, 19: 46551
boiling of, effects of surface conditions on nucleate, 19: 46549
determination in aluminum by flame photometry, 19: 46207
determination in biological materials, neutron activation, 19: 46165 (CEA-R-2837)
determination in beef heart, neutron activation, 19: 45753 (AE-191)
determination in carbonate, phosphate, silicate, and uranium rocks, flame photometric, 19: 46191
effects on distribution of strontium-90 in water-bearing strata by ground waters, 19: 46602
radiation effects on rat intestine metabolism of protective effects of AET and cysteamine against, 19: 46027
radiolysis of hexane in presence of, yields in, 19: 46324(R) (AGN-8132)
reactions with water in prototype boiler, analysis, 19: 46529 (APDA-175)
reactions with water, analysis of, 19: 46530(R) (BAW-1280-27)
reactions with water in boiler, engineering analysis, 19: 46531(R) (BAW-1280-28)
SODIUM ACETATES
reactions with sodium hydroxide to prepare methane, 19: 46319
SODIUM ALLOYS
Cs–K–Na, preparation and use for power production, 19: 47936(P)
K–Na, heat transfer during vertical upflow of, 19: 46528 (ANL-7038)
K–Na, heat transfer to, flowing through bundle of circular rods, 19: 46553
K–Na, performance in MHD cells, 19: 48053(R) (ANL-7090, pp 55-68)
SODIUM ARSENATES
effects on 4-aminobutyric acid content of brain in dogs, 19: 45979
SODIUM BROMIDES
radiation effects on absorption and luminescence spectra of nickel-, silver-, or tin-activated, 19: 47884(T) (IS-Trans-18)
$NdBr_3$–NaBr, complex formation in refractometric studies of, 19: 46254
SODIUM CARBONATES
reactions with rare earth oxides, properties and structure of compounds formed in, 19: 46241(R) (TID-22207, Paper A)
SODIUM CHLORIDES
molal volume and salt-induced structure transitions of aqueous, 19: 46237(R) (ORNL-3832, pp 76-99)
radiation effects on absorption and luminescence spectra of nickel-, silver-, or tin-activated, 19: 47884(T) (IS-Trans-18)
radioinduced luminescence in, de-excitation of light sums from x, 19: 46379(T)
$BaCl_2$–NaCl–H_2O, activity coefficient determination by ultracentrifugation, 19: 46237(R) (ORNL-3832, pp 76-99)
HCl–NaCl, thermodynamic properties of, 19: 46237(R) (ORNL-3832, pp 76-99)
KCl–NaCl–UF_4, uses in electrolytic processing of irradiated uranium fuels, 19: 46448
$NdCl_3$–NaCl, complex formation in, refractometric studies of, 19: 46254
SODIUM COMPOUNDS
organic, radiolysis yields in, 19: 46324(R) (AGN-8132)
SODIUM FLUORIDES
LiF–NaF, mixing enthalpies of molten, molar, 19: 46161(R) (ORNL-3832, pp 116-50)
SODIUM FLUOSILICATES
Na_2SiF_6, radiolysis yields in, 19: 46324(R) (AGN-8132)
SODIUM HYDROXIDES
corrosive effects on Croloy 2¼ steel, 19: 46478(R) (BAW-1280-25)
corrosive effects of aqueous solutions of, on Croloy 2¼ at high temperatures, 19: 46530(R) (BAW-1280-27)
reactions with sodium acetate to prepare methane, 19: 46319
SODIUM IODIDES
metabolism of iodine-131-labeled, by monkey respiratory tract and thyroid, 19: 45776
metabolism of iodine-125-labeled, in lactating cows, 19: 45781
SODIUM IONS
effects on sorptive properties of rhyodacite tuff for radioisotopes, 19: 48085
sorption of Amberlite, effects of anions on, 19: 46899(R) (ORNL-3832 pp 33-49)
SODIUM ISOTOPES Na-21
production in nitrogen-14 reactions on carbon-12, cross sections for, (E), 19: 47667
SODIUM ISOTOPES Na-22
content in atmosphere, 19: 46603
production in atmosphere, 19: 46603
production in nitrogen-14 reactions on oxygen-16, cross sections for, (E), 19: 47667
SODIUM ISOTOPES Na-23
deuteron reactions (d,α) at 4.9 to 5.5 Mev, neon-21 excited states from, (E), 19: 47633
neutron reactions (n,d) at 14 Mev, angular distributions from, (E/T), 19: 47644
SODIUM ISOTOPES Na-24
determination in aqueous solutions by detection of Cherenkov radiation, 19: 46215
production in nitrogen-14 reactions on carbon-12, cross sections for, (E), 19: 47667
use in medical diagnostics, 19: 46136
SODIUM LANTHANUM SULFATES
solubility in nitric acid and metathesis, 19: 46428(R) (ORNL-3847)
SODIUM OXIDES
thermal properties, 19: 47010(R) (ORNL-3832, pp 107-50)
SODIUM SELENITES
radioinduced paramagnetic centers in, ESR spectra of, 19: 46390
SODIUM SULFITES
effects of bactericidal activity of irradiated *p*-bromophenol, 19: 45834
effects on bactericidal activity in irradiated *p*-bromophenol, 19: 46007
SODIUM TETRAPHENYLBORATES
solvent properties for cesium, 19: 46441
SODIUM THIOSULFATES
complexes with cysteine, protective effects against radiation injuries in mice, 19: 46006
SODIUM YTTERBIUM OXIDES
preparation, properties, and structure of, 19: 46241(R) (TID-22207, Paper A)
SOILS
beryllium sorption in, effects of acidity on, 19: 45802
effects on strontium-90 content of alfalfa and grass in West Slovakia, USSR, 19: 45750
neutron activation of, gamma dose curves from, (T), 19: 46589 (UCRL-14332)
radiation effects on amino acids in, gamma, 19: 45941
radioactivity induced in, by Operation Bren, 19: 47569 (CEX-62-50)
radioactivity induced in, by underground explosions, 19: 46473 (UCRL-14249)
resistance to horizontal loading, lateral-plate bearing tests on mechanics of, 19: 46465 (AD-613991)
seismic wave attenuation in geologic discontinuity, acceleration, stresses, and velocity in, 19: 46580 (AD-613287)
sorptive properties for strontium, effects of aluminum oxides, calcium carbonates, and silicon oxides on, 19: 46434
strontium-90 content of, in German Democratic Republic, 1963, 19: 46610
strontium-90 uptake by plants from, effects of phosphate content on, 19: 45774
SOLAR BATTERIES

radiation effects on, in space vehicles, 19: 46875
SOLAR FLARES
data for fourth quarter, 1964, 19: 47468
effects on geomagnetic variations, 19: 47480
flash phase of, physical phenomenon in, (E), 19: 47188 (ADD-613636)
formation and properties of, model for, (T), 19: 47188 (AD-613636)
properties and localization of chromospheric, 19: 47191(T) (NASA-TT-F-250)
properties of weak chromospheric, 19: 47190(T) (NASA-TT-F-248)
radiation from, contribution of characteristic x rays to, (T), 19: 47197
radiation hazards to astronauts, 19: 45890
SOLAR RADIATION
effects of M-region, on geomagnetic pulsations, 19: 47454
effects of particle streams on atmospheric disturbances, 19: 47495
effects on ionosphere, 19: 47496
effects on threshold for magnetospheric transition-region plasma instability, (T), 19: 47460
electron production by x-, during solar flares, 19: 47480
intensity of extreme ultraviolet, (T), 19: 47210
neutron detection in, 19: 47279
radio emission in corona, determination of stream velocities by, 19: 47189(T) (N64-31082)
shock boundary in solar wind, 19: 47211
SOLENOIDS
connection of superconducting, with relay switch for electric energy storage, 19: 46475 (AD-612113)
design of, determination from specified magnetic fields, (T), 19: 47121 (UCRL-16080)
SOLIDS
book: *Mechanisms of Solid Friction*, 19: 47075
electron and lattice vibration correlations in, in terms of collective motions, 19: 47875 (AD-614136)
electron orbitals in, spin hamiltonian for nonorthogonal, (T), 19: 47254
neutron scattering by, 19: 47889
nucleation of precipitates from supersaturated solutions of, review on, 19: 47025(T) (ORNL-tr-637)
photon interactions in, properties of, (T), 19: 47332
SOLUTIONS
ion transport in aqueous, isotope effects in, 19: 46898 (HMI-B-44)
SOLVENT EXTRACTION PROCESSES
development of Talspeak, for separating actinides from lanthanides, 19: 46428(R) (ORNL-3847)
radiation effects on aromatic diluents and extractants for, gamma, 19: 46430 (ORNL-P-1601)
SOLVENTS
radiation effects on aromatic diluents for radiochemical processing, gamma, 19: 46430 (ORNL-P-1601)
SOUND
detection of h-f, superconducting diodes for, 19: 46739
SOVIET UNION
age estimation of Aldanian phlogopites in, 19: 46596
age estimation of upper anthropogenic layer in, 19: 46621
nuclear power stations in, economic aspects of, 19: 48014
strontium-90 content in alfalfa and grass in West Slovakia, 19: 45750
SOYBEANS
effects of protein from, on growth of chickens, 19: 45761(R) (ORO-631, pp 122-31)
SPACE
geodesics of space-time surface, gravitational effects on, (T), 19: 47192
hydrogen density in intergalactic, limits on ionized, (T), 19: 47196
remote handling in, evaluation of proposed methods for, 19: 46486 (CONF-640508, pp 233-47)
trajectory calculations for, computer program for generalized, 19: 48096 (SC-DR-65-271)
SPACE FLIGHT
book: *Geophysics and Space Data Bulletin No. 3*, 19: 47447 (AD-612083)
environmental problems of man in, conference on, 19: 45746
personnel protection against G forces, servo-restraint system for, 19: 46485 (CONF-640508, pp 210-23)
radiation hazards to man in, biological effects of, 19: 46001
radiation hazards, 19: 45890
radiobiology problems in, 19: 46000
SPACE MEDICINE
environmental problems of man in space, conference on, 19: 45746
SPACE POWER UNIT REACTOR
pump bearing development for, 19: 46458 (CNLM-6342)
SPACE VEHICLES
ablation and heating of cylindrical and spherical re-entry bodies, methods for predicting, 19: 46537 (SC-RR-65-187)
design of altimetric system for, 19: 46749(P)
handling of, equipment for remote, 19: 46500 (CONF-641120, pp 67-70)
maintenance of orbiting, remotely operated manipulator system for, 19: 46487 (CONF-640508, pp 248-303)
power plants for, analysis of nuclear Brayton-cycle, 19: 48048 (GE-65SD4251)
propulsion of, cavity nuclear reactors for, 19: 48046 (AD-613998)
radiation effects on components of, review of, 19: 46875
re-entry of, ablation testing of materials for, (E), 19: 47117(R) (SC-DC-65-1698)
re-entry of, plasma jet for simulating, 19: 46477 (ARL-65-121)
SPAIN
fallout monitoring at Moncloa Station, Madrid, 1964, 19: 46597
nuclear power development in, 19: 48011
SPARK CHAMBERS
data analysis system for, design of CHLOE, (E), 19: 46793
design of large, surrounded by magnetic fields, (E), 19: 46796
design of wide-gap track, (E), 19: 46779
design using magnetostrictive effect, (E), 19: 46783
development, 19: 46820
development, 19: 46643(R) (LAL-1136)
development and uses of wire, (E), 19: 46804
development for capture-to-fission ratio measurements, 19: 46766(R) (TID-22141, pp 67-79)
discharge planes for, design and operation of, (E), 19: 46784
operation and performance of wide-gap track, (E), 19: 46781
particle track analysis in photographs from, flying-spot systems for, (E), 19: 46787
particle track analysis in, system for, 19: 46789
particle track analysis in photographs from, (E), 19: 46790
particle track analysis in, review of systems for, (E), 19: 46791
particle track analysis in, use of AROMA code for, (E), 19: 46794
particle track analysis in photographs from, use of graph theory for, (T), 19: 46795
particle track analysis in photographs from, on-line computer system for, (E), 19: 46811
particle track analysis in, using raster-scan methods on photographs, (E), 19: 46786
performance for determining electron drift velocity variations in gases, 19: 47116 (BNL-9443)
performance for detection of electron showers at 0.5 to 8 Bev, 19: 47354
performance for discriminating electrons and pions, (E), 19: 46782
performance for electron spectroscopy from meson (μ) decay, 19: 46785
performance of sonic, for proton detection at 20 Bev, (E), 19: 46800
performance of wide-gap, for track analysis, (E), 19: 46780
performance with on-line computers for analyzing nuclear events, (E), 19: 46806
spark channel formation in air gap, 19: 47146
use in high-energy physics, 19: 46834
vidicon design for, (E), 19: 46788
SPECTROSCOPY
uses of atomic absorption, analytical, 19: 46166 (DP-980)
SPERM
radiosensitivity of Drosophila, 19: 45949
radiosensitivity of screw-worm fly, 19: 45950
SPERMATOGENESIS
radiosensitivity of, in domestic animals, 19: 45813(R) (ORO-631, pp 36-44)
SPHERES
electromagnetic wave scattering by, (T), 19: 47299(R) (AD-614046)
SPHINGOMYELIN
radioinduced in beef, chemical analysis of, 19: 46878 (NP-15455)
SPLEEN
nitrophenylbenzamine content in rat, 19: 46011
protective effects of injected tissues of, against radiation injuries in rats, 19: 46023
radiation effects on weight in mice of, genetic factors, 19: 45956
radiation effects on antibody production by transferred cells of, in mice, 19: 45986
radioinduced chromosomal aberrations in mouse, x, 19: 45911
thorium-228 decay in beagle, metabolism of bismuth-212, lead-212, and radium-224 from, 19: 45798
SPORES
radiosensitivity of *Bacillus subtilis*, effects of germination on uv, 19: 45848
radiosensitivity of pathological, 19: 46890
SQUIRRELS
radiation effects on glucose absorption by intestines in active and hibernating, 19: 45841
STAINLESS STEEL
burst and collapse pressures of tubes of AISI 304 L, 19: 46986 (KR-96)
corrosion of austenitic, by water, stress-, 19: 46959

mechanical properties at 75 to 1200°F, effects of heat treatment on, 19: 46913(R) (BMI-1733(Del.))
mechanical properties at cryogenic temperatures, 19: 47013 (PB-171809(Rev.)(Suppl.2))
radiation effects on 347, neutron, 19: 46912(R) (BMI-1727(Del.))
radiation effects on 347, fast neutron, 19: 46913(R) (BMI-1733(Del.))
radiation effects on stress corrosion of, in magnesium chloride, 19: 47079 (AERE-R-5014)
reactions with water at high temperatures during core meltdown, (E/T), 19: 47960(T) (ORNL-tr-694)
stress corrosion cracking of austenitic, by wetted thermal insulation, 19: 46949 (CONF-650905-2)
STANDARDS
for personnel working with ionizing radiations in Yugoslavia, 19: 46654(T) (JPRS-31993)
STARS
electron pressure ratio to gas pressure in atmospheres of, 19: 47187 (AD-612182)
element abundances in, 19: 47187 (AD-612182)
evolution of massive, helium burning in, (T), 19: 47202
evolution of quasars, gravitation theory for, 19: 47209
evolution of, through development phases and end state, (T), 19: 47201
gas clouds in dense clusters of, quasar model for, (T), 19: 47199
helium content of, 19: 47193
model of quasi-stellar radio source CTA 102, (T), 19: 47198
stability of supermassive, effects of magnetoturbulent energy on, 19: 47200
STATISTICS
criteria for differential cross section measurements with minimum uncertainty, (T), 19: 47601
STEAM
condensation in pool water, performance of pressure suppression containment system in, 19: 47927
heat transfer in subcooled, for high system pressures and hot surface charges, (T), 19: 46544
heat transfer in subcooled steam, for high system pressures and hot surface charges, (T), 19: 46544
superheaters for, review of developments in, 19: 48012
steam–water, analysis of boiling convection channel flows of, (E), 19: 46538(R) (TID-22148)
steam–water, two-phase flow at 1200 psig, orifice and venturi measurements of, 19: 46526 (AECL-2273)
STEARIC ACID, METHYL ESTER
radiolysis of clathrates containing tritium-labeled, self-, 19: 46359
radiolysis of tritium-labeled, self-, 19: 46360
STEEL
analysis of irradiated, for activation products, by ion-exchange separation and gamma spectrometry, 19: 46195
ductility of 1045, pressure effects on, 19: 46983 (AD-612159)
grain size in cast, titanium effects on control of, 19: 46980 (AD-611800)
mechanical properties at cryogenic temperatures, 19: 47013 (PB-171809(Rev.)(Suppl.2))
mechanical properties of electron-beam melted, 19: 46972
notch-brittleness during time-to-rupture tests, theory, 19: 47081 (EURAEC-1432)
properties for aerospace uses, 19: 47068
sorptive properties for tritium, effects of texture on, 19: 47018 (USNRDL-TR-890)
STELLARATORS (C)
plasma ion heating in, using ion-cyclotron-resonance, (E), 19: 47832
plasma particle losses and power balances in, (E), 19: 47854
STEROIDS
effects on strontium metabolism in man, 19: 45805
STIBINE, TRIPHENYL-
effects on scintillation quenching in benzene, 19: 46362
radiolysis of, in benzene, 19: 46362
STILBENE
radiolysis of *cis-* and *trans-*, spectra of yields in, 19: 46345
4,4'-STILBENEDIOL, α,α'-DIETHYL-
distribution in man of carbon-14-labeled, 19: 45797
uptake by cattle liver of carbon-14-labeled, 19: 45797
STRAIN GAGES
attachment of, using flame-spraying process, 19: 46723 (RFP-641)
cements for high-temperature, of tests, 19: 46715 (EUR-2473.f)
use in fuel assembly testing, in PWR, 19: 48000(R) (WCAP-3738)
STRESS ANALYSIS
book: *Thermal Stress Techniques in the Nuclear Industry*, 19: 47922 (TID-22119)
of perforated plates subjected to equal biaxial stress, 19: 46557 (NP-15459)
STRONTIUM
abundance in rocks, determination of rock origin from, 19: 46607
determination of, in presence of calcium, 19: 46197
effects on distribution of strontium-90 in water-bearing strata by ground waters, 19: 46602
metabolism, 19: 45729(R) (NYO-910-23, pp 1-111)
metabolism in man, effects of steroid hormones on, 19: 45805
preparation by reduction of barium salt using catalytic nascent hydrogen, 19: 46253(T) (ORNL-tr-803)
reactions with clays, exchange, 19: 46239(R) (ORO-631, pp 132-41)
separation from other fission products by solvent extraction using benzene–oxine solutions, 19: 46440
separation from yttrium by ion exchange, 19: 46196
separation from yttrium by chromatographic methods, 19: 46436
sorption from aqueous solutions by soils, 19: 46434
sorption from solutions by tuffs, 19: 48081 (RT/PROT(65)19)
STRONTIUM CARBONATES
reactions with rare earth oxides, ternary oxide formation in, 19: 46242(R) (TID-22207, Paper B)
reactions with rare earth oxides, ionic field strengths as criteria for compound formation in, 19: 46246(R) (TID-22207, Paper F)
STRONTIUM CHLORIDES
reduction by calcium carbide, 19: 46251(T) (ORNL-tr-673)
STRONTIUM FLUORIDES
reduction by calcium carbide, 19: 46251(T) (ORNL-tr-673)
STRONTIUM HAFNATES
growth of small single crystals of, 19: 47008(R) (NP-15429)
STRONTIUM IONS
displacement in soils by beryllium, 19: 45802
effects on radioinduced color center formation in potassium chloride crystals, 19: 46371
thermodynamic properties of aqueous, 19: 46282
STRONTIUM ISOTOPES
abundance in rocks from Réunion Island, 19: 46584
abundance ratios in rocks and rock derivates, effects of magmatic differentiation on, 19: 46600
STRONTIUM ISOTOPES Sr-85
diagnostic use for bone lesions, 19: 46133
diagnostic use for bone metastases, 19: 45729(R) (NYO-910-23, pp 1-111)
diagnostic use for bone lesions, 19: 45757(R) (NYO-910-23, pp 183-92)
uptake by tumorous bones, measurement of, 19: 45757(R) (NYO-910-23, pp 183-92)
STRONTIUM ISOTOPES Sr-86
abundance ratio to strontium-87 in oceanic and continental basalts, 19: 46607
energy level scheme for yttrium-86 decay-produced, (E/T), 19: 47584(R) (ORNL-3832, pp 1-28)
STRONTIUM ISOTOPES Sr-87
abundance ratio to strontium-86 in oceanic and continental basalts, 19: 46607
STRONTIUM ISOTOPES Sr-88
neutron capture by, radiation widths of gamma emission from, 19: 47115(R) (ANL-6983)
STRONTIUM ISOTOPES Sr-89
contamination of food by, after radiation accident, 19: 46694
effects on determination of strontium-90 in waste solutions, 19: 46196
leaching from vegetables, 19: 45758 (NYO-2598-24)
metabolism by vegetables, 19: 45758 (NYO-2598-24)
metabolism in chickens, 19: 45761(R) (ORO-631, pp 122-31)
radiation hazards of, released by accident, 19: 46696
STRONTIUM ISOTOPES Sr-90
body burden of, maximum permissible, 19: 46634 (AD-423463)
contamination of food by, after radiation accident, 19: 46694
content in biosphere, 1965, 19: 45748(R) (TID-22193)
content in bone samples in Australia, 19: 46595
content in bones of adults, effects of diet strontium-90 content on, 19: 45793
content in dust and precipitation, 19: 46632(R) (A/AC.82/G/L.987)
content in fallout over Australia, 1961 to 1963, 19: 46595
content in fish from lake waters in Finland, 1965, 19: 46587(R) (NYO-3446-3)
content in foods in Australia, 19: 46595
content in grass and milk, 1959 to 1962, 19: 45749
content in grass and alfalfa in West Slovakia, USSR, effect of plant calcium on, 19: 45750
content in milk, 19: 46632(R) (A/AC.82/G/L.987)
content in milk, effects of various foodstuffs on, 19: 45772
content in plants and soils of German Democratic Republic, 1963, 19: 46610
content in wheat in U. S., 1958 to 1964, 19: 46662
determination in food after incineration, 19: 46200

determination in urine using Cherenkov effect, 19: 46198
determination of, in presence of strontium-89, 19: 46196
distribution in water-bearing strata, effects of salt content of ground water on, 19: 46602
effectiveness in treatment of aviation tympanitis, 19: 46038(T) (JPRS-31602, pp 191-7)
effect on ovarian follicles in mice, 19: 45831
metabolism by man, 19: 45793
metabolism by plankton, 19: 45748(R) (TID-22193)
metabolism in animals and man, 19: 46634 (AD-423463)
metabolism in sheep, 19: 45759(R) (ORO-631, pp 77-82)
monitoring in Australia, 1963, 19: 46594
performance as heat source in Ripple I thermionic generator, 19: 46895
plant metabolism of, 19: 45804
plant uptake from soils of, effects of phosphate on, 19: 45774
radiation hazards of, released by accident, 19: 46696
toxic effects in sheep, 19: 45812(R) (ORO-631, pp 1-35)
uptake by tree branches, leaves, needles, roots, and stems from soil, 19: 45773
use in nuclear batteries, 19: 46897(P)

STRONTIUM OXIDES
reduction by aluminum carbide, catalytic effects of calcium fluoride on, 19: 46252(T) (ORNL-tr-683)

STRONTIUM ZIRCONATES
properties of, research program on thermal-mechanical, 19: 47008(R) (NP-15429)
$CaZrO_3$–$SrZrO_3$, stress-strain characteristics of, 19: 47008(R) (NP-15429)

STRUCTURAL COLUMNS
design for tank support, 19: 46524(P)

STRUCTURES
response spectra of single-degree-of-freedom dynamic, to large air-blast loads from nuclear explosions, 19: 46566 (AD-425747)

STYRENE
radioinduced grafting on polypropylene, 19: 46355

STYRENE POLYMERS
properties of, containing leuko compounds of triphenylmethane dyes as chemical dosimeters, 19: 46369

SUCCINIC ACID
effects on rate of reaction between uranium(IV) and thallium(III), 19: 46277

SULFATE COMPLEXES
with beryllium, ion exchange studies of, 19: 46230 (AAEC/E-136)

SULFATES
determination in scrubber solutions used in Dribble vent gas treatment plant, 19: 46471 (UCRL-14123)
effects on determination of strontium-90 in waste solutions, 19: 46196

SULFIDES
production, properties, and uses of refractory, 19: 47020(T) (AEC-tr-6616)

SULFITES
determination in scrubber solutions used in Dribble vent gas treatment plant, 19: 46471 (UCRL-14123)

SULFONATES
exchange of sodium ions with tetramethyl ammonium, in polystyrene, 19: 46237(R) (ORNL-3832, pp 76-99)

SULFUR
bremsstrahlung reactions (γ,t) at 37 Mev, yields in, (E), 19: 47596(R) (TID-22141, pp 94-7)
determination in arsenic, activation, 19: 46211

SULFUR COMPOUNDS
analytical uses of organic phosphorus-containing, 19: 46217
effects on muscular activity of guinea pig intestine, 19: 46005(T) (JPRS-31933, pp 6-12)
synthesis of, for use as radioprotective agents, 19: 46303(R) (NP-15409)

SULFUR DIOXIDES
radiation effects on gaseous, alpha, 19: 46332(R) (ORNL-3832, pp 50-65)

SULFUR IONS
production of, source for, 19: 47157 (AWRE-NR-1/65)

SULFUR ISOTOPES S-30
beta decay of, branching ratios, energies, and half lives, 19: 47603

SULFUR ISOTOPE S-31
magnetic moments and M1 transition probabilities in $2s_{1/2}$ $1d_{1/2}$ shell, (T), 19: 47641

SULFUR ISOTOPES S-32
bremsstrahlung reactions (γ,p) at 25.5 Mev, energy spectra from, (E), 19: 47699
deuteron reactions (d,p) with, coherent knockout amplitudes in, (T), 19: 47669
electron scattering by, energy levels and shell-model parameters from, (T), 19: 47677
neutron reactions (n,p) in soil, activity induced by, 19: 47569 (CEX-62-50)
yields from radiolysis of thiourea by neutrons, 19: 46365

SULFUR ISOTOPES S-33
magnetic moments and M1 transition probabilities in $2s_{1/2}$ $1d_{1/2}$ shell, (T), 19: 47641
production in iron meteorites by cosmic radiation, 19: 47195

SULFUR ISOTOPES S-35
determination in plant material by beta counting, 19: 46199
incorporation in barium sulfates and lead sulfates, effects of, solubility, 19: 46274
magnetic moments and M1 transition probabilities in $2s_{1/2}$ $1d_{1/2}$ shell, (T), 19: 47641
uptake by rat liver, histologic fixation and release of, 19: 45800

SULFUR ISOTOPES S-36
production in iron meteorites by cosmic radiation, 19: 47195

SULFUR OXIDES
effects on hydrogen yields in propane radiolysis, 19: 46396

SULFUR SYSTEMS
HF–S, radiolysis yields in, 19: 46324(R) (AGN-8132)

SULFURIC ACID
radiolysis of aqueous, products from gamma, 19: 46332(R) (ORNL-3832, pp, 50-65)

SUN
activity data for May, 1965, 19: 47468
activity of, effects on magnetic and ionospheric storms, 19: 47497
activity of, sudden ionospheric disturbances from, 19: 47494
corona of, velocity of corpuscular streams in, 19: 47189(T) (N64-31082)
coronal spectra during eclipse, (E), 19: 47451 (SC-M-65-419)
eclipse of, airborne observation of, 19: 47451 (SC-M-65-419)
gravitational radiation from thermal collisions in, quantum electrodynamics for, 19: 47204
helium content of, 19: 47193
magnetic field of large sunspots, model for solar flare production by, (T), 19: 47188 (AD-613636)
magnetic fields of, review on measurement of, 19: 47208
particle emissions from, relations of terrestrial disturbances to, 19: 47495
sunspot cycle effects on auroral activity, 19: 47472

SUPERCONDUCTIVITY
destruction in tin films by current, resistance changes on, (E), 19: 47530
Ginzburg-Landau equations for Abrikosov mixed state in, series solution of, 19: 47519
theory of, asymptotic exactness of BCS, (T), 19: 47509
theory of, nonlocal extension of Ginzburg-Landau equations in, 19: 47527

SUPERCONDUCTORS
critical current density and specific heat of niobium–tin intermetallic compounds, (E), 19: 47508
current decay propagation in niobium–zirconium alloy, persistent, (E), 19: 47507
currents in Josephson junctions of, persistent, (E), 19: 47521
design of, magnets of, for plasma research, 19: 47533
electron tunneling in junctions of, anomalous behavior of Josephson, 19: 47515
energy of rotating and stationary, free, (T), 19: 47504 (JPL-TR-32-650(Pt.2))
excitations in strong-coupling alloy, Fermi-liquid theory for collective, 19: 47518
Ginzburg-Landau equations for Abrikosov mixed state in, series solution of, 19: 47519
magnetic fields in dirty, anisotropic, temperature dependence of nucleation (T), 19: 47525
magnetic flux degradation phenomenon in coils, (E), 19: 47512
performance of tunnel diodes of, as high-frequency sound detector, 19: 46739
properties and longrange order of tantalum–tin alloy, processing effects on, (E), 19: 47513
properties for aerospace uses, 19: 47068
properties of type II, review of, 19: 47510
state density in, effects of magnetic impurities on, 19: 47535
superconducting transition temperature of thin films of, (E), 19: 47503 (BNL-9478)
thermodynamic properties of strong-coupling, 19: 47536
transition temperature of aluminum thin films, (E), 19: 47503 (BNL-9478)

SUPERFLUIDITY
theory of helium, microscopic, 19: 47506

SUPERHEATERS
design of sodium-heated, 19: 46478(R) (BAW-1280-25)

SUPERHEATERS (NUCLEAR)
development and use, review of, 19: 48012

SUPERSONIC FLOW

velocity distribution for compressible fluid, equation for stagnation-point, 19: 46956 (NP-15514(Vol.1))
SURFACE TENSION
measurement by pendant drop method, 19: 47065
measurement of liquid metal, review on, 19: 47064
SURFACE WATERS
radioactivity in Finland, 1965, 19: 46587(R) (NYO-3446-3)
radioactivity of, sources of errors in measurement of, 19: 46608
SURFACES
particle adhesion in gaseous and liquid environments to, decontamination methods for, 19: 46645 (ORNL-TM-1228)
SURGERY
for tumors of face and jaw, 19: 46074
of carcinoma of uterus, effects on urinary tract, 19: 46061
of carcinomas of esophagus, 19: 46051
of head in irradiated patients, 19: 46129
of neck in irradiated patients, 19: 46129
of radioinduced skin lesions after therapy, 19: 46085
of tumors of face and jaw, 19: 46075
pelvic exenteration for extensive visceral necrosis after radiotherapy of gynecologic cancer, 19: 46106
use of beta radiotherapy with, in treatment of glaucoma, 19: 46045
use of radiotherapy prior to, in treatment of breast cancer, 19: 46054
SWEDEN
radiation protection planning, 19: 46705
SWIMMING POOL REACTORS
design modifications to Avogadro RS1, at SORIN, 19: 48066
design of 100-kw Consort Mark-2, 19: 48067
SWINE
cerium-144 toxicology in, 19: 45759(R) (ORO-631, pp 77-82)
protection against fallout, 19: 46700
radiation effects on properdin content of blood serum of, ultraviolet, 19: 45919
radiation effects on molybdenum-99 metabolism in, 19: 45759(R) (ORO-631, pp 77-82)
radiation effects on tungsten-185 metabolism in, 19: 45759(R) (ORO-631, pp 77-82)
radiation effects on, delayed pathological, 19: 45812(R) (ORO-631, pp 1-35)
radiation effects on reproduction of, 19: 45813(R) (ORO-631, pp 36-44)
radiation effects on, pathological, 19: 45814(R) (ORO-631, pp 45-66)
radiation effects on, physiological, 19: 45815(R) (ORO-631, pp 67-76)
selenium-75 metabolism in, 19: 45759(R) (ORO-631, pp 77-82)
tellurium-127 metabolism in, 19: 45759(R) (ORO-631, pp 77-82)
zinc-65 metabolism in blood cells of, effects of dietary calcium, zinc, and fats on, 19: 45759(R) (ORO-631, pp 77-82)
SWITCHES
design of relay, connected with solenoid for electric energy storage, 19: 46475 (AD-612113)
development of high-power cyclotron resonance, 19: 46708(R) (AD-611560)
SWITZERLAND
fallout monitoring, 1963, 19: 46612
nuclear power development in, 19: 48009
SYNCHROCYCLOTRONS
design and operation at Harwell, 19: 48115
SYNCHROTRONS
development of pulsed, review of, 19: 47163 (BNL-9504)
vacuum system of Tokyo electron, design and performance of, 19: 47175
SYSTEMS FOR NUCLEAR AUXILIARY POWER
disassembly of, remote operations in, 19: 46504 (CONF-641120, pp 86-97)
performance of cobalt-60 fueled, 19: 46893 (DP-974)
SYSTEMS FOR NUCLEAR AUXILIARY POWER (SNAP-2)
temperature control coatings for 10A, development of, 19: 48050 (NAA-SR-9903)
SYSTEMS FOR NUCLEAR AUXILIARY POWER (SNAP-10)
temperature control coatings for 10A, development of, 19: 48050 (NAA-SR-9903)
SYSTEMS FOR NUCLEAR AUXILIARY POWER (SNAP-15)
design and performance of 15A, 19: 46894 (GA-5296)
SYSTEMS FOR NUCLEAR AUXILIARY POWER (SNAP-50)
pump bearing development for, 19: 46458 (CNLM-6342)
SZILARD-CHALMERS REACTIONS
use in production of high-specific-activity radioisotopes, problems in, 19: 46332(R) (ORNL-3832, pp 50-65)

T

TANKS
support device for, design of constant-height, 19: 46524(P)
TANTALUM
corrosion by mercury at 150°C, 19: 46428(R) (ORNL-3847)
crystal deformations in, analysis of double kink, (T), 19: 47011 (ORNL-3862)
determination in thorium oxide, spectrochemical, 19: 46226
determination in tantalum carbide–titanium carbide, method for, 19: 46941 (NP-15514(Vol.3))
determination in tantalum carbide–zirconium carbide, method for, 19: 46941 (NP-15514(Vol.3))
magnetic properties of superconducting, (E), 19: 47524
photoelectron production by 145, 280 and 320 kev gamma rays, cross sections for, (T), 19: 47329
properties for aerospace uses, 19: 47068
proton reactions at 660 Mev, holmium-162 production in, (E), 19: 47579 (JINR-P-2275)
reactions with plutonium and gallium–iron–plutonium fuels at 900 to 1150°C, 19: 46950 (LA-DC-7315)
separation from hydrochloric acid solutions by solvent extraction using tetrabutylpyrophosphate and tetrabutylhypophosphate, tracer studies of, 19: 46451
siliconizing by vapor deposition, mechanism of, 19: 47073
sorptive properties for cesium films, 19: 47900(T)
surface tension of, measurement by pendant drop method, 19: 47065
Ta–W, reactions with cesium at 3400°F, metallographic specimen preparation of, 19: 46954 (NMI-5025(Pt.I), pp 39-58)
TANTALUM ALLOYS
properties for aerospace uses, 19: 47068
Hf–Ta–W, reactions with cesium at 3400°C, metallographic specimen preparation of T-111, 19: 46954 (NMI-5025(Pt.I), pp 39-58)
Hf–Ta–W, reactions with uranium carbide, nitride, and dioxide, metallographic specimen preparation of T-111, 19: 46954 (NMI-5025 (Pt.I), pp 39-58)
Hf–Ta–W, weldability studies of T-111, 19: 46966(R) (WANL-PR(P)-007)
Mo–Nb–Ta–W, creep slip of solution-hardened, at 980 to 1370°C, 19: 47049
Nb–Ta–W, weldability studies of SCb-291, 19: 46966(R) (WANL-PR(P)-007)
Nb–Ta–W–Zr, weldability studies of FS-85, 19: 46966(R) (WANL-PR(P)-007)
Ta–Sn, superconducting properties and long range order of intermetallic compounds of, processing effects on, (E), 19: 47513
Ta–W, analysis by polarography, teflon electrode for, 19: 46157(R) (MLM-1254)
Ta–W, reactions with uranium carbide, nitride, and dioxide, metallographic specimen preparation of, 19: 46954 (NMI-5025(Pt.I), pp 39-58)
Ta–W, weldability studies of, 19: 46966(R) (WANL-PR(P)-007)
TANTALUM BORIDES
analysis for boron, method for, 19: 46941 (NP-15514(Vol.3))
corrosion by hydrogen chloride at 2250°C, 19: 46956 (NP-15514 (Vol.1))
electron emission from surfaces of, thermionic, 19: 46571 (HRL-5249-S)
lattice parameters and thermal expansion at 25 to 1700°C, 19: 47009 (NP-15514(Vol.2))
oxidation by carbon dioxide at 2250°C, 19: 46956 (NP-15514(Vol.1))
preparation and purification, 19: 46941 (NP-15514(Vol.3))
TANTALUM CARBIDES
corrosion by hydrogen chloride at 2250°C, 19: 46956 (NP-15514 (Vol.1))
oxidation by carbon dioxide at 2250°C, 19: 46956 (NP-15514(Vol.1))
preparation and purification, 19: 46941 (NP-15514(Vol.3))
sorptive properties for cesium films, 19: 47900(T)
thermal expansion at 25 to 2030°C, 19: 47009 (NP-15514(Vol.2))
Ag–TaC, production and properties of skeletal carbide composites of, 19: 46941 (NP-15514(Vol.3))
TaC–TiC, analysis for tantalum and titanium, method for, 19: 46941 (NP-15514(Vol.3))
TaC–ZrC, analysis for tantalum and zirconium, method for, 19: 46941 (NP-15514(Vol.3))
TANTALUM ISOTOPES Ta-181
gamma angular correlations from ammonium hafnium fluorides, (E), 19: 47607
TANTALUM OXIDES
reactions with copper oxides, structure of ABO_3 type compound formed in, 19: 46244(R) (TID-22207, Paper D)
thermodynamic properties of, at 500 to 1300°C, 19: 46297
TANTALUM SYSTEMS
C–Hf–Ta–W, weldability studies of T-222, 19: 46966(R) (WANL-PR(P)-007)
TARTARIC ACID
effects on rate of reaction between uranium(IV) and thallium(III),

19: 46277
TASTE
radiosensitivity in man, 19: 45825(T) (NSJ-tr-32)
TBP PROCESS
performance of 3 and 30%, at Savannah River Plant, 19: 46423 (DPSPU-64-30-28)
TECHNETIUM
electric conductivity and characteristic temperature of, (T), 19: 47063
separation from fission products by solvent extraction using cyclohexane, 19: 46160(R) (ORNL-3832, pp 29-32)
superconducting properties of, 19: 47536
thermal conductivity and diffusivity of electron-beam-melted, at room temperature to 575°C, 19: 46914(R) (BNWL-141)
toxic effects on chickens, 19: 45761(R) (ORO-631, pp 122-31)
TECHNETIUM ALLOYS
phase studies of, crystallochemical, 19: 47036
Tc–W, examination of arc-melted buttons of, 19: 46914(R) (BNWL-141)
TECHNETIUM CHLORIDES
benzene–iodopropane–$TeCl_4$, technetium-132 decay in, chemical reactions of iodine-132 from, 19: 46412
iodobenzene–iodopropane–$TeCl_4$, technetium-132 decay in, chemical reactions of iodine-132 from, 19: 46412
TECHNETIUM ISOTOPES Tc-94
energy level scheme, (E/T), 19: 47584(R) (ORNL-3832, pp 1-28)
TECHNETIUM ISOTOPES Tc-95
decay of, gamma spectra from metastable, 19: 47584(R) (ORNL-3832, pp 1-28)
TECHNETIUM ISOTOPES Tc-99
activation determination of, methods for, 19: 46160(R) (ORNL-3832, pp 29-32)
gamma spectra from irradiated, 19: 46160(R) (ORNL-3832, pp 29-32)
physical properties of, 19: 46139
preparation and properties for clinical uses, 19: 46140
use in liver scanning, 19: 46139
use in radiodiagnosis, 19: 46140
uses as radiation source for ionization detectors in gas chromatography, 19: 46887
TECHNETIUM ISOTOPES Tc-101
beta decay of, gamma coincidence measurements for, (E), 19: 47686
decay schemes, 19: 47584(R) (ORNL-3832, pp 1-28)
TECHNETIUM SYSTEMS
Si–Tc, crystal structure of $TcSi_2$ in, 19: 47055
TECHNICAL REPORTS
Air Force research objectives, 19: 48087 (AD-613537)
TEETH
lesions of, induced by radiomimetic substances in rats, 19: 45845
radiography of, radiation dose to gonads during, 19: 46107
radioinduced lesions of rat, 19: 45845
radiosensitivity of, in children, 19: 46074
TELEVISION EQUIPMENT
design for phase-contrast uv microbeam microscope, 19: 45891
vidicon design for use in spark chamber, (E), 19: 46788
TELLURIUM
separation from fission products, procedure for, 19: 46405
separation from fission products, method for, 19: 46169 (IDO-14664)
TELLURIUM ISOTOPES Te-124
energy levels from gamma-gamma angular correlations in, (E), 19: 47636
TELLURIUM ISOTOPES Te-127
metabolism in sheep and swine, 19: 45759(R) (ORO-631, pp 77-82)
TELLURIUM ISOTOPES Te-131
beta decay of isomeric, gamma spectra from, (E), 19: 47663
TELLURIUM ISOTOPES Te-132
beta decay of, in technetium chlorides in aliphatic-aromatic mixtures, chemical reaction of iodine-132 from, 19: 46412
TELLURIUM ISOTOPES Te-133
properties of short-lived, 19: 46405
TEMPERATURE
climatic, effects on iodine-131 metabolism by man, 19: 45779
effects on zinc-65 metabolism in dragonflies, 19: 45789
measurement of, engineering drawings of psychrometer probe for, 19: 46745
measurements in atmosphere, similarity with wind, 19: 47110 (RISO-100)
scale for, neodymium ethylsulfate, 19: 47883 (UCRL-16279)
TEMPERATURE CONTROL
methods for chromatographic columns, 19: 46157(R) (MLM-1254)
TENDONS
radiation effects on immunogenicity of grafts of, 19: 45964
radiation effects on immunogenicity of grafts of, 19: 45965
TENSILE PROPERTIES
measurement to 3000°F, design of equipment for, 19: 46712 (BNWL-SA-169)

TERBIUM
cohesive energy and ionization of, relation between, (T), 19: 47062
electric and thermal conductivity at low temperature, (E), 19: 47528
luminescence in zinc borate glass, 19: 46269
resonance absorption integrals, (E), 19: 47576(R) (IDO-17081, pp 49-76)
TERBIUM ALLOYS
Al–Tb, crystal structure of Laves phases in, 19: 47052
Co–Tb, crystal structure of Laves phases in, 19: 47052
Pd–Tb, phase studies, 19: 47051
TERBIUM BROMIDES
thermal decomposition of hydrates of, mechanisms of, 19: 46271
TERBIUM FERRATES(III)
crystal structure, 19: 46256
TERBIUM IONS
spectra in silicate glass, fluorescence, 19: 47886(T) (N64-21857, pp 1-6)
TERBIUM ISOTOPES Tb-159
neutron reactions (n,α) at 14.6 Mev, angular and energy distributions from, (E/T), 19: 47637
TERBIUM ISOTOPES Tb-162
decay of, gamma spectra in, 19: 47683
TERBIUM OXIDES
oxygen-18 exchange between molecular oxygen and, 19: 46266
TERPHENYL
effects of *para*-, on melting points of biphenyl–terphenyl mixtures, 19: 46300 (AECL-2261)
labeling with tritium, 19: 46313
mass spectra of, after electron bombardment, 19: 46328 (EUR-2227.e)
radioinduced luminescence in benzene, quenching effects of organometallics on, 19: 46362
toxic effects on blood, kidneys, and liver in rats, 19: 45769
use as a radical scavenger reagent to minimize radiation effects on TBP, 19: 46406(P)
biphenyl–terphenyl, melting points of, effects of *p*-terphenyl on, 19: 46300 (AECL-2261)
TETRACYCLINE
metabolism in blood, effects of calcium homostasis and malignant diseases on, 19: 45757(R) (NYO-910-23, pp 183-92)
TEXTILES
shielding properties of, thermal, 19: 45818 (TDCK-33500)
THALLIUM
determination by complexometric methods using EDTA, 19: 46219
superconducting transition temperature of, effect of mercury impurities on pressure effect on, (E), 19: 47529
THALLIUM ALLOYS
Hg–Tl, superconducting transition temperature of, pressure effect on, (E), 19: 47529
THALLIUM IONS
reactions with uranium ions, catalytic effects of dicarboxyl acids on, 19: 46277
THALLIUM ISOTOPES Tl-204
production, 19: 47576(R) (IDO-17081, pp 49-76)
THALLIUM ISOTOPES Tl-209
alpha spectra, (E), 19: 47576(R) (IDO-17081, pp 49-76)
THERMAL CONDUCTIVITY
measurement at high temperatures, apparatus for, 19: 46995 (EUR-2424.f)
measurement at high temperatures, theory and apparatus for, 19: 47009 (NP-15514(Vol.2))
THERMAL DIFFUSION
cascade for, hot-wire temperature vs current in, 19: 46157(R) (MLM-1254)
concentration of krypton-84 and -86 in krypton isotopic mixtures by, 19: 46157(R) (MLM-1254)
isotope separation by, 19: 46413
mass 17 methane separation by, 19: 46157(R) (MLM-1254)
THERMAL INSULATION
corrosive effects of wetted, on heated stressed alloys, 19: 46949 (CONF-650905-2)
development for SNAP systems, 19: 48050 (NAA-SR-9903)
THERMAL RADIATION
effects on serum denaturation, diagnostic value of, 19: 45924
effects on skin, pathological, 19: 45818 (TDCK-33500)
from nuclear explosions, hazards of, 19: 46671
THERMAL RADIATION SHIELDING
bibliography on, 19: 45818 (TDCK-33500)
THERMAL STRESSES
book: *Thermal Stress Techniques in the Nuclear Industry*, 19: 47922 (TID-22119)
THERMIONIC CELLS
development for direct conversion of heat to electricity, 19: 47286
development of in-pile, using liquid-metal electron collector, 19: 47281

(ANL-7039)
development of, without cesium reservoir, 19: 47282(R) (NYO-3429-4)
performance of cobalt-60 fueled, 19: 46893 (DP-974)
vacuum breakdown in presence of thermionic cathodes, 19: 46577
THERMOCOUPLES
development for in-pile measurements, 19: 46722 (PWAC-462)
properties of sintered molybdenum and tungsten alloys as, 19: 47019(T) (AD-619334)
THERMODYNAMIC PROPERTIES
of helium at 2,000 to 100,000°K, 19: 46235 (N64-26802)
THERMODYNAMICS
entropy production principle for non-equilibrium, (T), 19: 47551 (UJV-1354/65)
free energy of crystals in, nearest-neighbor approximation of quartic contributions to, (T), 19: 47878 (LA-3379)
vaporization at high temperatures, 19: 46234 (COO-1140-123)
THERMOELECTRIC CELLS
design of isotope-powered, for Ripple I, 19: 46895
development for direct conversion of heat to electricity, 19: 47286
plasma kinetics in, (T), 19: 47287(T)
transistor invertors for Ripple I and II, 19: 46896
radioinduced in lithium fluoride crystals, 19: 46762(R) (NYO-3474-1)
THERMOLUMINESCENT DETECTORS
performance for radiation dosimetry, 19: 46850
performance of calcium and lithium fluoride, 19: 46859
properties of lithium fluoride, 19: 46338 (UCRL-12367)
THERMOMETRY
thermomolecular pressure of helium-3 and -4 at 77°K, 19: 46157(R) (MLM-1254)
THERMONUCLEAR EXPLOSIONS
effects on fire spread, models for, (T), 19: 46638 (AD-613359)
fallout from, characteristics of, 19: 46585 (AD-410522)
fallout monitoring of high-altitude, 1962, 19: 46609
hazards of flashblindness from viewing radiations from, 19: 46655
radiation hazards from, 19: 46671
THERMONUCLEAR REACTIONS
particle injection in, high energy neutral, (E), 19: 47752
THERMONUCLEAR REACTORS
control of, (T), 19: 47816
control of, theta pinch approach to, 19: 47760
cyclotron radiation from plasma in, (T), 19: 47815
energy balance and heat transfer of pulsed, computer program for circulating, 19: 47720 (LA-3347)
neutron blankets for, materials evaluation for tritium-regenerating, 19: 47721 (LA-3385)
operation of scalloped torus-type, 19: 47779
plasma properties in Adiabatic Compression (AC) device, (E), 19: 47855
plasma stability in Zeta, (E), 19: 47856
plasma stability in Q machines, (T), 19: 47859
THERMONUCLEAR WEAPONS
book: *Nuclear Weapons—Physical Fundamentals*, 19: 46652(T) (JPRS-31842)
THICKNESS GAGES
performance of alpha, 19: 46888
THIOCYANATE COMPLEXES
with beryllium, ion exchange studies of, 19: 46230 (AAEC/E-136)
THIOCYANATE IONS
effects on contraction regulation by mechanical threshold in frog muscles, 19: 45736
THIOCYANATES
effects on iodine-131 metabolism in dairy cows, 19: 45760(R) (ORO-631, pp 83-121)
THIOCYANIC ACID
effects on metal extraction by tridodecylamine in organic diluent, 19: 46180 (UCRL-16254)
THIOLS
protective effects against radiation damage in mammals, review on, 19: 46010
THIOPENE, 2-CHLORO-
nuclear magnetic double resonance spectra, 19: 46247 (UCRL-16349)
THIOPHOSPHATES
properties and uses of trialkyl, 19: 46217
THORIUM
content in basalt from Mohole Project, 19: 46628
crystal structure of monolayers of, on tungsten surfaces, (E), 19: 47035
determination by complexometric methods using EDTA, 19: 46219
determination by isotopic dilution techniques, 19: 46204
determination of, use of Schiff's base in spectrophotometric, 19: 46206
determination using *N*-benzoyl-*N*-phenylhydroxylamine, gravimetric, 19: 46194
neutron resonance escape probability in aqueous solutions of, Monte Carlo calculation of, 19: 47970
neutron resonance escape probability in aqueous solutions of, 19: 47969
preparation of, by direct iodination of carbide, 19: 46969
separation from hydrochloric acid solution by solvent extraction using tetrabutylpyrophosphate and tetrabutylhypophosphate, tracer studies of, 19: 46451
separation from pitchblendes by solvent extraction and ion exchange, 19: 46606
separation from radium by ion exchange, 19: 47626
separation from siliceous materials, method for chemical, 19: 46190
spectra between 9960 and 2566 Å, interferometric wavelengths of emission, (E), 19: 47232
thermoelectric properties at 5 to 100°K, 19: 47042
THORIUM ALLOYS
Be–Th–U, preparation for metallography, 19: 46924 (NMI-4997, pp 55-61)
Ge–Th, vaporization of, stability of intermetallic compounds in, 19: 46298
Mg–Th, diffusion of beryllium to surface of, on heating at 300 to 500°C, 19: 47071
THORIUM BORIDES
preparation for metallography, 19: 46924 (NMI-4997, pp 56-61)
THORIUM CARBIDES
transformation temperatures of, thermal analysis of, 19: 47033
ThC_2–UC_2, diffusion of fission products from carbon-coated particulate, 19: 46913(R) (BMI-1733(Del.))
ThC_2–UC_2, preparation of carbon-coated particulate, for evaluation in BRR and ETR, 19: 46912(R) (BMI-1727(Del.))
ThC_2–UC_2, preparation of coated particulate, for evaluation in ETR, 19: 46913(R) (BMI-1733(Del.))
ThC–UC, preparation for metallography, 19: 46924 (NMI-4997, pp 55-61)
ThC_2–UC_2, radiation effects on coated particulate, 19: 46912(R) (BMI-1727(Del.))
THORIUM CHLORIDES
iodination of, to prepare pure thorium, 19: 46969
THORIUM(IV) CHLORIDES
effects on mast cell reactions in rat tissues, 19: 45766
THORIUM COMPLEXES
with alkylenepolyaminoacetic acid type chelating agents, preparation, 19: 46299(P)
THORIUM HYDRIDES
neutron inelastic scattering by, thermal, (E/T), 19: 47549(R) (TID-22141, pp 34-49)
THORIUM IONS
analytical uses in gravimetric determination of oxalic acid, 19: 46222
THORIUM ISOTOPES
content in pleistocene formations, 19: 46599
THORIUM ISOTOPES Th-227
half life determination from actinium-227 power growth curve, 19: 46157(R) (MLM-1254)
THORIUM ISOTOPES Th-228
neutron total cross section at ~2 ev, (E), 19: 47576(R) (IDO-17081, pp 49-76)
uptake and distribution in beagle bones, kidneys, liver, and spleen, 19: 45798
THORIUM ISOTOPES Th-229
alpha spectra, (E), 19: 47576(R) (IDO-17081, pp 49-76)
THORIUM ISOTOPES Th-230
content in pitchblende, of South Alligator River area, Australia, 19: 46606
THORIUM ISOTOPES Th-232
^{232}Th–^{238}U, neutron resonance absorption in mixtures of, (E/T), 19: 47575 (IDO-16986)
THORIUM MINERALS
gamma rays from, attenuation by air, 19: 46586 (NP-15361)
THORIUM OXIDES
analysis for hafnium, niobium, and tantalum, spectrochemical, 19: 46226
reactions with aqueous solutions, electrokinetics of, 19: 46281
spectra of vaporized oxygen-18 enriched, 19: 46982(R) (AD-611856)
THORIUM(IV) OXIDES
diffusion of non-volatile fission products in, 19: 47070
effects of injected, in man, pathological effects, 19: 46092
neutron irradiation of, for production of clean uranium-233, 19: 46900 (RL-SA-46-A)
pathological effects of deposited, in man, 19: 45980
pathological effects of, from deposited radiographic contrast media containing, 19: 45837
radiation dose calculations for, deposited in man, 19: 45837
vapor pressure at 2400 to 2900°K, 19: 46913(R) (BMI-1733(Del.)) (Del.))
BeO–PuO_2–ThO_2, melting point of, eutectic, 19: 46913(R) (BMI-1733

PbO_2–ThO_2, neutron resonance absorption in, (E/T), 19: 47575 (IDO-16986)
PuO_2–ThO_2, melting point of, eutectic, 19: 46913(R) (BMI-1733(Del.))
ThO_2–UO_2, neutron resonance absorption in, (E/T), 19: 47575 (IDO-16986)
ThO_2–UO_2, preparation of carbon-coated particulate, for evaluation in BRR and ETR, 19: 46912(R) (BMI-1727(Del.))
ThO_2–UO_2, preparation of coated particulate, for evaluation in ETR, 19: 46913(R) (BMI-1733)
ThO_2–UO_2, preparation of irradiated aluminum-clad lead-bonded, for metallography, 19: 47087 (NMI-4997, pp 189-97)

THORIUM SILICIDES
preparation for metallography, 19: 46924 (NMI-4997, pp 55-61)
vaporization, 19: 46298

THRESHOLD DETECTORS
performance for fast neutron spectra determination, 19: 46763 (RCN-37)

THULIUM
cohesive energy and ionization of, relation between, (T), 19: 47062
luminescence in zinc borate glass, 19: 46269
resonance absorption integrals, (E), 19: 47576(R) (IDO-17081, pp 49-76)
separation from aqueous chloride solutions by solvent extraction using di-n-octyl phosphinic acid, tracer studies of, 19: 46443

THULIUM ALLOYS
Al–Tm, crystal structure of Laves phases in, 19: 47052
Co–Tm, crystal structure of Laves phases in, 19: 47052

THULIUM BROMIDES
thermal decomposition of hydrates of, mechanisms of, 19: 46271

THULIUM FERRATES(III)
crystal structure, 19: 46256

THULIUM IONS
spectra in silicate glass, fluorescence, 19: 47886(T) (N64-21857, pp 1-6)

THULIUM ISOTOPES Tm-170
use in diagnosis of respiratory insufficiency, 19: 46118

THULIUM OXIDES
atomic charge and permittivity of, (E/T), 19: 47901(T)
oxygen-18 exchange between molecular oxygen and, 19: 46266

THYMIDINE
effects of tritium-labeled, on mutation induction in region of X chromosome in *D. melanogaster* DNA, 19: 45879
metabolism in deoxyribonucleic acid of tumor cells, tracer study, 19: 45791
radiation effects on metabolism of, by tumor cells in mice, tracer study, 19: 45936
radiation effects on metabolism in cell nuclei of, low-level beta, 19: 45808(R) (NYO-901-36)

THYMUS GLAND
effects on growth of tumor transplants in mice, 19: 45858
protective effects of injected tissues of, against radiation injuries in rats, 19: 46023
protective effects of, against carcinogenic effects of iodine-131 in mice, 19: 45808(R) (NYO-901-36)
radioinduced chromosomal aberrations in mouse, x, 19: 45911

THYROID DISEASES
radiodiagnosis, 19: 46081
radiodiagnosis of, using iodine-131, 19: 46072
radiodiagnosis using technetium-99, 19: 46140
radiotherapy of thyrotoxicosis using iodine-131, 19: 46122
radiotherapy of, during pregnancy, 19: 46049
radiotherapy of, use of iodine-131 for, 19: 45792

THYROID GLAND
analysis for iodine, x-ray spectrophotometric, 19: 46081
autoradiography of iodine-125 distribution in, 19: 45783
iodine metabolism in, tracer study in man, 19: 45754 (CEA-R-2787)
iodine metabolism in, tracer study, 19: 45792
iodine-125 and -131 content in, following uptake from milk, 19: 45782
iodine-125 metabolism in mouse, 19: 45783
iodine-131 metabolism in whole and sliced lobes of, from rats, 19: 45786
iodine-131 uptake in human, environmental, 19: 46035 (PHS-999-RM-14)
iodine-131 uptake by rat, effects of carbon monoxide exposure on, 19: 45770
iodine-131 uptake in monkey, following inhalation of labeled sodium iodide, 19: 45776
radiation effects on function of cells in, iodine-131, 19: 46082
radiation effects on weight in mice of, genetic factors, 19: 45956
radiation effects on metabolism in, from deposited iodine-131, 19: 45792
radioinduced ablation of, in chickens, 19: 45966
radioinduced carcinoma of, after radiotherapy, 19: 46069
radiosensitivity of cells of mouse, 19: 45871
radiosurgery of fish, beta, 19: 45972
radiotherapy of inoperable carcinoma of, evaluation of, 19: 46104
radiotherapy of thyrotoxicosis of, iodine-131, 19: 46082

THYRONINE, TRIIODO-
effects on growth of irradiated rat sarcoma, 19: 45943

THYROXINE
effects on iodine metabolism in lactating cows, 19: 45781
metabolism of iodine-131-labeled, in lactating cows, 19: 45781

TIMING CIRCUITS
design for pulse height-interval measurements, 19: 46724 (SC-TM-65-356)

TIN
bremsstrahlung reactions (γ,t) at 37 Mev, yields in, (E), 19: 47596(R) (TID-22141, pp 94-7)
determination by complexometric methods using EDTA, 19: 46219
electron beam backscattering at 4 to 14 Mev, effects on target current of, (E), 19: 47181
electron transport phenomena in, effects of magnetic fields on, 19: 47534
Mössbauer absorption spectra in metallic, oxide-impurity effects on tin-119m, (E), 19: 47654
neutron cross sections of, shell effects on thermal, (E), 19: 47618
photoelectron production by 145, 280 and 320 kev gamma rays, cross sections for, (T), 19: 47329
radioinduced reactions with bromobutane, effects of dose and other metals on, 19: 46912(R) (BMI-1727(Del.))
radioinduced reactions with 1-bromobutane, effects of heat on, 19: 46913(R) (BMI-1733(Del.))
reactions of, in liquid lead-tin alloys at 700, 800, and 900°C, 19: 46297
superconducting currents in junctions of, Josephson, 19: 47515
superconducting properties to 0.3°K, (E), 19: 47517
superconducting properties of, 19: 47536
superconductivity of films of, resistance changes on destruction by current of, (E), 19: 47530

TIN ALLOYS
Al–Cu–Fe–Sn–Ti–V, additive and alloying effects on mechanical properties of, 19: 46985 (AD-613651)
Ga–Sn, superconducting transition temperatures in, (E), 19: 47520
Nb–Sn, superconductivity of intermetallic compounds of, above 4.2°K, (E), 19: 47508
Nb–Sn, superconducting electromagnetic of, 19: 47526
Pb–Sn, thermodynamic properties, 19: 46297
Sn–U, vaporization of, stability of intermetallic compounds in, 19: 46298
Tu–Sn, superconducting properties and long range order of intermetallic compounds of, processing effects on, (E), 19: 47513

TIN CHLORIDES
effects on yields in gamma radiolysis of *cis*- and *trans*-stilbene, 19: 46345

TIN IONS
reactions of divalent, with uranium (VI), kinetics of, 19: 46292

TIN ISOTOPES
proton elastic scattering at 14.5 Mev, cross sections for, 19: 47705

TIN ISOTOPES Sn-116
alpha inelastic scattering at 44 Mev, cross section angular dependence in, 19: 47608
alpha scattering at 34.4 Mev, angular distributions for, (E), 19: 47623
meson (μ^-) capture by, K x ray energies from, 19: 47582 (NEVIS-129)
nuclear charge distribution radius, 19: 47582 (NEVIS-129)

TIN ISOTOPES Sn-117
alpha scattering at 34.4 Mev, angular distributions for, (E), 19: 47623

TIN ISOTOPES Sn-118
alpha scattering at 34.4 Mev, angular distributions for, (E), 19: 47623

TIN ISOTOPES Sn-119
alpha scattering at 34.4 Mev, angular distributions for, (E), 19: 47623
Mössbauer absorption spectra of isomeric, in metallic tin, oxide-impurity effects on, (E), 19: 47654

TIN ISOTOPES Sn-120
alpha scattering at 34.4 Mev, angular distributions for, (E), 19: 47623

TIN ISOTOPES Sn-124
meson (μ^-) capture by, K x ray energies from, 19: 47582 (NEVIS-129)
nuclear charge distribution radius, 19: 47582 (NEVIS-129)

TIN OXIDES
effects on Mössbauer absorption spectra of tin-119m in tin metal, (E), 19: 47654
radiation effects on, yields of antimony-125 from neutron, 19: 46388
thermodynamic properties of, at 500 to 1300°C, 19: 46297

TIN SYSTEMS
Al–C–Cu–H–N–Sn–Ti–V–Zr, mechanical properties of, 19: 46985 (AD-613651)

TIN, TETRAPHENYL-
effects on scintillation quenching in benzene, 19: 46362
radiation effects on, gamma, 19: 46761 (NYO-2979-34)
radiolysis of, in benzene, 19: 46362

TISSUE CULTURES

bone marrow, effects of ultrafiltrate from irradiated animals on, 19: 45815(R) (ORO-631, pp 67-76)
erythopoiesis maintenance in mouse marrow, method for, 19: 45740
of leukocytes, chromosome patterns of, 19: 45915
radiation effects on cell nuclei in Triton erythroblast, x, 19: 45925
radiation effects on poliovirus production by monkey-kidney, 19: 45955
radiation effects on mitotic activity of animal cells in, 19: 45867
radiation effects on desoxyribonucleic acid synthesis of animal cells in, 19: 45867
radiation effects on growth in HeLa, clone-size analysis of, 19: 45886
radiation effects on mammalian, 19: 45729(R) (NYO-910-23, pp 1-111)
radioinduced toxin effects on morphology and growth of tumor cells in, 19: 45946

TISSUE HOMOGENATES
protective effects of bovine liver, against radiation injuries in mice, 19: 46024

TISSUES
analysis for selenium by activation, 19: 46172 (KR-95)
effects of beryllium on guinea pig and rat, cytomorphology and histology of, 19: 45803
effects of thorium chloride on mast cell reactions in rat, 19: 45766
effects of uranyl acetate on induction of metachromasia in rat, 19: 45766
effects on phosphorus-32–chromium phosphate on rat, *in vitro*, 19: 45939
neutron dosimetry in, 19: 46121
radiation dosimetry for, from internal isotopes, 19: 46154
radiation effects on immune reactions to transplanted, 19: 45944
radiation effects on, bibliography, 19: 45807 (AED-C-04-17)
radiation effects on moisture content of rat, 19: 45896
radiation effects on response of salamander to grafts of, 19: 45897
radioinduced free radicals in rabbit muscle, ESR of gamma and x, 19: 45947
radiosterilization of, for use in homografting procedures, 19: 46879

TITANIUM
alpha attenuation by, energy-range relations in, 19: 46324(R) (AGN-8132)
analysis for thorium using *N*-benzoyl-*N*-phenylhydroxylamine, gravimetric, 19: 46194
determination by complexometric methods using EDTA, 19: 46219
determination in titanium carbide–zirconium carbide, method for, 19: 46941 (NP-15514(Vol.3))
determination in tantalum carbide–titanium carbide, method for, 19: 46941 (NP-15514(Vol.3))
effects on ductility of fissium–uranium–zirconium alloys, 19: 47004 (NMI-4997, pp 45-54)
effects on grain size control in cast steel, 19: 46980 (AD-611800)
heat of vaporization, 19: 46956 (NP-15514(Vol.1))
ionization on rhenium and tungsten, effects of condensed layers and residual gases on, 19: 47222(T) (ORNL-tr-679)
mechanical properties at cryogenic temperatures, 19: 47013 (PB-171809(Rev.)(Suppl.2))
properties for aerospace uses, 19: 47068
separation from other materials by electrolytic extraction, 19: 46454
sorptive properties of films of, for argon ions, (E), 19: 47072
surface tension of, measurement by pendant drop method, 19: 47065

TITANIUM ALLOYS
properties for aerospace uses, 19: 47068
Al–Cu–Fe–Sn–Ti–V, additive and alloying effects on mechanical properties of, 19: 46985 (AD-613651)
Al–Ti–V, interface friction in hot deformation of, 19: 46981(R) (AD-611821)
Mo–Ti, effects of protective coatings on oxidation and properties of, 19: 47061
Mo–Ti–Zr, reactions with cesium at 3400°F, metallographic specimen preparation of TZM, 19: 46954 (NMI-5025(Pt.I), pp 39-58)
Mo–Ti–Zr, reactions with uranium carbide, nitride, and dioxide, metallographic specimen preparation of TZM, 19: 46954 (NMI-5025 (Pt.I), pp 39-58)

TITANIUM BORIDES
analysis for boron, method for, 19: 46941 (NP-15514(Vol.3))
corrosion by hydrogen chloride at 2250°C, 19: 46956 (NP-15514 (Vol.1))
heat of formation and vaporization, 19: 46956 (NP-15514(Vol.1))
lattice parameters and thermal expansion at 25 to 2041°C, 19: 47009 (NP-15514(Vol.2))
oxidation by carbon dioxide at 2250°C, 19: 46956 (NP-15514(Vol.1))
preparation and purification, 19: 46941 (NP-15514(Vol.3))

TITANIUM CARBIDES
atomic vibrational amplitudes and Debye temperatures at 25 to 1600°C, 19: 47009 (NP-15514(Vol.2))
corrosion by hydrogen chloride at 2250°C, 19: 46956 (NP-15514 (Vol.1))
creep rate of polycrystalline, at 1890 to 2060°K, 19: 47009 (NP-15514(Vol.2))
oxidation by carbon dioxide at 2250°C, 19: 46956 (NP-15514(Vol.1))
preparation and purification, 19: 46941 (NP-15514(Vol.3))
thermal expansion coefficient of, x-ray determination of, 19: 47023(T) (LA-tr-65-20)
thermal expansion at 25 to 2080°C, 19: 47009 (NP-15514(Vol.2))
TaC–TiC, analysis for tantalum and titanium, method for, 19: 46941 (NP-15514(Vol.3))
TiC–ZrC, analysis for titanium and zirconium, method for, 19: 46941 (NP-15514(Vol.3))

TITANIUM COMPLEXES
with alkylenepolyaminoacetic acid type chelating agents, preparation, 19: 46299(P)

TITANIUM HYDRIDES
neutron inelastic scattering by, thermal, (E/T), 19: 47549(R) (TID-22141, pp 34-49)

TITANIUM ISOTOPES Ti-46
bremsstrahlung reactions (γ,pn) at 48 Mev, (E), 19: 47596(R) (TID-22141, pp 94-7)
deuteron reactions (d,He-3) with, residual nucleon interactions in, 19: 47115(R) (ANL-6983)

TITANIUM ISOTOPES Ti-49
proton elastic scattering at 14.5 Mev, cross sections for, 19: 47705

TITANIUM ISOTOPES Ti-50
proton inelastic scattering at 14.6 to 18.2 Mev, (E/T), 19: 47702

TITANIUM NITRIDES
atomic displacement amplitudes in defect structures of, nitrogen and titanium thermal and static, 19: 47009 (NP-15514(Vol.2))
atomic vibrational amplitudes and Debye temperatures at 25 to 1419°C, 19: 47009 (NP-15514(Vol.2))
lattice parameters and thermal expansion, effects of composition on, 19: 47009 (NP-15514(Vol.2))
preparation and purification, 19: 46941 (NP-15514(Vol.3))
spectra of vaporized, 19: 46982(R) (AD-611856)
thermal expansion at 25 to 1419°C, 19: 47009 (NP-15514(Vol.2))

TITANIUM OXIDES
TiO_2–U_3O_8, preparation and properties of $TiUO_5$ in, 19: 46272

TITANIUM STEEL
grain size in cast, 19: 46980 (AD-611800)
Cr–Ni–Ti, ageing of corrosion-resistant, structural changes in, 19: 47026(T) (ORNL-tr-795)

TITANIUM SULFIDES
intercalation of highly electropositive metals in, 19: 46265

TITANIUM SYSTEMS
Al–C–Cu–H–N–Sn–Ti–V–Zr, mechanical properties of, 19: 46985 (AD-613651)
C–N–Ti, Hall coefficients, 19: 47009 (NP-15514(Vol.2))

TITRATION EQUIPMENT
design of automatic potentiometric titrator, 19: 46162 (AECL-2262)
design of remotely operated, engineering drawings for, 19: 46225

TOBACCO
polonium-210 content in, from four countries, 19: 45801
radioinduced inactivation of necrosis virus of, ultraviolet, 19: 45962

TOKAI-MURA POWER REACTOR
shield cooling system for, calculation and design criteria for, 19: 48029

TOLUENE
effects on metal extraction by tridodecylamine in presence of hydrohalic or thiocyanic acid, 19: 46180 (UCRL-16254)
separation of tritiated, from tritiated pyridine, by gas chromatography, 19: 46213

TOLUENE, VINYL- POLYMERS
helium-ion absorption cross sections at 30 to 350 kev, (E), 19: 47871
proton absorption cross sections at 30 to 350 kev, (E), 19: 47871

TOXINS
radioinduced in rabbit liver, properties of, 19: 45946

TRACER TECHNIQUES
use in study of cesium reactions with materials in thermionic cells, 19: 47282(R) (NYO-3429-4)

TRACER TECHNIQUES (BIOLOGY)
method for, in electron microscope, 19: 45741

TRACER TECHNIQUES (MEDICINE)
calcium metabolic studies, 19: 46138
counters for, evaluation of whole-body, 19: 46137
counting statistics in, 19: 45742
data from, computer analysis of, 19: 46055
data from, computer analysis of, 19: 45735
diagnosis of respiratory insufficiency, 19: 46118
for bone lesion diagnosis, 19: 46133
for combined liver-lung scanning, 19: 46048

for kidney function tests in children, 19: 46109
for kidney function tests, 19: 46130
for kidney function tests, 19: 46079
for localization of intracranial vascular lesions, 19: 46086
for radiodiagnosis, 19: 46102
for study of blood circulation in lungs, 19: 46070
for thyroid function tests, 19: 46072
for vitamin B_{12} excretion, 19: 46083
liver scanning using molybdenum-99, 19: 46139
methods using iodine-131-labeled proteins and whole-body counting, 19: 46142
placenta localization during pregnancy, 19: 46117
short-lived radioisotopes for, 19: 46136
tracer for, properties of technetium-99, 19: 46140

TRAMEX PROCESS
curium-244 separation using, in Curium Recovery Facility, 19: 46428(R) (ORNL-3847)

TRANSDUCERS
development of eddy-current, for vibration sensing, 19: 46716(R) (IDO-17081, pp 77-123)
development of proximity, for fuel element deflection and vibration, 19: 46716(R) (IDO-17081, pp 77-123)

TRANSISTORS
performance of tunnel diode invertor, for thermoelectric generator, 19: 46896
radiation effects on, method for measuring, 19: 46871 (AD-614268)
use in fast switching circuits, 19: 46717 (INSJ-87)

TRANSURANIC ELEMENTS
neutron strength function for nuclei $220 \leq A \leq 248$, peak in s-wave, 19: 47115(R) (ANL-6983)
production on large scale, HFIR-TRU program on, 19: 46428(R) (ORNL-3847)

TRAPS
decontamination methods for helium-3 purification, 19: 46157(R) (MLM-1254)
materials for vacuum system, porous metal, 19: 46573 (UCRL-12393-T)

TREES
radioactivity from cesium-137, cobalt-60, iron-56, strontium-90, and zinc-65 uptake from soil, 19: 45773
radioinduced mutations of *Acer negundo*, 19: 45865
radiosensitivity of Pinus, genetic factors, 19: 45855

TRIDODECYLAMINE
solvent properties for metals in system with hydrohalic acid and organic diluent, 19: 46180 (UCRL-16254)

TRIETHYLAMINE
BF_3–triethylamine, boron isotopic exchange thermodynamics of, 19: 46899(R) (ORNL-3832, pp 33-49)

TRIMETHYLENE OXIDE
nuclear magnetic resonance spectra of, analysis, 19: 46247 (UCRL-16349)

TRIMETHYLENE SULFIDE
nuclear magnetic resonance spectra of, analysis, 19: 46247 (UCRL-16349)

TRIOCTYLAMINE
complexes with uranium, formation in solvent extraction processes, 19: 46447

TRITIUM
autoradiographic uses of, 19: 45729(R) (NYO-910-23, pp 1-111)
content in waste solutions, precipitation, ground water, and surface water at National Reactor Testing Station, 19: 46642 (IDO-12043)
deuteron reactions (d,n) with, level structure from, (T), 19: 47687
deuteron reactions (d,n) at 10 to 150 kev, α and neutron energies from, 19: 47568 (CEA-R-2779)
diffusion from electron-capture detectors, 19: 46670
electron elastic scattering by, nucleon structure from, (E), 19: 47565 (AD-614270)
incorporation in cholesterol esters of arachidonic and linoleic acids, 19: 46309
incorporation in organic acids at α-carbon atom, 19: 46306
incorporation in p-terphenyls, 19: 46313
incorporation in valine by Wilzbach method, 19: 46311
incorporation into linoleic acid of, 19: 45785
potential interactions in Λ hyperfragment of, neutron-proton tensor, (T), 19: 47657
production in fusion-reactor blankets, materials evaluation for, 19: 47721 (LA-3385)
separation by thermal diffusion and measurement of dated, 19: 46613
sorption on aluminum, brass, and steel surfaces, effects of texture on, 19: 47018 (USNRDL-TR-890)
use in drug-incorporated, in tumor radiotherapy, 19: 46125
uses as radiation source for ionization detectors in gas chromatography, 19: 46887

TRITIUM COMPOUNDS
synthesis of, methods for, 19: 45729(R) (NYO-910-23, pp 1-111)

TRITIUM IONS
reactions with butane at 2 to 6 kev, preparation of labeled hydrocarbons by, 19: 46415

TRITONS
emission from excited emulsion nuclei, (E), 19: 47651

TRYPSIN
radioinduced free radicals in, spectra of, 19: 46339 (UCRL-16358)

TRYPTOPHAN
metabolism in Pseudomonas, enzyme systems for, 19: 45808(R) (NYO-901-36)

TUBERCULOSIS
radiagnosis of, radiation hazards in, 19: 46110
radioinduced leukemia in patients with, 19: 45870

TUBES
boiling burnout in upward flow of Freon 12 through uniformly and non-uniformly heated, forced-convection, 19: 46527 (AEEW-R-426)
boiling instability in forced-convection flows through small, subcooled, 19: 46534 (NP-15437)
bowing in long, device for measuring, 19: 46710 (BNWL-59)
burnout in forced-convective boiling of water in, 19: 46541
burst and collapse pressures of stainless-steel, 19: 46986 (KR-96)
extrusion of, apparatus for, 19: 46979(P)
heat transfer by gas flow in horizontal, effects of buoyancy on, 19: 46545
particle deposition in long thin, 19: 46647 (RISO-104)

TUMORS
effects of chlorpromazine on respiration in, 19: 45862
effects of geological formations of incidence of malignant, 19: 45832
effects of radioinduced toxins on growth of cells from, in culture, 19: 45946
effects of transplanted, on liver enzyme systems in hamsters, 19: 45808(R) (NYO-901-36)
etiology, pathology, and treatment of, in man, 19: 45808(R) (NYO-901-36)
metabolism of desoxyribonucleic acid in, tracer study, 19: 45791
pathology of benzanthracene-induced in female mice, 19: 45808(R) (NYO-901-36)
pathology of melanomas in hamster skin, 19: 45906
pathology of methylcholanthrene-induced in mice, 19: 45808(R) (NYO-901-36)
production in rats by injected materials from irradiated donors, 19: 45815(R) (ORO-631, pp 67-76)
radiation effects on isoenzymes and lactate dehydrogenase in human, 19: 46124
radiation effects on desoxyribonucleic acid metabolism in, tracer study in mice, 19: 45936
radiation effects on morphology of lymphocytes in patients with Hodgkin's disease, 19: 46103
radiation effects on growth of transplanted, in mice, 19: 45858
radiation effects on respiration in, ultraviolet, 19: 45862
radiation effects on immune response and membrane permeability in Ehrlich ascites cells of, 19: 45914
radiation effects on growth of transplanted rat, 19: 45921
radiobiological aspects of, 19: 45743
radiodiagnosis of metastatic, by phosphorus-32 uptake, 19: 46098
radioinduced in domestic animals, 19: 45812(R) (ORO-631, pp 1-35)
radioinduced in lungs of mammals, 19: 45808(R) (NYO-901-36)
radioinduced in man, 19: 45996
radioinduced in man, 19: 45942
radioinduced in mice, antigenic adaptation in transplantable, 19: 45873
radioinduced in rats, effects of parabiosis on, 19: 45808(R) (NYO-901-36)
radioinduced in skin, 19: 45945
radioinduced, after injection of Thorotrast, 19: 46092
radioinduced, etiology of, 19: 45859
radioinduced, in residents of Hiroshima exposed to atomic explosion, 19: 45846
radioinduced, of breast, 19: 46090
radiosensitivity of tumors in rats, 19: 46022
radiosensitivity of implanted mouse, effects of oxygen on, 19: 46003
radiosensitivity of, effects of oxygen on, 19: 46097
radiosensitivity of metastatic, evaluated by phosphorus-32 uptake, 19: 46098
radiosensitivity of, factors in, 19: 45921
radiotherapy, 19: 46077
radiotherapy, 19: 46078
radiotherapy of bladder, x, 19: 46113
radiotherapy of bladder, 19: 46114
radiotherapy of bladder, gamma, 19: 46115
radiotherapy of ear, 19: 46084

radiotherapy of eye, 19: 46056
radiotherapy of face and jaw, 19: 46074
radiotherapy of facial in children, 19: 46075
radiotherapy of gynecological, using radioisotopes, 19: 46100
radiotherapy of head and neck, 19: 46129
radiotherapy of head and neck, synergistic effects of cytotoxic chemicals, 19: 46088
radiotherapy of melanoma of pectoral region, using iridium-192 wire applicator, 19: 46047
radiotherapy of metastatic, 19: 46101
radiotherapy of oral, 19: 46066
radiotherapy of pelvic, delayed radiation injury of intestine after, 19: 46065
radiotherapy of urinary bladder and rectum, gamma dosimetry in pendulum gamma, 19: 46093
radiotherapy of, biological factors in combined chemotherapy and, 19: 46096
radiotherapy of, dosimetry in neutron-capture, 19: 46121
radiotherapy of, electrophoretic study of effects on serum denaturation, 19: 45924
radiotherapy of, factors external and internal, 19: 46095
radiotherapy of, synergistic effects of 5-fluorouracil, 19: 46050
radiotherapy of, selection of energy for, 19: 46094
radiotherapy of, use of tritiated Synkayvite derivatives in, 19: 46125
research programs on, Great Britain, 1964, 19: 45744
separation of virus-like particles from human breast, by zone centrifuge, 19: 45730(R) (ORNL-3752)
surgical removal of face and jaw, 19: 46074
therapy of, radiobiological aspects of, 19: 45743
virus induced, etiology, 19: 45942

TUNGSTEN
atomic vibrational amplitudes and Debye temperatures at 25 to 1680°C, 19: 47009 (NP-15514(Vol.2))
coatings for high-temperature protection, restrictions on materials for, 19: 46911 (AFML-TR-64-392)
content and distribution in beef heart, 19: 45753 (AE-191)
corrosion by hydrogen chloride at 2250°C, 19: 46956 (NP-15514 (Vol.1))
crystal structure of, stacking faults in, 19: 47050
crystal structure of cavities in, 19: 47057
ductility of, pressure effects on, 19: 46983 (AD-612159)
effects on mechanical properties of sintered zirconium diboride, 19: 46907 (AD-456724)
elastic properties of, at 24 to 1800°C, 19: 47009 (NP-15514(Vol.2))
electron elastic scattering at 0 to 1.5 ev, 19: 47242
ionization of copper, silver, and titanium on, effects of condensed layers and residual gases on, 19: 47222(T) (ORNL-tr-679)
microstructure of single crystals of, electron diffraction study of, 19: 47022(T) (JPRS-31225, pp 1-5)
nitrogen-14 equilibration reaction with nitrogen-15 on, 19: 46289
oxidation at 1400 to 3150°K, reaction kinetics of, 19: 46956 (NP-15514(Vol.1))
oxidation by carbon dioxide at 2330 to 2850°K, reaction kinetics for, 19: 46956 (NP-15514(Vol.1))
properties for aerospace uses, 19: 47068
reactions with boron tetrafluoride and hydrogen fluoride, 19: 46956 (NP-15514(Vol.1))
reactions with cesium at 3400°F, metallographic specimen preparation of, 19: 46954 (NMI-5025(Pt.I), pp 39-58)
reactions with uranium carbide, nitride, and dioxide, metallographic specimen preparation of, 19: 46954 (NMI-5025(Pt.I), pp 39-58)
sintering in controlled reactive atmospheres, 19: 46960(R) (AD-611837)
surface tension of, measurement by pendent drop method, 19: 47065
thermal expansion at 25 to 1777°C, 19: 47009 (NP-15514(Vol.2)
thorium monolayers on surfaces of, crystal structure of, (E), 19: 47035
Re–W, reactions with cesium at 3400°F, metallographic specimen preparation of, 19: 46954 (NMI-5025(Pt.I), pp 39-58)
Ta–W, reactions with cesium at 3400°F, metallographic specimen preparation of, 19: 46954 (NMI-5025(Pt.I), pp 39-58)

TUNGSTEN ALLOYS
development with elevated temperature strength, 19: 46940(R) (NP-15444)
properties for aerospace uses, 19: 47068
thermoelectric properties of sintered, for use as thermocouples at high temperatures, 19: 47019(T) (AD-619334)
Ag–W, corrosion by dioxide at 2250°C, 19: 46956 (NP-15514(Vol.1))
Hf–Nb–W–Y, weldability studies of C-129Y, 19: 46966(R) (WANL-PR(P)-007)
Hf–Ta–W, reactions with cesium at 3400°C, metallographic specimen preparation of T-111, 19: 46954 (NMI-5025(Pt.I), pp 39-58)
Hf–Ta–W, reactions with uranium carbide, nitride, and dioxide, metallographic specimen preparation of T-111, 19: 46954 (NMI-5025 (Pt.I), pp 39-58)
Hf–Ta–W, weldability studies of T-111, 19: 46966(R) (WANL-PR(P)-007)
Mo–Nb–Ta–W, creep slip of solution-hardened, at 980 to 1370°C, 19: 47049
Mo–W, reactions with cesium at 3400°F, metallographic specimen preparation of, 19: 46954 (NMI-5025(Pt.I), pp 39-58)
Mo–W, reactions with uranium carbide, nitride, and dioxide, metallographic specimen preparation of, 19: 46954 (NMI-5025(Pt.I), pp 39-58)
Nb–Ta–W, weldability studies of SCb-291, 19: 46966(R) (WANL-PR(P)-007)
Nb–Ta–W–Zr, weldability studies of FS-85, 19: 46966(R) (WANL-PR(P)-007)
Nb–W, reactions with cesium at 3400°F, metallographic specimen preparation of, 19: 46954 (NMI-5025(Pt.I), pp 39-58)
Nb–W, reactions with uranium carbide, nitride, and dioxide, metallographic specimen preparation of, 19: 46954 (NMI-5025(Pt.I), pp 39-58)
Nb–W–Zr, weldability studies of Cb-752, 19: 46966(R) (WANL-PR(P)-007)
Re–W, reactions with uranium carbide, nitride, and dioxide, metallographic specimen preparation of, 19: 46954 (NMI-5025(Pt.I), pp 39-58)
Ta–W, analysis by polarography, teflon electrode for, 19: 46157(R) (MLM-1254)
Ta–W, reactions with uranium carbide, nitride, and dioxide metallographic specimen preparation of, 19: 46954 (NMI-5025(Pt.I), pp 39-58)
Ta–W, weldability studies of, 19: 46966(R) (WANL-PR(P)-007)
Tc–W, examination of arc-melted buttons of, 19: 46914(R) (BNWL-141)

TUNGSTEN CARBIDES
deformation of, interface friction in hot, 19: 46981(R) (AD-611821)

TUNGSTEN ISOTOPES W-182
neutron resonance parameters, (E), 19: 47595(R) (TID-22141, pp 50-66)

TUNGSTEN ISOTOPES W-183
neutron resonance parameters, (E), 19: 47595(R) (TID-22141, pp 50-66)

TUNGSTEN ISOTOPES W-184
neutron resonance parameters, (E), 19: 47595(R) (TID-22141, pp 50-66)

TUNGSTEN ISOTOPES W-185
metabolism in sheep and swine, 19: 45759(R) (ORO-631, pp 77-82)

TUNGSTEN ISOTOPES W-186
internal conversion coefficients for E2 transitions in, nuclear structure effects on, (T), 19: 47620
neutron resonance parameters, (E), 19: 47595(R) (TID-22141, pp 50-66)

TUNGSTEN OXIDES
thermal diffusivity at 1250 to 1650°C, 19: 46995 (EUR-2424.f)

TUNGSTEN SELENIDES
intercalation of strongly electropositive metals in, 19: 46265

TUNGSTEN SULFIDES
intercalation of highly electropositive metals in, 19: 46265

TUNGSTEN SYSTEMS
B–W–Zr, fabrication and mechanical properties of, 19: 46940(R) (NP-15444)
C–Hf–Nb–W, fabrication and mechanical properties of, 19: 46940(R) (NP-15444)
C–Hf–Ta–W, weldability studies of T-222, 19: 46966(R) (WANL-PR(P)-007)
C–Hf–W, fabrication and mechanical properties of, 19: 46940(R) (NP-15444)
C–Nb–W, fabrication and mechanical properties of, 19: 46940(R) (NP-15444)
C–Nb–W–Zr, fabrication and mechanical properties of, 19: 46940(R) (NP-15444)
C–Nb–W–Zr, weldability studies of D-43, 19: 46966(R) (WANL-PR(P)-007)
C–W–Zr, fabrication and mechanical properties of, 19: 46940(R) (NP-15444)

TURBINES
design, fabrication, and testing of closed cycle gas, 19: 47987 (AD-612409)

U

ULTRASONICS
effects on immune properties of gamma globulins, 19: 45860
equipment and techniques for fuel element flow detection, 19: 46716(R) (IDO-17081, pp 77-123)

ULTRAVIOLET RADIATION
carcinogenic effects in hamster skin, synergistic effects of chemicals, 19: 45906
dosimetry of, in biological system, 19: 45963
effects in algae, genetic, 19: 45842
effects in bacteriophage, inactivating, 19: 45961

effects in human skin, pathological, 19: 45907
effects in mice, carcinogenic, 19: 45827
effects in *Rhizobium trifolii*, inactivating, 19: 45961
effects on activation of guanidine- and puromycin-treated poliovirus infective centers, 19: 46032
effects on *Bacillus subtilis* spores, 19: 45848
effects on bacteria cells, damage repair in, 19: 45985
effects on cell membrane, morphological, 19: 45891
effects on desoxyribonucleic acid replication in bacteria, 19: 45909
effects on DNA priming ability in RNAse system, 19: 45849
effects on electroluminescent screens, (E), 19: 46341(T) (FTD-TT-65-24)
effects on *Escherichia coli* mutants, 19: 45948
effects on granular and transitional cell layers in human skin, 19: 45913
effects on human skin, dose determination for erythemal, 19: 45881
effects on luminescence of albumin solutions, effects of radioprotective compounds on, 19: 46342(T) (JPRS-31547, pp 6-12)
effects on mineral acid glasses, effects of iron ions and nitrous oxide on yields in, 19: 46394
effects on properdin content of blood serum of swine, 19: 45919
effects on proteins, inactivating, 19: 45839
effects on proteins, 19: 46382
effects on pyrimidine mutation induction in *Salmonella typhimurium*, genetic analysis of, 19: 45878
effects on replication of bacterial DNA, 19: 46002
effects on respiration in tumor cells and other biological systems, 19: 45862
effects on sea urchins, morphological, 19: 45840
effects on stomatal movement of Begonia leaves, 19: 45854
effects on *Streptomyces citreus*, genetic, 19: 45991
effects on tobacco necrosis virus, inactivating, 19: 45962
intensity of solar, (T), 19: 47210

ULTRAVIOLET SOURCES
design of microbeam, 19: 45891

ULTRAVIOLET SPECTROSCOPY
of biological polymers, 19: 48104 (UCRL-16278)

UNDERGROUND EXPLOSIONS
activation of terrestrial environment by, products of, 19: 46473 (UCRL-14249)
bibliography on cratering by nuclear, 19: 46466 (CEA-Bib-63)
determination using seismic wave amplitude and energy, 19: 46615 (AD-612033)
excavation by parallel rows of charges, small-scale study, 19: 46470 (SC-RR-65-303)
radial displacements and strains produced by contained nuclear, method for predicting, 19: 46467 (NVO-1163-43)
throwout from Danny Boy, measurements of, 19: 46468 (POR-1814)
use in mining ore bodies by caving, 19: 46472 (UCRL-14201)
vent gas treatment plant for Dribble, analytical systems for, 19: 46471 (UCRL-14123)

UNDERGROUND STRUCTURES
dynamic loading of strip footing of flexible arch structure in sand, simulation tests, 19: 46567 (NP-15396)
stresses on, compression wave, 19: 46569

UNION OF SOUTH AFRICA
atomic energy activities in, 1964 report on, 19: 48091(R) (NP-15418)

UNITED KINGDOM ATOMIC ENERGY AUTHORITY
Harwell facilities and research programs, 19: 48115

URACIL, 5-FLUORO-
effects combined with radiotherapy on palliative management of gastrointestinal cancer, 19: 46091
effects on radiosensitivity of tumors, 19: 46050

URANIUM
analysis for metallic impurities, atomic absorption spectroscopy for, 19: 46166 (DP-980)
analysis for thorium using *N*-benzoyl-*N*-phenylhydroxylamine, gravimetric, 19: 46194
content in basalt from Mohole Project, 19: 46628
crystal structure of, effects of aluminum and iron on precipitate growth in, 19: 46148
decay in minerals, measurement of radioactive halos from, 19: 46592(T) (ORNL-tr-701)
decomposition of beta and gamma phases in, alloying and heat treatment effects on network structures in, 19: 47060
determination by isotopic dilution techniques, 19: 46204
determination by potentiometric titration using potassium dichromate, 19: 46220
determination by potentiometric titration of acid liberated by complex formation, 19: 46205
determination in arc-fused urania, metallographic method for, 19: 46176 (NMI-4997, pp 110-23)
determination in hypostoichiometric uranium monocarbide, metallographic methods for, 19: 46177 (NMI-5025(Pt.I), pp 85-95)
determination of, in sea water, marine sediments, and monazites by ion exchange separation and fluorimetry, 19: 46223
dissolution in rocks, aqueous, 19: 46626
effects on mechanical properties of aluminum–copper–iron–tin–titanium–vanadium alloys, 19: 46985 (AD-613651)
effects on properties of carbon steel, 19: 47047
electron beam backscattering at 4 to 14 Mev, effects on target current of, (E), 19: 47181
electroplating of bars of, nickel plating bath for, 19: 46944(P)
emission from uranium-dioxide fissioning surfaces, model for, (T), 19: 47580 (LA-3352)
microstructure, effects of chemistry and casting history on, 19: 47007 (NMI-5025(Pt.I), pp 127-51)
neutron reactions (n,n′γ) at 14.8 Mev, differential cross sections for, (E/T), 19: 47594(R) (TID-22012, pp 176-205)
occurrence of, in German Federal Republic, 19: 46630
oxidation by carbon dioxide at 400 to 1000°C, 19: 46948 (CEA-R-2805)
phase transformations in, metallography of, 19: 47005 (NMI-4997, pp 76-84)
polishing of, etchants for electro-, 19: 46933 (NMI-4999, pp 78-84)
polishing of, technique for electro-, 19: 46920 (NMI-4996, pp 27-35c)
preparation for transmission electron microscopy, 19: 46933 (NMI-4999, pp 78-84)
processing of irradiated, by fused salt electrolysis, 19: 46448
purification by melting and solidification under a slag, 19: 46455(P)
radiation effects on swelling in alpha-, dislocation movement effects in, 19: 47100
radiation effects on thermal conductivity of, 19: 47101
radiography of cast bars and tubes, 19: 46562
radioinduced swelling in clad tubes of, effects of aluminum, iron, and silicon additions on, 19: 46917(R) (DP-975)
radioinduced swelling in, resistance to, 19: 47103
reactions with aluminum–silicon eutectic, metallographic and microauto-radiographic study of, 19: 46951 (NMI-4996, pp 19-26)
reactions with water at high temperatures during core meltdown, (E/T), 19: 47960(T) (ORNL-tr-694)
separation from high- and low-enrichment fuels, method for, 19: 47921(R) (ANL-7090, pp 30-54)
separation from irradiated fuels by fused salt electrolysis, 19: 46448
separation from nitric acid solutions by solvent extraction using TBP, 19: 46446
separation from nitric and sulfuric acid solutions by solvent extraction using TOA, complex formation in, 19: 46447
separation from nitric acid solutions by solvent extraction using tricaprylmethylammonium nitrate, 19: 46450
separation from rare earths by precipitation using dehydroxymaleic acid, 19: 46452
spectra of, isotope shifts in, 19: 47602
substructure of beta-quenched and recrystallized high-purity, 19: 46993 (CONF-650810-3)
surface tension of, measurement by pendant drop method, 19: 47065
Al–Si–U, radioinduced swelling in, resistance to, 19: 47103

URANIUM ALLOYS
grain size determination in, using crystallographic methods, 19: 47040
radiation effects on, bibliography on, 19: 47093 (VDDIT-16(5.2))
Al–Fe–U, radioinduced swelling in, resistance to, 19: 47103
Al–U, radiation effects on, 19: 48060(R) (IDO-17081, pp 1-47)
Be–Th–U, preparation for metallography, 19: 46924 (NMI-4997, pp 55-61)
Fe–Pu–U, properties and structure of, 19: 46992 (CEA-R-2792)
fissium–U–Zr, ductility of, effects of aluminum, silicon, titanium, and yttrium additions on, 19: 47004 (NMI-4997, pp 45-54)
Ga–U, vaporization of, stability of intermetallic compounds in, 19: 46298
In–U, vaporization of, stability of intermetallic compounds in, 19: 46298
Mo–U, fabrication into massive enriched core components for Super Kukla, safety in, 19: 46967 (Y-KB-62)
Mo–U, radioinduced swelling in clad tubular, 19: 46917(R) (DP-975)
Mo–U, separation of uranium from, by fused salt electrolysis, 19: 46448
Pb–U, vaporization of, stability of intermetallic compounds in, 19: 46298
Sn–U, vaporization of, stability of intermetallic compounds in, 19: 46298
U–Zr, phase diagram of uranium-rich, 19: 47014 (RT/MET(64)4)
U–Zr, radioinduced swelling in clad tubular, 19: 46917(R) (DP-975)
U–Zr, separation of uranium from, by fused salt electrolysis, 19: 46448
U–Zr, structure of, effects of heat treatment on, 19: 47014 (RT/MET 64)4)

URANIUM BORIDES
preparation for metallography, 19: 46924 (NMI-4997, pp 55-61)

URANIUM CARBIDES
analysis for uranium, metallographic methods for, 19: 46177 (NMI-5025(Pt.I), pp 85-95)

casting into bars, process using electron bombardment melting, 19: 46974(P)
corrosion by water vapor, 19: 46953 (NMI-4997, pp 62-75)
determination in arc-fused urania, metallographic method for, 19: 46176 (NMI-4997, pp 110-23)
fabrication of SAP-clad, 19: 47998(R) (SRO-118)
machining rods of, by continuous casting under electron bombardment, 19: 46963 (CEA-R-2733)
phase studies of, by radiocrystallographic methods, 19: 47041
preparation of carbon-coated particulate, for evaluation in BRR and ETR, 19: 46912(R) (BMI-1727(Del.))
preparation of coated particulate, for evaluation in BRR, 19: 46913(R) (BMI-1733(Del.))
preparation of pyrolytic carbon-coated and uncoated spheres of, for metallography, 19: 47006 (NMI-4997, pp 198-207)
radiation effects on coated particulate, 19: 46912(R) (BMI-1727(Del.))
radiation effects on structure of dispersion-type fuel elements of, metallography of, 19: 47084 (NMI-4997, pp 124-33)
reactions with refractory metal alloys, metallographic specimen preparation of, 19: 46954 (NMI-5025(Pt.I), pp 39-58)
reactions with refractory metal alloys, metallographic specimen preparation of, 19: 46954 (NMI-5025(Pt.I), pp 39-58)
sample preparation of irradiated, metallographic, 19: 47083 (NMI-4996, pp 77-85)
structure of pyrolytic carbon-coated and uncoated spheres of, metallography of, 19: 47006 (NMI-4997, pp 198-207)
thermionic work function measurements on sublimates from, (E), 19: 47038
PuC–UC, fabrication and properties for use as fuels, 19: 46999 (LA-DC-7297)
PuC–UC, performance as fast breeder reactor fuel, 19: 47993 (NAA-SR-10751)
ThC_2–UC_2, diffusion of fission products from carbon-coated particulate, 19: 46913(R) (BMI-1733(Del.))
ThC_2–UC_2, preparation of carbon-coated particulate, for evaluation in BRR and ETR, 19: 46912(R) (BMI-1727(Del.))
ThC_2–UC_2, preparation of coated particulate, for evaluation in ETR, 19: 46913(R) (BMI-1733)
ThC–UC, preparation for metallography, 19: 46924 (NMI-4997, pp 55-61)
ThC_2–UC_2, radiation effects on coated particulate, 19: 46912(R) (BMI-1727(Del.))
U–UC–UO_2, phase studies, 19: 46249(T) (LA-tr-65-15)

URANIUM(III) CHLORIDES
LiCl–KCl–UCl_3, uses in electrolytic processing of irradiated uranium fuels, 19: 46448

URANIUM COMPLEXES
with trioctylamine, composition and stability, 19: 46447

URANIUM COMPOUNDS
casting into bars, process using electron bombardment melting, 19: 46974(P)
radiation effects on, bibliography on, 19: 47093 (VDDIT-16(5.2))

URANIUM DEPOSITS
occurrence and economics of, in German Federal Republic, 19: 46630

URANIUM(IV) FLUORIDES
KCl–NaCl–UF_4, uses in electrolytic processing of irradiated uranium fuels, 19: 46448

URANIUM IONS
electrochemical properties of tetravalent, in ethanol–water systems, 19: 46292
reactions of hexavalent, with tin (II), kinetics of, 19: 46292
reactions with thallium ions, catalytic effects of dicarboxylic acids on, 19: 46277

URANIUM ISOTOPES U-232
neutron total cross at 0.01 to 10,000 ev, (E), 19: 47576(R) (IDO-17081, pp 49-76)
production in thoria irradiations, minimization, 19: 46900 (RL-SA-46-A)

URANIUM ISOTOPES U-233
fission of, zirconium-95 production from thermal neutron, (E), 19: 47584(R) (ORNL-3832, pp 1-28)
neutron capture-to-fission ratio in, engineering drawings of fission chamber for measuring, 19: 47713
neutron scattering and total cross sections of, (E), 19: 47595(R) (TID-22141, pp 50-66)
production by thoria irradiations, with minimum uranium-232 content, 19: 46900 (RL-SA-46-A)

URANIUM ISOTOPES U-234
content in pleistocene formations, 19: 46599

URANIUM ISOTOPES U-235
criticality studies, 19: 47967
determination in irradiated fuel slugs, nondestructive spectrometric, 19: 46178 (NP-15364)
fission fragments and neutron fission cross sections at 0.1 to 10 ev, 19: 47576(R) (IDO-17081, pp 49-76)
fission of, zirconium-95 production from thermal neutron, (E), 19: 47584(R) (ORNL-3832, pp 1-28)
fission product yield from, 19: 46585 (AD-410522)
neutron capture-to-fission ratio of, (E), 19: 47595(R) (TID-22141, pp 50-66)
neutron capture-to-fission ratio in, engineering drawings of fission chamber for measuring, 19: 47713
neutron fission cross section in fast reactors, method for measuring, 19: 47944 (ANL-7034)
neutron fission cross sections of, technique for measuring thermal, 19: 47567 (CEA-R-2775)
neutron fission of, yields of antimony-124 and -126 and implication on empirical Z_p function in, (E), 19: 47611
neutron scattering and total cross sections of, (E), 19: 47595(R) (TID-22141, pp 50-66)
production of, methods for, 19: 46413

URANIUM ISOTOPES U-238
content in pleistocene formations, 19: 46599
fission product yield from, 19: 46585 (AD-410522)
neutron capture cross section in fast reactors, method for measuring, 19: 47944 (ANL-7034)
neutron resonance absorption in heterogeneous media including moderator scattering, (T), 19: 47953 (BNL-9393)
^{232}Th–^{238}U, neutron resonance absorption in mixtures of, (E/T), 19: 47575 (IDO-16986)

URANIUM MINERALS
composition of vanadic, 19: 46627
conference on, Riverton, Wyoming, June 1965, 19: 46629
gamma rays from, attenuation by air, 19: 46586 (NP-15361)

URANIUM NITRIDES
determination in arc-fused urania, metallographic method for, 19: 46176 (NMI-4997, pp 110-23)
preparation for metallography, 19: 46924 (NMI-4997, pp 55-61)
preparation of coated particulate, for evaluation in ETR, 19: 46913(R) (BMI-1733(Del.))
reactions with refractory metal alloys, metallographic specimen preparation of, 19: 46954 (NMI-5025(Pt.I), pp 39-58)
reactions with refractory metal alloys, metallographic specimen preparation of, 19: 46954 (NMI-5025(Pt.I), pp 39-58)

URANIUM ORES
analysis for sodium, flame photometric, 19: 46191

URANIUM OXIDES
crystal structure of U_4O_9, 19: 46283
crystal structure on surface of pellets of sintered, x-ray diffraction studies of, 19: 47041
elasticity of, oxidation-reduction effects on Young's modulus for, 19: 47921(R) (ANL-7090, pp 30-54)
thermal capacity of U_4O_9, anomaly at 348°K in, 19: 46283

URANIUM(IV) OXIDES
analysis for carbides, excess oxygen, metallic uranium, and nitrides in arc-fused, metallographic, 19: 46176 (NMI-4997, pp 110-23)
diffusion of coated products from carbon-coated particulate, 19: 46913(R) (BMI-1733(Del.))
diffusion of fission fragments in, effects on grain growth and mass transport, 19: 46278
diffusion of fission products from alumina- and beryllia-coated, 19: 46913(R) (BMI-1733(Del.))
diffusion of non-volatile fission products in, 19: 47070
fabrication by vibratory compaction, 19: 46970
fabrication of Zircaloy-clad, 19: 47998(R) (SRO-118)
fission fragment energy deposition and range in cylindrical, slab, and spherical geometries of, 19: 46324(R) (AGN-8132)
fission products diffusion from carbon-coated particulate, effects of temperature on, 19: 46912(R) (BMI-1727(Del.))
preparation of aluminum-coated spheres of, in graphite for metallography, 19: 46925 (NMI-4997, pp 85-91)
preparation of beryllia-coated particulate, for evaluation in BRR and ETR, 19: 46912(R) (BMI-1727(Del.))
preparation of carbon-coated particulate, for evaluation in BRR and ETR, 19: 46912(R) (BMI-1727(Del.))
preparation of coated particulate, for evaluation in BRR, 19: 46913(R) (BMI-1733(Del.))
preparation of silicon carbide-coated particulate, for evaluation in BRR and ETR, 19: 46912(R) (BMI-1727(Del.))
preparation procedures, ceramographic, 19: 46937 (NMI-5025(Pt.I), pp 1-25)
radiation effects on coated particulate, 19: 46912(R) (BMI-1727(Del.))
radiation effects on Zircaloy-clad, at high exposures, 19: 46917(R) (DP-975)

radiolysis of thin films of, in fissiochemical loop, 19: 46324(R) (AGN-8132)
reactions with refractory metal alloys, metallographic specimen preparation of, 19: 46954 (NMI-5025(Pt.I), pp 39-58)
sintering properties of, effects of chromium oxide on, 19: 46971
thermal conductivity of sintered, at 1000 to 2000°C, 19: 46995 (EUR-2424.f)
thermal conductivity of single crystals of, at 1000 to 2200°C, 19: 46995 (EUR-2424.f)
uranium atom ejection from, by fission fragment emission, (T), 19: 47580 (LA-3352)
Al_2O_3–UO_2, radiation effects on fibrous fissiochemical fuels of, 19: 46324(R) (AGN-8132)
Al–UO_2, radiation effects on, 19: 48060(R) (IDO-17081, pp 1-47)
BeO–UO_2, diffusion of fission products from, 19: 46913(R) (BMI-1733 (Del.))
BeO–UO_2, meltdown studies in PBF, feasibility of, 19: 47952 (APDA-177)
BeO–UO_2, radiation effects on stability of, 19: 46912(R) (BMI-1727 (Del.))
BeO–UO_2–Y_2O_3, preparation procedures, ceramographic, 19: 46937 (NMI-5025(Pt.I), pp 1-25)
CaO–UO_2–ZrO_2, enthalpy and thermal conductivity at 100 to 2000°C, 19: 46912(R) (BMI-1727(Del.))
CeO_2–UO_2, radiation effects at high burnup, 19: 46912(R) (BMI-1727 (Del.))
Ni–UO_2, radiation effects on fibrous fissiochemical fuels of, 19: 46324(R) (AGN-8132)
PbO_2–UO_2, neutron resonance absorption in, (E/T), 19: 47575 (IDO-16986)
Pb–UO_2, use as radiation shielding, 19: 46916 (BNWL-IR-3)
PuO_2–UO_2, cost analysis for fuel rod fabrication of, 19: 47976 (BNWL-131A)
PuO_2–UO_2, developments in salt-cycle process for reprocessing, 19: 46422 (BNWL-SA-205)
PuO_2–UO_2, development as fast reactor fuel, 19: 46942(R) (NUMEC-3524-6)
PuO_2–UO_2, dissolution by nitric acid on irradiated stainless steel clad, 19: 46427 (ORNL-3754)
PuO_2–UO_2, fabrication into fuel rods for Saxton reactor, costs of, 19: 46962 (BNWL-131C)
PuO_2–UO_2, variable costs for fabricating fuel rods of, 19: 47977 (BNWL-131B)
ThO_2–UO_2, neutron resonance absorption in, (E/T), 19: 47575 (IDO-16986)
ThO_2–UO_2, preparation of carbon-coated particulate, for evaluation in BRR and ETR, 19: 46912(R) (BMI-1727(Del.))
ThO_2–UO_2, preparation of coated particulate, for evaluation in ETR, 19: 46913(R) (BMI-1733(Del.))
ThO_2–UO_2, preparation of irradiated aluminum-clad lead-bonded, for metallography, 19: 47087 (NMI-4997, pp 189-97)
UO_2–H_2O, critical and safe limits of slightly enriched, 19: 47955 (CONF-651103-6)
UO_2–H_2O, criticality calculations on, 19: 47959 (WCAP-3269-52)
UO_2–Y_2O_3–ZrO_2, preparation procedures, ceramographic, 19: 46937 (NMI-5025(Pt.I), pp 1-25)
UO_2–ZrO_2, crystal structure of calcia-stabilized, 19: 46913(R) (BMI-1733(Del.))
UO_2–ZrO_2, effects on calcia-stabilized at high burnup, 19: 46912(R) (BMI-1727(Del.))
UO_2–ZrO_2, enthalpy and thermal conductivity at 100 to 2000°C, 19: 46912(R) (BMI-1727(Del.))
UO_2–ZrO_2, radiation effects on fibrous fissiochemical fuels of, 19: 46324(R) (AGN-8132)
UO_2–ZrO_2, radiation effects on stability of, 19: 46912(R) (BMI-1727 (Del.))
UO_2–ZrO_2, radiation effects on calcia-stabilized, at high burnups, 19: 46913(R) (BMI-1733(Del.))
UO_2–ZrO_2, radiolysis in fissiochemical loop, 19: 46324(R) (AGN-8132)
U–UC–UO_2, phase studies, 19: 46249(T) (LA-tr-65-15)
U–UO_2, preparation procedures, ceramographic, 19: 46937 (NMI-5025 (Pt.I), pp 1-25)

URANIUM(IV-VI) OXIDES
fluorination of, bromine fluoride partial pressure effects on rate constant for, 19: 47921(R) (ANL-7090, pp 30-54)
radiation effects on structure of dispersion-type fuel elements of, metallography of, 19: 47084 (NMI-4997, pp 124-33)
TiO_2–U_3O_8, preparation and properties of $TiUO_5$ in, 19: 46272

URANIUM(VI) OXIDES
Al_2O_3–UO_3, radiation effects on fibrous fissiochemical fuels of, 19: 46324(R) (AGN-8132)
UO_3–ZrO_2, radiation effects on fibrous fissiochemical fuels of, 19: 46324(R) (AGN-8132)

URANIUM PHOSPHIDES
UP–US, melting point, 19: 47921(R) (ANL-7090, pp 30-54)

URANIUM SILICIDES
allotropic transformation of delta U_3Si, 19: 47024 (NLCO-tr-6)
vaporization, 19: 46298

URANIUM SULFIDES
mechanical properties, 19: 47921(R) (ANL-7090, pp 30-54)
UP–US, melting point, 19: 47921(R) (ANL-7090, pp 30-54)

URANIUM SYSTEMS
radiation effects on, bibliography on, 19: 47093 (VDDIT-16(5.2))
Al–Cr–Fe–Si–U, radioinduced swelling in, resistance to, 19: 47103
Al–Fe–Mo–Si–U, radioinduced swelling in, resistance to, 19: 47103
Al–Fe–Si–U, radioinduced swelling in, resistance to, 19: 47103
Al–Si–U, radiation effects on structure of dispersion-type fuel elements of, 19: 47084 (NMI-4997, pp 124-33)
C–U, atmospheric corrosion of, 19: 46947 (CEA-R-2732)
Fe–Si–U, radioinduced swelling in, resistance to, 19: 47103
Si–U, radioinduced swelling in, resistance to, 19: 47103
U–H_2O, critical and safe limits of slightly enriched, 19: 47955 (CONF-651103-6)
U–H_2O, criticality calculations on, 19: 47959 (WCAP-3269-52)
U–H_2O, neutron buckling in 3% enriched, Monte Carlo calculations of, 19: 47954 (BNWL-127)
U–UC–UO_2, phase studies, 19: 46249(T) (LA-tr-65-15)
U–UO_2, preparation procedures, ceramographic, 19: 46937 (NMI-5025 (Pt.I), pp 1-25)

URANYL ACETATES
effects on induction of metachromasia in rat tissues, 19: 45766
luminescence decay in, measurement, 19: 46737

URANYL IONS
effects on contraction regulation by action potential duration in frog muscles, 19: 45736
reduction of, in potassium halogenates solutions, polarographic, 19: 46260
separation from aqueous chloride solutions by solvent extraction using di-n-octyl phosphinic acid, tracer studies of, 19: 46443

URANYL NITRATES
crystal structure of hexahydrate, 19: 46255
crystal structure of hexahydrate, neutron diffraction studies of, 19: 46257
luminescence decay in, measurement, 19: 46737
separation from nitric acid solutions by solvent extraction using TBP, 19: 46446

URANYL SULFATES
luminescence decay in, measurement, 19: 46737

URANYL VANADATES
preparation and content in vanadic uranium minerals, 19: 46627

UREA
determination in aqueous solutions, methods for, 19: 46324(R) (AGN-8132)
radiation effects on permeability of plant cells by, 19: 45975

UREA, [3-(CHLOROMERCURI)-2-METHOXYPROPYL]-
labeling with mercury-203 for medical uses, 19: 46305

UREA, THIO-
radiolysis of, yields of compounds labeled with phosphorus-32 and sulfur-32 in neutron, 19: 46365

URIC ACID
electrochemical oxidation, 19: 46301 (COO-1148-97)

URINARY TRACT
radiation injuries in human, effects of prednisolone on, 19: 46033
radiation injuries of, induced by radiotherapy, 19: 46061
radiodiagnosis of diseases in children's, methods for reduction of exposure time, 19: 46108

URINE
analysis for glucuronides, 19: 45816(R) (ORO-631, pp 142-4)
analysis for strontium-90 and yttrium-90, use of Cherenkov effect in, 19: 46198
diethylstilbenediol uptake by human, 19: 45797
iodine content of, from children, 19: 45784
iodine-125 and -131 content in, following uptake from milk, 19: 45782
radiation effects on hippuric acid content of, whole-body, 19: 45815(R) (ORO-631, pp 67-76)
radiometric analysis of, use of immersible scintillation counter for, 19: 46083
separation of americium-241 alpha activity from plutonium in, method for, 19: 46187
zinc-65 excretion in human, effects of dietary calcium on, 19: 45787

UTERUS
inflammatory conditions of, late pathology of, 19: 46040

radiation response in patients with carcinomas of, 19: 45830
radiotherapy of carcinomas of, using cobalt-60 intercavitary applicators, 19: 46039(T) (JPRS-31667)
radiotherapy of carcinomas of, effects on urinary tract, 19: 46061
radiotherapy of carcinomas of, 19: 46064
radiotherapy of carcinomas of, effects on rectum, 19: 46099
radiotherapy of cervical carcinoma, pelvic exenteration for extensive visceral necrosis after, 19: 46106

V

VACCINES
preparation of *Brucella melitensis* and *Brucella abortus*, using irradiated bacteria, 19: 45868
VACUUM
photon interactions in, properties of, (T), 19: 47332
VACUUM GAGES
design and performance of diamagnetic suspension absolute, 19: 46579
use of cold and hot cathode, for low gas density measurements, 19: 46733
VACUUM SYSTEMS
hydrogen pressure measurement in ultrahigh, techniques for, 19: 46578
traps for, use of porous metal isolation, 19: 46573 (UCRL-12393-T)
VACUUM TECHNIQUES
for measurement of hydrogen pressure in ultrahigh vacuum systems, 19: 46578
VACUUM VESSELS
electron transfer in spherical, angular distribution in, (T), 19: 46824
VALERIC ACID
8-amino-, labeling with tritium at α-carbon atom, 19: 46306
VALINE
determination in mixture with isoleucine and leucine by infrared spectrometry, 19: 46184(T) (ORNL-tr-341)
labeling with tritium by Wilzbach method, 19: 46311
VALVES
acceleration switching, performance for machine tool control, 19: 48106 (Y-1488)
VAN ALLEN RADIATION BELTS
boundary during solar maximum, determination from energetic electron trapping, (E), 19: 47462
charged particle distribution in, 19: 47491
charged particle measurements in, from Vela Project, 19: 47450 (LA-DC-7365)
electromagnetic perturbation effects on particles trapped in, (T), 19: 47485
electron capture in outer, equatorial angle distribution between, (T), 19: 47474
electron energy distribution in outer, calculation based on modified Fermi heating, 19: 47487
neutron spectra in, 19: 47279
proton diffusion in outer, (T), 19: 47461
VAN DE GRAAFF ACCELERATORS
design and operation at Harwell, 19: 48115
electron dosimetry in 2-Mev, using cerium sulfate solution, 19: 47177
use as high-voltage source in 200-kev accelerator for generating 14-Mev neutrons, 19: 47176
VANADIUM
analysis for thorium using *N*-benzoyl-*N*-phenylhydroxylamine, gravimetric, 19: 46194
determination by complexometric methods using EDTA, 19: 46219
hydrolysis of pentavalent, scheme for, 19: 46237(R) (ORNL-3832, pp 76-99)
VANADIUM ALLOYS
Al–Cu–Fe–Sn–Ti–V, additive and alloying effects on mechanical properties of, 19: 46985 (AD-613651)
Al–Ti–V, interface friction in hot deformation of, 19: 46981(R) (AD-611821)
Mo–Nb–V–Zr, reactions with cesium at 3400°F, metallographic specimen preparation of B-66, 19: 46954 (NMI-5025(Pt.I), pp 39-58)
Mo–Nb–V–Zr, reactions with uranium carbide, nitride, and dioxide, metallographic specimen preparation of B-66, 19: 46954 (NMI-5025 (Pt.I), pp 39-58)
Mo–Nb–V–Zr, weldability studies of B-66, 19: 46966(R) (WANL-PR(P)-007)
Nb–V, interdiffusion in, 19: 47058
VANADIUM ISOTOPES V-48
separation from manganese-52, method for, 19: 46210
VANADIUM ISOTOPES V-51
bremsstrahlung reactions at 25, 29, and 37 Mev, (E), 19: 47596(R) (TID-22141, pp 94-7)
energy levels of, from chromium-51 decay, (E), 19: 47619
nitrogen-14 reactions with, excitation functions for one-neutron-transfer, (E/T), 19: 47586 (ORNL-TM-1218)
nitrogen-14 reactions at 20 to 42 Mev, excitation functions for, (E), 19: 47667
VANADIUM SYSTEMS
Al–C–Cu–H–N–Sn–Ti–V–Zr, mechanical properties of, 19: 46985 (AD-613651)
VAPORIZATION
at high temperatures, use in thermodynamic studies, 19: 46234 (COO-1140-123)
of metal from cylindrical cells, calculation of rates of, 19: 46943(T) (FTD-TT-65-611)
VEHICLES
design of remotely controlled mobile, with manipulators for recovery of aerospace nuclear power devices, 19: 46489 (CONF-640508, pp 327-33)
VELA PROJECT
data from Satellite program of, 19: 47450 (LA-DC-7365)
vent gas treatment plant for Dribble, analytical systems for, 19: 46471 (UCRL-14123)
VESSELS
design for high pressure infrared spectrometer, portable, 19: 46771
VIBRATING REED ELECTROMETERS
use in clinical dosimetry, 19: 46854
VIBRATIONS
effects on animal physiology, 19: 45824(T) (NASA-TT-F-354)
measurement in fuel assemblies, eddy-current transducers for, 19: 46716(R) (IDO-17081, pp 77-123)
VIRGINIA
deuterium content in rainfall in, Nov. 1 and 2, 1963, 19: 47112
gamma aeroradioactivity at 500 ft over, mapping of, 19: 46614
VIRUSES
carcinogenic effects of, 19: 45942
electrical birefringence of tobacco mosaic, 19: 48104 (UCRL-16278)
radiation effects on activation of guanidine- and puromycin-treated infective centers of polio, 19: 46032
radiation effects on production of polio, by monkey-kidney cells, 19: 45955
radiation effects on, and hosts, 19: 45974
radioinduced inactivation of tobacco necrosis, ultraviolet, 19: 45962
radiosensitivity of pathological, 19: 46890
role in leukemia etiology, 19: 45833
separation by centrifugation, engineering drawings of tubes for, 19: 46515
separation of, techniques for containment and sterilization in, 19: 45730(R) (ORNL-3752)
VISION
radiation effects on, of monkeys, 19: 45893
VITAMIN A
effects on polysaccharide metabolism in blood platelets of rats, 19: 45759(R) (ORO-631, pp 77-82)
VITAMIN B_{12}
measurement of cobalt-58-labeled, in urine, 19: 46083
use of cobalt-57-labeled, in radiodiagnosis, 19: 46128
VITAMINS
preparation of labeled, by microbial processes, 19: 46409

W

WASTE DISPOSAL
burial, evaluation of bentonite as moisture barrier in, 19: 48076 (DPSPU-62-30-3A)
economics of, in tanks, 19: 48080 (ORNL-2873)
injection of gases into lithosphere, appraisal at National Reactor Testing Station, 19: 48077 (IDO-12024)
methods of, following processing of irradiated fuel elements, 19: 46435
methods of, review of research and development activities on, 19: 48083
monitoring at Brookhaven, 1963, 19: 46640 (BNL-915)
monitoring in Clinch and Mohawk Rivers, 19: 46646(R) (PHS-999-RH-13)
radiation monitoring at Center for Nuclear Energy, Mol, 19: 46631 (A/AC.82/G/L.986)
research programs on, in Federal Republic of Germany, 19: 48112
system development for large closed-cycle pressurized-water reactors, 19: 48001(R) (WCAP-3743)
WASTE PROCESSING
coagulation precipitation methods of, effects of synthetic detergent on, 19: 48084
evaporation of, heat transfer properties of fluidized-bed spray-type evaporator for, 19: 48079(R) (NP-15371)
film evaporation methods of, design of plant for, 19: 48086
methods in Norway, 19: 48114
methods of, review of research and development activities on, 19: 48083
sorption of fission products by electrocoagulated aluminosilicates,

19: 48082 (UJV-1296/65)
WASTE SOLUTIONS
analysis for strontium-90 in presence of strontium-89, 19: 46196
cesium recovery from Purex Alkaline Supernate by solvent extraction using 4-*sec*-butyl-2(α-methylbenzyl)phenol, 19: 48075 (BNWL-68)
production in large closed-cycle pressurized-water reactors, 19: 48001(R) (WCAP-3743)
separation of rare earths from complexed, by solvent extraction using di(2-ethylhexyl)phosphoric acid, 19: 46432 (ORNL-P-1603)
sorption of radioisotopes from, by rhyodacite tuff, 19: 48085
treatment at Juelich research center, 19: 48078 (JUL-261-DE)
WATER
analysis for metallic impurities, atomic absorption spectroscopy for, 19: 46166 (DP-980)
boiling burnout in pressurized loops in natural circulation conditions, 19: 46536 (RT/ING(65)1)
boiling in heated tubes, burnout in, 19: 46541
boiling instability in forced-convection flows through small tubes, subcooled, 19: 46534 (NP-1543/)
corrosive effects on nickel-plated aluminum at 330°C, 19: 46945 (BNWL-98)
corrosive effects on superalloys at high temperatures, 19: 46946 (BNWL-100)
heat transfer to subcooled, effects of upstream compressibility on, 19: 46546
heat transfer to, at high pressures after critical heat flux, 19: 46554
molecular structure of, x-ray scattering determination of, 19: 46161(R) (ORNL-3832, pp 116-50)
neutron diffusion length in, from time-decaying fields, (E), 19: 47560
neutron energy spectra in, (T), 19: 47964
neutron inelastic scattering by, epithermal, (E/T), 19: 47549(R) (TID-22141, pp 34-49)
neutron spectra in, spatially dependent asymptotic, (T), 19: 47548(R) (TID-22141, pp 3-33)
neutron time-decay constants in, upper bounds for pulsed, (T), 19: 47553
purification for Dragon Reactor, 19: 48042
radioinduced ionization in, (T), 19: 46401
radiolysis, (T), 19: 46401
radiolysis of, acid-base dissociation constants for intermediates from, 19: 46343
radiolysis of, production of H_2O precursor to molecular hydrogen in, 19: 46332(R) (ORNL-3832, pp 50-65)
radiolysis of, reducing radical yields in gamma, 19: 46332(R) (ORNL-3832, pp 50-65)
radiosensitivity effects on peas, 19: 45863
reactions with metals at high temperatures during core meltdown, (E/T), 19: 47960(T) (ORNL-TR-694)
reactions with sodium in prototype boiler, analysis, 19: 46529 (APDA-175)
reactions with sodium in boiler, engineering analysis, 19: 46531(R) (BAW-1280-28)
reactions with water, analysis of, 19: 46530(R) (BAW-1280-27)
spectra in near-infrared at -20 to 250°C, absorption, 19: 46237(R) (ORNL-3832, pp 76-99)
$BaCl_2$–NaCl–H_2O, activity coefficient determination by ultracentrifugation, 19: 46237(R) (ORNL-3832, pp 76-99)
clay–H_2O, cation movement in, 19: 46239(R) (ORO-631, pp 132-41)
ethanol-H_2O, electrochemical properties of uranium (IV) in, 19: 46292
steam–water, analysis of boiling convection channel flows of, (E), 19: 46538(R) (TID-22148)
steam–water, two-phase flow at 1200 psig, orifice and venturi measurements of, 19: 46526 (AECL-2273)
U–H_2O, critical and safe limits of slightly enriched, 19: 47955 (CONF-651103-6)
U–H_2O, criticality calculations on, 19: 47959 (WCAP-3269-52)
U–H_2O, neutron buckling in 3% enriched, Monte Carlo calculations of, 19: 47954 (BNWL-127)
UO_2–H_2O, critical and safe limits of slightly enriched, 19: 47955 (CONF-651103-6)
UO_2–H_2O, criticality calculations on, 19: 47959 (WCAP-3269-52)
WATER-*d*
effects on growth of Agrostemma hypocotyl and Avena coleoptile cylinders, 19: 45763(T) (AD-468388)
WATER-d_2
analysis for metallic impurities, atomic absorption spectroscopy for, 19: 46166 (DP-980)
effects on thermal stability of proteins, 19: 46318
magnetic resonance of photolyzed single-crystal, 19: 46161(R) (ORNL-3832, pp 116-50)
management of, accounting systems at AECL for, 19: 47906 (AECL-2282)
neutron energy spectra in, (T), 19: 47964
neutron spectra in, time-dependent, (T), 19: 47548(R) (TID-22141, pp 3-33)
neutron thermalization in, interference scattering effects on, (T), 19: 47559
solvent properties for alcohols, amino acids and hydrocarbons, 19: 46318
spectra in near-infrared at -20 to 250°C, absorption, 19: 46237(R) (ORNL-3832, pp 76-99)
Fe–D_2O, neutron energy spectra in laminated, variations in, (E/T), 19: 47561
WATER COOLED REACTORS
core meltdown in, metal–water reactions in, (E/T), 19: 47960(T) (ORNL-tr-694)
WATER MODERATED REACTORS
design of experimental heterogeneous, 19: 48074(P)
neutron spectra in, calculation of thermal, 19: 47968
WATER SUPPLIES
fallout contamination of, radiation dose to man from, 19: 46633 (AD-276187)
monitoring of, at Juelich research center, 19: 48078 (JUL-261-DE)
WATER VAPOR
corrosive effects on uranium carbide metallographic specimens, 19: 46953 (NMI-4997, pp 62-75)
reactions with niobium, embrittling effects of, 19: 46296
WELDING
methods for reactor tube, remote gas tungsten-arc, 19: 46973
techniques for fabrication of thermionic cells, 19: 47282(R) (NYO-3429-4)
WELDS
inspection of, radiographic methods of, 19: 46564
WELL LOGGING
equipment for neutron-neutron, 19: 46622(P)
equipment for radiometric, 19: 46624(P)
method for gamma radiometric, 19: 46892(P)
radiometric equipment for, circuitry for, 19: 46623(P)
theory development and calculations for neutron, 19: 46619
WEST VIRGINIA
gamma aeroradioactivity at 500 ft over, mapping of, 19: 46614
WHEAT
strontium-90 content of U. S., 1958 to 1964, 19: 46662
WHISTLERS
power of magnetospheric electron velocity spectra from cyclotron absorption of, (E), 19: 47463
production of proton ion-cyclotron, in ionosphere, (E/T), 19: 47445 (AD-611828)
theory for, magnetoionic, (T), 19: 47464
WHITE OAK CREEK
cesium-137 distribution and fixation in sediments of lacustrine origin in, 19: 46681
WIND
measurements in atmosphere, similarity with temperature, 19: 47110 (RISO-100)
WINDOWS
radiation effects on glass hot-cell, gamma, 19: 47102
WINDSCALE ADVANCED GAS COOLED REACTOR
moderator radiation absorption rate in, calorimeter for determining, 19: 48031
WOOL
analysis for molybdenum, activation, 19: 46192
WOUNDS
radioactive contamination of, action levels in medical treatment of, 19: 46008
WYOMING
uranium occurrence in, survey of, 19: 46629

X

X RADIATION
absorption by fluoroscopic screens, 19: 46150
absorption by krypton and xenon, photoionization cross sections for, (T), 19: 47216 (AD-613675)
chimeras of mice, mortality from secondary disease in, 19: 45910
dose for mice, determination of lethal, 19: 45990
dose received by population from medical use of sources of, 19: 46112
dose reduction in diagnostic, use of, 19: 46146
dosimetry in diagnostic radiology, filtration and kilovoltage effects on depth, 19: 46144
dosimetry of diagnostic, collimation effects on, 19: 46145
dosimetry of diagnostic, ionization chambers for, 19: 46857
dosimetry of diagnostic, scintillator-photomultiplier combination for, 19: 46858
dosimetry of shell irradiation, phantom studies, 19: 46127
dosimetry of, from magnetrons in radar installations, 19: 46673
dosimetry of, photographic, 19: 46853

dosimetry using plastic scintillators, 19: 46105
effects in Drosophila, genetic, 19: 45949
effects in man, genetic, 19: 45967
effects in mice, immunological, 19: 45806 (AD-621543)
effects in mice, lethal, 19: 45982
effects in mice, leukemogenic, 19: 45911
effects in mice, pathological, 19: 45808(R) (NYO-901-36)
effects in rats, genetic, 19: 45808(R) (NYO-901-36)
effects on absorption and luminescence spectra of activated alkali halide phosphors, 19: 47884(T) (IS-Trans-18)
effects on acetylene, methylacetylene, and ethylacetylene, 19: 46334 (TID-22231)
effects on alkaline phosphatase production in mouse bones, 19: 45729(R) (NYO-910-23, pp 1-111)
effects on animal cells in tissue culture, mitotic, 19: 45867
effects on antibody production by transferred spleen cells in mice, 19: 45986
effects on aqueous solutions of DNA, 19: 45729(R) (NYO-910-23, pp 1-111)
effects on aqueous solutions of ADP, 19: 45729(R) (NYO-910-23, pp 1-111)
effects on barley seeds, genetic, 19: 45819(R) (TID-22176)
effects on behavior of rats, fetal exposure, 19: 45894
effects on blood circulation between parabiotic rats, 19: 45838
effects on blood-brain barriers in rabbits, 19: 45970
effects on cell nuclei, biological, 19: 45992
effects on chemiluminescence induction in organic compounds in presence of oxygen, 19: 46344
effects on chromosome aberrations in leukocytes, 19: 45915
effects on chromosomes of lymphocytes in man, morphological, 19: 45916
effects on chromosomes of lymphocytes in man, morphological, 19: 45917
effects on color center distribution in potassium chloride crystals, 19: 46371
effects on connective tissue cells, metabolic, 19: 45895
effects on *Cyathodium tuberosum*, mutagenic, 19: 45901
effects on D-glucose absorption by intestines in active and hibernating ground squirrels, 19: 45841
effects on DNA priming ability in RNAse system, 19: 45849
effects on dog heart, pathological, 19: 45835
effects on *E. coli* mutants, protective effects of phenylbenzamidine against, 19: 46012
effects on electroluminescent screens, (E), 19: 46341(T) (FTD-TT-65-24)
effects on enzyme content in rat intestine, 19: 45927
effects on erythropoiesis in rat embryos, 19: 45826
effects on *Escherichia freundii*, protective effects of fluoroacetate against x, 19: 46015
effects on *Escherichia coli* mutants, 19: 45948
effects on flour beetles, effects of pathogenic bacteria on, 19: 45908
effects on function of rat hematopoietic system, 19: 45984
effects on gaseous 1-butene and *cis* 2-butene, 19: 46335 (TID-22232)
effects on gaseous butadiene, 19: 46336 (TID-22236)
effects on gaseous propene, 19: 46337 (TID-22244)
effects on genetic loads and inbreeding in *D. melanogaster*, 19: 45952
effects on immune reactions in mice, 19: 45827
effects on immune response to transplanted kidneys in man, 19: 45888
effects on immunogenicity of tendon grafts, 19: 45964
effects on immunogenicity of tendon grafts, 19: 45965
effects on inactivation of papain coupled with poly-p-aminophenyl-alanine, 19: 45976
effects on lactic dehydrogenase activity in mouse blood plasma, 19: 45844
effects on leukemia induction, 19: 45915
effects on Lupinus, protective effects of moisture against mutagenic x, 19: 45847
effects on lysozyme activity in rat intestine, whole-body, 19: 45933
effects on mice, 19: 45990
effects on mice, genetic, 19: 45809(R) (NYO-1979-12)
effects on mice, protective effects of AET, glutathione, and serotonin against, 19: 46016
effects on mineral metabolism in mouse bones, 19: 45729(R) (NYO-910-23, pp 1-111)
effects on moisture content of rat tissues, 19: 45896
effects on mouse and rabbit ear, skin recovery processes in, 19: 45987
effects on mouse chromosomes during leukemia induction, 19: 45911
effects on mouse embryos, pathological, 19: 45852
effects on mouse life spans, effects of genetic damage on, 19: 45969
effects on mutation induction in region of X chromosome in *D. melanogaster* DNA, 19: 45879
effects on nuclei in Triton erythroblasts, 19: 45925
effects on nucleic acid content in liver of rat embryos, 19: 45826
effects on nucleic acid synthesis in ϕX174-infected *E. coli*, tracer study, 19: 45851
effects on nucleolar structures of *Cannabis sativa* seedlings, morphological, 19: 45940
effects on osteogenesis of long bones of mouse embryos, 19: 45872
effects on *Paramecium aurelia*, time course of recovery from lethal, 19: 45978
effects on performance capacity of mice and rats, 19: 45823(T) (JPRS-31933, pp 1-5)
effects on performance of tests requiring visual discrimination, by monkeys, 19: 45893
effects on phospholipase activity of intestinal mucosa of rats, 19: 45820(R) (TID-22227)
effects on poliovirus production by monkey-kidney cells, 19: 45955
effects on potassium chloride and sodium chloride phosphors, de-excitation of light sums from, 19: 46379(T)
effects on potatoes, genetic, 19: 45853
effects on proteins, inactivating, 19: 45839
effects on *Pseudomonas aeruginosa*, protective effects of acriflavin and diet against, 19: 46014
effects on pyrimidine mutation induction in *Salmonella typhimurium*, genetic analysis of, 19: 45878
effects on rabbit tibia, time factors for, 19: 45989
effects on rabbit muscle tissues, ESR of free radicals produced in, 19: 45947
effects on rabbit immunity to snake venom, 19: 45970
effects on rat body weight, heritable, 19: 45880
effects on rat skin, pathological, 19: 45957
effects on rectal mucosa of rats, whole-body, 19: 45918
effects on response of animal cells to virus infections, 19: 45974
effects on response of salamanders to tissue grafts, 19: 45897
effects on seeds of red clover, Ultuna, genetic, 19: 45882
effects on skin of guinea pigs, protective effects of chloroquinine, 19: 46019
effects on skin of guinea pigs, pathological, 19: 45869
effects on spleen weight in mice, genetic factors, 19: 45956
effects on suppressor genes in Drosophila, egg-irradiation, 19: 45968
effects on teeth of rats, pathological, 19: 45845
effects on thymus weight in mice, genetic factors, 19: 45956
effects on thymus gland in mice, cytological, 19: 45871
effects on tolerance to bovine serum albumin in rabbits, 19: 45902
effects on tumor implants in mice, effects of oxygen on, 19: 46003
effects on viruses, 19: 45974
effects on 2nd chromosomes in Drosophila, mutagenic, 19: 45876
effects on 4-aminobutyric acid content in brain of guinea pigs, 19: 45979
effects on 4-aminobutyric acid content of brain in dogs, 19: 45979
emission from auroral atmosphere, spatial asymmetry and time variation in microburst, (E), 19: 47470
emission from beta reactions with matter, 19: 47223
emission in solar flares, (T), 19: 47197
energy spectra in auroral zone atmosphere, (E), 19: 47471
intensity of solar, (T), 19: 47210
production by magnetrons in radar installations, 19: 46673
reactions with mercury vapor, electricity production in, (E), 19: 47283(T) (BNL-tr-8)
scattering by lithium deuterides, energy-gap determination from small-angle Compton, (E), 19: 46286
therapeutic use, 19: 46078
therapeutic use of, for carcinomas of esophagus, 19: 46051
therapeutic use of, for basal cell carcinoma, 19: 46059
therapeutic use of, for Hodgkin's disease, 19: 46067
use in astronomy, 19: 47207
use in radiography, preparation of exposure charts for, 19: 46561
use in therapy, 19: 46077
use in therapy of eyelid carcinomas, 19: 46052
use in therapy of metastatic tumors, dose factors, 19: 46101

X-RAY-ABSORPTION ANALYSIS
book: *Advances in X-Ray Analysis* Vol. 8, 19: 46185

X-RAY CAMERAS
photographs from, short-exposure-time, 19: 46729(T) (LA-tr-65-21)

X-RAY-DIFFRACTION ANALYSIS
book: *Advances in X-Ray Analysis* Vol. 8, 19: 46185
powder pattern generation and structure factor calculations for, computer program for, 19: 47877 (LA-3335)
statistical fluctuations in intensity, use in substructure measurements, 19: 46993 (CONF-650810-3)

X-RAY EQUIPMENT
conversion efficiencies of conventional image amplifiers, 19: 46151
design of furnace for intensity measurements on powders, 19: 47009 (NP-15514(Vol.2))
development at Grenoble Nuclear Center, 19: 46512

grid evaluation for diagnostic, 19: 46147
image quality and speed of film-screen combinations in diagnostic, 19: 46149
limitations of optical image intensification, technical, 19: 46744
performance of flash, 19: 46735
phosphors for diagnostic, efficiency of, 19: 46148
X-RAY FLUORESCENCE ANALYSIS
book: *Advances in X-Ray Analysis* Vol. 8, 19: 46185
radioisotope uses as radiation sources in, 19: 46201
X-RAY SOURCES
development of medical, using mercury-197, 19: 46141
energy spectra from, theoretical calculation of, 19: 45729(R) (NYO-910-23, pp 1-111)
preparation of beta-excited, 19: 47223
x-ray purity from gamma-excited, K, 19: 46407 (AAEC/TM-226(Suppl.1))
X-RAY SPECTRA
analysis and compilation of beta-stimulated, 19: 47223
XENON
content in samarskites, 19: 46598
effects on x radiolysis of acetylene, methylacetylene, and ethylacetylene, 19: 46334 (TID-22231)
electron drift velocity and mean energy in, determination of, 19: 47124(T) (SLAC-Trans-19)
exciton spectra in liquid and solid, (E), 19: 47893
ionization by, electron and proton impact at high energies, cross sections for, (T), 19: 47246
meson (π^-) reactions at 9 Bev/c, cross section for, (E), 19: 47689
meson (π^-) reactions at 9 Bev/c, neutron emission in high four-momentum transfer, (E), 19: 47698
photoionization cross sections for, calculation from model wave functions, (T), 19: 47216 (AD-613675)
XENON CHLORIDES
ionization potentials, calculated, 19: 46161(R) (ORNL-3832, pp 116-50)
XENON FLUORIDES
force constants of, calculation of molecular, 19: 46899(R) (ORNL-3832, pp 33-49)
ionization potentials, calculated, 19: 46161(R) (ORNL-3832, pp 116-50)
XENON IONS
beams of, analysis of duoplasmatron, 19: 47267
diffusion in aluminum at high bombardment energies, 19: 47080 (EUR-2478.e)
XENON ISOTOPES
abundance in meteorites, anomaly patterns in, 19: 47213
XENON ISOTOPES Xe-132
energy level schemes for cesium-132 and iodine-132 decay-produced, (E), 19: 47584(R) (ORNL-3832, pp 1-28)
XENON ISOTOPES Xe-133
separation from other fission products, 19: 46414
tracer use for measurement of blood circulation in lungs, 19: 46070
uses of, survey of, 19: 46414
XENON ISOTOPES Xe-135
separation from homogeneous suspension reactor fuels, method for, 19: 46426 (NP-15362)
XENON OXIDES
formation from beta decay of iodine-131 in potassium iodate, 19: 46411

Y

YANKEE POWER REACTOR
criticality calculations for, 19: 47959 (WCAP-3269-52)
YEASTS
growth cycle of *Schizosaccharomyces pombe*, 19: 45820(R) (TID-22227)
radiation effects on *Schizosaccharomyces pombe*, morphological, 19: 45820(R) (TID-22227)
survival of centrifugally frozen, effects of warming rate on, 19: 45730(R) (ORNL-3752)
YTTERBIUM
cohesive energy and ionization of, relation between, (T), 19: 47062
resonance absorption integrals, (E), 19: 47576(R) (IDO-17081, pp 49-76)
separation from aqueous chloride solutions by solvent extraction using di-n-octyl phosphinic acid, tracer studies of, 19: 46443
YTTERBIUM ALLOYS
Co–Yb, crystal structure of Laves phases in, 19: 47052
Pd–Y, phase studies, 19: 47051
Yb–Zn, crystal structure of intermetallic compound $YbZn_2$ in, 19: 47030
YTTERBIUM BROMIDES
thermal decomposition of hydrates of, mechanisms of, 19: 46271
YTTERBIUM FERRATES(III)
crystal structure, 19: 46256
YTTERBIUM IONS
spectra in silicate glass, fluorescence, 19: 47886(T) (N64-21857, pp 1-6)
YTTERBIUM ISOTOPES Yb-170
internal conversion coefficients for E2 transitions in, nuclear structure effects on, (T), 19: 47620
YTTERBIUM ISOTOPES Yb-173
gamma spectra from lutetium-173 decay, (E), 19: 47661
YTTERBIUM ISOTOPES Yb-174
energy levels from lutetium-174 decay, collective and two-particle, (E), 19: 47661
YTTERBIUM OXIDES
atomic charge and permittivity of, (E/T), 19: 47901(T)
oxygen-18 exchange between molecular oxygen and, 19: 46266
reactions with barium carbonates, ternary oxide formation in, 19: 46242(R) (TID-22207, Paper B)
YTTRIUM
effects on ductility of fission–uranium–zirconium alloys, 19: 47004 (NMI-4997, pp 45-54)
neutron scattering length of, 19: 47888
separation from aqueous chloride solutions by solvent extraction using di-n-octyl phosphinic acid, tracer studies of, 19: 46443
separation from other fission products by solvent extraction using benzene–oxine solutions, 19: 46440
separation from strontium by ion exchange, 19: 46196
separation from strontium by chromatographic methods, 19: 46436
UO_2–Y_2O_3–ZrO_2, preparation procedures, ceramographic, 19: 46937 (NMI-5025(Pt.I), pp 1-25)
YTTRIUM ALLOYS
Co–Y, phase diagram, 19: 47053
Cr–Y, fabrication for internal friction studies, 19: 46913(R) (BMI-1733 (Del.))
Hf–Nb–W–Y, weldability studies of C-129Y, 19: 46966(R) (WANL-PR(P)-007)
Mn–Y, phase studies by differential thermal, thermo-magnetical, and x-ray analysis of, 19: 46989 (AD-614466)
Mn–Y, preparation, phase studies, and properties of, 19: 46987 (AD-614462)
Y–Zr, oxidation in dry air at 1200 and 1600°C, 19: 47034
YTTRIUM BROMIDES
thermal decomposition of hydrates of, mechanisms of, 19: 46271
YTTRIUM FERRATES(III)
crystal structure, 19: 46256
YTTRIUM ISOTOPES Y-86
decay of, level scheme for strontium-86 from, (E), 19: 47584(R) (ORNL-3832, pp 1-28)
YTTRIUM ISOTOPES Y-89
production of isomeric, in neutron reactions with zirconium-90 at 14 Mev, (E), 19: 47566 (AERE-R-5009)
proton reactions (p,α) at 20.2 to 22.5 Mev, alpha angular distributions and spectra from, (E/T), 19: 47670
YTTRIUM ISOTOPES Y-90
determination by detection of Cherenkov radiation, 19: 46215
determination in urine using Cherenkov effect, 19: 46198
plant metabolism of, 19: 45804
YTTRIUM OXIDES
atomic charge and permittivity of, (E/T), 19: 47901(T)
crystal structure of, single-crystal x-ray diffraction studies of, 19: 47027
preparation and crystal structure of nonstoichiometric, 19: 46273
reactions with barium carbonates, ternary oxide formation in, 19: 46242(R) (TID-22207, Paper B)
BeO–UO_2–Y_2O_3, preparation procedures, ceramographic, 19: 46937 (NMI-5025(Pt.I), pp 1-25)
YUGOSLAVIA
potassium-40 activity in precipitation and waters in Vinca, 19: 46590(T) (JPRS-31469)
radiation protection standards, 19: 46654(T) (JPRS-31993)

Z

ZINC
content and distribution in beef heart, 19: 45753 (AE-191)
determination by potentiometric titration of acid liberated by complex formation, 19: 46205
dislocation mobility in pure single crystals of, basal, 19: 48089 (CALT-473-4)
erosion of electrodes of neutron-activated, in spark discharge, 19: 47134
neutron cross sections of, shell effects on thermal, (E), 19: 47618
ZINC ALLOYS
Ga–Zn, isotopic exchange of zinc-65 between aqueous solution and, 19: 46209

Mg–Zn, diffusion of beryllium to surface of, on heating at 300 to 500°C, 19: 47071
Yb–Zn, crystal structure of intermetallic compound $YbZn_2$, 19: 47030
ZINC BORATES
luminescence of rare earth ions in, 19: 46269
ZINC IODIDES
iodine exchange with alkyl iodides, 19: 46294
ZINC IONS
effects on contraction regulation by action potential duration in frog muscles, 19: 45736
ZINC ISOTOPES
proton elastic scattering at 14.5 Mev, cross sections for, 19: 47705
ZINC ISOTOPES Zn-64
deuteron inelastic scattering at 15 Mev, energy levels from, (E), 19: 47642
neutron reactions (n,2n) at 12.6 to 19.6 Mev, excitation function for, (E/T), 19: 47571 (EUR-2456.e)
proton scattering at 12 Mev, cross sections for, 19: 47585 (ORNL-3851)
ZINC ISOTOPES Zn-65
determination in shellfish by radiochemical techniques, 19: 46218
distribution in Columbia River effluent, 19: 46680
metabolism in blood cells of swine, effects of dietary calcium, zinc, and fats on, 19: 45759(R) (ORO-631, pp 77-82)
metabolism in dragonflies, effects of body size and temperature on, 19: 45789
metabolism in man, effects of dietary calcium on, 19: 45787
separation by isotopic exchange between aqueous solution and gallium-zinc alloy, 19: 46209
separation from manganese-52, method for, 19: 46210
uptake by tree branches, leaves, needles, roots, and stems from soil, 19: 45773
ZINC ISOTOPES Zn-66
deuteron inelastic scattering at 15 Mev, energy levels from, (E), 19: 47642
separation from zinc-67 by amalgam exchange, 19: 46899(R) (ORNL-3832, pp 33-49)
ZINC ISOTOPES Zn-67
deuteron inelastic scattering at 15 Mev, energy levels from, (E), 19: 47642
separation from zinc-66 by amalgam exchange, 19: 46899(R) (ORNL-3832, pp 33-49)
ZINC ISOTOPES Zn-68
deuteron inelastic scattering at 15 Mev, energy levels from, (E), 19: 47642
ZINC OXIDES
radiation effects on catalytic effects of, on gaseous reactions, 19: 46329 (EUR-2455.e)
ZINC PHOSPHATES
radiation effects on catalytic effects of, on gaseous reactions, 19: 46329 (EUR-2455.e)
ZINC SULFIDES
absorptive properties for x rays as function of photon energy, 19: 46150
ZIRCALOY-2
corrosion by coolant in HWCTR, 19: 46917(R) (DP-975)
corrosion in 8 *M* hydrochloric acid solution at 35 to 105°C, hydrogen pickup in, 19: 46428(R) (ORNL-3847)
radiation effects on corrosion of oxide films on, gamma and neutron, 19: 47099
strain behavior of round and sheet tensile specimens of, 19: 47012 (ORNL-TM-1226)
thickness measurement, autoradiographic technique for, 19: 46964 (NMI-4996, pp 149-63)
ZIRCALOY-4
Nb–Zircaloy-4–Zr, fabrication of tubular, methods for, 19: 47998(R) (SRO-118)
ZIRCONIUM
ablation during re-entry, device for testing, (E), 19: 47117(R) (SC-DC-65-1698)
alpha attenuation by, energy-range relations in, 19: 46324(R) (AGN-8132)
analysis for thorium using *N*-benzoyl-*N*-phenylhydroxylamine, gravimetric, 19: 46194
creep at 660-1425°C under tensile stress, 19: 47074
determination by complexometric methods using EDTA, 19: 46219
determination in niobium carbide–zirconium carbide, method for, 19: 46941 (NP-15514(Vol.3))
determination in titanium carbide–zirconium carbide, method for, 19: 46941 (NP-15514(Vol.3))
determination in tantalum carbide–zirconium carbide, method for, 19: 46941 (NP-15514(Vol.3))
determination using mandelic acid, 19: 46224
diffusion in thorium and uranium dioxides, 19: 47070
dissolution by hydrofluoric acid, effects of sulfuric acid on, 19: 46957(R) (ORNL-3832, pp 100-6)
effects on mechanical properties of aluminum–copper–iron–tin–titanium–vanadium alloys, 19: 46985 (AD-613651)
neutron cross sections of, shell effects on thermal, (E), 19: 47618
oxidation of, electron microscopy of thin films formed in, 19: 46958
precipitation by atrolactic acid and hexahydromandelic acid, 19: 46224
preparation of, by direct iodination of carbide, 19: 46969
radiation effects on corrosion by hydrofluoric acid, neutron, 19: 46957(R) (ORNL-3832, pp 100-6)
radiation effects on corrosion of oxide films on, gamma and neutron, 19: 47099
reactions with water at high temperatures during core meltdown, (E/T), 19: 47960(T) (ORNL-tr-694)
separation from hydrochloric acid solutions by solvent extraction using tetrabutylpyrophosphate and tetrabutylhypophosphate, tracer studies of, 19: 46451
separation from other fission products by solvent extraction using benzene–oxine solutions, 19: 46440
solvent extraction from nitric acid solutions, effects of solvent degradation on, 19: 46430 (ORNL-P-1601)
surface tension of, measurement by pendant drop method, 19: 47065
Nb–Zircaloy-4–Zr, fabrication of tubular, methods for, 19: 47998(R) (SRO-118)
UO_2–Y_2O_3–ZrO_2, preparation procedures, cermographic, 19: 46937 (NMI-5025(Pt.I), pp 1-25)
ZIRCONIUM ALLOYS
welding of Zircaloy sheet to hafnium plates, explosive, 19: 46961 (BMI-X-10139)
fissium–U–Zr, ductility of, effects of aluminum, silicon, titanium, and yttrium additions on, 19: 47004 (NMI-4997, pp 45-54)
Mg–Zr, diffusion of plutonium at 420 to 500°C in, 19: 47066
Mo–Nb–V–Zr, reactions with cesium at 3400°F, metallographic specimen preparation of B-66, 19: 46954 (NMI-5025(Pt.I), pp 39-58)
Mo–Nb–V–Zr, reactions with uranium carbide, nitride, and dioxide, metallographic specimen preparation of B-66, 19: 46954 (NMI-5025(Pt.I), pp 39-58)
Mo–Nb–V–Zr, weldability studies of B-66, 19: 46966(R) (WANL-PR(P)-007)
Mo–Ti–Zr, reactions with cesium at 3400°F, metallographic specimen preparation of TZM, 19: 46954 (NMI-5025(Pt.I), pp 39-58)
Mo–Ti–Zr, reactions with uranium carbide, nitride, and dioxide, metallographic specimen preparation of TZM, 19: 46954 (NMI-5025 (Pt.I), pp 39-58)
Nb–Ta–W–Zr, weldability studies of FS-85, 19: 46966(R) (WANL-PR(P)-007)
Nb–W–Zr, weldability studies of Cb-752, 19: 46966(R) (WANL-PR(P)-007)
Nb–Zr, critical currents in, effect of omega transformation on, (E), 19: 47511
Nb–Zr, current decay propagation in superconducting, persistent, (E), 19: 47507
Nb–Zr, electric conductivity at 200 to 1446°C, 19: 47015 (TIM-854)
Nb–Zr, magnetic flux degradation in superconducting coils of, (E), 19: 47512
Nb–Zr, pressure testing of tubular, 19: 47998(R) (SRO-118)
Nb–Zr, reactions with oxygen at 2000°F, 19: 47016 (TIM-901)
Nb–Zr, tensile properties of pressure tubing of, effects of hot working on, 19: 46539(R) (TID-22249)
Nb–Zr, thermal analysis of ω phase of, 19: 47037
U–Zr, phase diagram of uranium-rich, 19: 47014 (RT/MET(64)4)
U–Zr, radioinduced swelling in clad tubular, 19: 46917(R) (DP-975)
U–Zr, separation of uranium from, by fused salt electrolysis, 19: 46448
U–Zr, structure of, effects of heat treatment on, 19: 47014 (RT/MET 64)4)
Y–Zr, oxidation in dry air at 1200 and 1600°C, 19: 47034
ZIRCONIUM BORIDES
analysis for boron, method for, 19: 46941 (NP-15514(Vol.3))
binding of di-, by chromium, molybdenum, and tungsten, 19: 46907 (AD-456724)
corrosion by hydrogen chloride at 2250°C, 19: 46956 (NP-15514 (Vol.1))
lattice parameters and thermal expansion at 25 to 2020°C, 19: 47009 (NP-15514(Vol.2))
oxidation by carbon dioxide at 2250°C, 19: 46956 (NP-15514(Vol.1))
preparation and purification, 19: 46941 (NP-15514(Vol.3))
reactions with carbon, thermodynamic data for, 19: 46956 (NP-15514 (Vol.1))
thermodynamic properties, 19: 46956 (NP-15514(Vol.1))
vapor pressure at 2267 to 2445°K, 19: 46956 (NP-15514(Vol.1))
ZIRCONIUM CARBIDES

atomic vibrational amplitudes and Debye temperatures at 25 to 1700°C, 19: 47009 (NP-15514(Vol.2))
corrosion by hydrogen chloride at 2250°C, 19: 46956 (NP-15514 (Vol.1))
creep rate of polycrystalline, at 1960 to 2060°K, 19: 47009 (NP-15514 (Vol.2))
determination in niobium carbide–zirconium carbide, method for, 19: 46941 (NP-15514(Vol.3))
Fermi level, 19: 47009 (NP-15514(Vol.2))
iodination of, to prepare pure zirconium, 19: 46969
oxidation by carbon dioxide at 2250°C, 19: 46956 (NP-15514(Vol.1))
preparation and purification, 19: 46941 (NP-15514(Vol.3))
thermal expansion at 25 to 2040°C, 19: 47009 (NP-15514(Vol.2))
NbC–NbN–ZrC, Hall coefficient for solid solutions of, 19: 47009 (NP-15514(Vol.2))
NbC–ZrC, analysis for niobium and zirconium, method for, 19: 46941 (NP-15514(Vol.3))
NbC–ZrC, oxidation by carbon dioxide at 2250°C, 19: 46956 (NP-15514(Vol.1))
TaC–ZrC, analysis for tantalum and zirconium, method for, 19: 46941 (NP-15514(Vol.3))
TiC–ZrC, analysis for titanium and zirconium, method for, 19: 46941 (NP-15514(Vol.3))

ZIRCONIUM COMPLEXES
with alkylenepolyaminoacetic acid type chelating agents, preparation, 19: 46299(P)
with cupferron, radiation effects on, 19: 46761 (NYO-2979-34)

ZIRCONIUM FLUORIDES
complexes with hydrazine, preparation and stability of, 19: 46236 (NIJS-R-430)

ZIRCONIUM HYDRIDES
ablation during re-entry, device for testing, (E), 19: 47117(R) (SC-DC-65-1698)
hydrogen bonding in, neutron scattering study, 19: 46232 (BNWL-SA-239)
neutron inelastic scattering by, thermal, (E/T), 19: 47549(R) (TID-22141, pt 34-49)

ZIRCONIUM ISOTOPES
proton elastic scattering at 14.5 Mev, cross sections for, 19: 47705

ZIRCONIUM ISOTOPES Zr-90
alpha scattering at 34.4 Mev, angular distributions for, (E), 19: 47623
neutron reactions (n,pn) at 14 Mev, production of yttrium-89 isomers in, (E), 19: 47566 (AERE-R-5009)
proton reactions (p,α) at 20.2 to 22.5 Mev, alpha angular distributions and spectra from, (E/T), 19: 47670

ZIRCONIUM ISOTOPES Zr-91
alpha scattering at 34.4 Mev, angular distributions for, (E), 19: 47623

ZIRCONIUM ISOTOPES Zr-92
alpha scattering at 34.4 Mev, angular distributions for, (E), 19: 47623

ZIRCONIUM ISOTOPES Zr-95
beta decay of, β-γ circular polarization correlation in permitted transitions in, (E), 19: 47605
content in atmosphere and drinking water, Monclos Station, Spain, 1964, 19: 46597
content in holothuriae, western Mediterranean, 1962, 19: 46611
distribution in Columbia River effluent, 19: 46680
production by thermal neutron fission of uranium-233 and -235, (E), 19: 47584(R) (ORNL-3832, pp 1-28)

ZIRCONIUM NITRIDES
atomic vibrational amplitudes and Debye temperatures at 25 to 1426°C, 19: 47009 (NP-15514(Vol.2))
preparation and purification, 19: 46941 (NP-15514(Vol.3))
spectra of vaporized, 19: 46982(R) (AD-611856)
thermal expansion at 25 to 1426°C, 19: 47009 (NP-15514(Vol.2))

ZIRCONIUM OXIDES
crystal structure of, in thin films on zirconium, 19: 46958
preparation procedures, ceramographic, 19: 46937 (NMI-5025(Pt.I), pp 1-25)
$CaO–UO_2–ZrO_2$, enthalpy and thermal conductivity at 100 to 2000°C, 19: 46912(R) (BMI-1727(Del.))
$CaO–ZrO_2$, uses as electrolyte in oxygen concentration cells, 19: 46297
$HfO_2–ZrO_2$, thermal expansion of solid solutions of, at 900 to 2500°C, 19: 47045
$UO_2–ZrO_2$, crystal structure of calcia-stabilized, 19: 46913(R) (BMI-1733(Del.))
$UO_2–ZrO_2$, enthalpy and thermal conductivity at 100 to 2000°C, 19: 46912(R) (BMI-1727(Del.))
$UO_2–ZrO_2$, radiation effects on fibrous fissiochemical fuels of, 19: 46324(R) (AGN-8132)
$UO_3–ZrO_2$, radiation effects on fibrous fissiochemical fuels of, 19: 46324(R) (AGN-8132)
$UO_2–ZrO_2$, radiation effects on stability of, 19: 46912(R) (BMI-1727 (Del.))
$UO_2–ZrO_2$, radiation effects on calcia-stabilized, at high burnups, 19: 46913(R) (BMI-1733(Del.))
$UO_2–ZrO_2$, radiation effects on calcia-stabilized at high burnup, 19: 46912(R) (BMI-1727(Del.))
$UO_2–ZrO_2$, radiolysis in fissiochemical loop, 19: 46324(R) (AGN-8132)

ZIRCONIUM SILICATES
reactions with calcium oxide at 1300°C for 50 hr, 1200°C for 70 hr, or 1100°C for 120 hr, 19: 46267

ZIRCONIUM SYSTEMS
Al–C–Ca–H–N–Sn–Ti–V–Zr, mechanical properties of, 19: 46985 (AD-613651)
B–W–Zr, fabrication and mechanical properties of, 19: 46940(R) (NP-15444)
C–Nb–W–Zr, fabrication and mechanical properties of, 19: 46940(R) (NP-15444)
C–Nb–W–Zr, weldability studies of D-43, 19: 46966(R) (WANL-PR(P)-007)
C–W–Zr, fabrication and mechanical properties of, 19: 46940(R) (NP-15444)

REPORT NUMBER INDEX

Reports, conference papers and proceedings, numbered translations, and patents abstracted during the period are included in this index. Each item is listed by report number; this is followed by the abstract number and a brief notation regarding public availability. The index entries show, when known, which reports are on file in the depository libraries, which reports have been published in open-literature journals (journal citation given), and which reports can be purchased (source and price). Whenever a report is identified by more than one number, cross references from secondary to primary report numbers are cited.

The report number codes apply to AEC reports unless designated otherwise. Non-AEC reports are identified by parenthetical notes after the report codes; e.g., (non-AEC), (British), (Canadian), (French). The note (Misc.) identifies those codes used for both USAEC and non-AEC reports. Patents are listed under the heading "PATENTS"; the country of origin is included in parentheses.

A comprehensive listing of both AEC and non-AEC report codes is contained in TID-85(3rd Rev.), *Report Number Series Used by the Division of Technical Information in Cataloging Reports*. This information is also included in the Cumulative Report Number Index (issued annually).

Public Availability of USAEC Reports

All USAEC reports abstracted in *NSA* are available to the public through one or more of the following sources:

(1) Depository libraries in the United States, in other countries, and in international agencies. A list of these depositories appears on the inside covers of each issue of *NSA*.

(2) Scientific and technical journals or other publications.

(3) Microcard Editions, Inc., in Microcard and micronegative form. Orders and inquiries should be sent to: Accounting and Shipping Department, West Salem, Wisconsin 54669.

(4) Clearinghouse for Federal Scientific and Technical Information, U. S. Department of Commerce, Springfield, Virginia 22151.

(5) Superintendent of Documents, U. S. Government Printing Office, Washington, D. C. 20402.

Public Availability of Non-AEC Reports

U. S. Reports. Many reports of U. S. Government agencies are available to the public from the Clearinghouse for Federal Scientific and Technical Information (CFSTI). This availability is given when known. Such reports should be ordered by AD number or NASA-N number. If availability is not shown, inquiries may be directed to CFSTI. In the case of NP numbers, inquiries should be by title and author.

Non-U. S. Reports. Many reports of atomic energy establishments of other countries are deposited in the libraries listed on the inside covers of each issue of *NSA*.

Additionally, the following countries have made their reports available as indicated.

AUSTRALIA

Australian Atomic Energy Commission Research Establishment. Available upon request from the Library, Australian Atomic Research Establishment, Private Mail Bag, Sutherland, New South Wales, Australia.

BELGIUM

Centre d'Étude de l'Énergie Nucléaire. Available upon request to individuals and organizations, from the Centre d'Étude de l'Énergie Nucléaire (CEN), 31, Rue Belliard, Bruxelles, Belgium.

CANADA

Atomic Energy of Canada Limited. For sale by the Technical Information Officer, Atomic Energy of Canada Limited, Chalk River, Ontario, Canada. Copies are also deposited in libraries in the United Kingdom.

National Research Council of Canada. Available from the National Research Council of Canada, Ottawa 2, Ontario, Canada.

DENMARK

Atomic Energy Commission Research Establishment, Risø. Available on exchange from the Library, Danish Atomic Energy Commission, Risø, Roskilde, Denmark. Also for sale by Jul. Gjellerup, Booksellers, 87 Sölvgade, København K., Denmark.

Danatom. Available on loan from Research Establishment, Risø, Roskilde, Denmark. Copies are available from Danatom, Aurehøjvej 2, Hellerup, Denmark.

FRANCE

Commissariat à l'Énergie Atomique. Inquiries for reports numbered 1-2199 should be addressed to Commissariat à l'Énergie Atomique, Service Central de Documentation, Centre d'Études Nucléaires de Saclay, Boite Postale No. 2, Gif-sur-Yvette (S. et O.), France. Reports numbered 2200 and above are available from La Documentation Francaise, 16 Rue Lord-Byron, Paris VIII, France.

Service Central de Protection contre les Rayonnements Ionisants. Copies are available from Ministère de la Santé Publique, Service Central de Protection contre les Rayonnements Ionisants, B. P. n° 35–LE VESINET (S. et O.), France.

GERMANY

Deutsches Elektronen-Synchrotron DESY. Copies are available from Deutsches Elektronen-Synchrotron Desy, Dokumentation, 2000 Hamburg-Gr. Flottbek 1, Notkestieg 1, Germany.

Kernforschungsanlage. Copies may be ordered from Zentralbibliothek der Kernforschungsanlage Jülich, Jülich, Bundesrepublik Deutschland.

Hahn-Meitner-Institute für Kernforschung. Available without charge from Hahn-Meitner-Institute für Kernforschung Berlin, Bibliothek, Glienicker Strasse 100, 1 Berlin 39, Germany. Copies are deposited in many national nuclear centers in the world.

Johann-Wolfgang-Goethe Universität, Frankfurt Am Main, Institut für Kernphysik, (IKF). Copies are available from Gmelin Institut, 40-42 Varrentrappstrasse, Frankfurt (Main), West Germany.

ISRAEL

Israel Atomic Energy Commission. Available without charge from Ministry of Defence/Atomic Energy Com-

mission, Soreq Research Establishment, Yavne, Israel. Copies are deposited in libraries in Israel and in other countries.

ITALY

Centro Informazioni Studi Esperienze (CISE). For sale at CISE Press Office, Casella Postale 3986, Milano, Italy. Copies are deposited in libraries in Italy.

Comitato Nazionale per l'Energia Nucleare. Copies are available from Comitato Nazionale per l'Energia Nucleare, Divisione Affari Internazionali e Studi Economici, Ufficio Pubblicazioni, Via Belisario, 15, Roma, Italy.

JAPAN

Japan Atomic Energy Research Institute (JAERI). Available from the Staff Supply Cooperative of Japan Atomic Energy Research Institute (JAERI), 1-1 Tamura-Cho, Shiba, Minato-Ku, Tokyo, Japan. Copies are deposited in depositories in Tokyo, Nagoya, and Osaka.

Nagoya University. Copies are available from Research Information Center, Institute of Plasma Physics, Nagoya University, Nagoya, Japan.

University of Tokyo. Available free of charge from Institute for Nuclear Study, University of Tokyo, Tanashi-Machi, Kitatama-gun, Tokyo, Japan.

NETHERLANDS

Reactor Centrum Nederland. For sale by Reactor Centrum Nederland, 112 Scheveningseweg, 's-Gravenhage, The Netherlands. Copies are deposited in university libraries in Holland and in many national nuclear centers in the world.

NEW ZEALAND

Institute of Nuclear Sciences. Copies are available from Librarian, Institute of Nuclear Sciences, D.S.I.R., Private Bag, Lower Hutt, New Zealand. Copies are deposited in other countries.

NORWAY

Forsvarets Forskningsinstitutt. Copies available from Norwegian Defence Research Establishment, Library, P. O. Box 25, Kjeller, Norway.

Institutt for Atomenergi. "KR" reports are available on an exchange basis from the Library, Institutt for Atomenergi, Box 40, Kjeller, Norway. Other series are not generally available to the public.

Norwegian Reactor School. Copies are available from The Library, Institutt for Atomenergi, P. O. Box 40, Kjeller, Norway.

PAKISTAN

Atomic Energy Center. Copies are available from Atomic Energy Center, P. O. Box 658, Lahore, (West Pakistan).

POLAND

Reports of the Polish nuclear institutes are published by the Nuclear Energy Information Center of the Government Commissioner for Use of Nuclear Energy. Copies are available from Ośrodek Informacji o Energii Jądrowej, Warszawa, PKiN, Poland.

SPAIN

Junta de Energia Nuclear. "JEN" reports are available without charge from Servicio de Documentation, Junta de Energia Nuclear, Ciudad Universitaria, Madrid (3), Spain.

SWEDEN

Aktiebolaget Atomenergi. "AE" reports are for sale from Aktiebolaget Atomenergi, Library Section, Box 43041, Stockholm 43, Sweden. Bibliographies and literature surveys of the VDDIT- series may be obtained from Aktiebolaget Atomenergi, Information Office, Scientific and Technical Information, Box 43041, Stockholm 43, Sweden. Other series are not generally available to the public. Organizations in the atomic energy field may obtain copies from Aktiebolaget Atomenergi. Microcopy of AE reports is available from the International Documentation Centre, Tumba, Sweden.

SWITZERLAND

CERN European Organization for Nuclear Research. Available without charge from CERN European Organization for Nuclear Research, Geneva 23, Switzerland. Copies are deposited in libraries in 13 countries.

Eidgenössisches Institut für Reaktorforschung. "EIR" reports are available from Eidgenössiches Institut für Reaktorforschung, c/o Bibliothek, Würenlingen/Ag, Switzerland.

TURKEY

Turkish Atomic Energy Commission. Copies are available free of charge from T.A.E.C., Çekmece Nuclear Research Center, P. O. Box 1, Airport, Istanbul, Turkey.

UNITED KINGDOM

United Kingdom Atomic Energy Authority. Some reports are for sale in the United States by the British Information Service (BIS), 845 Third Avenue, New York, N. Y. 10022. United Kingdom reports generally may be purchased from Her Majesty's Stationery Office, London. Copies not for sale by Her Majesty's Stationery Office may be purchased in microcopy form from Micro Methods Limited, East Ardsley, Wakefield, Yorks, England. Report copies are deposited in a large number of libraries in England.

Conferences

Published conference proceedings as well as individual unpublished papers from conferences are included in this index. A CONF number is assigned to the conference if published proceedings are received and also if only a single paper is received. The base number used is year-month-sequence. Thus, the number CONF-650101 would indicate that the conference was held in 1965, in January, and that this was the first January 1965 conference so received. This number would be assigned to complete published proceedings, or if individual papers are received, the base number would be extended to include a paper number, i.e., CONF-650101-1. As additional papers are received, they will be assigned consecutive numbers in the series, CONF-650101-1, 2, 3, 4, etc. This numbering system ensures that all papers received from a conference will be associated with that conference in this index.

If published proceedings are received after the receipt of individual papers, the complete proceedings will be abstracted and the abstract number will appear in this index with the base CONF number.

Abbreviations Used in Availability Column

AECL	For sale by Atomic Energy of Canada Ltd., Chalk River, Ontario, Canada.
BIS	For sale by British Information Service, 845 Third Avenue, New York, N. Y. 10022
CFSTI	For sale by the Clearinghouse for Federal Scientific and Technical Information, U. S. Department of Commerce, Springfield, Virginia 22151. The symbol "cy" indicates that the format of the item sold may be either a printed document or a photographic reproduction (two-thirds of original size) depending upon the availability of printed stock. The indicated price is for either format. The symbol "mn" is used to indicate

that copy is available in the form of micronegatives (microfiche). The number preceding the "mn" symbol indicates the number of micronegatives in the set. Micronegatives are available at the following prices: One micronegative, $0.50; each additional micronegative of the set, $0.25. For additional micronegative copies of the same report requested at the time of the original order, $0.25 per micronegative. Prices are reduced on micronegatives if subscription distribution is purchased.

Dep. AEC reports: Full-size copy is on deposit in the depository libraries both inside and outside the United States. These reports are also for sale by Microcard Editions, Inc., Accounting and Shipping Department, West Salem, Wisconsin 54669.

Non-AEC reports: Full-size copy on deposit in the depository libraries in the United States only.

Dep.(mn) Same as for Dep., except copy is in micronegative (microfiche) form.

DSIR For sale by the National Lending Library for Science and Technology (D.S.I.R.), Boston Spa, Yorkshire, England.

DTI Extension Available from the U. S. Atomic Energy Commission, Division of Technical Information Extension, P. O. Box 62, Oak Ridge, Tennessee 37831.

EM Blueprints and Microcopy of AEC engineering drawings are available from Clearinghouse for Federal Scientific and Technical Information, U. S. Department of Commerce, Springfield, Virginia 22151. Current prices of the CAPE- packages may be obtained from this address. TID-4100, available from the Division of Technical Information Extension, P. O. Box 62, Oak Ridge, Tennessee 37831, contains information on all the CAPE- packages for sale.

Gmelin Available at a nominal charge and under the AED- number shown from Atomic Energy Documentation Center, Gmelin Institute, 40-42 Varrentrappstrasse, Frankfurt (Main), West Germany.

GPO For sale by the Superintendent of Documents, Government Printing Office, Washington, D. C. 20402.

HMSO Her Majesty's Stationery Office, London.

IAEA Available from the International Atomic Energy Agency, Vienna, Austria, and from its sales agencies in various countries throughout the world. A list of these agencies is found in each STI/DOC and STI/PUB publication.

JCL For sale by the Special Libraries Association Translation Center, John Crerar Library, 35 West 33rd Street, Chicago, Illinois 60616.

LC For sale by the Library of Congress, Photoduplication Service, Washington, D. C. 20540.

NAS National Academy of Sciences, National Research Council, Washington, D. C. 20418.

NRC For sale by the National Research Council of Canada, Ottawa, Ontario, Canada.

ORINS Available on interlibrary loan from the Library, Oak Ridge Institute of Nuclear Studies, Post Office Box 117, Oak Ridge, Tennessee 37831.

UKAEA, London Available from United Kingdom Atomic Energy Authority, 11 Charles II Street, London, S. W. 1.

UN United Nations Bookshop, United Nations Headquarters, New York, New York.

USGS Available free of charge from the U. S. Geological Survey, Washington, D. C. 20242.

[The symbols "ph," "mf," and "fs" are used to designate that copy is available only in photostat, microfilm, or facsimile form. The symbol "mn" is used to designate that copy is available in micronegative (microfiche) form. The symbol "cy" is used to designate full size or photographically enlarged copy (two-thirds of original size).]

Report No.	Abstract No.	Availability
A-AC–	**(Misc.)**	
82/G/L.986	19-46631	Dep. mn
82/G/L.987	19-46632	Dep. mn
AAEC-E–	**(Australian)**	
136	19-46230	Dep. mn
AAEC-TM–	**(Australian)**	
226(Suppl.1)	19-46407	Dep. mn
AD–	**(Misc.)**	
276187	19-46633	
410522	19-46585	
423463	19-46634	
425747	19-46566	CFSTI $2.60
425760	19-46456	CFSTI $3.60
456724	19-46907	Bureau of Mines Free
468299	19-46940	See NP-15444
468388	19-45763	CFSTI
611560	19-46708	CFSTI $2.00 cy, $0.50 mn
611629	19-47444	CFSTI $4.00 cy, $1.00 mn
611764	19-46635	CFSTI $3.00 cy, $0.75 mn
611765	19-46636	CFSTI $4.00 cy, $0.75 mn
611779	19-46321	CFSTI $3.00 cy, $0.75 mn
611800	19-46980	CFSTI $3.00 cy, $0.75 mn
611821	19-46981	CFSTI $1.00 cy, $0.50 mn
611828	19-47445	CFSTI $3.00 cy, $0.75 mn
611837	19-46960	CFSTI $1.00 cy, $0.50 mn
611856	19-46982	CFSTI $1.00 cy, $0.50 mn
612013	19-47446	CFSTI $4.00 cy, $1.00 mn
612033	19-46615	CFSTI $1.00 cy, $0.50 mn
612038	19-47564	CFSTI $1.00 cy, $0.50 mn
612070	19-46322	CFSTI $2.00 cy, $0.50 mn
612083	19-47447	CFSTI $5.00 cy, $1.25 mn
612090	19-47076	CFSTI $2.00 cy, $0.50 mn
612113	19-46475	CFSTI $1.00 cy, $0.50 mn
612119	19-47448	CFSTI $1.00 cy, $0.50 mn
612159	19-46983	CFSTI $1.00 cy, $0.50 mn
612182	19-47187	CFSTI $1.00 cy, $0.50 mn
612191	19-46870	CFSTI $1.00 cy, $0.50 mn
612197	19-47113	CFSTI $3.00 cy, $0.50 mn
612254	19-46637	CFSTI $6.00 cy, $1.50 mn
612275	19-46984	CFSTI $3.00 cy, $0.75 mn
612384	19-47873	CFSTI $3.00 cy, $0.75 mn
612409	19-47987	CFSTI $1.00 cy, $0.50 mn
612410	19-47214	CFSTI $1.00 cy, $0.50 mn
613199	19-47449	CFSTI $2.00 cy, $0.50 mn
613287	19-46580	CFSTI $3.00 cy, $0.75 mn
613307	19-47714	CFSTI $3.00 cy, $0.75 mn
613325	19-46876	CFSTI $5.00 cy, $1.25 mn
613358	19-47280	CFSTI $2.75 cy, $1.00 mn
613359	19-46638	CFSTI $5.00 cy, $1.25 mn
613375	19-47215	CFSTI $1.00 cy, $0.50 mn
613468	19-47537	CFSTI $1.00 cy, $0.50 mn
613471	19-47077	CFSTI $4.00 cy, $0.75 mn
613480	19-47863	CFSTI $4.00 cy, $0.75 mn
613529	19-46323	CFSTI $2.00 cy, $0.50 mn
613537	19-48087	CFSTI $3.00 cy, $0.75 mn
613575	19-47216	CFSTI $1.00 cy, $0.50 mn
613582	19-47217	CFSTI $7.00 cy, $1.75 mn
613606	19-47874	CFSTI $3.00 cy, $0.75 mn
613622	19-47715	CFSTI $1.00 cy, $0.50 mn
613636	19-47188	CFSTI $2.00 cy, $0.50 mn
613643	19-47078	CFSTI $1.00 cy, $0.50 mn
613651	19-46985	CFSTI $1.00 cy, $0.50 mn
613660	19-46231	CFSTI $2.00 cy, $0.50 mn
613674	19-46457	CFSTI $6.00 cy, $1.25 mn
613929	19-47218	CFSTI $1.00 cy, $0.50 mn
613934	19-47298	CFSTI $1.00 cy, $0.50 mn
613959	19-46476	CFSTI $6.00 cy, $1.50 mn
613991	19-46465	CFSTI $2.00 cy, $0.50 mn
613998	19-48046	CFSTI $1.00 cy, $0.50 mn
614046	19-47299	CFSTI $1.00 cy, $0.50 mn
614111	19-46570	CFSTI $3.00 cy, $0.75 mn
614118	19-46709	CFSTI $2.00 cy, $0.50 mn
614136	19-47875	CFSTI $1.00 cy, $0.50 mn
614253	19-47219	CFSTI $4.00 cy, $0.75 mn
614268	19-46871	CFSTI $1.00 cy, $0.50 mn
614270	19-47565	CFSTI $2.00 cy, $0.50 mn
614283	19-47716	CFSTI $1.00 cy, $0.50 mn
614285	19-47717	CFSTI $4.00 cy, $1.00 mn
614286	19-47114	CFSTI $3.00 cy, $0.75 mn
614435	19-47876	CFSTI $1.00 cy, $0.50 mn
614442	19-47718	CFSTI $5.00 cy, $1.25 mn
614462	19-46987	CFSTI $2.00 cy, $0.50 mn
614464	19-46908	CFSTI $3.00 cy, $0.75 mn
614465	19-46988	CFSTI $3.00 cy, $0.75 mn
614466	19-46989	CFSTI $2.00 cy, $0.50 mn
619323	19-46574	CFSTI
619334	19-47019	CFSTI
619382	19-46540	CFSTI
619512	19-46534	See NP-15437
620264	19-46909	
620589	19-46910	CFSTI $1.00 cy, $0.50 mn
621543	19-45806	CFSTI $1.00 cy, $0.50 mn
621549	19-46872	CFSTI $3.00 cy, $0.75 mn
AE–	**(Non-AEC)**	
191	19-45753	Dep. mn
AEC-tr–	**(For complete listing see TID-4025)**	
6487	19-48107	Dep. mn; CFSTI $3.00 cy, $0.75 mn
6570	19-46340	Dep.(mn); $1.00(cy), 1(mn) CFSTI; $1.60(fs), $0.80(mf) JCL
6615	19-46968	Dep. mn; CFSTI $1.00 cy, $0.50 mn; JCL $1.60 fs, $0.80 mf
6616	19-47020	Dep. mn; CFSTI $2.00 cy, $0.50 mn; JCL $2.60 fs, $0.83 mf
AECL–	**(Canadian)**	
2261	19-46300	Dep.; AECL $0.50 cy
2262	19-46162	Dep.; AECL $0.50
2263	19-46163	Dep.; AECL $0.50
2270	19-46750	Dep.; AECL $1.00
2273	19-46526	Dep.; AECL $1.50
2281	19-46639	Dep.; AECL $0.50
2282	19-47906	Dep.; AECL $1.00
AED-C–	**(Non-AEC)**	
04-17	19-45807	Dep. mn
AEEW-M–	**(British)**	
526	19-46751	Dep.; BIS $0.40; HMSO 2s.
AEEW-R–	**(British)**	
426	19-46527	Dep.; BIS $0.50; HMSO 2s. 6d.
AERE-M–	**(British)**	
1479	19-47064	J. Nucl. Mater., 16: 233-48(1965)
1564	19-46752	Dep.; BIS $0.50; HMSO 2s. 6d.
1581	19-47107	Phil. Mag. (8), 12: 427-30(1965)
AERE-R–	**(British)**	
4705	19-47098	J. Nucl. Mater., 16: 249-59(1965)
4752	19-47105	Phil. Mag. (8), 12: 261-72(1965)
4779	19-47099	J. Nucl. Mater., 16: 290-7(1965)
4782	19-47065	J. Nucl. Mater., 16: 260-70(1965)
4793	19-46278	J. Nucl. Mater., 16: 298-305(1965)
4800	19-47066	J. Nucl. Mater., 16: 271-89(1965)
4895	19-46753	Dep.; BIS $0.80; HMSO 4s.
5002	19-46164	Dep.; BIS $0.20; HMSO 1s. 2d.
5009	19-47566	Dep.; BIS $0.50; HMSO 2s. 6d.
5014	19-47079	Dep.; BIS $0.50; HMSO 2s. 6d.
AFCRL–	**(Non-AEC)**	
64-917	19-47444	See AD-611629
65-84	19-47718	See AD-614442
65-158	19-47219	See AD-614253
65-192	19-47716	See AD-614283
65-199	19-47299	See AD-614046
AFML-TR–	**(Non-AEC)**	
64-392	19-46911	
AFOSR–	**(Misc.)**	
65-0656	19-47875	See AD-614136
880	19-47298	See AD-613934
3031	19-47215	See AD-613375
3433	19-47187	See AD-612182

Report No.	Abstract No.	Availability
AFOSR-TR–	**(Non-AEC)**	
60-120	19-47714	See AD-613307
AGN–	**(Misc.)**	
8132	19-46324	Dep. mn; CFSTI $6.00 cy, $1.25 mn
AMRA-TR–	**(Non-AEC)**	
64-41	19-47078	See AD-613643
65-03	19-46985	See AD-613651
ANL–		
6776	19-47988	Dep. mn; CFSTI $2.00 cy, $0.50 mn
6983	19-47115	Dep. mn; CFSTI $3.00 cy, $0.75 mn
7013	19-46325	Dep. mn; CFSTI $2.00 cy, $0.50 mn
7034	19-47944	Dep. mn; CFSTI $2.00 cy, $0.50 mn
7038	19-46528	Dep. mn; CFSTI $2.00 cy, $0.50 mn
7039	19-47281	Dep. mn; CFSTI $1.00 cy, $0.50 mn
7050	19-47907	Dep. mn; CFSTI $6.00 cy, $2.50 mn
7061	19-47865	Dep. mn; CFSTI $1.00 cy, $0.50 mn
7090	19-47920	Dep. mn; CFSTI $3.00 cy, $0.75 mn
APDA–	**(Misc.)**	
173	19-47951	Dep. mn; CFSTI $2.00 cy, $0.50 mn
175	19-46529	Dep. mn; CFSTI $3.00 cy, $0.50 mn
177	19-47952	Dep. mn; CFSTI $3.00 cy, $0.75 mn
ARL–	**(Non-AEC)**	
65-121	19-46477	CFSTI
65-131	19-47719	
65-138	19-46990	
ASE–	**(Non-AEC)**	
759	19-47444	See AD-611629
AWRE-NR–	**(British)**	
1/65	19-47157	Dep.; BIS $0.30; HMSO 1s. 9d.
AWRE-O–	**(British)**	
47/65	19-46991	Dep.; BIS $0.90; HMSO 4s. 6d.
BAW–	**(Misc.)**	
1280-25	19-46478	Dep. mn; CFSTI $3.00 cy, $0.50 mn
1280-27	19-46530	Dep. mn; CFSTI $2.00 cy, $0.50 mn
1280-28	19-46531	Dep. mn; CFSTI $2.00 cy, $0.50 mn
BM-RI–	**(Misc.)**	
6549	19-46907	See AD-456724
BMI–	**(Misc.)**	
1727(Del.)	19-46912	Dep. mn; CFSTI $1.00 cy, $0.50 mn
1733(Del.)	19-46913	Dep. mn; CFSTI $1.00 cy, $0.50 mn
BMI-X–		
10139	19-46961	Dep. mn; CFSTI $2.00 cy, $0.50 mn
BNL–		
910	19-47158	Dep. mn; CFSTI $2.00 cy, $0.50 mn
915	19-46640	Dep. mn; CFSTI $1.00 cy, $0.50 mn
8116	19-46553	See CONF-650812-10
8308	19-46014	Intern. J. Radiation Biol., 9: 213-18(1965)
8447	19-45912	J. Pract. Nursing, 14: 24-6(1964)
8940	19-47625	J. Inorg. Nucl. Chem., 27: 1879-80(1965)
8957	19-46121	Radiology, 85: 555-64(1965)
9184	19-46806	IEEE (Inst. Elec. Electron. Engrs.), Trans. Nucl. Sci., NS-12: No. 4, 222-6(1965)
9248	19-47231	J. Geophys. Res., 70: 4992-4(1965)
9260	19-46784	IEEE (Inst. Elec. Electron. Engrs.), Trans. Nucl. Sci., NS-12: No. 4, 37-48(1965)
9308	19-48054	Dep. mn; CFSTI $3.00 cy, $0.75 mn
9388	19-47159	Dep. mn; CFSTI $1.00 cy, $0.50 mn
9393	19-47953	Dep. mn; CFSTI $1.00 cy, $0.50 mn
9402	19-48055	Dep. mn; CFSTI $1.00 cy, $0.50 mn
9443	19-47116	Dep. mn; CFSTI $1.00 cy, $0.50 mn
9450	19-47975	Dep. mn; CFSTI $1.00 cy, $0.50 mn
9478	19-47503	Dep. mn; CFSTI $1.00 cy, $0.50 mn
9482	19-47160	Dep. mn; CFSTI $2.00 cy, $0.50 mn
9483	19-47161	Dep. mn; CFSTI $1.00 cy, $0.50 mn
9488	19-45726	Dep. mn; CFSTI $1.00 cy, $0.50 mn
9492	19-46756	Dep. mn; CFSTI $1.00 cy, $0.50 mn
9503	19-47162	Dep. mn; CFSTI $1.00 cy, $0.50 mn
9504	19-47163	Dep. mn; CFSTI $1.00 cy, $0.50 mn
9506	19-45727	Dep. mn; CFSTI $1.00 cy, $0.50 mn
9510	19-48056	Dep. mn; CFSTI $2.00 cy, $0.50 mn
9520	19-47300	Dep. mn; CFSTI $2.00 cy, $0.50 mn
9535	19-46754	Dep. mn; CFSTI $1.00 cy, $0.50 mn
BNL-tr–		
8	19-47283	Dep. mn; JCL $1.00 fs, $0.80 mf
BNWL–		
59	19-46710	Dep. mn; CFSTI $2.00 cy, $0.50 mn
68	19-48075	Dep. mn; CFSTI $1.00 cy, $0.50 mn
70	19-46903	Dep. mn; CFSTI $2.00 cy, $0.50 mn
98	19-46945	Dep. mn; CFSTI $2.00 cy, $0.50 mn
100	19-46946	Dep. mn; CFSTI $3.00 cy, $0.75 mn
105	19-47990	Dep. mn; CFSTI $3.00 cy, $0.75 mn
109	19-48057	Dep. mn; CFSTI $3.00 cy, $0.75 mn
113-6	19-48088	Dep. mn; CFSTI $2.00 cy, $0.50 mn
116	19-46532	Dep. mn; CFSTI $2.00 cy, $0.50 mn
127	19-47954	Dep. mn; CFSTI $2.00 cy, $0.50 mn
130	19-48058	Dep. mn; CFSTI $1.00 cy, $0.50 mn
131A	19-47976	Dep. mn; CFSTI $2.00 cy, $0.50 mn
131B	19-47977	Dep. mn; CFSTI $2.00 cy, $0.50 mn
131C	19-46962	Dep. mn; CFSTI $2.00 cy, $0.50 mn
141	19-46914	Dep. mn; CFSTI $1.00 cy, $0.50 mn
144	19-46755	Dep. mn; CFSTI $1.00 cy, $0.50 mn
BNWL-C–		
27-7	19-46539	See TID-22249
BNWL-IR–		
2	19-46915	Dep. mn; CFSTI $1.00 cy, $0.50 mn
3	19-46916	Dep. mn; CFSTI $1.00 cy, $0.50 mn
BNWL-SA–		
115	19-47106	Phil. Mag. (8), 12: 419-21(1965)
161	19-46711	Dep. mn; CFSTI $1.00 cy, $0.50 mn
169	19-46712	Dep. mn; CFSTI $1.00 cy, $0.50 mn
205	19-46422	Dep. mn; CFSTI $1.00 cy, $0.50 mn
239	19-46232	Dep. mn; CFSTI $1.00 cy, $0.50 mn
CALT–		
473-4	19-48089	Dep. mn; CFSTI $3.00 cy, $0.75 mn
CAPE–		
1202	19-46866	
1203	19-48044	
1211	19-46863	
1213	19-46864	
1222	19-46745	
1223	19-46746	
1225	19-46225	
1226	19-46747	
1228	19-46865	
1229	19-47713	
1237	19-46515	
1242	19-46867	
CEA-Bib–	**(French)**	
63	19-46466	Dep. mn
CEA-R–	**(French)**	
2732	19-46947	Dep. mn
2733	19-46963	Dep. mn
2752	19-46233	Dep. mn
2771	19-46641	
2772	19-46757	Dep. mn
2775	19-47567	Dep. mn
2779	19-47568	Dep. mn
2782	19-47978	Dep. mn
2787	19-45754	Dep. mn
2792	19-46992	Dep. mn
2805	19-46948	Dep. mn
2809	19-45755	Dep. mn
2811	19-46713	Dep. mn
2837	19-46165	Dep. mn
CERN–	**(European Organization for Nuclear Research)**	

Report No.	Abstract No.	Availability
65-30	19-47301	Dep. mn
CEX-62-50	19-47569	Dep. mn; CFSTI $1.00 cy, $0.50 mn
CHAEM-28	(Turkish) 19-46326	Dep. mn
CHLM-6342	(Misc.) 19-46458	Dep. mn; CFSTI $3.00 cy, $0.75 mn
CONF-32-3	(Health Physics Society 7th Annual Meeting, Chicago, June 1962) 19-48076	See DPSPU-62-30-3A
CONF-105	19-46930	(17th Atomic Energy Commission Metallography Group Meeting, Los Alamos, N. Mex., May 1963) See NMI-4999
CONF-387	19-46291	(1st Australian Conference on Electrochemistry, Sydney, Feb. 1963)
CONF-550-99	(The International Conference on High-Energy Physics, Dubna, August 5–15, 1964) 19-46758	Dep. mn
CONF-607(Pt.I)	19-46936	(AEC Metallography Group 18th Meeting, Canoga Park, Calif., June 1964) See NMI-5025(Pt.I)
CONF-715	19-46185	(13th Annual Conference on Applications of X-Ray Analysis, Denver, Aug. 12–14, 1964)
CONF-600401	19-46919	(14th Metallographic Group Meeting, West Concord, Mass., Apr. 5–6, 1960) See NMI-4996
CONF-610501	19-46921	(15th Metallographic Group Meeting, Aiken, S. C., May 17–19, 1961) See NMI-4997
CONF-610601-1	(Health Physics Society Meeting, Las Vegas, Nev., June 12–16, 1961) 19-46633	See AD-276187
CONF-620301	19-46926	(16th Metallographic Group Meeting, Richland, Wash., Mar. 28–29, 1962) See NMI-4998
CONF-620302	19-46037	(Symposium on Technological Needs for Reduction of Patient Dosage from Diagnostic Radiology, Washington, D. C., Mar. 5–6, 1962)
CONF-620404-1	(Symposium on the Physics of Graphite Moderated Reactors, Bournemouth, England, Apr. 4–7, 1962) 19-47999	See TRG-Report-227
CONF-621006	19-45746	(1st International Symposium on Basic Environmental Problems of Man in Space, Paris, Oct. 29–Nov. 2, 1962)
CONF-630701-1	(6th International Conference on Ionization Phenomena in Gases, Paris, July 8–13, 1963) 19-47724	See MATT-267
CONF-630912	19-47075	(Conference on Mechanisms of Solid Friction, Kansas City, Mo., Sept. 16–18, 1963)
CONF-631105	19-46690	(Seminar on Protection of the Public in the Event of Radiation Accidents, Geneva, Nov. 18–22, 1963)
CONF-640508	19-46479	(Project Rose Seminar on Remotely Operated Special Equipment, Germantown, Md., May 26–27, 1964) Proceedings
CONF-640902	19-46732	(3rd International Measurement Conference, Stockholm, Sept. 14–19, 1964)
CONF-640918-1	(Symposium of High Energy Electrons, Montreux, Switzerland, Sept. 1964) 19-46714	Dep. mn; CFSTI $1.00 cy, $0.50 mn
CONF-641008	19-47802	(Seminar on Plasma Physics, Trieste, Italy, Oct. 5–31, 1964) See STI/PUB/89
CONF-641108-45	(American Physical Society, New York, Nov. 4–8, 1964) 19-47267	Gmelin, AED-CONF-64-196-78
CONF-641120	19-46491	(Project Rose Seminar on Remotely Operated Special Equipment, Jackass Flats, Nev., Nov. 4–5, 1964) Proceedings
CONF-641124-1	(International Conference on Applications of Fundamental Thermodynamics to Metallurgical Processes, Pittsburgh, Nov. 29–Dec. 1, 1964) 19-46234	See COO-1140-123
CONF-650101-3	(Mössbauer Symposium, New York, Jan. 26, 1965) 19-46748	Gmelin, AED-CONF-65-006-5
CONF-650115	19-46565	(11th National Symposium on Reliability Quality Control, Miami Beach, Fla., Jan. 12–14, 1965)
CONF-650219-1	(Canadian Assn. of Radiologists, 28th Annual Meeting, Toronto, Ont., Canada, Feb. 24–28, 1965) 19-46003	Gmelin, AED-CONF-65-043-1
CONF-650221-1	(Biophysical Society, 9th Annual Meeting, San Francisco, Feb. 24–26, 1965) 19-46034	ORINS
CONF-650311-3	(Conference on Analytical Chemistry and Applied Spectroscopy, Pittsburgh, Mar. 5, 1965) 19-46226	Gmelin, AED-CONF-65-025-2
CONF-650317-8	(American Physical Society Meeting, Kansas City, Mo., Mar. 25, 1965) 19-47536	Gmelin, AED-CONF-65-03[illegible]7
CONF-650327-2	(American Society of Tool and Mfg. Engineers, Annual Conference, Cleveland, Mar. 29–Apr. 2, 1965) 19-48098	See SC-R-65-902
CONF-650401-14	(American Chemical Society, Detroit, Apr. 4–9, 1965) 19-46181	See WAPD-T-1769
CONF-650405-10	(International Conference on Modern Trends in Activation Analysis, College Station, Tex., Apr. 19–22, 1965) 19-46228	Gmelin, AED-CONF-65-040-18
13	19-46229	Gmelin, AED-CONF-65-040-10
17	19-46227	Gmelin, AED-CONF-65-040-26
CONF-650410-41	(American Physical Society, Washington, D. C., Apr. 26–29, 1965) 19-47410	Gmelin, AED-CONF-65-073-77
44	19-47266	Gmelin, AED-CONF-65-073-80
CONF-650423-5	(International Conference on Physics of Solids and High Pressures, Tucson, Apr. 19–21, 1965) 19-47905	Gmelin, AED-CONF-65-058-12
CONF-650428-2	(Conference on Phenomena in the Neighborhood of the Critical Point, Washington, D. C., Apr. 5–8, 1965) 19-47904	Gmelin, AED-CONF-65-078-5
CONF-650436	19-47153	(6th Symposium on Engineering Aspects of Magnetohydrodynamics, Pittsburgh, Apr. 21–22, 1965)
CONF-650442-2	(2nd Space Congress, Cocoa Beach, Fla., Apr. 5–7, 1965) 19-48094	See SC-DC-65-1646
CONF-650501	19-47907	(The Application of Computing Methods to

Report No.	Abstract No.	Availability
		Reactor Problems, Argonne, Ill., May 17–19, 1965) See ANL-7050
CONF-650510	19-46778	(Purdue Conference on Instrumentation for High Energy Physics, Lafayette, Indiana, May 11–15, 1965)
CONF-650512	19-37944	(Symposium on Engineering Problems of Controlled Thermonuclear Research, Livermore, Calif., May 4–7, 1965)
9	19-46718	See LA-DC-7015
10	19-46719	See LA-DC-7030
11	19-47121	See UCRL-16080
CONF-650533–		(American Assn. on Contamination Control, Annual Meeting, Miami, Fla., May 25, 1965)
2	19-46645	See ORNL-TM-1228
CONF-650540–		(American Industrial Hygiene Assn. Meeting, Houston, Tex., May 4–7, 1965)
3	19-46707	Gmelin, AED-CONF-65-116-1
4	19-46706	Gmelin, AED-CONF-65-116-3
CONF-650552–		(Institute of Food Technologists, 25th Annual Meeting, Kansas City, Mo., May 16–20, 1965)
1	19-46877	Dep. mn; CFSTI $1.00 cy, $0.50 mn; Gmelin, AED-CONF-65-111
CONF-650556–		(Symposium on Electrical Methods and Principles in Molecular Biology, Jena, Germany, May 25–29, 1965)
1	19-46301	See COO-1148-97
CONF-650559	19-47991	(American Institute of Chemical Engineers, 56th National Meeting, San Francisco, Calif., May 16–19, 1965) See GA-6126
CONF-650631–		(International Powder Metallurgical Conference, New York, June 14–17, 1965)
2	19-46996	See EUR-2479.e
3	19-47080	See EUR-2478.e
CONF-650637–		(International Conference on Luminescent Dosimetry, Palo Alto, Calif., June 21–23, 1965)
3	19-46338	See UCRL-12367
CONF-650704–		(IAEA Symposium on Thermodynamics, Vienna, July 22–27, 1965)
15	19-46296	ORINS
16	19-46297	ORINS
22	19-46298	ORINS
CONF-650706–		(International Conference on the Study of Nuclear Structure with Neutrons, Antwerp, July 19–23, 1965)
23	19-47571	See EUR-2456.e
24	19-47581	See LA-DC-6730
CONF-650711–		(AIAA 2nd Annual Meeting and Technical Demonstration, San Francisco, July 26–29, 1965)
22	19-46547	ORINS
CONF-650803–		(IAEA Symposium on Nuclear Materials Management, Vienna, Aug. 30–Sept. 3, 1965)
8	19-47906	See AECL-2282
CONF-650804–		(5th Rare Earth Research Conference, Ames, Iowa, Aug. 30–Sept. 1, 1965)
8	19-46241	See TID-22207, Paper A
9	19-46994	See COO-1149-52
CONF-650806–		(7th International Conference on Phenomena in Ionized Gases, Belgrade, Aug. 22–27, 1965)
11	19-47723	See LA-DC-7112
13	19-47116	See BNL-9443
CONF-650810–		(Annual Conference on Applications of X-Ray Analysis, Denver, Aug. 25–27, 1965)
3	19-46993	Dep. mn; CFSTI $2.00 cy, $0.50 mn
CONF-650812–		(ASME–AIChE Heat Transfer Conference and Exhibit, Los Angeles, Aug. 8–11, 1965)
2	19-46546	ORINS
4	19-46549	ORINS
5	19-46548	ORINS
6	19-46550	ORINS
8	19-46554	ORINS
9	19-46551	ORINS
10	19-46553	ORINS
11	19-46552	ORINS
CONF-650816–		(Conference on Radiation Trapped in the Earth's Magnetic Field, Bergen, Norwry, Aug. 16–Sept. 3, 1965)
2	19-47450	See LA-DC-7365
CONF-650817–		(Gordon Research Conference on Ion Exchange, New London, N. H., Aug. 2–6, 1965)
1	19-46180	See UCRL-16254
CONF-650902–		(American Chemical Society, 150th National Meeting, Atlantic City, Sept. 12–17, 1965)
17	19-46422	See BNWL-SA-205
CONF-650905–		(American Institute of Chemical Engineers Symposia, Minneapolis, Sept. 26–29, 1965)
2	19-46949	Dep. mn; CFSTI $2.00 cy, $0.50 mn
CONF-650918–		(International Conference on the Chemistry of the Solvent Extraction of Metals, Harwell, Berks., England, Sept. 1965)
4	19-46423	See DPSPU-64-30-28
5	19-46430	See ORNL-P-1601
6	19-46431	See ORNL-P-1602
7	19-46432	See ORNL-P-1603
CONF-650919–		(Technicon Analytical Symposium, New York, Sept. 8–10, 1965)
3	19-46429	See ORNL-P-1522
CONF-650922–		(1st International Symposium on Magnet Technology, Stanford, Calif., Sept. 8–10, 1965)
3	19-47170	See UCRL-16384
8	19-47166	See ORNL-P-1605
9	19-47167	See ORNL-P-1619
11	19-46965	See UCRL-16383
CONF-650923–		(5th International Conference on High Energy Accelerators, Frascati, Italy, Sept. 9–16, 1965)
5	19-47161	See BNL-9483
7	19-47163	See BNL-9504
9	19-46756	See BNL-9492
11	19-47162	See BNL-9503
CONF-650924–		(Workshop Conference on Space Radiation Biology, Berkeley, Calif., Sept. 7–10, 1965)
2	19-46339	See UCRL-16358
3	19-46770	See UCRL-16354
CONF-650926–		(9th Meeting of the IMOG Subgroup on Environmental Testing, Amarillo, Tex., Sept. 14–15, 1965)
1	19-46723	See RFP-641
CONF-650928–		(International Conference on Polarization Phenomena of Nucleons, Karlsruhe, Germany, Sept. 6–10, 1965)
1	19-47570	See COO-7-0361
CONF-650932–		(Symposium on the Inelastic Scattering of Neutrons by Condensed Systems, Upton, N. Y., Sept. 1965)
1	19-46232	See BNWL-SA-239
2	19-47879	See LA-DC-7277
3	19-47572	See GA-6547
CONF-650933–		(Symposium on Advanced Problems and Methods in Fluid Dynamics, Jurata, Poland, Sept. 1–7, 1965)
1	19-46533	See LA-DC-7373
CONF-650935–		(2nd IAEA Conference on Plasma Physics and Controlled Nuclear Fusion Research, Culham, England, Sept. 6–10, 1965)
2	19-47722	See LA-DC-7039

Report No.	Abstract No.	Availability
3	19-47852	ORINS
4	19-47831	ORINS
5	19-47837	ORINS
7	19-47851	ORINS
8	19-47850	ORINS
9	19-47853	ORINS
10	19-47833	ORINS
11	19-47854	ORINS
12	19-47855	ORINS
13	19-47856	ORINS
14	19-47849	ORINS
16	19-47838	ORINS
18	19-47848	ORINS
21	19-47839	ORINS
22	19-47857	ORINS
23	19-47847	ORINS
24	19-47846	ORINS
25	19-47840	ORINS
27	19-47858	ORINS
28	19-47845	ORINS
29	19-47859	ORINS
30	19-47844	ORINS
32	19-47843	ORINS
33	19-47154	ORINS
34	19-47842	ORINS
37	19-47841	ORINS
38	19-47836	ORINS
40	19-47835	ORINS
41	19-47834	ORINS
42	19-47832	ORINS
CONF-650936–	**(1st International Symposium on Basic Problems in Thin Film Physics, Clausthal-Gottingen, Germany, Sept. 6–11, 1965)**	
2	19-47503	See BNL-9478
CONF-650937–	**(Conference on Megagauss Magnetic Field Generation by Explosives and Related Experiments, Frascati, Italy, Sept. 21–23, 1965)**	
1	19-47120	See UCRL-14349
CONF-650940–	**(Genetics Society of America, Mendel Centennial Conference, Fort Collins, Sept. 7–11, 1965)**	
1	19-45726	See BNL-9488
CONF-650942–	**(2nd Western Europe Conference on Photosynthesis, Zeist, Netherlands, Sept. 1965)**	
1	19-45727	See BNL-9506
CONF-650945–	**(International Conference on Elementary Particles, Oxford, Sept. 19–25, 1965)**	
1	19-47300	See BNL-9520
CONF-651001–	**(IEEE Nuclear Science Symposium, San Francisco, Oct. 1965)**	
2	19-46754	See BNL-9535
CONF-651004–	**(9th Conference on Analytical Chemistry in Nuclear Technology, Gatlinburg, Tenn., Oct. 12, 1965)**	
4	19-46510	See Y-DA-967
CONF-651011–	**(IMOG and Metrology Subgroup Meeting, Las Vegas, Nev., Oct. 11, 1965)**	
1	19-48093	See RFP-654
CONF-651101–	**(American Nuclear Society, Winter Meeting, Washington, D. C., Nov. 15–18, 1965) (Revised 11–8–65)**	
10	19-46644	See ORNL-P-1528
11	19-46721	See ORNL-P-1531
14	19-46711	See BNWL-SA-161
21	19-47975	See BNL-9450
22	19-46509	See UCRL-12497-T
23	19-46900	See RL-SA-46-A
25	19-47159	See BNL-9388
26	19-46506	Dep. mn; CFSTI $2.00 cy, $0.50 mn
27	19-48055	See BNL-9402
28	19-46950	See LA-DC-7315
29	19-47547	See LA-DC-7320
31	19-46712	See BNWL-SA-169
32	19-47953	See BNL-9393
33	19-46174	See LA-DC-7319
CONF-651102–	**(Royal Commonwealth Society, 3rd International Conference on Plutonium, London, Nov. 22–26, 1965)**	
7	19-46999	See LA-DC-7297
9	19-47880	See LA-DC-7353
CONF-651103–	**(IAEA Symposium on Criticality Control of Fissile Materials, Stockholm, Nov. 1–5, 1965)**	
3	19-46967	See Y-KB-62
6	19-47955	Dep. mn; CFSTI $1.00 cy, $0.50 mn
9	19-46433	See RL-SA-43
CONF-651105–	**(Conference on Nuclear Electronics, Bombay, India, Nov. 22–26, 1965)**	
2	19-48056	See BNL-9510
CONF-651108–	**(Symposium on Isotope Techniques, Urbana, Ill., Nov. 10–12, 1965)**	
1	19-46642	See IDO-12043
CONF-651110–	**(American Society of Mechanical Engineers, Annual Winter Meeting, Chicago, Nov. 7–11, 1965)**	
1	19-47925	See GA-6505
COO–		
7-0361	19-47570	Dep. mn; CFSTI $1.00 cy, $0.50 mn
35-78	19-47871	Phys. Rev., 140: A490-8(1965)
881-44	19-47351	Nuovo Cimento (10), 36: 1055-8(1965)
1001-3	19-46277	J. Inorg. Nucl. Chem., 27: 2119-21(1965)
1140-123	19-46234	Dep. mn; CFSTI $1.00 cy, $0.50 mn
1148-97	19-46301	Dep. mn; CFSTI $1.00 cy, $0.50 mn
1149-52	19-46994	Dep. mn; CFSTI $1.00 cy, $0.50 mn
1149-53	19-48090	Dep. mn; CFSTI $4.00 cy, $0.75 mn
1170-7	19-45756	Dep. mn; CFSTI $3.00 cy, $0.75 mn
1261-8	19-47370	Phys. Rev., 140: B463-5(1965)
1261-10	19-47344	Nuovo Cimento (10), 36: 965-7(1965)
1367-4	19-47095	Appl. Phys. Letters, 7: 190-2(1965)
CU–	**(Misc.)**	
235	19-47582	See NEVIS-129
1932-246	19-47302	Dep. mn; CFSTI $2.00 cy, $0.50 mn Phys. Rev., 140: B1328-34(1965)
DASA–	**(Misc.)**	
1540	19-47446	See AD-612013
1597	19-47449	See AD-613199
DESY–	**(German)**	
65/7	19-47303	Dep. mn
DP–		
974	19-46893	Dep. mn; CFSTI $1.00 cy, $0.50 mn
975	19-46917	Dep. mn; CFSTI $2.00 cy, $0.50 mn
977	19-46327	Dep. mn; CFSTI $1.00 cy, $0.50 mn
980	19-46166	Dep. mn; CFSTI $1.00 cy, $0.50 mn
DPSPU–		
62-30-3A	19-48076	Dep. mn; CFSTI $1.00 cy, $0.50 mn
64-30-28	19-46423	Dep. mn; CFSTI $2.00 cy, $0.50 mn
DUBNA REPORTS	**(Russian)**	
See JINR (Russian)		
EGG–		
1183-1017	19-46759	Dep. mn; CFSTI $2.00 cy, $0.50 mn
EUR–	**(European Atomic Energy Community)**	
1898.e	19-46167	Dep. mn
2227.e	19-46328	Dep. mn
2374	19-47081	See EURAEC-1432
2424.f	19-46995	Dep. mn
2425.f	19-45755	See CEA-R-2809
2437.e	19-46904	Dep. mn
2449.f	19-46992	See CEA-R-2792
2455.e	19-46329	Dep. mn
2456.e	19-47571	Dep. mn
2473.f	19-46715	Dep. mn
2478.e	19-47080	Dep. mn
2479.e	19-46996	Dep. mn

Report No.	Abstract No.	Availability
EURAEC–		
1432	19-47081	Dep. mn; CFSTI $3.00 cy, $0.75 mn
F–	**(Misc.)**	
B2098	19-46909	See AD-620264
FD–	**(Non-AEC)**	
22	19-46878	See NP-15455
FTD-MT–	**(Non-AEC)**	
63-246	19-46540	See AD-619382
FTD-TT–	**(Non-AEC)**	
65-24	19-46341	CFSTI
65-564	19-46574	See AD-619323
65-579	19-45763	See AD-468388
65-591	19-46248	CFSTI
65-611	19-46943	CFSTI
FZK–	**(Non-AEC)**	
202	19-47077	See AD-613471
GA–	**(Misc.)**	
5296	19-46894	Dep. mn; CFSTI $2.00 cy, $0.50 mn
6103	19-47559	Nukleonik, 7: 408-15(1965)
6126	19-47991	Dep. mn; CFSTI $1.00 cy, $0.50 mn; Gmelin, AED-Conf-65-086-16
6505	19-47925	Dep. mn; CFSTI $2.00 cy, $0.50 mn
6547	19-47572	Dep. mn; CFSTI $1.00 cy, $0.50 mn
GE–	**(Non-AEC)**	
65SD4251	19-48048	
HEPL–	**(Misc.)**	
355	19-47565	See AD-614270
HMI-B–	**(German)**	
44	19-46898	Dep. mn
HRL–	**(Non-AEC)**	
5249-S	19-46571	CFSTI $5.00 cy, $1.00 mn
I–	**(Misc.)**	
A2049-24	19-46462	See TID-22184
IA–	**(Non-AEC)**	
849	19-46168	Dep. mn
IAE–	**(Non-AEC)**	
700	19-47304	Dep. mn
717	19-47573	Dep. mn
723	19-47956	Dep. mn
724	19-47957	Dep. mn
836	19-47574	Dep. mn
IC–	**(Misc.)**	
65/57	19-47305	Dep. mn
IDO–		
12024	19-48077	Dep. mn; CFSTI $4.00 cy, $1.00 mn
12043	19-46642	Dep. mn; CFSTI $2.00 cy, $0.50 mn
14664	19-46169	Dep. mn; CFSTI $1.00 cy, $0.50 mn
16986	19-47575	Dep. mn; CFSTI $5.00 cy, $1.00 mn
17081	19-48059	Dep. mn; CFSTI $4.00 cy, $1.00 mn
17107	19-47577	Dep. mn; CFSTI $3.00 cy, $0.75 mn
IITRI–	**(Misc.)**	
A6034-2(App.I)	19-47655	Nuovo Cimento (10), 36: 1164-72(1965)
B6018-1	19-46918	CFSTI
INSJ–	**(Japanese)**	
86	19-47268	Dep. mn
87	19-46717	Dep. mn
IS–		
978	19-47062	J. Less-Common Metals, 9: 390-1(1965)
1000	19-47359	Nuovo Cimento (10), 36: 1303-15(1965)
1118	19-46273	J. Inorg. Nucl. Chem., 27: 1955-60(1965)
1131	19-47053	J. Less-Common Metals, 9: 281-8(1965)
IS-T–		
24	19-46424	Dep. mn; CFSTI $3.00 cy, $0.75 mn
28	19-47578	Dep. mn; CFSTI $4.00 cy, $1.00 mn
IS-Trans–		
18	19-47884	Dep. mn; CFSTI $1.00 cy, $0.50 mn; JCL $1.10 fs, $0.80 mf
JEN–	**(Spanish)**	
148-DQ/I-49	19-46170	Dep. mn
JINR–	**(Russian)**	
E-2343	19-47306	Dep. mn
P-2275	19-47579	Dep. mn
P-2278	19-47307	Dep. mn
P-2282	19-46997	Dep. mn
P-2284	19-47308	Dep. mn
P-2289	19-47309	Dep. mn
P-2313	19-47164	Dep. mn
JPL-TR–	**(Non-AEC)**	
32-650(Pt.2)	19-47504	
JPRS–	**(Non-AEC)**	
24372	19-47885	See N64-21857
27544	19-45764	CFSTI $1.00 cy, $0.50 mn
30979	19-46651	CFSTI $4.00 cy, $1.00 mn
31032	19-47122	CFSTI $3.00
31225	19-47021	CFSTI $1.00 cy, $0.50 mn
31469	19-46590	CFSTI $1.00 cy, $0.50 mn
31547	19-45731	CFSTI $1.00 cy, $0.50 mn
31602	19-45732	CFSTI $7.00 cy, $1.75 mn
31667	19-46039	CFSTI $1.00 cy, $0.50 mn
31822	19-45822	CFSTI $4.00 cy, $1.00 mn
31842	19-46652	CFSTI $4.00 cy, $0.75 mn
31843	19-46653	CFSTI $5.00 cy, $1.25 mn
31933	19-45733	CFSTI $1.00 cy, $0.50 mn
31993	19-46654	CFSTI $1.00 cy, $0.50 mn
JøL–	**(German)**	
261-DE	19-48078	Dep. mn
K-L–		
2012	19-46425	Dep. mn; CFSTI $1.00 cy, $0.50 mn
KAPL-M–		
6460	19-47866	Dep. mn; CFSTI $2.00 cy, $0.50 mn
6467	19-47544	Dep. mn; CFSTI $1.00 cy, $0.50 mn
6492	19-46171	Dep. mn; CFSTI $1.00 cy, $0.50 mn
6493	19-46555	Dep. mn; CFSTI $1.00 cy, $0.50 mn
KEA–	**(German)**	
311	19-47992	Dep. mn
KFK–	**(German)**	
297	19-47545	Dep. mn
298	19-47546	Dep. mn
KR–	**(Norwegian)**	
95	19-46172	Dep. mn
96	19-46986	Dep. mn
LA–		
3301	19-48049	Dep. mn; CFSTI $4.00 cy, $0.75 mn
3331	19-46998	Dep. mn; CFSTI $1.00 cy, $0.50 mn
3335	19-47877	Dep. mn; CFSTI $3.00 cy, $0.50 mn
3347	19-47720	Dep. mn; CFSTI $1.00 cy, $0.50 mn
3352	19-47580	Dep. mn; CFSTI $2.00 cy, $0.50 mn
3357	19-46173	Dep. mn; CFSTI $2.00 cy, $0.50 mn
3379	19-47878	Dep. mn; CFSTI $1.00 cy, $0.50 mn
3385	19-47721	Dep. mn; CFSTI $1.00 cy, $0.50 mn
LA-DC–		
6730	19-47581	Dep. mn; CFSTI $3.00 cy, $0.50 mn
6952	19-45969	Proc. Soc. Expt. Biol. Med., 119: 922-5 (1965)
7015	19-46718	Dep. mn; CFSTI $1.00 cy, $0.50 mn
7030	19-46719	Dep. mn; CFSTI $1.00 cy, $0.50 mn
7034	19-47505	Ann. Phys. (N. Y.), 34: 276-90(1965)
7039	19-47722	Dep. mn; CFSTI $1.00 cy, $0.50 mn

Report No.	Abstract No.	Availability
7112	19-47723	Dep. mn; CFSTI $2.00 cy, $0.50 mn
7277	19-47879	Dep. mn; CFSTI $1.00 cy, $0.50 mn
7297	19-46999	Dep. mn; CFSTI $1.00 cy, $0.50 mn
7315	19-46950	Dep. mn; CFSTI $1.00 cy, $0.50 mn
7319	19-46174	Dep. mn; CFSTI $1.00 cy, $0.50 mn
7320	19-47547	Dep. mn; CFSTI $1.00 cy, $0.50 mn
7352	19-47522	Phys. Rev. Letters, 15: 546-9(1965)
7353	19-47880	Dep. mn; CFSTI $2.00 cy, $0.50 mn
7365	19-47450	Dep. mn; CFSTI $2.00 cy, $0.50 mn
7373	19-46533	Dep. mn; CFSTI $2.00 cy, $0.50 mn
LA-tr-		
65-15	19-46249	Dep. mn; JCL $1.00 fs, $0.80 mf
65-20	19-47023	Dep. mn; CFSTI $1.00 cy, $0.50 mn; JCL $1.10 fs, $0.80 mf
65-21	19-46729	Dep. mn; CFSTI $1.00 cy, $0.50 mn; JCL $1.60 fs, $0.80 mf
LAL-	**(French)**	
1136	19-46643	Dep. mn
LMSD-	**(Non-AEC)**	
8-19-62-12	19-46871	See AD-614268
MATT-		
267	19-47724	Dep. mn; CFSTI $1.00 cy, $0.50 mn
294	19-47767	Nucl. Fusion, 5: 242-8(1965)
313	19-47750	J. Nuclear Energy Pt. C, 7: 399-417(1965)
MIT-	**(Misc.)**	
905-33	19-47663	Phys. Rev., 140: B268-76(1965)
ML-TDR-	**(Non-AEC)**	
64-280(Suppl.2)	19-47013	See PB-171809(Rev.)(Suppl.2)
MLM-		
1229]	19-47626	See TID-20867
1254	19-46157	Dep. mn; CFSTI $2.00 cy, $0.50 mn
1264	19-46175	Dep. mn; CFSTI $1.00 cy, $0.50 mn
1271	19-46302	Dep. mn; CFSTI $2.00 cy, $0.50 mn
N-	**(Misc.)**	
64-21857	19-47885	CFSTI $0.75 cy, $0.50 mn
64-26802	19-46235	
64-31082	19-47189	CFSTI $0.75 cy, $0.50 mn
64-32322	19-46873	
65-29716	19-46571	See HRL-5249-S
65-31176	19-46966	See WANL-PR-(P)-007
NAA-SR-		
9908	19-48050	Dep. mn; CFSTI $1.75 cy, $0.75 mn
10751	19-47993	Dep. mn; CFSTI $3.00 cy, $0.75 mn
NASA-CR-	**(Misc.)**	
304	19-47082	
54182	19-46571	See HRL-5249-S
54397	19-48048	See GE-65SD4251
54434	19-46966	See WANL-PR(P)-007
NASA-TM-	**(Misc.)**	
D-3006	19-46575	CFSTI $2.00
D-3041	19-46572	CFSTI $2.00 cy, $0.50 mn
NASA-TT-	**(Non-AEC)**	
F-204	19-47452	CFSTI $4.00
F-227	19-47189	For translation see N64-31082
F-248	19-47190	CFSTI $1.00 cy, $0.50 mn
F-250	19-47191	CFSTI $1.00 cy, $0.50 mn
F-354	19-45824	CFSTI $5.00 cy, $1.00 mn
NEVIS-	**(Misc.)**	
129	19-47582	
140	19-47302	See CU-1932-246
NIJS-R-	**(Yugoslavian)**	
430	19-46236	Dep. mn
NIRL-R-	**(British)**	
99	19-47165	Dep. mn; BIS $0.60; HMSO 3s.
NLCO-tr-		
6	19-47024	Dep. mn; JCL $1.10 fs, $0.80 mf
NMI-	**(Misc.)**	
4996	19-46919	Dep. mn; CFSTI $5.00 cy, $1.00 mn
4997	19-46921	Dep. mn; CFSTI $6.00 cy, $1.25 mn
4998	19-46926	Dep. mn; CFSTI $4.00 cy, $0.75 mn
4999	19-46930	Dep. mn; CFSTI $5.00 cy, $1.00 mn
5025(Pt.I)	19-46936	Dep. mn; CFSTI $2.25 cy, $1.25 mn
NP-	**(AEC File No. for Non-AEC Reports)**	
15175	19-47220	
15355	19-47725	Dep. mn
15361	19-46586	Bureau of Mines and Technical Surveys, Ottawa, $1.25
15362	19-46426	Dep. mn
15364	19-46178	Dep. mn
15370	19-46330	Dep. mn
15371	19-48079	Dep. mn
15376	19-47310	Dep. mn
15384	19-47867	Dep. mn
15393	19-47994	Dep.
15394	19-47726	Dep. mn
15396	19-46567	
15409	19-46303	
15418	19-48091	Dep. mn
15429	19-47008	
15431	19-46955	
15434	19-47727	
15437	19-46534	$5.00 cy, $1.00 mn CFSTI
15444	19-46940	
15454	19-47311	Dep. mn
15455	19-46878	
15459	19-46557	
15460	19-47312	Dep. mn
15462	19-46760	Dep. mn
15467	19-47583	Dep. mn
15473	19-47995	Dep. mn
15474	19-47996	Dep. mn
15477	19-48092	Dep. mn
15478	19-47997	Dep. mn
15486	19-47411	Dep. mn
15514(Vol.1)	19-46956	
15514(Vol.2)	19-47009	
15514(Vol.3)	19-46941	
NP-tr-	**(AEC File No. for Non-AEC Translations)**	
1275	19-46182	Dep. mn; JCL $1.60 fs, $0.80 mf
1282	19-47317	Dep. mn; CFSTI $1.00 cy, $0.50 mn; JCL $1.10 fs, $0.80 mf
1289	19-46183	Dep. mn; JCL $1.60 fs, $0.80 mf
NPCC-RKWP-	**(British)**	
P.435	19-47999	See TRG-Report-227
NSF-	**(Misc.)**	
7	19-46873	See N64-32322
NSJ-tr-	**(Japanese)**	
32	19-45825	Dep. mn; JCL $1.60 fs, $0.80 mf
30	19-46464	Dep. mn; JCL $2.60 fs, $1.07 mf
NUMEC-		
3524-6	19-46942	Dep. mn; CFSTI $1.00 cy, $0.50 mn
NYO-		
1163-43	19-46467	Dep. mn; CFSTI $2.00 cy, $0.50 mn
NYO-		
901-36	19-45808	Dep. mn; CFSTI $3.00 cy, $0.75 mn
910-23	19-45728	Dep. mn; CFSTI $5.00 cy, $1.00 mn
1858-1	19-46331	Dep. mn; CFSTI $1.00 cy, $0.50 mn
1979-12	19-45809	Dep. mn; CFSTI $1.00 cy, $0.50 mn
2403-8	19-47221	Dep. mn; CFSTI $1.00 cy, $0.50 mn
2598-24	19-45758	Dep. mn; CFSTI $3.00 cy, $0.75 mn
2979-34	19-46761	Dep. mn; CFSTI $3.00 cy, $0.50 mn
3394-2(Rev.)	19-45810	Dep. mn; CFSTI $5.00 cy, $1.00 mn
3406-2	19-46720	Dep. mn; CFSTI $2.00 cy, $0.50 mn
3429-4	19-47282	Dep. mn; CFSTI $4.00 cy, $0.75 mn
3446-3	19-46587	Dep. mn; CFSTI $1.00 cy, $0.50 mn

Report No.	Abstract No.	Availability
3474-1	19-46762	Dep. mn; CFSTI $1.00 cy, $0.50 mn
ORNL–		
2873	19-48080	Dep. mn; CFSTI $4.00 cy, $0.75 mn
3752	19-45730	Dep. mn; CFSTI $3.00 cy, $0.75 mn
3754	19-46427	Dep. mn; CFSTI $2.00 cy, $0.50 mn
3832	19-46159	Dep. mn; CFSTI $5.00 cy, $1.00 mn
3847	19-46428	Dep. mn; CFSTI $3.00 cy, $0.75 mn
3848	19-48061	Dep. mn; CFSTI $3.00 cy, $0.75 mn
3851	19-47585	Dep. mn; CFSTI $2.00 cy, $0.50 mn
3857	19-46588	Dep. mn; CFSTI $1.00 cy, $0.50 mn
3862	19-47011	Dep. mn; CFSTI $2.00 cy, $0.50 mn
ORNL-P–	**(Misc.)**	
158	19-46192	Anal. Chim. Acta, 33: 443-8(1965)
416	19-47685	Rev. Mod. Phys., 37: 679-708(1965)
585	19-47881	Dep. mn; CFSTI $1.00 cy, $0.50 mn
737	19-46681	Soil Sci. Soc. Am. Proc., 29: 383-7(1965)
1078	19-45910	J. Natl. Cancer Inst., 35: 227-34(1965)
1115	19-46217	Talanta, 12: 893-901(1965)
1189	19-46270	J. Electrochem. Soc., 112: 1032-40(1965)
1192	19-46281	J. Phys. Chem., 69: 3148-55(1965)
1296	19-47670	Phys. Rev., 140: B330-6(1965)
1300	19-47891	Phys. Rev., 140: A539-46(1965)
1315	19-47667	Phys. Rev., 140: B296-304(1965)
1402	19-47635	Nucl. Phys., 73: 529-38(1965)
1522	19-46429	Dep. mn; CFSTI $1.00 cy, $0.50 mn
1528	19-46644	Dep. mn; CFSTI $1.00 cy, $0.50 mn
1531	19-46721	Dep. mn; CFSTI $1.00 cy, $0.50 mn
1601	19-46430	Dep. mn; CFSTI $2.00 cy, $0.50 mn
1602	19-46431	Dep. mn; CFSTI $2.00 cy, $0.50 mn
1603	19-46432	Dep. mn; CFSTI $1.00 cy, $0.50 mn
1605	19-47166	Dep. mn; CFSTI $1.00 cy, $0.50 mn
1619	19-47167	Dep. mn; CFSTI $1.00 cy, $0.50 mn
ORNL-TM–		
1218	19-47586	Dep. mn; CFSTI $3.00 cy, $0.75 mn
1223	19-46568	Dep. mn; CFSTI $4.00 cy, $1.00 mn
1226	19-47012	Dep. mn; CFSTI $2.00 cy, $0.50 mn
1228	19-46645	Dep. mn; CFSTI $1.00 cy, $0.50 mn
1253	19-46238	Dep. mn; CFSTI $1.00 cy, $0.50 mn
1279	19-45747	Dep. mn; CFSTI $1.00 cy, $0.50 mn
ORNL-tr–		
623	19-46250	Dep. mn; JCL $1.10 fs, $0.80 mf
637	19-47025	Dep. mn; JCL $6.60 fs, $2.15 mf
642	19-46591	Dep. mn; CFSTI $1.00 cy, $0.50 mn; JCL $1.10 fs, $0.80 mf
668	19-47094	Dep. mn; JCL $9.10 fs, $3.50 mf
673	19-46251	Dep. mn; JCL $1.10 fs, $0.80 mf
679	19-47222	Dep. mn; JCL $3.60 fs, $1.13 mf
683	19-46252	Dep. mn; CFSTI $1.00 cy, $0.50 mn; JCL $1.60 fs, $0.80 mf
694	19-47960	Dep. mn; JCL $1.60 fs, $0.80 mf
701	19-46592	Dep. mn; JCL $1.60 fs, $0.80 mf
707	19-47599	Dep. mn; JCL $1.10 fs, $0.80 mf
710	19-47869	Dep. mn; JCL $1.60 fs, $0.80 mf
747	19-48002	Dep. mn; JCL $1.60 fs, $0.80 mf
748	19-46558	Dep. mn; JCL $1.10 fs, $0.80 mf
749	19-46559	Dep. mn; JCL $1.60 fs, $0.80 mf
754	19-48108	Dep. mn; CFSTI $1.00 cy, $0.50 mn; JCL $2.60 fs, $0.83 mf
755	19-46593	Dep. mn; JCL $3.60 fs, $1.28 mf
757	19-46625	Dep. mn; JCL $1.60 fs, $0.80 mf
758	19-46616	Dep. mn; JCL $2.60 fs, $0.89 mf
770	19-46408	Dep. mn; CFSTI $1.00 cy, $0.50 mn; JCL $2.60 fs, $0.89 mf
795	19-47026	Dep. mn; JCL $1.60 fs, $0.80 mf
803	19-46253	Dep. mn; JCL $1.10 fs, $0.80 mf
841	19-46184	Dep. mn; JCL $1.10 fs, $0.80 mf
ORO–		
631	19-45811	Dep. mn; CFSTI $5.00 cy, $1.00 mn
OTS–	**(Misc.)**	
64-31167	19-47885	See N64-21857
PATENTS	**(British)**	**(4s. 6d. each, U. K. Patent Office)**
997,190	19-47980	
997,197	19-46516	
1,000,777	19-46517	
1,000,798	19-46406	
1,000,931	19-47981	
1,000,933	19-47982	
1,000,982	19-48074	
1,002,078	19-47983	
1,002,171	19-46518	
1,002,601	19-46519	
1,002,794	19-46974	
1,002,842	19-47297	
1,002,900	19-46975	
1,003,244	19-46520	
1,003,395	19-47972	
1,003,714	19-47930	
1,003,964	19-47860	
1,004,046	19-46521	
PATENTS	**(German)**	
1,192,333	19-47931	
1,192,334	19-47932	
1,194,993	19-47933	
1,196,798	19-46868	
1,196,799	19-46869	
1,198,945	19-47934	
1,198,946	19-47935	
PATENTS	**(U. S.)**	**($0.25 each, U. S. Patent Office)**
3,193,385	19-46976	
3,195,304	19-47936	
3,196,271	19-46749	
3,197,185	19-46522	
3,197,640	19-46004	
3,198,817	19-46299	
3,200,041	19-47937	
3,200,043	19-47938	
3,200,044	19-47939	
3,200,251	19-46622	
3,200,269	19-46897	
3,200,937	19-46523	
3,201,076	19-46524	
3,201,318	19-47924	
3,201,319	19-47940	
3,201,320	19-47973	
3,201,321	19-48045	
3,201,322	19-47985	
3,201,947	19-46525	
3,202,580	19-47941	
3,202,584	19-47974	
3,202,619	19-46977	
3,202,822	19-46892	
3,202,852	19-47861	
3,202,915	19-47155	
3,203,086	19-46978	
3,203,217	19-46979	
3,203,877	19-46944	
3,204,098	19-46623	
3,204,103	19-47156	
3,205,068	19-46455	
3,205,142	19-47942	
3,205,148	19-47943	
3,205,174	19-47986	
3,205,338	19-47862	
3,205,356	19-46624	
PB–	**(Non-AEC)**	
166-166	19-46876	See AD-613325
171809(Rev.) (Suppl.2)	19-47013	CFSTI
PHS–	**(Misc.)**	
999-RH-13	19-46646	Public Health Service Free
999-RH-14	19-46035	Public Health Service Free
POR–	**(Misc.)**	
1814	19-46468	Dep. mn; CFSTI $5.00 cy, $1.00 mn
1815	19-46469	Dep. mn; CFSTI $4.00 cy, $0.75 mn
PR–	**(Non-AEC)**	
9	19-47725	See NP-15355

Report No.	Abstract No.	Availability
PWAC–	**(Misc.)**	
386	19-46535	Dep. mn; CFSTI $7.00 cy, $1.50 mn
462	19-46722	Dep. mn; CFSTI $2.00 cy, $0.50 mn
475	19-47958	Dep. mn; CFSTI $3.00 cy, $0.50 mn
R–	**(Misc.)**	
110	19-46586	See NP-15361
374	19-46465	See AD-613991
387	19-46567	See NP-15396
483	19-47582	See NEVIS-129
512	19-47302	See CU-1932-246
2298	19-46631	See A/AC.82/G/L.986
2302	19-46632	See A/AC.82/G/L.987
65SD8	19-47188	See AD-613636
RADC-TDR–	**(Misc.)**	
64-550	19-47717	See AD-614285
RADC-TR–	**(Non-AEC)**	
64-584	19-47114	See AD-614286
RCN–	**(Dutch)**	
37	19-46763	Dep. mn
RFP–		
562	19-46461	Dep. mn; CFSTI $1.00 cy, $0.50 mn
577	19-45762	Dep. mn; CFSTI $2.00 cy, $0.50 mn
618	19-46179	Dep. mn; CFSTI $1.00 cy, $0.50 mn
641	19-46723	Dep. mn; CFSTI $1.00 cy, $0.50 mn
654	19-48093	Dep. mn; CFSTI $1.00 cy, $0.50 mn
RISO–	**(Danish)**	
99	19-47109	Dep. mn
100	19-47110	Dep. mn
103	19-47882	Dep. mn
104	19-46647	Dep. mn
106	19-47894	Phys. Status Solidi, 11: 567-73(...)
RL-SA–		
43	19-46433	Dep. mn; CFSTI $1.00 cy, $0.50 mn
46-A	19-46900	Dep. mn; CFSTI $1.00 cy, $0.50 mn
RM–	**(Misc.)**	
4495-PR	19-47537	See AD-613468
RRA–	**(Misc.)**	
T52	19-47868	
RT-ING–	**(Italian)**	
(65)1	19-46536	Dep. mn
RT-MET–	**(Italian)**	
(64)4	19-47014	Dep. mn
RT-PROT–	**(Italian)**	
(65)19	19-48081	Dep. mn
SC–	**(Misc.)**	
4522(RR)	19-48062	Dep. mn; CFSTI $5.00 cy, $1.00 mn
SC-DC–		
65-1646	19-48094	Dep. mn; CFSTI $1.00 cy, $0.50 mn
65-1698	19-47117	Dep. mn; CFSTI $2.00 cy, $0.50 mn
SC-DR–		
64-539	19-48095	Dep. mn; CFSTI $1.00 cy, $0.50 mn
65-271	19-48096	Dep. mn; CFSTI $1.00 cy, $0.50 mn
65-338	19-48097	Dep. mn; CFSTI $1.00 cy, $0.50 mn
SC-M–		
65-419	19-47451	Dep. mn; CFSTI $2.00 cy, $0.50 mn
SC-R–		
65-902	19-48098	Dep. mn; CFSTI $1.00 cy, $0.50 mn
SC-RR–		
65-187	19-46537	Dep. mn; CFSTI $3.00 cy, $0.75 mn
65-303	19-46470	Dep. mn; CFSTI $3.00 cy, $0.75 mn
65-344	19-48063	Dep. mn; CFSTI $2.00 cy, $0.50 mn
65-464	19-46648	Dep. mn; CFSTI $1.00 cy, $0.50 mn
SC-T–		
65-749	19-48109	Dep. mn; JCL $1.10 fs, $0.80 mf
65-750	19-48110	JCL $1.10 fs, $0.80 mf
65-760	19-46730	Dep. mn; JCL $1.10 fs, $0.80 mf
SC-TM–		
64-653	19-48099	Dep. mn; CFSTI $3.00 cy, $0.75 mn
65-294	19-48100	Dep. mn; CFSTI $3.00 cy, $0.75 mn
65-332	19-48101	Dep. mn; CFSTI $1.00 cy, $0.50 mn
65-356	19-46724	Dep. mn; CFSTI $1.00 cy, $0.50 mn
SCTM–	**(Misc.)**	
167	19-46566	See AD-425747
169	19-46456	See AD-425760
SGAE-CH–	**(Austrian)**	
20/1965	19-46333	Dep. mn
SLAC-Trans–		
19	19-47124	Dep. mn; JCL $3.60 fs, $1.13 mf
21	19-46731	Dep. mn; JCL $1.10 fs, $0.80 mf
SM–	**(Misc.)**	
70/31	19-47955	See CONF-651103-6
70/44	19-46967	See Y-KB-62
SRO–		
118	19-47998	Dep. mn; CFSTI $1.00 cy, $0.50 mn
STI-PUB–	**(International Atomic Energy Agency)**	
89	19-47802	IAEA $13.00; S 273,-; £3.18.0; F.Fr. 52,-; DM 45.50 cy
94	19-46649	IAEA US $2.00; S 42,-; 12/-std; F.Fr.8,-; DM 6.40
95	19-46689	IAEA $1.00; S 21,- (6/-stg; F.Fr.4,-; DM 3.20)
SZS–	**(German)**	
6(1965)	19-46764	Dep. mn
TDCK–	**(Non-AEC)**	
33500	19-45818	Dep. mn
TID–		
20867	19-47626	J. Inorg. Nucl. Chem., 27: 1881-7(1965)
21477	19-47588	See TID-22012, pp 22-52
21602	19-47639	Nucl. Phys., 73: 579-87(1965)
21638	19-47962	IEEE (Inst. Elec. Electron. Engrs.), Trans. Nucl. Sci., NS-12: No. 4, 323-42(1965)
21746	19-47030	Acta Cryst., 19: 687-9(1965)
21760	19-47060	J. Less-Common Metals, 9: 338-53(1965)
21765	19-45889	J. Am. Assoc., 192: 357-64(1965)
21774	19-46366	J. Phys. Chem., 69: 3218-19(1965)
21905	19-47639	Nucl. Phys., 73: 579-87(1965)
21906	19-47638	Nucl. Phys., 73: 561-78(1965)
21954	19-45837	Am. J. Roentgenol., Radium Therapy Nucl. Med., 95: 479-93(1965)
21957	19-47179	Nucl. Phys., 73: 513-21(1965)
22012	19-47587	Dep.(mn); $7.00(cy), 6(mn) CFSTI
22092	19-46357	J. Am. Chem. Soc., 87: 4211-12(1965)
22116	19-47430	Proc. Natl. Acad. Sci. U. S., 54: 692-6 (1965)
22141	19-47092	Dep. mn; CFSTI $4.00 cy, $0.75 mn
22148	19-46538	Dep. mn; CFSTI $2.00 cy, $0.50 mn
22175	19-48102	Dep. mn; CFSTI $1.00 cy, $0.50 mn
22176	19-45819	Dep. mn; CFSTI $3.00 cy, $0.50 mn
22177	19-47168	Dep. mn; CFSTI $2.00 cy, $0.50 mn
22184	19-46462	Dep. mn; CFSTI $5.00 cy, $1.00 mn
22193	19-45748	Dep. mn; CFSTI $1.00 cy, $0.50 mn
22204	19-48064	Dep. mn; CFSTI $7.00 cy, $1.75 mn
22207	19-46240	Dep. mn; CFSTI $3.00 cy, $0.75 mn
22222	19-47313	Dep. mn; CFSTI $3.00 cy, $0.50 mn
22227	19-45820	Dep. mn; CFSTI $2.00 cy, $0.50 mn
22231	19-46334	Dep. mn; CFSTI $5.00 cy, $1.00 mn
22232	19-46335	Dep. mn; CFSTI $4.00 cy, $0.75 mn
22236	19-46336	Dep. mn; CFSTI $3.00 cy, $0.75 mn
22244	19-46337	Dep. mn; CFSTI $3.00 cy, $0.75 mn
22249	19-46539	Dep. mn; CFSTI $1.00 cy, $0.50 mn

Report No.	Abstract No.	Availability
22256	19-46767	Dep. mn; CFSTI $4.00 cy, $0.75 mn
TIM-	**(Misc.)**	
854	19-47015	Dep. mn; CFSTI $1.00 cy, $0.50 mn
901	19-47016	Dep. mn; CFSTI $1.00 cy, $0.50 mn
TRG-Report-	**(British)**	
227	19-47999	Dep. mn
TT-	**(Canadian)**	
64-11407/3	19-45734	CFSTI $4.00 cy, $1.00 mn
64-51793	19-45764	See JPRS-27544
65-31530	19-47122	See JPRS-31032
65-31722	19-47021	See JPRS-31225
65-31965	19-46590	See JPRS-31469
65-32043	19-45731	See JPRS-31547
65-32097	19-45732	See JPRS-31602
65-32162	19-46039	See JPRS-31667
65-32317	19-45822	See JPRS-31822
65-32337	19-46652	See JPRS-31842
65-32338	19-46653	See JPRS-31843
65-32427	19-45733	See JPRS-31933
65-32487	19-46654	See JPRS-31993
UCLA-		
12-542	19-45802	Soil Sci., 100: 210-17(1965)
UCRL-		
11218(Pt.II)	19-46726	Dep. mn; CFSTI $4.00 cy, $0.75 mn
11328	19-47648	Nucl. Phys., 73: 681-94(1965)
12018-T	19-47118	Dep. mn; CFSTI $2.00 cy, $0.50 mn
12246	19-46258	Acta Cryst., 19: 668-73(1965)
12277	19-47059	J. Less-Common Metals, 9: 321-37(1965)
12367	19-46338	Dep. mn; CFSTI $3.00 cy, $0.75 mn
12393-T	19-46573	Dep. mn; CFSTI $1.00 cy, $0.50 mn
12493	19-47239	Phys. Rev., 140: A432-6(1965)
12497-T	19-46509	Dep. mn; CFSTI $1.00 cy, $0.50 mn
14123	19-46471	Dep. mn; CFSTI $2.00 cy, $0.50 mn
14175	19-47775	Phys. Rev., 140: A466-70(1965)
14201	19-46472	Dep. mn; CFSTI $3.00 cy, $0.50 mn
14244	19-47119	Dep. mn; CFSTI $1.00 cy, $0.50 mn
14249	19-46473	Dep. mn; CFSTI $2.00 cy, $0.50 mn
14253	19-46768	Dep. mn; CFSTI $1.00 cy, $0.50 mn
14292	19-46581	Dep. mn; CFSTI $1.00 cy, $0.50 mn
14316	19-47017	Dep. mn; CFSTI $2.00 cy, $0.50 mn
14332	19-46589	Dep. mn; CFSTI $1.00 cy, $0.50 mn
14349	19-47120	Dep. mn; CFSTI $2.00 cy, $0.50 mn
16069	19-47662	Phys. Rev., 140: B264-7(1965)
16080	19-47121	Dep. mn; CFSTI $1.00 cy, $0.50 mn
16086	19-47664	Phys. Rev., 140: B277-82(1965)
16119	19-47069	Phys. Rev., 140: A648-50(1965)
16187	19-47597	Dep. mn; CFSTI $6.00 cy, $1.25 mn
16197	19-46727	Dep. mn; CFSTI $3.00 cy, $0.50 mn
16198	19-45968	Proc. Natl. Acad. Sci. U. S., 54: 736-41 (1965)
16204	19-47169	Dep. mn; CFSTI $1.00 cy, $0.50 mn
16254	19-46180	Dep. mn; CFSTI $2.00 cy, $0.50 mn
16260	19-48103	Dep. mn; CFSTI $1.00 cy, $0.50 mn
16278	19-48104	Dep. mn; CFSTI $6.00 cy, $1.25 mn
16279	19-47883	Dep. mn; CFSTI $4.00 cy, $0.75 mn
16290	19-48105	Dep. mn; CFSTI $4.00 cy, $1.00 mn
16297	19-47372	Phys. Rev. Letters, 15: 556-60(1965)
16325	19-46769	Dep. mn; CFSTI $3.00 cy, $0.75 mn
16336	19-46728	Dep. mn; CFSTI $1.00 cy, $0.50 mn
16349	19-46247	Dep. mn; CFSTI $4.00 cy, $1.00 mn
16354	19-46770	Dep. mn; CFSTI $1.00 cy, $0.50 mn
16358	19-46339	Dep. mn; CFSTI $2.00 cy, $0.50 mn
16383	19-46965	Dep. mn; CFSTI $1.00 cy, $0.50 mn
16384	19-47170	Dep. mn; CFSTI $1.00 cy, $0.50 mn
UCRL-Trans-		
1229(L)	19-47111	Dep. mn; JCL $2.60 fs, $0.89 mf
UJV-	**(Czechoslovakian)**	
1296/65	19-48082	Dep. mn
1354/65	19-47551	Dep. mn
URS-	**(Non-AEC)**	
641-6	19-46638	See AD-613359
USNRDL-TR-	**(Misc.)**	
876	19-47598	Dep. mn; CFSTI $3.00 cy, $0.75 mn
887	19-45806	See AD-621543
890	19-47018	
VDDIT-	**(Swedish)**	
16(5.2)	19-47093	Dep. mn
WANL-PR-	**(Misc.)**	
(P)-007	19-46966	CFSTI $3.00 cy, $0.50 mn
WAPD-T-		
1769	19-46181	Dep. mn; CFSTI $1.00 cy, $0.50 mn
WAPD-TM-	**(Misc.)**	
469	19-46463	Dep. mn; CFSTI $1.00 cy, $0.50 mn
WCAP-	**(Misc.)**	
1859(Rev.)	19-46650	
3269-52	19-47959	Dep. mn; CFSTI $3.00 cy, $0.50 mn
3738	19-48000	Dep. mn; CFSTI $4.00 cy, $1.00 mn
3743	19-48001	Dep. mn; CFSTI $6.00 cy, $1.50 mn
WL-TDR-	**(Non-AEC)**	
64-1(Suppl.1)	19-46870	See AD-612191
64-8	19-46580	See AD-613287
64-94	19-46476	See AD-613959
WL-TR-	**(Non-AEC)**	
64-136	19-47863	See AD-613480
64-148	19-46322	See AD-612070
64-152	19-47077	See AD-613471
65-26(Vol.1)	19-46457	See AD-613674
WT-	**(Misc.)**	
1814	19-46468	See POR-1814
1815	19-46469	See POR-1815
Y-		
1488	19-48106	Dep. mn; CFSTI $4.00 cy, $0.75 mn
Y-DA-		
967	19-46510	Dep. mn; CFSTI $1.00 cy, $0.50 mn
Y-KB-		
62	19-46967	Dep. mn; CFSTI $1.00 cy, $0.50 mn

UNITED STATES ATOMIC ENERGY COMMISSION

NUCLEAR SCIENCE ABSTRACTS

Volume 19

Numbers 19-24

Abstracts 35877-48118

October–December

1965

Division of Technical Information

STAFF OF NUCLEAR SCIENCE ABSTRACTS

MANAGING EDITOR

John W. Norris

ASSISTANT MANAGING EDITOR

Donald D. Davis

ASSOCIATE EDITORS

Lawrence T. Whitehead
David E. Bost
Robert C. Kelly
Lee M. Thompson

SUBJECT INDEX EDITOR

Everett J. Hoffman

EVALUATORS

William D. Matheny
John H. Mitchell
Mary H. Newman

ABSTRACTORS

F. S. Armstrong (AECL)
Jane G. Buchanan
D. Lamar Cason
Helen G. Donald
James R. Dulaney
Wells L. Green
Bernard O. Griggs
Mary Catherine Grissom
Fernando J. Hamilton
Phyllis C. Hansen
Thomas F. Heagerty
Carolyn D. Houston
Rose V. Jermain
Betty L. McDowell
Jean F. Peckham
Mona H. Raridon
Julia Redford
Lila B. Smith
Charles E. Stuber
Martha J. Thomas
Anne G. Ward
David C. West
Milton O. Whitson

SUBJECT HEADING SPECIALIST

Robert E. Upchurch

CORPORATE AUTHOR SPECIALIST

Clara L. Fox

DESCRIPTIVE CATALOGING SPECIALIST

J. Paul Meredith

SCHEDULING AND PUBLISHING COORDINATOR

Brainard L. Patton

Communication concerning the editorial policy and content of *NSA* should be addressed to the Managing Editor, *Nuclear Science Abstracts*, AEC Division of Technical Information Extension, P. O. Box 62, Oak Ridge, Tennessee 37831.

Use of funds for printing this publication approved by the Director of the Bureau of the Budget, May 20, 1963

DEPOSITORIES OF USAEC REPORTS

In Countries Other than the U.S.

ARGENTINA
Buenos Aires, Comisión Nacional de Energía Atómica
AUSTRALIA
Canberra, Australian National Library
Sutherland, New South Wales, Australian Atomic Energy Commission
AUSTRIA
Vienna, Zentral Bibliothek der Physikalischen Institute der Universität
BELGIUM
Mol-Donk, Centre d'Etude de l'Energie Nucleaire
BOLIVIA
La Paz, Comisión Nacional de Energia Nuclear
BRAZIL
Rio de Janeiro, Instituto Brasileiro de Bibliografia e Documentacao
São Paulo, Instituto de Energia Atomica, Cidade Universitaria São Paulo
BURMA
Rangoon, Union of Burma Applied Research Institute, Atomic Energy Center Library
CANADA
Hamilton, McMaster University
Ottawa, National Research Council Library
Vancouver, University of British Columbia
CHILE
Santiago, Instituto de Fisica y Matematicas, Universidad de Chile
CHINA
Hsinchu, Taiwan, Free China, National Tsing Hua University
COLOMBIA
Bogota, Instituto De Asuntos Nucleares
COSTA RICA
San Pedro, University of Costa Rica Library
DENMARK
Risö, Danish Atomic Energy Commission
ECUADOR
Quito, Escuela Politécnica Nacional
EL SALVADOR
San Salvador, Universidad de El Salvador, Biblioteca de Energia Nuclear
FINLAND
Helsinki, Teknillisen Korkeakoulun Kirjasto
FRANCE
Gif-sur-Yvette, Centre d'Etudes Nucléaires de Saclay
Paris, Académie des Sciences
GERMANY
Berlin, Hahn-Meitner-Institut für Kernforschung Berlin
Frankfurt/Main, Gmelin-Institut
Munich, Technische Hochschule, Bibliothek
GHANA
Accra, University College of Ghana
GREECE
Athens, Nuclear Research Center "Democritus"
GUATEMALA
Guatemala, Comisión Nacional de Energía Nuclear
INDIA
Bombay, Department of Atomic Energy
INDONESIA
Djogjakarta, Java, Science Faculty, Gadjah Mada University
IRAN
Tehran, Tehran University Nuclear Centre
IRAQ
Baghdad, Iraqi Atomic Energy Commission
IRELAND
Dublin, University College
ISRAEL
Rehovoth, Israel Atomic Energy Commission
ITALY
Rome, Centro di Studi Nucleari della Casaccia
Rome, Comitato Nazionale per l'Energia Nucleare
JAPAN
Tokyo, National Diet Library
KOREA
Seoul, Office of Atomic Energy
LEBANON
Beirut, Lebanese National Council for Scientific Research
LUXEMBOURG
Luxembourg, Ministry of Transport and Electricity
MALAYSIA
Kuala Lumpur, University of Malaysia
MEXICO
Mexico, D.F., Comisión Nacional de Energía Nuclear
NETHERLANDS
The Hague, Reactor Centrum Nederland
NEW ZEALAND
Lower Hutt, Institute of Nuclear Sciences
NIGERIA
Ibadan, University of Ibadan
NORWAY
Lillestrom, Institutt för Atomenergi
PAKISTAN
Lahore, West Pakistan, Atomic Energy Centre
PERU
Lima, Junta de Control de Energia Atomica
PHILIPPINE REPUBLIC
Manila, Philippine Atomic Energy Commission
POLAND
Warsaw, Biura Pelnomocnika Rzadu do Spraw Wykorzystania Energii Jadrowej
PORTUGAL
Sacavem, Junta de Energía Nuclear
REPUBLIC OF SOUTH AFRICA
Pretoria, Atomic Energy Board Library
REPUBLIC OF THE CONGO
Leopoldville, Université Lovanium
SPAIN
Madrid, Junta de Energía Nuclear, Biblioteca Documentación y Publicaciones, Ciudad Universitaria
SWEDEN
Nyköping, Aktiebolaget Atomenergi
SWITZERLAND
Zürich, Eidgenössische Technische Hochschule, Bibliothek
THAILAND
Bangkok, Office of the Thai Atomic Energy Commission, Department of Science
TURKEY
Ankara, Turkish Atomic Energy Commission, Atomic Energy Library
UNITED ARAB REPUBLIC
Cairo, Atomic Energy Commission
UNITED KINGDOM
Belfast, City Library
Birmingham, Central Library
Boston Spa, National Lending Library for Science and Technology
Bristol, Central Library
Glasgow, Mitchell Library
Kingston upon Hull, Central Library
Leeds, Central Library
Liverpool, Central Library
London, Central Library, Acton
London, Science Museum Library, South Kensington
Manchester, Central Library
Newcastle upon Tyne, Central Library
Nottingham, Central Library
Sheffield, Central Library
URUGUAY
Montevideo, Comision Nacional de Energia Atomica
VENEZUELA
Caracas, Instituto Venezolano de Investigaciones Científicas
VIET-NAM
Saigon, Atomic Energy Office
YUGOSLAVIA
Belgrade, Federal Commission for Nuclear Energy

In International Agencies

AUSTRIA
Vienna, International Atomic Energy Agency
BELGIUM
Brussels, La Bibliotheque EURATOM
FRANCE
Paris, European Nuclear Energy Agency, O.E.C.D.
ITALY
Ispra, EURATOM Research Center
SWITZERLAND
Geneva, United Nations Library

UNITED STATES
GOVERNMENT PRINTING OFFICE
DIVISION OF PUBLIC DOCUMENTS
WASHINGTON, D.C. 20402

OFFICIAL BUSINESS

POSTAGE AND FEES PAID
U.S. GOVERNMENT PRINTING OFFICE

MIAMI UNIVERSITY LIBRARY